AUTOANTIBODIES

EDITED BY: Rikard Holmdahl, Falk Nimmerjahn and Ralf J. Ludwig
PUBLISHED IN: Frontiers in Immunology and Frontiers in Medicine

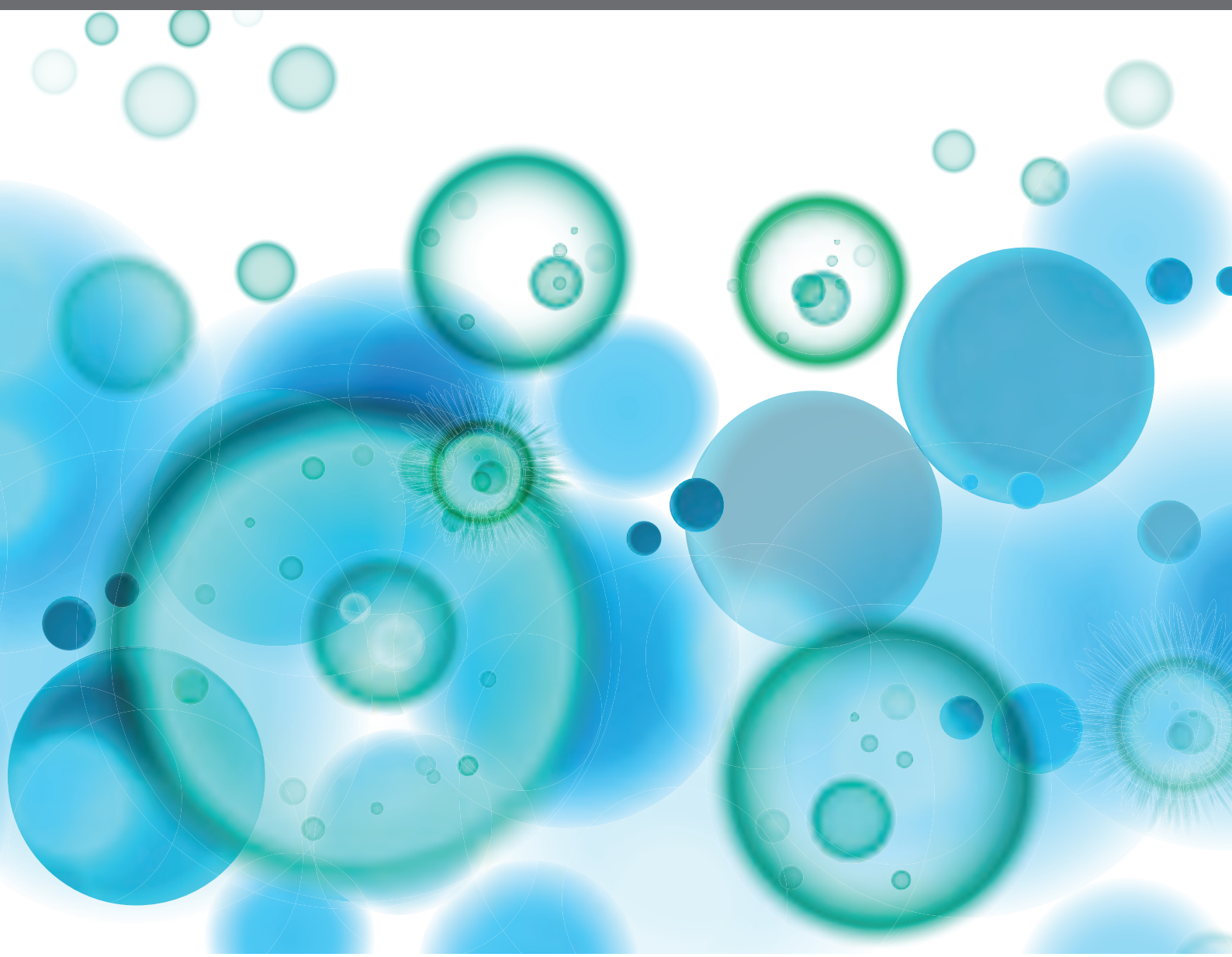

frontiers Research Topics

ISSN 1664-8714
ISBN 978-2-88945-874-5
DOI 10.3389/978-2-88945-874-5

About Frontiers

Frontiers is more than just an open-access publisher of scholarly articles: it is a pioneering approach to the world of academia, radically improving the way scholarly research is managed. The grand vision of Frontiers is a world where all people have an equal opportunity to seek, share and generate knowledge. Frontiers provides immediate and permanent online open access to all its publications, but this alone is not enough to realize our grand goals.

Frontiers Journal Series

The Frontiers Journal Series is a multi-tier and interdisciplinary set of open-access, online journals, promising a paradigm shift from the current review, selection and dissemination processes in academic publishing. All Frontiers journals are driven by researchers for researchers; therefore, they constitute a service to the scholarly community. At the same time, the Frontiers Journal Series operates on a revolutionary invention, the tiered publishing system, initially addressing specific communities of scholars, and gradually climbing up to broader public understanding, thus serving the interests of the lay society, too.

Dedication to Quality

Each Frontiers article is a landmark of the highest quality, thanks to genuinely collaborative interactions between authors and review editors, who include some of the world's best academicians. Research must be certified by peers before entering a stream of knowledge that may eventually reach the public - and shape society; therefore, Frontiers only applies the most rigorous and unbiased reviews.
Frontiers revolutionizes research publishing by freely delivering the most outstanding research, evaluated with no bias from both the academic and social point of view. By applying the most advanced information technologies, Frontiers is catapulting scholarly publishing into a new generation.

What are Frontiers Research Topics?

Frontiers Research Topics are very popular trademarks of the Frontiers Journals Series: they are collections of at least ten articles, all centered on a particular subject. With their unique mix of varied contributions from Original Research to Review Articles, Frontiers Research Topics unify the most influential researchers, the latest key findings and historical advances in a hot research area! Find out more on how to host your own Frontiers Research Topic or contribute to one as an author by contacting the Frontiers Editorial Office: researchtopics@frontiersin.org

AUTOANTIBODIES

Topic Editors:
Rikard Holmdahl, Karolinska Institutet, Sweden
Falk Nimmerjahn, University of Erlangen-Nürnberg, Germany
Ralf J. Ludwig, University of Lübeck, Germany

Citation: Holmdahl, R., Nimmerjahn, F., Ludwig, R. J., eds. (2019). Autoantibodies. Lausanne: Frontiers Media. doi: 10.3389/978-2-88945-874-5

Table of Contents

frontiers in Immunology

EDITORIAL
published: 02 April 2019
doi: 10.3389/fimmu.2019.00484

Editorial: Autoantibodies

Rikard Holmdahl[1]*, *Falk Nimmerjahn*[2]* and *Ralf J. Ludwig*[3]*

[1] Section of Medical Inflammation Research, Department of Medical Biochemistry and Biophysics, Karolinska Institute, Stockholm, Sweden, [2] Department of Biology, Institute of Genetics, University of Erlangen-Nürnberg, Erlangen, Germany, [3] Lübeck Institute of Experimental Dermatology and Center for Research on Inflammation of the Skin, University of Lübeck, Lübeck, Germany

Keywords: autoantibody, pemphigus, pemphigoid, arthritis, pathogenesis, biomarker, diagnos, treatment

Editorial on the Research Topic

Autoantibodies

AUTOANTIBODIES

Autoantibodies have become a popular research topic with a constantly growing number of research reports. The increasing interest from the scientific community is also reflected by the high number of articles within this Research Topic, which are illustrated by an interaction map that has been drawn by using the keywords of all articles from this collection (**Figure 1**). These articles, selected from the theme of this topic, cluster around "Autoantibodies" and "Autoimmunity." Clustering was also observed for specific diseases, namely, pemphigus and pemphigoid, lupus, arthritis, and neuroimmunology. Cytokines, B cells, cell signaling, and the complement cascade are the focus of many manuscripts within this Research Topic. This clustering was the basis for the selection of the manuscripts discussed in this editorial.

OPEN ACCESS

Edited and reviewed by:
Herman Waldmann,
University of Oxford, United Kingdom

***Correspondence:**
Rikard Holmdahl
Rikard.Holmdahl@ki.se
Falk Nimmerjahn
falk.nimmerjahn@fau.de
Ralf J. Ludwig
ralf.ludwig@uksh.de

Specialty section:
This article was submitted to Immunological Tolerance and Regulation, a section of the journal Frontiers in Immunology

Received: *24 January 2019*
Accepted: *22 February 2019*
Published: *02 April 2019*

Citation:
Holmdahl R, Nimmerjahn F and Ludwig RJ (2019) Editorial: Autoantibodies. Front. Immunol. 10:484. doi: 10.3389/fimmu.2019.00484

PEMPHIGUS AND PEMPHIGOID

We received a number of submissions on the topics of pemphigus and pemphigoid, which are characterized and caused by autoantibodies to structural proteins of the skin [(1, 2); Liu et al.]. After binding to their target antigens, these autoantibodies directly (in the case of pemphigus) or indirectly (in the case of pemphigoid) cause skin blistering, which is the common clinical denominator of these diseases. Diagnosis is based on the clinical presentation, the detection of autoantibodies and/or complement deposits in the skin (detected by direct immunofluorescent (IF) microscopy), as well as the serological detection of the autoantibodies (3). For both pemphigus and pemphigoid systemic immunosuppression corticosteroids are still the main treatment. However, the lack of efficacy and/or the adverse events contribute to the medical burden of these diseases, which have an overall high unmet medical need (4). Within this Research Topic "Autoantibodies," insights into the pathogenesis, as well as novel biomarkers and treatments, are presented with the prospect that they might improve the diagnosis and treatment of pemphigus and pemphigoid.

SYSTEMIC LUPUS ERYTHEMATOSUS

Systemic lupus erythematosus (SLE) is a complex and multifactorial systemic autoimmune disease that primarily affects young women. The chronic inflammatory processes triggered during this disease can affect a variety of organ systems, including the skin, blood vessels, kidneys, and joints. Loss of humoral tolerance toward nuclear antigens such as RNA, DNA, and histones is one hallmark of the disease, although the direct contribution of autoantibodies to the disease pathology in humans is still controversial.

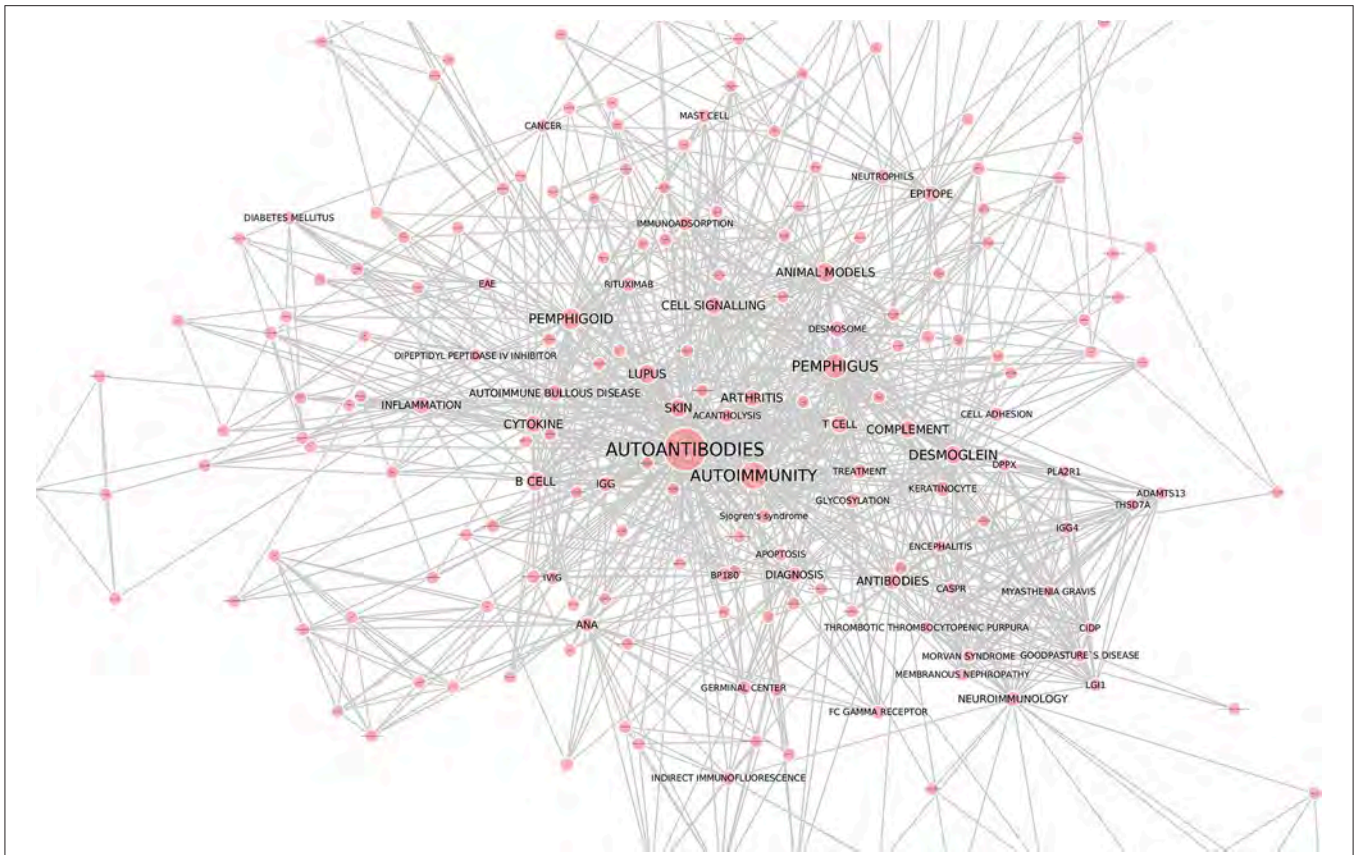

FIGURE 1 | Interaction network of articles within the Research Topic "Autoantibodies". Keywords of all 88 articles were downloaded from the website of the Research Topic "Autoantibodies" (https://www.frontiersin.org/research-topics/6220/autoantibodies). Cytoscape (https://cytoscape.org/) was used to draw the interaction map. Each line represents an interaction among the keywords, whereas the size of the red circles correlates to the number of times the respective keyword was mentioned. We thank Dr. Yask Guta (University of Lübeck) for generating this figure.

However, novel treatments targeting autoantibody-producing plasma cells have shown promising effects in patients with refractory SLE (5). In addition, novel insights into the activation and expansion of polyclonal autoreactive B cell responses during SLE in humans have emphasized the tight connection between the loss of humoral tolerance and disease activity (6). More direct evidence for the critical role of autoantibodies in SLE pathology is provided by animal model systems in the study of lupus nephritis, which have clearly demonstrated that the autoantibody-dependent activation of innate immune effector cells is a major factor for kidney and lung inflammation. With respect to the genetic factors involved in the loss of humoral tolerance to nuclear antigens, the loss or impaired signaling of the inhibitory effector FcgRIIb has been shown to lead to an increased level of autoantibody production by B cells and a decreased threshold for the activation of innate immune effector cells (7). In line with the studies in mice, a non-functional FcgRIIb variant has been shown to be a genetic risk factor for SLE development in humans (8, 9). However, it is also clear that multiple factors contribute to SLE development, including defects in apoptosis or enhanced TLR signaling (10, 11). Within the Research Topic "Autoantibodies," Weissenburger et al. provided new insights into how mutations in the deoxyribonuclease 1-like 3 gene lead to the massive production of autoantibodies against double stranded DNA. Moreover, Biermann et al. demonstrated that autoantibodies for secondary necrotic cells allow the identification of patients with SLE. With regard to innate immune effector cells, a decreased phagocytic capacity, resulting in the prolonged presence of dying cells in the body, has also been suggested to contribute to disease development (12). In summary, many pieces of the SLE puzzle have fallen into place and suggest that the loss of humoral tolerance is not simply a side effect of SLE but is rather an active player in the pathogenesis of SLE.

ARTHRITIS

Rheumatoid arthritis (RA) is one of the most common autoimmune diseases and has a large socioeconomic importance. The role of autoantibodies, such as rheumatoid factors (RF), has been instrumental in the classification and the investigation on the causes and pathogenesis of the disease. More recently, additional autoantibodies, such as antibodies to citrullinated

proteins (ACPA), have been described. The successful treatment with antibodies targeting B cells, reviewed by Hoffmann et al., have been key to the revival of the belief of the major role of B cells in RA and in several other autoimmune diseases. As in most autoimmune diseases, these autoantibodies appear years before the clinical onset of the disease. Sieghart et al. analyzed the isotype distribution of the different RA autoantibodies in early and established RA and showed that both the ACPA and RF of the IgG isotypes are specific for diagnosis but that the analysis of the IgM isotype increased the sensitivity of the test. RA has a high level of different antibodies, and the report emphasizes the value of analyzing different specificities for the diagnosis. Bitoun et al. immunized Macaque monkeys with citrullinated peptides and showed that the T cell response, but not the B cell response, was mainly directed to citrulline; this is similar to what has been observed in humans. However, in contrast to humans, monkeys with the MHC class II alleles (known to be associated with RA in humans) did not have predisposed T cell or B cell responses to citrullinated peptides. This indicates that we still lack an animal model that accurately reflects the autoimmune process leading to an ACPA response, which is known to occur in RA. Tong et al. highlights another autoantibody in RA, that are likely to also be pathogenic. The target antigen is type II collagen and in the report Tong defines and epitope targeted by such antibodies that is shared between type II and type XI collagen and they also show that both the native and the citrullinated form of the epitope is targeted by antibodies in RA.

AUTOIMMUNE NEUROLOGICAL DISEASES

Several articles also focused on autoimmune neurological diseases, mostly on improved diagnostics. Autoantibodies have been shown to be the cause of several neurological diseases, such as anti-NMDA receptor encephalitis (13) or myasthenia gravis. Within this article collection, the role of autoantibodies in "classical" neurodegenerative diseases, such as Parkinson's Disease, is discussed (Jiang et al.). This finding contributes to the current observations that autoantibodies to specific neuronal surface antigens are detected in a number of neuropsychiatric disorders (14). Functional validation of these autoantibodies would change the landscape of treatment for a number of neuropsychiatric diseases.

INSIGHTS INTO PATHOGENESIS

Animal model systems, even with their limitations (15), can significantly contribute to the understanding of disease pathogenesis. Within this Research Topic, two new animal models are described: Zheng et al. describe an immunization-based mouse model for primary Sjögren's Syndrome (Yin et al.). Tong et al. describe the shared epitopes among type XI and type II collagens in mice and humans with arthritis. Furthermore, an immunization-based arthritis model in the macaque (Bitoun et al.) and a model of feline limbic encephalitis (Tröscher et al.) are described within this Research Topic.

Large-scale genetic analyses, such as genome-wide association studies, have provided detailed insights into the underlying genetic association of autoimmune diseases, with the HLA locus as a major risk allele (16–19). Work summarized within this Research Topic demonstrates a co-occurrence of autoimmune diseases, namely, pemphigus and thyroid autoimmunity. Interestingly, the increased prevalence of anti-TPO autoantibodies was associated with the absence of certain HLA alleles and with the presence of non-desmoglein antibodies (Seiffert-Sinha et al.). Overlap at the mRNA expression level is also prevalent in different autoimmune diseases, specifically between pemphigus and systemic lupus erythematosus (SLE) (Sezin et al.). These comparative approaches may be useful to identify novel therapeutic targets that are either specific to one particular autoimmune disease or that may even be effective in the treatment of a specific cluster of autoimmune diseases. Examples of newly identified and validated risk alleles for SLE are described within this Research Topic: Gene expression in the B cells of quiescent SLE patients demonstrated an increased expression of *TRIB1*. To resolve the functional relevance of this gene for SLE pathogenesis, transgenic mice with the B cell-specific overexpression of *Trib1* were generated in the C57BL/6 genetic background. *Trib1* overexpression in B cells led to lower IgG1 concentrations under normal conditions. The immunization of mice with a T cell-dependent antigen also led to lower antigen-specific IgG titers, and the basal or forced anti-dsDNA IgM titers were lower in mice overexpressing *Trib1*. Collectively, these data point toward the *Trib1* regulatory role in autoantibody production in health and in disease (Simoni et al.). Based on the recent discovery of the rare null alleles of deoxyribonuclease 1-like 3 (*DNASE1L3*) and Fc gamma receptor IIB (*FCGR2B*) in SLE patients and genetic mouse models, Weisenburger et al. investigated the functional impact on these 2 genes in mice. For this purpose, mice deficient in both *Dnase1l3*- and *FcgR2b* were generated in the C57BL/6 genetic background. In these mice, high levels of anti-DNA IgG were observed as early as 10 weeks of age. Autoantibody titers in these mice exceeded those observed in 9-month-old NZB/W mice. In conclusion, both genes synergize to promote the IgG anti-DNA autoantibody production by B cells (Weisenburger et al.). For the organ-specific autoimmune disease pemphigus, novel associations with complement genes (Bumiller-Bini et al.) and within the neonatal Fc receptor are described within the Research Topic (Recke et al.).

However, genetics only partially explains disease susceptibility, and (at least in mice) the genetically determined disease susceptibility can be overcome by changing daily habits (20). Indeed, autoantibody production is modulated by environmental factors, such as the diet and the microbiota (Edwards et al.; Petta et al.). Furthermore, gender may have a greater impact on autoantibody production than previously appreciated (Edwards et al.). Within this Research Topic, several manuscripts addressed the contribution of environmental factors on the generation of autoantibodies and/or autoimmune diseases: In their study, Issac et al. showed that the mice who are unable to clear a *Salmonella* infection spontaneously develop anti-dsDNA autoantibodies. This was associated with an

increased CD25 expression for both CD4+ and CD8+ T cells. This effect was specific to *Salmonella* infections, as infections caused by other bacteria did not induce autoantibody production (Issac et al.). Two articles demonstrate that pemphigoid can be induced by treatment with gliptins or by physical triggers, such as burns (Gaudin et al.; Mai et al.).

Once autoantibodies are bound to their target antigen, they may induce disease through a variety of mechanisms (21). These are either direct (Fab-mediated effects), such as the induction of aberrant signaling, or alternatively, Fc-mediated events, such as the activation of complement and the engagement of activating Fc-receptors, that drive tissue damage.

In pemphigus, autoantibodies to the desmosomal proteins desmoglein (Dsg) 3 and (often) Dsg 1 cause intraepidermal blistering in the skin and mucous membranes (22). In addition to Dsg 1/3, a wide range of autoantibodies has been identified in pemphigus patients (Amber et al.). The pathogenic relevance of these autoantibodies is not as firmly established as it is for anti-Dsg1/3. However, the injection of IgG from a patient with Dsg 3-reactivity, but not Dsg 1-reactivity, into Dsg 3-deficient mice led to the induction of intraepidermal blistering (23). Recently, a model has been proposed to explain how Dsg- and non-Dsg autoantibodies can lead to intraepidermal blistering. In brief, this model proposes that, depending on the pathogenic activity of all autoantibodies toward the structures on keratinocytes, they are either capable of inducing disease alone or in combination with other autoantibodies (24). The precise mechanisms by which autoantibodies in pemphigus lead to desmosome dysfunction remain to be fully elucidated (Spindler and Waschke): Steric hindrance, i.e., the blockade of homophilic Dsg interactions within the desmosome through autoantibody binding, is believed to be one cause of blistering in pemphigus. Furthermore, Dsg3 is internalized after binding to anti-Dg3 autoantibodies (Schlögl et al.), a process that requires p38 MAPK activation (Cipolla et al.; Vielmuth et al.). In addition to Dsg3 internalization, keratin retraction, induced by pemphigus autoantibodies, has recently been demonstrated to be important in mediating autoantibody-induced cell dissociation (Schlögl et al.).

NOVEL DIAGNOSTICS / BIOMARKERS

Precise molecular diagnostics, paired with predictive biomarkers, form the basis of diagnosis as well as the selection of the appropriate treatment for each individual patient. Hence, almost 20% of the articles within the Research Topic "Autoantibodies" have focused on this topic.

The serological detection of autoantibodies is the basis of the diagnosis of many autoimmune diseases (21). Anti-nuclear antibodies (ANAs) are among the most-known autoantibodies. ANAs are associated with several rheumatic diseases, such as systemic lupus erythematosus and systemic sclerosis. However, low titers of ANAs are also present in healthy individuals (25). The gold standard for their detection is by indirect immunofluorescence and incubating the patient serum with Hep-2 cells (26). However, conventional ANA testing requires time, is laborious, and requires microscopy expertise. To overcome these limitations and to standardize and automate ANA indirect IF testing, a fully automated system, which includes staining pattern recognition, was recently developed (27). The workflow and performance characteristics of the fully automated ANA IIF system were compared to manual ANA testing by Ricchiuti et al. The use of fully automated ANA determination has significant labor savings and good concordance with manual ANA readings.

As mentioned above, ANAs are also found in quite a proportion of healthy individuals, ranging from 5 to 30% depending on the population and method used (25, 28–30). This by far exceeds the prevalence of ANA-associated rheumatic diseases. If the target antigen is identified, autoantibodies against DFS70 are often found Interestingly, isolated anti-DFS70 reactivity, which was observed in over 500 serum samples, was not associated with rheumatic disease. Hence, if the dense, fine speckled nuclear pattern, which corresponds to anti-DFS70 reactivity, is observed in Hep cells in ANA testing and anti-DFS70 reactivity is confirmed, then the presence of rheumatic disease is very unlikely (Carter et al.). In contrast, the detection of anti-cN-1A autoantibodies, which are found in 12% of patients with primary Sjögren's syndrome and in 10% of SLE patients, is associated with the presence of other autoimmune diseases (Rietveld et al.).

If an autoimmune disease is suspected but no autoantibodies can be detected by routine methods, these may be identified by applying novel techniques such as the determination of the specific isotypes of the autoantibodies in a suspected case of rheumatoid arthritis (Sieghart et al.) or by the use of a keratinocyte binding assay in a suspected case of pemphigus (Giurdanella et al.). In addition, autoantibodies are also found in certain diseases that are just beginning to be understood to be mediated by autoantibodies. These include neurological conditions (Scharf et al.), chronic obstructive pulmonary disease (Wen et al.), and cardiovascular diseases (Basavalingappa et al.; Ernst et al.; Meier and Binstadt). However, with few exceptions, such as anti-NMDA receptor autoantibodies (31), the pathogenic relevance of these autoantibodies needs to be determined.

Bullous pemphigoid (BP) is the most frequent type of pemphigoid disease (32). BP responds well to systemic (whole body) topical steroid treatment (33). After stopping steroid treatment, relapse occurs in 30–40% of patients (34). Hence, biomarkers that allow for the prediction of relapse would allow for patient selection for whom steroid treatment can be stopped or for determining which patients require prolonged steroid and/or adjuvant treatment. In a retrospective analysis of BP patients, Dr. Koga and colleagues demonstrated that high BP180 autoantibody levels were associated with future relapse. In contrast, age, BP230 antibodies or total IgE levels had no predictive value (35). Researchers from France described elevated anti-type VII collagen autoantibodies, which are the cause

of epidermolysis bullosa acquisita (36), in almost half of the BP patients at the time of relapse (Giusti et al.). This is also a retrospective chart analysis with a limited number of patients. However, both studies imply the possibility that predictive biomarkers for BP relapse can be identified. The steps toward this are a joint analysis of retrospective patient cohorts from several departments as well as a prospective diagnostic study.

NOVEL TREATMENTS

Based on the understanding of disease pathogenesis, novel treatment targets or therapeutic approaches for autoantibody-mediated diseases have emerged. Within the Research Topic "Autoantibodies," several articles have focused on new treatments.

The anti-CD20 antibody rituximab has dramatically improved the treatment of several autoantibody-mediated diseases, which was most recently demonstrated in a phase III clinical trial in pemphigus patients (37). Notably, the response to rituximab is not uniform across all autoantibody-mediated diseases, as was demonstrated by the lower efficacy of anti-CD20 treatment in pemphigoid patients when compared to that in pemphigus patients (Lamberts et al.). Rituximab and other emerging treatments to modulate B and plasma cells were the topic of three reviews within the Research Topic (Hofmann et al.; Malkiel et al.; Musette and, Bouaziz). In this Research Topic, Roders et al. also identified SYK as a regulator of B cell activation. Thus, targeting SYK not only affects the effector functions (see below) but also possibly affects the generation of autoantibodies. A different approach to modulate autoantibody concentrations may be to enhance their turnover by inhibiting the neonatal Fc receptor (38) or by selective immunoadsorption using recombinant antigens to specifically elute autoantibodies (Hofrichter et al.).

A blockade of autoantibody functions, either by targeting the Fab or Fc fragments, is another highly interesting treatment approach for autoantibody-mediated diseases. High doses of intravenous immunoglobulins (IVIG) are an effective second- or third-line treatment for a number of autoimmune diseases (39–41). How IVIG mediates the therapeutic effects is controversial (42): One hypothesis claims that all of the therapeutic effects of IVIG are mediated through the inhibition of the neonatal Fc receptor (FcRn) (43). By administering excess IgG, the FcRn becomes saturated, and thus, all IgG molecules (including the autoantibodies) are more rapidly cleared. Others provide compelling evidence that the anti-inflammatory effect of IVIG is mediated by regulating the activation threshold in myeloid effector cells by changing the ratio of activating versus inhibitory FcγR expression (44). This effect required both terminal sialic acid residues at the Fc portion of IgG, as well as the expression of the inhibitory molecule FcγRIIB (45). Finally, the presence of anti-idiotypic antibodies has been reported, specifically, the presence of anti-anti-Dsg 3 autoantibodies in IVIG preparations (46, 47). In this Research Topic, Kamaguchi et al. isolated anti-idiotypic antibodies against type XVII collagen, the major autoantigen in bullous pemphigoid (Liu et al.), and demonstrated a significant inhibitory activity of these antibodies against the pathogenic effects of BP patients' autoantibodies (Kamaguchi et al.).

In addition to the modulation of the Fab function of autoantibodies, their function can also be manipulated by changing the conserved N-linked Fc-glycan attached to the asparagine at position 297 in the constant region of the Fc heavy chain domains (Dekkers et al.). Indeed, the treatment of mice with endo-β-N-acetylglucosaminidase (EndoS), which hydrolyses the β-1,4-di-N-acetylchitobiose core of the N-linked complex type glycan on asparagine 297 (48), suppressed the induction of experimental arthritis (Nandakumar et al.), which was associated with the inhibition of the formation of large immune complexes and was independent of changes in the complement cascade or in antigen binding. The modulation of the conserved IgG's N-glycosylation site may have implications beyond the mere effector functions as was reported by Bartsch et al.: In their work, they demonstrate that antigen-specific sialylated autoantibodies but not non-specific sialylated IgG antibodies, attenuate disease manifestation in experimental lupus and arthritis. The antigen-specific sialylated autoantibodies modulated the B and T cell functions rather than modulating the effector functions of the autoantibodies.

In several autoimmune diseases, such as arthritis and pemphigoid disease, the activation of complement, the binding of immune cells to their immune complexes, and the subsequent intracellular signaling events are important for pathogenesis (21). The generalized inhibition of complement inhibition, which is achieved by the anti-C5 antibody eculizumab (49), is, however, associated with the risk of potentially life-threatening infections (50). These adverse effects could be reduced by restricting the complement inhibition at the site of complement activation or, even more ideally, at the site of pathologic tissue damage. By coupling a cyclic-RGD peptide to a function blocking C5 antibody, the construct is directed to the sites of the damaged endothelial cells. Thus, C5 inhibition preferentially occurs where endothelial damage is present (Durigutto et al.). In addition to the targeted delivery of C5-inhibitory compounds, selectivity may also be achieved by certain complement pathways, which are upregulated in specific diseases. The dissection of the individual contributions of the complement activation cascades in the pemphigoid disease epidermolysis bullosa acquisita [(51); Mihai et al.] demonstrated the predominant role of alternative complement activation and no contribution from the membrane attack complex. Thus, the selective targeting of C1q had therapeutic effects in an animal model of epidermolysis bullosa acquisita (Mihai et al.).

In addition to complement anaphylatoxins, cytokines recruit leukocytes to the sites of autoantibody-induced pathology. Thus, their inhibition has become a well-established therapeutic principle for several chronic inflammatory diseases (52). So far, however, each of the licensed biologics targets a single cytokine. To enhance the anti-inflammatory activity, Abraham et al. used phage display to identify promiscuous chemokine-binding peptides. These bind to a number of pro-inflammatory chemokines, such as CCL2, CCL5, and CXCL9-11. The use

of their selected lead compounds in models of autoimmune diseases ameliorated clinical disease manifestation (Abraham et al.). This approach may be applicable in endemic pemphigus foliaceus, where alterations in cytokine and chemokine serum concentrations have previously been noted (Timóteo et al).

Once bound to the immune complexes, a complex signaling cascade is triggered in the leukocytes, which ultimately leads to their activation and subsequent inflammation and tissue damage (53). By contrasting the mRNA expression between inflamed and healthy skin in experimental pemphigoid disease, several hub-genes that potentially contribute to tissue damage in pemphigoid were identified. The spleen tyrosine kinase was among the identified hub-genes. Both LysM-specific SYK knockout mice and mice treated with an inhibitor of the small molecule SYK were completely protected from the induction of experimental pemphigoid disease by autoantibody transfer [Samavedam et al.; (54)]. Corresponding findings were made in a mouse model of arthritis (Németh et al.). Taken together, these findings suggest that targeting SYK is a potential therapeutic approach for a number of autoantibody-mediated diseases. Furthermore, in the pemphigoid mouse model, the inhibition of PI3Kδ also prevented disease onset. Furthermore, pharmacological PI3Kδ inhibition improved clinical disease manifestation when applied in therapeutic, experimental settings (Koga et al.). In addition to these signaling pathways, others also contribute to the pathogenesis of pemphigoid disease, which has recently been reviewed elsewhere (53).

In pemphigus, in addition to the above-described alterations in cell signaling, several lines of evidence suggest that apoptosis contributes to the loss of keratinocyte adhesion and consequently intraepidermal blistering (55). Initially, the contribution of apoptosis was suggested by an increased expression of molecules involved in this process, i.e., different caspases, Fas, as well as FasL (56). Following this concept, the inhibition of the Fas-FasL interaction by a function blocking anti-FasL antibody can inhibit pemphigus IgG-induced pathology *in vitro*. Furthermore, mice lacking the expression of the secreted, soluble FasL do not develop intraepidermal blistering when injected with IgG antibodies from pemphigus patients (Lotti et al.).

All of the abovementioned treatments focused on targeting IgG-mediated autoimmunity. In addition to IgG-mediated autoimmunity, IgA autoantibodies have also long been recognized as pathogenic. However, only recently has attention been attributed to IgE-mediated autoimmunity (Maurer et al.). Despite their presence at high frequencies in many autoimmune diseases, the pathogenic relevance of IgE autoantibodies has thus far not been the focus of studies. In atopic dermatitis, a common, chronic inflammatory skin disease (57), the removal of immunoglobulins by immunoadsorption (and even the selective removal of IgE) has therapeutic effects [(58); Kasperkiewicz et al; Kasperkiewicz et al.], which are comparable to that of biological atopic dermatitis treatment (59). However, immunoadsorption is a very specialized procedure. In addition, especially in the *S. aureus*-colonized skin of atopic dermatitis patients, central intravenous lines may lead to severe infectious complications.

CONCLUDING REMARKS

"Autoantibodies" are a hot research topic, as was reflected by the articles of this Research Topic. Based on an enhanced understanding of disease pathogenesis, as well as the advancement of technology, we are at the verge of developing specific treatments for autoantibody-mediated diseases that may even be able to lead to a cure. This development is, for example, reflected by the use of chimeric autoantigen receptor T cells in the treatment of experimental pemphigus (60). In addition, novel developments in diagnostics now allow for the better diagnosis of patients as well as for the better understanding of the autoimmune nature of diseases, which had not been thought to be caused by an underlying autoimmune mechanism (Scharf et al.). Therefore, even if causal treatment is not possible, we may still be able to carefully select treatments that are tailored to each patient's needs based on the detected biomarkers.

AUTHOR CONTRIBUTIONS

All authors listed have made a substantial, direct and intellectual contribution to the work, and approved it for publication.

ACKNOWLEDGMENTS

We thank Dr. Yask Gupta (Lübeck Institute for Experimental Dermatology) for preparation of **Figure 1**. This word has been supported by the Clinical Research Unit Pemphigoid Diseases (KFO 303) and the Excellence Cluster Inflammation at Interfaces (EXC 306), all from the Deutsche Forschungsgemeinschaft.

REFERENCES

1. Schmidt E, Zillikens D. Pemphigoid diseases. *Lancet*. (2013) 381:320–32. doi: 10.1016/S0140-6736(12)61140-4
2. Hammers CM, Stanley JR. Mechanisms of disease: pemphigus and bullous pemphigoid. *Annu Rev Pathol*. (2016) 11:175–97. doi: 10.1146/annurev-pathol-012615-044313
3. Witte M, Zillikens D, Schmidt E. Diagnosis of autoimmune blistering diseases. *Front. Med*. (2018) 5:296. doi: 10.3389/fmed.2018.00296
4. Lamberts A, Yale M, Grando SA, Horváth B, Zillikens D, Jonkman MF. Unmet needs in pemphigoid diseases: an international survey amongst patients, clinicians and researchers. *Acta Derm Venereol*. (2018) 99:224–5. doi: 10.2340/00015555-3052
5. Alexander T, Sarfert R, Klotsche J, Kühl AA, Rubbert-Roth A, Lorenz HM et al. The proteasome inhibitior bortezomib depletes plasma cells and ameliorates clinical manifestations of refractory systemic lupus erythematosus. *Ann Rheum Dis*. (2015) 74:1474–8. doi: 10.1136/annrheumdis-2014-206016
6. Tipton CM, Fucile CF, Darce J, Chida A, Ichikawa T, Gregoretti I, et al. Diversity, cellular origin and autoreactivity of antibody-secreting cell population expansions in acute systemic lupus erythematosus. *Nat Immunol*. (2015) 16:755–65. doi: 10.1038/ni.3175

7. Bolland S, Yim YS, Tus K, Wakeland EK, Ravetch JV. Genetic modifiers of systemic lupus erythematosus in FcgammaRIIB(-/-) mice. *J Exp Med*. (2002) 195:1167–74. doi: 10.1084/jem.20020165
8. Willcocks LC, Carr EJ, Niederer HA, Rayner TF, Williams TN, Yang W, et al. A defunctioning polymorphism in FCGR2B is associated with protection against malaria but susceptibility to systemic lupus erythematosus. *Proc Natl Acad Sci USA*. (2010) 107:7881–5. doi: 10.1073/pnas.0915133107
9. Waisberg M, Tarasenko T, Vickers BK, Scott BL, Willcocks LC, Molina-Cruz A, et al. Genetic susceptibility to systemic lupus erythematosus protects against cerebral malaria in mice. *Proc Natl Acad Sci USA*. (2011) 108:1122–7. doi: 10.1073/pnas.1017996108
10. Yajima K, Nakamura A, Sugahara A, Takai T. FcgammaRIIB deficiency with Fas mutation is sufficient for the development of systemic autoimmune disease. *Eur J Immunol*. (2003) 33:1020–9. doi: 10.1002/eji.200323794
11. Pisitkun P, Deane JA, Difilippantonio MJ, Tarasenko T, Satterthwaite AB, Bolland S. Autoreactive B cell responses to RNA-related antigens due to TLR7 gene duplication. *Science*. (2006) 312:1669–72. doi: 10.1126/science.1124978
12. Herrmann M, Voll RE, Zoller OM, Hagenhofer M, Ponner BB, Kalden JR. Impaired phagocytosis of apoptotic cell material by monocyte-derived macrophages from patients with systemic lupus erythematosus. *Arthritis Rheum*. (1998) 41:1241–50. doi: 10.1002/1529-0131(199807)41:7<1241::AID-ART15>3.0.CO;2-H
13. Venkatesan A, Adatia K. Anti-NMDA-receptor encephalitis: from bench to clinic. *ACS Chem Neurosci*. (2017) 8:2586–95. doi: 10.1021/acschemneuro.7b00319
14. Zong S, Hoffmann C, Mané-Damas M, Molenaar P, Losen M, Martinez-Martinez P. Neuronal surface autoantibodies in neuropsychiatric disorders: are there implications for depression. *Front Immunol*. (2017) 8:752. doi: 10.3389/fimmu.2017.00752
15. Sundberg JP, Schofield PN. Living inside the box: environmental effects on mouse models of human disease. *Dis Model Mech*. (2018) 11:dmm035360. doi: 10.1242/dmm.035360
16. Vodo D, Sarig O, Sprecher E. The genetics of pemphigus vulgaris. *Front Med*. (2018) 5:226. doi: 10.3389/fmed.2018.00226
17. Sajda T, Hazelton J, Patel M, Seiffert-Sinha K, Steinman L, Robinson W, et al. Multiplexed autoantigen microarrays identify HLA as a key driver of anti-desmoglein and -non-desmoglein reactivities in pemphigus. *Proc Natl Acad Sci USA*. (2016) 113:1859–64. doi: 10.1073/pnas.1525448113
18. Kim K, Bang SY, Lee HS, Bae SC. Update on the genetic architecture of rheumatoid arthritis. *Nat Rev Rheumatol*. (2017) 13:13–24. doi: 10.1038/nrrheum.2016.176
19. Ghodke-Puranik Y, Niewold TB. Immunogenetics of systemic lupus erythematosus: A comprehensive review. *J Autoimmun*. (2015) 64:125–36. doi: 10.1016/j.jaut.2015.08.004
20. Aqel SI, Hampton JM, Bruss M, Jones KT, Valiente GR, Wu LC, et al. Daily moderate exercise is beneficial and social stress is detrimental to disease pathology in murine lupus nephritis. *Front Physiol*. (2017) 8:236. doi: 10.3389/fphys.2017.00236
21. Ludwig RJ, Vanhoorelbeke K, Leypoldt F, Kaya Z, Bieber K, McLachlan SM, et al. Mechanisms of autoantibody-induced pathology. *Front Immunol*. (2017) 8:603. doi: 10.3389/fimmu.2017.00603
22. Kasperkiewicz M, Ellebrecht CT, Takahashi H, Yamagami J, Zillikens D, Payne AS, et al. Pemphigus. *Nat Rev Dis Primers*. (2017) 3:17026. doi: 10.1038/nrdp.2017.26
23. Vu TN, Lee TX, Ndoye A, Shultz LD, Pittelkow MR, Dahl MV, et al. The pathophysiological significance of nondesmoglein targets of pemphigus autoimmunity. Development of antibodies against keratinocyte cholinergic receptors in patients with pemphigus vulgaris and pemphigus foliaceus. *Arch Dermatol*. (1998) 134:971–80.
24. Sinha AA, Sajda T. The evolving story of autoantibodies in Pemphigus vulgaris: development of the "super compensation hypothesis". *Front Med*. (2018) 5:218. doi: 10.3389/fmed.2018.00218
25. Prussmann J, Prussmann W, Recke A, Rentzsch K, Juhl D, Henschler R, et al. Co-occurrence of autoantibodies in healthy blood donors.[letter]. *Exp Dermatol*. (2014) 23:519–21. doi: 10.1111/exd.12445
26. Meroni PL, Schur PH. ANA screening: an old test with new recommendations. *Ann Rheum Dis*. (2010) 69:1420–2. doi: 10.1136/ard.2009.127100
27. Voigt J, Krause C, Rohwäder E, Saschenbrecker S, Hahn M, Danckwardt M, et al. Automated indirect immunofluorescence evaluation of antinuclear autoantibodies on HEp-2 cells. *Clin Dev Immunol*. (2012) 2012:651058. doi: 10.1155/2012/651058
28. Tan EM, Feltkamp TE, Smolen JS, Butcher B, Dawkins R, Fritzler MJ, et al. Range of antinuclear antibodies in "healthy" individuals. *Arthritis Rheum*. (1997) 40:1601–11. doi: 10.1002/1529-0131(199709)40:9<1601::AID-ART9>3.0.CO;2-T
29. Satoh M, Chan EK, Ho LA, Rose KM, Parks CG, Cohn RD, et al. Prevalence and sociodemographic correlates of antinuclear antibodies in the United States. *Arthritis Rheum*. (2012) 64:2319–27. doi: 10.1002/art.34380
30. Semchuk KM, Rosenberg AM, McDuffie HH, Cessna AJ, Pahwa P, Irvine DG. Antinuclear antibodies and bromoxynil exposure in a rural sample. *J Toxicol Environ Health A*. (2007) 70:638–57. doi: 10.1080/15287390600974593
31. Planagumà J, Leypoldt F, Mannara F, Gutiérrez-Cuesta J, Martín-García E, Aguilar E, et al. Human N-methyl D-aspartate receptor antibodies alter memory and behaviour in mice. *Brain*. (2015) 138:94–109. doi: 10.1093/brain/awu310
32. Hübner F, Recke A, Zillikens D, Linder R, Schmidt E. Prevalence and age distribution of pemphigus and pemphigoid diseases in Germany. *J Invest Dermatol*. (2016) 136:2495–8. doi: 10.1016/j.jid.2016.07.013
33. Joly P, Roujeau JC, Benichou J, Picard C, Dreno B, Delaporte E, et al. A comparison of oral and topical corticosteroids in patients with bullous pemphigoid. *N Engl J Med*. (2002) 346:321–7. doi: 10.1056/NEJMoa011592
34. Joly P, Roujeau JC, Benichou J, Delaporte E, D'Incan M, Dreno B et al. A comparison of two regimens of topical corticosteroids in the treatment of patients with bullous pemphigoid: a multicenter randomized study. *J Invest Dermatol*. (2009) 129:1681–7. doi: 10.1038/jid.2008.412
35. Koga H, Teye K, Ishii N, Ohata C, Nakama T. High index values of enzyme-linked immunosorbent assay for BP180 at baseline predict relapse in patients with bullous pemphigoid. *Front Med*. (2018) 5:139. doi: 10.3389/fmed.2018.00139
36. Koga H, Prost Squarcioni C, Iwata H, Jonkman MF, Ludwig RJ, Bieber K. Epidermolysis bullosa acquisita: The 2019 update. *Front Med*. (2018) 5:362. doi: 10.3389/fmed.2018.00362
37. Joly P, Maho-Vaillant M, Prost-Squarcioni C, Hebert V, Houivet E, Calbo S, et al. First-line rituximab combined with short-term prednisone versus prednisone alone for the treatment of pemphigus (Ritux 3): a prospective, multicentre, parallel-group, open-label randomised trial. *Lancet*. (2017) 389:2031–40. doi: 10.1016/S0140-6736(17)30070-3
38. Lee J, Werth VP, Hall RP, Eming R, Fairley JA, Fajgenbaum DC, et al. Perspective from the 5th International Pemphigus and Pemphigoid Foundation scientific conference. *Front Med*. (2018) 5:306. doi: 10.3389/fmed.2018.00306
39. Iwata H, Vorobyev A, Koga H, Recke A, Zillikens D, Prost-Squarcioni C, et al. Meta-analysis of the clinical and immunopathological characteristics and treatment outcomes in epidermolysis bullosa acquisita patients. *Orphanet J Rare Dis*. (2018) 13:153. doi: 10.1186/s13023-018-0896-1
40. Ishii N, Hashimoto T, Zillikens D, Ludwig RJ. High-dose intravenous immunoglobulin (IVIG) therapy in autoimmune skin blistering diseases. *Clin Rev Allergy Immunol*. (2010) 38:186–195. doi: 10.1007/s12016-009-8153-y
41. Amagai M, Ikeda S, Shimizu H, Iizuka H, Hanada K, Aiba S, et al. A randomized double-blind trial of intravenous immunoglobulin for pemphigus. *J Am Acad Dermatol*. (2009) 60:595–603. doi: 10.1016/j.jaad.2008.09.052
42. Schwab I, Nimmerjahn F. Intravenous immunoglobulin therapy: how does IgG modulate the immune system. *Nat Rev Immunol*. (2013) 13:176–89. doi: 10.1038/nri3401
43. Li N, Zhao M, Hilario-Vargas J, Prisayanh P, Warren S, Diaz LA, et al. Complete FcRn dependence for intravenous Ig therapy in autoimmune skin blistering diseases. *J Clin Invest*. (2005) 115:3440–50. doi: 10.1172/JCI24394
44. Kaneko Y, Nimmerjahn F, Ravetch JV. Anti-inflammatory activity of immunoglobulin G resulting from Fc sialylation. *Science*. (2006) 313:670–3. doi: 10.1126/science.1129594
45. Schwab I, Mihai S, Seeling M, Kasperkiewicz M, Ludwig RJ, Nimmerjahn F. Broad requirement for terminal sialic acid residues and FcgammaRIIB for the

preventive and therapeutic activity of intravenous immunoglobulins *in vivo*. *Eur J Immunol*. (2014) 44:1444–53. doi: 10.1002/eji.201344230
46. Mimouni D, Blank M, Payne AS, Anhalt GJ, Avivi C, Barshack I et al. Efficacy of intravenous immunoglobulin (IVIG) affinity-purified anti-desmoglein anti-idiotypic antibodies in the treatment of an experimental model of pemphigus vulgaris. *Clin Exp Immunol*. (2010) 162:543–9. doi: 10.1111/j.1365-2249.2010.04265.x
47. Mimouni D, Blank M, Ashkenazi L, Milner Y, Frusic-Zlotkin M, Anhalt GJ, et al. Protective effect of intravenous immunoglobulin (IVIG) in an experimental model of pemphigus vulgaris. *Clin Exp Immunol*. (2005) 142:426–32. doi: 10.1111/j.1365-2249.2005.02947.x
48. Collin M, Olsen A. EndoS, a novel secreted protein from Streptococcus pyogenes with endoglycosidase activity on human IgG. *EMBO J*. (2001) 20:3046–55. doi: 10.1093/emboj/20.12.3046
49. Zuber J, Fakhouri F, Roumenina LT, Loirat C, Frémeaux-Bacchi V, French SGFAHUS. Use of eculizumab for atypical haemolytic uraemic syndrome and C3 glomerulopathies. *Nat Rev Nephrol*. (2012) 8:643–57. doi: 10.1038/nrneph.2012.214
50. Benamu E, Montoya JG. Infections associated with the use of eculizumab: recommendations for prevention and prophylaxis. *Curr Opin Infect Dis*. (2016) 29:319–29. doi: 10.1097/QCO.0000000000000279
51. Mihai S, Chiriac MT, Takahashi K, Thurman JM, Holers MV, Zillikens D et al. The alternative pathway in complement activation is critical for blister induction in experimental epidermolysis bullosa acquisita. *J Immunol*. (2007) 178:6514–21. doi: 10.4049/jimmunol.178.10.6514
52. Reichert JM. Marketed therapeutic antibodies compendium. *MAbs*. (2012) 4:413–5. doi: 10.4161/mabs.19931
53. Ludwig RJ. Signaling and targeted-therapy of inflammatory cells in epidermolysis bullosa acquisita. *Exp Dermatol*. (2017). 26:1179–86. doi: 10.1111/exd.13335
54. Németh T, Virtic O, Sitaru C, Mócsai A. The Syk tyrosine kinase is required for skin inflammation in an *in vivo* mouse model of epidermolysis bullosa acquisita. *J Invest Dermatol*. (2017) 137:2131–9. doi: 10.1016/j.jid.2017.05.017
55. Schmidt E, Waschke J. Apoptosis in pemphigus. *Autoimmun Rev*. (2009) 8:533–7. doi: 10.1016/j.autrev.2009.01.011
56. Pacheco-Tovar MG, Avalos-Díaz E, Vega-Memije E, Bollain-y-Goytia JJ, López-Robles E, Hojyo-Tomoka MT, et al. The final destiny of acantholytic cells in pemphigus is Fas mediated. *J Eur Acad Dermatol Venereol*. (2009) 23:697–701. doi: 10.1111/j.1468-3083.2009.03162.x
57. Leung DY, Bieber T. Atopic dermatitis. *Lancet*. (2003) 361:151–160. doi: 10.1016/S0140-6736(03)12193-9
58. Wegner J, Weinmann-Menke J, von Stebut E. Immunoadsorption for treatment of severe atopic dermatitis. *Atheroscler Suppl*. (2017) 30:264–70. doi: 10.1016/j.atherosclerosissup.2017.05.043
59. Beck LA, Thaci D, Hamilton JD, Graham NM, Bieber T, Rocklin R, et al. Dupilumab treatment in adults with moderate-to-severe atopic dermatitis. *N Engl J Med*. (2014) 371:130–9. doi: 10.1056/NEJMoa1314768
60. Ellebrecht CT, Bhoj VG, Nace A, Choi EJ, Mao X, Cho MJ, et al. Reengineering chimeric antigen receptor T cells for targeted therapy of autoimmune disease. *Science*. (2016) 353:179–184. doi: 10.1126/science.aaf6756

Conflict of Interest Statement: RH has received honoraria and/or research grants from Lipum and Astrazeneca and is a founder of the small virtual company Vacara. RL has received honoraria and/or research grants from the following companies: Admirx, Almirall, Amryth, ArgenX, Biotest, Biogen, Euroimmun, Incyte, Immungenetics, Lilly, Novartis, UCB Pharma, Topadur, True North Therapeutics and Tx Cell.

The remaining author declares that the research was conducted in the absence of any commercial or financial relationships that could be construed as a potential conflict of interest.

frontiers in Immunology

ORIGINAL RESEARCH
published: 31 October 2018
doi: 10.3389/fimmu.2018.02362

Gene Expression Profiling of Lacrimal Glands Identifies the Ectopic Expression of MHC II on Glandular Cells as a Presymptomatic Feature in a Mouse Model of Primary Sjögren's Syndrome

*Junping Yin[1†], Junfeng Zheng[2†], Fengyuan Deng[1†], Wenjie Zhao[1], Yan Chen[2], Qiaoniang Huang[1], Renliang Huang[1], Lifang Wen[1], Xiaoyang Yue[3], Frank Petersen[3] and Xinhua Yu[1,3]**

[1] Xiamen-Borstel Joint Laboratory of Autoimmunity, The Medical College of Xiamen University, Xiamen, China, [2] Institute of Psychiatry and Neuroscience, Xinxiang Medical University, Xinxiang, China, [3] Priority Area Asthma & Allergy, Research Center Borstel, Airway Research Center North (ARCN), Members of the German Center for Lung Research (DZL), Borstel, Germany

Ectopic expression of MHC II molecules on glandular cells is a feature of primary Sjögren's syndrome (pSS). However, the cause of this ectopic expression and its potential role in the pathogenesis of the disease remains elusive. Here, we report that ectopic expression of MHC II molecules on glandular cells represents an early presymptomatic event in a mouse model of pSS induced by immunization of Ro60_316-335 peptide emulsified in TiterMax® as an adjuvant. Ectopic expression of MHC II was induced by TiterMax® but not by complete freund's adjuvant (CFA). Furthermore, immunization with Ro60_316-335 peptide emulsified in TiterMax®, but not in CFA, induced a pSS-like disease in mice. Our results suggests that ectopic expression of MHC II molecules on glandular cells represents a presymptomatic feature of pSS and that such ectopic expression can be induced by exogenous factors. In addition, this study also provides a novel mechanism how adjuvants can amplify immune responses.

Keywords: primary Sjögren's syndrome, mouse model, presymptomatic feature, MHC II ectopic expression, TiterMax®, adjuvant

OPEN ACCESS

Edited by:
Ralf J. Ludwig,
Universität zu Lübeck, Germany

Reviewed by:
Philippe Guilpain,
Université de Montpellier, France
Christoph M. Hammers,
Universität zu Lübeck, Germany
Unni Samavedam,
University of Cincinnati, United States

***Correspondence:**
Xinhua Yu
xinhuayu@fz-borstel.de

[†]These authors have contributed equally to this work

Specialty section:
This article was submitted to Immunological Tolerance and Regulation, a section of the journal Frontiers in Immunology

Received: *15 February 2018*
Accepted: *24 September 2018*
Published: *31 October 2018*

Citation:
Yin J, Zheng J, Deng F, Zhao W, Chen Y, Huang Q, Huang R, Wen L, Yue X, Petersen F and Yu X (2018) Gene Expression Profiling of Lacrimal Glands Identifies the Ectopic Expression of MHC II on Glandular Cells as a Presymptomatic Feature in a Mouse Model of Primary Sjögren's Syndrome. Front. Immunol. 9:2362. doi: 10.3389/fimmu.2018.02362

INTRODUCTION

Primary Sjögren's syndrome (pSS) is a systemic autoimmune disorder mainly targeting salivary and lacrimal glands (1). Clinically, pSS is characterized by hypofunction of salivary and lacrimal cells leading to xerostomia (dry mouth) and xerophthalmia (dry eyes) (1). Histologically, pSS is featured by lymphocytic foci in the salivary and lacrimal glands (2) as well as ectopic expression of MHC II molecules on the glandular epithelial cells of those glands (3). In addition, autoantibodies including anti-SSA/Ro and anti-SSB/La autoantibodies, rheumatoid factor and anti-nuclear antibodies (ANA) are also hallmarks for pSS (4). Despite to the well-known clinical, histological, and immunological features of the symptomatic phase of pSS, little is known about

the presymptomatic features of the disease. Currently, only autoantibodies such as anti-Ro60, anti-Ro52, and anti-La were described by Jonsson et al. in a large retrospective study (5) to be present in the presymptomatic phase of the disease.

Animal models are invaluable tools for the identification of relevant presymptomatic events in human autoimmune diseases (6, 7). With regard to pSS, presymptomatic events have been observed Non-obese diabetic (NOD) mice which develop a pSS-like disease spontaneously over time (8). Studies in this mouse strain revealed that the development the pSS-like disease consists of three sequential steps (9, 10). The first step is represented by intrinsic abnormalities in the exocrine glands, e.g., glandular cell apoptosis, followed by lymphocytes infiltration in the exocrine glands resulting in an impairment in secretion of saliva and tears. These observations in NOD mice suggest that intrinsic abnormalities in the exocrine glands and lymphocytic infiltration represent respective early and late presympomatic features in this mouse model.

Recently, we have established a novel mouse model for pSS by immunizing mice with human Ro60_316-335 peptide emulsified in TiterMax® as adjuvant (11). In this model, susceptible mice are characterized by generation of autoantibodies, lymphocytic infiltration and a decrease in tear secretion. By investigating gene expression profiles of lacrimal glands, we here aimed to identify the presymptomatic features of this novel mouse model of pSS.

METHODS AND MATERIALS

Mice and Immunization

Female Balb/c mice were purchased from Shanghai SLAC Laboratory Animal Co., Ltd (Shanghai, China). All mice were housed under the specific pathogen free condition in the animal facility of Xiamen University. Immunization was performed using the protocol described previously (11). Briefly, female Balb/c mice were immunized with Ro60_316-335 peptide or PBS control emulsified in the TiterMax® (Alexis Biochemicals, Lorrach, Germany) or complete Freund's adjuvant (CFA). Protocols of all animal experiments were approved by the Institutional Animal Care and Use Committee of Xiamen University.

Measurement of Tears and Saliva

Tears and saliva of mice were measured at week 0, 6, and 12 after immunization and further normalized to the bodyweight as described previously (11). Briefly, mice were starved for 16–18 h before the measurement, deeply anesthetized, and stimulated with pilocarpine hydrochloride (Sigma-Aldrich). Saliva was collected with a sponge immediately after the injection of pilocarpine for a time period of 20 min while tears were collected by using Phenol Red Thread (Jingming Ltd. Tianjin, China) at 10 min and 20 min time points after injection of pilocarpine. Both saliva and tear secretion volumes were normalized to individual mouse body weight.

Detection of Autoantibodies in Sera

Anti-Ro60_316-335 autoantibodies in murine sera were detected by ELISA as described previously (11). In brief, SSA peptides were absorbed onto Costar EIA/RIA Plates (Corning Icorporated, corning, NY, USA), washed and blocked with 3% BSA in PBS supplemented with 0.05% Tween-20 (PBS-T), incubated with the respective mouse sera (1:200 dilution), and further washed with PBS-T. Bound antibodies were detected by using peroxidase conjugated goat anti-mouse IgG antibodies (Sigma, USA) and tetramethylbenzidine (Solarbio, Beijing, China) as substrate.

Histopathological Assessment

Twelve weeks after immunization, mice were sacrificed and tissues were collected for histopathological evaluation. Histology of salivary and lacrimal glands was evaluated after Haematoxylin and Eosin (H&E) staining of 5-μm-thick sections derived from paraffin embedded tissue. Cryosections from salivary and lacrimal glands were used for direct or indirect immunofluorescence and immunohistochemical staining. Direct immunofluorescence staining was performed for the detection of $CD4^+$ T cell, $CD8^+$ T cell, $CD11c^+$ Dendritic cell and MHC II molecules by using Alexa-488 conjugated rat-anti-mouse CD4 (clone: RM4-5, Biolegend), Alexa-488 conjugated rat-anti-mouse CD8 (clone: 53-6.7, Biolegend), Alexa-488 conjugated Armenian Hamster-anti-Mouse CD11c antibody (clone: N418, Biolegend), and rat-anti-mouse I-A/I-E Antibody (clone: M5/114.15.2, Biolegend), respectively. Indirect Immunofluorescence staining was performed for the analysis of $CD3^+$ T cell and $CD19^+$ B cell by using rat-anti-mouse CD3 (clone: 17A2, Biolegend) and rat-anti-mouse CD19 (clone: 6D5, Biolegend), respectively, followed by using Alexa-488 conjugated goat-anti-rat IgG (clone: Poly4054, Biolegend). Immunohistochemistry was performed for the detection of MHC II molecules on lacrimal gland tissue cells by using rat-anti-mouse I-A/I-E antibody (clone: M5/114.15.2, Invitrogen) on cryosections.

Gene Expression Profiling Analysis

Total RNA was isolated from murine lacrimal glands at week 0, 2, and 6 after immunization using TRIzol Plus RNA Purification Kit (Invitrogen). The extracted total RNA from each sample was quantified by a NanoDrop ND-1000 spectrophotometer and RNA integrity was assessed by standard denaturing agarose gel electrophoresis. The double strand cDNA was synthesized by Invitrogen Superscript ds-cDNA synthesis kit (Invitrogen, USA) according to the manufacturer's protocol. cDNA was labeled with Cy3 using NimbleGen one-color DNA labeling kit (Roche NimbleGen Inc., USA). Labeled ds-cDNA samples were hybridized to NimbleGen Mouse 12x135K Gene Expression Microarray (Roche NimbleGen Inc., USA). Array scanning was done by the Axon GenePix 4000B microarray scanner (Molecular Devices Corporation, USA).

TIFF-files of scanned images were imported into NimbleScan software (version 2.5) for grid alignment and expression data analysis. Raw expression data were normalized through quantile normalization and the Robust Multichip Average (RMA) algorithm included in the NimbleScan software. Probe level (*_norm_RMA.pair) files and gene level (*_RMA.calls) files were generated after normalization. The gene level files were imported into Agilent GeneSpring GX software (version 11.5.1) for further analysis. Genes with values higher than or equal to lower cut-off:

100.0 in at least 3 out of 15 samples were chosen for further data analysis. Statistically significant differentially expressed genes (DEGs) were identified by Volcano Plot filtering (fold change $\geq$ 2.0, p-value $\leq$ 0.05). KEGG pathway analysis and Gene Ontology (GO) term enrichment analysis were applied to determine the roles of DEGs in various biological pathways and GO terms. To analyze the gene co-expression network, DEGs were submitted to the STRING database (version 10.5) for construction of a gene co-expression network. The constructed gene network was further edited by using the Cytoscape software platform (version: 3.6.1) (12).

Real Time Quantitative PCR

Total RNA was isolated and processed by real time quantitative PCR (RT-qPCR) for gene expression analysis. PCR was performed by the use of an Applied Biosystems 7500 Real-Time PCR System (Applied Biosystems). The *β-actin (Actb)* gene was used as internal control. Data was normalized using the $2^{-\Delta\Delta Ct}$ method. A list of primers used for the RT-qPCR was presented as **Supplementary Table 5**.

Statistical Analysis

Except gene expression profiling data, all data were analyzed by using GraphPad Prism software (GraphPad Software Inc.). *P*-values below 0.05 were considered as statistically significant.

RESULTS

Balb/c Mice Are Susceptible to Ro60_316-335 Peptide-Induced pSS-Like Disease

Previously, we have demonstrated that development of Ro60_316-335 peptide-induced pSS-like disease in mice depends on the genetic background of the mice, where C3H/He mice were found to be susceptible but DBA/1 and C57BL/6 mice were shown to be resistant to the disease (11). Here, we investigated whether Balb/c mice are susceptible to experimental pSS. As shown in **Figure 1A**, secretion of tears in mice immunized with Ro60_316-335 peptide emulsified in TiterMax® was significantly reduced as compared to mice immunized with PBS control at week 12 after immunization, while no reduction in secretion of saliva was observed (**Figure 1B**). Although no lymphocytic focus was observed in the histology of either salivary or lacrimal glands (**Figure 1C**), immunofluorescence staining revealed the infiltration of both $CD3^+$ T cells and $CD19^+$ B cells in lacrimal glands of Ro60_316-335-immunized mice but not in the control mice (**Figure 1D**). $CD3^+$ T cells, but not $CD19^+$ B cells, were also observed in the salivary glands of Ro60_316-335-immunized mice (**Supplementary Figure 1**). Analysis of the subtypes of T cells revealed that the infiltrated T cells in lacrimal glands were composed of both $CD4^+$ and $CD8^+$ T cells (**Supplementary Figure 2**). Collectively, Balb/c mice immunized with Ro60_316-335 peptide showed lymphocytes infiltration into the exocrine glands and impairment in tear secretion, demonstrating that this strain is susceptible to experimental pSS. Notably, immunization with a different peptide derived from Ro60 (Ro60_480-494) also emulsified in TiterMax® failed to induce corresponding disease symptoms (**Supplementary Figure 3**), indicating the specificity of this model for Ro60_316-335.

We next analyzed kinetics of T cell infiltration and autoantibody production in Ro60_316-335 peptide-immunized mice. As shown in **Figure 1E**, infiltration of $CD3^+$ T cells into the lacrimal gland was observed first at week 4 and reached a peak at week 6 after immunization. Moreover, anti-Ro60_316-335 peptide autoantibodies became detectable at day 10 and peaked at week 6 after immunization (**Figure 1F**). Kinetics of autoantibody production, lymphocytic infiltration, and impairment of tear secretion demonstrate that from week 0 to week 6 after the first immunization was the presymptomatic phase in Balb/c mice in this mouse model.

We then determined whether glandular cell apoptosis, a presymptomatic feature in NOD mouse model for pSS, exists also in the Ro60_316-335 peptide-induced model in Balb/c mice. As shown in **Supplementary Figure 4**, obvious glandular cell apoptosis was detected in lacrimal gland of neither Ro60_316-335 peptide-immunized mice nor control mice, suggesting that apoptosis is not a feature of this model.

Gene Expression Profiling of Lacrimal Glands From the Presymptomatic Phase of the Disease

Although our previous study has shown that C3H/He mice are also susceptible to the Ro60_316-335 peptide induced pSS-like disease (11), the time frame of the presymptomatic phase in Balb/c mice is better defined than that in C3H/He mice. Therefore we investigated the presymptomatic features in the lacrimal glands in the Balb/c strain. We determined gene expression profiling of the lacrimal glands in the presymptomatic phase, including the status prior to immunization (week 0), at week 2 and 6 weeks after immunization with Ro60_316-335 peptide emulsified in TiterMax®. Comparison were performed for peptide-immunized mice vs. untreated mice (week 0), peptide-immunized mice vs. PBS/ TiterMax®-treated control mice, and PBS/ TiterMax®-treated control mice vs. untreated mice. As shown in **Supplementary Figures 5**, **6**; **Supplementary Tables 1**, **2**, each comparison resulted in hundreds of upregulated or downregulated genes. To further characterize those differentially expressed genes, we performed gene ontology (GO) enrichment analysis (**Supplementary Table 3**), pathway enrichment analysis (**Supplementary Table 4**), and gene network analysis.

At week 6 after immunization, top enriched GO terms in upregulated genes in the lacrimal glands of Ro60_316-335 peptide-immunized mice as compared to untreated mice (week 0) belong to the gene groups of "immune system process," "T cell activation," "immune response," and "lymphocyte activation" (**Figure 2A**). These results were in line with findings of the pathway enrichment analysis, where those upregulated genes were allocated in the pathways "leukocyte transendothelial migration," "B cell receptor signaling," and "T cell receptor signaling" (**Figure 3A**). Interestingly, two infection related pathways, measles, and human T-cell lymphotropic virus type 1

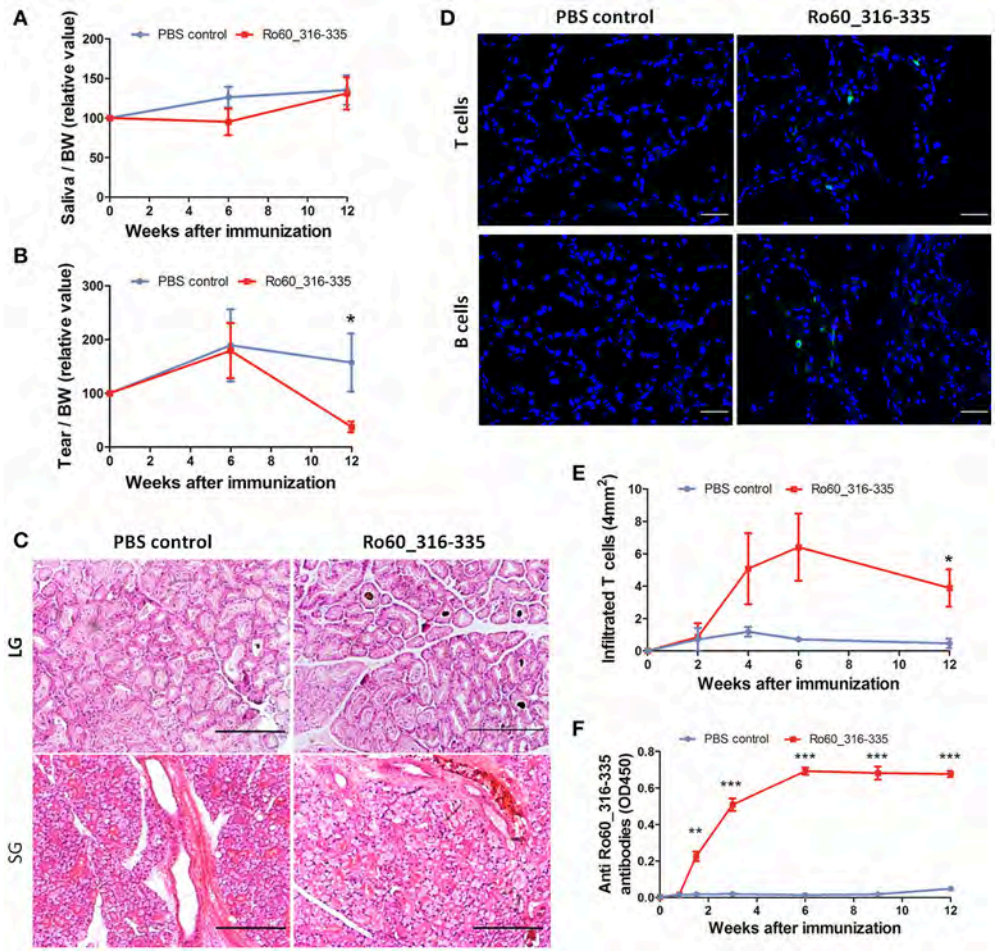

FIGURE 1 | Balb/c mice are susceptible to Ro60_316-335-induced pSS-like disease. Balb/c mice were treated with Ro60_316-335 peptide either emulsified in TiterMax® or PBS. Secretion of saliva **(A)** and tears **(B)** was determined after pilocarpine stimulation. Values were normalized to the respective body weights and subsequently to the levels of secretion determined before immunization. Results of two experiments were pooled and data presented as Mean ± SEM, statistically significant differences between peptide-immunized mice ($n = 11$) and controls ($n = 10$) were calculated by using Student's t-test (*$p < 0.05$). **(C)** Representative micrographs after H&E staining of sections derived from paraffin embedded lacrimal glands (upper) and salivary glands (lower) of mice immunized with Ro60_316-335 peptide or PBS control. Bars, 100um. **(D)** Representative immunofluorescence micrographs $CD3^+$ T cells (upper) and $CD19^+$ B cells (lower) in lacrimal glands of Ro60_316-335- or PBS-treated mice. Bars, 50um. **(E)** Time-kinetics of $CD3^+$ T cell infiltration in lacrimal glands of peptides immunized mice ($n = 4$) and controls ($n = 4$) at week 0, 2, 4, 6, and 12 after immunization. Data are presented as mean ± SEM, statistically significant differences between peptide- and PBS-treated mice were calculated by using Mann Whitney test (*$p < 0.05$). **(F)** Time-kinetics of anti-Ro60_316-335 autoantibodies production in the sera of Ro60_316-335 peptides immunized mice ($n = 13$) and controls ($n = 11$). Data presented as Mean ± SEM, statistically significant differences between peptide- and PBS- treated mice were calculated by using Mann Whitney test (**$p < 0.01$, ***$p < 0.001$).

(HTLV-1) infection, also appeared in the pathway enrichment analysis, suggesting that the immunization mediated immune responses within lacrimal glands was similar to those against infections. Furthermore, a gene network constructed on the basis of the identified upregulated gene showed that 7 out of top 10 central nodes belong to genes involved in "immune responses" (**Figure 4A**). Therefore, all three bioinformatic analysis strategies demonstrate that immune response associated genes were upregulated in lacrimal glands of Ro60_316-335 peptide-immunized mice compared to untreated mice. These findings are supported by our observation that infiltration of lymphocytes in the lacrimal glands reached the peak at 6 weeks after immunization. Notably, those immune response associated genes upregulated in lacrimal glands of peptide-immunized mice at week 6 after immunization were not seen in PBS/ TiterMax®-treated control mice (**Supplementary Tables 3**, **4**), suggesting that their upregulation was induced specifically by the peptide immunization.

Since gene expression data suggest that there were immune responses in the lacrimal glands of mice immunized with Ro60_316-335 peptide at 6 weeks after immunization, we next evaluated the gene expression profiling at 2 weeks after immunization in the early presymptomatic phase. As compared to week 0, top enriched GO terms of upregulated genes in

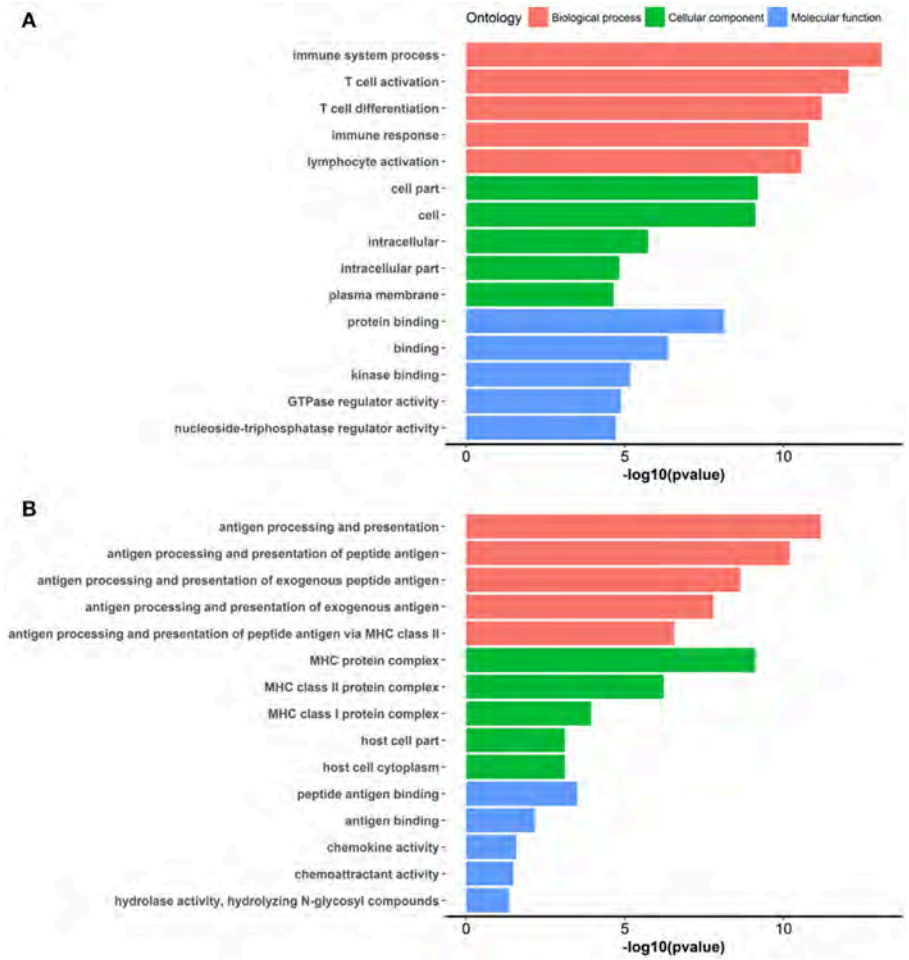

FIGURE 2 | Gene ontology (GO) enrichment of differentially expressed genes (DEGs) in the lacrimal glands of mice. **(A)** GO terms enriched in genes up-regulated in lacrimal glands of mice at week 6 after immunization with Ro60_316-335 peptide compared to untreated mice (week 0). **(B)** GO terms enriched in genes up-regulated in lacrimal glands of mice at week 2 after immunization with Ro60_316-335 peptide compared to untreated mice. The top 5 significantly enriched GO terms in "biological process," "cellular component," and "molecular function" are presented. Names of the GO terms are indicated in Y axis, while the X axis indicates *p*-values.

lacrimal glands at week 2 after immunization with the Ro60_316-335 peptide were "antigen processing and presentation," "MHC protein complex," and "peptide antigen binding" (**Figure 2B**), suggesting that genes involved in antigen presentation and processing were activated. This notion was confirmed by pathway enrichment analysis and gene network analysis, which showed that "antigen processing and presentation" was one of the top enriched pathways (**Figure 3B**) and that 5 out of top 10 central nodes consist of genes involved in antigen presentation and processing (**Figure 4B**), respectively. Therefore, our bioinformatic analysis demonstrate that in the lacrimal glands of mice at week 2 after immunization genes related to antigen presentation and processing were upregulated. Surprisingly, these genes were also found to be upregulated in mice treated PBS/TiterMax® as a control (**Supplementary Tables 3**, **4**), indicating that regulation to these genes was not driven by the antigen but by the adjuvant. Upregulated genes encompass several MHC I and MHC II genes, including *H2d1*, *H2eb1*, *H2ea1*, *H2k1*, *H2dmb1*, *H2q7*, *H2aa,* and *B2m* (**Figure 5A**). To confirm the upregulation of MHC genes, we performed real time quantitative PCR to determine the expression of *H2d1*, *H2k1*, *H2eb1,* and *H2aa*. As predicted, we found, all four MHC genes to be upregulated in the TiterMax®-treated groups in comparison to the respective untreated control group (**Figure 5B**).

Ectopic Expression of MHC II on Murine Lacrimal Glands

Under physiological condition, glandular cells express MHC I but not MHC II molecules. Thus, the upregulation of MHC II molecules observed here represent most likely an ectopic expression. Since such an ectopic expression of HLA II on epithelial cells of salivary glands is a feature of pSS patients (3, 13), we further characterized the expression of MHC II in lacrimal glands of the immunized mice. As expected, MHC II molecules were not expressed on glandular cells prior to immunization. However, ectopic expression of MHC II

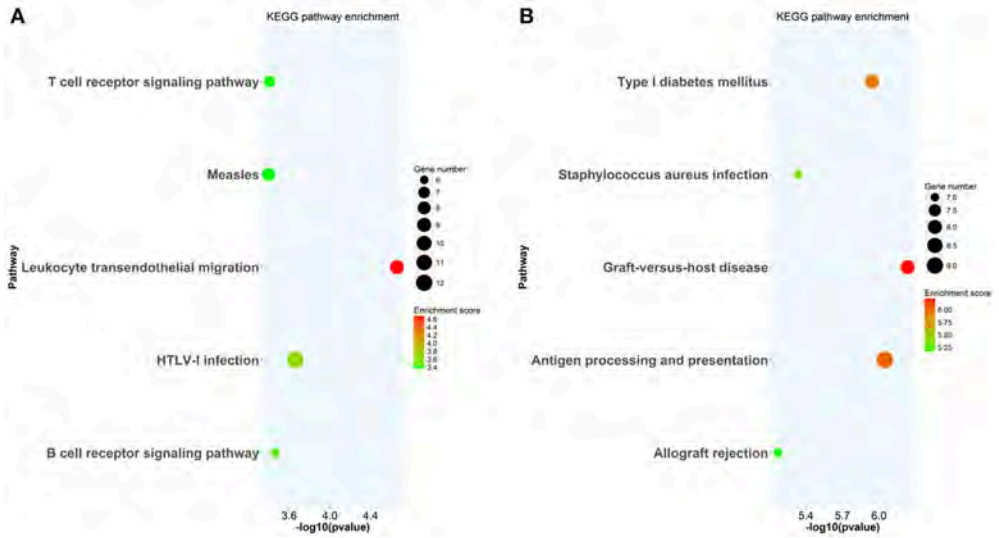

FIGURE 3 | KEGG pathway enrichment analysis of differentially expressed genes (DEGs) in lacrimal glands of mice. **(A)** KEGG pathways enriched in genes up-regulated in lacrimal glands of mice at week 6 after immunization with Ro60_316-335 peptide compared to untreated mice (week 0). **(B)** KEGG pathways enriched in genes up-regulated in lacrimal glands of mice at week 2 after immunization with Ro60_316-335 peptide compared to untreated mice. The top 5 significantly enriched KEGG pathways are shown. HTLV-1, Human T-cell lymphotropic virus type 1.

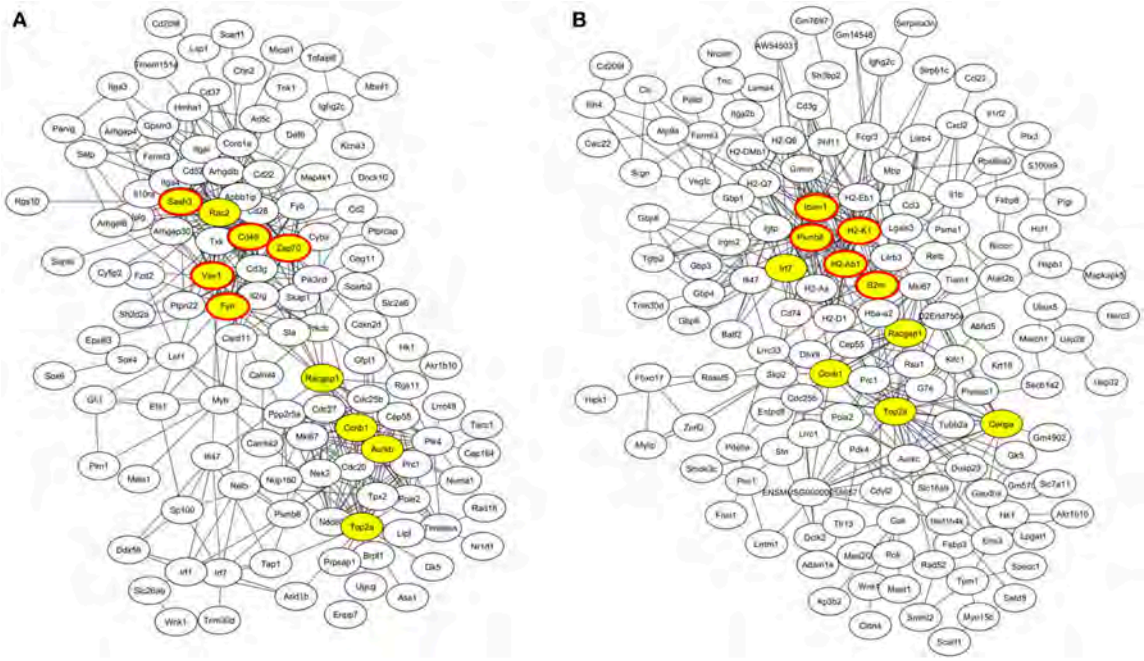

FIGURE 4 | Gene co-expression network of differentially expressed genes (DEGs) in lacrimal glands of mice. **(A)** Gene network of genes up-regulated in lacrimal glands of mice at week 6 after immunization with Ro60_316-335 peptide compared to untreated mice (week 0). The top 10 connected genes are labeled in yellow. Among the top ten connected genes, genes involved in immune responses are highlighted with red cycles. **(B)** Gene network of genes up-regulated in lacrimal glands of mice at week 2 after immunization with Ro60_316-335 peptide compared to untreated mice. The top 10 connected genes are labeled in yellow. Among the top ten connected genes, genes involved in antigen presentation are highlighted with red cycles.

molecules was observed at week 2, 6 and 12 after treatment with TiterMax®, irrespective whether a further antigen was co-applied or not (**Figure 6A** and **Supplementary Figure 7**). Immunohistochemical staining revealed further that MHC II molecules were ectopically expressed on both lacrimal acinar and ductal cells in the lacrimal glands of TiterMax®-treated mice

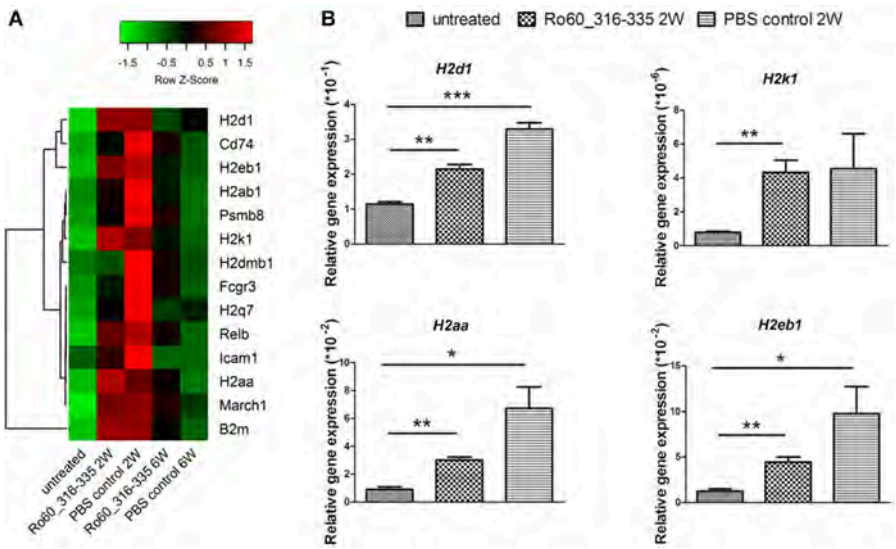

FIGURE 5 | Expression of genes involved in antigen processing and presentation in lacrimal glands of mice. **(A)** Heatmap of differentially expressed genes involved in antigen processing and presentation, with green and red color representing low and high gene expression, respectively. Signal intensity of gene expression was normalized by using the z-score and indicated in color from green (low) to red (high). Calculation and plotting were performed by using package *heatmap.2* in RStudio. **(B)** Validation of gene expression of *H2d1*, *H2k1*, *H2aa,* and *H2eb1* in lacrimal glands of mice at week 2 after immunization with Ro60_316-335 peptide, PBS/Titermax® control, and in untreated mice (week 0). The quantification of gene expression was determined by real time quantitative PCR with *β-actin* gene expression as internal control for normalization. Data are presented as mean ± SEM, statistical differences between groups were determined by using Student's *t*-test (*$p < 0.05$, **$p < 0.01$ and ***$p < 0.001$).

(**Figure 6B**). To confirm that elevated expression of MHC II molecules was associated with their upregulation on glandular cells but not by infiltration of professional APCs, we performed co-staining of tissue against MHC II in combination with CD11c. Although we could identify a small number of $CD11c^+MHCII^+$ APCs in the glandular tissue, the majority of MHC II^+ cells in the lacrimal glands of TiterMax®-treated mice scored negative for CD11c (**Figure 6C**).

To investigate whether the ectopic expression of MHC II molecules is limited to tissues of lacrimal glands, we determine the expression of MHC II in other organs including salivary glands, lung, kidney and heart. As shown in **Supplementary Figure 8**, ectopic expression of MHC II molecules could be detected in all analyzed organs in mice treated with TiterMax® but not in untreated controls.

To further examine whether MHC II expressing glandular cells interact with infiltrated $CD4^+$ T cells, we performed co-staining of MHC II molecules with CD4. As shown in **Figure 6D**, co-localization of $CD4^+$ T cells and MHC II expressing cells was observed in the lacrimal glands of mice immunized with Ro60_316-335 peptide, indicating that glandular cells may have the ability to present antigen to corresponding T cells. Noteworthy, no such interaction was observed in mice which received TiterMax® in the absence of the peptide.

CFA Does Not Induce Ectopic Expression of MHC II Molecules

Finally, we then investigated whether the adjuvant induced ectopic expression of MHC II molecules is specific for TiterMax® or a more general effect which can be mediated by other adjuvants too. However, treatment with CFA did not induce the ectopic expression of MHC II molecules in the lacrimal glands (**Figure 7A**) in Balb/c mice. Furthermore, immunization with Ro60_316-335 peptide emulsified in CFA failed to induce a pSS-like disease. Although these mice did produce autoantibodies against Ro60_316-335 peptide (**Figure 7E**), neither impairment in tears secretion (**Figures 7B,C**) nor lymphocytic infiltration (**Figure 7D**) was observed.

DISCUSSION

In this study, we could demonstrate that ectopic expression of MHC II molecules in lacrimal glands represents an early presymptomatic event in the Ro_316-335 peptide-induced model for pSS. Given that adjuvants are able to enhance maturation of dendritic cells and to increase antigen presentation, it is not surprising that application of an adjuvant mediates the upregulation of MHC molecules on professional APCs (14). However, the adjuvant-induced ectopic expression of MHC II molecules on glandular epithelial cells has not been observed so far. To our knowledge, this study reports for the first time on the ectopic expression of MHC II molecules as a presymptomatic feature of animal models of pSS.

In 1985, Lindahl et al. reported that HLA_DR molecules are ectopically expressed on the minor salivary gland epithelial cells around the dense lymphocytic infiltrates in pSS patients (13). Subsequent *in-situ* histological studies demonstrated that both salivary acinar and ductal cells ectopically express MHC II

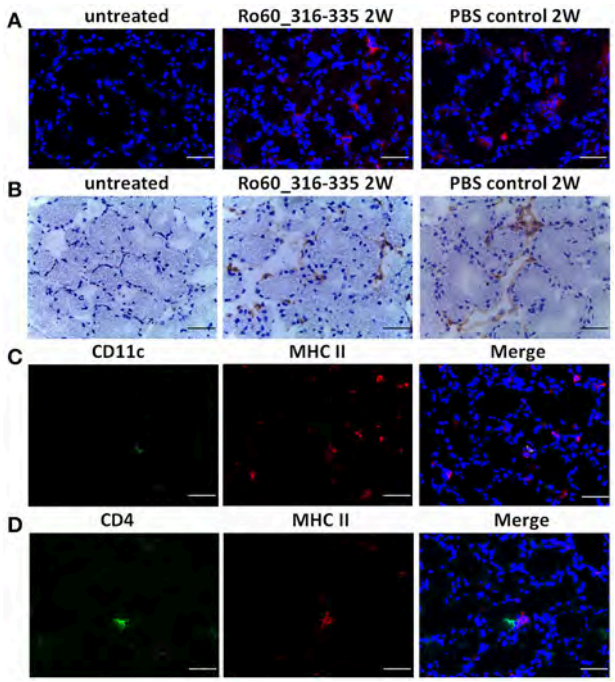

FIGURE 6 | Ectopic expression of MHC II molecules on glandular cells in lacrimal glands of TiterMax®-treated mice. **(A)** Representative micrographs of MHC II molecules on lacrimal glands from mice immunized with Ro60_316-335 peptides or PBS emulsified in TiterMax® at the week 2 after immunization and on untreated mice (week 0). MHC II molecules were detected on cryosections of the lacrimal glands by direct immunofluorescence staining using Alexa-647 conjugated rat-anti-mouse I-A/I-E Antibody. Bars, 50um. **(B)** Representative micrographs of MHC II molecules on lacrimal glands of mice. Expression of MHC II molecules was determined by immunohistochemistry on cryosections. Bars, 50um. **(C)** Co-staining for CD11c and MHC II molecules on cryosections of lacrimal glands from mice immunized with Ro60_316-335 peptides. CD11c and MHC II molecules on lacrimal gland tissue cells were detected by using Alexa-488 conjugated Armenian Hamster-anti-Mouse CD11c antibody and Alexa-647 conjugated rat-anti-mouse I-A/I-E Antibody, respectively. Bars, 50um. **(D)** Co-staining for CD4 and MHC II molecules on cryosections of lacrimal glands from mice immunized with Ro60_316-335 peptides. CD4 and MHC II molecules on lacrimal gland tissue cells were detected by Alexa-488 conjugated rat-anti-Mouse CD4 antibody and Alexa-647 conjugated rat-anti-mouse I-A/I-E Antibody, respectively. Bars, 50um.

molecules (3, 15). However, it is not clear whether this ectopic expression is a presymptomatic feature or already a consequence of the disease manifestation. So far, the only reported evidence for an ectopic expression of MHC II in an animal models for pSS derives from observations in *RbAp48* transgenic mice. In 2008, Ishimaru et al. reported that these mice develop a pSS-like disease spontaneously which is associated with an ectopic expression of MHC II molecules on glandular epithelial cells (16). Since in this study only the histology of exocrine gland of diseased mice was evaluated, it is not clear whether this ectopic expression of MHC II molecules is a presymptomatic feature of this model. By contrast, we here demonstrate that ectopic expression of MHC II molecules on both acinar and ductal cells is a true presymptomatic feature of Ro60_316-335 peptide-induced mouse model for pSS.

Although ectopic expression of MHC II molecules on glandular epithelial cell is a well-defined feature of pSS (13), it is not clear whether this abnormality is caused by a genetic dysregulation or by exogenous factors. In the *RbAp48* transgenic mouse model, ectopic expression of MHC II molecules is a clear consequence of a genetic modification and is mediated by the overepression of the *RbAp48* gene (16). In our study, ectopic expression of MHC II molecules is induced by application of TiterMax®, suggesting that the ectopic expression can be caused by an exogenous factor. Taken together, evidence from animal studies suggests that both genetic and environmental factors can mediate the ectopic expression of MHC II molecules on glandular epithelial cells in pSS.

Expression of MHC II genes are controlled by interferon regulatory factor 1 (IRF-1) and Class II Major histocompatibility complex transactivator (CIITA) as primary regulators of MHC II expression (17, 18). Moreover, it has been reported that IFN-γ regulate the expression of MHC II by acting on IRF-1 and CIITA (19). Consistently, IRF-1 has been reported to be highly expressed in the salivary gland from pSS patients (20), supporting the hypothesis that the ectopic expression of MHC II is regulated by IRF-1. With regard to the ectopic expression of MHC II on glandular epithelial cells in mice, Ishimaru et al. could demonstrate the production of IFN-γ by salivary gland epithelial cells which induces the upregulation of IRF-1 and CIITA and further leads to the ectopic expression of MHC II molecules in exocrine glands of the *RbAp48* transgenic mice (16). In line with these findings, we observed a significant upregulation of *IRF-1* and *CIITA* gene expression in the lacrimal gland of TiterMax® treated mice as compared to untreated mice (**Supplementary Figure 9**), providing indirect evidence that ectopic expression of MHC II molecules is likewise mediated by upregulation of these two molecules.

Since the MHC II molecules play a pivotal role in antigen presentation and subsequent $CD4^+$ T cell activation (21), it is conceivable that glandular epithelial cells expressing MHC II molecules might act as APCs and thus are involved in the initiation of the disease manifestation. This notion is supported by our observation that infiltrated $CD4^+$ T cells co-localized with glandular cells ectopically expressing MHC II molecules. Previously, Ishimaru et al. showed that salivary gland epithelial cells (SGEC) obtained from pSS patients express both MHC II molecules and co-stimulatory cytokines and are able to mediate the initiation, development and maintenance of inflammatory response as non-professional APCs *in vitro* (22), supporting a role of MHC II-expressing glandular epithelial cells as APCs.

Interestingly, TiterMax®, but not CFA, can induce ectopic expression of MHC II molecules. Furthermore, only TiterMax® but not CFA can be used as the effective adjuvant for Ro60_316-335 peptide-induced mouse model of pSS. This observation suggests that these two adjuvants are different in their actions in triggering immune responses, especially in triggering innate immune responses. Studies in which both adjuvants were compared have demonstrated that CFA is able to mediate stronger immune response than TiterMax® (23–26), in terms of antibody production and chronicity of inflammation. However,

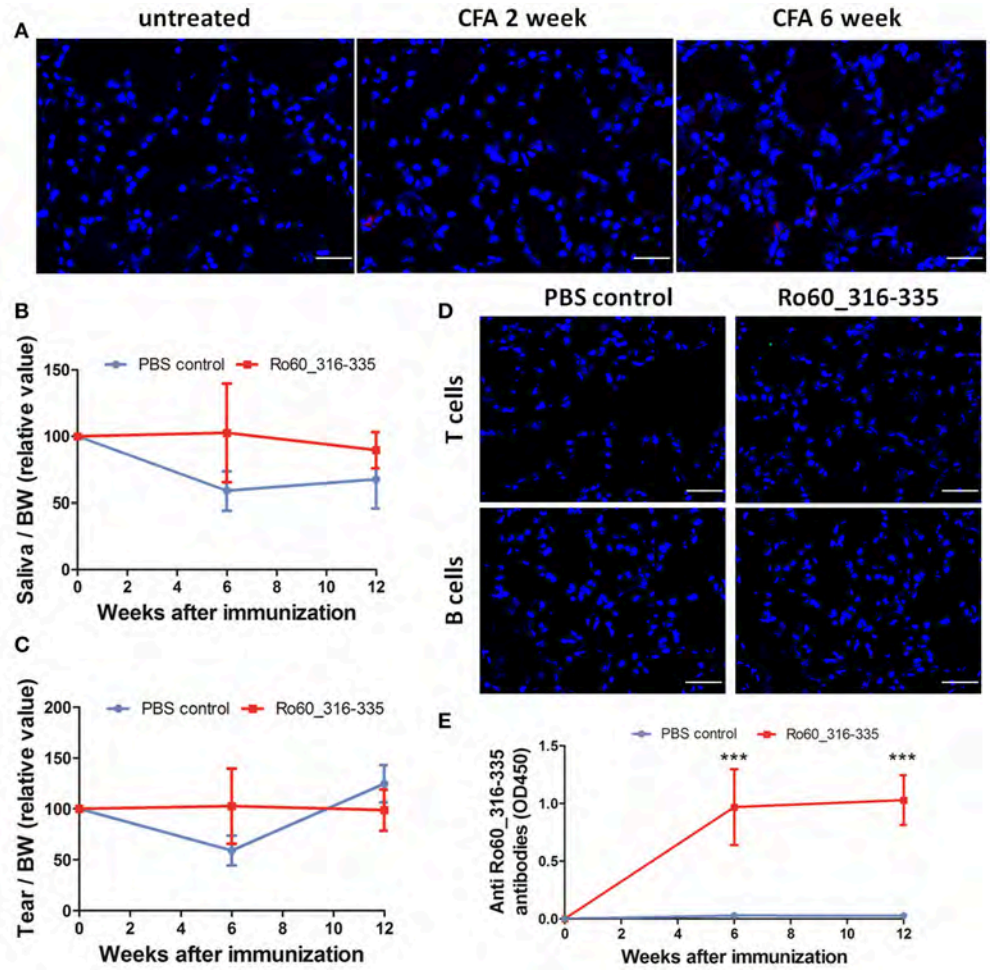

FIGURE 7 | Immunization with Ro60_316-335 peptide emulsified in complete freund's adjuvant (CFA) failed to induce pSS-like disease in Balb/c mice. **(A)** Representative immunofluorescence micrographs of MHC II molecules on cryosections of lacrimal glands from mice treated with PBS emulsified in CFA at week 0, 2, and 6 after immunization. Bars, 50 μm. Secretion of saliva **(B)** and tears **(C)** was determined after pilocarpine stimulation. Values were normalized to the respective body weights and subsequently to the levels of secretion determined before immunization. Data presented as mean± SEM, statistically significant differences between peptide-immunized mice ($n = 13$) and controls ($n = 8$) were determined using Student' *t*-test. **(D)** Representative immunofluorescence micrographs of $CD3^+$ T cells (upper) and $CD19^+$ B cells (lower) in lacrimal glands of Ro60_316-335-immunized mice or PBS-treated control mice. Bars, 50 μm. **(E)** Production of anti-Ro60_316-335 antibodies in the sera of mice immunized with Ro60_316-335 or PBS emulsified in CFA. Data are presented as mean ± SEM, statistically significant differences between peptide- and PBS- immunized mice were calculated by using Mann Whitney test (***$p < 0.001$).

the difference between CFA and TiterMax® in triggering innate immune responses was not clear so far.

Adjuvants are effective means to potentiate cellular and humoral immune responses in modeling human immune related diseases. The mode of action of adjuvants includes prolongation of the lifetime of (auto-)antigens, enhancement of antigen delivery to APC, and stimulation of the innate immune system (14, 27). The current study demonstrates that TiterMax® is able to induce ectopic expression of MHC II molecules on epithelial cells. Previously, Ishimaru and colleagues have shown that SGEC of pSS patient express beside MHC II molecules also antigen presenting-associated molecules such as CD86, CD80, and ICAM-1 (16). Moreover, SGEC are able to activate $CD4^+$ T cells, suggesting that they can function as antigen presenting cells (16). Therefore, the findings of the current study suggests a novel mechanism of adjuvant-mediated activation of the adaptive immune response by converting epithelial cells into APCs.

Although our results provide an idea on presymptomatic processes in experimental pSS, some limitations in this study have to be discussed. First, the Ro60_316-335 peptide-induced disease phenotypes in Balb/c mice are rather mild, which makes this model not ideal for all studies on this disease. Second, lymphocytic foci in the exocrine glands, a feature of pSS patients, are not present in Balb/c mice and only a rather mild infiltration of lymphocytes could be detected in lacrimal and salivary glands. It is not clear whether this limited number of infiltrated lymphocyte and their interaction with glandular cells are relevant to the development of disease. Third, given

that both lacrimal and salivary glands are characterized by mild lymphocytic infiltration and MHC II ectopic expression, it is unclear why only the secretion of tears is impaired. One possible explanation for this could be discrepant susceptibilities of both glands to autoimmune-mediated impairment. This idea is supported by observations in two other murine models of pSS. In thrombospondin-1-deficient mice impairment in tear secretion occurs without effect on the production of saliva (28) and in transgenic mice overexpressing retinoblastoma-associated protein 48 a more severe impairment of lacrimal gland function was seen than in the function of salivary glands (16). Finally, since TiterMax® represents a multi-component reagent, the identity of the defined substance relevant for the ectopic expression of the MHC II molecules has to be clarified.

In conclusion, the current study shows that TiterMax®-induced ectopic expression of MCH II molecules on exocrine glands is an important feature in the early presymptomatic phase of the Ro60 peptide-induced mouse model of pSS. These findings suggest that that ectopic expression of MHC II molecules in the exocrine glands might be a presymptomatic feature of pSS and such ectopic expression can be induced by exogenous factors. Furthermore, this study also suggests a novel mechanism of adjuvant action in potentiating immune responses.

AUTHOR CONTRIBUTIONS

JY, JZ, FD, WZ, YC, QH, RH, LW, XYue performed experiments, XYu conceived and supervised the project, JY, XYu, and FP wrote the manuscript.

FUNDING

This work was supported by the National Natural Science Foundation of China (No.81371325 and No. 81571593), the Deutsche Forschungsgemeinschaft, GRK1727 Modulation of Autoimmunity, and the German Center for Lung Research (DZL).

ACKNOWLEDGMENTS

We thank Guojun Geng (First Hospital Affiliated to Xiamen University) and Zhongjian Zhang (Xinxiang Medical University) for their help in the revision of the manuscript.

SUPPLEMENTARY MATERIAL

The Supplementary Material for this article can be found online at: https://www.frontiersin.org/articles/10.3389/fimmu.2018.02362/full#supplementary-material

REFERENCES

1. Fox RI. Sjogren's syndrome. *Lancet* (2005) 366:321–31. doi: 10.1016/S0140-6736(05)66990-5
2. Christodoulou MI, Kapsogeorgou EK, Moutsopoulos HM. Characteristics of the minor salivary gland infiltrates in Sjogren's syndrome. *J Autoimmun.* (2010) 34:400–7. doi: 10.1016/j.jaut.2009.10.004
3. Rowe D, Griffiths M, Stewart J, Novick D, Beverley PC, Isenberg DA. HLA class I and II, interferon, interleukin 2, and the interleukin 2 receptor expression on labial biopsy specimens from patients with Sjogren's syndrome. *Ann Rheum Dis.* (1987) 46:580–6. doi: 10.1136/ard.46.8.580
4. Kyriakidis NC, Kapsogeorgou EK, Tzioufas AG. A comprehensive review of autoantibodies in primary Sjogren's syndrome: clinical phenotypes and regulatory mechanisms. *J Autoimmun.* (2014) 51:67–74. doi: 10.1016/j.jaut.2013.11.001
5. Jonsson R, Theander E, Sjostrom B, Brokstad K, Henriksson G. Autoantibodies present before symptom onset in primary Sjogren syndrome. *JAMA* (2013) 310:1854–5. doi: 10.1001/jama.2013.278448
6. Petersen F, Yue X, Riemekasten G, Yu X. Dysregulated homeostasis of target tissues or autoantigens—A novel principle in autoimmunity. *Autoimmun Rev.* (2017) 16:602–11. doi: 10.1016/j.autrev.2017.04.006
7. Yu X, Petersen F. A methodological review of induced animal models of autoimmune diseases. *Autoimmun Rev.* (2018) 17:473–9. doi: 10.1016/j.autrev.2018.03.001
8. Robinson CP, Brayer J, Yamachika S, Esch TR, Peck AB, Stewart CA, et al. Transfer of human serum IgG to nonobese diabetic Igmu null mice reveals a role for autoantibodies in the loss of secretory function of exocrine tissues in Sjogren's syndrome. *Proc Natl Acad Sci USA.* (1998) 95:7538–43. doi: 10.1073/pnas.95.13.7538
9. Killedar SJ, Eckenrode SE, McIndoe RA, She JX, Nguyen CQ, Peck AB, et al. Early pathogenic events associated with Sjogren's syndrome (SjS)-like disease of the NOD mouse using microarray analysis. *Lab Invest.* (2006) 86:1243–60. doi: 10.1038/labinvest.3700487
10. Nguyen C, Singson E, Kim JY, Cornelius JG, Attia R, Doyle ME, et al. Sjogren's syndrome-like disease of C57BL/6.NOD-Aec1 Aec2 mice: gender differences in keratoconjunctivitis sicca defined by a cross-over in the chromosome 3 Aec1 locus. *Scand J Immunol.* (2006) 64:295–307. doi: 10.1111/j.1365-3083.2006.01828.x
11. Zheng J, Huang Q, Huang R, Deng F, Yue X, Yin J, et al. B Cells Are Indispensable for a Novel Mouse Model of Primary Sjogren's Syndrome. *Front Immunol.* (2017) 8:1384. doi: 10.3389/fimmu.2017.01384
12. Shannon P, Markiel A, Ozier O, Baliga NS, Wang JT, Ramage D, et al. Cytoscape: a software environment for integrated models of biomolecular interaction networks. *Genome Res.* (2003) 13:2498–504. doi: 10.1101/gr.1239303
13. Lindahl G, Hedfors E, Klareskog L, Forsum U. Epithelial HLA-DR expression and T lymphocyte subsets in salivary glands in Sjogren's syndrome. *Clin Exp Immunol.* (1985) 61:475–82.
14. Awate S, Babiuk LA, Mutwiri G. Mechanisms of action of adjuvants. *Front Immunol.* (2013) 4:114. doi: 10.3389/fimmu.2013.00114
15. Moutsopoulos HM, Hooks JJ, Chan CC, Dalavanga YA, Skopouli FN, Detrick B. HLA-DR expression by labial minor salivary gland tissues in Sjogren's syndrome. *Ann Rheum Dis.* (1986) 45:677–83. doi: 10.1136/ard.45.8.677
16. Ishimaru N, Arakaki R, Yoshida S, Yamada A, Noji S, Hayashi Y. Expression of the retinoblastoma protein RbAp48 in exocrine glands leads to Sjogren's syndrome-like autoimmune exocrinopathy. *J Exp Med.* (2008) 205:2915–27. doi: 10.1084/jem.20080174
17. Hobart M, Ramassar V, Goes N, Urmson J, Halloran PF. IFN regulatory factor-1 plays a central role in the regulation of the expression of class I and II MHC genes *in vivo*. *J Immunol.* (1997) 158:4260–9.
18. Harton JA, Ting JP. Class II transactivator: mastering the art of major histocompatibility complex expression. *Mol Cell Biol.* (2000) 20:6185–94. doi: 10.1128/MCB.20.17.6185-6194.2000
19. Steimle V, Siegrist CA, Mottet A, Lisowska-Grospierre B, Mach B. Regulation of MHC class II expression by interferon-gamma mediated by the transactivator gene CIITA. Science (1994) 265:106–9. doi: 10.1126/science.8016643
20. Wakamatsu E, Matsumoto I, Yasukochi T, Naito Y, Goto D, Mamura M, et al. Overexpression of phosphorylated STAT-1alpha in the labial salivary glands

of patients with Sjogren's syndrome. *Arthritis Rheum.* (2006) 54:3476–84. doi: 10.1002/art.22176
21. Germain RN. MHC-dependent antigen processing and peptide presentation: providing ligands for T lymphocyte activation. *Cell* (1994) 76:287–99. doi: 10.1016/0092-8674(94)90336-0
22. Tsunawaki S, Nakamura S, Ohyama Y, Sasaki M, Ikebe-Hiroki A, Hiraki A, et al. Possible function of salivary gland epithelial cells as nonprofessional antigen-presenting cells in the development of Sjogren's syndrome. *J Rheumatol.* (2002) 29:1884–96.
23. Bennett B, Check IJ, Olsen MR, Hunter RL. A comparison of commercially available adjuvants for use in research. *J Immunol Methods* (1992) 153:31–40. doi: 10.1016/0022-1759(92)90302-A
24. Lukic ML, Mensah-Brown E, Galadari S, Shahin A. Lack of apoptosis of infiltrating cells as the mechanism of high susceptibility to EAE in DA rats. *Dev Immunol.* (2001) 8:193–200. doi: 10.1155/2001/32636
25. Robinson K, Bellaby T, Wakelin D. Vaccination against the nematode *Trichinella spiralis* in high- and low-responder mice. Effects of different adjuvants upon protective immunity and immune responsiveness. *Immunology* (1994) 82:261–7.
26. Smith DE, O'Brien ME, Palmer VJ, Sadowski JA. The selection of an adjuvant emulsion for polyclonal antibody production using a low-molecular-weight antigen in rabbits. *Lab Anim Sci.* (1992) 42:599–601.
27. Billiau A, Matthys P. Modes of action of Freund's adjuvants in experimental models of autoimmune diseases. *J Leukoc Biol.* (2001) 70:849–60. doi: 10.1189/jlb.70.6.849
28. Turpie B, Yoshimura T, Gulati A, Rios JD, Dartt DA, Masli S. Sjogren's syndrome-like ocular surface disease in thrombospondin-1 deficient mice. *Am J Pathol.* (2009) 175:1136–47. doi: 10.2353/ajpath.2009.081058

Conflict of Interest Statement: The authors declare that the research was conducted in the absence of any commercial or financial relationships that could be construed as a potential conflict of interest.

frontiers in Immunology

REVIEW
published: 27 September 2018
doi: 10.3389/fimmu.2018.02047

The Challenge of the Pathogenesis of Parkinson's Disease: Is Autoimmunity the Culprit?

Tianfang Jiang[1], *Gen Li*[2], *Jun Xu*[3], *Shane Gao*[3]* *and Xu Chen*[1]*

[1] Department of Neurology, Shanghai Eighth People's Hospital Affiliated to Jiang Su University, Shanghai, China, [2] Department of Neurology & Institute of Neurology, Rui Jin Hospital Affiliated to Shanghai Jiao Tong University School of Medicine, Shanghai, China, [3] East Hospital, Tong Ji University School of Medicine, Shanghai, China

The role of autoimmunity in Parkinson's disease (PD), as one of the most popular research subjects, has been intensively investigated in recent years. Although the ultimate cause of PD is unknown, one major area of interest remains identifying new therapeutic targets and options for patients suffering from PD. Herein, we present a comprehensive review of the impacts of autoimmunity in neurodegenerative diseases, especially PD, and we have composed a logical argument to substantiate that autoimmunity is actively involved in the pathogenesis of PD through several proteins, including α-synuclein, DJ-1, PINK1, and Parkin, as well as immune cells, such as dendritic cells, microglia, T cells, and B cells. Furthermore, a detailed analysis of the relevance of autoimmunity to the clinical symptoms of PD provides strong evidence for the close correlation of autoimmunity with PD. In addition, the previously identified relationships between other autoimmune diseases and PD help us to better understand the disease pattern, laying the foundation for new therapeutic solutions to PD. In summary, this review aims to integrate and present currently available data to clarify the pathogenesis of PD and discuss some controversial but innovative research perspectives on the involvement of autoimmunity in PD, as well as possible novel diagnostic methods and treatments based on autoimmunity targets.

Keywords: autoimmunity, Parkinson's disease, α-synuclein, autoimmune diseases, neuroimmunology

OPEN ACCESS

Edited by:
Karsten Kretschmer, Technische Universität Dresden, Germany

Reviewed by:
Harley Y. Tse, Wayne State University, United States
Dan Lindholm, University of Helsinki, Finland

***Correspondence:**
Shane Gao
gaoshan2009@tongji.edu.cn
Xu Chen
cxwp65@163.com

Specialty section:
This article was submitted to Immunological Tolerance and Regulation, a section of the journal Frontiers in Immunology

Received: *25 January 2018*
Accepted: *20 August 2018*
Published: *27 September 2018*

Citation:
Jiang T, Li G, Xu J, Gao S and Chen X (2018) The Challenge of the Pathogenesis of Parkinson's Disease: Is Autoimmunity the Culprit? Front. Immunol. 9:2047. doi: 10.3389/fimmu.2018.02047

INTRODUCTION

The consensus is that under normal physiological conditions, the whole immune system fights against foreign antigens but not self-aggressors. Unfortunately, long-standing studies have revealed that immunological destruction may incite organisms to attack the self-antigens of cells or tissues, referred to as autoimmunity (1, 2). Failure to maintain the self-tolerance of lymphocytes is a fundamental explanation for the onset of autoimmune diseases. The pathogenesis of autoimmunity has been explored for many decades, and several relevant mechanisms have been confirmed to cause autoimmune diseases, which are summarized as follows: (1) genetic alterations in pattern recognition receptors (PRRs); (2) cross-reaction of immune cells with self-antigens (also called molecular mimicry); (3) epitope spreading or drifting; and (4) dysfunction of T cells and B cells. Specifically, Chastain and Schie have shown that genetic alterations in PRRs could increase the sensitivity threshold against harmless self-antigens. They also demonstrated that autoimmunity could result from cross-reactivity between a host cell receptor and the antibody induced by the antigenic epitope of an antiviral agent (3, 4).

Qiao et al. attributed the occurrence and development of an autoimmune disease to an imbalance between regulatory T cells (Tregs) plus suppressive cytokines and effector T cells plus pro-inflammatory cytokines (5). The powerful immune suppressive capacity of Tregs and their secreted cytokines could suppress not only effector T cells but also other immune cells, such as B cells and dendritic cells (DCs). Meanwhile, it has also been demonstrated that the assistance of $CD4^+$ cells (also known as helper T cells) is pivotal for the autoantibody response of B cells driven by autoantigens, which can also improve the outcome of immune reactions initiated by various antigen-presenting cells (APCs) as a secondary response to antigens (6, 7). This review mainly elaborates on how inappropriate immune responses in the central nervous system (CNS) contribute to the pathogenesis of a broad range of neurodegenerative disorders including but not be limited to Parkinson's disease (PD).

AUTOIMMUNITY IN NEURODEGENERATIVE DISEASES AND ITS RELEVANCE TO PD

The immune system always exerts intricate and reciprocal effects on the nervous system. Previous research considered brain cells safe from attack by the immune system because most neurons do not express antigens, which are markers specifically recognized by antibodies. Nevertheless, increasing data have indicated that autoimmunity causes neuronal demyelination, axonal damage, synaptic loss and further neurodegeneration (8). In fact, the CNS usually suffers from a chronic autoimmune attack. According to Kawai and Akira, inflammation is one of the first and most prominent events in this chronic process (9), which can last a decade or two, followed by the accumulation of neuronal injury, eventually resulting in irreversible neurodegeneration. When autoimmunity begins, some harmful cytokines are released, some of which further recruit immune cells to continuously attack neurons and nerve fibers (10–12). Multiple sclerosis is a torturous autoimmunity-related CNS disease with typical pathological variances that are usually clinically marked by oligoclonal bands and/or an increased immunoglobulin G index (13). As mentioned above, even though the damage associated with acute inflammatory lesions occurs first, the subsequent autoimmunity-induced neurodegeneration is linked with the progressive development of disability (14, 15). Overall, neurodegenerative diseases are irreversible, and the related deterioration might be due to the chronic, long-lasting, and autoimmunity-induced pathology transformation. Meanwhile, advanced age, one of the main risk factors of both neurodegeneration and autoimmune disease, is characterized by an erosion of tolerance and increased reactivity to self-antigens (16–19). As such, it is assumed that PD, as one of the most common neurodegenerative disorders ranking after Alzheimer's disease (AD), is also likely to be an autoimmune disease.

The pathogenesis, diagnosis and treatment of PD have received increasing interest due to the increasing morbidity and mortality, enervating features, irreversibility, and early-onset tendency of the disease. In terms of the mechanism of the death of dopaminergic neurons (DNs), no unanimous conclusion can yet be drawn. A growing number of published studies using cell culture systems and preclinical animal models have provided evidence for a role of the immune system in the etiology of PD (20–22). Some researchers had already begun to focus on the relationship between PD and autoimmunity as early in 1989; however, due to sample size limitations and immature experimental technology, they did not obtain reliable data showing a significant correlation between PD and autoimmunity (23). After nearly three decades, a series of research results have demonstrated that both the innate and adaptive immune systems are activated in PD. Significant increases in innate immune factors, including interleukin (IL)-1, IL-2, and IL-6 and tumor necrosis factor (TNF)-α, have been detected within the substantia nigra pars compacta (SNpc) and cerebrospinal fluid (CSF) of PD patients (24, 25), and γδ T cells, the first line of defense, have also been found to be elevated within the peripheral blood and CSF (26). For specific recognition, human catecholaminergic SNpc neurons express major histocompatibility complex I (MHC-I), which enables them to present autoantigens and be more susceptible to T cell-mediated cytotoxic attack (27). Increased levels of specific immunoglobulins in the peripheral blood and CSF of PD patients have further suggested that humoral autoimmunity is involved in the pathogenesis of PD (28–30). Additionally it became more convincing that post-mortem studies of PD brain tissue showed both $CD4^+$ and $CD8^+$ T cells in close proximity to DNs within the SNpc at levels 10-fold higher than in the control group (31). Analysis of the correlation between immunity and PD has demonstrated that immunoglobulin G (IgG) binds to DNs in PD (32). Moreover, an increase in $CD8^+$ T cells and a decrease in Tregs within the peripheral T lymphocyte populations of PD patients (33) indicated the downregulation of self-tolerance and upregulation of error recognition and self-attack, further corroborating the potential involvement of autoimmunity in PD progression. All of these reliable experimental data indicate that autoimmunity might play a key role in PD development. More in-depth studies are urgently needed to prove that autoimmunity is the main cause of PD and to explain the mechanism underlying the injury and selective loss of DNs. Autoimmunity contributes to the pathogenesis of PD in a multifactorial manner involving α-synuclein (α-syn) and immune cells (e.g., microglia and DCs) and the mutation of many genes (e.g., *PINK1*, *Parkin,* and *DJ-1*). These contributions produce varied and unique

Abbreviations: α-Syn, α-Synuclein; AD, Alzheimer's disease; APCs, antigen presenting cells; ARD, autoimmune rheumatic disease; BP, bullous pemphigoid; CNS, central nervous system; CSF, cerebrospinal fluid; DC, dendritic cell; DN, dopaminergic neuron; dsDNA, double-stranded deoxyribonucleic acid; GWAS, genome-wide association studies; HSV1, herpes simplex virus 1; Ig, immunoglobulin; IL, Interleukin; iTregs, induced regulatory T cells; LDLs, low-density lipoproteins; LPC, lipophosphatidylcholine; MAPK, mitogen-activated protein kinase; MDVs, mitochondria-derived vesicles; MHC, major histocompatibility complex; MitAP, mitochondrial antigens presentation; MPTP, 1-methyl-4-phenyl-1,2,3,6-tetrahydropyridine; NF-κB, nuclear factor kappaB; NM, neuromelanin; nTregs, natural regulatory T cells; PARK7, Parkinson's Disease Protein 7; PD, Parkinson's disease; PRRs, pattern recognition receptors; SIBO, small intestinal bacterial overgrowth; SLE, systemic lupus erythematous; SNpc, substantia nigra pars compacta; TNF, tumor necrosis factor; Tregs, regulatory T cells.

corresponding pathomechanisms and clinical features, which will be discussed at length in the following sections in sequence (**Figure 1**).

GENETIC REGULATION OF AUTOIMMUNITY IN PD

Some autoimmune diseases are frequently familial, while other autoimmune diseases are sporadic (34). Despite the proven genetic associations among distinct autoimmune diseases, much of the heritability remains unaccountable (35). Scientists have assumed that PD-related genes might be the key regulatory factors engaging the autoimmune system and their dysfunction would overshoot immunity either by lost tolerance or increased sensitivity thresholds to self-antigens (36). Undoubtedly, certain genes are closely related to PD, with two inheritance modes: autosomal dominant and autosomal recessive (37). Three genes, *PINK1*, *Parkin,* and *DJ-1*, are closely related to autosomal recessive genetics in early-onset PD. Meanwhile, mutations in *PINK1* and *Parkin*, which encode a mitochondrially targeted protein kinase and an E3 ubiquitin ligase, respectively, have been found in both familial and sporadic PD (38, 39). It was once believed that the dysfunction of these two genes would cause the failure to maintain normal mitochondrial function, leading to the loss of DNs and ultimately causing PD (39, 40). While in the past few years, it has been shown that *PINK1* and *Parkin*-related immune system disorders are indeed responsible for the upstream mechanism of mitochondrial aberrations. *PINK1*, a kinase stabilized at the surface of mitochondria, phosphorylates both ubiquitin and *Parkin* (41, 42). The reduced ability of *PINK1*$^{-/-}$ CD4^{+} T cells to suppress bystander T cell proliferation indicate that this pathological state could result in reduced immuno-surveillance or activated autoimmunity during PD progression (43). In addition, it has been reported that the loss of *PINK1*/*Parkin*-dependent mitochondrial quality control triggers a series of physiological events related to PD, including the abnormal initiation of innate immunity (44). The lack of *PINK1* and *Parkin* has been confirmed to induce high levels of mitochondrial antigen presentation (MitAP) MHC-I molecules in both macrophages and DCs, as well as accelerating the formation of mitochondria-derived vesicles (MDVs) on which MitAP depends both *in vitro* and *in vivo* (45). Data have also shown that *Parkin*$^{-/-}$ DNs with MitAP activation are recognized by established mitochondria antigen-specific T cells, accompanied by cytotoxic responses, including microglial activation and local inflammation, as well as a significant contribution of the immune system in the etiology of PD (34, 46). During the process of infection or inflammation, the presence of a lymphatic system in the CNS could facilitate the transportation of immune cells into the brain, subsequently destroying DNs expressing mitochondrial antigens on their surface. In other words, under these circumstances, mitochondrial antigen-expressing DNs are much more "visible" to autoimmunity (34, 47). As previously stated, elucidating the abnormal function of T cells in the absence of *PINK1* and/or *Parkin* may also help to unravel the role of autoimmunity in PD. Therefore, further investigations of T cell function in *PINK1* and/or *Parkin* mutation carriers are needed.

In addition to these observations, *DJ-1* (Parkinson's disease protein 7, *PARK7*) has also been reported to affect the development of natural Tregs (nTregs) and induced Tregs (iTregs, previously known as suppressor T cells). Mature Tregs with normal function, which modulate not only adaptive immunity but also innate immunity, are pivotal for maintaining thymic function, peripheral immune self-tolerance and immune system homeostasis. nTregs are generated in the thymus, while iTregs are derived from naïve CD4^{+} T cells encountering antigens in the peripheral organs. Both cell types are generally immunosuppressive through the suppression or downregulation of effector T cell proliferation (48). Their "self-check" function successfully prevents excessive effector cell reactions. On the other hand, the abnormal proliferation of both types of Tregs leads to the failure of self-/non-self-discrimination, resulting in autoimmune disease (49). Evidence reported by Singh et al. has demonstrated that *DJ-1*, one of the most classical key players responsible for PD pathogenesis, is strongly linked with neuroimmunology and multiple autoimmune responses in PD. In addition, *DJ-1*-deficient animal models have shown compromised iTreg induction, cell cycle progression, and cell survival and proliferation. *DJ-1*$^{-/-}$ iTregs are more proliferative, more susceptible to cell death signals and deficient in cell division compared with wild type counterparts, as analyzed by flow cytometry and Western blotting.

In conclusion, these discoveries provide a new perspective on the relationship between gene regulation and neuroimmunology. Consistent with previous reports, *PINK1*, *Parkin* and *DJ-1*, which have been cited as the three musketeers of neuroprotection (50), are beneficial to mammalian organisms. However, deficiency of these genes leads to a failure to maintain normal neuron function and prevent oxidative stress and inflammation damage in PD, which has also been confirmed by our previous studies (51, 52). Similarly, a failure to maintain the homeostatic immune system leads to a hyperactive autoimmune state and accelerates disease progression.

PATHOGENIC PROTEIN FUNCTION IN AUTOIMMUNITY-ASSOCIATED PD

α-Syn, a small synaptic protein and the primary component of Lewy bodies, if incorrectly modified or misfolded, can form soluble or insoluble aggregates and act as the neuropathological hallmark in the brain of patients with either sporadic or familial PD (53). α-Syn plays a leading role in the initiation and progression of Parkinson-like neurodegeneration because it can induce high neurotoxicity by diverse pathways, such as inflammation, oxidative stress and autophagy abnormalities (53, 54). The neurotoxicity of α-syn is largely attributed to its soluble or insoluble aggregates of oligomers or polymers, which are found throughout the SNpc in PD but are also found in other neurons. The hypothesis that α-syn is involved in the autoimmune process driving PD has been constantly

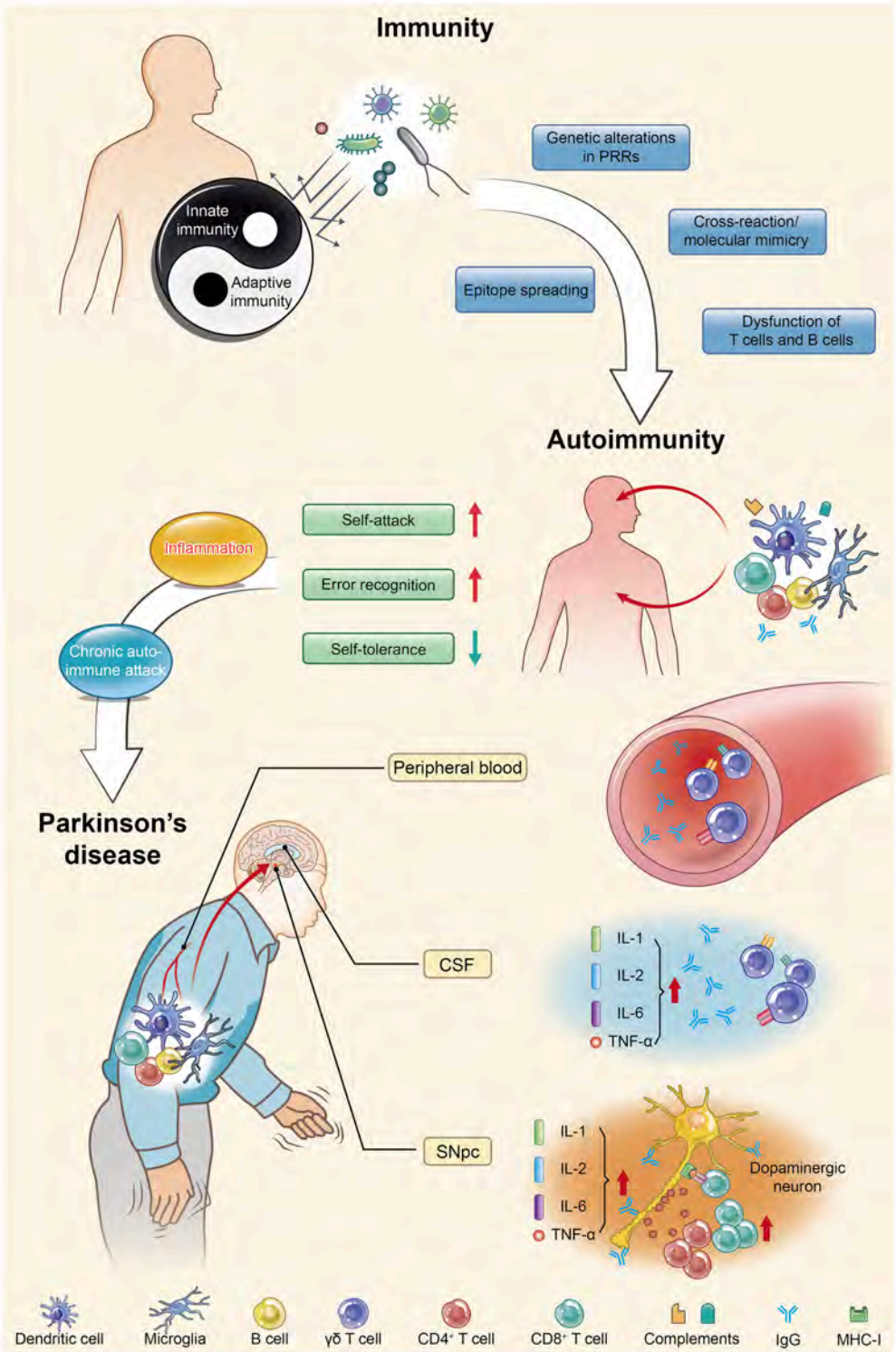

FIGURE 1 | Parkinson's disease (PD) is actually an autoimmune disease. Autoimmunity occurs when immune homeostasis is broken by several main mechanisms shown in this figure, which directly result in an increase in error recognition and self-attack and a decrease in self-tolerance to autoantigens. Regarding PD, chronic autoimmune attack is not only its pathogenesis but also always involved throughout the entire disease process. Inflammation is the first step of this attack, with the subsequent participation of various immune cells and immunoglobulins they produce, ultimately leading to the death of dopaminergic neurons. PRRs, pattern recognition receptors; CSF, cerebrospinal fluid; SNpc, substantia nigra pars compacta; IL, interleukin; TNF, tumor necrosis factor.

and widely debated. Prior experimental evidence in favor of α-syn as a self-antigen in PD is based on data reported by Benner et al., who found that effector T cells immunized by a self-antigen, nitrated-α-syn (typical neuropathology of PD), could exacerbate neuroinflammation and augment the neurodegeneration of SNpc DNs in an 1-methyl-4-phenyl-1,2,3,6-tetrahydropyridine (MPTP) mouse model (55). This finding indicates that nitrated-α-syn, as a self-protein and biomarker for the clinical diagnosis of PD, which was detected readily in cervical lymph nodes from MPTP-intoxicated mice, might break down immunological tolerance and induce the autoimmune responses that exacerbate the pathobiology of PD. This report led to an alternative theory that α-syn causes PD by triggering the immune system to attack the brain. Additionally, Cao et al. injected adeno-associated virus overexpressing α-syn into the SNpc of Fc-γ receptor$^{-/-}$ mice via a stereotaxic method and detected attenuated microglial activation and reduced dopaminergic neurodegeneration compared with non-injected controls (56). Over-abundance of α-Syn lead to the expression of a specific antigen, which further induces IgG generation. The Fc-γ receptor is expressed on the cell membrane of microglia, which binds IgG and triggers signal transduction events leading to microglial activation that eventually injures neurons in the SNpc. Therefore, α-syn is important for inducing an autoimmune response that leads to neurodegeneration. Upon further analysis, views from Heather's team have emphasized that in addition to nitration, another post-translational modification of α-Syn in PD, such as phosphorylation at serine 129 (S129), affects the toxicity, oligomerization, and immunogenicity of α-syn itself (57). Casein kinase-2 and G-protein-coupled receptor are two main kinases which influence the phosphorylation of α-syn (58, 59). Circumstance poisons such as MPTP and paraquat can also cause S129 of α-syn (60). Approximately 90% of α-syn in Lewy bodies is phosphorylated at S129 in PD in the brain, while it is relatively rare in human normal brain tissue (∼4%). Thus, researchers have speculated that the epitope of α-syn might not exist in the thymus when facing negative selection and would be erroneously recognized as a foreign antigen (61). In addition to the above findings and analysis, Li and Games and their colleagues found another way to change the antigenicity of α-syn both *in vitro* and *in vivo*. They passively immunized mice using α-syn antibodies designed to bind the gene's C-terminal fragments and successfully observed decreased α-syn aggregation, reduced DN loss, and alleviated movement disorder in the α-syn model of PD (62, 63). It could be concluded that the C-terminal truncation mutant of α-syn, identified in Lewy bodies and brain tissue with PD, possibly produces new antigens induced by altered α-syn processing.

As discussed above, molecular mimicry and cross immunoreactions are two of the primary mechanisms through which autoimmunity is triggered. Molecular mimicry between herpes simplex virus 1 (HSV1) and human α-syn was detected in PD patients in 2016. HSV1 infection could enhance the development of autoimmunity because autoreactive antibodies induced by HSV1 have the same response to the human α-syn homologous peptide bound to the membrane of DNs and lead to DN destruction (64). These results also support the assumption that α-syn participates in autoimmunity involved in the pathological progression of PD.

According to previous reports, MHC proteins are present on SNpc DNs and norepinephrine neurons in the locus coeruleus, and in the presence of the appropriate antigen and CD8$^+$ T cells (also known as cytotoxic T cells), MHC-I expressing SNpc murine neurons are more easily destroyed, suggesting that antigenic epitopes could activate CD8$^+$ T cells involved in the autoimmune response and cell death (27). In June 2017, Sulzer et al. concentrated on the characteristics of α-syn and tested whether it could be a target of T cells as a potential self-antigen (65). They detected the immune responses of peripheral blood mononuclear cells from 67 PD patients and 36 healthy controls that were exposed to a set of α-syn-derived peptides. It has been shown that the small stretches of α-syn around the Y39 and S129 phosphorylation regions successfully trigger the T cell response. Furthermore, the specific sets of T cells that respond to α-syn epitopes have also been identified to be mostly CD4$^+$ and partly CD8$^+$ T cells. This information could greatly benefit clinical diagnosis and treatment not only because T cell responsiveness might be a new biomarker for identifying individuals at risk or in the early stages of PD but also because of the potential for strategies for inhibiting the immune reaction or elevating the threshold of recognizing self-antigens, such as α-syn, as an attractive and promising therapeutic target in PD. However, there is still much more exploration to be done, as it is not yet clear if the autoimmune response is the initiator or an important pathogenic component of PD; in either case, it cannot be underestimated. Sulzer's team plans to block the autoimmune response in PD, e.g., by deleting certain T cell subpopulations, B cells or MHC, in an attempt to determine whether this will halt progression of the disease.

IMMUNE CELLS AND AUTOIMMUNITY IN PD

To date, numerous immune cells have been shown to be responsible for driving PD progression. DCs and microglia are two types of mammalian immune cells that act as the first and main forms of active immune defense in the CNS (66). They act first as APCs and then activate T cells to initiate the immune system to identify and attack extrinsic antigens. In essence, these immune cells lie at the intersection of the immune response and the neurodegenerative process—two primary aspects of CNS autoimmune disorders. DCs, the famous APCs (also known as accessory cells), serve as messengers between the innate and adaptive immune systems and can induce and even maintain self-tolerance (67). It is the differentiation/maturation rather than the haematopoietic origin or subset classification of DCs that determines their tolerogenic or immunogenic functions. Immature DCs can inhibit alloantigen-specific T cell responses to reverse autoimmune diseases in murine models but simultaneously induce antigen-specific T cell tolerance (68). The maturation of DCs into professional APCs via the upregulation of MHC expression enables DCs to capture antigens successfully (69). Based on these phenomena, Platt et al. proposed a theory

called "regulatory mechanisms by DCs" for immune responses against self-antigens. They concluded that the failure of DCs to control T cells via Treg differentiation and effector T cell clonal deletion leads to a direct attack on self-antigen-harboring target cells (70).

The progressive loss of neuromelanin (NM)-containing DNs in the SNpc is one of the predominant features of PD. Once produced by dopamine and norepinephrine via an interaction with cysteine as the inevitable by-product of aging (71), NM (the pigment) is no longer merely a spectator but an autoantigen released from dead DNs that stimulates the maturation and functional activation of DCs though being phagocytized by DCs, and then triggers an adaptive autoimmune response and finally leads to microglial activation, which enhances this autoimmunity via positive feedback (72). Subsequently, these mature DCs migrate from the CNS to cervical lymph nodes, resulting in the presentation of NM to naïve T and B cells in a highly immunogenic context (73). This autoimmune response might eventually lead to the death of NM-rich neurons in PD. Therefore, Oberlander and his colleagues inferred that NM is a potential target structure during autoimmune attack on DNs. This conclusion was later supported in 2009, as a relatively higher level of anti-NM antibodies was detected in the sera of PD patients (28). Consistently, a complement factor named C1q, which has been confirmed to be involved in the classical complement pathway and recognize antigen-bound IgG and IgM, was found to localize on the surface of extracellular NM in the brain of post-mortem PD patients (74). These data highlight the conclusion that NM is a potential target during the autoimmune-based pathogenesis of PD. Although DCs rarely exist in the healthy human brain, myeloid-derived DCs can still infiltrate the brain tissue during the process of neuroinflammation (75, 76). The exact mechanism by which NM activates DCs is by its peptide or lipid components, not by the dopamine melamine backbone, because DC maturation is due to the oxidized lipophosphatidylcholine (LPC) found in low-density lipoproteins (LDLs) (73). This point of view is supported by the increased lipid peroxidation in the SNpc detected in post-mortem PD patients.

In the context of autoimmune disorder-induced PD, the resulting antigens presented by microglia could promote self-antigen recognition by T cells, thus contributing to neuronal damage. The upregulation of MHC-II on microglia allowed microglia to present self-antigens to autoreactive T cells (77). This auto-aggressive loop initiated by DCs along with NM would be enhanced and amplified by microglial activation. Wilms et al. investigated the effects of NM on the release of neurotoxic mediators and the underlying signaling pathways through microglial culture in rats. NM augmented microglial activation by manipulating two signaling pathways, the p38 mitogen-activated protein kinase (MAPK) and nuclear factor kappa B (NF-κB) pathways (78). Similarly, NM injection into the rat SNpc induced microgliosis and the loss of tyrosine hydroxylase neurons *in vivo*, suggesting a close relationship between microglia and NM-associated DN degeneration in PD (79). As previously mentioned, inflammation acts as the first link between autoimmunity and its subsequent chronic damage, and our findings have suggested that the purinergic receptor P2Y6 mainly contributes to the activation and later phagocytosis of microglia in the CNS, resulting in an outbreak of inflammatory cytokines in the immune system (80). Hence, microglial activation is a downstream event in which microglia present an antigen (like NM) to DC-primed infiltrating T cells to direct the autoimmune response. Overall, DCs and microglia orchestrate the autoimmune response by executing different but cooperative functions during an autoimmune response (**Figure 2**).

CLINICAL FEATURES AND AUTOIMMUNITY IN PD

Dyskinesia, rest tremor, muscular rigidity, and gait disorder are the main motor symptoms of PD, while constipation, depression, hyposmia, and somnipathy are the main non-motor symptoms in a few PD patients. These symptoms indicate that there is much to translate from basic bench research into clinical treatment. Thus, the relationship between PD patients' clinical features and autoimmunity is also one of our interests in this review. There are three major, clinically relevant forms of PD: (1) tremor-dominant form; (2) rigidity-dominant form; and (3) gait difficulty form (81). Many clinical studies have provided solid evidence that autoimmunity participates in the pathogenesis of PD. Elevated serum levels of anti-α-syn antibodies have been found to be associated with familial variants of PD (29), and increased anti-GM1-ganglioside antibody levels have been detected in the tremor-dominant form of PD (82). As such, Benkler et al. analyzed 77 PD patients and 77 matched healthy controls and confirmed the presence of several autoantibodies previously shown to be involved with CNS manifestations (83). The anti-dsDNA seropositive PD patients had a significantly higher prevalence of dyskinesia than their control counterparts, and similar results were observed for anti-brain lysate antibodies. In terms of non-motor symptoms, depression is one of the most common symptoms in PD patients and has a strong positive correlation with the presence of anti-dsDNA and anti-brain lysate autoantibodies. Constipation is another well-known non-motor symptom of PD, and it has been reported to occur at median frequency of 40–50%, based on the definition (bowel movement frequency <1 per day) and clinical tools used (84). Among the indicators of impaired gastrointestinal motility in PD, only constipation may precede the onset of motor symptoms and can be an independent risk factor of PD (85), which may herald PD or related synucleinopathies neurodegenerative conditions by at least 5 years (86). Constipation has been confirmed to have an intimate relation with gut microbiota disorders. Evidence has shown that a pathogenic pathway exists between PD and small intestinal bacterial overgrowth (SIBO) (87), and the prevalence of SIBO is significantly higher in PD patients than in controls (88). Meanwhile, the "microbiome-gut-brain axis disorder" theory has been proposed to explain the pathogenesis of PD, which is significantly modulated by the gut microbiota via immunological and gut bacterial antigens exposed

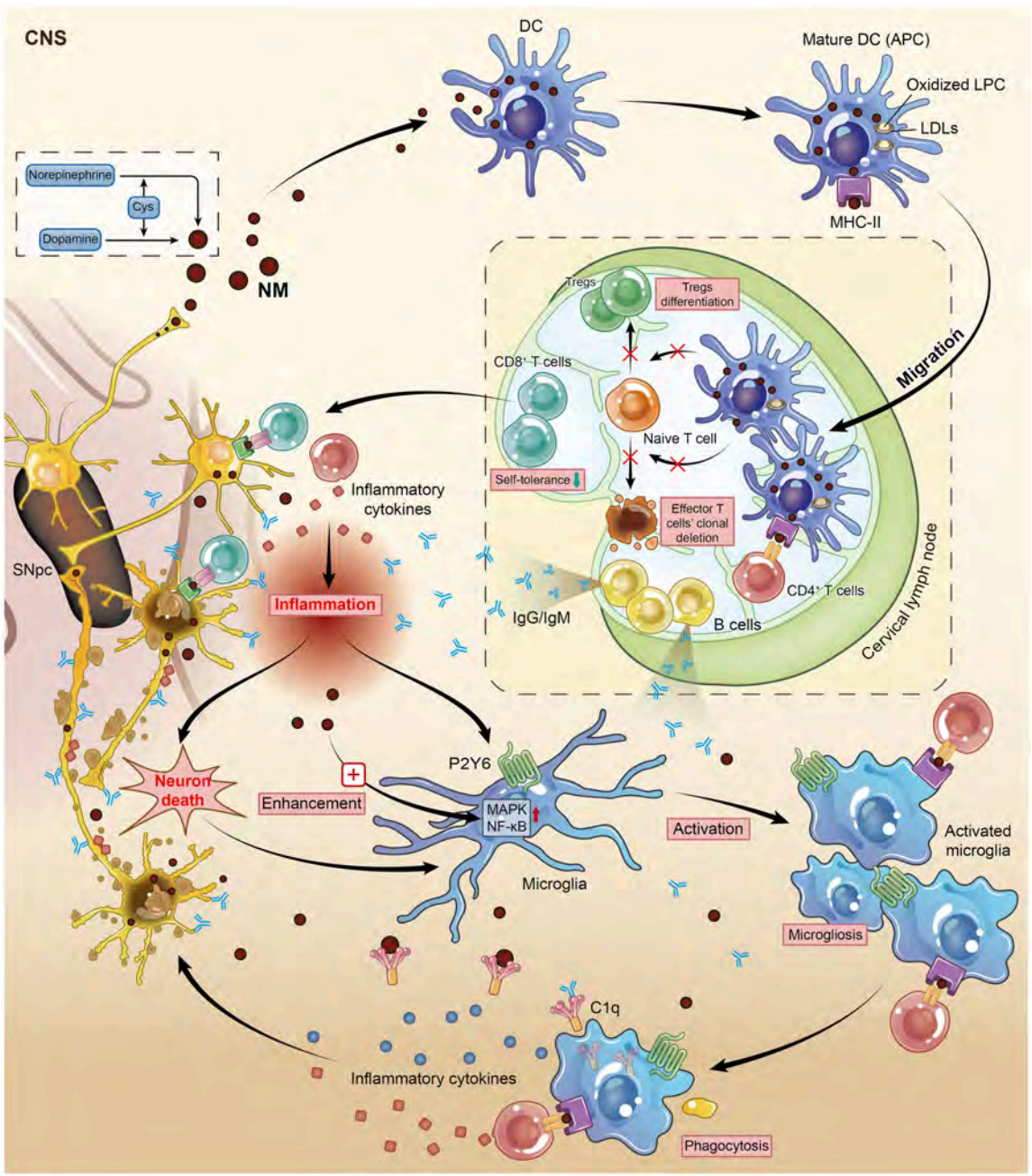

FIGURE 2 | Neuromelanin (NM) is one of the potential targets during the autoimmune-based pathogenesis of PD. This figure illustrates vividly how DCs and microglia, two kinds of mammalian immune cells, interact with each other and identify NM-rich cells as the object of autoimmune attack on DNs. Mature DCs migrate from the CNS to cervical lymph nodes, resulting in the presentation of NM to naïve T and B cells in a highly immunogenic context. This auto-aggressive loop initiated by DCs along with NM is enhanced and amplified by microglial activation. DC, dendritic cell; DN, dopaminergic neuron; CNS, central nervous system; APC, antigen-presenting cell; Cys, cysteine; Tregs, regulatory T cells.

to the immune system, which might also be autoimmunogenic (89). Dobbs et al. also proposed that gut microbiota disorders incur autoimmunity, ultimately resulting in neuronal damage and PD (90). Moreover, much research has provided new insights into the potential link between α-syn and the gut microbiota. Oueslati et al. described the appearance of α-syn-positive inclusions in the gastrointestinal track, notably in the colon, and elaborated the transmission of α-syn to the dorsal motor nucleus through the vagus nerve. This mechanism was further detailed by Braak's research showing that the α-syn pathology started in the submucosal plexus of the enteric nervous system and was propagated in a retrograde manner to the CNS (91). More specifically, α-syn aggregations reach the preganglionic cholinergic neurons of the dorsal motor nucleus and eventually

reaching the cerebral cortex via the retrograde axonal and transneuronal transport. In PD rat models, the increased expression of α-syn emerges earlier in the intestinal mucosa than in the brain (92). We observed intestinal flora variance in a PD mouse model induced by rotenone (data not published) and successfully detected and labeled α-syn in the intestinal mucosa to monitor its location and abnormal aggregation. All of these findings support the hypothesis that pathological progression spreads from the gut to the brain. In α-syn transgenic mice, intestinal flora disturbances have been observed and promoted constipation and motor dysfunction compared with the normal control mice. Furthermore, intestinal flora disturbances broke the immune tolerance mechanism of Tregs, leading to the activation of autoimmunity (93, 94). Excessive stimulation of the innate immune system caused by gut dysbiosis and/or SIBO might induce systemic inflammation, further incurring the activation of enteric glial cells and contributing to the initiation of α-syn misfolding, which is required for motor

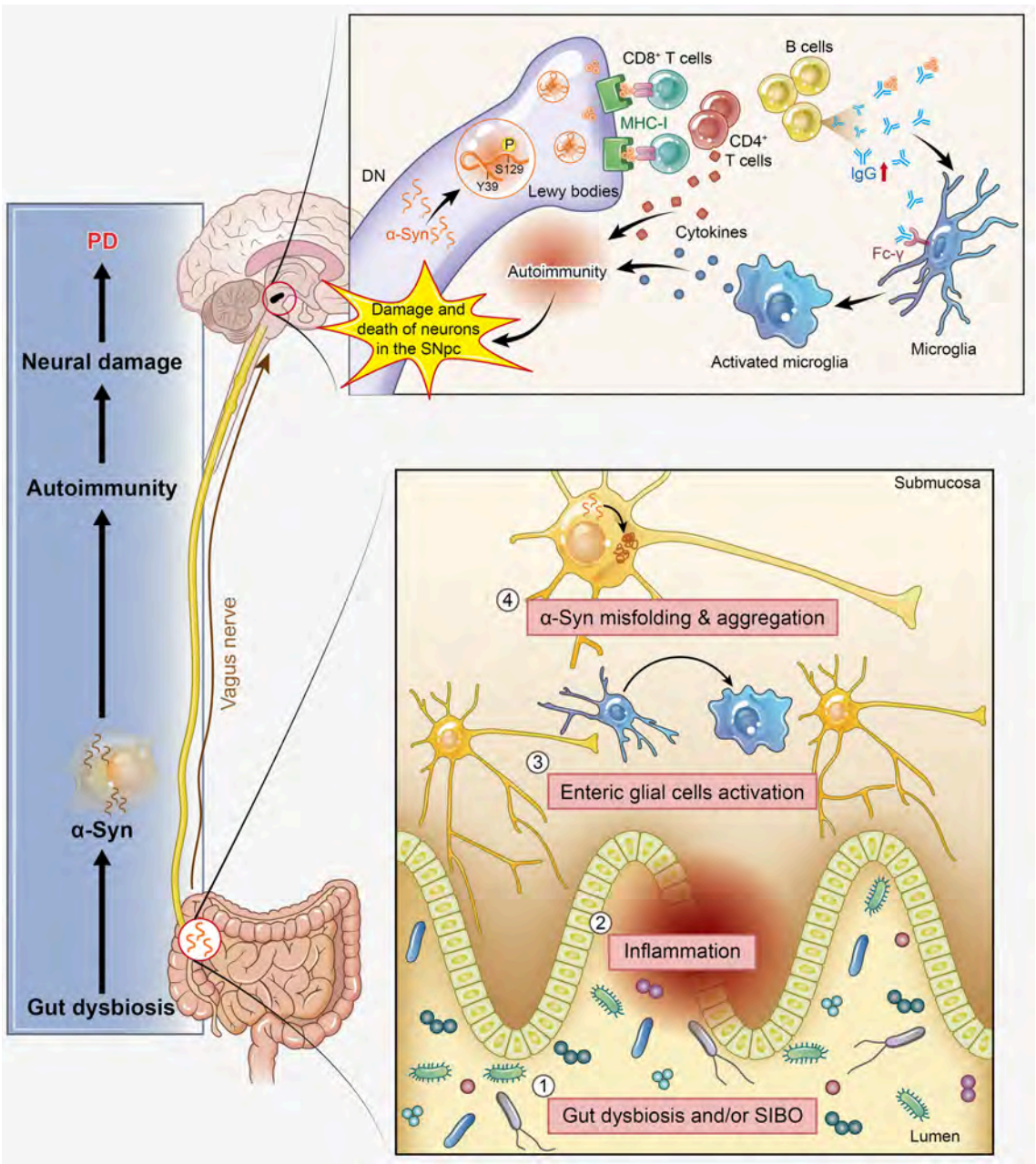

FIGURE 3 | α-Synuclein (α-syn) participates in autoimmunity and is involved in the pathological progression of PD. α-Syn, as the main disease-causing protein, first appears in the gut and is related to gut dysbiosis, which disturbs the intestinal immune system, leading to one of the main non-motor symptoms of PD: constipation. Then, this protein transmits to the dorsal motor nucleus through the vagus nerve and acts as a self-antigen targeted by effector T cells, B cells, and microglia. This autoimmunity attack finally results in the damage and death of DNs. SIBO, small intestinal bacterial overgrowth.

deficits (95). The involvement of α-syn in the autoimmunity-associated pathogenesis in the CNS of PD has been discussed in previous parts of this article; here, we provide additional evidence that α-syn-associated autoimmunity affects various aspects of PD, including both motor and non-motor symptoms, such as constipation. However, the exact mechanism driving α-syn aggregation in autoimmunity as well as its relationship with disease progression and neuronal degeneration remains unknown (**Figure 3**).

OTHER AUTOIMMUNE DISEASES COMBINED WITH PD

Autoimmunity can destroy the whole body, and at least 80 types of autoimmune diseases have been reported to date. There is no doubt that some of them tangle with each other and share a common pathogenesis. As early as 1999, Bonuccelli et al. reported that dyskinesias and "on-off" phenomena were abated when euthyroidism was restored in advanced PD accompanied by thyrotoxicosis (96). They further verified the possible neurological differences between PD and non-PD patients as being related to thyroid autoimmunity and function. Recently, increasing data have confirmed that hypo- and hyperthyroidism are more prevalent in PD patients than in normal controls because thyroperoxidase can influence PD nitrosative stress as well as serum α-syn nitrosylation (97). Likewise, in the last year, Bartkiewicz et al. confirmed that patients suffering bullous pemphigoid (BP), an autoimmune blistering dermatosis that occurs in the elderly, were more likely to suffer from neurological and psychiatric diseases, particularly prior to the diagnosis of BP (98). The autoantibodies bound two components of keratinocyte hemidesmosomal proteins, type XVII collagen/BPAG2 (BP180) and BPAG1 (BP230), as the autoantigens, which were also expressed in neuronal tissue. In addition, three types of autoantibodies, namely, anti-neuronal, anti-brain lysate, and anti-dsDNA antibodies, in patients with both PD and systemic lupus erythematous (SLE) were strongly associated with some clinical manifestations of PD, particularly dyskinesia and depression (99). A population-based case-control study in China last year also focused on the associations between autoimmune disease and PD (100). In this study, the overall incidence rate of PD was 30% higher in the autoimmune rheumatic disease (ARD) cohort than in the non-ARD cohort. Additional prospective studies should be conducted to confirm whether the activity and the severity of this autoimmune disease increase the risk of PD. Recent genome-wide association studies (GWAS) have tested the possible common genetic risk variants conveying risks for both PD and autoimmune diseases; 17 novel loci with overlap were identified, indicating that PD and other autoimmune diseases share genetic pathways (101). These results, from both fundamental and clinical studies, suggest that PD is closely associated with autoimmune diseases, further supporting the hypothesis that autoimmune mechanisms promote the development of PD.

Now that we have discussed this issue from a clinical perspective, immunotherapeutic strategies for PD cannot be neglected. Current treatments, including dopamine replacement therapy and alleviating the damage of oxidative stress and inflammation, seem insufficient and are limited in treating PD because most of them have only a therapeutic aim rather than both a therapeutic and prophylactic aim. The *in vivo* data presented by Zhu et al. demonstrated a significant

TABLE 1 | Autoimmunity can be a cause of PD.

Relationship	Research object	Evidence	References
Genetic regulation of autoimmunity in PD	*PINK1, Parkin*	Absence of *PINK1/Parkin* leads to the mitochondrial aberrations by triggering immune system disorders (reduced immuno-surveillance or activated autoimmunity).	(34, 43–47)
	DJ-1	Absence of *DJ-1* leads to abnormal proliferation of nTregs and iTregs, and result in autoimmunity.	(48, 49)
Pathogenic protein function in autoimmunity-associated PD	α-syn	Post-translational modifications and mutation of α-syn can be recognized as the autoantigen by the central immune system.	(55–57, 61, 63, 64)
Immune cells and autoimmunity in PD	DC	NM is an autoantigen released from dead DNs that stimulates the functional activation of DCs, triggering an autoimmune response and leading to microglial activation.	(28, 71–74)
	Microglia	Auto-aggressive loop initiated by DCs along with NM would be enhanced and amplified by microglial activation.	(77–79)
Clinical features and autoimmunity in PD	Tremor/dyskinesia/depression	Various autoantibodies have a strong positive correlation with these motor/non-motor symptoms.	(29, 82, 83)
	Constipation	Constipation is related to the gut dysbiosis and/or SIBO, which incurring the activation of enteric glial cells and contributing to the initiation of α-syn misfolding.	(89–92)
Other autoimmune diseases combined with PD	Hypothyroidism/hyperthyroidism/ BP/SLE/ARD	Other autoimmune diseases may share genetic pathways with PD and are correlated closely with some clinical manifestations of PD.	(96–101)

PD, Parkinson's disease; α-syn, α-synuclein; DC, dendritic cell; NM, neuromelanin; SIBO, small intestinal bacterial overgrowth; BP, bullous pemphigoid; SLE, systemic lupus erythematous; ARD, autoimmune rheumatic disease.

suppression of T cell mediated autoimmunity in carbidopa (one of the classical medicines against PD) treated mice compared with untreated mice (102). It revealed that to prevent autoimmune disorder in PD would be a new target for drug development. Meanwhile other new approaches for treating PD are also urgently needed. Accumulating data have shown that intracerebral injections of recombinant human α-syn can successfully expand nTreg and iTreg populations in a dose-dependent manner, accompanied by decreased α-syn aggregation in DNs and synapses and reduced neurodegeneration (103); this approach has potential as an immune therapy for PD. The exact mechanism might be that the induced α-syn-specific antibodies neutralize the α-syn deposits and harness the neuroinflammation by modulating the microglial phagocytosis of antibody-antigen complexes (104). Meanwhile, it has been proposed that the high affinity of α-syn antibodies to their α-syn antigen allows them to neutralize the neurotoxic α-syn aggregates without interfering with beneficial monomeric α-syn (105). In summary, an impaired capacity for immune clearance and blocking toxic α-syn aggregates might play critical roles in the pathogenesis of PD. Therefore, immunotherapy with α-syn antibodies could be a new alternative approach for effectively treating PD.

CONCLUSION

In all, autoimmunity disorders are one of the main mechanisms of PD pathogenesis and development and have gained increasing attention in recent years. Based on the latest research advances, including our laboratory data, conclusions can be drawn that both innate and adaptive immunity become pathogenic when self-antigen tolerance is lost. From all evidence, when facing an autoimmunity attack, the CNS cannot escape. To decipher the mechanisms of autoimmunity disorders involved in PD, the deletion or mutation of PD-related genes and the dysfunction of their encoded proteins should be studied. The involvement of α-syn provides strong evidence that this protein quite possibly acts as the first target of autoimmune attack, followed by the sustained activation of DCs and microglia, inflammation, and immune cell recruitment. Our review suggests that α-syn will no longer merely be the PD pathological hallmark but will also become one of the main targets of autoimmunity attack. In addition, NM, as another novel autoantigen released from dead DNs, is phagocytized by DCs and then induces the activation of microglia, contributing to the autoimmune aggravation of PD. Through developing neuroimmunoregulatory therapies, many new therapeutic options will become available to PD patients. These achievements will benefit both diagnostics and treatments. This review sheds light on autoimmunity associated with the etiology and pathogenesis of PD from a new perspective and further proposes some possible therapeutic targets and methods for PD (**Table 1**).

AUTHOR CONTRIBUTIONS

TJ and GL wrote the paper. JX supervised the figures. SG and XC supervised and wrote the paper.

ACKNOWLEDGMENTS

This work is supported by the Guangzhou Setzer biological Polytron Technologies Inc.

REFERENCES

1. Cardenas-Roldan J, Rojas-Villarraga A, Anaya JM. How do autoimmune diseases cluster in families? A systematic review and meta-analysis. *BMC Med.* (2013) 11:73. doi: 10.1186/1741-7015-11-73
2. Cooper GS, Bynum ML, Somers EC. Recent insights in the epidemiology of autoimmune diseases: improved prevalence estimates and understanding of clustering of diseases. *J Autoimmun.* (2009) 33:197–207. doi: 10.1016/j.jaut.2009.09.008
3. Chastain EM, Miller SD. Molecular mimicry as an inducing trigger for CNS autoimmune demyelinating disease. *Immunol Rev.* (2012) 245:227–38. doi: 10.1111/j.1600-065X.2011.01076.x
4. van Schie KA, Wolbink GJ, Rispens T. Cross-reactive and pre-existing antibodies to therapeutic antibodies–Effects on treatment and immunogenicity. *mAbs* (2015) 7:662–71. doi: 10.1080/19420862.2015.1048411
5. Qiao YC, Pan YH, Ling W, Tian F, Chen YL, Zhang XX, et al. The Yin and Yang of regulatory T cell and therapy progress in autoimmune disease. *Autoimmun Rev.* (2017) 16:1058–70. doi: 10.1016/j.autrev.2017.08.001
6. Iikuni N, Lourenco EV, Hahn BH, La Cava A. Cutting edge: regulatory T cells directly suppress B cells in systemic lupus erythematosus. *J Immunol.* (2009) 183:1518–22. doi: 10.4049/jimmunol.0901163
7. Mizoguchi A, Bhan AK. A case for regulatory B cells. *J Immunol.* (2006) 176:705–10. doi: 10.4049/jimmunol.176.2.705
8. Junker A, Bruck W. Autoinflammatory grey matter lesions in humans: cortical encephalitis, clinical disorders, experimental models. *Curr Opin Neurol.* (2012) 25:349–57. doi: 10.1097/WCO.0b013e3283534a8a
9. Kawai T, Akira S. Innate immune recognition of viral infection. *Nat Immunol.* (2006) 7:131–7. doi: 10.1038/ni1303
10. Doecke JD, Laws SM, Faux NG, Wilson W, Burnham SC, Lam CP, et al. Blood-based protein biomarkers for diagnosis of Alzheimer disease. *Arch Neurol.* (2012) 69:1318–25. doi: 10.1001/archneurol.2012.1282
11. Patejdl R, Zettl UK. Spasticity in multiple sclerosis: contribution of inflammation, autoimmune mediated neuronal damage and therapeutic interventions. *Autoimmun Rev.* (2017) 16:925–36. doi: 10.1016/j.autrev.2017.07.004
12. Ray S, Britschgi M, Herbert C, Takeda-Uchimura Y, Boxer A, Blennow K, et al. Classification and prediction of clinical Alzheimer's diagnosis based on plasma signaling proteins. *Nat Med.* (2007) 13:1359–62. doi: 10.1038/nm1653
13. Goris A, Pauwels I, Gustavsen MW, van Son B, Hilven K, Bos SD, et al. Genetic variants are major determinants of CSF antibody levels in multiple sclerosis. *Brain* (2015) 138:632–43. doi: 10.1093/brain/awu405
14. De Stefano N, Matthews PM, Fu L, Narayanan S, Stanley J, Francis GS, et al. Axonal damage correlates with disability in patients with relapsing-remitting multiple sclerosis. Results of a longitudinal magnetic resonance spectroscopy study. *Brain* (1998) 121:1469–77
15. Tallantyre EC, Bo L, Al-Rawashdeh O, Owens T, Polman CH, Lowe JS, et al. Clinico-pathological evidence that axonal loss underlies disability in progressive multiple sclerosis. *Mult. Scler.* (2010) 16:406–11. doi: 10.1177/1352458510364992
16. Agrawal A, Tay J, Ton S, Agrawal S, Gupta S. Increased reactivity of dendritic cells from aged subjects to self-antigen, the human DNA. *J Immunol.* (2009) 182:1138–45. doi: 10.4049/jimmunol.182.2.1138

17. Agrawal A, Tay J, Yang GE, Agrawal S, Gupta S. Age-associated epigenetic modifications in human DNA increase its immunogenicity. *Aging* (2010) 2:93–100. doi: 10.18632/aging.100121
18. Bueno V, Sant'Anna OA, Lord JM. Ageing and myeloid-derived suppressor cells: possible involvement in immunosenescence and age-related disease. *Age* (2014) 36:9729. doi: 10.1007/s11357-014-9729-x
19. Rosato E, Salsano F. Immunity, autoimmunity and autoimmune diseases in older people. *J Biol Regulat Homeostat Agents* (2008) 22:217.
20. De Virgilio A, Greco A, Fabbrini G, Inghilleri M, Rizzo MI, Gallo A, et al. Parkinson's disease: autoimmunity and neuroinflammation. *Autoimmun Rev.* (2016) 15:1005–11. doi: 10.1016/j.autrev.2016.07.022
21. Holmans P, Moskvina V, Jones L, Sharma M, Vedernikov A, Buchel F, et al. A pathway-based analysis provides additional support for an immune-related genetic susceptibility to Parkinson's disease. *Human Mol Genet.* (2013) 22:1039–49. doi: 10.1093/hmg/dds492
22. Kubo M, Kamiya Y, Nagashima R, Maekawa T, Eshima K, Azuma S, et al. LRRK2 is expressed in B-2 but not in B-1 B cells, and downregulated by cellular activation. *J Neuroimmunol.* (2010) 229:123–8. doi: 10.1016/j.jneuroim.2010.07.021
23. Moller A, Perrild H, Pedersen H, Hoier-Madsen M. Parkinson's disease and autoimmunity. *Acta Neurol Scand.* (1989) 79:173–5.
24. Liu B, Gao HM, Hong JS. Parkinson's disease and exposure to infectious agents and pesticides and the occurrence of brain injuries: role of neuroinflammation. *Environ Health Perspect.* (2003) 111:1065–73. doi: 10.1289/ehp.6361
25. Netea MG, Joosten LA, Latz E, Mills KH, Natoli G, Stunnenberg HG, et al. Trained immunity: a program of innate immune memory in health and disease. *Science* (2016) 352:aaf1098. doi: 10.1126/science.aaf1098
26. Fiszer U, Mix E, Fredrikson S, Kostulas V, Olsson T, Link H. gamma delta+ T cells are increased in patients with Parkinson's disease. *J Neurol Sci.* (1994) 121:39–45.
27. Cebrian C, Zucca FA, Mauri P, Steinbeck JA, Studer L, Scherzer CR, et al. MHC-I expression renders catecholaminergic neurons susceptible to T-cell-mediated degeneration. *Nat Commun.* (2014) 5:3633. doi: 10.1038/ncomms4633
28. Double KL, Rowe DB, Carew-Jones FM, Hayes M, Chan DK, Blackie J, et al. Anti-melanin antibodies are increased in sera in Parkinson's disease. *Exp Neurol* (2009) 217:297–301. doi: 10.1016/j.expneurol.2009.03.002
29. Papachroni KK, Ninkina N, Papapanagiotou A, Hadjigeorgiou GM, Xiromerisiou G, Papadimitriou A, et al. Autoantibodies to alpha-synuclein in inherited Parkinson's disease. *J Neurochem.* (2007) 101:749–56. doi: 10.1111/j.1471-4159.2006.04365.x
30. Yanamandra K, Gruden MA, Casaite V, Meskys R, Forsgren L, Morozova-Roche LA. alpha-synuclein reactive antibodies as diagnostic biomarkers in blood sera of Parkinson's disease patients. *PLoS ONE* (2011) 6:e18513. doi: 10.1371/journal.pone.0018513
31. Brochard V, Combadiere B, Prigent A, Laouar Y, Perrin A, Beray-Berthat V, et al. Infiltration of CD4+ lymphocytes into the brain contributes to neurodegeneration in a mouse model of Parkinson disease. *J Clin Invest.* (2009) 119:182–92. doi: 10.1172/jci36470
32. Orr CF, Rowe DB, Mizuno Y, Mori H, Halliday GM. A possible role for humoral immunity in the pathogenesis of Parkinson's disease. *Brain* (2005) 128:2665–74. doi: 10.1093/brain/awh625
33. Baba Y, Kuroiwa A, Uitti RJ, Wszolek ZK, Yamada T. Alterations of T-lymphocyte populations in Parkinson disease. *Parkinsonism Relat Dis.* (2005) 11:493–8. doi: 10.1016/j.parkreldis.2005.07.005
34. Mosley RL, Hutter-Saunders JA, Stone DK, Gendelman HE. Inflammation and adaptive immunity in Parkinson's disease. *Cold Spring Harb Persp Med* (2012) 2:a009381. doi: 10.1101/cshperspect.a009381
35. Cho JH, Gregersen PK. Genomics and the multifactorial nature of human autoimmune disease. *N Engl J Med.* (2011) 365:1612–23. doi: 10.1056/NEJMra1100030
36. Koutsilieri E, Lutz MB, Scheller C. Autoimmunity, dendritic cells and relevance for Parkinson's disease. *J Neural Trans.* (2013) 120:75–81. doi: 10.1007/s00702-012-0842-7
37. Houlden H, Singleton AB. The genetics and neuropathology of Parkinson's disease. *Acta Neuropathol.* (2012) 124:325–38. doi: 10.1007/s00401-012-1013-5
38. Narendra DP, Jin SM, Tanaka A, Suen DF, Gautier CA, Shen J, et al. PINK1 is selectively stabilized on impaired mitochondria to activate Parkin. *PLoS Biol.* (2010) 8:e1000298. doi: 10.1371/journal.pbio.1000298
39. Pickrell AM, Youle RJ. The roles of PINK1, parkin, and mitochondrial fidelity in Parkinson's disease. *Neuron* (2015) 85:257–73. doi: 10.1016/j.neuron.2014.12.007
40. Qu D, Hage A, Don-Carolis K, Huang E, Joselin A, Safarpour F, et al. BAG2 Gene-mediated regulation of pink1 protein is critical for mitochondrial translocation of parkin and neuronal survival. *J Biol Chem.* (2015) 290:30441–52. doi: 10.1074/jbc.M115.677815
41. Heo JM, Ordureau A, Paulo JA, Rinehart J, Harper JW. The PINK1-PARKIN mitochondrial ubiquitylation pathway drives a program of OPTN/NDP52 recruitment and TBK1 activation to promote mitophagy. *Mol Cell* (2015) 60:7–20. doi: 10.1016/j.molcel.2015.08.016
42. Lazarou M, Sliter DA, Kane LA, Sarraf SA, Wang C, Burman JL, et al. The ubiquitin kinase PINK1 recruits autophagy receptors to induce mitophagy. *Nature* (2015) 524:309–14. doi: 10.1038/nature14893
43. Ellis GI, Zhi L, Akundi R, Bueler H, Marti F. Mitochondrial and cytosolic roles of PINK1 shape induced regulatory T-cell development and function. *Eur J Immunol.* (2013) 43:3355–60. doi: 10.1002/eji.201343571
44. Mouton-Liger F, Jacoupy M, Corvol JC, Corti O. PINK1/Parkin-Dependent mitochondrial surveillance: from pleiotropy to parkinson's disease. *Front Mol Neurosci.* (2017) 10:120. doi: 10.3389/fnmol.2017.00120
45. Matheoud D, Sugiura A, Bellemare-Pelletier A, Laplante A, Rondeau C, Chemali M, et al. Parkinson's disease-related proteins pink1 and parkin repress mitochondrial antigen presentation. *Cell* (2016) 166:314–27. doi: 10.1016/j.cell.2016.05.039
46. Kannarkat GT, Boss JM, Tansey MG. The role of innate and adaptive immunity in Parkinson's disease. *J Parkinson's Dis.* (2013) 3:493–514. doi: 10.3233/jpd-130250
47. Louveau A, Smirnov I, Keyes TJ, Eccles JD, Rouhani SJ, Peske JD, et al. Structural and functional features of central nervous system lymphatic vessels. *Nature* (2015) 523:337–41. doi: 10.1038/nature14432
48. Bettelli E, Carrier Y, Gao W, Korn T, Strom TB, Oukka M, et al. Reciprocal developmental pathways for the generation of pathogenic effector TH17 and regulatory T cells. *Nature* (2006) 441:235–8. doi: 10.1038/nature04753
49. Sakaguchi S. Naturally arising Foxp3-expressing CD25+CD4+ regulatory T cells in immunological tolerance to self and non-self. *Nat Immunol.* (2005) 6:345–52. doi: 10.1038/ni1178
50. Trempe JF, Fon E. Structure and Function of Parkin, PINK1, and DJ-1, the three musketeers of neuroprotection. *Front Neurol.* (2013) 4:38. doi: 10.3389/fneur.2013.00038
51. Wang G, Pan J, Chen SD. Kinases and kinase signaling pathways: potential therapeutic targets in Parkinson's disease. *Progress Neurobiol.* (2012) 98:207–21. doi: 10.1016/j.pneurobio.2012.06.003
52. Yang H, Zhou HY, Li B, Niu GZ, Chen SD. Downregulation of parkin damages antioxidant defenses and enhances proteasome inhibition-induced toxicity in PC12 cells. *J Neuroimmune Pharmacol.* (2007) 2:276–83. doi: 10.1007/s11481-007-9082-2
53. Jiang T, Sun Q, Chen S. Oxidative stress: a major pathogenesis and potential therapeutic target of antioxidative agents in Parkinson's disease and Alzheimer's disease. *Progress Neurobiol.* (2016) 147:1–19. doi: 10.1016/j.pneurobio.2016.07.005
54. Jiang TF, Chen SD. Dysfunction of two lysosome degradation pathways of alpha-synuclein in Parkinson's disease: potential therapeutic targets? *Neurosci Bull.* (2012) 28:649–57. doi: 10.1007/s12264-012-1263-1
55. Benner EJ, Banerjee R, Reynolds AD, Sherman S, Pisarev VM, Tsiperson V, et al. Nitrated alpha-synuclein immunity accelerates degeneration of nigral dopaminergic neurons. *PLoS ONE* (2008) 3:e1376. doi: 10.1371/journal.pone.0001376
56. Cao S, Theodore S, Standaert DG. Fcgamma receptors are required for NF-kappaB signaling, microglial activation and dopaminergic neurodegeneration in an AAV-synuclein mouse model of Parkinson's disease. *Mol Neurodegenerat.* (2010) 5:42. doi: 10.1186/1750-1326-5-42
57. Allen Reish HE, Standaert DG. Role of alpha-synuclein in inducing innate and adaptive immunity in Parkinson disease. *J Parkinson's Dis.* (2015) 5:1–19. doi: 10.3233/jpd-140491

58. Hara S, Arawaka S, Sato H, Machiya Y, Cui C, Sasaki A, et al. Serine 129 phosphorylation of membrane-associated α-synuclein modulates dopamine transporter function in a G protein–coupled receptor kinase–dependent manner. *Mol Biol Cell* (2013) 24:1649–60. doi: 10.1091/mbc.E12-12-0903
59. Shahpasandzadeh H, Popova B, Kleinknecht A, Fraser PE, Outeiro TF, Braus GH. Interplay between sumoylation and phosphorylation for protection against α-synuclein inclusions. *J Biol Chem.* (2014) 289:31224–40. doi: 10.1074/jbc.M114.559237
60. Huang B, Wu S, Wang Z, Ge L, Rizak JD, Wu J, et al. Phosphorylated α-Synuclein accumulations and lewy body-like pathology distributed in parkinson's disease-related brain areas of aged rhesus monkeys treated with MPTP. *Neuroscience* (2018) 379:302–15. doi: 10.1016/j.neuroscience.2018.03.026
61. Anderson JP, Walker DE, Goldstein JM, de Laat R, Banducci K, Caccavello RJ, et al. Phosphorylation of Ser-129 is the dominant pathological modification of alpha-synuclein in familial and sporadic Lewy body disease. *J Biol Chem.* (2006) 281:29739–52. doi: 10.1074/jbc.M600933200
62. Games D, Seubert P, Rockenstein E, Patrick C, Trejo M, Ubhi K, et al. Axonopathy in an alpha-synuclein transgenic model of Lewy body disease is associated with extensive accumulation of C-terminal-truncated alpha-synuclein. *Am. J Pathol.* (2013) 182:940–53. doi: 10.1016/j.ajpath.2012.11.018
63. Li W, West N, Colla E, Pletnikova O, Troncoso JC, Marsh L, et al. Aggregation promoting C-terminal truncation of alpha-synuclein is a normal cellular process and is enhanced by the familial Parkinson's disease-linked mutations. *Proc Nat Acad Sci USA.* (2005) 102:2162–7. doi: 10.1073/pnas.0406976102
64. Caggiu E, Paulus K, Arru G, Piredda R, Sechi GP, Sechi LA. Humoral cross reactivity between alpha-synuclein and herpes simplex-1 epitope in Parkinson's disease, a triggering role in the disease? *J Neuroimmunol.* (2016) 291:110–4. doi: 10.1016/j.jneuroim.2016.01.007
65. Bandres-Ciga S, Cookson MR. Alpha-synuclein triggers T-cell response. Is Parkinson's disease an autoimmune disorder? *Mov Dis.* (2017) 32:1327. doi: 10.1002/mds.27116
66. Wlodarczyk A, Lobner M, Cedile O, Owens T. Comparison of microglia and infiltrating CD11c(+) cells as antigen presenting cells for T cell proliferation and cytokine response. *J Neuroinflammation* (2014) 11:57. doi: 10.1186/1742-2094-11-57
67. Bigley V, Barge D, Collin M. Dendritic cell analysis in primary immunodeficiency. *Curr Opin Allergy Clin Immunol.* (2016) 16:530–40. doi: 10.1097/aci.0000000000000322
68. Thomson AW, Robbins PD. Tolerogenic dendritic cells for autoimmune disease and transplantation. *Ann Rheum Dis.* (2008) 67 (Suppl. 3):iii90-6. doi: 10.1136/ard.2008.099176
69. Agrawal A, Sridharan A, Prakash S, Agrawal H. Dendritic cells and aging: consequences for autoimmunity. *Expert Rev Clin Immunol.* (2012) 8:73–80. doi: 10.1586/eci.11.77
70. Platt AM, Randolph GJ. Does deleting dendritic cells delete autoimmunity? *Immunity* (2010) 33:840–2. doi: 10.1016/j.immuni.2010.12.003
71. Ito S, Yamanaka Y, Ojika M, Wakamatsu K. The metabolic fate of ortho-quinones derived from catecholamine metabolites. *Int J Mol Sci.* (2016) 17:164. doi: 10.3390/ijms17020164
72. Haining R, Achat-Mendes C. Neuromelanin, one of the most overlooked molecules in modern medicine, is not a spectator. *Neural Regenerat Res.* (2017) 12:372–5. doi: 10.4103/1673-5374.202928
73. Oberlander U, Pletinckx K, Dohler A, Muller N, Lutz MB, Arzberger T, et al. Neuromelanin is an immune stimulator for dendritic cells in vitro. *BMC Neurosci.* (2011) 12:116. doi: 10.1186/1471-2202-12-116
74. Depboylu C, Schafer MK, Arias-Carrion O, Oertel WH, Weihe E, Hoglinger GU. Possible involvement of complement factor C1q in the clearance of extracellular neuromelanin from the substantia nigra in Parkinson disease. *J Neuropathol Exp Neurol.* (2011) 70:125–32. doi: 10.1097/NEN.0b013e31820805b9
75. Bailey SL, Schreiner B, McMahon EJ, Miller SD. CNS myeloid DCs presenting endogenous myelin peptides 'preferentially' polarize CD4+ T(H)-17 cells in relapsing EAE. *Nat Immunol.* (2007) 8:172–80. doi: 10.1038/ni1430
76. Zozulya AL, Ortler S, Lee J, Weidenfeller C, Sandor M, Wiendl H, et al. Intracerebral dendritic cells critically modulate encephalitogenic versus regulatory immune responses in the CNS. *J Neurosci.* (2009) 29:140–52. doi: 10.1523/jneurosci.2199-08.2009
77. Thompson KK, Tsirka SE. The diverse roles of microglia in the neurodegenerative aspects of central nervous system (CNS) autoimmunity. *Int J Mol Sci.* (2017) 18:504. doi: 10.3390/ijms18030504
78. Wilms H, Rosenstiel P, Sievers J, Deuschl G, Zecca L, Lucius R. Activation of microglia by human neuromelanin is NF-kappaB dependent and involves p38 mitogen-activated protein kinase: implications for Parkinson's disease. *FASEB J.* (2003) 17:500–2. doi: 10.1096/fj.020314fje
79. Zhang W, Phillips K, Wielgus AR, Liu J, Albertini A, Zucca FA, et al. Neuromelanin activates microglia and induces degeneration of dopaminergic neurons: implications for progression of Parkinson's disease. *Neurotox Res.* (2011) 19:63–72. doi: 10.1007/s12640-009-9140-z
80. Liu GD, Ding JQ, Xiao Q, Chen SD. P2Y6 receptor and immunoinflammation. *Neurosci Bull.* (2009) 25:161–4. doi: 10.1007/s12264009-0120-3
81. Thenganatt MA, Jankovic J. Parkinson disease subtypes. *JAMA Neurol.* (2014) 71:499–504. doi: 10.1001/jamaneurol.2013.6233
82. Zappia M, Crescibene L, Bosco D, Arabia G, Nicoletti G, Bagala A, et al. Anti-GM1 ganglioside antibodies in Parkinson's disease. *Acta Neurol Scand.* (2002) 106:54–7. doi: 10.1034/j.1600-0404.2002.01240.x
83. Benkler M, Agmon-Levin N, Hassin-Baer S, Cohen OS, Ortega-Hernandez OD, Levy A, et al. Immunology, autoimmunity, and autoantibodies in Parkinson's disease. *Clin Rev Allergy Immunol.* (2012) 42:164–71. doi: 10.1007/s12016-010-8242-y
84. Knudsen K, Krogh K, Ostergaard K, Borghammer P. Constipation in parkinson's disease: subjective symptoms, objective markers, and new perspectives. *Movement Dis.* (2017) 32:94–105. doi: 10.1002/mds.26866
85. Jost WH. Gastrointestinal dysfunction in Parkinson's Disease. *J Neurol Sci.* (2010) 289:69–73. doi: 10.1016/j.jns.2009.08.020
86. Goldman JG, Postuma R. Premotor and nonmotor features of Parkinson's disease. *Curr Opin Neurol.* (2014) 27:434–41. doi: 10.1097/wco.0000000000000112
87. Savica R, Carlin JM, Grossardt BR, Bower JH, Ahlskog JE, Maraganore DM, et al. Medical records documentation of constipation preceding Parkinson disease: a case-control study. *Neurology* (2009) 73:1752–8. doi: 10.1212/WNL.0b013e3181c34af5
88. Fasano A, Bove F, Gabrielli M, Petracca M, Zocco MA, Ragazzoni E, et al. The role of small intestinal bacterial overgrowth in Parkinson's disease. *Mov Dis.* (2013) 28:1241–9. doi: 10.1002/mds.25522
89. Negi S, Singh H, Mukhopadhyay A. Gut bacterial peptides with autoimmunity potential as environmental trigger for late onset complex diseases: in-silico study. *PLoS ONE* (2017) 12:e0180518. doi: 10.1371/journal.pone.0180518
90. Dobbs SM, Dobbs RJ, Weller C, Charlett A. Link between Helicobacter pylori infection and idiopathic parkinsonism. *Med Hypotheses* (2000) 55:93–8. doi: 10.1054/mehy.2000.1110
91. Braak H, de Vos RA, Bohl J, Del Tredici K. Gastric alpha-synuclein immunoreactive inclusions in Meissner's and Auerbach's plexuses in cases staged for Parkinson's disease-related brain pathology. *Neurosci Lett.* (2006) 396:67–72. doi: 10.1016/j.neulet.2005.11.012
92. Oueslati A, Ximerakis M, Vekrellis K. Protein Transmission, Seeding and degradation: key steps for alpha-synuclein prion-like propagation. *Exp Neurobiol.* (2014) 23:324–36. doi: 10.5607/en.2014.23.4.324
93. Cebula A, Seweryn M, Rempala GA, Pabla SS, McIndoe RA, Denning TL, et al. Thymus-derived regulatory T cells control tolerance to commensal microbiota. *Nature* (2013) 497:258–62. doi: 10.1038/nature12079
94. Sampson TR, Debelius JW, Thron T, Janssen S, Shastri GG, Ilhan ZE, et al. Gut microbiota regulate motor deficits and neuroinflammation in a model of parkinson’s disease. *Cell* (2016) 167:1469–80.e12. doi: 10.1016/j.cell.2016.11.018
95. Mulak A, Bonaz B. Brain-gut-microbiota axis in Parkinson's disease. *World J Gastroenterol.* (2015) 21:10609–20. doi: 10.3748/wjg.v21.i37.10609
96. Bonuccelli U, D'Avino C, Caraccio N, Del Guerra P, Casolaro A, Pavese N, et al. Thyroid function and autoimmunity in Parkinson's disease: a study of 101 patients. *Parkinsonism Relat Dis.* (1999) 5:49–53.
97. Fernandez E, Garcia-Moreno JM, Martin de Pablos A, Chacon J. May the thyroid gland and thyroperoxidase participate in nitrosylation of serum

proteins and sporadic Parkinson's disease? *Antioxid Redox Signal.* (2014) 21:2143–8. doi: 10.1089/ars.2014.6072

98. Bartkiewicz P, Gornowicz-Porowska J, Pietkiewicz PP, Swirkowicz A, Bowszyc-Dmochowska M, Dmochowski M. Neurodegenerative disorders, bullous pemphigoid and psoriasis: a comparative study in ethnic Poles indicates that Parkinson's disease is more relevant to bullous pemphigoid. *Postepy Dermatol Alergol.* (2017) 34:42–6. doi: 10.5114/ada.2017.65619
99. Liu FC, Huang WY, Lin TY, Shen CH, Chou YC, Lin CL, et al. Inverse association of parkinson disease with systemic lupus erythematosus: a nationwide population-based study. *Medicine* (2015) 94:e2097. doi: 10.1097/md.0000000000002097
100. Chang CC, Lin TM, Chang YS, Chen WS, Sheu JJ, Chen YH, et al. Autoimmune rheumatic diseases and the risk of Parkinson disease: a nationwide population-based cohort study in Taiwan. *Ann Med.* (2018) 50:83–90. doi: 10.1080/07853890.2017.1412088
101. Witoelar A, Jansen IE, Wang Y, Desikan RS, Gibbs JR, Blauwendraat C, et al. Genome-wide pleiotropy between parkinson disease and autoimmune diseases. *JAMA Neurolo.* (2017) 74:780–92. doi: 10.1001/jamaneurol.2017.0469
102. Zhu H, Lemos H, Bhatt B, Islam BN, Singh A, Gurav A, et al. Carbidopa, a drug in use for management of Parkinson disease inhibits T cell activation and autoimmunity. *PLoS ONE* (2017) 12:e0183484. doi: 10.1371/journal.pone.0183484
103. Christiansen JR, Olesen MN, Otzen DE, Romero-Ramos M, Sanchez-Guajardo V. Alpha-Synuclein vaccination modulates regulatory T cell activation and microglia in the absence of brain pathology. *J Neuroinflam.* (2016) 13:74. doi: 10.1186/s12974-016-0532-8
104. Brudek T, Winge K, Folke J, Christensen S, Fog K, Pakkenberg B, et al. Autoimmune antibody decline in Parkinson's disease and Multiple System Atrophy; a step towards immunotherapeutic strategies. *Mol Neurodegenerat.* (2017) 12:44. doi: 10.1186/s13024-017-0187-7
105. Emadi S, Barkhordarian H, Wang MS, Schulz P, Sierks MR. Isolation of a human single chain antibody fragment against oligomeric α-synuclein that inhibits aggregation and prevents α-synuclein induced toxicity. *J Mol Biol.* (2007) 368:1132–44. doi: 10.1016/j.jmb.2007.02.089

Conflict of Interest Statement: The authors declare that the research was conducted in the absence of any commercial or financial relationships that could be construed as a potential conflict of interest.

frontiers in Immunology

REVIEW
published: 12 September 2018
doi: 10.3389/fimmu.2018.01952

Tertiary Lymphoid Structures: Autoimmunity Goes Local

Elena Pipi[1,2†], Saba Nayar[1†], David H. Gardner[1], Serena Colafrancesco[3], Charlotte Smith[1] and Francesca Barone[1]*

[1] Rheumatology Research Group, Institute of Inflammation and Ageing, University of Birmingham, Birmingham, United Kingdom, [2] Experimental Medicine Unit, Immuno-Inflammation Therapeutic Area, GSK Medicines Research Centre, Stevenage, United Kingdom, [3] Reumatologia, University of Rome, Sapienza, Italy

Tertiary lymphoid structures (TLS) are frequently observed in target organs of autoimmune diseases. TLS present features of secondary lymphoid organs such as segregated T and B cell zones, presence of follicular dendritic cell networks, high endothelial venules and specialized lymphoid fibroblasts and display the mechanisms to support local adaptive immune responses toward locally displayed antigens. TLS detection in the tissue is often associated with poor prognosis of disease, auto-antibody production and malignancy development. This review focuses on the contribution of TLS toward the persistence of the inflammatory drive, the survival of autoreactive lymphocyte clones and post-translational modifications, responsible for the pathogenicity of locally formed autoantibodies, during autoimmune disease development.

Keywords: tertiary lymphoid structures (TLS), autoantibodies, germinal center response, glycosylation, B-cells

OPEN ACCESS

Edited by:
Ralf J. Ludwig, Universität zu Lübeck, Germany

Reviewed by:
Andreas Habenicht, Ludwig-Maximilians-Universität München, Germany
Karen Willard-Gallo, Free University of Brussels, Belgium

***Correspondence:**
Francesca Barone
f.barone@bham.ac.uk

† These authors have contributed equally to this work

Specialty section:
This article was submitted to Inflammation, a section of the journal Frontiers in Immunology

Received: *11 February 2018*
Accepted: *07 August 2018*
Published: *12 September 2018*

Citation:
Pipi E, Nayar S, Gardner DH, Colafrancesco S, Smith C and Barone F (2018) Tertiary Lymphoid Structures: Autoimmunity Goes Local. Front. Immunol. 9:1952. doi: 10.3389/fimmu.2018.01952

INTRODUCTION

The polyclonal expansion of autoreactive B cells is a cardinal feature of autoimmune conditions. Whether directed against a single antigen or playing part in a poly-specific response, autoreactive B cells support the persistence of the autoimmune process and, in several cases are directly pathogenic.

The development of an autoreactive B cell repertoire during the natural history of the autoimmune condition is regulated by the process of affinity maturation against single or multiple autoantigens that occurs within the inner part of the B cell follicles, classically within secondary lymphoid organs (SLOs) (1). Formation of B cell follicles and germinal centers (GC) has been also described in ectopic or tertiary lymphoid structures (TLS) in a process defined "ectopic lymphoneogenesis." TLS form at target organs of chronic inflammatory/autoimmune process, localized infections and in the areas surrounding solid tumors (2–11). The prognostic value of these structures is debated. TLS formation in target organs autoimmune disease is classically associated with disease persistence and worst clinical manifestations. In solid tumors TLS have instead been associated with the generation of an anti-tumor response, however in some cases the ability of tumor cells to induce T regulatory cells (Treg) and suppress the host immune response has been described **Table 1**.

Often indicated as "tertiary lymphoid organs," TLS fail to adhere to the proper definition of organs as they lack a stable structural organization, including a capsule, and are better classified as "tertiary lymphoid structures" or TLS (97). TLS are not present in embryonic life and form in adult life to support local aggregation of lymphocytes at the target organ of disease. Other terms

TABLE 1 | TLS in different conditions.

Disease	Type	Localization	Specific antigens identified?	Role/prognosis	Human studies	Mouse studies
GPA/WG	AID	Lungs	ANCAs	pathogenic	(12, 13)	
Hashimoto's Thyroiditis	AID	Thyroid	Thyroglobulin, Thyroperoxidase	pathogenic	(14, 15)	(16, 17)
MS	AID	CNS	Myelin (in mice)	pathogenic	(18–21)	(22–28)
Myasthenia gravis	AID	Thymus	Acetylcholine receptor	pathogenic	(29, 30)	(31)
Primary biliary cirrhosis,	AID	Liver	No	N/A	(32)	
Rheumatoid Arthritis	AID	Synovium	RF, Citrullinated proteins	pathogenic	(33, 34)	(33, 35)
Sjogren's Syndrome	AID	Salivary/Lachrymal glands, Lung	SSA/Ro & SSB/La	pathogenic	(36–38)	(39, 40)
SLE	AID	Kidneys	No	pathogenic	(41)	(42, 43)
Breast cancer	Can	Breast	Tumor associated antigens	favorable	(44–47)	
Colorectal cancer	Can	Colon	No	favorable	(48, 49)	(49)
Lung cancer	Can	Lung	No	favorable	(50, 51)	
Ovarian cancer	Can	Ovarian	No	favorable	(52)	
Melanoma	Can	Skin	No	favorable	(53)	
PCD	Can	Pancreas	No	favorable	(54)	
Prostate cancer	Can	Prostate	No	favorable	(55)	
Atherosclerosis	CID	Arteries	No	protective (in mice)	(56, 57)	(58, 59)
COPD	CID	Lung	No	pathogenic (in mice)	(60–64)	(60, 62, 65)
IBD	CID	Gut	No	pathogenic (in mice)	(66–69)	(70–74)
PSC	CID	Liver	No	N/A	(75)	
Lyme disease	Inf	Joints	No direct evidence	N/A	(76)	
HCV	Inf	Liver	No direct evidence	N/A	(77–80)	
Heliobacter pylori	Inf	Gastric wall	No direct evidence	Pathogenic	(81–83)	(84)
Mycobacterium tuberculosis	Inf	Lungs	No direct evidence	Protection against pathogen	(85–87)	(85, 86, 88)
Allograft transplants	Tra	Heart, lung, kidney	Allo-antigens	Highly controversial	(89–94)	(95, 96)

GPA/WG, Granulomatosis polyangiitis/Wegener's granulomatosis; COPD, Chronic Obstructive Pulmonary Disease; IBD, Inflammatory Bowel Disease; PSC, Primary Sclerosing Cholangitis AID, Autoimmune disease; CID, Chronic inflammatory disease; PDC, Pancreatic duct carcinoma; HCV, Hepatitis C virus; Can, Cancer; Tran, Transplantation; Inf, Infection. (Note: Studies on mice are presented only if there is evidence from human studies for the presence of TLSs in these different conditions).

including "ectopic lymphoid structures" (ELS) or "ectopic germinal centers". The latter, however, should only be used when GC formation is determined histologically within the ectopic lymphoid tissue (97–101). The cross-over between TLS and SLO is the subject of debate and has been reviewed by ourselves and others in recent publications (9, 98).

The term "tertiary lymphoid" tissue in the literature dates back to 1992 and was introduced by Louis Picker and Eugene Butcher (102) to describe the formation of extra-lymphoid sites, where memory lymphocytes and/or precursors can be re-stimulated by antigen to induce further clonal expansion or terminal effector responses. By definition, TLS arise in tissues whose main function is other than the generation of immune cells or the initiation of an adaptive immune response. This excludes the bone marrow and thymus, (as primary lymphoid organs) and spleen, lymph nodes and Peyer's patches (which are defined as SLOs). The kidneys, heart, pancreas, synovium and salivary glands are not embryologically predisposed to host the presence of lymphoid tissue therefore lymphocyte assembly at these sites should be considered TLS. The liver provides a hematopoietic function during embryonic development (103) however, this function is lost postnatally, thus including this organ among those that host TLS in adult life (97).

TLS form in response to a series of pro-inflammatory cytokines and TNF receptor family members following the local cross-talk between inflammatory immune cells and resident stromal cells. Fibroblasts, perivascular myo-fibroblasts and resident mesenchymal cells have been differently implicated in TLS development (39, 75, 104–112). Their role has been recently reviewed elsewhere (97, 113, 114). Probably evolved before SLO, TLS might have developed in ectopic tissues to fulfill the survival need of aggregated leucocytes, prior to placentation and development of SLOs. As such, the ability of TLS to be initiated independently from Lymphotoxin (LT) upon the expression of inflammatory cytokines and in absence of lymphoid tissue inducer cells (LTi) might

have remained as heritage of their developmental ancestry (97).

Physiologically, the generation of a humoral response requires the physical interaction of naïve B cells with antigen experienced T cells within the confined space of a microenvironment rich in survival and chemotactic factors (115). Lymphocytes are recruited from the bloodstream to the SLO in response to a chemotactic gradient that regulates cell positioning and interactions (116, 117). CXCL13 and CCL19/CCL21, ligands for the chemokine receptors CXCR5 and CCR7, respectively, regulate the recirculation of naïve B cells between the inner part of the B cell follicle to the outer area of the T/B cell boundary (118), thus enabling the contact of B cells with antigen-experienced, activated T cells (119). Within the follicles, antigen-experienced B cells migrate toward the dark zone of the GC, a highly hypoxic CXCL12-rich area. Within this area they become highly proliferating centroblasts and upregulate the enzyme activation-induced cytidine deaminase (AID) (120, 121), that regulates the introduction of single base-pair substitutions of antibody gene segments in the immunoglobulin (Ig) variable-region genes, in a process defined as somatic hypermutation (SHM) (122).

Following SHM, B cells stop proliferating and undergo the process of affinity maturation (123). Differentiated, non-dividing B cells (centrocytes) upregulate CXCR5 and migrate along the CXCL13 gradient toward the GC light zone (120), herby establishing connections with the network of follicular dendritic cells (FDC) that provide survival factors (124, 125) and antigen presentation via the CR2 receptor (125, 126). Within the light zone, centrocytes also encounter mature T follicular helper cells (T_{fh}), known to provide signals for selection and terminal differentiation into long-lived plasma cells or memory B cells (127–130). Once exited from the GC, affinity matured B cells undergo the process of class switch recombination (CSR), that regulates isotype switching and ultimate effector function of the immunoglobulins (Igs). This latter process is also regulated by AID (130–142) (**Figure 1A**).

This organizational program in SLOs is maintained by the anatomical differentiation of specialized, resident stromal cells that regulate migration and functional activation of the immune cells in the different part of the follicle (138, 143–149). The development of this stromal network and the signals required for his homeostasis have been reviewed elsewhere (150). TLS display a similar anatomical structure to support naïve B and T cell recirculation, including the expression of homeostatic lymphoid chemokines CXCL13, CCL21 and CCL19 and the molecular complex peripheral node addressin (PNAd) (97, 98, 151, 152). However, the complex anatomical compartmentalization displayed in SLO is rarely acquired in TLS. While the majority of reports on TLS describe a certain degree of T/B cell segregation, vascular/stromal cell specialization and expression of lymphoid chemokines, the presence of a more complex organization of the TLS and the formation of functional GC is highly variable within and amongst diseases (4, 153–155). In TLS that form during chronic autoimmune processes, the establishment of such disorganized microenvironment, rich in survival factors and pro-inflammatory cytokines, but likely missing key checkpoints for autoreactive cells screening, is likely responsible for the local generation of pathogenic autoantibody specificities and oncogenic mutations, ultimately favoring disease progression (1, 9, 97, 98).

TLS IN AUTOIMMUNE CONDITIONS: A LESSON FROM RHEUMATOID ARTHRITIS AND SJÖGREN'S SYNDROME

In 1996, Nancy Ruddle described the presence of a "structural chronic inflammatory process" caused by ectopic production of lymphotoxin, in the context of chronic inflammation of the pancreas (156). Since then, TLS formation has been associated with a localized process of inflammation at sites of infection, autoimmunity, cancer, and allograft rejection. The ultimate pathogenic role of TLS is still debated (98, 151) and most likely depends on the context, organ and type of disease. For the scope of this review we will focus on the role of TLS in supporting the autoimmune process in chronic autoimmune conditions and we will discuss the role of TLS in Rheumatoid Arthritis (RA) and primary Sjögren's Syndrome (pSS) (33, 36, 135, 151, 157–162).

RA is the most common rheumatic autoimmune condition, affecting 0.5–1% of the global adult population. The pathological features of the disease include severe inflammation of the synovial membrane that, in some cases, leads to tissue destruction and subchondral bone erosions (163–166). Histologically, the disease can be classified in 3 main histopathological subtypes: a lymphoid type, mainly characterized by T and B cell aggregates that form TLS; a myeloid type, characterized by diffuse infiltration of prevalent monocyte and macrophages; and the fibroid type, defined by scarce or no immune cell infiltration and prevalent synovial fibroblast hyperplasia (151).

The presence of a "…marked infiltration of chronic inflammatory cells *(lymphocytes or plasma cells predominating) with tendency to form "lymphoid nodules"* was recognized already in the 1957 RA classification criteria (167). In 1972, Munthe and Natvig suggested that the RA synovial membrane is similar to an active lymphoid organ*, containing many lymphoid follicles with GC that undergo local division and differentiation into plasma cells with restricted Ig production* (168). Later, Steere and colleagues described "*elements found in normal organized lymphoid tissue*" in synovial lesions from both RA and Lyme disease patients (169); suggesting that the formation of GC-like structures in the synovium is not specific for RA and can be driven by the local antigenic stimulation. It took, however, more than 40 years after these first descriptions to introduce the concept that B-cell affinity maturation could arise within the inflamed synovium (170). It is now accepted that TLS are present in less than half of RA patients who display so called "lymphoid" synovitis (151) and that, in those patients, the presence of TLS is associated with differential prognosis and disease manifestations (151). TLS formation in the synovia have been also identified in patients with psoriatic arthritis (171) and ankylosing spondylitis (172, 173).

A similar phenomenon of leucocyte aggregation in lymphoid like structures occurs in the salivary glands of patients affected

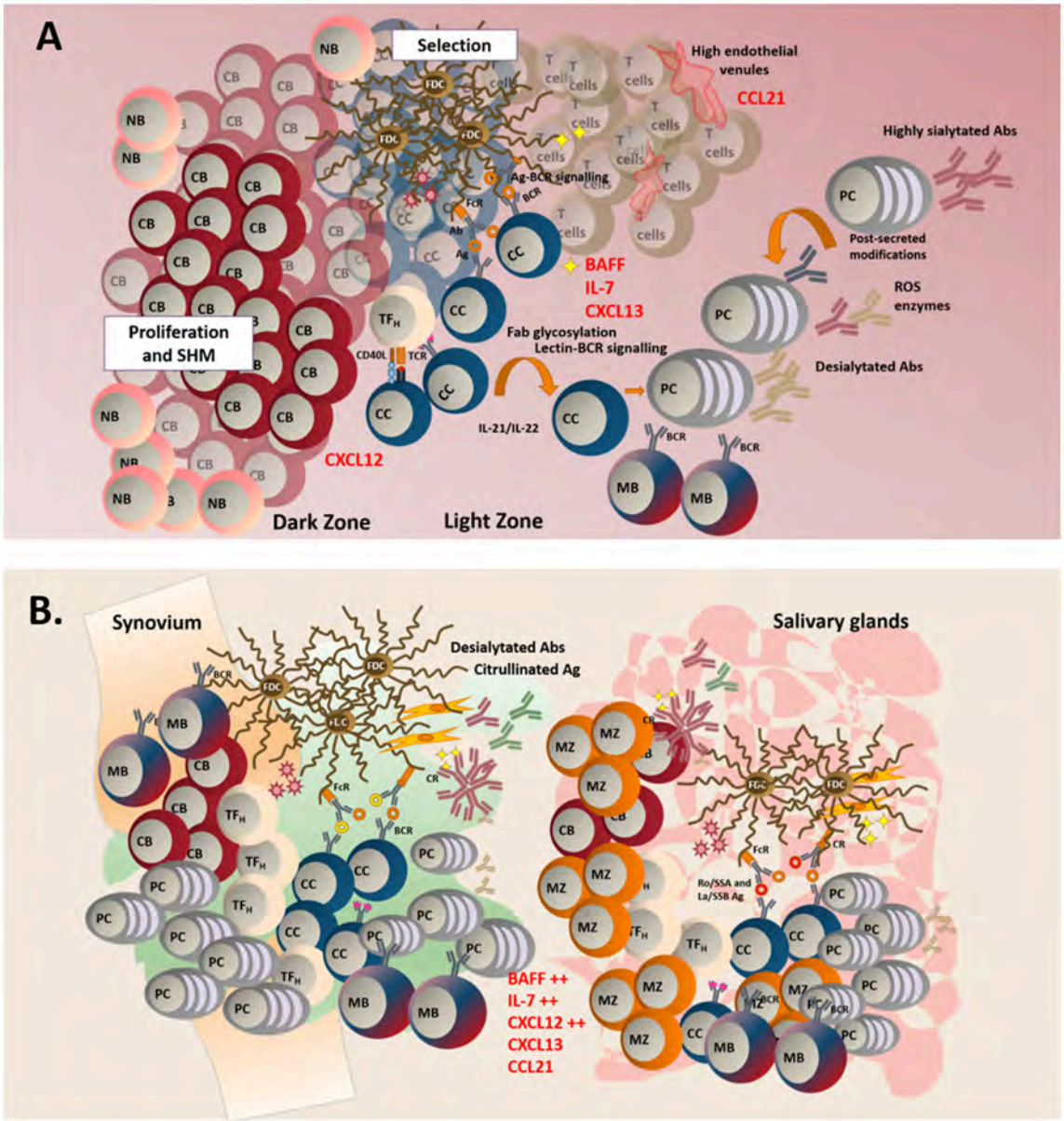

FIGURE 1 | (A) In TLS, naïve B cells (NB), enter the follicle to initiate a classical germinal center reaction. In the dark zone, centroblasts (CB) proliferate and acquire somatic hypermutations in their variable region. In the light zone, centrocytes (CC) are selected after their interaction with specific antigen found on the surface of follicular dendritic cells (FDCs). Lectin-BCR signaling can potentially result in enhanced selection of B cells. Failure to receive survival signals from either TF_H (T follicular helper cells) or FDCs leads to B cell apoptosis. Successful affinity maturation results in either mature B cell (MB) of plasma cells generation. GC microenvironment can control the outcome of the immune response by regulating the glycosylation profile of the antibodies. **(B)** TLS display a less organized anatomical structure and a predominant infiltration of MB and marginal zone B cells (MB). Aberrant production of survival and chemoattractant signals is observed at these sites.

by pSS, a disease characterized by chronic inflammation of the exocrine glands, with progressive loss of function (sicca syndrome) and systemic activation of the humoral response (174). Excessive B cell hyperactivity and extra-glandular manifestation are observed in ∼30% of pSS patients and an increased risk for lymphoma development has been described in this condition. In 1974, Chused et al. first described the presence of lymphoid-like structures in the salivary glands of patients with pSS (175). This was followed by the report of local antigenic stimulation within GC-like structures in the salivary glands (176) and, 10 years later, by the description of FDC network formation within the aggregates (177). In 1998, Stott and colleagues provided the first experimental evidence of an antigen-driven GC response, defined by clonal B cell proliferation and clone hypermutation within the salivary gland inflammatory foci (37), and, since then, several features associated with

lymphoneogenesis have been reported within pSS aggregates (157, 178).

It is now recognized that during pSS, TLS form in the minor salivary and/or parotid gland in around 30–40% of patients (151) and those structures host a phenomenon of oligoclonal B cell expansion and SHM of the Ig variable genes (37). The formation of TLS in pSS salivary glands correlates with increased B cell hyperactivity, the presence of anti-SSA and anti-SSB autoantibodies, hypergammaglobulinemia and cryoglobulinemia, supporting the hypothesis that TLS persistence contributes to disease progression in pSS (179). Our group has contributed to these reports, describing both the expression of lymphoid chemokines and of AID within highly organized aggregates that harbor in the salivary gland of patients with pSS and MALT lymphoma (135, 180). The relationship between TLS formation and disease progression in pSS is still debated. TLS detection has been associated with high antibody titer, systemic manifestations and lymphoma development. However, the direct correlation between GC formation in the salivary glands and lymphoma formation has not been demonstrated, suggesting that the development of GC+ TLS within the salivary glands represent one of the stages in the process of lymphomagenesis but is not *per se* sufficient to induce lymphoma (135, 154, 161, 180–182).

In order to better understand the pathogenic effect that TLS play in disease it is important to dissect the elements, present within these structures that contribute to their function and persistence in the tissue.

STRUCTURAL ELEMENTS OF TLS

Antigen

There is enough evidence to support the hypothesis that TLS form to provide an immune response against locally displayed antigens. There are suggestions that TLS formation is an antigen (Ag)-driven process. In the mucosal associated lymphoid tissue that forms during Helicobacter *Pilori* gastritis antigen clearance following antibiotic treatment impacts on TLS maintenance and progression to lymphoma (183), similarly inducible bronchial associated lymphoid tissue can dissolve upon antigen clearance (184). Maffia and colleagues explored the properties of Ag presentation within TLS (58, 185) demonstrating that Ag presentation is regulated by a random process of diffusion, rather than selective Ag uptake by DCs. Those data are reinforced by the anatomical structure of TLS where conduits, able to support Ag movement and APC migration have been described (186). In this context, the absence of a capsule could favor not only the initial Ag delivery in the tissue, but the progressive accumulation of new antigen specificities during the course of the immune response, favoring the persistence of these structures in the tissue.

During a classical immune response, the antigens are collected by antigen presenting cells in the periphery and moved, via a complex network of lymphatic vessels, to draining lymph nodes (LNs) (187–189). LN space is pre-formed during the embryonic development and anatomically set before the generation of the immune response to accommodate optimal interaction between APC, Ag and immune cells. Differently by SLOs, TLS organization is not anatomically predisposed to organize such a response and Ag presentation is often provided by non-immune cells, such as stromal cells and epithelial cells (190–193).

Lack of Ag drainage could mechanistically explain TLS formation. TLS form spontaneously in the lungs of mice deficient for CCR7, a chemokine receptor required for the migration of antigen-charged dendritic cells (DCs) to draining lymph nodes (194). However, the reconstitution of these animals with CCR7-sufficient cells is enough to re-establish the physiological delivery of the antigen to the lymph node and to induce TLS resolution in the tissue. This evidence appears to suggest that an intrinsic defect in DCs is sufficient to trigger TLS establishment. However, it is not clear whether this phenomenon could be also supported by a defect of lymphatic drainage from the inflamed tissue.

The expansion of a functional network of lymphatic vessels is required for appropriate antigen delivery to the SLOs. There are several reports describing the dramatic remodeling of the lymphatic vessels during inflammation, whereby the activation of NF-κB pathway supported by the expression of LT, IL-1 and TNFα, stimulates the expression of Prox1 and increases the transcripts for the VEGF-R3, both of which are factors involved in lymphoangiogenesis (195–201). TLS lack the presence of an organized lymphatic system such as the one described in SLOs (152). However, the expansion of the lymphatic vascular system has been observed in these structures, in response to the same cytokine milieu that regulates the maturation of the non-vascular stroma at these sites (97, 105). It is not clear whether these newly formed vascular structures are, however, able to establish viable connections with pre-existing lymphatics. The failure to do so would prevent efficient drainage of the antigen to the SLOs and support the excessive antigenic stimulation in the peripheral tissue (89, 202–206).

Lymphangiogenesis associated with tertiary lymphoid structure (TLS) has been reported in numerous studies. Defects in lymphangiogenesis in RA present with a reduction in lymphatic flow, absence of lymphatic pulse and collapse of draining LNs is observed during disease and is associated with flare onsets as has been shown *in vivo* and *ex vivo* studies performed by Schwarz and colleagues (207). Accordingly, effective therapeutic approaches in RA, including anti-TNF and B cell have been associated with the expansion of the lymphatic bed (208) and increase in cell drainage from the synovium (209).

In a model of pSS our group demonstrated that during TLS assembly an expansion of the lymphatic vascular network takes place and this is regulated by the sequential engagement of IL-7 and LTβR signaling; suggesting the presence of a natural pro-resolving mechanism for lymphocyte exit from the tissues during TLS establishment (105).

The open questions related to the mobilization of Ag loaded APC to the draining SLOs could be addressed in the future by inducing TLS formation and tracking the movement of labeled antigen-loaded DCs across vessels. The possibility to interfere pharmacologically or genetically with the process of lymphoangiogenesis and with the molecules responsible for cell migration across these structures, is likely to elucidate this complex phenomenon and to provide evidences on the role of

aberrant antigen presentation and vascular disturbances in TLS establishment and persistence.

Both RA and pSS are characterized by antibody production against a discrete set of autoantigens and a large body of research in this area has been focused around the identification of antigen specificities within the TLS in the context of these diseases. The presence of citrullinated proteins has been reported within the synovia of RA patients by Baeten (210) and others, and associated with the local expression of the enzyme peptidyl arginine deiminase (PAD) in patients characterized by high systemic and local levels of anti-citrullinated antibodies (APCA) (211). This report fails to demonstrate the presence of the citrullinated proteins within the synovial TLS and is in disagreement with other studies reporting the detection of citrullinated proteins in non-RA synovium lacking classical TLS (212); casting doubts on the exclusive association between citrullinated protein expression and TLS development in RA. Additional evidence that associate the presence of TLS with the generation of auto-antibody specificity against citrullinated peptides (but not necessarily local display of the defined antigen) will be discussed in a different section of this review.

Stronger evidences supporting the link between TLS and local auto-antigen presentation have been provided in pSS. Ro/SSA 52 kDa, Ro/SSA 60 kDa and La/SSB belong to a intracellular complex of RNA binding proteins that is physiologically involved in the intrinsic response to viruses (213). The aberrant expression of Ro and La has been reported in pSS patients upon cellular apoptosis or extracellular transport in vesicles (214–216). Moreover, the presence of anti-Ro52/TRIM21 specific plasma cells has been demonstrated, at the boundaries of well-organized TLS in pSS salivary glands, establishing a clear connection between local antigen presentation and TLS formation in this disease (158). The presence of extractable nuclear antigen (ENA) antibodies against these two ribonucleoproteins is pathognomonic for Sjogren's and associated with more severe systemic manifestation and worst prognosis (214, 216, 217).

Lymphocytic Components of TLS

We have recently reviewed the role of non-haematopoietic cells in TLS establishment and organization (97, 98) and for the scope of this issue focused on autoantibodies, we will limit the discussion in this manuscript to the lymphocytic compartment.

Whilst mainly constituted of B cells and associated with aberrant humoral responses and GC formation, TLS establishment and maintenance strongly relies on T cells. In humans, the presence of a shared TCR specificity among different follicles in the RA synovium, has been described, suggesting the presence of a common antigen for different TLS that form within the synovial tissue (218). In line with this finding, depletion of CD8+ T cells in human synovium-SCID mouse chimeras hinders the formation on TLS (218).

Recently, efforts have been made to identify the cells and signals required for TLS establishment and a series of reports have highlighted the important role of IL-17+ T cells. Th17 cells are required for iBALT formation (219) and for TLS establishment in a model of experimental autoimmune encephalomyelitis (EAE); the latter, dependent on the production of LT-αβ, IL-17 and IL-22 (22, 23, 220, 221). In human renal allograft rejection, Th17 cells have been shown to promote ectopic GC formation in an IL-21 dependent manner (222). Aberrant differentiation of Th17 cells in the absence of IL-27 has been also associated with aberrant TLS formation in an experimental model of arthritis and in a model of pSS (223, 224).

Our group has recently demonstrated the requirement of IL-22 producing T cells in the early phases of TLS establishment in murine salivary glands (39). In this model, IL-22 production, similarly to the IL-17 production in the lungs and brain, appears to regulate, independently but also in synergy with lymphotoxin and TNF, the ectopic production of lymphoid chemokines that defines TLS formation (97). These studies demonstrate that T cells, and in particular Th17/Th22 cells, play an important role in shaping the constituents of TLS in a manner that can support subsequent B cell recruitment and germinal center formation.

Whether TLS provide a site of aggregation for naïve T cell is not clear and whilst naïve T cell recruitment and priming has been reported within TLS that form in pancreatic tissue in NOD mice (225), it is more likely that effector T cells and central memory recirculate in these structures, in particular in the earliest phases of TLS assembly. On the contrary it is now well accepted that TLS function as a site for functional T cell polarization. TLS maintenance appears to hinge on the functional relationship between T-follicular helper cells and regulatory T cell populations. T cells displaying a T_{fh} phenotype have been described in TLS, where they are expected to regulate the GC reaction and the activation of resident proliferating B cells (1). In the TLS that form outside the arterial wall and control the atherosclerotic plaque development, the presence of T_{fh} correlates with the organization and maintenance of the ectopic B cell clusters (226). Functional interference of the T_{fh} by ICOS-L blockade results in decreased TLS formation and aberrant atherosclerotic plaque formation. The opposite effect is obtained by depletion of T regulatory cells, previously demonstrated to play a critical role in the homeostatic control of the TLS and in the atherosclerotic process (58).

The developmental program of T_{fh} in TLS is debated. There are suggestions that this population in TLS derives from a population of peripheral $CXCR5^+$ T cells that migrate to the peripheral tissue following the newly established CXCL13 gradient. These circulating CXCR5+ cells do not bear classical signs of activation and would, by definition, preferentially migrate to SLOs; however, the local differentiation of HEVs and the expression of PNAd (the ligand for L-selectin) supports their homing to the TLS (227). Others suggest that, within TLS, T_{fh} locally differentiate from other T cell subpopulations, including Th17. In support of this hypothesis, in EAE, Th17 cells appear to acquire some characteristics of T_{fh} including the expression of CXCR5, ICOS and Bcl6 (23). Similarly, within the inflamed joints of RA patients, a population of $PD1^{hi}CXCR5^{-}CD4^{+}$ T cells termed "peripheral helpers" has been described that appear to fulfill the function of T_{fh} within the periphery (228). In pSS the expansion of T_{fh} cells has been reported and correlates with the increasing frequency of memory B and plasma cells in the tissue and blood (229, 230).

Genetic manipulation in conditional knockouts is currently in use to induce TLS formation in mice deficient for specific T cell populations and will allow better definition of cellular requirements for TLS formation.

Classically, fully established TLS are mainly characterized by B cell infiltration and the inversion of the B/T cell ratio within TLS has been used as an index of disease severity (231, 232). In SLO, naïve B cells are known to receive antigen education and co-stimulation; however, whether a similar phenomenon would regularly occur in TLS is debated. Patients with pSS display altered peripheral blood B cell frequencies with a predominance of $CD27^-$ naïve B cells, diminished frequencies/absolute numbers of $CD27^+$ memory B cells in the periphery, and an enrichment of mature B cells in the salivary glands (233, 234). The presence of $CD20^+CD27^+$ B cells and plasmablasts is a consistent finding in pSS salivary glands biopsies (235). Whilst we have reported the presence of IgD^+ naïve B cells, in particular in large TLS (180), memory B cells remain the predominant component of the infiltrates (180, 236). This casts doubts over the possibility that naïve B cells are primed within the TLS (235). In support of this hypothesis, *bona fide* GC B cells ($CD10^+CD21^{+/-}CD24^{+/-}CD27^-CD38^+IgD^-$ that express AID) are rarely found within the B cell aggregates of TLS, that are mainly inhabited by $CD10^-CD21^+CD24^+CD27^{\pm}CD38^-IgD^+$ marginal zone-like type II transitional B cells (159) (**Figure 1B**).

The connection between the marginal zone (MZ) and TLS establishment is also not clear. There are several evidences supporting the involvement of MZ B cells in autoimmunity, including reports of preferential SHM and B cell proliferation in MRL Fas/lpr mice spleen (237) and the presence of RF^+ cells in the splenic marginal sinus bridging channels (238). The low threshold of BCR activation, the numerous effector functions of MZ B cells and the link between autoimmunity, TLS and MZ lymphoma development in pSS suggests a direct involvement of this population in TLS pathology (239, 240). However, the origin of the MZ-like B cells and the relationship between those and the ectopic GC has not been proven. In humans, MZ B cells are allegedly able to recirculate and carry a highly mutated B cell receptor (241–243), thus suggesting a post-GC origin of this population. This is not the case in mice, where MZ B cells are stable and permanently located in the spleen (242–244). Interestingly, however, MZ-B cells in humans share some phenotypic features of transitional B cells, a highly autoreactive B cell population that emerge from the BM and mature inside the spleen before entering the follicle (245–248), suggesting the possibility that transitional immature autoreactive cells are inhabiting the ectopic follicles. The recirculation pattern and screening of transitional B cells has been described from Spencer and co-authors in an elegant work that describes the migration and BCR editing of this population in the gut-associated lymphoid tissue (GALT) (245). This process, aimed at modifying the specificity of autoreactive clones, is altered in systemic lupus erythematosus (SLE), resulting in the expansion of the autoreactive B cell repertoire (245). In diseases characterized by TLS formation, such as pSS and RA, this recirculation pathway could be also altered, favoring the migration of autoreactive clones from the lymphoid organs to the TLS. Hereby, the aberrant expression of survival factors and chemokines would support clonal expansion in the absence of BCR editing and support persistence of autoimmunity.

The use of mass cytometry on digested tissue and sections are needed to better characterize in humans the phenotype and functional features of the B cells inhabiting the TLS. The use of transgenic mice engineered to track cells *in vivo* (249) will be useful in inducible models of TLS to perform migration studies *in vivo*.

TLS AS ABERRANT MICROENVIRONMENTS FOR AUTOREACTIVE B CELL SURVIVAL AND DIFFERENTIATION

More than simply acting as a hub for lymphocyte migration, TLS have also been shown to provide critical survival signals for incoming lymphocytes and differentiated long-lived plasma cells such as BAFF, IL-7, and CXCL12 (98, 250). The persistence of TLS in the tissue, despite peripheral B cell depletion of post Rituximab, has been reported in RA (251), SS and lymphoma (252) and, more recently in peri-bronchial TLS described in two patients with cystic fibrosis and chronic Pseudomonas aeruginosa infection treated with B cell depletion therapy before transplantation. The reason for this persistence most probably resides on the excess survival factors, such as B cell activating factor (BAFF) or IL-7 present within the TLS that protects tissue infiltrating cells.

BAFF is a potent B-cell survival factor produced within SLO GCs and in the periphery by fibroblasts and epithelial cells (159, 248–253) Excess BAFF is known to rescue self-reactive B-cells from peripheral deletion and allows their entry into forbidden follicular and marginal zone niches (253). The connection between BAFF, MZ B cells, loss of tolerance and TLS emerged from studies in mice transgenic for BAFF (BAFF-Tg), that develop a lupus-like syndrome followed by infiltration of MZ-like B cells within salivary glands TLS (254). Interestingly, BAFF-Tg asplenic mice that lack MZ-B and B1a cells, but retain normal B1b cell numbers, develop lupus nephritis but lack TLS in the salivary glands, suggesting that both BAFF and MZ-B cells are required for TLS establishment in this model (255).

Other lymphoid survival cytokines including IL-7 have been described in association with TLS establishment in chronic diseases (162, 256–258). Gene expression levels of IL-7, IL-7 receptor (both IL-7Rα and IL-2Rγ subunits) and its downstream signaling gene JAK3 are significantly elevated in RA patient biopsies displaying TLS (259). Similarly, engagement of the IL-7/IL-7R axis has been linked to formation of TLS in salivary glands and associated with pSS pathology (22, 23, 33, 36, 37, 39, 58, 75, 89, 102–112, 112–262). Among other critical homeostatic functions, IL-7 can abrogate the suppressive ability of Treg, altering the balance between pro-inflammatory effector cells vs. suppressive T cells (162, 256, 258). Consistent with these observations, *in vivo* studies demonstrated the ability of IL-7 to induce TLS formation (263–265). The reciprocal expression of T and B cell survival factors in TLS is somehow strictly regulated by

the critical balance between infiltrating T and B cells, probably in response to gradients of lymphotoxin and TNF family members. The mechanism regulating this production and the resulting segregation of lymphocytes in T or B cell rich areas is still under investigation (266).

We and others have provided evidence that a functional GC response takes place within these structures. This supports the concept that even if TLS do not initiate disease they are involved in its progression. In particular, we have demonstrated that AID is expressed in pSS salivary gland TLS in association with networks of follicular dendritic cells (135) and that its expression is retained in the large GCs found in parotid pSS-MALT lymphomas. On the contrary, neoplastic B cells are found to be consistently negative for AID expression (135). AID expression in GC B cells controls susceptibility to apoptosis, ultimately regulating the magnitude of the GC response (267). In SLO, low levels of AID expression have been associated with defective somatic hypermutation and decreased peripheral B cell tolerance (268). AID expression in TLS is consistently low (as compared to SLOs), thus potentially explaining the aberrant survival and lack of selection of autoreactive B-cell clones in ectopic GCs.

Other data have been generated supporting the functional role of TLS in sustaining the generation of novel antibody specificities. Transplantation of TLS from pSS salivary glands infected with Epstein-Barr virus (EBV) into SCID mice have been shown to support the production of anti-Ro 52/anti-La 48 and anti-EBV antibodies and the survival of autoreactive B cell clones (158). Similar data have been produced for RA. The presence of $CD138^+$ plasma cells, characterized by immune reactivity against citrullinated fibrinogen, has been described within $AID^+/CD21^+$ follicular structures (33). Moreover, the survival of these clones in a transfer model of human biopsies in SCID mice, alongside the detection of gamma-Cmu circular transcripts in synovial grafts, has been reported. These observations provide evidence that synovial TLS represents an independent compartment for B cell maturation (33).

AUTOANTIBODY PRODUCTION GOES LOCAL

The contribution of the immune response that arises within TLS toward disease severity, including the production of autoantibodies, remains controversial (151). Nonetheless there are substantial evidences in support of local antibody production within the inflamed synovium and convincing documentation that the synovial microenvironment could independently favor the production of RA specific antibodies (33)

Mellors et al. firstly described the presence of "plasma B cells" that are able to react with FITC-labeled human IgG, interpreting this result as evidence of synovial production of rheumatoid factors (RF) by tissue-resident plasma cells (269). The first solid indication of local IgG production in RA is dated to 1968 with the report of Ig synthesis in rheumatoid synovium *in vitro* (270). Further studies supported this observation suggesting that gene selection, usage of kappa/lambda chains and class switching follows a non-stochastic process in the RA synovium (168). Similarly, the enrichment in RF^+ B cells producing mono-reactive, affinity matured, class switched antibodies in the RA synovium is highly suggestive of a local process of affinity maturation (271–273). On the contrary, clones producing mono-reactive RF have not been obtained from the synovial tissue of patients with osteoarthritis, where TLS do not form, supporting the link between chronic autoimmune diseases and TLS (271–275).

The production of anti-citrullinated protein antibodies (ACPA) has been firmly associated with RA development (276) and there are convincing evidences that these specificities can be locally produced in the RA synovium within the TLS (277, 278). Both anti-cyclic citrullinated peptide (CCP) antibodies (279) and anti-CCP producing B cells (280) have been detected in the synovial fluid of RA patients and antibodies against different citrullinated RA candidate antigens (vimentin, type II collagen, fibrinogen and α-enolase) appear to be enriched in the joint compared to paired serum (281). Notably, the presence of anti-CCP antibodies in the synovium has been also reported in RA seronegative patients (279, 282), thus highlighting the dissociation between the systemic and local autoimmune response. In support of this notion, the presence of $FcRL4^+$ ACPA producing IgA-B has been reported in the synovium, but not in the blood of RA patients (283). This observation provides an indication that inflammatory joints provide a specific microenvironment able to shape and influence B cell immune phenotype and output.

The ability of TLS to sustain the whole autoimmune process in the absence of SLO is debated. However, cloning of the local B cell repertoire isolated from inflamed organs bearing TLS is highly suggestive of the presence of a functional and SLO-independent process of affinity maturation. Terminally differentiated $CD20^-CD38^+$ cells, rheumatoid factor (RF) producing B cells have been detected in the inflamed joints of RA patients (284). Moreover, clonal analysis has provided evidence of an antigen-dependent process of SHM, selection and isotype switching in TLS positive RA synovium, indicating that a dominant antigen-specific local immune response shapes the synovial plasma cell repertoire (170, 285–290). Similarly, in pSS, the multiclonal expansion of B cells within the salivary glands has been described. Expansion of B cell clones bearing Humkv325, a conserved V kappa gene usually associated with lymphomas, was described previously in 1989 (291). Additional studies further supported the notion that an antigen-driven germinal center-type B cell response and somatic hypermutation occurs within the salivary glands (37, 292, 293). The presence of clones that expand and mature in the TLS does not prove that the autoimmune process is initiated within the TLS, or that the presence of TLS is causative of disease. However, a certain degree of antigen-experience and affinity maturation of the B cell repertoire undoubtedly occurs within TLS (33, 135, 153, 160, 294–296) and, whilst the causal role of these structures in disease initiation cannot be proved, TLS certainly display the ability to host and perpetuate the autoimmune process. Production of Ig and RF has been shown in other tissues, in addition to the synovium, including rheumatoid pericardium (297), pleura (298), muscles (299), and in the inducible bronchus-associated lymphoid tissue

(iBALT) in patients with pulmonary complications of RA (219). The presence of sputum autoantibodies in the absence of systemic seropositivity, and the increased autoantibody:total Ig ratio in the sputum (300) suggest that lymphoid tissue present in the bronchi of RA lungs can also act as sites of antibody development.

Independent IgG and IgM synthesis has been also described in pSS salivary glands (301) with later studies confirming the presence of RF^+ clones in ∼43% of patients with pSS (302) and with the ability of salivary gland infiltrating B cells to secrete antibodies specific for the Ro52/TRIM21, Ro60 and La autoantigens (36, 179, 217, 303). *In vitro* expression of recombinant antibodies derived from either newly emigrant/transitional mature naïve B cells from pSS patients and healthy individuals confirmed the presence of high frequencies of autoreactive antibodies in both populations. This suggests a general defective peripheral B cell tolerance in this condition (304).

Analysis of Ig levels in different compartments (blood, saliva) has further contributed to our understanding of the ability of TLS to independently produce antibodies. Increased levels of IgA, but not IgG- and IgM-RF, has been detected in the saliva of patients with pSS (305). A study on isotype distribution of anti-Ro/SS-A and anti-La/SS-B antibodies in the plasma and saliva of patients with pSS demonstrated a correlation between the focus score (the measured degree of salivary gland inflammation) and autoantibody titers in saliva or blood. This report establishes a pathogenic link between locally displayed autoantigens, presence of antigen specific B cells in the inflamed tissue and autoreactive Ig levels (306).

IMMUNOGLOBULINS AND GLYCOSYLATION: THE SWEETER THE BETTER?

It is becoming increasingly clear that antibody post-translational modifications, in particular glycosylation, can influence their function and pathogenicity. However, a relationship between the pathogenic microenvironment established in the TLS and the progressive acquisition of pathogenic post-translational modifications has not been demonstrated.

Glycosylation is the process by which glycans are attached to proteins, lipids and other molecules, thereby altering their structure and influencing their biological activity. Whilst IgG presents a single conserved N glycosylation site within the Fc region, other subclasses are more heavily glycosylated (307). IgG Fc glycosylation determines the binding of the globulins to their receptors, FcRs type I (FcgammaRs) and II (SIGN-R1, DC-SIGN, DCIR, CD22, and CD23), thereby influencing Ig downstream pro-inflammatory, anti-inflammatory or immunomodulatory effects (308, 309). In addition to conserved IgG Fc glycans, ∼15–25% of serum IgG contain glycans within the Fab domain. Intriguingly, the attachment sites for N-glycans to the Fab portion is determined by the process of somatic hypermutation and, accordingly, Fab glycosylation could influence antibody binding, activity, half-life, formation of immunocomplexes and strength of BCR signaling [extensively reviewed in (310)].

The presence of altered glycosylation in RA was suggested in the 1970s, but it wasn't until 1985 when two studies from Oxford and Japan demonstrated different galactosylation profiles between normal individuals and patients with RA or OA (311). Later, Axford and colleagues reported the presence of reduced circulating B cell galactosyltransferase activity in RA (312), which was later confirmed in other studies (313–315). Other post-translational modifications have been described in RA. Several studies have demonstrated the presence of an altered overall glycosylation status within specific Ig subclasses (316) that can be detected before disease onset (317). This correlates with measures of disease activity (318, 319) and decreased sialylation of RF-IgG, but not in non-RF-IgG (318, 320, 321).

More recently, the degree of IgG glycosylation has been used to monitor treatment effectiveness (321) and, whilst no differences have been observed in the Fc glycosylation pattern between ACPA-IgG1 and total IgG1 in arthralgia patients, a decrease in galactose residues have been observed in patients with preclinical synovitis before the onset of RA; a change probably supported by the increasingly inflammatory microenvironment (322). The increased presence of agalactosylated IgG in the synovial fluid as compared to serum samples of RA has also been reported (323). Finally, Scherer et al. recently demonstrated the presence of autoreactive IgG in synovial fluid with decreased number of galactosylation and sialylation sites as compared to serum. This latter difference appeared to be specific for autoreactive specificities as no difference was observed in total IgG glycosylation (324).

Elevated levels of asialylated IgG have been detected in 60% of pSS patients and those appear to correlate with clinical manifestations, such as Raynaud's phenomenon and arthritis. A strong correlation with rheumatoid factor or IgA-containing immune complexes was reported (325). Based on IgG galactosylation, the pSS patients can be classified into two groups: one with comparable galactosylation status as in RA patients with the presence of RF, and the other similar to healthy individuals, and RF seronegative (326).

More recently, studies on Fab glycosylation and disease have been performed. Corsiero and colleagues reported the relationship between increased molecular weight of anti-NET antibodies and the presence of N-glycans onto the Fab domain of autoreactive clones in RA, suggesting that the process of SHM occurring in the synovium is responsible for the acquisition of-N glycosylation sites (286). Acquisition of N-glycosylation sites and subsequent enrichment in Fab-glycans in the variable domain of ACPA-IgG has been further confirmed (327, 328). On a similar note, it has been reported that there is a selective increase in Fab-N glycosylation sites in ACPA specific clones. However, the presence of those glycans didn't appear to significantly alter the antigen binding of the APCA. Accordingly, *in silico* analysis suggested that the added glycans were not located on the antibody binding sites (329). Moreover, an increased frequency of N-glycans in the Fab ACPA domain, but in association with altered antibody affinity, has been also reported (330). Interestingly, this enrichment was more prominent on ACPA isolated from synovial fluid compared with peripheral blood (264), providing evidence that the local microenvironment

influences the immunoglobulin glycosylation pattern. Hamza *et al*. recently reported the high prevalence of acquired IgG N-glycosylation sites in pSS suggesting a hypothesis that in pSS, the selection pressures that shape the antibody repertoire in the parotid glands results from an antigen-independent mechanism and is driven by interactions between glycosylated B cell receptors and lectins within the microenvironment (328). In summary, the glycan composition can have different associations with the disease, depending on the site of glycosylation. Decreased and increased glycosylation for the Fc and Fab portion, respectively, have been associated with RA and SS.

A relationship between post-translational modifications and antibody pathogenicity has been proposed. Leader et al. reported the presence of agalactosylated IgG in synovial immunocomplexes, suggesting a pathogenic role for agalactosylated IgG (331). However, the relationship between glycosylation and RF activity is debated (318, 332). The presence of N-linked glycosylation sites within the Fc portion of target IgG has been also shown to markedly reduce RF binding *in vitro* (333) whilst the ability of rheumatoid factors to selectively bind hypogalactosylated IgG has been suggested (334). In mice, desialylated but not sialylated immune complexes appear to enhance osteoclastogenesis *in vitro* (335). Accordingly, artificial sialylation of anti-type II collagen antibodies, including ACPAs, but not other IgG can supress the development of collagen-induced arthritis (CIA) (320, 336).

A potential pathogenic role of IgG glycosylation in pSS pathogenesis, to our knowledge, has not been addressed yet. A recent study pointed out that the Fc-mucin binding is enhanced when antibodies are agalactosylated, offering a mechanistic concept for increased binding on mucosal surfaces of the inflammatory agalocysylated antibodies and potential antibody pathogenicity (337).

Agalactosylated IgG levels were not found to be correlated in twin pairs indicating a low influence from genetic factors for IgG glycosylation (338). However, four loci contained genes for glycosyltransferases (ST6GAL1, B4GALT1, FUT8, and MGAT3) have been highlighted in genome-wide association studies for loci associated with IgG N-glycosylation (339). There is evidence to support the notion that the microenvironment can influence Fc IgG glycosylation. A recent study illustrates the ability of CpG, IFN-gamma and IL-21 to increase Fc-linked galactosylation and reduce bisecting N-acetylglucosamine levels (340). Stimulation of a mouse B cell lymphoma line with IL-4 and IL-5, but not LPS, has been shown to significantly decrease the terminal glycosylation of secreted IgA (341) and IgM (342), but substantially increase the terminal glycosylation of MHC Class-I (342), suggesting that the glycosylation machinery works in a protein-specific manner.

A mechanistic link between inflammation and post-translational modification has been recently established by G. Schett's group in a manuscript illustrating the ability of IL-21 and IL-22 to regulate the expression of α2,6-sialyltransferase-1 in newly differentiating plasma cells, thus controlling the glycosylation profile of secreted IgG (320). Interestingly, both T cell-independent B cell activation (343) and tolerance induction with T cell-dependent protein antigens (344) results in the production of sialylated IgG. However, T cell independent vaccination seems to result in a stronger induction of sialylated antigen specific antibodies (345).

IgG glycosylation can also be controlled at an extracellular level. IgG sialylation has been reported in the bloodstream, through secreted ST6Gal1 (326). S-glycosyltransferases have also been shown to alter the IgG molecule at sites of inflammation with local platelets serving as nucleotide-sugar donors (346). Other reports link the process of altered glycosylation to a post-secretory degradative process involving oxygen free radicals (347). All together these reports suggest the possibility that the site of antibody synthesis can profoundly affect the post-translational profile of the immunoglobulins.

Due to technological limitations, the extent of the disease-related glycan alterations and the role of these modifications in disease pathophysiology has not been thoroughly addressed. A novel microfluidic-based method to identify trace sulphated IgG N-glycans as biomarkers for rheumatoid arthritis has been recently described (348) and high-throughput methods for analysing IgG glycosylation have also been introduced (349). These tools have been only used in selected populations and their application on a larger scale could, in the future, unveil differences and patterns not yet captured.

To our knowledge, there has been no attempt to use these stratification tools in the context of TLS associated pathologies. The differential profile of glycosylation observed in Ig isolated, respectively from serum and synovial compartments suggest the fascinating hypothesis that SLO and TLS differentially regulate these post-translational modifications (323, 324, 350). However, the possibility that Ig derived from SLO and TLS present substantially different "sugary fingerprints" and that those patterns correlate with a certain degree of tissue involvement and disease progression has still to be proven.

TLS AND LYMPHOMAGENESIS

If the concept of an association between progressive post-translational modifications of the Ig repertoire and continuous antigen exposure within a highly inflammatory environment is true, we should be able to detect progressive accumulation of Ig in patients undergoing malignant transformation through the course of autoimmunity. The occurrence of non-Hodgkin's lymphoma (NHL) is pathogenically linked to TLS and represents the most serious complication of pSS, but not RA (351).

B cell VH and VL gene analysis for pSS patients with lymphoma revealed several point mutations in the germline genes and intra-clonal sequence heterogeneity, in line with an ongoing somatic hypermutation process sustaining lymphoma growth (352, 353). It is believed that the emergence of monoclonal RF B cells within the polyclonal infiltrate of the salivary gland TLS represents a key developmental step in lymphomagenesis. Chromosomal abnormalities and mutation eventually converge in these B clones that present a proliferative advantage, ultimately converting them into malignant clones. Indeed, there is a strong bias for RF specific B cells in the salivary gland MALT-type lymphoma (354–356), whilst alternative

analysis of the B cell repertoire in micro dissected labial salivary glands could not convincingly demonstrate predominance of RF reactivity in the infiltrating clones (357). The relationship between GC formation and lymphomagenesis has been recently challenged and further studies will be required to clarify the pathogenic link between TLS persistence and emergency of malignant clones (161, 182, 358, 359).

The high incidence of acquired N-glycosylation sites found in follicular lymphoma (360) would be suggestive of a similar phenomenon in pSS associated MALT lymphoma; however, contrary to these expectations, patients with MALT lymphoma present low frequency of N-glycosylation sites (161, 182, 358, 359, 361). Longitudinal analysis of the glycosylation and sialylation profile in patients with TLS undergoing lymphoma transformations are needed to address these questions.

FUTURE PROSPECTIVE AND CONCLUSIONS

In conclusion, TLS formation can be easily considered as a hallmark of tissue autoimmunity. In the past few years a large body of work has been generated aimed at dissecting key aspects of TLS biology, however, many areas have to be further addressed. The inter-dependency between SLOs and TLS has to be better dissected in order to understand whether these immune hubs are functional, both in the early phases as tolerance is broken and, later, during disease progression. The signals regulating migration pathways and differentiation of immune cells within the TLS should also be investigated *in vivo* with the prospective to target these pathways therapeutically. A better knowledge around the signals involved in TLS establishment and maturation, but in particular, the mechanisms regulating GC formation and regulation should be acquired. Moreover, a specific effort should be made to dissect the functional role of TLS GCs in the development of lymphoma. Finally, key questions should be answered around the cross-talk between the TLS and their surrounding environment, dissecting the permissive factors for TLS formation and persistence in the tissue.

The acquired knowledge on the role of non-haematopoietic stromal cells in TLS biology has been critically important in explaining why these structures are resistant to classical immune cell therapy. In the future, potential combined therapy could be utilized to interfere with the microenvironment alongside targeting immune cells in TLS associated disease that is non-responsive to classical immunosuppression.

AUTHOR CONTRIBUTIONS

EP and FB defined the content of the manuscript, contributed to literature search and manuscript writing. SN, DG and SC contributed to literature search and manuscript writing. CS contributed to manuscript writing. EP and FB created graphical illustrations. All authors approved the final version of the manuscript.

FUNDING

FB is supported by ARUK.

REFERENCES

1. Pitzalis C, Jones GW, Bombardieri M, Jones SA. Ectopic lymphoid-like structures in infection, cancer and autoimmunity. *Nat Rev Immunol*. (2014) 14:447–62. doi: 10.1038/nri3700
2. Engelhard VH, Rodriguez AB, Mauldin IS, Woods AN, Peske JD, Slingluff, et al. Immune cell infiltration and tertiary lymphoid structures as determinants of antitumor immunity. *J Immunol*. (2018) 200:432–42. doi: 10.4049/jimmunol.1701269
3. Teillaud JL, Dieu-Nosjean MC. Tertiary lymphoid structures: an anti-tumor school for adaptive immune cells and an antibody factory to fight cancer? *Front Immunol*. (2017) 8:830. doi: 10.3389/fimmu.2017.00830
4. Jing F, Choi EY. Potential of Cells and Cytokines/Chemokines to Regulate Tertiary Lymphoid Structures in Human Diseases. *Immune Netw*. (2016) 16:271–80. doi: 10.4110/in.2016.16.5.271
5. Alsughayyir J, Pettigrew GJ, Motallebzadeh R. Spoiling for a fight: b lymphocytes as initiator and effector populations within tertiary lymphoid organs in autoimmunity and transplantation. *Front Immunol*. (2017) 8:1639. doi: 10.3389/fimmu.2017.01639
6. Sautes-Fridman C, Lawand M, Giraldo NA, Kaplon H, Germain C, Fridman WH, et al. Tertiary lymphoid structures in cancers: prognostic value, regulation, and manipulation for therapeutic intervention. *Front Immunol*. (2016) 7:407. doi: 10.3389/fimmu.2016.00407
7. Germain C, Gnjatic S, Dieu-Nosjean MC. Tertiary lymphoid structure-associated b cells are key players in anti-tumor immunity. *Front Immunol*. (2015) 6:67. doi: 10.3389/fimmu.2015.00067
8. Mitsdoerffer M, Peters A. Tertiary lymphoid organs in central nervous system autoimmunity. *Front Immunol*. (2016) 7:451. doi: 10.3389/fimmu.2016.00451
9. Jones GW, Hill DG, Jones SA. Understanding immune cells in tertiary lymphoid organ development: it is all starting to come together. *Front Immunol*. (2016) 7:401. doi: 10.3389/fimmu.2016.00401
10. Buettner M, Lochner M. Development and function of secondary and tertiary lymphoid organs in the small intestine and the colon. *Front Immunol*. (2016) 7:342. doi: 10.3389/fimmu.2016.00342
11. Neyt K, Perros F, GeurtsvanKessel CH, Hammad H, Lambrecht BN. Tertiary lymphoid organs in infection and autoimmunity. *Trends Immunol*. (2012) 33:297–305. doi: 10.1016/j.it.2012.04.006
12. Voswinkel J, Assmann G, Held G, Pitann S, Gross WL, Holl-Ulrich K, et al. Single cell analysis of B lymphocytes from Wegener's granulomatosis: B cell receptors display affinity maturation within the granulomatous lesions. *Clin Exp Immunol*. (2008) 154:339–45. doi: 10.1111/j.1365-2249.2008.03775.x
13. Voswinkel J, Mueller A, Kraemer JA, Lamprecht P, Herlyn K, Holl-Ulrich K, et al. B lymphocyte maturation in Wegener's granulomatosis: a comparative analysis of VH genes from endonasal lesions. *Ann Rheum Dis*. (2006) 65:859–64. doi: 10.1136/ard.2005.044909
14. Armengol MP, Cardoso-Schmidt CB, Fernandez M, Ferrer X, Pujol-Borrell R, Juan M. Chemokines determine local lymphoneogenesis and a reduction of circulating $CXCR4^{+}$ T and CCR7 B and T lymphocytes in thyroid autoimmune diseases. *J Immunol*. (2003) 170:6320–8. doi: 10.4049/jimmunol.170.12.6320
15. Armengol MP, Juan M, Lucas-Martin A, Fernandez-Figueras MT, Jaraquemada D, Gallart T, et al. Thyroid autoimmune disease: demonstration of thyroid antigen-specific B cells and recombination-activating gene

expression in chemokine-containing active intrathyroidal germinal centers. *Am J Pathol*. (2001) 159:861–73. doi: 10.1016/S0002-9440(10)61762-2
16. Furtado GC, Marinkovic T, Martin AP, Garin A, Hoch B, Hubner W, et al. Lymphotoxin beta receptor signaling is required for inflammatory lymphangiogenesis in the thyroid. *Proc Natl Acad Sci USA*. (2007) 104:5026–31. doi: 10.1073/pnas.0606697104
17. Martin AP, Coronel EC, Sano G, Chen SC, Vassileva G, Canasto-Chibuque C, et al. A novel model for lymphocytic infiltration of the thyroid gland generated by transgenic expression of the CC chemokine CCL21. *J Immunol*. (2004) 173:4791–8. doi: 10.4049/jimmunol.173.8.4791
18. Howell OW, Reeves CA, Nicholas R, Carassiti D, Radotra B, Gentleman SM, et al. Meningeal inflammation is widespread and linked to cortical pathology in multiple sclerosis. *Brain* (2011) 134:2755–71. doi: 10.1093/brain/awr182
19. Lovato L, Willis SN, Rodig SJ, Caron T, Almendinger SE, Howell OW, et al. Related B cell clones populate the meninges and parenchyma of patients with multiple sclerosis. *Brain* (2011) 134:534–41. doi: 10.1093/brain/awq350
20. Magliozzi R, Howell O, Vora A, Serafini B, Nicholas R, Puopolo M, et al. Meningeal B-cell follicles in secondary progressive multiple sclerosis associate with early onset of disease and severe cortical pathology. *Brain* (2007) 130:1089–104. doi: 10.1093/brain/awm038
21. Serafini B, Rosicarelli B, Magliozzi R, Stigliano E, Aloisi F. Detection of ectopic B-cell follicles with germinal centers in the meninges of patients with secondary progressive multiple sclerosis. *Brain Pathol*. (2004) 14:164–74. doi: 10.1111/j.1750-3639.2004.tb00049.x
22. Pikor NB, Astarita JL, Summers-Deluca L, Galicia G, Qu J, Ward LA, et al. Integration of Th17- and lymphotoxin-derived signals initiates meningeal-resident stromal cell remodeling to propagate neuroinflammation. *Immunity* (2015) 43:1160–73. doi: 10.1016/j.immuni.2015.11.010
23. Peters A, Pitcher LA, Sullivan JM, Mitsdoerffer M, Acton SE, Franz B, et al. Th17 cells induce ectopic lymphoid follicles in central nervous system tissue inflammation. *Immunity* (2011) 35:986–96. doi: 10.1016/j.immuni.2011.10.015
24. Lehmann-Horn K, Wang SZ, Sagan SA, Zamvil SS, von Budingen HC. B cell repertoire expansion occurs in meningeal ectopic lymphoid tissue. *JCI Insight*. (2016) 1:e87234. doi: 10.1172/jci.insight.87234
25. Dang AK, Tesfagiorgis Y, Jain RW, Craig HC, Kerfoot SM. Meningeal infiltration of the spinal cord by non-classically activated B cells is associated with Chronic disease course in a spontaneous B cell-dependent model of CNS Autoimmune disease. *Front Immunol*. (2015) 6:470. doi: 10.3389/fimmu.2015.00470
26. Kuerten S, Schickel A, Kerkloh C, Recks MS, Addicks K, Ruddle NH, et al. Tertiary lymphoid organ development coincides with determinant spreading of the myelin-specific T cell response. *Acta Neuropathol*. (2012) 124:861–73. doi: 10.1007/s00401-012-1023-3
27. Bettelli E, Baeten D, Jager A, Sobel RA, Kuchroo VK. Myelin oligodendrocyte glycoprotein-specific T and B cells cooperate to induce a Devic-like disease in mice. *J Clin Invest*. (2006) 116:2393–402. doi: 10.1172/JCI28334
28. Magliozzi R, Columba-Cabezas S, Serafini B, Aloisi F. Intracerebral expression of CXCL13 and BAFF is accompanied by formation of lymphoid follicle-like structures in the meninges of mice with relapsing experimental autoimmune encephalomyelitis. *J Neuroimmunol*. (2004) 148:11–23. doi: 10.1016/j.jneuroim.2003.10.056
29. Hill ME, Shiono H, Newsom-Davis J, Willcox N. The myasthenia gravis thymus: a rare source of human autoantibody-secreting plasma cells for testing potential therapeutics. *J Neuroimmunol*. (2008) 201-202:50–56. doi: 10.1016/j.jneuroim.2008.06.027
30. Sims GP, Shiono H, Willcox N, Stott DI. Somatic hypermutation and selection of B cells in thymic germinal centers responding to acetylcholine receptor in myasthenia gravis. *J Immunol*. (2001) 167:1935–44. doi: 10.4049/jimmunol.167.4.1935
31. Robinet M, Villeret B, Maillard S, Cron MA, Berrih-Aknin S, Le Panse R. Use of toll-like receptor agonists to induce ectopic lymphoid structures in myasthenia gravis mouse models. *Front Immunol*. (2017) 8:1029. doi: 10.3389/fimmu.2017.01029
32. Sharifi S, Murphy M, Loda M, Pinkus GS, Khettry U. Nodular lymphoid lesion of the liver: an immune-mediated disorder mimicking low-grade malignant lymphoma. *Am J Surg Pathol*. (1999) 23:302–8. doi: 10.1097/00000478-199903000-00009
33. Humby F, Bombardieri M, Manzo A, Kelly S, Blades MC, Kirkham B, et al. Ectopic lymphoid structures support ongoing production of class-switched autoantibodies in rheumatoid synovium. *PLoS Med*. (2009) 6:e1. doi: 10.1371/journal.pmed.0060001
34. Takemura S, Braun A, Crowson C, Kurtin PJ, Cofield RH, O'Fallon WM, et al. Lymphoid neogenesis in rheumatoid synovitis. *J Immunol*. (2001) 167:1072–80. doi: 10.4049/jimmunol.167.2.1072
35. Croia C, Serafini B, Bombardieri M, Kelly S, Humby F, Severa M, et al. Epstein-Barr virus persistence and infection of autoreactive plasma cells in synovial lymphoid structures in rheumatoid arthritis. *Ann Rheum Dis*. (2013) 72:1559–68. doi: 10.1136/annrheumdis-2012-202352
36. Salomonsson S, Jonsson MV, Skarstein K, Brokstad KA, Hjelmstrom P, Wahren-Herlenius M, et al. Cellular basis of ectopic germinal center formation and autoantibody production in the target organ of patients with Sjogren's syndrome. *Arthritis Rheum*. (2003) 48:3187–201. doi: 10.1002/art.11311
37. Stott DI, Hiepe F, Hummel M, Steinhauser G, Berek C. Antigen-driven clonal proliferation of B cells within the target tissue of an autoimmune disease. *The salivary glands of patients with Sjogren's syndrome J Clin Invest*. (1998) 102:938–46. doi: 10.1172/JCI3234
38. Rangel-Moreno J, Hartson L, Navarro C, Gaxiola M, Selman M, Randall TD. Inducible bronchus-associated lymphoid tissue. (iBALT) in patients with pulmonary complications of rheumatoid arthritis. *J Clin Invest*. (2006) 116:3183–94. doi: 10.1172/JCI28756
39. Barone F, Nayar S, Campos J, Cloake T, Withers DR, Toellner KM, et al. IL-22 regulates lymphoid chemokine production and assembly of tertiary lymphoid organs. *Proc Natl Acad Sci USA*. (2015) 112:11024–9. doi: 10.1073/pnas.1503315112
40. Bombardieri M, Barone F, Lucchesi D, Nayar S, van den Berg WB, Proctor G, et al. Inducible tertiary lymphoid structures, autoimmunity, and exocrine dysfunction in a novel model of salivary gland inflammation in C57BL/6 mice. *J Immunol*. (2012) 189:3767–76. doi: 10.4049/jimmunol.1201216
41. Chang A, Henderson SG, Brandt D, Liu N, Guttikonda R, Hsieh C, et al. *In situ* B cell-mediated immune responses and tubulointerstitial inflammation in human lupus nephritis. *J Immunol*. (2011) 186:1849–60. doi: 10.4049/jimmunol.1001983
42. Dorraji SE, Hovd AK, Kanapathippillai P, Bakland G, Eilertsen GO, Figenschau SL, et al. Mesenchymal stem cells and T cells in the formation of Tertiary Lymphoid Structures in Lupus Nephritis. *Sci Rep*. (2018) 8:7861. doi: 10.1038/s41598-018-26265-z
43. Kang S, Fedoriw Y, Brenneman EK, Truong YK, Kikly K, Vilen BJ. BAFF induces tertiary lymphoid structures and positions t cells within the glomeruli during lupus nephritis. *J Immunol*. (2017) 198:2602–11. doi: 10.4049/jimmunol.1600281
44. Gu-Trantien C, Loi S, Garaud S, Equeter C, Libin M, de Wind A, et al. $CD4^+$ follicular helper T cell infiltration predicts breast cancer survival. *J Clin Invest*. (2013) 123:2873–92. doi: 10.1172/JCI67428
45. Martinet L, Garrido I, Filleron T, Le Guellec S, Bellard E, Fournie JJ, et al. Human solid tumors contain high endothelial venules: association with T- and B-lymphocyte infiltration and favorable prognosis in breast cancer. *Cancer Res*. (2011) 71:5678–87. doi: 10.1158/0008-5472.CAN-11-0431
46. Kotlan B, Simsa P, Teillaud JL, Fridman WH, Toth J, McKnight M, et al. Novel ganglioside antigen identified by B cells in human medullary breast carcinomas: the proof of principle concerning the tumor-infiltrating B lymphocytes. *J Immunol*. (2005) 175:2278–85. doi: 10.4049/jimmunol.175.4.2278
47. Nzula S, Going JJ, Stott DI. Antigen-driven clonal proliferation, somatic hypermutation, and selection of B lymphocytes infiltrating human ductal breast carcinomas. *Cancer Res*. (2003) 63:3275–80.
48. Coppola D, Nebozhyn M, Khalil F, Dai H, Yeatman T, Loboda A, et al. Unique ectopic lymph node-like structures present in human primary colorectal carcinoma are identified by immune gene array profiling. *Am J Pathol*. (2011) 179:37–45. doi: 10.1016/j.ajpath.2011.03.007
49. Bergomas F, Grizzi F, Doni A, Pesce S, Laghi L, Allavena P, et al. Tertiary intratumor lymphoid tissue in colo-rectal cancer. *Cancers. (Basel)*. (2011) 4:1–10. doi: 10.3390/cancers4010001

50. de Chaisemartin L, Goc J, Damotte D, Validire P, Magdeleinat P, Alifano M, et al. Characterization of chemokines and adhesion molecules associated with T cell presence in tertiary lymphoid structures in human lung cancer. *Cancer Res*. (2011) 71:6391–9. doi: 10.1158/0008-5472.CAN-11-0952
51. Dieu-Nosjean MC, Antoine M, Danel C, Heudes D, Wislez M, Poulot V, et al. Long-term survival for patients with non-small-cell lung cancer with intratumoral lymphoid structures. *J Clin Oncol*. (2008) 26:4410–7. doi: 10.1200/JCO.2007.15.0284
52. Kroeger DR, Milne K, Nelson BH. Tumor-infiltrating plasma cells are associated with tertiary lymphoid Structures, cytolytic T-cell responses, and superior prognosis in ovarian cancer. *Clin Cancer Res*. (2016) 22:3005–15. doi: 10.1158/1078-0432.CCR-15-2762
53. Martinet L, Le Guellec S, Filleron T, Lamant L, Meyer N, Rochaix P, et al. High endothelial venules. (HEVs) in human melanoma lesions: major gateways for tumor-infiltrating lymphocytes. *Oncoimmunology* (2012) 1:829–39. doi: 10.4161/onci.20492
54. Hiraoka N, Ino Y, Yamazaki-Itoh R, Kanai Y, Kosuge T, Shimada K. Intratumoral tertiary lymphoid organ is a favourable prognosticator in patients with pancreatic cancer. *Br J Cancer* (2015) 112:1782–90. doi: 10.1038/bjc.2015.145
55. Garcia-Hernandez ML, Uribe-Uribe NO, Espinosa-Gonzalez R, Kast WM, Khader SA, Rangel-Moreno J. A unique cellular and molecular microenvironment is present in tertiary lymphoid organs of patients with spontaneous prostate cancer regression. *Front Immunol*. (2017) 8:563. doi: 10.3389/fimmu.2017.00563
56. Houtkamp MA, de Boer OJ, van der Loos CM, van der Wal AC, Becker AE. Adventitial infiltrates associated with advanced atherosclerotic plaques: structural organization suggests generation of local humoral immune responses. *J Pathol*. (2001) 193:263–9. doi: 10.1002/1096-9896(2000)9999:9999<::AID-PATH774>3.0.CO;2-N
57. Ramshaw AL, Parums DV. Immunohistochemical characterization of inflammatory cells associated with advanced atherosclerosis. *Histopathology* (1990) 17:543–52. doi: 10.1111/j.1365-2559.1990.tb00794.x
58. Hu D, Mohanta SK, Yin C, Peng L, Ma Z, Srikakulapu P, et al. Artery tertiary lymphoid organs control aorta immunity and protect against atherosclerosis via vascular smooth muscle cell lymphotoxin beta receptors. *Immunity* (2015) 42:1100–15. doi: 10.1016/j.immuni.2015.05.015
59. Grabner R, Lotzer K, Dopping S, Hildner M, Radke D, Beer M, et al. Lymphotoxin beta receptor signaling promotes tertiary lymphoid organogenesis in the aorta adventitia of aged ApoE-/- mice. *J Exp Med*. (2009) 206:233–48. doi: 10.1084/jem.20080752
60. Seys LJ, Verhamme FM, Schinwald A, Hammad H, Cunoosamy DM, Bantsimba-Malanda C, et al. Role of B Cell-activating factor in chronic obstructive pulmonary disease. *Am J Respir Crit Care Med*. (2015) 192:706–18. doi: 10.1164/rccm.201501-0103OC
61. Polverino F, Cosio BG, Pons J, Laucho-Contreras M, Tejera P, Iglesias A, et al. B cell-activating factor. An orchestrator of lymphoid follicles in severe chronic obstructive pulmonary disease. *Am J Respir Crit Care Med*. (2015) 192:695–705. doi: 10.1164/rccm.201501-0107OC
62. Roos AB, Sanden C, Mori M, Bjermer L, Stampfli MR, Erjefalt JS. IL-17A is elevated in end-stage chronic obstructive pulmonary disease and contributes to cigarette smoke-induced lymphoid neogenesis. *Am J Respir Crit Care Med*. (2015) 191:1232–41. doi: 10.1164/rccm.201410-1861OC
63. Van Pottelberge G R, Bracke KR, Van den Broeck S, Reinartz SM, van Drunen CM, Wouters EF, et al. Plasmacytoid dendritic cells in pulmonary lymphoid follicles of patients with COPD. *Eur Respir J*. (2010) 36:781–91. doi: 10.1183/09031936.00140409
64. Hogg JC, Chu F, Utokaparch S, Woods R, Elliott WM, Buzatu L, et al. The nature of small-airway obstruction in chronic obstructive pulmonary disease. *N Engl J Med*. (2004) 350:2645–53. doi: 10.1056/NEJMoa032158
65. Bracke KR, Verhamme FM, Seys LJ, Bantsimba-Malanda C, Cunoosamy DM, Herbst R, et al. Role of CXCL13 in cigarette smoke-induced lymphoid follicle formation and chronic obstructive pulmonary disease. *Am J Respir Crit Care Med*. (2013) 188:343–55. doi: 10.1164/rccm.201211-2055OC
66. Carlsen HS, Baekkevold ES, Johansen FE, Haraldsen G, Brandtzaeg P. B cell attracting chemokine 1 (CXCL13) and its receptor CXCR5 are expressed in normal and aberrant gut associated lymphoid tissue. *Gut* (2002) 51:364–71. doi: 10.1136/gut.51.3.364
67. Kaiserling E. Newly-formed lymph nodes in the submucosa in chronic inflammatory bowel disease. *Lymphology* (2001) 34:22–9.
68. Fujimura Y, Kamoi R, Iida M. Pathogenesis of aphthoid ulcers in Crohn's disease: correlative findings by magnifying colonoscopy, electron microscopy, and immunohistochemistry. *Gut* (1996) 38:724–32. doi: 10.1136/gut.38.5.724
69. Surawicz CM, Belic L. Rectal biopsy helps to distinguish acute self-limited colitis from idiopathic inflammatory bowel disease. *Gastroenterology* (1984) 86:104–13.
70. Olivier BJ, Cailotto C, van der Vliet J, Knippenberg M, Greuter MJ, Hilbers FW, et al. Vagal innervation is required for the formation of tertiary lymphoid tissue in colitis. *Eur J Immunol*. (2016) 46:2467–80. doi: 10.1002/eji.201646370
71. McNamee EN, Masterson JC, Jedlicka P, Collins CB, Williams IR, Rivera-Nieves J. Ectopic lymphoid tissue alters the chemokine gradient, increases lymphocyte retention and exacerbates murine ileitis. *Gut*. (2013) 62:53–62. doi: 10.1136/gutjnl-2011-301272
72. Lochner M, Ohnmacht C, Presley L, Bruhns P, Si-Tahar M, Sawa S, et al. Microbiota-induced tertiary lymphoid tissues aggravate inflammatory disease in the absence of RORgamma t and LTi cells. *J Exp Med*. (2011) 208:125–34. doi: 10.1084/jem.20100052
73. Kawamura T, Kanai T, Dohi T, Uraushihara K, Totsuka T, Iiyama R, et al. Ectopic CD40 ligand expression on B cells triggers intestinal inflammation. *J Immunol*. (2004) 172:6388–97. doi: 10.4049/jimmunol.172.10.6388
74. Spahn TW, Herbst H, Rennert PD, Lugering N, Maaser C, Kraft M, et al. Induction of colitis in mice deficient of Peyer's patches and mesenteric lymph nodes is associated with increased disease severity and formation of colonic lymphoid patches. *Am J Pathol*. (2002) 161:2273–82. doi: 10.1016/S0002-9440(10)64503-8
75. Grant AJ, Goddard S, Ahmed-Choudhury J, Reynolds G, Jackson DG, Briskin M, et al. Hepatic expression of secondary lymphoid chemokine (CCL21) promotes the development of portal-associated lymphoid tissue in chronic inflammatory liver disease. *Am J Pathol*. (2002) 160:1445–55. doi: 10.1016/S0002-9440(10)62570-9
76. Ghosh S, Steere AC, Stollar BD, Huber BT. *In situ* diversification of the antibody repertoire in chronic Lyme arthritis synovium. *J Immunol*. (2005) 174:2860–9. doi: 10.4049/jimmunol.174.5.2860
77. Racanelli V, Sansonno D, Piccoli C, D'Amore FP, Tucci FA, Dammacco F. Molecular characterization of B cell clonal expansions in the liver of chronically hepatitis C virus-infected patients. *J Immunol*. (2001) 167:21–9. doi: 10.4049/jimmunol.167.1.21
78. Murakami J, Shimizu Y, Kashii Y, Kato T, Minemura M, Okada K, et al. Functional B-cell response in intrahepatic lymphoid follicles in chronic hepatitis C. *Hepatology* (1999) 30:143–50. doi: 10.1002/hep.510300107
79. Magalini AR, Facchetti F, Salvi L, Fontana L, Puoti M, Scarpa A. Clonality of B-cells in portal lymphoid infiltrates of HCV-infected livers. *J Pathol*. (1998) 185:86–90. doi: 10.1002/(SICI)1096-9896(199805)185:1<86::AID-PATH59>3.0.CO;2-R
80. Sansonno D, De Vita S, Iacobelli AR, Cornacchiulo V, Boiocchi M, Dammacco F. Clonal analysis of intrahepatic B cells from HCV-infected patients with and without mixed cryoglobulinemia. *J Immunol*. (1998) 160:3594–601.
81. Mazzucchelli L, Blaser A, Kappeler A, Scharli P, Laissue JA, Baggiolini M, et al. BCA-1 is highly expressed in Helicobacter pylori-induced mucosa-associated lymphoid tissue and gastric lymphoma. *J Clin Invest*. (1999) 104:R49–54. doi: 10.1172/JCI7830
82. Zaitoun AM. The prevalence of lymphoid follicles in Helicobacter pylori associated gastritis in patients with ulcers and non-ulcer dyspepsia. *J Clin Pathol*. (1995) 48:325–9. doi: 10.1136/jcp.48.4.325
83. Genta RM, Hamner HW. The significance of lymphoid follicles in the interpretation of gastric biopsy specimens. *Arch Pathol Lab Med*. (1994) 118:740–3.
84. Winter S, Loddenkemper C, Aebischer A, Rabel K, Hoffmann K, Meyer TF, et al. The chemokine receptor CXCR5 is pivotal for ectopic mucosa-associated lymphoid tissue neogenesis in chronic Helicobacter pylori-induced inflammation. *J Mol Med. (Berl)*. (2010) 88:1169–80. doi: 10.1007/s00109-010-0658-6

85. Slight SR, Rangel-Moreno J, Gopal R, Lin Y, Fallert Junecko BA, Mehra S, et al. CXCR5(+) T helper cells mediate protective immunity against tuberculosis. *J Clin Invest*. (2013) 123:712–26. doi: 10.1172/JCI65728
86. Tsai MC, Chakravarty S, Zhu G, Xu J, Tanaka K, Koch C, et al. Characterization of the tuberculous granuloma in murine and human lungs: cellular composition and relative tissue oxygen tension. *Cell Microbiol*. (2006) 8:218–32. doi: 10.1111/j.1462-5822.2005.00612.x
87. Ulrichs T, Kosmiadi GA, Trusov V, Jorg S, Pradl L, Titukhina M, et al. Human tuberculous granulomas induce peripheral lymphoid follicle-like structures to orchestrate local host defence in the lung. *J Pathol*. (2004) 204:217–28. doi: 10.1002/path.1628
88. Maglione PJ, Xu J, Chan J. B cells moderate inflammatory progression and enhance bacterial containment upon pulmonary challenge with Mycobacterium tuberculosis. *J Immunol*. (2007) 178:7222–34. doi: 10.4049/jimmunol.178.11.7222
89. Kerjaschki D, Regele HM, Moosberger I, Nagy-Bojarski K, Watschinger B, Soleiman A, et al. Lymphatic neoangiogenesis in human kidney transplants is associated with immunologically active lymphocytic infiltrates. *J Am Soc Nephrol*. (2004) 15:603–12. doi: 10.1097/01.ASN.0000113316.52371.2E
90. Sato M, Hirayama S, Matsuda Y, Wagnetz D, Hwang DM, Guan Z, et al. Stromal activation and formation of lymphoid-like stroma in chronic lung allograft dysfunction. *Transplantation* (2011) 91:1398–405. doi: 10.1097/TP.0b013e31821b2f7a
91. Cheng J, Torkamani A, Grover RK, Jones TM, Ruiz DI, Schork NJ, et al. Ectopic B-cell clusters that infiltrate transplanted human kidneys are clonal. *Proc Natl Acad Sci USA*. (2011) 108:5560–5. doi: 10.1073/pnas.1101148108
92. Thaunat O, Patey N, Caligiuri G, Gautreau C, Mamani-Matsuda M, Mekki Y, et al. Chronic rejection triggers the development of an aggressive intragraft immune response through recapitulation of lymphoid organogenesis. *J Immunol*. (2010) 185:717–28. doi: 10.4049/jimmunol.0903589
93. Thaunat O, Patey N, Gautreau C, Lechaton S, Fremeaux-Bacchi V, Dieu-Nosjean MC, et al. B cell survival in intragraft tertiary lymphoid organs after rituximab therapy. *Transplantation* (2008) 85:1648–53. doi: 10.1097/TP.0b013e3181735723
94. Zarkhin V, Kambham N, Li L, Kwok S, Hsieh SC, Salvatierra O, et al. Characterization of intra-graft B cells during renal allograft rejection. *Kidney Int*. (2008) 74:664–73. doi: 10.1038/ki.2008.249
95. Li W, Bribriesco AC, Nava RG, Brescia AA, Ibricevic A, Spahn JH, et al. Lung transplant acceptance is facilitated by early events in the graft and is associated with lymphoid neogenesis. *Mucosal Immunol*. (2012) 5:544–54. doi: 10.1038/mi.2012.30
96. Brown K, Sacks SH, Wong W. Tertiary lymphoid organs in renal allografts can be associated with donor-specific tolerance rather than rejection. *Eur J Immunol*. (2011) 41:89–96. doi: 10.1002/eji.201040759
97. Barone F, Gardner DH, Nayar S, Steinthal N, Buckley CD, Luther SA. Stromal fibroblasts in tertiary lymphoid structures: a novel target in chronic inflammation. *Front Immunol*. (2016) 7:477. doi: 10.3389/fimmu.2016.00477
98. Buckley CD, Barone F, Nayar S, Benezech C, Caamano J. Stromal cells in chronic inflammation and tertiary lymphoid organ formation. *Annu Rev Immunol*. (2015) 33:715–45. doi: 10.1146/annurev-immunol-032713-120252
99. Barone F, Nayar S, Buckley CD. The role of non-hematopoietic stromal cells in the persistence of inflammation. *Front Immunol*. (2012) 3:416. doi: 10.3389/fimmu.2012.00416
100. Carragher DM, Rangel-Moreno J, Randall TD. Ectopic lymphoid tissues and local immunity. *Semin Immunol*. (2008) 20:26–42. doi: 10.1016/j.smim.2007.12.004
101. Jones GW, Jones SA. Ectopic lymphoid follicles: inducible centres for generating antigen-specific immune responses within tissues. *Immunology* (2016) 147:141–51. doi: 10.1111/imm.12554
102. Picker LJ, Butcher EC. Physiological and molecular mechanisms of lymphocyte homing. *Ann Rev Immunol*. (1992) 10:561–91. doi: 10.1146/annurev.iy.10.040192.003021
103. Golub R, Cumano A. Embryonic hematopoiesis. *Blood Cells Mol Dis*. (2013) 51:226–31. doi: 10.1016/j.bcmd.2013.08.004
104. Manzo A, Bugatti S, Caporali R, Prevo R, Jackson DG, Uguccioni M, et al. CCL21 expression pattern of human secondary lymphoid organ stroma is conserved in inflammatory lesions with lymphoid neogenesis. *Am J Pathol*. (2007) 171:1549–62. doi: 10.2353/ajpath.2007.061275
105. Nayar S, Campos J, Chung MM, Navarro-Nunez L, Chachlani M, Steinthal N, et al. bimodal expansion of the lymphatic vessels is regulated by the sequential expression of il-7 and lymphotoxin alpha1beta2 in newly formed tertiary lymphoid structures. *J Immunol*. (2016) 197:1957–67. doi: 10.4049/jimmunol.1500686
106. Dutertre CA, Clement M, Morvan M, Schakel K, Castier Y, Alsac JM, et al. Deciphering the stromal and hematopoietic cell network of the adventitia from non-aneurysmal and aneurysmal human aorta. *PLoS ONE* (2014) 9:e89983. doi: 10.1371/journal.pone.0089983
107. Cupovic J, Onder L, Gil-Cruz C, Weiler E, Caviezel-Firner S, Perez-Shibayama C, et al. Central Nervous System Stromal Cells Control Local CD8(+) T Cell Responses during Virus-Induced Neuroinflammation. *Immunity* (2016) 44:622–33. doi: 10.1016/j.immuni.2015.12.022
108. Barone F, Bombardieri M, Manzo A, Blades MC, Morgan PR, Challacombe SJ, et al. Association of CXCL13 and CCL21 expression with the progressive organization of lymphoid-like structures in Sjogren's syndrome. *Arthritis Rheum*. (2005) 52:1773–84. doi: 10.1002/art.21062
109. Manzo A, Paoletti S, Carulli M, Blades MC, Barone F, Yanni G, et al. Systematic microanatomical analysis of CXCL13 and CCL21 *in situ* production and progressive lymphoid organization in rheumatoid synovitis. *Eur J Immunol*. (2005) 35:1347–59. doi: 10.1002/eji.200425830
110. Park YE, Woo YJ, Park SH, Moon YM, Oh HJ, Kim JI, et al. IL-17 increases cadherin-11 expression in a model of autoimmune experimental arthritis and in rheumatoid arthritis. *Immunol Lett*. (2011) 140:97–103. doi: 10.1016/j.imlet.2011.07.003
111. Lotzer K, Dopping S, Connert S, Grabner R, Spanbroek R, Lemser B, et al. Mouse aorta smooth muscle cells differentiate into lymphoid tissue organizer-like cells on combined tumor necrosis factor receptor-1/lymphotoxin beta-receptor NF-kappaB signaling. *Arterioscler Thromb Vasc Biol*. (2010) 30:395–402. doi: 10.1161/ATVBAHA.109.191395
112. Luther SA, Bidgol A, Hargreaves DC, Schmidt A, Xu Y, Paniyadi J, et al. Differing activities of homeostatic chemokines CCL19, CCL21, and CXCL12 in lymphocyte and dendritic cell recruitment and lymphoid neogenesis. *J Immunol*. (2002) 169:424–33. doi: 10.4049/jimmunol.169.1.424
113. Stranford S, Ruddle NH. Follicular dendritic cells, conduits, lymphatic vessels, and high endothelial venules in tertiary lymphoid organs: parallels with lymph node stroma. *Front Immunol*. (2012) 3:350. doi: 10.3389/fimmu.2012.00350
114. Ruddle NH. Lymphatic vessels and tertiary lymphoid organs. *J Clin Invest*. (2014) 124:953–9. doi: 10.1172/JCI71611
115. Janeway Jr CA, Bottomly K. Signals and signs for lymphocyte responses. *Cell* (1994) 76:275–85. doi: 10.1016/0092-8674(94)90335-2
116. Ansel KM, Ngo VN, Hyman PL, Luther SA, Forster R, Sedgwick JD, et al. A chemokine-driven positive feedback loop organizes lymphoid follicles. *Nature* (2000) 406:309–14. doi: 10.1038/35018581
117. Cyster JG, Ngo VN, Ekland EH, Gunn MD, Sedgwick JD, Ansel KM. Chemokines and B-cell homing to follicles. *Curr Top Microbiol Immunol*. (1999) 246, 87–92; discussion 93. doi: 10.1007/978-3-642-60162-0_11
118. Pereira JP, Kelly LM, Cyster JG. Finding the right niche: B-cell migration in the early phases of T-dependent antibody responses. *Int Immunol*. (2010) 22:413–9. doi: 10.1093/intimm/dxq047
119. Wolniak KL, Shinall SM, Waldschmidt TJ. The germinal center response. *Crit Rev Immunol*. (2004) 24:39–65. doi: 10.1615/CritRevImmunol.v24.i1.20
120. Allen CD, Ansel KM, Low C, Lesley R, Tamamura H, Fujii N, et al. Germinal center dark and light zone organization is mediated by CXCR4 and CXCR5. *Nat Immunol*. (2004) 5:943. doi: 10.1038/ni1100
121. Bannard O, Horton RM, Allen CD, An J, Nagasawa T, Cyster JG. Germinal center centroblasts transition to a centrocyte phenotype according to a timed program and depend on the dark zone for effective selection. *Immunity* (2013) 39:912–24. doi: 10.1016/j.immuni.2013.08.038
122. Nagaoka H, Muramatsu M, Yamamura N, Kinoshita K, Honjo T. Activation-induced deaminase. (AID)-directed hypermutation in the immunoglobulin Sμ region: implication of AID involvement in a common step of class switch recombination and somatic hypermutation. *J Exp Med*. (2002) 195:529–34. doi: 10.1084/jem.20012144
123. MacLennan IC. Germinal centers. *Ann Rev Immunol*. (1994) 12:117–39. doi: 10.1146/annurev.iy.12.040194.001001

124. Haberman AM, Shlomchik MJ. Reassessing the function of immune-complex retention by follicular dendritic cells. *Nat Rev Immunol*. (2003) 3:757. doi: 10.1038/nri1178
125. Wang X, Cho B, Suzuki K, Xu Y, Green JA, An J, et al. Follicular dendritic cells help establish follicle identity and promote B cell retention in germinal centers. *J Exp Med*. (2011) 208:2497–510. doi: 10.1084/jem.20111449
126. Allen CD, Cyster JG. Follicular dendritic cell networks of primary follicles and germinal centers: Phenotype and function. *Semin Immunol*. (2008) 20:14-25. doi: 10.1016/j.smim.2007.12.001
127. Zhang Y, Garcia-Ibanez L, Toellner KM. Regulation of germinal center B-cell differentiation. *Immunol Rev*. (2016) 270, 8–19. doi: 10.1111/imr.12396
128. Vinuesa CG, Cyster JG. How T cells earn the follicular rite of passage. *Immunity* (2011) 35:671–80. doi: 10.1016/j.immuni.2011.11.001
129. Vinuesa CG, Linterman MA, Yu D, MacLennan IC. Follicular Helper T Cells. *Annu Rev Immunol*. (2016) 34:335–68. doi: 10.1146/annurev-immunol-041015-055605
130. Ise W, Fujii K, Shiroguchi K, Ito A, Kometani K, Takeda K, et al. T follicular helper cell-germinal center B cell interaction strength regulates entry into plasma cell or recycling germinal center cell fate. *Immunity* (2018) 48:702–15 e4. doi: 10.1016/j.immuni.2018.03.027
131. Berek C, Berger A, Apel M. Maturation of the immune response in germinal centers. *Cell*. (1991) 67:1121–9. doi: 10.1016/0092-8674(91)90289-B
132. Jacob J, Kelsoe G, Rajewsky K, Weiss U. Intraclonal generation of antibody mutants in germinal centres. *Nature* (1991) 354:389–92. doi: 10.1038/354389a0
133. Muramatsu M, Kinoshita K, Fagarasan S, Yamada S, Shinkai Y, Honjo T. Class switch recombination and hypermutation require activation-induced cytidine deaminase. (AID), a potential RNA editing enzyme. *Cell* (2000) 102:553–63. doi: 10.1016/S0092-8674(00)00078-7
134. Muramatsu M, Sankaranand VS, Anant S, Sugai M, Kinoshita K, Davidson NO, et al. Specific expression of activation-induced cytidine deaminase (AID), a novel member of the RNA-editing deaminase family in germinal center B cells. *J Biol Chem*. (1999) 274:18470–6. doi: 10.1074/jbc.274.26.18470
135. Bombardieri M, Barone F, Humby F, Kelly S, McGurk M, Morgan P, et al. Activation-induced cytidine deaminase expression in follicular dendritic cell networks and interfollicular large B cells supports functionality of ectopic lymphoid neogenesis in autoimmune sialoadenitis and MALT lymphoma in Sjogren's syndrome. *J Immunol*. (2007) 179:4929–38. doi: 10.4049/jimmunol.179.7.4929
136. Eisen HN, Siskind GW. Variations in Affinities of Antibodies during the Immune Response. *Biochemistry*. (1964) 3:996–1008. doi: 10.1021/bi00895a027
137. Allen CD, Okada T, Cyster JG. Germinal-center organization and cellular dynamics. *Immunity*. (2007) 27:190–202. doi: 10.1016/j.immuni.2007.07.009
138. Moser K, Tokoyoda K, Radbruch A, MacLennan I, Manz RA. Stromal niches, plasma cell differentiation and survival. *Curr Opin Immunol*. (2006) 18:265–70. doi: 10.1016/j.coi.2006.03.004
139. Oropallo MA, Cerutti A. Germinal center reaction: antigen affinity and presentation explain it all. *Trends Immunol*. (2014) 35:287–9. doi: 10.1016/j.it.2014.06.001
140. Mesin L, Ersching J, Victora GD. Germinal center B cell dynamics. *Immunity* (2016) 45:471–82. doi: 10.1016/j.immuni.2016.09.001
141. Victora GD, Schwickert TA, Fooksman DR, Kamphorst AO, Meyer-Hermann M, Dustin ML, et al. Germinal center dynamics revealed by multiphoton microscopy with a photoactivatable fluorescent reporter. *Cell* (2010) 143:592–605. doi: 10.1016/j.cell.2010.10.032
142. Bannard O, Cyster JG. Germinal centers: programmed for affinity maturation and antibody diversification. *Curr Opin Immunol*. (2017) 45:21–30. doi: 10.1016/j.coi.2016.12.004
143. Cupedo T, Lund FE, Ngo VN, Randall TD, Jansen W, Greuter MJ, et al. Initiation of cellular organization in lymph nodes is regulated by non-B cell-derived signals and is not dependent on CXC chemokine ligand 13. *J Immunol*. (2004) 173:4889–96. doi: 10.4049/jimmunol.173.8.4889
144. Rodda LB, Bannard O, Ludewig B, Nagasawa T, Cyster JG. Phenotypic and morphological properties of germinal center dark zone Cxcl12-expressing reticular cells. *J Immunol*. (2015) 195:4781–91. doi: 10.4049/jimmunol.1501191
145. Roozendaal R, Mebius RE. Stromal cell-immune cell interactions. *Annu Rev Immunol*. (2011) 29:23–43. doi: 10.1146/annurev-immunol-031210-101357
146. Cyster JG, Ansel KM, Reif K, Ekland EH, Hyman PL, Tang HL, et al. Follicular stromal cells and lymphocyte homing to follicles. *Immunol Rev*. (2000) 176:181–93. doi: 10.1034/j.1600-065X.2000.00618.x
147. Kranich J, Krautler NJ. How Follicular Dendritic Cells Shape the B-Cell Antigenome. *Front Immunol*. (2016) 7:225. doi: 10.3389/fimmu.2016.00225
148. Denton AE, Linterman MA. Stromal networking: cellular connections in the germinal centre. *Curr Opin Immunol*. (2017) 45:103–11. doi: 10.1016/j.coi.2017.03.001
149. Yi T, Wang X, Kelly LM, An J, Xu Y, Sailer AW, et al. Oxysterol gradient generation by lymphoid stromal cells guides activated B cell movement during humoral responses. *Immunity* (2012) 37:535–48. doi: 10.1016/j.immuni.2012.06.015
150. Hughes CE, Benson RA, Bedaj M, Maffia P. Antigen-presenting cells and antigen presentation in tertiary lymphoid organs. *Front Immunol*. (2016) 7:481. doi: 10.3389/fimmu.2016.00481
151. Bombardieri M, Lewis M, Pitzalis C. Ectopic lymphoid neogenesis in rheumatic autoimmune diseases. *Nat Rev Rheumatol*. (2017) 13:141–54. doi: 10.1038/nrrheum.2016.217
152. Ruddle NH. High endothelial venules and lymphatic vessels in tertiary lymphoid organs: characteristics, functions, and regulation. *Front Immunol*. (2016) 7:491. doi: 10.3389/fimmu.2016.00491
153. Corsiero E, Nerviani A, Bombardieri M, Pitzalis C. Ectopic lymphoid structures: powerhouse of autoimmunity. *Front Immunol*. (2016) 7:430. doi: 10.3389/fimmu.2016.00430
154. Bombardieri M, Pitzalis C. Ectopic lymphoid neogenesis and lymphoid chemokines in Sjogren's syndrome: at the interplay between chronic inflammation, autoimmunity and lymphomagenesis. *Curr Pharm Biotechnol*. (2012) 13:1989–96. doi: 10.2174/138920112802273209
155. Weyand CM, Goronzy JJ. Ectopic germinal center formation in rheumatoid synovitis. *Ann N Y Acad Sci*. (2003) 987:140–9. doi: 10.1111/j.1749-6632.2003.tb06042.x
156. Kratz A, Campos-Neto A, Hanson MS, Ruddle NH. Chronic inflammation caused by lymphotoxin is lymphoid neogenesis. *J Exp Med*. (1996) 183:1461–72. doi: 10.1084/jem.183.4.1461
157. Amft N, Curnow SJ, Scheel-Toellner D, Devadas A, Oates J, Crocker J, et al. Ectopic expression of the B cell-attracting chemokine BCA-1. (CXCL13) on endothelial cells and within lymphoid follicles contributes to the establishment of germinal center-like structures in Sjogren's syndrome. *Arthritis Rheum*. (2001) 44:2633–41. doi: 10.1002/1529-0131(200111)44:11<2633::AID-ART443>3.0.CO;2-9
158. Croia C, Astorri E, Murray-Brown W, Willis A, Brokstad KA, Sutcliffe N, et al. Implication of Epstein-Barr virus infection in disease-specific autoreactive B cell activation in ectopic lymphoid structures of Sjogren's syndrome. *Arthritis Rheumatol*. (2014) 66:2545–57. doi: 10.1002/art.38726
159. Daridon C, Pers JO, Devauchelle V, Martins-Carvalho C, Hutin P, Pennec YL, et al. Identification of transitional type II B cells in the salivary glands of patients with Sjogren's syndrome. *Arthritis Rheum*. (2006) 54:2280–8. doi: 10.1002/art.21936
160. Hansen A, Lipsky PE, Dorner T. B cells in Sjogren's syndrome: indications for disturbed selection and differentiation in ectopic lymphoid tissue. *Arthritis Res Ther*. (2007) 9:218. doi: 10.1186/ar2210
161. Theander E, Vasaitis L, Baecklund E, Nordmark G, Warfvinge G, Liedholm R, et al. Lymphoid organisation in labial salivary gland biopsies is a possible predictor for the development of malignant lymphoma in primary Sjogren's syndrome. *Ann Rheum Dis*. (2011) 70:1363–8. doi: 10.1136/ard.2010.144782
162. Finke D, Schmutz S. Interleukin 7-induced lymphoid neogenesis in arthritis: recapitulation of a fetal developmental programme? *Swiss Med Wkly*. (2008) 138:500–5.
163. Martin L. Rheumatoid arthritis: symptoms, diagnosis, and management. *Nurs Times*. (2004) 100:40–4.
164. Tak, P. P., and Bresnihan, B.. (2000). The pathogenesis and prevention of joint damage in rheumatoid arthritis: advances from synovial biopsy and tissue analysis. *Arthritis Rheum* 43:2619–33. doi: 10.1002/1529-0131(200012)43:12<2619::AID-ANR1>3.0.CO;2-V
165. Targonska-Stepniak B. [Rheumatoid arthritis as a connective tissue disease]. *Wiad Lek*. (2018) 71:47–51.

166. Smolen JS, Aletaha D, Barton A, Burmester GR, Emery P, Firestein GS, et al. Rheumatoid arthritis. *Nat Rev Dis Primers*. (2018) 4:18001. doi: 10.1038/nrdp.2018.1
167. Ropes MW, Bennett GA, Cobb S, Jacox R, Jessar RA. Proposed diagnostic criteria for rheumatoid arthritis. *Ann Rheum Dis*. (1957) 16:118–25. doi: 10.1136/ard.16.1.118
168. Munthe E, Natvig JB. Immunglobulin classes, subclasses and complexes of IgG rheumatoid factor in rheumatoid plasma cells. *Clin Exp Immunol*. (1972) 12:55–70.
169. Steere AC, Duray PH, Butcher EC. Spirochetal antigens and lymphoid cell surface markers in Lyme synovitis. Comparison with rheumatoid synovium and tonsillar lymphoid tissue. *Arthritis Rheum*. (1988) 31:487–95. doi: 10.1002/art.1780310405
170. Schroder AE, Greiner A, Seyfert C, Berek C. Differentiation of B cells in the nonlymphoid tissue of the synovial membrane of patients with rheumatoid arthritis. *Proc Natl Acad Sci USA*. (1996) 93:221–5. doi: 10.1073/pnas.93.1.221
171. Canete JD, Santiago B, Cantaert T, Sanmarti R, Palacin A, Celis R, et al. Ectopic lymphoid neogenesis in psoriatic arthritis. *Ann Rheum Dis*. (2007) 66:720–6. doi: 10.1136/ard.2006.062042
172. Voswinkel J, Weisgerber K, Pfreundschuh M, Gause A. B lymphocyte involvement in ankylosing spondylitis: the heavy chain variable segment gene repertoire of B lymphocytes from germinal center-like foci in the synovial membrane indicates antigen selection. *Arthritis Res*. (2001) 3:189–95. doi: 10.1186/ar297
173. Krenn V, Hensel F, Kim HJ, Souto Carneiro MM, Starostik P, Ristow G, et al. Molecular IgV(H) analysis demonstrates highly somatic mutated B cells in synovialitis of osteoarthritis: a degenerative disease is associated with a specific, not locally generated immune response. *Lab Invest*. (1999) 79:1377–84.
174. Campos J, Hillen MR, Barone F. Salivary Gland Pathology in Sjogren's Syndrome. *Rheum Dis Clin North Am*. (2016) 42:473–83. doi: 10.1016/j.rdc.2016.03.006
175. Chused TM, Hardin JA, Frank MM, Green I. Identification of cells infiltrating the minor salivary glands in patients with Sjogren's syndrome. *J Immunol*. (1974) 112:641–8.
176. Nair PN, Schroeder HE. Duct-associated lymphoid tissue. (DALT) of minor salivary glands and mucosal immunity. *Immunology* (1986) 57:171–80.
177. Aziz KE, McCluskey PJ, Wakefield D. Characterisation of follicular dendritic cells in labial salivary glands of patients with primary Sjogren syndrome: comparison with tonsillar lymphoid follicles. *Ann Rheum Dis*. (1997) 56:140–3. doi: 10.1136/ard.56.2.140
178. Xanthou G, Polihronis M, Tzioufas AG, Paikos S, Sideras P, Moutsopoulos HM. "Lymphoid" chemokine messenger RNA expression by epithelial cells in the chronic inflammatory lesion of the salivary glands of Sjogren's syndrome patients: possible participation in lymphoid structure formation. *Arthritis Rheum* (2001) 44:408–18. doi: 10.1002/1529-0131(200102)44:2<408::AID-ANR60>3.0.CO;2-0
179. Salomonsson S, Wahren-Herlenius M. Local production of Ro/SSA and La/SSB autoantibodies in the target organ coincides with high levels of circulating antibodies in sera of patients with Sjogren's syndrome. *Scand J Rheumatol*. (2003) 32:79–82. doi: 10.1080/03009740310000076
180. Barone F, Bombardieri M, Rosado MM, Morgan PR, Challacombe SJ, De Vita S, et al. CXCL13, CCL21, and CXCL12 expression in salivary glands of patients with Sjogren's syndrome and MALT lymphoma: association with reactive and malignant areas of lymphoid organization. *J Immunol*. (2008) 180:5130–40. doi: 10.4049/jimmunol.180.7.5130
181. Alunno A, Leone MC, Giacomelli R, Gerli R, Carubbi F. Lymphoma and lymphomagenesis in primary sjogren's syndrome. *Front Med. (Lausanne)*. (2018) 5:102. doi: 10.3389/fmed.2018.00102
182. Haacke, EA, van der Vegt B, Vissink AF, Spijkervet KL, Bootsma HF, Kroese GM. Germinal centres in diagnostic labial gland biopsies of patients with primary Sjogren's syndrome are not predictive for parotid MALT lymphoma development. *Ann Rheum Dis.* (2017) 76:1781–4. doi: 10.1136/annrheumdis-2017-211290
183. Pereira MI, Medeiros JA. Role of Helicobacter pylori in gastric mucosa-associated lymphoid tissue lymphomas. *World J Gastroenterol*. (2014) 20:684–98. doi: 10.3748/wjg.v20.i3.684
184. Halle S, Dujardin HC, Bakocevic N, Fleige H, Danzer H, Willenzon S, et al. Induced bronchus-associated lymphoid tissue serves as a general priming site for T cells and is maintained by dendritic cells. *J Exp Med*. (2009) 206:2593–601. doi: 10.1084/jem.20091472
185. Macritchie N, Grassia G, Sabir SR, Maddaluno M, Welsh P, Sattar N, et al. Plasmacytoid dendritic cells play a key role in promoting atherosclerosis in apolipoprotein E-deficient mice. *Arterioscler Thromb Vasc Biol*. (2012) 32:2569–79. doi: 10.1161/ATVBAHA.112.251314
186. Link A, Hardie DL, Favre S, Britschgi MR, Adams DH, Sixt M, et al. Association of T-zone reticular networks and conduits with ectopic lymphoid tissues in mice and humans. *Am J Pathol*. (2011) 178:1662–75. doi: 10.1016/j.ajpath.2010.12.039
187. Drayton DL, Liao S, Mounzer RH, Ruddle NH. Lymphoid organ development: from ontogeny to neogenesis. *Nat Immunol*. (2006) 7:344–53. doi: 10.1038/ni1330
188. Junt T, Scandella E, Ludewig B. Form follows function: lymphoid tissue microarchitecture in antimicrobial immune defence. *Nat Rev Immunol*. (2008) 8:764–75. doi: 10.1038/nri2414
189. Neely HR, Flajnik MF. Emergence and evolution of secondary lymphoid organs. *Annu Rev Cell Dev Biol*. (2016) 32:693–711. doi: 10.1146/annurev-cellbio-111315-125306
190. Lukacs-Kornek V, Turley SJ. Self-antigen presentation by dendritic cells and lymphoid stroma and its implications for autoimmunity. *Curr Opin Immunol*. (2011) 23:138–45. doi: 10.1016/j.coi.2010.11.012
191. Malhotra D, Fletcher AL, Turley SJ. Stromal and hematopoietic cells in secondary lymphoid organs: partners in immunity. *Immunol Rev*. (2013) 251:160–76. doi: 10.1111/imr.12023
192. Turley SJ, Fletcher AL, Elpek KG. The stromal and haematopoietic antigen-presenting cells that reside in secondary lymphoid organs. *Nat Rev Immunol*. (2010) 10:813–25. doi: 10.1038/nri2886
193. van de Pavert SA, Mebius RE. New insights into the development of lymphoid tissues. *Nat Rev Immunol*. (2010) 10:664–74. doi: 10.1038/nri2832
194. Kocks JR, Davalos-Misslitz AC, Hintzen G, Ohl L, Forster R. Regulatory T cells interfere with the development of bronchus-associated lymphoid tissue. *J Exp Med*. (2007) 204:723–34. doi: 10.1084/jem.20061424
195. Alitalo K. The lymphatic vasculature in disease. *Nat Med*. (2011) 17:1371–80. doi: 10.1038/nm.2545
196. Alitalo K, Tammela T, Petrova TV. Lymphangiogenesis in development and human disease. *Nature* (2005) 438:946–53. doi: 10.1038/nature04480
197. Flister MJ, Wilber A, Hall KL, Iwata C, Miyazono K, Nisato RE, et al. Inflammation induces lymphangiogenesis through up-regulation of VEGFR-3 mediated by NF-kappaB and Prox1. *Blood* (2010) 115:418–29. doi: 10.1182/blood-2008-12-196840
198. Mounzer RH, Svendsen OS, Baluk P, Bergman CM, Padera TP, Wiig H, et al. Lymphotoxin-alpha contributes to lymphangiogenesis. *Blood* (2010) 116:2173–82. doi: 10.1182/blood-2009-12-256065
199. Kunder CA, St John AL, Abraham SN. Mast cell modulation of the vascular and lymphatic endothelium. *Blood* (2011) 118:5383–93. doi: 10.1182/blood-2011-07-358432
200. Cursiefen C, Chen L, Borges LP, Jackson D, Cao J, Radziejewski C, et al. VEGF-A stimulates lymphangiogenesis and hemangiogenesis in inflammatory neovascularization via macrophage recruitment. *J Clin Invest*. (2004) 113:1040–50. doi: 10.1172/JCI20465
201. Hamrah P, Chen L, Zhang Q, Dana MR. Novel expression of vascular endothelial growth factor receptor. (VEGFR)-3 and VEGF-C on corneal dendritic cells. *Am J Pathol*. (2003) 163:57–68. doi: 10.1016/S0002-9440(10)63630-9
202. Thaunat O, Kerjaschki D, Nicoletti A. Is defective lymphatic drainage a trigger for lymphoid neogenesis? *Trends Immunol*. (2006) 27:441–5. doi: 10.1016/j.it.2006.08.003
203. Burman A, Haworth O, Hardie DL, Amft EN, Siewert C, Jackson DG, et al. A chemokine-dependent stromal induction mechanism for aberrant lymphocyte accumulation and compromised lymphatic return in rheumatoid arthritis. *J Immunol*. (2005) 174:1693–700. doi: 10.4049/jimmunol.174.3.1693
204. von der Weid PY, Rehal S, Ferraz JG. Role of the lymphatic system in the pathogenesis of Crohn's disease. *Curr Opin Gastroenterol*. (2011) 27:335–41. doi: 10.1097/MOG.0b013e3283476e8f

205. Kajiya K, Detmar M. An important role of lymphatic vessels in the control of UVB-induced edema formation and inflammation. *J Invest Dermatol.* (2006) 126:919–21. doi: 10.1038/sj.jid.5700126
206. Wilkinson LS, Edwards JC. Demonstration of lymphatics in human synovial tissue. *Rheumatol Int.* (1991) 11:151–5. doi: 10.1007/BF00332553
207. Bouta EM, Wood RW, Brown EB, Rahimi H, Ritchlin CT, Schwarz EM. *In vivo* quantification of lymph viscosity and pressure in lymphatic vessels and draining lymph nodes of arthritic joints in mice. *J Physiol.* (2014) 592:1213–23. doi: 10.1113/jphysiol.2013.266700
208. Polzer K, Baeten D, Soleiman A, Distler J, Gerlag DM, Tak PP, et al. Tumour necrosis factor blockade increases lymphangiogenesis in murine and human arthritic joints. *Ann Rheum Dis.* (2008) 67:1610–6. doi: 10.1136/ard.2007.083394
209. Li J, Ju Y, Bouta EM, Xing L, Wood RW, Kuzin I, et al. Efficacy of B cell depletion therapy for murine joint arthritis flare is associated with increased lymphatic flow. *Arthritis Rheum.* (2013) 65:130–8. doi: 10.1002/art.37709
210. Baeten, D, Peene I, Union A, Meheus L, Sebbag M, Serre G, et al. Specific presence of intracellular citrullinated proteins in rheumatoid arthritis synovium: relevance to antifilaggrin autoantibodies. *Arthritis Rheum.* (2001) 44:2255–62.
211. De Rycke L, Nicholas AP, Cantaert T, Kruithof E, Echols JD, Vandekerckhove B, et al. Synovial intracellular citrullinated proteins colocalizing with peptidyl arginine deiminase as pathophysiologically relevant antigenic determinants of rheumatoid arthritis-specific humoral autoimmunity. *Arthritis Rheum.* (2005) 52:2323–30. doi: 10.1002/art.21220
212. Vossenaar ER, Smeets TJ, Kraan MC, Raats JM, van Venrooij WJ, Tak PP. The presence of citrullinated proteins is not specific for rheumatoid synovial tissue. *Arthritis Rheum.* (2004) 50:3485–94. doi: 10.1002/art.20584
213. Keene JD. Molecular structure of the La and Ro autoantigens and their use in autoimmune diagnostics. *J Autoimmun.* (1989) 2:329–34. doi: 10.1016/0896-8411(89)90160-1
214. Tzioufas AG, Hantoumi I, Polihronis M, Xanthou G, Moutsopoulos HM. Autoantibodies to La/SSB in patients with primary Sjogren's syndrome (pSS) are associated with upregulation of La/SSB mRNA in minor salivary gland biopsies (MSGs). *J Autoimmun.* (1999) 13:429–34. doi: 10.1006/jaut.1999.0333
215. de Wilde, PC, Kater L, Bodeutsch C, van den Hoogen FH, van de Putte LB, van Venrooij WJ. Aberrant expression pattern of the SS-B/La antigen in the labial salivary glands of patients with Sjogren's syndrome. *Arthritis Rheum.* (1996) 39:783–91. doi: 10.1002/art.1780390510
216. Barcellos KS, Nonogaki S, Enokihara MM, Teixeira MS, Andrade LE. Differential expression of Ro/SSA 60 kDa and La/SSB, but not Ro/SSA 52 kDa, mRNA and protein in minor salivary glands from patients with primary Sjogren's syndrome. *J Rheumatol.* (2007) 34:1283–92.
217. Tengner, P, Halse AK, Haga HJ, Jonsson R, Wahren-Herlenius M. Detection of anti-Ro/SSA and anti-La/SSB autoantibody-producing cells in salivary glands from patients with Sjogren's syndrome. *Arthritis Rheum.* (1998) 41:2238–48. doi: 10.1002/1529-0131(199812)41:12<2238::AID-ART20>3.0.CO;2-V
218. Kang YM, Zhang X, Wagner UG, Yang H, Beckenbaugh RD, Kurtin PJ, et al. CD8 T cells are required for the formation of ectopic germinal centers in rheumatoid synovitis. *J Exp Med.* (2002) 195:1325–36. doi: 10.1084/jem.20011565
219. Rangel-Moreno J, Carragher DM, de la Luz Garcia-Hernandez M, Hwang JY, Kusser K, Hartson L, et al. The development of inducible bronchus-associated lymphoid tissue depends on IL-17. *Nat Immunol.* (2011) 12:639–46. doi: 10.1038/ni.2053
220. Chiang EY, Kolumam GA, Yu X, Francesco M, Ivelja S, Peng I, et al. Targeted depletion of lymphotoxin-alpha-expressing TH1 and TH17 cells inhibits autoimmune disease. *Nat Med.* (2009) 15:766–73. doi: 10.1038/nm.1984
221. Chiang EY, Kolumam G, McCutcheon KM, Young J, Lin Z, Balazs M, et al. *In vivo* depletion of lymphotoxin-alpha expressing lymphocytes inhibits xenogeneic graft-versus-host-disease. *PLoS ONE* (2012) 7:e33106. doi: 10.1371/journal.pone.0033106
222. Deteix C, Attuil-Audenis V, Duthey A, Patey N, McGregor B, Dubois V, et al. Intragraft Th17 infiltrate promotes lymphoid neogenesis and hastens clinical chronic rejection. *J Immunol.* (2010) 184:5344–51. doi: 10.4049/jimmunol.0902999
223. Lucchesi D, Pontarini E, Coleby R, Jones GW, Hill DG, Pitzalis C, et al. Interleukin-27 Regulates the magitude of the ectopic germinal centre response in a viral inducible model of sialadenitis. *Ann Rheumatic Dis.* (2018) 77. doi: 10.1136/annrheumdis-2018-EWRR2018.96
224. Jones GW, Bombardieri M, Greenhill CJ, McLeod L, Nerviani A, Rocher-Ros V, et al. Interleukin-27 inhibits ectopic lymphoid-like structure development in early inflammatory arthritis. *J Exp Med.* (2015) 212:1793–802. doi: 10.1084/jem.20132307
225. Lee Y, Chin RK, Christiansen P, Sun Y, Tumanov AV, Wang J, et al. Recruitment and activation of naive T cells in the islets by lymphotoxin beta receptor-dependent tertiary lymphoid structure. *Immunity.* (2006) 25:499–509. doi: 10.1016/j.immuni.2006.06.016
226. Clement M, Guedj K, Andreata F, Morvan M, Bey L, Khallou-Laschet J, et al. Control of the T follicular helper-germinal center B-cell axis by $CD8^+$ regulatory T cells limits atherosclerosis and tertiary lymphoid organ development. *Circulation* (2015) 131:560–70. doi: 10.1161/CIRCULATIONAHA.114.010988
227. Schmitt N, Bentebibel SE, Ueno H. Phenotype and functions of memory Tfh cells in human blood. *Trends Immunol.* (2014) 35:436–42. doi: 10.1016/j.it.2014.06.002
228. Rao DA, Gurish MF, Marshall JL, Slowikowski K, Fonseka CY, Liu Y, et al. Pathologically expanded peripheral T helper cell subset drives B cells in rheumatoid arthritis. *Nature* (2017) 542:110–4. doi: 10.1038/nature20810
229. Jin L, Yu D, Li X, Yu N, Li X, Wang Y, et al. $CD4^+CXCR5^+$ follicular helper T cells in salivary gland promote B cells maturation in patients with primary Sjogren's syndrome. *Int J Clin Exp Pathol.* (2014) 7:1988–96.
230. Kang KY, Kim HO, Kwok SK, Ju JH, Park KS, Sun DI, et al. Impact of interleukin-21 in the pathogenesis of primary Sjogren's syndrome: increased serum levels of interleukin-21 and its expression in the labial salivary glands. *Arthritis Res Ther.* (2011) 13:R179. doi: 10.1186/ar3504
231. Voulgarelis M, Tzioufas AG. Pathogenetic mechanisms in the initiation and perpetuation of Sjogren's syndrome. *Nat Rev Rheumatol.* (2010) 6:529–37. doi: 10.1038/nrrheum.2010.118
232. Christodoulou MI, Kapsogeorgou EK, Moutsopoulos HM. Characteristics of the minor salivary gland infiltrates in Sjogren's syndrome. *J Autoimmun.* (2010) 34:400–7. doi: 10.1016/j.jaut.2009.10.004
233. Bohnhorst JO, Thoen JE, Natvig JB, Thompson KM. Significantly depressed percentage of $CD27^+$ (memory) B cells among peripheral blood B cells in patients with primary Sjogren's syndrome. *Scand J Immunol.* (2001) 54:421–7. doi: 10.1046/j.1365-3083.2001.00989.x
234. Bohnhorst JO, Bjorgan MB, Thoen JE, Jonsson R, Natvig JB, Thompson KM. Abnormal B cell differentiation in primary Sjogren's syndrome results in a depressed percentage of circulating memory B cells and elevated levels of soluble CD27 that correlate with Serum IgG concentration. *Clin Immunol.* (2002) 103:79–88. doi: 10.1006/clim.2002.5199
235. Larsson A, Bredberg A, Henriksson G, Manthorpe R, Sallmyr A. Immunohistochemistry of the B-cell component in lower lip salivary glands of Sjogren's syndrome and healthy subjects. *Scand J Immunol.* (2005) 61:98–107. doi: 10.1111/j.0300-9475.2005.01540.x
236. Hansen A, Odendahl M, Reiter K, Jacobi AM, Feist E, Scholze J, et al. Diminished peripheral blood memory B cells and accumulation of memory B cells in the salivary glands of patients with Sjogren's syndrome. *Arthritis Rheum.* (2002) 46:2160–71. doi: 10.1002/art.10445
237. William J, Euler C, Christensen S, Shlomchik MJ. Evolution of autoantibody responses via somatic hypermutation outside of germinal centers. *Science* (2002) 297:2066–70. doi: 10.1126/science.1073924
238. William J, Euler C, Shlomchik MJ. Short-lived plasmablasts dominate the early spontaneous rheumatoid factor response: differentiation pathways, hypermutating cell types, and affinity maturation outside the germinal center. *J Immunol.* (2005) 174:6879–87. doi: 10.4049/jimmunol.174.11.6879
239. Nocturne G, Mariette X. B cells in the pathogenesis of primary Sjogren syndrome. *Nat Rev Rheumatol.* (2018) 14:133–45. doi: 10.1038/nrrheum.2018.1
240. Nocturne G, Mariette X. Sjogren Syndrome-associated lymphomas: an update on pathogenesis and management. *Br J Haematol.* (2015) 168:317–27. doi: 10.1111/bjh.13192

241. Reynaud CA, Descatoire M, Dogan I, Huetz F, Weller S, Weill JC. IgM memory B cells: a mouse/human paradox. *Cell Mol Life Sci*. (2012) 69:1625–34. doi: 10.1007/s00018-012-0971-z
242. Steiniger B, Timphus EM, Barth PJ. The splenic marginal zone in humans and rodents: an enigmatic compartment and its inhabitants. *Histochem Cell Biol*. (2006) 126:641–8. doi: 10.1007/s00418-006-0210-5
243. Vossenkamper A, Spencer J. Transitional B cells: how well are the checkpoints for specificity understood? *Arch Immunol Ther Exp. (Warsz)*. (2011) 59:379–84. doi: 10.1007/s00005-011-0135-0
244. Mebius RE, Kraal G. Structure and function of the spleen. *Nat Rev Immunol*. (2005) 5:606–16. doi: 10.1038/nri1669
245. Vossenkamper A, Blair PA, Safinia N, Fraser LD, Das L, Sanders TJ, et al. A role for gut-associated lymphoid tissue in shaping the human B cell repertoire. *J Exp Med*. (2013) 210:1665–74. doi: 10.1084/jem.20122465
246. Mietzner B, Tsuiji M, Scheid J, Velinzon K, Tiller T, Abraham K, et al. Autoreactive IgG memory antibodies in patients with systemic lupus erythematosus arise from nonreactive and polyreactive precursors. *Proc Natl Acad Sci USA*. (2008) 105:9727–32. doi: 10.1073/pnas.0803644105
247. Meffre E, Wardemann H. B-cell tolerance checkpoints in health and autoimmunity. *Curr Opin Immunol*. (2008) 20:632–8. doi: 10.1016/j.coi.2008.09.001
248. Bemark M, Holmqvist J, Abrahamsson J, Mellgren K. Translational Mini-Review Series on B cell subsets in disease. Reconstitution after haematopoietic stem cell transplantation - revelation of B cell developmental pathways and lineage phenotypes. *Clin Exp Immunol*. (2012) 167:15–25. doi: 10.1111/j.1365-2249.2011.04469.x
249. Tomura M, Yoshida N, Tanaka J, Karasawa S, Miwa Y, Miyawaki A, et al. Monitoring cellular movement *in vivo* with photoconvertible fluorescence protein "Kaede" transgenic mice. *Proc Natl Acad Sci USA*. (2008) 105:10871–6. doi: 10.1073/pnas.0802278105
250. Szyszko EA, Brokstad KA, Oijordsbakken G, Jonsson MV, Jonsson R, Skarstein K. Salivary glands of primary Sjogren's syndrome patients express factors vital for plasma cell survival. *Arthritis Res Ther*. (2011) 13:R2. doi: 10.1186/ar3220
251. Vos K, Thurlings RM, Wijbrandts CA, van Schaardenburg D, Gerlag DM, Tak PP. Early effects of rituximab on the synovial cell infiltrate in patients with rheumatoid arthritis. *Arthritis Rheum*. (2007) 56:772–8. doi: 10.1002/art.22400
252. Quartuccio L, Fabris M, Moretti M, Barone F, Bombardieri M, Rupolo M, et al. Resistance to rituximab therapy and local BAFF overexpression in Sjogren's syndrome-related myoepithelial sialadenitis and low-grade parotid B-cell lymphoma. *Open Rheumatol J*. (2008) 2:38–43. doi: 10.2174/1874312900802010038
253. Thien M, Phan TG, Gardam S, Amesbury M, Basten A, Mackay F, et al. Excess BAFF rescues self-reactive B cells from peripheral deletion and allows them to enter forbidden follicular and marginal zone niches. *Immunity*. (2004) 20:785–98. doi: 10.1016/j.immuni.2004.05.010
254. Groom J, Kalled SL, Cutler AH, Olson C, Woodcock SA, Schneider P, et al. Association of BAFF/BLyS overexpression and altered B cell differentiation with Sjogren's syndrome. *J Clin Invest*. (2002) 109:59–68. doi: 10.1172/JCI0214121
255. Fletcher CA, Groom JR, Woehl B, Leung H, Mackay C, Mackay F. Development of autoimmune nephritis in genetically asplenic and splenectomized BAFF transgenic mice. *J Autoimmun*. (2011) 36:125–34. doi: 10.1016/j.jaut.2010.12.002
256. Hartgring SA, Bijlsma JW, Lafeber FP, van Roon JA. Interleukin-7 induced immunopathology in arthritis. *Ann Rheum Dis*. (2006) 65(Suppl. 3):iii69–74. doi: 10.1136/ard.2006.058479
257. Hartgring SA, Willis CR, Alcorn D, Nelson LJ, Bijlsma JW, Lafeber FP, et al. Blockade of the interleukin-7 receptor inhibits collagen-induced arthritis and is associated with reduction of T cell activity and proinflammatory mediators. *Arthritis Rheum*. (2010) 62:2716–25. doi: 10.1002/art.27578
258. Huang HY, Luther SA. Expression and function of interleukin-7 in secondary and tertiary lymphoid organs. *Semin Immunol*. (2012) 24:175–89. doi: 10.1016/j.smim.2012.02.008
259. Timmer TC, Baltus B, Vondenhoff M, Huizinga TW, Tak PP, Verweij CL, et al. Inflammation and ectopic lymphoid structures in rheumatoid arthritis synovial tissues dissected by genomics technology: identification of the interleukin-7 signaling pathway in tissues with lymphoid neogenesis. *Arthritis Rheum*. (2007) 56:2492–502. doi: 10.1002/art.22748
260. Harada S, Yamamura M, Okamoto H, Morita Y, Kawashima M, Aita T, et al. Production of interleukin-7 and interleukin-15 by fibroblast-like synoviocytes from patients with rheumatoid arthritis. *Arthritis Rheum*. (1999) 42:1508–16. doi: 10.1002/1529-0131(199907)42:7<1508::AID-ANR26>3.0.CO;2-L
261. Van Roon JA, Verweij MC, Wijk MW, Jacobs KM, Bijlsma JW, Lafeber FP. Increased intraarticular interleukin-7 in rheumatoid arthritis patients stimulates cell contact–dependent activation of CD4+ T cells and macrophages. *Arthritis Rheumatol*. (2005) 52:1700–10. doi: 10.1002/art.21045
262. Hikida M, Nakayama Y, Yamashita Y, Kumazawa Y, Nishikawa SI, Ohmori H. Expression of recombination activating genes in germinal center B cells: involvement of interleukin 7 (IL-7) and the IL-7 receptor. *J Exp Med*. (1998) 188:365–72. doi: 10.1084/jem.188.2.365
263. Watanabe M, Ueno Y, Yajima T, Okamoto S, Hayashi T, Yamazaki M, et al. Interleukin 7 transgenic mice develop chronic colitis with decreased interleukin 7 protein accumulation in the colonic mucosa. *J Exp Med*. (1998) 187:389–402. doi: 10.1084/jem.187.3.389
264. Uehira M, Matsuda H, Hikita I, Sakata T, Fujiwara H, Nishimoto H. The development of dermatitis infiltrated by gamma delta T cells in IL-7 transgenic mice. *Int Immunol*. (1993) 5:1619–27. doi: 10.1093/intimm/5.12.1619
265. Meier D, Bornmann C, Chappaz S, Schmutz S, Otten LA, Ceredig R, et al. Ectopic lymphoid-organ development occurs through interleukin 7-mediated enhanced survival of lymphoid-tissue-inducer cells. *Immunity*. (2007) 26:643–54. doi: 10.1016/j.immuni.2007.04.009
266. Hillen MR, Radstake TR, Hack CE, van Roon JA. Thymic stromal lymphopoietin as a novel mediator amplifying immunopathology in rheumatic disease. *Rheumatology (Oxford)*. (2015) 54:1771–9. doi: 10.1093/rheumatology/kev241
267. Zaheen A, Boulianne B, Parsa JY, Ramachandran S, Gommerman JL, Martin A. AID constrains germinal center size by rendering B cells susceptible to apoptosis. *Blood* (2009) 114:547–54. doi: 10.1182/blood-2009-03-211763
268. Cantaert T, Schickel JN, Bannock JM, Ng YS, Massad C, Delmotte FR, et al. Decreased somatic hypermutation induces an impaired peripheral B cell tolerance checkpoint. *J Clin Invest*. (2016) 126:4289–302. doi: 10.1172/JCI84645
269. Mellors RC, Heimer R, Corcos J, Korngold L. Cellular Origin of Rheumatoid Factor. *J Exp Med*. (1959) 110:875–86. doi: 10.1084/jem.110.6.875
270. Smiley JD, Sachs C, Ziff M. *In vitro* synthesis of immunoglobulin by rheumatoid synovial membrane. *J Clin Invest*. (1968) 47:624–32. doi: 10.1172/JCI105758
271. Randen I, Brown D, Thompson KM, Hughes-Jones N, Pascual V, Victor K, et al. Clonally related IgM rheumatoid factors undergo affinity maturation in the rheumatoid synovial tissue. *J Immunol*. (1992) 148:3296–301.
272. Thompson KM, Borretzen M, Randen I, Forre O, Natvig JB. V-gene repertoire and hypermutation of rheumatoid factors produced in rheumatoid synovial inflammation and immunized healthy donors. *Ann N Y Acad Sci*. (1995) 764:440–9. doi: 10.1111/j.1749-6632.1995.tb55861.x
273. Koopman WJ, Schrohenloher RE, Crago SS, Spalding DM, Mestecky J. IgA rheumatoid factor synthesis by dissociated synovial cells. Characterization and relationship to IgM rheumatoid factor synthesis. *Arthritis Rheum*. (1985) 28:1219–27. doi: 10.1002/art.1780281105
274. Hakoda M, Ishimoto T, Hayashimoto S, Inoue K, Taniguchi A, Kamatani N, et al. Selective infiltration of B cells committed to the production of monoreactive rheumatoid factor in synovial tissue of patients with rheumatoid arthritis. *Clin Immunol Immunopathol*. (1993) 69:16–22. doi: 10.1006/clin.1993.1144
275. Thompson KM, Randen I, Borretzen M, Forre O, Natvig JB. Variable region gene usage of human monoclonal rheumatoid factors derived from healthy donors following immunization. *Eur J Immunol*. (1994) 24:1771–8. doi: 10.1002/eji.1830240808
276. van Venrooij WJ, van Beers JJ, Pruijn GJ. Anti-CCP antibodies: the past, the present and the future. *Nat Rev Rheumatol*. (2011) 7:391–8. doi: 10.1038/nrrheum.2011.76

277. Amara K, Steen J, Murray F, Morbach H, Fernandez-Rodriguez BM, Joshua V, et al. Monoclonal IgG antibodies generated from joint-derived B cells of RA patients have a strong bias toward citrullinated autoantigen recognition. *J Exp Med*. (2013) 210:445–55. doi: 10.1084/jem.20121486
278. Masson-Bessiere C, Sebbag M, Durieux JJ, Nogueira L, Vincent C, Girbal-Neuhauser E, et al. In the rheumatoid pannus, anti-filaggrin autoantibodies are produced by local plasma cells and constitute a higher proportion of IgG than in synovial fluid and serum. *Clin Exp Immunol*. (2000) 119:544–52. doi: 10.1046/j.1365-2249.2000.01171.x
279. Caspi D, Anouk M, Golan I, Paran D, Kaufman I, Wigler I, et al. Synovial fluid levels of anti-cyclic citrullinated peptide antibodies and IgA rheumatoid factor in rheumatoid arthritis, psoriatic arthritis, and osteoarthritis. *Arthritis Rheum*. (2006) 55:53–6. doi: 10.1002/art.21691
280. Reparon-Schuijt C C, van Esch WJ, van Kooten C, Schellekens GA, de Jong BA, van Venrooij WJ, et al. Secretion of anti-citrulline-containing peptide antibody by B lymphocytes in rheumatoid arthritis. *Arthritis Rheum*. (2001) 44:41–7. doi: 10.1002/1529-0131(200101)44:1<41::AID-ANR6>3.0.CO;2-0
281. Snir O, Widhe M, Hermansson M, von Spee C, Lindberg J, Hensen S, et al. Antibodies to several citrullinated antigens are enriched in the joints of rheumatoid arthritis patients. *Arthritis Rheum*. (2010) 62:44–52. doi: 10.1002/art.25036
282. Spadaro A, Riccieri V, Scrivo R, Alessandri C, Valesini G. Anti-cyclic citrullinated peptide antibody determination in the synovial fluid of patients with rheumatoid arthritis: comment on the article by Caspi et al. *Arthritis Rheum*. (2006) 55:681–2; author reply 682. doi: 10.1002/art.22113
283. Amara K, Clay E, Yeo L, Ramskold D, Spengler J, Sippl N, et al. Immunoglobulin characteristics and RNAseq data of FcRL4+ B cells sorted from synovial fluid and tissue of patients with rheumatoid arthritis. *Data Brief*. (2017) 13:356–70. doi: 10.1016/j.dib.2017.06.009
284. Reparon-Schuijt C C, van Esch WJ, van Kooten C, Levarht EW, Breedveld FC, Verweij CL. Functional analysis of rheumatoid factor-producing B cells from the synovial fluid of rheumatoid arthritis patients. *Arthritis Rheum* (1998) 41:2211–20. doi: 10.1002/1529-0131(199812)41:12<2211::AID-ART17>3.0.CO;2-O
285. Van Esch WJ, Reparon-Schuijt CC, Hamstra HJ, Van Kooten C, Logtenberg T, Breedveld FC, et al. Human IgG Fc-binding phage antibodies constructed from synovial fluid $CD38^+$ B cells of patients with rheumatoid arthritis show the imprints of an antigen-dependent process of somatic hypermutation and clonal selection. *Clin Exp Immunol*. (2003) 131:364–76. doi: 10.1046/j.1365-2249.2003.02068.x
286. Corsiero E, Bombardieri M, Carlotti E, Pratesi F, Robinson W, Migliorini P, et al. Single cell cloning and recombinant monoclonal antibodies generation from RA synovial B cells reveal frequent targeting of citrullinated histones of NETs. *Ann Rheum Dis*. (2016) 75:1866–75. doi: 10.1136/annrheumdis-2015-208356
287. Gause A, Gundlach K, Carbon G, Daus H, Trumper L, Pfreundschuh M. Analysis of VH gene rearrangements from synovial B cells of patients with rheumatoid arthritis reveals infiltration of the synovial membrane by memory B cells. *Rheumatol Int*. (1997) 17:145–50. doi: 10.1007/s002960050026
288. Gause A, Gundlach K, Zdichavsky M, Jacobs G, Koch B, Hopf T, et al. The B lymphocyte in rheumatoid arthritis: analysis of rearranged V kappa genes from B cells infiltrating the synovial membrane. *Eur J Immunol*. (1995) 25:2775–82. doi: 10.1002/eji.1830251010
289. Voswinkel J, Trumper L, Carbon G, Hopf T, Pfreundschuh M, Gause A. Evidence for a selected humoral immune response encoded by VH4 family genes in the synovial membrane of a patient with rheumatoid arthritis. (RA). *Clin Exp Immunol*. (1996) 106:5–12. doi: 10.1046/j.1365-2249.1996.d01-806.x
290. Voswinkel J, Weisgerber K, Pfreundschuh M, Gause A. The B lymphocyte in rheumatoid arthritis: recirculation of B lymphocytes between different joints and blood. *Autoimmunity* (1999) 31:25–34. doi: 10.3109/08916939908993856
291. Kipps TJ, Tomhave E, Chen PP, Fox RI. Molecular characterization of a major autoantibody-associated cross-reactive idiotype in Sjogren's syndrome. *J Immunol*. (1989) 142:4261–8.
292. Gellrich S, Rutz S, Borkowski A, Golembowski S, Gromnica-Ihle E, Sterry W, et al. Analysis of V(H)-D-J(H) gene transcripts in B cells infiltrating the salivary glands and lymph node tissues of patients with Sjogren's syndrome. *Arthritis Rheum*. (1999) 42:240–7. doi: 10.1002/1529-0131(199902)42:2<240::AID-ANR5>3.0.CO;2-I
293. Maier-Moore JS, Koelsch KA, Smith K, Lessard CJ, Radfar L, Lewis D, et al. Antibody-secreting cell specificity in labial salivary glands reflects the clinical presentation and serology in patients with Sjogren's syndrome. *Arthritis Rheumatol*. (2014) 66:3445–56. doi: 10.1002/art.38872
294. Manzo A, Bombardieri M, Humby F, Pitzalis C. Secondary and ectopic lymphoid tissue responses in rheumatoid arthritis: from inflammation to autoimmunity and tissue damage/remodeling. *Immunol Rev*. (2010) 233:267–85. doi: 10.1111/j.0105-2896.2009.00861.x
295. Astorri E, Bombardieri M, Gabba S, Peakman M, Pozzilli P, Pitzalis C. Evolution of ectopic lymphoid neogenesis and *in situ* autoantibody production in autoimmune nonobese diabetic mice: cellular and molecular characterization of tertiary lymphoid structures in pancreatic islets. *J Immunol*. (2010) 185:3359–68. doi: 10.4049/jimmunol.1001836
296. Le Pottier L, Devauchelle V, Fautrel A, Daridon C, Saraux A, Youinou P, et al. Ectopic germinal centers are rare in Sjogren's syndrome salivary glands and do not exclude autoreactive B cells. *J Immunol*. (2009) 182:3540–7. doi: 10.4049/jimmunol.0803588
297. Spalding DM, Haber P, Schrohenloher RE, Koopman WJ. Production of immunoglobulin and rheumatoid factor by lymphoid cells in rheumatoid pericardium. *Arthritis Rheum*. (1985) 28:1071–4. doi: 10.1002/art.1780280917
298. Halla JT, Koopman WJ, Schrohenloher RE, Darby WL, Heck LW. Local synthesis of IgM and IgM rheumatoid factor in rheumatoid pleuritis. *J Rheumatol*. (1983) 10:204–9.
299. Halla JT, Koopman WJ, Fallahi S, Oh SJ, Gay RE, Schrohenloher RE. Rheumatoid myositis. Clinical and histologic features and possible pathogenesis. *Arthritis Rheum*. (1984) 27:737–43. doi: 10.1002/art.1780270703
300. Willis VC, Demoruelle MK, Derber LA, Chartier-Logan CJ, Parish MC, Pedraza IF, et al. Sputum autoantibodies in patients with established rheumatoid arthritis and subjects at risk of future clinically apparent disease. *Arthritis Rheum*. (2013) 65:2545–54. doi: 10.1002/art.38066
301. Talal N, Asofsky R, Lightbody P. Immunoglobulin synthesis by salivary gland lymphoid cells in Sjogren's syndrome. *J Clin Invest*. (1970) 49:49–54. doi: 10.1172/JCI106221
302. Anderson LG, Cummings NA, Asofsky R, Hylton MB, Tarpley TMJr, Tomasi TBJr, et al. Salivary gland immunoglobulin and rheumatoid factor synthesis in Sjogren's syndrome. *Natural history and response to treatment Am J Med*. (1972) 53:456–63. doi: 10.1016/0002-9343(72)90141-6
303. Halse A, Harley JB, Kroneld U, Jonsson R. Ro/SS-A-reactive B lymphocytes in salivary glands and peripheral blood of patients with Sjogren's syndrome. *Clin Exp Immunol*. (1999) 115:203–7. doi: 10.1046/j.1365-2249.1999.00778.x
304. Glauzy S, Sng J, Bannock JM, Gottenberg JE, Korganow AS, Cacoub P, et al. Defective Early B Cell Tolerance Checkpoints in Sjogren's Syndrome Patients. *Arthritis Rheumatol*. (2017) 69:2203–8. doi: 10.1002/art.40215
305. Markusse HM, Otten HG, Vroom TM, Smeets TJ, Fokkens N, Breedveld FC. Rheumatoid factor isotypes in serum and salivary fluid of patients with primary Sjogren's syndrome. *Clin Immunol Immunopathol*. (1993) 66:26–32. doi: 10.1006/clin.1993.1004
306. Halse AK, Marthinussen MC, Wahren-Herlenius M, Jonsson R. Isotype distribution of anti-Ro/SS-A and anti-La/SS-B antibodies in plasma and saliva of patients with Sjogren's syndrome. *Scand J Rheumatol*. (2000) 29:13–9. doi: 10.1080/030097400750001752
307. Maverakis E, Kim K, Shimoda M, Gershwin ME, Patel F, Wilken R, et al. Glycans in the immune system and The Altered Glycan Theory of Autoimmunity: a critical review. *J Autoimmun*. (2015) 57:1–13. doi: 10.1016/j.jaut.2014.12.002
308. Bruckner C, Lehmann C, Dudziak D, Nimmerjahn F. Sweet SIGNs: IgG glycosylation leads the way in IVIG-mediated resolution of inflammation. *Int Immunol*. (2017) 29:499–509. doi: 10.1093/intimm/dxx053
309. Pincetic A, Bournazos S, DiLillo DJ, Maamary J, Wang TT, Dahan R, et al. Type, I., and type II Fc receptors regulate innate and adaptive immunity. *Nat Immunol*. (2014) 15:707–16. doi: 10.1038/ni.2939

310. van de Bovenkamp, F S, Hafkenscheid L, Rispens T, Rombouts Y. The Emerging Importance of IgG Fab Glycosylation in immunity. *J Immunol.* (2016) 196:1435–41. doi: 10.4049/jimmunol.1502136
311. Parekh RB, Dwek RA, Sutton BJ, Fernandes DL, Leung A, Stanworth D, et al. Association of rheumatoid arthritis and primary osteoarthritis with changes in the glycosylation pattern of total serum IgG. *Nature* (1985) 316:452–7. doi: 10.1038/316452a0
312. Axford JS, Mackenzie L, Lydyard PM, Hay FC, Isenberg DA, Roitt IM. Reduced B-cell galactosyltransferase activity in rheumatoid arthritis. *Lancet* (1987) 2:1486–8. doi: 10.1016/S0140-6736(87)92621-3
313. Keusch J, Lydyard PM, Berger EG, Delves PJ. B lymphocyte galactosyltransferase protein levels in normal individuals and in patients with rheumatoid arthritis. *Glycoconj J*. (1998) 15:1093–7. doi: 10.1023/A:1006957711557
314. Furukawa K, Matsuta K, Takeuchi F, Kosuge E, Miyamoto T, Kobata A. Kinetic study of a galactosyltransferase in the B cells of patients with rheumatoid arthritis. *Int Immunol*. (1990) 2:105–12. doi: 10.1093/intimm/2.1.105
315. Axford JS. Decreased B-cell galactosyltransferase activity in rheumatoid arthritis. *Br J Rheumatol.* (1988) 27(Suppl. 2):170. doi: 10.1093/rheumatology/XXVII.suppl_2.170
316. Kratz EM, Borysewicz K, Katnik-Prastowska I. Terminal monosaccharide screening of synovial immunoglobulins G and A for the early detection of rheumatoid arthritis. *Rheumatol Int*. (2010) 30:1285–92. doi: 10.1007/s00296-009-1139-5
317. Tomana M, Schrohenloher R, Bennett P, Del Puente A, Koopman W. Occurrence of deficient galactosylation of serum IgG prior to the onset of rheumatoid arthritis. *Rheumatol Int*. (1994) 13:217–20. doi: 10.1007/BF00290198
318. Matsumoto A, Shikata K, Takeuchi F, Kojima N, Mizuochi T. Autoantibody activity of IgG rheumatoid factor increases with decreasing levels of galactosylation and sialylation. *J Biochem*. (2000) 128:621–8. doi: 10.1093/oxfordjournals.jbchem.a022794
319. Parekh RB, Roitt IM, Isenberg DA, Dwek RA, Ansell BM, Rademacher TW. Galactosylation of IgG associated oligosaccharides: reduction in patients with adult and juvenile onset rheumatoid arthritis and relation to disease activity. *Lancet* (1988) 1:966–9. doi: 10.1016/S0140-6736(88)91781-3
320. Pfeifle R, Rothe T, Ipseiz N, Scherer HU, Culemann S, Harre U, et al. Regulation of autoantibody activity by the IL-23-TH17 axis determines the onset of autoimmune disease. *Nat Immunol*. (2017) 18:104–13. doi: 10.1038/ni.3579
321. Gindzienska-Sieskiewicz E, Radziejewska I, Domyslawska I, Klimiuk PA, Sulik A, Rojewska J, et al. Changes of glycosylation of IgG in rheumatoid arthritis patients treated with methotrexate. *Adv Med Sci.* (2016) 61:193–7. doi: 10.1016/j.advms.2015.12.009
322. Rombouts Y, Ewing, E, van de Stadt LA, Selman MH, Trouw LA, Deelder AM, et al.. Anti-citrullinated protein antibodies acquire a pro-inflammatory Fc glycosylation phenotype prior to the onset of rheumatoid arthritis. *Ann Rheum Dis.* (2015) 74:234–41. doi: 10.1136/annrheumdis-2013-203565
323. Tsuchiya N, Endo T, Matsuta K, Yoshinoya S, Takeuchi F, Nagano Y, et al. Detection of glycosylation abnormality in rheumatoid IgG using N-acetylglucosamine-specific Psathyrella velutina lectin. *J Immunol*. (1993) 151:1137–46.
324. Scherer HU, van der Woude D, Ioan-Facsinay A, el Bannoudi, H, Trouw LA, Wang J, et al. Glycan profiling of anti-citrullinated protein antibodies isolated from human serum and synovial fluid. *Arthritis Rheum.* (2010) 62:1620–9. doi: 10.1002/art.27414
325. Youinou P, Pennec YL, Casburn-Budd R, Dueymes M, Letoux G, Lamour A. Galactose terminating oligosaccharides of IgG in patients with primary Sjogren's syndrome. *J Autoimmun*. (1992) 5:393–400. doi: 10.1016/0896-8411(92)90151-F
326. Kuroda Y, Nakata M, Makino A, Matsumoto A, Ohashi K, Itahashi K, et al. Structural studies on IgG oligosaccharides of patients with primary Sjogren's syndrome. *Glycoconj J*. (2002) 19:23–31. doi: 10.1023/A:1022528829799
327. Kempers AC, Hafkenscheid L, Dorjee AL, Moutousidou E, van de Bovenkamp FS, Rispens T, et al. The extensive glycosylation of the ACPA variable domain observed for ACPA-IgG is absent from ACPA-IgM. *Ann Rheum Dis*. (2017) 77:1087–8. doi: 10.1136/annrheumdis-2017-211533
328. Hamza N, Hershberg U, Kallenberg CG, Vissink A, Spijkervet FK, Bootsma H, et al. Ig gene analysis reveals altered selective pressures on Ig-producing cells in parotid glands of primary Sjogren's syndrome patients. *J Immunol*. (2015) 194:514–21. doi: 10.4049/jimmunol.1302644
329. Lloyd KA, Steen J, Titcombe PJ, Mueller DL, Klareskog L, Malmström V, et al. 08.19 Variable domain n-linked glycosylation is a key feature of monoclonal acpa-igg. *Ann Rheum Dis*. (2017) 76:A82–3. doi: 10.1136/annrheumdis-2016-211055.19
330. Rombouts Y, Willemze A, van Beers JJ, Shi J, Kerkman PF, van Toorn L, et al. Extensive glycosylation of ACPA-IgG variable domains modulates binding to citrullinated antigens in rheumatoid arthritis. *Ann Rheum Dis*. (2016) 75:578–85. doi: 10.1136/annrheumdis-2014-206598
331. Leader KA, Lastra GC, Kirwan JR, Elson CJ. Agalactosyl IgG in aggregates from the rheumatoid joint. *Br J Rheumatol*. (1996) 35:335–41. doi: 10.1093/rheumatology/35.4.335
332. Falkenburg WJJ, Kempers AC, Dekkers G, Ooijevaar-de Heer P, Bentlage AE, Vidarsson G, et al. Rheumatoid factors do not preferentially bind to ACPA-IgG or IgG with altered galactosylation. *Rheumatology. (Oxford)* (2017) 56:2025–30. doi: 10.1093/rheumatology/kex284
333. al-Balaghi S, Abedi-Valugerdi M, Moller E. Binding specificities of a polyreactive and a monoreactive human monoclonal IgG rheumatoid factor: role of oligosaccharides. *Scand J Immunol.* (1996) 44:470–7. doi: 10.1046/j.1365-3083.1996.d01-338.x
334. Soltys AJ, Hay FC, Bond A, Axford JS, Jones MG, Randen I, et al. The binding of synovial tissue-derived human monoclonal immunoglobulin M rheumatoid factor to immunoglobulin G preparations of differing galactose content. *Scand J Immunol.* (1994) 40:135–43. doi: 10.1111/j.1365-3083.1994.tb03442.x
335. Harre U, Lang SC, Pfeifle R, Rombouts Y, Fruhbeisser S, Amara K, et al. Glycosylation of immunoglobulin G determines osteoclast differentiation and bone loss. *Nat Commun*. (2015) 6:6651. doi: 10.1038/ncomms7651
336. Ohmi Y, Ise W, Harazono A, Takakura D, Fukuyama H, Baba Y, et al. Sialylation converts arthritogenic IgG into inhibitors of collagen-induced arthritis. *Nat Commun*. (2016) 7:11205. doi: 10.1038/ncomms11205
337. Gunn B, Schneider J, Shansab M, Bastian AR, Fahrbach K, Smith A, Mahan A, et al. Enhanced binding of antibodies generated during chronic HIV infection to mucus component MUC16. *Mucosal Immunol.* (2016) 9:1549–58. doi: 10.1038/mi.2016.8
338. Azuma K, Shinzaki S, Asazawa H, Kuroki E, Kawamoto S, Kamada Y, et al. Twin studies on the effect of genetic factors on serum agalactosyl immunoglobulin G levels. *Biomed Rep*. (2014) 2:213–6. doi: 10.3892/br.2014.216
339. Lauc G, Huffman JE, Pucic M, Zgaga L, Adamczyk B, Muzinic A, et al. Loci associated with N-glycosylation of human immunoglobulin G show pleiotropy with autoimmune diseases and haematological cancers. *PLoS Genet*. (2013) 9:e1003225. doi: 10.1371/journal.pgen.1003225
340. Wang J, Balog CI, Stavenhagen K, Koeleman CA, Scherer HU, Selman MH, et al. Fc-glycosylation of IgG1 is modulated by B-cell stimuli. *Mol Cell Proteomics*. (2011) 10:M110.004655. doi: 10.1074/mcp.M110.004655
341. Chintalacharuvu SR, Emancipator SN. The glycosylation of IgA produced by murine B cells is altered by Th2 cytokines. *J Immunol*. (1997) 159:2327–33.
342. Chintalacharuvu SR, Emancipator SN. Differential glycosylation of two glycoproteins synthesized by murine B cells in response to IL-4 plus IL-5. *Cytokine* (2000) 12:1182–8. doi: 10.1006/cyto.2000.0699
343. Hess C, Winkler A, Lorenz AK, Holecska V, Blanchard V, Eiglmeier S, et al. T cell-independent B cell activation induces immunosuppressive sialylated IgG antibodies. *J Clin Invest*. (2013) 123:3788–96. doi: 10.1172/JCI65938
344. Oefner CM, Winkler A, Hess C, Lorenz AK, Holecska V, Huxdorf M, et al. Tolerance induction with T cell-dependent protein antigens induces regulatory sialylated IgGs. *J Allergy Clin Immunol.* (2012) 129:1647–55 e13. doi: 10.1016/j.jaci.2012.02.037
345. Kao D, Lux A, Schaffert A, Lang R, Altmann F, Nimmerjahn F. IgG subclass and vaccination stimulus determine changes in antigen specific antibody glycosylation in mice. *Eur J Immunol*. (2017) 47:2070–9. doi: 10.1002/eji.201747208
346. Pagan JD, Kitaoka M, Anthony RM. Engineered sialylation of pathogenic antibodies *in vivo* attenuates Autoimmune disease. *Cell* (2018) 172, 564–577 e13. doi: 10.1016/j.cell.2017.11.041

347. Griffiths HR, Lunec J. The effects of oxygen free radicals on the carbohydrate moiety of IgG. *FEBS Lett*. (1989) 245:95–9. doi: 10.1016/0014-5793(89)80199-1
348. Wang JR, Gao WN, Grimm R, Jiang S, Liang Y, Ye H, et al. A method to identify trace sulfated IgG N-glycans as biomarkers for rheumatoid arthritis. *Nat Commun*. (2017) 8:631. doi: 10.1038/s41467-017-00662-w
349. Trbojevic-Akmacic I, Vilaj M, Lauc G. High-throughput analysis of immunoglobulin G glycosylation. *Expert Rev Proteomics*. (2016) 13:523–34. doi: 10.1080/14789450.2016.1174584
350. Hafkenscheid L, Bondt A, Scherer HU, Huizinga TW, Wuhrer M, Toes RE, et al. Structural analysis of variable domain glycosylation of anti-citrullinated protein antibodies in rheumatoid arthritis reveals the presence of highly sialylated glycans. *Mol Cell Proteomics*. (2017) 16:278–87. doi: 10.1074/mcp.M116.062919
351. Royer B, Cazals-Hatem D, Sibilia J, Agbalika F, Cayuela JM, Soussi T, et al. Lymphomas in patients with Sjogren's syndrome are marginal zone B-cell neoplasms, arise in diverse extranodal and nodal sites, and are not associated with viruses. *Blood* (1997) 90:766–75.
352. Lasota J, Miettinen MM. Coexistence of different B-cell clones in consecutive lesions of low-grade MALT lymphoma of the salivary gland in Sjogren's disease. *Mod Pathol*. (1997) 10:872–8.
353. Bahler DW, Miklos JA, Swerdlow SH. Ongoing Ig gene hypermutation in salivary gland mucosa-associated lymphoid tissue-type lymphomas. *Blood* (1997) 89:3335–44.
354. Bende RJ, Aarts WM, Riedl RG, de Jong D, Pals ST, van Noesel CJ. Among B cell non-Hodgkin's lymphomas, MALT lymphomas express a unique antibody repertoire with frequent rheumatoid factor reactivity. *J Exp Med*. (2005) 201:1229–41. doi: 10.1084/jem.20050068
355. De Re V, De Vita S, Gasparotto D, Marzotto A, Carbone A, Ferraccioli G, et al. Salivary gland B cell lymphoproliferative disorders in Sjogren's syndrome present a restricted use of antigen receptor gene segments similar to those used by hepatitis C virus-associated non-Hodgkins's lymphomas. *Eur J Immunol*. (2002) 32:903–10. doi: 10.1002/1521-4141(200203)32:3<903::AID-IMMU903>3.0.CO;2-D
356. Martin T, Weber JC, Levallois H, Labouret N, Soley A, Koenig S, et al. Salivary gland lymphomas in patients with Sjogren's syndrome may frequently develop from rheumatoid factor B cells. *Arthritis Rheum*. (2000) 43:908–16. doi: 10.1002/1529-0131(200004)43:4<908::AID-ANR24>3.0.CO;2-K
357. Bende RJ, Slot LM, Hoogeboom R, Wormhoudt TA, Adeoye AO, Guikema JE, et al. Stereotypic rheumatoid factors that are frequently expressed in mucosa-associated lymphoid tissue-type lymphomas are rare in the labial salivary glands of patients with Sjogren's syndrome. *Arthritis Rheumatol*. (2015) 67:1074–83. doi: 10.1002/art.39002
358. Risselada AP, Kruize AA, Bijlsma JW. Clinical features distinguishing lymphoma development in primary Sjogren's Syndrome–a retrospective cohort study. *Semin Arthritis Rheum*. (2013) 43:171–7. doi: 10.1016/j.semarthrit.2013.03.001
359. Voulgarelis M, Dafni UG, Isenberg DA, Moutsopoulos HM. Malignant lymphoma in primary Sjogren's syndrome: a multicenter, retrospective, clinical study by the European Concerted Action on Sjogren's Syndrome. *Arthritis Rheum*. (1999) 42:1765–72. doi: 10.1002/1529-0131(199908)42:8<1765::AID-ANR28>3.0.CO;2-V
360. Zhu D, McCarthy H, Ottensmeier CH, Johnson P, Hamblin TJ, Stevenson FK. Acquisition of potential N-glycosylation sites in the immunoglobulin variable region by somatic mutation is a distinctive feature of follicular lymphoma. *Blood* (2002) 99:2562–8. doi: 10.1182/blood.V99.7.2562
361. Zhu D, Ottensmeier CH, Du MQ, McCarthy H, Stevenson FK. Incidence of potential glycosylation sites in immunoglobulin variable regions distinguishes between subsets of Burkitt's lymphoma and mucosa-associated lymphoid tissue lymphoma. *Br J Haematol*. (2003) 120:217–22. doi: 10.1046/j.1365-2141.2003.04064.x

Conflict of Interest Statement: The authors declare that the research was conducted in the absence of any commercial or financial relationships that could be construed as a potential conflict of interest.

frontiers in Immunology

ORIGINAL RESEARCH
published: 03 September 2018
doi: 10.3389/fimmu.2018.01935

Immunoadsorption of Desmoglein-3-Specific IgG Abolishes the Blister-Inducing Capacity of Pemphigus Vulgaris IgG in Neonatal Mice

Maxi Hofrichter[1†], Jenny Dworschak[2†], Shirin Emtenani[1], Jana Langenhan[2], Fanny Weiß[1], Lars Komorowski[2], Detlef Zillikens[3], Winfried Stöcker[2], Christian Probst[2], Enno Schmidt[1,3‡] and Stephanie Goletz[1‡]*

[1] Lübeck Institute of Experimental Dermatology, University of Lübeck, Lübeck, Germany, [2] Institute of Experimental Immunology, Euroimmun AG, Lübeck, Germany, [3] Department of Dermatology, University of Lübeck, Lübeck, Germany

Pemphigus vulgaris (PV) is a potentially life-threatening autoimmune blistering disease which is associated with autoantibodies directed against two desmosomal proteins, desmoglein (Dsg) 3 and 1. Treatment of PV is rather challenging and relies on the long-term use of systemic corticosteroids and additional immunosuppressants. More recently, autoantibody-depleting therapies such as rituximab, high-dose intravenous immunoglobulins, and immunoadsorption were shown to be valuable treatment options in PV. Specific removal of pathogenic autoantibodies would further increase efficacy and usability of immunoadsorption. Here, we tested the capacity of our recently developed prototypic Dsg1- and Dsg3-specific adsorbers to remove circulating pathogenic autoantibodies from three different PV patients. The pathogenic potential of the Dsg3/1-depleted IgG fractions and the anti-Dsg3-specific IgG was explored in two different *in vitro* assays based on cultured human keratinocytes, the desmosome degradation assay and the dispase-based dissociation assay. In addition, the neonatal mouse model of PV was used. In both *in vitro* assays, no difference between the pathogenic effect of total PV IgG and anti-Dsg3-specific IgG was seen, while Dsg3/1-depleted and control IgG were not pathogenic. For the samples of all 3 PV patients, depletion of anti-Dsg3/1 IgG resulted in a complete loss of pathogenicity when injected into neonatal mice. In contrast, injection of anti-Dsg3-specific IgG, eluted from the column, induced gross blistering in the mice. Our data clearly show that anti-Dsg3-specific IgG alone is pathogenic *in vitro* and *in vivo,* whereas Dsg3/1-depletion results in a complete loss of pathogenicity. Furthermore, our data suggest that Dsg-specific adsorption may be a suitable therapeutic modality to efficiently reduce pathogenic autoantibodies in patients with severe PV.

Keywords: acantholysis, autoantibody, desmoglein, desmosome, immunoadsorption, pemphigus, skin, treatment

OPEN ACCESS

Edited by:
David William Scott, Uniformed Services University of the Health Sciences, United States

Reviewed by:
Cornelia Deeg, Ludwig-Maximilians-Universität München, Germany
Robert Gniadecki, University of Alberta, Canada
David Andrew Fulcher, Australian National University, Australia

***Correspondence:**
Enno Schmidt
enno.schmidt@uksh.de

†These authors have contributed equally to this work as first authors

‡These authors have contributed equally to this work as last authors

Specialty section:
This article was submitted to Immunological Tolerance and Regulation, a section of the journal Frontiers in Immunology

Received: *12 December 2017*
Accepted: *06 August 2018*
Published: *03 September 2018*

Citation:
Hofrichter M, Dworschak J, Emtenani S, Langenhan J, Weiß F, Komorowski L, Zillikens D, Stöcker W, Probst C, Schmidt E and Goletz S (2018) Immunoadsorption of Desmoglein-3-Specific IgG Abolishes the Blister-Inducing Capacity of Pemphigus Vulgaris IgG in Neonatal Mice. Front. Immunol. 9:1935. doi: 10.3389/fimmu.2018.01935

INTRODUCTION

Pemphigus vulgaris (PV) is a potentially life-threatening intraepidermal blistering autoimmune disease (1–4). Desmoglein 3 (Dsg3) and desmoglein 1 (Dsg1) have been identified as autoantigens in PV (5–8). Dsg1 and Dsg3 are desmosomal transmembrane cadherins that mediate intercellular adhesion of keratinocytes in the skin and surface-close epithelia (3, 6, 9). In PV patients with exclusive mucosal involvement (mPV), autoantibodies are restricted to Dsg3, whereas autoantibodies against both Dsg3 and Dsg1 are associated with skin and mucosal lesions (mucocutaneous type of PV, mcPV) (10–12). In pemphigus foliaceus (PF), autoantibody reactivity is limited to Dsg1 and patients only develop skin lesions. In addition to Dsg1 and Dsg3, a variety of other target antigens have been described in PV including muscarinic and nicotinic acethylcholine receptors, annexins, thyroid peroxidase, desmocollins, and mitochondrial proteins (13–15). While good, albeit not undisputed, evidence for the pathogenic effect of anti-Dsg1/3 antibodies has been provided, less data were reported about the pathogenicity of non-Dsg antibodies (13, 15–20).

Treatment of PV is challenging and has required the long-term use of prednisolone and other immunosuppressants such as azathioprine and mycophenoles (4, 21, 22). Very recently, first-line rituximab, an anti-CD20 antibody that depletes B cells from the circulation for 3–9 months, in conjunction with the short term use of prednisolone has been shown to be significantly more effective and safe compared to the long term use of prednisolone alone (23). High-dose intravenous immunoglobulin and immunoadsorption are two other treatment modalities that reduce serum anti-Dsg autoantibodies and are recommended in refractory and/or severely affected PV patients (21, 22, 24). The reduction of serum autoantibodies in PV appears to be a particularly attractive therapeutic approach since the direct pathogenic importance of pemphigus autoantibodies has been shown in various experimental settings *in vitro* and *in vivo* (13, 25).

Whereas plasmapheresis requires substitution with fresh-frozen plasma or human albumin, immunoadsorption specifically removes antibodies from the circulation (24). Unfortunately, the use of immunoadsorption is limited by the increased risk of infections due to the parallel reduction of protective immunoglobulins. Thus, removal of Dsg-specific antibodies appeared to be advantageous leading to the recent development of prototypic anti-Dsg1 and anti-Dsg3 adsorbers. The Dsg1/3-specific adsorbers are based on the recombinant Dsg ectodomains coupled to sepharose and allowed the effective removal of anti-Dsg reactivity from PV and PF serum samples *in vitro* (26). The aim of the present study was to show that by the use of the Dsg1/3-specific adsorbers removal of anti-Dsg antibodies from PV sera is sufficient to abolish the pathogenic effect of pemphigus IgG not only *in vitro* but also *in vivo* in neonatal mice. We now also show that anti-Dsg3-specific IgG is sufficient for acantholysis in cultured keratinocytes and blister formation in neonatal mice.

Abbreviations: Dsg, desmoglein; IF, immunofluorescence; NH IgG, normal human immunoglobulin G; PF, pemphigus foliaceus; PV, pemphigus vulgaris; mPV, mucosal pemphigus vulgaris; mcPV, mucocutaneous pemphigus vulgaris.

MATERIAL AND METHODS

Patients

IgG from 3 PV patients (PV1, PV2, PV3) that were treated with conventional protein A immunoadsorption at the Department of Dermatology, Lübeck, was used (27, 28). The clinical phenotype, age, sex, indirect immunofluorescence (IF) serum titers on monkey esophagus, and anti-Dsg1/3 IgG serum levels by ELISA (Euroimmun, Lübeck, Germany) are shown in **Table 1**. IgG bound to protein A was eluted by glycine buffer (pH 2.8) and immediately neutralized with 1M Tris pH 9.0 followed by precipitation with ammonium sulfate and dialysis against PBS. As no immunoadsorption material from healthy donors is available, we use affinity-purified IgG from sera of healthy volunteers as control. The study was performed following the Declaration of Helsinki. Pathogenicity experiments were positively reviewed by the ethics committees of the University of Lübeck, Germany (file reference, 09-090).

Affinity Purification of Dsg-Specific PV IgG Using the Entire Ectodomain of Dsg3 and Dsg1

For antigen-specific immunoaffinity purification of anti-Dsg3 and anti-Dsg1 IgG, the entire ectodomains of Dsg3 and Dsg1, respectively, were immobilized on N-hydroxysuccinimide-activated Sepharose 4 Fast Flow (GE Healthcare, Buckinghamshire, UK) as previously described (26). Immunoaffinity purifications were performed as follows. The immobilized protein matrix was transferred into microcentrifuge spin columns (Thermo Fisher Scientific, Darmstadt, Germany) and washed three times with tris-buffered saline supplemented with 5 mM $CaCl_2$ (Ca^{2+}-TBS). The concentrated IgG of the PV patients was diluted 1:1 with Ca^{2+}-TBS and incubated with the immobilized protein for 30 min at room temperature. The flow-through fraction was collected by centrifugation at 500x g for 30 s. After several washing steps with Ca^{2+}-TBS (until $OD_{280} < 0.05$) the anti-Dsg3 and anti-Dsg1 IgG fractions were eluted from the matrix with IgG elution buffer (Thermo Fisher Scientific) until the OD_{280} was below 0.05, and immediately neutralized with 1M Tris pH 9.0. All eluted fractions were pooled and buffer was exchanged to PBS using Vivaspin 500 centrifugal filter units (Sartorius AG, Göttingen, Germany). Finally, Dsg3/1-depleted PV IgG (flow-through fractions) and anti-Dsg3 PV IgG (eluted fractions) were analyzed for anti-Dsg3 and anti-Dsg1 autoantibody reactivity by ELISA (Euroimmun).

Immunoblotting With HaCaT Extract

HaCaT cells were grown in low calcium Keratinocyte Growth Medium 2, KGM2 (Promocell, Heidelberg, Germany) containing 0.06 mM CaCl2 to confluence and lysed in Laemmli sample buffer. Lysates were fractionated by SDS-PAGE, transferred to nitrocellulose membrane and immunoblotted as reported (29). After blocking, nitrocellulose membranes were incubated

TABLE 1 | Pemphigus vulgaris (PV) patients' characteristics.

Patient no.	Sex	Age (years)	Clinical phenotype	Monkey esophagus (serum)	Anti-Dsg1 serum level (U/ml)	Anti-Dsg3 serum level (U/ml)
PV1	M	70	mcPV	1:2,560	1,045	3,572
PV2	M	44	mcPV	1:1,280	103	9,748
PV3	F	72	mPV	1:320	–	6,001

mcPV, mucocutaneous PV; mPV, mucosal PV.

with anti-Dsg3 specific IgG (2 μg/ml), a monoclonal anti-Dsg3 antibody (1:100, Bio-Rad, Munich, Germany), control IgG (2 μg/ml) from a healthy donor and IVIg (2 μg/ml, Biotest, Dreieich, Germany) diluted in TBST containing 5% skimmed milk powder plus 1% BSA. As secondary antibodies a horseradish peroxidase (HRP)-conjugated polyclonal goat anti-human IgG antibody (1:1,000, DAKO, Hamburg, Germany,) and a polyclonal rabbit anti-mouse IgG antibody (1:1,000; DAKO) were used. The proteins were visualized using Super Signal West Femto (Thermo Fisher Scientific).

Desmosome Degradation Assay

The desmosome degradation assay was performed as described previously (26, 30, 31). In brief, HaCaT cells were grown in 8-well chamber slides (BDBiosciences, Heidelberg, Germany) to confluent monolayers. Low calcium Keratinocyte Growth Medium 2, KGM2 (Promocell) containing 0.06 mM $CaCl_2$ was changed to high calcium medium by adding sterile 0.15 M $CaCl_2$ to a final concentration of 1.5 mM calcium. Monolayers were treated with PV IgG, control IgG and IgG fractions collected from Dsg3 and Dsg1 immunoaffinity purification as indicated in the results part. After 24 h incubation at 37°C in a humidified atmosphere, culture medium was removed and monolayers were washed with DPBS (Thermo Fisher Scientific) and subsequently fixed with 4% paraformaldehyde. After washing, monolayers were treated with 0.1% Triton X-100 (Sigma Aldrich, Steinheim, Germany), incubated with 10% normal goat serum (DAKO) plus 1% BSA (Carl Roth, Karlsruhe, Germany) and then with mouse anti-human Dsg3 IgG1 (1:100 in PBS, clone 5G11; Acris, Herford, Germany) for 30 min at 37°C and after three times washing with Cy3-labeled goat anti-mouse IgG (1:100 in PBS; Dianova, Hamburg, Germany). Slides were mounted with ProLong R Gold antifade reagent (Life Technologies, Carlsbad, USA) and examined microscopically (BZ-9000, Keyence, Neu-Isenburg, Germany).

Dispase-Based Dissociation Assay

The assay was performed as reported previously (26, 30–32) with minor modifications. In brief, HaCaT cells were cultivated in 12-well-plates (Greiner Bio-One, Solingen, Germany) with KGM2 (Promocell) containing 0.06 mM $CaCl_2$ in a humidified atmosphere (5 CO_2) at 37°C. At confluence, fresh KGM2 containing 1.5 mM $CaCl_2$ was added. PV IgG (2 mg/mL), control IgG (2 mg/mL), anti-Dsg3-specific IgG fractions collected from Dsg3- and Dsg1-specific affinity purification (20 μg/mL) and anti-Dsg3/1-depleted IgG (2 mg/mL), respectively were added and incubated for 24 h. Subsequently, the cells were treated with dispase solution (2.5 U/ml for 30 min; Stemcell Techn., Vancouver, Canada) and subjected to mechanical stress by pipetting 10 times (5 times moderate, 5 times strong) with a 1 ml pipette. Cell fragments were fixed and stained with crystal violet (Sigma Aldrich). Photos were taken from each well and cell fragments were counted manually. Every experiment was performed at least in triplicate.

Passive Transfer Neonatal Mouse Model

Neonatals from C57BL/6 mice (Charles River Laboratories, Sulzfeld, Germany) were injected subcutaneously <24 h after birth with the respective PV IgG fraction at doses of 3–7 mg/g of total and anti-Dsg3/1-depleted IgG and 300 μg/g anti-Dsg3-specific IgG (each IgG batch was applied in 3 mice) with or without exfoliative toxin A (ETA; Toxin Technology Inc., Sarasota, USA) as described in parts previously (33, 34). ETA is a serine protease produced from *Staphylococcus aureus* which specifically degrades Dsg1 (35). Due to the different expression patterns of Dsg1 and Dsg3 in mucous membranes and the skin, anti-Dsg3 IgG is only pathogenic in the skin when Dsg1 is graded concomitantly (either by anti-Dsg1 IgG or ETA). In contrast, in mucous membranes, anti-Dsg3 antibodies alone are sufficient to induce intraepithelial splitting (12). Here, half of the minimum ETA dose was applied that in preliminary experiments had induced clinical blistering (usually 0.1 μg/g bodyweight). After 16–24 h, the mice were clinically evaluated before and after application of mechanical stress at the back and sides of mice (Nikolsky phenomenon). Blood was obtained as well as biopsies from the back for histopathology (H&E staining) and direct IF microscopy. All animal experiments were approved by the Animal Rights Commission of the Ministry of Agriculture and Environment, Schleswig Holstein (98-8/14).

Immunofluorescence Microscopy

For direct IF microscopy, a polyclonal rabbit anti-human IgG-FITC antibody (Bio-Rad, Hercules, USA) at a dilution of 1:50 in PBS was used for 1 h at room temperature. For indirect IF microscopy, 6 μm sections of monkey esophagus were incubated with human IgG and mouse sera in a dilution range of 1:20–1:5120 in PBS for 1 h at room temperature. For detection, a FITC-labeled polyclonal anti-human IgG (DAKO) at 1:50 in PBS was employed for 30 min at room temperature.

Statistics

Graphpad Prism 6 was used for the statistical analysis. The dispase assay data across different groups within each patient was

compared for its statistical significance using the Kruskal-Wallis test. For all three patients, correction for multiple comparisons was done by *post-hoc* Dunn's tests to identify significant pairwise differences between the groups.

RESULTS

Dsg1- and Dsg3-Specific Adsorption of PV Patient IgG

Anti-Dsg3-specific IgG was immunoadsorbed from total PV IgG in all three PV patients as previously described in Langenhan et al. (26). In addition, in PV1 and PV2, the present Dsg1-reactivity was removed by Dsg1-specific immunoadsorption. To study the effect of Dsg-specific IgG we focused on anti-Dsg3-specific IgG since only two of the three PV patients revealed Dsg1-specifc IgG. Characteristics of patient IgG after Dsg3/1-specific adsorption are summarized in **Tables 2**, **3**. Western blot analysis of cellular extracts of cultured human keratinocytes confirmed the specific purification of anti-Dsg3 PV IgG (**Figure 1**). Indirect IF microscopy on monkey esophagus revealed that total IgG from PV patients as well as Dsg3-specific IgG, but not Dsg3/1-depleted IgG and control IgG from a healthy blood donor, showed the PV-typical intercellular staining of the stratified squamous epithelium (**Figure 2**, **Table 2**).

Dsg3/1-Specific Depletion of PV IgG Abolishes Pathogenicity *in vitro*

To evaluate the pathogenicity of the Dsg3-specific PV IgG and anti-Dsg3/1 IgG-depleted fractions *in vitro,* the desmosome degradation assay and the dispase-based dissociation assay were performed. The PV IgG-induced loss of Dsg3 expression on the keratinocyte cell surface due to internalization of Dsg3 into endosomes and degradation was determined microscopically. Incubation of HaCaT cell monolayers with either total PV patient IgG or anti-Dsg3-specific IgG resulted in an equivalent discontinuous Dsg3 staining at the keratinocyte cell borders (**Figure 3**). In contrast, when cells were treated with anti-Dsg3/1 IgG-depleted fractions and normal human IgG, respectively, Dsg3 staining was uniformly localized to the cell membrane of keratinocytes (**Figure 3**).

In the dispase-based dissociation assay, treatment with PV1, PV2, and PV3 IgG, respectively, as expected resulted in significantly more keratinocyte fragments compared to incubation with normal human IgG (PV1: $p = 0.0011$; PV2: $p = 0.0045$; PV3: $p = 0.003$; **Figure 4**). Incubation of monolayers with purified Dsg3-specific PV IgG from the three patients generated a significantly higher fragmentation level compared to incubation with anti-Dsg3/1-depleted IgG (PV1: $p = 0.046$; PV2:

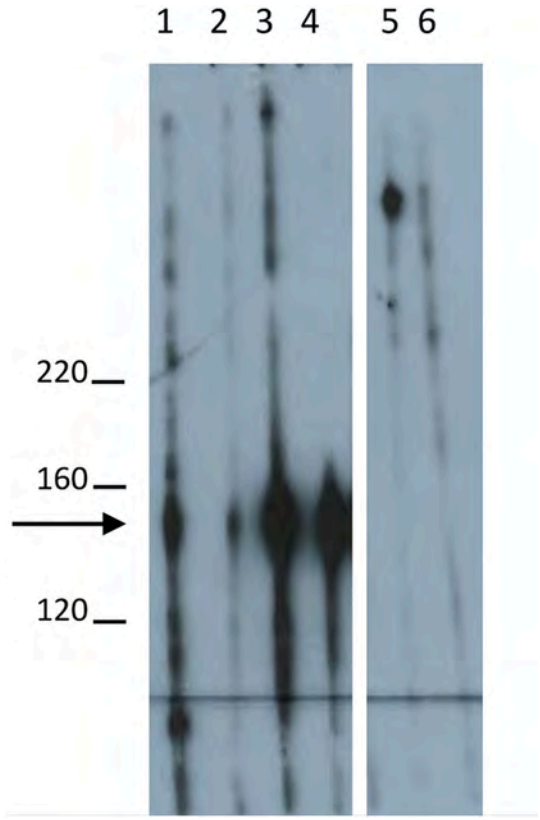

FIGURE 1 | Desmoglein3-specific IgG reactivity in Western blot using extract of cultured keratinocytes. Western blotting of a monoclonal anti-Dsg3 antibody (lane 1; Bio-Rad, Munich, Germany), Dsg3-specific IgG (2 μg/ml) from pemphigus vulgaris (PV) patient PV1 (lane 2), PV2 (lane 3), and PV3 (lane 4) with extract of cultured HaCaT keratinocytes. IgG affinity purified from a healthy volunteer (2 μg/ml) and IVIg (2 μg/ml, Biotest, Dreieich, Germany) are shown in lanes 5 and 6. Molecular weight markers are shown to the left (kDa). The arrow indicates the migration position of desmoglein 3.

TABLE 2 | Characteristics of pemphigus vulgaris (PV) IgG fractions.

Patient no.	PV IgG[a]			Purified anti-Dsg3 PV IgG			Anti-Dsg3/1 depleted PV IgG		
	Dsg3 (U/ml)[b]	Dsg1 (U/ml)[b]	IIF (titer)[c]	Dsg3 (U/ml)[b]	Dsg1 (U/ml)[b]	IIF (titer)[c]	Dsg3 (U/ml)[b]	Dsg1 (U/ml)[b]	IIF (titer)[c]
PV1	49,446	16,933	>1:5,120	9,463	Neg.	1:640	Neg.	Neg.	Neg.
PV2	29,526	27	>1:5,120	19,034	Neg.	1:1,280	Neg.	Neg.	Neg.
PV3	11,773	Neg.	>1:5,120	1,691	Neg.	1:320	Neg.	Neg.	Neg.

[a] *Before subjection to Dsg-specific adsorption.*
[b] *By ELISA (Euroimmun; lower cut-off 20 U/ml).*
[c] *By indirect immunofluorescence (IIF) microscopy on monkey esophagus.*
Dsg, desmoglein; neg., negative.

TABLE 3 | Characteristics of pemphigus vulgaris (PV) IgG fractions (dispase-based dissociation assay).

Patient no.	PV IgG[a]		Purified anti-Dsg3 PV IgG		Anti-Dsg3/1 depleted PV IgG	
	Dsg3 (U/ml)[b]	Dsg1 (U/ml)[b]	Dsg3 (U/ml)[b]	Dsg1 (U/ml)[b]	Dsg3 (U/ml)[b]	Dsg1 (U/ml)[b]
PV1	1,776	44	139	Neg.	Neg.	Neg.
PV2	3,217	Neg.	1,446	Neg.	Neg.	Neg.
PV3	2,274	Neg.	752	Neg.	Neg.	Neg.

[a] *Before subjection to Dsg-specific adsorption.*
[b] *By ELISA (Euroimmun; lower cut-off 20 U/ml).*
Dsg, desmoglein; neg., negative.

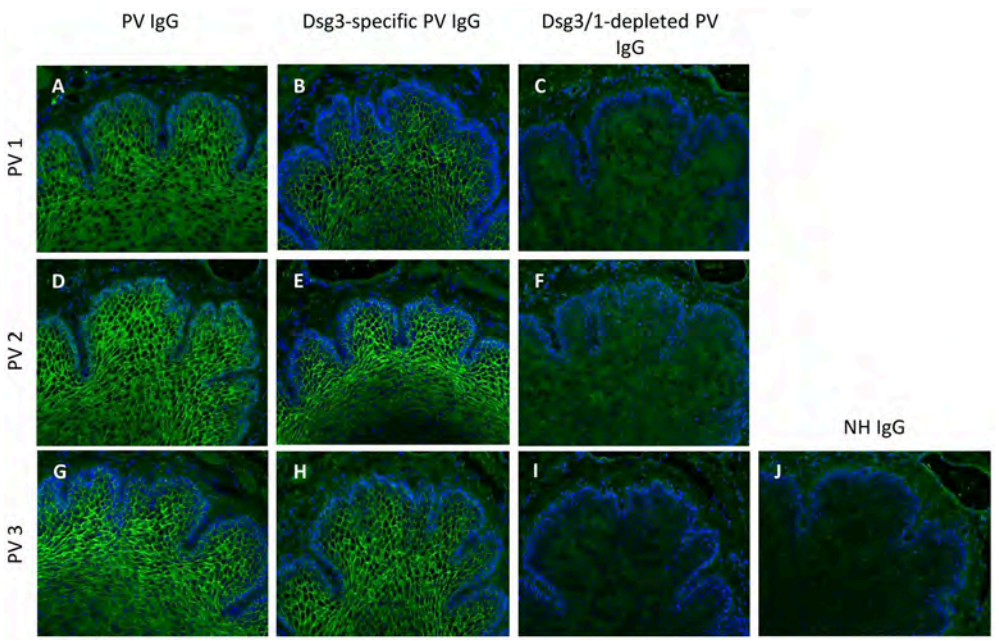

FIGURE 2 | Indirect immunofluorescence (IF) microscopy on monkey esophagus confirms Dsg3/1-specific depletion of IgG from pemphigus vulgaris (PV) IgG. Total PV IgG from three different pemphigus vulgaris (PV) patients (PV1 **(A)**, PV2 **(D)**, PV3 **(G)**) and the respective anti-Dsg3-specific IgG **(B,E,H)** but not the anti-Dsg3/1 IgG-depleted IgG fractions **(C,F,I)** and normal human IgG (NH IgG; **J**) revealed the characteristic intercellular epithelial staining. Nuclei were counterstained with DAPI.

$p = 0.011$; PV3: $p = 0.02$; **Figure 4**). No difference was observed between treatment with anti-Dsg3/1-depleted IgG and normal human IgG (**Figure 4**).

Anti-Dsg3/1 IgG-Depleted PV IgG Prevents Pathogenicity While Anti-Dsg3-Specific IgG Results in Blister Formation in Neonatal Mice

When injected into neonatal mice, only total PV1 IgG contained enough anti-Dsg1 antibodies for the induction of skin blisters without co-injection of a subclinical dose of ETA (**Figure 5A,** lane 1). For mice injected with PV2 or PV3 IgG, gentle mechanical friction was required to obtain macroscopic blistering (**Figure 5A,** lanes 4 and 7). The injection of anti-Dsg3-specific IgG fractions from all three PV patients (combined with subclinical ETA doses) induced gross skin blistering (**Figure 5A,** lanes 2, 5, and 8). In contrast, anti-Dsg3/1 IgG-depleted IgG from all three PV patients (combined with subclinical ETA doses) failed to induce blistering in neonatal mice (**Figure 5A,** lanes 3, 6, and 9). Lesional skin biopsies revealed suprabasal acantholysis, the characteristic histological finding of PV, after injection of PV IgG and anti-Dsg3-specific IgG, but not after injection of Dsg3/1-depleted PV IgG fractions or ETA alone (**Figure 5D**). By direct IF microscopy, intercellular IgG depositions were found in the epidermis in all PV IgG and anti-Dsg3-specific IgG-injected mice, but not in mice injected with anti-Dsg3/1 IgG-depleted PV IgG or ETA alone (**Figure 5B**). By indirect IF microscopy on monkey esophagus, the characteristic intercellular staining was seen with sera of mice injected with PV IgG and anti-Dsg3 specific PV IgG, but not after injection of anti-Dsg1/3-depleted IgG or ETA alone (**Figure 5C**).

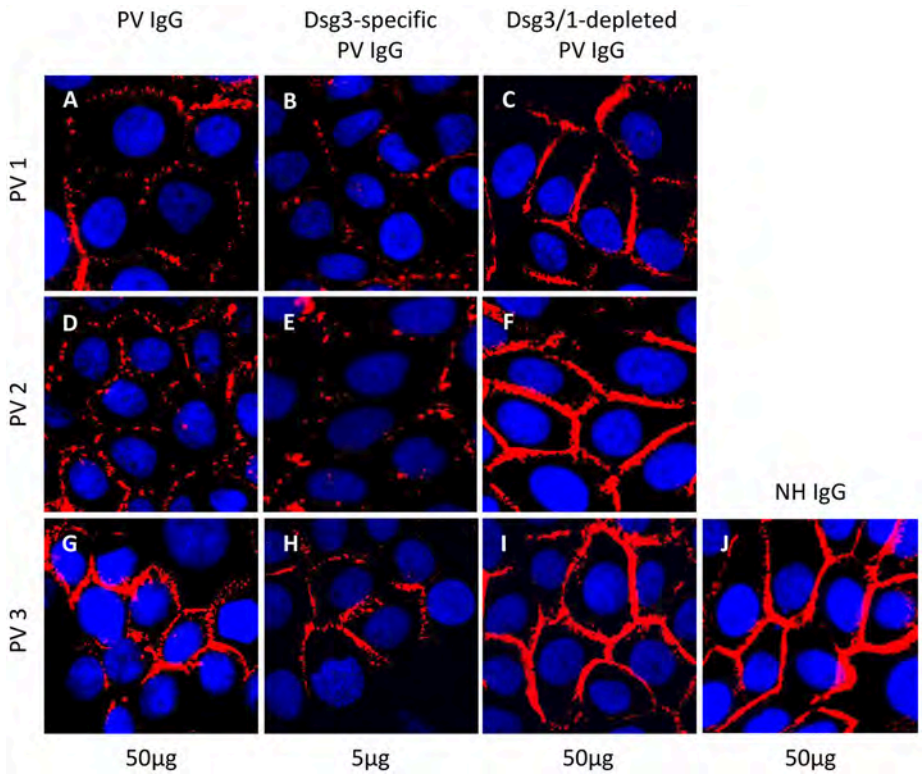

FIGURE 3 | Desmosome degradation assay. HaCaT keratinocytes were treated with 50 µg/ml total pemphigus vulgaris (PV) IgG, 5 µg/ml anti-Dsg3-specific and 50 µg/ml anti-Dsg3/1 IgG-depleted PV IgG from three different pemphigus vulgaris (PV) patients (PV1, PV2, PV3) before immunostaining with anti-Dsg3 IgG. Dsg3 degradation was detected after incubation with total PV IgG **(A,D,G)** and Dsg3-specific IgG **(B,E,H)** but not with the PV IgG fractions depleted of anti-Dsg1/3 IgG **(C,F,I)** and normal human IgG (50 µg/ml; NH IgG; **J**).

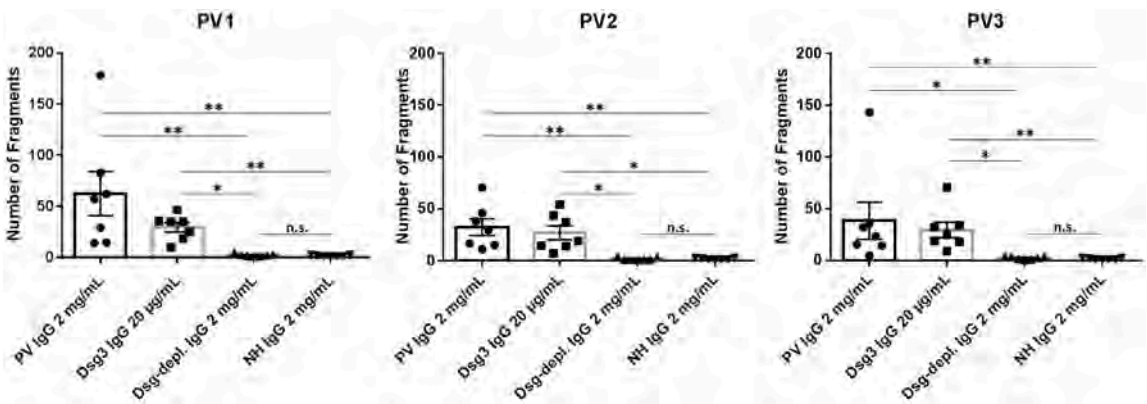

FIGURE 4 | Dispase-based dissociation assay. Incubation of keratinocyte monolayers with total pemphigus vulgaris (PV) IgG and anti-Dsg3-specific IgG from three different PV patients (PV1, PV2, PV3) showed a significantly higher fragmentation compared to treatment with normal human IgG (NH IgG) and the anti-Dsg3/1-depleted PV IgG (Dsg-depl. IgG), respectively. No difference between incubation with NH IgG and anti-Dsg3/1-depleted IgG was observed. In addition, incubation with Dsg3-specific IgG resulted in significantly higher fragmentations compared to both Dsg-depleted PV IgG and NH IgG, respectively. Data show the mean and standard error of the mean (error bars) of seven independent experiments. *, $p < 0.05$; **, $p < 0.01$; n.s., not significant.

DISCUSSION

Adjuvant immunoadsorption is a well-established treatment option in a variety of autoantibody-mediated diseases including PV. So far, more than 100 pemphigus patients were reported to have been subjected to immunoadsorption which has been recommended in the guideline of the German Dermatological Society for the treatment of refractory or severe PV (21, 36).

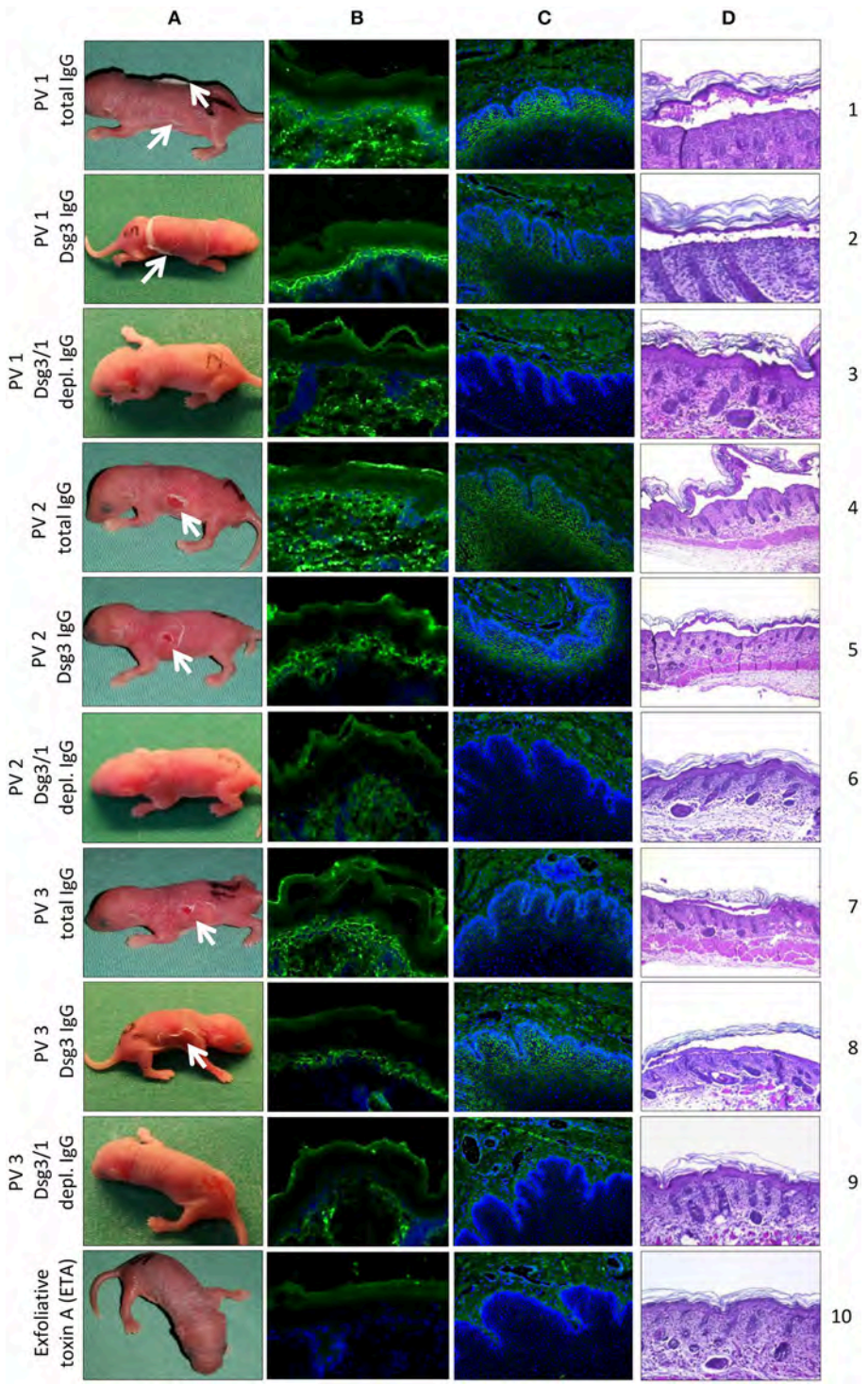

FIGURE 5 | *In vivo* pathogenicity of pemphigus vulgaris (PV) IgG fractions. Injection of neonatal mice ($n = 3$/ group) with PV IgG and anti-Dsg3-specific IgG purified from three different PV patients PV1, PV2, PV3) induced flaccid macroscopic blisters (**A**; lanes 1, 2, 4, 5, 7, and 8; white arrows) and suprabasal splitting as seen by lesional histopathology (**D**; lanes 1, 2, 4, 5, 7, and 8). No macroscopic and microscopic blistering was induced by PV IgG depleted of anti-Dsg3/1 IgG from the three PV patients (**A,D**; lanes 3, 6, and 9) or ETA alone (**A,D**; lane 10). By direct immunofluorescence (IF) microscopy of back skin, an intercellular epidermal staining was observed in mice injected with PV IgG (**B**; lanes 1, 4, and 7) or anti-Dsg3-specific IgG (**B**; lanes 2, 5, and 8) but not after injection of anti-Dsg3/1 IgG-depleted IgG (**B**; lanes 3, 6, and 9) or ETA alone (**B**, lane 10). By indirect IF microscopy on monkey esophagus, the characteristic intercellular staining (1:80 dilutions are shown) was seen with sera of mice injected with PV IgG (**C**; lanes 1, 4, and 7) and anti-Dsg3-specific PV IgG (**C**; lanes 2, 5, and 8), but not after injection of PV IgG depleted of Dsg3-specific IgG (**C**; lanes 3, 6, and 9) or ETA alone (**C**, lane 10). Nuclei were counterstained with DAPI.

Furthermore, the results of a randomized control trial comparing the efficacy and safety of immunoadsorption plus best medical treatment with best medical treatment alone in pemphigus are currently evaluated. In PV, it may be of particular value to rapidly reduce the amount of circulating autoantibodies at the beginning of treatment at a stage when other therapies, i.e., corticosteroids, azathioprine, and rituximab, are not yet effective. This assumption is supported by the clear evidence of a direct pathogenic effect of pemphigus autoantibodies as demonstrated by the occurrence of transient pemphigus in neonates of mothers with PV, the correlation of disease activity with serum levels of anti-Dsg1/3 IgG and various experimental models *in vitro* and *in vivo* (2, 15, 20, 33). Conventional immunoadsorption is, however, limited due to the risk of hypogammaglobulinaemia and the subsequent risk of infections. This disadvantage would not be applicable for the use of autoantibody-specific adsorbers. Therefore, we have recently developed Dsg1- and Dsg3-specific adsorbers based on the recombinant Dsg ectodomains. We could show that the prototypic adsorbers effectively removed anti-Dsg1/3 IgG from PV and PF sera and eliminated the pathogenic effect of PV and PF IgG *in vitro* (26).

In the present study, the prototypic adsorbers were employed to investigate whether Dsg1/3-specific adsorption can also abolish the pathogenic effect of PV IgG *in vivo*. Extending our previous studies (26), we asked the question whether anti-Dsg3-specific IgG alone, i.e., without the addition of non-desmoglein antibodies, is sufficient to induce pathogenic effects *in vitro* and intraepidermal blistering in mice. Our experiments are of particular importance since the concept that in the great majority of PV patients, the pathogenic effects of autoantibodies are mediated by anti-Dsg antibodies is challenged (13, 16). Furthermore, although Amagai et al. previously showed that affinity-purified anti-Dsg3 IgG prevented pathogenicity *in vivo* (37), there are still doubts about the specificity of the affinity purification as the recombinant Dsg3 fragment used for this process contained the constant region of human IgG1 that might have also bound to non-Dsg PV autoantibodies (13, 38). In our Dsg1/3-specific adsorbers, only the ectodomains of Dsg1 and 3 were used (26).

Here, we initially demonstrated the high efficiency of the Dsg3/1-specific adsorbers since no anti-Dsg3 or anti-Dsg1 IgG antibodies could be detected in the Dsg3/1-depleted IgG fraction by ELISA. This result was corroborated by Western blotting of anti-Dsg1/3-specific IgG and anti-Dsg1/3 IgG-depleted PV IgG fractions with extract of human keratinocytes. In line, by indirect IF microscopy on monkey esophagus both, total PV IgG and anti-Dsg3-specific IgG but not anti-Dsg3/1 IgG-depleted PV IgG and normal human IgG stained the epithelium.

Next, we demonstrated in two different *in vitro* assays that PV IgG, depleted from anti-Dsg1/3 reactivity by the use of the Dsg1/3-specific adsorbers, lost their pathogenic effect. No difference between anti-Dsg1/3 IgG-depleted IgG and normal human IgG was observed in both, the desmosome degradation assay and the dispase-based dissociation assay. In contrast, PV IgG and anti-Dsg3-specific IgG obtained after elution from our Dsg1/3-specific adsorbers led to increased desmosome degradation and keratinocyte dissociation, respectively. It has already previously been shown that human keratinocytes loose Dsg3 expression on their cell surface after incubation with PV IgG (39, 40). Nevertheless, we observed that total PV IgG and anti-Dsg3-specific IgG from PV3 resulted in less Dsg3 degradation (**Figures 3G,H**) compared to the IgG fractions of PV1 and PV2. We hypothesize that the weaker desmosome-degrading capacity of both PV3 IgG and PV3 anti-Dsg3-specific IgG may be explained by the lower anti-Dsg3 IgG titers in this patient (**Table 2**).

Furthermore, the different PV IgG fractions were also assayed in the neonatal mouse model of PV. Initially, Anhalt and coworkers reported that the injection of PV serum in neonatal mice recapitulated major clinical and immunopathological characteristics of the human diseases, i.e., flaccid blisters that easily erode when mechanical friction is applied, intraepidermal split formation as detected by histopathology, and the intercellular binding of PV antibodies in the epidermis as seen by direct IF microscopy (33). In the present study, the injection of PV IgG and Dsg1/3-specific IgG led to macroscopic and microscopic blisters indicating that anti-Dsg1/3 IgG alone is pathogenic and does not require the presence of non-Dsg PV autoantibodies. These data are supported by the previous observations that injection of the monoclonal anti-Dsg3 antibody AK23 resulted in blister formation in neonatal as well as in adult mice (41, 42). More important for the future use of the Dsg1/3-specific adsorbers in the treatment of PV patients is our observation that PV IgG fractions depleted from anti-Dsg1/3 reactivity did not induce skin lesions when injected into neonatal mice. These results unequivocally show that non-Dsg antibodies that had been previously described in PV sera directed e.g., against muscarinic and nicotinic acethylcholine receptors, annexins, thyroid peroxidase, and mitochondrial proteins are not a prerequisite for blister formation in PV. In line, these non-Dsg antibodies have not yet been described to be pathogenic *in vivo* while co-pathogenic effects have been reported *in vitro* (13, 15, 17, 18, 20, 43, 44). One may speculate that the previously proposed pathogenic effect of non-Dsg antibodies in PV is not a key element for the initiation of blister formation.

In contrast, anti-desmocollin autoantibodies that have been described in pemphigus sera caused desmosome degradation in the desmosome degradation assay, cell fragmentation in the dispase-based dissociation assay, and suprabasal splitting in an *ex vivo* skin model (45–47). In line, desmocollin 3-deficient mice present with skin erosions and suprabasal intraepidermal blistering (48). However, evidence is accumulating that anti-desmocollin autoantibodies may be more relevant in paraneoplastic and atypical pemphigus than in PV and PF (49–51). In fact, in a large prospective study with more than 330 pemphigus patients, only 4% of all pemphigus sera and 2.7% of PV and PF sera exhibited anti-desmocollin reactivity, while 98% of sera contained anti-Dsg3 and/or anti-Dsg1 IgG (52). These data indicate that only in a small number of PV and PF patients, Dsg1/3-specific immunoadsorption may not be clinically effective although anti-Dsg1/3 antibodies have effectively been decreased. Future studies now aim at

applying the Dsg3/1-specific adsorbers in a clinical trial with PV patients.

AUTHOR CONTRIBUTIONS

MH contributed to the performance of the experiments and the writing of the manuscript. JD contributed to the planning of the project and the performance of the experiments. SE and JL contributed to the performance of the experiments and to the revision of the manuscript. FW contributed to the performance of the experiments and to the revision of the manuscript. LK contributed to the planning of the project. DZ contributed to the planning of the project and to the revision of the manuscript. WS contributed to the planning of the project and to the revision of the manuscript. CP contributed to the planning of the project and to the revision of the manuscript. ES contributed to the planning of the project and to the writing of the manuscript. SG contributed to the planning of the project and to the writing of the manuscript.

FUNDING

This work was supported by the European Regional Development Fund (project no. 122-09-017) and the Excellence Cluster *Inflammation@Interfaces* (DFG EXC306/2).

REFERENCES

1. Schmidt E, Zillikens, D. The diagnosis and treatment of autoimmune blistering skin diseases. *Dtsch Arztebl Int.* (2011) 108:399–405. doi: 10.3238/arztebl.2011.0405
2. Kasperkiewicz M, Ellebrecht CT, Takahashi H, Yamagami J, Zillikens D, Payne AS, et al. Pemphigus. *Nat Rev Dis Primers.* (2017) 3:17026. doi: 10.1038/nrdp.2017.26
3. Ludwig RJ, Vanhoorelbeke K, Leypoldt F, Kaya Z, Bieber K, McLachlan SM, et al. Mechanisms of autoantibody-induced pathology. *Front Immunol.* (2017) 8:603. doi: 10.3389/fimmu.2017.00603
4. Schmidt E. Rituximab as first-line treatment of pemphigus. *Lancet* (2017) 389:1956–8. doi: 10.1016/S0140-6736(17)30787-0
5. Koch PJ, Walsh MJ, Schmelz M, Goldschmidt MD, Zimbelmann R, Franke WW. Identification of desmoglein, a constitutive desmosomal glycoprotein, as a member of the cadherin family of cell adhesion molecules. *Eur J Cell Biol.* (1990) 53:1–12.
6. Amagai M, Klaus-Kovtun V, Stanley JR. Autoantibodies against a novel epithelial cadherin in pemphigus vulgaris, a disease of cell adhesion. *Cell* (1991) 67:869–77.
7. Wheeler GN, Parker AE, Thomas CL, Ataliotis P, Poynter D, Arnemann J, et al. Desmosomal glycoprotein DGI, a component of intercellular desmosome junctions, is related to the cadherin family of cell adhesion molecules. *Proc Natl Acad Sci USA.* (1991) 88:4796–800.
8. Ishii K, Amagai M, Hall RP, Hashimoto T, Takayanagi A, Gamou S, et al. Characterization of autoantibodies in pemphigus using antigen-specific enzyme-linked immunosorbent assays with baculovirus-expressed recombinant desmogleins. *J Immunol.* (1997) 159:2010–7.
9. Eyre RW, Stanley JR. Identification of pemphigus vulgaris antigen extracted from normal human epidermis and comparison with pemphigus foliaceus antigen. *J Clin Invest.* (1988) 81:807–12. doi: 10.1172/JCI113387
10. Ding X, Aoki V, Mascaro JM Jr, Lopez-Swiderski A, Diaz LA, Fairley JA. Mucosal and mucocutaneous (generalized) pemphigus vulgaris show distinct autoantibody profiles. *J Invest Dermatol.* (1997) 109:592–6.
11. Amagai M, Komai A, Hashimoto T, Shirakata Y, Hashimoto K, Yamada T, et al. Usefulness of enzyme-linked immunosorbent assay using recombinant desmogleins 1 and 3 for serodiagnosis of pemphigus. *Br J Dermatol.* (1999) 140:351–7.
12. Mahoney MG, Wang Z, Rothenberger K, Koch PJ, Amagai M, Stanley JR. Explanations for the clinical and microscopic localization of lesions in pemphigus foliaceus and vulgaris. *J Clin Invest.* (1999) 103:461–8. doi: 10.1172/JCI5252
13. Ahmed AR, Carrozzo M, Caux F, Cirillo N, Dmochowski M, Alonso AE, et al. Monopathogenic vs multipathogenic explanations of pemphigus pathophysiology. *Exp Dermatol.* (2016) 25:839–46. doi: 10.1111/exd.13106
14. Sajda T, Hazelton J, Patel M, Seiffert-Sinha K, Steinman L, Robinson W, et al. Multiplexed autoantigen microarrays identify HLA as a key driver of anti-desmoglein and -non-desmoglein reactivities in pemphigus. *Proc Natl Acad Sci USA.* (2016) 113:1859–64. doi: 10.1073/pnas.1525448113
15. Schmidt E, Spindler V, Eming R, Amagai M, Antonicelli F, Baines JF, et al. Meeting report of the pathogenesis of pemphigus and pemphigoid meeting in munich, september 2016. *J Invest Dermatol.* (2017) 137:1199–203. doi: 10.1016/j.jid.2017.01.028
16. Amagai M, Ahmed AR, Kitajima Y, Bystryn JC, Milner Y, Gniadecki R, et al. Are desmoglein autoantibodies essential for the immunopathogenesis of pemphigus vulgaris, or just "witnesses of disease"? *Exp Dermatol* (2006) 15:815–31. doi: 10.1111/j.1600-0625.2006.00499_1.x
17. Chernyavsky AI, Arredondo J, Piser T, Karlsson E, Grando SA. Differential coupling of M1 muscarinic and alpha7 nicotinic receptors to inhibition of pemphigus acantholysis. *J Biol Chem.* (2008) 283:3401–8. doi: 10.1074/jbc.M704956200
18. Kalantari-Dehaghi M, Chen Y, Deng W, Chernyavsky A, Marchenko S, Wang PH, et al. Mechanisms of mitochondrial damage in keratinocytes by pemphigus vulgaris antibodies. *J Biol Chem.* (2013) 288:16916–25. doi: 10.1074/jbc.M113.472100
19. Cipolla GA, Park JK, Lavker RM, Petzl-Erler ML. Crosstalk between signaling pathways in pemphigus: a role for endoplasmic reticulum stress in p38 mitogen-activated protein kinase activation? *Front Immunol.* (2017) 8:1022. doi: 10.3389/fimmu.2017.01022
20. Spindler V, Eming R, Schmidt E, Amagai M, Grando S, Jonkman MF, et al. Mechanisms causing loss of keratinocyte cohesion in pemphigus. *J Invest Dermatol.* 138:32–7. (2017). doi: 10.1016/j.jid.2017.06.022
21. Eming R, Sticherling M, Hofmann SC, Hunzelmann N, Kern JS, Kramer H, et al. S2k guidelines for the treatment of pemphigus vulgaris/foliaceus and bullous pemphigoid. *J Dtsch Dermatol Ges.* (2015) 13:833–44. doi: 10.1111/ddg.12606
22. Hertl M, Jedlickova H, Karpati S, Marinovic B, Uzun S, Yayli S, et al. Pemphigus. S2 Guideline for diagnosis and treatment–guided by the European Dermatology Forum (EDF) in cooperation with the European Academy of Dermatology and Venereology (EADV). *J Eur Acad Dermatol Venereol.* (2015) 29:405–14. doi: 10.1111/jdv.12772
23. Joly P, Maho-Vaillant M, Prost-Squarcioni C, Hebert V, Houivet E, Calbo S, et al. First-line rituximab combined with short-term prednisone versus prednisone alone for the treatment of pemphigus (Ritux 3): a prospective, multicentre, parallel-group, open-label randomised trial. *Lancet* (2017) 389:2031–40. doi: 10.1016/S0140-6736(17)30070-3
24. Schmidt E, Zillikens D. Immunoadsorption in dermatology. *Arch Dermatol Res.* (2010) 302:241–53. doi: 10.1007/s00403-009-1024-9
25. Waschke J, Spindler V. Desmosomes and extradesmosomal adhesive signaling contacts in pemphigus. *Med Res Rev.* (2014) 34:1127–45. doi: 10.1002/med.21310
26. Langenhan J, Dworschak J, Saschenbrecker S, Komorowski L, Schlumberger W, Stocker W, et al. Specific immunoadsorption of pathogenic autoantibodies in pemphigus requires the entire ectodomains of desmogleins. *Exp Dermatol.* (2014) 23:253–9. doi: 10.1111/exd.12355
27. Schmidt E, Klinker E, Opitz A, Herzog S, Sitaru C, Goebeler M, et al. Protein A immunoadsorption: a novel and effective adjuvant treatment of severe pemphigus. *Br J Dermatol.* (2003) 148:1222–9. doi: 10.1046/j.13652133.2003.05302.x

28. Kasperkiewicz M, Shimanovich I, Meier M, Schumacher N, Westermann L, Kramer J, et al. Treatment of severe pemphigus with a combination of immunoadsorption, rituximab, pulsed dexamethasone and azathioprine/mycophenolate mofetil: a pilot study of 23 patients. *Br J Dermatol.* (2012) 166:154–60. doi: 10.1111/j.1365-2133.2011.10585.x
29. Groth S, Recke A, Vafia K, Ludwig RJ, Hashimoto T, Zillikens D, et al. Development of a simple enzyme-linked immunosorbent assay for the detection of autoantibodies in anti-p200 pemphigoid. *Br J Dermatol.* (2011) 164:76–82. doi: 10.1111/j.1365-2133.2010.10056.x
30. Schmidt E, Gutberlet J, Siegmund D, Berg D, Wajant H, Waschke J. Apoptosis is not required for acantholysis in pemphigus vulgaris. *Am J Physiol Cell Physiol.* (2009) 296:C162–72. doi: 10.1152/ajpcell.00161.2008
31. Spindler V, Rotzer V, Dehner C, Kempf B, Gliem M, Radeva M, et al. Peptide-mediated desmoglein 3 crosslinking prevents pemphigus vulgaris autoantibody-induced skin blistering. *J Clin Invest.* (2013) 123:800–11. doi: 10.1172/JCI60139
32. Payne AS, Ishii K, Kacir S, Lin C, Li H, Hanakawa Y, et al. Genetic and functional characterization of human pemphigus vulgaris monoclonal autoantibodies isolated by phage display. *J Clin Invest.* (2005) 115:888–99. doi: 10.1172/JCI24185
33. Anhalt GJ, Labib RS, Voorhees JJ, Beals TF, Diaz LA. Induction of pemphigus in neonatal mice by passive transfer of IgG from patients with the disease. *N Engl J Med.* (1982) 306:1189–96. doi: 10.1056/NEJM198205203062001
34. Dworschak J, Recke A, Freitag M, Ludwig RJ, Langenhan J, Kreuzer OJ, et al. Mapping of B cell epitopes on desmoglein 3 in pemphigus vulgaris patients by the use of overlapping peptides. *J Dermatol Sci.* (2012) 65:102–9. doi: 10.1016/j.jdermsci.2011.11.012
35. Amagai M, Matsuyoshi N, Wang ZH, Andl C, Stanley JR. Toxin in bullous impetigo and staphylococcal scalded-skin syndrome targets desmoglein 1. *Nat Med.* (2000) 6:1275–7. doi: 10.1038/81385
36. Meyersburg D, Schmidt E, Kasperkiewicz M, Zillikens D. Immunoadsorption in dermatology. *Ther Apher Dial.* (2012) 16:311–20. doi: 10.1111/j.1744-9987.2012.01075.x
37. Amagai M, Hashimoto T, Shimizu N, Nishikawa T. Absorption of pathogenic autoantibodies by the extracellular domain of pemphigus vulgaris antigen (Dsg3) produced by baculovirus. *J Clin Invest.* (1994) 94:59–67. doi: 10.1172/JCI117349
38. Grando SA. Pemphigus autoimmunity: hypotheses and realities. *Autoimmunity* (2012) 45:7–35. doi: 10.3109/08916934.2011.606444
39. Mao X, Choi EJ, Payne AS. Disruption of desmosome assembly by monovalent human pemphigus vulgaris monoclonal antibodies. *J Invest Dermatol.* (2009) 129:908–18. doi: 10.1038/jid.2008.339
40. Jennings JM, Tucker DK, Kottke MD, Saito M, Delva E, Hanakawa Y, et al. Desmosome disassembly in response to pemphigus vulgaris IgG occurs in distinct phases and can be reversed by expression of exogenous Dsg3. *J Invest Dermatol.* (2011) 131:706–18. doi: 10.1038/jid.2010.389
41. Tsunoda K, Ota T, Aoki M, Yamada T, Nagai T, Nakagawa T, et al. Induction of pemphigus phenotype by a mouse monoclonal antibody against the amino-terminal adhesive interface of desmoglein 3. *J Immunol.* (2003) 170:2170–8. doi: 10.4049/jimmunol.170.4.2170
42. Schulze K, Galichet A, Sayar BS, Scothern A, Howald D, Zymann H, et al. An adult passive transfer mouse model to study desmoglein 3 signaling in pemphigus vulgaris. *J Invest Dermatol.* (2012) 132:346–55. doi: 10.1038/jid.2011.299
43. Nguyen VT, Ndoye A, Grando SA. Pemphigus vulgaris antibody identifies pemphaxin. a novel keratinocyte annexin-like molecule binding acetylcholine. *J Biol Chem.* (2000) 275:29466–76. doi: 10.1074/jbc.M003174200
44. Nguyen VT, Ndoye A, Grando SA. Novel human alpha9 acetylcholine receptor regulating keratinocyte adhesion is targeted by Pemphigus vulgaris autoimmunity. *Am J Pathol.* (2000) 157:1377–91. doi: 10.1016/S0002-9440(10)64651-2
45. Spindler V, Heupel WM, Efthymiadis A, Schmidt E, Eming R, Rankl C, et al. Desmocollin 3-mediated binding is crucial for keratinocyte cohesion and is impaired in pemphigus. *J Biol Chem.* (2009) 284:30556–64. doi: 10.1074/jbc.M109.024810
46. Mao X, Nagler AR, Farber SA, Choi EJ, Jackson LH, Leiferman KM, et al. Autoimmunity to desmocollin 3 in pemphigus vulgaris. *Am J Pathol.* (2010) 177:2724–30. doi: 10.2353/ajpath.2010.100483
47. Rafei D, Muller R, Ishii N, Llamazares M, Hashimoto T, Hertl M, et al. IgG autoantibodies against desmocollin 3 in pemphigus sera induce loss of keratinocyte adhesion. *Am J Pathol.* (2011) 178:718–23. doi: 10.1016/j.ajpath.2010.10.016
48. Chen J, Den Z, Koch PJ. Loss of desmocollin 3 in mice leads to epidermal blistering. *J Cell Sci.* (2008) 121(Pt. 17):2844–9. doi: 10.1242/jcs.031518
49. Muller R, Heber B, Hashimoto T, Messer G, Mullegger R, Niedermeier A, et al. Autoantibodies against desmocollins in European patients with pemphigus. *Clin Exp Dermatol.* (2009) 34:898–903. doi: 10.1111/j.1365-2230.2009.03241.x
50. Brandt O, Rafei D, Podstawa E, Niedermeier A, Jonkman MF, Terra JB, et al. Differential IgG recognition of desmoglein 3 by paraneoplastic pemphigus and pemphigus vulgaris sera. *J Invest Dermatol.* (2012) 132:1738–41. doi: 10.1038/jid.2012.1
51. Ishii N, Teye K, Fukuda S, Uehara R, Hachiya T, Koga H, et al. Anti-desmocollin autoantibodies in nonclassical pemphigus. *Br J Dermatol.* (2015) 173:59–68. doi: 10.1111/bjd.13711
52. Mindorf S, Dettmann IM, Kruger S, Fuhrmann T, Rentzsch K, Karl I, et al. Routine detection of serum antidesmocollin autoantibodies is only useful in patients with atypical pemphigus. *Exp Dermatol.* (2017) 26:1267–70. doi: 10.1111/exd.13409

Conflict of Interest Statement: JD, JL, LK, and CP are employees of Euroimmun AG. Winfried Stöcker is board members of Euroimmun AG. DZ and ES have a research cooperation with Euroimmun.

The remaining authors declare that the research was conducted in the absence of any commercial or financial relationships that could be construed as a potential conflict of interest.

frontiers in Immunology

ORIGINAL RESEARCH
published: 10 August 2018
doi: 10.3389/fimmu.2018.01833

Flightless I Alters the Inflammatory Response and Autoantibody Profile in an OVA-Induced Atopic Dermatitis Skin-Like Disease

Zlatko Kopecki†, Natalie E. Stevens, Heng T. Chong, Gink N. Yang and Allison J. Cowin†*

Regenerative Medicine, Future Industries Institute, University of South Australia, Adelaide, SA, Australia

Atopic dermatitis (AD) is a chronic pruritic inflammatory skin disease characterized by excessive inflammation and disrupted skin barrier function. Although the etiology of AD is not completely understood, clinical and basic studies suggest increasing involvement of autoantibodies against intracellular proteins. An actin remodeling protein, Flightless I (Flii), has been shown to promote development of inflammatory mediated skin conditions and impairment of skin barrier development and function. Here, we sought to determine the effect of altering *Flii* expression on the development of AD and its contribution to autoimmune aspects of inflammatory skin conditions. Ovalbumin (OVA)-induced AD skin-like disease was induced in *Flii* heterozygous (*Flii*$^{+/-}$), wild-type (*Flii*$^{+/+}$), and *Flii* transgenic (*Flii*$^{Tg/Tg}$) mice by epicutaneous exposure to OVA for 3 weeks; each week was separated by 2-week resting period. Reduced *Flii* expression resulted in decreased disease severity and tissue inflammation as determined by histology, lymphocytic, and mast cell infiltrate and increased anti-inflammatory IL-10 cytokine levels and a marked IFN-γ Th_1 response. In contrast, *Flii* over-expression lead to a Th_2 skewed response characterized by increased pro-inflammatory TNF-α cytokine production, Th_2 chemokine levels, and Th_2 cell numbers. Sera from OVA-induced AD skin-like disease *Flii*$^{+/-}$ mice showed a decreased level of autoreactivity while sera from *Flii*$^{Tg/Tg}$ mice counterparts showed an altered autoantibody profile with strong nuclear localization favoring development of a more severe disease. These findings demonstrate autoimmune responses in this model of OVA-induced AD-like skin disease and suggest that Flii is a novel target, whose manipulation could be a potential approach for the treatment of patients with AD.

Keywords: atopic dermatitis, flightless I, autoantibody, inflammation, skin barrier

OPEN ACCESS

Edited by:
Ralf J. Ludwig, Universität zu Lübeck, Germany

Reviewed by:
Luciana D'Apice, Consiglio Nazionale Delle Ricerche (CNR), Italy
Kentaro Izumi, Hokkaido University, Japan

****Correspondence:***
Zlatko Kopecki
zlatko.kopecki@unisa.edu.au

†These authors have contributed equally to this work.

Specialty section:
This article was submitted to Cytokines and Soluble Mediators in Immunity, a section of the journal Frontiers in Immunology

Received: *21 December 2017*
Accepted: *25 July 2018*
Published: *10 August 2018*

Citation:
Kopecki Z, Stevens NE, Chong HT, Yang GN and Cowin AJ (2018) Flightless I Alters the Inflammatory Response and Autoantibody Profile in an OVA-Induced Atopic Dermatitis Skin-Like Disease. Front. Immunol. 9:1833. doi: 10.3389/fimmu.2018.01833

INTRODUCTION

Atopic dermatitis (AD) is one of the most common heterogeneous inflammatory skin diseases affecting 20% of children and 1–3% of adults worldwide (1). The disease is associated with impairments in the skin barrier and variable clinical indicators including occurrence of eczematous lesions, pruritus, and cheilitis (1). The etiology of AD is complex and is often characterized by abnormal immunological pathways that manifest in an imbalance of T-helper ($Th)_1$ and Th_2 responses (2). Typically, AD is described as having a biphasic course consisting of an acute inflammatory Th_2-dominated phase associated with IgE production and a chronic phase distinguished by reappearance

of Th_1 responses, tissue remodeling, and dermal thickening (3). Histopathologically, AD is characterized by an inflammatory infiltrate consisting of $CD4^+$ memory T cells, mast cells, and eosinophils and a controlled temporal-spatial expression of pro-inflammatory cytokines and chemokines driving atopic inflammation of the skin (4).

Research within the last decade has found an association between AD and autoantibody development, suggesting the contribution of autoantibodies to the pathogenesis of AD (3, 5–8). It is proposed that tissue damage induced by AD allows exposure of intracellular antigens that are normally inaccessible by antibodies to the extracellular space, where they can interact with B cells and antibodies (9). A broad spectrum of IgE targeting self-antigens have been identified in above 90% of severe AD patients and high-avidity IgG autoantibodies have been proposed as potential diagnostic markers for severe AD (5, 10–12). The fact that these autoantibodies are associated with disease severity implicates their role in both humoral and cellular immunity in AD pathogenesis (5, 12). Antinuclear antibodies have been shown to have both biological and clinical significance acting as sensors of cellular stress and inflammation associated with environmental factors (13). While the presence of autoantibodies can have a protective role as natural autoantibodies (14), the presence of nuclear autoantibodies in AD has been suggested to lead to the continual provocation of the immune system hence contributing to the severity and chronicity of disease.

Flightless I (Flii) is a highly conserved and unique member of the gelsolin family of actin remodeling proteins and a nuclear receptor activator affecting the transcriptional activity of many modulators of tissue remodeling and inflammation (15, 16). Flii has been demonstrated to regulate cytokine secretion and cellular inflammatory responses *via* its intracellular and extracellular effects on toll-like receptors (17–20). Flii expression increases in skin during development and in response to inflammation, injury, skin cancer development, wound healing, and skin blistering (21–23). Over-expression of *Flii* delays the development of an intact skin barrier in the embryonic skin of mice and impairs the recovery of the epidermal barrier post injury *via* its effects on tight-junction formation (22). A recent study has shown that reducing Flii levels either genetically or using Flii neutralizing antibodies decreases erythema, inflammatory cell infiltrate, and pro-inflammatory cytokine secretion in a mouse model of psoriasiform dermatitis (24). Taken together, these findings suggest a possible role for Flii in inflammatory responses mediating AD. Using an OVA-induced AD-like skin mouse model (25), this study aimed to investigate the effect of differential *Flii* gene expression on development of AD *via* characterization of inflammatory and autoimmune responses responsible for AD pathogenesis.

MATERIALS AND METHODS

Animal Studies

Mice were maintained according to the Australian Code for the Care and Use of Animals for Scientific Purposes under protocols approved by the Child Youth and Women's Health Service Animal Ethics Committee (AEC916/06/2015). Mice with the BALB/c background and wild-type controls were obtained from inbred litters. *Flii*-deficient heterozygous null mice ($Flii^{+/-}$) and mice carrying the complete human *Flii* gene on a cosmid transgene were maintained as described previously (26, 27). Heterozygous transgenic mice $Flii^{Tg/+}$ were made by crossing $Flii^{+/+}$ with cosmid transgene $Flii^{+/-}$. These transgenic mice were intercrossed to obtain animals homozygous for the transgene $Flii^{Tg/Tg}$ which carry two copies of the mouse *Flii* gene and two copies of the human *Flii* transgene.

Atopic dermatitis was induced *via* epicutaneous exposure of mice to OVA as previously described (25). Briefly, 10- to 12-week-old female wild-type ($Flii^{+/+}$), *Flii* heterozygous ($Flii^{+/-}$), and *Flii* transgenic ($Flii^{Tg/Tg}$) mice ($n = 8$/genotype) were anesthetized using isoflurane inhalation, the skin on the back of mice was shaved and then tape stripped four times by a transparent adhesive tape (Tegaderm) to introduce a standardized skin injury. A gauze patch (1×1 cm^2) soaked with 100 µl of 0.1% OVA (OVA group) in saline or 0.9% saline (control group) was placed on the back skin and secured with Tegaderm dressing. The experiment comprised three 1-week exposures with a 2-week interval between each exposure week (**Figure 1A**). Clinical images of affected skin, transepidermal water loss (TEWL), and erythema measurements were recorded at the end of the third sensitization week. The level of skin erythema was measured daily using a handheld DermaLab Unit (Cortex Technology) following manufacturer's instructions. This instrument uses skin reflectance spectroscopy to determine the redness of inflamed skin. The instrument was blanked prior to placing a probe directly onto the inflamed AD-like lesions on dorsal skin and a reading obtained as previously described (24). Measurements of TEWL were obtained with a calibrated Vapometer evaporimeter (Delfin Technologies, Finland). The probe was allowed to equilibrate for approximately 30 s before a brief measurement period (8 s) as indicated in manufacturer's guidelines. The Vapometer was placed directly onto the inflamed AD-like lesions on dorsal skin (using an 11-mm adaptor) and held there securely for the duration of the measurement. For both erythema and TEWL analysis, three separate measurements were taken per mouse to ensure the entire region of AD-like inflamed back skin was assessed as previously described (24). Mice were then euthanized and skin biopsies collected for histology analysis, immunohistochemistry, and mRNA extraction. Blood was collected for autoimmunity experiments.

Histology and Immunohistochemistry

Paraffin-embedded fixed tissue samples were stained with hematoxylin and eosin or toluidine blue following established protocols (28). Level of skin inflammation was assessed using skin thickness measurements, and analysis of inflammatory and mast cell numbers in lesional skin of OVA-induced AD-like skin lesions of $Flii^{+/-}$, wild-type, and $Flii^{Tg/Tg}$ mice using high magnification images and light microscopy using optimized protocols using Image Pro-Plus 5.1 program (MediaCybernetics Inc.) as previously described (24). Skin thickness included epidermal and dermal measurements of OVA-induced AD-like lesions; inflammatory cell number was assessed by counting total inflammatory cells in 10 different HPF of view in OVA-induced AD-like lesions, and mast cell analysis included counting toludine blue positive

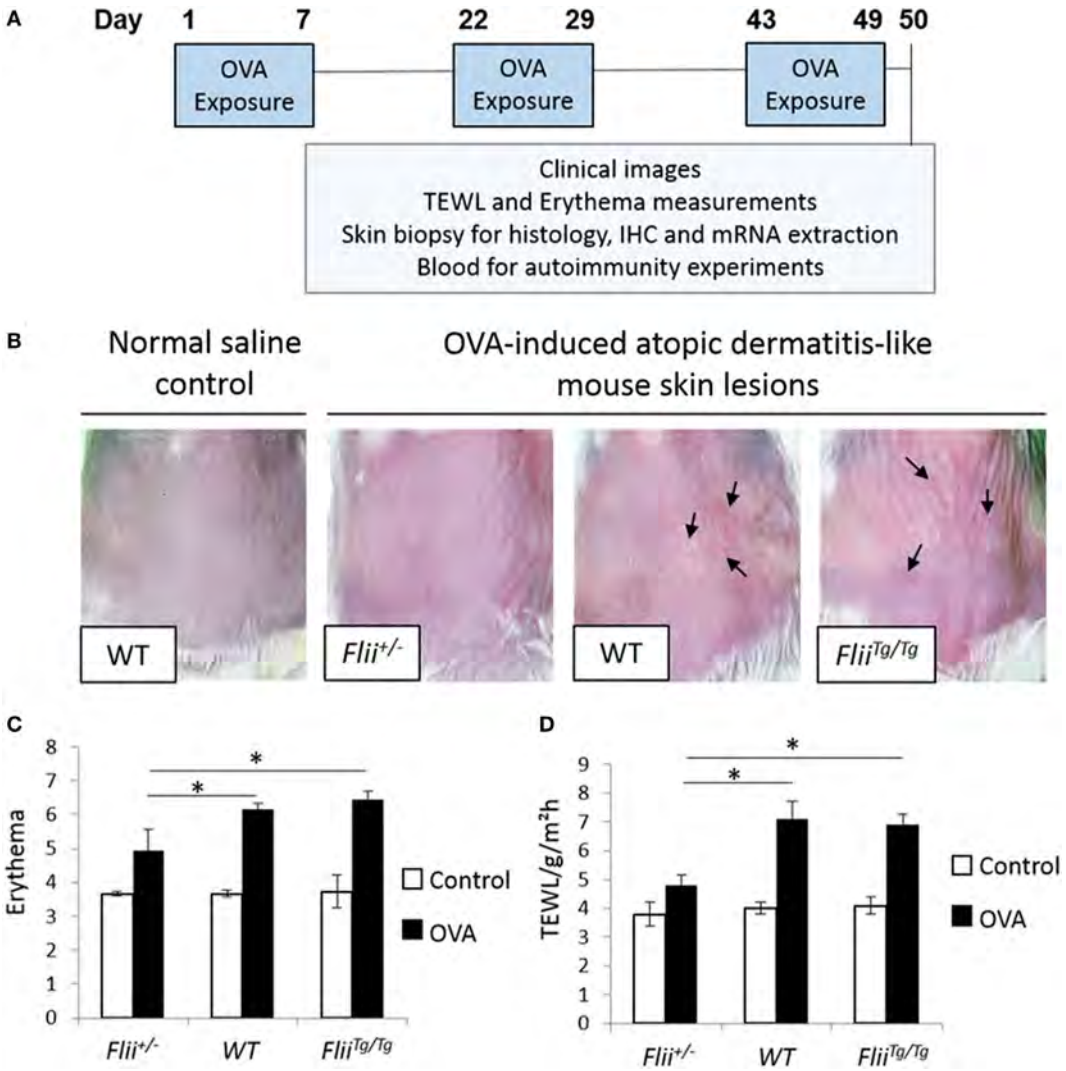

FIGURE 1 | Reduced *Flii* expression leads to decreased development of OVA-induced atopic dermatitis (AD)-like lesions. **(A)** Ovalbumin (OVA) exposure protocol, including a total of three 1-week exposures to 100 µl 0.1% OVA or saline control on patches separated from each other by 2-week resting interval. **(B)** Representative clinical images of OVA-induced AD-like skin lesions in mice differential *Flii* expression illustrating high degree of erythema, skin thickening, and scaling (black arrowhead) in WT and *Flii*$^{Tg/Tg}$ mice exposed to OVA. **(C,D)** OVA exposure leads to development of AD-like lesions demonstrated by increased erythema and transepidermal water loss (TEWL). Decreasing *Flii* expression reduces development of AD-like lesions with significantly decreased erythema and TEWL measurements compared to OVA exposed skin of WT and *Flii*$^{Tg/Tg}$ animals. $n = 8$. Mean ± SEM. *<0.05.

mast cells in entire sections of OVA-induced AD-like skin lesions per mm^2. Immunohistochemistry was also performed on paraffin-embedded fixed AD-like skin lesions following antigen retrieval according to the manufacturer's protocols (DAKO Corporation, Glostrup, Denmark). Following blocking in 3% normal goat serum, primary antibodies against CD4 [rat monoclonal, #14-9766-82 (Thermo Scientific, Australia) (1:200)], T-bet [rabbit polyclonal, #PA5-40573 (Thermo Scientific, Australia) (1:100)], GATA-3 [rabbit polyclonal, #ab106625 (Abcam Australia) (1:100)], and ROR-γ [rabbit monoclonal, #ab207082 (Abcam Australia) (1:3,000)] were applied and slides were incubated at 4°C overnight in a humidified chamber before application of species-specific, Alexa Flour-488 or Alexa Flour-594 secondary antibodies (Invitrogen, Australia) for 1 h at room temperature. Finally, slides were washed and mounted in Fluorescence Mounting Medium (Dako, Australia). Images were captured on Olympus microscope and CellSense Live Science Imaging Software program (Olympus, Germany) used for counting the positive cells in the AD-like lesions of *Flii*$^{+/-}$, wild-type, and *Flii*$^{Tg/Tg}$ mice. Negative controls included replacing primary antibodies with normal rabbit IgG, or normal mouse IgG. For verification of staining, non-specific binding was determined by omitting primary or secondary antibodies. All control sections had negligible immunofluorescence.

RTq-PCR

Harvested tissue was snap-frozen in liquid nitrogen and total RNA was isolated using Ultraclean Tissue and Cell RNA Isolation

Kit (MoBio Laboratories, Carlsbad, CA, USA) according to the manufacturer's protocol. Total cDNA was synthesized using iScript cDNA Synthesis Kit (Bio-Rad Laboratories, Hercules, CA, USA) according to manufacturer's protocol. Quantitative PCR was performed using iQ SYBR Green Supermix (Bio-Rad Laboratories, Hercules, CA, USA) in triplicate reactions. The plates were placed in a CFX Connect Real-Time PCR Detection System (Bio-Rad Laboratories, Hercules, CA, USA). Reactions underwent 30 s at 95°C, then 40 cycles of 5 s at 95°C, 20 s at 60°C, and 10 s at 95°C before determination of melt curve between 65 and 95°C. GAPDH and CyPA were used as reference genes and inter-reaction calculator method was applied for all plates. For relative comparison, the cycle threshold value (Ct) was analyzed using the ΔΔCt method and data reported as Ct normalized to reference genes. Sequences for PCR primers are listed in Table S1 in Supplementary Material.

Autoantibody Immunofluorescence

In order to assess the degree of autoimmunity in OVA-induced AD-like skin of *Flii*$^{+/-}$, wild-type, and *Flii*$^{Tg/Tg}$ mice, sub-confluent primary wild-type mouse keratinocytes were stained with mouse sera of AD-induced mice following established protocols (13, 29). Briefly, primary keratinocytes were isolated from murine epidermis as previously described (30), grown on glass coverslips and washed in 1× phosphate-buffered saline before paraformaldehyde (4%) fixation (10 min at room temperature). Fixed cells were subsequently permeabilized using 0.2% Triton-X-100 and 0.5% BSA in 1× phosphate-buffered saline (5 min at room temperature) before incubation with pooled murine serum ($n = 3$) diluted (1 in 10) in 0.5% BSA in 1× phosphate-buffered saline for 1 h. Bound murine IgG was detected with Alexa Flour 633 goat anti-mouse IgG (1 in 1,000; #A21050; Invitrogen, Mulgrave, VIC, Australia) in 1× phosphate-buffered saline for 1 h at room temperature. Following repeated 2 min washes with 1× phosphate-buffered saline, cells were stained with DAPI nucleic acid stain (Sigma-Aldrich) for 5 min at room temperature before washing and mounting for imaging. Negative controls included omitting the incubation with mouse serum. All control sections had negligible immunofluorescence. Staining pattern of autoantibodies was assessed using the Olympus microscope and CellSense Live Science Imaging Software program (Olympus, Germany).

Immunoblot Analysis of AD Serum Autoreactive Antibodies

Protein was extracted from *WT* murine keratinocytes using standard protein extraction protocols (31). Samples of extracted protein (20 μg) were run on 10% SDS-PAGE gels (30 min; 200V) and transferred to nitrocellulose by wet transfer (1 h; 100V). Membranes were cut into strips, blocked in 3% bovine serum albumin (Sigma) for 30 min, and probed with murine serum diluted (1 in 10) in tris-buffered saline containing 3% BSA and 0.1% Tween overnight. After washing, horseradish peroxidase-conjugated goat anti-murine immunoglobulin secondary antibody was added for a further 1 h at room temperature. Stringent washes were performed before detection of horseradish peroxidase and exposure using GeneSnap analysis program (SynGene, Frederick, MD, USA).

Statistical Analysis

Statistical differences were determined using the Student's *t*-test or one-way ANOVA. For data not following a normal distribution, the Mann–Whitney *U* test was performed. A *P* value of less than 0.05 was considered significant.

RESULTS

Flii-Deficient Mice Exhibit Reduced OVA-Induced AD-Like Skin Disease

The repeated epicutaneous exposure of OVA (**Figure 1A**) on mouse skin results in an AD-like skin disease with histological and phenotypic features of human AD, including erythema, skin thickening, and a localized immune response (25). *Flii* homozygous (*Flii*$^{-/-}$) mice are embryonic lethal (26); therefore, using the OVA-induced AD-like skin mouse model, the severity of OVA-induced AD-like lesions was determined in response to different *Flii* gene levels in *Flii* heterozygous (*Flii*$^{+/-}$), normal (*Flii*$^{+/+}$), and *Flii* transgenic (*Flii*$^{Tg/Tg}$) mice. All three mice genotypes developed localized inflammation which increased following each week of OVA exposure. *Flii*-deficient mice showed reduced levels of inflammation and scaling (**Figure 1B**). Spectrophotometric measurement of the redness of the OVA exposed skin showed that *Flii*-deficient mice had significantly less erythema (**Figure 1B**) than wild-type and *Flii*$^{Tg/Tg}$ counterparts at day 50 of the experiment. Similarly, the degree of TEWL was also significantly reduced in *Flii*$^{+/-}$ mice and very similar to that observed in control animals (**Figure 1C**). Control mice administered saline only showed no evidence of AD-like inflammation macroscopically or any development of erythema or TEWL (**Figures 1B–D**).

A hallmark of AD is skin thickening with a marked influx of leukocyte and mast cell inflammatory infiltrate. All OVA-induced AD-like skin sections showed evidence of AD compared to control saline exposed skin including a degree of epidermal hyperplasia and edema coupled with inflammatory lymphocytic and mast cell dermal infiltrate (**Figures 2A–C**). Examining the skin thickness in OVA-induced AD-like skin lesions revealed that deficient *Flii* mice had significantly thinner skin than OVA-induced AD-like skin lesions of wild-type and *Flii*$^{Tg/Tg}$ mice (**Figure 2A**). Assessment of lymphocytic and mast cell dermal infiltrate showed that *Flii* deficiency consistently resulted in significantly decreased inflammatory cell numbers (**Figures 2B,C**). In contrast, both normal and increased *Flii* gene expression resulted in thickened epidermis, increased numbers of inflammatory cells (**Figure 2B**) and mast cells (**Figure 2C**). Control mice skin exposed to saline only gauze patch showed no evidence of AD-like dermatitis features microscopically and had low levels of inflammatory infiltrate in the dermis (**Figures 2A–C**).

Anti-Inflammatory Cytokine mRNA Profiles Are Increased in OVA-Induced AD-Like Skin of *Flii*-Deficient Mice

OVA-induced AD-like skin lesions of *Flii*$^{+/-}$, wild-type, and *Flii*$^{Tg/Tg}$ mice were assessed for *Flii* and levels of cytokines and chemokines mediating the Th_1 and Th_2 inflammatory responses

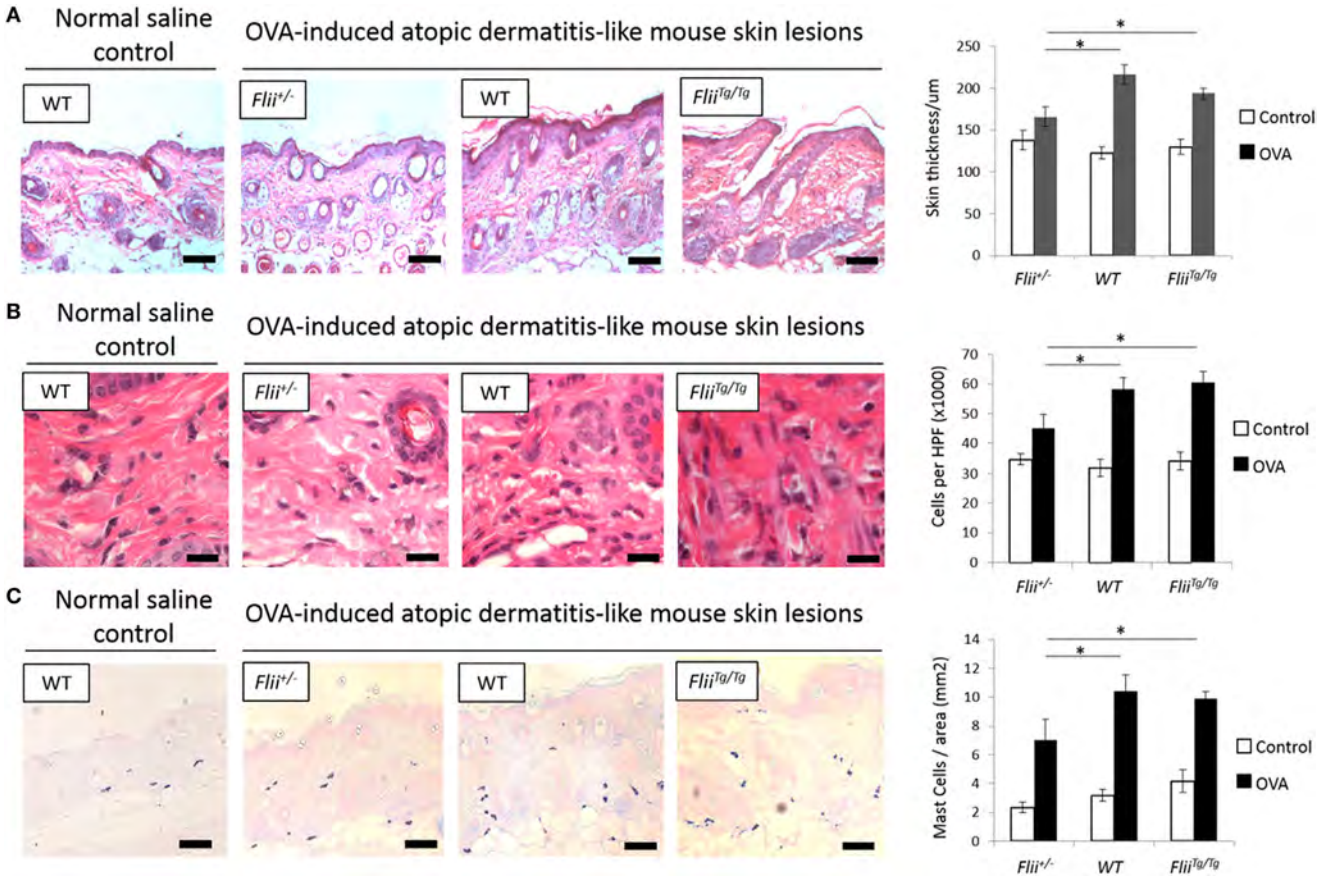

FIGURE 2 | Mice with reduced *Flii* expression develop less severe OVA-induced atopic dermatitis (AD) skin-like lesions and tissue inflammation. **(A)** Representative images and graphical analysis of skin thickness in *Flii*$^{+/-}$, WT, and *Flii*$^{Tg/Tg}$ mice with OVA-induced AD skin-like lesions illustrating evidence of epidermal hyperplasia, edema, and lymphocytic infiltrate. Magnification 4× scale bar 200 μm. **(B)** Representative images and graphical analysis of lymphocytic inflammatory infiltrate in in *Flii*$^{+/-}$, WT, and *Flii*$^{Tg/Tg}$ mice with OVA-induced AD skin-like lesions illustrating decreased inflammation in *Flii*$^{+/-}$ mice skin. Magnification 1,000× scale bar 25 μm. **(C)** Representative images and graphical analysis of mast cells numbers in *Flii*$^{+/-}$, WT, and *Flii*$^{Tg/Tg}$ mice with OVA-induced AD skin-like lesions illustrating decreased inflammation in *Flii*$^{+/-}$ mice skin. Magnification 4× scale bar 200 μm. $n = 8$. Mean ± SEM. *<0.05.

during AD pathogenesis. *Flii*-deficient mice showed approximately 25% decrease in *Flii* levels, while *Flii* over-expressing mice had a twofold increase in *Flii* levels compared to wild-type counterparts (**Figure 3**). *Flii* gene levels were found to affect number of key cytokines and chemokines responsible for development of AD-like lesions. Notably, main *Flii* deficiency favored a Th_1 immune response and decreased inflammation with significant threefold increase in IFN-γ mRNA levels compared to *Flii*$^{Tg/Tg}$ mice, decreased pro-inflammatory IL-4, and increased anti-inflammatory IL-10 mRNA levels compared to both wild-type and *Flii*$^{Tg/Tg}$ mice (**Figure 3**). Interestingly, *Flii*$^{+/-}$ OVA-induced AD-like skin lesions also showed increased IL-5 and IL-6 mRNA levels when compared to *Flii*$^{Tg/Tg}$ mice but not wild-type counterparts (**Figure 3**). In contrast, over-expression of *Flii* resulted in similar cytokine levels to wild-type counterparts, except significantly increased TNF-α mRNA expression and significantly reduced IFN-γ mRNA expression when compared to both *Flii*-deficient and wild-type mice, which would favor more severe AD manifestation. Cytokine mRNA levels of IL-13, IL-23, and IL-17A did not differ between OVA-induced AD-like skin lesions of three genotypes (**Figure 3**). Expression of CCL22 mRNA was significantly increased in OVA-induced AD-like skin lesions of *Flii*$^{Tg/Tg}$ mice compared to wild-type mice, while OVA-induced AD-like skin lesions of *Flii*$^{+/-}$ mice showed elevated CCL17 chemokine mRNA expression compared to *Flii*$^{Tg/Tg}$ mice (**Figure 4**). CXCL9 chemokine mRNA levels were found to be similar in all three genotypes (**Figure 4**). The unbalanced skewed ratio of Th1/Th2 response in *Flii*$^{Tg/Tg}$ mice was confirmed by immunohistochemical co-staining of T cell subset markers, namely Th1 (CD4 and T-bet), Th2 (CD4 and GATA-3), and Th17 (CD4 and ROR-γ) showing increased Th2 cell numbers in dermal area of *Flii*$^{Tg/Tg}$ mice (**Figures 5A–D**).

Flii$^{Tg/Tg}$ OVA-Induced AD-Like Disease Mice Have Altered Autoreactivity Profiles Compared With WT and *Flii*$^{-/-}$ Mice

To compare autoantibody formation in the OVA-induced AD-like disease model between *Flii*-deficient, wild-type, and *Flii*-overexpressing mice, serum samples collected at day 50

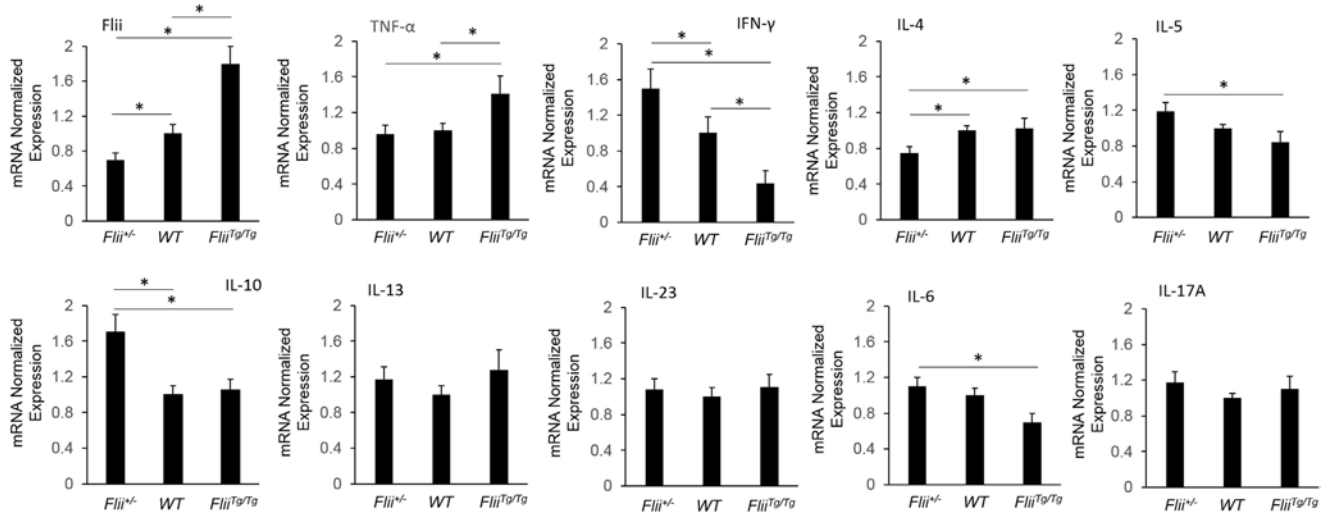

FIGURE 3 | OVA-induced atopic dermatitis (AD) skin-like lesions of *Flii*-deficient mice exhibit increased anti-inflammatory cytokine levels. mRNA levels of Flii, pro-inflammatory, and anti-inflammatory cytokines responsible for manifestation of AD were analyzed in the OVA-induced AD skin-like lesions of $Flii^{+/-}$, wild-type, and $Flii^{Tg/Tg}$ animals. OVA-induced AD skin-like lesions of *Flii*-deficient mice have significantly higher IFN-γ, reduced IL-4 signaling, and significantly higher levels of anti-inflammatory IL-10 while the *Flii* transgenic counterparts show significantly increased TNF-α and significantly reduced IFN-γ compared to wild-type animals. $n = 6$. Mean ± SEM. *<0.05.

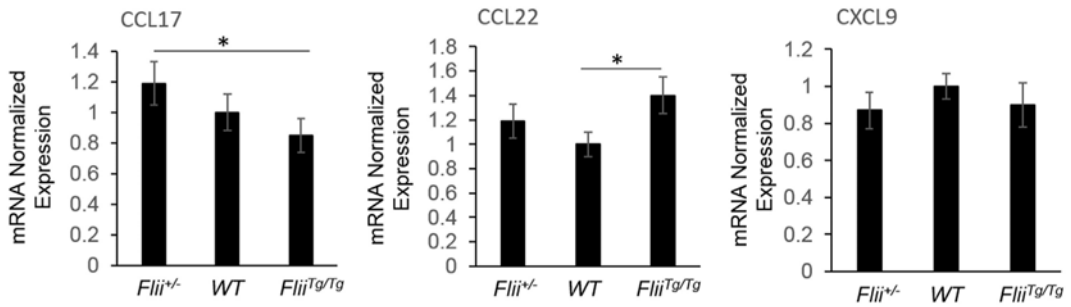

FIGURE 4 | *Flii* expression affects Th_2 chemokine levels in OVA-induced atopic dermatitis (AD) skin-like lesions. mRNA levels of CCL17, CCL22, and CXCL9 chemokines responsible for manifestation of AD were analyzed in the OVA-induced AD skin-like lesions of $Flii^{+/-}$, wild-type, and $Flii^{Tg/Tg}$ animals. OVA-induced AD skin-like lesions of $Flii^{+/-}$ mice have significantly higher levels of CCL17 compared to $Flii^{Tg/Tg}$ counterparts, while CCL22 was significantly increased in OVA-induced AD skin-like lesions of $Flii^{Tg/Tg}$ mice compared to wild-type controls. $n = 6$. Mean ± SEM. *<0.05.

were assessed by immunofluorescence and immunoblot analysis. Primary keratinocytes from wild-type mice were fixed and probed with pooled sera from experimental mice and staining patterns analyzed using fluorescence microscopy. Cytoplasmic and perinuclear staining within keratinocytes was apparent after incubation with sera from all three genotypes, however, only sera from OVA-induced AD-like disease $Flii^{Tg/Tg}$ mice produced strong nuclear staining patterns (**Figure 6A**). To further elucidate autoreactivity in these samples, keratinocyte whole-cell lysates were separated *via* SDS-PAGE, transferred to nitrocellulose membrane, and probed with pooled sera (**Figure 6B**). Additionally, autoreactivity patterns of individual mouse sera are shown in Figure S1 in Supplementary Material. Regions of differential autoreactivity were detected at 145, 70, 60, and 43 kDa band sizes (black arrows). Immunoblot analysis of sera (**Figure 6C**) from individual mice found that autoreactivity was highest in wild-type mice (50%) and $Flii^{Tg/Tg}$ mice (43%), while Flii-deficient ($Flii^{+/-}$) mice showed the lowest degree of autoreactivity (25%). Positive autoreactive bands at 70 kDa were also different in $Flii^{Tg/Tg}$ mice compared to the two other genotypes, which may be responsible for the nuclear staining pattern observed in immunofluorescence analysis. Immunoblot analysis of sera from normal non-dermatitis mice from each genotype were also analyzed; no autoreactivity was detected (Figure S2 in Supplementary Material).

DISCUSSION

Flii is a cytoskeletal protein with important roles in skin development, tight junction function, skin barrier establishment, and recovery post injury which is upregulated in response to tissue

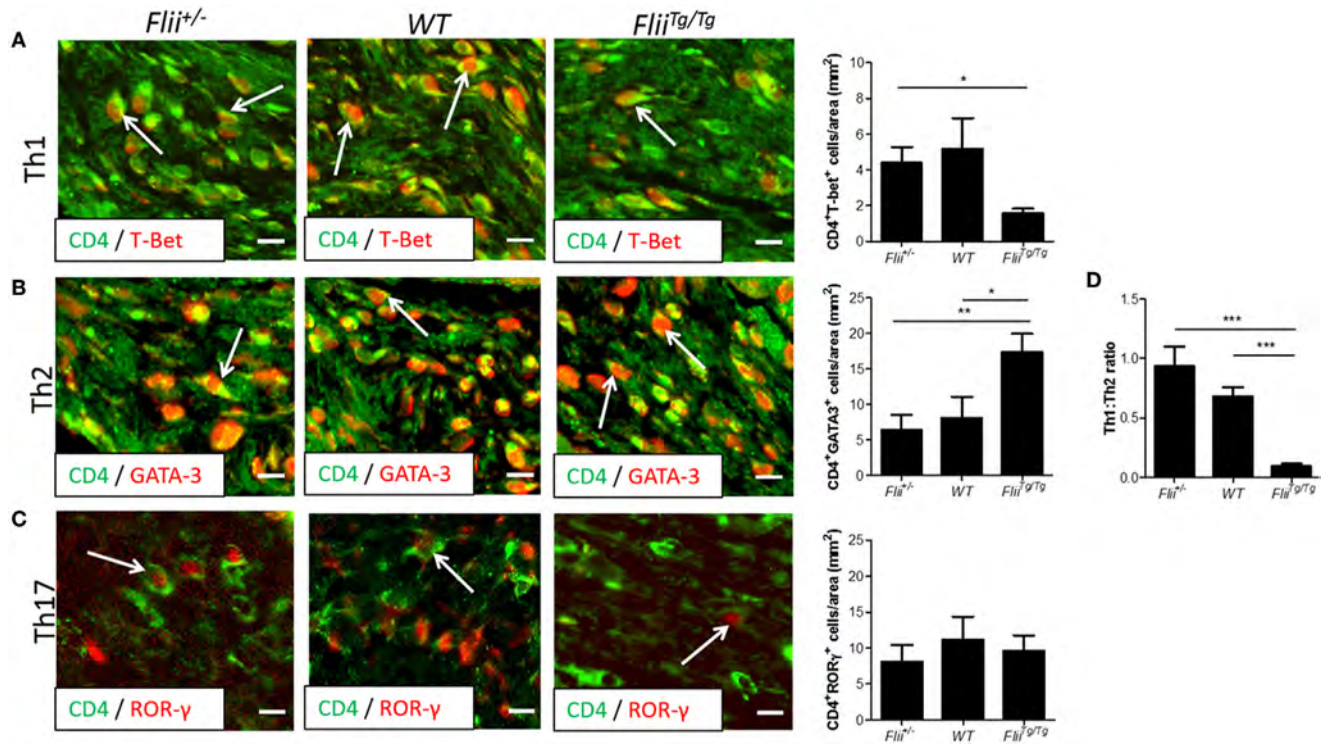

FIGURE 5 | Mice with increased Flii expression exhibit increased Th2 cell numbers within OVA-induced atopic dermatitis (AD) skin-like lesions. **(A)** Representative images and graphical analysis of Th1 ($CD4^+T\text{-}bet^+$) cell numbers in AD skin-like lesions within $Flii^{+/-}$, WT, and $Flii^{Tg/Tg}$ mice. **(B)** Representative images and graphical analysis of Th2 ($CD4^+GATA\text{-}3^+$) cell numbers in AD skin-like lesions within $Flii^{+/-}$, WT, and $Flii^{Tg/Tg}$ mice. **(C)** Representative images and graphical analysis of Th17 ($CD4^+ROR\gamma^+$) cell numbers in AD skin-like lesions within $Flii^{+/-}$, WT, and $Flii^{Tg/Tg}$ mice. **(D)** Ratio of Th1 to Th2 cells within AD skin-like lesions of $Flii^{+/-}$, WT, and $Flii^{Tg/Tg}$ mice. Magnification 4× scale bar 200 μm. $n = 6$. Mean ± SEM. *<0.05.

inflammation and wounding (22, 31). The secreted form of Flii has been shown to affect innate immune signaling pathways and modulate cell activity and cytokine secretion from fibroblasts and macrophages *in vitro* (17, 20). Recent studies have described the contribution of *Flii* over-expression in exacerbation of inflammatory conditions, including psoriasiform dermatitis (24) and an autoimmune inflammation-mediated epidermolysis bullosa acquisita (23, 32).

To determine if Flii affects AD development and severity, mice with low ($Flii^{+/-}$), normal ($Flii^{+/+}$), and high ($Flii^{Tg/Tg}$) expression of the *Flii* gene were exposed to repeated epicutaneous exposure to OVA and induced to form AD-like skin lesions. In contrast to our original hypothesis, *Flii* over-expression did not result in a more exacerbated development of erythema and AD-like skin lesions. However, reduced Flii levels in *Flii*-deficient mice led to significantly decreased development of AD-like skin lesions as marked by decreased erythema, TEWL, epidermal hyperplasia, and lymphocytic and mast cell tissue infiltrate compared to both wild-type and $Flii^{Tg/Tg}$ mice. Despite increased IFN-γ levels, the AD lesions of $Flii^{+/-}$ mice had reduced IL-4, which may contribute significantly to the reduced skin thickening in this model of AD (33). These findings are in agreement with studies which demonstrated that reducing Flii expression, either genetically or using Flii neutralizing antibodies, decreased tissue inflammation, and disease severity in mouse models of psoriasiform dermatitis and epidermolysis bullosa acquisita (23, 24, 32).

Genetically modified mice engineered to over-express Th_2 cytokines develop skin barrier defects and AD spontaneously (34). The formation of AD lesions is known to be triggered by production of Th_2 cytokines by mast cells and $CD4^+$ T cells which also promote IgE production by B cells, while Th_1 cells secrete IFN-γ to suppress proliferation of Th_2 cells and IgE synthesis (35, 36). The dominance of Th_2 cytokines in AD cause decreased expression of fillagrin and other barrier promoting molecules found in the skin (3). Examining the levels of cytokines and chemokines produced in AD-like lesional skin of $Flii^{+/-}$, wild-type, and $Flii^{Tg/Tg}$ mice revealed decreased IFN-γ levels in $Flii^{Tg/Tg}$ mice suggestive of Th_2 immune responses, while $Flii^{+/-}$ had increased IFN-γ levels and decreased clinical AD severity suggestive of potential Flii effect on IgE synthesis, however, this is yet to be investigated. Analysis of T-helper subsets within lesional skin showed a significantly Th_2 skewed response in OVA-induced AD-like lesions of $Flii^{Tg/Tg}$ mice with higher numbers of $CD4^+GATA3^+$ cells compared to AD-like lesions of $Flii^{+/-}$ or wild-type counterparts who showed significantly higher Th_1:Th_2 ratio. Additionally, AD-like lesions of $Flii^{Tg/Tg}$ mice showed increased pro-inflammatory TNF-α cytokine levels and while TNF-α has been demonstrated to promote the AD development (37) we did not observe increased

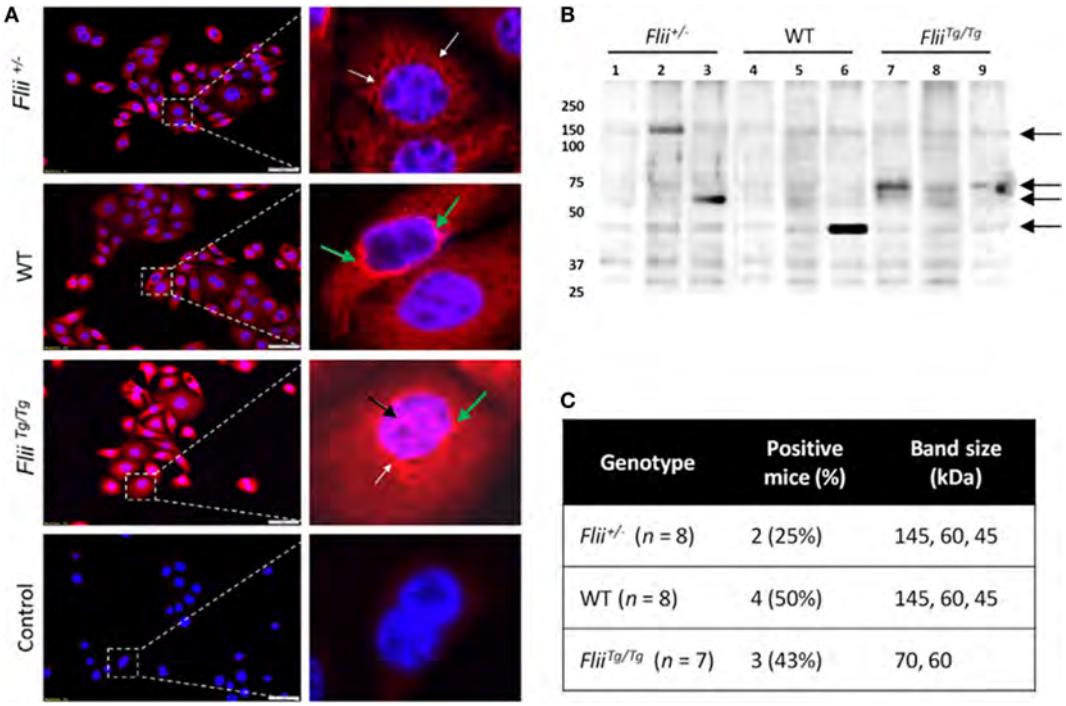

FIGURE 6 | Over-expression of *Flii* produces an altered autoantibody profile in murine OVA-induced atopic dermatitis (AD) skin-like disease. **(A)** Representative images of IF microscopy staining patterns produced by mouse autoreactive IgG (red) and DAPI nuclear counterstaining (blue) in primary mouse keratinocytes. Magnification 20×; scale bar 50 μm. Antibodies from OVA-induced AD skin-like lesions of *Flii*$^{+/-}$ and WT mice producing a predominantly cytoplasmic (white arrow) and perinuclear (green arrow) staining patterns, while antibodies from OVA-induced AD skin-like lesions of *Flii*$^{Tg/Tg}$ mice produce a strong cytoplasmic, perinuclear (green arrow), and nuclear (black arrow) staining patterns. **(B)** Western blot analysis of murine keratinocyte proteins probed with pooled sera from OVA-induced AD-like mice (2–3 mice per lane); black arrows represent regions of autoreactivity. **(C)** Autoreactivity summary of Western blot results from murine keratinocyte lysate probed with sera from individual mice.

AD severity in these mice in this model of OVA-induced AD. As mast cell numbers were not significantly increased in *Flii*$^{Tg/Tg}$ mice, and T-helper cells were heavily skewed toward a Th2 phenotype within *Flii*$^{Tg/Tg}$ lesions, excess TNF-α was likely produced by other cell types such as macrophages, which is further supported by increased CCL22 chemokine levels observed in *Flii*$^{Tg/Tg}$ mice. Interestingly, previous studies have shown that secreted Flii reduces macrophage secretion of TNF-α *in vitro* (20) while *in vivo* studies using a mouse model of psoriasiform dermatitis showed reduced TNF-α levels in response to reduced Flii (24) which was not observed in this model of OVA-induced AD. These findings may reflect inherent differences between *in vivo* and *in vitro* studies, for example differences in complex *in vivo*, multicellular environments, as well as differences in different models of inflammatory skin diseases.

In agreement with previous studies demonstrating decreased tissue inflammation and inflammatory cytokine secretion in *Flii*-deficient mice (24, 32), OVA-induced AD-like skin lesions of *Flii*$^{+/-}$ mice showed a reduced inflammatory response marked by significantly increased anti-inflammatory IL-10 secretion as well as significantly increased IFN-γ and significantly reduced IL-4 levels. Indeed, IL-4 has been shown to be essential for eosinophil recruitment, Th_2 cell differentiation, and IgE production (38). The increased CCL17 expression observed in AD lesions of *Flii*$^{+/-}$ mice compared to *Flii*$^{Tg/Tg}$ mice may be a potential mechanism to restore Th_1/Th_2 balance, as CCL17 has previously been shown to induce a Th_2-dominated inflammatory reaction (39). Reduction of *Flii* levels did not alter IL-23 and IL-17A cytokine levels as previously observed in psoriasiform dermatitis (24) suggesting that Th_{17} responses are not involved in this model of AD. Despite significant differences in IFN-γ levels between three genotypes, CXCL9 chemokine levels were not altered between genotypes in this model of AD. IL-13 levels were also not significantly different between three genotypes, however, there was a trend to higher levels in *Flii*$^{Tg/Tg}$ mice OVA-induced AD-like skin lesions and IL-13 cytokine has previously been linked to autoantibody production in early rheumatoid arthritis (40).

Autoimmunity has been increasingly recognized to play part in exacerbating the severity of AD (6, 9, 12) as a consequence of both humoral and cellular and immunity (6). It is postulated that IFN-γ signaling during AD pathogenesis may promote the development of autoimmunity as IFN-γ overexpressing mice spontaneously develop autoantibodies (41, 42) and deletion of the IFN-γ receptor inhibits autoantibody production in lupus-prone mice (43). On the basis of our findings showing altered AD severity and altered Th_1/Th_2 responses including significantly altered IFN-γ expression with different *Flii* genotypes, we examined the effect of Flii levels on autoimmunity in OVA-induced

AD-like skin lesions. The decreased severity of AD observed in *Flii*$^{+/-}$ mice also correlated with the reduced degree of autoreactivity (50% reduction vs WT), and further studies are required to investigate whether the autoantibodies from OVA induced AD-like skin mice contribute to or are a product of the observed AD-like symptoms. Immunoblot analysis of sera from normal non-dermatitis mice showed no autoreactivity suggesting that autoantibody development was disease-specific. Interestingly, both *Flii*$^{+/-}$ and wild-type mice showed similar autoantibody staining patterns and regions of differential autoreactivity. *Flii*$^{Tg/Tg}$ mice showed similar levels of autoreactivity compared to wild-type mice, however, in addition to the cytoplasmic and perinuclear staining pattern observed in all genotypes, the sera of these mice had a strong nuclear staining pattern. This pattern may indicate the presence of disease-mediating antinuclear antibodies which have been clinically associated with AD and other inflammatory skin disorders (44–46). Flii has previously been shown to affect TLR signaling pathways, both intracellularly and extracellularly, hence modulating innate inflammatory responses and directly impacting immune signaling, however, the potential role of Flii in autoimmunity has not been explored to date. Further studies are required to determine if autoreactivity in *Flii* genetic mice is a direct result of the impact of *Flii* on immune signaling or if it is secondary to increased pathology observed in these animals. In addition, determining the subtype of autoreactive immunoglobulins developed in the OVA-challenged murine model of AD would allow more comparison to be drawn to findings of previous clinical cohorts (10, 47).

While major differences between human AD and murine models have been demonstrated (47, 48), models of AD promote our understanding of the complex pathogenesis of human AD, and identify potential novel targets for design of targeted biologics (49). Here, we have demonstrated that Flii is a novel target in AD and that reducing its levels decreased the severity of AD in the ovalbumin-challenged murine model of AD. Additionally, we have examined the role of autoimmunity in this model of AD and while the exact mechanisms are yet to be identified, our results suggest that the effects of Flii upon Th_1/Th_2 balance and autoimmunity are important during AD pathogenesis.

ETHICS STATEMENT

Mice were maintained according to the Australian Code for the Care and Use of Animals for Scientific Purposes under protocols approved by the Child Youth and Women's Health Service Animal Ethics Committee (AEC916/06/2015).

AUTHOR CONTRIBUTIONS

AC and ZK conceived all the experiments with assistance from NS. ZK and NS carried out experiments and analysis with the assistance of HC and GY. ZK, NS, and AC wrote the manuscript and all authors contributed to the manuscript preparation and approved the final submitted and published versions.

ACKNOWLEDGMENTS

AC is supported by NHMRC Senior Research Fellowship (GNT#1102617) and ZK is supported by a Future Industries Institute Foundation Fellowship.

SUPPLEMENTARY MATERIAL

The Supplementary Material for this article can be found online at https://www.frontiersin.org/articles/10.3389/fimmu.2018.01833/full#supplementary-material.

TABLE S1 | Primer sequences used in real-time qPCR.

REFERENCES

1. Plotz SG, Wiesender M, Todorova A, Ring J. What is new in atopic dermatitis/eczema? *Expert Opin Emerg Drugs* (2014) 19(4):441–58. doi:10.1517/14728214.2014.953927
2. D'Auria E, Banderali G, Barberi S, Gualandri L, Pietra B, Riva E, et al. Atopic dermatitis: recent insight on pathogenesis and novel therapeutic target. *Asian Pac J Allergy Immunol* (2016) 34(2):98–108. doi:10.12932/AP0732.34.2.2016
3. Avena-Woods C. Overview of atopic dermatitis. *Am J Manag Care* (2017) 23 (8 Suppl):S115–23.
4. Homey B, Steinhoff M, Ruzicka T, Leung DY. Cytokines and chemokines orchestrate atopic skin inflammation. *J Allergy Clin Immunol* (2006) 118(1):178–89. doi:10.1016/j.jaci.2006.03.047
5. Cipriani F, Ricci G, Leoni MC, Capra L, Baviera G, Longo G, et al. Autoimmunity in atopic dermatitis: biomarker or simply epiphenomenon? *J Dermatol* (2014) 41(7):569–76. doi:10.1111/1346-8138.12464
6. Navarrete-Dechent C, Perez-Mateluna G, Silva-Valenzuela S, Vera-Kellet C, Borzutzky A. Humoral and cellular autoreactivity to epidermal proteins in atopic dermatitis. *Arch Immunol Ther Exp (Warsz)* (2016) 64(6):435–42. doi:10.1007/s00005-016-0400-3
7. Tang TS, Bieber T, Williams HC. Does "autoreactivity" play a role in atopic dermatitis? *J Allergy Clin Immunol* (2012) 129(5):1209–15e2. doi:10.1016/j.jaci.2012.02.002
8. Watanabe K, Muro Y, Sugiura K, Tomita Y. IgE and IgG(4) autoantibodies against DFS70/LEDGF in atopic dermatitis. *Autoimmunity* (2011) 44(6):511–9. doi:10.3109/08916934.2010.549157
9. Muro Y. Autoantibodies in atopic dermatitis. *J Dermatol Sci* (2001) 25(3):171–8. doi:10.1016/S0923-1811(01)00084-6
10. Watanabe K, Muro Y, Sugiura K, Akiyama M. High-avidity IgG autoantibodies against DFS70/LEDGF in atopic dermatitis. *J Clin Cell Immunol* (2013) 4:170. doi:10.4172/2155-9899.1000170
11. Ohkouchi K, Mizutani H, Tanaka M, Takahashi M, Nakashima K, Shimizu M. Anti-elongation factor-1alpha autoantibody in adult atopic dermatitis patients. *Int Immunol* (1999) 11(10):1635–40. doi:10.1093/intimm/11.10.1635
12. Mittermann I, Aichberger KJ, Bunder R, Mothes N, Renz H, Valenta R. Autoimmunity and atopic dermatitis. *Curr Opin Allergy Clin Immunol* (2004) 4(5):367–71. doi:10.1097/00130832-200410000-00007
13. Ochs RL, Mahler M, Basu A, Rios-Colon L, Sanchez TW, Andrade LE, et al. The significance of autoantibodies to DFS70/LEDGFp75 in health and disease: integrating basic science with clinical understanding. *Clin Exp Med* (2016) 16(3):273–93. doi:10.1007/s10238-015-0367-0
14. Silosi I, Silosi CA, Boldeanu MV, Cojocaru M, Biciusca V, Avramescu CS, et al. The role of autoantibodies in health and disease. *Rom J Morphol Embryol* (2016) 57(2 Suppl):633–8.
15. Chan H, Kopecki Z, Waters J, Powell BC, Arkell R, Cowin AJ. Cytoskeletal protein Flightless I differentially affects TGF-β isoform expression in both in vitro and in vivo wound models. *Wound Pract Res* (2014) 22(3):169–81.

16. Choi JS, Choi SS, Kim ES, Seo YK, Seo JK, Kim EK, et al. Flightless-1, a novel transcriptional modulator of PPARgamma through competing with RXRalpha. *Cell Signal* (2015) 27(3):614–20. doi:10.1016/j.cellsig.2014.11.035
17. Cowin AJ, Lei N, Franken L, Ruzehaji N, Offenhauser C, Kopecki Z, et al. Lysosmal secretion of Flightless I upon injury has the potential to alter inflammation. *Commun Integr Biol* (2012) 5(6):546–9. doi:10.4161/cib.21928
18. Ruzehaji N, Mills SJ, Melville E, Arkell R, Fitridge R, Cowin AJ. The influence of Flightless I on toll-like-receptor-mediated inflammation in a murine model of diabetic wound healing. *Biomed Res Int* (2013) 2013:389792. doi:10.1155/2013/389792
19. Wang T, Chuang TH, Ronni T, Gu S, Du YC, Cai H, et al. Flightless I homolog negatively modulates the TLR pathway. *J Immunol* (2006) 176(3):1355–62. doi:10.4049/jimmunol.176.3.1355
20. Lei N, Franken L, Ruzehaji N, Offenhauser C, Cowin AJ, Murray RZ. Flightless, secreted through a late endosome/lysosome pathway, binds LPS and dampens cytokine secretion. *J Cell Sci* (2012) 125(Pt 18):4288–96. doi:10.1242/jcs.099507
21. Kopecki Z, Yang GN, Jackson JE, Melville EL, Calley MP, Murrell DF, et al. Cytoskeletal protein Flightless I inhibits apoptosis, enhances tumor cell invasion and promotes cutaneous squamous cell carcinoma progression. *Oncotarget* (2015) 6(34):36426–40. doi:10.18632/oncotarget.5536
22. Kopecki Z, Yang GN, Arkell RM, Jackson JE, Melville E, Iwata H, et al. Flightless I over-expression impairs skin barrier development, function and recovery following skin blistering. *J Pathol* (2014) 232(5):541–52. doi:10.1002/path.4323
23. Kopecki Z, Arkell RM, Strudwick XL, Hirose M, Ludwig RJ, Kern JS, et al. Overexpression of the Flii gene increases dermal-epidermal blistering in an autoimmune ColVII mouse model of epidermolysis bullosa acquisita. *J Pathol* (2011) 225(3):401–13. doi:10.1002/path.2973
24. Chong HT, Yang GN, Sidhu S, Ibbetson J, Kopecki Z, Cowin AJ. Reducing Flightless I expression decreases severity of psoriasis in an imiquimod-induced murine model of psoriasiform dermatitis. *Br J Dermatol* (2017) 176(3):705–12. doi:10.1111/bjd.14842
25. Wang G, Savinko T, Wolff H, Dieu-Nosjean MC, Kemeny L, Homey B, et al. Repeated epicutaneous exposures to ovalbumin progressively induce atopic dermatitis-like skin lesions in mice. *Clin Exp Allergy* (2007) 37(1):151–61. doi:10.1111/j.1365-2222.2006.02621.x
26. Campbell HD, Fountain S, McLennan IS, Berven LA, Crouch MF, Davy DA, et al. Fliih, a gelsolin-related cytoskeletal regulator essential for early mammalian embryonic development. *Mol Cell Biol* (2002) 22(10):3518–26. doi:10.1128/MCB.22.10.3518-3526.2002
27. Cowin AJ, Adams DH, Strudwick XL, Chan H, Hooper JA, Sander GR, et al. Flightless I deficiency enhances wound repair by increasing cell migration and proliferation. *J Pathol* (2007) 211(5):572–81. doi:10.1002/path.2143
28. Kajisa T, Yamaguchi T, Hu A, Suetake N, Kobayashi H. Hydrogen water ameliorates the severity of atopic dermatitis-like lesions and decreases interleukin-1beta, interleukin-33, and mast cell infiltration in NC/Nga mice. *Saudi Med J* (2017) 38(9):928–33. doi:10.15537/smj.2017.9.20807
29. Ochs RL, Muro Y, Si Y, Ge H, Chan EK, Tan EM. Autoantibodies to DFS 70 kd/transcription coactivator p75 in atopic dermatitis and other conditions. *J Allergy Clin Immunol* (2000) 105(6 Pt 1):1211–20. doi:10.1067/mai.2000.107039
30. Kopecki Z, Arkell R, Powell BC, Cowin AJ. Flightless I regulates hemidesmosome formation and integrin-mediated cellular adhesion and migration during wound repair. *J Invest Dermatol* (2009) 129(8):2031–45. doi:10.1038/jid.2008.461
31. Kopecki Z, Cowin AJ. Flightless I: an actin-remodelling protein and an important negative regulator of wound repair. *Int J Biochem Cell Biol* (2008) 40(8):1415–9. doi:10.1016/j.biocel.2007.04.011
32. Kopecki Z, Ruzehaji N, Turner C, Iwata H, Ludwig RJ, Zillikens D, et al. Topically applied Flightless I neutralizing antibodies improve healing of blistered skin in a murine model of epidermolysis bullosa acquisita. *J Invest Dermatol* (2012) 133(4):1008–16. doi:10.1038/jid.2012.457
33. Matsunaga MC, Yamauchi PS. IL-4 and IL-13 inhibition in atopic dermatitis. *J Drugs Dermatol* (2016) 15(8):925–9.
34. Vestergaard C, Yoneyama H, Murai M, Nakamura K, Tamaki K, Terashima Y, et al. Overproduction of Th2-specific chemokines in NC/Nga mice exhibiting atopic dermatitis-like lesions. *J Clin Invest* (1999) 104(8):1097–105. doi:10.1172/JCI7613
35. Matsuda H, Watanabe N, Geba GP, Sperl J, Tsudzuki M, Hiroi J, et al. Development of atopic dermatitis-like skin lesion with IgE hyperproduction in NC/Nga mice. *Int Immunol* (1997) 9(3):461–6. doi:10.1093/intimm/9.3.461
36. Yamanaka K, Mizutani H. The role of cytokines/chemokines in the pathogenesis of atopic dermatitis. *Curr Probl Dermatol* (2011) 41:80–92. doi:10.1159/000323299
37. Danso MO, van Drongelen V, Mulder A, van Esch J, Scott H, van Smeden J, et al. TNF-alpha and Th2 cytokines induce atopic dermatitis-like features on epidermal differentiation proteins and stratum corneum lipids in human skin equivalents. *J Invest Dermatol* (2014) 134(7):1941–50. doi:10.1038/jid.2014.83
38. Nedoszytko B, Sokolowska-Wojdylo M, Ruckemann-Dziurdzinska K, Roszkiewicz J, Nowicki RJ. Chemokines and cytokines network in the pathogenesis of the inflammatory skin diseases: atopic dermatitis, psoriasis and skin mastocytosis. *Postepy Dermatol Alergol* (2014) 31(2):84–91. doi:10.5114/pdia.2014.40920
39. Vestergaard C, Deleuran M, Gesser B, Larsen CG. Thymus- and activation-regulated chemokine (TARC/CCL17) induces a Th2-dominated inflammatory reaction on intradermal injection in mice. *Exp Dermatol* (2004) 13(4):265–71. doi:10.1111/j.0906-6705.2004.00149.x
40. Silosi I, Boldeanu MV, Cojocaru M, Biciusca V, Padureanu V, Bogdan M, et al. The relationship of cytokines IL-13 and IL-17 with autoantibodies profile in early rheumatoid arthritis. *J Immunol Res* (2016) 2016:3109135. doi:10.1155/2016/3109135
41. Seery JP. IFN-gamma transgenic mice: clues to the pathogenesis of systemic lupus erythematosus? *Arthritis Res* (2000) 2(6):437–40. doi:10.1186/ar124
42. Watt FM. Transgenic mice expressing IFN-gamma in the epidermis are a model of inflammatory skin disease and systemic lupus erythematosus. *Ernst Schering Res Found Workshop* (2005) (50):277–91. doi:10.1007/3-540-26811-1_16
43. Haas C, Ryffel B, Le Hir M. IFN-gamma receptor deletion prevents autoantibody production and glomerulonephritis in lupus-prone (NZB x NZW)F1 mice. *J Immunol* (1998) 160(8):3713–8.
44. Higashi N, Niimi Y, Aoki M, Kawana S. Clinical features of antinuclear antibody-positive patients with atopic dermatitis. *J Nippon Med Sch* (2009) 76(6):300–7. doi:10.1272/jnms.76.300
45. Wozniacka A, Salamon M, McCauliffe D, Sysa-Jedrzejowska A. Antinuclear antibodies in rosacea patients. *Postepy Dermatol Alergol* (2013) 30(1):1–5. doi:10.5114/pdia.2013.33372
46. Silvy F, Bertin D, Bardin N, Auger I, Guzian MC, Mattei JP, et al. Antinuclear antibodies in patients with psoriatic arthritis treated or not with biologics. *PLoS One* (2015) 10(7):e0134218. doi:10.1371/journal.pone.0134218
47. Ewald DA, Noda S, Oliva M, Litman T, Nakajima S, Li X, et al. Major differences between human atopic dermatitis and murine models, as determined by using global transcriptomic profiling. *J Allergy Clin Immunol* (2017) 139(2):562–71. doi:10.1016/j.jaci.2016.08.029
48. Martel BC, Lovato P, Baumer W, Olivry T. Translational animal models of atopic dermatitis for preclinical studies. *Yale J Biol Med* (2017) 90(3):389–402.
49. Kabashima K, Nomura T. Revisiting murine models for atopic dermatitis and psoriasis with multipolar cytokine axes. *Curr Opin Immunol* (2017) 48:99–107. doi:10.1016/j.coi.2017.08.010

Conflict of Interest Statement: IP associated with this project has been filed by AbRegen Pty Ltd., of which AC is a shareholder and both AC and ZK are named inventors on associated patents.

The handling Editor declared a past co-authorship with one of the authors AC.

frontiers in Immunology

ORIGINAL RESEARCH
published: 02 August 2018
doi: 10.3389/fimmu.2018.01788

The p.Arg435His Variation of IgG3 With High Affinity to FcRn Is Associated With Susceptibility for Pemphigus Vulgaris—Analysis of Four Different Ethnic Cohorts

Andreas Recke[1,2], Sarah Konitzer[1], Susanne Lemcke[1], Miriam Freitag[1], Nele Maxi Sommer[1], Mohammad Abdelhady[3], Mahsa M. Amoli[4], Sandrine Benoit[5], Farha El-Chennawy[6], Mohammad Eldarouti[3], Rüdiger Eming[7], Regine Gläser[8], Claudia Günther[9], Eva Hadaschik[10], Bernhard Homey[11], Wolfgang Lieb[12,13], Wiebke K. Peitsch[14,15], Claudia Pföhler[16], Reza M. Robati[17], Marjan Saeedi[17], Miklós Sárdy[18], Michael Sticherling[19], Soner Uzun[20], Margitta Worm[21], Detlef Zillikens[2], Saleh Ibrahim[1], Gestur Vidarsson[22], Enno Schmidt[1]* and the German AIBD Genetic Study Group[†]*

[1] Lübeck Institute of Experimental Dermatology (LIED), University of Lübeck, Lübeck, Germany, [2] Department of Dermatology, Allergology and Venereology, University of Lübeck, Lübeck, Germany, [3] Department of Dermatology, Faculty of Medicine, Cairo University, Giza, Egypt, [4] Metabolic Disorders Research Center, Endocrinology and Metabolism Molecular – Cellular Sciences Institute, Tehran University of Medical Sciences, Tehran, Iran, [5] Department of Dermatology, Venereology and Allergology, University Hospital Würzburg, Würzburg, Germany, [6] Department of Clinical Pathology, Mansoura Faculty of Medicine, Mansoura University, Mansoura, Egypt, [7] Department of Dermatology and Allergology, Phillips-Universität Marburg, Marburg, Germany, [8] Department of Dermatology, Venereology and Allergology, Christian Albrecht University, Kiel, Germany, [9] Department of Dermatology, University Hospital of Dresden, Dresden, Germany, [10] Department of Dermatology, Ruprecht-Karls-University of Heidelberg, Heidelberg, Germany, [11] Department of Dermatology, Heinrich Heine University, Düsseldorf, Germany, [12] Institute of Epidemiology, Christian-Albrechts-University, Kiel, Germany, [13] Popgen Biobank, Christian-Albrechts-University, Kiel, Germany, [14] Department of Dermatology, University Medical Center Mannheim, Heidelberg University, Mannheim, Germany, [15] Department of Dermatology, Vivantes Klinikum im Friedrichshain, Berlin, Germany, [16] Department of Dermatology, Saarland University Medical School, Homburg/Saar, Germany, [17] Skin Research Center, Shahid Beheshti University of Medical Sciences, Tehran, Iran, [18] Department of Dermatology, Ludwig Maximilian University Munich, Munich, Germany, [19] Department of Dermatology, University of Erlangen-Nuremberg, Erlangen, Germany, [20] Department of Dermatology, Faculty of Medicine, Akdeniz University, Antalya, Turkey, [21] Department of Dermatology, Venerology and Allergology, Allergy Center Charité, Charité-Medical University Berlin, Berlin, Germany, [22] Department of Experimental Hematology, Sanquin Research Institute, Amsterdam, Netherlands

IgG3 is the IgG subclass with the strongest effector functions among all four IgG subclasses and the highest degree of allelic variability among all constant immunoglobulin genes. Due to its genetic position, IgG3 is often the first isotype an antibody switches to before IgG1 or IgG4. Compared with the other IgG subclasses, it has a reduced half-life which is probably connected to a decreased affinity to the neonatal Fc receptor (FcRn). However, a few allelic variants harbor an amino acid replacement of His435 to Arg that reverts the half-life of the resulting IgG3 to the same level as the other IgG subclasses. Because of its functional impact, we hypothesized that the p.Arg435His variation could be associated with susceptibility to autoantibody-mediated diseases like pemphigus vulgaris (PV) and bullous pemphigoid (BP). Using a set of samples from German, Turkish, Egyptian, and Iranian patients and controls, we were able to demonstrate a genetic association of the p.Arg435His variation with PV risk, but not with BP risk. Our results suggest a hitherto unknown role for the function of IgG3 in the pathogenesis of PV.

Keywords: immunology, dermatology, autoantibodies, allotype, pemphigus, pemphigoid, half-life, functional genetics

OPEN ACCESS

Edited by:
Antony Basten, Garvan Institute of Medical Research, Australia

Reviewed by:
Paul Anthony Gleeson, University of Melbourne, Australia
Derry Charles Roopenian, Jackson Laboratory, United States

****Correspondence:***
Andreas Recke
andreas.recke@uksh.de;
Enno Schmidt
enno.schmidt@uksh.de

[†]A complete list of the members of German AIBD Genetic Study Group appears in the "The German AIBD Genetic Study group members."

Specialty section:
This article was submitted to Immunological Tolerance and Regulation, a section of the journal Frontiers in Immunology

Received: *28 February 2018*
Accepted: *19 July 2018*
Published: *02 August 2018*

Citation:
Recke A, Konitzer S, Lemcke S, Freitag M, Sommer NM, Abdelhady M, Amoli MM, Benoit S, El-Chennawy F, Eldarouti M, Eming R, Gläser R, Günther C, Hadaschik E, Homey B, Lieb W, Peitsch WK, Pföhler C, Robati RM, Saeedi M, Sárdy M, Sticherling M, Uzun S, Worm M, Zillikens D, Ibrahim S, Vidarsson G, Schmidt E and the German AIBD Genetic Study Group (2018) The p.Arg435His Variation of IgG3 With High Affinity to FcRn Is Associated With Susceptibility for Pemphigus Vulgaris—Analysis of Four Different Ethnic Cohorts. Front. Immunol. 9:1788. doi: 10.3389/fimmu.2018.01788

INTRODUCTION

Of the four human IgG subclasses, IgG3 (gene IGHG3) exhibits the strongest capabilities to activate complement and effector cells of the innate immune system (1). Compared with the other IgG subclasses, IgG3 has a reduced half-life which is probably caused by a decreased affinity to FcRn (2). FcRn is involved in IgG transport across mucosal cells and the placenta. Moreover, FcRn is responsible for the exceptionally long half-life of IgG, and it rescues IgG from lysosomal degradation by recycling it back to the surface in endothelial cells. It further appears to be involved in IgG-mediated phagocytosis (3). The reduced half-life of IgG3 appears to be caused by an amino acid replacement at residue 435, where this IgG subclass typically carries an arginine instead of a histidine like the other IgG subclasses. From the 19 different alleles that the IMGT (ImMunoGeneTics information) database[1] lists for IGHG3, 3 alleles contain a histidine instead of an arginine at this position (IgG3:p.Arg435His variation, NG_001019.5:g.1053927G>A, RefSNP rs4042056, **Figure 1**). These three alleles are associated with the G3m15 and G3m16 allotypes which are quite rare in the European population and more frequent in Asia and Africa (4). The histidine residue at position 435 leads to a higher affinity of IgG3 to FcRn and, consequently, to a prolonged half-life and most likely to an increased bioavailability in extravascular tissues (2).

Immunoglobulin allotypes represent serological features of genetic variations within the constant domains. Gm–Am allotypes are inherited as fixed combination, also termed Gm–Am haplotypes (5). They have been associated with various autoimmune diseases and different immune responses to bacterial infections (6). Of note, an association with immunoglobulin kappa light chain allotypes (Km allotypes) has been described for bullous pemphigoid (BP) but not for pemphigus vulgaris (PV) (7). However, the underlying mechanisms remain unexplained. Genetic polymorphisms with functional impact like the p.Arg435His variation of IgG3 might affect the etiology and pathogenesis of associated diseases, including autoantibody-mediated diseases. Therefore, this study was conducted to elucidate a possible association of the p.Arg435His variation with PV. PV is a severe autoimmune blistering disorder of the skin and surface-close mucous membranes, characterized by autoantibodies against desmosomal proteins of the epidermis and epithelia of mucosal membranes: desmoglein 3 and, in the mucocutaneous variant of PV, also desmoglein 1. IgG1 and IgG4, the most frequent IgG subclasses, have been demonstrated to cause acantholysis (8, 9). IgG3, however, is often the first IgG subclass that appears immediately after the B cell switch from IgM (10). IgG anti-Dsg3 autoantibodies lead to steric hindrance in desmoglein interaction, altered cellular signaling, and aberrant cellular distribution of desmogleins resulting in acantholysis, the formation of flaccid blisters and erosions (11, 12). The events that lead to the irregular production of autoantibodies are largely unknown. While PV is known to be strongly associated with certain HLA alleles, such as DRB1*0402 and DQB1*0503, we have recently described an association with the first non-HLA gene, ST18, in PV patients from Egypt and Israel, but not from Germany (13, 14). Moreover, PV susceptibility was found to be

[1]http://www.imgt.org (Accessed: 25 January, 2017).

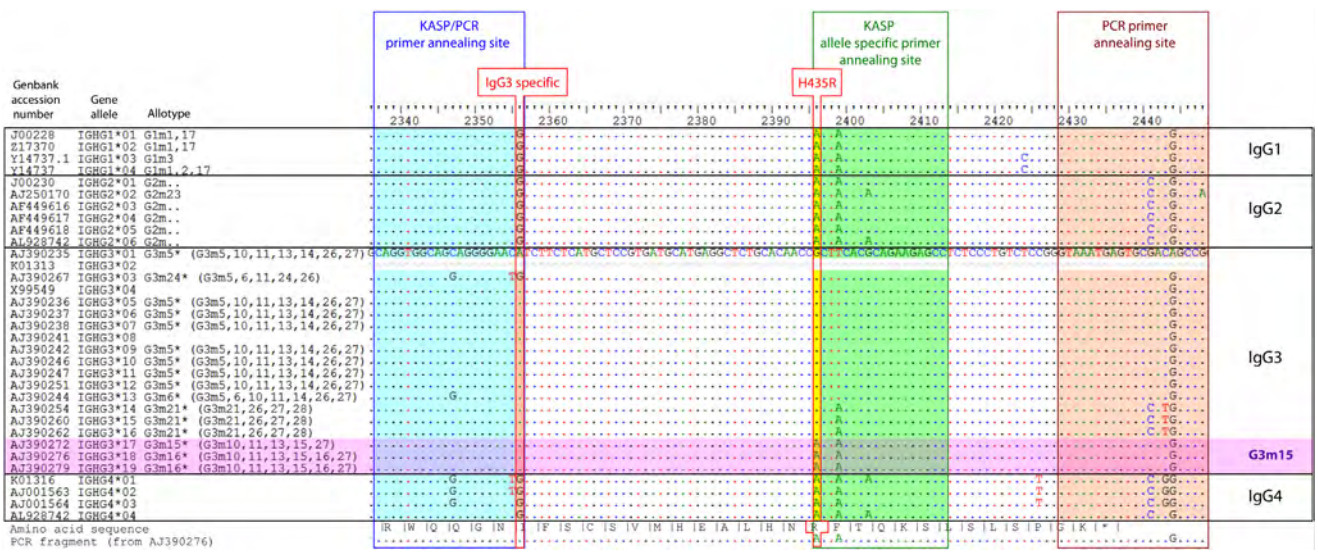

FIGURE 1 | Alignment of human IgG gene alleles. Alignment of all human IgG alleles listed in IMGT [http://www.imgt.org (Accessed: 15 March, 2015)], including GenBank accession number, gene names, isotype, allele numbering, and allotype numbering. Primer annealing sites for KASP and IgG3-specific PCR are shaded in blue, green, and red, respectively. Nucleotides unique in IgG3 (IgG3 specific) and the g.1053927G>A variation (p.Arg435His) are indicated with a red border. The full DNA sequence is shown for the reference sequence (AJ390235), for all other sequences, all bases except those that differ from the reference are masked by a dot. The amino acid sequence of the reference sequence is shown on the bottom site, together with the PCR fragment amplified for Sanger sequencing. The IGHG3 alleles that contain the g.1053927G>A variation are highlighted in pink (G3m15). A marker for DNA positions within the alignment set is given on the top scale.

associated with certain polymorphisms of FcγRIIb and FcγRIIc, indicating a role of peripheral tolerance in this disease (15). Here, we followed up on the idea of non-HLA susceptibility genes in pemphigus and investigated a possible association with the functionally important p.Arg435His variation of IgG3.

MATERIALS AND METHODS

Description of Cohorts

Samples and controls were stored and analyzed in the order in which they were collected, irrespective of age and gender. The inclusion criteria for PV and BP followed the recent guidelines of the German Society of Dermatology and European Academy of Dermatology and Venereology (16–18). In brief, PV was diagnosed based on the clinical picture with flaccid blisters and/or erosions on the skin and/or surface-close mucous membranes, intercellular IgG and/or C3 deposition in the epidermis/epithelia by direct immunofluorescence and/or detection of circulating anti-desmoglein 3 autoantibodies. In BP, diagnosis was made in patients with compatible clinical picture, i.e., tense blisters, erosions, prurigo-type lesions, and urticarial or eczematous lesions (19), deposition of IgG and/or C3 at the dermal–epidermal junction by direct immunofluorescence microscopy, and/or detection of serum BP180 NC16A IgG. The respective diagnosis was re-evaluated in the Department of Dermatology, Lübeck, Germany. Normal healthy controls were defined not to match any of the above criteria.

Allotype-Specific ELISA

The G3m15 allotype was detected with a sandwich ELISA using the same single chain Fv (scFv) for capture and detection, as described (2). Briefly, microtiter plates (Nalge Nunc International, Rochester, NY, USA) were coated with anti-hIgG3 G3m15 scFv [1.5A10 anti G3m(s,t)] at 5 µg/ml in carbonate buffer, pH 9.6. After washing with phosphate-buffered saline (PBS)/0.05% Tween-20 (PBST), plates were blocked with 1% biotin-free BSA (Carl Roth GmbH, Karlsruhe, Germany) in PBST (1% BSA in PBST). After washing, serum samples and the positive control G3m15 diluted in 1% BSA in PBST were loaded onto the plates and incubated for 2 h. For detection, plates were incubated with biotin-conjugated anti-hIgG3 G3m15 scFv, diluted at 5 µg/ml in 1% BSA in PBST, followed by peroxidase-conjugated streptavidin (Dako Deutschland GmbH, Hamburg, Germany) diluted 1:2,000 in 1% BSA in PBST. For colorimetric detection, plates were developed using TurboTMB (Perbio Science Deutschland GmbH, Bonn, Germany) and stopped with 1 M H_2SO_4 solution. OD values were measured at 450 nm using a VICTOR 3™ reader (PerkinElmer Inc., Waltham, MA, USA).

Determination of the rs4042056 Genotype by KASP Assay

The genotype of the rs4042056 was determined with the KASP method (LGC Genomics GmbH, Berlin, Germany), using a customized assay on a realplex[2] Mastercycler (Eppendorf AG, Hamburg, Germany), followed by fluorescence end-point reading with an Applied Biosystems 7800 Real-Time PCR system (Life Technologies GmbH, Darmstadt, Germany). For each sample, 10 ng of genomic DNA was used and mixed with KASP reagents according to the manufacturer. The KASP assay contained the allele-specific HEX-conjugated primer 5′-ggc tct tct gcg tga agc-3′, the FAM-conjugated primer 5′-ggc tct tct gcg tga agt-3′, and the common primer 5′-cag gtg gca gca ggg gaa ca-3′.

Amplification of the rs4042056 Flanking Sequence

The gene sequence flanking the rs4042056 in the human IgG3 gene was amplified by PCR using the forward primer 5′-cag gtg gca gca ggg gaa ca-3′ and the reverse primer 5′-cgg ccg tcg cac tca ttt ac-3′, resulting in a 112 bp product (Figure S1 in Supplementary Material). After agarose gel purification with the QIAquick Gel Extraction Kit (Qiagen, Hilden, Germany), this product was subjected to Sanger sequencing at Eurofins Genomics, Ebersberg, Germany, using the same primers. For PCR, HotStart Phusion polymerase (Life Technologies GmbH, Darmstadt, Germany) was used with Phusion HiFidelity buffer, 1% DMSO and 10 pmol of each primer. PCR program: 98°C for 30 s; 10 cycles of 98°C for 5 s, 75°C (−1.0°C/cycle) for 20 s, 72°C 10 s; 25 cycles of 98°C for 5 s, 65°C for 20 s, 72°C 10 s; final elongation for 5 min at 72°C.

Statistical Analysis

The open-source software GNU R version 3.15[2] was used for statistical analysis, together with the package *lme4* for generalized linear mixed effects regression of co-dominant, recessive and dominant genetic effects, including stratification by ethnic cohort. For cohort-wise analyses, Lidstone additive smoothing was applied by addition of a pseudocount of $\alpha = 0.5$.

For combined analyses of serum and DNA samples, the generalized linear mixed effects regression was extended by using both sample type and ethnic cohort as stratification factors.

For comparison of genotyping results between different methods, Cohen's weighted kappa was calculated using the function *cohen.kappa* in package *psych*. Hardy–Weinberg equilibrium was checked with the function *HWAlltests* from the R package *HardyWeinberg*.

To compare genotype frequencies determined in sera or DNA samples, we used a logistic regression with the risk allotype/allele as response variable and sample type (or genotyping method), ethnic origin and disease state (PV vs. healthy control) as covariates, including all two- and three-way interactions. For calculation of likelihood-ratio test *p* values, the function *Anova* from R package *car* was applied.

RESULTS

We collected genomic DNA or serum samples from 516 PV patients and 555 population-matched healthy controls from Germany ($n = 137$ patients, $n = 259$ controls), Iran ($n = 78$ patients, $n = 90$ controls), Turkey ($n = 148$ patients, $n = 19$ controls), and Egypt ($n = 153$ patients, 197 controls) (**Table 1**). Furthermore, DNA or serum from 173 German patients with

[2]http://www.R-project.org/ (Accessed: 27 February, 2018).

BP, another autoimmune blistering skin disease associated with autoantibodies against BP180 (collagen type XVII), was analyzed (**Table 2**) (20). Separate cohorts were applied for serum and DNA samples.

Designing a PCR-based genotyping method for processing large sample numbers turned out to be challenging. The primer combination had to be specific for the IgG3 subclass and at the same time, should amplify most of the known allotypes and differentiate between the two allelic variants of the rs4042056 SNP (minor allele: g.1053927G>A, **Figure 1**). For this purpose, the *Kompetitive Allele-Specific PCR* method (KASP™) appeared to be appropriate. The selectivity for the IgG3 gene is provided by a 3′ base (G/A) mismatch of the common primer with the sequence of IgG1, IgG2, and IgG4 gene. This mismatch also suppresses amplification in case of the IGHG3*03 allele [rs79545032, g.105769317A>G, minor allele frequency (MAF) 4% in and 16% in African populations (21)], but 17 of the 19 IgG3 gene alleles listed in the IMGT database were matching the primer sequence sufficiently. To verify the results of the KASP assay we amplified the region flanking the g.1053927G>A variation in the IgG3 gene by PCR in a small number of samples representing the different genotypes. The genotype of this SNP was determined using Sanger sequencing (Figure S1 in Supplementary Material). The comparison showed that both methods were correlating well [Table S1 in Supplementary Material, Cohen's weighted kappa = 0.62 (95% CI: 0.39–0.85), Fisher's exact test $p = 0.0054$]. Furthermore, we used a fully saturated logistic regression model to evaluate the dependency of genotype frequencies on disease status, genotyping method, ethnic origin and all possible interactions between those. The likelihood ratio test revealed that only disease status ($p = 0.002$) and ethnic origin ($p = 0.0095$) show a significant influence on the genotype frequency, while the genotyping method—and any interaction of genotyping method with the other covariates—did not have an effect. This confirms that both genotyping methods are equivalent, and it indicates the frequency of the p.Arg435His variation is more common in MENA countries.

For serum samples ($n = 177$ patients, $n = 136$), we used a sandwich ELISA to serologically determine the G3m15 allotype that is described to be linked to the p.Arg435His variation (2) (**Table 1**). The MAF estimation for the p.Arg435His variation did not differ significantly between the results from the KASP assay (3.3% in cases and 0.5% in controls) and the ELISA (2% in cases and 1.1% in controls). Moreover, the frequencies of the G3m15 allotype and the p.Arg435His variation were different in cases and controls especially in the Egyptian and the Turkish populations. The distribution of genotypes was not in Hardy–Weinberg equilibrium for all cohorts of PV cases and in the Iranian cohort of controls.

To test if our finding for p.Arg435His variation in PV was a general phenomenon for all autoimmune blistering diseases (20) a cohort of $n = 173$ German patients with BP was used. In this cohort of BP patients, no significant association of disease risk with the p.Arg435His or the G3m15 allotype was observed (**Table 2**). The genotype distribution of BP cases had no Hardy-Weinberg equilibrium.

DISCUSSION

Allotypic variation has been associated with various autoimmune diseases including autoimmune blistering skin diseases (6, 7). However, the functional role of allotypic variation is mostly unknown with the exception of the p.Arg435His variation which has been demonstrated to affect the half-life of IgG3 (2). We hypothesized that such a functionally relevant variation should be important for the susceptibility of autoantibody-mediated diseases like PV and BP.

High-throughput genotyping of the p.Arg435His variation is hampered by a high variability of the target gene region on the one hand, and a high degree of homology between IgG3 and the other three IgG subclass genes. We were able to design a genotyping method based on KASP technology, but this method did not discriminate heterozygotes from homozygotes. To check the results of this method in a subset of samples representing all detectable genotypes, we used PCR amplification and Sanger sequencing which overall confirmed the validity of the KASP assay. Using the KASP assay, we could demonstrate an association between the p.Arg435His variation and PV in the combined analyses of all ethnic groups, and within the group of German patients. Analysis within the other ethnic groups showed no significant association. This is most probably related to smaller cohort sizes, compared with the German one, because the odds ratio ranged between 1 and 3 in all ethnic cohorts.

As a secondary method for genotyping, we used an ELISA method that detects an amino acid variation which is, according to IMGT databases, linked to the p.Arg435His variation. Using this method alone, we could not find any association with PV disease, which might be explained by the overall lower number of available serum samples in the cohort. However, combining ELISA with KASP genotyping data, using genotyping method and ethnic origin for stratification in a mixed effects logistic regression analysis, reaffirmed the results gained by KASP assay alone. Furthermore, the genotype frequencies of cohorts did not differ significantly between the genotyping methods. Therefore, our results confirm that both genotyping by KASP assay and ELISA lead to equivalent results.

The IgG subclass of autoantibodies in PV is most frequently IgG4, followed by IgG1 (9). IgG2 and IgG3 are found in only sporadically. However, this does not exclude the possibility that the prolonged half-life of IgG3 with the p.Arg435His variation could affect very early preclinical stages of PV. IgG3 is the often first IgG subclass a B cell switches to from IgM, before IgG1 and IgG4 (10). Very early autoantibodies are possibly involved in feedback loops that self-promote autoimmune responses (22). In this scenario, the p.Arg435His variation might enhance these feedback loops by its ability to increase the half-life and biodistribution of these autoantibodies as well as the processing of IgG3-bound autoantigen by enhanced phagocytosis (3). We may speculate that the higher susceptibility to PV associated with the p.Arg435His variation is related to the altered promotion of preclinical PV to the clinically manifest disease. As an alternative explanation, the genomic region flanking the p.Arg435His variation might lead to a changed class switching behavior, as it has been shown for the G3m(b) (**Figure 1**, G3m5* allotype in current nomenclature)

TABLE 1 | IgG3 rs4042056 variation in pemphigus vulgaris by KASP assay.

KASP[a]	Cases				Controls				Recessive[c]		Dominant[c]		Co-dominant[c]	
rs4042056	**AA**	**AG**	**GG**	**MAF (%)[b]**	**AA**	**AG**	**GG**	**MAF (%)[b]**	**OR (95% CI)**	***p***	**OR (95% CI)**	***p***	**OR (95% CI)**	***p***
Germany	4 4.6%	0 0%	83 95%	4.6*	0 0%	1 0.55%	180 99%	0.28	19 (1–350)	0.0074	5.2 (1–27)	0.037	3.2 (1.1–9.5)	0.014
Iran	5 6.4%	1 1.3%	72 92%	7.1*	3 3.3%	0 0%	87 97%	3.3*	1.9 (0.5–7.4)	0.37	2.1 (0.6–7.5)	0.24	1.4 (0.7–2.8)	0.28
Turkey	9 12%	1 1.4%	63 86%	13*	0 0%	0 0%	19 100%	0	5.8 (0.33–100)	0.12	3.4 (0.4–28)	0.19	2.2 (0.6–7.6)	0.15
Egypt	2 2%	0 0%	99 98%	2*	0 0%	0 0%	126 100%	0	6.4 (0.3–130)	0.16	6.4 (0.3–130)	0.16	2.5 (0.6–12)	0.16
Total[g]	20 5.9%	2 0.6%	317 94%	6.2	3 0.7%	1 0.2%	412 99%	0.84	4.28 (1.6–11.9)	0.0051	3.7 (1.5–9)	0.0038	2.78 (1.0–7.6)	0.047

ELISA[d]	Cases			Controls			Dominant[c]		ELISA/KASP combined dominant[h]	
G3m15	**Positive**	**Negative**	**MAF (%)[e]**	**Positive**	**Negative**	**MAF (%)[e]**	**OR (95% CI)**	***p***	**OR (95% CI)**	***p***
Germany	*1* *2.0%*	*49* *98.0%*	*1.0*	1 1.3%	77 98.7%	0.6	1.6 (0.2–15)	0.7	*4.9 (0.9–25.4)*	*0.061*
Iran	n.a.[f]	n.a.[f]	n.a.[f]	n.a.[f]	n.a.[f]	n.a.[f]	n.a.	n.a.	n.a.	n.a.
Turkey	4 5.3%	71 94.7%	2.7	n.a.[f]	n.a.[f]	n.a.[f]	n.a.	n.a.	n.a.	n.a.
Egypt	2 3.8%	50 96.2%	1.9	2 3.3%	59 96.7%	1.7	1.6 (0.33–8)	0.54	*2.5 (0.4–13.7)*	*0.298*
Total[g]	7 4%	170 96%	*2*	3 2.2%	136 97.8%	*1.1*	1.75 (0.4–7.6)	0.83	3.6 (1.5–8.8)	0.0041

[a]The KASP assay directly determined the genotype of rs4042056 SNP that corresponds to the amino acid at residue 435. The minor A allele (g.1053927G>A) allele corresponds to p.Arg435His.

[b]MAF, minor allele frequency, i.e., frequency of the A allele. An asterisk (*) indicates that the respective genotype distribution is not in Hardy–Weinberg equilibrium.

[c]Logistic regression (recessive, dominant, and co-dominant models) stratified by ethnic cohort. The 95% confidence interval is given for the odds ratio (OR); the p value (p) is given for the likelihood ratio test (LR test) on the genotype. For origin-wise models, the raw ORs are shown. In the combined analysis, a generalized linear mixed effects (with implicit adjustment) model with logit link function was applied. In case of 0 values in corresponding data, Lidstone additive smoothing was used to allow calculation of ORs and ensure convergence of the fitting routine.

[d]The ELISA detects the G3m15 allotype of IgG3 that is linked to the p.Arg435His variation.

[e]MAF, minor allele frequency, i.e., frequency of the allele encoding the G3m15 allotype, inferred assuming Hardy–Weinberg equilibrium.

[f]n.a., no serum samples available.

[g]Regression calculated with a generalized linear mixed effects model (uncorrelated intercept and genotype effect as random effects).

[h]Logistic regression of combined ELISA and KASP results. The genotyping method was used for stratification in a random effects model (compare table footnote c). For the calculation across all ethnicities, ethnic origin was used together the genotyping method for stratification.

TABLE 2 | IgG3 rs4042056 variation and G3m15 allotype in bullous pemphigoid.

KASP[a]	Cases				Controls				Recessive[c]		Dominant[c]		Co-dominant[c]	
rs4042056	AA	AG	GG	MAF (%)[d]	AA	AG	GG	MAF (%)[d]	OR (95% CI)	*p*	OR (95% CI)	*p*	OR (95% CI)	*p*
Germany	1 1.2%	1 1.2%	84 97.8%	0.58*	0 0%	1 0.6%	180 99.4%	0.3	6.3 (0.3–160)	0.22	3.2 (0.5–20)	0.2	2.4 (0.7–8.8)	0.16
ELISA[b]	**Cases**				**Controls**						**Dominant[c]**		**ELISA/KASP combined dominant[f]**	
G3m15	**Positive**		**Negative**	**MAF (%)[e]**	**Positive**		**Negative**	**MAF (%)[e]**			**OR (95% CI)**	***p***	**OR (95% CI)**	***p***
Germany	0 0%		87 100%	*0.0*	1 1.3%		77 98.7%	0.6			0.3 (0.01–7.4)	0.42	1.7 (0.2–12.5)	0.61

*[a]Results from the KASP assay, respectively (for comparison of values and footnote comments see **Table 1**).*

*[b]Results from the ELISA allotype determination (for comparison of values and footnote comments see **Table 1**).*

[c]Logistic regression (recessive, dominant, and co-dominant models) stratified by ethnic cohort. The 95% confidence interval is given for the odds ratio (OR); the p value (p) is given for the likelihood ratio test (LR test) on the genotype. In case of 0 values in corresponding data, Lidstone additive smoothing was used to allow calculation of ORs and ensure convergence of the fitting routine.

[d]MAF, minor allele frequency, i.e., frequency of the A allele. An asterisk (*) indicates that the respective genotype distribution is not in Hardy–Weinberg equilibrium.

[e]MAF, minor allele frequency, i.e., frequency of the allele encoding the G3m15 allotype, inferred assuming Hardy–Weinberg equilibrium.

*[f]Logistic regression of combined ELISA and KASP results. The genotyping method was used for stratification in a random effects model (compare table footnote h of **Table 1**).*

and G3m(g) (**Figure 1**, G3m21* allotype in current nomenclature) allotype (23). This alternative explanation assumes that the antibody repertoire is changed generally in way that promotes development of PV, but does not require the existence of early IgG3 autoantibodies.

In case of BP, other mechanisms might be important for the disease development. This is not only reflected by differences between PV and BP concerning associations with FcγR polymorphisms (15), but also, as found here, concerning the p.Arg435His variation that does not appears to be associated with BP susceptibility.

A study with individuals from malaria-endemic regions in Benin showed that anti-malaria IgG3 is transferred from pregnant mothers with the p.Arg435His variation to their unborn children and that these children have an improved immunoprotection against malaria (24). In our cohorts, we could find an increased frequency of the minor g.1053927G>A (p.Arg435His) allele in the patient cohorts from Iran and Turkey, in contrast to Egypt and Germany. Iran and Turkey are denoted as malaria-endemic countries from the U.S. Centers of Disease Control, while Egypt and Germany are not (25). A connection between malaria and pemphigus diseases has not been described, yet. Malaria is transmitted by stinging insects. This is remarkable, because in endemic Pemphigus foliaceus in Brazil, a connection to stinging insects has been described: autoantibodies against desmoglein 1 from affected patients cross-react with a salivary protein of a biting fly (26, 27). A genetic test does not allow to distinguish a direct effect of variation on susceptibility to a disease from a population effect. Our data show that the frequency of the p.Arg435His variation is higher in Iran and Turkey, favors the assumption of Dechavanne et al., that this variation could be an evolutionary adaption to malaria (24). Though highly speculative, a link between malaria and PV, be it genetic or environmental, would provide an alternative or additional explanation for the association between PV and the p.Arg435His variation: PV patients might preferably come from malaria-endemic areas within the investigated countries, while controls do not have this preference, leading to an increased frequency of the p.Arg435His variation. Such a population effect cannot be distinguished with the data available. However, a population effect would not imply any direct functional effect of the p.Arg435His variation on PV susceptibility or a theoretical involvement of IgG3 in PV.

The Hardy–Weinberg equilibrium assumption did not hold in any of the PV case cohorts. Next to the above described technical challenges, population effects as described above and the known high degree of consanguinity in the investigated populations could explain this phenomenon (28).

In summary, we found an association of PV but not of BP with a genetic variation that is known to change half-life and effector functions of IgG3. These data suggest that IgG3 may play a role in the pathogenesis of PV or that there may be a link between malaria or malaria-transmitting mosquitoes and PV in MENA countries.

THE GERMAN AIBD GENETIC STUDY GROUP MEMBERS

Alexander Kreuter, Department of Dermatology, Venereology and Allergology, University of Bochum, Bochum, Germany

(current affiliation: Department of Dermatology, Venereology and Allergology, HELIOS St. Elisabeth Klinik Oberhausen, Oberhausen, Germany); **Christos C. Zouboulis**, Department of Dermatology, Venereology, Allergology and Immunology, Dessau Medical Center, Dessau, Germany; **Georg Däschlein**, Department of Dermatology, University of Greifswald, Greifswald, Germany; **Kerstin Steinbrink**, Department of Dermatology, University Medical Center Mainz, University of Mainz, Mainz, Germany; **Manfred Kunz**, Department of Dermatology, Venereology and Allergology, University of Leipzig, Leipzig, Germany; **Nicolas Hunzelmann**, Department of Dermatology, University of Cologne, Cologne, Germany; **Steven Goetze**, Department of Dermatology, University Hospital Jena, Jena, Germany.

ETHICS STATEMENT

This study was carried out in accordance with the recommendations of institutional review board of the University of Lübeck and the review boards of the collaborating centers. The protocol was approved by the institutional review board of the University of Lübeck (File No. 08-156) and the review boards of the collaborating centers. All subjects gave written informed consent in accordance with the Declaration of Helsinki. Samples and demographic data of patients and controls were collected in adherence to ethics and German privacy protection regulations.

AUTHOR CONTRIBUTIONS

AR designed research, performed experiments, analyzed data, interpreted results, and wrote the manuscript; SK performed experiments, analyzed data, and wrote the manuscript; SL interpreted results and wrote the manuscript; MF performed experiments and analyzed data; NS, MA, SB, FE-C, ME, RE, RG, CG, EH, BH, WL, WP, RR, MSaeedi, MSárdy, MSticherling, SU, MW, and DZ recruited patients and organized sample collections; SI designed research, interpreted results, and wrote the manuscript; GV designed research, interpreted results, and wrote the manuscript; ES recruited patients, interpreted results, and wrote the manuscript; the German AIBD Genetic Study Group organized sample collections.

ACKNOWLEDGMENTS

We thank everybody involved in the collection of blood samples and all volunteers and patients who donated blood for this study. This work received infrastructural support from the Deutsche Forschungsgemeinschaft Cluster of Excellence Inflammation at Interfaces (Cluster 306/2).

SUPPLEMENTARY MATERIAL

The Supplementary Material for this article can be found online at https://www.frontiersin.org/articles/10.3389/fimmu.2018.01788/full#supplementary-material.

REFERENCES

1. Recke A, Sitaru C, Vidarsson G, Evensen M, Chiriac MT, Ludwig RJ, et al. Pathogenicity of IgG subclass autoantibodies to type VII collagen: induction of dermal-epidermal separation. *J Autoimmun* (2010) 34:435–44. doi:10.1016/j.jaut.2009.11.003
2. Stapleton NM, Andersen JT, Stemerding AM, Bjarnarson SP, Verheul RC, Gerritsen J, et al. Competition for FcRn-mediated transport gives rise to short half-life of human IgG3 and offers therapeutic potential. *Nat Commun* (2011) 2:599. doi:10.1038/ncomms1608
3. Stapleton NM, Einarsdóttir HK, Stemerding AM, Vidarsson G. The multiple facets of FcRn in immunity. *Immunol Rev* (2015) 268:253–68. doi:10.1111/imr.12331
4. Lefranc G, Chaabani H, Van Loghem E, Lefranc MP, De Lange G, Helal AN. Simultaneous absence of the human IgG1, IgG2, IgG4 and IgA1 subclasses: immunological and immunogenetical considerations. *Eur J Immunol* (1983) 13:240–4. doi:10.1002/eji.1830130312
5. Lefranc M-P, Lefranc G. Human Gm, Km, and Am allotypes and their molecular characterization: a remarkable demonstration of polymorphism. *Methods Mol Biol* (2012) 882:635–80. doi:10.1007/978-1-61779-842-9_34
6. Pressler T, Pandey JP, Espersen F, Pedersen SS, Fomsgaard A, Koch C, et al. Immunoglobulin allotypes and IgG subclass antibody response to *Pseudomonas aeruginosa* antigens in chronically infected cystic fibrosis patients. *Clin Exp Immunol* (1992) 90:209–14.
7. Zitouni M, Martel P, Ben Ayed M, Raux G, Gilbert D, Joly P, et al. Pemphigus is not associated with allotypic markers of immunoglobulin kappa. *Genes Immun* (2002) 3:50–2. doi:10.1038/sj.gene.6363817
8. Funakoshi T, Lunardon L, Ellebrecht CT, Nagler AR, O'Leary CE, Payne AS. Enrichment of total serum IgG4 in patients with pemphigus. *Br J Dermatol* (2012) 167:1245–53. doi:10.1111/j.1365-2133.2012.11144.x
9. Futei Y, Amagai M, Ishii K, Kuroda-Kinoshita K, Ohya K, Nishikawa T. Predominant IgG4 subclass in autoantibodies of pemphigus vulgaris and foliaceus. *J Dermatol Sci* (2001) 26:55–61. doi:10.1016/S0923-1811(00)00158-4
10. Jackson KJL, Wang Y, Collins AM. Human immunoglobulin classes and subclasses show variability in VDJ gene mutation levels. *Immunol Cell Biol* (2014) 92:729–33. doi:10.1038/icb.2014.44
11. Stanley JR, Amagai M. Pemphigus, bullous impetigo, and the staphylococcal scalded-skin syndrome. *N Engl J Med* (2006) 355:1800–10. doi:10.1056/NEJMra061111
12. Kasperkiewicz M, Ellebrecht CT, Takahashi H, Yamagami J, Zillikens D, Payne AS, et al. Pemphigus. *Nat Rev Dis Primers* (2017) 3:17026. doi:10.1038/nrdp.2017.26
13. Sarig O, Bercovici S, Zoller L, Goldberg I, Indelman M, Nahum S, et al. Population-specific association between a polymorphic variant in ST18, encoding a pro-apoptotic molecule, and pemphigus vulgaris. *J Invest Dermatol* (2012) 132:1798–805. doi:10.1038/jid.2012.46
14. Sinha AA, Brautbar C, Szafer F, Friedmann A, Tzfoni E, Todd JA, et al. A newly characterized HLA DQ beta allele associated with pemphigus vulgaris. *Science* (1988) 239:1026–9. doi:10.1126/science.2894075
15. Recke A, Vidarsson G, Ludwig RJ, Freitag M, Möller S, Vonthein R, et al. Allelic and copy-number variations of FcγRs affect granulocyte function and susceptibility for autoimmune blistering diseases. *J Autoimmun* (2015) 61:36–44. doi:10.1016/j.jaut.2015.05.004
16. Feliciani C, Joly P, Jonkman MF, Zambruno G, Zillikens D, Ioannides D, et al. Management of bullous pemphigoid: the European Dermatology Forum consensus in collaboration with the European Academy of Dermatology and Venereology. *Br J Dermatol* (2015) 172:867–77. doi:10.1111/bjd.13717
17. Hertl M, Jedlickova H, Karpati S, Marinovic B, Uzun S, Yayli S, et al. Pemphigus. S2 guideline for diagnosis and treatment – guided by the European Dermatology Forum (EDF) in cooperation with the European Academy of Dermatology and Venereology (EADV). *J Eur Acad Dermatol Venereol* (2015) 29:405–14. doi:10.1111/jdv.12772
18. Schmidt E, Goebeler M, Hertl M, Sárdy M, Sitaru C, Eming R, et al. S2k guideline for the diagnosis of pemphigus vulgaris/foliaceus and bullous pemphigoid. *J Dtsch Dermatol Ges* (2015) 13:713–27. doi:10.1111/ddg.12612

19. Schmidt E, della Torre R, Borradori L. Clinical features and practical diagnosis of bullous pemphigoid. *Dermatol Clin* (2011) 29:427–438,viii–ix. doi:10.1016/j.det.2011.03.010
20. Schmidt E, Zillikens D. Pemphigoid diseases. *Lancet* (2013) 381:320–32. doi:10.1016/S0140-6736(12)61140-4
21. Clarke L, Fairley S, Zheng-Bradley X, Streeter I, Perry E, Lowy E, et al. The international Genome sample resource (IGSR): a worldwide collection of genome variation incorporating the 1000 Genomes Project data. *Nucleic Acids Res* (2017) 45:D854–9. doi:10.1093/nar/gkw829
22. Hjelm F, Carlsson F, Getahun A, Heyman B. Antibody-mediated regulation of the immune response. *Scand J Immunol* (2006) 64:177–84. doi:10.1111/j.1365-3083.2006.01818.x
23. Pan Q, Rabbani H, Mills FC, Severinson E, Hammarström L. Allotype-associated variation in the human gamma3 switch region as a basis for differences in IgG3 production. *J Immunol* (1997) 158:5849–59.
24. Dechavanne C, Dechavanne S, Sadissou I, Lokossou AG, Alvarado F, Dambrun M, et al. Associations between an IgG3 polymorphism in the binding domain for FcRn, transplacental transfer of malaria-specific IgG3, and protection against *Plasmodium falciparum* malaria during infancy: a birth cohort study in Benin. *PLoS Med* (2017) 14:e1002403. doi:10.1371/journal.pmed.1002403
25. Brunette GW, Centers for Disease Control (U.S.). *CDC Yellow Book 2018: Health Information for International Travel*. Oxford, UK: Oxford University Press (2017).
26. Aoki V, Millikan RC, Rivitti EA, Hans-Filho G, Eaton DP, Warren SJP, et al. Environmental risk factors in endemic pemphigus foliaceus (fogo selvagem). *J Investig Dermatol Symp Proc* (2004) 9:34–40. doi:10.1111/j.1087-0024.2004.00833.x
27. Qian Y, Jeong JS, Maldonado M, Valenzuela JG, Gomes R, Teixeira C, et al. Cutting edge: Brazilian pemphigus foliaceus anti-desmoglein 1 autoantibodies cross-react with sand fly salivary LJM11 antigen. *J Immunol* (2012) 189:1535–9. doi:10.4049/jimmunol.1200842
28. Barbouche M-R, Mekki N, Ben-Ali M, Ben-Mustapha I. Lessons from genetic studies of primary immunodeficiencies in a highly consanguineous population. *Front Immunol* (2017) 8:737. doi:10.3389/fimmu.2017.00737

Conflict of Interest Statement: The authors declare that the research was conducted in the absence of any commercial or financial relationships that could be construed as a potential conflict of interest.

frontiers in Immunology

HYPOTHESIS AND THEORY
published: 18 July 2018
doi: 10.3389/fimmu.2018.01189

Reversing Autoimmunity Combination of Rituximab and Intravenous Immunoglobulin

A. Razzaque Ahmed[1,2]* *and Srinivas Kaveri*[3]

[1] Department of Dermatology, Tufts University School of Medicine, Boston, MA, United States, [2] Center for Blistering Diseases, Boston, MA, United States, [3] INSERM U1138 Centre de Recherche des Cordeliers, Paris, France

In this concept paper, the authors present a unique and novel protocol to treat autoimmune diseases that may have the potential to reverse autoimmunity. It uses a combination of B cell depletion therapy (BDT), specifically rituximab (RTX) and intravenous immunoglobulin (IVIg), based on a specifically designed protocol (Ahmed Protocol). Twelve infusions of RTX are given in 6–14 months. Once the $CD20^+$ B cells are depleted from the peripheral blood, IVIg is given monthly until B cells repopulation occurs. Six additional cycles are given to end the protocol. During the stages of B cell depletion, repopulation and after clinical recovery, IVIg is continued. Along with clinical recovery, significant reduction and eventual disappearance of pathogenic autoantibody occurs. Administration of IVIg in the post-clinical period is a crucial part of this protocol. This combination reduces and may eventually significantly eliminates inflammation in the microenvironment and facilitates restoring immune balance. Consequently, the process of autoimmunity and the phenomenon that lead to autoimmune disease are arrested, and a sustained and prolonged disease and drug-free remission is achieved. Data from seven published studies, in which this combination protocol was used, are presented. It is known that BDT does not affect check points. IVIg has functions that mimic checkpoints. Hence, when inflammation is reduced and the microenvironment is favorable, IVIg may restore tolerance. The authors provide relevant information, molecular mechanism of action of BDT, IVIg, autoimmunity, and autoimmune diseases. The focus of the manuscript is providing an explanation, using the current literature, to demonstrate possible pathways, used by the combination of BDT and IVIg in providing sustained, long-term, drug-free remissions of autoimmune diseases, and thus reversing autoimmunity, albeit for the duration of the observation.

Keywords: reversal of autoimmunity, autoimmune diseases, autoantibodies, B cell development, B cell depletion therapy, intravenous immunoglobulin, rituximab, autoimmune blistering diseases

OPEN ACCESS

Edited by:
Ralf J. Ludwig,
Universität zu Lübeck, Germany

Reviewed by:
Hiroaki Iwata,
Hokkaido University, Japan
Khalaf Kridin,
Rambam Health Care Campus, Israel

***Correspondence:**
A. Razzaque Ahmed
arahmedmd@msn.com

Specialty section:
This article was submitted to Immunological Tolerance and Regulation, a section of the journal Frontiers in Immunology

Received: *12 January 2018*
Accepted: *14 May 2018*
Published: *18 July 2018*

Citation:
Ahmed AR and Kaveri S (2018) Reversing Autoimmunity Combination of Rituximab and Intravenous Immunoglobulin. Front. Immunol. 9:1189. doi: 10.3389/fimmu.2018.01189

INTRODUCTION

The treatment of autoimmune disease is a challenge and priority as they affect 50 million individuals in the United States, and currently they collectively are the third most common disease category (1, 2). This importance is further emphasized by the fact, that many people may be affected for a significant portion of their lives (1, 2). Historically, their prognosis dramatically improved with the advent and use of systematic corticosteroids (CS). Unfortunately, the much-needed long-term use of high dose systemic CS resulted in serious, and catastrophic, side effects, which caused morbidity

and mortality (3). Consequently, immunosuppressive agents (ISA) in combination with CS became the major treatment modality (3, 4). The long-term use of this combination resulted in profound immune suppression, resulting in fatal opportunistic infections. B cells are considered the key participants in autoimmune diseases, since they produce pathogenic autoantibodies (5). Recently, B cell depletion therapy (BDT), specifically rituximab (RTX), has gained enormous popularity in the treatment of autoimmune diseases (6, 7).

B cell depletion therapy produces rapid clinical remissions in 70–80% of patients (8). However, majority if not most patients, develop relapses. Benefits from a single infusion usually last 9–18 months (9, 10). The reported rate of relapse depends on the duration of follow-up (11–15). As the effect of the BDT wears off clinical disease recurs, suggesting that BDT may not produce long-term sustained clinical remissions, without its continued use.

UNMET NEEDS

The preferable drug(s) to treat autoimmune disease would be whose use requires a defined protocol, grounded in scientific fact, with predictors of progress, discernible end point, produces long-term sustained clinical remission, without need for continued or additional therapy. It must be safe, have minimal immediate and long-term adverse events, readily available, easy to administer, and produce a good quality of life. Currently, no such drugs or agent(s) are available. To fulfill this unmet need, based on scientific literature, presented in this manuscript, a protocol was developed, and is the focus on this paper.

THE CONCEPT

Autoimmune diseases that are associated with the autoantibodies are presumed to be B cell driven (5). Therefore, BDT was used. Since use of RA protocol, in which 1 g of RTX is given 15 days apart, was associated with high relapse rates, multiple infusions were given (12). The rationale being that multiple infusions may delete $CD20^+$ B cells (10). Repeated infusions would capture those cells residing at immune privileged sites, subsequently leave, enter peripheral circulation, and are lysed (16). Removal of autoreactive B cells would decrease inflammations in the microenvironment and eventually reduce pathogenic autoantibody production (9).

Intravenous immunoglobulin has multiple effects on the immune and inflammatory pathways (17–19). The properties used in this concept are those that act synergistically with BDT. IVIg would enhance and complement the anti-inflammatory effects of BDT (20–22). Once inflammation is significantly reduced or eliminated, IVIg might restore immune balance to normal homeostasis (23, 24). During BDT induced B cells depletion, IVIg provides immunoprophylaxis. Simultaneously, the multiple IVIg infusions produce sustained long-term clinical remissions, decrease and possibly eliminate pathogenic autoantibody (25).

Commercial preparations of IVIg in addition to IgG, contain small amounts of several molecules, playing a vital role in its biologic and pharmacological functions (24). Many have not been identified, and amongst others include cytokines, cytokine receptors, molecular markers, antibodies against T cells determinants, such as CD4 CD8, HLA antigens, super antigens, and anti-idiotypic antibodies (24). Their amounts are not constant and vary among batches, from the same manufacturer. Their relative amounts vary among brand names, since the patents used, have different biochemical methodologies and industrial processes (26). One of clinical implications of these variabilities is that, patients need multiple infusions to demonstrate clinical benefit, and subsequently additional infusions to retain the benefit obtained. Critical level of biochemical molecules or receptors may only be obtained from multiple infusions. Single or limited infusion may not provide the pharmacodynamics necessary for producing desired clinical response. Another explanation for multiple infusions is that antibodies in commercial preparations compete with pathological autoantibodies for neonatal Fc receptor (FcRn) binding (27). One recent clinical study highlights the long-term benefits of multiple infusions. In patients with chronic inflammatory demyelinating polyneuropathy, limited infusions of IVIg provide significant clinical relief because of its anti-inflammatory effect. Durations of remission are limited, relapse occurs, requiring repeat infusion (28). Recent study demonstrated that multiple infusions during the post-inflammatory recovery period provided prolonged remission lasting up to 52 weeks, in 70% of patients (28). This study demonstrated that it was multiple infusions, at defined intervals, after clinical recovery that produced a sustained prolonged clinical remission (28).

THE PROTOCOL

The protocol that has produced sustained clinical remissions without need for subsequent systemic therapy is presented in **Figure 1** (Ahmed Protocol) (29). It has three phases. In phase 1, patient received a cycle of IVIg before receiving RTX, then eight infusions of RTX in eight consecutive weeks, at a dose of 375 mg/m^2 per infusion. Thereafter, four additional infusions of RTX either at monthly or preferably at 3 months interval are administered. Patients are disease free during this period. These repeated infusions will enhance the penetration of RTX into bone marrow (BM), lymph nodes (LNs), and spleen, eliminates those $CD20^+$ B cells that freshly migrate into the peripheral blood (PB) from these sites. The $CD20^+$ B cell count is zero usually by the second or third infusion. Since the half-life of IVIg is usually 3 weeks, it is administered monthly (30). During phase 1, previous initiated treatments with CS and ISA have no demonstrable pharmacologic benefit or need, are tapered and discontinued.

Phase 2, is the period of continued B cell depletion. IVIg infusions are continued until B cells repopulate.

In phase 3, IVIg is used according to an established protocol (31), developed by a Consensus Development Committee on the use of IVIg therapy for the treatment of autoimmune mucocutaneous blistering diseases, in which it initially produced 36 months sustained remissions, without any additional systemic therapy (31, 32). Twenty years later, these patients are still in remission (unpublished data). In these patients, pathogenic autoantibody levels declined and were non-detectable during follow-up periods (33–38). These results were demonstrated in

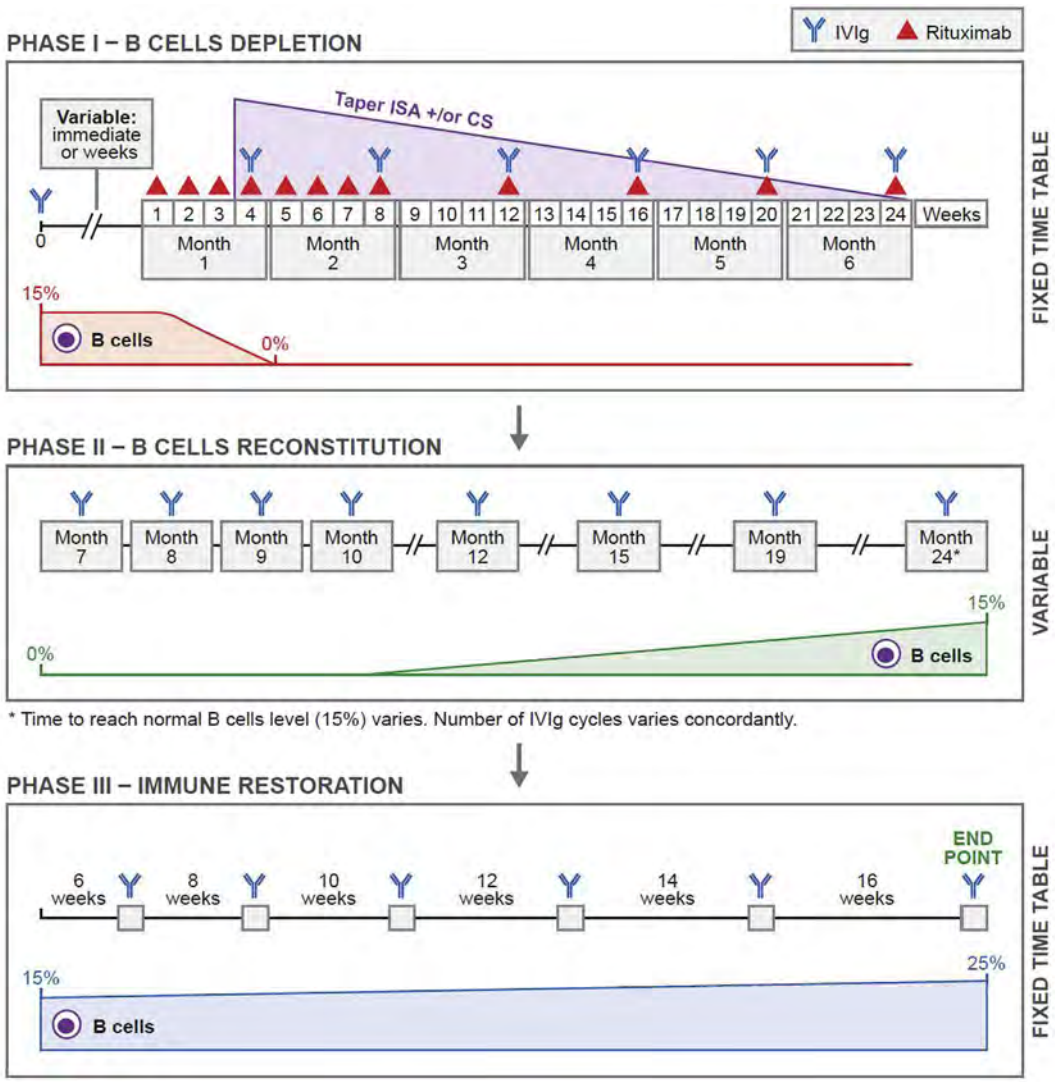

FIGURE 1 | Novel protocol using a combination of rituximab (RTX) and intravenous immunoglobulin (IVIg). In phase 1, before initiating RTX, patients were given one cycle of IVIg (2 g/kg/cycle) for immunoprophylaxis. Thereafter, they were given weekly infusions of RTX (375 mg/m^2) for eight consecutive weeks. Additional RTX infusions were given once a month for four consecutive months. Thus, the patients received 12 infusions of RTX during a 6-month period. IVIg was given at monthly intervals during phase 1 for continuing immunoprophylaxis. In phase 2, patients received multiple cycles of IVIg at monthly intervals. The number of cycles depended on the repopulation of B cells. The CD19$^+$ B-cell count was 0 at the beginning. Phase 2 ended when the CD19$^+$ B-cell count was 15%. Phase 3 was based on a published protocol and was consistent in all patients. Each patient received a total of six cycles of IVIg given at 6-, 8-, 10-, 12-, and 14-week intervals. The last cycle was at 16-week interval. Thus phase 3 lasted 16.5 months. This was the end of the protocol. Abbreviations: CS, corticosteroids; ISA, immunosuppressive agents. Reprinted from Ref. (29), with permission from Elsevier.

patients with pemphigus vulgaris (PV), pemphigus foliaceus, bullous pemphigoid (BP), mucous membrane pemphigoid (MMP) aka cicatrical pemphigoid, oral pemphigoid, ocular cicatrical pemphigoid (OCP), epidermolysis bullosa acquisita (EBA), and pemphigoid gestationis (33–38). Collectively, the data strongly suggest that, these last seven infusions during phase 3, most likely affected multiple cells, molecules, mediators, and receptors, causing a restoration of immune balance, return to hemostasis and possibly re-institution of tolerance.

The beneficial effects of IVIg, its anti-inflammatory actions and influence on the microenvironment, are best understood from situations where clinical failure or lack of response was observed. In such situations, the inflammatory influences are excessive. Wherein the microenvironment does not allow IVIg to exert immune-regulatory effects. Beneficial effects of IVIg can be influenced by mediators of inflammation, such granulocyte-colony stimulating factor (G-CSF), IL-1β, and IL6 (39). Threefold higher levels of G-CSF were observed in patients nonresponsive to IVIg compared to responders. G-CSF uses signaling pathways of STAT3 for induction of granulopoiesis and differentiation of granulocytes (39). Resultant high levels of neutrophils in the microenvironment, possibly inhibit many functions of IVIg. Interestingly, BDT

can significantly inhibit STAT3 activity, resulting in reduction of granulopoiesis, neutrophil production, and decrease in inflammation in the microenvironment of the tissues (40). This supports the concept of synergistic effects of RTX and IVIg.

PROOF OF CONCEPT

The authors combined RTX with IVIg in a specific protocol (Ahmed Protocol) (**Figure 1**). All patients that are reported by our group completed the protocol. Limited aspects, relevant features including the results of treatment of severe recalcitrant patients with pemphigus vulgaris, bullous pemphigoid, mucous membrane pemphigus, ocular cicatrical pemphigoid, and epidermolysis bullosa acquisita (EBA) are presented in **Table 1** (29, 41–45).

Into October 2006, we reported successful clinical outcomes in 11 patients with severe widespread PV involving the skin and multiple mucosae (41). These patients were previously treated with long-term high dose prednisone, 4–8 ISA and IVIg. The duration of all systemic therapy prior to combination therapy was mean of 68.8 months (range 31–219). The mean duration of follow-up after discontinuation of combination therapy was a mean of 31.7 months (range 22–37). None of the patients had any serious infection, were hospitalized for disease- or treatment-related issues, and remained in complete clinical remission, off therapy, with no detectable autoantibody and normal B cells.

In 2015, follow-up study reported that the patients continued to remain in complete clinical remission, off systemic therapy, with serological and immunopathological remission, and normal levels of B cells (42). The serum IgM levels reduced after a RTX therapy, became normal. They were carefully monitored, did not develop malignancies or other auto-immune disease. Hence, for 12–15 years post therapy a prolonged sustained clinical, serological, and immuno-pathological remission resulted from the combination therapy (42).

Ten patients with severe and widespread PV with contraindications for CS and ISA, treated with the combination of IVIg and RTX, using the same protocol, were reported in 2016 (43). Combination therapy was first-line treatment. Clinical response and complete disease resolution was rapid. During the follow-up of 131.7 months (10.97 years), the patients were in complete clinical remission, off therapy, with accompanying serological and immune-pathological remission, no relapses, infections, hospitalizations, or serious adverse events. An approximately, 10-year later the remissions remain.

Twelve patients with recalcitrant bullous pemphigoid (BP) who had failed CS and ISA, had multiple relapses on them, some had already received RTX by RA protocol, were treated by the combination of RTX and IVIg and followed for a mean of 73.8 months (6 years) post therapy were reported in 2015 (29). The patients remained in complete clinical remission off therapy, in serological and immune-pathological remission with normal levels of B cells in PB. They experienced no serious adverse events, infections, or hospitalizations and enjoyed a high quality of life. These remissions remain in a current follow-up of 9 years.

The combination of RTX and IVIg used to treat patients with recalcitrant ocular cicatrical pemphigoid (CP) and MMP has been reported in a controlled trial (44). These patients had MMP with multiple mucosal involvements, but the urgent issue was impending total blindness. 12 patients were divided into two groups. The control group had six patients, blind in one eye, with rapidly progressive OCP in the second eye, were treated with conventional therapy with ISA. All six patients became blind in both eyes. In the study group, four patients blind in one eye and two had persistent bilateral severe non-responsive conjunctival

TABLE 1 | Relevant data from autoimmune bullous diseases treated with rituximab (RTX) and intravenous immunoglobulin (IVIg).

	Pemphigus vulgaris		Bullous pemphigoid	Mucous membrane pemphigoid	Epidermolysis bullosa aquisita
No of patients	11	10	12	6	5
Mean age at onset	38 (15–68)	47.8 (35–64)	68.25 (60–76)	74 (69–79)	50.6 (31–61)
Mean duration of disease before combined therapy	68.8 months (32–219 months)	None	36.5 months (2.7–72 months)	7 years (4.5–9.6 years)	8.8 years (2–20 years)
Duration of combined therapy	28 months (22–40 months)	32 months (17–52 months)	23.8 months (20–30 months)	24.6 months (18–29 months)	25 months (18–23 months)
Time to B cell depletion	4 weeks (3–6)	1.5 weeks (0.5–2.5)	2.3 weeks (0.5–3.9)	1.8 weeks (0.5–3.1 weeks)	2.0 weeks (0.6–3.4 weeks)
Time to B cell repopulation	12 months (18–26 months)	22.6 months (14–28 months)	70 months (17–31 months)	22 months (16–36 months)	18 months (12–28 months)
Time to serological remission	18 months (14–22 months)	11 months (9–14 months)	14 months (10–18 months)	14 months (12–18 months)	N/A
Clinical outcome	CCR	CCR	CCR	CCR	CR
SAE infection	None	None	None	None	None
SAE cardiac	None	None	None	None	None
SAE deaths	None	None	None	None	None
Mean total duration of follow-up	132.5 months (15–37 months)	131.7 months (111–136 months)	73 months (48–144 months)	9.8 years (99–115 months)	26 months (10–29 months)
Relapse reported, since discontinuation of combined treatment	None	None	None	None	None

CCR = complete clinical remission = no disease, no drug.
CR, clinical remission on therapy; NA, not available.

inflammation, were treated with RTX and IVIg. There best-corrected visual acuity and Foster OCP staging of the study group recovered and stabilized. Blindness was prevented. They had no serious adverse events to RTX or IVIg, no infections, no hospitalizations and a good quality of life. Initially followed for 1-year post therapy (44) and now for additional 8 years, these six patients with recalcitrant OCP, had complete clinical and serological remission, with normal levels of B cells, and a good quality of life and most importantly preventions of blindness.

Investigators from Turkey reported five patients with cutaneous and mucosal epidermolysis bullosa acquisita (EBA), resistant to conventional therapy, who were treated with combination of RTX and IVIg in 2017 (45). The published protocol for the combination of RTX and IVIg (29) was not followed. Modified protocol was used. Patients did have a positive clinical response, but still were under treatment 22 months post therapy.

A British group in 2016 reported three patients with MMP and one with linear IgA bullous disease, non-responsive to conventional therapy, all four blind in one eye, treated with two cycles of RTX and 2–9 monthly infusions of IVIg (46). Ahmed protocol (41) was not used. Visual acuity stabilized in all patients and progression of scarring ceased. Three of the four patients continued to require conventional immunosuppressive therapy after discontinuing IVIg and RTX. Follow-up post combination therapy was limited. One patient developed pneumonia followed by life-threatening septicemia and corneal infections, 3 and 6 weeks, respectively, after RTX infusions.

This rather limited sample of studies on autoimmune blistering disease, adds an extremely important dimension to the "Concept," *albeit* a little early in the overall scheme. In the two studies (45, 46) in which the Ahmed protocol was not followed, the outcomes were not as favorable compared to outcomes where the protocol was followed (29, 41–44). These limited observations validate its potential to produce long-term sustained clinical and serological remission.

It needs to be highlighted that autoimmune mucocutaneous blistering diseases are used as for proof of concept, only because published data, though limited, was available, and complete to validate the principle. The data lack experiments that would have given a molecular and cellular basis to the concept. The purpose of the authors is to encourage other investigators to emulate the concept and use the Ahmed protocol. It is interesting to note that BDT has shown to be effective in autoimmune diseases generally considered to be T cell mediated, such as type 1 diabetes, multiple sclerosis, and thrombocytopenic purpura (TTP) (47–50).

Certain features in the clinical profile and course give evidence for recalcitrant disease. Diseases were present for several years, failed high doses of CS and multiple ISA, IVIg and in some one cycle of RTX, had turbulent clinical course with multiple relapses and remissions, and numerous significant or catastrophic side effects, resulting in frequent hospitalization, poor quality of life, and frequent loss of employment. Combination therapy was used as a treatment of last resort.

In addition to sustained long-term clinical remission, serological and tissue immunopathology, this combination has additional benefits. Patients with MMP, oral pemphigoid (OP), OCP, and EBA ceased to have disease progression.

The authors recognize that data presented have definitive limitations. Number of patients and diseases are limited. Studies are retrospective and lack controls. Control group of similar recalcitrant patients are difficult to obtain, specially is rare and orphan diseases. Controlled studies on such sick patients could be unethical.

DISCUSSION

The authors provide the molecular and cellular basis from relevant studies in the literature, to provide the basis for reported observations. The mechanism of action of IVIg, and the effects of BDT on the immune system are presented. To put the "concept" into proper perspective, certain features of autoimmunity and autoimmune disease are discussed, only to demonstrate how and where these biologic agents have the potential to influence them. The attempts of the authors are to demonstrate the mechanism by which the combination of IVIg and BDT influences the clinical course and positive outcome. Ultimately, there could be reversal of autoimmunity, *albeit* only for the duration of the reported follow-up period.

It needs to be emphasized that this discussion is not focused or targeted to a specific autoimmune disease. This data derived from multiple sources, human and animal, *in vitro* and *in vivo* studies, is solely to present cellular and molecular evidence for the "concept."

The illustrations in this manuscript taken from publications, with the permission of the publishers, utilize known facts to provide a foundation for the "concept." Legends accompanying the illustrations have been included because they contain messages and valuable information to understand immunology germane to the "concept."

TOLERANCE AND AUTOIMMUNITY

A detailed and comprehensive discussion on tolerance and autoimmunity is beyond the scope of this manuscript. Limited and relevant literature on both, specifically those directly impacting the proposed "concept," and possible mechanism involved in producing the positive clinical outcomes observed.

Two features are pivotal. First, the importance of the microenvironment and processes within it that influence disease manifestation, and response to therapy. Second, inflammation is central to the pathogenesis and persistence of autoimmune diseases. The best proof of this comes from the fact, that if not all, most autoimmune diseases respond to CS (3). Frequently, as doses are reduced or discontinued, relapses occur. When the dosages are increased, clinical remissions are restored.

Tolerance is a state of natural equilibrium, wherein the body does not permit development of detrimental phenomena, and eliminates whichever occur (51, 52). Alteration or loss of tolerance results in autoimmunity (53). The progression from autoimmunity to autoimmune disease is complex, and multi-factorial, dependent on autoreactive B cells, T cells, plasma cells, and many other cells and molecules involved in inflammatory pathways and the immune system. These include several cytokines, leukotrienes, lymphokines, growth factors, and signaling pathways (51–56).

B Cell Development—Role of Checkpoints

Checkpoints that play a significant role in the process of B cell tolerance have been characterized (56) (**Figure 2**). Checkpoints 1 and 2, located in the BM influence pre B cells and B cell receptor (BCR). At checkpoint 3, between BM and PB, reactivity of the BCR develops and can respond to self-antigens. At checkpoint 4,

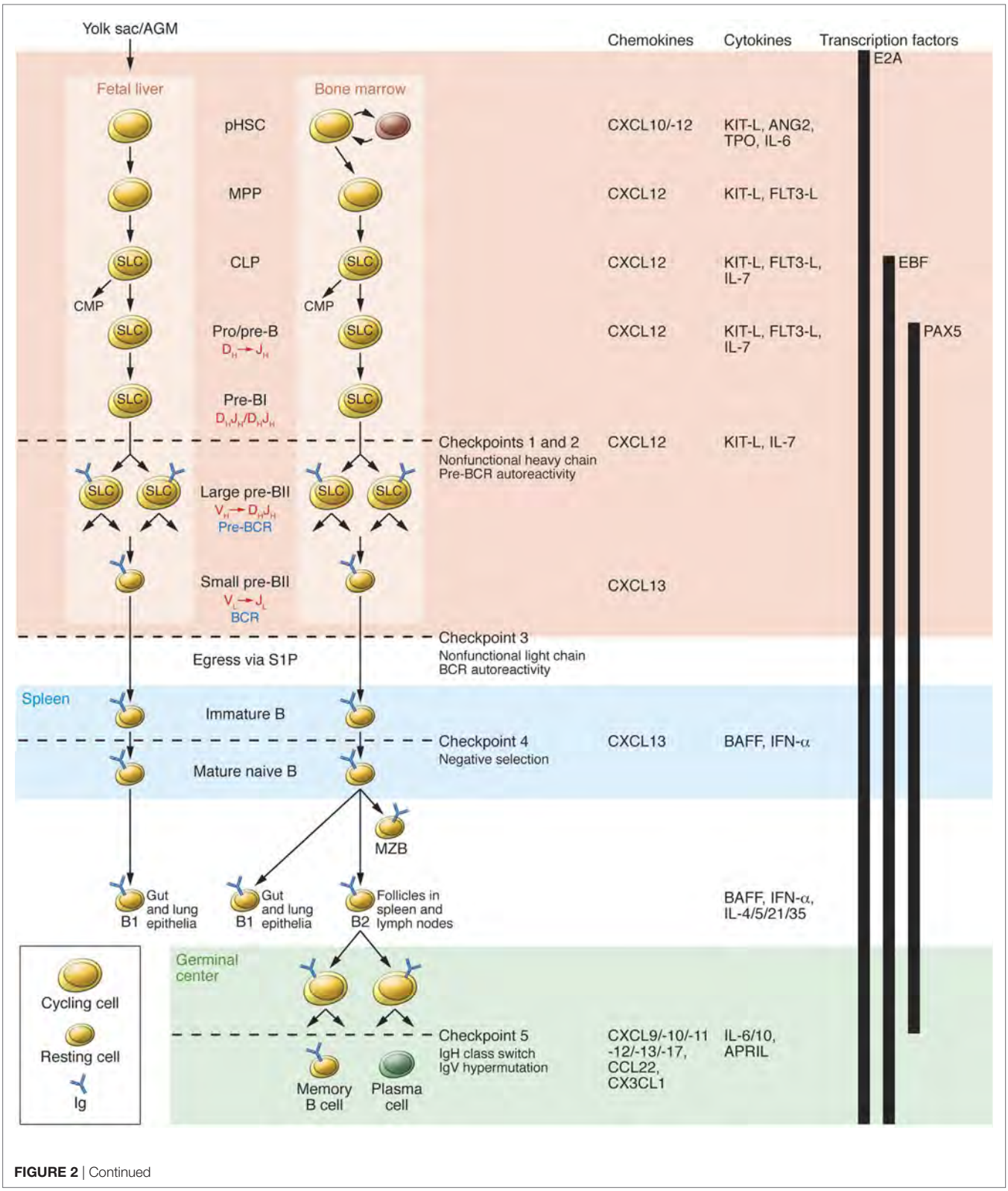

FIGURE 2 | Continued

FIGURE 2 | B cell development in fetal liver and bone marrow (BM). pHSC progenitors originate extraembyronically from yolk sac and, at later stages of development, intraembyronically from the aorta-gonad-mesonephros region. pHSCs develop in the fetal liver prenatally and in BM postnatally; both of these environments (pink region) provide crucial transcription factors, chemokines, cytokines, and cell contacts that regulate differentiation. Additionally, pHSCs localize to specialized niches that allow for their long-term survival in BM but not in fetal liver. Expression of the transcription factor E2A and the V(D)J rearrangement machinery RAG1/2 restricts CLPs from developing into B lineage cells. B cell receptors (BCRs) are generated by stepwise rearrangements of Ig segments. Pre-B cells that have undergone productive $V_HD_HJ_H$ rearrangement express an Igμ chain that can pair with SLC to form a pre-BCR, which stimulates large pre-B cell proliferation. lastly, V_L-to-J_L rearrangement occurs in small pre-BII cells, which become surface BCR-expressing immature B cells. They then enter the spleen (blue region), where fetal liver-derived BI cells predominately populate the gut and lung epithelia as mature B cells. BM-derived B cells mature in spleen to BI cells, which populate the lung and epithelia; MZB cells, which populate the marginal zone; and BII cells, which are organized in B cell-rich follicles where T cell-dependent antigenic stimulation promotes development of germinal centers (green region). Antigen-specific follicular helper T cells induce B cell Ig class-switching and IgV-region hypermutation and help to develop memory B cells and plasma cells. The developing B cell repertoires are monitored for structural fitness and autoreactivity at five checkpoints. Abbreviation: CMP, common myeloid progenitor. Reprinted from Ref. (56) with permission from American Society for Clinical Investigation.

in the spleen, positive or negative selection of B cells occurs. At checkpoint 5, mature B cells undergo somatic hypermutation. Deletion of genes can downgrade serum light chains, leading to continued pre BCR expression, resulting in pre B cell hyperplasia. These mutations can influence emergent self IgH-repertoire, maintaining the presence of autoreactive pre B cells. At checkpoint 5 present in the germinal centers of the LNs and spleen. B cells encounter auto-antigens, in the context of the MHC class II gene products, and can possibly produce autoreactive memory B cells (57). Checkpoints 1, 2, and 3 are referred to as central tolerance and checkpoints 4 and 5 to as peripheral tolerance (56).

At checkpoints 4 and 5 there is a potential influence from toll-like receptor (TLR) (58, 59). Negative selection of autoreactive B cells prevents autoreactivity by process of deletion, receptor editing, and anergy. In contrast, positive selection occurs due to clonal expansion of transitional B cells, in the periphery and is affected by interaction with BCR signaling, B cell activating factor receptor (BAFFR), CD40, and the TLRs (57, 60). When tolerance is effective there is an equal balance between negative and positive selection. In autoimmune diseases, this immune balance is lost and favors negative selection. Excessive amount of BAFF can result in negative selection and consequent produce autoimmunity is depicted in **Figure 3**. Transitional B cells mature and populate the follicular mature (FM) compartment or the marginal zone (MZ) and germinal centers of LNs and spleen (61). While majority of the autoreactive BCR specificities are deleted by negative selection, some in the MZ compartment survive and may contribute to autoimmunity (56). High levels of BAFF can rescue low affinity autoreactive B cells from negative selections. It is usually believed that more than 90% of autoreactive B cells are eliminated by checkpoints. Alterations in checkpoints have been associated with high levels of autoreactive B cells, T cells, and autoimmune disease (53, 56). During remissions, checkpoints resume normal functions, reduce autoreactive cells, and return to pre-disease or physiological status (62).

B Cells and Plasma Cells

B cells and plasma cells residing in specific niches, differentiate by a sequential processes, aided by growth and survival factors and their signals. Upon leaving the BM, B cells circulate through PB, reach the LNs and spleen, encounter cognitive antigens, costimulatory signals, and dendritic cells, proliferate and differentiate into plasmablasts and plasma cells (63). Short-lived plasma cells have a lifespan of approximately 3 weeks, while long-lived plasma cells may survive for 6 months or more (63). While majority reside in the BM, a smaller population may reside in the spleen (63). Their longevity is influenced by the microenvironment, including specific survival signals from BM and inflamed tissues (63).

Autoreactive B Cells

Autoreactive B cells play a significant role in propelling from autoimmunity to autoimmune disease. They act as antigen-presenting cells, interact with T cells in the germinal centers or target tissues, and may undergo somatic hypermutation and class-switch recombination (64). They amplify the inflammatory response and play a significant role in generating autoimmune pathogenic memory B cells (64). Certain subsets of B cells that express specific factors, can convert them to pathogenic autoantibody secreting cells, in the presence of tolerance checkpoints (63, 64). Some of those reported include overexpression of CD19, reduced expression of CD21 (63, 64), upregulation of CD95 and BAFF.

The maintenance of autoimmunity is facilitated, in part by the large plasma cells, prone to apoptosis, but thrive in disease microenvironments, because of survival and growth factors (56). For example, BAFF provides survival signals for immature B cells, mature NFB cells, plasma cells in the BM, and $CD27^+$ memory cells (65). In the BM there is a feedback loop between pre B cells and plasma cells. Cytokines such as IL5, IL6, TNFα, and SDF-1a that can modulate inflammation and affect longevity of plasma cells (66). In this survival niche, these long-lived memory plasma cells are frequently protected from the effects of ISA and may play a role in disease progression or relapse (16). During relapse, emergence of $CD20^+CD27^+$ memory cells, in association with costimulatory T cells, provide signals to plasma cells so that they can produce more autoantibodies and cause disease (67). In addition, newly generated naive B cells ($CD10^+/IGD^+$) exiting the BM, with T dependent or independent signals, may have the capacity to undergo differentiation and become autoreactive plasma cells (68–70).

T Cells

T cell tolerance plays a critical and vital role in the generation and persistence of autoimmunity. (**Figure 4**) The authors have not provided as much information on T cell tolerance, as on B cell tolerance, because of their focus on B cell development and BDT. In the thymus, T cells encounter several self-peptides, in the context of MHC class II gene products, Foxp3 expression on regulatory T cells ($CD4^-$, CD25-CTLA4) and proliferate and differentiate

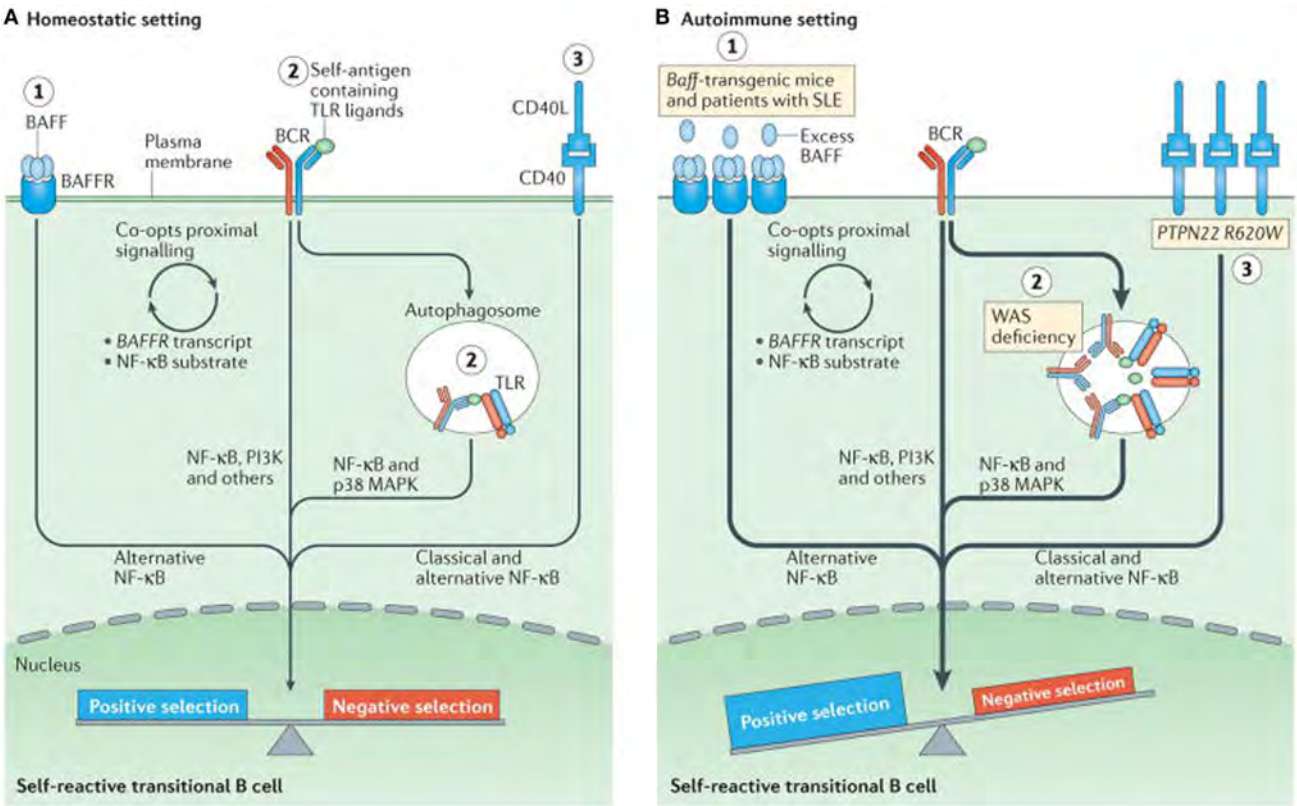

FIGURE 3 | Altered B cell receptor (BCR) and co-receptor signaling promotes increased autoreactivity within the naive B cell repertoire. **(A)** Under homeostatic conditions, self-reactive B cells are subjected to both positive and negative selection mechanisms as they transit into the naive B cell pool and establish the naive repertoire. Whereas, tonic BCR signaling and BCR engagement with self-antigen primarily regulate these events, synergy between the BCR and co-receptors fine-tunes the tolerance program within a given B cell. Among these co-receptors, B cell activating factor receptor (BAFFR) signaling (1) synergizes with BCR signaling during late bone marrow and transitional development through a series of complex events, including proximal biochemical crosstalk and the downstream transcriptional regulation of both receptor and substrate expression. Dual BCR and toll-like receptor (TLR) signaling (2) is mediated by internalization and delivery of self-antigens that contain TLR ligands to autophagosomes, which contain endosome-resident TLRs. CD40 signaling (3), which is triggered by interaction with CD40 ligand (CD40L) on T cells and possibly other cell types, also integrates with the BCR signaling pathway. Although BCR signaling can modulate CD40 expression, other biochemical or transcriptional events that affect this crosstalk are less well understood. **(B)** In genetic (or environmental) settings that promote an increased risk of developing autoimmunity, the homeostatic signaling thresholds are modulated, and self-reactive B cells exhibit greater positive selection, and/or reduced negative selection, leading to a naive repertoire that is skewed toward autoreactivity. For example, excess amounts of B cell-activating factor (BAFF 1) in the *Baff*-transgenic mouse model rescue low-affinity self-reactive B cells from negative selection. A similar mechanism has been proposed to exist in individuals with systemic lupus erythematosus (SLE). Similarly, in mouse and human settings of Wiskott–Aldrich syndrome (WAS) deficiency (2), hyper-responsive dual BCR and TLR signaling promotes the positive selection of transitional B cells with BCRs that use a limited subset of genes that encode self-reactive heavy-chain variable (VH) domains. Healthy individuals with the autoimmunity-associated variant *PTPN22*^{R620W} (3) exhibit altered BCR and CD40 signaling, and have an enrichment of self-reactive BCR specificities within the naive B cell compartment. Although it has not yet been definitively demonstrated, it is likely that enhanced positive selection, rather than relaxed negative selection, predominantly mediates this change. The thickness of the arrows indicates the strength of pathway activation. Abbreviations: MAPK, mitogen-activated protein kinase; NF-κB, nuclear factor-κB; PI3K, phosphatidylinositol 3-kinase. Reprinted from Ref. (60) with permission from Springer Nature.

into cytotoxic T cells, but most importantly eliminate potentially autoreactive T cells (71). Studies in mice and humans, have demonstrated that T cells proliferate upon contact with dendritic cells and self-antigens, but are promptly eliminated by the processes of deletion or anergy and thus maintain tolerance (71). However, when these T cells are in contact with the inappropriate dendritic cells or an inappropriate self-antigen, they undergo a process of defective deletion or loss of anergy, and consequently became autoreactive and can produce autoimmunity (71).

Autoantibodies can be generated from autoreactive B cells, when activated by T independent signals some of which may act through toll-like receptors. Toll-like receptor 7 (TLR7) has promotional, while TLR9 has a regulatory role (72). Some other molecules that influence this process are CD38, CD40, CD40L, TLR7, 9, IFN-γ, IL6, IL10, IL21, CD86 (72). Dendritic cells often vital in autoimmunity can act independently or in collaboration with several cytokines, some of which are CXL2, 3 BAFF, BAFF-R, FCγR, APRIL, and interferon γ (71, 73).

Interestingly, active T cells can inhibit further T cell stimulation using dendritic cells and IL10 as a mediator, while simultaneously they are known to facilitate, T cell activation through IL6 (74) Therefore, it appears that they can simultaneously exert opposite effects on immune responses, indicating that their biological activities depend on their microenvironment. This has clinical

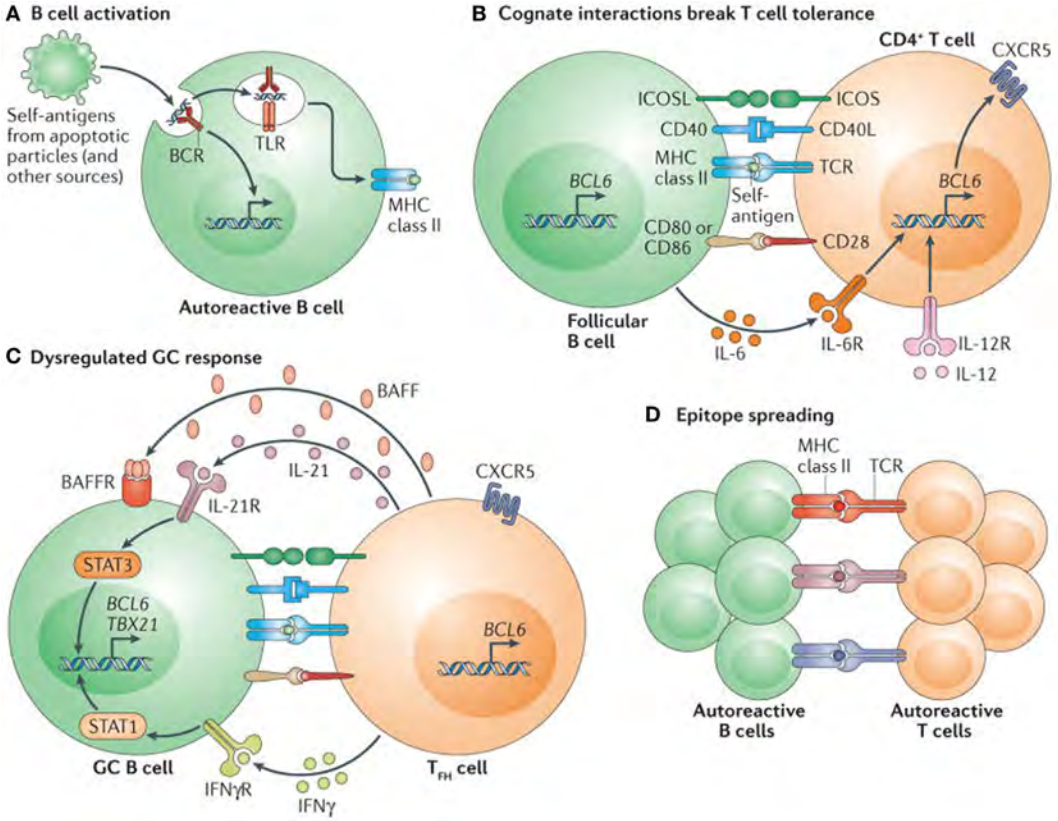

FIGURE 4 | Self reactive B cells initiate autoimmune germinal center (GC) formation by facilitating breaks in T cell tolerance. **(A)** After binding to self-antigen (either soluble or bound to antigen-presenting cells) derived from apoptotic particles or other disease-specific targets, autoreactive B cell receptors (BCRs) traffic nuclear antigens to the endosomal receptors toll-like receptor 7 (TLR7) and TLR9, resulting in initial B cell activation in response to integrated BCR-dependent and TLR-dependent signaling. In parallel, endolysosomal enzymes also process internalized self-antigens (including a broad range of nucleic acid-associated proteins) into peptides for loading onto MHC class II. **(B)** B cells function as antigen-presenting cells to present MHC class II-bound peptides to cognate self-reactive $CD4^+$ T cells at the T cell–B cell border of lymphoid follicles. Together with co-stimulatory signals provided by CD80 and/or CD86 and inducible T cell co-stimulator ligand (ICOSL), self-reactive B cells initiate breaks in $CD4^+$ T cell tolerance. Activated $CD4^+$ T cells subsequently express CXC-chemokine receptor 5 and B cell lymphoma 6 (BCL-6), resulting in their migration to the B cell follicle as early T follicular helper (T_{FH}) cells (not shown). Activated B cells also produce interleukin-6 (IL-6), which may facilitate T_{FH} cell differentiation by inducing BCL-6 expression, although this has not yet been directly tested. **(C)** T_{FH} cells promote GC formation through the production of IL-21, which sustains B cell BCL-6 expression and promotes B cell activation, class-switch recombination and plasma cell differentiation. In autoimmune settings, interferon-γ (IFNγ; probably derived from activated $CD4^+$ T cells) drives GC formation in a B cell-intrinsic, signal transducer and activator of transcription 1-dependent manner, in part by enhancing BCL-6 expression. IFNγ also promotes B cell-intrinsic expression of the transcription factor T-bet (encoded by *TBX21*), which is required for class-switch recombination to pathogenic IgG2a and IgG2c isotypes, but is redundant for IFNγ-driven GC formation. Although not yet directly tested in autoimmune models, this dysregulated GC response is probably affected by additional cytokines, including B cell-activating factor (BAFF), which promotes the selection of high-affinity GC B cell clones, and IL-12, which facilitates T cell IFNγ production and T_{FH} cell differentiation. **(D)** Iterative interactions between GCB cells and cognate T_{FH} cells within ongoing autoimmune GCs probably result in epitope spreading and the recruitment of additional autoreactive T cell and B cell clones. Abbreviations: BAFFR, BAFF receptor; CD40L, CD40 ligand; ICOS, inducible T cell co-stimulator; IFNγR, IFNγ receptor; IL-6R, IL-6 receptor; TCR, T cell receptor. Reprinted from Ref. (60) with permission from Springer Nature.

relevance because the clinical course of many autoimmune diseases has multiple stages and phases, and microenvironments may significantly influence them (74).

Recent studies suggest that regulatory B cells (B_{regs}) that produce IL10 or TGFβ, capable of preventing or suppressing autoimmunity, may do so by introducing anergy in T cells (74).

The anatomical microenvironment of the germinal centers, considered essential for B cell differentiation and maintenance of homeostasis, may also facilitate induction of effector T cell function (75). B cells can influence maintenance and development of effector $CD4^+$ memory T cells, induction of peripheral tolerance, and regulation of the balance of helper T cells (75, 76). In germinal centers, B cells can present antigens to memory T cells and elicit cytokine production (77). They provide a second activation signal to follicular $CD4^+$ T cells, previously activated by dendritic cells (75, 76). Consequently, IL4 produced within the germinal centers can provide a microenvironment for Th2 development (77).

B CELL DEPLETION THERAPY

The concepts that guided initial investigations to use BDT in treating autoimmune disease, were primarily to provide the

immune system reinstallation of regulating of emerging autoreactive B lymphocytes and establish a normal B cell repertoire (i.e., restoration of tolerance) (78).

B cell depletion therapy agents consist are hybridomas, produce IgG1 monoclonal antibodies that specifically target the CD20 molecule (78). The presence on mature B cells, but not on stem cells, plasmablasts, and plasma cells (79) significantly influences the pharmacokinetics and biopharmacology of BDT. Its efficacy depends on dosage, diffusion into the tissues, kinetics of elimination, and frequency of administration (80).

Mechanism of Action

The binding of BDT to the CD20 molecule leads to cell lysis and subsequently their disappearance from PB. Some depletion mechanisms include antibody dependent cellular cytotoxicity (ADCC), complement dependent cytotoxicity, phagocytosis by the reticuloendothelial system, and apoptosis of B cells by crosslinking CD20 molecules (80).

The clinical benefits of BDT were based on the "Road Block Hypothesis" (81). In the road from physiologic to autoimmune state, the autoreactive B cells may play a significant role in producing inflammation and pathogenesis by shifting the repertoire toward antigen-specific autoreactive B cells and BCR. Therefore, the hypotheses proposed that, depleting these autoreactive B cells, could eliminate interactions between costimulatory signals and pro-inflammatory mediators (81). Consequently, the "road" to autoimmunity would be blocked; local inflammation would be eliminated, resulting in clinical recovery.

Effects on Different Compartments of Immune System

B cells depletion is not universal, differs significant in different compartments of the immune system which has implication on clinical outcomes. 100% depletion is observed in the PB, compared to 32% in the BM, perhaps lower levels in germinal centers and marginal zones of LNs and spleen (82, 83). Furthermore, PB $CD20^+$ cells account for approximately 2% of the total B cell population (84). Usually B cells differentiation and maturation occurs in the BM, where stromal cells produce factors promoting their survival and growth (85).

Role of Memory B Cells

The role of memory B cells in the clinical responses, final clinical outcome, notably relapse, cannot be overemphasized. Clinical response is observed with depletion of $CD19^+$, $CD27^+$ memory cells from the PB and BM (86). Studies demonstrate that pretherapy levels of $CD27^+$ memory cells may predict clinical response. Better responses are observed in patients with lower levels than with higher levels (87, 88). Clinical response is also influenced by the pre and post treatment levels of long-lived plasma cells and levels of survival factors (87, 88). After BDT infusion, there is a repopulation of naïve B cells that are CD38 high, CD27 high, and $sIgD^-$. There is a decrease in the number of non-class-switched (IgD^+, $CD27^+$) and class-switched (IgD^-, $CD27^+$) memory B cells (86, 89). A gradual decrease in levels of naïve B cells and a progressive increase in $CD27^+$ memory B cells occur as the pharmacological effects BDT begin to diminish (86).

Patients that do not demonstrate a favorable clinical response to the initial treatment with RTX, may have high levels of plasmablasts/plasma cells. Additional cycles, before complete repopulation occurs, could increase chances of good clinical response (86).

Several patients in clinical remission may have demonstrable levels of autoantibodies, because long-lived plasma cells, unaffected by BDT, produce them (90).

After depletion, return to normal levels is observed in all B cell compartments. Simultaneously, return to balance and appropriate ratios of Th1/Th2, increased numbers of helper T cells and T regulatory (T_{reg}) cells occurs (91). Increase in T_{regs} is reported in ITP and systemic lupus erythematosus but not in RA patients, may be because they are simultaneously treated with methotrexate (91–93). This observation puts into focus the effects and influence of CS and ISA used as concomitant therapy with RTX. In many studies, "concomitant therapy" after RTX is continued, albeit in lower dosages.

Duration of Remission

The duration of clinical remission following BDT depends on known and unknown factors. A key factor is the duration required for $CD27^+$ memory B cells to exit the BM, reach the spleen and LNs, and become autoreactive (88). Naïve memory cells are more susceptible than long-lived memory B cells (88). It is reported that, if at 2 years post-RTX, the levels of memory cells are less than 50% of their pretreatment levels, remissions are longer (94, 95). The process of conversions into memory cell phenotype occurs by somatic hyper-mutation, during highly variable periods, and can take up to 6 years after a single cycle of BDT (89). Longer remission occurs when fewer memory cells enter germinal centers of LNs and spleen and become plasmablasts and plasma cells (94).

Repopulation

Almost complete depletion of $CD20^+$ B cells in the PB occurs within 3–7 days after the first infusion of BDT. Repopulation to normal levels in the PB, minimally requires between 6 and 12 months and could be 3 years (84). Repopulation influences clinical course, outcome, need for future therapy, and depends on extent of depletion, clearance of BDT and BM capacity to regenerate (84). A factor that has not received attention is presence of comorbidities, specially coexisting autoimmune diseases.

Formed inside and outside germinal centers, several subpopulations of memory cells, with different phenotypes develop during repopulation (88). In autoimmune diseases, there are greater expansions in $IgD^-IgM^+CD27^+$ and IgG^-CD27^+ phenotypes (96–98), that predominantly use IgG1 and IgG3, potent activators of complement and involved in target killing by ADCC (99).

During the process of repopulation, $CD27^+IgD^-IgM^-CD38^+$ plasmablasts undergo differentiation, maturation, somatic mutation, and eventually become plasma cells (100, 101). $CD20^-$ plasma cells not detected in the PB during depletion are detected during repopulation (102, 103). Not infrequently, measurable levels of pathological autoantibodies are detected when repopulation reaches pretreatment levels, since long-lived plasma cells, repopulate (104) consequent to increased production of BAFF by the spleen (105).

This is a paradoxical effect of BDT. It depletes $CD20^+$ B cells, but facilitates the differentiation and growth of short-lived plasma cells to become long-lived plasma cells in the spleen (105–107).

Relapse After BDT

Rheumatoid arthritis (RA) was the first autoimmune disease, in which multiple trials showed significant clinical benefit after two infusions of 1 g of RTX, 15 days apart, mostly in 6–12 months follow up studies (108). In RA, the high incidence of relapse requires multiple cycles to maintain clinical remissions (12, 15), having influence on cellular and humoral immune responses (74). Incidence of relapse is directly related to the duration of follow-up reported in the study (11). Longer follow-ups have higher incidence, reaching 70–85% (11).

Usually relapse does not occur until repopulation of $CD20^+$ B cells reach pretreatment level (86, 101, 109), and with increase in B cells exiting the BM into the microenvironment (90, 110), where with appropriate signals they differentiate into autoreactive B cells (90).

Levels of BAFF and autoreactive plasmablast are high in the PB during active disease (111). BAFF-R expression is reduced on naïve and memory B cells during relapse, regardless of serum BAFF levels (110).

Repopulation of autoreactive memory B cells and/or plasmablasts accompany relapse, and may be predictors of relapse (88). Soluble-free light chains and CD23 affect differentiation of plasmablasts present in early phase of relapse (90, 111). During relapse $CD95^+CD27^+$ cells that produce proinflammatory TNFa and IL10 have higher ratios compared to transitional cell in PB (112).

In the microenvironment of the germinal center, maintenance of memory B cells is independent of T cell interaction (75), but necessary for their differentiation into long-lived plasma cells (75, 113).

Proinflammatory autoreactive B cells in the microenvironment are characterized by the Ki67 marker present on pre B and immature B cells leaving the BM, while kappa-deleting recombination excision circles characterize migrating transitional cells (114, 115). Autoreactive B cells demonstrate high proportions of Hep2 autoreactive antibodies and have high prevalence of T1858, PTPN22 risk alleles (55, 64).

B cell depletion therapy has several serious adverse events, notable infection, due to immune suppression, resulting in septicemia and death (116). IVIg can reduce this risk. Late onset neutropenia associated with pneumonia (12, 116, 117) and cardiac issues (117) is of significant concern.

From a panoramic perspective, some investigators have suggested the following, "the evidence therefore indicates that currently used anti-CD20 treatments do not return the patient to an earlier state of immunity akin to the 'tabula rasa' (that is a blank slate), in which all the past levels reminiscent of memory and proves (auto) immune responses have been excised" (100).

Processes vital to central and peripheral tolerance, such as anergy, receptor editing, and deletion among others, are not affected or restored by BDT (118), consequently it cannot eliminate autoimmunity for sustained durations. Eventually, autoreactive B cells with the cooperation of autoreactive T cells produce inflammation giving the microenvironment a pathologic profile and autoimmune disease return (118).

IVIg THERAPY

Intravenous immunoglobulin has been used in treating immuno-deficiencies for more than six decades. It has to be used as monotherapy, or as an adjunct with other drugs, in treating autoimmune and inflammatory disease for several years (17). It influences almost every component of the immune and inflammatory systems, producing multiple beneficial results.

Mechanism of Action

Intravenous immunoglobulin's has multiple mechanism of action (17). In **Figure 5**, the influence of IVIg on innate and adaptive immunity is presented. The $(Fab)_2$ fragment and Fc fragment of the molecule, are known to have different functions and effects. The $(Fab)_2$ fragment plays a vital role in killing of target cells, the blockade of cell–cell interactions mediated by cell-surface receptors, such as CD95 and CD95 ligand; the neutralization of cytokines; the neutralization of autoantibodies by anti-idiotypic antibodies; and the scavenging of the anaphylotoxins C3a and C5a (17, 18). The Fc portion may play a vital role in Fc-dependent pathways include; the saturation of the FcRn; the expansion of regulatory T (T_{reg}) cell populations; the blockade of immune complex binding to low-affinity Fcy receptors (FcyR); the modulation of dendritic cell activation *via* FcyRIII; and the modulation of activating and inhibitory FcyR expression on innate immune effector cells and B cells (19, 20). IVIg regulates FcyRIIIa and IFN-yR2 on circulating dendritic cells and by stimulating production of IL-33 by human macrophages (119). This provides an important anti-inflammatory effect of IVIg through the IL1 receptor antagonist levels (120).

Its anti-inflammatory effects and its ability to regulate immune balance are its most important functions (21–23, 121–125). Therefore, IVIg has the capacity to eliminate clinical autoimmunity, restore a state of tolerance, and reinstate physiologic homeostasis (17, 18).

Role in Autoimmunity and Autoimmune Disease

Intravenous immunoglobulin can influence repertoire of mature B cells, including their heterogeneity, and consequently plasma cells (17), which affect the persistence of autoimmunity, and possibly its elimination (24, 126–129).

Intravenous immunoglobulin facilitates the migration of immature plasmablasts and naïve plasma cells from BM into PB and eventually the microenvironment of diseased tissue (129, 130). These cells differentiate into $CD138^+$ plasma cells that produce normal or physiologic antibodies that play a critical role in restoring immune balance (18). In the diseased microenvironment, previously present pathogenic autoantibody producing plasma cells compete with these new normal plasma cells for survival and growth factors (131). Positive clinical response to IVIg correlates with increased number of normal $CD138^+$ plasma cells (130).

The effects of IVIg on regulatory T cells (T_{regs}) eventually decrease inflammation resulting from Th1 and Th17 cells (23). IVIg imposes a tolerogenic state to the dendritic cells accompanied

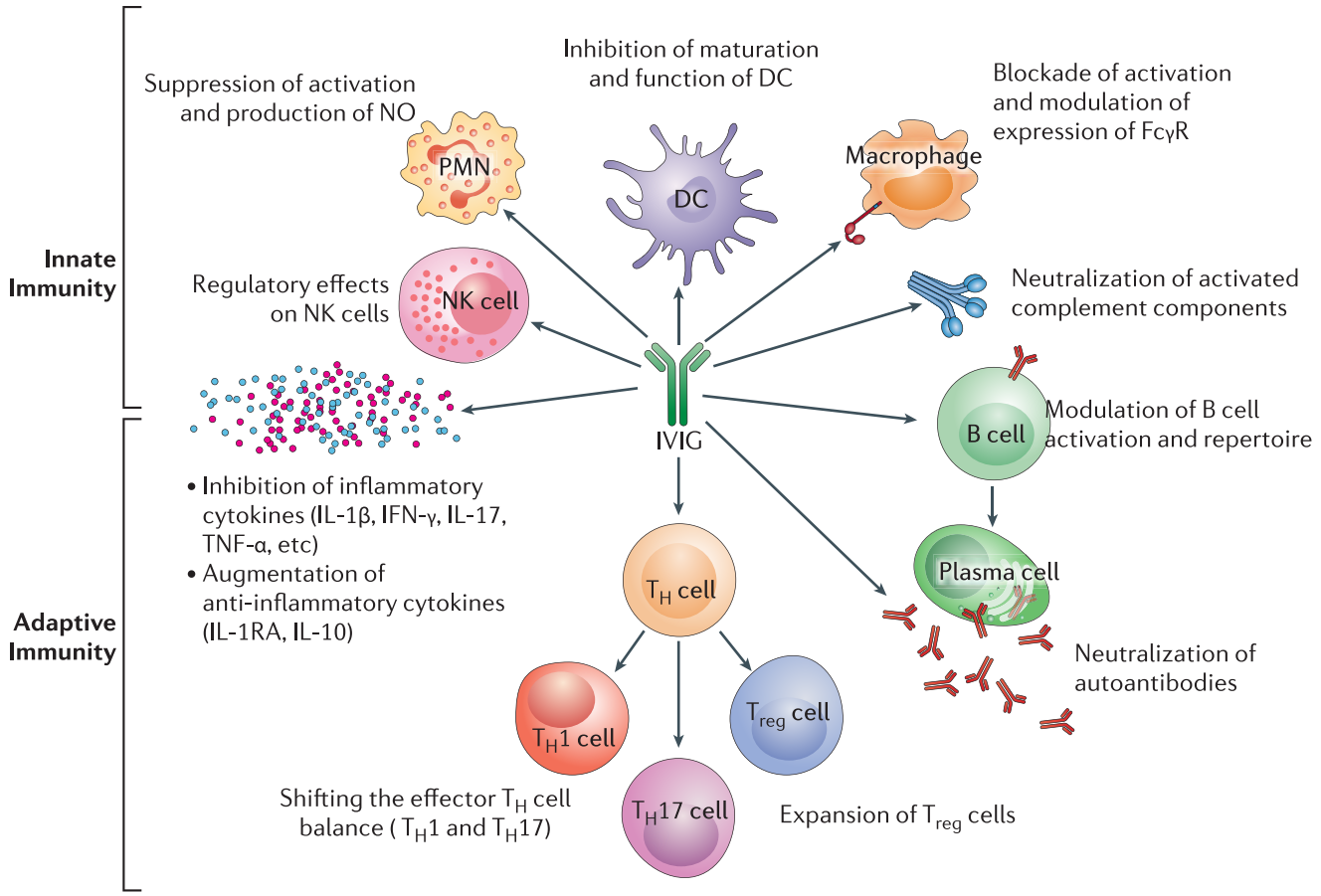

FIGURE 5 | The impact of intravenous immunoglobulin (IVIg) on the innate and the adaptive immune compartments in the context of autoimmune and inflammatory diseases. IVIg inhibits activation and function of various innate immune cells, such as DCs, monocytes, macrophages (MΦ), neutrophils [polymorphonuclear cells (PMN)], and NK cells. It neutralizes activated complement components. In addition, IVIg modulates B-cell functions and plasma cells (Pl), reciprocally regulates T_{reg} cells and effector T cells, such as T_h1 and T_h17 subsets and downregulates the production of inflammatory cytokines. Reprinted from Ref. (16) with permission from Oxford University Press.

by an expansion of antigen-specific T_{regs} which are ultimately capable of decreasing inflammation in the microenvironment (23, 132).

Several lines of evidence indicate that IVIg establishes a physiologic homeostasis in tissue environments, by multiple mechanisms such as anti-idiotypic antibodies (127, 133, 134), increasing the population of T_{regs} and normal BCR, the TGF_B receptor of T and B cells, downregulating TNFα. IL-1, 2, 3, 4, 5, 6, 8, 11, and 17 and CXL2, 3, and 5 decreasing amounts of BAFF/APRIL and modulating FcyR (18–20, 119, 127, 133–138). Decrease in tissue inflammation occurs because IVIg maneuvers the functionally aberrant lymphocytes, neutrophils, macrophages, and other cells toward their normal physiologic states (18–20, 119, 127, 134–138). IVIg facilitates the development and proliferation of regulatory T_{regs} and B_{regs} (20, 23, 127, 132, 134–139).

Influence on Checkpoints

The role of checkpoints is crucial in maintaining the state of tolerance and is detailed in **Figure 2** (56). Through the process of somatic mutation in naïve B cells, IVIg enhances the expression of IgD on the cells surface (140), which is implicated in the induction of anergy. Continued anergy eventually silences autoreactive B cells (56, 64). Receptor editing of BCR in autoreactive B cells is facilitated by the interaction between IVIg and CD22 (141). IVIg influences normal B cell by enhancing Vh germ line usage, and VDJ recombination process, which indirectly affects autoreactive B cells (142). IVIg promotes increased usage of Vh3–30 and 3–23 gene segments during the VDJ recombination process. This promotes the increased production of a normal B cell repertoire (142–144). It induces apoptosis of many cells *via* either Fas–FasL pathways or through anti-idiotypic antibodies (145, 146). Thus the cumulative evidence demonstrates that IVIg can induce and promote processes that mimic the actions and functions of physiologic checkpoints and thus has the capacity and efficacy to eliminate autoreactive T and B cells (57, 59).

Role of IVIg in Immunoprophylaxis

One of the most important aspects and secondary benefits of the Ahmed protocol is the role of IVIg in providing immunoprophylaxis, as evident by the fact that none of patients, in their studies

had serious infections, were hospitalized or died from infectious etiologies (29, 41–44). Prolonged B cell depletion can induce immunosuppression by several mechanisms (147). In RA, it has been reported that 10% patients have hypogammaglobulinemia after first course of RTX and 30% after fourth course (148), becoming a risk factor for infection (147). RTX induced prolonged B cell depletion impairs T cell-mediated immunity with decreased risk for viral and fungal interferons (147). The issue of infection during immunosuppression is more significant in blistering disease, because denuded epithelium is more susceptible to infection. Indeed currently, the commonest cause of death in blistering diseases is infection (149).

There is significant body of evidence that documents the ability of IVIg therapy to prevent and fight serious infections and potentially fatal infections (150). An extensive or detailed validation of this is beyond the scope of this concept paper. Examples of such situations are as follows. Patients with RTX-induced hypogammaglobulinemia have serious, multiple, or recurrent infection for which IVIg therapy has been used (151–153). IVIg is a valuable therapeutic agent in several serious infections (154–156) and its use resulted in decrease of duration of hospitalization (157). It is considered standard therapy in patients with sepsis (150, 158, 159) including neonatal sepsis (160) and especially in post-surgical sepsis (161–163). It has been frequently used to treat immunosuppression in patients with malignancy, wherein the cancer itself or to its treatment produced it (164), and with significant benefits in multiple myeloma (165).

Intravenous immunoglobulin is also routinely used in protocols for bone marrow or solid organ transplants (166, 167). A meta-analysis of nine randomized trials, involving 435 patients using several objective parameters for assessment, in patients with severe sepsis and septic shock, IVIg not only was more effective clinically but also more cost-effective (168).

In **Table 2,** the authors have presented a synopsis of how the various compartments of the immune system are affected in autoimmunity. It is not all inclusive or exhaustive. Its purpose is to demonstrate some of the influence of BDT and IVIg on these compartments.

SELECTED RECENT STUDIES AND RELATIONSHIP TO "CONCEPT"

Several recently published studies have impact and influence on the "concept." However, two publications warrant mention because of their content and immediacy of impact.

First is a recent study involving 90 untreated PV patients, by 36 investigators, from 25 centers in France, in which RTX is recommended as first-line treatment (169). The control group had 44 patients, who received only prednisone, dose of 1 mg/kg/day, for moderate disease, for 12 months, and 1.5 mg/kg/day, for

TABLE 2 | Mechanisms of immuno-regulation in the microenvironment in an autoimmune disease state and post-therapy.

	Microenvironment, tolerance, checkpoints	Ig, autoAbs, BCR, and Fc receptor	B cells, memory cells, and plasma cells	Cellular and complement pathways	Cytokines
Autoimmunity (lifelong)	– Chronic inflammation – Loss tolerance – Defective checkpoints	– Increased IgG class switching – Elevated levels autoAbs – Formation immune complexes – Activation FcγRI/FcγRIII loss regulatory FcγRIIB	– Increase autoreactive B cells – Induction of short- and long-lived autoreactive memory and plasma cells	– Increased neutrophil/ monocytes/macrophages activation – Activation complement cascade – Activation autoreactive T cells – Imbalance ratio of Th/Tregs Cells	Inflammatory: – IL1–10, INFγ, TNFa, TGF-b CXCL3, CXCL5, CCL13, XCL2 IL10: – Loss of protective effect – Production B cell autoAbs – Favors class switch to IgG4
B cell depletion (repeated infusions)	– Rapid, temporary depletion CD20+ B cells decrease inflammation – No effect on tolerance – No effect on checkpoints	– Downregulation BCR – Decreased autoAbs levels – Inhibition of FcRs – Repeated infusion reduces Serum IgM, IgA, and IgG	– Increase transitional cells – Increase Bregs – Decrease short-lived autoreactive cells – Expansion autoreactive memory B-cells – No effect on long-lived autoreactive plasma cells	– Neutropenia – Decreased monocytes/ macrophage/DC activity – Complement consumption – Restoration Th1/Th2 ratio – Increase Tregs – Inhibit CD4 + T cells	– Decreased IL activity – Increased BAFF/APRIL levels – Increased transitional Anti-inflammatory IL-10
Intravenous Ig (repeated infusions)	– Sustained, decreased inflammation – Restores tolerance – Mimics checkpoints	– Inhibit FcγRI/FcγRIII – Upregulate FcγRIIB – Edit autoreactive BCR – Deletes autoreactive BCR – Deactivate autoreactive BCR – Increased production new non-self-reactive IgG, IgM	– Inhibition autoreactive B-cell differentiation – Induction B-cell apoptosis – Regulation B-cell subsets – Production of new, naïve non-autoreactive plasma/ memory cells	– Neutrophil apoptosis – Reduction complement levels – Modulation CD4 + – T cell differentiation – Suppress Ag-specific T cells – Upregulation Tregs population	– Inhibition selective IL activity, – Decrease BAFF/APRIL levels – Increase regulatory anti-inflammatory IL-10 production

Abs, antibodies; Ag, antigen; APRIL, a proliferation ligand; BAFF, B cell activating factor; BCR, B cell receptor; Bregs, B regulatory cells; DC, dendritic cell; Ig, immunoglobulin; IL, interleukin; R, receptor; Th, T helper cell; Treg, T regulatory cell.

severe disease, for 18 months. The study group of 46 patients was treated as follows. Initially, moderately severe patients received 0.5 mg/kg/day for 3 months and patients with severe diseases got 1.0 mg/kg/day for 6 months. They received 1 g of RTX at day 1 and 15, followed two prophylactic doses of 500 mg each, at month 12 and 18. This was done, although in an earlier report, the lack of benefit from "prophylactic" use of RTX in preventing relapses had been demonstrated (170). A statistically significant difference in benefits was observed in the RTX (study) group.

There are certain grave concerns regarding this study. The initial design of 2 years follow-up was extended to 3 years, with only one visit at month 36. Surprisingly, 79 of 90 patients (88%) with severe disease were never treated. Usually patients in countries with or without socialized medicine, with PV, would have been treated soon, and not have allowed to progress to untreated severe disease.

Incidence of relapse is vital to any RTX study on PV and reflects its validity and utility. Information on relapses is presented at multiple sites. The authors state that at month 24, 11 out of 44 patients (25%) had relapses, 4 (10%) of which were severe and 7 (15%) were moderate. Careful reading showed that 8 of 11 occurred in 6–12 months and three during 12–24 months. However, at month 36 only 2 of 41 patients (2%) had a relapse. Yet the authors report that 41 of 44 (89.8%) patients were in complete remission, off therapy at month 24. What is lacking is information on duration and treatment of the relapses, since there is no mention of additional RTX treatment. In the patients who relapsed within 6–12 months, were their B cells completely deleted by the two RTX infusion, prior to their developing a relapse? Did their B-cells repopulate within 6–12 months? How successful is a therapy when 25% of patients, relapses in less than 1 year? Since relapses were accompanied with increase in anti-desmoglein autoantibody titers, the critical question is, after initial RTX therapy did anti-desmoglein antibodies decrease, disappear, or remain unchanged. This would also be a valuable index of efficacy. The relapses in this study further support the inability of the "prophylactic" use of RTX to prevent relapses.

The issue of relapse and its management is critical to RTX therapy and to physicians using it. In these PV patients more detailed and clear information was needed.

It is difficult to duplicate or verify such a study based on patient selection. Finding 79 patients with severe untreated disease is a daunting task. Similarly, administering only high dose systemic corticosteroids, without any ISA is unlikely, especially when their significant and catastrophic adverse events are known and especially in patients with severe disease. In most instances, patients, their relatives, or their primary care physicians would not permit this option. It is also unclear that how many patients had more than one serious adverse event. The authors report that from a total of 80 patients, 20 patients (25%) had significant infections, 10 patients (13%) cardiovascular disorders, 6 patients (8%) psychiatric disorders, 10 patients (13%) bone disorders including fractures and osteoporosis 17 patients (21%) diabetes and endocrine disorders, while 13 patients (16%) developed steroid myopathy. It appears that these data were collected at month 24, and are very significant and concerning. What about month 36?

The manufacturer provided the drug. Based on this specific study, RTX has been granted Expedited Review or Fast Track Approval by the Food and Drug Administration of the US. Most investigators would consider a confirmation of this study in the US, essential. In studies with long-term follow-up, multiple relapses are reported (11). It would be important to know of the 44 study group, French patients develop relapses on longer observation periods. In spite of these comments, it needs to be recognized that this is the only randomized controlled trial (RCT) examining the efficacy and safety profile of RTX in PV. Recent studies indicate multiple infusions of BDT are necessary for rheumatoid arthritis patients to maintain a comfortable clinical condition (92). Consequences of large numbers of infusion, on the immune and inflammatory systems, could possibly emerge 20–30 years later.

An interesting and relevant clinical trial is currently in progress. A total of 124 patients with moderate to severe PV will be enrolled at 60 centers worldwide, to evaluate the efficacy and safety of RTX versus mycophenolate mofetil. It will involve a 52-week double blind treatment period and a 48-week post-treatment discontinuation safety follow-up period. Since the follow-up period is limited, it may not address its impact on the clinical course, especially production of long-term sustained clinical remissions or the issue of later relapses. Information on this clinical trial is available at clinicaltrials.gov identifier NCT02383589.

The second study, from the October 2017 issue of Frontiers in Immunology (84) examines what has been learnt from therapies that target CD20 and future trends. Most importantly, it addresses a vital issue, the need to enhance the efficacy of current BDT. This efficacy depends on its ability to penetrate lymphoid tissues (171). Studies in mice and primate indicate that B cell depletion in the BM, spleen, and lymphoid tissues frequently require larger amount of anti CD20 antibody. If not eradicated, there is a potential for such sites to act as reservoirs, from where autoreactive B cells can emerge leading to relapse (84). This may account for inability of a single cycle of RTX, to produce long-term remissions and also cause for frequent relapses in many patients (84). Cumulatively, these studies explain why frequent multiple doses given initially are more effective. Indirectly they also provide support for the initial and 1-year systematic use of RTX in the Ahmed Protocol.

Information on enhancing efficacy of BDT therapies is still evolving. Glycoengineering and Fc engineering have shown benefits (84). Several new immunomodulatory molecules are being developed for use with anti CD20 therapy. Some of these are STING antagonist which increases expression of activated FcγR's crucial for antibody mediated therapy (84). Ibrutinib, an irreversible inhibitor of Btk, idelalisib targets the delta form of lipid kinase phosphoinositide-3-kinase expressed on leukocytes, Ventoclax an inhibitor that targets Bcl-2 (84). Bispecific antibodies are emerging (84). Investigators have combined antibodies to CD19 and CD3, CD20 and CD22, and a tribody which combine two CD20 antibodies with antibody to Fcγ RIIIA (84). Lenalidomide combined with anti-CD20 has greater benefit than anti-CD20 alone (84).

Decrelizumab as an anti-CD20 antibody has been effective in progressive multiple sclerosis (MS) and Ublituximab, a glycoengineering anti-CD20 mAb also helps MS patients. Some investigators recommend antibodies to BAFF to be more effective than RTX alone in autoimmune disease (84).

Autoreactive B cells and T cells have multiple participants during their development and functional processes. Blocking a single or limited number, may cause the human body to find the alternative pathways to bypass the block. Since IVIg influences many pathways of the immune and inflammatory system. (**Table 1**), it is entirely possible that IVIg may already contain some of these pharmacologically active agents under investigation and more. Their concentration may be low and variable. Further such studies on IVIg are, therefore, warranted.

SYNERGISTIC EFFECT OF IVIg WITH RTX

Based on the Ahmed protocol presented in this manuscript (**Figure 1**), the preceding discussion provides some mechanisms that account for the positive clinical outcome and prolonged remissions.

Rituximab eliminates autoreactive B cells from the PB shortly after its initiation. As BM and possibly the spleen and LNs expunge their autoreactive cells, subsequent periodic infusions eliminate them. Reduction of inflammation in the microenvironment, results from elimination of autoreactive B cells and proinflammatory mediators. These processes were enhanced by the anti-inflammatory effects of IVIg used simultaneously. This process continues during the B cell depletion phase. Inspite of lack of B cells, and prolonged immune suppression, there were no serious infections, because of immunoprophylaxis was provided by IVIg. In addition, when the effects of RTX begin to wear off, IVIg exerts immune restoration by increasing T_{reg}, B_{reg}, macrophages, dendritic cells, and promoting more $CD138^+$, normal plasma cells. It decreases population of autoreactive B cells in the microevironment, decreases BAFF, other growth factors, neutralizes cytokines like IL4, IL6, and IL10 among others. Anti-HLA antibodies could reduce presentation of autoantigens to T cell receptors. In the reduction and absence of inflammation, the tissue microenvironment now has the opportunity to return to physiologic homeostasis, since IVIg continued in phase 3 of the protocol, accomplishes this by mimicking the function of checkpoints. In doing so, IVIg reduces emergence of autoreactive B and T cells, possibly decreasing chance for relapse. RTX's inability to influence checkpoints is compensated by IVIg. The gradual withdrawal of IVIg allows the dysfunctional immune regulation to slowly return to normality until fully restored, and retain it for the foreseeable future.

FUTURE STUDY DESIGN

One of the objectives of this concept paper is to stimulate investigators to treat larger cohorts of patients with autoimmune blistering diseases with this combination treatment (Ahmed protocol), and investigate its potential benefit in other autoimmune diseases. Patients who are non-responsive to conventional therapy should be studied first, especially those with recalcitrant diseases. Defined inclusion criteria are essential. Four groups with reasonably similar disease severity would be required (i) RTX^+ IVIg, (ii) RTX only, (iii) IVIg only, and (iv) CS and ISA. Careful monitoring of clinical disease with an objective scoring system, repeated serological testing, evaluation of lymphocytes subsets in PB at pre-determined time interval, memory B cells (CD27), T_{regs}, and B_{regs} plasma cells and regular assessment of several serological markers, such as BAFF, BAFFR, IL1, ILRA, IL4, IL6, IL10, and others. Likewise serum IgG, IgA, and IgM should be evaluated as designated intervals. When possible, various microarrays, proteomics, and other developing assays and technologies could be used to distinguish responders from non-responders. It would be essential to have the number of patients in each category sufficient for statistical analysis. One of the most important and key element would be a follow-up of 5 years or more. Without a long follow-up, the impact of the treatment on the clinical course and relapse cannot be completely assessed. The authors realize that obtaining funding for such a study could be a great challenge.

CONCLUSION

In conclusion, the authors consider that the combination of IVIg and BDT (Ahmed Protocol) could be a very valuable modality to treat patients with autoimmune diseases, especially those who are non-responsive to conventional immunosuppressive therapy or to BDT, and especially those with recalcitrant disease. The authors are not recommending this as standard of care or first-line therapy. Instead, it should be a treatment of last resort. Its initial and limited use has demonstrated that in patients with recalcitrant severe wide spread autoimmune mucocutaneous diseases, prolonged sustained disease and drug-free remissions, without relapse, infections, mortality, or hospitalization have been reported. The authors cannot predict whether factor(s) that initiated or precipitated autoimmune disease cannot recur in the future, or that reversal of autoimmunity would last lifelong. These patients enjoy a high quality of life they had never experienced, nor such a complete remission. These clinical observations provide the foundation and opportunity to conduct research which could produce meaningful insights into central and peripheral tolerance and mechanism for its restoration. Clinical recovery, accompanied by serological and immuno-pathologic remission, persistent normal levels of B cells, and lack of other immune abnormalities, would strongly suggest that, in this patient population, combined treatment with RTX and IVIg, possibly resulted in the reversal of autoimmunity and autoimmune disease.

AUTHOR NOTE

Since the submission and acceptance of this manuscript in May 2018, the Food & Drug Administration of the US has approved the use of rituximab in the treatment of pemphigus vulgaris.

AUTHOR CONTRIBUTIONS

ARA and SK: both authors contributed equally to the entire process.

ACKNOWLEDGMENTS

The authors are grateful to Dr. Yana Turkowski and Dr. Shawn Shetty for their valuable help in preparing the manuscript. This study was supported in part by an unrestricted educational grant from the Dysimmune Diseases Foundation, Plantation, FL.

REFERENCES

1. American Autoimmune Related Diseases Association. *Autoimmune Disease Statistics*. Available from: https://www.aarda.org/news-information/statistics/#1488234345468-3bf2d325-1052.2017
2. Wang L, Wang FS, Gershwin ME. Human autoimmune diseases: a comprehensive update. *J Intern Med* (2015) 278:369–95. doi:10.1111/joim.12395
3. Truhan AP, Ahmed AR. Corticosteroids: a review with emphasis on complications of prolonged systematic therapy. *Ann Allergy* (1989) 62:375–91.
4. Bijlsma JW, Van Everdingen AA, Huisman M, De Nijs RN, Jacobs JW. Glucocorticoids in rheumatoid arthritis: effects on erosions and bone. *Ann N Y Acad Sci* (2002) 966:82–90. doi:10.1111/j.1749-6632.2002.tb04205.x
5. Zhang J, Jacobi AM, Wang T, Diamond B. Pathogenic autoantibodies in systemic lupus erythematosus are derived from both self-reactive and non-self–reactive B cells. *Mol Med* (2008) 14:675–81. doi:10.2119/2008-00066.Zhang
6. Tandan R, Hehir MK, Waheed W, Howard DB. Rituximab treatment of myasthenia gravis: a systematic review. *Muscle Nerve* (2017) 56:185–96. doi:10.1002/mus.25597
7. Moreno Torres I, García-Merino A. Anti-CD20 monoclonal antibodies in multiple sclerosis. *Expert Rev Neurother* (2017) 17:359–71. doi:10.1080/14737175.2017.1245616
8. Arnold DM, Dentali F, Crowther MA, Meyer RM, Cook RJ, Sigouin C, et al. Systematic review: efficacy and safety of rituximab for adults with idiopathic thrombocytopenic purpura. *Ann Intern Med* (2007) 146:25–33. doi:10.7326/0003-4819-146-1-200701020-00006
9. Caporali R, Caprioli M, Bobbio-Pallavicini F, Bugatti S, Montecucco C. Long term treatment of rheumatoid arthritis with rituximab. *Autoimmun Rev* (2009) 8:591–4. doi:10.1016/j.autrev.2009.02.008
10. Edwards JC, Cambridge G, Leandro MJ. Repeated B-cell depletion in clinical practice. *Rheumatology* (2007) 46:1509–14. doi:10.1093/rheumatology/kem164
11. Wang HH, Liu CW, Li YC, Huang YC. Efficacy of rituximab for pemphigus: a systematic review and meta-analysis of different regimens. *Acta Derm Venereol* (2015) 95:928–32. doi:10.2340/00015555-2116
12. van Vollenhoven RF, Emery P, Bingham CO, Keystone EC, Fleischmann RM, Furst DE, et al. Long-term safety of rituximab in rheumatoid arthritis: 9.5-year follow-up of the global clinical trial programme with a focus on adverse events of interest in RA patients. *Ann Rheum Dis* (2013) 72:1496–502. doi:10.1136/annrheumdis-2012-201956
13. Routy B, Boulassel MR, Spurll GM, Warner MN, Routy JP. Multiple cycles of rituximab therapy in chronic refractory immune thrombocytopenia: a case report with a 10-year follow-up. *Am J Ther* (2013) 20:219–22. doi:10.1097/MJT.0b013e318258905e
14. Rommer PS, Dörner T, Freivogel K, Haas J, Kieseier BC, Kümpfel T, et al. Safety and clinical outcomes of rituximab treatment in patients with multiple sclerosis and neuromyelitis optica: experience from a national online registry (GRAID). *J Neuroimmune Pharmacol* (2016) 11:1–8. doi:10.1007/s11481-015-9646-5
15. Anderson D, Phan C, Johnston WS, Siddiqi ZA. Rituximab in refractory myasthenia gravis: a prospective, open-label study with long-term follow-up. *Ann Clin Transl Neurol* (2016) 3:552–5. doi:10.1002/acn3.314
16. Winter O, Dame C, Jundt F, Hiepe F. Pathogenic long-lived plasma cells and their survival niches in autoimmunity, malignancy, and allergy. *J Immunol* (2012) 189:5105–11. doi:10.4049/jimmunol.1202317
17. Galeotti C, Kaveri SV, Bayry J. IVIG-mediated effector functions in autoimmune and inflammatory diseases. *Int Immunol* (2017) 29(11):491–8. doi:10.1093/intimm/dxx039
18. Schwab I, Nimmerjahn F. Intravenous immunoglobulin therapy: how does IgG modulate the immune system? *Nat Rev Immunol* (2013) 13:176–89. doi:10.1038/nri3401
19. Nagelkerke SQ, Kuijpers TW. Immunomodulation by IVIg and the role of Fc-gamma receptors: classic mechanisms of action after all? *Front Immunol* (2015) 5:674. doi:10.3389/fimmu.2014.00674
20. Samuelsson A, Towers TL, Ravetch JV. Anti-inflammatory activity of IVIG mediated through the inhibitory Fc receptor. *Science* (2001) 291:484–6. doi:10.1126/science.291.5503.484
21. Arumugam TV, Tang SC, Lathia JD, Cheng A, Mughal MR, Chigurupati S, et al. Intravenous immunoglobulin IVIG protects the brain against experimental stroke by preventing complement-mediated neuronal cell death. *Proc Natl Acad Sci U S A* (2007) 104:L14104–9. doi:10.1073/pnas.0700506104
22. Ruiz de Souza V, Carreno MP, Kaveri SV, Ledur A, Sadeghi H, Cavaillon JM, et al. Selective induction of interleukin-1 receptor antagonist and interleukin-8 in human monocytes by normal polyspecific IgG (intravenous immunoglobulin). *Eur J Immunol* (1995) 25:1267–73. doi:10.1002/eji.1830250521
23. Kaufman GN, Massoud AH, Dembele M, Yona M, Piccirillo CA, Mazer BD. Induction of regulatory T cells by intravenous immunoglobulin: a bridge between adaptive and innate immunity. *Front Immunol* (2015) 6:469. doi:10.3389/fimmu.2015.00469
24. Kazatchkine MD, Kavery SV. Immunomodulation of autoimmune and inflammatory diseases with intravenous immune globulin. *N Engl J Med* (2001) 345:747–55. doi:10.1056/NEJMra993360
25. Ahmed AR. Treatment of autoimmune mucocutaneous blistering diseases with intravenous immunoglobulin therapy. *Expert Opin Investig Drugs* (2005) 13(8):1019–32. doi:10.1517/13543784.13.8.1019
26. Martin TD. IVIg: contents, properties and methods of industrial production—evolving closer to a more physiologic product. *Int Immunopharmacol* (2006) 6:517–22. doi:10.1016/j.intimp.2005.11.005
27. Wang Y, Tian Z, Thirumalai D, Zhang X. Neonatal Fc receptor (FcRn): a novel target for therapeutic antibodies and antibody engineering. *J Drug Target* (2014) 22(4):269–78. doi:10.3109/1061186X.2013.875030
28. Kuwabara S, Mori M, Misawa S, Suzuki M, Nishiyama K, Mutoh T, et al. Intravenous immunoglobulin for maintenance treatment of chronic inflammatory demyelinating polyneuropathy: a multicentre, open-label, 52-week phase III trial. *J Neurol Neurosurg Psychiatry* (2017) 88:832–8. doi:10.1136/jnnp-2017-316427
29. Ahmed AR, Shetty S, Kaveri S, Spigelman Z. Treatment of recalcitrant bullous pemphigoid (BP) with a novel protocol: a retrospective study with a 6-year follow-up. *J Am Acad Dermatol* (2016) 74:700–8. doi:10.1016/j.jaad.2015.11.030
30. Bonilla FA. Pharmacokinetics of immunoglobulin administered via intravenous or subcutaneous routes. *Immunol Allergy Clin North Am* (2008) 28(4):803–19. doi:10.1016/j.iac.2008.06.006
31. Ahmed AR, Dahl MV. Consensus statement on the use of intravenous immunoglobulin therapy in the treatment of autoimmune mucocutaneous blistering diseases. *Arch Dermatol* (2003) 139:1051–9. doi:10.1001/archderm.139.8.1051
32. Gürcan HM, Jeph S, Ahmed AR. Intravenous immunoglobulin therapy in autoimmune mucocutaneous blistering diseases: a review of the evidence for its efficacy and safety. *Am J Clin Dermatol* (2010) 11:315–26. doi:10.2165/11533290-000000000-00000
33. Sami N, Ali S, Bhol KC, Ahmed AR. Influence of intravenous immunoglobulin therapy of autoantibody titres to BP Ag1 and BP Ag2 in patients with bullous pemphigoid. *J Eur Acad Dermatol Venereol* (2003) 17:641–5. doi:10.1046/j.1468-3083.2003.00714.x
34. Sami N, Bhol KC, Ahmed AR. Influence of intravenous immunoglobulin therapy on autoantibody titers to desmoglein 3 and desmoglein 1 in pemphigus vulgaris. *Eur J Dermatol* (2003) 13:377–81.
35. Sami N, Bhol KC, Ahmed AR. Influence of IVIg therapy on autoantibody titers to desmoglein 1 in patients with pemphigus foliaceus. *Clin Immunol* (2002) 105:192–8. doi:10.1006/clim.2002.5278
36. Sami N, Bhol KC, Ahmed AR. Treatment of oral pemphigoid with intravenous immunoglobulin as monotherapy. Long-term follow-up: influence of treatment on antibody titres to human α6 integrin. *Clin Exp Immunol* (2002) 129:533–40. doi:10.1046/j.1365-2249.2002.01942.x
37. Letko E, Bhol K, Foster CS, Ahmed AR. Influence of intravenous immunoglobulin therapy on serum levels of anti-β4 antibodies in ocular cicatricial pemphigoid. A correlation with disease activity. *Curr Eye Res* (2000) 21:646–54. doi:10.1076/0271-3683(200008)2121-VFT646
38. Nguyen T, Alraqum E, Razzaque Ahmed A. Positive clinical outcome with IVIg as monotherapy in recurrent pemphigoid gestationis. *Int Immunopharmacol* (2015) 26:1–3. doi:10.1016/j.intimp.2015.02.038
39. Galeotti C, Kaveri SV, Bayry J. Molecular and immunological biomarkers to predict IVIg response. *Trends Mol Med* (2015) 21:145–7. doi:10.1016/j.molmed.2015.01.005

40. Zhao T, Ren H, Wang X, Liu P, Yan F, Jiang W, et al. Rituximab-induced HMGB1 release is associated with inhibition of STAT3 activity in human diffuse large B-cell lymphoma. *Oncotarget* (2015) 6:27816–31. doi:10.18632/oncotarget.4816
41. Ahmed AR, Spigelman Z, Cavacini L, Posner M. Treatment of pemphigus vulgaris with rituximab and intravenous immune globulin. *N Engl J Med* (2006) 355:1772–3. doi:10.1056/NEJMoa062930
42. Ahmed AR, Kaveri S, Spigelman Z. Long-term remissions in recalcitrant pemphigus vulgaris. *N Engl J Med* (2015) 373:2693–4. doi:10.1056/NEJMc1508234
43. Ahmed AR, Nguyen T, Kaveri S, Spigelman Z. First line treatment of pemphigus vulgaris with a novel protocol in patients with contraindications to systemic corticosteroids and immunosuppressive agents: preliminary retrospective study with a seven year follow-up. *Int Immunopharmacol* (2016) 34:25–31. doi:10.1016/j.intimp.2016.02.013
44. Foster C, Chang P, Ahmed AR. Combination of rituximab and intravenous immunoglobulin for recalcitrant ocular cicatricial pemphigoid. *Ophtomology* (2010) 117(5):861–9. doi:10.1016/j.ophtha.2009.09.049
45. Oktem A, Bengu N, Ayse B, NIhal K, Cengizhan E, Seher B, et al. Long term results of rituximab-intravenous immunoglobulin combination therapy in patients with epidermolysis bullosa acquisita resistant to conventional therapy. *J Dermatolog Treat* (2017) 28(1):50–4. doi:10.1080/09546634.2016.1179711
46. Steger B, Madhusudan S, Kaye SB, Stylianides A, Romano V, Maqsood SE, et al. Combined use of rituximab and intravenous immunoglobulin for severe autoimmune cicatricial conjunctivitis – an interventional case series. *Cornea* (2016) 35:1611–4. doi:10.1097/ICO.0000000000001024
47. Pescovitz MD, Greenbaum CJ, Krause-Steinrauf H, Becker DJ, Gitelman SE, Goland R, et al. Rituximab, B-lymphocyte depletion, and preservation of beta-cell function. *N Engl J Med* (2009) 361:2143–52. doi:10.1056/NEJMoa0904452
48. Castillo-Trivino T, Braithwaite D, Bacchetti P, Waubant E. Rituximab in relapsing and progressive forms of multiple sclerosis: a systematic review. *PLoS One* (2013) 8(7):e66308. doi:10.1371/journal.pone.0066308
49. Chen H, Fu A, Wang J, Wu T, Li Z, Tang J, et al. Rituximab as first-line treatment for acquired thrombotic thrombocytopenic purpura. *J Int Med Res* (2017) 45(3):1253–60. doi:10.1177/0300060517695646
50. Palanichamy A, Jahn S, Nickles D, Derstine M, Abounasr A, Hauser SL, et al. Rituximab efficiently depletes increased CD20-expressing T cells in multiple sclerosis patients. *J Immunol* (2014) 193:580–6. doi:10.4049/jimmunol.1400118
51. Theofilopoulos AN, Kono DH, Baccala R. The Multiple Pathways to Autoimmunity. *Nat Immunol* (2017) 18:716–24. doi:10.1038/ni.3731
52. Manjarrez-Orduño N, Quách TD, Sanz I. B cells and immunological tolerance. *J Invest Dermatol* (2009) 129:278–88. doi:10.1038/jid.2008.240
53. Mackay IR. Science, medicine, and the future: tolerance and autoimmunity. *BMJ* (2000) 321:93–6. doi:10.1136/bmj.321.7253.93
54. Wardemann H, Yurasov S, Schaefer A, Young JW, Meffre E, Nussenzweig MC. Predominant autoantibody production by early human B cell precursors. *Science* (2003) 301:1374–7. doi:10.1126/science.1086907
55. Menard L, Saadoun D, Isnardi I, Ng YS, Meyers G, Massad C, et al. The PTPN22 allele encoding an R620W variant interferes with the removal of developing autoreactive B cells in humans. *J Clin Invest* (2011) 121:3635–44. doi:10.1172/JCI45790
56. Melchers F. Checkpoints that control B cell development. *J Clin Invest* (2015) 125:2203–10. doi:10.1172/JCI78083
57. Salinas GF, Braza F, Brouard S, Tak PP, Baeten D. The role of B lymphocytes in the progression from autoimmunity to autoimmune disease. *Clin Immunol* (2013) 146:34–45. doi:10.1016/j.clim.2012.10.005
58. Mårtensson IL, Almqvist N, Grimsholm O, Bernardi AI. The pre-B cell receptor checkpoint. *FEBS Lett* (2010) 584:2572–9. doi:10.1016/j.febslet.2010.04.057
59. Yurasov S, Wardemann H, Hammersen J, Tsuiji M, Meffre E, Pascual V, et al. Defective B cell tolerance checkpoints in systemic lupus erythematosus. *J Exp Med* (2005) 201:703–11. doi:10.1084/jem.20042251
60. Pelanda R, Torres RM. Central B-cell tolerance: where selection begins. *Cold Spring Harb Perspect Biol* (2012) 4:a007146. doi:10.1101/cshperspect.a007146
61. Kolhatkar NS, Brahmandam A, Thouvenel CD, Becker-Herman S, Jacobs HM, Schwartz MA, et al. Altered BCR and TLR signals promote enhanced positive selection of autoreactive transitional B cells in Wiskott-Aldrich syndrome. *J Exp Med* (2015) 212:1663–77. doi:10.1084/jem.20150585
62. Alexander T, Arnold R, Hiepe F, Radbruch A. Resetting the immune system with immunoablation and autologous haematopoietic stem cell transplantation in autoimmune diseases. *Clin Exp Rheumatol* (2006) 34:53–7.
63. Manz RA, Arce S, Cassese G, Hauser AE, Hiepe F, Radbruch A. Humoral immunity and long-lived plasma cells. *Curr Opin Immunol* (2002) 14:517–21. doi:10.1016/S0952-7915(02)00356-4
64. Rawlings DJ, Metzler G, Wray-Dutra M, Jackson SW. Altered B cell signaling in autoimmunity. *Nat Rev Immunol* (2017) 17:421–36. doi:10.1038/nri.2017.24
65. Flint SM, Gibson A, Lucas G, Nandigam R, Taylor L, Provan D, et al. A distinct plasmablast and naïve B-cell phenotype in primary immune thrombocytopenia. *Haematologica* (2016) 101:698–706. doi:10.3324/haematol.2015.137273
66. Cassese G, Arce S, Hauser AE, Lehnert K, Moewes B, Mostarac M, et al. Plasma cell survival is mediated by synergistic effects of cytokines and adhesion – dependent signals. *J Immunol* (2003) 171:1684–90. doi:10.4049/jimmunol.171.4.1684
67. Hoffman W, Lakkis FG, Chalasani G. B cells, antibodies, and more. *Clin J Am Soc Nephrol* (2016) 11:137–54. doi:10.2215/CJN.09430915
68. Hutloff A, Büchner K, Reiter K, Baelde HJ, Odendahl M, Jacobi A, et al. Involvement of inducible costimulator in the exaggerated memory B cell and plasma cell generation in systemic lupus erythematosus. *Arthritis Rheum* (2004) 50:3211–20. doi:10.1002/art.20519
69. Bemark M. Translating transitions – how to decipher peripheral human B cell development. *J Biomed Res* (2015) 29:264–84. doi:10.7555/JBR.29.20150035
70. Shlomchik MJ. Sites and stages of autoreactive B cell activation and regulation. *Immunity* (2008) 28:18–28. doi:10.1016/j.immuni.2007.12.004
71. Ohashi PS. T-cell signalling and autoimmunity: molecular mechanisms of disease. *Nat Rev Immunol* (2002) 2:427–38. doi:10.1038/nri822
72. Lampropoulou V, Calderon-Gomez E, Roch T, Neves P, Shen P, Stervbo U, et al. Suppressive functions of activated B cells in autoimmune diseases reveal the dual roles of toll-like receptors in immunity. *Immunol Rev* (2010) 233:146–61. doi:10.1111/j.0105-2896.2009.00855.x
73. Rochas C, Hillion S, Saraux A, Mageed RA, Youinou P, Jamin C, et al. Transmembrane BAFF from rheumatoid synoviocytes requires interleukin-6 to induce the expression of recombination-activating gene in B lymphocytes. *Arthiritis Rheum* (2009) 60(5):1261–71. doi:10.1002/art.24498
74. Mauri C, Menon M. Human regulatory B cells in health and disease: therapeutic potential. *J Clin Invest* (2017) 127:772–9. doi:10.1172/JCI85113
75. Johansson-Lindbom B, Borrebaeck CA. Germinal center B cells constitute a predominant physiological source of IL-4: implication for Th2 development in vivo. *J Immunol* (2002) 168:3165–9. doi:10.4049/jimmunol.168.7.3165
76. Naradkian MS, Scholz JL, Oropallo MA, Cancro MP. Understanding B cell biology drugs targeting B cells in autoimmune diseases. In: Bosch X, Ramos-Casals M, Khamashta M, editors. *Milestones in Drug Therapy*. Basel: Spring (2014). p. 11–35.
77. Harris DP, Haynes L, Sayles PC, Duso DK, Eaton SM, Lepak NM, et al. Reciprocal regulation of polarized cytokine production by effector B and T cells. *Nat Immun* (2000) 1:475–82. doi:10.1038/82717
78. Anolik JH, Barnard J, Cappione A, Pugh-Bernard AE, Felgar RE, Looney RJ, et al. Rituximab improves peripheral B cell abnormalities in human systemic lupus erythematosus. *Arthritis Rheum* (2004) 50:3580–90. doi:10.1002/art.20592
79. Uchida J, Lee Y, Hasegawa M, Liang Y, Bradney A, Oliver JA, et al. Mouse CD20 expression and function. *Int Immunol* (2004) 16:119–29. doi:10.1093/intimm/dxh009
80. Maloney DG, Smith B, Rose A. Rituximab: mechanism of action and resistance. *Semin Oncol* (2002) 29(1 Suppl 2):2–9. doi:10.1053/sonc.2002.30156
81. Silverman GJ, Boyle DL. Understanding the mechanistic basis in rheumatoid arthritis for clinical response to anti-CD20 therapy: the B-cell roadblock hypothesis. *Immunol Rev* (2008) 223:175–85. doi:10.1111/j.1600-065X.2008.00627.x
82. Leandro MJ. B-cell subpopulations in humans and their differential susceptibility to depletion with anti-CD20 monoclonal antibodies. *Arthritis Res Ther* (2013) 15(Suppl 1):S3. doi:10.1186/ar3908

83. Nakou M, Katsikas G, Sidiropoulos P, Bertsias G, Papadimitraki E, Raptopoulou A, et al. Rituximab therapy reduces activated B cells in both the peripheral blood and bone marrow of patients with rheumatoid arthritis: depletion of memory B cells correlates with clinical response. *Arthritis Res Ther* (2009) 11:R131. doi:10.1186/ar2798
84. Marshall MJE, Stopforth RS, Cragg MS. Therapeutic antibodies: what have we learnt from targeting CD20 and where are we going? *Front Immunol* (2017) 8:1245. doi:10.3389/fimmu.2017.01245
85. Moser K, Tokoyoda K, Radbruch A, MacLennan I, Manz RA. Stromal niches, plasma cell differentiation and survival. *Curr Opin Immunol* (2006) 18:265–70. doi:10.1016/j.coi.2006.03.004
86. Benucci M, Manfredi M, Puttini PS, Atzeni F. Predictive factors of response to rituximab therapy in rheumatoid arthritis: what do we know today? *Autoimmun Rev* (2010) 9:801–3. doi:10.1016/j.autrev.2010.07.006
87. Leandro MJ, Cambridge G, Ehrenstein MR, Edwards JC. Reconstitution of peripheral blood B cells after depletion with rituximab in patients with rheumatoid arthritis. *Arthritis Rheum* (2006) 54:613–20. doi:10.1002/art.21617
88. Roll P, Dörner T, Tony HP. Anti-CD20 therapy in patients with rheumatoid arthritis: predictors of response and B cell subset regeneration after repeated treatment. *Arthritis Rheum* (2008) 58:1566–75. doi:10.1002/art.23473
89. Muhammad K, Roll P, Einsele H, Dörner T, Tony HP. Delayed acquisition of somatic hypermutations in repopulated IGD+CD27+ memory B cell receptors after rituximab treatment. *Arthritis Rheum* (2009) 60:2284–93. doi:10.1002/art.24722
90. Cambridge G, Perry HC, Nogueira L, Serre G, Parsons HM, De La Torre I, et al. The effect of B-cell depletion therapy on serological evidence of B-cell and plasmablast activation in patients with rheumatoid arthritis over multiple cycles of rituximab treatment. *J Autoimmun* (2014) 50:67–76. doi:10.1016/j.jaut.2013.12.002
91. Chavele KM, Ehrenstein MR. Regulatory T-cells in systemic lupus erythematosus and rheumatoid arthritis. *FEBS Lett* (2011) 585:3603–10. doi:10.1016/j.febslet.2011.07.043
92. van Vollenhoven RF, Emery P, Bingham CO, Keystone EC, Fleischmann R, Furst DE, et al. Longterm safety of patients receiving rituximab in rheumatoid arthritis clinical trials. *J Rheumatol* (2010) 37:558–67. doi:10.3899/jrheum.090856
93. Stasi R, Cooper N, Del Poeta G, Stipa E, Laura Evangelista M, Abruzzese E, et al. Analysis of regulatory T-cell changes in patients with idiopathic thrombocytopenic purpura receiving B cell–depleting therapy with rituximab. *Blood* (2008) 112:1147–50. doi:10.1182/blood-2007-12-129262
94. Rehnberg M, Amu S, Tarkowski A, Bokarewa MI, Brisslert M. Short- and long-term effects of anti-CD20 treatment on B cell ontogeny in bone marrow of patients with rheumatoid arthritis. *Arthritis Res Ther* (2009) 11:R123. doi:10.1186/ar2789
95. Anolik JH, Barnard J, Owen T, Zheng B, Kemshetti S, Looney RJ, et al. Delayed memory B cell recovery in peripheral blood and lymphoid tissue in systemic lupus erythematosus after B cell depletion therapy. *Arthritis Rheum* (2007) 56:3044–56. doi:10.1002/art.22810
96. Weller S, Braun MC, Tan BK, Rosenwald A, Cordier C, Conley ME, et al. Human blood IgM "memory" B cells are circulating splenic marginal zone B cells harboring a prediversified immunoglobulin repertoire. *Blood* (2004) 104:3647–54. doi:10.1182/blood-2004-01-0346
97. Fecteau JF, Cote G, Neron S. A new memory CD27-IgG+ B cell population in peripheral blood expressing VH genes with low frequency of somatic mutation. *J Immunol* (2006) 177:3728–36. doi:10.4049/jimmunol.177.6.3728
98. Wei C, Anolik J, Cappione A, Zheng B, Pugh-Bernard A, Brooks J, et al. A new population of cells lacking expression of CD27 represents a notable component of the B cell memory compartment in systemic lupus erythematosus. *J Immunol* (2007) 178:6624–33. doi:10.4049/jimmunol.178.10.6624
99. Berkowska MA, Driessen GJ, Bikos V, Grosserichter-Wagener C, Stamatopoulos K, Cerutti A, et al. Human memory B cells originate from three distinct germinal center-dependent and -independent maturation pathways. *Blood* (2011) 118:2150–8. doi:10.1182/blood-2011-04-345579
100. Silverman GJ. Therapeutic B cell depletion and regeneration in rheumatoid arthritis: emerging patterns and paradigms. *Arthritis Rheum* (2006) 54:2356–67. doi:10.1002/art.22020
101. Roll P, Palanichamy A, Kneitz C, Dorner T, Tony HP. Regeneration of B cell subsets after transient B cell depletion using anti-CD20 antibodies in rheumatoid arthritis. *Arthritis Rheum* (2006) 54:2377–86. doi:10.1002/art.22019
102. Teng YK, Wheater G, Hogan VE, Stocks P, Levarht EW, Huizinga TW, et al. Induction of long-term B-cell depletion in refractory rheumatoid arthritis patients preferentially affects autoreactive more than protective humoral immunity. *Arthritis Res Ther* (2012) 14:R57. doi:10.1186/ar3770
103. Huang H, Benoist C, Mathis D. Rituximab specifically depletes short-live dautoreactive plasma cells in a mouse model of inflammatory arthritis. *Proc Natl Acad Sci U S A* (2010) 107:4658–63. doi:10.1073/pnas.1001074107
104. Mahévas M, Michel M, Weill JC, Reynaud CA. Long-lived plasma cells in autoimmunity: lessons from B-cell depleting therapy. *Front Immunol* (2013) 4:494. doi:10.3389/fimmu.2013.00494
105. Mahévas M, Michel M, Vingert B, Moroch J, Boutboul D, Audia S, et al. Emergence of long-lived autoreactive plasma cells in the spleen of primary warm auto-immune hemolytic anemia patients treated with rituximab. *J Autoimmun* (2015) 62:22–30. doi:10.1016/j.jaut.2015.05.006
106. Cheng Q, Mumtaz IM, Khodadadi L, Radbruch A, Hoyer BF, Hiepe F. Autoantibodies from long-lived 'memory' plasma cells of NZB/W mice drive immune complex nephritis. *Ann Rheum Dis* (2013) 72:2011–7. doi:10.1136/annrheumdis-2013-203455
107. Hoyer BF, Moser K, Hauser AE, Peddinghaus A, Voigt C, Eilat D, et al. Short-lived plasmablasts and long-lived plasma cells contribute to chronic humoral autoimmunity in NZB/W mice. *J Exp Med* (2004) 199:1577–84. doi:10.1084/jem.20040168
108. Shetty S, Fischer MC, Ahmed AR. Review on the influence of protocol design on clinical outcomes in rheumatoid arthritis treated with rituximab. *Ann Pharmacother* (2013) 47:311–23. doi:10.1345/aph.1R574
109. Cambridge G, Leandro MJ, Edwards JC, Ehrenstein MR, Salden M, Bodman-Smith M, et al. Serologic changes following B lymphocyte depletion therapy for rheumatoid arthritis. *Arthritis Rheum* (2003) 48:2146–54. doi:10.1002/art.11181
110. Becerra E, Scully MA, Leandro MJ, Heelas EO, Westwood JP, De La Torre I, et al. Effect of rituximab on B cell phenotype and serum B cell-activating factor levels in patients with thrombotic thrombocytopenic purpura. *Clin Exp Immunol* (2015) 179:414–25. doi:10.1111/cei.12472
111. Ehrenstein MR, Wing C. The BAFFling effects of rituximab in lupus: danger ahead? *Nat Rev Rheumatol* (2016) 12:367–72. doi:10.1038/nrrheum.2016.18
112. Brezinschek HP, Rainer F, Brickmann K, Graninger WB. B lymphocytetyping for prediction of clinical response to rituximab. *Arthritis Res Ther* (2012) 14:R161. doi:10.1186/ar3901
113. de la Torre I, Moura RA, Leandro MJ, Edwards J, Cambridge G. B-cell activating factor receptor expression on naive and memory B cells: relationship with relapse in patients with rheumatoid arthritis following B-cell depletion therapy. *Ann Rheum Dis* (2010) 69:2181–8. doi:10.1136/ard.2010.131326
114. Van Zelm MC, van der Burg M, Langerak AW, van Dongen JJ. PID comes full circle: applications of V(D)J recombination excision circles in research, diagnostics and newborn screening of primary immunodeficiency disorders. *Front Immunol* (2011) 2:12. doi:10.3389/fimmu.2011.00012
115. Shahaf G, Zisman-Rozen S, Benhamou D, Melamed D, Mehr R. B cell development in the bone marrow is regulated by homeostatic feedback exerted by mature B cells. *Front Immunol* (2016) 7:77. doi:10.3389/fimmu.2016.00077
116. Shetty S, Ahmed AR. Preliminary analysis of mortality associated with rituximab use in autoimmune diseases. *Autoimmunity* (2013) 46:487–96. doi:10.3109/08916934.2013.838563
117. Kasi PM, Tawbi HA, Oddis CV, Kulkarni HS. Clinical review serious adverse events associated with the use of rituximab – a critical care perspective. *Crit Care* (2012) 16:231–41. doi:10.1186/cc11304
118. Chamberlain N, Massad C, Oe T, Cataert T, Herold KC, Meffre S. Rituximab does not reset defective early B cell tolerance checkpoint. *J Clin Invest* (2016) 126(1):282–7. doi:10.1172/JCI83840
119. Tjon AS, van Gent R, Jaadar H, Martin van Hagen P, Mancham S, van der Laan LJ, et al. Intravenous immunoglobulin treatment in humans suppresses dendritic cell function via stimulation of IL-4 and IL-13 production. *J Immunol* (2014) 192:5625–34. doi:10.4049/jimmunol.1301260
120. Bhol KC, Desai S, Kumari S, Colon JS, Ahmed AR. Pemphigus vulgaris: the role of IL-1 and IL-1 receptor antagonist in pathogenesis and effects of intravenous immunoglobulin on their production. *Clin Immunol* (2001) 100:172–80. doi:10.1006/clim.2001.5061
121. Basta M, Dalakas MC. High-dose intravenous immunoglobulin exerts its beneficial effects in patients with dermatomyositis by blocking endomysial

deposition of activated complement fragments. *J Clin Invest* (1994) 94:1729–35. doi:10.1172/JCI117520
122. Basta M, Van Goor F, Luccioli S, Billings EM, Vortmeyer AO, Baranyi L, et al. F(ab)'2-mediated neutralization of C3a and C5a anaphylatoxins: a novel effector function of immunoglobulins. *Nat Med* (2003) 9:431–8. doi:10.1038/nm836
123. Bayry J, Lacroix-Desmazes S, Carbonneil C, Misra N, Donkova V, Pashov A, et al. Inhibition of maturation and function of dendritic cells by intravenous immunoglobulin. *Blood* (2003) 101:758–65. doi:10.1182/blood-2002-05-1447
124. Ephrem A, Chamat S, Miguel C, Fisson S, Mouthon L, Caligiuri G, et al. Expansion of CD4+CD25+ regulatory T cells by intravenous immunoglobulin: a critical factor in controlling experimental autoimmune encephalomyelitis. *Blood* (2008) 111:715–22. doi:10.1182/blood-2007-03-079947
125. Othy S, Hegde P, TOpcu S, Sharma M, Maddur MS, Lacroix-Desmazes S, et al. Intravenous gammaglobulin inhibits encephalitogenic potential of pathogenic T ells and interferes with their trafficking to the central nervous system, implicating sphingosine-1tareget of rapamycin axis. *J Immunol* (2013) 190:4535–41. doi:10.4049/jimmunol.1201965
126. Dietrich G, Varela F, Hurez V, Bouanani M, Kaatchkine ME. Selection of the expressed B cell repertoire by infusion of normal immunoglobulin G in a patient with autoimmune thyroiditis. *Eur J Immunol* (1993) 23:2945. doi:10.1002/eji.1830231133
127. Kazatchkine MD, Dietrich G, Hurez V, Ronda N, Bellon B, Rossi F, et al. Region meditated selection of autoreactive repertoire by intravenous immunoglobulin IVIG. *Immunol Rev* (1994) 139:79–107. doi:10.1111/j.1600-065X.1994.tb00858.x
128. Varela F, Andersson A, Dietrich G, Sundbald A, Holmberg D, Kazatchkine MD, et al. The population dynamics of antibodies in normal and autoimmune individuals. *Proc Natl Acad Sci U S A* (1991) 88:5917. doi:10.1073/pnas.88.13.5917
129. Marchlonis JJ, Kaveri S, Lacroix-Desmazes S, Kazatchkine MD. Natural recognition repertoire and the evolutionary emergence of the combinatorial immune system. *FASEB J* (2002) 8:842–8. doi:10.1096/fj.01-0953hyp
130. Dussault N, Ducas E, Racine C, Jacques A, Paré I, Côté S, et al. Immunomodulation of human B cells following treatment with intravenous immunoglobulins involves increased phosphorylation of extracellular signal regulated kinases 1 and 2. *Int Immunol* (2008) 20:1369–79. doi:10.1093/intimm/dxn090
131. O'Connor BP, Gleeson MW, Noelle RJ, Erickson LD. The rise and fall of long-lived humoral immunity: terminal differentiation of plasma cells in health and disease. *Immunol Rev* (2003) 194:61–76. doi:10.1034/j.1600-065X.2003.00055.x
132. Crow AR, Brinc D, Lazarus AH. New insight into the mechanism of action of IVIg: the role of dendritic cells. *J Thromb Haemost* (2009) 7:245–8. doi:10.1111/j.1538-7836.2009.03420.x
133. Dietrich G, Kazatchkine MD. Normal immunoglobulin for therapeutic use contain antiidiotypic specificities against and immunoglobulin antibodies. *J Clin Invest* (1990) 85:620–5. doi:10.1172/JCI114483
134. Sultan Y, Kazatchkine MD, Maisonneuve P, Nydegger UE. Anti-idiotypic suppression of autoantibodies to factor VIII by high dose intravenous immunoglobulin. *Lancet* (1984) 2:765–8. doi:10.1016/S0140-6736(84)90701-3
135. Mariño E, Grey ST. B cells as effectors and regulators of autoimmunity. *Autoimmunity* (2012) 45:377–87. doi:10.3109/08916934.2012.665527
136. Aschermann S, Lux A, Baerenwaldt A, Biburger M, Nimmerjahn F. The other side of immunoglobulin G: suppressor of inflammation. *Clin Exp Immunol* (2010) 160:161–7. doi:10.1111/j.1365-2249.2009.04081.x
137. Lux A, Aschermann S, Biburger M, Nimmerjahn F. The pro and anti-inflammatory activities of immunoglobulin G. *Ann Rheum Dis* (2010) 69:i92–6. doi:10.1136/ard.2009.117101
138. Le Pottier L, Bendaoud B, Dueymes M, Daridon C, Youinoi P, Shoenfeld Y, et al. BAFF, a new target for intravenous immunoglobulin in autoimmunity and cancer. *J Clin Immunol* (2007) 27:257–65. doi:10.1007/s10875-007-9082-2
139. Maddur MS, Othy S, Hegde P, Vani J, Lacroix-Desmazes S, Bayry J, et al. Immunomodulation by intravenous immunoglobulin: role of regulatory T cells. *J Clin Immunol* (2010) 30(Suppl 1):S4–8. doi:10.1007/s10875-010-9394-5
140. Sabouri Z, Perotti S, Spierings E, Humburg P, Yabas M, Bergmann H, et al. IgD attenuates the IgM-induced anergy response in transitional and mature B cells. *Nat Commun* (2016) 7:13381–7. doi:10.1038/ncomms13381
141. Séïté JF, Cornec D, Renaudineau Y, Youinou P, Mageed RA, Hillion S. IVIg modulates BCR signaling through CD22 and promotes apoptosis in mature human B lymphocytes. *Blood* (2010) 116:1698–704. doi:10.1182/blood-2009-12-261461
142. Rao SP, Riggs JM, Friedman DF, Scully MS, LeBien TW, Silberstein LE. Biased VH gene usage in early lineage human B cells: evidence for preferential Ig gene rearrangement in the absence of selection. *J Immunol* (1999) 163:2732–40.
143. Hoffmann M, Uttenreuther-Fischer MM, Lerch H, Gaedicke G, Fischer P. IVIG-bound IgG and IgM cloned by phage display from a healthy individual reveal the same restricted germ-line gene origin as in autoimmune thrombocytopenia. *Clin Exp Immunol* (2000) 121:37–46. doi:10.1046/j.1365-2249.2000.01229.x
144. Osei A, Uttenreuther-Fischer MM, Lerch H, Gaedicke G, Fischer P. Restricted VH3 gene usage in phage-displayed Fab that are selected by intravenous immunoglobulin. *Arthritis Rheum* (2000) 43:2722–32. doi:10.1002/1529-0131(200012)43:12<2722::AID-ANR12>3.0.CO;2-N
145. Shoenfeld Y, Rauova L, Gilburd B, Kvapil F, Goldberg I, Kopolovic J, et al. Efficacy of IVIG affinity-purified anti-double-stranded DNA anti-idiotypic antibodies in the treatment of an experimental murine model of systemic lupus erythematosus. *Int Immunol* (2002) 14:1303–11. doi:10.1093/intimm/dxf099
146. Lee CH, Suh CH, Lee J, Kim YT, Lee SK. The effects of anti-idiotypic antibody on antibody production and apoptosis of anti-dsDNA antibody producing cells. *Clin Exp Rheumatol* (2003) 21:291–300.
147. Kelesidis T, Daikos G, Boumpas D, Tsiodras S. Does rituximab increase the incidence of infectious complications? A narrative review. *Int J Infect Dis* (2011) 15(1):e2–16. doi:10.1016/j.ijid.2010.03.025
148. Samson M, Audia S, Lakomy D, Bonnotte B, Tavernier C, Ornetti P. Diagnostic strategy for patients with hypogammaglobulinemia in rheumatology. *Joint Bone Spine* (2011) 78(3):241–5. doi:10.1016/j.jbspin.2010.09.016
149. Kridin K, Sagi S, Berman R. Mortality and cause of death in patients with pemphigus. *Acta Derm Venereol* (2017) 97:607–11. doi:10.2340/00015555-2611
150. Hemming VG. Use of intravenous immunoglobulins for prophylaxis or treatment of infectious diseases. *Clin Diagn Lab Immunol* (2001) 8(5):859–63. doi:10.1128/CDLI.8.5.859-863.2001
151. Roberts DM, Jones RB, Smith RM, Alberici F, Kumaratne DS, Burns S, et al. Rituximab-associated hypogammaglobulinemia: incidence, predictors and outcomes in patients with multi-system autoimmune disease. *J Autoimmun* (2015) 57:60–5. doi:10.1016/j.jaut.2014.11.009
152. Roberts DM, Smith RM, Alberici F, Kumaratne DS, Burns S, Jayne DR. Immunoglobulin G replacement for the treatment of infective complications of rituximab-associated hypogammaglobulinemia in autoimmune disease: a case series. *J Autoimmun* (2015) 57:24–9. doi:10.1016/j.jaut.2014.11.004
153. Casulo C, Maragulia J, ZeLenetz AD. Incidence of hypogammaglobulinemia in patients receiving rituximab and the use of intravenous immunoglobulin for recurrent infections. *Clin Lymphoma Myeloma Leuk* (2013) 13:106–11. doi:10.1016/j.clml.2012.11.011
154. Shimizu M, Katoh H, Hamaoka S, Kinoshita M, Akiyama K, Naito Y, et al. Protective effects of intravenous immunoglobulin and antimicrobial agents on acute pneumonia in leukopenic mice. *J Infect Chemother* (2016) 22:240–7. doi:10.1016/j.jiac.2016.01.006
155. Koch C, Hecker A, Grau V, Padberg W, Wolff M, Henrich M. Intravenous immunoglobulin in necrotizing fasciitis – a case report and review of recent literature. *Ann Med Surg (Lond)* (2015) 4:260–3. doi:10.1016/j.amsu.2015.07.017
156. Hsu JL, Safdar N. Polyclonal immunoglobulins and hyperimmune globulins in prevention and management of infectious diseases. *Infect Dis Clin North Am* (2011) 25:773–88. doi:10.1016/j.idc.2011.07.005
157. Aghamohammadi A, Moin M, Farhoudi A, Rezaei N, Pourpak Z, Movahedi M, et al. Efficacy of intravenous immunoglobulin on the prevention of pneumonia in patients with agammaglobulinemia. *FEMS Immunol Med Microbiol* (2004) 40:113–8. doi:10.1016/S0928-8244(03)00304-3
158. Di Rosa R, Pietrosanti M, Luzi G, Salemi S, D'Amelio R. Polyclonal intravenous immunoglobulin: an important additional strategy in sepsis? *Eur J Intern Med* (2014) 25:511–6. doi:10.1016/j.ejim.2014.05.002

159. Bermejo-Martin JF, Giamarellos-Bourboulis EJ. Endogenous immunoglobulins and sepsis: new perspectives for guiding replacement therapies. *Int J Antimicrob Agents* (2015) 46(Suppl 1):S25–8. doi:10.1016/j.ijantimicag.2015.10.013
160. Capasso L, Borrelli AC, Ferrara T, Coppola C, Cerullo J, Izzo F, et al. Immunoglobulins in neonatal sepsis: has the final word been said? *Early Hum Dev* (2014) 90(Suppl 2):S47–9. doi:10.1016/S0378-3782(14)50013-8
161. Buda S, Riefolo A, Biscione R, Goretti E, Cattabriga I, Grillone G, et al. Clinical experience with polyclonal IgM-enriched immunoglobulins in a group of patients affected by sepsis after cardiac surgery. *J Cardiothorac Vasc Anesth* (2005) 19:440–5. doi:10.1053/j.jvca.2005.05.003
162. Kukic BP, Savic NB, Stevanovic KS, Trailovic RD, Cvetkovic S, Davidovic LB. Effect of IgM-enriched immunoglobulin as adjunctive therapy in a patient following sepsis after open thoracoabdominal aortic aneurysm repair. *J Cardiothorac Vasc Anesth* (2016) 30:746–8. doi:10.1053/j.jvca.2015.08.025
163. Tagami T, Matsui H, Fushimi K, Yasunaga H. Intravenous immunoglobulin use in septic shock patients after emergency laparotomy. *J Infect* (2015) 71:158–66. doi:10.1016/j.jinf.2015.04.003
164. Windegger TM, Lambooy CA, Hollis L, Morwood K, Weston H, Fung YL. Subcutaneous immunoglobulin therapy for hypogammaglobulinemia secondary to malignancy or related drug therapy. *Transfus Med Rev* (2017) 31:45–50. doi:10.1016/j.tmrv.2016.06.006
165. Chapel HM, Lee M, Hargreaves R, Pamphilon DH, Prentice AG. Randomised trial of intravenous immunoglobulin as prophylaxis against infection in plateau-phase multiple myeloma. The UK group for immunoglobulin replacement therapy in multiple myeloma. *Lancet* (1994) 343:1059–63. doi:10.1016/S0140-6736(94)90180-5
166. Ueda M, Bergerb M, Galec RP, Lazarusd HM. Immunoglobulin therapy in hematologic neoplasms and after hematopoietic cell transplantation. *Blood Rev* (2018) 32:106–15. doi:10.1016/j.blre.2017.09.003
167. Staak A, Renner F, Suesal C, Dietrich H, Rainer L, Kamali-Ernst S, et al. Immunoglobulin induction therapy in renal transplant recipients: effects on immunoglobulin and regulatory antibody levels. *Transplant Proc* (2006) 38:3483–5. doi:10.1016/j.transproceed.2006.10.041
168. Neilson AR, Burchardib H, Schneidera H. Cost-effectiveness of immunoglobulin M-enriched immunoglobulin (pentaglobin) in the treatment of severe sepsis and septic shock. *J Crit Care* (2005) 20:239–49. doi:10.1016/j.jcrc.2005.03.003
169. Joly P, Maho-Vaillant M, Prost-Squarcioni C, Hebert V, Houviet E, Calbo S, et al. First line rituximab combined with short term prednisone versus prednisone alone for the treatment of pemphigus (ritux 3); a prospective multicentre, parallet-group, open label randomized trial. *Lancet* (2017) 389:2031–40. doi:10.1016/S0140-6736(17)30070-3
170. Gregoriou S, Giatrakou S, Theodoropoulos K, Katoulis A, Loumou P, Toumbis-Ioannou E, et al. Pilot study of 19 patients with severe pemphigus: prophylactic treatment with rituximab does not appear to be beneficial. *Dermatology* (2014) 228:158–65. doi:10.1159/000357031
171. Blum KS, Pabst R. Lymphocyte numbers and subsets in human blood. Do they mirror the situation in all organs? *Immunol Lett* (2007) 108:45–51. doi:10.1016/j.imlet.2006.10.009

Conflict of Interest Statement: The authors declare that the research was conducted in the absence of any commercial or financial relationships that could be construed as a potential conflict of interest.

frontiers in Immunology

ORIGINAL RESEARCH
published: 16 July 2018
doi: 10.3389/fimmu.2018.01623

Streptococcal Endo-β-*N*-Acetylglucosaminidase Suppresses Antibody-Mediated Inflammation *In Vivo*

Kutty Selva Nandakumar[1,2], Mattias Collin[3], Kaisa E. Happonen[4,5], Susanna L. Lundström[6], Allyson M. Croxford[7], Bingze Xu[2], Roman A. Zubarev[6], Merrill J. Rowley[7], Anna M. Blom[4], Christian Kjellman[8] and Rikard Holmdahl[1,2]*

[1] School of Pharmaceutical Sciences, Southern Medical University, Guangzhou, China, [2] Medical Inflammation Research, Department of Medical Biochemistry and Biophysics, Karolinska Institute, Stockholm, Sweden, [3] Division of Infection Medicine, Department of Clinical Sciences, Lund University, Lund, Sweden, [4] Department of Translational Medicine, Lund University, Lund, Sweden, [5] Molecular Neurobiology Laboratory, Salk Institute for Biological Studies, La Jolla, CA, United States, [6] Division of Physiological Chemistry I, Department of Medical Biochemistry and Biophysics, Karolinska Institute, Stockholm, Sweden, [7] Department of Biochemistry and Molecular Biology, Monash University, Clayton, VIC, Australia, [8] Hansa Medical AB, Lund, Sweden

OPEN ACCESS

Edited by:
Piotr Trzonkowski, Gdańsk Medical University, Poland

Reviewed by:
SunAh Kang, University of North Carolina at Chapel Hill, United States
Lennart T. Mars, Institut National de la Santé et de la Recherche Médicale (INSERM), France

***Correspondence:**
Kutty Selva Nandakumar
nandakumar@smu.edu.cn

Specialty section:
This article was submitted to Immunological Tolerance and Regulation, a section of the journal Frontiers in Immunology

Received: 30 November 2017
Accepted: 02 July 2018
Published: 16 July 2018

Citation:
Nandakumar KS, Collin M, Happonen KE, Lundström SL, Croxford AM, Xu B, Zubarev RA, Rowley MJ, Blom AM, Kjellman C and Holmdahl R (2018) Streptococcal Endo-β-N-Acetylglucosaminidase Suppresses Antibody-Mediated Inflammation In Vivo. Front. Immunol. 9:1623. doi: 10.3389/fimmu.2018.01623

Endo-β-*N*-acetylglucosaminidase (EndoS) is a family 18 glycosyl hydrolase secreted by *Streptococcus pyogenes*. Recombinant EndoS hydrolyzes the β-1,4-di-*N*-acetylchitobiose core of the N-linked complex type glycan on the asparagine 297 of the γ-chains of IgG. Here, we report that EndoS and IgG hydrolyzed by EndoS induced suppression of local immune complex (IC)-mediated arthritis. A small amount (1 μg given i.v. to a mouse) of EndoS was sufficient to inhibit IgG-mediated arthritis in mice. The presence of EndoS disturbed larger IC lattice formation both *in vitro* and *in vivo*, as visualized with anti-C3b staining. Neither complement binding *in vitro* nor antigen-antibody binding *per se* were affected. Thus, EndoS could potentially be used for treating patients with IC-mediated pathology.

Keywords: endoglycosidase, arthritis, rheumatoid, glycosylation, mouse models, complement, immunoglobulin G, immunohistochemistry

INTRODUCTION

Endoglycosidases form a group (E.C.3.2 subclass) of enzymes that hydrolyze non-terminal glycosidic bonds in oligosaccharides or polysaccharides. Endo-β-*N*-acetylglucosaminidase (EndoS) is a member of the GlcNAc polymer hydrolyzing glycosyl hydrolases of family 18 (FGH18) secreted by group A β-hemolytic *Streptococcus pyogenes*. It exclusively hydrolyzes the β-1,4-di-*N*-acetylchitobiose core of the asparagine-linked complex-type glycan on Asn-297 of the γ-chains of IgG (1). The crystal structure of EndoS revealed that it contains five distinct protein domains (glycosidase, leucine-rich repeat, hybrid Ig, carbohydrate-binding module, and three-helix bundle domains) (2) and concerted conformational changes in both the enzyme and substrate are required for subsequent antibody deglycosylation (2, 3). Recently, functionally and structurally related enzymes have been identified in certain serotypes of *S. pyogenes*, *Streptococcus dysgalactiae*, and *Corynebacterium pseudotuberculosis* (4–6).

Glycosylation is an important post-translational modification affecting the structure and biological properties of proteins. Subtle changes in IgG N-glycome could alter Fc conformation

with dramatic consequences for IgG effector functions (7). Extensive non-covalent interactions between the carbohydrate and the protein moiety in the IgG-Fc region result in reciprocal influences on conformation (8). NMR studies suggested a significant role for Fc-glycan dynamics in Fc receptor (FcR) interactions (9). The minimal oligosaccharide structure in IgG is a hexasaccharide (GlcNAc2Man3GlcNAc) with variable sugar residues attached resulting in the generation of many different glycoforms. Altered IgG glycoforms lacking terminal sialic acid and galactose residues were identified to be more common on IgG from RA patients (10). Differential sialylation was reported to regulate the inflammatory property of IgG (11). Furthermore, a single molecule Förster resonance energy transfer study has shown that Fc deglycosylation resulting from EndoS treatment led to wide changes in Fc conformation, which enhanced its flexibility (12).

Antibodies such as anti-citrullinated protein antibodies (ACPA), rheumatoid factors (RF), anti-type II collagen antibodies, and immune complexes (ICs) are prevalent in RA. ACPA and RF also precede disease development (13, 14). IC-mediated pathology is evident in several autoimmune diseases. Importantly, the pathogenic effect of circulating IC was shown to be dependent on their size and composition (15). Both antigen-driven (soluble and target tissue-bound) and RF containing ICs present in RA patients are of intermediate (6S–19S) to large (22S–30S) size. The larger ICs containing RF (>22S) are implicated in extra-articular manifestations in RA (16). Furthermore, CII containing ICs from RA synovial fluid were shown to induce production of inflammatory cytokines (TNF-α, IL-1β, and IL-8) from peripheral blood mononuclear cells *via* FcγRIIA (17).

Antibodies from RA patients upon passive transfer induced arthritis in mice (18, 19). The effector phase of arthritis is optimally studied using the collagen antibody-induced arthritis (CAIA) model, which is induced by anti-CII IgG mAbs (20). This model exhibits features of bone and cartilage erosion, major infiltration of granulocytes, and deposition of IgG and complement factors on the cartilage surface. CAIA is characteristic of RA and is dependent on complement, FcγRs, TNF-α, IL-1β, and neutrophils as well as macrophages (20). Furthermore, it should be mentioned that human intravenous immunoglobulins (hIVIg) were earlier used at very high concentrations (1 g/kg) and 1 h before arthritogenic serum transfer to attenuate joint inflammation and the anti-inflammatory property of IgG was shown to be mainly due to Fc sialylation (11). Interestingly, removal of the N-linked glycan by EndoS treatment abrogated the pathogenic potential of antibodies (21–23) and abolished all the pro-inflammatory properties of IC from SLE patients (24). In addition, EndoS-hydrolyzed IgG ameliorated several antibody-mediated diseases in mice, including arthritis (22). Attenuation of inflammation was reported to be dependent on IgG_1 and IgG_{2b} subclasses but the mechanisms were not clarified. EndoS hydrolyzes all the IgG subclasses in man and mice but no effects on the other isotypes have been detected under physiological conditions. Here, we demonstrate suppression of inflammatory arthritis by minimal amounts of EndoS, an effect which is dominant and mediated through disturbances in the formation of ICs on the cartilage surface.

MATERIALS AND METHODS

Mice

The B10.Q founder mice were obtained originally from Professor Jan Klein (Tubingen, Germany) and have been maintained in our laboratory for more than 20 years. The BALB/c founder mice were obtained from Jackson laboratories (Bar Harbor, ME, USA). (BALB/c × B10.Q) F1 mice, short named as QB, were bred in the Medical Inflammation Research animal house facility in Lund and Stockholm. For *in vivo* experiments shown in **Figure 2**, arthritis was induced in male BALB/c mice obtained from Harlan, Denmark. The animals were kept in a specific pathogen free (Felasa II) animal facility with a climate controlled environment having 12-h light/dark cycles in polystyrene cages containing wood shavings and were fed standard rodent chow and water *ad libitum*. Two- to four-months-old male mice were used in all the experiments, with the experimental groups matched for age, mixed in cages, and run blindly. Splenectomy or sham operation was done under isoflurane anesthesia. Two- to three-days-old pups were used for immunohistochemical studies. Local animal welfare authorities approved the animal experiments.

Antibodies

The CII-specific hybridomas (M2139, M284, CIIC1, CIIC2, CB20, and UL1) were generated and characterized as described (26–28). ACC4 antibody recognizes the citrullinated CII epitope, C1 (29). A mouse anti-trinitrophenol (anti-TNP) antibody-producing hybridoma (Hy2.15) was a gift from Georges Köhler (30). A mouse monoclonal hybridoma recognizing trophozoite antigens (2B5.3; CRL-1960) and human HLA-DR α-chain specific antibody clone (L243) were obtained from ATCC (Rockville, MD, USA). M284 and CB20 mAbs (31) bind CII epitopes, J1 and C1, respectively. Mouse intravenous immunoglobulins (mIVIg; Equitech-Bio Inc.) and hIVIg (Octagam, Octapharma AB) were used. All the hybridomas were cultured in ultra-low bovine IgG-containing DMEM Glutamax-I culture medium (Gibco BRL, Invitrogen AB, Sweden) with 100 mg/l of kanamycin monosulfate (Sigma, St. Louis, MO, USA). MAbs were generated on a large scale as culture supernatant using Integra cell line 1000 (CL-1000) flasks (Integra Biosciences, Switzerland). Antibodies were purified using γ-bind plus affinity gel matrix (GE Healthcare, Sweden) and the Äkta purification system (GE Healthcare, Sweden) as described (20). Briefly, culture supernatants were centrifuged at 12,500 rpm for 30 min, filtered, and degassed before applying to the gel matrix. The gel was washed extensively and the antibodies were eluted using acetic acid buffer at pH 3.0 and neutralized with 1 M Tris–HCl, pH 9.0. The peak fractions were pooled and dialyzed extensively against PBS, pH 7.0 with or without azide. The IgG content was determined by freeze drying. The antibody solutions were sterilized using 0.2-μm syringe filters (Dynagard, Spectrum Laboratories, CA, USA), aliquoted, and stored at −70°C.

EndoS Hydrolysis of IgG

IgGs (CIIC1, M2139, M284, CIIC2, UL1, CB20, ACC4, Hy2.15, L243, CRL-1960, mIVIg and hIVIg) were hydrolyzed with recombinant EndoS fused to GST (GST-EndoS) as previously

described (1). Five micrograms of GST-EndoS in PBS were added per milligram of mAb followed by incubation for 16 h at 37°C. GST-EndoS was removed by three serial passages over Glutathione-Sepharose 4B columns with a 1,000-fold over-capacity of GST-binding (GE Healthcare, Uppsala, Sweden). SDS-PAGE and *Lens culinaris* agglutinin (LCA) lectin blotting were used to assess the purity and efficacy of EndoS cleavage. Briefly, 2 µg of EndoS hydrolyzed and unhydrolyzed IgG were separated on 10% SDS-PAGE followed by staining with PageBlue protein stain (Thermo Fisher Scientific), or blotted to PVDF using TransBlot Turbo transfer packs and apparatus (Bio-Rad, Hercules, CA, USA). Membranes were blocked with 10 mM HEPES (pH 7.5) with 0.15 M NaCl, 0.01 mM $MnCl_2$, 0.1 mM $CaCl_2$, and 0.1% Tween-20 (HBST) and incubated with 1 µg/ml of biotinylated LCA lectin (Vector Laboratories, Burlingame, CA, USA). After washing in HBST, membranes were incubated with 50 ng/ml of peroxidase-labeled streptavidin (Vector Laboratories), and developed using Super Signal West Pico Chemiluminescent Substrate (Thermo Fisher Scientific) and a ChemiDoc XRS imaging system (Bio-Rad). The DeGlycIt treatment was performed following the manufacturer's instructions (Genovis AB, Lund, Sweden). Briefly, antibodies were added to a column with immobilized EndoS, the column was incubated for 30 min under rotation, and the deglycosylated antibodies were eluted by centrifugation.

Glycopeptide Identification

Endo-β-*N*-acetylglucosaminidase hydrolyzed or unhydrolyzed antibodies (15 µg) were trypsin digested similar to what has been previously described (32). Samples were analyzed using a reversed phase liquid chromatography system (Easy-nLC, Proxeon) connected to a Velos Orbitrap mass spectrometer (Thermo Fisher Scientific). The MS was operated in positive mode, and the survey MS scan in the range of *m/z* 300–2,000 was obtained at a resolution of 60,000. MS/MS was performed using CID and ETD fragmentation. IgG Fc glycopeptides were identified in LC-MS/MS datasets by their characteristic retention times and accurate monoisotopic masses (within <10 ppm from the theoretical values) of doubly and triply charged ions from M2139: EDYNSTIR, CIIC1, and L243: EDYNSTLR as well as Hy2.15: EEQFNSTFR, respectively. Protein identity was confirmed using MASCOT search engine (V.2.3.2) using IPI mouse concatenated database. Search parameters were as follows: MS mass error tolerance at 10 ppm, MS/MS mass accuracy at 0.5 Da, tryptic digestion with a maximum of two missed-cleavages, carbamidomethylation of cysteine as a fixed modification, asparagine and glutamine deamidation, methionine oxidation as well as N-glycosylation (HexNAc[n]dHex[n]Hex[n]) as variable modifications.

Rabbit IgG Cleavage Assay

This *in vitro* assay made use of rabbit IgG as a reporter for EndoS activity in combination with another streptococcal enzyme, IgG-degrading enzyme of *Streptococcus pyogenes* (IdeS). IdeS has the ability to efficiently cleave human (33) and rabbit IgG (34) while leaving mouse IgG_1 and IgG_{2b} intact (35). After IdeS treatment, deglycosylated rabbit Fc-fragment was possible to distinguish from the non-deglycosylated part using SDS-PAGE (i.e., a 25-kDa fragment with and without glycosylation). The reactions contained 5 µg of the EndoS-treated mouse antibodies and 5 µg of rabbit gamma globulin (Jackson ImmunoResearch) and were incubated at 37°C for 60 min during which potentially remaining EndoS will deglycosylate rabbit IgG, the reporter in this assay. After this incubation, IdeS (1 µg) was added and the reaction was allowed to continue for an additional 45 min. SDS loading buffer was added, and one-third of the reaction mixture was separated on SDS-PAGE (4–20% TGX, Bio-Rad), stained, and visualized.

Particle Size Measurement Using Dynamic Light Scattering (DLS)

To determine the size of ICs by EndoS-hydrolyzed IgGs we used DLS. Briefly, CII purified from rat chondrosarcoma dissolved in 0.1 M acetic acid at 5 mg/ml was diluted further in PBS (1 mg/ml) and anti-CII mAb (high affinity M2139 or low affinity CB20; 1 mg/ml) in PBS were mixed together at 1:1 ratio and incubated for 30 min at 37°C, followed by addition of either unhydrolyzed (Hy2.15) or EndoS-hydrolyzed (Hy2.15H) anti-hapten IgG at the ratio 1:1:1. Twenty microliters of this mixture were loaded on to the capillary tube in the DLS instrument (Precision Detectors Inc., Bellingham, MA, USA). The particle sizes expressed as the apparent *Z*-average (or intensity-weighted) hydrodynamic diameter (dH) and polydispersity index, which provides information on the deviation from monodispersity were measured (36) and compared between the groups.

Surface Plasmon Resonance (SPR) Analysis

Surface Plasmon Resonance (Biacore 2000; Biacore) analysis was performed using the standard procedure (37). Briefly, CII was immobilized on the surface of CM5 sensor chips. EndoS-hydrolyzed and unhydrolyzed IgGs were injected at different concentrations through flow cells in the running buffer (10 mM HEPES, pH 7.4, 150 mM NaCl, 3.4 mM EDTA, and 0.005% surfactant P20) at a flow rate of 30 µl/min. Antibodies were injected for 3 min and dissociation of bound molecules was observed for 7 min. Background binding to control flow cells was subtracted automatically. The chips were regenerated using pulse injection of 100% ethylene glycol followed by 2 M NaCl and 100 mM HCl.

Collagen Antibody-Induced Arthritis

Endo-β-*N*-acetylglucosaminidase-hydrolyzed and unhydrolyzed, two or four arthritogenic mAb combinations were studied: M2139 (γ2b), CIIC1 (γ2a), CIIC2 (γ2b), and UL1 (γ2b) bind to triple helical J1 (MP*GERGAAGIAGPK—P* indicates hydroxyproline), $C1^1$ (GARGLTGRO) (38), D3 (RGAQGPOGATGF), and U1 (GLVGPRGERGF) CII epitopes, respectively. The cocktail of the mAbs (9 or 4 mg/mouse) was prepared by mixing equal concentrations of each of the sterile filtered antibody solutions. Mice were injected i.v. with 250–500 µl solution. All the mice received LPS (25 µg/mice/i.p.) at day 5 as described earlier (39). CAIA experiment shown in **Figure 2** was done as follows: mice were administered with 2 mg/mouse of CII-specific mAb cocktail (MD Biosciences) i.p. on day 0 followed by 50 µg/mouse

of LPS (*E. coli* 055:B5) on day 5. The animals were divided into different groups ($n = 8–10$ mice/group), and different substances were administered i.v. on day 0 and the arthritic score of the animals were followed between days 0 and 14. Mice were examined daily for development of arthritis. Scoring of the inflammation was done blindly using a scoring system based on the number of inflamed joints in each paw, inflammation being defined by swelling and redness. In all the arthritis experiments, the maximum score given was 15/paw, 60 for all 4 paws (25), except in **Figure 2**, where arthritis was evaluated using a scoring scale of 0–16 (25).

Histological Preparations

Paws were dissected from each group of mice (3–4 mice/group), fixed in 4% phosphate buffered paraformaldehyde solution (pH 7.0) for 24 h, decalcified for 3–4 weeks in a solution containing EDTA, polyvinylpyrrolidone, and Tris–HCl, pH 6.95 followed by dehydration and embedding in paraffin. Sections of 6 µm were stained with hematoxylin-eosin to determine cellular infiltrations and, bone and cartilage morphology. Joint sections were scored as follows: score 0, normal joints. Score 1, mild synovitis with hyperplastic synovial membrane and small focal infiltration of inflammatory cells, increased numbers of vessels in the synovium and a villous formation of synovium but without any bone or cartilage erosions. Score 2, moderate synovitis with pannus formation, bone and cartilage erosions limited to discrete foci and undisturbed joint architecture. Score 3, severe pannus formation with extensive erosions of bone and cartilage with disrupted joint architecture.

For immunohistochemistry, 2–3 days old QB pups (3–4 mice/group) were injected with 1 mg each of a unhydrolyzed antibody cocktail containing M2139 + CIIC2 + UL1 antibodies, EndoS-hydrolyzed IgG (M2139H + CIIC2H + UL1H), or a mixture of unhydrolyzed and EndoS-hydrolyzed IgG at 1:1 ratio. Twenty-four hours later, mice were sacrificed, and paw samples were snap frozen in OCT compound using cold isopentane and dry ice. Sections of 6 µm were stained with biotinylated anti-kappa (clone: 187.1) or goat anti-mouse anti-C3c antibodies (Nordic Immunological Laboratories, Tilburg, The Netherlands). Extravidin-peroxidase and diaminobenzidine were used for detection. CIIC1 mAb was excluded from this cocktail because of their inability to activate complement after binding to CII. Histology scoring of joint sections after anti-C3c antibodies was done as follows: 0, no staining; 1, staining only at sub-chondral bone junction area; 2, weak; and 3, strong staining uniformly on the cartilage surface.

Complement Activation and RF-Like Activity of CII-Binding Antibodies

Microtiter plates were coated with 3 µg/ml M2139 or CIIC1 alone or in combination with 3, 6, and 12 µg/ml of EndoS-hydrolyzed or unhydrolyzed Hy2.15, L243, M2139, and CIIC1 IgG in 75 mM sodium carbonate buffer pH 9.6 overnight at 4°C. Plates were washed between each step with 50 mM Tris–HCl, 150 mM NaCl, 0.1% Tween-20, pH 8.0. Wells were blocked with 1% BSA in PBS for 2 h at RT to prevent unspecific binding. Serum was diluted to 0.5% in GVB^{++} (5 mM veronal buffer pH 7.4, 144 mM NaCl, 1 mM $MgCl_2$, 0.15 mM $CaCl_2$, and 1% gelatin) and added to the plates, followed by 1 h incubation at 37°C. Deposited C3b was detected using a goat anti-C3 antibody (ICN pharmaceuticals/Cappel, Aurora, OH, USA) and a rabbit anti-goat HRP conjugate (Dako Denmark A/S, Glostrup, Denmark). Deposited C1q was detected using a biotinylated mouse anti-C1q (clone JL-1) antibody (Hycult Biotech, Uden, The Netherlands) and a streptavidin-HRP conjugate (Thermo Fisher Scientific). The plates were developed using *O*-phenylenediamine substrate (Dako) and H_2O_2 and the absorbance at 490 nm was measured.

To study complement activation on CII-bound antibodies, microtiter plates were coated with 10 µg/ml CII in 75 mM sodium carbonate buffer pH 9.6 overnight at 4°C. The wells were blocked using 3% fish gelatin in 50 mM Tris–HCl, 150 mM NaCl, 0.1% Tween-20, pH 8.0 (blocking buffer). M2139 mAb alone at a concentration of 10 µg/ml or in combination with 10, 20, and 40 µg/ml of EndoS-hydrolyzed or unhydrolyzed Hy2.15, L243, or M2139 IgG diluted in blocking buffer was added and the plates were incubated at 4°C overnight. Serum diluted to 4% in $DGVB^{++}$ (2.5 mM veronal buffer pH 7.35, 72 mM NaCl, 0.1% gelatin, 1 mM $MgCl_2$, 0.15 mM $CaCl_2$, 2.5% glucose) was added to the wells and complement activation was allowed to proceed for 1 h at 37°C. Deposited C3b was detected as above. RF-like activity of CIIC1 antibodies was determined as described earlier (40). Biotin labeled CIIC1 was detected by europium-conjugated streptavidin using the dissociation-enhanced lanthanide fluoroimmunoassay system.

Analysis of the *In Vitro* Effects of mAbs Using Bovine Cartilage Explants

Articular cartilage samples extracted from adult bovine metacarpophalangeal joints and cartilage shavings (5 mm × 5 mm × 1 mm) were cultured for up to 14 days in DMEM with 20% (v/v) FCS and 25 µg/ml ascorbic acid, having 100 µg/ml of mAb or in medium alone. Medium was changed every 2 day, and fresh ascorbic acid and mAb were added at each change. Cartilage samples were tested in duplicate, and all experiments were performed at least twice. On day 14, cartilage explants were fixed in 4% paraformaldehyde and embedded in paraffin for Fourier transform infrared microspectroscopy (FTIRM). Sections (5 µm) were placed onto MirrIR low-e microscope slides (Kevley Technologies, Chesterland, OH, USA), and adjacent sections were stained with toluidine blue. FTIR images were recorded with a Stingray Digilab FTS 7000 series spectrometer coupled to a UMA 600 microscope equipped with a 64 × 64 focal plane array detector. For each spectrum, 16 scans were co-added at a resolution of 6/cm. The spectra were analyzed using CytoSpec imaging software (41). Raw chemical maps were generated from the integrated intensities of specific functional groups identified in the spectra, and 10 spectra from the surface of the explant and 10 from the interior were extracted from the raw chemical maps. The mean spectra for "surface" and "interior" were calculated to assess the effects of antibody penetration on the peaks characteristic of CII and proteoglycans. Analysis was performed on the location of the amide 1 peak (1,640–1,670/cm), which represents total protein, which for cartilage, is primarily CII. For proteoglycans, analysis was based on the height of the

peak at 1,076/cm, within the region of 1,175–960/cm derived from carbohydrate moieties.

Collagen-Induced Arthritis

Arthritis was induced in male (BALB/c × B10.Q) F1 mice with 100 µg of rat CII/CFA per mouse by i.d. immunization on day 0 and treated i.v. with different test substances on days 14, 21, 28, and 35. Development of clinical arthritis was followed through visual scoring of the animals based on the number of inflamed joints in each paw, starting 2 weeks postimmunization and continuing until the end of the experiment. An extended scoring protocol (25) ranging from 1 to 15 for each paw with a maximum score of 60/mouse was used. The mice were scored three times per week after immunization.

Statistical Analyses

All the mice with arthritis were included for calculation of severity. The severity of arthritis was analyzed by Mann–Whitney

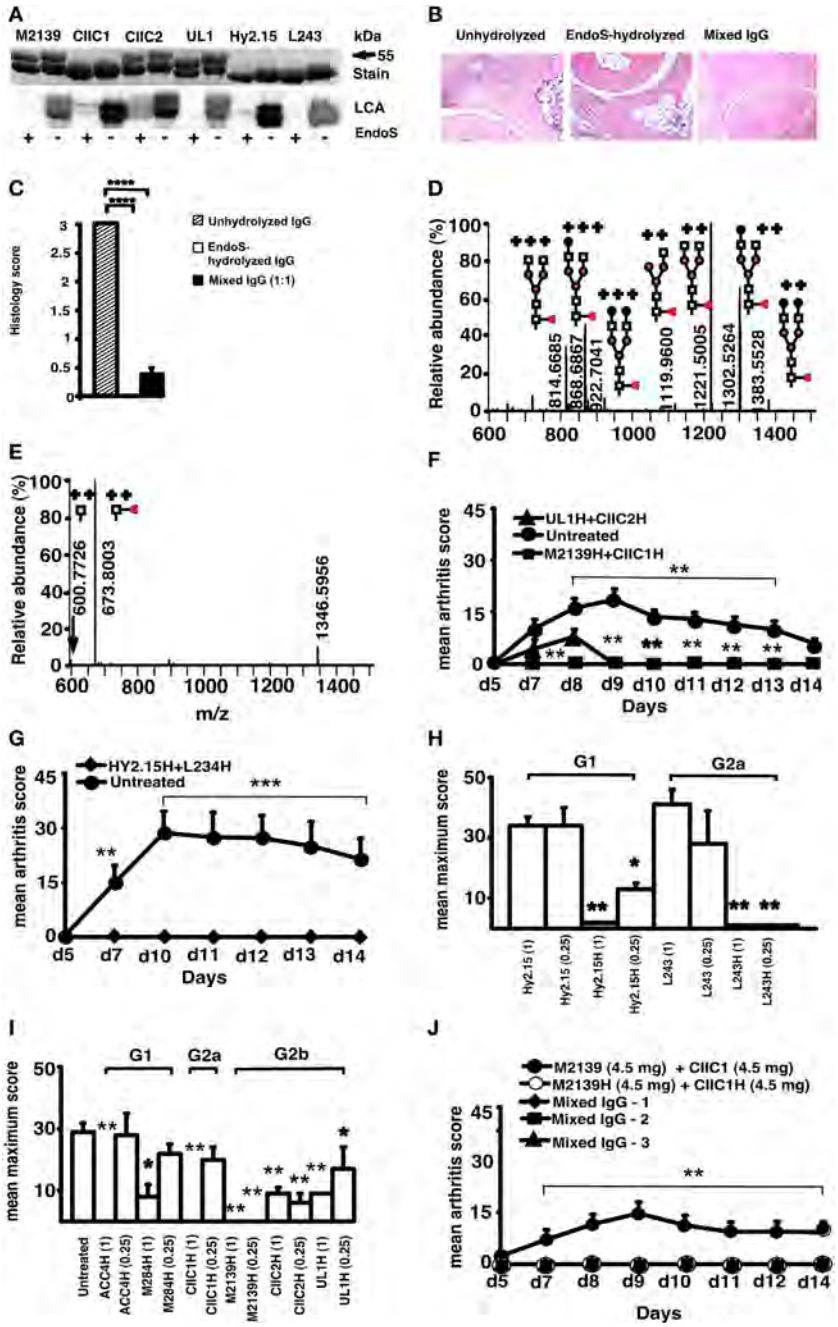

FIGURE 1 | Continued

FIGURE 1 | Endo-β-*N*-acetylglucosaminidase (EndoS) and enzyme-hydrolyzed IgG inhibit inflammation. **(A)** SDS/PAGE and lectin blot analysis of mAbs incubated with (+) or without (–) EndoS hydrolysis and separated by 10% SDS/PAGE. The proteins were detected by PageBlue stain (Stain) or by blotting onto a PVDF membrane probed with *Lens culinaris* agglutinin (LCA). **(B)** Representative figures of H&E-stained ankle joints of mice (n = 3–4/group) injected with anti-CII mAbs; unhydrolyzed (*Left*), EndoS-hydrolyzed (*Center*), or mixed IgG (*Right*) on day 9. Magnification 10×. **(C)** Joint sections were scored under the microscope based on the scoring scale as described in Section "Materials and Methods." In each group, at least five sections were scored for each mouse. ****$p < 0.0001$. Error bars indicate ± SEM. **(D)** Mass spectrometric analysis of Hy2.15 and **(E)** EndoS-treated Hy2.15. Shown spectra were acquired during the time period for which the majority of glycosylated peptides from EEQFNSTFR (21.5–23.0 min) elute. Doubly and triply charged ions as well as predicted glycan structures are shown. All numbers given are for the monoisotopic mass charge. In all of the animal experiments, male (BALB/c × B10.Q) F1 mice were used. Unless otherwise stated all of the mice received antibodies i.v. (d 0) and 25 μg of LPS i.p. (d 5). For arthritis induction in experiments shown in **(F,G,J)**, 9 mg of two anti-CII mAb mixtures (M2139 + CIIC1) were used, whereas for experiments in **(H,I)** 4 mg of four anti-CII mAb mixture (M2139 + CIIC1 + CIIC2 + UL1) was used. Antigen specificity is not required for inhibition. Mice (n = 42) were injected with 4 mg of EndoS-hydrolyzed IgG **(F)** M2139H + CIIC1H or UL1H + CIIC2H or **(G)** Hy2.15H + L243H followed by anti-CII mAb. Dose and subclass dependency. **(H)** Mice (n = 39) were injected with EndoS-hydrolyzed or unhydrolyzed IgG1 (Hy2.15) or IgG2a (L243) mAb binding to joint unrelated antigens at two different concentrations (1 and 0.25 mg), followed by anti-CII mAb. **(I)** Mice (n = 65) were injected with different subclasses of EndoS-hydrolyzed anti-CII (M284H, M2139H, CIIC1H, CIIC2H, and UL1H) or anti-citrullinated CII peptide IgG (ACC4H) at two different concentrations (1 and 0.25 mg), followed by anti-CII mAb. **(J)** Mice (n = 25) were injected with a mixture of EndoS-hydrolyzed and/or unhydrolyzed anti-CII IgG at different combinations. In mixed IgG groups, group 1 received 4.5 mg of unhydrolyzed and 4.5 mg of EndoS-hydrolyzed IgG, group 2 had 6.8 mg of unhydrolyzed and 2.3 mg of EndoS-hydrolyzed IgG, and group 3 received 7.9 mg of unhydrolyzed and 1.1 mg of EndoS-hydrolyzed IgG. Error bars indicate ± SEM. Arthritis scoring scale of 0–60 was used (25). All the groups were compared with the untreated group for statistical analysis. *$p < 0.05$; **$p < 0.01$; ***$p < 0.001$.

TABLE 1 | IgG glycoforms before and after endo-β-*N*-acetylglucosaminidase (EndoS) hydrolyzation.

Antibody		**M2139**	**M2139H**	**CIIC1**	**CIIC1H**
Sequence		**EDYNSTIR**	**EDYNSTIR**	**EDYNSTLR**	**EDYNSTLR**
Glycan[a]	HexNAc(1)	–	2.6%	–	3.8%
	HexNAc(1)dHex(1)	–	97%	–	95%
	HexNAc(4)Hex(3)	–	–	–	–
	HexNAc(4)Hex(4)	–	–	–	–
	HexNAc(3)Hex(3)dHex(1)	1.5%	–	6.5%	–
	HexNAc(3)Hex(4)dHex(1)	0.4%	–	1.3%	–
	HexNAc(4)Hex(3)dHex(1)	48%	–	35%	0.7%
	HexNAc(4)Hex(4)dHex(1)	43%	–	42%	0.5%
	HexNAc(4)Hex(5)dHex(1)	4.3%	–	4.4%	–
	HexNAc(4)Hex(6)dHex(1)	0.3%	–	0.2%	–
	HexNAc(3)Hex(4)dHex(1)NeuGc(1)	–	–	5.0%	–
	HexNAc(4)Hex(4)dHex(1)NeuGc(1)	0.5%	–	3.2%	–
	HexNAc(4)Hex(5)dHex(1)NeuGc(1)	1.8%	–	1.8%	–
	HexNAc(4)Hex(6)dHex(1)NeuGc(1)	–	–	0.3%	–

[a]*HexNAc, N-acetylhexoseamine; dHex, deoxy-hexose; Hex, hexose; NeuGc, N-glycolylneuraminic acid; H, EndoS-hydrolyzed.*

*Relative abundances (%) of the main Fc IgG glycoforms found in the antibodies and EndoS treated antibodies, respectively. Glycopeptides were identified by their characteristic retention times and accurate monoisotopic masses (within <10 ppm from the theoretical values) of doubly and triply charged ions. Peptide sequences and glycan compositions are indicated. Glycans substituting EDY**N**STIR and EDY**N**STLR eluted at approximately 18–20 min and EEQF**N**STFR at approximately 21–23 min, respectively.*

U test and the incidence by Chi Square or Fisher exact test using Statview (version 5.0.1) and Prism software. Two-way ANOVA and two-tailed Student's *t*-test were also used for statistical analysis. Significance was considered when $p < 0.05$, for a 95% confidence interval.

RESULTS

Small Amounts of EndoS Inhibit IgG-Mediated Inflammation

Endo-β-*N*-acetylglucosaminidase treatment specifically cleaved the Asn-297 glycan on IgG (**Figure 1A**), which removed almost all (99%) of the variable glycan chains attached to the first *N*-acetylglucosamine (GlcNAc) residue of the Fc region (**Figures 1D,E**; **Tables 1** and **2**). Injection of anti-CII mAb (EndoS-unhydrolyzed IgG) induced typical CAIA. Arthritis developed in mice as early as 48 h with 100% incidence at day 10. Massive infiltration of immune cells, pannus formation, and distinct bone and cartilage erosions were observed in this group of mice (**Figure 1B**). Injection of EndoS-hydrolyzed IgG, irrespective of CII epitope specificity, did not lead to any signs of arthritis (**Figures 1B,F–J**) resulting in normal joint architecture. Interestingly, mice treated with a mixture of unhydrolyzed and EndoS-hydrolyzed IgG potently blocked the development of arthritis. EndoS-hydrolyzed antibodies against trinitrophenol (TNP) (Hy2.15) and against human HLA-DR (L243), which are commonly used as control antibodies in the mouse, also completely inhibited CAIA when mixed with the anti-CII antibodies used for induction (**Figure 1G**). Inhibition of arthritis occurred irrespective of the IgG subclass, or the antigen specificity (**Figures 1H,I**). When we analyzed the

TABLE 2 | Joint unrelated antigen(s)-specific IgG glycoforms before and after endo-β-*N*-acetylglucosaminidase (EndoS) hydrolyzation.

Antibody		L243	L243H	Hy2.15	Hy2.15H
Sequence		**EDYNSTLR**	**EDYNSTLR**	**EEQFNSTFR**	**EEQFNSTFR**
Glycan[a]	HexNAc(1)	–	2.6%	–	15%
	HexNAc(1)dHex(1)	–	97%	–	84%
	HexNAc(4)Hex(3)	–	–	3.4%	–
	HexNAc(4)Hex(4)	–	–	1.3%	–
	HexNAc(3)Hex(3)dHex(1)	4.6%	–	2.5%	–
	HexNAc(3)Hex(4)dHex(1)	3.3%	–	0.7%	–
	HexNAc(4)Hex(3)dHex(1)	22%	–	46%	0.1%
	HexNAc(4)Hex(4)dHex(1)	50%	–	27%	0.5%
	HexNAc(4)Hex(5)dHex(1)	10%	–	5.0%	0.2%
	HexNAc(4)Hex(6)dHex(1)	4.6%	–	0.1%	–
	HexNAc(3)Hex(4)dHex(1)NeuGc(1)	2.6%	–	2.5%	–
	HexNAc(4)Hex(4)dHex(1)NeuGc(1)	0.3%	–	5.9%	–
	HexNAc(4)Hex(5)dHex(1)NeuGc(1)	1.7%	–	4.5%	–
	HexNAc(4)Hex(6)dHex(1)NeuGc(1)	0.7%	–	1.5%	–

[a]*HexNAc, N-acetylhexoseamine; dHex, deoxy-hexose; Hex, hexose; NeuGc, N-glycolylneuraminic acid; H, EndoS-hydrolyzed.*

*Relative abundances (%) of the main Fc IgG glycoforms found in the antibodies and EndoS treated antibodies, respectively. Glycopeptides were identified by their characteristic retention times and accurate monoisotopic masses (within <10 ppm from the theoretical values) of doubly and triply charged ions. Peptide sequences and glycan compositions are indicated. Glycans substituting EDY**N**STIR and EDY**N**STLR eluted at approximately 18–20 min and EEQF**N**STFR at approximately 21–23 min, respectively.*

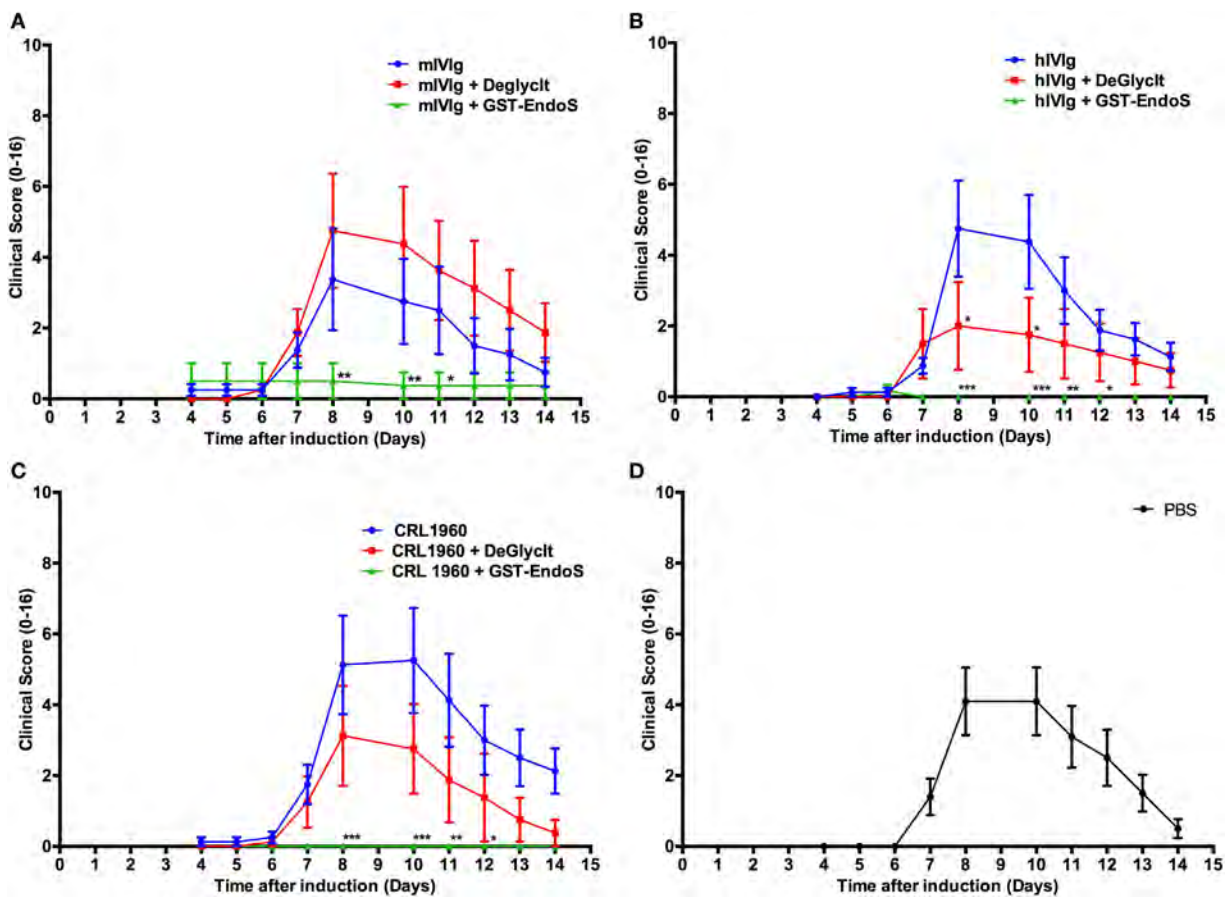

FIGURE 2 | Analysis of endo-β-*N*-acetylglucosaminidase (EndoS) effects *in vivo*. Arthritic score (mean ± SEM) of collagen antibody-induced arthritis animals (n = 8–10 mice/group) treated with different antibody preparations that were either untreated or deglycosylated with GST-tagged EndoS (GST-EndoS) or EndoS immobilized to sepharose beads (DeGlycIt). Arthritis was induced on day 0 by i.p. administration of 2 mg/mouse of anti-collagen antibody cocktail followed by administration of 50 µg LPS on day 5. The test substances (1 mg/mouse) were injected i.v. on day 0. DeGlycIT or GST-EndoS treated mouse intravenous immunoglobulins (mIVIg) **(A)**, human intravenous immunoglobulins (hIVIg) **(B)** or mouse monoclonal antibody recognizing trophozoite antigens (2B5.3; CRL-1960) **(C)** were used as test substances and PBS was injected as control **(D)**. Error bars indicate ± SEM. Arthritis scoring scale (0–16) was used (25). All the groups were compared with the untreated group for statistical analysis. *$p < 0.05$; **$p < 0.01$; ***$p < 0.001$.

dose dependence of the arthritis suppressive effect, we found that 1 mg of EndoS-hydrolyzed IgG present in the mixture of 9 mg of antibodies completely inhibited arthritis (**Figure 1J**), whereas 3 mg of unmodified anti-CII mAb was sufficient to induce arthritis (20).

We have earlier reported our results interpreted as dominant suppression of inflammation by glycan hydrolyzed IgG (42) but we withdrew this report as we discovered that we could not rule out that small amounts of EndoS, undetectable on PageBlue stained gels, remained after hydrolysis *in vitro*. Consequently, when we used DeglycIT column for cleaving the N-linked sugars instead of GST-EndoS treatment and serial passage through glutathione-Sepharose 4B columns (DeglycIT spin column contains EndoS immobilized on agarose, which facilitates complete removal of the enzyme in one step instead of two step process with GST-EndoS treatment and purification using glutathione-Sepharose 4B), we observed no inhibition of arthritis (**Figures 2A–C**) compared with the control mice (**Figure 2D**). We rechecked our GST-EndoS treated purified IgG samples used in the above experiments by Western blot and in most (12/14) of the samples we could still not detect the presence of EndoS. In the remaining two samples, we found very low level of residual enzyme, <0.02% of total protein (data not shown).

To find whether the residual EndoS present in the IgG preparation had any enzymatic activity, we designed a new rabbit IgG cleavage assay using another streptococcal enzyme, IdeS. With this assay, it is now possible to detect the presence of residual activity of EndoS in the IgG preparation treated with EndoS even after three serial passages over Glutathione-Sepharose 4B columns with a 1,000-fold overcapacity of GST binding but not after treatment with DeglycIT column (**Figure 3A**).

To further investigate if the level of residual EndoS activity was sufficient to deglycosylate the mouse endogenous IgG pool *in vivo*, mice were injected with 1 mg of untreated hIVIg (Octagam) or GST-EndoS treated Octagam. IgG was purified from the mouse serum (collected 18 h later) using protein G Sepharose and the samples were treated with IdeS to cleave the human IgG. The results indicate that the intact (i.e., of mouse origin) IgG heavy chain band migrates a longer distance (indicating a decreased molecular size) in the sample purified from the mouse injected with the GST-EndoS treated Octagam

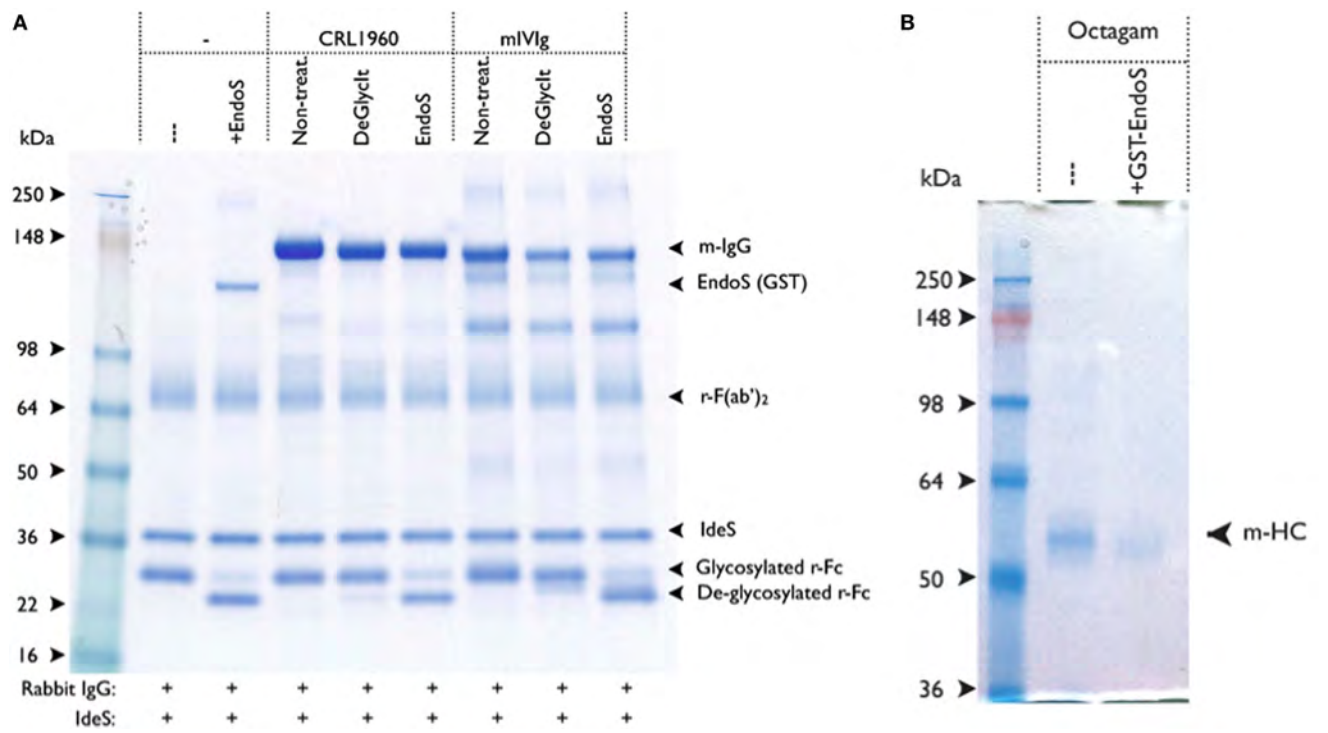

FIGURE 3 | IgG treated with GST-endo-β-*N*-acetylglucosaminidase (EndoS) contains residual enzyme activity. **(A)** EndoS treated antibody preparations were tested for residual EndoS activity by using rabbit IgG cleavage assay. Rabbit IgG was used as a reporter for EndoS activity, in which ability of IdeS to efficiently cleave the heavy chain of rabbit IgG was used. After IdeS treatment, the deglycosylated rabbit Fc-fragment was distinguished from the non-deglycosylated rabbit Fc-fragment using SDS-PAGE (i.e., a 25-kDa fragment ± glycosylation). Rabbit IgG (1.7 μg) and IdeS (0.3 μg) were added to each of the sample. Molecular weight markers (lane 1); without EndoS (lane 2); with EndoS (0.5 μg, lane 3); 1.7 μg of CRL-1940 untreated (lane 4); CRL-1940 DeGlycIT treated (lane 5); CRL-1940 GST-EndoS treated (lane 6); mouse intravenous immunoglobulins (mIVIg) untreated (lane 7); mIVIg DeGlycIT treated (lane 8); mIVIg GST-EndoS treated (lane 9). m-IgG: mouse IgG, r-Fc: monomeric rabbit Fc-fragment. The gel shown was run under non-reducing condition. **(B)** BALB/c mice were intravenously injected with untreated control Octagam (human intravenous immunoglobulins, 1 mg) or GST-EndoS treated Octagam (1 mg). Serum was collected 18 h after injection and IgG was purified from serum using protein G sepharose. Samples were treated with IdeS to cleave remaining Octagam and the samples were analyzed on SDS-PAGE. m-HC, mouse heavy chain. IgG purified from mice injected with untreated control Octagam (lane 1) or GST-EndoS treated Octagam (lane 2) were shown. The gel shown was run under reducing condition.

compared with the heavy chain band from the mouse injected with the untreated control Octagam (**Figure 3B**). Hence, deglycosylation is a likely explanation for this shift in size on SDS-PAGE. As a next step, we titrated the amount (100 µg to 1 ng) of EndoS needed for inhibiting antibody-mediated inflammation (**Table 3**). Our results show that intravenous injection of as low as 1 µg EndoS was sufficient to completely inhibit antibody-initiated inflammation and even lower when mixed with DeglycIT treated anti-CII antibody, 0.1 µg EndoS (**Table 3**). As a next step, we incubated antibodies with recombinant EndoS at two different concentrations (0.1 or 1 µg) and after incubation for 1 h antibodies were purified using affinity column or left unpurified (**Figure 4**). These antibodies were injected into mice before arthritogenic monoclonal antibodies were transferred into them. Interestingly, as observed earlier, 1 µg but not 0.1 µg of EndoS added to the purified DeglycIT treated antibody was sufficient to inhibit arthritis, whether it underwent one more cycle of affinity purification after incubation with EndoS or not (**Table 3**). However, deglycIT purified M2139 added with 1 µg of GST-EndoS was found to be inferior to GST-EndoS hydrolyzed M2139 in attenuating joint inflammation (**Table 3**).

From these results, we concluded that the small amount of residual EndoS present in enzyme treated IgG fractions is a requirement for the observed hydolyzed antibody-mediated arthritis inhibition. To determine whether this small amount of EndoS was sufficient to cleave the sugars from IgG *in vivo* we injected small amounts of EndoS and analyzed the presence of glycan on circulating IgG. As shown in **Figure 5**, it is clear that 0.1 µg of EndoS injected *in vivo* was capable of specifically cleaving most of the carbohydrates present on all the IgG subclasses, whereas only at 1 µg concentration all the carbohydrates present in the Fc region of IgG were cleaved.

To find the effective therapeutic window, EndoS-hydrolyzed IgG was administered to groups of mice at different concentrations and time points and one group of mice was left untreated in each experiment. Dose titration of the EndoS-hydrolyzed IgG separately showed that complete inhibition of arthritis was achieved down to 250 µg (**Figure 6A**). In the time titration experiments, antibody cocktail and then LPS were injected at 0 and 3 h, respectively. In the 0 h treatment group, EndoS-hydrolyzed IgG was injected initially, followed by an injection of mAb cocktail. Unlike −48 h time, complete blocking of arthritis was observed when the treatment with EndoS-hydrolyzed IgG was done 3 h before or after the arthritogenic cocktail injection (**Figure 6B**). However, when EndoS-hydrolyzed IgG was injected 48 h after mAb injection (+48 h group), significant blocking of arthritis was observed ($p < 0.05$ to $p < 0.01$ for different time points), which increases the therapeutic value of the EndoS. Since anti-CII antibodies are bound to cartilage within 30 min after injection as detected by immunohistochemistry (43), we concluded that EndoS and the enzyme hydrolyzed IgG could block the disease most effectively if injected within 48 h after antibody binding or during the time when antibodies start binding to the cartilage surface. However, we did not find any role for the spleen (mice splenectomized or sham operated 2 weeks earlier were used for this purpose) in EndoS and enzyme-hydrolyzed IgG induced arthritis inhibition (**Figure 6C**).

TABLE 3 | Titration of inhibitory dose of endo-β-*N*-acetylglucosaminidase (EndoS) using antibody-mediated inflammation.

Groups[a]	Incidence	Maximum arthritis score[b] (mean ± SEM)
PBS	16/18	21 ± 7
GST-EndoS (100 µg)	0/4**	0**
GST-EndoS (10 µg)	0/4**	0**
GST-EndoS (1 µg)	0/13****	0****
GST-EndoS (0.1 µg)	13/15[n.s.]	18 ± 9[n.s.]
M2139-E[c]	0/4**	0**
M2139-D[d]	14/14[n.s.]	18 ± 6[n.s.]
M2139-D + GST-EndoS (1 µg)[e]	4/9*	10 ± 6*
M2139-D + GST-EndoS (0.1 µg)[e]	9/13[n.s.]	23 ± 4[n.s.]
M2139-D + GST-EndoS (1 µg)[f]	6/9[n.s.]	12 ± 6*
M2139-D + GST-EndoS (0.1 µg)[f]	8/9[n.s.]	21 ± 5[n.s.]

[a]All the mice received 9 mg of arthritogenic two mAb cocktail (M2139, CIIC1) i.v. on day 0 and 25 µg of LPS was injected i.p. on day 5. Four-month-old male (BALB/c × B10.Q) F1 mice (n = 112) were used in all these experiments.

[b]Arthritis severity was scored using the scale 0–60. Mice with arthritis only were included for calculations.

[c]M2139 antibodies (250 µg) treated with GST-EndoS was injected i.v. on day 0.

[d]M2139 antibodies (250 µg) treated with DeglycIT and purified was injected i.v. on day 0.

[e]M2139 antibodies (250 µg) treated with DeglycIT and purified were incubated with indicated concentrations of GST-EndoS for 1 h at RT before i.v. injection on day 0.

[f]M2139 antibodies (250 µg) treated with DeglycIT and purified were incubated with indicated concentrations of GST-EndoS for 1 h at RT. Antibodies were further purified using HiTrap Protein G HP column before i.v. injection on day 0.

**p < 0.05; **p < 0.01; ****p < 0.0001; n.s., not significant.*

EndoS Hydrolysis of IgG Does Not Affect Antigen Binding

Biacore analysis of the antigen-antibody binding in the presence or absence of EndoS and enzyme-hydrolyzed IgG clearly demonstrated that removal of carbohydrate moieties from mAbs did not affect their high affinity binding to CII epitopes (**Figure 6D**). We have earlier shown antibody-mediated damage in cartilage explants cultured *in vitro* with the mAb to CII used in this study: this pre-inflammatory effect does not require live cells, is mediated by F_{ab} and is epitope dependent (44). To test whether EndoS hydrolysis could change this effect, FTIRM was used for chemical analysis of cartilage (41) cultured in the presence of 100 µg/ml EndoS-hydrolyzed IgG containing minor amounts of the enzyme or unhydrolyzed mAb (**Figures 6E–H**). The height and location of the amide 1 peak, representing protein, predominantly collagen, and the height of the proteoglycan peak at 1,076/cm were examined at the cartilage surface, where the mAb penetrates, and in the interior of cartilage explants (**Figure 6E**). After 14 days, the amide 1 peak at the surface and in the interior of the control cartilage cultured without mAb was at 1,659/cm (range 1,655–1,666/cm). There were striking changes in spectra from cartilage cultured in the presence of unhydrolyzed M2139 mAb (**Figure 6F**). However, the spectra [amide 1 peak representing mainly collagen (**Figure 6G**) and proteoglycan peak at 1,076/cm (**Figure 6H**)] obtained were similar when the cartilage was cultured with Endo-S hydrolyzed IgG containing minor

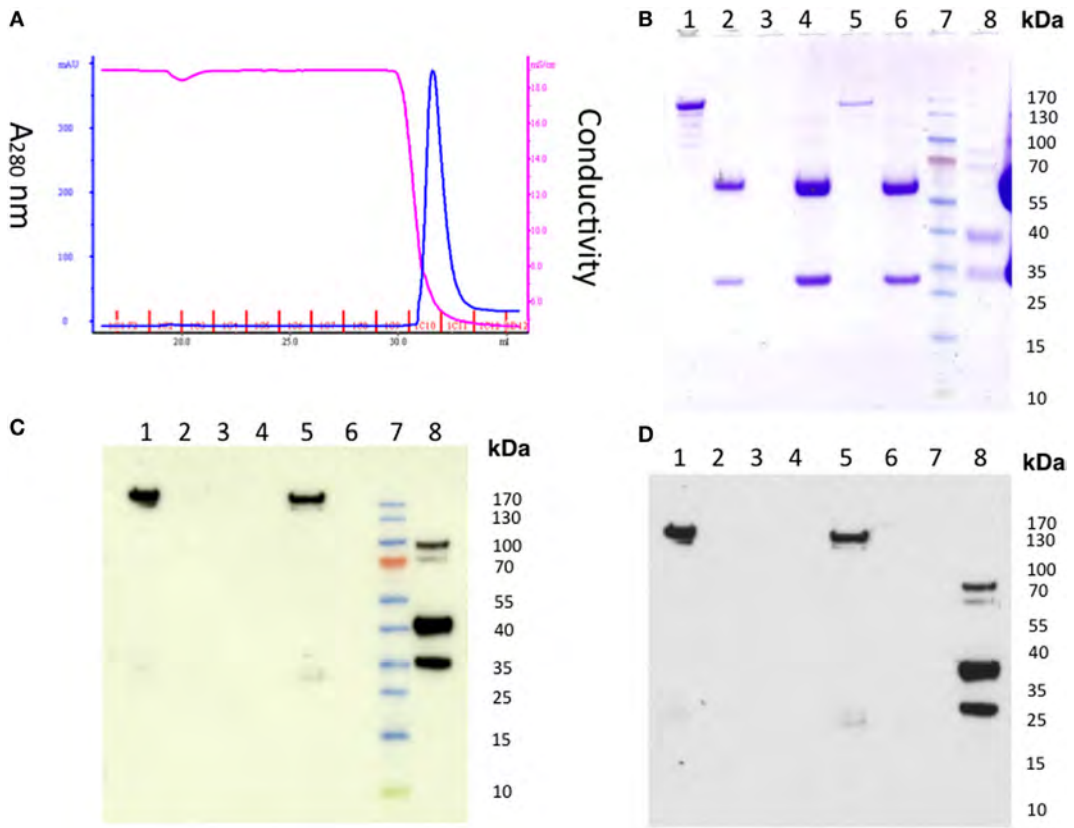

FIGURE 4 | Detection of residual endo-β-*N*-acetylglucosaminidase (EndoS) in the GST-EndoS treated IgG after protein G purification. M2139 antibody (2 mg) was incubated with 0.1 μg or 1 μg of EndoS in PBS at 37°C for 1 h followed by immediate purification on HiTrap Protein G HP column **(A)** Chromatogram. The flow through fraction and the eluate were analyzed by SDS-PAGE followed by Western blot. **(B)** SDS-PAGE and Western blot using **(C)** alkaline phosphatase or **(D)** peroxidase conjugate as secondary antibody. Flow-through samples were concentrated before loading on to SDS-PAGE. After transfer, the Western blot membrane was incubated with Eu-N1-labeled anti-GST antibody, followed by donkey anti-goat AP or anti-goat HRP conjugate. For the AP conjugate, the positive bands were visualized using 1-Step TM NBT/BCIP substrate. For the HRP conjugate, the light emission was enhanced using ECL followed by film exposure. Lane 1, EndoS; lane 2, M2139; lane 3, concentrated flow through (0.1 mg group); lane 4, eluate (0.1 mg group); lane 5, concentrated flow through (1 mg group), lane 6, eluate (1 mg group); lane 7, protein standard; lane 8, control GST-fusion protein.

amounts of the enzyme or unhydrolyzed anti-CII IgG. Beyond the region of penetration by mAb, the spectra were generally similar to those of controls cultured without mAb, but spectra from the surface of the cartilage showed substantial changes (**Figures 6E,F**). For both unhydrolyzed and EndoS-hydrolyzed anti-CII containing minor amounts of the enzyme, there was a shift in the location of the amide 1 peak from 1,659/cm to as low as 1,643/cm (**Figure 6G**). This shift is indicative of denaturation of the CII and accompanied by substantial decreases in the height of the amide 1 peak, as well as the proteoglycan peak at 1,076/cm, indicating a total loss of matrix (**Figure 6H**). These data confirm that the EndoS-hydrolyzed IgG retained its antibody reactivity.

EndoS and Enzyme Hydrolyzed IgG Disrupt Larger IC Formation

As a next step, we analyzed whether the EndoS and EndoS-hydrolyzed antibodies can disrupt the growth of Fc-dependent ICs. For this we used DLS technique and analyzed the formation of IC by CII and anti-CII mAb in the presence of EndoS-hydrolyzed IgG, which contain minor amounts of the enzyme or unhydrolyzed IgG. As shown in **Figures 7A,B**, larger IC formation was clearly disturbed by the presence of EndoS and enzyme-hydrolyzed IgG. Interestingly, disturbance of large IC was more prominent in the presence of low affinity (**Figure 7A**) than high affinity IgG (**Figure 7B**). It has earlier been shown that the binding to low affinity Fc-receptors is decreased by EndoS modification (21). However, the binding is directly related to IC formation. Different data have been reported regarding complement binding after EndoS hydrolysis (21, 22). To directly investigate this, we analyzed complement fixation using either immobilized EndoS-hydrolyzed IgG containing residual amount of EndoS or unhydrolyzed IgG, or CII-anti-CII ICs. The presence of the enzyme and EndoS-hydrolyzed IgG did not interfere with the ability of antibodies to stimulate complement deposition, when bound to immobilized CII (**Figure 7C**). Furthermore, presence of the enzyme and EndoS-hydrolyzed IgG did not interfere with the ability of antibodies to stimulate complement deposition,

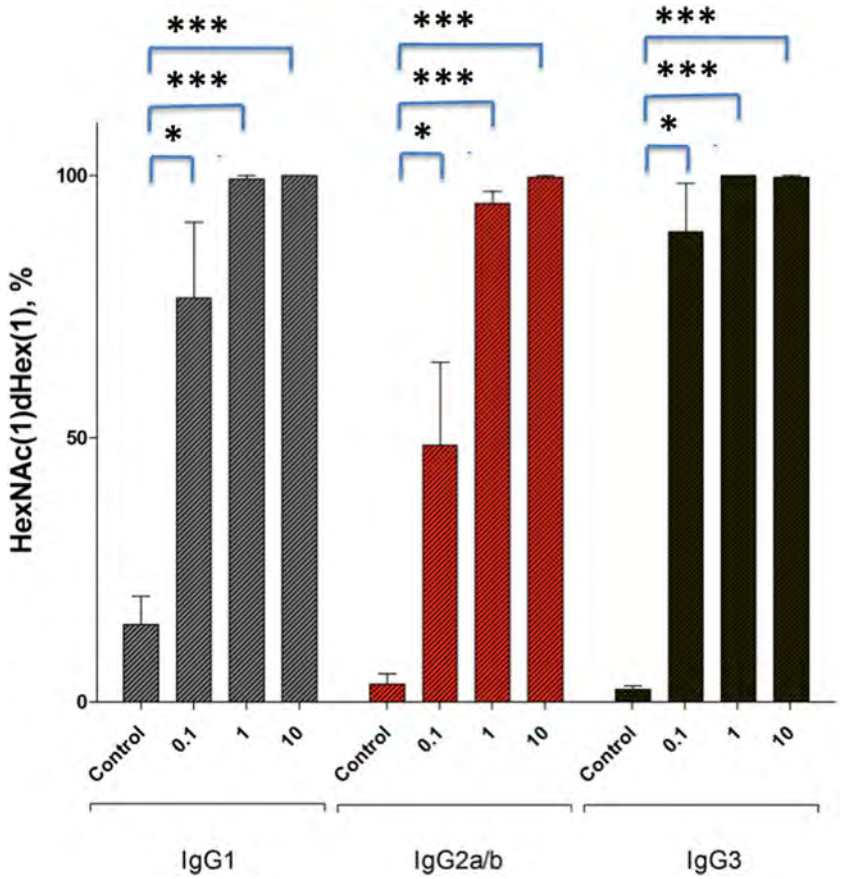

FIGURE 5 | Relative abundance of dHex-HexNAc after endo-β-*N*-acetylglucosaminidase (EndoS) treatment *in vivo*. Male (BALB/c × B10.Q) F1 mice ($n = 12$) were injected with GST- recombinant protein (control), 0.1 μg, 1 μg, or 10 μg of GST-EndoS. Serum samples were collected before and 18 h after the injection. Even at 0.1 μg of EndoS injection the majority of the found glycopeptides, for all IgG types are the truncated dHex-HexNAc variants. The bar graph shows mean ± SEM of the relative abundance of dHex-HexNAc compared with other Fc-glycopeptides. dHex(1)-HexNAc (1), dHex (1)Hex (3)HexNac (4), dHex (1)Hex (4)HexNAc (4), dHex (1)Hex (5)HexNAc (4) sugars present on IgG1 (EEQFNSTFR), IgG2b (EDYNSTIR)/IgG2a (EDYNSTLR), and IgG3 (EAQYNSTFR) peptides, respectively. Glycopeptides were analyzed using mass spectrometry. $^{*}p < 0.05$; $^{****}p < 0.0005$.

when antibodies were immobilized directly on the plate (data not shown).

The presence of EndoS-hydrolyzed IgG did not affect complement activation but did affect IC stability *in vitro*; hence, we further analyzed deposition of C3b, the activated product of complement factor C3, on the cartilage of mice as a measure of IC deposition and complement activation *in vivo*. Twenty-four hours after the injection of EndoS-hydrolyzed, unhydrolyzed or mixed anti-CII IgG, mouse paws were analyzed for the binding of mAbs to cartilage using anti-kappa antibodies as well as for deposited C3b. The mAbs readily bound to the cartilage surface, but the pattern of C3b deposition between the groups was entirely different (**Figures 7D,E**). Minimal C3b staining was observed, only on the sub-chondral bone junction area of the joints from mice injected with EndoS-hydrolyzed IgG compared with a significant level of deposition throughout the cartilage surface in the unhydrolyzed IgG injected group. In mice injected with mixed IgG, staining on the sub-chondral bone junction area was more intense with weak staining on the cartilage surface.

Previously, we reported RF-like activity of one of the mAbs (CIIC1) present in the arthritogenic cocktail (40); hence, it might be possible that the observed inhibition of arthritis by EndoS hydrolyzed IgG might be due to this property of CIIC1 antibodies. However, we did not observe any difference in CIIC1 mAb binding activity to EndoS hydrolyzed and unhydrolyzed IgG (**Figure 8**), thereby ruling out the contribution of RF-like activity of CIIC1 in the inhibition of antibody-initiated inflammation. Though EndoS is highly potent in inhibiting antibody-mediated inflammation, we did not find any arthritis inhibitory activity of EndoS-hydrolyzed IgG (**Figure 9A**) or direct injection of the enzyme (**Figure 9B**) using collagen-induced arthritis model.

DISCUSSION

Cleavage of the Fc glycan by the streptococcal enzyme EndoS leads to severely impaired effector functions. Here, we show that very small amounts of EndoS injected *in vivo* in the mouse blocks the development of CAIA. Based on our findings, we

propose that EndoS and enzyme treated IgG disrupted larger IC lattice formation through destabilization of all the Fc effector functions including Fc–Fc interactions between pathogenic and deglycosylated Fc domains but without involving changes in C1q and C3b binding, leading to attenuation of joint inflammation.

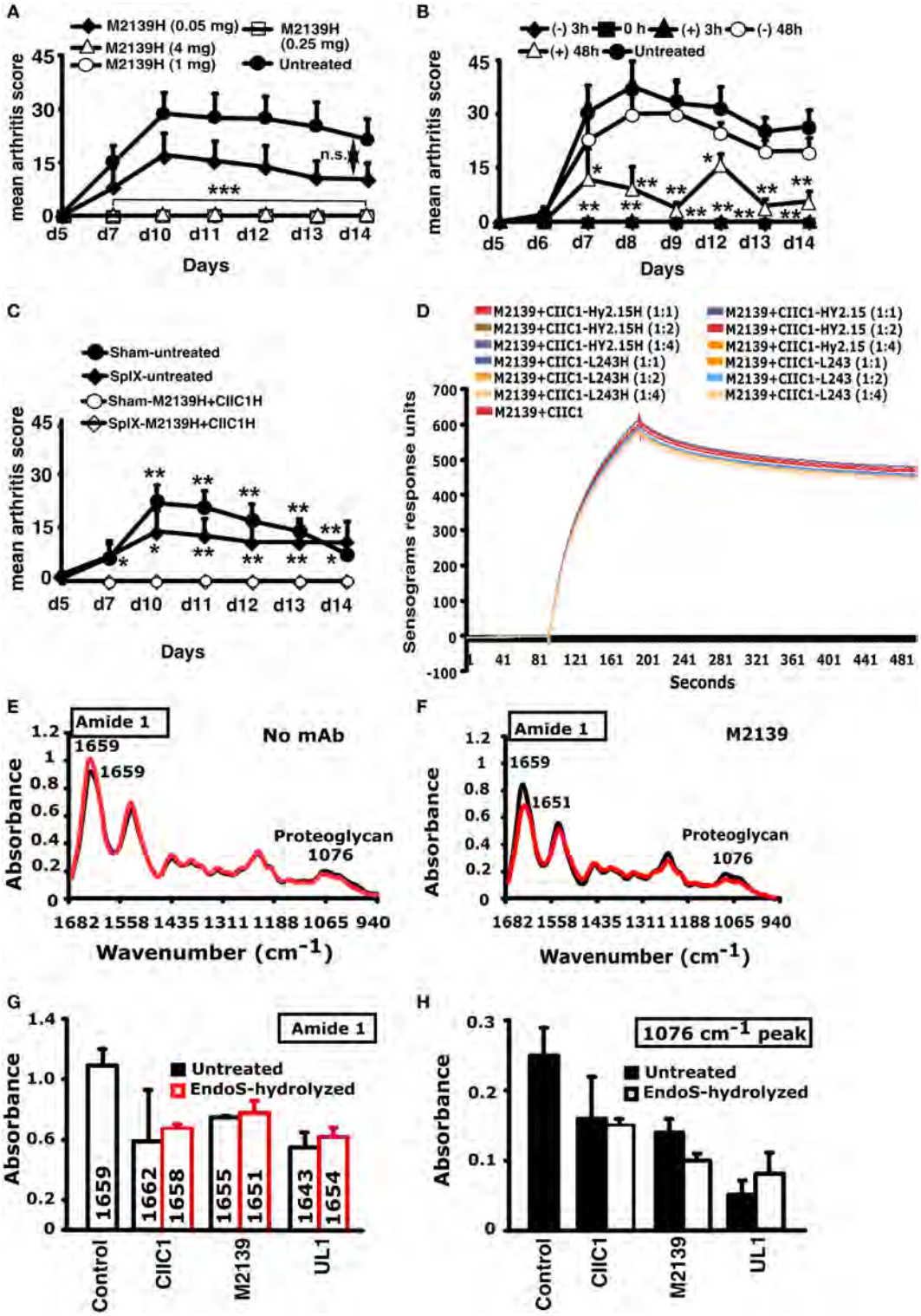

FIGURE 6 | Continued

FIGURE 6 | Inhibition of inflammation and Surface Plasmon Resonance (SPR) and Fourier transform infrared microspectroscopy (FTIRM) analysis. **(A)** Mice ($n = 25$) were injected with different concentrations (50–4,000 μg) of endo-β-*N*-acetylglucosaminidase (EndoS)-hydrolyzed single anti-CII IgG (M2139H), followed by anti-CII mAb. Three hours after the antibody transfer, LPS was injected. H denotes EndoS-hydrolyzed IgG. Hy2.15 and L243 represent mAbs binding to TNP hapten and human HLA-DR antigen, respectively. **(B)** Mice ($n = 30$) were injected with 1 mg of EndoS-hydrolyzed anti-CII IgG (M2139H + CIIC1H + CIIC2H + UL1H) at different time points (−48, −3, 0, +3, or +48 h). At 0 and 3 h, anti-CII mAb (M2139 + CIIC1 + CIIC2 + UL1) and then LPS were injected. One group of mice received no treatment. **(C)** Effect of splenectomy. Mice ($n = 21$) were either splenectomized (Splx) or sham-operated (Sham). Three weeks later, they were injected with 4 mg of EndoS-hydrolyzed IgG (M2139H + CIICH) or left untreated, followed by anti-CII mAb (M2139 + CIIC1). Panel **(H)** denotes EndoS-hydrolyzed IgG. Error bars indicate ± SEM. **(D)** SPR (Biacore) analysis of antibody binding capacity of EndoS-hydrolyzed and unhydrolyzed IgG was performed using CII immobilized on CM5 sensor chip. MAbs were injected at different concentrations through flow cells at a flow rate of 30 μl/min. Antibodies were injected for 3 min and dissociation of bound molecules was observed for 7 min. There was no difference in antibody binding when EndoS-hydrolyzed or unhydrolyzed IgGs were added at different ratios to anti-CII mAb mixture. **(E,F)** Changes in the chemical composition of the cartilage were assessed using FTIRM analysis. Representative mean spectra are shown from cartilage cultures without antibody **(E)**, and from cartilage cultured for 14 days with 100 μg/ml of unhydrolyzed mAb M2139 **(F)**. The results shown are the mean of 10 measurements taken from the central areas (red line) and near the surface of the tissue (black line). The mean spectra for surface and interior were calculated to assess the effects of antibody penetration on the peaks characteristic of CII and of proteoglycans. **(G,H)** The mean peaks from the surface cartilage were compared with those from antibody-exposed surface of cartilage exposed to the EndoS-hydrolyzed or unhydrolyzed IgG. Cartilage exposed to either EndoS-hydrolyzed or unhydrolyzed IgG (CIIC1, M2139, and UL1) showed similar changes. **(G)** The height and location of the amide 1 peak, which represents the total protein content of the tissue, in the region 1,600–1,700/cm. **(H)** The height of the peak at 1,076/cm represents proteoglycans. All the groups were compared with the untreated group for statistical analysis. $^{*}p < 0.05$; $^{**}p < 0.01$; $^{***}p < 0.001$; n.s., not significant.

It has earlier been reported that treatment of mice with higher doses (10–100 μg) of EndoS can suppress many antibody-mediated autoimmune disease models [thrombocytopenic purpura (23), arthritis (22), glomerulonephritis (45, 46), encephalomyelitis (47), hemolytic anemia (48), and epidermolysis bullosa acquisita (49)]. By contrast, we found that EndoS treatment of CIA could not affect the disease development although treatment was done with high EndoS doses (200 μg). However, CIA is a complex disease in which not only pathogenic antibodies are of importance and in addition, initiation and duration of arthritogenic antibody synthesis in the CIA model is likely to be highly variable. By contrast, in the CAIA model, we found that EndoS had a potent therapeutic effect. This was dependent on a strict time window indicating that EndoS is effective during the formation of ICs and also after 48 h of antibody transfer. In addition, we found that though the EndoS was effective in very low doses on CAIA, the same treatment protocols, with EndoS or with hydrolyzed IgG containing small amounts of EndoS had no effect on CIA.

Binding of the arthritogenic antibodies to the cartilage matrix happens within minutes after intravenous injection as detected using positron emission tomography (50) and the subsequent formation of ICs on the joint surface is likely to be the major factor leading to the clinically apparent inflammation and arthritis. In the process of local IC formation, Fc:Fc interactions play an important role (51), and the specific glycans present in the CH2 domain of IgG might have a vital function in this process. Since the suppression seems to be mediated through more acute effects during the binding of antibodies to the cartilage, we hypothesized this might be due to the instability of ICs formed within the target tissue, the articular joints (as illustrated in **Figure 7F**). Specific IgG glycan hydrolysis alters both murine and human IgG–FcγR interactions (21, 22) and, removal of outer-arm sugar residues affects the thermal stability and functionality of the CH2 domains of IgGs (52). However, the length and nature of residual carbohydrate structures could also affect Fc:Fc interactions and thereby IC formation, complement binding and FcR binding capacities. It is of interest to note that EndoS hydrolysis of IgG does not influence the interactions with the neonatal FcR; hence, overall circulation time of antibodies should be unaffected. However, after EndoS treatment of IgG binding to the other FcRs is affected to varying extent *in vitro* (21), which indeed could attenuate cell-mediated pathology and possibly also clearance of dead cells. Interestingly, it has been shown that IgG maintains several of its FcR-dependent activities with just a mono- or disaccharides present on the Fc glycan *in vivo* (53).

Anti-inflammatory property of terminal sialic acids present on IgG-Fc was demonstrated earlier (11). C-type lectin receptor SIGN-R1 (CD209) expressed on macrophages in the splenic marginal zone is required for recognition of such sialic acids (54), which results in the production of IL-33 and expansion of IL-4-producing basophils promoting increased expression of the inhibitory FcγRIIb on effector macrophages leading to attenuation of inflammation (55). However, in this study, splenectomy did not alter the inhibitory capacity of EndoS-hydrolyzed IgG suggesting involvement of other mechanisms than the SIGN-R1 pathway.

Analysis of immunohistochemical staining of the EndoS and enzyme-hydrolyzed and unhydrolyzed antibody-injected joints for complement activation has led to the conclusion that the presence of small amounts of EndoS and EndoS-hydrolyzed IgG indeed decreased the formation of larger IC *in situ*, most likely by *in vivo* cleaving of IgG sugars and through the disturbance of Fc:Fc-interactions. Significance of Fc:Fc interactions in precipitation (56) and formation of insoluble ICs (51) are early wisdoms. In addition, dinitrophenol specific non-precipitating antibodies were shown to inhibit as well as solubilize IC between antigen and precipitating antibodies (57) that might involve Fc:Fc interactions. Later, structural evidence for such interactions involving the glycosylation loop of one Fc-fragment dimer binding to the CH2–CH3 interface of another Fc fragment has been demonstrated (58). Although oligosaccharides have been reported not to be involved in direct contacts with symmetry-related molecules (58), their interactions with the protein moiety in the IgG–Fc region could very well affect the reciprocal influences on conformation (8). Recent studies also showed

that reduced Fc/FcγR interactions through Fc deglycosylation by treatment with EndoS led to improvement of imaging specificity (59) as well as reduction in IC-mediated neutrophil activation (60). Importance of the size of the IC on its effector functions possibly by changes in its interactions with FcγRs has been documented (61).

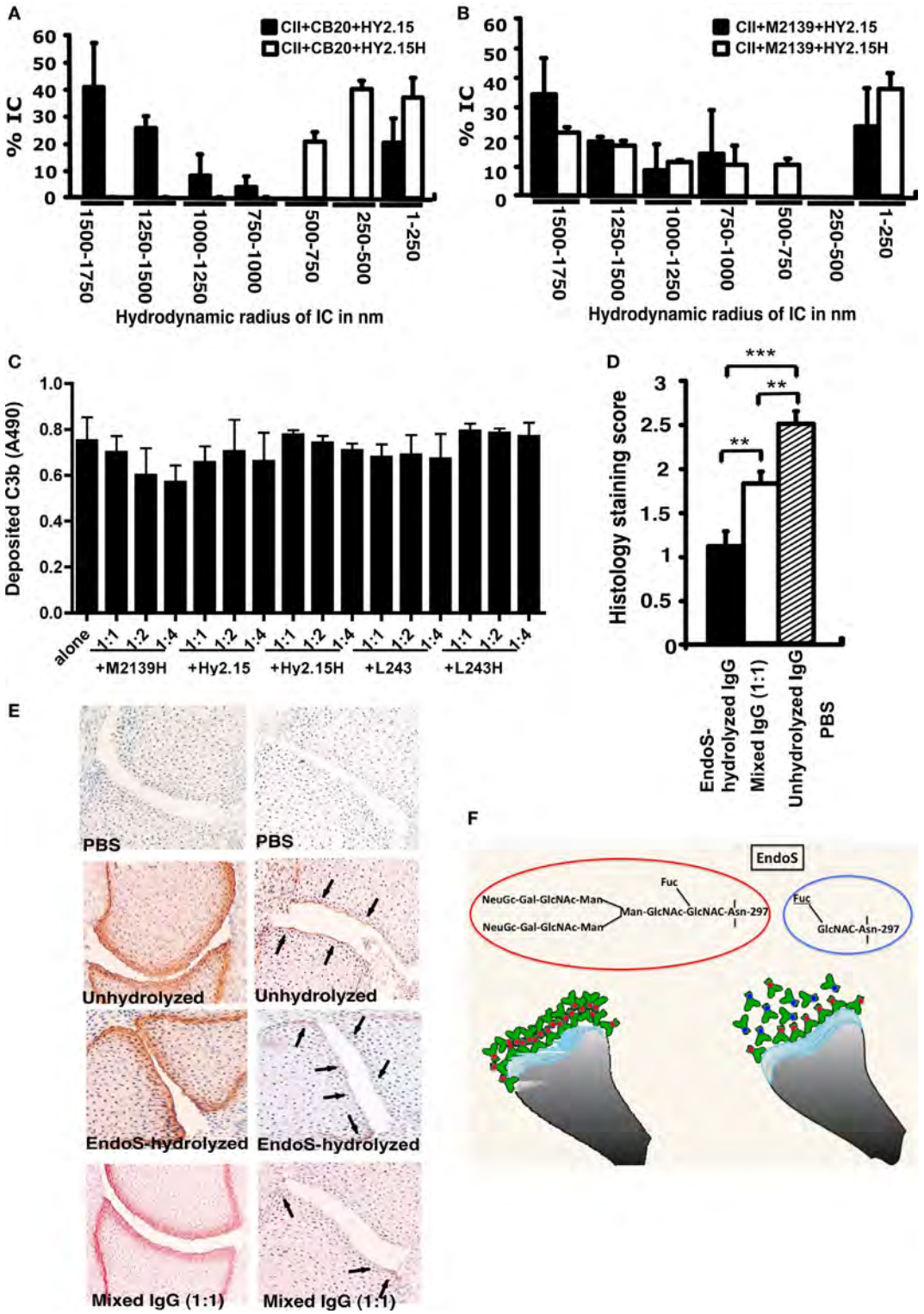

FIGURE 7 | Continued

FIGURE 7 | Disturbance of stable ICs and complement activation. Collagen type II (CII; 1 mg/ml) and anti-CII mAb CB20 [low affinity; **(A)**] or M2139 [high affinity; **(B)**] at 1 mg/ml were mixed together at 1:1 ratio and incubated for 30 min at 37°C, followed by addition of anti-hapten IgG, either unhydrolyzed (Hy2.15) or endo-β-*N*-acetylglucosaminidase (EndoS)-hydrolyzed IgG (Hy2.15H) containing minor amounts of EndoS at the ratio 1:1:1. Twenty microliters of this mixture were loaded on to capillary tube in the Dynamic Light Scattering instrument. Relative sizes of ICs present in the solution are indicated in the X-axis and Y-axis denotes percentage of ICs present in the solution. Each sample was measured 5–7 times and the bars represent mean values from two experiments. Error bars indicate ± SEM. **(C)** Complement activation on CII bound anti-CII antibodies (M2139H) were monitored by measuring C3b deposition. Each bar represents mean values from three experiments ± SD. **(D)** Deposition of C3b on the cartilage of mice was used as a measure of IC deposition and complement activation after the injection of EndoS-hydrolyzed containing minor amounts of EndoS, unhydrolyzed or mixed anti-CII IgG. Two- to three-day-old mouse pups (3–4 mice/group) were injected with 1 mg each of unhydrolyzed IgG (M2139 + CIIC2 + UL1), EndoS-hydrolyzed IgG (M2139H + CIIC2H + UL1H) containing minor amounts of EndoS or a mixture of IgGs at 1:1 ratio. In each group, 26–44 joints were scored in total. $^{**}p < 0.01$; $^{***}p < 0.005$. Error bars indicate ± SEM. **(E)** Paw samples collected 24 h later were stained with biotinylated anti-kappa (left column) or goat anti-mouse anti-C3c antibodies (right column). Joint sections from PBS (first row), unhydrolyzed (second row), EndoS-hydrolyzed containing minor amounts of EndoS (third row), or a mixture (1:1) of IgG (fourth row) injected mice is shown. Magnification 20×. Arrows indicate C3b deposition within ICs formed on the joint cartilage surface. **(F)** Diagram illustrating possible binding mechanisms involved in the suppression of arthritis by EndoS-hydrolyzed antibodies containing minor amounts of EndoS.

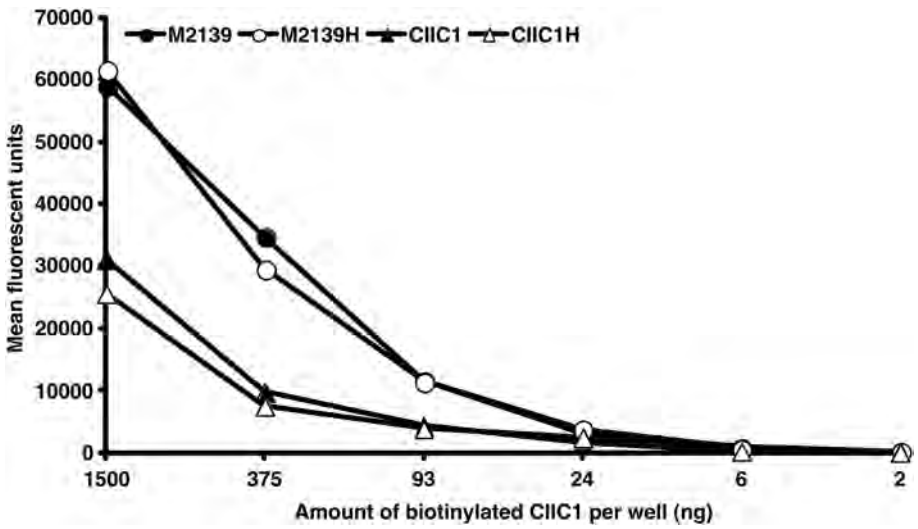

FIGURE 8 | Disturbance of IC formation by rheumatoid factor (RF)-like activity of CIIC1 mAb. Endo-β-*N*-acetylglucosaminidase (EndoS) hydrolyzed (M2139H, CIIC1H) or unhydrolyzed (M2139, CIIC1) antibody coated (10 μg/well) ELISA plates after blocking with BSA were incubated with different concentrations of biotinylated CIIC1 antibody. Europium-conjugated streptavidin and the dissociation-enhanced lanthanide fluoroimmunoassay system were used for detection of biotinylated antibody. There was no significant difference in biotinylated CIIC1 antibody binding to EndoS hydrolyzed or unhydrolyzed M2139 and CIIC1 mAbs demonstrating negligible contribution of RF like activity of CIIC1 mAb in disturbing IC formation.

Our present data clearly demonstrate that EndoS is the causal factor in preventing antibody-mediated inflammation. As shown in **Figure 5**, 0.1 μg of EndoS injected *in vivo* was capable of specifically cleaving most of the carbohydrates present on all the IgG subclasses, whereas EndoS at 1 μg concentration cleaved all the carbohydrates present in the Fc region of IgG. After intravenous injection, antibodies are present in the circulation for at least 14 days, and the binding of antibodies to the cartilage surface is a dynamic process; hence, it is plausible that the small amounts of EndoS is sufficient to deglycosylate at least part of the injected antibodies, which in turn through destabilization of all the Fc effector functions including Fc–Fc interactions between glycosylated and deglycosylated antibodies could lead to disruption of the formation of larger CII-specific antibody immune-complexes on the joints.

Streptococcus pyogenes secretes several enzymes and proteins that bind and modulate the functions of Igs as a part of its strategy for evading the immune system (62). Disruption of the development of larger IC lattices by EndoS and enzyme-cleaved IgG could very well be one such strategy. Conversely, antibodies as a constituent of ICs play an important role in promoting various inflammatory processes. Neutrophils play a vital part during this process, and sequential complement fixation generating C5a and direct engagement of Fcγ receptors are needed to initiate and sustain such neutrophil recruitment *in vivo* and subsequent inflammation (63). Bidirectional regulation of C5aR and FcγRs, which could significantly influence effector functions, was reported earlier (64). At the same time, IgG_1 containing ICs could also suppress C5a-dependent inflammatory response. This suppression is dependent on high galactosylation of IgG N-glycans, because it promotes the association between FcγRIIB and dectin-1 (65).

In conclusion, very small amounts of residual EndoS present along with the glycan hydrolyzed IgG, but not the IgG with truncated sugars *per se*, inhibits arthritis. It highlights the extreme potency of EndoS *in vivo* and that the potency of

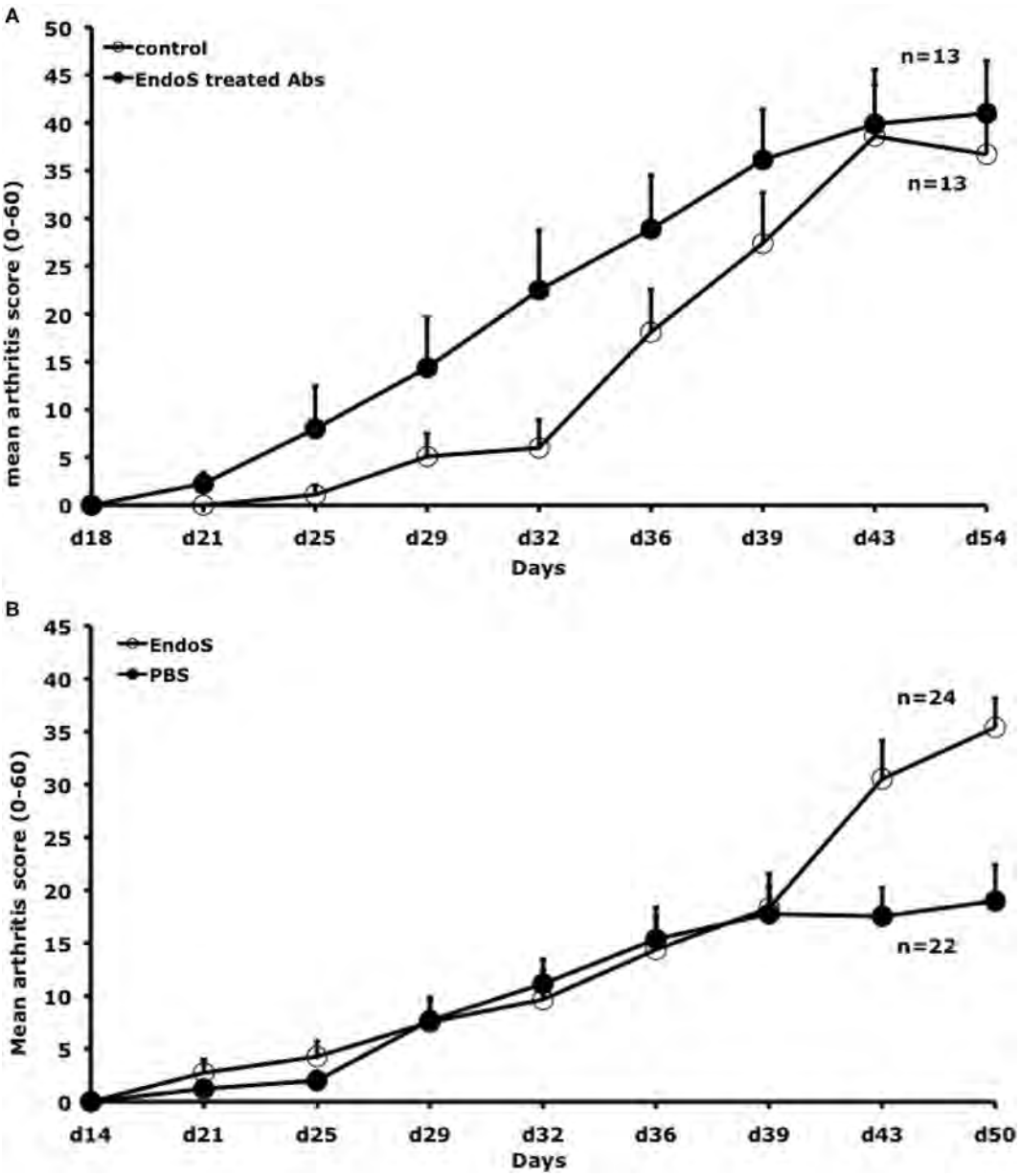

FIGURE 9 | Neither endo-β-*N*-acetylglucosaminidase (EndoS) treated IgG nor EndoS inhibits collagen-induced arthritis. **(A)** Mean arthritis score in male (BALB/c × B10.Q) F1 mice (n = 26, 13 mice/group) is shown. Arthritis was induced with rat CII/CFA immunization on day 0 and treated i.v. with 2 mg of EndoS-hydrolyzed antibodies (1 mg each of M2139 and CIIC1) or PBS on days 14, 21, 28, and 35. Error bars indicate ± SEM. **(B)** Mean arthritis score in male (BALB/c × B10.Q) F1 mice (n = 46, 22–24 mice/group) were shown. Arthritis was induced with rat CII/CFA immunization on day 0 and treated i.v. with 50 μg of EndoS or PBS on days 14, 21, 28, and 35. Error bars indicate ± SEM.

EndoS is confined to a local effect on the formation and functions of ICs.

ETHICS STATEMENT

This study was carried out in accordance with the recommendations of "Regional ethical committee, Malmö-Lund region" and Regional ethical committee Stockholm (North), Sweden. The protocol was approved by the "Regional ethical committee, Malmö-Lund region" and Regional ethical committee Stockholm (North), Sweden.

AUTHOR CONTRIBUTIONS

KSN participated in the conception and design of the study, acquisition, analysis, and interpretation of the data, and wrote the manuscript. MC, KH, SL, AC, and BX participated in the acquisition, analysis, and interpretation of the data, manuscript

preparation, and final approval. RZ participated in the design of the study, manuscript preparation, and final approval. MR, AB, and CK participated in the design of the study, interpretation of the data, manuscript preparation, and final approval. RH participated in the conception and design of the study, interpretation of the data, manuscript preparation, and final approval.

ACKNOWLEDGMENTS

We thank Dr. Rajesh Ponnusamy for his help in measuring the sizes of ICs by DLS. We also would like to thank Emma Mondoc for performing histology and Carlos Palestro for taking care of animals. This study was supported by grants from King Gustaf V:s 80 years foundation, Swedish Rheumatism Association, Åke Wiberg, Alfred Österlund, Petrus and Augusta Hedlund, Clas Groschinsky, Torsten och Ragnar Söderberg, the Swedish Society for Medicine, the Royal Physiografic Society in Lund, the KA Wallenberg foundation, The Swedish Strategic Science Foundation (SSF), the Swedish governmental funding for clinical research (ALF), Hansa Medical AB, Swedish Research Council (2009-2338; 2010-57X-20240; K2012-66X-14928-09-5), EU MasterSwitch project (grant number: HEALTH-F2-2008-223404), Guangdong province (201001Y04675344), matching grant from Dongguan city, Southern Medical University, Guangzhou, start up grant (No: C1034211), and the National Health and Medical Research Council of Australia, an Arthritis Australia Project Grant. The funders had no role in preparation of the manuscript or decision to publish.

REFERENCES

1. Collin M, Olsén A. EndoS, a novel secreted protein from *Streptococcus pyogenes* with endoglycosidase activity on human IgG. *EMBO J* (2001) 20:3046–55. doi:10.1093/emboj/20.12.3046
2. Trastoy B, Lomino JV, Pierce BG, Carter LG, Gunther S, Giddens JP, et al. Crystal structure of *Streptococcus pyogenes* EndoS, an immunomodulatory endoglycosidase specific for human IgG antibodies. *Proc Natl Acad Sci U S A* (2014) 111:6714–9. doi:10.1073/pnas.1322908111
3. Dixon EV, Claridge JK, Harvey DJ, Baruah K, Yu X, Vesiljevic S, et al. Fragments of bacterial endoglycosidase s and immunoglobulin g reveal subdomains of each that contribute to deglycosylation. *J Biol Chem* (2014) 289:13876–89. doi:10.1074/jbc.M113.532812
4. Sjögren J, Cosgrave EF, Allhorn M, Nordgren M, Bjork S, Olsson F, et al. EndoS and EndoS2 hydrolyze Fc-glycans on therapeutic antibodies with different glycoform selectivity and can be used for rapid quantification of high-mannose glycans. *Glycobiology* (2015) 25:1053–63. doi:10.1093/glycob/cwv047
5. Shadnezhad A, Naegeli A, Collin M. CP40 from *Corynebacterium pseudotuberculosis* is an endo-beta-N-acetylglucosaminidase. *BMC Microbiol* (2016) 16:261. doi:10.1186/s12866-016-0884-3
6. Shadnezhad A, Naegeli A, Sjögren J, Adamczyk B, Leo F, Allhorn M, et al. EndoSd: an IgG glycan hydrolyzing enzyme in *Streptococcus dysgalactiae* subspecies dysgalactiae. *Future Microbiol* (2016) 11:721–36. doi:10.2217/fmb.16.14
7. Ferrara C, Grau S, Jager C, Sondermann P, Brunker P, Waldhauer I, et al. Unique carbohydrate-carbohydrate interactions are required for high affinity binding between FcgammaRIII and antibodies lacking core fucose. *Proc Natl Acad Sci U S A* (2011) 108:12669–74. doi:10.1073/pnas.1108455108
8. Deisenhofer J. Crystallographic refinement and atomic models of a human Fc fragment and its complex with fragment B of protein A from *Staphylococcus aureus* at 2.9- and 2.8-A resolution. *Biochemistry* (1981) 20:2361–70. doi:10.1021/bi00512a001
9. Barb AW, Prestegard JH. NMR analysis demonstrates immunoglobulin G N-glycans are accessible and dynamic. *Nat Chem Biol* (2011) 7:147–53. doi:10.1038/nchembio.511
10. Parekh RB, Dwek RA, Sutton BJ, Fernandes DL, Leung A, Stanworth D, et al. Association of rheumatoid arthritis and primary osteoarthritis with changes in the glycosylation pattern of total serum IgG. *Nature* (1985) 316:452–7. doi:10.1038/316452a0
11. Kaneko Y, Nimmerjahn F, Ravetch JV. Anti-inflammatory activity of immunoglobulin G resulting from Fc sialylation. *Science* (2006) 313:670–3. doi:10.1126/science.1129594
12. Piraino MS, Kelliher MT, Aburas J, Southern CA. Single molecule Forster resonance energy transfer studies of the effect of EndoS deglycosylation on the structure of IgG. *Immunol Lett* (2015) 167:29–33. doi:10.1016/j.imlet.2015.06.011
13. Rantapaa-Dahlqvist S, De Jong BA, Berglin E, Hallmans G, Wadell G, Stenlund H, et al. Antibodies against cyclic citrullinated peptide and IgA rheumatoid factor predict the development of rheumatoid arthritis. *Arthritis Rheum* (2003) 48:2741–9. doi:10.1002/art.11223
14. Nielen MM, Van Schaardenburg D, Reesink HW, Van De Stadt RJ, Van Der Horst-Bruinsma IE, De Koning MH, et al. Specific autoantibodies precede the symptoms of rheumatoid arthritis: a study of serial measurements in blood donors. *Arthritis Rheum* (2004) 50:380–6. doi:10.1002/art.20018
15. Cochrane CG, Hawkins D. Studies on circulating immune complexes. 3. Factors governing the ability of circulating complexes to localize in blood vessels. *J Exp Med* (1968) 127:137–54. doi:10.1084/jem.127.1.137
16. Mageed RA, Kirwan JR, Thompson PW, Mccarthy DA, Holborow EJ. Characterisation of the size and composition of circulating immune complexes in patients with rheumatoid arthritis. *Ann Rheum Dis* (1991) 50:231–6. doi:10.1136/ard.50.4.231
17. Mullazehi M, Mathsson L, Lampa J, Ronnelid J. Surface-bound anti-type II collagen-containing immune complexes induce production of tumor necrosis factor alpha, interleukin-1beta, and interleukin-8 from peripheral blood monocytes via Fc gamma receptor IIA: a potential pathophysiologic mechanism for humoral anti-type II collagen immunity in arthritis. *Arthritis Rheum* (2006) 54:1759–71. doi:10.1002/art.21892
18. Wooley PH, Luthra HS, Singh SK, Huse AR, Stuart JM, David CS. Passive transfer of arthritis to mice by injection of human anti-type II collagen antibody. *Mayo Clin Proc* (1984) 59:737–43. doi:10.1016/S0025-6196(12)65583-9
19. Petkova SB, Konstantinov KN, Sproule TJ, Lyons BL, Awwami MA, Roopenian DC. Human antibodies induce arthritis in mice deficient in the low-affinity inhibitory IgG receptor Fc gamma RIIB. *J Exp Med* (2006) 203:275–80. doi:10.1084/jem.20051951
20. Nandakumar KS, Svensson L, Holmdahl R. Collagen type II-specific monoclonal antibody-induced arthritis in mice: description of the disease and the influence of age, sex, and genes. *Am J Pathol* (2003) 163:1827–37. doi:10.1016/S0002-9440(10)63542-0
21. Nandakumar KS, Collin M, Olsén A, Nimmerjahn F, Blom AM, Ravetch JV, et al. Endoglycosidase treatment abrogates IgG arthritogenicity: importance of IgG glycosylation in arthritis. *Eur J Immunol* (2007) 37:2973–82. doi:10.1002/eji.200737581
22. Albert H, Collin M, Dudziak D, Ravetch JV, Nimmerjahn F. In vivo enzymatic modulation of IgG glycosylation inhibits autoimmune disease in an IgG subclass-dependent manner. *Proc Natl Acad Sci U S A* (2008) 105:15005–9. doi:10.1073/pnas.0808248105
23. Collin M, Shannon O, Björck L. IgG glycan hydrolysis by a bacterial enzyme as a therapy against autoimmune conditions. *Proc Natl Acad Sci U S A* (2008) 105:4265–70. doi:10.1073/pnas.0711271105
24. Lood C, Allhorn M, Lood R, Gullstrand B, Olin AI, Rönnblom L, et al. IgG glycan hydrolysis by endoglycosidase S diminishes the proinflammatory properties of immune complexes from patients with systemic lupus erythematosus: a possible new treatment? *Arthritis Rheum* (2012) 64:2698–706. doi:10.1002/art.34454
25. Holmdahl RCS, Mikulowska A, Vestberg M, Brunsberg U, Hansson a-S, Sundvall M, et al. Genetic analysis of murine models for rheumatoid arthritis.

In: Adolpho K, editor. *Human Genome Methods*. New York: CRC Press (1998). p. 215–38.
26. Holmdahl R, Rubin K, Klareskog L, Larsson E, Wigzell H. Characterization of the antibody response in mice with type II collagen-induced arthritis, using monoclonal anti-type II collagen antibodies. *Arthritis Rheum* (1986) 29:400–10. doi:10.1002/art.1780290314
27. Schulte S, Unger C, Mo JA, Wendler O, Bauer E, Frischholz S, et al. Arthritis-related B cell epitopes in collagen II are conformation-dependent and sterically privileged in accessible sites of cartilage collagen fibrils. *J Biol Chem* (1998) 273:1551–61. doi:10.1074/jbc.273.3.1551
28. Bajtner E, Nandakumar KS, Engstrom A, Holmdahl R. Chronic development of collagen-induced arthritis is associated with arthritogenic antibodies against specific epitopes on type II collagen. *Arthritis Res Ther* (2005) 7:R1148–57. doi:10.1186/ar1800
29. Uysal H, Bockermann R, Nandakumar KS, Sehnert B, Bajtner E, Engstrom A, et al. Structure and pathogenicity of antibodies specific for citrullinated collagen type II in experimental arthritis. *J Exp Med* (2009) 206:449–62. doi:10.1084/jem.20081862
30. Shulman M, Wilde CD, Kohler G. A better cell line for making hybridomas secreting specific antibodies. *Nature* (1978) 276:269–70. doi:10.1038/276269a0
31. Mo JA, Bona CA, Holmdahl R. Variable region gene selection of immunoglobulin G-expressing B cells with specificity for a defined epitope on type II collagen. *Eur J Immunol* (1993) 23:2503–10. doi:10.1002/eji.1830231019
32. Lundstrom SL, Fernandes-Cerqueira C, Ytterberg AJ, Ossipova E, Hensvold AH, Jakobsson PJ, et al. IgG antibodies to cyclic citrullinated peptides exhibit profiles specific in terms of IgG subclasses, Fc-glycans and a fab-peptide sequence. *PLoS One* (2014) 9:e113924. doi:10.1371/journal.pone.0113924
33. Von Pawel-Rammingen U, Johansson BP, Bjorck L. IdeS, a novel streptococcal cysteine proteinase with unique specificity for immunoglobulin G. *EMBO J* (2002) 21:1607–15. doi:10.1093/emboj/21.7.1607
34. Johansson BP, Shannon O, Björck L. IdeS: a bacterial proteolytic enzyme with therapeutic potential. *PLoS One* (2008) 3:e1692. doi:10.1371/journal.pone.0001692
35. Nandakumar KS, Johansson BP, Björck L, Holmdahl R. Blocking of experimental arthritis by cleavage of IgG antibodies in vivo. *Arthritis Rheum* (2007) 56:3253–60. doi:10.1002/art.22930
36. Long Y, Philip JY, Schillen K, Liu F, Ye L. Insight into molecular imprinting in precipitation polymerization systems using solution NMR and dynamic light scattering. *J Mol Recognit* (2011) 24:619–30. doi:10.1002/jmr.1097
37. Sjöberg AP, Trouw LA, Clark SJ, Sjölander J, Heinegard D, Sim RB, et al. The factor H variant associated with age-related macular degeneration (His-384) and the non-disease-associated form bind differentially to C-reactive protein, fibromodulin, DNA, and necrotic cells. *J Biol Chem* (2007) 282:10894–900. doi:10.1074/jbc.M610256200
38. Dobritzsch D, Lindh I, Uysal H, Nandakumar KS, Burkhardt H, Schneider G, et al. Crystal structure of an arthritogenic anticollagen immune complex. *Arthritis Rheum* (2011) 63:3740–8. doi:10.1002/art.30611
39. Nandakumar KS, Holmdahl R. Efficient promotion of collagen antibody induced arthritis (CAIA) using four monoclonal antibodies specific for the major epitopes recognized in both collagen induced arthritis and rheumatoid arthritis. *J Immunol Methods* (2005) 304:126–36. doi:10.1016/j.jim.2005.06.017
40. Uysal H, Sehnert B, Nandakumar KS, Boiers U, Burkhardt H, Holmdahl R, et al. The crystal structure of the pathogenic collagen type II-specific mouse monoclonal antibody CIIC1 Fab: structure to function analysis. *Mol Immunol* (2008) 45:2196–204. doi:10.1016/j.molimm.2007.12.005
41. Croxford AM, Nandakumar KS, Holmdahl R, Tobin MJ, Mcnaughton D, Rowley MJ. Chemical changes demonstrated in cartilage by synchrotron infrared microspectroscopy in an antibody-induced murine model of rheumatoid arthritis. *J Biomed Opt* (2011) 16:066004. doi:10.1117/1.3585680
42. Nandakumar KS, Collin M, Happonen KE, Croxford AM, Lundström SL, Zubarev RA, et al. Dominant suppression of inflammation by glycan-hydrolyzed IgG. *Proc Natl Acad Sci U S A* (2013) 110:10252–7. doi:10.1073/pnas.1301480110
43. Holmdahl R, Mo JA, Jonsson R, Karlstrom K, Scheynius A. Multiple epitopes on cartilage type II collagen are accessible for antibody binding in vivo. *Autoimmunity* (1991) 10:27–34. doi:10.3109/08916939108997144
44. Amirahmadi SF, Pho MH, Gray RE, Crombie DE, Whittingham SF, Zuasti BB, et al. An arthritogenic monoclonal antibody to type II collagen, CII-C1, impairs cartilage formation by cultured chondrocytes. *Immunol Cell Biol* (2004) 82:427–34. doi:10.1111/j.0818-9641.2004.01267.x
45. Van Timmeren MM, Van Der Veen BS, Stegeman CA, Petersen AH, Hellmark T, Collin M, et al. IgG glycan hydrolysis attenuates ANCA-mediated glomerulonephritis. *J Am Soc Nephrol* (2010) 21:1103–14. doi:10.1681/ASN.2009090984
46. Yang R, Otten MA, Hellmark T, Collin M, Bjorck L, Zhao MH, et al. Successful treatment of experimental glomerulonephritis with IdeS and EndoS, IgG-degrading streptococcal enzymes. *Nephrol Dial Transplant* (2010) 25:2479–86. doi:10.1093/ndt/gfq115
47. Benkhoucha M, Molnarfi N, Santiago-Raber ML, Weber MS, Merkler D, Collin M, et al. IgG glycan hydrolysis by EndoS inhibits experimental autoimmune encephalomyelitis. *J Neuroinflammation* (2012) 9:209. doi:10.1186/1742-2094-9-209
48. Allhorn M, Briceno JG, Baudino L, Lood C, Olsson ML, Izui S, et al. The IgG-specific endoglycosidase EndoS inhibits both cellular and complement-mediated autoimmune hemolysis. *Blood* (2010) 115:5080–8. doi:10.1182/blood-2009-08-239020
49. Hirose M, Vafia K, Kalies K, Groth S, Westermann J, Zillikens D, et al. Enzymatic autoantibody glycan hydrolysis alleviates autoimmunity against type VII collagen. *J Autoimmun* (2012) 39:304–14. doi:10.1016/j.jaut.2012.04.002
50. Wipke BT, Wang Z, Kim J, McCarthy TJ, Allen PM. Dynamic visualization of a joint-specific autoimmune response through positron emission tomography. *Nat Immunol* (2002) 3:366–72. doi:10.1038/ni775
51. Easterbrook-Smith SB, Vandenberg RJ, Alden JR. The role of Fc:Fc interactions in insoluble immune complex formation and complement activation. *Mol Immunol* (1988) 25:1331–7. doi:10.1016/0161-5890(88)90048-X
52. Mimura Y, Church S, Ghirlando R, Ashton PR, Dong S, Goodall M, et al. The influence of glycosylation on the thermal stability and effector function expression of human IgG1-Fc: properties of a series of truncated glycoforms. *Mol Immunol* (2000) 37:697–706. doi:10.1016/S0161-5890(00)00105-X
53. Kao D, Danzer H, Collin M, Groß A, Eichler J, Stambuk J, et al. A monosaccharide residue is sufficient to maintain mouse and human IgG subclass activity and directs IgG effector functions to cellular Fc receptors. *Cell Rep* (2015) 13:2376–85. doi:10.1016/j.celrep.2015.11.027
54. Anthony RM, Wermeling F, Karlsson MC, Ravetch JV. Identification of a receptor required for the anti-inflammatory activity of IVIG. *Proc Natl Acad Sci U S A* (2008) 105:19571–8. doi:10.1073/pnas.0810163105
55. Anthony RM, Kobayashi T, Wermeling F, Ravetch JV. Intravenous gammaglobulin suppresses inflammation through a novel T(H)2 pathway. *Nature* (2011) 475:110–3. doi:10.1038/nature10134
56. Moller NP. Fc-mediated immune precipitation. I. A new role of the Fc-portion of IgG. *Immunology* (1979) 38:631–40.
57. Cosio FG, Birmingham DJ, Sexton DJ, Hebert LA. Interactions between precipitating and nonprecipitating antibodies in the formation of immune complexes. *J Immunol* (1987) 138:2587–92.
58. Kolenko P, Dohnalek J, Duskova J, Skalova T, Collard R, Hasek J. New insights into intra- and intermolecular interactions of immunoglobulins: crystal structure of mouse IgG2b-Fc at 2.1-A resolution. *Immunology* (2009) 126:378–85. doi:10.1111/j.1365-2567.2008.02904.x
59. Gao P, Pinkston KL, Wilganowski N, Robinson H, Azhdarinia A, Zhu B, et al. Deglycosylation of mAb by EndoS for improved molecular imaging. *Mol Imaging Biol* (2015) 17:195–203. doi:10.1007/s11307-014-0781-9
60. Yu X, Zheng J, Collin M, Schmidt E, Zillikens D, Petersen F. EndoS reduces the pathogenicity of anti-mCOL7 IgG through reduced binding of immune complexes to neutrophils. *PLoS One* (2014) 9:e85317. doi:10.1371/journal.pone.0085317
61. Lux A, Yu X, Scanlan CN, Nimmerjahn F. Impact of immune complex size and glycosylation on IgG binding to human FcgammaRs. *J Immunol* (2013) 190:4315–23. doi:10.4049/jimmunol.1200501
62. Collin M, Björck L. Toward clinical use of the IgG specific enzymes IdeS and EndoS against antibody-mediated diseases. *Methods Mol Biol* (2017) 1535:339–51. doi:10.1007/978-1-4939-6673-8_23
63. Sadik CD, Kim ND, Iwakura Y, Luster AD. Neutrophils orchestrate their own recruitment in murine arthritis through C5aR and FcgammaR signaling. *Proc Natl Acad Sci U S A* (2012) 109:E3177–85. doi:10.1073/pnas.1213797109

64. Karsten CM, Kohl J. The immunoglobulin, IgG Fc receptor and complement triangle in autoimmune diseases. *Immunobiology* (2012) 217:1067–79. doi:10.1016/j.imbio.2012.07.015
65. Karsten CM, Pandey MK, Figge J, Kilchenstein R, Taylor PR, Rosas M, et al. Anti-inflammatory activity of IgG1 mediated by Fc galactosylation and association of FcgammaRIIB and dectin-1. *Nat Med* (2012) 18:1401–6. doi:10.1038/nm.2862

Conflict of Interest Statement: Hansa Medical AB (HMAB) holds patents for using EndoS as a treatment for antibody-mediated diseases. MC is listed as one of the inventors on these applications and has a royalty and consultancy agreement with HMAB. Genovis AB holds patents for the biotechnological use of EndoS on which MC is listed as an inventor.

frontiers in Immunology

ORIGINAL RESEARCH
published: 12 July 2018
doi: 10.3389/fimmu.2018.01558

Therapeutic Effect of a Novel Phosphatidylinositol-3-Kinase δ Inhibitor in Experimental Epidermolysis Bullosa Acquisita

Hiroshi Koga[1†], Anika Kasprick[1‡], Rosa López[2], Mariona Aulí[3], Mercè Pont[2], Núria Godessart[2], Detlef Zillikens[4], Katja Bieber[1], Ralf J. Ludwig[1,4‡] and Cristina Balagué[2*‡]*

[1] Lübeck Institute of Experimental Dermatology, University of Lübeck, Lübeck, Germany, [2] Skin Biology and Pharmacology, Almirall R&D, Barcelona, Spain, [3] Preclinical Safety and Toxicology, Almirall R&D, Barcelona, Spain, [4] Department of Dermatology University of Lübeck, Lübeck, Germany

OPEN ACCESS

Edited by:
Massimo Gadina,
National Institute of Arthritis and Musculoskeletal and Skin Diseases (NIAMS), United States

Reviewed by:
Attila Mocsai,
Semmelweis University, Hungary
Zhi Liu,
University of North Carolina at Chapel Hill, United States

***Correspondence:**
Ralf J. Ludwig
ralf.ludwig@uksh.de;
Cristina Balagué
cristina.balague@almirall.com

†Present address:
Hiroshi Koga,
Department of Dermatology, Kurume University School of Medicine, Kurume, Japan

‡These authors have contributed equally to this work.

Specialty section:
This article was submitted to Inflammation, a section of the journal Frontiers in Immunology

Received: 29 November 2017
Accepted: 25 June 2018
Published: 12 July 2018

Citation:
Koga H, Kasprick A, López R, Aulí M, Pont M, Godessart N, Zillikens D, Bieber K, Ludwig RJ and Balagué C (2018) Therapeutic Effect of a Novel Phosphatidylinositol-3-Kinase δ Inhibitor in Experimental Epidermolysis Bullosa Acquisita. Front. Immunol. 9:1558. doi: 10.3389/fimmu.2018.01558

Epidermolysis bullosa acquisita (EBA) is a rare, but prototypical, organ-specific autoimmune disease, characterized and caused by autoantibodies against type VII collagen (COL7). Mucocutaneous inflammation, blistering, and scarring are the clinical hallmarks of the disease. Treatment of EBA is difficult and mainly relies on general immunosuppression. Hence, novel treatment options are urgently needed. The phosphatidylinositol-3-kinase (PI3K) pathway is a putative target for the treatment of inflammatory diseases, including EBA. We recently discovered LAS191954, an orally available, selective PI3Kδ inhibitor. PI3Kδ has been shown to be involved in B cell and neutrophil cellular functions. Both cell types critically contribute to EBA pathogenesis, rendering LAS191954 a potential drug candidate for EBA treatment. We, here, demonstrate that LAS191954, when administered chronically, dose-dependently improved the clinical phenotype of mice harboring widespread skin lesions secondary to immunization-induced EBA. Direct comparison with high-dose corticosteroid treatment indicated superiority of LAS191954. Interestingly, levels of circulating autoantibodies were unaltered in all groups, indicating a mode of action independent of the inhibition of B cell function. In line with this, LAS191954 also hindered disease progression in antibody transfer-induced EBA, where disease develops dependent on myeloid, but independent of B cells. We further show that, *in vitro*, LAS191954 dose-dependently impaired activation of human myeloid cells by relevant disease stimuli. Specifically, immune complex-mediated and C5a-mediated ROS release were inhibited in a PI3Kδ-dependent manner. Accordingly, LAS191954 also modulated the dermal–epidermal separation induced *in vitro* by co-incubation of immune complexes with polymorph nuclear cells, thus pointing to an important role of PI3Kδ in EBA effector functions. Altogether, these results suggest a new potential mechanism for the treatment of EBA and potentially also other autoimmune bullous diseases.

Keywords: phosphatidylinositol-3-kinase, skin, autoimmunity, animal models, treatment, preclinical testing, pemphigoid, epidermolysis bullosa acquisita

INTRODUCTION

Pemphigoid diseases comprise a group of autoimmune disorders with a high, and so far, unmet medical need. They are clinically characterized by chronic (muco)-cutaneous inflammation and subepidermal blistering, and are caused by autoantibodies targeting structural proteins of the dermal–epidermal junction (1–4). Pemphigoid diseases pose an immense burden on the affected patients, including an increased mortality (5), and are difficult to treat. For example, bullous pemphigoid, characterized

by autoantibodies targeting type XVII collagen (COL17) respond well to corticosteroid treatment, but after stopping treatment, the disease frequently relapses (6). This requires prolonged, and often systemic, corticosteroid treatment. In contrast, the pemphigoid disease epidermolysis bullosa acquisita (EBA), characterized by autoantibodies against type VII collagen (COL7), is notoriously refractory to many treatments. Even after prolonged immunosuppressive treatment, many patients fail to reach a clinical remission (7, 8). Hence, there is a yet high unmet medical need for the development of novel treatments for pemphigoid diseases, especially EBA (3).

Animal models of EBA have provided detailed insights into the disease pathogenesis (9, 10). During the induction phase of the disease, COL7-autoreactive plasma cells are generated in a CD4-dependent fashion (11), which lead to the production of antibodies to COL7. In the effector phase, these autoantibodies bind to their cognate target antigen at the dermal–epidermal junction and trigger a cascade of events that include the activation of the complement network, recruitment of myeloid cells (12, 13), and engagement of Fcγ receptors (14). This in turn leads to the activation of signal transduction pathways downstream of Syk (15) and Src kinases (16), which also include PI3Kβ (17, 18), resulting in the release of potent inflammatory mediators, such as cytokines, reactive oxygen species, and proteases, which combined are instrumental for lesion formation.

The PI3Kδ-dependent pathways are activated in various inflammatory and cancerous conditions, and pharmacological inhibition or genetic inactivation of this pathway has demonstrated efficacy in several preclinical models of inflammation as well as in lymphoma patients (19). We hypothesized that the role of PI3Kδ could be critical in the context of the postulated EBA pathogenesis by directly impacting in the function of critical cellular players. On the one hand, genetic and pharmacological studies with specific PI3Kδ inhibitors have shown that antibody responses to T cell-dependent antigens as well as the production of autoantibodies in some models are PI3Kδ dependent (20–22). In addition, PI3Kδ is required for distinct neutrophil functions *in vitro* and *in vivo* such as neutrophil directional migration and degranulation in response to distinct receptor activations (23–25). Hence, pharmacological targeting of the PI3Kδ pathway could block two crucial pathways in EBA pathogenesis, namely autoantibody formation and production, and FcγR-mediated myeloid cell activation.

Based on the above considerations, we here evaluated the effect of LAS191954, a recently described novel selective PI3Kδ inhibitor (26), on clinical aspects of distinct experimental EBA mouse models. Our results indicate that the compound can reverse established immunization-induced disease and prevent disease induced by anti-COL7 antibody transfer. Further assessment of the mechanism of action suggests that these effects are greatly contributed by the inhibition of myeloid cell function in a predominantly PI3Kδ-dependent manner.

MATERIALS AND METHODS

Experiments With Human Biomaterials

Foreskin and blood collections from healthy volunteers were performed after written informed consent was obtained. All experiments with human samples were approved by the ethical committee of the Medical Faculty of the University of Lübeck and were performed in accordance with the Declaration of Helsinki.

Laboratory Animals

C57Bl/6 (B6) and B6.SJL-H2s (B6.s) mice were obtained from colonies held at the animal facility at the University of Lübeck. Mice were housed under specific pathogen-free conditions and provided standard mouse chow and acidified drinking water *ad libitum*. Mice aged 6–10 weeks were used for the experiments. All clinical examinations, biopsies, and bleedings were performed under anesthesia with i.p. administration of a mixture of ketamine (100 μg/g) and xylazine (15 μg/g). Evaluation of skin lesions was performed as described (10). Animal experiments were approved by local authorities of the Animal Care and Use Committee (Kiel, Germany) and performed by certified personnel. For KLH immunization studies, male Crl:CD1 (ICR) mice were purchased from Charles River. Female MRL/MpJ-Faslpr/J mice were purchased from The Jackson Laboratory (Bar Harbor, ME, USA). Animals were housed in polycarbonate cages, with free access to water and non-purified stock diet and allowed to condition for 2 weeks in their new environment at 22 ± 2°C, 40–70% relative humidity, and 12 h:12 h light:dark cycles. All animal care and experimental procedures followed the European Community Directive 86/609/CEE and the Autonomous Catalan law (Decret 214/1997) for the use of laboratory animals and were approved by the Almirall Animal Experimentation Ethical Committee.

Chemicals

LAS191954 was synthesized as previously described (26). For *in vivo per os* administration, LAS191954 was suspended in 0.5% methylcellulose, 0.1% Tween80. This mixture was stable for at least a week at 4°C. For chronic studies, compound was prepared once a week and kept at 4°C in the dark. Methylprednisolone (MP) (Urbason®) used in the EBA experiments was purchased from Sanofi-Aventis (Frankfurt, Germany). For KLH immunization and MRL/lpr studies, MP succinate and prednisolone was purchased from Sigma. All corticoids were dissolved in the vehicle described above for each model. Phorbol 12-myristate 13-acetate (PMA; Sigma-Aldrich, Munich, Germany) and *N*-formyl-L-methionyl-L-leucyl-L-phenylalanine (fMLP; Sigma-Aldrich, Munich, Germany) were dissolved in Aqua ad injectable and PBS/2% ethanol, respectively.

Generation of the vWFA2 Recombinant Protein and Anti-Murine vWFA2 IgG

Recombinant murine von Willebrand factor A-like domain 2 (vWFA2) of the NC1 of COL7 [aa 1048–1238 with five additional amino acids (GRAMG) at the N-terminus] were produced as previously described using prokaryotic expression (27). Rabbit anti-murine vWFA2 IgG was generated as previously described (28). IgG from rabbit serum was isolated using Protein G Sepharose Fast Flow affinity column chromatography (Amersham Biosciences, Freiburg, Germany) as described (28). Reactivity of IgG fractions was analyzed by IF microscopy on murine skin. Concentrations of the purified rabbit IgG were measured at 280 nm by spectrophotometer.

Animal Models of EBA

For induction of experimental EBA by immunization in B6.s mice, we followed previously published protocols (11). Mice were monitored weekly for presence of skin lesions. If in an individual mouse, skin lesions affected 2% or more of the body surface area, it was randomized to one of the four treatment groups: (i) vehicle (0.5% methylcellulose, 0.1% Tween80 once daily by oral gavage), (ii) MP (20 mg/kg once daily by oral gavage), (iii/iv) LAS191954 at 1 or 3 mg/kg (once daily by oral gavage). Mice that did not reach this inclusion criterion 8 weeks after immunization were not considered further. Treatments were carried out for a total period of 6 weeks. Each week mice were clinically evaluated and the percentage of the affected body surface area determined by an investigator unaware of the treatment. At randomization and at the end of the treatment period, serum was obtained for determination of circulating antigen-specific IgG, which was performed as described (11). Compound plasma levels were determined by spectrometry as described (26) on samples obtained 1 h after the last compound administration. This time point corresponds approximately to the Cmax of the compound in plasma as determined in healthy mouse PK studies (data not shown). At the same time, ears of the mice were fixed in paraformaldehyde for later H&E staining for semiquantitative evaluation of the dermal leukocyte infiltration.

Induction of experimental EBA by antibody transfer in B6 mice was performed as described earlier (28). Same treatments as above were started one day before the first IgG injection and maintained throughout the 12-day experiment. Mice were clinically evaluated every fourth day, and the percentage of affected body surface area was noted.

Assessment of T-Cell-Dependent Antibody Responses (TDAR) in Mice

Immunizations with KLH were performed as described (29) and the effect of compounds on the primary specific IgG subsequently assessed on day 15. Groups of six animals received LAS191954 (0.1, 0.3, 1, and 3 mg/kg) or MP (1, 3, and 10 mg/kg) or vehicle daily by oral gavage starting on the day of sensitization (day 1) until day 14. Terminal blood samples were collected 24 h after the last treatment administration (day 15) into EDTA tubes for anti-KLH antibody testing as described (29).

MRL/lpr Studies

Baseline antibody measurements were determined at weeks 9–10 of age and used to randomize animals to experimental groups using QuickCalcs tool from GraphPad (http://www.graphpad.com/quickcalcs/randomize2/). Each group consisted of a minimum of eight animals. Animals were orally administered vehicle, LAS191954 or prednisolone. All test solutions were analyzed after each period of administration to recheck stability and compound concentration. On weeks 2 and 4, blood was sampled by submandibular bleeding for antibody level determination. Samples from all time points were analyzed for anti-dsDNA levels and anti-desmoglein 3 antibody levels. Antibodies to dsDNA and Dsg3 were determined using the Mouse anti-dsDNA total Ig ELISA Kit (Alpha Diagnostic Cat#5110) and the Mouse Desmoglein 3 Antibody ELISA kit (MBL International Cat#7597), respectively.

ROS Release by Polymorph Nuclear Cells (PMN) and Monocytes

Polymorph nuclear cells are isolated from freshly drawn, heparin-anticoagulated blood from healthy volunteers by using PolymorphPrep™ (Axis-Shield GmbH, Heidelberg, Germany) according to the manufacturer's protocol. Stock solutions of LAS191954 were prepared in DMSO at different concentrations starting at 3×10^{-3} M and following a fourfold bank dilution and stored at −80°C. For every experiment, LAS191954 was further diluted 1:250 in modified dye-free RPMI 1640 medium (Genaxxon, Ulm, Germany) containing 1% fetal calf serum and 25 mM HEPES to a fourfold assay concentration. MP was dissolved in modified dye-free RPMI 1640 medium containing 1% fetal calf serum and 25 mM HEPES to a fourfold assay concentration (2.0×10^{-3}, 4.0×10^{-4}, and 2.0×10^{-4} M). For release of ROS, PMA (10 ng/mL), fMLP (1 μM), and human recombinant C5a (100 nM; Hycultec, Beutelsbach, Germany) were prepared at a twofold assay concentration on white microwell plates (Greiner BioOne, Frickenhausen, Germany). For immune complex-induced activation, white microwell plates were coated with recombinant human COL7 (10 μg/mL), and after blocking with 1% bovine serum albumin (BSA), monoclonal anti-human COL7 IgG1 was added (2 μg/mL). Isolated PMN (4×10^6 cells/mL) were diluted 1:2 with different concentrations (fourfold) of LAS191954 or (fourfold) of MP, and preincubated for 15 min at room temperature before added to the different stimuli on the assay plate. Untreated and DMSO-treated cells served as controls. By using the luminol (5-amino-2,3-dihydro-1,4-phthalazindione)-amplified chemiluminescence assay, released ROS was measured at a VICTOR™ 3 reader (PerkinElmer Inc., Waltham, MA, USA) over a period ranging from 60 to 180 min as described in detail elsewhere (30). For monocyte isolation, human peripheral blood mononuclear cells (PBMCs) were isolated from heparin-anticoagulated blood samples using the Ficoll density gradient (GE Healthcare, Freiburg, Germany) according to the manufacturer's instructions. In a next step, human monocytes were purified from the isolated PBMCs with the magnetic cell separation (MACS) method using the monocyte isolation kit II human (Miltenyi, Bergisch- Gladbach, Germany) according to the manufacturer's instructions. The purity of monocytes and neutrophils was evaluated by fluorescent staining with PE/Cy7 anti- human CD14 antibody (clone HCD14, Biolegend, Kobenz, Germany) and FITC anti-human CD16 antibody (BD Biosciences, Heidelberg, Germany) in a flow cytometer measurement (MACSQuant® Analyzer 10, Miltenyi). ROS release assay using monocytes was performed as described above.

Ex Vivo Dermal–Epidermal Separation (DES) Assay

Cryosections of human skin were incubated with rabbit anti-human $COL7^{FNIII8\text{-}FNIII9}$, followed by the addition of human PMN as described (31). To evaluate the potential effect of LAS191954, the compound or vehicle (0.1% DMSO) was added at varying concentrations along with the PMN onto the skin sections. Separation of the dermal–epidermal junction was calculated as length of separation divided by total length of the dermal–epidermal junction

on skin section measured with BZ-9000 fluorescence microscope (Keyence, Frankfurt, Germany). Evaluation was conducted by an investigator unaware of the section's treatments.

Chemotaxis of PMN

Polymorph nuclear cells were prepared from citrated blood of healthy donors by a combination of sedimentation and Ficoll density gradient centrifugation as described (10). Sedimented cells were incubated with ice-cold aqua dest for lysis of erythrocytes, washed in ice-cold phosphate buffered saline (PBS), and suspended in PBS at 4×10^6 cells/mL. To determine the effect of the PI3Kδ inhibitor LAS191954 on neutrophilic chemotaxis, stock solutions of the inhibitor stored at −80°C (prepared in DMSO at different concentrations starting at 3×10^{-3} M and following a fourfold bank dilution) were further diluted 1:500 in PBS containing 1% BSA to a twofold assay concentration and tested in a slightly modified chemotaxis assay (32). In brief, interleukine (IL)-8 (6 nM; Peprotech, Hamburg, Germany), fMLP (10 nM), and human recombinant C5a (12 nM) were diluted in PBS with Ca^{2+}, Mg^{2+}/0.1% BSA and added to the bottom wells of the chamber. After covering the bottom wells with a polycarbonate membrane (pore size: 5 µm, Costar Nucleopore GmbH, Tübingen, Germany), the top wells were filled with 1×10^5 freshly prepared neutrophils in PBS with Ca^{2+}, Mg^{2+}/1% BSA that were preincubated with different concentrations of the PI3Kδ inhibitor LAS191954 (10 min, 37°C). After incubation for 1 h at 37°C, migration was terminated by removing the cells from the top wells. Migrated cells were transferred from the bottom wells to a microtiter plate and lysed with 0.1% hexabromide solution. Number of migrated neutrophils was determined *via* endogenous myeloperoxidase activity by adding myeloperoxidase substrate tetramethylbenzidine (Life Technologies, Paisley, UK). The redox reaction was stopped by 0.9 M sulfuric acid and oxidized tetramethylbenzidine measured at $\lambda = 450$ nm. The number of migrated neutrophils was calculated from a standard curve of cell lysates run in parallel.

Statistical Analysis

Statistical analysis was performed using SigmaPlot 13.0. Used tests are indicated at each figure legend. A p-value of <0.05 was considered significant. If not otherwise indicated, mean and SEM are presented.

RESULTS

LAS191954 Ameliorates Already Established Disease in Immunization-Induced EBA

LAS191954 is a specific and potent inhibitor of the p110δ catalytic isoform of PI3K with a reported enzymatic potency of 2.6 nM (26). The compound is 30-fold selective versus the p110β (IC50 94.2 nM) and p110γ (IC50 71.7 nM) isoforms and 3,000-fold over the p110α isoform (IC50 8226 nM). A similar selectivity profile as in the enzymatic assays has been observed in PI3Kδ-dependent (human anti-IgD activated PBMC) or PI3Kβ-dependent (S1P-activated HUVEC) cellular assays, with reported IC50 of 4.6 nM and 295 nM, respectively. No off-target activity has been reported in a panel of GPCRs, transporter, and kinases up to 10 µM. *In vivo*, LAS191954 shows excellent oral bioavailability in preclinical species and demonstrates pharmacological activity in both acute and chronic settings (26).

We took advantage of the above selective and potent compound profile to first evaluate the therapeutic effect of pharmacological PI3Kδ inhibition in EBA, by treating mice with active disease with two different doses of LAS191954 daily for 6 weeks. Allocation to treatment was performed when skin lesions affected 2% or more of the body surface area in individual mice. To rule out a potential allocation bias, the time after immunization and the affected body surface area were analyzed in each group. Both, time after immunization (Figure S1A in Supplementary Material) and affected body surface area at time of allocation (Figure S1B in Supplementary Material) showed no significant differences in all groups. In vehicle-treated animals, affected body surface area increased twofold within the first week, remained constant until week 4, and then gradually decreased until the end of the 6-week treatment period. As shown in **Figures 1A,B**, in mice treated with LAS191954 at 1 mg/kg, disease progression was impaired, without a statistical significant difference between vehicle and the LAS191954-treated (1 mg/kg) group during individual time points of the 6-week observation period. Of note, a higher dose of LAS191954 (3 mg/kg) completely abolished disease progression and even improved disease (defined as less body surface area affected by skin lesions) starting from week 4. In line with the dose-dependent clinical effects, compound plasma exposures increased proportionally with the dose in the treated animals as assessed at the 1 h post-administration time point (corresponding to the Cmax) on the last day of the study. Free plasma levels were 575 ± 245 nM for the 3 mg/kg- and 135 ± 71 nM for the 1 mg/kg-treated group. These results were in agreement with oral pharmacokinetic studies performed in healthy mice (data not shown). High-dose corticosteroid treatment (20 mg/kg MP) was used as a reference treatment in a head-to-head comparison, because previous work demonstrated beneficial effects of high-dose MP treatment in this model (33). In line with previous data (where MP was given i.p.), orally administered MP hindered disease progression (with significant differences observed at week 4), but failed to improve skin blistering (**Figures 1A,B**). Investigation of the dermal leukocyte infiltrate, evaluated in ears of mice at the end of the treatment period, did not show any differences among the groups (**Figures 1C,D**).

LAS191954 Does Not Modify Circulating Autoantibody Titer in Experimental EBA

In order to ascertain whether the mechanism of action of LAS191954 in experimental EBA involves the antibody response, we first assessed whether chronic treatment with the compound had an effect on circulating autoantibody concentrations. To address this, we determined the levels of anti-COL7 specific IgG in mice treated for 6 weeks with LAS191954 at the end of the treatment period (same experiment as in **Figure 1**). Of note, a similar decrease of COL7-specific IgG was observed in all treatment groups (**Figure 2**), suggesting that LAS191954 had no impact on autoantibody levels over this time period in this model.

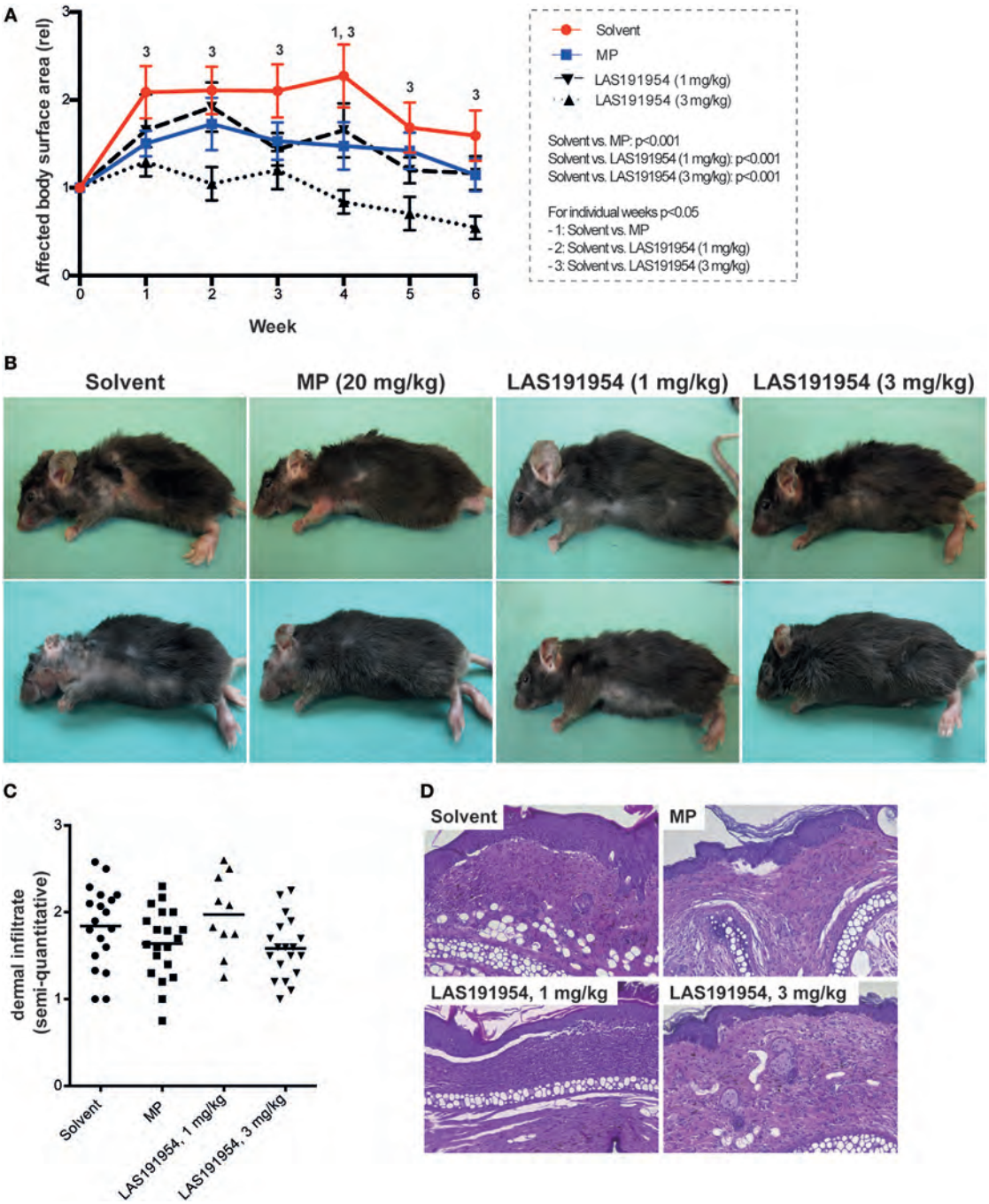

FIGURE 1 | Pharmacological PI3Kδ inhibition improves already clinically manifested experimental Epidermolysis bullosa acquisita (EBA). B6.s mice were immunized with COL7 for induction of experimental EBA. When skin lesions affected 2% or more of the body surface area, individual mice were randomly allocated to one of the four treatment groups. **(A)** Clinical disease severity, expressed as affected body surface area in relation to the time of allocation to treatment (week 0). Data are based on 11 mice per group, with the exception of LAS191954 1 mg/kg [$n = 6$; two-way ANOVA (taking time and treatment as variables) with Holm-Sidak posttest]. The global p values of testing solvent versus the treatments is given in the box on the left. For the posttest, p values < 0.05 are indicated by numbers, whereas "1" indicates a difference between solvent and methylprednisolone (MP), "2" a difference between solvent and LAS191954 (1 mg/kg), and "3" a difference between solvent and LAS191954 (3 mg/kg). **(B)** Representative clinical images of two mice from each group taken at the end of the experiment. **(C)** Semiquantitative evaluation of the dermal infiltrate of the ears at week 6 of the experiment, with 0 indicating no, 1 mild, 2 moderate, and 3 severe infiltration. While a tendency toward lower infiltration scores was noted in MP and LAS191954 (3 mg/kg), this was not statistically significant. Each datapoint represents one ear per group (if possible, both ears were evaluated). Statistical significance was calculated using ANOVA. **(D)** Representative H&E-stained sections from all treatment groups at week 6 of treatment. Original magnification 200×.

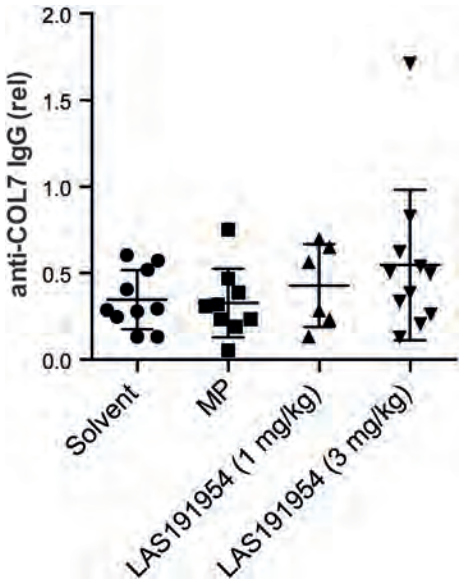

FIGURE 2 | Circulating anti-COL7 IgG remains unaltered after treatment with either LAS191954 or methylprednisolone. At randomization (week 0) and at the end of the treatment (week 6), serum was obtained from selected mice. The graph shows the mean and STW of the relative serum concentration of anti-COL7 IgG antibodies at week 6 in relation to week 0. In all groups, a decrease of COL7-specifig IgG was noted, with no statistically difference observed among the groups. Data are based on 6–11 mice per group. Each dot represents the data from one animal. Statistical analysis was performed using one-way ANOVA.

This result was in contrast with the reported role of PI3Kδ in TDAR and B cell function (20). To further study the effect of LAS191954 on humoral responses, we checked whether LAS191954 could prevent antibody responses to a model immunogen like KLH in CD1 mice. In this setting, the response is elicited in the absence of potent adjuvants, unlike in the EBA model. Indeed, LAS191954 dose-dependently inhibited the primary IgG response with a maximal response attained at 0.3 mg/kg (Figure S2 in Supplementary Material). We further tested whether LAS191954 could reduce the spontaneous production of autoantibodies in MRL/lpr mice, a mouse strain showing an autoimmune lymphoproliferative disorder with autoantibodies to various antigens including the skin-specific antigen, desmoglein (Dsg) 3 (34). Chronic treatment of mice daily for 4 weeks progressively and dose-dependently decreased the titer of circulating dsDNA-specific and Dsg3-specific autoantibodies (Figure S3 in Supplementary Material) with the dose of 1 mg/kg being maximal and similar to the effect of prednisolone in this model.

Taken together, these results indicate that the observed therapeutic effect of LAS191954 in immunization-induced EBA seems to be independent of modulatory effects on antibody responses, despite LAS191954 being able to modulate antibody responses in other induced and spontaneous mouse models at similar or lower doses, suggesting that differences in the way the immune response is elicited in all models may account for the results observed.

LAS191954 Prevents Onset of Inflammation in Antibody Transfer-Induced EBA

We next evaluated the effect of LAS191954 on antibody transfer-induced EBA. This model recapitulates the effector phase of the disease, as it is induced by direct transfer of anti-COL7 IgG and requires myeloid cell activation through activating FcγR (9). The same doses of LAS191954 and MP as in the immunization-induced EBA model above were administered to groups of mice following a preventive scheme as described in Section "Materials and Methods." The results show that small but significant effects of both MP and LAS191954 were obtained at reducing blistering versus vehicle-treated mice (**Figure 3**) suggesting a potential effect of the compound in the effector phase.

Taken together, the above results indicate that LAS191954 has a pharmacological effect in two different EBA mouse models at similar effective doses and suggest that inhibition of pathogenic myeloid cell activation rather than blocking autoantibody production accounts for the observed therapeutic effect.

LAS191954 Inhibits Myeloid Cell Function *In Vitro*

To validate these assumptions, we next set out to determine whether the mechanism of action of LAS191954 may be driven by effects on myeloid cells. For this, we isolated PMN from human volunteers' peripheral blood and assessed the effect of LAS191954 on the release of ROS induced by immune complexes. LAS191954 dose-dependently reduced the immune complex-induced ROS release from human PMN with an IC50 of 11 nM (**Figure 4A**). These findings were validated by use of another PI3Kδ-selective inhibitor (IC-87114) (23), which also dose-dependently and well within the reported IC50, reduced the immune complex-induced ROS release from human PMN (not shown). Furthermore, we investigated the impact of LAS191954 on immune complex-induced ROS release from human monocytes, which recently has been shown to contribute to EBA pathogenesis (13). Like in PMN, LAS191954 also impaired the immune complex-induced ROS release from human monocytes (Figure S4 in Supplementary Material). The effect of MP on immune complex-induced ROS release was also investigated in parallel. As reported earlier, when MP was given at the same dose (35), MP impaired the immune complex-induced ROS release from PMN. Yet, and in contrast to LAS191954, higher concentrations were required, consistent with the high doses that are used *in vivo* (**Figures 4B,C**). To test if also other known inducers of PMN activation are sensitive to LAS191954 treatment, PMN were activated using PMA, fMLP, or C5a. While LAS191954 had no impact on PMA-induced ROS release (**Figure 4E**), C5a-induced and fMLP-induced ROS release was dose-dependently inhibited with IC50s of 19 and 7.6 nM, respectively (**Figures 4D,F**). Based

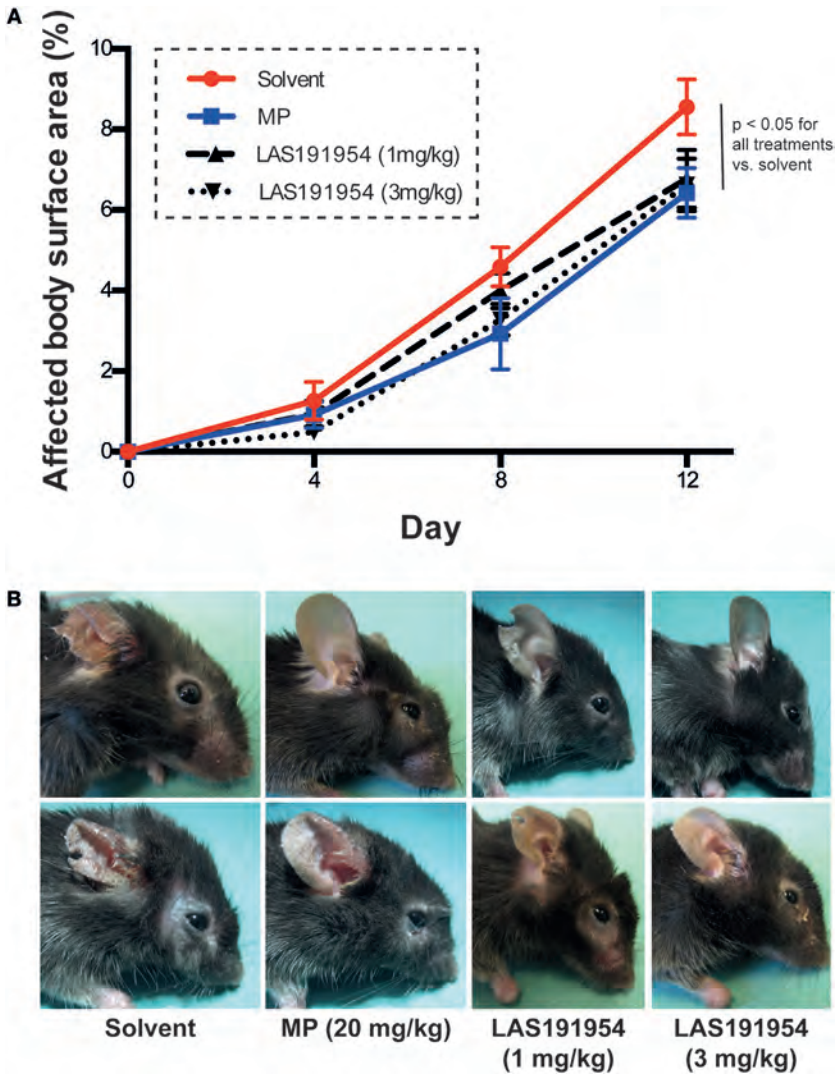

FIGURE 3 | LAS191954 treatment prevents the onset of antibody transfer-induced Epidermolysis bullosa acquisita (EBA). Experimental EBA was induced in B6 mice by repetitive injections of anti-COL7 IgG. Simultaneously, mice were treated with the indicated compounds. **(A)** In all groups, experimental EBA was induced. Data are based on 10 mice per group. Statistical analysis was performed using two-way ANOVA (taking time and treatment as variables) with Holm-Sidak posttest. **(B)** Representative clinical images of two mice from each group taken at the end of the experiment.

on the potency and selectivity profile described for the compound [see above and Ref. (26)], these results suggest that inhibition of PI3Kδ is the mechanism that accounts for the observed inhibition of ROS release.

In order to evaluate if LAS191954 can prevent a detrimental downstream effect of ROS on skin, we made use of a ROS-dependent *in vitro* model of human EBA. This model emulates the EBA prototypical DES on cryosections of human skin co-incubated with human COL7 antibodies bound to human PMN, reflecting IC-induced PMN activation (12). We measured the epidermolytic effect in the presence of different compound concentrations. In line with the previous results, LAS191954 dose-dependently and almost completely abolished *ex vivo* dermal-epidermal separation at and above concentrations of 47 nM (**Figures 4G,H**), suggesting that this process was also dependent on PI3Kδ activation.

In experimental EBA, the crucial CD18-dependent myeloid extravasation into the skin is partially driven by IL-8 mouse homolog cytokines and the complement cascade component, C5a (36, 37). We, therefore, next evaluated the effect of LAS191954 on human PMN migration induced by fMLP, IL-8, or C5a. Compared to the fMLP-induced ROS release, the impact of LAS191954 on fMLP-induced myeloid cell migration was minimal, albeit significant at the highest tested dose (**Figure 5A**). Similarly, C5a-induced migration was unaffected (**Figure 5C**). In contrast, LAS191954 completely abolished

the IL-8 induced migration of human PMN with an IC50 of 93 nM (**Figure 5B**). Altogether, these results demonstrate that LAS191954 can efficiently modulate distinct human myeloid cell functions.

DISCUSSION

The aim of this study was to test whether pharmacological inhibition of PI3Kδ with a novel selective inhibitor can modulate the

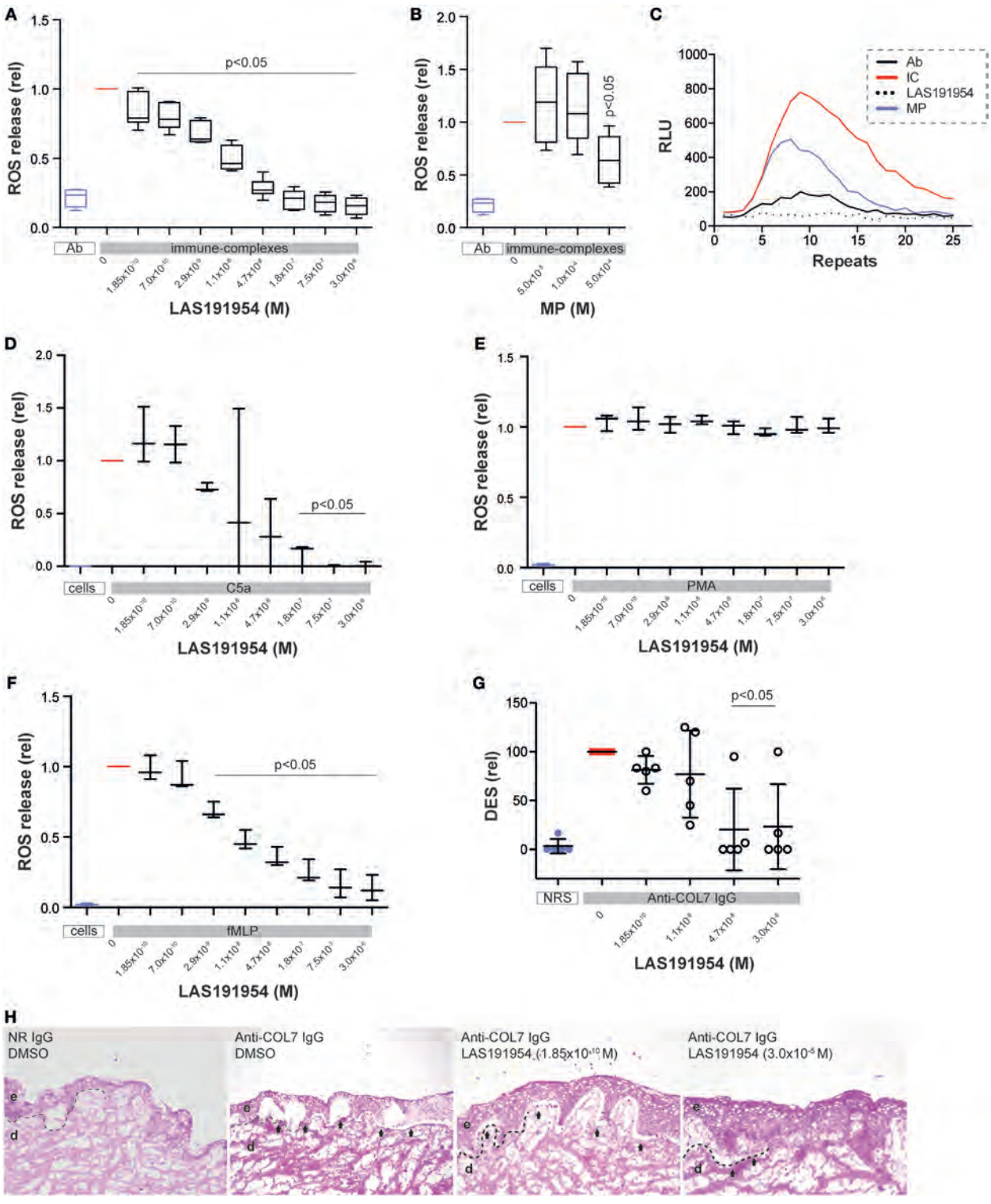

FIGURE 4 | Continued

FIGURE 4 | PI3Kδ is predominantly required for immune complex-induced ROS release from human polymorph nuclear cells (PMN). **(A–C)** Human PMNs were activated using immune complexes and their activation was determined by measuring ROS release over time in **(A)** the absence or presence of LAS191954. The graph shows the ROS release in relation to the vehicle control (n = 6/group). **(B)** In the same experimental setting, methylprednisolone was used as a reference treatment (n = 6/group). **(C)** Example of ROS release. The y-axis shows the relative light units, which correspond to the ROS release. Repeats indicate the time; one repeat approximately corresponds to 2.4 min. Human PMN were activated by **(D)** C5a, **(E)** PMA, and **(F)** fMLP, respectively, in absence or presence of LAS191954. All data in graphs **(D–F)** is based on three experiments per group. **(G)** Cryosections of human skin were incubated with rabbit anti-human COL7 and human PMN from healthy donors. This leads to dermal–epidermal separation (DES), which is shown in relation to vehicle-treated sections. Data are based on five experiments per group. **(H)** Representative, H&E-stained sections of human skin sections incubated with anti-human COL7 and human PMN from healthy donors. For all panels, one-way ANOVA with Holm-Sidak posttest was used for statistical analysis. Abbreviations: e, epidermis; d, dermis, arrows indicate DES, dotted line indicates location of dermal–epidermal junction.

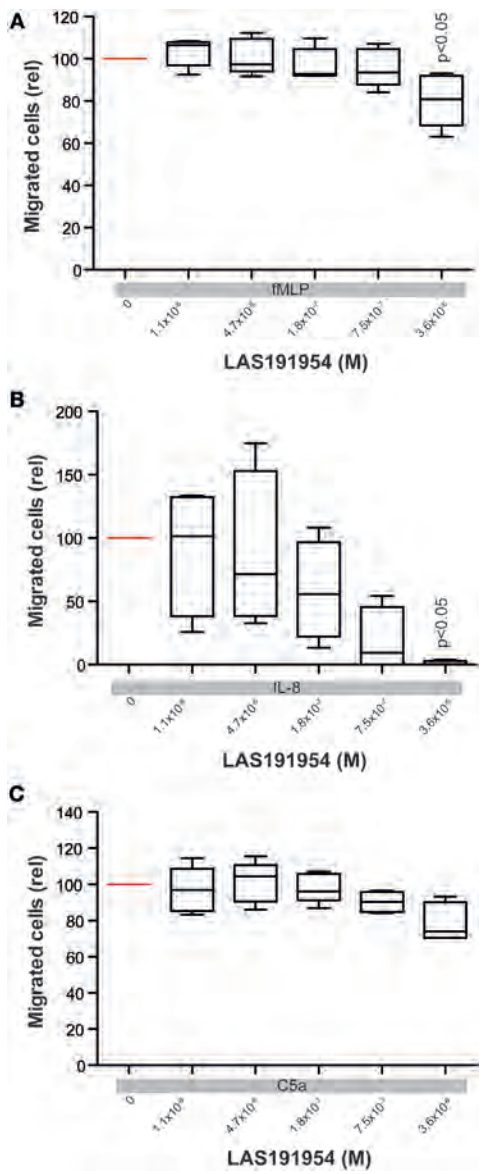

FIGURE 5 | Blockade of PI3Kδ mainly blocks IL-8 induced polymorph nuclear cells (PMN) migration. Migration of human PMN was induced using **(A)** fMLP, **(B)** IL-8, or **(C)** C5a in the presence of LAS191954. All panels show migrated cells in relation to the positive control (vehicle, no LAS191954). Data are based on five experiments per group, with the exception of C5a-induced migration (n = 4). For all panels, one-way ANOVA with Holm-Sidak posttest was used for statistical analysis.

progression of experimental EBA in mice. We demonstrate that chronic administration of this compound using a therapeutic scheme (i.e., in established clinical disease induced by COL7 immunization) improves and even normalizes the cutaneous clinical manifestations in a dose-dependent fashion. This effect is superior to that obtained with a high dose of corticosteroid and does not seem to be mediated by modulation of antibody responses. Furthermore, in an antibody transfer-induced model of EBA reproducing the effector phase of the disease, the compound can prevent the blistering induced by pathogenic antibody transfer in a similar way as corticosteroids.

Myeloid cells are essential for experimental EBA development in mice and distinct contributions of different PI3K isoforms to neutrophil function have been described. In this regard, previous studies have shown that loss of PI3Kβ expression conferred a substantial, but incomplete, protection from inflammation in antibody transfer-induced EBA. Furthermore, chimeric mice created by adoptive transfer of PI3Kβ-deficient bone marrow cells into irradiated wild-type mice were similarly protected from EBA induction. Further *in vitro* experiments indicated that PI3Kβ and PI3Kδ may act synergistically to release ROS from immune complex-activated murine and human myeloid cells (17, 38). Similarly, combined pharmacological inhibition or genetic deficiency of PI3Kβ and PI3Kδ were found to be necessary to inhibit the mouse neutrophil ROS response to *Aspergillus fumigatus* hyphae (39). Hence, both, PI3Kβ and δ seem to be the driving forces for immune complex and pathogen-driven ROS release in neutrophils.

The differential potency of our compound in each PI3K isoform allows us to further assess the contribution of each isoform in the biological process studied. *In vitro*, the compound inhibits ROS release from human PMN stimulated with immune complexes or other physiologically relevant inducers (fMLP, C5a) and does so at concentrations expecting to inhibit mainly the PI3Kδ isoform while sparing the other class I PI3K isoforms. In addition, the epidermal–dermal separation promoted by immune complex-induced ROS release also occurs at nanomolar concentrations at which the δ isoform is predominantly inhibited. Conversely, several neutrophil responses were insensitive (i.e., C5a-induced PMN migration) to the compound or only at very high concentrations (i.e., fMLP-induced PMN migration) indicating that either no PI3K isoform is involved or only the α isoform is playing a role in those pathways, in agreement with previous reports (40, 41). We further corroborated these findings with IC-87114, another highly PI3Kδ inhibitor that is >50 times selective over PI3Kβ (23). IC87114 dose-dependently reduced

the immune complex-induced ROS release from human PMN at concentrations exclusively covering the PI3Kδ (not shown). Considering these results along with our findings of an unaltered dermal neutrophil infiltrate at the end of the LAS191954 treatment (**Figures 1C,D**), this indicates that the PI3Kδ is predominantly required for ROS release from PMN, while having less pronounced effects on PMN migration.

When analyzing the *in vivo* situation, the calculated unbound compound concentrations in plasma (575 ± 245 nM) for the dose at which the compound exerts its maximum efficacy (3 mg/kg) in the experimental EBA model do not allow to attribute the observed effects solely to the inhibition of PI3Kδ. Whereas this dose may have ensured an extended inhibition period for PI3Kδ, partial and transient coverage of PI3Kβ and γ may also have occurred during the dosing period, suggesting that inhibition of more than one isoform may be necessary for full efficacy in the EBA models. This hypothesis is aligned with the reported PI3Kδ and PI3Kβ essential roles in the IC-induced neutrophil response. In addition, a predominant use of PI3Kβ by mouse neutrophils and of PI3Kδ by human neutrophils for the production of ROS in response to immune complexes was reported (41), indicating that species-specific differences in the usage of distinct PI3K isoforms in mouse and human neutrophils may be possible. However, an additional, highly selective PI3Kδ inhibitor, IC-87114, also impaired the induction of antibody transfer-induced EBA (data not shown), thus further supporting PI3Kδ as a key PI3K isoform in this model. This would be in agreement with our *in vivo* observations and also with our results in human PMN where PI3Kδ seems to be the only isoform required for the functions studied. Furthermore, our finding of an unaltered dermal neutrophil infiltrate at the end of the treatment with LAS191954 in the immunization-induced EBA model indicates that the PI3Kδ isoform is not essential for PMN migration while being required for IC-activated ROS release.

We found that the autoantibody response to COL7 was not altered by the chronic administration of the compound as determined by IgG levels on the last day of the experimental EBA study, ruling out the potential modulation of the adaptive response as a contributor to the therapeutic effect. Based on the biology of the target, this result was unexpected and is in contrast with the compound's observed inhibitory effect on the antibody response to T-cell-dependent antigens and on the autoantibody titer in a spontaneous autoimmunity mouse strain (MRL/lpr) at doses similar or below the ones used in the EBA study. Although not a clear explanation can be put forward for this discrepancy, a potential difference may lie in the way the antibody response is elicited in the EBA model with the use of a very potent adjuvant and inducer of IgG production (unpublished observations). Alternatively, it is possible that effects of PI3Kδ inhibition on B cells may not have become evident during the 6-week observation period because of the 7-week autoreactive plasma cells half-life in this model (42). In addition, as we observed a decrease of anti-COL7 IgG in all groups, including the control group, the potential effects of PI3Kδ inhibition could have been masked. Finally, the particular T cell-dependent autoantibody generation in immunization-induced EBA (11) may be insensitive to pharmacological PI3Kδ inhibition.

Taken together, our results provide new evidence that targeting the PI3Kδ pathway may be a suitable approach for the treatment of EBA, and possibly also other pemphigoid diseases such as bullous pemphigoid in which activation of myeloid cells has a key pathogenic role.

ETHICS STATEMENT

Foreskin and blood collections from healthy volunteers were performed after written informed consent was obtained. All experiments with human samples were approved by the ethical committee of the Medical Faculty of the University of Lübeck and were performed in accordance with the Declaration of Helsinki. *Laboratory animals*: C57Bl/6 (B6) and B6.SJL-H2s (B6.s) mice were obtained from colonies held at the animal facility at the University of Lübeck. Mice were housed under specific pathogen-free conditions and provided standard mouse chow and acidified drinking water *ad libitum*. Mice aged 6–10 weeks were used for the experiments. All clinical examinations, biopsies, and bleedings were performed under anesthesia with i.p. administration of a mixture of ketamine (100 μg/g) and xylazine (15 μg/g). Evaluation of skin lesions was performed as described (10). Animal experiments were approved by local authorities of the Animal Care and Use Committee (Kiel, Germany) and performed by certified personnel. For KLH immunization studies, male Crl:CD1 (ICR) mice were purchased from Charles River. Female MRL/MpJ-Faslpr/J mice were purchased from The Jackson Laboratory (Bar Harbor, ME, USA). Animals were housed in polycarbonate cages, with free access to water and non-purified stock diet and allowed to condition for 2 weeks in their new environment at 22 ± 2°C, 40–70% relative humidity and 12 h:12 h light:dark cycles. All animal care and experimental procedures followed the European Community Directive 86/609/CEE and the Autonomous Catalan law (Decret 214/ 1997) for the use of laboratory animals and were approved by the Almirall Animal Experimentation Ethical Committee.

AUTHOR CONTRIBUTIONS

HK, AK, NG, RL, MP, MA, KB, and CB performed experiments. DZ, RL, and CB analyzed the data and wrote the manuscript. NG, RL, and CB designed the study. All authors read, commented, and approved the final version of the manuscript.

ACKNOWLEDGMENTS

The authors acknowledge María Domínguez and Peter Eichhorn for compound plasma level quantification, as well as Claudia Kauderer, Astrid Fischer, Jose Luis Gómez, and Laia Benavent for excellent technical assistance. The study was supported by the Excellence Cluster "Inflammation at Interfaces" (EXC 306/2), the Research Training Groups "Genes, Environment, and Inflammation" (GRK 1743/1) and "Modulation of

Autoimmunity" (GRK1727/1 and 2), the Clinical Research Unit "Pemphigoid Diseases" (KFO 303/1) all from the Deutsche Forschungsgemeinschaft, the Uehara Memorial Foundation as well as from a research agreement between Almirall and the University of Lübeck.

SUPPLEMENTARY MATERIAL

The Supplementary Material for this article can be found online at https://www.frontiersin.org/articles/10.3389/fimmu.2018.01558/full#supplementary-material.

REFERENCES

1. Schmidt E, Zillikens D. Pemphigoid diseases. *Lancet* (2013) 381:320–32. doi:10.1016/S0140-6736(12)61140-4
2. Ludwig RJ, Kalies K, Köhl J, Zillikens D, Schmidt E. Emerging treatments for pemphigoid diseases. *Trends Mol Med* (2013) 19:501–12. doi:10.1016/j.molmed.2013.06.003
3. Ludwig RJ, Vanhoorelbeke K, Leypoldt F, Kaya Z, Bieber K, McLachlan SM, et al. Mechanisms of autoantibody-induced pathology. *Front Immunol* (2017) 8:603. doi:10.3389/fimmu.2017.00603
4. Goletz S, Zillikens D, Schmidt E. Structural proteins of the dermal-epidermal junction targeted by autoantibodies in pemphigoid diseases. *Exp Dermatol* (2017) 26(12):1154–62. doi:10.1111/exd.13446
5. Langan SM, Smeeth L, Hubbard R, Fleming KM, Smith CJ, West J. Bullous pemphigoid and pemphigus vulgaris – incidence and mortality in the UK: population based cohort study. *BMJ* (2008) 337:a180. doi:10.1136/bmj.a180
6. Joly P, Roujeau JC, Benichou J, Delaporte E, D'Incan M, Dreno B, et al. A comparison of two regimens of topical corticosteroids in the treatment of patients with bullous pemphigoid: a multicenter randomized study. *J Invest Dermatol* (2009) 129:1681–7. doi:10.1038/jid.2008.412
7. Kim JH, Kim YH, Kim SC. Epidermolysis bullosa acquisita: a retrospective clinical analysis of 30 cases. *Acta Derm Venereol* (2011) 91:307–12. doi:10.2340/00015555-1065
8. Ludwig RJ. Clinical presentation, pathogenesis, diagnosis, and treatment of epidermolysis bullosa acquisita. *ISRN Dermatol* (2013) 2013:812029. doi:10.1155/2013/812029
9. Kasperkiewicz M, Sadik CD, Bieber K, Ibrahim SM, Manz RA, Schmidt E, et al. Epidermolysis bullosa acquisita: from pathophysiology to novel therapeutic options. *J Invest Dermatol* (2016) 136:24–33. doi:10.1038/JID.2015.356
10. Bieber K, Koga H, Nishie W. In vitro and in vivo models to investigate the pathomechanisms and novel treatments for pemphigoid diseases. *Exp Dermatol* (2017) 26(12):1163–70. doi:10.1111/exd.13415
11. Iwata H, Bieber K, Tiburzy B, Chrobok N, Kalies K, Shimizu A, et al. B cells, dendritic cells, and macrophages are required to induce an autoreactive CD4 helper T cell response in experimental epidermolysis bullosa acquisita. *J Immunol* (2013) 191:2978–88. doi:10.4049/jimmunol.1300310
12. Chiriac MT, Roesler J, Sindrilaru A, Scharffetter-Kochanek K, Zillikens D, Sitaru C. NADPH oxidase is required for neutrophil-dependent autoantibody-induced tissue damage. *J Pathol* (2007) 212:56–65. doi:10.1002/path.2157
13. Hirose M, Kasprick A, Beltsiou F, Dieckhoff Schulze K, Schulze FS, Samavedam UK, et al. Reduced skin blistering in experimental epidermolysis bullosa acquisita after anti-TNF treatment. *Mol Med* (2016) 23. doi:10.2119/molmed.2015.00206
14. Kasperkiewicz M, Nimmerjahn F, Wende S, Hirose M, Iwata H, Jonkman MF, et al. Genetic identification and functional validation of FcγRIV as key molecule in autoantibody-induced tissue injury. *J Pathol* (2012) 228:8–19. doi:10.1002/path.4023
15. Németh T, Virtic O, Sitaru C, Mócsai A. The Syk tyrosine kinase is required for skin inflammation in an in vivo mouse model of epidermolysis bullosa acquisita. *J Invest Dermatol* (2017) 137:2131–9. doi:10.1016/j.jid.2017.05.017
16. Kovács M, Németh T, Jakus Z, Sitaru C, Simon E, Futosi K, et al. The Src family kinases Hck, Fgr, and Lyn are critical for the generation of the in vivo inflammatory environment without a direct role in leukocyte recruitment. *J Exp Med* (2014) 211:1993–2011. doi:10.1084/jem.20132496
17. Kulkarni S, Sitaru C, Jakus Z, Anderson KE, Damoulakis G, Davidson K, et al. PI3Kβ plays a critical role in neutrophil activation by immune complexes. *Sci Signal* (2011) 4:ra23. doi:10.1126/scisignal.2001617
18. Ludwig RJ. Signaling and targeted-therapy of inflammatory cells in epidermolysis bullosa acquisita. *Exp Dermatol* (2017) 26:1179–86. doi:10.1111/exd.13335
19. Puri KD, Gold MR. Selective inhibitors of phosphoinositide 3-kinase delta: modulators of B-cell function with potential for treating autoimmune inflammatory diseases and B-cell malignancies. *Front Immunol* (2012) 3:256. doi:10.3389/fimmu.2012.00256
20. Koyasu S. The role of PI3K in immune cells. *Nat Immunol* (2003) 4:313–9. doi:10.1038/ni0403-313
21. Durand CA, Hartvigsen K, Fogelstrand L, Kim S, Iritani S, Vanhaesebroeck B, et al. Phosphoinositide 3-kinase p110 delta regulates natural antibody production, marginal zone and B-1 B cell function, and autoantibody responses. *J Immunol* (2009) 183:5673–84. doi:10.4049/jimmunol.0900432
22. Maxwell MJ, Tsantikos E, Kong AM, Vanhaesebroeck B, Tarlinton DM, Hibbs ML. Attenuation of phosphoinositide 3-kinase δ signaling restrains autoimmune disease. *J Autoimmun* (2012) 38:381–91. doi:10.1016/j.jaut.2012.04.001
23. Sadhu C, Masinovsky B, Dick K, Sowell CG, Staunton DE. Essential role of phosphoinositide 3-kinase delta in neutrophil directional movement. *J Immunol* (2003) 170:2647–54. doi:10.4049/jimmunol.170.5.2647
24. Sadhu C, Dick K, Tino WT, Staunton DE. Selective role of PI3K delta in neutrophil inflammatory responses. *Biochem Biophys Res Commun* (2003) 308:764–9. doi:10.1016/S0006-291X(03)01480-3
25. Puri KD, Doggett TA, Douangpanya J, Hou Y, Tino WT, Wilson T, et al. Mechanisms and implications of phosphoinositide 3-kinase delta in promoting neutrophil trafficking into inflamed tissue. *Blood* (2004) 103:3448–56. doi:10.1182/blood-2003-05-1667
26. Erra M, Taltavull J, Gréco A, Bernal FJ, Caturla JF, Gràcia J, et al. Discovery of a potent, selective, and orally available PI3Kδ inhibitor for the treatment of inflammatory diseases. *ACS Med Chem Lett* (2017) 8:118–23. doi:10.1021/acsmedchemlett.6b00438
27. Leineweber S, Schonig S, Seeger K. Insight into interactions of the von-Willebrand-factor-A-like domain 2 with the FNIII-like domain 9 of collagen VII by NMR and SPR. *FEBS Lett* (2011) 585:1748–52. doi:10.1016/j.febslet.2011.04.071
28. Iwata H, Witte M, Samavedam UK, Gupta Y, Shimizu A, Ishiko A, et al. Radiosensitive hematopoietic cells determine the extent of skin inflammation in experimental epidermolysis bullosa acquisita. *J Immunol* (2015) 195:1945–54. doi:10.4049/jimmunol.1501003
29. Aulí M, Domènech A, Andrés A, Orta M, Salvà M, Descotes J, et al. Multiparametric immunotoxicity screening in mice during early drug development. *Toxicol Lett* (2012) 214:200–8. doi:10.1016/j.toxlet.2012.08.020
30. Yu X, Holdorf K, Kasper B, Zillikens D, Ludwig RJ, Petersen F. FcgammaRIIA and FcgammaRIIIB Are required for autoantibody-induced tissue damage in experimental human models of bullous pemphigoid. *J Invest Dermatol* (2010) 130:2841–4. doi:10.1038/jid.2010.230
31. Vorobyev A, Ujiie H, Recke A, Buijsrogge JJA, Jonkman MF, Pas HH, et al. Autoantibodies to multiple epitopes on the non-collagenous-1 domain of type VII collagen induce blisters. *J Invest Dermatol* (2015) 135:1565–73. doi:10.1038/jid.2015.51
32. Ludwig A, Schiemann F, Mentlein R, Lindner B, Brandt E. Dipeptidyl peptidase IV (CD26) on T cells cleaves the CXC chemokine CXCL11 (I-TAC) and abolishes the stimulating but not the desensitizing potential of the chemokine. *J Leukoc Biol* (2002) 72:183–91. doi:10.1189/jlb.72.1.183
33. Hirose M, Tiburzy B, Ishii N, Pipi E, Wende S, Rentz E, et al. Effects of intravenous immunoglobulins on mice with experimental epidermolysis bullosa acquisita. *J Invest Dermatol* (2015) 135:768–75. doi:10.1038/jid.2014.453
34. Nishimura H, Strominger JL. Involvement of a tissue-specific autoantibody in skin disorders of murine systemic lupus erythematosus and autoinflammatory diseases. *Proc Natl Acad Sci U S A* (2006) 103:3292–7. doi:10.1073/pnas.0510756103
35. Hellberg L, Samavedam UK, Holdorf K, Hänsel M, Recke A, Beckmann T, et al. Methylprednisolone blocks autoantibody-induced tissue damage through

inhibition of neutrophil activation. *J Invest Dermatol* (2013) 133:2390–9. doi:10.1038/jid.2013.91

36. Witte M, Koga H, Hashimoto T, Ludwig RJ, Bieber K. Discovering potential drug-targets for personalized treatment of autoimmune disorders – what we learn from epidermolysis bullosa acquisita. *Expert Opin Ther Targets* (2016) 19:1–14. doi:10.1517/14728222.2016.1148686
37. Deng F, Chen Y, Zheng J, Huang Q, Cao X, Zillikens D, et al. CD11b-deficient mice exhibit an increased severity in the late phase of antibody transfer-induced experimental epidermolysis bullosa acquisita. *Exp Dermatol* (2017) 26:1175–8. doi:10.1111/exd.13434
38. Chu JY, Dransfield I, Rossi AG, Vermeren S. Non-canonical PI3K-Cdc42-Pak-Mek-Erk signaling promotes immune-complex-induced apoptosis in human neutrophils. *Cell Rep* (2016) 17:374–86. doi:10.1016/j.celrep.2016.09.006
39. Boyle KB, Gyori D, Sindrilaru A, Scharffetter-Kochanek K, Taylor PR, Mócsai A, et al. Class IA phosphoinositide 3-kinase beta and delta regulate neutrophil oxidase activation in response to *Aspergillus fumigatus* hyphae. *J Immunol* (2011) 186:2978–89. doi:10.4049/jimmunol.1002268
40. Helmer E, Watling M, Jones E, Tytgat D, Jones M, Allen R, et al. First-in-human studies of seletalisib, an orally bioavailable small-molecule PI3Kδ inhibitor for the treatment of immune and inflammatory diseases. *Eur J Clin Pharmacol* (2017) 73:581–91. doi:10.1007/s00228-017-2205-7
41. Heit B, Liu L, Colarusso P, Puri KD, Kubes P. PI3K accelerates, but is not required for, neutrophil chemotaxis to fMLP. *J Cell Sci* (2008) 121:205–14. doi:10.1242/jcs.020412
42. Tiburzy B, Szyska M, Iwata H, Chrobok N, Kulkarni U, Hirose M, et al. Persistent autoantibody-production by intermediates between short-and long-lived plasma cells in inflamed lymph nodes of experimental epidermolysis bullosa acquisita. *PLoS One* (2013) 8:e83631. doi:10.1371/journal.pone.0083631

Conflict of Interest Statement: RL, MA, MP, NG, and CB are employees of Almirall S.A. Costs for this research were in part covered by a research agreement between Almirall and the University of Lübeck. The remaining authors declare that the research was conducted in the absence of any commercial or financial relationships that could be construed as a potential conflict of interest.

frontiers in Immunology

ORIGINAL RESEARCH
published: 09 July 2018
doi: 10.3389/fimmu.2018.01447

A Spectrum of Neural Autoantigens, Newly Identified by Histo-Immunoprecipitation, Mass Spectrometry, and Recombinant Cell-Based Indirect Immunofluorescence

Madeleine Scharf†, Ramona Miske*†, Stephanie Kade, Stefanie Hahn, Yvonne Denno, Nora Begemann, Nadine Rochow, Christiane Radzimski, Stephanie Brakopp, Christian Probst, Bianca Teegen, Winfried Stöcker and Lars Komorowski*

Institute of Experimental Immunology, EUROIMMUN AG, Lübeck, Germany

OPEN ACCESS

Edited by:
Herman Waldmann, University of Oxford, United Kingdom

Reviewed by:
David Cameron Wraith, University of Birmingham, United Kingdom
Lucienne Chatenoud, Université Paris Descartes, France

***Correspondence:**
Madeleine Scharf
m.scharf@euroimmun.de;
Ramona Miske
r.miske@euroimmun.de

†These authors have contributed equally to this work.

Specialty section:
This article was submitted to Immunological Tolerance and Regulation, a section of the journal Frontiers in Immunology

Received: *02 November 2017*
Accepted: *11 June 2018*
Published: *09 July 2018*

Citation:
Scharf M, Miske R, Kade S, Hahn S, Denno Y, Begemann N, Rochow N, Radzimski C, Brakopp S, Probst C, Teegen B, Stöcker W and Komorowski L (2018) A Spectrum of Neural Autoantigens, Newly Identified by Histo-Immunoprecipitation, Mass Spectrometry, and Recombinant Cell-Based Indirect Immunofluorescence. Front. Immunol. 9:1447. doi: 10.3389/fimmu.2018.01447

Background: A plurality of neurological syndromes is associated with autoantibodies against neural antigens relevant for diagnosis and therapy. Identification of these antigens is crucial to understand the pathogenesis and to develop specific immunoassays. Using an indirect immunofluorescence assay (IFA)-based approach and applying different immunoprecipitation (IP), chromatographic and mass spectrometric protocols was possible to isolate and identify a spectrum of autoantigens from brain tissue.

Methods: Sera and CSF of 320 patients suspected of suffering from an autoimmune neurological syndrome were comprehensively investigated for the presence of anti-neural IgG autoantibodies by IFA using mosaics of biochips with brain tissue cryosections and established cell-based recombinant antigen substrates as well as immunoblots. Samples containing unknown brain tissue-specific autoantibodies were subjected to IP with cryosections of cerebellum and hippocampus (rat, pig, and monkey) immobilized to glass slides or with lysates produced from homogenized tissue, followed by sodium dodecyl sulfate-polyacrylamide gel electrophoresis, tryptic digestion, and matrix-assisted laser desorption/ionization–time of flight mass spectrometry analysis. Identifications were confirmed by IFA with recombinant HEK293 cells and by neutralizing the patients' autoantibodies with the respective recombinantly expressed antigens in the tissue-based immunofluorescence test.

Results: Most samples used in this study produced speckled, granular, or homogenous stainings of the hippocampal and cerebellar molecular and/or granular layers. Others exclusively stained the Purkinje cells. Up to now, more than 20 different autoantigens could be identified by this approach, among them ATP1A3, CPT1C, Flotillin1/2, ITPR1, NBCe1, NCDN, RGS8, ROCK2, and Syntaxin-1B as novel autoantigens.

Discussion: The presented antigen identification strategy offers an opportunity for identifying up to now unknown neural autoantigens. Recombinant cell substrates containing

the newly identified antigens can be used in serology and the clinical relevance of the autoantibodies can be rapidly evaluated in cohort studies.

Keywords: neural autoantibodies, immunoprecipitation, antigen identification, autoantigens, indirect immunofluorescence

INTRODUCTION

In autoimmune diseases, an abnormal response of the immune system attacks the body's own cells causing malfunction or injury. The immune response is often associated with the appearance of autoreactive antibodies (=autoantibodies) that bind specifically to the body's own structures (=autoantigens). In neurological autoimmune diseases the nervous system is affected as a result. The spectrum of diagnoses of neurological autoimmune disorders has expanded rapidly in the recent years due to the discovery of new anti-neural antibodies.

Most of the initially described anti-neural autoantibodies are directed against intracellular proteins like Hu, Yo, Ri, Ta, GAD, and amphiphysin (1). They are generally considered to be epiphenomena of a T-cell-driven reaction against tumor cells expressing neuronal antigens. Because of their limited access to their target antigens, they probably bear no pathogenic potential *in vivo* though anti-Hu has recently been shown to activate neurons (2). They are crucial biomarkers for the diagnosis of paraneoplastic autoimmune disorders and often lead to very early diagnosis of the corresponding cancers.

In the past years, a significant number of pathogenic autoantibodies against neural surface-associated proteins have been described, including AQP4, NMDAR, LGI1, CASPR2, AMPAR1, and AMPAR2, GABA-A and -B receptors, glycin receptor, DPPX, mGluR5, IgLON5, and neurexin-3-alpha (1, 3–7). These autoantibodies are frequently non-paraneoplastic, generally occur in association with inflammatory damage to the brain and can trigger seizures, impairment of visual acuity, psychosis-like symptoms, and/or movement disorders.

Most notably, anti-neural autoantibodies are not only important diagnostic markers. Knowing the identity of the corresponding autoantigens also helps to determine the treatment strategy. Patients with antibodies targeting intracellular proteins generally respond poorly to immunosuppressive treatments but need fast onset of oncotherapy in most cases. In contrast, antibodies targeting cell surface proteins can have direct pathogenic effects, and patients' symptoms often improve after immunotherapy.

The most frequently used method for neural cell surface antigen identification has been immunoprecipitation after antibody binding to live primary hippocampal neurons (5–11). The neuronal cells used for these experiments are isolated from rat embryos and need to be cultivated for at least 14 days to allow differentiation before patient antibodies are applied to the culture. Preparation and cultivation of the cells are elaborate, thus hampering their use for screening of autoantibodies in clinical diagnostics. Moreover, the method is limited as it can only be used if the antigenic target is presented at the surface of the cultivated neurons.

For identification of intracellular antigens, immunoscreening of cDNA expression libraries (12, 13) or libraries of purified recombinant proteins (14) has been used successfully. Other strategies rely on the separation of brain tissue extracts in one- or two-dimensional gel electrophoresis followed by transfer of the separated proteins onto membranes and incubation with patient antibodies (15, 16). In these experiments, the frequency of irrelevant positive results is high because revelation of hidden epitopes may lead to unspecific binding of antibodies to unfolded and/or electrophoretically concentrated proteins. At the same time, these methods often denature the three-dimensional structure of protein antigens. Since autoantibodies sometimes do not bind to structurally non-authentic antigens in these setups, their usefulness is further limited.

Here, we report on an antigen identification strategy that is derived from indirect immunofluorescence assay (IFA) using brain tissue cryosections which is still one of the most versatile screening procedures for anti-neural autoantibodies, especially against up to now unspecified target antigens. Cryosectioning generally conserves the microenvironment of tissues such that protein structures are stabilized and epitopes presented nearly authentical.

MATERIALS AND METHODS

In the first step, the immunocomplexes formed by the patient's autoantibodies and the animal tissue cryosections were analyzed in an immunocomplex extraction assay. A combination of histo- or tissue-immunoprecipitation (HIP/TIP), chromatography, and mass spectrometry was used for antigen identification. Correct antigen identification was verified by IFA using the respective antigen recombinantly expressed in HEK293 cells and by neutralizing the autoantibodies' tissue reaction with the recombinant antigen.

Reagents

Reagents were obtained from Merck, Darmstadt, Germany, or Sigma-Aldrich, Heidelberg, Germany if not specified otherwise.

Human Samples

An ethics approval was not required as per institutional and national guidelines. The serum samples were collected by the clinical immunological laboratory Stöcker, Lübeck (Germany) for the purpose of autoantibody testing and were provided to the authors in an anonymized form. Hence, the authors did not

Abbreviations: EDTA, ethylenediamine tetraacetic acid; FITC, fluorescein isothiocyanate; HIP, histo-immunoprecipitation; IFA, indirect immunofluorescence assay; MALDI–TOF MS, matrix-assisted laser desorption/ionization–time of flight mass spectrometry; PAGE, polyacrylamide gel electrophoresis; PMF, peptide mass fingerprint; RC-IFA, recombinant cell-based indirect immunofluorescence assay; SDS, sodium dodecyl sulfate; TIP, tissue-immunoprecipitation.

have access to identifiable information. After use for clinical diagnostics the samples were coded and stored at −20°C until first research use after which they were stored at +4°C for further experiments to avoid repeated freeze/thaw cycles. Stored sera samples were used as sources of IgG antibodies.

Control collectives included healthy blood donors and patients with defined autoantibody-associated neurological syndromes.

Indirect Immunofluorescence Assay

Indirect immunofluorescence assay was conducted using slides with a diagnostic biochip screening array of brain tissue cryosections (hippocampus of rat, cerebellum of rat and monkey) combined with recombinant HEK293 cells, each biochip separately expressing the following 30 brain antigens: Hu, Yo, Ri, CV2, SOX1, PNMA1, PNMA2, ARHGAP26, Homer3, CARP VIII, ZIC4, DNER/Tr, GAD65, GAD67, amphiphysin, recoverin, GABAB receptor, glycine receptor, DPPX, glutamate receptors (types NMDA, AMPA, mGluR1, mGluR5), LGI1, CASPR2, AQP4 (M1 and M23), MOG, MP-0, and MAG. Each biochip mosaic was incubated with 70 µL of PBS-diluted sample at room temperature for 30 min, washed with PBS-Tween for 5 min. In the second step, either Alexa488-labeled goat anti-human IgG (Jackson Research, Suffolk, United Kingdom), or fluorescein isothiocyanate-labeled goat anti-human IgG (Euroimmun) were applied and incubated at room temperature for 30 min. Slides were washed again with PBS-Tween for 5 min. Slides were embedded in PBS-buffered, DABCO containing glycerol, and examined by fluorescence microscopy. Positive and negative controls were included. Samples were classified as positive or negative based on fluorescence reactivity of the transfected cells in direct comparison with mock-transfected cells and control samples. Cell nuclei were visualized by DNA staining with TO-PRO3 iodide (dilution 1:2,000) (ThermoFisher Scientific, Schwerte, Germany). In neutralization experiments, recombinant antigens were mixed with diluted serum samples 1 h prior to the IFA as described in Stöcker et al. (17). Results were evaluated independently by two observers using a laser scanning microscope (LSM700, Zeiss, Jena, Germany).

Immunocomplex Extraction Assay

The assay was performed using slides with a biochip array of brain tissue cryosections (rat hippocampus, rat cerebellum, and monkey cerebellum). Each biochip mosaic was incubated with PBS-diluted sample at room temperature for 30 min, washed with PBS-Tween, and immersed in PBS-Tween for 5 min. In the second step, the slides were incubated either in extraction buffer [100 mmol/L Tris–HCl pH 7.4, 150 mmol/L sodium chloride, 2.5 mmol/L ethylenediamine tetraacetic acid (EDTA), 0.5% (w/v) deoxycholate, and 1% (w/v) Triton X-100 containing protease inhibitors] or in detergent-free control buffer for 30 min at room temperature while gently shaking. After washing with PBS-Tween, the incubation with secondary antibody, washing, and preparation of slides fluorescence microscopy was performed as described for IFA. Extraction of the immunocomplexes was estimated by direct comparison of the signal intensity of the biochip mosaics incubated with extraction buffer or with the control buffer.

Histo-Immunoprecipitation

Cerebellum from rat or pig was dissected and shock-frozen in −160°C isopentane. The tissue was cryosectioned (4 µm) with a SM2000R microtome (Leica Microsystems, Nussloch, Germany), placed on the entire surface of glass slides, and dried. Whole slides were then incubated with patient's serum (diluted 1:100) at 4°C for 3 h followed by three washing steps with PBS containing 0.2% (w/v) Tween 20. Immunocomplexes were extracted from the sections by incubation in extraction buffer [100 mmol/L Tris–HCl pH 7.4, 150 mmol/L sodium chloride, 2.5 mmol/L EDTA, 0.5% (w/v) deoxycholate, and 1% (w/v) Triton X-100 containing protease inhibitors] at room temperature for 30 min. Detached material was homogenized and centrifuged at 16,000 × *g* at 4°C for 15 min. The clear supernatants were then incubated with Protein G Dynabeads (ThermoFisher Scientific, Dreieich, Germany) at 4°C overnight to capture immunocomplexes. The beads were washed three times with PBS and eluted with NuPage LDS sample buffer (ThermoFisher Scientific, Schwerte, Germany) containing 25 mmol/L dithiothreitol at 70°C for 10 min. Carbamidomethylation with 59 mM iodoacetamide (Bio-Rad, Hamburg, Germany) was performed prior to sodium dodecyl sulfate (SDS)-polyacrylamide gel electrophoresis (PAGE) (NuPAGE, ThermoFisher Scientific, Schwerte, Germany). Separated proteins were visualized with Coomassie Brilliant Blue (G-250) (Merck) and identified by mass spectrometric (MS) analysis (see below for details).

Tissue-Immunoprecipitation

Hippocampus or cerebellum from rat was dissected and shock-frozen in liquid nitrogen. The tissues were homogenized in extraction buffer [100 mmol/L Tris–HCl pH 7.4, 150 mmol/L sodium chloride, 2.5 mmol/L EDTA, 0.5% (w/v) sodium deoxycholate, and 1% (w/v) Triton X-100] containing protease inhibitors (Complete mini, Roche Diagnostics, Penzberg, Germany) with a Miccra D-8 (Roth, Karlsruhe, Germany) and a hand homogenizer (Sartorius, Göttingen, Germany) at 4°C. The tissue lysates was centrifuged at 21,000 × *g* at 4°C for 15 min and clear supernatants were incubated with patient's serum (diluted 1:33) at 4°C for 3 h. Pulldown of immunocomplexes and analysis of eluate fractions was performed as described for HIP.

Mass Spectrometry

Mass spectrometry sample preparation was performed similar to Koy et al. (18). Unless otherwise indicated, hardware, software, MALDI targets, peptide standards, and matrix reagents were obtained from Bruker Daltonics, Bremen, Germany.

Briefly, visible protein bands were excised from Coomassie Brilliant Blue G-250 stained gels. After destaining and tryptic digestion peptides were extracted and spotted with α-cyano-4-hydroxycinnamic acid onto a MTP AnchorChip™ 384 TF target.

Matrix-assisted laser desorption/ionization–time of flight mass spectrometry/TOF measurements were performed with an Autoflex III smartbeam TOF/TOF200 System using flexControl 3.0, 3.3, or 3.4 software. MS spectra for peptide mass fingerprinting (PMF) were recorded in positive ion reflector mode with 4,000–10,000 shots and in a mass range from 600 to 4,000 Da. Spectra were calibrated externally with the commercially available

Peptide Calibration Standard II, processed with flexAnalysis 3.0, 3.3, or 3.4 and peak lists were analyzed with BioTools 3.2.

The Mascot search engine Mascot Server 2.3 (Matrix Science, London, UK) was used for protein identification by searching against the NCBI or SwissProt database limited to Mammalia. Search parameters were as follows: mass tolerance was set to 80 ppm, one missed cleavage site was accepted, and carbamidomethylation of cysteine residues as well as oxidation of methionine residues were set as fixed and variable modifications, respectively. To evaluate the protein hits, a significance threshold of $p < 0.05$ was chosen.

For further confirmation of the PMF hits two to five peptides of each identified protein were selected for MS/MS measurements using the WARP feedback mechanism of BioTools. Parent and fragment masses were recorded with 400 and 1,000 shots, respectively. Spectra were processed and analyzed as described above with a fragment mass tolerance of 0.7 Da.

Recombinant Expression of Antigens in HEK293 Cells

For cloning details see Table S1 in Supplementary Material. The antigens were expressed in the human cell line HEK293 after ExGen500-mediated transfection (ThermoFisher Scientific) according to the manufacturer's instructions.

For the preparation of IFA substrates, HEK293 were grown on sterile cover glasses, transfected, and allowed to express the recombinant antigens for 48 h. Cover glasses were washed with PBS, fixed with acetone for 10 min at room temperature, air-dried, cut into 2 mm × 2 mm-sized fragments (biochips) and used as substrates in IFA as described. Alternatively, cells were transfected in standard T-flasks and the cells harvested after 48 h. The cell suspension was centrifuged at 1,500 × *g*, 4°C for 20 min and the resulting sediment extracted with 20 mmol/L Tris–HCl pH 7.4, 50 mmol/L potassium chloride, 5 mmol/L EDTA. The extracts were stored in aliquots at −80°C until further use.

RESULTS

Results of Serum Prescreening by IFA

The samples used in this study had originally been sent to the Clinical Immunological Laboratory for determination of anti-neural autoantibodies between 01/2011 and 07/2016. The 320 sera included in this study showed different IgG staining patterns on brain tissue cryosections (hippocampus of rat, cerebellum of rat and monkey) with a minimum endpoint titer of 1:100 (Figure S1 in Supplementary Material). Most samples ($n = 261$) produced speckled, granular, or homogenous staining of the hippocampal and cerebellar molecular and granular layers. Others ($n = 59$) stained cerebellar Purkinje cells. None of these sera revealed reactivity with the monospecific biochips of the diagnostic biochip screening array.

Immunocomplex Extractability

The extractability of immunocomplexes from cryosections bound to the glass slide surface was determined for each serum sample prior to immunoprecipitation. For sera which showed medium to high extractability ($n = 182$), HIP was applied, while for the other sera TIP was used ($n = 138$) (**Figure 1**).

Some sera did not show any differences in the signal intensities after using extraction and control buffer, while other sera showed slight or even strong reduction of signal intensity after incubation with extraction buffer (**Figure 2**). A strong decrease of signal

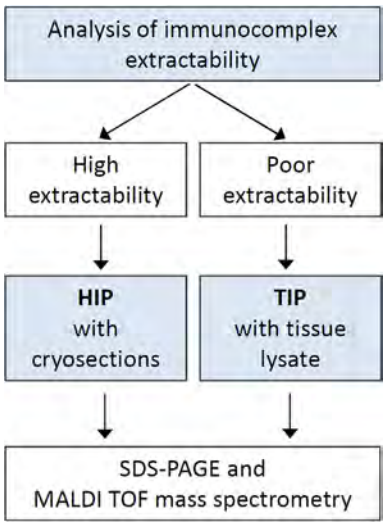

FIGURE 1 | Procedure diagram. Schematic representation of the steps of antigen identification. Abbreviations: HIP, histo-immunoprecipitation; TIP, tissue-immunoprecipitation.

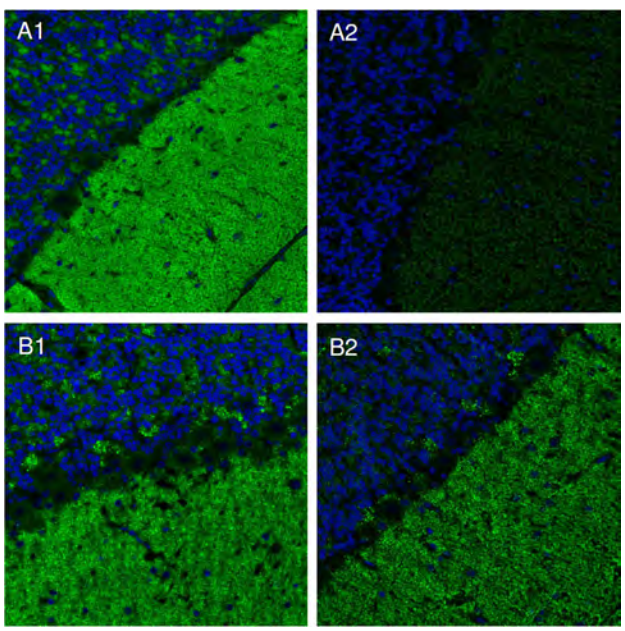

FIGURE 2 | Immunocomplex extraction. Slides with cerebellum cryosections were incubated with patients' sera and subsequently with either extraction [100 mmol/L Tris–HCl pH 7.4, 150 mmol/L sodium chloride, 2.5 mmol/L ethylenediamine tetraacetic acid, 0.5% (w/v) deoxycholate, 1% (w/v) Triton X-100] **(A2,B2)**, or detergent-free control buffer **(A1,B1)**. Bound IgG was visualized by Alexa488-labeled goat anti-human IgG. Nuclei were counterstained by incubation with TO-PRO-3 iodide (blue). Examples of soluble **(A)** and insoluble **(B)** immunocomplexes are shown.

intensity was interpreted as high extractability of the respective immunocomplexes.

Identified Autoantigens

Coomassie stained SDS-PAGE of eluate fractions obtained from HIP preparations generally showed lower numbers of protein bands and less IgG compared to TIP eluate fractions (**Figure 3B**), because washing the cryosections attached to glass coverslides removed more effectively unbound antibodies (**Figure 3A**). Specific antigen bands and unspecific protein bands were discriminated by comparison with eluate fractions of control sera. Using matrix-assisted laser desorption/ionization–time of flight mass spectrometry (MALDI–TOF MS), several antigens could be identified, among them: AP3B2, ATP1A3, CLIP1, CNTN1/CASPR1, CPT1C, ERC1, Flotillin1/2, GLURD2, GRIPAP1, Hexokinase-1, Homer 3, ITPR1, KCNA2, NBCe1, Neurochondrin, RGS8, ROCK2, RyR2, and STX1b (**Table 1**). The immunoprecipitation method which was performed for the identification of each antigen is indicated in **Table 2**.

Verification

As a proof for correct antigen identification, the patients' samples were then tested by IFA using transfected HEK293 cells which expressed the new target antigens (**Figure 4A**). Characteristic staining patterns were obtained on all cellular substrates containing the respective recombinant target antigens, while there were no corresponding stainings of mock-transfected cells or cells expressing the other target antigens.

The reaction of the patients' autoantibodies on brain tissue sections could be abolished or significantly reduced in all cases by pre-incubation with HEK293 lysate containing the respective recombinant antigen (**Figure 4B**). Antibody binding was unaffected when a comparable fraction from mock-transfected HEK293 cells was used.

Sera from patients with various anti-neural autoantibodies as disease controls (anti-NMDAR, anti-Hu, anti-Yo, anti-Ri, anti-AQP4, anti-LGI1, and anti-CASPR2), and sera from healthy blood donors were analyzed by IFA or ELISA with the recombinant antigens in parallel to the samples of the index patients. 18 of the 24 recombinant substrates showed no positive reactions with control sera. With five recombinant antigens only around 1–2% of the healthy blood donor sera reacted in a 1:10 dilution (**Table 2**).

DISCUSSION

Here, we describe a potent strategy to discover new neural autoantigens. Starting point is the definition of a characteristic IFA staining pattern on neural tissue. In sera of patients with putative neurological autoimmune diseases reacting with cryosections of cerebellum or hippocampus by indirect immunofluorescence but

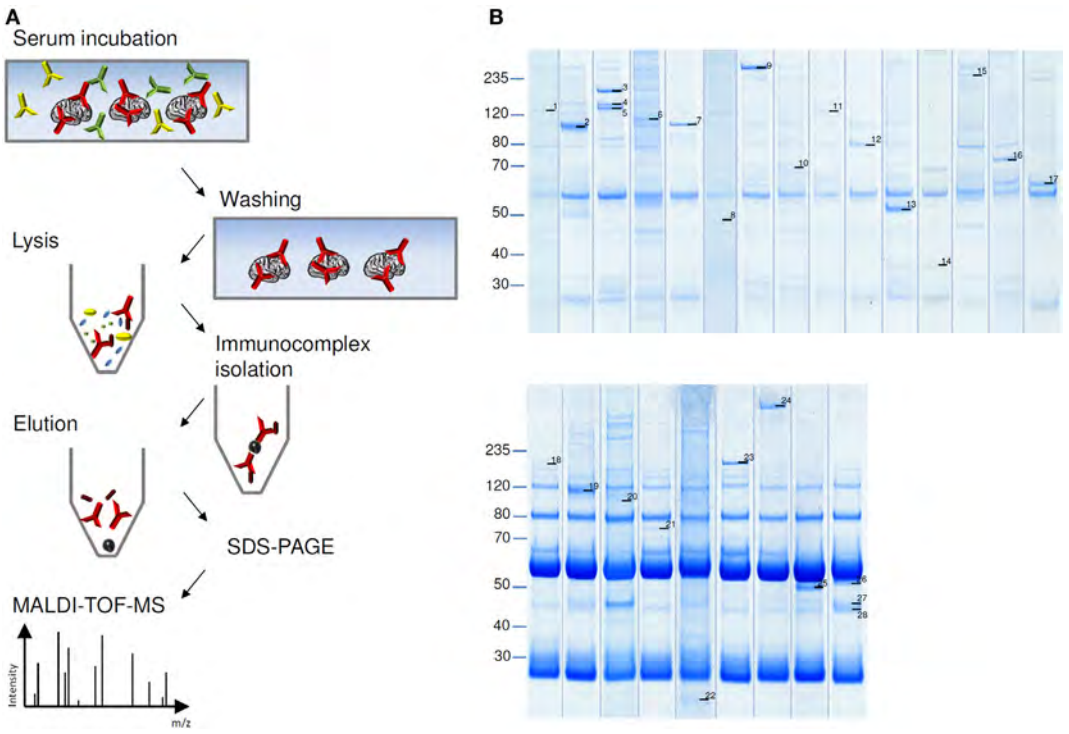

FIGURE 3 | Immunoprecipitation of autoantigens. **(A)** Schema of histo-immunoprecipitation (HIP) with cerebellum cryosections immobilized on glass slides. Slides were incubated with patient's serum followed by washing and removal of unbound antibodies. Cells were lysed and soluble immunocomplexes were isolated by protein-G-coated magnetic beads. Sodium dodecyl sulfate (SDS)-eluted proteins were separated by SDS-polyacrylamide gel electrophoresis and visualized by staining with colloidal coomassie blue. Antigen bands were prepared and analyzed with matrix-assisted laser desorption/ionization–time of flight mass spectrometry (MALDI–TOF MS). **(B)** Examples of HIP (upper panel) and tissue-immunoprecipitation (lower panel). Labeled protein bands were analyzed in MALDI–TOF MS. Results are listed in **Table 1**.

TABLE 1 | Proteins identified from immunoprecipitates using matrix-assisted laser desorption/ionization–time of flight mass spectrometry by peptide mass fingerprinting.

Band	Protein name/Entry name (UniProt)	Accession number	Cutoff	Score	Sequence coverage (%)	Mass[c] (kDa)
1	AP-3 complex subunit beta-2 (**AP3B2_MOUSE**)	Q9JME5	61	78	19	119.7
2	Sodium/potassium-transporting ATPase subunit alpha-3 (**AT1A3_RAT**)	P06687	61	169	35	113.0
3	Contactin-associated protein 1 (**CNTP1_RAT**)	P97846	61	243	34	157.7
4	Contactin-associated protein 1 (**CNTP1_RAT**)	P97846	61	185	25	157.7
5	Contactin-1 (**CNTN1_RAT**)	Q63198	61	212	44	114.2
6	Glutamate receptor ionotropic, delta-2 (**GRID2_RAT**)	Q63226	61	164	36	114.0
7	Hexokinase-1 (**HXK1_RAT**)	P05708	61	154	31	103.5
8	Homer protein homolog 3 (**HOME3_RAT**)	Q9Z2X5	61	54[a]	29	39.8
9	Inositol 1,4,5-trisphosphate receptor type 1 (**ITPR1_RAT**)	P29994	61	357	34	316.4
10	Potassium voltage-gated channel subfamily A member 2 (**KCNA2_RAT**)	P63142	61	105	27	57.1
11	Electrogenic sodium bicarbonate cotransporter 1 (**S4A4_RAT**)	Q9JI66	61	69	15	122.1
12	Carnitine O-palmitoyltransferase 1, brain isoform (**CPT1C_RAT**)	F1LN46	61	211	52	91.0
13	Flotillin-2 (**FLOT2_RAT**)	Q9Z2S9	61	123	52	47.4
	Flotillin-1 (**FLOT1_RAT**)	Q9Z1E1	61	112	57	47.7
14	Syntaxin-1B (**STX1B_RAT**)	P61265	61	78	44	33.4
15	p229[b]		61	59	11	231.2
16	p75[b]		61	241	58	74.9
17	p58[b]		61	111	38	59.2
18	CAP-Gly domain-containing linker protein 1 (**CLIP1_RAT)**	Q9JK25	61	63	14	148.8
19	ELKS/Rab6-interacting/CAST family member 1 (**RB6I2_RAT**)	Q811U3	61	108	30	108.9
20	Regulator of G-protein signaling 8 (**RGS8_RAT**)	P49804	61	110	57	21.2
21	Neurochondrin (**NCDN_RAT**)	O35095	61	160	41	80.4
22	GRIP1-associated protein 1 (**GRAP1_RAT**)	Q9JHZ4	61	75	25	96.3
23	Rho-associated protein kinase 2 (**ROCK2_RAT**)	Q62868	61	225	33	161.4
24	Ryanodine receptor 2 (**RYR2_RAT**)	B0LPN4	61	376	25	567.8
25	**p48**[b]		61	188	52	47.1
26	**p51**[b]		61	119	50	50.8
27	**p43**[b]		61	87	45	43.3
28	**p41**[b]		61	95	56	40.9

Database: SwissProt, taxonomy Mammalia.

All results were confirmed by mass spectrometry (MS)/MS.

[a]*MS results not significant, antigen was confirmed by recombinant cell-based indirect immunofluorescence assay.*

[b]*Publication in progress.*

[c]*Fixed modification: carbamidomethyl (cystein); variable modification: oxidation (methionin).*

not with established brain autoantigens, we were able to identify more than 20 different target antigens. We verified all antigen identifications by (1) specific immunostaining of HEK293 cells expressing the respective recombinant antigens by the patient's IgG and (2) specific competitive inhibition of the patient's IgG antibody by pre-incubation with the antigen extracted from recombinant HEK293 cells.

In the first step, we analyzed the immunocomplex extractability, which determined the immunoprecipitation approach. Analyzing immunocomplex extractability rather than antigen extractability is beneficial, as autoantibody binding in first step of our HIP protocol might influence antigen solubility. The extraction buffer contained 0.5% (w/v) deoxycholate and 1% (w/v) Triton X-100 as detergents. Other solubilization agents like 0.1% SDS, as well as increased salt-concentration or pH variations could be used to adjust optimal extraction conditions for individual immunocomplexes.

In the second step, HIP was performed for extractable immunocomplexes. The antibodies bind to their targets, which are presented in their natural environment and conformation on cryosections of rat or primate cerebellum immobilized on glass slides. If HIP was not performed because of poor immunocomplex extractability, we were successful in nine cases using a classical immunoprecipitation approach by incubating tissue lysates with patients' sera (TIP) (**Table 2**). In TIP, the antigens were solubilized prior to antibody binding, avoiding antigen insolubility by antibody cross linkage.

A number of techniques for the identification of autoantigens have been in use, since the discovery of autoantibodies. One approach that has been used for the discovery of neuronal surface-autoantigens in the past years relies on cultivated intact primary hippocampal neurons of rat embryos as antigen source followed by immunoprecipitation and mass spectrometry like in our protocol. Though it is focused on antibody-accessible surface proteins, and thus promises the discovery of immunosuppressable disease phenotypes it also has limitations. In particular, isolation and cultivation of these cells requires sophisticated technical skills and is highly labor-intensive. Moreover, intracellular antigens cannot be discovered by living cell-based immunoprecipitation. HIP provides better temporal flexibility as substrates can be prepared in bulk amounts and stored in aliquots for later use. In addition, cell surface and intracellular antigens are presented in their natural conformation and are accessible to antibody binding.

Compared to TIP, HIP immunoprecipitates showed fewer background bands and only weak IgG bands due to removal of unbound antibodies. This simplifies the selection of bands to be

TABLE 2 | Antigens identified using histo-immunoprecipitation (HIP) or tissue-immunoprecipitation (TIP).

Protein name/Entry name (UniProt)	Gene name and/or short name	Identification method	Subcellular localization	Reactivity of control sera in RC-indirect immunofluorescence assay	%	Publication
AP-3 complex subunit beta-2 (**AP3B2_HUMAN**)	AP3B2	HIP	Cytoplasm, membrane associated	0/149 HC	0%	(19)
Sodium/potassium-transporting ATPase subunit alpha-3 (**AT1A3_RAT**)	ATP1A3	HIP	Plasma membrane	0/37 HC	0%	(20)
CAP-Gly domain-containing linker protein 1 (**CLIP1_RAT**)	CLIP1	TIP	Cytoplasm	0/49 HC[a]	0%	(21)
Contactin-1 (**CNTN1_RAT**)/Contactin-associated protein 1 (**CNTP1_RAT**)	CNTN1/ CASPR1	HIP	Plasma membrane	0/48 HC 0/29 DC	0% 0%	(22)
Carnitine O-palmitoyltransferase 1, brain isoform (**CPT1C_RAT**)	CPT1C	HIP	Endoplasmic reticulum	0/44 HC	0%	
ELKS/Rab6-interacting/CAST family member 1 (**RB6I2_RAT**)	ERC1	TIP	Cytoplasm	0/49 HC 0/26 DC	0% 0%	(23)
Flotillin-1 (**FLOT1_RAT**) Flotillin-2 (**FLOT2_RAT**)	Flotillin1/2	HIP	Plasma membrane associated	0/226 HC 0/34 DC	0% 0%	(24)
Glutamate receptor ionotropic, delta-2 (**GRID2_HUMAN**)	GLURD2	HIP	Plasma membrane	0/205 HC	0%	(25)
GRIP1-associated protein 1 (**GRAP1_RAT**)	GRIPAP1	TIP	Cytoplasm, endosomes	0/50 HC[a]	0%	(26)
Hexokinase-1 (**HXK1_HUMAN**)	HK-1	HIP	Outer mitochondrial membrane	2/235 HC	0.85%	(27) (28)
Homer protein homolog 3 (**HOME3_RAT**)	HOMER3, Homer-3	HIP	Cytoplasm, plasma membrane associated	1/46 HC	2.17%	(29) (30)
Inositol 1,4,5-trisphosphate receptor type 1 (**ITPR1_RAT**)	ITPR1, IP3R1	HIP	Endoplasmic reticulum membrane	0/37 HC 0/34 DC	0% 0%	(31)
Potassium voltage-gated channel subfamily A member 2 (**KCNA2_RAT**)	KCNA2, Kv1.2	HIP	Plasma membrane	1/52 HC	1.92%	(32)
Electrogenic sodium bicarbonate cotransporter 1 (**S4A4_RAT**)	SCL4A4, NBCe1	HIP	Plasma membrane	19/235 HC 3/34 DC	8.08% 8.82%	
Neurochondrin (**NCDN_RAT**)	NCDN	TIP	Cytoplasm, partially plasma membrane associated	0/37 HC 0/33 DC	0% 0%	(33)
Regulator of G-protein signaling 8 (**RGS8_RAT**)	RGS8	TIP	Cytoplasm, plasma membrane associated	0/50 HCs[a] 0/14 DC[a]	0% 0%	
Rho-associated protein kinase 2 (**ROCK2_RAT**)	ROCK2	TIP	Cytoplasm	0/49 HC 0/39 DC	0% 0%	(24)
Ryanodine receptor 2 (**RYR2_RAT**)	RYR2	TIP	Endoplasmic reticulum membrane	0/50 HC[a]	0%	(34)
Syntaxin-1B (**STX1B_RAT**)	STX1b	HIP	Plasma membrane associated	0/45 HC 0/33 DC	0% 0%	
p229[b]		HIP	Cytoplasm	1/148 HC	0.68%	
p75[b]		HIP	Inner mitochondrial membrane	0/48 HC 0/42 DC	0% 0%	
p58[b]		HIP	Outer mitochondrial membrane	0/44 HC	0%	
p48[b]		TIP	Cell nuclei and cytoplasm	0/48 HC 0/33 DC	0% 0%	
p41/p43/p51 complex[b]		TIP	Cytoplasm	1/49 HC[a]	2.04%	

[a]*Analyzed via ELISA with purified recombinant antigen.*

[b]*Publication in progress.*

HC, healthy control; DC, disease control (sera with autoantibodies against known neuronal antigens).

analyzed in MALDI–TOF MS and reduces false identifications. HIP also has the potential to be used for target antigen identification in patients with other organ-specific or not organ-specific autoimmune diseases.

Using HIP, five cell surface proteins could be identified (**Table 2**). Among them GLURD2, KCNA2, and CNTN1/CASPR1 have previously been reported as neuronal autoantigens (22, 32, 35). Out of the 19 identified intracellular antigens 7 are known

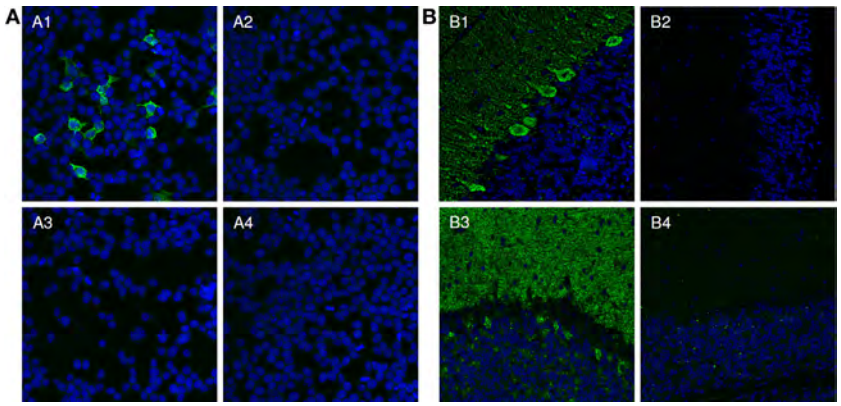

FIGURE 4 | Verification of identified antigens by indirect immunofluorescence. **(A)** Indirect immunofluorescence analysis of transfected HEK293 cells. Acetone-fixed recombinant HEK293 cells expressing the protein of interest (1, 3) or a mock-transfected control (2, 4) were incubated with patient serum (1, 2) or with control serum (3, 4) (both 1:1,000). Cell nuclei were counterstained with TO-PRO-3 iodide (blue). Only HEK293-expressing the protein of interest reacted with the patient sera (green). **(B)** Two examples for the neutralization of immunofluorescence reaction on neuronal tissues. Serum 1 and 2 (green) were pre-incubated with extracts of HEK293 cells transfected with empty control vector (1, 3) or the plasmid harboring the cDNA of interest and analyzed in an indirect immunofluorescence assay with rat cerebellar cryosections (2, 4). The extract containing the protein of interest greatly reduced or abolished the immune reaction of the serum on rat cerebellum (2, 4). The control extracts had no effect (1, 3). Nuclei were counterstained by incubation with TO-PRO-3 iodide (blue).

antigenic targets in autoimmune diseases (19, 21, 23, 26–29, 34). Moreover, we were able to identify 14 novel autoantigens. Not all of the antigens we identified are exclusively expressed in neural tissues. For some antigens like ATP1A3, ITPR1, or ROCK2 an expression in tumor samples of the respective index patient was observed, pointing to a paraneoplastic autoimmune background (20, 31, 36). Antigens like Flotillin1/2, GRIPAP1, or CLIP1 are also expressed in non-neural tissues without a tumor association (21, 24, 26). However, other autoantibodies, like AQP4 or DPPX which are established markers for neurological autoimmune diseases (37, 38) show also expression in non-neuronal tissues.

Following the successful identification of target autoantigens based on index samples, cohort studies including patients with similar neurological symptoms and disease as well as healthy controls must validate whether the discovered autoantibodies appear rarely or are common markers for specific phenotypes like autoantibody-mediated brain disorders or paraneoplastic neurological syndromes. For autoantibodies against ATP1A3, ITPR1, NCDN, and ROCK2 an association to autoimmune cerebellar syndromes has already been demonstrated by the authors (20, 31, 33, 36). Moreover, anti-Flotillin1/2 autoantibodies were found to be present in multiple sclerosis patients (24). Thus, the antigen identification strategy that we present offers a potent instrument for identifying unknown autoantigens and contributes to better diagnosis of autoimmune diseases.

AUTHOR CONTRIBUTIONS

MS, SK, SH, and RM were involved in immunoprecipitation, interpretation of data, antibody testing, and microscopy. MS and RM were involved in writing of the manuscript. NB and YD performed mass spectrometric analysis. NR, CR, SB, and CP performed molecular biology work. BT and WS were involved in supervising of antibody testing and microscopy. WS and LK were involved in the conception and organization of the research project and in writing of the manuscript.

ACKNOWLEDGMENTS

We thank Susann Satow, Laura Olejko, Jonas Joneleit, and Beatrice Witt for their excellent technical assistance.

SUPPLEMENTARY MATERIAL

The Supplementary Material for this article can be found online at https://www.frontiersin.org/articles/10.3389/fimmu.2018.01447/full#supplementary-material.

REFERENCES

1. Probst C, Saschenbrecker S, Stoecker W, Komorowski L. Anti-neuronal autoantibodies: current diagnostic challenges. *Mult Scler Relat Disord* (2014) 3(3):303–20. doi:10.1016/j.msard.2013.12.001
2. Li Q, Michel K, Annahazi A, Demir IE, Ceyhan GO, Zeller F, et al. Anti-Hu antibodies activate enteric and sensory neurons. *Sci Rep* (2016) 6:38216. doi:10.1038/srep38216
3. Lennon VA, Kryzer TJ, Pittock SJ, Verkman AS, Hinson SR. IgG marker of optic-spinal multiple sclerosis binds to the aquaporin-4 water channel. *J Exp Med* (2005) 202(4):473–7. doi:10.1084/jem.20050304
4. Dalmau J, Gleichman AJ, Hughes EG, Rossi JE, Peng X, Lai M, et al. Anti-NMDA-receptor encephalitis: case series and analysis of the effects of antibodies. *Lancet Neurol* (2008) 7(12):1091–8. doi:10.1016/S1474-4422(08)70224-2
5. Boronat A, Gelfand JM, Gresa-Arribas N, Jeong HY, Walsh M, Roberts K, et al. Encephalitis and antibodies to dipeptidyl-peptidase-like protein-6, a subunit of Kv4.2 potassium channels. *Ann Neurol* (2013) 73(1):120–8. doi:10.1002/ana.23756
6. Petit-Pedrol M, Armangue T, Peng X, Bataller L, Cellucci T, Davis R, et al. Encephalitis with refractory seizures, status epilepticus, and antibodies to the GABAA receptor: a case series, characterisation of the antigen, and analysis

of the effects of antibodies. *Lancet Neurol* (2014) 13(3):276–86. doi:10.1016/S1474-4422(13)70299-0
7. Sabater L, Gaig C, Gelpi E, Bataller L, Lewerenz J, Torres-Vega E, et al. A novel non-rapid-eye movement and rapid-eye-movement parasomnia with sleep breathing disorder associated with antibodies to IgLON5: a case series, characterisation of the antigen, and post-mortem study. *Lancet Neurol* (2014) 13(6):575–86. doi:10.1016/S1474-4422(14)70051-1
8. Lai M, Hughes EG, Peng X, Zhou L, Gleichman AJ, Shu H, et al. AMPA receptor antibodies in limbic encephalitis alter synaptic receptor location. *Ann Neurol* (2009) 65(4):424–34. doi:10.1002/ana.21589
9. Lai M, Huijbers MG, Lancaster E, Graus F, Bataller L, Balice-Gordon R, et al. Investigation of LGI1 as the antigen in limbic encephalitis previously attributed to potassium channels: a case series. *Lancet Neurol* (2010) 9(8):776–85. doi:10.1016/S1474-4422(10)70137-X
10. Lancaster E, Lai M, Peng X, Hughes E, Constantinescu R, Raizer J, et al. Antibodies to the GABA(B) receptor in limbic encephalitis with seizures: case series and characterisation of the antigen. *Lancet Neurol* (2010) 9(1):67–76. doi:10.1016/S1474-4422(09)70324-2
11. Gresa-Arribas N, Planaguma J, Petit-Pedrol M, Kawachi I, Katada S, Glaser CA, et al. Human neurexin-3alpha antibodies associate with encephalitis and alter synapse development. *Neurology* (2016) 86(24):2235–42. doi:10.1212/WNL.0000000000002775
12. Gure AO, Stockert E, Scanlan MJ, Keresztes RS, Jager D, Altorki NK, et al. Serological identification of embryonic neural proteins as highly immunogenic tumor antigens in small cell lung cancer. *Proc Natl Acad Sci U S A* (2000) 97(8):4198–203. doi:10.1073/pnas.97.8.4198
13. Bataller L, Sabater L, Saiz A, Serra C, Claramonte B, Graus F. Carbonic anhydrase-related protein VIII: autoantigen in paraneoplastic cerebellar degeneration. *Ann Neurol* (2004) 56(4):575–9. doi:10.1002/ana.20238
14. Jarius S, Wandinger KP, Horn S, Heuer H, Wildemann B. A new Purkinje cell antibody (anti-Ca) associated with subacute cerebellar ataxia: immunological characterization. *J Neuroinflammation* (2010) 7:21. doi:10.1186/1742-2094-7-21
15. Dalmau J, Furneaux HM, Gralla RJ, Kris MG, Posner JB. Detection of the anti-Hu antibody in the serum of patients with small cell lung cancer – a quantitative western blot analysis. *Ann Neurol* (1990) 27(5):544–52. doi:10.1002/ana.410270515
16. Honnorat J, Antoine JC, Derrington E, Aguera M, Belin MF. Antibodies to a subpopulation of glial cells and a 66 kDa developmental protein in patients with paraneoplastic neurological syndromes. *J Neurol Neurosurg Psychiatry* (1996) 61(3):270–8. doi:10.1136/jnnp.61.3.270
17. Stöcker W, Otte M, Ulrich S, Normann D, Finkbeiner H, Stocker K, et al. Autoimmunity to pancreatic juice in Crohn's disease. Results of an autoantibody screening in patients with chronic inflammatory bowel disease. *Scand J Gastroenterol Suppl* (1987) 139:41–52. doi:10.3109/00365528709089774
18. Koy C, Mikkat S, Raptakis E, Sutton C, Resch M, Tanaka K, et al. Matrix-assisted laser desorption/ionization-quadrupole ion trap-time of flight mass spectrometry sequencing resolves structures of unidentified peptides obtained by in-gel tryptic digestion of haptoglobin derivatives from human plasma proteomes. *Proteomics* (2003) 3(6):851–8. doi:10.1002/pmic.200300381
19. Darnell RB, Furneaux HM, Posner JB. Antiserum from a patient with cerebellar degeneration identifies a novel protein in Purkinje cells, cortical neurons, and neuroectodermal tumors. *J Neurosci* (1991) 11(5):1224–30. doi:10.1523/JNEUROSCI.11-05-01224.1991
20. Scharf M, Miske R, Heidenreich F, Giess R, Landwehr P, Blocker IM, et al. Neuronal Na+/K+ ATPase is an autoantibody target in paraneoplastic neurologic syndrome. *Neurology* (2015) 84(16):1673–9. doi:10.1212/WNL.0000000000001493
21. Griffith KJ, Ryan JP, Senecal JL, Fritzler MJ. The cytoplasmic linker protein CLIP-170 is a human autoantigen. *Clin Exp Immunol* (2002) 127(3):533–8. doi:10.1046/j.1365-2249.2002.01756.x
22. Querol L, Nogales-Gadea G, Rojas-Garcia R, Martinez-Hernandez E, Diaz-Manera J, Suarez-Calvet X, et al. Antibodies to contactin-1 in chronic inflammatory demyelinating polyneuropathy. *Ann Neurol* (2013) 73(3):370–80. doi:10.1002/ana.23794
23. Huijbers MG, Lipka AF, Potman M, Hensbergen PJ, Titulaer MJ, Niks EH, et al. Antibodies to active zone protein ERC1 in Lambert-Eaton myasthenic syndrome. *Hum Immunol* (2013) 74(7):849–51. doi:10.1016/j.humimm.2013.03.004
24. Hahn S, Trendelenburg G, Scharf M, Denno Y, Brakopp S, Teegen B, et al. Identification of the flotillin-1/2 heterocomplex as a target of autoantibodies in bona fide multiple sclerosis. *J Neuroinflammation* (2017) 14(1):123. doi:10.1186/s12974-017-0900-z
25. Miske R, Hahn S, Rosenkranz T, Müller M, Dettmann IM, Mindorf S, et al. Autoantibodies against glutamate receptor δ2 after allogenic stem cell transplantation. *Neurol Neuroimmunol Neuroinflamm* (2016) 3(4):e255. doi:10.1212/NXI.0000000000000255
26. Stinton LM, Selak S, Fritzler MJ. Identification of GRASP-1 as a novel 97 kDa autoantigen localized to endosomes. *Clin Immunol* (2005) 116(2):108–17. doi:10.1016/j.clim.2005.03.021
27. Gonzalez-Gronow M, Cuchacovich M, Francos R, Cuchacovich S, Fernandez Mdel P, Blanco A, et al. Antibodies against the voltage-dependent anion channel (VDAC) and its protective ligand hexokinase-I in children with autism. *J Neuroimmunol* (2010) 227(1–2):153–61. doi:10.1016/j.jneuroim.2010.06.001
28. Norman GL, Yang CY, Ostendorff HP, Shums Z, Lim MJ, Wang J, et al. Anti-kelch-like 12 and anti-hexokinase 1: novel autoantibodies in primary biliary cirrhosis. *Liver Int* (2015) 35(2):642–51. doi:10.1111/liv.12690
29. Zuliani L, Sabater L, Saiz A, Baiges JJ, Giometto B, Graus F. Homer 3 autoimmunity in subacute idiopathic cerebellar ataxia. *Neurology* (2007) 68(3):239–40. doi:10.1212/01.wnl.0000251308.79366.f9
30. Höftberger R, Sabater L, Ortega A, Dalmau J, Graus F. Patient with homer-3 antibodies and cerebellitis. *JAMA Neurol* (2013) 70(4):506–9. doi:10.1001/jamaneurol.2013.1955
31. Jarius S, Scharf M, Begemann N, Stocker W, Probst C, Serysheva II, et al. Antibodies to the inositol 1,4,5-trisphosphate receptor type 1 (ITPR1) in cerebellar ataxia. *J Neuroinflammation* (2014) 11:206. doi:10.1186/s12974-014-0206-3
32. Hart IK, Waters C, Vincent A, Newland C, Beeson D, Pongs O, et al. Autoantibodies detected to expressed K+ channels are implicated in neuromyotonia. *Ann Neurol* (1997) 41(2):238–46. doi:10.1002/ana.410410215
33. Miske R, Gross CC, Scharf M, Golombeck KS, Hartwig M, Bhatia U, et al. Neurochondrin is a neuronal target antigen in autoimmune cerebellar degeneration. *Neurol Neuroimmunol Neuroinflamm* (2017) 4(1):e307. doi:10.1212/NXI.0000000000000307
34. Mygland A, Tysnes OB, Matre R, Volpe P, Aarli JA, Gilhus NE. Ryanodine receptor autoantibodies in myasthenia gravis patients with a thymoma. *Ann Neurol* (1992) 32(4):589–91. doi:10.1002/ana.410320419
35. Shiihara T, Kato M, Konno A, Takahashi Y, Hayasaka K. Acute cerebellar ataxia and consecutive cerebellitis produced by glutamate receptor delta2 autoantibody. *Brain Dev* (2007) 29(4):254–6. doi:10.1016/j.braindev.2006.09.004
36. Popkirov S, Ayzenberg I, Hahn S, Bauer J, Denno Y, Rieckhoff N, et al. Rho-associated protein kinase 2 (ROCK2): a new target of autoimmunity in paraneoplastic encephalitis. *Acta Neuropathol Commun* (2017) 5(1):40. doi:10.1186/s40478-017-0447-3
37. Radicke S, Cotella D, Graf EM, Ravens U, Wettwer E. Expression and function of dipeptidyl-aminopeptidase-like protein 6 as a putative beta-subunit of human cardiac transient outward current encoded by Kv4.3. *J Physiol* (2005) 565(Pt 3):751–6. doi:10.1113/jphysiol.2005.087312
38. Zhu C, Chen Z, Jiang Z. Expression, distribution and role of aquaporin water channels in human and animal stomach and intestines. *Int J Mol Sci* (2016) 17(9):E1399. doi:10.3390/ijms17091399

Conflict of Interest Statement: MS, RM, SK, SH, YD, NB, NR, CR, SB, CP, BT, and LK are employees of the Euroimmun AG, a company that develops, produces, and manufactures immunoassays for the detection of disease-associated antibodies. WS is member of the Board of the Euroimmun AG.

frontiers in Immunology

ORIGINAL RESEARCH
published: 05 July 2018
doi: 10.3389/fimmu.2018.01551

Epistatic Interactions Between Mutations of Deoxyribonuclease 1-Like 3 and the Inhibitory Fc Gamma Receptor IIB Result in Very Early and Massive Autoantibodies Against Double-Stranded DNA

*Thomas Weisenburger[1], Bettina von Neubeck[1], Andrea Schneider[1], Nadja Ebert[1], Daniel Schreyer[1], Andreas Acs[1] and Thomas H. Winkler[1,2]**

[1] Department of Biology, Nikolaus-Fiebiger-Center for Molecular Medicine, Friedrich-Alexander-University Erlangen-Nuremberg, Erlangen, Germany, [2] Medical Immunology Campus Erlangen, Friedrich-Alexander-University Erlangen-Nuremberg, Erlangen, Germany

OPEN ACCESS

Edited by:
Ralf J. Ludwig, Universität zu Lübeck, Germany

Reviewed by:
SunAh Kang, University of North Carolina at Chapel Hill, United States
Rudolf Armin Manz, Universität zu Lübeck, Germany

***Correspondence:**
Thomas H. Winkler
thomas.winkler@fau.de

Specialty section:
This article was submitted to Immunological Tolerance and Regulation, a section of the journal Frontiers in Immunology

Received: *03 February 2018*
Accepted: *22 June 2018*
Published: *05 July 2018*

Citation:
Weisenburger T, von Neubeck B, Schneider A, Ebert N, Schreyer D, Acs A and Winkler TH (2018) Epistatic Interactions Between Mutations of Deoxyribonuclease 1-Like 3 and the Inhibitory Fc Gamma Receptor IIB Result in Very Early and Massive Autoantibodies Against Double-Stranded DNA. Front. Immunol. 9:1551. doi: 10.3389/fimmu.2018.01551

Autoantibodies against double-stranded DNA (anti-dsDNA) are a hallmark of systemic lupus erythematosus (SLE). It is well documented that anti-dsDNA reactive B lymphocytes are normally controlled by immune self-tolerance mechanisms operating at several levels. The evolution of high levels of IgG anti-dsDNA in SLE is dependent on somatic hypermutation and clonal selection, presumably in germinal centers from non-autoreactive B cells. Twin studies as well as genetic studies in mice indicate a very strong genetic contribution for the development of anti-dsDNA as well as SLE. Only few single gene defects with a monogenic Mendelian inheritance have been described so far that are directly responsible for the development of anti-dsDNA and SLE. Recently, among other mutations, rare null-alleles for the deoxyribonuclease 1 like 3 (*DNASE1L3*) and the Fc gamma receptor IIB (*FCGR2B*) have been described in SLE patients and genetic mouse models. Here, we demonstrate that double Dnase1l3- and FcgR2b-deficient mice in the C57BL/6 background exhibit a very early and massive IgG anti-dsDNA production. Already at 10 weeks of age, autoantibody production in double-deficient mice exceeds autoantibody levels of diseased 9-month-old NZB/W mice, a long established multigenic SLE mouse model. In single gene-deficient mice, autoantibody levels were moderately elevated at early age of the mice. Premature autoantibody production was accompanied by a spontaneous hyperactivation of germinal centers, early expansions of T follicular helper cells, and elevated plasmablasts in the spleen. Anti-dsDNA hybridomas generated from double-deficient mice show significantly elevated numbers of arginines in the CDR3 regions of the heavy-chain as well as clonal expansions and diversification of B cell clones with moderate numbers of somatic mutations. Our findings show a strong epistatic interaction of two SLE-alleles which prevent early and high-level anti-dsDNA autoantibody production. Both genes apparently synergize to keep in check excessive germinal center reactions evolving into IgG anti-dsDNA antibody producing B cells.

Keywords: Dnase1l3, anti-DNA autoantibodies, systemic lupus erythematosus, Fcgr2b, germinal center

INTRODUCTION

The formation of antibodies against DNA is considered to be the serologic hallmark of systemic lupus erythematosus (SLE). Autoantibodies against double-stranded DNA (anti-dsDNA) antibodies are the most studied and the most enigmatic autoantibodies in SLE. Their presence correlates with nephritis both in human SLE patients and in mice with a spontaneous lupus-like disease (1–3).

Systemic lupus erythematosus has a strong genetic component as demonstrated by high concordance rates for disease manifestation as well as autoantibody development in monozygotic twins (4, 5). In rare cases, a monogenic cause for the development of SLE-like disease and autoantibody production illustrates the pathways that predispose for SLE. The strongest associations were found to loss of function of genes that are involved in clearance of apoptotic cells, chromatin, and nucleic acids (6). Homozygous mutations in the *C1q* genes are responsible for SLE or SLE-like disease (7) and *C1q*-deficient mice accumulate apoptotic cells in several tissues and develop anti-DNA autoantibodies and SLE in certain genetic backgrounds but not in the C57BL/6 background (8, 9). Homozygous mutations in the *TREX1* gene encoding a DNA exonuclease present in the cytoplasm are associated with the Aicardi–Goutieres syndrome-1 with increased systemic type I interferon levels and antinuclear autoantibodies (10). Likewise, *Trex1*-deficient mice develop autoantibodies and SLE-like disease.

Other apparently monogenic causes of SLE-like disease and anti-DNA autoantibodies were described in mutant mice. The deficiency of the IgG inhibitory Fc γ receptor IIB (FcγRIIB) is associated with the development of SLE in mice with a strong influence of background genes, however (11, 12). In the absence of FcγRIIB, autoreactive B cells are found in the germinal centers and somatic hypermutation contributed to anti-DNA reactivity (13). In mice, a promoter variant in the *Fcgr2b* gene results in enhanced germinal center responses and autoantibody production (14). A defunctioning single nucleotide polymorphism (SNP) in the human *FCGR2B* gene is associated with susceptibility to SLE (15) and the upregulation of FcγRIIB in memory B cells is decreased in SLE patients (16). In addition, FcγRIIB plays an important regulatory function on dendritic cells (DCs), macrophages, and neutrophils [reviewed in Ref. (17)].

Another single gene defect leading to anti-DNA production and SLE-like disease is demonstrated by the observation that milk fat globule-EGF factor 8 has a critical role in removing apoptotic B cells in the germinal centers and that its absence can lead to autoimmune diseases (18).

More recently, deficiency in the *Deoxyribonuclease 1 like 3* gene (*DNASE1L3*) was associated with SLE-like disease in Arabian, Turkish, and Italian families (19–21). SLE-like symptoms were associated with a hypocomplementemic urticarial vasculitis syndrome in several clinical cases. In *Dnase1l3*-deficient mice, anti-dsDNA autoantibodies develop, followed by a late onset of SLE-like disease (22). Dnase1l3 is part of four homologous mammalian extracellular deoxyribonucleases of the Dnase1 family, Dnase1, Dnase1l1, Dnase1l2, and Dnase1l3 (23).

Here, we describe a new conditional mouse model for Dnase1l3 deficiency and confirm the early appearance of IgG anti-dsDNA autoantibodies at moderate levels in the serum of these mice. The development of anti-dsDNA antibodies does not require the presence of toll-like receptor 9 (TLR9) but a strong epistatic interaction with a mutation in the Fcgr2b gene leads to strikingly early and high anti-dsDNA serum levels accompanied by spontaneous hyperactivation of germinal centers.

MATERIALS AND METHODS

Mice

Mice were maintained in SPF conditions at the animal facility of the Friedrich-Alexander-University, Erlangen. C57BL/6 mice were obtained from Charles River, Sulzfeld, Germany. TLR9-deficient mice (24) were a kind gift of H. Wagner, Munich. Fcgr2b-deficient mice (25) backcrossed for 12 generations to C57BL/6 were obtained from Taconic and the *yaa* mutation was introduced by breeding in the *yaa* mutation from male B6.SB-Yaa/J mice obtained from the Jackson laboratory. For the generation of Dnase1l3-deficient mice, a targeting vector was obtained from the KOMP consortium (project CSD48807, clone HTGRS01006_A_B09) and partially re-sequenced. Standard techniques were used to transfect the V6.5 embryonic stem cell line (kindly provided by R. Jaenisch, Boston) derived from a C57BL/6x129Sv F1 cross (26). Homologous recombination was screened with left arm and right arm primers by PCR using LongAmp® Taq (New England Biolabs) according to the instructions of the manufacturer. Primers are listed in the Primer List in Data Sheet S2 in Supplementary Material. Correct integration was further verified by sequencing of the PCR products from both sides of the genomic integration. ES cells were injected into C57BL/6 blastocysts and chimeric mice were crossed with C57BL/6 mice. After germline transmission, one line was kept on C57BL/6x129sv mixed background. A pure backcross to C57BL/6 background was obtained by marker-assisted speed-congenics using 74 genomic SNP markers (LGC Genomics, KASP genotyping) covering all mouse chromosomes. After five generations, heterozygous offspring mice containing all marker loci from C57BL/6 were intercrossed to obtain C57BL/6 "knockout-first" Dnase1l3-deficient mice. After crossing with flp-deleter mice (27), Dnase1l3-deficient mice with a deleted exon 2 were created. For the establishment of Dnase1l3/Fcgr2b double-deficient mice, male Fcgr2b$^{-/-}$ *yaa* mice were intercrossed with C57BL/6 "knockout-first" Dnase1l3-deficient mice. In the F2 generation, homozygous Dnase1l3/Fcgr2b double-deficient male and female mice were selected and used for further breeding. Animal care and experiments were approved by the animal ethics committee of Regierung von Mittelfranken (Animal Ethics Number: 54-2532.1-21/09 and TS-05/5).

Flow Cytometric Analysis

For cell sorting of macrophage and DC cell populations, spleen, liver, lung, brain, and lamina propria tissue from 8- to 14-week-old C57BL/6 mice was mechanically dissociated with a gentle MACS™ and the respective tissue dissociation kit (Miltenyi Biotec). Bone marrow cells were flushed from femurs of C57BL/6 mice. For analysis of germinal center cells and myeloid cells, spleens were harvested, crushed through a 100 μM nylon mesh filter and resuspended in RPMI 1640 medium (PAN-Biotech) supplemented with

10% FCS. After erythrocyte lysis (5 min at room temperature in 0.15 M NH_4Cl, 0.02 M HEPES, 0.1 mM EDTA), cells were washed two times and resuspended in FACS buffer (PBS, 2% FCS, 1 mM EDTA) for staining with directly conjugated antibodies. For intracellular IFN-γ staining, cells were treated with Cell Stimulation Cocktail + Protein Transport Inhibitors (eBioscience) for 2 h at 37°C. Cells were stained extracellularly for T_{FH} markers and were fixed and permeabilized with the FIX & PERM Kit (Nordic-MUbio) according to the manufacturer's protocol. The following antibody conjugates were obtained from BioLegend: CD45-BV421, CD19-BV421, CD38-PE, GL7-APC, CD95-PECy7, CD11b-BV510, CD11b-PECy7, CD11c-APCCy7, LY6C-PerCPCy5.5, LY6G-FITC, CXCR5-BV421, and PD1-PECy7. The following antibody conjugates were obtained from eBioscience: MHCII-PE, CD4-FITC, CD44-APC, CD8-FITC, B220-PerCPCy5.5, IgD-PE, IgM-FITC, CD21-FITC, CD23-PE, and F4/80-AF647. BV510-conjugated anti-PSGL-1 and BV421-conjugated anti-F4/80 were obtained from BD Biosciences. APC-conjugated anti-Siglec-H was obtained from Miltenyi Biotec. Flow cytometry analysis was performed on a Cytoflex instrument (Beckman Coulter) and FlowJo v10.4 analysis software (FlowJo, LLC).

ELISA for Anti-dsDNA Autoantibodies

Levels of anti-dsDNA were measured by ELISA. 20 µg/ml % poly-L-lysine (Sigma-Aldrich) was used to precoat MaxiSorp plates (Nunc). After 2 h at RT, plates were coated with dsDNA from calf thymus (20 µg/ml; Sigma-Aldrich) in TE (pH 7.5) buffer overnight at 4°C. Plates were washed with PBS/0.05% Tween 20 and sera was added in 1/2 serial dilutions starting at 1/100. A serum pool obtained from 9-month-old diseased NZB/W mice served as internal standard. The starting dilution of 1/200 of the NZB/W serum was arbitrarily assigned to 100 relative units. Goat-anti-mouse IgG or goat-anti-mouse IgM, Fc-specific, coupled to horseradish peroxidase was used for detection (Jackson ImmunoResearch).

Gene Expression by Quantitative RT-PCR (qRT-PCR)

For qRT-PCR, RNA from FACS sorted cells was isolated by the RNeasy kit (QIAGEN) according to the manufacturer's instructions. cDNA was synthesized by SCRIPTUM reverse transcriptase (Bio&Sell), and qRT-PCR was performed on a quantitative PCR system (Biorad CFX96) with Absolute qPCR SYBR Green Mix 2× (Thermo Scientific) using intron-spanning primers for Dnase1l3 and HPRT (see Primer List in Data Sheet S2 in Supplementary Material). In a second set of experiments, TaqMan® Assays for Dnase1l3 and GAPDH were performed on an Applied Biosystems 7500 machine. Calculation of relative expression levels were performed according to the relative ΔCt-method (28).

Hybridoma Production and Sequencing of V Region Genes

Hybridomas were generated from three female double-deficient mice that previously had a rise of IgG anti-dsDNA autoantibodies in the serum. As a fusion partner, SP2/0 cells obtained originally from F. Melchers, Basel were used. Standard techniques were applied and hybridoma supernatants were tested on day 10 after fusion for IgG anti-dsDNA antibodies by ELISA. Hybridoma cells from positive wells were expanded and subcloned by single cell sorting at least once.

Total RNA was isolated from the hybridomas with RNeasy (Qiagen) and variable genes of the hybridomas were cloned with RT-PCR using universal V_H- and V_L-primers (see Primer List in Data Sheet S2 in Supplementary Material) and the StrataClone PCR Cloning Kit. Inserts were Sanger sequenced with M13 primers annealing to the plasmid vector (LGC Genomics). The analysis for VH and VL gene usage, CDR-assignment and for potential somatic mutations was performed by V-QUEST (29) at the IMGT website.[1] Sequence alignment was created with the Geneious Software (Biomatters Ltd.).

RESULTS

Expression of *Dnase1l3* in Hematopoietic Cells

It was described that *Dnase1l3* is primarily expressed in macrophages in liver and spleen (30). To obtain a more detailed view of the expression pattern of *Dnase1l3* in hematopoietic cells in different tissues, we isolated lymphocyte, monocyte, macrophage, and DC populations from blood, bone marrow, spleen, lymph node, peritoneal cavity, liver, lung, brain, and lamina propria of the colon by FACS sorting and analyzed expression of *Dnase1l3* by quantitative real-time PCR. The results are summarized in **Table 1**. Among lymphocytes, a low-level expression of *Dnase1l3* was found in B1a B cells and marginal zone B cells, whereas conventional B cells as well as T cells did show no detectable expression. We did not detect any expression of *Dnase1l3* in different blood or tissue monocytes, including inflammatory monocytes from mice infected with the murine cytomegalovirus. Also, granulocytes did not exhibit detectable expression. As described before (22), conventional DCs in the spleen but also in liver and lamina propria expressed the highest levels of *Dnase1l3*. Among tissue resident macrophages, we detected a more complex expression pattern. Red pulp macrophages from spleen, Kupffer cells from liver, as well as macrophages from the lamina propria expressed very high levels, whereas macrophages isolated from the bone marrow, the peritoneum, the brain (microglia), and lung (alveolar macrophages) showed no detectable expression. Lower levels were detected in subcapsular sinus macrophages as well as plasmacytoid DCs. In summary, we detected Dnase1l3 expression mainly in antigen-presenting cell populations like conventional DCs and B1a and marginal zone B cells as well as in some tissue resident macrophages.

Generation of Conditional Dnase 1l3-Deficient Mice

To study the physiological function of Dnase1l3, we generated Dnase1l3-deficient mice using the "knockout-first" strategy as described by Skarnes et al. (31). The knockout-first allele is initially a non-expressive form, but can be converted to a conditional allele after recombination with Flp recombinase (Figure S1A in

[1] www.imgt.org (Accessed: April, 2016–March, 2018).

TABLE 1 | Expression levels of Dnase1l3 in mouse hematopoietic cells.

Cell population; organ	Phenotype used for FACS sorting	Relative expression levels[a]
Pre/pro B cells, bone marrow	$B220^+$ IgM^-	–
Immature B cells, bone marrow	$B220^+$ IgM^+ IgD^-	–
Follicular B cells, spleen	$B220^+$ $CD21^{lo}$ $CD23^{hi}$	–
Marginal zone B cells, spleen	$B220^+$ $CD21^{hi}$ $CD23^{lo}$	+
B1a B cells, peritoneum	$B220^+$ $CD11b^+$ $CD5^+$	+
T cells, spleen	$B220^-$ $CD3^+$	–
Monocytes, non-classical, blood	$CD45^+$ $CD11b^+$ $Ly6C^+$ $MHCII^{lo}$	–
Monocytes, classical, blood	$CD45^+$ $CD11b^+$ $Ly6C^-$ $MHCII^{lo}$	–
Monocytes, peritoneum	$CD45^+$ $CD11b^{hi}$ $F4/80^{lo}$ $MHCII^+$	–
Monocytes, spleen	$CD45^+$ $CD11b^+$ $Ly6C^+$ $MHCII^{lo}$	–
Monocytes, lung	$CD45^+$ $CD11b^+$ $LY6C^+$ $MHCII^{lo}$	–
Monocytes, bone marrow	$CD45^+$ $CD11b^+$ $Ly6C^+$ $MHCII^{lo}$	–
Monocytes, lung, mCMV infection	$CD45^+$ $CD11b^+$ $LY6C^+$ $MHCII^+$	–
Neutr. granulocytes, bone marrow	$CD45^+$ $Ly\text{-}6G^{hi}$	–
Plasmacytoid dendritic cells (DCs)	$CD45^+$ $CD11c^{lo}$ $SiglecH^+$	+
Myeloid DCs, spleen	$CD11c^{++}$ MHC^{++} $CD11b^+$ $CD8^-$	+++
Lymphoid DCs, spleen	$CD11c^{++}$ MHC^{++} $CD11b^-$ $CD8^+$	+++
DCs, liver	$CD11b^+$ $CD11c^+$ $Ly6C^-$ $MHCII^{++}$	++
DCs, lamina propria colon	$CD11b^+$ $CD11c^+$ $Ly6C^-$ $MHCII^{++}$	+++
Microglia, brain	$CD45^{lo}$ $F4/80^+$ $CD11b^+$	–
Macrophages, bone marrow	$CD45^+$ $F4/80^+$ $CD11b^{low}$ $CD11c^-$	–
Macrophages, peritoneum	$CD45^+$ $F4/80^{++}$ $CD11b^+$ $CD11c^{lo}$	–
Alveolar macrophages, lung	$CD45^+$ $F4/80^+$ $CD11b^{low}$ $CD11c^{++}$	–
Macrophages, spleen	$CD45^+$ $F4/80^+$ $CD11b^{low}$ $CD11c^-$	+++
Kupffer cells, liver	$CD45^+$ $F4/80^+$ $CD11b^{low}$ $CD11c^-$	+++
Macrophages, lamina propria colon	$CD45^+$ $F4/80^+$ $CD11b^{low}$ $CD11c^-$	++
Subcapsular sinus macrophages, LN	$CD11b^+$ $CD169^+$ $CD11c^-$ $F4/80^-$	+

Relative expression levels as determined by quantitative real-time PCR from sorted cells. Summary of two to five individual experiments, each.

[a]*Relative expression levels as compared to expression levels in spleen $CD11c^{hi}$ DCs.*

–, not detectable; +, 1–5% of DCs; ++, 5–20% of DCs; +++, 20–100% of DCs.

Supplementary Material). Transcripts are forced to be spliced from exon 1 of the Dnase1l3 gene to the splice acceptor side of a lacZ reporter and terminated by the downstream polyA sides. This should result in a knockout allele, as downstream exons are not transcribed (Figures S1A,B in Supplementary Material). To verify that downstream exons are not transcribed from the knockout-first allele [allele name termed $Dnase1l3^{tm1a(KOMP)Wtsi}$ according to Skarnes et al. (31), abbreviated as $Dnase1l3^{tm1a}$], we used cDNA from MACS-enriched DCs from spleens of homozygous and littermate mice in an RT-PCR reaction using primers located in downstream exons 5 and 7 (Figure S1B in Supplementary Material). As shown in Figure S1C in Supplementary Material, transcripts from the mutated allele were undetectable by this sensitive PCR reaction. This shows that the knockout-first allele is a null allele, as expected from the analysis of many similar alleles generated by the KOMP program (32). We also crossed mice with the knockout-first allele with E2a-Cre deleter mice (33) to obtain an exon 2 knockout allele missing exon 2 which will be termed $Dnase1l3^{\Delta ex2}$.

Development of Anti-dsDNA Autoantibodies in Dnase1l3-Deficient Mice

We analyzed serum IgG anti-dsDNA autoantibodies from groups of mice at different ages. As shown in **Figure 1A**, homozygous Dnase1l3-deficient mice showed significantly elevated IgG anti-dsDNA antibody levels already at young age (3–4 months). At later time points (**Figures 1B–D**), these titers show only a moderate increase. Dnase1l3-deficient mice at 1-year of age still have significantly, but modestly increased IgG anti-dsDNA titers. All groups except group 4 in **Figure 1B** are derived from mice in a mixed 129 × C57BL/6 background. For the group of mice at the age of 18–26 weeks fully congenic C57BL/6 mice have similar anti-dsDNA antibody levels, suggesting that the mixed genetic background of the mice had little if any influence on the development of anti-dsDNA antibodies (**Figure 1B**). For a cohort of 16- to 28-week-old mice, the influence of the sex on the development of autoantibodies was analyzed. As shown in Figure S2 in Supplementary Material a tendency for higher anti-dsDNA autoantibodies in female versus male mice was observed, which was not statistically significant. In addition, we analyzed homozygous $Dnase1l3^{\Delta ex2}$ mice with a complete deletion of exon 2 of *Dnase1l3* and found similar levels of anti-dsDNA autoantibodies as compared to mice with a homozygous $Dnase1l3^{tm1a}$ mutation, further supporting the notion that $Dnase1l3^{tm1a}$ mutation is a null mutation (**Figure 2A**). Thus, Dnase1l3-deficient mice spontaneously develop moderate levels of anti-DNA autoantibodies already at 3-month of age which are not increasing significantly upon aging. Neither a significant contribution of residual 129 genetic background nor any significant influence of the sex of the mice influenced anti-dsDNA autoantibodies.

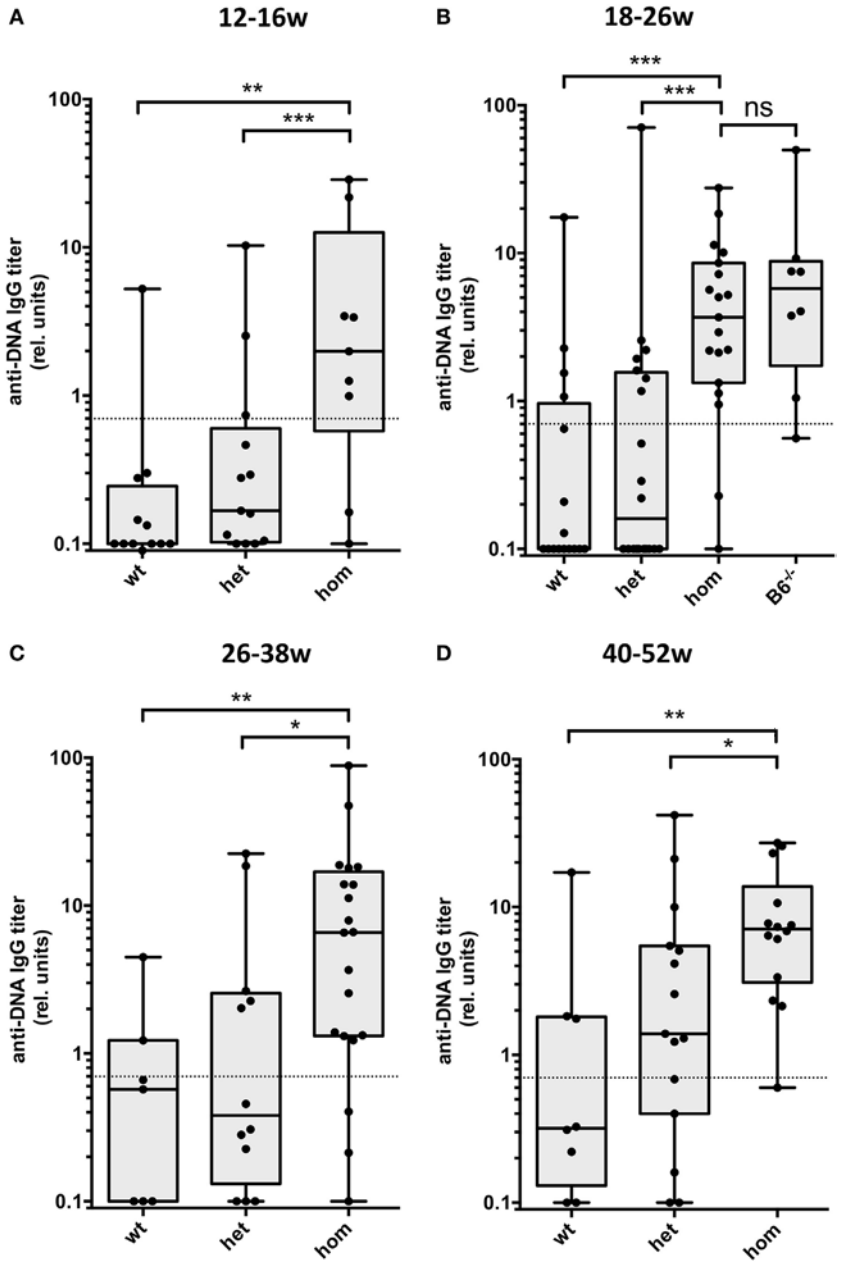

FIGURE 1 | Development of IgG autoantibodies against double-stranded DNA (anti-dsDNA) antibodies in Dnase1l3-deficient mice. Sera from mice at the age of **(A)** 12–16 weeks, **(B)** 18–26 weeks, **(C)** 26–38 weeks, and **(D)** 40–52 weeks were tested for IgG anti-dsDNA antibodies by ELISA. The mice are grouped according to the genotype of the Dnase1l3^{tm1a} mutation. All cohorts of mice are derived from 129 × C57BL/6 mixed background except homozygous mutant mice in **(B)** which are backcrossed to pure C57BL/6 background (B6$^{-/-}$). Relative binding units are presented as compared to a standard serum pool from 9-month-old NZB/W mice. The dotted lines represent a cutoff derived from a panel of sera from C57BL/6 mice. Data are presented as box plot with individual data represented by filled circles (*$p < 0.05$; **$p < 0.01$; ***$p < 0.001$ Mann–Whitney *U* test).

Epistatic Interactions With Other Mutations Involved in the Generation of Anti-dsDNA Antibodies

As anti-dsDNA autoantibody levels remained moderately elevated in Dnase1l3-deficient mice up to an age of 1 year, we asked the question whether other relevant single mutations might influence anti-dsDNA autoantibody titers. First, we intercrossed Dnase1l3-deficient mice with TLR9-deficient mice to obtain double-deficient mice. As demonstrated in **Figure 2A**, additional TLR9-deficiency had no significant influence on anti-dsDNA titers in Dnase1l3-deficient mice. We also generated double-deficient mice for *Dnase1l3* and Fcgr2b in which male mice in addition contain the *yaa* mutation accelerating SLE-like disease

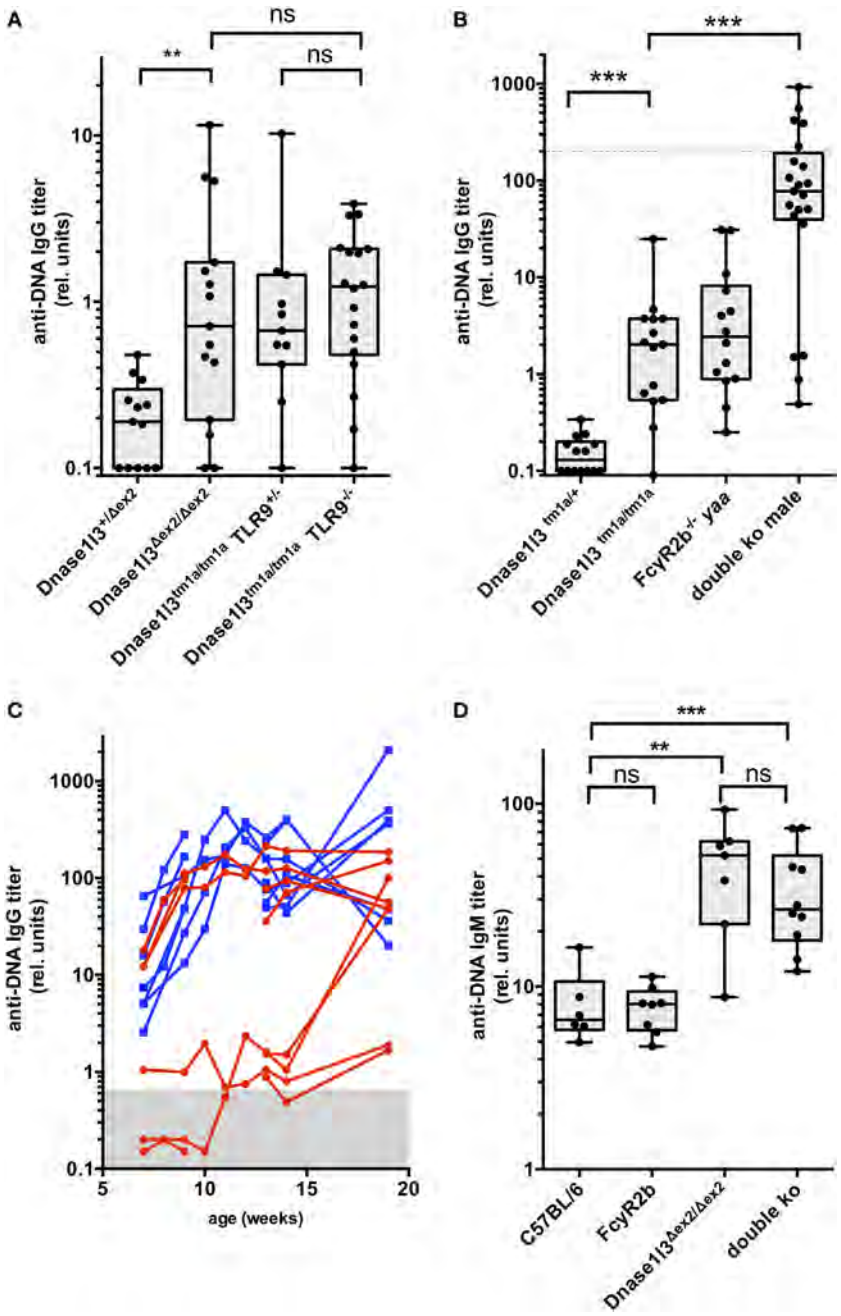

FIGURE 2 | Development of IgG and IgM autoantibodies against double-stranded DNA (anti-dsDNA) antibodies in double-deficient mice. In **(A)**, the results from 3- to 4-month-old toll-like receptor 9 (TLR9) × Dnase1l3 mice are displayed. The genotypes of the mice are denoted at the axis. In **(B)**, the results from 3-month-old FcgR2b × Dnase1l3 mice are displayed. The genotypes of the mice are denoted at the axis. The dotted lines represent anti-dsDNA antibody levels of a serum pool of 9-month-old female NZB/W mice. Data are presented as box plot with individual data represented by filled circles. **(C)** Follow-up of IgG anti-dsDNA autoantibody levels in individual female FcgR2b × Dnase1l3 double-deficient mice (red) and male FcgR2b *yaa* × Dnase1l3 double-deficient mice (blue). In **(D)**, the IgM anti-dsDNA levels from a cohort of 2- to 3-month-old FcgR2b × Dnase1l3 mice are displayed. The genotypes of the mice are denoted at the axis. Data are presented as box plot with individual data represented by filled circles (*$p < 0.05$; **$p < 0.01$; ***$p < 0.001$ Mann–Whitney *U* test).

in the FcγRIIB-deficient background (12). As shown in **Figure 2B**, we observed extremely high anti-dsDNA titers in double-deficient male mice at the age of 3-month reaching anti-dsDNA levels similar to 9-month-old NZB/W female mice. At this age, FcγRIIB$^{-/-}$ *yaa* male mice had anti-dsDNA titers comparable to single Dnase1l3-deficient mice which were around 50-fold lower than in male double-deficient mice (**Figure 2B**).

Since these anti-dsDNA antibody levels in double-deficient male mice were higher than in any other SLE-prone strain of mice including MRL/lpr and NZB/W mice at the same age, we weekly

analyzed anti-dsDNA antibodies in sera starting at the age of 7 weeks. We included also female mice in this analysis. As shown in **Figure 2C**, already at the age of 7 weeks all male mice (blue curves in **Figure 2C**) had clearly elevated anti-dsDNA serum levels that might have be transferred from the double-deficient mothers *via* placental transfer. We consider this unlikely, however, as some female littermate mice at the same age had normal levels of anti-dsDNA antibodies in their sera (**Figure 2C**). In all male mice of this cohort and in three out of six female mice which we analyzed at this young age, IgG anti-dsDNA antibody levels massively increased within 3–5 weeks up to 50-fold, reaching a maximum level around 10–12 weeks of age. Most of the other female mice developed these maximum levels of autoantibodies at the age of 15–20 weeks. Thus, mutations in *Dnase1l3* and Fcgr2b show strong epistasis and the *yaa* mutation further increases the penetrance of early hyperproduction of anti-dsDNA antibodies in male mice in this model.

As IgM anti-DNA autoantibodies typically develop early in SLE models, we analyzed IgM anti-dsDNA levels in a cohort of 2- to 3-month-old animals of the different genotypes. Interestingly, Dnase1l3 single-deficient mice show highly elevated IgM anti-dsDNA autoantibodies comparable to double-deficient mice, whereas FcγRIIB-knockout mice had normal IgM anti-dsDNA levels (**Figure 2D**). Thus, loss of tolerance toward DNA is an early event in Dnase1l3-deficient mice.

Spontaneous Germinal Center Formation and Elevated Production of Anti-dsDNA Secreting Cells in Dnase1l3 and FcγRIIB Double-Deficient Mice

We have proposed earlier that anti-dsDNA antibodies evolve from non-autoreactive progenitors in germinal centers (34, 35) and strong evidence has been accumulated that the FcγRIIB plays an important role in B cell tolerance in the GC (17). We therefore analyzed spontaneous germinal center development in double-deficient mice at the age of 9–14 weeks. As shown in **Figure 3A**, all male double-deficient mice had elevated frequencies of $CD38^{lo}$, $GL7^{+}$, Fas^{+} GC B cells in the spleen when compared to both single deficient male or female mice or wild-type C57BL/6 mice. In this cohort, one out of five female double-deficient mice showed a dramatically elevated GC B cell frequency. Therefore, the early and strong anti-dsDNA antibody response is accompanied by GC hyperactivation in double-deficient mice.

The activation of B cells in the spleens of double-deficient mice is also accompanied by high frequencies of IgG—antibody secreting plasma blasts or plasma cells (**Figure 3B**). Up to 3% of all B cells were found to be IgG antibody secreting cells, suggesting a considerable hyperactivation of the B cell compartment. Only a fraction of these IgG secreting B cells was anti-dsDNA specific (0.6–3.8% of all IgG secreting cells, **Figures 3B,C**).

Analysis of Somatic Hypermutation in IgG Anti-dsDNA Hybridomas

To gain further insight into the mechanism of anti-dsDNA development in double-deficient mice, we prepared hybridomas from spleens of unimmunized mice and selected IgG anti-dsDNA hybridomas for the sequence analysis of V_H- and in selected case also V_L-genes. For this analysis, we focused on female double-deficient mice that were selected for previous rise of IgG anti-dsDNA autoantibodies before fusion. Data for the V_H-genes are summarized in **Table 2**. Most hybridoma clones used the IgG2c isotype (25/31 clones) followed by a few IgG2b and one IgG3 anti-dsDNA hybridoma, similar to anti-DNA autoantibodies in other SLE-prone mice (36). In all three mice that were used for the generation of hybridomas we observed clonally related hybridomas clearly derived from one B cell and diversified by somatic mutations. We detected somatic mutations in the heavy chains of all hybridomas (**Table 2**; Figure S3 in Supplementary Material). In many cases, the numbers of mutations within the V_H and V_L gene region were relatively low with few replacement mutations present. For those clones that contributed with three or more individual hybridomas, we analyzed the diversification from the germline sequence as well as intraclonal diversification in more detail. Very few shared mutations were observed within the clonal relatives as shown in Figure S3 in Supplementary Material suggesting a "bush-like" diversification by somatic hypermutation from a single B cell rather than a stepwise maturation with intermediate selection.

We found that the CDR3 regions of the heavy chains of the hybridomas have an unusually high frequency of arginines, as it has been noted before in collections of anti-dsDNA hybridomas from SLE-prone mouse strains (39). Whereas 6,203 arginines can be found among 166,000 amino acids (3.7%) in the CDR3 region of mouse antibodies in the large abYsis antibody database,[2] all anti-dsDNA hybridomas together described here have a frequency of 16.2% (47 arginines among 289 CDR3 amino acids; $p < 0.001$, Chi-Square). Interestingly, we found a recurrent usage of one V_H gene (VH5-17) among expanded clones in all three independent mice (shaded in **Table 2**). In summary, sequence analysis of anti-dsDNA hybridomas showed clear evidence for clonal expansion and somatic mutation among the anti-dsDNA hybridomas from double-deficient mice.

Early Expansion of T Follicular Helper (T_{FH}) Cells in Dnase1l3 and FcγRIIB Double-Deficient Mice

To get some mechanistic insight into the early spontaneous formation of germinal centers, we analyzed cohorts of young (8–9 weeks of age) and older mice (14–19 weeks) of single- and double-knockout mice for myeloid cell populations as well as T helper cell subpopulations in the spleen. The analysis of the frequency of monocytes, DCs, plasmacytoid DCs, and macrophages in the spleen did not reveal significant changes among single- or double-mutant mice as compared to C57BL/6 mice of similar age (data not shown). We observed an increase of Ly6G-positive neutrophils in the spleen of older FcγRIIB- as well as double-knockout mice, most likely reflecting inflammatory activity (**Figure 4A**). General activation of the $CD4^{+}$ T cell compartment as evidenced by high levels of CD44 expression was observed in older FcγRIIB- as well as in double-knockout

[2] http://www.bioinf.org.uk/abysis3.1 (Accessed: November 12, 2017).

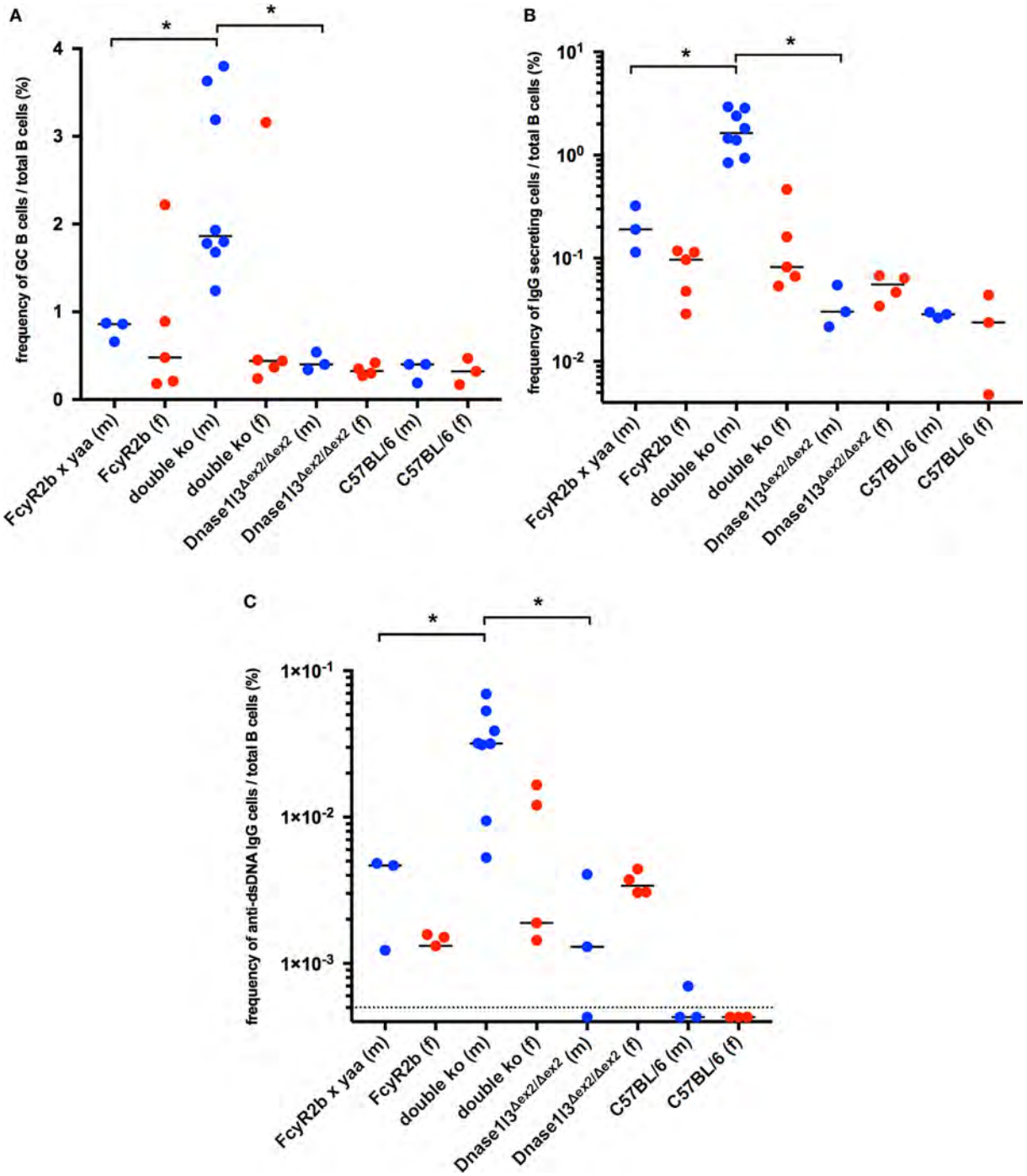

FIGURE 3 | Spontaneous germinal center development and elevated production of autoantibodies against double-stranded DNA (anti-dsDNA) secreting cells in Dnase1l3 and FcgR2b double-deficient mice. **(A)** Analysis of splenic B cells from 9- to 14-week-old mice by flow cytometry. The frequency of GL7$^+$, Fas$^+$ germinal center B cells among all CD19$^+$ B cells is displayed. The frequency of total IgG **(B)** and IgG anti-dsDNA **(C)** secreting B cells was determined by Elispot. Blue circles represent male mice, red circles represent female mice; dotted line in **(C)** represents the limit of detection (*$p < 0.05$; Mann–Whitney *U* test).

mice, but interestingly not in older Dnase1l3 single knockout animals (**Figure 4B**). Expansions of CD44^{hi} T_H cells were not observed in any cohort of young mice. T cell hyperactivation was particularly high in male animals carrying the *yaa* allele as denoted by the blue symbols but not restricted to *yaa*-animals in the cohorts (**Figure 4B**). We observed an expansion of the PD1^{hi} PSGL-1^{lo} T_{FH} cells in older FcγRIIB-knockout mice and particularly striking in double-knockout mice (**Figure 4C**).

TABLE 2 | Summary of V region gene analysis from autoantibodies against double-stranded DNA hybridomas.

Hybridoma	Clone[a]	Isotype	VH gene	JH gene	Mutations: total/non-silent	CDR3[b]	Number of Arg in CDR3[c]
Mouse 1, female 14w							
4B10.1	#1	IgG2c	V5-17	J4	4/3	ARRKLRNYYAMDY	2
6B9.1	#1	IgG2c	V5-17	J4	3/2	ARRKLRNYYAMDY	2
7F4.1	#2	IgG2b	V1-82	J2	1/1	ARPGRRGRYYFDY	3
3C5.2	#2	IgG2c	V1-82	J2	2/0	ARPGRRGRYYFDY	3
3F5.1	#3	IgG2c	V1-7	J3	4/2	ARSYYGSKGWFTY	0
3E2.1	#4	IgG2c	V1-26	J2	6/2	ASGDSSGPFDY	0
1E7.1	#5	IgG2c	V2-2	J4	1/0	ARNRLRRGLDY	3
2B11.1	#6	IgG2c	V1-81	J2	9/6	AGEHAGPYYFDY	0
10A12.1	#7	IgG2c	V5-9-1	J3	5/3	TRGGDSSGYRFAY	1
Mouse 2, female 12w							
1E5	#1	IgG2c	V5-17	J4	1/1	ARRGLRGVMDY	2
8F4	#1	IgG2c	V5-17	J4	7/5	VRRGLRGAMDY	2
8H4	#1	IgG2c	V5-17	J4	4/1	VRRGLRGAMDY	2
1G2.1	#1	IgG2c	V5-17	J4	4/3	ARRGLRGAMNY	2
2C1.2	#1	IgG2c	V5-17	J4	4/2	VRRGLRGAMDY	2
4H2.1	#1	IgG2c	V5-17	J4	2/0	ARRGLRGAMDY	2
5G3	#2	IgG2b	V5-17	J4	6/4	AKQLRLRYYAMDY	2
6E5	#2	IgG2b	V5-17	J4	4/3	SKQLRLRYYAMDY	2
9A10	#2	IgG2b	V5-17	J4	6/5	AKQLRLRYYAMDY	2
3C5	#3	IgG2b	V9-4	J4	1/1	ARDGNSYEGFAY	0
Mouse 3, female 24w							
5G12	#1	IgG2c	V1-81	J3	7/6	AEDGYAWFTY	0
5F11	#1	IgG2c	V1-81	J3	4/4	AEDGYVWFAY	0
4C2	#1	IgG2c	V1-81	J3	13/10	AEDGYVWFAY	0
3B7	#2	IgG2c	V1-9	J3	9/4	ARERNYITGFAY	1
1F10	#2	IgG2c	V1-9	J3	9/7	ARERNYITGFAY	1
1D12	#2	IgG2c	V1-9	J3	2/1	ARERNYITGFAY	1
2A2	#3	IgG2c	V7-3	J2	1/1	ARFPAGTRRYYFDY	2
5B4	#3	IgG2c	V7-3	J2	4/2	ARFPAGTRRYYFDY	2
3A9	#3	IgG2c	V7-3	J2	3/2	ARFPAGTRRYYFDY	2
1G1	#4	IgG2c	V5-17	J3	7/6	ARNYYVNRRGFAY	2
1G5	#5	IgG2c	V5-17	J3	8/6	TSRQLRLRRVAY	4
3F12	#6	IgG3	V1-26	J3	3/2	TRKGWDDAY	0

Orange shaded, recurrent VH gene; blau coloured, arginine residues in CDR3.

[a]*Clonally related hybridomas as defined by identical VH, D, and JH usage, identical CDR3 length and >95% nucleotide identity in CDR3.*

[b]*CDR3 as defined by IMGT (37).*

[c]*CDR3 as defined by Kabat et al. (38).*

Notably, T_{FH} cell are significantly expanded already in young double-knockout mice (**Figure 4C**). The frequency of IFN-γ producing $CD4^+$ T cells was elevated in both single-knockout strains of older age and strongly elevated in older double-knockout animals (**Figure 4D**). Thus, early expansion of T_{FH} cells in the spleen correlates with the enhanced spontaneous germinal center development and high-level IgG anti-dsDNA production in double-deficient mice.

DISCUSSION

The results described in this study reveal a strong genetic interaction of two individual susceptibility genes for anti-dsDNA autoantibody production in SLE that have been described in familiar lupus, as well as in knockout mouse models. Null mutations in the *DNASE1L3* gene were described in familial forms of SLE in Saudi Arabia, Turkey, and Italy (19–21). Anti-dsDNA autoantibodies were observed in almost all of the cases reported. In addition, a potentially defunctioning missense SNP present in relatively high frequency in the Caucasian population (40) shows a very high association with anti-centromere antibody-positive systemic sclerosis (41). For FCGR2B a SNP with considerable variation in frequency among human populations results in threonine replacing isoleucine in the transmembrane domain of the receptor (15). This causes the variant receptor to be excluded from sphingolipid rafts, resulting in a malfunctioning receptor (15). As both SNPs have a relatively high frequency within the Caucasian and Asian population (the missense SNP in Dnase1l3 is rare among populations with African origin[3]), we consider it highly worthwhile to analyze the frequency of these two variations among SLE patients. Current GWAS studies can explain only a minority of the heritability of complex diseases, a phenomenon that has been termed missing heritability (42). Epistatic interactions would be difficult to detect in GWAS studies because of computational challenges and low statistical power (43). We are currently analyzing such a possible epistatic interaction of *Dnase1l3* and *FcγRIIB* in a German/French SLE cohort from the upper Rhine.

[3]http://phase3browser.1000genomes.org (Accessed: February 15, 2018).

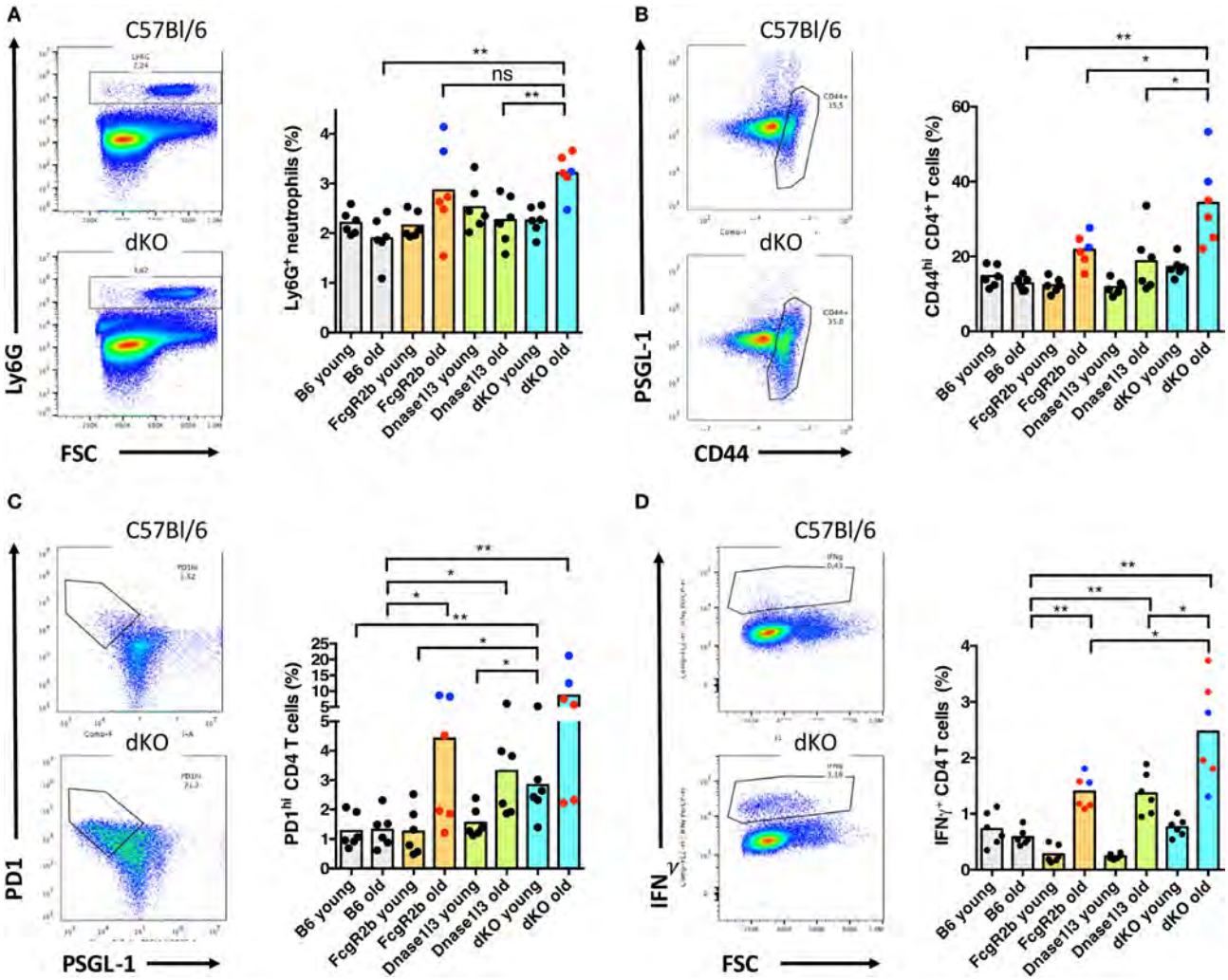

FIGURE 4 | Early expansion of T follicular helper (T_{FH}) cells and elevated levels of neutrophils in older Dnase1l3 and FcgR2b double-deficient mice. **(A)** Analysis of the expansion of Ly6G-positive neutrophils in the spleen of young (8–9 weeks old) and older (14–19 weeks old) mice. The genotypes of the mice are denoted at the axis. In **(B)**, activation of the CD4+ T cell compartment is displayed by the frequency of $CD44^{hi}$ CD4 cells. **(C)** Analysis of the expansions of $PD1^{hi}$ $PSGL\text{-}1^{lo}$ T_{FH} cells. In **(D)**, the frequency of IFN-γ producing CD4+ T cells is displayed. As an example for each analysis, a density plot is shown for wild-type and double-deficient mice. Blue circles specifically highlight male mice, red circles represent female mice (*$p < 0.05$; **$p < 0.01$; Mann–Whitney *U* test).

In our analysis of cohorts of double-mutant mice, we also introduced the *yaa* allele that results in a *TLR7* gene-duplication (44, 45). The analysis of female double-mutant mice and male double-mutant carrying the *yaa* mutation clearly revealed an influence of *yaa* on the penetrance of development of high levels of anti-dsDNA antibodies very early. Only approximately 50% of female mice developed high levels of anti-dsDNA antibodies at the age of 13 weeks. This is in accordance with the notion that *yaa* accelerates systemic autoimmunity as a genetic modifier in a context of a coexisting SLE background (44, 46). Also, the penetrance of early hyperactivation of germinal centers is much lower in female double-deficient mice, consistent with the described role of the *yaa* allele for defective germinal center selection in SLE (47). Importantly, double-deficient *yaa* male mice at the age of 3 months showed about 40 times higher anti-dsDNA levels when compared to *FcγRIIb*$^{-/-}$ *yaa* male mice of the same age.

Double-mutant mice showed a hyperactivation of spontaneously developing germinal centers which correlates with an early expansion of T_{FH} cells in the spleen. Expansions of T_{FH} cells were first noted in *sanroque* mutant mice with a lupus-like disease and autoantibody production (48) and later also in some SLE patients with severe disease (49). As T_{FH} cells are essential for germinal center responses (50), our findings here in the context of two epistatically acting mutations in the C57BL/6 genetic background further strengthen the model that dysregulated germinal center reactions are crucially involved in the early phases of the generation of IgG anti-dsDNA autoantibodies and the development of SLE (35, 50).

In *FcγRIIB*-deficient mice, an increase in anti-DNA reactive GC B cells was observed and somatic mutations contributed to the generation of highly autoreactive IgG antibodies (13). Opposite to the findings in single *Fcgr2b*-deficient mice, however, we observed clonal expansions of anti-DNA reactive B cells as well as

concomitant expansion of anti-DNA plasmablasts or plasma cells. These combined observations prompt a further development of our model of the evolution of anti-DNA autoantibodies in germinal centers (35). FcγRIIB and potentially other negative regulators for B cell signaling (51) might play a major role in the regulation of autoreactive GC B cells which otherwise would develop from non-self-reactive or low-level self-reactive precursors by somatic mutations (34). We now propose that the deficiency to eliminate nuclear material would drive such autoreactive B cell from the germinal center into clonal expansion and plasma cell differentiation, presumably outside of the germinal center. Our sequence analysis points in the direction that these B cells mutated only for limited periods of time. The "bush-like" diversification by somatic hypermutation from a single B cell rather than a stepwise maturation with intermediate selection is compatible with this model. Similar "bush-like" genealogies were also observed in SLE-prone mice (52, 53). An extraordinary high content of arginine residues in the CDR3 region of the heavy chain, which is also observed in our study here, apparently is a very common prerequisite for such an evolution of anti-dsDNA antibodies (39). Recent work attributed removal of apoptotic microparticles from the circulation as a major role of Dnase1l3 to prevent loss of tolerance to chromatin (22). We suggest an alternative explanation which is mutually not exclusive and might operate at local sites, particularly in the liver, the spleen, and lymph nodes. We found the highest levels of Dnase1l3 expression in cells with excellent antigen-presenting competence, high expression of scavenging receptors and TLRs, i.e., DCs and Kupffer cells in the liver. Local secretion of Dnase1l3 might function as a kind of shield to prevent these cells from being activated by damage-associated molecular patterns *via* TLRs and other receptors (54, 55).

In the same direction, local Dnase1l3 secretion might eliminate or lower the activation of DCs after uptake of DNA-containing immune complexes *via* Fc receptors which has the potential to trigger maturation and interferon production of DCs (17). Under non-inflammatory conditions, the inhibitory FcγRIIB would dominate activating signals from activating Fcγ receptors on DCs (17), however. This could reflect the situation in our single Dnase1l3-deficient mouse, in which anti-dsDNA production is stalled at relatively moderate levels. When FcγRIIB is blocked on human DCs, high levels of IL-12p70 can be induced when antibody coated tumor cells are delivered to the DCs (56) and type I interferon is induced after delivery of immune complexes to DCs (57). This scenario might explain the phenotype of Dnase1l3/FcγRIIB double-deficient animals described here. Under these circumstances, any DNA-containing immune complex could potentially trigger DC maturation and production of type I interferon and stimulate T_H1 driven responses. A self-perpetuating feedback loop would result when anti-dsDNA autoantibodies have evolved in such a scenario (58). For the initial trigger, IgG anti-dsDNA antibodies are not an essential content in the stimulating immune complexes. Pathogen-derived DNA together with pathogen-specific antibodies would be sufficient for starting such a DC-initiated self-perpetuating feedback loop.

Our conditional Dnase1l3 allele as well as conditional deletion of FcγRIIB will allow the detailed analysis of the cell types that are essential for the protection against uncontrolled evolution of anti-dsDNA autoantibodies in germinal centers. Potentially, comprehensive understanding of this regulation might allow the development of new targeted therapies for SLE.

ETHICS STATEMENT

Animal care and experiments were approved by the animal ethics committee of Regierung von Mittelfranken (Animal Ethics Number: 54-2532.1-21/09 and TS-05/5).

AUTHOR CONTRIBUTIONS

TW and BN performed experiments, analyzed data, and interpreted data. AS, NE, DS, and AA performed experiments and analyzed data. THW performed experiments, conceived the experiments, analyzed data, interpreted data, and wrote the manuscript. All authors were involved in critically reading of the manuscript and approved the final version to be published.

ACKNOWLEDGMENTS

The authors wish to thank Stefanie Brey for expert technical assistance. We also thank Uwe Appelt and Markus Mroz (FACS core facility at the Nikolaus-Fiebiger-Center for Molecular Medicine, FAU, Erlangen) for cell sorting. We also thank Natalya Seredkina and Ole-Petter Rekvig (The Arctic University of Norway, Tromsø, Norway) for helpful discussions. The vector used for this research project was generated by the trans-NIH Knock-Out Mouse Project (KOMP) and obtained from the KOMP Repository (www.komp.org).

FUNDING

This work was funded by the Deutsche Forschungsgemeinschaft through the grant TRR130 (project P11 and C03) to THW.

SUPPLEMENTARY MATERIAL

The Supplementary Material for this article can be found online at https://www.frontiersin.org/articles/10.3389/fimmu.2018.01551/full#supplementary-material.

REFERENCES

1. Ter Borg EJ, Horst G, Hummel EJ, Limburg PC, Kallenberg CG. Measurement of increases in anti-double-stranded DNA antibody levels as a predictor of disease exacerbation in systemic lupus erythematosus. A long-term, prospective study. *Arthritis Rheum* (1990) 33:634–43. doi:10.1002/art.1780330505
2. Ehrenstein MR, Katz DR, Griffiths MH, Papadaki L, Winkler TH, Kalden JR, et al. Human IgG anti-DNA antibodies deposit in kidneys and induce proteinuria in SCID mice. *Kidney Int* (1995) 48:705–11. doi:10.1038/ki.1995.341
3. Manson JJ, Ma A, Rogers P, Mason LJ, Berden JH, Van Der Vlag J, et al. Relationship between anti-dsDNA, anti-nucleosome and anti-alpha-actinin antibodies and markers of renal disease in patients with lupus nephritis: a prospective longitudinal study. *Arthritis Res Ther* (2009) 11:R154. doi:10.1186/ar2831

4. Deapen D, Escalante A, Weinrib L, Horwitz D, Bachman B, Roy-Burman P, et al. A revised estimate of twin concordance in systemic lupus erythematosus. *Arthritis Rheum* (1992) 35:311–8. doi:10.1002/art.1780350310
5. Reichlin M, Harley JB, Lockshin MD. Serologic studies of monozygotic twins with systemic lupus erythematosus. *Arthritis Rheum* (1992) 35:457–64. doi:10.1002/art.1780350416
6. Munoz LE, Lauber K, Schiller M, Manfredi AA, Herrmann M. The role of defective clearance of apoptotic cells in systemic autoimmunity. *Nat Rev Rheumatol* (2010) 6:280–9. doi:10.1038/nrrheum.2010.46
7. Topaloglu R, Bakkaloglu A, Slingsby JH, Mihatsch MJ, Pascual M, Norsworthy P, et al. Molecular basis of hereditary C1q deficiency associated with SLE and IgA nephropathy in a Turkish family. *Kidney Int* (1996) 50:635–42. doi:10.1038/ki.1996.359
8. Botto M, Dell'agnola C, Bygrave AE, Thompson EM, Cook HT, Petry F, et al. Homozygous C1q deficiency causes glomerulonephritis associated with multiple apoptotic bodies. *Nat Genet* (1998) 19:56–9. doi:10.1038/ng0598-56
9. Mitchell DA, Pickering MC, Warren J, Fossati-Jimack L, Cortes-Hernandez J, Cook HT, et al. C1q deficiency and autoimmunity: the effects of genetic background on disease expression. *J Immunol* (2002) 168:2538–43. doi:10.4049/jimmunol.168.5.2538
10. Lee-Kirsch MA, Gong M, Chowdhury D, Senenko L, Engel K, Lee YA, et al. Mutations in the gene encoding the 3'-5' DNA exonuclease TREX1 are associated with systemic lupus erythematosus. *Nat Genet* (2007) 39:1065–7. doi:10.1038/ng2091
11. Bolland S, Ravetch JV. Spontaneous autoimmune disease in Fc(gamma) RIIB-deficient mice results from strain-specific epistasis. *Immunity* (2000) 13:277–85. doi:10.1016/S1074-7613(00)00027-3
12. Bolland S, Yim YS, Tus K, Wakeland EK, Ravetch JV. Genetic modifiers of systemic lupus erythematosus in FcgammaRIIB(-/-) mice. *J Exp Med* (2002) 195:1167–74. doi:10.1084/jem.20020165
13. Tiller T, Kofer J, Kreschel C, Busse CE, Riebel S, Wickert S, et al. Development of self-reactive germinal center B cells and plasma cells in autoimmune Fc gammaRIIB-deficient mice. *J Exp Med* (2010) 207:2767–78. doi:10.1084/jem.20100171
14. Espeli M, Clatworthy MR, Bokers S, Lawlor KE, Cutler AJ, Kontgen F, et al. Analysis of a wild mouse promoter variant reveals a novel role for FcgammaRIIb in the control of the germinal center and autoimmunity. *J Exp Med* (2012) 209:2307–19. doi:10.1084/jem.20121752
15. Willcocks LC, Carr EJ, Niederer HA, Rayner TF, Williams TN, Yang W, et al. A defunctioning polymorphism in FCGR2B is associated with protection against malaria but susceptibility to systemic lupus erythematosus. *Proc Natl Acad Sci U S A* (2010) 107:7881–5. doi:10.1073/pnas.0915133107
16. Mackay M, Stanevsky A, Wang T, Aranow C, Li M, Koenig S, et al. Selective dysregulation of the FcgammaIIB receptor on memory B cells in SLE. *J Exp Med* (2006) 203:2157–64. doi:10.1084/jem.20051503
17. Espeli M, Smith KG, Clatworthy MR. FcgammaRIIB and autoimmunity. *Immunol Rev* (2016) 269:194–211. doi:10.1111/imr.12368
18. Hanayama R, Tanaka M, Miyasaka K, Aozasa K, Koike M, Uchiyama Y, et al. Autoimmune disease and impaired uptake of apoptotic cells in MFG-E8-deficient mice. *Science* (2004) 304:1147–50. doi:10.1126/science.1094359
19. Al-Mayouf SM, Sunker A, Abdwani R, Abrawi SA, Almurshedi F, Alhashmi N, et al. Loss-of-function variant in DNASE1L3 causes a familial form of systemic lupus erythematosus. *Nat Genet* (2011) 43:1186–8. doi:10.1038/ng.975
20. Ozcakar ZB, Foster J II, Diaz-Horta O, Kasapcopur O, Fan YS, Yalcinkaya F, et al. DNASE1L3 mutations in hypocomplementemic urticarial vasculitis syndrome. *Arthritis Rheum* (2013) 65:2183–9. doi:10.1002/art.38010
21. Carbonella A, Mancano G, Gremese E, Alkuraya FS, Patel N, Gurrieri F, et al. An autosomal recessive DNASE1L3-related autoimmune disease with unusual clinical presentation mimicking systemic lupus erythematosus. *Lupus* (2017) 26:768–72. doi:10.1177/0961203316676382
22. Sisirak V, Sally B, D'agati V, Martinez-Ortiz W, Ozcakar ZB, David J, et al. Digestion of chromatin in apoptotic cell microparticles prevents autoimmunity. *Cell* (2016) 166:88–101. doi:10.1016/j.cell.2016.05.034
23. Keyel PA. Dnases in health and disease. *Dev Biol* (2017) 429:1–11. doi:10.1016/j.ydbio.2017.06.028
24. Hemmi H, Takeuchi O, Kawai T, Kaisho T, Sato S, Sanjo H, et al. A toll-like receptor recognizes bacterial DNA. *Nature* (2000) 408:740–5. doi:10.1038/35047123
25. Takai T, Ono M, Hikida M, Ohmori H, Ravetch JV. Augmented humoral and anaphylactic responses in Fc gamma RII-deficient mice. *Nature* (1996) 379:346–9. doi:10.1038/379346a0
26. Eggan K, Akutsu H, Loring J, Jackson-Grusby L, Klemm M, Rideout WM III, et al. Hybrid vigor, fetal overgrowth, and viability of mice derived by nuclear cloning and tetraploid embryo complementation. *Proc Natl Acad Sci U S A* (2001) 98:6209–14. doi:10.1073/pnas.101118898
27. Rodriguez CI, Buchholz F, Galloway J, Sequerra R, Kasper J, Ayala R, et al. High-efficiency deleter mice show that FLPe is an alternative to Cre-loxP. *Nat Genet* (2000) 25:139–40. doi:10.1038/75973
28. Schmittgen TD, Livak KJ. Analyzing real-time PCR data by the comparative C(T) method. *Nat Protoc* (2008) 3:1101–8. doi:10.1038/nprot.2008.73
29. Brochet X, Lefranc MP, Giudicelli V. IMGT/V-QUEST: the highly customized and integrated system for IG and TR standardized V-J and V-D-J sequence analysis. *Nucleic Acids Res* (2008) 36:W503–8. doi:10.1093/nar/gkn316
30. Liu QY, Pandey S, Singh RK, Lin W, Ribecco M, Borowy-Borowski H, et al. DNaseY: a rat DNaseI-like gene coding for a constitutively expressed chromatin-bound endonuclease. *Biochemistry* (1998) 37:10134–43. doi:10.1021/bi9800597
31. Skarnes WC, Rosen B, West AP, Koutsourakis M, Bushell W, Iyer V, et al. A conditional knockout resource for the genome-wide study of mouse gene function. *Nature* (2011) 474:337–42. doi:10.1038/nature10163
32. White JK, Gerdin AK, Karp NA, Ryder E, Buljan M, Bussell JN, et al. Genome-wide generation and systematic phenotyping of knockout mice reveals new roles for many genes. *Cell* (2013) 154:452–64. doi:10.1016/j.cell.2013.06.022
33. Lakso M, Pichel JG, Gorman JR, Sauer B, Okamoto Y, Lee E, et al. Efficient in vivo manipulation of mouse genomic sequences at the zygote stage. *Proc Natl Acad Sci U S A* (1996) 93:5860–5. doi:10.1073/pnas.93.12.5860
34. Wellmann U, Letz M, Herrmann M, Angermuller S, Kalden JR, Winkler TH. The evolution of human anti-double-stranded DNA autoantibodies. *Proc Natl Acad Sci U S A* (2005) 102:9258–63. doi:10.1073/pnas.0500132102
35. Schroeder K, Herrmann M, Winkler TH. The role of somatic hypermutation in the generation of pathogenic antibodies in SLE. *Autoimmunity* (2013) 46:121–7. doi:10.3109/08916934.2012.748751
36. Andrews BS, Eisenberg RA, Theofilopoulos AN, Izui S, Wilson CB, Mcconahey PJ, et al. Spontaneous murine lupus-like syndromes. Clinical and immunopathological manifestations in several strains. *J Exp Med* (1978) 148:1198–215. doi:10.1084/jem.148.5.1198
37. Lefranc MP, Giudicelli V, Ginestoux C, Bodmer J, Muller W, Bontrop R, et al. IMGT, the international ImMunoGeneTics database. *Nucleic Acids Res* (1999) 27:209–12. doi:10.1093/nar/27.1.209
38. Kabat EA, Wu TT, Perry HM, Gottesman KS, Foeller C. *Sequences of Proteins of Immunological Interest*. Washington, DC: NIH Publication (1991).
39. Radic MZ, Weigert M. Genetic and structural evidence for antigen selection of anti-DNA antibodies. *Annu Rev Immunol* (1994) 12:487–520. doi:10.1146/annurev.iy.12.040194.002415
40. Ueki M, Kimura-Kataoka K, Takeshita H, Fujihara J, Iida R, Sano R, et al. Evaluation of all non-synonymous single nucleotide polymorphisms (SNPs) in the genes encoding human deoxyribonuclease I and I-like 3 as a functional SNP potentially implicated in autoimmunity. *FEBS J* (2014) 281:376–90. doi:10.1111/febs.12608
41. Mayes MD, Bossini-Castillo L, Gorlova O, Martin JE, Zhou X, Chen WV, et al. Immunochip analysis identifies multiple susceptibility loci for systemic sclerosis. *Am J Hum Genet* (2014) 94:47–61. doi:10.1016/j.ajhg.2013.12.002
42. Manolio TA, Collins FS, Cox NJ, Goldstein DB, Hindorff LA, Hunter DJ, et al. Finding the missing heritability of complex diseases. *Nature* (2009) 461:747–53. doi:10.1038/nature08494
43. Crawford L, Zeng P, Mukherjee S, Zhou X. Detecting epistasis with the marginal epistasis test in genetic mapping studies of quantitative traits. *PLoS Genet* (2017) 13:e1006869. doi:10.1371/journal.pgen.1006869
44. Pisitkun P, Deane JA, Difilippantonio MJ, Tarasenko T, Satterthwaite AB, Bolland S. Autoreactive B cell responses to RNA-related antigens due to TLR7 gene duplication. *Science* (2006) 312:1669–72. doi:10.1126/science.1124978
45. Subramanian S, Tus K, Li QZ, Wang A, Tian XH, Zhou J, et al. A Tlr7 translocation accelerates systemic autoimmunity in murine lupus. *Proc Natl Acad Sci U S A* (2006) 103:9970–5. doi:10.1073/pnas.0603912103

46. Izui S, Merino R, Fossati L, Iwamoto M. The role of the Yaa gene in lupus syndrome. *Int Rev Immunol* (1994) 11:211–30. doi:10.3109/08830189409061728
47. Woods M, Zou YR, Davidson A. Defects in germinal center selection in SLE. *Front Immunol* (2015) 6:425. doi:10.3389/fimmu.2015.00425
48. Vinuesa CG, Cook MC, Angelucci C, Athanasopoulos V, Rui L, Hill KM, et al. A RING-type ubiquitin ligase family member required to repress follicular helper T cells and autoimmunity. *Nature* (2005) 435:452–8. doi:10.1038/nature03555
49. Simpson N, Gatenby PA, Wilson A, Malik S, Fulcher DA, Tangye SG, et al. Expansion of circulating T cells resembling follicular helper T cells is a fixed phenotype that identifies a subset of severe systemic lupus erythematosus. *Arthritis Rheum* (2010) 62:234–44. doi:10.1002/art.25032
50. Craft JE. Follicular helper T cells in immunity and systemic autoimmunity. *Nat Rev Rheumatol* (2012) 8:337–47. doi:10.1038/nrrheum.2012.58
51. Jellusova J, Wellmann U, Amann K, Winkler TH, Nitschke L. CD22 x Siglec-G double-deficient mice have massively increased B1 cell numbers and develop systemic autoimmunity. *J Immunol* (2010) 184:3618–27. doi:10.4049/jimmunol.0902711
52. Shlomchik M, Mascelli M, Shan H, Radic MZ, Pisetsky D, Marshak-Rothstein A, et al. Anti-DNA antibodies from autoimmune mice arise by clonal expansion and somatic mutation. *J Exp Med* (1990) 171:265–92. doi:10.1084/jem.171.1.265
53. Guo W, Smith D, Aviszus K, Detanico T, Heiser RA, Wysocki LJ. Somatic hypermutation as a generator of antinuclear antibodies in a murine model of systemic autoimmunity. *J Exp Med* (2010) 207:2225–37. doi:10.1084/jem.20092712
54. Venereau E, Ceriotti C, Bianchi ME. DAMPs from cell death to new life. *Front Immunol* (2015) 6:422. doi:10.3389/fimmu.2015.00422
55. Mahajan A, Herrmann M, Munoz LE. Clearance deficiency and cell death pathways: a model for the pathogenesis of SLE. *Front Immunol* (2016) 7:35. doi:10.3389/fimmu.2016.00035
56. Dhodapkar KM, Kaufman JL, Ehlers M, Banerjee DK, Bonvini E, Koenig S, et al. Selective blockade of inhibitory Fcgamma receptor enables human dendritic cell maturation with IL-12p70 production and immunity to antibody-coated tumor cells. *Proc Natl Acad Sci U S A* (2005) 102:2910–5. doi:10.1073/pnas.0500014102
57. Dhodapkar KM, Banerjee D, Connolly J, Kukreja A, Matayeva E, Veri MC, et al. Selective blockade of the inhibitory Fcgamma receptor (FcgammaRIIB) in human dendritic cells and monocytes induces a type I interferon response program. *J Exp Med* (2007) 204:1359–69. doi:10.1084/jem.20062545
58. Marshak-Rothstein A. Toll-like receptors in systemic autoimmune disease. *Nat Rev Immunol* (2006) 6:823–35. doi:10.1038/nri1957

Conflict of Interest Statement: No potential conflict of interest relevant to this publication is reported.

The reviewer, RM and the handling Editor declared their shared affiliation.

frontiers in Immunology

ORIGINAL RESEARCH
published: 20 June 2018
doi: 10.3389/fimmu.2018.01384

Induction of Hypergammaglobulinemia and Autoantibodies by *Salmonella* Infection in MyD88-Deficient Mice

*Jincy M. Issac[1†], Yassir A. Mohamed[1], Ghada Hassan Bashir[1], Ashraf Al-Sbiei[2], Walter Conca[3†], Taj A. Khan[4], Asif Iqbal[5], Gabriela Riemekasten[6], Katja Bieber[7], Ralf J. Ludwig[7], Otavio Cabral-Marques[6†], Maria J. Fernandez-Cabezudo[2] and Basel K. al-Ramadi[1]**

[1] Department of Medical Microbiology and Immunology, College of Medicine and Health Sciences, United Arab Emirates University, Al Ain, United Arab Emirates, [2] Department of Biochemistry, College of Medicine and Health Sciences, United Arab Emirates University, Al Ain, United Arab Emirates, [3] Department of Internal Medicine, College of Medicine and Health Sciences, United Arab Emirates University, Al Ain, United Arab Emirates, [4] Department of Microbiology, Kohat University of Science and Technology, Kohat, Pakistan, [5] Department of Pharmacology, University of Illinois at Chicago, Chicago, IL, United States, [6] Department of Rheumatology, University of Lübeck, Lübeck, Germany, [7] Lübeck Institute of Experimental Dermatology, University of Lübeck, Lübeck, Germany

Growing evidence indicates a link between persistent infections and the development of autoimmune diseases. For instance, the inability to control *Salmonella* infection due to defective toll-like receptor (TLR)/myeloid differentiation primary response 88 (MyD88) signaling has linked the development of persistent infections to a breakdown in B cell tolerance. However, the extent of immune dysregulation in the absence of TLR-MyD88 signaling remains poorly characterized. Here, we show that MyD88$^{-/-}$ mice are unable to eliminate attenuated *Salmonella enterica* serovar Typhimurium, even when challenged with a low-dose inoculum (200 CFUs/mouse), developing a persistent and progressive infection when compared to wild-type (MyD88$^{+/+}$) animals. The splenic niche of MyD88$^{-/-}$ mice revealed increased counts of activated, Sca-1-positive, myeloid subpopulations highly expressing BAFF during persistent *Salmonella* infection. Likewise, the T cell compartment of *Salmonella*-infected MyD88$^{-/-}$ mice showed increased levels of CD4^{+} and CD8^{+} T cells expressing Sca-1 and CD25 and producing elevated amounts of IL-4, IL-10, and IL-21 in response to CD3/CD28 stimulation. This was associated with increased Tfh cell differentiation and the presence of CD4^{+} T cells co-expressing IFN-γ/IL-4 and IFN-γ/IL-10. Noteworthy, infected MyD88$^{-/-}$ mice had enhanced serum titers of both anti-*Salmonella* antibodies as well as autoantibodies directed against double-stranded DNA, thyroglobulin, and IgG rheumatoid factor, positive nuclear staining with HEp-2 cells, and immune complex deposition in the kidneys of MyD88$^{-/-}$ mice infected with live but not heat-killed *Salmonella*. Infection with other microorganisms (*Acinetobacter baumanii*, *Streptococcus agalactiae*, or *Escherichia coli*) was unable to trigger the autoimmune phenomenon. Our findings suggest that dysregulation of the immune response in the absence of MyD88 is pathogen-dependent and highlight potentially important genotype–environmental factor correlations.

Keywords: MyD88 deficiency, autoantibodies, *Salmonella typhiumrium*, hypergammaglobulinemia, Tfh cells

OPEN ACCESS

Edited by:
Falk Nimmerjahn, Friedrich-Alexander-Universität Erlangen-Nürnberg, Germany

Reviewed by:
Thomas H. Winkler, Friedrich-Alexander-Universität Erlangen-Nürnberg, Germany
Roland Lang, Universitätsklinikum Erlangen, Germany

****Correspondence:***
Basel K. al-Ramadi
ramadi.b@uaeu.ac.ae

†Present address:
Jincy M. Issac, Department of Medicine, Faculty of Medicine, Kuwait University, Kuwait City, Kuwait; Walter Conca, Department of Medicine, King Faisal Specialist Hospital and Research Center, Riyadh, Saudi Arabia; Otavio Cabral-Marques, Center for Chronic Immunodeficiency, Medical Center-University of Freiburg, Faculty of Medicine, University of Freiburg, Freiburg, Germany

Specialty section:
This article was submitted to Immunological Tolerance and Regulation, a section of the journal Frontiers in Immunology

Received: *07 December 2017*
Accepted: *04 June 2018*
Published: *20 June 2018*

Citation:
Issac JM, Mohamed YA, Bashir GH, Al-Sbiei A, Conca W, Khan TA, Iqbal A, Riemekasten G, Bieber K, Ludwig RJ, Cabral-Marques O, Fernandez-Cabezudo MJ and al-Ramadi BK (2018) Induction of Hypergammaglobulinemia and Autoantibodies by Salmonella Infection in MyD88-Deficient Mice. Front. Immunol. 9:1384. doi: 10.3389/fimmu.2018.01384

INTRODUCTION

The innate immune sensing apparatus, as originally proposed by Janeway (1), serves two important functions: first, it is a means through which the host can recognize and respond rapidly to microbial pathogens; second, the innate immune machinery directs and regulates the ensuing adaptive immune responses so as to achieve maximum efficiency against the invading pathogens. Over the past 25 years, extensive experimental evidence has been amassed in support of both of these essential functions (2). Particularly, recognition of conserved structures of pathogens by pattern recognition receptors such as toll-like receptors (TLRs) have been demonstrated to orchestrate both innate and adaptive immune responses (3, 4). Upon binding to pathogen-associated molecular patterns, most TLRs signal through myeloid differentiation primary response 88 (MyD88), an essential cytoplasmic adaptor protein that links triggering of TLRs and IL-1/IL-18 receptors to downstream activation of IL-1 receptor-associated kinases (IRAKs) and the nuclear factor-kappa B (NF-κB) (5). In turn, this initiates the production of various pro-inflammatory and immunoregulatory cytokines that control the subsequent development of antimicrobial B and T cell responses (6, 7). However, the requirement of TLR/MyD88 pathway for antibody responses has been challenged by several studies demonstrating T-cell-dependent antibody synthesis in the absence of TLR/MyD88 signaling (8).

The importance of the TLR-MyD88 pathway in host defense against a variety of microbial pathogens has been extensively demonstrated (9–20). Despite this critical requirement for TLR/MyD88 pathway for host defense against microbial infections, other studies demonstrated that it is dispensable for the generation of antibody responses, particularly in response to experimental infections by *Salmonella enterica* serovar Typhimurium (hereafter referred to as *S. typhimurium*) (17, 21, 22) and *Borrelia burgdorferi* (23). These apparently conflicting findings even extend to the requirement of MyD88/TLR pathway for protective adaptive immunity to *Salmonella* infection. While one study reported that MyD88 deficiency had little effect on protection (22), we and others have shown that MyD88-deficient mice are profoundly susceptible to infection (17, 21). *Salmonella typhimurium* bacteria are Gram-negative, food and water-borne pathogens that cause annually millions of cases of acute gastroenteritis, fever, and septicemia, representing a significant public-health problem worldwide (24, 25). Notably, damage of host tissues during *Salmonella* infections has provided a link between *Salmonella* outbreaks and the development of autoimmune diseases (26–28). However, the mechanisms behind these phenomena remain poorly understood, necessitating a better understanding of the host protective mechanisms in *Salmonella* infections.

To gain further insight into the role of TLR-MyD88 signaling in the immune response against *Salmonella*, we previously demonstrated that the inherent susceptibility of MyD88-deficient ($MyD88^{-/-}$) mice to *Salmonella* infection is linked to a defective production of inflammatory cytokines and impaired recruitment of immune cells to the infection site (17). Despite the observed defects, $MyD88^{-/-}$ mice produced increased levels of anti-*Salmonella* IgG antibodies (17), suggesting that *Salmonella* dysregulates the adaptive immune response. Here, we report a follow-up of our previous findings in which we characterized the activation state of innate (myeloid cells) and adaptive (T and B lymphocytes) immune responses from $MyD88^{-/-}$ mice in response to an attenuated strain of *S. typhimurium*, designated BRD509E (29, 30). Furthermore, we determined the underlying mechanism of the hypergammaglobulinemia response in BRD509E-infected $MyD88^{-/-}$ mice as well as its implications for autoreactive B cell responses.

MATERIALS AND METHODS

Bacterial Strains

For the current studies, we have used an attenuated $aroA^{-}/aroD^{-}$ double auxotrophic mutant strain of *S. typhimurium* (BRD509E) cultured and prepared as previously described (30, 31). Where indicated, we also utilized a strain of *Acinetobacter baumanii* (designated NM97), a clinical isolate from Tawam hospital, which was kindly provided by Dr. Tibor Pal (Department of Medical Microbiology and Immunology, College of Medicine and Health Sciences, United Arab Emirates University). Heat-killed (HK) *Salmonella* was prepared by incubating log-phase bacterial suspension at 65°C for 1 h.

Mice

C57BL/6 wild-type mice ($MyD88^{+/+}$) were purchased from the Jackson Laboratory (Bar Harbor, ME, USA). MyD88-deficient mice ($MyD88^{-/-}$) were generously provided by Dr. Shizuo Akira (Osaka University, Japan) (32) through Dr. Richard Flavell (Yale University School of Medicine, USA). Mice were bred in our animal facility and maintained in filter-topped isolator cages on Bactrim-supplemented water. Mice were taken off antibiotic for at least 7–10 days before use in any experiment. All animals were routinely used at 8–12 weeks of age when the bacteria were inoculated intraperitoneally (i.p.). All studies involving animals were conducted in accordance with and after approval of the animal research ethics committee of the College of Medicine and Health Sciences, United Arab Emirates University. In some experiments, sera from 8-week-old female autoimmune MRL/MpJ-Fas^{lpr} (MRL-lpr) mice (Jackson Laboratory) were used for comparative determination of anti-double-stranded DNA (dsDNA) titers.

Enumeration of Bacteria in Target Organs and Fecal Pellets

Procedures for determination of bacterial loads have been detailed elsewhere (17, 33). Fecal CFUs were determined at the indicated time points by streaking fecal suspension on *Salmonella–Shigella* agar plates containing ampicillin and streptomycin. Similarly, bacterial CFUs were also determined in spleen and liver homogenates prepared in cold sterile saline.

Spleen Cell Preparation and Enrichment

Erythrocyte-depleted spleen single cell suspensions were prepared as described previously (31). Purification of $CD4^{+}$ T cells and $CD11b^{+}$ myeloid subpopulations was done using magnetic bead separation on an autoMACS cell sorter (Miltenyi Biotec,

Germany) according to manufacturer's instructions. The purity of $CD4^+$ T cells was always between 90 and 95% and myeloid cells between 80 and 85%.

Phenotyping of Splenic Immune Cell Subsets

Processing of spleen cells for flow cytometric analysis was carried out as detailed previously (34). Immunophenotyping of splenic myeloid cells was done using the following panel of conjugated mAbs: CD11b-eFluor780, Gr-1-FITC, Sca-1-PE, and CD80-APC (all from Biolegend or eBioscience, San Diego, CA, USA). For the analysis of splenic T population, we used a panel of mAbs consisting of CD3-FITC, CD4-PE-Cy7, CD8α-APC-Cy7, CD25-APC, and Sca-1-PE. Splenic B lymphocytes were analyzed using the following mAb panel: CD19-PE-Cy7, Sca-1-PE, CD80-APC, and CD86-FITC. In all staining groups, 7-AAD dye was included in order to exclude non-viable cells from the analysis. Data were collected on 30,000 cells using BD FACSCantoII cytometer and analyzed using BD FACSDiva software.

Analysis of Intracellular Cytokine Levels

The levels of intracellular cytokines were assessed as recently described (35), with minor modifications. Briefly, spleen cell suspensions were seeded in 24-well plates and remained unstimulated or were stimulated with anti-CD3 (clone 2C11) mAb (5 μg/well) plus 100 μl of anti-CD28 (clone 37.N.51) at 20 μg/well for 24 h at 37°C in the presence of brefeldin A for the last 4 h of culture (GolgiPlug; BDcytofix/cytoperm plusTM solution kit, BD Biosciences). After overnight incubation, cells were harvested, stained with CD4-APC-Cy7 mAb (Biolegend), and intracellularly (BD Cytofix/Cytoperm Plus #555028) with anti-IFNγ-PE-Cy7 plus anti-IL4-APC or anti-IFNγ-PE-Cy7 plus anti-IL10-PE or isotype controls (all from Biolegend). Cells were read on a BD FACSCanto II and the data analyzed using BD FACSDiva software.

Cytokine Release

Purified splenic $CD4^+$ T cells were cultured in the presence or absence of plate-bound mAbs specific to murine CD3 and CD28 molecules, as described above. After overnight incubation, supernatants were harvested and analyzed for IFNγ, IL-4, and IL-10 cytokines by ELISA following the manufacturer's instructions (BD Biosciences).

Gene Expression Analysis

Expression of target gene from purified and $CD11b^+$ myeloid and $CD4^+$ T cells was evaluated using qRT-PCR as previously described (34) using TaqMan reverse transcription reagents (Applied Biosystems, Foster City, CA, USA) and following the manufacturer's protocol. Briefly, TaqMan primers and probes (all from Applied Biosystems) were used to study the expression of various cytokines (including BAFF, IL-4, IL-6, IL-10, IL-12p35, IL-17F, IL-21, IFN-γ, and TGF-β), transcription factors (T-bet, GATA-3, RoRγ, Bcl-6, Foxp3), inducible nitric oxide synthase (iNOS), and the checkpoint protein PD-1. The levels of transcripts were normalized according to the ΔCq method to respective mRNA levels of the housekeeping gene hypoxanthine guanine phosphoribosyltransferase (HPRT).

Measurement of Antibacterial Antibodies

Serum samples were obtained at the indicated time points post i.p. infection with 200 CFUs/mouse (for live *Salmonella*), 2×10^5 CFUs/mouse (for HK *Salmonella*), or 1×10^5 CFUs/mouse of *A. baumanii*. The presence of *Salmonella*-specific or *Acinetobacter*-specific antibodies of IgG1, IgG2c, IgG3, and IgM isotypes were determined by ELISA as previously described (17, 31). Maxisorb microplates (Nunc, Roskilde, Denmark) were coated with 1×10^6/ml HK BRD509E overnight. After blocking (1% BSA, 5% sucrose, 0.05% NaN_3 in 1XPBS, pH 7.2–7.4), serum samples were titrated serially in the reagent diluent (1% BSA in 1XPBS, pH: 7.2–7.4) and incubated at room temperature (RT) for 2 h. After washing, the plates were incubated for 2 h with the respective biotin-conjugated anti-mouse Ig isotypes (goat anti-IgM, Jackson Immunoresearch, West Grove, PA, USA; goat anti-IgG1, goat anti-IgG2c, and rat anti-IgG3, all from Southern Biotech, Birmingham, AL, USA) followed by Streptavidin-HRP. The plates were developed using TMB substrate and read at 450 nm using a TECAN microplate reader (Maennedorf, Switzerland). For the quantitative determination of anti-*Salmonella* Ab concentrations, wells were coated with 0.1 μg/ml of goat anti-mouse Ig (H + L) Ab (Southern Biotech). After blocking with 2% BSA/PBS (pH 7.2) buffer, the standard curve was generated using specific mouse isotype Abs (IgG1 or IgG2c; starting concentration 50 ng/ml). For the rest of the plate, serum samples from individual animals were serially titrated in duplicate. The test plate was then incubated at RT for 2 h, washed extensively, and received appropriate secondary Abs (biotin-conjugated, isotype-specific Abs) and incubated for an additional 2 h at RT. After another series of washings, streptavidin-HRP was added and the plates developed using TMB, as described above.

Determination of Serum Autoantibodies

The levels of autoantibodies directed against dsDNA, thyroglobulin, and mouse IgG rheumatoid factor (RF) were assessed by ELISA following a published method with modifications (36). For the detection of dsDNA-specific Abs, Maxisorp plates were coated with 1 μg/ml of dsDNA (from calf thymus; Sigma) diluted in borate-buffered saline (BBS) overnight at 4°C. After three wash cycles, wells were blocked for 1 h at RT with BBS supplemented with 0.4% Tween 20 and 1.0% BSA. Serum samples (1/500 to 1/1,000 final dilutions) were then added and incubated for 2 h. After washing with BBS, the plates were incubated with biotin-conjugated goat-anti-mouse IgG, Fcγ-specific Ab (Jackson Immunoresearch) for 2 h at RT. Finally, the plates were incubated with Streptavidin-HRP and developed with TMB, as described above. For the detection of RF and anti-thyroglobulin antibodies, Maxisorp plates were coated overnight at 4°C with 1 μg/ml of either mouse IgG (Jackson Immunoresearch) for RF assay or thyroglobulin (from bovine thyroid; Sigma) diluted in 0.05 M carbonate buffer (pH = 9.6). Following three washes with PBS containing 0.05% Tween, the wells were blocked with PBS/Tween/1% BSA for 2 h at RT. Serum samples, diluted to 1/1,000, were added in duplicate and incubated for 2 h at RT. The plates

were then washed and developed using the same procedure described above.

Detection of Antinuclear Antibodies (ANA) by Immunofluorescence Using HEp-2 Cells

Serum ANA were detected by indirect immunofluorescence using a fluorescence-based HEp-2 ANA kit, according to the manufacturer's protocol (INOVA Diagnostics, San Diego, CA, USA). Diluted serum samples (1/80) and controls were incubated for 30 min at RT in a moist chamber. After gently rinsing with PBS, FITC-conjugated goat anti-mouse IgG (Pierce,) was added and incubated for 30 min, following which the mounting media was added and coverslip placed. The fluorescence was visualized at 40× magnification using an Olympus BX51 fluorescent microscope (Olympus Corporation, Japan).

Histopathological Kidney Analysis

Kidney biopsies were fixed in 4% paraformaldehyde, embedded in paraffin, and assayed for immune complex deposition. Tissue sections were stained with biotin-goat anti-mouse IgG (Fcγ-specific; 1/2,000 dilution) for 2 h followed by streptavidin-HRP (BD Biosciences) for 1 h. The peroxidase activity was determined using DAB chromogen (BD Biosciences). After washing, hematoxylin was added and sections were then rehydrated, mounted with DPX, and viewed under 20× and 40× light microscope.

Statistical Analysis

Statistical significance was analyzed using Student's *t*-test, using the statistical program of GraphPad Prism software (San Diego, CA, USA). Differences between experimental groups were considered significant when p values were <0.05.

RESULTS

Persistent Infection by Attenuated *Salmonella* Strain in MyD88$^{-/-}$ Mice

We have previously demonstrated that MyD88$^{-/-}$ mice are susceptible to infection by an attenuated strain of *S. typhimurium* (BRD509E) (17, 30). While the lethal dose 50 (LD_{50}) of the BRD509E strain in C57BL/6 mice, when given i.p., is ~5×10^6 CFUs per mouse, the equivalent LD_{50} in MyD88$^{-/-}$ mice is ~400 CFUs/mouse, more than 10,000-fold lower than that of C57BL/6 mice. In this context, while i.p. inoculation of BRD509E (at doses as low as 4×10^2 CFUs/mouse) resulted in high mortality rates in MyD88$^{-/-}$ mice, its oral administration led to the establishment of a chronic infection that lasted for more than 6 months (17). Here, we examined further the extent of the susceptibility to BRD509E in MyD88$^{-/-}$ mice. We first followed the bacterial shedding in the feces over a 4-week period after the animals were infected i.p. with a low dose of BRD509E (200 CFUs/mouse). In wild-type MyD88$^{+/+}$ mice, only a low level of fecal shedding of *S. typhimurium* organisms (~10 CFUs/g feces) was observed 2 weeks postinfection (**Figure 1A**). By day 21, as the infection was phenotypically resolved, a minimal fecal shedding of *S. typhimurium* organisms was observed. In contrast, MyD88$^{-/-}$ mice exhibited a persistent, progressively worsening infection accompanied by increasing levels of bacterial shedding over the 4-week observation period, reaching $>10^5$ CFUs/g feces (**Figure 1A**). This observation correlated with significantly elevated bacterial burden in the spleen and liver of infected MyD88$^{-/-}$ mice, where the bacteria recovered was 158- and 240-fold greater, respectively, than in infected MyD88$^{+/+}$ mice (**Figures 1B,C**). Thus, MyD88$^{-/-}$ mice fail to control the replication of BRD509E strain irrespective of the challenge dose.

Increased Counts and Activation of Splenic Myeloid Cells Following *Salmonella* Infection in MyD88$^{-/-}$ Mice

To gain novel insights into the role of MyD88 in the immune response against *Salmonella*, MyD88$^{-/-}$ mice were infected with ~3×10^3 CFUs/mouse of BRD509E strain, which corresponds to an intermediate dose when compared to our previous report (17), and changes in spleen cellularity were analyzed at day 21 postinfection. MyD88$^{-/-}$ mice exhibited a protracted state of splenomegaly, ~3.8-fold larger than in wild-type counterparts (**Figures 1D,E**). Analysis of splenic immune cells demonstrated that MyD88$^{-/-}$ mice displayed a significant increase in the number of CD11b$^+$ myeloid cells in comparison to infected MyD88$^{+/+}$ counterparts (**Figure 1F**). Meanwhile, no change was observed in absolute counts of T and B lymphocytes (**Figures 1G,H**).

To characterize the different subpopulations of CD11b$^+$ myeloid cells in the spleen of infected animals, we performed flow cytometric analysis using a combination of mAbs to CD11b and Gr-1 proteins as well as the activation markers Sca-1, CD80, and MHC class II. Based on staining with mAbs to CD11b and Gr-1, three CD11b$^+$ myeloid subpopulations (Gr-1^{high}, Gr-1^{low}, and Gr-1$^-$) could be discerned (**Figures 1I–L**). The Gr-1^{high} cells represent granulocytes and are negative for MHC class II and CD80 expression (data not shown). The CD11b$^+$Gr-1^{low} and Gr-1$^-$ cells represent monocyte lineage cells and are positive for MHC class II (data not shown). By day 21 postinfection, the levels of splenic Gr-1^{high}, and Gr-1^{low} subpopulations were still elevated in both infected MyD88$^{-/-}$ and MyD88$^{+/+}$ mice as compared to non-infected (NI) counterparts (**Figures 1J,L**). Splenic Gr-1^{low} monocytes were the predominant cell type in infected MyD88$^{-/-}$ mice (**Figure 1M**), accounting for the observed protracted splenomegaly (**Figure 1D**). Sca-1 is an IFNγ-inducible activation marker on myeloid and lymphoid cells (37) and it has been shown to be upregulated in *Salmonella* infections (29). Analysis of Sca-1 expression on splenic myeloid cells confirmed its upregulation on all three subpopulations (**Figures 1I–L,N**) with the extent of activation being consistently higher in infected MyD88$^{-/-}$ mice. This is most likely a reflection of the chronicity of *Salmonella* infection in these mice.

Given the persistent infection and increased infiltration of inflammatory myeloid cells into the spleens of MyD88$^{-/-}$ mice at day 21 of infection, CD11b$^+$ cells were purified from different experimental groups and assessed for the expression of inflammatory mediators. We observed an elevated iNOS transcriptional activity in myeloid cells which reached >1,000-fold higher levels in both MyD88$^{+/+}$ and MyD88$^{-/-}$ myeloid cells compared to NI

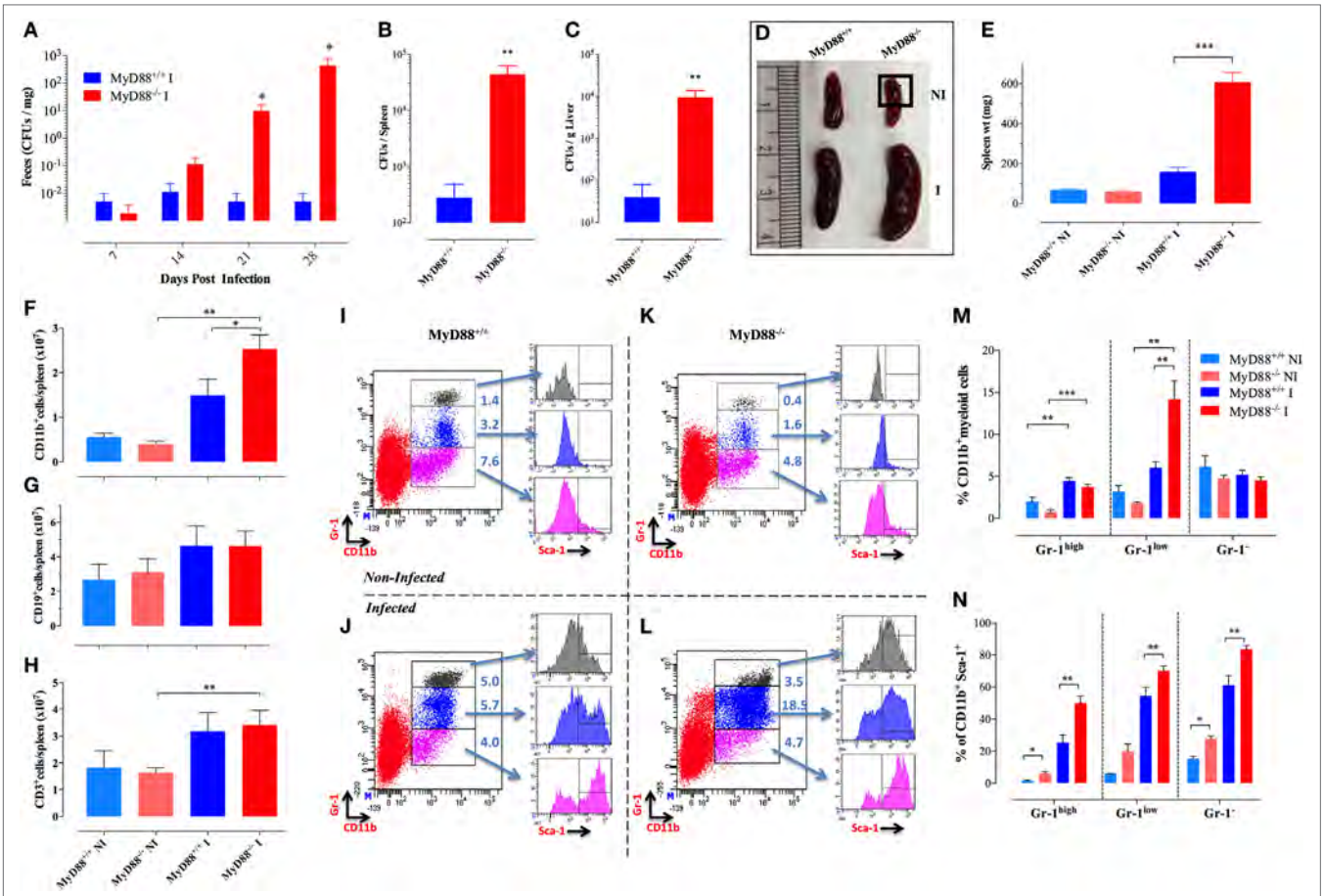

FIGURE 1 | Splenomegaly and inflammatory myeloid cell influx in *Salmonella*-infected MyD88$^{-/-}$ mice. **(A–C)** WT (MyD88$^{+/+}$) and MyD88$^{-/-}$ mice were infected i.p. with BRD509 (200 CFUs/mouse). Bacterial shedding in the feces was followed for 4 weeks **(A)**. Bacterial loads in spleen **(B)** and liver **(C)** at day 28 postinfection are shown. **(D,E)** Mice were infected with BRD509 (3,000 CFUs/mouse) and sacrificed at day 21. **(D)** Spleens of non-infected (NI) and infected (I) groups are shown. **(E)** Spleen weights of the different experimental groups. Each data point represents the mean ± SEM of 6–10 mice per group. **(F–H)** Absolute cell counts of CD11b^{+} myeloid cells **(F)**, CD19^{+} B lymphocytes **(G)** and CD3^{+} T lymphocytes **(H)** per spleen. **(I–N)** Flow cytometric analysis of splenic myeloid cells and activation status. Splenocytes of NI **(I,K)** or *Salmonella*-infected **(J,L)** MyD88$^{+/+}$ **(I,J)** or MyD88$^{-/-}$ **(K,L)** mice were analyzed for CD11b and Gr-1 positivity. Based on Gr-1 expression levels, three distinct CD11b^{+} populations could be discerned, CD11b^{+}Gr-1^{high} (top panel), CD11b^{+}Gr-1^{low} (middle panel), and CD11b^{+}Gr-1^{-} (bottom panel). Each of these subpopulations was further analyzed for the expression of Sca-1 activation marker. Results of individual mice are shown. **(M)** Percentage of CD11b^{+} cells expressing high, low, or negative levels of Gr-1 protein in NI or BRD509-infected MyD88$^{+/+}$ or MyD88$^{-/-}$ mice. **(N)** Alterations in expression of Sca-1 protein in the different myeloid subpopulations. The results are representative of at least three to four independent experiments. Asterisks denote statistically significant differences between MyD88$^{-/-}$ and MyD88$^{+/+}$ mice (*$p < 0.05$; **$p < 0.01$; ***$p < 0.001$).

animals (**Figure 2A**), indicative of an ongoing pro-inflammatory milieu in both mouse strains. In agreement, equivalent levels of IL-12p35 and IL-6 were also evident in both NI and infected MyD88$^{+/+}$ and MyD88$^{-/-}$ mice (**Figure 2B**). Of note, a significantly enhanced BAFF expression level was observed in infected MyD88$^{-/-}$ mice compared to wild-type mice (**Figure 2C**). Given the important role of BAFF in driving autoreactive B cell responses (38, 39), we also determined the levels of BAFF cytokine in mouse sera. Measurement of systemic BAFF levels revealed a 4.9-fold increase in BAFF in infected MyD88$^{-/-}$ mice compared to infected MyD88$^{+/+}$ animals (**Figure 2D**). Interestingly, this analysis also showed significantly higher (threefold) BAFF serum levels in uninfected MyD88$^{-/-}$ mice compared to their wild-type counterpart (**Figure 2D**). Additionally, *Salmonella* infection induced significant elevation (2.5-fold) in serum BAFF levels in MyD88$^{-/-}$ mice compared to uninfected counterpart (**Figure 2D**). Collectively, these findings suggest a hyperinflammatory state of myeloid cells from MyD88$^{-/-}$ mice in the context of a chronic infection with attenuated *Salmonella*. This is also combined with significantly elevated serum BAFF levels in MyD88$^{-/-}$ mice.

Enhanced T Lymphocyte Activation in the Spleens of *Salmonella*-Infected MyD88$^{-/-}$ Mice

Considering the interconnection between innate and adaptive immune responses (3, 40), the abnormal activation displayed by splenic myeloid cells of MyD88$^{-/-}$ animals suggested the possibility that *Salmonella* infection could also affect the activation

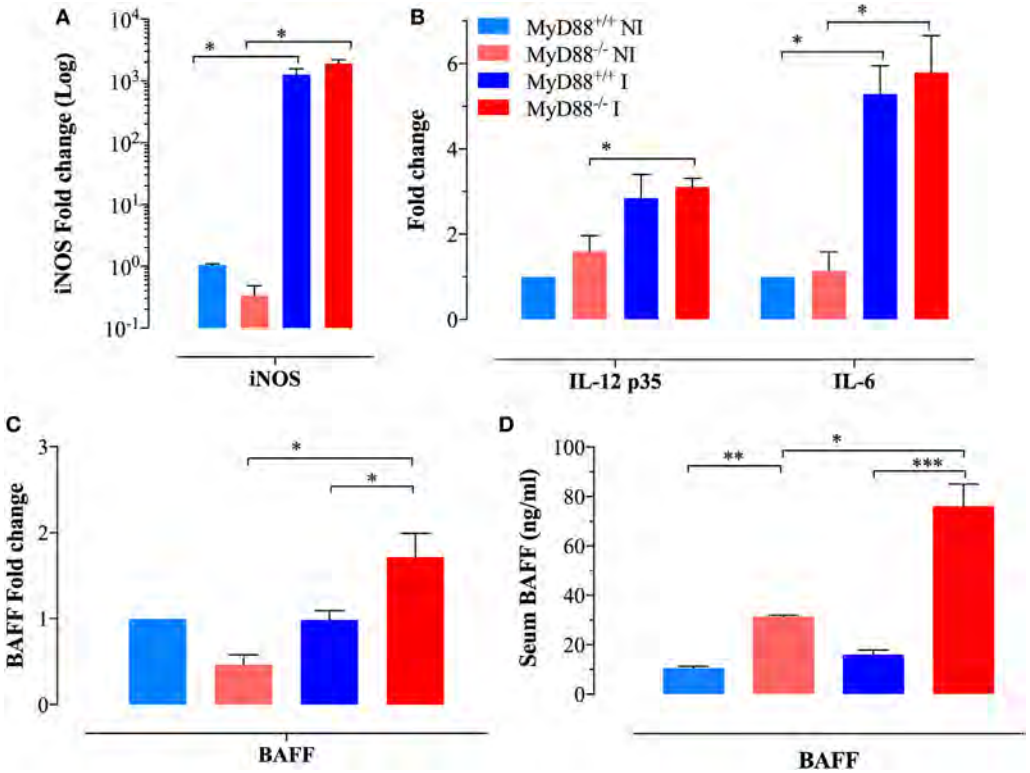

FIGURE 2 | Analysis of cytokine gene expression and serum levels in myeloid cells. Gene expression levels of **(A)** inducible nitric oxide synthase (iNOS) and **(B)** IL-12p35 and IL-6 in CD11b$^+$ splenic myeloid cells purified from the different experimental groups. Each data point represents the mean ± SEM of three to four mice per group. **(C)** Analysis of BAFF gene expression in purified myeloid cells [$n = 3$ for non-infected (NI) groups and $n = 8$ for infected groups]. Alterations in gene expression are depicted as fold-change compared to NI WT mice. **(D)** Analysis of systemic BAFF levels in mouse sera by ELISA. Each data point represents the mean ± SEM of three (NI) or eight (infected) mice per group. Analysis was done on whole sera or purified myeloid cells obtained from NI or *Salmonella*-infected mice at day 21 postinfection. Data are compiled from two independent experiments (*$p < 0.05$; **$p < 0.01$; ***$p < 0.001$).

of adaptive immune cells. The frequency of CD3$^+$ T cells in NI wild-type mice was 33.1 ± 2.1 and was essentially unchanged (34.9 ± 2.2) at day 21 postinfection (**Figures 3A–C**). Despite no changes in the absolute lymphocyte counts when comparing infected MyD88$^{+/+}$ with MyD88$^{-/-}$ mice (**Figure 1H**), the latter showed a slightly lower frequency of CD3$^+$ cells (25.9 ± 1.5) in the T lymphocyte compartment (**Figure 3B**). Since the frequency of CD4$^+$ T cells was not abnormal in MyD88$^{-/-}$ mice, the reduced CD3$^+$ cells in the T lymphocyte compartment was probably due to low percentage of CD8$^+$ T cells (**Figure 3D**). Most important, phenotypic analysis of T cells upon *Salmonella* infection demonstrated an increased expression of Sca-1 on CD4$^+$ and CD8$^+$ T cells from both mice strains (**Figures 3E,F**; Figure S1 in Supplementary Material). However, the upregulation of Sca-1 expression was significantly higher on T cells from MyD88$^{-/-}$ mice compared to wild-type mice. Furthermore, while we did not detect increased CD25 expression on T cells from infected wild-type mice when compared to NI animals, the absence of MyD88 resulted in a strong upregulation of this activation marker (**Figures 3G,H**; Figure S1 in Supplementary Material). Therefore, the incapacity to control *S. typhimurium* infection in MyD88$^{-/-}$ mice leads to a hyperactivation of innate and adaptive immune cells.

Abnormalities in T Helper Subsets in MyD88$^{-/-}$ Mice

We sought to further characterize the immunopathological mechanisms behind the abnormal adaptive immune cells during uncontrolled *S. typhimurium* infection. Considering the pivotal role of CD4$^+$ T lymphocytes in the global control of immune responses including the host resistance against *Salmonella* (41, 42), we evaluated the gene expression in purified splenic CD4$^+$ T cells of cytokines and transcription factors that specify the program of T helper cells in MyD88$^{+/+}$ and MyD88$^{-/-}$ mice. Transcription of IFN-γ, the main cytokine that defines the Th1 signature, was significantly elevated (27- to 32-fold) upon *Salmonella* infection in both MyD88$^{+/+}$ and MyD88$^{-/-}$ mice (**Figure 4A**). Noteworthy, CD4$^+$ T cells from MyD88$^{-/-}$ spontaneously expressed increased levels of IL-4 and IL-21 when compared to wild-type mice, which are pivotal cytokines that define Th2 (43–45) and Tfh (follicular Th cells) (46, 47) profiles, respectively. After *Salmonella* infection, the amount of IL-4 and IL-21 was strongly upregulated in CD4$^+$ T cells of MyD88$^{-/-}$, but not MyD88$^{+/+}$, mice (**Figure 4A**). The expression level of IL-10, another Th2 cytokine (48), was also elevated (~14-fold) in infected MyD88$^{-/-}$ mice (**Figure 4A**). Interestingly, the enhanced Tfh-specific transcriptional signature was mirrored

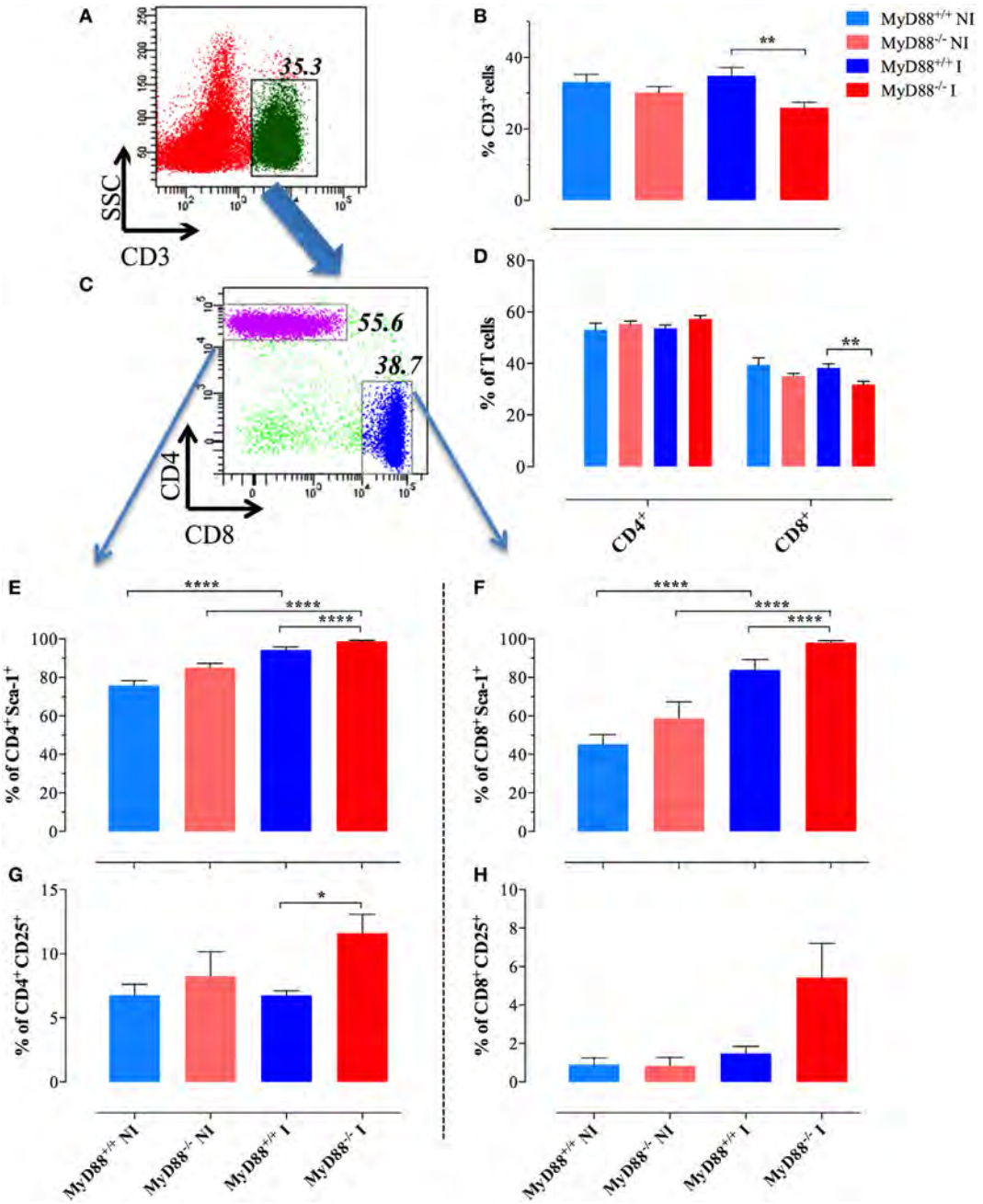

FIGURE 3 | Changes in splenic T lymphocyte populations following infection. A representative dot plot of non-infected (NI) WT splenocytes showing gated CD3+ T lymphocytes **(A)** and CD4 and CD8 subpopulations **(C)** within gated CD3+ cells. **(B)** Changes in the percent of CD3+ lymphoid cells in the whole spleen. **(D)** Changes in the ratios of CD4+ and CD8+ cells within the T cell populations. Analysis was done on day 21 postinfection with BRD509 (n = 4–6 for NI and 8–10 for infected groups). Changes in the percent of CD4+ **(E,G)** and CD8+ **(F,H)** T cells positive for Sca-1 **(E,F)** or CD25 **(G,H)** are shown (*$p < 0.05$, **$p < 0.01$, ***$p < 0.001$). The results are representative of three independent experiments.

by significant upregulation in BAFF (5.3-fold) and PD-1 (39.2-fold) gene transcription compared to control (**Figure 4A**). The increase in IL-4, IL-21, IL-10, BAFF, and PD-1 gene transcription was significantly higher in infected MyD88$^{-/-}$ compared to infected MyD88$^{+/+}$ mice. On the other hand, no significant changes were observed in the expression of IL-17 or TGF-β in CD4+ T cells from any mouse strain (data not shown) Overall, our data suggest that *S. typhimurium* infection exacerbates Th2 and Tfh transcriptional signatures, which are essential for the modulation of antibody production (49, 50).

In order to validate our gene expression approach, we purified CD4+ T cells from NI and infected mice and analyze the

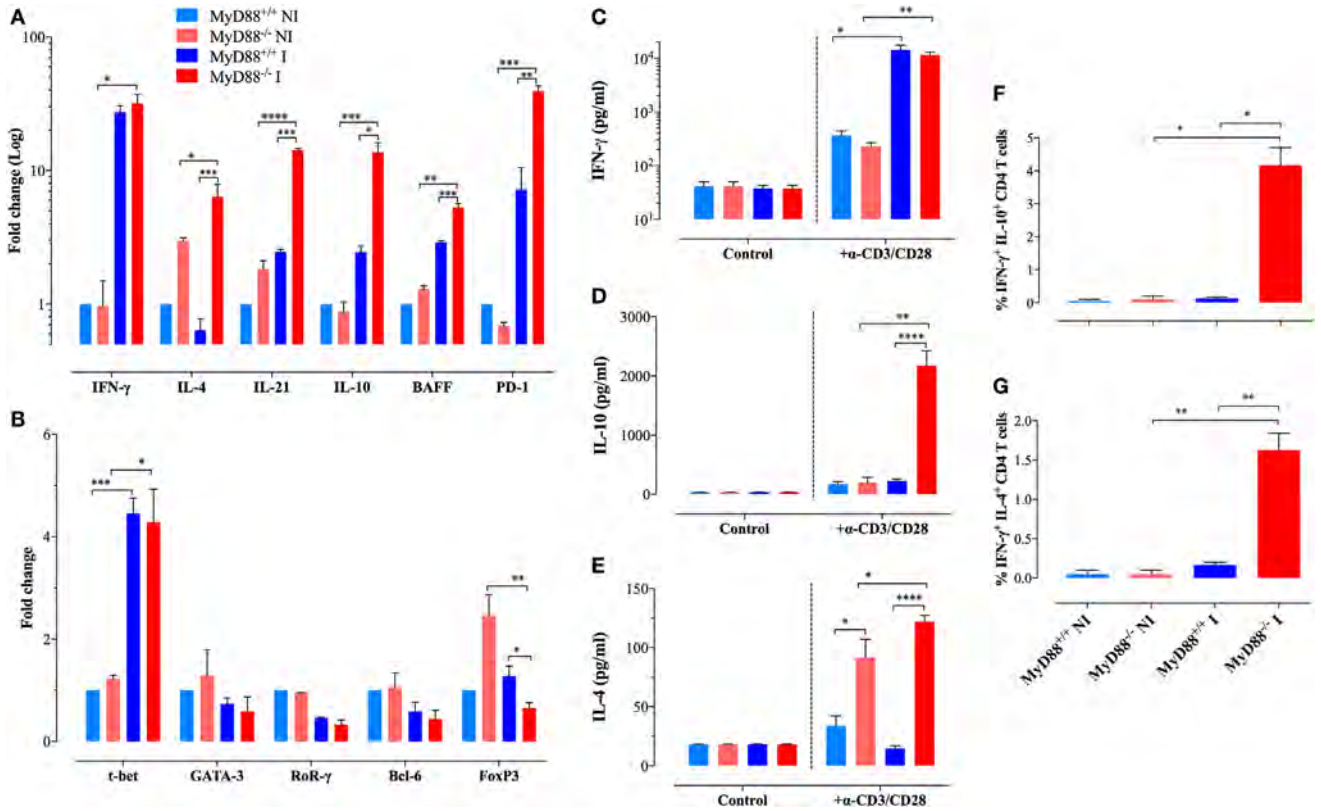

FIGURE 4 | Analysis of gene expression and cytokine production profiles in purified CD4+ T lymphocytes. **(A,B)** Gene expression levels of key cytokines **(A)** and transcription factors **(B)** in purified CD4+ T cells of different experimental groups were analyzed by quantitative real-time PCR (n = 3–6 per group). Alterations in gene expression are depicted as fold-change compared to non-infected (NI) WT mice. Analysis was done on CD4+ T cells purified from NI or *Salmonella*-infected mice at day 21 postinfection. **(C–E)** Secretion of IFN-γ **(C)**, IL-10 **(D)**, and IL-4 **(E)** by purified CD4+ T cells after stimulation with plate-bound anti-CD3/CD28 antibodies. Data are compiled from two independent experiments (n = 3–6 per group). **(F,G)** Intracellular cytokine staining of purified CD4+ T cells. The graphs depict cumulative data showing the percent of CD4+ T cells co-expressing IFN-γ plus IL-10 **(F)** or IFN-γ plus IL-4 cytokines **(G)**. All determinations were done in triplicates. The data are representative of three independent experiments (*p < 0.05, **p < 0.01, ***p < 0.001, ****p < 0.0001).

secretion of cytokines upon stimulation with a combination of plate-bound anti-CD3/CD28 mAbs. Both MyD88$^{+/+}$ and MyD88$^{-/-}$ mice secreted abundant and comparable levels of IFN-γ (**Figure 4C**). IL-10 secretion was only strongly detected in the supernatants of CD4+ T cells from infected MyD88$^{-/-}$ mice (**Figure 4D**). Moreover, IL-4 secretion was detected only from MyD88$^{-/-}$ CD4+ T cells, which is in agreement with the gene expression findings (**Figure 4E**). Interestingly, CD4+ T cells from uninfected MyD88$^{-/-}$, but not MyD88$^{+/+}$, mice could also secrete IL-4 upon induction *via* the TCR, suggesting an endogenous predisposition to Th2 responses in these mice (**Figure 4E**). Next, intracellular staining of cytokines in anti-CD3/CD28-activated CD4+ T cells was performed by flow cytometric analysis. The data revealed that while CD4+ T cells from infected MyD88$^{+/+}$ mice follow the traditional Th1/Th2 polarized model, CD4+ T cells from MyD88$^{-/-}$ mice co-expressed IFN-γ and IL-4 or IFN-γ and IL-10 (**Figures 4F,G**; Figure S2 in Supplementary Material). The rather heterogeneous cytokine profile observed in MyD88$^{-/-}$ T cells is typical of the cytokine pattern expressed by Tfh cells (51). Recently, it was reported that naïve Th21 cells, which are implicated in autoimmune disease, do also express a combination of cytokines (IL-21 and IFNγ) typically associated with different Th cell lineages (52).

Underlying the findings described above, we observed an upregulated expression of T-bet, the transcriptional factor responsible for Th1 differentiation, in CD4+ T cells from both mice strains (**Figure 4B**). Meanwhile, NI MyD88$^{-/-}$ mice displayed a higher spontaneous gene expression of FoxP3, the transcription factor responsible for the differentiation of T regulatory (T reg) cells, compared to wild-type mice. However, following infection, the expression of FoxP3 was downregulated to levels comparable to those from wild-type mice. No changes were observed in the expression of GATA-3, RoRγ, or Bcl-6, which are responsible for the commitment of Th2, Th17, and Tfh cells, respectively (**Figure 4B**). Thus, despite the skilled T lymphocytes hyperactivation profile for Th2 and Tfh signatures, suggesting unique Th cell differentiation in infected MyD88$^{-/-}$ mice, transcription factor expression profiling in total CD4+ T cells showed no substantial differences between MyD88$^{+/+}$ and MyD88$^{-/-}$ mice, most likely due to the low sensitivity of the assay.

MyD88$^{-/-}$ Mice Exhibit Dysregulated Antibody Responses When Challenged With *S. typhimurium*

Apart from hyperactivation of myeloid cells including the increased expression of BAFF, a well-known factor associated with abnormal B cell responses and autoimmune diseases (53–56), we demonstrate here that MyD88$^{-/-}$ mice develop hyperactivation of Th2 and Tfh cells. While the role of IL-4 producing cells (Th2) is still a paradox due to pro- or anti-inflammatory effects associated with the development or prevention of autoimmune diseases (57), respectively, it is clear that Tfh cells are key players for the development of humoral immunity and associated autoimmune diseases (52). Although NI and *Salmonella*-infected MyD88$^{+/+}$ and MyD88$^{-/-}$ mice showed similar percentages of splenic B cells (Figure S3A in Supplementary Material), B cells of MyD88$^{-/-}$ mice exhibited higher Sca-1 expression (Figures S3B,C in Supplementary Material), suggesting hyperactivation. Analysis of costimulatory molecules on the surface of B cells demonstrated elevated levels of CD86 expression from infected MyD88$^{-/-}$ mice when compared to MyD88$^{+/+}$ animals (Figure S3E in Supplementary Material), while no differences were observed in the expression of CD80 molecule (Figure S3D in Supplementary Material). Thus, B lymphocytes from MyD88$^{-/-}$ mice appear to be hyper-responsive to *Salmonella* infection.

In accordance, even at a low dose of infection (equivalent to <1 LD_{50}), MyD88$^{-/-}$ mice displayed high serum levels of anti-*Salmonella* antibodies of IgM as well as IgG3 and IgG2c and IgG1 isotypes in comparison to wild-type mice (**Figures 5A–D**). The absolute levels of *Salmonella*-specific IgG2c and IgG1 were also measured and the data confirmed the serum titers (**Figures 5E,F**). The high IgG serum levels of anti-*Salmonella* antibodies in infected MyD88$^{-/-}$ mice first became evident as early as 21 days post *Salmonella* inoculation (**Figures 5G–I**) and was still significantly elevated up to 2 months later, the longest period of observation (data not shown). We also measured total IgG levels and observed that in NI animals, relatively low and comparable levels of serum IgG3 and IgG2c were detected in both MyD88$^{+/+}$ and MyD88$^{-/-}$ mouse strains (Figures S4A,B in Supplementary Material), while IgG1 amounts in uninfected MyD88$^{-/-}$ mice were significantly elevated compared to MyD88$^{+/+}$

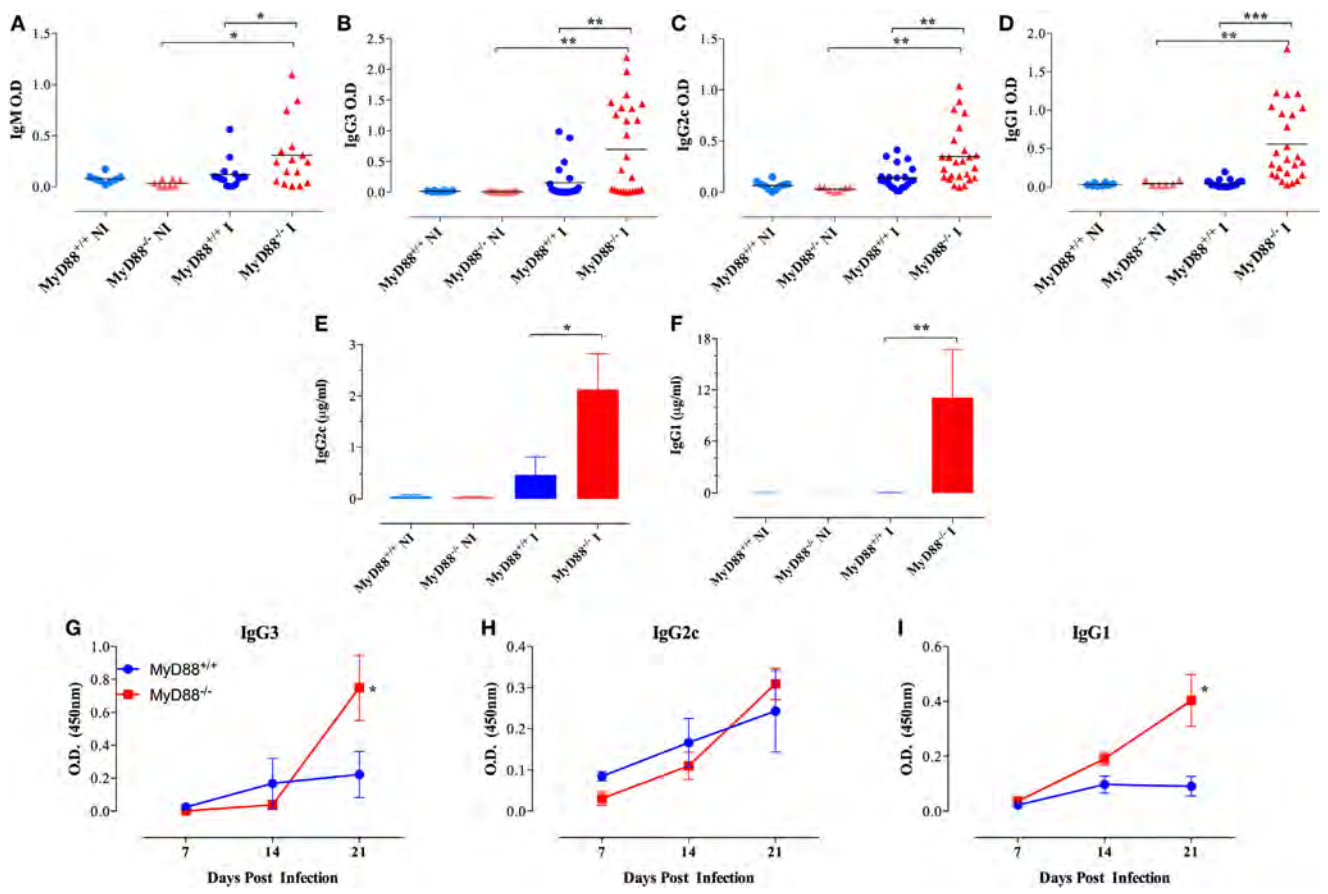

FIGURE 5 | Hypergammaglobulinemia in *Salmonella*-infected MyD88$^{-/-}$ mice. Mice were inoculated i.p. with BRD509 (~200 CFUs/mouse) and sera collected at 4 weeks and analyzed for the presence of *Salmonella*-specific IgM **(A)**, IgG3 **(B)**, IgG2c **(C)**, and IgG1 **(D)** isotypes. Quantification of *Salmonella*-specific serum IgG2c **(E)** and IgG1 **(F)** antibodies in non-infected (NI) and 3-week infected **(I)** mice. Absolute antibody levels are expressed in micrograms per milliliter serum (n = 3–6 per group). **(G–I)** The kinetics of development of antibodies to *Salmonella* infection was evaluated during the first 3 weeks post i.p. infection with a dose of 4,000 CFUs/mouse. *Salmonella*-specific IgG3, IgG2c, and IgG1 were determined (n = 3–6 per group per time point). Asterisks denote statistically significant differences between MyD88$^{-/-}$ and MyD88$^{+/+}$ mice (*p < 0.05; **p < 0.01; ***p < 0.001). Data are compiled from three independent experiments.

mice (2,303 ± 740 vs 626 ± 95 μg/ml, respectively; Figure S4C in Supplementary Material). In *Salmonella*-infected mice, serum IgG3 and IgG2c concentrations were significantly increased, by an average of threefold to fivefold over those in uninfected controls, in both mouse strains (Figures S4A,B in Supplementary Material), while no significant changes in serum IgG1 concentrations were observed upon infection with *Salmonella* in both mouse strains. Noteworthy, the serum levels of all three IgG subclasses in infected MyD88$^{-/-}$ mice were higher in relation to MyD88$^{+/+}$. Hence, in addition to showing a humoral immune response that is constitutively skewed to Th2-induced IgG isotypes, MyD88$^{-/-}$ mice challenged with attenuated *Salmonella* display hypergammaglobulinemia due to unresolved infection.

Presence of Self-Reactive B Cells in MyD88$^{-/-}$ Mice Following Systemic *Salmonella* Infection

Considering the immune hyperactivation and potential etiological link between *Salmonella* infections and the development of autoimmune diseases (26–28), we analyzed the generation of autoantibodies in response to BRD509E. Mouse sera were collected 4–6 weeks following i.p. infection and tested for reactivity against dsDNA, thyroglobulin, and IgG. To rule out non-specific cross-reactivity, all autoantibody ELISAs were determined at a serum dilution of 1/1,000 or greater. Moreover, since all ELISAs were run using IgG-specific secondary antibodies, all observed reactivities reflect IgG isotype autoantibodies. No significant levels of autoreactive antibodies were detectable in wild-type (MyD88$^{+/+}$) mice before or after infection. Similarly, sera from NI MyD88$^{-/-}$ mice had no reactivity to any of the autoantigens. On the other hand, *Salmonella*-infected MyD88$^{-/-}$ mice displayed increased titers of autoantibodies directed against dsDNA (i.e., ANA), thyroglobulin, and IgG RF (**Figures 6A–C**). In order to gain further insight about the physiological significance of the observed autoantibody levels, we compared the sera of *Salmonella*-infected MyD88$^{-/-}$ mice with that of autoimmune MRL-lpr mice for reactivity to dsDNA. The MRL-lpr serum samples were collected from 8-week-old female mice and were positive at 1/100 dilution for

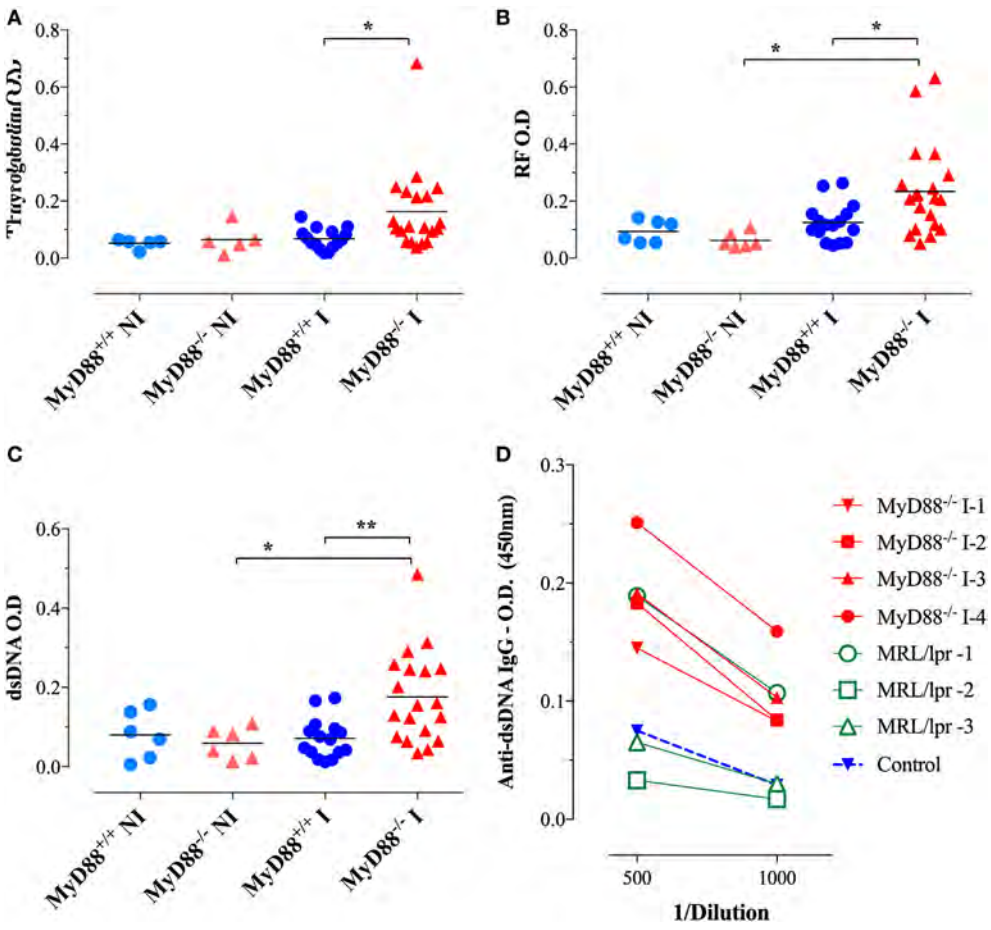

FIGURE 6 | Autoantibody reactivity of MyD88$^{-/-}$ sera after systemic *Salmonella* infection. Sera were collected 4–6 weeks following i.p. infection with BRD509 (~200 CFUs/mouse) and tested for reactivity with thyroglobulin **(A)**, rheumatoid factor [RF; **(B)**], and double-stranded DNA (dsDNA) **(C)** by specific ELISA. The cutoff for the detection of these autoantibodies was determined at 1/1,000 dilution. Data are compiled from three independent experiments. **(D)** Comparison of anti-dsDNA reactivity in sera of MRL-lpr (n = 3) and infected MyD88$^{-/-}$ mice (n = 4). Serum reactivity with dsDNA was done at the indicated final dilutions (1/500 to 1/1,000). Non-infected sera are represented by the "Control" group. Data are representative of two independent experiments (*p < 0.05; **p < 0.01; ***p < 0.001).

ANA using the Euroimmun IIFT:HEp-20-10 cell test kit (data not shown). As shown in **Figure 6D**, a comparison of randomly selected individual serum samples showed that the levels of dsDNA-specific IgG autoantibodies in infected MyD88$^{-/-}$ mice were comparable to, or higher than, those of MRL-lpr mice. Taken together, the data confirm that *Salmonella* infection of MyD88$^{-/-}$ mice induces significant levels of autoantibodies of multiple specificities.

Sera were also tested for reactivity to fixed HEp-2 cells by immunofluorescence. Sera from infected MyD88$^{-/-}$ mice exhibited different patterns of reactivity to dsDNA, ranging from homogenous to fine/coarse speckled (**Figures 7A–C**). Importantly, sera from uninfected mice from both groups were negative for HEp-2 staining (**Figures 7D,E**). While only 8% of the sera from infected MyD88$^{+/+}$ mice (1 out of 12) were positive for HEp-2 staining (**Figure 7F**), approximately 53% of sera (8 out of 15) collected from infected MyD88$^{-/-}$ mice showed strong reactivity to dsDNA in HEp-2 cells (**Figure 7G**). These data suggest that different nuclear antigens are being recognized by the autoantibodies produced in infected MyD88$^{-/-}$ mice.

Given the state of hypergammaglobulinemia and the increased levels of serum IgG autoantibodies in infected MyD88$^{-/-}$ mice, we next evaluated whether this fact was associated with more abundant immune complex deposition in kidney glomeruli. No evidence of staining was detected in the glomeruli of NI MyD88$^{+/+}$ or MyD88$^{-/-}$ mice (**Figures 8A,D**). In sharp contrast, much brighter staining, indicating more deposits of immune complexes,

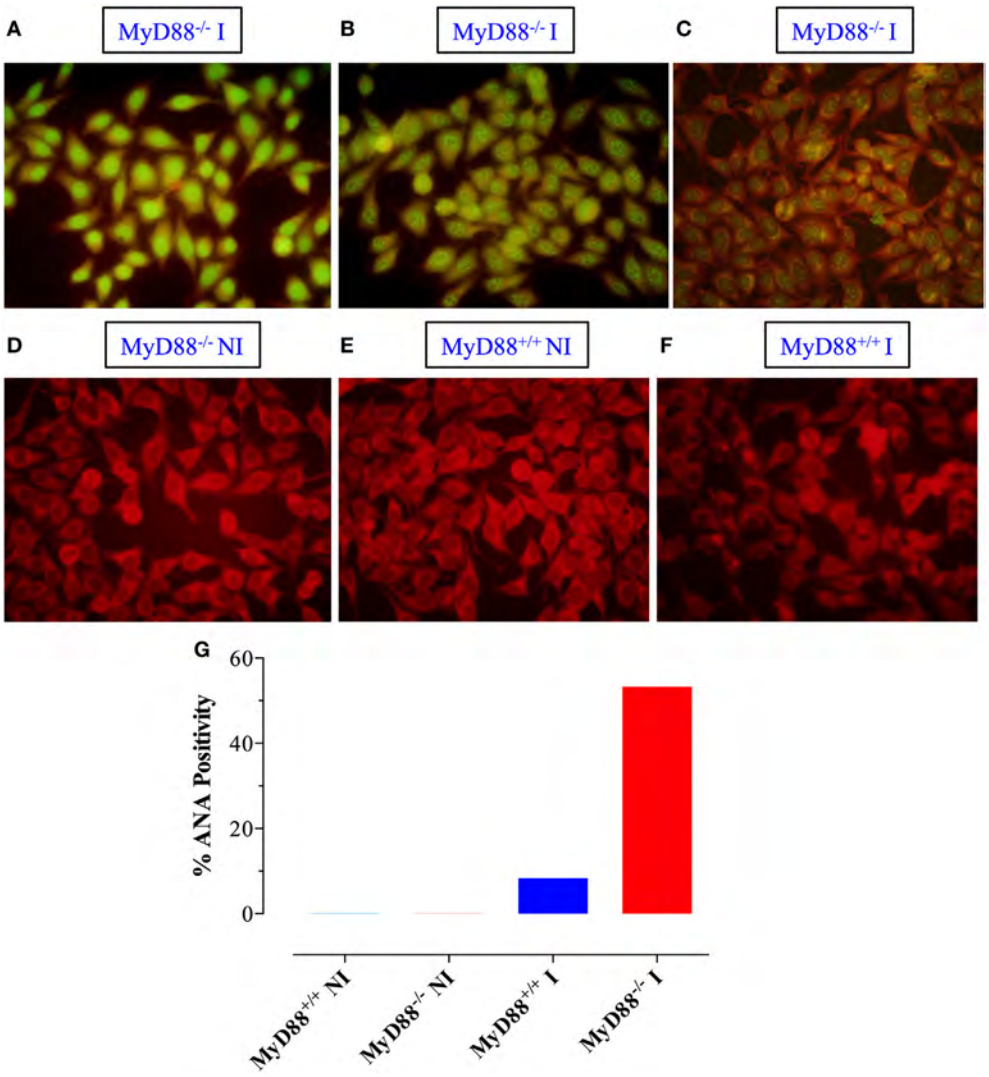

FIGURE 7 | Qualitative detection of antinuclear antibodies (ANA) by immunoflurosence on HEp-2 cells. Sera from *Salmonella*-infected **(A–C)** or non-infected (NI) **(D)** MyD88$^{-/-}$ mice were incubated with HEp-2 cells, as described in Section "Materials and Methods." Positive staining showing homogenous **(A)**, speckled **(B)**, and cytoplasmic **(C)** patterns is shown. As a control, reactivity of sera from NI **(E)** or infected **(F)** MyD88$^{+/+}$ mice is also shown. The percentage of sera from the different experimental groups (n = 5–15 mice/group) that was positive for ANA is summarized in panel **(G)**. The fluorescence was visualized at 40× magnification using an Olympus fluorescent microscope. Data are compiled from three independent experiments.

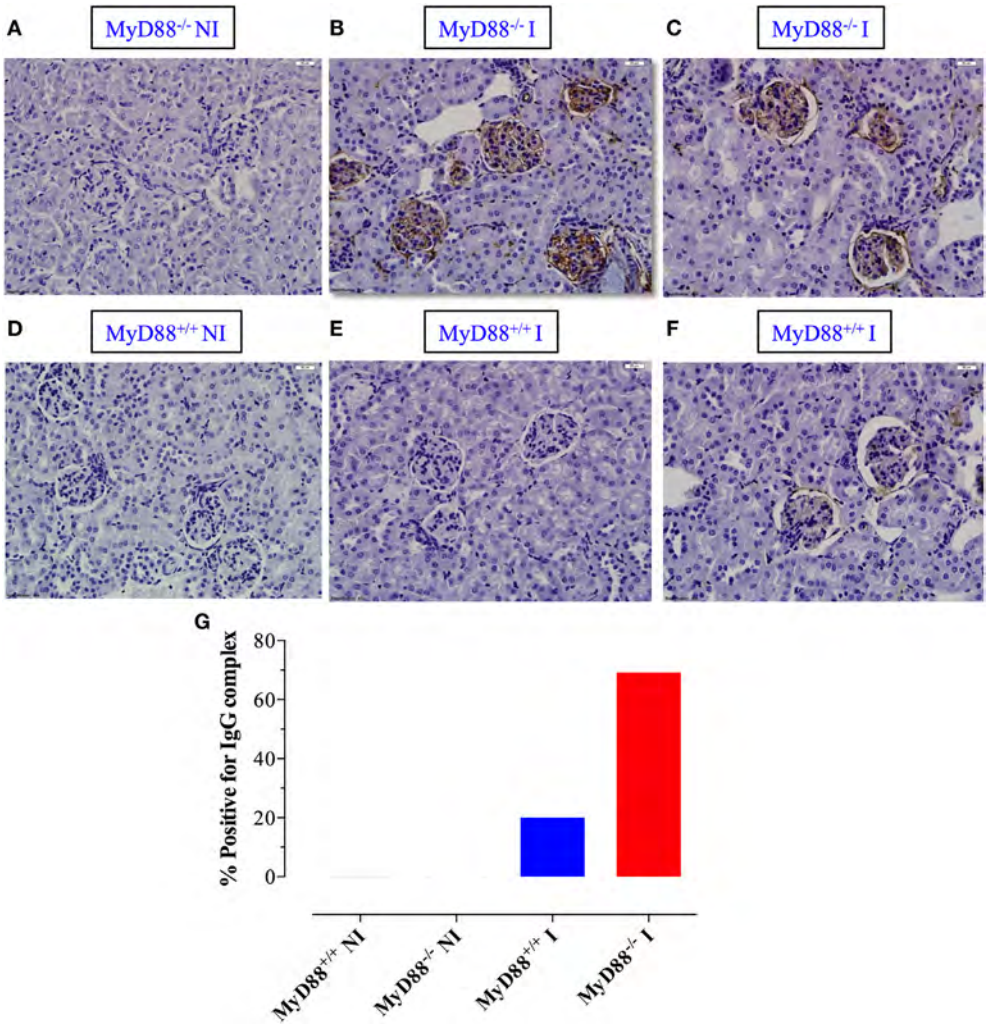

FIGURE 8 | Deposition of immune complexes in *Salmonella*-infected MyD88$^{-/-}$ mice. **(A–F)** Kidney sections were prepared from non-infected (NI) **(A,D)** and infected (I) MyD88$^{-/-}$ **(B,C)** and MyD88$^{+/+}$ **(E,F)** mice and stained with anti-IgG antibody, as described in Section "Materials and Methods" (n = 5–15 mice/group). **(G)** The percentage of mice whose kidney sections scored positive for the presence of immune deposits by DAB staining. Images were taken at 40× magnification. Data are compiled from three independent experiments.

was detected in ~69% of *Salmonella*-infected MyD88$^{-/-}$ mice (**Figures 8B,C,G**) while about 20% of infected MyD88$^{+/+}$ mice showed positive staining of glomeruli but those were generally of low level of intensity (**Figures 8E,F**). Taken together, our data suggest that the absence of MyD88 predisposes animals to hypergammaglobulinemia, production of autoantibodies, and deposition of immune complexes in kidney glomeruli following infection with *S. typhimurium*.

Requirements for Infection-Induced Hypergammaglobulinemia and Autoantibody Production

The next series of experiments were designed to study the requirements for the observed hypergammaglobulinemia and autoantibody synthesis in MyD88$^{-/-}$ mice. We first asked whether infection with another Gram-negative bacterium, *A. baumanii* (strain NM970), could lead to similarly dysregulated antibody production in MyD88$^{-/-}$ mice. Two months following inoculation, MyD88$^{-/-}$ mice exhibited higher bacterial loads in spleen and liver when compared to MyD88$^{+/+}$ mice (**Figures 9A,B**). Infected MyD88$^{-/-}$ mice developed mainly IgG3 antibodies specific to *Acinetobacter*, but they were significantly lower (fourfold) than those observed in infected MyD88$^{+/+}$ mice (**Figure 9C**). No significant bacteria-specific IgG2c or IgG1 antibodies were detected (**Figures 9D,E**). In addition, *A. baumanii* did not induce antibodies directed against dsDNA and thyroglobulin (**Figures 9F,G**). Furthermore, there was no evidence of antibody dysregulation or autoantibody production in MyD88$^{-/-}$ mice infected with the Gram-negative pathogen, *Escherichia coli* or with the Gram-positive bacterium Group B *Streptococcus* (*Streptococcus agalactiae*) (data not shown). Therefore, the development of

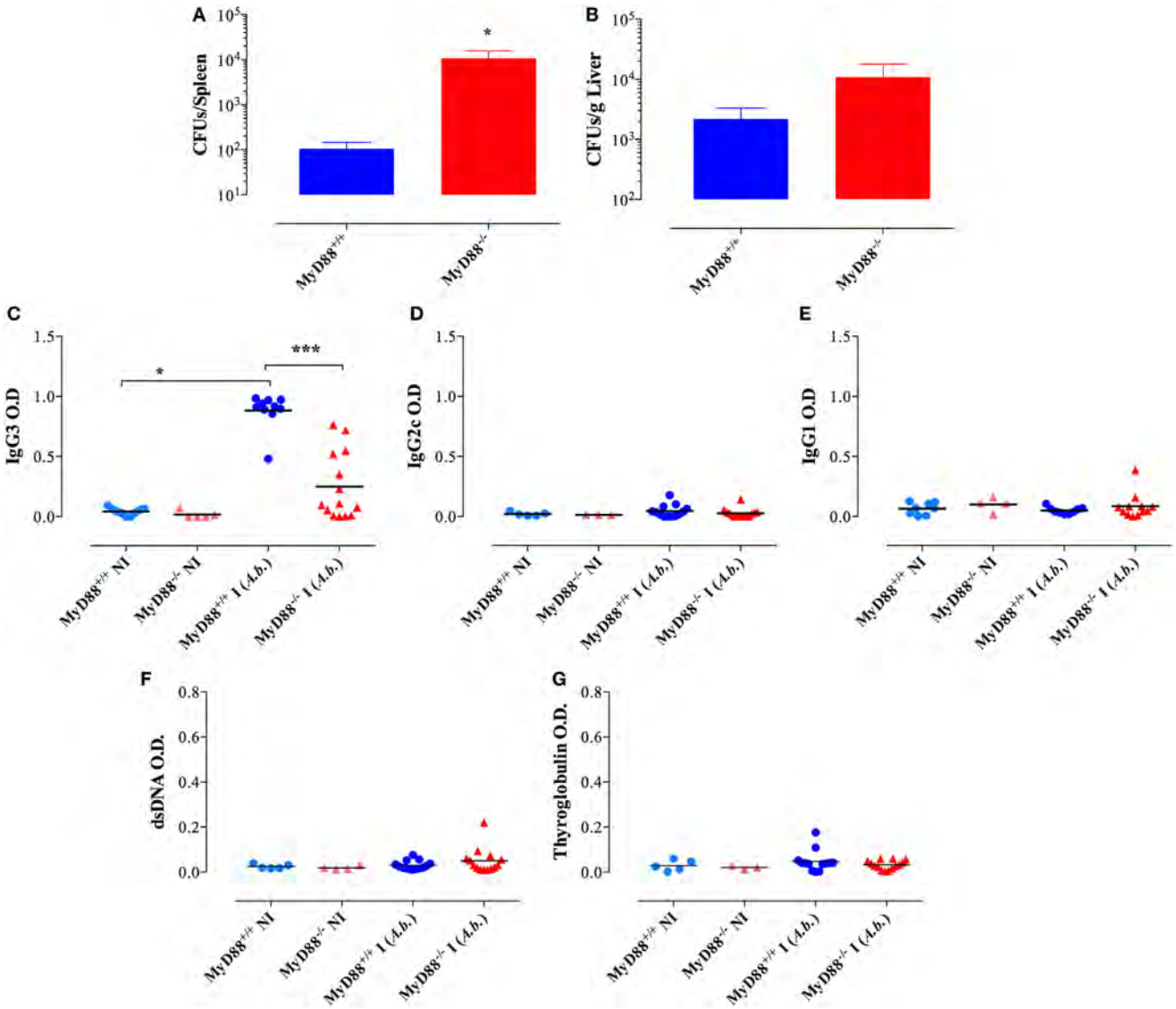

FIGURE 9 | No evidence for immunoglobulin dysregulation in MyD88$^{-/-}$ mice following infection with *Acinetobacter baumanii.* Two months post i.p. infection with a dose of ~1 × 10^5 CFUs/mouse of *A. baumanii*, bacterial counts in spleen **(A)** and liver **(B)** were enumerated (n = 6–7 mice/group). Serum levels of anti-*Acinetobacter* IgG3 **(C)**, IgG2c **(D)**, and IgG1 **(E)** isotypes. **(F,G)** Serum reactivity to double-stranded DNA (dsDNA) and thyroglobulin. The cutoff for the detection of these autoantibodies was determined at 1/1,000 dilution (*$p < 0.05$, ****$p < 0.0001$). Data are compiled from two independent experiments.

autoreactive B cells in infected MyD88$^{-/-}$ mice is dependent on the pathogen with which the animals are challenged.

We also tested the capacity of HK *Salmonella* (strain BRD509E) to induce hypergammaglobulinemia. Although triggering a larger production of IgG1 subclass in MyD88$^{-/-}$ mice in comparison to wild-type mice, the antibody levels in sera were lower than those induced when MyD88$^{-/-}$ mice were infected with live bacteria. HK *Salmonella* was unable to significantly trigger the production of IgG3 and IgG2 subclasses (**Figures 10A–C**) as well as ANA antibodies in both wild-type and MyD88$^{-/-}$ mice (**Figure 10D**). These results indicate that the nature of *Salmonella* antigens is critical for the breakdown in B cell self-tolerance in MyD88$^{-/-}$ mice.

DISCUSSION

After penetration of epithelial barrier through M cells overlying the lymphoid follicles of Peyer's patches, *S. typhimurium,* which is an important model commonly used to study human immune responses to *S. typhi* (58), typically infect macrophages, causing a self-limiting infection in the lamina propria. However, an impaired immune response can result in uncontrolled spread of bacteria into deeper organs such as spleen and liver, where the immune responses try to control the massive bacterial proliferation (22, 59, 60). Here, we show that even low doses (~2 × 10^2 CFUs/mouse) of an attenuated strain of *S. typhimurium* (29, 31) can cause a disseminated disease in MyD88$^{-/-}$ mice, as

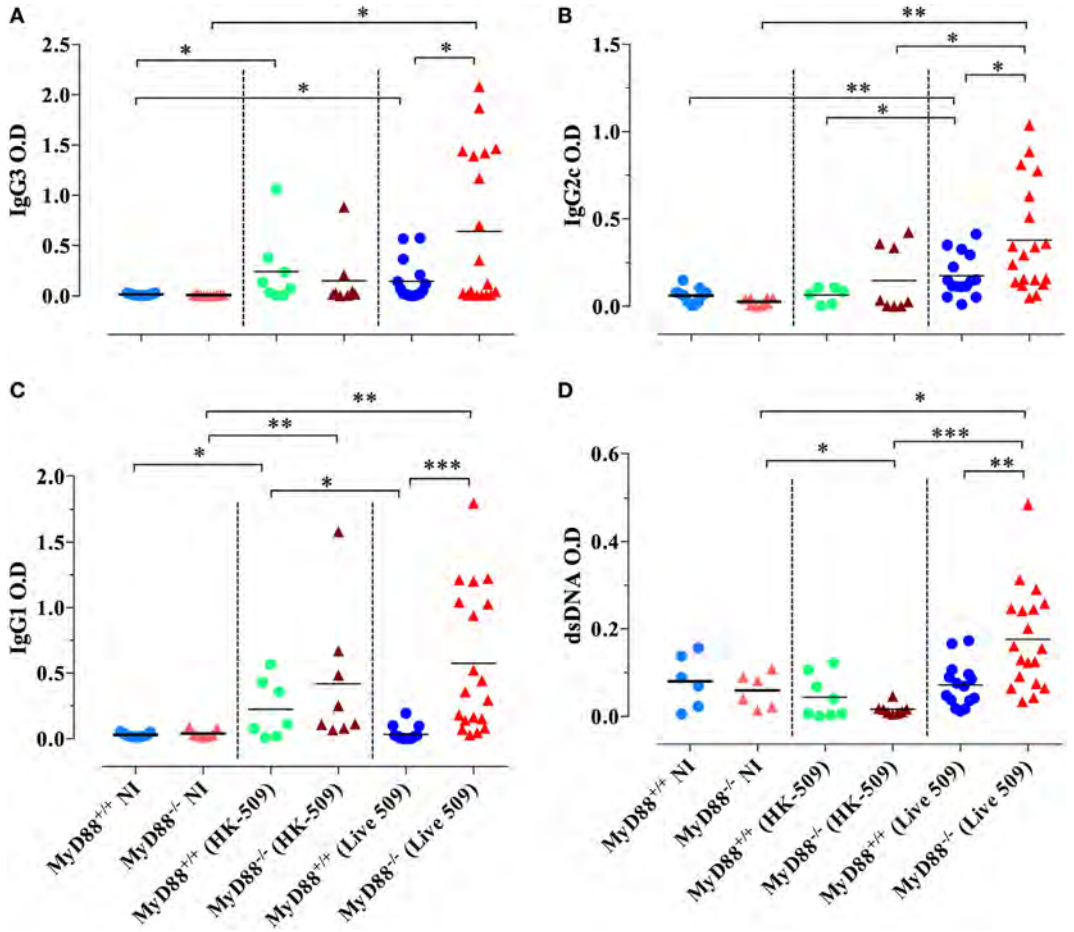

FIGURE 10 | Absence of immunoglobulin dysregulation and autoantibodies in MyD88$^{-/-}$ mice following injection of heat-killed (HK) BRD509. Serum levels of *Salmonella*-specific IgG3 **(A)**, IgG2c **(B)**, and IgG1 **(C)** antibodies were determined at 8 weeks post i.p. inoculation of 2×10^5 HK BRD509. For comparison, antibody production in response to low dose infection with live BRD509E strain, at 3 weeks postinfection, is shown. **(D)** Serum reactivity to double-stranded DNA (dsDNA) in HK vs live *Salmonella*-infected mice. The cutoff for the detection of dsDNA was determined at 1/1,000 dilution. Data are compiled from two independent experiments (*$p < 0.05$; **$p < 0.01$; ***$p < 0.001$).

detected by shedding of bacteria in their stools, splenomegaly, and significantly elevated bacterial burden in spleen and liver compared to MyD88$^{+/+}$ mice. Our data are in agreement with Seibert et al. (22) who reported a defective control of bacterial spread in response to the attenuated *Aro*$^-$ strain SL7207 and Ko et al. (21) who demonstrated that MyD88-dependent innate immune responses are indispensable for protection against another attenuated strain of *S. typhimurium*. Taken together, the data described above suggest that despite the well-characterized phenotypic differences between MyD88-deficient mice and humans, both species are naturally highly susceptible to invasive *Salmonella* infections (16, 17). Importantly, different attenuated bacteria have been designed to effectively work as live vaccines by inducing protection against invasive *Salmonella* diseases (61). Moreover, recombinant strains of *Salmonella* engineered to express immunomodulatory cytokines have been shown to boost innate and adaptive immune responses in normal as well as in immunodeficient hosts (13, 18, 29, 33, 62, 63). The success of these preclinical studies promises to improve the public-health problems caused by *Salmonella* infections, such as those caused by multidrug-resistant strains (64–69) and the high mortality of infected children (70, 71). However, adverse side effects of live vaccines in MyD88-deficient patients have been reported (72). Thereby, the translation of *Salmonella* live vaccines to the clinical routine will need to be carefully monitored to avoid severe adverse effects in infants with inborn errors of TLR signaling.

The establishment of persistent infections by bacterial species, such as *S. typhimurium*, is associated with considerable tissue damage, leading to hyperactivation of immune responses (28). In this context, the characterization of dysregulated adaptive immune responses, including hypergammaglobulinemia, in MyD88$^{-/-}$ mice remains to be explored. Seibert et al. (22) reported a reduced accumulation of CD11b$^+$Gr1$^+$ myeloid cells in spleens of infected MyD88$^{-/-}$ mice, which are unable to clear *S. typhimurium* (SL7207 strain). However, with the exception of elevated *Salmonella*-specific IgG1 antibodies, the authors found

normal levels of anti-*Salmonella* IgM, IgG2b, and IgG2c as well as apparently no abnormalities in T cell responses, suggesting a minimal alteration of humoral and cellular immunity against *S. typhimurium*. On the other hand, Ko et al. reported that *S. typhimurium*-infected (RASV strain) MyD88$^{-/-}$ mice display expanded numbers of B cells, CD4^{+} T cells, and CD11b^{+}Gr1^{+} myeloid cells in their spleen (73). Furthermore, MyD88$^{-/-}$ mice develop dysregulated antibody responses characterized by increased serum levels of IgG, IgA, and IgM *Salmonella*-specific antibodies, production of anti-dsDNA autoantibodies, and deposition of immune complexes in kidneys in a T_{FH} cell-dependent manner.

The apparent differences between the aforementioned studies could be due to different approaches such as the route of bacterial administration (17) and/or the bacterial strains used (74), thus requiring further investigation. Our present findings indicate that abnormalities of myeloid and T cells from MyD88$^{-/-}$ mice contribute systemically to the development of an abnormal humoral immunity characterized by high serum levels of *Salmonella*-specific IgM, IgG3, IgG2c, and IgG1 antibodies and enhanced levels of anti-dsDNA, anti-thyroglobulin, and IgG RF. Our data also suggest that the *Salmonella*-driven B cell activation (73, 75) is dependent upon the establishment of a chronic infection, since only live bacteria were able to induce hypergammaglobulinemia and autoantibody production in MyD88$^{-/-}$ mice. Interestingly, the dysregulation of humoral immune responses in MyD88$^{-/-}$ mice seem to be dependent upon the species of pathogen that mice are challenged with. Thus, while MyD88$^{-/-}$ mice infected with different attenuated *Salmonella* strains or with *B. burgdorferi* (23) developed extreme hypergammaglobulinemia compared to MyD88$^{+/+}$ animals, other bacterial species (*A. baumanii*, *S. agalactiae*, and *E. coli*) were unable to trigger the same phenomenon. Therefore, our findings provide an important link between environmental factor, genetic background, and the potential development of autoimmune diseases.

The hyperactivation of B cell responses in the context of a chronic infection in MyD88$^{-/-}$ mice correlates with aberrant activation of myeloid cells and Tfh cells and the production of BAFF cytokine. Increased levels of BAFF breach B cell tolerance by enhancing survival of self-reactive B cells, thus allowing their abnormal entry into the mature follicular compartment where they can receive T cell help (76). A suppressive role for B cell-intrinsic MyD88 expression has also been proposed (77), which may well underlie the breakdown of B cell self-tolerance in our *Salmonella* infection model. Our current findings show that the autoantibody levels produced in chronically infected MyD88$^{-/-}$ mice are comparable to, or higher than, those in autoimmune MRL-lpr mice. An inflammatory positive-feedback loop involving activated BAFF-producing myeloid cells and IFNγ-secreting T cells has been shown to play an important role in driving autoantibody production in autoimmune-prone mice (78). Purified T cells of infected MyD88$^{-/-}$ mice exhibited a heterogeneous cytokine expression pattern, including IL-21, IL-4, BAFF, IL-10, and IFN-γ and upregulated PD-1. Moreover, intracellular cytokine staining confirmed the increased presence of splenic T cells co-expressing IFN-γ plus IL-4 or IFN-γ plus IL-10 in *Salmonella*-infected MyD88$^{-/-}$ mice. This heterogeneous cytokine expression profile is typical of Tfh cells (51). Collectively, in the absence of MyD88, a persistent infection induces hypergammaglobulinemia and autoantibody development driven by the aberrant activation of myeloid cells and BAFF secretion. This, in turn, activates Tfh cells which consequently drive aberrant B cell responses.

In an attempt to translate our findings to humans, during approximately 10 years after the first report suggesting that the MyD88 signaling pathway is essential for the removal of autoreactive B cells, paradoxically neither autoreactive antibodies were identified in the serum of MyD88-deficient patients nor these subjects were reported to develop autoimmune diseases (72, 79). However, very few MyD88-deficient patients have been characterized so far (72). The clinical spectrum of MyD88-deficiency remains to be determined in different geographic regions of the world where MyD88-deficient subjects will enter in contact with different pathogens that could trigger the development of self-reactive B cells. In line with this hypothesis, during the time of manuscript preparation, a single Myd88-deficient patient and four with IRAK4 deficiency were reported to develop a particular pattern of self-reactive B cells, which are expanded during lupus flares, and speculated to be modulated by alterations in human microbiome (80). This indicates that patients with MyD88 deficiency must be monitored for the development of autoreactive B cells and that improvement in the genetic diagnosis of this primary immunodeficiency worldwide could provide a priceless opportunity to uncover new MyD88-dependent mechanisms that orchestrate the adaptive immune response.

In conclusion, our findings expand the knowledge about the role of the TLR-MyD88 pathway in the host protection against *Salmonella* infections. Importantly, these data further characterize the dysregulation of adaptive immune system triggered by *S. typhimurium* in MyD88$^{-/-}$ mice. Considering the link between *Salmonella* infections and the development of autoimmune diseases (26, 27, 81, 82), future studies to further investigate the nature of immune dysregulation induced by *Salmonella* species in immunocompromised and immunocompetent hosts could reveal several novel important immunological mechanisms that can be explored as new therapeutic targets.

ETHICS STATEMENT

All studies involving animals were conducted in accordance with and after approval of the animal research ethics committee of the College of Medicine and Health Sciences, United Arab Emirates University.

AUTHOR CONTRIBUTIONS

JI performed experiments and analyzed data. YM provided valuable suggestions and support for all molecular studies. GB provided valuable support for histological studies. AA-S performed ELISA experiments and analyzed data. WC contributed to the design of the study. TK and AI performed bioinformatics analysis. GR contributed to the discussion. KB and RL provided valuable

reagents. OC-M contributed to data analysis and interpretation and to manuscript writing. MF-C supervised the project and wrote the final manuscript. Ba-R designed the study, supervised the project, analyzed data, and wrote the final manuscript. All authors read and approved the final manuscript.

ACKNOWLEDGMENTS

The authors wish to thank Dr. S. Akira (Osaka University, Osaka, Japan) and Dr. Richard Flavell (Yale University School of Medicine, New Haven, CT, USA) for providing the MyD88$^{-/-}$ mice and Dr. Tibor Pal (CMHS, UAE University) for the *A. baumanii* NM97 strain. The authors also thank Dr. Maryem Rabah (Habib Bourguiba Hospital, Sfax, Tunisia) for valuable assistance with autoantibody assays. This work formed part of the thesis dissertation for the award of the Ph.D. degree to JI (83).

FUNDING

This work was funded by grants from the Research Grants Committee of the College of Medicine and Health Sciences, United Arab Emirates (UAE) University (to Ba-R), the Scientific Research Council, UAE University (to WC and Ba-R) and, in part, by a UAEU Program for Advanced Research grant, University Research Council, UAE University (to Ba-R). JI was supported through a scholarship from the Office of the Deputy Vice Chancellor for Research and Graduate Studies of UAE University.

SUPPLEMENTARY MATERIAL

The Supplementary Material for this article can be found online at https://www.frontiersin.org/articles/10.3389/fimmu.2018.01384/full#supplementary-material.

REFERENCES

1. Janeway CA. Approaching the asymptote? Evolution and revolution in immunology. *Cold Spring Harb Symp Quant Biol* (1989) 54:1–13. doi:10.1101/SQB.1989.054.01.003
2. Iwasaki A, Medzhitov R. Control of adaptive immunity by the innate immune system. *Nat Immunol* (2015) 16(4):343–53. doi:10.1038/ni.3123
3. Loures FV, Pina A, Felonato M, Feriotti C, de Araujo EF, Calich VL. MyD88 signaling is required for efficient innate and adaptive immune responses to *Paracoccidioides brasiliensis* infection. *Infect Immun* (2011) 79(6):2470–80. doi:10.1128/IAI.00375-10
4. Vajjhala PR, Ve T, Bentham A, Stacey KJ, Kobe B. The molecular mechanisms of signaling by cooperative assembly formation in innate immunity pathways. *Mol Immunol* (2017) 86:23–37. doi:10.1016/j.molimm.2017.02.012
5. Akira S, Takeda K. Toll-like receptor signalling. *Nat Rev Immunol* (2004) 4:499–511. doi:10.1038/nri1391
6. Pasare C, Medzhitov R. Toll-dependent control mechanisms of CD4 T cell activation. *Immunity* (2004) 21(5):733–41. doi:10.1016/j.immuni.2004.10.006
7. Pasare C, Medzhitov R. Control of B-cell responses by toll-like receptors. *Nature* (2005) 438(7066):364–8. doi:10.1038/nature04267
8. Gavin AL, Hoebe K, Duong B, Ota T, Martin C, Beutler B, et al. Adjuvant-enhanced antibody responses in the absence of toll-like receptor signaling. *Science* (2006) 314(5807):1936–8. doi:10.1126/science.1135299
9. Scanga CA, Aliberti J, Jankovic D, Tilloy F, Bennouna S, Denkers EY, et al. Cutting edge: MyD88 is required for resistance to *Toxoplasma gondii* infection and regulates parasite-induced IL-12 production by dendritic cells. *J Immunol* (2002) 168(12):5997–6001. doi:10.4049/jimmunol.168.12.5997
10. Scanga CA, Bafica A, Feng CG, Cheever AW, Hieny S, Sher A. MyD88-deficient mice display a profound loss in resistance to *Mycobacterium tuberculosis* associated with partially impaired Th1 cytokine and nitric oxide synthase 2 expression. *Infect Immun* (2004) 72(4):2400–4. doi:10.1128/IAI.72.4.2400-2404.2004
11. Campos MA, Closel M, Valente EP, Cardoso JE, Akira S, Alvarez-Leite JI, et al. Impaired production of proinflammatory cytokines and host resistance to acute infection with *Trypanosoma cruzi* in mice lacking functional myeloid differentiation factor 88. *J Immunol* (2004) 172(3):1711–8. doi:10.4049/jimmunol.172.3.1711
12. Weiss DS, Raupach B, Takeda K, Akira S, Zychlinsky A. Toll-like receptors are temporally involved in host defense. *J Immunol* (2004) 172(7):4463–9. doi:10.4049/jimmunol.172.7.4463
13. al-Ramadi BK, Fernandez-Cabezudo MJ, Mustafa N, Xu D. Activation of innate immune responses by IL-2-expressing *Salmonella typhimurium* is independent of toll-like receptor 4. *Mol Immunol* (2004) 40(10):671–9. doi:10.1016/j.molimm.2003.09.005
14. Roy MF, Lariviere L, Wilkinson R, Tam M, Stevenson MM, Malo D. Incremental expression of Tlr4 correlates with mouse resistance to *Salmonella* infection and fine regulation of relevant immune genes. *Genes Immun* (2006) 7(5):372–83. doi:10.1038/sj.gene.6364309
15. Bretz C, Gersuk G, Knoblaugh S, Chaudhary N, Randolph-Habecker J, Hackman RC, et al. MyD88 signaling contributes to early pulmonary responses to *Aspergillus fumigatus*. *Infect Immun* (2008) 76(3):952–8. doi:10.1128/IAI.00927-07
16. von Bernuth H, Picard C, Puel A, Casanova JL. Experimental and natural infections in MyD88- and IRAK-4-deficient mice and humans. *Eur J Immunol* (2012) 42(12):3126–35. doi:10.1002/eji.201242683
17. Issac JM, Sarawathiamma D, Al-Ketbi MI, Azimullah S, Al-Ojali SM, Mohamed YA, et al. Differential outcome of infection with attenuated *Salmonella* in MyD88-deficient mice is dependent on the route of administration. *Immunobiology* (2013) 218(1):52–63. doi:10.1016/j.imbio.2012.02.001
18. Al-Ojali SM, Tara Moore CB, Fernandez-Cabezudo MJ, Al-Ramadi BK. IFNgamma expression by an attenuated strain of *Salmonella enterica* serovar Typhimurium improves vaccine efficacy in susceptible TLR4-defective C3H/HeJ mice. *Med Microbiol Immunol* (2013) 202(1):49–61. doi:10.1007/s00430-012-0248-z
19. Bello-Irizarry SN, Wang J, Johnston CJ, Gigliotti F, Wright TW. MyD88 signaling regulates both host defense and immunopathogenesis during pneumocystis infection. *J Immunol* (2014) 192(1):282–92. doi:10.4049/jimmunol.1301431
20. Coady A, Sil A. MyD88-dependent signaling drives host survival and early cytokine production during *Histoplasma capsulatum* infection. *Infect Immun* (2015) 83(4):1265–75. doi:10.1128/IAI.02619-14
21. Ko HJ, Yang JY, Shim DH, Yang H, Park SM, Curtiss R III, et al. Innate immunity mediated by MyD88 signal is not essential for induction of lipopolysaccharide-specific B cell responses but is indispensable for protection against *Salmonella enterica* serovar Typhimurium infection. *J Immunol* (2009) 182(4):2305–12. doi:10.4049/jimmunol.0801980
22. Seibert SA, Mex P, Kohler A, Kaufmann SH, Mittrucker HW. TLR2-, TLR4- and Myd88-independent acquired humoral and cellular immunity against *Salmonella enterica* serovar Typhimurium. *Immunol Lett* (2010) 127(2):126–34. doi:10.1016/j.imlet.2009.10.008
23. Woods A, Soulas-Sprauel P, Jaulhac B, Arditi B, Knapp AM, Pasquali JL, et al. MyD88 negatively controls hypergammaglobulinemia with autoantibody production during bacterial infection. *Infect Immun* (2008) 76(4):1657–67. doi:10.1128/IAI.00951-07
24. Diamond CE, Leong KWK, Vacca M, Rivers-Auty J, Brough D, Mortellaro A. *Salmonella typhimurium*-induced IL-1 release from primary human monocytes requires NLRP3 and can occur in the absence of pyroptosis. *Sci Rep* (2017) 7(1):6861. doi:10.1038/s41598-017-07081-3
25. Wotzka SY, Nguyen BD, Hardt WD. *Salmonella typhimurium* diarrhea reveals basic principles of enteropathogen infection and disease-promoted DNA exchange. *Cell Host Microbe* (2017) 21(4):443–54. doi:10.1016/j.chom.2017.03.009
26. Hannu T, Mattila L, Siitonen A, Leirisalo-Repo M. Reactive arthritis following an outbreak of *Salmonella typhimurium* phage type 193 infection. *Ann Rheum Dis* (2002) 61(3):264–6. doi:10.1136/ard.61.3.264
27. Locht H, Molbak K, Krogfelt KA. High frequency of reactive joint symptoms after an outbreak of *Salmonella* enteritidis. *J Rheumatol* (2002) 29(4):767–71.

28. Monack DM, Mueller A, Falkow S. Persistent bacterial infections: the interface of the pathogen and the host immune system. *Nat Rev Microbiol* (2004) 2(9):747–65. doi:10.1038/nrmicro955
29. al-Ramadi BK, Al-Dhaheri MH, Mustafa N, Abouhaidar M, Xu D, Liew FY, et al. Influence of vector-encoded cytokines on anti-*Salmonella* immunity: divergent effects of interleukin-2 and tumor necrosis factor alpha. *Infect Immun* (2001) 69(6):3980–8. doi:10.1128/IAI.69.6.3980-3988.2001
30. al-Ramadi BK, Bashir G, Rizvi TA, Fernandez-Cabezudo MJ. Poor survival but high immunogenicity of IL-2-expressing *Salmonella typhimurium* in inherently resistant mice. *Microbes Infect* (2004) 6(4):350–9. doi:10.1016/j.micinf.2003.12.012
31. al-Ramadi BK, Fernandez-Cabezudo MJ, Ullah A, El-Hasasna H, Flavell RA. CD154 is essential for protective immunity in experimental *Salmonella* infection: evidence for a dual role in innate and adaptive immune responses. *J Immunol* (2006) 176(1):496–506. doi:10.4049/jimmunol.176.1.496
32. Adachi O, Kawai T, Takeda K, Matsumoto M, Tsutsui H, Sakagami M, et al. Targeted disruption of the MyD88 gene results in loss of IL-1- and IL-18-mediated function. *Immunity* (1998) 9(1):143–50. doi:10.1016/S1074-7613(00)80596-8
33. al-Ramadi BK, Adeghate E, Mustafa N, Ponery AS, Fernandez-Cabezudo MJ. Cytokine expression by attenuated intracellular bacteria regulates the immune response to infection: the *Salmonella* model. *Mol Immunol* (2002) 38(12–13):931–40. doi:10.1016/S0161-5890(02)00020-2
34. Kaimala S, Mohamed YA, Nader N, Issac J, Elkord E, Chouaib S, et al. *Salmonella*-mediated tumor regression involves targeting of tumor myeloid suppressor cells causing a shift to M1-like phenotype and reduction in suppressive capacity. *Cancer Immunol Immunother* (2014) 63(6):587–99. doi:10.1007/s00262-014-1543-x
35. George JA, Bashir G, Qureshi MM, Mohamed YA, Azzi J, al-Ramadi BK, et al. Cholinergic stimulation prevents the development of autoimmune diabetes: evidence for the modulation of Th17 effector cells via an IFNγ-dependent mechanism. *Front Immunol* (2016) 7:419. doi:10.3389/fimmu.2016.00419
36. Chen F, Maldonado MA, Madaio M, Eisenberg RA. The role of host (endogenous) T cells in chronic graft-versus-host autoimmune disease. *J Immunol* (1998) 161(11):5880–5.
37. LeClair KP, Bridgett MM, Dumont FJ, Palfree RGE, Hammerling U, Bothwell ALM. Kinetic analysis of Ly-6 gene induction in a T lymphoma by interferons and interleukin-1 and demonstration of Ly-6 inducibility in diverse cell types. *Eur J Immunol* (1989) 19:1233–9. doi:10.1002/eji.1830190713
38. Mackay F, Silveira PA, Brink R. B cells and the BAFF/APRIL axis: fast-forward on autoimmunity and signaling. *Curr Opin Immunol* (2007) 19(3):327–36. doi:10.1016/j.coi.2007.04.008
39. Stadanlick JE, Cancro MP. BAFF and the plasticity of peripheral B cell tolerance. *Curr Opin Immunol* (2008) 20(2):158–61. doi:10.1016/j.coi.2008.03.015
40. Ito T, Connett JM, Kunkel SL, Matsukawa A. The linkage of innate and adaptive immune response during granulomatous development. *Front Immunol* (2013) 4:10. doi:10.3389/fimmu.2013.00010
41. Hess J, Ladel C, Miko D, Kaufmann SH. *Salmonella typhimurium* aroA$^-$ infection in gene-targeted immunodeficient mice: major role of CD4$^+$ TCR-ab cells and IFN-g in bacterial clearance independent of intracellular location. *J Immunol* (1996) 156(9):3321–6.
42. Ziegler SF. Division of labour by CD4(+) T helper cells. *Nat Rev Immunol* (2016) 16(7):403. doi:10.1038/nri.2016.53
43. Cabral-Marques O, Arslanian C, Ramos RN, Morato M, Schimke L, Soeiro Pereira PV, et al. Dendritic cells from X-linked hyper-IgM patients present impaired responses to *Candida albicans* and *Paracoccidioides brasiliensis*. *J Allergy Clin Immunol* (2012) 129(3):778–86. doi:10.1016/j.jaci.2011.10.026
44. Guenova E, Skabytska Y, Hoetzenecker W, Weindl G, Sauer K, Tham M, et al. IL-4 abrogates T(H)17 cell-mediated inflammation by selective silencing of IL-23 in antigen-presenting cells. *Proc Natl Acad Sci U S A* (2015) 112(7):2163–8. doi:10.1073/pnas.1416922112
45. Lopez-Bravo M, Minguito de la Escalera M, Dominguez PM, Gonzalez-Cintado L, del Fresno C, Martin P, et al. IL-4 blocks TH1-polarizing/inflammatory cytokine gene expression during monocyte-derived dendritic cell differentiation through histone hypoacetylation. *J Allergy Clin Immunol* (2013) 132(6):1409–19. doi:10.1016/j.jaci.2013.08.039
46. Vogelzang A, McGuire HM, Yu D, Sprent J, Mackay CR, King C. A fundamental role for interleukin-21 in the generation of T follicular helper cells. *Immunity* (2008) 29(1):127–37. doi:10.1016/j.immuni.2008.06.001
47. Lu KT, Kanno Y, Cannons JL, Handon R, Bible P, Elkahloun AG, et al. Functional and epigenetic studies reveal multistep differentiation and plasticity of in vitro-generated and in vivo-derived follicular T helper cells. *Immunity* (2011) 35(4):622–32. doi:10.1016/j.immuni.2011.07.015
48. Bashyam H. Th1/Th2 cross-regulation and the discovery of IL-10. *J Exp Med* (2007) 204(2):237. doi:10.1084/jem.2042fta
49. Ettinger R, Sims GP, Fairhurst AM, Robbins R, da Silva YS, Spolski R, et al. IL-21 induces differentiation of human naive and memory B cells into antibody-secreting plasma cells. *J Immunol* (2005) 175(12):7867–79. doi:10.4049/jimmunol.175.12.7867
50. Kohm AP, Sanders VM. Suppression of antigen-specific Th2 cell-dependent IgM and IgG1 production following norepinephrine depletion in vivo. *J Immunol* (1999) 162(9):5299–308.
51. Crotty S. T follicular helper cell differentiation, function, and roles in disease. *Immunity* (2014) 41(4):529–42. doi:10.1016/j.immuni.2014.10.004
52. Marnik EA, Wang X, Sproule TJ, Park G, Christianson GJ, Lane-Reticker SK, et al. Precocious interleukin 21 expression in naive mice identifies a natural helper cell population in autoimmune disease. *Cell Rep* (2017) 21(1):208–21. doi:10.1016/j.celrep.2017.09.036
53. Bermejo DA, Amezcua-Vesely MC, Montes CL, Merino MC, Gehrau RC, Cejas H, et al. BAFF mediates splenic B cell response and antibody production in experimental Chagas disease. *PLoS Negl Trop Dis* (2010) 4(5):e679. doi:10.1371/journal.pntd.0000679
54. Groom JR, Fletcher CA, Walters SN, Grey ST, Watt SV, Sweet MJ, et al. BAFF and MyD88 signals promote a lupus-like disease independent of T cells. *J Exp Med* (2007) 204(8):1959–71. doi:10.1084/jem.20062567
55. Shlomchik MJ. Sites and stages of autoreactive B cell activation and regulation. *Immunity* (2008) 28(1):18–28. doi:10.1016/j.immuni.2007.12.004
56. Steri M, Orru V, Idda ML, Pitzalis M, Pala M, Zara I, et al. Overexpression of the cytokine BAFF and autoimmunity risk. *N Engl J Med* (2017) 376(17):1615–26. doi:10.1056/NEJMoa1610528
57. Biedermann T, Rocken M. Pro- and anti-inflammatory effects of IL-4: from studies in mice to therapy of autoimmune diseases in humans. *Ernst Schering Res Found Workshop* (2005) 50:235–42. doi:10.1007/3-540-26811-1_13
58. Stecher B, Macpherson AJ, Hapfelmeier S, Kremer M, Stallmach T, Hardt WD. Comparison of *Salmonella enterica* serovar Typhimurium colitis in germfree mice and mice pretreated with streptomycin. *Infect Immun* (2005) 73(6):3228–41. doi:10.1128/IAI.73.6.3228-3241.2005
59. Monack DM, Bouley DM, Falkow S. *Salmonella typhimurium* persists within macrophages in the mesenteric lymph nodes of chronically infected Nramp1+/+ mice and can be reactivated by IFNgamma neutralization. *J Exp Med* (2004) 199(2):231–41. doi:10.1084/jem.20031319
60. Vazquez-Torres A, Jones-Carson J, Baumler AJ, Falkow S, Valdivia R, Brown W, et al. Extraintestinal dissemination of *Salmonella* by CD18-expressing phagocytes. *Nature* (1999) 401:804–8. doi:10.1038/44593
61. Hoiseth SK, Stocker BAD. Aromatic-dependent *Salmonella typhimurium* are non-virulent and effective as live vaccines. *Nature* (1981) 291:238–9. doi:10.1038/291238a0
62. al-Ramadi BK, Mustafa N, AbouHaidar M, Fernandez-Cabezudo MJ. Induction of innate immunity by IL-2-expressing *Salmonella* confers protection against lethal infection. *Mol Immunol* (2003) 39(13):763–70. doi:10.1016/S0161-5890(03)00005-1
63. Al-Ojali SM, Moore CB, Fernandez-Cabezudo MJ, Al-Ramadi BK. Enhancement of the anti-*Salmonella* immune response in CD154-deficient mice by an attenuated, IFN-gamma-expressing, strain of *Salmonella enterica* serovar Typhimurium. *Microb Pathog* (2012) 52(6):326–35. doi:10.1016/j.micpath.2012.03.002
64. Brunelle BW, Bearson BL, Bearson SMD, Casey TA. Multidrug-resistant *Salmonella enterica* serovar Typhimurium isolates are resistant to antibiotics that influence their swimming and swarming motility. *mSphere* (2017) 2(6). doi:10.1128/mSphere.00306-17
65. Brunelle BW, Bearson SM, Bearson BL. Tetracycline accelerates the temporally-regulated invasion response in specific isolates of multidrug-resistant *Salmonella enterica* serovar Typhimurium. *BMC Microbiol* (2013) 13:202. doi:10.1186/1471-2180-13-202
66. Carroll LM, Wiedmann M, den Bakker H, Siler J, Warchocki S, Kent D, et al. Whole-genome sequencing of drug-resistant *Salmonella enterica* isolates from dairy cattle and humans in New York and Washington States reveals source and Geographic Associations. *Appl Environ Microbiol* (2017) 83(12). doi:10.1128/AEM.00140-17

67. Elshayeb AA, Ahmed AA, El Siddig MA, El Hussien AA. Prevalence of current patterns and predictive trends of multidrug-resistant *Salmonella typhi* in Sudan. *Ann Clin Microbiol Antimicrob* (2017) 16(1):73. doi:10.1186/s12941-017-0247-4
68. Martinez MC, Retamal P, Rojas-Aedo JF, Fernandez J, Fernandez A, Lapierre L. Multidrug-resistant outbreak-associated *Salmonella* strains in irrigation water from the metropolitan region, Chile. *Zoonoses Public Health* (2017) 64(4):299–304. doi:10.1111/zph.12311
69. Zhang CZ, Ren SQ, Chang MX, Chen PX, Ding HZ, Jiang HX. Resistance mechanisms and fitness of *Salmonella typhimurium* and *Salmonella* enteritidis mutants evolved under selection with ciprofloxacin in vitro. *Sci Rep* (2017) 7(1):9113. doi:10.1038/s41598-017-09151-y
70. MacLennan CA, Martin LB, Micoli F. Vaccines against invasive *Salmonella* disease: current status and future directions. *Hum Vaccin Immunother* (2014) 10(6):1478–93. doi:10.4161/hv.29054
71. McGregor AC, Waddington CS, Pollard AJ. Prospects for prevention of *Salmonella* infection in children through vaccination. *Curr Opin Infect Dis* (2013) 26(3):254–62. doi:10.1097/QCO.0b013e32835fb829
72. Picard C, von Bernuth H, Ghandil P, Chrabieh M, Levy O, Arkwright PD, et al. Clinical features and outcome of patients with IRAK-4 and MyD88 deficiency. *Medicine (Baltimore)* (2010) 89(6):403–25. doi:10.1097/MD.0b013e3181fd8ec3
73. Ko HJ, Yang H, Yang JY, Seo SU, Chang SY, Seong JK, et al. Expansion of Tfh-like cells during chronic *Salmonella* exposure mediates the generation of autoimmune hypergammaglobulinemia in MyD88-deficient mice. *Eur J Immunol* (2012) 42(3):618–28. doi:10.1002/eji.201141748
74. Litrup E, Torpdahl M, Malorny B, Huehn S, Helms M, Christensen H, et al. DNA microarray analysis of *Salmonella* serotype Typhimurium strains causing different symptoms of disease. *BMC Microbiol* (2010) 10:96. doi:10.1186/1471-2180-10-96
75. Di Niro R, Lee SJ, Vander Heiden JA, Elsner RA, Trivedi N, Bannock JM, et al. *Salmonella* infection drives promiscuous B cell activation followed by extrafollicular affinity maturation. *Immunity* (2015) 43(1):120–31. doi:10.1016/j.immuni.2015.06.013
76. Thien M, Phan TG, Gardam S, Amesbury M, Basten A, Mackay F, et al. Excess BAFF rescues self-reactive B cells from peripheral deletion and allows them to enter forbidden follicular and marginal zone niches. *Immunity* (2004) 20(6):785–98. doi:10.1016/j.immuni.2004.05.010
77. Neves P, Lampropoulou V, Calderon-Gomez E, Roch T, Stervbo U, Shen P, et al. Signaling via the MyD88 adaptor protein in B cells suppresses protective immunity during *Salmonella typhimurium* infection. *Immunity* (2010) 33(5):777–90. doi:10.1016/j.immuni.2010.10.016
78. Scapini P, Hu Y, Chu CL, Migone TS, Defranco AL, Cassatella MA, et al. Myeloid cells, BAFF, and IFN-gamma establish an inflammatory loop that exacerbates autoimmunity in Lyn-deficient mice. *J Exp Med* (2010) 207(8):1757–73. doi:10.1084/jem.20100086
79. Isnardi I, Ng YS, Srdanovic I, Motaghedi R, Rudchenko S, von Bernuth H, et al. IRAK-4- and MyD88-dependent pathways are essential for the removal of developing autoreactive B cells in humans. *Immunity* (2008) 29(5):746–57. doi:10.1016/j.immuni.2008.09.015
80. Schickel JN, Glauzy S, Ng YS, Chamberlain N, Massad C, Isnardi I, et al. Self-reactive VH4-34-expressing IgG B cells recognize commensal bacteria. *J Exp Med* (2017) 214(7):1991–2003. doi:10.1084/jem.20160201
81. Soloski MJ, Metcalf ES. *Salmonella* as an inducer of autoimmunity. *EcoSal Plus* (2007) 2(2). doi:10.1128/ecosalplus.8.8.13
82. Kerstein A, Schuler S, Cabral-Marques O, Fazio J, Hasler R, Muller A, et al. Environmental factor and inflammation-driven alteration of the total peripheral T-cell compartment in granulomatosis with polyangiitis. *J Autoimmun* (2017) 78:79–91. doi:10.1016/j.jaut.2016.12.004
83. Issac JM. *Role of MyD88 Protein in the Maintenance of Immunological Self-Tolerance: Induction of Autoimmunity by Salmonella Infection Consequent to MyD88 Deficiency*. Dissertation thesis, Al-Ain: United Arab Emiraets University (2014).

Conflict of Interest Statement: The authors declare that the research was conducted in the absence of any commercial or financial relationships that could be construed as a potential conflict of interest.

The reviewer TW and the handling Editor declared their shared affiliation.

frontiers in Immunology

ORIGINAL RESEARCH
published: 06 June 2018
doi: 10.3389/fimmu.2018.01183

Sialylated Autoantigen-Reactive IgG Antibodies Attenuate Disease Development in Autoimmune Mouse Models of Lupus Nephritis and Rheumatoid Arthritis

Yannic C. Bartsch[1†], Johann Rahmöller[1,2†], Maria M. M. Mertes[3†], Susanne Eiglmeier[3], Felix K. M. Lorenz[3], Alexander D. Stoehr[3], Dominique Braumann[1,4], Alexandra K. Lorenz[3], André Winkler[3], Gina-Maria Lilienthal[1], Janina Petry[1], Juliane Hobusch[1], Moritz Steinhaus[1], Constanze Hess[3], Vivien Holecska[3], Carolin T. Schoen[3], Carolin M. Oefner[3], Alexei Leliavski[1], Véronique Blanchard[4] and Marc Ehlers[1,3,5]**

[1] Laboratories of Immunology and Antibody Glycan Analysis, Institute for Nutrition Medicine, University of Lübeck and University Medical Center Schleswig-Holstein, Lübeck, Germany, [2] Department of Anesthesiology and Intensive Care, University of Lübeck and University Medical Center Schleswig Holstein, Lübeck, Germany, [3] Laboratory of Tolerance and Autoimmunity, German Rheumatism Research Center, An Institute of the Leibniz Association, Berlin, Germany, [4] Laboratory of Glycodesign and Glycoanalytics, Institute for Laboratory Medicine, Clinical Chemistry and Pathobiochemistry, Charité – University Medicine Berlin, Berlin, Germany, [5] Airway Research Center North (ARCN), University of Lübeck, German Center for Lung Research (DZL), Lübeck, Germany

Pro- and anti-inflammatory effector functions of IgG antibodies (Abs) depend on their subclass and Fc glycosylation pattern. Accumulation of non-galactosylated (agalactosylated; G0) IgG Abs in the serum of rheumatoid arthritis and systemic lupus erythematosus (SLE) patients reflects severity of the diseases. In contrast, sialylated IgG Abs are responsible for anti-inflammatory effects of the intravenous immunoglobulin (pooled human serum IgG from healthy donors), administered in high doses (2 g/kg) to treat autoimmune patients. However, whether low amounts of sialylated autoantigen-reactive IgG Abs can also inhibit autoimmune diseases is hardly investigated. Here, we explore whether sialylated autoantigen-reactive IgG Abs can inhibit autoimmune pathology in different mouse models. We found that sialylated IgG auto-Abs fail to induce inflammation and lupus nephritis in a B cell receptor (BCR) transgenic lupus model, but instead are associated with lower frequencies of pathogenic Th1, Th17 and B cell responses. In accordance, the transfer of small amounts of immune complexes containing sialylated IgG Abs was sufficient to attenuate the development of nephritis. We further showed that administration of sialylated collagen type II (Col II)-specific IgG Abs attenuated the disease symptoms in a model of Col II-induced arthritis and reduced pathogenic Th17 cell and autoantigen-specific IgG Ab responses. We conclude that sialylated autoantigen-specific IgG Abs may represent a promising tool for treating pathogenic T and B cell immune responses in autoimmune diseases.

Keywords: autoimmunity, IgG glycosylation, sialylation, ST6gal1, systemic lupus erythematosus, rheumatoid arthritis, immunosuppression, Th17

Abbreviations: Ab, antibody; autoAb, autoantibody; BCR, B cell receptor; CFA, complete Freund's adjuvant; CIA, collagen-induced arthritis; DC, dendritic cell; eCFA, enriched complete Freund's adjuvant; IC, immune complex; IFA, incomplete Freund's adjuvant; OVA, ovalbumin; PC, plasma cell; RA, rheumatoid arthritis; SLE, systemic lupus erythematosus; St6gal1, beta-galactoside alpha2,6-sialyltransferase 1; TCR, T cell receptor; TNP, 2,4,6-trinitrophenyl.

OPEN ACCESS

Edited by:
Lucienne Chatenoud,
Université Paris Descartes
France

Reviewed by:
Lennart T. Mars,
Institut National de la Santé et de la Recherche Médicale (INSERM), France
Maria Cecilia G. Marcondes,
San Diego Biomedical Research Institute, United States

***Correspondence:**
Véronique Blanchard
veronique.blanchard@charite.de;
Marc Ehlers
marc.ehlers@uksh.de

†These authors have contributed equally to this work.

Specialty section:
This article was submitted to Immunological Tolerance and Regulation, a section of the journal Frontiers in Immunology

Received: 29 November 2017
Accepted: 11 May 2018
Published: 06 June 2018

Citation:
Bartsch YC, Rahmöller J, Mertes MMM, Eiglmeier S, Lorenz FKM, Stoehr AD, Braumann D, Lorenz AK, Winkler A, Lilienthal G-M, Petry J, Hobusch J, Steinhaus M, Hess C, Holecska V, Schoen CT, Oefner CM, Leliavski A, Blanchard V and Ehlers M (2018) Sialylated Autoantigen-Reactive IgG Antibodies Attenuate Disease Development in Autoimmune Mouse Models of Lupus Nephritis and Rheumatoid Arthritis. Front. Immunol. 9:1183. doi: 10.3389/fimmu.2018.01183

INTRODUCTION

The ability of IgG antibodies (Abs) to modulate immune responses depends on the Ab subclass and the structure of the N-glycan attached to Asn-297 in the Fc region that affect IgG binding to activating and inhibitory Fcγ receptors (FcγRs) on effector cells (1, 2). The biantennary core of the Fc glycan consists of four N-acetylglucosamines (GlcNAcs) and three mannoses, which can be further modified with fucose, bisecting GlcNAc, galactose and terminal sialic acid residues (Figure S1 in Supplementary Material).

The abundance of non-galactosylated (agalctosylated; G0) serum IgG Abs that lack galactose and terminal sialic acid residues positively correlates with the disease severity in rheumatoid arthritis (RA) and systemic lupus erythematosus (SLE) (3–25), whereas alleviated disease activity in RA patients during pregnancy or after anti-TNF treatment is associated with increased levels of sialylated IgG Ab (6, 17, 20, 26–28). Intriguingly, this correlation is especially prominent when only autoreactive IgG Abs are analyzed (22), suggesting that G0 IgG Abs may exacerbate autoimmune inflammation in an antigen-specific manner. Indeed, agalactosylated, but not sialylated, IgG autoantibodies (autoAbs) are able to induce disease symptoms in passive models of arthritis (9, 24).

With regard to the development of differently Fc glycosylated IgG Abs, it has been shown that immune responses under inflammatory conditions induce plasma cells (PCs) that generate G0 IgG, whereas immune responses under tolerogenic conditions induce more galactosylated and sialylated IgG Abs (29–32).

The anti-inflammatory effects of sialylated IgG Abs have first been reported for the intravenous immunoglobulin (IVIG)—pooled human serum IgG from healthy donors (33–35). The sialylated IVIG fraction attenuates arthritis in mice *via* its binding to the C-type lectin receptor SIGN-R1 (specific ICAM-3 grabbing non-integrin-related 1) on regulatory marginal-zone macrophages (36), and thereby induces an anti-inflammatory environment and upregulates the inhibitory Fcγ receptor FcγRIIB on effector macrophages (37). Moreover, sialylated IVIG is able to inhibit dendritic cell (DC) maturation through an FcγRIIB-independent mechanism (29, 38–40). Together, these data suggest that the sialylated IVIG fraction exerts anti-inflammatory effects on both innate and adaptive immune cells.

Under physiological conditions, IgG Abs mediate their effector functions through the formation of immune complexes (ICs) with an antigen (29–32, 41). Recent reports suggest that sialylation of antigen-specific IgG Abs affects their effector functions and the course of an immune response (29, 30). In the context of autoimmunity, application of small amounts of sialylated IgG autoAbs has reduced joint swelling in the collagen-induced arthritis (CIA) model (24). Furthermore, endogenous sialylation of IgG Abs have attenuated disease development in mouse models of nephritis and arthritis through a pathway similar to IVIG (42). Finally, ICs containing sialylated antigen-specific IgG Abs have inhibited LPS-induced IL-6 production by DCs *in vitro* (29).

To further investigate the protective effect of sialylated autoantigen-specific IgG Abs on the development of autoimmune pathology, here we studied the disease course in lupus nephritis-prone FcγRIIB-deficient (Fcgr2b$^{-/-}$) mice and in 56R$^{+/-}$Fcgr2b$^{-/-}$ mice that express a transgenic self- and polyreactive B cell receptor (BCR) (43–46) and produce T cell-independent sialylated IgG2a and IgG2b autoAbs (47). We further tested how sialylated collagen type II (Col II)-reactive monoclonal murine IgG Abs influence the development of Col II-induced arthritis (CIA), accumulation of Th1 and Th17 cells, and autoAb production. Our results suppose that sialylated IgG autoAbs attenuate the development of pathogenic autoimmune conditions and might affect inflammatory T and B cell responses.

MATERIALS AND METHODS

Mice

C57BL/6 wt mice were purchased from Charles River Laboratories (Bar Harbor, ME, USA). Fcgr2b$^{-/-}$ mice and 56R$^{+/-}$Fcgr2b$^{-/-}$ mice with the transgenic VDJ4 heavy (H) chain knock-in (56R) (43, 44) on the C57BL/6 background have been described previously (45, 46, 48–50). Ovalbumin (OVA)-specific TCR transgenic OT-II$^{+/+}$ mice (B6.Cg-Tg(TcraTcrb)425Cbn/J; stock no. 004194) (51) and Thy1.1$^{+/+}$ mice (B6.PL-Thy1a/CyJ; stock no. 000406) on the C57BL/6 background were purchased from Jackson Laboratories. F1 offsprings of OT-II$^{+/+}$ × Thy1.1$^{+/+}$ breedings were used for cell transfer experiments. Genotypes were determined *via* PCR amplification of tail DNA (46). The mice were bred and maintained in accordance with federal laws and institutional guidelines.

Reagents

For the experiments, ovalbumin (OVA) was purchased from Sigma-Aldrich (Steinheim, Germany) and 2,4,6-Trinitrophenyl (TNP)(12)-coupled bovine serum albumin (TNP(12)-BSA) and TNP(5)OVA were purchased from Biosearch Technologies (Novato, CA, USA or Petaluma, CA, USA). TNP-sheep IgG was prepared using TNP-e-aminocaproyl-OSu (Biosearch Technologies) and sheep IgG (Sigma-Aldrich) in the laboratory. IVIG (Intratect) was obtained from Biotest Pharma GmbH (Dreieich, Germany). Complete Freund's adjuvant [CFA; 1 mg Mycobacterium tuberculosis (*Mtb*)/ml; #F5881] and incomplete Freund's adjuvant (IFA; #F5506) were purchased from Sigma-Aldrich. Enriched CFA (eCFA) was prepared by adding heat-killed *Mtb.*H37 RA (BD Biosciences, San Diego, CA, USA) to IFA (5 mg *Mtb*/ml) (30).

Detection of Proteinuria

Urine samples were tested on Multistix 10 Visual strips (Bayer, Leverkusen, Germany). Proteinuria was scored as follows: 0 = negative, 1 = ≤ 75 mg/dl, 2 = ≤ 125 mg/dl, 3 = > 125 mg/dl.

Kidney Histology

Kidney specimens of lupus-prone Fcgr2b$^{-/-}$ or 56R$^{+/-}$Fcgr2b$^{-/-}$ mice were embedded in Tissue-Tek OCT compound immediately after removal and snap frozen on dry ice. Sections (7 µm) were fixed in ice-cold acetone and stained with FITC-conjugated anti-mouse IgG2a$_a$ or IgG2a$_b$ (Bethyl Laboratories; Montgomery, TX,

USA), Cy5-conjugated anti-mouse Mac-1 (M1/70.15.11) and Cy5-conjugated anti-mouse macrophage marker (F4/80).

HEp-2 Cell Staining

Sera (1:100 dilution) from lupus-prone Fcgr2b$^{-/-}$ or 56R$^{+/-}$Fcgr2b$^{-/-}$ mice were added to commercially available HEp-2 slides (Orgentec, Mainz, Germany). The captured Abs were detected with a FITC-conjugated anti-mouse IgG2a$_a$ or IgG2a$_b$ Ab (Bethyl Laboratories).

Flow Cytometric Analysis

Indicated organs from immunized and untreated mice were prepared for flow cytometric analysis (LSRII, BD Biosciences or Attune; Thermo Fisher Scientific, Waltham, MA, USA) on the indicated days. The following biotin- or fluorochrome-coupled Abs were used for staining at 4°C: anti-CD138 (clone 218-2), anti-B220 (RA3-6B2), anti TCRbeta (H5-590), anti-CD95 (Jo-2), anti-CD4 (RM4-5), anti-IgM$_a$ (DS-1), anti-IgM$_b$ (AF6-78), anti-IL-17A (TC11-18H10), anti-IFNγ (XMG1.2) (all purchased from BD Biosciences), anti-CD8 (53-6.7), anti-GL-7 (GL-7), anti-IgG1 (RMG1-1), anti-CD90.1/Thy1.1 (Ox-7) (all purchased from Biolegend, San Diego, CA, USA), anti-Foxp3 (FJK16s), anti-IgM (eB121-15F9) (all purchased from Thermo Fisher Scientific), anti-IgG (polyclonal; Bethyl Laboratories), anti-St6gal1 (polyclonal; R&D Systems, Minneapolis, MN, USA), anti-CD44 (IM7) and anti-CD62L (MEL14) (all of which were generated in the laboratory). Fluorochrome-coupled OVA was purchased from Thermo Fisher Scientific and streptavidin reagents from Biolegend. For intracellular staining, the samples were fixed with Cytofix/Cytoperm according to the manufacturer's instructions (BD Biosciences) followed by permeabilization with Perm/Wash Buffer (own preparation, 0.05% saponin in 0.05× PBS). For intranuclear Foxp3 staining, samples were fixed and permeabilized with the Foxp3 Fix/Perm buffer set according to the manufacturer's instructions (Thermo Fisher Scientific). For intracellular cytokine analysis, cells were re-stimulated with PMA (10 ng/ml) and ionomycin (1 μg/ml) (Sigma-Aldrich) for 4 h, whereby Brefeldin A (Sigma-Aldrich) was added after 1 h of stimulation to facilitate the accumulation of cytokines in the interior of the cell.

Enzyme-Linked Immunofluorescence Assays (ELISAs)

Abs specific for double-stranded DNA were detected as described previously (46). Briefly, ELISA plates were precoated with 5 μg/ml of methylated BSA (Sigma-Aldrich), followed by overnight incubation at 4°C with 50 μg/ml of calf thymus DNA (Sigma-Aldrich). After washing, the plates were blocked (PBS, 3% BSA, 1 mM EDTA, 0.1% gelatin) and subsequently incubated with 1/100 diluted serum. Captured Abs were detected with horseradish peroxidase-coupled goat anti-mouse IgG, IgG1, IgG2a$_a$, IgG2a$_b$ or IgG2b secondary Abs (Bethyl Laboratories), followed by incubation with a 3,3′,5,5′-tetramethylbenzidine substrate solution (BD Biosciences); the optical density was measured at 450 nm. Abs against nucleosomes were detected in 1/100 diluted sera using nucleosome-coupled ELISA plates (Orgentec). For the detection of TNP- or Col II-reactive Abs, ELISA plates were coated with 5 μg/ml of TNP-BSA or 2 μg/ml of Col II in 0.05 M Carbonate/Bicarbonate buffer, pH 9.6 (Sigma-Aldrich).

Depletion of CD4$^+$ T Cells

For depletion of CD4$^+$ T cells, mice were injected intraperitoneally (i.p.) with 250 μg of anti-mouse CD4 (GK1.5) every 4 days for the indicated period of time. GK1.5 hybridoma Abs were purified from hybridoma cultures using protein G Sepharose. The depletion of CD4$^+$ T cells (blood samples) was verified *via* flow cytometry (Figure S2 in Supplementary Material).

Sialylation Analysis of Serum IgG Abs From wt, Fcgr2b$^{-/-}$ and 56R$^{+/-}$Fcgr2b$^{-/-}$ Mice

Serum IgG Abs from the indicated wt, Fcgr2b$^{-/-}$ and 56R$^{+/-}$Fcgr2b$^{-/-}$ mice were purified using protein G Sepharose. To characterize the sialylation of purified IgG Abs, the GlykoScreen™ Sialic Acid Quantification Kit (Prozyme, Hayward, CA, USA) was utilized according to the manufacturer's instructions. In brief, sialic acid molecules were enzymatically released from the purified IgG Abs by incubation with sialidase A for 2 h at 37°C. Released sialic acid molecules were enzymatically converted in a two-step process to acetylphosphate and hydrogen peroxide. Addition of HRP catalyzed a reaction of hydrogen peroxide with another added substrate into a fluorescent dye, which was quantified at 590 nm.

Purification of Polyreactive Serum IgG Abs From 56R$^{+/-}$Fcgr2b$^{-/-}$ Mice

Serum IgG Abs from 56R$^{+/-}$Fcgr2b$^{-/-}$ mice were purified with Protein-G-Sepharose. Purified IgG Abs were applied to TNP(12)-BSA-coupled cyanogen bromide-activated Sepharose 4B (GE Healthcare, Fairfield, CT, USA) columns (prepared in the laboratory) for purification of polyreactive IgG Abs. Reactivity against various autoantigens was verified *via* ELISA (data not shown) and IgG N-glycosylation was characterized through MALDI-TOF mass spectrometry (MS).

In Vitro De-Sialylation of IgG Abs

De-sialylation of purified polyreactive serum IgG Abs was performed with the Prozyme Sialidase kit (Prozyme).

In Vitro Galactosylation and/or Sialylation of IgG Abs

In vitro galactosylation and/or sialylation of monoclonal anti-TNP murine IgG1 (clone H5) and anti-Thy1.1 murine IgG1 (clone OX-7) hybridoma Abs (52, 53) and cloned and produced anti-Col II murine IgG1 Abs (see below) were performed as described previously (29, 35). Briefly, Abs were galactosylated with human beta1,4-galactosyltransferase and UDP-Galactose and/or sialylated with human beta-galactoside alpha2,6-sialyltransferase (St6gal1) and CMP-sialic acid (all reagents were obtained from Calbiochem, Darmstadt, Germany). Antigen-reactivity was verified *via* ELISA, and IgG N-glycosylation was analyzed through MALDI-TOF MS or HPLC (32).

Glycan Analysis of Polyreactive Serum IgG Abs From 56R$^{+/-}$Fcgr2b$^{-/-}$ Mice and Monoclonal IgG Abs *via* MALDI-TOF MS

N-glycans were isolated from purified IgG samples *via* hydrolysis with recombinantly expressed endoglycosidase S (EndoS) from

Streptococcus pyogenes (54). EndoS cleaves the Fc N-glycans of IgG Abs between the first and second GlcNAc (Figure S1 in Supplementary Material). The resulting N-glycans were purified through solid phase extraction using reversed-phase C18 and graphitized carbon columns (Alltech, Deerfield, IL, USA). The samples were then permethylated according to standard protocols (30, 55) and further investigated *via* MALDI-TOF MS in duplicate. The spectra were recorded on an Ultraflex III mass spectrometer (Bruker Daltonics Corporation, Billerica, MA, USA) equipped with a Smartbeam laser. Calibration was performed on a glucose ladder, and 2,5-dihydroxybenzoic acid was used as the matrix. Spectra were recorded in reflector positive ionization mode, and mass spectra from 3,000 laser shots were accumulated. Based on the terminal sugar moiety, the EndoS resulting peaks were assigned to one of the following nine groups: G0+ bisecting GlcNAc, G0 w/o bisecting GlcNAc, G1+ bisecting GlcNAc, G1 w/o bisecting GlcNAc, G2+ bisecting GlcNAc, G2 w/o bisecting GlcNAc, G1S1, G2S1 and G2S2 (Figure S1 in Supplementary Material). Peaks containing both sialic acid and bisecting GlcNAc were not detected. In general, murine IgG Abs hardly showed bisecting GlcNAc structures. However, the calculated proportions of the bisecting GlcNAc versions of G0, G1 and G2 were added to the percentages of the G0, G1 and G2 versions without bisecting GlcNAc, respectively, to get six groups totaling 100%: G0, G1, G2, G1S1, G2S1 and G2S2. In some figures the percentages of S1 (G1S1 + G2S1) and S2 (G2S2) glycans are presented.

Nephrotoxic Nephritis-Induced Mouse Model

Nephritis was induced by injection of 100 µg of sheep IgG Abs in CFA on day 0, followed by intravenous (i.v.) injection of 80 µl of sheep anti-glomerular basement membrane (anti-GBM) nephrotoxic serum (NTS) 4 days later (56). Development of nephritis was verified by the detection of proteinuria as described above.

Cloning and Production of Col II-Reactive Murine IgG1 Abs

The variable VDJ heavy chain and VJ light chain DNA sequences of Col II-reactive murine IgG2b, clone M2139 (VDJ heavy chain: NCBI accession number Z72462; VJ light chain: NCBI accession number Z72463) (57) and IgG2a, clone CII 1-5 (VDJ heavy chain: NCBI accession number MMU69538; VJ light chain: NCBI accession number MMU69539) (58), were synthesized (Mr. Gene, Germany) with flanking restriction sites and cloned into previously described eukaryotic IgH and IgL expression vectors (59, 60), which were modified to include the murine C57BL/6 IgG1 heavy chain or kappa light chain constant region, respectively (Figure S4 in Supplementary Material). The constant heavy and light chain regions were amplified from C57BL/6 splenic cDNA *via* RT-PCR (IgG1 forward primer, 5′-GCGTCGACGACACCCCCATCTGTCTATCCACTGGCCC and reverse primer, 5′-TTATTCGGCGTACGCGTCATTTAC CAGGAGAGTGGGAG; kappa forward primer, 5′-GCCGTACG GATGCTGCACCAACTGTATCCAT and reverse primer, 5′-TTATTCGGAAGCTTTCAACACTCATTCCTGTTGAAG). Col II-reactive monoclonal IgG1 Abs were produced *via* polyethylenimine (PEI; Sigma-Aldrich)-mediated cotransfection of human embryonic kidney 293 cells with plasmid DNA encoding the IgH and IgL chains (Figure S4 in Supplementary Material). IgG Ab integrity was analyzed through SDS gel electrophoresis, while Ab reactivity was controlled *via* ELISA, and IgG Fc N-glycosylation was analyzed using MALDI-TOF MS.

Chicken COL2-Induced Arthritis (CIA) Mouse Model

Chicken type II collagen (Col II; Sigma-Aldrich) was dissolved at 2 mg/ml in 0.05 M acetic acid and emulsified in an equal volume of enriched CFA (see reagents). Then, 8–10-week-old Fcgr2b$^{-/-}$ mice were immunized subcutaneously (s.c.) with 100 µl of the emulsion (equivalent to 100 µg of Col II). On day 21, a booster s.c. injection of 100 µg of chicken Col II in IFA was administered. Mice were monitored for swelling encompassing the paw and ankle or ankylosis of the limb to determine the onset and severity of the disease in a blinded manner. The swelling of each foot was scored as follows: healthy paws and ankles (score 0) showed no abnormal swelling, redness, contact sensitivity or motor activity alterations. Low swelling of paws and/or ankles was scored with 1, pronounced swelling with 2 and severe balloon-like whole swelling (ankylosis) with 3; thus, each mouse could achieve a maximum score of 12. The mean clinical score was calculated by totaling the scores of all mice in a group and dividing by the number of mice in that group. Prevalence indicates the percentage of animals in an individual group with a score >0 on the indicated time point. Onset of disease was specified at the indicated day, at which an animal reached score >0 for the first time.

Ankle Histology

Ankle samples were embedded in paraffin and sections were stained with hematoxylin and eosin (H&E) or anti-CD3. Immunofluorescence was detected using a Leica DM IRE confocal laser scanning microscope.

OT-II Cell Transfer Experiments

Purified splenocytes of OT-II$^{+/-}$ × Thy1.1$^{+/-}$ donor mice (8–12-week-old mice) were labeled with the CellTrace Violet Cell Proliferation Kit according to the manufacturer's protocol (Thermo Fisher Scientific). 3×10^7 labeled cells were transferred i.v. in naive recipient C57BL/6 wt or Fcgr2b$^{-/-}$ mice (8–12-week-old mice). One hour later the recipient mice were injected i.p. with 90 µg of low-sialylated or *in vitro* galactosylated plus sialylated anti-TNP IgG1 (H5) Abs or PBS. On the following day, 200 µl of an 1:1 water-in-oil emulsion of enriched CFA and PBS containing 30 µg of TNP(5)-OVA (Biosearch Technologies) or OVA (Sigma-Aldrich) was injected into each of the recipient mice. After 4 days, the mice were sacrificed and splenic and mesenteric lymphnode cells were analyzed *via* flow cytometry.

DC Culture

Bone marrow (BM)-derived DCs were generated over 8 days in IMDM (Thermo Fisher Scientific) containing 10% FCS, 10 ng/ml IL-4, 20 ng/ml GM-CSF (R&D Systems) and 50 µM 2-mercaptoethanol. Subsequently, the cells were cultured in 96-well plates with

ICs containing 10 μg of chicken Col II and different proportions of non-sialylated (<1% sialylation) and sialylated (46% sialylation) Col II-specific IgG1 (clone M2139; total amount per well: 40 μg/ml) in medium containing 10% IgG-depleted FCS. The IL-6 concentration was detected after 36 h *via* ELISA (BD Biosciences).

Statistical Analysis

Statistical analyses unless otherwise stated, were performed using Student's *t*-test comparing two groups or One-way ANOVA for more groups, respectively, or the logrank test for survival curves: $*P < 0.05$, $**P < 0.01$, and $***P < 0.001$. If not stated otherwise, murine data were taken from one representative out of 2–5 individual experiments or combined from multiple experiments and are presented as the mean or median (median fluorescence intensity) values as indicated ±SEM; each data point represents an individual animal.

RESULTS

56R-Derived IgG2a and IgG2b autoAbs Fail to Induce Disease Symptoms in Lupus-Prone Mice

To study how IgG Fc glycosylation is associated with the development of autoimmune pathology, we first used lupus-prone FcγRIIB knockout mice, a model of spontaneous lupus nephritis (Fcgr2b$^{-/-}$ females on the C57BL/6, haplotype b, background) (46, 48–50). By 4–5 months of age, more than a half of Fcgr2b$^{-/-}$ mice developed DNA-, nucleosome- and poly (here shown for anti-TNP reactivity)-reactive IgG2a and IgG2b autoAbs, which accumulated in the kidney (**Figure 1**; Figure S2 in Supplementary Material) (46, 49, 50, 60–64).

Fcgr2b$^{-/-}$ mice positive for IgG autoAbs started to develop proteinuria by the age of 6 months, and about a half of the Fcgr2b$^{-/-}$ mice died due to severe nephritis by the age of 9 months (**Figures 1A,B** and data not shown) (46, 49, 50). Mice developing nephritis showed, in addition to IgG Ab depositions, also macrophage infiltrations in the kidney (**Figure 1A**). Inversely, mice with IgG Ab depositions in the kidney, but without macrophage infiltrations, did not show proteinuria and nephritis (**Figure 1A**).

In comparison, we analyzed nephritis development in female Fcgr2b$^{-/-}$ mice that expressed one "knock-in" allele of the self- and polyreactive 56R VDJ4 Ig heavy chain (haplotype a) (56R$^{+/-}$Fcgr2b$^{-/-}$ mice; **Figure 1**) (43–46). About 90–95% of all B cells in 56R$^{+/-}$Fcgr2b$^{-/-}$ mice expressed a 56R-based BCR (**Figure 1D**).

Earlier studies have shown that 56R$^{+/-}$ mice on the C57BL/6 wt background produce autoreactive IgM and some IgG Abs (47), and that the introduction of the 56R allele into lupus-prone Fcgr2b$^{-/-}$ mice lead to increased IgG class switched autoAbs, particular of the 56R allele (45, 46). Whereas the generation of IgG2a and IgG2b autoAbs in Fcgr2b$^{-/-}$ mice requires T cell help (50, 60), autoAbs in 56R$^{+/-}$ wt mice largely develop in a T-cell-independent manner (47). Because we recently demonstrated that T cell-independent B cell activation induces immunosuppressive sialylated IgG Abs *in vivo* (30), we wondered whether the introduction of the 56R allele into lupus-prone Fcgr2b$^{-/-}$ mice may lead to T cell-independent IgG autoAbs and provide a disease-protective effect.

In line with previous reports, 56R$^{+/-}$Fcgr2b$^{-/-}$ mice generated high serum titers of class-switch DNA-, nucleosome- and poly-reactive IgG2a$_a$ and IgG2b Abs, which formed depositions in the kidney (**Figure 1**; Figure S2 in Supplementary Material) (45, 46). In contrast to Fcgr2b$^{-/-}$ mice, all 56R$^{+/-}$Fcgr2b$^{-/-}$ mice developed IgG2a$_a$ and IgG2b autoAbs already by the age of 2 months (45, 46), which (IgG2a$_a$, but not IgG2b) only slightly further increased until the age of 6 months (**Figure 1E**). We also found comparable anti-nuclear reactivity of IgG2a Abs in the sera of 5–7 months old Fcgr2b$^{-/-}$ and 56R$^{+/-}$Fcgr2b$^{-/-}$ mice (**Figure 1F**). However, despite the early presence of IgG Abs of similar antigen specificity and subclass, and IgG Ab deposition in the kidney, none of the 56R$^{+/-}$Fcgr2b$^{-/-}$ mice showed macrophage infiltration into the kidney and proteinuria by the age of 9 months (**Figures 1A,B**).

56R$^{+/-}$Fcgr2b$^{-/-}$ Mice Do Not Develop Splenomegaly and Do Not Accumulate Th1 and Th17 Cells and PCs Seen in Fcgr2b$^{-/-}$ Mice

In Fcgr2b$^{-/-}$ mice, the development of IgG2a and IgG2b autoAbs was associated with splenomegaly, increased frequencies of Th1 and PCs and IC accumulation in the kidneys (**Figures 1A** and **2A,B**). The subsequent development of lupus nephritis (manifested by proteinuria) was additionally associated with further enhanced splenomegaly, increased frequencies of Th17 cells and infiltration of macrophages into the kidneys (**Figures 1A,B** and **2A,B**). These findings confirm recent studies showing that the IL-17 signaling pathway is important for the development of disease in lupus-prone mice (50).

In contrast, 56R$^{+/-}$Fcgr2b$^{-/-}$ mice showed no signs of autoimmune inflammation (**Figures 2A,B**). Together these findings suggest that 56R-derived IgG autoAbs may be able to actively protect lupus-prone FcγRIIB-deficient mice from developing autoimmune inflammation.

56R-Derived IgG2a and IgG2b autoAbs Develop T Cell Independently in 56R$^{+/-}$Fcgr2b$^{-/-}$ Mice

Next, we analyzed whether IgG2a and IgG2b autoAbs in 56R$^{+/-}$Fcgr2b$^{-/-}$ mice developed independently of T cell help as described for 56R$^{+/-}$ mice on the C57BL/6 wt background (**Figures 3A,B**; Figure S2 in Supplementary Material) (47). While in Fcgr2b$^{-/-}$ mice, depletion of CD4 cells reduced the IgG2a and IgG2b autoAb titers and enhanced frequencies of splenic and BM PCs, which is in line with reported observations (50, 60), depletion of CD4 cells in 56R$^{+/-}$Fcgr2b$^{-/-}$ mice with the same anti-CD4 doses failed to reduce IgG2a and IgG2b autoAb titers (**Figures 3A,B**; Figure S2 in Supplementary Material).

Although, it has been mentioned that autoAbs develop more or less independently of Toll-like receptor (TLR) 9 in 56R$^{+/-}$ mice (47), it has been shown that the accumulation of class switched IgG2a and IgG2b autoAbs in 56R$^{+/-}$Fcgr2b$^{-/-}$ mice depends at least partially on TLR9 and particularly on MyD88 signaling (46). Hence, B cell activation and IgG2a and IgG2b class switching

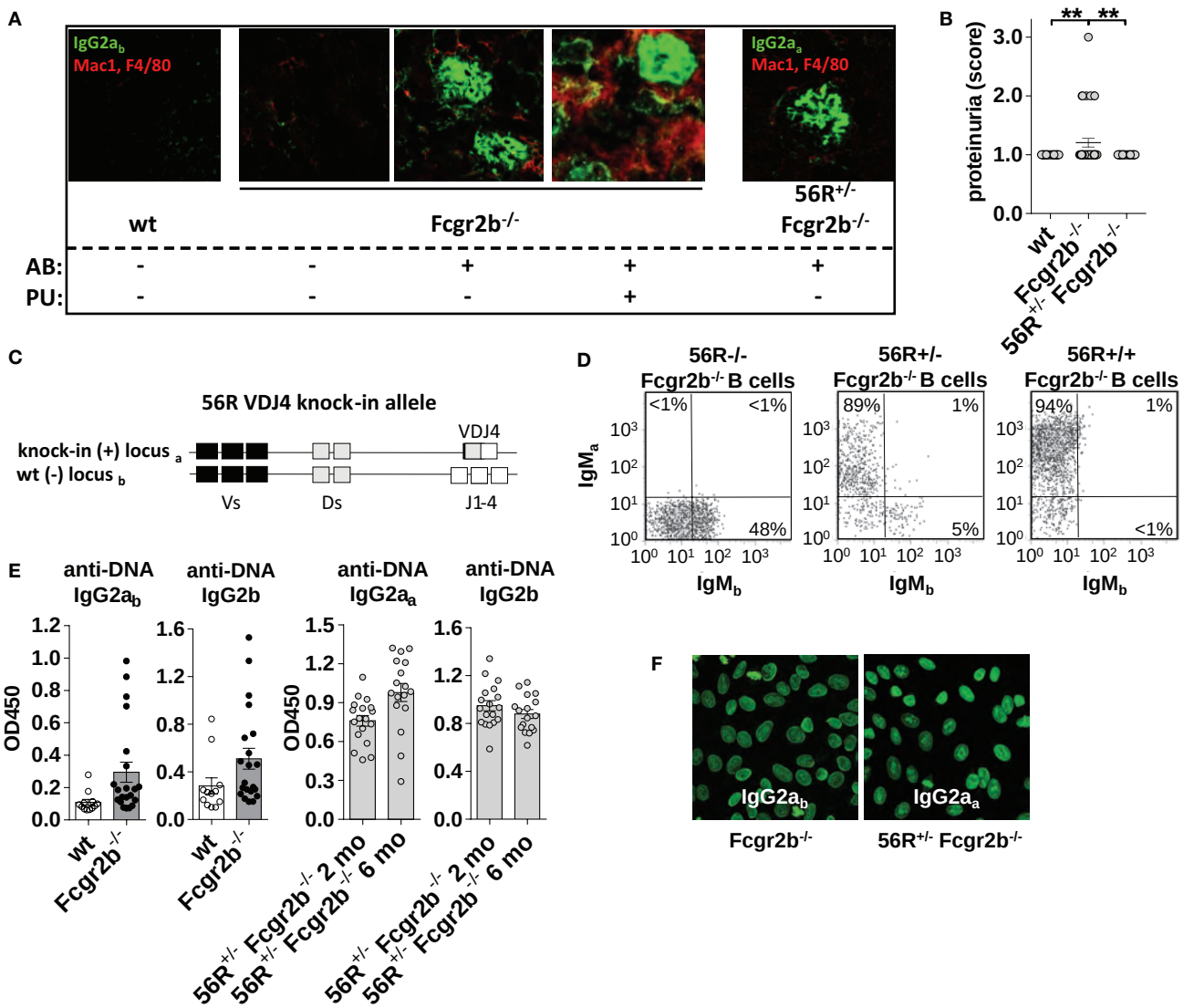

FIGURE 1 | 56R$^{+/-}$Fcgr2b$^{-/-}$ mice develop self- and polyreactive IgG2a and IgG2b autoantibodies (autoAbs) earlier than Fcgr2b$^{-/-}$ but show no signs of renal inflammation. **(A)** Indirect immunofluorescence analysis of IgG2a immune complex (IC) depositions and macrophage infiltration in kidney sections from 6-month-old wt mice, IgG autoAb (AB)-negative and proteinuria (PU)-negative (AB^{-}PU^{-}), AB^{+}PU^{-} and AB^{+}PU^{+}Fcgr2b$^{-/-}$ mice (all IgG2a$_b$) and 56R$^{+/-}$Fcgr2b$^{-/-}$ mice (IgG2a$_a$). The presented immunofluorescence images are representative of at least five mice per group. **(B)** PU scores for 5–6-month-old wt (n = 30), Fcgr2b$^{-/-}$ (n = 39) and 56R$^{+/-}$Fcgr2b$^{-/-}$ (n = 30) mice. Each data point represents an individual animal; horizontal lines represent mean values. **(C)** Schematic representation of the self- and polyreactive 56R VDJ4 knock-in (haplotype a) and the wt (haplotype b) heavy chain loci. The 56R VDJ4 knock-in replaced the endogenous IgH Js and can class-switch to all Ab isotypes (43–46). **(D)** The frequencies of B220+ B cells expressing the knock-in allele (a) or the wt allele (b) were analyzed by flow cytometry of splenocytes from 2-month-old 56R$^{-/-}$, 56R$^{+/-}$ or 56R$^{+/+}$Fcgr2b$^{-/-}$ mice. About 5–10% of B cells in 56R$^{+/-}$Fcgr2b$^{-/-}$ mice expressed the wt (IgM$_b$+) BCR. **(E)** Anti-DNA IgG2a$_b$, IgG2b or IgG2a$_a$ subclass Abs in sera of 5–7-month-old wt and Fcgr2b$^{-/-}$ mice and 2- or 6-month-old 56R$^{+/-}$Fcgr2b$^{-/-}$ mice were determined *via* enzyme-linked immunofluorescence assay. Each data point represents an individual animal. Bars indicate mean values. **(F)** IgG2a$_b$ and IgG2a$_a$ Ab binding to HEp-2 slides from sera of 6-month-old Fcgr2b$^{-/-}$ and 56R$^{+/-}$Fcgr2b$^{-/-}$ mice, respectively.

might take place T cell independently *via* 56R BCR and TLR/MyD88 signaling in 56R$^{+/-}$Fcgr2b$^{-/-}$ mice (65).

Lupus-Resistant 56R$^{+/-}$Fcgr2b$^{-/-}$ Mice Generate Sialylated IgG Abs

Next we studied whether the serum IgG glycosylation differs between lupus-prone Fcgr2b$^{-/-}$ mice and 56R$^{+/-}$Fcgr2b$^{-/-}$ mice. Autoimmune-prone MRL-Fas(lpr) mice and SLE patients show increased levels of pro-inflammatory agalactosylated (G0) IgGs in serum, compared to healthy controls (8, 12, 15). In line with that, serum IgG Abs from lupus-prone Fcgr2b$^{-/-}$ mice were less sialylated, compared to wild-type controls (**Figures 3C,D**; Figure S1 in Supplementary Material). Reduced IgG sialylation was especially evident in Fcgr2b$^{-/-}$ mice that developed signs of lupus nephritis (proteinuria and kidney inflammation) (**Figure 3D**).

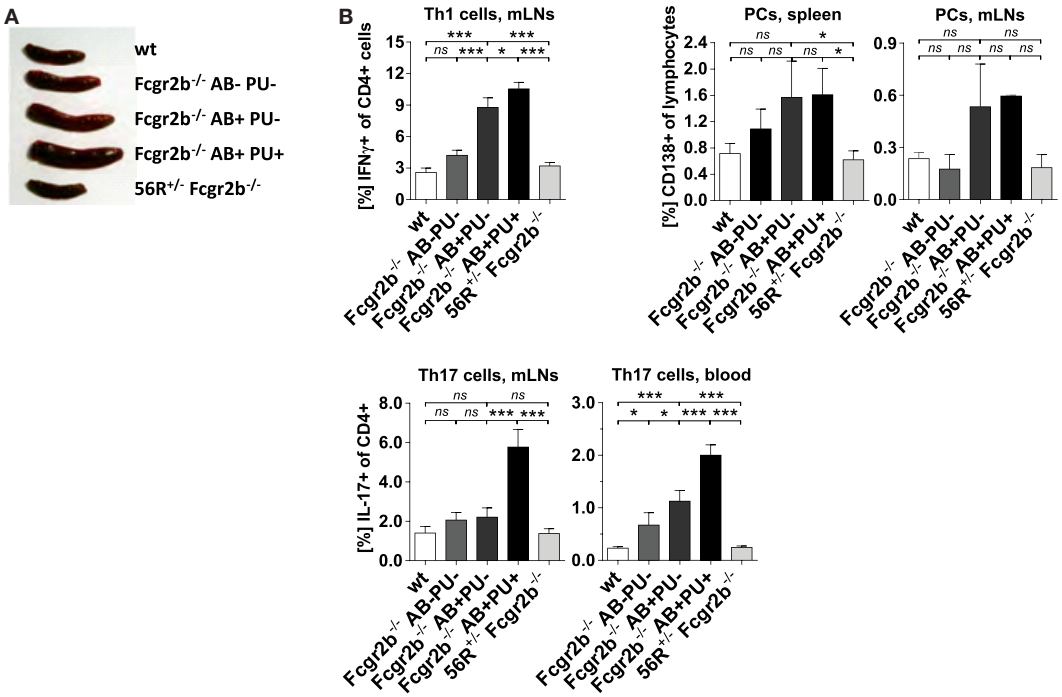

FIGURE 2 | Absence of splenomegaly and no accumulation of Th1, Th17 and plasma cells (PCs) in 56R$^{+/-}$Fcgr2b$^{-/-}$ mice. **(A)** Spleen sizes of 5–7-month-old wt mice, Fcgr2b$^{-/-}$ mice in the following disease states: IgG autoAb (AB)-negative and proteinuria (PU)-negative (AB^{-}PU^{-}), AB^{+}PU^{-} and AB^{+}PU^{+}, and 56R$^{+/-}$Fcgr2b$^{-/-}$ mice. The presented organ sizes are representative of a minimum of five mice per group. **(B)** The frequency of mesenteric lymph node (mLN) CD4^{+} IFNγ^{+} Th1 cells, splenic and mLN CD138^{+}PCs and mLN and blood CD4^{+} IL-17^{+} Th17 cells of 5–7-month-old wt mice (Th1 cells, mLNs, n = 8/PCs, spleen, n = 3/PCs, mLNs, n = 3/Th17 cells, mLNs, n = 8/Th17 cells, blood, n = 15), Fcgr2b$^{-/-}$ mice [AB^{-}PU^{-} (n = 12/3/3/12/10), AB^{+}PU^{-} (n = 12/3/3/21/17) and AB^{+}PU^{+} (n = 11/3/3/13/7)] and 56R$^{+/-}$Fcgr2b$^{-/-}$ mice (n = 12/12/3/12/26), as measured by flow cytometry. The bars indicate the mean values.

In contrast, serum IgG sialylation in 56R$^{+/-}$Fcgr2b$^{-/-}$ mice was comparable to that of healthy wild-type animals (**Figure 3D**).

Notably, the protein expression level of the alpha2,6-sialyltransferase 1 (St6gal1), which is responsible for terminal sialylation of IgG Fc glycan (24, 29–31), was reduced in total and IgG-switched PCs (IgG^{+}PC) of Fcgr2b$^{-/-}$ mice with nephritis, but not in PCs of 56R$^{+/-}$Fcgr2b$^{-/-}$ mice (**Figures 3E,F**). These data are consistent with our recent findings that T cell independent B cell activation leads to the development of PCs expressing high levels of St6gal1 and producing sialylated IgG Abs (30).

Transfer of ICs Containing Sialylated IgG Abs Inhibit Nephritis in Fcgr2b$^{-/-}$ Mice

To address such a possible ameliorating effect, we next tested whether ICs containing sialylated IgG autoAbs from 56R$^{+/-}$Fcgr2b$^{-/-}$ mice can directly attenuate the onset of nephritis in an induced nephritis model (53). We purified polyreactive TNP-binding (Figure S2 in Supplementary Material) IgG Abs from sera of 56R$^{+/-}$Fcgr2b$^{-/-}$ mice and generated ICs with TNP-coupled sheep (TNP-sheep) IgG Abs using either the purified native (sialylated) or *in vitro* sialidase-treated (de-sialylated) polyreactive IgG Abs (**Figures 4A,B**). The ICs were then transferred to Fcgr2b$^{-/-}$ mice and, 2 weeks later, the nephritis was induced by injecting TNP-sheep IgG Abs in CFA followed by i.v. injection of sheep anti-GBM NTS 4 days later (**Figure 4**) (56).

The ICs containing de-sialylated polyreactive IgG Abs increased nephritis-induced mortality when compared to a positive control (**Figure 4C**). In contrast, the ICs containing native sialylated polyreactive IgG Abs attenuated nephritis-induced mortality in Fcgr2b-/- mice (**Figure 4C**). Similarly, ICs containing *in vitro* sialylated anti-TNP monoclonal murine IgG1 (clone H5) Abs, but neither native non-sialylated anti-TNP monoclonal nor sialylated antigen-unspecific monoclonal murine IgG1 Abs, reduced mortality in this nephritis model (**Figures 4D–F**; Figure S3 in Supplementary Material). In summary, these results showed that only antigen-specific sialylated IgG Abs were able to attenuate disease development.

Sialylated Collagen-Specific IgG autoAbs Attenuate Autoimmune Inflammation in the CIA Model Independent of FcγRIIB

In order to see whether these sialylation dependent attenuating effects are detectable in a broader spectrum of autoimmune disease models, we further analyzed whether sialylated IgG autoAbs are able to attenuate autoimmune pathology and inflammation also in the collagen type II-induced arthritis (CIA) model. In contrast to earlier studies (24) we chose FcγRIIB-deficient mice for our experiments (66), because the observed inhibitory effect of sialylated IgG autoAbs in the former experiments was FcγRIIB-independent.

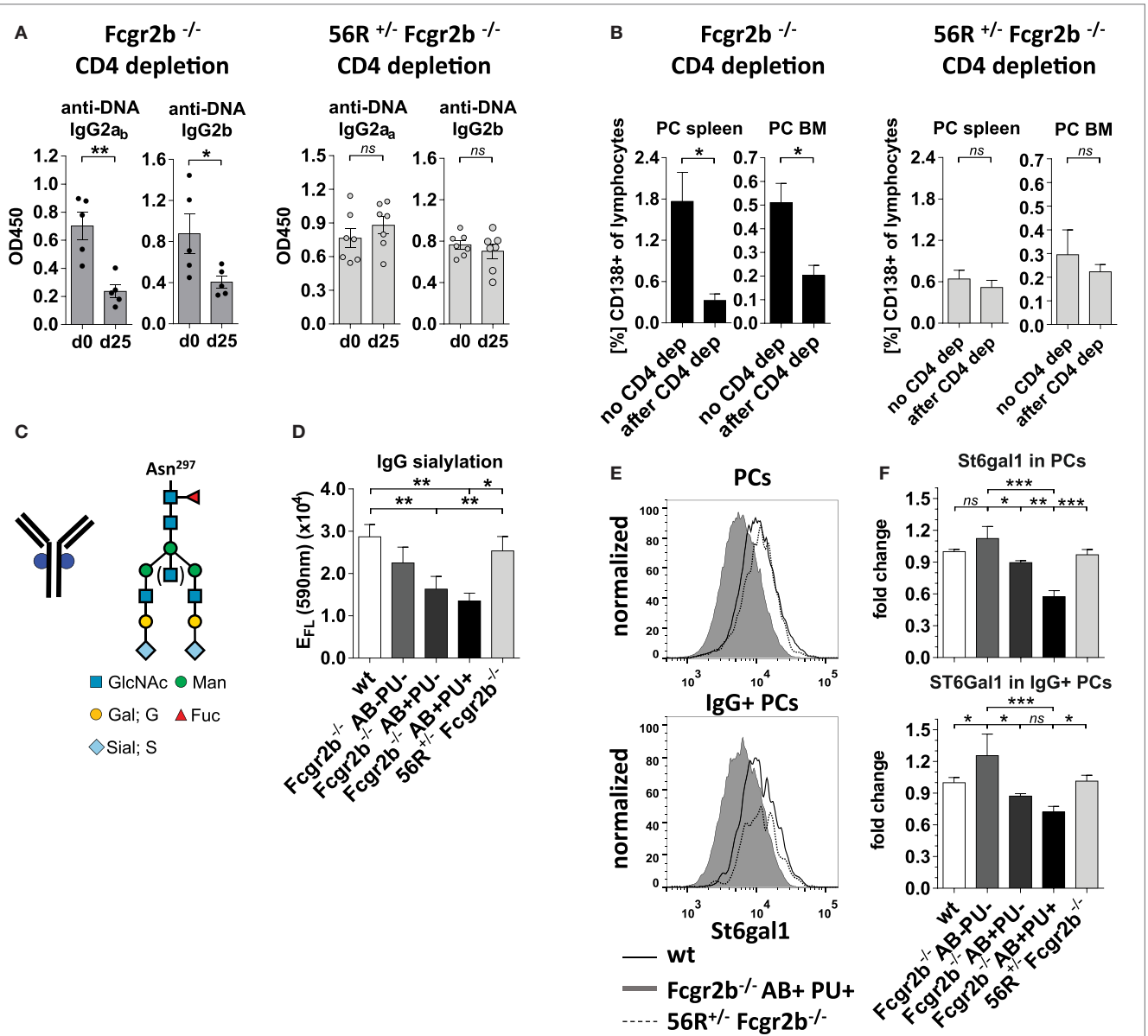

FIGURE 3 | Self- and polyreactive IgG2a and IgG2b autoantibodies (autoAbs) in 56R$^{+/-}$Fcgr2b$^{-/-}$ mice develop T cell independently and are sialylated. **(A,B)** AutoAb-positive 5-month-old Fcgr2b$^{-/-}$ mice or 2.5-month-old 56R$^{+/-}$Fcgr2b$^{-/-}$ mice received i.p. injections of anti-mouse CD4 (GK1.5) every 4 days for 25 days to deplete CD4$^+$ T cells (Figure S2 in Supplementary Material). **(A)** Serum anti-DNA IgG2a$_b$, IgG2b and IgG2a$_a$ levels before and after CD4 depletion. **(B)** The frequencies of CD138$^+$ PCs in the spleen and bone marrow (BM) of untreated (n = 6) versus CD4-depleted (n = 4) Fcgr2b$^{-/-}$ mice, and untreated (spleen, n = 13; BM, n = 3) versus CD4 depleted (n = 4) 56R$^{+/-}$Fcgr2b$^{-/-}$ mice were analyzed *via* FACS. One representative experiment is shown. **(C)** The biantennary core of the glycan structure linked to Asn 297 in the Fc region of IgG Abs consists of four N-acetylglucosamines (GlcNAc; blue) and three mannoses (Man), which can be further modified with fucose, bisecting GlcNAc and terminal galactose (G) and sialic acid (S) residues. **(D)** The sialic acid content in serum IgG Abs of 5–6-month-old autoAb (AB)-negative and proteinuria (PU)-negative [AB$^-$PU$^-$ (n = 8), AB$^+$PU$^-$ (n = 6) and AB$^+$PU$^+$ (n = 4)] Fcgr2b$^{-/-}$ mice and 56R$^{+/-}$Fcgr2b$^{-/-}$ mice (n = 11) compared to wt mice (n = 10) were analyzed with the GlykoScreen™ Sialic Acid Quantification Kit (Prozyme) (Efl: fluorescence emission at 590 nm). **(E,F)** St6gal1 protein expression in splenic total and IgG$^+$ PCs of 6–7-month-old AB$^-$PU$^-$ (n = 4), AB$^+$PU$^-$ (n = 5) and AB$^+$PU$^+$ (n = 9) Fcgr2b$^{-/-}$ mice and 56R$^{+/-}$Fcgr2b$^{-/-}$ mice (n = 6), compared to wt mice (n = 5). **(E)** Representative intracellular staining of St6gal1 protein expression levels in splenic PCs of wt, AB$^+$PU$^+$Fcgr2b$^{-/-}$ and 56R$^{+/-}$Fcgr2b$^{-/-}$ mice measured by flow cytometry. **(F)** Relative median fluorescence levels of St6gal1 protein expression. Median St6gal1 protein expression levels in total or IgG$^+$ PCs of three independent experiments were measured by flow cytometry and normalized (fold change) to the expression in wt controls (=1) in the respective experiments. The normalized data of three independent experiments were summarized (mean) in the graphs.

We produced two monoclonal murine Col II-reactive murine IgG1 Abs (clones M2139 and CII 1–5; 57, 58) in a native, very low-sialylated form and then generated sialylated forms of these Abs by *in vitro* galactosylation and sialylation (**Figures 5A,B**; Figures S1 and S5 in Supplementary Material), which do not affect antigen reactivity (Figure S5 in Supplementary Material).

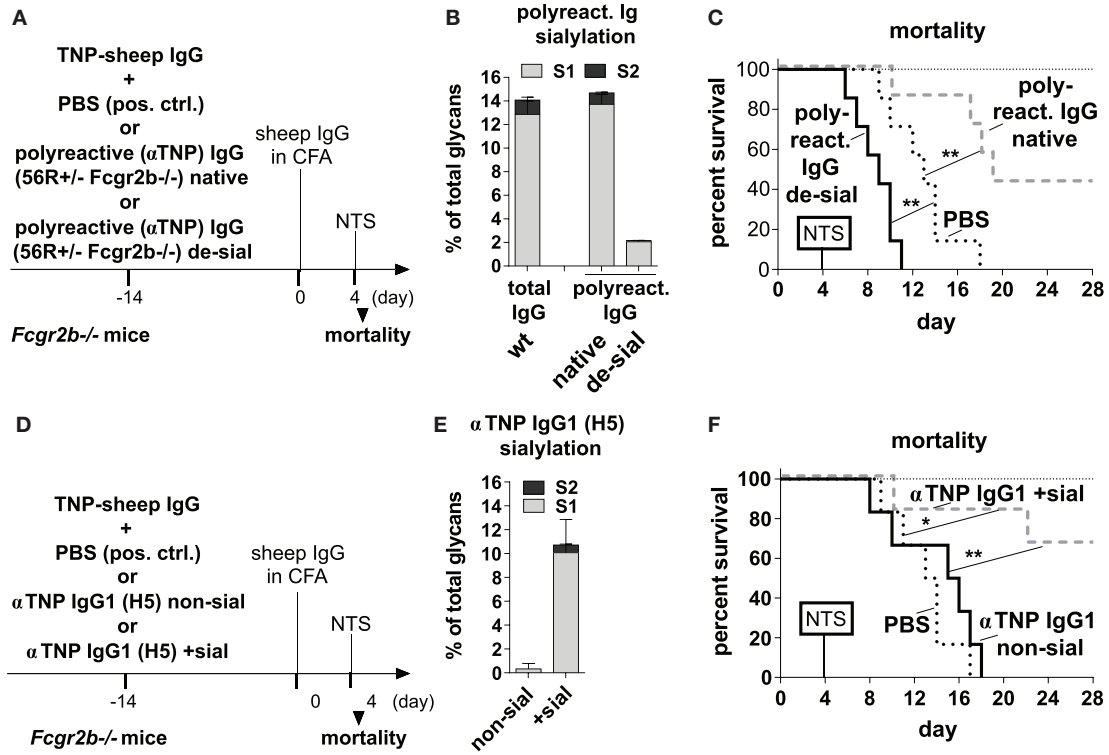

FIGURE 4 | Transfer of sialylated polyreactive IgG antibodies (Abs) derived from 56R$^{+/-}$Fcgr2b$^{-/-}$ mice or administration of sialylated antigen-specific monoclonal IgG Abs reduces nephritis-induced mortality in Fcgr2b$^{-/-}$ mice. **(A–C)** Transfer of sialylated polyreactive IgG Abs from 56R$^{+/-}$Fcgr2b$^{-/-}$ mice reduces nephritis-induced mortality. **(A)** Graphical representation of the experimental strategy. Fcgr2b$^{-/-}$ mice received ICs containing 100 µg of TNP-sheep IgG and 200 µg of either sialylated (native) or sialidase-treated de-sialylated (de-sial) polyreactive IgG Abs derived from 2–3-month-old 56R$^{+/-}$Fcgr2b$^{-/-}$ mice. The positive control (pos. ctrl.) group was treated with PBS and TNP-sheep IgG only. After 14 days, nephritis was induced by injection of sheep IgG in CFA and subsequent intravenous injection of sheep anti-glomerular basement membrane nephrotoxic serum (NTS) 4 days later. **(B)** Fc sialylation of purified total serum IgG Abs from wt mice and purified polyreactive IgG Abs from 56R$^{+/-}$Fcgr2b$^{-/-}$ mice before and after sialidase treatment was determined through EndoS-treatment and MALDI-TOF mass spectrometry (MS) (percentage of glycans with one or two sialic acid residues: S1 and S2; Figure S1 in Supplementary Material). **(C)** Kaplan-Meier survival analysis of the indicated groups. **(D–F)** Application of sialylated antigen-specific monoclonal IgG Abs reduces nephritis-induced mortality. **(D)** Graphical representation of the experimental strategy as described in **(A)**. Fcgr2b$^{-/-}$ mice were treated with ICs containing 100 µg of TNP-sheep IgG and 100 µg of either native non-sialylated (αTNP murine IgG1 non-sial) or *in vitro* sialylated (αTNP IgG1 +sial) monoclonal anti-TNP murine IgG1 (clone H5) Abs. After 14 days, nephritis was induced as described above. **(E)** Fc sialylation of the monoclonal anti-TNP murine IgG 1 Abs (clone H5) before and after *in vitro* sialylation was determined through EndoS-treatment and MALDI-TOF MS (the percentage of one or two sialic acid residues coupled to the glycan: S1, S2; Figure S1 in Supplementary Material). **(F)** Kaplan–Meier survival analysis for the indicated groups. One representative experiment out of two independent experiments is shown.

CIA was induced *via* s.c. injection of chicken Col II in enriched CFA and challenged with Col II in IFA 3 weeks later (**Figure 5A**).

100 µg of the Col II-reactive IgG1 Abs (either the low-sialylated or the sialylated form) were administered twice –1 day before and 9 days after the first immunization (**Figure 5A**). Foot swelling (clinical scores of 0–3 per foot with a maximum clinical score of 12 per mouse) was used as the marker to assess the CIA reaction.

The sialylated, but not the low-sialylated, Col II-reactive IgG Abs significantly reduced the mean clinical score of foot swelling, as compared to a PBS-treated control group (**Figures 5C,D**). In detail, only about 50% of the mice treated with the sialylated Col II-specific IgG1 Abs started to develop foot swelling (clinical score > 0 per mouse), whereas more than 80% of the mice treated with low-sialylated Col II-specific IgG Abs or with PBS developed foot swelling (**Figures 5D,E**). No significant differences in the timing of the disease onset were observed between the groups (**Figure 5F**). Together, these data are consistent with recent findings that sialylated Col II-specific IgG1 Abs can attenuate CIA in DBA/1 mice (24). Their studies further showed that the suppressive effect of sialylated IgG autoAbs was autoantigen-specific; an antigen-unspecific sialylated IgG1 Ab failed to attenuate CIA in their model (24). Here, we further show, that the attenuation of CIA with sialylated IgG autoAbs is independent of FcγRIIB.

Furthermore, the effect of 100 µg of the different sialylated Col II-specific IgG1 Abs was compared to the effect of high (50 mg; approximately 2 g/kg) and low (100 µg; approximately 4 mg/kg) doses of IVIG on the induction of CIA and particular inflammatory T and B cell responses in the CIA model (Figure S5 in Supplementary Material). We found that high doses of IVIG attenuated the mean clinical score and the prevalence of CIA such as low amounts (1/500 compared to high dose IVIG) of sialylated IgG autoAbs (Figure S5 in Supplementary Material), whereas administration of equal amounts of non-specific (sialylated) IgG

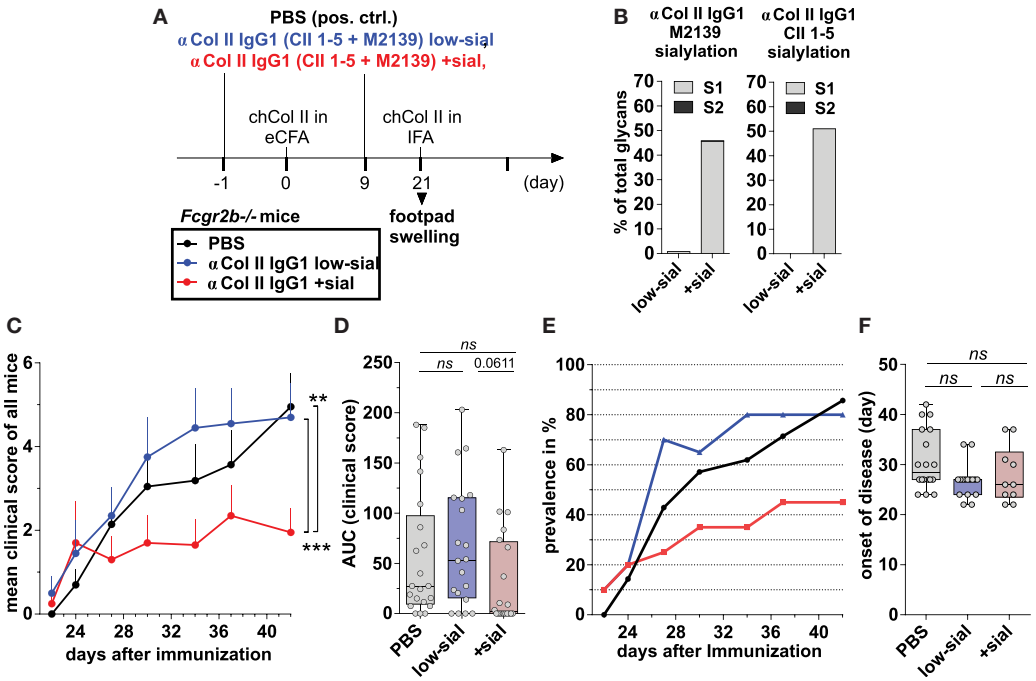

FIGURE 5 | Sialylated collagen type II (Col II)-reactive monoclonal IgG antibodies (Abs) suppress collagen-induced arthritis (CIA). **(A)** Graphical representation of the experimental strategy. CIA was induced in Fcgr2b$^{-/-}$ mice by subcutaneous injection of Col II in enriched CFA (eCFA) and subsequent challenge with Col II in incomplete Freund's adjuvant (IFA) on day 21. One day before and 9 days after the first immunization, the mice received 100 µg of either low-sialylated (low-sial) or *in vitro* galactosylated plus sialylated (+sial) anti-Col II murine IgG1 Abs (clones M2139 and CII 1–5; 50 µg each) The positive control group received PBS instead of Abs. **(B)** Fc sialylation of native (low-sial) and *in vitro* galactosylated plus sialylated (+ sial) anti-Col II M2139 and CII 1–5 murine IgG1 Abs measured by EndoS-treatment and MALDI-TOF mass spectrometry (MS) (percentage of glycans with one or two sialic acid residues: S1 and S2; Figure S1 in Supplementary Material). **(C–F)** Combined clinical data of two independent CIA experiments (PBS: $n = 21$; low-sial: 21; +sial; $n = 20$). Foot swelling was scored on the indicated days from 0 to 3 per foot resulting in a maximal clinical score of 12 per mouse. The **(C)** mean clinical score of all mice and the **(E)** prevalence (percentage of affected animals with a score > 0) are shown for all groups on the indicated days. **(D)** The area under the curve (AUC) of the clinical score over the time was calculated for each mouse. AUC = 0 indicates that the animal never developed foot swelling (mice with score 0: PBS: $n = 3$; low-sial: $n = 4$; +sial: $n = 10$). **(F)** The day of disease onset shown only of the mice that developed foot swelling (score > 0) during the experiment. Differences in disease evolution (C) were analyzed using two-way ANOVA.

(low doses of IVIG) was insufficient to alleviate autoimmune inflammation. Random analysis of ankle sections by histology H&E and anti-CD3 staining showed no differences between mice from different groups with identical foot scores (Figure S5 in Supplementary Material and data not shown).

Also, high, but not low, doses of IVIG and sialylated, but not low-sialylated, Col II-reactive IgG autoAbs reduced by trend the accumulation of Th1 cells and significantly the accumulation of inflammatory Th17 cells, which are known for their important role also in the pathogenesis of CIA (**Figure 6A**) (67–71). Interestingly, unlike sialylated Col II-specific IgG1 Abs, the high doses of IVIG failed to inhibit the generation of Col II-specific IgG2 autoAbs (**Figure 6B**) suggesting a different or additional mechanism of low doses of sialylated Col II-specific IgG Abs as compared to high doses of IVIG.

We could not detect a significant influence of sialylated or low-sialylated anti-Col II IgG Abs on the frequency of total Foxp3$^+$ regulatory CD4 T (Treg) cells in the CIA model (data not shown). However, we observed an increase in antigen-specific Foxp3$^+$Treg frequencies and a tendency toward a reduction of antigen-specific CD4 T cell proliferation with sialylated IgG Abs as compared to low-sialylated IgG Abs in a transfer model with OVA-specific (OT-II) CD4 T cells in C57BL/6 wt and Fcgr2b$^{-/-}$ mice (Figure S6 in Supplementary Material).

Also, the induction of OVA-specific Foxp3$^+$Tregs by sialylated monoclonal TNP-specific IgG Abs seemed to be antigen-specific, as mice immunized with OVA (in contrast to TNP-OVA) failed to elicit a comparable increase in Foxp3$^+$Treg frequencies (Figures S6D,E in Supplementary Material).

These data further suggested an effect of sialylated antigen-specific IgG Abs on the adaptive immune response through an FcγRIIB-independent mechanism.

Matured dendritic cells (DCs) that produce inflammatory cytokines are a prerequisite for induction of inflammatory T and B cell responses and there is evidence that ICs containing sialylated IgG Abs can inhibit DC activation (29). We assessed how IgG sialylation modulates the capacity of ICs to suppress IL-6 production, a cytokine critical for Th17 generation (72, 73) and CIA development (70, 71, 74, 75), by BM-derived FcγRIIB-deficient DCs *in vitro* (**Figure 6C**). IL-6 secretion induced by treating DCs with ICs containing asialylated Col II-reactive IgG1 autoAbs was dramatically reduced by adding sialylated IgG Abs (**Figure 6C**).

In summary, the data suggest that ICs containing antigen and sialylated antigen-specific IgG Abs can influence DC

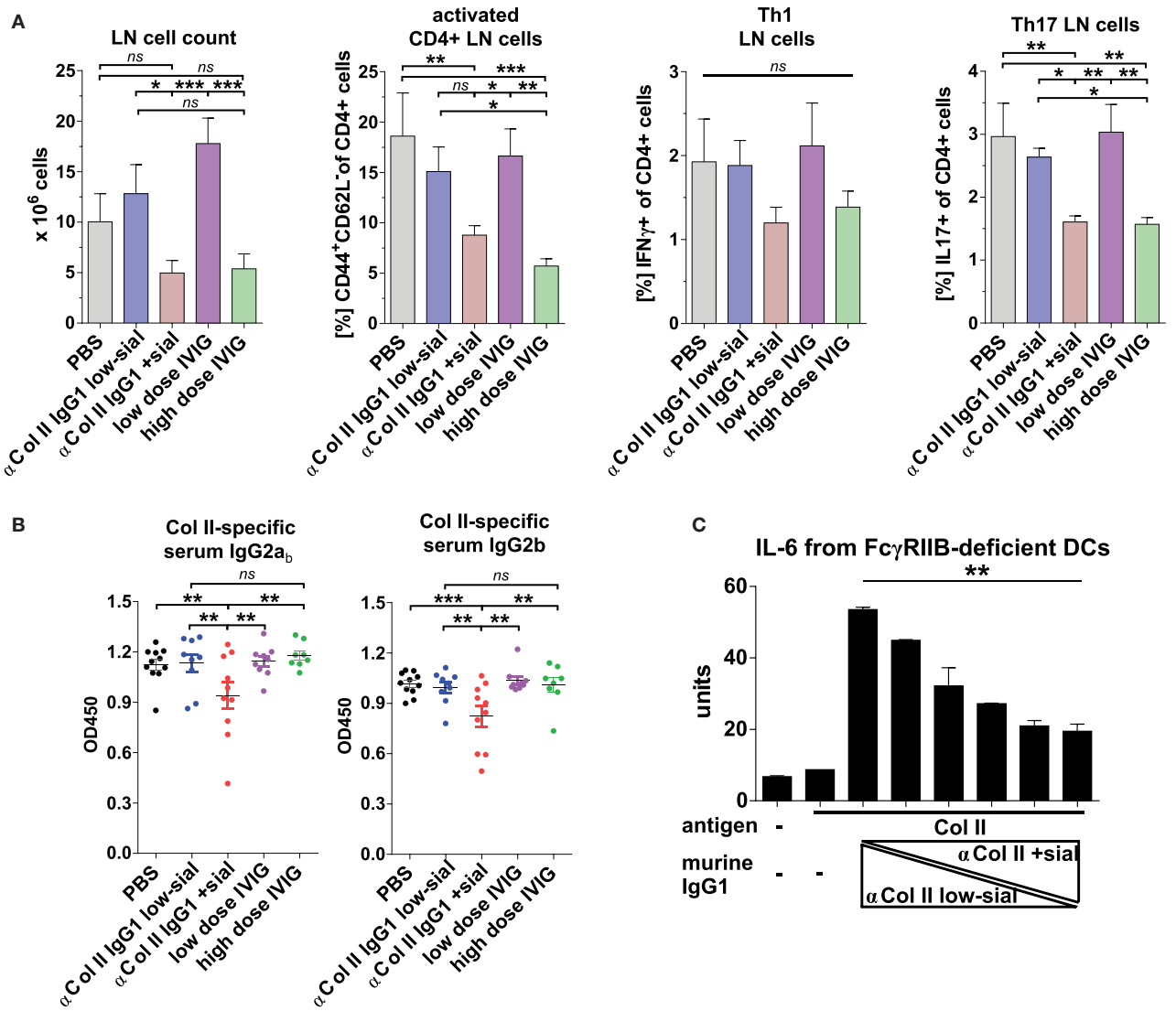

FIGURE 6 | Sialylated collagen type II (Col II)-reactive monoclonal IgG antibodies (Abs) reduce the accumulation of proinflammatory Th17 cells and IgG autoAbs. Collagen-induced arthritis (CIA) was induced in Fcgr2b$^{-/-}$ mice as described in **Figure 5** and Figure S5C in Supplementary Material. One day before and 9 days after the first immunization, the mice received 100 µg of either low-sialylated (low-sial; $n = 10$) or *in vitro* galactosylated plus sialylated (+sial; $n = 9$) anti-Col II murine IgG1 Abs (clones M2139 and CII 1–5; 50 µg each) or high dose (50 mg; $n = 10$) or low dose (100 µg; $n = 10$) of intravenous immunoglobulin (IVIG) (Figure S5B in Supplementary Material). The positive control group received PBS instead of Abs ($n = 10$). **(A)** Pooled popliteal and brachial lymph nodes (LN) of each mouse from the indicated groups were analyzed on day 47 to determine total cell counts and the frequencies of activated CD4$^+$CD44$^+$CD62L$^-$ T cells, CD4$^+$IFNγ$^+$ Th1 cells and CD4$^+$IL-17$^+$ Th17 cells. **(B)** Col II-reactive IgG2a$_b$ and IgG2b serum Ab levels measured on day 42 by enzyme-linked immunofluorescence assay (ELISA). One representative experiment out of two independent experiments is shown. **(C)** Sialylation of Col II-specific IgG1 Abs inhibits IL-6 secretion by dendritic cells (DCs). Bone marrow-derived DCs from Fcgr2b$^{-/-}$ mice were cultured in the presence of ICs containing 1 µg of Col II and 4 µg of different ratios of low-sialylated (< 1% sialylation; **Figure 5B**) and *in vitro* galactosylated and sialylated (46% sialylation; **Figure 5B**) Col II-specific IgG1 Abs (clone M2139; % of sialylation from left to right: <1, 3, 6, 12, 23, 46%). The IL-6 concentration in the supernatant was analyzed after 36 h *via* ELISA. The presented data are representative of four independent experiments.

activation and thereby regulate antigen-specific T and finally B cell responses.

DISCUSSION

Fc glycosylation of IgG molecules regulates their effector functions and thereby may critically contribute to development of autoimmune pathology. On the one hand, agalactosylated IgG autoAbs are associated with severity of autoimmune disorders, such as RA and SLE (3–25), and able to induce disease symptoms in mouse models of RA (9, 24). On the other hand, the presence of autoAbs in sera of many healthy humans (76–79) implies that additional factors, including Fc glycosylation, seem crucial for rendering autoAbs pathogenic. For instance, RA patients develop

IgG autoAbs long before clinical symptoms (21, 80), and the glycosylation patterns of these early autoAbs are less inflammatory compared to IgG Abs detected in patients with the manifested disease (21, 25).

Another unexplored possibility is that anti-inflammatory sialylated autoAbs not only lack pathogenic activity, but may be responsible for inducing immune tolerance to autoantigens in healthy animals and humans. Indeed, we have recently demonstrated that T-cell-independent antigens promote generation of immunosuppressive sialylated IgG molecules (30), whereas T-cell-dependent immunizations can induce antigen-specific IgG Abs with pro- or anti-inflammatory glycosylation patterns depending on the co-stimuli (29, 30). Our present study further suggests that sialylated IgG2a and IgG2b autoAbs produced by 56R BCR-expressing B cells in a T-cell-independent manner are able to attenuate development of nephritis in lupus-prone FcγRIIB-deficient mice. These findings therefore would extend the existing knowledge that B cells regulate immune responses and inhibit autoimmune pathology *via* secretion of immunosuppressive cytokines, such as IL-10 and IL-35 (81).

Antigen specificity of sialylated IgG Abs may play a critical role in exerting their anti-inflammatory effect. Indeed, the transfer of ICs containing sialylated polyreactive IgG autoAbs from $56R^{+/-}Fcgr2b^{-/-}$ mice or sialylated antigen-specific monoclonal IgG Abs attenuated the development of the induced nephritis (**Figure 4**), whereas antigen-unspecific sialylated monoclonal IgG Abs failed to reach the inhibitory potential of antigen-specific sialylated IgG Abs.

In the arthritis model, sialylated Col II-specific IgG Abs reduced arthritis symptoms (**Figure 5**), whereas administration of equal amounts of non-specific (sialylated) IgG (low dose of IVIG) was insufficient to alleviate autoimmune inflammation. These data are well consistent with recent reports showing that sialylated Col II-specific IgG1 Abs can inhibit CIA in DBA/1 mice (24). Importantly, Ohmi et al. demonstrated that the inhibitory effect of sialylated IgG autoAbs in the CIA model is autoantigen-specific, since non-specific sialylated IgG1 failed to suppress CIA (24). We cannot exclude, however, that the suppressive effects of sialylated IgG autoAbs observed here are only partially mediated in an antigen specific manner.

Mouse studies that used IVIG and sialylated Fc fragments suggest that antigen specificity is not essential for the anti-inflammatory action of the sialylated subfraction of IVIG (35). By comparing the effects of high doses of (sialylated) IVIG and sialylated collagen-specific IgG Abs, our data suggest that antigen specificity might significantly enhance the capacity of sialylated Abs to inhibit immune reactions. In accordance, we found that small amounts of collagen-specific sialylated IgG1 Abs, but not high doses of IVIG, were able to inhibit the development of IgG2 autoAbs in the CIA model. Since antigen specificity is necessary for IC formation, antigen-specific sialylated IgG Abs might inhibit IgG autoAb production *via* an alternative pathway that potentially requires IC formation.

Extensive evidence suggest that generation of Th17 cells plays a crucial role in pathogenesis of many autoimmune disorders and mouse models of SLE and CIA are dependent on IL-17 (50, 67, 70, 71). Moreover, IL-17 is necessary for development of pathogenic G0 IgG Abs (30). IL-6 skews T cell differentiation toward IL-17A-producing Th17 cells, suppressing the generation of $Foxp3^{+}$Treg cells (72, 73). In line, we showed that sialylation of IgG autoAbs reduces IL-6 production by DCs *in vitro* and Th17 cell accumulation in autoimmune models. Moreover, we observed that only the formation of sialylated IgG ICs increases the frequencies of antigen-specific $Foxp3^{+}$Treg cells in the OT-II^{+}T cell transfer model.

In summary, we suppose that ICs containing autoantigen-specific sialylated IgG Abs influence inflammatory DC activation and IL-6 production in a FcγRIIB-independent manner and thereby downregulate Th17 generation, formation of pathogenic G0 autoAbs and, hence, alleviate clinical signs of autoimmune pathology.

ETHICS STATEMENT

All of the mice were bred and maintained at the German Rheumatism Research Center in Berlin or the University of Lübeck, Germany and all experiments were conducted with the approval of and in accordance with regulatory guidelines and ethical standards set by both institutions and the Ministry of Berlin or Schleswig-Holstein, Germany.

AUTHOR CONTRIBUTIONS

YCB, JR and MMMM conducted key experiments. SE and FKML performed the chicken collagen induced arthritis mouse experiments. ADS, DB, AKL, AW, G-ML, JP, JH, MS, CH, VH, CTS, CMO and AL performed some of the *in vivo* and *in vitro* experiments. YCB, DB and VB performed IgG glycan analysis. ME coordinated and supervised the experiments and wrote the manuscript.

ACKNOWLEDGMENTS

We thank Angelina Jahn, Heidi Hecker-Kia, Heidi Schliemann, Tuula Geske, Toralf Kaiser, Detlef Grunow, Katja Grollich, Anja A. Kühl, and Robina Thurmann for technical assistance. We thank Michael Madaio for the support with NTS, Mattias Collin for the EndoS and Birgitta Heyman for the anti-TNP IgG1 H5 hybridoma cells.

FUNDING

ME's laboratories were supported by the Else-Kröner-Fresenius Foundation (2014_A91) and the German Research Foundation [EH 221/4-1, EH 221/5-1, EH 221/8-1, EH 221/9-1, Research Training Group (GRK) 1727, international GRK1911, Clinical Research Unit (CRU) 303, SFB/TR 654 and Excellence cluster 306]. ME was a fellow of the Claussen-Simon-Foundation. AL was supported by the German Research Foundation (excellence cluster 306, junior grant) and the University of Lübeck (junior grant) and VB was supported by the German Ministry of Research and Education (03IP511) and the Sonnenfeld Foundation. We acknowledge financial support by Land Schleswig-Holstein (funding program: "Open Access Publikationsfonds").

SUPPLEMENTARY MATERIAL

The Supplementary Material for this article can be found online at https://www.frontiersin.org/articles/10.3389/fimmu.2018.01183/full#supplementary-material.

FIGURE S1 | EndoS-released glycan structures. **(A)** The biantennary core of the glycan structure linked to Asn 297 in the Fc region of IgG antibodies (Abs) consists of four N-acetylglucosamines (GlcNAc; blue) and three mannoses (Man), which can be further modified with fucose, bisecting GlcNAc and terminal galactose (G) and sialic acid [S; human (purple) – N-acetylneuraminic acid (Neu5Ac) or murine (light-blue) – N-glycolylneuraminic acid (Neu5Gc)] residues. MALDI-TOF mass spectrometry (MS) of N-glycans linked to Asn 297 at IgG Fc fragments was performed through EndoS-treatment; the endoglycosidase S (EndoS) cleavage site is indicated with an arrow. **(B)** Possible human and murine Fc glycan structures released from Asn 297 using EndoS. The patterns include glycan structures with human (blue) sialic acid (Neu5Ac) residues or murine (red) sialic acid residues (Neu5Gc). The numbers represent the molecular mass (*m/z*) of the possible Fc glycan structures (permethylated) released upon EndoS treatment.

FIGURE S2 | Early development of self- and polyreactive IgG2a and IgG2b autoAbs in 56R$^{+/-}$Fcgr2b$^{-/-}$ mice is T cell independent. These data are part of the analyses described in **Figures 1–3**. **(A)** Anti-nucleosome (nuc) and **(B)** anti-TNP (polyreactive) IgG2a$_b$, IgG2b or IgG2a$_a$ serum subclass antibodies (Abs) of 5–7-month-old wt and Fcgr2b$^{-/-}$ mice and 2- or 6-month-old 56R$^{+/-}$Fcgr2b$^{-/-}$ mice were determined *via* enzyme-linked immunofluorescence assay (ELISA). Each data point represents an individual animal. Bars indicate mean values. **(C,D)** AutoAb-positive 5-month-old Fcgr2b$^{-/-}$ mice or 2.5-month-old 56R$^{+/-}$Fcgr2b$^{-/-}$ mice were treated every 4 days (d) with i.p. injections of anti-mouse CD4 (GK1.5) to deplete CD4$^+$ T cells for 25 days. **(C)** The efficacy of CD4$^+$TCRbeta$^+$ cell depletion *via* anti-CD4 Ab treatment was monitored through FACS analysis of peripheral blood samples from C57BL/6 wt mice on days 2 and 5 after a single injection of 250 µg of anti-CD4. **(D)** Serum anti-nucleosome (nuc) IgG2a$_b$, IgG2b and IgG2a$_a$ autoAb levels before and after CD4 depletion were determined *via* ELISA. Data from the same representative experiment as described in **Figures 3A,B** are shown. **(E)** Representative intracellular staining of St6gal1 protein expression levels in splenic plasma cells (PCs) of a wt and AB$^+$PU$^+$Fcgr2b$^{-/-}$ mouse and an isotype control staining of the same AB$^+$PU$^+$Fcgr2b$^{-/-}$ mouse analyzed by flow cytometry.

FIGURE S3 | Sialylated antigen-specific IgG antibodies (Abs) protect significant better from mortality in the nephrotoxic nephritis model than sialylated IgG Abs with an irrelevant specificity. **(A)** The data in **(A)** are also part of the experiment described in **Figures 4D–F**. TNP-specific enzyme-linked immunofluorescence assay (ELISA); the Fc glycosylation pattern of anti-TNP murine IgG1 Abs (clone H5) has no influence on TNP recognition. **(B)** Graphical representation of the experimental strategy. C57BL/6 wt mice received 100 µg of TNP-sheep IgG and 100 µg of either sialylated antigen-specific anti-TNP murine IgG1 (clone: H5; H5 + sial; $n = 6$) or sialylated antigen-unspecific anti-Thy1.1 murine IgG1 (clone: OX-7; OX-7 + sial; $n = 4$) Abs. After 14 days, nephritis was induced by injection of sheep IgG in complete Freund's adjuvant (CFA) and subsequent intravenous treatment with sheep anti-glomerular basement membrane nephrotoxic serum (NTS) 4 days later. **(C)** Fc sialylation of the monoclonal anti-TNP murine IgG 1 (clone H5) and anti-Thy1.1 murine IgG1 (clone OX-7) Abs was determined through EndoS-treatment and MALDI-TOF mass spectrometry (MS) (percentage of glycans with one or two sialic acid residues: S1 and S2). **(D)** Kaplan–Meier survival analysis of the indicated groups. One representative experiment is shown.

FIGURE S4 | Sequences and cloning of the CII-reactive monoclonal murine IgG1 antibodies used in the experiments shown in **Figures 5 and 6** and Figure S5 in Supplementary Material. The start and stop codons are colored in red. The restriction sites used for cloning are highlighted in yellow. The first box (blue) represents the leader sequence. The second box (yellow) shows the variable VDJ or VJ sequence whereas the third box (gray) is the constant IgG1-Fc or kappa chain sequence, respectively. **(A) Col II-reactive (clone M2139) murine IgG1 heavy chain** (accession number: MH208236). The 43 bold and underlined bases behind the leader sequence were missing in the original sequence description (NCBI Z72462) (57) and completed here by the J558.2.88 (NCBI BN000872) sequence because of its highest homology to the original sequence observed after NCBI, IgBlast alignment. The C57BL/6 IgG1 heavy chain constant region starts two bases in front of the *SalI* restriction site. Because of the introduction of the *SalI* restriction site, the constant IgG1 heavy chain sequence starts with the amino acids (A)STT… instead of (A)KTT…, which had no functional influence (60). **(B) Col II-reactive (clone M2139) murine kappa chain** (accession number: MH208237). The first 27 bold and underlined bases behind the leader sequence were missing in the original sequence description (NCBI Z72463) (57) and were completed here by the 21-1 (NCBI X16955) sequence because of its highest homology to the original sequence observed after NCBI, IgBlast alignment. The IGKJ2 sequence in the original sequence description was incomplete and completed here with bold and underlined letters representing the IGKJ2 sequence (accession number V00777) identified on the ImMunoGeneTics (IMGT) Marie-Paule homepage (http://www.imgt.org). The C57BL/6 constant light chain region starts with the *BsiWI* restriction site. Because of the introduction of the *BsiWI* restriction site, the constant kappa light chain sequence starts with the amino acids (R)TDA… instead of (R)ADA…, which had no functional influence (60). **(C) Col II-reactive (clone CII 1-5) murine IgG1 heavy chain** (accession number: MH208238). The IGHJ2 sequence in the original sequence description (NCBI MMU69538) (58) was incomplete and completed here with bold and underlined letters representing the IGHJ2 sequence (accession number V00770) identified on the ImMunoGeneTics (IMGT) Marie-Paule homepage (http://www.imgt.org). The C57BL/6 IgG1 heavy chain constant region starts two bases in front of the *SalI* restriction site. Because of the introduction of the *SalI* restriction site, the constant IgG heavy chain sequence starts with the amino acids (A)STT… instead of (A)KTT…, which had no functional influence (60). **(D) Col II-reactive (clone CII 1-5) murine kappa chain** (accession number: MH208239). The four bold and underlined bases behind the leader sequence were corrected from the original sequence description (NCBI MMU69539) (58) because of its obvious mismatching from the highly homologous 12-44 (NCBI AJ235955) sequence observed after NCBI, IgBlast alignment probably resulting by sequencing/analyzing mistakes. The exchanges were from g to c, c to a, c to g and a to g. The IGKJ1 sequence in the original sequence description was incomplete and completed here with bold and underlined letters representing the IGKJ1 sequence (accession number V00777) identified on the ImMunoGeneTics (IMGT) Marie-Paule homepage (http://www.imgt.org). The C57BL/6 constant light chain region starts with the *BsiWI* restriction site. Because of the introduction of the *BsiWI* restriction site the constant kappa light chain sequence starts with the amino acids (R)TDA… instead of (R)ADA…, which had no functional influence (60).

FIGURE S5 | Low doses of sialylated Col II-reactive monoclonal IgG antibodies (Abs) and high doses of intravenous immunoglobulin (IVIG) attenuate collagen-induced arthritis (CIA). These data are parts of the experiments described in **Figures 5 and 6**. **(A)** Col II reactivities of native low-sialylated (low-sial) and *in vitro* galactosylated plus sialylated (+sial) M2139 and CII 1-5 IgG1 Abs and of an antigen-unspecific, TNP-specific murine IgG1 hybridoma Ab (clone H5; negative control) (52) were determined through ELISA. **(B)** Graphical representation of the experimental strategy used in **Figure 6**. CIA was induced in Fcgr2b$^{-/-}$ mice as described in **Figure 5A**. One day before and 9 days after the first immunization the mice received 100 µg of either non-sialylated (low-sial; $n = 10$) or *in vitro* galactosylated plus sialylated (+sial; $n = 9$) anti-Col II murine IgG1 Abs (clones M2139 and CII 1-5; 50 µg each) or high dose (50 mg; $n = 10$) or low dose (100 µg; $n = 10$) IVIG. The positive control group received PBS instead of Abs ($n = 10$). **(C)** Foot swelling was scored on the indicated days from 0 to 3 per foot resulting in a maximal clinical score of 12 per mouse. The mean clinical score of all mice and the prevalence (percentage of affected animals with a score > 0) are shown for all groups on the indicated days. **(D)** Representative foot ankle sections of representative mice with CIA score 0 (left; healthy mouse) or score 2 (right; mouse with a swollen ankle) were stained with hematoxylin and eosin (H&E) or anti-CD3. One representative experiment out of two independent experiments is shown. Differences in disease evolution were calculated using two-way ANOVA.

FIGURE S6 | Application of sialylated antigen-specific murine IgG1 antibodies (Abs) enhances the development of antigen-specific Foxp3$^+$Tregs. **(A)** Graphical representation of the experimental strategy. On day −1, C57BL/6 wt or Fcgr2b$^{-/-}$ mice were treated intravenous with 3×10^7 labeled splenocytes from OT-II$^{+/-}$ × Thy1.1$^{+/-}$ mice and subsequently treated i.p. with 90 µg of low-sialylated (low-sial) or *in vitro* galactosylated plus sialylated (sial) monoclonal murine anti-TNP IgG1 Abs (clone H5) or no Ab. On day 0, mice were immunized

i.p. with 30 µg of TNP(5)-OVA or OVA (antigen-unspecific control) in enriched CFA (eCFA) and on day 4, mice were sacrificed for flow cytometry analysis of mesenteric lymph node (mLN) cells and splenocytes. **(B)** Fc sialylation of low-sialylated or *in vitro* galactosylated plus sialylated anti-TNP IgG1 Abs (H5) was determined through EndoS-treatment and MALDI-TOF mass spectrometry (MS) (percentage of glycans with one or two sialic acid residues: S1, S2; Figure S1 in Supplementary Material). **(C)** Representative Foxp3 expression analysis of gated, proliferating (as a marker for antigen-specific activation) OT-II$^{+/-}$ × Thy1.1$^{+/-}$CD4^{+} mLN cells of all three groups treated with TNP-OVA by flow cytometry on day four. **(D,E)** Foxp3^{+}cell frequencies of transferred proliferating OT-II$^{+/-}$ × Thy1.1$^{+/-}$ mLN and spleen cells from C57BL/6 wt mice after immunization with **(D)** TNP-OVA or **(E)** OVA in eCFA as determined by flow cytometry. **(F)** Percentage of proliferating OT-II$^{+/-}$ × Thy1.1$^{+/-}$ of all CD4^{+} spleen cells from C57BL/6 wt mice after immunization with TNP-OVA in eCFA. One representative out of two independent experiments is shown. **(G)** Foxp3^{+} cell frequencies of transferred proliferating OT-II$^{+/-}$ × Thy1.1$^{+/-}$ mLN and spleen cells from Fcgr2b$^{-/-}$ mice after immunization with TNP-OVA in eCFA. One representative out of two independent experiments is shown.

REFERENCES

1. Nimmerjahn F, Ravetch JV. Divergent immunoglobulin g subclass activity through selective Fc receptor binding. *Science* (2005) 310(5753):1510–2. doi:10.1126/science.1118948
2. Nimmerjahn F, Ravetch JV. Fcgamma receptors as regulators of immune responses. *Nat Rev Immunol* (2008) 8(1):34–47. doi:10.1038/nri2206
3. Parekh RB, Dwek RA, Sutton BJ, Fernandes DL, Leung A, Stanworth D, et al. Association of rheumatoid arthritis and primary osteoarthritis with changes in the glycosylation pattern of total serum IgG. *Nature* (1985) 316(6027):452–7. doi:10.1038/316452a0
4. Parekh RB, Roitt IM, Isenberg DA, Dwek RA, Ansell BM, Rademacher TW. Galactosylation of IgG associated oligosaccharides: reduction in patients with adult and juvenile onset rheumatoid arthritis and relation to disease activity. *Lancet* (1988) 1(8592):966–9. doi:10.1016/S0140-6736(88)91781-3
5. Parekh R, Isenberg D, Rook G, Roitt I, Dwek R, Rademacher T. A comparative analysis of disease-associated changes in the galactosylation of serum IgG. *J Autoimmun* (1989) 2(2):101–14. doi:10.1016/0896-8411(89)90148-0
6. Rook GA, Steele J, Brealey R, Whyte A, Isenberg D, Sumar N, et al. Changes in IgG glycoform levels are associated with remission of arthritis during pregnancy. *J Autoimmun* (1991) 4(5):779–94. doi:10.1016/0896-8411(91)90173-A
7. Bodman KB, Sumar N, Mackenzie LE, Isenberg DA, Hay FC, Roitt IM, et al. Lymphocytes from patients with rheumatoid arthritis produce agalactosylated IgG in vitro. *Clin Exp Immunol* (1992) 88(3):420–3. doi:10.1111/j.1365-2249.1992.tb06465.x
8. Tomana M, Schrohenloher RE, Reveille JD, Arnett FC, Koopman WJ. Abnormal galactosylation of serum IgG in patients with systemic lupus erythematosus and members of families with high frequency of autoimmune diseases. *Rheumatol Int* (1992) 12(5):191–4. doi:10.1007/BF00302151
9. Rademacher TW, Williams P, Dwek RA. Agalactosyl glycoforms of IgG autoantibodies are pathogenic. *Proc Natl Acad Sci U S A* (1994) 91(13):6123–7. doi:10.1073/pnas.91.13.6123
10. van Zeben D, Rook GA, Hazes JM, Zwinderman AH, Zhang Y, Ghelani S, et al. Early agalactosylation of IgG is associated with a more progressive disease course in patients with rheumatoid arthritis: results of a follow-up study. *Br J Rheumatol* (1994) 33(1):36–43. doi:10.1093/rheumatology/33.1.36
11. Malhotra R, Wormald MR, Rudd PM, Fischer PB, Dwek RA, Sim RB. Glycosylation changes of IgG associated with rheumatoid arthritis can activate complement via the mannose-binding protein. *Nat Med* (1995) 1(3):237–43. doi:10.1038/nm0395-237
12. Pilkington C, Yeung E, Isenberg D, Lefvert AK, Rook GA. Agalactosyl IgG and antibody specificity in rheumatoid arthritis, tuberculosis, systemic lupus erythematosus and myasthenia gravis. *Autoimmunity* (1995) 22(2):107–11. doi:10.3109/08916939508995306
13. Williams PJ, Rademacher TW. Analysis of murine IgG isotype galactosylation in collagen-induced arthritis. *Scand J Immunol* (1996) 44(4):381–7. doi:10.1046/j.1365-3083.1996.d01-323.x
14. Dong X, Storkus WJ, Salter RD. Binding and uptake of agalactosyl IgG by mannose receptor on macrophages and dendritic cells. *J Immunol* (1999) 163(10):5427–34.
15. Kuroda Y, Nakata M, Nose M, Kojima N, Mizuochi T. Abnormal IgG galactosylation and arthritis in MRL-Fas(lpr) or MRL-FasL(gld) mice are under the control of the MRL genetic background. *FEBS Lett* (2001) 507(2):210–4. doi:10.1016/S0014-5793(01)02974-X
16. Axford JS, Cunnane G, Fitzgerald O, Bland JM, Bresnihan B, Frears ER. Rheumatic disease differentiation using immunoglobulin G sugar printing by high density electrophoresis. *J Rheumatol* (2003) 30(12):2540–6.
17. Pasek M, Duk M, Podbielska M, Sokolik R, Szechiński J, Lisowska E, et al. Galactosylation of IgG from rheumatoid arthritis (RA) patients – changes during therapy. *Glycoconj J* (2006) 23(7–8):463–71. doi:10.1007/s10719-006-5409-0
18. Arnold JN, Wormald MR, Sim RB, Rudd PM, Dwek RA. The impact of glycosylation on the biological function and structure of human immunoglobulins. *Annu Rev Immunol* (2007) 25:21–50. doi:10.1146/annurev.immunol.25.022106.141702
19. Nimmerjahn F, Anthony RM, Ravetch JV. Agalactosylated IgG antibodies depend on cellular Fc receptors for in vivo activity. *Proc Natl Acad Sci U S A* (2007) 104(20):8433–7. doi:10.1073/pnas.0702936104
20. van de Geijn FE, Wuhrer M, Selman MH, Willemsen SP, de Man YA, Deelder AM, et al. Immunoglobulin G galactosylation and sialylation are associated with pregnancy-induced improvement of rheumatoid arthritis and the postpartum flare: results from a large prospective cohort study. *Arthritis Res Ther* (2009) 11(6):R193. doi:10.1186/ar2892
21. Ercan A, Cui J, Chatterton DE, Deane KD, Hazen MM, Brintnell W, et al. Aberrant IgG galactosylation precedes disease onset, correlates with disease activity, and is prevalent in autoantibodies in rheumatoid arthritis. *Arthritis Rheum* (2010) 62(8):2239–48. doi:10.1002/art.27533
22. Scherer HU, van der Woude D, Ioan-Facsinay A, el Bannoudi H, Trouw LA, Wang J, et al. Glycan profiling of anti-citrullinated protein antibodies isolated from human serum and synovial fluid. *Arthritis Rheum* (2010) 62(6):1620–9. doi:10.1002/art.27414
23. Troelsen LN, Jacobsen S, Abrahams JL, Royle L, Rudd PM, Narvestad E, et al. IgG glycosylation changes and MBL2 polymorphisms: associations with markers of systemic inflammation and joint destruction in rheumatoid arthritis. *J Rheumatol* (2012) 39(3):463–9. doi:10.3899/jrheum.110584
24. Ohmi Y, Ise W, Harazono A, Takakura D, Fukuyama H, Baba Y, et al. Sialylation converts arthritogenic IgG into inhibitors of collagen-induced arthritis. *Nat Commun* (2016) 7:11205. doi:10.1038/ncomms11205
25. Pfeifle R, Rothe T, Ipseiz N, Scherer HU, Culemann S, Harre U, et al. Regulation of autoantibody activity by the IL-23-TH17 axis determines the onset of autoimmune disease. *Nat Immunol* (2017) 18(1):104–13. doi:10.1038/ni.3579
26. Alavi A, Arden N, Spector TD, Axford JS. Immunoglobulin G glycosylation and clinical outcome in rheumatoid arthritis during pregnancy. *J Rheumatol* (2000) 27(6):1379–85.
27. Förger F, Ostensen M. Is IgG galactosylation the relevant factor for pregnancy-induced remission of rheumatoid arthritis? *Arthritis Res Ther* (2010) 12(1):108. doi:10.1186/ar2919
28. Van Beneden K, Coppieters K, Laroy W, De Keyser F, Hoffman IE, Van den Bosch F, et al. Reversible changes in serum immunoglobulin galactosylation during the immune response and treatment of inflammatory autoimmune arthritis. *Ann Rheum Dis* (2009) 68(8):1360–5. doi:10.1136/ard.2008.089292
29. Oefner CM, Winkler A, Hess C, Lorenz AK, Holecska V, Huxdorf M, et al. Tolerance induction with T cell-dependent protein antigens induces regulatory sialylated IgGs. *J Allergy ClinImmunol* (2012) 129(6):1647–55. doi:10.1016/j.jaci.2012.02.037
30. Hess C, Winkler A, Lorenz AK, Holecska V, Blanchard V, Eiglmeier S, et al. T cell-independent B cell activation induces immunosuppressive sialylated IgG antibodies. *J Clin Invest* (2013) 123(9):3788–96. doi:10.1172/JCI65938
31. Collin M, Ehlers M. The carbohydrate switch between pathogenic and immunosuppressive antigen-specific antibodies. *Exp Dermatol* (2013) 22(8):511–4. doi:10.1111/exd.12171
32. Epp A, Hobusch J, Bartsch YC, Petry J, Lilienthal GM, Koeleman CAM, et al. Sialylation of IgG antibodies inhibits IgG-mediated allergic reactions. *J Allergy Clin Immunol* (2017) 141(1):399–402.e8. doi:10.1016/j.jaci.2017.06.021

33. Kaneko Y, Nimmerjahn F, Ravetch JV. Anti-inflammatory activity of immunoglobulin G resulting from Fc sialylation. *Science* (2006) 313(5787):670–3. doi:10.1126/science.1129594
34. Nimmerjahn F, Ravetch JV. Anti-inflammatory actions of intravenous immunoglobulin. *Annu Rev Immunol* (2008) 26:513–33. doi:10.1146/annurev.immunol.26.021607.090232
35. Anthony RM, Nimmerjahn F, Ashline DJ, Reinhold VN, Paulson JC, Ravetch JV. Recapitulation of IVIG anti-inflammatory activity with a recombinant IgG Fc. *Science* (2008) 320(5874):373–6. doi:10.1126/science.1154315
36. Anthony RM, Wermeling F, Karlsson MC, Ravetch JV. Identification of a receptor required for the anti-inflammatory activity of IVIG. *Proc Natl Acad Sci U S A* (2008) 105(50):19571–8. doi:10.1073/pnas.0810163105
37. Anthony RM, Kobayashi T, Wermeling F, Ravetch JV. Intravenous gammaglobulin suppresses inflammation through a novel T(H)2 pathway. *Nature* (2011) 475(7354):110–3. doi:10.1038/nature10134
38. Bayry J, Lacroix-Desmazes S, Delignat S, Mouthon L, Weill B, Kazatchkine MD, et al. Intravenous immunoglobulin abrogates dendritic cell differentiation induced by interferon-alpha present in serum from patients with systemic lupus erythematosus. *Arthritis Rheum* (2003) 48(12):3497–502. doi:10.1002/art.11346
39. Aubin E, Lemieux R, Bazin R. Indirect inhibition of in vivo and in vitro T-cell responses by intravenous immunoglobulins due to impaired antigen presentation. *Blood* (2010) 115(9):1727–34. doi:10.1182/blood-2009-06-225417
40. Massoud AH, Yona M, Xue D, Chouiali F, Alturaihi H, Ablona A, et al. Dendritic cell immunoreceptor: a novel receptor for intravenous immunoglobulin mediates induction of regulatory T cells. *J Allergy Clin Immunol* (2014) 133(3):853–63.e5. doi:10.1016/j.jaci.2013.09.029
41. Karsten CM, Pandey MK, Figge J, Kilchenstein R, Taylor PR, Rosas M, et al. Anti-inflammatory activity of IgG1 mediated by Fc galactosylation and association of Fc gamma RIIB and dectin-1. *Nat Med* (2012) 18(9):1401–6. doi:10.1038/nm.2862
42. Pagan JD, Kitaoka M, Anthony RM. Engineered sialylation of pathogenic antibodies in vivo attenuates autoimmune disease. *Cell* (2017) 72(3):564–77.e13. doi:10.1016/j.cell.2017.11.041
43. Chen C, Nagy Z, Prak EL, Weigert M. Immunoglobulin heavy chain gene replacement: a mechanism of receptor editing. *Immunity* (1995) 3(6):747–55. doi:10.1016/1074-7613(95)90064-0
44. Li H, Jiang Y, Prak EL, Radic M, Weigert M. Editors and editing of anti-DNA receptors. *Immunity* (2001) 15(6):947–57. doi:10.1016/S1074-7613(01)00251-5
45. Fukuyama H, Nimmerjahn F, Ravetch JV. The inhibitory Fcgamma receptor modulates autoimmunity by limiting the accumulation of immunoglobulin G+ anti-DNA plasma cells. *Nat Immunol* (2005) 6(1):99–106. doi:10.1038/ni1151
46. Ehlers M, Fukuyama H, McGaha T, Aderem A, Ravetch J. TLR9/MyD88 signaling is required for class switching to pathogenic IgG2a and 2b autoantibodies in SLE. *J Exp Med* (2006) 203(3):553–61. doi:10.1084/jem.20052438
47. Tsao PY, Jiao J, Ji MQ, Cohen PL, Eisenberg RA. T cell-independent spontaneous loss of tolerance by anti-double-stranded DNA B cells in C57BL/6 mice. *J Immunol* (2008) 181(11):7770–7. doi:10.4049/jimmunol.181.11.7770
48. Takai T, Ono M, Hikida M, Ohmori H, Ravetch JV. Augmented humoral and anaphylactic responses in Fc gamma RII-deficient mice. *Nature* (1996) 379(6563):346–9. doi:10.1038/379346a0
49. Bolland S, Ravetch JV. Spontaneous autoimmune disease in Fc(gamma) RIIB-deficient mice results from strain-specific epistasis. *Immunity* (2000) 13(2):277–85. doi:10.1016/S1074-7613(00)00027-3
50. Stoehr AD, Schoen CT, Mertes MMM, Eiglmeier S, Holecska V, Lorenz AK, et al. TLR9 in peritoneal B-1b cells is essential for production of protective self-reactive IgM to control Th17 cells and severe autoimmunity. *J Immunol* (2011) 187(6):2953–65. doi:10.4049/jimmunol.1003340
51. Barnden MJ, Allison J, Heath WR, Carbone FR. Defective TCR expression in transgenic mice constructed using cDNA-based alpha- and beta-chain genes under the control of heterologous regulatory elements. *Immunol Cell Biol* (1998) 76(1):34–40. doi:10.1046/j.1440-1711.1998.00709.x
52. Wernersson S, Karlsson MC, Dahlström J, Mattsson R, Verbeek JS, Heyman B. IgG-mediated enhancement of antibody responses is low in Fc receptor gamma chain-deficient mice and increased in Fc gamma RII-deficient mice. *J Immunol* (1999) 163(2):618–22.
53. Mason DW, Williams AF. The kinetics of antibody binding to membrane antigens in solution and at the cell surface. *Biochem J* (1980) 187(1):1–20. doi:10.1042/bj1870001
54. Collin M, Olsén A. Effect of SpeB and EndoS from *Streptococcus pyogenes* on human immunoglobulins. *Infect Immun* (2001) 69(11):7187–9. doi:10.1128/IAI.69.11.7187-7189.2001
55. Wedepohl S, Kaup M, Riese SB, Berger M, Dernedde J, Tauber R, et al. N-glycan analysis of recombinant L-selectin reveals sulfated GalNAc and GalNAc-GalNAc motifs. *J Proteome Res* (2010) 9(7):3403–11. doi:10.1021/pr100170c
56. Madaio MP, Salant DJ, Adler S, Darby C, Couser WG. Effect of antibody charge and concentration on deposition of antibody to glomerular basement membrane. *Kidney Int* (1984) 26(4):397–403. doi:10.1038/ki.1984.188
57. Nandakumar KS, Andrén M, Martinsson P, Bajtner E, Hellström S, Holmdahl R, et al. Induction of arthritis by single monoclonal IgG anti-collagen type II antibodies and enhancement of arthritis in mice lacking inhibitory FcgammaRIIB. *Eur J Immunol* (2003) 33(8):2269–77. doi:10.1002/eji.200323810
58. Iribe H, Kabashima H, Ishii Y, Koga T. Epitope specificity of antibody response against human type II collagen in the mouse susceptible to collagen-induced arthritis and patients with rheumatoid arthritis. *Clin Exp Immunol* (1988) 73(3):443–8.
59. Wardemann H, Yurasov S, Schaefer A, Young JW, Meffre E, Nussenzweig MC. Predominant autoantibody production by early human B cell precursors. *Science* (2003) 301(5638):1374–7. doi:10.1126/science.1086907
60. Tiller T, Kofer J, Kreschel C, Busse C, Riebel S, Wickert S, et al. Development of self-reactive germinal center B cells and plasma cells in autoimmune Fc gamma RIIB-deficient mice. *J Exp Med* (2010) 207(12):2767–78. doi:10.1084/jem.20100171
61. Pankewycz OG, Migliorini P, Madaio MP. Polyreactive autoantibodies are nephritogenic in murine lupus nephritis. *J Immunol* (1987) 139(10):3287–94.
62. Deshmukh US, Bagavant H, Fu SM. Role of anti-DNA antibodies in the pathogenesis of lupus nephritis. *Autoimmun Rev* (2006) 5(6):414–8. doi:10.1016/j.autrev.2005.10.010
63. Ehlers M, Ravetch J. Opposing effects of toll-like receptor stimulation induce autoimmunity or tolerance. *Trends Immunol* (2007) 28(2):74–9. doi:10.1016/j.it.2006.12.006
64. Fischer M, Ehlers M. Toll-like receptors in autoimmunity. *Ann N Y Acad Sci* (2008) 1143:21–34. doi:10.1196/annals.1443.012
65. Leadbetter EA, Rifkin IR, Hohlbaum AM, Beaudette BC, Shlomchik MJ, Marshak-Rothstein A. Chromatin-IgG complexes activate B cells by dual engagement of IgM and toll-like receptors. *Nature* (2002) 416(6881):603–7. doi:10.1038/416603a
66. Yuasa T, Kubo S, Yoshino T, Ujike A, Matsumura K, Ono M, et al. Deletion of fcgamma receptor IIB renders H-2(b) mice susceptible to collagen-induced arthritis. *J Exp Med* (1999) 189(1):187–94. doi:10.1084/jem.189.1.187
67. Nakae S, Nambu A, Sudo K, Iwakura Y. Suppression of immune induction of collagen-induced arthritis in IL-17-deficient mice. *J Immunol* (2003) 171(11):6173–7. doi:10.4049/jimmunol.171.11.6173
68. Leipe J, Grunke M, Dechant C, Reindl C, Kerzendorf U, Schulze-Koops H, et al. Role of Th17 cells in human autoimmune arthritis. *Arthritis Rheum* (2010) 62(10):2876–85. doi:10.1002/art.27622
69. Arroyo-Villa I, Bautista-Caro MB, Balsa A, Aguado-Acín P, Nuño L, Bonilla-Hernán MG, et al. Frequency of Th17 CD4+ T cells in early rheumatoid arthritis: a marker of anti-CCP seropositivity. *PLoS One* (2012) 7(8):e42189. doi:10.1371/journal.pone.0042189
70. Sarkar S, Justa S, Brucks M, Endres J, Fox DA, Zhou X, et al. Interleukin (IL)-17A, F and AF in inflammation: a study in collagen-induced arthritis and rheumatoid arthritis. *Clin Exp Immunol* (2014) 177(3):652–61. doi:10.1111/cei.12376
71. Lubberts E, Koenders MI, van den Berg WB. The role of T-cell interleukin-17 in conducting destructive arthritis: lessons from animal models. *Arthritis Res Ther* (2005) 7:29–37. doi:10.1186/ar1550
72. Bettelli E, Carrier Y, Gao W, Korn T, Strom TB, Oukka M, et al. Reciprocal developmental pathways for the generation of pathogenic effector TH17 and regulatory T cells. *Nature* (2006) 441(7090):235–8. doi:10.1038/nature04753
73. Bettelli E, Oukka M, Kuchroo VK. T(H)-17 cells in the circle of immunity and autoimmunity. *Nat Immunol* (2007) 8:345–50. doi:10.1038/ni0407-345

74. Ohshima S, Saeki Y, Mima T, Sasai M, Nishioka K, Nomura S, et al. Interleukin 6 plays a key role in the development of antigen-induced arthritis. *Proc Natl Acad Sci U S A* (1998) 95(14):8222–6. doi:10.1073/pnas.95.14.8222
75. Sasai M, Saeki Y, Ohshima S, Nishioka K, Mima T, Tanaka T, et al. Delayed onset and reduced severity of collagen-induced arthritis in interleukin-6-deficient mice. *Arthritis Rheum* (1999) 42(8):1635–43. doi:10.1002/1529-0131(199908)42:8<1635::AID-ANR11>3.0.CO;2-Q
76. Egner W. The use of laboratory tests in the diagnosis of SLE. *J Clin Pathol* (2000) 53(6):424–32. doi:10.1136/jcp.53.6.424
77. Tiller T, Tsuiji M, Yurasov S, Velinzon K, Nussenzweig MC, Wardemann H. Autoreactivity in human IgG+ memory B cells. *Immunity* (2007) 26(2): 205–13. doi:10.1016/j.immuni.2007.01.009
78. Olsen NJ, Karp DR. Autoantibodies and SLE: the threshold for diseases. *Nat Rev Rheumatol* (2014) 10(3):181–6. doi:10.1038/nrrheum.2013.184
79. Nagele EP, Han M, Acharya NK, DeMarshall C, Kosciuk MC, Nagele RG. Natural IgG autoantibodies are abundant and ubiquitous in human sera, and their number is influenced by age, gender, and disease. *PLoS One* (2013) 8(4):e60726. doi:10.1371/journal.pone.0060726
80. Majka DS, Deane KD, Parrish LA, Lazar AA, Barón AE, Walker CW, et al. Duration of preclinical rheumatoid arthritis-related autoantibody positivity increases in subjects with older age at time of disease diagnosis. *Ann Rheum Dis* (2008) 67(6):801–7. doi:10.1136/ard.2007.076679
81. Fillatreau S, Gray D, Anderton SM. Not always the bad guys: B cells as regulators of autoimmune pathology. *Nat Rev Immunol* (2008) 8(5):391–7. doi:10.1038/nri2315

Conflict of Interest Statement: The authors declare that the research was conducted in the absence of any commercial or financial relationships that could be construed as a potential conflict of interest.

frontiers in Immunology

ORIGINAL RESEARCH
published: 05 June 2018
doi: 10.3389/fimmu.2018.01200

Autoantibodies to Cytosolic 5′-Nucleotidase 1A in Primary Sjögren's Syndrome and Systemic Lupus Erythematosus

Anke Rietveld[1], Luuk L. van den Hoogen[2], Nicola Bizzaro[3], Sofie L. M. Blokland[2], Cornelia Dähnrich[4], Jacques-Eric Gottenberg[5], Gunnar Houen[6], Nora Johannsen[4], Thomas Mandl[7], Alain Meyer[5], Christoffer T. Nielsen[8], Peter Olsson[7], Joel van Roon[2], Wolfgang Schlumberger[4], Baziel G. M. van Engelen[1], Christiaan G. J. Saris[1] and Ger J. M. Pruijn[9]*

[1] Department of Neurology, Center for Neuroscience, Donders Institute for Brain, Cognition and Behaviour, Radboud University Medical Center, Nijmegen, Netherlands, [2] Laboratory of Translational Immunology, Department of Rheumatology and Clinical Immunology, University Medical Center Utrecht, Utrecht University, Utrecht, Netherlands, [3] Laboratorio di Patologia Clinica, Ospedale San Antonio, Azienda Sanitaria Universitaria Integrata di Udine, Tolmezzo, Italy, [4] Institute for Experimental Immunology, Euroimmun AG, Lübeck, Germany, [5] Service de physiologie et d'explorations fonctionnelles, Service de rhumatologie, Centre de référence des maladies auto-immunes rares and Fédération de médecine translationnelle de Strasbourg, Université de Strasbourg, Strasbourg, France, [6] Department of Autoimmunology and Biomarkers, Statens Serum Institut, Copenhagen, Denmark, [7] Department of Clinical Sciences Malmö, Lund University, Malmö, Sweden and Department of Rheumatology, Skåne University Hospital, Malmö, Sweden, [8] Copenhagen Lupus and Vasculitis Clinic, Centre for Rheumatology and Spine Disease, Rigshospitalet, Copenhagen University Hospital, Copenhagen, Denmark, [9] Department of Biomolecular Chemistry, Radboud Institute for Molecular Life Sciences and Institute for Molecules and Materials, Radboud University, Nijmegen, Netherlands

OPEN ACCESS

Edited by:
Falk Nimmerjahn, Friedrich-Alexander-Universität Erlangen-Nürnberg, Germany

Reviewed by:
Ralf J. Ludwig, Universität zu Lübeck, Germany
Luz Pamela Blanco, National Institutes of Health (NIH), United States
Yolande Richard, Institut National de la Santé et de la Recherche Médicale (INSERM), France

***Correspondence:**
Anke Rietveld
anke.rietveld@radboudumc.nl

Specialty section:
This article was submitted to Inflammation, a section of the journal Frontiers in Immunology

Received: *24 November 2017*
Accepted: *14 May 2018*
Published: *05 June 2018*

Citation:
Rietveld A, van den Hoogen LL, Bizzaro N, Blokland SLM, Dähnrich C, Gottenberg J-E, Houen G, Johannsen N, Mandl T, Meyer A, Nielsen CT, Olsson P, van Roon J, Schlumberger W, van Engelen BGM, Saris CGJ and Pruijn GJM (2018) Autoantibodies to Cytosolic 5′-Nucleotidase 1A in Primary Sjögren's Syndrome and Systemic Lupus Erythematosus. Front. Immunol. 9:1200. doi: 10.3389/fimmu.2018.01200

Introduction: Autoantibodies to cytosolic 5′-nucleotidase 1A (cN-1A; NT5C1A) have a high specificity when differentiating sporadic inclusion body myositis from polymyositis and dermatomyositis. In primary Sjögren's syndrome (pSS) and systemic lupus erythematosus (SLE) anti-cN-1A autoantibodies can be detected as well. However, various frequencies of anti-cN-1A reactivity have been reported in SLE and pSS, which may at least in part be explained by the different assays used. Here, we determined the occurrence of anti-cN-1A reactivity in a large number of patients with pSS and SLE using one standardized ELISA.

Methods: Sera from pSS (n = 193) and SLE patients (n = 252) were collected in five European centers. Anti-cN-1A, anti-Ro52, anti-nucleosome, and anti-dsDNA reactivities were tested by ELISA (Euroimmun AG) in a single laboratory. Correlations of anti-cN-1A reactivity with demographic data and clinical data (duration of disease at the moment of serum sampling, autoimmune comorbidity and presence of muscular symptoms) were analyzed using SPSS software.

Results: Anti-cN-1A autoantibodies were found on average in 12% of pSS patients, with varying frequencies among the different cohorts (range: 7–19%). In SLE patients, the anti-cN-1A positivity on average was 10% (range: 6–21%). No relationship was found between anti-cN-1A reactivity and the presence or absence of anti-Ro52, anti-nucleosome, and anti-dsDNA reactivity in both pSS and SLE. No relationship between anti-cN-1A reactivity and duration of disease at the moment of serum sampling and the duration of serum storage was observed. The frequency of muscular symptoms or

viral infections did not differ between anti-cN-1A-positive and -negative patients. In both disease groups anti-cN-1A-positive patients suffered more often from other autoimmune diseases than the anti-cN-1A-negative patients (15 versus 5% ($p = 0.05$) in pSS and 50 versus 30% ($p = 0.02$) in SLE).

Conclusion: Our results confirm the relatively frequent occurrence of anti-cN-1A in pSS and SLE patients and the variation in anti-cN-1A reactivity between independent groups of these patients. The explanation for this variation remains elusive. The correlation between anti-cN-1A reactivity and polyautoimmunity should be evaluated in future studies. We conclude that anti-cN-1A should be classified as a myositis-associated-, not as a myositis-specific-autoantibody based on its frequent presence in SLE and pSS.

Keywords: Cytosolic 5′-nucleotidase 1A, anti-cN-1A, NT5C1A, autoantibodies, inclusion body myositis, Sjögren's syndrome, systemic lupus erythematosus

INTRODUCTION

Autoantibodies are often helpful in the diagnosis and follow up of patients with inflammatory myopathies. Traditionally these antibodies are characterized as myositis-specific (MSA) or myositis-associated antibodies (MAA), according to their specificity. In 2013, two independent research groups described a novel antibody in sporadic inclusion body myositis (IBM): anti-cytosolic 5′-nucleotidase 1A (anti-cN-1A; anti-NT5C1A) (1, 2). cN-1A is an enzyme involved in the conversion of adenosine monophosphate to adenosine, and it has a role in the dephosphorylation of nucleotides to nucleosides (1). IBM is a slowly progressive muscle disease with a late onset. Its cause is yet unknown; inflammation, degeneration, and mitochondrial dysfunction all seem to play a role in the pathogenesis of IBM. Anti-cN-1A is present in 33–76% of IBM patients, and the variation is probably not only due to differences between cohorts, but is also dependent on the detection method and cutoff values that are used (1). Anti-cN-1A testing can improve the diagnostic process in IBM, and it can be used as a marker of expected disease severity. Anti-cN-1A positive IBM patients have more pronounced bulbar weakness and a higher mortality rate (2, 3). The presence or absence of anti-cN-1A antibodies in IBM is not related to the duration of symptoms or to the presence or absence of other autoimmune diseases or other autoantibodies (2). The specificity of anti-cN-1A antibodies has been established in previous studies. In healthy controls and in patients with polymyositis, dermatomyositis, and other neurological diseases, the prevalence of anti-cN-1A is low (0–4%) (4). However, in the systemic autoimmune diseases primary Sjögren's syndrome (pSS) and systemic lupus erythematosus (SLE) anti-cN-1A autoantibodies have been detected at various frequencies with different methods of detection (4–7). We aimed to establish the occurrence of anti-cN-1A reactivity in multiple independent groups of European pSS and SLE patients using a single standardized detection method.

MATERIALS AND METHODS

Patients

Sera from pSS ($n = 193$) and SLE patients ($n = 252$) were collected in five different European centers: Tolmezzo, Italy; Strasbourg, France; Utrecht, The Netherlands; Malmö, Sweden and Copenhagen, Denmark. The patients were enrolled in biobanks in each of the participating centers, for which ethical permission was obtained. The SLE patients were diagnosed using the 1997 American College of Rheumatology criteria; pSS patients fulfilled the American-European Consensus Classification Criteria (8, 9). Demographic data (age and sex of the patient), clinical data (duration of disease at the moment of serum sampling, autoimmune co-morbidity, and presence of muscular symptoms) and the total duration of storage of the sample were retrieved from the respective biobank databases by the local researcher blinded for anti-cN-1A status. Muscular symptoms were defined as myalgia and muscle weakness, autoimmune comorbidity was defined as the presence of any other autoimmune disease. Patients with Sjögren's syndrome secondary to SLE were classified as SLE.

Laboratory Analysis

Anti-cN-1A, anti-dsDNA, anti-nucleosomes, and anti-Ro52 reactivities were tested by ELISA in a single laboratory. The anti-cN-1A, anti-dsDNA-NcX, and anti-nucleosomes ELISA are commercially available ELISAs and were performed according to the manufacturer's instructions (respective order numbers EA 1675-4801G, EA 1572-9601G, and EA 1574-9601G, Euroimmun AG, Lübeck, Germany). The anti-cN-1A ELISA is based on recombinant full-length cN-1A antigen as described earlier (7). Results were evaluated semi-quantitatively as a ratio (optical density (OD) 450 sample/OD450 calibrator, ratio ≥ 1 positive). The anti-dsDNA-NcX ELISA utilizes native dsDNA (isolated from calf thymus) as antigen, which is immobilized via highly purified mononucleosomes free of histone H1, Scl-70, and other non-histone components (cutoff: ≥ 100 IU/ml) (10). The anti-nucleosomes ELISA is based on native mononucleosomes free of histone H1, Scl-70 and non-histone components (cutoff: ≥ 20 RU/ml) (11).

Determination of anti-Ro52 reactivity was performed using an in-house ELISA (Euroimmun). Microtiter plates (Nunc, Denmark) were coated with 1 μg/ml recombinant Ro52 in PBS, pH 7.5 overnight at 4°C, washed with PBS-0.05% (w/v) Tween-20, and blocked for 2 h with PBS-0.1% (w/v) casein, followed by washing. Sera diluted 1:200 in PBS-0.1% (w/v) casein were incubated for 30 min before washing. Bound antibodies were detected

using anti-human IgG peroxidase conjugate (Euroimmun) and stained with tetramethylbenzidine (Euroimmun) for 15 min. OD was determined at 450 nm (reference 620 nm) using an automated spectrophotometer (Spectra Mini, Tecan, Germany). All procedures were carried out at room temperature. The cutoff of the anti-Ro52 ELISA was defined at the 99% percentile based on samples from healthy blood donors ($n = 100$), anti-nuclear antibodies-negative patients ($n = 52$) and rheumatoid arthritis patients ($n = 40$). Results were evaluated semi-quantitatively as a ratio (OD450 sample/OD450 calibrator, ratio ≥ 1 positive).

Statistics

IBM SPSS for Windows version 22 (IBM Corp., Armonk, NY, USA) was used for statistical analyses. Chi-square tests and Fisher's exact test (categorical variables) and Mann–Whitney *U* test (continuous, non-parametric variables) were used for pair-wise comparisons between groups. Correlations between autoantibody titers and other variables (e.g., duration of storage) were analyzed using Spearman ranking. A 2-sided *p*-value of 0.05 or less was deemed statistically significant in this exploratory study.

RESULTS

Anti-cN-1A antibodies were found in 12% of the pSS patients (23/193) and in 10% of all SLE patients (26/252). The prevalence of anti-cN-1A showed some variation between countries in both diseases (**Tables 1** and **2**). The distribution of the levels of anti-cN-1A antibodies did not appear to differ between the groups from different countries and between pSS and SLE (**Figure 1**).

The associations between anti-cN-1A reactivity and clinical, demographic, and laboratory findings are presented in **Tables 1** and **2**. A trend toward gender-association of anti-cN-1A reactivity did not reach statistical significance (18% of men in pSS and 17% in SLE showed anti-cN-1A reactivity, versus 12 ($p = 0.5$) and 10% ($p = 0.2$), respectively, of women). No association between anti-cN-1A and duration of disease or sample storage duration was found. Muscular complaints were almost equal for anti-cN-1A-positive and -negative patients, with myalgia being the most frequently reported symptom. One of the pSS patients had a biopsy-proven polymyositis, but this patient had no anti-cN-1A antibodies. In the anti-cN-1A-positive patients, a higher rate of autoimmune co-morbidity was seen: 15% of the anti-cN-1A-positive pSS and 50% of the anti-cN-1A-positive SLE patients suffered from one or more other autoimmune diseases, whereas autoimmune comorbidity was observed in 5 and 30%, respectively, of the anti-cN-1A-negative patients ($p = 0.05$ in pSS, $p = 0.02$ in SLE). The presence or absence of other antibodies did not differ between the anti-cN-1A-positive and -negative patients in both disease groups.

DISCUSSION

The current cohort with anti-cN-1A reactivity in 12% of pSS and 10% of SLE patients confirm the relatively high prevalence of anti-cN-1A in these diseases. In addition, a range of frequencies was observed in the groups from various European countries (pSS: 7–19%; SLE:

TABLE 1 | Clinico-demographic correlations: anti-cN-1A in primary Sjögren's syndrome (pSS).

pSS	Anti-cN-1A positive 12% (23/193)	Anti-cN-1A negative 88% (170/193)	*p*-Value
Provenance of the serum			0.21
– Italy	7%	93%	
– The Netherlands	8%	92%	
– France	19%	81%	
– Sweden	15%	85%	
Female/male	12%/18%	88%/82%	0.63
Presence of muscular complaints[b]	33% (4/12)	27% (20/74)	0.80
Presence of autoimmune co-morbidity[c] (number of patients)	15% (3/20)	5% (7/135)	0.05[a]
– Antiphospholipid syndrome	– 4% (1)	– 0% (0)	
– Rheumatoid arthritis	– 4% (1)	– 2% (4)	
– Other	– 4% (1)	– 2% (3)	
Presence of current or past viral infection[d]	5% (1/19)	3% (4/128)	0.51
Presence of other antibodies			
– dsDNA	0% (0/23)	6% (11/170)	0.37
– anti-nucleosomes	0% (0/23)	6% (11/170)	0.37
– Ro52	65% (15/23)	68% (115/170)	0.82

[a]*Statistically significant ($p \leq 0.05$).*
[b]*Missing data in 55% of patients.*
[c]*Missing data in 20% of patients.*
[d]*Missing data in 24% of patients.*

TABLE 2 | Clinico-demographic correlations: anti-cN-1A in systemic lupus erythematosus (SLE).

SLE	Anti-cN-1A positive 10% (26/252)	Anti-cN-1A negative 90% (226/252)	*p*-Value
Provenance of the serum			0.03[a]
– Italy	6%	94%	
– The Netherlands	12%	88%	
– France	21%	79%	
– Denmark	6%	94%	
Female/male	10%/17%	91%/83%	0.27
Presence of muscular complaints[b]	0% (0/19)	1% (2/160)	1.0
Presence of autoimmune co-morbidity[c] (number of patients)	46% (11/24)	30% (58/195)	0.02[a]
– sSS	– 15% (4)	– 5% (10)	
– Antiphospholipid syndrome	– 19% (5)	– 19% (38)	
– Rheumatoid arthritis	– 12% (3)	– 2% (4)	
– Other	– 0% (0)	– 2% (4)	
– Combination	– 0% (0)	– 1% (2)	
Presence of current or past viral infection[d]	9% (2/23)	6% (10/177)	0.88
Presence of other antibodies			
– dsDNA	31% (8/26)	39% (88/226)	0.52
– anti-nucleosomes	23% (6/26)	31% (71/226)	0.50
– Ro52	42% (11/26)	32% (73/226)	0.38

[a]*Statistically significant ($p \leq 0.05$).*
[b]*Missing data in 29% of patients.*
[c]*Missing data in 13% of patients.*
[d]*Missing data in 21% of patients.*

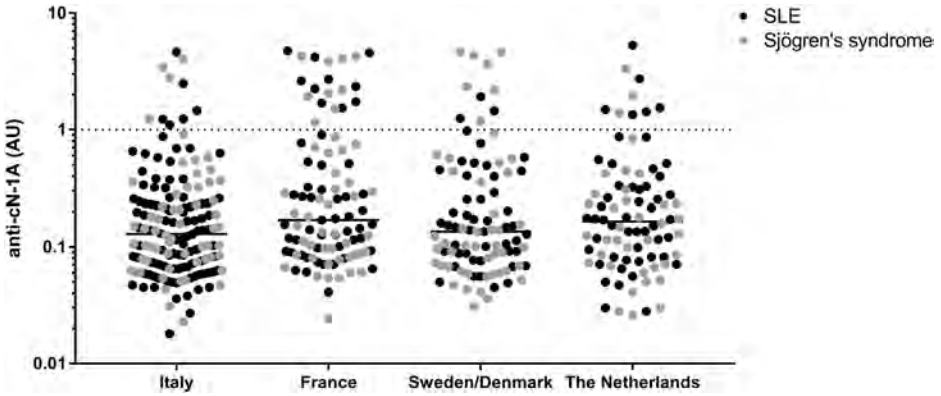

FIGURE 1 | Distribution of anti-cN-1A reactivity in primary Sjögren's syndrome and systemic lupus erythematosus (SLE) patients from different countries. Dotted line = cutoff of anti-cN-1A reactivity (1.0 AU).

TABLE 3 | Anti-cN-1A reactivity among systemic lupus erythematosus (SLE) and primary Sjögren's syndrome (pSS) cohorts in former and current studies.

Cohort	Technique	Origin of samples	Disease	Number of patients	Anti-cN-1A positivity (%)
Herbert et al. (4)	ELISA with 3 synthetic peptides	The Netherlands	SLE	44	20
			pSS	22	36
Kramp et al. (7)	ELISA with recombinant full-length protein[a]	North American	SLE	33	6
			pSS	20	0
Lloyd et al. (6)	Immunoblotting against NT5C1A (full-length)-transfected and nontransfected HEK 293 cell lysates	USA	SLE	96	14
			pSS	44	23
Muro et al. (5)	ELISA with recombinant full-length protein	Japan	SLE	50	6
			pSS	50	4
Rietveld et al. (current study)	ELISA with recombinant full-length protein[a]	Europe	SLE	252	10
			pSS	193	12

[a]*The same standardized ELISA was used in these studies.*

6–21%), which seems to be consistent with the variation in anti-cN-1A reactivity that was observed in these diseases in previous studies. However, it should be noted that the results of these studies were obtained with various in-house assays. Our study is the first to analyze anti-cN-1A in pSS and SLE patients from different centers in parallel using a single, standardized assay at a single laboratory. The current study does not offer an explanation for the relatively frequent presence of anti-cN-1A in pSS and SLE sera, nor for the variation in the frequency of anti-cN-1A among different countries.

Table 3 summarizes the results reported in four previous publications on anti-cN-1A reactivity in pSS and SLE. The largest cohort thus far consisted of 96 SLE and 44 pSS patients and the study included a comparison with clinical data as well. The subset of SLE patients with myositis (5%) did not show anti-cN-1A reactivity, and no correlation was found between anti-cN-1A reactivity and Raynaud's phenomenon or interstitial lung disease. Similarly, among pSS patients no correlation could be found between anti-cN-1A status and clinical and laboratory features, and none of the pSS patients had any muscular complaints (6). Muro and coworkers reported concomitant positivity for anti-dsDNA and anti-Ro/SSA in the pSS and SLE patients with anti-cN-1A reactivity (5). The clinical and laboratory features of the two other reported cohorts are not described in detail (4, 7).

Currently, IBM diagnosis is based on the combination of clinical features, laboratory findings, and muscle biopsy results (12). Unfortunately, application of the diagnostic criteria does not always lead to a quick and definite diagnosis. Although no treatment is yet available for IBM, a correct diagnosis is important, as for example misclassification as polymyositis and subsequent treatment with steroids can negatively influence the IBM disease course (13). The detection of anti-cN-1A antibodies could accelerate and improve the diagnosis of IBM. The presence of anti-cN-1A reactivity in a subset of SLE and pSS patients does not interfere with the clinical usefulness of anti-cN-1A testing in myositis due to the phenotypic differences between IBM and systemic autoimmune diseases. A standardized assay to detect anti-cN-1A antibodies, with clearly defined sensitivity and specificity, is of great importance before starting to use anti-cN-1A detection in clinical practice.

The large variation in the frequencies of anti-cN-1A in SLE and pSS reported in the aforementioned previous studies might be due to the different techniques that were used: western blotting and ELISA with the full-length recombinant protein produced in different host cells, and ELISA with three synthetic peptides [**Table 3**, reviewed in detail in Ref. (1, 14)]. The ELISA using three synthetic peptides is based on epitope mapping that has shown three regions of cN-1A that are targeted most frequently by autoantibodies. In that study,

different patterns of reactivity with these three linear epitopes were observed (4). However, the use of small synthetic peptides does not allow the detection of antibodies against discontinuous or conformational epitopes. IBM sera reactive with one of these epitopes were not always positive when using full-length recombinant protein as antigen, whereas other sera were not reactive with any of the epitopes, but were positive when assessed using the full-length cN-1A ELISA (1). Variable seropositivity was seen in IBM patients dependent upon which isotype (IgG, IgA, or IgM) of anti-cN-1A antibody was tested (15, 16). In general, immunoblotting with full-length cN-1A expressed in transfected HEK293 cells showed a higher sensitivity and lower specificity than the three-peptide cN-1A ELISAs (1, 7). A direct comparison of the methodologies to detect anti-cN-1A antibodies has not yet been undertaken.

The role of cN-1A in the pathophysiology of IBM and the possible pathways of anti-cN-1A antibody induced pathology are not yet fully elucidated, although a recent study confirmed a role of anti-cN-1A antibodies in the onset of IBM (14, 17). *In vitro* and *in vivo* (in mice) passive immunization with anti-cN-1A–positive IgG leads to histological changes in the muscle fibers resembling the changes in IBM: an increase of p62 aggregates and an associated macrophage infiltration was seen in the *in vivo* model (17). Whether passive immunization led to pathophysiological changes as seen in SLE and pSS, is not stated. The variation in anti-cN-1A reactivity between the different countries included in our current study might be due to the different genetic backgrounds of the patients, although HLA-association studies in IBM did not show a difference between anti-cN-1A-positive and -negative patients (18).

The retrospective nature of our study led to some difficulties in the interpretation of the clinical data. First of all, for some items a large subset of data is lacking, for example regarding the presence or absence of muscular complaints. Furthermore, the presence or absence of muscular symptoms might be subject to reporting bias of patients: fatigue and diffuse pain in patients with systemic autoimmune diseases could be reported as myalgia. Autoimmune comorbidity might have been reported in different ways and antiphospholipid syndrome, for example, might not have been reported in a subset of patients. This means that the finding of an increased rate of autoimmune comorbidity in the anti-cN-1A-positive patients should be interpreted with caution. A prospective study with standardized clinical data collection and a broader panel of autoantibodies (including for example anti-CCP, anti-thyroid, and anti-skin autoantibodies) should clarify the relationship between anti-cN-1A reactivity and the presence of comorbidities, in particular other autoimmune diseases. A former study on IBM, using standardized data extraction sheets, did not show such a correlation (2). The included sera were provided by European centers only, meaning that comparisons with cohorts with other ethnical backgrounds can be difficult. We did not test healthy subjects in parallel with the SLE and pSS patients, but two independent laboratories have previously evaluated healthy subjects using the same ELISA as we have used in this study, showing anti-cN-1A reactivity in 2 and 3% (1/52 and 7/202) (7).

This retrospective study confirms the relatively high prevalence and substantial variation in anti-cN-1A reactivity in different cohorts of pSS and SLE patients. Based on this, we conclude that anti-cN-1A should be classified as a MAA, not as a MSA. Prospective studies should shed more light on the role of anti-cN-1A in pSS and SLE to elucidate its pathophysiological role and to further explore its potential correlation with clinical features.

ETHICS STATEMENT

Local ethics committee approval concerning the pSS and SLE biobanks is present in each of the participating centers (Lund University 2012/98; UMC Utrecht METC 12-296; Strasbourg CCP Est IV 09-02-2010, Italy: Authorization of the Privacy Guarantor No. 9, December 12th, 2013).

AUTHOR CONTRIBUTIONS

Initiation and design of this research: AR, CS, BE, and GP. Clinical data collection, establishment of the patient groups, and contribution of cases: NB, AM, LH, SB, JR, JG, GH, CN, PO, and TM. Establishment of the antibody detection method and laboratory analysis: WS, NJ, CD, BE, and GP. Statistical analysis: AR and LH. Draft manuscript preparation: AR. All authors were involved with the review of the manuscript and approved the final version.

FUNDING

AR, BE, and GP received a grant from Prinses Beatrix Spierfonds (W.OR12-15). The laboratory analysis was performed by Euroimmun AG, Lübeck.

REFERENCES

1. Herbert MK, Pruijn GJ. Novel serology testing for sporadic inclusion body myositis: disease-specificity and diagnostic utility. *Curr Opin Rheumatol* (2015) 27(6):595–600. doi:10.1097/BOR.0000000000000216
2. Lilleker JB, Rietveld A, Pye SR, Mariampillai K, Benveniste O, Peeters MT, et al. Cytosolic 5'-nucleotidase 1A autoantibody profile and clinical characteristics in inclusion body myositis. *Ann Rheum Dis* (2017) 76(5):862–8. doi:10.1136/annrheumdis-2016-210282
3. Goyal NA, Cash TM, Alam U, Enam S, Tierney P, Araujo N, et al. Seropositivity for NT5c1A antibody in sporadic inclusion body myositis predicts more severe motor, bulbar and respiratory involvement. *J Neurol Neurosurg Psychiatry* (2016) 87(4):373–8. doi:10.1136/jnnp-2014-310008
4. Herbert MK, Stammen-Vogelzangs J, Verbeek MM, Rietveld A, Lundberg IE, Chinoy H, et al. Disease specificity of autoantibodies to cytosolic 5'-nucleotidase 1A in sporadic inclusion body myositis versus known autoimmune diseases. *Ann Rheum Dis* (2016) 75(4):696–701. doi:10.1136/annrheumdis-2014-206691
5. Muro Y, Nakanishi H, Katsuno M, Kono M, Akiyama M. Prevalence of anti-NT5C1A antibodies in Japanese patients with autoimmune rheumatic diseases in comparison with other patient cohorts. *Clin Chim Acta* (2017) 472:1–4. doi:10.1016/j.cca.2017.07.002
6. Lloyd TE, Christopher-Stine L, Pinal-Fernandez I, Tiniakou E, Petri M, Baer A, et al. Cytosolic 5'-nucleotidase 1A as a target of circulating autoantibodies in autoimmune diseases. *Arthritis Care Res* (2016) 68(1):66–71. doi:10.1002/acr.22600
7. Kramp SL, Karayev D, Shen G, Metzger AL, Morris RI, Karayev E, et al. Development and evaluation of a standardized ELISA for the determination

of autoantibodies against cN-1A (Mup44, NT5C1A) in sporadic inclusion body myositis. *Auto Immun Highlights* (2016) 7(1):16. doi:10.1007/s13317-016-0088-8
8. Hochberg MC. Updating the American college of rheumatology revised criteria for the classification of systemic lupus erythematosus. *Arthritis Rheum* (1997) 40(9):1725. doi:10.1002/art.1780400928
9. Vitali C, Bombardieri S, Jonsson R, Moutsopoulos HM, Alexander EL, Carsons SE, et al. Classification criteria for Sjogren's syndrome: a revised version of the European criteria proposed by the American-European Consensus Group. *Ann Rheum Dis* (2002) 61(6):554–8. doi:10.1136/ard.61.6.554
10. Biesen R, Dahnrich C, Rosemann A, Barkhudarova F, Rose T, Jakob O, et al. Anti-dsDNA-NcX ELISA: dsDNA-loaded nucleosomes improve diagnosis and monitoring of disease activity in systemic lupus erythematosus. *Arthritis Res Ther* (2011) 13(1):R26. doi:10.1186/ar3250
11. Suer W, Dahnrich C, Schlumberger W, Stocker W. Autoantibodies in SLE but not in scleroderma react with protein-stripped nucleosomes. *J Autoimmun* (2004) 22(4):325–34. doi:10.1016/j.jaut.2004.02.002
12. Rose MR, Group EIW. 188th ENMC International workshop: inclusion body myositis, 2–4 December 2011, Naarden, The Netherlands. *Neuromuscul Disord* (2013) 23(12):1044–55. doi:10.1016/j.nmd.2013.08.007
13. Benveniste O, Guiguet M, Freebody J, Dubourg O, Squier W, Maisonobe T, et al. Long-term observational study of sporadic inclusion body myositis. *Brain* (2011) 134(Pt 11):3176–84. doi:10.1093/brain/awr213
14. Ludwig RJ, Vanhoorelbeke K, Leypoldt F, Kaya Z, Bieber K, McLachlan SM, et al. Mechanisms of autoantibody-induced pathology. *Front Immunol* (2017) 8:603. doi:10.3389/fimmu.2017.00603
15. Greenberg SA. Cytoplasmic 5'-nucleotidase autoantibodies in inclusion body myositis: isotypes and diagnostic utility. *Muscle Nerve* (2014) 50(4):488–92. doi:10.1002/mus.24199
16. Limaye VS, Lester S, Blumbergs P, Greenberg SA. Anti-cn1a antibodies in south australian patients with inclusion body myositis. *Muscle Nerve* (2016) 53(4):654–5. doi:10.1002/mus.24989
17. Tawara N, Yamashita S, Zhang X, Korogi M, Zhang Z, Doki T, et al. Pathomechanisms of anti-cytosolic 5'-nucleotidase 1A autoantibodies in sporadic inclusion body myositis. *Ann Neurol* (2017) 81(4):512–25. doi:10.1002/ana.24919
18. Rothwell S, Cooper RG, Lundberg IE, Gregersen PK, Hanna MG, Machado PM, et al. Immune-array analysis in sporadic inclusion body myositis reveals HLA-DRB1 amino acid heterogeneity across the myositis spectrum. *Arthritis Rheumatol* (2017) 69(5):1090–9. doi:10.1002/art.40045

Conflict of Interest Statement: GP and BE are inventors of a patent (EP20120740236) licensed to Euroimmun AG and GP received financial support from Euroimmun for his research programme. CD, NJ, and WS are employees of Euroimmun AG. WS is a board member of Euroimmun AG. WS and CD are shareholders of Euroimmun AG. The remaining authors declare that the research was conducted in the absence of any commercial or financial relationships that could be construed as a potential conflict of interest.

frontiers in Immunology

REVIEW
published: 04 June 2018
doi: 10.3389/fimmu.2018.01190

Non-Desmoglein Antibodies in Patients With Pemphigus Vulgaris

Kyle T. Amber[1]*, *Manuel Valdebran*[1] and *Sergei A. Grando*[1,2,3]*

[1] Department of Dermatology, University of California Irvine, Irvine, CA, United States, [2] Department of Dermatology, Institute for Immunology, University of California Irvine, Irvine, CA, United States, [3] Department of Biological Chemistry, Institute for Immunology, University of California Irvine, Irvine, CA, United States

Pemphigus vulgaris (PV) is a potentially life-threatening mucocutaneous autoimmune blistering disease. Patients develop non-healing erosions and blisters due to cell–cell detachment of keratinocytes (acantholysis), with subsequent suprabasal intraepidermal splitting. Identified almost 30 years ago, desmoglein-3 (Dsg3), a Ca^{2+}-dependent cell adhesion molecule belonging to the cadherin family, has been considered the "primary" autoantigen in PV. Proteomic studies have identified numerous autoantibodies in patients with PV that have known roles in the physiology and cell adhesion of keratinocytes. Antibodies to these autoantibodies include desmocollins 1 and 3, several muscarinic and nicotinic acetylcholine receptor subtypes, mitochondrial proteins, human leukocyte antigen molecules, thyroid peroxidase, and hSPCA1—the Ca^{2+}/Mn^{2+}-ATPase encoded by ATP2C1, which is mutated in Hailey–Hailey disease. Several studies have identified direct pathogenic roles of these proteins, or synergistic roles when combined with Dsg3. We review the role of these direct and indirect mechanisms of non-desmoglein autoantibodies in the pathogenesis of PV.

Keywords: pemphigus, autoantibodies, secretory pathway Ca^{2+} ATPase, ATP2C1, acantholysis, keratinocyte, acetylcholine

OPEN ACCESS

Edited by:
Falk Nimmerjahn, Friedrich-Alexander-Universität Erlangen-Nürnberg, Germany

Reviewed by:
Francisco Javier Sánchez-García, Instituto Politécnico Nacional, Mexico
Zrinka Bukvic Mokos, University Hospital Center Zagreb, Croatia

***Correspondence:**
Kyle T. Amber
kamber@uci.edu;
Sergei A. Grando
sgrando@uci.edu

Specialty section:
This article was submitted to Immunological Tolerance and Regulation, a section of the journal Frontiers in Immunology

Received: *02 December 2017*
Accepted: *14 May 2018*
Published: *04 June 2018*

Citation:
Amber KT, Valdebran M and Grando SA (2018) Non-Desmoglein Antibodies in Patients With Pemphigus Vulgaris. Front. Immunol. 9:1190. doi: 10.3389/fimmu.2018.01190

INTRODUCTION

Pemphigus vulgaris (PV) is a potentially life-threatening mucocutaneous autoimmune blistering disease. Patients develop non-healing erosions and blisters due to cell–cell detachment of keratinocytes (acantholysis), with subsequent suprabasal intraepidermal splitting. Identified more than 25 years ago, desmoglein-3 (Dsg3), a Ca^{2+}-dependent cell adhesion molecule belonging to the cadherin family, has been considered the "primary" autoantigen in PV.

While convincing evidence has supported the pathogenic role of anti-Dsg antibody-mediated acantholysis, there has been a shift in our understanding of the disease from steric hindrance by autoantibodies to modification of cell metabolism and signaling, and structural alterations in the desmosome affecting cell adhesion (1–3).

Abbreviations: ACh, acetylcholine; AChR, acetylcholine receptor; AMA, anti-mitochondrial antibodies; CytC, cytochrome *c*; DIF, direct immunofluorescence; Dsc, desmocollin; Dsg, desmoglein; FcRn, neonatal Fc receptor; HHD, Hailey–Hailey disease; HLA, human leukocyte antigen; mAChR, muscarinic acetylcholine receptor; mcPV, mucocutaneous pemphigus vulgaris; MHC, major histocompatibility complex; mPTP, mitochondrial permeability transition pore; nAChR, nicotinic acetylcholine receptor; PF, pemphigus foliaceus; PH, pemphigus herpetiformis; PKP3, plakophilin-3; PNP/PAMS, paraneoplastic pemphigus/paraneoplastic autoimmune multiorgan syndrome; PV, pemphigus vulgaris; PVeg, pemphigus vegetans; PV IgG, IgG from pemphigus vulgaris patients; PX, pemphaxin.

Proteomic studies have identified numerous autoantibodies in patients with PV that have known roles in the physiology and cell adhesion of keratinocytes. These autoantibodies include desmocollins (Dsc) 1 and 3, several muscarinic and nicotinic acetylcholine receptor (nAChR) subtypes, mitochondrial proteins, human leukocyte antigen (HLA) molecules, thyroid peroxidase (TPO), and hSPCA1—the Ca^{2+}/Mn^{2+}-ATPase encoded by ATP2C1, which is mutated in Hailey–Hailey disease (HHD).

The presence of numerous potentially pathogenic autoantibodies in pemphigus points toward a need to understand these non-Dsg antibodies. While several of the most prevalent non-Dsg autoantibodies have been characterized regarding their effect on keratinocyte biology, a majority of identified autoantibodies remain poorly understood. We review the direct and indirect pathogenic mechanisms of non-Dsg autoantibodies in PV.

MAJOR DEFINED AUTOANTIGENS

Desmocollins

Desmocollins (Dsc) and Dsgs are two specialized Ca^{2+}-dependent cadherin subfamilies that provide structure to the desmosomes (4). On the cell surface, Dsc and Dsg bind to each other, providing support, and meditating connections between intermediate filaments of neighboring cells (5, 6). In addition, this cadherin complex forms an anchor for keratin intermediate filaments which attach to the inner cytoplasmic surface (6).

Desmocollins play an important role in cell-to-cell adhesion. This role was demonstrated by Spindler et al. (7) through the application of monoclonal antibodies against extracellular domains of Dsc3 in human skin model which resulted in intraepidermal blister formation. They also provided evidence of homophilic and heterophilic trans-interaction of Dsc3 with Dsg1. Their data showed that Dsg-1 IgG antibodies reduces the adhesion of Dsc-3 to the surface of keratinocytes, possibly by targeting the Dsc3/Dsg1 binding on keratinocyte cell surface (7).

Previously, IgA autoantibodies to Dsc1 were identified in subcorneal pustular dermatosis (8). However, various reports of IgG autoantibodies against the three different Dsc have been found in paraneoplastic pemphigus/paraneoplastic autoimmune multiorgan syndrome (PNP/PAMS), PV, pemphigus foliaceus (PF), pemphigus vegetans (PVeg), and pemphigus herpetiformis (PH) (9).

In a study of a large cohort of pemphigus patients, autoantibodies to Dsc 1 and 3 were present in 44% of patients, with only 7% in matched controls (10). Ishii et al. reported their findings related to the detection of anti-Dsc antibodies in a series of 164 pemphigus cases. Anti-Dsc antibodies were found in 3 of 22 PV cases (13%) and 3 of 18 PF cases (18%). By contrast, 53 of 79 PNP/PAMS cases (67%) demonstrated anti-Dsc 1–3 antibodies. Specifically, Dsc3 antibodies were detected in roughly 60% of the cases, Dsc 2 in 37%, and Dsc 3 in 16.5% of cases. In PH and PVeg, around 40% of sera showed strong reactivity with Dsc1–3 (11).

Dettmann et al. studied serum reactivity with Dsc 1, 2, and 3 serum autoantibodies in various groups of patients with pemphigus. In their first cohort consisting of 102 PV patients with oral lesions with positive direct immunofluorescence (DIF) and the presence of anti-Dsg3 IgG, no antibodies were found against Dsc 1, 2, and 3. The second cohort was composed of 24 patients with oral lesions but no detectable Dsg3 autoantibodies; therein IgG antibodies against Dsc 3 were found in one case. The third cohort composed of 23 patients with PNP/PAMS mostly reactive against anti-Dsg3 and envoplakin, from whom anti-Dsc 2 and anti-Dsc 3 IgG autoantibodies were identified in two patients, respectively (9). A fourth cohort consisting of sera from 749 patients of the International Autoimmune Bullous Diseases Study Group was also analyzed for reactivity with epitopes of Dsc. Of these patients, 333 were diagnosed with pemphigus. Investigators found 14 (4%) Dsc reactive cases; 3 were from patients with PNP/PAMS, 2 from patients with PVeg. 2 of 14 sera were from PV patients in whom no Dsg 1 or 3 reactivity was found. Three reactive cases of PF showed Dsc 1-specific IgG. Of 5 Dsg3-negative sera, 333 (40%) showed reactivity with Dsc 1. Thus, testing for autoantibodies against Dscs was only recommended in patients with atypical pemphigus (9).

hSPCA1

The ATP2C1 gene codes for a magnesium-dependent enzyme that catalyzes the hydrolysis of Ca^{2+}-transport ATP. This secretory pathway Ca^{2+} ATPase pump is expressed in the Golgi apparatus (GA) which is involved in the transport of calcium and manganese ions from the cytosol to the lumen of the GA. Mutations in ATP2C1 results in depletion of Ca^{2+} stores in the GA with increased Ca^{2+} in the cytosol (12). Low Ca^{2+} concentration in the GA could impair posttranslational processing of important desmosomal proteins such as Dsg and Dsc. As a result, acantholysis develops. These mutations have been found in HHD (12, 13).

Clinical and pathological similarities between HHD and PV exist. Clinically, vesicle and bulla formation may be present in early lesions of HHD. However, features of established lesions include eroded scaly plaques in symmetrical and intertriginous distribution, commonly in axillae, groin, neck, inframammary fold, and perineum (14). On the other hand, features of PV include flaccid blisters and erosions on mucosa and sometime also skin. Histologically, in PV, suprabasal acantholysis is present with intraepidermal bulla formation and a tombstone pattern of the remaining cells of the basal layer. Although acantholysis is also present in HHD, it involves all epidermal layers resembling the dilapidated brick wall (14). Invariably, DIF is negative in HHD.

Over 125 pathogenic mutations through the ATP2C1 gene have been described in HHD (15, 16). Approximately 20% are nonsense mutations, 30% are frame-shift mutations with premature termination codons, and 28% are missense mutations (17). Investigators suggest that haploinsufficiency is the mechanism of dominant inheritance observed in this entity (18).

Autoantibodies against hSPCA1 are seen in 43% of patients with PV compared to 8% in matched controls (OR = 8.51) (10). Given the similarities in clinical phenotype and role of cell disadhesion in both of these diseases, it is tempting to suspect that anti-hSPCA1 autoantibodies have an active role in PV. To date, however, there have been no studies assessing the pathogenic role of these autoantibodies.

Cholinergic Receptors

The human epidermis has an elaborate non-neuronal cholinergic system composed of an axis that involves keratinocyte

acetylcholine (ACh) enzymes involved in ACh synthesis and degradation, and nicotinic and muscarinic acetylcholine receptors (AChRs) (19). Keratinocyte ACh plays a role in the regulation of cell–cell and cell–matrix adhesion. This mechanism is accomplished through AChR signaling. These receptors have a regulatory effect by activation or inhibition of kinase cascades. Resulting outcome will lead to either upregulation or downregulation of the expression of cell adhesion molecules such as cadherins and integrins (19).

Muscarinic acetylcholine receptors (mAChRs) are single-subunit transmembrane glycoproteins composed of five receptor subtypes (M_1–M_5). Odd-numbered mAChRs bind to pertussis toxin-insensitive G proteins stimulating phospholipase C enzymes that hydrolyze phosphatidylinositol 4,5-bisphosphate, yielding the second messenger molecules inositol 1,4,5-trisphosphate (IP3) and diacyl glycerol which in turn control intracellular levels of Ca^{2+} and protein kinase C activity, respectively. Even-numbered mAChR subtypes couple to pertussis toxin-sensitive G proteins ultimately leading to inhibition of adenyl cyclase, and weakly stimulating phospholipase C; they also rectify K^+ channels, and augment arachidonic acid release (19). *In vitro* experiments have shown that mAChR activation may prevent, stop, and reverse acantholysis mediated by pemphigus antibodies (20). Autoantibodies against mAChRs have been identified in the serum of 85–100% of pemphigus patients (21, 22). Lakshmi et al. prospectively evaluated the disease severity of 45 patients with pemphigus who were followed up at baseline, 3 months, and 15 months. They collected sera from these patients to assess the titers of antibodies against Dsg1/Dsg3 and anti-M3 mAChR to correlate them with disease severity and response to therapy. They found that antibody titers correlated significantly with disease activity and that anti-M3 mAChR antibodies were present in all cases (22).

Nicotinic acetylcholine receptors are members of the superfamily of ligand-gated ion channel proteins, mediating Na^+ and Ca^{2+} influx and K^+ efflux. These receptors are not only present on the surface of keratinocytes but also on the mitochondrial outer membrane (23). Mitochondrial-nAChRs inhibit mitochondrial permeability transition pore (mPTP) opening, restraining cytochrome *c* (CytC) release, thereby preventing apoptosis (24). IgG from patients with PV bind to several mitochondrial-nAChR subtypes (α3, α5, α7, α9, α10, β2, and β4), resulting in swelling of mitochondria, rupture of outer membrane, and release of CytC caused by mPTP opening. Moreover, CytC induces apoptosome formation with activation of caspase-9 with subsequent induction of apoptosis (25).

Pemphaxin (PX) is a 75-kDa annexin also known as annexin 31 or ANXA9 (26) which was discovered by screening of keratinocyte λgt11 cDNA expression library with PVIgG antibodies. PX acts as an AChR with dual muscarinic and nicotinic pharmacology. *In vitro* studies demonstrated that anti-PX antibodies induced acantholysis in keratinocyte monolayers; confirmation was done with immunofluorescence studies showing positivity in a net-like pattern. *In vivo* experiments demonstrated that while adsorption of anti-PX autoantibody abolished acantholytic activity of PV IgG fraction, adding it back to the preabsorbed fraction restored the acantholytic activity of PV IgG fraction, although anti-PX autoantibody alone did not cause clinically evident skin blisters (27). This finding indicates that PV results from synergistic action of several antibodies to different self-antigens, including AChRs (28). Simultaneous and synergistic action of PV IgGs against the cell membrane and mitochondrial-nAChRs inactivates adhesion molecules and opening of mPTP. Affected keratinocytes shrink and detach from neighboring cells. Therein, antibodies to desmosomal components prevent keratinocyte from re-attachment making keratinocyte detachment irreversible (29).

Anti-Mitochondrial Proteins

Anti-mitochondrial antibodies (AMA) play an important role in the pathogenesis of PV as they can trigger the intrinsic apoptotic pathway. Adsorption of AMA prevents acantholysis (30). Autoantibodies against numerous mitochondrial antigens are seen in patients with PV, as summarized in **Table 1**. Other studies evaluating AMA in patients with pemphigus included that by Marchenko et al., which found AMA in 100% (6/6) of sera of patients with PV when studying penetration of PVIgG into the subcellular mitochondrial fraction (30). Experiments conducted by Chernyavsky et al. (25) found AMA against different subunits of mitochondrial ACh receptors in 100% (5/5) sera from patients who had anti-nAChR antibodies.

Anti-mitochondrial antibodies bind mitochondrial proteins eliciting the opening of the mPMP which cause massive swelling of mitochondria, rupture of outer membrane, release of CytC, and subsequent activation of caspase-9 (31). In so doing, AMA can complement pro-acantholytic actions of other types

TABLE 1 | Mitochondrial autoantibodies in patients with PV with an incidence greater than 5% and OR > 2 when compared with healthy controls (10).

Antigen	Symbol	Incidence in PV (%)	Incidence in controls (%)	OR
Mitochondrial processing peptidase beta subunit	PMPCB	31	4	8.47
Cytochrome b5 outer mitochondrial membrane isoform precursor	CYB5B	19	1	13.07
Carnitine *O*-palmitoyltransferase I, mitochondrial muscle isoform	CPT1B	18	5	3.51
Peptidase (mitochondrial processing) alpha	PMPCA	16	4	3.75
Mitochondrial import inner membrane translocase subunit TIM13 B	TIMM13	16	4	4.50
Carnitine *O*-palmitoyltransferase I, mitochondrial liver isoform	CPT1A	13	4	3.05
Mitochondrial uncoupling protein 2 (UCP20)	UCP20	10	5	2.02
Solute carrier family 25 (mitochondrial carrier; citrate transporter, member 5)	SLC25A5	10	4	2.27
Solute carrier family 25 (mitochondrial carrier; peroxisomal membrane protein) member 17	SLC25A5	8	1	5.75
Mitochondrial intermediate peptidase	MIPEP	7	1	9.93
Mitochondrial import inner membrane translocase subunit	TIMM22	6	1	3.92

of non-Dsg antibodies launching a downstream signaling event involving Src, epidermal growth factor receptor kinase, p38 mitogen-activated protein kinase (p38MAPK), and c-Jun N-terminal kinase (30).

Chen et al. (29) demonstrated that PV IgGs including AMA couple with neonatal Fc receptor (FcRn) on the cell membrane. The PV IgGs–FcRn complex allows the entrance of AMA to the keratinocyte. Once in the cytosol, they dissociate and are trafficked to the mitochondria where they trigger proapoptotic events with subsequent CytC release and activation of caspase-9 (25, 30). These events correlate with the shrinkage of basal keratinocytes seen in histologic sections (29).

Upon recovery, new desmosomes are extended toward neighboring keratinocytes; however, anti-Dsg antibodies prevent bonding of new desmosomes due to steric hindrance, thereby acantholysis becomes an irreversible process (29). The term "apoptolysis" has been introduced to denote these apoptotic and acantholytic events (30).

Overexpression of suppression of tumorigenicity 18 gene (ST18) in keratinocytes of predisposed individuals appears to increase susceptibility of cells to apoptosis and immune dysregulation (32–34). Interestingly, ST18 is overexpressed in PV non-lesional skin when compared with the skin of healthy individuals, indicating a possible predisposition to pemphigus (32). A variant in the promoter region drives increased gene transcription in a p53/p63-dependent manner. This polymorphism, however, appears to be most associated with PV arising in Jewish and Egyptian patients, rather than German, or Chinese (32, 35). Sarig et al. did, however, note an increase of ST18 in patients with psoriasis. Thus, it unclear whether ST18 overexpression simply is associated with inflammatory processes.

Thyroid Peroxide Antibodies

Thyroid peroxidase (TPO), originally described as thyroid microsomal antigen, is a member of the thyroid autoantigens which includes thyroglobulin and thyroid-stimulating hormone receptor (36). TPO is a glycoprotein present on the apical surface of thyroid follicular cells (36); it is involved in the synthesis of T3 and T4, catalyzing several steps in the process (37). Approximately 85–90% of patients with chronic thyroiditis have anti-TPO antibodies (38); therefore, these antibodies are considered to be the hallmark of autoimmune thyroid disease (ATD), particularly, Hashimoto's thyroiditis, postpartum thyroiditis, and Grave's disease (37).

Several studies have documented the association between PV and the presence of anti-TPO antibodies as it is summarized in **Table 2**. The mean percentage of pemphigus patient with anti-TPO antibodies among all these studies was 19% (3.6–40%), which is well above the standard incidence of anti-TPO autoantibodies. Nevertheless, larger prospective multi-centric studies are needed to further characterize this association.

The link between thyroid and skin development and homeostasis has been well documented (47–49). This relationship correlates with the ability of thyroid hormones to bind nuclear receptors with consequent effects on proliferation of keratinocytes and fibroblasts (50, 51). However, the role of thyroid proteins in cell-to-cell adhesion remains poorly understood (51).

TABLE 2 | Current studies on the incidence of thyroid autoantibodies and thyroid disease in patients with pemphigus.

Study	Country	Patients	Incidence
Pitoia et al. (39)	Argentina	PV (n = 15)	
		Anti-TPO	6 (40%)
		Hashimoto thyroiditis	1 (6.6%)
Michailidou et al. (40)	Greece	PV (n = 129)	
		Incidence of Thyroid disease	2 (2.6%)
Ansar et al. (41)	Iran	PV (n = 22)	
		Anti-TPO	5 (22%)
Daneshpazhooh et al. (42)	Iran	PV (n = 75)	
		Anti-TPO	12 (16%)
Leshem et al. (43)	Israel	PV and PF (n = 110)	
		Anti-TPO	4 (3.6%)
Kavala et al. (44)	Turkey	PV (n = 80)	
		Altered thyroid function test and anti-thyroid Ab	13 (16%)
		Anti-TPO	6 (8%)
		Anti-Tg	2 (2.5%)
		Primary thyroid disease (PTD)	13 (16%)
		Hashimoto thyroiditis	7 (9%)
Ameri et al. (45)	Italy	PV (n = 25)	
		Anti-TPO	6 (24%)
Parameswaran et al. (46)	USA	PV (n = 230)	
		Group database	
		ATD	23 (10%)
		PV (n = 171)	
		Online survey	
		ATD	16 (9.36%)
		PV (n = 393)	
		IPPF registry	
		ATD	36 (9.16%)

PV, pemphigus vulgaris; anti-TPO, anti-thyroid peroxidase; anti-Tg, anti-thyroglobulin; TSH, thyroid-stimulating hormone; IPPF, International Pemphigus and Pemphigoid Foundation; ATD, autoimmune thyroid disease.

Plakophilin 3

Plakophilin 3 is a member of the armadillo family of proteins; this protein has an important role in the generation of a stable desmosome due to its multiple interactions with several proteins such as desmosomal cadherins, Dsg1, Dsg3, desmoplakin, plakoglobins, and epithelial keratin 18 (52, 53).

Autoreactivity against plakophilin-3 (PKP3) has been demonstrated by Lambert et al. in five PNP/PAMS (100%) sera and in one PV (25%) serum in a series that evaluated sera from five PNP, four PV, two PF, five bullous pemphigoid (BP), one cicatricial pemphigoid, and one linear IgA dermatosis (53). In a large study of PV patients using proteomic technique, 43% of PV patients had autoantibodies targeting plakophilin 3, compared with 7% of matched controls (OR = 6.56) (10).

Preliminary experiments done by Sklyarova et al. have demonstrated that mice deficient in PKP3 show alteration and rearrangement of desmosomes in the epidermis and hair follicles (54). While desmosomes and adherens junctions were significantly altered, compensatory changes in junctional proteins were seen, with upregulation of desmoplakin, plakophilin 1 and 2, E-cadherin, and β-catenin. These mice were also prone to dermatitis. Thus, while it appears unlikely that loss of PKP3 can

lead to the clinical phenotype in pemphigus, it is one key to a dense network of proteins that stabilize desmosomes.

E-Cadherin

E-cadherins along with P-cadherin are the classical cadherins forming adherens junctions, which in conjunction with desmosomes mediate cell-to-cell adhesion (55). Overexpression of E-cadherin has been observed as a result of disruption of desmosomes by PV autoantibodies. E-cadherin partially compensates for loss of cell cohesion, rescuing the cell but also attenuating activation of p38MAPK. E-cadherin is required to assemble Dsg3 into desmosomes (55).

Oliveira et al. and Evangelista et al. have demonstrated antibodies targeting E-cadherin in sera of pemphigus patients (56, 57). One study identified autoantibodies in 78% of mucocutaneous pemphigus vulgaris (mcPV) ($n = 62$) and 33% ($n = 18$) of those with mucosal involvement. Moderate correlation was found between the index values of E-cadherin and Dsg1 antigen/antibody, but no correlation with Dsg3; this finding suggested that antibodies against E-cadherin might cross-react with Dsg1 (or *vice versa*) (57). Similar findings were reported by Evangelista et al. who demonstrated anti-E-cadherin antibodies in 100% of sera of patients with pemphigus foliaceus ($n = 13$) and fogo selvagem ($n = 15$); autoantibodies were observed in 79% of those with mcPV and none of the mucosal-type PV ($n = 7$) (56). More recent proteomic studies of patients with PV demonstrate autoantibodies against E-cadherin in 31% of pemphigus patients compared with 7% of healthy controls (OR = 4.29) (10). Thus, while further pathogenicity studies are needed, the already published data suggests an important synergistic role of E-cadherin autoantibodies in the pathogenesis of pemphigus.

Plakoglobin

Plakoglobin is a member of the Armadillo family of adhesion and signaling proteins. It has a key role in the organization of desmosomes (58, 59). The highly conserved intracytoplasmic–cadherin-like segment of Dsgs is required for direct binding of Dsgs to plakoglobin (60). Silencing of plakoglobin results in p38MAPK-dependent cell disadhesion in cultured keratinocytes. Plakoglobin additionally regulates levels of Dsg3 (61). Interestingly, inhibition of p38MAPK can prevent PV IgG-induced blistering (62). In PV, there is an accumulation of c-Myc, due to a decrease in plakoglobin-mediated suppression of c-Myc (63). Plakoglobin is a principle effector of PV IgG downstream signaling (64–66). Plakoglobin can additionally regulate the promoters of Dsc2 and Dsc3 (67). While a compensatory increase in beta-catenin can be seen in the setting of plakoglobin silencing, it is insufficient for maintaining normal levels of plakophilin-1 or desmoplakin in the desmosomal plaque (68).

Plakoglobin is precipitated from sera of PV and PF patients, linked to Dsgs (69). It is internalized in combination with Dsg3 and PV IgG, resulting in retraction of keratin filaments (70). PV IgG may also promote separation of Dsg3 and plakoglobin (71). This is consistent with immunohistochemical studies in PV, in which plakoglobin staining was displaced toward the nucleus in comparison to healthy control (72).

Larger studies of autoantibodies in patients with PV demonstrated that 26% of patients carried autoantibodies against junctional plakoglobin, compared with 5% of controls (OR = 5.15) (10). Ishii et al. likewise described a patient with PNP/PAMS who had immunoreactivity against plakoglobin (73). Whether these anti-plakoglobin autoantibodies participate in the plakoglobin-Dsg3 dissociation remains to be determined.

FcεRI

Human immunoglobulin E (IgE) molecules bind with very high affinity to receptors on the surface of basophils and mast cells. As a result, mast cells release histamine, leukotrienes, prostaglandins, and cytokines (74). Basophils and mast cells can be activated by cross-linking of IgE interacting with antigens (direct anaphylaxis) or by antibodies directed against Fcε chain of IgE, or against the epitopes of α chain of FcεRI or anti-IgG acting on IgG–IgE complexes bound to FcεRI (74).

Tissue specific or systemic autoimmunity might lower the threshold of immunocompetent cells to recognize FcεRI. For this reason, Fiebiger et al. (75) in their study on anti-FcεRIα autoantibodies in chronic urticaria, included sera from patients with systemic and skin-specific autoimmune diseases including systemic lupus erythematosus, dermatomyositis, BP, and PV. Interestingly, anti-FcεRIα antibodies were found in all groups. As opposed to chronic urticaria, antibodies from the autoimmune cutaneous diseases group lacked complement-activation properties, potentially limiting the activation of basophils and subsequent histamine release (75). Sera from 28 PV patients were analyzed by ELISA, of which 39% were positive for anti-FCεR1 antibodies. Pronounced IgG reactivity against Western-blotted recombinant soluble FcεRIα was found in sera of 2 PV patients. Particularly, IgG2 and IgG4 subtypes were found in these patients (75).

The significance of the anti-FcεRIα antibodies in pemphigus remains unclear.

Other Autoantibodies

While the above discussed non-Dsg autoantibodies target known participants in cell disadhesion and autoimmunity, numerous other autoantibodies have been detected in patients with pemphigus (10). A better understanding of these and other non-Dsg antibodies will provide significant insight into the pathogenesis of pemphigus.

HLA AS A LINK BETWEEN DIFFERENT IMPLICATED AUTOANTIGENS

The HLA region is located on chromosome 6, present only in humans coding for the major histocompatibility complex (MHC) genes. MHC class I genes are known as HLA-A, HLA-B, and HLA-C; coding for proteins present on the surface of almost all cells. MHC class II genes are located within the HLA-D region on chromosome 6 which contains three subregions: DP, DQ, and DR. Each subregion has one expressed α and β chain gene. Six genes are contained: HLA-DPA1, HLA-DPB1, HLA-DQA1, HLA-DQB1, HLA-DRA, and HLA-DRB1 (76).

There is a strong association between PV and HLA class II genes, especially DR4 and DR14. Further analyses on particular allele

subtypes have demonstrated an association with the DRB1*0402, DRB1*1401, DRB1*1404, DRB1*1454, DQB1*0503, and DQB1*0302 alleles. In fact, more than 95% of PV patients carry one the following alleles: DRB1*0402 or DQB1*0503 (2, 77, 78). Particularly, these last two alleles are strongly associated with the Ashkenazi Jewish population (79). PV has been associated with HLA class I including those with HLA-A3, A10, A26, B15, B35, B38, B44, and B60; however, their significance is yet to be elucidated (77). Susceptibility to PF has been linked to the presence of DR4, DR14, and DR1, although no single DR4 or DR14 allele was associated with the PF (80).

High-risk HLA alleles can efficiently accommodate autoantigen-derived peptides, thus eliciting a T-cell-mediated response (78). At the same time, B-cells can be activated by anti-desmosomal CD4 T effector cells.

In contrast to antigen presentation, MHC II autoantibodies can be seen in up to 45% of patients with PV compared 7% in healthy controls (OR = 6.22), with autoantibodies against numerous MHC I and MHC II molecules (10). The functional role of these autoantibodies remains unclear.

Sajda et al. studied a panel of different autoantibodies present in sera of 40 PV patients, 20 healthy relatives, and 20 unrelated controls. Among these antibodies, they identified five which were more significantly associated with PV including Dsg3, mAChR3, mAChR4, mAChR5, and TPO. Of particular interest, non-Dsg autoantibodies in sera of healthy relatives of patients with PV were also seen. Subsequently, they performed HLA analysis clustering the patients into those who had presence or absence of PV-associated HLA alleles DRB1*0402 and/or DQB1*0503. Interestingly, most healthy relatives who presented with these alleles had similar antibody profiles to that of active pemphigus patients, whereas relatives who were negative for the risk alleles had antibody profiles similar to those of unrelated controls (81). Further findings revealed that autoantibody levels on HLA+ and HLA− relatives were comparable, thus implying that further genetic and environmental factors may lead to clinical pathology and remains to be studied (81). These data highlight the importance of HLA as a driver for the breakdown of self-tolerance and the specificity of the autoimmune response.

CONCLUSION

The pathogenesis of pemphigus is a complex process involving autoantibodies against numerous structural and metabolic proteins that regulate keratinocyte adhesion and survival. Several of these autoantibodies have been confirmed to have a pathogenic role in pemphigus, by altering the desmosomal plaque, synergistically complementing classic anti-Dsg autoantibody action, or altering mitochondrial physiology. In light of the hundreds of autoantibodies present in patients with PV, only few remain characterized. Thus, significant work is needed to determine the pathogenicity of these autoantibodies.

AUTHOR CONTRIBUTIONS

Substantial contributions to the conception or design of the work; or the acquisition, analysis, or interpretation of data for the work; drafting the work or revising it critically for important intellectual content; final approval of the version to be published; agreement to be accountable for all aspects of the work in ensuring that questions related to the accuracy or integrity of any part of the work are appropriately investigated and resolved: KA, MV, and SG.

REFERENCES

1. Nguyen VT, Arredondo J, Chernyavsky AI, Kitajima Y, Pittelkow M, Grando SA. Pemphigus vulgaris IgG and methylprednisolone exhibit reciprocal effects on keratinocytes. *J Biol Chem* (2004) 279(3):2135–46. doi:10.1074/jbc.M309000200
2. Di Zenzo G, Amber KT, Sayar BS, Muller EJ, Borradori L. Immune response in pemphigus and beyond: progresses and emerging concepts. *Semin Immunopathol* (2016) 38(1):57–74. doi:10.1007/s00281-015-0541-1
3. Spindler V, Eming R, Schmidt E, Amagai M, Grando S, Jonkman MF, et al. Mechanisms causing loss of keratinocyte cohesion in pemphigus. *J Invest Dermatol* (2017) 138(1):32–7. doi:10.1016/j.jid.2017.06.022
4. Chitaev NA, Troyanovsky SM. Direct Ca^{2+}-dependent heterophilic interaction between desmosomal cadherins, desmoglein and desmocollin, contributes to cell-cell adhesion. *J Cell Biol* (1997) 138(1):193–201. doi:10.1083/jcb.138.1.193
5. Garrod DR, Merritt AJ, Nie Z. Desmosomal cadherins. *Curr Opin Cell Biol* (2002) 14(5):537–45. doi:10.1016/S0955-0674(02)00366-6
6. Kitajima Y. New insights into desmosome regulation and pemphigus blistering as a desmosome-remodeling disease. *Kaohsiung J Med Sci* (2013) 29(1):1–13. doi:10.1016/j.kjms.2012.08.001
7. Spindler V, Heupel WM, Efthymiadis A, Schmidt E, Eming R, Rankl C, et al. Desmocollin 3-mediated binding is crucial for keratinocyte cohesion and is impaired in pemphigus. *J Biol Chem* (2009) 284(44):30556–64. doi:10.1074/jbc.M109.024810
8. Hashimoto T, Kiyokawa C, Mori O, Miyasato M, Chidgey MA, Garrod DR, et al. Human desmocollin 1 (Dsc1) is an autoantigen for the subcorneal pustular dermatosis type of IgA pemphigus. *J Invest Dermatol* (1997) 109(2):127–31. doi:10.1111/1523-1747.ep12319025
9. Dettmann IM, Kruger S, Fuhrmann T, Rentzsch K, Karl I, Probst C, et al. Routine detection of serum antidesmocollin autoantibodies is only useful in patients with atypical pemphigus. *Exp Dermatol* (2017) 26(12):1267–70. doi:10.1111/exd.13409
10. Kalantari-Dehaghi M, Anhalt GJ, Camilleri MJ, Chernyavsky AI, Chun S, Felgner PL, et al. Pemphigus vulgaris autoantibody profiling by proteomic technique. *PLoS One* (2013) 8(3):e57587. doi:10.1371/journal.pone.0057587
11. Ishii N, Teye K, Fukuda S, Uehara R, Hachiya T, Koga H, et al. Anti-desmocollin autoantibodies in nonclassical pemphigus. *Br J Dermatol* (2015) 173(1):59–68. doi:10.1111/bjd.13711
12. Zhang F, Yan X, Jiang D, Tian H, Wang C, Yu L. Eight novel mutations of ATP2C1 identified in 17 Chinese families with Hailey-Hailey disease. *Dermatology* (2007) 215(4):277–83. doi:10.1159/000107620
13. Btadini W, Abou Hassan OK, Saadeh D, Abbas O, Ballout F, Kibbi AG, et al. Identification of several mutations in ATP2C1 in Lebanese families: insight into the pathogenesis of Hailey-Hailey disease. *PLoS One* (2015) 10(2):e0115530. doi:10.1371/journal.pone.0115530
14. Chiaravalloti A, Payette M. Hailey-Hailey disease and review of management. *J Drugs Dermatol* (2014) 13(10):1254–7.
15. Shi BJ, Xiao S, Zhang Z, Lu J, Xue M, Jiang Y, et al. The ATP2C1 gene in Hailey-Hailey disease patients: one novel deletion and one novel splicing mutation. *J Eur Acad Dermatol Venereol* (2015) 29(12):2495–7. doi:10.1111/jdv.12398
16. Micaroni M, Giacchetti G, Plebani R, Xiao GG, Federici L. ATP2C1 gene mutations in Hailey-Hailey disease and possible roles of SPCA1 isoforms in membrane trafficking. *Cell Death Dis* (2016) 7(6):e2259. doi:10.1038/cddis.2016.147
17. Szigeti R, Kellermayer R. Autosomal-dominant calcium ATPase disorders. *J Invest Dermatol* (2006) 126(11):2370–6. doi:10.1038/sj.jid.5700447

18. Shibata A, Sugiura K, Kimura U, Takamori K, Akiyama M. A novel ATP2C1 early truncation mutation suggests haploinsufficiency as a pathogenic mechanism in a patient with Hailey-Hailey disease. *Acta Derm Venereol* (2013) 93(6):719–20. doi:10.2340/00015555-1551
19. Grando SA. Cholinergic control of epidermal cohesion. *Exp Dermatol* (2006) 15(4):265–82. doi:10.1111/j.0906-6705.2006.00410.x
20. Grando SA, Dahl MV. Activation of keratinocyte muscarinic acetylcholine receptors reverses pemphigus acantholysis. *J Eur Acad Dermatol Venereol* (1993) 2(2):72–86. doi:10.1111/j.1468-3083.1993.tb00016.x
21. Vu TN, Lee TX, Ndoye A, Shultz LD, Pittelkow MR, Dahl MV, et al. The pathophysiological significance of nondesmoglein targets of pemphigus autoimmunity. Development of antibodies against keratinocyte cholinergic receptors in patients with pemphigus vulgaris and pemphigus foliaceus. *Arch Dermatol* (1998) 134(8):971–80.
22. Lakshmi MJD, Jaisankar TJ, Rajappa M, Thappa DM, Chandrashekar L, Divyapriya D, et al. Correlation of antimuscarinic acetylcholine receptor antibody titers and antidesmoglein antibody titers with the severity of disease in patients with pemphigus. *J Am Acad Dermatol* (2017) 76(5):895–902. doi:10.1016/j.jaad.2016.11.039
23. Kalashnyk OM, Gergalova GL, Komisarenko SV, Skok MV. Intracellular localization of nicotinic acetylcholine receptors in human cell lines. *Life Sci* (2012) 91(21–22):1033–7. doi:10.1016/j.lfs.2012.02.005
24. Lykhmus O, Gergalova G, Koval L, Zhmak M, Komisarenko S, Skok M. Mitochondria express several nicotinic acetylcholine receptor subtypes to control various pathways of apoptosis induction. *Int J Biochem Cell Biol* (2014) 53:246–52. doi:10.1016/j.biocel.2014.05.030
25. Chernyavsky A, Chen Y, Wang PH, Grando SA. Pemphigus vulgaris antibodies target the mitochondrial nicotinic acetylcholine receptors that protect keratinocytes from apoptolysis. *Int Immunopharmacol* (2015) 29(1):76–80. doi:10.1016/j.intimp.2015.04.046
26. Lanza A, Cirillo N, Femiano F, Gombos F. How does acantholysis occur in pemphigus vulgaris: a critical review. *J Cutan Pathol* (2006) 33(6):401–12. doi:10.1111/j.0303-6987.2006.00523.x
27. Nguyen VT, Ndoye A, Grando SA. Pemphigus vulgaris antibody identifies pemphaxin. A novel keratinocyte annexin-like molecule binding acetylcholine. *J Biol Chem* (2000) 275(38):29466–76. doi:10.1074/jbc.M003174200
28. Grando SA. Autoimmunity to keratinocyte acetylcholine receptors in pemphigus. *Dermatology* (2000) 201(4):290–5. doi:10.1159/000051540
29. Chen Y, Chernyavsky A, Webber RJ, Grando SA, Wang PH. Critical role of the neonatal Fc receptor (FcRn) in the pathogenic action of antimitochondrial autoantibodies synergizing with anti-desmoglein autoantibodies in pemphigus vulgaris. *J Biol Chem* (2015) 290(39):23826–37. doi:10.1074/jbc.M115.668061
30. Marchenko S, Chernyavsky AI, Arredondo J, Gindi V, Grando SA. Antimitochondrial autoantibodies in pemphigus vulgaris: a missing link in disease pathophysiology. *J Biol Chem* (2010) 285(6):3695–704. doi:10.1074/jbc.M109.081570
31. Arredondo J, Chernyavsky AI, Karaouni A, Grando SA. Novel mechanisms of target cell death and survival and of therapeutic action of IVIg in pemphigus. *Am J Pathol* (2005) 167(6):1531–44. doi:10.1016/S0002-9440(10)61239-4
32. Sarig O, Bercovici S, Zoller L, Goldberg I, Indelman M, Nahum S, et al. Population-specific association between a polymorphic variant in ST18, encoding a pro-apoptotic molecule, and pemphigus vulgaris. *J Invest Dermatol* (2012) 132(7):1798–805. doi:10.1038/jid.2012.46
33. Grando SA. The mitochondrion is a common target of disease pathophysiology in pemphigus and pemphigoid. *Exp Dermatol* (2015) 24(9):655–6. doi:10.1111/exd.12772
34. Vodo D, Sarig O, Geller S, Ben-Asher E, Olender T, Bochner R, et al. Identification of a functional risk variant for pemphigus vulgaris in the ST18 gene. *PLoS Genet* (2016) 12(5):e1006008. doi:10.1371/journal.pgen.1006008
35. Yue Z, Fu X, Chen M, Wang Z, Wang C, Yang B, et al. Lack of association between the single nucleotide polymorphism of ST18 and pemphigus in Chinese population. *J Dermatol* (2014) 41(4):353–4. doi:10.1111/1346-8138.12363
36. Sinclair D. Clinical and laboratory aspects of thyroid autoantibodies. *Ann Clin Biochem* (2006) 43(Pt 3):173–83. doi:10.1258/000456306776865043
37. Sheehan MT. Biochemical testing of the thyroid: TSH is the best and, oftentimes, only test needed – a review for primary care. *Clin Med Res* (2016) 14(2):83–92. doi:10.3121/cmr.2016.1309
38. Kotani T. [Anti-TPO autoantibodies]. *Rinsho Byori* (1998) 46(4):324–30.
39. Pitoia F, Moncet D, Glorio R, Graciela Diaz A, Rodriguez Costa G, Carbia S, et al. Prevalence of thyroid autoimmunity in patients with pemphigus vulgaris. *Medicina (B Aires)* (2005) 65(4):307–10.
40. Michailidou EZ, Belazi MA, Markopoulos AK, Tsatsos MI, Mourellou ON, Antoniades DZ. Epidemiologic survey of pemphigus vulgaris with oral manifestations in northern Greece: retrospective study of 129 patients. *Int J Dermatol* (2007) 46(4):356–61. doi:10.1111/j.1365-4632.2006.03044.x
41. Ansar A, Farshchian M, Farahnaki S, Farshchian M. Thyroid autoimmunity in Iranian patients with pemphigus vulgaris. *J Eur Acad Dermatol Venereol* (2009) 23(6):719–20. doi:10.1111/j.1468-3083.2009.03172.x
42. Daneshpazhooh M, Behjati J, Hashemi P, Shamohammadi S, Mortazavi H, Nazemi MJ, et al. Thyroid autoimmunity and pemphigus vulgaris: is there a significant association? *J Am Acad Dermatol* (2010) 62(2):349–51. doi:10.1016/j.jaad.2009.05.024
43. Leshem YA, Katzenelson V, Yosipovitch G, David M, Mimouni D. Autoimmune diseases in patients with pemphigus and their first-degree relatives. *Int J Dermatol* (2011) 50(7):827–31. doi:10.1111/j.1365-4632.2010.04818.x
44. Kavala M, Kural E, Kocaturk E, Zindanci I, Turkoglu Z, Can B. The evaluation of thyroid diseases in patients with pemphigus vulgaris. *ScientificWorldJournal* (2012) 2012:146897. doi:10.1100/2012/146897
45. Ameri P, Cinotti E, Mussap M, Murialdo G, Parodi A, Cozzani E. Association of pemphigus and bullous pemphigoid with thyroid autoimmunity in Caucasian patients. *J Am Acad Dermatol* (2013) 68(4):687–9. doi:10.1016/j.jaad.2012.11.022
46. Parameswaran A, Attwood K, Sato R, Seiffert-Sinha K, Sinha AA. Identification of a new disease cluster of pemphigus vulgaris with autoimmune thyroid disease, rheumatoid arthritis and type I diabetes. *Br J Dermatol* (2015) 172(3):729–38. doi:10.1111/bjd.13433
47. Tomic-Canic M, Day D, Samuels HH, Freedberg IM, Blumenberg M. Novel regulation of keratin gene expression by thyroid hormone and retinoid receptors. *J Biol Chem* (1996) 271(3):1416–23. doi:10.1074/jbc.271.3.1416
48. Leonhardt JM, Heymann WR. Thyroid disease and the skin. *Dermatol Clin* (2002) 20(3):473–81. doi:10.1016/S0733-8635(02)00009-8
49. Burman KD, McKinley-Grant L. Dermatologic aspects of thyroid disease. *Clin Dermatol* (2006) 24(4):247–55. doi:10.1016/j.clindermatol.2006.04.010
50. Slominski A, Wortsman J. Neuroendocrinology of the skin. *Endocr Rev* (2000) 21(5):457–87. doi:10.1210/er.21.5.457
51. Cianfarani F, Baldini E, Cavalli A, Marchioni E, Lembo L, Teson M, et al. TSH receptor and thyroid-specific gene expression in human skin. *J Invest Dermatol* (2010) 130(1):93–101. doi:10.1038/jid.2009.180
52. Bonne S, Gilbert B, Hatzfeld M, Chen X, Green KJ, van Roy F. Defining desmosomal plakophilin-3 interactions. *J Cell Biol* (2003) 161(2):403–16. doi:10.1083/jcb.200303036
53. Lambert J, Bracke S, van Roy F, Pas HH, Bonne S, De Schepper S. Serum plakophilin-3 autoreactivity in paraneoplastic pemphigus. *Br J Dermatol* (2010) 163(3):630–2. doi:10.1111/j.1365-2133.2010.09845.x
54. Sklyarova T, Bonne S, D'Hooge P, Denecker G, Goossens S, De Rycke R, et al. Plakophilin-3-deficient mice develop hair coat abnormalities and are prone to cutaneous inflammation. *J Invest Dermatol* (2008) 128(6):1375–85. doi:10.1038/sj.jid.5701189
55. Rotzer V, Hartlieb E, Vielmuth F, Gliem M, Spindler V, Waschke J. E-cadherin and Src associate with extradesmosomal Dsg3 and modulate desmosome assembly and adhesion. *Cell Mol Life Sci* (2015) 72(24):4885–97. doi:10.1007/s00018-015-1977-0
56. Evangelista F, Dasher DA, Diaz LA, Prisayanh PS, Li N. E-cadherin is an additional immunological target for pemphigus autoantibodies. *J Invest Dermatol* (2008) 128(7):1710–8. doi:10.1038/sj.jid.5701260
57. Oliveira ME, Culton DA, Prisayanh P, Qaqish BF, Diaz LA. E-cadherin autoantibody profile in patients with pemphigus vulgaris. *Br J Dermatol* (2013) 169(4):812–8. doi:10.1111/bjd.12455
58. Yin T, Getsios S, Caldelari R, Godsel LM, Kowalczyk AP, Muller EJ, et al. Mechanisms of plakoglobin-dependent adhesion: desmosome-specific functions in assembly and regulation by epidermal growth factor receptor. *J Biol Chem* (2005) 280(48):40355–63. doi:10.1074/jbc.M506692200
59. Yin T, Getsios S, Caldelari R, Kowalczyk AP, Muller EJ, Jones JC, et al. Plakoglobin suppresses keratinocyte motility through both cell-cell adhesion-dependent and -independent mechanisms. *Proc Natl Acad Sci U S A* (2005) 102(15):5420–5. doi:10.1073/pnas.0501676102

60. Roh JY, Stanley JR. Plakoglobin binding by human Dsg3 (pemphigus vulgaris antigen) in keratinocytes requires the cadherin-like intracytoplasmic segment. *J Invest Dermatol* (1995) 104(5):720–4. doi:10.1111/1523-1747.ep12606963
61. Spindler V, Dehner C, Hubner S, Waschke J. Plakoglobin but not desmoplakin regulates keratinocyte cohesion via modulation of p38MAPK signaling. *J Invest Dermatol* (2014) 134(6):1655–64. doi:10.1038/jid.2014.21
62. Egu DT, Walter E, Spindler V, Waschke J. Inhibition of p38MAPK signaling prevents epidermal blistering and alterations of desmosome structure induced by pemphigus autoantibodies in human epidermis. *Br J Dermatol* (2017) 177(6):1612–8. doi:10.1111/bjd.15721
63. Williamson L, Raess NA, Caldelari R, Zakher A, de Bruin A, Posthaus H, et al. Pemphigus vulgaris identifies plakoglobin as key suppressor of c-Myc in the skin. *EMBO J* (2006) 25(14):3298–309. doi:10.1038/sj.emboj.7601224
64. Muller E, Caldelari R, De Bruin A, Baumann D, Bierkamp C, Balmer VV, et al. Pathogenesis in pemphigus vulgaris: a central role for the armadillo protein plakoglobin. *J Invest Dermatol* (2000) 115(2):332. doi:10.1046/j.1523-1747.2000.00abs-2.x
65. Caldelari R, de Bruin A, Baumann D, Suter MM, Bierkamp C, Balmer V, et al. A central role for the armadillo protein plakoglobin in the autoimmune disease pemphigus vulgaris. *J Cell Biol* (2001) 153(4):823–34. doi:10.1083/jcb.153.4.823
66. de Bruin A, Caldelari R, Williamson L, Suter MM, Hunziker T, Wyder M, et al. Plakoglobin-dependent disruption of the desmosomal plaque in pemphigus vulgaris. *Exp Dermatol* (2007) 16(6):468–75. doi:10.1111/j.1600-0625.2007.00557.x
67. Tokonzaba E, Chen J, Cheng X, Den Z, Ganeshan R, Muller EJ, et al. Plakoglobin as a regulator of desmocollin gene expression. *J Invest Dermatol* (2013) 133(12):2732–40. doi:10.1038/jid.2013.220
68. Acehan D, Petzold C, Gumper I, Sabatini DD, Muller EJ, Cowin P, et al. Plakoglobin is required for effective intermediate filament anchorage to desmosomes. *J Invest Dermatol* (2008) 128(11):2665–75. doi:10.1038/jid.2008.141
69. Korman NJ, Eyre RW, Klaus-Kovtun V, Stanley JR. Demonstration of an adhering-junction molecule (plakoglobin) in the autoantigens of pemphigus foliaceus and pemphigus vulgaris. *N Engl J Med* (1989) 321(10):631–5. doi:10.1056/NEJM198909073211002
70. Calkins CC, Setzer SV, Jennings JM, Summers S, Tsunoda K, Amagai M, et al. Desmoglein endocytosis and desmosome disassembly are coordinated responses to pemphigus autoantibodies. *J Biol Chem* (2006) 281(11):7623–34. doi:10.1074/jbc.M512447200
71. Aoyama Y, Owada MK, Kitajima Y. A pathogenic autoantibody, pemphigus vulgaris-IgG, induces phosphorylation of desmoglein 3, and its dissociation from plakoglobin in cultured keratinocytes. *Eur J Immunol* (1999) 29(7):2233–40. doi:10.1002/(SICI)1521-4141(199907)29:07<2233::AID-IMMU2233>3.0.CO;2-4
72. Lo Muzio L, Pannone G, Staibano S, Mignogna MD, Rubini C, Farronato G, et al. Strict correlation between uPAR and plakoglobin expression in pemphigus vulgaris. *J Cutan Pathol* (2002) 29(9):540–8. doi:10.1034/j.1600-0560.2002.290906.x
73. Ishii M, Izumi J, Fujiwara H, Ito M, Hamada M. Immunoblotting detection of gamma-catenin (plakoglobin) antibody in the serum of a patient with paraneoplastic pemphigus. *Br J Dermatol* (2001) 144(2):377–9. doi:10.1046/j.1365-2133.2001.04031.x
74. Marone G, Spadaro G, Palumbo C, Condorelli G. The anti-IgE/anti-FcepsilonRIalpha autoantibody network in allergic and autoimmune diseases. *Clin Exp Allergy* (1999) 29(1):17–27. doi:10.1046/j.1365-2222.1999.00441.x
75. Fiebiger E, Hammerschmid F, Stingl G, Maurer D. Anti-FcepsilonRIalpha autoantibodies in autoimmune-mediated disorders. Identification of a structure-function relationship. *J Clin Invest* (1998) 101(1):243–51. doi:10.1172/JCI511
76. Todd JA, Acha-Orbea H, Bell JI, Chao N, Fronek Z, Jacob CO, et al. A molecular basis for MHC class II–associated autoimmunity. *Science* (1998) 240(4855):1003–9.
77. Sinha AA. The genetics of pemphigus. *Dermatol Clin* (2011) 29(3):381–91. doi:10.1016/j.det.2011.03.020
78. Amber KT, Staropoli P, Shiman MI, Elgart GW, Hertl M. Autoreactive T cells in the immune pathogenesis of pemphigus vulgaris. *Exp Dermatol* (2013) 22(11):699–704. doi:10.1111/exd.12229
79. Slomov E, Loewenthal R, Goldberg I, Korostishevsky M, Brenner S, Gazit E. Pemphigus vulgaris in Jewish patients is associated with HLA-A region genes: mapping by microsatellite markers. *Hum Immunol* (2003) 64(8):771–9. doi:10.1016/j.humimm.2003.09.008
80. Tron F, Gilbert D, Mouquet H, Joly P, Drouot L, Makni S, et al. Genetic factors in pemphigus. *J Autoimmun* (2005) 24(4):319–28. doi:10.1016/j.jaut.2005.03.006
81. Sajda T, Hazelton J, Patel M, Seiffert-Sinha K, Steinman L, Robinson W, et al. Multiplexed autoantigen microarrays identify HLA as a key driver of anti-desmoglein and -non-desmoglein reactivities in pemphigus. *Proc Natl Acad Sci U S A* (2016) 113(7):1859–64. doi:10.1073/pnas.1525448113

Conflict of Interest Statement: The authors declare that the research was conducted in the absence of any commercial or financial relationships that could be construed as a potential conflict of interest.

frontiers in Immunology

ORIGINAL RESEARCH
published: 24 May 2018
doi: 10.3389/fimmu.2018.01030

Gliptin Accountability in Mucous Membrane Pemphigoid Induction in 24 Out of 313 Patients

*Olivier Gaudin[1], Vannina Seta[1,2], Marina Alexandre[1], Gérôme Bohelay[1], Françoise Aucouturier[3], Sabine Mignot-Grootenboer[4], Saskia Ingen-Housz-Oro[5], Céline Bernardeschi[2], Pierre Schneider[6], Benoît Mellottee[1], Frédéric Caux[1] and Catherine Prost-Squarcioni[1,7,8]**

[1] Department of Dermatology, Referral Center for Autoimmune Bullous Diseases (MALIBUL), Avicenne Hospital, Assistance Publique Hôpitaux De Paris (AP-HP), Paris 13 University, Bobigny, France, [2] Department of Dermatology, Referral Center for Autoimmune Bullous Diseases (MALIBUL), Cochin Hospital, Assistance Publique Hôpitaux De Paris (AP-HP), Université Paris Descartes, Paris, France, [3] Department of Immunology, Referral Center for Autoimmune Bullous Diseases (MALIBUL), Saint-Louis Hospital, Assistance Publique Hôpitaux De Paris (AP-HP), Paris, France, [4] Department of Immunology, Referral Center for Autoimmune Bullous Diseases (MALIBUL), Bichat Hospital, Assistance Publique Hôpitaux De Paris (AP-HP), Paris, France, [5] Department of Dermatology, Referral Center for Autoimmune Bullous Diseases (MALIBUL), Henri-Mondor Hospital, Assistance Publique Hôpitaux De Paris (AP-HP), Créteil, France, [6] Department of Dermatology, Referral Center for Autoimmune Bullous Diseases (MALIBUL), Saint-Louis Hospital, Assistance Publique Hôpitaux De Paris (AP-HP), Paris, France, [7] Department of Histology, UFR Léonard de Vinci, Paris 13 University, Bobigny, France, [8] Department of Pathology, Avicenne Hospital, Assistance Publique Hôpitaux De Paris (AP-HP), Paris 13 University, Bobigny, France

OPEN ACCESS

Edited by:
Ralf J. Ludwig,
Universität zu Lübeck,
Germany

Reviewed by:
Takashi Hashimoto,
Osaka City University
Graduate School of Medicine,
Japan
Kentaro Izumi,
Hokkaido University,
Japan

***Correspondence:**
Catherine Prost-Squarcioni
catherine.prost@aphp.fr

Specialty section:
This article was submitted to
Immunological Tolerance
and Regulation, a section
of the journal
Frontiers in Immunology

Received: 28 February 2018
Accepted: 24 April 2018
Published: 24 May 2018

Citation:
Gaudin O, Seta V, Alexandre M,
Bohelay G, Aucouturier F, Mignot-
Grootenboer S, Ingen-Housz-Oro S,
Bernardeschi C, Schneider P,
Mellottee B, Caux F and
Prost-Squarcioni C (2018) Gliptin
Accountability in Mucous Membrane
Pemphigoid Induction
in 24 Out of 313 Patients.
Front. Immunol. 9:1030.
doi: 10.3389/fimmu.2018.01030

Mucous membrane pemphigoids (MMPs) and bullous pemphigoid (BP) are autoimmune bullous diseases that share physiopathological features: both can result from autoantibodies directed against BP180 or BP230 antigens. An association has been reported between BP and intake of gliptins, which are dipeptidyl peptidase-IV inhibitors used to treat type 2 diabetes mellitus. Clinical and immunological differences have been reported between gliptin-induced BPs and classical BPs: mucosal involvement, non-inflammatory lesions, and target BP180 epitopes other than the NC16A domain. Those findings accorded gliptins extrinsic accountability in triggering MMP onset. Therefore, we examined gliptin intrinsic accountability in a cohort of 313 MMP patients. To do so, we (1) identified MMP patients with gliptin-treated (challenge) diabetes; (2) selected those whose interval between starting gliptin and MMP onset was suggestive or compatible with gliptin-induced MMP; (3) compared the follow-ups of patients who did not stop (no dechallenge), stopped (dechallenge) or repeated gliptin intake (rechallenge); (4) compared the clinical and immunological characteristics of suggestive-or-compatible-challenge patients to 121 never-gliptin-treated MMP patients serving as controls; and (5) individually scored gliptin accountability as the trigger of each patient's MMP using the World Health Organization-Uppsala Monitoring Center, Naranjo- and Begaud-scoring systems. 17 out of 24 gliptin-treated diabetic MMP patients had suggestive (≤12 weeks) or compatible challenges. Complete remission at 1 year of follow-up was more frequent in the 11 dechallenged patients. One rechallenged patient's MMP relapsed. These 17 gliptin-treated diabetic MMP patients differed significantly from the MMP controls by more cutaneous, less buccal, and less severe involvements and no direct immunofluorescence IgA labeling of the basement membrane zone. Multiple autoantibody-target antigens/epitopes (BP180–NC16A, BP180 mid- and C-terminal parts, integrin α6β4) could be detected, but not laminin 332. Last, among the 24 gliptin-treated diabetic MMP patients, five had high (I4–I3), 12 had low (I2-I1) and 7 had I0 Begaud

intrinsic accountability scores. These results strongly suggest that gliptins are probably responsible for some MMPs. Consequently, gliptins should immediately be discontinued for patients with a positive accountability score. Moreover, pharmacovigilance centers should be notified of these events.

Keywords: autoimmune bullous diseases, mucous membrane pemphigoid, fibrosis, dipeptidyl peptidase IV inhibitor, gliptin, diabetes mellitus, adverse drug reaction, drug-accountability study

INTRODUCTION

Mucous membrane pemphigoids (MMPs) are rare diseases with very low annual incidences worldwide, ranging from 0.07 million inhabitants in Kuwait to 2 million inhabitants in Germany, and intermediate, with 1.25 million inhabitants, in France (1). These diseases are defined clinically. They cover a heterogeneous group of subepithelial autoimmune blistering diseases that predominantly affect the mucous membranes (2). They include the classical MMP, formerly called cicatricial pemphigoid, laminin 332 MMP, α6β4 integrin MMP, mucous membrane dominant epidermolysis bullosa acquisita (MM-EBA), and mucous membrane dominant linear IgA disease [MM-linear IgA bullous dermatosis (LABD)]. Abnormal scarring is the hallmark of MMPs: lesions heal *via* a fibrosing process leading to cicatricial lesions that can cause severe impairment of the eyes or can be life-threatening in larynx or esophagus.

Although MMP clinical characteristics differ from those of bullous pemphigoid (BP) (younger patients, mucous membrane involvement, bullous cutaneous lesions predominantly on the head-and-neck, cicatricial evolution) (3), classical MMP, and BP share physiopathological features: both result from the activity of autoantibodies directed against hemidesmosomal proteins of basal keratinocytes, BP 230 (BP230) and BP 180 (BP180) antigens, predominantly the C-terminal region and BP180–NC16A epitopes in MMP and BP, respectively (2, 4, 5).

An association between BP and the intake of several drugs (spironolactone, amiodarone, sulfasalazine, allopurinol, furosemide, etc.) has been reported, since 1970 (6–8), and most recently with gliptins, which are dipeptidyl peptidase-IV (DPPIV) inhibitors used to treat type 2 diabetes mellitus. Three gliptins are currently available in France: sitagliptin and vildagliptin, since 2007, and saxagliptin, since 2009. The first BP cases associated with gliptin intake were described in 2011. Since then, 42 cases of gliptin-associated BP have been published as case reports or in short series (9–23), 37 in two case-control studies (20, 24), and 208 identified in pharmacovigilance databases (16, 25). A study comparing 3,397 BP patients to 12,941 basocellular carcinoma controls from the Finnish nationwide registry and showing that vidagliptine increases the risk of BP has also been partially published very recently (26). Several authors have highlighted different clinical and immunological phenotypes of these gliptin-associated BPs: mucosal involvement (15), non-inflammatory lesions (18, 23), and target BP180 epitopes outside the NC16A domain (18, 23).

Because the role of gliptins in MMP had never been investigated, we examined gliptin accountability in MMP induction in 24 gliptin-treated diabetic MMP patients in our center cohort of 313 MMP patients. Our primary objective was to identify patients with a first gliptin-intake-to-MMP-onset interval "suggestive" or "compatible" with MMP induction. Then we analyzed clinical and immunological findings and outcomes of these selected patients to evaluate other accountability criteria of gliptin MMP induction and, finally, indicate prognosis.

MATERIALS AND METHODS

Referral Center Database

This single-multisite-center retrospective study (January 2007–June 2016), approved by our local Institutional Review Board (IRB 00003835 no. 2013/39NI), was conducted using the database of our Referral Center for autoimmune bullous diseases. The following information was systematically recorded in each patient's standardized medical chart. During their first consultation at our Center, all patients were asked about their medical history and treatments, evaluated by a multidisciplinary team that noted all cutaneous and mucous membrane lesions, clearly distinguishing MMP reversible "active" mucous membrane lesions from irreversible "cicatricial" mucous membrane lesions (27–29). Skin and/or mucous membrane biopsy findings and immunoserological results at diagnosis yielding a definite diagnosis were also recorded: direct immunofluorescence (DIF) immune-deposit pattern at the dermal–epidermal junction (linear) and Ig class(es) (IgA, IgG, IgM), ±C3 deposits; ultrastructural immune-deposit location by direct immunoelectron microscopy (IEM; when done, according to availability in each department); standard indirect immunofluorescence (IIF) on rat or monkey esophagus and 1 M NaCl-treated human or commercially available (Euroimmun, Lübeck, Germany) monkey salt-split skin (SSS), using polyvalent anti-IgG, IgA, IgM as secondary antibodies; commercially available BP180–NC16A and BP230 enzyme-linked immunosorbent assays (ELISAs) using anti-IgG secondary antibodies (MBL, Nagoya, Japan and/or Euroimmun, Lübeck, Germany); and immunoblot on amniotic membrane extracts (when done, according to availability in each department). In patients with a subepithelial autoimmune blistering disease [i.e., linear immunoglobulin (Ig) deposits along the basement membrane zone (BMZ) in DIF], diagnoses of MMP and BP were retained

Abbreviations: BMZ, basement membrane zone; BP, bullous pemphigoid; DIF, direct immunofluorescence; DPPIV, dipeptidyl peptidase-IV; EBA, epidermolysis bullosa acquisita; ELISA, enzyme-linked immunosorbent assay; IEM, immunoelectron microscopy; IIF, indirect immunofluorescence; LABD, linear IgA bullous dermatosis; MMP, mucous membrane pemphigoid; SSS, salt-split skin; WHO–UMC, World Health Organization–Uppsala Monitoring Center.

on clinical criteria: the first when lesions predominantly affected the mucous membranes (2) and the second in patients who fulfilled criteria of Vaillant (3). Diagnoses of LABD and EBA were retained on immunological criteria: the first on class IgA of autoantibodies and the second when autoantibodies targeted type VII collagen (by ELISA and/or immunoblot) and/or are located in anchoring-fibril zone (AFz) (by IEM). Diagnosis of MM-LABD or MM-EBA was retained in patients with predominant mucous membrane lesions and respectively a LABD or an EBA. Other MMP subgroups have been diagnosed according to the target antigen of autoantibodies (by IEM, IIF on SSS, ELISA, and/or immunoblot). In particular, the immunoblot on amniotic extract allowed the detection of antibodies to laminin 332 and α6/β4 integrin (30). Last, MMP was classified as severe or not according to Chan criteria (2, 27–29).

Gliptin-Treated MMP Patients

First, we identified all consecutive patients with a definite MMP diagnosis, then selected those with diabetes mellitus, and, finally, included MMP patients prescribed gliptins to treat their diabetes.

Chronology of Gliptin Intake and MMP Onset

Using Begaud's updated nomenclature (**terms in bold type;** 31) to impute a potential gliptin role in triggering MMP, dates of gliptin introduction (**challenge**), discontinuation (**dechallenge**), reintroduction (if any) (**rechallenge**), and the first MMP symptoms were extracted from the Center's database, collected from patient's chart and/or by contacting the patient's general practitioner. Diabetics who started taking a gliptin before MMP onset and had a first gliptin-intake-to-MMP-onset interval suggestive or compatible with MMP induction formed the **suggestive-or-compatible challenge** group (**Figure 1**). Those who discontinued gliptin during the first year of MMP follow-up formed the dechallenge group and those who did not comprised the **no-dechallenge** group.

Clinical and Immunological Findings and MMP Follow-Up

Clinical and immunological characteristics at MMP diagnosis were extracted from the Center's database. Observation end points were collected retrospectively from patients' charts: time to first MMP complete remission (CR), CR rate at 1 year of MMP follow-up, and relapse rates at 1 year and the end of MMP follow-up (1–3 years), according to Murrell et al.'s criteria (31).

Reference Series of MMP Patients Without Gliptin Intake

One hundred and twenty-one consecutive MMP patients who had never taken a gliptin and had at least 1 year of follow-up served as controls. Patients with MM-LABD were excluded, as were those with MM-EBA. Clinical and immunological findings at diagnosis and CR and relapse rates at 1 year of follow-up were extracted from the Center's database and/or collected from each patient's chart.

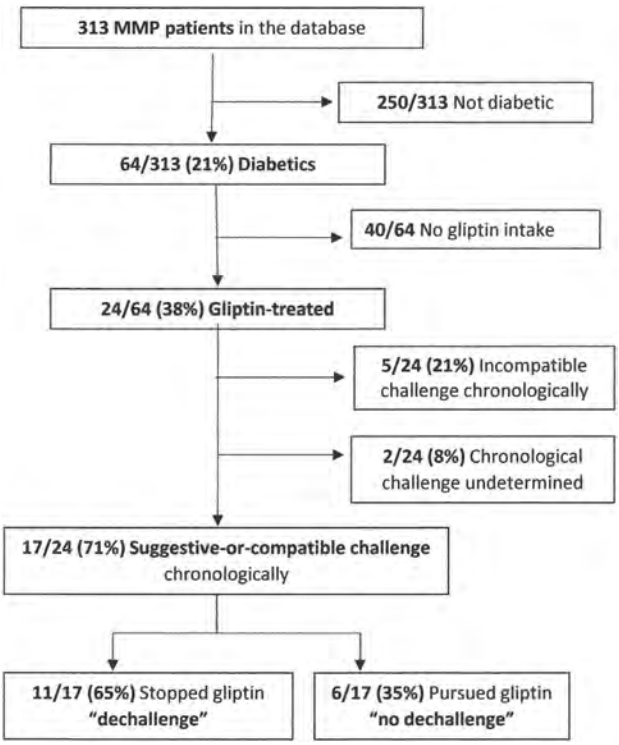

FIGURE 1 | Flowchart. Abbreviation: MMP, mucous membrane pemphigoid.

Statistical Analyses

Quantitative variables, reported as mean ± SD or medians (range), were compared with Mann–Whitney *U*-tests. Qualitative parameters, expressed as numbers (%) were compared with chi^2 or Fisher's exact tests, as appropriate. Two-tailed *p*-values less than 0.05 were considered statistically significant. Statistical analyses were computed with R version 3.4.3 (R Foundation for statistical Computing, Vienna, Austria).

Accountability Scoring

Accountability criteria were analyzed and scored using Begaud's system, updated in 2011 (32, 33), Naranjo's method (34) and the World Health Organization–Uppsala Monitoring Center's (WHO–UMC) assessment (35).

RESULTS

Gliptin-Treated MMP Patients

Among the 313 MMP patients seen in our Center between January 2007 and June 2016, 64 (20%; 39 F/25 M) were diabetics and 24 (38%) of them were treated with gliptin (**Figure 1**). All but four of them (patients 7, 10, 13, and 14) had >1 year of follow-up in our Center.

Chronological Data on Gliptin Use

17 (71%) of the 24 MMP patients started taking a gliptin to treat their diabetes before MMP onset (**suggestive-or-compatible**

challenge group), with the median first gliptin-intake-to-MMP-onset interval of 136 (range 4–588) weeks (**Table 1**). Arbitrarily, ≤12 weeks to MMP onset was considered **suggestive** of gliptin induction for patients 1–4 and >12 weeks considered **compatible** for patients 5–17. Patients 1–11 (11, 65%) of the 17 had discontinued gliptin because of uncontrolled diabetes (**dechallenge** group) and patients 12–17 (6, 35%) did not (**no-dechallenge** group). 5 (21%) of the 24 gliptin-treated MMP diabetics started taking it after MMP onset (**incompatible-challenge** group). For the remaining two patients, the date of gliptin introduction could not be determined (**undetermined-challenge** group). No other therapeutic agent was suspected in MMP onset.

Clinical and Immunological MMP Data

Among the 17 **suggestive-or-compatible-challenge** group patients (nine women; eight men), patient 1 took saxagliptin, 11 vildagliptin (patients 2–7 and 12–16), and five sitagliptin (patients 8–11, 17) (**Table 1**) alone or combined with metformin. At MMP diagnosis, their ages ranged from 48 to 81 (mean 69, median 71) years, 48–75 (mean 66, median 71) years for women and 60–81 (mean 71, median 74) years for men (**Figure 2**), their weight from 55 to 154 (mean 87, median 80) kg and their body mass indexes from 24 to 45 (mean 32, median 29). Three (18%) of them had exclusively mucous membrane involvement, and 14 had (82%) mucous membrane and cutaneous involvements. A median of three sites per patient were involved (**Figure 3**): skin (14, 82%), mouth (11, 65%), larynx (6, 35%), genitals and/or anus (8, 47%), and conjunctiva (2, 12%); none had esophageal involvement. Last, patients 1, 4, 6, 9, 12, 13, and 17 [seven, 41%] had severe MMP involvement, with more than three involved sites for patient 12, and laryngeal involvement in the other six associated with severe conjunctival fibrosis in patients 1 and 6. Initial treatment chosen according to the MMP severity and the patients' comorbidities was dapsone, alone or in association with 11 patients, doxycycline with 6, cyclophosphamide with 5, and rituximab with two (**Table 1**).

Direct immunofluorescence microscopy of tissue samples from 14 (82%) of the 17 of suggestive-or-compatible-challenge group patients had linear IgG deposits and 15 (88%) linear C3 deposits along the BMZ; none had IgA deposits (**Table 2**). IEM (**Figure 4**) of nine patients' biopsies were positive for eight (89%): immune deposits were located on the lamina densa with/without the lamina lucida (LL) in seven (78%) of them and exclusively on the upper LL in the last one (11%); none had deposits under the lamina densa in the AFz. Autoantibodies directed against BMZ antigens were detected in 8 (47%) of the 17 patients whose sera were tested by IIF on rat or monkey esophagus. IIF on SSS was positive for 4 out of 15 patients and autoantibodies always labeled the cleavage roof; none labeled the cleavage floor. ELISA BP180 and BP230 were positive for 7 (47%) and 3 (20%) of the 15 patients tested, respectively. Immunoblots on amniotic membrane extract (**Figure 5**) of sera from seven of the nine ELISA BP180–NC16A-negative patients were negative for three patients and positive for four, detecting: a 200-kDa band consistent with the β4 chain of α6β4 integrin (patient 8), whose immune deposits were located on hemidesmosomes by direct IEM; a 180-kDa band (patient 3); a 120-kDa band (patient 11); and 180- and 120-kDa bands (patient 7).

Follow-Up of the Suggestive-or-Compatible-Challenge Group

Overall, median follow-up was 40 (range 0–164) weeks and median time to CR 8 (range 0–36) weeks. After the first year of follow-up, CR and relapse rates were 82 and 31%, respectively (**Table 3**). No patient died.

When **dechallenge** (patients 1–11) and **no-dechallenge** (patients 12–17) groups were compared, respectively, the CR rate was higher for the former than latter (88 vs. 66%). Conversely the follow-up durations [32 (0–104) vs. 78 (4–164) weeks], times to first (CR) [8 (2–16) vs. 18 (0–36) weeks] and relapse rates of 22 vs. 50% were lower in **dechallenge** group than in **no-dechallenge** one. It is worth noting that **dechallenge** group patient 6 relapsed before gliptin withdrawal and patient 4 after it, and patient 8 relapsed 17 months after MMP diagnosis and 1 month after gliptin **rechallenge**.

Last, for the **dechallenge** group, MMP evolution was **suggestive** of gliptin imputability for six (1, 2, 5, 8, 9, and 11) of the seven patients who obtained CR, **non-suggestive** for the patient who did not, **inconclusive** for patient 4 in CR at 1 year of follow-up but who relapsed, and for patients 3, 7, and 10, with <1 year of follow-up, and patient 3 not seen at 1 year. For the **no-dechallenge** group, at 1 year of follow-up, MMP evolution was **non-suggestive** for patients 15 and 16 in CR, **suggestive** for patient 12 who had not achieved CR and **inconclusive** for remaining patients 13, 14, because of too short follow-up, and 17, who was not seen at 1 year.

Control MMP Patients Without Gliptin Use

Our controls were 121 patients with MMP (excluding MM-EBA and MM-LABD) seen consecutively in our Center, who had never taken a gliptin and were followed for at least 1 year (**Table 4**). At MMP diagnosis (baseline), their ages ranged from 38 to 96 years, weights from 44 to 114 kg, and body mass indexes from 18 to 40. Half of them had only mucous membrane involvement and the other half had cutaneous and mucous membrane involvements, and 78 had severe MMP. Controls had a median of 2 (1–5) involved sites: 50% skin, 89% mouth, 30% larynx, 31% genitals/anus, 25% conjunctiva, and 31% esophagus. Immunologically, by DIF microscopy, 74% controls had linear IgG deposits along the BMZ, 71% had linear C3 deposits, and 26% had linear IgA deposits which were neither isolated nor predominate over IgG. Immune deposits were located on the lamina densa with/without the LL in 60% of them and on the upper LL in 13%. IIF microscopy of their biopsies identified circulating autoantibodies labeling the cleavage roof of SSS in 21%, the cleavage floor 2%, both sides in 3%, and no labeling of 74%. Control MMP patients whose sera labeled the cleavage floor in IIF on SSS had deposits on the lamina densa, but not the AFz by IEM, thereby excluding EBA and consistent with a laminin 332 MMP diagnosis. ELISA detected circulating anti-BP180 autoantibodies in 43 (51%) and anti-BP230 in 10 (13%) control sera. At 1 year of follow-up, 56% of the controls were in CR, 23% suffered relapses/flares, and 2% had died.

Comparing the **suggestive-or-compatible-challenge** group's characteristics to those of the MMP controls, most were comparable, especially the relapse and CR rates at 1 year of follow-up.

TABLE 1 | Clinical characteristics of the 17 MMP patients with suggestive-or-compatible gliptin challenges.

Challenge	Sex/age (years)	Weight (kg)/BMI (kg/m²)	1st gliptin-dose-to-MMP-onset interval (weeks)	MM sites involved						MMP severity		Initial treatment	1-year MMP follow-up	
Gliptin patient				Total*n*	Skin	Mouth	Genitals/anus	Eyes	NT/larynx	Mild	Severe		Relapse	CR
Dechallenge														
Saxagliptin														
1	M/79	65/24	4	4	+	+	−	+	+/+	−	+	Dap, RTX	No	Yes
Vildagliptin														
2	F/71	68/27	4	2	−	+	+	−	−/−	+	−	Dap	No	Yes
3	M/60	75/29	4	3	+	+	+	−	−/−	+	−	Doxy	No[a]	Unknown
4	F/71	Unknown	12	2	−	+	−	−	+/+	−	+	Dap, CyP	Yes	Yes
5	M/77	80/27	36	3	+	+	−	−	+/−	+	−	Dap	No	Yes
6	F/61	92/36	36	5	+	+	+	+	+/+	−	+	Dap, RTX	Yes[b]	No
7	M/81	80/30	144	2	+	−	−	−	+/−	+	−	Doxy	Unknown[c]	Unknown
Sitagliptin														
8	M/62	91/29	104	3	−	+	+	−	+/−	+	−	Dap	Yes[d]	Yes
9	F/57	Unknown	136	3	+	+	−	−	+/+	−	+	Dap, CyP	No	Yes
10	F/74	55/25	144	3	+	+	−	−	+/−	+	−	Dap	Unknown[c]	Unknown
11	M/76	Unknown	232	2	+	−	+	−	−/−	+	−	tCTC	No	Yes
No dechallenge														
Vildagliptin														
12	M/72	70/25	72	4	+	+	+	−	+/−	−	+	Dap, CyP	Yes	No
13	F/75	105/41	148	3	+	−	+	−	+/+	−	+	CyP, Doxy	Unknown[c]	Unknown
14	F/48	100/33	236	2	+	−	−	−	+/−	+	−	Dap	Unknown[c]	Unknown
15	F/71	77/nd	244	2	+	−	+	−	−/−	+	−	Unknown	No	Yes
16	F/65	100/43	588	3	+	+	−	−	+/−	+	−	Dap	No	Yes
Sitagliptin														
17	M/64	154/45	144	2	+	−	−	−	+/+	−	+	CyP, Doxy	Yes[a]	Unknown

MMP, mucous membrane pemphigoid; BMI, body mass index; MM, mucous membrane; NT, nose and throat; CR, complete remission; +, positive; –, negative; Dap, dapsone; RTX, rituximab; Doxy, doxycyclin; CyP, cyclophosphamide; tCTC, topical corticosteroid.

[a]*These patients were followed for >1 year but were not examined at 1 year, so exact status at 1 year is unknown.*

[b]*Relapse on gliptin.*

[c]*Follow-up <1 year, with no additional information about outcome.*

[d]*Relapse after rechallenge.*

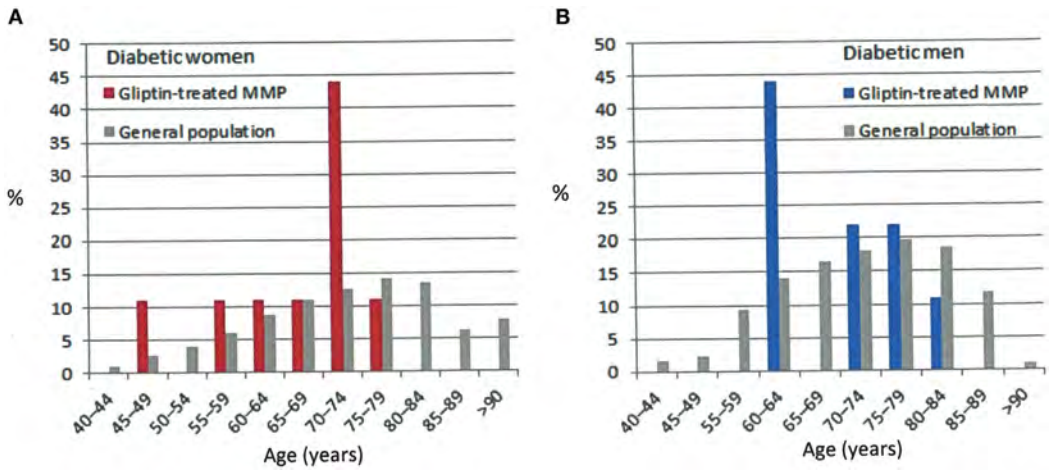

FIGURE 2 | Percentage of patients by age group in the general diabetic population and our suggestive-or-compatible gliptin-induced mucous membrane pemphigoid group: **(A)** in women, **(B)** in men, diabetic patients (36).

The **suggestive-or-compatible-challenge** patients were older than controls but not significantly so. However, **suggestive-or-compatible-challenge** group differed significantly from controls by weighing more, having higher body mass indexes, with more frequent cutaneous involvement, less frequent buccal, and severe involvements, and no IgA deposits.

Accountability Scoring

Using Begaud's scoring system, **extrinsic accountability** was rated B2 (sparse and/or unreliable publications) for all our gliptin-treated MMP patients, in analogy with reported gliptin-induced BP, a similar autoimmune bullous disease (**Table 5**). For the **suggestive-or-compatible-challenge** group, the **chronological accountability** criterion was scored C3 (**likely**): for patients 1 and 2 because of their **suggestive** times to MMP onset and **suggestive** outcomes after gliptin **dechallenge**, and patient 8 because of the **compatible** time to MMP onset, positive **rechallenge**, and **suggestive** outcome; C2 (**plausible**): for patients 3 and 4 with **suggestive** times to MMP onset and **inconclusive** outcomes, and patients 5, 9, 11, 12, and 17 with **compatible** times to MMP onset and **suggestive** outcomes; and C1 (**doubtful**) for the seven others because of **compatible** times to MMP onset but **inconclusive** or **non-suggestive** outcomes.

The **symptomatological accountability** criterion was scored: S2 (**evocative**) for five patients whose clinical (cutaneous lesions, no buccal disease, no severe involvement) and immunological features (no IgA deposits), which differed significantly from controls; and S1 (**not evocative**) for the 12 other patients. No specific laboratory test can prove the link between gliptin intake and MMP.

Finally, the **intrinsic accountability** (combining C and S scores) was rated I4 for three patients, I3 for two patients, I2 for eight, I1 for four, and I0 for the seven patients with chronologically incompatible or undetermined challenge.

Naranjo's accountability score assigns points according to the following information: (1) previous reports described a similar adverse drug reaction (ADR) (gliptin-induced BP) (1 point); (2) MMP appeared after gliptin intake (2 points); (3) MMP regressed faster after gliptin withdrawal (1 point) (patients 1–4, 8, 9, 11); (4) the adverse event appeared when the drug was readministered (2 points) (patient 8); (5) MMP that could have been idiopathic (−1 point); (6) no placebo was given (0 points); (7) the drug concentration in blood was not tested (0 points); (8) no dose-related reaction was sought (0 points); (9) a patient had the same reaction as when previously exposed (1 point) (patient 8); (10) no objective test assessed the adverse event (0 points). The Naranjo's score was 6 for patient 8, meaning a **probable** ADR, but 3 for 5 patients and 2 for 11 patients meaning **possible** ADRs.

According to WHO–UMC accountability criteria, gliptin was **probably** responsible for triggering MMP for all patients of **the suggestive-or-compatible-challenge** group, a reasonable time relationship between drug intake and first MMP manifestations; MMP regressed after gliptin withdrawal and relapsed after readministration; and because MMP could have been spontaneous.

DISCUSSION

Our novel study on gliptin accountability in MMP induction was undertaken because of their extrinsic accountability, based on the following reports: MMP and BP have clinical and immunological similarities (4), a demonstrated significant association between gliptin intake and BP onset in diabetic patients (16, 24, 25) and some gliptin-associated BPs have atypical clinical and immunological phenotypes (15, 18, 23, 25).

Mucous membrane pemphigoid and BP are subepithelial AIBDs, characterized by linear immune deposits along the BMZ, but have different clinical features. MMP is clinically defined by the predominance of mucous membrane lesions over skin lesions (2) and healing of its lesions leads to characteristic cicatricial scarring. BP, on the other hand, is typified by the absence of mucous membrane lesions, absence of predominant head-and-neck involvement, and absence of scars, and older age at onset (>70 years) (3).

FIGURE 3 | Typical patterns and locations of active and cicatricial mucous membrane pemphigoid lesions in patients 10 **(A)**, 13 **(B,E,F)**, 16 **(C)**, 8 **(D)**, and 3 **(G)**. **(A)** Active buccal mucosa lesions: erosions covered by pseudomembranes or yellowish slough, surrounded by inflammatory erythema. **(B)** Cicatricial cutaneous lesions: atrophic scars and milia on the upper back. **(C)** Active and cicatricial lesions: post-bullous erosion and atrophic scars on the breast. **(D)** Post-bullous erosions and synechiae between the prepuce and the glans penis. **(E)** Disappearance of the balanopreputial furrow. **(F)** Synechiae in perianal area and atrophic scars on the skin. **(G)** Perianal linear erosion and atrophic scars.

Mucous membrane pemphigoid and BP share two autoantibody-target antigens, BP230 and BP180, but the dominant BP180 epitopes differ (4). The majority of MMP patients' sera react with the C-terminal domain of BP180, located in the lamina densa, combined or not with reactivity against the NC16A epitope, which is the membrane-proximal non-collagenous region of the BP180 ectodomain in upper LL (5, 38, 39). Conversely, 80–90% of BP patients have IgG autoantibodies directed against the NC16A domain (40–42). Moreover, many authors reported that variable percentages (10–50%, depending on the study) of BP autoantibodies targeted BP180 regions outside the NC16A domain (23, 43–49). Notably, that reactivity with extracellular epitopes of the BP180 C-terminal domain appeared suggestive of atypical BP, i.e., with skin and MM involvements (44, 46) or lesions limited to the lower legs and scarring of the toenail beds (49).

Other target antigens associated with the clinical MMP phenotype have been characterized molecularly: laminin 332, both α6β4 integrin subunits, and type VII collagen (4), respectively defining laminin 332 MMP, α6β4 integrin MMP, and MM-EBA. MMP also includes MM-LABD, with predominant IgA immune deposits along the BMZ.

Potential drug induction of autoimmune bullous diseases has been known for decades. Although autoimmune bullous diseases are rare diseases with low annual incidences, among which BP is the least rare, associations have been published between drug intake and many BP (6–8) and LABD cases (50) but only a few MMPs (51). Since 2011, an increasing number of reports have suggested that gliptins trigger BP (9–15, 17–23). Last, very recently, four comparative case–non-case studies demonstrated a significant association between gliptin intake and BP onset in

TABLE 2 | Immunological findings of the 17 gliptin-treated MMP patients with suggestive-or-compatible challenges.

Patient	Immune deposits on						IIF anti-BMZ IgG (esophagus)		IIF on SSS		ELISA (nl <9 AU)		Blot[a] (kDa)
	DIF BMZ			Direct IEM			Rat	Monkey	Roof	Floor	BP230	BP180	
	IgA	IgG	C3	LD ± LL	Upper LL ± HD	AFz							
1	–	+	+	nd	nd	nd	–	–	–	–	<9	189	nd
2	–	+	+	–	–	–	–	–	–	–	1	0	nd
3	–	+	+	+	–	–	–	1/100	–	–	7	10	180
4	–	+	+	nd	nd	nd	1,280	–	+	–	61	149	nd
5	–	+	+	+	–	–	–	nd	–	–	0	1	–
6	–	–	+	+	–	–	200	nd	+	–	2	136	nd
7	–	+	+	+	–	–	–	50	–	–	0	1	180, 120
8	–	+	–	–	+	–	–	–	–	–	nd	nd	200
9	–	+	+	nd	nd	nd	–	20	+	–	2	1	–
10	–	+	+	+	–	–	200	nd	nd	nd	10	68	nd
11	–	+	+	nd	nd	nd	640	nd	+	–	–	–	120
12	–	+	+	nd	nd	nd	100	100	–	–	6	24	nd
13	–	–	+	nd	nd	nd	–	–	nd	nd	nd	nd	nd
14	–	–	+	nd	nd	nd	–	–	–	–	2	109	nd
15	–	+	+	+	–	–	–	–	–	–	8	2	nd
16	–	+	–	+	–	–	–	–	–	–	12	62	nd
17	–	+	+	nd	nd	nd	–	–	–	–	0	1	–

MMP, mucous membrane pemphigoid; DIF, direct immunofluorescence; BMZ, basement membrane zone; Ig, immunoglobulin; IEM, immunoelectron microscopy; LD, lamina densa; LL, lamina lucida; ±, with or without; HD, hemidesmosome; AFz, anchoring-fibril zone; IIF, indirect immunofluorescence; SSS, salt-split skin; ELISA, enzyme-linked immunosorbent assay; nl, normal; AU, arbitrary unit; nd: not determined; +, positive; –, negative.

[a]*Immunoblot on amniotic membrane extract.*

diabetic patients (16, 24–26). To the best of our knowledge, possible gliptin-induced MMP has not been described to date.

Gliptins are DPPIV inhibitors used to treat diabetes, since 2007 in France (52, 53). They inhibit incretin degradation, which improves β-cell function in diabetics (54) by increasing insulin-secretory tone (55). Their HbA1c-lowering ability is less than that of hypoglycemic sulfonamides and glucagon-like peptide-1 inhibitor but they carry a lower risk of hypoglycemia (56).

Dipeptidyl peptidase-IV is not specific to insulinotropic hormones. It is abundantly distributed, notably in the skin, on the surface of keratinocytes, sebocytes, fibroblasts, and T cells. DPPIV is involved in the regulation of DNA synthesis and cytokine production by those cells, for example, CCL11/eotaxin (57) and transforming growth factor-β1 (TGF-β1) (58–60). DPPIV is also a cell-surface plasminogen receptor that activates plasminogen conversion leading to more plasmin (61), which is a major serine protease known to cleave the 120-kDa ectodomain of BP180, thereby generating LABD-97 antigen (62). Role of eotaxin and plasminogen–plasmin system is well known in BP pathogenesis (63, 64) and that of TGF-β1 in MMP is suspected (65). How gliptins induce BP or MMP by acting as DPPIV inhibitors on eotaxin, TGF-β1, and/or plasminogen/plasmin system remains to be elucidated.

Between 2011 and 2017, 14 case reports or small series reported 42 patients who developed BP while taking gliptins for their diabetes (Table S1 in Supplementary Material). The authors of those original articles individually scored gliptin accountability for each patient with the WHO–UMC system for 17 of them (10, 15, 20) and Naranjo's score for 6 (19), Karch-Lasagna system for 1 (16), and accountability was assigned *a posteriori* for the remaining 18 (9, 11–14, 17, 18, 21, 22) (See Table S1 in Supplementary Material). 17 BPs were **probable** gliptin-induced ADRs, 23 were **possible** ADRs, and 2 BPs were most likely not gliptin-induced because of long interval (>48 months) between gliptin intake and BP onset.

19 (45%) out of those 40 **probable**-or-**possible** gliptin-induced BPs appeared to be associated with vildagliptin, 10 (24%) with sitagliptin, 8 (19%) with linagliptin, and 5 (12%) with another gliptin (See Table S2 in Supplementary Material). Their overall characteristics were as follows: 19 women and 21 men (F/M sex ratio 0.90), median age 76 (59–93) years, and median gliptin-intake-to-BP-onset interval 32 (4–192) weeks. Gliptin **dechallenge** for 33 had favorable outcomes for 26 and were, therefore, considered **suggestive** of gliptin imputability. One patient died 14 days after starting corticosteroids. Information on evolution after **dechallenge** was not available for five.

The first two comparative case–non-case studies were published in 2016, after analysis of pharmacovigilance databases (16, 25). Comparing French patients with BP ADRs to those with non-BP ADRs, Béné et al. showed that the former were associated more significantly and frequently with gliptin exposure (odds ratio 67.5; 95% CI 47.1–96.9) and vildagliptin carried a higher risk than other gliptins. The individual gliptin accountability for those 42 BPs was rated as **probable** for 10 and**possible** for 31, and not reported for one (Table S2 in Supplementary Material). In the European pharmacovigilance database, Garcia et al. identified 166 BPs reportedly induced by gliptin exposure. Using proportional reporting ratios, they found that BP was relatively more frequently associated with gliptins than with other drugs, again with vildagliptin being most strongly associated. Unfortunately, detailed clinical features were not reported.

Recently, a third well-designed case–non-case study was published (24). Comparing 61 diabetic BP patients to 122 age- and

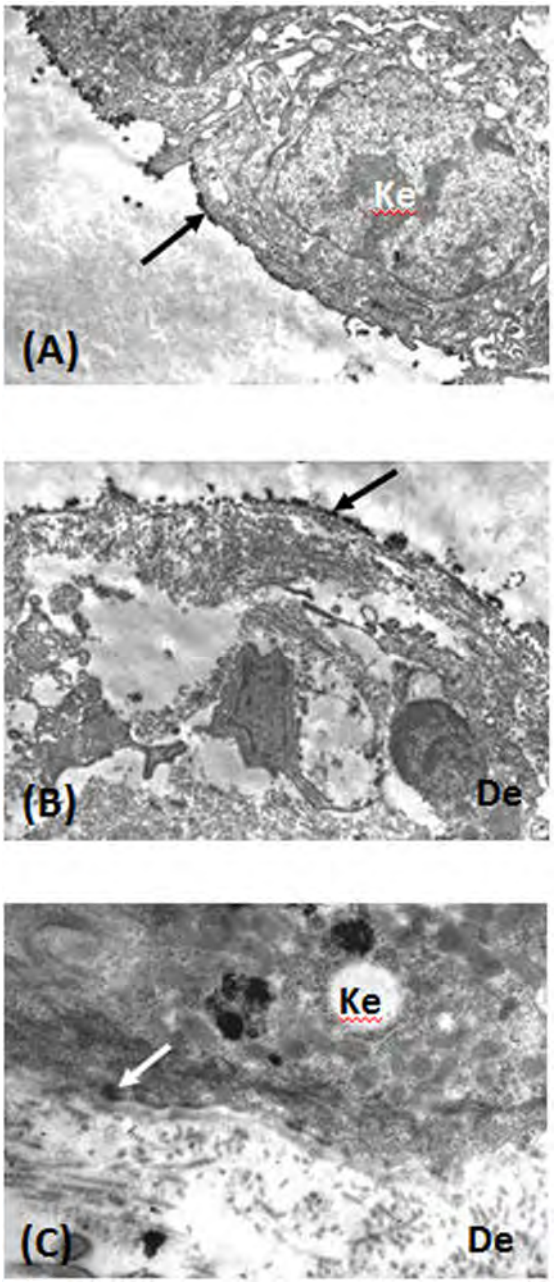

FIGURE 4 | Direct immunoelectron microscopy of tissue sections from patients 10 **(A,B)** and 8 **(C)** was performed as previously described (37). **(A)** Immune deposits (arrow) on the lamina lucida (LL) cleavage roof. **(B)** Immune deposits (arrow) in the lower LL and lamina densa at the cleavage floor. **(C)** Immune deposits (arrow) in the upper LL, close to hemidesmosomes. Abbreviations: Ke, keratinocyte; De, dermis.

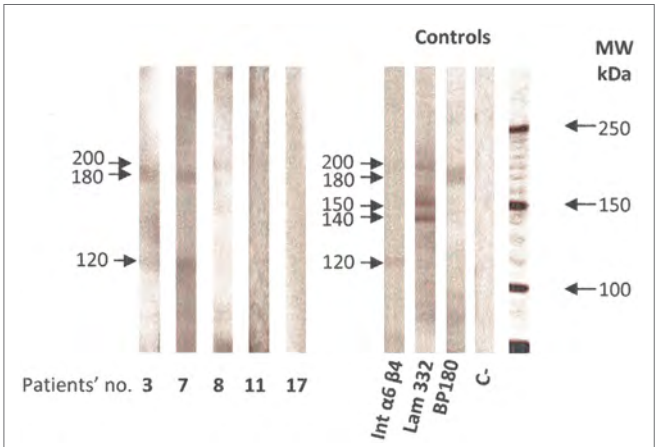

FIGURE 5 | Immunoblot on amniotic membrane extract with sera from patients 3, 7, 8, 11, and 17 of the suggestive-or-compatible gliptin-induced mucous membrane pemphigoid group, was performed as previously described (30). Positive controls were α6 β4 integrin, laminin 332, and BP 180 antigen; C– was a negative control with normal human serum. Abbreviation: MW, molecular mass.

sex-matched diabetic controls, those authors demonstrated a significant association between gliptin use and BP onset in univariate analysis and after adjustment: 28 (46%) of the 61 diabetic BP patients took gliptins vs. 18% of the diabetic controls (odds ratio 2.64, 95% CI 1.19–5.85; $p = 0.02$ in multivariable analysis). Stratified analyses showed a stronger association for men and patients ≥80 years old. Once again, vildagliptin had a stronger association but the study was underpowered to detect differences among the other gliptins.

Very recently, a study comparing 3,397 BP patients with 12,941 basocellular carcinoma controls from the Finnish nationwide registry has shown that vidagliptine and BP are significantly associated with an adjusted odds ratio of 10.4 (4.56; 23.80) (26). The Gliptin-onset-to-BP-diagnosis interval was of 449 days. Clinical and immunological data were not available in this study.

Another case-control study (20) comparing gliptin-treated diabetic patients with BP to diabetic patients without skin diseases found more frequent gliptin use among BP diabetics [9/23 (39.1%) vs. 57/170 (33.5%)], but not significantly so.

Last, some reportedly gliptin-associated BPs had atypical clinical and/or immunological phenotypes, raising doubts about the BP diagnosis. Izumi et al. (23) described seven gliptin-associated BPs and showed they differed significantly from conventional BP by the absences of inflammatory lesions and circulating autoantibodies targeting the BP180–NC16A epitope and the presence of autoantibodies targeting the mid-portion of BP180 (120-kDa ectodomain and LABD-97). However, those patients had no autoantibodies targeting the BP180 C-terminal domain, which could have suggested an MMP diagnosis. Sakai et al. (18) also had a patient with similar gliptin-associated BP. Mendoça et al. (15) reported a patient with mucous membrane involvement at diagnosis, including arytenoid edema with several ulcerated lesions covered with fibrin, raising the question of gliptin-induced MMP rather than BP.

Finally, seven cases reported in the French pharmacovigilance database as BP ADRs to gliptin were excluded from Béné et al.'s study (25) because they did not meet Kershenovich BP, and Vaillant BP criteria, suggesting that they might really have been MMP.

TABLE 3 | Evolutive characteristics of the suggestive-or-compatible challenge MMP patients who discontinued gliptin (dechallenge) vs. those who continued it (no dechallenge).[a]

Characteristic	Overall		Dechallenge		No dechallenge	
	n = 17	Missing	*n* = 11	Missing	*n* = 6	Missing
Weeks, median (range)						
Gliptin-onset-to-MMP-diagnosis interval	136 (4–588)	0	36 (4–232)	0	136 (4–588)	0
Time to first complete remission	8 (0–36)	7	8 (2–16)	3	18 (0–36)	4
Length of follow-up	40 (0–164)	0	32 (0–104)	0	78 (4–164)	0
Initial treatment	17	1	11	0	5	1
Dapsone	11		8 (73%)		3 (50%)	
Doxycyclin	6		4 (36%)		2 (33%)	
Cyclophosphamide	5		2 (18%)		3 (50%)	
Rituximab	2		2 (18%)		0	
At the first year of follow-up, patients, n (%)						
Relapses/flares						
Yes	4 (31%)	4	2[b] (22%)	2	2 (50%)	2
No	9 (69%)		7[c] (78%)		2 (50%)	
Complete remission						
Yes	9 (82%)	6	7 (88%)	3	2 (66%)	3
No	2 (18%)		1 (13%)		1 (33%)	
Deaths						
Yes	0	6	0	3	0	3
No	11 (100%)		(100%)		3 (100%)	

MMP, mucous membrane pemphigoid.

[a]*The dechallenge group stopped gliptin intake during the first year of follow-up; the no-dechallenge group was still taking gliptin at 1 year of follow-up.*

[b]*One relapsed before and one after stopping gliptin.*

[c]*One relapsed after 1 year of follow-up and a rechallenge.*

This retrospective, monocenter study on a historical cohort was limited by MMP rarity. However, because our Center recruits patients with autoimmune bullous diseases, our findings should provide a fairly accurate appreciation of this population. Its retrospective design often means that data collection was incomplete and, indeed, some patients immunological test results are missing. In addition, we did not compare diabetic MMP cases to diabetic controls and epitope mapping of autoantibody-targeted antigens was not done.

The potential of gliptins to induce MMP was not investigated previously. We identified 24 gliptin-treated diabetic MMP patients, representing 38% of all MMP diabetic patients, a rate similar to that of gliptin-triggered BP in diabetics (24). We evaluated chronological gliptin accountability in MMP induction case by case: it was **incompatible**, excluding gliptin's role, for 5 patients but **suggestive or compatible** for 17.

Vildagliptin was the most frequently incriminated gliptin for our 17 MMP diabetic patients, as for BP in the literature (Table S2 in Supplementary Material), but the highest intrinsic accountability scores were equally distributed among gliptins. It is worth noting that sitagliptin (and not vildagliptin) is the most prescribed in France, and the rest of Europe (66), suggesting that vildagliptin has a greater capacity to induce autoimmune bullous diseases.

The female/male ratio of these 17 MMP diabetics was higher than that of the general diabetic population and BP diabetics (1.1 vs. 0.7 vs. 0.65–0.83, respectively) but similar to that of our MMP controls (**Table 4**). MMP diabetics were younger than the general diabetic population (36) and BP diabetics tended to be older than our MMP controls. Median time to MMP onset was longer, with a wider range, than for gliptin-induced BP, which can be explained by the insidious evolution of mucous membrane lesions in MMP. The arbitrarily chosen time to distinguish **suggestive** (4 patients) from **compatible** (13 patients) chronology was ≤12 weeks; the 13 patients with **compatible** chronologies had intervals exceeding 36 weeks.

At MMP diagnosis, most of our 17 MMP diabetics did not have severe involvement. They differed significantly from MMP controls by their higher weights and their body mass indexes. Indeed, overweight and obesity is known to be a risk factor for type 2 diabetes. This difference was, therefore, expected from our population of type 2 diabetic MMP patients. They also had more frequent cutaneous involvement, less buccal involvement, and absence of DIF-detectable IgA deposits along the BMZ. The MMP outcomes of these 17 patients, during and at the end of the first year of follow-up, were the same as that for MMP controls. Indeed, gliptin-associated MMPs responded well to usual treatments after gliptin withdrawal. Intriguingly, the endocrinologists had discontinued gliptins for all the 11 patients because of insufficient diabetes control. Gliptin-triggering of MMP had never been suspected by dermatologists treating MMP patients.

Our immunological study results suggested that *in vivo*-fixed and circulating autoantibodies targeted multiple BMZ antigens/epitopes. IEM showed immune deposits in the lamina densa with/without the LL as in "classical MMP" in seven patients, four of them ELISA BP180–NC16A-positive. The three BP180–NC16A-negative ELISAs were immunoblot-positive

TABLE 4 | Characteristics and comparisons of suggestive-or-compatible challenge vs. never-gliptin-treated control MMP groups.

Characteristic	Suggestive-or-compatible challenge		Controls		*p*
	n = 17	Missing	*n* = 121	Missing	
Age, mean/median (range), years	69/71 (48–81)		66.4/66 (38–96)		0.46
Weight, mean/median (range), kg	87/80 (55–154)		72.6/73 (44–114)		0.02
BMI, mean/median (range), kg/m^2	32/29 (24–45)		26.1/25 (18–40)		0.01
Female/male, *n* (%); sex ratio	9 (53%)/8 (47%); 1.1	0	69 (57%)/52 (43%); 1.3	0	
Involved sites, mean/median (range), *n*	2.8/3 (2–5)		2.2/2 (1–5)		
MMP involvement, *n* (%)		0		2	
Isolated MM	3 (18%)		59 (50%)		
MM and cutaneous	14 (82%)		60 (50%)		
DIF, yes/no, *n* (%)					
IgA deposits	0	0	26 (22%)/94 (78%)	1	0.04
IgG deposits	14 (82%)/3 (18%)	0	89 (74%)/31 (26%)	1	
C3 deposits	14 (82%)/3 (18%)	0	85 (71%)/35 (29%)	1	
Direct IEM, *n* (%)					
LD ± LL	7 (87%)	9	62 (60%)	18	
Upper LL ± HD	1 (13%)		13 (13%)		
IIF on SSS, *n* (%)					
Roof	4 (27%)	2	22 (21%)	18	
Floor	0		2 (2%)		
Mixed	0		3 (3%)		
Negative	11 (73%)		76 (74%)		
ELISA, positive/negative, *n* (%)					
BP230	3 (20%)/13 (80%)	2	10 (13%)/68 (87%)	43	
BP180	7 (47%)/8 (53%)	2	43 (51%)/41 (49%)	37	
Involvement, yes/no, *n* (%)					
Cutaneous	14 (82%)/3 (18%)		60 (50%)/59 (50%)		0.02
Buccal	11 (65%)/6 (35%)	0	101 (89%)/12 (11%)	8	0.01
Laryngeal	6 (35%)/11 (65%)	0	34 (30%)/79 (70%)	8	
Genital and/or anal	8 (47%)/9 (53%)	0	35 (31%)/78 (69%)	8	
Conjunctival	2 (12%)/15 (88%)	0	28 (25%)/85 (75%)	8	0.36
Esophageal	0	0	6 (5%)/107 (95%)	8	
Severe	7 (41%)/10 (59%)	0	78 (67%)/39 (33%)	8	0.05
At 1 year of follow-up, yes/no, *n* (%)					
Complete remission	9 (82%)/2 (18%)	6	68 (56%)/53 (44%)	0	0.12
Relapses/flares	4 (33%)/8 (67%)	5	28 (23%)/93 (77%)	0	
Deaths	0/17 (100%)	0	2 (2%)/119 (98%)	0	

MMP, mucous membrane pemphigoid; BMI, body mass index; MM, mucous membrane; DIF, direct immunofluorescence; Ig, immunoglobulin; IEM, immunoelectron microscopy; LD, lamina densa; LL, lamina lucida; ±, with or without; HD, hemidesmosome; IIF, indirect immunofluorescence; SSS, salt-split skin; ELISA, enzyme-linked immunosorbent assay.

on amniotic membrane extract, detecting each with band(s) at 180, 120, or 180 and 120 kDa. These serological findings along with IEM observations showed that gliptin-associated MMP autoantibodies could target the NC16A epitope, the mid-portion and the C-terminal domain of BP180. IEM of patient 8's biopsy showed deposits exclusively at the upper LL, his BP180–NC16A ELISA was negative and immunoblotting detected a 200-kDa band consistent with the β4 chain of α6β4 integrin. Laminin 332 MMP, MM-EBA, and MM-LABD were excluded for all gliptin-associated MMPs.

Using three accountability methods, WHO–UMC's criteria, Naranjo's score (most used worldwide), and Begaud's method (most used in France and Europe), we assessed gliptin imputability in MMP induction. With the WHO–UMC accountability criteria, gliptin triggering of MMP was **probable** for 17 patients and **unlikely** for 7. With Naranjo's system, ADRs were considered **probable for** only 1 patient, **possible** for 16, and **doubtful** for 7 patients. Last, according to Begaud's method, with scores ranging from I0 to I6, only 5 patients (I4 for three, I3 for two) were given **high accountability** scores, 12 had low **accountability** (I2 for eight, I1 for four), and 7 were scored I0, meaning chronologically **incompatible** or **undetermined** challenge.

The results of this study demonstrated that gliptins are probably responsible for some MMPs. Hence, all doctors prescribing gliptins must be made aware of this potential toxicity. The practical consequence of that finding is that, as soon as a positive accountability score is established, by precaution, gliptins, which can be easily switched in the case of inefficacy or ADR, should be replaced by another antidiabetic drug. Importantly, all such cases must be reported as possible ADRs to a pharmacovigilance center.

Large case–non-case comparative studies need to be performed to confirm or refute MMP induction by gliptins and better understand their pathogenic mechanism. Target-epitope mapping might help to determine whether a particular immune response occurs in drug-induced MMP.

TABLE 5 | Gliptin accountability scores for suggestive-or-compatible MMP-induction patients.

Challenge	1st gliptin dose to MMP onset (wk)	Challenge[a]	Dechallenge		Rechallenge R0/R+/R−	Begaud's accountability scores[b]			Naranjo's score[c]	
gliptin patient			Yes/no	Outcome		C1–C3	S1–S3	I1–16	0–13	ADR
Dechallenge										
Saxagliptin										
1	4	Suggestive	Yes	Suggestive	R0	C3	S1	I4	3	Possible
Vildagliptin										
2	4	Suggestive	Yes	Suggestive	R0	C3	S1	I4	3	Possible
3	4	Suggestive	Yes	Inconclusive	R0	C2	S1	I2	2	Possible
4	12	Suggestive	Yes	Inconclusive	R0	C2	S1	I2	2	Possible
5	36	Compatible	Yes	Suggestive	R0	C2	S1	I2	3	Possible
6	36	Compatible	Yes	Not suggestive	R0	C1	S1	I1	2	Possible
7	144	Compatible	Yes	Inconclusive	R0	C1	S2	I2	2	Possible
Sitagliptin										
8	104	Compatible	Yes	Suggestive	R+	C3	S1	I4	6	Probable
9	136	Compatible	Yes	Suggestive	R0	C2	S1	I2	3	Possible
10	144	Compatible	Yes	Inconclusive	R0	C1	S1	I1	2	Possible
11	232	Compatible	Yes	Suggestive	R0	C2	S2	I3	3	Possible
No dechallenge										
Vildagliptin										
12	72	Compatible	No	Suggestive	R0	C2	S1	I2	2	Possible
13	148	Compatible	No	Inconclusive	R0	C1	S1	I1	2	Possible
14	236	Compatible	No	Inconclusive	R0	C1	S2	I2	2	Possible
15	244	Compatible	No	Not suggestive	R0	C1	S2	I2	2	Possible
16	588	Compatible	No	Not suggestive	R0	C1	S1	I1	2	Possible
Sitagliptin										
17	144	Compatible	No	Inconclusive	R0	C2	S2	I3	2	Possible

MMP, mucous membrane pemphigoid; wk, week; R0, no rechallenge; R+, positive rechallenge; R−, negative rechallenge; ADR, adverse drug reaction.

[a]*Suggestive, time to onset ≤12 weeks; compatible, time to onset >12 weeks.*

[b]*Chronological score: C1, doubtful; C2, plausible; C3, likely. Symptomatological scoring: S1, doubtful; S2, plausible; S3, likely. Intrinsic accountability scoring [combining chronological (C) and symptomatological (S) scores]: I1 (C1S1), I2 (C1S2 or C2S1), I3 (C2S2), I4 (C1S3 or C3S1), I5 (C2S3 or C3S2), and I6 (C3S3) (32).*

[c]*Narango's score: >9, definite ADR; 5–8, probable ADR; 1–4, possible ADR; 0, doubtful ADR (34).*

ETHICS STATEMENT

This study was approved by our local Institutional Review Board (IRB 00003835 no. 2013/39NI). All subjects gave written informed consent in accordance with the Declaration of Helsinki.

AUTHOR CONTRIBUTIONS

OG, VS, FC, and CP-S conceived and designed the study. MA, GB, SI-H-O, CB, PS, and CP-S collected clinical data. FA and SM-G conducted the immunological studies. OG, VS, BM, and CP-S organized the database. VS and OG conducted the statistical analyses. OG wrote the first draft of the manuscript. OG and CP-S rewrote sections of the manuscript. All authors contributed to manuscript revision, and read and approved the submitted version.

ACKNOWLEDGMENTS

We thank physicians who referred patients to our Referral Center for autoimmune bullous diseases and the Center's physicians who assured multidisciplinary patient management (Drs. Francis Pascal, Isaac Soued, and Serge Doan); Mrs. Nicole Lièvre and Mr. Michel Heller for their technical assistance; and Janet Jacobson for editorial assistance.

SUPPLEMENTARY MATERIAL

The Supplementary Material for this article can be found online at https://www.frontiersin.org/articles/10.3389/fimmu.2018.01030/full#supplementary-material.

REFERENCES

1. Bernard P, Vaillant L, Labeille B, Bedane C, Arbeille B, Denoeux JP, et al. Incidence and distribution of subepidermal autoimmune bullous skin diseases in three French regions. Bullous Diseases French Study Group. *Arch Dermatol* (1995) 131:48–52. doi:10.1001/archderm.1995.01690130050009
2. Chan LS, Ahmed AR, Anhalt GJ, Bernauer W, Cooper KD, Elder MJ, et al. The first international consensus on mucous membrane pemphigoid: definition, diagnostic criteria, pathogenic factors, medical treatment, and prognostic indicators. *Arch Dermatol* (2002) 138:370–9. doi:10.1001/archderm.138.3.370
3. Vaillant L, Bernard P, Joly P, Prost C, Labeille B, Bedane C, et al. Evaluation of clinical criteria for diagnosis of bullous pemphigoid. French Bullous Study Group. *Arch Dermatol* (1998) 134:1075–80. doi:10.1001/archderm.134.9.1075
4. Schmidt E, Zillikens D. Pemphigoid diseases. *Lancet* (2013) 381:320–32. doi:10.1016/S0140-6736(12)61140-4
5. Murakami H, Nishioka S, Setterfield J, Bhogal BS, Black MM, Zillikens D, et al. Analysis of antigens targeted by circulating IgG and IgA autoantibodies

in 50 patients with cicatricial pemphigoid. *J Dermatol Sci* (1998) 17:39–44. doi:10.1016/S0923-1811(97)00067-4
6. Bastuji-Garin S, Joly P, Picard-Dahan C, Bernard P, Vaillant L, Pauwels C, et al. Drugs associated with bullous pemphigoid. A case-control study. *Arch Dermatol* (1996) 132:272–6. doi:10.1001/archderm.1996.03890270044006
7. Bastuji-Garin S, Joly P, Lemordant P, Sparsa A, Bedane C, Delaporte E, et al. Risk factors for bullous pemphigoid in the elderly: a prospective case-control study. *J Invest Dermatol* (2011) 131:637–43. doi:10.1038/jid.2010.301
8. Stavropoulos PG, Soura E, Antoniou C. Drug-induced pemphigoid: a review of the literature. *J Eur Acad Dermatol Venereol* (2014) 28:1133–40. doi:10.1111/jdv.12366
9. Pasmatzi E, Monastirli A, Habeos J, Georgiou S, Tsambaos D. Dipeptidyl peptidase-4 inhibitors cause bullous pemphigoid in diabetic patients: report of two cases. *Diabetes Care* (2011) 34:e133. doi:10.2337/dc11-0804
10. Skandalis K, Spirova M, Gaitanis G, Tsartsarakis A, Bassukas ID. Drug-induced bullous pemphigoid in diabetes mellitus patients receiving dipeptidyl peptidase-IV inhibitors plus metformin: bullous pemphigoid and dipeptidyl peptidase-IV inhibitors. *J Eur Acad Dermatol Venereol* (2012) 26:249–53. doi:10.1111/j.1468-3083.2011.04062.x
11. Aouidad I, Fite C, Marinho E, Deschamps L, Crickx B, Descamps V. A case report of bullous pemphigoid induced by dipeptidyl peptidase-4 inhibitors. *JAMA Dermatol* (2013) 149:243–5. doi:10.1001/jamadermatol.2013.1073
12. Attaway A, Mersfelder TL, Vaishnav S, Baker JK. Bullous pemphigoid associated with dipeptidyl peptidase IV inhibitors. A case report and review of literature. *J Dermatol Case Rep* (2014) 31:24–8. doi:10.3315/jdcr.2014.1166
13. Béné J, Jacobsoone A, Coupe P, Auffret M, Babai S, Hillaire-Buys D, et al. Bullous pemphigoid induced by vildagliptin: a report of three cases. *Fundam Clin Pharmacol* (2015) 29:112–4. doi:10.1111/fcp.12083
14. Haber R, Fayad AM, Stephan F, Obeid G, Tomb R. Bullous pemphigoid associated with linagliptin treatment. *JAMA Dermatol* (2016) 152:224. doi:10.1001/jamadermatol.2015.2939
15. Mendonça FMI, Martín-Gutierrez FJ, Ríos-Martín JJ, Camacho-Martinez F. Three cases of bullous pemphigoid associated with dipeptidyl peptidase-4 inhibitors – one due to linagliptin. *Dermatology* (2016) 232:249–53. doi:10.1159/000443330
16. García M, Aranburu MA, Palacios-Zabalza I, Lertxundi U, Aguirre C. Dipeptidyl peptidase-IV inhibitors induced bullous pemphigoid: a case report and analysis of cases reported in the European pharmacovigilance database. *J Clin Pharm Ther* (2016) 41:368–70. doi:10.1111/jcpt.12397
17. Keseroglu HO, Taş-Aygar G, Gönül M, Gököz O, Ersoy-Evans S. A case of bullous pemphigoid induced by vildagliptin. *Cutan Ocul Toxicol* (2017) 36:201–2. doi:10.1080/15569527.2016.1211670
18. Sakai A, Shimomura Y, Ansai O, Saito Y, Tomii K, Tsuchida Y, et al. Linagliptin-associated bullous pemphigoid that was most likely caused by IgG autoantibodies against the midportion of BP180. *Br J Dermatol* (2017) 176:541–3. doi:10.1111/bjd.15111
19. Fania L, Salemme A, Provini A, Pagnanelli G, Collina MC, Abeni D, et al. Detection and characterization of IgG, IgE and IgA autoantibodies in patients with bullous pemphigoid associated with dipeptidyl peptidase-IV inhibitors. *J Am Acad Dermatol* (2018) 78:592–5. doi:10.1016/j.jaad.2017.09.051
20. Schaffer C, Buclin T, Jornayvaz FR, Cazzaniga S, Borradori L, Gilliet M, et al. Use of dipeptidyl-peptidase IV inhibitors and bullous pemphigoid. *Dermatology* (2017) 233(5):401–3. doi:10.1159/000480498
21. Yoshiji S, Murakami T, Harashima SI, Ko R, Kashima R, Yabe D, et al. Bullous pemphigoid associated with dipeptidyl peptidase-4 inhibitors: report of five cases. *J Diabetes Investig* (2018) 9:445–7. doi:10.1111/jdi.12695
22. Harada M, Yoneda A, Haruyama S, Yabuki K, Honma Y, Hiura M, et al. Bullous pemphigoid associated with the dipeptidyl peptidase-4 inhibitor sitagliptin in a patient with liver cirrhosis complicated with rapidly progressive hepatocellular carcinoma. *Intern Med* (2017) 56:2471–4. doi:10.2169/internalmedicine.8703-16
23. Izumi K, Nishie W, Mai Y, Wada M, Natsuga K, Ujiie H, et al. Autoantibody profile differentiates between inflammatory and noninflammatory bullous pemphigoid. *J Invest Dermatol* (2016) 136:2201–10. doi:10.1016/j.jid.2016.06.622
24. Benzaquen M, Borradori L, Berbis P, Cazzaniga S, Valero R, Richard MA, et al. Dipeptidyl peptidase-IV inhibitors, a risk factor for bullous pemphigoid. Retrospective multicenter case–control study in France and Switzerland. *J Am Acad Dermatol* (2017). doi:10.1016/j.jaad.2017.12.038
25. Béné J, Moulis G, Bennani I, Auffret M, Coupe P, Babai S, et al. Bullous pemphigoid and dipeptidyl peptidase IV-inhibitors: a case/non-case study in the French Pharmacovigilance Database. *Br J Dermatol* (2016) 175:296–301. doi:10.1111/bjd.14601
26. Varpuluoma O, Försti AK, Jokelainen K, Turpeinen M, Timonen M, Huilaja L, et al. Vildagliptin significantly increases the risk of bullous pemphigoid: a Finnish Nationwide Registry Study. *J Invest Dermatol* (2018). doi:10.1016/j.jid.2018.01.027
27. Tauber J, Sainz de la Maza M, Foster CS. Systemic chemotherapy for ocular cicatricial pemphigoid. *Cornea* (1991) 10:185–95. doi:10.1097/00003226-199105000-00001
28. Setterfield J, Shirlaw PJ, Kerr-Muir M, Neill S, Bhogal BS, Morgan P, et al. Mucous membrane pemphigoid: a dual circulating antibody response with IgG and IgA signifies a more severe and persistent disease. *Br J Dermatol* (1998) 138:602–10. doi:10.1046/j.1365-2133.1998.02168.x
29. Le Roux-Villet C, Prost-Squarcioni C, Alexandre M, Caux F, Pascal F, Doan S, et al. Rituximab for patients with refractory mucous membrane pemphigoid. *Arch Dermatol* (2011) 147:843–9. doi:10.1001/archdermatol.2011.54
30. Grootenboer-Mignot S, Descamps V, Picard-Dahan C, Nicaise-Roland P, Prost-Squarcioni C, Leroux-Villet C, et al. Place of human amniotic membrane immunoblotting in the diagnosis of autoimmune bullous dermatoses. *Br J Dermatol* (2010) 162:743–50. doi:10.1111/j.1365-2133.2009.09566.x
31. Murrell DF, Marinovic B, Caux F, Prost C, Ahmed R, Wozniak K, et al. Definitions and outcome measures for mucous membrane pemphigoid: recommendations of an international panel of experts. *J Am Acad Dermatol* (2015) 72:168–74. doi:10.1016/j.jaad.2014.08.024
32. Miremont-Salamé G, Théophile H, Haramburu F, Bégaud B. Causality assessment in pharmacovigilance: the French method and its successive updates. *Thérapie* (2016) 71:179–86. doi:10.1016/j.therap.2016.02.010
33. Arimone Y, Bidault I, Dutertre J-P, Gérardin M, Guy C, Haramburu F, et al. Réactualisation de la méthode française d'imputabilité des effets indésirables des médicaments. *Thérapie* (2011) 66:517–25. doi:10.2515/therapie/2011073
34. Naranjo CA, Busto U, Sellers EM, Sandor P, Ruiz I, Roberts EA, et al. A method for estimating the probability of adverse drug reactions. *Clin Pharmacol Ther* (1981) 30:239–45. doi:10.1038/clpt.1981.154
35. *The Use of the WHO-UMC System for Standardised Case Causality Assessment*. (2017). Available from: https://www.who-umc.org/media/2768/standardised-case-causality-assessment.pdf (Accessed: June 25, 2017).
36. Ricci P, Blotière PO, Weill A, Simon D, Tuppin P, Ricordeau P, et al. Diabète traité: quelles évolutions entre 2000 et 2009 en France. *Bull Epidemiol Hebd* (2010) 42–43:425–31.
37. Prost C, Labeille B, Chaussade V, Guillaume JC, Martin N, Dubertret L. Immunoelectron microscopy in subepidermal autoimmune bullous diseases: a prospective study of IgG and C3 bound in vivo in 32 patients. *J Invest Dermatol* (1987) 89:567–73. doi:10.1111/1523-1747.ep12461226
38. Balding SD, Prost C, Diaz LA, Bernard P, Bedane C, Aberdam D, et al. Cicatricial pemphigoid autoantibodies react with multiple sites on the BP180 extracellular domain. *J Invest Dermatol* (1996) 106:141–6. doi:10.1111/1523-1747.ep12329728
39. Bédane C, McMillan JR, Balding SD, Bernard P, Prost C, Bonnetblanc JM, et al. Bullous pemphigoid and cicatricial pemphigoid autoantibodies react with ultrastructurally separable epitopes on the BP180 ectodomain: evidence that BP180 spans the lamina lucida. *J Invest Dermatol* (1997) 108:901–7. doi:10.1111/1523-1747.ep12292701
40. Giudice GJ, Emery DJ, Zelickson BD, Anhalt GJ, Liu Z, Diaz LA. Bullous pemphigoid and herpes gestationis autoantibodies recognize a common non-collagenous site on the BP180 ectodomain. *J Immunol* (1993) 151:5742–50.
41. Matsumura K, Amagai M, Nishikawa T, Hashimoto T. The majority of bullous pemphigoid and herpes gestationis serum samples react with the NC16a domain of the 180-kDa bullous pemphigoid antigen. *Arch Dermatol Res* (1996) 288:507–9. doi:10.1007/BF02505245
42. Kobayashi M, Amagai M, Kuroda-Kinoshita K, Hashimoto T, Shirakata Y, Hashimoto K, et al. BP180 ELISA using bacterial recombinant NC16A protein as a diagnostic and monitoring tool for bullous pemphigoid. *J Dermatol Sci* (2002) 30:224–32. doi:10.1016/S0923-1811(02)00109-3
43. Perriard J, Jaunin F, Favre B, Büdinger L, Hertl M, Saurat JH, et al. IgG autoantibodies from bullous pemphigoid (BP) patients bind antigenic sites on both

the extracellular and the intracellular domains of the BP antigen 180. *J Invest Dermatol* (1999) 112:141–7. doi:10.1046/j.1523-1747.1999.00497.x
44. Hofmann S, Thoma-Uszynski S, Hunziker T, Bernard P, Koebnick C, Stauber A, et al. Severity and phenotype of bullous pemphigoid relate to autoantibody profile against the NH_2- and COOH-terminal regions of the BP180 ectodomain. *J Invest Dermatol* (2002) 119:1065–73. doi:10.1046/j.1523-1747.2002.19529.x
45. Mariotti F, Grosso F, Terracina M, Ruffelli M, Cordiali-Fei P, Sera F, et al. Development of a novel ELISA system for detection of anti-BP180 IgG and characterization of autoantibody profile in bullous pemphigoid patients. *Br J Dermatol* (2004) 151:1004–10. doi:10.1111/j.1365-2133.2004.06245.x
46. Di Zenzo G, Grosso F, Terracina M, Mariotti F, De Pità O, Owaribe K, et al. Characterization of the anti-BP180 autoantibody reactivity profile and epitope mapping in bullous pemphigoid patients. *J Invest Dermatol* (2004) 122:103–10. doi:10.1046/j.0022-202X.2003.22126.x
47. Thoma-Uszynski S, Uter W, Schwietzke S, Schuler G, Borradori L, Hertl M. Autoreactive T and B cells from bullous pemphigoid (BP) patients recognize epitopes clustered in distinct regions of BP180 and BP230. *J Immunol* (2006) 176:2015–23. doi:10.4049/jimmunol.176.3.2015
48. Di Zenzo G, Thoma-Uszynski S, Calabresi V, Fontao L, Hofmann SC, Lacour JP, et al. Demonstration of epitope-spreading phenomena in bullous pemphigoid: results of a prospective multicenter study. *J Invest Dermatol* (2011) 131:2271–80. doi:10.1038/jid.2011.180
49. Fairley JA, Bream M, Fullenkamp C, Syrbu S, Chen M, Messingham KN. Missing the target: characterization of bullous pemphigoid patients who are negative using the BP180 enzyme-linked immunosorbent assay. *J Am Acad Dermatol* (2013) 68:395–403. doi:10.1016/j.jaad.2012.09.012
50. Chanal J, Ingen-Housz-Oro S, Ortonne N, Duong T-A, Thomas M, Valeyrie-Allanore L, et al. Linear IgA bullous dermatosis: comparison between the drug-induced and spontaneous forms. *Br J Dermatol* (2013) 169:1041–8. doi:10.1111/bjd.12488
51. Vassileva S. Drug-induced pemphigoid: bullous and cicatricial. *Clin Dermatol* (1998) 16:379–87. doi:10.1016/S0738-081X(98)00008-X
52. Inzucchi SE, Bergenstal RM, Buse JB, Diamant M, Ferrannini E, Nauck M, et al. Management of hyperglycemia in type 2 diabetes, 2015: a patient-centered approach: update to a position statement of the American Diabetes Association and the European Association for the Study of Diabetes. *Diabetes Care* (2015) 38:140–9. doi:10.2337/dc14-2441
53. Thrasher J. Pharmacologic management of type 2 diabetes mellitus: available therapies. *Am J Cardiol* (2017) 120:S4–16. doi:10.1016/j.amjcard.2017.05.009
54. Mari A, Sallas WM, He YL, Watson C, Ligueros-Saylan M, Dunning BE, et al. Vildagliptin, a dipeptidyl peptidase-IV inhibitor, improves model-assessed β-cell function in patients with type 2 diabetes. *J Clin Endocrinol Metab* (2005) 90:4888–94. doi:10.1210/jc.2004-2460
55. Vella A, Bock G, Giesler PD, Burton DB, Serra DB, Saylan ML, et al. Effects of dipeptidyl peptidase-4 inhibition on gastrointestinal function, meal appearance, and glucose metabolism in type 2 diabetes. *Diabetes* (2007) 56:1475–80. doi:10.2337/db07-0136
56. Ali S, Fonseca V. Saxagliptin overview: special focus on safety and adverse effects. *Expert Opin Drug Saf* (2013) 12:103–9. doi:10.1517/14740338.2013.741584
57. Forssmann U, Stoetzer C, Stephan M, Kruschinski C, Skripuletz T, Schade J, et al. Inhibition of CD26/dipeptidyl peptidase IV enhances CCL11/eotaxin-mediated recruitment of eosinophils *in vivo*. *J Immunol* (2008) 181:1120–7. doi:10.4049/jimmunol.181.2.1120
58. Reinhold D, Bank U, Bühling F, Lendeckel U, Faust J, Neubert K, et al. Inhibitors of dipeptidyl peptidase IV induce secretion of transforming growth factor-beta 1 in PWM-stimulated PBMC and T cells. *Immunology* (1997) 91:354–60. doi:10.1046/j.1365-2567.1997.d01-2258.x
59. Thielitz A, Reinhold D, Vetter R, Bank U, Helmuth M, Hartig R, et al. Inhibitors of dipeptidyl peptidase IV and aminopeptidase N target major pathogenetic steps in acne initiation. *J Invest Dermatol* (2007) 127:1042–51. doi:10.1038/sj.jid.5700439
60. Thielitz A, Vetter RW, Schultze B, Wrenger S, Simeoni L, Ansorge S, et al. Inhibitors of dipeptidyl peptidase IV-like activity mediate antifibrotic effects in normal and keloid-derived skin fibroblasts. *J Invest Dermatol* (2008) 128:855–66. doi:10.1038/sj.jid.5701104
61. Gonzalez-Gronow M, Kaczowka S, Gawdi G, Pizzo SV. Dipeptidyl peptidase IV (DPP IV/CD26) is a cell-surface plasminogen receptor. *Front Biosci* (2008) 13:1610–8. doi:10.2741/2785
62. Hofmann SC, Voith U, Schönau V, Sorokin L, Bruckner-Tuderman L, Franzke CW. Plasmin plays a role in the in vitro generation of the linear IgA dermatosis antigen LABD97. *J Invest Dermatol* (2009) 129:1730–9. doi:10.1038/jid.2008.424
63. Günther C, Wozel G, Meurer M, Pfeiffer C. Up-regulation of CCL11 and CCL26 is associated with activated eosinophils in bullous pemphigoid. *Clin Exp Immunol* (2011) 166:145–53. doi:10.1111/j.1365-2249.2011.04464.x
64. Liu Z, Li N, Diaz LA, Shipley M, Senior RM, Werb Z. Synergy between a plasminogen cascade and MMP-9 in autoimmune disease. *J Clin Invest* (2005) 115:879–87. doi:10.1172/JCI23977
65. Caproni M, Calzolari A, Salvatore E, Giomi B, Volpi W, D'Agata A, et al. Cytokine profile and supposed contribution to scarring in cicatricial pemphigoid. *J Oral Pathol Med* (2003) 32:34–40. doi:10.1034/j.1600-0714.2003.00028.x
66. IMS Health. *Launch Excellence in the Diabetes Market*. London: IMS Health (2012). Available from: https://www.yumpu.com/en/document/view/9195817/launch-excellence-in-the-diabetes-market-lessons-from-ims-health

Conflict of Interest Statement: The authors declare that the research was conducted in the absence of any commercial or financial relationships that could be construed as a potential conflict of interest.

frontiers in Immunology

CASE REPORT
published: 07 May 2018
doi: 10.3389/fimmu.2018.00994

Clinical and Immunological Study of 30 Cases With Both IgG and IgA Anti-Keratinocyte Cell Surface Autoantibodies Toward the Definition of Intercellular IgG/IgA Dermatosis

Takashi Hashimoto[1,2], Kwesi Teye[3], Koji Hashimoto[4], Katarzyna Wozniak[5], Daisuke Ueo[6], Sakuhei Fujiwara[7], Kazuhiro Inafuku[8], Yorihisa Kotobuki[9], Ines Lakos Jukic[10], Branka Marinović[10], Anna Bruckner[11], Daisuke Tsuruta[1], Tamihiro Kawakami[12] and Norito Ishii[13]*

[1] Department of Dermatology, Osaka City University Graduate School of Medicine, Osaka, Japan, [2] Kurume University School of Medicine, Kurume, Japan, [3] Kurume University Institute of Cutaneous Cell Biology, Kurume, Japan, [4] Department of Life Sciences, Graduate School of Arts and Sciences, University of Tokyo, Tokyo, Japan, [5] Department of Dermatology and Immunodermatology, Medical University of Warsaw, Warsaw, Poland, [6] Ueo Dermatology Clinic, Saiki, Japan, [7] Department of Dermatology, Faculty of Medicine, Oita University, Yufu, Japan, [8] Department of Dermatology, Kimitsu Chuo Hospital, Kimitsu, Japan, [9] Department of Dermatology, Osaka University Graduate School of Medicine, Suita, Japan, [10] University Hospital Centre Zagreb, Department of Dermatology and Venereology, School of Medicine, University of Zagreb, Zagreb, Croatia, [11] Pediatric Dermatology, University of Colorado School of Medicine, Children's Hospital Colorado, Denver, CO, United States, [12] Department of Dermatology, St. Marriana Medical University, Kawasaki, Japan, [13] Department of Dermatology, Kurume University School of Medicine, Fukuoka, Japan

OPEN ACCESS

Edited by:
Falk Nimmerjahn, Friedrich-Alexander-Universität Erlangen-Nürnberg, Germany

Reviewed by:
Frank Antonicelli, Université de Reims Champagne Ardenne, France
Marian Dmochowski, Poznan University of Medical Sciences, Poland

***Correspondence:**
Takashi Hashimoto
hashyt@gmail.com

Specialty section:
This article was submitted to Immunological Tolerance and Regulation, a section of the journal Frontiers in Immunology

Received: *13 December 2017*
Accepted: *20 April 2018*
Published: *07 May 2018*

Citation:
Hashimoto T, Teye K, Hashimoto K, Wozniak K, Ueo D, Fujiwara S, Inafuku K, Kotobuki Y, Jukic IL, Marinović B, Bruckner A, Tsuruta D, Kawakami T and Ishii N (2018) Clinical and Immunological Study of 30 Cases With Both IgG and IgA Anti-Keratinocyte Cell Surface Autoantibodies Toward the Definition of Intercellular IgG/IgA Dermatosis. Front. Immunol. 9:994. doi: 10.3389/fimmu.2018.00994

Several sporadic cases, in which direct and indirect immunofluorescence studies simultaneously detected IgG and IgA autoantibodies to keratinocyte cell surfaces, have been reported mainly under the name of IgG/IgA pemphigus. However, there have been no systematic studies for this condition. In this study, we collected 30 cases of this condition from our cohort of more than 5,000 autoimmune bullous disease cases, which were consulted for our diagnostic methods from other institutes, and summarized their clinical and immunological findings. Clinically, there was no male–female prevalence, mean age of disease onset was 55.6 years, and mean duration before this condition was suspected was 18 months. The patients showed clinically bullous and pustular skin lesions preferentially on the trunk and extremities, and histopathologically intraepidermal pustules and blisters with infiltration of neutrophils and eosinophils. Immunologically, ELISAs frequently detected IgG and IgA autoantibodies to both desmogleins and desmocollins. From the characteristic clinical, histopathological, and immunological features, which are considerably different from those in classical IgG types of pemphigus, we propose this disease as a new disease entity with preferential name of intercellular IgG/IgA dermatosis (IGAD). This was the largest study of IGAD to date.

Keywords: autoimmune bullous diseases, desmocollin, desmoglein, ELISA, intercellular IgG/IgA dermatosis

INTRODUCTION

Autoimmune bullous disease (AIBD) is divided into pemphigus group with autoantibodies to keratinocyte cell surfaces (CSs) and pemphigoid group with autoantibodies to epidermal basement membrane zone (BMZ) (1, 2). Two representative classical IgG types of pemphigus are pemphigus vulgaris (PV) and pemphigus foliaceus (PF), which react with desmoglein 3 (Dsg3) and Dsg1,

respectively, although there are many other forms of pemphigus (3, 4). Among them, cases with anti-CS antibodies exclusively of IgA class had been called as IgA pemphigus (5–8), for which we proposed intercellular IgA dermatosis (IAD) as a preferable name (5, 7, 8).

IgG/IgA pemphigus is the name given to an atypical form of pemphigus characterized by *in vivo* bound and/or circulating anti-keratinocyte CS antibodies of both IgG and IgA classes (1). The results in approximately 20 reports indicated that IgG/IgA pemphigus is an atypical form of pemphigus with heterogeneous clinical and histopathological features (9–30). However, because this condition is extremely rare, there is no systematic study and disease entity of this condition has not been established. At Kurume University, we have examined more than 5,000 cases of various AIBDs, which were consulted at other institutes for our diagnostic studies (1, 31). Therefore, in this study, we attempted to determine the characteristic clinical, histopathological, and immunological features of all patients with both IgG and IgA anti-keratinocyte CS antibodies as the first step to establish this disease entity.

In this retrospective study, we selected 30 cases with IgG and IgA anti-CS antibodies from our AIBD cohort, and characterized them clinically, histopathologically, and immunologically. Considerably distinct features found in these cases indicated this condition as a new disease entity, and we propose the term "intercellular IgG/IgA dermatosis (IGAD)" to this disorder, following the designation of IAD.

MATERIALS AND METHODS

This study was performed following Declaration of Helsinki and guidelines of local ethics committees of Kurume University School of Medicine. Informed consents were provided by all patients and normal individuals.

Cases and Sera

In this study, we used our AIBD cohort of 5,402 cases. Information and sera for these cases were sent to us from other institutes in either Japan or other countries between 1996 and 2015. Information of clinical and histopathological findings and direct immunofluorescence (IF) was obtained from consultation letters.

Various Immunological Methods

IF Studies

Direct IF for IgG, IgA, IgM, and C3 using skin biopsies was performed mainly at other institutes. Indirect IF studies of normal human skin and monkey esophagus for both IgG and IgA antibodies were performed by standard method. In cases with autoimmune reactivity with epidermal BMZ, indirect IF of 1 M NaCl-split normal human skin for IgG and IgA antibodies were also performed (32).

Immunoblotting Studies

Immunoblotting of normal human epidermal extract was performed as described previously (33, 34). In cases with reactivity with BMZ, we also performed IB analyses using BP180 NC16a domain recombinant protein (RP) (35), BP180 C-terminal domain RP (36), concentrated culture supernatant of HaCaT cells (37), normal human dermal extract (38), and purified human laminin-332 (39) for both IgG and/or IgA antibodies.

ELISA Studies

Commercially available IgG ELISAs of Dsg1 and Dsg3 (cutoff: <index 12) (MESACUP, MBL, Nagoya, Japan) (40) were conducted according to the manufacturer's instruction. Using the same ELISA kits, IgA antibodies to Dsg1 and Dsg3 (cutoff: <OD 0.15) were also examined (41). In addition, ELISAs of mammalian RPs of human desmocollin 1 (Dsc1)-Dsc3 were performed for both IgG antibodies (42) and IgA antibodies (43). Cutoff OD values were 0.2 for Dsc1, 0.07 for Dsc2, and 0.12 for Dsc3 for IgG antibodies, and 0.123 for Dsc1, 0.048 for Dsc2, and 0.074 for Dsc3 for IgA antibodies. Furthermore, in cases with reactivity with BMZ, we performed IgG ELISAs of BP180 NC16a domain RP (cutoff: <index 15) (44), BP230 RPs (cutoff values: <index 9) (45), and type VII collagen RP (MBL) (46). OD at 490 nm was measured by ELISA reader.

COS-7 Cell cDNA Transfection Method

COS-7 cell cDNA transfection method using cDNAs of human Dsc1–Dsc3 was performed as described previously (47).

Statistical Analyses

We statistically analyzed correlations between the results in Dsg and Dsc ELISAs and clinical parameters. Differences among qualitative results were compared using the chi-square test. Differences among quantitative parameters between groups were assessed using the Mann–Whitney *U* test. p Values less than 0.05 were considered significant.

RESULTS

Diagnoses

In this study, we suspected the diagnosis of IGAD for 30 cases, which showed simultaneous IgG and IgA immunoreactivity with keratinocyte CS antigens in direct IF and various serological studies (whole clinical and immunological data are shown in Tables S1 and S2 in Supplementary Material, respectively). In addition, four cases showed IgG and/or IgA anti-BMZ immunoreactivity by IF and/or molecular studies.

Clinical diagnosis in the consultation letters for the 30 cases included IGAD (12 cases), IAD (9 cases), and other AIBDs (7 cases), while no clinical diagnosis was given in 2 cases (Table S3A in Supplementary Material).

Regarding the diagnoses after the characterization, 26 IGAD cases had sole IGAD, while bullous pemphigoid, linear IgA bullous dermatosis, and linear IgA/IgG bullous dermatosis were concomitant in 1, 1, and 2 cases, respectively (Table S3B in Supplementary Material). In addition, one case each was suggested to be named as IgG/IgA PF and IgG/IgA PV.

Because of the large cohort size and long surveillance time, most of the clinical, histopathological, and immunological results were not obtained from all cases. Therefore, we summarize only available results for each parameter in the following sections.

Detailed Reports for Six New IGAD Cases

Clinical and histopathological findings and disease courses for six patients are described in Supplementary data (cases 17, 22, 23, 25, 27, and 29 in Tables S1 and S2 in Supplementary Material), as well as corresponding figures (Figures S1–S6 in Supplementary Material). Clinical, histopathological, and IF features in representative IGAD cases are also depicted in **Figure 1**.

Clinical Findings in 30 IGAD Cases

Backgrounds of the Cases

The 30 IGAD cases included 18 Japanese, 6 European, 3 US, 2 Indian, and 1 Australian. There were 15 males and 13 females, with 2 cases without information of gender. Mean ages of 30 cases were 55.6 years (53.4 years for males and 57.8 years for females). The durations between the disease onset and the consultation to us for 21 cases were from 2 weeks to 10 years (mean 18 months).

Before the cases visited the practitioners, who consulted us, one each case was treated with systemic steroid, antihistamine, combination of systemic steroid and antihistamine, and minocycline. Administration of vancomycin was not reported.

Underlying diseases included six malignant tumors, i.e., two cases of lung cancer and one case each of uterus carcinoma, breast carcinoma, gallbladder carcinoma, and malignant lymphoma. In addition, one case each had diabetes mellitus, IgA nephropathy, myasthenia gravis, Sweet's syndrome, Sjogren's syndrome, and PV.

Clinical Manifestations

Involved sites available from consultation letters for the 30 IGAD cases were the whole body (2 cases), the trunk (19 cases), the extremities (17 cases), the intertriginous areas (4 cases), and the head/face (6 cases) (**Figure 1**; Table S1 in Supplementary Material). Mucosal lesions were found in oral mucosae (11 cases) and conjunctiva (2 cases), with 1 case each with genital, nasal, and esophageal mucosae.

Regarding clinical manifestations, 19 cases showed blister formation with vesicles (5 cases), tense bullae (2 cases) and flaccid bullae (3 cases), 10 cases showed pustule formation, 10 cases showed erosions, and 17 cases showed erythemas with annular erythemas (9 cases). Other clinical manifestations were crust formation (3 cases), pigmentation (2 cases), and vegetating lesions (1 case). Itch was complained by 6 patients.

Histopathological Features

Among 23 IGAD cases with histopathological information for skin biopsies, 10 cases showed intraepidermal blister formation at

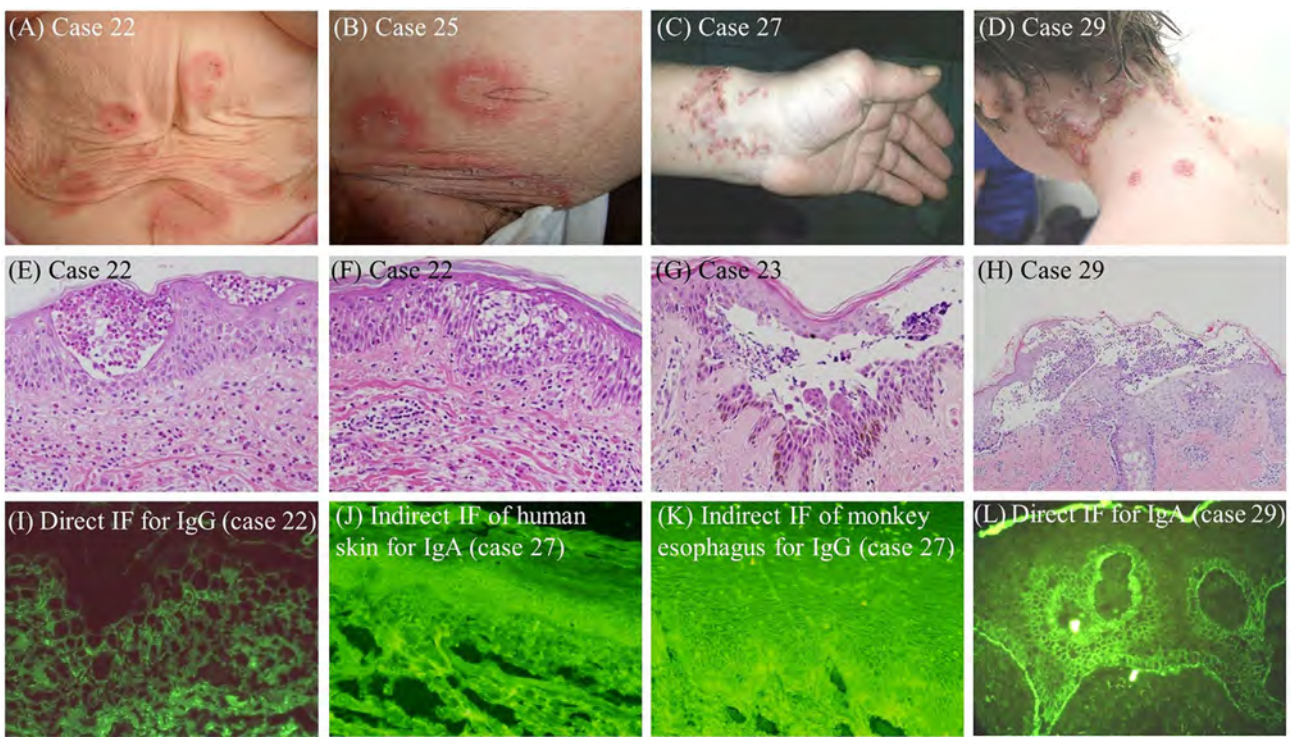

FIGURE 1 | Clinical **(A–D)**, histopathological **(E–H)**, and IF **(I–L)** features in representative IGAD cases examined in this study. **(A)** Vesicles were seen on the peripheries of annular erythemas on the abdomen (case 22). **(B)** Annular erythemas with superficial pustules and desquamation were seen (case 25). **(C)** Erythematous skin lesions with pustules and crusts on the left wrist were seen (case 27). **(D)** Pustular skin lesions on the peripheries of annular erythemas were seen (case 29). **(E,F)** Eosinophilic pustules in the upper epidermis **(E)** and eosinophilic spongiosis in the middle epidermis **(F)** were seen (case 22). **(G)** Acantholytic blisters and pustules in the middle epidermis were seen (case 23). **(H)** Subcorneal pustules with predominant neutrophils and a few eosinophils were seen. **(I)** The result of direct IF for IgG (case 22). **(J)** The result of indirect IF of normal human skin for IgA antibodies (case 27). **(K)** The results of indirect IF of monkey esophagus for IgG antibodies (case 27). **(L)** The result of direct IF for C3 (case 29).

the upper epidermis or middle epidermis, while 12 cases showed intraepidermal pustules at the upper epidermis, middle or lower epidermis (**Figure 1**; Table S1 in Supplementary Material). Spongiosis and acantholysis were observed in three and four cases, respectively. Intraepidermal infiltrations of neutrophils, eosinophils, and lymphocytes were found in 11, 8, and 4 cases, respectively. Presence and absence of acantholysis were described in one and three cases, respectively. Two cases showed subepidermal blisters.

Treatments, Responsiveness, and Complications

Sole therapy of oral steroids, dapsone (DDS), minocycline, and combinations of these drugs and other treatments were performed as described in 13 cases (Tables S1 and S4 in Supplementary Material). The responsiveness to these therapies was variable (Table S4 in Supplementary Material).

Immunological Findings

Direct IF

The results of direct IF were described in the consulting letters for 22 patients. IgG, IgA, and C3 depositions to keratinocyte CSs were positive in 17, 17, and 5 cases, respectively (**Table 1**A). IgG deposition was seen at upper epidermis in one case, lower epidermis in two cases, and entire epidermis in two cases. IgA deposition was seen at upper epidermis in one cases, lower epidermis in four cases, and entire epidermis in four cases. IgG, IgA, and C3 depositions to epidermal BMZ were observed in one, one, and two cases, respectively.

TABLE 1 | Results of various immunofluorescence (IF) studies.

		Positive	Total	Positive rates (%)
(A) Direct IF for skin biopsy				
Cell surface (CS)	IgG	17	22	77.27
Upper epidermis		1		5.88
Lower epidermis		2		11.76
Entire epidermis		2		11.76
CS	IgA	17	22	77.27
Upper epidermis		1		5.88
Lower epidermis		4		23.53
Entire epidermis		4		23.53
CS	C3	5	6	83.33
BMZ	IgG	1	21	4.76
	IgA	1	21	4.76
	C3	2	5	66.67
(B) Indirect IF using normal human skin as a substrate				
IgG	CS	17	29	58.6
IgA	CS	20	29	69.0
(C) Indirect IF using monkey esophagus as a substrate				
IgG	CS	14	18	77.8
IgA	CS	14	18	77.8
(D) Indirect IF using 1 M NaCl-split normal human skin as a substrate				
IgG	Epidermal side	2	16	12.5
	Dermal side	0	16	0.0
IgA	Epidermal side	3	16	18.8
	Dermal side	0	16	0.0

CS, keratinocyte cell surface; BMZ, basement membrane zones.

Indirect IF

In indirect IF of normal human skin performed for 29 IGAD cases, IgG and IgA anti-keratinocyte CS antibodies were positive in 17 and 20 cases, respectively (Figure S3 in Supplementary Material) (**Table 1**B–D). In addition, two and one cases showed IgG and IgA anti-BMZ antibodies, respectively. Indirect IF of monkey esophagus performed for 18 cases detected anti-epithelial CS antibodies of both IgG and IgA classes in 14 cases. In addition, two cases each showed IgG and IgA anti-BMZ antibodies. In indirect IF of 1 M NaCl-split human skin performed for 16 cases, IgG and IgA reactivity with epidermal side was found in two and three cases, respectively.

IB Studies of Normal Human Epidermal Extract and Other Substrates for BMZ Autoantigens

In immunoblotting of normal human epidermal extract performed for all 30 IGAD cases, few cases showed positive reactivity with various epidermal autoantigens for both IgG and IgA classes (Table S5 in Supplementary Material). For IgG antibodies, three cases each reacted with Dsg1 and Dsg3 and one case each reacted with both a and b forms of Dsc. One case each reacted with desmoplakin I, BP230, and envoplakin. For IgA antibodies, one case reacted with Dsg3 and two cases each reacted with both a and b forms of Dsc.

The four cases with positive reactivity with BMZ in IF studies were further examined by immunoblotting for the reactivity with various BMZ autoantigens. Two cases showed positive IgG, but not IgA, reactivity with BP180 NC16a domain RP, while none reacted with BP180 C-terminal domain RP for either IgG or IgA antibodies. One case was positive for IgG, but not IgA, for the 120-kDa LAD-1 in concentrated culture supernatant of HaCaT cells. No positive reactivity was found in immunoblotting of both purified human laminin-332 and normal human dermal extracts for either IgG or IgA antibodies.

ELISAs

In commercially available IgG ELISAs for Dsg1 and Dsg3 for all 30 cases, 19 (63.6%) and 14 (46.7%) cases showed IgG reactivity with Dsg1 and Dsg3, respectively, and 19 (63.3%) and 13 (43.3%) cases showed IgA reactivity with Dsg1 and Dsg3, respectively (**Table 2**A). In ELISAs of mammalian RPs of Dsc1–Dsc3, 6 (20.0%), 7 (23.3%), and 11 (36.7%) cases showed IgG reactivity with Dsc1, Dsc2, and Dsc3, respectively, while 5 (16.7%), 8 (26.7%), and 7 (23.3%) cases showed IgA reactivity with Dsc1, Dsc2, and Dsc3, respectively (**Table 2**B).

Interestingly, there were very high association of detection of IgG and IgA antibodies to the same Dsgs, i.e., 18 (94.7%) of 19 cases with IgG antibodies to Dsg1 had IgA antibodies to Dsg1, 18 (94.7%) of 19 cases with IgA anti-Dsg1 antibodies had IgG anti-Dsg1 antibodies, 11 (78.6%) of 14 cases with IgG anti-Dsg3 antibodies had IgA anti-Dsg3 antibodies, and 11 (84.6%) of 13 cases with IgA anti-Dsg3 antibodies had IgA anti-Dsg3 antibodies. By contrast, rates of coexistence of IgG and IgA antibodies to Dsc1–Dsc3 were not very high, i.e., only 50.0% (3/6), 57.1% (4/7), and 54.5% (6/11) of cases with IgG antibodies to Dsc1, Dsc2, and Dsc3 had IgA antibodies to the same Dscs (Table S2 in Supplementary Material).

TABLE 2 | Results of various ELISAs and COS7 cell cDNA transfection.

	Positive	Total	Positive rates (%)
(A) ELISAs for Dsg1 and Dsg3 for IgG and IgA antibodies			
ELISA Dsg1 (IgG)	19	30	63.3
ELISA Dsg3 (IgG)	14	30	46.3
ELISA Dsg1 (IgA)	19	30	63.3
ELISA Dsg3 (IgA)	13	30	43.3
(B) ELISAs for desmocollin 1 (Dsc1)-Dsc3 for IgG and IgA antibodies			
ELISA Dsc1 (IgG)	6	30	20.0
ELISA Dsc2 (IgG)	7	30	23.3
ELISA Dsc3 (IgG)	11	30	36.7
ELISA Dsc1 (IgA)	5	30	16.7
ELISA Dsc2 (IgA)	8	30	26.7
ELISA Dsc3 (IgA)	7	30	23.3
(C) COS-7 cell cDNA transfection methods for Dsc1-Dsc3 for IgG and IgA antibodies			
COS-7 Dsc1 (IgG)	0	23	0.0
COS-7 Dsc2 (IgG)	0	23	0.0
COS-7 Dsc3 (IgG)	1	23	4.3
COS-7 Dsc1 (IgA)	1	24	4.2
COS-7 Dsc2 (IgA)	0	24	0.0
COS-7 Dsc3 (IgA)	2	24	8.3

One of the four cases with positive reactivity with BMZ in IF studies was positive in IgG ELISA of BP180 NC16a RP (data not shown).

COS-7 Cell cDNA Transfection Methods

In COS-7 cell cDNA transfection method performed for 23 and 24 cases for IgG and IgA antibodies, respectively, one case showed IgG reactivity with Dsc3, and one and two cases showed IgA reactivity with Dsc1 and Dsc3, respectively (**Table 2**C).

Statistical Analyses Between the Dsg and Dsc ELISAs and Clinical Parameters

The case with positive reactivity with Dsg3 for both IgG ($p = 0.0103$) and IgA antibodies had oral mucosal lesions significantly more frequently. Female cases had both IgA anti-Dsg1 antibodies ($p = 0.0351$) and IgG anti-Dsc1 antibodies ($p = 0.0409$) more frequently (chi-square for independence test). No statistically significant correlations were found for any other clinical parameters, including ages, disease durations, sites and manifestations of skin lesions, and responses to various treatments, as well as histopathological features.

DISCUSSION

In this study, although the diagnosis of IGAD was suspected by atypical clinico-histopathological features, we made possible diagnosis of IGAD for patients showing simultaneously IgG and IgA reactivity in various immunological examinations, including IF, immunoblotting, ELISA, and cDNA transfection studies. Particularly, ELISAs were sensitive and detected IgG and IgA antibodies to Dsgs and Dscs in considerable numbers of patients. Finally, using the tentative diagnostic criteria, we diagnosed 30 patients as IGAD.

Clinically, skin lesions developed mainly on the trunk and extremities, and 11 cases showed oral mucosal lesions. Most patients showed blisters, erosions, and/or pustules with erythematous lesions. In most cases, histopathology showed intraepidermal blister and/or pustules at various layers in the epidermis. The major infiltrating cells were neutrophils, followed by eosinophils and lymphocytes. Acantholysis was not clearly seen in some of the patients. Spongiosis were seen occasionally. These clinico-histopathological findings were generally compatible with those in previously reported cases (9–30). In 11 cases, various therapies, mainly oral steroids and DDS, were performed with different efficacy.

Immunologically, direct IF and indirect IF of normal human skin and monkey esophagus were the most sensitive methods with positive rates from 60 to 80%. Regarding antigen detection methods, IgG and IgA ELISAs for Dsgs and Dscs were very sensitive. The IgG and IgA ELISAs detected antibodies to Dsg1 and Dsg3 in 63 and 45% of the patients, respectively, and antibodies to Dsc1–Dsc3 in 20–40% of the patients. Because anti-Dsc antibodies are rarely detected in classical IgG type pemphigus diseases (42), the frequent detection of anti-Dsc antibodies for both IgG and IgA antibodies was considered the significant feature in IGAD. The presence of autoantibodies to other than Dsgs may account for the absence of acantholysis in some patients.

By contrast, sensitivity of immunoblotting of normal epidermal extract and cDNA transfection was very low.

Statistical analyses revealed that anti-Dsg3 antibodies of both IgG and IgA classes were more frequently detected in the cases with oral mucosal lesions. Because Dsg3 is autoantigens found in mucosal-type PV, the results further suggested the significant involvement of IgG anti-Dsg3 antibodies in oral involvement in IGAD. This result may also suggest the pathogenic role of IgA anti-Dsg3 antibodies in development of oral lesions. However, because of the high rates of simultaneous detection of IgG and IgA anti-Dsg3 antibodies in the same sera, the oral lesions might be produced by IgG, but not IgA, anti-Dsg3 antibodies.

Thus, IGAD patients tended to show clinico-histopathological features of both blisters and pustules. IgG-type pemphigus usually shows blisters, while IAD shows pustules. Therefore, IGAD seems to show mixed features of IgG-type pemphigus and IAD. Immunologically, IgG and IgA antibodies tended to react with both Dsgs and Dscs, which also indicates mixed immunological features of IgG-type pemphigus and IAD. These clinical, histopathological, and immunological features are different from either IgG-type pemphigus or IAD. Therefore, we concluded that IGAD is a distinct clinical entity with unique clinical and immunological features.

In this study, we performed no disease model experiments for the pathogenic role of IgG and IgA antibodies in IGAD. However, several IGAD cases showed clear acantholytic histology, suggesting that IgG antibodies to Dsg1 and/or Dsg3 induced the cell detachment similar to IgG-type pemphigus. In addition, because most IGAD cases showed extensive pustular lesions, IgA antibodies to either Dsgs or Dscs may produce the pustular lesions similar to IAD.

We should also consider the molecular mechanisms of simultaneous production of autoantibodies of IgG and IgA classes to various keratinocyte CS antigens, particularly class switch recombination (CSR) for antibody class switching (48, 49). CSR occurs through a genomic rearrangement within constant region locus of

immunoglobulin heavy chain, where gene segments of all immunoglobulin classes are tandemly located downstream of the VDJ variable region locus (Figure S7 in Supplementary Material). The upstream classes are looped out through the CSR and the downstream class is docked into the VDJ region (Figure S7 in Supplementary Material). Thus, the class switching is irreversible and a class must be switched from left to right. Although a class has been considered to be switched from IgM/IgD-producing B-cells to IgG-, IgA-, and IgE-producing B-cells (50), a recent study of comprehensive antibody repertoire sequencing followed by lineage tracing revealed more variable class switch pathways, including pathway from IgG1 to IgA1 (Figure S7 in Supplementary Material) (51).

The extremely high rates of simultaneous detection of IgG and IgA anti-Dsg3 antibodies in the same sera found in this study may indicate that IgG-producing B-cells converted to IgA-producing B-cells. Although we could not determine the ancestral class, predominance of IgG1 class in human serum may suggest that the autoantibody switch from IgG1 to IgA1. By contrast, concurrence of IgG and IgA antibodies to the same Dscs was not very high, suggesting that different immunological IgG and IgA autoantibodies may develop by different molecular mechanisms between Dsgs and Dscs. In future studies, these CSR-related molecular mechanisms in IGAD should be examined more extensively using subclass-specific secondary antibodies or methods to detect the epitopes in more detail.

In conclusion, the present study was the first systematic study for IGAD, and suggested that IGAD is a distinct disease entity with characteristic clinical, histopathological, and immunological features. Combination methods of direct IF, indirect IF of normal human skin/monkey esophagus and ELISAs of Dsgs and Dscs are useful to make the diagnosis of IGAD.

AUTHOR CONTRIBUTIONS

TH, DT, and NI designed the study. KW, DU, SF, KI, YK, IJ, BM, AB, and TK gave clinical and histopathological information of the patients. KT and NI performed the experiments. TH, DT, KT, and NI analyzed the data. TH and KH prepared the figures. TK performed the statistical analyses. TH, KT, KH, DT, and NI wrote the paper.

ACKNOWLEDGMENTS

We gratefully appreciate Ms. Tomoko Tashima and Ms. Shinobu Ide for secretarial work and Ms. Michiru Kubo and Ms. Kyoko Hiromatsu for conducting experiments. We thank all patients for their participation, all members at both Department of Dermatology, Kurume University School of Medicine, and Kurume University Institute of Cutaneous Cell Biology for long lasting efforts for this study, and all researchers and practitioners in other institutes for generously sending us sera and information of the patients.

FUNDING

This study was supported by Grants-in-Aid for Scientific Research (No. 20390308, 20591331, 21659271, 23591634, 23791298, 23791299, 23791300, 23791301, 24659534, 24591672, 24591640, 24791185), and Supported Program for the Strategic Research Foundation at Private Universities from the Ministry of Education, Culture, Sports, Science and Technology; and by "Research on Measures for Intractable Diseases" Project: matching fund subsidy to Takashi Hashimoto and Masayuki Amagai from the Ministry of Health, Labor and Welfare. The study was also supported by grants from Takeda Science Foundation.

SUPPLEMENTARY MATERIAL

The Supplementary Material for this article can be found online at https://www.frontiersin.org/articles/10.3389/fimmu.2018.00994/full#supplementary-material.

REFERENCES

1. Hashimoto T, Tsuruta D, Koga H, Fukuda S, Ohyama B, Komai A, et al. Summary of results of serological tests and diagnoses for 4774 cases of various autoimmune bullous diseases consulted to Kurume University. *Br J Dermatol* (2016) 175:953–65. doi:10.1111/bjd.14692
2. Hashimoto T, Ishii N, Ohata C, Furumura M. Pathogenesis of epidermolysis bullosa acquisita, an autoimmune subepidermal bullous disease. *J Pathol* (2012) 228:1–7. doi:10.1002/path.4062
3. Hashimoto T. Treatment strategies for pemphigus vulgaris in Japan. *Expert Opin Pharmacother* (2008) 9:1519–30. doi:10.1517/14656566.9.9.1519
4. Tsuruta D, Ishii N, Hashimoto T. Diagnosis and treatment of pemphigus. *Immunotherapy* (2012) 4:735–45. doi:10.2217/imt.12.67
5. Nishikawa T, Shimizu H, Hashimoto T. Role of IgA intercellular antibodies: report of clinically and immunopathologically atypical cases. *Proc XVII World Congr Dermatol* (1987):383–4.
6. Hashimoto T. Immunopathology of IgA pemphigus. *Clin Dermatol* (2001) 19:683–9. doi:10.1016/S0738-081X(00)00193-0
7. Hashimoto T, Nishikawa T. Nomenclature for diseases with IgA antikeratinocyte cell surface autoantibodies. *Br J Dermatol* (2015) 173:868–9. doi:10.1111/bjd.13813
8. Hashimoto T, Teye K, Ishii N. Clinical and immunological studies of 49 cases of various types of intercellular IgA dermatosis and 13 cases of classical subcorneal pustular dermatosis examined at Kurume University. *Br J Dermatol* (2017) 176:168–75. doi:10.1111/bjd.14780
9. Chorzelski TP, Hashimoto T, Nishikawa T, Ebihara T, Dmochowski M, Ismail M, et al. Unusual acantholytic bullous dermatosis associated with neoplasia and IgG and IgA antibodies against bovine desmocollins I and II. *J Am Acad Dermatol* (1994) 31:351–5. doi:10.1016/S0190-9622(94)70171-7
10. Ohno H, Miyagawa S, Hashimoto T, Nakagawa A, Watanabe K, Nishikawa T, et al. Atypical pemphigus with concomitant IgG and IgA anti-intercellular autoantibodies associated with monoclonal IgA gammopathy. *Dermatology* (1994) 189(Suppl 1):115–6. doi:10.1159/000246948
11. Oiso N, Yamashita C, Yoshioka K, Amagai M, Komai A, Nagata Y, et al. IgG/IgA pemphigus with IgG and IgA antidesmoglein 1 antibodies detected by enzyme-linked immunosorbent assay. *Br J Dermatol* (2002) 147:1012–7. doi:10.1046/j.1365-2133.2002.04984.x
12. Kozlowska A, Hashimoto T, Jarzabek-Chorzelska M, Amagai A, Nagata Y, Strasz Z, et al. Pemphigus herpetiformis with IgA and IgG antibodies to desmoglein 1 and IgG antibodies to desmocollin 3. *J Am Acad Dermatol* (2003) 48:117–22. doi:10.1067/mjd.2003.23
13. Bruckner AL, Fitzpatrick JE, Hashimoto T, Weston WL, Morelli JG. Atypical IgA/IgG pemphigus involving the skin, oral mucosa, and colon in a child: a novel variant of IgA pemphigus? *Pediatr Dermatol* (2005) 22:321–7. doi:10.1111/j.1525-1470.2005.22408.x

14. Morizane S, Yamamoto T, Hisamatsu Y, Tsuji K, Oono T, Hashimoto T, et al. Pemphigus vegetans with IgG and IgA antidesmoglein 3 antibodies. *Br J Dermatol* (2005) 153:1236–7. doi:10.1111/j.1365-2133.2005.06956.x
15. Heng A, Nwaneshiudu A, Hashimoto T, Amagai M, Stanley JR. Intraepidermal neutrophilic IgA/IgG antidesmocollin 1 pemphigus. *Br J Dermatol* (2006) 154:1018–20. doi:10.1111/j.1365-2133.2006.07226.x
16. Kowalewski C, Hashimoto T, Amagai M, Jablonska S, Mackiewicz W, Wozniak K. IgA/IgG pemphigus: a new atypical subset of pemphigus? *Acta Derm Venereol* (2006) 86:357–8. doi:10.2340/00015555-0060
17. Maruyama H, Kawachi Y, Fujisawa Y, Itoh S, Furuta J, Ishii Y, et al. IgA/IgG pemphigus positive for anti-desmoglein 1 autoantibody. *Eur J Dermatol* (2007) 17:94–5. doi:10.1684/ejd.2007.0176
18. Nakajima K, Hashimoto T, Nakajima H, Yokogawa M, Ikeda M, Kodama H. IgG/IgA pemphigus with dyskeratotic acantholysis and intraepidermal neutrophilic microabscesses. *J Dermatol* (2007) 34:757–60. doi:10.1111/j.1346-8138.2007.00378.x
19. Mentink LF, de Jong MC, Kloosterhuis GJ, Zuiderveen J, Jonkman MF, Pas HH. Coexistence of IgA antibodies to desmogleins 1 and 3 in pemphigus vulgaris, pemphigus foliaceus and paraneoplastic pemphigus. *Br J Dermatol* (2007) 156:635–41. doi:10.1111/j.1365-2133.2006.07717.x
20. Tajima M, Mitsuhashi Y, Irisawa R, Amagai M, Hashimoto T, Tsuboi R. IgA pemphigus reacting exclusively to desmoglein 3. *Eur J Dermatol* (2010) 20:626–9. doi:10.1684/ejd.2010.1021
21. Santiago-et-Sanchez-Mateos D, Juarez Martin A, Gonzalez De Arriba A, Delgado Jimenez Y, Fraga J, Hashimoto T, et al. IgG/IgA pemphigus with IgA and IgG antidesmoglein 1 antibodies detected by enzyme-linked immunosorbent assay: presentation of two cases. *J Eur Acad Dermatol Venereol* (2011) 25:110–2. doi:10.1111/j.1468-3083.2010.03686.x
22. Hosoda S, Suzuki M, Komine M, Murata S, Hashimoto T, Ohtsuki M. A case of IgG/IgA pemphigus presenting malar rash-like erythema. *Acta Derm Venereol* (2012) 92:164–6. doi:10.2340/00015555-1258
23. Ueda A, Ishii N, Temporin K, Yamazaki R, Murakami F, Fukuda S, et al. IgA pemphigus with paraneoplastic pemphigus-like clinical features showing IgA antibodies to desmoglein 1/3 and desmocollin 3, and IgG and IgA antibodies to the basement membrane zone. *Clin Exp Dermatol* (2013) 38:370–3. doi:10.1111/ced.12050
24. Uchiyama R, Ishii N, Arakura F, Kiniwa Y, Nakazawa K, Uhara H, et al. IgA/IgG pemphigus with infiltration of neutrophils and eosinophils in an ulcerative colitis patient. *Acta Derm Venereol* (2014) 94:737–8. doi:10.2340/00015555-1836
25. Furuya A, Takahashi E, Ishii N, Hashimoto T, Satoh T. IgG/IgA pemphigus recognizing desmogleins 1 and 3 in a patient with Sjogren's syndrome. *Eur J Dermatol* (2014) 24:512–3. doi:10.1684/ejd.2014.2391
26. Watkins C, West C, Kosari P, Ali S, Sangüeza O, Huang W. IgG/IgA pemphigus: report of a rare variant of atypical pemphigus and a review of the literature. *J Dermatol Clin Res* (2014) 2:1011.
27. Lane N, Parekh P. IgG/IgA pemphigus. *Am J Dermatopathol* (2014) 36:1002–4. doi:10.1097/DAD.0000000000000058
28. Cetkovska P, Komorousova M, Lomicova I. Management of a pemphigus with IgA and IgG antibodies and coexistent lung cancer. *Dermatol Ther* (2014) 27:236–9. doi:10.1111/dth.12126
29. Kanwar AJ, Vinay K, Saikia UN, Koga H, Teye K, Tsuruta D, et al. IgG/IgA pemphigus reactive with desmoglein 1 with additional undetermined reactivity with epidermal basement membrane zone. *Indian J Dermatol Venereol Leprol* (2014) 80:46–50. doi:10.4103/0378-6323.125499
30. Inoue-Nishimoto T, Hanafusa T, Hirohata A, Mabuchi-Kiyohara E, Mizoguchi N, Matsumoto K, et al. IgG/IgA pemphigus representing pemphigus vegetans caused by low titres of IgG and IgA antibodies to desmoglein 3 and IgA antibodies to desmocollin 3. *J Eur Acad Dermatol Venereol* (2016) 30:1229–31. doi:10.1111/jdv.13158
31. Ohzono A, Sogame R, Li X, Teye K, Tsuchisaka A, Numata S, et al. Clinical and immunological findings in 104 cases of paraneoplastic pemphigus. *Br J Dermatol* (2015) 173:1447–52. doi:10.1111/bjd.14162
32. Woodley DT. Immunofluorescence on salt-split skin for the diagnosis of epidermolysis bullosa acquisita. *Arch Dermatol* (1990) 126:229–31. doi:10.1001/archderm.126.2.229
33. Sugi T, Hashimoto T, Hibi T, Nishikawa T. Production of human monoclonal anti-basement membrane zone (BMZ) antibodies from a patient with bullous pemphigoid (BP) by Epstein-Barr virus transformation. Analyses of the heterogeneity of anti-BMZ antibodies in BP sera using them. *J Clin Invest* (1989) 84:1050–5. doi:10.1172/JCI114266
34. Hashimoto T, Ogawa MM, Konohana A, Nishikawa T. Detection of pemphigus vulgaris and pemphigus foliaceus antigens by immunoblot analysis using different antigen sources. *J Invest Dermatol* (1990) 94:327–31. doi:10.1111/1523-1747.ep12874456
35. Matsumura K, Amagai M, Nishikawa T, Hashimoto T. The majority of bullous pemphigoid and herpes gestationis serum samples react with the NC16a domain of the 180-kDa bullous pemphigoid antigen. *Arch Dermatol Res* (1996) 288:507–9. doi:10.1007/BF02505245
36. Nie Z, Hashimoto T. IgA antibodies of cicatricial pemphigoid sera specifically react with C-terminus of BP180. *J Invest Dermatol* (1999) 112:254–5. doi:10.1046/j.1523-1747.1999.00501.x
37. Ishii N, Ohyama B, Yamaguchi Z, Hashimoto T. IgA autoantibodies against the NC16a domain of BP180 but not 120-kDa LAD-1 detected in a patient with linear IgA disease. *Br J Dermatol* (2008) 158:1151–3. doi:10.1111/j.1365-2133.2008.08492.x
38. Ishii N, Yoshida M, Hisamatsu Y, Ishida-Yamamoto A, Nakane H, Iizuka H, et al. Epidermolysis bullosa acquisita sera react with distinct epitopes on the NC1 and NC2 domains of type VII collagen: study using immunoblotting of domain-specific recombinant proteins and postembedding immunoelectron microscopy. *Br J Dermatol* (2004) 150:843–51. doi:10.1111/j.1365-2133.2004.05933.x
39. Hisamatsu Y, Nishiyama T, Amano S, Matsui C, Ghohestani R, Hashimoto T. Usefulness of immunoblotting using purified laminin 5 in the diagnosis of anti-laminin 5 cicatricial pemphigoid. *J Dermatol Sci* (2003) 33:113–9. doi:10.1016/S0923-1811(03)00158-0
40. Ishii K, Amagai M, Hall RP, Hashimoto T, Takayanagi A, Gamou S, et al. Characterization of autoantibodies in pemphigus using antigen-specific enzyme-linked immunosorbent assays with baculovirus-expressed recombinant desmogleins. *J Immunol* (1997) 159:2010–7.
41. Hashimoto T, Komai A, Futei Y, Nishikawa T, Amagai M. Detection of IgA autoantibodies to desmogleins by an enzyme-linked immunosorbent assay: the presence of new minor subtypes of IgA pemphigus. *Arch Dermatol* (2001) 137:735–8. doi:10-1001/pubs.Arch Dermatol
42. Ishii N, Teye K, Fukuda S, Uehara R, Hachiya T, Koga H, et al. Anti-desmocollin autoantibodies in nonclassical pemphigus. *Br J Dermatol* (2015) 173:59–68. doi:10.1111/bjd.13711
43. Teye K, Numata S, Ohzono A, Ohyama B, Tsuchisaka A, Koga H, et al. Establishment of IgA ELISAs of mammalian recombinant proteins of human desmocollins 1-3. *J Dermatol Sci* (2016) 83:75–7. doi:10.1016/j.jdermsci.2016.04.001
44. Kobayashi M, Amagai M, Kuroda-Kinoshita K, Hashimoto T, Shirakata Y, Hashimoto K, et al. BP180 ELISA using bacterial recombinant NC16a protein as a diagnostic and monitoring tool for bullous pemphigoid. *J Dermatol Sci* (2002) 30:224–32. doi:10.1016/S0923-1811(02)00109-3
45. Yoshida M, Hamada T, Amagai M, Hashimoto K, Uehara R, Yamaguchi K, et al. Enzyme-linked immunosorbent assay using bacterial recombinant proteins of human BP230 as a diagnostic tool for bullous pemphigoid. *J Dermatol Sci* (2006) 41:21–30. doi:10.1016/j.jdermsci.2005.11.002
46. Saleh MA, Ishii K, Kim YJ, Murakami A, Ishii N, Hashimoto T, et al. Development of NC1 and NC2 domains of type VII collagen ELISA for the diagnosis and analysis of the time course of epidermolysis bullosa acquisita patients. *J Dermatol Sci* (2011) 62:169–75. doi:10.1016/j.jdermsci.2011.03.003
47. Hashimoto T, Kiyokawa C, Mori O, Miyasato M, Chidgey MA, Garrod DR, et al. Human desmocollin 1 (Dsc1) is an autoantigen for the subcorneal pustular dermatosis type of IgA pemphigus. *J Invest Dermatol* (1997) 109:127–31. doi:10.1111/1523-1747.ep12319025
48. Muramatsu M, Kinoshita K, Fagarasan S, Yamada S, Shinkai Y, Honjo T. Class switch recombination and hypermutation require activation-induced cytidine deaminase (AID), a potential RNA editing enzyme. *Cell* (2000) 102:553–63. doi:10.1016/S0092-8674(00)00078-7
49. Stavnezer J, Guikema JE, Schrader CE. Mechanism and regulation of class switch recombination. *Annu Rev Immunol* (2008) 26:261–92. doi:10.1146/annurev.immunol.26.021607.090248

50. Tangye SG, Hodgkin PD. Divide and conquer: the importance of cell division in regulating B-cell responses. *Immunology* (2004) 112:509–20. doi:10.1111/j.1365-2567.2004.01950.x
51. Horns F, Vollmers C, Croote D, Mackey SF, Swan GE, Dekker CL, et al. Lineage tracing of human B cells reveals the in vivo landscape of human antibody class switching. *Elife* (2016) 5. doi:10.7554/eLife.23066

Conflict of Interest Statement: The authors declare that the research was conducted in the absence of any commercial or financial relationships that could be construed as a potential conflict of interest.

The reviewer MD declared a past co-authorship with one of the authors KW to the handling Editor.

frontiers in Immunology

ORIGINAL RESEARCH
published: 07 May 2018
doi: 10.3389/fimmu.2018.00989

Autoantibodies Recognizing Secondary NEcrotic Cells Promote Neutrophilic Phagocytosis and Identify Patients With Systemic Lupus Erythematosus

*Mona H. C. Biermann[1†], Sebastian Boeltz[1†], Elmar Pieterse[2], Jasmin Knopf[1], Jürgen Rech[1], Rostyslav Bilyy[1,3], Johan van der Vlag[2], Angela Tincani[4], Jörg H. W. Distler[1], Gerhard Krönke[1], Georg Andreas Schett[1], Martin Herrmann[1] and Luis E. Muñoz[1]**

[1] Department of Internal Medicine 3 – Rheumatology and Immunology, Friedrich-Alexander-Universität Erlangen-Nürnberg (FAU) and Universitätsklinikum Erlangen, Erlangen, Germany, [2] Department of Nephrology, Radboud University Medical Centre, Nijmegen, Netherlands, [3] Danylo Halytsky Lviv National Medical University, Lviv, Ukraine, [4] Division of Rheumatology and Clinical Immunology, Department of Clinical and Experimental Sciences, Spedali Civili and University of Brescia, Brescia, Italy

OPEN ACCESS

Edited by:
Ralf J. Ludwig,
Universität zu Lübeck,
Germany

Reviewed by:
Jason S. Knight,
University of Michigan,
United States
Constantinos Petrovas,
National Institutes of Health
(NIH), United States

***Correspondence:**
Luis E. Muñoz
luis.munoz@uk-erlangen.de

[†]These authors have contributed equally to this work.

Specialty section:
This article was submitted to Immunological Tolerance and Regulation, a section of the journal Frontiers in Immunology

Received: 02 February 2018
Accepted: 20 April 2018
Published: 07 May 2018

Citation:
Biermann MHC, Boeltz S, Pieterse E, Knopf J, Rech J, Bilyy R, van der Vlag J, Tincani A, Distler JHW, Krönke G, Schett GA, Herrmann M and Muñoz LE (2018) Autoantibodies Recognizing Secondary NEcrotic Cells Promote Neutrophilic Phagocytosis and Identify Patients With Systemic Lupus Erythematosus. Front. Immunol. 9:989. doi: 10.3389/fimmu.2018.00989

Deficient clearance of apoptotic cells reportedly contributes to the etiopathogenesis of the autoimmune disease systemic lupus erythematosus (SLE). Based on this knowledge, we developed a highly specific and sensitive test for the detection of SLE autoantibodies (AAb) utilizing secondary NEcrotic cell (SNEC)-derived material as a substrate. The goal of the present study was to validate the use of SNEC as an appropriate antigen for the diagnosis of SLE in large cohort of patients. We confirmed the presence of apoptotically modified autoantigens on SNEC (dsDNA, high mobility group box 1 protein, apoptosis-associated chromatin modifications, e.g., histones H3-K27-me3; H2A/H4 AcK8,12,16; and H2B-AcK12). Anti-SNEC AAb were measured in the serum of 155 patients with SLE, 89 normal healthy donors (NHD), and 169 patients with other autoimmune connective tissue diseases employing SNEC-based indirect enzyme-linked immunosorbent assay (SNEC ELISA). We compared the test performance of SNEC ELISA with the routine diagnostic tests dsDNA Farr radioimmunoassay (RIA) and nucleosome-based ELISA (*anti-dsDNA-NcX-ELISA*). SNEC ELISA distinguished patients with SLE with a specificity of 98.9% and a sensitivity of 70.6% from NHD clearly surpassing RIA and *anti-dsDNA-NcX-ELISA*. In contrast to the other tests, SNEC ELISA significantly discriminated patients with SLE from patients with rheumatoid arthritis, primary anti-phospholipid syndrome, spondyloarthropathy, psoriatic arthritis, and systemic sclerosis. A positive test result in SNEC ELISA significantly correlated with serological variables and reflected the uptake of opsonized SNEC by neutrophils. This stresses the relevance of SNECs in the pathogenesis of SLE. We conclude that SNEC ELISA allows for the sensitive detection of pathologically relevant AAb, enabling its diagnostic usage. A positive SNEC test reflects the opsonization of cell remnants by AAb, the neutrophil recruitment to tissues, and the enhancement of local and systemic inflammatory responses.

Keywords: systemic lupus erythematosus, secondary necrosis, autoimmunity, autoantibodies, inflammation, connective tissue diseases

INTRODUCTION

Systemic lupus erythematosus (SLE) is a chronic inflammatory autoimmune disease. Its pathogenesis is multifactorial including the involvement of genetic (1), hormonal (2), immunologic (3), and environmental factors like infections (4, 5). The appearance of autoantibodies (AAb) is the hallmark of systemic autoimmunity in SLE and results from a series of immune-mediated events that typically precede the onset of clinical symptoms by several years. The development of autoimmunity is considered to be partly triggered by impaired clearance of apoptotic cells in the germinal centers of the lymph nodes (6–9). Apoptotic cells that are not cleared rapidly by professional phagocytes lose their membrane integrity and, consequently, release cytoplasmic and nuclear autoantigens. These antigens are usually connected to damage-associated molecular patterns (DAMPs) like the high mobility group box 1 protein (HMGB1) (10). The material generated in the absence of a proper clearance is designated as secondary NEcrotic cells (SNECs) (11–13). The concomitant release of DAMPs and nucleic acids triggers an inflammatory response (14, 15) which, in combination with the accessibility of autoantigens, precipitates the production of SNEC-specific AAb (16). After autoimmunity is established uncleared post-apoptotic material serves as autoantigen repository for the formation of pathogenic immune complexes (ICs) (17, 18). These complexes form *in situ* or deposit in various tissues, especially in the kidney, skin, and joints, where they trigger inflammation and tissue damage (19, 20).

In 1948, Hargraves discovered the LE cell as first test for diagnosing SLE [reviewed in Ref. (21)] representing a phagocytic cell that has ingested the secondary necrotic nucleus of another cell closely resembling SNEC (22). AAb against nuclear proteins are essential to form LE cells (23, 24) suggesting recognition of SNEC in the context of autoimmunity in SLE (25, 26). Accordingly, LE cells reportedly indicate serologically and clinically active disease with major organ involvement. After several decades, the LE cell test was replaced by serum autoantibody testing in 1997, not least because LE cell testing is time consuming and challenging (27, 28). The presence of AAb increases the risk for clinical disease by at least 40-fold (29). A plethora of autoantibody specificities can be detected in patients with SLE that comprise reactivities against dsDNA, nucleosomes, RNA-protein complexes, Smith antigen (Sm), and ribosomal proteins (30).

Considering the aforementioned pathophysiologic events, we hypothesized that the detection of anti-SNEC AAb is a highly specific and potentially sensitive tool for the classification of SLE. Thus, the goal of the present study was to validate the use of SNEC as an appropriate antigen for the diagnosis of SLE in large cohort of patients. Employing SNEC as antigen, we developed a specific and sensitive high-throughput test to identify patients with pathogenic AAb against post-apoptotic cells. This anti-SNEC enzyme-linked immunosorbent assay (ELISA) discriminated SLE patients from healthy individuals and patients with other autoimmune connective tissue diseases with a specificity and sensitivity of 98.9 and 70.6%, respectively, surpassing currently used standard detection methods.

MATERIALS AND METHODS

Patient and Normal Healthy Donor (NHD) Serum Samples

This study was carried out in accordance with the recommendations of institutional guidelines and the approval of the ethical committee of the Universitätsklinikum Erlangen (permit # 54_14B). The protocol was approved by the ethical committee of the Universitätsklinikum Erlangen (permit # 54_14B). Written informed consent was given by each donor in accordance with the Declaration of Helsinki. Serum samples from NHD and patients with SLE, RA, SpA, PsA, and SSc, fulfilling the 1997 American College of Rheumatology criteria, were obtained at the Department of Rheumatology and Immunology of the Universitätsklinikum Erlangen. Sera from patients with primary anti-phospholipid syndrome (PAPS) were obtained from the Department Rheumatology and Clinical Immunology of the Spedali Civili and University of Brescia. Samples were stored at −20°C until analysis.

Preparation of SNECs

Peripheral blood mononuclear cells (PMBC) were obtained from heparinized whole NHD blood and isolated by density gradient-based isolation using Lymphoflot (Bio-Rad, Dreieich, Germany) as previously described (31). Isolated PBMCs were adjusted to a concentration of 5×10^6 cells/ml in PBS and irradiated using 240 mJ/cm^2 UVB light for 90 s. After incubation for 24 h at 37°C and antigen retrieval at 56°C, SNEC was stored at −20°C containing 5 mM EDTA. Before coating, SNEC was washed in 10 mM Tris buffer containing 1 mM EDTA (pH 8.0). For *ex vivo* phagocytosis assays, SNEC was concentrated to 15×10^7 cells/ml and labeled with propidium iodide (PI).

Ex Vivo Phagocytosis Assays

Fresh heparinized whole blood from NHD was added to polystyrene tubes and 12% serum of NHD or patients with SLE and 10% PI-stained SNEC (15×10^7/ml) was added. Samples were incubated for 4 h at 37°C to allow uptake of SNEC by phagocytes and stained for HLA-DR (FITC), CD16 (APC), and DNA (Hoechst33342) for 30 min at 4°C in the dark. After hypotonic lysis of erythrocytes and fixation of the cells, samples were measured by flow cytometry (Gallios™ Beckman Colter, Krefeld, Germany) and analyzed using Kaluza 1.5 software (Beckmann Colter). Uptake of SNEC is presented as *phagocytosis index* calculated using the percentage of PI-positive cells and the mean fluorescent intensity.

SNEC ELISA

The serum of NHD and patients affected by several pathological conditions was analyzed by ELISA for the presence of anti-SNEC IgG AAb. 96-well microtiter plates (Nunc-Immuno™Maxisorp) were coated overnight at 4°C with 50 µl of Poly-L-Lysine (20 µg/ml) in 10 mM Tris buffer containing 1 mM EDTA (pH 8.0). Plates were washed three times with 200 µl of washing buffer [phosphate-buffered saline (PBS), 0.05% Tween 20, pH 7.4] after each incubation step. After coating overnight at 4°C with SNEC in 10 mM Tris buffer containing 1 mM EDTA (pH 8.0), plates were

blocked for 1 h at room temperature (RT) with 100 µl blocking agent (2% BSA in PBS) per well, 50 µl of serum per well (1:200 in PBS-T) was added and incubated for 1 h at RT. Next, 50 µl of goat anti-human IgG Fc HRP-conjugated (Southern Biotech, Birmingham, AL, USA) antibody (1:50,000 in washing buffer) was added and incubated for 1 h at RT. Finally, plates were incubated with 50 µl of substrate solution [substrate buffer (0.1 M Na_2HPO_4, 0.05 M citrate acid, pH 5.0), 10% TMB, and 0.02% H_2O_2 (30%)] for 5 to 10 min. The reaction was stopped with 50 µl of H_2SO_4 (25%) and absorbances were read at 450 and 620 nm reference wavelength. To account for differences between plates, values were corrected using a standard serum applied on each plate.

Characterization of SNEC Autoantigens by ELISA

ELISA was performed as described above. Antibodies detecting several autoantigens [mAb #34: mouse anti-histone H3 (32); mAb #42: mouse anti-DNA; mAb BT131: mouse anti-apoptotic nucleosome (33); mAb BT164: mouse anti-H3-K27me3 (34); mAb KM-2: mouse anti-H4-AcK8,12,16 (35); mAb LG11-2: mouse anti-H2B-AcK12 (36); rabbit anti-HMGB1 (Abcam, Cambridge, UK)] were added at the indicated concentrations in PBS-T (containing 1% BSA) and incubated for 1 h at RT. The respective secondary antibodies, goat anti-mouse IgG Fc HRP-conjugated (Jackson ImmunoResearch, Suffolk, UK), goat anti-rabbit IgG Fc HRP-conjugated (Southern Biotech, Birmingham, AL, USA), and goat anti-human IgG Fc HRP-conjugated (Southern Biotech, Birmingham, AL, USA) were added (1:10,000 in PBS-T, 1% BSA) for 1 h at RT.

Immunofluorescence Staining

Eight-well Nunc chamber slides (VWR, Darmstadt, Germany) were coated, washed, and blocked as described above. Wells were incubated with the serum of one NHD with a low SNEC ELISA value and the serum of one SLE patient with a high SNEC ELISA value (1:200 in PBS-T) or antibodies detecting histone H3 (mAb #34) and mouse anti-H3-K27me3 (mAb BT164). Goat anti-human IgG FITC (Jackson ImmunoResearch, Suffolk, UK), goat anti-mouse IgG Cy®5 (Jackson ImmunoResearch, Suffolk, UK), and goat anti-rabbit IgG Cy®5 (Jackson ImmunoResearch, Suffolk, UK) were added and incubated for 1 h in the dark. A control staining lacking a primary antibody was included. Finally, slides were washed with PBS and H_2O, embedded in DAKO fluorescent mounting medium (Agilent Technologies, Santa Clara, CA, USA) and analyzed using the Eclipse Ni-U (Nikon Corporation, Tokyo, Japan).

Live Fluorescence Microscopy

Fresh heparinized whole blood from NHD was obtained and 12% serum of patients with SLE and 10% PI-stained SNEC (150×10^6 cells/ml) were added. The samples were incubated for 1 h at 37°C. After hypotonic lysis of erythrocytes and fixation with 4% PFA, cells were deposited on chamber slides. Slides were blocked with 10% FCS and stained for CD15 (APC) and DNA (Hoechst33342) and the respective isotype control antibody for 2 h at RT in the dark and analyzed using the Eclipse Ni-U.

Adsorption of Anti-SNEC AAb From SLE Serum

Serum C-reactive protein (CRP) was purified using immobilized p-Aminophenyl Phosphoryl Choline agarose gel (Thermofisher) as per the manufacturer's instructions. CRP bound to agarose was incubated with SNEC for 1 h at RT (13). Anti-SNEC AAb were removed from SLE serum by incubation with SNEC-bound CRP agarose by incubation for 1 h at RT.

Statistical Data Analysis

Age, sex, comorbidities, organ involvement, and disease onset were recorded for all patients. CRP levels, erythrocyte sedimentation rate (ESR), rheumatoid factor (RF), dsDNA radioimmunoassay (RIA), anti-dsDNA-NcX-ELISA, extractable nuclear antigen (ENA) profiles, and complement levels (C3 and C4) were measured on the same day of serum collection. Disease activity score European Consensus Lupus Activity Measurement Manifestation (ECLAM) was calculated. For comparisons between two groups, Mann–Whitney *U*-tests for numerical variables and exact χ^2-tests for nominal characteristics were employed. ANOVA with Bonferroni *Post Hoc* correction was employed for comparisons among several groups. Associations among clinical and laboratory variables were measured by Bravais-Pearson correlation coefficients and corrected after Bonferroni. The discriminatory power of a test was evaluating calculating the receiver operating characteristic (ROC) method. Cumulative predicted probabilities [the area under the curve, positive predictive value (PPV), negative predictive value (NPV), diagnostic odds ratio (DOR), cutoff, sensitivity, specificity] were calculated for numeric comparison of ROC curves. All statistical analyzes were performed using IBM SPSS Software (version 21) and GraphPad Prism 5.03 software. A p value ≤ 0.05 was considered statistically significant.

RESULTS

AAb From Patients With SLE Recognize SNEC-Borne Autoantigens Modified During Apoptosis

We employed SNEC as immobilized antigen in an indirect ELISA (Figure S1A in Supplementary Material) to detect SLE-specific antibodies. We demonstrated the availability of specific apoptotically modified nuclear autoantigens on SNEC (**Figure 1A**) and confirmed the presence of DNA, histone H3, nucleosomes, and histones carrying several apoptotic modifications (histone H3 K27-me3; histone H2A/H4 AcK8,12,16, histone H2B-AcK12). Representative pictures of repeated SNEC antigen characterization are shown. Analyzes by immunofluorescence revealed that autoreactive IgG present in the sera of patients with SLE strongly bound to immobilized SNEC, whereas sera of NHD lacked reactivity (**Figure 1B**). SNEC was recognized by DNA- and nucleosome-specific AAb in a particular manner (**Figure 1C**) resembling the recognition pattern of SLE serum-derived AAb (**Figure 1C**). These monoclonal antibodies also recognized antigens on HEp-2 cells; however, apoptotically modified histone H3 was recognized to a lesser extent (**Figure 1D**). HMGB1 was also found on immobilized SNEC linked to apoptotic DNA (Figure S1B

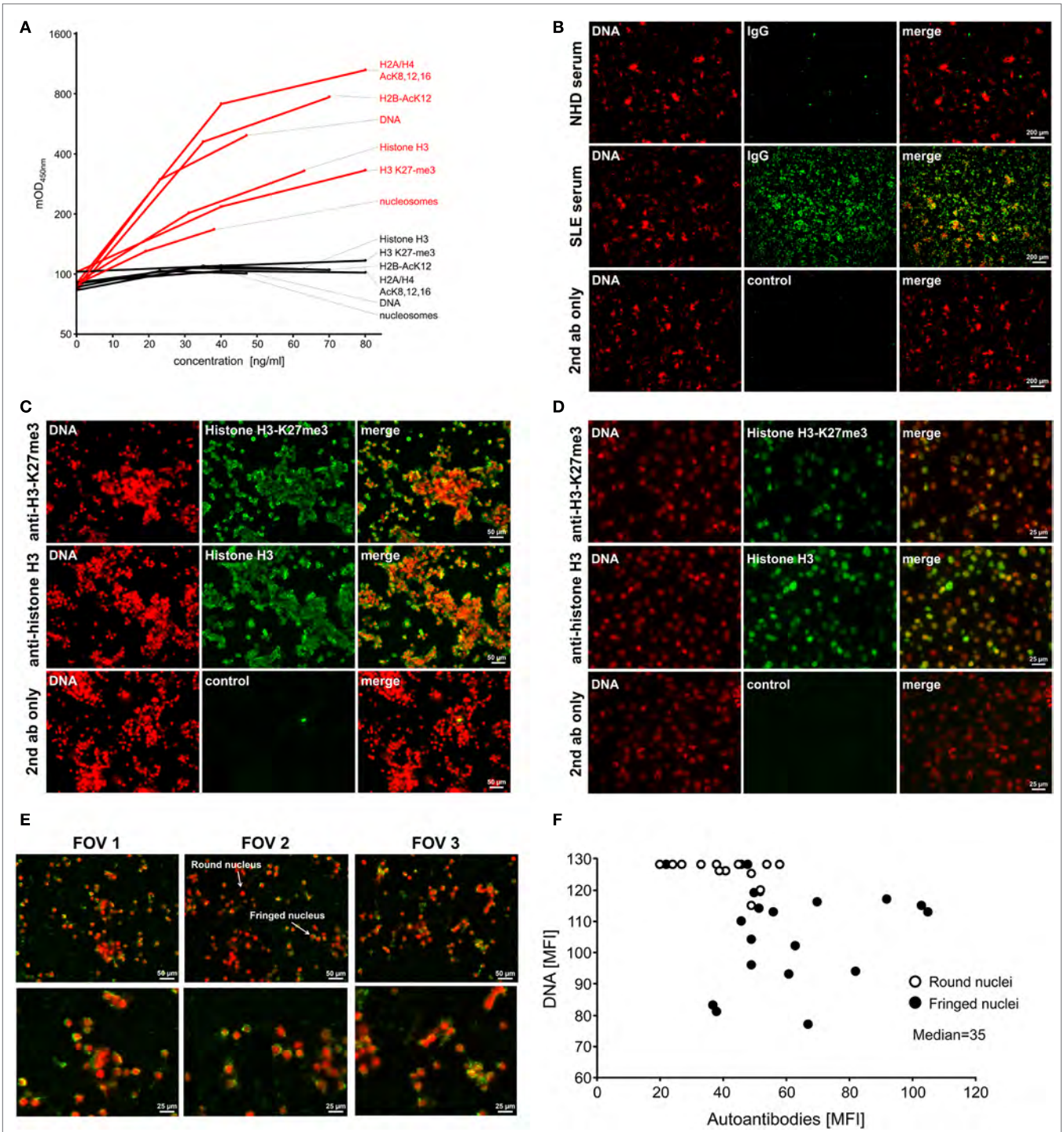

FIGURE 1 | Immobilized secondary NEcrotic cells (SNECs) expose naïve and modified nuclear autoantigens. **(A)** Recognition of immobilized autoantigens on SNEC by specific antibodies. Coated material contained histone H3 (#34), DNA (#42), nucleosomes (BT131), and the apoptotically modified histones H3 K27-me3 (BT164), H2A/H4 AcK8,12,16, (KM-2), and H2B-AcK15 (LG11-2). Respective isotype control antibodies (iso) displayed background signals. **(B)** Immunofluorescence of SLE-borne IgG autoantibodies (AAb) binding immobilized SNEC counter-stained for DNA by propidium iodide (PI). NHD, normal healthy donor; SLE, systemic lupus erythematosus; magnification 20×. **(C)** Immunofluorescence of histone H3 and modified histone H3 K27-me3 on immobilized SNEC counter-stained for DNA by PI; magnification 40×. **(D)** Immunofluorescence staining of histone H3 and modified histone H3 K27-me3 on HEp-2 cells. **(E)** Immunofluorescence of binding pattern of IgG autoantibodies present in the serum of patients with SLE to immobilized SNEC stained for DNA by PI; FOV, field of view. **(F)** Morphometric evaluation of **(E)**, intensity of DNA staining versus the intensity of IgG staining.

in Supplementary Material). Murine AAb bound SNEC in a unique pattern preferentially targeting cells with low DNA densities (**Figure 1C**). Morphometry confirmed that human SLE AAb showed a similar binding pattern preferring cells with fringed nuclei and decondensed chromatin when compared to targets with bright round nuclei (**Figures 1E,F**).

The Test Performance of SNEC ELISA Surpasses That of Current Routine Assays

To establish a reproducible assay, we tested the linearity of SNEC ELISA employing serial dilutions of positive and negative sera (Figure S1C in Supplementary Material). For further analyzes, we used a serum dilution factor of 200 lying in the linear detection range. Comparison of different apoptosis stimuli resulted in comparable autoantibody detection for UVB- or Dexamethasone-induced apoptosis (Figure S1D in Supplementary Material). To assess the performance of SNEC ELISA, we studied 155 patients with SLE [median age 44.5 years (inter quartile range (IQR) 22–42)] and 89 normal healthy donors (NHD) [median age 27.5 years (IQR 25–33)] (**Table 1**). A summary of demographical, serological, and clinical data of all study cohorts is presented in **Tables 1** and **2**. The reproducibility of SNEC ELISA in terms of batch variability was tested and corrected using a standard serum, which revealed reproducible signals.

Secondary NEcrotic cell ELISA values from individuals of the NHD and SLE cohorts were not dependent on age (Figures S1F,G in Supplementary Material). ROC analyzes using the NHD sera as control cohort determined positive sera above the cutoff of 246 mOD (**Figure 2A**). 70.6% of patients with SLE showed seropositivity in SNEC ELISA, whereas just 1.1% of NHD were positive (**Figure 2A**). Patients with secondary anti-phospholipid syndrome (sAPS, 72.7%) are depicted additionally in a separate cohort and are undistinguishable from the patients with SLE without sAPS (**Figure 2A**). We employed sera from patients with other connective tissue disorders, namely PAPS (0%), rheumatoid arthritis (RA, 1.9%), spondyloarthropathy (SpA, 0%), psoriatic arthritis (PsA, 0%), or systemic sclerosis (SSc, 3.4%) (**Figure 2A**) showing cumulatively only 1.2% seropositivity in SNEC ELISA (**Figure 2A**).

Receiver operating characteristic analysis showed a specificity of 98.9% at a sensitivity of 70.6% for SNEC ELISA (**Figure 2B**) surpassing current routine assays like the *anti-dsDNA-NcX-ELISA* (EUROIMMUN) and the Farr radioimmunoassay (IBL International) in our cohort (**Figure 2B**). Analysis of the ROC curves of combined results of RIA and ENA nucleosome or ENA histone revealed that the sensitivity of SNEC ELISA also outperformed the combination of these tests (Figure S1E and Table S1 in Supplementary Material). A PPV of 99.1% for SNEC ELISA confirmed the high accuracy of the assay (**Figure 2B**), comparable to RIA and *anti-dsDNA-NcX-ELISA* (98.3 and 98.5%, respectively). The NPV, indicating the percentage of true negative test results, was 66.2% for SLE, clearly exceeding RIA and *anti-dsDNA-NcX-ELISA* (NPV: 30.1 and 41.2%). SNEC ELISA was the most effective test with a DOR of 211.2, performing better than RIA (DOR 25.0) and *anti-dsDNA-NcX-ELISA* (DOR 46.3) (**Figure 2B**).

The most frequently affected organs in our study cohort were joints (62.1%), skin (60.1%), and kidneys (40.5%) (**Table 3**), a distribution similar to previous reports. None of the employed diagnostic tests [anti-nuclear antigen (ANA), *anti-dsDNA-NcX-ELISA*, RIA, and SNEC ELISA] predicted enhanced risks for any organ involvement (**Figure 2C**). Interestingly, the number of patients with photosensitivity or SLE-related central nervous system involvement was significantly lower if SNEC ELISA was positive (**Figure 2C**, red). Correlation analyzes demonstrated further associations of anti-SNEC antibodies with serological variables of SLE (**Figure 3**; Tables S2 and S3 in Supplementary Material).

Anti-SNEC Antibodies Correlate With Serological Variables of SLE

In order to explore the degree of association between SNEC ELISA, *anti-dsDNA-NcX-ELISA*, RIA, and serological variables commonly used for monitoring SLE disease activity, we analyzed complement levels (C3 and C4), markers of inflammation (CRP and ESR), and levels of AAb (ANA and ENA profiles) (**Figure 3**; Tables S2 and S3 in Supplementary Material). One-way ANOVA analyzes revealed that the levels of anti-SNEC and *anti-dsDNA-NcX* antibodies significantly correlated with increasing titers of ANA on HEp-2 ($p = 0.1 \times 10^{-26}$ and 0.4×10^{-8}, respectively) (Table S2 in Supplementary Material). Bonferroni *post hoc* testing

TABLE 1 | Demographical and serological characteristics of the study cohorts.

		NHD	SLE	PAPS	RA	SpA	PsA	SSc
n		89	155	37	53	20	30	29
Sex	(Female/male)	52/33	133/22	28/9	40/13	7/13	14/16	19/9
Current age (years)	Median/IQR	27.5/25–33	44.5/22–42	47/37–40	62.8/53–71	46.2/36–57	54.1/46–63	55.3/50–72
Age at diagnosis (years)	Median/IQR	na	29.2/10–76	na	45.3/36–57	31.6/18.5–41.6	40.2/33–53	47.9/42–62
CRP (mg/dl) [<5 mg/L]	Median/IQR	na	3.7/2.2–6.2	na	3.5/2.3–8.3	4.9/2.55–9.5	5.0/2.1–7.0	6.3/2.8–9.4
RF (IE/ml) [0–20 IE/ml]	Median/IQR	na	na	na	25.5/0–183	na	na	na
ACPA (U/ml) [<10 U/ml]	Median/IQR	na	na	na	57.5/3.6–294.3	na	na	na
a-SNEC IgG (mOD) [<246 mOD]	Median/IQR	85.0/64.0–121.5	309.8/239.4–375.3	61.0/12.4–94.0	85.9/42.0–148.8	50.6/38.5–86.4	52.0/34.6–92.9	109.0/89.9–122.1
SNEC ELISA positivity	%	1.1	70.6	0.0	1.9	0.0	0.0	3.4

ACPA, anti-citrullinated peptide antibody; a-SNEC IgG, anti-secondary necrotic cell-IgG antibody; CRP, C-reactive Protein; IE, Internationale Einheit (engl. International units); IQR, interquartile range; mOD, mean optical density; na, not available; PAPS, primary anti-phospholipid syndrome; PsA, psoriatic arthritis; RA, rheumatoid arthritis; RF, rheumatoid factor; SLE, systemic lupus erythematosus; SpA, spondyloarthropathy; SSc, systemic sclerosis; U, unit; NHD, normal healthy donor.

TABLE 2 | Serological and clinical characteristics of the SLE cohort.

	Variable	*n*	Mean ± SD	Frequency altered (%)
Serology	ANA on HEp-2 (1/) [≥1/320]	152	1544.2 ± 3389.3	71.2
	Radioimmunoassay (RIA) dsDNA (U/ml) [0–7 U/ml]	153	22.3 ± 79.2	39
	C3 (mg/dl) [81.1–157 mg/dl]	153	87.6 ± 21.3	63
	C4 (mg/dl) [12.9–39.2 mg/dl]	153	15.4 ± 5.7	14
	CRP (mg/l) [<5 mg/L]	152	5.4 ± 6.20	17
	Anti-CL IgG [0–14 GPL U/ml]	56	28.0 ± 56.2	37.5
	Anti-β2GP IgG [0–10 U/ml]	56	12.3 ± 25.3	21.4
	ESR (mm/60min) [<20 *F*; <15 M mm/60 min]	146	18.7 ± 13.5	42
	a-SNEC IgG [mean optical density (mOD)] [<246 mOD]	153	264.5 ± 100.6	71
	Ncx dsDNA ELISA (IE/ml) [<100 IE/ml]	153	146.9 ± 187.6	43
ENA [0–3]	Histones	155	0.72 ± 1.05	41
	Nucleosomes	155	0.74 ± 1.06	44
	Ro-52 (52 kDa)	155	0.85 ± 1.29	36
	SS-A (60 kDa)	155	0.99 ± 1.34	39
	RNP/Sm	155	0.71 ± 1.21	31
	AMA-M2	155	0.15 ± 0.54	11
	Ribosomal P protein	155	0.21 ± 0.57	17
	PCNA	155	0.05 ± 0.20	6
	Centromer B	155	0.04 ± 0.24	4
	Jo-1	155	0.03 ± 0.20	3
	PM-Scl	155	0.08 ± 0.26	13
	Scl-70	155	0.07 ± 0.36	5
	SS-B	155	0.25 ± 0.78	12
	RNP C	155	0.09 ± 0.37	9
	RNP A	155	0.31 ± 0.83	15
	RNP 70	155	0.25 ± 0.73	12
	Sm	155	0.20 ± 0.64	12
Clinic	SLEDAI (0–105)	84	2.82 ± 2.65	
	ECLAM (1–10)	153	5.73 ± 2.51	

C3/C4; complement factor 3/4; Anti-β2GP1 IgG, anti-β2 glycoprotein1 IgG; anti-CL, anti-cardiolipin IgG; ANA, anti-nuclear antigen; ENA, extractable nuclear antigen; CRP, C-reactive protein; ESR, erythrocyte sedimentation rate; ECLAM, European Consensus Lupus Activity Measurement Manifestation; SLEDAI, SLE disease activity index.

confirmed significantly increased values of anti-SNEC antibodies for ANA titers above 1:1,000 (**Figure 3A**). The levels of anti-dsDNA antibodies detected by RIA did not increase proportionally with ANA titers (Table S2 in Supplementary Material). We found a significant negative correlation between complement C3 levels and all anti-nuclear antibody tests (RIA Person's $r = -0.223$, $p = 0.006$; SNEC $r = -0.259$, $p = 0.001$; dsDNA-NcX $r = -0.238$, $p = 0.003$) (Table S2 in Supplementary Material). While CRP levels did not correlate with any of the tests, C4 negatively correlated with RIA and ESR with SNEC ELISA and anti-dsDNA-NcX ELISA (Table S3 in Supplementary Material). The anti-SNEC antibody levels correlated with 2 out of the 17 markers of the ENA profile: histone and nucleosome, both considered specific for SLE (**Figure 3B**). Taken together, anti-SNEC autoantibody levels significantly correlated with the most important canonical serological variables. The anti-SNEC antibody levels and the RIA assay were independent of SLE disease activity (**Figure 3D**; Table S3 in Supplementary Material). Approximately 50% of the patients tested showed low ECLAM values between 4 and 7 most likely due to permanent therapeutic treatment (Figure S1H in Supplementary Material).

Phagocytosis of SNEC by Neutrophils Is Mediated by SNEC-Specific AAb

We investigated the uptake of SNEC opsonized by anti-SNEC AAb (SNEC immune complexes: SNEC-IC) in a whole blood phagocytosis assay. We observed a positive correlation of uptake of fluorescent SNEC into neutrophils ($CD16^{POS}$-$HLA\text{-}DR^{NEG}$) in the presence of sera from SLE patients measured by flow cytometry (Spearman's $r = 0.5103$; $p < 0.0001$) (**Figure 4A**). Consistent with published data, NHD with low levels of autoreactive IgG showed very low uptake of SNEC into neutrophils (**Figure 4A**). *Z*-stack series of immunofluorescence images confirmed the uptake of SNEC into $CD15^{POS}$ neutrophils in the presence of a high anti-SNEC IgG SLE serum (**Figure 4B**). SNEC was only sporadically present in neutrophils when NHD serum was employed. Uptake of SNEC was also visible in $CD15^{NEG}$ monocytes in the presence of both SLE and NHD sera (**Figure 4B**, red arrow). $CD16^{POS}$-$HLA\text{-}DR^{NEG}$ neutrophils displayed a substantially diminished uptake of SNEC when anti-SNEC antibodies were adsorbed from SLE serum (SNEC, adsorbed) suggesting that the uptake of SNEC by neutrophils is mainly mediated by opsonizing AAb (**Figure 4C**). We confirmed this result for 12 different SLE sera (**Figure 4D**). Despite achieving moderate (3–48%) anti-SNEC autoantibody adsorption, SNEC phagocytosis was reduced up to 85% (**Figure 4E**). This suggests that SNEC preferentially catches the high-affine pathologically relevant AAb from sera of patients with SLE.

DISCUSSION

Patients with SLE are classified based on a combination of clinical and laboratory findings. Importantly, the sole presence of biopsy-proven lupus nephritis together with positivity for ANA or anti-dsDNA antibodies is declared as sufficient for a definite diagnosis (37) emphasizing the pivotal role of circulating pathogenic AAb for classification of SLE. However, current tests employing nuclear material derived from cell lysates or recombinant proteins for the detection of SLE-specific AAb disregard the apoptotic nature of these antigens. This is particularly critical since a clearance deficiency of apoptotic cells contributes to the etiopathogenesis of SLE (6, 38).

Considering the pathophysiological events in SLE, we developed a high-throughput assay employing SNEC as target for autoreactive IgG. The major goal of our study was to establish a reproducible substrate for the sensitive detection of SLE-typical AAb. The selection of PBMCs for the production of SNEC was based on the fact that the accumulation of apoptotic material in germinal centers is the main driving force leading to the break of self-tolerance. Since lymphocytes have the capacity to proliferate and die by canonical apoptosis, we supposed that these cells are likely to mainly expose pathogenically relevant autoantigens in the context of SLE.

Our test distinguished patients with SLE from NHD with high specificity and sensitivity of 98.9 and 70.6%, respectively. In the same study cohort, *anti-dsDNA-NcX-ELISA*, and RIA, commonly used for routine testing, showed sensitivities of 43.1 or 37.9%, respectively. Although, RIA is considered the gold standard for

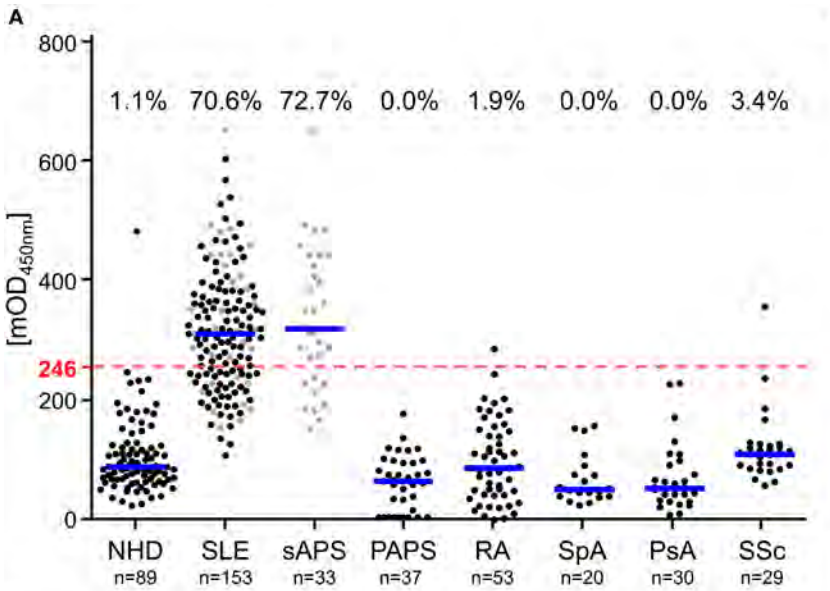

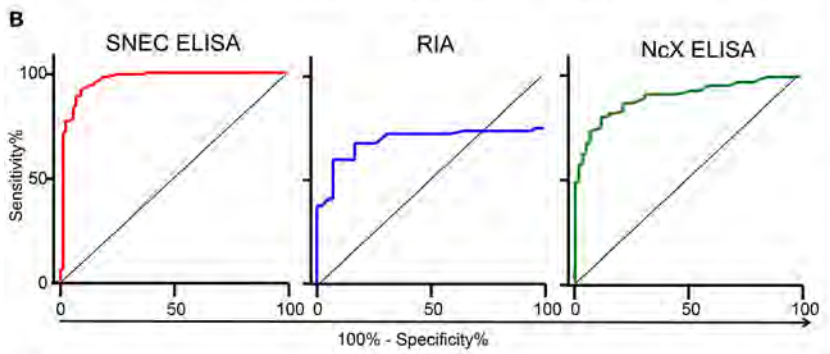

	SNEC ELISA	RIA	NcX ELISA
Cases studied (NHD+SLE)	242 (89 + 153)	195 (42 + 153)	215 (62 + 153)
Sensitivity	70.6	37.9	43.1
Specificity	98.9	97.6	98.4
Negative predictive value	66.2	30.1	41.2
Positive predictive value	99.1	98.3	98.5
Test performance (diagnostic odds ratio, DOR)	211.2	25.0	46.3

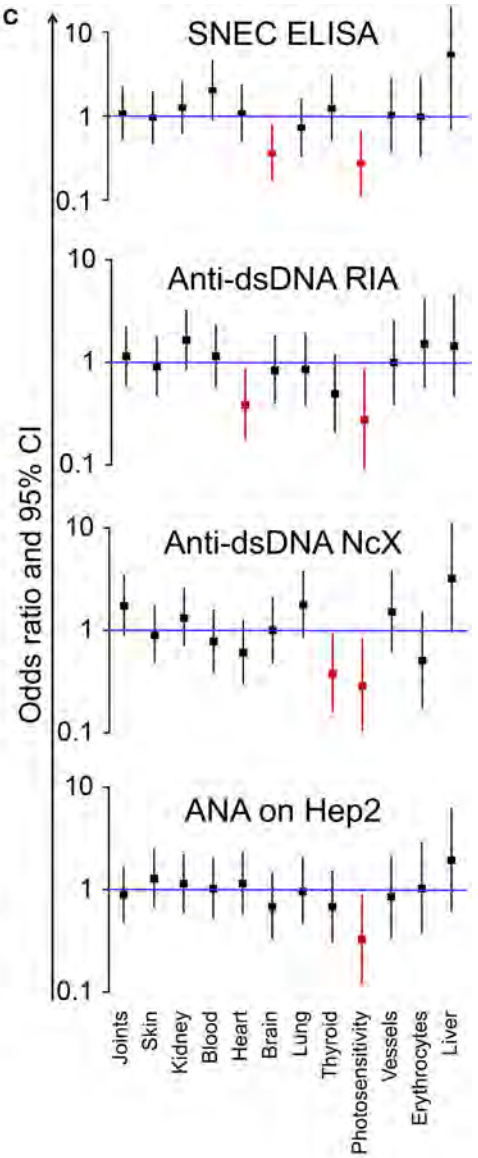

FIGURE 2 | SLE-derived AAb are specifically and sensitively detected by secondary NEcrotic cell (SNEC) ELISA. **(A)** Reactivity of sera from normal healthy donors (NHD) and patients with SLE, secondary anti-phospholipid syndrome (sAPS, gray dots in the SLE cohort), primary anti-phospholipid syndrome (PAPS), spondyloarthropathy (SpA), psoriatic arthritis (PsA), and systemic sclerosis (SSc) against SNEC were assessed by ELISA. Using receiver operating characteristic (ROC) analysis, the cut-off for positive values was calculated at 246 mean optical density (dashed red line). Frequencies of SNEC positivity are displayed above the respective cohort in percent (%). **(B)** The overall test performance of the SNEC ELISA (left), radioimmunoassay (RIA) dsDNA Farr assay (center), and anti-dsDNA-NcX-ELISA (right) was evaluated employing ROC analysis. The respective diagnostic parameters (specificity, sensitivity, negative predictive value, positive predictive value, and diagnostic odds ratio) were calculated and are displayed below. **(C)** Organ involvement was analyzed by comparison of odds ratios for SNEC ELISA, anti-dsDNA RIA, anti-dsDNA-NcX ELISA, and anti-nuclear antigen on HEp-2 titers. The depicted odd ratios are within the 95% confidence interval.

SLE serology it does not detect low affinity AAb. Since positive test results correlate with disease severity, it is suitable for monitoring of SLE disease course and lupus nephritis in individual patients (39). Another routine diagnostic assay, the *Crithidia luciliae* immunofluorescence test, turned out to not be a reliable screening tool in unselected patients with rheumatic symptoms, although it has diagnostic value for a limited number of key SLE manifestations such as proteinuria (40). In comparison to these, SNEC ELISA appears suitable for broad, quick and cost-efficient screening of populations with presumptive diagnosis of SLE. It specifically discriminates patients with SLE from those with other rheumatic diseases such as RA, SpA, PsA, SSc, or PAPS.

TABLE 3 | Frequencies of organ affection by autoantibody test and statistics from contingency tables.

		n	Frequency (%)	SNEC ELISA		Anti-dsDNA RIA		Anti-dsDNA NcX	
				χ^2	*p*	χ^2	*p*	χ^2	*p*
Arthritis	Yes	95	62.1	0.03	0.853	0.15	0.697	2.58	0.108
	No	58							
Rash	Yes	92	60.1	0.02	0.893	0.06	0.805	0.10	0.751
	No	61							
Renal	Yes	62	40.5	0.37	0.545	2.18	0.140	0.70	0.401
	No	91							
Cardiovascular	Yes	43	28.1	0.03	0.859	5.64	**0.018**	1.78	0.182
	No	110							
Leukopenia	Yes	47	30.7	2.82	0.093	0.15	0.700	0.49	0.482
	No	106							
Cerebral	Yes	38	24.8	6.87	**0.009**	0.19	0.663	0.00	0.980
	No	115							
Lung	Yes	35	22.9	0.63	0.427	0.15	0.696	2.18	0.139
	No	118							
Thyroid	Yes	31	20.3	0.19	0.666	2.52	0.113	4.92	**0.027**
	No	122							
Photosensitivity	Yes	24	15.7	8.81	**0.003**	5.58	**0.018**	5.92	**0.015**
	No	129							
Vasculitis	Yes	21	13.7	0.00	0.967	0.00	0.995	0.80	0.372
	No	132							
Liver	Yes	13	8.5	3.12	0.077	0.39	0.535	3.85	0.050
	No	140							
Hemolysis	Yes	17	11.1	0.00	0.964	0.64	0.423	1.53	0.216
	No	136							
MOF	Yes	2	1.3	0.83	0.361	0.12	0.734	1.57	0.210
	No	150							

Anti-dsDNA, anti-double stranded deoxyribonucleic acid antibodies; NcX, nucleosomes; RIA, radio immunosorbent assay; SNEC, secondary NEcrotic cells; MOF, multiple organ failure.

The bold fond indicates p value ≤ 0.05.

Anti-dsDNA AAb do not only recognize helical B-DNA but also bent DNA present in the large intergenic regions of chromatin (41, 42). The *anti-dsDNA-NcX-ELISA* utilizes dsDNA complexed with nucleosomes for the detection of anti-nuclear antibodies. However, considering our findings, this substrate might not completely reflect the full arsenal of (apoptosis-associated) autoantigens recognized by SLE AAb. We confirmed the presence in SNEC of apoptosis-associated chromatin modifications reportedly associated with SLE (43) such as H3-K27me3, H2A/H4-AcK8,12,16, and H2B-AcK12. Consistently, standard serological variables such as ENA and ANA reactivity significantly correlated with SNEC positivity. Likewise, nucleosomes and dsDNA, representing classical autoantigenic targets for SLE-specific AAb, were accessible. We observed that HMGB1 is present in SNEC extending the repertoire of apoptosis-related autoantigens. HMBG1 reportedly to co-precipitates with anti-histone and anti-dsDNA antibodies and appears complexed with free nucleosomes in the circulation of patients with SLE (10). HMGB1-containing nucleosomes from apoptotic cells induce anti-dsDNA and anti-histone IgG-mediated responses in a toll-like receptor 2-dependent manner (44). The accessibility of HMGB1-containing nucleosomes in our assay highlights the importance of SNEC material in the pathogenesis of SLE (45).

Deposition of circulating and *in situ* formed ICs is known to be a critical factor triggering inflammation and tissue damage in SLE. They consist of assorted intracellular material exposing various modified epitopes to AAb (46, 47). Evidence that cellular debris accumulates as extracellular material in tissues exclusively in SLE patients goes back to the 50 s (48–50) and was revisited recently (51). The uptake of these ICs into phagocytes has been shown to bepro-inflammatory and mediated by FcγR (12, 18). We observed a significant correlation between the presence of anti-SNEC AAb and the uptake of SNEC into $CD16^{POS}$ granulocytes. Some of the SLE sera employed did not facilitate phagocytosis of SNEC, although anti-SNEC IgG was measured by SNEC ELISA. Since the employed phagocytosis assay is a complex biological system, it might be less sensitive than SNEC ELISA. Thus, low amounts of AAb which can already be detected by SNEC ELISA, do not facilitate the uptake of measurable amounts of SNEC by neutrophils. Adsorption of anti-SNEC AAb from serum resulted in substantial reduction of SNEC uptake into granulocytes. Even a mild reduction of anti-SNEC autoantibody levels resulted in strongly diminished phagocytosis. Thus, we suggest that SNEC ELISA enables the detection of pathogenic AAb in SLE sera.

We hypothesize that the AAb measured by SNEC ELISA induce the pathomechanism depicted in **Figure 5**. In healthy individuals

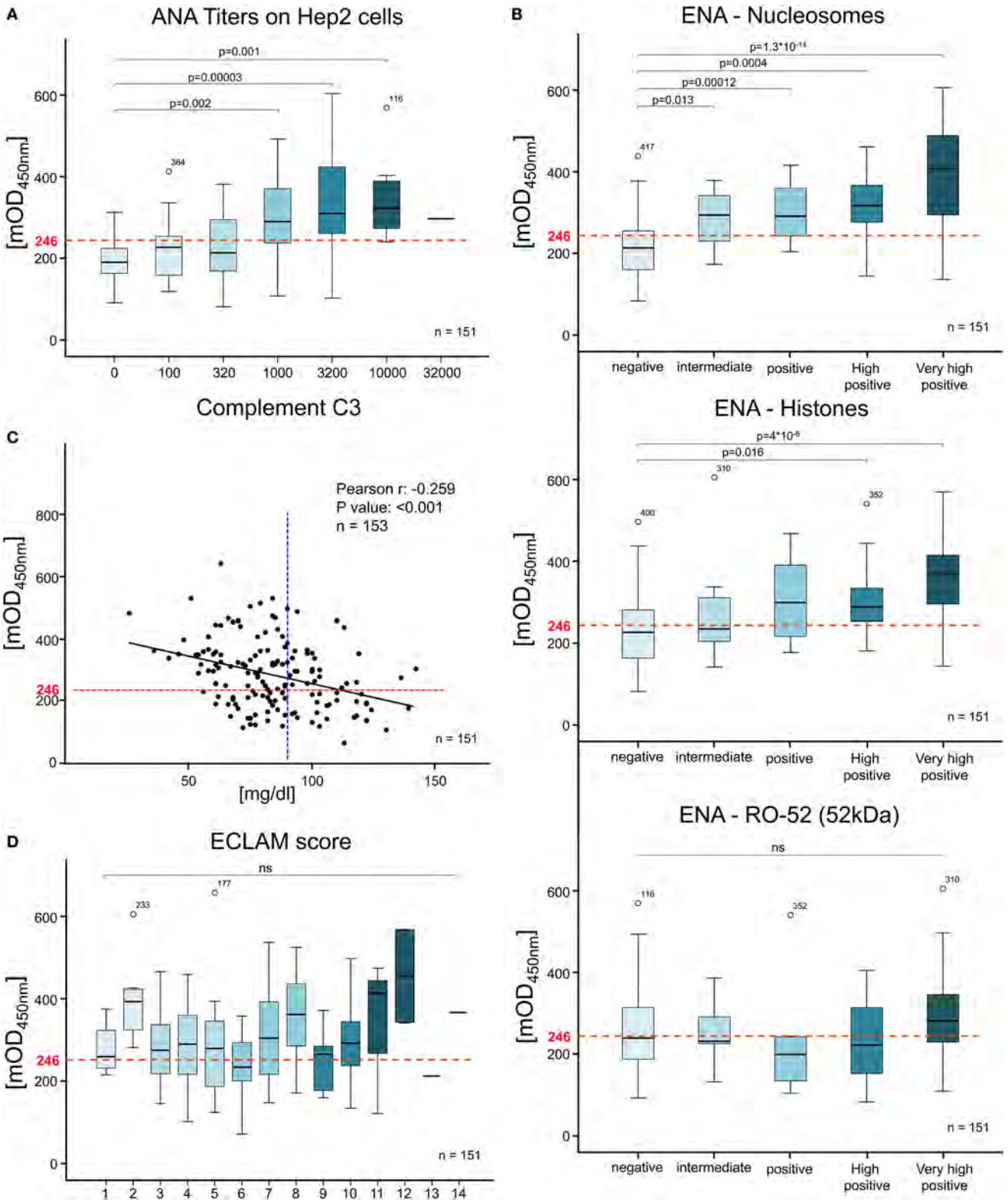

FIGURE 3 | Anti-secondary NEcrotic cell (SNEC) IgG correlates with serological disease variables but not with the disease activity. The correlation of SNEC ELISA levels with serological and clinical variables was evaluated by Bravais-Pearson correlation coefficients and corrected after Bonferroni. SNEC positivity was compared to **(A)** anti-nuclear antigen on HEp-2 cell titers, **(B)** extractable nuclear antigen positivity (Nucleosomes, Histones, Ro52), **(C)** Complement C3 levels (cut off C3 levels at 90 mg/ml indicated as blue dotted line), **(D)** European Consensus Lupus Activity Measurement Manifestation Score and others (see also Tables 1, 2 and S1, S2 in Supplementary Material). The SNEC ELISA cut-off at 246 mean optical density is depicted as a red dotted line.

(NHD), apoptotic cells are swiftly engulfed by phagocytes without the induction of inflammatory responses, a process referred to as efferocytosis (**Figure 5**) (15). The recognition of phosphatidylserine on the outer surface of the dead or dying cell is a key step in this process. It engages several different proteins and lipids including $\alpha_V\beta_3$ integrin, TAM receptors (Tryo3, Axl, Mer), milk fat globule-EGF factor 8 protein (MFG-E8), growth arrest-specific protein 6 (Gas6), protein S and phosphatidylserine (15). Upon recognition,

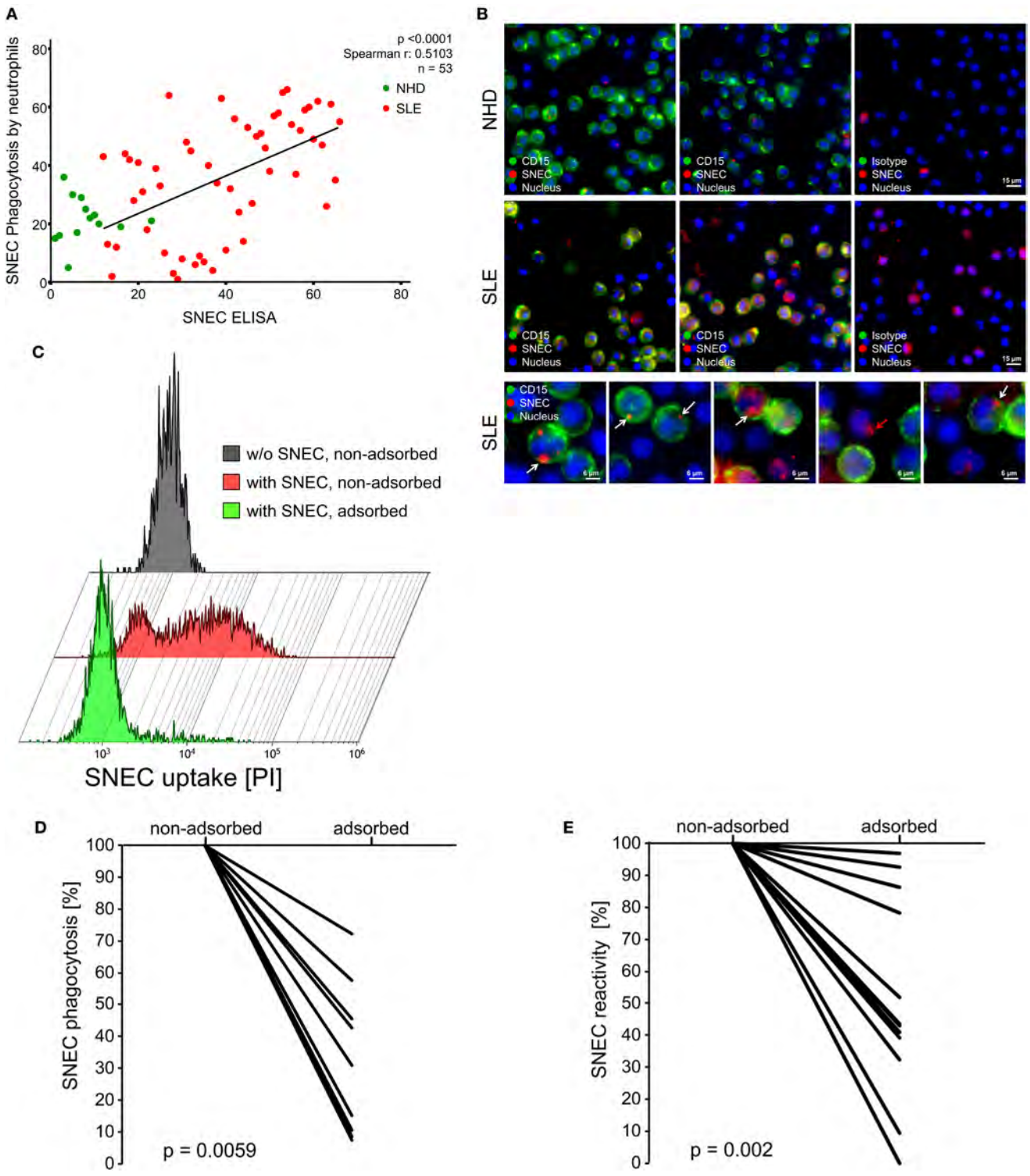

FIGURE 4 | Continued

FIGURE 4 | Secondary NEcrotic cell (SNEC) positivity correlates with uptake of SNEC into blood-borne neutrophils. **(A)** Correlation of SNEC uptake by neutrophils assessed by flow cytometry with anti-SNEC IgG. Values are displayed as ranks. Spearman's rank correlation coefficient was calculated using the values of patients with SLE. **(B)** Representative microphotographs of *z*-stack series showing that PI-stained SNEC (red) was taken up by neutrophils with a segmented nucleus (CD15POS; displayed in green; Hoechst 33342POS; displayed in blue). White arrows indicate SNEC taken up by neutrophils. SNEC phagocytosed by a CD15NEG mononuclear phagocyte is indicated by a red arrow. **(C)** Uptake of PI-stained SNEC by CD16POS HLA-DRNEG granulocytes in whole blood assessed by flow cytometry in the presence (+SNEC, non-adsorbed) or absence (+SNEC, adsorbed) of anti-SNEC autoantibodies. CD16POS HLA-DRNEG granulocytes in whole blood without addition of SNEC served as negative control (–SNEC). Shown is the uptake of SNEC in the presence of a representative adsorbed and non-adsorbed SLE serum. **(D)** Percentage of SNEC uptake into CD16POSHLA-DRNEG granulocytes in the presence of 10 anti-SNEC antibody adsorbed SLE sera relative to the corresponding non-adsorbed sera. **(E)** Percentage of residual anti-SNEC IgG in adsorbed relative to the corresponding non-adsorbed sera assessed by SNEC ELISA.

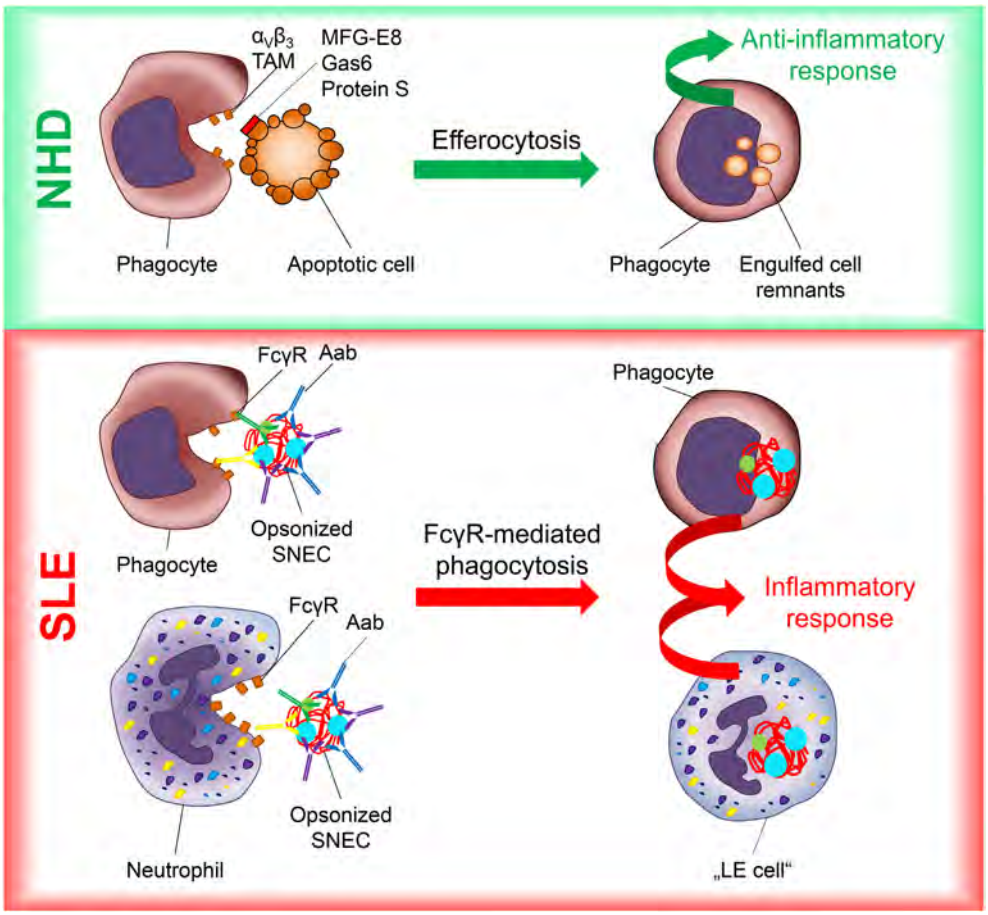

FIGURE 5 | Inflammation in SLE is driven by FcγR-mediated uptake into phagocytes of secondary NEcrotic cell (SNEC) opsonized by autoantibodies (AAb). In healthy individuals (NHD), apoptotic cells are cleared rapidly and silently by professional phagocytes involving a plethora receptors and bridging molecules such as $\alpha_v\beta_3$ integrin, Tryo3–Axl–Mer (TAM), milk fat globule-EGF factor 8 protein (MFG-E8), growth arrest-specific protein 6 (Gas6), and Proteins S. This marked redundancy avoids disintegration of apoptotic cells and the generation of SNEC. In patients with systemic lupus erythematosus (SLE), the concurrence of AAb and SNEC results in the opsonization and Fcγ Receptor (FcγR)-mediated uptake of SNEC into phagocytes, especially neutrophils. This perpetuates inflammatory responses and causes tissue damage. Lupus erythematosus (LE) cell.

phagocytes release immunomodulatory factors including TGFβ suppressing the inflammatory responses by surrounding cells. This enables the silent clearance of billions of dead and dying cells daily. In systemic lupus erythematosus (SLE), AAb recognize nuclear material derived from apoptotic cells that had escaped canonical clearance (SNEC) (**Figure 5**). It is known that the formation of ICs composed of SNEC and AAb activates complement and induces inflammation *via* uptake of these opsonized complexes (12, 13, 52). Blood-borne phagocytes, especially Neutrophils, taking up opsonized SNEC have formerly been described as LE cells. In contrast to the silent efferocytosis, Fc gamma receptor (FcγR)-dependent uptake of nucleic acid containing SNEC favors the release of pro-inflammatory mediators (15, 53). It was demonstrated that FcγRIIA-mediated contact with soluble ICs results in formation of NETs *in vivo* (54). Although we did not observe release of NETs in response to anti-SNEC antibody-mediated IC uptake employing life cell imaging phagocytosis experiments, it poses an interesting topic for future investigations.

Secondary NEcrotic cell-autoantibody complexes carry DNA, which is considered a danger signal by the immune system confusing them with opsonized virus particles (*virus-mimetic*), and consequently triggers DNA sensing proinflammatory pathways. The latter include TLR-9, cyclic GMP-AMP synthase, DNA-dependent activator of IFN-regulatory factors, absent in melanoma 2, STING, gamma-interferon inducible protein-16, nucleotide-binding domain leucine-rich repeat containing protein family pyrin domain containing 3, DEAD/H-box helicase 41, and meiotic recombination 11 protein [summarized in Ref. (55)]. These molecules stimulate type I IFN expression, referred to as the IFN signature, shared by most patients with SLE, which correlates with the clinical appearance and severity of SLE (56).

This study gives insight into the mechanism of SLE etiopathogenesis with respect to autoantibody pathogenicity in terms of FcγR-mediated phagocytosis and provides the basis for improved serological screening of SLE. However, limitations of the study have to be considered. First, SLE patients were under treatment and thus often showed low disease activity. The lack of a full range ECLAM distribution might create a bias that partially explains the absence of an association of anti-nuclear antibody tests with disease activity scores. Moreover, it was demonstrated that anti-nucleosome antibodies present in serologically active but clinically quiescent patients predicted future flares (57). SNEC ELISA might detect AAb which did not result in increased disease activity yet. In fact, that the test performance is not affected by the patients' clinical status renders SNEC ELISA a robust screening test for patients with suspected SLE. Second, our study analyzed patients from a single center. Investigations of several patient groups from different study centers (multicenter study) are required to confirm applicability to different ethnicities. The investigations of specific intracellular DNA-sensors and related signaling pathways in neutrophils will provide further insights in the pathogenesis of SLE with potential therapeutic applications. In conclusion, in this study, we confirm that SNEC uptake is intimately linked with the pathogenesis of the disease. We also demonstrate that the detection of anti-SNEC antibodies is a powerful tool supporting the diagnosis of SLE and the exclusion of other autoimmune connective tissue diseases.

ETHICS STATEMENT

This study was carried out in accordance with the recommendations of institutional guidelines and the approval of the ethical committee of the Universitätsklinikum Erlangen. The protocol was approved by the ethical committee of the Universitätsklinikum Erlangen (permit # 54_14B). Written informed consent was given by each donor in accordance with the Declaration of Helsinki.

AUTHOR CONTRIBUTIONS

MB and JK planned and performed ELISA and phagocytosis experiments and conducted data analysis. SB and LM coordinated clinical data mining and performed statistical analysis. EP and JV performed monoclonal ELISA experiments and provided scientific input. JR, BH, RB, GS, and GK collected clinical data and provided scientific input. MH and LM supervised the project, planned experiments, and conducted data analysis. All authors wrote, read, and approved the manuscript.

ACKNOWLEDGMENTS

The present work was performed in (partial) fulfillment of the requirements for obtaining the degree "Dr. med."/"Dr. rer. biol. hum." to SB. The authors acknowledge support by Deutsche Forschungsgemeinschaft and Friedrich-Alexander- Universität Erlangen-Nürnberg (FAU) within the funding program Open Access Publishing. We would like to thank Veronika Gröger, Ferdinand Reiser, and Christine Schülein for their excellent technical assistance.

FUNDING

This work was partially supported by the German Research Foundation (DFG) to MH (CRC1181-C03, KFO257), by the EU H2020-MSCE-RISE-2015 project Nr. 690836 PANG to LM and RB, by the Volkswagen-Stiftung grant# 90361 to MH and RB, by grants from the Dutch Arthritis Association (grant 09-1-308; JV), by the Dutch Kidney Foundation (KSBS 12.073; EP/JV), by the RadboudUMC Honors Academy (EP), by the doctoral training program GK1660 of the DFG (JK), and by Ardea Biosciences, Inc. to MH and LM.

SUPPLEMENTARY MATERIAL

The Supplementary Material for this article can be found online at https://www.frontiersin.org/articles/10.3389/fimmu.2018.00989/full#supplementary-material.

REFERENCES

1. Harley JB, Kelly JA, Kaufman KM. Unraveling the genetics of systemic lupus erythematosus. *Springer Semin Immunopathol* (2006) 28(2):119–30. doi:10.1007/s00281-006-0040-5
2. Costenbader KH, Feskanich D, Stampfer MJ, Karlson EW. Reproductive and menopausal factors and risk of systemic lupus erythematosus in women. *Arthritis Rheum* (2007) 56(4):1251–62. doi:10.1002/art.22510
3. Hahn BH, Ebling F, Singh RR, Singh RP, Karpouzas G, La Cava A. Cellular and molecular mechanisms of regulation of autoantibody production in lupus. *Ann N Y Acad Sci* (2005) 1051:433–41. doi:10.1196/annals.1361.085
4. Cooper GS, Dooley MA, Treadwell EL, St Clair EW, Gilkeson GS. Risk factors for development of systemic lupus erythematosus: allergies, infections, and family history. *J Clin Epidemiol* (2002) 55(10):982–9. doi:10.1016/S0895-4356(02)00429-8
5. Lehmann P, Holzle E, Kind P, Goerz G, Plewig G. Experimental reproduction of skin lesions in lupus erythematosus by UVA and UVB radiation. *J Am Acad Dermatol* (1990) 22(2 Pt 1):181–7. doi:10.1016/0190-9622(90)70020-I
6. Baumann I, Kolowos W, Voll RE, Manger B, Gaipl U, Neuhuber WL, et al. Impaired uptake of apoptotic cells into tingible body macrophages in germinal centers of patients with systemic lupus erythematosus. *Arthritis Rheum* (2002) 46(1):191–201. doi:10.1002/1529-0131(200201)46:1<191::AID-ART10027>3.0.CO;2-K
7. Munoz LE, Gaipl US, Franz S, Sheriff A, Voll RE, Kalden JR, et al. SLE – a disease of clearance deficiency? *Rheumatology* (2005) 44(9):1101–7. doi:10.1093/rheumatology/keh693

8. Gaipl US, Munoz LE, Grossmayer G, Lauber K, Franz S, Sarter K, et al. Clearance deficiency and systemic lupus erythematosus (SLE). *J Autoimmun* (2007) 28(2–3):114–21. doi:10.1016/j.jaut.2007.02.005
9. Schulze C, Munoz LE, Franz S, Sarter K, Chaurio RA, Gaipl US, et al. Clearance deficiency – a potential link between infections and autoimmunity. *Autoimmun Rev* (2008) 8(1):5–8. doi:10.1016/j.autrev.2008.07.049
10. Urbonaviciute V, Furnrohr BG, Meister S, Munoz L, Heyder P, De Marchis F, et al. Induction of inflammatory and immune responses by HMGB1-nucleosome complexes: implications for the pathogenesis of SLE. *J Exp Med* (2008) 205(13):3007–18. doi:10.1084/jem.20081165
11. Kuhn A, Herrmann M, Kleber S, Beckmann-Welle M, Fehsel K, Martin-Villalba A, et al. Accumulation of apoptotic cells in the epidermis of patients with cutaneous lupus erythematosus after ultraviolet irradiation. *Arthritis Rheum* (2006) 54(3):939–50. doi:10.1002/art.21658
12. Munoz LE, Janko C, Grossmayer GE, Frey B, Voll RE, Kern P, et al. Remnants of secondarily necrotic cells fuel inflammation in systemic lupus erythematosus. *Arthritis Rheum* (2009) 60(6):1733–42. doi:10.1002/art.24535
13. Janko C, Franz S, Munoz LE, Siebig S, Winkler S, Schett G, et al. CRP/anti-CRP antibodies assembly on the surfaces of cell remnants switches their phagocytic clearance toward inflammation. *Front Immunol* (2011) 2:70. doi:10.3389/fimmu.2011.00070
14. Matzinger P. The danger model: a renewed sense of self. *Science* (2002) 296(5566):301–5. doi:10.1126/science.1071059
15. Birge RB, Boeltz S, Kumar S, Carlson J, Wanderley J, Calianese D, et al. Phosphatidylserine is a global immunosuppressive signal in efferocytosis, infectious disease, and cancer. *Cell Death Differ* (2016) 23(6):962–78. doi:10.1038/cdd.2016.11
16. Munoz LE, Lauber K, Schiller M, Manfredi AA, Herrmann M. The role of defective clearance of apoptotic cells in systemic autoimmunity. *Nat Rev Rheumatol* (2010) 6(5):280–9. doi:10.1038/nrrheum.2010.46
17. Pieterse E, van der Vlag J. Breaking immunological tolerance in systemic lupus erythematosus. *Front Immunol* (2014) 5:164. doi:10.3389/fimmu.2014.00164
18. Munoz LE, Janko C, Schulze C, Schorn C, Sarter K, Schett G, et al. Autoimmunity and chronic inflammation – two clearance-related steps in the etiopathogenesis of SLE. *Autoimmun Rev* (2010) 10(1):38–42. doi:10.1016/j.autrev.2010.08.015
19. Obermoser G, Pascual V. The interferon-alpha signature of systemic lupus erythematosus. *Lupus* (2010) 19(9):1012–9. doi:10.1177/0961203310371161
20. Mayadas TN, Tsokos GC, Tsuboi N. Mechanisms of immune complex-mediated neutrophil recruitment and tissue injury. *Circulation* (2009) 120(20):2012–24. doi:10.1161/CIRCULATIONAHA.108.771170
21. Hargraves MM. Discovery of the LE cell and its morphology. *Mayo Clin Proc* (1969) 44(9):579–99.
22. Hepburn AL. The LE cell. *Rheumatology* (2001) 40(7):826–7. doi:10.1093/rheumatology/40.7.826
23. Schett G, Steiner G, Smolen JS. Nuclear antigen histone H1 is primarily involved in lupus erythematosus cell formation. *Arthritis Rheum* (1998) 41(8):1446–55. doi:10.1002/1529-0131(199808)41:8<1446::AID-ART15>3.0.CO;2-6
24. Schett G, Rubin RL, Steiner G, Hiesberger H, Muller S, Smolen J. The lupus erythematosus cell phenomenon: comparative analysis of antichromatin antibody specificity in lupus erythematosus cell-positive and -negative sera. *Arthritis Rheum* (2000) 43(2):420–8. doi:10.1002/1529-0131(200002)43:2<420::AID-ANR24>3.0.CO;2-Z
25. Schmidt-Acevedo S, Perez-Romano B, Ruiz-Arguelles A. 'LE cells' result from phagocytosis of apoptotic bodies induced by antinuclear antibodies. *J Autoimmun* (2000) 15(1):15–20. doi:10.1006/jaut.2000.0381
26. Schett G, Smole J, Zimmermann C, Hiesberger H, Hoefler E, Fournel S, et al. The autoimmune response to chromatin antigens in systemic lupus erythematosus: autoantibodies against histone H1 are a highly specific marker for SLE associated with increased disease activity. *Lupus* (2002) 11(11):704–15. doi:10.1191/0961203302lu247oa
27. Piette JC. Updating the American College of Rheumatology criteria for systemic lupus erythematosus: comment on the letter by Hochberg. *Arthritis Rheum* (1998) 41(4):751. doi:10.1002/1529-0131(199804)41:4<751::AID-ART30>3.0.CO;2-W
28. Quismorio FP. Clinical application of serologic abnormalities in systemic lupus erythematosus. 7th ed. In: Wallace DJ, Bevra H, editors. *Dubois' Lupus Erythematosus*. Philadelphia: Lippincott Williams & Wilkins (2007). p. 933–55.
29. Arbuckle MR, McClain MT, Rubertone MV, Scofield RH, Dennis GJ, James JA, et al. Development of autoantibodies before the clinical onset of systemic lupus erythematosus. *N Engl J Med* (2003) 349(16):1526–33. doi:10.1056/NEJMoa021933
30. Dema B, Charles N. Autoantibodies in SLE: specificities, isotypes and receptors. *Antibodies* (2016) 5(1):2. doi:10.3390/antib5010002
31. Noble PB, Cutts JH. Separation of blood leukocytes by Ficoll gradient. *Can Vet J* (1967) 8(5):110–1.
32. van der Heijden GW, Dieker JW, Derijck AA, Muller S, Berden JH, Braat DD, et al. Asymmetry in histone H3 variants and lysine methylation between paternal and maternal chromatin of the early mouse zygote. *Mech Dev* (2005) 122(9):1008–22. doi:10.1016/j.mod.2005.04.009
33. van Bavel CC, Dieker JW, Tamboer WP, van der Vlag J, Berden JH. Lupus-derived monoclonal autoantibodies against apoptotic chromatin recognize acetylated conformational epitopes. *Mol Immunol* (2010) 48(1–3):248–56. doi:10.1016/j.molimm.2010.08.003
34. van Bavel CC, Dieker JW, Kroeze Y, Tamboer WP, Voll R, Muller S, et al. Apoptosis-induced histone H3 methylation is targeted by autoantibodies in systemic lupus erythematosus. *Ann Rheum Dis* (2011) 70(1):201–7. doi:10.1136/ard.2010.129320
35. Dieker JW, Fransen JH, van Bavel CC, Briand JP, Jacobs CW, Muller S, et al. Apoptosis-induced acetylation of histones is pathogenic in systemic lupus erythematosus. *Arthritis Rheum* (2007) 56(6):1921–33. doi:10.1002/art.22646
36. van Bavel CC, Dieker J, Muller S, Briand JP, Monestier M, Berden JH, et al. Apoptosis-associated acetylation on histone H2B is an epitope for lupus autoantibodies. *Mol Immunol* (2009) 47(2–3):511–6. doi:10.1016/j.molimm.2009.08.009
37. Petri M, Orbai AM, Alarcon GS, Gordon C, Merrill JT, Fortin PR, et al. Derivation and validation of the systemic lupus international collaborating clinics classification criteria for systemic lupus erythematosus. *Arthritis Rheum* (2012) 64(8):2677–86. doi:10.1002/art.34473
38. Herrmann M, Voll RE, Zoller OM, Hagenhofer M, Ponner BB, Kalden JR. Impaired phagocytosis of apoptotic cell material by monocyte-derived macrophages from patients with systemic lupus erythematosus. *Arthritis Rheum* (1998) 41(7):1241–50. doi:10.1002/1529-0131(199807)41:7<1241::AID-ART15>3.0.CO;2-H
39. Egner W. The use of laboratory tests in the diagnosis of SLE. *J Clin Pathol* (2000) 53(6):424–32. doi:10.1136/jcp.53.6.424
40. Compagno M, Rekvig OP, Bengtsson AA, Sturfelt G, Heegaard NH, Jonsen A, et al. Clinical phenotype associations with various types of anti-dsDNA antibodies in patients with recent onset of rheumatic symptoms. Results from a multicentre observational study. *Lupus Sci Med* (2014) 1(1):e000007. doi:10.1136/lupus-2013-000007
41. Herrmann M, Winkler TH, Fehr H, Kalden JR. Preferential recognition of specific DNA motifs by anti-double-stranded DNA autoantibodies. *Eur J Immunol* (1995) 25(7):1897–904. doi:10.1002/eji.1830250716
42. Richmond TJ, Davey CA. The structure of DNA in the nucleosome core. *Nature* (2003) 423(6936):145–50. doi:10.1038/nature01595
43. Dieker J, Berden JH, Bakker M, Briand JP, Muller S, Voll R, et al. Autoantibodies against modified histone peptides in SLE patients are associated with disease activity and lupus nephritis. *PLoS One* (2016) 11(10):e0165373. doi:10.1371/journal.pone.0165373
44. Urbonaviciute V, Starke C, Pirschel W, Pohle S, Frey S, Daniel C, et al. Toll-like receptor 2 is required for autoantibody production and development of renal disease in pristane-induced lupus. *Arthritis Rheum* (2013) 65(6):1612–23. doi:10.1002/art.37914
45. Scaffidi P, Misteli T, Bianchi ME. Release of chromatin protein HMGB1 by necrotic cells triggers inflammation. *Nature* (2002) 418(6894):191–5. doi:10.1038/nature00858
46. Munoz LE, van Bavel C, Franz S, Berden J, Herrmann M, van der Vlag J. Apoptosis in the pathogenesis of systemic lupus erythematosus. *Lupus* (2008) 17(5):371–5. doi:10.1177/0961203308089990
47. Rosen A, Casciola-Rosen L, Ahearn J. Novel packages of viral and self-antigens are generated during apoptosis. *J Exp Med* (1995) 181(4):1557–61. doi:10.1084/jem.181.4.1557
48. Klemperer P, Gueft B, Lee S, Leuchtenberger C, Pollister A. Cytochemical changes of acute lupus erythematosus. *Arch Pathol* (1950) 49(5):503–16.
49. Worthington JW Jr, Baggenstoss AH, Hargraves MM. Significance of hematoxylin bodies in the necropsy diagnosis of systemic lupus erythematosus. *Am J Pathol* (1959) 35:955–69.

50. Gueft B, Laufer A. Further cytochemical studies in systemic lupus erythematosus. *AMA Arch Pathol* (1954) 57(3):201–26.
51. Munoz LE, Leppkes M, Fuchs TA, Hoffmann M, Herrmann M. Missing in action-the meaning of cell death in tissue damage and inflammation. *Immunol Rev* (2017) 280(1):26–40. doi:10.1111/imr.12569
52. Munoz LE, Janko C, Chaurio RA, Schett G, Gaipl US, Herrmann M. IgG opsonized nuclear remnants from dead cells cause systemic inflammation in SLE. *Autoimmunity* (2010) 43(3):232–5. doi:10.3109/08916930903510930
53. Sachet M, Liang YY, Oehler R. The immune response to secondary NEcrotic cells. *Apoptosis* (2017) 22(10):1189–204. doi:10.1007/s10495-017-1413-z
54. Chen K, Nishi H, Travers R, Tsuboi N, Martinod K, Wagner DD, et al. Endocytosis of soluble immune complexes leads to their clearance by FcgammaRIIIB but induces neutrophil extracellular traps via Fcgamma-RIIA in vivo. *Blood* (2012) 120(22):4421–31. doi:10.1182/blood-2011-12-401133
55. Bai Y, Tong Y, Liu Y, Hu H. Self-dsDNA in the pathogenesis of systemic lupus erythematosus. *Clin Exp Immunol* (2017) 191(1):1–10. doi:10.1111/cei.13041
56. Crow MK. Type I interferon in the pathogenesis of lupus. *J Immunol* (2014) 192(12):5459–68. doi:10.4049/jimmunol.1002795
57. Ng KP, Manson JJ, Rahman A, Isenberg DA. Association of antinucleosome antibodies with disease flare in serologically active clinically quiescent patients with systemic lupus erythematosus. *Arthritis Rheum* (2006) 55(6):900–4. doi:10.1002/art.22356

Conflict of Interest Statement: The authors declare that the research was conducted in the absence of any commercial or financial relationships that could be construed as a potential conflict of interest.

frontiers in Immunology

TECHNOLOGY REPORT
published: 04 May 2018
doi: 10.3389/fimmu.2018.00927

Automated Processing and Evaluation of Anti-Nuclear Antibody Indirect Immunofluorescence Testing

Vincent Ricchiuti[1], Joseph Adams[1], Donna J. Hardy[1], Alexander Katayev[2] and James K. Fleming[2]*

[1] North Central Division, Laboratory Corporation of America Holdings (LabCorp), Dublin, OH, United States, [2] Department of Science and Technology, Laboratory Corporation of America Holdings (LabCorp), Elon, NC, United States

Indirect immunofluorescence (IIF) is considered by the American College of Rheumatology (ACR) and the international consensus on ANA patterns (ICAP) the gold standard for the screening of anti-nuclear antibodies (ANA). As conventional IIF is labor intensive, time-consuming, subjective, and poorly standardized, there have been ongoing efforts to improve the standardization of reagents and to develop automated platforms for assay incubation, microscopy, and evaluation. In this study, the workflow and performance characteristics of a fully automated ANA IIF system (Sprinter XL, EUROPattern Suite, IFA 40: HEp-20-10 cells) were compared to a manual approach using visual microscopy with a filter device for single-well titration and to technologist reading. The Sprinter/EUROPattern system enabled the processing of large daily workload cohorts in less than 8 h and the reduction of labor hands-on time by more than 4 h. Regarding the discrimination of positive from negative samples, the overall agreement of the EUROPattern software with technologist reading was higher (95.6%) than when compared to the current method (89.4%). Moreover, the software was consistent with technologist reading in 80.6–97.5% of patterns and 71.0–93.8% of titers. In conclusion, the Sprinter/EUROPattern system provides substantial labor savings and good concordance with technologist ANA IIF microscopy, thus increasing standardization, laboratory efficiency, and removing subjectivity.

Keywords: anti-nuclear antibodies, autoimmune rheumatic diseases, automation, computer-aided immunofluorescence microscopy, EUROPattern Suite, HEp-20-10 cells, indirect immunofluorescence, standardization

OPEN ACCESS

Edited by:
Ralf J. Ludwig, Universität zu Lübeck, Germany

Reviewed by:
Anil Chauhan, Saint Louis University, United States
Otavio Cabral-Marques, Universität zu Lübeck, Germany

****Correspondence:***
Vincent Ricchiuti
ricchiv@labcorp.com

Specialty section:
This article was submitted to Immunological Tolerance and Regulation, a section of the journal Frontiers in Immunology

Received: *24 November 2017*
Accepted: *13 April 2018*
Published: *04 May 2018*

Citation:
Ricchiuti V, Adams J, Hardy DJ, Katayev A and Fleming JK (2018) Automated Processing and Evaluation of Anti-Nuclear Antibody Indirect Immunofluorescence Testing. Front. Immunol. 9:927. doi: 10.3389/fimmu.2018.00927

INTRODUCTION

Anti-nuclear antibodies (ANA) represent important diagnostic markers in various autoimmune rheumatic conditions (e.g., systemic lupus erythematosus (SLE), Sjögren's syndrome, systemic sclerosis, dermato/poly myositis, mixed connective tissue diseases, and rheumatoid arthritis), with an increasingly recognized relevance to disease prediction and prognosis (1–6). Low-titer ANA may also be detected in healthy individuals (7–9). The term "ANA" is commonly used *sensu lato* to encompass not only antibodies directed against nuclear antigens, but also those binding to constituents of the nuclear envelope, mitotic spindle apparatus, or cytoplasm.

In 1957, the first ANA was demonstrated by indirect immunofluorescence (IIF) in the serum of SLE patients, followed by the discovery and characterization of extractable nuclear antigens in 1959 (10–12). IIF testing has since become the standard method for ANA screening in patient sera, using human epithelial cells (HEp-2) or variants of this laryngeal carcinoma cell line as the

preferred cell substrate (13, 14). Hep-2 cells present a very broad spectrum of 100–150 cell antigens at different stages of the cell cycle, allowing the sensitive detection of numerous clinically relevant autoantibodies. However, conventional ANA IIF testing is time-consuming, laborious, and burdened by the need for microscopy expertise, subjectivity of interpretation, lack of automation, and a low degree of standardization leading to high intra- and inter-laboratory variance (15–18). As the demand for ANA testing has increased considerably over the past decades and pushed large service laboratories to provide high throughput, reduced turnaround time-consuming and cost-saving diagnostics, there has been a movement from IIF to largely automated screening methods, in particular ELISA and flow cytometric bead-based ("multiplex") immunoassays that are based on a limited number of purified and/or recombinant antigenic substrates. Examples for multiplex assays include the BioPlex 2200 ANA screen(Bio-Rad), Athena Multi-Lyte (ZEUS Scientific), Quanta Plex (INOVA Diagnostics), and FIDIS (BMD) (13, 16, 19–30). Samples classified as positive through screening by ELISA or multiplex are usually reflexed to IIF to confirm the result and to determine the titer and associated ANA pattern(s), while samples devoid of reactivity against the antigenic panel are reported as negative. Although this approach is time-consuming and cost-saving and provides a high specificity for each single antigen, the use of screening panels has slightly less sensitivity than HEp-2-based IIF. In 2007, the American College of Rheumatology setup a task force which soon after released a position statement recommending IIF as the "gold standard" for ANA testing (13, 31). This concept was adopted later by international organizations and, along with advances in IIF automation, led to a "renaissance" of IIF (16, 32). In current practice, a two-step strategy is commonly applied, where initial ANA IIF screening provides information on antibody patterns and titers, followed by a confirmatory monospecific test (e.g., ELISA, Multiplex, and immunoblot) to identify the autoantibody (33), or in many laboratories, the reverse algorithm is also performed, where enzyme immunoassay positivity is reflexed to IIF.

In 2015, the persisting lack of inter-laboratory standardization and other problems in ANA IIF testing and reporting put forth an International Consensus on ANA patterns (ICAP) (34, 35). Beside the main objective of (i) standardizing the categorization and nomenclature of HEp-2 cell ANA patterns, the ICAP consensus also recommended (ii) endpoint titration of positive samples. The relevance of this point becomes clear considering that single-well testing of high-titer sera bears the risk of antibody masking. Masking may occur when a diagnostically relevant autoantibody is indiscernible due to the presence of further dominant or unspecific antibodies or when hook/prozone effects from antibody excess cause atypical, diffuse, faint, or negative IIF staining (36, 37). (iii) Clinically relevant mixed patterns should be discriminated accurately considering the possibility of antibody masking. (iv) The ICAP intention is to differentiate patterns that should be readily recognized (competent-level) from patterns that would be more challenging and distinguishable only when observers or technologists have attained a expert-level proficiency. Reporting should include all competent-level nuclear and cytoplasmic patterns. Optimally, all patterns seen in a positive sample should be reported regardless of the clinical relevance. (v) Transfected HEp-2 cells for general pattern definition should not be used.

Additionally, the biomedical industry has improved IIF standardization for the preparation of substrates and slides, the automation of slide incubation, software-based image acquisition and interpretation (computer-aided IF microscopy) (38–44), as well as the automated transfer of results. Different commercial systems for automated ANA IIF testing have recently been developed and evaluated (17, 29, 30, 45–55). The Sprinter XL and the EUROPattern Suite (Euroimmun, Lübeck, Germany) have been designed to provide a high-throughput platform for automated specimen processing and slide incubation as well as for automated microscopy, titer, and pattern interpretation (23, 56).

In this study, the ANA IIF workflow characteristics and analytical performance of the Sprinter/EUROPattern system were evaluated against manual processing and visual microscopy with or without titration support.

METHODS

Human Sera

Analysis of the workflow and of labor savings was calculated on consecutive serum samples representing the daily workload cohorts for routine ANA analysis at the respective laboratories within Laboratory Corporation of America® Holdings (LabCorp) reference laboratory network in the USA. For the evaluation of assay performance, we used 97 ANA negative samples and 176 patient samples pre-characterized as ANA positive using the PolyTiter immunofluorescence system (Polymedco, Inc., Cortland Manor, NY, USA) and ANAFLUOR Hep-2 reagent kit (DiaSorin, Stillwater, MN, USA). These samples had been sent to the LabCorp Dublin Regional Laboratory (OH) for routine antibody screening. The cohort of 176 positive samples was grouped according to the ANA pattern detected by the manual protocol [68 homogeneous, 41 granular (speckled), 20 centromere, 22 nucleolar, and 25 mixed patterns]. In accordance with the Declaration of Helsinki (1964) ethical guidelines, samples were blinded for analysis to maintain confidentiality. The study protocol was determined to be exempt by the Institutional Review Board (Western Institutional Review Board®, Puyallup, WA, USA).

Data Collection

Workflow data were collected at LabCorp laboratories in Birmingham (AL), Burlington (NC), Dallas (TX), Dublin (OH), Houston (TX), Phoenix (AZ), Raritan (NJ), and Tampa (FL). Analyses to evaluate diagnostic performance were performed in Dublin LabCorp Laboratory.

IIF Testing for ANA Using Three Approaches

Current Method: ANAFLUOR Hep-2 Reagent Kit (DiaSorin, Stillwater, MN, USA)

Sample preparation and slide incubation were processed according to the manufacturer's procedure. Only one serum dilution (1:40) is required for the titer determination. Each processed slide

was read independently under fluorescent microscopy by three experienced technologists complemented with an immunofluorescent titration system: PolyTiter immunofluorescence system (Polymedco, Inc., Cortland Manor, NY, USA). The latter uses filter-controlled light attenuation to determine semiquantitatively the ANA endpoint titer from a single serum dilution by relating the intensity of fluorescent staining to reference calibrators. The titration system is comprised of hardware (digital control pad, filter unit, and microscope adapters), software, and pre-diluted calibrator solutions with endpoint titer values of 1:40, 1:160, 1:640, and1:2,560. Diluted patient sera, kit controls, and calibrators are assayed according to the manufacturer's instructions. Results for ANA patterns and calculated titers were entered into laboratory information system (LIS) and reviewed manually by two technologists.

Conventional Visual IIF Microscopy

If PolyTiter results were questionable, sample preparation and slide incubation were performed manually using the ANAFLUOR Hep-2 reagent kit. Serum sample titers were manually prepared using the following dilutions: 1:40, 1:80, 1:160, 1:320, 1:640, and 1:1,280. Experienced technologists using fluorescent microscopy read each slide independently, and results were entered manually.

Automated ANA IIF Protocol: Sprinter/EUROPattern System

Samples and slides were processed using the Sprinter XL (Euroimmun AG, Lübeck, Germany), followed by automated evaluation using the EUROPattern Suite (Euroimmun AG, Lübeck, Germany). ANA detection was performed by the IFA 40: HEp-20-10 kit assay according to the manufacturer's instructions (Euroimmun AG, Lübeck, Germany) (57). The IFA 40: HEp-20-10 allows for easier evaluation due to an increased spectrum of cells in the mitotic phase and of human nuclear antigens when compared to traditional Hep-2 cells. The increase of cells in the mitotic phase offers easy confirmation of reactions (**Figure 1**). The slides have 10-reaction fields, each containing a biochip coated with HEp-20-10 cells. Serum samples were diluted in PBS-Tween and screened for ANA at 1:40. Positive samples (1:80 and above) were reflexed for titers at three dilutions (1:80, 1:320, and 1:1,280) by automated dilution using Sprinter XL system. The fluorescein isothiocyanate-labeled anti-human IgG conjugate solution contains propidium iodide as counterstain for image segmentation by EUROPattern.

The Sprinter XL provides automated processing of IIF tests, including sample identification, dilution, and dispensing, followed by slide incubation and washing (**Figure 2A**). The Sprinter XL system has a loading capacity of up to 240 samples and 30 slides,

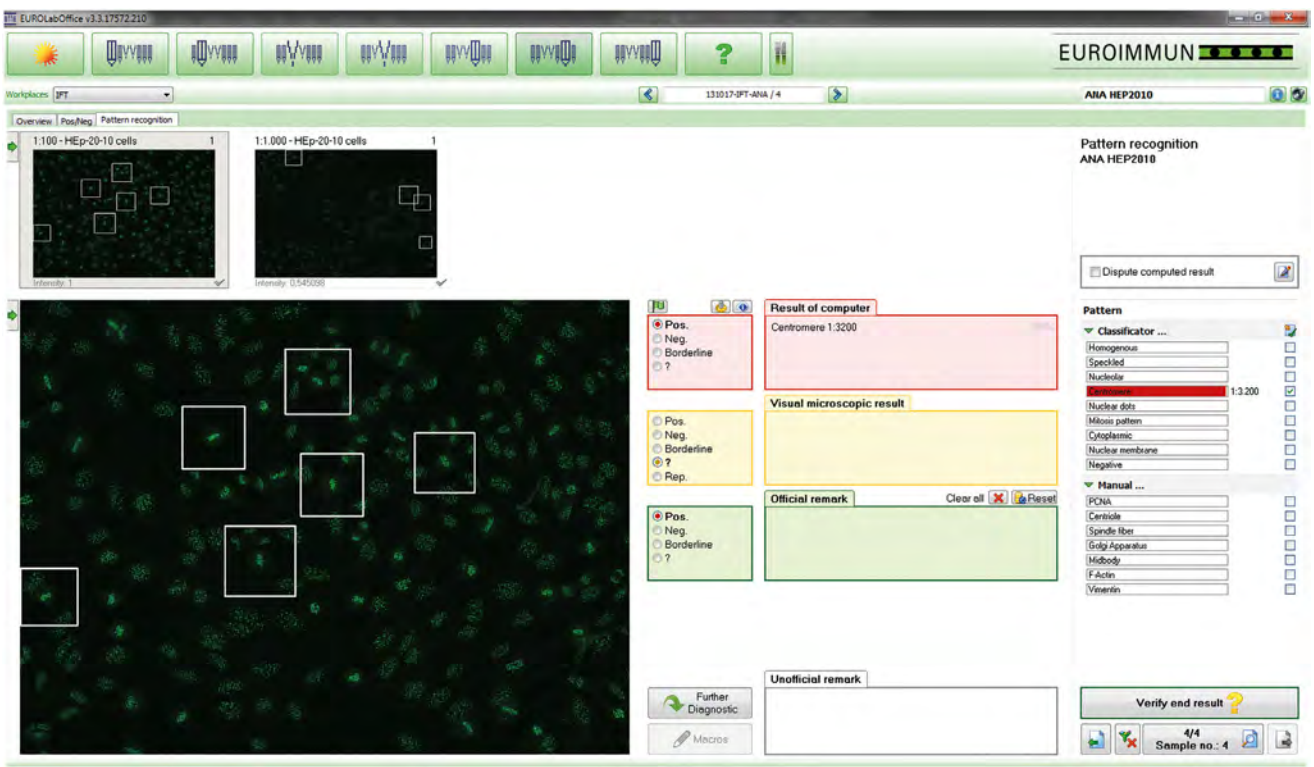

FIGURE 1 | EUROPattern Suite graphical user interface. For each sample classified as positive, the system displays the indirect immunofluorescence (IIF) images for different dilutions/substrates (left) and the proposed results of automated interpretation (right), merging all proposed results (classification, titer, confidence value) into one report per patient. To support pattern interpretation, mitotic cells and late metaphase chromosomes can be highlighted. The proposed results are to be confirmed (or modified) interactively by the technologist. Negative results are displayed in a small-format scroll-down register and can be verified batch-wise (data not shown).

which are identified through barcode and matrix code readers, respectively. The pipetting unit comprises two arms and four washable needles. Washing is based on slide flooding. The EUROPattern Suite is a system to record, evaluate, and archive digital images of IIF slides. It is based on a combination of several hardware and software modules, as described elsewhere (23, 56, 58–60). In brief, the EUROPattern fluorescent microscope (**Figure 2B**) is equipped with a 20× objective, two high-resolution cameras, LEDs for fluorescence or transmitted light with a lifespan of >50,000 h, and a matrix code reader for slide identification. The slide magazine has a loading capacity of 500 reaction fields that can be processed within 2.5 h (18 s per analysis). The digital images undergo positive/negative classification by the EUROpattern software, capable of discriminating homogeneous, centromeres, speckled, nuclear dots, nucleolar, nuclear membrane, cytoplasmic, and negative/unspecific patterns (**Figure 3**). Mixed patterns with varying antibody titers can also be identified. In samples classified as positive, interpretation of the fluorescence pattern is based on the *k*-nearest neighbor algorithm, comparing the image features with a reference database based on more than 5,000 images (115,000 cell references). If a patient sample is analyzed in different dilutions, EUROPattern merges all images into one report containing the proposed pattern/s, titer/s, and the corresponding confidence value/s (**Figure 1**). Results must be

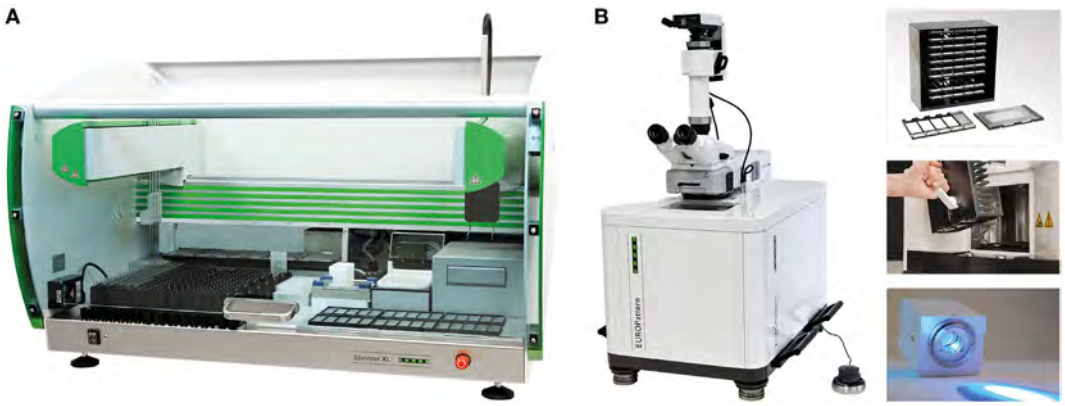

FIGURE 2 | Automation of anti-nuclear antibodies indirect immunofluorescence (IIF). **(A)** Sprinter XL for fully automated processing of IIF tests from the dilution and dispensing of samples to the incubation and washing of microscope slides. In addition, the system is capable of running ELISA microplates. Capacity: 160–240 sample tubes, 30 ten-field IIF slides, six microplates. **(B)** The EUROPattern Suite microscope is equipped, among others, a customized set of autofocusing objectives (10×/20×/40×), oculars (optional), two high-resolution cameras, long-life cLED, 3D manual controller, matrix code reader, and slide magazine plus carrier. Capacity: 50 ten-field slides (500 analyses), 18 sec/analysis.

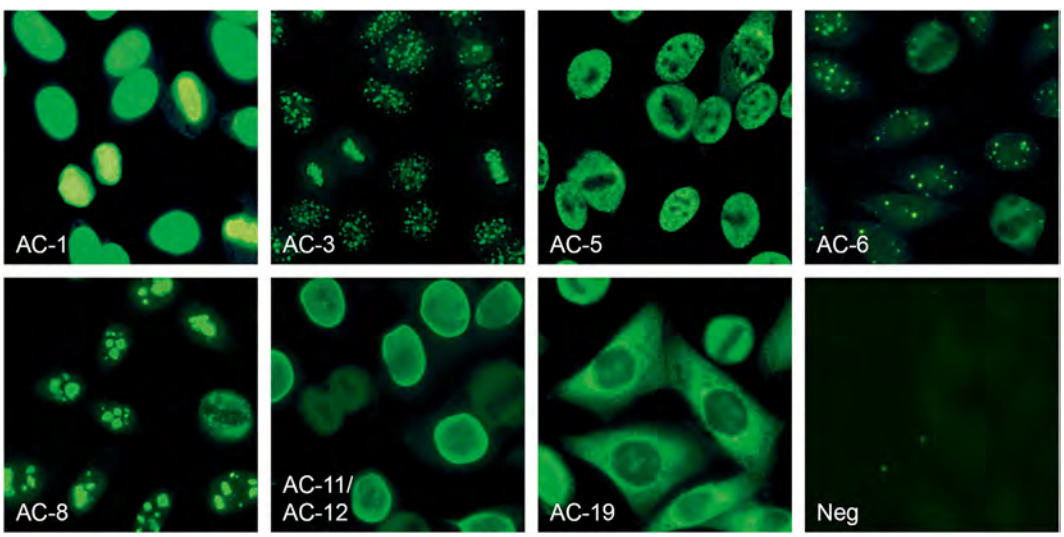

FIGURE 3 | Anti-nuclear antibodies (ANA) patterns recognized by the EUROPattern Suite software (numbering according to International consensus on ANA patterns): homogeneous (AC-1), centromere (AC-3), speckled (AC-5), nuclear dots (AC-6), nucleolar (AC-8), nuclear membrane (AC-11, AC-12), cytoplasmic (AC-19), and negative/unspecific (Neg). Mixed patterns with varying titers can also be identified (data not shown).

confirmed or may be modified by laboratory personnel, either one by one (positive samples) or batch-wise (negative samples). The EUROPattern graphical user interface is incorporated into the superordinate laboratory management software EUROLabOffice, which allows the EUROPattern system to exchange data with the LIS. Additionally, EUROLabOffice is capable of compiling worklists, interconnecting with other laboratory devices (e.g., Sprinter XL), consolidating the results of different techniques (IFA, ELISA, immunoblot) into one report per patient, and paperless data archiving.

The EUROPattern microscope and software, in combination with the IFA 40: HEP-20-10 EUROPattern assay, has received FDA 510(*k*) clearance (No. k141827).

Evaluation Criteria

The purpose of this study was to evaluate a new automated ANA IIF protocol (Sprinter/EUROPattern system) as an alternative for a method that was discontinued. Some criteria were considered to evaluate the new IIF protocol: FDA-approved system, automated platform, high-throughput, positive ID throughout the process, workflow compatibility with 8 h shift, LIS interface, reliable pattern recognition, and batch reporting of negatives.

Statistical Methods

Statistical analyses were performed using GraphPadPrism 6 (GraphPad Software Inc., La Jolla, San Jose, CA, USA). The degree of inter-rater agreement between visual and automated antibody pattern interpretation was assessed by the percentage of concordance and by kappa coefficients. According to Altmann (61), kappa (κ) values were interpreted as follows: ≤0.20 poor, 0.21–0.40 fair, 0.41–0.60 moderate, 0.61–0.80 good, and 0.81–1.00 very good agreement. Confidence intervals (CI 95%) were calculated according to the modified Wald method.

RESULTS

Characteristics of HEp-20-10 Slides

Throughout this study, the biochip slides coated with HEp-20-10 cells were of consistent quality. The number of mitotic cells per reaction field exceeded that of standard Hep-2 cells by 10-fold.

Workflow Evaluation

Run times for daily workload cohorts were surveyed at eight LabCorp laboratories using the Sprinter XL for sample preparation and slide processing, followed by EUROPattern-based image acquisition and evaluation. According to the individual number of samples, up to three screening and titer runs were conducted per laboratory, using three dilutions for the determination of endpoint titers in positive samples. The total time requirement was between 06:00 and 07:00 h (**Table 1**), thus conforming to an 8-h shift. **Figure 4** depicts the workflow recorded at the Dublin laboratory, where the processing of 400 samples in two screen and two titer runs took a total time of 07:10 h or approximately 1 min per sample.

Labor Savings

The demand for labor was compared between the automated Sprinter/EUROPattern system and the manual procedure that was in use. The Sprinter/EUROPattern method comprises two analytical runs: (1) screening for the purpose of positive/negative discrimination at a single dilution, (2) determination of patterns and endpoint titers in positive samples using three dilutions (three-well approach). In contrast, the previous method provided endpoint titers from a single dilution (single-well approach). Calculations for an average of 400 samples per day revealed a total hands-on time of 98 min (01:38 h) for the Sprinter/EUROPattern system, and 355 min (5:55 h) for the previous method, corresponding to a total of 4:20 h labor savings (**Table 2**).

If a single-well approach was used for each of the methods, the labor hands-on time would amount to 82 min (1:22 h) for the Sprinter/EUROPattern system and 355 min (5:55 h) for the current method. The difference in labor savings between the Sprinter/EUROPattern three-well and single-well approach was only 16 min for an 8-h shift (**Table 3**).

Evaluation of ANA Patterns and Titers

Diagnostic performance for ANA patterns and endpoint titers using the EUROPattern Suite was evaluated using 176 positive and 97 negative samples. The results were compared to the PolyTiter system with or without a technologist reading the slides for both EUROPattern and PolyTiter systems. The number of times the technologist agreed with the initial instrument call for pattern or titer is expressed in % (**Table 4**).

TABLE 1 | Workflow analysis for anti-nuclear antibodies indirect immunofluorescence testing in average daily workload cohorts at eight LabCorp laboratories (fiscal year 2016).

Laboratory site	Samples (*n*)	Number of devices (*n*)		Runs per day (*n*)		Approximately overall time requirement
		Sprinter XL	EUROPattern	Screening	Titer	
Houston, TX, USA	141	1	1	1	1	06:00 h
Tampa, FL, USA	134	1	1	1	1	06:10 h
Dallas, TX, USA	187	1	1	1	1	06:40 h
Phoenix, AZ, USA	231	1	1	1	1	07:10 h
Birmingham, AL, USA	236	2	2	2	1	06:30 h
Burlington, NC, USA	471	2	2	2	2	07:10 h
Dublin, OH, USA	330	2	2	2	2	07:10 h
Raritan, NJ, USA	568	3	3	3	3	07:05 h

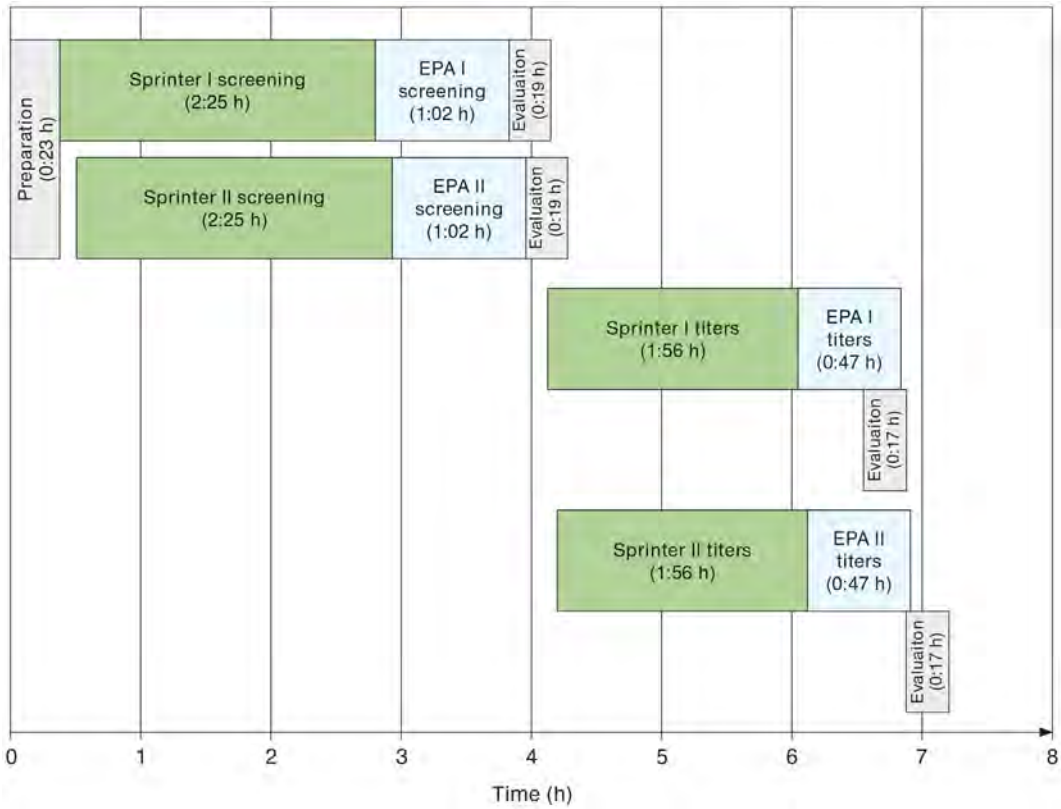

FIGURE 4 | Exemplary schematic workflow of automated anti-nuclear antibodies indirect immunofluorescence as determined at the LabCorp laboratory Dublin (OH, USA) for a daily workload cohort comprising 388 samples. Two Sprinter XL devices were used for sample/slide incubation and two EUROPattern (EPA) devices for image acquisition and interpretation. Initial screening aimed at discriminating negative from positive samples. Only the 194 positive samples were further analyzed for patterns and endpoint titers using three dilutions per sample.

Positive/negative classification by EUROPattern and technologist reading with the PolyTiter system without technologist demonstrated a total agreement rate of 89.4% ($\kappa = 0.780$) (**Table 4**, EUROPattern vs. current method) and 92.3% ($\kappa = 0.838$) when technologist was reading slides on EUROPattern Suite vs. the PolyTiter (**Table 4**, Technologist vs. current method). Highest overall agreement of 95.6% ($\kappa = 0.905$) was found when we compared the reading between EUROPattern and a technologist (**Table 4**, EUROPattern vs. technologist). In each pattern group (except for the granular group), the highest degree of positive agreement was found between EUROPattern and technologist reading, declining in the following order: centromere and mixed patterns (100%), granular patterns (97.6%), homogenous patterns (92.6%), and nucleolar patterns (86.4%) (**Table 4**).

Pattern assignment using the PolyTiter system showed similar concordance rates for EUROPattern (68.4–100%) and for PolyTiter reading (76.3–100%), with least pattern matches observed among samples with nucleolar or mixed patterns. Endpoint titer agreement (within ±1 dilutions) with the current method varied depending on the pattern type between 5.0 and 72.1% by the EUROPattern Suite and between 35.0 and 73.5% by technologist reading, with lowest rates obtained in the centromere pattern group. High pattern correlation (80.6–97.5%) in combination with the highest endpoint titer agreement rates (71.0–93.8%) were found when comparing EUROPattern vs. technologist reading, indicating that the three-well approach provides higher overall accuracy (**Table 5**). The PolyTiter method (single-well approach) is at disadvantage when evaluating mixed patterns because it only distinguishes between two patterns.

If patterns and titers were determined at a single dilution (1:80), 100% correlation was observed between EUROPattern and technologist reading. In contrast, the correlation values between EUROPattern and the PolyTiter method were lower (pattern 75.3%, titer 57.1%) (**Table 6**).

DISCUSSION

This study examined the workflow and performance characteristics of the automated Sprinter/EUROPattern IIF system as an alternative to the two methods described herein. It was not the purpose of the study to evaluate the diagnostic performance of the Sprinter/EUROPattern IIF system, therefore, we did not use well-defined characterized patient population, such as (1) autoimmune rheumatic disease patient cohort, (2) non-ARD diseased cohort, and (3) healthy control group in our study, but just negative or positive serum specimen for ANA. Overall, the evaluation

TABLE 2 | Comparison of labor hands-on time between the current LabCorp method (single-well) and the Sprinter/EUROPattern system (two runs, three-well dilution).

	Current method		Sprinter/EUROPattern	
	Details	**Total time (min)**	**Details**	**Total time (min)**
I. Anti-nuclear antibodies (ANA) indirect immunofluorescence screening (on average 400 screens per day, single dilution)				
Set-up	7 s/sample, manual	47	5.8 s/sample, incl. reagents	39
Pipetting	7.7 s/sample, manual	51	Sprinter XL	0
Washing	10 s/slide, manual	6	Sprinter XL	0
Conjugate	16 s/slide, manual	9	Sprinter XL	0
Washing	10 s/slide, manual	6	Sprinter XL	0
Coverslip	10 s/slide, manual	6.7	6 s/slide (titerplane)	4.0
Slide evaluation	Read in dark room: negative 7.5 s, positive 30 s, mixed positive 45 s	94	Read and release negatives on computer: negative 3 s, borderline 20 s; positives: titer estimation (II)	18
Slide manipulation, focus, writing results	15.2 s/slide, manual	101	EUROPattern	0
Clean-up		5		5
Result entry into computer		30	EUROPattern	0
Total labor for screens (min)		355		65
II. ANA IIF titers (on average 100 titers per day, three dilutions)				
Set-up		0	2.5 s/sample, incl. reagents	4
Pipetting		0	Sprinter XL	0
Washing		0	Sprinter XL	0
Conjugate		0	Sprinter XL	0
Washing			Sprinter XL	0
Coverslip		0	6 s/slide (titerplane)	1
Read slides		0	Read slides on computer: positive titer = 10.5 s/patient (all titers displayed on 1 screen)	18
Slide manipulation, focus, writing results		0	EUROPattern	0
Clean-up		0	Daily maintenance, shutdown	10
Result entry into computer		0		0
Total labor for titer (min)		0		33
III. ANA IIF screening and titers				
Total labor hands-on time (min)		355		98
Savings EUROPattern (min)				257 (4 h 17 min)

TABLE 3 | Comparison of labor hands-on time between the current LabCorp method (single-well) and the Sprinter/EUROPattern system (single-well).

	Current method		Sprinter/EUROPattern	
	Details	**Total time (min)**	**Details**	**Total time (min)**
I. Anti-nuclear antibodies (ANA) indirect immunofluorescence (IIF) screening (on average 400 screens per day, single dilution)				
Set-up	7 s/sample, manual	47	5.8 s/sample, incl. reagents	39
Pipetting	7.7 s/sample, manual	51	Sprinter XL	0
Washing	10 s/slide, manual	6	Sprinter XL	0
Conjugate	16 s/slide, manual	9	Sprinter XL	0
Washing	10 s/slide, manual	6	Sprinter XL	0
Coverslip	10 s/slide, manual	6.7	6 s/slide (titerplane)	4.0
Slide evaluation	Read in dark room: negative 7.5 s, positive 30 s, mixed positive 45 s	94	Read and release negatives on computer: negative 3 s, borderline 20 s; positives 10.5 s	34
Slide manipulation, focus, writing results	15.2 s/slide, manual	101	EUROPattern	0
Clean-up		5		5
Result entry into computer		30	EUROPattern	0
Total labor for screens (min)		355		82
II. ANA IIF single-well analysis				
Total labor hands-on time (min)		355		82
Savings EUROPattern (min)				273 (4 h 33 min)

criteria for a new automated ANA IIF approach (see Evaluation Criteria) were either met or exceeded. The automated approach completed the daily workload within an 8-h shift and reduced the labor hands-on time for screening and titer runs by more than 4 h. Applying automation in a single-well approach resulted in further labor savings of 16 min. However, this slight reduction should not justify an overall application of the single-well approach considering the associated risk of interferences (masking, prozone

TABLE 4 | Agreement (positive/negative results) between EUROPattern, the current LabCorp method, and technologist reading.

Specimens	*n*	Sample agreement (95% CI)		
		EUROPattern vs. current method	Technologist vs. current method	EUROPattern vs. technologist
Homogenous pattern	68	79.4% (68.2–87.4%)	83.8% (73.1–90.9%)	92.6% (83.5–97.2%)
Granular pattern	41	97.6% (86.3–100%)	100% (89.8–100%)	97.6% (86.3–100%)
Centromere pattern	20	95.0% (74.6–100%)	95.0% (74.6–100%)	100% (81.0–100%)
Nucleolar pattern	22	63.6% (42.9–80.4%)	81.8% (60.9–93.3%)	86.4% (65.8–96.1%)
Mixed patterns	25	92.0% (73.9–98.9%)	92.0% (73.9–98.9%)	100% (84.2–100%)
Positive agreement	176	85.2% (79.2–89.8%)	89.8% (84.3–93.5%)	94.9% (90.4–97.4%)
Negative agreement	97	96.9% (90.9–99.3%)	96.9% (90.9–99.3%)	96.9% (90.9–99.3%)
Overall agreement	273	89.4% (85.1–92.5%)	92.3% (88.5–95.0%)	95.6% (92.4–97.6%)
κ-Value		0.780 (0.705–0.854)	0.838 (0.772–0.904)	0.905 (0.853–0.958)

TABLE 5 | Pattern and titer agreement between EUROPattern, the current LabCorp method, and technologist reading.

Specimens	*n*	EUROPattern vs. current method		Technologist vs. current method		EUROPattern vs. technologist	
		Pattern	Titer[a,b]	Pattern	Titer[b]	Pattern	Titer[a,b]
Homogenous pattern	68	85.3%	72.1%	85.3%	73.5%	97.5%	93.8%
Granular pattern	41	92.7%	61.0%	92.7%	63.4%	90.7%	85.2%
Centromere pattern	20	100%	5.0%	100%	35.0%	80.6%	74.2%
Nucleolar pattern	22	68.2%	59.1%	77.3%	59.1%	80.6%	71.0%
Mixed patterns	25	68.4%	52.6%	76.3%	55.3%	89.7%	84.6%

[a]*Endpoint titers by EUROPattern were based on a three-well dilution protocol (1:80, 1:320, 1:1,280).*
[b]*Titer agreement within ±1 dilution.*

TABLE 6 | Comparison of single-well analysis between EUROPattern and the current LabCorp method or technologist reading.

Dilution	*n*	EUROPattern vs. current method		EUROPattern vs. technologist	
		Pattern	Titer[a]	Pattern	Titer[a]
1:40	179	73.3%	59.5%	N/A	N/A
1:80	115	75.3%	57.1%	100%	100%

[a]*Titer agreement within ±1 dilution.*

effect) and reduced accuracy. Longer walk-away times may contribute to greater laboratory productivity with the gain in higher throughput. In addition, the Sprinter/EUROPattern system is less prone to error in barcode-based sample/slide identification and the use of positive patient IDs throughout the process. The graphical user interface displays all results and the corresponding images, allowing for fast interactive validation of individual positive or batches of negative reports. Since the software-proposed results require verified (or possibly modified) by the operator, subjectivity cannot be completely removed, but the system has the potential to reach 100% concordance with visual microcopy.

The performance of the EUROPattern Suite is in accordance with the ICAP guidelines (34), including the distinction of several nuclear, but also cytoplasmic patterns on native HEp-20 or HEp-2010 cells, the identification of mixed patterns, and the calculation of semi-quantitative endpoint titers on the basis of several dilutions. Sample titration is highly relevant for the discrimination of mixed ANA patterns (60, 62). Using IIF screening at only a single titer, masked patterns can be missed, resulting in incomplete reporting of diagnostically relevant antibodies. According to Carter et al., distinct masked patterns were observed in 1% (29 out of 3,000) of routine ANA samples (63). Similarly, prozone ANA patterns may be indiscernible if the patient sample is not sufficiently diluted, resulting in false-negative results (36, 37). Thus, systems that provide pattern and titer proposals from single-well estimations may be at a disadvantage.

According to our data, the EUROPattern system provided overall improvement with respect to the recognition of ANA patterns and the determination of endpoint titers. Overall highest correlation values resulted from comparing EUROPattern vs. technologist reading, either based on a three-dilution protocol (patterns, 80.6–97.5%; titers, 71.0–93.8%) or on single-well analysis (patterns, 100%; titers, 100%). Lower correlation values with the current method derived (patterns, 68.2–100%; titers, 5.0–72.1%) may be due to inherent flaws such as the utilization of a speckled standard curve only, the occurrence of masking effects, and standardization of the slide manufacturing process.

These findings are consistent with recent literature revealing good performance characteristics of the EUROPattern Suite. For example, Voigt et al. analyzed a total of 351 serum samples to compare the performance of the EUROPattern software-based evaluation with technologist visual interpretation by expert technologists. They also found 99.4% concordant results for positive/negative discrimination with a sensitivity and specificity of the EUROPattern Suite of 100 and 97.5%, respectively. The agreement in main pattern recognition (including mixed patterns) amounted to 94.0% (56). Yoo et al. used the same approach based on 104 samples, reporting a sensitivity and specificity of 94.3 and 94.1%, respectively, and concordance in negative/positive classification of 94.2%. Matching of major patterns occurred in 83.7% of samples with simple and 95.2% with mixed ANA patterns. Comparison of simple pattern titers revealed 82.9% agreement between both methods (59). Tozzoli et al. reported 100% diagnostic sensitivity of the EUROPattern system with reference to manual IFA (16). Bizzaro et al. compared the EUROPattern Suite to five other automated systems (AKLIDES, NOVA View, Zenit G-Sight, Helios, and Image Navigator) using 126 manually

pre-characterized sera. This study, which was the first to compare the diagnostic accuracy of six systems for automated ANA-IIF reading on the same series of sera, showed that all systems are able to perform very well the task for which they were created. Overall sensitivity of the six automated systems was 96.7% and overall specificity was 89.2%. Most false negatives were recorded for cytoplasmic patterns, whereas among nuclear patterns those with a low level of fluorescence (i.e., multiple nuclear dots, mid-body, and nuclear rim) were sometimes missed. The intensity values of the light signal of various instruments showed a good correlation with the titer obtained by manual reading (Spearman's rho between 0.672 and 0.839; $P < 0.0001$ for all the systems). Imprecision ranged from 1.99 to 25.2% and, for all the systems, it was lower than that obtained by the manual IIF test (39.1%). The accuracy of pattern recognition, which is for now restricted to the most typical patterns (homogeneous, speckled, nucleolar, centromere, multiple nuclear dots, and cytoplasmic) was limited, ranging from 52 to 79%. The systems demonstrated overall concordance rates for the classification of positive and negative results of 93.7–96.8% (EUROPattern: 93.7%), and correct pattern assignment in 52–79% (EUROPattern: 79%) (30).

Like similar automated instruments for ANA reading and interpretation, the EUROPattern Suite is a closed system, i.e., neither microscope nor software is interchangeable with other analogous devices (23, 30). The EUROPattern Suite is restricted to the use of Euroimmun IIF kits as this is the only way to guarantee high quality of results. For EUROPattern-based evaluation, Euroimmun offers not only slides coated with HEp-2 or HEp-20-10 cells, but also several other cell substrates for other diagnostic purposes (e.g., *Crithidia luciliae*, ethanol-fixed and formalin-fixed human granulocytes, transfected cells, and infected cells). Noteworthy, IFA40: HEp-20-10 kits contribute to the standardization of EUROPattern-based ANA testing. Constant quality of the substrate is ensured by quality control measures throughout the production of the HEp-20-10-coated biochips. Reliability of the assay has been demonstrated by validation studies (57).

In conclusion, the EUROPattern Suite, along with the Sprinter IIF slide processor, is a fully automated solution for ANA IIF testing on HEp-20-10 cells, allowing laboratories to perform testing on hundreds of samples per day. The Sprinter/EUROPattern system enables substantially reduced hands-on time and high correlation with technologist visual IIF microscopy, thus supporting high throughput, labor savings, and standardized operations.

ETHICS STATEMENT

In accordance with the Declaration of Helsinki (1964) ethical guidelines, samples were blinded for analysis to maintain confidentiality. The study protocol was determined to be exempt by the Institutional Review Board.

AUTHOR CONTRIBUTIONS

All authors designed, analyzed data, and wrote the manuscript.

ACKNOWLEDGMENTS

We gratefully acknowledge for the technical support of Michelle Campo from Euroimmun AG, Lübeck, Germany for assisting and guidance performing the analytical component of the study.

REFERENCES

1. Bizzaro N. Autoantibodies as predictors of disease: the clinical and experimental evidence. *Autoimmun Rev* (2007) 6:325–33. doi:10.1016/j.autrev.2007.01.006
2. Harel M, Shoenfeld Y. Predicting and preventing autoimmunity, myth or reality? *Ann N Y Acad Sci* (2006) 1069:322–45. doi:10.1196/annals.1351.031
3. Damoiseaux J, Andrade LE, Fritzler MJ, Shoenfeld Y. Autoantibodies 2015: from diagnostic biomarkers toward prediction, prognosis and prevention. *Autoimmun Rev* (2015) 14:555–63. doi:10.1016/j.autrev.2015.01.017
4. Klareskog L, Gregersen PK, Huizinga TW. Prevention of autoimmune rheumatic disease: state of the art and future perspectives. *Ann Rheum Dis* (2010) 69:2062–6. doi:10.1136/ard.2010.142109
5. Arbuckle MR, McClain MT, Rubertone MV, Scofield RH, Dennis GJ, James JA, et al. Development of autoantibodies before the clinical onset of systemic lupus erythematosus. *N Engl J Med* (2003) 349:1526–33. doi:10.1056/NEJMoa021933
6. Wiik AS. Anti-nuclear autoantibodies: clinical utility for diagnosis, prognosis, monitoring, and planning of treatment strategy in systemic immunoinflammatory diseases. *Scand J Rheumatol* (2005) 34:260–8. doi:10.1080/03009740500202664
7. Tan EM, Feltkamp TE, Smolen JS, Butcher B, Dawkins R, Fritzler MJ, et al. Range of antinuclear antibodies in "healthy" individuals. *Arthritis Rheum* (1997) 40:1601–11. doi:10.1002/art.1780400909
8. Vrethem M, Skogh T, Berlin G, Ernerudh J. Autoantibodies versus clinical symptoms in blood donors. *J Rheumatol* (1992) 19:1919–21.
9. Solomon DH, Kavanaugh AJ, Schur PH. Evidence-based guidelines for the use of immunologic tests: antinuclear antibody testing. *Arthritis Rheum* (2002) 47:434–44. doi:10.1002/art.10561
10. Friou GJ, Finch SC, Detre KD. Interaction of nuclei and globulin from lupus erythematosis serum demonstrated with fluorescent antibody. *J Immunol* (1958) 80:324–9.
11. Holborow EJ, Weir DM, Johnson GD. A serum factor in lupus erythematosus with affinity for tissue nuclei. *Br Med J* (1957) 2:732–4. doi:10.1136/bmj.2.5047.732
12. Holman HR, Deicher HR, Kunkel HG. The L. E. cell and the L. E. serum factors. *Bull N Y Acad Med* (1959) 35:409–18.
13. Meroni PL, Schur PH. ANA screening: an old test with new recommendations. *Ann Rheum Dis* (2010) 69:1420–2. doi:10.1136/ard.2009.127100
14. Sack U, Conrad K, Csernok E, Frank I, Hiepe F, Krieger T, et al. Autoantibody detection using indirect immunofluorescence on HEp-2 cells. *Ann N Y Acad Sci* (2009) 1173:166–73. doi:10.1111/j.1749-6632.2009.04735.x
15. Ulvestad E. Performance characteristics and clinical utility of a hybrid ELISA for detection of ANA. *APMIS* (2001) 109:217–22. doi:10.1034/j.1600-0463.2001.090305.x
16. Tozzoli R, Bonaguri C, Melegari A, Antico A, Bassetti D, Bizzaro N. Current state of diagnostic technologies in the autoimmunology laboratory. *Clin Chem Lab Med* (2013) 51:129–38. doi:10.1515/cclm-2012-0191
17. Hiemann R, Buttner T, Krieger T, Roggenbuck D, Sack U, Conrad K. Challenges of automated screening and differentiation of non-organ specific autoantibodies on HEp-2 cells. *Autoimmun Rev* (2009) 9:17–22. doi:10.1016/j.autrev.2009.02.033
18. Copple SS, Giles SR, Jaskowski TD, Gardiner AE, Wilson AM, Hill HR. Screening for IgG antinuclear autoantibodies by HEp-2 indirect fluorescent antibody assays and the need for standardization. *Am J Clin Pathol* (2012) 137:825–30. doi:10.1309/AJCPICNFG7UCES1S
19. Bruner BF, Guthridge JM, Lu R, Vidal G, Kelly JA, Robertson JM, et al. Comparison of autoantibody specificities between traditional and bead-based assays in a large, diverse collection of patients with systemic lupus

erythematosus and family members. *Arthritis Rheum* (2012) 64:3677–86. doi:10.1002/art.34651
20. Shovman O, Gilburd B, Barzilai O, Shinar E, Larida B, Zandman-Goddard G, et al. Evaluation of the BioPlex 2200 ANA screen: analysis of 510 healthy subjects: incidence of natural/predictive autoantibodies. *Ann N Y Acad Sci* (2005) 1050:380–8. doi:10.1196/annals.1313.120
21. Desplat-Jego S, Bardin N, Larida B, Sanmarco M. Evaluation of the BioPlex 2200 ANA screen for the detection of antinuclear antibodies and comparison with conventional methods. *Ann N Y Acad Sci* (2007) 1109:245–55. doi:10.1196/annals.1398.030
22. Op De Beeck K, Vermeersch P, Verschueren P, Westhovens R, Marien G, Blockmans D, et al. Antinuclear antibody detection by automated multiplex immunoassay in untreated patients at the time of diagnosis. *Autoimmun Rev* (2012) 12:137–43. doi:10.1016/j.autrev.2012.02.013
23. Krause C, Ens K, Fechner K, Voigt J, Fraune J, Rohwäder E, et al. EUROPattern suite technology for computer-aided immunofluorescence microscopy in autoantibody diagnostics. *Lupus* (2015) 24:516–29. doi:10.1177/0961203314559635
24. Binder SR. Autoantibody detection using multiplex technologies. *Lupus* (2006) 15:412–21. doi:10.1191/0961203306lu2326oa
25. Zandman-Goddard G, Gilburd B, Shovman O, Blank M, Berdichevski S, Langevitz P, et al. The homogeneous multiplexed system – a new method for autoantibody profile in systemic lupus erythematosus. *Clin Dev Immunol* (2005) 12:107–11. doi:10.1080/17402520500116723
26. Fritzler MJ, Fritzler ML. The emergence of multiplexed technologies as diagnostic platforms in systemic autoimmune diseases. *Curr Med Chem* (2006) 13:2503–12. doi:10.2174/092986706778201639
27. Fenger M, Wiik A, Hoier-Madsen M, Lykkegaard JJ, Rozenfeld T, Hansen MS, et al. Detection of antinuclear antibodies by solid-phase immunoassays and immunofluorescence analysis. *Clin Chem* (2004) 50:2141–7. doi:10.1373/clinchem.2004.038422
28. Eissfeller P, Sticherling M, Scholz D, Hennig K, Luttich T, Motz M, et al. Comparison of different test systems for simultaneous autoantibody detection in connective tissue diseases. *Ann N Y Acad Sci* (2005) 1050:327–39. doi:10.1196/annals.1313.035
29. Mahler M, Meroni PL, Bossuyt X, Fritzler MJ. Current concepts and future directions for the assessment of autoantibodies to cellular antigens referred to as anti-nuclear antibodies. *J Immunol Res* (2014) 2014:315179. doi:10.1155/2014/315179
30. Bizzaro N, Antico A, Platzgummer S, Tonutti E, Bassetti D, Pesente F, et al. Automated antinuclear immunofluorescence antibody screening: a comparative study of six computer-aided diagnostic systems. *Autoimmun Rev* (2014) 13:292–8. doi:10.1016/j.autrev.2013.10.015
31. American College of Rheumatology. *American College of Rheumatology Position Statement: Methodology of Testing for Antinuclear Antibodies*. (2009). Available from: https://www.rheumatology.org/Portals/0/Files/Methodology%20of%20Testing%20Antinuclear%20Antibodies%20Position%20Statement.pdf
32. Agmon-Levin N, Damoiseaux J, Kallenberg C, Sack U, Witte T, Herold M, et al. International recommendations for the assessment of autoantibodies to cellular antigens referred to as anti-nuclear antibodies. *Ann Rheum Dis* (2014) 73:17–23. doi:10.1136/annrheumdis-2013-203863
33. Tozzoli R, Bizzaro N, Tonutti E, Villalta D, Bassetti D, Manoni F, et al. Guidelines for the laboratory use of autoantibody tests in the diagnosis and monitoring of autoimmune rheumatic diseases. *Am J Clin Pathol* (2002) 117: 316–24. doi:10.1309/Y5VF-C3DM-L8XV-U053
34. Chan EK, Damoiseaux J, Carballo OG, Conrad K, de Melo CW, Francescantonio PL, et al. Report of the first international consensus on standardized nomenclature of antinuclear antibody HEp-2 cell patterns 2014-2015. *Front Immunol* (2015) 6:412. doi:10.3389/fimmu.2015.00412
35. Chan EK, Damoiseaux J, de Melo Cruvinel W, Carballo OG, Conrad K, Francescantonio PL, et al. Report on the second international consensus on ANA pattern (ICAP) workshop in Dresden 2015. *Lupus* (2016) 25:797–804. doi:10.1177/0961203316640920
36. Dubois-Galopin F, Beauvillain C, Dubois D, Pillet A, Renier G, Jeannin P, et al. New markers and an old phenomenon: prozone effect disturbing detection of filaggrin (keratin) autoantibodies. *Ann Rheum Dis* (2007) 66:1121–2. doi:10.1136/ard.2006.066027
37. Linder E, Miettinen A. Prozone effects in indirect immunofluorescence. *Scand J Immunol* (1976) 5:513–9. doi:10.1111/j.1365-3083.1976.tb00306.x
38. Benammar Elgaaied A, Cascio D, Bruno S, Ciaccio MC, Cipolla M, Fauci A, et al. Computer-assisted classification patterns in autoimmune diagnostics: the AIDA project. *Biomed Res Int* (2016) 2016:2073076. doi:10.1155/2016/2073076
39. Hobson P, Lovell BC, Percannella G, Saggese A, Vento M. Computer aided diagnosis for anti-nuclear antibodies HEp-2 images: progress and challenges. *Pattern Recognit Lett* (2016) 82:3–11. doi:10.1016/j.patrec.2016.06.013
40. Di Cataldo S, Tonti S, Bottino A, Ficarra E. ANAlyte: a modular image analysis tool for ANA testing with indirect immunofluorescence. *Comput Methods Programs Biomed* (2016) 128:86–99. doi:10.1016/j.cmpb.2016.02.005
41. Rigon A, Soda P, Zennaro D, Iannello G, Afeltra A. Indirect immunofluorescence in autoimmune diseases: assessment of digital images for diagnostic purpose. *Cytometry B Clin Cytom* (2007) 72:472–7. doi:10.1002/cyto.b.20356
42. Glory E, Murphy RF. Automated subcellular location determination and high-throughput microscopy. *Dev Cell* (2007) 12:7–16. doi:10.1016/j.devcel.2006.12.007
43. Sack U, Knoechner S, Warschkau H, Pigla U, Emmrich F, Kamprad M. Computer-assisted classification of HEp-2 immunofluorescence patterns in autoimmune diagnostics. *Autoimmun Rev* (2003) 2:298–304. doi:10.1016/S1568-9972(03)00067-3
44. Hu Y, Murphy RF. Automated interpretation of subcellular patterns from immunofluorescence microscopy. *J Immunol Methods* (2004) 290:93–105. doi:10.1016/j.jim.2004.04.011
45. Alsuwaidi M, Dollinger M, Fleck M, Ehrenstein B. The reliability of a novel automated system for ANA immunofluorescence analysis in daily clinical practice. *Int J Rheumatol* (2016) 2016:6019268. doi:10.1155/2016/6019268
46. Copple SS, Jaskowski TD, Giles R, Hill HR. Interpretation of ANA indirect immunofluorescence test outside the darkroom using NOVA view compared to manual microscopy. *J Immunol Res* (2014) 2014:149316. doi:10.1155/2014/149316
47. Meroni PL, Bizzaro N, Cavazzana I, Borghi MO, Tincani A. Automated tests of ANA immunofluorescence as throughput autoantibody detection technology: strengths and limitations. *BMC Med* (2014) 12:38. doi:10.1186/1741-7015-12-38
48. Bossuyt X, Cooreman S, De Baere H, Verschueren P, Westhovens R, Blockmans D, et al. Detection of antinuclear antibodies by automated indirect immunofluorescence analysis. *Clin Chim Acta* (2013) 415:101–6. doi:10.1016/j.cca.2012.09.021
49. Bonroy C, Verfaillie C, Smith V, Persijn L, De Witte E, De Keyser F, et al. Automated indirect immunofluorescence antinuclear antibody analysis is a standardized alternative for visual microscope interpretation. *Clin Chem Lab Med* (2013) 51:1771–9. doi:10.1515/cclm-2013-0016
50. Tozzoli R, Antico A, Porcelli B, Bassetti D. Automation in indirect immunofluorescence testing: a new step in the evolution of the autoimmunology laboratory. *Auto Immun Highlights* (2012) 3:59–65. doi:10.1007/s13317-012-0035-2
51. Willitzki A, Hiemann R, Peters V, Sack U, Schierack P, Rodiger S, et al. New platform technology for comprehensive serological diagnostics of autoimmune diseases. *Clin Dev Immunol* (2012) 2012:284740. doi:10.1155/2012/284740
52. Melegari A, Bonaguri C, Russo A, Luisita B, Trenti T, Lippi G. A comparative study on the reliability of an automated system for the evaluation of cell-based indirect immunofluorescence. *Autoimmun Rev* (2012) 11:713–6. doi:10.1016/j.autrev.2011.12.010
53. Rigon A, Buzzulini F, Soda P, Onofri L, Arcarese L, Iannello G, et al. Novel opportunities in automated classification of antinuclear antibodies on HEp-2 cells. *Autoimmun Rev* (2011) 10:647–52. doi:10.1016/j.autrev.2011.04.022
54. Egerer K, Roggenbuck D, Hiemann R, Weyer MG, Buttner T, Radau B, et al. Automated evaluation of autoantibodies on human epithelial-2 cells as an approach to standardize cell-based immunofluorescence tests. *Arthritis Res Ther* (2010) 12:1–9. doi:10.1186/ar2949
55. Kivity S, Gilburd B, Agmon-Levin N, Carrasco MG, Tzafrir Y, Sofer Y, et al. A novel automated indirect immunofluorescence autoantibody evaluation. *Clin Rheumatol* (2012) 31:503–9. doi:10.1007/s10067-011-1884-1
56. Voigt J, Krause C, Rohwäder E, Saschenbrecker S, Hahn M, Danckwardt M, et al. Automated indirect immunofluorescence evaluation of antinuclear

autoantibodies on HEp-2 cells. *Clin Dev Immunol* (2012) 2012:651058. doi:10.1155/2012/651058
57. Rohwäder E, Locke M, Fraune J, Fechner K. Diagnostic profile on the IFA 40: HEp-20-10 – an immunofluorescence test for reliable antinuclear antibody screening. *Expert Rev Mol Diagn* (2015) 15:451–62. doi:10.1586/14737159.2015.993612
58. Gerlach S, Affeldt K, Pototzki L, Krause C, Voigt J, Fraune J, et al. Automated evaluation of *Crithidia luciliae* based indirect immunofluorescence tests: a novel application of the EUROPattern-suite technology. *J Immunol Res* (2015) 2015:742402. doi:10.1155/2015/742402
59. Yoo IY, Oh JW, Cha HS, Koh EM, Kang ES. Performance of an automated fluorescence antinuclear antibody image analyzer. *Ann Lab Med* (2017) 37:240–7. doi:10.3343/alm.2017.37.3.240
60. Jacobs JF, van der Molen RG, Bossuyt X, Damoiseaux J. Antigen excess in modern immunoassays: to anticipate on the unexpected. *Autoimmun Rev* (2015) 14:160–7. doi:10.1016/j.autrev.2014.10.018
61. Altman DG. *Practical Statistics for Medical Research*. London: Chapman & Hall (1991). p. 403–9.
62. Tate J, Ward G. Interferences in immunoassay. *Clin Biochem Rev* (2004) 25:105–20.
63. Carter S, Carter JB. Recognition and significance of masked ANA patterns. *Scientific Presentation at the 29th Association of Medical Laboratory Immunologists (AMLI) Annual Meeting, Pittsburgh, USA*. (2017).

Conflict of Interest Statement: Reagent and instrumentation were provided by Euroimmun for validation purpose.

The reviewer OC and handling Editor declared their shared affiliation.

frontiers in Immunology

REVIEW
published: 30 April 2018
doi: 10.3389/fimmu.2018.00880

Emerging Concepts in Immune Thrombocytopenia

*Maurice Swinkels[1], Maaike Rijkers[2], Jan Voorberg[2], Gestur Vidarsson[3], Frank W. G. Leebeek[1] and A. J. Gerard Jansen[1,2]**

[1] Department of Hematology, Erasmus University Medical Centre, Rotterdam, Netherlands, [2] Department of Plasma Proteins, AMC-Sanquin Landsteiner Laboratory, Amsterdam, Netherlands, [3] Department of Experimental Immunohematology, AMC-Sanquin Landsteiner Laboratory, Amsterdam, Netherlands

Immune thrombocytopenia (ITP) is an autoimmune disease defined by low platelet counts which presents with an increased bleeding risk. Several genetic risk factors (e.g., polymorphisms in immunity-related genes) predispose to ITP. Autoantibodies and cytotoxic CD8$^+$ T cells (Tc) mediate the anti-platelet response leading to thrombocytopenia. Both effector arms enhance platelet clearance through phagocytosis by splenic macrophages or dendritic cells and by induction of apoptosis. Meanwhile, platelet production is inhibited by CD8$^+$ Tc targeting megakaryocytes in the bone marrow. CD4$^+$ T helper cells are important for B cell differentiation into autoantibody secreting plasma cells. Regulatory Tc are essential to secure immune tolerance, and reduced levels have been implicated in the development of ITP. Both Fcγ-receptor-dependent and -independent pathways are involved in the etiology of ITP. In this review, we present a simplified model for the pathogenesis of ITP, in which exposure of platelet surface antigens and a loss of tolerance are required for development of chronic anti-platelet responses. We also suggest that infections may comprise an important trigger for the development of auto-immunity against platelets in ITP. Post-translational modification of autoantigens has been firmly implicated in the development of autoimmune disorders like rheumatoid arthritis and type 1 diabetes. Based on these findings, we propose that post-translational modifications of platelet antigens may also contribute to the pathogenesis of ITP.

Keywords: immune thrombocytopenia, immune thrombocytopenic purpura, autoantibodies, CD8$^+$ T cells, autoimmunity, ITP

OPEN ACCESS

Edited by:
Falk Nimmerjahn, Friedrich-Alexander-Universität Erlangen-Nürnberg, Germany

Reviewed by:
Matthew Cook, Australian National University, Australia
Pawel R. Kiela, University of Arizona, United States

***Correspondence:**
A. J. Gerard Jansen
a.j.g.jansen@erasmusmc.nl

Specialty section:
This article was submitted to Immunological Tolerance and Regulation, a section of the journal Frontiers in Immunology

Received: *30 November 2017*
Accepted: *09 April 2018*
Published: *30 April 2018*

Citation:
Swinkels M, Rijkers M, Voorberg J, Vidarsson G, Leebeek FWG and Jansen AJG (2018) Emerging Concepts in Immune Thrombocytopenia. Front. Immunol. 9:880. doi: 10.3389/fimmu.2018.00880

INTRODUCTION

Immune thrombocytopenia (ITP) is an autoimmune disease characterized by low platelet counts and increased bleeding risk (1–4). The initial event(s) leading to anti-platelet autoimmunity remains unclear, but strong evidence exists that autoantibodies and autoreactive CD8$^+$ cytotoxic T cells (Tc) trigger enhanced platelet destruction and impair platelet production by megakaryocytes (MKs) in the bone marrow. We will briefly discuss the clinical aspects of this heterogeneous disease, followed by an overview of the mechanisms and pathways by which autoreactive B and Tc engage in anti-platelet immunity, with a particular focus on their specificity for platelet autoantigens. We will postulate a general model for ITP pathophysiology and finally highlight opportunities in ITP research, which can be derived from studies on other autoimmune diseases.

Epidemiology and Clinical Features

Immune thrombocytopenia is a diagnosis of exclusion: patients who develop thrombocytopenia (defined as platelet counts below 100,000 platelets per microliter) with no clear underlying cause

are currently diagnosed with (isolated) primary ITP (1, 4). Secondary ITP is defined as an ITP induced by other diseases or treatments. These include autoimmune disorders, lymphoproliferative disorders, infectious agents, transfusion, or induction by drugs, accounting in total for 20% of ITP cases (5, 6). In total, the incidence of ITP is approximately 1.9–6.4 per 100,000 children/year and 3.3–3.9 per 100,000 adults/year (6–8), and this number is increasing (6, 9). ITP can be classified in a transient form termed newly diagnosed ITP (up until 3 months), or persistent ITP (up until 12 months) that is more prevalent in children, or a chronic form (longer than 12 months) that does not resolve on itself and is more prevalent in adult patients (1, 6, 7). The acronym "ITP" should not be confused with the outdated definition of "idiopathic thrombocytopenic purpura" that has been used previously (1, 4). ITP is no longer considered an idiopathic disease and a proportion of patients do not present with purpura (see below). In this review, we discuss both adult and pediatric ITP studies and highlight discrepancies between both groups where necessary.

Bleeding symptoms in ITP patients typically present as either a mild form, such as bleeding in skin and mucosal regions, or a more severe, life-threatening form, such as bleeding in gastrointestinal or intracranial areas (6, 10). Patients with ITP have varying platelet counts as a result of the disease. Those with platelet counts above 50,000 per microliter rarely bleed, but below this "threshold" value, there are large differences in clinical phenotypes between patients that are as of yet unexplained (2, 3, 10). Platelet function testing appears successful in predicting bleeding risk in patients (11–13). However, no clear-cut diagnostic tools exist as associations between biomarkers and ITP remain limited, and no markers exist that may predict treatment responses (2, 3). The most common therapeutic options are based on immunosuppression [by corticosteroids, intravenous immunoglobulin (IVIg), or rituximab], or stimulation of platelet production [by thrombopoietin receptor agonists (TPO-RAs), see below].

Platelet Life Cycle

On average, the human body produces around 100 billion platelets per day resulting in a concentration of ~150,000–400,000 platelets per microliter blood (14). Platelets circulate for approximately 7–10 days, slowly undergoing age-related changes in morphology, activation, and surface receptor density (15–18). Platelets are produced by MKs in the bone marrow (19). MKs are polynuclear cells that protrude extensions in the blood, termed proplatelets, and eventually bud off platelets from these extensions (20, 21). Recent findings show that MKs may also reside in the lung, facilitating platelet production in lung tissues (22), although the relevance of platelet production at this site is currently unclear.

Thrombopoietin (TPO) is the key hormone responsible for platelet production. It is primarily synthesized in the liver and promotes MKs to produce platelets in the bone marrow *via* the TPO receptor, Mpl (23–25). As newly made TPO is released in the bloodstream by hepatocytes, it is also incorporated into circulating platelets *via* Mpl. This constitutes an inhibitory feedback loop in which platelet counts inversely correlate with the amount of TPO reaching the bone marrow to stimulate new platelet production (23, 26). Recent evidence suggests that the Ashwell-Morrell receptor (AMR) on hepatocytes plays an important role in this physiological process. Normally, as platelets age terminal sialic acid is gradually lost from the surface, which exposes the underlying galactose residues. This allows for their clearance by the AMR (27). AMR-mediated platelet clearance triggers hepatic TPO transcription and translation, and new TPO is released (27). Several other physiological clearance mechanisms exist that control platelet numbers, such as platelet apoptosis (28) and possibly phagocytosis by αMβ2 integrins on hepatic and splenic macrophages [for a review, see Ref. (29)].

In ITP, this normal platelet life cycle is disturbed by autoantibodies and platelet-reactive $CD8^+$ Tc as summarized in **Figure 1**. Autoantibodies and $CD8^+$ Tc may interfere with multiple aspects of the platelet life cycle, including their production and clearance that result in thrombocytopenia. In such thrombocytopenic conditions, the small amount of circulating Mpl-containing platelets often leads to high TPO levels (30, 31). Interestingly, only slightly elevated TPO levels are observed in ITP; likely because platelets with incorporated TPO are rapidly cleared (31). Therefore, one of the therapeutic options for ITP patients involves stimulation of the TPO receptor on MKs by TPO-RAs, which proves to be successful in many patients (32). Not all patients are equally responsive to TPO-RAs and poor responders likely suffer from a prolonged autoimmune response against platelets that cannot be resolved by increasing the platelet production.

Genetic Risk Factors

As mentioned, autoreactive B and Tc have been firmly implicated in the pathophysiology of ITP. Consequently, many studies have reported associations between ITP and single nucleotide polymorphisms (SNP) in immunity-related genes. Polymorphisms in genes encoding specific cyto- or chemokines, such as interleukin (IL)-1, IL-2, IL-4, IL-6, IL-10, IL-17, TNF-α, TGF-β, and IFN-γ, have been associated with ITP (33–37). Several studies have also investigated whether specific HLA class I or II alleles are elevated in patients with ITP (38–45); current findings suggest that polymorphic sites within the HLA locus are not linked to ITP as studies have reported both significant and nonsignificant findings (37–44). The variation in studies could potentially be explained by small sample size, ethnic variability, or differences in diagnosis, yet does not allow to reach a consensus. New biomarkers such as miRNAs regulating levels of cytokines or other immune components are also increasingly recognized as potential risk factors for ITP (46). Classically, polymorphisms in Fcγ receptors (FcγRs) have been associated with the onset and pathogenesis of ITP (47–54) and are therefore further discussed below. Most of the reported association studies performed in ITP patients were conducted in small cohorts and in specific ethnic subgroups, and thus should be interpreted with caution. Additionally, many of the identified associations are not found in all patients and are commonly observed in other autoimmune diseases as well and are therefore general predisposing factors and not specific for ITP. Advances in (epi)genomics are likely to identify additional genetic risk factors for the development of ITP (55, 56).

Environmental Risk Factors

For a long time, the occurrence of specific infections has been associated with ITP, particularly in children (5–7). Some of

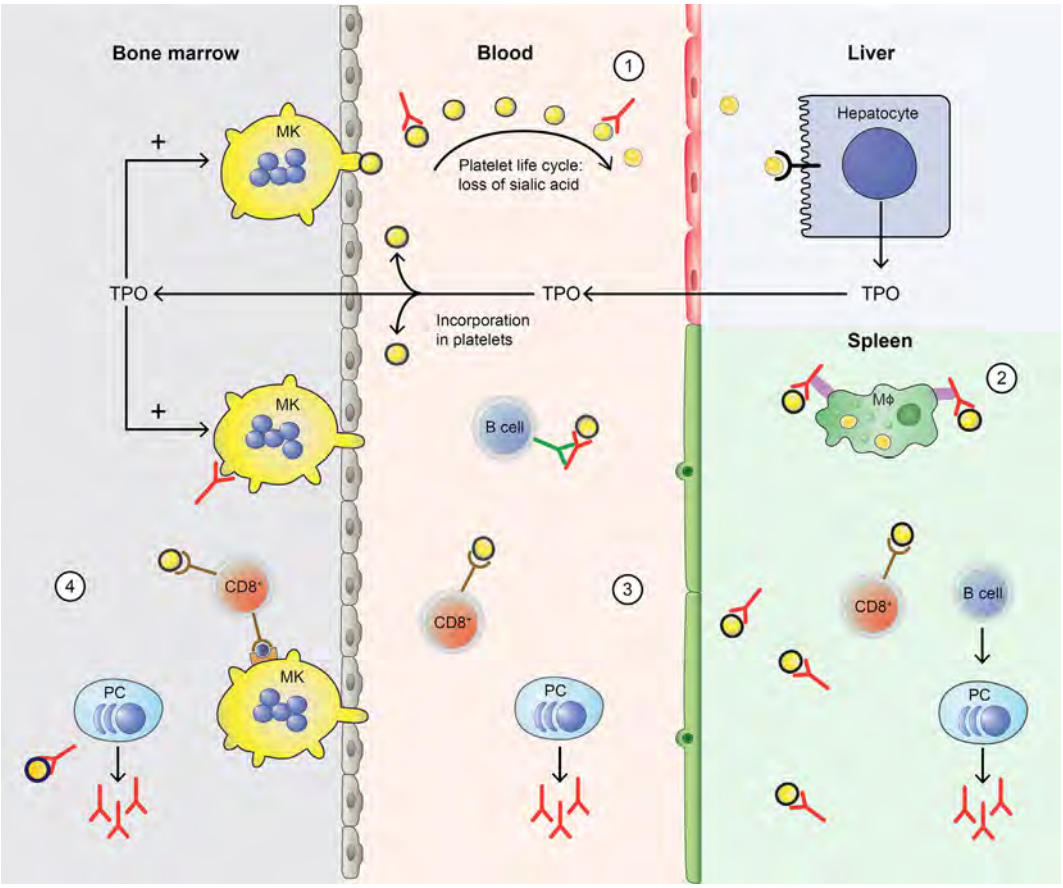

FIGURE 1 | Disturbance of the platelet life cycle in immune thrombocytopenia (ITP). (1) Platelets (yellow) are normally produced by megakaryocytes (MKs, yellow) in the bone marrow. Aging platelets undergo apoptosis but also gradually lose terminal sialic acid from the surface (indicated by black circles). This allows for their clearance in the liver. Liver-mediated platelet clearance triggers hepatic TPO transcription and translation, and new TPO is released. This process is disrupted by autoantibodies in ITP, which are hypothesized to enhance platelet desialylation leading to enhanced clearance. (2) Macrophages (MF, green) can phagocytose platelets; meanwhile, platelet antigens are presented in the spleen to immune cells, such as $CD4^+$ T helper (Th) cells. With $CD4^+$ T cell help, B cells (B cell, dark blue) are able to differentiate into platelet-reactive plasma cells (PC, light blue) that can secrete autoantibodies (red). Cytotoxic T cells (Tc) ($CD8^+$, red) can directly lyse platelets. (3) In peripheral blood, plasma cells and cytotoxic Tc further induce autoimmune responses against platelets. Cytotoxic Tc may also induce desialylation leading to enhanced clearance. In addition, platelet-reactive memory B cells may be present in the blood. (4) Plasma cells and cytotoxic Tc are also present in the bone marrow, where they can inhibit platelet production by targeting MKs.

the most occurring and most studied infectious agents are *Helicobacter pylori* (57, 58), Hepatitis C virus (59, 60) and human immunodeficiency virus (61–67). Evidence also exists for Cytomegalovirus (68, 69), Epstein Barr Virus (69), and some other viruses (70, 71). Although individual cases of ITP have been reported after vaccination, this is exceedingly rare (72, 73). One of the suggested mechanisms by which infections lead to autoimmunity is the occurrence of molecular mimicry. In this case, viral proteins resemble platelet receptors to evade the immune system (74). In case of an immune response against these viral proteins, cross reactivity may occur against platelet receptors, which subsequently lead to autoantibodies specific for both the viral protein and platelet receptors. This could explain the initiation of ITP in some cases (60–63, 66), which can be resolved by clearance of the infectious agent after which autoantibodies diminish (57, 58). Besides a transient decrease in platelet counts, infections sometimes elicit strong immune responses that can perpetuate and develop into chronic ITP, resulting in sustained platelet clearance.

Toll-like receptors are present on various innate immune cells, including platelets, and are suggested to mediate some of the microbial-platelet interactions that can trigger and/or aggravate autoimmunity (75). Immune-mediated thrombocytopenia may also occur as a result of other autoimmune diseases, drugs, transfusion, and in lymphoproliferative disorders (76, 77). Often, these cases are also diagnosed as secondary ITP, but may greatly differ in etiology. As our review focuses on primary ITP, we refer readers to Ref. (77) for more information on the underlying pathophysiology of these forms of secondary ITP.

ETIOLOGY

Autoantibodies

In approximately 60% of all ITP patients, autoantibodies are found, predominantly against platelet glycoprotein (GP) IIb/IIIa (~70%) and/or the GP Ib–IX–V complex (~25%) (78–81). Antibodies against GPIa–IIa or GPVI are also detected in

sporadic cases (~5%) (80, 82, 83). While it is not entirely clear how autoantibodies against platelet antigens are generated, their effect on platelet clearance and production have now been fully elucidated (**Figure 1**). When microbial-antigens mimicking platelet autoantigens, or the platelet antigens themselves, are presented to B cells, these can develop into autoantibody-secreting plasma cells. The spleen has been implied as an organ where immune cells are primarily presented with platelet autoantigens, and where platelet clearance takes place most (84, 85). Particularly splenic macrophages and dendritic cells (DCs) can present platelet antigens to T helper (Th) cells that provide help to B cells that differentiate into antibody-secreting plasma cells (86, 87). Plasma cells secreting platelet-reactive autoantibodies are present in peripheral blood and bone marrow, where they can further generate autoantibodies that can sequester platelets and MKs (88–90). In addition, memory B cells activated in the spleen are also released in the circulation (**Figure 2**) (85). Autoantibodies accelerate platelet clearance by removal *via* splenic macrophages and DCs (87), complement deposition (91–93) and platelet apoptosis (94), or by inhibiting megakaryocytic platelet production (88–90).

Autoantibody and B Cell Classification

Initial studies investigating autoantibodies in ITP identified high levels of platelet-associated IgGs (PAIgGs) in nearly all patients, and they were soon thought to be the causative factor of the autoimmune response. However, it was found that PAIgGs bound nonspecifically to platelets and were detected in other non-ITPs as well (95), likely because platelets themselves can bind circulating IgG *via* FcγRIIa (96). PAIgGs thus proved to be a poor predictor of the disease [for a review, see Ref. (95)]. Although it is interesting that PAIgGs levels are higher in ITP and other thrombocytopenic patients (consisting of different IgG subclasses compared to healthy individuals), their usefulness in investigating ITP remains limited and can be largely subscribed to the state of thrombocytopenia rather than the autoimmune conditions. Following the introduction of the MAIPA and immunobead assays in 1987 (79, 97), investigators were able to detect and further study platelet-specific autoantibodies in ITP (98, 99).

Most autoantibodies found in chronic ITP patients are of the IgG class, but IgM and sporadically IgA antibodies are also detected (100–102). IgM antibodies were shown to fix complement on platelets which could facilitate clearance, but this has not been further investigated; IgG autoantibodies seem to be the main mediator of antibody-driven autoimmunity (100). Most prevalent are IgGs of the IgG1 subclass, and while IgG2, IgG3, and IgG4 subclass autoantibodies can be also found in patients, they are often accompanied by IgG1 antibodies (103, 104). Autoantibody allotypes and Fc-glycosylation are important determinants in antibody-mediated immunity and immunological disorders related to ITP (105–107), yet have been scarcely investigated.

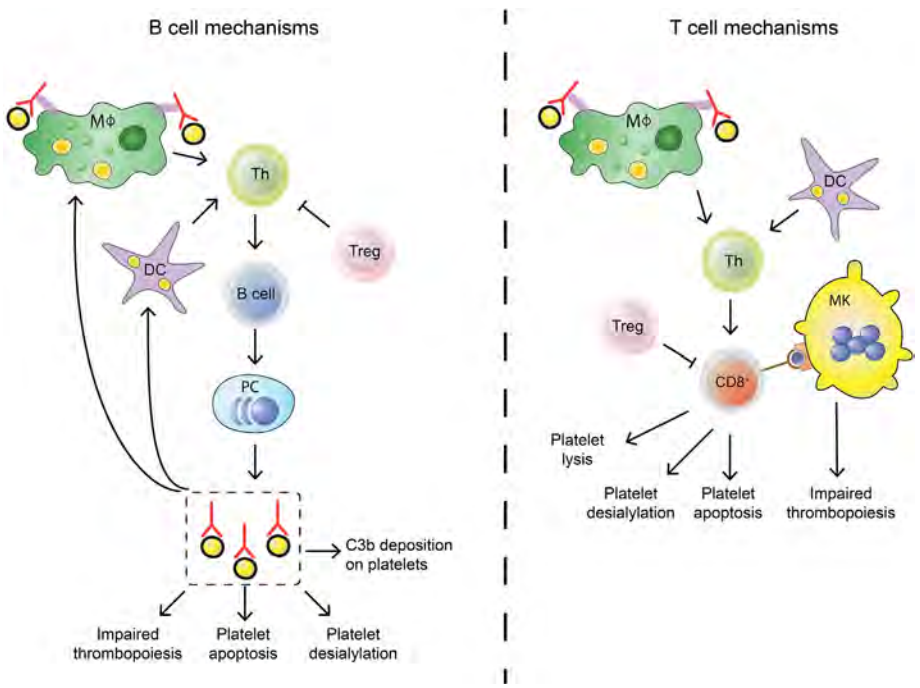

FIGURE 2 | Differences in B cell and T cell mechanisms in immune thrombocytopenia (ITP). B cells (left) differ from cytotoxic T cells (Tc) (right) in their autoimmune response against platelets in ITP. Stimulation of the adaptive immune response is similar: splenic macrophages (green) and dendritic cells (DCs, purple) can phagocytose platelet fragments to present to T helper (Th, light green) cells. Th cells are able to induce B cell development into autoantibody secreting plasma cells and can also stimulate cytotoxic Tc effector mechanisms. This process is regulated by regulatory Tc (Treg, pink), but regulatory T cell levels are imbalanced in ITP patients which leads to insufficient control of the autoimmune response. Shared effector functions of B cell-produced autoantibodies and cytotoxic Tc include impairing thrombopoiesis by targeting megakaryocytes (MKs), inducing platelet apoptosis and enhancing platelet desialylation. Autoantibodies can further stimulate C3b deposition on platelets to initiate complement activation, while cytotoxic Tc can directly lyse platelets.

In the majority of ITP patients, B cells producing platelet-binding antibodies have been identified in clinical samples from different sources, such as peripheral blood, spleen, and bone marrow (108–115). However, not all patients have platelet-reactive B cells (108, 109, 112–114), suggesting that B cell independent autoimmune mechanisms (such as $CD8^+$ T cell mediated autoimmunity) exist. A landmark study by Roark and co-workers employed repertoire cloning to clone platelet autoantibodies from the spleen of two patients with chronic ITP (110). Sequence analysis of Ig heavy chain arrangements revealed that these anti-platelet antibodies evolved from a restricted number of B cell clones and provided evidence for extensive modification of heavy chain segments by somatic hypermutation (110). Overall, these findings provide evidence for a $CD4^+$ T cell-driven antigen-specific response in patients with ITP. Evidence for the selective incorporation of the VH3-30 variable heavy chain gene segment was noted in this study providing additional evidence for a restricted, oligoclonal B cell response targeting a limited number of epitopes on platelet antigens in ITP patients (110).

Autoepitope Specificity of Antibodies

As the predominant source of epitopes for autoantibodies in ITP, the GP IIb/IIIa receptor, or integrin $\alpha_{IIb}\beta_3$, has been studied most frequently. Reports have shown that autoantibodies can bind epitopes in both the extracellular- and cytoplasmic domain of GPIIb/IIIa (80, 116). However, autoantibodies targeting the cytoplasmic domain are likely to be generated during platelet destruction rather than being pathogenic, but their significance remains unclear (80). Subsequent studies have shown that autoantibodies particularly bind to the IIb subunit (117, 118), or contradictory, the IIIa subunit of the dimer (119). Eventually, several investigators have demonstrated that specific portions of the protein are preferred autoepitopes in ITP, often near ligand binding sites (81, 120). The vitronectin ($\alpha_v\beta_3$) receptor shares the β_3 integrin with GPIIb/IIIa and was shown to be an important autoantigen in ITP as well (121). However, this has not been further investigated.

Less is known about relevant autoepitopes on GP complex Ib-IX-V, although most antibodies are directed against the GPIb part of the receptor complex (78, 98, 122). Interestingly, patients with autoantibodies against GPIb are often less responsive to immunosuppressive therapy with corticosteroids or IVIg when compared to patients with GPIIb/IIIa autoantibodies (122–124). This could be explained by specific epitopes on GPIb, relative receptor abundance on the platelet surface or differences between both protein complexes.

B Cell Help by $CD4^+$ T Cells

B cells require help by $CD4^+$ Tc to efficiently develop into antibody-secreting plasma cells (**Figure 2**). As the development of autoantibodies is a hallmark of ITP, several studies have explored the involvement of $CD4^+$ Tc in the pathogenesis of ITP. Initial observational studies showed that cytokines necessary for Th functions (such as IL-2, IL-10, IFN-γ) are increased in ITP patients (125, 126). Further evidence came from studies that identified a T cell imbalance in ITP: patients have a disturbed Th1/Th2 subset ratio, which trends toward a Th1 phenotype (127–129). Both rituximab and splenectomy seemed to resolve this polarization in responding patients, indicating the importance of balancing different populations of $CD4^+$ Tc in ITP (128, 130). Pioneering work by Kuwana and co-workers have provided firm evidence for the presence of auto-reactive $CD4^+$ Tc that target epitopes on GPIIb/IIIa (131, 132).

Recently, pro-inflammatory Th17 cells have emerged as a critical player in development of autoimmunity (133). Higher levels of Th17 cells were observed in several ITP cohorts (134, 135), but not in all studies (136). Several studies have found higher levels of both Th1 and Th17, compared to Th2 (137–141). The potential involvement of another subset of Th cells, Th22, was also investigated in ITP. Th22 cells typically promote protective and regenerative responses with predominant effects on epithelial cells (142–144). Increased levels IL-22 and elevated levels of the Th22 T cell subset have been observed in patients with ITP suggesting a role for this population of Tc in ITP pathogenesis (145, 146). In line with its established role in B cell help, splenic follicular Th (T_{FH}) cells have also been implicated in the pathogenesis of ITP (147). These findings show that multiple Th populations including Th1/Th17/Th22/T_{FH} contribute to the pathogenesis of ITP (127, 129, 135, 137, 145–147). We anticipate that the observed skewing toward Th1/Th17/Th22/T_{FH} populations is not specific for ITP as similar Th polarization profiles are observed in other autoimmune diseases.

$CD8^+$ T Cells

Besides autoreactive B cells, $CD8^+$ Tc have also been implicated in ITP pathogenesis (126, 148, 149). Evidence from association studies shows that patients with ITP more often present with polymorphisms in $CD8^+$ related cytokines (126, 150, 151), have increased granzyme levels (152), and have imbalanced ratios of $CD8^+$ Tc cell subsets (137, 140). As $CD8^+$ Tc are also dependent on help of $CD4^+$ Th cells to efficiently perform effector functions, the polarization of $CD4^+$ Th cells probably also affects the $CD8^+$ Tc cell response (137, 140).

T cells are part of cell-mediated immunity and have different effector functions compared to antibody-secreting B cells. In ITP, B cells and Tc thus elicit different forms of anti-platelet immunity (**Figure 2**). $CD8^+$ Tc have been shown to directly lyse platelets (148, 153–155), induce platelet apoptosis (153), and inhibit thrombopoiesis by MKs (156). $CD8^+$ Tc can further inhibit platelet production by inhibiting MK apoptosis (157).

Increased levels of $CD8^+$ Tc were found in patients without autoantibodies (154), suggesting that $CD8^+$ Tc cell-mediated autoimmunity can be elicited separately from autoantibody-mediated autoimmunity. Evidence of a T cell response separate from antibody-mediated autoimmunity was further shown in ITP patients who did not respond to the anti-$CD20^+$ B cell-depleting antibody rituximab, in whom increased levels of splenic $CD8^+$ Tc were detected (158). In contrast, $CD8^+$ Tc were found to be protective and required for effective steroid therapy in a murine model of ITP, although these findings are counterintuitive and not supported by observations in other autoimmune diseases (159).

It is unclear how the B cell depletion and repopulation effects of rituximab alter T cell subsets in responding patients. Possibly, the altered cytokine environment as a result of B cell depletion affects T cell subsets, as the B-T cell interplay is essential in a

systemic autoimmune response (160). A recent study showed that rituximab could suppress murine $CD8^+$ T-cell mediated immune responses (161), suggesting that B cells may regulate the $CD8^+$ T-cell response in ITP. In fact, ITP patients present with lower levels of regulatory B cells (162). However, the effect of rituximab treatment in ITP remains difficult to interpret as B cell depletion may also affect $CD20^+$ regulatory B cells, which can secrete IL-10 and other suppressive cytokines to induce immune tolerance (163), as suggested previously.

As of yet, the target peptides expressed on MHC class I recognized by platelet specific $CD8^+$ Tc have not been identified. Interestingly, no clear HLA association is found in ITP patients (38–45), as opposed to other autoimmune diseases. In *H. pylori*-mediated ITP, HLA associations were also unclear (114, 164). Platelets are capable of presenting non-renewable MK-derived peptides on MHC class I, and it is likely that these peptides are being recognized by $CD8^+$ Tc that develop in patients with ITP (165). More recently, it was proposed that platelets have the propensity to activate naïve $CD8^+$ Tc and that platelets can present pathogen-derived peptides in the context of MHC class I (166). In this context, it is interesting to note that following dengue infection the MHC class I density on platelets increases, suggesting an active role of platelets in combatting infections (166, 167). Under resting conditions, platelets do not express MHC class II molecules on their surface, but several reports suggested platelets to express MHCII complexes during infection (164, 168). Whether antigen presentation on MHC class I by platelets has a role in the pathogenesis of ITP has not been demonstrated. In view of the established role of $CD8^+$ Tc in this autoimmune disorder, this will be an interesting area for further research.

Regulatory T Cells

Tregs are a crucial checkpoint to limit immunity and secure immune tolerance. As such, they are important regulators that keep both B- and T cell-mediated autoimmunity in check (**Figure 2**). The importance of Tregs for the pathogenesis of ITP is evidenced by their reduced numbers and function in patients (169–173). The pivotal role of immune regulation in ITP, particularly by Tregs, was further shown by phenotypic and Treg profiling studies of treated versus untreated ITP patients. Treatment with corticosteroids and/or rituximab in responding patients both improved Treg levels as well as their activity (130, 174–178), indicating that loss of tolerance is essential for the pathogenesis of ITP. In an experimental murine model of ITP, Tregs were retained in the thymus. This was resolved by IVIg treatment, which normalized Tregs in the periphery (179). Additionally, transferring retained thymocytes delayed the onset of ITP, suggesting Tregs actively prevent ITP development at least in mice (179). Interestingly, TPO-RAs improved Treg activity indicating that platelets could directly or indirectly play a regulatory role in ITP by affecting Treg levels (175). As such, it is clear that ITP patients present with lower Treg levels which are restored upon successful treatment (see above). However, it is still unclear whether restoring Treg functionality directly alleviates the disease or is simply a marker of restored immune tolerance. Potentially involved pathways are further discussed below.

Tregs can interact with DCs to induce a tolerogenic phenotype. Two studies found that the interplay between Tregs and DCs is impaired in ITP (178, 180). As Treg levels are lower in ITP, this leads to a reduced expression of immunomodulatory enzyme indoleamine 2,3-dioxygenase 1 (IDO1) by DCs, and increased levels of mature DCs that can present (auto)antigens to other immune cells (178, 180). The important role of tolerance induction by DCs in ITP was further suggested by another study, in which IVIg was shown to mediate its effect *via* DCs in a murine model (181). The interplay between Tregs and DCs and immunomodulation *via* IL-10 is not only important in ITP but was also found essential in antibody-mediated acute lung injury (182, 183). As such, the Treg-DC-axis may be particularly important in autoantibody-mediated ITP, but this remains to be investigated.

Other Immune Cells

Several other immune cells may modulate autoimmune responses in ITP but have been investigated sparsely. Neutrophils have been found to line MKs in ITP bone marrow (184), but their role in ITP has not been further investigated. A subset of $CD16^+$ monocytes derived from patients with ITP has shown to promote the proliferation of IFN-γ^+ $CD4^+$ Tc (185). Shifts in the balance of inhibitory and activating FcγRs were observed on monocytes following treatment with high-dose corticosteroid dexamethason as well as following *H. pylori* eradication in ITP (186, 187) (further discussed below). Additionally, they were found to be involved in T cell development (185). Both increased and decreased levels of NK cells have been found in ITP patients (188–190). The significance of these observations is unclear since NK cells are not able to lyse platelets (148).

Finally, platelets themselves may be able to affect the autoimmune response in ITP, as they are increasingly recognized as mediators of immunity and inflammation [for a recent review, see Ref. (191)]. Evidence for such an autoregulatory loop was found in ITP patients responding to TPO-RAs, who not only had increased platelet counts but also correlating higher TGF-β plasma levels (175). Presumably, increased plasma TGF-β levels derive from an increased platelet mass (175). Furthermore, TPO-RAs reduced both autoantibody and T cell responses in a mouse model, which also lead to elevated TGF-β plasma levels (192). Interestingly, TPO-RAs may induce remission in a subset of patients whom then no longer needed therapy to maintain platelet levels (193–195). This would imply that immune tolerance can be restored in certain patient subsets by enhancing platelet numbers. Another mechanism by which platelets regulate immune responses occurs *via* CD40L. Activated Tc can stimulate B cell proliferation and differentiation *via* CD40L interactions with CD40 on B cells (196). Platelets normally express CD40L only upon activation, but higher baseline levels are observed in ITP patients (13). Furthermore, activated platelets from ITP patients were shown to stimulate autoreactive B cells by CD40L (197). Interestingly, CD40L inhibition was successful in suppressing T cell-assisted B cell-mediated autoantibody production in ITP, even in treatment of refractory ITP (198, 199). However, whether this is similarly successful affecting a potential B cell-platelet interaction remains unknown.

PATHWAYS INVOLVED IN PLATELET CLEARANCE

FcγR-Mediated Eradication of Platelets

FcγRs have long been implicated in ITP etiology. These receptors are differentially expressed on immune cells and are the primary receptor for IgG. FcγRs mediate different functions, including phagocytosis, antibody dependent cellular cytotoxicity, and release of cytokines [reviewed in detail in Ref. (96)]. Most FcγRs are involved in activating the immune system, whereas FcγRIIb is the only inhibitory FcγR. Platelets only express FcγRIIa on their surface, while myeloid cells, such as granulocytes, monocytes, macrophages, and DCs express several FcγRs (96). In liver and particularly spleen, monocytes and macrophages have been suggested to bind and phagocytose Ig-opsonized platelets by FcγRs, explicitly contributing to platelet clearance and autoantigen presentation (85, 87). As such, polymorphisms in several FcγRs have been associated with ITP (47–54). The low affinity FcγRIIa, FcγRIIIb on granulocytes, and FcγRIIIa on NK cells, monocytes, and macrophages all contain SNP that affect binding affinity to IgG (200).

For FcγRIIa, one polymorphism at position 131 (R/H, with H having higher affinity) most strongly or exclusively affects IgG2 binding (200), and the higher-affinity allele was found to be associated with ITP (48, 51–54). However, these studies had inconsistent outcomes. A recent meta-analysis indicated that the R131H polymorphism might be associated with a subgroup of childhood-onset ITP, but this should be interpreted with caution (54). In accordance with the notion that FcγRIIIa$^+$ splenic monocytes are particularly important for the clearance of platelets, only the higher affinity-allele of the FcγRIIIa polymorphism at position 158 [F/V, with 158 V having higher affinity for IgG1 and IgG3 (200)] has been found to be associated with ITP (48, 50–53). Intriguingly, one study found that a polymorphism in the transmembrane region of the inhibitory FcγRIIb (232I/T) is associated with the onset of newly diagnosed ITP in children (49). This polymorphism (232T) has been found to negatively affect the capacity of this receptor to downregulate immune responses (201) and could point at an immunomodulatory role of FcγRIIb. Intriguingly, eradication of *H. pylori* (a potential molecular mimicry causative of the onset of ITP) was found to shift monocyte FcγR expression toward an inhibitory FcγRIIb phenotype (187). Finally, the FcγRIIc has also been associated with ITP (50). FcγRIIc is a pseudogene in most individuals, but having FcγRIIc most likely predisposes individuals to stronger immune responses (202, 203). While the extracellular IgG-binding domain of FcγRIIc is identical to the inhibitory FcγRIIb, the intracelllular tail is identical to FcγRIIa and contains an activating motif (202). Due to the proposed expression of FcγRIIc on B cells, it may downregulate the negative feedback provided by FcγRIIb (202). Interestingly, FcγRs are known to crosstalk with Toll-like receptors, particularly during bacterial infections. This leads to T cell polarization (204), but it is unclear if this crosstalk is in any way relevant for platelets and/or in the context of ITP. Considering the strong correlation with infections in the onset of ITP, investigating the FcγR-TLR crosstalk could be interesting.

Additional evidence that FcγR-mediated pathways are important in ITP pathogenesis was shown by the therapeutic use of IVIg, which may bind FcγRs by its Fc-portion (205), and is one of the successful cornerstone treatments for ITP to rapidly increase platelet counts. It was recently shown that IVIg does not modulate FcγR expression directly but inhibits the phagocytic capabilities of splenic macrophages (206). In addition, a previous pilot study has also shown that Syk-inhibitors, which affect downstream FcγR signaling, can improve ITP (207). While IVIg does not work in all patients, the efficacy may be predicted by specific FcγR polymorphisms (208). As such, various FcγR polymorphisms provide the most compelling evidence that genetics may affect ITP, both by predicting higher risk of disease development and treatment outcomes. In addition, the role of FcγRs on platelets and other immune cells has now been firmly implicated in ITP pathogenesis. Nevertheless, FcγR-independent mechanisms may exist as well.

FcγR-Independent Eradication of Platelets

A recent study has implicated a FcγR-independent pathway in an experimental mouse model (209), which was hypothesized to occur simultaneously aside FcγR-mediated clearance by splenic macrophages. Autoreactive antibodies against GPIb were hypothesized to induce platelet activation and degranulation, which leads to sialidase release (210). This induces desialylation of platelet membrane glycans, which can subsequently lead to recognition of platelets by the AMR in the liver thereby accelerating platelet clearance (27, 209). Interestingly, there are a few cases of ITP patients with abnormal platelet surface sialic acid levels (211, 212). Oseltamivir, which is a sialidase inhibitor used to treat influenza, has been found to increase platelet sialic acid content (213) and in two cases was successful in ameliorating thrombocytopenia whereas conventional therapy was not (212, 214). Platelet desialylation was also found to correlate with non-responsiveness to first-line therapies in ITP (215). Finally, CD8$^+$ Tc have also been suggested to induce platelet desialylation and to facilitate platelet clearance similar to the earlier mentioned mechanisms (155). While the importance of sialic acid in the platelet life cycle has long been established (14), it is unclear whether the experimental findings in mice can be translated to a human and/or clinical setting. Ongoing studies are needed to establish the importance of platelet desialylation in ITP.

C-Reactive Protein and Reactive Oxygen Species

Recently, a role for inflammatory acute-phase protein C-reactive protein (CRP) has also been implied in ITP pathogenesis (216). CRP levels were elevated in ITP patients and enhanced platelet phagocytosis in presence of anti-platelet antibodies *in vitro* and *in vivo*. This effect was ameliorated by IVIg treatment, suggesting that this mechanism may at least in part be mediated *via* FcγRs (216). Phosphorylcholine, a CRP ligand present on cell surfaces, was exposed after antibody-induced oxidative stress. Oxidative stress induced by ITP autoantibodies has also been shown in two separate studies on ITP (217, 218) and appears to be a suitable biomarker for ITP (219). Additionally, the pathophysiological role of reactive oxygen species has long been implied in a model of

HIV-initiated ITP (64, 65, 67). In this model, reactive oxygen species induced by platelet antibodies were able to directly lyse platelets, leading to platelet fragmentation. This appears to involve the platelet NADPH pathway and is complement independent (65). Interestingly, treating platelets with dexamethasone was shown to inhibit NADPH oxidase components that partially prevented induction of reactive oxygen species (67). Further studies will be required to elucidate the exact role of CRP, oxidative stress, and autoantibodies or autoreactive $CD8^+$ Tc in ITP.

MODEL FOR ITP PATHOGENESIS

As knowledge on the pathogenesis of ITP develops, definitions become outdated, and lines between primary and secondary ITP are beginning to blur. In other autoimmune diseases, infections are increasingly recognized as one of the primary initiating events that can lead to an autoimmune response. This is not the case for ITP, where it is regarded as a secondary form. However, even in what is called primary ITP, there must be some sort of initiating event that triggers the autoimmune response and exposes platelet antigens. This initiating event will obviously still have consequences for clinical treatment of ITP, whether it is an infection, blood transfusion, drug, or an unknown other trigger. Nonetheless, infections should no longer simply be regarded as a secondary form considering their potential as an initiating event or trigger to expose platelet antigens.

The number of people developing ITP directly after an infection is small, which suggests that additional factors have to be present during an infection to develop persistent autoimmunity. Individuals with a known autoimmune disease are more prone to develop ITP, indicating that dysregulation of immune homeostasis may contribute to the onset of ITP. Interestingly, most pediatric patients only develop transient thrombocytopenia, which is eventually resolved when the viral antigen is cleared. Meanwhile, similar to other autoimmune disorders, chronic ITP is more prevalent in adult patients, and the incidence increases with age. Based on the currently available data, we propose a simplified model of ITP in which both exposure of platelet antigens and loss of tolerance are required to induce ITP (**Figure 3**). The specific type of trigger likely determines whether a $CD4^+$ T cell-assisted B cell response develops or whether $CD8^+$ Tc targeting platelets are induced. Transient forms of ITP may develop if insufficient $CD4^+$ T cell help is available for the generation of class-switched, fully affinity matured, strongly binding anti-platelet antibodies. Such antibodies are likely produced by bone marrow-residing plasma cells in a fully developed $CD4^+$ T cell-assisted B cell response. We furthermore propose that platelet directed $CD8^+$ T cell responses develop following presentation of pathogen-derived peptides on MHC class I that may evoke the formation of $CD8^+$ Tc that (cross) react with peptides presented on MHC class I on platelets.

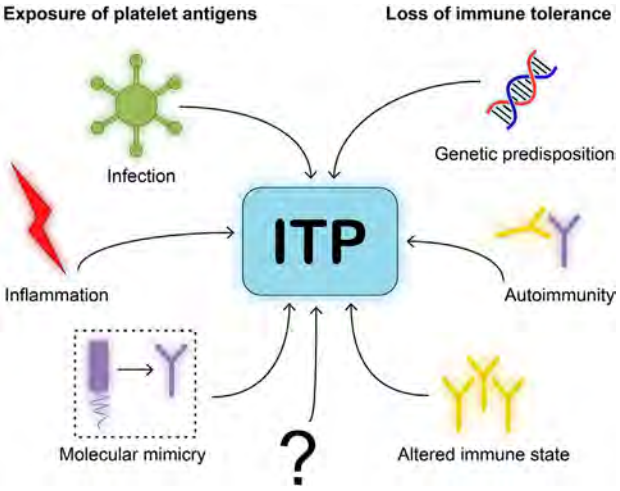

FIGURE 3 | Model for immune thrombocytopenia (ITP) pathogenesis. We postulate a simplified model for the pathogenesis of ITP. One, neo-epitopes on platelet antigens need to be exposed to immune cells. This requires an initiating event or trigger, such as infection, inflammation, or molecular mimicry of viral antigens to resemble platelet glycoproteins. Two, immune cells will need to be able to develop self-reactivity due to loss of immune tolerance. This requires either genetic disposition in immune related-genes, autoimmunity by comorbidities that implies a central dysfunction in tolerance, or an altered immune state such as after organ transplantation.

FUTURE RESEARCH

Emerging Concepts and Opportunities to Unravel the Pathogenesis of ITP

Limited information is available on the autoantigens in ITP and their importance for recognition by immune cells once bound by autoantibodies. Epitopes targeted by platelet autoantibodies seem to differ between patients, coinciding with different responses to therapy and different bleeding phenotypes. The molecular basis for the variable bleeding diathesis in patients with ITP has not yet been fully elucidated. Investigators have primarily made use of ITP sera or plasmas to study the role of autoantibodies. However, these can contain multiple autoantibodies, some potentially undetected by the current methods. Similar to the elegant studied by Roark and co-workers (110), specific autoantibodies should be isolated to further study their effects on platelets, possibly combining characteristics like subclass characterization, epitope specificity, and glycosylation patterns.

ITP Versus Other Autoimmune Diseases: Lessons to Be Learnt

In other autoimmune disorders such as rheumatoid arthritis, systemic lupus erythematosus, or type 1 diabetes, it has been shown that post-translational modifications of autoantigens can elicit the formation of $CD4^+$ T cell responses as well as create neo-epitopes that are recognized by B cells. In view of the common mechanisms involved in loss of tolerance against self, these findings may open novel avenues for dissecting pathways contributing to the onset of ITP.

Evidence has been obtained for post-translational modifications of platelet proteins. Phosphorylation and particularly glycosylation of platelets have been well studied (29, 210, 220, 221), and the importance of platelet glycans is increasingly appreciated. Furthermore, platelets and peripheral blood contain different glycosyltransferases to modify platelet glycans (221), but their relevance in normal platelet physiology is still unclear and their

potential relevance for the onset of ITP has not been established. A role for desialylation triggered by platelet autoantibodies or $CD8^+$ Tc has been postulated, but it is unknown if this can also lead to the generation of neo-epitopes on the platelet surface (155, 209). Recently, it was also shown that formation of oxidative stress induced neo-epitopes on platelets promotes binding of the acute phase protein CRP resulting in enhanced phagocytosis of IgG-coated platelets (216). It is unclear whether the autoantibodies found in ITP patients are able to recognize such neo-epitopes in similar fashion.

Besides post-translational modifications, platelet membranes are highly dynamic with respect to the expression of cell-surface receptors. GP expression on the platelet surface is tightly regulated by different metalloproteases, such as ADAM10 and ADAM 17 that facilitate receptor shedding (222, 223). Additionally, platelet granules release their content to rapidly increase receptor density on the membrane, such as the well-established activation marker P-selectin (223). These processes are important in both health and disease (224); however, it is unknown if the dynamic shuffling of receptors on the platelet surface is in any way relevant to formation of neo-epitopes in ITP.

The difference between post-translational modifications in other autoimmune diseases and ITP is that most of the modifications mentioned above are induced by autoantibodies in ITP, while modifications in for example the autoantigens that are implicated in rheumatoid arthritis precede the formation of autoantibodies (225–227) and are postulated to be one of the key events that triggers their generation. In fact, infection-induced post-translational modifications of target proteins, such as citrullination of fibrin, are thought to initiate a continuous inflammatory environment, which eventually leads to autoimmunity (225–227). Interestingly, the autoantigens in rheumatoid arthritis are usually located on "static" long-lived cartilage and/or joint proteins, such as fibrin. This is different in ITP, where the autoantigens are located on GPs on platelets that have a limited lifespan. Currently, no information is available with respect to the potential of post-translational modifications of platelet antigens to trigger autoimmune responses. In view of the prominent role of post-translational modifications in the onset of autoimmunity, we speculate that this will provide a novel and interesting avenue for future research to dissect the mechanisms that contribute to the onset of ITP.

CONCLUSION

We suggest a simplified model of ITP in which both exposure of platelet antigens and loss of tolerance are required for the onset of ITP, thereby promoting $CD4^+$ T cell-assisted B cell responses against platelets. Additionally, we propose that infections resulting in the presentation of pathogen-derived peptides on MHC class I may induce the formation of $CD8^+$ Tc that (cross) react with peptides presented on MHC class I on platelets. Specific triggers likely determine the type of autoimmune response against platelets. We speculate that post-translational modifications of platelet antigens harbor potential to generate neo-epitopes that trigger autoimmune responses in ITP, as they do in other autoimmune disorders. Future studies interrogating these hypotheses may yield novel insights into the mechanisms that underlie the development of ITP.

AUTHOR CONTRIBUTIONS

MS wrote the manuscript. MR, JV, GV, FL and AJ provided input, made suggestions for improvement, and approved the final version for submission.

ACKNOWLEDGMENTS

We would like to thank Egied Simons (Department of Hematology, Erasmus Medical Centre, Rotterdam) for his help in digitalizing **Figures 1–3**.

FUNDING

Supported by grant PPOC-2013-019 and PPOC-2015-024P (Netherlands Ministry of Health). AJGJ is supported by a Clinical Fellowship of the European Hematology Association.

REFERENCES

1. Rodeghiero F, Stasi R, Gernsheimer T, Michel M, Provan D, Arnold DM, et al. Standardization of terminology, definitions and outcome criteria in immune thrombocytopenic purpura of adults and children: report from an international working group. *Blood* (2009) 113(11):2386–93. doi:10.1182/blood-2008-07-162503
2. Provan D, Stasi R, Newland AC, Blanchette VS, Bolton-Maggs P, Bussel JB, et al. International consensus report on the investigation and management of primary immune thrombocytopenia. *Blood* (2010) 115(2):168–86. doi:10.1182/blood-2009-06-225565
3. Neunert C, Lim W, Crowther M, Cohen A, Solberg L Jr, Crowther MA, et al. The American Society of Hematology 2011 evidence-based practice guideline for immune thrombocytopenia. *Blood* (2011) 117(16):4190–207. doi:10.1182/blood-2010-08-302984
4. Michel M. Immune thrombocytopenia nomenclature, consensus reports, and guidelines: what are the consequences for daily practice and clinical research? *Semin Hematol* (2013) 50(Suppl 1):S50–4. doi:10.1053/j.seminhematol.2013.03.008
5. Cines DB, Bussel JB, Liebman HA, Luning Prak ET. The ITP syndrome: pathogenic and clinical diversity. *Blood* (2009) 113(26):6511–21. doi:10.1182/blood-2009-01-129155
6. Moulis G, Palmaro A, Montastruc JL, Godeau B, Lapeyre-Mestre M, Sailler L. Epidemiology of incident immune thrombocytopenia: a nationwide population-based study in France. *Blood* (2014) 124(22):3308–15. doi:10.1182/blood-2014-05-578336
7. Terrell DR, Beebe LA, Vesely SK, Neas BR, Segal JB, George JN. The incidence of immune thrombocytopenic purpura in children and adults: a critical review of published reports. *Am J Hematol* (2010) 85(3):174–80. doi:10.1002/ajh.21616
8. Bennett CM, Neunert C, Grace RF, Buchanan G, Imbach P, Vesely SK, et al. Predictors of remission in children with newly diagnosed immune thrombocytopenia: data from the Intercontinental Cooperative ITP Study Group Registry II participants. *Pediatr Blood Cancer* (2018) 65(1):e26736. doi:10.1002/pbc.26736
9. An R, Wang PP. Length of stay, hospitalization cost, and in-hospital mortality in US adult inpatients with immune thrombocytopenic purpura, 2006-2012. *Vasc Health Risk Manag* (2017) 13:15–21. doi:10.2147/VHRM.S123631

10. Neunert C, Noroozi N, Norman G, Buchanan GR, Goy J, Nazi I, et al. Severe bleeding events in adults and children with primary immune thrombocytopenia: a systematic review. *J Thromb Haemost* (2015) 13(3):457–64. doi:10.1111/jth.12813
11. Panzer S, Rieger M, Vormittag R, Eichelberger B, Dunkler D, Pabinger I. Platelet function to estimate the bleeding risk in autoimmune thrombocytopenia. *Eur J Clin Invest* (2007) 37(10):814–9. doi:10.1111/j.1365-2362.2007.01855.x
12. Greene LA, Chen S, Seery C, Imahiyerobo AM, Bussel JB. Beyond the platelet count: immature platelet fraction and thromboelastometry correlate with bleeding in patients with immune thrombocytopenia. *Br J Haematol* (2014) 166(4):592–600. doi:10.1111/bjh.12929
13. Frelinger AL III, Grace RF, Gerrits AJ, Berny-Lang MA, Brown T, Carmichael SL, et al. Platelet function tests, independent of platelet count, are associated with bleeding severity in ITP. *Blood* (2015) 126(7):873–9. doi:10.1182/blood-2015-02-628461
14. Li R, Hoffmeister KM, Falet H. Glycans and the platelet life cycle. *Platelets* (2016) 27(6):505–11. doi:10.3109/09537104.2016.1171304
15. Shrivastava M. The platelet storage lesion. *Transfus Apher Sci* (2009) 41(2):105–13. doi:10.1016/j.transci.2009.07.002
16. Devine DV, Serrano K. The platelet storage lesion. *Clin Lab Med* (2010) 30(2):475–87. doi:10.1016/j.cll.2010.02.002
17. Rijkers M, van den Eshof BL, van der Meer PF, van Alphen FPJ, de Korte D, Leebeek FWG, et al. Monitoring storage induced changes in the platelet proteome employing label free quantitative mass spectrometry. *Sci Rep* (2017) 7(1):11045. doi:10.1038/s41598-017-11643-w
18. Rijkers M, van der Meer PF, Bontekoe IJ, Daal BB, de Korte D, Leebeek FW, et al. Evaluation of the role of the GPIb-IX-V receptor complex in development of the platelet storage lesion. *Vox Sang* (2016) 111(3):247–56. doi:10.1111/vox.12416
19. Stegner D, vanEeuwijk JMM, Angay O, Gorelashvili MG, Semeniak D, Pinnecker J, et al. Thrombopoiesis is spatially regulated by the bone marrow vasculature. *Nat Commun* (2017) 8(1):127. doi:10.1038/s41467-017-00201-7
20. Italiano JE Jr, Lecine P, Shivdasani RA, Hartwig JH. Blood platelets are assembled principally at the ends of proplatelet processes produced by differentiated megakaryocytes. *J Cell Biol* (1999) 147(6):1299–312. doi:10.1083/jcb.147.6.1299
21. Thon JN, Montalvo A, Patel-Hett S, Devine MT, Richardson JL, Ehrlicher A, et al. Cytoskeletal mechanics of proplatelet maturation and platelet release. *J Cell Biol* (2010) 191(4):861–74. doi:10.1083/jcb.201006102
22. Lefrancais E, Ortiz-Munoz G, Caudrillier A, Mallavia B, Liu F, Sayah DM, et al. The lung is a site of platelet biogenesis and a reservoir for haematopoietic progenitors. *Nature* (2017) 544(7648):105–9. doi:10.1038/nature21706
23. Gurney AL, Carver-Moore K, de Sauvage FJ, Moore MW. Thrombocytopenia in c-mpl-deficient mice. *Science* (1994) 265(5177):1445–7. doi:10.1126/science.8073287
24. Alexander WS, Roberts AW, Nicola NA, Li R, Metcalf D. Deficiencies in progenitor cells of multiple hematopoietic lineages and defective megakaryocytopoiesis in mice lacking the thrombopoietic receptor c-Mpl. *Blood* (1996) 87(6):2162–70.
25. Varghese LN, Defour JP, Pecquet C, Constantinescu SN. The thrombopoietin receptor: structural basis of traffic and activation by ligand, mutations, agonists, and mutated calreticulin. *Front Endocrinol* (2017) 8:59. doi:10.3389/fendo.2017.00059
26. de Sauvage FJ, Carver-Moore K, Luoh SM, Ryan A, Dowd M, Eaton DL, et al. Physiological regulation of early and late stages of megakaryocytopoiesis by thrombopoietin. *J Exp Med* (1996) 183(2):651–6. doi:10.1084/jem.183.2.651
27. Grozovsky R, Begonja AJ, Liu K, Visner G, Hartwig JH, Falet H, et al. The Ashwell-Morell receptor regulates hepatic thrombopoietin production via JAK2-STAT3 signaling. *Nat Med* (2015) 21(1):47–54. doi:10.1038/nm.3770
28. Mason KD, Carpinelli MR, Fletcher JI, Collinge JE, Hilton AA, Ellis S, et al. Programmed anuclear cell death delimits platelet life span. *Cell* (2007) 128(6):1173–86. doi:10.1016/j.cell.2007.01.037
29. Grozovsky R, Giannini S, Falet H, Hoffmeister KM. Regulating billions of blood platelets: glycans and beyond. *Blood* (2015) 126(16):1877–84. doi:10.1182/blood-2015-01-569129
30. Tahara T, Usuki K, Sato H, Ohashi H, Morita H, Tsumura H, et al. A sensitive sandwich ELISA for measuring thrombopoietin in human serum: serum thrombopoietin levels in healthy volunteers and in patients with haemopoietic disorders. *Br J Haematol* (1996) 93(4):783–8. doi:10.1046/j.1365-2141.1996.d01-1741.x
31. Kosugi S, Kurata Y, Tomiyama Y, Tahara T, Kato T, Tadokoro S, et al. Circulating thrombopoietin level in chronic immune thrombocytopenic purpura. *Br J Haematol* (1996) 93(3):704–6. doi:10.1046/j.1365-2141.1996.d01-1702.x
32. Rodeghiero F, Carli G. Beyond immune thrombocytopenia: the evolving role of thrombopoietin receptor agonists. *Ann Hematol* (2017) 96(9):1421–34. doi:10.1007/s00277-017-2953-6
33. Wu KH, Peng CT, Li TC, Wan L, Tsai CH, Lan SJ, et al. Interleukin 4, interleukin 6 and interleukin 10 polymorphisms in children with acute and chronic immune thrombocytopenic purpura. *Br J Haematol* (2005) 128(6):849–52. doi:10.1111/j.1365-2141.2005.05385.x
34. Emmerich F, Bal G, Barakat A, Milz J, Muhle C, Martinez-Gamboa L, et al. High-level serum B-cell activating factor and promoter polymorphisms in patients with idiopathic thrombocytopenic purpura. *Br J Haematol* (2007) 136(2):309–14. doi:10.1111/j.1365-2141.2006.06431.x
35. Rocha AM, De Souza C, Rocha GA, De Melo FF, Saraiva IS, Clementino NC, et al. IL1RN VNTR and IL2-330 polymorphic genes are independently associated with chronic immune thrombocytopenia. *Br J Haematol* (2010) 150(6):679–84. doi:10.1111/j.1365-2141.2010.08318.x
36. Pehlivan M, Okan V, Sever T, Balci SO, Yilmaz M, Babacan T, et al. Investigation of TNF-alpha, TGF-beta 1, IL-10, IL-6, IFN-gamma, MBL, GPIA, and IL1A gene polymorphisms in patients with idiopathic thrombocytopenic purpura. *Platelets* (2011) 22(8):588–95. doi:10.3109/09537104.2011.577255
37. Saitoh T, Tsukamoto N, Koiso H, Mitsui T, Yokohama A, Handa H, et al. Interleukin-17F gene polymorphism in patients with chronic immune thrombocytopenia. *Eur J Haematol* (2011) 87(3):253–8. doi:10.1111/j.1600-0609.2011.01651.x
38. Kuwana M, Kaburaki J, Pandey JP, Murata M, Kawakami Y, Inoko H, et al. HLA class II alleles in Japanese patients with immune thrombocytopenic purpura. Associations with anti-platelet glycoprotein autoantibodies and responses to splenectomy. *Tissue Antigens* (2000) 56(4):337–43. doi:10.1034/j.1399-0039.2000.560405.x
39. Leung AY, Hawkins BR, Chim CS, Kwong YY, Liang RH. Genetic analysis of HLA-typing in Chinese patients with idiopathic thrombocytopenic purpura. *Haematologica* (2001) 86(2):221–2.
40. Stanworth SJ, Turner DM, Brown J, McCloskey D, Brown C, Provan D, et al. Major histocompatibility complex susceptibility genes and immune thrombocytopenic purpura in Caucasian adults. *Hematology* (2002) 7(2):119–21. doi:10.1080/10245330290028605
41. El Neanaey WA, Barakat SS, Ahmed MA, El Nabie WM, Ahmed ME. The relation between HLA-DRB1 alleles and the outcome of therapy in children with idiopathic thrombocytopenic purpura. *Egypt J Immunol* (2005) 12(2):29–38.
42. Hopkins LM, Davis JM, Buchli R, Vangundy RS, Schwartz KA, Gerlach JA. MHC class I-associated peptides identified from normal platelets and from individuals with idiopathic thrombocytopenic purpura. *Hum Immunol* (2005) 66(8):874–83. doi:10.1016/j.humimm.2005.06.004
43. Maia MH, Peixoto Rde L, de Lima CP, Magalhaes M, Sena L, Costa Pdo S, et al. Predisposition to idiopathic thrombocytopenic purpura maps close to the major histocompatibility complex class I chain-related gene A. *Hum Immunol* (2009) 70(3):179–83. doi:10.1016/j.humimm.2009.01.011
44. Negi RR, Bhoria P, Pahuja A, Saikia B, Varma N, Malhotra P, et al. Investigation of the possible association between the HLA antigens and idiopathic thrombocytopenic purpura (ITP). *Immunol Invest* (2012) 41(2):117–28. doi:10.3109/08820139.2011.593218
45. Ho WL, Lu MY, Hu FC, Lee CC, Huang LM, Jou ST, et al. Clinical features and major histocompatibility complex genes as potential susceptibility factors in pediatric immune thrombocytopenia. *J Formos Med Assoc* (2012) 111(7):370–9. doi:10.1016/j.jfma.2011.06.025
46. Jernas M, Hou Y, Stromberg Celind F, Shao L, Nookaew I, Wang Q, et al. Differences in gene expression and cytokine levels between newly diagnosed and chronic pediatric ITP. *Blood* (2013) 122(10):1789–92. doi:10.1182/blood-2013-05-502807
47. Foster CB, Zhu S, Erichsen HC, Lehrnbecher T, Hart ES, Choi E, et al. Polymorphisms in inflammatory cytokines and Fcgamma receptors in childhood chronic immune thrombocytopenic purpura: a pilot study. *Br J Haematol* (2001) 113(3):596–9. doi:10.1046/j.1365-2141.2001.02807.x

48. Carcao MD, Blanchette VS, Wakefield CD, Stephens D, Ellis J, Matheson K, et al. Fcgamma receptor IIa and IIIa polymorphisms in childhood immune thrombocytopenic purpura. *Br J Haematol* (2003) 120(1):135–41. doi:10.1046/j.1365-2141.2003.04033.x
49. Bruin M, Bierings M, Uiterwaal C, Revesz T, Bode L, Wiesman ME, et al. Platelet count, previous infection and FCGR2B genotype predict development of chronic disease in newly diagnosed idiopathic thrombocytopenia in childhood: results of a prospective study. *Br J Haematol* (2004) 127(5):561–7. doi:10.1111/j.1365-2141.2004.05235.x
50. Breunis WB, van Mirre E, Bruin M, Geissler J, de Boer M, Peters M, et al. Copy number variation of the activating FCGR2C gene predisposes to idiopathic thrombocytopenic purpura. *Blood* (2008) 111(3):1029–38. doi:10.1182/blood-2007-03-079913
51. Amorim DM, Silveira Vda S, Scrideli CA, Queiroz RG, Tone LG. Fcgamma receptor gene polymorphisms in childhood immune thrombocytopenic purpura. *J Pediatr Hematol Oncol* (2012) 34(5):349–52. doi:10.1097/MPH.0b013e3182580908
52. Eyada TK, Farawela HM, Khorshied MM, Shaheen IA, Selim NM, Khalifa IA. FcgammaRIIa and FcgammaRIIIa genetic polymorphisms in a group of pediatric immune thrombocytopenic purpura in Egypt. *Blood Coagul Fibrinolysis* (2012) 23(1):64–8. doi:10.1097/MBC.0b013e32834ddf2f
53. Papagianni A, Economou M, Tragiannidis A, Karatza E, Samarah F, Gombakis N, et al. FcgammaRIIa and FcgammaRIIIa polymorphisms in childhood primary immune thrombocytopenia: implications for disease pathogenesis and outcome. *Blood Coagul Fibrinolysis* (2013) 24(1):35–9. doi:10.1097/MBC.0b013e328359bc3b
54. Wang D, Hu SL, Cheng XL, Yang JY. FCGR2A rs1801274 polymorphism is associated with risk of childhood-onset idiopathic (immune) thrombocytopenic purpura: evidence from a meta-analysis. *Thromb Res* (2014) 134(6):1323–7. doi:10.1016/j.thromres.2014.10.003
55. Simeoni I, Stephens JC, Hu F, Deevi SV, Megy K, Bariana TK, et al. A high-throughput sequencing test for diagnosing inherited bleeding, thrombotic, and platelet disorders. *Blood* (2016) 127(23):2791–803. doi:10.1182/blood-2015-12-688267
56. Bariana TK, Ouwehand WH, Guerrero JA, Gomez K; BRIDGE Bleeding, Thrombotic and Platelet Disorders and ThromboGenomics Consortia. Dawning of the age of genomics for platelet granule disorders: improving insight, diagnosis and management. *Br J Haematol* (2017) 176(5):705–20. doi:10.1111/bjh.14471
57. Takahashi T, Yujiri T, Shinohara K, Inoue Y, Sato Y, Fujii Y, et al. Molecular mimicry by *Helicobacter pylori* CagA protein may be involved in the pathogenesis of *H. pylori*-associated chronic idiopathic thrombocytopenic purpura. *Br J Haematol* (2004) 124(1):91–6. doi:10.1046/j.1365-2141.2003.04735.x
58. Stasi R, Sarpatwari A, Segal JB, Osborn J, Evangelista ML, Cooper N, et al. Effects of eradication of *Helicobacter pylori* infection in patients with immune thrombocytopenic purpura: a systematic review. *Blood* (2009) 113(6):1231–40. doi:10.1182/blood-2008-07-167155
59. Rajan SK, Espina BM, Liebman HA. Hepatitis C virus-related thrombocytopenia: clinical and laboratory characteristics compared with chronic immune thrombocytopenic purpura. *Br J Haematol* (2005) 129(6):818–24. doi:10.1111/j.1365-2141.2005.05542.x
60. Zhang W, Nardi MA, Borkowsky W, Li Z, Karpatkin S. Role of molecular mimicry of hepatitis C virus protein with platelet GPIIIa in hepatitis C-related immunologic thrombocytopenia. *Blood* (2009) 113(17):4086–93. doi:10.1182/blood-2008-09-181073
61. Hohmann AW, Booth K, Peters V, Gordon DL, Comacchio RM. Common epitope on HIV p24 and human platelets. *Lancet* (1993) 342(8882):1274–5. doi:10.1016/0140-6736(93)92363-X
62. Bettaieb A, Oksenhendler E, Duedari N, Bierling P. Cross-reactive antibodies between HIV-gp120 and platelet gpIIIa (CD61) in HIV-related immune thrombocytopenic purpura. *Clin Exp Immunol* (1996) 103(1):19–23. doi:10.1046/j.1365-2249.1996.917606.x
63. Dominguez V, Gevorkian G, Govezensky T, Rodriguez H, Viveros M, Cocho G, et al. Antigenic homology of HIV-1 GP41 and human platelet glycoprotein GPIIIa (integrin beta3). *J Acquir Immune Defic Syndr Hum Retrovirol* (1998) 17(5):385–90. doi:10.1097/00042560-199804150-00001
64. Nardi M, Tomlinson S, Greco MA, Karpatkin S. Complement-independent, peroxide-induced antibody lysis of platelets in HIV-1-related immune thrombocytopenia. *Cell* (2001) 106(5):551–61. doi:10.1016/S0092-8674(01)00477-9
65. Nardi M, Feinmark SJ, Hu L, Li Z, Karpatkin S. Complement-independent Ab-induced peroxide lysis of platelets requires 12-lipoxygenase and a platelet NADPH oxidase pathway. *J Clin Invest* (2004) 113(7):973–80. doi:10.1172/JCI20726
66. Li Z, Nardi MA, Karpatkin S. Role of molecular mimicry to HIV-1 peptides in HIV-1-related immunologic thrombocytopenia. *Blood* (2005) 106(2):572–6. doi:10.1182/blood-2005-01-0243
67. Nardi MA, Gor Y, Feinmark SJ, Xu F, Karpatkin S. Platelet particle formation by anti GPIIIa49-66 Ab, Ca2+ ionophore A23187, and phorbol myristate acetate is induced by reactive oxygen species and inhibited by dexamethasone blockade of platelet phospholipase A2, 12-lipoxygenase, and NADPH oxidase. *Blood* (2007) 110(6):1989–96. doi:10.1182/blood-2006-10-054064
68. DiMaggio D, Anderson A, Bussel JB. Cytomegalovirus can make immune thrombocytopenic purpura refractory. *Br J Haematol* (2009) 146(1):104–12. doi:10.1111/j.1365-2141.2009.07714.x
69. Wu Z, Zhou J, Wei X, Wang X, Li Y, Peng B, et al. The role of Epstein-Barr virus (EBV) and cytomegalovirus (CMV) in immune thrombocytopenia. *Hematology* (2013) 18(5):295–9. doi:10.1179/1607845413Y.0000000084
70. Wright JF, Blanchette VS, Wang H, Arya N, Petric M, Semple JW, et al. Characterization of platelet-reactive antibodies in children with varicella-associated acute immune thrombocytopenic purpura (ITP). *Br J Haematol* (1996) 95(1):145–52. doi:10.1046/j.1365-2141.1996.d01-1872.x
71. Musaji A, Cormont F, Thirion G, Cambiaso CL, Coutelier JP. Exacerbation of autoantibody-mediated thrombocytopenic purpura by infection with mouse viruses. *Blood* (2004) 104(7):2102–6. doi:10.1182/blood-2004-01-0310
72. Mantadakis E, Farmaki E, Buchanan GR. Thrombocytopenic purpura after measles-mumps-rubella vaccination: a systematic review of the literature and guidance for management. *J Pediatr* (2010) 156(4):623–8. doi:10.1016/j.jpeds.2009.10.015
73. Grimaldi-Bensouda L, Michel M, Aubrun E, Leighton P, Viallard JF, Adoue D, et al. A case-control study to assess the risk of immune thrombocytopenia associated with vaccines. *Blood* (2012) 120(25):4938–44. doi:10.1182/blood-2012-05-431098
74. Rose NR. Negative selection, epitope mimicry and autoimmunity. *Curr Opin Immunol* (2017) 49:51–5. doi:10.1016/j.coi.2017.08.014
75. Aslam R, Speck ER, Kim M, Crow AR, Bang KW, Nestel FP, et al. Platelet toll-like receptor expression modulates lipopolysaccharide-induced thrombocytopenia and tumor necrosis factor-alpha production in vivo. *Blood* (2006) 107(2):637–41. doi:10.1182/blood-2005-06-2202
76. Aster RH, Bougie DW. Drug-induced immune thrombocytopenia. *N Engl J Med* (2007) 357(6):580–7. doi:10.1056/NEJMra066469
77. Cines DB, Liebman H, Stasi R. Pathobiology of secondary immune thrombocytopenia. *Semin Hematol* (2009) 46(1 Suppl 2):S2–14. doi:10.1053/j.seminhematol.2008.12.005
78. van Leeuwen EF, van der Ven JT, Engelfriet CP, von dem Borne AE. Specificity of autoantibodies in autoimmune thrombocytopenia. *Blood* (1982) 59(1):23–6.
79. McMillan R, Tani P, Millard F, Berchtold P, Renshaw L, Woods VL Jr. Platelet-associated and plasma anti-glycoprotein autoantibodies in chronic ITP. *Blood* (1987) 70(4):1040–5.
80. He R, Reid DM, Jones CE, Shulman NR. Spectrum of Ig classes, specificities, and titers of serum antiglycoproteins in chronic idiopathic thrombocytopenic purpura. *Blood* (1994) 83(4):1024–32.
81. Kiyomizu K, Kashiwagi H, Nakazawa T, Tadokoro S, Honda S, Kanakura Y, et al. Recognition of highly restricted regions in the beta-propeller domain of alphaIIb by platelet-associated anti-alphaIIbbeta3 autoantibodies in primary immune thrombocytopenia. *Blood* (2012) 120(7):1499–509. doi:10.1182/blood-2012-02-409995
82. Beer JH, Rabaglio M, Berchtold P, von Felten A, Clemetson KJ, Tsakiris DA, et al. Autoantibodies against the platelet glycoproteins (GP) IIb/IIIa, Ia/IIa, and IV and partial deficiency in GPIV in a patient with a bleeding disorder and a defective platelet collagen interaction. *Blood* (1993) 82(3):820–9.
83. Boylan B, Chen H, Rathore V, Paddock C, Salacz M, Friedman KD, et al. Anti-GPVI-associated ITP: an acquired platelet disorder caused by autoantibody-mediated clearance of the GPVI/FcRgamma-chain complex from the human platelet surface. *Blood* (2004) 104(5):1350–5. doi:10.1182/blood-2004-03-0896
84. Najean Y, Rain JD, Billotey C. The site of destruction of autologous 111In-labelled platelets and the efficiency of splenectomy in children

and adults with idiopathic thrombocytopenic purpura: a study of 578 patients with 268 splenectomies. *Br J Haematol* (1997) 97(3):547–50. doi:10.1046/j.1365-2141.1997.832723.x

85. Kuwana M, Okazaki Y, Kaburaki J, Kawakami Y, Ikeda Y. Spleen is a primary site for activation of platelet-reactive T and B cells in patients with immune thrombocytopenic purpura. *J Immunol* (2002) 168(7):3675–82. doi:10.4049/jimmunol.168.7.3675
86. Catani L, Fagioli ME, Tazzari PL, Ricci F, Curti A, Rovito M, et al. Dendritic cells of immune thrombocytopenic purpura (ITP) show increased capacity to present apoptotic platelets to T lymphocytes. *Exp Hematol* (2006) 34(7):879–87. doi:10.1016/j.exphem.2006.03.009
87. Kuwana M, Okazaki Y, Ikeda Y. Splenic macrophages maintain the anti-platelet autoimmune response via uptake of opsonized platelets in patients with immune thrombocytopenic purpura. *J Thromb Haemost* (2009) 7(2):322–9. doi:10.1111/j.1538-7836.2008.03161.x
88. Chang M, Nakagawa PA, Williams SA, Schwartz MR, Imfeld KL, Buzby JS, et al. Immune thrombocytopenic purpura (ITP) plasma and purified ITP monoclonal autoantibodies inhibit megakaryocytopoiesis in vitro. *Blood* (2003) 102(3):887–95. doi:10.1182/blood-2002-05-1475
89. McMillan R, Wang L, Tomer A, Nichol J, Pistillo J. Suppression of in vitro megakaryocyte production by antiplatelet autoantibodies from adult patients with chronic ITP. *Blood* (2004) 103(4):1364–9. doi:10.1182/blood-2003-08-2672
90. Lev PR, Grodzielski M, Goette NP, Glembotsky AC, Espasandin YR, Pierdominici MS, et al. Impaired proplatelet formation in immune thrombocytopenia: a novel mechanism contributing to decreased platelet count. *Br J Haematol* (2014) 165(6):854–64. doi:10.1111/bjh.12832
91. Tsubakio T, Tani P, Curd JG, McMillan R. Complement activation in vitro by antiplatelet antibodies in chronic immune thrombocytopenic purpura. *Br J Haematol* (1986) 63(2):293–300. doi:10.1111/j.1365-2141.1986.tb05552.x
92. Peerschke EI, Andemariam B, Yin W, Bussel JB. Complement activation on platelets correlates with a decrease in circulating immature platelets in patients with immune thrombocytopenic purpura. *Br J Haematol* (2010) 148(4):638–45. doi:10.1111/j.1365-2141.2009.07995.x
93. Najaoui A, Bakchoul T, Stoy J, Bein G, Rummel MJ, Santoso S, et al. Autoantibody-mediated complement activation on platelets is a common finding in patients with immune thrombocytopenic purpura (ITP). *Eur J Haematol* (2012) 88(2):167–74. doi:10.1111/j.1600-0609.2011.01718.x
94. Goette NP, Glembotsky AC, Lev PR, Grodzielski M, Contrufo G, Pierdominici MS, et al. Platelet apoptosis in adult immune thrombocytopenia: insights into the mechanism of damage triggered by auto-antibodies. *PLoS One* (2016) 11(8):e0160563. doi:10.1371/journal.pone.0160563
95. George JN. Platelet immunoglobulin G: its significance for the evaluation of thrombocytopenia and for understanding the origin of alpha-granule proteins. *Blood* (1990) 76(5):859–70.
96. Nagelkerke SQ, Kuijpers TW. Immunomodulation by IVIg and the role of Fc-gamma receptors: classic mechanisms of action after all? *Front Immunol* (2014) 5:674. doi:10.3389/fimmu.2014.00674
97. Kiefel V, Santoso S, Weisheit M, Mueller-Eckhardt C. Monoclonal antibody-specific immobilization of platelet antigens (MAIPA): a new tool for the identification of platelet-reactive antibodies. *Blood* (1987) 70(6):1722–6.
98. Fujisawa K, Tani P, O'Toole TE, Ginsberg MH, McMillan R. Different specificities of platelet-associated and plasma autoantibodies to platelet GPIIb-IIIa in patients with chronic immune thrombocytopenic purpura. *Blood* (1992) 79(6):1441–6.
99. Crossley A, Calvert JE, Taylor PR, Dickinson AM. A comparison of monoclonal antibody immobilization of platelet antigen (MAIPA) and immunobead methods for detection of GPIIb/IIIa antiplatelet antibodies in immune thrombocytopenic purpura. *Transfus Med* (1997) 7(2):127–34. doi:10.1046/j.1365-3148.1997.d01-15.x
100. Cines DB, Wilson SB, Tomaski A, Schreiber AD. Platelet antibodies of the IgM class in immune thrombocytopenic purpura. *J Clin Invest* (1985) 75(4):1183–90. doi:10.1172/JCI111814
101. Winiarski J. IgG and IgM antibodies to platelet membrane glycoprotein antigens in acute childhood idiopathic thrombocytopenic purpura. *Br J Haematol* (1989) 73(1):88–92. doi:10.1111/j.1365-2141.1989.tb00225.x
102. Nishioka T, Yamane T, Takubo T, Ohta K, Park K, Hino M. Detection of various platelet-associated immunoglobulins by flow cytometry in idiopathic thrombocytopenic purpura. *Cytometry B Clin Cytom* (2005) 68(1):37–42. doi:10.1002/cyto.b.20067
103. Chan H, Moore JC, Finch CN, Warkentin TE, Kelton JG. The IgG subclasses of platelet-associated autoantibodies directed against platelet glycoproteins IIb/IIIa in patients with idiopathic thrombocytopenic purpura. *Br J Haematol* (2003) 122(5):818–24. doi:10.1046/j.1365-2141.2003.04509.x
104. Hymes K, Schur PH, Karpatkin S. Heavy-chain subclass of round antiplatelet IgG in autoimmune thrombocytopenic purpura. *Blood* (1980) 56(1):84–7.
105. Vidarsson G, Dekkers G, Rispens T. IgG subclasses and allotypes: from structure to effector functions. *Front Immunol* (2014) 5:520. doi:10.3389/fimmu.2014.00520
106. Sonneveld ME, Natunen S, Sainio S, Koeleman CA, Holst S, Dekkers G, et al. Glycosylation pattern of anti-platelet IgG is stable during pregnancy and predicts clinical outcome in alloimmune thrombocytopenia. *Br J Haematol* (2016) 174(2):310–20. doi:10.1111/bjh.14053
107. Sonneveld ME, de Haas M, Koeleman C, de Haan N, Zeerleder SS, Ligthart PC, et al. Patients with IgG1-anti-red blood cell autoantibodies show aberrant Fc-glycosylation. *Sci Rep* (2017) 7(1):8187. doi:10.1038/s41598-017-08654-y
108. Christie DJ, Sauro SC, Fairbanks KD, Kay NE. Detection of clonal platelet antibodies in immunologically-mediated thrombocytopenias: association with circulating clonal/oligoclonal B cells. *Br J Haematol* (1993) 85(2):277–84. doi:10.1111/j.1365-2141.1993.tb03167.x
109. Kim J, Park CJ, Chi HS, Kim MJ, Seo JJ, Moon HN, et al. Idiopathic thrombocytopenic purpura: better therapeutic responses of patients with B- or T-cell clonality than patients without clonality. *Int J Hematol* (2003) 78(5):461–6. doi:10.1007/BF02983822
110. Roark JH, Bussel JB, Cines DB, Siegel DL. Genetic analysis of autoantibodies in idiopathic thrombocytopenic purpura reveals evidence of clonal expansion and somatic mutation. *Blood* (2002) 100(4):1388–98.
111. Stockelberg D, Hou M, Jacobsson S, Kutti J, Wadenvik H. Evidence for a light chain restriction of glycoprotein Ib/IX and IIb/IIIa reactive antibodies in chronic idiopathic thrombocytopenic purpura (ITP). *Br J Haematol* (1995) 90(1):175–9. doi:10.1111/j.1365-2141.1995.tb03397.x
112. Stockelberg D, Hou M, Jacobsson S, Kutti J, Wadenvik H. Light chain-restricted autoantibodies in chronic idiopathic thrombocytopenic purpura, but no evidence for circulating clone B-lymphocytes. *Ann Hematol* (1996) 72(1):29–34. doi:10.1007/BF00663013
113. van der Harst D, de Jong D, Limpens J, Kluin PM, Rozier Y, van Ommen GJ, et al. Clonal B-cell populations in patients with idiopathic thrombocytopenic purpura. *Blood* (1990) 76(11):2321–6.
114. Veneri D, De Matteis G, Solero P, Federici F, Zanuso C, Guizzardi E, et al. Analysis of B- and T-cell clonality and HLA class II alleles in patients with idiopathic thrombocytopenic purpura: correlation with *Helicobacter pylori* infection and response to eradication treatment. *Platelets* (2005) 16(5):307–11. doi:10.1080/09537100400028685
115. Voelkerding KV, Sandhaus LM, Belov L, Frenkel L, Ettinger LJ, Raska K Jr. Clonal B-cell proliferation in an infant with congenital HIV infection and immune thrombocytopenia. *Am J Clin Pathol* (1988) 90(4):470–4. doi:10.1093/ajcp/90.4.470
116. Fujisawa K, O'Toole TE, Tani P, Loftus JC, Plow EF, Ginsberg MH, et al. Autoantibodies to the presumptive cytoplasmic domain of platelet glycoprotein IIIa in patients with chronic immune thrombocytopenic purpura. *Blood* (1991) 77(10):2207–13.
117. Kosugi S, Tomiyama Y, Honda S, Kato H, Kiyoi T, Kashiwagi H, et al. Platelet-associated anti-GPIIb-IIIa autoantibodies in chronic immune thrombocytopenic purpura recognizing epitopes close to the ligand-binding site of glycoprotein (GP) IIb. *Blood* (2001) 98(6):1819–27. doi:10.1182/blood.V98.6.1819
118. McMillan R, Lopez-Dee J, Loftus JC. Autoantibodies to alpha(IIb)beta(3) in patients with chronic immune thrombocytopenic purpura bind primarily to epitopes on alpha(IIb). *Blood* (2001) 97(7):2171–2. doi:10.1182/blood.V97.7.2171
119. Kekomaki R, Dawson B, McFarland J, Kunicki TJ. Localization of human platelet autoantigens to the cysteine-rich region of glycoprotein IIIa. *J Clin Invest* (1991) 88(3):847–54. doi:10.1172/JCI115386
120. McMillan R, Wang L, Lopez-Dee J, Jiu S, Loftus JC. Many alphaIIbbeta3 autoepitopes in chronic immune thrombocytopenic purpura are localized to alphaIIb between amino acids L1 and Q459. *Br J Haematol* (2002) 118(4):1132–6. doi:10.1046/j.1365-2141.2002.03751.x

121. Kosugi S, Tomiyama Y, Honda S, Kashiwagi H, Shiraga M, Tadokoro S, et al. Anti-alphavbeta3 antibodies in chronic immune thrombocytopenic purpura. *Thromb Haemost* (2001) 85(1):36–41. doi:10.1055/s-0037-1612660
122. Berchtold P, Wenger M. Autoantibodies against platelet glycoproteins in autoimmune thrombocytopenic purpura: their clinical significance and response to treatment. *Blood* (1993) 81(5):1246–50.
123. Zeng Q, Zhu L, Tao L, Bao J, Yang M, Simpson EK, et al. Relative efficacy of steroid therapy in immune thrombocytopenia mediated by anti-platelet GPIIbIIIa versus GPIbalpha antibodies. *Am J Hematol* (2012) 87(2):206–8. doi:10.1002/ajh.22211
124. Peng J, Ma SH, Liu J, Hou Y, Liu XM, Niu T, et al. Association of autoantibody specificity and response to intravenous immunoglobulin G therapy in immune thrombocytopenia: a multicenter cohort study. *J Thromb Haemost* (2014) 12(4):497–504. doi:10.1111/jth.12524
125. Semple JW, Freedman J. Increased antiplatelet T helper lymphocyte reactivity in patients with autoimmune thrombocytopenia. *Blood* (1991) 78(10):2619–25.
126. Semple JW, Milev Y, Cosgrave D, Mody M, Hornstein A, Blanchette V, et al. Differences in serum cytokine levels in acute and chronic autoimmune thrombocytopenic purpura: relationship to platelet phenotype and antiplatelet T-cell reactivity. *Blood* (1996) 87(10):4245–54.
127. Ogawara H, Handa H, Morita K, Hayakawa M, Kojima J, Amagai H, et al. High Th1/Th2 ratio in patients with chronic idiopathic thrombocytopenic purpura. *Eur J Haematol* (2003) 71(4):283–8. doi:10.1034/j.1600-0609.2003.00138.x
128. Panitsas FP, Mouzaki A. Effect of splenectomy on type-1/type-2 cytokine gene expression in a patient with adult idiopathic thrombocytopenic purpura (ITP). *BMC Blood Disord* (2004) 4(1):4. doi:10.1186/1471-2326-4-4
129. Wang T, Zhao H, Ren H, Guo J, Xu M, Yang R, et al. Type 1 and type 2 T-cell profiles in idiopathic thrombocytopenic purpura. *Haematologica* (2005) 90(7):914–23.
130. Stasi R, Del Poeta G, Stipa E, Evangelista ML, Trawinska MM, Cooper N, et al. Response to B-cell depleting therapy with rituximab reverts the abnormalities of T-cell subsets in patients with idiopathic thrombocytopenic purpura. *Blood* (2007) 110(8):2924–30. doi:10.1182/blood-2007-02-068999
131. Kuwana M, Kaburaki J, Ikeda Y. Autoreactive T cells to platelet GPIIb-IIIa in immune thrombocytopenic purpura. Role in production of anti-platelet autoantibody. *J Clin Invest* (1998) 102(7):1393–402. doi:10.1172/JCI4238
132. Kuwana M, Kaburaki J, Kitasato H, Kato M, Kawai S, Kawakami Y, et al. Immunodominant epitopes on glycoprotein IIb-IIIa recognized by autoreactive T cells in patients with immune thrombocytopenic purpura. *Blood* (2001) 98(1):130–9. doi:10.1182/blood.V98.1.130
133. Chen X, Oppenheim JJ. Th17 cells and Tregs: unlikely allies. *J Leukoc Biol* (2014) 95(5):723–31. doi:10.1189/jlb.1213633
134. Ma D, Zhu X, Zhao P, Zhao C, Li X, Zhu Y, et al. Profile of Th17 cytokines (IL-17, TGF-beta, IL-6) and Th1 cytokine (IFN-gamma) in patients with immune thrombocytopenic purpura. *Ann Hematol* (2008) 87(11):899–904. doi:10.1007/s00277-008-0535-3
135. Guo ZX, Chen ZP, Zheng CL, Jia HR, Ge J, Gu DS, et al. The role of Th17 cells in adult patients with chronic idiopathic thrombocytopenic purpura. *Eur J Haematol* (2009) 82(6):488–9. doi:10.1111/j.1600-0609.2009.01229.x
136. Sollazzo D, Trabanelli S, Curti A, Vianelli N, Lemoli RM, Catani L. Circulating CD4+CD161+CD196+ Th17 cells are not increased in immune thrombocytopenia. *Haematologica* (2011) 96(4):632–4. doi:10.3324/haematol.2010.038638
137. Zhang J, Ma D, Zhu X, Qu X, Ji C, Hou M. Elevated profile of Th17, Th1 and Tc1 cells in patients with immune thrombocytopenic purpura. *Haematologica* (2009) 94(9):1326–9. doi:10.3324/haematol.2009.007823
138. Zhu X, Ma D, Zhang J, Peng J, Qu X, Ji C, et al. Elevated interleukin-21 correlated to Th17 and Th1 cells in patients with immune thrombocytopenia. *J Clin Immunol* (2010) 30(2):253–9. doi:10.1007/s10875-009-9353-1
139. Rocha AM, Souza C, Rocha GA, de Melo FF, Clementino NC, Marino MC, et al. The levels of IL-17A and of the cytokines involved in Th17 cell commitment are increased in patients with chronic immune thrombocytopenia. *Haematologica* (2011) 96(10):1560–4. doi:10.3324/haematol.2011.046417
140. Hu Y, Ma DX, Shan NN, Zhu YY, Liu XG, Zhang L, et al. Increased number of Tc17 and correlation with Th17 cells in patients with immune thrombocytopenia. *PLoS One* (2011) 6(10):e26522. doi:10.1371/journal.pone.0026522
141. Ji L, Zhan Y, Hua F, Li F, Zou S, Wang W, et al. The ratio of Treg/Th17 cells correlates with the disease activity of primary immune thrombocytopenia. *PLoS One* (2012) 7(12):e50909. doi:10.1371/journal.pone.0050909
142. Eyerich K, Dimartino V, Cavani A. IL-17 and IL-22 in immunity: driving protection and pathology. *Eur J Immunol* (2017) 47(4):607–14. doi:10.1002/eji.201646723
143. Eyerich S, Eyerich K, Cavani A, Schmidt-Weber C. IL-17 and IL-22: siblings, not twins. *Trends Immunol* (2010) 31(9):354–61. doi:10.1016/j.it.2010.06.004
144. Eyerich S, Eyerich K, Pennino D, Carbone T, Nasorri F, Pallotta S, et al. Th22 cells represent a distinct human T cell subset involved in epidermal immunity and remodeling. *J Clin Invest* (2009) 119(12):3573–85. doi:10.1172/JCI40202
145. Cao J, Chen C, Zeng L, Li L, Li X, Li Z, et al. Elevated plasma IL-22 levels correlated with Th1 and Th22 cells in patients with immune thrombocytopenia. *Clin Immunol* (2011) 141(1):121–3. doi:10.1016/j.clim.2011.05.003
146. Hu Y, Li H, Zhang L, Shan B, Xu X, Li H, et al. Elevated profiles of Th22 cells and correlations with Th17 cells in patients with immune thrombocytopenia. *Hum Immunol* (2012) 73(6):629–35. doi:10.1016/j.humimm.2012.04.015
147. Audia S, Rossato M, Santegoets K, Spijkers S, Wichers C, Bekker C, et al. Splenic TFH expansion participates in B-cell differentiation and antiplatelet-antibody production during immune thrombocytopenia. *Blood* (2014) 124(18):2858–66. doi:10.1182/blood-2014-03-563445
148. Olsson B, Andersson PO, Jernas M, Jacobsson S, Carlsson B, Carlsson LM, et al. T-cell-mediated cytotoxicity toward platelets in chronic idiopathic thrombocytopenic purpura. *Nat Med* (2003) 9(9):1123–4. doi:10.1038/nm921
149. Ware RE, Howard TA. Phenotypic and clonal analysis of T lymphocytes in childhood immune thrombocytopenic purpura. *Blood* (1993) 82(7):2137–42.
150. Shenoy S, Mohanakumar T, Chatila T, Tersak J, Duffy B, Wang R, et al. Defective apoptosis in lymphocytes and the role of IL-2 in autoimmune hematologic cytopenias. *Clin Immunol* (2001) 99(2):266–75. doi:10.1006/clim.2001.5017
151. Olsson B, Andersson PO, Jacobsson S, Carlsson L, Wadenvik H. Disturbed apoptosis of T-cells in patients with active idiopathic thrombocytopenic purpura. *Thromb Haemost* (2005) 93(1):139–44. doi:10.1160/TH04-06-0385
152. Olsson B, Jernas M, Wadenvik H. Increased plasma levels of granzymes in adult patients with chronic immune thrombocytopenia. *Thromb Haemost* (2012) 107(6):1182–4. doi:10.1160/TH12-01-0012
153. Zhang F, Chu X, Wang L, Zhu Y, Li L, Ma D, et al. Cell-mediated lysis of autologous platelets in chronic idiopathic thrombocytopenic purpura. *Eur J Haematol* (2006) 76(5):427–31. doi:10.1111/j.1600-0609.2005.00622.x
154. Zhao C, Li X, Zhang F, Wang L, Peng J, Hou M. Increased cytotoxic T-lymphocyte-mediated cytotoxicity predominant in patients with idiopathic thrombocytopenic purpura without platelet autoantibodies. *Haematologica* (2008) 93(9):1428–30. doi:10.3324/haematol.12889
155. Qiu J, Liu X, Li X, Zhang X, Han P, Zhou H, et al. CD8(+) T cells induce platelet clearance in the liver via platelet desialylation in immune thrombocytopenia. *Sci Rep* (2016) 6:27445. doi:10.1038/srep27445
156. Olsson B, Ridell B, Carlsson L, Jacobsson S, Wadenvik H. Recruitment of T cells into bone marrow of ITP patients possibly due to elevated expression of VLA-4 and CX3CR1. *Blood* (2008) 112(4):1078–84. doi:10.1182/blood-2008-02-139402
157. Li S, Wang L, Zhao C, Li L, Peng J, Hou M. CD8+ T cells suppress autologous megakaryocyte apoptosis in idiopathic thrombocytopenic purpura. *Br J Haematol* (2007) 139(4):605–11. doi:10.1111/j.1365-2141.2007.06737.x
158. Audia S, Samson M, Mahevas M, Ferrand C, Trad M, Ciudad M, et al. Preferential splenic CD8(+) T-cell activation in rituximab-nonresponder patients with immune thrombocytopenia. *Blood* (2013) 122(14):2477–86. doi:10.1182/blood-2013-03-491415
159. Ma L, Simpson E, Li J, Xuan M, Xu M, Baker L, et al. CD8+ T cells are predominantly protective and required for effective steroid therapy in murine models of immune thrombocytopenia. *Blood* (2015) 126(2):247–56. doi:10.1182/blood-2015-03-635417

160. Shlomchik MJ, Craft JE, Mamula MJ. From T to B and back again: positive feedback in systemic autoimmune disease. *Nat Rev Immunol* (2001) 1(2):147–53. doi:10.1038/35100573
161. Guo L, Kapur R, Aslam R, Speck ER, Zufferey A, Zhao Y, et al. CD20+ B-cell depletion therapy suppresses murine CD8+ T-cell-mediated immune thrombocytopenia. *Blood* (2016) 127(6):735–8. doi:10.1182/blood-2015-06-655126
162. Li X, Zhong H, Bao W, Boulad N, Evangelista J, Haider MA, et al. Defective regulatory B-cell compartment in patients with immune thrombocytopenia. *Blood* (2012) 120(16):3318–25. doi:10.1182/blood-2012-05-432575
163. Mauri C, Menon M. Human regulatory B cells in health and disease: therapeutic potential. *J Clin Invest* (2017) 127(3):772–9. doi:10.1172/JCI85113
164. Veneri D, Gottardi M, Guizzardi E, Zanuso C, Krampera M, Franchini M. Idiopathic thrombocytopenic purpura, *Helicobacter pylori* infection, and HLA class II alleles. *Blood* (2002) 100(5):1925–6; author rely 6–7. doi:10.1182/blood-2002-05-1348
165. Gouttefangeas C, Diehl M, Keilholz W, Hornlein RF, Stevanovic S, Rammensee HG. Thrombocyte HLA molecules retain nonrenewable endogenous peptides of megakaryocyte lineage and do not stimulate direct allocytotoxicity in vitro. *Blood* (2000) 95(10):3168–75.
166. Chapman LM, Aggrey AA, Field DJ, Srivastava K, Ture S, Yui K, et al. Platelets present antigen in the context of MHC class I. *J Immunol* (2012) 189(2):916–23. doi:10.4049/jimmunol.1200580
167. Trugilho MRO, Hottz ED, Brunoro GVF, Teixeira-Ferreira A, Carvalho PC, Salazar GA, et al. Platelet proteome reveals novel pathways of platelet activation and platelet-mediated immunoregulation in dengue. *PLoS Pathog* (2017) 13(5):e1006385. doi:10.1371/journal.ppat.1006385
168. Boshkov LK, Kelton JG, Halloran PF. HLA-DR expression by platelets in acute idiopathic thrombocytopenic purpura. *Br J Haematol* (1992) 81(4):552–7. doi:10.1111/j.1365-2141.1992.tb02991.x
169. Fahim NM, Monir E. Functional role of CD4+CD25+ regulatory T cells and transforming growth factor-beta1 in childhood immune thrombocytopenic purpura. *Egypt J Immunol* (2006) 13(1):173–87.
170. Sakakura M, Wada H, Tawara I, Nobori T, Sugiyama T, Sagawa N, et al. Reduced Cd4+Cd25+ T cells in patients with idiopathic thrombocytopenic purpura. *Thromb Res* (2007) 120(2):187–93. doi:10.1016/j.thromres.2006.09.008
171. Liu B, Zhao H, Poon MC, Han Z, Gu D, Xu M, et al. Abnormality of CD4(+) CD25(+) regulatory T cells in idiopathic thrombocytopenic purpura. *Eur J Haematol* (2007) 78(2):139–43. doi:10.1111/j.1600-0609.2006.00780.x
172. Yu J, Heck S, Patel V, Levan J, Yu Y, Bussel JB, et al. Defective circulating CD25 regulatory T cells in patients with chronic immune thrombocytopenic purpura. *Blood* (2008) 112(4):1325–8. doi:10.1182/blood-2008-01-135335
173. Zhang XL, Peng J, Sun JZ, Liu JJ, Guo CS, Wang ZG, et al. De novo induction of platelet-specific CD4(+)CD25(+) regulatory T cells from CD4(+) CD25(-) cells in patients with idiopathic thrombocytopenic purpura. *Blood* (2009) 113(11):2568–77. doi:10.1182/blood-2008-03-148288
174. Stasi R, Cooper N, Del Poeta G, Stipa E, Laura Evangelista M, Abruzzese E, et al. Analysis of regulatory T-cell changes in patients with idiopathic thrombocytopenic purpura receiving B cell-depleting therapy with rituximab. *Blood* (2008) 112(4):1147–50. doi:10.1182/blood-2007-12-129262
175. Bao W, Bussel JB, Heck S, He W, Karpoff M, Boulad N, et al. Improved regulatory T-cell activity in patients with chronic immune thrombocytopenia treated with thrombopoietic agents. *Blood* (2010) 116(22):4639–45. doi:10.1182/blood-2010-04-281717
176. Audia S, Samson M, Guy J, Janikashvili N, Fraszczak J, Trad M, et al. Immunologic effects of rituximab on the human spleen in immune thrombocytopenia. *Blood* (2011) 118(16):4394–400. doi:10.1182/blood-2011-03-344051
177. Li Z, Mou W, Lu G, Cao J, He X, Pan X, et al. Low-dose rituximab combined with short-term glucocorticoids up-regulates Treg cell levels in patients with immune thrombocytopenia. *Int J Hematol* (2011) 93(1):91–8. doi:10.1007/s12185-010-0753-z
178. Ling Y, Cao X, Yu Z, Ruan C. Circulating dendritic cells subsets and CD4+Foxp3+ regulatory T cells in adult patients with chronic ITP before and after treatment with high-dose dexamethasome. *Eur J Haematol* (2007) 79(4):310–6. doi:10.1111/j.1600-0609.2007.00917.x
179. Aslam R, Hu Y, Gebremeskel S, Segel GB, Speck ER, Guo L, et al. Thymic retention of CD4+CD25+FoxP3+ T regulatory cells is associated with their peripheral deficiency and thrombocytopenia in a murine model of immune thrombocytopenia. *Blood* (2012) 120(10):2127–32. doi:10.1182/blood-2012-02-413526
180. Catani L, Sollazzo D, Trabanelli S, Curti A, Evangelisti C, Polverelli N, et al. Decreased expression of indoleamine 2,3-dioxygenase 1 in dendritic cells contributes to impaired regulatory T cell development in immune thrombocytopenia. *Ann Hematol* (2013) 92(1):67–78. doi:10.1007/s00277-012-1556-5
181. Siragam V, Crow AR, Brinc D, Song S, Freedman J, Lazarus AH. Intravenous immunoglobulin ameliorates ITP via activating Fc gamma receptors on dendritic cells. *Nat Med* (2006) 12(6):688–92. doi:10.1038/nm1416
182. Kapur R, Kim M, Rebetz J, Rondina MT, Porcelijn L, Semple JW. Low levels of interleukin-10 in patients with transfusion-related acute lung injury. *Ann Transl Med* (2017) 5(16):339. doi:10.21037/atm.2017.04.37
183. Kapur R, Kim M, Aslam R, McVey MJ, Tabuchi A, Luo A, et al. T regulatory cells and dendritic cells protect against transfusion-related acute lung injury via IL-10. *Blood* (2017) 129(18):2557–69. doi:10.1182/blood-2016-12-758185
184. Houwerzijl EJ, Blom NR, van der Want JJ, Esselink MT, Koornstra JJ, Smit JW, et al. Ultrastructural study shows morphologic features of apoptosis and para-apoptosis in megakaryocytes from patients with idiopathic thrombocytopenic purpura. *Blood* (2004) 103(2):500–6. doi:10.1182/blood-2003-01-0275
185. Zhong H, Bao W, Li X, Miller A, Seery C, Haq N, et al. CD16+ monocytes control T-cell subset development in immune thrombocytopenia. *Blood* (2012) 120(16):3326–35. doi:10.1182/blood-2012-06-434605
186. Liu XG, Ma SH, Sun JZ, Ren J, Shi Y, Sun L, et al. High-dose dexamethasone shifts the balance of stimulatory and inhibitory Fcgamma receptors on monocytes in patients with primary immune thrombocytopenia. *Blood* (2011) 117(6):2061–9. doi:10.1182/blood-2010-07-295477
187. Asahi A, Nishimoto T, Okazaki Y, Suzuki H, Masaoka T, Kawakami Y, et al. *Helicobacter pylori* eradication shifts monocyte Fcgamma receptor balance toward inhibitory FcgammaRIIB in immune thrombocytopenic purpura patients. *J Clin Invest* (2008) 118(8):2939–49. doi:10.1172/JCI34496
188. Semple JW, Bruce S, Freedman J. Suppressed natural killer cell activity in patients with chronic autoimmune thrombocytopenic purpura. *Am J Hematol* (1991) 37(4):258–62. doi:10.1002/ajh.2830370409
189. Garcia-Suarez J, Prieto A, Reyes E, Manzano L, Merino JL, Alvarez-Mon M. Severe chronic autoimmune thrombocytopenic purpura is associated with an expansion of CD56+ CD3- natural killer cells subset. *Blood* (1993) 82(5):1538–45.
190. Ebbo M, Audonnet S, Grados A, Benarous L, Mahevas M, Godeau B, et al. NK cell compartment in the peripheral blood and spleen in adult patients with primary immune thrombocytopenia. *Clin Immunol* (2017) 177:18–28. doi:10.1016/j.clim.2015.11.005
191. Koupenova M, Clancy L, Corkrey HA, Freedman JE. Circulating platelets as mediators of immunity, inflammation, and thrombosis. *Circ Res* (2018) 122(2):337–51. doi:10.1161/CIRCRESAHA.117.310795
192. Nishimoto T, Numajiri M, Nakazaki H, Okazaki Y, Kuwana M. Induction of immune tolerance to platelet antigen by short-term thrombopoietin treatment in a mouse model of immune thrombocytopenia. *Int J Hematol* (2014) 100(4):341–4. doi:10.1007/s12185-014-1661-4
193. Ghadaki B, Nazi I, Kelton JG, Arnold DM. Sustained remissions of immune thrombocytopenia associated with the use of thrombopoietin receptor agonists. *Transfusion* (2013) 53(11):2807–12. doi:10.1111/trf.12139
194. Thachil J, Salter I, George JN. Complete remission of refractory immune thrombocytopenia (ITP) with a short course of Romiplostim. *Eur J Haematol* (2013) 91(4):376–7. doi:10.1111/ejh.12165
195. Mahevas M, Fain O, Ebbo M, Roudot-Thoraval F, Limal N, Khellaf M, et al. The temporary use of thrombopoietin-receptor agonists may induce a prolonged remission in adult chronic immune thrombocytopenia. Results of a French observational study. *Br J Haematol* (2014) 165(6):865–9. doi:10.1111/bjh.12888

196. Grewal IS, Flavell RA. CD40 and CD154 in cell-mediated immunity. *Annu Rev Immunol* (1998) 16:111–35. doi:10.1146/annurev.immunol.16.1.111
197. Solanilla A, Pasquet JM, Viallard JF, Contin C, Grosset C, Dechanet-Merville J, et al. Platelet-associated CD154 in immune thrombocytopenic purpura. *Blood* (2005) 105(1):215–8. doi:10.1182/blood-2003-07-2367
198. Kuwana M, Nomura S, Fujimura K, Nagasawa T, Muto Y, Kurata Y, et al. Effect of a single injection of humanized anti-CD154 monoclonal antibody on the platelet-specific autoimmune response in patients with immune thrombocytopenic purpura. *Blood* (2004) 103(4):1229–36. doi:10.1182/blood-2003-06-2167
199. Kuwana M, Kawakami Y, Ikeda Y. Suppression of autoreactive T-cell response to glycoprotein IIb/IIIa by blockade of CD40/CD154 interaction: implications for treatment of immune thrombocytopenic purpura. *Blood* (2003) 101(2):621–3. doi:10.1182/blood-2002-07-2157
200. Bruhns P, Iannascoli B, England P, Mancardi DA, Fernandez N, Jorieux S, et al. Specificity and affinity of human Fcgamma receptors and their polymorphic variants for human IgG subclasses. *Blood* (2009) 113(16):3716–25. doi:10.1182/blood-2008-09-179754
201. Kono H, Kyogoku C, Suzuki T, Tsuchiya N, Honda H, Yamamoto K, et al. FcgammaRIIB Ile232Thr transmembrane polymorphism associated with human systemic lupus erythematosus decreases affinity to lipid rafts and attenuates inhibitory effects on B cell receptor signaling. *Hum Mol Genet* (2005) 14(19):2881–92. doi:10.1093/hmg/ddi320
202. Li X, Wu J, Ptacek T, Redden DT, Brown EE, Alarcon GS, et al. Allelic-dependent expression of an activating Fc receptor on B cells enhances humoral immune responses. *Sci Transl Med* (2013) 5(216):216ra175. doi:10.1126/scitranslmed.3007097
203. Stegmann TC, Veldhuisen B, Nagelkerke SQ, Winkelhorst D, Schonewille H, Verduin EP, et al. RhIg-prophylaxis is not influenced by FCGR2/3 polymorphisms involved in red blood cell clearance. *Blood* (2017) 129(8):1045–8. doi:10.1182/blood-2016-05-716365
204. van Egmond M, Vidarsson G, Bakema JE. Cross-talk between pathogen recognizing toll-like receptors and immunoglobulin Fc receptors in immunity. *Immunol Rev* (2015) 268(1):311–27. doi:10.1111/imr.12333
205. Schwab I, Nimmerjahn F. Intravenous immunoglobulin therapy: how does IgG modulate the immune system? *Nat Rev Immunol* (2013) 13(3):176–89. doi:10.1038/nri3401
206. Audia S, Santegoets K, Laarhoven AG, Vidarsson G, Facy O, Ortega-Deballon P, et al. Fcgamma receptor expression on splenic macrophages in adult immune thrombocytopenia. *Clin Exp Immunol* (2017) 188(2):275–82. doi:10.1111/cei.12935
207. Podolanczuk A, Lazarus AH, Crow AR, Grossbard E, Bussel JB. Of mice and men: an open-label pilot study for treatment of immune thrombocytopenic purpura by an inhibitor of Syk. *Blood* (2009) 113(14):3154–60. doi:10.1182/blood-2008-07-166439
208. Heitink-Polle KMJ, Laarhoven AG, Bruin MCA, Veldhuisen B, Nagelkerke SQ, Kuijpers T, et al. Fc-gamma receptor polymorphisms are associated with susceptibility to and recovery from pediatric immune thrombocytopenia. *Blood* (2016) 128(22):867.
209. Li J, van der Wal DE, Zhu G, Xu M, Yougbare I, Ma L, et al. Desialylation is a mechanism of Fc-independent platelet clearance and a therapeutic target in immune thrombocytopenia. *Nat Commun* (2015) 6:7737. doi:10.1038/ncomms8737
210. Jansen AJ, Josefsson EC, Rumjantseva V, Liu QP, Falet H, Bergmeier W, et al. Desialylation accelerates platelet clearance after refrigeration and initiates GPIbalpha metalloproteinase-mediated cleavage in mice. *Blood* (2012) 119(5):1263–73. doi:10.1182/blood-2011-05-355628
211. Li J, Callum JL, Lin Y, Zhou Y, Zhu G, Ni H. Severe platelet desialylation in a patient with glycoprotein Ib/IX antibody-mediated immune thrombocytopenia and fatal pulmonary hemorrhage. *Haematologica* (2014) 99(4):e61–3. doi:10.3324/haematol.2013.102897
212. Shao L, Wu Y, Zhou H, Qin P, Ni H, Peng J, et al. Successful treatment with oseltamivir phosphate in a patient with chronic immune thrombocytopenia positive for anti-GPIb/IX autoantibody. *Platelets* (2015) 26(5):495–7. doi:10.3109/09537104.2014.948838
213. Jansen AJ, Peng J, Zhao HG, Hou M, Ni H. Sialidase inhibition to increase platelet counts: a new treatment option for thrombocytopenia. *Am J Hematol* (2015) 90(5):E94–5. doi:10.1002/ajh.23953
214. Alioglu B, Tasar A, Ozen C, Selver B, Dallar Y. An experience of oseltamivir phosphate (tamiflu) in a pediatric patient with chronic idiopathic thrombocytopenic purpura: a case report. *Pathophysiol Haemost Thromb* (2010) 37(2–4):55–8. doi:10.1159/000321379
215. Tao L, Zeng Q, Li J, Xu M, Wang J, Pan Y, et al. Platelet desialylation correlates with efficacy of first-line therapies for immune thrombocytopenia. *J Hematol Oncol* (2017) 10(1):46. doi:10.1186/s13045-017-0413-3
216. Kapur R, Heitink-Polle KM, Porcelijn L, Bentlage AE, Bruin MC, Visser R, et al. C-reactive protein enhances IgG-mediated phagocyte responses and thrombocytopenia. *Blood* (2015) 125(11):1793–802. doi:10.1182/blood-2014-05-579110
217. Zhang B, Lo C, Shen L, Sood R, Jones C, Cusmano-Ozog K, et al. The role of vanin-1 and oxidative stress-related pathways in distinguishing acute and chronic pediatric ITP. *Blood* (2011) 117(17):4569–79. doi:10.1182/blood-2010-09-304931
218. Jin CQ, Dong HX, Cheng PP, Zhou JW, Zheng BY, Liu F. Antioxidant status and oxidative stress in patients with chronic ITP. *Scand J Immunol* (2013) 77(6):482–7. doi:10.1111/sji.12048
219. Elsalakawy WA, Ali MA, Hegazy MG, Farweez BA. Value of vanin-1 assessment in adult patients with primary immune thrombocytopenia. *Platelets* (2014) 25(2):86–92. doi:10.3109/09537104.2013.782484
220. Premsler T, Lewandrowski U, Sickmann A, Zahedi RP. Phosphoproteome analysis of the platelet plasma membrane. *Methods Mol Biol* (2011) 728:279–90. doi:10.1007/978-1-61779-068-3_19
221. Lee-Sundlov MM, Ashline DJ, Hanneman AJ, Grozovsky R, Reinhold VN, Hoffmeister KM, et al. Circulating blood and platelets supply glycosyltransferases that enable extrinsic extracellular glycosylation. *Glycobiology* (2017) 27(2):188–98. doi:10.1093/glycob/cww108
222. Fong KP, Barry C, Tran AN, Traxler EA, Wannemacher KM, Tang HY, et al. Deciphering the human platelet sheddome. *Blood* (2011) 117(1):e15–26. doi:10.1182/blood-2010-05-283838
223. Andrews RK, Gardiner EE. Basic mechanisms of platelet receptor shedding. *Platelets* (2017) 28(4):319–24. doi:10.1080/09537104.2016.1235690
224. Au AE, Josefsson EC. Regulation of platelet membrane protein shedding in health and disease. *Platelets* (2017) 28(4):342–53. doi:10.1080/09537104.2016.1203401
225. Doyle HA, Mamula MJ. Post-translational protein modifications in antigen recognition and autoimmunity. *Trends Immunol* (2001) 22(8):443–9. doi:10.1016/S1471-4906(01)01976-7
226. Zavala-Cerna MG, Martinez-Garcia EA, Torres-Bugarin O, Rubio-Jurado B, Riebeling C, Nava A. The clinical significance of posttranslational modification of autoantigens. *Clin Rev Allergy Immunol* (2014) 47(1):73–90. doi:10.1007/s12016-014-8424-0
227. Klareskog L, Ronnelid J, Lundberg K, Padyukov L, Alfredsson L. Immunity to citrullinated proteins in rheumatoid arthritis. *Annu Rev Immunol* (2008) 26:651–75. doi:10.1146/annurev.immunol.26.021607.090244

Conflict of Interest Statement: AJ has received travel funding for hematological conferences from Novartis, not specifically for the subject of the manuscript. FL has received an unrestricted grant outside the submitted work from CSL Behring and Shire, and is a consultant for UniQure, NovoNordisk, and Shire, of which the fees go to Erasmus University. JV is a consultant for BioTest. The other authors report no conflict of interest.

frontiers in Immunology

CLINICAL TRIAL
published: 27 April 2018
doi: 10.3389/fimmu.2018.00906

Exercise Increases Insulin Sensitivity and Skeletal Muscle AMPK Expression in Systemic Lupus Erythematosus: A Randomized Controlled Trial

Fabiana B. Benatti[1,2], Cíntia N. H. Miyake[1], Wagner S. Dantas[1], Vanessa O. Zambelli[3], Samuel K. Shinjo[1], Rosa M. R. Pereira[1], Maria Elizabeth R. Silva[4], Ana Lúcia Sá-Pinto[1], Eduardo Borba[1], Eloisa Bonfá[1] and Bruno Gualano[1]*

[1] Rheumatology Division, Hospital das Clinicas HCFMUSP, Faculdade de Medicina FMUSP, Universidade de Sao Paulo, Sao Paulo, Brazil, [2] School of Applied Sciences, Universidade Estadual de Campinas (UNICAMP), Limeira, Sao Paulo, Brazil, [3] Butantan Institute, Sao Paulo, Brazil, [4] Endocrinology Division, Hospital das Clinicas HCFMUSP, Faculdade de Medicina FMUSP, Universidade de Sao Paulo, Sao Paulo, Brazil

OPEN ACCESS

Edited by:
Ralf J. Ludwig, Universität zu Lübeck, Germany

Reviewed by:
Leonardo Roever, Federal University of Uberlandia, Brazil
Junjie Xiao, Shanghai University, China

***Correspondence:**
Fabiana B. Benatti
fabiana.benatti@fca.unicamp.br

Specialty section:
This article was submitted to Inflammation, a section of the journal Frontiers in Immunology

Received: *31 December 2017*
Accepted: *11 April 2018*
Published: *27 April 2018*

Citation:
Benatti FB, Miyake CNH, Dantas WS, Zambelli VO, Shinjo SK, Pereira RMR, Silva MER, Sá-Pinto AL, Borba E, Bonfá E and Gualano B (2018) Exercise Increases Insulin Sensitivity and Skeletal Muscle AMPK Expression in Systemic Lupus Erythematosus: A Randomized Controlled Trial. Front. Immunol. 9:906. doi: 10.3389/fimmu.2018.00906

Systemic lupus erythematosus (SLE) patients may show increased insulin resistance (IR) when compared with their healthy peers. Exercise training has been shown to improve insulin sensitivity in other insulin-resistant populations, but it has never been tested in SLE. Therefore, the aim of the present study was to assess the efficacy of a moderate-intensity exercise training program on insulin sensitivity and potential underlying mechanisms in SLE patients with mild/inactive disease. A 12-week, randomized controlled trial was conducted. Nineteen SLE patients were randomly assigned into two groups: trained (SLE-TR, $n = 9$) and non-trained (SLE-NT, $n = 10$). Before and after 12 weeks of the exercise training program, patients underwent a meal test (MT), from which surrogates of insulin sensitivity and beta-cell function were determined. Muscle biopsies were performed after the MT for the assessment of total and membrane GLUT4 and proteins related to insulin signaling [Akt and AMP-activated protein kinase (AMPK)]. SLE-TR showed, when compared with SLE-NT, significant decreases in fasting insulin [−39 vs. +14%, $p = 0.009$, effect size (ES) = −1.0] and in the insulin response to MT (−23 vs. +21%, $p = 0.007$, ES = −1.1), homeostasis model assessment IR (−30 vs. +15%, $p = 0.005$, ES = −1.1), a tendency toward decreased proinsulin response to MT (−19 vs. +6%, $p = 0.07$, ES = −0.9) and increased glucagon response to MT (+3 vs. −3%, $p = 0.09$, ES = 0.6), and significant increases in the Matsuda index (+66 vs. −31%, $p = 0.004$, ES = 0.9) and fasting glucagon (+4 vs. −8%, $p = 0.03$, ES = 0.7). No significant differences between SLT-TR and SLT-NT were observed in fasting glucose, glucose response to MT, and insulinogenic index (all $p > 0.05$). SLE-TR showed a significant increase in AMPK Thr 172 phosphorylation when compared to SLE-NT (+73 vs. −12%, $p = 0.014$, ES = 1.3), whereas no significant differences between groups were observed in Akt Ser 473 phosphorylation, total and membrane GLUT4 expression, and GLUT4 translocation (all $p > 0.05$). In conclusion, a 12-week moderate-intensity aerobic

exercise training program improved insulin sensitivity in SLE patients with mild/inactive disease. This effect appears to be partially mediated by the increased insulin-stimulated skeletal muscle AMPK phosphorylation.

Clinical Trial Registration: www.ClinicalTrials.gov, identifier NCT01515163.

Keywords: aerobic exercise, insulin resistance, glucagon, GLUT4, inflammatory rheumatic disease

INTRODUCTION

Insulin resistance (IR) is a condition of decreased sensitivity or responsiveness of insulin-sensitive tissues to insulin (1). It is an independent risk factor for type 2 diabetes (T2D) and cardiovascular diseases (CVD), and has been suggested to play a central role in the increased risk of CVD morbidity and mortality in systemic lupus erythematosus (SLE) (2).

We have recently shown that non-T2D SLE patients with mild/inactive disease have increased IR when compared with healthy controls matched by age, gender, body composition, physical activity levels, and food intake (3). Notably, this was despite normal glucose tolerance, as evidenced by normal fasting and postprandial glycemia, as well as preserved skeletal muscle total GLUT4 content and translocation to the membrane in response to a meal. This suggests that SLE patients are capable of overcoming IR in peripheral tissues, preserving glucose uptake at the expense of increased fasting and postprandial insulin secretion, which could lead to β-cell dysfunction and T2D in the long run, increasing CVD risk (4). Patients with SLE also show a state of hyperglucagonemia, both at fasting and postprandially (3). Increased glucagon levels are commonly observed in T2D (5, 6) and have been independently associated with IR in non-T2D individuals (7), suggesting that SLE patients may show at least some level of pancreatic α-cell dysfunction, which could further increase the risk of T2D (8).

Physical exercise is considered a cornerstone for both the prevention and treatment of T2D, as it exerts both acute and chronic beneficial effects on insulin sensitivity (9). A bout of exercise leads to translocation of the glucose transporter GLUT4 from intracellular vesicles to the membrane, facilitating glucose transport into skeletal muscle in an insulin-independent manner (10). Moreover, exercise enhances insulin sensitivity in skeletal muscle, an effect that can last up to 48 h after cessation of exercise (11). If habitually repeated, these bouts of exercise (i.e., exercise training) may further improve insulin sensitivity by enhancing insulin-stimulated glucose transport capacity *via* increases in the expression and/or activity of proteins involved in intracellular insulin signaling pathways, such as protein kinase B (Akt) and AMP-activated protein kinase (AMPK), two important regulators of insulin action in muscle (9, 12).

Exercise has been shown to improve important CVD risk factors in SLE, such as aerobic deconditioning, endothelial function, and autonomic dysfunction (13–17). However, when compared with healthy and T2D individuals, SLE patients are less responsive to the effects of exercise upon lipid profile (18), potentially due to features inherent to the disease, such as persistent inflammation (19). As chronic inflammation can also aggravate IR (20), it is possible that these patients could also be resistant to the beneficial effects of exercise on insulin sensitivity. To our knowledge, there are no studies examining whether, and to what extent, exercise improves IR in SLE and the possible mechanisms involved.

The main aim of the present study was to assess the efficacy of an aerobic training program on insulin sensitivity in SLE patients with mild/inactive disease. Additionally, proteins related to insulin signaling were examined to unravel potential mechanisms underlying exercise-induced improvements in insulin sensitivity in SLE.

MATERIALS AND METHODS

Study Design and Patients

This was a 12-week, randomized controlled trial conducted in the Laboratory of Physical Conditioning for Rheumatologic Patients of the School of Medicine (LACRE), University of São Paulo, Brazil. The manuscript was reported according to the CONSORT statement guidelines. This is the final study that comprised a large clinical trial which aimed to comprehensively investigate the effects of exercise training on the autonomic function, cardiorespiratory parameters, inflammatory markers, and cardiometabolic risk factors in SLE patients (registered at http://clinicaltrials.gov as NCT01515163) (15, 17, 18, 21).

Nineteen adult women with SLE were randomly assigned to participate in a supervised exercise training program (TR; $n = 9$) or to be part of a non-exercised control group (NT; $n = 10$). All SLE patients fulfilled the revised American College of Rheumatology criteria for SLE (22) and were consecutively selected from our outpatient Lupus clinic of the Clinical Hospital at the School of Medicina, University of São Paulo (Hospital das Clinicas HCFMUSP, Faculdade de Medicina, Universidade de Sao Paulo). Disease activity was measured by Systemic Lupus Erythematosus Disease Activity Index (SLEDAI) 2000 scores (23). Exclusion criteria were as follows: age >45 years, body mass index (BMI) ≥35 kg/m^2, SLEDAI >4, prednisone dose >10 mg/day, menopause, diagnosed T2DM, cardiovascular dysfunction, rhythm and conduction disorders, musculoskeletal disturbances, current kidney and pulmonary involvements, peripheral neuropathy, tobacco use, use of statins, fibrate, insulin or insulin sensitizers, and other systemic autoimmune diseases.

At baseline (Pre), physical activity levels were assessed for characterization purposes using accelerometers, as described elsewhere (24). Patients were strongly instructed to maintain their usual living activities throughout the study. At Pre and after 12 weeks of the intervention (Post), patients underwent a meal test (MT) and were assessed for insulin sensitivity and beta-cell function. Muscle biopsies were performed after the MT for the assessment of total and membrane GLUT4, as well as two

candidate proteins related to insulin signaling (Akt and AMPK). Aerobic capacity (using a graded exercise test), body composition [using dual X-ray absorptiometry (DXA)], food intake, and laboratory parameters were also assessed. Post assessments were performed 60–72 h after the last training session in the trained group to avoid any carryover effect associated with the last exercise bout. This study was approved by the Ethics Committee for Analysis of Research Projects of the General Hospital, School of Medicine, University of São Paulo, affiliated to the National Committee for Ethics in Research of Brazil. All subjects signed an informed consent prior to participation.

Exercise Training Program

Systemic lupus erythematosus patients in the TR group underwent a 12-week, twice-a-week, supervised exercise training program in an intra-hospital gymnasium (Laboratory of Assessment and Conditioning in Rheumatology, School of Medicine, University of São Paulo). The training sessions consisted of a 5-min warm-up followed by 30–50 min of treadmill walking, and a 5-min cooling-down period. The walking duration was gradually increased every 4 weeks, from 30 to 50 min. The intensity of the exercise sessions was set at the heart rate (HR) corresponding to the interval between the ventilatory anaerobic threshold (VAT) and 10% below the respiratory compensation point (RCP), both determined as described in the subsequent subsection.

Aerobic Capacity

Maximal graded exercise tests were performed on a treadmill (Centurion 200, Micromed, Brazil), with increments in velocity and grade at every minute until volitional exhaustion. Oxygen uptake (VO_2) and carbon dioxide output (VCO_2) were obtained through breath-by-breath sampling and expressed as a 30-s average using an indirect calorimetric system (Cortex—model Metalyzer IIIB, Leipzig, Germany). HR was continuously recorded at rest, during exercise and during recovery, using a 12-lead electrocardiogram (Ergo PC Elite, Inc., Micromed, Brazil). Cardiopulmonary exercise test was considered maximal when one of the following criteria were met: VO_2 plateau (i.e., <150 ml/min increase between two consecutive stages); respiratory exchange ratio value above 1.10; HR no less than 10 beats below age-predicted maximal HR. Peak oxygen consumption (VO_{2peak}) was considered as the average of the final 30 s of the test. Ventilatory thresholds were identified as follows: VAT was determined when ventilatory equivalent for VO_2 (VE/VO_2) increased without a concomitant increase in ventilatory equivalent for carbon dioxide (VE/VCO_2), whereas the RCP was determined when VE/VO_2 and VE/VCO_2 increased simultaneously.

Meal Test

After an overnight fast, participants were given a 3-h mixed meal challenge (500 kcal, 60% CHO, 20% fat, and 20% protein). Blood samples were collected at 0, 30, 60, 90, 120, and 180 min for plasma glucose, insulin, proinsulin, triglycerides, and glucagon measurements. Glucose was assessed using a glucose-oxidase method (GOD/PAP, Roche Diagnostics, Germany). Insulin was assessed by a chemiluminescent method (Roche Diagnostics, Germany). Proinsulin and glucagon were assessed by a double-antibody radioimmunoassay (Linco Research, USA). Free fatty acid fasting levels were assessed by a colorimetric assay (Wako, USA). Subjects were instructed to refrain from physical exercise, alcohol, and caffeine intake 24 h prior to the test.

Surrogates of Insulin Sensitivity

Area under the curve (AUC) of glucose, insulin, glucagon, and proinsulin were calculated using the trapezoidal rule. Whole-body insulin sensitivity surrogate, Matsuda Index, was also calculated from the MT (25); the homeostasis model assessment (HOMA IR) was calculated from fasting glucose and insulin levels (26). Beta-cell function was estimated using the Insulinogenic Index, calculated as the ratio of the incremental insulin and glucose responses at 30 min in response to the MT (27).

Muscle Biopsies

Muscle samples were obtained from the midportion of the *m. vastus lateralis* of the right limb using the percutaneous needle biopsy technique with suction in a subgroup of patients (SLE-TR, $n = 4$; SLE-NT, $n = 5$) 30 min after the MT. An aliquot of each muscle sample was immediately frozen in liquid nitrogen and stored at −80°C for subsequent analyses.

Western Blotting

Muscle samples were homogenized and centrifuged in order to isolate the membrane fraction and the cytoplasmatic compartment as previously described (28). Total and membrane fraction protein concentration was determined using the Bradford assay. Samples were subjected to SDS-PAGE in polyacrylamide gel with equal loading (30 μg). Internal loading control was carried out to control for gel-to-gel variability. After electrophoresis, proteins were electrotransferred to a nitrocellulose membrane and monitored with the use of 0.5% Ponceau S staining of the blot membrane. Primary antibodies were incubated overnight at 4°C (GLUT4, 1:1,000, #07-1404, Millipore, Billerica, MA, USA; phospho-Akt Ser 473, 1:1,000, #4058; phospho-AMPK Thr 172, 1:1,000, #2535; GAPDH, 1:1,000, #2118, Cell Signaling Technology, Danvers, MA, USA). Binding of the primary antibody was detected by using peroxidase-conjugated secondary anti-rabbit and mouse antibodies using chemiluminescence (SuperSignal West Femto Chemilumininescent Substrate, Thermo Scientific®) detected by ImageQuant LAS 4000 (GE Healthcare®) and quantified by densitometry (Scion Image®), and normalized to housekeeping (GAPDH). GLUT4 translocation was defined as the ratio of membrane GLUT4 to total GLUT4 (29).

Body Composition

Body composition (lean, total, and trunk fat mass) was assessed by DXA using Hologic densitometry equipment (Discovery model; Hologic, Inc., USA).

Food Intake

Food intake was assessed using three 24-h dietary recalls undertaken on separate days (two weekdays and one weekend day) using a visual aid photo album of real foods. Energy and macronutrient intake were analyzed by the Brazilian software Virtual Nutri®.

Statistical Analysis

To minimize the impact of inter-individual variability, all values were converted into delta scores (i.e., Post − Pre values) and thereafter tested by a mixed model, considering Pre values from all dependent variables as covariates. Tukey *post hoc* was used for multiple comparisons. Baseline data were compared using Fisher's exact tests and unpaired Student's *t*-tests. Cohen's *d* was used to determine between-group effect sizes for dependent variables (30). The significance level was previously set at $p \leq 0.05$, with a trend toward significance being accepted at $p \leq 0.1$. All analyses were performed using SAS 9.2, SAS Institute Inc., Cary, NC, USA. Data are presented as means ± SDs.

Post hoc power analyses were performed with the assistance of the G-Power® software (version 3.1.2) and demonstrated a power of 70 and 60% at an alpha level of 5% to detect significant differences in insulin sensitivity (assessed by the HOMA IR and $AUC_{insulin}$ in response to the MT) between SLE-TR and SLE-NT, with effect sizes (ES) of −1.0 and −0.8.

RESULTS

Patients

Approximately 900 adult SLE patients were initially screened for participation and 192 were eligible. Sixty-three patients initially agreed to take part in the study. Thirty-four patients withdrew from the study before baseline assessments. Thus, 29 patients were randomly assigned to either SLE-TR ($n = 14$) or SLE-NT ($n = 15$). Six patients withdrew from the study for personal reasons (three from SLE-TR and three from SLE-NT), one patient became pregnant (SLE-NT), one patient fractured her limb outside training sessions (SLE-TR), and two patients had disease flare (one from SLE-TR and one from SLE-NT). Thus, the 19 patients who completed the study were analyzed (SLE-TR = 9, SLE-NT = 10) (**Figure 1**). We opted for a "per protocol" approach instead of an intention-to-treat (ITT) analysis as the primary research goal of our study was to determine the potential efficacy of exercise training on insulin sensitivity and not its effectiveness (31). In this context, ITT analysis has been regarded as more susceptible to type II error (32, 33), as the treatment effect may be diluted due to drop-outs (33). Importantly, baseline comparisons using Fisher's exact tests and unpaired *T* tests analyses of those who were lost to follow-up and those who retained in each group did not show any drop-out bias (data not shown). Due to technical issues, four patients (one from SLE-TR and three from SLE-NT) were not assessed for glucagon and two patients from SLE-NT were not assessed for proinsulin levels.

Table 1 shows demographic data of the patients. Groups were similar regarding age, BMI, body composition, physical activity levels, current clinical treatment, disease activity status, and disease duration (all $p > 0.05$).

Surrogates of Insulin Sensitivity

Systemic lupus erythematosus-trained group showed, in comparison with SLE-NT, greater decreases in fasting insulin (−39 vs. +14%, $p = 0.009$, ES = −1.0), $AUC_{insulin}$ (−23 vs. +21%, $p = 0.007$, ES = −1.1), HOMA IR (−30 vs. +15%, $p = 0.005$, ES = −1.1), and fasting free fatty acids (−11 vs. +17%, $p = 0.02$, ES = −1.2); a tendency toward decreased $AUC_{proinsulin}$ (−19 vs. +6%, $p = 0.07$, ES = −0.9) and increased $AUC_{glucagon}$ (+3 vs. −3%, $p = 0.09$, ES = 0.6); and greater increases in Matsuda index of whole-body insulin sensitivity (+66 vs. −31%, $p = 0.004$, ES = 0.9) and fasting glucagon (+4 vs. −8%, $p = 0.03$, ES = 0.7). By contrast, no significant differences between SLT-TR and SLT-NT were observed in

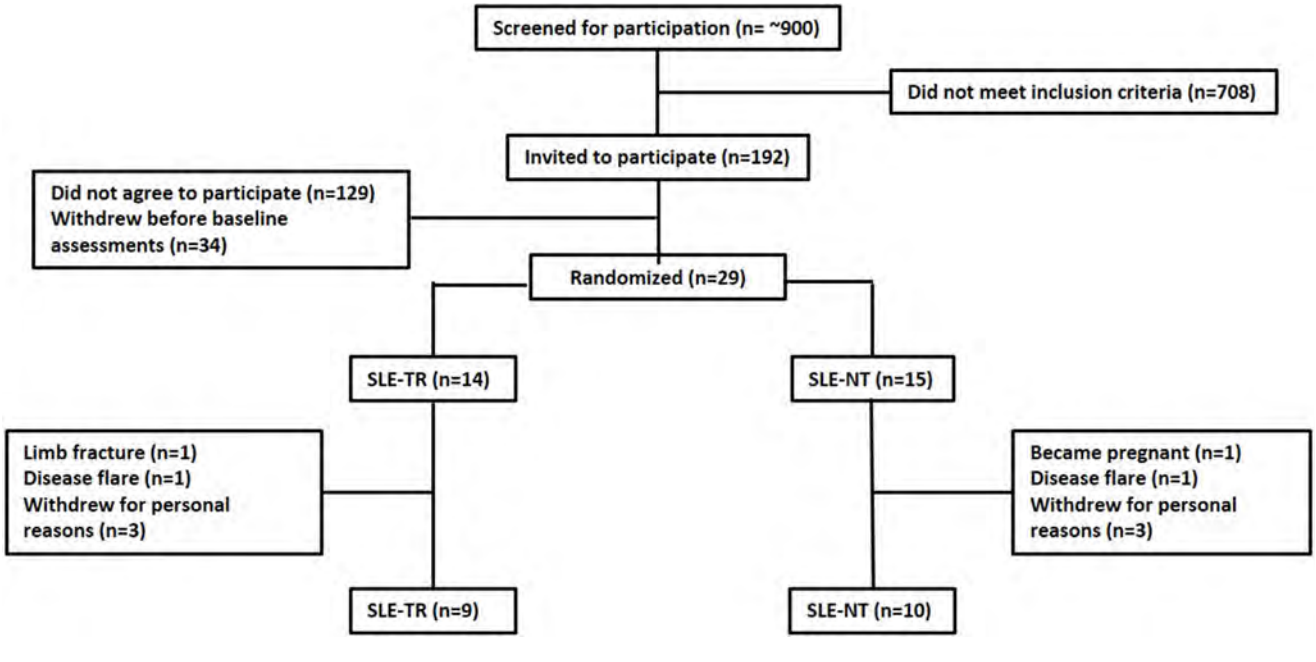

FIGURE 1 | Flow diagram of patients.

fasting glucose (−2 vs. +2%, $p = 0.25$, ES = −0.6), $AUC_{glucose}$ (−2 vs. 0%, $p = 0.28$, ES = −0.5), fasting proinsulin (−12 vs. +1%, $p = 0.39$, ES = −0.5), and insulinogenic index (−37 vs. +8%, $p = 0.23$, ES = −0.6) (**Table 2**; **Figure 2**).

TABLE 1 | Demographic, current clinical and treatment data and physical activity levels in SLE patients at baseline.

	SLE-TR ($n = 9$)	SLE-NT ($n = 10$)	CI (95%)	p
Age (years)	34.8 ± 4.1	32.4 ± 6.50	−4.8 to 9.5	0.19
BMI (kg/m^2)	26.3 ± 3.4	26.2 ± 3.8	−4.6 to 4.8	0.94
Total fat (%)	33.5 ± 5.4	34.9 ± 4.5	−8.9 to 6.2	0.60
Trunk fat (%)	30.0 ± 7.3	33.8 ± 7.1	−14.8 to 7.2	0.32
SLEDAI	0.22 ± 0.67	0.40 ± 1.26	−1.3 to 0.9	0.71
Disease duration (years)	9.8 ± 4.1	8.5 ± 5.9	−6.3 to 3.7	0.59
Drugs				
Current glucocorticoid use (mg)	1.7 ± 3.5	2.0 ± 4.2	−5.0 to 4.3	0.85
Cumulative glucocorticoid (g/kg)	42.1 ± 31.8	32.4 ± 19.1	−34.8 to 15.4	0.42
Glucocorticoid [no. (%)]	2 (22)	2 (20)	–	1.0
Hydroxychloroquine [no. (%)]	5 (56)	7 (70)	–	0.65
Methotrexate [no. (%)]	2 (22)	2 (20)	–	1.0
Azathioprine [no. (%)]	5 (56)	4 (40)	–	0.66
Mycophenolate [no. (%)]	1 (11)	2 (20)	–	1.0
Cyclophosphamide [no. (%)]	0 (0)	0 (0)	–	1.0
Oral contraceptive [no. (%)]	6 (67)	6 (60)	–	1.0
Physical activity level				
Sedentary time (% of day)	56.2 (9.6)	59.4 (8.4)	−20.3 to 11.7	0.49
Total MVPA (min/day)	29.1 (13.7)	25.4 (17.4)	−18.8 to 29.3	0.65
MVPA (min/day in ≥10-min bouts)	8.6 (7.7)	6.8 (8.5)	−12.3 to 15.5	0.68
Counts/day	607,873 (210,321)	605,455 (185,164)	−207,687 to 376,189	0.45

Data are expressed as mean ± SD or no. (%) and 95% confidence interval (CI).
SLE, systemic lupus erythematosus; SLE-TR, trained group; SLE-NT, non-trained group; BMI, body mass index; SLEDAI, Systemic Lupus Erythematosus Disease Activity Index; MVPA, moderate to vigorous physical activity.
Fisher exact tests and unpaired T-tests were used to assess possible differences between SLE groups (SLE-TR vs. SLE-NT).

Skeletal Muscle Protein Expression and GLUT4 Translocation in Response to the MT

Systemic lupus erythematosus-trained group showed a significant increase in AMPK Thr 172 phosphorylation when compared with SLE-NT (+73 vs. −12%, $p = 0.014$, ES = 1.3). By contrast, no significant differences between groups were observed in Akt Ser 473 phosphorylation (+16 vs. −12%, $p = 0.5$, ES = 0.7), total GLUT4 expression (+31 vs. +13%, $p = 0.8$, ES = 0.7), membrane GLUT4 expression (+78 vs. +7%, $p = 0.37$, ES = 1.0), and GLUT4 translocation (+9 vs. −5%, $p = 0.7$, ES = 0.6) (**Figure 3**).

Aerobic Capacity

Systemic lupus erythematosus-trained group showed significant increases in time at VAT (+35 vs. −6%, $p = 0.01$, ES = 1.2), time at RCP (+21 vs. +10%, $p = 0.04$, ES = 0.9), time to exhaustion (+18 vs. +5%, $p = 0.008$, ES = 1.1), and heart rate peak (+5 vs. +1%, $p = 0.007$, ES = 0.85), whereas no between-group differences were observed in VO_2peak (+5 vs. +4%, $p = 0.9$, ES = −0.01) (**Table 3**).

Body Composition

No significant between-group differences were observed in body weight, fat mass, lean mass, and trunk fat after the intervention (SLE-TR vs. SLE-NT, $p > 0.05$) (**Table 3**).

Food Intake

There were no significant differences in total energy or macronutrient intake between groups ($p > 0.05$ for all variables, **Table 3**).

Laboratory Parameters

No significant differences in any of the laboratory parameters were observed between SLE-TR and SLE-NT ($p > 0.05$ for all variables; **Table 3**).

DISCUSSION

To the best of our knowledge, this was the first study to investigate the efficacy of an exercise training program as well as its potential

TABLE 2 | Insulin sensitivity and beta-cell function estimates in trained and non-trained SLE patients before and after the exercise intervention.

	SLE-TR ($n = 9$)		SLE-NT ($n = 10$)				
	Pre	Δ (95% CI)	Pre	Δ (95% CI)	Δ diff (95% CI)	p	ES
Fasting glucose levels (mg/dL)	79.9 ± 8.20	−1.5 (−5.2 to 2.2)	81.2 ± 9.9	1.4 (−2.1 to 4.8)	−2.8 (−7.9 to 2.2)	0.25	−0.6
$AUC_{glucose}$ (mg/dL)	16,000 ± 2,406	−335 (−184 to 117)	16,425 ± 3,034	73 (−69 to 215)	−1,066 (−3,132 to 1,000)	0.28	−0.5
Fasting insulin levels (μU/mL)	10.0 ± 6.0	−3.9 (−6.7 to −1.1)	10.8 ± 6.0	1.5 (−1.1 to 4.2)	−4.5 (−7.5 to −1.4)	0.009	−1.0
$AUC_{insulin}$ (μU/mL)	8,817 ± 5,638	−2,068 (−3,933 to −204)	8,374 ± 4,589	1,728 (−41 to 3,498)	−3,797 (−6,367 to −1,227)	0.007	−1.1
Fasting glucagon levels (pg/mL)	133.1 ± 38.2	5.9 (−3.3 to 15.2)	114.2 (29.9)	−9.7 (−19.8 to 0.4)	15.6 (1.9 to 29.3)	0.03	0.7
$AUC_{glucagon}$ (pg/mL)	23,108 ± 6,954	681 (−449 to 1,812)	20,166 ± 4,653	−712 (−1,965 to 541)	1,393 (−294 to 3,081)	0.09	0.6
HOMA IR	2.05 ± 1.39	−0.62 (−1.07 to −0.16)	2.21 ± 1.40	0.34 (−0.09 to 0.76)	−0.95 (−1.57 to −0.32)	0.005	−1.1
Matsuda Index	8.1 ± 7.1	5.4 (1.9 to 8.8)	7.3 ± 5.6	−2.3 (−5.6 to 0.9)	7.7 (2.9 to 12.5)	0.004	0.9
Free fatty acids (mEq/L)	0.7 ± 0.3	−0.1 (−0.2 to 0.0)	0.6 ± 0.1	0.1 (−0.0 to 0.2)	−0.2 (−0.3 to 0.0)	0.02	−1.2
Fasting proinsulin	11.3 ± 4.3	−1.4 (−4.0 to 1.2)	14.5 ± 6.0	0.1 (−2.6 to 2.8)	−1.5 (−5.3 to 2.2)	0.39	−0.5
$AUC_{proinsulin}$	6,495 ± 2,220	−1,259 (−2,572 to 53)	6,941 ± 2,831	392 (−919 to 1,704)	−165 (−351 to 20)	0.07	−0.9
Insulinogenic index	3.4 (3.0)	−1.3 (−5.8 to 3.3)	2.9 (2.1)	−0.2 (−1.4 to 0.9)	−1.1 (−2.8 to 0.7)	0.23	−0.6

Data expressed as mean ± SD. Delta change (Δ) and 95% confidence interval (95% CI), estimated difference between delta changes (Δ difference) and 95% CI, and level of significance (p) calculated using a mixed model adjusted by Pre values; effect size (ES).
SLE, systemic lupus erythematosus; SLE-TR, trained group; SLE-NT, non-trained group; AUC, area under the curve calculated from the response to the meal test; HOMA, homeostasis model assessment.

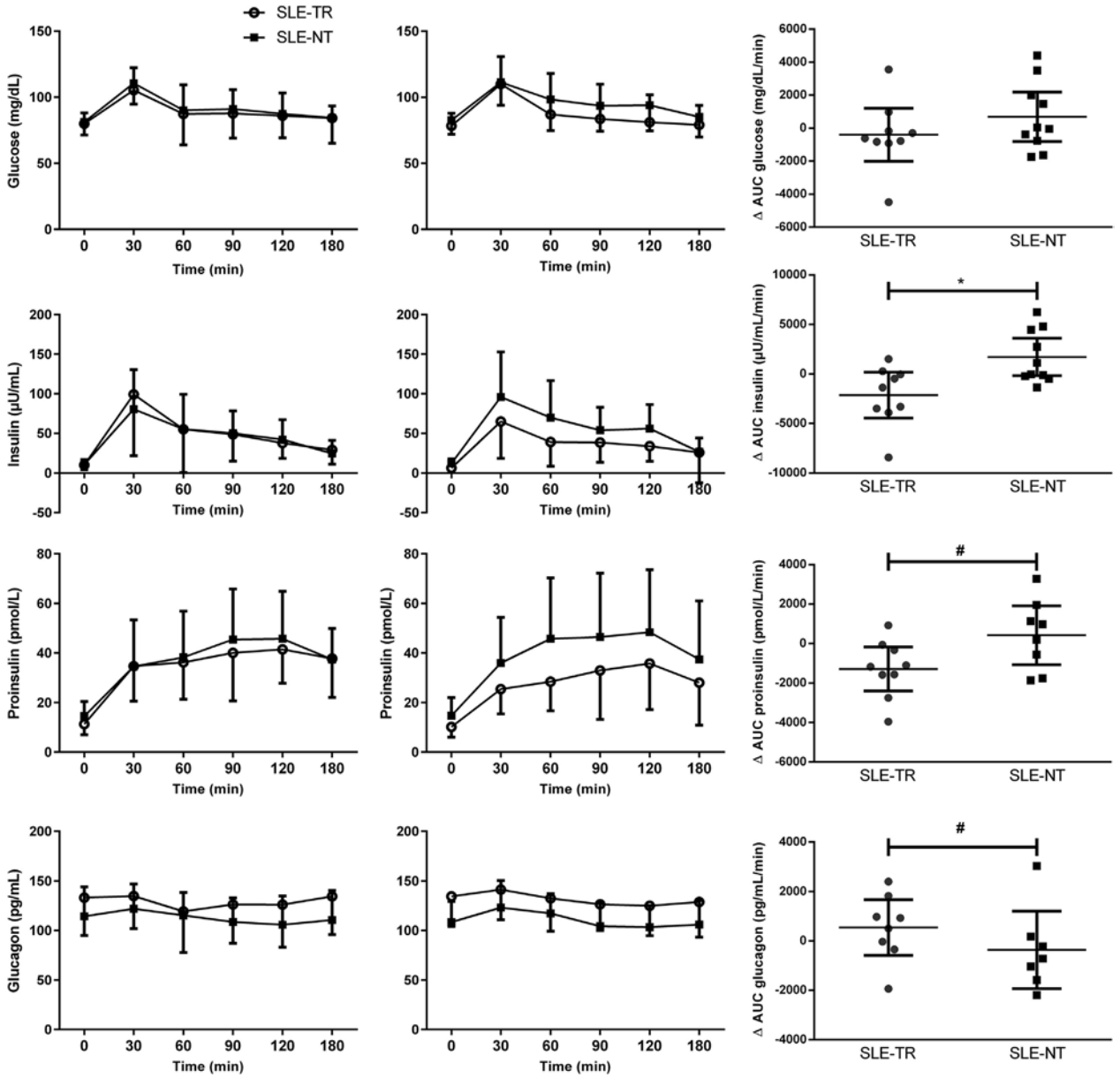

FIGURE 2 | Insulin sensitivity and beta-cell function estimates in SLE-TR and SLE-NT (Pre and Post data and delta changes). Data are expressed as mean ± SD. SLE, systemic lupus erythematosus; SLE-TR, trained group (open circles); SLE-NT, non-trained group (black squares); AUC, area under the curve calculated from the response to the meal test. Mixed model tests adjusted by Pre values were used to assess possible differences in delta changes between groups. $^{*}p < 0.05$, SLE-TR vs. SLE-NT; $^{\#}p < 0.09$, SLE-TR vs. SLE-NT.

underlying molecular mechanisms on insulin sensitivity in SLE patients. The main finding of this study was that a 12-week aerobic exercise training program improved insulin sensitivity in patients with mild/inactive SLE. We also identified that this improvement may be associated with increased insulin-stimulated skeletal muscle AMPK phosphorylation, a master regulator of insulin action in muscle.

Systemic lupus erythematosus patients may have increased IR when compared with their healthy peers (3), which is an important risk factor for T2D and CVD (2, 34). In this study, aerobic exercise elicited greater improvements (vs. control) in insulin sensitivity in SLE patients, as reflected by improved HOMA IR (an index based on fasting steady-state parameters which primarily reflects hepatic IR) (26), fasting insulin, insulin response to the MT, and the Matsuda Index (an estimate of whole-body insulin sensitivity derived from the MT) (25). Importantly, these beneficial responses were observed despite no changes in fasting glucose or glucose response to a meal load. These findings were unsurprising because these patients may not have glucose intolerance (3). Thus, the overall improvements in insulin sensitivity

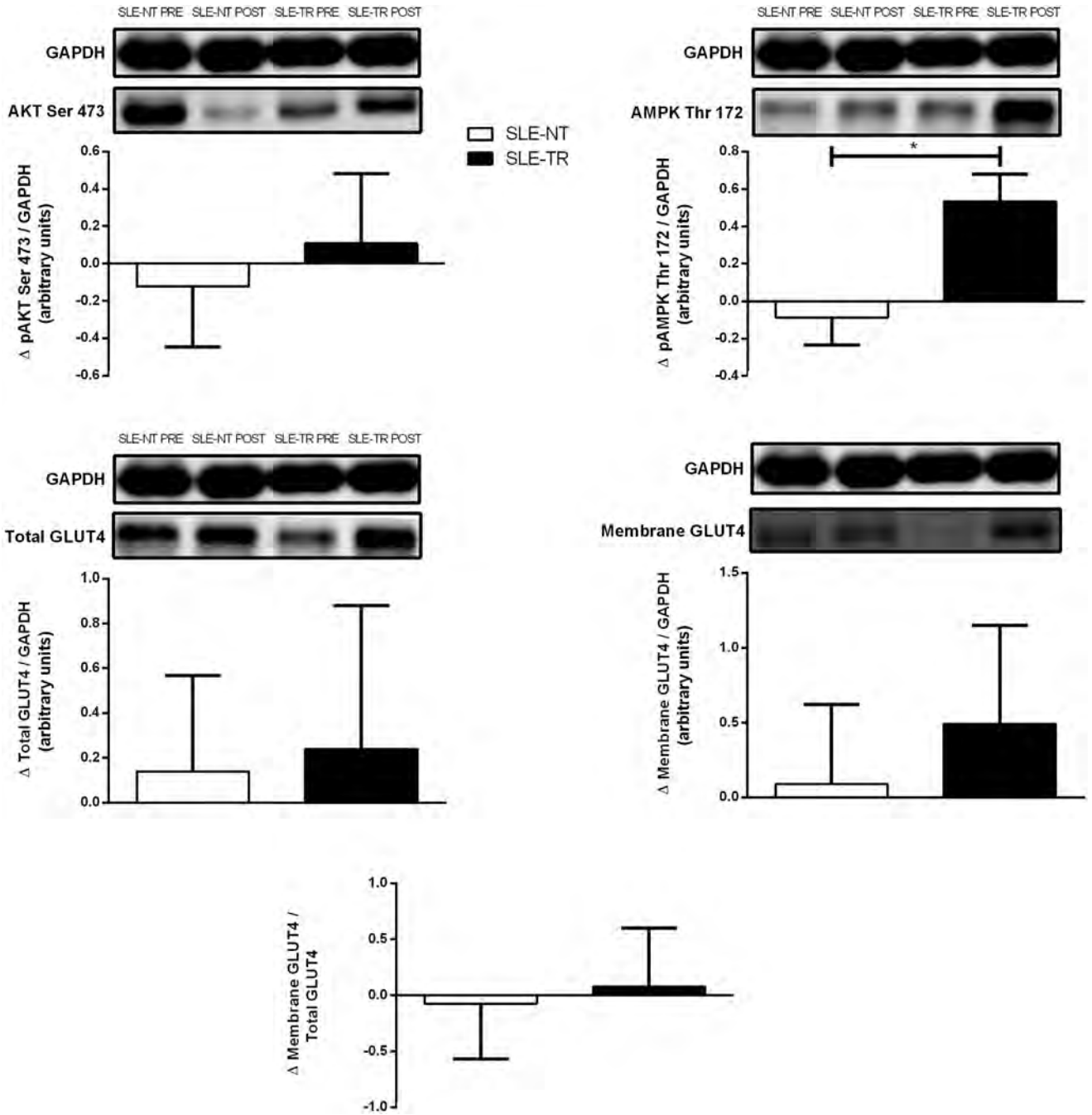

FIGURE 3 | Delta changes for protein expression of skeletal muscle phosphorylated AKT Ser 273, phosphorylated AMP-activated protein kinase (AMPK) Thr 172, total GLUT4, membrane GLUT4, and GLUT4 translocation in response to a meal test in SLE-TR and SLE-NT. SLE, systemic lupus erythematosus; SLE-TR, trained group ($n = 4$); SLE-NT, non-trained group ($n = 5$). Mixed model tests adjusted by Pre values were used to assess possible differences in delta changes between groups. *$p < 0.05$, SLE-TR vs. SLE-NT.

should be attributed to the lower secretion of insulin required to maintain glucose levels both at fasting and following nutrient intake. Interestingly, we also observed that fasting free fatty acids levels were diminished after 12 weeks of exercise training, which suggests decreased lipolysis despite lower levels of insulin. Because a major effect of insulin on adipose tissue is to inhibit lipolysis (35), it is likely that insulin sensitivity in adipose tissue was also improved after training. Altogether, these findings suggest that exercise was able to improve hepatic and peripheral insulin sensitivity in SLE patients.

It is noteworthy that improvements in insulin sensitivity in the trained group were shown regardless of any changes in dietary

TABLE 3 | Body composition, physical capacity, blood parameters, and food intake in trained and non-trained SLE patients before and after the exercise intervention.

	SLE-TR (n = 9)		SLE-NT (n = 10)				
	Pre	Δ (95% CI)	Pre	Δ (95% CI)	Δ diff (95% CI)	p	ES
Body composition							
Body weight (kg)	65.0 ± 10.5	−0.3 (−1.7 to 1.1)	67.6 ± 8.8	0.2 (−1.2 to 1.5)	−0.4 (−2.3 to 1.5)	0.6	−0.1
Fat mass (kg)	21.7 ± 6.5	0.1 (−0.9 to 1.1)	22.8 ± 4.8	−0.2 (−1.3 to 0.9)	0.3 (−1.3 to 1.8)	0.7	0.26
Lean mass (kg)	42.0 ± 4.8	0.4 (−1.0 to 1.7)	42.2 ± 5.7	0.3 (−1.1 to 1.8)	0.02 (−1.9 to 2.0)	0.9	0.02
Trunk fat (%)	30.0 ± 7.3	0.4 (−0.7 to 1.4)	33.8 ± 7.1	−0.8 (−1.9 to 0.4)	1.2 (−0.4 to 2.8)	0.13	0.9
Physical capacity							
Time at VAT (min)	4.9 ± 1.5	1.7 (0.7 to 2.7)	5.2 ± 0.9	−0.3 (−1.4 to 0.9)	2.0 (0.5 to 3.6)	0.01	1.2
Time at RCP (min)	9.6 ± 1.5	2.0 (1.3 to 2.7)	8.9 ± 1.6	0.9 (0.1 to 1.7)	1.1 (0.0 to 2.1)	0.04	0.92
Time to exhaustion (min)	11.5 ± 1.5	2.1 (1.4 to 2.8)	11.0 ± 1.6	0.6 (−0.2 to 1.4)	1.5 (0.5 to 2.5)	0.008	1.1
VO_2peak (mL/kg/min)	23.5 ± 4.7	1.1 (−1.2 to 3.4)	22.9 ± 4.6	0.9 (−1.7 to 3.6)	0.2 (−3.3 to 3.7)	0.9	−0.01
HRpeak (bpm)	171 ± 14	9.2 (5.7 to 12.6)	174 ± 11	1.4 (−2.6 to 5.3)	7.8 (2.5 to 13.0)	0.007	0.85
Blood parameters							
C3 (90–180 mg/dL)	95 ± 17	−1.6 (−10.9 to 7.7)	101 ± 13	−2.6 (−10.3 to 5.1)	0.9 (−11.2 to 13.1)	0.8	0.26
C4 (10–40 mg/dL)	16.2 ± 4.6	−0.9 (−3.1 to 1.4)	16.8 ± 7.3	−0.3 (−2.1 to 1.5)	1.3 (−3.4 to 2.3)	0.7	0.05
CPK (26–192 U/L)	97 ± 34	−0.5 (−31.3 to 30.2)	114 ± 62	−14.0 (−37.2 to 9.2)	13.5 (−25.0 to 52.0)	0.5	0.44
Creatinine (0.50–0.90 mg/dL)	0.74 ± 0.11	−0.01 (−0.09 to 0.07)	0.67 ± 0.10	−0.01 (−0.07 to 0.06)	−0.00 (−0.11 to 0.10)	0.9	0.24
Urea (10–50 mg/dL)	22.6 ± 4.6	1.0 (−3.4 to 5.5)	27.0 ± 7.2	−1.4 (−4.8 to 2.0)	2.4 (−3.2 to 8.0)	0.4	0.7
Erythrocytes (4.0–5.4 million/mm^3)	4.0 ± 0.3	−0.1 (−0.3 to 0.1)	4.3 ± 0.2	0.1 (−0.1 to 0.2)	−0.2 (−0.4 to 0.1)	0.14	−0.6
Hematocrit (35–47%)	37.1 ± 1.5	−1.3 (−2.5 to −0.1)	37.6 ± 2.0	0.2 (−0.9 to 1.3)	−1.5 (−3.1 to 0.1)	0.08	−0.7
Leukocytes (4.0–11.0 mil/mm^3)	4.4 ± 1.6	−0.4 (−1.6 to 0.9)	6.2 ± 2.6	−0.6 (−0.2 to 1.3)	−0.9 (−2.4 to 0.6)	0.2	0.11
Platelets (140–450 mil/mm^3)	237 ± 49	3.9 (−26.1 to 33.9)	233 ± 49	−0.3 (−27.1 to 26.5)	4.2 (−36.0 to 44.5)	0.8	0.11
CRP (<5 mg/L)	2.3 ± 2.3	−0.3 (−1.9 to 1.3)	3.4 ± 2.8	−0.2 (−1.6 to 1.2)	−0.1 (−2.3 to 1.9)	0.9	0.19
ESR (5.6–11.0 mm)	14.6 ± 12.0	3.1 (−4.3 to 10.6)	15.1 ± 10.4	1.2 (−5.8 to 8.2)	2.0 (−8.2 to 12.2)	0.7	0.22
Dietary intake							
Total energy (kcal)	2,022 ± 695	−5 (−696 to 686)	1,885 ± 572	−113 (−769 to 543)	108 (−845 to 1,061)	0.8	0.01
Protein (g)	83.1 ± 35.2	−1.3 (−32.6 to 30.0)	75.3 ± 24.7	1.3 (−28.6 to 31.1)	−2.6 (−45.8 to 40.7)	0.9	−0.15
Protein (%)	20.2 ± 12.6	−4.0 (−6.9 to 1.2)	19.3 ± 9.1	−2.8 (−5.5 to −0.1)	−1.3 (−5.2 to 2.7)	0.5	−0.2
Carbohydrate (g)	258 ± 112	17 (−80 to 113)	239 ± 76	3 (−89 to 96)	13 (−121 to 147)	0.8	0.04
Carbohydrate (%)	47.4 ± 12.6	6.9 (2.7 to 11.1)	47.8 ± 14.8	6.7 (2.8 to 10.7)	0.1 (−5.6 to 5.9)	0.9	0.04
Fat (g)	73.1 ± 28.3	−6.9 (−28.6 to 14.7)	69.8 ± 29.6	−15.6 (−36.2 to 4.9)	8.7 (−21.2 to 38.5)	0.5	0.26
Fat (%)	32.4 ± 7.5	−2.7 (−5.6 to 0.1)	32.9 ± 9.9	−4.2 (−6.9 to −1.5)	1.4 (−2.5 to 5.4)	0.5	0.26

Data expressed as mean ± SD. Delta change (Δ) and 95% confidence interval (95% CI), estimated difference between delta changes (Δ difference) and 95% CI, and level of significance (p) calculated using a mixed model adjusted by Pre values; effect size (ES).

SLE, systemic lupus erythematosus; SLE-TR, trained group; SLE-NT, non-trained group; VAT, ventilatory anaerobic threshold; RCP, respiratory compensation point; VO_2 peak, oxygen uptake peak; Hrpeak, heart rate peak; CPK, creatine phosphokinase; CRP, C-reactive protein; ESR, erythrocytes sedimentation rate.

intake or body composition. It is well known that changes in dietary intake, as well as body fat, may impact insulin sensitivity (36–38). Importantly, the current data indicate that exercise *per se*, independent of any concomitant modification in body composition or food intake, can improve insulin action in SLE. It remains to be determined whether interventions resulting in amelioration of eating habits and body fat mass would promote more pronounced enhancements in insulin sensitivity.

The mechanisms by which exercise training enhances insulin sensitivity in skeletal muscle may be associated with increased skeletal muscle GLUT4 content and/or activation of proteins involved in skeletal muscle insulin signal transduction, namely, Akt and AMPK, which can both increase insulin-stimulated GLUT4 translocation (9, 12). To gather some mechanistic insights, we took muscle biopsies and assessed candidate proteins involved in insulin signaling. Although we did not observe any differences in Akt phosphorylation or total skeletal muscle GLUT4 content, we did show a greater increase in AMPK phosphorylation after a meal load in the trained SLE patients. AMPK is a cellular energy sensor and a master regulator of insulin action in muscle. Its activation has been linked to improvements in insulin sensitivity and inflammation (39). However, in the current study, increased AMPK expression did not lead to enhanced GLUT4 translocation, since the higher total GLUT4 expression and membrane GLUT4 expression in trained SLE did not reach statistical significance. The low number of muscle biopsies may have precluded the detection of significant changes. Alternatively, the absence of improvement may be related to the fact that insulin-stimulated GLUT4 translocation is preserved in SLE patients, as previously demonstrated by our group (3). Larger studies are warranted to further clarify the molecular mechanisms underlying the exercise-induced improvement in insulin sensitivity in SLE, as well as the influence of exercise-induced AMPK overexpression upon insulin sensitivity and inflammatory responses.

We have previously shown that SLE patients with mild/inactive disease show preserved beta-cell function as reflected by similar proinsulin-to-insulin ratios and a higher insulinogenic index when compared with their healthy peers (3). The latter surrogate pinpoints the higher insulin secretion needed to overcome IR in SLE patients, which could predispose β-cell dysfunction (4).

In the present study, reductions in proinsulin levels paralleled those in insulin levels after the exercise training program, indicating a still preserved beta-cell function. Although the insulinogenic index was reduced in the trained group by 37% (vs. +8% in the non-trained group), this difference did not reach statistical significance. It is possible that the decrease in insulin secretion upon nutrient stimulus after exercise training may not have been enough to incite detectable reductions in the insulinogenic index in the trained group.

We expected any improvements in insulin sensitivity to improve the pancreatic α-cell response to insulin, thus leading to decreased glucagonemia in the trained group. In contrast, exercise training elicited slightly increased glucagon levels at fasting (+4%) and in response to the MT (+3%). This suggests that exercise does not enhance pancreatic α-cell sensitivity to insulin, and that the decreased insulin levels at fasting and in response to a meal load possibly led to a lower suppression of glucagon secretion. We have shown positive correlations between glucagon levels and erythrocytes sedimentation rate (ERS) and interleukin-6 (IL-6) in SLE patients with mild/inactive disease (3), suggesting that these inflammatory markers could partially explain hyperglucagonemia (40). There is evidence that an exercise intervention with similar characteristics to the current one fails to reduce ERS and IL-6 in SLE patients with mild disease (21). Thus, it is possible that greater improvements in systemic inflammation may be necessary to elicit reductions in glucagonemia in these patients, although this emerging hypothesis remains to be examined.

In addition to the positive effects on insulin sensitivity, the exercise training program led to significant improvements in physical capacity, without affecting laboratory and clinical disease-related parameters, in accordance with previous literature (13–16, 21, 41). This further reinforces the notion that exercise is a safe and effective tool in improving CVD risks in mild/inactive SLE. In a clinical setting, therefore, exercise emerges as a valid intervention which should be recommended to treat IR in this disease.

Limitations

First, we cannot extrapolate our findings to SLE patients with different characteristics, including disease severity, comorbidities, and drug regimens. Regarding the latter, it is well known that some drugs can alter glucose homeostasis (e.g., hydroxychloroquine and glucocorticoid) (42, 43). Since this was a small-scale study, larger trials are necessary to determine whether sub-samples of SLE patients taking specific medications, such as those aforementioned, respond to exercise differently. Second, the methods used to assess insulin sensitivity in this study permitted the calculation of hepatic and whole-body insulin sensitivity estimates, but not the direct assessment of hepatic, peripheral insulin sensitivity, or skeletal muscle glucose uptake. Finally, the small sample size may have limited the power to detect potentially statistically significant changes, particularly for the secondary outcomes.

Future Directions

This study is the first to demonstrate the value of exercise in improving IR in SLE. *In vitro* and experimental studies are necessary to validate the role of the AMPK pathway and to investigate the role of further canonical pathways not examined in this study (e.g., PPAR-gamma and MAPK) in the improvements of insulin sensitivity in response to exercise in SLE. Moreover, molecular array studies are warranted to explore further potential mechanisms underlying this response, which could lead to potential therapeutic targets. Perhaps more importantly, long-term, well-powered, clinical trials remain necessary to examine the chronic effect of exercise, along with the usual pharmacological treatment, on the prevention of T2DM and CVD in this disease.

In conclusion, a 12-week moderate-intensity aerobic exercise training program can improve insulin sensitivity in patients with mild/inactive SLE. Importantly, this response appears to be associated with increased insulin-stimulated skeletal muscle AMPK phosphorylation.

AUTHOR CONTRIBUTIONS

FB, BG, and EB conceived the study. FB analyzed and interpreted the data and drafted the manuscript. CM, WD, VZ, SS, RP, ES AS-P, and EB acquired data. All authors revised and approved the final version of the manuscript and are, thus, accountable for its content.

ACKNOWLEDGMENTS

Authors thank FAPESP (2011/24093-2; 2011/08302-0; 2015/03756-4; 2017/02546-1) and CNPq (150737/2015-7 and 305068/2014-8) for the financial support. We are grateful to Rosa Fukui and William Neves for technical assistance. We would like to thank Dr. Bryan Saunders for proofreading the manuscript.

REFERENCES

1. Muniyappa R, Lee S, Chen H, Quon MJ. Current approaches for assessing insulin sensitivity and resistance in vivo: advantages, limitations, and appropriate usage. *Am J Physiol Endocrinol Metab* (2008) 294(1):E15–26. doi:10.1152/ajpendo.00645.2007
2. Yang G, Li C, Gong Y, Fang F, Tian H, Li J, et al. Assessment of insulin resistance in subjects with normal glucose tolerance, hyperinsulinemia with normal blood glucose tolerance, impaired glucose tolerance, and newly diagnosed type 2 diabetes (prediabetes insulin resistance research). *J Diabetes Res* (2016) 2016:9270768. doi:10.1155/2016/9270768
3. Miyake CNH, Gualano B, Dantas WS, Pereira RT, Neves W, Zambelli VO, et al. Increased insulin resistance and glucagon levels in mild/inactive systemic lupus erythematosus patients despite normal glucose tolerance. *Arthritis Care Res (Hoboken)* (2018) 70(1):114–24. doi:10.1002/acr.23237
4. Kahn SE. Clinical review 135: the importance of beta-cell failure in the development and progression of type 2 diabetes. *J Clin Endocrinol Metab* (2001) 86(9):4047–58. doi:10.1210/jcem.86.9.7713
5. Baron AD, Schaeffer L, Shragg P, Kolterman OG. Role of hyperglucagonemia in maintenance of increased rates of hepatic glucose output in type II diabetics. *Diabetes* (1987) 36(3):274–83. doi:10.2337/diabetes.36.3.274
6. Reaven GM, Chen YD, Golay A, Swislocki AL, Jaspan JB. Documentation of hyperglucagonemia throughout the day in nonobese and obese patients with noninsulin-dependent diabetes mellitus. *J Clin Endocrinol Metab* (1987) 64(1):106–10. doi:10.1210/jcem-64-1-106
7. Ferrannini E, Muscelli E, Natali A, Gabriel R, Mitrakou A, Flyvbjerg A, et al. Association of fasting glucagon and proinsulin concentrations with insulin resistance. *Diabetologia* (2007) 50(11):2342–7. doi:10.1007/s00125-007-0806-x
8. Ferrannini E, Natali A, Muscelli E, Nilsson PM, Golay A, Laakso M, et al. Natural history and physiological determinants of changes in glucose

tolerance in a non-diabetic population: the RISC Study. *Diabetologia* (2011) 54(6):1507–16. doi:10.1007/s00125-011-2112-x
9. Bird SR, Hawley JA. Update on the effects of physical activity on insulin sensitivity in humans. *BMJ Open Sport Exerc Med* (2016) 2(1):e000143. doi:10.1136/bmjsem-2016-000143
10. Sylow L, Kleinert M, Richter EA, Jensen TE. Exercise-stimulated glucose uptake – regulation and implications for glycaemic control. *Nat Rev Endocrinol* (2017) 13(3):133–48. doi:10.1038/nrendo.2016.162
11. Mikines KJ, Sonne B, Farrell PA, Tronier B, Galbo H. Effect of physical exercise on sensitivity and responsiveness to insulin in humans. *Am J Physiol* (1988) 254(3 Pt 1):E248–59. doi:10.1152/ajpendo.1988.254.3.E248
12. Frosig C, Rose AJ, Treebak JT, Kiens B, Richter EA, Wojtaszewski JF. Effects of endurance exercise training on insulin signaling in human skeletal muscle: interactions at the level of phosphatidylinositol 3-kinase, Akt, and AS160. *Diabetes* (2007) 56(8):2093–102. doi:10.2337/db06-1698
13. Ramsey-Goldman R, Schilling EM, Dunlop D, Langman C, Greenland P, Thomas RJ, et al. A pilot study on the effects of exercise in patients with systemic lupus erythematosus. *Arthritis Care Res* (2000) 13(5):262–9. doi:10.1002/1529-0131(200010)13:5<262::AID-ANR4>3.0.CO;2-8
14. Carvalho MR, Sato EI, Tebexreni AS, Heidecher RT, Schenkman S, Neto TL. Effects of supervised cardiovascular training program on exercise tolerance, aerobic capacity, and quality of life in patients with systemic lupus erythematosus. *Arthritis Rheum* (2005) 53(6):838–44. doi:10.1002/art.21605
15. Miossi R, Benatti FB, Luciade de Sa Pinto A, Lima FR, Borba EF, Prado DM, et al. Using exercise training to counterbalance chronotropic incompetence and delayed heart rate recovery in systemic lupus erythematosus: a randomized trial. *Arthritis Care Res (Hoboken)* (2012) 64(8):1159–66. doi:10.1002/acr.21678
16. dos Reis-Neto ET, da Silva AE, Monteiro CM, de Camargo LM, Sato EI. Supervised physical exercise improves endothelial function in patients with systemic lupus erythematosus. *Rheumatology (Oxford)* (2013) 52(12):2187–95. doi:10.1093/rheumatology/ket283
17. Prado DM, Benatti FB, de Sa-Pinto AL, Hayashi AP, Gualano B, Pereira RM, et al. Exercise training in childhood-onset systemic lupus erythematosus: a controlled randomized trial. *Arthritis Res Ther* (2013) 15(2):R46. doi:10.1186/ar4205
18. Benatti FB, Miossi R, Passareli M, Nakandakare ER, Perandini L, Lima FR, et al. The effects of exercise on lipid profile in systemic lupus erythematosus and healthy individuals: a randomized trial. *Rheumatol Int* (2015) 35(1):61–9. doi:10.1007/s00296-014-3081-4
19. Sabry A, Sheashaa H, El-Husseini A, Mahmoud K, Eldahshan KF, George SK, et al. Proinflammatory cytokines (TNF-alpha and IL-6) in Egyptian patients with SLE: its correlation with disease activity. *Cytokine* (2006) 35(3–4):148–53. doi:10.1016/j.cyto.2006.07.023
20. Plomgaard P, Bouzakri K, Krogh-Madsen R, Mittendorfer B, Zierath JR, Pedersen BK. Tumor necrosis factor-alpha induces skeletal muscle insulin resistance in healthy human subjects via inhibition of Akt substrate 160 phosphorylation. *Diabetes* (2005) 54(10):2939–45. doi:10.2337/diabetes.54.10.2939
21. Perandini LA, Sales-de-Oliveira D, Mello SB, Camara NO, Benatti FB, Lima FR, et al. Exercise training can attenuate the inflammatory milieu in women with systemic lupus erythematosus. *J Appl Physiol (1985)* (2014) 117(6):639–47. doi:10.1152/japplphysiol.00486.2014
22. Hochberg MC. Updating the American college of rheumatology revised criteria for the classification of systemic lupus erythematosus. *Arthritis Rheum* (1997) 40(9):1725. doi:10.1002/art.1780400928
23. Gladman DD, Ibanez D, Urowitz MB. Systemic lupus erythematosus disease activity index 2000. *J Rheumatol* (2002) 29(2):288–91.
24. Pinto AJ, Miyake CN, Benatti FB, Silva CA, Sallum AM, Borba E, et al. Reduced aerobic capacity and quality of life in physically inactive patients with systemic lupus erythematosus with mild or inactive disease. *Arthritis Care Res (Hoboken)* (2016) 68(12):1780–6. doi:10.1002/acr.22905
25. Matsuda M, DeFronzo RA. Insulin sensitivity indices obtained from oral glucose tolerance testing: comparison with the euglycemic insulin clamp. *Diabetes Care* (1999) 22(9):1462–70. doi:10.2337/diacare.22.9.1462
26. Matthews DR, Hosker JP, Rudenski AS, Naylor BA, Treacher DF, Turner RC. Homeostasis model assessment: insulin resistance and beta-cell function from fasting plasma glucose and insulin concentrations in man. *Diabetologia* (1985) 28(7):412–9. doi:10.1007/BF00280883
27. Tura A, Kautzky-Willer A, Pacini G. Insulinogenic indices from insulin and C-peptide: comparison of beta-cell function from OGTT and IVGTT. *Diabetes Res Clin Pract* (2006) 72(3):298–301. doi:10.1016/j.diabres.2005.10.005
28. Dantas WS, Marcondes JA, Shinjo SK, Perandini LA, Zambelli VO, Neves WD, et al. GLUT4 translocation is not impaired after acute exercise in skeletal muscle of women with obesity and polycystic ovary syndrome. *Obesity (Silver Spring)* (2015) 23(11):2207–15. doi:10.1002/oby.21217
29. Gualano B, de Salles Painneli V, Roschel H, Artioli GG, Neves M Jr, De Sa Pinto AL, et al. Creatine in type 2 diabetes: a randomized, double-blind, placebo-controlled trial. *Med Sci Sports Exerc* (2011) 43(5):770–8. doi:10.1249/MSS.0b013e3181fcee7d
30. Cohen J. *Statistical Power Analysis for the Behavioral Sciences*. Hillsdale, USA: Lawrence Erlbaum Associates (1998).
31. Victora CG, Habicht JP, Bryce J. Evidence-based public health: moving beyond randomized trials. *Am J Public Health* (2004) 94(3):400–5. doi:10.2105/AJPH.94.3.400
32. Hollis S, Campbell F. What is meant by intention to treat analysis? Survey of published randomised controlled trials. *BMJ* (1999) 319(7211):670–4. doi:10.1136/bmj.319.7211.670
33. Fergusson D, Aaron SD, Guyatt G, Hebert P. Post-randomisation exclusions: the intention to treat principle and excluding patients from analysis. *BMJ* (2002) 325(7365):652–4. doi:10.1136/bmj.325.7365.652
34. Baron AD. Insulin resistance and vascular function. *J Diabetes Complications* (2002) 16(1):92–102. doi:10.1016/S1056-8727(01)00209-4
35. Chakrabarti P, Kim JY, Singh M, Shin YK, Kim J, Kumbrink J, et al. Insulin inhibits lipolysis in adipocytes via the evolutionarily conserved mTORC1-Egr1-ATGL-mediated pathway. *Mol Cell Biol* (2013) 33(18):3659–66. doi:10.1128/MCB.01584-12
36. Orchard TJ, Temprosa M, Goldberg R, Haffner S, Ratner R, Marcovina S, et al. The effect of metformin and intensive lifestyle intervention on the metabolic syndrome: the diabetes prevention program randomized trial. *Ann Intern Med* (2005) 142(8):611–9. doi:10.7326/0003-4819-142-8-200504190-00009
37. Due A, Larsen TM, Hermansen K, Stender S, Holst JJ, Toubro S, et al. Comparison of the effects on insulin resistance and glucose tolerance of 6-mo high-monounsaturated-fat, low-fat, and control diets. *Am J Clin Nutr* (2008) 87(4):855–62. doi:10.1093/ajcn/87.4.855
38. Due A, Larsen TM, Mu H, Hermansen K, Stender S, Astrup A. Comparison of 3 ad libitum diets for weight-loss maintenance, risk of cardiovascular disease, and diabetes: a 6-mo randomized, controlled trial. *Am J Clin Nutr* (2008) 88(5):1232–41. doi:10.3945/ajcn.2007.25695
39. Hardie DG, Ross FA, Hawley SA. AMPK: a nutrient and energy sensor that maintains energy homeostasis. *Nat Rev Mol Cell Biol* (2012) 13(4):251–62. doi:10.1038/nrm3311
40. Ellingsgaard H, Hauselmann I, Schuler B, Habib AM, Baggio LL, Meier DT, et al. Interleukin-6 enhances insulin secretion by increasing glucagon-like peptide-1 secretion from L cells and alpha cells. *Nat Med* (2011) 17(11):1481–9. doi:10.1038/nm.2513
41. Tench CM, McCarthy J, McCurdie I, White PD, D'Cruz DP. Fatigue in systemic lupus erythematosus: a randomized controlled trial of exercise. *Rheumatology (Oxford)* (2003) 42(9):1050–4. doi:10.1093/rheumatology/keg289
42. McDonough AK, Curtis JR, Saag KG. The epidemiology of glucocorticoid-associated adverse events. *Curr Opin Rheumatol* (2008) 20(2):131–7. doi:10.1097/BOR.0b013e3282f51031
43. Chen YM, Lin CH, Lan TH, Chen HH, Chang SN, Chen YH, et al. Hydroxychloroquine reduces risk of incident diabetes mellitus in lupus patients in a dose-dependent manner: a population-based cohort study. *Rheumatology (Oxford)* (2015) 54(7):1244–9. doi:10.1093/rheumatology/keu451

Conflict of Interest Statement: The authors declare that the research was conducted in the absence of any commercial or financial relationships that could be construed as a potential conflict of interest.

frontiers in Immunology

REVIEW
published: 27 April 2018
doi: 10.3389/fimmu.2018.00911

The Contribution of Autoantibodies to Inflammatory Cardiovascular Pathology

*Lee A. Meier and Bryce A. Binstadt**

Center for Immunology, Department of Pediatrics, University of Minnesota Medical School, Minneapolis, MN, United States

Chronic inflammation and resulting tissue damage underlie the vast majority of acquired cardiovascular disease (CVD), a general term encompassing a widely diverse array of conditions. Both innate and adaptive immune mechanisms contribute to chronic inflammation in CVD. Although maladies, such as atherosclerosis and cardiac fibrosis, are commonly conceptualized as disorders of inflammation, the cellular and molecular mechanisms that promote inflammation during the natural history of these diseases in human patients are not fully defined. Autoantibodies (AAbs) with specificity to self-derived epitopes accompany many forms of CVD in humans. Both adaptive/induced iAAbs (generated following cognate antigen encounter) and also autoantigen-reactive natural antibodies (produced independently of infection and in the absence of T cell help) have been demonstrated to modulate the natural history of multiple forms of CVD including atherosclerosis (atherosclerotic cardiovascular disease), dilated cardiomyopathy, and valvular heart disease. Despite the breadth of experimental evidence for the role of AAbs in CVD, there is a lack of consensus regarding their specific functions, primarily due to disparate conclusions reached, even when similar approaches and experimental models are used. In this review, we seek to summarize the current understanding of AAb function in CVD through critical assessment of the clinical and experimental evidence in this field. We additionally highlight the difficulty in translating observations made in animal models to human physiology and disease and provide a summary of unresolved questions that are critical to address in future studies.

Keywords: cardiovascular, inflammation, autoantibodies, atherosclerosis, autoimmunity

OPEN ACCESS

Edited by:
Ralf J. Ludwig, Universität zu Lübeck, Germany

Reviewed by:
Torsten Witte, Hannover Medical School, Germany
Jocelyne Demengeot, Instituto Gulbenkian de Ciência (IGC), Portugal

***Correspondence:**
Bryce A. Binstadt
binstadt@umn.edu

Specialty section:
This article was submitted to Immunological Tolerance and Regulation, a section of the journal Frontiers in Immunology

Received: *16 January 2018*
Accepted: *12 April 2018*
Published: *27 April 2018*

Citation:
Meier LA and Binstadt BA (2018) The Contribution of Autoantibodies to Inflammatory Cardiovascular Pathology. Front. Immunol. 9:911. doi: 10.3389/fimmu.2018.00911

INTRODUCTION

Cardiovascular (CV) disease (CVD) has been the most significant cause of morbidity and mortality worldwide for over a century and will continue to be for the foreseeable future (1). CVDs are heterogeneous and include coronary heart disease (CHD), peripheral vascular disease (PVD), valvular heart disease (VHD), and stroke. The main pathological process that underlies the majority of these CVD manifestations is atherosclerosis, a chronic inflammatory response to lipid products in the walls of large and medium arteries. Atherosclerosis is the single most significant contributor to human mortality (2). It has long been hypothesized that immune dysregulation and chronic inflammation contribute to the development of CV pathology independently of traditional atherosclerotic cardiovascular disease (ASCVD) risk factors (3). Until recently, however, there was no direct clinical evidence supporting the detrimental role for inflammation in this process. Outcomes from

the randomized, multicenter Canakinumab Anti-inflammatory Thrombosis Outcome Study (CANTOS), completed in late 2017, provide the strongest evidence to date in support of the pro-atherogenic role for inflammation in humans. Canakinumab, a monoclonal antibody (mAb) directed against interleukin-1β (IL-1β), significantly reduced adverse CV outcomes in patients with a history of myocardial infarction (MI) and elevated C-reactive protein (CRP) (4). While, CANTOS focused solely on the effects of IL-1β blockade in secondary CV prevention, this intervention represents only one from many potential therapeutic approaches. The CANTOS trial provides confirmation of the "inflammation hypothesis" in CVD through robust clinical analysis, a critical milestone on the path toward a more comprehensive understanding of the role of inflammation in CV pathology. Although the additional clinical trials are currently underway that target other inflammatory mediators in CVD (5, 6), many unresolved questions remain regarding the specific cellular and molecular immune mechanisms that promote chronic CV inflammation. Therefore, a significant challenge facing the field of CVD research is to define these critical immune mediators, particularly those that can be targeted therapeutically.

The specific contributions that humoral immunity (e.g., complement, antibodies (Ab), etc.) provides during the natural history of CVD remain unresolved. Multiple clinical studies have demonstrated correlative evidence in favor of a CVD-promoting role for Abs, and this topic has been reviewed extensively elsewhere (7–10). Despite this, no current therapeutic approaches are designed to improve CVD outcomes by reducing Ab production or activity. Ab with reactivity to self-epitopes [autoantibodies (AAbs)] have been observed in many forms of CVD, and have diverse epitope reactivities, binding affinities, and isotypes. Abs specific to multiple varieties of cardiac/myocardium- and blood vessel-related epitopes have been characterized in human CVD, including those demonstrating binding affinity to antigens that are cardiac-specific [e.g., cardiac troponin-I (cTnI) (11)], cardiac-associated [e.g., oxidized apolipoproteins (12)], and ones that are ubiquitously expressed [e.g., heat-shock proteins (HSPs) (13)]. Despite the breadth of evidence demonstrating correlations between serum AAb titers and CVD severity, there is no consensus on the specific roles that AAbs play in CVD progression or whether they might be appropriate targets for CVD treatment. In short, contradictory evidence exists. In addition, determining whether AAbs represent causative agents rather than passive bystanders during the natural history of CVD is a challenging task, particularly in the context of highly heterogeneous manifestations of CVD in humans.

The potential mechanisms by which AAbs may promote CVD include target opsonization and subsequent recognition and activation of immune cells bearing antibody-recognizing Fc receptors (i.e., type II hypersensitivity), leukocyte activation following immune complex deposition and complement fixation (i.e., type III hypersensitivity), and target neutralization/inhibition. The purpose of this review is to summarize the current understanding how AAbs contribute to specific forms of CV pathology including ASCVD, dilated cardiomyopathy (DCM), and VHD. In addition, we highlight the key recent experimental and clinical findings in this field. Finally, we discuss a number of the remaining unresolved questions this field faces in pursuit of future clinical translation.

THE RESPONSE TO CV DAMAGE HAS GENETIC AND ENVIRONMENTAL CONTRIBUTIONS

The induction of an immune response to autoantigens in the setting of human CVD is thought to occur as a result of CV insults (e.g., MI and atherosclerotic plaque necrosis). Self-antigens that are normally sequestered within the cardiac parenchyma and vascular walls are liberated and/or produced during the course of an inflammatory response and its resolution. Exposure of these immunogenic elements induces innate and adaptive immune activation. Coupled with the potent inflammatory signals that invariably accompany tissue damage, robust immunopathology of CV tissue can ensue, including AAb production. Because these self-antigens are present in virtually unlimited supply, chronic autoimmunity and tissue inflammation can result.

The primary determinants of the magnitude of the induced response to self-antigens include the characteristics of the tissue insult (e.g., infarct size and microbial burden) and the affected individual's degree of genetic predisposition to autoimmunity (14). Experimental studies in mice have provided evidence for the contribution of genetics to the development of CV pathology. For example, the A/J mouse strain is highly susceptible to enterovirus-induced experimental myocarditis whereas C57BL/6 mice are protected (15). Juvenile male BALB/c mice develop more dramatic experimental enterovirus-induced myocarditis than females (16), and atherosclerosis occurs most readily in the C57BL/6 background whereas the CH3 and BALB/c backgrounds are protected from this disease (17). The homogeneous genetic backgrounds in inbred mouse strains amplify the genetic contribution to experimental CVD initiation and progression while minimizing the contribution of environmental factors, as opposed to the diverse forms of CVD that occur in the extensively outbred human population. For example, monozygotic human twins generally develop autoimmune disease with much less than 50% concordance, underscoring the putative role for environmental factors (18). In addition, experimental animal housing conditions generally involve isolation from environmental inputs. While this strict environmental control improves the reliability and reproducibility of animal studies, and it does not accurately represent the diverse environmental stimuli that humans encounter.

The hypothesis that CV damage is a critical predecessor of AAb generation in CVD is widely accepted and supported by experimental and clinical evidence. However, this hypothesis is complicated by the observation that cardiac AAbs can also be found in apparently healthy individuals without a personal history of CVD, and the presence of these AAbs predicts the development of CVD later in life (19). In addition, the presence of CV-reactive natural antibodies (NAbs) in the general population (elaborated upon later) further complicates the understanding of the role for AAbs in CV pathology (20).

ATHEROSCLEROSIS IS DRIVEN BY INFLAMMATION

Atherosclerosis is a chronic reaction to lipid- and cholesterol-rich lipoprotein deposits (i.e., lipid- and cholesterol-rich plaques) in the sub-endothelium of large and medium arteries, and it has been reviewed extensively (3). It is the main driver of coronary artery disease (CAD), peripheral artery disease, and stroke. Of note, "cholesterol" refers to a specific chemical entity [i.e., (3β)-cholest-5-en-3-ol] but it is often conflated, out of convenience, with either low- or high-density lipoproteins (LDL and HDL, respectively). In fact, LDL and HDL are heterogeneous particles containing variable amounts of lipids and phospholipids (PLs) packaged within a combination of protein carriers (i.e., apolipoproteins). Circulating LDL and HDL have well-substantiated direct and inverse correlations, respectively, with CVD risk; because of this, significant efforts have been put into understanding the specific cellular mechanisms that underpin these observations.

The inflammatory nature of atherosclerosis is undisputed and supported by a breadth of experimental and clinical observations. It is well known that patients with systemic inflammatory diseases develop accelerated and more aggressive forms of ASCVD than the general population (21). Despite this, the mechanisms governing ASCVD initiation and progression are incompletely understood, particularly with respect to AAb generation and function. ASCVD often begins in early adolescence and is initiated by endothelial dysfunction arising primarily from disturbed hemodynamics and lipid-induced inflammation, in addition to additional environmental factors and the individual's genetic susceptibility. The formation of macroscopic "fatty streaks" at arterial branch points and other sites of turbulence heralds the early stages of ASCVD. Fatty streaks are primarily composed of oxidized lipoprotein particles [including oxidized low-density lipoprotein (oxLDL)], foam cells (lipid-laden macrophages), vascular smooth muscle cells (vSMCs), and lymphocytes. Over an individual's lifetime, the streak composition and structural features evolve due to chronic superimposed inflammatory and healing responses. Late-stage disease ultimately results in formation of an atheromatous plaque (22). Atherosclerosis manifests clinically due to the effects of tissue ischemia and/or infarction caused by partial or complete plaque occlusion of arterial lumens. While most commonly associated with the myocardium, atherosclerotic ischemia and infarction can affect any of the body's tissues (e.g., in the setting of PVD).

Efforts to understand the pathophysiology of ASCVD have largely relied on one of two mouse models of the disease based on genetic disruption of lipid clearance: apolipoprotein-E- and LDL receptor-deficient mice (*ApoE*$^{-/-}$ and *Ldlr*$^{-/-}$, respectively). When placed on a high-fat ("Western") diet, these mice rapidly develop extreme hyperlipidemia, and lipid-rich plaques form shortly thereafter in a predictable distribution. Genetic manipulation of these mouse models has provided significant insight into the underlying inflammatory mechanisms that promote ASCVD, with the caveat that experimental atherosclerosis in mice exhibits substantial differences from the disease in humans (23).

B CELLS ALTER THE TRAJECTORY OF ASCVD

The role of B cells during ASCVD initiation and progression has been studied extensively and is reviewed in detail elsewhere (24). A 2013 genome-wide association study compared 188 patients with CHD with 188 healthy controls. Gene ontology enrichment analysis demonstrated that B cell activation, differentiation, and signaling genes were among the most prominently enriched in patients with CHD (25).

The predominant B cell subsets in mice and humans are B-1 and B-2 cells that produce NAbs and induced (adaptive) antibodies (iAb, iAAb when reactive with self-antigens), respectively. The dominant paradigm for understanding the role that B cells play during the natural history of ASCVD is based on opposing functions of B-1 and B-2 cells, with the former generally being disease-ameliorating and the latter disease-promoting. A schematic of how B-1 cell-derived NAbs and B-2 cell-derived iAAbs contribute to CAD is shown in **Figure 1**. The majority of studies that have contributed to construction of this paradigm have been derived from experimental atherosclerosis in mice, but clinical observations do indeed support this diametric model and are described in the following sections.

A comparison of B-1 and B-2 cells is shown in **Figure 2**. In mice, B-1 cells are identified and distinguished from the more common B-2 B cells based on lower expression of B220 and by the presence of CD43 (26). B-1 cells can be further subdivided into B-1a and B-1b subsets based on the presence or absence of CD5 expression, respectively (27). An analogous population of innate-like B-1 cells in humans that appears to have similar functional properties to those in mice is identified based on the following surface marker profile: $CD20^{+}CD27^{+}CD43^{+}CD70^{-}$ (28). Importantly, in humans, CD5 is promiscuously expressed on B-1 and B-2 cells in multiple contexts and is not a reliable distinguishing feature of these lineages (29). It is thought that in mice all three B cell subsets (B-1a, B-1b, and B-2) originate from distinct lineages (30), and are thus theoretically targetable through conditional and constitutive gene knockout studies to dissect their discrete functional differences. Clarifying the role of B cells in atherogenesis will require understanding the distinct versus overlapping functions of each subset in ASCVD. **Table 1** provides a summary of the heterogeneous AAbs that are most actively studied in ASCVD with putative functional roles in the disease course highlighted.

NAbs RESTRAIN ATHEROSCLEROSIS

Cardiovascular-reactive AAbs are produced in both homeostatic and disease states. NAbs are an important class of AAbs produced during homeostasis in the absence of cognate antigen encounter or infection. The biology of NAbs has been reviewed extensively elsewhere (31). In multiple experimental ASCVD models, NAbs have been shown to be disease-restraining (20, 32–35).

Natural antibodies are derived from B-1 cells (36) that are enriched in the spleen, bone marrow (BM), and body cavities (e.g., pleural and peritoneal) (31). In the absence of infection, the vast majority of serum IgM Ab in mice (between 80 and 90%) are

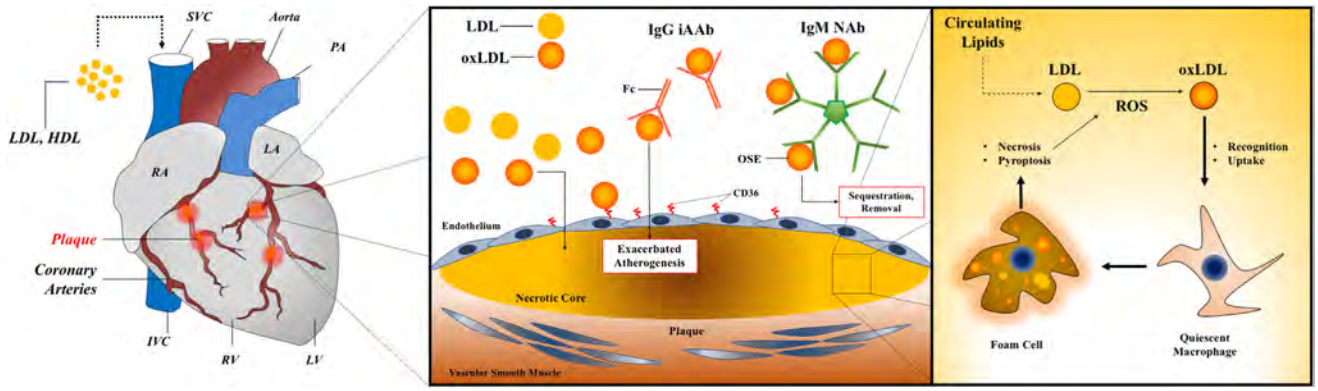

FIGURE 1 | AAbs in myocarditis and dilated cardiomyopathy. Left panel: a diagram of cardiac anatomy with relevant structures labeled, including the coronary arteries and associated plaques. Middle panel: a generalized schematic for AAbs in atherogenesis showing opposing roles for B-1 cell-derived IgM NAb and B-2 cell-derived IgG iAAb. Right panel: foam cell formation and feed-forward inflammatory activation within vessel plaques through enhanced uptake of oxidized lipids during atherogenesis. Abbreviations: LDL, low-density lipoprotein; HDL, high-density lipoprotein; NAbs, natural antibodies; iAAb, induced autoantibodies; Ig, immunoglobulin; oxLDL, oxidized low-density lipoprotein; OSE, oxidation-specific epitope; RA, right atrium; LA, left atrium; IVC, inferior vena cava; SVC, superior vena cava; RV, right ventricle; LV, left ventricle; PA, pulmonary artery.

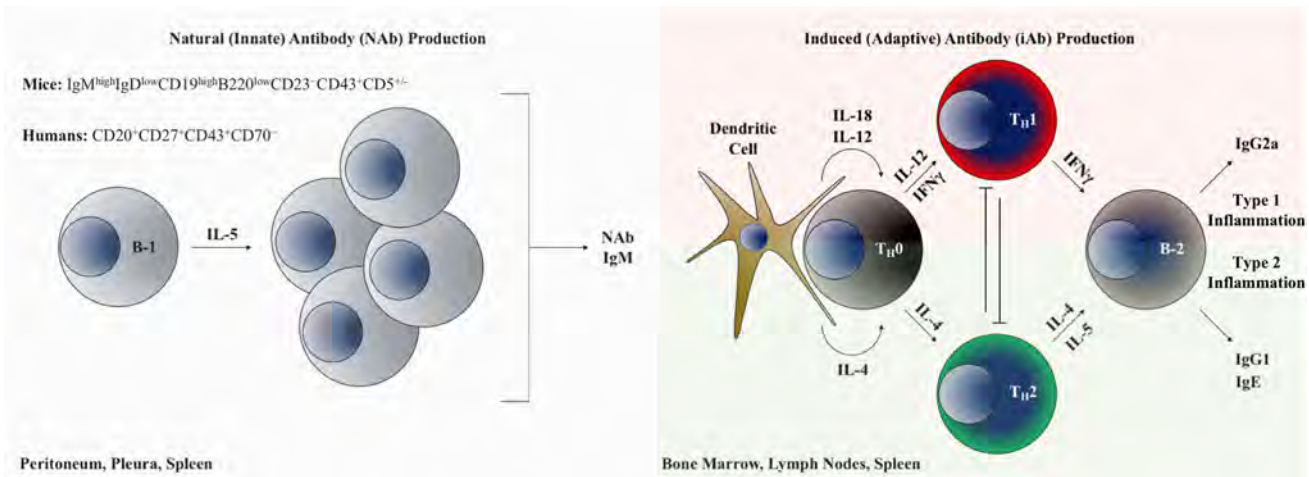

FIGURE 2 | B-1 and B-2 cells as modulators of cardiovascular inflammation through AAb production. Left panel: B-1 B cells inhabiting the body cavities are interleukin-5 dependent and produce polyreactive natural antibodies, predominantly of the IgM isotype. Right panel: B-2 lymphocytes generate adaptive immunoglobulin under the control of inflammatory cytokine programming. Abbreviations: T_H0, naive CD4+ T lymphocyte; T_H1, type 1 inflammation-polarized CD4+ helper T lymphocyte; T_H2, type 2 inflammation-polarized CD4+ helper T lymphocyte; IFN-γ, interferon gamma.

NAbs (37). Characteristics of NAbs include (a) low-affinity for their target antigens relative to those resulting from the germinal center (GC) reaction and (b) polyreactivity with a wide array of structurally distinct cellular elements including autoantigens (e.g., elements of apoptotic cells and cell membrane components) and evolutionarily conserved microbial products (31). Of note, NAbs generally exhibit immunoglobulin-encoding gene segments in the germline configuration, indicating that their production is independent of somatic recombination and hypermutation (38, 39). Optimal development and production of NAb from B-1 cells requires IL-5 signaling (40, 41). The association between *Il5* gene hypomorphisms in humans with ASCVD provides a putative link to B-1 B cells and NAbs in this disease process (42). NAb reactivity with multiple self-derived antigens has been implicated in conferring this benefit, with many experimental studies focusing on NAb reactive to LDL derivatives (20, 32, 43–46). Despite multiple clinical studies supporting the ASCVD-restraining role for NAbs, studies demonstrating disease-promoting activity of NAbs have also been reported in both humans and in experimental ASCVD (47–50). Thus, it is not possible to reach generalizable conclusions regarding the role for NAb during the initiation and progression of ASCVD. With this caveat in mind, selected key findings that contribute to the understanding of NAb function in ASCVD are described below.

Plaque-accumulated lipid and cholesterol deposits are prone to oxidation, both spontaneously and enzymatically. Oxidation of plaque constituents renders them antigenic through formation of oxidation-specific (neo)epitopes (OSEs) when adducted to

TABLE 1 | Summary of commonly studied autoantibodies in atherosclerotic cardiovascular disease.

Ab type	Antigen	Predominant isotype	Type of antigen	Promoting or restraining	References
Natural	Phosphatidylcholine	IgM	Oxidized phospholipid	Restraining	(64–69)
	Malondialdehyde-LDL	IgM >> IgG		Restraining	(48, 49)
	Phosphorylcholine (PC)	IgM (E06) and IgA (T15)		Restraining	(78–80)
	Cardiolipin	IgM and IgA >> IgG		Restraining	(52)
Induced	Endothelial cells (AECA[1])	IgG	Unknown	Promoting	(138, 146, 147)
	Heat-shock protein-60/65	IgG	Protein metabolites	Promoting	(96–98)
	Apolipoprotein A-1	IgG		Promoting	(102, 103)

[1]*AECA, anti-endothelial cell antibody.*

proteins within the plaques (51, 52). OSEs have been implicated in a variety of disease states, reviewed elsewhere (53). Some of the most widely studied endogenous OSEs within the context of ASCVD are derived from PL oxidation, including malondialdehyde (MDA) and phosphocholine (phosphorylcholine when functionally adducted) (53). These immunogenic OSEs subsequently induce an inflammatory reaction within the plaque and vessel wall vicinity. Employing a reductionist approach based on these observations, researchers have generated OSEs *in vitro,* such as copper-oxidized LDL (CuOxLDL), a model antigen containing heterogeneous OSEs generated through reacting purified LDL particles with copper sulfate ($CuSO_4$) (54–56). CuOxLDL reagents have been useful for standardizing assays OSE-reactive AAb detection assays (56) and for clarifying OSE-induced immune responses through immunization in experimental models of ASCVD (57).

Phosphatidylcholine is ubiquitous in mice and humans and is a component of cell membranes and cholesterol particles (both HDL and LDL). It readily undergoes enzymatic oxidation by platelet-activating factor-acetylhydrolase (LP-PLA2) to yield immunogenic phosphorylcholine (PC) (58), an OSE that has been demonstrated to be an important inflammatory mediator in the setting of ASCVD, functioning through activation of T cells, monocytes, and endothelial cells following protein adduction (51, 59–63). In humans, serum levels of PC-reactive natural IgM (anti-PC-IgM) were inversely correlated with the risk of atherosclerosis, vein-graft stenosis, and stroke in the general population and also in patients with systemic lupus erythematosus (64–69). Additional studies in humans have demonstrated associations between alternative OSEs and their role in atherogenesis. For example, MDA, an OSE produced from the breakdown of polyunsaturated fatty acids, is a highly reactive moiety that readily forms immunogenic protein adducts and is recognized by circulating IgM AAbs. Multiple observational studies in humans have demonstrated inverse correlations between MDA-reactive IgM AAbs and atherosclerotic disease. Specifically, low levels of MDA-reactive NAbs are correlated with increased carotid intima-to-media thickness (IMT, a clinical measure of atherosclerosis determined using angiography) and increased risk of coronary artery stenosis (35, 48). These studies provide preliminary evidence that strategies for enhancing NAb production may be beneficial for combatting ASCVD.

Studies in *Apoe*$^{-/-}$ and *Ldlr*$^{-/-}$ mice have provided evidence for the disease-restraining role for NAbs during atherosclerosis initiation and progression and provide researchers with the ability to dissect the cellular and molecular pathways mediating their production. Splenectomized *Apoe*$^{-/-}$ mice developed more aggressive lesions than intact *Apoe*$^{-/-}$ control mice, a phenotype that could be rescued through adoptive transfer of B-1a cells (34). Importantly, this protection depended on the ability of the transferred B-1 cells to secrete IgM. Recently, B-1b cells were shown to be sufficient for atheroprotection in *Apoe*$^{-/-}$ mice *via* OSE-specific NAb production (70). The authors provided evidence implicating DNA-binding protein inhibitor 3 (Id3) as a negative regulator of B-1b cell development–conditional deletion of *Id3* in B cells using *Cd19-Cre* on the *Apoe*$^{-/-}$ background led to increased B-1b cell numbers, increased titers of oxLDL-NAb, and decreased atherosclerotic lesion formation. The study was buttressed by the authors' identification of a hypomorphic *Id3* polymorphism in humans that leads to elevated B-1 cell numbers and oxLDL-NAb levels. Interestingly, the same group previously reported that *constitutive* deficiency of *Id3* significantly exacerbated atherogenesis (71), thus implicating potential alternative functions for *Id3* in non-B cell populations during the natural history of ASCVD.

Using spleens from *Apoe*$^{-/-}$ mice, researchers cloned of 13 oxLDL-reactive NAb (designated "E0" Ab) (44). The E06 antibody generated from these studies recognizes phosphorylcholine-adducted oxidized phospholipids (oxPL) and not free PC or reduced/native PLs (72). *In vitro* studies using the E06 antibody demonstrated its ability to prevent macrophage uptake of oxLDL, an important element of foam cell formation during atherogenesis (73, 74). Clone E06 was later shown to competitively inhibit CuOxLDL binding to CD36 [a member of the scavenger receptor (SR) family of proteins that mediates oxLDL uptake], demonstrating not only that CD36 is a receptor for oxPL but also that oxPL-specific NAbs inhibit CD36-mediated oxLDL uptake (75), which may then interfere with CD36-mediated foam cell formation (74). The more recent observation that CD36 ligands promote inflammatory responses through activation of a TLR4/6 signaling cascade provides further insight into potential pathways by which NAb (E06 in particular) may mediate ASCVD-protective effects (76).

The B-1 cell-derived T15 IgA NAb clone has been studied extensively and was previously shown to confer enhanced *Streptococcus pneumoniae* immunity in mice through recognition of PC in the *Streptococcus* capsule (77, 78). Intriguingly, the antigen-binding domains of E06 and T15 are identical and differ only in isotype (79). Immunizing *Ldlr*$^{-/-}$ mice with preparations of *S. pneumoniae* significantly elevated NAb IgM titers and

reduced plaque development, thus demonstrating the presence of molecular mimicry between *S. pneumoniae* and oxLDL in addition to a potential mechanism by which NAbs generally restrain ASCVD progression. In addition, this and other studies have provided evidence for a potential vaccine for atherosclerosis prevention based on enhancing NAb production (80). Later studies showed that passive immunization of *Apoe*$^{-/-}$ mice with monoclonal T15 antibody resulted in significant reductions in the development of vein-graft atherosclerosis without altering serum cholesterol levels (81), establishing the potential efficacy of NAb-based therapies as a treatment for ASCVD.

Many of the molecular and cellular mechanisms that underlie the association between NAb and atheroprotection still need more investigation. A number of putative, and non-mutually exclusive, mechanisms have been proposed based on experimental observations. These include binding and recognition of oxidized lipid adducts on the surface of apoptotic cells, thereby promoting plaque macrophage- and/or dendritic cell-mediated recognition of dead/dying cell debris (43), potentially in a process dependent on the complement component, C1q (82). Others have demonstrated a role for oxLDL-reactive NAb-mediated inhibition of endothelial cell (EC) activation and IL-8 (CXCL8) secretion in response to stimulation by dying cells (83). EC expression of CD36 has emerged as a potential target in vascular disease due to its ability to mediate pro-inflammatory activation, and immune cell recruitment (84, 85). It is likely that endothelial CD36 is involved in the ameliorative effects of NAbs in atherogenesis. One report indicates that oxLDL-NAbs restrain atherogenesis in the absence of altered plaque apoptotic cell clearance (34). Thus, it is highly likely that NAbs have additional functions in ASCVD that remain to be defined.

iAAbs MAY PROMOTE ATHEROSCLEROSIS

The most prevalent antibody isotype in human serum is adaptive/induced IgG produced by B-2 cells. Within the context of CVD, iAAbs of the IgG isotype have been studied extensively (24). Like atherosclerosis-associated NAb produced during homeostatic conditions, iAAbs produced in the setting of inflammation and/or infection also play a role in atherogenesis. The specific functions of iAAbs are much less clear, due partly to contradictory conclusions within the literature. Unlike homeostatically produced NAb, production of iAAbs requires the concerted interaction of multiple cell types (namely B- and T-lymphocytes and antigen presenting cells) and inflammatory signals (cytokines) to transform a naive B cell into a class-switched, somatically hypermutated, and antibody-secreting plasma cell.

By contrast to the relative breadth of data demonstrating an atheroprotective role for B-1 cell-derived NAb, the role for B-2 cell-derived iAAb in atherosclerotic disease remains unresolved. Early studies of B cells in ASCVD initially implicated a disease-restraining role for B-2 cells: splenectomized *Apoe*$^{-/-}$ mice displayed an exaggerated atherosclerotic phenotype that could be rescued through adoptive transfer of splenocytes (86). In agreement with these observations, it was also shown that atherogenesis was amplified in *Ldlr*$^{-/-}$ mice reconstituted with BM from B cell-deficient animals (*Ighm*$^{-/-}$, encoding μMT), relative to those reconstituted with B cell-replete, wild-type BM (87). In contradiction to the disease-restraining role for B-2 cells suggested by these studies, it was later shown that systemic B-2 cell depletion with anti-CD20 mAb in either *Apoe*$^{-/-}$ or *Ldlr*$^{-/-}$ mice significantly reduced atherosclerotic lesion formation (88, 89). While multiple explanations could explain these disparate observations, including differences in housing conditions and microbiota (90), contradictory conclusions exist and are in need of further study. It is important to acknowledge the phenotypic and functional diversity of B-2 cells, which include marginal zone, follicular, and regulatory B cell (B_{regs}) subsets (91). Clarification of the disparate observations highlighted above will likely involve determining the discrete roles each of these B-2 cell subsets plays during the natural history of ASCVD.

Similar to B-1 cell-derived NAb, iAAbs reactive to OSE have been reported in both human atherosclerosis and animal models of it (92–95). Demonstration of a clear correlation between serum OSE-reactive IgG and disease severity in humans has been challenging; while some studies have shown weak positive correlations, and others have shown none. In experimental murine atherosclerosis, OSE-reactive IgG titers correlate with plaque burden, increasing during plaque growth and decreasing during plaque regression (94). This correlative observation says little about the specific role for OSE-reactive IgG AAbs throughout the disease course, however. While many experimental observations have demonstrated a pro-atherogenic role for OSE-reactive IgG AAbs, their functional roles in ASCVD are far from resolved.

In addition, strategies investigating vaccination for generating adaptive antibody responses to ASCVD-associated epitopes have also shown observations that conflict with the putative disease-promoting role for iAAbs in ASCVD (49, 57). Repeated immunization of *Ldlr*$^{-/-}$ mice with MDA-adducted LDL (MDA-LDL) or native LDL over a period of 7 weeks followed by atherogenesis induction using a high-fat diet demonstrated a significant reduction in atherosclerotic lesion formation in both cases (49). While less dramatic in the setting of native LDL immunization, both immunization strategies significantly reduced lesion formation relative to saline-injected control animals. Significantly elevated titers of isotype-switched Ab with specificity to oxidized lipid products were only observed in the setting of MDA-LDL immunization. Both type 1 inflammation-polarized CD4+ helper T lymphocyte- and type 2 inflammation-polarized CD4+ helper T lymphocyte-associated antibody titers (IgG2a and IgG1, respectively) were increased in this setting, and were inversely correlated lesion development. Thus, these observations complicate assigning an ASCVD-promoting role for iAAbs.

In addition to OSEs, HSP-60 is an autoantigen that has been of interest to the atherosclerosis field. In the setting of atherosclerotic inflammation, endothelial cells upregulate expression of HSP-60 which displays structural similarity (i.e., molecular mimicry) with HSP-65 from *Mycobacterium* and *Chlamydia spp*. (13). In the context of before exposure or infection, the existence of an anti-HSP-65 antibody response provides a mechanism for induction of autoimmunity in the setting of atherosclerotic inflammation leading to upregulation of endothelial HSP-60. In support

of a pro-inflammatory role for HSP-65 AAbs in atherogenesis, induction of arterial inflammation in normocholesterolemic rabbits was observed following immunization with HSP-65 without alterations in serum cholesterol (96). In addition, *Ldlr*$^{-/-}$ mice on regular chow developed atherosclerotic lesions following intraperitoneal injections of anti-HSP-65-IgG (97). While one epidemiological study in humans demonstrated HSP-65-reactive IgG titers correlated with atherosclerosis severity (as measured by carotid IMT) (98), and another demonstrated no correlation (99). Further exploration is needed to clarify these disparate observations.

Antibodies against apolipoprotein A-1 (ApoA1), a main protein constituent of HDL, were initially observed in patients with systemic inflammatory diseases such as right atrium (RA) (100). While HDL levels are commonly thought of as being atheroprotective, induced IgG antibody responses to immunogenic products of ApoA1 degradation have demonstrated positive correlations with atherogenesis. HDL promotes lipid clearance and disposal through reverse cholesterol transport. Whether anti-ApoA1 Ab interfere with this process has not been determined. It was shown in patients with RA that circulating ApoA1-reactive IgG antibody titers are superior predictors of major cardiac events relative to more than 15 biomarkers tested in the study including serum HDL, LDL, triglycerides, and CRP (101). Using patient studies, it has been hypothesized that anti-ApoA1 IgG promotes inflammatory activation through stimulation of a toll-like receptor 2-TLR4-NFκB signaling axis in innate immune cell populations (102). Later, it was observed in humans that resting heart rate (a prognostic marker used in assessing patients following MI) was inversely correlated with anti-ApoA1 IgG titers. Expanding on these observations, when rat cardiomyocytes were cultured in the presence of aldosterone with or without anti-ApoA1 IgG Ab, and spontaneous contraction was shown to decrease in an anti-ApoA1 IgG dose-dependent fashion (103). While additional studies are necessary to dissect the mechanisms that underlie these observations, anti-ApoA1 IgG AAbs also appear to be a potential therapeutic target in ASCVD treatment.

A hallmark of late-stage atherosclerotic disease in humans and experimental atherosclerosis is the development of arterial tertiary lymphoid organs (ATLOs) in the adventitia at the sites of plaque formation (104–106). An attractive hypothesis to explain their genesis rests on a compensatory response to chronic inflammatory stimulation. The definitive functional role of ATLOs in the context of atherosclerotic disease has long eluded the CV research community. Recently, multiple studies have attempted to address this. Using *Apoe*$^{-/-}$ mice on a Western diet, the authors elegantly demonstrate that ATLO contain a T-follicular-helper (T_{FH})-GC B cell-axis that that governs lesion formation and promotes exacerbated disease. The authors additionally demonstrated the ATLO T_{FH}-GC B cell-axis is restrained through $CD8^+$ regulatory T cells that are restricted to the non-classical major histocompatibility complex Qa-1 [the mouse ortholog of human leukocyte antigen-E] (105). Another study from the same year reached the opposite conclusion about the function of ATLO in *Apoe*$^{-/-}$ mice (106). Therein, the authors concluded that ATLO formation restrains atherosclerosis; disruption of ATLO formation through conditional deletion of the lymphotoxin-β receptor in vSMCs exacerbated lesion formation (106). The humoral consequences of disrupting ATLO formation were beyond the scope of the study in question. Nonetheless, the opposing conclusions reached by these two studies are in need of further clarification. Resolving the role of ATLO in ASCVD will contribute to the understanding of humoral immunity and AAbs in this context.

MYOCARDITIS AND DCM: THE ROLE OF AAbs

Myocarditis is inflammation of the myocardium and its most common sequela is DCM (107). DCM is the most common cause of heart failure in children and young adults, and it is thought that as many as one in three cases of myocarditis progress to DCM (108). While not all cases of myocarditis result in DCM and while not all cases of DCM are the result of myocarditis, there exists a clear link between the two disease manifestations in a significant proportion of cases. Due to this connection, substantial research emphasis has been placed on understanding DCM immunopathogenesis and how it progresses from myocarditis. It is currently believed that autoimmune-mediated DCM represents the major subtype of the disease (109) with emerging evidence that type 3 inflammatory signals [i.e., those mediating $CD4^+$ T-helper (T_H) polarization toward a T_H17 phenotype] play a critical role in its pathogenesis (110–114).

Clinical studies have associated multiple AAbs with myocarditis and DCM. This topic has been reviewed in extensive detail elsewhere (115). IgG AAbs directed against the β1-adrenergic receptor (β1AR) were detected in the sera of DCM patients and shown to inhibit catecholamine binding when cultured with rat cardiomyocytes *in vitro*, whereas sera from patients with ischemic CM, VHD, and healthy controls demonstrated no effect (116). A later study using a synthetic peptide derived from an extracellular domain of β1AR demonstrated elevated anti-β1AR AAbs in the sera of DCM patients relative to controls (31 versus 12%, respectively) (117). Interestingly, anti-β1AR AAbs were also detectable in the healthy control group, demonstrating that the mere presence of anti-β1AR is not predictive of pathology. When Japanese white rabbits were immunized with a synthetic peptide corresponding to an extracellular domain of the β1AR, induction of anti-β1AR IgG production was observed (118). Purified anti-β1AR IgG from these animals inhibited catecholamine responsiveness when cultured on rabbit cardiomyocytes. At 6-months post-immunization, cardiac hypertrophy and abnormal hemodynamics were seen. Additional analyses indicated evidence of anti-β1AR AAb-mediated adrenergic overstimulation leading to compensatory downregulation of β1AR expression, and concomitant upregulation of proteins that inhibit β-adrenergic signaling, thus laying the groundwork for a disease-exacerbating positive feedback loop. An additional study in a limited patient population demonstrated that a significant proportion (36%) of DCM patients with circulating anti-β1AR IgG also exhibited elevated anti-M2-muscarinic receptor (M2AChR) IgG AAbs (119). Relative to serum samples from control patients, anti-M2AChR IgG AAbs were significantly elevated in the context of DCM (39% in DCM versus 8% in

controls) (119). In the myocardium, muscarinic and adrenergic signaling exert opposing effects, with muscarinic signaling exhibiting negative inotropic and chronotropic effects and adrenergic signaling doing the opposite. Overstimulation and desensitization of each pathway have been postulated as a functional consequence of circulating anti-M2AChR and anti-β1AR AAbs, ultimately leading to heart failure (118, 120). Additional studies confirming these hypotheses are needed, however. Additional cardiac-related autoantigens with established AAb reactivity in human DCM include cTnI (11, 121–123), mitochondrial M7 (124), adenine-nucleotide transporter (ANT) (125), Na-K ATPase (126), actin (127), acetylcholine receptor (128), α/β Myosin heavy chain (129, 130), myosin light chain-1 (127), HSP-60 (131), sarcoplasmic reticulum Ca^{2+}-ATPase (SR-Ca^{2+}-ATPase) (132), laminin (133), and tropomyosin (127). A summary of the most studied antigens observed in myocarditis and cardiomyopathy can be found in **Table 2**. The primary mechanism by which AAbs exacerbate disease in DCM remains unknown, however, and alternative explanations exist to explain their roles that include to target neutralization and adaptation to persistent stimulation.

Again, underscoring the inflammatory nature of this DCM, as many as one out of three cases of myocarditis ultimately progresses to DCM. The concept of molecular mimicry is central to the understanding of autoimmune responses to cardiac antigens and multiple infectious agents have been identified with elements bearing epitope similarity to them (134). Known infectious causes of human myocarditis that exhibit molecular mimicry of cardiac antigens include *Trypanosoma cruzi* (135), parvovirus B19 (136), coxsackievirus (15), and *Borrelia* spp. (137). In each case, cardiac myosin appears to contain dominant epitopes bearing structural similarity to pathogen-derived antigens.

Rheumatic heart disease (RHD) provides a prototypical example of molecular mimicry in CM. In RHD, untreated and repeated infections with *Streptococcus pyogenes* [group A strep (GAS)] may lead to acute rheumatic fever characterized by a constellation of symptoms resembling many rheumatic conditions including polyarthritis, in addition to carditis (138). RF progresses to chronic RHD in as many as 50% of patients (139). Cross-reactivity between GAS and components of cardiac proteins is currently accepted as a key driver of RHD (140). Determination that M proteins (one of the major virulence factors expressed by GAS) exhibit structural similarity with cardiac myosin provided critical insight into the nature of RHD (141). Since, it has been shown that components of GAS [including its carbohydrate antigen and *N*-acetyl-β-D-glucosamine (GlcNAc) (142, 143)] display molecular mimicry with additional cardiac antigens, such as laminin (144), tropomyosin (145), the endothelium (146–148), and others, including those restricted to the cardiac valves (144). Generation of adaptive Ab responses to infections with cross-reactivity to cardiac antigens is a critical element of post-infectious myocarditis and its common sequela DCM.

Much of the understanding of infectious myocarditis and DCM has been garnered from animal models of experimental autoimmune myocarditis (EAM). Inflammatory HD with many histologic features of RHD (including pan-carditis, granulomatous lesion formation, the presence of Anitschkow cells, and late-stage valvular scarring) was accomplished by immunizing mice *via* intraperitoneal injections of a sonicated preparation of GAS (149). Refining the experimental approach, the Cunningham group developed a rat model of RF/RHD based on immunization of Lewis rats with purified M protein (150–152). In addition to myocardial inflammation, cardiac valve pathology was also observed in these studies. In addition, identification of $CD4^+$ T cells with M protein cross-reactivity lent further insight into mechanisms by which infection may induce an adaptive AAb response *via* the support of $CD4^+$ T cell help. The specific cellular and molecular mechanisms by which cardiac-reactive AAbs mediate tissue destruction in these model systems (and in human RHD) remain unclear, however. Future investigation of EAM models that utilize conditional and constitutive gene deletion will be useful for mechanistic studies and clarification of these observations.

Multiple viruses (enteroviruses, most commonly) have been established as causative agents of myocarditis/DCM. The most well-studied of these is coxsackievirus B3 (CVB3), a cytolytic enterovirus with cardiotropism (153). The presence of detectable enteroviral genomic material and enteroviral-reactive Ab has been observed in as many as 70% of DCM patients (15). In CVB-induced EAM, it has long been known that anti-cardiac myosin AAbs are generated during the disease course and that cardiac myosin-reactive AAb titers correlate with myocarditis severity (154). It is unclear what functional role anti-cardiac myosin AAbs play during the course of viral myocarditis/DCM; a lack of cross-reactivity between cardiac myosin-reactive AAbs and CVB3 was reported, thus contradicting the mimicry hypothesis as a driver of CVB3-myocarditis/DCM (155). It has been postulated that, rather than participating as active promoters of enteroviral-induced cardiac damage, AAbs generated during CVB3 infection are bystanders in the disease process, with their titers reflecting the degree of tissue damage (153). CVB3 has also been shown

TABLE 2 | Summary of the most commonly studied cardiac-related autoantibodies in myocarditis and cardiomyopathy.

Antigen	Proposed pathological mechanism	References
Acetylcholine receptor	Negative inotropy and bradycardia	(128)
Actin	Undefined	(127)
Adenine-nucleotide transporter	Metabolism inhibition	(125)
β1-adrenergic-R	Negative inotropy	(116, 117)
Heat-shock protein-60	Increased recognition clearance of stressed cardiomyocytes	(127, 131)
Laminin	Undefined	(133)
M2 muscarinic AChR	Negative inotropy	(119, 120)
Mitochondrial M7	Undefined	(124)
α/β Myosin heavy chain	Negative inotropy and failure of thymic self-tolerance	(129, 130)
Myosin light chain-1	Undefined	(127)
Na-K ATPase	Arrhythmogenicity	(126)
Sarcoplasmic reticulum-Ca-ATPase	Metabolism alterations	(132)
Tropomyosin	Undefined	(127)
Troponin	Negative inotropy	(11, 121–123)

to share moderate sequence homology to mitochondrial ANT, a postulated alternative target of molecular mimicry during CVB3-induced EAM (156). In a limited cohort, anti-ANT AAbs were observed in 94% of DCM patients (125). Additional work is needed to determine whether this represents a clinically relevant antigen for AAb targeting in viral myocarditis/DCM.

Spontaneous endocarditis and valvular carditis occur with complete penetrance in the T cell receptor (TCR) transgenic K/B.g7 mouse line (also referred to as K/BxN in some studies), without immunization or infection (157). Thus, this model provides a useful tool for dissecting the cellular and molecular mechanisms that underpin cardiac pathology in the setting of sterile systemic inflammation. K/B.g7 mice exhibit expression of a transgenic TCR termed "KRN" that recognizes a peptide derived from the self-protein glucose-6-phosphate-isomerase (GPI, a ubiquitous metabolic enzyme) presented in the context of the I-A^{g7} major histocompatibility complex II molecule from the non-obese-diabetic mouse strain (158–160). Systemic GPI-specific T cell activation leads to production of high-titer anti-GPI IgG AAbs. K/B.g7 mice develop erosive polyarthritis, endocarditis, and fibrotic valvular carditis with a left-sided predilection, primarily affecting the mitral valve (MV) (157, 161). It was demonstrated that macrophages are the key cellular mediators of valve pathology in K/B.g7 mice; animals treated systemically with macrophage-depleting clodronate liposomes were protected from MV disease (MVD) (161). Using constitutive gene deletion approaches, our group demonstrated that activating IgG receptors (FcγRs), specifically FcγRIII (CD16) and FcγRIV (CD16.2), act redundantly and are required for MVD; protection from disease occurs only in the absence of both (161). These results support a model whereby circulating IgG AAbs mediate cardiac inflammation through macrophage activation downstream of activating FcγR-mediated recognition of circulating IgG AAbs. Additional studies employing conditional gene deletions to dissect the key functional consequences induced in macrophages following IgG AAb recognition have provided important insight into mechanisms by which AAbs contribute to experimental VHD (162). Samples from patients with RHD were used to demonstrate correlations of the authors' experimental observations to human inflammatory VHD.

FUTURE DIRECTIONS

Mechanistic insight is needed to better understand the role for AAbs in CV pathology. Studies pursuing mechanistic rather than descriptive and/or correlative insight will be critical for rectification of the seemingly conflicting observations, and conclusions that have been seen and reached. Identification of therapeutically targetable elements of AAb generation in CVD will require cellular and molecular mechanistic insight. Gene deletion approaches, both constitutive and conditional, for experimental dissection of the pathways by which AAbs function in the heterogeneous manifestations of CVD will likely prove useful to this field. Significant questions that remain unanswered include: what determines the quality (i.e., isotype and affinity) and quantity (i.e., circulating titers) of an Ab response in the setting of CV inflammation, and how do these antibody responses engage additional immune cells to restrain or promote CV immunopathology. Finally, how does the interplay between CVD-associated Ab and the discrete inflammatory lineages with which they engage ultimately interface with the underlying tissue parenchyma (e.g., myocardium and blood vessel wall) to promote or restrain detrimental CV remodeling (e.g., plaque formation and fibrosis). Employing lineage-specific gene deletion approaches (e.g., Cre-loxP recombination) will undoubtedly prove illuminating. Finally, progress within this field will be well served by demonstrating clinical relevance through correlation of experimental observations to human disease. In addition to their rarity, samples from human disease states are often logistically complicated to acquire. Despite this, the potential insight that can be gained from correlations between experimental disease models and human pathology cannot be underscored. Future progress in this field will ultimately be made through clinical translation. Thus, complementing mechanistic work in experimental models with observations in inflammatory human CV pathology will be critical.

CONCLUSION

There is substantial evidence for the disease-modulating role that AAbs have in CVD. Despite the breadth of evidence, there is little consensus regarding the specific functions that AAbs have in the various forms of CVD in which they are implicated, and numerous conflicting observations and hypotheses have been reported. A large majority of studies have been observational or correlative, rather than mechanistic, and therefore have not translated into therapeutic strategies for human CVD. The field now needs to focus on how these AAbs engage particular molecular and cellular immune components to influence disease severity; the insights provided by this approach will point the way to new therapeutic options.

AUTHOR CONTRIBUTIONS

LM and BB determined the scope of this review, wrote the manuscript, and revised the manuscript. LM generated the figures and tables.

FUNDING

The following funding sources supported this work: NIH (R01-HL121093, T32-AI007313, T32-GM008244).

REFERENCES

1. Mozaffarian D, Benjamin EJ, Go AS, Arnett DK, Blaha MJ, Cushman M, et al. Heart disease and stroke statistics – 2015 update: a report from the American heart association. *Circulation* (2015) 131(4):e29–322. doi:10.1161/cir.0000000000000152
2. Lozano R, Naghavi M, Foreman K, Lim S, Shibuya K, Aboyans V, et al. Global and regional mortality from 235 causes of death for 20 age groups in 1990 and 2010: a systematic analysis for the global burden of disease study 2010. *Lancet* (2012) 380(9859):2095–128. doi:10.1016/S0140-6736(12)61728-0
3. Viola J, Soehnlein O. Atherosclerosis – a matter of unresolved inflammation. *Semin Immunol* (2015) 27(3):184–93. doi:10.1016/j.smim.2015.03.013

4. Ridker PM, Everett BM, Thuren T, MacFadyen JG, Chang WH, Ballantyne C, et al. Antiinflammatory therapy with canakinumab for atherosclerotic disease. *N Engl J Med* (2017) 377(12):1119–31. doi:10.1056/NEJMoa1707914
5. Sparks JA, Barbhaiya M, Karlson EW, Ritter SY, Raychaudhuri S, Corrigan CC, et al. Investigating methotrexate toxicity within a randomized double-blinded, placebo-controlled trial: rationale and design of the cardiovascular inflammation reduction trial-adverse events (CIRT-AE) study. *Semin Arthritis Rheum* (2017) 47(1):133–42. doi:10.1016/j.semarthrit.2017.02.003
6. ClinicalTrials.gov [Internet]. *Colchicine Cardiovascular Outcomes Trial (COLCOT)*. NCT02551094. Bethesda, MD: National Library of Medicine (US) (2000). [cited 2018 April 15]. Available from: https://clinicaltrials.gov/ct2/show/study/NCT02551094
7. Madrigal-Matute J, Martin-Ventura JL, Blanco-Colio LM, Egido J, Michel JB, Meilhac O. Heat-shock proteins in cardiovascular disease. *Adv Clin Chem* (2011) 54:1–43. doi:10.1016/B978-0-12-387025-4.00001-7
8. Nussinovitch U, Shoenfeld Y. The diagnostic and clinical significance of anti-muscarinic receptor autoantibodies. *Clin Rev Allergy Immunol* (2012) 42(3):298–308. doi:10.1007/s12016-010-8235-x
9. Nussinovitch U, Shoenfeld Y. The clinical significance of anti-beta-1 adrenergic receptor autoantibodies in cardiac disease. *Clin Rev Allergy Immunol* (2013) 44(1):75–83. doi:10.1007/s12016-010-8228-9
10. Nussinovitch U, Shoenfeld Y. The clinical and diagnostic significance of anti-myosin autoantibodies in cardiac disease. *Clin Rev Allergy Immunol* (2013) 44(1):98–108. doi:10.1007/s12016-010-8229-8
11. Leuschner F, Li J, Goser S, Reinhardt L, Ottl R, Bride P, et al. Absence of auto-antibodies against cardiac troponin I predicts improvement of left ventricular function after acute myocardial infarction. *Eur Heart J* (2008) 29(16):1949–55. doi:10.1093/eurheartj/ehn268
12. Karthikeyan G, Teo KK, Islam S, McQueen MJ, Pais P, Wang X, et al. Lipid profile, plasma apolipoproteins, and risk of a first myocardial infarction among Asians: an analysis from the interheart study. *J Am Coll Cardiol* (2009) 53(3):244–53. doi:10.1016/j.jacc.2008.09.041
13. Heltai K, Kis Z, Burian K, Endresz V, Veres A, Ludwig E, et al. Elevated antibody levels against *Chlamydia pneumoniae*, human HSP60 and mycobacterial HSP65 are independent risk factors in myocardial infarction and ischaemic heart disease. *Atherosclerosis* (2004) 173(2):339–46. doi:10.1016/j.atherosclerosis.2003.12.026
14. Rosenblum MD, Remedios KA, Abbas AK. Mechanisms of human autoimmunity. *J Clin Invest* (2015) 125(6):2228–33. doi:10.1172/JCI78088
15. Gangaplara A, Massilamany C, Brown DM, Delhon G, Pattnaik AK, Chapman N, et al. Coxsackievirus B3 infection leads to the generation of cardiac myosin heavy chain-alpha-reactive CD4 T cells in a/j mice. *Clin Immunol* (2012) 144(3):237–49. doi:10.1016/j.clim.2012.07.003
16. Fairweather D, Rose NR. Coxsackievirus-induced myocarditis in mice: a model of autoimmune disease for studying immunotoxicity. *Methods* (2007) 41(1):118–22. doi:10.1016/j.ymeth.2006.07.009
17. Paigen B, Holmes PA, Mitchell D, Albee D. Comparison of atherosclerotic lesions and HDL-lipid levels in male, female, and testosterone-treated female mice from strains C57bl/6, BALB/c, and C3H. *Atherosclerosis* (1987) 64(2–3):215–21. doi:10.1016/0021-9150(87)90249-8
18. Bogdanos DP, Smyk DS, Rigopoulou EI, Mytilinaiou MG, Heneghan MA, Selmi C, et al. Twin studies in autoimmune disease: genetics, gender and environment. *J Autoimmun* (2012) 38(2–3):J156–69. doi:10.1016/j.jaut.2011.11.003
19. Caforio AL, Mahon NG, Baig MK, Tona F, Murphy RT, Elliott PM, et al. Prospective familial assessment in dilated cardiomyopathy: cardiac autoantibodies predict disease development in asymptomatic relatives. *Circulation* (2007) 115(1):76–83. doi:10.1161/CIRCULATIONAHA.106.641472
20. Chou MY, Fogelstrand L, Hartvigsen K, Hansen LF, Woelkers D, Shaw PX, et al. Oxidation-specific epitopes are dominant targets of innate natural antibodies in mice and humans. *J Clin Invest* (2009) 119(5):1335–49. doi:10.1172/jci36800
21. Prasad M, Hermann J, Gabriel SE, Weyand CM, Mulvagh S, Mankad R, et al. Cardiorheumatology: cardiac involvement in systemic rheumatic disease. *Nat Rev Cardiol* (2015) 12(3):168–76. doi:10.1038/nrcardio.2014.206
22. Kumar V, Abbas AK, Aster JC, Cotran RS, Robbins SL. *Robbins and Cotran Pathologic Basis of Disease*. Philadelphia, PA: Elsevier (2015).
23. Getz GS, Reardon CA. Animal models of atherosclerosis. *Arterioscler Thromb Vasc Biol* (2012) 32(5):1104–15. doi:10.1161/ATVBAHA.111.237693
24. Kyaw T, Tipping P, Bobik A, Toh BH. Opposing roles of B lymphocyte subsets in atherosclerosis. *Autoimmunity* (2017) 50(1):52–6. doi:10.1080/08916934.2017.1280669
25. Huan T, Zhang B, Wang Z, Joehanes R, Zhu J, Johnson AD, et al. A systems biology framework identifies molecular underpinnings of coronary heart disease. *Arterioscler Thromb Vasc Biol* (2013) 33(6):1427–34. doi:10.1161/ATVBAHA.112.300112
26. Tsiantoulas D, Diehl CJ, Witztum JL, Binder CJ. B cells and humoral immunity in atherosclerosis. *Circ Res* (2014) 114(11):1743–56. doi:10.1161/CIRCRESAHA.113.301145
27. Stall AM, Adams S, Herzenberg LA, Kantor AB. Characteristics and development of the murine B-1b (ly-1 B sister) cell population. *Ann N Y Acad Sci* (1992) 651:33–43. doi:10.1111/j.1749-6632.1992.tb24591.x
28. Griffin DO, Holodick NE, Rothstein TL. Human B1 cells in umbilical cord and adult peripheral blood express the novel phenotype CD20+ CD27+ CD43+ CD70. *J Exp Med* (2011) 208(1):67–80. doi:10.1084/jem.20101499
29. Lee J, Kuchen S, Fischer R, Chang S, Lipsky PE. Identification and characterization of a human CD5+ pre-naive B cell population. *J Immunol* (2009) 182(7):4116–26. doi:10.4049/jimmunol.0803391
30. Tornberg UC, Holmberg D. B-1a, B-1b and B-2 B cells display unique VHDJH repertoires formed at different stages of ontogeny and under different selection pressures. *EMBO J* (1995) 14(8):1680–9.
31. Holodick NE, Rodriguez-Zhurbenko N, Hernandez AM. Defining natural antibodies. *Front Immunol* (2017) 8:872. doi:10.3389/fimmu.2017.00872
32. Binder CJ, Hartvigsen K, Chang MK, Miller M, Broide D, Palinski W, et al. IL-5 links adaptive and natural immunity specific for epitopes of oxidized LDL and protects from atherosclerosis. *J Clin Invest* (2004) 114(3):427–37. doi:10.1172/JCI20479
33. Perry HM, Oldham SN, Fahl SP, Que X, Gonen A, Harmon DB, et al. Helix-loop-helix factor inhibitor of differentiation 3 regulates interleukin-5 expression and B-1a B cell proliferation. *Arterioscler Thromb Vasc Biol* (2013) 33(12):2771–9. doi:10.1161/ATVBAHA.113.302571
34. Kyaw T, Tay C, Krishnamurthi S, Kanellakis P, Agrotis A, Tipping P, et al. B1a B lymphocytes are atheroprotective by secreting natural IgM that increases IgM deposits and reduces necrotic cores in atherosclerotic lesions. *Circ Res* (2011) 109(8):830–40. doi:10.1161/CIRCRESAHA.111.248542
35. Karvonen J, Paivansalo M, Kesaniemi YA, Horkko S. Immunoglobulin M type of autoantibodies to oxidized low-density lipoprotein has an inverse relation to carotid artery atherosclerosis. *Circulation* (2003) 108(17):2107–12. doi:10.1161/01.CIR.0000092891.55157.A7
36. Casali P, Notkins AL. CD5+ B lymphocytes, polyreactive antibodies and the human B-cell repertoire. *Immunol Today* (1989) 10(11):364–8. doi:10.1016/0167-5699(89)90268-5
37. Baumgarth N, Herman OC, Jager GC, Brown L, Herzenberg LA, Herzenberg LA. Innate and acquired humoral immunities to influenza virus are mediated by distinct arms of the immune system. *Proc Natl Acad Sci U S A* (1999) 96(5):2250–5. doi:10.1073/pnas.96.5.2250
38. Rose NR. The concept of immunodiagnosis. 3rd ed. In: Gershwin YSLME, editor. *Autoantibodies*. (Chap. 1), San Diego: Elsevier (2014). p. 3–10.
39. McCoy KD, Harris NL, Diener P, Hatak S, Odermatt B, Hangartner L, et al. Natural IgE production in the absence of MHC class II cognate help. *Immunity* (2006) 24(3):329–39. doi:10.1016/j.immuni.2006.01.013
40. Erickson LD, Foy TM, Waldschmidt TJ. Murine B1 B cells require IL-5 for optimal T cell-dependent activation. *J Immunol* (2001) 166(3):1531–9. doi:10.4049/jimmunol.166.3.1531
41. Horikawa K, Takatsu K. Interleukin-5 regulates genes involved in B-cell terminal maturation. *Immunology* (2006) 118(4):497–508. doi:10.1111/j.1365-2567.2006.02382.x
42. Consortium IKC. Large-scale gene-centric analysis identifies novel variants for coronary artery disease. *PLoS Genet* (2011) 7(9):e1002260. doi:10.1371/journal.pgen.1002260
43. Chang MK, Bergmark C, Laurila A, Horkko S, Han KH, Friedman P, et al. Monoclonal antibodies against oxidized low-density lipoprotein bind to apoptotic cells and inhibit their phagocytosis by elicited macrophages: evidence that oxidation-specific epitopes mediate macrophage recognition. *Proc Natl Acad Sci U S A* (1999) 96(11):6353–8. doi:10.1073/pnas.96.11.6353
44. Palinski W, Horkko S, Miller E, Steinbrecher UP, Powell HC, Curtiss LK, et al. Cloning of monoclonal autoantibodies to epitopes of oxidized lipoproteins

from apolipoprotein E-deficient mice. Demonstration of epitopes of oxidized low density lipoprotein in human plasma. *J Clin Invest* (1996) 98(3):800–14. doi:10.1172/JCI118853
45. Shaw PX, Horkko S, Tsimikas S, Chang MK, Palinski W, Silverman GJ, et al. Human-derived anti-oxidized LDL autoantibody blocks uptake of oxidized LDL by macrophages and localizes to atherosclerotic lesions *in vivo*. *Arterioscler Thromb Vasc Biol* (2001) 21(8):1333–9. doi:10.1161/hq0801.093587
46. Frostegard J, Tao W, Georgiades A, Rastam L, Lindblad U, Lindeberg S. Atheroprotective natural anti-phosphorylcholine antibodies of IgM subclass are decreased in Swedish controls as compared to non-westernized individuals from New Guinea. *Nutr Metab (Lond)* (2007) 4:7. doi:10.1186/1743-7075-4-7
47. Mayr M, Kiechl S, Tsimikas S, Miller E, Sheldon J, Willeit J, et al. Oxidized low-density lipoprotein autoantibodies, chronic infections, and carotid atherosclerosis in a population-based study. *J Am Coll Cardiol* (2006) 47(12):2436–43. doi:10.1016/j.jacc.2006.03.024
48. Tsimikas S, Brilakis ES, Lennon RJ, Miller ER, Witztum JL, McConnell JP, et al. Relationship of IgG and IgM autoantibodies to oxidized low density lipoprotein with coronary artery disease and cardiovascular events. *J Lipid Res* (2007) 48(2):425–33. doi:10.1194/jlr.M600361-JLR200
49. Freigang S, Horkko S, Miller E, Witztum JL, Palinski W. Immunization of LDL receptor-deficient mice with homologous malondialdehyde-modified and native LDL reduces progression of atherosclerosis by mechanisms other than induction of high titers of antibodies to oxidative neoepitopes. *Arterioscler Thromb Vasc Biol* (1998) 18(12):1972–82. doi:10.1161/01.ATV.18.12.1972
50. Palinski W, Tangirala RK, Miller E, Young SG, Witztum JL. Increased autoantibody titers against epitopes of oxidized LDL in LDL receptor-deficient mice with increased atherosclerosis. *Arterioscler Thromb Vasc Biol* (1995) 15(10):1569–76. doi:10.1161/01.ATV.15.10.1569
51. Palinski W, Rosenfeld ME, Yla-Herttuala S, Gurtner GC, Socher SS, Butler SW, et al. Low density lipoprotein undergoes oxidative modification *in vivo*. *Proc Natl Acad Sci U S A* (1989) 86(4):1372–6. doi:10.1073/pnas.86.4.1372
52. Horkko S, Miller E, Dudl E, Reaven P, Curtiss LK, Zvaifler NJ, et al. Antiphospholipid antibodies are directed against epitopes of oxidized phospholipids. Recognition of cardiolipin by monoclonal antibodies to epitopes of oxidized low density lipoprotein. *J Clin Invest* (1996) 98(3):815–25. doi:10.1172/JCI118854
53. Weismann D, Binder CJ. The innate immune response to products of phospholipid peroxidation. *Biochim Biophys Acta* (2012) 1818(10):2465–75. doi:10.1016/j.bbamem.2012.01.018
54. Steinbrecher UP, Parthasarathy S, Leake DS, Witztum JL, Steinberg D. Modification of low density lipoprotein by endothelial cells involves lipid peroxidation and degradation of low density lipoprotein phospholipids. *Proc Natl Acad Sci U S A* (1984) 81(12):3883–7. doi:10.1073/pnas.81.12.3883
55. Virella G, Koskinen S, Krings G, Onorato JM, Thorpe SR, Lopes-Virella M. Immunochemical characterization of purified human oxidized low-density lipoprotein antibodies. *Clin Immunol* (2000) 95(2):135–44. doi:10.1006/clim.2000.4857
56. Lopes-Virella MF, Koskinen S, Mironova M, Horne D, Klein R, Chassereau C, et al. The preparation of copper-oxidized LDL for the measurement of oxidized LDL antibodies by EIA. *Atherosclerosis* (2000) 152(1):107–15. doi:10.1016/S0021-9150(99)00456-6
57. Ameli S, Hultgardh-Nilsson A, Regnstrom J, Calara F, Yano J, Cercek B, et al. Effect of immunization with homologous LDL and oxidized LDL on early atherosclerosis in hypercholesterolemic rabbits. *Arterioscler Thromb Vasc Biol* (1996) 16(8):1074–9. doi:10.1161/01.ATV.16.8.1074
58. Steinbrecher UP, Pritchard PH. Hydrolysis of phosphatidylcholine during LDL oxidation is mediated by platelet-activating factor acetylhydrolase. *J Lipid Res* (1989) 30(3):305–15.
59. Frostegard J, Nilsson J, Haegerstrand A, Hamsten A, Wigzell H, Gidlund M. Oxidized low density lipoprotein induces differentiation and adhesion of human monocytes and the monocytic cell line U937. *Proc Natl Acad Sci U S A* (1990) 87(3):904–8. doi:10.1073/pnas.87.3.904
60. Frostegard J, Wu R, Giscombe R, Holm G, Lefvert AK, Nilsson J. Induction of T-cell activation by oxidized low density lipoprotein. *Arterioscler Thromb* (1992) 12(4):461–7. doi:10.1161/01.ATV.12.4.461
61. Stemme S, Faber B, Holm J, Wiklund O, Witztum JL, Hansson GK. T lymphocytes from human atherosclerotic plaques recognize oxidized low density lipoprotein. *Proc Natl Acad Sci U S A* (1995) 92(9):3893–7. doi:10.1073/pnas.92.9.3893
62. Ragab MS, Selvaraj P, Sgoutas DS. Oxidized lipoprotein (a) induces cell adhesion molecule Mac-1 (CD 11b) and enhances adhesion of the monocytic cell line U937 to cultured endothelial cells. *Atherosclerosis* (1996) 123(1–2):103–13. doi:10.1016/0021-9150(95)05790-0
63. Wu R, Giscombe R, Holm G, Lefvert AK. Induction of human cytotoxic T lymphocytes by oxidized low density lipoproteins. *Scand J Immunol* (1996) 43(4):381–4. doi:10.1046/j.1365-3083.1996.d01-51.x
64. Su J, Georgiades A, Wu R, Thulin T, de Faire U, Frostegard J. Antibodies of IgM subclass to phosphorylcholine and oxidized LDL are protective factors for atherosclerosis in patients with hypertension. *Atherosclerosis* (2006) 188(1):160–6. doi:10.1016/j.atherosclerosis.2005.10.017
65. Sjoberg BG, Su J, Dahlbom I, Gronlund H, Wikstrom M, Hedblad B, et al. Low levels of IgM antibodies against phosphorylcholine-A potential risk marker for ischemic stroke in men. *Atherosclerosis* (2009) 203(2):528–32. doi:10.1016/j.atherosclerosis.2008.07.009
66. Fiskesund R, Stegmayr B, Hallmans G, Vikstrom M, Weinehall L, de Faire U, et al. Low levels of antibodies against phosphorylcholine predict development of stroke in a population-based study from northern Sweden. *Stroke* (2010) 41(4):607–12. doi:10.1161/STROKEAHA.109.558742
67. Frostegard J. Low level natural antibodies against phosphorylcholine: a novel risk marker and potential mechanism in atherosclerosis and cardiovascular disease. *Clin Immunol* (2010) 134(1):47–54. doi:10.1016/j.clim.2009.08.013
68. Sobel M, Moreno KI, Yagi M, Kohler TR, Tang GL, Clowes AW, et al. Low levels of a natural IgM antibody are associated with vein graft stenosis and failure. *J Vasc Surg* (2013) 58(4):997–1005.e1001–2. doi:10.1016/j.jvs.2013.04.042
69. Anania C, Gustafsson T, Hua X, Su J, Vikstrom M, de Faire U, et al. Increased prevalence of vulnerable atherosclerotic plaques and low levels of natural IgM antibodies against phosphorylcholine in patients with systemic lupus erythematosus. *Arthritis Res Ther* (2010) 12(6):R214. doi:10.1186/ar3193
70. Rosenfeld SM, Perry HM, Gonen A, Prohaska TA, Srikakulapu P, Grewal S, et al. B-1b cells secrete atheroprotective IgM and attenuate atherosclerosis. *Circ Res* (2015) 117(3):e28–39. doi:10.1161/CIRCRESAHA.117.306044
71. Doran AC, Lehtinen AB, Meller N, Lipinski MJ, Slayton RP, Oldham SN, et al. Id3 is a novel atheroprotective factor containing a functionally significant single-nucleotide polymorphism associated with intima-media thickness in humans. *Circ Res* (2010) 106(7):1303–11. doi:10.1161/CIRCRESAHA.109.210294
72. Friedman P, Horkko S, Steinberg D, Witztum JL, Dennis EA. Correlation of antiphospholipid antibody recognition with the structure of synthetic oxidized phospholipids. Importance of Schiff base formation and aldol condensation. *J Biol Chem* (2002) 277(9):7010–20. doi:10.1074/jbc.M108860200
73. Horkko S, Bird DA, Miller E, Itabe H, Leitinger N, Subbanagounder G, et al. Monoclonal autoantibodies specific for oxidized phospholipids or oxidized phospholipid-protein adducts inhibit macrophage uptake of oxidized low-density lipoproteins. *J Clin Invest* (1999) 103(1):117–28. doi:10.1172/JCI4533
74. Rahaman SO, Lennon DJ, Febbraio M, Podrez EA, Hazen SL, Silverstein RL. A CD36-dependent signaling cascade is necessary for macrophage foam cell formation. *Cell Metab* (2006) 4(3):211–21. doi:10.1016/j.cmet.2006.06.007
75. Boullier A, Gillotte KL, Hörkkö S, Green SR, Friedman P, Dennis EA, et al. The binding of oxidized low density lipoprotein to mouse CD36 is mediated in part by oxidized phospholipids that are associated with both the lipid and protein moieties of the lipoprotein. *J Biol Chem* (2000) 275(13):9163–9. doi:10.1074/jbc.275.13.9163
76. Stewart CR, Stuart LM, Wilkinson K, van Gils JM, Deng J, Halle A, et al. CD36 ligands promote sterile inflammation through assembly of a toll-like receptor 4 and 6 heterodimer. *Nat Immunol* (2010) 11(2):155–61. doi:10.1038/ni.1836
77. Masmoudi H, Mota-Santos T, Huetz F, Coutinho A, Cazenave PA. All T15 Id-positive antibodies (but not the majority of VHT15+ antibodies) are produced by peritoneal CD5+ B lymphocytes. *Int Immunol* (1990) 2(6):515–20. doi:10.1093/intimm/2.6.515
78. Briles DE, Forman C, Hudak S, Claflin JL. Anti-phosphorylcholine antibodies of the T15 idiotype are optimally protective against *Streptococcus pneumoniae*. *J Exp Med* (1982) 156(4):1177–85. doi:10.1084/jem.156.4.1177
79. Shaw PX, Horkko S, Chang MK, Curtiss LK, Palinski W, Silverman GJ, et al. Natural antibodies with the T15 idiotype may act in atherosclerosis, apoptotic

clearance, and protective immunity. *J Clin Invest* (2000) 105(12):1731–40. doi:10.1172/JCI8472
80. Binder CJ, Horkko S, Dewan A, Chang MK, Kieu EP, Goodyear CS, et al. Pneumococcal vaccination decreases atherosclerotic lesion formation: molecular mimicry between *Streptococcus pneumoniae* and oxidized LDL. *Nat Med* (2003) 9(6):736–43. doi:10.1038/nm876
81. Faria-Neto JR, Chyu KY, Li X, Dimayuga PC, Ferreira C, Yano J, et al. Passive immunization with monoclonal IgM antibodies against phosphorylcholine reduces accelerated vein graft atherosclerosis in apolipoprotein E-null mice. *Atherosclerosis* (2006) 189(1):83–90. doi:10.1016/j.atherosclerosis.2005.11.033
82. Chen Y, Park YB, Patel E, Silverman GJ. IgM antibodies to apoptosis-associated determinants recruit C1q and enhance dendritic cell phagocytosis of apoptotic cells. *J Immunol* (2009) 182(10):6031–43. doi:10.4049/jimmunol.0804191
83. Huber J, Vales A, Mitulovic G, Blumer M, Schmid R, Witztum JL, et al. Oxidized membrane vesicles and blebs from apoptotic cells contain biologically active oxidized phospholipids that induce monocyte-endothelial interactions. *Arterioscler Thromb Vasc Biol* (2002) 22(1):101–7. doi:10.1161/hq0102.101525
84. Ramakrishnan DP, Hajj-Ali RA, Chen Y, Silverstein RL. Extracellular vesicles activate a CD36-dependent signaling pathway to inhibit microvascular endothelial cell migration and tube formation. *Arterioscler Thromb Vasc Biol* (2016) 36(3):534–44. doi:10.1161/ATVBAHA.115.307085
85. Cho S. CD36 as a therapeutic target for endothelial dysfunction in stroke. *Curr Pharm Des* (2012) 18(25):3721–30. doi:10.2174/138161212802002760
86. Caligiuri G, Nicoletti A, Poirier B, Hansson GK. Protective immunity against atherosclerosis carried by B cells of hypercholesterolemic mice. *J Clin Invest* (2002) 109(6):745–53. doi:10.1172/JCI7272
87. Major AS, Fazio S, Linton MF. B-lymphocyte deficiency increases atherosclerosis in LDL receptor-null mice. *Arterioscler Thromb Vasc Biol* (2002) 22(11):1892–8. doi:10.1161/01.ATV.0000039169.47943.EE
88. Ait-Oufella H, Herbin O, Bouaziz JD, Binder CJ, Uyttenhove C, Laurans L, et al. B cell depletion reduces the development of atherosclerosis in mice. *J Exp Med* (2010) 207(8):1579–87. doi:10.1084/jem.20100155
89. Kyaw T, Tay C, Khan A, Dumouchel V, Cao A, To K, et al. Conventional B2 B cell depletion ameliorates whereas its adoptive transfer aggravates atherosclerosis. *J Immunol* (2010) 185(7):4410–9. doi:10.4049/jimmunol.1000033
90. Jonsson AL, Backhed F. Role of gut microbiota in atherosclerosis. *Nat Rev Cardiol* (2017) 14(2):79–87. doi:10.1038/nrcardio.2016.183
91. Pieper K, Grimbacher B, Eibel H. B-cell biology and development. *J Allergy Clin Immunol* (2013) 131(4):959–71. doi:10.1016/j.jaci.2013.01.046
92. Miller YI, Choi SH, Wiesner P, Fang L, Harkewicz R, Hartvigsen K, et al. Oxidation-specific epitopes are danger-associated molecular patterns recognized by pattern recognition receptors of innate immunity. *Circ Res* (2011) 108(2):235–48. doi:10.1161/CIRCRESAHA.110.223875
93. Binder CJ, Chang MK, Shaw PX, Miller YI, Hartvigsen K, Dewan A, et al. Innate and acquired immunity in atherogenesis. *Nat Med* (2002) 8(11):1218–26. doi:10.1038/nm1102-1218
94. Tsimikas S, Palinski W, Witztum JL. Circulating autoantibodies to oxidized LDL correlate with arterial accumulation and depletion of oxidized LDL in LDL receptor-deficient mice. *Arterioscler Thromb Vasc Biol* (2001) 21(1):95–100. doi:10.1161/01.ATV.21.1.95
95. Yla-Herttuala S, Palinski W, Butler SW, Picard S, Steinberg D, Witztum JL. Rabbit and human atherosclerotic lesions contain IgG that recognizes epitopes of oxidized LDL. *Arterioscler Thromb* (1994) 14(1):32–40. doi:10.1161/01.ATV.14.1.32
96. Xu Q, Dietrich H, Steiner HJ, Gown AM, Schoel B, Mikuz G, et al. Induction of arteriosclerosis in normocholesterolemic rabbits by immunization with A1 shock protein 65. *Arterioscler Thromb* (1992) 12(7):789–99. doi:10.1161/01.ATV.12.7.789
97. George J, Afek A, Gilburd B, Shoenfeld Y, Harats D. Cellular and humoral immune responses to heat shock protein 65 are both involved in promoting fatty-streak formation in LDL-receptor deficient mice. *J Am Coll Cardiol* (2001) 38(3):900–5. doi:10.1016/S0735-1097(01)01440-1
98. Xu Q, Willeit J, Marosi M, Kleindienst R, Oberhollenzer F, Kiechl S, et al. Association of serum antibodies to heat-shock protein 65 with carotid atherosclerosis. *Lancet* (1993) 341(8840):255–9. doi:10.1016/0140-6736(93)92613-X
99. Knoflach M, Kiechl S, Kind M, Said M, Sief R, Gisinger M, et al. Cardiovascular risk factors and atherosclerosis in young males: army study (atherosclerosis risk-factors in male youngsters). *Circulation* (2003) 108(9):1064–9. doi:10.1161/01.CIR.0000085996.95532.FF
100. Vuilleumier N, Bas S, Pagano S, Montecucco F, Guerne PA, Finckh A, et al. Anti-apolipoprotein A-1 IgG predicts major cardiovascular events in patients with rheumatoid arthritis. *Arthritis Rheum* (2010) 62(9):2640–50. doi:10.1002/art.27546
101. Finckh A, Courvoisier DS, Pagano S, Bas S, Chevallier-Ruggeri P, Hochstrasser D, et al. Evaluation of cardiovascular risk in patients with rheumatoid arthritis: do cardiovascular biomarkers offer added predictive ability over established clinical risk scores? *Arthritis Care Res (Hoboken)* (2012) 64(6):817–25. doi:10.1002/acr.21631
102. Pagano S, Satta N, Werling D, Offord V, de Moerloose P, Charbonney E, et al. Anti-apolipoprotein A-1 IgG in patients with myocardial infarction promotes inflammation through TLR2/CD14 complex. *J Intern Med* (2012) 272(4):344–57. doi:10.1111/j.1365-2796.2012.02530.x
103. Vuilleumier N, Rossier MF, Pagano S, Python M, Charbonney E, Nkoulou R, et al. Anti-apolipoprotein A-1 IgG as an independent cardiovascular prognostic marker affecting basal heart rate in myocardial infarction. *Eur Heart J* (2010) 31(7):815–23. doi:10.1093/eurheartj/ehq055
104. Grabner R, Lotzer K, Dopping S, Hildner M, Radke D, Beer M, et al. Lymphotoxin beta receptor signaling promotes tertiary lymphoid organogenesis in the aorta adventitia of aged ApoE-/- mice. *J Exp Med* (2009) 206(1):233–48. doi:10.1084/jem.20080752
105. Clement M, Guedj K, Andreata F, Morvan M, Bey L, Khallou-Laschet J, et al. Control of the T follicular helper-germinal center B-cell axis by CD8(+) regulatory T cells limits atherosclerosis and tertiary lymphoid organ development. *Circulation* (2015) 131(6):560–70. doi:10.1161/circulationaha.114.010988
106. Hu D, Mohanta SK, Yin C, Peng L, Ma Z, Srikakulapu P, et al. Artery tertiary lymphoid organs control aorta immunity and protect against atherosclerosis via vascular smooth muscle cell lymphotoxin beta receptors. *Immunity* (2015) 42(6):1100–15. doi:10.1016/j.immuni.2015.05.015
107. Cihakova D, Rose NR. Pathogenesis of myocarditis and dilated cardiomyopathy. *Adv Immunol* (2008) 99:95–114. doi:10.1016/S0065-2776(08)00604-4
108. Dimas VV, Denfield SW, Friedman RA, Cannon BC, Kim JJ, Smith EO, et al. Frequency of cardiac death in children with idiopathic dilated cardiomyopathy. *Am J Cardiol* (2009) 104(11):1574–7. doi:10.1016/j.amjcard.2009.07.034
109. Nussinovitch U, Shoenfeld Y. Autoimmunity and heart diseases: pathogenesis and diagnostic criteria. *Arch Immunol Ther Exp (Warsz)* (2009) 57(2):95–104. doi:10.1007/s00005-009-0013-1
110. Baldeviano GC, Barin JG, Talor MV, Srinivasan S, Bedja D, Zheng D, et al. Interleukin-17A is dispensable for myocarditis but essential for the progression to dilated cardiomyopathy. *Circ Res* (2010) 106(10):1646–55. doi:10.1161/CIRCRESAHA.109.213157
111. Wu L, Ong S, Talor MV, Barin JG, Baldeviano GC, Kass DA, et al. Cardiac fibroblasts mediate IL-17A-driven inflammatory dilated cardiomyopathy. *J Exp Med* (2014) 211(7):1449–64. doi:10.1084/jem.20132126
112. Myers JM, Cooper LT, Kem DC, Stavrakis S, Kosanke SD, Shevach EM, et al. Cardiac myosin-Th17 responses promote heart failure in human myocarditis. *JCI Insight* (2016) 1(9):e85851. doi:10.1172/jci.insight.85851
113. Huang Y, Wu W, Wang Y. Expression or secretion of IL-17 in the peripheral blood mononuclear cells from patients with dilated cardiomyopathy. *Acta Cardiol* (2009) 64(2):201–5. doi:10.2143/AC.64.2.2036138
114. Barin JG, Baldeviano GC, Talor MV, Wu L, Ong S, Fairweather D, et al. Fatal eosinophilic myocarditis develops in the absence of IFN-gamma and IL-17A. *J Immunol* (2013) 191(8):4038–47. doi:10.4049/jimmunol.1301282
115. Kaya Z, Leib C, Katus HA. Autoantibodies in heart failure and cardiac dysfunction. *Circ Res* (2012) 110(1):145–58. doi:10.1161/CIRCRESAHA.111.243360
116. Limas CJ, Goldenberg IF, Limas C. Autoantibodies against beta-adrenoceptors in human idiopathic dilated cardiomyopathy. *Circ Res* (1989) 64(1):97–103. doi:10.1161/01.RES.64.1.97
117. Magnusson Y, Marullo S, Hoyer S, Waagstein F, Andersson B, Vahlne A, et al. Mapping of a functional autoimmune epitope on the beta 1-adrenergic receptor in patients with idiopathic dilated cardiomyopathy. *J Clin Invest* (1990) 86(5):1658–63. doi:10.1172/JCI114888
118. Iwata M, Yoshikawa T, Baba A, Anzai T, Nakamura I, Wainai Y, et al. Autoimmunity against the second extracellular loop of beta(1)-adrenergic receptors induces beta-adrenergic receptor desensitization and myocardial

hypertrophy in vivo. *Circ Res* (2001) 88(6):578–86. doi:10.1161/01.RES.88.6.578
119. Fu LX, Magnusson Y, Bergh CH, Liljeqvist JA, Waagstein F, Hjalmarson A, et al. Localization of a functional autoimmune epitope on the muscarinic acetylcholine receptor-2 in patients with idiopathic dilated cardiomyopathy. *J Clin Invest* (1993) 91(5):1964–8. doi:10.1172/jci116416
120. Stavrakis S, Kem DC, Patterson E, Lozano P, Huang S, Szabo B, et al. Opposing cardiac effects of autoantibody activation of beta-adrenergic and M2 muscarinic receptors in cardiac-related diseases. *Int J Cardiol* (2011) 148(3):331–6. doi:10.1016/j.ijcard.2009.11.025
121. Doesch AO, Mueller S, Nelles M, Konstandin M, Celik S, Frankenstein L, et al. Impact of troponin I-autoantibodies in chronic dilated and ischemic cardiomyopathy. *Basic Res Cardiol* (2011) 106(1):25–35. doi:10.1007/s00395-010-0126-z
122. Kaya Z, Goser S, Buss SJ, Leuschner F, Ottl R, Li J, et al. Identification of cardiac troponin I sequence motifs leading to heart failure by induction of myocardial inflammation and fibrosis. *Circulation* (2008) 118(20):2063–72. doi:10.1161/CIRCULATIONAHA.108.788711
123. Goser S, Andrassy M, Buss SJ, Leuschner F, Volz CH, Ottl R, et al. Cardiac troponin I but not cardiac troponin T induces severe autoimmune inflammation in the myocardium. *Circulation* (2006) 114(16):1693–702. doi:10.1161/CIRCULATIONAHA.106.635664
124. Klein R, Maisch B, Kochsiek K, Berg PA. Demonstration of organ specific antibodies against heart mitochondria (anti-M7) in sera from patients with some forms of heart diseases. *Clin Exp Immunol* (1984) 58(2):283–92.
125. Schultheiss HP, Bolte HD. Immunological analysis of auto-antibodies against the adenine nucleotide translocator in dilated cardiomyopathy. *J Mol Cell Cardiol* (1985) 17(6):603–17. doi:10.1016/S0022-2828(85)80029-8
126. Baba A, Yoshikawa T, Ogawa S. Autoantibodies produced against sarcolemmal Na-K-ATPase: possible upstream targets of arrhythmias and sudden death in patients with dilated cardiomyopathy. *J Am Coll Cardiol* (2002) 40(6):1153–9. doi:10.1016/S0735-1097(02)02075-2
127. Latif N, Baker CS, Dunn MJ, Rose ML, Brady P, Yacoub MH. Frequency and specificity of antiheart antibodies in patients with dilated cardiomyopathy detected using SDS-PAGE and western blotting. *J Am Coll Cardiol* (1993) 22(5):1378–84. doi:10.1016/0735-1097(93)90546-D
128. Goin JC, Borda ES, Auger S, Storino R, Sterin-Borda L. Cardiac M(2) muscarinic cholinoceptor activation by human chagasic autoantibodies: association with bradycardia. *Heart* (1999) 82(3):273–8. doi:10.1136/hrt.82.3.273
129. Caforio AL, Grazzini M, Mann JM, Keeling PJ, Bottazzo GF, McKenna WJ, et al. Identification of alpha- and beta-cardiac myosin heavy chain isoforms as major autoantigens in dilated cardiomyopathy. *Circulation* (1992) 85(5):1734–42. doi:10.1161/01.CIR.85.5.1734
130. Lv H, Havari E, Pinto S, Gottumukkala RV, Cornivelli L, Raddassi K, et al. Impaired thymic tolerance to alpha-myosin directs autoimmunity to the heart in mice and humans. *J Clin Invest* (2011) 121(4):1561–73. doi:10.1172/JCI44583
131. Lin L, Kim SC, Wang Y, Gupta S, Davis B, Simon SI, et al. HSP60 in heart failure: abnormal distribution and role in cardiac myocyte apoptosis. *Am J Physiol Heart Circ Physiol* (2007) 293(4):H2238–47. doi:10.1152/ajpheart.00740.2007
132. Khaw BA, Narula J, Sharaf AR, Nicol PD, Southern JF, Carles M. SR-Ca2+ ATPase as an autoimmunogen in experimental myocarditis. *Eur Heart J* (1995) 16:92–6. doi:10.1093/eurheartj/16.suppl_O.92
133. Wolff PG, Kuhl U, Schultheiss HP. Laminin distribution and autoantibodies to laminin in dilated cardiomyopathy and myocarditis. *Am Heart J* (1989) 117(6):1303–9. doi:10.1016/0002-8703(89)90410-9
134. Myers JM, Fairweather D, Huber SA, Cunningham MW. Autoimmune myocarditis, valvulitis, and cardiomyopathy. *Curr Protoc Immunol* (2013) Chapter 15:.11–.51. doi:10.1002/0471142735.im1514s101
135. Higuchi Mde L, Benvenuti LA, Martins Reis M, Metzger M. Pathophysiology of the heart in Chagas' disease: current status and new developments. *Cardiovasc Res* (2003) 60(1):96–107. doi:10.1016/S0008-6363(03)00361-4
136. Breinholt JP, Moulik M, Dreyer WJ, Denfield SW, Kim JJ, Jefferies JL, et al. Viral epidemiologic shift in inflammatory heart disease: the increasing involvement of parvovirus B19 in the myocardium of pediatric cardiac transplant patients. *J Heart Lung Transplant* (2010) 29(7):739–46. doi:10.1016/j.healun.2010.03.003
137. Raveche ES, Schutzer SE, Fernandes H, Bateman H, McCarthy BA, Nickell SP, et al. Evidence of Borrelia autoimmunity-induced component of Lyme carditis and arthritis. *J Clin Microbiol* (2005) 43(2):850–6. doi:10.1128/JCM.43.2.850-856.2005
138. Scalzi V, Hadi HA, Alessandri C, Croia C, Conti V, Agati L, et al. Anti-endothelial cell antibodies in rheumatic heart disease. *Clin Exp Immunol* (2010) 161(3):570–5. doi:10.1111/j.1365-2249.2010.04207.x
139. Marijon E, Mirabel M, Celermajer DS, Jouven X. Rheumatic heart disease. *Lancet* (2012) 379(9819):953–64. doi:10.1016/S0140-6736(11)61171-9
140. Rush CM, Govan BL, Sikder S, Williams NL, Ketheesan N. Animal models to investigate the pathogenesis of rheumatic heart disease. *Front Pediatr* (2014) 2:116. doi:10.3389/fped.2014.00116
141. Dell A, Antone SM, Gauntt CJ, Crossley CA, Clark WA, Cunningham MW. Autoimmune determinants of rheumatic carditis: localization of epitopes in human cardiac myosin. *Eur Heart J* (1991) 12(Suppl D):158–62. doi:10.1093/eurheartj/12.suppl_D.158
142. Shikhman AR, Greenspan NS, Cunningham MW. A subset of mouse monoclonal antibodies cross-reactive with cytoskeletal proteins and group A streptococcal M proteins recognizes N-acetyl-beta-D-glucosamine. *J Immunol* (1993) 151(7):3902–13.
143. Skyllouriotis P, Skyllouriotis-Lazarou M, Natter S, Steiner R, Spitzauer S, Kapiotis S, et al. IgG subclass reactivity to human cardiac myosin in cardiomyopathy patients is indicative of a Th1-like autoimmune disease. *Clin Exp Immunol* (1999) 115(2):236–47. doi:10.1046/j.1365-2249.1999.00807.x
144. Galvin JE, Hemric ME, Ward K, Cunningham MW. Cytotoxic mAb from rheumatic carditis recognizes heart valves and laminin. *J Clin Invest* (2000) 106(2):217–24. doi:10.1172/jci7132
145. Fenderson PG, Fischetti VA, Cunningham MW. Tropomyosin shares immunologic epitopes with group A streptococcal M proteins. *J Immunol* (1989) 142(7):2475–81.
146. D'Cruz DP, Houssiau FA, Ramirez G, Baguley E, McCutcheon J, Vianna J, et al. Antibodies to endothelial cells in systemic lupus erythematosus: a potential marker for nephritis and vasculitis. *Clin Exp Immunol* (1991) 85(2):254–61. doi:10.1111/j.1365-2249.1991.tb05714.x
147. Savage CO, Gaskin G, Pusey CD, Pearson JD. Anti-neutrophil cytoplasm antibodies can recognize vascular endothelial cell-bound anti-neutrophil cytoplasm antibody-associated autoantigens. *Exp Nephrol* (1993) 1(3):190–5.
148. Renaudineau Y, Grunebaum E, Krause I, Praprotnik S, Revelen R, Youinou P, et al. Anti-endothelial cell antibodies (AECA) in systemic sclerosis – increased sensitivity using different endothelial cell substrates and association with other autoantibodies. *Autoimmunity* (2001) 33(3):171–9. doi:10.3109/08916930109008045
149. Cromartie WJ, Craddock JG. Rheumatic-like cardiac lesions in mice. *Science* (1966) 154(3746):285–7. doi:10.1126/science.154.3746.285
150. Quinn A, Kosanke S, Fischetti VA, Factor SM, Cunningham MW. Induction of autoimmune valvular heart disease by recombinant streptococcal M protein. *Infect Immun* (2001) 69(6):4072–8. doi:10.1128/iai.69.6.4072-4078.2001
151. Huang J, Xie X, Lin ZF, Luo MQ, Yu BY, Gu JR. Induction of myocarditis lesions in Lewis rats by formalin-killed cells of group A *Streptococcus*. *J Int Med Res* (2009) 37(1):175–81. doi:10.1177/147323000903700121
152. Xie X, Zhou H, Huang J, Huang H, Feng Z, Mei K, et al. An animal model of chronic rheumatic valvulitis induced by formalin-killed streptococci. *Rheumatol Int* (2010) 30(12):1621–5. doi:10.1007/s00296-009-1246-3
153. Fujinami RS, von Herrath MG, Christen U, Whitton JL. Molecular mimicry, bystander activation, or viral persistence: infections and autoimmune disease. *Clin Microbiol Rev* (2006) 19(1):80–94. doi:10.1128/CMR.19.1.80-94.2006
154. Wolfgram LJ, Beisel KW, Rose NR. Heart-specific autoantibodies following murine coxsackievirus B3 myocarditis. *J Exp Med* (1985) 161(5):1112–21. doi:10.1084/jem.161.5.1112
155. Neu N, Craig SW, Rose NR, Alvarez F, Beisel KW. Coxsackievirus induced myocarditis in mice: cardiac myosin autoantibodies do not cross-react with the virus. *Clin Exp Immunol* (1987) 69(3):566–74.
156. Schwimmbeck PL, Schwimmbeck NK, Schultheiss HP, Strauer BE. Mapping of antigenic determinants of the adenine-nucleotide translocator and coxsackie B3 virus with synthetic peptides: use for the diagnosis of viral heart disease. *Clin Immunol Immunopathol* (1993) 68(2):135–40. doi:10.1006/clin.1993.1109
157. Binstadt BA, Hebert JL, Ortiz-Lopez A, Bronson R, Benoist C, Mathis D. The same systemic autoimmune disease provokes arthritis and endocarditis

via distinct mechanisms. *Proc Natl Acad Sci U S A* (2009) 106(39):16758–63. doi:10.1073/pnas.0909132106

158. Kouskoff V, Korganow AS, Duchatelle V, Degott C, Benoist C, Mathis D. Organ-specific disease provoked by systemic autoimmunity. *Cell* (1996) 87(5):811–22. doi:10.1016/S0092-8674(00)81989-3
159. Korganow AS, Ji H, Mangialaio S, Duchatelle V, Pelanda R, Martin T, et al. From systemic T cell self-reactivity to organ-specific autoimmune disease via immunoglobulins. *Immunity* (1999) 10(4):451–61. doi:10.1016/S1074-7613(00)80045-X
160. Maccioni M, Zeder-Lutz G, Huang H, Ebel C, Gerber P, Hergueux J, et al. Arthritogenic monoclonal antibodies from K/BxN mice. *J Exp Med* (2002) 195(8):1071–7. doi:10.1084/jem.20011941
161. Hobday PM, Auger JL, Schuneman GR, Haasken S, Verbeek JS, Binstadt BA. Fcgamma receptor III and Fcgamma receptor IV on macrophages drive autoimmune valvular carditis in mice. *Arthritis Rheumatol* (2014) 66(4): 852–62. doi:10.1002/art.38311
162. Meier LA, Auger JL, Engelson BJ, Cowan HM, Breed ER, Gonzalez-Torres MI, et al. CD301b/MGl2(+) mononuclear phagocytes orchestrate autoimmune cardiac valve inflammation and fibrosis. *Circulation* (2018). doi:10.1161/CIRCULATIONAHA.117.033144

Conflict of Interest Statement: The authors affirm that this manuscript was generated in the absence of any material or financial conflict of interest that may have potentially influenced its content.

frontiers in Immunology

ORIGINAL RESEARCH
published: 25 April 2018
doi: 10.3389/fimmu.2018.00858

Keratin Retraction and Desmoglein3 Internalization Independently Contribute to Autoantibody-Induced Cell Dissociation in Pemphigus Vulgaris

*Elisabeth Schlögl[1], Mariya Y. Radeva[1], Franziska Vielmuth[1], Camilla Schinner[1], Jens Waschke[1] and Volker Spindler[1,2]**

[1] *Chair of Vegetative Anatomy, Faculty of Medicine, Institute of Anatomy, Ludwig Maximilian University of Munich, Munich, Germany,* [2] *Department of Biomedicine, University of Basel, Basel, Switzerland*

Pemphigus vulgaris (PV) is a potentially lethal autoimmune disease characterized by blister formation of the skin and mucous membranes and is caused by autoantibodies against desmoglein (Dsg) 1 and Dsg3. Dsg1 and Dsg3 are linked to keratin filaments in desmosomes, adhering junctions abundant in tissues exposed to high levels of mechanical stress. The binding of the autoantibodies leads to internalization of Dsg3 and a collapse of the keratin cytoskeleton—yet, the relevance and interdependence of these changes for loss of cell–cell adhesion and blistering is poorly understood. In live-cell imaging studies, loss of the keratin network at the cell periphery was detectable starting after 60 min of incubation with immunoglobulin G fractions of PV patients (PV-IgG). These rapid changes correlated with loss of cell–cell adhesion detected by dispase-based dissociation assays and were followed by a condensation of keratin filaments into thick bundles after several hours. Dsg3 internalization started at 90 min of PV-IgG treatment, thus following the early keratin changes. By inhibiting casein kinase 1 (CK-1), we provoked keratin alterations resembling the effects of PV-IgG. Although CK-1-induced loss of peripheral keratin network correlated with loss of cell cohesion and Dsg3 clustering in the membrane, it was not sufficient to trigger the internalization of Dsg3. However, additional incubation with PV-IgG was effective to promote Dsg3 loss at the membrane, indicating that Dsg3 internalization is independent from keratin alterations. *Vice versa*, inhibiting Dsg3 internalization did not prevent PV-IgG-induced keratin retraction and only partially rescued cell cohesion. Together, keratin changes appear very early after autoantibody binding and temporally overlap with loss of cell cohesion. These early alterations appear to be distinct from Dsg3 internalization, suggesting a crucial role for initial loss of cell cohesion in PV.

Keywords: pemphigus, keratin filaments, desmosome, cell adhesion, keratinocytes

OPEN ACCESS

Edited by:
Anne Fletcher, Monash University, Australia

Reviewed by:
Carlo Pincelli, University of Modena and Reggio Emilia, Italy
Animesh A. Sinha, University at Buffalo, United States

****Correspondence:***
Volker Spindler
volker.spindler@unibas.ch

Specialty section:
This article was submitted to Immunological Tolerance and Regulation, a section of the journal Frontiers in Immunology

Received: *30 November 2017*
Accepted: *06 April 2018*
Published: *25 April 2018*

Citation:
Schlögl E, Radeva MY, Vielmuth F, Schinner C, Waschke J and Spindler V (2018) Keratin Retraction and Desmoglein3 Internalization Independently Contribute to Autoantibody-Induced Cell Dissociation in Pemphigus Vulgaris. Front. Immunol. 9:858. doi: 10.3389/fimmu.2018.00858

INTRODUCTION

Pemphigus vulgaris (PV) is a severe autoimmune disease affecting the skin and mucous membranes (1). The disease is caused by autoantibodies developing against the transmembrane, cadherin-type cell adhesion molecules desmoglein (Dsg)3 and Dsg1, leading to loss of cell–cell adhesion. This results in blisters predominantly in the mucosa of the oral cavity and the epidermis. Together with

desmocollins, Dsgs build up the core of desmosomes, cell–cell adhesion structures abundant in tissues exposed to high degrees of mechanical stress (2). In desmosomes, the transmembrane adhesion molecules form clusters in the membrane and bind extracellularly to their counterparts in the membrane of opposing cells. Intracellularly, they are connected to the intermediate filament network through the linker molecules plakoglobin (Pg), plakophilins (Pkp), and desmoplakin (Dp). This arrangement represents a mechanically stable yet tunable meshwork stabilizing entire tissues (3). The mechanisms leading to loss of cell cohesion in PV are complex as autoantibodies interfere with turnover of desmosomal molecules and desmosome-associated proteins (4, 5). The internalization and depletion of Dsg3 together with other desmosomal components as well as alterations of the keratin intermediate filament (KIF) network are two hallmarks of the disease detectable in biopsies of patient skin and reproduced in disease models (6).

Dsg3 membrane depletion is thought to occur on two levels (4, 5): (i) molecules already transported to the membrane but not yet incorporated into desmosomes are endocytosed leading to interference with desmosome assembly and (ii) existing desmosomes are disassembled and desmosomal molecules or even "half desmosomes" are internalized. The altered turnover of desmosomal molecules is connected to a variety of signaling events in response to autoantibody binding and depends on sufficient lipid rafts. Desmosomal molecules are located in these lipid-enriched membrane domains and both the assembly and disassembly of desmosomes are disturbed upon application of cholesterol-depleting agents (7, 8). Furthermore, p38MAPK, a central molecule deregulated in pemphigus, was shown to be essential for Dsg3 internalization (9) as well as for the KIF network alterations in response to PV-IgG treatment (10, 11).

Keratin intermediate filaments are not static structures but are continuously remodeled to adapt to environmental cues (3, 12). KIFs are nucleated in the cell periphery, elongated and transported toward the nucleus, and disassembled in a perinuclear area to allow reassembly in the cell cortex (13). With regard to turnover rates, it was suggested that a dynamic, quickly changing pool can be distinguished from a stable pool of KIFs inserting in the desmosomal or hemi-desmosomal plaque (14). KIF network dynamics are highly regulated by posttranscriptional modifications, especially phosphorylations (12, 15). *Vice versa*, KIFs regulate the activity of kinases at least in part through scaffolding functions. As an example, KIFs sequester PKCα through the adapter protein RACK1 and stabilize desmosomes by suppressing PKCα activity (16), which was also shown to be disturbed in response to pemphigus autoantibodies (17). Recently, it was demonstrated that casein kinase 1α (CK-1α) localizes to KIFs through FAMH83, which is important for KIF bundling and desmosome turnover (18, 19).

The changes of the KIF network in pemphigus, summarized as "keratin retraction," are incompletely understood. Early ultrastructural work in patient biopsies demonstrated reduced amounts of KIFs in the cell periphery (20). KIFs condensate to thicker bundles clustering in the perinuclear area and lose contact to the desmosomal plaque. However, it is unclear whether this phenomenon and internalization of desmosomal molecules in response to autoantibodies are linked. Furthermore, it is unknown whether KIF alterations are the cause or rather the consequence of Dsg3 depletion and loss of cell cohesion in PV.

To address these questions, we applied live imaging approaches and biochemical assays to define the temporal relationship between Dsg3 internalization and keratin retraction and to determine how these changes of the cytoskeleton contribute to loss of cell adhesion in PV.

MATERIALS AND METHODS

Cell Culture, Test Reagents, and Constructs

The immortalized human keratinocyte cell line HaCaT and HaCaT cells stably expressing human cytokeratin5 (CK5) fused to Yellow Fluorescent Protein (YFP, kind gift of Reinhard Windoffer and Nicole Schwarz, Institute of Molecular and Cellular Anatomy, RWTH Aachen University) were cultured in Dulbecco's Modified Eagle Medium supplemented with 10% FCS (Biochrom, Berlin, Germany), 50 U/ml penicillin and 50 U/ml streptomycin (both AppliChem, Darmstadt, Germany), and 0.5 mg/ml G418 in the case of HaCaT-CK5-YFP for selection. Cells were grown in a humidified atmosphere containing 5% CO_2 at 37°C. Cells were used 24 h after reaching confluency. Medium was changed the day before experiments were performed. Incubations were carried out for the indicated period of time. Casein kinase 1 (CK-1) inhibitor D4476 (Abcam, Cambridge, UK) was used at a concentration of 100 μM. Methyl-β-cyclodextrin (Sigma Aldrich, Munich, Germany), referred to as β-MCD, was applied in a concentration of 1 mM.

pDEST-mDsg3-mCherry-N1 was constructed using the Gateway recombinational cloning system (ThermoFisher, Waltham, MA, USA). In brief, the full-length nucleotide sequence encoding mouse Dsg3 was amplified by PCR using primers carrying attB-specific sites. The primers used were as follow: mDsg3-FW, 5′-GGGGACAAGTTTGTACAAAAAAGCAGGCTTCGAAGGAGATAGAACCatgacctgcctcttcc-3′ and mDsg3-Rev, 5′GGGGACCACTTTGTACAAGAAAGCTGGGTCtagatgggaacaggtttc, where the gateway recombination sequences (including attB sites) are present in capital letters and the lower case letters indicate the sequence complementary to the mouse Dsg3 cDNA. The attB-flanked PCR amplicon was inserted into attP-containing pDONR vector (ThermoFisher) and thus the entry clone was generated. Following the manufacturer's instruction, the insert was subcloned into a destination vector (pDEST-mCherry-N1, Plasmid #31907, Addgene). As a result, mDsg3 was fused to mCherry on its C-terminus.

Pemphigus Sera and IgG Purification

Pemphigus sera (PV-IgG) were provided by Enno Schmidt (Lübeck Institute of Experimental Dermatology, University of Lübeck Germany). ELISA titers were as follows: PV1-IgG: anti-Dsg3: 181.44, anti-Dsg1 212.27; PV2-IgG: anti-Dsg3: 206.21, and anti-Dsg1: 182.15. Use of patients' IgG was approved by the ethics committee (AZ12-178). Additional approval of the study was not required according to the local and national

guidelines. Both PV-IgG and an IgG fraction pooled from three different healthy donators (Control-IgG) were purified as described previously (21). In brief, immunoglobulin fractions were extracted from sera through immobilization to protein A agarose (ThermoFisher) in purification columns for 3 h at room temperature. After centrifugation, the serum was removed and the agarose was washed with phosphate-buffered saline (PBS). After elution of the antibodies by sodium citrate buffer (20 mM, pH 2.4) and neutralization with Na_2CO_3, a filter unit (Amicon Ultra–4, 100k; Merck Millipore, Darmstadt, Germany) allowed concentration of the IgG fraction at 19,000 *g* for 20 min. IgG was stored in PBS and used in a concentration of 250 µg/ml. AK23, a monoclonal antibody derived from a PV mouse model (Biozol, Eching, Germany) was used in a concentration of 75 µg/ml.

Immunostaining

HaCaT cells stably expressing CK5-YFP were grown on glass cover slips and fixed with 2% formalin in PBS (freshly prepared from paraformaldehyde) for 10 min at room temperature before being treated with 0.1% Triton X-100 for 5 min to guarantee permeabilization. Subsequently, cells were blocked with 1% normal goat serum and 3% BSA in PBS for 45 min. Cells were incubated with an anti-Dsg3 antibody (clone 5G11, sc-53487, Santa Cruz Biotechnology, Heidelberg, Germany) at 4°C overnight. A Cy3-conjugated secondary goat-anti-mouse antibody (Dianova, Hamburg, Germany) was applied for 1 h at room temperature. 1.5% *N*-propyl gallate was used as an antifading compound to embed the glass dish with cultured cells on glass slides. Images were acquired using a Leica SP5 confocal microscope with a 63× NA 1.4 PL APO objective. Confocal microscopy was performed using lasers with 514 and 543 nm wavelengths for excitation. Analysis was performed using ImageJ (www.nih.gov). The straight bar tool was used to plot intensity profiles of regions of interest. A straight bar of 15 µm length and 20 px width was placed perpendicularly over the cell border of two adjacent cells. Dsg3 was used to indicate the cell border. The position of the bar was not altered for plotting the intensity profile of the respective CK5 image. Resulting intensity profiles indicating the distribution of the protein of interest were compiled in Excel (Microsoft, Redmond, WA, USA) and subsequently normalized to the baseline.

Western Blot and Lysates

Cells were washed with PBS and subsequently lysed with SDS-lysis buffer (25 mmol/l HEPES, 2 mmol/l EDTA, 25 mmol/l NaF and 1% SDS, pH 7.4) followed by sonification. Protein amount was determined using the BCA method (ThermoFisher, USA). A mixture of lysate and Laemmli buffer containing 50 mM dithiothreitol was prepared and 10 µg of protein were loaded on a gel for electrophoresis. Electrophoresis and western blotting were carried out according to standard procedures. Membranes were blocked in either 5% skim milk powder dissolved in Tris-buffered-saline containing 0.05% tween (TBS-T) or 5% BSA in TBS-T at room temperature for 1 h. The following antibodies were applied in BSA in TBS-T at 4°C overnight: Dsg3 pAb (ELA-EAP3816-120, Biozol), Desmoplakin I/II pAb (H-300) (sc-33555, Santa Cruz), CK14 mAB (LL002) (ab7800, Abcam, Cambridge, UK), GAPDH mAb (0411) (sc-47724, Santa Cruz), phospho-p38 MAPK pAb (Thr180/Tyr182, D3F9) (#4511, Cell Signaling Cambridge, UK), and p38 MAPK pAb (#9212, Cell Signaling). HRP-coupled goat-anti-mouse Ab or goat-anti-rabbit Ab (both Dianova) were applied as secondary antibodies at room temperature. Membranes were developed using the ECL system (GE Healthcare, Munich, Germany). Western blots were analyzed by measuring the integrated density of bands after background subtraction using ImageJ.

Triton X-100 Protein Fractionation

HaCaT-CK5 cells were put on ice and washed with ice-cold PBS. Extraction buffer (0.5% Triton X-100, 50 mmol/l MES, 25 mmol/l EGTA, 5 mmol/l $MgCl_2$) containing 0.1% leupeptin, aprotinin, and pepstatin as well as 1% phenylmethylsulfonyl fluoride was applied for 10 min under gentle shaking on ice followed by scraping to retrieve lysates. Centrifugation at 19,000 *g* for 10 min at 4°C enabled the separation of the cytoskeletal insoluble fraction from the triton-soluble non-cytoskeletal-bound fraction. The Triton X-100 soluble fraction was harvested and processed separately for blotting. The obtained pellet representing the insoluble fraction was suspended in SDS-lysis buffer (25 mmol/l HEPES, 2 mmol/l EDTA, 25 mmol/l NaF, and 1% SDS, pH 7.4) and sonicated. Protein levels of both fractions were measured using the BCA method (ThermoFisher). 5 or 10 µg of each fraction were mixed with Laemmli buffer and subjected to Western blotting.

Biotinylation Assay

After incubation, HaCaT-CK5 cells were put on ice and thoroughly washed with HbSS. This step was followed by a 1 h incubation with 0.25 mM membrane-impermeable EZ-Link Sulfo-NHS-Biotin (ThermoFisher). To remove excess biotin, cells were washed with ice-cold HbSS containing 100 mM Glycin and plain HbSS afterward. Under gentle shaking, cells were incubated with cooled lysis buffer (50 mM NaCl, 10 mM PIPES, 3 mM $MgCl_2$, 1% Triton X-100, 1% phenylmethylsulfonyl fluoride, 0.1% of each leupetin, aprotinin, and pepstatin) for 20 min on ice. Lysates were acquired through scraping and subsequently centrifuging at 19,000 *g* for 5 min. Supernatant was retrieved and protein concentrations were measured using the BCA method (ThermoFisher). 250 µg of protein were mixed with 70 µl of NeutrAvidin (HighCapacity)-agarose (ThermoFisher) and put on a rotator overnight at 4°C. The next day, agarose beads were washed five times with cold lysis buffer. Biotinylated-protein attached to the agarose was suspended in 3× Laemmli buffer containing 50 mM dithiotreitol (AppliChem). Lysates were loaded on gels and Western blotting was carried out as described above. Biotin of the biotin-bound fraction was detected using streptavidin-HRP (Cell Signaling), the integrated density of the entire lane of each condition was measured and used as a loading control. Representative sections of the membranes are shown in the figures. The whole lysate was normalized to GAPDH.

Phos-tag™ Assay

To determine the phosphorylation state of a protein, a Manganese (II)-Phos-tag™ SDS-PAGE (Wako Chemicals GmbH, Steinbach, Germany) was carried out. The Phos-tag component which is incorporated in the gel reduces the migration speed of phosphorylated proteins in the electrophoresis process. The imbalance of migration speed between phosphorylated proteins and their lower or non-phosphorylated counterparts enables the detection of a phosphorylation state. After the indicated treatment of cells with D4476 reagent, HaCaT-CK5 cells were put on ice and washed with prechilled TBS and lysed in Laemmli buffer supplemented with 0.1% of each leupeptin, pepstatin, and aprotinin, 1% of phenylmethylsulfonyl fluoride, phosphatase inhibitor (Roche), and 50 mM dithiotreitol. Manganese (II)-Phos-tag™ SDS-PAGE was performed according to the manufacturer's instructions. For electrophoresis 6% polyacrylamide gels were freshly prepared containing either 0 mM (control gel) or 30 mM Phos-tag™ ALL-107 (Wako Chemicals). Lysates were sonicated and loaded on the gels. Mn^{2+} was removed from the gels by washing twice for 10 min in transfer buffer containing 30 mM EDTA. A third washing step followed in transfer buffer without EDTA equally for 10 min. Proteins were transferred to a PVDF-membrane (Bio-Rad Laboratories, Munich, Germany). Antibodies were applied as detailed in the Western blot section.

Dispase-Based Dissociation Assay

HaCaT keratinocytes were seeded in duplicate for each condition and grown for 24 h after reaching confluency. Cells were washed with prewarmed PBS and subsequently incubated with HbSS containing Dispase II (>2.4 U/ml; Sigma Aldrich) for 20 min at 37°C in order to detach the cell monolayer from the well bottom. Dispase II solution was replaced by HbSS. A defined sheer stress was applied to the cell sheets by pipetting the monolayer 10 times using an electrical 1 ml pipet. Increased numbers of fragments, counted under a binocular microscope, compared to control conditions indicated the loss of intercellular adhesion. For better display of the fragments, 10 µM thiazolyl blue tetrazolium bromide (MTT) (SigmaAldrich) were added to the vials for 20 min to obtain staining of viable cells.

Live Cell Imaging

HaCaT-CK5 cells were seeded in µ-slide eight-well imaging chambers (Ibidi, Martinsried, Germany) and grown to confluency. Dulbecco's Modified Eagle Medium with supplements was replaced with Dulbecco's Modified Eagle Medium without phenol red. Transfection with pDest-mDsg3-mCherry for double transfection experiments was carried out 3 days after cell seeding at a confluency of 90% with Lipofectamine LTX with Plus Reagent (ThermoFisher). The transfection was performed according to the manufacturer's protocol, incubating the cells with a final concentration of 3 µg plasmid DNA, 3 µl Plus-Reagent and 5 µl of LTX-Reagent per milliliter for 4 h. Experiments were carried out 24 h after transfection. Live Cell Imaging experiments were performed using a Leica SP5 confocal microscope with a 63× NA 1.2 PL APO water or a 63× NA 1.4 PL APO oil objective. An incubator housing (OKOLAB, Pozzuoli, Italy) guaranteed a constant humidified atmosphere at 37°C with 5% CO_2.

Untransfected HaCaT CK5-YFP cells were imaged with a 20-mW argon laser at 514 nm wavelength and 3% laser power. A stack was created covering the entire z-dimension of the monolayer in 0.5 µm steps and 512 × 512 pixel stacks were acquired every 30 s. Z-stacks of HaCaT CK5-YFP cells transfected with Dsg3-mCherry were generated by sequential imaging using the 514 nm argon laser and a 10-mW 543 nm laser line at 20% power. Images were acquired every 2 min.

Live Cell Imaging Analysis

All stacks were deconvolved using the software Huygens Essentials (Scientific Volume Imaging, Hilversum, The Netherlands) at a signal to noise ratio of 10 and a maximum of 30 iterations. Further analysis of otherwise raw image data was performed with ImageJ, unless specified otherwise.

To analyze the number of keratin bridges of adjacent cells, a maximum intensity projection of all layers was used. KIFs "bridging" two neighboring cells were manually counted and put in relation to the length of the respective cell border area. For intensity measurement in the cell periphery, a projection of layers covering the lower 4 µm of the cell was applied. The mesh size of KIFs differs from the cell periphery toward the nucleus (22), a phenomenon which was also evident in HaCaTs expressing CK5-YFP. Following this indication, the mean intensity of the cell periphery with a large mesh size and the mean intensity of the dense perinuclear KIF network were independently analyzed using the drawing tool of ImageJ. To quantify loss of keratins in the cell periphery, the peripheral KIF intensity values were divided by the perinuclear intensity values.

Keratin thickening was quantified in maximum intensity projections. Intensity levels of independent experiments were adjusted to the same baseline and further processed with the software CellProfiler (23). In a first step, the tubeness filter was applied. A threshold of 0.2 was defined through empiric trials and applied to the images in a next step. Bridging and cleaning filters were applied to close small gaps between KIF bundles or to remove one-pixel error signals, respectively. Resulting images depicted high intensity KIF signals as white, corresponding to thickened keratin bundles. The mean intensity of these images was used as measure for KIF thickening.

The intensity of Dsg3 in the membrane was analyzed using a projection of three layers (1.5 µm) located above and below the plane with the largest nuclear diameter. Only cells with clear membrane localization were included for imaging. The mean intensity of a 2 µm wide region of interest containing the entire cell circumference was compared with the intensity of the remaining cytoplasm (excluding the nucleus region devoid of any signals). We used this index to detect an intensity switch from the cell border into the cytoplasm as an indicator for Dsg3 internalization.

To determine Dsg3 membrane clustering, a bar of 10 µm length and 10 px width was drawn over the Dsg3 signal at the membrane and the intensity profile was plotted every 12 min at the same region. Clustering was indicated by intensity peaks in the profile developing over time. These were quantified as follows: First, the average intensity value of the initial 0 min profile was calculated. This value was multiplied by 1.5 and used as threshold

for the subsequent time points. To detect newly occurring peaks in the profiles, we calculated the area under the curve above this threshold.

Data Processing and Statistics

Photoshop CC 2017 (Adobe Systems, San Jose, CA, USA) was used for image processing and compilation. We used Excel (Microsoft, Redmond, WA, USA) for data analysis. Statistical significance was determined using paired Student's *t*-test for two-group comparisons in Excel or one-way ANOVA followed by Bonferroni correction using Graphpad Prism (Graphpad Software, LaJolla, CA, USA) for comparison of more than two groups. Significance was presumed with $p < 0.05$. Data shown are mean ± SEM.

RESULTS

Pemphigus Autoantibodies Induced Dsg3 Depletion and Keratin Retraction *In Vitro*

Initially, we characterized changes in Dsg3 and keratin distribution under static conditions in cultured human keratinocytes. HaCaT keratinocytes stably expressing YFP-tagged CK5 were incubated with PV1-IgG for 2, 12, and 24 h (**Figures 1A,B**). After 12 h and even more so after 24 h incubation, the keratin cytoskeleton appeared retracted from the cell periphery (arrows) and Dsg3 clustering together with reduced localization along the cell border was visible. In line with previous data (24), Dsg3 was linearized in arrays perpendicular to the cell border and intracellular Dsg3 clusters (arrowheads) reminiscent of internalization were present. At 2 h, the distribution of Dsg3 showed subtle changes and a beginning reduction of keratin intensity at cell borders was detectable. At 24 h, the amount of CK5 and Dsg3 was reduced in the cytoskeletal (Triton X-100 insoluble) pool (**Figure 1B**). This indicates disassembly of the KIF network after longer periods of PV-IgG treatment.

Despite only minor detectable changes by immunostaining at 2 h of PV1-IgG incubation, cell–cell adhesion was compromised as revealed by dispase-based dissociation assays (**Figure 1C**). In agreement with the structural changes, cell cohesion was more strongly impaired at later time points. Together, the cell line applied here demonstrates the typical hallmarks of the disease also evident in keratinocytes from pemphigus patient skin (25).

The time course of KIF changes in response to PV-IgG is largely unknown. Using atomic force microscopy imaging, an altered cytoskeletal meshwork in living keratinocytes within the first 2 h was demonstrated recently (26). Because KIF and Dsg3 changes started around 2 h after autoantibody addition in static experiments, we next performed live cell imaging in the first 2 h using HaCaT keratinocytes stably expressing CK5-YFP to detect potential discrete changes in the same cells. In this approach, we carried out high resolution three-dimensional confocal time-lapse microscopy. Z-stacks spanning the entire cell height were acquired in 30-s intervals and changes in response to PV1-IgG were analyzed in maximum intensity projections. We first investigated the number of filaments running perpendicular to the cell membrane (**Figure 2A**). Interestingly, these structures known to be relatively stable did not change within 2 h in absence or presence of PV-IgG. To detect potential effects which might be concealed in maximum intensity projections, we separately analyzed the bottom 4 µm of the keratinocyte monolayer, in which the KIF network was most volatile (**Figure 2B**; see Video S1 in Supplementary Material). Indeed, these image series showed a significant loss of keratin fluorescence in the cell periphery starting around 60 min of PV-IgG incubation. At these early time points, the overall extent of the observed changes was rather moderate but clearly detectable by analyzing the signal intensities in the cell periphery. To evaluate the distribution in longer time courses, we performed overview experiments in lower magnification for up to 12 h with a reduced temporal resolution. Interestingly, KIFs condensed into thicker bundles which became visible after around 6 h of PV1-IgG treatment and progressed further on (**Figure 2C**). For analysis, a thresholding step was applied and the amount of signal exceeding this threshold was analyzed (see Materials and Methods).

Together, the live cell imaging experiments suggest a biphasic impact of autoantibody binding on keratin filament distribution. Initially, a pool located in the cell periphery and potentially being responsible for KIF assembly is reduced which is followed by condensation of more stable filaments anchoring desmosomes.

Keratin Changes Paralleled Dsg3 Clustering and Preceded Dsg3 Internalization

Next, we further investigated the temporal relationship between keratin alterations and Dsg3 internalization. We generated a Dsg3 construct C-terminally fused with mCherry and used it for transfections of HaCaT cells stably expressing CK5-YFP. Similar to the experiments without double transfection, a reduction of the keratin network in the cell periphery became evident starting at 60 min of PV1-IgG incubation, indicating that Dsg3 overexpression did not alter keratin dynamics (**Figures 3A,B**; see Video S1 in Supplementary Material). Dsg3 signals at cell borders were stable for 90 min of PV1-IgG incubation and were starting to become reduced afterward as demonstrated by analysis of membrane intensities (**Figures 3A,C**). Thus, the amount of Dsg3 in the membrane appeared to be reduced later than the CK5 changes. The exogenous CK5 expression was not protective with regard to Dsg3 internalization, as wild-type HaCaT cells transfected with Dsg3-GFP displayed similar results (Figure S1 in Supplementary Material). To support these imaging data, we performed cell surface biotinylation assays to biochemically determine the extent of Dsg3 membrane depletion (**Figure 3D**). In agreement with live imaging data, only a minor reduction of Dsg3 membrane levels was detectable after 2 h, whereas depletion from the membrane was pronounced after 12 and 24 h of PV2-IgG incubation, respectively. Stable Dsg3 membrane levels do not rule out alterations in the distribution of the molecules. Clustering of Dsg3 molecules within the membrane in response to PV-IgG was shown to precede internalization (24). We thus analyzed Dsg3 clustering in live cell experiments which was detectable first after 60 min of PV-IgG incubation and proceeding over time (**Figures 3A,E**, arrowheads). In parallel to these experiments, we closely monitored cell cohesion by dispase-based dissociation

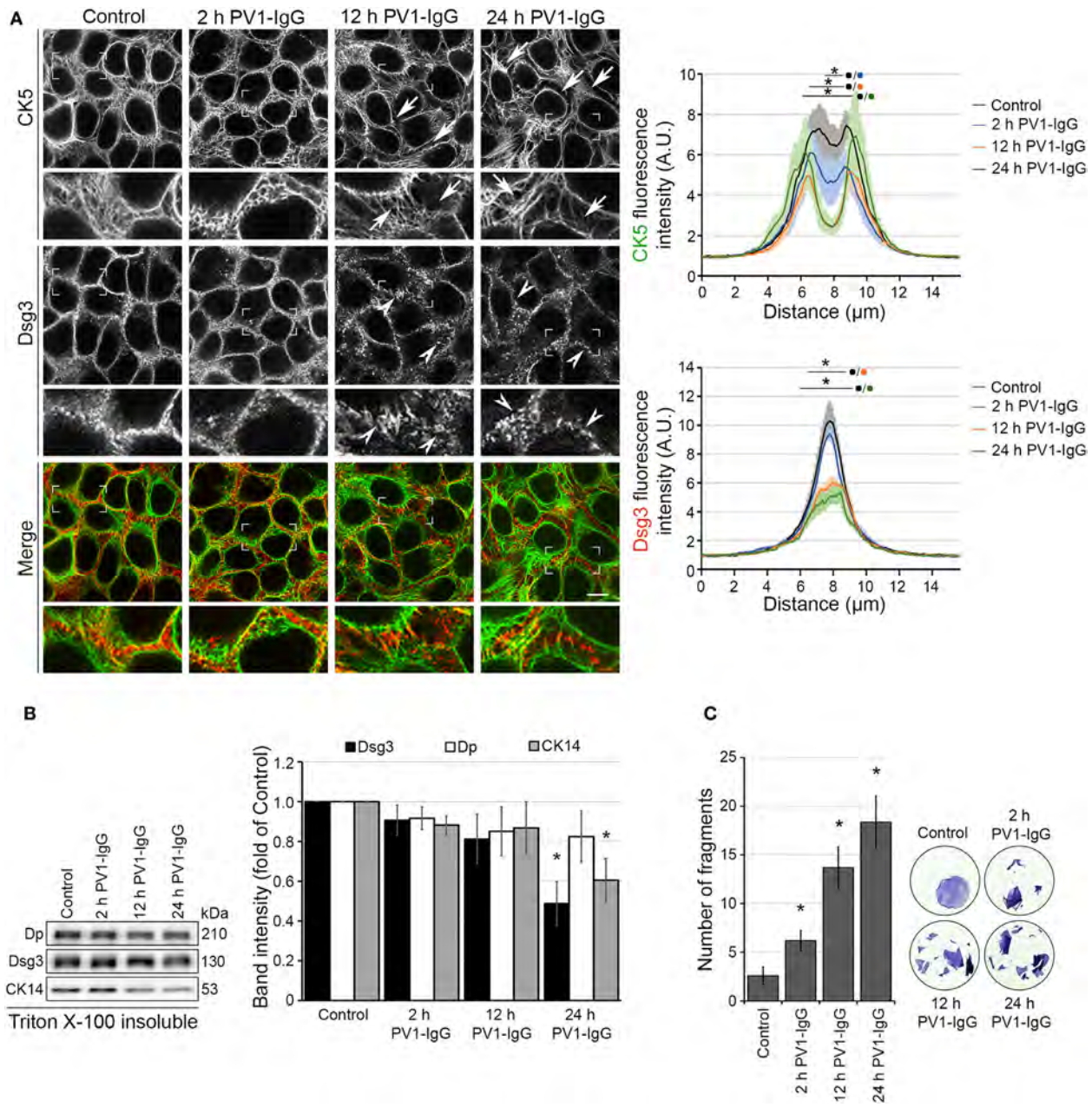

FIGURE 1 | Structural changes of human keratinocytes in response to pemphigus vulgaris (PV) antibody exposure. HaCaT keratinocytes expressing cytokeratin5 (CK5)-YPF (HaCaT-CK5) were incubated with PV1-IgG for 2, 12, or 24 h. Images shown are representatives of >3 independent experiments. **(A)** Desmoglein (Dsg)3 staining and CK5 expression in response to the antibody binding. Loss of keratin filaments in the cell periphery is marked by arrows and Dsg3 alterations by arrowheads. Comparison of fluorescence profiles on a 15 µm line perpendicularly to the membrane of two adjacent cells ($n = 75$ cells from three independent experiments, $^*p < 0.05$ vs. control). Bar represents 10 µm. **(B)** Triton X-100 insoluble fraction, representing the cytoskeletal-bound fraction, of HaCaT-CK5 lysates after incubation with PV1-IgG for the indicated period of time ($n = 6$). Densitometric analysis of structure proteins shown as fold of control ($n = 6$, $^*p < 0.05$ vs. control). **(C)** Dispase-based dissociation assays in HaCaT-CK5 keratinocytes after PV1-IgG treatment ($n = 5$, $^*p < 0.05$ vs. control). Representative images of cell sheets after applied sheer stress stained with 10 µM MTT for better visibility.

assays (**Figure 3F**). Compared to the gross disruption of the monolayer typically evident at 24 h of incubation, at these early time points the monolayer fragmentation was mainly detectable at the periphery presumably because cells are slightly less dense in this region. Compared to Control-IgG, fragmentation and thus loss of cell–cell adhesion was significantly increased beginning at 30 min of PV2-IgG incubation and increased further on.

These results demonstrate that changes in KIF distribution parallel loss of cell cohesion and Dsg3 clustering but precede a morphologically and biochemically detectable Dsg3 internalization.

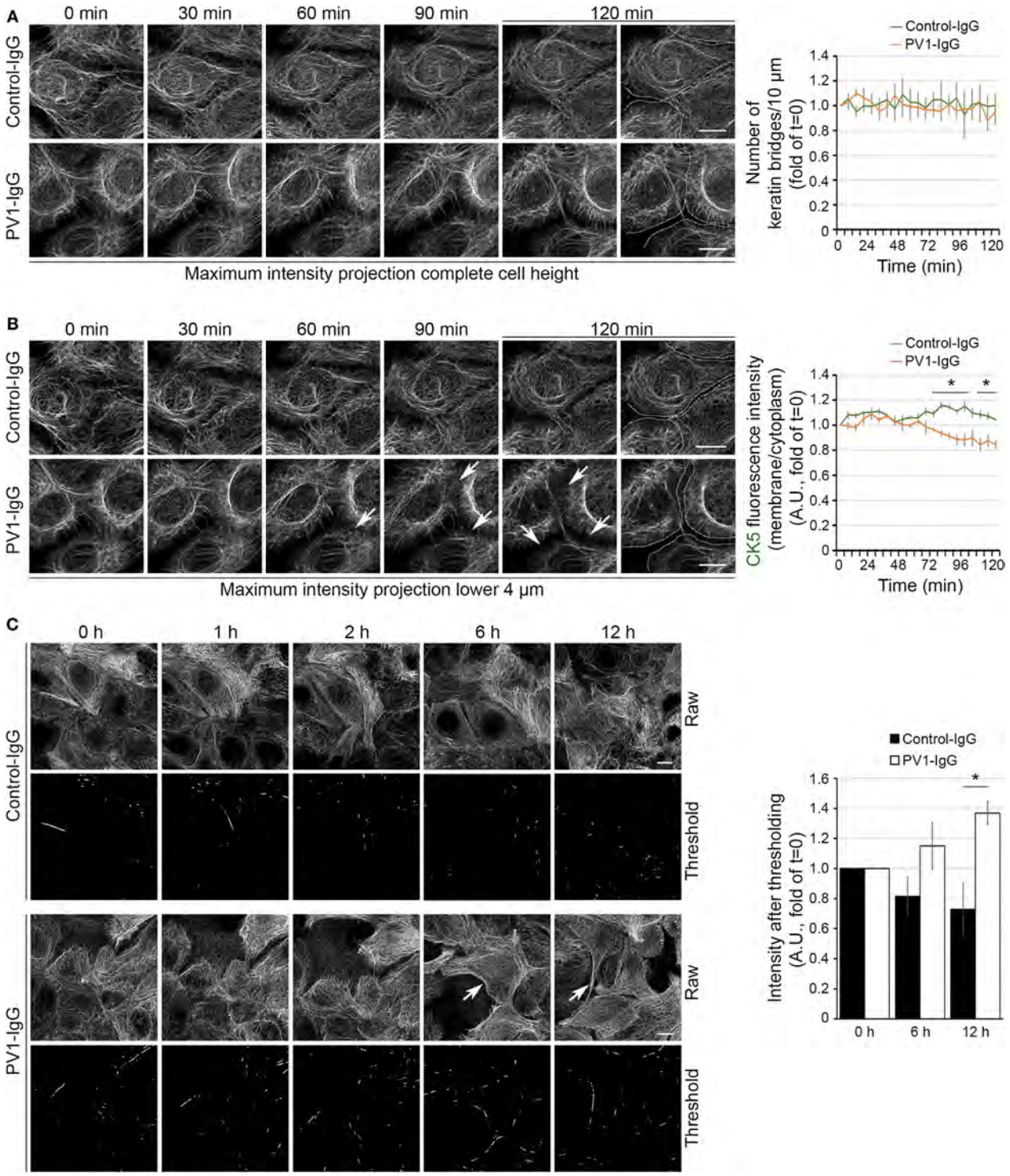

FIGURE 2 | Time course of keratin changes after antibody binding. Representative image sequence of high resolution three-dimensional confocal time-lapse microscopy as a maximum intensity projection of the complete HaCaT-CK5 cell height **(A)**. Images were acquired in 30-s intervals and number of keratin bridges was assessed every 6 min after PV1-IgG addition (n = 8–10 cells from three to four independent experiments, $^*p < 0.05$ vs. Control-IgG at respective time point). **(B)** In a maximum intensity projection containing the lower 4 µm of the cell body, the ratio of fluorescence intensity in the cell periphery to fluorescence intensity in the cytoplasm was analyzed every 6 min. Arrows mark loss of fluorescence intensity in the cell periphery. Dashed lines indicate the cell border area and were drawn for better visualization (n = 8–10 cells from three to four independent experiments, $^*p < 0.05$ vs. Control-IgG at respective time point). **(C)** Keratin bundling (arrows) was caused by PV1-IgG exposure. Bundling was visualized by putting a threshold on raw data and measuring the remaining intensity (n = 3–4, $^*p < 0.05$ vs. Control-IgG at respective time point). Bars represent 10 µm.

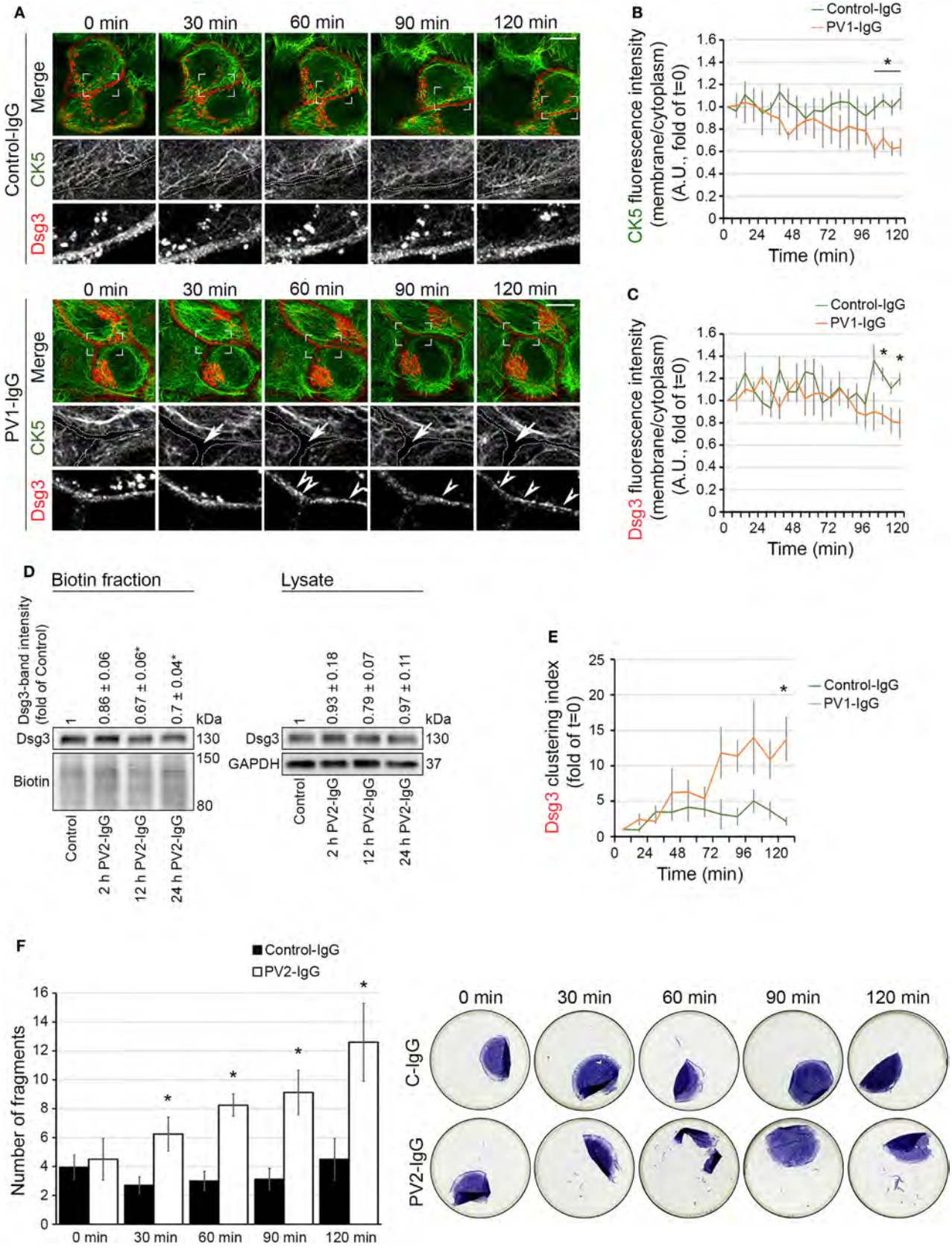

FIGURE 3 | Continued

FIGURE 3 | Keratin changes and Dsg3 clustering occurred in parallel and preceded Dsg3 internalization. HaCaT keratinocytes expressing CK5-YFP were transfected with Dsg3-mCherry. In three-dimensional confocal time-lapse microscopy experiments, cells were incubated with either PV1-IgG or Control-IgG and imaged every 2 min for 120 min. Dashed lines indicate cell border areas **(A)**. Ratio of CK5 fluorescence intensity and in the cell periphery vs. intensity in the cytoplasm was assessed **(B)** (n = 5–6 cells, each from an independent experiment, $^*p < 0.05$ vs. Control-IgG at respective time point). Ratio of Dsg3 distribution in the membrane vs. the cytoplasm **(C)** (n = 5–6, $^*p < 0.05$ vs. Control-IgG). Streptavidin pulldown of biotinylated membrane Dsg3 after 2, 12, and 24 h of PV2-IgG incubation and densitometric analysis of protein levels (n = 3–4, $^*p < 0.05$ vs. control) **(D)**. Dsg3 clustering was evaluated with intensity profile plotting linearly along the membrane (n = 5–6, $^*p < 0.05$ vs. Control-IgG at respective time point) **(E)**. Loss of cell adhesion caused by incubation with PV2-IgG was measured in parallel to structural changes at early time points by dispase-based dissociation assay **(F)** (n = 4–5, $^*p < 0.05$ vs. respective Control-IgG incubation).

CK-1 Inhibition Altered Keratin Distribution Similar to PV-IgG

The observation that KIF changes correspond to Dsg3 clustering but precede Dsg3 depletion from the membrane is suggestive of a keratin-dependent regulation of Dsg3 turnover. To test this hypothesis, an approach to induce keratin retraction independent from autoantibody binding to Dsg3 is required. Recently, CK-1α was identified to mediate keratin cytoskeleton organization in a FAM83H-dependent manner (18). CK-1α regulates the filamentous state of keratin filaments and its inhibition promotes keratin bundling in proximity to the nucleus. The phenotype of keratin reorganization under CK-1α inhibition closely matched the one that is observable in PV.

We visualized the effect of the CK-1 inhibitor D4476 on HaCaT cells expressing CK5-YFP. Inhibition of CK-1 induced peripheral keratin filament loss after 1 h, resembling PV-IgG-induced keratin retraction (**Figure 4A**). In line with a regulation of KIFs by CK-1, D4476-induced dephosphorylation of CK14 as indicated by Phos-Tag experiments (**Figure 4B**). Keratin retraction in response to autoantibody binding in PV is associated with a rapid increase of p38MAPK signaling. Inhibition of p38MAPK prevents keratin cytoskeleton rearrangement and loss of cell cohesion (10). Also, the PV-IgG fraction applied here induced p38MAPK activation (Figure S1B in Supplementary Material; See also **Figure 6C**). Similar to the effects of PV-IgG, phospho-p38MAPK levels were increased in response to D4476 incubation for 1 h compared to control conditions (**Figure 4C**). Finally, D4476 incubation induced loss of cell cohesion which was prevented by inhibition of p38MAPK through SB203580 (**Figure 4D**; Figure S1C in Supplementary Material). Nevertheless, reduced cell cohesion in response to D4476 was further impaired by additional application of AK23, a monoclonal anti-Dsg3 autoantibody derived from a pemphigus mouse model (**Figure 4E**; Figure S1D in Supplementary Material). Taken together, KIF alterations in response to CK-1 inhibition through D4476 resemble PV-IgG-induced keratin retraction.

Keratin Retraction Did Not Induce Dsg3 Internalization

To elucidate a possible dependence of keratin retraction on Dsg3 distribution, we applied D4476 in live cell imaging experiments with human keratinocytes expressing CK5-YFP transfected with Dsg3-mCherry. Cells were pre-incubated with either D4476 or DMSO, followed by 3 h of PV2-IgG incubation (see Video S2 in Supplementary Material). Image analysis showed a drastic reduction of keratin cytoskeleton fluorescence in the cell periphery when inhibiting CK-1 which did not occur under control conditions with DMSO (**Figure 5A**, arrows). Interestingly, the retraction of the keratin cytoskeleton was not paralleled by internalization of Dsg3. However, additional incubation with PV2-IgG promoted internalization of Dsg3 when the cytoskeleton was already altered (arrowheads). We further substantiated these findings by immunostaining under conditions without Dsg3 overexpression (**Figure 5B**). Similar to the live cell experiments, Dsg3 appeared unaffected under conditions of D4476-mediated keratin retraction. Nevertheless, Dsg3 clustering and intracellular Dsg3 vesicles were found in both conditions after additional incubation with PV1-IgG (arrowheads). In support of these data, streptavidin pull down of biotinylated surface molecules confirmed the absence of Dsg3 depletion from the membrane in D4476-treated cultures which was induced upon additional 3 h incubation with PV2-IgG (**Figure 5C**).

Interestingly, although overall membrane levels were not altered, the analysis of Dsg3 distribution revealed Dsg3 clustering in the membrane after 60 min of D4476 treatment (**Figure 5D**). These data show that D4476-mediated KIF redistribution did not induce Dsg3 internalization but contributed to clustering in the membrane. This suggests that Dsg3 clustering and internalization of Dsg3 are distinct events and demonstrate the dependence of Dsg3 clustering on correct distribution of the KIF network. By contrast, Dsg3 internalization appears to be independent from KIF alterations and may be a result of other mechanisms elicited by autoantibody binding to Dsg3.

Inhibition of Dsg3 Internalization Did Not Prevent Keratin Retraction

Desmosome assembly and disassembly were shown to be dependent on lipid-raft integrity (7, 27), which can be disturbed by the cholesterol-depleting agent methyl-β-cyclodextrin (β-MCD). In this regard, it was shown that disruption of lipid raft formation restrains Dsg3 endocytosis following PV antibody exposure (7). We used β-MCD to investigate the dependence of keratin alterations triggered by PV-IgG on Dsg3 internalization. Immunostaining and biotinylation assays of human keratinocytes expressing CK5-YFP revealed that 1 h pre-incubation with β-MCD largely prevented Dsg3 internalization after autoantibody exposure (**Figures 6A,B**). However, keratin retraction was still present under these conditions, indicating independency of Dsg3 alterations. Despite the restriction of Dsg3 internalization through lipid raft disruption and in line with a p38MAPK-dependent regulation of the keratin network, p38MAPK activation by PV1-IgG was not abolished (**Figure 6C**). In dispase-based dissociation

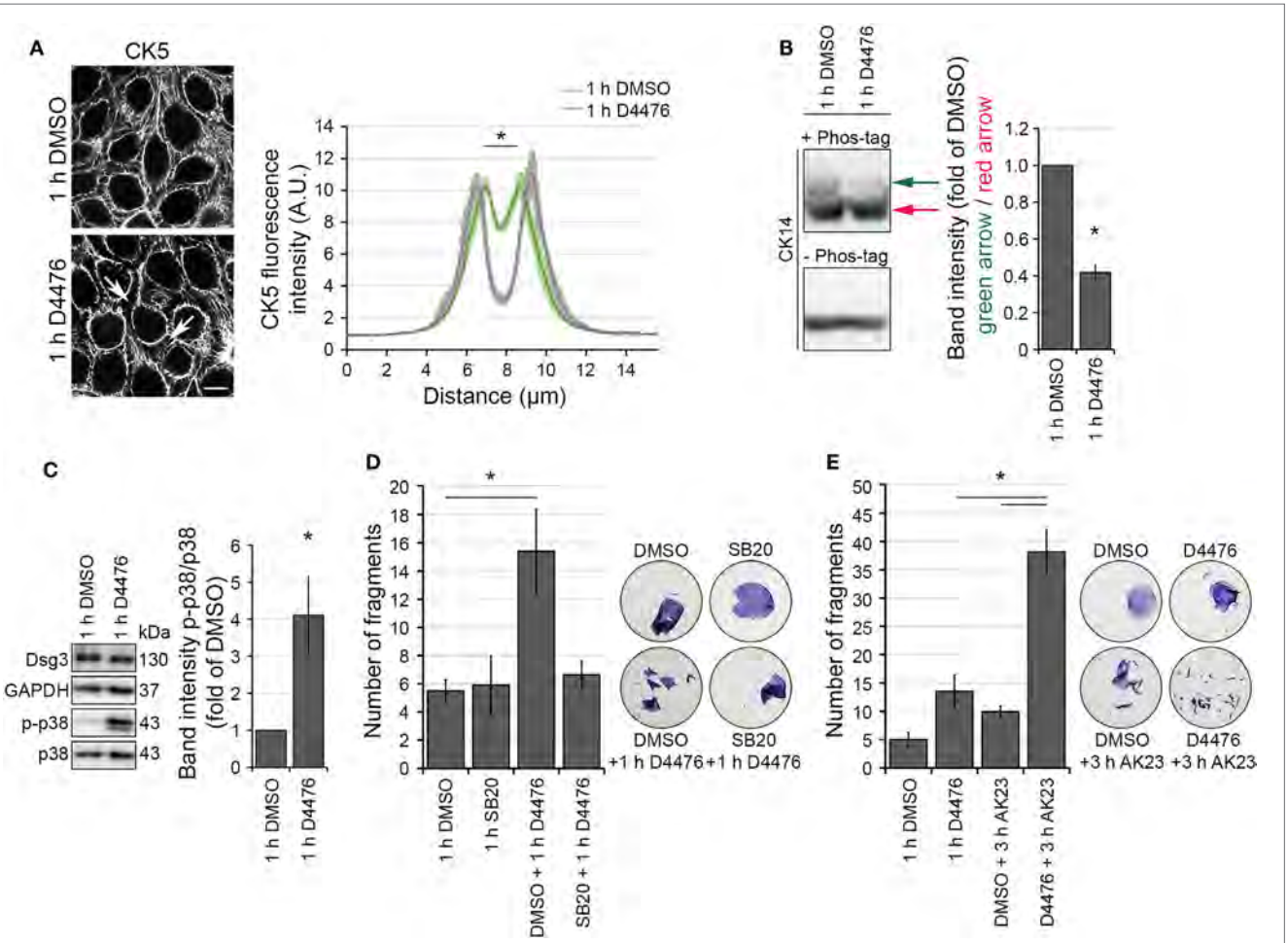

FIGURE 4 | Casein kinase 1 inhibition provoked keratin alterations resembling the PV-IgG-induced phenotype. HaCaT-CK5 cells were incubated with CK-1 inhibitor D4476 for 1 h. The resulting keratin retraction (arrows) was measured with a bar of 15 µm length perpendicular to the cell border of two adjacent cells **(A)** (n = 75–100 cells from three to four independent experiments, $^*p < 0.05$ vs. 1 h DMSO). Bar is 10 µm. **(B)** Phos-tag™ was incorporated in a 6% Western blot gel (+ Phos-tag) to detect the phosophorylation status of CK14 in HaCaT-CK5 cells. Control gel without Phos-tag (– Phos-tag) excluded protein fragmentation. Band intensity of both phosphorylation sites was measured and the first phosphorylation site (green arrow) was divided by the basal phosphorylation site (red arrow) (n = 4, $^*p < 0.05$ vs. 1 h DMSO). **(C)** SDS lysates were generated from cells treated with 1 h D4476 or 1 h DMSO and p38MAPK phosphorylation was evaluated. Densitometric results were normalized to total p38 levels as a loading control (n = 6, $^*p < 0.05$ vs. 1 h DMSO) Cell adhesion was quantified in HaCaT keratinocytes by dispase-based dissociation assays. Pre-incubation with SB203580 (SB20) as a specific inhibitor of p38MAPK or DMSO as a control for 1 h was followed by D4476 incubation for 1 h (n = 4–5, $^*p < 0.05$) **(D)**. Pre-incubation with D4476 or DMSO for 1 h followed by 3 h incubation with AK23, a pathogenic monoclonal desmoglein (Dsg)3 antibody **(E)** (n = 4, $^*p < 0.05$). Remaining cell sheets and fragments were stained with 10 µM MTT for visualization.

assays, loss of cell–cell adhesion caused by PV2-IgG was ameliorated through lipid raft disruption (**Figure 6D**). Taken together, these results suggest that keratin alterations are independent from Dsg3 endocytosis following PV-IgG incubation. Moreover, both effects apparently contribute to loss of cell cohesion. This suggests different mechanisms driving keratin alterations and Dsg3 internalization.

DISCUSSION

In the present study, we show a precise time course of Dsg3 endocytosis and keratin retraction in response to PV-IgG, dissecting the temporal relationship of two hallmarks of PV. Our results demonstrate that both mechanisms contribute to loss of cell cohesion but appear to be largely independent of each other. Based on the observation that cell dissociation is correlating with keratin changes before onset of Dsg3 internalization, these results suggest an important role of keratin retraction for loss of cell cohesion and blistering.

Keratin Alterations Precede Dsg3 Internalization

It is a matter of debate whether KIF alterations in response to pemphigus autoantibodies are secondary to changes of the desmosomes or rather cause and contribute to altered desmosome composition and turnover. Indeed, in early ultrastructural studies, it was suggested that the initial changes affect KIFs (20, 28). We here demonstrated that changes of the KIF

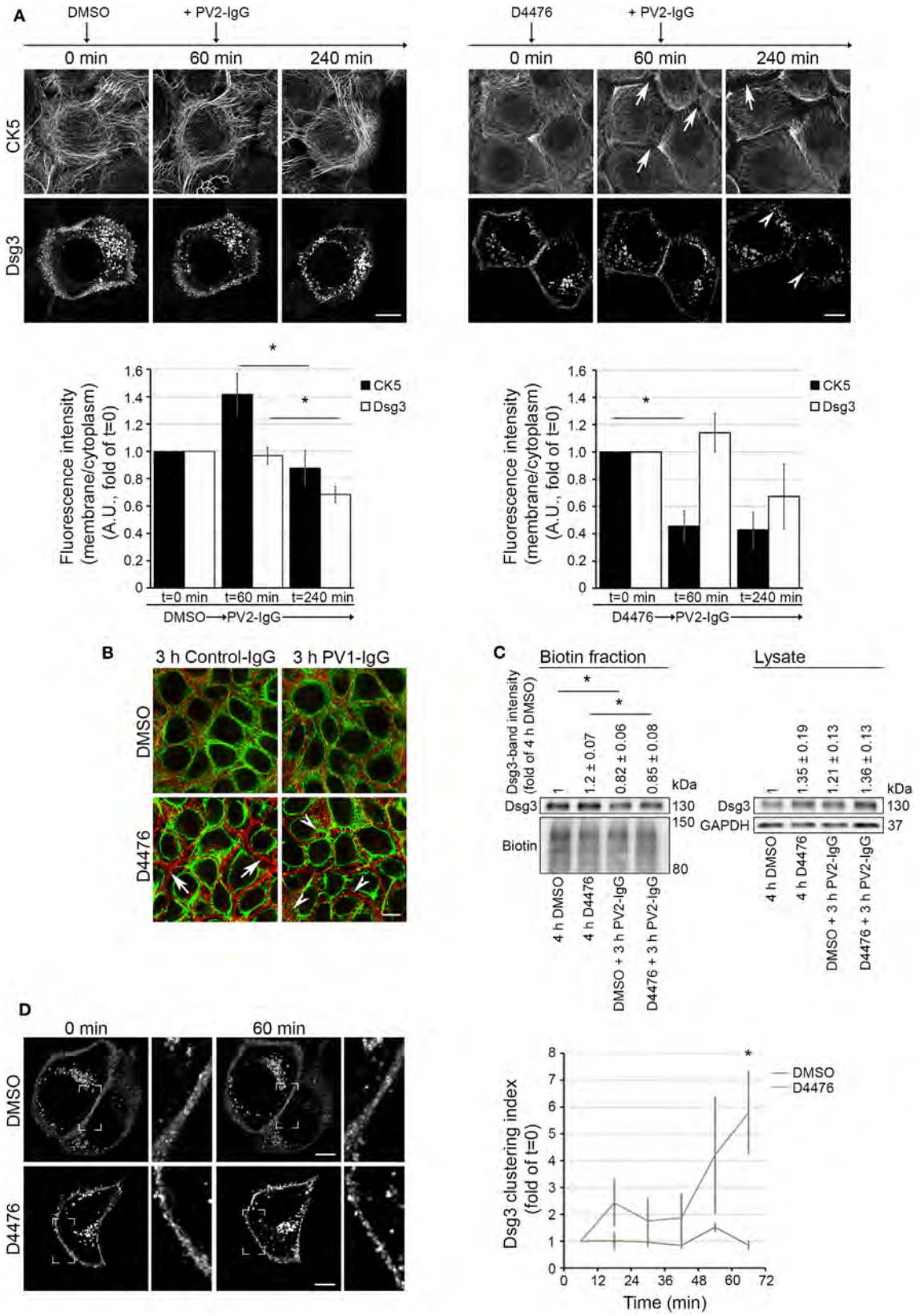

FIGURE 5 | Continued

FIGURE 5 | D4476-induced keratin changes did not induce Dsg3 internalization. HaCaT-CK5 keratinocytes were transfected with pDest-mDsg3-mCherry, incubated with D4476 or DMSO and followed up by three-dimensional confocal time-lapse microscopy **(A)**. D4476 caused keratin retraction after 60 min (arrows) but did not lead to internalization of Dsg3. Subsequent addition of PV2-IgG caused Dsg3 membrane depletion (arrowheads). Bar represents 10 µm ($n = 4$ cells from 4 independent experiments, $^*p < 0.05$). **(B)** Immunostaining of HaCaT-CK5 keratinocytes and Dsg3. Keratin changes occurred under D4476 treatment (arrows) and signs of Dsg3 fragmentation and internalization were visible in response to PV1-IgG treatment only (arrowheads). Images shown are representative for three to four independent experiments. Bar represents 10 µm. **(C)** Streptavidin pulldown of biotinylated Dsg3 in HaCaT-CK5 cells incubated with DMSO or D4476 for 4 h as a control and 1 h incubation followed by a 3 h PV2-IgG incubation. Dsg3 membrane levels were densitometrically assessed ($n = 3$–5, $^*p < 0.05$ vs. respective control condition). **(D)** Dsg3-clustering was analyzed in 1 h live cell imaging sequence of DMSO or D4476 incubation. Clustering was detected using a bar of 10 µm applied linearly on the membrane ($n = 4$, $^*p < 0.05$ vs. DMSO at respective time point). Bar represents 10 µm.

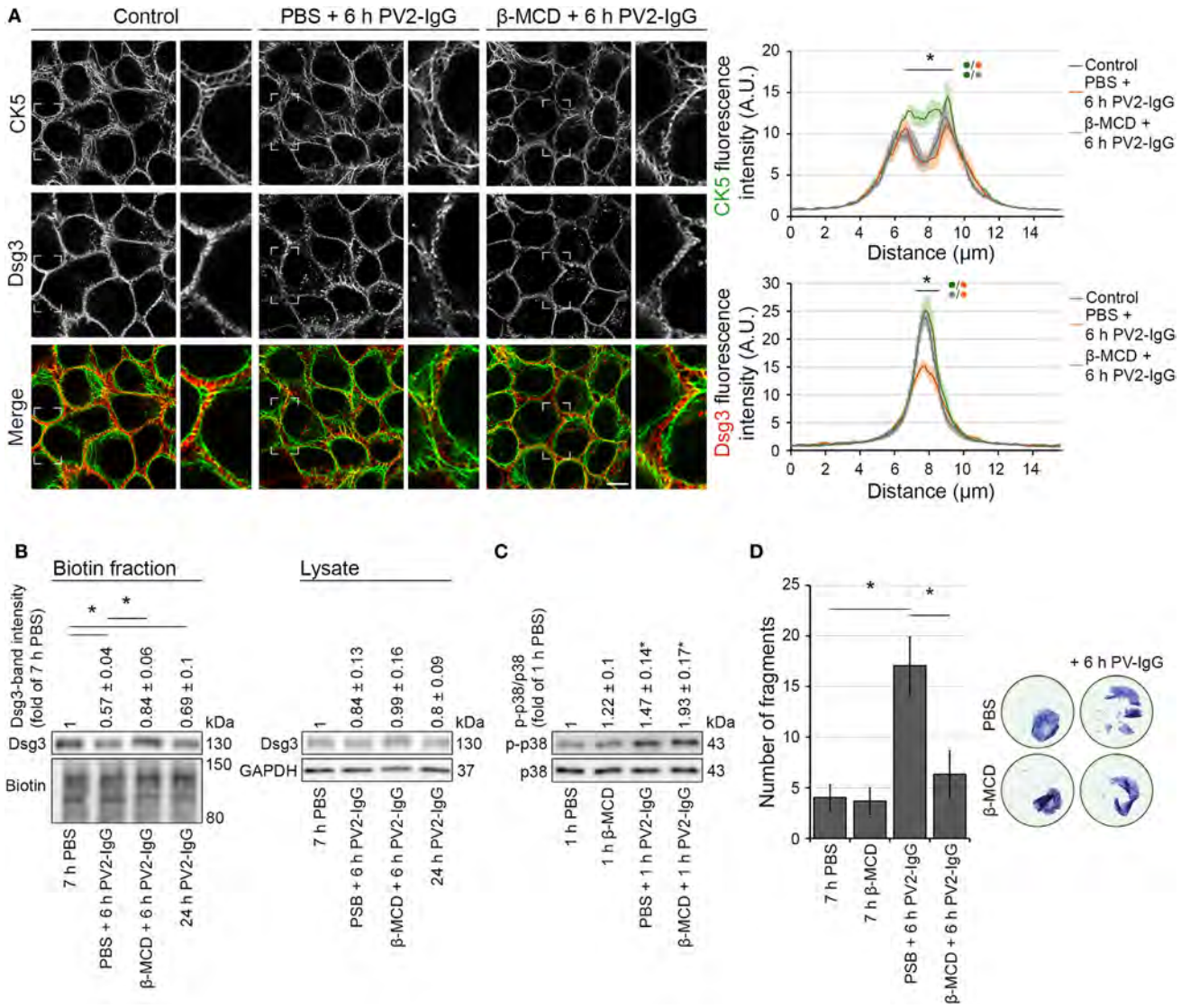

FIGURE 6 | Inhibition of Dsg3 internalization through cholesterol depletion did not prevent PV-IgG-driven keratin alterations. HaCaT-CK5 keratinocytes were pre-incubated with either PBS or β-MCD as a cholesterol-depleting agent for 1 h and then exposed to PV2-IgG for 6 h. Images shown **(A)** are representative for four independent experiments. For analysis a bar of 15 µm was applied perpendicularly over the cell border of two adjacent cells and the fluorescence intensity was plotted for both Dsg3 and CK5 ($n = 100$ cells from four independent experiments; $^*p < 0.05$). Bar represents 10 µm. **(B)** Streptavidin pulldown of biotinylated membrane Dsg3 was performed with HaCaT-CK5 keratinocytes ($n = 3$–5, $^*p < 0.05$). **(C)** Phosphorylation of p38MAPK was determined by densitometry. **(D)** Intercellular adhesion was determined by dispase-based dissociation assays in HaCaT keratinocytes ($n = 8$, $^*p < 0.05$).

cytoskeleton are visible in HaCaT keratinocytes starting at 60 min after application of autoantibodies. Reduced cell–cell adhesion is detectable even earlier, at least under mechanical stress, whereas endocytosis of Dsg3 is not apparent before 90 min of autoantibody exposure. Interestingly, these changes do not affect the amounts of long filaments running perpendicular to

the cell membrane presumably anchoring desmosomes. Rather, the amounts of KIFs in basal and peripheral areas of the cell were reduced. These areas are known to be regions of KIF assembly. It is conceivable that binding of autoantibodies interferes with KIF cycling by limiting the assembly which, in the longer run, would then affect the entire network integrity. This is supported by the notion that the levels of CK14 are getting reduced after several hours. In this context, the thickening of remaining bundles after several hours may be interpreted as a cellular response to the failing adhesion (3). It has to be noted that in primary keratinocytes Dsg3 internalization was shown to occur after 60 min (29). This difference might be related to different maturation states of desmosomes in HaCaT vs. primary keratinocytes (30) or differences in the pathogenicity of the autoantibody fractions applied. For the current study, we relied on the HaCaT cell line for better expression efficiencies of two large proteins compared to primary keratinocytes.

Importantly, it cannot be ruled out that the overexpression approach applied in the current study affects the turnover of the respective molecules. For instance, it was shown that Dsg3 overexpression slows down its internalization and degradation and reduces monolayer fragmentation in response to pemphigus antibodies (24). In our study, the time frame of Dsg3 internalization of transfected and untransfected cells appeared to be at least largely similar as judged from the comparison of fixed, untransfected cells in **Figure 1A** and live cell imaging with Dsg3 overexpression in **Figure 3A**. Nevertheless, it is possible that Dsg3 internalization occurs faster in untransfected cells. Dsg3 internalization showed a similar time frame in HaCaT cells expressing CK5-YFP compared to cells with endogenous keratins only (compare **Figure 3A**; Figure S1A in Supplementary Material). This indicates that keratin overexpression does not alter Dsg3 internalization in response to PV-IgG but does not rule out an effect on keratin changes which may also occur faster in untransfected cells. At least under conditions in which both Dsg3 and keratins are overexpressed, the initial keratin changes precede the internalization of Dsg3.

It is unclear whether the KIFs in the basal cell periphery, which are depleted early in response to PV-IgG, are connected to desmosomes. Instead, the consequences on cell adhesion might be indirect. The desmosomal plaque proteins Dp and Pkp isoforms assemble in a juxtamembranous region together with already attached keratin filaments and are then transported to nascent desmosomes (31, 32). It is possible that this process is compromised by autoantibody-mediated reduced KIF assembly. Alternatively, the phenomenon of interdesmosomal widening may be connected to KIF alterations. It is known that the membranes of adjacent keratinocytes separate between the desmosomes at very early stages following autoantibody incubation (33, 34). As the KIF network is a major determinant of keratinocyte stiffness (35, 36), it is possible that a reduction in the cell periphery favors membrane separation in the interdesmosomal areas. Also, a weakening of the subplasmalemmal network of KIFs that may stabilize interdesmosomal membrane areas may contribute (37). This is supported by observations that p38MAPK inhibition, which blocks keratin retraction as detected in static images, is also reducing interdesmosomal widening (38). This suggests that the interdesmosomal membrane areas contribute to overall cell adhesion.

The observation that the alterations of the KIF cytoskeleton, in comparison to Dsg3 internalization, better correlate with loss of cell cohesion indicates a major contribution to PV-IgG-induced cell dissociation. This mechanism may contribute to the initial loss of cell cohesion that may be conferred through steric hindrance of Dsg3 interactions by PV-IgG. Indeed, it can be concluded from knockout studies that keratins are essential for strong cell–cell adhesion *in vivo* and *in vitro* (16, 39). Furthermore, it was shown that in cells lacking keratins, the forces by which two Dsg3 molecules trans-interact were reduced in a p38MAPK-dependent manner (40).

Based on these results, KIF changes appear not to be secondary to alterations of desmosomal adhesion molecules but to contribute to loss of cell cohesion even in the very early responses to PV-IgG challenge.

Dsg3 Depletion and Keratin Changes May Be Regulated Independently

Given the temporal relationship of KIF alterations and Dsg3 internalization, it may be suggested that these two events are causally connected and Dsg3 membrane depletion is a consequence of altered KIF distribution. However, our results with the CK-1 inhibitor D4476 do not support this hypothesis. CK-1 inhibition resulted in a KIF phenotype resembling the effect of PV-IgG incubation. Under these conditions, no Dsg3 internalization or depletion was detectable whereas additional incubation with PV-IgG induced Dsg3 endocytosis. This supports a model in which Dsg3 membrane localization is independent from KIF changes. In line with these observations, keratinocytes derived from keratin knockout animals exhibit smaller desmosomes and reduced levels of some desmosomal molecules such as Dsg2 but have elevated levels of Dsg3 and unaltered plakoglobin content (16, 39, 40). Hence, the impact of keratins on desmosomal proteins is not uniformly affecting all molecules, which may be related to the observations that desmosomal molecules differentially contribute to cell cohesion (41, 42).

However, although the levels of Dsg3 in the membrane were unaltered, Dsg3 clustering was increased under conditions of D4476-mediated KIF reorganization. Together with the notion from previous data showing that Dsg3 mobility in the membrane is elevated in keratinocytes devoid of KIFs (40), this may indicate that Dsg3 is excluded from desmosomes and forms clusters that are subject to internalization. Indeed, such a model is supported by pulse-chase studies and live cell experiments (24, 43) of Dsg3 trafficking in response to PV-IgG. In this scenario, PV-IgG-induced Dsg3 endocytosis would require a first clustering step, which is normally suppressed by keratins or keratin insertion, and a second internalization step which is independent from keratins. For the latter step, lipid rafts may be essential (7).

Based on these observations, we inhibited Dsg3 endocytosis by interference with lipid raft composition through application of β-MCD. Interestingly, this abrogated Dsg3 endocytosis but did not prevent KIF alterations, indicating that these occur independently of Dsg3 internalization.

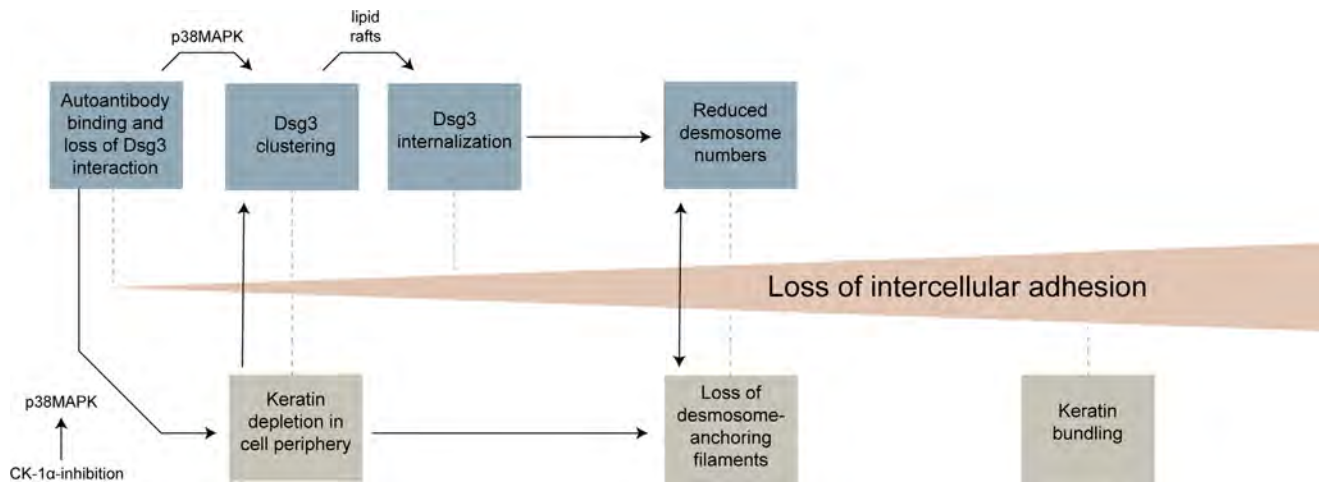

FIGURE 7 | Overview of morphological changes leading to loss of keratinocyte adhesion in response to pemphigus vulgaris-IgG.

Toward a Sequence of Structural Changes Resulting in Cell Dissociation

The results of this study and previous work from several groups can be integrated into a model in which distinct morphological hallmarks are merging to gradually increase cell dissociation (**Figure 7**). Anti-Dsg3 antibodies were shown to sterically inhibit Dsg3 trans-interactions (26, 44) which may contribute to initial loss of cell cohesion and represent a trigger for activation of p38MAPK (11). This, together with crosslinking effects of polyvalent anti-Dsg3 autoantibodies, induces an early clustering of Dsg3 molecules in the cell membrane (24, 45). Early alterations in keratin assembly may contribute to this effect, which also appear to be p38MAPK mediated and which were reproduced by CK-1 inhibition in this study. Dsg3 clustering is then followed by Dsg3 internalization, a process which is dependent on lipid rafts (7). Dsg3 endocytosis together with the internalization of other desmosomal molecules leads to destabilization of desmosomes. Importantly, internalization of desmosomal molecules affects both the assembly and the disassembly of desmosomes, leading to a reduction of desmosome size and numbers (4, 5). KIF loss or uncoupling from desmosomes, possibly bolstered by the altered keratin turnover, contribute to desmosome destabilization and *vice versa* (39, 40). Finally, the thickening of keratin filaments observed at later stages may represent a general cellular stress response or can be interpreted as futile attempt to strengthen cell–cell adhesion by better anchoring the remaining desmosomes. Other mechanisms so far described in pemphigus such as diverse alterations in intracellular signaling, the occurrence of non-desmosomal autoantibodies, or the genetic background (6), may contribute by modulating these morphological changes. It is conceivable that several of these steps need to occur to induce full loss of cell cohesion and blistering. Depending on the experimental setup (e.g., IgG fraction, Ca^{2+} dependency of desmosomes, model system), some of these steps may be more important than others. This may explain some of the controversies existing in the field of pemphigus research.

ETHICS STATEMENT

The sera used in the present study were collected in accordance with the recommendations of ethic committee of University of Lübeck, AZ12-178; name of project: Autoantikörperreaktivität und Pathophysiologie bei blasenbildenden Autoimmunerkrankungen (Pemphigoid und Pemphigus).

AUTHOR CONTRIBUTIONS

ES performed experiments and analyzed data. MR created constructs. FV and CS supervised experiments and analyzed data. JW and VS analyzed data and interpreted results. VS designed the study. ES and VS wrote the manuscript.

FUNDING

The study was supported by grants of the Deutsche Forschungsgemeinschaft SP1300/1-3 and SP1300/3-1 to VS as well as the Föfole program of the LMU.

SUPPLEMENTARY MATERIAL

The Supplementary Material for this article can be found online at https://www.frontiersin.org/articles/10.3389/fimmu.2018.00858/full#supplementary-material.

VIDEO S1 | HaCaT-CK5 cells transfected with pDest-mDsg3-mCherry and incubated with PV1-IgG for 120 min. Images were acquired every 2 min.

VIDEO S2 | 60 min D4476 incubation in HaCaT-CK5 cells transfected with pDest-mDsg3-mCherry followed by 180 min of PV2-IgG incubation. Images were collected every 2 min.

FIGURE S1 | **(A)** HaCaT wild-type keratinocytes showed a similar time course of Dsg3 internalization as HaCaTs expressing cytokeratin5 (CK5)-yellow fluorescent protein ($n = 4$, $^*p < 0.05$). **(B)** HaCaT-CK5 lysates were processed into a TX-100 insoluble and soluble pool showing p38MAPK activation ($n = 4$). **(C,D)** p38MAPK activation and protein levels in HaCaT-CK5 cells after the indicated treatment which correlate to **Figures 4D,E**. Cells were processed for Western blotting as SDS lysates [panel (C): n = 4, panel (D): n = 3–5].

REFERENCES

1. Kasperkiewicz M, Ellebrecht CT, Takahashi H, Yamagami J, Zillikens D, Payne AS, et al. Pemphigus. *Nat Rev Dis Primers* (2017) 3:17026. doi:10.1038/nrdp.2017.26
2. Stahley SN, Kowalczyk AP. Desmosomes in acquired disease. *Cell Tissue Res* (2015) 360:439–56. doi:10.1007/s00441-015-2155-2
3. Hatzfeld M, Keil R, Magin TM. Desmosomes and intermediate filaments: their consequences for tissue mechanics. *Cold Spring Harb Perspect Biol* (2017) 9(6). doi:10.1101/cshperspect.a029157
4. Kitajima Y. 150(th) anniversary series: desmosomes and autoimmune disease, perspective of dynamic desmosome remodeling and its impairments in pemphigus. *Cell Commun Adhes* (2014) 21:269–80. doi:10.3109/15419061.2014.943397
5. Spindler V, Waschke J. Pemphigus – a disease of desmosome dysfunction caused by multiple mechanisms. *Front Immunol* (2018) 9:136. doi:10.3389/fimmu.2018.00136
6. Spindler V, Eming R, Schmidt E, Amagai M, Grando S, Jonkman MF, et al. Mechanisms causing loss of keratinocyte cohesion in pemphigus. *J Invest Dermatol* (2018) 138(1):32–7. doi:10.1016/j.jid.2017.06.022
7. Stahley SN, Saito M, Faundez V, Koval M, Mattheyses AL, Kowalczyk AP. Desmosome assembly and disassembly are membrane raft-dependent. *PLoS One* (2014) 9:e87809. doi:10.1371/journal.pone.0087809
8. Vollner F, Ali J, Kurrle N, Exner Y, Eming R, Hertl M, et al. Loss of flotillin expression results in weakened desmosomal adhesion and pemphigus vulgaris-like localisation of desmoglein-3 in human keratinocytes. *Sci Rep* (2016) 6:28820. doi:10.1038/srep28820
9. Jolly PS, Berkowitz P, Bektas M, Lee H-E, Chua M, Diaz LA, et al. p38MAPK signaling and desmoglein-3 internalization are linked events in pemphigus acantholysis. *J Biol Chem* (2010) 285:8936–41. doi:10.1074/jbc.M109.087999
10. Berkowitz P, Hu P, Liu Z, Diaz LA, Enghild JJ, Chua MP, et al. Desmosome signaling. Inhibition of p38MAPK prevents pemphigus vulgaris IgG-induced cytoskeleton reorganization. *J Biol Chem* (2005) 280:23778–84. doi:10.1074/jbc.M501365200
11. Spindler V, Rotzer V, Dehner C, Kempf B, Gliem M, Radeva M, et al. Peptide-mediated desmoglein 3 crosslinking prevents pemphigus vulgaris autoantibody-induced skin blistering. *J Clin Invest* (2013) 123:800–11. doi:10.1172/JCI60139
12. Sawant MS, Leube RE. Consequences of keratin phosphorylation for cytoskeletal organization and epithelial functions. *Int Rev Cell Mol Biol* (2017) 330:171–225. doi:10.1016/bs.ircmb.2016.09.005
13. Kolsch A, Windoffer R, Wurflinger T, Aach T, Leube RE. The keratin-filament cycle of assembly and disassembly. *J Cell Sci* (2010) 123:2266–72. doi:10.1242/jcs.068080
14. Leube RE, Moch M, Kolsch A, Windoffer R. "Panta rhei": perpetual cycling of the keratin cytoskeleton. *Bioarchitecture* (2011) 1:39–44. doi:10.4161/bioa.1.1.14815
15. Loschke F, Seltmann K, Bouameur JE, Magin TM. Regulation of keratin network organization. *Curr Opin Cell Biol* (2015) 32:56–64. doi:10.1016/j.ceb.2014.12.006
16. Kröger C, Loschke F, Schwarz N, Windoffer R, Leube RE, Magin TM. Keratins control intercellular adhesion involving PKC-α-mediated desmoplakin phosphorylation. *J Cell Biol* (2013) 201:681–92. doi:10.1083/jcb.201208162
17. Dehner C, Rotzer V, Waschke J, Spindler V. A desmoplakin point mutation with enhanced keratin association ameliorates pemphigus vulgaris autoantibody-mediated loss of cell cohesion. *Am J Pathol* (2014) 184:2528–36. doi:10.1016/j.ajpath.2014.05.016
18. Kuga T, Kume H, Kawasaki N, Sato M, Adachi J, Shiromizu T, et al. A novel mechanism of keratin cytoskeleton organization through casein kinase Ialpha and FAM83H in colorectal cancer. *J Cell Sci* (2013) 126:4721–31. doi:10.1242/jcs.129684
19. Kuga T, Sasaki M, Mikami T, Miake Y, Adachi J, Shimizu M, et al. FAM83H and casein kinase I regulate the organization of the keratin cytoskeleton and formation of desmosomes. *Sci Rep* (2016) 6:26557. doi:10.1038/srep26557
20. Wilgram GF, Caulfield JB, Lever WF. An electron microscopic study of acantholysis in pemphigus vulgaris. *J Invest Dermatol* (1961) 36:373–82. doi:10.1038/jid.1961.58
21. Waschke J, Bruggeman P, Baumgartner W, Zillikens D, Drenckhahn D. Pemphigus foliaceus IgG causes dissociation of desmoglein 1-containing junctions without blocking desmoglein 1 transinteraction. *J Clin Invest* (2005) 115:3157–65. doi:10.1172/JCI23475
22. Sivaramakrishnan S, DeGiulio JV, Lorand L, Goldman RD, Ridge KM. Micromechanical properties of keratin intermediate filament networks. *Proc Natl Acad Sci U S A* (2008) 105:889–94. doi:10.1073/pnas.0710728105
23. Carpenter AE, Jones TR, Lamprecht MR, Clarke C, Kang IH, Friman O, et al. CellProfiler: image analysis software for identifying and quantifying cell phenotypes. *Genome Biol* (2006) 7:R100. doi:10.1186/gb-2006-7-10-r100
24. Jennings JM, Tucker DK, Kottke MD, Saito M, Delva E, Hanakawa Y, et al. Desmosome disassembly in response to pemphigus vulgaris IgG occurs in distinct phases and can be reversed by expression of exogenous Dsg3. *J Invest Dermatol* (2011) 131:706–18. doi:10.1038/jid.2010.389
25. Waschke J. The desmosome and pemphigus. *Histochem Cell Biol* (2008) 130:21–54. doi:10.1007/s00418-008-0420-0
26. Vielmuth F, Waschke J, Spindler V. Loss of desmoglein binding is not sufficient for keratinocyte dissociation in pemphigus. *J Invest Dermatol* (2015) 135:3068–77. doi:10.1038/jid.2015.324
27. Resnik N, Sepčić K, Plemenitaš A, Windoffer R, Leube R, Veranič P. Desmosome assembly and cell-cell adhesion are membrane raft-dependent processes. *J Biol Chem* (2011) 286:1499–507. doi:10.1074/jbc.M110.189464
28. Stoughton RB. Mechanisms of blister formation. *AMA Arch Derm* (1957) 76:584–90. doi:10.1001/archderm.1957.01550230050008
29. Calkins CC, Setzer SV, Jennings JM, Summers S, Tsunoda K, Amagai M, et al. Desmoglein endocytosis and desmosome disassembly are coordinated responses to pemphigus autoantibodies. *J Biol Chem* (2006) 281:7623–34. doi:10.1074/jbc.M512447200
30. Spindler V, Endlich A, Hartlieb E, Vielmuth F, Schmidt E, Waschke J. The extent of desmoglein 3 depletion in pemphigus vulgaris is dependent on Ca(2+)-induced differentiation: a role in suprabasal epidermal skin splitting? *Am J Pathol* (2011) 179:1905–16. doi:10.1016/j.ajpath.2011.06.043
31. Albrecht LV, Zhang L, Shabanowitz J, Purevjav E, Towbin JA, Hunt DF, et al. GSK3- and PRMT-1-dependent modifications of desmoplakin control desmoplakin-cytoskeleton dynamics. *J Cell Biol* (2015) 208:597–612. doi:10.1083/jcb.201406020
32. Godsel LM, Hsieh SN, Amargo EV, Bass AE, Pascoe-McGillicuddy LT, Huen AC, et al. Desmoplakin assembly dynamics in four dimensions. *J Cell Biol* (2005) 171:1045–59. doi:10.1083/jcb.200510038
33. Diercks GF, Pas HH, Jonkman MF. The ultrastructure of acantholysis in pemphigus vulgaris. *Br J Dermatol* (2009) 160:460–1. doi:10.1111/j.1365-2133.2008.08971.x
34. Hashimoto K, Lever WF. An ultrastructural study of cell junctions in pemphigus vulgaris. *Arch Dermatol* (1970) 101:287–98. doi:10.1001/archderm.1970.04000030031005
35. Ramms L, Fabris G, Windoffer R, Schwarz N, Springer R, Zhou C, et al. Keratins as the main component for the mechanical integrity of keratinocytes. *Proc Natl Acad Sci U S A* (2013) 110:18513–8. doi:10.1073/pnas.1313491110
36. Seltmann K, Fritsch AW, Kas JA, Magin TM. Keratins significantly contribute to cell stiffness and impact invasive behavior. *Proc Natl Acad Sci U S A* (2013) 110:18507–12. doi:10.1073/pnas.1310493110
37. Quinlan RA, Schwarz N, Windoffer R, Richardson C, Hawkins T, Broussard JA, et al. A rim-and-spoke hypothesis to explain the biomechanical roles for cytoplasmic intermediate filament networks. *J Cell Sci* (2017) 130:3437–45. doi:10.1242/jcs.202168
38. Egu DT, Walter E, Spindler V, Waschke J. Inhibition of p38MAPK signalling prevents epidermal blistering and alterations of desmosome structure induced by pemphigus autoantibodies in human epidermis. *Br J Dermatol* (2017) 177(6):1612–8. doi:10.1111/bjd.15721
39. Bar J, Kumar V, Roth W, Schwarz N, Richter M, Leube RE, et al. Skin fragility and impaired desmosomal adhesion in mice lacking all keratins. *J Invest Dermatol* (2014) 134:1012–22. doi:10.1038/jid.2013.416
40. Vielmuth F, Wanuske MT, Radeva MY, Hiermaier M, Kugelmann D, Walter E, et al. Keratins regulate the adhesive properties of desmosomal cadherins through signaling. *J Invest Dermatol* (2018) 138(1):121–31. doi:10.1016/j.jid.2017.08.033

41. Hartlieb E, Kempf B, Partilla M, Vigh B, Spindler V, Waschke J. Desmoglein 2 is less important than desmoglein 3 for keratinocyte cohesion. *PLoS One* (2013) 8:e53739. doi:10.1371/journal.pone.0053739
42. Keil R, Rietscher K, Hatzfeld M. Antagonistic regulation of intercellular cohesion by plakophilins 1 and 3. *J Invest Dermatol* (2016) 136:2022–9. doi:10.1016/j.jid.2016.05.124
43. Aoyama Y, Nagai M, Kitajima Y. Binding of pemphigus vulgaris IgG to antigens in desmosome core domains excludes immune complexes rather than directly splitting desmosomes. *Br J Dermatol* (2010) 162:1049–55. doi:10.1111/j.1365-2133.2010.09672.x
44. Heupel WM, Zillikens D, Drenckhahn D, Waschke J. Pemphigus vulgaris IgG directly inhibit desmoglein 3-mediated transinteraction. *J Immunol* (2008) 181:1825–34. doi:10.4049/jimmunol.181.3.1825
45. Saito M, Stahley SN, Caughman CY, Mao X, Tucker DK, Payne AS, et al. Signaling dependent and independent mechanisms in pemphigus vulgaris blister formation. *PLoS One* (2012) 7:e50696. doi:10.1371/journal.pone.0050696

Conflict of Interest Statement: The authors declare that the research was conducted in the absence of any commercial or financial relationships that could be construed as a potential conflict of interest.

frontiers in Immunology

ORIGINAL RESEARCH
published: 24 April 2018
doi: 10.3389/fimmu.2018.00839

Keratinocyte Binding Assay Identifies Anti-Desmosomal Pemphigus Antibodies Where Other Tests Are Negative

*Federica Giurdanella, Albertine M. Nijenhuis, Gilles F. H. Diercks, Marcel F. Jonkman and Hendri H. Pas**

Department of Dermatology, University of Groningen, University Medical Center Groningen, Center for Blistering Diseases, Groningen, Netherlands

The serological diagnosis of pemphigus relies on the detection of IgG autoantibodies directed against the epithelial cell surface by indirect immunofluorescence (IIF) on monkey esophagus and against desmoglein 1 (Dsg1) and Dsg3 by ELISA. Although being highly sensitive and specific tools, discrepancies can occur. It is not uncommon that sera testing positive by ELISA give a negative result by IIF and *vice versa*. This brings diagnostic challenges wherein pemphigus has to be ascertained or ruled out, especially when no biopsy is available. We utilized the ability of anti-Dsg3 and anti-Dsg1 IgG to bind in specific desmosomal patterns to living cells to investigate these discrepancies between IIF and ELISA. Living cultured primary normal human keratinocytes were grown under differentiating conditions to induce adequate expression of Dsg1 and Dsg3, incubated with patient serum for 1 h, and then stained to visualize bound IgG. We investigated two different groups; sera from patients with a positive direct immunofluorescence (DIF) and inconsistent serological findings (n = 43) and sera with positive ELISA or IIF but with negative DIF (n = 60). As positive controls we used 50 sera from patients who fulfilled all diagnostics criteria, and 10 sera from normal human subjects served as negative controls. In the DIF positive group, IgG from 39 of the 43 sera bound to the cells in a desmosomal pattern while in the DIF negative group none of the 60 sera bound to the cells. This shows that for pemphigus patients, ELISA and IIF can be negative while anti-desmosomal antibodies are present and *vice versa* that ELISA and IIF can be positive in non-pemphigus cases. In absence of a biopsy for DIF, such findings may lead to misdiagnosis.

Keywords: pemphigus, diagnosis, autoantibodies, desmosomes, desmogleins, keratinocyte

OPEN ACCESS

Edited by:
Falk Nimmerjahn, Friedrich-Alexander-Universität Erlangen-Nürnberg, Germany

Reviewed by:
Christian David Sadik, Universität zu Lübeck, Germany
Xinhua Yu, Forschungszentrum Borstel (LG), Germany

***Correspondence:**
Hendri H. Pas
h.h.pas@umcg.nl

Specialty section:
This article was submitted to Immunological Tolerance and Regulation, a section of the journal Frontiers in Immunology

Received: *30 November 2017*
Accepted: *05 April 2018*
Published: *24 April 2018*

Citation:
Giurdanella F, Nijenhuis AM, Diercks GFH, Jonkman MF and Pas HH (2018) Keratinocyte Binding Assay Identifies Anti-Desmosomal Pemphigus Antibodies Where Other Tests Are Negative. Front. Immunol. 9:839. doi: 10.3389/fimmu.2018.00839

INTRODUCTION

The autoimmune bullous disease pemphigus is caused by the loss of cell–cell adhesion between keratinocytes, induced by autoantibodies mainly directed against the desmosomal cadherins desmoglein 1 (Dsg1) and/or 3 (Dsg3). The serological diagnosis of pemphigus relies on the demonstration of circulating anti-Dsg1 and anti-Dsg3 by ELISA and/or by indirect immunofluorescence (IIF) on monkey esophagus substrate (1). In the pemphigus foliaceus (PF) subgroup, only

antibodies against Dsg1 are present, whereas in pemphigus vulgaris (PV) antibodies against Dsg3 are found in mucosal dominant PV (mdPV), or together with anti-Dsg1 in mucocutaneous PV (mcPV) (2). Apart from antibodies to Dsg 1 and 3 also antibodies to desmocollins (Dsc) 1, 2, and 3 are found, but these are more prevalent in atypical pemphigus diseases as paraneoplastic pemphigus, pemphigus herpetiformis, and pemphigus vegetans but are only found sporadically in classical PV and PF (3, 4). In addition to cadherins, dozens of other proteins were shown to be recognized by pemphigus IgG, including muscarinic and nicotinic acetylcholine receptors, the neonatal Fc receptor, and mitochondrial proteins but proof that these non-desmosomal antibodies have a role in acantholysis is lacking (5). Although being a highly sensitive and specific tool, the ELISA for Dsg1 and Dsg3 ectodomains can be positive without clinical or other laboratory evidence for actual pemphigus, and a number of reports documenting a lack of concordance between positive ELISA and the final diagnosis of the patient can be found in the literature (6). Also, we recently reported the possibility of discrepancies for biopsy proven pemphigus patients, where we found that 9% of positive ELISA sera tested negative by IIF, while 6% of IIF positive sera were negative by ELISA and 5% of pemphigus patient had completely negative serology (7). The latter can be due to a low level of antibodies that is not detectable by IIF or ELISA, to the cessation of antibody production while the skin is still loaded with IgG or that the disease is driven by non-desmosomal antibodies. Inconsistent findings during the diagnostic process bring decision-making challenges wherein the diagnosis of pemphigus needs to be confirmed or ruled out, especially when no biopsy is available. Here, we employed as a new method the ability of pemphigus serum IgG to bind to living cultured keratinocytes to understand discrepancies in currently used diagnostic serum assays.

MATERIALS AND METHODS

Human Sera

From our database of the Center for Blistering Diseases in the Netherlands, we retrospectively selected sera from patients that had pemphigus in the differential diagnosis and at least one positive test, direct immunofluorescence (DIF), IIF on monkey esophagus, or Dsg ELISA. This retrospective study with leftover sera from diagnostic tests does not need approval of the ethics committee in the Netherlands. We included 103 sera and divided them in two groups according to the positive or negative result at DIF analysis for IgG deposits at the epithelial cell surface (ECS). Each group was subsequently branched in subgroups according to the results obtained by IIF and by ELISA as routinely performed in the diagnostic work up of autoimmune bullous diseases (**Figure 1**). As double check, all sera were retested by both IIF on monkey esophagus and, to avoid false positives due to precursor epitopes, also by MBL MESACUP-2 Dsg ELISA. In the DIF negative group, 18 sera were positive for anti-Dsg1 antibodies (median 36.5, Q1 30, Q3 43), and 14 sera were positive for anti-Dsg3 antibodies (median 34.5, Q1 29, Q3 45). Of the 60 DIF negative patients, the final diagnosis was available for 49 patients and included among others 10 cases of lichen planus and 7 cases of pemphigoid but no case of pemphigus (**Table 1**). For the validation of the *in vitro* assay, we used as positive controls sera from 50 PV and PF patients whose diagnosis had been ascertained by concordance between DIF, IIF, ELISA, and clinical and histopathological findings. Sera from 10 healthy human subjects served as negative controls.

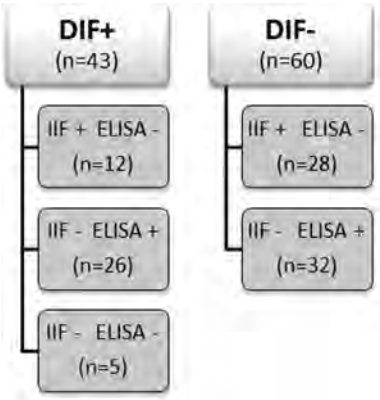

FIGURE 1 | Groups' characteristics and sampling number.

TABLE 1 | Final diagnoses of patients in the direct immunofluorescence negative group.

Definite diagnosis	No. of cases
Lichen planus	10
Bullous pemphigoid	7
Pruritus sine materia	4
Aphthosis	3
Eczema	3
Impetigo bullosa	2
Pityriasis rubra pilaris	2
Prurigo nodularis	2
Pseudoporphyria	2
Vasculitis	2
Brachioradial pruritus	1
Dermatitis factitia	1
Erosive pustular scalp dermatosis	1
Genital ulcer	1
Gingivitis	1
Graft versus host disease	1
Lichen planus pemphigoid	1
Lupus erythematosus	1
Mucous membrane pemphigoid	1
Nummular eczema	1
Urticaria	1
Vulvar carcinoma	1

Final diagnoses were unavailable in 11 sera that were sent from different hospitals for a second opinion.

Keratinocyte Binding Assay (KBA)

NHK were isolated from redundant healthy skin obtained from breast reduction surgery upon written informed consent and grown on glass coverslips in 24-well plates using CnT-Prime and CnT-Prime 2D Differentiation medium (CELLnTEC, Switzerland) at 37°C and 5% CO_2. When shifted to 1.2 mM calcium medium,

desmosomes are induced that initially contain Dsg3 but not Dsg1. After prolonged incubation, cells start to differentiate and to synthesize Dsg1. Hence, we used cells 4 days after calcium shift to test binding of patient IgG to desmosomal proteins. NHK on coverslips were incubated with 2.5% serum in culture medium for 1 h at 37°C after which the cells were fixed in 2% formaldehyde and stored frozen at −80°C until staining. Fixed keratinocytes were stained using DyLight488-labeled goat-anti-human IgG and DAPI for the nuclear staining. The KBA was scored positive for anti-Dsg1 antibodies if IgG bound only to large differentiated cells, and positive for anti-Dsg3 antibodies if IgG bound to all cells. If all cells bind IgG then it is impossible to assess the presence of concomitant anti-Dsg1 IgG as the large differentiated cells also express a high level of Dsg3. Hence, the term "not determinable." The KBA was scored negative if no binding to human IgG was observed. Coverslips were examined under a Leica DMRA fluorescence microscope and images acquired by a Leica DFC350 FX digital camera (Leica, Germany).

Dsg1 and Dsg3 ELISA

All sera were tested by the MESACUP-2 ELISA test for anti-Dsg1 and anti-Dsg3 antibodies (MBL, Japan). As a second means of comparison of the negative ELISA results of sera that tested positive in the KBA ($n = 13$), the anti-Dsg1 and anti-Dsg3 microplate ELISA (EUROIMMUN AG, Germany) was used. Both tests were performed according to the manufacturers' respective protocols, and a cutoff value of 20 U/ml was used to define positivity.

RESULTS

Keratinocyte Binding Assay

IgG from anti-Dsg3 containing sera binds to all keratinocytes in a typical desmosomal pattern (**Figure 2A**). IgG directed against Dsg1 binds in a desmosomal pattern to differentiated cells only that are easily recognizable as they are much larger than undifferentiated cells and lie on top of them (**Figure 2B**). All PF sera and all PV sera of the positive control group bound to the cells in the expected patterns, and of the 10 normal human sera not one serum bound to the cells.

In the DIF+ groups 91% of the sera reacted with cultured keratinocytes by binding of IgG in a desmosomal pattern. Other patterns were not observed. In the IIF+ group, 10 of the 12 sera tested positive for desmosomal IgG binding (Table S1 in Supplementary Material). In the ELISA+ group, all 26 sera tested positive for desmosomal binding. Interestingly, two sera (Table S1 in Supplementary Material, #30, #32) positive for both anti-Dsg1 and anti-Dsg3 IgG showed binding in the Dsg1 pattern only, which was in line with the clinical presentation of both patients that suggested PF instead of PV. IgG from one serum positive for anti-Dsg1 (Table S1 in Supplementary Material, #34) and one serum positive for anti-Dsg3 (Table S1 in Supplementary Material, #36) bound in a converse pattern to the cells; in the first case, erosive lesions limited to the foreskin were present, while in the second case both skin and oral involvement were noted. In the serologically negative group, two sera bound to the cells in the Dsg1 pattern (Table S1 in Supplementary Material, #39, #42) and in one case in the Dsg3 pattern (Table S1 in Supplementary Material, #43). None of the DIF− sera showed a desmosomal binding to cells. Results are summarized in the Table S2 in Supplementary Material.

Dsg1 and Dsg3 ELISA

The sera that bound to cells but were negative by routine MBL ELISA were also assayed by a Dsg ELISA kit from another manufacturer. Although one serum tested positive with this kit, the other 12 remained negative. Complete ELISA results are listed in **Table 2**.

DISCUSSION

Here, we developed a KBA as an additional test based on the ability of pemphigus IgG to bind to desmosomes of living keratinocytes. The KBA discriminates PV from PF but cannot discriminate between mdPV and mcPV as differentiated cells also express Dsg3. Although not qualitative it is a very sensitive assay as in the developing phase of the KBA, we found that when titers decrease and the ELISA turns negative the KBA remains positive (data not shown). Furthermore, similar to ELISA, the assay does not

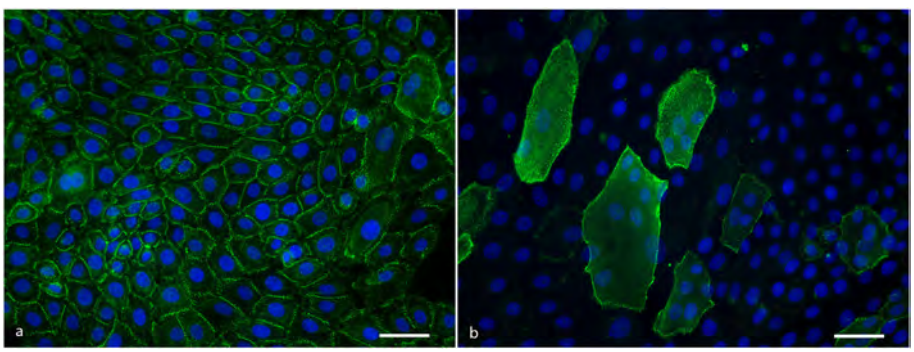

FIGURE 2 | **(A)** Anti-Dsg3 IgG binding pattern to cultured keratinocytes showing desmosomal distribution at cell–cell contacts. Scale bar is 50 µm. **(B)** Anti-desmoglein 1 IgG binding pattern to cultured keratinocytes showing a desmosomal distribution at the cell periphery of differentiated cells. Scale bar is 50 µm.

TABLE 2 | Alternative ELISA results for sera testing positive for keratinocyte binding but negative on first ELISA.

Group	Sample	MBL ELISA desmoglein 1 (Dsg1)	MBL ELISA Dsg3	EU ELISA Dsg1	EU ELISA Dsg3	KBA Dsg1	KBA Dsg3
D+ I+ E–	1	1	3	2	2	nd	+
D+ I+ E–	2	3	2	2	3	nd	+
D+ I+ E–	3	1	4	2	3	+	–
D+ I+ E–	4	2	17	2	6	nd	+
D+ I+ E–	5	19	13	2	15	nd	+
D+ I+ E–	6	9	5	–14	–4	nd	+
D+ I+ E–	7	8	14	3	8	nd	+
D+ I+ E–	8	3	16	1	10	nd	+
D+ I+ E–	10	6	5	**34**	**45**	nd	+
D+ I+ E–	12	4	1	2	2	nd	+
D+ I–E–	38	17	1	6	2	+	–
D+ I– E–	41	1	0	–11	–7	+	–
D+ I– E–	42	6	2	–10	–3	nd	+

Values are expressed in U/mL.
Positive results are in bold.
D, direct immunofluorescence; I, indirect immunofluorescence; E, Dsg ELISA; EU, euroimmun; KBA, keratinocyte binding assay; nd, not determinable.

TABLE 3 | Values of sensitivity and specificity calculated for positive and negative controls, biopsy proven pemphigus patients and negative DIF patients groups.

Group	*n*	KBA+	Sensitivity (%)	Specificity (%)
Positive controls	50	50	100	–
D+ I+ E–	12	10	83.3	–
D+ I– E+	26	26	100	–
D+ I– E–	5	3	60	–
NHS	10	0	–	100
D– I+ E–	28	0	–	100
D– I– E+	32	0	–	100

D, direct immunofluorescence; I, indirect immunofluorescence; E, Dsg ELISA; NHS, normal human subjects; KBA, keratinocyte binding assay.

discriminate between pathogenic and non-pathogenic antibodies as sera from patients in remission off-medication with positive anti-Dsg3 titers also bound to the cells (unpublished results).

Our results show that the KBA has a high correlation with the DIF, we tested in total here 93 sera with positive DIF and 97% of the sera bound to the cells in the specific desmosomal patterns (for details see **Table 3**). This is a higher sensitivity than IIF and ELISA which we recently calculated to be, respectively, 86 and 89% (7). However, in contrast to IIF and ELISA, the KBA is labor intensive and also not quantitative and therefore not a suitable replacement for either IIF or ELISA. Of the 60 sera with negative DIF, none of the sera bound to the cells. As we reported before, a negative DIF is extremely rare in pemphigus and therefore pemphigus is not expected for this group, and indeed the final diagnosis that we could retrieve for 49 of these patients differed from pemphigus.

Interestingly, in two cases, we observed binding in a converse pattern than the antibodies' profile determined by ELISA. In the first case (#34), only anti-Dsg1 IgG were detected by ELISA, but lesions were confined to the foreskin and the histopathology showed a suprabasal intraepidermal split, fitting a diagnosis of PV and presence of anti-Dsg3 antibodies as detected by KBA. The second case (#36) was a patient presenting with mucocutaneous involvement but both ELISA and KBA detected a different antibody profile than expected. The reason for this discrepancy is unclear.

A few reports in literature describe the existence of antibodies against Dsg1 and/or Dsg3 in patients affected by skin conditions other than pemphigus especially patients affected by lichen planus. Given explanations vary between these antibodies having an actual role in the pathogenesis of oral lichen planus or that they would be non-pathogenic (8–10). DIF was only performed in one of these studies, and both patients had no ECS IgG deposition (10). Most of the our lichen planus patients had a DIF with fibrin deposition along the BMZ, but no deposition in ECS pattern although in one case some irregular IgG deposition was seen in the epidermis. Four sera displayed anti-ECS antibodies and six were positive in ELISA, either for anti-Dsg1 or anti-Dsg3, or for both anti-Dsg1 and anti-Dsg3. Although positive in ELISA, they did not bind to cells. Seen that in actual active pemphigus, we clearly found binding when ELISAs became negative (values below 9) the question evolves to what these antibodies bind on the ELISA plates. As we used MESACUP-2 ELISA, it cannot be to the precursor form of Dsg. If they are non-pathogenic antibodies, then they differ from non-pathogenic antibodies in pemphigus patients in complete remission off therapy as these do bind to the cells. It could be that the antibodies are directed to a cryptotope that becomes unmasked in recombinant Dsg present on the ELISA plate. A last explanation is that they are just false positives caused by IgG binding to some other non-Dsg component on the plate, although we then would have expected them to be positive in both ELISAs. Interestingly, 10 sera that bound to the cells (KBA+) were IIF positive but were negative in ELISA kits from different manufacturers. Some patients had positive ELISAs at start of the disease but these turned negative during the course of disease, while IIF stayed positive. Other patients never developed a positive ELISA. As the binding patterns were desmosomal the underlying protein must be desmosomal or desmosome associated. Prime candidates are Dsc and seen the binding of nine sera to all cells, Dsc3 would be the prime suspect. However, eight of these sera were included in a previous study on anti-Dsc3 antibodies, and only one of these was positive in an assay on transfected HEK cells that expressed the ectodomain of Dsc3 on the cell surface (4). In this same study, all eight sera tested also negative for anti-Dsc1 and anti-Dsc2 antibodies. Other antigens have been suggested to serve as pemphigus antigens including muscarinic and nicotinic acetylcholine receptors, pemphaxin, and mitochondrial proteins (11–14). But these antigens are non-desmosomal and therefore cannot explain the observed desmosomal binding patterns. Despite being negative in the Dsg3 ELISA, we feel that Dsg3 is still the prime candidate as antigen. It is possible that we are dealing with low titer high avidity anti-Dsg3 antibodies here that have index values below the cutoff of the ELISA. We have observed patients with active disease that during titer monitoring occasionally had ELISA values just above the cutoff value but mostly, under still active disease, under the cutoff value (unpublished results).

For daily practice of diagnosis, our binding assay results indicate that ELISA and IIF should be interpreted with care as they are positive in a considerable number of cases without other laboratory or clinical evidence of pemphigus. We estimated that in our database for the period 1 January 2002 until 1 January 2017, about 13% of patients with positive ELISAs for Dsg did not have pemphigus. Therefore, taking serum but no biopsy for diagnosis, which is a regularly encountered procedure in the consulting room, bears a risk to reach a false conclusion. In our database, we found 32 sera with no concomitant biopsy that tested positive in either IIF or ELISA, while only 2 (6%) were capable of binding to cells in the KBA (Table S3 in Supplementary Material).

The KBA we demonstrate here is extremely sensitive and reliable. For specialized laboratories, it can provide additional information in challenging cases where the diagnosis of pemphigus cannot be decisively confirmed nor ruled out by routine serological analysis. Furthermore, it is an additional research tool to investigate the nature of pemphigus antibodies.

AUTHOR CONTRIBUTIONS

FG, HP, and MJ contributed to the design of the study. FG and AN performed the experiments. FG and HP wrote the manuscript. GD and MJ revised the manuscript.

ACKNOWLEDGMENTS

The authors would like to thank L. van Nijen-Vos, H. J. Meijer, and S. M. van der Molen (Laboratory of Immunodermatology, Center for Blistering Diseases, UMCG, Groningen, the Netherlands) for their invaluable help with the laboratory analysis performed in this study.

SUPPLEMENTARY MATERIAL

The Supplementary Material for this article can be found online at https://www.frontiersin.org/articles/10.3389/fimmu.2018.00839/full#supplementary-material.

REFERENCES

1. Hertl M, Jedlickova H, Karpati S, Marinovic B, Uzun S, Yayli S, et al. Pemphigus. S2 guideline for diagnosis and treatment – guided by the European Dermatology Forum (EDF) in cooperation with the European Academy of Dermatology and Venereology (EADV). *J Eur Acad Dermatol Venereol* (2015) 29(3):405–14. doi:10.1111/jdv.12772
2. Hashimoto T, Ogawa MM, Konohana A, Nishikawa T. Detection of pemphigus vulgaris and pemphigus foliaceus antigens by immunoblot analysis using different antigen sources. *J Invest Dermatol* (1990) 94(3):327–31. doi:10.1111/1523-1747.ep12874456
3. Ishii N, Teye K, Fukuda S, Uehara R, Hachiya T, Koga H, et al. Anti-desmocollin autoantibodies in nonclassical pemphigus. *Br J Dermatol* (2015) 173(1):59–68. doi:10.1111/bjd.13711
4. Dettmann IM, Krüger S, Fuhrmann T, Rentzsch K, Karl I, Probst C, et al. Routine detection of serum antidesmocollin autoantibodies is only useful in patients with atypical pemphigus. *Exp Dermatol* (2017) 26(12):1267–70. doi:10.1111/exd.13409
5. Kalantari-Dehaghi M, Anhalt GJ, Camilleri MJ, Chernyavsky AI, Chun S, Felgner PL, et al. Pemphigus vulgaris autoantibody profiling by proteomic technique. *PLoS One* (2013) 8(3):e57587. doi:10.1371/journal.pone.0057587
6. Barnadas MA, Rubiales MV, Gich I, Gelpí C. Usefulness of specific anti-desmoglein 1 and 3 enzyme-linked immunoassay and indirect immunofluorescence in the evaluation of pemphigus activity. *Int J Dermatol* (2015) 54(11):1261–8. doi:10.1111/ijd.12768
7. Giurdanella F, Diercks GFH, Jonkman MF, Pas HH. Laboratory diagnosis of pemphigus: direct immunofluorescence remains the gold standard. *Br J Dermatol* (2016) 175(1):185–6. doi:10.1111/bjd.14408
8. Lukac J, Brozović S, Vucicević-Boras V, Mravak-Stipetić M, Malenica B, Kusić Z, et al. Serum autoantibodies to desmogleins 1 and 3 in patients with oral lichen planus. *Croat Med J* (2006) 47(1):53–8.
9. Gholizadeh N, Khoini Poorfar H, TaghaviZenouz A, Vatandoost M, Mehdipour M. Comparison of serum autoantibodies to desmogleins I, III in patients with oral lichen planus and healthy controls. *Iran J Pathol* (2015) 10(2):136–40.
10. Muramatsu K, Nishie W, Natsuga K, Fujita Y, Iwata H, Yamada T, et al. Two cases of erosive oral lichen planus with autoantibodies to desmoglein 3. *J Dermatol* (2016) 43(11):1350–3. doi:10.1111/1346-8138.13493
11. Chen Y, Chernyavsky A, Webber RJ, Grando SA, Wang PH. Critical role of the neonatal Fc receptor (FcRn) in the pathogenic action of antimitochondrial autoantibodies synergizing with anti-desmoglein autoantibodies in pemphigus vulgaris. *J Biol Chem* (2015) 290(39):23826–37. doi:10.1074/jbc.M115.668061
12. Lakshmi MJD, Jaisankar TJ, Rajappa M, Thappa DM, Chandrashekar L, Divyapriya D, et al. Correlation of antimuscarinic acetylcholine receptor antibody titers and antidesmoglein antibody titers with the severity of disease in patients with pemphigus. *J Am Acad Dermatol* (2017) 76(5):895–902. doi:10.1016/j.jaad.2016.11.039
13. Marchenko S, Chernyavsky AI, Arredondo J, Gindi V, Grando SA. Antimitochondrial autoantibodies in pemphigus vulgaris: a missing link in disease pathophysiology. *J Biol Chem* (2010) 285(6):3695–704. doi:10.1074/jbc.M109.081570
14. Nguyen VT, Arredondo J, Chernyavsky AI, Pittelkow MR, Kitajima Y, Grando SA. Pemphigus vulgaris acantholysis ameliorated by cholinergic agonists. *Arch Dermatol* (2004) 140(3):327–34. doi:10.1001/archderm.140.3.327

Conflict of Interest Statement: The authors declare that the research was conducted in the absence of any commercial or financial relationships that could be construed as a potential conflict of interest.

frontiers in Immunology

ORIGINAL RESEARCH
published: 24 April 2018
doi: 10.3389/fimmu.2018.00876

Determination of Autoantibody Isotypes Increases the Sensitivity of Serodiagnostics in Rheumatoid Arthritis

Daniela Sieghart[1†], Alexander Platzer[1†], Paul Studenic[1], Farideh Alasti[1], Maresa Grundhuber[2], Sascha Swiniarski[2], Thomas Horn[3], Helmuth Haslacher[4], Stephan Blüml[1], Josef Smolen[1] and Günter Steiner[1]*

[1] Division of Rheumatology, Department of Internal Medicine III, Medical University of Vienna, Vienna, Austria, [2] Thermo Fisher Scientific, Phadia GmbH, Freiburg, Germany, [3] Thermo Fisher Scientific, Phadia Austria GmbH, Vienna, Austria, [4] Department of Laboratory Medicine, Medical University of Vienna, Vienna, Austria

OPEN ACCESS

Edited by:
Philippe Saas, INSERM UMR1098 Interactions Hôte-Greffon-Tumeur & Ingénierie Cellulaire et Génique, France

Reviewed by:
Yasser El-Sherbiny, University of Leeds, United Kingdom
Willem Falkenburg, Sanquin, Netherlands

***Correspondence:**
Günter Steiner
guenter.steiner@meduniwien.ac.at

[†]These authors have contributed equally to this work.

Specialty section:
This article was submitted to Inflammation, a section of the journal Frontiers in Immunology

Received: *15 January 2018*
Accepted: *09 April 2018*
Published: *24 April 2018*

Citation:
Sieghart D, Platzer A, Studenic P, Alasti F, Grundhuber M, Swiniarski S, Horn T, Haslacher H, Blüml S, Smolen J and Steiner G (2018) Determination of Autoantibody Isotypes Increases the Sensitivity of Serodiagnostics in Rheumatoid Arthritis. Front. Immunol. 9:876. doi: 10.3389/fimmu.2018.00876

Anti-citrullinated protein antibodies (ACPA) and rheumatoid factor (RF) are the most commonly used diagnostic markers of rheumatoid arthritis (RA). These antibodies are predominantly of the immunoglobulin (Ig) M (RF) or IgG (ACPA) isotype. Other subtypes of both antibodies—particularly IgA isotypes and other autoantibodies—such as RA33 antibodies—have been repeatedly reported but their diagnostic value has still not been fully elucidated. Here, we investigated the prevalence of IgA, IgG, and IgM subtypes of RF, ACPA, and RA33 antibodies in patients with RA. To determine the diagnostic specificity and sensitivity sera from 290 RA patients (165 early and 125 established disease), 261 disease controls and 100 healthy subjects were tested for the presence of IgA, IgG, and IgM isotypes of RF, ACPA, and RA33 by EliA™ platform (Phadia AB, Uppsala, Sweden). The most specific antibodies were IgG-ACPA, IgA-ACPA, and IgG-RF showing specificities >98%, closely followed by IgG- and IgA-RA33 while IgM subtypes were somewhat less specific, ranging from 95.8% (RA33) to 90% (RF). On the other hand, IgM-RF was the most sensitive subtype (65%) followed by IgG-ACPA (59.5%) and IgA-RF (50.7%). Other subtypes were less sensitive ranging from 35 (IgA-ACPA) to 6% (IgA-RA33). RA33 antibodies as well as IgA-RF and IgA-ACPA were found to increase the diagnostic sensitivity of serological testing since they were detected also in seronegative patients reducing their number from 109 to 85. Moreover, analyzing IgM-RF by EliA™ proved more sensitive than measuring RF by nephelometry and further reduced the number of seronegative patients to 76 individuals. Importantly, among antibody positive individuals, RA patients were found having significantly more antibodies (≥3) than disease controls which generally showed one or two antibody species. Thus, increasing the number of autoantibodies in serological routine testing provides valuable additional information allowing to better distinguish between RA and other rheumatic disorders, also in patients not showing antibodies in current routine diagnostics. In conclusion, testing for multiple autoantibody specificities increases the diagnostic power of autoimmune diagnostics and could further support physicians in clinical decision-making.

Keywords: autoantibodies, rheumatoid factor, anti-citrullinated protein antibodies, RA33 antibodies, immunoglobulin isotypes, rheumatoid arthritis

INTRODUCTION

Rheumatoid arthritis (RA) is a systemic autoimmune disease characterized by chronic joint inflammation which leads to structural damage of bone and cartilage (1). Besides joint inflammation, duration of symptoms and acute-phase reactants, autoantibodies—rheumatoid factor (RF) and anti-citrullinated protein antibodies (ACPA)—are important diagnostic tools that are also used for classification of RA (2). RF is directed against the Fc portion of immunoglobulin (Ig) G and is usually measured by nephelometry, which captures all classes of Igs but mainly large molecules like IgM. ACPA are the most specific markers for RA and like RF appear early in the disease process and may precede clinical symptoms by several years (3). They are predominantly of the IgG isotype and are commonly measured by assays employing a cyclic citrullinated peptide (CCP) as antigen.

Despite the high sensitivity of the assays used in routine diagnostics still about one-third of RA patients are negative for IgG-ACPA and RF. It has been proposed by several authors that additional testing for other RF and ACPA isotypes—particularly IgA—might increase the sensitivity of RA serodiagnostics (4–8) or predict the development of disease (9), but clear-cut evidence is still scarce. Therefore, routine diagnostics are commonly restricted to measuring IgG-ACPA (usually by ELISA) and the determination of IgM-RF. RA33 antibodies (which are directed to the nuclear antigen hnRNP-A2/B1) were also found to be fairly specific for RA and testing for RA33 antibodies could be of additional diagnostic usefulness because they are also detected in RF/ACPA negative RA patients. However, published data on RA33 antibodies so far refer only to the IgG isotype and their use in routine diagnostics has not yet been widely established (10–13).

It was therefore the aim of this study to measure the IgG, IgA, and IgM isotypes of RF, ACPA, and RA33 in patients with RA and related rheumatic diseases in order to assess their diagnostic sensitivity and specificity. In particular, this study aimed to explore if testing for multiple antibody species can increase the power of RA serodiagnostics by reducing the number of seronegative patients, thereby allowing an earlier diagnosis and treatment of patients negative for the routinely measured antibodies.

MATERIALS AND METHODS

Patients

To determine the sensitivity and specificity of autoantibodies, sera were obtained from 290 RA patients, classified according to the 2010 EULAR/American College of Rheumatology criteria (2). Among these, 165 patients were early RA (inception cohort) receiving their first treatment with methotrexate (MTX) and 125 patients were established RA receiving their first treatment with a TNF inhibitor. The antibody measurements were in general performed at the time of therapy induction or maximum 2 months before or 2 weeks thereafter if a baseline sample was not available (38 patients) because antibody titers are quite stable and seroconversion is rarely observed before or shortly after start of treatment. Disease control samples were collected from 100 patients with osteoarthritis (OA), 50 patients with systemic lupus erythematosus (SLE), 50 patients with ankylosing spondylitis, 13 patients with reactive arthritis (reA), 15 patients with dermatomyositis-polymyositis, 14 patients with granulomatosis with polyangiitis, and 19 osteoporosis patients. In addition, 100 sera from healthy subjects were analyzed for the presence of autoantibodies. Descriptive statistics for the Vienna inception ($n = 165$) and established RA ($n = 125$) cohort are summarized in **Table 1**. Disease controls had a median age of 55 (43–64) and 68.8% were females. Healthy subjects had a median age of 50 (42.5–55) and 72% were females. An informed consent was obtained from all patients as well as healthy subjects and the study was approved by the ethics committee of the Medical University of Vienna (ethics vote number: 559/2005).

Detection of Autoantibodies

Serum samples were tested for the presence of IgA, IgG, and IgM isotypes of RF, ACPA, and RA33 by EliA™ platform (Phadia AB, Uppsala, Sweden). Of note, the anti-RA33 EliA™ is a prototype assay that is not yet commercially available (14) but is designed according to the same principle as the commercial assays available for the EliA platform (Phadia AB, Uppsala, Sweden). In this assay, recombinant human hnRNP-A2/B1 expressed in a eukaryotic expression system is used as antigen and a monospecific serum used as standard. According to our established standard protocols, a calibration curve for each isotype is determined during each measurement. This is used to calculate the defined units of the antibodies measured with commercially available assays or the concentration of the antibodies measured with prototype assays (research use only, IgM-CCP, IgA-, IgG-, and IgM-RA33) which have no defined units. Cutoffs for RF IgM, IgA, and IgG as well as ACPA IgG and IgA were employed according to the manufacturer's instructions. The cutoff for IgG-ACPA used in this study was 7 U/ml, which is (according to the manufacturer) the "equivocal cutoff" while in routine diagnostics the "positive cutoff" of 10 U/ml is used. However, since even at the lower cutoff the assay showed a specificity versus disease controls of 99% also

TABLE 1 | Descriptive characteristics of rheumatoid arthritis (RA) patients.

	RA (inception)	RA (established)
Age (years)	57.4 (47.2–66.2)	53.2 (44.1–63.3)
Female%	74.2	83.8
Disease duration (years)	**0.1 (0–0.3)**	**6.5 (2.5–12)*** **
Simplified disease activity index	15.6 (9.3–24.2)	14.4 (8.7–21)
Clinical disease activity index	14.2 (8.5–22.1)	12 (7–18.2)
Disease activity score	4.4 (3.4–5.2)	4.2 (3.3–4.8)
C-reactive protein [mg/dl]	0.8 (0.3–1.6)	0.4 (0.2–1.3)
Pain	43 (18–56)	36 (18–56.5)
Patient global disease activity	40 (19.5–60.5)	41 (21–60)
Evaluator's global disease activity	20 (9.5–35)	21.5 (10–35)
Health access and quality index (HAQ)	**0.4 (0–1)**	**0.8 (0.25–1.5)***
Swollen joint count 28	3 (2–6)	3 (2–6)
Tender joint count 28	3 (1–7)	3 (0–6)
Corticosteroids (mg)	6.3 (5–10.5)	6.3 (5–9.8)

*Descriptive characteristics of inception and established RA were calculated at treatment start (baseline), i.e., MTX treatment in the inception cohort and anti-TNF treatment in patients with established RA. Values are medians and lower and the upper quartiles provided in brackets. Disease duration was calculated from the date of diagnosis. The corticosteroid dose also refers only to the baseline visit and gives no information about earlier prescriptions. Significant differences between the inception and established RA cohort are shown in bold numbers. Corr. p-values for disease duration was ***$p < 0.0001$ and HAQ was *$p = 0.012$.*

patients with equivocal IgG-ACPA levels were included in our analysis. Cutoffs for prototype anti-RA33 (IgA, IgG, and IgM) and the IgM-ACPA EliA™ were calculated by receiver operating characteristic (ROC) curve analysis (15) against disease controls and healthy subjects. Area under the curve (AUC) values for the ROC curves are shown in **Table 2**, see Figure S1 in Supplementary Material for the ROC diagrams [made with the R package pROC (16)]. In addition, RF and ACPA had been routinely measured by nephelometry using the N Latex RF kit (employing human IgG as antigen) on a BN II system (Siemens Healthcare GmbH, Germany) and the anti-CCP EliA™ (Thermo Fisher Scientific), respectively.

Statistical Analysis

For comparison of two groups of numeric values a two-tailed Mann–Whitney *U*-test was performed using R (version 3.2.3). For comparison of two groups of nominal values (gender) Fisher's exact test was used. If a correction for multiple testing was done (written as "corr. *p*-values"), it was the Bonferroni correction. A *p*-value of <0.05 was considered significant. To distinguish between the *p*-value levels they are depicted as $^{*}p \leq 0.05$, $^{**}p \leq 0.01$, and $^{***}p \leq 0.001$.

RESULTS

Cutoffs, Sensitivities, and Specificities of Autoantibodies

To determine their diagnostic sensitivity and specificity, the nine autoantibody species were measured in 290 patients with RA, 261 disease controls, and 100 healthy subjects. Cutoffs were used either according to the manufacturer or determined by ROC curve analysis (RA33 antibodies and IgM-ACPA). Positive predictive values of antibodies against disease controls or healthy subjects were also calculated. The data are summarized in **Table 2**. Among the three RF isotypes, IgM-RF showed the highest sensitivity (64.8%) followed by IgA-RF (50.7%) and IgG-RF (14.4%).

Specificities versus disease controls were 95.3% for IgA-RF, 98.6% for IgG-RF, and 90% for IgM-RF, the latter being comparable to the specificity of nephelometric RF (89%) determined in previous studies (11, 17). Of note, testing for IgM-RF proved more sensitive than nephelometric RF determination (64.8 vs 59%; **Table 2**). Of the 171 patients positive for RF by nephelometry only three were negative by EliA™ and overall the titers of both assays correlated with a coefficient of determination (R^2) of 0.78 and an intraclass correlation of 0.79 (Figure S2 in Supplementary Material). Despite the good correlation, a few discrepant results were obtained which can be explained by methodological differences between the two assays employing antigens (IgG) of human (nephelometry) or rabbit (EliA™) origin which may occasionally cause discrepancies (18).

Among the ACPA isotypes, IgG-ACPA was by far the most sensitive marker (57.9%) and also the most specific one (99.4%). A similar specificity was found for IgA-ACPA (98.6%) which, however, was much less prevalent showing a sensitivity of only 34.1%. IgM-ACPA was the least sensitive (28.6%) and the least specific subtype (95.6%).

To define positivity of RA33 antibodies, cutoffs for prototype RA33 EliA™ were calculated by ROC curve analysis and set to reach at least 95% specificity against disease controls and 98% against healthy subjects. Using these criteria, 4.5 (IgA-RA33), 12 (IgG-RA33), and 32 µg/l (IgM-RA33) were defined as cutoffs for the three anti-RA33 subtypes which showed sensitivities of 6, 6.2, and 17.7%, respectively. Both IgA- and IgG-RA33 showed high specificity (97.5 and 97.2%) while the specificity of IgM-RA33 was 95.8% and thus comparable to IgM-ACPA but superior to IgM-RF (**Table 2**).

Thus, not surprisingly the IgM isotypes of all three antibodies proved less specific than IgG and IgA isotypes. However, of the three measured IgM isotypes (RF, ACPA, and RA33), the titers of IgM-RF and IgM-ACPA were significantly higher in RA patients than in disease controls and healthy subjects (**Figure 1**). Among the 261 disease controls, false positive results were obtained particularly in patients with OA, ankylosing spondylitis and SLE

TABLE 2 | Specificity and sensitivity of rheumatoid factor (RF), anti-citrullinated protein antibodies (ACPA), and RA33 isotypes for the diagnosis of rheumatoid arthritis (RA).

	IgA-RF	IgG-RF	IgM-RF	IgA-ACPA	IgG-ACPA	IgM-ACPA	IgA-RA33	IgG-RA33	IgM-RA33	RA33 (total)	IgA-RF/ACPA (total)	RF (routine)	ACPA (routine)
Cutoff	14 IU/ml	28 IU/ml	3.5 IU/ml	7 U/ml	7 U/ml	116.7 µg/l	4.5 µg/l	12 µg/l	32 µg/l			15.9 IU/ml	10 U/ml
Specificity (healthy)	98%	98%	92%	99%	99%	95%	98%	98%	98%	94%	97%	n.d.	n.d.
Specificity (disease controls)	95.3%	98.6%	90%	98.6%	99.4%	95.6%	97.5%	97.2%	95.8%	90%	94.2%	n.d.	n.d.
Patients with RA (*n*)	290	290	290	290	290	290	235	290	243	290	290	290	290
Sensitivity (% positive patients)	50.7%	14.4%	64.8%	34.1%	57.9%	28.6%	6%	6.2%	17.7%	22%	55.2%	59%	55.2%
PPV (healthy)	95.4%	85.4%	86.8%	96.5%	97.9%	82.3%	63.1%	71.6%	84.2%	74.9%	93.7%		
PPV (disease controls)	89.8%	89.3%	84%	95.2%	98.7%	84.1%	57.8%	64.3%	71.7%	64.1%	88.5%		
AUC (RA vs healthy)	0.775	0.643	0.785	0.742	0.754	0.67	0.55	0.608	0.481				
AUC (RA vs disease controls)	0.725	0.643	0.784	0.704	0.777	0.687	0.646	0.47	0.537				

Antibodies were measured in sera of 290 RA patients, 261 disease controls and 100 healthy subjects. Cutoffs for RF isotypes and for IgA- and IgG-ACPA were used according to the manufacturer's instructions (U = unit; IU = international unit). Cutoffs for IgM-ACPA and prototype RA33 EliA™ were calculated by receiver operating characteristic (ROC) curve analysis. The total number of RA33 positive patients and IgA-RF and/or IgA-ACPA positive patients are summarized in the last two columns. The data obtained with routinely measured RF (nephelometry) and IgG-ACPA (EliA™) are shown for comparison. Specificity, sensitivity, and positive predictive values are showing the performance of each Ig. The area under the ROC curve (area under the curve [AUC]) values measure the performance without a particular cutoff. An AUC of 0.5 would be random when not choosing the cutoff carefully. The higher an AUC value is, the better is the performance. See also Figure S1 in Supplementary Material for a visualization of the ROCs.

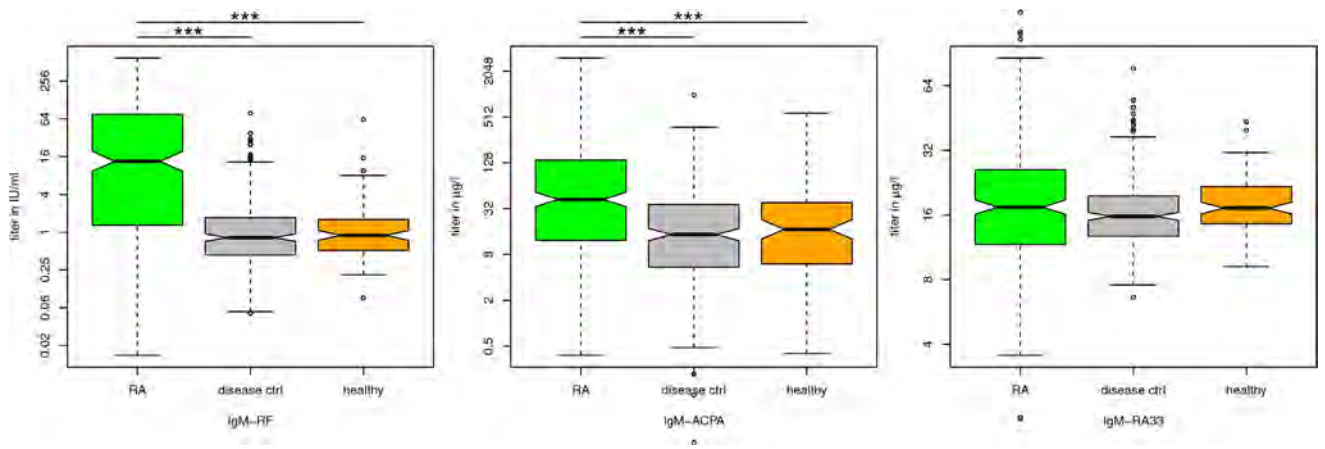

FIGURE 1 | Immunoglobulin (Ig) titers of rheumatoid arthritis (RA) patients vs healthy and disease control patients. The significance corresponds fairly to the overlap of the notches in the boxplots: IgM-rheumatoid factor (RF) and IgM-ACPA are significantly ($p \leq 0.001$) different between RA patients and disease controls or healthy subjects, whereas IgM-RA33 titers did not significantly differ between the three groups.

TABLE 3 | Antibody profile of healthy subjects and disease controls.

	Tested patients	IgA-RF	IgG-RF	IgM-RF	RF total	IgA-ACPA	IgG-ACPA	IgM-ACPA	ACPA total	IgA-RA33	IgG-RA33	IgM-RA33	RA33 total
Healthy	100	2	2	8	11	1	1	5	6	2	2	2	6
SLE	50	11	3	13	18					3	3	6	11
Ankylosing spondylitis	50		1	3	4	3	1	5	8	2	3	5	10
Osteoarthritis	100	3		13	16	1		9	10	1	1	3	6
Reactive arthritis	13	1		1	1	1	1	1	1	1			1
Osteoporosis	19	2	1	3	4			1	1		1	1	2
Dermatomyositis-polymyositis	15			2	2					1	1		2
Granulomatosis with polyangiitis	14			1	1					1	1		2
Total	361	19	7	44	57	6	3	21	26	11	12	17	40
Total excluding SLE	311	8	4	31	39	6	3	21	26	8	9	11	29

100 healthy subjects as well as 50 patients with systemic lupus erythematosus (SLE), 50 patients with ankylosing spondylitis, 100 patients with osteoarthritis (OA), 13 patients with reactive arthritis (reA), 19 osteoporosis patients, 15 dermatomyositis–polymyositis patients, and 14 patients with granulomatosis with polyangiitis (Wegener's granulomatosis) were tested for the presence of IgA, IgG, and IgM of RF, ACPA, and RA33. Total numbers of positive patients including or excluding patients with SLE are indicated.

(**Table 3**). Since SLE patients are rarely seen in an early arthritis clinic, the number of positive disease controls excluding SLE is additionally indicated in **Table 3**. Of note, in disease controls, there was hardly any overlap of antibodies with the majority of patients being positive for only one or two antibody species (see added diagnostic value).

Distribution of Autoantibody Isotypes in RA Patients

The cohort of 290 RA patients consisted of 165 patients with early RA who had started their first MTX treatment at the Division of Rheumatology and 125 RA patients with established disease who had started their first treatment with TNF inhibitors. No major differences in autoantibody titers were observed between patients with early and established RA (Figure S3 in Supplementary Material). As expected, IgM-RF was the major subtype and also the most sensitive of all nine autoantibody species tested. Thus, 188 patients were positive for IgM-RF, 147 for IgA-RF, and only 42 for IgG-RF. These two isotypes largely overlapped with IgM-RF and only 12 patients were solely positive for either IgA-RF ($n = 9$) or IgG-RF ($n = 3$), while in 44 patients IgM-RF was the only isotype. In total, 200 patients (69%) were RF positive and in 33 patients all three isotypes were detected (**Figure 2A**).

With respect to ACPA, 168 patients were positive for IgG-ACPA and 99 for IgA-ACPA while IgM-ACPA was found in only 83 patients. Both IgA- and IgM-ACPA largely overlapped with the IgG isotype and only 9 patients were solely positive for IgM- and a single patient was solely positive for IgA-ACPA as compared to IgG-ACPA which in 49 patients was the only ACPA species. In total, 178 patients were ACPA positive and in 53 patients all three isotypes were detected (**Figure 2B**).

Concerning RA33 antibodies, 14 patients were positive for IgA- and 18 for IgG-RA33. Interestingly, the major RA33 subtype was IgM which was detected in 43 patients. Prevalence of IgG-RA33 was lower but specificity was markedly higher than reported in previous studies (10–13). In total, 64 patients were RA33 positive. However, in contrast to RF and ACPA, the overlap between the RA33 isotypes was marginal (**Figure 2C**). Thus,

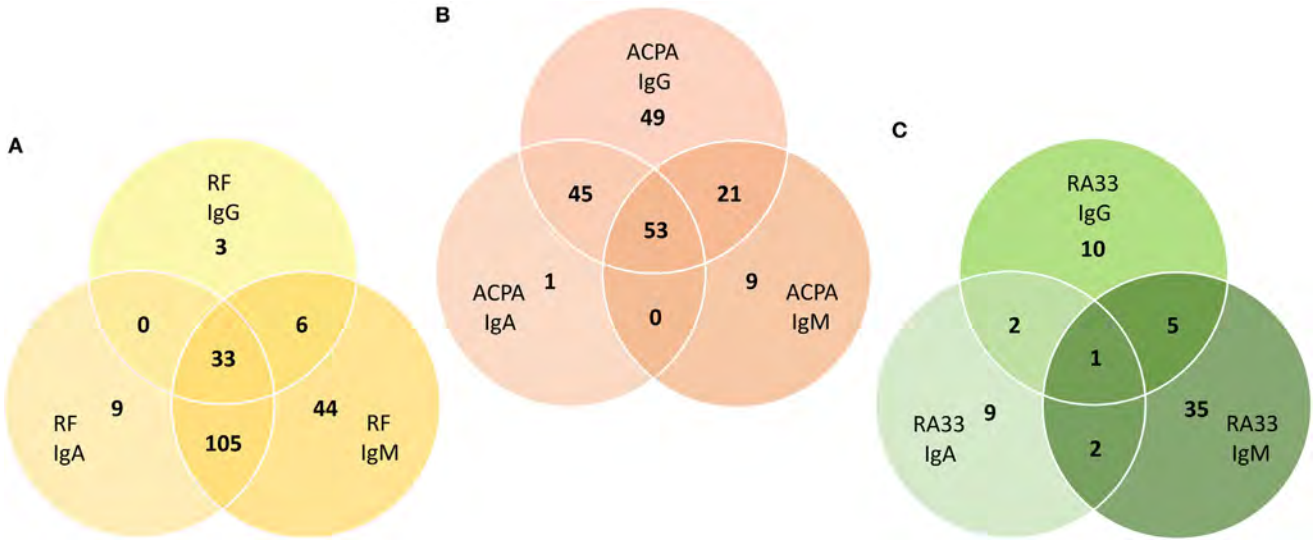

FIGURE 2 | Isotype distribution of rheumatoid factor (RF), anti-citrullinated protein antibodies (ACPA), and RA33 antibodies among antibody positive patients. Venn diagrams visualizing the overlap between **(A)** RF, **(B)** ACPA, and **(C)** RA33 IgA, IgG, and IgM isotypes. The major RF subtype is IgM largely overlapping with IgA and IgG subtypes. The major ACPA subtype is IgG largely overlapping with IgA and IgM subtypes. The major RA33 subtype is IgM but there is little overlap with the IgA and IgG subtypes.

only nine patients tested positive for two isotypes and in a single patient co-occurrence of all three isotypes was seen.

Added Diagnostic Value of Testing for Multiple Isotypes

Among the 290 RA patients, 150 (51.7%) were positive for both RF and ACPA by routine diagnostics, while 21 (7.2%) and 10 (3.4%), respectively, were solely positive for either RF or ACPA (**Figure 2A**); 109 (37.6%) patients were negative for both antibodies and are therefore referred to as seronegative. Out of these, 13 (4.5%) patients showed at least one RA33 subtype and 15 (5.2%) patients were positive for either IgA-RF ($n = 14$) and/or IgA-ACPA ($n = 4$), whereas IgG-RF and IgM-ACPA did not further increase the sensitivity of autoantibody diagnostics. In addition, 14 (4.8%) RF negative patients (as determined by nephelometry) tested positive for IgM-RF by EliA™ (**Figure 3A**).

The majority of antibody positive RA patients was found to be triple positive for (nephelometric) RF, IgG-ACPA and either IgA-RF or IgA-ACPA. Interestingly, among the 64 RA33 positive patients 48 were also positive for IgA-RF and/or IgA-ACPA (**Figure 3B**). Concerning the added diagnostic value of testing for multiple antibodies, 24 (8.3%) formerly seronegative patients were positive for either IgA-RF/ACPA or RA33 antibodies. Therefore, additional testing for IgA-RF/ACPA and RA33 reduced the number of seronegative patients by approximately 22% (**Figure 3B**). Additional specification of IgM-RF further reduced the number of seronegative patients resulting in a total reduction of 30%. Importantly, with respect to the diagnostic value of the IgM-RF determination, the majority of patients negative for nephelometric RF but positive for IgM-RF were low-titered but showed additional reactivities (including IgG-ACPA), in contrast to the controls which were usually monospecific for IgM-RF.

Typically, RA patients were positive for multiple antibody species, which was in sharp contrast to the disease controls (**Table 3**). Among the 81 antibody positive disease controls, 73% showed only one antibody species whereas the majority of antibody positive RA patients (74%) had at least three antibodies with only 14% of the patients showing singular positivities, mostly of the IgM or IgA isotype (**Figure 4**). Thus, the presence of three antibodies had a specificity of 94% and the presence of four antibodies was almost 99% specific for RA, even in IgG-ACPA negative patients among which eight showed four or more antibodies and four were triple positive. Double positive disease control usually showed only IgM antibodies with the notable exception of SLE patients in which IgM-RF and IgA-RF commonly occurred together, whereas none of them showed any ACPA isotype.

There were no major differences in clinical parameters between antibody negative and positive patients, except that TJC28 is significantly ($p = 0.04$) lower in patients with 4 or more antibodies compared to seronegative patients (**Table 4**).

DISCUSSION

Approximately one-third of RA patients are commonly negative for RF and ACPA, the two serological marker antibodies which are routinely determined in RA serodiagnostics. However, it is still not fully clarified whether these patients are completely negative for autoantibodies or may rather generate antibody species that are not covered by routine diagnostics where usually IgG-ACPA (by ELISA) and RF (by nephelometry or ELISA) are determined. This issue has been in addressed in several previous studies in which especially IgA subtypes of RF and ACPA were found to occur mainly in seropositive patients. However, in none of these studies, all three ACPA and RF isotypes were investigated in parallel and

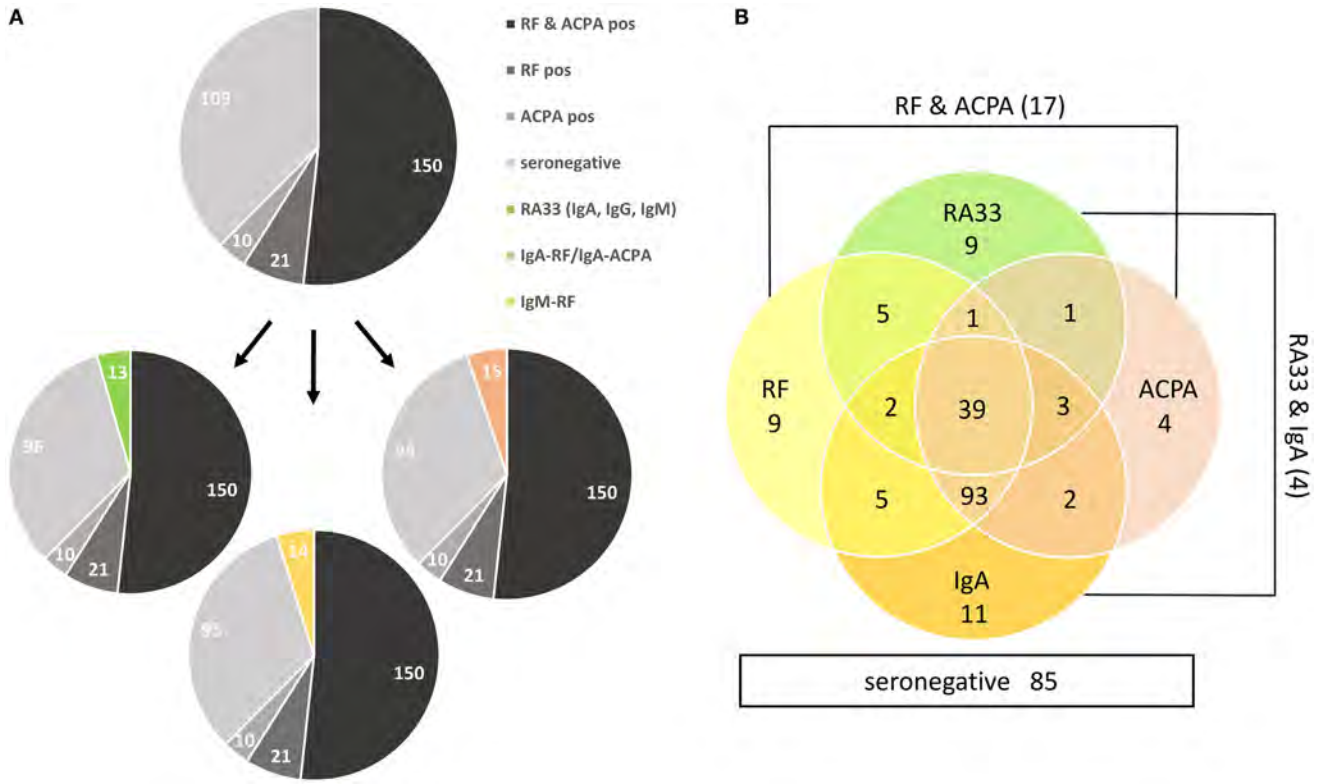

FIGURE 3 | Added diagnostic value of IgA-rheumatoid factor (RF)/anti-citrullinated protein antibodies (ACPA), IgM-RF and RA33 antibodies. **(A)** Numbers of patients tested positive by routine diagnostics (RF nephelometry, IgG-ACPA) and seronegative patients (upper pie chart) showing additional RA33 antibodies (lower left pie chart), IgM-RF (lower middle pie chart) or IgA-RF/ACPA (lower right pie chart). **(B)** Venn chart visualizing the diagnostic overlap of RA33 and IgA antibodies with routine diagnostics (RF nephelometry, IgG-ACPA). The numbers of seronegative patients (n = 85), RF, and IgG-ACPA positive but RA33 and IgA-RF/ACPA negative patients (n = 17) as well as patients positive for both RA33 and IgA-RF/ACPA but negative for RF and ACPA (n = 4) are also indicated.

disease controls were usually not included (4–6, 8). The results obtained in our comprehensive analysis in which three isotypes of RF, ACPA, and RA33 were determined in a large number of RA patients, disease controls, and healthy subjects (651 individuals in total) show that about one-third of "seronegative" patients generate antibodies known to be highly associated with RA including IgA isotypes of RF and ACPA as well as RA33 antibodies. Although RA33 antibodies were much less prevalent than the other antibodies and also proved less specific, they nevertheless contributed to the reduction of the serological gap being present in 12% of seronegative patients usually in conjunction with other antibody species. A similar number of seronegative patients were positive in the IgM-RF assay which proved slightly more sensitive than the nephelometric assay (Figure S2 in Supplementary Material). Most of the additionally detected IgM-RF were of low titer but usually co-occurred with other antibody species, in contrast to (seropositive) healthy or disease controls in which IgM-RF was usually the only species. Only three sera positive by nephelometry were negative in the IgM-RF assay (Figure S2 in Supplementary Material), which may be explained by the use of antigens from different species (18). Of note, most of the seronegative RA patients showed multiple reactivities, whereas controls were usually monospecific for a single antibody species and showed predominantly one or two IgM reactivities, particularly patients with OA or ankylosing spondylitis. While low titer IgM antibodies occurring as single entities are of limited diagnostic usefulness they can nevertheless be helpful markers when co-occurring with other antibody species such as IgA-RF/ACPA isotypes or RA33 antibodies, which proved also less specific for RA than IgG-ACPA.

IgG-RA33 has been described in several studies to have a prevalence of 20–30% and a specificity of approximately 90% (13, 19). Although in our cohort the newly developed IgG-RA33 EliA™ prototype proved less sensitive, specificity was better than 97% and similar values were obtained for IgA-RA33. However, due to the modest sensitivity, the positive predictive values of RA33 antibodies were lower than those of the other antibodies investigated (**Table 2**). Interestingly, IgM-RA33 was the most prevalent RA33 subtype and showed similar specificity as IgM-ACPA while IgM-RF was the least specific of all nine isotypes investigated. In contrast to RF and ACPA, RA33 isotypes showed little overlap and therefore, despite their modest sensitivities, RA33 antibodies were seen in more than 20% of RA patients including, as mentioned above, a substantial number of seronegative ones. Importantly, RA33 antibodies commonly co-occurred with other antibody species such as IgM-RF or IgM-ACPA, which are also less specific than IgG-ACPA.

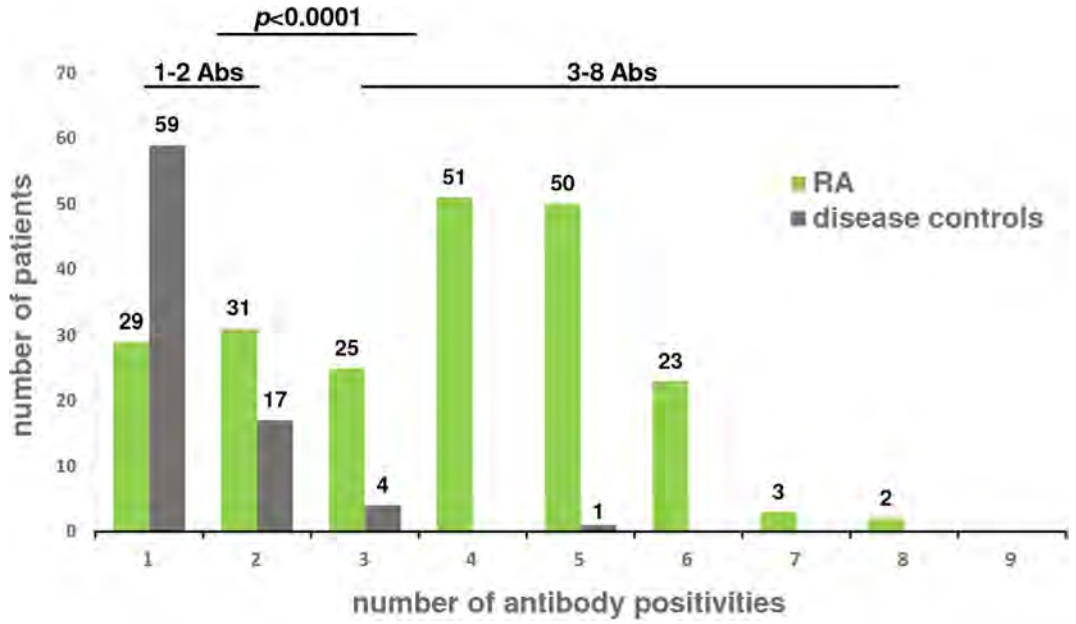

FIGURE 4 | Number of antibody positivities in rheumatoid arthritis (RA) patients and disease controls. 290 RA patients and 261 disease controls were tested for the presence of IgA, IgG, and IgM isotypes of rheumatoid factor, anti-citrullinated protein antibodies and RA33. The number of antibodies detected in a patient's serum is indicated on the *x*-axis; the number of patients is indicated on the *y*-axis. Disease controls were found to have significantly ($p < 0.001$) fewer antibody positivities (1–2 Abs) compared to RA patients who commonly had more than two antibodies (3–8 Abs).

TABLE 4 | Clinical parameters of rheumatoid arthritis patients with none, 1–3, and 4 or more positive Igs.

	Seronegative	1–3 antibodies	4 or more antibodies
Number of patients	78	88	124
Age (years)	53.4 (44.2–65.7)	57.2 (46.8–66.3)	56.6 (46.6–63.6)
Female%	80.8%	85%	75%
Disease duration (years)	0.3 (0.025–2.1)	0.5 (0–6.1)	1 (0.1–8.3)
Simplified disease activity index	16.6 (9.9–25.1)	13.6 (9.3–23.3)	14.8 (8.7–22)
Clinical disease activity index	14.9 (9.2–22.7)	12 (8.5–20.2)	12.7 (7.4–19.25)
Disease activity score	4.4 (3.7–5.1)	4.3 (3.1–5.1)	4.2 (3.4–5)
C-reactive protein [mg/dl]	0.5 (0.2–1.2)	0.5 (0.2–1.3)	0.8 (0.3–1.7)
Pain	41 (22–58)	40 (20.5–60.5)	35 (15–52)
Patient global disease activity	40 (23–58)	45 (20–61.5)	38 (19–60)
Evaluator's global disease activity (EGA)	21 (10–34)	20 (10–29.5)	24 (10–38)
Health access and quality index	0.8 (0.125–1.5)	0.8 (0.25–1.25)	0.6 (0.125–1.1)
Swollen joint count 28	3 (2–4)	3 (2–5)	4 (2–7)
Tender joint count 28	**4 (2–8)**	3 (0–7)	**2 (0–5)***
Corticosteroids (mg)	6.3 (5–12.5)	6.3 (5–10)	6.3 (5–6.3)

*Values are medians and lower and the upper quartiles are indicated in brackets. Disease duration was calculated from the date of diagnosis. TJC28 was found to be significantly (*corr. p = 0.04) lower in patients with 4 or more antibodies compared to seronegative patients.*

Remarkably, co-occurrence of these antibodies was very specific for RA and not observed in disease controls or healthy subjects. In fact, co-occurrence of IgM-RA33 with other antibodies was seen in only 8 out of 261 disease controls and in a single healthy subject. Hence, determination of RA33 antibodies and RF/ACPA isotypes, especially IgA- and IgM-RF, reduced the number of seronegative patients by approximately 30%. Another important aspect of this study is the observation that sera of RA patients generally contained multiple reactivities, in contrast to sera from disease controls and healthy subjects. However, no major differences in clinical parameters were seen at baseline between seronegative patients, patients with 1–3 antibodies and patients with 4 or more antibodies—a pattern highly specific for RA, even in the absence of IgG-ACPA—except that TJC28 was significantly lower in patients with 4 or more antibodies compared to seronegative patients. We have not yet analyzed disease progression and outcome or response to therapy but it has recently been shown by other investigators that patients with multiple antibodies are at increased risk for relapse when tapering DMARD therapy (20, 21).

Therefore, the determination of multiple antibodies and isotypes, even if they are not highly specific for RA, does not only reduce the number of seronegative (i.e., IgG-ACPA and RF

negative) patients but seems to have also prognostic value with respect to disease progression and response to therapy, a matter that is currently under investigation. Thus, it is conceivable that patients with a high number of autoantibodies and hence a high level of autoimmunity may be more responsive to therapies targeting B- and T-lymphocytes such as the anti-CD20 antibody rituximab or the CTLA4-Ig construct abatacept (22). In this sense, it is certainly worthwhile to search for additional antibodies (23) or subtypes (24) and other disease markers (including miRNAs and genetics) that together may help to further stratify RA patients with the aim to treat them more efficiently in a personalized way.

CONCLUSION

Testing for multiple autoantibody specificities adds diagnostic value in covering more RA patients and reducing the diagnostic gap left by routine RF and IgG-ACPA determination. Furthermore, the number of antibodies co-occurring in a patient's serum might provide some prognostic value allowing further subclassification of patients.

ETHICS STATEMENT

This study was carried out in accordance with the recommendations of the "guidelines for storing and using patients samples" of the Ethical Committee of the Medical University of Vienna. With written informed consent from all subjects. All subjects gave written informed consent in accordance with the Declaration of Helsinki that their blood and urine samples can be stored and used for scientific purposes. The protocol was approved by the Ethical Committee of the Medical University of Vienna (ethics vote number: 559/2005).

AUTHOR CONTRIBUTIONS

All authors participated in drafting the article or revising it critically for important intellectual content, and all authors gave final approval of the version to be submitted. Study conception and design: DS, AP, and GS. Acquisition of data: DS, AP, HH, MG, SS, and TH. Analysis and interpretation of data: DS, AP, FA, PS, SB, JS, and GS.

FUNDING

This work was supported by the Innovative Medicines Initiative Joint Undertaking under grant agreement no 115142 (BTCure) and no 777357 (RTCure).

SUPPLEMENTARY MATERIAL

The Supplementary Material for this article can be found online at https://www.frontiersin.org/articles/10.3389/fimmu.2018.00876/full#supplementary-material.

REFERENCES

1. Malmstrom V, Catrina AI, Klareskog L. The immunopathogenesis of seropositive rheumatoid arthritis: from triggering to targeting. *Nat Rev Immunol* (2017) 17(1):60–75. doi:10.1038/nri.2016.124
2. Aletaha D, Neogi T, Silman AJ, Funovits J, Felson DT, Bingham CO III, et al. 2010 rheumatoid arthritis classification criteria: an American College of Rheumatology/European League against rheumatism collaborative initiative. *Ann Rheum Dis* (2010) 69(9):1580–8. doi:10.1136/ard.2010.138461
3. Rantapaa-Dahlqvist S, de Jong BA, Berglin E, Hallmans G, Wadell G, Stenlund H, et al. Antibodies against cyclic citrullinated peptide and IgA rheumatoid factor predict the development of rheumatoid arthritis. *Arthritis Rheum* (2003) 48(10):2741–9. doi:10.1002/art.11223
4. Bas S, Genevay S, Meyer O, Gabay C. Anti-cyclic citrullinated peptide antibodies, IgM and IgA rheumatoid factors in the diagnosis and prognosis of rheumatoid arthritis. *Rheumatology* (2003) 42(5):677–80. doi:10.1093/rheumatology/keg184
5. Conrad K, Roggenbuck D, Reinhold D, Dorner T. Profiling of rheumatoid arthritis associated autoantibodies. *Autoimmun Rev* (2010) 9(6):431–5. doi:10.1016/j.autrev.2009.11.017
6. Falkenburg WJ, van Schaardenburg D, Ooijevaar-de Heer P, Wolbink G, Rispens T. IgG subclass specificity discriminates restricted IgM rheumatoid factor responses from more mature anti-citrullinated protein antibody-associated or Isotype-switched IgA responses. *Arthritis Rheumatol* (2015) 67(12):3124–34. doi:10.1002/art.39299
7. Gilliam BE, Chauhan AK, Moore TL. Evaluation of anti-citrullinated type II collagen and anti-citrullinated vimentin antibodies in patients with juvenile idiopathic arthritis. *Pediatr Rheumatol Online J* (2013) 11(1):31. doi:10.1186/1546-0096-11-31
8. Infantino M, Manfredi M, Meacci F, Sarzi-Puttini P, Ricci C, Atzeni F, et al. Anti-citrullinated peptide antibodies and rheumatoid factor isotypes in the diagnosis of rheumatoid arthritis: an assessment of combined tests. *Clin Chim Acta* (2014) 436:237–42. doi:10.1016/j.cca.2014.05.019
9. Brink M, Hansson M, Mathsson-Alm L, Wijayatunga P, Verheul MK, Trouw LA, et al. Rheumatoid factor isotypes in relation to antibodies against citrullinated peptides and carbamylated proteins before the onset of rheumatoid arthritis. *Arthritis Res Ther* (2016) 18:43. doi:10.1186/s13075-016-0940-2
10. Hassfeld W, Steiner G, Graninger W, Witzmann G, Schweitzer H, Smolen JS. Autoantibody to the nuclear antigen RA33: a marker for early rheumatoid arthritis. *Br J Rheumatol* (1993) 32(3):199–203. doi:10.1093/rheumatology/32.3.199
11. Nell VP, Machold KP, Stamm TA, Eberl G, Heinzl H, Uffmann M, et al. Autoantibody profiling as early diagnostic and prognostic tool for rheumatoid arthritis. *Ann Rheum Dis* (2005) 64(12):1731–6. doi:10.1136/ard.2005.035691
12. Nell-Duxneuner V, Machold K, Stamm T, Eberl G, Heinzl H, Hoefler E, et al. Autoantibody profiling in patients with very early rheumatoid arthritis: a follow-up study. *Ann Rheum Dis* (2010) 69(1):169–74. doi:10.1136/ard.2008.100677
13. Yang X, Wang M, Zhang X, Li X, Cai G, Xia Q, et al. Diagnostic accuracy of anti-RA33 antibody for rheumatoid arthritis: systematic review and meta-analysis. *Clin Exp Rheumatol* (2016) 34(3):539–47.
14. Ball EM, Tan AL, Fukuba E, McGonagle D, Grey A, Steiner G, et al. A study of erosive phenotypes in lupus arthritis using magnetic resonance imaging and anti-citrullinated protein antibody, anti-RA33 and RF autoantibody status. *Rheumatology* (2014) 53(10):1835–43. doi:10.1093/rheumatology/keu215
15. Hajian-Tilaki K. Receiver operating characteristic (ROC) curve analysis for medical diagnostic test evaluation. *Caspian J Intern Med* (2013) 4(2):627–35.
16. Robin X, Turck N, Hainard A, Tiberti N, Lisacek F, Sanchez JC, et al. pROC: an open-source package for R and S+ to analyze and compare ROC curves. *BMC Bioinformatics* (2011) 17(12):77. doi:10.1186/1471-2105-12-77
17. Ingegnoli F, Castelli R, Gualtierotti R. Rheumatoid factors: clinical applications. *Dis Markers* (2013) 35(6):727–34. doi:10.1155/2013/726598
18. Falkenburg WJ, von Richthofen HJ, Koers J, Weykamp C, Schreurs MWJ, Bakker-Jonges LE, et al. Clinically relevant discrepancies between different rheumatoid factor assays. *Clin Chem Lab Med* (2018). doi:10.1515/cclm-2017-0988
19. Lee YH, Bae SC. Diagnostic accuracy of anti-Sa and anti-RA33 antibodies in rheumatoid arthritis: a meta-analysis. *Z Rheumatol* (2017) 76(6):535–8. doi:10.1007/s00393-016-0134-y

20. Trouw LA, Toes RE. Rheumatoid arthritis: autoantibody testing to predict response to therapy in RA. *Nat Rev Rheumatol* (2016) 12(10):566–8. doi:10.1038/nrrheum.2016.151
21. Figueiredo CP, Bang H, Cobra JF, Englbrecht M, Hueber AJ, Haschka J, et al. Antimodified protein antibody response pattern influences the risk for disease relapse in patients with rheumatoid arthritis tapering disease modifying antirheumatic drugs. *Ann Rheum Dis* (2017) 76(2):399–407. doi:10.1136/annrheumdis-2016-209297
22. Gottenberg JE, Courvoisier DS, Hernandez MV, Iannone F, Lie E, Canhao H, et al. Brief report: association of rheumatoid factor and anti-citrullinated protein antibody positivity with better effectiveness of abatacept: results from the Pan-European Registry Analysis. *Arthritis Rheumatol* (2016) 68(6):1346–52. doi:10.1002/art.39595
23. Trouw LA, Rispens T, Toes REM. Beyond citrullination: other post-translational protein modifications in rheumatoid arthritis. *Nat Rev Rheumatol* (2017) 13(6):331–9. doi:10.1038/nrrheum.2017.15
24. Cabrera-Villalba S, Gomara MJ, Cañete JD, Ramírez J, Salvador G, Ruiz-Esquide V, et al. Differing specificities and isotypes of anti-citrullinated peptide/protein antibodies in palindromic rheumatism and rheumatoid arthritis. *Arthritis Res Ther* (2017) 19(1):141. doi:10.1186/s13075-017-1329-6

Conflict of Interest Statement: MG, SS, and TH are employees of Thermo Fisher Scientific—Phadia GmbH. All other authors declare that the research was conducted in the absence of any commercial or financial relationships that could be construed as a potential conflict of interest.

frontiers in Immunology

ORIGINAL RESEARCH
published: 24 April 2018
doi: 10.3389/fimmu.2018.00787

SYK Inhibition Induces Apoptosis in Germinal Center-Like B Cells by Modulating the Antiapoptotic Protein Myeloid Cell Leukemia-1, Affecting B-Cell Activation and Antibody Production

Nathalie Roders[1,2,3†], Florence Herr[1,2,3†], Gorbatchev Ambroise[2,3], Olivier Thaunat[4,5,6], Alain Portier[2,3], Aimé Vazquez[2,3‡] and Antoine Durrbach[1,2,3‡]*

[1] Institut Francilien de Recherche en Nephrologie et Transplantation (IFRNT), Service de Néphrologie, Hôpital Bicêtre, Le Kremlin Bicêtre, France, [2] INSERM UMRS-MD 1197, Villejuif, France, [3] Université Paris Sud, Orsay, France, [4] French National Institute of Health and Medical Research (INSERM) Unit 1111, Lyon, France, [5] Department of Transplantation, Nephrology and Clinical Immunology, Edouard Herriot University Hospital, Lyon, France, [6] Claude Bernard University Lyon 1, Lyon, France

OPEN ACCESS

Edited by:
Jen Anolik,
University of Rochester,
United States

Reviewed by:
Paolo Casali,
The University of Texas Health Science Center San Antonio,
United States
Masaki Hikida,
Akita University, Japan

***Correspondence:**
Antoine Durrbach
a.durrbach@gmail.com

†Joint first authors.

‡Joint last authors.

Specialty section:
This article was submitted to B Cell Biology, a section of the journal Frontiers in Immunology

Received: 06 November 2017
Accepted: 29 March 2018
Published: 24 April 2018

Citation:
Roders N, Herr F, Ambroise G, Thaunat O, Portier A, Vazquez A and Durrbach A (2018) SYK Inhibition Induces Apoptosis in Germinal Center-Like B Cells by Modulating the Antiapoptotic Protein Myeloid Cell Leukemia-1, Affecting B-Cell Activation and Antibody Production. Front. Immunol. 9:787. doi: 10.3389/fimmu.2018.00787

B cells play a major role in the antibody-mediated rejection (AMR) of solid organ transplants, a major public health concern. The germinal center (GC) is involved in the generation of donor-specific antibody-producing plasma cells and memory B cells, which are often poorly controlled by current treatments. Myeloid cell leukemia-1 (Mcl-1), an antiapoptotic member of the B-cell lymphoma-2 family, is essential for maintenance of the GC reaction and B-cell differentiation. During chronic AMR (cAMR), tertiary lymphoid structures resembling GCs appear in the rejected organ, suggesting local lymphoid neogenesis. We report the infiltration of the kidneys with B cells expressing Mcl-1 in patients with cAMR. We modulated GC viability by impairing B-cell receptor signaling, by spleen tyrosine kinase (SYK) inhibition. SYK inhibition lowers viability and Mcl-1 protein levels in Burkitt's lymphoma cell lines. This downregulation of Mcl-1 is coordinated at the transcriptional level, possibly by signal transducer and activator of transcription 3 (STAT3), as shown by (1) the impaired translocation of STAT3 to the nucleus following SYK inhibition, and (2) the lower levels of Mcl-1 transcription upon STAT3 inhibition. Mcl-1 overproduction prevented cells from entering apoptosis following SYK inhibition. *In vitro* studies with primary tonsillar B cells confirmed that SYK inhibition impaired cell survival and decreased Mcl-1 protein levels. It also impaired B-cell activation and immunoglobulin G secretion by tonsillar B cells. These findings suggest that the SYK–Mcl-1 pathway could be targeted, to improve graft survival by manipulating the humoral immune response.

Keywords: germinal center B-cells, spleen tyrosine kinase inhibition, myeloid cell leukemia-1, apoptosis, antibody-mediated rejection

INTRODUCTION

B cells play a major role in acute and chronic antibody-mediated rejection (AMR) and allograft survival. AMR after solid organ transplantation is associated with a high frequency of organ deterioration and graft loss, despite the availability of treatment. Current therapies include plasmapheresis (1, 2), high-dose intravenous immunoglobulin (3, 4), monoclonal anti-CD20 antibodies

(5, 6), proteasome inhibitors (4, 7), and complement inhibitors (8, 9). However, these treatments frequently fail to control AMR, donor-specific antibody (DSA) production, and memory B-cell formation.

B-cell activation through B-cell receptor (BCR) signaling drives B-cell survival, differentiation, anergy, or apoptosis, depending on the other signals received by the cell. Antigen (Ag)-dependent BCR activation leads to the recruitment and activation of spleen tyrosine kinase (SYK) (10, 11). Active SYK induces the formation of a signalosome, containing kinases and adaptor proteins, which sets in motion signaling cascades, such as those involving AKT, mitogen-activated protein kinases, nuclear factor of activated T cells, and nuclear factor-κB (NFκB), resulting in translational modifications (12). Germinal centers (GC) play an important role in driving the differentiation of B cells into DSA-producing plasma and memory B cells (13). In solid organ transplantation, the development of tertiary lymphoid structures (TLS) sustaining a functional ectopic germinal center reaction has been demonstrated in human grafts displaying chronic AMR (cAMR) (14, 15). Following T cell-dependent B-cell activation and GC formation, B cells undergo clonal expansion, isotype class switching, somatic hypermutation (16–18), and affinity maturation and selection (19–21). They leave the GC as highly specific long-lived memory B-cells and antibody (Ab)-producing plasma cells.

The persistence of the GC and the selection of high-affinity effector B cells are regulated by pro- and antiapoptotic signals influenced by Ag binding and cell-mediated interactions (20, 22, 23). The members of the B-cell lymphoma-2 (Bcl-2) protein family maintain the delicate balance between cell survival and apoptotic death. The proteins of this family form three groups: (i) antiapoptotic proteins, including myeloid cell leukemia-1 (Mcl-1), Bcl-2, and Bcl-xs/l, which play an essential role in cell survival; (ii) proapoptotic proteins, BAX and BAK, required to trigger downstream apoptotic processes, such as cytochrome *c* release from the mitochondria, and subsequent caspase activation; (iii) the so-called "BH-3-only" proteins, including Puma, Noxa, Bad, Bid, and Bim, which interact with the other members of the family to control their activity (24–26). Vikstrom et al. (27) showed that no GCs or memory B-cells developed in the absence of Mcl-1, highlighting the importance of Mcl-1 for GC maintenance and B-cell differentiation. In a previous study of the role of PUMA in regulating mitogen-activated B cells and memory B cells, we observed that both PUMA and Mcl-1 were expressed in GCs *in vivo* (28), suggesting a possible key role in the maintenance and development of GC and memory B cells.

In kidneys displaying cAMR, we observed an infiltration of B cells expressing Mcl-1, like pre-GC and GC B cells. We investigated the relationship between BCR signaling and B-cell survival and differentiation, by inhibiting SYK. Using Burkitt's lymphoma-derived cells as a model for GC centroblasts, we showed that SYK inhibition decreased cell viability. SYK inhibition reduced Mcl-1 gene expression *via* signal transducer and activator of transcription 3 (STAT3). Immunoglobulin (Ig) synthesis was also impaired by SYK inhibition in primary B cells *in vitro*; these cells were also less viable, less strongly activated, and had lower Mcl-1 protein levels.

MATERIALS AND METHODS

Reagents and Antibodies

The following reagents were used: BAY61-3606 (Merck Millipore), Stattic (Torcis), Q-VD-Oph (Sigma), MG-132 (Calbiochem), and cycloheximide (Sigma).

We used the following primary Abs: hCD19-APD-Cy-7 (SJ25C1; BD Biosciences Cat# 557791 RRID:AB_396873), hCD38-BV421 (HIT2; BD Biosciences Cat# 562445 RRID:AB_11153870) hsIgD-Pe-Cy7 (IA6-2; BD Biosciences Cat# 561314 RRID:AB_10642457), hCD80-BV605 (L307.4; BD Biosciences Cat# 563315), hPhospho-SYK-AF488 (C87C1; Cell Signaling Technology Cat# 4349), and hMcl-1-FITC (Biorbyt Cat# orb15956 RRID:AB_10747574) for flow cytometry. Anti-Mcl-1 (S-19; Santa Cruz Biotechnology Cat# sc-819 RRID:AB_2144105), anti-Bcl-2 (C-2; Santa Cruz Biotechnology Cat# sc-819 RRID:AB_2144105), anti-Bcl-$x_{S/L}$ (S-18; Santa Cruz Biotechnology Cat# sc-819 RRID:AB_2144105), anti-GAPDH (Sigma-Aldrich Cat# G9545 RRID:AB_796208), and anti-PARP (Cell Signaling Technology Cat# 9542 also 9542S, 9542L, 9542P RRID:AB_2160739) antibodies were used for immunoblotting and anti-hCD19 (HIB19; BD Biosciences Cat# 555409 RRID:AB_395809), anti-hMcl-1 (Sigma-Aldrich Cat# HPA008455 RRID:AB_1079334), and anti-STAT3 (K-15; Santa Cruz Biotechnology Cat# sc-483 RRID:AB_632441) Abs were used for immunohistology.

Retroviral particles were generated with the following plasmids: the expression plasmid pBabe-Flag-hMcl-1, a gift from Roger Davis (29) (Addgene plasmid # 25371), the empty vector control plasmid pBabe-puro-IRES-EGFP, a gift from L. Miguel Martins (Addgene plasmid # 14430), the envelope-expressing plasmid pCMV-VSV-G, a gift from Bob Weinberg (Addgene plasmid # 8454), and the packaging plasmid pCL-Eco (Novus Biologicals).

Cell Culture

BL41, RAMOS, and BL2 Burkitt's lymphoma cells were cultured in complete RPMI medium: RPMI-1640 (Sigma) supplemented with 10% heat-inactivated fetal bovine serum (FBS, Dominique Dutscher), 100 U/ml penicillin and 100 µg/ml streptomycin (Sigma).

HEK 293T and CD40 ligand/CD32 ligand-expressing murine fibroblasts were cultured in complete Dulbecco's modified Eagle medium (DMEM; Sigma) supplemented with 10% FBS, 100 U/ml penicillin, 100 µg/ml streptomycin, and 0.1 mg/ml Normocin™ (InvivoGen).

Renal biopsy specimens and detransplanted kidneys were obtained from transplant recipients presenting end-stage renal failure due to cAMR, who gave written informed consent, in accordance with the Helsinki Declaration, for the use of part of their biopsy specimens for research on renal transplantation. The samples were stored at the Biological Resource Center of Paris-South University. This collection has been declared to the French Ministry of Research: AC-2017-2991.

Cells were isolated from detransplanted kidneys by separating the cortex from adipose tissue and the medulla. The tissue was dissected and added to enzyme buffer (70% DMEM, 1% BSA, 2.4 mM $CaCl_2$, 0.4 mg/ml liberase, and 240 U DNase) and dissociated

with a GentleMACS™ Dissociator (Miltenyi Biotech). The cell suspension was incubated for 45 min at 37°C, with shaking. Cells were separated from the tissue with a stainless-steel strainer and a glass grinder. Cells were washed with HEPES Eagle's medium buffer (70% DMEM, 1% BSA, 2.4 mM $CaCl_2$,). Mononuclear cells were isolated from the cell suspension by centrifugation on a Pancoll (Human; PAN™ Biotech) gradient (2:1 ratio of diluted cells to Pancoll) at 600 × *g* for 20 min. Mononuclear cells were isolated and washed in complete RPMI.

Primary cells were isolated from tonsillar tissue removed from patients during tonsillectomy. The tonsils were dissected and pushed through a stainless-steel strainer with a glass grinder. Cells were collected and washed with complete RPMI, then homogenized by passage through a nylon cell strainer with 100 µm pores (BD Bioscience).

Tonsillar cells were cocultured in complete RPMI, with CD40 ligand/CD32 ligand-expressing fibroblasts, in the presence of anti-µ Abs (Jackson Immunoresearch), LPS (Sigma), and BAY61-3606. Fibroblast growth was blocked by incubation with mitomycin C (10 µg/ml, Roche) for 30 min at 37°C, under an atmosphere containing 5% CO_2, before the addition of tonsillar cells.

Retrovirus Production and Cell Transduction

Retroviruses were generated by the transient cotransfection of HEK 293T cells with a three-plasmid combination, by the calcium phosphate coprecipitation method, as previously described (30). After 3 days of culture in cells, the retroviral particles were collected and concentrated with 5× PEG IT™ viral precipitation solution (System Biosciences).

For retroviral transduction, 2×10^6 BL41 cells were collected and mixed with a suspension of retroviral particles in the presence of Polybrene (Santa Cruz Biotechnology). The resulting suspension was then centrifuged at 300 × *g* for 90 min. Cells were incubated at 37°C under an atmosphere containing 5% CO_2 for 2 h, and fresh complete RPMI was then added. Transduced cells were selected by a series of puromycin (1 µg/ml; InvivoGen) treatments.

Western Blotting

Whole-cell lysates were prepared in lysis buffer [50 mM Tris–HCl, pH 7.4, 150 mM NaCl, 2 mM EDTA (ethylenediaminetetraacetic acid), 1% Triton X-100, and 1% Igepal/NP-40, supplemented with Halt™ Protease inhibitor cocktail (Thermo Scientific)]. For phosphorylation analysis, the phosphatase inhibitors ß-glycerophosphate (12.5 nM), sodium orthovanadate (10 µM), sodium fluoride (0.1 mM), and *N*-ethylmaleimide (30 µM) were added before cell lysis. Protein determinations were performed with the micro-BCA protein assay kit (Thermo Scientific). Protein samples (equal masses) were heated for 5 min at 99°C after the addition of Tris–glycine SDS sample buffer (Life Technologies) containing 10% ß-mercaptoethanol (Sigma). They were subjected to polyacrylamide gel electrophoresis and the protein bands were transferred onto nitrocellulose membranes (Santa Cruz). The membranes were incubated with primary Abs, and Ab binding was visualized by chemiluminescence with horseradish peroxide (HRP)-conjugated secondary Abs (Jackson Immunoresearch), the Immobilon HRP chemiluminescence substrate for western blots (Millipore) and a DDC camera (LAS-4000 mini, Fujifilm).

Flow Cytometry

We assessed the viability of BL41, RAMOS, and BL2 cells by flow cytometry, with a BD Accuri C6 flow cytometer (BD Biosciences). Viability was assessed by expressing the proportion of viable cells (excluding granular and shrunken cells) as a percentage of the total cell population, based on forward (fw) and side light scattering profiles.

Apoptotic cells were identified with the Pacific Blue Annexin V Apoptosis detection kit and 7-AAD (Biolegend), according to the manufacturer's protocol. Cells were analyzed in a BD LSRFortessa flow cytometer (BD Biosciences).

For extracellular staining, cells were incubated with fvs620 (1:1,000 dilution; BD Biosciences) in 1× PBS for 15 min at room temperature. Non-specific binding was blocked with human BD FC block (2.5 µg/1×10^6 cells; BD Biosciences) in 1× PBS supplemented with 2.5% FCS and 0.1% sodium azide, and cells were then incubated with fluorescent Abs. Intracellular staining for non-phosphorylated proteins was performed as follows: cells were fixed in 4% paraformaldehyde (PFA, Alfa Aesar), then incubated with NH_4Cl (100 mM) for quenching, permeabilized with 0.15% saponin (VWR), and incubated with conjugated Abs in the presence of saponin.

For intracellular staining for phosphorylation analysis, saponin was replaced with 0.1% Triton X-100 (Sigma) and 50% methanol was added, and the cells were then left on ice for permeabilization. The cells were then incubated with fluorochrome-conjugated Abs and analyzed in a BD LSRFortessa flow cytometer (BD Biosciences). All flow cytometry data were analyzed with FlowJo^{tm} (FlowJo Treestar, RRID:SCR_008520) software.

Enzyme-Linked Immunosorbent Assay

Total immunoglobulin G (IgG) secretion by tonsillar B cells was assessed with the Human IgG Total ELISA Ready-SET-Go!® kit (Affymetrix, eBioscience) according to the manufacturer's protocol, with undiluted supernatant. Absorbance was read at 450 and 570 nm, with a FLUOstar Omega microplate reader (BMG Labtech). Secreted IgG was quantified by comparison with a standard curve.

Immunofluorescence

The paraffin was removed from the sections by three sequential washes in xylene (Sigma). The sections were then rehydrated by passage through a series of ethanol solutions in water (100, 90, and 70% ethanol in distilled water). Ags were retrieved by boiling samples twice, for 5 min each, in citrate buffer (pH 6) supplemented with 0.05% Tween-20 (Sigma) in a microwave oven, and allowing the sample to cool to room temperature. Non-specific binding to FC receptors was blocked by incubating slides for 1 h at room temperature in blocking buffer (1× PBS, 1% FBS, 1% BSA, 1% human AB serum) supplemented with 0.1% Triton X-100, and then incubating them with primary Abs followed by AF488- or AF594-conjugated secondary Abs (Life Technologies).

BL41 cells were attached to poly-L-lysine slides (Thermo Scientific), fixed in 4% PFA and permeabilized by incubation

with 0.15% Triton X-100. Samples were blocked by incubation with 10% FBS in 1× PBS and quenched with NH_4Cl (100 mM). Samples were incubated with primary Abs and then with AF488-conjugated secondary Abs (Life Technologies).

Nuclei were stained with DAPI (4,6 diamidino-2-phenylindole, 1:10,000; Life Technologies) and the sections were mounted on slides in Fluoromount-G™ slide-mounting medium (Beckman Coulter) and covered with a coverslip.

Images were acquired with a Leica SP5 confocal microscope (Leica Microsystems) equipped with a 63× oil immersion fluorescence objective.

Gene Expression Analysis

RNA was extracted from BL41, RAMOS, and BL2 cells with the RNeasy plus mini kit (Qiagen), according to the manufacturer's protocol, including lysate homogenization with QIAshredder spin columns (Qiagen). We then generated cDNA from 1 µg of RNA, with the RevertAid H Minus First Strand cDNA Synthesis Kit (Thermo Scientific), according to the manufacturer's protocol.

Real-time quantitative PCR was performed with cDNA diluted 1:10, primers (0.75 µM final concentration) and the QuantiNova SYBR Green PCR Kit (Qiagen). The following primers were used: Mcl-1 (fw 5′-ATGCTTCGGAAACTGGACAT-3′; reverse (rv) 5′-TCCTGATGCCACCTTCTAGG-3′) as the target gene and GAPDH (fw 5′-AATCCCATCACCATCTTCCA-3′; rv 5′-TGGACTCCACGACGTACTCA-3′), 18 s (fw 5'-AGAAACGGCTACCACATCCA-3'; rv: 5'-CACCAGACTTGCCCTCCA-3′) and RPS13 (5'-CGAAAGCATCTTGAGAGGAACA-3'; rv: 5'-TCGAGCCAAACGGTGAATC-3') as housekeeping genes (Sigma). PCR was performed with the Mx3005P qPCR System (Agilent Technologies).

PCR efficiency was determined with 10-fold dilutions, according to the following equation: efficiency $(E) = 10^{(-1/\text{slope})}$. Cq values were determined with the following equation: $Cq = Ct\log_2(E)$. The Mcl-1 expression ratio was determined as follows: $\text{Ratio} = \left((2)^{\Delta CqMcl-1}\right) / \left((2)^{\Delta CqHK}\right)$, where $\Delta Cq = Cq_{\text{untreated}} - Cq_{\text{treated}}$.

Statistical Analysis

We analyzed the data for BL41, RAMOS, and BL2 cells in multiple *t*-tests, with Holm-Sidak correction for multiple testing, in Prism (Graphpad Prism, RRID:SCR_002798). Data for tonsillar B cells were analyzed by paired *t*-test/within-subject analysis, in InVivoStat.

RESULTS

Infiltrating B Cells Expressing Mcl-1 Are Observed in Kidney Grafts Displaying Chronic Antibody-Mediated Rejection

Myeloid cell leukemia-1 has been shown to be important for GC maintenance and B-cell differentiation (27). According to the mature B-cell (BM) 1-BM5 classification [expression of surface IgD (sIgD) and CD38 (31)], we determined Mcl-1 expression profiles for different B-cell populations based on the expression of sIgD and CD38: $sIgD^+CD38^{-/low}$ cells are naïve B cells that are undifferentiated or in the early stages of differentiation (BM1-BM2), $sIgD^+CD38^{high}$ cells are pre-GC cells (BM2'), $sIgD^-CD38^{high}$ cells are GC cells (BM3 + BM4), and $sIgD^-CD38^{-/low}$ cells are terminally differentiated B cells (early BM5-BM5). In tonsillar B cells, Mcl-1 levels were high in the early GC and GC populations (**Figure 1A**).

In kidney grafts displaying cAMR, infiltrating B cells were detected by the immunostaining of histological sections for CD19. Counterstaining for Mcl-1 revealed the colocalization of this protein with CD19. Histological sections of non-rejected human kidneys were stained in the same way, and no infiltrating B cells were observed on sections of these kidneys. However, Mcl-1 is not exclusive to B cells and was also observed in tubular structures (**Figure 1B**). A flow cytometry analysis of mononuclear cells isolated from kidneys detransplanted due to cAMR revealed the presence of a large proportion of infiltrating memory B cells ($CD19^+CD27^+$) and plasma cells ($CD138^+$) (Figure S1 in Supplementary Material).

These results indicate that cAMR is associated with an infiltration of differentiated B cells into the kidney graft and that some of the B cells infiltrating the graft express Mcl-1, like GC cells.

Inhibiting SYK Activity Decreases Viability and Mcl-1 Protein Levels in Germinal Center-Like Cells

We then investigated ways of disrupting GC B-cell responses. Given the key role of SYK downstream from the BCR, we treated BL41 cells, a Burkitt's lymphoma cell line used as a model of GC centroblasts (32), with the SYK inhibitor BAY61-3606 (33), to inhibit BCR signaling. We assessed the effect of SYK inhibition on cell viability. Shrinkage and blebbing are two characteristic features of apoptotic cells (34). We therefore identified dead cells on the basis of their small size and high granularity. Cell viability was decreased in a dose-dependent manner by BAY61-3606 treatment, with a 70% decrease observed in the presence of 5 µM BAY61-3606 (**Figure 2A**). We confirmed that BAY61-3606 reduced the level of SYK phosphorylation at TYR525/526, which is located in the activation loop of the kinase (11), in unstimulated BL41 cells (**Figure 2B**).

We then analyzed the levels of the antiapoptotic proteins Mcl-1, Bcl-2, and Bcl-xl. SYK inhibition resulted in lower levels of Mcl-1 protein, whereas the levels of the Bcl-2 and Bcl-xl proteins were unaffected. Mcl-1 may be cleaved by activated caspases (35) or degraded by the proteasome (36). We assessed the possible caspase-dependent degradation of Mcl-1, by treating cells with the caspase inhibitor Q-VD-Oph and BAY61-3606. This treatment resulted in only a partial rescue of Mcl-1 levels, but with the successful inhibition of caspase activation and the induction of cell death, as shown by FACS analysis and the cleavage pattern of PARP, a known substrate of caspase-3 (**Figure 2C**). Similar profiles for Mcl-1 and viability following SYK inhibition in the presence of Q-VD-Oph were observed with the Burkitt's lymphoma cell lines RAMOS and BL2 (Figure S2A in Supplementary Material).

The inhibition of proteasome activity by MG132 led to an increase in Mcl-1 protein levels in control cells. However, Mcl-1

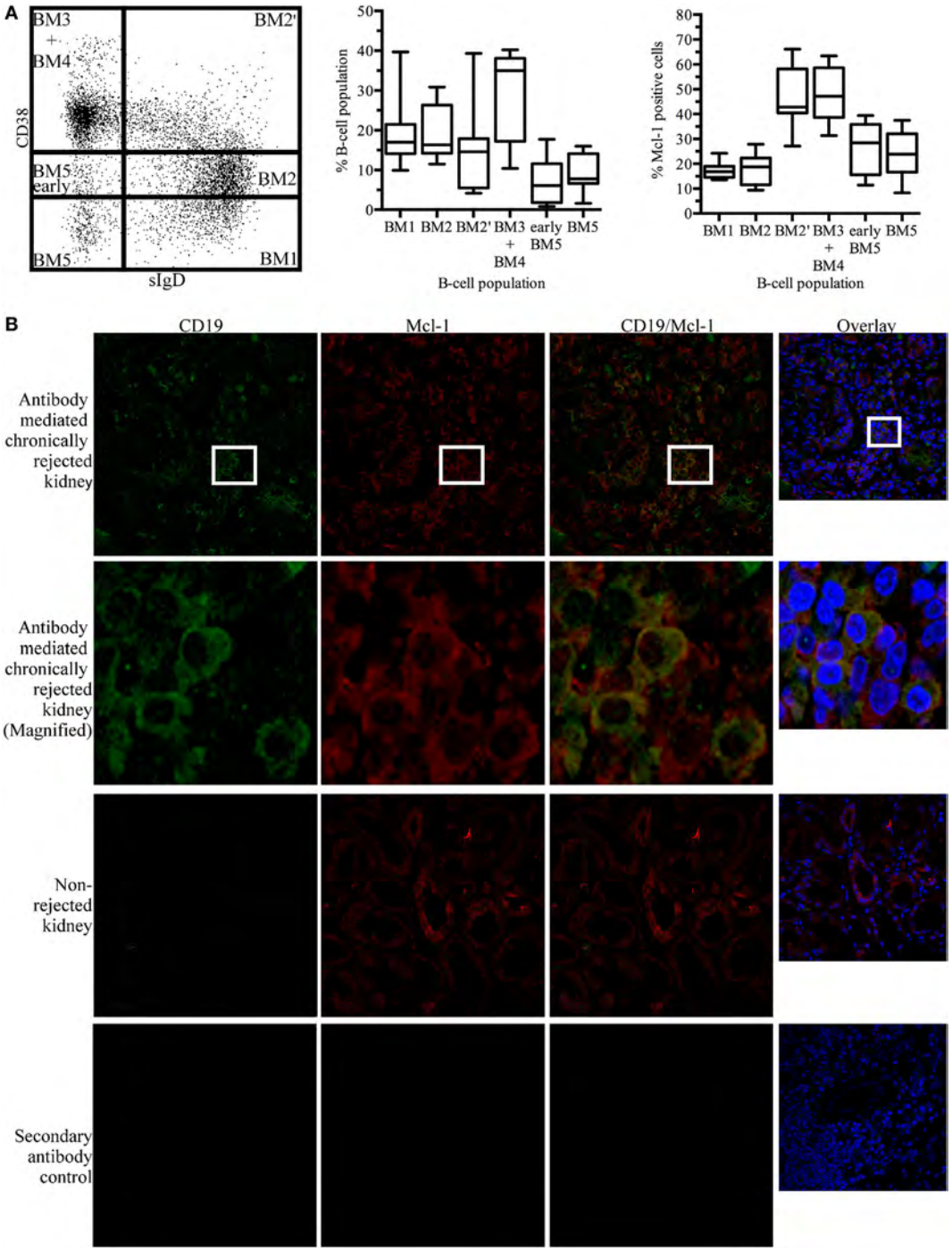

FIGURE 1 | Myeloid cell leukemia-1 (Mcl-1)-expressing B cells are found in kidney grafts in cases of chronic antibody-mediated rejection **(A)** Unstimulated tonsillar cells were stained for CD19, sIgD, CD38, and Mcl-1 and analyzed by flow cytometry. B-cell populations were identified according to the BM1-BM5 classification, based on the expression of CD19, sIgD, and CD38, and additional staining for Mcl-1 was performed. The boxplot shows the distribution between donors and the quadrant indicates the values between the fifth and ninety-fifth percentiles, $n = 7$. **(B)** Immunofluorescence staining of paraffin-embedded chronically rejected kidney with anti-CD19 and anti-Mcl-1 antibodies. Images were obtained with a Leica confocal microscope fitted with a 63× objective. sIgD, surface IgD; CD, cluster of differentiation; BM, mature B cell.

levels in cells treated with BAY61-3606 and MG132 remained similar to those in control cells (**Figure 2D**), suggesting that SYK inhibition does not modify the rate of Mcl-1 protein degradation. RAMOS and BL2 cells treated with BAY61-3606 and MG132 had similar Mcl-1 expression profiles (Figure S2B in Supplementary Material).

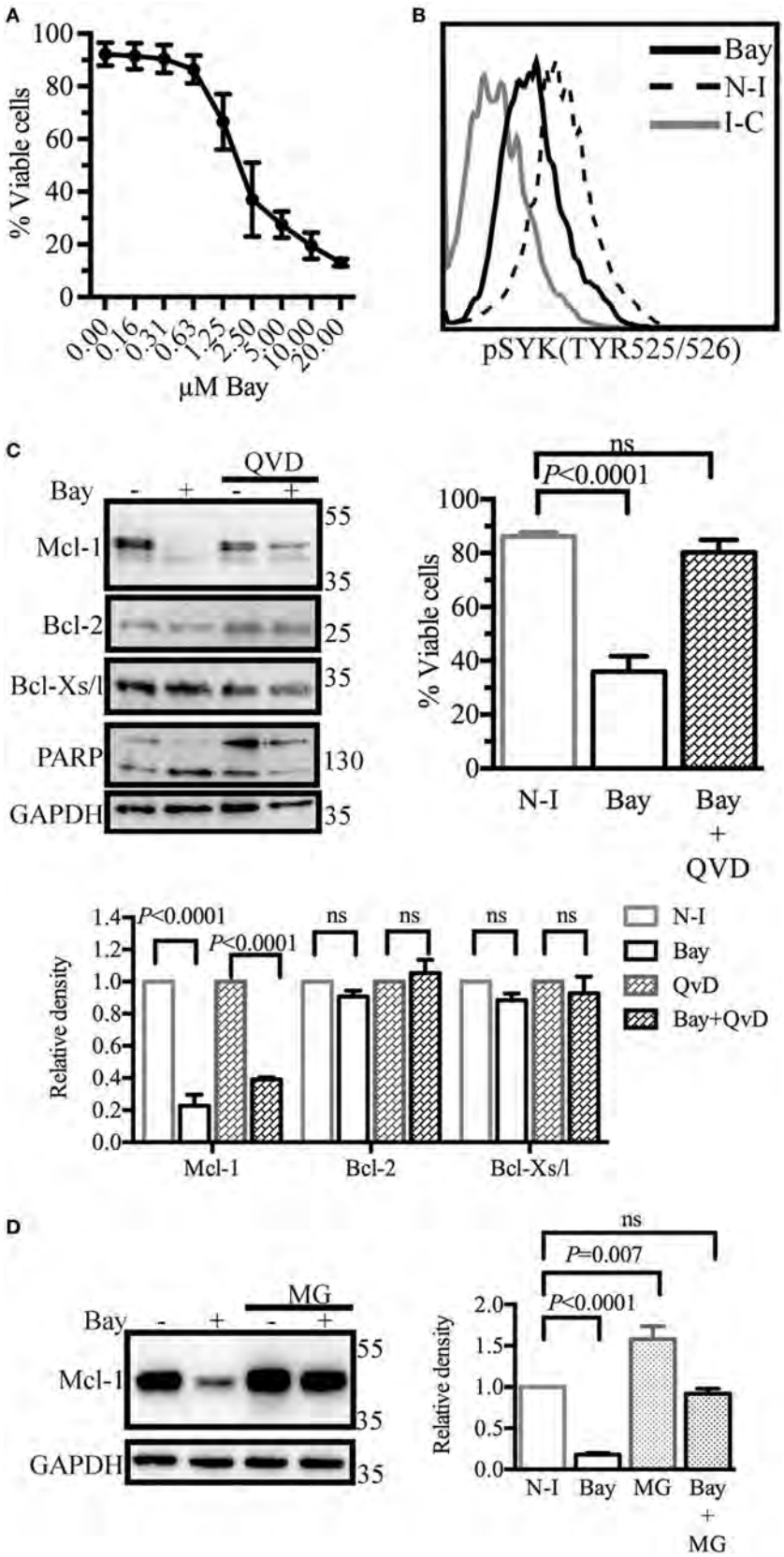

FIGURE 2 | Continued

FIGURE 2 | Spleen tyrosine kinase (SYK) inhibition in BL41 cells (Burkitt's lymphoma cells) reduces viability and decreases levels of the antiapoptotic protein myeloid cell leukemia-1 (Mcl-1). **(A)** Cell viability was determined by flow cytometry analyses of cell morphology (forward and side scatter) following dose-gradient treatment with BAY61-3606 for 16 h. The data shown are mean values (±SEM, $n = 3$). **(B)** The phosphorylation status of SYK was determined by flow cytometry following SYK inhibition with BAY61-3606 (5 μM; 20 min). **(C)** BL41 cells were treated with BAY61-3606 (5 μM; 4 h) and Q-VD-Oph (10 μM; 4 h). Levels of the antiapoptotic proteins Mcl-1, B-cell lymphoma-2 (Bcl-2) and Bcl-xl were determined by western blotting, with quantification by protein densitometry and normalization against GAPDH levels. The data shown are mean values (±SEM, $n = 3$). Q-VD-Oph efficiency was determined by western-blot analysis of PARP cleavage (4 h) and cell death inhibition (16 h). The data shown are mean values (±SEM, $n = 5$). **(D)** BL41 cells were treated with BAY61-3606 (5 μM; 4 h) and MG-132 (10 μM; 4 h) and Mcl-1 protein levels were determined by western blotting, with quantification by protein densitometry and normalization against GAPDH levels. The data shown are mean values (±SEM, $n = 5$). Bay, BAY61-3606; N-I, non-inhibited; I-C, isotype control; QVD, Q-VD-Oph; ns, not significant; MG, MG132.

SYK Inhibition Modulates Mcl-1 Gene Expression and Alters the Cellular Distribution of STAT3

As SYK inhibition did not accelerate Mcl-1 protein degradation in BL41 cells, we hypothesized that the lower levels of Mcl-1 protein observed in BL41 cells exposed to BAY61-3606 might result from lower levels of *de novo* protein synthesis. We tested this hypothesis by determining Mcl-1 mRNA levels by RT-qPCR. BAY61-3606 treatment substantially decreased Mcl-1 gene expression in BL41 cells, for up to 4 h after treatment. Lower levels of Mcl-1 mRNA were also observed in RAMOS and BL2 cells exposed to BAY61-3606 (Figure S3A in Supplementary Material). The short turnover of the Mcl-1 protein in BL41 cells was confirmed by blocking protein synthesis with cycloheximide, which resulted in lower levels of Mcl-1 protein after 2 h, supporting the hypothesis that SYK inhibition affects *de novo* protein synthesis (**Figure 3A**).

Signal transducer and activator of transcription 3 (STAT3) has been identified as a major regulator of Mcl-1 gene transcription (37, 38). Immunohistological analysis in basal conditions showed STAT3 to be present in the nucleus of BL41 cells, where it can mediate Mcl-1 gene transcription. BAY61-3606 inhibited the translocation of STAT3 from the cytoplasm to the nucleus (**Figure 3B**), suggesting a role for STAT3 in the regulation of Mcl-1 gene expression by BCR signaling. Incubation with the STAT3 inhibitor Stattic resulted in a 70% decrease in cell viability associated with the lower levels of Mcl-1 protein. Caspase inhibition by Q-VD-Oph rescued the cells from the cell death induced by Stattic, whereas Mcl-1 protein levels were only partially rescued, suggesting that STAT3 inhibition does not result in a caspase-dependent cleavage of Mcl-1 similar to that observed with BAY61-3606. The lack of PARP cleavage confirmed the effectiveness of Q-VD-Oph, as shown in **Figure 2C**. Similarly, Stattic treatment decreased Mcl-1 protein levels in both RAMOS and BL2 cells. Caspase inhibition with Q-VD-Oph in the presence of Stattic did not affect Mcl-1 levels, as already observed in BL41 cells (Figure S3B in Supplementary Material). We assessed Mcl-1 gene expression by RT-qPCR. We found that 4 h of treatment with Stattic decreased the level of Mcl-1 gene expression (**Figure 3C**). Treatment with Stattic in RAMOS and BL2 cells also decreased Mcl-1 transcript levels (Figure S3B in Supplementary Material).

Taken together, these results indicate that STAT3 is involved in regulating Mcl-1 gene expression in BL41, RAMOS, and BL2 cells.

Overexpression of the Mcl-1 Gene Counteracts the Inhibition of Both SYK and STAT3

We investigated whether Mcl-1 gene overexpression could rescue BL41 cells from apoptosis. Cells were transduced with retroviral particles containing an Mcl-1 construct, or with control particles lacking this construct. As expected, the Mcl-1 overexpression induced by retroviral particles was not influenced by BAY61-3606 or Stattic in transduced BL41 cells (**Figure 4A**). A similar effect was observed for levels of Mcl-1 gene expression (**Figure 4B**). The effect of BAY61-3606 and Stattic on apoptosis was then assessed in both types of BL41 cells, in a flow cytometry assay based on the extracellular expression of phosphatidylserine and 7-AAD uptake. The proportion of apoptotic cells increased in cells transduced with the empty vector, whereas no such increase upon SYK or STAT3 inhibition was observed in cells overexpressing Mcl-1 (**Figure 4C**). We conclude that the downregulation of Mcl-1 in BL41 cells following SYK inhibition is required to induce apoptotic cell death.

SYK Inhibition in Tonsillar B Cells Decreases Viability, Activation, and Mcl-1 Expression, Resulting in Lower Levels of Ig Secretion

We then sought to confirm the general effect of SYK inhibition on primary B cells activated *in vitro*. An analysis of SYK phosphorylation revealed that BAY61-3606 reduced the phosphorylation state of SYK in activated B cells (**Figure 5A**).

Flow cytometry analyses were performed on tonsillar B cells ($CD19^+$) after 3 days in culture. The viability of activated B cells in which BCR signaling was impaired by BAY61-3606 was 60% lower than that of control cells. Non-activated cells were not viable in culture, and no difference was observed between non-activated cells in the presence and absence of Bay61-3606 (**Figure 5B**).

Lower B-cell viability was associated with lower levels of Mcl-1 protein and of B-cell activation, as assessed by monitoring CD80 expression. This effect was observed in total B cells and in the pre-GC and GC (BM2′ and BM3 + BM4) populations identified on the basis of the BM1–BM5 classification (**Figure 5C**).

We then investigated the effects of SYK inhibition on Ig production, by assessing IgG secretion after 3 days in culture. Activated cells secreted about 150 ng of IgG per ml, whereas activated cells treated with BAY61-3606 secreted smaller amounts of IgG (**Figure 5D**).

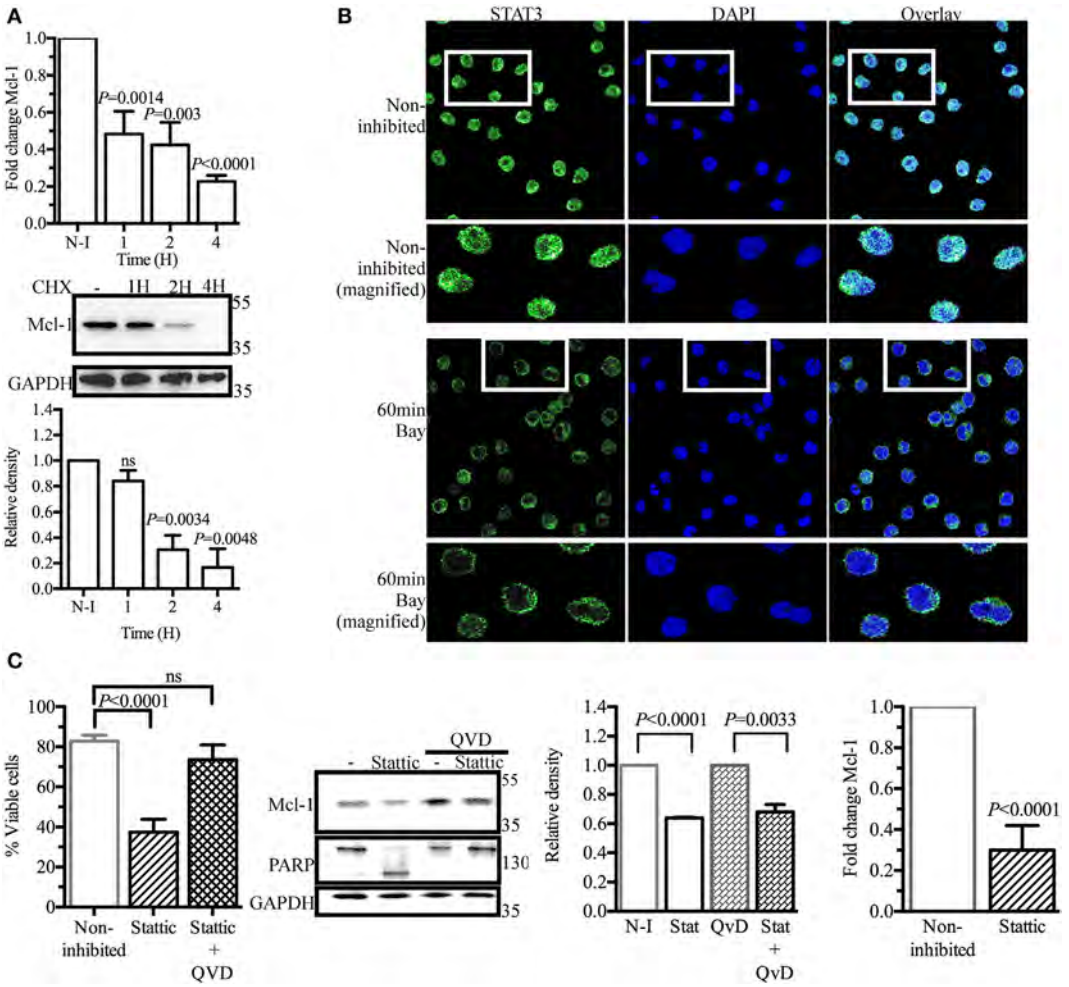

FIGURE 3 | Signal transducer and activator of transcription 3 (STAT3) as a potential regulator of myeloid cell leukemia-1 (Mcl-1) gene transcription in BL41 cells (Burkitt's lymphoma cells) upon spleen tyrosine kinase inhibition. **(A)** BL41 cells were treated with BAY61-3606 (5 μM) for 1, 2, and 4 h and expression of the Mcl-1 gene was assessed by RT-qPCR. Mean values are shown (±SEM, $n = 5$), and significant P-values are indicated for comparisons with cells not treated with BAY61-3606. BL41 cells were treated with cycloheximide (10 μM) for 1, 2, and 4 h and Mcl-1 protein levels were determined by western blotting, with quantification by protein densitometry and normalization against GAPDH levels. Mean values are shown (±SEM, $n = 3$), and significant P-values are indicated for comparisons with cells not treated with BAY61-3606. **(B)** BL41 cells were treated with BAY61-3606 (5 μM; 60 min), and the cellular location of STAT3 was determined by immunofluorescence analyses. Images were obtained with a Leica confocal microscope equipped with a 63× objective. **(C)** The viability of BL41 cells was determined by flow cytometry analysis in cells treated with the STAT3 inhibitor Stattic (5 μM; 16 h) in the presence or absence of Q-VD-Oph (10 μM). Apoptotic cells were identified on the basis of their size and granularity, as assessed by forward and side light scattering. The data shown are mean values (±SEM, $n = 6$). Mcl-1 protein levels were assessed by western blotting after treatment with Stattic (5 μM; 4 h) and Q-VD-Oph (10 μM); Mcl-1 levels were quantified by protein densitometry and normalized against GAPDH levels. The data shown are mean values (±SEM, $n = 3$). Q-VD-Oph efficiency was determined by western blotting to analyze PARP cleavage (4 h) and cell death inhibition (16 h). Mean values are shown (±SEM, $n = 6$). Mcl-1 gene expression levels were determined by RT-qPCR. Mean values are shown (±SEM, $n = 4$), and significant P-values are shown for comparisons with cells not treated with BAY61-3606. CHX, cycloheximide; N-I, non-inhibited; Bay, BAY61-3606; QVD, Q-VD-Oph; ns, not significant.

These results suggest that SYK inhibition reduces cell viability and Mcl-1 protein levels and impairs B-cell activation and IgG secretion.

DISCUSSION

The GC reaction is important for the generation of effector B cells with a high Ag affinity. During the GC reaction, apoptosis is required to eliminate B cells with low Ag affinity and self-reactive B cells (19, 39, 40).

Conversely, the positive selection of GC B cells with a high Ag affinity and the promotion of their survival are essential for the generation of effector B cells (19, 20). The role of antiapoptotic Bcl-2 family members, including Bcl-2, Mcl-1, and Bcl-xl, in the GC reaction has been investigated. Yoshino et al. (41) observed that resting and mantle-zone B cells expressed Bcl-2, whereas GC B cells did not. This finding was confirmed by the identification of Bcl-6 as a repressor of Bcl-2 transcription (42, 43). We confirmed, in a previous study based on the *in situ* staining of human lymphocytes, that GC cells do not express Bcl-2, whereas

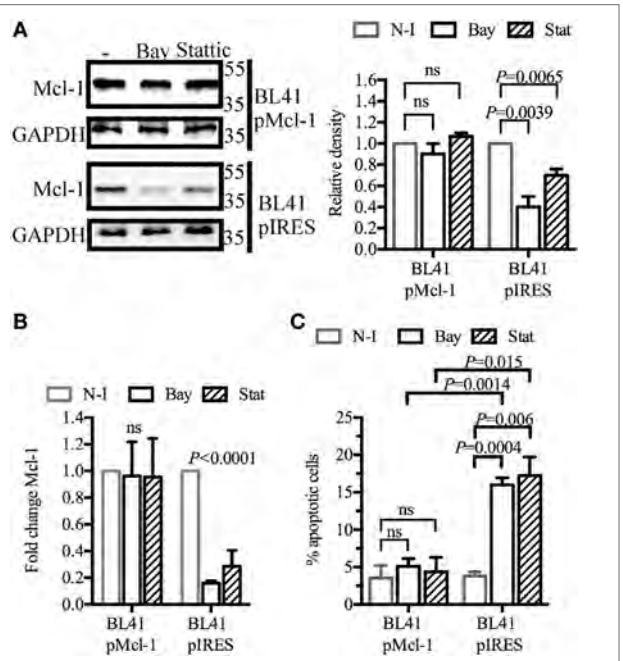

FIGURE 4 | Myeloid cell leukemia-1 (Mcl-1) overexpression protects BL41 cells against BAY61-3606-induced apoptosis BL41 cells were transduced with retroviral particles containing an Mcl-1 construct (pMcl-1), or an empty vector (pIRES) as a control. **(A)** The transduced cells were treated with BAY61-3606 or Stattic (5 μM; 4 h). Mcl-1 protein levels were determined by western blotting, with quantification by protein densitometry and normalization against GAPDH levels. Mean values are shown (±SEM, $n = 3$). **(B)** Mcl-1 gene expression was determined by RT-qPCR after treatment with BAY61-3606 (5 μM; 4 h) or Stattic (5 μM; 4 h). Mean values are shown (±SEM, $n = 4$), and significant P-values are shown for comparisons with cells not treated with inhibitor. **(C)** Apoptotic cells were identified on the basis of their extracellular expression of phosphatidylserine, detected by Annexin V staining, and their plasma membrane permeability, assessed by monitoring their uptake of 7-AAD after treatment with BAY61-3606 (5 μM; 8 h) or Stattic (5 μM; 8 h). Mean values are shown (±SEM, $n = 4$). Bay, BAY61-3606; N-I, non-inhibited; ns, not significant; Stat, Stattic.

Mcl-1 is co-expressed with PUMA and Bcl-xl in these cells (28). There is growing evidence to suggest that Mcl-1 is a key player in the survival of activated B cells. Vikstrom et al. (27) showed, with a conditional Mcl-1 knockout model in mice, that the absence of Mcl-1 resulted in the defective development of GC and memory cells and impaired Ig secretion. In the same study, memory B-cell formation had no effect on the GC reaction in Bcl-xl knockout mice. We confirm here that Mcl-1 is strongly expressed in the BM3 + BM4 population of tonsillar B cells corresponding to GC B cells (31).

A recent study showed that GCs may develop outside secondary lymphoid organs and form TLS, which generate effector and memory B cells. Such TLS have been reported in cases of persistent inflammation (44, 45). Thaunat et al. (14) detected TLS in kidney allografts in cases of cAMR, in which infiltrating B cells, T cells, and follicular dendritic cells were identified. GC B-cell characteristics, such as clonality, high levels of proliferation, and the upregulation of GC-related genes, have been observed in these infiltrations (14, 46–48). We found that the B cells infiltrating kidneys displaying cAMR expressed Mcl-1, consistent with the notion that the B cells infiltrating grafted organs are part of the TLS and are involved in the local immune response and effector B-cell production. Various immunosuppressive treatments have been developed to prevent and treat acute cellular rejection, but these treatments are clearly ineffective against cAMR, which remains a leading cause of chronic organ failure (49–51). There is, therefore, an urgent need to develop new treatments that effectively alter GC-like cell viability and differentiation, to reduce the prevalence of cAMR.

B-cell receptor signaling during B-cell development leads to the elimination of self-reactive B cells by programmed cell death (52, 53), whereas Ag affinity-linked BCR engagement later in the GC reaction leads to the apoptosis of cells with a low Ag affinity and the differentiation of cells with a high Ag affinity into effector B cells (19–21). SYK acts very early in the signaling chain, and is, therefore, an attractive candidate regulator of BCR signaling. In this study, we aimed to impair BCR signaling by inhibiting the kinase activity of SYK, to decrease GC B-cell viability. In GC centroblast cell lines, inhibition of the constitutively active SYK kinase resulted in the downregulation of Mcl-1 and a decrease in cell viability. We show that preventing Mcl-1 protein degradation with caspase or proteasome inhibitors only partially rescues Mcl-1 protein levels, and our RT-qPCR experiments confirmed the downregulation of Mcl-1 gene transcription.

Akgul et al. (54) identified several binding sites for transcription factors, including STAT3, within the promotor region of the Mcl-1 gene. The role of STAT3 in the GC response remains unclear, but this transcription factor has been shown to influence the T cell-dependent IgG response, and STAT3 deficiencies impair the generation of human memory B cells (55, 56). Ding et al. (57) recently showed, with a STAT3 knockout mouse model, that STAT3 is dispensable for GC initiation but essential for the maintenance of the GC reaction. Immunized STAT3 knockout mice had larger numbers of apoptotic GC B cells than normal mice, and this higher level of apoptosis was associated with lower levels of Mcl-1 gene expression (57). STAT3 has already been reported to be involved in Mcl-1 regulation, but mostly on the basis of observations from experiments in which the JAK/STAT pathway was activated by cytokine- and growth factor-induced signaling (58–60). We show here, in BL41 cells, that SYK inhibition impairs the translocation of STAT3 to the nucleus, preventing its binding to the promoter of the Mcl-1 gene, whereas this transcription factor remains constitutively nuclear in the absence of treatment. STAT3 inhibition mimicked the effects of SYK inhibition in terms of Mcl-1 expression and cell death. We show here that BCR signaling is associated with the STAT3-modulated regulation of Mcl-1 protein levels. The modulation of STAT3 levels by the BCR is supported by data from studies reporting a JAK-independent link between BCR signaling and STAT3 (61, 62). We also show that Mcl-1 overexpression prevents cells from entering apoptosis in the presence of inhibitors of both SYK and STAT3. These results suggest that Mcl-1 downregulation is required to induce apoptosis, confirming the key role of Mcl-1 in maintaining the GC reaction, as reported in previous studies (27, 28, 63).

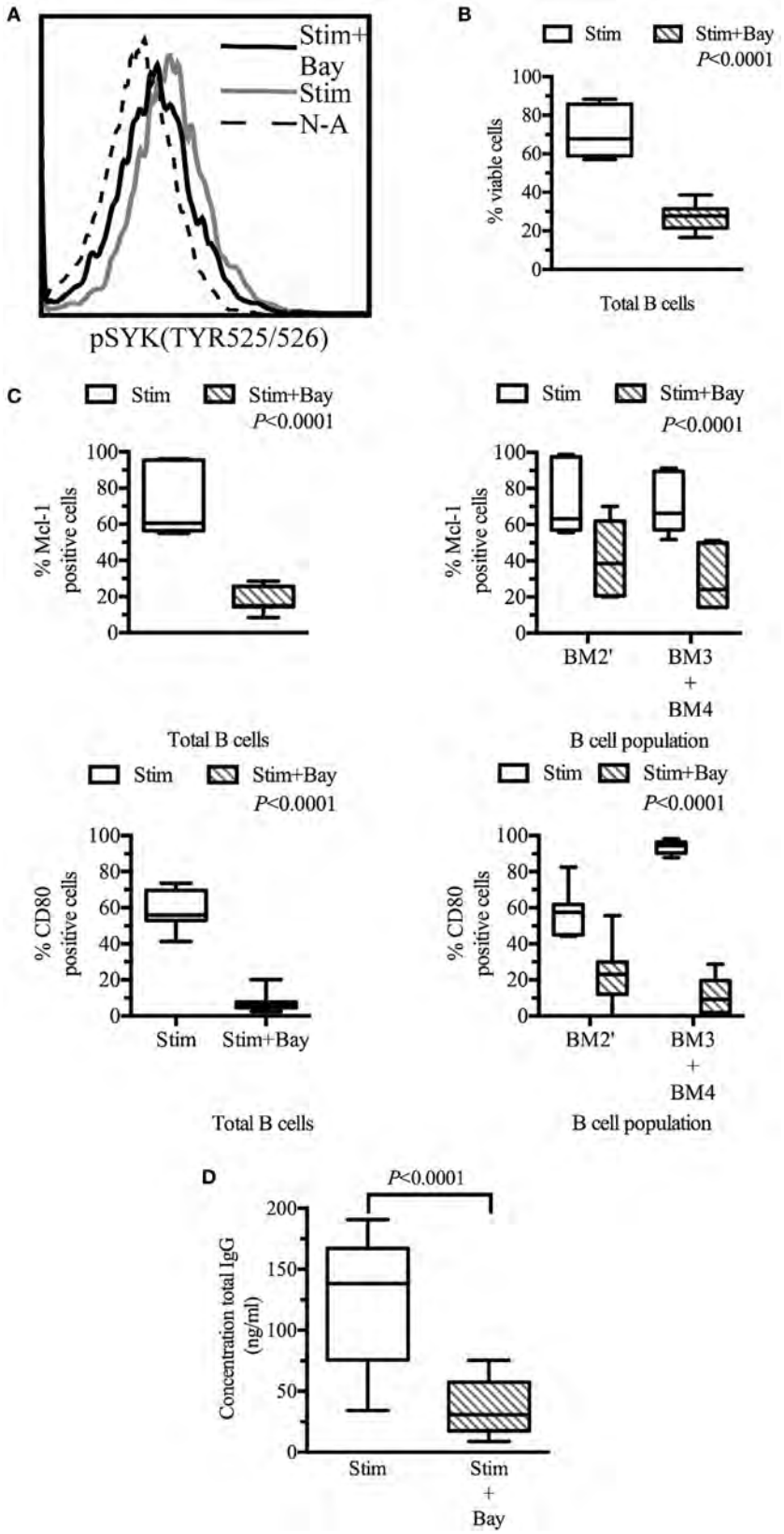

FIGURE 5 | Continued

FIGURE 5 | Spleen tyrosine kinase (SYK) inhibition in tonsillar B cells decreases viability, activation, and effector functions. Tonsillar cells activated *in vitro* by incubation with CD40L fibroblasts (1:10 ratio, fibroblasts: tonsillar cells), anti-μ antibody (10 μg/ml) and LPS (1 μg/ml) Non-activated tonsillar cells were cultured with CD32L fibroblasts (1:10 ratio, fibroblasts: tonsillar cells). **(A)** Following incubation for 20 min in the presence or absence of BAY61-3606 (5 μM), B cells were identified on the basis of their expression of CD19, and SYK phosphorylation status was determined by flow cytometry. **(B)** Following 3 days of culture, cells were stained with a fixable viability stain and identified on the basis of their CD19 expression status, by flow cytometry. Dead B cells were identified with a fixable viability stain. The boxplot shows the distribution between donors, and the quadrant indicates the values between the fifth and ninety-fifth percentiles, $n = 7$. **(C)** Following 3 days of culture, cells were stained with fixable viability stain, and for CD19, sIgD, CD38, CD80, and myeloid cell leukemia-1 (Mcl-1), and analyzed by flow cytometry. Viable cells were identified as fixable viability stain-negative. Mcl-1 levels were determined in CD19-positive cells and in pre-GC (BM2′) and GC B cells (BM3 + BM4) identified on the basis of sIgD and CD38 expression profiles. Activation state was determined by assessing CD80 expression in CD19-positive cells and in pre-GC (BM2′) and GC B-cells (BM3 + BM4). The boxplot represents the distribution between donors and the quadrant indicates the values between the fifth and ninety-fifth percentiles; significant *P* values are shown on the graphs for comparisons between all stimulated cells and those treated with BAY61-3606, $n = 7$. **(D)** The total immunoglobulin G (IgG) secreted by the cells during 3 days of culture was analyzed by ELISA. The boxplot represents the distribution between donors and the quadrant indicates the values between the fifth and ninety-fifth percentiles, $n = 9$. stim, stimulated; Bay, BAY61-3606; N-A, non-activated; CD, cluster of differentiation.

Le Huu et al. (64) observed an increase in SYK phosphorylation in B cells following allogeneic bone marrow transplantation in mice. In human patients with graft versus host disease (GVDH), total SYK levels were found to be higher than those in healthy patients. In the same study, PBMCs isolated from GVDH patients were found to have a higher BCR responsiveness following BCR engagement than PBMCs from healthy patients. SYK inhibition reduced BCR responsiveness in these cells (65). These findings suggest that activated SYK plays a role in GVDH. We show here that SYK inhibition in activated B cells reduces cell viability *in vitro*. Our results are consistent with those of Flynn et al. (66), showing that SYK inhibition induces apoptosis more strongly in B cells isolated from the PBMCs of patients with active GVDH than in those from patients with inactive or no GVDH. We found that this lower viability was associated with Mcl-1 downregulation in BL41 cells, a finding confirmed by our experiments with primary tonsillar B cells. We also show that SYK inhibition is associated with weaker activation, as shown by the level of CD80 expression.

The damaging role of the DSAs produced following organ transplantation has been studied in detail. Preexisting and *de novo* IgG DSAs are associated with acute and chronic solid graft injury (51, 67, 68), whereas DSAs of the IgM and IgA types are not in themselves damaging (69, 70). We showed that SYK inhibition in primary cells activated *in vitro* abolished all IgG secretion. These results therefore suggest that SYK inhibition affects the GC reaction and GC B-cell responsiveness.

In conclusion, our data show that SYK inhibition affects BCR signaling-mediated cell survival through the downregulation of Mcl-1 gene transcription. We demonstrate that SYK inhibition impairs B-cell responses by altering B-cell reactivity to Ags and decreasing Ab production. These results suggest that, in cases of cAMR, SYK could be targeted by new therapeutic tools, to improve graft survival by manipulating the humoral immune response.

ETHICS STATEMENT

Renal biopsy specimens and detransplanted kidneys were obtained from transplant recipients with end-stage renal failure due to cAMR, who gave written informed consent in accordance with the Declaration of Helsinki for the use of part of their biopsy specimens for research on renal transplantation. The samples were stored at the Biological Resource Center of Paris-South University and the collection has been declared to the French Ministry of Research: AC-2017-2991. The tonsil used were collected 5 years ago from children with tonsillar hypertrophy. Tonsils removed from children in this context are generally considered to be waste and are normally immediately destroyed in the operating room without histological analysis. We have such tonsils, before their destruction. The project and the protocol were submitted to the ED468 (Biosigne) doctoral school for approval.

AUTHOR CONTRIBUTIONS

AD, AV, and NR designed the study; NR, FH, GA, and AP performed experiments; FH and GA contributed to study design; OT helped to obtain histological slides for cAMR kidney samples; NR prepared the manuscript; and the other authors commented on the manuscript.

ACKNOWLEDGMENTS

We thank Catherine Nowak for providing tonsils and Celine Verstuyft from the Biological Resource Center CRB PARIS SUD (BB-0033-00089) for help and technological support.

FUNDING

This study was supported by grants from DIM Biothérapie and Vaincre le cancer-NRB.

SUPPLEMENTARY MATERIAL

The Supplementary Material for this article can be found online at https://www.frontiersin.org/articles/10.3389/fimmu.2018.00787/full#supplementary-material.

FIGURE S1 | Unstimulated B-cells isolated from mononuclear cells extracted from transplant recipients presenting end-stage renal failure due to chronic AMR were stained for CD19, CD27 and CD138 and analyzed by flow cytometry. Memory B-cells were identified based on the expression of CD19 and CD27. Plasma cells were identified based on the expression of CD138, $n = 4$.

FIGURE S2 | **(A)** BL2 and RAMOS cells were treated with BAY61-3606 (5 μM; 4 h) and Q-VD-Oph (10 μM; 4 h). Levels of the antiapoptotic proteins myeloid cell leukemia-1 (Mcl-1), were determined by western blotting. Q-VD-Oph efficiency was determined by western-blot analysis of PARP cleavage (4 h) and cell death inhibition (16 h). The data shown are mean values (±SEM, $n = 3$). **(B)** BL2 and RAMOS cells were treated with BAY61-3606 (5 μM; 4 h) or MG-132 (10 μM; 4 h)

and Mcl-1 protein levels were determined by western blotting, with quantification by protein densitometry and normalization against GAPDH levels ($n = 1$). Bay: BAY61-3606, N-I: non-inhibited, QVD: Q-VD-Oph, MG: MG132.

FIGURE S3 | **(A)** BL2 and RAMOS cells were treated with BAY61-3606 (5 μM; 4 h) and expression of the myeloid cell leukemia-1 (Mcl-1) gene was assessed by RT-qPCR. Mean values are shown (±SEM, $n = 3$). **(B)** Mcl-1 protein levels were assessed by western blotting after treatment with Stattic (5 μM; 4 h) and Q-VD-Oph (10 μM). Q-VD-Oph efficiency was determined by western blotting to analyze PARP cleavage (4 h) Mcl-1 gene expression levels were determined by RT-qPCR. Mean values are shown (±SEM, $n = 3$). Bay: BAY61-3606, QVD: Q-VD-Oph.

REFERENCES

1. Bonomini V, Vangelista A, Frascà GM, Di Felice A, Liviano D, Arcangelo G. Effects of plasmapheresis in renal transplant rejection. A controlled study. *Trans Am Soc Artif Intern Organs* (1985) 31:698–703.
2. Slatinska J, Honsova E, Burgelova M, Slavcev A, Viklicky O. Plasmapheresis and intravenous immunoglobulin in early antibody-mediated rejection of the renal allograft: a single-center experience. *Ther Apher Dial* (2009) 13(2): 108–12. doi:10.1111/j.1744-9987.2009.00664.x
3. Jordan SC, Vo A, Tyan D, Toyota M. Desensitization therapy with intravenous gammaglobulin (IVIG): applications in solid organ transplantation. *Trans Am Clin Climatol Assoc* (2006) 117:199–211.
4. Waiser J, Duerr M, Schönemann C, Rudolph B, Wu K, Halleck F, et al. Rituximab in combination with bortezomib, plasmapheresis, and high-dose IVIG to treat antibody-mediated renal allograft rejection. *Transplant Direct* (2016) 2(8):e91. doi:10.1097/TXD.0000000000000604
5. Faguer S, Kamar N, Guilbeaud-Frugier C, Fort M, Modesto A, Mari A, et al. Rituximab therapy for acute humoral rejection after kidney transplantation. *Transplantation* (2007) 83(9):1277–80. doi:10.1097/01.tp.0000261113.30757.d1
6. Mulley WR, Hudson FJ, Tait BD, Skene AM, Dowling JP, Kerr PG, et al. A single low-fixed dose of rituximab to salvage renal transplants from refractory antibody-mediated rejection. *Transplantation* (2009) 87(2):286–9. doi:10.1097/TP.0b013e31819389cc
7. Kizilbash S, Claes D, Ashoor I, Chen A, Jandeska S, Matar RB, et al. Bortezomib in the treatment of antibody-mediated rejection in pediatric kidney transplant recipients: A Multicenter Midwest Pediatric Nephrology Consortium study. *Pediatr Transplant* (2017) 21(3):e12873. doi:10.1111/petr.12873
8. Orandi BJ, Zachary AA, Dagher NN, Bagnasco SM, Garonzik-Wang JM, Van Arendonk KJ, et al. Eculizumab and splenectomy as salvage therapy for severe antibody-mediated rejection after HLA-incompatible kidney transplantation. *Transplantation* (2014) 98(8):857–63. doi:10.1097/TP.0000000000000298
9. Yelken B, Arpalı E, Görcin S, Kocak B, Karatas C, Demiralp E, et al. Eculizumab for treatment of refractory antibody-mediated rejection in kidney transplant patients: a single-center experience. *Transplant Proc* (2015) 47(6):1754–9. doi:10.1016/j.transproceed.2015.06.029
10. Cornall RJ, Cheng AM, Pawson T, Goodnow CC. Role of Syk in B-cell development and antigen-receptor signaling. *Proc Natl Acad Sci U S A* (2000) 97(4):1713–8. doi:10.1073/pnas.97.4.1713
11. Tsang E, Giannetti AM, Shaw D, Dinh M, Tse JKY, Gandhi S, et al. Molecular mechanism of the Syk activation switch. *J Biol Chem* (2008) 283(47):32650–9. doi:10.1074/jbc.M806340200
12. Dal Porto JM, Gauld SB, Merrell KT, Mills D, Pugh-Bernard AE, Cambier J. B cell antigen receptor signaling 101. *Mol Immunol* (2004) 41(6–7):599–613. doi:10.1016/j.molimm.2004.04.008
13. Jacob J, Kelsoe G, Rajewsky K, Weiss U. Intraclonal generation of antibody mutants in germinal centres. *Nature* (1991) 354(6352):389–92. doi:10.1038/354389a0
14. Thaunat O, Field A-C, Dai J, Louedec L, Patey N, Bloch M-F, et al. Lymphoid neogenesis in chronic rejection: evidence for a local humoral alloimmune response. *Proc Natl Acad Sci U S A* (2005) 102(41):14723–8. doi:10.1073/pnas.0507223102
15. Koenig A, Thaunat O. Lymphoid neogenesis and tertiary lymphoid organs in transplanted organs. *Front Immunol* (2016) 7:646. doi:10.3389/fimmu.2016.00646
16. Berek C, Berger A, Apel M. Maturation of the immune response in germinal centers. *Cell* (1991) 67(6):1121–9. doi:10.1016/0092-8674(91)90289-B
17. Jacob J, Kassir R, Kelsoe G. *In situ* studies of the primary immune response to (4-hydroxy-3-nitrophenyl)acetyl. I. The architecture and dynamics of responding cell populations. *J Exp Med* (1991) 173(5):1165–75. doi:10.1084/jem.173.5.1165
18. Muramatsu M, Kinoshita K, Fagarasan S, Yamada S, Shinkai Y, Honjo T. Class switch recombination and hypermutation require activation-induced cytidine deaminase (AID), a potential RNA editing enzyme. *Cell* (2000) 102(5):553–63. doi:10.1016/S0092-8674(00)00078-7
19. Liu YJ, Joshua DE, Williams GT, Smith CA, Gordon J, MacLennan ICM. Mechanism of antigen-driven selection in germinal centres. *Nature* (1989) 342(6252):929–31. doi:10.1038/342929a0
20. Tarlinton DM, Smith KGC. Dissecting affinity maturation: a model explaining selection of antibody-forming cells and memory B cells in the germinal centre. *Immunol Today* (2000) 21(9):436–41. doi:10.1016/S0167-5699(00)01687-X
21. Meyer-Hermann ME, Maini PK, Iber D. An analysis of B cell selection mechanisms in germinal centers. *Math Med Biol* (2006) 23(3):255–77. doi:10.1093/imammb/dql012
22. Billian G, Mondière P, Berard M, Bella C, Defrance T. Antigen receptor-induced apoptosis of human germinal center B cells is targeted to a centrocytic subset. *Eur J Immunol* (1997) 27(2):405–14. doi:10.1002/eji.1830270210
23. Fischer SF, Bouillet P, O'Donnell K, Light A, Tarlinton DM, Strasser A. Proapoptotic BH3-only protein Bim is essential for developmentally programmed death of germinal center-derived memory B cells and antibody-forming cells. *Blood* (2007) 110(12):3978–84. doi:10.1182/blood-2007-05-091306
24. Youle RJ, Strasser A. The BCL-2 protein family: opposing activities that mediate cell death. *Nat Rev Mol Cell Biol* (2008) 9(1):47–59. doi:10.1038/nrm2308
25. Shamas-Din A, Kale J, Leber B, Andrews DW. Mechanisms of action of Bcl-2 family proteins. *Cold Spring Harb Perspect Biol* (2013) 5(4):a008714. doi:10.1101/cshperspect.a008714
26. Siddiqui WA, Ahad A, Ahsan H. The mystery of BCL2 family: Bcl-2 proteins and apoptosis: an update. *Arch Toxicol* (2015) 89(3):289–317. doi:10.1007/s00204-014-1448-7
27. Vikstrom I, Carotta S, Lüthje K, Peperzak V, Jost PJ, Glaser S, et al. Mcl-1 is essential for germinal center formation and B cell memory. *Science* (2010) 330(6007):1095–9. doi:10.1126/science.1191793
28. Clybouw C, Fischer S, Auffredou MT, Hugues P, Alexia C, Bouillet P, et al. Regulation of memory B-cell survival by the BH3-only protein Puma. *Blood* (2011) 118(15):4120–8. doi:10.1182/blood-2011-04-347096
29. Morel C, Carlson SM, White FM, Davis RJ. Mcl-1 integrates the opposing actions of signaling pathways that mediate survival and apoptosis. *Mol Cell Biol* (2009) 29(14):3845–52. doi:10.1128/MCB.00279-09
30. Gavrilescu LC, Van Etten RA. Production of replication-defective retrovirus by transient transfection of 293T cells. *J Vis Exp* (2007) 10:550. doi:10.3791/550
31. Pascual V, Liu YJ, Magalski A, Bouteiller OD, Banchereau J, Capra JD. Analysis of somatic mutation in five B cell subsets of human tonsil. *J Exp Med* (1994) 180(1):329–39. doi:10.1084/jem.180.1.329
32. Küppers R, Klein U, Hansmann M-L, Rajewsky K. Cellular origin of human B-cell lymphomas. *N Engl J Med* (1999) 341(20):1520–9. doi:10.1056/NEJM199911113412007
33. Yamamoto N, Takeshita K, Shichijo M, Kokubo T, Sato M, Nakashima K, et al. The orally available spleen tyrosine kinase inhibitor 2-[7-(3,4-dimethoxyphenyl)-imidazo[1,2-c]pyrimidin-5-ylamino]nicotinamide dihydrochloride (BAY 61-3606) blocks antigen-induced airway inflammation in rodents. *J Pharmacol Exp Ther* (2003) 306(3):1174–81. doi:10.1124/jpet.103.052316
34. Krysko DV, Vanden Berghe T, D'Herde K, Vandenabeele P. Apoptosis and necrosis: detection, discrimination and phagocytosis. *Methods* (2008) 44(3):205–21. doi:10.1016/j.ymeth.2007.12.001
35. Michels J, O'Neill JW, Dallman CL, Mouzakiti A, Habens F, Brimmell M, et al. Mcl-1 is required for Akata6 B-lymphoma cell survival and is converted to a cell death molecule by efficient caspase-mediated cleavage. *Oncogene* (2004) 23(28):4818–27. doi:10.1038/sj.onc.1207648
36. Nencioni A, Hua F, Dillon CP, Yokoo R, Scheiermann C, Cardone MH, et al. Evidence for a protective role of Mcl-1 in proteasome inhibitor-induced apoptosis. *Blood* (2005) 105(8):3255–62. doi:10.1182/blood-2004-10-3984

37. Bhattacharya S, Ray RM, Johnson LR. STAT3-mediated transcription of Bcl-2, Mcl-1 and c-IAP2 prevents apoptosis in polyamine-depleted cells. *Biochem J* (2005) 392(2):335–44. doi:10.1042/BJ20050465
38. Thomas LW, Lam C, Edwards SW. Mcl-1; the molecular regulation of protein function. *FEBS Lett* (2010) 584(14):2981–9. doi:10.1016/j.febslet.2010.05.061
39. Han S, Zheng B, Porto JD, Kelsoe G. *In situ* studies of the primary immune response to (4-hydroxy-3-nitrophenyl)acetyl. IV. Affinity-dependent, antigen-driven B cell apoptosis in germinal centers as a mechanism for maintaining self-tolerance. *J Exp Med* (1995) 182(6):1635–44. doi:10.1084/jem.182.6.1635
40. Shokat KM, Goodnow CC. Antigen-induced B-cell death and elimination during germinal-centre immune responses. *Nature* (1995) 375(6529):334–8. doi:10.1038/375334a0
41. Yoshino T, Kondo E, Cao L, Takahashi K, Hayashi K, Nomura S, et al. Inverse expression of bcl-2 protein and Fas antigen in lymphoblasts in peripheral lymph nodes and activated peripheral blood T and B lymphocytes. *Blood* (1994) 83(7):1856–61.
42. Ci W, Polo JM, Cerchietti L, Shaknovich R, Wang L, Yang SN, et al. The BCL6 transcriptional program features repression of multiple oncogenes in primary B cells and is deregulated in DLBCL. *Blood* (2009) 113(22):5536–48. doi:10.1182/blood-2008-12-193037
43. Saito M, Novak U, Piovan E, Basso K, Sumazin P, Schneider C, et al. BCL6 suppression of BCL2 via Miz1 and its disruption in diffuse large B cell lymphoma. *Proc Nat Acad Sci U S A* (2009) 106(27):11294–9. doi:10.1073/pnas.0903854106
44. Kratz A, Campos-Neto A, Hanson MS, Ruddle NH. Chronic inflammation caused by lymphotoxin is lymphoid neogenesis. *J Exp Med* (1996) 183(4): 1461–72. doi:10.1084/jem.183.4.1461
45. Takemura S, Klimiuk PA, Braun A, Goronzy JJ, Weyand CM. T cell activation in rheumatoid synovium is B-cell dependent. *J Immunol* (2001) 167(8):4710–8. doi:10.4049/jimmunol.167.8.4710
46. Kerjaschki D, Regele HM, Moosberger I, Nagy-Bojarski K, Watschinger B, Soleiman A, et al. Lymphatic neoangiogenesis in human kidney transplants is associated with immunologically active lymphocytic infiltrates. *J Am Soc Nephrol* (2004) 15(3):603–12. doi:10.1097/01.ASN.0000113316.52371.2E
47. Thaunat O, Patey N, Caligiuri G, Gautreau C, Mamani-Matsuda M, Mekki Y, et al. Chronic rejection triggers the development of an aggressive intragraft immune response through recapitulation of lymphoid organogenesis. *J Immunol* (2010) 185(1):717–28. doi:10.4049/jimmunol.0903589
48. Cheng J, Torkamani A, Grover RK, Jones TM, Ruiz DI, Schork NJ, et al. Ectopic B-cell clusters that infiltrate transplanted human kidneys are clonal. *Proc Natl Acad Sci U S A* (2011) 108(14):5560–5. doi:10.1073/pnas.1101148108
49. Durrbach A, Francois H, Beaudreuil S, Jacquet A, Charpentier B. Advances in immunosuppression for renal transplantation. *Nat Rev Nephrol* (2010) 6(3):160–7. doi:10.1038/nrneph.2009.233
50. Lodhi SA, Lamb KE, Meier-Kriesche HU. Solid organ allograft survival improvement in the United States: the long-term does not mirror the dramatic short-term success. *Am J Transplant* (2011) 11(6):1226–35. doi:10.1111/j.1600-6143.2011.03539.x
51. Loupy A, Hill GS, Jordan SC. The impact of donor-specific anti-HLA antibodies on late kidney allograft failure. *Nat Rev Nephrol* (2012) 8(6):348–57. doi:10.1038/nrneph.2012.81
52. Yurasov S, Nussenzweig MC. Regulation of autoreactive antibodies. *Curr Opin Rheumatol* (2007) 19(5):421–6. doi:10.1097/BOR.0b013e328277ef3b
53. Yarkoni Y, Getahun A, Cambier JC. Molecular underpinning of B-cell anergy. *Immunol Rev* (2010) 237(1):249. doi:10.1111/j.1600-065X.2010.00936.x
54. Akgul C, Turner PC, White MRH, Edwards SW. Functional analysis of the human MCL-1 gene. *Cell Mol Life Sci* (2000) 57(4):684–91. doi:10.1007/PL00000728
55. Fornek JL, Tygrett LT, Waldschmidt TJ, Poli V, Rickert RC, Kansas GS. Critical role for Stat3 in T-dependent terminal differentiation of IgG B cells. *Blood* (2006) 107(3):1085–91. doi:10.1182/blood-2005-07-2871
56. Avery DT, Deenick EK, Ma CS, Suryani S, Simpson N, Chew GY, et al. B cell–intrinsic signaling through IL-21 receptor and STAT3 is required for establishing long-lived antibody responses in humans. *J Exp Med* (2010) 207(1):155–71. doi:10.1084/jem.20091706
57. Ding C, Chen X, Dascani P, Hu X, Bolli R, Zhang H-G, et al. STAT3 signaling in B cells is critical for germinal center maintenance and contributes to the pathogenesis of murine models of lupus. *J Immunol* (2016) 196(11):4477–86. doi:10.4049/jimmunol.1502043
58. Puthier D, Bataille R, Amiot M. IL-6 up-regulates mcl-1 in human myeloma cells through JAK/STAT rather than ras/MAP kinase pathway. *Eur J Immunol* (1999) 29(12):3945–50. doi:10.1002/(SICI)1521-4141(199912)29:12<3945::AID-IMMU3945>3.0.CO;2-O
59. Epling-Burnette PK, Liu JH, Catlett-Falcone R, Turkson J, Oshiro M, Kothapalli R, et al. Inhibition of STAT3 signaling leads to apoptosis of leukemic large granular lymphocytes and decreased Mcl-1 expression. *J Clin Invest* (2001) 107(3):351–62. doi:10.1172/JCI9940
60. Mott JL, Kobayashi S, Bronk SF, Gores GJ. mir-29 regulates Mcl-1 protein expression and apoptosis. *Oncogene* (2007) 26(42):6133–40. doi:10.1038/sj.onc.1210436
61. Wang L, Kurosaki T, Corey SJ. Engagement of the B-cell antigen receptor activates STAT through Lyn in a Jak-independent pathway. *Oncogene* (2006) 26(20):2851–9. doi:10.1038/sj.onc.1210092
62. Uckun FM, Qazi S, Ma H, Tuel-Ahlgren L, Ozer Z. STAT3 is a substrate of SYK tyrosine kinase in B-lineage leukemia/lymphoma cells exposed to oxidative stress. *Proc Natl Acad Sci U S A* (2010) 107(7):2902–7. doi:10.1073/pnas.0909086107
63. Vikstrom I, Slomp A, Carrington EM, Moesbergen LM, Chang C, Kelly GL, et al. MCL-1 is required throughout B-cell development and its loss sensitizes specific B-cell subsets to inhibition of BCL-2 or BCL-XL. *Cell Death Dis* (2016) 7(8):e2345. doi:10.1038/cddis.2016.237
64. Le Huu D, Kimura H, Date M, Hamaguchi Y, Hasegawa M, Hau KT, et al. Blockade of Syk ameliorates the development of murine sclerodermatous chronic graft-versus-host disease. *J Dermatol Sci* (2014) 74(3):214–21. doi:10.1016/j.jdermsci.2014.02.008
65. Allen JL, Tata PV, Fore MS, Wooten J, Rudra S, Deal AM, et al. Increased BCR responsiveness in B cells from patients with chronic GVHD. *Blood* (2014) 123(13):2108–15. doi:10.1182/blood-2013-10-533562
66. Flynn R, Allen JL, Luznik L, MacDonald KP, Paz K, Alexander KA, et al. Targeting Syk-activated B cells in murine and human chronic graft-versus-host disease. *Blood* (2015) 125(26):4085–94. doi:10.1182/blood-2014-08-595470
67. Lee P-C, Terasaki PI, Takemoto SK, Lee P-H, Hung C-J, Chen Y-L, et al. All chronic rejection failures of kidney transplants were preceded by the development of HLA antibodies. *Transplantation* (2002) 74(8):1192–4. doi:10.1097/01.TP.0000031249.33030.FB
68. Kaneku H, O'Leary JG, Banuelos N, Jennings LW, Susskind BM, Klintmalm GB, et al. *De novo* donor-specific HLA antibodies decrease patient and graft survival in liver transplant recipients. *Am J Transplant* (2013) 13(6):1541. doi:10.1002/ajt.12212
69. Arnold ML, Heinemann FM, Horn P, Ziemann M, Lachmann N, Mühlbacher A, et al. 16th IHIW: anti-HLA alloantibodies of the of IgA isotype in re-transplant candidates. *Int J Immunogenet* (2013) 40(1):17–20. doi:10.1111/iji.12032
70. Everly MJ, Rebellato LM, Haisch CE, Briley KP, Bolin P, Kendrick WT, et al. Impact of IgM and IgG3 anti-HLA alloantibodies in primary renal allograft recipients. *Transplantation* (2014) 97(5):494–501. doi:10.1097/01.TP.0000441362.11232.48

Conflict of Interest Statement: The authors declare that the research was conducted in the absence of any commercial or financial relationships that could be construed as a potential conflict of interest.

frontiers in Immunology

REVIEW
published: 23 April 2018
doi: 10.3389/fimmu.2018.00835

Targeting B Cells and Plasma Cells in Autoimmune Diseases

Katharina Hofmann, Ann-Katrin Clauder and Rudolf Armin Manz*

Institute for Systemic Inflammation Research, University of Luebeck, Luebeck, Schleswig-Holstein, Germany

Success with B cell depletion using rituximab has proven the concept that B lineage cells represent a valid target for the treatment of autoimmune diseases, and has promoted the development of other B cell targeting agents. Present data confirm that B cell depletion is beneficial in various autoimmune disorders and also show that it can worsen the disease course in some patients. These findings suggest that B lineage cells not only produce pathogenic autoantibodies, but also significantly contribute to the regulation of inflammation. In this review, we will discuss the multiple pro- and anti-inflammatory roles of B lineage cells play in autoimmune diseases, in the context of recent findings using B lineage targeting therapies.

Keywords: B cells, IL-10$^+$ B cell, autoantibodies, autoimmune disease, rheumatoid arthritis, rituximab, bortezomib

OPEN ACCESS

Edited by:
Duncan Howie,
University of Oxford,
United Kingdom

Reviewed by:
Andrew L. Snow,
Uniformed Services University of the Health Sciences,
United States
Raymond John Steptoe,
The University of Queensland,
Australia
Adriana Gruppi,
Centro de Investigaciones en Bioquímica Clínica e Inmunología (CIBICI CONICET), Argentina

****Correspondence:***
Katharina Hofmann
katharina.hofmann@outlook.com

Specialty section:
This article was submitted to Immunological Tolerance and Regulation, a section of the journal Frontiers in Immunology

Received: *17 December 2017*
Accepted: *05 April 2018*
Published: *23 April 2018*

Citation:
Hofmann K, Clauder A-K and Manz RA (2018) Targeting B Cells and Plasma Cells in Autoimmune Diseases. Front. Immunol. 9:835. doi: 10.3389/fimmu.2018.00835

INTRODUCTION

The presence of autoantibodies is characteristic of most autoimmune diseases and has been widely used for diagnosis. Despite this, within the last 10–15 years B cells have been recognized as therapeutic targets for the treatment of autoimmune diseases. B cell subtypes, and the mechanisms of antibody production and maintenance, are highly diverse, and likewise the susceptibility of autoantibody-secreting plasma cells to therapies seems to be dependent on their tissue localization (1). Generally, conventional immunosuppressive therapy, using either steroids or cytostatic drugs, is commonly used in many autoimmune diseases and partly inhibits autoantibody production (2–5). At present, several drugs that specifically target B cells or plasma cells are either in clinical use or under development and promise to be very efficient for the treatment of various autoimmune diseases (6–8). Among them are (I) monoclonal antibodies against CD19, CD20, and CD22 that can directly target multiple B cell subtypes, but not or only to a lesser extent mature antibody-secreting plasma cells, (II) inhibitors of B cell activating factor (BAFF) and A proliferation-inducing ligand (APRIL), two cytokines which are very important survival factors for B cells and plasma cells, respectively, and (III) velcade/bortezomib, a small molecule proteasome inhibitor that spares B cells but eliminates both short-lived and long-lived plasma cells (9).

B cell directed therapies have proven not only to be therapeutically effective in classic B cell/autoantibody-driven disorders, such as autoimmune blistering skin diseases, myasthenia gravis, or antibody/immune-complex-mediated systemic lupus erythematosus (SLE), but also in diseases that are believed to be mainly driven by T cells, most prominently rheumatoid arthritis (RA) or multiple sclerosis (MS) (10–12). By contrast, in some cases, therapeutic B cell depletion results in the aggravation of symptoms. These findings emphasize that B cells play multiple roles that are relevant for the onset and clinical outcomes of autoimmune inflammatory disorders.

In this review, we will discuss how B cell targeting therapies may affect distinct B cell and plasma cell subpopulations, and how this depletion modulates the outcome of autoimmune diseases.

B CELLS, PLASMA CELLS, AND THEIR IMPACT ON AUTOIMMUNE DISEASES

B Cell Maturation and Subsets

In humans and mice, there are three known functionally and phenotypically distinct B cell subsets: B-1, B-2, and marginal zone (MZ) B cells (13). While B-1 and MZ B cells can contribute to innate and adaptive immunity, "conventional" B-2 cells provide adaptive humoral immunity.

B-1 cells arise already early in embryonic development and comprised about 5% of all B cells in mice and humans. The B-1 population is the major source of natural IgM antibodies that exhibit reactivity to self and common microbial antigens (14). B-2 cells are activated in T-dependent immune responses and produce antibodies of all subclasses, and are capable of forming memory B cells with increased antibody affinity. MZ B cells are found in the marginal sinus of the white pulp of the spleen and predominantly produce antibodies that are specific for carbohydrate antigens.

While autoantibodies contribute to the pathogenesis of many autoimmune disorders, natural autoantibodies can be protective (14–16), suggesting that the various B cell subsets play multifaceted roles in autoimmune diseases (17).

After birth, large numbers of immature B-2 B cells are continuously formed within the bone marrow (18). During the stepwise differentiation of B cell precursors into immature B cells, the genes encoding the B cell receptor are reorganized, which at the population level generates a heavily diverse antibody repertoire. Immature B cells express high levels of functional antigen receptors (antibodies) of the IgM subclass on their surface (19). Thereafter, based on the specificity and affinity of their individual B cell receptors, immature B cell clones are either negatively or positively selected (20).

Some immature B cells bearing an autoreactive B cell receptor become deleted by central tolerance mechanisms operative in the bone marrow. The immigration of immature B cells into the spleen occurs through the terminal branches of the central arteriole that drains into sinusoids of the MZ (21). After migration to the splenic follicles, non-self-reactive IgM^+/IgD^- immature B cells penetrate the MZ sinus to migrate through the interface between the periarteriolar lymphoid sheaths and B cell follicles, and eventually become IgM^+/IgD^+ naive mature B-2 or MZ B cells. This process is strongly dependent on high concentrations of the cytokine BAFF, which is expressed in splenic follicles. Most self-reactive immature B cells that passed central tolerance induction are energized or deleted in the spleen before they reach the BAFF-rich follicles. This peripheral tolerance mediating process relies on the activation of self-reactive B cells by autoantigens, which results in arrest of migration before these cells can enter the splenic follicle, and as a consequence they die as a result of BAFF-deprivation (21). Despite this, autoantibodies are also found in healthy individuals (22, 23), suggesting that some autoreactive B cells escape both the central and peripheral tolerance inducing mechanisms.

Mature B cells recirculate through the blood and accumulate in the follicles of secondary lymphoid tissues (24). Interestingly enough, mature B cells express a certain degree of migrational diversity. While all mature B cells are found in systemic and mucosal secondary lymphoid tissues, only a subpopulation of mature B cells recirculate through the bone marrow, a process of unknown biological significance, but which is clearly well controlled. In mice, these B cells express CD22, an Ig superfamily member serving as an adhesion receptor for sialic acid-bearing ligands. CD22 binds to CD22-ligands specifically present on sinusoidal endothelial cells in the bone marrow, but not on endothelial cells in other lymphoid tissues (25). A heterogeneous population of B cells also recirculates through the skin, as has been shown in animal models (26). These B cells express typical skin-homing receptors, e.g., ligands for E-selectin and α-4 and β-1 integrins, and exhibit a different immunophenotype than lymph node B cells. It is thought that these cells activate T cells at the site of inflammation and can increase local antibody production (26). However, the possibility that skin-homing B cells contribute to autoimmune skin diseases remains to be established.

After stimulation with their cognate (self-) antigen, mature B cells eventually may form short-lived plasma cells, memory B cells, or long-lived plasma cells (27, 28). As discussed below, these cell types markedly contribute to the pathogenesis of autoimmune diseases and exhibit a specific response to distinct therapeutic approaches.

Memory B Cells

Memory B cells are formed within germinal centers and differ from naive B cells with respect to several features. While many human and murine memory B cells still express IgM, a significant proportion has already switched to the production of downstream antibody subclasses, mainly IgA and IgGs (29–31). Antigen-mediated crosslinking of membrane IgG provides a much stronger activation signal than IgM (32), which contributes to the reduced activation threshold observed for memory B cells and their capacity to quickly give rise to antibody-secreting plasma cells (33–36). Independent from their subclass, memory B cells have down-regulated the expression of genes that negatively control BCR signaling and have up-regulated the expression of their counterparts (37, 38). Moreover, memory B cells also express higher affinity B cell receptors, which not only strengthens the effector functions of the antibodies secreted by their plasma cell progeny, but also allows memory B cells to sense very low antigen doses. Consequently, memory B cells resemble very powerful antigen-presenting cells (APCs) (39, 40). While dendritic cells definitively represent the most important APC during the initiation of the immune response, memory B cells may take over later. Hence, antigen-presentation by memory B cells might be of particular importance during the later phases of chronic immune reactions, such as autoimmune diseases. Human, but not murine, memory B cells show increased expression of CD27. The interaction of CD27 with its ligand on T cells, CD70, promotes the differentiation of activated memory B cells into plasma cells (41). Compared with naive cells, human memory B cells also exhibit a distinct expression profile of homing molecules; these molecules help B cells to interact with T cells and present their cognate antigen in the context of MHC class II in an optimal manner (42–47). The capacity to efficiently interact with T cells is crucial to quickly boosting both the formation of plasma cells

and antibody secretion, but likely also increases the capacity of memory B cells to modulate T cell responses.

In conclusion, memory B cells are optimized to interact with T cells and to yield strong antibody responses even in response to relatively little stimulation. Autoreactive memory antibodies are likely to contribute to the chronic and progressive course typically observed for autoimmune disorders (48). High frequencies of memory B cells are associated with poor clinical responses to RTX treatment (49). RTX treatment results in the efficient depletion of memory B cells in peripheral blood, and relapse after this treatment is thought to be associated with the repopulation of IgD-CD27$^-$ and IgD-CD27$^+$ memory B cells (50). However, RTX may not deplete the whole B cell memory compartment. RTX-treated patients can generate robust recall responses to repeated influenza vaccination, as indicated by the increase in serum antibody levels and peripheral blood plasmablast frequencies (51). This memory response is comparable to that observed in healthy controls. Hence, a significant fraction of memory B cells seems to be resistant to RTX treatment and is most likely localized in lymphoid or inflamed tissues (51). In mice, distinct layers of memory B cells have been identified, suggesting that the memory compartment is much more complex and diverse than expected (52, 53). Similarly, in human donors, distinct subpopulations of memory B cells that distinctly express homing receptors, such as CXCR3, have been observed in blood (46, 54). In response to IFN-γ, activated B cells upregulate CXCR3, which thereafter is stably expressed on their memory B cell progeny (46, 54). These findings may indicate that a subpopulation of memory B cells is formed under inflammatory conditions, such as during an autoimmune disease flare-up, which then might be able to migrate into inflammatory tissues where they are relatively protected from therapeutic intervention.

Short-Lived and Long-Lived Plasma Cells

Successful activation of naive B cells leads to a massive clonal expansion and eventually the formation of short-lived plasma cells in the extra-follicular areas of secondary lymphoid tissues (55). In mice, these cells exhibit lifetimes of less than a week (56). Cytostatic drugs, such as cyclophosphamide, prevent B proliferation and the formation of new antibody-secreting cells, hence eliminating the short-lived plasma cell compartment (57). Simultaneous to the formation of short-lived plasma cells, germinal centers may give rise to both memory B cells and long-lived plasma cells. For a brief period following vaccination, precursors of long-lived plasma cells (plasmablasts) are found in human peripheral blood (54); these cells then give home to deposit tissues, such as bone marrow, mucosal tissue, or sites of inflammation. The tissue homing of these cells is tightly regulated by adhesion molecules, chemokines, and their receptors (58–60). In peripheral blood, plasma cell subpopulations are found that exhibit different expression profiles of homing receptors. For example, migratory plasmablasts, induced by intracutaneous vaccination, express L-selectin, which are associated with homing to peripheral lymph nodes (61, 62). Similar to the return of locally activated plasma cell precursors to mucosal sites, cells that are activated in the context of a pro-inflammatory response seem to be programmed to relocate to inflamed tissues. Here, the high levels of inflammatory cytokines can support plasma cell survival, likely enabling these cells survive for the period of inflammation (60). These data suggest that plasma cells formed in the course of an inflammation-associated immune response can maintain the production of antibodies but will disappear when the cause of inflammation has resolved (46, 63).

In human tissues, various plasma cell subpopulations exist which exhibit different phenotypes and stages of differentiation (46, 64, 65). Some plasma cell stages still express CD20, indicating that they might be susceptible to RTX treatment. However, mature human plasma cells have lost CD20 expression (66–68). Accordingly, even B cell depletion has been found to have no impact on the production of human memory antibodies, e.g., specific for tetanus toxoid (63). In general, serum antibodies of different specificities show a great variety of responses following B cell depletion, ranging from no response to depletion below the detection limit (69), possibly suggesting that antibodies are maintained by various mechanisms, including short-lived plasma cell populations that are replenished by various memory B cell subsets and by long-lived plasma cells. The notion that long-lived plasma cells contribute to the production of autoantibodies (57), but are not affected by conventional immunosuppressive drugs such as steroids or cyclophosphamide, or by B cell depletion, has identified them as a novel target cell requiring specific therapeutic approaches (70).

B Lineage Cells Exert Multiple Roles That Drive Pathogenesis but Also Control the Severity of Inflammation

B cells play multiple functions. Following differentiation into plasma cells, they secrete huge amounts of antibodies into the body fluids. Autoantibodies can contribute to the pathogenesis of autoimmune diseases in multiple ways (71). They can initiate immune-complex-mediated inflammation, deplete specific cell types or modulate important signaling pathways, relevant in SLE, antibody-mediated hemolytic anemia or Hashimoto's thyroiditis and Graves' disease, respectively (72–75). However, more recent studies indicate that antibodies can also exert significant anti-inflammatory effects, which limit or even inhibit autoimmune pathogenesis. The pro- and anti-inflammatory effects of antibodies depend on their isotype (76) and on their Fc *N*-linked glycosylation patterns (77, 78). While IgGs with low levels of galactosylation promote inflammation, sialylated IgGs have a strong anti-inflammatory capacity (79, 80). Highly glycosylated IgG antibodies have been shown to inhibit autoimmune inflammation in mouse models (76, 81, 82). Changes in autoantibody glycosylation have been observed during the course of human autoimmune diseases, possibly providing an interesting novel diagnostic tool, but also suggesting that the antibody glycosylation pattern can alter the clinical course of autoimmune disorders (83).

B lineage cells can also present antigens in the context of MHC II and secrete immunomodulatory cytokines, thereby playing a prominent role for the modulation of antigen-specific T cell responses (84–86). B cells probably only play a minor role in T cell priming. However, during secondary or chronic immune reactions B cells resemble very potent APCs that drive the expansion

of activated T helper cells (87–90). Hence, B cells are likely to be both important antigen-presenting and T cell promoting cells during chronic and repeated immune reactions, such as occurs during the course of autoimmune diseases.

In addition, various B lineage cells, including those with a $CD138^+$ plasmablast/plasma cell phenotype, have been shown to express a variety of pro-inflammatory cytokines that can stimulate innate effector cells and significantly contribute to inflammation and immune protection in murine models (91–93). Moreover, while some B lineage cells promote inflammation, others exhibit profound immunosuppressive capacities (94). As shown in many models, B cells and plasma cells can also suppress autoimmune inflammation through the production of cytokines, such as IL-10, TGF-beta, or IL-35 (86, 95–98). Interestingly, IL-10 and IL-35 are produced by B cells that have different phenotypes (98). As discussed below, the therapeutic induction of immunosuppressive B lineage cells may be an interesting direction for the development of future therapies.

LESSONS FROM RTX TREATMENT OF AUTOIMMUNE DISEASES

Regarding the clinical use of B cell targeting therapies, the majority of the information comes from studies using RTX. This chimeric mouse/human monoclonal antibody targets the pan B cell marker CD20, a transmembrane protein expressed on all B lineage cells, from early pre-B to mature B and memory B cells. CD20 has been shown to mediate Ca^{2+} influx across plasma membranes and is important in maintaining intracellular Ca^{2+} concentration and activation of B cells (99). RTX was the first anti-CD20 antibody approved by the U.S. Food and Drug Administration for medical use in 1997 as Rituxan®, originally to treat B cell non-Hodgkin lymphomas (100). Later it was also approved for use in RA, granulomatosis with polyangiitis, and microscopic polyangiitis and there is growing clinical use of RTX in other autoimmune diseases, such as MS, SLE, and autoimmune blistering skin diseases (101–105).

Mode of Action of RTX

After binding of RTX to membrane bound CD20 it mediates strong complement-dependent cytotoxicity directed to its target cell due to the enhanced clustering of antibody Fc regions (106, 107). Based on its ability to redistribute CD20 into lipid rafts, which provides the molecular basis for RTXs engagement of complement factors, RTX is classified as a type I anti-CD20 antibody. By contrast, type II antibodies cannot cause this redistribution of CD20 (108–111), do not induce complement-dependent cytotoxicity to the same extent (111), but appear to induce a greater degree of directly induced, non-apoptotic cell death, upon binding to target cells (112).

CD20 expression is lost during differentiation into mature antibody-secreting plasma cells (66–68). This lack of CD20, particularly on long-lived plasma cells, explains why RTX treatment does not interfere with the production of memory antibodies, such as anti-tetanus/-measles/-mumps/-rubella (63, 113). Depending on the stage of plasma cell differentiation and tissue localization, early plasma cells (plasmablasts) exhibit various levels of CD20 expression (114). While mature long-lived plasma cells are apparently not depleted by RTX, it is not known to which extent earlier plasma cell stages are affected.

Independent of disease, RTX leads to the depletion of peripheral B cells from approximately 90% to close to 100% (**Table 1**). Despite this fact, the clinical efficacy of RTX varies broadly among different autoimmune diseases, and also among individual patients. Following withdrawal of RTX treatment, B cell levels recover within 6–20 months, with the rate of recovery greatly varying between individual patients (115).

Use of RTX in Pemphigus Vulgaris (PV)

RTX has shown promising results in the treatment of PV, an autoantibody-driven blistering skin disease. In three independent clinical studies, comprising a total of 43 patients with this rare autoimmune disorder, RTX treatment achieved a complete remission in over 80–95% of patients (103, 116, 117) who, importantly, were refractory to steroid therapy. This impressive clinical outcome was achieved in parallel with B cell depletion close to undetectable levels in almost all patients. One study showed that in most, but not all patients, the levels of anti-keratinocyte cell-surface IgG4 autoantibodies dropped to undetectable levels (116). In another study, anti-desmoglein 1 and 3 (Dsg1/3) autoantibodies were measured and found to be reduced on average by 65–80% (103). Generally, the response to RTX treatment seems to correlate with the extent of B cell depletion. However, two treated patients showed clinical remission despite persistent high levels of anti-Dsg1/3 autoantibodies, although remission was delayed compared with that in patients who showed remarkably reduced autoantibody levels (103). Hence, a reduction in the levels of autoantibodies seems to be a major factor in the success of RTX in treating PV. Nevertheless, the finding that RTX can improve clinical symptoms in patients that still exhibit high levels of anti-Dsg1/3 autoantibodies, suggests that RTX can also act *via* additional mechanisms. It would be interesting to consider this concept while designing future clinical studies.

Use of RTX in RA

Studies using RTX in RA have provided additional evidence that its therapeutic efficacy is not merely based on the reduction of autoantibody levels. In this disease, RTX is recommended for use in patients refractory to standard therapy (118). Although the B cell depletion rate is almost 100%, a clinical response was observed in approximately 60–70% of patients (11, 105, 119). Considering that these patients did not respond to other therapies, this was deemed to be a significant success. Results from more recent studies have suggested that RTX has better long-term efficacy when used in patients with fewer previous treatments and lower disease activity (120). Interestingly, the clinical response to RTX in RA positively correlates with the presence of anti-CCP autoantibodies, but is inversely correlated with the IgG-levels present before treatment (121–124). Autoantibodies and IgG-levels together with serum IL-33 have also been reported to predict the clinical response to RTX (125).

Based on the correlation between serum autoantibodies and response to RTX, on first view it seems possible that suppression

TABLE 1 | Efficacy of RTX treatment varies.

		RA		SLE		PV	MS		
Reference		Emery et al. (11); Rubbert-Roth et al. (105); Haraoui et al. (119)	Rovin et al. (145)	Leandro et al. (146); Albert et al. (147)	Lu et al. (148)	Ahmed et al. (116); Joly et al. (103); Pfütze et al. (117)	Dunn et al. (150); Cross et al. (104)	Hauser et al. (149)	Hawker et al. (151)
Patient no.		120/346/465	144	24	50	11/21/11	16/399	104	439
Dose and duration		1 mg for 24/48 weeks	1 mg for 52 weeks	1 mg for 6 months	1 mg for 6 months	375 mg/m^2 for 6 months	375 mg/m^2/0.5–1 mg for 6 months	1 mg for 48 weeks	1 mg for 96 weeks
Clinical improvement	Partial	*ACR20/50/70:* in 54–72/27–48/7–23%	*Proteinurea:* in 26.4%	*Proteinurea/BILAG/ SLEDAI:* in 65–70%	*BILAG:* in 42%	*Skin lesions:* in 8.2–20%	*EDSS:* in 12.5–63.2%	*GELN:* in 80.3%	*CDP:* –
	Complete	–	in 30.6%	–	–	in 80–95%	–	in 19.7%	–
	No	in 5%	in 43.1%	–	–	–	in 36.8–81.25%: worse in 6.25%	–	in 100%
B cell depletion efficacy in periphery		Significant depletion to 6 cells/μL	Complete depletion in 99%	Almost complete depletion in 94–96% of patients	Complete depletion in 42%; partial depletion in 47% and no depletion in 11% of patients	In almost all patients complete B cell depletion	Depletion by 95–99.8% in all patients; 90% depletion in spinal fluid	Over 95% depletion in all patients	
Autoantibody involvement		Anti-CCP aab and RF reduced by 45%	Anti-dsDNA aab reduced by 75%	Anti-dsDNA aab reduced by 35%	Anti-dsDNA aab reduced by 60%	In 81.8% IgG/IgG4 anti-keratinocyte cell-surface aab undetectable; dramatic decrease of IgG/IgG4 anti-Dsg1 (by 80%) and Dsg3 (by 65%) aab	Elevated serum anti-MOG aab	–	
Remark		HACA in 2.3–7.3%	–	HACA in 33%, correlating with B cell depletion rate		Clear correlation between aab and disease	HACA in 24.1–37%, correlates with B cell depletion rate	HACA in 24.1% of patients	

RA, rheumatoid arthritis; SLE, systemic lupus erythematosus; PV, Pemphigus vulgaris; MS, multiple sclerosis; ACR, American College of Rheumatology Criteria, standard criteria to measure the effectiveness of arthritis treatments in clinical trials for rheumatoid arthritis, 20/50/70 refers to the improvement in tender or swollen joint counts as a percentage; HACA, human anti-chimeric antibodies; CCP, cyclic citrullinated peptides; RF, rheumatoid factor; MTX, methotrexate; MMF, methyl mofetil; Std, standard therapy; BILAG, British Isles Lupus Activity Group, organ-specific 86-question assessment based on the principle of the clinical intent to treat; SLEDAI, SLE Disease Activity Index, a list of 24 items (16 clinical items including seizure, psychosis, organic brain syndrome, visual disturbance, other neurological problems, hair loss, new rash, muscle weakness, arthritis, blood vessel inflammation, mouth sores, chest pain that worsens with deep breathing, and manifestations of pleurisy and/or pericarditis and fever, and eight laboratory results, including urinalysis testing, blood complement levels, increased anti-DNA antibody levels, low platelet count, and low white blood cell count); EDSS, Expanded Disability Status Scale is a method of quantifying disability in multiple sclerosis and monitoring changes in the level of disability; CDP, delayed time to confirmed disease progression; Dsg, desmoglein; cANCA, anti-neutrophil cytoplasmic antibodies; MOG, myelin oligodendrocyte glycoprotein; aab, autoantibodies; dsDNA, double-stranded DNA.

of autoantibodies is a relevant mechanism by which RTX affects the clinical outcome of RA. The presence of autoantibodies such as rheumatoid factor (RF) and anti-CCP correlate well with disease activity in RA patients and indicate the presence and activation of autoreactive B cells. Moreover, anti-CCP and IgM-RF can enhance pro-inflammatory macrophage functions *in vitro* (126), supporting the idea that these autoantibodies may also contribute to RA pathogenesis *in vivo.* However, the reduction of serum autoantibody levels in RTX-treated responders is only very moderate, i.e., approximately 50 and 30%, for anti-CCP and RF, respectively, with a high degree of variation being observed (69). It seems questionable that such minor reductions in autoantibody levels cause the clinical response. Moreover, the absolute autoantibody levels persisting in responders after treatment were still two to fivefold higher than in non-responders (69). If autoantibodies in responders and non-responders exhibit similar pathogenicity, the moderate depletion of autoantibodies in responders to levels above of non-responders would not explain the success of the therapy. Other studies have also shown very moderate RTX effects on IgA and IgG anti-CCP autoantibodies, suggesting that a significant proportion is produced by long-lived plasma cells (127). The question of whether these antibodies contribute to RA pathogenicity remains to be addressed.

RTX Effects on CD4 T Cells

Alternative explanations for the anti-inflammatory effects of RTX in RA patients include the suppression of inflammatory T cells in favor of regulatory T cells subsets, possibly in combination with an induction of high galactosylated anti-inflammatory antibodies. There is good evidence that CD4 T cells can activate myeloid and synovial cells, which in turn activate and recruit macrophages to synovial tissue, eventually leading to joint inflammation and cartilage destruction, whereas regulatory T cells are protective (128–131).

The production of pro- and anti-inflammatory cytokines such IFN-γ, IL-17, or IL-10 seems to be key for T cell mediated control of RA pathogenesis. There is evidence that the clinical response to RTX therapy in RA is associated with lower IFN-γ levels (132). Moreover, a study including 52 patients showed that RTX often induces a reduction in the number of peripheral blood CD4 T cells, an effect that was strongly associated with the clinical response (133). It is possible that the depletion of a small subpopulation of $CD20^+$ T cells contributes to this effect (134).

However, there is good evidence that B cells can efficiently promote CD4 T cell functions through antigen-presentation and cytokine release. As discussed above, while B cells may play only a minor role in T cell priming, during secondary or chronic immune reactions, B cells can act as very potent APCs that drive the expansion of activated T helper cells (87–89, 135). Hence, B cell depletion may impair the formation, clonal expansion, and function of T memory cells.

Accordingly, T cell activation in the synovium of RA patients has been reported to be dependent on B cells (136). Hence, it is highly likely that RTX mediates its beneficial effects in RA at least partly through the depletion of T cell stimulating B lineage cells, although this remains to be studied further.

Effects of RTX Mediated B Cell Depletion on Cytokines

Of note, under certain conditions, B cells can also directly promote innate inflammatory effector cells through the production of cytokines such as IFN-γ, IL-6, granulocyte-macrophage colony-stimulating factor, and IL-17 (91, 93, 137, 138). In mice, B cell ablation has been shown to ameliorate autoimmune diseases by depleting IL-6-producing B cells (93). Moreover, a recent study has provided evidence that B cells from RA patients show abnormal IL-6 signaling and altered cytokine production, and that this may contribute to disease (139). Hence, B cells resemble an underestimated source of inflammatory cytokines and the depletion of such pro-inflammatory cytokine producing B cells is likely to contribute to the therapeutic outcome of RTX treatment.

RTX Effects on Antibody Glycosylation

T cell help in germinal centers has been found to be important for the induction of inflammatory low-glycosylated IgG antibodies (82). In particular, the T cell-derived cytokines such as IFN-γ and IL-17 are capable of synergistically promoting the production of low-sialylated, and potentially pathogenic, antibodies (82, 139). Based on the notion that the clinical response to RTX in RA is associated with lower IFN-γ levels (132), it is possible that a reduction in IFN-γ levels, in turn, leads to alterations in antibody glycosylation.

In accordance with the idea that these processes are of pathophysiological relevance, reduced antibody glycosylation has been reported to precede disease onset and to correlate with disease activity in RA patients (140). This phenotype is highly prevalent in, but not restricted to, autoantibodies (141). Hence, it is possible that acting through a reduction in IFN-γ levels, RTX corrects the shift toward the production of pro-inflammatory antibodies that is observed in RA. Of note, high-glycosylated antibodies can mediate anti-inflammatory effects independent of their specificity, as indicated by the therapeutic effects of intravenously administered immunoglobulins (142), although antigen-specific effects might be considerably stronger and require lower antibody concentrations (79, 81, 143). Accordingly, highly glycosylated IgGs have been reported to induce antigen-specific tolerance (78). Hence, RTX may partly mediate its beneficial effects through changes in antibody glycosylation, either *via* a reduction in autoantibody pathogenicity, through the generation of anti-inflammatory autoantibodies, or by the induction of persistent high levels of anti-inflammatory total IgGs that mimic continuous IVIG treatment.

Effects of RTX in MS and SLE

Similar to what has been observed in RA, the therapeutic effect of RTX in SLE and MS is variable. Its impact on total antibody levels as well as on autoantibody levels shows a high degree of diversity (**Table 1**). In a recent study, only 11 out of 32 SLE patients with IgG hypergammaglobulinemia before treatment showed reduced IgG-levels after 12 months of treatment (144). Likewise, a reduction in anti-double-stranded DNA levels was incomplete, with high inter-individual variety and differences between antibody subclasses (145–148). Despite homogenous

B cell depletion rates in MS of over 90 and 95% in spinal fluid and in the periphery, respectively, the disease outcome showed great variation (104, 149–151). Interestingly, RTX has even been found to worsen the clinical outcome of MS (104).

These variable results might be not be surprising in the light of the finding that B lineage cells play multiple pro-and anti-inflammatory roles in experimental autoimmune encephalomyelitis (EAE), a murine model of MS. B cell-derived IL-6 has been shown to be crucial for the initiation of EAE, suggesting that B cells can promote MS pathogenesis through the production of this pro-inflammatory cytokine (93). However, there is an abundance of evidence that anti-inflammatory B cell subsets can also efficiently suppress CD4 T cells mediating neuroinflammation, and that these effects are mediated by B lineage-derived IL-10, TGF-β, and IL-35 (98, 152). These findings led to the concept of regulatory B cells (Bregs), which, however, have never been clearly defined. Recent results indicate that these IL-10$^+$ B lineage cells have a plasmablast phenotype (98, 153). Similarly, investigations conducted by our group have identified plasmablasts/plasma cells as an important source of IL-10, capable of suppressing skin inflammation in a murine model of epidermolysis bullosa acquisita (EBA) (85). In EAE, B lineage-derived IL-6 and IL-10 were shown to have an impact on the induction and resolution of inflammation, respectively (93, 98, 153). These findings may partly explain the heterogeneity of the clinical response to RTX observed in MS. Depending on the major role of B lineage cells as drivers or inhibitors of inflammation in individual patients, and possibly related to timing, RTX may be either beneficial or worse for the clinical course of MS.

ALTERNATIVE B CELL TARGETING APPROACHES

Second Generation Anti-CD20 Antibodies

The great clinical success of the chimeric antibody, RTX, has stimulated the development of the second generation anti-CD20 antibodies, ocrelizumab, obinutuzumab, veltuzumab, and ofatumumab (154). These second generation anti-CD20 antibodies are humanized or even fully human, exhibit improved effector functions, and compared with rituximab show greater potential *in vitro*. Due to these properties, they are expected to be more effective, to exhibit lower immunogenicity, and to be better tolerated. However, these expectations, which may be validated by head-to-head trials of these second generation anti-CD20 antibodies and RTX, have not been confirmed till date.

Ocrelizumab has recently been approved for the treatment of relapsing-remitting MS, and is the first approved treatment for primary progressive MS. In RA, however, ocrelizumab seems to have no benefit over current treatments, leading to a halt in the development of ocrelizumab for the treatment of RA (155).

Clinical trials exploring the use of obinutuzumab, veltuzumab, and ofatumumab in autoimmune disorders are at various stages of development and have been extensively reviewed by Du and colleagues (154). In general, it appears that the new anti-CD20 antibodies are effective against autoimmune diseases, against which RTX is also beneficial, but more studies are needed to evaluate their efficiency and long-term safety profiles in greater detail.

Antibodies Targeting CD19

Other B cell depleting reagents that promise a great potential for the treatment of autoimmune diseases are a series of reagents targeting CD19, which are currently under development. These include humanized antibodies, "bi-specific T cell engagers," and antibody-drug conjugates, such as inebilizumab, blinatumomab, and SAR3419, among several others (156, 157).

CD19 targeting therapeutics generally exhibit a broader target spectrum than anti-CD20 based reagents. CD19 is expressed very early in B cell development, being evident already on pro-B cells and on all later B cell stages, whereas CD20 is expressed later, starting at the immature B cell stage. Possibly of greater importance for the treatment of autoimmune diseases, in addition to all mature B cell subsets, CD19 is expressed on a significant proportion of plasmablasts and plasma cells, particularly outside the bone marrow (64, 114). Accordingly, CD19 targeting reagents have been reported to deplete pre-existing peripheral antibody-secreting cells, at least in humanized mouse models (158). Hence, CD19 targeting reagents might be not only suitable for treating B cell malignancies, but also exhibit great potential for therapeutic use in autoimmune diseases, particularly for those diseases with a strong involvement of pathogenic antibodies, e.g., SLE, pemphigus, and neuromyelitis optica.

BAFF/APRIL Antagonists

An alternative therapeutic strategy to target B cells is the blockade of B lineage survival factors, such as BAFF and its homolog APRIL and their receptors (159). Together, BAFF and APRIL along with their receptors form a complex system, which is very important for the survival of mature B cells and plasma cells. There are three receptors that bind BAFF and APRIL with different affinities. BAFF binds to BAFF-R, transmembrane activator and calcium modulator and cyclophilin ligand interactor, and B cell maturation protein. These three receptors are differentially expressed at various times during B cell ontogeny (160). Most BAFF circulates as a soluble active homo-trimer (161) that binds to BAFF-R and this interaction is required for survival of late transitional, MZ, and mature naive B cells, all of which are depleted by BAFF-blockade (162, 163).

Several BAFF/APRIL targeting drugs are currently under development. The humanized anti-BAFF antibody belimumab has already been approved in the EU and the USA for the treatment of adult patients with active, autoantibody-positive, and SLE despite standard therapy. It is generally well tolerated with low rates of immunogenicity. Belimumab in combination with standard therapy reduces the overall disease activity and the incidence and severity of flares, has steroid-sparing effects, and can maintain disease control for at least 10 years (164). Interestingly, despite its clinical efficiency, belimumab only partly inhibits the production of IgG-autoantibodies. While some studies found no reduction of IgG-autoantibody levels following treatment with belimumab, others have reported a decline of 40–60% within 2–7 years of treatment (165–167). This is in accordance with the finding that belimumab depletes both naive and activated B cells, but not memory B cells (165, 167).

Similar to what has been observed with RTX, B cell targeting by blockade of BAFF and APRIL using belimumab, tabalumab, or atacicept also shows greatly variable effects on the levels of autoantibodies and the clinical outcome of autoimmune diseases (118, 168–181), and of note, seem to have only limited effects on the production of (auto)antibodies (**Table 2**).

Generally, B cell targeting represents a powerful strategy for the treatment of autoimmune diseases. Its mechanism of action seems to be diverse and complex, and needs further elucidation.

DIRECT TARGETING OF PLASMA CELLS BY BORTEZOMIB

As originally shown by us and others, in mice, memory antibodies are secreted by long-lived plasma cells (182, 183). The notion that these cells can contribute to the production of autoantibodies but do not respond to current therapeutic approaches (57), has led to the search for novel plasma cell targeting agents.

The small molecule proteasome inhibitor bortezomib promotes plasma cell apoptosis and is approved for the treatment of multiple myeloma. Nearly a decade ago, Voll and colleagues reported that this drug could also be useful for the treatment of antibody-mediated autoimmune diseases. They demonstrated that bortezomib efficiently depletes both short-lived and long-lived plasma cells and protects mice with lupus-like disease from nephritis (70). Its efficacy was later proven in various models of antibody-mediated autoimmune diseases (184–186). There is now increasing evidence that bortezomib can also efficiently deplete autoantibodies in patients, resulting in the improvement of clinical symptoms, as has been described for refractory primary Sjögren's syndrome, refractory SLE, thrombotic thrombocytopenic purpura, and among others (9, 187–197). The potential development of severe side effects, such as peripheral neuropathies may limit the use of bortezomib in autoimmune diseases. However, its unique capacity to deplete antibody-producing plasma cells suggests that the safety and efficacy of bortezomib should be evaluated in clinical trials including more patients who are refractory to standard therapeutic approaches.

INDUCTION OF ANTI-INFLAMMATORY B LINEAGE CELLS: A PROMISING THERAPEUTIC TREATMENT OPTION?

IL-10$^+$ B lineage cells have been known as potent suppressors of autoimmune inflammation for decades (198). Over the last decade, the expansion of IL-10$^+$ B cells using various approaches has been shown to efficiently suppress both autoimmune and allergic inflammation in numerous models (85, 199, 200). The first report that IL-10$^+$ B cells exert a suppressive function was in 2002 by Fillatreau and colleagues (86), who showed that chimeric mice with a B cell specific IL-10 deficiency do not recover from EAE. Later, IL-10$^+$ B cells were termed as Bregs or B10 cells. However, no surface marker or transcription factor unique to these cells has been identified to date. These cells are only functionally defined by their production of anti-inflammatory cytokines such as IL-10, and more recently IL-35, and the resulting suppression of inflammation and autoimmune diseases (201, 202).

Phenotype and Origin of Human IL-10-Producing B Cells

The combination of markers used to describe "regulatory B cells" in human and mice is controversial. The phenotypic identification of these B cells and their possible origin and development have been excellently reviewed elsewhere (198, 203). In humans, the ability to produce anti-inflammatory IL-10 has been reported in B cells at various stages of development: immature/transitional B cells (CD19$^+$ CD38^{hi} CD24^{hi}) (204), plasmablasts (CD27^{int} CD38^{hi}) (153, 205), and memory B cells (CD19$^+$ CD27$^+$) (206, 207). It is likely that IL-10$^+$ B cells represent a transient stage with a functional program rather than a terminally differentiated stage, and that any B cell can acquire suppressive properties within a certain environment. Nevertheless, it is debatable if these cells arise from a single shared progenitor, from individual progenitors, or are induced under certain environmental stimuli (198, 203). Interestingly, in this context autocrine IL-10 can promote human IL-10$^+$ B cells to differentiate into IgG- and IgM-secreting plasma cells (208).

IL-10-Producing B Cells in Patients Suffering from Autoimmune Diseases

The first report describing human IL-10-producing B lineage cells in autoimmune diseases was in 2010 by Iwata et al. (207), who described abnormally high frequencies of peripheral IL-10$^+$ B cells in various autoimmune diseases, such as SLE, RA, MS, Sjögren's syndrome, and blistering skin diseases. An increase in the number of blood IL-10$^+$ CD19$^+$ CD24^{hi} CD38^{hi} cells was also found in PV patients, but these B cells were functionally unable to suppress Th1 immune responses (209). By contrast, several studies on RA (206, 210–212), SLE (204), systemic sclerosis (SSc) (213, 214), and MS (215–217) patients have shown a reduced number of peripheral IL-10-producing B cells compared with that in the controls. This was often accompanied by an impaired suppressive capacity of CD4 T cells. An overview describing the modulation of human IL-10-producing B lineage cells in different autoimmune diseases has been provided by Miyagaki et al. (218).

IL-10-Producing B Cell Dynamics Following B Cell Targeting Therapy

In myasthenia gravis, depletion of B cells with RTX showed that IL-10$^+$ B cells can be found to have repopulated in the periphery after several months (219). Immunosuppressive treatments, TNF-therapy, and BAFF-blockade in RA (206), SSc (213), and experimental diabetes mellitus type 1 (220), respectively, have shown that IL-10-producing B lineage cells enrich after treatment and that their frequency is even higher than before treatment. In relapsing-remitting MS, the frequencies of IL-10$^+$ CD19$^+$ B cells were significantly reduced in patients experiencing a relapse compared with that in patients in remission (217), indicating that the clinical outcome of the disease also depends on the availability of IL-10-producing B cells.

Moreover, a "good responder" to RTX in myasthenia gravis showed a rapid repopulation of CD19$^+$ IL-10$^+$ B cells after

TABLE 2 | Efficacy of belimumab, tabalumab, and atacicept.

		RA			SLE				SS	MS
		Atacicept	**Belimumab**	**Tabalumab**	**Atacicept**	**Belimumab**	**Blisibimod**	**Tabalumab**	**Belimumab**	**Atacicept**
Patient no.		311	415	1,041	47/6	1,353	547	1,124	30	255
Duration		38 weeks	24/48 weeks	52 weeks	9/52 weeks	52–76 weeks	24 weeks	52 weeks	52 weeks	36 weeks
Clinical improvement	Partial Complete No	– – *ACR20*	*ACR20*:in 41% – *ACR50+70*	*ACR20/50/70*:in 70/36/13% – –	in 22.2% in 44.5% worse in 33% stopped	*SELENA–SLEDAI/ BILAG*:in 46.5/58.6% – –	*Proteinurea*:reduced – –	*SRI-4*:in 49.2% – secondary end point	*EULAR*:in 86.7% – –	– – Failed and even worse
B cell depletion efficacy in periphery		Circulating mature B and plasma cells reduced	B cell depletion 16–48%; no depletion of memory B cells and plasma cells	B cell reduction by 18–40%; no depletion of memory B cells	Reduction by 60%; plasma cells depleted	Reduction by 55.7%	Significant reduction	Significant reduction	Significant reduction	Significant reduction
Autoantibody involvement		RF but not anti-CCP levels reduced	Reduction of RF by 30%	CRP reduced		Reduction of anti-dsDNA aab by 44–49%	Anti-dsDNA decreasedC3 increased	Anti-dsDNA aab significantly decreased	Reduction of RF by 30%	
Remark		Serum IgA+M (by 19.4%) and IgG (by 8.6%) modestly reduced	Moderate change of total Ig; better response in RF+ or ACPA+ patients	Total serum Ig decline by 11% Phase III study in RA terminated		Seropositive and highly diseased patients respond better; total serum Ig modestly reduced by 16%		C3 + C4 increased; total serum Ig reduced; development was stopped	Total Ig not changed	Severe adverse events; higher relapse rate in treated group compared to controls
References		Genovese et al. (170); van Vollenhoven et al. (171)	Stohl et al. (181)	Smolen et al. (168); Greenwald et al. (169)	Dall'Era et al. (176); Lenert et al. (177); Ginzler et al. (178)	Navarra et al. (172); Furie et al. (173)	Furie et al. (175)	Merrill et al. (174)	Mariette et al. (179)	Kappos et al. (180)

RA, rheumatoid arthritis; SLE, systemic lupus erythematosus; SS, Sjörgen's syndrome; MS, multiple sclerosis; ACR, American College of Rheumatology Criteria, standard criteria to measure the effectiveness of arthritis treatments in clinical trials for rheumatoid arthritis, 20/50/70 refers to the improvement in tender or swollen joint counts as a percentage; CCP, cyclic citrullinated peptides; RF, rheumatoid factor; MMF, methyl mofetil; std, standard therapy; BILAG, British Isles Lupus Activity Group, organ-specific 86-question assessment based on the principle of the clinical intent to treat; SELENA, Safety of Estrogens in Systemic Lupus Erythematosus National Assessment; SLEDAI, SLE Disease Activity Index, a list of 24 items (16 clinical items, including seizure, psychosis, organic brain syndrome, visual disturbance, other neurological problems, hair loss, new rash, muscle weakness, arthritis, blood vessel inflammation, mouth sores, chest pain that worsens with deep breathing, and manifestations of pleurisy and/or pericarditis and fever, and eight laboratory results, including urinalysis testing, blood complement levels, increased anti-DNA antibody levels, low platelet count, and low white blood cell count); EDSS, Expanded Disability Status Scale is a method of quantifying disability in multiple sclerosis and monitoring changes in the level of disability; aab, autoantibodies; C3 + 4, Complement factors 3 and 4; ACPA, Anti-citrullinated peptide/protein antibodies; CRP, C-reactive protein; SRI-4, Systemic Lupus Erythematosus Responder Index for 4-point reduction due to SLEDAI; EULAR SS, The European League Against Rheumatism for Sjörgen's Syndrome; Ig, immunoglobulins; dsDNA, double-stranded DNA.

from 8 to 9 months compared with a "non-responder," where repopulation was delayed (219). This shows that the kinetics of the IL-10$^+$ B cell repopulation is related to the responsiveness to RTX. Similarly, Colliou et al. (221) have shown that RTX-treated PV patients in complete remission had fourfold higher numbers of IL-10$^+$ CD19$^+$ B cells compared with patients in incomplete remission. In SLE patients responding well to RTX treatment, IL-10$^+$ CD24^{hi} CD38^{hi} B cells were found to repopulate and exhibited a restored suppressive function compared to non-responders (222).

Differences in IL-10-producing B cells in individual patients and types of autoimmune diseases could explain the differential outcome and benefit of B cell specific therapies. For example, in SLE and lupus nephritis, pan B cell therapies, such as RTX, show only moderate or even no benefit, despite the significant role of B cells in this disease (145, 223). The depletion of anti-inflammatory B cells could contribute to this unexpected result. Very few studies to date have included an analysis of the kinetics and function of IL-10-producing B cells after B cell depleting therapy. To better understand the individual clinical outcome of the patients and the differences between certain autoimmune diseases treated with the same B cell targeting agent, it would be of great benefit to include an analysis of IL-10$^+$ B lineage cells in further studies.

Challenges Hampering the Development of IL-10$^+$ B Cell-Based Therapies

Restoring the regulatory capacity and the number of IL-10$^+$ B cells is a promising therapeutic goal for the treatment of autoimmune diseases. However, currently two unsolved problems hamper the development of a therapy based on IL-10$^+$ B cells. First, the methods used to generate IL-10$^+$ B cells for therapeutic approaches are not suitable for a clinical setting. Second, the identity and phenotype of IL-10$^+$ B cells remain uncertain. Nevertheless, recent progress has been made with respect to both issues. Giacomini et al. (224) have shown that stimulation of peripheral blood mononuclear cells (PBMCs) from MS patients with thymosin-α1 (Tα1) increases IL-10 and IL-35 secretion and expands transitional- and plasmablast-like B cell populations. Upon exposure to pro-inflammatory cytokines, such as IL-21, IL-6, and IL-1β, an expansion of IL-10$^+$ B cell population has been observed. In RA patients, IL-21 increases the number of IL-10-producing B cells in the memory compartment and induces IL-10$^+$ plasmablasts (206), whereas in mice, gut microbiota-derived IL-1β and IL-6 promote the formation of various IL-10$^+$ B lineage cells in the spleen and lymph nodes (225). By contrast, the anti-inflammatory cytokine IL-35 can also induce human B cells to produce IL-10 and IL-35 (226). Nevertheless, inducing anti-inflammatory B cells *in vivo via* inflammatory cytokines bears the risk of undesirable pathogenic side effects by also activating other effector cell types. If not expanded *in vivo*, IL-10$^+$ B cells could be also induced from patient PBMCs *in vitro* and transferred back. Here, the questions of the amount of B cells required to improve clinical symptoms and the stability of the IL-10$^+$ phenotype and function arise. The difficulties and potential of these therapies were recently discussed by Mauri and Menon (227).

Induction of IL-10-Producing Plasma Cells/Plasmablasts: Potential as a Novel Treatment Option

Progress has been made in defining the identity of IL-10$^+$ B cells that could be used to develop a novel therapeutic strategy. During the last decade, several phenotypically distinct murine B cell subsets have been described that produce IL-10 upon *in vitro* stimulation, which was able to limit autoimmune diseases (198). These cells include B cells with a CD5$^+$ CD1d^{hi} phenotype (B10) (228), CD5$^+$ B cells (B1-a) (229), transitional type 2-MZ precursors (230), and MZ B cells (231).

Of note, the surface markers used to characterize the identity of the IL-10$^+$ B cells change following activation and might be not suitable to define a specific B cell subtype under inflammatory conditions. Interestingly in this context, it has been shown that "B10" cells upregulate the expression of the transcription factors Blimp1 and IRF4 while downregulating that of Pax5, suggesting that these cells undergo plasma cell differentiation. Moreover, upon transfer into recipient mice, "B10" cells become antibody-secreting cells (232). More recently, CD138^{hi} plasmablasts in murine spleen (98) or lymph nodes (153) were described as the major producer of anti-inflammatory IL-10 and IL-35 *in vivo* with the ability to limit EAE. In accordance with these findings, we found that IL-10$^+$ plasma cells exhibit profound anti-inflammatory activities in a model of EBA, a rare autoimmune skin disease (85). These cells induce IL-10 expression but reduce IFN-γ production in CD4 T cells, promote IL-10 production by CD4$^+$/Foxp3$^+$ Tregs and suppress neutrophil functions. Hence, IL-10$^+$ plasmablasts/plasma cells represent an important anti-inflammatory B cell subtype.

Identification of the identity of IL-10$^+$ B lineage cells may help to develop a novel method to induce these cells in a therapeutic setting. Stimulation of B cells with CpG-oligonucleotides induces both plasma cell differentiation and IL-10 expression. Accordingly, experimental induction of IL-10$^+$ B lineage cells by adaptive transfer of CpG-stimulated B cells has recently been shown to suppress ongoing EAE inflammation in a therapeutic setting (200). This approach may open a novel perspective for the treatment of inflammatory autoimmune diseases.

CONCLUDING REMARKS

The success of current B cell targeting therapies emphasizes the important roles B cells play in the pathogenesis of autoimmune diseases. There is overwhelming evidence from animal models indicating that B lineage cells exhibit multiple powerful pro- and anti-inflammatory capacities. The current experience with B cell targeting therapies suggests that these findings also hold true in the clinic. Hence, therapies that specifically deplete pathogenic B cells and plasma cells, or generate immunosuppressive B cells/plasma cells could hold great potential for the treatment of autoimmune diseases. In an optimal setting, the therapy would be tailored to the individual patient based on his/her predicted needs, benefits, and risks.

AUTHOR CONTRIBUTIONS

KH, A-KC, and RM contributed to reviewing the current literature and writing of the manuscript.

FUNDING

KH was supported by the Research Training Group 1727 "Modulation of Autoimmunity" (GRK 1727). A-KC was founded by the Clinical Research Unit 303 "Pemphigoid Diseases – Molecular Pathways and their Therapeutic Potential" (CRU303). RM was supported by the Excellence Cluster "Inflammation at Interfaces" (EXC 306/2).

REFERENCES

1. Manz RA, Hauser AE, Hiepe F, Radbruch A. Maintenance of serum antibody levels. *Annu Rev Immunol* (2005) 23:367–86. doi:10.1146/annurev.immunol.23.021704.115723
2. Yan SX, Deng XM, Wang QT, Sun XJ, Wei W. Prednisone treatment inhibits the differentiation of B lymphocytes into plasma cells in MRL/MpSlac-lpr mice. *Acta Pharmacol Sin* (2015) 36:1367–76. doi:10.1038/aps.2015.76
3. Cupps TR, Gerrard TL, Falkoff RJ, Whalen G, Fauci AS. Effects of in vitro corticosteroids on B cell activation, proliferation, and differentiation. *J Clin Invest* (1985) 75:754–61. doi:10.1172/JCI111757
4. Zhu LP, Cupps TR, Whalen G, Fauci AS. Selective effects of cyclophosphamide therapy on activation, proliferation, and differentiation of human B cells. *J Clin Invest* (1987) 79:1082–90. doi:10.1172/JCI112922
5. Glaesener S, Quach TD, Onken N, Weller-Heinemann F, Dressler F, Huppertz HI, et al. Distinct effects of methotrexate and etanercept on the B cell compartment in patients with juvenile idiopathic arthritis. *Arthritis Rheumatol* (2014) 66:2590–600. doi:10.1002/art.38736
6. Liu Z, Davidson A. BAFF inhibition: a new class of drugs for the treatment of autoimmunity. *Exp Cell Res* (2011) 317:1270–7. doi:10.1016/j.yexcr.2011.02.005
7. Marshall MJE, Stopforth RJ, Cragg MS. Therapeutic antibodies: what have we learnt from targeting CD20 and where are we going? *Front Immunol* (2017) 8:1245. doi:10.3389/fimmu.2017.01245
8. Zhao Q, Chen X, Li J, Jiang J, Li M, Zhong W, et al. Pharmacokinetics, pharmacodynamics and preliminary observations for clinical activity and safety of multiple doses of human mouse chimeric anti-CD22 monoclonal antibody (SM03) in Chinese patients with systemic lupus erythematosus. *Clin Drug Investig* (2016) 36:889–902. doi:10.1007/s40261-016-0426-7
9. Alexander T, Sarfert R, Klotsche J, Kuhl AA, Rubbert-Roth A, Lorenz HM, et al. The proteasome inhibitior bortezomib depletes plasma cells and ameliorates clinical manifestations of refractory systemic lupus erythematosus. *Ann Rheum Dis* (2015) 74:1474–8. doi:10.1136/annrheumdis-2014-206016
10. Emery P, Gottenberg JE, Rubbert-Roth A, Sarzi-Puttini P, Choquette D, Taboada VM, et al. Rituximab versus an alternative TNF inhibitor in patients with rheumatoid arthritis who failed to respond to a single previous TNF inhibitor: SWITCH-RA, a global, observational, comparative effectiveness study. *Ann Rheum Dis* (2015) 74:979–84. doi:10.1136/annrheumdis-2013-203993
11. Emery P, Fleischmann R, Filipowicz-Sosnowska A, Schechtman J, Szczepanski L, Kavanaugh A, et al. The efficacy and safety of rituximab in patients with active rheumatoid arthritis despite methotrexate treatment: results of a phase IIB randomized, double-blind, placebo-controlled, dose-ranging trial. *Arthritis Rheum* (2006) 54:1390–400. doi:10.1002/art.21778
12. Moreno Torres I, Garcia-Merino A. Anti-CD20 monoclonal antibodies in multiple sclerosis. *Expert Rev Neurother* (2017) 17:359–71. doi:10.1080/14737175.2017.1245616
13. Allman D, Pillai S. Peripheral B cell subsets. *Curr Opin Immunol* (2008) 20:149–57. doi:10.1016/j.coi.2008.03.014
14. Ehrenstein MR, Notley CA. The importance of natural IgM: scavenger, protector and regulator. *Nat Rev Immunol* (2010) 10:778–86. doi:10.1038/nri2849
15. Gronwall C, Vas J, Silverman GJ. Protective roles of natural IgM antibodies. *Front Immunol* (2012) 3:66. doi:10.3389/fimmu.2012.00066
16. Holodick NE, Zeumer L, Rothstein TL, Morel L. Expansion of B-1a cells with germline heavy chain sequence in lupus mice. *Front Immunol* (2016) 7:108. doi:10.3389/fimmu.2016.00108
17. Viau M, Zouali M. B-lymphocytes, innate immunity, and autoimmunity. *Clin Immunol* (2005) 114:17–26. doi:10.1016/j.clim.2004.08.019
18. Hardy RR, Li YS, Allman D, Asano M, Gui M, Hayakawa K. B-cell commitment, development and selection. *Immunol Rev* (2000) 175:23–32. doi:10.1111/j.1600-065X.2000.imr017517.x
19. King LB, Monroe JG. Immunobiology of the immature B cell: plasticity in the B-cell antigen receptor-induced response fine tunes negative selection. *Immunol Rev* (2000) 176:86–104. doi:10.1034/j.1600-065X.2000.00609.x
20. George J, Claflin L. Selection of B cell clones and memory B cells. *Semin Immunol* (1992) 4:11–7.
21. Cyster JG. Chemokines and cell migration in secondary lymphoid organs. *Science* (1999) 286:2098–102. doi:10.1126/science.286.5447.2098
22. Lang K, Pruss H. Frequencies of neuronal autoantibodies in healthy controls: estimation of disease specificity. *Neurol Neuroimmunol Neuroinflamm* (2017) 4:e386. doi:10.1212/NXI.0000000000000386
23. Pisetsky DS. Antinuclear antibody testing – misunderstood or misbegotten? *Nat Rev Rheumatol* (2017) 13:495–502. doi:10.1038/nrrheum.2017.74
24. Perez-Andres M, Paiva B, Nieto WG, Caraux A, Schmitz A, Almeida J, et al. Human peripheral blood B-cell compartments: a crossroad in B-cell traffic. *Cytometry B Clin Cytom* (2010) 78(Suppl 1):S47–60. doi:10.1002/cyto.b.20547
25. Nitschke L, Floyd H, Ferguson DJ, Crocker PR. Identification of CD22 ligands on bone marrow sinusoidal endothelium implicated in CD22-dependent homing of recirculating B cells. *J Exp Med* (1999) 189:1513–8. doi:10.1084/jem.189.9.1513
26. Geherin SA, Fintushel SR, Lee MH, Wilson RP, Patel RT, Alt C, et al. The skin, a novel niche for recirculating B cells. *J Immunol* (2012) 188:6027–35. doi:10.4049/jimmunol.1102639
27. Dufaud CR, McHeyzer-Williams LJ, McHeyzer-Williams MG. Deconstructing the germinal center, one cell at a time. *Curr Opin Immunol* (2017) 45:112–8. doi:10.1016/j.coi.2017.03.007
28. Ribatti D. The discovery of plasma cells: an historical note. *Immunol Lett* (2017) 188:64–7. doi:10.1016/j.imlet.2017.06.006
29. Luo Y, Yoshihara A, Oda K, Ishido Y, Suzuki K. Excessive cytosolic DNA fragments as a potential trigger of Graves' disease: an encrypted message sent by animal models. *Front Endocrinol* (2016) 7:144. doi:10.3389/fendo.2016.00144
30. Klein U, Goossens T, Fischer M, Kanzler H, Braeuninger A, Rajewsky K, et al. Somatic hypermutation in normal and transformed human B cells. *Immunol Rev* (1998) 162:261–80. doi:10.1111/j.1600-065X.1998.tb01447.x
31. Seifert M, Przekopowitz M, Taudien S, Lollies A, Ronge V, Drees B, et al. Functional capacities of human IgM memory B cells in early inflammatory responses and secondary germinal center reactions. *Proc Natl Acad Sci U S A* (2015) 112:E546–55. doi:10.1073/pnas.1416276112
32. Wienands J, Engels N. Control of memory B cell responses by extrinsic and intrinsic mechanisms. *Immunol Lett* (2016) 178:27–30. doi:10.1016/j.imlet.2016.05.010
33. Vitetta ES, Berton MT, Burger C, Kepron M, Lee WT, Yin XM. Memory B and T cells. *Annu Rev Immunol* (1991) 9:193–217. doi:10.1146/annurev.iy.09.040191.001205
34. Arpin C, de Bouteiller O, Razanajaona D, Briere F, Banchereau J, Lebecque S, et al. Human peripheral B cell development. sIgM-IgD+CD38+ hypermutated germinal center centroblasts preferentially express Ig lambda light chain and have undergone mu-to-delta switch. *Ann N Y Acad Sci* (1997) 815:193–8. doi:10.1111/j.1749-6632.1997.tb52060.x
35. Tangye SG, Avery DT, Deenick EK, Hodgkin PD. Intrinsic differences in the proliferation of naive and memory human B cells as a mechanism for enhanced secondary immune responses. *J Immunol* (2003) 170:686–94. doi:10.4049/jimmunol.170.2.686
36. Deenick EK, Avery DT, Chan A, Berglund LJ, Ives ML, Moens L, et al. Naive and memory human B cells have distinct requirements for STAT3 activation to differentiate into antibody-secreting plasma cells. *J Exp Med* (2013) 210:2739–53. doi:10.1084/jem.20130323
37. Feldhahn N, Schwering I, Lee S, Wartenberg M, Klein F, Wang H, et al. Silencing of B cell receptor signals in human naive B cells. *J Exp Med* (2002) 196:1291–305. doi:10.1084/jem.20020881

38. Klein U, Tu Y, Stolovitzky GA, Keller JL, Haddad J Jr, Miljkovic V, et al. Transcriptional analysis of the B cell germinal center reaction. *Proc Natl Acad Sci U S A* (2003) 100:2639–44. doi:10.1073/pnas.0437996100
39. Nowosad CR, Spillane KM, Tolar P. Germinal center B cells recognize antigen through a specialized immune synapse architecture. *Nat Immunol* (2016) 17:870–7. doi:10.1038/ni.3458
40. Sacquin A, Gador M, Fazilleau N. The strength of BCR signaling shapes terminal development of follicular helper T cells in mice. *Eur J Immunol* (2017) 47:1295–304. doi:10.1002/eji.201746952
41. Agematsu K, Nagumo H, Oguchi Y, Nakazawa T, Fukushima K, Yasui K, et al. Generation of plasma cells from peripheral blood memory B cells: synergistic effect of interleukin-10 and CD27/CD70 interaction. *Blood* (1998) 91: 173–80.
42. Maurer D, Holter W, Majdic O, Fischer GF, Knapp W. CD27 expression by a distinct subpopulation of human B lymphocytes. *Eur J Immunol* (1990) 20:2679–84. doi:10.1002/eji.1830201223
43. Bar-Or A, Oliveira EM, Anderson DE, Krieger JI, Duddy M, O'Connor KC, et al. Immunological memory: contribution of memory B cells expressing costimulatory molecules in the resting state. *J Immunol* (2001) 167:5669–77. doi:10.4049/jimmunol.167.10.5669
44. Liu YJ, Barthelemy C, de Bouteiller O, Arpin C, Durand I, Banchereau J. Memory B cells from human tonsils colonize mucosal epithelium and directly present antigen to T cells by rapid up-regulation of B7-1 and B7-2. *Immunity* (1995) 2:239–48. doi:10.1016/1074-7613(95)90048-9
45. Roy MP, Kim CH, Butcher EC. Cytokine control of memory B cell homing machinery. *J Immunol* (2002) 169:1676–82. doi:10.4049/jimmunol.169.4.1676
46. Muehlinghaus G, Cigliano L, Huehn S, Peddinghaus A, Leyendeckers H, Hauser AE, et al. Regulation of CXCR3 and CXCR4 expression during terminal differentiation of memory B cells into plasma cells. *Blood* (2005) 105:3965–71. doi:10.1182/blood-2004-08-2992
47. Ubillos I, Campo JJ, Requena P, Ome-Kaius M, Hanieh S, Rose H, et al. Chronic exposure to malaria is associated with inhibitory and activation markers on atypical memory B cells and marginal zone-like B cells. *Front Immunol* (2017) 8:966. doi:10.3389/fimmu.2017.00966
48. Manz RA, Moser K, Burmester GR, Radbruch A, Hiepe F. Immunological memory stabilizing autoreactivity. *Curr Top Microbiol Immunol* (2006) 305:241–57.
49. Reddy V, Klein C, Isenberg DA, Glennie MJ, Cambridge G, Cragg MS, et al. Obinutuzumab induces superior B-cell cytotoxicity to rituximab in rheumatoid arthritis and systemic lupus erythematosus patient samples. *Rheumatology (Oxford)* (2017) 56:1227–37. doi:10.1093/rheumatology/kex067
50. Muto K, Matsui N, Unai Y, Sakai W, Haji S, Udaka K, et al. Memory B cell resurgence requires repeated rituximab in myasthenia gravis. *Neuromuscul Disord* (2017) 27:918–22. doi:10.1016/j.nmd.2017.06.012
51. Cho A, Bradley B, Kauffman R, Priyamvada L, Kovalenkov Y, Feldman R, et al. Robust memory responses against influenza vaccination in pemphigus patients previously treated with rituximab. *JCI Insight* (2017) 2:e93222. doi:10.1172/jci.insight.93222
52. Budeus B, Schweigle de Reynoso S, Przekopowitz M, Hoffmann D, Seifert M, Kuppers R. Complexity of the human memory B-cell compartment is determined by the versatility of clonal diversification in germinal centers. *Proc Natl Acad Sci U S A* (2015) 112:E5281–9. doi:10.1073/pnas.1511270112
53. Dogan I, Bertocci B, Vilmont V, Delbos F, Megret J, Storck S, et al. Multiple layers of B cell memory with different effector functions. *Nat Immunol* (2009) 10:1292–9. doi:10.1038/ni.1814
54. Odendahl M, Mei H, Hoyer BF, Jacobi AM, Hansen A, Muehlinghaus G, et al. Generation of migratory antigen-specific plasma blasts and mobilization of resident plasma cells in a secondary immune response. *Blood* (2005) 105:1614–21. doi:10.1182/blood-2004-07-2507
55. Young KH, Chan WC, Fu K, Iqbal J, Sanger WG, Ratashak A, et al. Mantle cell lymphoma with plasma cell differentiation. *Am J Surg Pathol* (2006) 30:954–61. doi:10.1097/00000478-200608000-00004
56. Hiepe F, Alexander T, Voll RE. [Plasma cells]. *Z Rheumatol* (2015) 74:20–5. doi:10.1007/s00393-014-1438-4
57. Hoyer BF, Moser K, Hauser AE, Peddinghaus A, Voigt C, Eilat D, et al. Short-lived plasmablasts and long-lived plasma cells contribute to chronic humoral autoimmunity in NZB/W mice. *J Exp Med* (2004) 199:1577–84. doi:10.1084/jem.20040168
58. Hargreaves DC, Hyman PL, Lu TT, Ngo VN, Bidgol A, Suzuki G, et al. A coordinated change in chemokine responsiveness guides plasma cell movements. *J Exp Med* (2001) 194:45–56. doi:10.1084/jem.194.1.45
59. Kabashima K, Haynes NM, Xu Y, Nutt SL, Allende ML, Proia RL, et al. Plasma cell S1P1 expression determines secondary lymphoid organ retention versus bone marrow tropism. *J Exp Med* (2006) 203:2683–90. doi:10.1084/jem.20061289
60. Moser K, Tokoyoda K, Radbruch A, MacLennan I, Manz RA. Stromal niches, plasma cell differentiation and survival. *Curr Opin Immunol* (2006) 18:265–70. doi:10.1016/j.coi.2006.03.004
61. Quiding-Jarbrink M, Nordstrom I, Granstrom G, Kilander A, Jertborn M, Butcher EC, et al. Differential expression of tissue-specific adhesion molecules on human circulating antibody-forming cells after systemic, enteric, and nasal immunizations. A molecular basis for the compartmentalization of effector B cell responses. *J Clin Invest* (1997) 99:1281–6. doi:10.1172/JCI119286
62. Quiding-Järbrink M, Lakew M, Nordström I, Banchereau J, Butcher E, Holmgren J, et al. Human circulating specific antibody-forming cells after systemic and mucosal immunizations: differential homing commitments and cell surface differentiation markers. *Eur J Immunol* (1995) 25:322–7. doi:10.1002/eji.1830250203
63. Ferraro AJ, Drayson MT, Savage CO, MacLennan IC. Levels of autoantibodies, unlike antibodies to all extrinsic antigen groups, fall following B cell depletion with Rituximab. *Eur J Immunol* (2008) 38:292–8. doi:10.1002/eji.200737557
64. Arce S, Luger E, Muehlinghaus G, Cassese G, Hauser A, Horst A, et al. CD38 low IgG-secreting cells are precursors of various CD38 high-expressing plasma cell populations. *J Leukoc Biol* (2004) 75:1022–8. doi:10.1189/jlb.0603279
65. Rodriguez-Bayona B, Ramos-Amaya A, Bernal J, Campos-Caro A, Brieva JA. Cutting edge: IL-21 derived from human follicular helper T cells acts as a survival factor for secondary lymphoid organ, but not for bone marrow, plasma cells. *J Immunol* (2012) 188:1578–81. doi:10.4049/jimmunol.1102786
66. Kehrl JH, Riva A, Wilson GL, Thevenin C. Molecular mechanisms regulating CD19, CD20 and CD22 gene expression. *Immunol Today* (1994) 15:432–6. doi:10.1016/0167-5699(94)90273-9
67. Mei HE, Schmidt S, Dorner T. Rationale of anti-CD19 immunotherapy: an option to target autoreactive plasma cells in autoimmunity. *Arthritis Res Ther* (2012) 14(Suppl 5):S1. doi:10.1186/ar3909
68. Leandro MJ. B-cell subpopulations in humans and their differential susceptibility to depletion with anti-CD20 monoclonal antibodies. *Arthritis Res Ther* (2013) 15(Suppl 1):S3. doi:10.1186/ar3908
69. Fabris M, De Vita S, Blasone N, Visentini D, Pezzarini E, Pontarini E, et al. Serum levels of anti-CCP antibodies, anti-MCV antibodies and RF IgA in the follow-up of patients with rheumatoid arthritis treated with rituximab. *Auto Immun Highlights* (2010) 1:87–94. doi:10.1007/s13317-010-0013-5
70. Neubert K, Meister S, Moser K, Weisel F, Maseda D, Amann K, et al. The proteasome inhibitor bortezomib depletes plasma cells and protects mice with lupus-like disease from nephritis. *Nat Med* (2008) 14:748–55. doi:10.1038/nm1763
71. Ludwig RJ, Vanhoorelbeke K, Leypoldt F, Kaya Z, Bieber K, McLachlan SM, et al. Mechanisms of autoantibody-induced pathology. *Front Immunol* (2017) 8:603. doi:10.3389/fimmu.2017.00603
72. Toriani-Terenzi C, Fagiolo E. IL-10 and the cytokine network in the pathogenesis of human autoimmune hemolytic anemia. *Ann N Y Acad Sci* (2005) 1051:29–44. doi:10.1196/annals.1361.044
73. Boi F, Pani F, Mariotti S. Thyroid autoimmunity and thyroid cancer: review focused on cytological studies. *Eur Thyroid J* (2017) 6:178–86. doi:10.1159/000468928
74. Rose T, Dorner T. Drivers of the immunopathogenesis in systemic lupus erythematosus. *Best Pract Res Clin Rheumatol* (2017) 31:321–33. doi:10.1016/j.berh.2017.09.007
75. Frohlich E, Wahl R. Thyroid autoimmunity: role of anti-thyroid antibodies in thyroid and extra-thyroidal diseases. *Front Immunol* (2017) 8:521. doi:10.3389/fimmu.2017.00521
76. Strait RT, Posgai MT, Mahler A, Barasa N, Jacob CO, Kohl J, et al. IgG1 protects against renal disease in a mouse model of cryoglobulinaemia. *Nature* (2015) 517:501–4. doi:10.1038/nature13868
77. Nimmerjahn F, Ravetch JV. Fcgamma receptors as regulators of immune responses. *Nat Rev Immunol* (2008) 8:34–47. doi:10.1038/nri2206

78. Oefner CM, Winkler A, Hess C, Lorenz AK, Holecska V, Huxdorf M, et al. Tolerance induction with T cell-dependent protein antigens induces regulatory sialylated IgGs. *J Allergy Clin Immunol* (2012) 129:1647–55.e13. doi:10.1016/j.jaci.2012.02.037
79. Karsten CM, Pandey MK, Figge J, Kilchenstein R, Taylor PR, Rosas M, et al. Anti-inflammatory activity of IgG1 mediated by Fc galactosylation and association of FcgammaRIIB and dectin-1. *Nat Med* (2012) 18:1401–6. doi:10.1038/nm.2862
80. Anthony RM, Ravetch JV. A novel role for the IgG Fc glycan: the anti-inflammatory activity of sialylated IgG Fcs. *J Clin Immunol* (2010) 30 (Suppl 1):S9–14. doi:10.1007/s10875-010-9405-6
81. Hess C, Winkler A, Lorenz AK, Holecska V, Blanchard V, Eiglmeier S, et al. T cell-independent B cell activation induces immunosuppressive sialylated IgG antibodies. *J Clin Invest* (2013) 123:3788–96. doi:10.1172/JCI65938
82. Pfeifle R, Rothe T, Ipseiz N, Scherer HU, Culemann S, Harre U, et al. Regulation of autoantibody activity by the IL-23-TH17 axis determines the onset of autoimmune disease. *Nat Immunol* (2017) 18:104–13. doi:10.1038/ni.3579
83. Seeling M, Bruckner C, Nimmerjahn F. Differential antibody glycosylation in autoimmunity: sweet biomarker or modulator of disease activity? *Nat Rev Rheumatol* (2017) 13:621–30. doi:10.1038/nrrheum.2017.146
84. Claes N, Fraussen J, Stinissen P, Hupperts R, Somers V. B cells are multifunctional players in multiple sclerosis pathogenesis: insights from therapeutic interventions. *Front Immunol* (2015) 6:642. doi:10.3389/fimmu.2015.00642
85. Kulkarni U, Karsten CM, Kohler T, Hammerschmidt S, Bommert K, Tiburzy B, et al. IL-10 mediates plasmacytosis-associated immunodeficiency by inhibiting complement-mediated neutrophil migration. *J Allergy Clin Immunol* (2016) 137:1487–97.e6. doi:10.1016/j.jaci.2015.10.018
86. Fillatreau S, Sweenie CH, McGeachy MJ, Gray D, Anderton SM. B cells regulate autoimmunity by provision of IL-10. *Nat Immunol* (2002) 3:944–50. doi:10.1038/ni833
87. Crawford A, Macleod M, Schumacher T, Corlett L, Gray D. Primary T cell expansion and differentiation in vivo requires antigen presentation by B cells. *J Immunol* (2006) 176:3498–506. doi:10.4049/jimmunol.176.6.3498
88. Rodriguez-Pinto D, Moreno J. B cells can prime naive CD4+ T cells in vivo in the absence of other professional antigen-presenting cells in a CD154-CD40-dependent manner. *Eur J Immunol* (2005) 35:1097–105. doi:10.1002/eji.200425732
89. Secrist H, DeKruyff RH, Umetsu DT. Interleukin 4 production by CD4+ T cells from allergic individuals is modulated by antigen concentration and antigen-presenting cell type. *J Exp Med* (1995) 181:1081–9. doi:10.1084/jem.181.3.1081
90. Krieger J, Jenis DM, Chesnut RW, Grey HM. Studies on the capacity of intact cells and purified Ia from different B cell sources to function in antigen presentation to T cells. *J Immunol* (1988) 140:388–94.
91. Bermejo DA, Jackson SW, Gorosito-Serran M, Acosta-Rodriguez EV, Amezcua-Vesely MC, Sather BD, et al. Trypanosoma cruzi trans-sialidase initiates a program independent of the transcription factors RORgammat and Ahr that leads to IL-17 production by activated B cells. *Nat Immunol* (2013) 14:514–22. doi:10.1038/ni.2569
92. Lino AC, Dorner T, Bar-Or A, Fillatreau S. Cytokine-producing B cells: a translational view on their roles in human and mouse autoimmune diseases. *Immunol Rev* (2016) 269:130–44. doi:10.1111/imr.12374
93. Barr TA, Shen P, Brown S, Lampropoulou V, Roch T, Lawrie S, et al. B cell depletion therapy ameliorates autoimmune disease through ablation of IL-6-producing B cells. *J Exp Med* (2012) 209:1001–10. doi:10.1084/jem.20111675
94. Shen P, Fillatreau S. Antibody-independent functions of B cells: a focus on cytokines. *Nat Rev Immunol* (2015) 15:441–51. doi:10.1038/nri3857
95. Anderton SM, Fillatreau S. Activated B cells in autoimmune diseases: the case for a regulatory role. *Nat Clin Pract Rheumatol* (2008) 4:657–66. doi:10.1038/ncprheum0950
96. Dang VD, Hilgenberg E, Ries S, Shen P, Fillatreau S. From the regulatory functions of B cells to the identification of cytokine-producing plasma cell subsets. *Curr Opin Immunol* (2014) 28:77–83. doi:10.1016/j.coi.2014.02.009
97. Fillatreau S. B cells and their cytokine activities implications in human diseases. *Clin Immunol* (2017) 186:26–31. doi:10.1016/j.clim.2017.07.020
98. Shen P, Roch T, Lampropoulou V, O'Connor RA, Stervbo U, Hilgenberg E, et al. IL-35-producing B cells are critical regulators of immunity during autoimmune and infectious diseases. *Nature* (2014) 507:366–70. doi:10.1038/nature12979
99. Walshe CA, Beers SA, French RR, Chan CH, Johnson PW, Packham GK, et al. Induction of cytosolic calcium flux by CD20 is dependent upon B cell antigen receptor signaling. *J Biol Chem* (2008) 283:16971–84. doi:10.1074/jbc.M708459200
100. Jonas C. Rituxan: the new kid on the block. *Oncol Nurs Forum* (1998) 25:669.
101. Tandan R, Hehir MK II, Waheed W, Howard DB. Rituximab treatment of myasthenia gravis: a systematic review. *Muscle Nerve* (2017) 56:185–96. doi:10.1002/mus.25597
102. Schioppo T, Ingegnoli F. Current perspective on rituximab in rheumatic diseases. *Drug Des Devel Ther* (2017) 11:2891–904. doi:10.2147/DDDT.S139248
103. Joly P, Mouquet H, Roujeau JC, D'Incan M, Gilbert D, Jacquot S, et al. A single cycle of rituximab for the treatment of severe pemphigus. *N Engl J Med* (2007) 357:545–52. doi:10.1056/NEJMoa067752
104. Cross AH, Stark JL, Lauber J, Ramsbottom MJ, Lyons JA. Rituximab reduces B cells and T cells in cerebrospinal fluid of multiple sclerosis patients. *J Neuroimmunol* (2006) 180:63–70. doi:10.1016/j.jneuroim.2006.06.029
105. Rubbert-Roth A, Tak PP, Zerbini C, Tremblay JL, Carreno L, Armstrong G, et al. Efficacy and safety of various repeat treatment dosing regimens of rituximab in patients with active rheumatoid arthritis: results of a phase III randomized study (MIRROR). *Rheumatology (Oxford)* (2010) 49:1683–93. doi:10.1093/rheumatology/keq116
106. Degn SE, Thiel S. Humoral pattern recognition and the complement system. *Scand J Immunol* (2013) 78:181–93. doi:10.1111/sji.12070
107. Wang SY, Weiner G. Complement and cellular cytotoxicity in antibody therapy of cancer. *Expert Opin Biol Ther* (2008) 8:759–68. doi:10.1517/14712598.8.6.759
108. Deans JP, Robbins SM, Polyak MJ, Savage JA. Rapid redistribution of CD20 to a low density detergent-insoluble membrane compartment. *J Biol Chem* (1998) 273:344–8. doi:10.1074/jbc.273.1.344
109. Cragg MS, Glennie MJ. Antibody specificity controls in vivo effector mechanisms of anti-CD20 reagents. *Blood* (2004) 103:2738–43. doi:10.1182/blood-2003-06-2031
110. Lim SH, Beers SA, French RR, Johnson PW, Glennie MJ, Cragg MS. Anti-CD20 monoclonal antibodies: historical and future perspectives. *Haematologica* (2010) 95:135–43. doi:10.3324/haematol.2008.001628
111. Oldham RJ, Cleary KLS, Cragg MS. CD20 and its antibodies: past, present, and future. *For Immunopathol Dis Therap* (2014) 5:7–23. doi:10.1615/ForumImmunDisTher.2015014073
112. Chan HT, Hughes D, French RR, Tutt AL, Walshe CA, Teeling JL, et al. CD20-induced lymphoma cell death is independent of both caspases and its redistribution into triton X-100 insoluble membrane rafts. *Cancer Res* (2003) 63:5480–9.
113. Teng YK, Wheater G, Hogan VE, Stocks P, Levarht EW, Huizinga TW, et al. Induction of long-term B-cell depletion in refractory rheumatoid arthritis patients preferentially affects autoreactive more than protective humoral immunity. *Arthritis Res Ther* (2012) 14:R57. doi:10.1186/ar3770
114. Medina F, Segundo C, Campos-Caro A, Gonzalez-Garcia I, Brieva JA. The heterogeneity shown by human plasma cells from tonsil, blood, and bone marrow reveals graded stages of increasing maturity, but local profiles of adhesion molecule expression. *Blood* (2002) 99:2154–61. doi:10.1182/blood.V99.6.2154
115. Cambridge G, Leandro MJ, Edwards JC, Ehrenstein MR, Salden M, Bodman-Smith M, et al. Serologic changes following B lymphocyte depletion therapy for rheumatoid arthritis. *Arthritis Rheum* (2003) 48:2146–54. doi:10.1002/art.11181
116. Ahmed AR, Spigelman Z, Cavacini LA, Posner MR. Treatment of pemphigus vulgaris with rituximab and intravenous immune globulin. *N Engl J Med* (2006) 355:1772–9. doi:10.1056/NEJMoa062930
117. Pfütze M, Eming R, Kneisel A, Kuhlmann U, Hoyer J, Hertl M. Clinical and immunological follow-up of pemphigus patients on adjuvant treatment with immunoadsorption or rituximab. *Dermatology* (2009) 218:237–45. doi:10.1159/000187431
118. Smolen JS, Landewe R, Bijlsma J, Burmester G, Chatzidionysiou K, Dougados M, et al. EULAR recommendations for the management of rheumatoid arthritis with synthetic and biological disease-modifying antirheumatic drugs: 2016 update. *Ann Rheum Dis* (2017) 76:960–77. doi:10.1136/annrheumdis-2016-210715

119. Haraoui B, Bokarewa M, Kallmeyer I, Bykerk VP; RESET Investigators. Safety and effectiveness of rituximab in patients with rheumatoid arthritis following an inadequate response to 1 prior tumor necrosis factor inhibitor: the RESET Trial. *J Rheumatol* (2011) 38:2548–56. doi:10.3899/jrheum.110444
120. De Keyser F, Hoffman I, Durez P, Kaiser MJ, Westhovens R; MIRA Study Group. Longterm followup of rituximab therapy in patients with rheumatoid arthritis: results from the Belgian MabThera in Rheumatoid Arthritis registry. *J Rheumatol* (2014) 41:1761–5. doi:10.3899/jrheum.131279
121. Gardette A, Ottaviani S, Tubach F, Roy C, Nicaise-Roland P, Palazzo E, et al. High anti-CCP antibody titres predict good response to rituximab in patients with active rheumatoid arthritis. *Joint Bone Spine* (2014) 81:416–20. doi:10.1016/j.jbspin.2014.06.001
122. Couderc M, Mathieu S, Pereira B, Glace B, Soubrier M. Predictive factors of rituximab response in rheumatoid arthritis: results from a French university hospital. *Arthritis Care Res (Hoboken)* (2013) 65:648–52. doi:10.1002/acr.21865
123. Lal P, Su Z, Holweg CT, Silverman GJ, Schwartzman S, Kelman A, et al. Inflammation and autoantibody markers identify rheumatoid arthritis patients with enhanced clinical benefit following rituximab treatment. *Arthritis Rheum* (2011) 63:3681–91. doi:10.1002/art.30596
124. Chatzidionysiou K, Lie E, Nasonov E, Lukina G, Hetland ML, Tarp U, et al. Highest clinical effectiveness of rituximab in autoantibody-positive patients with rheumatoid arthritis and in those for whom no more than one previous TNF antagonist has failed: pooled data from 10 European registries. *Ann Rheum Dis* (2011) 70:1575–80. doi:10.1136/ard.2010.148759
125. Sellam J, Riviere E, Courties A, Rouzaire PO, Tolusso B, Vital EM, et al. Serum IL-33, a new marker predicting response to rituximab in rheumatoid arthritis. *Arthritis Res Ther* (2016) 18:294. doi:10.1186/s13075-016-1190-z
126. Sokolove J, Johnson DS, Lahey LJ, Wagner CA, Cheng D, Thiele GM, et al. Rheumatoid factor as a potentiator of anti-citrullinated protein antibody-mediated inflammation in rheumatoid arthritis. *Arthritis Rheumatol* (2014) 66:813–21. doi:10.1002/art.38307
127. Cambridge G, Perry HC, Nogueira L, Serre G, Parsons HM, De La Torre I, et al. The effect of B-cell depletion therapy on serological evidence of B-cell and plasmablast activation in patients with rheumatoid arthritis over multiple cycles of rituximab treatment. *J Autoimmun* (2014) 50:67–76. doi:10.1016/j.jaut.2013.12.002
128. Strober S, Holoshitz J. Mechanisms of immune injury in rheumatoid arthritis: evidence for the involvement of T cells and heat-shock protein. *Immunol Rev* (1990) 118:233–55. doi:10.1111/j.1600-065X.1990.tb00818.x
129. Roberts CA, Dickinson AK, Taams LS. The interplay between monocytes/macrophages and CD4(+) T cell subsets in rheumatoid arthritis. *Front Immunol* (2015) 6:571. doi:10.3389/fimmu.2015.00571
130. Diogo D, Okada Y, Plenge RM. Genome-wide association studies to advance our understanding of critical cell types and pathways in rheumatoid arthritis: recent findings and challenges. *Curr Opin Rheumatol* (2014) 26:85–92. doi:10.1097/BOR.0000000000000012
131. Esensten JH, Wofsy D, Bluestone JA. Regulatory T cells as therapeutic targets in rheumatoid arthritis. *Nat Rev Rheumatol* (2009) 5:560–5. doi:10.1038/nrrheum.2009.183
132. Benucci M, Manfredi M, Puttini PS, Atzeni F. Predictive factors of response to rituximab therapy in rheumatoid arthritis: what do we know today? *Autoimmun Rev* (2010) 9:801–3. doi:10.1016/j.autrev.2010.07.006
133. Melet J, Mulleman D, Goupille P, Ribourtout B, Watier H, Thibault G. Rituximab-induced T cell depletion in patients with rheumatoid arthritis: association with clinical response. *Arthritis Rheum* (2013) 65:2783–90. doi:10.1002/art.38107
134. Wilk E, Witte T, Marquardt N, Horvath T, Kalippke K, Scholz K, et al. Depletion of functionally active CD20+ T cells by rituximab treatment. *Arthritis Rheum* (2009) 60:3563–71. doi:10.1002/art.24998
135. Barr TA, Brown S, Mastroeni P, Gray D. TLR and B cell receptor signals to B cells differentially program primary and memory Th1 responses to *Salmonella enterica*. *J Immunol* (2010) 185:2783–9. doi:10.4049/jimmunol.1001431
136. Takemura S, Klimiuk PA, Braun A, Goronzy JJ, Weyand CM. T cell activation in rheumatoid synovium is B cell dependent. *J Immunol* (2001) 167:4710–8. doi:10.4049/jimmunol.167.8.4710
137. Agrawal S, Gupta S. TLR1/2, TLR7, and TLR9 signals directly activate human peripheral blood naive and memory B cell subsets to produce cytokines, chemokines, and hematopoietic growth factors. *J Clin Immunol* (2011) 31:89–98. doi:10.1007/s10875-010-9456-8
138. Rauch PJ, Chudnovskiy A, Robbins CS, Weber GF, Etzrodt M, Hilgendorf I, et al. Innate response activator B cells protect against microbial sepsis. *Science* (2012) 335:597–601. doi:10.1126/science.1215173
139. Fleischer S, Ries S, Shen P, Lheritier A, Cazals F, Burmester GR, et al. Anti-interleukin-6 signalling therapy rebalances the disrupted cytokine production of B cells from patients with active rheumatoid arthritis. *Eur J Immunol* (2017) 48(1):194–203. doi:10.1002/eji.201747191
140. Parekh RB, Roitt IM, Isenberg DA, Dwek RA, Ansell BM, Rademacher TW. Galactosylation of IgG associated oligosaccharides: reduction in patients with adult and juvenile onset rheumatoid arthritis and relation to disease activity. *Lancet* (1988) 1:966–9. doi:10.1016/S0140-6736(88)91781-3
141. Ercan A, Cui J, Chatterton DE, Deane KD, Hazen MM, Brintnell W, et al. Aberrant IgG galactosylation precedes disease onset, correlates with disease activity, and is prevalent in autoantibodies in rheumatoid arthritis. *Arthritis Rheum* (2010) 62:2239–48. doi:10.1002/art.27533
142. Kaneko Y, Nimmerjahn F, Ravetch JV. Anti-inflammatory activity of immunoglobulin G resulting from Fc sialylation. *Science* (2006) 313:670–3. doi:10.1126/science.1129594
143. Collin M, Ehlers M. The carbohydrate switch between pathogenic and immunosuppressive antigen-specific antibodies. *Exp Dermatol* (2013) 22:511–4. doi:10.1111/exd.12171
144. Reddy V, Martinez L, Isenberg DA, Leandro MJ, Cambridge G. Pragmatic treatment of patients with systemic lupus erythematosus with rituximab: long-term effects on serum immunoglobulins. *Arthritis Care Res (Hoboken)* (2017) 69:857–66. doi:10.1002/acr.22993
145. Rovin BH, Furie R, Latinis K, Looney RJ, Fervenza FC, Sanchez-Guerrero J, et al. Efficacy and safety of rituximab in patients with active proliferative lupus nephritis: the lupus nephritis assessment with rituximab study. *Arthritis Rheum* (2012) 64:1215–26. doi:10.1002/art.34359
146. Leandro MJ, Cambridge G, Edwards JC, Ehrenstein MR, Isenberg DA. B-cell depletion in the treatment of patients with systemic lupus erythematosus: a longitudinal analysis of 24 patients. *Rheumatology (Oxford)* (2005) 44:1542–5. doi:10.1093/rheumatology/kei080
147. Albert D, Dunham J, Khan S, Stansberry J, Kolasinski S, Tsai D, et al. Variability in the biological response to anti-CD20 B cell depletion in systemic lupus erythaematosus. *Ann Rheum Dis* (2008) 67:1724–31. doi:10.1136/ard.2007.083162
148. Lu TY, Ng KP, Cambridge G, Leandro MJ, Edwards JC, Ehrenstein M, et al. A retrospective seven-year analysis of the use of B cell depletion therapy in systemic lupus erythematosus at University College London Hospital: the first fifty patients. *Arthritis Rheum* (2009) 61:482–7. doi:10.1002/art.24341
149. Hauser SL, Waubant E, Arnold DL, Vollmer T, Antel J, Fox RJ, et al. B-cell depletion with rituximab in relapsing-remitting multiple sclerosis. *N Engl J Med* (2008) 358:676–88. doi:10.1056/NEJMoa0706383
150. Dunn N, Juto A, Ryner M, Manouchehrinia A, Piccoli L, Fink K, et al. Rituximab in multiple sclerosis: frequency and clinical relevance of anti-drug antibodies. *Mult Scler* (2017):1352458517720044. doi:10.1177/1352458517720044
151. Hawker K, O'Connor P, Freedman MS, Calabresi PA, Antel J, Simon J, et al. Rituximab in patients with primary progressive multiple sclerosis: results of a randomized double-blind placebo-controlled multicenter trial. *Ann Neurol* (2009) 66:460–71. doi:10.1002/ana.21867
152. Fillatreau S, Gray D, Anderton SM. Not always the bad guys: B cells as regulators of autoimmune pathology. *Nat Rev Immunol* (2008) 8:391–7. doi:10.1038/nri2315
153. Matsumoto M, Baba A, Yokota T, Nishikawa H, Ohkawa Y, Kayama H, et al. Interleukin-10-producing plasmablasts exert regulatory function in autoimmune inflammation. *Immunity* (2014) 41:1040–51. doi:10.1016/j.immuni.2014.10.016
154. Du FH, Mills EA, Mao-Draayer Y. Next-generation anti-CD20 monoclonal antibodies in autoimmune disease treatment. *Auto Immun Highlights* (2017) 8:12. doi:10.1007/s13317-017-0100-y
155. Emery P, Rigby W, Tak PP, Dorner T, Olech E, Martin C, et al. Safety with ocrelizumab in rheumatoid arthritis: results from the ocrelizumab phase III program. *PLoS One* (2014) 9:e87379. doi:10.1371/journal.pone.0087379
156. Hammer O. CD19 as an attractive target for antibody-based therapy. *MAbs* (2012) 4:571–7. doi:10.4161/mabs.21338

157. Jabbour E, Ravandi F, Kebriaei P, Huang X, Short NJ, Thomas D, et al. Salvage chemoimmunotherapy with inotuzumab ozogamicin combined with mini-hyper-CVD for patients with relapsed or refractory philadelphia chromosome-negative acute lymphoblastic leukemia: a phase 2 clinical trial. *JAMA Oncol* (2018) 4:230–4. doi:10.1001/jamaoncol.2017.2380
158. Tedder TF. CD19: a promising B cell target for rheumatoid arthritis. *Nat Rev Rheumatol* (2009) 5:572–7. doi:10.1038/nrrheum.2009.184
159. Gopaluni S, Smith RM, Lewin M, McAlear CA, Mynard K, Jones RB, et al. Rituximab versus azathioprine as therapy for maintenance of remission for anti-neutrophil cytoplasm antibody-associated vasculitis (RITAZAREM): study protocol for a randomized controlled trial. *Trials* (2017) 18:112. doi:10.1186/s13063-017-1857-z
160. Bossen C, Schneider P. BAFF, APRIL and their receptors: structure, function and signaling. *Semin Immunol* (2006) 18:263–75. doi:10.1016/j.smim.2006.04.006
161. Gross JA, Johnston J, Mudri S, Enselman R, Dillon SR, Madden K, et al. TACI and BCMA are receptors for a TNF homologue implicated in B-cell autoimmune disease. *Nature* (2000) 404:995–9. doi:10.1038/35010115
162. Condon MB, Ashby D, Pepper RJ, Cook HT, Levy JB, Griffith M, et al. Prospective observational single-centre cohort study to evaluate the effectiveness of treating lupus nephritis with rituximab and mycophenolate mofetil but no oral steroids. *Ann Rheum Dis* (2013) 72:1280–6. doi:10.1136/annrheumdis-2012-202844
163. Ramos-Casals M, Garcia-Hernandez FJ, de Ramon E, Callejas JL, Martinez-Berriotxoa A, Pallares L, et al. Off-label use of rituximab in 196 patients with severe, refractory systemic autoimmune diseases. *Clin Exp Rheumatol* (2010) 28:468–76.
164. Blair HA, Duggan ST. Belimumab: a review in systemic lupus erythematosus. *Drugs* (2018) 78:355–66. doi:10.1007/s40265-018-0872-z
165. Jacobi AM, Huang W, Wang T, Freimuth W, Sanz I, Furie R, et al. Effect of long-term belimumab treatment on B cells in systemic lupus erythematosus: extension of a phase II, double-blind, placebo-controlled, dose-ranging study. *Arthritis Rheum* (2010) 62:201–10. doi:10.1002/art.27189
166. Ginzler EM, Wallace DJ, Merrill JT, Furie RA, Stohl W, Chatham WW, et al. Disease control and safety of belimumab plus standard therapy over 7 years in patients with systemic lupus erythematosus. *J Rheumatol* (2014) 41:300–9. doi:10.3899/jrheum.121368
167. Stohl W, Hiepe F, Latinis KM, Thomas M, Scheinberg MA, Clarke A, et al. Belimumab reduces autoantibodies, normalizes low complement levels, and reduces select B cell populations in patients with systemic lupus erythematosus. *Arthritis Rheum* (2012) 64:2328–37. doi:10.1002/art.34400
168. Smolen JS, Weinblatt ME, van der Heijde D, Rigby WF, van Vollenhoven R, Bingham CO III, et al. Efficacy and safety of tabalumab, an anti-B-cell-activating factor monoclonal antibody, in patients with rheumatoid arthritis who had an inadequate response to methotrexate therapy: results from a phase III multicentre, randomised, double-blind study. *Ann Rheum Dis* (2015) 74:1567–70. doi:10.1136/annrheumdis-2014-207090
169. Greenwald M, Szczepanski L, Kennedy A, Veenhuizen M, Komocsar WJ, Polasek E, et al. A 52-week, open-label study evaluating the safety and efficacy of tabalumab, an anti-B-cell-activating factor monoclonal antibody, for rheumatoid arthritis. *Arthritis Res Ther* (2014) 16:415. doi:10.1186/s13075-014-0415-2
170. Genovese MC, Kinnman N, de La Bourdonnaye G, Pena Rossi C, Tak PP. Atacicept in patients with rheumatoid arthritis and an inadequate response to tumor necrosis factor antagonist therapy: results of a phase II, randomized, placebo-controlled, dose-finding trial. *Arthritis Rheum* (2011) 63:1793–803. doi:10.1002/art.30373
171. van Vollenhoven RF, Kinnman N, Vincent E, Wax S, Bathon J. Atacicept in patients with rheumatoid arthritis and an inadequate response to methotrexate: results of a phase II, randomized, placebo-controlled trial. *Arthritis Rheum* (2011) 63:1782–92. doi:10.1002/art.30372
172. Navarra SV, Guzman RM, Gallacher AE, Hall S, Levy RA, Jimenez RE, et al. Efficacy and safety of belimumab in patients with active systemic lupus erythematosus: a randomised, placebo-controlled, phase 3 trial. *Lancet* (2011) 377:721–31. doi:10.1016/S0140-6736(10)61354-2
173. Furie R, Petri M, Zamani O, Cervera R, Wallace DJ, Tegzova D, et al. A phase III, randomized, placebo-controlled study of belimumab, a monoclonal antibody that inhibits B lymphocyte stimulator, in patients with systemic lupus erythematosus. *Arthritis Rheum* (2011) 63:3918–30. doi:10.1002/art.30613
174. Merrill JT, van Vollenhoven RF, Buyon JP, Furie RA, Stohl W, Morgan-Cox M, et al. Efficacy and safety of subcutaneous tabalumab, a monoclonal antibody to B-cell activating factor, in patients with systemic lupus erythematosus: results from ILLUMINATE-2, a 52-week, phase III, multicentre, randomised, double-blind, placebo-controlled study. *Ann Rheum Dis* (2016) 75:332–40. doi:10.1136/annrheumdis-2015-207654
175. Furie RA, Leon G, Thomas M, Petri MA, Chu AD, Hislop C, et al. A phase 2, randomised, placebo-controlled clinical trial of blisibimod, an inhibitor of B cell activating factor, in patients with moderate-to-severe systemic lupus erythematosus, the PEARL-SC study. *Ann Rheum Dis* (2015) 74:1667–75. doi:10.1136/annrheumdis-2013-205144
176. Dall'Era M, Chakravarty E, Wallace D, Genovese M, Weisman M, Kavanaugh A, et al. Reduced B lymphocyte and immunoglobulin levels after atacicept treatment in patients with systemic lupus erythematosus: results of a multicenter, phase Ib, double-blind, placebo-controlled, dose-escalating trial. *Arthritis Rheum* (2007) 56:4142–50. doi:10.1002/art.23047
177. Lenert P, Icardi M, Dahmoush L. ANA (+) ANCA (+) systemic vasculitis associated with the use of minocycline: case-based review. *Clin Rheumatol* (2013) 32:1099–106. doi:10.1007/s10067-013-2245-z
178. Ginzler EM, Wax S, Rajeswaran A, Copt S, Hillson J, Ramos E, et al. Atacicept in combination with MMF and corticosteroids in lupus nephritis: results of a prematurely terminated trial. *Arthritis Res Ther* (2012) 14:R33. doi:10.1186/ar3738
179. Mariette X, Seror R, Quartuccio L, Baron G, Salvin S, Fabris M, et al. Efficacy and safety of belimumab in primary Sjogren's syndrome: results of the BELISS open-label phase II study. *Ann Rheum Dis* (2015) 74:526–31. doi:10.1136/annrheumdis-2013-203991
180. Kappos L, Hartung HP, Freedman MS, Boyko A, Radu EW, Mikol DD, et al. Atacicept in multiple sclerosis (ATAMS): a randomised, placebo-controlled, double-blind, phase 2 trial. *Lancet Neurol* (2014) 13:353–63. doi:10.1016/S1474-4422(14)70028-6
181. Stohl W, Merrill JT, McKay JD, Lisse JR, Zhong ZJ, Freimuth WW, et al. Efficacy and safety of belimumab in patients with rheumatoid arthritis: a phase II, randomized, double-blind, placebo-controlled, dose-ranging study. *J Rheumatol* (2013) 40:579–89. doi:10.3899/jrheum.120886
182. Manz RA, Thiel A, Radbruch A. Lifetime of plasma cells in the bone marrow. *Nature* (1997) 388:133–4. doi:10.1038/40540
183. Slifka MK, Antia R, Whitmire JK, Ahmed R. Humoral immunity due to long-lived plasma cells. *Immunity* (1998) 8:363–72. doi:10.1016/S1074-7613(00)80541-5
184. Bontscho J, Schreiber A, Manz RA, Schneider W, Luft FC, Kettritz R. Myeloperoxidase-specific plasma cell depletion by bortezomib protects from anti-neutrophil cytoplasmic autoantibodies-induced glomerulonephritis. *J Am Soc Nephrol* (2011) 22:336–48. doi:10.1681/ASN.2010010034
185. Gomez AM, Vrolix K, Martinez-Martinez P, Molenaar PC, Phernambucq M, van der Esch E, et al. Proteasome inhibition with bortezomib depletes plasma cells and autoantibodies in experimental autoimmune myasthenia gravis. *J Immunol* (2011) 186:2503–13. doi:10.4049/jimmunol.1002539
186. Taddeo A, Khodadadi L, Voigt C, Mumtaz IM, Cheng Q, Moser K, et al. Long-lived plasma cells are early and constantly generated in New Zealand Black/New Zealand White F1 mice and their therapeutic depletion requires a combined targeting of autoreactive plasma cells and their precursors. *Arthritis Res Ther* (2015) 17:39. doi:10.1186/s13075-015-0551-3
187. Rosenberg AS, Pariser AR, Diamond B, Yao L, Turka LA, Lacana E, et al. A role for plasma cell targeting agents in immune tolerance induction in autoimmune disease and antibody responses to therapeutic proteins. *Clin Immunol* (2016) 165:55–9. doi:10.1016/j.clim.2016.02.009
188. Mehta B, Mahadeo K, Zaw R, Tang S, Kapoor N, Abdel-Azim H. Bortezomib for effective treatment of a child with refractory autoimmune hemolytic anemia post allogeneic hematopoietic stem cell transplant. *Pediatr Blood Cancer* (2014) 61:2324–5. doi:10.1002/pbc.25172
189. Jakez-Ocampo J, Atisha-Fregoso Y, Llorente L. Refractory primary Sjogren syndrome successfully treated with bortezomib. *J Clin Rheumatol* (2015) 21:31–2. doi:10.1097/RHU.0000000000000210
190. Verbrugge SE, Scheper RJ, Lems WF, de Gruijl TD, Jansen G. Proteasome inhibitors as experimental therapeutics of autoimmune diseases. *Arthritis Res Ther* (2015) 17:17. doi:10.1186/s13075-015-0529-1
191. Khandelwal P, Davies SM, Grimley MS, Jordan MB, Curtis BR, Jodele S, et al. Bortezomib for refractory autoimmunity in pediatrics. *Biol Blood Marrow Transplant* (2014) 20:1654–9. doi:10.1016/j.bbmt.2014.06.032

192. Yates S, Matevosyan K, Rutherford C, Shen YM, Sarode R. Bortezomib for chronic relapsing thrombotic thrombocytopenic purpura: a case report. *Transfusion* (2014) 54:2064–7. doi:10.1111/trf.12614
193. van Balen T, Schreuder MF, de Jong H, van de Kar NC. Refractory thrombotic thrombocytopenic purpura in a 16-year-old girl: successful treatment with bortezomib. *Eur J Haematol* (2014) 92:80–2. doi:10.1111/ejh.12206
194. Gomez AM, Willcox N, Molenaar PC, Buurman W, Martinez-Martinez P, De Baets MH, et al. Targeting plasma cells with proteasome inhibitors: possible roles in treating myasthenia gravis? *Ann N Y Acad Sci* (2012) 1274:48–59. doi:10.1111/j.1749-6632.2012.06824.x
195. Danchaivijitr P, Yared J, Rapoport AP. Successful treatment of IgG and complement-mediated autoimmune hemolytic anemia with bortezomib and low-dose cyclophosphamide. *Am J Hematol* (2011) 86:331–2. doi:10.1002/ajh.21950
196. Hiepe F, Radbruch A. Plasma cells as an innovative target in autoimmune disease with renal manifestations. *Nat Rev Nephrol* (2016) 12:232–40. doi:10.1038/nrneph.2016.20
197. Hiepe F, Dorner T, Hauser AE, Hoyer BF, Mei H, Radbruch A. Long-lived autoreactive plasma cells drive persistent autoimmune inflammation. *Nat Rev Rheumatol* (2011) 7:170–8. doi:10.1038/nrrheum.2011.1
198. Mauri C, Menon M. The expanding family of regulatory B cells. *Int Immunol* (2015) 27:479–86. doi:10.1093/intimm/dxv038
199. van der Vlugt LE, Labuda LA, Ozir-Fazalalikhan A, Lievers E, Gloudemans AK, Liu KY, et al. Schistosomes induce regulatory features in human and mouse CD1d(hi) B cells: inhibition of allergic inflammation by IL-10 and regulatory T cells. *PLoS One* (2012) 7:e30883. doi:10.1371/journal.pone.0030883
200. Korniotis S, Gras C, Letscher H, Montandon R, Megret J, Siegert S, et al. Treatment of ongoing autoimmune encephalomyelitis with activated B-cell progenitors maturing into regulatory B cells. *Nat Commun* (2016) 7:12134. doi:10.1038/ncomms12134
201. Mauri C, Bosma A. Immune regulatory function of B cells. *Annu Rev Immunol* (2012) 30:221–41. doi:10.1146/annurev-immunol-020711-074934
202. Egwuagu CE, Yu CR. Interleukin 35-producing B cells (i35-Breg): a new mediator of regulatory B-cell functions in CNS autoimmune diseases. *Crit Rev Immunol* (2015) 35:49–57. doi:10.1615/CritRevImmunol.2015012558
203. Rosser EC, Mauri C. Regulatory B cells: origin, phenotype, and function. *Immunity* (2015) 42:607–12. doi:10.1016/j.immuni.2015.04.005
204. Blair PA, Norena LY, Flores-Borja F, Rawlings DJ, Isenberg DA, Ehrenstein MR, et al. CD19(+)CD24(hi)CD38(hi) B cells exhibit regulatory capacity in healthy individuals but are functionally impaired in systemic lupus erythematosus patients. *Immunity* (2010) 32:129–40. doi:10.1016/j.immuni.2009.11.009
205. de Masson A, Bouaziz JD, Le Buanec H, Robin M, O'Meara A, Parquet N, et al. CD24(hi)CD27(+) and plasmablast-like regulatory B cells in human chronic graft-versus-host disease. *Blood* (2015) 125:1830–9. doi:10.1182/blood-2014-09-599159
206. Banko Z, Pozsgay J, Szili D, Toth M, Gati T, Nagy G, et al. Induction and differentiation of IL-10-producing regulatory B cells from healthy blood donors and rheumatoid arthritis patients. *J Immunol* (2017) 198:1512–20. doi:10.4049/jimmunol.1600218
207. Iwata Y, Matsushita T, Horikawa M, Dilillo DJ, Yanaba K, Venturi GM, et al. Characterization of a rare IL-10-competent B-cell subset in humans that parallels mouse regulatory B10 cells. *Blood* (2011) 117:530–41. doi:10.1182/blood-2010-07-294249
208. Heine G, Drozdenko G, Grun JR, Chang HD, Radbruch A, Worm M. Autocrine IL-10 promotes human B-cell differentiation into IgM- or IgG-secreting plasmablasts. *Eur J Immunol* (2014) 44:1615–21. doi:10.1002/eji.201343822
209. Zhu HQ, Xu RC, Chen YY, Yuan HJ, Cao H, Zhao XQ, et al. Impaired function of CD19(+) CD24(hi) CD38(hi) regulatory B cells in patients with pemphigus. *Br J Dermatol* (2015) 172:101–10. doi:10.1111/bjd.13192
210. Daien CI, Gailhac S, Mura T, Audo R, Combe B, Hahne M, et al. Regulatory B10 cells are decreased in patients with rheumatoid arthritis and are inversely correlated with disease activity. *Arthritis Rheumatol* (2014) 66:2037–46. doi:10.1002/art.38666
211. Salomon S, Guignant C, Morel P, Flahaut G, Brault C, Gourguechon C, et al. Th17 and CD24hiCD27+ regulatory B lymphocytes are biomarkers of response to biologics in rheumatoid arthritis. *Arthritis Res Ther* (2017) 19:33. doi:10.1186/s13075-017-1244-x
212. Flores-Borja F, Bosma A, Ng D, Reddy V, Ehrenstein MR, Isenberg DA, et al. CD19+CD24hiCD38hi B cells maintain regulatory T cells while limiting TH1 and TH17 differentiation. *Sci Transl Med* (2013) 5:173ra23. doi:10.1126/scitranslmed.3005407
213. Matsushita T, Hamaguchi Y, Hasegawa M, Takehara K, Fujimoto M. Decreased levels of regulatory B cells in patients with systemic sclerosis: association with autoantibody production and disease activity. *Rheumatology (Oxford)* (2016) 55:263–7. doi:10.1093/rheumatology/kev331
214. Aravena O, Ferrier A, Menon M, Mauri C, Aguillon JC, Soto L, et al. TIM-1 defines a human regulatory B cell population that is altered in frequency and function in systemic sclerosis patients. *Arthritis Res Ther* (2017) 19:8. doi:10.1186/s13075-016-1213-9
215. Duddy M, Niino M, Adatia F, Hebert S, Freedman M, Atkins H, et al. Distinct effector cytokine profiles of memory and naive human B cell subsets and implication in multiple sclerosis. *J Immunol* (2007) 178:6092–9. doi:10.4049/jimmunol.178.10.6092
216. Bar-Or A, Fawaz L, Fan B, Darlington PJ, Rieger A, Ghorayeb C, et al. Abnormal B-cell cytokine responses a trigger of T-cell-mediated disease in MS? *Ann Neurol* (2010) 67:452–61. doi:10.1002/ana.21939
217. Knippenberg S, Peelen E, Smolders J, Thewissen M, Menheere P, Cohen Tervaert JW, et al. Reduction in IL-10 producing B cells (Breg) in multiple sclerosis is accompanied by a reduced naive/memory Breg ratio during a relapse but not in remission. *J Neuroimmunol* (2011) 239:80–6. doi:10.1016/j.jneuroim.2011.08.019
218. Miyagaki T, Fujimoto M, Sato S. Regulatory B cells in human inflammatory and autoimmune diseases: from mouse models to clinical research. *Int Immunol* (2015) 27:495–504. doi:10.1093/intimm/dxv026
219. Sun F, Ladha SS, Yang L, Liu Q, Shi SX, Su N, et al. Interleukin-10 producing-B cells and their association with responsiveness to rituximab in myasthenia gravis. *Muscle Nerve* (2014) 49:487–94. doi:10.1002/mus.23951
220. Wang Q, Racine JJ, Ratiu JJ, Wang S, Ettinger R, Wasserfall C, et al. Transient BAFF blockade inhibits type 1 diabetes development in nonobese diabetic mice by enriching immunoregulatory B lymphocytes sensitive to deletion by anti-CD20 cotherapy. *J Immunol* (2017) 199:3757–70. doi:10.4049/jimmunol.1700822
221. Colliou N, Picard D, Caillot F, Calbo S, Le Corre S, Lim A, et al. Long-term remissions of severe pemphigus after rituximab therapy are associated with prolonged failure of desmoglein B cell response. *Sci Transl Med* (2013) 5:175ra30. doi:10.1126/scitranslmed.3005166
222. Menon M, Blair PA, Isenberg DA, Mauri C. A regulatory feedback between plasmacytoid dendritic cells and regulatory B cells is aberrant in systemic lupus erythematosus. *Immunity* (2016) 44:683–97. doi:10.1016/j.immuni.2016.02.012
223. Merrill JT, Burgos-Vargas R, Westhovens R, Chalmers A, D'Cruz D, Wallace DJ, et al. The efficacy and safety of abatacept in patients with non-life-threatening manifestations of systemic lupus erythematosus: results of a twelve-month, multicenter, exploratory, phase IIb, randomized, double-blind, placebo-controlled trial. *Arthritis Rheum* (2010) 62:3077–87. doi:10.1002/art.27601
224. Giacomini E, Rizzo F, Etna MP, Cruciani M, Mechelli R, Buscarinu MC, et al. Thymosin-alpha1 expands deficient IL-10-producing regulatory B cell subsets in relapsing-remitting multiple sclerosis patients. *Mult Scler* (2017) 24(2):127–39. doi:10.1177/1352458517695892
225. Rosser EC, Oleinika K, Tonon S, Doyle R, Bosma A, Carter NA, et al. Regulatory B cells are induced by gut microbiota-driven interleukin-1beta and interleukin-6 production. *Nat Med* (2014) 20:1334–9. doi:10.1038/nm.3680
226. Wang RX, Yu CR, Dambuza IM, Mahdi RM, Dolinska MB, Sergeev YV, et al. Interleukin-35 induces regulatory B cells that suppress autoimmune disease. *Nat Med* (2014) 20:633–41. doi:10.1038/nm.3554
227. Mauri C, Menon M. Human regulatory B cells in health and disease: therapeutic potential. *J Clin Invest* (2017) 127:772–9. doi:10.1172/JCI85113
228. Yanaba K, Bouaziz JD, Haas KM, Poe JC, Fujimoto M, Tedder TF. A regulatory B cell subset with a unique CD1dhiCD5+ phenotype controls T cell-dependent inflammatory responses. *Immunity* (2008) 28:639–50. doi:10.1016/j.immuni.2008.03.017
229. O'Garra A, Chang R, Go N, Hastings R, Haughton G, Howard M. Ly-1 B (B-1) cells are the main source of B cell-derived interleukin 10. *Eur J Immunol* (1992) 22:711–7. doi:10.1002/eji.1830220314

230. Evans JG, Chavez-Rueda KA, Eddaoudi A, Meyer-Bahlburg A, Rawlings DJ, Ehrenstein MR, et al. Novel suppressive function of transitional 2 B cells in experimental arthritis. *J Immunol* (2007) 178:7868–78. doi:10.4049/jimmunol.178.12.7868
231. Gray M, Miles K, Salter D, Gray D, Savill J. Apoptotic cells protect mice from autoimmune inflammation by the induction of regulatory B cells. *Proc Natl Acad Sci U S A* (2007) 104:14080–5. doi:10.1073/pnas.0700326104
232. Maseda D, Smith SH, DiLillo DJ, Bryant JM, Candando KM, Weaver CT, et al. Regulatory B10 cells differentiate into antibody-secreting cells after transient IL-10 production in vivo. *J Immunol* (2012) 188:1036–48. doi:10.4049/jimmunol.1102500

Conflict of Interest Statement: The authors declare that the research was conducted in the absence of any commercial or financial relationships that could be construed as a potential conflict of interest.

frontiers in Immunology

REVIEW
published: 19 April 2018
doi: 10.3389/fimmu.2018.00692

Autoantibody Signaling in Pemphigus Vulgaris: Development of an Integrated Model

*Thomas Sajda and Animesh A. Sinha**

Department of Dermatology, Jacobs School of Medicine and Biomedical Sciences, University at Buffalo, Buffalo, NY, United States

Pemphigus vulgaris (PV) is an autoimmune skin blistering disease effecting both cutaneous and mucosal epithelia. Blister formation in PV is known to result from the binding of autoantibodies (autoAbs) to keratinocyte antigens. The primary antigenic targets of pathogenic autoAbs are known to be desmoglein 3, and to a lesser extent, desmoglein 1, cadherin family proteins that partially comprise the desmosome, a protein structure responsible for maintaining cell adhesion, although additional autoAbs, whose role in blister formation is still unclear, are also known to be present in PV patients. Nevertheless, there remain large gaps in knowledge concerning the precise mechanisms through which autoAb binding induces blister formation. Consequently, the primary therapeutic interventions for PV focus on systemic immunosuppression, whose side effects represent a significant health risk to patients. In an effort to identify novel, disease-specific therapeutic targets, a multitude of studies attempting to elucidate the pathogenic mechanisms downstream of autoAb binding, have led to significant advancements in the understanding of autoAb-mediated blister formation. Despite this enhanced characterization of disease processes, a satisfactory explanation of autoAb-induced acantholysis still does not exist. Here, we carefully review the literature investigating the pathogenic disease mechanisms in PV and, taking into account the full scope of results from these studies, provide a novel, comprehensive theory of blister formation in PV.

Keywords: pemphigus vulgaris, autoantibodies, signaling pathways, p38MAPK, calcium, epidermal growth factor receptor, Rho GTPases

OPEN ACCESS

Edited by:
Ralf J. Ludwig, Universität zu Lübeck, Germany

Reviewed by:
Robert Gniadecki, University of Alberta, Canada
Sergei Grando, University of California, Irvine, United States

***Correspondence:**
Animesh A. Sinha
aasinha@buffalo.edu

Specialty section:
This article was submitted to Immunological Tolerance and Regulation, a section of the journal Frontiers in Immunology

Received: *01 February 2018*
Accepted: *21 March 2018*
Published: *19 April 2018*

Citation:
Sajda T and Sinha AA (2018) Autoantibody Signaling in Pemphigus Vulgaris: Development of an Integrated Model. Front. Immunol. 9:692. doi: 10.3389/fimmu.2018.00692

INTRODUCTION

Pemphigus vulgaris (PV) is an autoimmune skin blistering disease characterized by the presence of autoantibodies (autoAbs) directed against keratinocyte surface antigens. It has been well established that autoAbs alone are capable of driving blister formation in PV. Early studies identified the primary target of pathogenic autoAbs as desmoglein 3 (Dsg3) and to a lesser extent, desmoglein 1 (Dsg1). More recently, additional autoAbs specificities have been identified in PV patients that could potentially also contribute to disease pathogenicity (1, 2). Despite extensive research, the exact mechanisms through which autoAbs induce a loss of cell–cell adhesion (also termed acantholysis) are not well understood.

Since the primary target of PV autoAbs was shown to be a desmosomal protein, most of the earliest theories of acantholysis suggested that the loss of cell adhesion was simply the result of

autoAbs sterically hindering the homo- and heterophillic binding of desmosomal proteins between neighboring cells (3, 4). Studies showing that staphylococcal exfoliative toxins, which cleave Dsg1, could produce blisters similar to those seen in PF, indicated that disturbance of desmosomal proteins was capable of causing a loss of cell–cell adhesion (5, 6). The relationship between desmoglein expression and cell adhesion was further supported by the observation that Dsg3-deficient mice develop mucosal lesions similar to those seen in PV patients (7). Together, these data demonstrated that interference with desmoglein interactions was sufficient to drive a loss of cell–cell adhesion.

The observation by multiple groups that PVIgG was seen only to bind at desmosomal areas also supported the idea that autoAb interference of desmosomal interaction drives blister formation (8–10). In addition, in areas of acantholysis, PVIgG was seen to bind to both desmosomal plaques and split desmosomes (11), indicating that PVIgG could access desmosome-associated desmogleins.

Further support for the steric hindrance theory came from later studies attempting to characterize the fine-epitope specificity of anti-Dsg3 autoAbs. It was shown that autoAbs primarily target the amino terminal of Dsg3 which, based on the crystal structure of other classical cadherins, was predicted to facilitate trans-interaction (12–17). Furthermore, only anti-Dsg3 autoAbs targeting the amino terminal EC1-2 of Dsg3 could illicit blister formation when passively transferred to neonatal mice, not anti-Dsg3 autoAbs targeting the more carboxyl domains EC3-5. Another study demonstrated that anti-Dsg3 autoAbs preferentially recognize the mature form of Dsg3, but not an immature form, which requires additional proteolytic processing to participate in adhesion (18, 19). It was also shown that autoAb binding was dependent on the proper calcium stabilized formation of Dsg3, which is known to be required for proper adhesive functioning (13, 20, 21). Later experiments using atomic force microscopy (AFM) were able to demonstrate that PVIgG could directly interfere with Dsg3 trans-interaction (22).

One potential liability of the steric hindrance theory was the possibility that blistering effects were mediated by the constant regions of the Abs. However, experiments showing that Fab and $F(ab_2)$ fragments, as well as single-chain variable fragments which lack the Fc domain, were able to induce blister formation *in vitro* proved that Fc-dependent mechanisms were not necessary for blister formation (23–26). Additional experiments demonstrating the pathogenicity of PVIgG in C5a-deficient mice indicated that compliment activation was not required for acantholysis (23).

Over time, evidence has accumulated suggesting steric hindrance may not be the primary or sole pathogenic mechanism operative in PV. One of the earliest indications that alternative mechanisms may drive pathogenesis was the observation that IgG from PF patients could induce disease in mice without interfering with trans-adhesion of Dsg1 (27). It was noted in multiple studies that PVIgG was seen to bind extra-desmosomal spaces on the surface of keratinocytes, allowing for the possibility that binding of autoAbs outside of desmosomes may affect disease (3, 28). It was also shown that PVIgG binding induced cytoskeletal changes and the retraction of keratin intermediate filaments before any visible changes in desmosomes (29–33). It was also noted that in early PV lesions keratinocytes first separate at inter-desmosomal areas and desmosomes are still intact and interacting with neighboring desmosomes (29, 34–36). Together, these findings suggested that desmosomal separation may be downstream of other processes induced by the binding of autoAbs. Recently, one research group used AFM to demonstrate that the loss of Dsg3 binding alone was not sufficient to cause a loss of cell adhesion, strongly indicating that steric hindrance by itself cannot sufficiently explain acantholysis in PV (37).

An early alternative to the steric hindrance theory was suggested by results showing that the binding of autoAbs initiated the activation of proteases which in turn degraded Dsg3 and inhibited cell–cell adhesion. Specifically, plasminogen activator was thought to play a role in disease (38). PVIgG was shown to induce signaling that led to increased production of plasminogen activator (39, 40). Furthermore, PVIgG induced keratinocyte expression of plasminogen activator receptor (38, 41). However, inhibition of plasminogen *via* dexamethasone did not prevent PVIgG-induced acantholysis (42). The role of other proteases was also shown not to be essential in disease by the failure of protease inhibitors and gene ablation to prevent blister formation (43, 44).

One of the earliest studies that indicated that autoAbs may exert their pathogenic effect through the activation of intracellular cascades demonstrated that plakoglobin (Pkg)-deficient mice were protected from PVIgG-induced blister formation (45). Pkg, an armadillo family protein, is well established as a major signaling molecule involved in the regulation of cell adhesion (46, 47). The inability of PVIgG to induce blisters in the absence of Pkg strongly suggests that alteration of Pkg signaling is a primary pathogenic mechanism of PVIgG. In addition, keratinocytes incubated at 4°C did not show any effects of PVIgG on cell adhesion, suggesting that the mechanisms underlying blister formation are energy dependent (48).

Identification and characterization of the precise signaling pathways driving autoAb-induced acantholysis has been a significant focus for PV research. As a result, large amounts of (often conflicting) information concerning the signaling alterations downstream of anti-Dsg and PVIgG binding have been characterized. Moreover, studies showing that autoAbs in PV sera directed at non-desmoglein antigens can also elicit intracellular signaling have further complicated efforts to elicit the precise mechanisms driving disease (49, 50). The primary signaling pathways and the evidence that supports their role in PV pathogenesis are reviewed below (see **Table 1** for evidence supporting steric hindrance vs. intracellular signaling).

SIGNALING PATHWAYS IMPLICATED IN PV

p38MAPK

p38 is one of the three major families of mitogen-activated protein kinases (MAPK), which are known to play a prominent role in a wide range of cellular pathways (51). In general, p38MAPK proteins can be activated by environmental stress and regulate the transcription of inflammatory cytokines (52). All MAPKs require dual phosphorylation for enzymatic activity, and each contains a

TABLE 1 | Evidence supporting steric hindrance vs. intracellular signaling.

Evidence supporting the steric hindrance theory
• Desmoglein 3 (Dsg3)/desmoglein 1 (Dsg1), the primary targets of pathogenic autoantibodies (autoAbs), directly mediate cell adhesion
• Enzymatic cleavage of Dsg1 is sufficient to cause a loss of cell adhesion
• Pathogenic anti-Dsg3 autoAbs preferentially target the EC regions thought to mediate trans-adhesion
• Pathogenic anti-Dsg3 autoAbs preferentially recognize Dsg3 in the calcium bound, functional competent conformation
• Anti-Dsg3 autoAbs can access and bind Dsg3 molecules in intact desmosomes
Evidence indicating a role for intracellular signaling
• In PF, a related disease, autoAbs targeting Dsg regions that do not mediate trans-adhesion can induce a loss of cell adhesion
• After exposure to PVIgG, cytoskeletal changes occur before impairment of desmosomal adhesion
• In early pemphigus vulgaris lesions, inter-desmosomal contacts are impaired while desmosomal contacts remain intact
• Studies using atomic force microscopy have shown that blocking of trans-adhesion alone does not induce a loss of cell adhesion
• PVIgG-induced acantholysis is impaired at low temperatures, suggesting an energy requiring process is involved
• Inhibition of multiple signaling pathways can inhibit PVIgG-induced acantholysis both *in vitro* and *in vivo*

characteristic dual phosphorylation sequence which affect both the substrate specificity and ability to auto-phosphorylate (53, 54). There are four types of p38MAPK: α, β, γ, and δ, each displaying unique patterns of tissue expression (52). Only p38MAPK α, β, and δ are known to be expressed in keratinocytes (52, 54–58) and have been primarily associated with differentiation and apoptosis (59).

The significance of p38MAPK signaling in PV pathogenesis was first suggested by a study which observed that PVIgG induced significant increases in the phosphorylation of p38MAPK, MAPKAP2 (MK2), and heat-shock protein (Hsp)27 (60). The degree of phosphorylation was shown to increase when cells were treated with higher concentrations of PVIgG. In addition, treatment of cells with p38MAPK inhibitors was able to prevent PVIgG-induced acantholysis as well as changes in the actin cytoskeleton and the retraction of KIFs from desmosomal attachments, both of which are hallmarks of acantholysis in PV. Inhibition of p38MAPK also prevented PVIgG-induced phosphorylation of MK2, Hsp27, and p38MAPK (60).

Other studies assessing the role of PVIgG on p38MAPK activation identified that PVIgG causes keratin retraction and p38MAPK activation within 30 min, and another peak at 6–10 h in cultured human keratinocytes. Only inhibition at the earlier time point was associated with prevention of blister formation and keratin retraction (61). Another study showed that AK23, a mouse-derived monoclonal anti-Dsg3 antibody, could also activate p38MAPK, demonstrating that autoAb binding to Dsg3 specifically can lead to p38MAPK activation (62).

The relevance of p38MAPK in disease was emphasized by findings that both p38MAPK and Hsp27 are phosphorylated in the lesional skin of PV patients (63). Further studies demonstrated that p38MAPK inhibitor blocks acantholysis *in vivo*, as well as p38MAPK activation, suggesting auto-phosphorylation of p38MAPK (64). p38MAPK activation was also shown to cause Dsg3 internalization, and p38MAPK inhibition can prevent this phenomenon *in vivo* (65). A more detailed assessment of the effects of p38MAPK showed that p38 depletes extra-desmosomal Dsg3 early as 30 min, and also is responsible for later depletion (2–24 h) of other desmosomal cadherins as well as DP (66–70).

The regulation of cytoskeletal changes by p38MAPK is especially relevant in understanding how p38MAPK plays a role in PV pathogenesis. In epithelial cells, cell detachment has been shown to induce p38MAPK activation (71), indicating a close relationship between p38MAPK and cellular adhesion. Furthermore, p38MAPK activation can lead to phosphorylation, and subsequent destabilization of keratin intermediate filaments (72), which could be one explanation for the characteristic retraction of KIFs seen in PV. p38MAPK is known to regulate actin filaments as well (73). Since extra-desmosomal Dsg3 complexes with actin cytoskeleton and is required to bring DP to desmosomal plaques (74, 75), it is possible that PVIgG-induced dysregulation of p38MAPK could interfere with proper desmosome assembly.

MAPKAP2 is phosphorylated and activated by p38MAPK (76, 77). The activation of MK2 has been associated with cell cycle control, cytokine production, and regulation of the keratin and actin cytoskeletons (78–80). The inhibition of MK2 has been shown to prevent PVIgG-induced spontaneous blister formation in mice, but not blistering solicited *via* the application of mechanical stress (81). This suggests that while MK2 may mediate some of the pathogenic effects of PVIgG, additional pathways downstream of p38MAK are likely also contributing to acantholysis.

Heat-shock protein 27 is another signaling molecule activated by MK2 (82). Hsp27 regulates both actin (83–85) and keratin cytoskeleton (86, 87). Both p38MAPK and MK2 regulate the effect of Hsp27 on the cytoskeleton *via* phosphorylation (88–90). Taken together, these findings demonstrate that one possible pathogenic mechanism of PVIgG-induced p38MAPK activation could be the perversion of typical cytoskeletal regulation, resulting in impaired cell adhesion.

The degree of evidence supporting a role for p38MAPK activation in the pathogenesis of PV has led researchers to investigate the utility of p38MAPK inhibition for the clinical treatment of PV. In a small clinical trial, 15 PV patients were treated with KC-706, a small molecule allosteric inhibitor of p38MAPK. Unfortunately, the trial was terminated before completion due to severe side effects of the drug. At the time of cessation, half of the patients were seen to exhibit at least a partial response to treatment, whereas the other half showed no improvement or a worsening of symptoms (91). Hopefully, the development of newer, more specific inhibitors of p38MAPK and other downstream targets will allow for effective pathway inhibition while avoiding serious side effects (92).

In addition to the effects listed above, p38MAPK can affect epidermal growth factor receptor (EGFR) signaling (93), RhoA activation (60, 68, 94, 95), and various apoptotic pathways (96). All of these pathways have been implicated in PV pathogenesis and are discussed in greater detail below.

Calcium/Protein Kinase C (PKC)/ Phospholipase C (PLC)

The role of calcium signaling in keratinocyte differentiation and adhesion is well established. Increasing the Ca^{2+} concentration in keratinocyte culture medium increases intracellular calcium which in turn induces cell–cell contact (mainly adherens junctions) within 5 min, and formation of desmosomes within 2 h (97–104). PLC, an isoenzyme that is responsible for the cleavage of phosphatidylinositol 4,5-bisphosphate (PIP_2) into inositol 1,4,5-triphosphate (IP_3) and diacylglycerol (DAG), plays a significant role in calcium-induced keratinocyte differentiation (103, 105–108). PKC is a downstream target of PLC and is activated by calcium and DAG. Of the five isoforms known to be expressed in keratinocytes, PKC-alpha has been shown to play a major role in epidermal differentiation and proliferation (109–112).

Early studies showing that PVIgG leads to a rapid increase in intracellular calcium in keratinocytes were the first to implicate calcium signaling as a pathogenic signaling pathway in PV (113, 114). Additional studies demonstrated that PKC was activated within 30 s of treatment of PVIgG (115). A significant role for calcium signaling in PV pathogenesis was strengthened by studies which showed inhibition of PKC could prevent acantholysis both *in vitro* and *in vivo* (116, 117). It was also shown that inhibition of PLC prevented PVIgG-induced acantholysis, as well as increases in intracellular calcium and PKC activation (118). These results suggest that PVIgGs may exert their pathogenic effect by eliciting an increase in intracellular calcium, which leads to the activation of downstream signaling pathways.

The identification of PKC as a potential driver of PVIgG-induced pathogenesis is especially interesting due to the well-established role of PKC in cell adhesion. It has been shown that PKC activation leads to weakened cell–cell adhesion, whereas PKC inhibition results in increased adhesion (119, 120). In addition, PKC is known to be required for desmosome assembly and disassembly (41, 97, 121–126). The association of PKC with cell adhesion and desmosomal regulation may provide insight to help identify exactly how PVIgG induced PKC activation results in a loss of cell adhesion. One study showed that PVIgG-induced activation of PKC leads to its dissociation from KIFs and subsequent phosphorylation of DP, which resulted in desmosomal instability (127, 128). Another mechanism through which PKC activation may contribute to disease pathogenesis is by its effect on KIF turnover. It has been shown that PKC directly phosphorylates keratin molecules, leading to a turnover in KIFs (129, 130). This phenomenon may also explain the mechanistic background for the detachment of KIFs which is the hallmark of acantholysis.

Epidermal Growth Factor Receptor

Epidermal growth factor receptor is a well-studied signaling pathway that impacts a multitude of cellular processes either through the direct binding of its ligand, epidermal growth factor, or by cross-activation from a number of other signaling pathways (131–134). EGFR signaling has been shown to impact cell adhesion *via* both adherens junctions and desmosomes (135–137). Specifically, association with Dsg1 has been shown to suppress EGFR extracellular signal-regulated kinase 1/2 signaling in skin (138). In addition, it has been shown that EGFR activation can induce the phosphorylation of Pkg and decrease the association of desmoplakin with the desmosome, resulting in weakened cellular adhesion (139). In general, these studies associate an activation of EGFR signaling with destabilization of desmosomal adhesion.

The association between EGFR signaling and cell adhesion provided a rationale for researchers to investigate if EGFR signaling played a role in acantholysis, and it was eventually shown that PVIgG led to the activation of EGFR in keratinocytes (49, 93). Further studies determined that the activation of EGFR could be detected as early as 30 min after exposure to PVIgG, but the activation occurred downstream of p38MAPK activation (49, 66, 67, 140). Another group was able to show that anti-Dsg3 autoAbs could also lead to EGFR activation (14). Multiple studies then showed that the inhibition of EGFR could prevent PVIgG-induced skin blistering both *in vivo* and in human skin explants (66, 93, 141).

In addition, EGFR is implicated in PV pathogenesis *via* a second signaling axis independent of p38MAPK. PVIgG binding induces secretion of EGF and related mediators from basal keratinocytes, which in turn activate Src, focal adhesion kinase, and mammalian target of rapamycin (mTOR) *via* EGFR and nitric oxide synthase. The end result is the activation of caspases 3 and 9, which have been proposed to contribute to bister formation (142–145). The role for traditional apoptosis in PV pathogenesis is currently unclear; our group showed that the induction of apoptosis-related mechanisms after anti-Dsg antibody binding is reversible and independent of the Fas/FasL axis (146). However, studies showing that inhibition of the low level caspase-3 induction caused by PVIgG prevented acantholysis *in vitro* and *in vivo* suggest that caspase-3 activation does indeed play a role in disease (147).

Rho Family GTPases

Rho and Rac are both members of the Rho small GTPases family, which are known to play a role cytoskeletal reorganization, cell polarity, morphogenesis, and cell migration (61). These Rho family GTPases are known to affect the turnover of adherens junctions through multiple pathways (148). Both Rho and Rac are required for the establishment of adherens junctions (149, 150), and the activation of Rac has also been shown inhibit desmosomal adhesion in human keratinocytes (151).

The first association of Rho GTPases with PV pathogenesis was seen in experiments which demonstrated that the activation of Rho GTPases could prevent PVIgG-induced blister formation in human skin. Additional studies were able to show that RhoA activation was able to block the PVIgG-induced retraction of KIFs as well as loss of cell adhesion in HaCaT cells (41). Also, it was observed that HaCaT cells treated with PVIgG demonstrated a reduction in RhoA activity. In addition, p38MAPK inhibitors were shown to block the PVIgG-induced reduction of RhoA activity (94). These results suggest that PVIgG-induced activation of p38MAPK may induce blister formation, at least in part, by inhibiting the activity of RhoA. Given that the formation of adherens junctions has been shown to be necessary for proper assembly and disassembly of desmosomes (47, 152, 153), the loss

of desmosomal adhesion seen in PV may be secondary to the inhibition of adherens junctions caused by RhoA inhibition.

For a summary of evidence in support of PV-associated signaling pathways, see **Table 2**.

INTEGRATED MODEL OF PV autoAb-INDUCED SIGNALING

The pathogenic processes following the binding of autoAbs that eventually drive the loss of cell adhesion are diverse and complex. Taken together, the above data suggest that the disease mechanisms underlying PV are the result of both the direct steric interference of adhesion molecule interaction by autoAb binding *and* the activation of intracellular signaling pathways elicited *via* autoAb binding. A viewpoint that could tie both these mechanisms together is to see the desmosome/keratin intermediate filament complex as a signaling complex which participates in mechanosensing in addition to providing structural stability. Although desmosomal proteins have not yet been shown to function in this manner, a wealth of data exists which describes a similar function in adherens junctions (154). If this was shown to be the case with desmosomal proteins as well, it would be reasonable to assume that, in addition to physically interfering with desmosomal adhesion, the binding of autoAbs in PV may alter signaling pathways associated with the desmosomal complex, such as p38MAPK, EGFR, and PKC that ultimately interfere with the structural stability of keratinocytes.

Taking into consideration the breadth of experimental data detailing autoAb-induced activation of intracellular signaling pathways, we propose that blister formation in PV may result from the following mechanism: (1) binding of autoAbs to target desmosomal antigens (either desmosomal or extra-desmosomal) induces the activation of PLC, leading to the activation of PKC *via* Ca^{2+} and DAG, which in turn activates p38MAPK *via* MAP3ks [such as Ask1 (155, 156)]; (2) activated PKC (either through direct phosphorylation of keratin filaments or DP) and p38MAPK (*via* MK2 and Hsp27 phosphorylation) then induce the retraction of the KIFs as well as the turnover of the actin cytoskeleton; (3) the retraction of KIFs from the desmosomal plaques, as well as cytoskeletal rearrangements, then cause a destabilization of desmosomes, and a weakening of cell adhesion; (4) finally, the weakening of cell adhesion, coupled with the mechanical stress induced by cytoskeletal rearrangements, induces a cellular stress response, resulting in the activation of Src, EGFR, and Rac1 (as well as other pathways), and re-initiation/perpetuation of the pathological cycle (**Figure 1**).

A primary advantage of this model is the ability to provide a mechanistic framework for understanding how the widely variegated set of factors that have been implicated across multiple studies may be contributing to PV pathogenesis. For example, multiple studies have linked increased levels of reactive oxygen species (ROS) to PV (157–161), but a potential mechanistic contribution to disease has not been well defined. Using our model, however, the known ability of ROS to affect KIF and actin cytoskeletons as well as PKC, Src, p38MAPK, and RhoA signaling (162–167) potentially demonstrates how ROS may contribute to blister formation in a number of ways. As a result, our model can also explain how anti-mitochondrial autoAbs, which have been suggested to play a role in PV and shown to increase ROS production, can directly mediate disease pathogenesis (50, 168–172). Furthermore, the activation of pro-apoptotic pathways by autoAb binding has been shown to modulate p38MAPK (50) and may further contribute to the signaling pathologies that drive acantholysis.

Although this model lays a comprehensive framework for the mechanism of blister formation incorporating all of the major signaling pathways implicated in pathogenesis by the literature, future experiments are required to test the validity of this model and more precisely define the series of signaling events which occur downstream of autoAb binding. Determining the degree to which both desmosomal and extra-desmosomal Dsg proteins associate with signaling molecules and whether or not the binding of autoAbs to these proteins is sufficient to elicit intracellular signaling is a high priority to ascertain if these molecules could function as signal transducers and if so, through which pathways. Immunofluorescent studies of keratinocyte monolayers before and after PVIgG treatment may be one way to determine which molecules are physically associated with desmosomal proteins and determine if autoAb

TABLE 2 | Evidence in support of pemphigus vulgaris (PV)-associated signaling pathways.

p38MAPK	Ca/protein kinase C (PKC)	Epidermal growth factor receptor (EGFR)	Rho GTPases
– PVIgG induces significant increases in the phosphorylation of p38MAPK, MAPKAP2, and heat-shock protein (Hsp)27 – Treatment of cells with p38MAPK inhibitors prevents PVIgG-induced acantholysis as well as changes in the actin cytoskeleton and the retraction of KIFs from desmosomal attachments – Inhibition of p38MAPK prevents PVIgG-induced phosphorylation of MAPKAP2, Hsp27, and p38MAPK *in vivo* – p38MAPK and Hsp27 are phosphorylated in the lesional skin of PV patients	– PVIgG leads to a rapid increase in intracellular calcium in keratinocytes – Inhibition of PKC prevents acantholysis both *in vitro* and *in vivo* – Inhibition of phospholipase C prevents PVIgG-induced acantholysis, as well as increases in intracellular calcium and PKC activation	– PVIgG leads to the activation of EGFR in keratinocytes – Anti-Dsg3 autoantibodies can also lead to EGFR activation – Inhibition of EGFR prevents PVIgG-induced skin blistering both *in vivo* and in human skin explants	– Activation of Rho GTPases prevents PVIgG-induced blister formation in human skin – Cells treated with PVIgG demonstrate a reduction in RhoA activity – p38MAPK inhibitors block PVIgG-induced reduction of RhoA activity – RhoA activation blocks PVIgG-induced retraction of KIFs as well as loss of cell adhesion in HaCaT cells

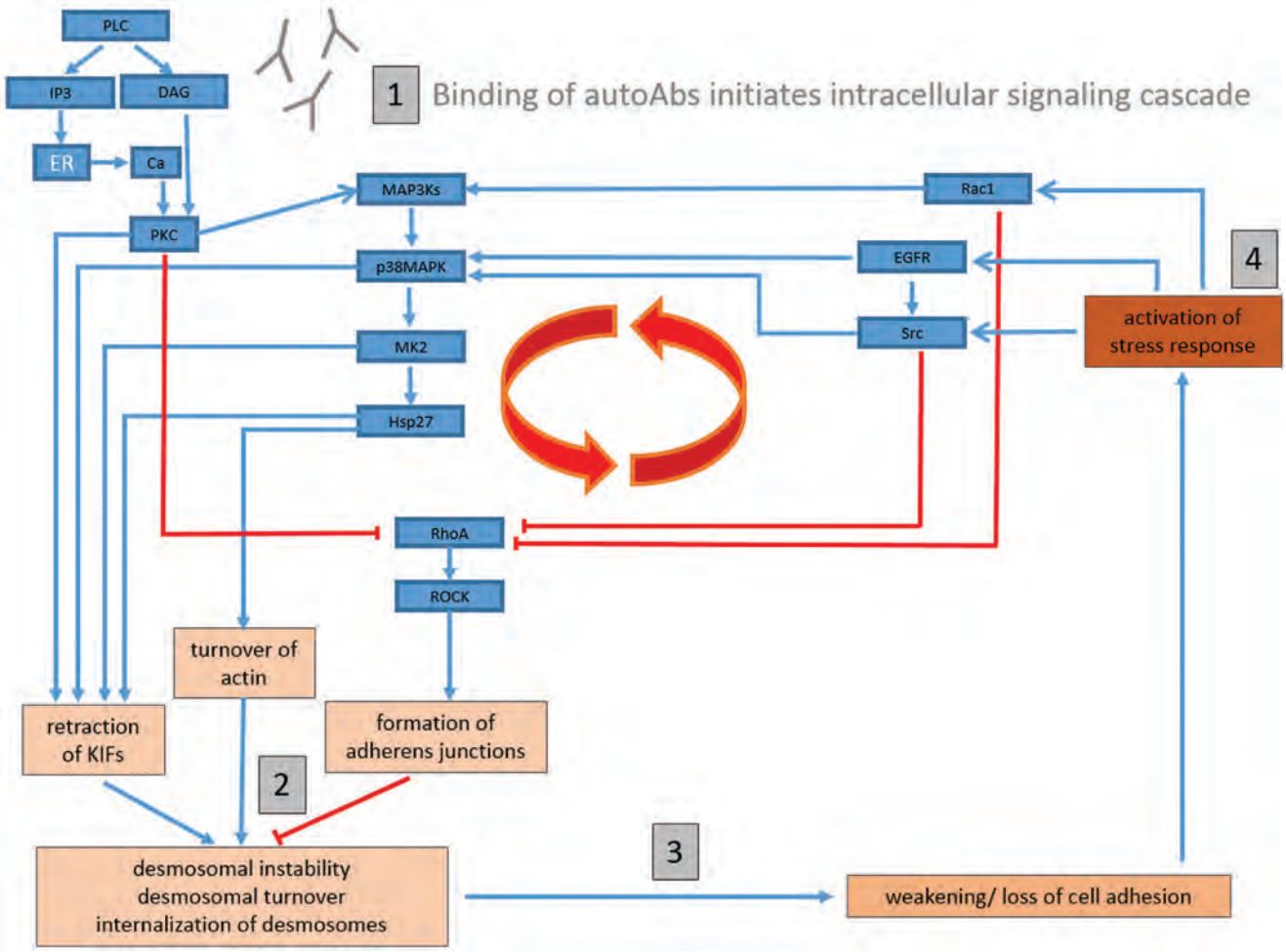

FIGURE 1 | Proposed comprehensive model of signaling mechanisms underlying blister formation in pemphigus vulgaris. (1) Binding of autoantibodies (autoAbs) to target keratinocyte antigens (either desmosomal or extra-desmosomal) induces the activation of phospholipase C (PLC), and subsequently the activation of protein kinase C (PKC) *via* Ca^{2+} and diacylglycerol (DAG), which then activates p38MAPK *via* MAP3ks (such as Ask1); (2) activated PKC {either through direct phosphorylation of keratin filaments or DP} and p38MAPK {*via* MAPKAP2 (MK2) and heat-shock protein (Hsp)27 phosphorylation} then induce the retraction of the KIFs as well as the turnover of the actin cytoskeleton; (3) the retraction of KIFs from the desmosomal plaques, as well as cytoskeletal rearrangements, then cause a destabilization of desmosomes, and a weakening of cell adhesion; (4) finally, the weakening of cell adhesion, coupled with the mechanical stress induced by cytoskeletal rearrangements, induces a cellular stress response, resulting in the activation of Src, epidermal growth factor receptor (EGFR), and Rac1 (as well as other pathways), and re-initiation/perpetuation of the pathological cycle. RhoA is inhibited by multiple pathways (such as PKC, EGFR/Src, and Rac1). As RhoA activation has been shown to inhibit PVIgG-induced acantholysis, an inhibition of RhoA would promote cell dissociation. Blue arrow-headed lines indicate activation, while red bar-headed lines indicate inhibition of selected molecules/pathways.

binding leads to their activation/translocation. Another important step would be to more precisely define the upstream MAPK cascade that leads to p38MAPK activation. There are multiple upstream signaling molecules which are known to activate p38MAPK and the characterization of the molecules involved in this process could allow for a better understanding of how autoAbs, or additional factors such as hormones or cytokines (which are known to utilize specific cascades) could activate p38MAPK (173–175). Protein microarray analysis, which allows for rapid, highly specific, multiplexed analysis of the signal transduction pathways (176, 177), would be well suited for this task.

Desmosomal proteins as a mechanosensing signaling complex would provide a logical intersection between the two primary theories of autoAb-induced blister formation in PV. Although future studies are still needed, there exists a great potential to significantly and directly affect the development of future treatments in PV. Identification of the signals transduced by autoAb binding could lead to the identification of potentially novel drug targets, or, at the very least allow researchers to focus on disease-specific signaling pathologies, resulting in small molecule inhibitors with a lower chance of harmful side effects and the ability to minimize systemic suppression of the immune system. In addition, large scale profiling of the signal

transduction pathways upstream of MAPK may represent an especially beneficial endeavor as such studies could identify cytokines or hormones which may be contributing to disease process. In addition to facilitating the use of disease specific anti-cytokine or hormonal therapies which may already be in use for other disease modalities, such information could be individualized to the specific pathologies driving disease in a given patient, informing more tailored and effective treatment strategies and greatly enhancing clinical management of disease.

AUTHOR CONTRIBUTIONS

AS and TS contributed to the conceptualization and writing of the manuscript.

ACKNOWLEDGMENTS

We thank K. Seiffert-Sinha for critical review of the manuscript. We thank B.K.S. and M.S. for their continued guidance and support.

REFERENCES

1. Amagai M, Klaus-Kovtun V, Stanley JR. Autoantibodies against a novel epithelial cadherin in pemphigus vulgaris, a disease of cell adhesion. *Cell* (1991) 67:869–77. doi:10.1016/0092-8674(91)90360-B
2. Ahmed AR, Carrozzo M, Caux F, Cirillo N, Dmochowski M, Alonso AE, et al. Monopathogenic vs multipathogenic explanations of pemphigus pathophysiology. *Exp Dermatol* (2016) 25:839–46. doi:10.1111/exd.13106
3. Patel HP, Diaz LA, Anhalt GJ, Labib RS, Takahashi Y. Demonstration of pemphigus antibodies on the cell surface of murine epidermal cell monolayers and their internalization. *J Invest Dermatol* (1984) 83:409–15. doi:10.1111/1523-1747.ep12273480
4. Jones JC, Yokoo KM, Goldman RD. Further analysis of pemphigus autoantibodies and their use in studies on the heterogeneity, structure, and function of desmosomes. *J Cell Biol* (1986) 102:1109–17. doi:10.1083/jcb.102.3.1109
5. Amagai M, Matsuyoshi N, Wang ZH, Andl C, Stanley JR. Toxin in bullous impetigo and staphylococcal scalded-skin syndrome targets desmoglein 1. *Nat Med* (2000) 6:1275–7. doi:10.1038/81385
6. Hanakawa Y, Schechter NM, Lin C, Nishifuji K, Amagai M, Stanley JR. Enzymatic and molecular characteristics of the efficiency and specificity of exfoliative toxin cleavage of desmoglein 1. *J Biol Chem* (2004) 279:5268–77. doi:10.1074/jbc.M311087200
7. Koch PJ, Mahoney MG, Ishikawa H, Pulkkinen L, Uitto J, Shultz L, et al. Targeted disruption of the pemphigus vulgaris antigen (desmoglein 3) gene in mice causes loss of keratinocyte cell adhesion with a phenotype similar to pemphigus vulgaris. *J Cell Biol* (1997) 137:1091–102. doi:10.1083/jcb.137.5.1091
8. Shimizu H, Masunaga T, Ishiko A, Kikuchi A, Hashimoto T, Nishikawa T. Pemphigus vulgaris and pemphigus foliaceus sera show an inversely graded binding pattern to extracellular regions of desmosomes in different layers of human epidermis. *J Invest Dermatol* (1995) 105:153–9. doi:10.1111/1523-1747.ep12316695
9. Akiyama M, Hashimoto T, Sugiura M, Nishikawa T. Ultrastructural localization of pemphigus vulgaris and pemphigus foliaceus antigens in cultured human squamous carcinoma cells. *Br J Dermatol* (1991) 125:233–7. doi:10.1111/j.1365-2133.1991.tb14746.x
10. Karpati S, Amagai M, Prussick R, Cehrs K, Stanley JR. Pemphigus vulgaris antigen, a desmoglein type of cadherin, is localized within keratinocyte desmosomes. *J Cell Biol* (1993) 122:409–15. doi:10.1083/jcb.122.2.409
11. Shimizu A, Ishiko A, Ota T, Tsunoda K, Amagai M, Nishikawa T. IgG binds to desmoglein 3 in desmosomes and causes a desmosomal split without keratin retraction in a pemphigus mouse model. *J Invest Dermatol* (2004) 122:1145–53. doi:10.1111/j.0022-202X.2004.22426.x
12. Li N, Aoki V, Hans-Filho G, Rivitti EA, Diaz LA. The role of intramolecular epitope spreading in the pathogenesis of endemic pemphigus foliaceus (fogo selvagem). *J Exp Med* (2003) 197:1501–10. doi:10.1084/jem.20022031
13. Sekiguchi M, Futei Y, Fujii Y, Iwasaki T, Nishikawa T, Amagai M. Dominant autoimmune epitopes recognized by pemphigus antibodies map to the N-terminal adhesive region of desmogleins. *J Immunol* (2001) 167:5439–48. doi:10.4049/jimmunol.167.9.5439
14. Tsunoda K, Ota T, Aoki M, Yamada T, Nagai T, Nakagawa T, et al. Induction of pemphigus phenotype by a mouse monoclonal antibody against the amino-terminal adhesive interface of desmoglein 3. *J Immunol* (2003) 170:2170–8. doi:10.4049/jimmunol.170.4.2170
15. Shapiro L, Fannon AM, Kwong PD, Thompson A, Lehmann MS, Grubel G, et al. Structural basis of cell-cell adhesion by cadherins. *Nature* (1995) 374:327–37. doi:10.1038/374327a0
16. Nagar B, Overduin M, Ikura M, Rini JM. Structural basis of calcium-induced E-cadherin rigidification and dimerization. *Nature* (1996) 380:360–4. doi:10.1038/380360a0
17. Boggon TJ, Murray J, Chappuis-Flament S, Wong E, Gumbiner BM, Shapiro L. C-cadherin ectodomain structure and implications for cell adhesion mechanisms. *Science* (2002) 296:1308–13. doi:10.1126/science.1071559
18. Yokouchi M, Saleh MA, Kuroda K, Hachiya T, Stanley JR, Amagai M, et al. Pathogenic epitopes of autoantibodies in pemphigus reside in the amino-terminal adhesive region of desmogleins which are unmasked by proteolytic processing of prosequence. *J Invest Dermatol* (2009) 129:2156–66. doi:10.1038/jid.2009.61
19. Ozawa M, Kemler R. Correct proteolytic cleavage is required for the cell adhesive function of uvomorulin. *J Cell Biol* (1990) 111:1645–50. doi:10.1083/jcb.111.4.1645
20. Eyre RW, Stanley JR. Human autoantibodies against a desmosomal protein complex with a calcium-sensitive epitope are characteristic of pemphigus foliaceus patients. *J Exp Med* (1987) 165:1719–24. doi:10.1084/jem.165.6.1719
21. Kamiya K, Aoyama Y, Shirafuji Y, Hamada T, Morizane S, Fujii K, et al. A higher correlation of the antibody activities against the calcium-dependent epitopes of desmoglein 3 quantified by ethylenediaminetetraacetic acid-treated enzyme-linked immunosorbent assay with clinical disease activities of pemphigus vulgaris. *J Dermatol Sci* (2013) 70:190–5. doi:10.1016/j.jdermsci.2013.02.011
22. Heupel WM, Zillikens D, Drenckhahn D, Waschke J. Pemphigus vulgaris IgG directly inhibit desmoglein 3-mediated transinteraction. *J Immunol* (2008) 181:1825–34. doi:10.4049/jimmunol.181.3.1825
23. Anhalt GJ, Till GO, Diaz LA, Labib RS, Patel HP, Eaglstein NF. Defining the role of complement in experimental pemphigus vulgaris in mice. *J Immunol* (1986) 137:2835–40.
24. Mascaro JM Jr, Espana A, Liu Z, Ding X, Swartz SJ, Fairley JA, et al. Mechanisms of acantholysis in pemphigus vulgaris: role of IgG valence. *Clin Immunol Immunopathol* (1997) 85:90–6. doi:10.1006/clin.1997.4408
25. Payne AS, Ishii K, Kacir S, Lin C, Li H, Hanakawa Y, et al. Genetic and functional characterization of human pemphigus vulgaris monoclonal autoantibodies isolated by phage display. *J Clin Invest* (2005) 115:888–99. doi:10.1172/JCI24185
26. Rock B, Labib RS, Diaz LA. Monovalent Fab' immunoglobulin fragments from endemic pemphigus foliaceus autoantibodies reproduce the human disease in neonatal Balb/c mice. *J Clin Invest* (1990) 85:296–9. doi:10.1172/JCI114426
27. Waschke J, Bruggeman P, Baumgartner W, Zillikens D, Drenckhahn D. Pemphigus foliaceus IgG causes dissociation of desmoglein 1-containing junctions without blocking desmoglein 1 transinteraction. *J Clin Invest* (2005) 115:3157–65. doi:10.1172/JCI23475
28. Bedane C, Prost C, Thomine E, Intrator L, Joly P, Caux F, et al. Binding of autoantibodies is not restricted to desmosomes in pemphigus vulgaris: comparison of 14 cases of pemphigus vulgaris and 10 cases of pemphigus foliaceus studied by western immunoblot and immunoelectron microscopy. *Arch Dermatol Res* (1996) 288:343–52.
29. Wilgram GF, Caulfield JB, Lever WF. An electron microscopic study of acantholysis in pemphigus vulgaris. *J Invest Dermatol* (1961) 36:373–82. doi:10.1038/jid.1961.58

30. Baroni A, Buommino E, Paoletti I, Orlando M, Ruocco E, Ruocco V. Pemphigus serum and captopril induce heat shock protein 70 and inducible nitric oxide synthase overexpression, triggering apoptosis in human keratinocytes. *Br J Dermatol* (2004) 150:1070–80. doi:10.1111/j.1365-2133.2004.05919.x
31. Jinbu Y, Kitajima Y, Koto S, Akasaka Y, Yaoita H. Different effects of pemphigus antibody and plasmin on the distribution of keratin intermediate filaments and desmoplakins between cultured oral and epidermal keratinocytes. *J Dermatol Sci* (1992) 3:6–12. doi:10.1016/0923-1811(92)90003-T
32. Kitajima Y, Inoue S, Yaoita H. Effects of pemphigus antibody on the organization of microtubules and keratin-intermediate filaments in cultured human keratinocytes. *Br J Dermatol* (1986) 114:171–9. doi:10.1111/j.1365-2133.1986.tb02795.x
33. Lever WF. *Pemphigus and Pemphigoid*. Springfield, IL: Thomas (1965).
34. Hashimoto K, Lever WF. An electron microscopic study on pemphigus vulgaris of the mouth and the skin with special reference to the intercellular cement. *J Invest Dermatol* (1967) 48:540–52. doi:10.1038/jid.1967.86
35. Hashimoto K, Lever WF. The intercellular cement in pemphigus vulgaris, an electron microscopic study. *Dermatologica* (1967) 135:27–34. doi:10.1159/000254157
36. Sams WM Jr, Gammon WR. Mechanism of lesion production in pemphigus and pemphigoid. *J Am Acad Dermatol* (1982) 6:431–52. doi:10.1016/S0190-9622(82)70036-2
37. Vielmuth F, Waschke J, Spindler V. Loss of desmoglein binding is not sufficient for keratinocyte dissociation in pemphigus. *J Invest Dermatol* (2015) 135:3068–77. doi:10.1038/jid.2015.324
38. Hashimoto K, Shafran KM, Webber PS, Lazarus GS, Singer KH. Anti-cell surface pemphigus autoantibody stimulates plasminogen activator activity of human epidermal cells. A mechanism for the loss of epidermal cohesion and blister formation. *J Exp Med* (1983) 157:259–72. doi:10.1084/jem.157.1.259
39. Schaefer BM, Jaeger CJ, Kramer MD. Plasminogen activator system in pemphigus vulgaris. *Br J Dermatol* (1996) 135:726–32. doi:10.1046/j.1365-2133.1996.d01-1070.x
40. Feliciani C, Toto P, Wang B, Sauder DN, Amerio P, Tulli A. Urokinase plasminogen activator mRNA is induced by IL-1alpha and TNF-alpha in in vitro acantholysis. *Exp Dermatol* (2003) 12:466–71. doi:10.1034/j.1600-0625.2002.120415.x
41. Seishima M, Satoh S, Nojiri M, Osada K, Kitajima Y. Pemphigus IgG induces expression of urokinase plasminogen activator receptor on the cell surface of cultured keratinocytes. *J Invest Dermatol* (1997) 109:650–5. doi:10.1111/1523-1747.ep12337662
42. Anhalt GJ, Patel HP, Labib RS, Diaz LA, Proud D. Dexamethasone inhibits plasminogen activator activity in experimental pemphigus in vivo but does not block acantholysis. *J Immunol* (1986) 136:113–7.
43. Schuh T, Besch R, Braungart E, Flaig MJ, Douwes K, Sander CA, et al. Protease inhibitors prevent plasminogen-mediated, but not pemphigus vulgaris-induced, acantholysis in human epidermis. *Biol Chem* (2003) 384:311–5. doi:10.1515/BC.2003.035
44. Mahoney MG, Wang ZH, Stanley JR. Pemphigus vulgaris and pemphigus foliaceus antibodies are pathogenic in plasminogen activator knockout mice. *J Invest Dermatol* (1999) 113:22–5. doi:10.1046/j.1523-1747.1999.00632.x
45. Caldelari R, de Bruin A, Baumann D, Suter MM, Bierkamp C, Balmer V, et al. A central role for the armadillo protein plakoglobin in the autoimmune disease pemphigus vulgaris. *J Cell Biol* (2001) 153:823–34. doi:10.1083/jcb.153.4.823
46. Zhurinsky J, Shtutman M, Ben-Ze'ev A. Plakoglobin and beta-catenin: protein interactions, regulation and biological roles. *J Cell Sci* (2000) 113(Pt 18):3127–39.
47. Getsios S, Huen AC, Green KJ. Working out the strength and flexibility of desmosomes. *Nat Rev Mol Cell Biol* (2004) 5:271–81. doi:10.1038/nrm1356
48. Calkins CC, Setzer SV, Jennings JM, Summers S, Tsunoda K, Amagai M, et al. Desmoglein endocytosis and desmosome disassembly are coordinated responses to pemphigus autoantibodies. *J Biol Chem* (2006) 281:7623–34. doi:10.1074/jbc.M512447200
49. Chernyavsky AI, Arredondo J, Kitajima Y, Sato-Nagai M, Grando SA. Desmoglein versus non-desmoglein signaling in pemphigus acantholysis: characterization of novel signaling pathways downstream of pemphigus vulgaris antigens. *J Biol Chem* (2007) 282:13804–12. doi:10.1074/jbc.M611365200
50. Marchenko S, Chernyavsky AI, Arredondo J, Gindi V, Grando SA. Antimitochondrial autoantibodies in pemphigus vulgaris: a missing link in disease pathophysiology. *J Biol Chem* (2010) 285:3695–704. doi:10.1074/jbc.M109.081570
51. Johnson GL, Lapadat R. Mitogen-activated protein kinase pathways mediated by ERK, JNK, and p38 protein kinases. *Science* (2002) 298:1911–2. doi:10.1126/science.1072682
52. Dashti SR, Efimova T, Eckert RL. MEK7-dependent activation of p38 MAP kinase in keratinocytes. *J Biol Chem* (2001) 276:8059–63. doi:10.1074/jbc.C000862200
53. Hanks SK, Hunter T. Protein kinases 6. The eukaryotic protein kinase superfamily: kinase (catalytic) domain structure and classification. *FASEB J* (1995) 9:576–96. doi:10.1096/fasebj.9.8.7768349
54. Han J, Lee JD, Jiang Y, Li Z, Feng L, Ulevitch RJ. Characterization of the structure and function of a novel MAP kinase kinase (MKK6). *J Biol Chem* (1996) 271:2886–91. doi:10.1074/jbc.271.6.2886
55. Lechner C, Zahalka MA, Giot JF, Moller NP, Ullrich A. ERK6, a mitogen-activated protein kinase involved in C2C12 myoblast differentiation. *Proc Natl Acad Sci U S A* (1996) 93:4355–9. doi:10.1073/pnas.93.9.4355
56. Li Z, Jiang Y, Ulevitch RJ, Han J. The primary structure of p38 gamma: a new member of p38 group of MAP kinases. *Biochem Biophys Res Commun* (1996) 228:334–40. doi:10.1006/bbrc.1996.1662
57. Court NW, dos Remedios CG, Cordell J, Bogoyevitch MA. Cardiac expression and subcellular localization of the p38 mitogen-activated protein kinase member, stress-activated protein kinase-3 (SAPK3). *J Mol Cell Cardiol* (2002) 34:413–26. doi:10.1006/jmcc.2001.1523
58. Kumar S, McDonnell PC, Gum RJ, Hand AT, Lee JC, Young PR. Novel homologues of CSBP/p38 MAP kinase: activation, substrate specificity and sensitivity to inhibition by pyridinyl imidazoles. *Biochem Biophys Res Commun* (1997) 235:533–8. doi:10.1006/bbrc.1997.6849
59. Eckert RL, Efimova T, Dashti SR, Balasubramanian S, Deucher A, Crish JF, et al. Keratinocyte survival, differentiation, and death: many roads lead to mitogen-activated protein kinase. *J Investig Dermatol Symp Proc* (2002) 7:36–40. doi:10.1046/j.1523-1747.2002.19634.x
60. Berkowitz P, Hu P, Liu Z, Diaz LA, Enghild JJ, Chua MP, et al. Desmosome signaling. Inhibition of p38MAPK prevents pemphigus vulgaris IgG-induced cytoskeleton reorganization. *J Biol Chem* (2005) 280:23778–84. doi:10.1074/jbc.M501365200
61. Lee HE, Berkowitz P, Jolly PS, Diaz LA, Chua MP, Rubenstein DS. Biphasic activation of p38MAPK suggests that apoptosis is a downstream event in pemphigus acantholysis. *J Biol Chem* (2009) 284:12524–32. doi:10.1074/jbc.M808204200
62. Kawasaki Y, Aoyama Y, Tsunoda K, Amagai M, Kitajima Y. Pathogenic monoclonal antibody against desmoglein 3 augments desmoglein 3 and p38 MAPK phosphorylation in human squamous carcinoma cell line. *Autoimmunity* (2006) 39:587–90. doi:10.1080/08916930600971943
63. Berkowitz P, Diaz LA, Hall RP, Rubenstein DS. Induction of p38MAPK and HSP27 phosphorylation in pemphigus patient skin. *J Invest Dermatol* (2008) 128:738–40. doi:10.1038/sj.jid.5701080
64. Berkowitz P, Hu P, Warren S, Liu Z, Diaz LA, Rubenstein DS. p38MAPK inhibition prevents disease in pemphigus vulgaris mice. *Proc Natl Acad Sci U S A* (2006) 103:12855–60. doi:10.1073/pnas.0602973103
65. Jolly PS, Berkowitz P, Bektas M, Lee HE, Chua M, Diaz LA, et al. p38MAPK signaling and desmoglein-3 internalization are linked events in pemphigus acantholysis. *J Biol Chem* (2010) 285:8936–41. doi:10.1074/jbc.M109.087999
66. Saito M, Stahley SN, Caughman CY, Mao X, Tucker DK, Payne AS, et al. Signaling dependent and independent mechanisms in pemphigus vulgaris blister formation. *PLoS One* (2012) 7:e50696. doi:10.1371/journal.pone.0050696
67. Schulze K, Galichet A, Sayar BS, Scothern A, Howald D, Zymann H, et al. An adult passive transfer mouse model to study desmoglein 3 signaling in pemphigus vulgaris. *J Invest Dermatol* (2012) 132:346–55. doi:10.1038/jid.2011.299
68. Mao X, Choi EJ, Payne AS. Disruption of desmosome assembly by monovalent human pemphigus vulgaris monoclonal antibodies. *J Invest Dermatol* (2009) 129:908–18. doi:10.1038/jid.2008.339
69. Jennings JM, Tucker DK, Kottke MD, Saito M, Delva E, Hanakawa Y, et al. Desmosome disassembly in response to pemphigus vulgaris IgG occurs in distinct phases and can be reversed by expression of exogenous Dsg3. *J Invest Dermatol* (2011) 131:706–18. doi:10.1038/jid.2010.389

70. Oktarina DA, van der Wier G, Diercks GF, Jonkman MF, Pas HH. IgG-induced clustering of desmogleins 1 and 3 in skin of patients with pemphigus fits with the desmoglein nonassembly depletion hypothesis. *Br J Dermatol* (2011) 165:552–62. doi:10.1111/j.1365-2133.2011.10463.x
71. Rosen K, Shi W, Calabretta B, Filmus J. Cell detachment triggers p38 mitogen-activated protein kinase-dependent overexpression of Fas ligand. A novel mechanism of anoikis of intestinal epithelial cells. *J Biol Chem* (2002) 277:46123–30. doi:10.1074/jbc.M207883200
72. Ku NO, Azhar S, Omary MB. Keratin 8 phosphorylation by p38 kinase regulates cellular keratin filament reorganization: modulation by a keratin 1-like disease causing mutation. *J Biol Chem* (2002) 277:10775–82. doi:10.1074/jbc.M107623200
73. Gliem M, Heupel WM, Spindler V, Harms GS, Waschke J. Actin reorganization contributes to loss of cell adhesion in pemphigus vulgaris. *Am J Physiol Cell Physiol* (2010) 299:C606–13. doi:10.1152/ajpcell.00075.2010
74. Tsang SM, Brown L, Gadmor H, Gammon L, Fortune F, Wheeler A, et al. Desmoglein 3 acting as an upstream regulator of Rho GTPases, Rac-1/Cdc42 in the regulation of actin organisation and dynamics. *Exp Cell Res* (2012) 318:2269–83. doi:10.1016/j.yexcr.2012.07.002
75. Godsel LM, Dubash AD, Bass-Zubek AE, Amargo EV, Klessner JL, Hobbs RP, et al. Plakophilin 2 couples actomyosin remodeling to desmosomal plaque assembly via RhoA. *Mol Biol Cell* (2010) 21:2844–59. doi:10.1091/mbc.E10-02-0131
76. Freshney NW, Rawlinson L, Guesdon F, Jones E, Cowley S, Hsuan J, et al. Interleukin-1 activates a novel protein kinase cascade that results in the phosphorylation of Hsp27. *Cell* (1994) 78:1039–49. doi:10.1016/0092-8674(94)90278-X
77. Rouse J, Cohen P, Trigon S, Morange M, Alonso-Llamazares A, Zamanillo D, et al. A novel kinase cascade triggered by stress and heat shock that stimulates MAPKAP kinase-2 and phosphorylation of the small heat shock proteins. *Cell* (1994) 78:1027–37. doi:10.1016/0092-8674(94)90277-1
78. Han J, Lee JD, Bibbs L, Ulevitch RJ. A MAP kinase targeted by endotoxin and hyperosmolarity in mammalian cells. *Science* (1994) 265:808–11. doi:10.1126/science.7914033
79. Piotrowicz RS, Hickey E, Levin EG. Heat shock protein 27 kDa expression and phosphorylation regulates endothelial cell migration. *FASEB J* (1998) 12:1481–90. doi:10.1096/fasebj.12.14.1481
80. Rousseau S, Houle F, Landry J, Huot J. p38 MAP kinase activation by vascular endothelial growth factor mediates actin reorganization and cell migration in human endothelial cells. *Oncogene* (1997) 15:2169–77. doi:10.1038/sj.onc.1201380
81. Mao X, Li H, Sano Y, Gaestel M, Mo Park J, Payne AS. MAPKAP kinase 2 (MK2)-dependent and -independent models of blister formation in pemphigus vulgaris. *J Invest Dermatol* (2014) 134:68–76. doi:10.1038/jid.2013.224
82. Rogalla T, Ehrnsperger M, Preville X, Kotlyarov A, Lutsch G, Ducasse C, et al. Regulation of Hsp27 oligomerization, chaperone function, and protective activity against oxidative stress/tumor necrosis factor alpha by phosphorylation. *J Biol Chem* (1999) 274:18947–56. doi:10.1074/jbc.274.27.18947
83. Benndorf R, Hayess K, Ryazantsev S, Wieske M, Behlke J, Lutsch G. Phosphorylation and supramolecular organization of murine small heat shock protein HSP25 abolish its actin polymerization-inhibiting activity. *J Biol Chem* (1994) 269:20780–4.
84. Geum D, Son GH, Kim K. Phosphorylation-dependent cellular localization and thermoprotective role of heat shock protein 25 in hippocampal progenitor cells. *J Biol Chem* (2002) 277:19913–21. doi:10.1074/jbc.M104396200
85. Panasenko OO, Kim MV, Marston SB, Gusev NB. Interaction of the small heat shock protein with molecular mass 25 kDa (hsp25) with actin. *Eur J Biochem* (2003) 270:892–901. doi:10.1046/j.1432-1033.2003.03449.x
86. Perng MD, Cairns L, van den IP, Prescott A, Hutcheson AM, Quinlan RA. Intermediate filament interactions can be altered by HSP27 and alphaB-crystallin. *J Cell Sci* (1999) 112(Pt 13):2099–112.
87. Evgrafov OV, Mersiyanova I, Irobi J, Van Den Bosch L, Dierick I, Leung CL, et al. Mutant small heat-shock protein 27 causes axonal Charcot-Marie-Tooth disease and distal hereditary motor neuropathy. *Nat Genet* (2004) 36:602–6. doi:10.1038/ng1354
88. Guay J, Lambert H, Gingras-Breton G, Lavoie JN, Huot J, Landry J. Regulation of actin filament dynamics by p38 map kinase-mediated phosphorylation of heat shock protein 27. *J Cell Sci* (1997) 110(Pt 3):357–68.
89. Lavoie JN, Hickey E, Weber LA, Landry J. Modulation of actin microfilament dynamics and fluid phase pinocytosis by phosphorylation of heat shock protein 27. *J Biol Chem* (1993) 268:24210–4.
90. Lavoie JN, Lambert H, Hickey E, Weber LA, Landry J. Modulation of cellular thermoresistance and actin filament stability accompanies phosphorylation-induced changes in the oligomeric structure of heat shock protein 27. *Mol Cell Biol* (1995) 15:505–16. doi:10.1128/MCB.15.1.505
91. Schultz HY, Diaz LA, Sirois DA, Werth VP, Grando SA. Generating consensus research goals and treatment strategies for pemphigus and pemphigoid: the 2010 JC Bystryn Pemphigus and Pemphigoid Meeting. *J Invest Dermatol* (2011) 131:1395–9. doi:10.1038/jid.2011.120
92. Cohen P. Targeting protein kinases for the development of anti-inflammatory drugs. *Curr Opin Cell Biol* (2009) 21:317–24. doi:10.1016/j.ceb.2009.01.015
93. Bektas M, Jolly PS, Berkowitz P, Amagai M, Rubenstein DS. A pathophysiologic role for epidermal growth factor receptor in pemphigus acantholysis. *J Biol Chem* (2013) 288:9447–56. doi:10.1074/jbc.M112.438010
94. Waschke J, Spindler V, Bruggeman P, Zillikens D, Schmidt G, Drenckhahn D. Inhibition of Rho A activity causes pemphigus skin blistering. *J Cell Biol* (2006) 175:721–7. doi:10.1083/jcb.200605125
95. Spindler V, Rotzer V, Dehner C, Kempf B, Gliem M, Radeva M, et al. Peptide-mediated desmoglein 3 crosslinking prevents pemphigus vulgaris autoantibody-induced skin blistering. *J Clin Invest* (2013) 123:800–11. doi:10.1172/JCI60139
96. Wu NL, Lee TA, Tsai TL, Lin WW. TRAIL-induced keratinocyte differentiation requires caspase activation and p63 expression. *J Invest Dermatol* (2011) 131:874–83. doi:10.1038/jid.2010.402
97. Sheu HM, Kitajima Y, Yaoita H. Involvement of protein kinase C in translocation of desmoplakins from cytosol to plasma membrane during desmosome formation in human squamous cell carcinoma cells grown in low to normal calcium concentration. *Exp Cell Res* (1989) 185:176–90. doi:10.1016/0014-4827(89)90047-5
98. Kitajima Y, Aoyama Y, Seishima M. Transmembrane signaling for adhesive regulation of desmosomes and hemidesmosomes, and for cell-cell datachment induced by pemphigus IgG in cultured keratinocytes: involvement of protein kinase C. *J Investig Dermatol Symp Proc* (1999) 4:137–44. doi:10.1038/sj.jidsp.5640197
99. Sharpe GR, Gillespie JI, Greenwell JR. An increase in intracellular free calcium is an early event during differentiation of cultured human keratinocytes. *FEBS Lett* (1989) 254:25–8. doi:10.1016/0014-5793(89)81002-6
100. Tu CL, Oda Y, Bikle DD. Effects of a calcium receptor activator on the cellular response to calcium in human keratinocytes. *J Invest Dermatol* (1999) 113:340–5. doi:10.1046/j.1523-1747.1999.00698.x
101. Oda Y, Tu CL, Chang W, Crumrine D, Komuves L, Mauro T, et al. The calcium sensing receptor and its alternatively spliced form in murine epidermal differentiation. *J Biol Chem* (2000) 275:1183–90. doi:10.1074/jbc.275.2.1183
102. Tu CL, Chang W, Bikle DD. The extracellular calcium-sensing receptor is required for calcium-induced differentiation in human keratinocytes. *J Biol Chem* (2001) 276:41079–85. doi:10.1074/jbc.M107122200
103. Xie Z, Bikle DD. The recruitment of phosphatidylinositol 3-kinase to the E-cadherin-catenin complex at the plasma membrane is required for calcium-induced phospholipase C-gamma1 activation and human keratinocyte differentiation. *J Biol Chem* (2007) 282:8695–703. doi:10.1074/jbc.M609135200
104. Berridge MJ, Irvine RF. Inositol trisphosphate, a novel second messenger in cellular signal transduction. *Nature* (1984) 312:315–21. doi:10.1038/312315a0
105. Punnonen K, Denning M, Lee E, Li L, Rhee SG, Yuspa SH. Keratinocyte differentiation is associated with changes in the expression and regulation of phospholipase C isoenzymes. *J Invest Dermatol* (1993) 101:719–26. doi:10.1111/1523-1747.ep12371682
106. Homma Y, Emori Y, Shibasaki F, Suzuki K, Takenawa T. Isolation and characterization of a gamma-type phosphoinositide-specific phospholipase C (PLC-gamma 2). *Biochem J* (1990) 269:13–8. doi:10.1042/bj2690013
107. Meldrum E, Parker PJ, Carozzi A. The PtdIns-PLC superfamily and signal transduction. *Biochim Biophys Acta* (1991) 1092:49–71. doi:10.1016/0167-4889(91)90177-Y
108. Suh PG, Ryu SH, Choi WC, Lee KY, Rhee SG. Monoclonal antibodies to three phospholipase C isozymes from bovine brain. *J Biol Chem* (1988) 263:14497–504.

109. Cataisson C, Joseloff E, Murillas R, Wang A, Atwell C, Torgerson S, et al. Activation of cutaneous protein kinase C alpha induces keratinocyte apoptosis and intraepidermal inflammation by independent signaling pathways. *J Immunol* (2003) 171:2703–13. doi:10.4049/jimmunol.171.5.2703
110. Hara T, Saito Y, Hirai T, Nakamura K, Nakao K, Katsuki M, et al. Deficiency of protein kinase Calpha in mice results in impairment of epidermal hyperplasia and enhancement of tumor formation in two-stage skin carcinogenesis. *Cancer Res* (2005) 65:7356–62. doi:10.1158/0008-5472.CAN-04-4241
111. Wang HQ, Smart RC. Overexpression of protein kinase C-alpha in the epidermis of transgenic mice results in striking alterations in phorbol ester-induced inflammation and COX-2, MIP-2 and TNF-alpha expression but not tumor promotion. *J Cell Sci* (1999) 112(Pt 20):3497–506.
112. Jansen AP, Dreckschmidt NE, Verwiebe EG, Wheeler DL, Oberley TD, Verma AK. Relation of the induction of epidermal ornithine decarboxylase and hyperplasia to the different skin tumor-promotion susceptibilities of protein kinase C alpha, -delta and -epsilon transgenic mice. *Int J Cancer* (2001) 93:635–43. doi:10.1002/ijc.1395
113. Lyubimov H, Goldshmit D, Michel B, Oron Y, Milner Y. Pemphigus – identifying the autoantigen and its possible induction of epidermal acantholysis via Ca^{2+} signalling. *Isr J Med Sci* (1995) 31:42–8.
114. Seishima M, Esaki C, Osada K, Mori S, Hashimoto T, Kitajima Y. Pemphigus IgG, but not bullous pemphigoid IgG, causes a transient increase in intracellular calcium and inositol 1,4,5-triphosphate in DJM-1 cells, a squamous cell carcinoma line. *J Invest Dermatol* (1995) 104:33–7. doi:10.1111/1523-1747.ep12613469
115. Kitajima Y. New insights into desmosome regulation and pemphigus blistering as a desmosome-remodeling disease. *Kaohsiung J Med Sci* (2013) 29:1–13. doi:10.1016/j.kjms.2012.08.001
116. Cirillo N, Lanza A, Prime SS. Induction of hyper-adhesion attenuates autoimmune-induced keratinocyte cell-cell detachment and processing of adhesion molecules via mechanisms that involve PKC. *Exp Cell Res* (2010) 316:580–92. doi:10.1016/j.yexcr.2009.10.005
117. Spindler V, Endlich A, Hartlieb E, Vielmuth F, Schmidt E, Waschke J. The extent of desmoglein 3 depletion in pemphigus vulgaris is dependent on $Ca^{(2+)}$-induced differentiation: a role in suprabasal epidermal skin splitting? *Am J Pathol* (2011) 179:1905–16. doi:10.1016/j.ajpath.2011.06.043
118. Esaki C, Seishima M, Yamada T, Osada K, Kitajima Y. Pharmacologic evidence for involvement of phospholipase C in pemphigus IgG-induced inositol 1,4,5-trisphosphate generation, intracellular calcium increase, and plasminogen activator secretion in DJM-1 cells, a squamous cell carcinoma line. *J Invest Dermatol* (1995) 105:329–33. doi:10.1111/1523-1747.ep12319948
119. Kimura TE, Merritt AJ, Garrod DR. Calcium-independent desmosomes of keratinocytes are hyper-adhesive. *J Invest Dermatol* (2007) 127:775–81. doi:10.1038/sj.jid.5700643
120. Hobbs RP, Amargo EV, Somasundaram A, Simpson CL, Prakriya M, Denning MF, et al. The calcium ATPase SERCA2 regulates desmoplakin dynamics and intercellular adhesive strength through modulation of PKCα signaling. *FASEB J* (2011) 25:990–1001. doi:10.1096/fj.10-163261
121. Godsel LM, Hsieh SN, Amargo EV, Bass AE, Pascoe-McGillicuddy LT, Huen AC, et al. Desmoplakin assembly dynamics in four dimensions: multiple phases differentially regulated by intermediate filaments and actin. *J Cell Biol* (2005) 171:1045–59. doi:10.1083/jcb.200510038
122. Bass-Zubek AE, Hobbs RP, Amargo EV, Garcia NJ, Hsieh SN, Chen X, et al. Plakophilin 2: a critical scaffold for PKC alpha that regulates intercellular junction assembly. *J Cell Biol* (2008) 181:605–13. doi:10.1083/jcb.200712133
123. Thomason HA, Cooper NH, Ansell DM, Chiu M, Merrit AJ, Hardman MJ, et al. Direct evidence that PKCalpha positively regulates wound re-epithelialization: correlation with changes in desmosomal adhesiveness. *J Pathol* (2012) 227:346–56. doi:10.1002/path.4016
124. Wallis S, Lloyd S, Wise I, Ireland G, Fleming TP, Garrod D. The alpha isoform of protein kinase C is involved in signaling the response of desmosomes to wounding in cultured epithelial cells. *Mol Biol Cell* (2000) 11:1077–92. doi:10.1091/mbc.11.3.1077
125. Osada K, Seishima M, Kitajima Y. Pemphigus IgG activates and translocates protein kinase C from the cytosol to the particulate/cytoskeleton fractions in human keratinocytes. *J Invest Dermatol* (1997) 108:482–7. doi:10.1111/1523-1747.ep12289726
126. Aoyama Y, Yamamoto Y, Yamaguchi F, Kitajima Y. Low to high Ca^{2+}-switch causes phosphorylation and association of desmocollin 3 with plakoglobin and desmoglein 3 in cultured keratinocytes. *Exp Dermatol* (2009) 18:404–8. doi:10.1111/j.1600-0625.2008.00814.x
127. Kroger C, Loschke F, Schwarz N, Windoffer R, Leube RE, Magin TM. Keratins control intercellular adhesion involving PKC-alpha-mediated desmoplakin phosphorylation. *J Cell Biol* (2013) 201:681–92. doi:10.1083/jcb.201208162
128. Hobbs RP, Green KJ. Desmoplakin regulates desmosome hyperadhesion. *J Invest Dermatol* (2012) 132:482–5. doi:10.1038/jid.2011.318
129. Sivaramakrishnan S, Schneider JL, Sitikov A, Goldman RD, Ridge KM. Shear stress induced reorganization of the keratin intermediate filament network requires phosphorylation by protein kinase C zeta. *Mol Biol Cell* (2009) 20:2755–65. doi:10.1091/mbc.E08-10-1028
130. Ridge KM, Linz L, Flitney FW, Kuczmarski ER, Chou YH, Omary MB, et al. Keratin 8 phosphorylation by protein kinase C delta regulates shear stress-mediated disassembly of keratin intermediate filaments in alveolar epithelial cells. *J Biol Chem* (2005) 280:30400–5. doi:10.1074/jbc.M504239200
131. Hackel PO, Zwick E, Prenzel N, Ullrich A. Epidermal growth factor receptors: critical mediators of multiple receptor pathways. *Curr Opin Cell Biol* (1999) 11:184–9. doi:10.1016/S0955-0674(99)80024-6
132. Keely SJ, Uribe JM, Barrett KE. Carbachol stimulates transactivation of epidermal growth factor receptor and mitogen-activated protein kinase in T84 cells. Implications for carbachol-stimulated chloride secretion. *J Biol Chem* (1998) 273:27111–7. doi:10.1074/jbc.273.42.27111
133. Li X, Lee JW, Graves LM, Earp HS. Angiotensin II stimulates ERK via two pathways in epithelial cells: protein kinase C suppresses a G-protein coupled receptor-EGF receptor transactivation pathway. *EMBO J* (1998) 17:2574–83. doi:10.1093/emboj/17.9.2574
134. Tsai W, Morielli AD, Peralta EG. The m1 muscarinic acetylcholine receptor transactivates the EGF receptor to modulate ion channel activity. *EMBO J* (1997) 16:4597–605. doi:10.1093/emboj/16.15.4597
135. Hoschuetzky H, Aberle H, Kemler R. Beta-catenin mediates the interaction of the cadherin-catenin complex with epidermal growth factor receptor. *J Cell Biol* (1994) 127:1375–80. doi:10.1083/jcb.127.5.1375
136. Yin T, Getsios S, Caldelari R, Godsel LM, Kowalczyk AP, Muller EJ, et al. Mechanisms of plakoglobin-dependent adhesion: desmosome-specific functions in assembly and regulation by epidermal growth factor receptor. *J Biol Chem* (2005) 280:40355–63. doi:10.1074/jbc.M506692200
137. Miravet S, Piedra J, Castano J, Raurell I, Franci C, Dunach M, et al. Tyrosine phosphorylation of plakoglobin causes contrary effects on its association with desmosomes and adherens junction components and modulates beta-catenin-mediated transcription. *Mol Cell Biol* (2003) 23:7391–402. doi:10.1128/MCB.23.20.7391-7402.2003
138. Getsios S, Simpson CL, Kojima S, Harmon R, Sheu LJ, Dusek RL, et al. Desmoglein 1-dependent suppression of EGFR signaling promotes epidermal differentiation and morphogenesis. *J Cell Biol* (2009) 185:1243–58. doi:10.1083/jcb.200809044
139. Gaudry CA, Palka HL, Dusek RL, Huen AC, Khandekar MJ, Hudson LG, et al. Tyrosine-phosphorylated plakoglobin is associated with desmogleins but not desmoplakin after epidermal growth factor receptor activation. *J Biol Chem* (2001) 276:24871–80. doi:10.1074/jbc.M102731200
140. Frusic-Zlotkin M, Raichenberg D, Wang X, David M, Michel B, Milner Y. Apoptotic mechanism in pemphigus autoimmunoglobulins-induced acantholysis – possible involvement of the EGF receptor. *Autoimmunity* (2006) 39:563–75. doi:10.1080/08916930600971836
141. Sanchez-Carpintero I, Espana A, Pelacho B, Lopez Moratalla N, Rubenstein DS, Diaz LA, et al. In vivo blockade of pemphigus vulgaris acantholysis by inhibition of intracellular signal transduction cascades. *Br J Dermatol* (2004) 151:565–70. doi:10.1111/j.1365-2133.2004.06147.x
142. Pretel M, Espana A, Marquina M, Pelacho B, Lopez-Picazo JM, Lopez-Zabalza MJ. An imbalance in Akt/mTOR is involved in the apoptotic and acantholytic processes in a mouse model of pemphigus vulgaris. *Exp Dermatol* (2009) 18:771–80. doi:10.1111/j.1600-0625.2009.00893.x
143. Gil MP, Modol T, Espana A, Lopez-Zabalza MJ. Inhibition of FAK prevents blister formation in the neonatal mouse model of pemphigus vulgaris. *Exp Dermatol* (2012) 21:254–9. doi:10.1111/j.1600-0625.2012.01441.x
144. Espana A, Modol T, Gil MP, Lopez-Zabalza MJ. Neural nitric oxide synthase participates in pemphigus vulgaris acantholysis through upregulation of

Rous sarcoma, mammalian target of rapamycin and focal adhesion kinase. *Exp Dermatol* (2013) 22:125–30. doi:10.1111/exd.12088
145. Marquina M, Espana A, Fernandez-Galar M, Lopez-Zabalza MJ. The role of nitric oxide synthases in pemphigus vulgaris in a mouse model. *Br J Dermatol* (2008) 159:68–76. doi:10.1111/j.1365-2133.2008.08582.x
146. Seiffert-Sinha K, Yang R, Fung CK, Lai KW, Patterson KC, Payne AS, et al. Nanorobotic investigation identifies novel visual, structural and functional correlates of autoimmune pathology in a blistering skin disease model. *PLoS One* (2014) 9:e106895. doi:10.1371/journal.pone.0106895
147. Luyet C, Schulze K, Sayar BS, Howald D, Muller EJ, Galichet A. Preclinical studies identify non-apoptotic low-level caspase-3 as therapeutic target in pemphigus vulgaris. *PLoS One* (2015) 10:e0119809. doi:10.1371/journal.pone.0119809
148. Braga VM. Cell-cell adhesion and signalling. *Curr Opin Cell Biol* (2002) 14:546–56. doi:10.1016/S0955-0674(02)00373-3
149. Braga VM, Machesky LM, Hall A, Hotchin NA. The small GTPases Rho and Rac are required for the establishment of cadherin-dependent cell-cell contacts. *J Cell Biol* (1997) 137:1421–31. doi:10.1083/jcb.137.6.1421
150. Ehrlich JS, Hansen MD, Nelson WJ. Spatio-temporal regulation of Rac1 localization and lamellipodia dynamics during epithelial cell-cell adhesion. *Dev Cell* (2002) 3:259–70. doi:10.1016/S1534-5807(02)00216-2
151. Braga VM, Betson M, Li X, Lamarche-Vane N. Activation of the small GTPase Rac is sufficient to disrupt cadherin-dependent cell-cell adhesion in normal human keratinocytes. *Mol Biol Cell* (2000) 11:3703–21. doi:10.1091/mbc.11.11.3703
152. Gumbiner B, Stevenson B, Grimaldi A. The role of the cell adhesion molecule uvomorulin in the formation and maintenance of the epithelial junctional complex. *J Cell Biol* (1988) 107:1575–87. doi:10.1083/jcb.107.4.1575
153. Vasioukhin V, Bauer C, Yin M, Fuchs E. Directed actin polymerization is the driving force for epithelial cell-cell adhesion. *Cell* (2000) 100:209–19. doi:10.1016/S0092-8674(00)81559-7
154. Hatzfeld M, Keil R, Magin TM. Desmosomes and intermediate filaments: their consequences for tissue mechanics. *Cold Spring Harb Perspect Biol* (2017) 9(6):a029157. doi:10.1101/cshperspect.a029157
155. Ammoun S, Lindholm D, Wootz H, Akerman KE, Kukkonen JP. G-protein-coupled OX1 orexin/hcrtr-1 hypocretin receptors induce caspase-dependent and -independent cell death through p38 mitogen-/stress-activated protein kinase. *J Biol Chem* (2006) 281:834–42. doi:10.1074/jbc.M508603200
156. Salvador JM, Mittelstadt PR, Guszczynski T, Copeland TD, Yamaguchi H, Appella E, et al. Alternative p38 activation pathway mediated by T cell receptor-proximal tyrosine kinases. *Nat Immunol* (2005) 6:390–5. doi:10.1038/ni1177
157. Javanbakht MH, Djalali M, Daneshpazhooh M, Zarei M, Eshraghian MR, Derakhshanian H, et al. Evaluation of antioxidant enzyme activity and antioxidant capacity in patients with newly diagnosed pemphigus vulgaris. *Clin Exp Dermatol* (2015) 40:313–7. doi:10.1111/ced.12489
158. Shah AA, Dey-Rao R, Seiffert-Sinha K, Sinha AA. Increased oxidative stress in pemphigus vulgaris is related to disease activity and HLA-association. *Autoimmunity* (2016) 49:248–57. doi:10.3109/08916934.2016.1145675
159. Shah AA, Sinha AA. Oxidative stress and autoimmune skin disease. *Eur J Dermatol* (2013) 23:5–13. doi:10.1684/ejd.2012.1884
160. Yesilova Y, Ucmak D, Selek S, Dertlioglu SB, Sula B, Bozkus F, et al. Oxidative stress index may play a key role in patients with pemphigus vulgaris. *J Eur Acad Dermatol Venereol* (2013) 27:465–7. doi:10.1111/j.1468-3083.2012.04463.x
161. Naziroglu M, Kokcam I, Simsek H, Karakilcik AZ. Lipid peroxidation and antioxidants in plasma and red blood cells from patients with pemphigus vulgaris. *J Basic Clin Physiol Pharmacol* (2003) 14:31–42. doi:10.1515/JBCPP.2003.14.1.31
162. Zeller KS, Riaz A, Sarve H, Li J, Tengholm A, Johansson S. The role of mechanical force and ROS in integrin-dependent signals. *PLoS One* (2013) 8:e64897. doi:10.1371/journal.pone.0064897
163. Hancock JT, Desikan R, Neill SJ. Role of reactive oxygen species in cell signalling pathways. *Biochem Soc Trans* (2001) 29:345–50. doi:10.1042/bst0290345
164. Aslan M, Ozben T. Oxidants in receptor tyrosine kinase signal transduction pathways. *Antioxid Redox Signal* (2003) 5:781–8. doi:10.1089/152308603770380089
165. Dalle-Donne I, Rossi R, Milzani A, Di Simplicio P, Colombo R. The actin cytoskeleton response to oxidants: from small heat shock protein phosphorylation to changes in the redox state of actin itself. *Free Radic Biol Med* (2001) 31:1624–32. doi:10.1016/S0891-5849(01)00749-3
166. Chiarugi P. Reactive oxygen species as mediators of cell adhesion. *Ital J Biochem* (2003) 52:28–32.
167. Huot J, Houle F, Marceau F, Landry J. Oxidative stress-induced actin reorganization mediated by the p38 mitogen-activated protein kinase/heat shock protein 27 pathway in vascular endothelial cells. *Circ Res* (1997) 80:383–92. doi:10.1161/01.RES.80.3.383
168. Grando SA. The mitochondrion is a common target of disease pathophysiology in pemphigus and pemphigoid. *Exp Dermatol* (2015) 24:655–6. doi:10.1111/exd.12772
169. Chen Y, Chernyavsky A, Webber RJ, Grando SA, Wang PH. Critical role of the neonatal Fc receptor (FcRn) in the pathogenic action of antimitochondrial autoantibodies synergizing with anti-desmoglein autoantibodies in pemphigus vulgaris. *J Biol Chem* (2015) 290:23826–37. doi:10.1074/jbc.M115.668061
170. Chernyavsky A, Chen Y, Wang PH, Grando SA. Pemphigus vulgaris antibodies target the mitochondrial nicotinic acetylcholine receptors that protect keratinocytes from apoptolysis. *Int Immunopharmacol* (2015) 29:76–80. doi:10.1016/j.intimp.2015.04.046
171. Kalantari-Dehaghi M, Chen Y, Deng W, Chernyavsky A, Marchenko S, Wang PH, et al. Mechanisms of mitochondrial damage in keratinocytes by pemphigus vulgaris antibodies. *J Biol Chem* (2013) 288:16916–25. doi:10.1074/jbc.M113.472100
172. Saleh MA, Salem H, El Azizy H. Autoantibodies other than anti-desmogleins in pemphigus vulgaris patients. *Indian J Dermatol* (2017) 62:47–51. doi:10.4103/0019-5154.198032
173. Kaur R, Liu X, Gjoerup O, Zhang A, Yuan X, Balk SP, et al. Activation of p21-activated kinase 6 by MAP kinase kinase 6 and p38 MAP kinase. *J Biol Chem* (2005) 280:3323–30. doi:10.1074/jbc.M406701200
174. Vergarajauregui S, San Miguel A, Puertollano R. Activation of p38 mitogen-activated protein kinase promotes epidermal growth factor receptor internalization. *Traffic* (2006) 7:686–98. doi:10.1111/j.1600-0854.2006.00420.x
175. Mittelstadt PR, Salvador JM, Fornace AJ Jr, Ashwell JD. Activating p38 MAPK: new tricks for an old kinase. *Cell Cycle* (2005) 4:1189–92. doi:10.4161/cc.4.9.2043
176. Chruscinski AJ, Singh H, Chan SM, Utz PJ. Broad-scale phosphoprotein profiling of beta adrenergic receptor (beta-AR) signaling reveals novel phosphorylation and dephosphorylation events. *PLoS One* (2013) 8:e82164. doi:10.1371/journal.pone.0082164
177. Chan SM, Ermann J, Su L, Fathman CG, Utz PJ. Protein microarrays for multiplex analysis of signal transduction pathways. *Nat Med* (2004) 10:1390–6. doi:10.1038/nm1139

Conflict of Interest Statement: The authors declare that the research was conducted in the absence of any commercial or financial relationships that could be construed as a potential conflict of interest.

frontiers in Immunology

OPINION
published: 18 April 2018
doi: 10.3389/fimmu.2018.00810

Ultra-Low Dosage Regimen of Rituximab in Autoimmune Blistering Skin Conditions

*Mauro Alaibac**

Unit of Dermatology, Department of Medicine, University of Padua, Padua, Italy

Keywords: rituximab, autoimmune blistering conditions, skin, pemphigus, B-cells

Rituximab is a chimeric human-mouse monoclonal anti-CD20 antibody initially developed to treat B cell lymphoproliferative disorders (1). It is now increasingly being used for the treatment of B cell-mediated skin autoimmune disorders, including autoimmune blistering skin diseases (2, 3). Rituximab targets all CD20 expressing B-cells, including precursor B cells and mature and memory B cells, whereas it does not interact with CD20-negative early pre-B cells and terminally differentiated plasma cells. Consequently, it completely depletes peripheral memory B cells, but it does not affect preexisting titers of serum antibody produced by long-lived antibody-secreting plasma cells (4). Rituximab mainly acts through antibody-dependent cell-mediated cytotoxicity, although alternative mechanisms may also be involved in complement-dependent cytotoxicity and in direct effect of the drug leading to apoptosis (5). Peripheral B cell depletion by rituximab treatment is usually observed for 6–9 months. After 1 year, many patients show complete mature B cell recovery, whereas the population of circulating memory B cells may be slow to recover after treatment (6). On the other hand, it is plausible that rituximab treatment does not completely eliminate memory B-cells which could be responsible for subsequent disease relapse.

Autoimmune blistering skin diseases are a group of heterogeneous skin conditions characterized by the presence of serum autoantibodies targeting desmosomal structural proteins (pemphigus group) or the hemidesmosomal anchoring complex (pemphigoides group) (7, 8). These disorders are generally treated with systemic corticosteroids which are often combined with other immunosuppressive and/or immunomodulatory approaches, notably azathioprine, mycophenolate mofetil, dapsone, tetracyclines, plasmapheresis, immunoadsorption, and high-dose intravenous immunoglobulins (9). These treatments may not be effective for either induction or maintenance of remission or, alternatively, need to be discontinued because of unmanageable adverse effects. B-cells play a central role in the pathogenesis of autoimmune blistering disorders and rituximab, which selectively targets B cells, has proven to be an effective and safe therapeutic agent in patients with autoimmune blistering skin disorders refractory to conventional treatments (9). To this regard, the recent published randomized controlled trial of rituximab and short-course prednisone versus standard-dose prednisone in new-onset pemphigus has clearly demonstrated that rituximab with short-course prednisone was a more effective treatment than the high-dose prednisone regimen used in this trial, which has been the mainstay of therapy for pemphigus over the years (10). Furthermore, rituximab associated with short-course prednisone showed lower rates of grade 3 or 4 adverse events compared with standard-dose prednisone (10). These results indicate that rituximab associated with short-course prednisone should be considered the first-line therapy for new-onset pemphigus.

The optimal dosing of rituximab in autoimmune blistering skin conditions is currently poorly defined. Initially, rituximab was used for the treatment of pemphigus following the lymphoma dosing regimen (375 mg/m^2 weekly for 4 weeks) (11). However, given the fact that B-cell burden in autoimmune blistering skin diseases is much lower than that in lymphoproliferative disorders, several studies have investigated lower dosage. Horwath et al. treated patients with pemphigus with a single course of two infusions of rituximab (500 mg each) at an interval of 2 weeks with

OPEN ACCESS

Edited by:
Randy Q. Cron, University of Alabama at Birmingham, United States

Reviewed by:
Pui Y. Lee, Harvard University, United States
Matthew Stoll, University of Alabama at Birmingham, United States

***Correspondence:**
Mauro Alaibac
mauro.alaibac@unipd.it

Specialty section:
This article was submitted to Autoimmune and Autoinflammatory Disorders, a section of the journal Frontiers in Immunology

Received: *05 March 2018*
Accepted: *03 April 2018*
Published: *18 April 2018*

Citation:
Alaibac M (2018) Ultra-Low Dosage Regimen of Rituximab in Autoimmune Blistering Skin Conditions. Front. Immunol. 9:810. doi: 10.3389/fimmu.2018.00810

satisfactory responses and relapses generally occurring at the end of the second year (12). Several low-dose protocols for the treatment of pemphigus have been reviewed in a recent meta-analysis, such as the rheumatoid arthritis protocol (2 × 1,000 mg doses at a 2-week interval) and the standard low-dose rituximab (2 × 500 mg doses at a 2-week interval) with the concomitant use of immunoadsorption or high-dose intravenous immunoglobulins (13). Moreover, a very recent investigation has shown impressive results in healthy volunteers treated with ultra-low dosage of rituximab. In this study, the authors demonstrated that <1% of the conventional rituximab doses induced a nearly complete depletion of circulating B lymphocytes (1 mg/m^2 rituximab depleted 97% of all B-cells and doses of 0.3 mg and 0.1 mg/m^2 depleted, respectively 75 and 66% of circulating B-lymphocytes) (14). After 4 weeks from the infusion of rituximab circulating B-cells returned to approximately 60% of normal levels in the 1 mg/m^2 dose group, whereas recovery was completed by 9 months after infusion in the 1 mg/m^2 dose group and about 1 month after infusion in the 0.3 mg and 0.1 mg/m^2 dose groups. From the data of the study, the authors extrapolated that 100 mg rituximab may be sufficient to induce a depletion of B-cells for 3 months and, consequently, two doses of 100 mg every 3 months could deplete the B-cell population for 6 months. Thus, alternative ultra-low dosing schedules for rituximab could be proposed for antibody-dependent autoimmune diseases, including autoimmune blistering skin disorders, as they may provide a considerable improvement of the cost effectiveness. Moreover, well-designed clinical trials are warranted to determine the efficacy of ultra-low dosage rituximab and to assess whether there are other potential advantages over conventional low-dose protocols, in particular lower risk for infection and lower risk for infusion reaction.

AUTHOR CONTRIBUTIONS

MA conceived and wrote the manuscript.

REFERENCES

1. Salles G, Barrett M, Foà R, Maurer J, O'Brien S, Valente N, et al. Rituximab in B-cell hematologic malignancies: a review of 20 years of clinical experience. *Adv Ther* (2017) 34:2232–73. doi:10.1007/s12325-017-0612-x
2. Franks SE, Getahun A, Hogarth PM, Cambier JC. Targeting B cells in treatment of autoimmunity. *Curr Opin Immunol* (2016) 43:39–45. doi:10.1016/j.coi.2016.09.003
3. Huang A, Madan RK, Levitt J. Future therapies for pemphigus vulgaris: rituximab and beyond. *J Am Acad Dermatol* (2016) 74:746–53. doi:10.1016/j.jaad.2015.11.008
4. Marshall MJE, Stopforth RJ, Cragg MS. Therapeutic antibodies: what have we learnt from targeting CD20 and where are we going? *Front Immunol* (2017) 8:1245. doi:10.3389/fimmu.2017.01245
5. Abulayha A, Bredan A, El Enshasy H, Daniels I. Rituximab: modes of action, remaining dispute and future perspective. *Future Oncol* (2014) 10:2481–92. doi:10.2217/fon.14.146
6. Leandro MJ. B-cell subpopulations in humans and their differential susceptibility to depletion with anti-CD20 monoclonal antibodies. *Arthritis Res Ther* (2013) 15:S3. doi:10.1186/ar3908
7. Baum S, Sakka N, Artsi O, Trau H, Barzilai A. Diagnosis and classification of autoimmune blistering diseases. *Autoimmun Rev* (2014) 13:482–9. doi:10.1016/j.autrev.2014.01.047
8. Kershenovich R, Hodak E, Mimouni D. Diagnosis and classification of pemphigus and bullous pemphigoid. *Autoimmun Rev* (2014) 13:477–81. doi:10.1016/j.autrev.2014.01.011
9. Amber KT, Murrell DF, Schmidt E, Joly P, Borradori L. Autoimmune subepidermal bullous diseases of the skin and mucosa: clinical featur s, diagnosis, and management. *Clin Rev Allergy Immunol* (2018) 54:26–51. doi:10.1007/s12016-017-8633-4
10. Joly P, Maho-Vaillant M, Post-Squarcioni C, Hebert V, Houivet E, Calbo S, et al. First-line rituximab combined with short-term prednisone versus prednisone alone for the treatment of pemphigus (Ritux 3): a prospective, multicentre, parallel-group, open-label randomised trial. *Lancet* (2017) 389:2031–40. doi:10.1016/S0140-6736(17)30070-3
11. Ahmed AR, Shetty S. The emerging role of rituximab in autoimmune blistering diseases. *Am J Clin Dermatol* (2015) 16:167–77. doi:10.1007/s40257-015-0121-0
12. Horváth B, Huizinga J, Pas HH, Mulder AB, Jonkman MF. Low-dose rituximab is effective in pemphigus. *Br J Dermatol* (2012) 166:405–12. doi:10.1111/j.1365-2133.2011.10663.x
13. Wang HH, Liu CW, Li YC, Huang YC. Efficacy of rituximab for pemphigus: a systematic review and meta-analysis of different regimens. *Acta Derm Venereol* (2015) 95:928–32. doi:10.2340/00015555-2116
14. Schoergenhofer C, Schwameis M, Firbas C, Bartko J, Derhaschnig U, Mader RM, et al. Single, very low rituximab doses in healthy volunteers – a pilot and a randomized trial: implications for dosing and biosimilarity testing. *Sci Rep* (2018) 8:124. doi:10.1038/s41598-017-17934-6

Conflict of Interest Statement: The author declares that the research was conducted in the absence of any commercial or financial relationships that could be construed as a potential conflict of interest.

The reviewer MS and handling Editor declared their shared affiliation.

frontiers in Immunology

REVIEW
published: 17 April 2018
doi: 10.3389/fimmu.2018.00779

Humoral Epitope Spreading in Autoimmune Bullous Diseases

*Dario Didona[1] and Giovanni Di Zenzo[2]**

[1] Clinic for Dermatology and Allergology, University Hospital Marburg, University of Marburg, Marburg, Germany, [2] Molecular and Cell Biology Laboratory, Istituto Dermopatico dell'Immacolata (IDI)-IRCCS, Rome, Italy

Autoimmune blistering diseases are characterized by autoantibodies against structural adhesion proteins of the skin and mucous membranes. Extensive characterization of their autoantibody targets has improved understanding of pathogenesis and laid the basis for the study of antigens/epitopes diversification, a process termed epitope spreading (ES). In this review, we have reported and discussed ES phenomena in autoimmune bullous diseases and underlined their functional role in disease pathogenesis. A functional ES has been proposed: (1) in bullous pemphigoid patients and correlates with the initial phase of the disease, (2) in pemphigus vulgaris patients with mucosal involvement during the clinical transition to a mucocutaneous form, (3) in endemic pemphigus foliaceus, underlining its role in disease pathogenesis, and (4) in numerous cases of disease transition associated with an intermolecular diversification of immune response. All these findings could give useful information to better understand autoimmune disease pathogenesis and to design antigen/epitope specific therapeutic approaches.

Keywords: autoantibody, antigen, epitope, epitope spreading, pathogenesis, specific therapy, desmoglein, BP180

OPEN ACCESS

Edited by:
Ralf J. Ludwig, Universität zu Lübeck, Germany

Reviewed by:
Abhigyan Satyam, Harvard Medical School, United States
Jens Waschke, Ludwig-Maximilians-Universität München, Germany

****Correspondence:***
Giovanni Di Zenzo
g.dizenzo@idi.it

Specialty section:
This article was submitted to Immunological Tolerance and Regulation, a section of the journal Frontiers in Immunology

Received: *25 January 2018*
Accepted: *28 March 2018*
Published: *17 April 2018*

Citation:
Didona D and Di Zenzo G (2018) Humoral Epitope Spreading in Autoimmune Bullous Diseases. Front. Immunol. 9:779. doi: 10.3389/fimmu.2018.00779

INTRODUCTION

Autoimmune diseases are caused by dysregulation of the immune system or arise as a consequence of microbial infection (1–3). In human, many antigens have been identified in patients and several studies have demonstrated that autoantigens, autoantibody, or related autoreactive lymphocytes can transfer autoimmune disease in animal models. Autoantigens are often clustered on the basis of tissue-specific expression or their structural organization. Several studies conducted in animal models and patients with autoimmune disease suggest that epitope spreading (ES) is the probable explanation for this clustering of specificities in human autoimmune diseases. The ES is an important component of the protective immune responses that acts to enhance its efficiency.

The dynamics of autoimmune response has been investigated both in patients and in animal models. However, although several animal models of autoimmune disease have demonstrated the functional value of ES, in patients limited data are available. A possible explanation could be the early occurrence of ES before the diagnosis and the inhibitory effect of therapy on the autoimmune response.

Autoimmune bullous diseases are organ-specific diseases of the skin and mucous membranes characterized by circulating and tissue bound autoantibodies to structural proteins that maintain cell–cell and cell–matrix adhesions. Studies on prospective cohort of patients have allowed to characterize the dynamics of humoral response and have provided in some studies and reports evidence of the functional role of ES.

Abbreviations: ES, epitope spreading; IIF, indirect immunofluorescence; DIF, direct immunofluorescence; IB, immunoblotting; BMZ, basement membrane zone; Dsg, desmoglein; Coll VII, collagen VII; PV, pemphigus vulgaris; PF, pemphigus foliaceus; EPF, endemic pemphigus foliaceus; MMP, mucous membrane pemphigoid; PNP, paraneoplastic pemphigus; EBA, epidermolysis bullosa acquisita; BP, bullous pemphigoid.

To study ES can give a better insight into the autoimmune response elucidating: (i) the initiation and progression of the disease and (ii) the meaning of the autoantigen clustering and specific reactivity profile in patients. Furthermore, to understand the possible influence of ES in autoimmune progression and to gain knowledge of relevant autoantigen and epitopes could be crucial for diagnosis and for designing antigen-specific treatments.

Here, we summarize the significance and mechanism of ES and review current literature on humoral ES in the autoimmune bullous diseases that are paradigmatic autoantibody mediated disorders.

ES: DEFINITION AND SIGNIFICANCE

Epitope spreading represents the process of diversification of B and/or T-cell response from the initial dominant epitope to a secondary epitope over time. To expand the antigenic epitopes corresponds to optimizing the Ag recognition, to enhancing the neutralization function of antibodies and, in general, to contributing to the efficiency of the immune response.

Epitope spreading that occurs within a single antigen or involves different antigens is termed intramolecular and intermolecular ES, respectively. The intramolecular ES consists of the diversification of immune response in the same autoantigen; the intermolecular ES commonly involves different antigens of a single macromolecular complex or that colocalize in the same anatomical site.

The reactivity that spreads from a single autoantigen to multiple antigens through cross-reactivity is not authentic ES. However, the cross-reactivity could be an initial step to ES. In systemic lupus erythematosus (SLE), autoreactivity to three ribosomal P protein (P_1, P_2, and P_3) is due to a cross-reactive C-terminal epitope present in all three molecules (4). Nevertheless, additional ES phenomenon has been described (5). In this context, the cross-reactivity at the base of molecular mimicry phenomenon can initiate the spreading of an autoimmune response in genetically susceptible hosts. In multiple sclerosis (MS), the initial inflammatory response to a virus infecting the central nervous system can be the triggering factor that induces ES toward autoantigens (6). Similarly, patients with infectious mononucleosis possess circulating IgM to p542, a hematopoietic cell antigen that cross-reacts with Epstein–Barr virus (EBV) nuclear antigen. Afterward, they develop also IgM autoantibodies to p554 that do not cross-react with EBV antigens and that probably arise through ES (7, 8).

In autoimmune response against molecular targets, ES can vary between patients and sometimes reveals a predictable hierarchy. The hierarchy of dominant and secondary epitopes is due to a differential protein processing and presentation, MHC restriction, and to the availability of epitope-specific T and B cells, taking into account central and peripheral tolerance mechanisms.

The predictable sequential ES cascade can present a clinical value. In a subset of patients with mild SLE and relevant skin involvement, autoantibody responses are directed only to the 60 kDa RoAg. In contrast, many patients with primary Sjogren's syndrome and SLE possess IgG autoantibodies for both Ro and La Ag (9, 10).

The functional value of ES in disease development and progression has been clearly demonstrated in immune response in animal models with autoimmune disease. In relapsing experimental autoimmune encephalomyelitis (EAE), an experimental animal model for MS, the contribution to the pathogenesis and specifically to the relapsing clinical episodes of T cell response against epitopes released as a result of tissue damage *via* ES is evident. Specifically, emerging responses to myelin epitopes are clearly able to mediate disease relapse in this mouse model (11, 12). The measles virus infections in Lewis rats are a further example of the causative role of ES in disease induction. This infection induces inflammatory demyelinating lesions in central nervous system. T cells from rats have been reported to proliferate in response to myelin basic protein (MBP) and no cross-reactivity between MBP and virus was demonstrated (13, 14). T cells activated with MBP and adoptively transferred in recipient rats induce lesions resembling those of EAE model (15). Interesting data on functional ES are also provided in non-obese diabetic (NOD) mice, a model of type 1 diabetes where destruction of pancreatic β cells is mediated by CD4 and CD8 T cells specific for numerous epitopes expressed on insulin (Ins) and other autoantigens. Using NOD splenocytes coupled with intact Ins and several additional diabetogenic epitopes Prasad et al. have demonstrated that Ins B9–23 is a dominant initiating epitope, but autoimmune responses to Ins epitope(s) distinct from Ins B9–23 are driven by ES (16). In this context, the progression to overt disease is associated with responses to epitopes distinct from the initiating B9–23 region (16).

However, a pathological role for ES was not always demonstrated in human diseases. Limited data on the functional relation between ES, clinical severity, and disease pathogenesis have been reported. One reason may be that published studies were small in scale (17–19) or that at the time of the diagnosis the ES phenomenon might already have occurred (20, 21). In addition, since treatments are based on inhibition of autoimmune response ES, could be negatively modulated. Indeed, some interesting data on functional value of ES are reported in patients affected by autoimmune blistering diseases. In bullous pemphigoid (BP), the ES phenomenon seems to be associated with disease severity at diagnosis (22). Furthermore, several reports describe a transition from a certain bullous disease to another one due to an intermolecular ES phenomenon that involves a different disease specific antigen. Maeda et al. described a patient who developed BP 12 years after pemphigus foliaceus (PF) being diagnosed (23). Another example of ES occurred during the progression to SLE. Patient autoantibody profiles showed a target diversification over time. Specifically, anti-nRNP-A antibodies bind to the N-terminus of the protein more frequently in later stages when compared to the diagnosis suggesting a role of this diversification in the progression of autoimmune disease (24).

Finally, further evidence of a functional ES in humans is associated with transplantation of allografts. In several cases, ES of the host response to the allograft and organ allograft rejection are clearly correlated (25, 26).

MECHANISM OF ES

Immune responses are characterized by the immunodominance of epitopes within antigens and a great diversity of T- and B-cell

epitope specificity. The broadening of the immune response in autoimmune diseases is induced by tissue damage and inflammation, endocytic processing, antigen presentation, and somatic hypermutation (SHM).

There are two major mechanisms at the base of B cell ES in autoimmune diseases: the first is independent of a physical association of antigens while the second is dependent (27). In the "independent" mechanism, tissue damage inflammation and cytokines induce T cells to recognize cryptic epitopes and activate B cells. On the other hand, a "dependent" response relies on the activation of T and B cells by processing and presentation of physical associated antigens.

Mechanism Independent of Physical Association of Antigens

The development of secondary epitopes in the initial autoantigen or in different autoantigens can depend on the release of antigens or the disclosure of part of antigens during a chronic autoimmune or inflammatory response. In this context, a chronic tissue damage can induce the activation and recruitment of autoreactive lymphocytes specific for epitopes, which are distinct from and non-cross-reactive with the disease-inducing epitope.

An example is the spreading from viral to self epitopes that is shown to play a pathological role in several virus-induced autoimmune disease models (28). A persistent infection can cause the activation of microorganism-specific T cells which mediates tissue damage and release of self peptides (29). Moreover, the induced inflammation can also result in an increased infiltration of T cells at the site of infection and a non-specific activation of self-reactive T cells. Another possible scenario during microbial infection is driven by the IFN-γ secreted by both activated T cells and infected tissue cells. This cytokine can activate antigen presenting cells (APC) and lead to the engulfment of self-antigens. Increased protease production and different processing of captured self-antigens can result in presentation of cryptic self-epitopes that possibly activate autoimmune T and B cells (29). One example of molecular mimicry involves the relation between EBV infection and the development of SLE. The EBV nuclear Ag-1 (EBNA-1) contains a peptide sequence that closely resembles a region on the Smith Ag (Sm) targeted by autoantibodies in SLE patients. Immunization of rabbits with EBNA-1 peptide leads to development of cross-reactivity to Sm antigen that spreads toward an immune response to Sm and nRNP complexes (30). A prospective study on BP patients showed that the autoimmune response starts with autoantibodies specific for an extracellular antigen and then spreads to an intracellular one, suggesting that tissue damage and inflammation play a role in the dynamics of the response (22).

Mechanism Dependent of Physical Association of Antigens

Autoantigens are frequently part of multiantigen complexes. T cells specific for one epitope of an antigen can activate B cells that are specific for other different antigens of the complex, allowing production of autoantibodies even against antigens/epitopes not originally targeted by the immune response (31). In this case, B cells directed against disease-initiating epitopes mediate antigen-specific uptake of large protein complexes leading to the efficient presentation of self-epitopes from distinct proteins. Immune responses are initiated by presentation of immunodominant epitopes to CD4 T cells by APC such as dendritic cells. The primed CD4 helper T cells then activate antigen-specific B cells. The APC function of B cells induce an increased uptake of antigen that leads to a stimulation of CD4 T cell also by peptides that weakly bind MHC class II molecules. In this context, the processing of antigens is directed by the specificity of the immunoglobulin receptor on B cells. In fact, the epitope bound by the immunoglobulin is protected from proteolysis, and this alters the array of peptides presented to naive CD4 T cells (31). An example of ES dependent of physical association of antigens is the development of autoantibodies to multiple components of the La/Ro ribonucleoprotein complex in SLE and SS. The initiation of an immune response on a single component is at the base of the appearance of mixed autoantibody patterns in these systemic autoimmune diseases (32). The splicesome consists of multiple proteins and nucleic acids associated with each other. Thus, immunization with various SmD peptides leads to the development of autoantibodies not only against regions of the SmD protein but also against the U1-associated ribonucleoprotein (A-RNP) and induces lupus-like symptoms in a mouse model (33).

The mechanism at the base of inter- and intramolecular ES dependent on physical association of antigens can be associated with endocytic processing and SHM. After binding to B cell receptors, the antigen is endocytosed, cleaved and loaded into a compatible MHC class II complex on the cell surface (34). This process can allow the presentation of previously unrecognized epitopes or, in case of endocytosis of multi-antigen complex, the presentation of novel antigen (27, 35). On the other hand, after B cells activation in response to Ag, they undergo SHM in germinal centers. IgV gene experiences single nucleotide substitutions at a frequency of about 10^{-3} per base pair in each B lymphocyte generation (36). Thereafter an affinity maturation process allows a selection of cells with a higher affinity for the Ag. In the context of cell selection, intramolecular ES can occur during the selection of B cells with higher affinity for a different epitope of the Ag or also different Ag (37). Autoantibodies specific for dsDNA can be generated through SHM in developing SLE (38).

Finally, several factors that could influence the ES in the physically linked antigens have been described. In SLE, the strength of non-covalent interactions between Ku antigen and the DNA protein kinase catalytic subunit (p350) is stabilized by autoantibodies that may enhance ES to the p350 antigen (39). In addition, antibody binding of autoantigens may mask some epitopes during antigen presentation or also facilitate presentation of poorly tolerized epitopes (40, 41). In organ-specific autoimmunity, the anatomical isolation of antigens is presumably associated with a less efficient central or thymic T-cell tolerance requiring intrathymic antigen presentation during development of the T-cell repertoire. This partial central tolerance to tissue specific antigens could facilitate the ES. Finally, ES may also be determined by MHC genes, as observed in the experimental model of La/Ro autoimmunity (27).

HUMORAL ES IN AUTOIMMUNE BULLOUS DISEASES

Autoimmune bullous diseases of the skin and mucosae constitute a large group of diseases, including BP, pemphigus vulgaris (PV), PF, paraneoplastic pemphigus (PNP), epidermolysis bullosa acquisita (EBA), linear IgA bullous disease, dermatitis herpetiformis (DH), mucous membrane pemphigoid (MMP), lichen planus pemphigoid (LPP), and others. Their clinical presentation is polymorphic and the pathogenesis is mainly associated with autoantibodies targeting distinct components of the basement membrane zone (BMZ) and desmosome of stratified epithelia. These autoantigens represent structural proteins important for maintenance of epidermal and dermoepidermal integrity. Over the past few decades, identification of autoantigens and relative autoantibodies has improved understanding of the pathogenesis laying the foundation for the study of the dynamics of humoral ES.

Bullous Pemphigoid

Bullous pemphigoid, the most frequent autoimmune bullous disease, typically affects the elderly and is associated with a significant morbidity and mortality. The cutaneous manifestations of BP are protean. In the prodromal, non-bullous phase, patients complain of severe itch sometimes accompanied by eczematiform, papular, and or urticarial lesions. In the bullous stage, vesicles and bullae develop on apparently normal or erythematous skin. Involvement of the oral cavity is observed in 10–30% of cases (42). BP is associated with autoantibody to BP antigen 1 and 2 (BPAG 1 and BPAG2) also known as BP230 and BP180, two components of junctional adhesion complexes in human skin. The diagnosis is based on clinical evaluation and detection by direct immunofluorescence (DIF) of IgG and/or complement deposition along the BMZ in a linear pattern. Serological tests such as indirect immunofluorescence (IIF) and antigen-based ELISAs have a confirmatory value (42). The vast majority of BP sera react with an immunodominant extracellular domain of BP180, termed non-collagenous 16A (NC16A) domain (43, 44). The pathogenic relevance of autoantibodies to NC16A is supported by several experimental evidences (43, 45–47). Although *in vitro* and *in vivo* animal models have shown that IgG autoantibodies to BP180 are pathogenic, the role of anti-BP230 antibodies is only partially clear (48, 49). Several studies in BP patients demonstrated that, in addition to the NC16A domain, other epitopes of BP180 and BP230 are targeted by both autoaggressive B and T cells (50–57). To study the dynamics of IgG reactivity against different BP180 epitopes, Di Zenzo et al. have employed a mouse model in which skin obtained from transgenic mice expressing human BP180 was grafted on the back of wild-type mice. The grafting induced an immune response to BP180 perfectly located in its natural molecular context (58). Interestingly, the IgG reactivity with extracellular epitopes preceded IgG recognition of intracellular domain. Indeed, the spread of humoral immune responses in this graft model was exclusively target specific and the kinetics of graft loss is completely different from alloantigen-related graft rejection previously described in this model (59). A possible interpretation of these data is that antibodies directed against extracellular epitopes of BP180 may have induced tissue damage with consequent exposure of intracellular epitopes (**Figure 1**). These findings were in accord with a previous study by Di Zenzo et al. on the analysis of the humoral response in a large cohort of BP patients. Reactivity results obtained on a vast array of BP230 and BP180 epitopes demonstrated that the IgG recognition of intracellular epitopes was already present at an early stage of the disease (52). Data from mouse model and BP patients raise the possibility that the development of IgG against intracellular epitopes or antigens may correlate with the initial phase of the disease when the tissue damage starts occurring (**Figure 1**).

In order to assess the evolution of IgG autoantibodies, a multicenter prospective study in 35 BP patients over a 12-month observation period was performed (22). ELISA and immunoblotting (IB) assays were utilized to assess circulating autoantibodies to BP180 and BP230 peptides. In particular, ES events were detected in 17 of 35 patients and preferentially occurred at an early stage of the disease. The functional role of ES was supported by its significant relation to disease severity at diagnosis. Moreover, in line with data obtained by Di Zenzo et al. in mice grafted with human BP180, in three patients the spreading of IgG reactivity to intracellular epitopes of BP180 and BP230 (an intracellular antigen) was preceded by recognition of the BP180 ectodomain (**Figure 1**).

All these findings suggest that IgG recognition of the BP180 ectodomain is an early event, followed by intra- and intermolecular ES events, which shape the individual course of BP. In addition, these data could give useful information for design therapeutical approaches. In particular, to deplete pathogenic autoantibodies, other pathogenic region of BP180 (in addition to NC16A) should be considered as possible therapy using decoy peptides to block autoantibody binding *in vivo*. However, this approach may require early and massive administration of several different peptides.

Several cases of automimmune bullous disease patients indicate that an ES phenomenon often leads to a disease transition. Recently, Sardy et al. reported an interesting case of an 18-year-old Caucasian woman, affected by BP, who showed clinical and laboratory transition to MMP 5 years after the BP diagnosis (60). The patient developed a severe esophageal stenosis, that was not present at the time of the BP diagnosis. DIF detected linear IgG and C3 fluorescence along the mucosal side of the BMZ. Furthermore, IgG autoantibodies directed against the immunodominan epitope of BP180 (NC16A domain) and the BP230 COOH-terminal were identified. Laminin 332 ELISA was positive. Immunoblot studies showed presence of IgG4 autoantibodies to laminin 332, and both IgA and IgG against desmoglein 3 (Dsg3). Collagen VII (Coll VII) autoantibodies were detected neither by ELISA nor by immunoblot. At the time of BP diagnosis, no evidence of MMP have been detected, and anti-laminin 332, autoantibodies were not tested. In addition, retrospective analysis of the serum samples showed no reactivity. After the BP diagnosis, the patient was started on topical steroid therapy and a short course of oral prednisolone obtaining a partial BP remission. The authors postulated that insufficient immunosuppressive treatment of BP might facilitate ES, and lead to a more complex clinical course (60). Another interesting

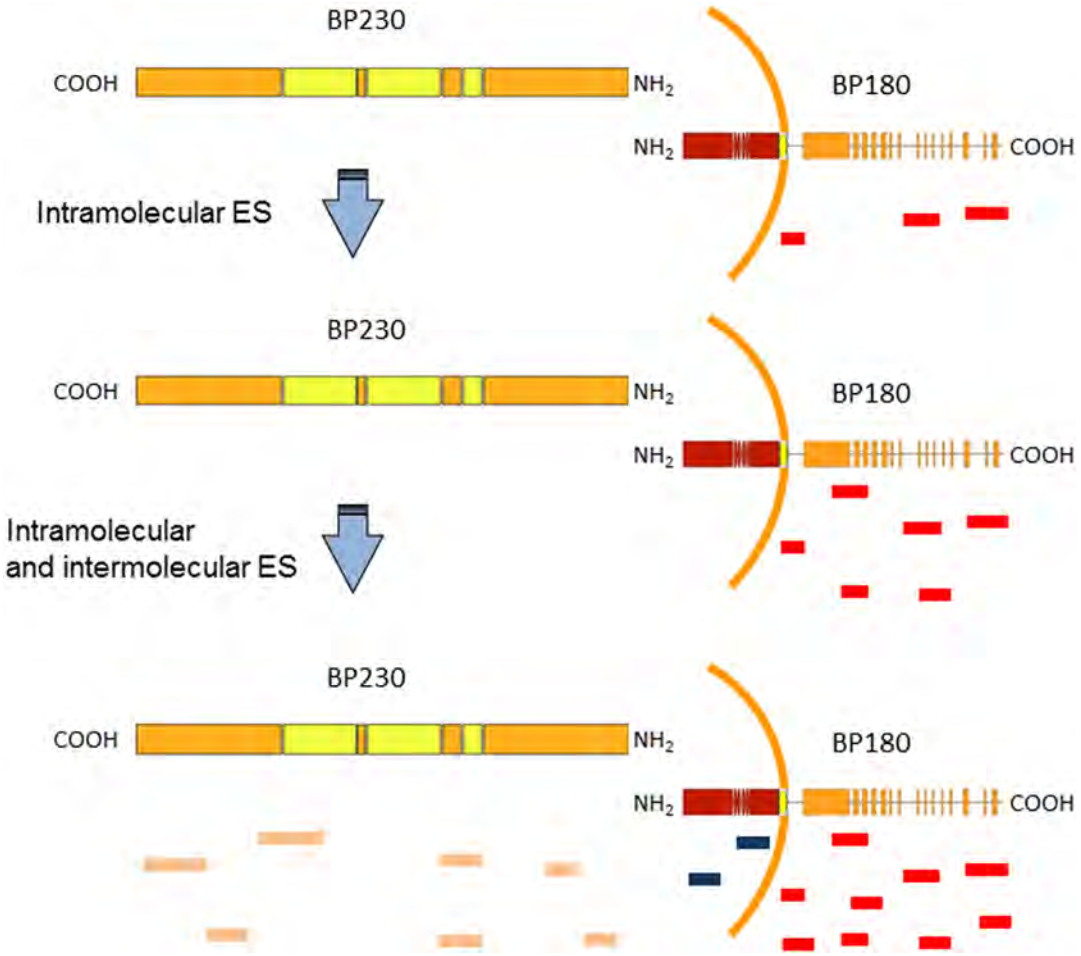

FIGURE 1 | Epitope spreading (ES) in bullous pemphigoid (BP) patients. A schematic representation of BP antigens (BP180 and BP230). Findings support the idea that IgG recognition of the BP180 ectodomain is an early event in BP disease, followed by variable intramolecular ES (red and blue lines in BP180 ectodomain) and intermolecular ES events (orange lines), which likely shape the individual course of BP (22, 58).

case was reported by Kasperkiewicz et al. In a 70-year-old man with hemorrhagic blisters, widespread crusted erosions, and the immunopathological characteristics of anti-p200 (γ1 laminin subunit) pemphigoid, treatment with doxycycline, topical corticosteroids and immunoadsorption led to rapid clinical remission. Nineteen weeks later, a relapse occurred with an altered clinical phenotype together with autoantibodies against both p200 and NC16A suggested a functional role of ES in the disease transition (61). Autoimmune bullous diseases often develop in patients with psoriasis. BP was the most prevalent followed by antilaminin γ1 pemphigoid (62). A possible explanation of the development of BP in psoriatic patients is provided by previous studies that have shown that laminin 1 and laminin α1 within BMZ are disrupted in both involved and uninvolved psoriatic lesions (63, 64). In general, the damage to BMZ in patients with psoriasis may induce the development of several antibodies such as anti-laminin γ1 and -BP180. However, although a Taiwanese population study disclosed that psoriasis occurred significantly more in patients with BP than that in the control group, large population studies in each country are necessary to support this association (65).

Pemfigus Vulgaris

Pemphigus includes a group of potential life-threatening autoimmune blistering diseases of the skin and mucous membranes. These diseases are characterized by autoimmune responses mainly directed against two transmembrane components of desmosomes, Dsg3 and Dsg1 (66). Similar to other cadherins, Dsg3 and Dsg1 comprise five extracellular subdomains of approximately equal size (EC1–EC5). Several distinct forms of pemphigus have been reported (PV, PF, PNP, and others); the most common is PV. In PV, the critical role of autoantibodies to Dsg3 is largely demonstrated (67–71). The diagnosis clinical and histopathological findings are supported by demonstration of the IgG deposition on the surface of the epithelial cells by DIF. Detection of circulating autoantibodies against the cell surface by IIF and/or to recombinant Dsgs by ELISA can confirm the diagnosis (69). Usually, the oral mucosa is first involved and then blisters arise on the whole body. In the skin, Dsg3 is mainly expressed in the basal and suprabasal layers, while Dsg1 is predominantly expressed in the upper epidermal layers. However, in oral mucosa Dsg3 is highly expressed throughout the epithelium,

while Dsg1 is less expressed. According with "Dsg compensation" theory, the Dsg3/Dsg1 autoantibody profile is at the base of different clinical variants of pemphigus depending on differential expression pattern of Dsg1 and Dsg3 (72). More specifically, in PV patients antibodies to Dsg3 cause mucosal disease due to lack of compensation by Dsg1, while they don't induce cutaneous disease because of compensation by Dsg1. In PV, patients who acquire antibodies to Dsg1, compensation is no longer possible, resulting in cutaneous as well as mucosal disease (67, 73, 74). On the other hand, in PF antibodies to Dsg1 cause cutaneous disease, while they cannot cause mucosal disease, because Dsg3 is present at high levels throughout the epithelium (75). In accord with this theory are the results obtained in a mouse model by Ding et al. The authors showed that the passive transfer of PV anti-Dsg1 and -Dsg3 antibodies were able to generate cutaneous lesion while anti-Dsg3 antibodies alone were not (73).

To investigate the ES phenomenon in PV and to identify the basis of clinical transition from mucosal to mucocutaneous involvement, Salato et al. analyzed sera from PV patients taken at various times during the course of disease (76). A subset of PV patients transitioned from mucosal PV to mucocutaneous PV and their autoantibodies profile were evaluated. One representative patient, with only mucosal involvement at an early PV stage, had autoantibodies specific for C-terminal region of Dsg3 ectodomain in the EC5 subdomain. At this time the circulating autoantibodies were not able to bind human skin by IIF (76) (**Figure 2**). Several years later, the patient produced autoantibodies directed to EC1 subdomain of Dsg3 demonstrating an intramolecular ES phenomenon. Interestingly, the autoantibodies started to bind the human skin by IIF and an intermolecular ES toward Dsg1 occurred (**Figure 2**). At this stage, the patient exhibited non-cross-reactive autoimmunity to both Dsg3 and Dsg1 and developed cutaneous as well as mucosal blisters (**Figure 2**). In this context, it is important to underline that the pathogenic activity of anti-Dsg1 autoantibodies affinity purified from a PV patient serum was previously demonstrated in a mouse model

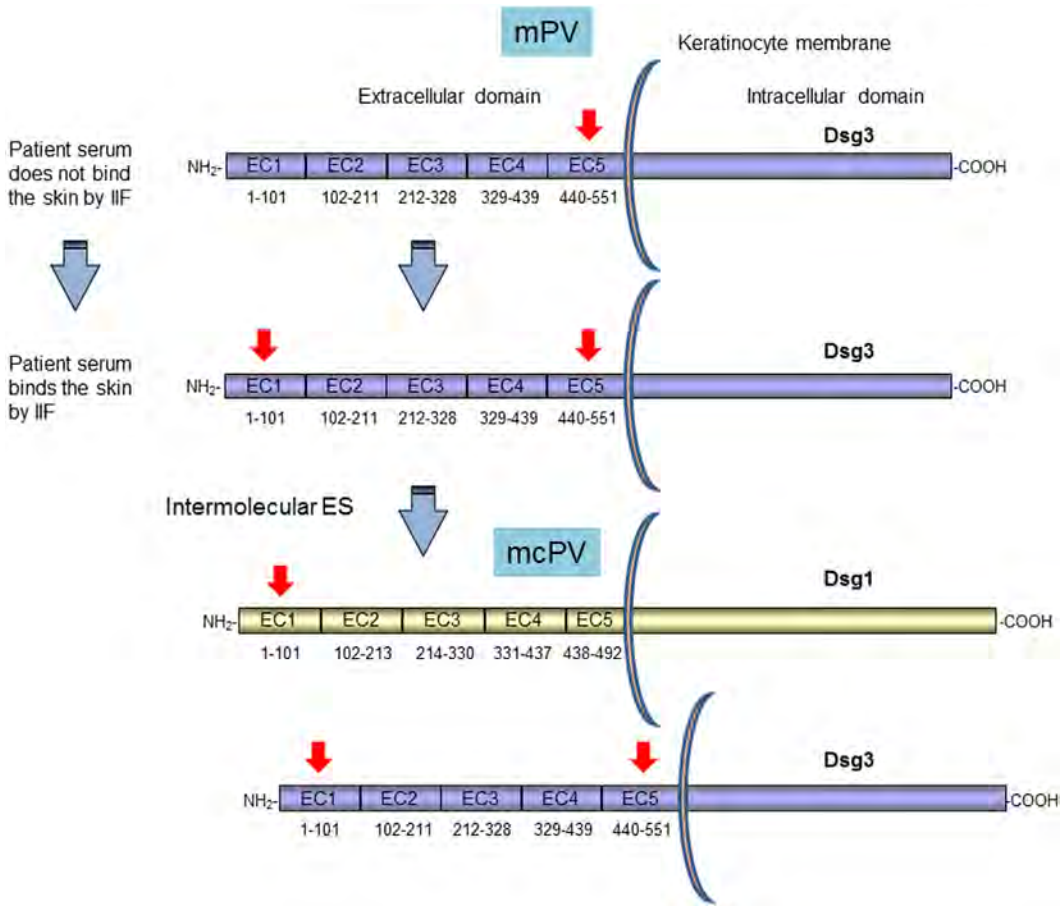

FIGURE 2 | Clinical transition between mucosal pemphigus vulgaris (PV) to mucocutaneous PV as proposed by Salato et al. Survey and schematic representation of the antigenic regions recognized by autoantibodies of a representative PV patient with only mucosal involvement (mPV) that shift clinical phenotype to mucocutaneous one (mcPV) (76). PV antigens (Dsg1 and Dsg3) with relative subdomains (EC1–EC5) of Dsg1 and 3 and their amino acid sequences are illustrated. Red arrows indicate the regions recognized by patient autoantibodies during the course of the disease (76). The mPV patient at an early stage of disease has autoantibodies specific for ectodomain (EC5) subdomain. At this time the circulating autoantibodies are not able to bind human skin by [indirect immunofluorescence (IIF)]. Several years later, the patient produces autoantibodies directed to EC1 by an intramolecular ES phenomenon. At this stage the autoantibodies start to bind the human skin and an intermolecular ES toward Dsg1 occurred with development of cutaneous as well as mucosal blisters (76).

based on antibody passive transfer (77). Previous cases with mucosal involvement and anti-Dsg3 autoantibodies that spread to Dsg1 with cutaneous involvement in addition to mucosal one were also reported (73, 78). A major limitation of study from Salato et al. was the use of Dsg1/Dsg3 swapping domains approach for the epitope mapping of autoantibody reactivity. In fact, although the majority of anti-Dsg3 IgG autoantibodies in PV did not cross-react with Dsg1, in mucocutaneous-type PV, with both anti-Dsg1 and anti-Dsg3, autoantibodies mapping results from this approach, may be less reliable, because of the sequence homology of two cadherins. In addition, the exclusive presence of autoantibody to the C-terminal domain of Dsg3 in PV patients with mucosal lesions appeared in contrast with several studies that showed that the vast majority of PV sera react with the N-terminal portion of Dsg3 and rarely bind the C-terminal one (79, 80). On the other hand, the fact that an intermolecular ES from Dsg3 to Dsg1 and not the presence of cross-reactive antibodies is at the base of clinical phenotype transition in PV was demonstrated by an inhibition assay in PV patients with mucocutaneous lesions (67). However, it could be hypothesized the presence of few cross-reactive not detectable antibodies that shift the reactivity from Dsg3 to Dsg1 possibly followed by an intramolecular ES event in the Dsg1 molecule. Indeed, the isolation from PV patients with Dsg1/Dsg3 cross-reactive monoclonal autoantibodies could corroborate this hypothesis (42, 81).

In contrast with data from Salato et al., another study using the same approach has reported a stable epitope profile during disease course in four PV patients (80). A further study analyzed ES events in a larger cohort of PV patients (53 patients) at multiple disease stages (20). In this case, a different system based on Dsg3 (or Dsg1)/Dsg2 domain-swapped molecules was employed. In this approach using Dsg2 cadherin as the backbone of the domain-swapped molecules, the epitopes recognized by anti-Dsg3 IgG could be analyzed without the influence of anti-Dsg1 IgG autoantibodies and vice versa, because PV sera showed no reactivity with Dsg2. As previously reported, the major epitopes recognized by PV sera were calcium-dependent and mapped at the N-terminal region of Dsgs (**Figure 3A**). Interestingly, the recognized region appeared to be unchanged over the course of disease in both anti-Dsg3 mucosal dominant-type PV and anti-Dsg3/Dsg1 mucocutaneous-type PV (20). Intramolecular epitope shift was not evident in the vast majority of PV cases and only two patients of 53 showed an intramolecular ES event in the Dsg3 during the disease course. Specifically, a PV patient (PV1) in active stage reacted to EC1/4 and shifted to EC2/3 during remission, strongly reducing the anti-EC1 reactivity, and another one (PV2) showed a transition from active to moderate disease characterized by a stable anti-EC1 reactivity and the appearance of anti-EC2/4 antibodies (**Figure 3A**) (20). Independent of disease stage, in most PV patients the major Dsg3 epitopes are localized in the EC1–2 subdomains, while in PV with cutaneous involvement dominant epitopes of Dsg1 are in addition present in EC1 but not in the EC2–5 subdomains (**Figure 3A**) (20). In contrast to the results of Salato et al., no mucosal dominant-type PV sera reacted only with the EC4 or EC5 subdomain of Dsg3. Further studies with larger cohort of well characterized patients with only mucosal and mucocutaneous phenotype are needed to clarify the relation between recognized epitope and clinical phenotype and to better understand the role of ES in this phenotype transition. All these studies show three major limitations (i) it was impossible to evaluate ES before the onset of disease, (ii) treatment could influence the ES during the course of the disease, and (iii) a possible intradomain ES was not investigated.

In addition to Dsg3 and Dsg1, several other organ-specific non-Dsg autoantibodies in pemphigus patient sera could be involved in an intermolecular ES phenomenon. For example, antibodies against an acetylcholine receptor and pemphaxin that are not pathogenic alone, but may act synergistically with pathogenic anti-Dsg3 antibodies (82–85). Another example are antibodies targeting keratinocyte mitochondria that contribute to the process of acantholysis and could be also involved in ES phenomena associated with the tissue damage induced by pathogenic autoantibodies (85, 86). Other autoantibodies specific for intracellular domains of Dsgs, a calcium pump encoded by ATP2C1, desmocollin 1, BP230, periplakin, E-cadherin, Dsg4, desmoplakin 1, and desmoplakin 2 have been detected in pemphigus patients (69). However, since their pathogenic role has not been demonstrated they could be considered a result of an intermolecular ES phenomenon without any functional role in the disease. According with this possible interpretation are findings from our study on the presence of other non-disease specific autoantibodies in autoimmune bullous disease such as anti-BP180, BP230 and Coll VII autoantibodies in PV patients or anti-Dsg3 autoantibodies in BP. Interestingly, the reactivity against additional non disease-specific antigens was rare and remained stable during disease course, while in the same patients reactivity against disease-specific antigens fluctuated in parallel with disease severity. This atypical reactivity possibly represented an epiphenomenon unrelated to the evolution and progression of the autoimmune disease (87). Further studies are needed to understand the possible role of ES in the generation of these autoantibodies and their role in disease pathogenesis.

In a recent study, Cho et al. have postulated a functional role of ES in the pathogenesis of PV. In particular, they have isolated cross-reactive rotavirus/Dsg3 antibodies from PV patients. A subset of these antibodies had the potential to confer protection against rotavirus infection but also to cause pathogenic effects on skin, suggesting a role of molecular mimicry in the disease pathogenesis (88). In this context, the authors speculate that even in the presence of non-pathogenic and cross-reactive antibodies, the activation of a cross-reactive B cell could stimulate Dsg3-reactive T cells to trigger a broader anti-Dsg3 B cell response, that react to other and possibly pathogenic epitopes leading to PV (88).

Pemfigus Foliaceus

Pemphigus foliaceus is an autoimmune blistering skin disease characterized by superficial cutaneous erosions. Tissue bound and circulating autoantibodies that react to Dsg1 have shown a pathogenic role in the disease (75, 89) and provide important diagnostic clues in addition to clinical evaluation. The most common subtype is sporadic PF occurring all over the world, whereas endemic PF (EPF) is found in rural areas of Brazil, where the disease is known as fogo selvagem (90–92).

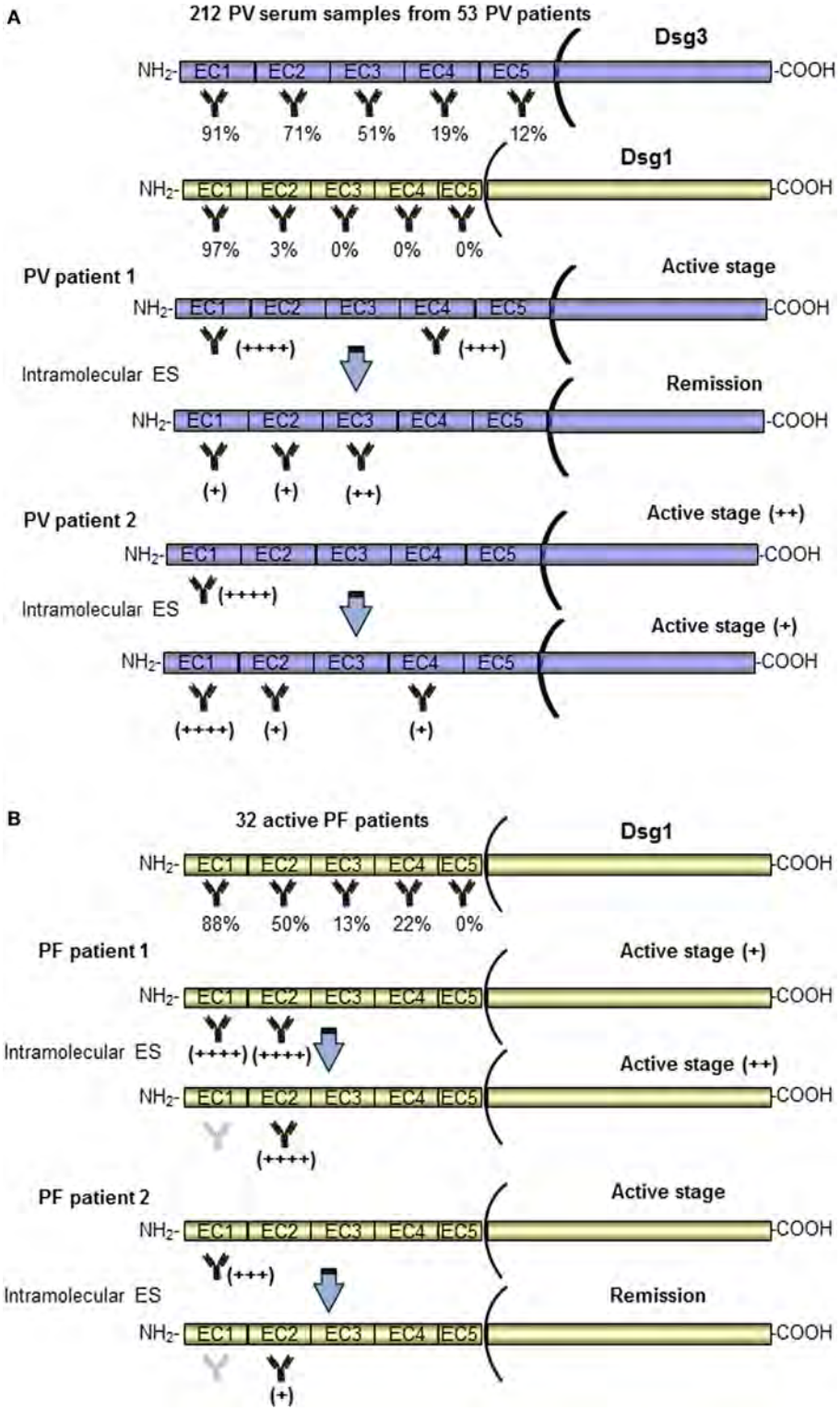

FIGURE 3 | Pemphigus vulgaris (PV) and pemphigus foliaceus (PF) patients present Dsg3 and Dsg1 epitope profiles stable over the disease course. A schematic representation of the antigenic regions recognized by autoantibodies of a PV **(A)** and PF **(B)** patients at diagnosis, with relative percentage of reactivity, and during the disease course (20, 21). Only two patients (for PV and PF) in whom epitope spreading (ES) phenomenon occurred have been shown. In most PV and PF patients, the major Dsg3 and Dsg1 epitopes are localized in the EC1–2 subdomains. In the vast majority of PV and PF patients, the epitope profile remained stable during the course of the disease. Of note, two patients (PV patient 1 and PF patient 2) in active stage reacted to EC1 and shifted with an intramolecular ES to other subdomains (EC2/EC3 and EC2) (20, 21).

In 2010, Chan et al. have characterized the dynamics of immunoreactivity to various Dsg1 extracellular subdomains in non-endemic PF patients during the course of the disease by using the Dsg1/Dsg2 domain-swapped molecules approach. According to data obtained on PV patients, most of the anti-Dsg1 antibodies bind to the N-terminus region of Dsg1 (**Figure 3B**), and this reactivity prevails across various activity stages. Only two PF patients lost their EC1 reactivity upon remission and in one case shifting to EC2 (**Figure 3B**) (21). Thus, in PV such as in PF patients, the Dsg3 and Dsg1 epitope profiles remained stable over the disease course and, because of the rarity of ES, treatments based on the depletion or abrogation of autoantibodies to the N-terminal domains of Dsg3/Dsg1 should be promising (**Figure 3B**). Another possible involvement of ES is described in a previous study from Ishii et al. that have isolated several pathogenic and non-pathogenic monoclonal antibodies from PF patients (93). Some non-pathogenic antibodies bound to the proprotein of Dsg1, which are thought to be synthesized as intracellular inactive precursor proteins with prosequences that are cleaved to yield mature and extracellular adhesive molecules. Similarly, non-pathogenic autoantibodies from PV patients were also able to bind the precursor of Dsg3 (94, 95). Interestingly, these findings could suggest that PV and PF patients at first develop non-pathogenic antibodies against the intracellular Dsg precursor to which they would not be expected to have tolerance, and in some susceptible patients the antibody response might shift through ES to pathogenic autoantibodies specific for the mature molecule (93–95). Further studies are needed to confirm this hypothesis.

Although the sporadic PF and EPF form share similar immunological and clinical features, the latter presents peculiar characteristics. Specifically, a clinical study suggests that intramolecular ES could be the cause for the development of EPF (96). Patients in the preclinical stage and healthy individuals from endemic areas possessed IgG1 circulating autoantibodies that recognize non-pathogenic epitopes in the C-terminal domain of the Dsg1 ectodomain (EC5), whereas when the disease developed in individuals with certain HLA susceptibility genes pathogenic antibodies directed against the N-terminal region of Dsg1 ectodomain (EC1 and EC2) appeared. Concomitantly a possible antibody subclass switching from IgG1 to IgG4 seemed to occur (**Figure 4A**) (96–98). In this context, Warren et al. have previously shown that up to 55% of healthy individuals living in endemic areas have low levels of anti-Dsg1 antibodies (97). In addition, a strong relationship has been found between infestation with hematophagous insects, certain HLA susceptibility genes and the occurrence of fogo selvagem, suggesting a role of environmental factors in development of the disease (99). In accord with this idea, Qian et al. have found in patients IgG4 and IgE autoantibodies that cross-reacted with a salivary antigen (LJM11) from sand flies targeting a shared conformational epitope in the EC1-EC2 subdomains (100). Compared to normal controls, individuals before and after onset of fogo selvagem have significantly higher IgE anti-LJM11 and anti-Dsg1 antibodies, suggesting that the IgE antibodies develop before the onset of EPF (100). However, individuals have significantly lower levels of anti-Dsg1 IgE before fogo selvagem onset than after the development of the disease, suggesting that LJM11 might be the initial target of IgE response (101) (**Figure 4B**). In order to further investigate this cross-reactive immune response and to clarify whether it represents a non-specific activation of the immune system or an antigen-selected response, an antibody phage display library approach was employed. Qian et al. generated libraries comprising only IgG4 subclass from three EPF patients and 14 clonally independent IgG4 monoclonal antibodies were isolated and analyzed (102). Noteworthy, all of these IgG4 monoclonal antibodies were cross-reactive to both Dsg1 and LJM11 and extensively mutated. Furthermore, the revertant monoclonal antibodies, which represent the germline configuration, also recognized both Dsg1 and LJM11 (102). Collectively, these findings suggest that the development of anti-Dsg1 IgG4 antibody in EPF patients could be the result of initial IgE response to the environmental antigen (such as LJM11). In this context, a chronic stimulation of LJM11 antigen and the production of IL10 by the immune system promote the development of pathogenic IgG4 antibodies, which are cross-reactive to both LJM11 and Dsg1 (**Figure 4B**). Very recently, Evangelista et al. have demonstrated that fogo selvagem is mediated by pathogenic IgG4 autoantibodies against the EC1 subdomain of Dsg1 (103). However, whether the epitope on LJM11 shares its conformational structure with this pathogenic epitope or with a non-pathogenic epitope on Dsg1 that through an intradomain ES could generate pathogenic autoantibodies has not been investigated (103). Thus, putting the evidences all together, IgG4 pathogenic autoantibodies in EPF could be the result of an intramolecular ES event from non-pathogenic autoantibody specific for EC5 subdomain of Dsg1 to a pathogenic one against EC1 subdomain (**Figure 4A**). In parallel, antigen mimicry that induces with or without ES an antibody switch from an epitope of salivary gland fly antigen to a pathogenic epitope on the EC1 subdomain of Dsg1 has been demonstrated (**Figure 4B**).

As postulated, for the clinical transition from mucous to mucocutaneous PV an intermolecular ES phenomenon could also be at the base of disease transition. In particular, transition from PV to PF and *vice versa* is a well-documented phenomenon (**Table 1**). In most cases, PV patient shift to PF, although some cases where PF patients switched to PV have been described (104–120). The mechanism of transition between PV and PF is unclear, and a possible role of ES in this phenomenon has been postulated (**Table 1**). In cases of PV transforming from PF, anti-Dsg1 autoantibodies were initially present (108, 109). Dsg3 may be released from skin lesions leading to the production of anti-Dsg3 autoantibodies and a phenotype switch. It is unclear if transition from PV to PF is permanent or whether it is due to preferential suppression of Dsg3 antibodies caused by the immunosuppressive therapy (114). Indeed, only in few cases the transition was reported in patients without therapy (104, 113). Rarely, pemphigus and the pemphigoid group of diseases may develop in the same patient (121). Up to date, only four reports about PF to BP transition have been reported (23, 122–124). Usually, the IgG detected in those patients belongs to IgG1 or IgG4. However, Recke et al. reported the presence of IgG3 in their patient. In all the cases described, the transition to BP was associated with a complete disappearance of anti-Dsg autoantibodies highlighting a functional role of ES in these cases (124).

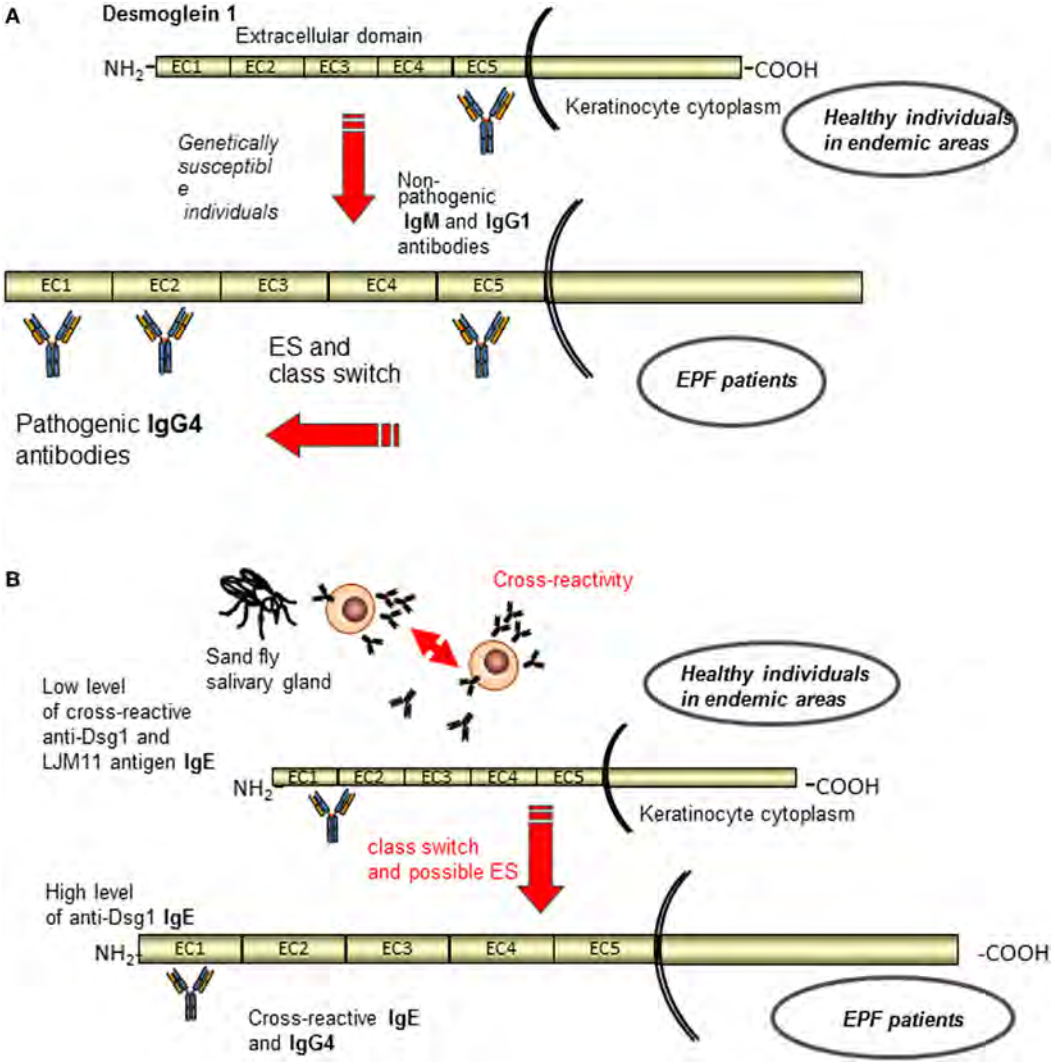

FIGURE 4 | Current etiopathogenetic model for endemic pemphigus foliaceus (EPF). A schematic representation of the antigenic regions recognized by autoantibodies of normal individuals and EPF patients. **(A)** Patients in the preclinical stage and healthy individuals from endemic areas possess IgG1 circulating autoantibodies that recognize non-pathogenic epitopes in the EC5, whereas when the disease developed appeared pathogenic IgG4 antibodies to EC1 and EC2 through class switch and ES (96–98). **(B)** In parallel, antigen mimicry that induces with or without ES an antibody switch from an epitope of salivary gland fly antigen (IgE) to a pathogenic epitope on the EC1 subdomain of Dsg1 (IgG4) is shown (102).

Paraneoplastic Pemphigus

Paraneoplastic pemphigus is a rare autoimmune bullous disease that is always associated with neoplasm (125, 126). Typically, PNP patients show autoantibodies directed against the plakin family, including antibodies against envoplakin, periplakin, desmoplakins I and II, plectin, the hemidesmosomal protein BP180 and BP230 (125, 126), and the protease inhibitor alpha-2-macroglobulin-like-1 (127). Furthermore, antibodies against plakophilin 3, desmocollins 1, desmocollins 3, Dsg1, and 3 have also been detected in PNP (125, 126). Clinically, patients are characterized by the presence of severe mucocutaneous lesions and sometimes respiratory failure, and they are refractory to standard treatment. Diagnosis mainly based on DIF, relies also on the demonstration of autoantibodies in serum, assessed by IB, ELISA, IIF on rat bladder and immunoprecipitation with radioactive keratinocyte extracts. IIF on rat bladder epithelium that expresses plakins and not Dsg is useful for differential diagnosis with pemphigus. However, this approach is not completely reliable considering that some pemphigus patient reacts with plakins in addition to Dsgs (128–131).

Bowen et al. suggested that ES might play a role in the pathogenesis of PNP (132). They described five PNP patients showing clinical and pathological features of lichen planus (LP) (132). Among them, one showed initially negative results by IIF on rat bladder epithelium; however, one year after, positive IIF staining was observed. Furthermore, the same patient showed initially only autoantibodies against alpha-2-macroglobulin-like-1 of 170 kDa and desmoplakin I; after one year, IB detected

TABLE 1 | Cases of pemphigus with clinical shifting between PF and PV.

Reference	Transition	Age	Sex	Initial Ab	Transition period (years)	Ab after transition
Iwatsuki et al. (104)	PV to PF	36	F	NP	3	Dsg 1[a]
	PV to PF	58	F	NP	1	NP
Kawana et al. (105)	PV to PF	57	F	Dsg 3[a]	3	Dsg 1[a]
	PV to PF	46	F	Dsg 3[a]	3	Dsg 1[a]
Chang et al. (106)	PV to PF	47	M	NP	4	Dsg 1[a] Dsg 3[a]
Mendiratta et al. (107)	PV to PF	46	W	NP	NP	NP
Ishii et al. (108)	PF to PV	35	M	Dsg 1[b]	6	Dsg 1[b] Dsg 3[b]
Komai et al. (109)	PF to PV	40	NP	Dsg 1[b]	0.5	Dsg 1[a] Dsg 3[a,b]
	PV to PF and again to PV	38	NP	Dsg 1[a,b] Dsg 3[a,b]	1	Dsg 3[a,b] Dgs 1[a] Dsg 3[a,b]
Kimoto et al. (110)	PV to PF	77	F	Dsg 3[b]	5	Dsg 1[b]
Tsuji et al. (111)	PV to PF	55	M	Dsg 3[b]	3	Dsg 1[b]
Harman et al. (112)	PV to PF	44	F	Dsg 1[b] Dsg 3[b]	5	Dsg 1[b]
Toth et al. (113)	PV to PF	28	M	Dsg 1[b] Dsg 3[b]	2	Dsg 1[b]
Ng et al. (114)	PV to PF	29	M	NP	4	Dsg 1[b]
	PV to PF	56	M	NP	3	Dsg 1[b]
	PV to PF	45	F	NP	3	Dsg 1[b]
Park et al. (115)	PF to PV	48	M	Negative[a]	5	Dsg 1[b] Dsg 3[b]
Awazawa et al. (116)	PF to PV	79	F	Dsg 1[b]	1.5	Dsg 3[b]
Pigozzi et al. (117)	PF to PV	90	F	Dsg1[b]	0.7	Dsg3[b]
Lévy-Sitbon et al. (118)	PV to PF	47	M	NP	2.7	NP
España et al. (119)	PV to PF	49	M	Dsg 1[a]	2	Dsg 1[a]
	PV to PF	35	M	Dsg 3[a] Dsg 3[a]	3.8	Dsg 1[a] Dsg 3[a]
Ito et al. (120)	PV to PF	57	M	Dsg 1[b] Dsg 3[b]	0.2	Dsg 1[b]

[a]*Immunoblot.*
[b]*ELISA.*
Ab, antibodies; PV, pemphigus vulgaris; PF, pemphigus foliaceus; NP, not provided; Dsg, desmoglein.

also desmoplakin II, BP230, and periplakin (132). Therefore, it has been postulated that the lichenoid eruption, which led to necrosis of keratinocytes, might be a mechanism for exposing previously masked antigens to autoreactive T cells, leading to an intermolecular ES that involves other skin antigens. Another PNP case, in which ES might be involved, was reported by Okahashi et al. (133). They described a 41-year-old patient who initially showed only mucosal lesion; however, 3 months after PNP diagnosis, he also developed toxic epidermal necrolysis (TEN)-like cutaneous lesions. IgG against envoplakin and periplakin were detected by IB both at the time of PNP diagnosis and when the patient developed cutaneous lesion. Contrarywise, ELISA detected anti-Dsg1 and three IgG only after the arise of cutaneous lesion. Therefore, the authors proposed that autoimmune response led initially to interface and lichenoid dermatitis, which exposed self-antigens developing humoral autoimmunity mediated by ES (133).

In 2012 cloning monoclonal antibodies from a PNP patient by using phage display approach, the pathogenic activity of anti-Dsg3 autoantibodies has been demonstrated (134). Epitope mapping using domain-swapped Dsg3/Dsg2 showed that these monoclonal antibodies bound conformational epitopes in the EC2 and EC3 domains. In parallel, to study the Dsg3 epitope profile in PNP Ohyama et al. (20) tested sera from 14 patients. Interestingly, in addition to the reactivity against the EC1 subdomain of Dsg3 detected in all patients, 57%, 71%, and 86% of PNP sera reacted with the EC2, EC3, and EC4 subdomain, respectively. Thus, circulating antibodies in PNP had unique epitope profile, although, such as in PV and PF, the most recognized region is the Dsg N-terminal one. These findings were consistent with a previous study (135) and suggested that the typical autoantibody profile may have contributed to their unique clinical and histopathological features.

Several theories have been proposed to explain the association between bullous disease and tumor. One theory proposed that immune response against tumor antigens cross-reacting with epithelial antigen can lead to an autoimmune response against skin and mucous membrane (136). Another theory proposed that the tumors may have caused cytokine dysregulation leading to autoimmunity to Dsgs with subsequent tissue damage and intermolecular ES toward intracellular proteins of the plakin family and or hemidesmosomal proteins. However, although the pathogenic role of anti-Dsg3 autoantibodies has been demonstrated (134), autoantibodies to Dsg3 are not detected in all patients and not always detected at the beginning of the disease onset (133). Another possible explanation is that the cellular damage induced by tumor specific immune response could expose intracellular antigen, such as plakins, and lead to an autoimmune response to the skin and mucous membrane and a possible intermolecular ES toward other antigens such as Dsgs.

Indeed, with the exception of few case reports, the dynamics of humoral response during disease course was not reported in PNP patients and could be the objective of future studies.

Epidermolysis Bullosa Acquisita

Epidermolysis bullosa acquisita is an acquired, subepidermal bullous disease. The main feature of EBA is autoimmunity to Col VII with consequent reduction of anchoring fibrils (137). On the one hand, a classical "mechanobullous" form has been described, which is characterized by blistering, erosions with milia formation, and scarring over trauma exposed sites (138). On the other hand, several patients with an "inflammatory" form of EBA mimicking BP, characterized by blisters on intertriginous areas that heal without scars, have been reported (138). Clinical diagnosis is confirmed by demonstration of IgG and/or IgA and C3 deposits at the BMZ by DIF. In EBA, IIF performed on salt-split skin (SSS) usually shows binding of antibodies to the dermal side of the blister and circulating autoantibodies bind to Coll VII by ELISA or IB (139). Specifically, EBA is mainly characterized by IgG autoantibodies to the non-collagenous domain (NC1) of Coll VII (137, 139). However, no evidence of intramolecular and intermolecular ES in an active mouse model of EBA was found. Reactivity to additional regions outside Coll VII did not occur in mouse suggesting that ES does not contribute to EBA development in this mouse model (140).

Epitope spreading that involves EBA antigen is reported in sera from patients with SLE that contain autoantibodies to Coll VII (141, 142). Chan et al. reported the case of a 15-year-old patient, who showed IgA and IgG circulating autoantibodies against BP230, as well as against the full-length native form and the recombinant NC1 domain of Coll VII (143). In addition, IgG autoantibodies against laminin 332 and laminin 311 have been detected in the same patient. These findings could be explained by an intermolecular ES phenomenon. Indeed, because the NC1 domain of Coll VII bound to the β3 chain of laminin 332, it was thought that the initial autoimmune reaction against Coll VII led to secondary damage of laminin 332 and other adjacent BMZ component, like laminin 311 and BP230 (144). In addition, several reports of EBA patients who subsequently developed SLE or vice versa have been described and could represent the effect of an ES phenomenon (141, 143, 145–150) (**Table 2**). Dotson et al. were the first to describe a 19-year-old EBA patient, who developed clinical and serologic evidence of SLE five years after the diagnosis of EBA (145). Cutaneous lesions examined by electron microscopy before and after the development of SLE

TABLE 2 | Patient showing coexistence of EBA and SLE disease and/or antigens.

Reference	Number of patients	First diagnosed disease	Age and sex	Laboratory findings	Method	Note
Dotson et al. (145)	1	EBA	19, F	ANA (1:2560), anti-U1RNP Ab	–	SLE diagnosis 5 years after EBA diagnosis
Barton et al. (146)	1	BSLE	18, F	IgG against COLVII	IB	–
Gammon et al. (141)	4	1 Pt SLE; 3 Pt BSLE	3 Pt 20–23, 1 Pt 50; 3 F, 1 M	IgG against COLVII	WB	–
Kettler et al. (147)	1	EBA/BSLE?	8, F	ANA (1:2560), anti-U1RNP Ab, anti-Sm Ab	–	–
Boh et al. (148)	3	EBA	34, F	Homogeneous ANA (1:160) anti-dsDNA Ab (1:640), anti-U1RNP Ab	–	SLE diagnosis 2 years after EBA diagnosis
			51, F	Speckled ANA (1:640), low C3, anti-dsDNA Ab (1:40), anti-U1RNP Ab		SLE diagnosis 3 years after EBA diagnosis
			57, F	Speckled ANA (1:640), anti-ds-DNA Ab, anti-U1RNP Ab, anti-Sm Ab		SLE diagnosis 14 years after EBA diagnosis
McHenry et al. (149)	1	SLE	77, M	–	–	EBA diagnosis 6 years after SLE diagnosis
Yoon et al. (150)	1	EBA	38, F	–	–	EBA preceded a dramatic SLE flare with fatal cerebral vasculitis
Chan et al. (143)	1	BSLE	15, F	IgA and IgG against BP230, NCA1 domain of COLVII; IgG against LAM5 and LAM6	IB	–

Ab, antibodies; BSLE, bullous systematic lupus erythematosus; COLVII, collagen VII; F, female; IB, immunoblotting; LAM, laminin; M, male; Pt, patient; SLE, systematic lupus erythematosus; WB, Western blot.

showed characteristics previously reported by electron microscopy in patients with EBA. DIF before and after the diagnosis of SLE highlighted linear depositions of immunoglobulin and complement; IIF findings showed no abnormalities.

It has also been reported that EBA is associated with inflammatory bowel disease (IBD) in up to 50% of patients (151). Indeed, a high prevalence of circulating antibodies against Coll VII in IBD patients has been detected (151, 152). Furthermore, Lohi et al. evidenced the presence of Coll VII in the intestinal epithelium (153). Therefore, it has been speculated that autoimmunity to Coll VII, which is present in both gut and skin, might justify the frequent association between EBA and IBD. Moreover, Coll VII antibodies in Crohn's disease patients may be an ES phenomenon. Veritably, inflammation provoked by Crohn's disease may alter the intestinal epithelial BMZ, leading to an ongoing autoimmunity to Coll VII (154).

A few cases of psoriasis associated with EBA have been reported (155–161). In these cases, the role of ES is not clear and it could be postulated that its involvement is due to the long-lasting psoriasis lesions. Specifically, a damage to the BMZ could induce circulating non-pathogenic autoantibodies that lead to development of immunobullous diseases (161).

Epitope spreading phenomenon has been thought also as the leading cause of the concomitant presence of two different autoimmune bullous skin diseases in the same patient (162–167) (**Table 3**). As reported by Yang et al. ES phenomenon could be the explanation of a case of typical pemphigoid gestationis with IgG antibodies to Coll VII (167). In this report, the patient showed a rash on the trunk and limbs with intense erythema, vesicles, and bullae one month postpartum. IB detected IgG autoantibodies reacting against BP230 in the epidermal extracts and 290 kDa Coll VII in the dermal extracts; BP180 antibodies were detected only using an ELISA based on BP180 antigen. Therefore, the authors concluded that these immunopathological findings could be explained by intermolecular ES phenomenon (167). Jonkman et al. described recently a female patient with inflammatory EBA showing non-scarring oral and vaginal involvement (163). Circulating IgG autoantibodies to Coll VII and α3 chain of laminin 332 were simultaneously detected by IB. To further confirm the simultaneous presence of autoantibodies against laminin 332 and Coll VII, IIF on skin substrates lacking BMZ molecules was performed. IgG bound to the BMZ of specimens lacking laminin 332 and Coll VII, revealing the simultaneous presence of two autoantibodies. Therefore, a simultaneous diagnosis of EBA and anti-laminin 332 MMP was made. The significance of the anti-laminin 332 antibodies remains obscure, but it may be determined by the pathogenic presence of anti-Coll VII autoantibodies; indeed, cryptic laminin 332 epitopes could be uncovered in lesional skin, leading to intermolecular ES. The fact that laminin 332 and Coll VII are intimately connected, because the β3 chain of the former binds the NC1 domain of the latter, could suggest a mechanism dependent of physical association of antigens.

Linear IgA Bullous Dermatosis (LABD)

Linear IgA bullous dermatosis is an autoimmune subepidermal bullous disease that may be idiopathic or drug-induced (168). Pathologically, LABD is characterized by linear deposition of IgA at the BMZ (168). Dermal and epidermal antigens are identified by IgA, IgG, and by both antibody isotypes (169, 170). Proteolytic cleavage product of BP180 are the major antigen, but also BP230 and Coll VII are less commonly detected (169, 170). In the epidermis, BP180 is the major and possibly initiating antigen (169, 170). Indeed, different binding sites for the LABD antibodies have been reported on BP180 in studies in which the full-length protein, the 120-/97-kDa fragments of its soluble ectodomain and the immunodominant NC16A domain were employed (169–175). These studies showed that intramolecular ES could occur within BP180 leading to the simultaneous binding of IgA antibodies to intact BP180 and its soluble ectodomain. Allen et al. reported in a recent study that no sera identified the dermal 97-kDa protein, while they detected antibody response to a 285 kDa antigen (LABD285) and BP180, suggesting that intermolecular ES of the antigens of the extracellular matrix/dermal components of the basement membrane plays a role in LABD etiopathology (169). In another study, Allen et al. reported that 35% of LABD sera targeted single antigens and 42% targeted two or more antigens with IgA antibodies (170). The presence of multiple epidermal antigens was commoner in adults (51%) than in children (25%), and might be due to a continual antigenic stimulation. Therefore, they suggested that both intra- and intermolecular ES led to the multiplicity of IgA target antigens (170). Indeed, they reported that 34 of 72 IgA antibodies binding BP180 also bound BP230. In addition, they showed that of 72 LABD sera binding BP180, 23 bound also both BP230 and LABD285, and two bound LABD285. Intramolecular ES within BP180 was reported more rarely, with 19 of 72 sera also binding the 97-kDa soluble ectodomain. In contrast to IgA, intermolecular ES with IgG antibodies was rarely reported, and did not involve LABD285. In conclusion, Allen et al. have proposed that the intermolecular ES is frequent in LABD, is age related, and is associated with IgA antibodies rather than IgG antibodies (170). Recently, Sakaguchi et al. described three patients, in whom ELISA detected IgG and IgA antibodies

TABLE 3 | EBA associated with other autoimmune bullous disease.

Reference	Number of patients	Age and sex	Other disease	Laboratory findings	Method
Kawachi et al. (162)	1	1, M	BP	IgG against BP180 NC16A domain	IB
Jonkman et al. (163)	1	64, F	MMP	IgG against laminin α3 subunit	IB
Furukawa et al. (164)	1	29, F	Anti-p200 pemphigoid	IgG against γ1 subunit	IB
Buijsrogge et al. (165)	1	70, M	EBA	IgA against plectin	IB
Osawa et al. (166)	1	75, M	LABD	IgG against 120 kDa antigen	IB
Yang et al. (167)	1	22, F	PG	IgG against BP180 and BP230	IB

BP, bullous pemphigoid; EBA, epidermolysis bullosa acquisita; F, female; IB, immunoblotting; LABD, linear IgA bullous dermatosis; M, male; PG, pemphigoid gestationis.

to various subunits of laminin 332, in addition to IgG and IgA reactivity to Coll VII, γ1 subunit, and BP230 and BP180 recombinant proteins (176). A strong IgG and IgA reactivity to laminin 332 has been seldom described in the literature. The authors postulated that the production of autoantibodies against different BMZ antigens was led by ES. Even if the original epitopes in these cases were not detectable, the first immune response might be directed to laminin 332 because of the marked and constant reactivity. Nevertheless, because of the variegated antigen subset in LABD, several patients with peculiar laboratory findings whose epitope/antigen pattern could be due to ES have been described in the literature (177–199) (**Table 4**).

The ES phenomenon has been also proposed to be involved in LABD patients with psoriasis (200, 201). Cooke et al. reported the case of a 29-year-old man with plaque psoriasis who developed LABD after herpes zoster infection. IB detected IgA antibodies

TABLE 4 | Characteristics of LABD patients with peculiar laboratory findings.

Reference	Number of patients	Findings	Method	Note
Kanitakis et al. (177)	1	IgA against BP230	WB	–
Zambruno et al. (178)	1	IgA against 290 kDa antigen of anchoring fibrils	WB	40 years old, M
Berard et al. (179)	1	IgA against BP230	WB	18 months old, F
Hashimoto et al. (180)	1	IgA against CollVII	IB	–
Kawahara et al. (181)	2	IgG and IgA antibodies on dermal side of SSS	IIF	–
Ghohestani et al. (182)	6	IgA against BP230	IB	–
	5	IgA against BP180		
Honoki et al. (183)	1	IgG against a 230 kDa epidermal antigen	IB	54 years old, F
Wakelin et al. (184)	1	IgA against CollVII	WB	76 years old, M
Nie et al. (185)	14	IgA against the XV collagenous domain of BP180, and NC16A of BP180	IB	–
Lin et al. (186)	4	IgA against NC16A domain of BP180	IB	–
Metz et al. (187)	1	IgA and IgG against BP180	WB	39 years old, F
Shimizu et al. (188)	1	Linear deposition of IgA and IgG along the BMZ	DIF	78 years old, M; localized IgA/IgG LABD
Passos et al. (189)	1	Linear deposition of IgA and IgG along the BMZ	DIF	21 years old, F
Yanagihara et al. (190)	1	Linear deposition of IgA and IgG along the BMZ	DIF	35 years old, M; Vogt-Koyanagi-Harada disease
Sakaguchi et al. (176)	3	Pt 1 IgG against laminin α3, laminin β3, laminin γ2; IgA against laminin α3, laminin β3, laminin γ2, Coll VII, Laminin γ1, BP180-C	IB	81 years old, F; K pancreas
		Pt 2 IgG against laminin α3, laminin γ2; IgA against lamininα3, laminin γ2, BP230, BP180-C		88 years old, M; K colon
		Pt 3 IgG against laminin γ2, BP180-N; IgA against laminin α3,		64 years old, M
Kern et al. (191)	1	IgA against the 120 kDa ectodomain of BP180 and Dsg3		48 years old, M; Ulcerative colitis; Overlap LABD and IgA Pemphigus?
Tashima et al. (192)	1	IgA against BP180 NC16A	IB	84 years old, M
Zenke et al. (193)	1	IgA against the 145- and 165-kDa α3 subunits of laminin 332	IB	62 years old, M
Izaki et al. (194)	1	IgA and IgG against the 165-kDa and 145-kDa forms of α3 subunit and the 105-kDa γ2 subunit of laminin 332	IB	53 years old, M
Li et al. (195)	1	IgG and IgA against laminin α 3, laminin-β3 and laminin γ2; IgG and IgA against α6 and β4 subunit of integrin	IB	80 years old, M
Fernandes et al. (196)	1	Linear deposition of IgA and IgG along the BMZ	DIF	7 years old, M
Izaki et al. (197)	1	Linear deposition of IgA and IgG along the BMZ	DIF	5 months old, M
Koga et al. (198)	1	IgG against desmocollin 1	ELISA	70 years old, M; transition from LABD to PH/coexistence of both LABD and PH
Matsuura et al. (199)	1	IgA against NC16A domain of BP180; no reaction to LAD1 shed ectodomains of BP180	IB	29 years old, F; pregnancy (38th week)

BMZ, basal membrane zone; BP, bullous pemphigoid; K, carcinoma; COLL, collagen; DIF, direct immunofluorescence; Dsg, desmoglein; F, female; IB, immunoblotting; IIF, indirect immunofluorescence; M, male; PT, patient; PH, pemphigus herpetiformis; SSS, salt-split skin; WB, Western blot.

against BP180 and BP230 antigens, and IgG autoantibodies that reacted weakly to the BP180 antigen (200). A similar case was previously reported by Takagi et al. who described the simultaneous presence of psoriasis and LABD in a 68-year-old man after an active hepatitis C infection. In this case, IB detected IgA antibodies against a 97-kDa target antigen in epidermal extracts (201).

LABD has been also reported in association with autoimmune rheumatic diseases, including dermatomyositis, rheumatoid arthritis, and Sjögren's syndrome (202–206). However, the role of ES in these associations is under debate.

The association between LABD and ulcerative colitis (UC) has been widely reported. Indeed, Paige et al. reported that 8 out 70 LABD patients were also affected by UC (207). In all cases, UC preceded LABD onset by a median of 6.5 years. In addition, a few single cases of LABD associated with UC have been reported (191, 207–211) (**Table 5**). The reason for this association is unclear, but alteration in colonic mucosal B cell and IgA production may play a pivotal role in LABD onset.

Dermatitis Herpetiformis

In gluten sensitive individuals, gluten can lead to pathological immune responses against both gluten components and transglutaminases (TGs). DH belongs to gluten-induced autoimmune diseases. DH is characterized by chronic, pruritic, polymorphic, papulovesicular, or rarely blistering lesions. Histologically DH, such as other subepidermal autoimmune diseases, presents subepidermal blisters neutrophil and eosinophil infiltration and granular IgA deposition in the dermal papilla by DIF. DH patients show circulating IgA to TG3, which is the pivotal autoantigen (212, 213). In most of DH patients, IgA to TG2 are detected, indicating an underlying, usually latent or mild celiac disease (CD) (212, 213). A TG6 autoimmunity may also be detected in some DH patients (212, 213). Furthermore, in a few DH patients, no circulating IgA to TG3 have been reported, but only circulating TG3-IgA immune complexes (212, 213). All three enzymes (TG2, TG3, and TG6) bind deamidate gliadin or other gluten peptides. This diversification of autoimmune antigens could be explained by intermolecular ES. Indeed, it has been postulated that a continued exposure to gliadin could lead to development of IgA anti-TG3 antibodies in patients who already have IgA anti-TG2 antibodies; a subgroup of those who develop IgA anti-TG3 antibodies then develop DH (214). The presence of IgA anti-TG2 antibodies in most DH patients and a higher prevalence of IgA anti-TG3 antibodies in adults than in children with CD are two of the main findings in support of the ES phenomenon (213). In fact, it has been thought that ES could be an explanation for the DH late onset in comparison to CD, which often involves pediatric patients. In this regard, it has been hypothesized that ES and/or cross-reactivity between TG2 and TG3 could lead to TG3 autoimmunity, leading to circulating IgA-TG3 immune complexes formation, which determines skin features in some CD patients (213). However, the possible mechanism of a directly gluten-induced TG3 autoimmunity could not be excluded (213).

Several cases of patients with a history of DH and BP have been reported (215–228) (**Table 6**). Van der Meer was the first to describe a patient showing clinically both DH and BP features, but only pathological and DIF BP features were found (215). In six cases, DH preceded BP by 4 months to 11 years (223–225). Ameen et al. reported a case of DH that evolved into BP 11 years after its original diagnosis (225). Initially, DIF showed linear BMZ staining with IgG and C3, associated with intensefibrillar IgA staining in the dermal papillae. IIF detected circulating anti-BMZ IgG with epidermal binding on SSS. After 11 years, the response to dapsone and gluten-free diet failed, and a new skin biopsy was performed, revealing overlapping BP/DH immune-histochemical features. Therefore, the authors concluded that the evolution from DH into BP was due to intermolecular ES phenomenon, postulating that neutrophilic infiltrate of DH caused BMZ disruption, leading to the exposure of BP antigens to autoreactive lymphocytes (155, 225). In 11 cases, dual findings for BP and DH were detected by DIF (220–227). On the one hand, BP and DH were described as concomitant in nine cases (220, 221, 223–227); on the other hand, in two patients, DIF was performed at different time, showing only one disease per biopsy (222, 228). In five of the nine patients, serum antibodies were directed against the BMZ, and in one patient only antiendomysial antibodies were highlighted at the DH onset (223). Only two patients with serum autoantibodies compatible with both BP and DH have been described, however, sera were not taken at the same time (222, 228). Indeed, only Schulze et al. detected both BP and DH serum autoantibodies at the same time (227). In addition, Vaira et al. analyzed the HLA profile in a patient, who developed DH several years after the BP diagnosis. HLA alleles were HLA-DQB1 03:01 (predisposing to BP), HLA-DQA1 05:05/05:01 (predisposing to CD) and HLA-DQB1 02:01 (predisposing to CD and to DH) (228). The authors concluded that those findings highlighted a specific genetic susceptibility to both diseases in the same patient (228).

TABLE 5 | LABD patients with UC.

Reference	Number of patients	Sex	Age at UC diagnosis	Age at LABD diagnosis
Chan et al. (208)	1	M	76	80
Paige et al. (207)	8	M	12	20
		M	36	41
		M	52	60
		F	30	38
		M	59	60
		F	21	64
		F	7	8
		M	45	47
De Simone et al. (209)	1	–	–	–
Chi et al. (210)	1	F	11	41
Keller et al. (211)	1	M	54	54
Kern et al. (191)	1	M	-	48

F, female; LABD, linear IgA bullous disease; M, male; UC, ulcerative colitis.

Mucous Membrane Pemphigoid

Mucous membrane pemphigoid includes different autoimmune subepithelial blistering diseases mainly involving mucous membranes, including the mouth, ocular mucosae, and mucous membranes of the nose (229). Several epithelial basement membrane components have been reported as potential targets of

TABLE 6 | Patients with a history of DH and BP.

Reference	Number of patient	Clinic	Pathology	DIF positive for both BP and DH	Note
Van der Meer et al. (215)	1	DH + BP	BP	–	BP features detected by DIF
Honeyman et al. (216)	1	Switch from DH to BP	Switch from DH to BP	–	–
Jablonska et al. (217)	9	Concomitant DH and BP	Concomitant DH and BP	–	–
Bean et al. (218)	7	DH	Concomitant DH and BP	–	–
Honeyman et al. (219)	1	Concomitant DH and BP	Concomitant DH and BP	–	Initially negative, later circulating BP antibodies
Jolliffe et al. (220)	1	Concomitant DH and BP	BP	+	57 years old, F
De Jong et al. (221)	1	Concomitant DH and BP	Concomitant DH and BP	+	–
Jawitz et al. (222)	1	DH	BP; only DH 5 years later	+	41 years old, F
Sander et al. (223)	1	First DH; BP after 5 years	First DH; BP after 5 years	+	68 years old, M
Setterfield et al. (224)	1	First DH; both DH and BP 25 years after	First DH; both DH and BP 25 years after	+	58 years old, M
Ameen et al. (225)	1	First DH; BP 11 years after	First DH; both DH and BP 11 years after	+	84 years old, F
Murphy et al. (226)	3	First DH; DH and BP later (4 months, 1 and 11 years)	-	+	83 years old, 2 M; 84 years old, F
Schultze et al. (227)	1	DH	Non-specific for BP or DH	+	77 years old, M; BP and DH serum autoantibodies simultaneously
Vaira et al. (228)	1	First BP; later DH	DH during the follow-up	+	48 years old, M

BP, bullous pemphigoid; DH, dermatitis herpetiformis; DIF, direct immunofluorescence; F, female; M, male.

MMP, including BP180, BP230, Coll VII, laminin 332, laminin 311, α6 and β4 integrin subunits (229). The main MMP features is the presence of linear deposits of immunoglobulins (IgG and/or IgA), and/or complement fragments at the dermal–epidermal and/or chorioepithelial BMZ (230). Due to low circulating autoantibodies titers IIF is often negative. For diagnosis detection by ELISA or IB of two major targets of MMP BP180, principally its extracellular domain (231–233), and laminin 332, which are both constitutive elements of anchoring filaments can be of confirmatory value. Therefore, MMP is divided into two major types, anti-BP180-MMP and anti-laminin332-type MMP (234).

The involvement of ES phenomenon in MMP has been postulated in several studies (235–238). It has been thought that in BP180-MMP the development of autoantibodies to laminin 332, which has a pathogenic role in the disease (239), is produced *via* ES from BP180 C terminal domain to laminin 332, because of physical interaction of BP180 C terminal domain and laminin 332 in epidermal BMZ (238). Indeed, Yasukochi et al. reported that IgG or IgA antibodies against various subunits of laminin 332 were detected in 54 of 332 cases of BP180-MMP (238). Bernard et al. presumed the involvement of ES phenomenon in a recent study on laminin 332-MMP, which has reported to be associated with a raised relative risk for neoplastic diseases (235). On the one hand, anti-BP180 auto-antibodies have been detected in up to 75% MMP patients (240); on the other hand, autoantibodies against BP230 have only been occasionally identified in MMP serum, as reported also by Bernard et al. (235). Furthermore, anti-BP230 antibodies have been more oftenly detected in anti-laminin 332 MMP patients (235). This association has been described as determined by ES phenomenon. In point of fact, it has been postulated that damage to BMZ might lead to an abnormal exposure of intracellular antigens such as BP230. In addition, Bernard et al. concluded that the phenomenon of ES could be also postulated for the NC16A domain of BP180, which is strongly immunogenic (231, 235). Another interesting case of possible intermolecular ES was reported by Inoue et al. (104). The authors described one MMP patient, who showed only anti-BP230 autoantibodies. Indeed, IgG antibodies reacted neither with the BP180 NC16A domain nor with the C-terminal domain. Moreover, IB and ELISA identified exclusively anti-BP230 antibodies in the patient's serum. Furthermore, patient serum did not show reactivity either with any subunits of laminin 332 or with the 120-kDa fragments of BP180 (LAD1). Since the release of autoantibodies to the cytoplasmic protein BP230 is considered a secondary phenomenon, the authors speculated that intermolecular ES could occur because of the oral mucosa ulcerations that led to IgG anti-BP230 production (241). In this context, Hayashi et al. described a MMP patient with blisters who showed IgA and IgG autoantibodies that targeted both laminin 332 and BP180 (242).

The ES phenomenon may be also involved in MMP patients with a history of different autoimmune diseases that involve skin, mucous membrane or different organs (243–251) (**Table 7**). In a recent study on 6 MMP patients, Zakka et al. postulated the involvement of ES phenomenon in patient with both MMP and mixed connective tissue disease (MCTD) (244). MCTD is a systemic autoimmune disease with mixed features of SLE, dermatomyositis, rheumatoid arthritis, scleroderma, and polymyositis (252). The target antigen is a complex of small nuclear ribonucleoproteins (snRNPs), including a 70 kDa polypeptide (snRNP70) (252). The authors observed that all the 6 MMP patients, which showed antibodies against BP180, BP230, and subunit of human β4 integrin, showed antibodies also to snRNP70 (244). Moreover, they reported that all MMP patients carried either the HLA II alleles DQb1*0301, *0302, or *0603 that have been described as associated with MMP (244). However, only three of six patients carried the HLA alleles associated with MCTD (HLADR4). Although the remaining three patients did

not have any allele associated with MCTD, they had MCTD clinical features and serological markers (244). The presence of one autoimmune disease could induce tissue damage and exposure to the immune system of a previously masked epitope. Therefore, the authors concluded that it was possible for the patients who lacked the HLA II genes related to MCTD to produce autoantibodies to snRNP70 as result of an ES phenomenon. In addition, Malik et al. described 8 patients who showed an association of MMP with SLE, MCTD, or both (243). Among them, four patients developed MMP and SLE or MCTD simultaneously, while the other four patients developed SLE, MCTD or both after the MMP diagnosis in a period ranging from 2 to 10 years. ES phenomenon could be also involved in the association between subepidermal autoimmune blistering diseases and IBD, as postulated by Shipman et al. (245). In a recent article, the authors reviewed the literature about this association, finding out 48 cases of IBD patients who showed also a subepidermal blistering disease. More specifically, they reported two female patients who developed MMP several years after the first IBD diagnosis. In both cases, DIF showed linear staining for IgG and C3 at the BMZ. However, only in one case IB detected IgG antibodies to the BP180 antigen. Therefore, the authors theorized that exposure to antigens in the gastro-intestinal tract eventually led to cutaneous disease, which was also supported by the positive DIF in the colon in two LAD patients (253) (**Table 7**). A supposed intermolecular ES was reported by Ohata et al., who described a singular patient who was affected simultaneously by pemphigus herpetiformis (PH) and MMP with autoantibodies to the laminin γ2 subunit, Dsc1, and BP180 C-terminus (249). Therefore, the authors postulated that ES from Dsc1 to BMZ antigens might lead to the simultaneous occurrence of PH and MMP, although such phenomenon was not demonstrated (249). Kaune et al. described an 87-year old Caucasian female patient with complete symblepharon and dysphagia who showed by IB IgG4 autoantibodies both to the 200 kDa antigen and to the C-terminus of laminin γ1 subunit; in addition, IgA autoantibodies to the C-terminal fragment of BP180 4575-antigens and IgG autoantibodies to BP180 NC16A have been detected in the same patient by IB (250). The authors postulated the involvement of ES, describing the coexistence of p200/laminin γ1 subunit-pemphigoid and MMP. Monshi et al. reported the case of a Caucasian woman affected by anti-p200 pemphigoid who developed antiepiligrin cicatricial pemphigoid, a rare and major subtype of MMP, 17 months after the first diagnosis (247). However, this patient never developed mucosal lesions. In these cases, the ES phenomenon could be postulated but not demonstrated as the cause of two concomitant diseases.

On the contrary, when the transition from one disease to another is accompanied by shifting of reactivity from one antigen to another, the ES phenomenon is strongly probable. Several cases of clinical switch from a skin disease to MMP have been reported in the literature (60, 254–257) (**Table 8**). Chan et al. reported in 1991 five Steven-Johnson's syndrome (SJS) patients, who

TABLE 7 | MMP patients associated with other autoimmune diseases.

Reference	Number of patients and disease	Multiple antigens	Method	Note
Malik et al. (243)	2 concomitant MMP + SLE 2 concomitant MMP + MCTD 2 MMP who developed SLE 1 MMP who developed MCTD 1 MMP who developed SLE/MCTD	Ab against β4 integrin subunit (8 Pt); Ab against BP180 (6 Pt); Ab against BP180 and a 240 kDa antigen (2 Pt)	IB	Coexistence of MMP, SLE and/or MCTD
Zakka et al. (244)	3 MMP	Ab against snRNP70	ELISA	Pt who lacked any HLA II genes associated with MCTD may produce *via* epitope spreading Ab against snRNP70
Shipman et al. (245)	1 UC; 1 CD	Linear staining for IgG and C3 at the BMZ IgG anti-BMZ on the dermal side of SSS	DIF IIF	IB showed IgG against BP180 only in Pt with Crohn's disease
Takegami et al. (246)	1 concomitant MMP + LAD + SS	IgG and IgA against laminin α3 subunit; IgA against 120 kDa antigen	IB	Simultaneous diagnosis of MMP, LAD, and SS
Monshi et al. (247)	1 anti-p200/anti-LAM γ1 pemphigoid	IgG against α3 chain of laminin 332	IB	86 years old, F; no mucosal involvement
Yamada et al. (248)	1 PNP	IgG against γ2 subunit of laminin 332	IB	68 years old, M; K thyroid, kidney CCK, follicular dendritic cell sarcoma in the retroperitoneal area.
Ohata et al. (249)	1 PH	IgG and IgA against BP180 C-terminus; IgG against γ2 subunit of laminin 332	IB	63 years old, M; no mucosal involvement
Li et al. (250)	1 anti-p200/anti-LAM γ1 pemphigoid	IgG against γ1, α3 and β3 subunit of laminin 332	IB	72 years old, M; psoriasis
Kaune et al. (251)	1 anti-p200/anti-LAM γ1 pemphigoid	IgA against C-terminal fragment of BP180; IgG against BP180 NC16A	IB	87 years old, F

Ab, antibody; BMZ, basal membrane zone; CD, Crohn's disease; DIF, direct immunofluorescence; F, female; M, male; IIF, indirect immunofluorescence; IB, immunoblotting; LAD, linear IgA dermatosis; MCTD, mixed connective tissue disease; MMP, mucous membrane pemphigoid; Pt, patient; SLE, systemic lupus erythematosus; SS, Sjögren syndrome; UC, ulcerative colitis; BP, bullous pemphigoid; K, carcinoma; CCK, clear cell carcinoma; PH, pemphigus herpetiformis; PNP, paraneoplastic pemphigus.

TABLE 8 | Reported case of switch to MMP.

Reference	Number of patients and disease	DIF (number of patients)	IIF (number of patients)	ELISA (number of patients)	IB (number of patients)	Note	Clinical switch
Chan et al. (254)	5 SJS	Performed (5/5)	Performed (2/5)	NP	Pt 1 120 and 140 kDa epidermal antigen Pt 2 120 kDa epidermal antigen	Pt 1 59 years old, M; MMP onset 6 months after SJS Pt 2 6 years old, M; MMP onset 31 years after SJS Pt 3 22 years old, M; MMP onset 14 months after SJS Pt 4 33 years old, F; MMP onset 2 years after SJS Pt 5 34 years old, F; MMP onset 2 years after SJS	From SJS to MMP
De Rojas et al. (255)	5 LS	Performed (1/5)	NP	NP	NP	–	From LS to MMP
Mignogna et al. (256)	2 OLP	Performed (2/2)	Performed (2/2)	Ab against BP180	NP	Pt 1 72 years old, F Pt 2 64 years old, F	From OLP to MMP
Fania et al. (257)	2 LS	Performed (2/2)	Performed (2/2)	Performed (2/2)	NP	Pt 1 80 years old, M; MMP onset 6 months after LS Pt 2 60 years old, M; MMP onset 2 months after LS	From LS to MMP
Sardy et al. (60)	BP	Performed	NP	IgG against laminin 332	IgG4 against laminin 332	18 years old, F; MMP transition 5 years after the BP diagnosis	From BP to MMP

BP, bullous pemphigoid; DIF, direct immunofluorescence; F, female; IIF, indirect immunofluorescence; IB, immunoblotting; LS, Lyell's syndrome; M, male; MMP, mucous membrane pemphigoid; NP, not performed; OLP, oral lichen planus; Pt, patient; SJS, Steven-Johnson's syndrome.

developed MMP (254). SJS is a life-threatening dermatosis with high morbidity and mortality. These patients developed MMP, characterized by chronic ocular mucosal scarring lesions. The linear immune deposits along the oral or ocular mucosal BMZ in all five patients fulfilled the diagnostic criteria for MMP. In addition, immunoblot analysis of the serum of two of five patients identified a 120-kDa epidermal antigen, which may represent one of the MMP autoantigens (258). The authors concluded that the mucosal injury occurred in SJS resulted in ES phenomenon involving the 120-kDa epithelial antigen (254). Similarly, Fania et al. described two male patients who developed MMP with chronic ocular mucosal scarring lesions after TEN (257). In both patients, DIF on perilesional conjunctiva showed IgG and C3 deposits along the BMZ in a linear pattern, while IIF and ELISA for BP180 and BP230 were negative. Although the association between TEN and MMP may be coincidental, the authors hypothesized that chronic eye surface injury might represent an immunologic trigger, leading to the ES phenomenon. Moreover, five cases similar to those reported by Fania et al. were described by De Rojas et al. (255) (**Table 8**).

Finally, it has been also reported that MMP can arise in patient with hematological disease or solid malignancies, possibly involving the ES phenomenon (259–267). It has been postulated that the massive alteration of tumoral cells or tissues could lead to an autoimmune disease through cross-reactive antigens or exposure of criptic epitopes followed by an ES phenomenon.

Lichen Planus Pemphigoides

Lichen planus pemphigoides is a rare autoimmune blistering disease that occurs in association with LP. DIF shows linear deposits of IgG and C3 along the BMZ with fibrillary deposits of fibrin at the epithelial/lamina propria junction. By IB and ELISA LPP sera are strongly reactive with BP180. More specifically, LPP sera reacted with AA 46–59 of NC16A domain, previously shown to be unreactive with BP sera (268). Mignogna et al. reported two cases of oral lichen planus (OLP) who switched to MMP in a period ranging from 3 to 11 years (256). They hypothesized that the patients might be an example of the ES phenomenon suggesting that LPP might not exist as a separate disease, but might be the result of the ES from one disease (OLP) to another (BP/MMP), where the lichenoid papules arise before the vesciculobullous lesions or vice versa. In particular, the BMZ break, due to mast cell degranulation, might have continuously exposed BMZ proteins, such as BP180 and laminin-322, that may lead to an autoimmune humoral response (256). Another case from Sekiya et al. presented at first LP lesions on the hands, and than developed blisters on her limbs and erosions of the buccal mucosa (269). The patient's serum reacted to IgG autoantibodies against the BP180 NC16A domain, the BP180 C-terminal domain and Dsg1. However, a serum sampled one and a half years before the diagnosis of LP did not shown activity to BP180 domains. These findings may evidence that the damage to the basal cells in LP exposed a sequestered antigen or formed neoantigens, producing pathogenic autoantibodies that lead to LPP. Most of the previous LPP cases showed autoantibodies to the NC16A domain of BP180. This report demonstrates the presence of circulating autoantibodies to BP180 only after the development of blisters, suggesting the role of sequestered antigen exposure or neoantigens in the LPP etiopathogenesis.

IMPLICATIONS FOR THERAPY

Treatment regimens for autoimmune blistering skin diseases rely on general immunosuppression, typically with corticosteroids, steroid-sparing immunosuppressive drugs, and/or adjunctive treatments such as intravenous immunoglobulins or plasmapheresis. The B cell-depleting anti-CD20 antibody (rituximab) has emerged as a major option for pemphigus patients with steroid-resistant disease or when there are adverse effects with conventional therapies. Data from a recent clinical trial suggest that first-line use of rituximab plus short-term prednisone is safe and more effective than using prednisone alone (270). However, these approaches impair the efficiency of the immune response and render the treated subjects to be more susceptible to the infections. In addition, since patient morbidity and even mortality results from side effects of treatment, the development of more targeted therapies that leave the immune system functional and able to neutralize pathogens is desirable.

To overcome this problems therapy for autoimmune diseases should eliminate only pathogenic autoimmune cells such as performed by Ellebrecht et al. for pemphigus therapy. They have recently demonstrated that autoantigen-based chimeric immunoreceptors can direct T cells to kill Dsg3-specific B cells *in vivo* (271). Another target specific approach could be based on therapeutical peptides (such as decoy peptides) able to specifically deplete pathogenic autoantibodies (45). The association of PV with human leukocyte antigen class II alleles has highlighted the role of the presentation of immunodominant peptides to autoreactive T helper cells. In parallel, the correlation of disease activity and autoantibodies of the IgG4 and IgE subclasses underlines the role of T helper 2 cells as critical regulators of pemphigus pathogenesis. In this context, novel therapeutic approaches that target autoreactive T cells functions could be also relevant in future. In this context, therapeutic peptide vaccine approach for the restoration of immune tolerance is currently investigated (272, 273). An interesting study on MS, which has led to a phase I clinical trial in humans, has used peripheral blood mononuclear cells chemically engineered to present peptides (274). Thus, the evidence that an ES phenomenon may change the epitope/antigen profile during the course of the disease and the demonstration of its pathological role could make the development of epitope/antigen-specific therapies more difficult.

An ideal therapeutic approach should be able to eliminate not only specific pathogenic autoantibodies present at disease onset but also those arising during the course of disease through the ES phenomenon. In addition, it should be considered that whereas the epitope/antigen specific therapeutic approaches involve untreated bullous disease patients, the performed studies involving treated patients could have underestimated the impact of ES in disease progression.

In the light of published data on ES in the autoimmune blistering disease, the possible therapeutic use of decoy peptides to block autoantibody binding *in vivo* may require early and aggressive administration of several different peptides. For example, as for BP, other pathogenic regions of BP180, in addition to NC16A, should be considered (22). On the other hand, in pemphigus disease, the hypothesis that multiple antigens could be sequentially involved by ES in the pathogenesis of disease (85) could suggest an antigen specific approach based on multiple antigens and not only on the major one. On the other hand, the static nature of the Dsg3-reactive B cell repertoire that persists over time and causes disease relapse in PV patients suggests that Dsg3 ectodomain could be an effective target for PV therapy (20, 271, 275–278). In addition, although autoimmune response may spread to new epitopes during the course of disease, specific epitope/antigen therapies show considerable efficacy in epitope-induced mouse models of autoimmunity (272, 273, 279, 280) suggesting that epitope-specific therapies could also operate at the level of regulating mechanisms of immune tolerance rather than depending only on the interference with specific autoaggressive B and T cells.

CONCLUDING REMARKS

To get insights into the dynamics and role of sequential immune responses to newly arising epitopes/antigens is crucial to understand autoimmune disease pathogenesis. Moreover, this knowledge could be used to design antigen-specific therapies.

Although definition of hierarchy and functional significance of ES in human disease is difficult, this knowledge in animal models of autoimmune disease has been partially obtained. The difficulty to investigate ES in patients is probably due to the immunosuppressive treatments that could impair the diversification of the immune response and the time of ES appearance that, such as occurred in several mouse models, could become detectable before disease onset. However, despite these limitations, in patients affected by autoimmune bullous diseases the functional role of ES has been demonstrated. In particular, in BP patients a significant relation of ES with disease severity at diagnosis has been reported (22). Moreover, data from mouse model and BP patients raise the possibility that the development of autoantibodies against intracellular targets may follow extracellular one and correlates with the initial phase of the disease when the tissue damage starts occurring (22, 58). Although in PV the ES has been rarely found (20), in the clinical transition between mucosal form to the mucocutaneous one seems to have a major role (73, 76). In addition, the growing body of evidences on the existence of other pathogenic autoantibodies targeting non-Dsg antigens located on cell membrane (83, 84) and/or intracellular compartments (85) suggests a role of autoantibody diversification in PV pathogenesis. In parallel, in EPF the role of ES appears to be crucial for the establishment of the autoimmune response (102). Moreover, several reported cases in which a disease transition is preceded by an intermolecular ES phenomenon further underlines the functional role of ES in autoimmune blistering disease.

Autoantigens targeted by ES phenomena in autoimmune blistering disease are often physically linked (for example BP180 and BP230, Laminin 332 and BP180; laminin 332 and Coll VII), Thus, a mechanism dependent on physical association seems to be involved in the disease pathogenesis. In addition, a mechanism independent by physical association, such as tissue damage

followed by the exposure of cryptic epitope, at least in BP and PNP, has been postulated.

In conclusion, the definition of hierarchy and functional significance of ES in autoimmune bullous diseases is partially known at present. An important improvement of knowledge on ES phenomenon could be achieved by dissecting the process in active mouse models that are available for the majority of autoimmune blistering diseases (43, 45, 82, 281–285).

AUTHOR CONTRIBUTIONS

GZ and DD have designed and written the manuscript.

FUNDING

The present work has been supported by the Italian Ministry of Health (Ricerca Corrente 2017, to GZ).

REFERENCES

1. Oldstone MB. Molecular mimicry and autoimmune disease. *Cell* (1987) 51(5):878.
2. Gianani R, Sarvetnick N. Viruses, cytokines, antigens, and autoimmunity. *Proc Natl Acad Sci U S A* (1996) 93(6):2257–9. doi:10.1073/pnas.93.6.2257
3. Yang SH, Gao CY, Li L, Chang C, Leung PSC, Gershwin ME. The molecular basis of immune regulation in autoimmunity. *Clin Sci (Lond)* (2018) 132(1):43–67. doi:10.1042/CS20171154
4. Elkon K, Skelly S, Parnassa A, Moller W, Danho W, Weissbach H, et al. Identification and chemical synthesis of a ribosomal protein antigenic determinant in systemic lupus erythematosus. *Proc Natl Acad Sci U S A* (1986) 83(19):7419–23. doi:10.1073/pnas.83.19.7419
5. Gordon TP, Wolfson-Reichlin M, Blalock D, Deveshwar S, Reichlin M. Humoral response in spontaneous and experimental autoimmunity to the ribosomal P proteins. *Lupus* (1996) 5(4):340–1. doi:10.1177/096120339600500418
6. Kurtzke JF. Epidemiologic evidence for multiple sclerosis as an infection. *Clin Microbiol Rev* (1994) 7(1):141. doi:10.1128/CMR.7.1.141
7. Vaughan JH, Valbracht JR, Nguyen MD, Handley HH, Smith RS, Patrick K, et al. Epstein-Barr virus-induced autoimmune responses. I. Immunoglobulin M autoantibodies to proteins mimicking and not mimicking Epstein-Barr virus nuclear antigen-I. *J Clin Invest* (1995) 95(3):1306–15. doi:10.1172/JCI117781
8. Vaughan JH, Nguyen MD, Valbracht JR, Patrick K, Rhodes GH. Epstein-Barr virus-induced autoimmune responses. II. Immunoglobulin G autoantibodies to mimicking and nonmimicking epitopes. Presence in autoimmune disease. *J Clin Invest* (1995) 95(3):1316–27. doi:10.1172/JCI117782
9. Hendrick JP, Wolin S, Rinke J, Lerner MR, Steitz JA. Ro small cytoplasmic rihonudeoproteins are a subclass of La ribonndeoproteins: further characterization of the Ro and La small ribontxcleop rote ins from uninfected mammahan cells. *Mol Cell Biol* (1981) 1(12):1138–49. doi:10.1128/MCB.1.12.1138
10. Reichlin M. Significance of the Ro antigen system. *J Clin Iramtinol* (1986) 6(5):339–48. doi:10.1007/BF00915372
11. McRae BL, Vanderlugt CL, Dal Canto MC, Miller SD. Functional evidence for epitope spreading in the relapsing pathology of experimental autoimmune encephalomyelitis. *J Exp Med* (1995) 182(1):75–85. doi:10.1084/jem.182.1.75
12. Miller SD, Vanderlugt CL, Lenschow DJ, Pope JG, Karandikar NJ, Dal Canto MC, et al. Blockade of CD28/B7-1 interaction prevents epitope spreading and clinical relapses of murine EAE. *Immunity* (1995) 3(6):739–45. doi:10.1016/1074-7613(95)90063-2
13. Liebert UG, Linington C, Ter Meulen V. Induction of autoimmune reactions to myelin basic protein in measles virus encephalitis in Lewis rats. *J Neuroimmunol* (1988) 17(2):103–18. doi:10.1016/0165-5728(88)90018-5
14. Liebert UG, Hashim GA, Ter Meulen V. Characterization of measles virus-induced cellular autoimmune reactions against myelin basic protein in Lewis rats. *J Neuroimmunol* (1990) 29(1–3):139–47. doi:10.1016/0165-5728(90)90156-H
15. Liebert UG, Ter Meulen V. Synergistic interaction between measles virus infection and myelin basic protein peptide-specific T cells in the induction of experimental allergic encephalomyelitis in Lewis rats. *J Neuroimmunol* (1993) 46(1–2):217–23. doi:10.1016/0165-5728(93)90252-T
16. Prasad S, Kohm AP, McMahon JS, Luo X, Miller SD. Pathogenesis of NOD diabetes is initiated by reactivity to the insulin B chain 9-23 epitope and involves functional epitope spreading. *J Autoimmun* (2012) 39(4):347–53. doi:10.1016/j.jaut.2012.04.005
17. Tuohy VK, Yu M, Weinstock-Guttman B, Kinkel RP. Diversity and plasticity of self recognition during the development of multiple sclerosis. *J Clin Invest* (1997) 99(7):1682–90. doi:10.1172/JCI119331
18. Goebels N, Hofstetter H, Schmidt S, Brunner C, Wekerle H, Hohlfeld R. Repertoire dynamics of autoreactive T cells in multiple sclerosis patients and healthy subjects: epitope spreading versus clonal persistence. *Brain* (2000) 123(Pt 3):508–18. doi:10.1093/brain/123.3.508
19. O'Connor KC, Appel H, Bregoli L, Call ME, Catz I, Chan JA, et al. Antibodies from inflamed central nervous system tissue recognize myelin oligodendrocyte glycoprotein. *J Immunol* (2005) 175(3):1974–82. doi:10.4049/jimmunol.175.3.1974
20. Ohyama B, Nishifuji K, Chan PT, Kawaguchi A, Yamashita T, Ishii N, et al. Epitope spreading is rarely found in pemphigus vulgaris by large-scale longitudinal study using desmoglein 2-based swapped molecules. *J Invest Dermatol* (2012) 132(4):1158–68. doi:10.1038/jid.2011.448
21. Chan PT, Ohyama B, Nishifuji K, Yoshida K, Ishii K, Hashimoto T, et al. Immune response towards the amino-terminus of desmoglein 1 prevails across different activity stages in nonendemic pemphigus foliaceus. *Br J Dermatol* (2010) 162(6):1242–50. doi:10.1111/j.1365-2133.2010.09696.x
22. Di Zenzo G, Thoma-Uszynski S, Calabresi V, Fontao L, Hofmann SC, Lacour JP, et al. Demonstration of epitope-spreading phenomena in bullous pemphigoid: results of a prospective multicenter study. *J Invest Dermatol* (2011) 131(11):2271–80. doi:10.1038/jid.2011.180
23. Maeda JY, Moura AK, Maruta CW, Santi CG, Prisayanh PS, Aoki V. Changes in the autoimmune blistering response: a clinical and immunopathological shift from pemphigus foliaceus to bullous pemphigoid. *Clin Exp Dermatol* (2006) 31(5):653–5. doi:10.1111/j.1365-2230.2006.02174.x
24. Poole BD, Schneider RI, Guthridge JM, Velte CA, Reichlin M, Harley JB, et al. Early targets of nuclear RNP humoral autoimmunity in human systemic lupus erythematosus. *Arthritis Rheum* (2009) 60(3):848–59. doi:10.1002/art.24306
25. Ciubotariu R, Liu Z, Colovai AI, Ho E, Itescu S, Ravalli S, et al. Persistent allopeptide reactivity and epitope spreading in chronic rejection of organ allografts. *J Clin Invest* (1998) 101(2):398–395. doi:10.1172/JCI1117
26. Liu ZR, Colovai AI, Tugulea S, Reed EF, Fisher PE, Mancini D, et al. Indirect allorecognidon of donor HLA-DR peptides in organ allograft rejection. *J Clin Invest* (1996) 98:1150–7. doi:10.1172/JCI118898
27. McCluskey J, Farris AD, Keech CL, Purcell AW, Rischmueller M, Kinoshita G, et al. Determinant spreading: lessons from animal models and human disease. *Immunol Rev* (1998) 164:209–29. doi:10.1111/j.1600-065X.1998.tb01222.x
28. Olson JK, Croxford JL, Miller SD. Virus-induced autoimmunity: potential role of viruses in initiation, perpetuation, and progression of T cell-mediated autoimmune diseases. *Viral Immunol* (2001) 14(3):227–50. doi:10.1089/088282401753266756
29. Vanderlugt CL, Miller SD. Epitope spreading in immune-mediated diseases: implications for immunotherapy. *Nat Rev Immunol* (2002) 2(2):85–95. doi:10.1038/nri724
30. Poole BD, Scofield RH, Harley JB, James JA. Epstein–Barr virus and molecular mimicry in systemic lupus erythematosus. *Autoimmunity* (2006) 39(1):63–70. doi:10.1080/08916930500484849
31. Cornaby C, Gibbons L, Mayhew V, Sloan CS, Welling A, Poole BD. B cell epitope spreading: mechanisms and contribution to autoimmune diseases. *Immunol Lett* (2015) 163(1):56–68. doi:10.1016/j.imlet.2014.11.001
32. Topfer F, Gordon T, McCluskey J. Intra- and intermolecular spreading of autoimmunity involving the nuclear self-antigens La (SS-B) and Ro (SS-A). *Proc Nat Acad Sci U S A* (1995) 92(3):875–9. doi:10.1073/pnas.92.3.875

33. Deshmukh US, Bagavant H, Sim D, Pidiyar V, Fu SM. A SmD peptideinduces better antibody responses to other proteins within the small nuclearribonucleoprotein complex than to SmD protein via intermolecular epitopespreading. *J Immunol* (2007) 178(4):2565–71. doi:10.4049/jimmunol.178.4.2565
34. Amigorena S, Bonnerot C. Fc receptor signaling and trafficking: a connection-for antigen processing. *Immunol Rev* (1999) 172:279–84. doi:10.1111/j.1600-065X.1999.tb01372.x
35. Lake P, Mitchison NA. Regulatory mechanisms in the immune response tocell-surface antigens. *Cold Spring Harbor Symp Quantitat Biol* (1977) 41(Pt2):589–95. doi:10.1101/SQB.1977.041.01.068
36. Di Noia JM, Neuberger MS. Molecular mechanisms of antibody somatic hyper-mutation. *Annu Rev Biochem* (2007) 76:1–22. doi:10.1146/annurev.biochem.76.061705.090740
37. Deshmukh US, Bagavant H, Lewis J, Gaskin F, Fu SM. Epitope spreading within lupus-associated ribonucleoprotein antigens. *Clin Immunol* (2005) 117(2):112–20. doi:10.1016/j.clim.2005.07.002
38. Ray SK, Putterman C, Diamond B. Pathogenic autoantibodies are routinely generated during the response to foreign antigen: a paradigm for autoimmune disease. *Proc Natl Acad Sci U S A* (1996) 93(5):2019–24. doi:10.1073/pnas.93.5.2019
39. Satoh M, Ajmani AK, Stojanov L, Langdon JJ, Ogasawara T, Wang J, et al. Autoantibodies that stabilize the molecular interaction of Ku antigen with DNA-dependent protein kinase catalytic subunit. *Clin Exp Immunol* (1996) 105(3):460–7. doi:10.1046/j.1365-2249.1996.d01-775.x
40. Simetsek PD, Campbell DG, Lanzavecchia A, Eairweather N, Watts C. Modulation of antigen processing by bound antibodies can boost or suppress class II major histocompatibility complex presentation of different T cell determinants. *J Exp Med* (1995) 181(6):1957–63. doi:10.1084/jem.181.6.1957
41. Watts C, Lanzavecchia A. Suppressive effect of antibody on processing of T cell epitopes. *J Exp Med* (1993) 178(4):1459–63. doi:10.1084/jem.178.4.1459
42. Di Zenzo G, Della Torre R, Zambruno G, Borradori L. Bullous pemphigoid: from the clinic to the bench. *Clin Dermatol* (2012) 30:3–16. doi:10.1016/j.clindermatol.2011.03.005
43. Ujiie H, Shibaki A, Nishie W, Sawamura D, Wang G, Tateishi Y, et al. A novel active mouse model for bullous pemphigoid targeting humanized pathogenic antigen. *J Immunol* (2010) 184(4):2166–74. doi:10.4049/jimmunol.0903101
44. Zillikens D, Rose PA, Balding SD, Liu Z, Olague-Marchan M, Diaz LA, et al. Tight clustering of extracellular BP180 epitopes recognized by bullous pemphigoid autoantibodies. *J Invest Dermatol* (1997) 109(4):573–9. doi:10.1111/1523-1747.ep12337492
45. Nishie W, Sawamura D, Goto M, Ito K, Shibaki A, McMillan JR, et al. Humanization of autoantigen. *Nat Med* (2007) 13(3):378–83. doi:10.1038/nm1496
46. Yamamoto K, Inoue N, Masuda R, Fujimori A, Saito T, Imajoh-Ohmi S, et al. Cloning of hamster type XVII collagen cDNA, and pathogenesis of anti-type XVII collagen antibody and complement in hamster bullous pemphigoid. *J Invest Dermatol* (2002) 118(3):485–92. doi:10.1046/j.0022-202x.2001.01683.x
47. Liu Z, Diaz LA, Troy JL, Taylor AF, Emery DJ, Fairley JA, et al. A passive transfer model of the organspecific autoimmune disease, bullous pemphigoid, using antibodies generated against the hemidesmosomal antigen, BP180. *J Clin Invest* (1993) 92(5):2480–8. doi:10.1172/JCI116856
48. Kiss M, Husz S, Jánossy T, Marczinovits I, Molnár J, Korom I, et al. Experimental bullous pemphigoid generated in mice with an antigenic epitope of the human hemidesmosomal protein BP230. *J Autoimmun* (2005) 24(1):1–10. doi:10.1016/j.jaut.2004.09.007
49. Feldrihan V, Licarete E, Florea F, Cristea V, Popescu O, Sitaru C, et al. IgG antibodies against immunodominant C-terminal epitopes of BP230 do not induce skin blistering in mice. *Hum Immunol* (2014) 75(4):354–63. doi:10.1016/j.humimm.2014.01.005
50. Murakami H, Nishioka S, Setterfield J, Bhogal BS, Black MM, Zillikens D, et al. Analysis of antigens targeted by circulating IgG and IgA autoantibodies in 50 patients with cicatricial pemphigoid. *J Dermatol Sci* (1998) 17(1):39–44. doi:10.1016/S0923-1811(97)00067-4
51. Di Zenzo G, Grosso F, Terracina M, Mariotti F, De Pità O, Owaribe K, et al. Characterization of the anti-BP180 autoantibody reactivity profile and epitope mapping in bullous pemphigoid patients. *J Invest Dermatol* (2004) 122(1):103–10. doi:10.1046/j.0022-202X.2003.22126.x
52. Di Zenzo G, Thoma-Uszynski S, Fontao L, Calabresi V, Hofmann SC, Hellmark T, et al. Multicenter prospective study of the humoral autoimmune response in bullous pemphigoid. *Clin Immunol* (2008) 128(3):415–26. doi:10.1016/j.clim.2008.04.012
53. Tanaka M, Hashimoto T, Amagai M, Shimizu N, Ikeguchi N, Tsubata T, et al. Characterization of bullous pemphigoid antibodies by use of recombinant bullous pemphigoid antigen proteins. *J Invest Dermatol* (1991) 97(4):725–8. doi:10.1111/1523-1747.ep12484223
54. Perriard J, Jaunin F, Favre B, Büdinger L, Hertl M, Saurat JH, et al. IgG autoantibodies from bullous pemphigoid (BP) patients bind antigenic sites on both the extracellular and the intracellular domains of the BP antigen 180. *J Invest Dermatol* (1999) 112(2):141–7. doi:10.1046/j.1523-1747.1999.00497.x
55. Skaria M, Jaunin F, Hunziker T, Riou S, Schumann H, Bruckner-Tuderman L, et al. IgG autoantibodies from bullous pemphigoid patients recognize multiple antigenic reactive sites located predominantly within the B and C subdomains of the COOH-terminus of BP230. *J Invest Dermatol* (2000) 114(5):998–1004. doi:10.1046/j.1523-1747.2000.00893.x
56. Mariotti F, Grosso F, Terracina M, Ruffelli M, Cordiali-Fei P, Sera F, et al. Development of a novel ELISA system for detection of anti-BP180 IgG and characterization of autoantibody profile in bullous pemphigoid patients. *Br J Dermatol* (2004) 151(5):1004–10. doi:10.1111/j.1365-2133.2004.06245.x
57. Thoma-Uszynski S, Uter W, Schwietzke S, Schuler G, Borradori L, Hertl M. Autoreactive T and B cells from bullous pemphigoid (BP) patients recognize epitopes clustered in distinct regions of BP180 and BP230. *J Immunol* (2006) 176(3):2015–23. doi:10.4049/jimmunol.176.3.2015
58. Di Zenzo G, Calabresi V, Olasz EB, Zambruno G, Yancey KB. Sequential intramolecular epitope spreading of humoral responses to human BPAG2 in a transgenic model. *J Invest Dermatol* (2010) 130(4):1040–7. doi:10.1038/jid.2009.309
59. Olasz EB, Roh J, Yee CL, Arita K, Akiyama M, Shimizu H. Human bullous pemphigoid antigen 2 transgenic skin elicits specific IgG in wildtype mice. *J Invest Dermatol* (2007) 127(12):2807–17. doi:10.1038/sj.jid.5700970
60. Sárdy M, Borovaya A, Horváth ON, Folwaczny C, Schmitt W, Schmidt T, et al. Successful rituximab treatment of juvenile bullous pemphigoid with esophageal scarring due to epitope spreading. *J Dtsch Dermatol Ges* (2016) 14(6):618–21. doi:10.1111/ddg.12902
61. Kasperkiewicz M, Hoppe U, Zillikens D, Schmidt E. Relapse-associated autoantibodies to BP180 in a patient with anti-p200 pemphigoid. *Clin Exp Dermatol* (2010) 35(6):614–7. doi:10.1111/j.1365-2230.2009.03731.x
62. Ohata C, Ishii N, Koga H, Fukuda S, Tateishi C, Tsuruta D, et al. Coexistence of autoimmune bullous diseases (AIBDs) and psoriasis: a series of 145 cases. *J Am Acad Dermatol* (2015) 73(1):50–5. doi:10.1016/j.jaad.2015.03.016
63. Mondello MR, Magaudda L, Pergolizzi S, Santoro A, Vaccaro M, Califano L, et al. Behavior of laminin 1 and type IV collagen in uninvolved psoriatic skin. Immunohistochemical study using confocal laser scanning microscopy. *Arch Dermatol Res* (1996) 288(9):527–31. doi:10.1007/BF02505249
64. Vaccaro M, Magaudda L, Cutroneo G, Trimarchi F, Barbuzza O, Guarneri F, et al. Changes in the distribution of laminin alpha1 chain in psoriatic skin: immunohistochemical study using confocal laser scanning microscopy. *Br J Dermatol* (2002) 146(3):392–8. doi:10.1046/j.1365-2133.2002.04637.x
65. Chen YJ, Wu CY, Lin MW, Chen TJ, Liao KK, Chen YC, et al. Comorbidity profiles among patients with bullous pemphigoid: a nationwide population-based study. *Br J Dermatol* (2011) 165(3):593–9. doi:10.1111/j.1365-2133.2011.10386.x
66. Amagai M, Klaus-Kovtun V, Stanley JR. Autoantibodies against a novel epithelial cadherin in pemphigus vulgaris, a disease of cell adhesion. *Cell* (1991) 67(5):869–77. doi:10.1016/0092-8674(91)90360-B
67. Ishii K, Amagai M, Hall RP, Hashimoto T, Takayanagi A, Gamou S, et al. Characterization of autoantibodies in pemphigus using antigen-specific enzyme-linked immunosorbent assays with baculovirus-expressed recombinant desmogleins. *J Immunol* (1997) 159(4):2010–7.
68. Ruach M, Ohel G, Rahav D, Samueloff A. Pemphigus vulgaris and pregnancy. *Obstet Gynecol Surv* (1995) 50(10):755–60. doi:10.1097/00006254-199510000-00023

69. Di Zenzo G, Amber KT, Sayar BS, Müller EJ, Borradori L. Immune response in pemphigus and beyond: progresses and emerging concepts. *Semin Immunopathol* (2016) 38(1):57–74. doi:10.1007/s00281-015-0541-1
70. Di Zenzo G, Borradori L, Muller EJ. The pathogenesis of pemphigus: controversy versus complexity. *Exp Dermatol* (2017) 26(12):1271–3. doi:10.1111/exd.13176
71. Anhalt GJ, Labib RS, Voorhees JJ, Beals TF, Diaz LA. Induction of pemphigus in neonatal mice by passive transfer of IgG from patients with the disease. *N Engl J Med* (1982) 306(20):1189–96. doi:10.1056/NEJM198205203062001
72. Mahoney MG, Wang Z, Rothenberger K, Koch PJ, Amagai M, Stanley JR. Explanations for the clinical and microscopic localization of lesions in pemphigus foliaceus and vulgaris. *J Clin Invest* (1999) 103(4):461–8. doi:10.1172/JCI5252
73. Ding X, Aoki V, Mascaro JM Jr, Lopez-Swiderski A, Diaz LA, Fairley JA. Mucosal and mucocutaneous (generalized) pemphigus vulgaris show distinct autoantibody profiles. *J Invest Dermatol* (1997) 109(4):592–6. doi:10.1111/1523-1747.ep12337524
74. Harman KE, Gratian MJ, Bhogal BS, Challacombe SJ, Black MM. A study of desmoglein 1 autoantibodies in pemphigus vulgaris: racial differences in frequency and the association with a more severe phenotype. *Br J Dermatol* (2000) 143(2):343–8. doi:10.1046/j.1365-2133.2000.03660.x
75. Amagai M, Hashimoto T, Green KJ, Shimizu N, Nishikawa T. Antigen-specific immunoadsorption of pathogenic autoantibodies in pemphigus foliaceus. *J Invest Dermatol* (1995) 104(6):895–901. doi:10.1111/1523-1747.ep12606168
76. Salato VK, Hacker-Foegen MK, Lazarova Z, Fairley JA, Lin MS. Role of intramolecular epitope spreading in pemphigus vulgaris. *Clin Immunol* (2005) 116(1):54–64. doi:10.1016/j.clim.2005.03.005
77. Ding X, Diaz LA, Fairley JA, Giudice GJ, Liu Z. The anti-desmoglein 1 autoantibodies in pemphigus vulgaris sera are pathogenic. *J Invest Dermatol* (1999) 112(5):739–43. doi:10.1046/j.1523-1747.1999.00585.x
78. Miyagawa S, Amagai M, Iida T, Yamamoto Y, Nishikawa T, Shirai T. Late development of antidesmoglein 1 antibodies in pemphigus vulgaris: correlation with disease progression. *Br J Dermatol* (2000) 142(4):849.
79. Sekiguchi M, Futei Y, Fujii Y, Iwasaki T, Nishikawa T, Amagai M. Dominant autoimmune epitopes recognized by pemphigus antibodies map to the N-terminal adhesive region of desmogleins. *J Immunol* (2001) 167(9):5439–48. doi:10.4049/jimmunol.167.9.5439
80. Futei Y, Amagai M, Sekiguchi M, Nishifuji K, Fujii Y, Nishikawa T. Use of domain-swapped molecules for conformational epitope mapping of desmoglein 3 in pemphigus vulgaris. *J Invest Dermatol* (2000) 115(5):829–34. doi:10.1046/j.1523-1747.2000.00137.x
81. Payne AS, Ishii K, Kacir S, Lin C, Li H, Hanakawa Y, et al. Genetic and functional characterization of human pemphigus vulgaris monoclonal autoantibodies isolated by phage display. *J Clin Invest* (2005) 115(4):888–9. doi:10.1172/JCI24185
82. Tsunoda K, Ota T, Aoki M, Yamada T, Nagai T, Nakagawa T, et al. Induction of pemphigus phenotype by a mouse monoclonal antibody against the amino-terminal adhesive interface of desmoglein 3. *J Immunol* (2003) 170(4):2170–8. doi:10.4049/jimmunol.170.4.2170
83. Nguyen VT, Ndoye A, Grando SA. Novel human alpha 9 acetylcholine receptor regulating keratinocyte adhesion is targeted by Pemphigus vulgaris autoimmunity. *Am J Pathol* (2000) 157(4):1377–91. doi:10.1016/j.bcp.2009.05.020
84. Nguyen VT, Ndoye A, Grando SA. Pemphigus vulgaris antibody identifies pemphaxin. A novel keratinocyte annexinlike molecule binding acetylcholine. *J Biol Chem* (2000) 275(38):29466–76. doi:10.1074/jbc.M003174200
85. Ahmed AR, Carrozzo M, Caux F, Cirillo N, Dmochowski M, Alonso AE, et al. Monopathogenic vs multipathogenic explanations of pemphigus pathophysiology. *Exp Dermatol* (2016) 25(11):839–46. doi:10.1111/exd.13106
86. Marchenko S, Chernyavsky AI, Arredondo J, Gindi V, Grando SA. Antimitochondrial autoantibodies in pemphigus vulgaris: a missing link in disease pathophysiology. *J Biol Chem* (2010) 285(6):3695–704. doi:10.1074/jbc.M109.081570
87. Calabresi V, Mariotti F, Pacifico V, Didona B, Zambruno G, Di Zenzo G. Reactivity against non disease-specific antigens in autoimmune bullous disease is rare and may represent an epiphenomenon. ESDR Annual Meeting; 2014 September 11-13; Copenhagen, Denmark. *J Invest Dermatol* (2014) 134:s14.
88. Cho MJ, Ellebrecht CT, Hammers CM, Mukherjee EM, Sapparapu G, Boudreaux CE, et al. Determinants of VH1-46 cross-reactivity to pemphigus vulgaris autoantigen desmoglein 3 and rotavirus antigen VP6. *J Immunol* (2016) 197(4):1065–73. doi:10.4049/jimmunol.1600567
89. Stanley JR, Koulu L, Thivolet C. Distinction between epidermal antigens binding pemphigus vulgaris and pemphigus foliaceus autoantibodies. *J Clin Invest* (1984) 74:313–20. doi:10.1172/JCI111426
90. Diaz LA, Sampaio SAP, Rivitti EA, Martins CR, Cunha PR, Lombardi C, et al. Endemic pemphigus foliaceus (fogo selvagem): II. Current and historic epidemiologic studies. *J Invest Dermatol* (1989) 92(1):4–12. doi:10.1111/1523-1747.ep13070394
91. Abrèu-Velez AM, Hashimoto T, Bollag WB, Tobón Arroyave S, Abrèu-Velez CE, Londoño ML, et al. A unique form of endemic pemphigus in northern Colombia. *J Am Acad Dermatol* (2003) 49(4):599–608. doi:10.1067/S0190-9622(03)00851-X
92. Di Zenzo G, Zambruno G, Borradori L. Endemic pemphigus foliaceus: towards understanding autoimmune mechanisms of disease development. *J Invest Dermatol* (2012) 132:2499–502. doi:10.1038/jid.2012.369
93. Ishii K, Lin C, Siegel DL, Stanley JR. Isolation of pathogenic monoclonal anti-desmoglein 1 human antibodies by phage display of pemphigus foliaceus autoantibodies. *J Invest Dermatol* (2008) 128(4):939–48. doi:10.1038/sj.jid.5701132
94. Yokouchi M, Saleh MA, Kuroda K, Hachiya T, Stanley JR, Amagai M, et al. Pathogenic epitopes of autoantibodies in pemphigus reside in the amino-terminal adhesive region of desmogleins which are unmasked by proteolytic processing of prosequence. *J Invest Dermatol* (2009) 129(9):2156–66. doi:10.1038/jid.2009.61
95. Sharma PM, Choi EJ, Kuroda K, Hachiya T, Ishii K, Payne AS. Pathogenic anti-desmoglein MAbs show variable ELISA activity because of preferential binding of mature versus proprotein isoforms of desmoglein 3. *J Invest Dermatol* (2009) 129(9):2309–12. doi:10.1038/jid.2009.41
96. Li N, Aoki V, Hans-Filho G, Rivitti EA, Diaz LA. The role of intramolecular epitope spreading in the pathogenesis of endemic pemphigus foliaceus (fogo-selvagem). *J Exp Med* (2003) 197(11):1501–10. doi:10.1084/jem.20022031
97. Warren SJ, Arteaga LA, Rivitti EA, Aoki V, Hans-Filho G, Qaqish BF, et al. The role of subclass switching in the pathogenesis of endemic pemphigus foliaceus. *J Invest Dermatol* (2003) 120:104–8. doi:10.1046/j.1523-1747.2003.12017.x
98. Aoki V, Rivitti EA, Diaz LA. Update on fogo selvagem, an endemic form of pemphigus foliaceus. *J Dermatol* (2015) 42(1):18–26. doi:10.1111/1346-8138.12675
99. Aoki V, Millikan RC, Rivitti EA, Hans-Filho G, Eaton DP, Warren SJ, et al. Environmental risk factors in endemic pemphigus foliaceus (fogo selvagem). *J Investig Dermatol Symp Proc* (2004) 9(1):34–40. doi:10.1111/j.1087-0024.2004.00833.x
100. Qian Y, Jeong JS, Maldonado M, Valenzuela JG, Gomes R, Teixeira C. Cutting edge: brazilian pemphigus foliaceus anti-desmoglein 1 autoantibodies cross-react with sand fly salivary LJM11. *Antigen J Immunol* (2012) 189(4):1535–9. doi:10.4049/jimmunol.1200842
101. Qian Y, Jeong JS, Abdeladhim M, Valenzuela JG, Aoki V, Hans-Filhio G, et al. IgE anti-LJM11 sand fly salivary antigen may herald the onset of Fogo selvagem in endemic Brazilian regions. *J Invest Dermatol* (2015) 135(3):913–5. doi:10.1038/jid.2014.430
102. Qian Y, Jeong JS, Ye J, Dang B, Abdeladhim M, Aoki V, et al. Overlapping IgG4 responses to self- and environmental antigens in endemic pemphigus foliaceus. *J Immunol* (2016) 196(5):2041–50. doi:10.4049/jimmunol.1502233
103. Evangelista F, Roth AJ, Prisayanh P, Temple BR, Li N, Qian Y, et al. Pathogenic IgG4 autoantibodies from endemic pemphigus foliaceus recognize a desmoglein-1 conformational epitope. *J Autoimmun* (2018). doi:10.1016/j.jaut.2017.12.017
104. Iwatsuki K, Takigawa M, Hashimoto T, Nishikawa T, Yamada M. Can pemphigus vulgaris become pemphigus foliaceus? *J Am Acad Dermatol* (1991) 25(5 Pt 1):797–800. doi:10.1016/S0190-9622(08)80971-1
105. Kawana S, Hashimoto T, Nishikawa T, Nishiyama S. Shift in clinical features, histologic findings and antigen profiles from pemphigus vulgaris to pemphigus foliaceus – two case studies. *Dermatology* (1994) 189(Suppl 1):57–9. doi:10.1159/000246931
106. Chang SN, Kim SC, Lee IJ, Seo SJ, Hong CK, Park WH. Transition from pemphigus vulgaris to pemphigus foliaceus. *Br J Dermatol* (1997) 137(2):303–5.

107. Mendiratta V, Sarkar R, Sharma RC, Korann RV. Transition of pemphigus vulgaris to pemphigus foliaceus. *Indian J Dermatol Venereol Leprol* (2000) 66(2):85–6.
108. Ishii K, Amagai M, Ohata Y, Shimizu H, Hashimoto T, Ohya K, et al. Development of pemphigus vulgaris in a patient with pemphigus foliaceus: antidesmoglein antibody profile shift confirmed by enzyme-linked immunosorbent assay. *J Am Acad Dermatol* (2000) 42(5 Pt 2):859–61. doi:10.1016/S0190-9622(00)90253-6
109. Komai A, Amagai M, Ishii K, Nishikawa T, Chorzelski T, Matsuo I, et al. The clinical transition between pemphigus foliaceus and pemphigus vulgaris correlates well with the changes in autoantibody profile assessed by an enzyme-linked immunosorbent assay. *Br J Dermatol* (2001) 144(6):1177–82. doi:10.1046/j.1365-2133.2001.04227.x
110. Kimoto M, Ohyama M, Hata Y, Amagai M, Nishikawa T. A case of pemphigus foliaceus which occurred after five years of remission from pemphigus vulgaris. *Dermatology* (2001) 203(2):174–6. doi:10.1159/000051737
111. Tsuji Y, Kawashima T, Yokota K, Tateish Y, Tomita Y, Matsumura T, et al. Clinical and serological transition from pemphigus vulgaris to pemphigus foliaceus demonstrated by desmoglein ELISA system. *Arch Dermatol* (2002) 138(1):95–6. doi:10.1001/archderm.138.1.95
112. Harman KE, Gratian MJ, Shirlaw PJ, Bhogal BS, Challacombe SJ, Black MM. The transition of pemphigus vulgaris into pemphigus foliaceus: a reflection of changing desmoglein 1 and 3 autoantibody levels in pemphigus vulgaris. *Br J Dermatol* (2002) 146(4):684–7. doi:10.1046/j.1365-2133.2002.04608.x
113. Tóth GG, Pas HH, Jonkman MF. Transition of pemphigus vulgaris into pemphigus foliaceus confirmed by antidesmoglein ELISA profile. *Int J Dermatol* (2002) 41(8):525–7. doi:10.1046/j.1365-4362.2002.15452.x
114. Ng PP, Thng ST. Three cases of transition from pemphigus vulgaris to pemphigus foliaceus confirmed by desmoglein ELISA. *Dermatology* (2005) 210(4):319–21. doi:10.1159/000084757
115. Park SG, Chang JY, Cho YH, Kim SC, Lee MG. Transition from pemphigus foliaceus to pemphigus vulgaris: case report with literature review. *Yonsei Med J* (2006) 47(2):278–81. doi:10.3349/ymj.2006.47.2.278
116. Awazawa R, Yamamoto Y, Gushi M, Taira K, Yagi N, Asato Y, et al. Case of pemphigus foliaceus that shifted into pemphigus vulgaris after adrenal tumor resection. *J Dermatol* (2007) 34(8):549–55. doi:10.1111/j.1346-8138.2007.00329.x
117. Pigozzi B, Peserico A, Schiesari L, Alaibac M. Pemphigus foliaceus evolving into pemphigus vulgaris: a probable example of 'intermolecular epitope spreading' confirmed by enzyme-linked immunosorbent assay study. *J Eur Acad Dermatol Venereol* (2008) 22(2):242–4. doi:10.1111/j.1468-3083.2007.02298.x
118. Lévy-Sitbon C, Reguiaï Z, Durlach A, Goeldel AL, Grange F, Bernard P. Transition from pemphigus vulgaris to pemphigus foliaceus: a case report. *Ann Dermatol Venereol* (2013) 140(12):788–92. doi:10.1016/j.annder.2013.07.013
119. España A, Koga H, Suárez-Fernández R, Ohata C, Ishii N, Irarrazaval I, et al. Antibodies to the amino-terminal domain of desmoglein 1 are retained during transition from pemphigus vulgaris to pemphigus foliaceus. *Eur J Dermatol* (2014) 24(2):174–9. doi:10.1684/ejd.2014.2277
120. Ito T, Moriuchi R, Kikuchi K, Shimizu S. Rapid transition from pemphigus vulgaris to pemphigus foliaceus. *J Eur Acad Dermatol Venereol* (2016) 30(3):455–7. doi:10.1111/jdv.12832
121. Sami N, Ahmed AR. Dual diagnosis of pemphigus and pemphigoid. Retrospective review of thirty cases in the literature. *Dermatology* (2001) 202(4):293–301. doi:10.1159/000051661
122. Korman NJ, Stanley JR, Woodley DT. Coexistence of pemphigus foliaceus and bullous pemphigoid. Demonstration of autoantibodies that bind to both the pemphigus foliaceus antigen complex and the bullous pemphigoid antigen. *Arch Dermatol* (1991) 127(3):387–90. doi:10.1001/archderm.127.3.387
123. Peterson JD, Chang AJ, Chan LS. Clinical evidence of an intermolecular epitope spreading in a patient with pemphigus foliaceus converting into bullous pemphigoid. *Arch Dermatol* (2007) 143(2):272–4. doi:10.1001/archderm.143.2.272
124. Recke A, Rose C, Schmidt E, Bröcker EB, Zillikens D, Sitaru C. Transition from pemphigus foliaceus to bullous pemphigoid: intermolecular B-cell epitope spreading without IgG subclass shifting. *J Am Acad Dermatol* (2009) 61(2):333–6. doi:10.1016/j.jaad.2008.10.061
125. Didona D, Didona B, Richetta AG, Cantisani C, Moliterni E, Calvieri S, et al. Paraneoplastic pemphigus: a trait d'union between dermatology and oncology. *Adv Mod Oncol Res* (2015) 1(2):97–103. doi:10.18282/amor.v1.i2.42
126. Paolino G, Didona D, Magliulo G, Iannella G, Didona B, Mercuri SR, et al. Paraneoplastic pemphigus: insight into the autoimmune pathogenesis, clinical features and therapy. *Int J Mol Sci* (2017) 18(12):E2532. doi:10.3390/ijms18122532
127. Schepens I, Jaunin F, Begre N, Läderach U, Marcus K, Hashimoto T, et al. The protease inhibitor alpha-2-macroglobulin-like-1 is the p170 antigen recognized by paraneoplastic pemphigus autoantibodies in human. *PLoS One* (2010) 5(8):e12250. doi:10.1371/journal.pone.0012250
128. Mimouni D, Foedinger D, Kouba DJ, Orlow SJ, Rappersberger K, Sciubba JJ, et al. Mucosal dominant pemphigus vulgaris with anti-desmoplakin autoantibodies. *J Am Acad Dermatol* (2004) 51(1):62–7. doi:10.1016/j.jaad.2003.11.051
129. Cozzani E, Dal Bello MG, Mastrogiacomo A, Drosera M, Parodi A. Antidesmoplakin antibodies in pemphigus vulgaris. *Br J Dermatol* (2006) 154(4):624–8. doi:10.1111/j.1365-2133.2005.06987.x
130. Ortolan DG, Souza DP, Aoki V, Santi CG, Gabbi TV, Ichimura LM, et al. Analysis of the reactivity of indirect immunofluorescence in patients with pemphigus foliaceus and pemphigus vulgaris using rat bladder epithelium as a substrate. *Clinics (Sao Paulo)* (2011) 66(12):2019–23. doi:10.1590/S1807-59322011001200004
131. Watanabe T, Kato M, Yoshida Y, Fukuda S, Hashimoto T, Yamamoto O. Mucocutaneous-type pemphigus vulgaris with anti-desmoplakin autoantibodies. *Eur J Dermatol* (2011) 21(2):299–300. doi:10.1684/ejd.2011.1307
132. Bowen GM, Peters NT, Fivenson DP, Su LD, Nousari HC, Anhalt GJ, et al. Lichenoid dermatitis in paraneoplastic pemphigus: a pathogenic trigger of epitope spreading? *Arch Dermatol* (2000) 136(5):652–6. doi:10.1001/archderm.136.5.652
133. Okahashi K, Oiso N, Ishii N, Miyake M, Uchida S, Matsuda H, et al. Paraneoplastic pemphigus associated with Castleman disease: progression from mucous to mucocutaneous lesions with epitope-spreading phenomena. *Br J Dermatol* (2017) 176(5):1406–9. doi:10.1111/bjd.15389
134. Saleh MA, Ishii K, Yamagami J, Shirakata Y, Hashimoto K, Amagai M. Pathogenic anti-desmoglein 3 mAbs cloned from a paraneoplastic pemphigus patient by phage display. *J Invest Dermatol* (2012) 132(4):1141–8. doi:10.1038/jid.2011.449
135. Futei Y, Amagai M, Hashimoto T, Nishikawa T. Conformational epitope mapping and IgG subclass distribution of desmoglein 3 in paraneoplastic pemphigus. *J Am Acad Dermatol* (2003) 49(6):1023–8. doi:10.1016/s0190
136. Robinson N, Hashimoto T, Amagai M, Chan LS. The new pemphigus variants. *J Am Acad Dermatol* (1999) 40(5 Pt 1):649–71. doi:10.1016/S0190-9622(99)70145-3 quiz 672-3,
137. Woodley DT, Briggaman RA, O'Keefe EJ, Inman AO, Queen LL, Gammon WR. Identification of the skin basement-membrane autoantigen in epidermolysis bullosa acquisita. *N Engl J Med* (1984) 310(16):1007–13. doi:10.1056/NEJM198404193101602
138. Gammon WR. Epidermolysis bullosa acquisita: a disease of autoimmunity to type VII collagen. *J Autoimmun* (1991) 4(1):59–71. doi:10.1016/0896-8411(91)90007-Y
139. Calabresi V, Sinistro A, Cozzani E, Cerasaro C, Lolicato F, Muscianese M, et al. Sensitivity of different assays for the serological diagnosis of epidermolysis bullosa acquisita: analysis of a cohort of 24 Italian patients. *J Eur Acad Dermatol Venereol* (2014) 28(4):483–90. doi:10.1111/jdv.12129
140. Ludwig RJ, Recke A, Bieber K, Müller S, Marques Ade C, Banczyk D, et al. Generation of antibodies of distinct subclasses and specificity is linked to H2s in an active mouse model of epidermolysis bullosa acquisita. *J Invest Dermatol* (2011) 131(1):167–76. doi:10.1038/jid.2010.248
141. Gammon WR, Briggaman RA. Epidermolysis bullosa acquisita and bullous systemic lupus erythematosus. *Dermat Clin* (1993) 11(3):535–47.
142. Lapiere JC, Woodley DT, Parente MG, Iwasaki T, Wynn KC, Christiano AM, et al. Epitope mapping of type VII collagen. Identification of discrete peptide sequences recognized by sera from patients with acquired epidermolysis bullosa. *J Clin Invest* (1993) 92(4):1831–9. doi:10.1172/JCI116774
143. Chan LS, Lapiere JC, Chen M, Traczyk T, Mancini AJ, Paller AS, et al. Bullous systemic lupus erythematosus with autoantibodies recognizing multiple skin basement membrane components, bullous pemphigoid antigen 1, laminin-5, laminin-6, and type VII collagen. *Arch Dermatol* (1999) 135(5):569–73. doi:10.1001/archderm.135.5.569

144. Chen M, Marinkovich MP, Jones JC, O'Toole EA, Li YY, Woodley DT. NC1 domain of type VII collagen binds to the beta3 chain of laminin 5 via a unique subdomain within the fibronectin-like repeats. *J Invest Dermatol* (1999) 112(2):177–83. doi:10.1046/j.1523-1747.1999.00491.x
145. Dotson AD, Raimer SS, Pursley TV, Tschen J. Systemic lupus erythematosus occurring in a patient with epidermolysis bullosa acquisita. *Arch Dermatol* (1981) 117(7):422–6. doi:10.1001/archderm.1981.01650070050025
146. Barton DD, Fine JD, Gammon WR, Sams WM Jr. Bullous systemic lupus erythematosus: an unusual clinical course and detectable circulating autoantibodies to the epidermolysis bullosa acquisita antigen. *J Am Acad Dermatol* (1986) 15(2 Pt 2):369–73. doi:10.1016/S0190-9622(86)70181-3
147. Kettler AH, Bean SF, Duffy JO, Gammon WR. Systemic lupus erythematosus presenting as a bullous eruption in a child. *Arch Dermatol* (1988) 124(7):1083–7. doi:10.1001/archderm.124.7.1083
148. Boh E, Roberts LJ, Lieu TS, Gammon WR, Sontheimer RD. Epidermolysis bullosa acquisita preceding the development of systemic lupus erythematosus. *J Am Acad Dermatol* (1990) 22(4):587–93. doi:10.1016/0190-9622(90)70077-U
149. McHenry PM, Dagg JH, Tidman MJ, Lever RS. Epidermolysis bullosa acquisita occurring in association with systemic lupus erythematosus. *Clin Exp Dermatol* (1993) 18(4):378–80. doi:10.1111/j.1365-2230.1993.tb02224.x
150. Yoon J, Moon TK, Lee KH, Kim SC. Fatal vascular involvement in systemic lupus erythematosus following epidermolysis bullosa acquisita. *Acta Derm Venereol* (1995) 75(2):143–6.
151. Chen M, O'Toole EA, Sanghavi J, Mahmud N, Weir D, Kelleher D, et al. Type VII collagen exists in human intestine and serves as an antigenic target in patients with inflammatory bowel disease. *J Eur Acad Dermatol Venereol* (1997) 108:542.
152. Licarete E, Ganz S, Recknagel M, Di Zenzo G, Hashimoto T, Hertl M, et al. Prevalence of collagen VII-specific autoantibodies in patients with autoimmune and inflammatory diseases. *BMC Immunol* (2012) 13:16. doi:10.1186/1471-2172-13-16
153. Lohi J, Leivo I, Tani T, Kiviluoto T, Kivilaakso E, Burgeson RE, et al. Laminins, tenascin and type VII collagen in colorectal mucosa. *Histochem J* (1996) 28(6):431–40. doi:10.1007/BF02331434
154. Chan LS, Vanderlugt CJ, Hashimoto T, Nishikawa T, Zones JJ, Black MM, et al. Epitope spreading: lessons from autoimmune skin diseases. *J Invest Dermatol* (1998) 110(2):103–9. doi:10.1046/j.1523-1747.1998.00107.x
155. Kirtschig G, Chow ET, Venning VA, Wojnarowska FT. Acquired subepidermal bullous diseases associated with psoriasis: a clinical, immunopathological and immunogenetic study. *Br J Dermatol* (1996) 135(5):738–45. doi:10.1111/j.1365-2133.1996.tb03883.x
156. Saeki H, Hayashi N, Komine M, Soma Y, Shimada S, Watanabe K, et al. A case of generalized pustular psoriasis followed by bullous disease: an atypical case of bullous pemphigoid or a novel bullous disease? *Br J Dermatol* (1996) 134(1):152–5. doi:10.1046/j.1365-2133.1996.d01-758.x
157. Endo Y, Tamura A, Ishikawa O, Miyachi Y, Hashimoto T. Psoriasis vulgaris coexistent with epidermolysis bullosa acquisita. *Br J Dermatol* (1997) 137(5):783–6. doi:10.1111/j.1365-2133.1997.tb01119.x
158. Hoshina D, Sawamura D, Nomura T, Tanimura S, Abe M, Onozuka T, et al. Epidermolysis bullosa acquisita associated with psoriasis vulgaris. *Clin Exp Dermatol* (2007) 32(5):516–8. doi:10.1111/j.1365-2230.2007.02430.x
159. Kabashima R, Hino R, Bito T, Kabashima K, Nakamura M, Bungo O, et al. Epidermolysis bullosa acquisita associated with psoriasis. *Acta Derm Venereol* (2010) 90(3):314–6. doi:10.2340/00015555-0832
160. Min L, Kensuke M, Takashi H, Naoyuki H. Epidermolysis bullosa acquisita in a patient with psoriasis vulgaris. *Eur J Dermatol* (2015) 25(5):499–500. doi:10.1684/ejd.2015.2623
161. Moon SY, Eun DH, Jung HJ, Kim JY, Park TI, Lee WJ, et al. Coexistence of psoriasis and epidermolysis bullosa acquisita: evaluation of the integrity of the basement membrane. *J Cutan Pathol* (2017) 44(6):602–3. doi:10.1111/cup.12940
162. Kawachi Y, Ikegami M, Hashimoto T, Matsumura K, Tanaka T, Otsuka F. Autoantibodies to bullous pemphigoid and epidermolysis bullosa acquisita antigens in an infant. *Br J Dermatol* (1996) 135(3):443–7. doi:10.1111/j.1365-2133.1996.tb01511.x
163. Jonkman MF, Schuur J, Dijk F, Heeres K, de Jong MC, van der Meer JB, et al. Inflammatory variant of epidermolysis bullosa acquisita with IgG autoantibodies against type VII collagen and laminin alpha3. *Arch Dermatol* (2000) 136(2):227–31. doi:10.1001/archderm.136.2.227
164. Furukawa H, Miura T, Takahashi M, Nakamura K, Kaneko F, Ishii F, et al. A case of anti-p200 pemphigoid with autoantibodies against both a novel 200-kD dermal antigen and the 290-kD epidermolysis bullosa acquisita antigen. *Dermatology* (2004) 209(2):145–8. doi:10.1159/000079601
165. Buijsrogge JJ, de Jong MC, Meijer HJ, Dijk F, Jonkman MF, Pas HH. Inflammatory epidermolysis bullosa acquisita with coexistent IgA antibodies to plectin. *Clin Exp Dermatol* (2005) 30(5):531–4. doi:10.1111/j.1365-2230.2005.01854.x
166. Osawa M, Demitsu T, Toda S, Yokokura H, Umemoto N, Yamada T, et al. A case of mixed bullous disease of epidermolysis bullosa acquisita and linear IgA bullous dermatosis. *Dermatology* (2005) 211(2):146–8. doi:10.1159/000086445
167. Yang B, Wang C, Wu M, Du D, Yan X, Zhou G, et al. A case of pemphigoid gestationis with concurrent IgG antibodies to BP180, BP230 and type VII collagen. *Australas J Dermatol* (2014) 55(1):e15–8. doi:10.1111/j.1440-0960.2012.00960.x
168. Marathe K, Lu J, Morel KD. Bullous diseases: kids are not just little people. *Clin Dermatol* (2015) 33(6):644–56. doi:10.1016/j.clindermatol.2015.09.007
169. Allen J, Wojnarowska F. Linear IgA disease: the IgA and IgG response to dermal antigens demonstrates a chiefly IgA response to LAD285 and a dermal 180-kDa protein. *Br J Dermatol* (2003) 149(5):1055–8. doi:10.1111/j.1365-2133.2003.05647.x
170. Allen J, Wojnarowska F. Linear IgA disease: the IgA and IgG response to the epidermal antigens demonstrates that intermolecular epitope spreading is associated with IgA rather than IgG antibodies, and is more common in adults. *Br J Dermatol* (2003) 149(5):977–85. doi:10.1111/j.1365-2133.2003.05648.x
171. Zillikens D, Herzele K, Georgi M, Schmidt E, Chimanovitch I, Schumann H, et al. Autoantibodies in a subgroup of patients with linear IgA disease react with the NC16A domain of BP180. *J Invest Dermatol* (1999) 113(6):947–53. doi:10.1046/j.1523-1747.1999.00808.x
172. Marinkovich P, Taylor T, Keene D, Burgeson RE, Zone JJ. LAD-1, the linear IgA bullous dermatosis autoantigen, is a novel 120kDa anchoring filament protein synthesized by epidermal cells. *J Invest Dermatol* (1996) 106(4):734–8. doi:10.1111/1523-1747.ep12345782
173. Zone JJ, Taylor TB, Meyer LJ, Petersen MJ. The 97 kDa linear IgA bullous disease antigen is identical to a portion of the extracellular domain of the 180 kDa bullous pemphigoid antigen, BPAg2. *J Invest Dermatol* (1998) 110(3):207–10. doi:10.1046/j.1523-1747.1998.00129.x
174. Roh JY, Yee C, Lazarova Z, Hall RP, Yancey KB. The 120-kDa soluble ectodomain of type XVII collagen is recognized by autoantibodies in patients with pemphigoid and linear IgA dermatosis. *Br J Dermatol* (2000) 143(1):104–11. doi:10.1046/j.1365-2133.2000.03598.x
175. Christophoridis S, Budinger L, Borradori L, Hunziker T, Merk HF, Hertl M. IgG, IgA and IgE autoantibodies against the ectodomain of BP180 in patients with bullous and cicatricial pemphigoid, and linear IgA bullous dermatosis. *Br J Dermatol* (2000) 143(2):349–55. doi:10.1046/j.1365-2133.2000.03661.x
176. Sakaguchi M, Bito T, Oda Y, Kikusawa A, Nishigori C, Munetsugu T, et al. Three cases of linear IgA/IgG bullous dermatosis showing IgA and IgG reactivity with multiple antigens, particularly laminin-332. *JAMA Dermatol* (2013) 149(11):1308–13. doi:10.1001/jamadermatol.2013.5691
177. Kanitakis J, Mauduit G, Cozzani E, Badinand P, Faure M, Claudy A. Linear IgA bullous dermatosis of childhood with autoantibodies to a 230 kDa epidermal antigen. *Pediatr Dermatol* (1994) 11(2):139–44. doi:10.1111/j.1525-1470.1994.tb00568.x
178. Zambruno G, Manca V, Kanitakis J, Cozzani E, Nicolas JF, Giannetti A. Linear IgA bullous dermatosis with autoantibodies to a 290 kd antigen of anchoring fibrils. *J Am Acad Dermatol* (1994) 31(5 Pt 2):884–8. doi:10.1016/S0190-9622(94)70252-7
179. Bérard F, Kanitakis J, Di Maio M, Ghohestani R, Hermier C, David L, et al. Linear IgA bullous dermatosis in children with autoantibodies against 180 kDa pemphigoid antigen. *Arch Pediatr* (1996) 3(4):345–7.
180. Hashimoto T, Ishiko A, Shimizu H, Tanaka T, Dodd HJ, Bhogal BS, et al. A case of linear IgA bullous dermatosis with IgA anti-type VII collagen autoantibodies. *Br J Dermatol* (1996) 134(2):336–9. doi:10.1111/j.1365-2133.1996.tb07624.x
181. Kawahara Y, Hashimoto T, Watanabe K, Kurihara S, Matsuo I, Nishikawa T. Two cases of atypical bullous disease showing linear IgG and IgA deposition in

the basement membrane zone. *J Dermatol* (1996) 23(4):254–8. doi:10.1111/j.1346-8138.1996.tb04008.x
182. Ghohestani RF, Nicolas JF, Kanitakis J, Claudy A. Linear IgA bullous dermatosis with IgA antibodies exclusively directed against the 180- or 230-kDa epidermal antigens. *J Invest Dermatol* (1997) 108(6):854–8. doi:10.1111/1523-1747.ep12292581
183. Honoki K, Muramatsu T, Tsubakimoto A, Shirai T. Linear IgA bullous dermatosis with circulating IgG autoantibodies to the 230 kD epidermal antigen. *J Dermatol* (1998) 25(8):503–9. doi:10.1111/j.1346-8138.1998.tb02444.x
184. Wakelin SH, Allen J, Zhou S, Wojnarowska F. Drug-induced linear IgA disease with antibodies to collagen VII. *Br J Dermatol* (1998) 138(2):310–4. doi:10.1046/j.1365-2133.1998.02081.x
185. Nie Z, Nagata Y, Joubeh S, Hirako Y, Owaribe K, Kitajima Y, et al. IgA antibodies of linear IgA bullous dermatosis recognize the 15th collagenous domain of BP180. *J Invest Dermatol* (2000) 115(6):1164–6. doi:10.1046/j.1523-1747.2000.0202a-7.x
186. Lin MS, Fu CL, Olague-Marchan M, Hacker MK, Zillikens D, Giudice GJ, et al. Autoimmune responses in patients with linear IgA bullous dermatosis: both autoantibodies and T lymphocytes recognize the NC16A domain of the BP180 molecule. *Clin Immunol* (2002) 102(3):310–9. doi:10.1006/clim.2001.5177
187. Metz BJ, Ruggeri SY, Hsu S, Reed JA, Ghohestani AS, Uitto J, et al. Linear IgA dermatosis with IgA and IgG autoantibodies to the 180 kDa bullous pemphigoid antigen (BP180): evidence for a distinct subtype. *Int J Dermatol* (2004) 43(6):443–6. doi:10.1111/j.1365-4632.2004.02016.x
188. Shimizu S, Natsuga K, Shinkuma S, Yasui C, Tsuchiya K, Shimizu H. Localized linear IgA/IgG bullous dermatosis. *Acta Derm Venereol* (2010) 90(6):621–4. doi:10.2340/00015555-0985
189. Passos L, Rabelo RF, Matsuo C, Santos M, Talhari S, Talhari C. Linear IgA/IgG bullous dermatosis: successful treatment with dapsone and mycophenolate mofetil. *An Bras Dermatol* (2011) 86(4):747–50. doi:10.1590/S0365-05962011000400018
190. Yanagihara S, Mizuno N, Naruse A, Tateishi C, Tsuruta D, Ishii M. Linear immunoglobulin A/immunoglobulin G bullous dermatosis associated with Vogt-Koyanagi-Harada disease. *J Dermatol* (2011) 38(8):798–791. doi:10.1111/j.1346-8138.2011.01221.x
191. Kern JS, Gehring W, Kreisel W, Hertl M, Technau-Hafsi K, Bruckner-Tuderman L, et al. Overlap of IgA pemphigus and linear IgA dermatosis in a patient with ulcerative colitis: a mere coincidence? *Acta Derm Venereol* (2014) 94(2):228–30. doi:10.2340/00015555-1658
192. Tashima S, Konishi K, Koga H, Hashimoto T. A case of vancomycin-induced linear IgA bullous dermatosis with circulating IgA antibodies to the NC16a domain of BP180. *Int J Dermatol* (2014) 53(3):e207–9. doi:10.1111/ijd.12047
193. Zenke Y, Nakano T, Eto H, Koga H, Hashimoto T. A case of vancomycin-associated linear IgA bullous dermatosis and IgA antibodies to the α3 subunit of laminin-332. *Br J Dermatol* (2014) 170(4):965–9. doi:10.1111/bjd.12720
194. Izaki S, Mitsuya J, Okada T, Koga H, Hashimoto T, Terui T. A case of linear IgA/IgG bullous dermatosis with anti-laminin-332 autoantibodies. *Acta Derm Venereol* (2015) 95(3):359–60. doi:10.2340/00015555-1923
195. Li X, Tsuchisaka A, Qian H, Teye K, Ishii N, Sogame R, et al. Linear IgA/IgG bullous dermatosis reacts with multiple laminins and integrins. *Eur J Dermatol* (2015) 25(5):418–23. doi:10.1684/ejd.2015.2555
196. Fernandes KA, Galvis KH, Gomes AC, Nogueira OM, Felix PA, Vargas TJ. Linear IgA and IgG bullous dermatosis. *An Bras Dermatol* (2016) 91(5 Suppl 1):32–4. doi:10.1590/abd1806-4841.20164630
197. Izaki S, Ito K, Ishii N, Hashimoto T, Fujita H, Terui T. Infantile linear IgA/IgG bullous dermatosis. *Eur J Dermatol* (2016) 26(1):96–8. doi:10.1684/ejd.2015.2667
198. Koga H, Ishii N, Hashimoto T, Nakama T. Case of shift from linear immunoglobulin A bullous dermatosis to pemphigus herpetiformis for a short period of time. *J Dermatol* (2017) 44(2):189–93. doi:10.1111/1346-8138.13677
199. Matsuura K, Ujiie H, Hayashi M, Muramatsu K, Yoshizawa J, Ito T, et al. Linear IgA bullous dermatosis in a pregnant woman with autoantibodies to the non-collagenous 16A domain of type XVII collagen. *Acta Derm Venereol* (2017) 97(3):404–5. doi:10.2340/00015555-2557
200. Cooke N, Jenkinson H, Wojnarowska F, McKenna K, Alderdice J. Coexistence of psoriasis and linear IgA disease in a patient with recent herpes zoster infection. *Clin Exp Dermatol* (2005) 30(6):643–5. doi:10.1111/j.1365-2230.2005.01872.x
201. Takagi Y, Sawada S, Yamauchi M, Amagai M, Niimura M. Coexistence of psoriasis and linear IgA bullous dermatosis. *Br J Dermatol* (2000) 142(3):513–6. doi:10.1046/j.1365-2133.2000.03367.x
202. Barrows-Wade L, Jordon RE, Arnett FC Jr. Linear IgA bullous dermatosis associated with dermatomyositis. *Arch Dermatol* (1992) 128(3):413–4. doi:10.1001/archderm.128.3.413
203. Hayakawa K, Shiohara T, Yagita A, Nagashima M. Linear IgA bullous dermatosis associated with rheumatoid arthritis. *J Am Acad Dermatol* (1992) 26(1):110–3. doi:10.1016/0190-9622(92)70017-A
204. Alba D, Alvarez-Doforno R, Casado M, Borbujo J. Linear bullous IGA dermatosis and systemic lupus erythematosus. *Med Clin (Barc)* (1995) 105(2):77–8.
205. Tobón GJ, Toro CE, Bravo JC, Cañas CA. Linear IgA bullous dermatosis associated with systemic lupus erythematosus: a case report. *Clin Rheumatol* (2008) 27(3):391–3. doi:10.1007/s10067-007-0752-5
206. Mavragani CP, Asvesti K, Moutsopoulos HM. Linear IgA dermatosis in a patient with primary Sjogren's syndrome. *Rheumatology (Oxford)* (2013) 52(2):403–4. doi:10.1093/rheumatology/kes148
207. Paige DG, Leonard JN, Wojnarowska F, Fry L. Linear IgA disease and ulcerative colitis. *Br J Dermatol* (1997) 136(5):779–82. doi:10.1046/j.1365-2133.1997.6751622.x
208. Chan LS, Regezi JA, Cooper KD. Oral manifestations of linear IgA disease. *J Am Acad Dermatol* (1990) 22(2 Pt 2):362–5. doi:10.1016/0190-9622(90)70049-N
209. De Simone C, Guerriero C, Pellicano R. Linear IgA disease and ulcerative colitis. *Eur J Dermatol* (1998) 8(1):48–50.
210. Chi HI, Arai M. Linear IgA bullous dermatosis associated with ulcerative colitis. *J Dermatol* (1999) 26(3):150–3. doi:10.1111/j.1346-8138.1999.tb03445.x
211. Keller AS, Bouldin MB, Drage LA, Hauser SC, Davis MD. Linear IgA bullous dermatosis: an association with ulcerative colitis versus renal cell carcinoma. *Dig Dis Sci* (2003) 48(4):783–9. doi:10.1023/A:1022805329847
212. Eckert RL, Sturniolo MT, Broome AM, Ruse M, Rorke EA. Transglutaminase function in epidermis. *J Invest Dermatol* (2005) 124(3):481–92. doi:10.1111/j.0022-202X.2005.23627.x
213. Kárpáti S, Sárdy M, Németh K, Mayer B, Smyth N, Paulsson M, et al. Transglutaminases in autoimmune and inherited skin diseases: the phenomena of epitope spreading and functional compensation. *Exp Dermatol* (2017). doi:10.1111/exd.13449
214. Mendes FB, Hissa-Elian A, Abreu MA, Gonçalves VS. Review: dermatitis herpetiformis. *An Bras Dermatol* (2013) 88(4):594–5. doi:10.1590/abd1806-4841.20131775
215. Van der Meer JB. Granular deposits of immunoglobulins in the skin of patients with dermatitis herpetiformis, an immunofluorescence study. *Br J Dermatol* (1969) 81(7):493–493. doi:10.1111/j.1365-2133.1969.tb16024.x
216. Honeyman JF, Honeyman A, Lobitz WC, Storrs FJ. The enigma of bullous pemphigoid and dermatitis herpetiformis. *Arch Dermatol* (1972) 106(1):22–5. doi:10.1001/archderm.1972.01620100010002
217. Jablonska S, Chorzelski TP, Beutner E, Maciejowska E, Rzsa G. Dermatitis herpetiformis and bullous pemphigoid. Intermediate and mixed forms. *Arch Dermatol* (1976) 112:45–8. doi:10.1001/archderm.112.1.45
218. Bean SF, Michel B, Furey N, Thorne EG, Meltzer L. Vesicular pemphigoid. *Arch Dermatol* (1976) 112(10):1402–4. doi:10.1001/archderm.112.10.1402
219. Honeyman JF, Honeyman AR, De la Parra MA, Pinto A, Eguiguren GJ. Polymorphic pemphigoid. *Arch Dermatol* (1979) 115(4):423–7. doi:10.1001/archderm.115.4.423
220. Jolliffe DS, Sarkany I. Mixed bullous disease. *Clin Exp Dermatol* (1983) 8(1):113–6. doi:10.1111/j.1365-2230.1983.tb01752.x
221. de Jong MC, van der Meer JB, de Nijs JA, van der Putte SC. Concomitant immunohistochemical characteristics of pemphigoid and dermatitis herpetiformis in a patient with atypical bullous dermatosis. *Acta Derm Venereol* (1983) 63(6):476–82.
222. Jawitz J, Kumar V, Nigra TP, Beutner EH. Vesicular pemphigoid versus dermatitis herpetiformis. *J Am Acad Dermatol* (1984) 10(5 Pt 2):892–6. doi:10.1016/S0190-9622(84)80441-7
223. Sander HM, Utz MMP, Peters MS. Bullous pemphigoid and dermatitis herpetiformis: mixed bullous disease or coexistence of two separate entities? *J Cutan Pathol* (1989) 16(6):370–4. doi:10.1111/j.1600-0560.1989.tb00588.x

224. Setterfield J, Bhogal B, Black MM, McGibbon DH. Dermatitis herpetiformis and bullous pemphigoid: a developing association confirmed by immunoelectronmicroscopy. *Br J Dermatol* (1997) 136(2):253–6. doi:10.1046/j.1365-2133.1997.d01-1181.x
225. Ameen M, Bhogal BS, Black MM. Dermatitis herpetiformis evolving into bullous pemphigoid: a probable example of epitope spreading. *Clin Exp Dermatol* (2000) 25(5):398–400. doi:10.1046/j.1365-2230.2000.00673.x
226. Murphy LA, Bhogal BS, Banerjee P, Black MM. Dermatitis herpetiformis converting into bullous pemphigoid: a study of three cases. *Br J Dermatol* (2003) 149(Suppl 64):17.
227. Schulze F, van Beek N, Terheyden P, Zillikens D, Schmidt E. Concomitant bullous pemphigoid and dermatitis herpetiformis. *Dermatology* (2013) 226(3):217–21. doi:10.1159/000349982
228. Vaira F, Della Valle V, Fanoni D, Pontini P, Muratori S. Bullous pemphigoid and dermatitis herpetiformis association: a genetic predisposition. *J Dermatol* (2013) 40(11):940–1. doi:10.1111/1346-8138.12262
229. Chan LS. Ocular and oral mucous membrane pemphigoid (cicatricial pemphigoid). *Clin Dermatol* (2012) 30(1):34–7. doi:10.1016/j.clindermatol.2011.03.007
230. Bruch-Gerharz D, Hertl M, Ruzicka T. Mucous membrane pemphigoid: clinical aspects, immunopathological features and therapy. *Eur J Dermatol* (2007) 17(3):191–200. doi:10.1684/ejd.2007.0148
231. Balding SD, Prost C, Diaz LA, Bernard P, Bedane C, Aberdam D, et al. Cicatricial pemphigoid autoantibodies react with multiple sites on the BP180 extracellular domain. *J Invest Dermatol* (1996) 106(1):141–6. doi:10.1111/1523-1747.ep12329728
232. Calabresi V, Carrozzo M, Cozzani E, Arduino P, Bertolusso G, Tirone F, et al. Oral pemphigoid autoantibodies preferentially target BP180 ectodomain. *Clin Immunol* (2007) 122:207–13. doi:10.1016/j.clim.2006.10.007
233. Cozzani E, Di Zenzo G, Calabresi V, Carrozzo M, Burlando M, Longanesi L, et al. Autoantibody profile of a cohort of 78 Italian patients with mucous membrane pemphigoid: correlation between reactivity profile and clinical involvement. *Acta Derm Venereol* (2016) 96:768–73. doi:10.2340/00015555-2311
234. Murrell DF, Marinovic B, Caux F, Prost C, Ahmed R, Wozniak K, et al. Definitions and outcome measures for mucous membrane pemphigoid: recommendations of an international panel of experts. *J Am Acad Dermatol* (2015) 72(1):168–74. doi:10.1016/j.jaad.2014.08.024
235. Bernard P, Antonicelli F, Bedane C, Joly P, Le Roux-Villet C, Duvert-Lehembre S, et al. Prevalence and clinical significance of anti-laminin 332 autoantibodies detected by a novel enzyme-linked immunosorbent assay in mucous membrane pemphigoid. *JAMA Dermatol* (2013) 149(5):533–40. doi:10.1001/jamadermatol.2013.1434
236. Setterfield J, Shirlaw PJ, Kerr-Muir M, Neill S, Bhogal BS, Morgan P, et al. Mucous membrane pemphigoid: a dual circulating antibody response with IgG and IgA signifies a more severe and persistent disease. *Br J Dermatol* (1998) 138(4):602–10. doi:10.1046/j.1365-2133.1998.02168.x
237. Egan CA, Hanif N, Taylor TB, Meyer LJ, Petersen MJ, Zone JJ. Characterization of the antibody response in oesophageal cicatricial pemphigoid. *Br J Dermatol* (1999) 140(5):859–64. doi:10.1046/j.1365-2133.1999.03159.x
238. Yasukochi A, Teye K, Ishii N, Hashimoto T. Clinical and immunological studies of 332 Japanese patients tentatively diagnosed as anti-BP180-type mucous membrane pemphigoid: a novel BP180 C-terminal domain enzyme-linked immunosorbent assay. *Acta Derm Venereol* (2016) 96(6):762–7. doi:10.2340/00015555-2407
239. Lazarova Z, Hsu R, Yee C, Yancey KB. Human anti-laminin 5 autoantibodies induce subepidermal blisters in an experimental human skin graft model. *J Invest Dermatol* (2000) 114(1):178–84. doi:10.1046/j.1523-1747.2000.00829.x
240. Oyama N, Setterfield JF, Powell AM, Sakuma-Oyama Y, Albert S, Bhogal BS, et al. Bullous pemphigoid antigen II (BP180) and its soluble extracellular domains are major autoantigens in mucous membrane pemphigoid: the pathogenic relevance to HLA class II alleles and disease severity. *Br J Dermatol* (2006) 154(1):90–8. doi:10.1111/j.1365-2133.2005.06998.x
241. Inoue T, Yagami A, Iwata Y, Ishii N, Hashimoto T, Matsunaga K. Mucous membrane pemphigoid reactive only with BP230. *J Dermatol* (2016) 43(10):1228–9. doi:10.1111/1346-8138.13361
242. Hayashi I, Shinkuma S, Shimizu S, Natsuga K, Ujiie H, Yasui C, et al. Mucous membrane pemphigoid with generalized blisters: IgA and IgG autoantibodies target both laminin-332 and type XVII collagen. *Br J Dermatol* (2012) 166(5):1116–20. doi:10.1111/j.1365-2133.2011.10776.x
243. Malik M, Gürcan HM, Ahmed AR. Coexistence of mucous membrane pemphigoid and connective-tissue disease. *Clin Exp Dermatol* (2010) 35(2):156–9. doi:10.1111/j.1365-2230.2009.03222.x
244. Zakka LR, Reche PA, Ahmed AR. The molecular basis for the presence of two autoimmune diseases occurring simultaneously – preliminary observations based on computer analysis. *Autoimmunity* (2012) 45(3):253–63. doi:10.3109/08916934.2011.632454
245. Shipman AR, Reddy H, Wojnarowska F. Association between the subepidermal autoimmune blistering diseases linear IgA disease and the pemphigoid group and inflammatory bowel disease: two case reports and literature review. *Clin Exp Dermatol* (2012) 37(5):461–8. doi:10.1111/j.1365-2230.2012.04383.x
246. Takegami Y, Makino T, Matsui K, Ueda C, Fukuda S, Hashimoto T, et al. Coexistence of antilaminin-332-type mucous membrane pemphigoid, lamina lucida-type linear IgA bullous dermatosis and Sjögren syndrome. *Clin Exp Dermatol* (2013) 38(2):194–6. doi:10.1111/ced.12030
247. Monshi B, Groth S, Richter L, Schmidt E, Zillikens D, Rappersberger K. A long-term study of a patient with anti-p200 pemphigoid: correlation of autoantibody levels with disease activity and an example of epitope spreading. *Br J Dermatol* (2012) 167(5):1179–83. doi:10.1111/j.1365-2133.2012.11076.x
248. Yamada H, Nobeyama Y, Matsuo K, Ishiji T, Takeuchi T, Fukuda S, et al. A case of paraneoplastic pemphigus associated with triple malignancies in combination with antilaminin-332 mucous membrane pemphigoid. *Br J Dermatol* (2012) 166(1):230–1. doi:10.1111/j.1365-2133.2011.10520.x
249. Ohata C, Higashi Y, Yamagami J, Koga H, Ishii N, Kanekura T, et al. Coexistence of pemphigus herpetiformis with IgG antibodies to desmocollin 1 and pemphigoid with IgG antibodies to BP180 C-terminal domain and laminin γ2. *JAMA Dermatol* (2013) 149(4):502–4. doi:10.1001/jamadermatol.2013.1916
250. Li X, Qian H, Ishii N, Yamaya M, Fukuda H, Mukai H, et al. A case of concurrent antilaminin γ1 pemphigoid and antilaminin-332-type mucous membrane pemphigoid. *Br J Dermatol* (2014) 171(5):1257–9. doi:10.1111/bjd.13107
251. Kaune KM, Kasperkiewicz M, Tams D, Bergmann M, Zutt M. Anti-p200/anti-laminin γ1 pemphigoid and BP180 NC16A/4575-positive mucous membrane pemphigoid: late diagnosis in a patient with disease-related loss of vision and multiple previous surgical interventions. *Hautarzt* (2015) 66(1):60–4. doi:10.1007/s00105-014-3529-1
252. Swanton J, Isenberg D. Mixed connective tissue disease: still crazy after all these years. *Rheum Dis Clin North Am* (2005) 31:421–36. doi:10.1016/j.rdc.2005.04.009
253. Cowan CG, Lamey PJ, Walsh M, Irwin ST, Allen G, McKenna KE. Linear IgA disease (LAD): immunoglobulin deposition in oral and colonic lesions. *J Oral Pathol Med* (1995) 24(8):374–8. doi:10.1111/j.1600-0714.1995.tb01202.x
254. Chan LS, Soong HK, Foster CS, Hammerberg C, Cooper KD. Ocular cicatricial pemphigoid occurring as a sequela of Stevens-Johnson syndrome. *JAMA* (1991) 266(11):1543–6. doi:10.1001/jama.1991.03470110089038
255. De Rojas MV, Dart JK, Saw VP. The natural history of Stevens Johnson syndrome: patterns of chronic ocular disease and the role of systemic immunosuppressive therapy. *Br J Ophthalmol* (2007) 91(8):1048–53. doi:10.1136/bjo.2006.109124
256. Mignogna MD, Fortuna G, Leuci S, Stasio L, Mezza E, Ruoppo E. Lichen planus pemphigoides, a possible example of epitope spreading. *Oral Surg Oral Med Oral Pathol Oral Radiol Endod* (2010) 109(6):837–43. doi:10.1016/j.tripleo.2009.12.044
257. Fania L, Giannico MI, Fasciani R, Zampetti A, Ambrogio S, Balestrazzi E, et al. Ocular mucous membrane pemphigoid after Lyell syndrome: occasional finding or predisposing event? *Ophthalmology* (2012) 119(4):688–93. doi:10.1016/j.ophtha.2011.09.038
258. Sarret Y, Reano A, Nicolas JF, Su H, Thivolet J. Bullous pemphigoid and cicatricial pemphigoid: immunoblotting detection of involved autoantigens. *Autoimmunity* (1989) 2(2):145–53. doi:10.3109/08916938909019951
259. Shannon JF, Mackenzie-Wood A, Wood G, Goldstein D. Cicatricial pemphigoid in non-Hodgkin's lymphoma. *Intern Med J* (2003) 33(8):396–7. doi:10.1046/j.1445-5994.2003.t01-1-00430.x
260. Aisa Y, Mori T, Nakazato T, Yamazaki R, Yamagami J, Amagai M, et al. Cicatricial pemphigoid of the oropharynx after allogeneic stem cell

transplantation for relapsed follicular lymphoma. *Int J Hematol* (2005) 82(3):266–9. doi:10.1532/IJH97.05061
261. Takahara M, Tsuji G, Ishii N, Dainichi T, Hashimoto T, Kohno K, et al. Mucous membrane pemphigoid with antibodies to the beta (3) subunit of Laminin 332 in a patient with acute myeloblastic leukemia and graft-versus-host disease. *Dermatology* (2009) 219(4):361–4. doi:10.1159/000243807
262. Mahmood S, Lim ZY, Benton E, du Vivier A, Bhogal B, Mufti GJ, et al. Mucous membrane pemphigoid following reduced intensity conditioning allogeneic haematopoietic SCT for biphenotypic leukaemia. *Bone Marrow Transplant* (2010) 45(1):195–6. doi:10.1038/bmt.2009.98
263. Masunaga K, Toyoda M, Kokuba H, Takahara M, Ohyama B, Hashimoto T, et al. Mucous membrane pemphigoid with antibodies to the β3 subunit of laminin 332. *J Dermatol* (2011) 38(11):1082–4. doi:10.1111/j.1346-8138.2010.01185.x
264. Hirakawa Y, Oiso N, Ishii N, Koga H, Tatebayashi M, Uchida S, et al. Mucous membrane pemphigoid with IgG autoantibodies to the 120-kDa ectodomain of type XVII collagen (BP180/linear IgA dermatosis antigen) in a patient with idiopathic thrombocytopenic purpura. *Acta Derm Venereol* (2015) 95(4):493–4. doi:10.2340/00015555-1964
265. Endo Y, Tsuji M, Shirase T, Fukuda S, Hashimoto T, Miyachi Y, et al. Angioimmunoblastic T-cell lymphoma presenting with both IgA-related leukocytoclastic vasculitis and mucous membrane pemphigoid. *Eur J Dermatol* (2011) 21(2):274–6. doi:10.1684/ejd.2010.1227
266. Okada R, Yamaguchi Y, Sawaki H, Hashimoto T, Aihara M. Development of mucous membrane pemphigoid with antibodies to the β3 subunit of laminin 332 and bronchiolitis obliterans in a patient with chronic graft-versus-host disease. *Eur J Dermatol* (2015) 25(5):505–6. doi:10.1684/ejd.2015.2622
267. Young AL, Bailey EE, Colaço SM, Engler DE, Grossman ME. Anti-laminin-332 mucous membrane pemphigoid associated with recurrent metastatic prostate carcinoma: hypothesis for a paraneoplastic phenomenon. *Eur J Dermatol* (2011) 21(3):401–4. doi:10.1684/ejd.2011.1360
268. Zillikens D, Caux F, Mascaro JM, Wesselmann U, Schmidt E, Prost C, et al. Autoantibodies in lichen planus pemphigoides react with a novel epitope within the C-terminal NC16A domain of BP180. *J Invest Dermatol* (1999) 113(1):117–21. doi:10.1046/j.1523-1747.1999.00618.x
269. Sekiya A, Kodera M, Yamaoka T, Iwata Y, Usuda T, Ohzono A, et al. A case of lichen planus pemphigoides with autoantibodies to the NC16a and C-terminal domains of BP180 and to desmoglein-1. *Br J Dermatol* (2014) 171(5):1230–5. doi:10.1111/bjd.13097
270. Joly P, Maho-Vaillant M, Prost-Squarcioni C, Hebert V, Houivet E, Calbo S, et al. First-line rituximab combined with short-term prednisone versus prednisone alone for the treatment of pemphigus (Ritux 3): a prospective, multicentre, parallel-group, open-label randomised trial. *Lancet* (2017) 389(10083):2031–40. doi:10.1016/S0140-6736(17)30070-3
271. Ellebrecht CT, Bhoj VG, Nace A, Choi EJ, Mao X, Cho MJ, et al. Reengineering chimeric antigen receptor T cells for targeted therapy of autoimmune disease. *Science* (2016) 353(6295):179–84. doi:10.1126/science.aaf6756
272. Serr I, Fürst RW, Achenbach P, Scherm MG, Gökmen F, Haupt F, et al. Type 1 diabetes vaccine candidates promote human Foxp3(+) Treg induction in humanized mice. *Nat Commun* (2016) 7:10991. doi:10.1038/ncomms10991
273. Mikecz K, Glant TT, Markovics A, Rosenthal KS, Kurko J, Carambula RE, et al. An epitope-specific DerG-PG70 LEAPS vaccine modulates T cell responses and suppresses arthritis progression in two related murine models of rheumatoid arthritis. *Vaccine* (2017) 35(32):4048–56. doi:10.1016/j.vaccine.2017.05.009
274. Lutterotti A, Yousef S, Sputtek A, Stürner KH, Stellmann JP, Breiden P, et al. Antigen-specific tolerance by autologous myelin peptide-coupled cells: a phase 1 trial in multiple sclerosis. *Sci Transl Med* (2013) 5(188):188ra75. doi:10.1126/scitranslmed.3006168
275. Hammers CM, Chen J, Lin C, Kacir S, Siegel DL, Payne AS, et al. Persistence of anti-desmoglein 3 IgG (+) B-cell clones in pemphigus patients over years. *J Invest Dermatol* (2015) 135(3):742–9. doi:10.1038/jid.2014.291
276. Di Zenzo G, Zambruno G. Clonal analysis of B-cell response in pemphigus course: toward more effective therapies. *J Invest Dermatol* (2015) 135:651–4. doi:10.1038/jid.2014.499
277. Ellebrecht CT, Payne AS. Setting the target for pemphigus vulgaris therapy. *JCI Insight* (2017) 2(5):e92021. doi:10.1172/jci.insight.92021
278. Chen J, Zheng Q, Hammers CM, Ellebrecht CT, Mukherjee EM, Tang HY, et al. Proteomic analysis of pemphigus autoantibodies indicates a larger, more diverse, and more dynamic repertoire than determined by B cell genetics. *Cell Rep* (2017) 18(1):237–47. doi:10.1016/j.celrep.2016.12.013
279. Acha-Orbea H, Mitchell DJ, Timmerman L, Wraith DC, Waldor MK, Tausch GS, et al. Limited heterogeneity of T cell receptors from lymphocytes mediating autoimmune encephalomyelitis allows specific immune intervention. *Cell* (1988) 54:263–73. doi:10.1016/0092-8674(88)90558-2
280. Brocke S, Gijbels K, Allegretta M, Ferber I, Piercy C, Blankenstein T, et al. Treatment of experimental encephalomyelitis with a peptide analogue of myelin basic protein. *Nature* (1996) 379:343–5. doi:10.1038/379343a0
281. Amagai M, Tsunoda K, Suzuki H, Nishifuji K, Koyasu S, Nishikawa T. Use of autoantigen-knockout mice in developing an active autoimmune disease model for pemphigus. *J Clin Invest* (2000) 105(5):625–31. doi:10.1172/JCI8748
282. Sitaru C, Chiriac MT, Mihai S, Büning J, Gebert A, Ishiko A, et al. Induction of complement-fixing autoantibodies against type VII collagen results in subepidermal blistering in mice. *J Immunol* (2006) 177(5):3461–8. doi:10.4049/jimmunol.177.5.3461
283. Takahashi H, Kouno M, Nagao K, Wada N, Hata T, Nishimoto S, et al. Desmoglein 3-specific CD4+ T cells induce pemphigus vulgaris and interface dermatitis in mice. *J Clin Invest* (2011) 121(9):3677–88. doi:10.1172/JCI57379
284. Hirose M, Recke A, Beckmann T, Shimizu A, Ishiko A, Bieber K, et al. Repetitive immunization breaks tolerance to type XVII collagen and leads to bullous pemphigoid in mice. *J Immunol* (2011) 187(3):1176–83. doi:10.4049/jimmunol.1100596
285. Hurskainen T, Kokkonen N, Sormunen R, Jackow J, Löffek S, Soininen R, et al. Deletion of the major bullous pemphigoid epitope region of collagen XVII induces blistering, autoimmunization, and itching in mice. *J Invest Dermatol* (2015) 135(5):1303–10. doi:10.1038/jid.2014.443

Conflict of Interest Statement: The authors declare that the research was conducted in the absence of any commercial or financial relationships that could be construed as a potential conflict of interest.

frontiers in Immunology

REVIEW
published: 16 April 2018
doi: 10.3389/fimmu.2018.00765

Are Anti-Retinal Autoantibodies a Cause or a Consequence of Retinal Degeneration in Autoimmune Retinopathies?

*Grazyna Adamus**

School of Medicine, Casey Eye Institute, Oregon Health & Science University, Portland, OR, United States

Autoantibodies (AAbs) against various retinal proteins have been associated with vision loss in paraneoplastic and non-paraneoplastic autoimmune retinopathies (AR). There are two major paraneoplastic syndromes associated anti-retinal AAbs, cancer-associated retinopathy (CAR), and melanoma-associated retinopathy. Some people without a cancer diagnosis may present symptoms of CAR and have anti-retinal AAbs. The etiology and pathogenesis of those entities are not fully understood. In this review, we provide evidence for the role of AAbs in retinal death and degeneration. Studies of epitope mapping for anti-recoverin, anti-enolase, and anti-carbonic anhydrase II revealed that although patients' AAbs may recognize the same retinal protein as normal individuals they bind to different molecular domains, which allows distinguishing between normal and diseased AAbs. Given the great diversity of anti-retinal AAbs, it is likely some antibodies have greater pathogenic potential than others. Pathogenic, but not normal antibodies penetrate the target cell, reach their specific antigen, induce apoptosis, and impact retinal pathophysiology. Photoreceptors, dying by apoptosis, induced by other than immunologic mechanisms produce substantial amounts of metabolic debris, which consequently leads to autoimmunization and enhanced permeability of the blood–retinal barrier. AAbs that were made as a part of anti-cancer response are likely to be the cause of retinal degeneration, whereas others, generated against released antigens from damaged retina, contribute to the progression of retinopathy. Altogether, AAbs may trigger retinal degeneration and may also exacerbate the degenerative process in response to the release of sequestered antigens and influence disease progression.

Keywords: autoantibody, retinal degeneration, cancer-associated retinopathy, melanoma-associated retinopathy, recoverin, enolase, transient receptor potential channel protein 1, epitope mapping

OPEN ACCESS

Edited by:
Rachel R. Caspi, National Institutes of Health (NIH), United States

Reviewed by:
Lennart T. Mars, Institut National de la Santé et de la Recherche Médicale (INSERM), France
Raymond John Steptoe, The University of Queensland, Australia

***Correspondence:**
Grazyna Adamus
adamusg@ohsu.edu

Specialty section:
This article was submitted to Immunological Tolerance and Regulation, a section of the journal Frontiers in Immunology

Received: *30 November 2017*
Accepted: *27 March 2018*
Published: *16 April 2018*

Citation:
Adamus G (2018) Are Anti-Retinal Autoantibodies a Cause or a Consequence of Retinal Degeneration in Autoimmune Retinopathies? Front. Immunol. 9:765. doi: 10.3389/fimmu.2018.00765

INTRODUCTION

Autoantibodies (AAbs) against retinal proteins have been associated with vision disturbance in paraneoplastic and non-paraneoplastic autoimmune retinopathies (AR). Cancer-associated retinopathy (CAR), a visual paraneoplastic syndrome, is characterized by sudden and unexplained loss of vision associated with distant cancer and the presence of AAbs (1, 2). Those

Abbreviations: AAbs, autoantibodies; AR, autoimmune retinopathy; CAR, cancer-associated retinopathy; MAR, melanoma-associated retinopathy; RCS, Royal College of Surgeons; RPE, retinal pigment epithelium; APC, antigen-presenting cells; GCAP, guanylate cyclase-activating protein; TULP1, tubby-like protein 1; IRBP, interphotoreceptor retinoid-binding protein; HSP27, heat shock protein 27; CAII, carbonic anhydrase II; TRPM1, transient receptor potential channel protein 1; TULP1, tubby-like protein 1; ERG, electroretinogram.

AAbs bind to various antigens present in the retina and are collectively called anti-retinal AAbs. CAR can be associated with any cancer and dysfunction of photoreceptor cells and other retinal cells (3). A disorder that affects people with metastatic skin melanoma and vision loss related to the dysfunction of retinal bipolar cells has been separated from CAR syndrome and was named melanoma-associated retinopathy (MAR) (4–6). Autoimmune retinopathy (AR) concerns people with acute or subacute vision loss who present symptoms of CAR and have anti-retinal AAbs but without a cancer diagnosis at presentation (7). Autoimmune retinopathies commonly affect individuals of over 50 years old. As the general population grows older, the number of seropositive patients for anti-retinal AAbs increases with complaints of vision loss. In this review, we will provide evidence for autoimmunity as a primary contributing mechanism underlying retinal cell death or as a secondary role in exacerbating the degenerative processes in response to antigens being released from the degenerating retina, thus influencing the progression of AR. Even if AAbs did not initiate the pathogenic processes, they could still drastically impact the progression of AR. Pathology of retinal degeneration in human tissue is illustrated in **Figure 1**.

AUTOIMMUNE RETINAL DEGENERATION SYNDROMES

Paraneoplastic (CAR, MAR) and non-paraneoplastic (AR) disorders are immunologically and symptomatically heterogeneous. CAR is characterized by sudden and progressive loss of vision associated with photosensitivity, reduced visual acuity, defects in color vision, constriction of visual fields, ring scotoma, and attenuated retinal arteriole (1, 2). The function of both cone and rod photoreceptor cells can be affected. In the case of cone-related dysfunction, patients present with photosensitivity, photopsias, glare, severely reduced central vision, and impaired color perception. Rod dysfunction manifests with night blindness, impaired dark adaptation, and peripheral visual field loss, e.g., ring scotoma.

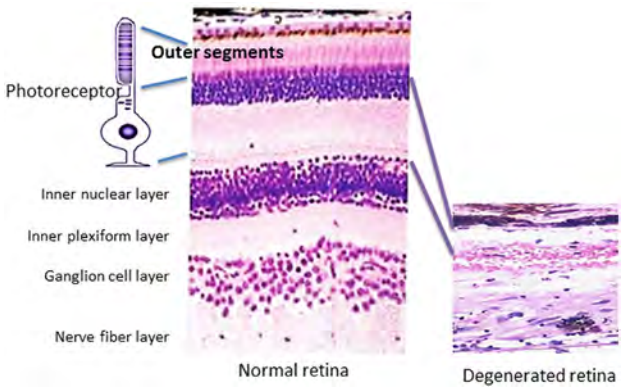

FIGURE 1 | Pathology of retinal degeneration. A picture that illustrates a rod photoreceptor cell next to normal human retina (on the left) that is composed of several cell layers as follows: inner and outer segments of rod and cones of photoreceptors cells, outer nuclear layer, outer plexiform layer, inner nuclear layer, inner plexiform layer, ganglion cells layer, nerve fiber layer (axons of ganglion cells), and outer limiting membrane that neighbors with vitreous. A photograph of degenerated retina from a patient who lost completely photoreceptor cell layer (on the right), only inner part of the retina remained unaffected.

Melanoma-associated retinopathy is characterized by symptoms of acquired night blindness, light sensations, visual loss, defect in visual fields, and reduced b-waves in the electroretinogram (ERG) (8). It primarily affects bipolar cell function, but photoreceptors can also be damaged in MAR patients (9, 10). Despite significant variations in signs and symptoms, we and others have found some similarities in the clinical presentation of retinopathy associated with AAbs of the same specificity. For example, the clinical phenotype for anti-recoverin-associated retinopathy appears to be different from the retinopathy that is associated with anti-enolase antibodies (11–13). These disorders are rare. The low incidence of CAR and MAR could be related to the fact that most patients with carcinomas or melanoma do not perceive that their eye problems could be connected to their distant malignancy. It may also be possible that substantial subjective vision loss only occurs after a critical number of rod and cone photoreceptors are destroyed (14–16). Retinal autoimmunity can also contribute to photoreceptor cell loss in hereditary retinitis pigmentosa (RP) and possibly other inherited retinal dystrophies.

GENERATION OF ANTI-RETINAL AAbs

Autoantibodies against a variety of retinal antigens have been detected in patients' blood but the precise mechanism for AAb origination remains unclear. Specifically, the question is whether the antibodies are involved in the initial pathogenesis of retinal disease or if they develop during the course of the disease as a secondary event. We contemplate three possible causes of AAb formation in retinal degenerative diseases: (A) the antitumor response, (B) the anti-microbial response, or (C) the autoimmune response against self-antigens that are released from a damaged retina (**Figure 2**).

(A) There is evidence that CAR antibodies are produced as a part of antitumor response (17–22). Both malignant and benign tumors are capable of inducing a humoral immune response (23, 24). During antitumor response, released antigens are picked up and processed by antigen-presenting cells, which eventually leads to the production of AAbs that may cross-react with protein antigens in the retina. Some retinal antigens are identical or partially identical to the antigens present in cancer cells that are upregulated during tumorigenesis. An example of such a response are AAbs against recoverin, a protein normally sequestered in the retina but it is also produced in small cell carcinoma of the lung and other cancers (25–29). The process of AAb formation likely starts in the pre-malignant phase and may serve to limit the tumor growth (30, 31). Anti-recoverin AAbs were also found in patients that initially presented with ocular disturbances—without cancer; however, a malignancy was later discovered (25, 32, 33).

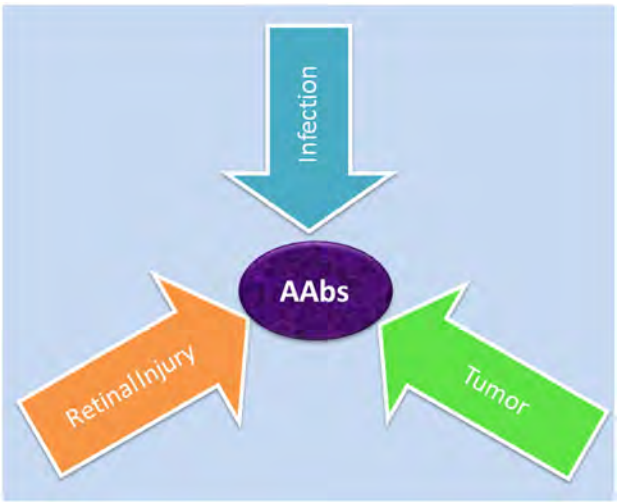

FIGURE 2 | Possible causes for generation of autoantibodies reacted with retinal antigens: anti-microbial responses (infection) against similar antigens released after infection, antitumor responses (tumor) against upregulated similar proteins, or anti-retinal responses to released sequestered proteins (retinal injury) from dying retinal cells.

(B) The second possibility for AAb generation is an anti-microbial response, since there are putative similarities between proteins that exist in pathogens and the retina. An autoimmune response can emerge following infection by a microbial pathogen, whose proteins have structural similarities to human proteins (34). Proteins, to which the immune system is normally self-tolerant, might elicit autoimmune responses. Thus, antibodies evoked against pathogenic proteins can cross-react with retinal proteins and act as AAbs and the implicated autoantigens then provide a source for persistent stimulation. Exposure to infections by bacteria and viruses throughout the entire life of the host induces memory microbe-specific T and B cells, which then recognize self-antigens of the eye, leading to autoimmune processes. Cross-reactive microbial AAbs with retinal antigens, in particular, against conserved proteins with important physiological functions can cross the blood–retinal barrier (BRB) and access similar or identical antigens in retinal cells (35–37). An example of such cross-reactive antibodies is AAb against glycolytic enzymes, which have important metabolic functions in both microbial and retinal cells. Moreover, glycolytic proteins are multifunctional, they not only exist in the cytosol, but are also exposed on the membrane of microbes, making them easily accessible to the immune system (36).

(C) The third mechanism for antibody production can be explained by the availability of retinal antigens during retinal degeneration initiated by some other the immunological processes. There is evidence for the activation of autoimmune responses secondary to retinal degeneration, due to the genetic mutation in different forms of RP (38–40). Causative mutations may initiate cellular stress in photoreceptor cells through the secretion of chemokines and the recruitment of microglia into the outer retina (41). It has been hypothesized that retinal proteins that are sequestered under normal physiological conditions, and protected from immune recognition, are released from the damaged tissue and become targets of the immune effector functions once exposed to the immune system (42, 43). The concept that new AAbs are produced in response to debris from regions of pathology implies that these AAbs function in the clearance of debris from the tissue (44). A variety of AAbs have been detected in patients with retinal diseases, but not all of them are against proteins that are normally present in photoreceptor cells, especially in outer segments. The potential antigenic proteins participate in the phototransduction process, by which the photoreceptor cells generate electrical signals in response to the absorption of photons (45). Photoreceptor cells are post-mitotic, terminally differentiated retinal cells that have no regenerative ability under normal physiological conditions, whose number inversely decreases with age—presumably due to cell death (46). Retinal cell death is also associated with increased numbers of subretinal microglial accumulation and complement activation (47). Although the eye has an immune privileged status, it is still susceptible to immune-mediated inflammatory disease, both by infectious and autoimmune stimuli (48, 49). A crucial step in the activation process is the recruitment of inflammatory cells, such as macrophages and microglia, to the local injured area/retina; which leads to the release of pro-inflammatory cytokines and amplifies the disease's process (50). The accumulation of debris in the outer segment provides a signaling mechanism for the activation and chemotaxis of microglial cells (41). Such processes may enhance disease progression by augmenting apoptotic photoreceptor cell death, disrupting the BRB, and attracting blood macrophages into the retina (51, 52). Excessive deposition of complement components at the retinal pigment epithelial/outer segments of photoreceptor cell space, particularly when concentrated in deposits of metabolic debris, may act as a trigger for inflammatory macrophage activation.

The research using the dystrophic Royal College of Surgeons (RCS) rat model showed that anti-retinal AAbs and T cells were generated, with distinctive activation trends, in response to the availability of antigenic material being released from dying photoreceptor cells during retinal degeneration (53). A strong initial response in anti-photoreceptor antibodies declined about the rat age 40 days, but later, there was a rebound, with a subsequent wave of antibody production, caused by an additional antigenic re-stimulation as more cells died and remained measurable until photoreceptor cells disappeared and self-antigens that were being released from dying cells were no longer available (53). This suggests that, even if AAbs did not initiate the pathogenic processes, they could still drastically influence their progression. Moreover, the adoptive transfer of anti-retinal AAbs obtained from RCS rats with inherited retinal degeneration induced disruption of the blood–retinal barrier, upregulation of MCP-1 (CCL2) chemokine, and attracted macrophages/microglia into the retina. This additional influx of microglia correlated with

increased levels of photoreceptor apoptosis, thus influencing the long-term photoreceptor survival (53). It is likely that early on, the same anti-retinal AAbs could contribute to the cell death, and later, to the progression of retinal degeneration by recruiting activated macrophages/microglia into the retina and production of new AAbs.

Although AAbs are frequently found in the circulation of patients with loss of vision, it is difficult to determine the primary mechanism of antibody formation. Assessing the cross-reactivity between cancer-retina and microbial-retinal antigens, using tissue samples or purified antigens helps with identification of the source of antigenic stimulation. However, identifying AAbs that were generated as a result of retinal death is much more difficult task. Regardless of the origination of anti-retinal AAbs, they are found to persist over time in the circulation and are associated with a stable or progressive course of vision loss (11). Due to the chronic nature of retinal autoimmunity, AAbs are likely to appear before manifestation of clinical symptoms though it is not possible to test non-symptomatic patients. Such AAbs could provide a good predictive biomarker for the potential development of retinal disease and neoplasm.

RETINAL AUTOANTIGENS

Patients with CAR, MAR, and AR have AAbs that generally target intracellular proteins, and only a few that are directed against membrane proteins, located in various retinal cell types (**Figure 3**) (54–58). Some of the first AAbs found in association with CAR are AAbs against recoverin, a calcium-binding protein that plays an important function in visual phototransduction (6, 59–61). Initially, only patients who had been diagnosed with small cell carcinoma of the lung were found to be seropositive for anti-recoverin AAbs (62, 63). However, in subsequent years, other malignancies were found to be associated with anti-recoverin AAbs (64). Anti-recoverin AAbs were also detected in patients with different cancers without visual presentation, but were not reported in healthy individuals without cancer, suggesting that AAbs are mainly generated against the cancer-expressed recoverin (65). Recoverin has been considered a main biomarker for CAR syndrome but anti-recoverin AAb presence is infrequent; in fact, only about 5% of CAR patients possess anti-recoverin antibodies (66). However, the absence of AAbs against recoverin does not exclude a diagnosis of paraneoplastic syndrome. Thus far, over 30 different antigens in the retina have been identified in association of vision loss (67–70).

Presumed targets in retinal degeneration are photoreceptor cells, the outer layer of the retina (**Figure 1**). Recoverin is a photoreceptor cell protein, in addition to several other photoreceptor antigens found, including arrestin, guanylate cyclase-activating protein, transducin-α and transducin-β, TULP1, Rab6, rhodopsin, and interphotoreceptor retinoid-binding protein (IRBP) (10, 22, 28, 54, 55, 66, 71, 72). However, sera of patients with CAR possess AAbs that not only react with photoreceptor cell antigens but also with bipolar and ganglion cells of the retina (62, 66, 73, 74). AAbs against glycolytic enzymes, such as enolase, aldolase, glyceraldehyde-3-phosphate dehydrogenase, and pyruvate kinase M2, dominate in sera of patients with AR (36). Antibodies against heat shock proteins, such as heat shock protein 27 (HSP27) and HSP65, have also been detected in patients with CAR and AR (66, 75, 76). Carbonic anhydrase II (CAII) is one of the major target proteins in prostate cancer-CAR and AR (77).

In MAR, transient receptor potential channel protein 1 (TRPM1), a membrane autoantigen is associated with retinal ON bipolar cell dysfunction (57, 58, 78–80). TRPM1 is also found in melanocytes (57, 58). The epitope of the TRPM1 AAbs is localized to the short intracellular domain in the amino terminal part of TRPM1 sequence (58, 80). It is hypothesized that TRPM1 AAbs are generated in response to abnormal TRPM1 polypeptides, encoded by an alternate mRNA splice variant that is expressed by malignant melanocytes (56). These AAbs are infrequent, found in less than 5% of MAR patients. More often, AAbs against proteins involved in phototransduction have been detected, likely because human melanoma cells *in vitro* express rhodopsin, transducin, and cyclic guanosine 3′,5′-monophosphate phosphodiesterase 6, guanylyl cyclase 1, recoverin, and arrestin (81). In fact, AAbs against transducin, rhodopsin, arrestin, and IRBP have been found in MAR in addition to α-enolase, CAII, myelin basic protein, mitofilin, and titin (4, 22, 28, 82, 83). In recent years, there have been multiple reports of a MAR-like retinopathy with associated detachments of the retinal pigment epithelium (RPE) and neurosensory retina. Such a clinical presentation is termed paraneoplastic vitelliform

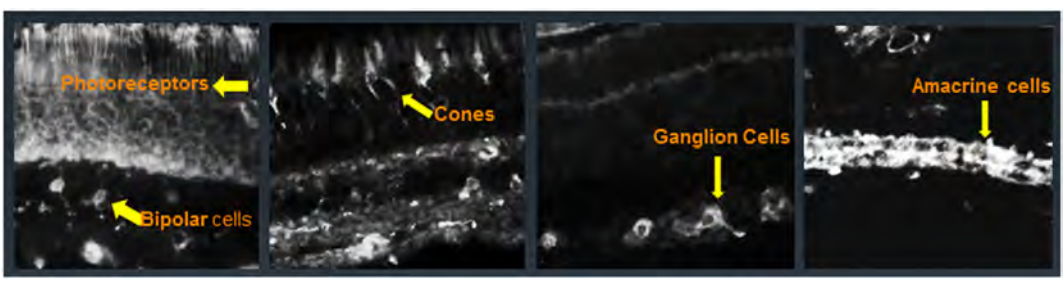

FIGURE 3 | Immunofluorescent labeling of the human retina with cancer-associated retinopathy patients' anti-retinal autoantibodies (AAbs) specific for different cellular structures. From left to right: AAbs label photoreceptor cells and bipolar cells, cone photoreceptors, ganglion cells, and amacrine cells; arrows point at immunofluorescent cells.

retinopathy. In some cases, three additional proteins, besides the usual anti-enolase-α, anti-bestrophin, and anti-peroxiredoxin, were detected in the serum (84–86).

Autoantibodies with similar specificities were found in patients with AR who do not have a previous history of visual problems and develop a sudden onset of photopsias, night blindness, scotomata, and visual field loss (39, 87). AAbs against recoverin, α-enolase, aldolase, and CAII as well as AAbs against heat shock proteins (HSP27, HSP60) and CRMP2 were identified in patients with AR (66, 76, 88, 89). It has been speculated that AR can also be a secondary complication of other conditions such as RP, birdshot retinopathy, or acute zonal occult outer retinopathy (AZOOR). RP patients with cystoid macular edema often have antibodies against CAII (90). High incidence of AAbs has been observed in patients with AZOOR but it is not clear whether this condition is autoimmune mediated (91, 92).

IMPORTANCE OF EPITOPE MAPPING IN AR

It has been assumed that autoimmunity starts with an immune response to a single antigen, and it subsequently extends to other proteins in the same tissue, or amino acid sequence within the same molecule (epitopes) by a process called "epitope spreading" (93, 94). Testing for epitopes for major AAbs that play a role in the autoimmunity of retinopathy is important because it could potentially distinguish normal from pathogenic antibodies. There is evidence that epitope spreading plays a role in the formation of anti-retinal T cells and in antibody responses associated with ocular immunity (95). The first indication of different epitopes in the same antigenic protein involved in autoimmune uveitis was demonstrated using experimental autoimmune uveitis (EAU), a model for autoimmune noninfectious uveitis in humans. Two proteins were found to be major antigens in humans and experimental animals: IRBP, also known as retinol binding protein-3, and arrestin, also known as S-Antigen (96–99). By the use of synthetic peptides of the human IRBP, the sequence within amino acids 1–20 was identified as a major uveitogenic epitope for the T cell response, which is widely recognized by different species (100). Two other IRBP epitopes, residues 461–480 and 651–670, are also uveitogenic (101). The study of EAU have shown that it is important to use human protein sequences in epitope mapping for human immune responses because the amino acid differences between experimental animals and human sequences may affect the identification of novel pathogenic epitopes and the determination of epitope spreading. In the EAU model, epitope spreading from the immunizing to the non-immunizing peptide was demonstrated for both IRBP 1–20 and 629–643 sequences and was consistent with the destruction of retinal tissue, increasing repertoire of antigen-specific effector T-cell with disease progression (102).

Arrestin epitopes were studied in patients with uveitis, using linear synthetic peptides, spanning the entire sequence of the protein. Two synthetic peptides, amino acid regions 286–305 and 306–325 are uveitogenic in the rat model of uveitis (103). Human patients respond to the arrestin peptides 61–80 and other arrestin peptides with high frequencies (104). These results further confirm that autoimmunity to arrestin is crucial for the pathology of uveitis (104). In the case of IRBP and arrestin proteins, the demonstration of epitope spreading is correlated with clinical disease, which implies that an evolving immune response plays an important part in progression of chronic autoimmune ocular inflammation. AAbs to arrestin and IRBP are not only important in autoimmune uveitis but they are detected in AR and CAR (105).

Recoverin was one of the first presumed autoantigen in CAR. It has been demonstrated in *in vitro* and *in vivo* studies that this protein is immunogenic and induces the production of pathogenic antibodies and T cells (59, 62, 106–108). In epitope mapping experiments, using synthetic peptides that overlap the entire recoverin sequence, two major epitopes for human AAbs have been found within the residues 38–43 (QFQSI) and 64–70 (KAYAQHV), in proximity to the calcium-binding domain EF-hand 2 (25, 107). Both mapped regions of recoverin can be accessible to the immune system because they exist on the surface of the molecule. AAb binding was found to be dependent on recoverin calcium-binding properties, which induce conformational changes in the recoverin protein, and enhance binding of AAbs to recoverin (107). The majority of antibodies to recoverin, both in human disease and in animals that are immunized with recoverin, are directed against the same major immunodominant region, the sequence 64–70 (107, 109). An immunization of animals, with the peptide 64–70, induced EAU in rats and the antibodies that were generated affected photoreceptor cell function, which in turn produced an activation of the caspase-dependent apoptotic pathways *in vitro* (25, 106, 109, 110).

Cancer-associated retinopathy patients possess recoverin-specific cytotoxic T lymphocytes (CTLs) in the peripheral blood, which can recognize aberrantly expressing recoverin in cancer cells (109, 111). In the study of recoverin-derived HLA class I—A24-binding peptides to generate antitumor-recoverin CTLs, the investigators identified three recoverin epitopes: R49 (QFQSIYAKF), R49.2 (QFQSIYAKFF), and R64 (AYAQHVFRSF) (109). In part, these CTL epitope sequences (QFQS and AYAQHV) correspond to the major binding sites for anti-recoverin AAbs in humans (107). Overall, it suggested that the capacity to induce the pathogenic effects is dependent on the region of the antigenic protein that is being recognized by the immune system.

Enolase-α is a major antigen in CAR and AR. Soon after its discovery, there was a concern about a broad association of anti-enolase-α AAbs in an autoimmunity that is not restricted to any particular disease, and is occasionally found in sera of normal individuals (36, 112). Epitope mapping of CAR and normal sera revealed three binding regions of enolase within the amino acid residues 31–38 (FRAAVPSG), 176–183 (ANFREAMR), and 421–428 (AKFAGRNF), and these epitopes were common for all AAbs tested, independent of disease status (113). However, the enolase sequence 56–63 (RYMGKGVS) is uniquely recognized by CAR sera. There are also differences in *in vitro* cytotoxic activities and cell-death-promoting activities between anti-enolase AAbs of healthy and CAR affected individuals (113). Anti-enolase-α AAbs from patients with CAR and healthy individuals did not

bind to the epitope involved in the plasminogen binding of enolase-α sequence 250—256 (FFRSGKY), suggesting that these conditions are not associated with distresses of the intravascular and pericellular fibrinolytic system (114).

Anti-enolase AAbs have been associated with a number of cancer and autoimmune diseases but there is limited information about the fine recognition of this antigen. Anti-enolase AAbs of patients with endometrial adenocarcinoma, but not from healthy individuals, were found to recognize 2 regions of enolase sequence: 53–87 and 207–238 (115). The first epitope that was associated with endometriosis, sequence 53–87, overlaps with the presumed pathogenic epitope related to CAR, sequence 56–63 (115). One study showed that the common human enolase sequence 257–272 (DLDFKSPDDPSRYISP), spanning amino acids located within an external loop of the molecule, showed similarities between α-enolase and α-ERM molecule (116). The high specificity of antibodies to the NH_2-terminal region of enolase-α in patients with Hashimoto's encephalopathy suggests that this is the most immunogenic site and that AAbs against N-terminal enolase can serve as diagnostic biomarkers for the disease (117). The NH_2-terminal region of α-enolase is located on the external part of the enzyme and is important for intermolecular interactions (118). The overall conclusion, based on those findings, is that in spite of recognition of enolase-α, AAbs that are found in different diseases and in normal individuals are not the same—they can bind to different parts of molecule.

The study of fine specificity of AAbs generated against CAII further confirms that AAbs against common proteins are distinctive. During the course of retinal disease from non-paraneoplastic (AR) to paraneoplastic stage (CAR), sera bind to different domains of CAII and differ from healthy control sera (33). The AR sera predominantly react with the following N-terminal epitopes: 22–26 (IAKGE) and 85–90 (DGTYRL), which corresponded to the catalytic core of the enzyme. The major epitopes for CAR AAbs are found to be reactive with the peptide 201–208 (CVTWIV) and 218–222 (SSEQVL) clustered with the α-helix, and the last sheet strand 17, the peptide 254–258 (RQIKA). It is important to note that the N-terminal epitope 85–90 is recognized by 91% of AR patients and the major epitope for CAR is the sequence 218–222 that reacts with 77% of patients. The analysis of epitope location in a 3D molecular structure of the native CAII reveals their partial or full exposure on the protein surface. Anti-CAII AAbs from normal healthy controls do not share the major determinants with CAR and AR patients. This remarkable finding showed the shift in epitope recognition from the primary AR-like epitope profile to the secondary CAR-like antibody profile in a patient who developed cancer 2 years after initial symptoms of vision loss (33). The detailed knowledge of epitopes recognized by anti-retinal AAbs that are associated with retinal paraneoplastic syndromes is valuable for development of new diagnostic assays for CAR, MAR, and AR, and for the study of mechanisms involved in pathogenesis of retinopathy.

PATHOGENICITY OF ANTI-RETINAL AAbs

Autoantibody-mediated retinal injury can be mediated by cytotoxic T cells and AAbs to detect self-antigens in the cell (109). The perceived inability of anti-retinal AAbs to get to the retina and cross cell membranes to access their target intracellular antigens diminished the understanding of their role in the pathogenicity of retinopathy (**Figure 4**). However, a number of studies have demonstrated that anti-retinal AAbs can indeed penetrate the cells and affect their viability and cellular function (74, 80, 108, 113, 119–123). Given the great diversity of anti-retinal AAbs, it is likely some antibodies have greater pathogenic potential than others to impact retinal pathophysiology.

It has been suggested that the AAbs reactivity with target cells depends on the microenvironment and genetic traits of individual (108, 119, 122, 124). AAbs alone might have little or no effect on healthy cells, but can be highly cytotoxic when coupled with other damaging conditions, like inflammation or cancer treatment. The first step in antibody pathogenicity is the ability to get to the antigen. As majority of antigens are intracellular, AAbs have to penetrate the tissue to get to the target cells. The fact that they can penetrate into living cells can explain their pathogenic potential, functioning through the activation of cell apoptosis after prolonged exposure of the retina to such antibodies from the circulation (125). Not only anti-recoverin IgGs but also their Fab fragments penetrate into retinal cells *in vitro* and *in vivo* by an active process and induce apoptosis through the caspase 3 pathway (108, 122, 126). One study showed that the mechanism of cellular entry by an AAb can be mediated by a membrane proxy protein for the target antigen, e.g., the cell surface molecules, calreticulin, and myosin-1 can serve as surrogate antigens for penetrating anti-double-stranded DNA antibodies (127).

In retinopathy, AAbs have different antigenic specificities and may affect different metabolic pathways, including phototransduction for recoverin, glycolysis for enolase, and pH control for

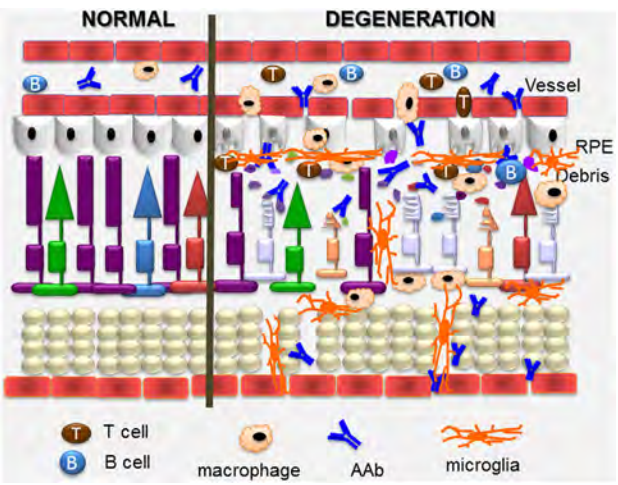

FIGURE 4 | Overview of pathogenic autoimmune processes on the retina. Anti-retinal autoantibodies (AAbs) can provoke and can be a consequence of retinal degeneration. AAbs attract activated microglia/microphages that produce pro-inflammatory cytokines and chemokines, and induce apoptosis of cone and rod photoreceptor cells (showing on the right), resulting in retinal degeneration. Inflammatory cytokines and chemokines, activation of microglia and photoreceptor apoptosis can trigger secondary autoimmunity, and production of new anti-retinal AAbs. Cytotoxic T cells specific for retinal antigens are likely also involved in the pathogenic process.

CAII, they all cause an increase in the intracellular calcium (**Table 1**), which may be an initial step that triggers cell death (36, 128). Such a calcium-induced cytotoxicity seems to play a major role in AR and several other diseases.

It is conceivable that after cellular entry, anti-recoverin AAbs bind the antigen and block its function, which regulates rhodopsin phosphorylation in a Ca^{2+}-dependent manner (129). Interestingly, the anti-recoverin antibody promotes rhodopsin phosphorylation when added to rod outer segments of photoreceptor cells *in vitro* (123). Similar effects on rhodopsin phosphorylation are observed in rat eyes treated with anti-recoverin antibody, which in effect impairs the ERG responses. Co-injection of caspase inhibitors with anti-recoverin significantly suppresses the antibody-induced enhancement of rhodopsin phosphorylation, suggesting that these antibodies dysregulate cellular function. After anti-retinal antibody entry, there is a rapid increase in the intracellular [Ca^{2+}], which results in the activation of the mitochondrial apoptotic pathway followed by cell death (128, 130). Not only anti-recoverin but also anti-rhodopsin, anti-arrestin, and anti-enolase AAbs have the ability to induce the influx of intracellular calcium and cytotoxicity (128). In consequence, AAbs could influence cell activation, proliferation, and death and induce expression of pro-inflammatory cytokines (131). It was also reported that anti-recoverin antibodies were found in the aqueous humor and vitreous cavity beyond the BRB in a patient with CAR. Altogether, the experimental findings suggest that antibody-mediated retinal cell death involves multistep process, in which anti-recoverin AAbs must reach the retina from the circulation and then penetrate photoreceptor cells, block the recoverin function, increase intracellular calcium, and enhance of rhodopsin phosphorylation, which in effect activates apoptosis (108, 122, 123, 132).

In addition to anti-recoverin AAbs, anti-enolase and anti-CAII antibodies also block the function of their corresponding proteins. Most anti-enolase antibodies bind to Müller cells and ganglion cells and they act on those cells, inducing apoptotic death (74). After anti-enolase antibody cellular internalization, the antibody inactivates the enzyme (133). However, the enzymatic activity of enolase is not inhibited when the retinal cells are treated with endocytosis inhibitor cytochalasin B, which blocks antibody entry into the cells. The anti-enolase antibody blocks the catalytic function and likely inhibits glycolysis by reducing glycolytic ATP. Such changes in ATP, as an effect of antibody action, over the lifetime of a patient, may slowly damage neuronal cells and lead to retinal degeneration. In fact, in some patients with anti-enolase AAbs, visual impairment has a slow progression of central vision loss (11). In experiments using *ex vivo* eye explants and intravitreal injections of anti-enolase AAbs, the enolase antibodies are also capable of penetrating retinal tissue to target ganglion cells and inner nuclear layers and consequently induce cell-containing antigen apoptosis (62). The apoptotic nuclei detected by a DNA fragmentation assay and caspase 3-positive cells are co-localized to their targeted retinal layers—the ganglion cell layer and inner nuclear layer. Normal AAbs without specificity to retinal antigens did not induce pathogenic processes in retinal cells. A similar mechanism may occur in patients with CAR, which may lead to visual loss and blindness. **Figure 4** illustrates the presumed autoimmune pathogenic process in retinal degeneration.

Anti-CAII AAbs have also the capacity to induce cellular damage by impairing CAII cellular function through inhibiting the catalytic activity of CAII in a dose-dependent manner, decreasing intracellular pH, and increasing intracellular calcium, which in effect decreases retinal cell viability and survival (134). The decrease of intracellular pH, related to the function of the enzyme in the cell could cause acidification by changes in CO_2/H_2CO_3 metabolism and in proton pump activity, the Na^+/H^+ exchanger. Some anti-CAII AAbs cause a decrease of pH to below pH 6.8, which could lead to caspase activation in those retinal cells. The destabilized catalytic function of CAII and alterations in cytosolic pH occur very early in the process, suggesting that AAbs are the inducers of apoptosis (77).

In addition to the *in vitro* studies (above), animal investigations further confirmed that anti-recoverin antibodies have pathogenic potential. After intravitreal injection into the eye, anti-recoverin antibodies are capable of penetrating photoreceptor and bipolar cells, the normal site of recoverin expression in the retina, and then they induce apoptotic cell death as detected by an increased number of TdT-dUTP terminal nick-end labeling (TUNEL)-positive cells, fragmentation of DNA in a DNA ladder electrophoresis, and structural changes observed in electron

TABLE 1 | Effects of major CAR autoantibodies (AAbs) on retinal cell function *in vitro*.

AAb	Autoantigen	Effect on function	Mechanism
Anti-recoverin	23-kDa calcium-binding protein present in photoreceptor cells; regulates rhodopsin phosphorylation in a calcium-dependent manner in phototransduction cascade	AAbs deregulate the phototransduction, leading to retinal degeneration in CAR when access retinal cells	Inhibition of calcium-binding function Elevation of intracellular calcium Deregulation of phototransduction
Anti-α-enolase (likely anti-GAPDH, anti-aldolase, anti-PKM2)	46-kDa enzyme present in every cell; coverts 2-phosphoglycerate into phosphoenolpyruvate in glycolytic pathway leading to ATP production	AAbs deregulate the glucose metabolism, leading apoptotic death when access retinal cells	Inhibition enolase catalytic function Depletion of ATP Elevation of intracellular calcium Lowering intracellular pH
Anti-carbonic anhydrase II (CAII)	30-kDa enzyme present in the retina; catalyzes a reversible conversion of carbon dioxide to bicarbonate and participle in pH control and ion transport	AAbs impair the pH control and ion transport, leading to cell dysfunction and death when access cells	Inhibition of catalytic activity of CAII in a dose-dependent manner Decrease of intracellular pH Increasing intracellular calcium
Normal Abs	Unknown	None	None

microscopy (107). Intravitreal injection of AAbs against recoverin, together with anti-heat shock cognate protein 70 (HSP70) that co-exist in patients with CAR, cause a decrease in ERG amplitudes and apoptotic cell death in the outer nuclear layer in Lewis rat eyes (113). Internalization of anti-HSP70 AAbs into photoreceptor cells likely blocks the biologic protection of HSP70 chaperon functions to suppress protein aggregation, denaturation, and misfolding, which in effect may promote anti-recoverin antibody-mediated retinal degeneration. Synergetic autoimmune responses against recoverin and HSP70 suggest their involvement in the pathogenesis of CAR (62).

In the recent years, AAbs associated with retinopathy in melanoma patients (MAR) caught the attention of scientists. In the study of ret-transgenic mice that spontaneously develop melanoma, the investigators observed that those transgenic mice frequently developed retinopathy (28). Passive transfer of MAR sera or spleen cells also induce morphological changes in the retina and stimulates functional changes as measured by the ERG in recipient mice (28). These pathological changes reveal degeneration of photoreceptors, bipolar cells, and pigment epithelium as well as produce retinal detachment. Some of the mice with melanoma tumors also had AAbs against arrestin and transducin.

Investigations of TRPM1 AAbs have shown that incubation of living retinal neurons with TRPM1-positive MAR serum cause accumulation of IgGs in ON bipolar cells isolated from TRPM1-positive mice, but not knockout TRPM1$^{-/-}$ mice, suggesting that the uptake of AAbs targets the intracellular antigen, which in effect reduces the ON bipolar cell response to light (58, 80). MAR AAbs reduce the b-wave amplitude of the ERG by targeting a key component of the ON bipolar cell signal transduction pathway (80). After intravitreal administration of TRMP1-positive serum into mice eyes, the ERGs are altered acutely and antibodies are detected in bipolar cells, but only in wild-type and not in TRPM1-knockout mice (79). Moreover, the bipolar cells appear apoptotic within 5 h after the injection and in 3 months, the inner nuclear layer was thinner and the amplitudes of the ERGs were more reduced. Recently published studies revealed cross-reactivity of TRPM1 with TRPM3, which is present in the RPE, suggesting that such AAbs could contribute to pathology of MAR, possibly inducing retinal and RPE detachments (56).

It has been argued that if healthy individuals and affected patients are seropositive for the same AAbs, those AAbs cannot be pathogenic. However, studies on epitope mapping for anti-recoverin, anti-enolase, and anti-CAII reveal that although different AAbs recognize the same protein, they bind to a different immunogenic domain on the molecule (33, 107, 113). Epitope mapping shows that natural antibodies may have similar antigenic specificity to CAR and AR AAbs, but they can still be distinguished based on their fine epitope recognition pattern (see above). Natural antibodies are IgM and IgG classes, are usually cross-reactive with antigens of different origin (polyspecific) and recognize non-self-antigens of pathogens as well as self-related antigens (135, 136). It is important to appreciate that natural antibodies provide various essential functions within the immune system, such as providing protection against infections and removing cellular debris (137).

FINAL REMARKS

A number of studies have revealed the existence of various retinal autoantigens that specifically interact with AAbs in patients with autoimmune retinopathies. Such a vast repertoire of anti-retinal AAbs observed in patients with CAR, AR, and AR is not surprising because other autoimmune diseases are associated with multiple AAbs. Anti-retinal AAbs, especially those that were made against cancer or microbial cross-reactive antigens, are likely to play a primary causative role in retinal degeneration, whereas others can contribute to disease progression and promote damage of retinal cells. It has been argued that anti-retinal AAbs are a result of retinal demise rather than a direct cause (epiphenomenon) of retinopathy. Thus, dying photoreceptors by apoptosis that is initiated by some other mechanisms (hereditary), produce substantial amounts of debris, containing high concentrations of antigens discharged from dying outer segments, and which may lead to autoimmunization and the enhanced permeability of the blood–retinal barrier (138, 139). Although not all antigens have been identified and are known only by their molecular mass, they can be used to follow the progression of retinopathy and the effects of treatment. It is important to remember that some anti-retinal AAbs can occur before the diagnosis of cancer, so they could be used in early cancer detection, e.g., anti-recoverin AAbs (25). Moreover, they can also serve as biomarkers in the context of ocular presentation and findings, despite the fact that the pathogenicity has not been conclusively proven.

AUTHOR CONTRIBUTIONS

The sole author is totally responsible for the design and writing of the review.

FUNDING

This work was supported by grant P30 EY010572 from the National Institutes of Health (Bethesda, MD, USA) and by unrestricted departmental funding from Research to Prevent Blindness (New York, NY, USA).

REFERENCES

1. Chan JW. Paraneoplastic retinopathies and optic neuropathies. *Surv Ophthalmol* (2003) 48:12–38. doi:10.1016/S0039-6257(02)00416-2
2. Rahimy E, Sarraf D. Paraneoplastic and non-paraneoplastic retinopathy and optic neuropathy: evaluation and management. *Surv Ophthalmol* (2013) 58:430–58. doi:10.1016/j.survophthal.2012.09.001
3. Kornguth SE, Klein R, Appen R, Choate J. Occurrence of anti-retinal ganglion cell antibodies in patients with small cell carcinoma of the lung. *Cancer* (1982) 50:1289–93. doi:10.1002/1097-0142(19821001)50:7<1289::AID-CNCR2820500711>3.0.CO;2-9
4. Milam AH, Saari JC, Jacobson SG, Lubinski WP, Feun LG, Alexander KR. Autoantibodies against retinal bipolar cells in cutaneous melanoma-associated retinopathy. *Invest Ophthalmol Vis Sci* (1993) 34:91–100.

5. Borkowski LM, Grover S, Fishman GA, Jampol LM. Retinal findings in melanoma-associated retinopathy. *Am J Ophthalmol* (2001) 132:273–5. doi:10.1016/S0002-9394(01)00915-1
6. Keltner JL, Thirkill CE, Yip PT. Clinical and immunologic characteristics of melanoma-associated retinopathy syndrome: eleven new cases and a review of 51 previously published cases. *J Neuroophthalmol* (2001) 21:173–87. doi:10.1097/00041327-200109000-00004
7. Mizener JB, Kimura AE, Adamus G, Thirkill CE, Goeken JA, Kardon RH. Autoimmune retinopathy in the absence of cancer. *Am J Ophthalmol* (1997) 123:607–18. doi:10.1016/S0002-9394(14)71073-6
8. Ladewig G, Reinhold U, Thirkill CE, Kerber A, Tilgen W, Pfohler C. Incidence of antiretinal antibodies in melanoma: screening of 77 serum samples from 51 patients with American Joint Committee on Cancer stage I-IV. *Br J Dermatol* (2005) 152:931–8. doi:10.1111/j.1365-2133.2005.06480.x
9. Alexander KR, Fishman GA, Peachey NS, Marchese AL, Tso MOM. "On" response defect in paraneoplastic night blindness with cutaneous malignant melanoma. *Invest Ophthalmol Vis Sci* (1992) 33:477–83.
10. Potter MJ, Adamus G, Szabo SM, Lee R, Mohaseb K, Behn D. Autoantibodies to transducin in a patient with melanoma-associated retinopathy. *Am J Ophthalmol* (2002) 134:128–30. doi:10.1016/S0002-9394(02)01431-9
11. Weleber RG, Watzke RC, Shults WT, Trzupek KM, Heckenlively JR, Egan RA, et al. Clinical and electrophysiologic characterization of paraneoplastic and autoimmune retinopathies associated with antienolase antibodies. *Am J Ophthalmol* (2005) 139:780–94. doi:10.1016/j.ajo.2004.12.104
12. Ohguro H, Yokoi Y, Ohguro I, Mamiya K, Ishikawa F, Yamazaki H, et al. Clinical and immunologic aspects of cancer-associated retinopathy. *Am J Ophthalmol* (2004) 137:1117–9. doi:10.1016/j.ajo.2004.01.010
13. Jacobson DM. Paraneoplastic disorders of neuro-ophthalmologic interest. *Curr Opin Ophthalmol* (1996) 7:30–8. doi:10.1097/00055735-199612000-00005
14. Geller AM, Sieving PA. Assessment of foveal cone photoreceptors in Stargardt's macular dystrophy using a small dot detection task. *Vision Res* (1993) 33:1509–24. doi:10.1016/0042-6989(93)90144-L
15. Delyfer M-N, Léveillard T, Mohand-Saïd S, Hicks D, Picaud S, Sahel J-A. Inherited retinal degenerations: therapeutic prospects. *Biol Cell* (2004) 96:261–9. doi:10.1111/j.1768-322X.2004.tb01414.x
16. Narayan DS, Wood JPM, Chidlow G, Casson RJ. A review of the mechanisms of cone degeneration in retinitis pigmentosa. *Acta Ophthalmol* (2016) 94:748–54. doi:10.1111/aos.13141
17. Polans AS, Adamus G. Recoverin is the tumor antigen in cancer-associated retinopathy. *Behav Brain Sci* (1995) 18:483–5. doi:10.1017/S0140525X00039406
18. Adamus G, Amundson D, MacKay C, Gouras P. Long-term persistence of anti-recoverin autoantibodies in endometrial cancer-associated retinopathy. *Arch Ophthalmol* (1998) 116:251–3.
19. Maeda A, Ohguro H, Maeda T, Wada I, Sato N, Kuroki Y, et al. Aberrant expression of photoreceptor-specific calcium-binding protein (recoverin) in cancer cell lines. *Cancer Res* (2000) 60:1914–20.
20. Bazhin AV, Savchenko MS, Shifrina ON, Demoura SA, Chikina SY, Jaques G, et al. Recoverin as a paraneoplastic antigen in lung cancer: the occurrence of anti-recoverin autoantibodies in sera and recoverin in tumors. *Lung Cancer* (2004) 44:193–8. doi:10.1016/j.lungcan.2003.10.006
21. Dot C, Guigay J, Adamus G. Anti-alpha-enolase antibodies in cancer-associated retinopathy with small cell carcinoma of the lung. *Am J Ophthalmol* (2005) 139:746–7. doi:10.1016/j.ajo.2004.10.044
22. Bazhin AV, Schadendorf D, Willner N, Smet CD, Heinzelmann A, Tikhomirova NK, et al. Photoreceptor proteins as cancer-retina antigens. *Int J Cancer* (2007) 120:1268–76. doi:10.1002/ijc.22458
23. Comtesse N, Zippel A, Walle S, Monz D, Backes C, Fischer U, et al. Complex humoral immune response against a benign tumor: frequent antibody response against specific antigens as diagnostic targets. *Proc Natl Acad Sci U S A* (2005) 102:9601–6. doi:10.1073/pnas.0500404102
24. Tanaka A, Takase H, Adamus G, Mochizuki M. Cancer-associated retinopathy caused by benign thymoma. *Br J Ophthalmol* (2010) 94:526–8. doi:10.1136/bjo.2008.151563
25. Polans A, Witkowska D, Haley T, Amundson D, Baizer L, Adamus G. Recoverin, a photoreceptor-specific calcium-binding protein, is expressed by the tumor of a patient with cancer-associated retinopathy. *Proc Natl Acad Sci U S A* (1995) 92:9176–80. doi:10.1073/pnas.92.20.9176
26. Matsubara S, Yamaji Y, Soto M, Fujita J, Takahara J. Expression of a photoreceptor protein, recoverin, as a cancer-associated retinopathy autoantigen in human lung cancer cell lines. *Br J Cancer* (1996) 74:1419–22. doi:10.1038/bjc.1996.558
27. Bazhin AV, Savchenko MS, Belousov EV, Jaques G, Philippov PP. Stimulation of the aberrant expression of a paraneoplastic antigen, recoverin, in small cell lung cancer cell lines. *Lung Cancer* (2004) 45:299–305. doi:10.1016/j.lungcan.2004.02.015
28. Bazhin AV, Dalke C, Willner N, Abschütz O, Wildberger HGH, Philippov PP, et al. Cancer-retina antigens as potential paraneoplastic antigens in melanoma-associated retinopathy. *Int J Cancer* (2009) 124:140–9. doi:10.1002/ijc.23909
29. Ohguro H, Odagiri H, Miyagawa Y, Ohguro I, Sasaki M, Nakazawa M. Clinicopathological features of gastric cancer cases and aberrantly expressed recoverin. *Tohoku J Exp Med* (2004) 202:213–9. doi:10.1620/tjem.202.213
30. Darnell RB, Deangelis LM. Regression of small-cell carcinoma in patients with paraneoplastic neuronal antibodies. *Lancet* (1993) 341:21–2. doi:10.1016/0140-6736(93)92485-C
31. Matsuo S, Ohguro H, Ohguro I, Nakazawa M. Clinicopathological roles of aberrantly expressed recoverin in malignant tumor cells. *Ophthalmic Res* (2010) 43:139–44. doi:10.1159/000253486
32. Kornguth SE, Kalinke T, Grunwald GB, Schutta H, Dahl D. Anti-neurofilament antibodies in sera of patients with small cell carcinoma of the lung and with visual paraneoplastic syndrome. *Cancer Res* (1986) 46:2588–95.
33. Adamus G, Yang S, Weleber RG. Unique epitopes for carbonic anhydrase II autoantibodies related to autoimmune retinopathy and cancer-associated retinopathy. *Exp Eye Res* (2016) 147:161–8. doi:10.1016/j.exer.2016.05.012
34. Atassi MZ, Casali P. Molecular mechanisms of autoimmunity. *Autoimmunity* (2008) 41:123–32. doi:10.1080/08916930801929021
35. Novack GD, Leopold IH. The blood-aqueous and blood-brain barriers to permeability. *Am J Ophthalmol* (1988) 105:412–6. doi:10.1016/0002-9394(88)90308-X
36. Adamus G. Impact of autoantibodies against glycolytic enzymes on pathogenicity of autoimmune retinopathy and other autoimmune disorders. *Front Immunol* (2017) 8:505. doi:10.3389/fimmu.2017.00505
37. de Andrade FA, Fiorot SHS, Benchimol EI, Provenzano J, Martins VJ, Levy RA. The autoimmune diseases of the eyes. *Autoimmun Rev* (2016) 15:258–71. doi:10.1016/j.autrev.2015.12.001
38. Heckenlively JR, Aptsiauri N, Nusinowitz S, Peng C, Hargrave PA. Investigations of antiretinal antibodies in pigmentary retinopathy and other retinal degenerations. *Trans Am Ophthalmol Soc* (1996) 94:179–200.
39. Heckenlively J, Ferreyra H. Autoimmune retinopathy: a review and summary. *Semin Immunopathol* (2008) 30:127–34. doi:10.1007/s00281-008-0114-7
40. Gupta N, Brown KE, Milam AH. Activated microglia in human retinitis pigmentosa, late-onset retinal degeneration, and age-related macular degeneration. *Exp Eye Res* (2003) 76:463–71. doi:10.1016/S0014-4835(02)00332-9
41. Roque RS, Rosales AA, Jingjing L, Agarwal N, Al-Ubaidi MR. Retina-derived microglial cells induce photoreceptor cell death in vitro. *Brain Res* (1999) 836:110–9. doi:10.1016/S0006-8993(99)01625-X
42. Suurmond J, Diamond B. Autoantibodies in systemic autoimmune diseases: specificity and pathogenicity. *J Clin Invest* (2015) 125:2194–202. doi:10.1172/JCI78084
43. Taylor AW. Ocular immune privilege. *Eye* (2009) 23:1885–9. doi:10.1038/eye.2008.382
44. DeMarshall C, Sarkar A, Nagele EP, Goldwaser E, Godsey G, Acharya NK, et al. Chapter one – utility of autoantibodies as biomarkers for diagnosis and staging of neurodegenerative diseases. In: Hurley MJ, editor. *International Review of Neurobiology*. Academic Press (2015). p. 1–51.
45. Hargrave PA, McDowell JH. Rhodopsin and phototransduction. *Int Rev Cytol* (1993) 137B:49–97. doi:10.1016/S0074-7696(08)62600-5
46. Grossniklaus HE, Geisert EE, Nickerson JM. Chapter twenty-two – introduction to the retina. In: Hejtmancik JF, John MN, editors. *Progress in Molecular Biology and Translational Science*. Academic Press (2015). p. 383–96.
47. Zipfel PF, Lauer N, Skerka C. The role of complement in AMD. In: Lambris JD, Adamis AP, editors. *Inflammation and Retinal Disease: Complement Biology and Pathology*. New York: Springer (2010). p. 9–24.
48. Niederkorn JY. See no evil, hear no evil, do no evil: the lessons of immune privilege. *Nat Immunol* (2006) 7:354–9. doi:10.1038/ni1328
49. Forrester JV, Xu H. Good news–bad news: the Yin and Yang of immune privilege in the eye. *Front Immunol* (2012) 3:338. doi:10.3389/fimmu.2012.00338

50. Zhao L, Zabel MK, Wang X, Ma W, Shah P, Fariss RN, et al. Microglial phagocytosis of living photoreceptors contributes to inherited retinal degeneration. *EMBO Mol Med* (2015) 7:1179–97. doi:10.15252/emmm.201505298
51. Karlstetter M, Ebert S, Langmann T. Microglia in the healthy and degenerating retina: insights from novel mouse models. *Immunobiology* (2010) 215:685–91. doi:10.1016/j.imbio.2010.05.010
52. Joly S, Francke M, Ulbricht E, Beck S, Seeliger M, Hirrlinger P, et al. Resident microglia and bone marrow immigrants remove dead photoreceptors in retinal lesions. *Am J Pathol* (2009) 174:2310–23. doi:10.2353/ajpath.2009.090023
53. Kyger M, Worley A, Adamus G. Autoimmune responses against photoreceptor antigens during retinal degeneration and their role in macrophage recruitment into retinas of RCS rats. *J Neuroimmunol* (2013) 254:91–100. doi:10.1016/j.jneuroim.2012.10.007
54. Adamus G. Autoantibody targets and their cancer relationship in the pathogenicity of paraneoplastic retinopathy. *Autoimmun Rev* (2009) 8:410–4. doi:10.1016/j.autrev.2009.01.002
55. Kikuchi T, Arai J, Shibuki H, Kawashima H, Yoshimura N. Tubby-like protein 1 as an autoantigen in cancer-associated retinopathy. *J Neuroimmunol* (2000) 103:26–33. doi:10.1016/S0165-5728(99)00163-0
56. Duvoisin RM, Haley TL, Ren G, Strycharska-Orczyk I, Bonaparte JP, Morgans CW. Autoantibodies in melanoma-associated retinopathy recognize an epitope conserved between TRPM1 and TRPM3. *Invest Ophthalmol Vis Sci* (2017) 58:2732–8. doi:10.1167/iovs.17-21443
57. Kondo M, Sanuki R, Ueno S, Nishizawa Y, Hashimoto N, Ohguro H, et al. Identification of autoantibodies against TRPM1 in patients with paraneoplastic retinopathy associated with ON bipolar cell dysfunction. *PLoS One* (2011) 6:e19911. doi:10.1371/journal.pone.0019911
58. Dhingra A, Fina ME, Neinstein A, Ramsey DJ, Xu Y, Fishman GA, et al. Autoantibodies in melanoma-associated retinopathy target TRPM1 cation channels of retinal ON bipolar cells. *J Neurosci* (2011) 31:3962–7. doi:10.1523/JNEUROSCI.6007-10.2011
59. Thirkill CE, Tait RC, Tyler NK, Roth AM, Keltner JL. The cancer-associated retinopathy antigen is a recoverin-like protein. *Invest Ophthalmol Vis Sci* (1992) 33:2768–72.
60. Polans AS, Buczylko J, Crabb J, Palczewski K. A photoreceptor calcium binding protein is recognized by autoantibodies obtained from patients with cancer-associated retinopathy. *J Cell Biol* (1991) 112:981–9. doi:10.1083/jcb.112.5.981
61. McGinnis JF, Stepanik PL, Baehr W, Subbaraya I, Lerious V. Clonning and sequencing of the 23-kDa mouse photoreceptor cell-specific protein. *FEBS Lett* (1992) 302:172–7. doi:10.1016/0014-5793(92)80433-H
62. Adamus G, Guy J, Schmied JL, Arendt A, Hargrave PA. Role of anti-recoverin autoantibodies in cancer-associated retinopathy. *Invest Ophthalmol Vis Sci* (1993) 34:2626–33.
63. Thirkill CE, Keltner JL, Tyler NK, Roth AM. Antibody reactions with retina and cancer-associated antigens in 10 patients with cancer-associated retinopathy. *Arch Ophthalmol* (1993) 111:931–7. doi:10.1001/archopht.1993.01090070049018
64. Adamus G. The role of recoverin in autoimmunity. In: Philippov PP, Koch KW, editors. *Neuronal Calcium Sensor Protein*. New York: Nova Science Publisher, Inc. (2006). p. 181–200.
65. Bazhin AV, Shifrina ON, Savchenko MS, Tikhomirova NK, Goncharskaia MA, Gorbunova VA, et al. Low titre autoantibodies against recoverin in sera of patients with small cell lung cancer but without a loss of vision. *Lung Cancer* (2001) 34:99–104. doi:10.1016/S0169-5002(01)00212-4
66. Yang S, Dizhoor A, Wilson DJ, Adamus G. GCAP1, Rab6, and HSP27: novel autoantibody targets in cancer-associated retinopathy and autoimmune retinopathy. *Transl Vis Sci Technol* (2016) 5:1. doi:10.1167/tvst.5.3.1
67. Adamus G, Ren G, Weleber RG. Autoantibodies against retinal proteins in paraneoplastic and autoimmune retinopathy. *BMC Ophthalmol* (2004) 4:5. doi:10.1186/1471-2415-4-5
68. Morohoshi K, Goodwin AM, Ohbayashi M, Ono SJ. Autoimmunity in retinal degeneration: autoimmune retinopathy and age-related macular degeneration. *J Autoimmun* (2009) 33:247–54. doi:10.1016/j.jaut.2009.09.003
69. Adamus G, Choi D, Raghunath A, Schiffman J. Significance of anti-retinal autoantibodies in cancer-associated retinopathy with gynecological cancers. *J Clin Exp Ophthalmol* (2013) 4:307. doi:10.4172/2155-9570.1000307
70. ten Berge JC, van Rosmalen J, Vermeer J, Hellström C, Lindskog C, Nilsson P, et al. Serum autoantibody profiling of patients with paraneoplastic and non-paraneoplastic autoimmune retinopathy. *PLoS One* (2016) 11:e0167909. doi:10.1371/journal.pone.0167909
71. Adamus G. Paraneoplastic retinal degeneration. In: Levin L, Albert DM, editors. *Ocular Disease: Mechanisms and Management*. Saunders Elsevier, Inc. (2010). p. 599–608.
72. Adamus G, Brown L, Weleber RG. Molecular biomarkers for autoimmune retinopathies: significance of anti-transducin-alpha autoantibodies. *Exp Mol Pathol* (2009) 87:195–203. doi:10.1016/j.yexmp.2009.08.003
73. Milam AH, Dacey DM, Dizhoor AM. Recoverin immunoreactivity in mammalian cone bipolar cells. *Vis Neurosci* (1992) 10:1–10. doi:10.1017/S0952523800003175
74. Ren G, Adamus G. Cellular targets of anti-alpha-enolase autoantibodies of patients with autoimmune retinopathy. *J Autoimmun* (2004) 23:161–7. doi:10.1016/j.jaut.2004.06.003
75. Ohguro H, Ogawa K, Nakagawa T. Recoverin and Hsc 70 are found as autoantigens in patients with cancer-associated retinopathy. *Invest Ophthalmol Vis Sci* (1999) 40:82–9.
76. Adamus G, Bonnah R, Brown L, David L. Detection of autoantibodies against heat shock proteins and collapsin response mediator proteins in autoimmune retinopathy. *BMC Ophthalmol* (2013) 13:48. doi:10.1186/1471-2415-13-48
77. Adamus G, Karren L. Autoimmunity against carbonic anhydrase II affects retinal cell functions in autoimmune retinopathy. *J Autoimmun* (2009) 32:133–9. doi:10.1016/j.jaut.2009.02.001
78. Irie S, Furukawa T. TRPM1. In: Nilius B, Flockerzi V, editors. *Mammalian Transient Receptor Potential (TRP) Cation Channels: Volume I*. Berlin, Heidelberg: Springer (2014). p. 387–402.
79. Ueno S, Nishiguchi KM, Tanioka H, Enomoto A, Yamanouchi T, Kondo M, et al. Degeneration of retinal ON bipolar cells induced by serum including autoantibody against TRPM1 in mouse model of paraneoplastic retinopathy. *PLoS One* (2013) 8:e81507. doi:10.1371/journal.pone.0081507
80. Xiong WH, Duvoisin RM, Adamus G, Jeffrey BG, Gellman C, Morgans CW. Serum TRPM1 autoantibodies from melanoma associated retinopathy patients enter retinal on-bipolar cells and attenuate the electroretinogram in mice. *PLoS One* (2013) 8:e69506. doi:10.1371/journal.pone.0069506
81. Bazhin AV, Schadendorf D, Owen RW, Zernii EY, Philippov PP, Eichmuller SB. Visible light modulates the expression of cancer-retina antigens. *Mol Cancer Res* (2008) 6:110–8. doi:10.1158/1541-7786.MCR-07-0140
82. Hartmann TB, Bazhin AV, Schadendorf D, Eichmuller SB. SEREX identification of new tumor antigens linked to melanoma-associated retinopathy. *Int J Cancer* (2005) 114:88–93. doi:10.1002/ijc.20762
83. Pföhler C, Preuss K-D, Tilgen W, Stark A, Regitz E, Fadle N, et al. Mitofilin and titin as target antigens in melanoma-associated retinopathy. *Int J Cancer* (2007) 120:788–95. doi:10.1002/ijc.22384
84. Eksandh L, Adamus G, Mosgrove L, Andreasson S. Autoantibodies against bestrophin in a patient with vitelliform paraneoplastic retinopathy and a metastatic choroidal malignant melanoma. *Arch Ophthalmol* (2008) 126:432–5. doi:10.1001/archopht.126.3.432
85. van Dijk EH, van Herpen CM, Marinkovic M, Haanen JB, Amundson D, Luyten GP, et al. Serous retinopathy associated with mitogen-activated protein kinase kinase inhibition (binimetinib) for metastatic cutaneous and uveal melanoma. *Ophthalmology* (2015) 122:1907–16. doi:10.1016/j.ophtha.2015.05.027
86. Koreen L, He SX, Johnson MW, Hackel RE, Khan NW, Heckenlively JR. Anti-retinal pigment epithelium antibodies in acute exudative polymorphous vitelliform maculopathy: a new hypothesis about disease pathogenesis. *Arch Ophthalmol* (2011) 129:23–9. doi:10.1001/archophthalmol.2010.316
87. Fox AR, Gordon LK, Heckenlively JR, Davis JL, Goldstein DA, Lowder CY, et al. Consensus on the diagnosis and management of nonparaneoplastic autoimmune retinopathy using a modified Delphi approach. *Am J Ophthalmol* (2016) 168:183–90. doi:10.1016/j.ajo.2016.05.013
88. Ohta K, Kikuchi T, Yoshida N. Slowly progressive non-neoplastic autoimmune-like retinopathy. *Graefes Arch Clin Exp Ophthalmol* (2011) 249:155–8. doi:10.1007/s00417-010-1436-4
89. Choi EY, Kim M, Adamus G, Koh HJ, Lee SC. Non-paraneoplastic autoimmune retinopathy: the first case report in Korea. *Yonsei Med J* (2016) 57:527–31. doi:10.3349/ymj.2016.57.2.527

90. Heckenlively JR, Jordan BL, Aptsiauri N. Association of antiretinal antibodies and cystoid macular edema in patients with retinitis pigmentosa. *Am J Ophthalmol* (1999) 127:565–73. doi:10.1016/S0002-9394(98)00446-2
91. Adamus G. Is zonal occult outer retinopathy an autoimmune disease? *J Clin Exp Ophthalmol* (2011) 2:9. doi:10.4172/2155-9570.1000104e
92. Qian CX, Wang A, DeMill DL, Jayasundera T, Branham K, Abalem MF, et al. Prevalence of antiretinal antibodies in acute zonal occult outer retinopathy: a comprehensive review of 25 cases. *Am J Ophthalmol* (2017) 176: 210–8. doi:10.1016/j.ajo.2016.12.001
93. Lehmann PV, Forsthuber T, Miller A, Sercarz EE. Spreading of T-cell autoimmunity to cryptic determinants of an autoantigen. *Nature* (1992) 358:155–8. doi:10.1038/358155a0
94. Vanderlugt CL, Miller SD. Epitope spreading in immune-mediated diseases: implications for immunotherapy. *Nat Rev Immunol* (2002) 2:85–95. doi:10.1038/nri724
95. Moticka EJ, Adamus G. Specificity of T and B cell responses to bovine rhodopsin in Lewis rats. *Cell Immunol* (1991) 138:175–84. doi:10.1016/0008-8749(91)90142-X
96. Adamus G, Chan CC. Experimental autoimmune uveitides: multiple antigens, diverse diseases. *Int Rev Immunol* (2002) 21:209–29. doi:10.1080/08830180212068
97. Descamps FJ, Kangave D, Cauwe B, Martens E, Geboes K, Abu El-Asrar A, et al. Interphotoreceptor retinoid-binding protein as biomarker in systemic autoimmunity with eye inflictions. *J Cell Mol Med* (2008) 12:2449–56. doi:10.1111/j.1582-4934.2008.00264.x
98. Dua HS, Abrams M, Barrett JA, Gregerson DS, Forrester JV, Donoso LA. Epitopes and idiotypes in experimental autoimmune uveitis: a review. *Curr Eye Res* (1992) 11:59–65. doi:10.3109/02713689208999512
99. Takeuchi M, Usui Y, Okunuki Y, Zhang L, Ma J, Yamakawa N, et al. Immune responses to interphotoreceptor retinoid-binding protein and S-antigen in Behçet's patients with uveitis. *Invest Ophthalmol Vis Sci* (2010) 51:3067–75. doi:10.1167/iovs.09-4313
100. Avichezer D, Silver PB, Chan CC, Wiggert B, Caspi RR. Identification of a new epitope of human IRBP that induces autoimmune uveoretinitis in mice of the H-2b haplotype. *Invest Ophthalmol Vis Sci* (2000) 41:127–31.
101. Cortes LM, Mattapallil MJ, Silver PB, Donoso LA, Liou GI, Zhu W, et al. Repertoire analysis and new pathogenic epitopes of IRBP in C57BL/6 (H-2b) and B10.RIII (H-2r) mice. *Invest Ophthalmol Vis Sci* (2008) 49:1946–56. doi:10.1167/iovs.07-0868
102. Boldison J, Khera TK, Copland DA, Stimpson ML, Crawford GL, Dick AD, et al. A novel pathogenic RBP-3 peptide reveals epitope spreading in persistent experimental autoimmune uveoretinitis. *Immunology* (2015) 146: 301–11. doi:10.1111/imm.12503
103. Donoso LA, Yamaki K, Merryman CF, Shinohara T, Yue S, Sery TW. Human S-antigen: characterization of uveitopathogenic sites. *Curr Eye Res* (1988) 7:1077–85. doi:10.3109/02713688809001879
104. Rai G, Saxena S, Kumar H, Singh VK. Human retinal S-antigen: T cell epitope mapping in posterior uveitis patients. *Exp Mol Pathol* (2001) 70:140–5. doi:10.1006/exmp.2000.2338
105. ten Berge JC, Schreurs MW, Vermeer J, Meester-Smoor MA, Rothova A. Prevalence and clinical impact of antiretinal antibodies in uveitis. *Acta Ophthalmol* (2016) 94:282–8. doi:10.1111/aos.12939
106. Adamus G, Ortega H, Witkowska D, Polans A. Recoverin: a potent uveitogen for the induction of photoreceptor degeneration in Lewis rats. *Exp Eye Res* (1994) 59:447–56. doi:10.1006/exer.1994.1130
107. Adamus G, Amundson D. Epitope recognition of recoverin in cancer associated retinopathy: evidence for calcium-dependent conformational epitopes. *J Neurosci Res* (1996) 45:863–72. doi:10.1002/(SICI)1097-4547(19960915)45:6<863::AID-JNR23>3.0.CO;2-V
108. Adamus G, Machnicki M, Seigel GM. Apoptotic retinal cell death induced by autoantibodies of cancer associated retinopathy. *Invest Ophthalmol Vis Sci* (1997) 38:283–91.
109. Maeda A, Ohguro H, Nabeta Y, Hirohashi Y, Sahara H, Maeda T, et al. Identification of human antitumor cytotoxic T lymphocytes epitopes of recoverin, a cancer-associated retinopathy antigen, possibly related with a better prognosis in a paraneoplastic syndrome. *Eur J Immunol* (2001) 31:563–72. doi:10.1002/1521-4141(200102)31:2<563::AID-IMMU563>3.0.CO;2-D
110. Gery I, Chanaud NP III, Anglade E. Recoverin is highly uveitogenic in Lewis rats. *Invest Ophthalmol Vis Sci* (1994) 35:3342–5.
111. Maeda A, Maeda T, Liang Y, Yenerel M, Saperstein DA. Effects of cytotoxic T lymphocyte antigen 4 (CTLA4) signaling and locally applied steroid on retinal dysfunction by recoverin, cancer-associated retinopathy antigen. *Mol Vis* (2006) 12:885–91.
112. Adamus G, Aptsiauri N, Guy J, Heckenlively J, Flannery J, Hargrave PA. The occurrence of serum autoantibodies against enolase in cancer-associated retinopathy. *Clin Immunol Immunopathol* (1996) 78:120–9. doi:10.1006/clin.1996.0021
113. Adamus G, Amundson D, Seigel GM, Machnicki M. Anti-enolase alpha autoantibodies in cancer-associated retinopathy: epitope mapping and cytotoxicity on retinal cells. *J Autoimmun* (1998) 11:671–7. doi:10.1006/jaut.1998.0239
114. Terrier B, Degand N, Guilpain P, Servettaz A, Guillevin L, Mouthon L. Alpha-enolase: a target of antibodies in infectious and autoimmune diseases. *Autoimmun Rev* (2007) 6:176–82. doi:10.1016/j.autrev.2006.10.004
115. Walter M, Berg H, Leidenberger FA, Schweppe K-W, Northermann W. Autoreactive epitopes within the human apha-enolase and their recognition by sera from patients with endometriosis. *J Autoimmun* (1995) 8:931–45. doi:10.1016/S0896-8411(95)80027-1
116. Arza B, Felez J, Lopez-Alemany R, Miles LA, Munoz-Canoves P. Identification of an epitope of alpha-enolase (a candidate plasminogen receptor) by phage display. *Thromb Haemost* (1997) 78:1097–103.
117. Fujii A, Yoneda M, Ito T, Yamamura O, Satomi S, Higa H, et al. Autoantibodies against the amino terminal of α-enolase are a useful diagnostic marker of Hashimoto's encephalopathy. *J Neuroimmunol* (2005) 162:130–6. doi:10.1016/j.jneuroim.2005.02.004
118. Lebioda L, Stec B. Mapping of isozymic differences in enolase. *Int J Biol Macromol* (1991) 13:97–100. doi:10.1016/0141-8130(91)90055-Y
119. Alarcon-Segovia D, Ruiz-Arguelles A, Llorente L. Broken dogma: penetration of autoantibodies into living cells. *Immunol Today* (1996) 17:163–4.
120. Golan TD, Gharavi AE, Elkon KB. Penetration of autoantibodies into living epithelial cells. *J Invest Dermatol* (1993) 100:316–22. doi:10.1111/1523-1747.ep12469994
121. Zack DJ, Stempniak M, Wong AL, Taylor C, Weisbart RH. Mechanism of cellular penetration and nuclear localization of an anti-double strand DNA autoantibody. *J Immunol* (1996) 157:2082–8.
122. Shiraga S, Adamus G. Mechanism of CAR syndrome: anti-recoverin antibodies are the inducers of retinal cell apoptotic death via the caspase 9- and caspase 3-dependent pathway. *J Neuroimmunol* (2002) 132:72–82. doi:10.1016/S0165-5728(02)00314-4
123. Maeda T, Maeda A, Maruyama I, Ogawa KI, Kuroki Y, Sahara H, et al. Mechanisms of photoreceptor cell death in cancer-associated retinopathy. *Invest Ophthalmol Vis Sci* (2001) 42:705–12.
124. Noble PW, Bernatsky S, Clarke AE, Isenberg DA, Ramsey-Goldman R, Hansen JE. DNA-damaging autoantibodies and cancer: the lupus butterfly theory. *Nat Rev Rheumatol* (2016) 12:429–34. doi:10.1038/nrrheum.2016.23
125. Adamus G. Autoantibody-induced apoptosis as a possible mechanism of autoimmune retinopathy. *Autoimmun Rev* (2003) 2:63–9. doi:10.1016/S1568-9972(02)00127-1
126. Adamus G, Machnicki M, Elerding H, Sugden B, Blocker YS, Fox DA. Antibodies to recoverin induce apoptosis of photoreceptor and bipolar cells in vivo. *J Autoimmun* (1998) 11:523–33. doi:10.1006/jaut.1998.0221
127. Marchenko S, Chernyavsky AI, Arredondo J, Gindi V, Grando SA. Antimitochondrial autoantibodies in pemphigus vulgaris. *J Biol Chem* (2010) 285:3695–704. doi:10.1074/jbc.M109.081570
128. Adamus G, Webb S, Shiraga S, Duvoisin RM. Anti-recoverin antibodies induce an increase in intracellular calcium in retinal cells. *J Autoimmun* (2006) 26:146–53. doi:10.1016/j.jaut.2005.11.007
129. Ohguro H, Maruyama I, Nakazawa M, Oohira A. Antirecoverin antibody in the aqueous humor of a patient with cancer-associated retinopathy. *Am J Ophthalmol* (2002) 134:605–7. doi:10.1016/S0002-9394(02)01633-1
130. Chen W, Elias RV, Cao W, Lerious V, McGinnis JF. Anti-recoverin antibodies cause the apoptotic death of mammalian photoreceptor cells in vitro. *J Neurosci Res* (1999) 57:706–18. doi:10.1002/(SICI)1097-4547(19990901)57:5<706::AID-JNR12>3.0.CO;2-G

131. Lim P-L, Zouali M. Pathogenic autoantibodies: emerging insights into tissue injury. *Immunol Lett* (2006) 103:17–26. doi:10.1016/j.imlet.2005.10.023
132. Ohguro H, Ogawa K, Maeda T, Maeda A, Maruyama I. Cancer-associated retinopathy induced by both anti-recoverin and anti-hsc70 antibodies in vivo. *Invest Ophthalmol Vis Sci* (1999) 40:3160–7.
133. Magrys A, Anekonda T, Ren G, Adamus G. The role of anti-alpha-enolase autoantibodies in pathogenicity of autoimmune-mediated retinopathy. *J Clin Immunol* (2007) 27:181–92. doi:10.1007/s10875-006-9065-8
134. Adamus G, Karren L. Relevance of anti-carbonic anhydrase II autoantibodies in autoimmune retinopathy. *9th International Ocular Inflammation Society Congress*. Paris, France (2007). 43 p.
135. Baumgarth N, Tung JW, Herzenberg LA. Inherent specificities in natural antibodies: a key to immune defense against pathogen invasion. *Springer Semin Immunopathol* (2005) 26:347–62. doi:10.1007/s00281-004-0182-2
136. Nagele EP, Han M, Acharya NK, DeMarshall C, Kosciuk MC, Nagele RG. Natural IgG autoantibodies are abundant and ubiquitous in human sera, and their number is influenced by age, gender, and disease. *PLoS One* (2013) 8:e60726. doi:10.1371/journal.pone.0060726
137. Holodick NE, Rodríguez-Zhurbenko N, Hernández AM. Defining natural antibodies. *Front Immunol* (2017) 8:872. doi:10.3389/fimmu.2017.00872
138. Neumann H, Kotter MR, Franklin RJM. Debris clearance by microglia: an essential link between degeneration and regeneration. *Brain* (2009) 132:288–95. doi:10.1093/brain/awn109
139. Nagata S, Hanayama R, Kawane K. Autoimmunity and the clearance of dead cells. *Cell* (2010) 140:619–30. doi:10.1016/j.cell.2010.02.014

Conflict of Interest Statement: The author declares that the research was conducted in the absence of any commercial or financial relationships that could be construed as a potential conflict of interest.

frontiers in Immunology

MINI REVIEW
published: 13 April 2018
doi: 10.3389/fimmu.2018.00622

B Cell Modulation Strategies in Autoimmune Diseases: New Concepts

Philippe Musette[1] and Jean David Bouaziz[2]**

[1] Dermatology Department, INSERM U976, Rouen University Hospital, Rouen, France, [2] Dermatology Department, INSERM U976, Saint Louis University Hospital, Paris, France

B cells are major effector cells in autoimmunity through antibody production, T cell help and pro-inflammatory cytokine production. Major advances have been made in human B cell biology knowledge using rituximab and type II new anti-CD20 antibodies, anti-CD19 antibodies, anti-CD22 antibodies, autoantigen specific B cell depleting therapy (chimeric antigen receptor T cells), and B cell receptor signaling inhibition (Bruton's tyrosine kinase inhibitors). However, in certain circumstances B cell depleting therapy may lead to the worsening of the autoimmune disease which is in accordance with the existence of a regulatory B cell population. Current concepts and future directions for B cell modulating therapies in autoimmune diseases with a special focus on pemphigus are discussed.

Keywords: autoimmunity, autoantibodies, B cell, B cell depletion, regulatory B cell

OPEN ACCESS

Edited by:
Ralf J. Ludwig,
University of Lübeck, Germany

Reviewed by:
John Stanley,
University of Pennsylvania, United States
Aimee S. Payne,
University of Pennsylvania, United States

****Correspondence:***
Philippe Musette
philippe.musette@chu-rouen.fr;
Jean David Bouaziz
jean-david.bouaziz@aphp.fr

Specialty section:
This article was submitted to Immunological Tolerance and Regulation, a section of the journal Frontiers in Immunology

Received: *12 January 2018*
Accepted: *13 March 2018*
Published: *13 April 2018*

Citation:
Musette P and Bouaziz JD (2018) B Cell Modulation Strategies in Autoimmune Diseases: New Concepts. Front. Immunol. 9:622. doi: 10.3389/fimmu.2018.00622

INTRODUCTION

B cells were primary identified for their key role as enhancers of the immune response in autoimmunity, because they give rise to autoantibody producing plasma cells and promote $CD4^+$ T cell responses by antigen presentation. The B cells bearing these functions are usually considered as effector B cells. Recently published studies indicate that B cells can also act as negative sensors of the immune response in autoimmunity, these regulatory properties are mainly attributed to the recently identified interleukin 10 (IL-10) regulatory B cell compartment (Breg) (1–3). New therapies target these B cell populations with drugs directed against B cell surface markers (CD20, CD22), activating factors (BAFF, TACI), or cytokines (IL-6, TNFα, IFNα) (4, 5). The most focused strategy to target B cells in autoimmune diseases would be to specifically remove autoreactive effector B cells, and amplify autoantigen driven Bregs, while maintaining immune surveillance. Such a strategy is difficult to achieve especially because antigen specific targeting is challenging and, the relative contribution of B cells to the pathogenesis of autoimmune disease might differ considerably from one disease to another.

Autoreactive B cells give rise to autoreactive plasma cells whose pathogenicity might be direct through production of IgG^+ autoantibodies that bind to specific target molecules (e.g., acetylcholine receptor on the motor end plate in myasthenia gravis; desmoglein 1 and 3 on keratinocyte in pemphigus) or through the formation of immune complexes in tissues that locally activate the complement cascade. B cells are also important effector cells in autoimmune diseases because

Abbreviations: CAR, chimeric antigen receptor; CAAR, chimeric autoantibody receptor; BTK, Bruton's tyrosine kinase.

they regulate lymphoid tissue structure, contribute to antigen presentation and costimulation (6), regulate dendritic cell function and pathways of T helper cell differentiation, and release inflammatory cytokines including IL-8, IL-6, LT-α, and TNF-α (7–10). Our review will focus on B cell therapies in various autoimmune disorders with a special focus on pemphigus (an autoimmune blistering skin disease). **Table 1** summarizes recent studies in pemphigus that target B cells or their pathogenic antibodies.

ANTI-CD20 mAb

B cell depletion using type 1 anti-CD20 monoclonal antibodies (rituximab, ofatumumab, ocrelizumab) has shown varying degrees of efficacy in some human autoimmune diseases ranging from dramatic efficacy to sometimes worsening of symptoms (4, 11). Rituximab has been proved to be highly efficient in rheumatoid arthritis, pemphigus (12, 13), granulomatosis with polyangiitis, and microscopic polyangiitis (14). Ocrelizumab was recently proved to be efficient and FDA approved in relapsing multiple sclerosis (15, 16).

The limited efficacy or adverse effects of B cell depleting therapies in some diseases may be partially explained by the fact that rituximab also depletes the Breg compartment. IL-10-producing Bregs were first identified in mice and shown to downregulate immune response and inflammation, making them probably instrumental for maintenance of self tolerance. Numerous recent studies have also characterized IL-10-producing Bregs in humans and have started to decipher their phenotype and mode of suppression. The cell surface phenotype of human Bregs is mainly composed of $CD24^{high}CD27^{+}$ B cell subpopulation (17, 18) and $CD24^{high}CD38^{high}$ transitional B cell subpopulation (19). Mechanisms of suppression include inhibition of $CD4^{+}$ T proliferation, associated with induction and expansion of regulatory T cells, inhibition of Th1 differentiation, and also suppression of monocyte activation. The decreased frequency and/or decreased suppressive activity of Bregs have been recently shown in patients with lupus (19), immune thrombocytopenia (20), rheumatoid arthritis (21), ANCA-associated vasculitis (22), pemphigus (23), and systemic sclerosis (24). In addition an increase in Bregs is associated with better prognosis or complete remission in certain autoimmune diseases (25, 26). B cell depletion therapy using rituximab in systemic lupus erythematosus (SLE) (26, 27) and pemphigus (25) patients may also promote the emergence of a functional transitional Breg pool upon B cell reconstitution which may contribute to the long-term efficacy of rituximab in these diseases. Indeed rituximab induces a prolonged and continuous repopulation with naive B cells with a new repertoire (25, 28) after the initial B-cell depletion, whereas the reappearance of memory B cells is markedly delayed (25, 26). This blockage of B cell maturation is associated with a blockage of the auto-reactive IgM to IgG class switching process (25). Finally, B cell depletion induces a two step mechanism of immunosupression by eliminating the autoreactive B cells involved in the production of pathogenic IgG^{+} autoantibodies (28, 29) and by promoting the appearance of Bregs (25) (**Figure 1**). Rituximab therapy may, however, decrease the humoral immune response to recall antigens (30) which may increase the risk of patient infection including hepatitis B reactivation and progressive multifocal leukoencephalopathy (polyomavirus JC), whereas long-term anti tetanus and anti-pneumococcal antibody response is maintained (25). It also seems conceivable that, given the role of B cells in generating antitumor responses (31), B cell depletion using rituximab may contribute to long-term expansion of uncontrolled tumor cells (32). B cell depletion therapy using rituximab may be particularly efficient in pemphigus because it depletes memory B cells that give rise to short-lived plasma cells that produce pathogenic autoantibodies. Rituximab preserves long-lived plasma cells that may be more important for "natural" protection against infection. Pathogenic autoantibodies may be the result of a temporary breakdown of immune tolerance giving rise to pathogenic B cells clones that are abrogated using rituximab (33). B cell-activating factor (BAFF) and a proliferation-inducing ligand are important B cell differentiation and survival factors. Their targeting could also be interesting for pemphigus treatment.

A new class of "type II" anti-CD20 antibodies (obinutuzumab) that induce little complement-dependent cytotoxicity but induce signaling-dependent B cell death is under development (34). This type II class is particularly interesting because, contrary to rituximab, it may be more efficient at depleting organ resident B cells.

New strategies will require specific targeting of the pathogenic effector functions of B cells and if possible the promotion of their regulatory function without modifying B cell dependent immune surveillance.

TABLE 1 | Current ongoing studies in pemphigus that target B cells or their pathogenic antibodies (excluding studies with rituximab).

A Long-Term Extension Study of Ofatumumab (**type I anti-CD20**) Injection for Subcutaneous Use in Subjects With Pemphigus Vulgaris *ClinicalTrials.gov identifier: NCT02613910*
Efficacy and Safety of Ofatumumab (**type I anti-CD20**) in Treatment of Pemphigus Vulgaris *ClinicalTrials.gov identifier: NCT01920477*
Study of Efficacy and Safety of VAY736 (**anti-BAFF-R**) in Patients With Pemphigus Vulgaris *ClinicalTrials.gov identifier: NCT01930175*
A Study to Evaluate the Safety, PD, PK and Efficacy of ARGX-113 (**human IgG1-derived Fc fragment that binds to FcRn**) in Patients With Pemphigus *ClinicalTrials.gov identifier: NCT03334058*
A Safety Study of SYNT001 (**A Humanized IgG4 Monoclonal Antibody That Disrupts the Interaction of FcRn and IgG**) in Subjects With Pemphigus (Vulgaris or Foliaceus) *ClinicalTrials.gov identifier: NCT03075904*
A Study of PRN1008 (**Bruton's tyrosine kinase inhibitor**) in Adult Patients With Pemphigus Vulgaris *ClinicalTrials.gov identifier: NCT02704429*

Bold represents mechanisms of action of the drug.
FcRn, neonatal Fc Receptors.
New therapies seek to disrupt the IgG–FcRn interaction to increase the clearance of pathogenic IgG antibodies from the body.

ANTI-CD19 AND ANTI-CD22 mAbs

Anti-CD20 mAbs efficiently deplete mature naive and memory B cells, inhibit the development of short-lived plasma cells, but spare long-lived plasma cells and previously produced protective antibodies acquired during infection or vaccination. Contrary to

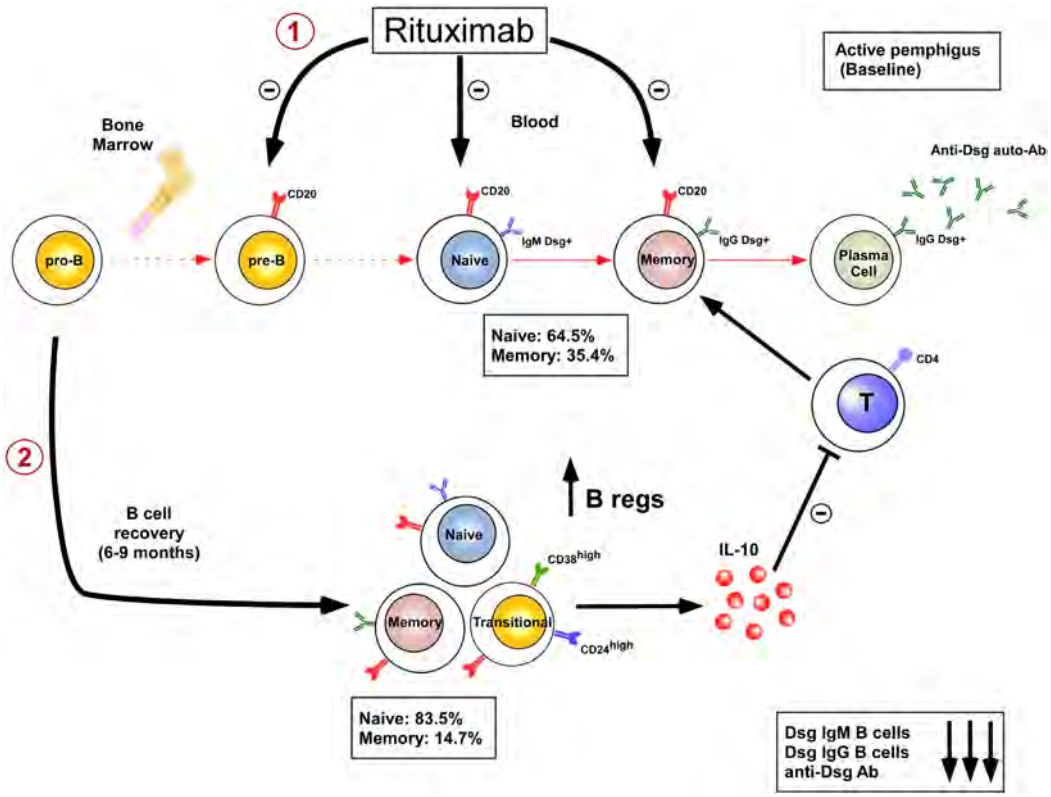

FIGURE 1 | Dual mechanisms of B cell depletion: 1: elimination of autoreactive B cells; 2: induction of regulatory B cells.

CD20, CD19 is expressed from early B cell development (pro-B stage) to the last differentiation stage including plasma cells. These features make CD19 an attractive target for B cell depletion. MEDI-551 (inebilizumab) is a human IgG1 anti-CD19 mAb that was developed for the treatment of multiple sclerosis (35). Interestingly, bispecific antibodies (blinatumomab) that redirect T cells to CD19 have been developed and have shown efficacy for the treatment of acute lymphoblastic leukemia (36). Such bispecific antibodies that target leukemic and normal B cells could be an interesting approach for the treatment of autoimmune diseases in the future.

Epratuzumab is a humanized monoclonal antibody that binds to the glycoprotein CD22 (an inhibitory C-type lectin) expressed on mature and malignant B cells. Epratuzumab has completed phase III trials for the treatment of SLE (37). Although endpoints were not reached in this study, the drug was well tolerated. Epratuzumab diminishes B-cell receptor activation (38) and induces only partial B-cell depletion (39).

ANTIGEN SPECIFIC B CELL DEPLETION USING CHIMERIC AUTOANTIBODY RECEPTOR (CAAR) T CELLS

Targeting antigen specific immune response represents a very interesting strategy. In this respect a promising strategy has been developed for the treatment of pemphigus vulgaris, a blistering autoimmune skin disease, in which autoimmune B cells produce autoantibodies against the desmoglein 1 and 3 antigens present in the skin. Until recently, different approaches including immunoabsorption of Dsg autoantibodies *ex vivo* (40), or anti idiotype antibodies directed against Dsg3 specific autoantibodies (41) were developed without clinical impact. Recently, alive T cells that express a chimeric antigen receptor (CAR) composed of an antibody structure fused to the CD3 signaling domain engineered to recognize tumor-associated antigens have shown remarkable efficacy in B cell leukemia (42). Moreover CAR T cells are able to proliferate and expand *in vivo*. A new approach is now being developed with a CAAR including truncated fragments of the Dsg3 extracellular domain fused to CD137/CD3 signaling domains expressed on T cells. This CAAR is able to recognize autoantibodies against Dsg3 fixed on the B cell membrane (**Figure 2**). CAAR T cells have shown efficacy in eliminating anti-Dsg3 specific B cells *in vitro* and in a pemphigus mice model (43).

INHIBITION OF B CELL RECEPTOR SIGNALING

Activation of the B cell receptor induces downstream signaling of multiple kinases crucial for B cell activation. Among them, Lyn, Syk, PI3K, and Bruton' tyrosine kinase (BTK) are potential therapeutic targets for autoreactive B cell silencing and depletion.

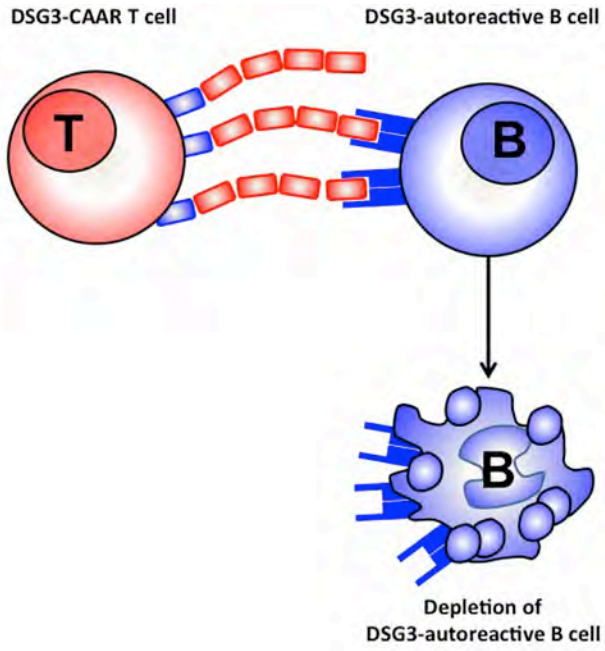

FIGURE 2 | Chimeric auto antibody receptor (CAAR) T cell.

Among the potential drugs, ibrutinib, a pharmacological BTK inhibitor has been developed and licensed for the treatment of chronic lymphocytic leukemia. Targeting BTK using ibrutinib may be an interesting approach to treat autoimmune diseases. Indeed, transgenic mice overexpressing BTK in B cells manifested SLE-like autoimmune disease involving kidneys, lungs, and salivary glands (44). Recently, ibrutinib has shown efficacy in chronic graft versus host disease the physiopathology of which involves allo-reactive B and T cells. Based on these results, ibrutinib was approved in the US for treatment of adult patients with GVHD after failure of one or more lines of systemic therapy (45). A new BTK inhibitor known as PRN1008 is under evaluation for the treatment of pemphigus in humans (ClinicalTrials.gov Identifier: NCT02704429).

CONCLUSION

Much progress has been made in depleting circulating and resident B cells present in inflamed tissue and secondary lymphoid organs. An ideal strategy in the future will require specific targeting of the pathogenic effector functions of B cells and if possible the promotion of their regulatory function without modifying B cell-dependent immune surveillance. More targeted therapies on specific B cell populations and functions will allow better patient management.

AUTHOR CONTRIBUTIONS

PM and JDB contributed equally to the manuscript.

ACKNOWLEDGMENTS

The authors are grateful to Nikki Sabourin-Gibbs (Rouen University Hospital) for her help in editing the manuscript.

FUNDING

The paper was funded by INSERM.

REFERENCES

1. Fillatreau S, Sweenie CH, McGeachy MJ, Gray D, Anderton SM. B cells regulate autoimmunity by provision of IL-10. *Nat Immunol* (2002) 3:944–50. doi:10.1038/ni833
2. Mauri C, Bosma A. Immune regulatory function of B cells. *Annu Rev Immunol* (2012) 30:221–41. doi:10.1146/annurev-immunol-020711-074934
3. Bouaziz JD, Yanaba K, Tedder TF. Regulatory B cells as inhibitors of immune responses and inflammation. *Immunol Rev* (2008) 224:201–14. doi:10.1111/j.1600-065X.2008.00661.x
4. Townsend MJ, Monroe JG, Chan AC. B-cell targeted therapies in human autoimmune diseases: an updated perspective. *Immunol Rev* (2010) 237:264–83. doi:10.1111/j.1600-065X.2010.00945.x
5. Jordan N, Lutalo PMK, D'Cruz DP. Novel therapeutic agents in clinical development for systemic lupus erythematosus. *BMC Med* (2013) 11:120. doi:10.1186/1741-7015-11-120
6. Ronchese F, Hausmann B. B lymphocytes in vivo fail to prime naive T cells but can stimulate antigen-experienced T lymphocytes. *J Exp Med* (1993) 177:679–90. doi:10.1084/jem.177.3.679
7. Harris DP, Haynes L, Sayles PC, Duso DK, Eaton SM, Lepak NM, et al. Reciprocal regulation of polarized cytokine production by effector B and T cells. *Nat Immunol* (2000) 1(6):475–82. doi:10.1038/82717
8. Defuria J, Belkina AC, Jagannathan-Bogdan M, Snyder-Cappione J, Carr JD, Nersesova YR, et al. B cells promote inflammation in obesity and type 2 diabetes through regulation of T cell function and inflammatory cytokine profile. *Proc Natl Acad Sci U S A* (2013) 110:5133–8. doi:10.1073/pnas.1215840110
9. Hamze M, Desmetz C, Guglielmi P. B cell-derived cytokines in diseases. *Eur Cytokine Netw* (2013) 24:20–6. doi:10.1684/ecn.2013.0327
10. Barr TA, Shen P, Brown S, Lampropoulou V, Roch T, Lawrie S, et al. B cell depletion therapy ameliorates autoimmune disease through ablation of IL-6-producing B cells. *J Exp Med* (2012) 209:1001–10. doi:10.1084/jem.20111675
11. Thaunat O, Morelon E, Defrance T. Am"B"valent: anti CD20 antibodies unravel the dual role of B cells in immunopathogenesis. *Blood* (2010) 116:515–21. doi:10.1182/blood-2010-01-266668
12. Cohen MD, Keystone E. Rituximab for rheumatoid arthritis. *Rheumatol Ther* (2015) 2:99–111. doi:10.1007/s40744-015-0016-9
13. Joly P, Maho-Vaillant M, Prost-Squarcioni C, Hebert V, Houivet E, Calbo S, et al. First-line rituximab combined with short-term prednisone versus prednisone alone for the treatment of pemphigus (Ritux3): a prospective, multicentre, parallel-group, open-label randomised trial. *Lancet* (2017) 389:2031–40. doi:10.1016/S0140-6736(17)30070-3
14. Guillevin L, Pagnoux C, Karras A. Rituximab versus azathioprine for maintenance in ANCA associated vasculitis. *N Engl J Med* (2014) 371:1771–80. doi:10.1056/NEJMoa1404231
15. Hauser SL, Bar-Or A, Comi G, Giovannoni G, Hartung HP, Hemmer B, et al. Ocrelizumab versus interferon beta-1a in relapsing multiple sclerosis. *N Engl J Med* (2017) 376:221–34. doi:10.1056/NEJMoa1601277
16. Montalban X, Hauser SL, Kappos L, Arnold DL, Bar-Or A, Comi G, et al. Ocrelizumab versus placebo in primary progressive multiple sclerosis. *N Engl J Med* (2017) 376:209–20. doi:10.1056/NEJMoa1606468
17. Bouaziz JD, Calbo S, Maho-Vaillant M, Saussine A, Bagot M, Bensussan A, et al. IL10 produced by activated human B cells regulates CD4(+) T-cell activation in vitro. *Eur J Immunol* (2010) 40:2686–91. doi:10.1002/eji.201040673
18. Iwata Y, Matsushita T, Horikawa M, Dilillo DJ, Yanaba K, Venturi GM, et al. Characterization of a rare IL10-competent B-cell subset in humans that parallels mouse regulatory B10 cells. *Blood* (2011) 117:530–41. doi:10.1182/blood-2010-07-294249

19. Blair PA, Noreña LY, Flores-Borja F, Rawlings DJ, Isenberg DA, Ehrenstein MR, et al. CD19(+)CD24(hi)CD38(hi) B cells exhibit regulatory capacity in healthy individuals but are functionally impaired in systemic lupus erythematosus patients. *Immunity* (2010) 32:129–40. doi:10.1016/j.immuni.2009.11.009
20. Li X, Zhong H, Bao W, Boulad N, Evangelista J, Haider MA, et al. Defective regulatory B-cell compartment in patients with immune thrombocytopenia. *Blood* (2012) 120(16):3318–25. doi:10.1182/blood-2012-05-432575
21. Flores-Borja F, Bosma A, Ng D, Reddy V, Ehrenstein MR, Isenberg DA, et al. CD19+CD24hiCD38hi B cells maintain regulatory T cells while limiting TH1 and TH2 differentiation. *Sci Transl Med* (2013) 5:173ra23. doi:10.1126/scitranslmed.3005407
22. Wilde B, Thewissen M, Damoiseaux J, Knippenberg S, Hilhorst M, van Paassen P, et al. Regulatory B cells in ANCA-associated vasculitis. *Ann Rheum Dis* (2013) 72:1416–9. doi:10.1136/annrheumdis-2012-202986
23. Zhu HQ, Xu RC, Chen YY, Yuan HJ, Cao H, Zhao XQ, et al. Impaired function of CD19(+) CD24(hi) CD38(hi) regulatory B cells in patients with pemphigus. *Br J Dermatol* (2015) 172(1):101–10. doi:10.1111/bjd.13192
24. Matsushita T, Hamaguchi Y, Hasegawa M, Takehara K, Fujimoto M. Decreased levels of regulatory B cells in patients with systemic sclerosis: association with autoantibody production and disease activity. *Rheumatology (Oxford)* (2016) 55(2):263–7. doi:10.1093/rheumatology/kev331
25. Colliou N, Picard D, Caillot F, Calbo S, Le Corre S, Lim A, et al. Long-Term remissions of severe pemphigus after rituximab therapy are associated with prolonged failure of desmoglein B cell response. *Sci Transl Med* (2013) 5(175):175ra30. doi:10.1126/scitranslmed.3005166
26. Anolik JH, Barnard J, Owen T, Zheng B, Kemshetti S, Looney RJ, et al. Delayed memory B cell recovery in peripheral blood and lymphoid tissue in systemic lupus erythematosus after B cell depletion therapy. *Arthritis Rheum* (2007) 56:3044–56. doi:10.1002/art.22810
27. Palanichamy A, Barnard J, Zheng B, Owen T, Quach T, Wei C, et al. Novel human transitional B cell populations revealed by B cell depletion therapy. *J Immunol* (2009) 182:5982–93. doi:10.4049/jimmunol.0801859
28. Mouquet H, Musette P, Gougeon ML, Jacquot S, Lemercier B, Lim A, et al. B-cell depletion immunotherapy in pemphigus: effects on cellular and humoral immune responses. *J Invest Dermatol* (2008) 128:2859–69. doi:10.1038/jid.2008.178
29. Joly P, Mouquet H, Roujeau JC, D'Incan M, Gilbert D, Jacquot S, et al. A single cycle of rituximab for the treatment of severe pemphigus. *N Engl J Med* (2007) 357:545–52. doi:10.1056/NEJMoa067752
30. van der Kolk LE, Baars JW, Prins MH, Van Oers MH. Rituximab treatment results in impaired secondary humoral immune responsiveness. *Blood* (2002) 100:2257–9.
31. Li Q, Teitz-Tennenbaum S, Donald EJ, Li M, Chang AE. In vivo sensitized and in vitro activated B cells mediate tumor regression in cancer adoptive immunotherapy. *J Immunol* (2009) 183(5):3195–203. doi:10.4049/jimmunol.0803773
32. Tarella C, Passera R, Magni M, Benedetti F, Rossi A, Gueli A, et al. Risk factors for the development of secondary malignancy after high-dose chemotherapy and autograft, with or without rituximab: a 20-year retrospective follow-up study in patients with lymphoma. *J Clin Oncol* (2011) 29(7):814–24. doi:10.1200/JCO.2010.28.9777
33. Hammers CM, Chen J, Lin C, Kacir S, Siegel DL, Payne AS, et al. Persistence of anti-desmoglein 3 IgG(+) B-cell clones in pemphigus patients over years. *J Invest Dermatol* (2015) 135(3):742–9. doi:10.1038/jid.2014.291
34. Niederfellner G, Lammens A, Mundigl O, Georges GJ, Schaefer W, Schwaiger M, et al. Epitope characterization and crystal structure of GA101 provide insights into the molecular basis for type I/II distinction of anti CD20 antibodies. *Blood* (2011) 118:358–67. doi:10.1182/blood-2010-09-305847
35. Agius MA, Klodowska-Duda G, Maciejowski M, Potemkowski A, Li J, Patra K, et al. Safety and tolerability of inebilizumab (MEDI-551) an anti-CD19 monoclonal antibody, in patients with relapsing forms of multiple sclerosis: results from a phase 1 randomised, placebo-controlled, escalating intravenous and subcutaneous dose study. *Mult Scler* (2017). doi:10.1177/1352458517740641
36. Velasquez MP, Bonifant C, Gottschalk S. Redirecting T cells to hematological malignancies with bispecific antibodies. *Blood* (2018) 131:30–8. doi:10.1182/blood-2017-06-741058
37. Wallace DJ, Gordon C, Strand V, Hobbs K, Petri M, Kalunian K, et al. Efficacy and safety of epratuzumab in patients with moderate/severe flaring systemic lupus erythematosus from two randomized, double-blind, placebo-controlled multicentre studies (ALLEVIATE) and follow-up. *Rheumatology* (2013) 52:1313–22. doi:10.1093/rheumatology/ket129
38. Sieger N, Fleischer SJ, Mei HE. CD22 ligation inhibits downstream B cell receptor signaling and downstream Ca^{2+} flux upon activation. *Arthritis Rheum* (2013) 65:770–9. doi:10.1002/art.37818
39. Wallace DJ, Kalunian K, Petri MA. Efficacy and safety of eprazumab in patients with moderate/severe active systemic lupus erythematous: results from EMBLEM, a phase IIb, randomized, double-blind, placebo-controlled, multicentrestudy. *Ann Rheum Dis* (2014) 73:183–90. doi:10.1136/annrheumdis-2012-202760
40. Amagai M, Hashimoto T, Shimizu N, Nishikawa T. Absorption of pathogenic autoantibodies by the extracellular domain of pemphigus vulgaris antigen (Dsg3) produced by baculovirus. *J Clin Invest* (1994) 94:919–26. doi:10.1172/JCI117349
41. Payne AS, Siegel DL, Stanley JR. Targeting pemphigus autoantibodies through their heavy-chain variable region genes. *J Invest Dermatol* (2007) 127:1681–91. doi:10.1038/sj.jid.5700790
42. Porter DL, Levine BL, Kalos M, Bagg A, June CH. Chimeric antigen receptor-modified T cells in chronic lymphoid leukemia. *N Engl J Med* (2011) 365:725–33. doi:10.1056/NEJMoa1103849
43. Ellebrecht CT, Bhoj VG, Nace A, Choi EJ, Mao X, Cho MJ, et al. Reengineering chimeric antigen receptor T cells for targeted therapy of autoimmune disease. *Science* (2016) 353:179–84. doi:10.1126/science.aaf6756
44. Kil LP, de Bruijn MJ, Van Nimwegen M, Corneth OB, van Hamburg JP, Dingjan GM, et al. Btk levels set the threshold for B-cell activation and negative selection of autoreactive B cells in mice. *Blood* (2012) 119:3744–56. doi:10.1182/blood-2011-12-397919
45. Miklos D, Corey S, Arora M, Waller EK, Jagasia M, Pusic I, et al. Ibrutinib for chronic graft versus host disease after failure of prior therapy. *Blood* (2017) 130(21):2243–50. doi:10.1182/blood-2017-07-793786

Conflict of Interest Statement: The authors declare that the research was conducted in the absence of any commercial or financial relationships that could be construed as a potential conflict of interest.

frontiers in Immunology

CASE REPORT
published: 12 April 2018
doi: 10.3389/fimmu.2018.00542

Bullous Pemphigoid Triggered by Thermal Burn Under Medication With a Dipeptidyl Peptidase-IV Inhibitor: A Case Report and Review of the Literature

Yosuke Mai[1], Wataru Nishie[1], Kazumasa Sato[2], Moeko Hotta[1], Kentaro Izumi[1], Kei Ito[2], Kazuyoshi Hosokawa[3] and Hiroshi Shimizu[1]*

[1] Department of Dermatology, Hokkaido University Graduate School of Medicine, Sapporo, Japan, [2] Department of Dermatology, JR Sapporo Hospital, Sapporo, Japan, [3] Department of Dermatology, Shinkotoni Skin Care Clinic, Sapporo, Japan

Bullous pemphigoid (BP) is a common autoimmune blistering disease in which autoantibodies mainly target the hemidesmosomal component BP180 (also known as type XVII collagen) in basal keratinocytes. Various triggering factors are known to induce BP onset, including radiotherapy, burns, ultraviolet exposure, surgery, and the use of dipeptidyl peptidase-IV inhibitors (DPP4i), which are widely used antihyperglycemic drugs. Here, we present a case of BP triggered by a thermal burn under medication with DPP4i. A 60-year-old man with type II diabetes had been treated with the DPP4i linagliptin for 1 year. After the right forearm experienced a thermal burn, blisters developed around the burned area and gradually spread over the whole body with the production of autoantibodies targeting the non-NC16A domain of BP180. The diagnosis of BP was confirmed by immunohistopathological examination. Upon withdrawal of linagliptin and treatment with topical steroid and minocycline, complete remission was achieved after 4 months. Previously, 13 cases of BP that developed after thermal burns have been reported, and our case shared some of the clinical features of these thermal burn-induced BP cases. Interestingly, the present case also showed the typical clinical, histopathological, and immunological features of the non-inflammatory type of DPP4i-associated BP (DPP4i-BP). Although the pathogenesis of BP remains uncertain, the present case suggests that DPP4i may trigger the onset of BP similarly to a thermal burn. In addition, the clinical and histopathological features of DPP4i-BP may be distinct from other types of BP.

Keywords: bullous pemphigoid, dipeptidyl peptidase-IV inhibitor, dipeptidyl peptidase-IV inhibitor-associated bullous pemphigoid, burn, cellulitis, autoimmune disease, autoantibodies, physical factors

OPEN ACCESS

Edited by:
Ralf J. Ludwig, University of Lübeck, Germany

Reviewed by:
Jean Kanitakis, Hospices Civils de Lyon, France
Cezary Kowalewski, Medical University of Warsaw, Poland

****Correspondence:***
Wataru Nishie
nishie@med.hokudai.ac.jp

Specialty section:
This article was submitted to Immunological Tolerance and Regulation, a section of the journal Frontiers in Immunology

Received: *15 November 2017*
Accepted: *02 March 2018*
Published: *12 April 2018*

Citation:
Mai Y, Nishie W, Sato K, Hotta M, Izumi K, Ito K, Hosokawa K and Shimizu H (2018) Bullous Pemphigoid Triggered by Thermal Burn Under Medication With a Dipeptidyl Peptidase-IV Inhibitor: A Case Report and Review of the Literature. Front. Immunol. 9:542. doi: 10.3389/fimmu.2018.00542

CASE PRESENTATION

A 60-year-old man with type II diabetes was referred to our department due to blisters and erosions over the whole body. He had been treated with linagliptin, a dipeptidyl peptidase-IV inhibitor (DPP4i), for 1 year. Two months before the referral, he had suffered a deep, 7-cm-long dermal burn on the right forearm from a kitchen accident. Within 2 days after the burn, blisters had appeared

Abbreviations: BP, bullous pemphigoid; DPP4i, dipeptidyl peptidase-IV inhibitor; DPP4i-BP, dipeptidyl peptidase-IV inhibitor-associated bullous pemphigoid; CLEIA, chemiluminescent enzyme immunoassay; ELISA, enzyme-linked immunosorbent assay; HLA, human leukocyte antigen.

on the right forearm, which were treated with a topical antibiotic ointment. However, multiple blisters and erosions gradually developed over the body over the course of 2 months. Physical examination revealed tense blisters and erosions of 5 mm to 2 cm in diameter with circumscribed erythematous lesions predominantly on the right forearm (**Figure 1A**). Blisters and erosions less than 5 mm in diameter without erythema were found on the face, the trunk, and the left leg (**Figure 1B**). Although BP180 NC16A chemiluminescent enzyme immunoassay (CLEIA) was negative (5.9 U/mL; normal, <9.0 U/mL), histopathological examination of the blister showed sub-epidermal blister formation with some eosinophilic infiltration in the dermis (**Figure 1C**). Direct immunofluorescence showed linear deposition of IgG autoantibodies along the dermal–epidermal junction (**Figure 1D**), and 1 M NaCl-split skin indirect immunofluorescence revealed circulating IgG autoantibodies reacting with the epidermal side of the artificial blisters (not shown). Notably, enzyme-linked immunosorbent assay (ELISA) using full-length recombinant BP180 was positive (index value, 41.8; normal, <4.64) (1). Based on these findings, the diagnosis of bullous pemphigoid (BP) was made. Linagliptin was withdrawn 2 days after the referral, and treatment with a topical steroid and minocycline at 100 mg/day was started. His skin lesions gradually improved, and ELISA with full-length recombinant BP180 became negative (index value, 1.03). Complete remission off therapy was achieved 4 months later (**Figure 2**). Although no DPP4i was re-administered, blisters appeared on the left forearm 16 months later, when he developed cellulitis on the right leg. The histopathology of the blister showed sub-epidermal blistering with scant eosinophilic infiltration in the dermis (not shown), which was consistent with BP. BP180 NC16A CLEIA was still negative (<3 U/mL). Topical steroid, minocycline at 200 mg/day, and nicotinamide at 1,500 mg/day were initiated, and the lesions completely resolved 2 months later. At 2 months after the cessation of treatment, no recurrence was observed (**Figure 2**).

INTRODUCTION

Bullous pemphigoid is a common autoimmune blistering disease in which autoantibodies target the hemidesmosomal components BP180 (also known as type XVII collagen) and/or BP230 at the dermal–epidermal junction (3). Clinically, tense blister formation associated with itchy urticarial erythema is typically observed in BP patients, and sub-epidermal blister formation with eosinophilic infiltration is histopathologically observed (3). Although the etiology of BP remains unclear, various factors, including radiotherapy, burns, ultraviolet (UV) exposure, trauma, surgical procedures, topical medications, and infections are known to trigger the onset of the disease (4, 5). Recently, emerging evidence reports that the use of DPP4i, which are widely used to treat patients with diabetes mellitus, increases the risk of BP onset (6–9).

DISCUSSION

Herein, we report a case of BP in which a thermal burn triggered the onset of the disease. As shown in **Table 1**, various BP-inducing physical factors, including radiation (5, 10–18), UV radiation

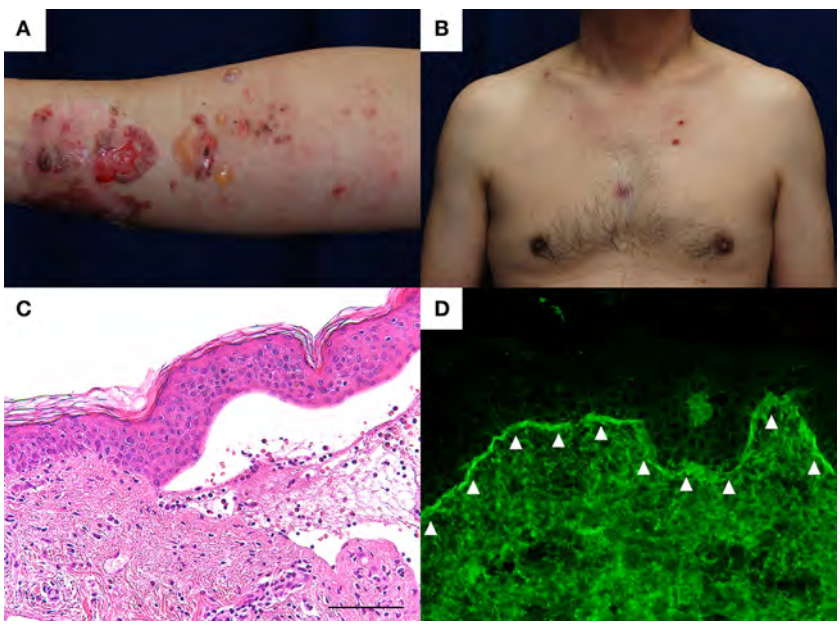

FIGURE 1 | **(A)** Tense blisters and erosions of less than 2 cm in diameter developed over the thermal burn scar on the right forearm. Circumscribed erythematous lesions were also found. **(B)** Small erosions of less than 5 mm in diameter were found on the trunk without erythema. **(C)** Histopathological examination of the blister shows sub-epidermal blistering with some eosinophilic infiltration in the dermis. Scale bar: 100 μm. **(D)** Direct immunofluorescence shows linear IgG autoantibody deposits at the basement membrane zone (arrowheads).

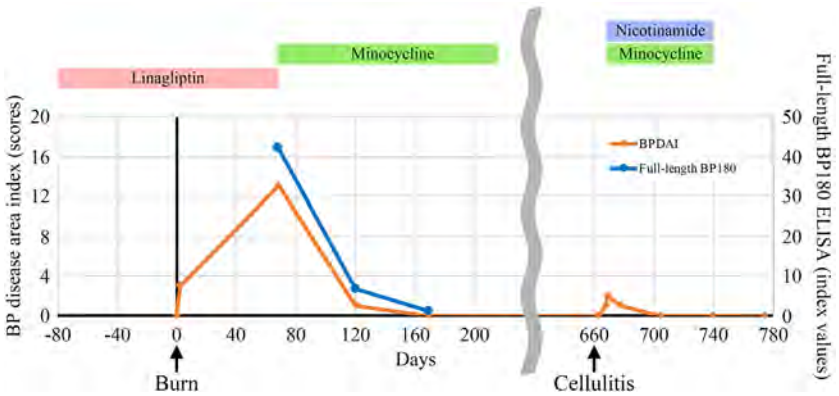

FIGURE 2 | Indices of the bullous pemphigoid (BP) disease area index scores (2) and enzyme-linked immunosorbent assay (ELISA) using full-length recombinant BP180 during the clinical course.

TABLE 1 | List of physical triggering factors for bullous pemphigoid.

Triggering factor	No. of cases
Radiation	38
UV	37
PUVA	13
UVB	5
Goeckerman	4
PUVA and UVB	3
UVA	3
Sunlight	2
PUVA and sunlight	1
PUVASOL	1
Ingram	1
Unknown wavelength	4
Surgical wound	22
Ostomy	19
Colostomy	10
Gastrostomy	5
Ileostomy	2
Urostomy	2
Burn	14
Thermal burn	13
Chemical burn	1
Skin graft	6
Other	11
Scratching	3
Injury	2
Dye injection	1
Mechanical trauma	1
Insect bite	1
Revascularization	1
Photodynamic therapy	1
Hernia	1

UV, ultraviolet; PUVA, psoralen-ultraviolet A; UVB, ultraviolet B; UVA, ultraviolet A; PUVASOL, psoralen-ultraviolet A and sunlight exposure.

(5, 19–30), surgical wounds (5, 31–45), ostomy (31, 46–51), burns (5, 52–62), skin grafts (59, 63–67), and other trauma (5, 68–72) have been reported in the English literature. Regarding thermal burns, 13 cases have been reported (**Table 2**) (5, 52–61). Notably, in contrast to the present case, none of those 13 cases relapsed (5, 52–61) suggesting that the present case had a unique clinical course.

Interestingly, linagliptin, which is a DPP4i, was administered to our case until the onset of BP. DPP4i-associated BP (DPP4i-BP) is a unique, recently reported subtype of BP that develops with the administration of DPP4i medications such as vildagliptin, sitagliptin, and linagliptin (6–9). DPP4i-BP tends to show scant erythema and low levels of autoantibodies targeting the NC16A domain of BP180 or the absence of such autoantibodies (1, 73). In our case, BP developed after 1 year of DPP4i administration, in which erythema was scantly observed and autoantibodies specifically targeted the non-NC16A domain of BP180. In addition, complete remission was achieved after the withdrawal of DPP4i and the initiation of treatment with topical steroid and systemic minocycline. Histopathologically, eosinophilic infiltration was not evident. These characteristics closely resembled those of the non-inflammatory type of DPP4i-BP (1, 73); therefore, DPP4i use may also be involved in the development of the disease. It should be noted that a recent study reported that 18% of DPP4i-BP cases relapsed even after the withdrawal of DPP4i (7). Although the immunohistopathological results were uncertain, the present case developed BP-like blisters when he suffered from cellulitis 16 months after complete remission, indicating that DPP4i was also associated with the BP onset in the present case.

The pathogenic mechanisms of the physical trigger for BP onset remain elusive. The physical factors cause tissue destruction that activates the inflammatory process, which may result in the observed auto-reactivity to basement membrane proteins, including BP180 (5). Alternatively, basement membrane proteins may be altered as a result of physical factors (74) resulting in immunogenicity with increased affinity to certain human leukocyte antigen (HLA) alleles (75). Notably, 86% of cases of the non-inflammatory type of DPP4i-BP carried HLA-DQB1*03:01 (73). Although the HLA allele was not examined, it is likely that the present case had a genetic propensity to the breakdown of self-tolerance to BP180.

TABLE 2 | Overview of thermal burn-induced bullous pemphigoid (BP) cases.

No.	Age	Sex	BP180	BP230	Diagnosis	Eruption	Delay after burn	Relapse	Reference
1	80	M			HE, DIF, IIF	Localized	2 weeks	Not mentioned	Jevtic and Grigoris (52)
2	69	M			HE	Generalized	3 weeks	Not mentioned	Quartey-Papafio and Hudson (53)
3	75	F			HE	Generalized	10 weeks	No	Balato et al. (54)
4	79	M			HE. DIF, sslIF	Localized	1 month	No	Vassileva et al. (55)
5	49	F			HE, DIF	Localized	5 weeks	Not mentioned	Wagner et al. (56)
6	67	M			HE, DIF	Generalized	8 months	No	Wagner et al. (56)
7	51	M	NC16A	(–)	HE, DIF, sslIF	Generalized	6 weeks	No	Xu et al. (57)
8	68	F			HE, DIF, sslIF	Generalized	A few days	No	Korfitis et al. (38)
9	74	M			HE, DIF	Generalized	2 weeks	Not mentioned	Bachmeyer et al. (58)
10	85	F	NC16A		HE, DIF	Localized	20 months	No	Neri et al. (60)
11	73	F			HE, DIF	Generalized	6 weeks	Not mentioned	Damevska et al. (60)
12	89	F	(–)	(+)	HE, DIF, sslIF	Localized	69 years	No	Morita et al. (61)
13	76	M	NC16A	(+)	HE, DIF	Generalized	A few hours	Not mentioned	Dănescu et al. (5)
Our case	60	M	Non-NC16A		HE, DIF, sslIF	Generalized	2 days	Yes	

M, male; F, female; HE, hematoxylin and eosin stain; DIF, direct immunofluorescence; IIF, indirect immunofluorescence; sslIF, 1 M NaCl-split skin indirect immunofluorescence.

CONCLUDING REMARKS

In conclusion, we reported a case of BP induced by a thermal burn. Interestingly, the patient received DPP4i and showed the typical clinical, histopathological, and immunological characteristics of the non-inflammatory type of DPP4i-BP. Although the pathogenesis of thermal burn-induced BP and DPP4i-BP remains uncertain, BP may occur due to various triggering factors.

ETHICS STATEMENT

This report on a single patient complies with the Declaration of Helsinki. The patient gave written informed consent for the publication of this report.

AUTHOR CONTRIBUTIONS

YM, WN, and KIzumi drafted the paper. KS, MH, KIto, and KH were involved in treating the patient and collecting the clinical data. HS supervised the writing of the manuscript.

ACKNOWLEDGMENTS

The authors thank the patient and express their appreciation to Hiroko Azuma for her technical assistance.

FUNDING

This work was supported in part by a Grant-in-Aid for Scientific Research (B) (#24390274 to WN) and Challenging Exploratory Research (#15K15409 to WN).

REFERENCES

1. Izumi K, Nishie W, Mai Y, Wada M, Natsuga K, Ujiie H, et al. Autoantibody profile differentiates between inflammatory and noninflammatory bullous pemphigoid. *J Invest Dermatol* (2016) 136:2201–10. doi:10.1016/j.jid.2016.06.622
2. Murrell DF, Daniel BS, Joly P, Borradori L, Amagai M, Hashimoto T, et al. Definitions and outcome measures for bullous pemphigoid: recommendations by an international panel of experts. *J Am Acad Dermatol* (2012) 66:479–85. doi:10.1016/j.jaad.2011.06.032
3. Schmidt E, Zillikens D. Pemphigoid diseases. *Lancet* (2013) 26:320–32. doi:10.1016/S0140-6736(12)61140-4
4. Lo SA, Ruocco E, Brancaccio G, Caccavale S, Ruocco V, Wolf R. Bullous pemphigoid: etiology, pathogenesis, and inducing factors: facts and controversies. *Clin Dermatol* (2013) 31:391–9. doi:10.1016/j.clindermatol.2013.01.006
5. Dănescu S, Chiorean R, Macovei V, Sitaru C, Baican A. Role of physical factors in the pathogenesis of bullous pemphigoid: case report series and a comprehensive review of the published work. *J Dermatol* (2016) 43:134–40. doi:10.1111/1346-8138.13031
6. Skandalis K, Spirova M, Gaitanis G, Tsartsarakis A, Bassukas ID. Drug-induced bullous pemphigoid in diabetes mellitus patients receiving dipeptidyl peptidase-IV inhibitors plus metformin. *J Eur Acad Dermatol Venereol* (2012) 26:249–53. doi:10.1111/j.1468-3083.2011.04062.x
7. Attaway A, Mersfelder TL, Vaishnav S, Baker JK. Bullous pemphigoid associated with dipeptidyl peptidase IV inhibitors. A case report and review of literature. *J Dermatol Case Rep* (2014) 8:24–8. doi:10.3315/jdcr.2014.1166
8. Béné J, Moulis G, Bennani I, Auffret M, Coupe P, Babai S, et al. Bullous pemphigoid and dipeptidyl peptidase IV inhibitors: a case-noncase study in the French pharmacovigilance database. *Br J Dermatol* (2016) 175:296–301. doi:10.1111/bjd.14601
9. Sakai A, Shimomura Y, Ansai O, Saito Y, Tomii K, Tsuchida Y, et al. Linagliptin-associated bullous pemphigoid that was most likely caused by IgG autoantibodies against the midportion of BP180. *Br J Dermatol* (2017) 176:541–3. doi:10.1111/bjd.15111
10. Mul VE, van Geest AJ, Pijls-Johannesma MC, Theys J, Verschueren TA, Jager JJ, et al. Radiation-induced bullous pemphigoid: a systematic review of an unusual radiation side effect. *Radiother Oncol* (2007) 82:5–9. doi:10.1016/j.radonc.2006.11.014
11. Cabrera-Rodríguez JJ, Muñoz-García JL, Quirós Rivero J, Ropero Carmona F, Ríos Kavadoy Y. Radio-induced bullous pemphigoid. *Clin Transl Oncol* (2010) 12:66–8. doi:10.1007/s12094-010-0469-9
12. Olsha O, Lijoretzky G, Grenader T. Bullous pemphigoid following adjuvant radiotherapy for breast cancer. *Breast J* (2011) 17:204–5. doi:10.1111/j.1524-4741.2010.01060.x
13. Zhou X, Velez NF, Farsani T, Tsiaras W, Laga AC, Werchniak AE, et al. Multiple tense bullae localized to the right breast in a woman in her seventies. *JAMA Dermatol* (2013) 149:1427–8. doi:10.1001/jamadermatol.2013.4704
14. Nieder C, Al-Shibli K, Tollåli T. Nontargeted effect after radiotherapy in a patient with non-small cell lung cancer and bullous pemphigoid. *Case Rep Oncol Med* (2015) 2015:964687. doi:10.1155/2015/964687
15. Campa M, Mansouri B, Wilcox B, Griffin JR. Radiation-induced localized bullous pemphigoid in a patient with breast carcinoma. *Dermatol Online J* (2016) 22.

16. Shon W, Wada DA, Kalaaji AN. Radiation-induced pemphigus or pemphigoid disease in 3 patients with distinct underlying malignancies. *Cutis* (2016) 97:219–22.
17. Hirotsu K, Chiou AS, Chiang A, Kim J, Kwong BY, Pugliese S. Localized bullous pemphigoid in a melanoma patient with dual exposure to PD-1 checkpoint inhibition and radiation therapy. *JAAD Case Rep* (2017) 3:404–6. doi:10.1016/j.jdcr.2017.06.004
18. Kluger N, Mandelin J, Santti K, Jeskanen L, Nuutinen P. Bullous pemphigoid triggered by radiotherapy for breast cancer. *Presse Med* (2017) 46:128–30. doi:10.1016/j.lpm.2016.09.019
19. George PM. Bullous pemphigoid possibly induced by psoralen plus ultraviolet A therapy. *Photodermatol Photoimmunol Photomed* (1996) 11:185–7. doi:10.1111/j.1600-0781.1995.tb00166.x
20. Roeder C, Driesch PV. Psoriatic erythroderma and bullous pemphigoid treated successfully with acitretin and azathioprine. *Eur J Dermatol* (1999) 9:537–9.
21. Denli YG, Uslular C, Acar MA. Bullous pemphigoid in a psoriatic patient. *J Eur Acad Dermatol Venereol* (2000) 14:316–7. doi:10.1046/j.1468-3083.2000.00059-4.x
22. Salmhofer W, Soyer HP, Wolf P, Födinger D, Hödl S, Kerl H. UV light-induced linear IgA dermatosis. *J Am Acad Dermatol* (2004) 50:109–15. doi:10.1016/S0190-9622(03)02120-0
23. Washio H, Hara H, Suzuki H, YoshidA M, Hashimoto T. Bullous pemphigoid on psoriasis lesions after UVA radiation. *Acta Derm Venereol* (2005) 85:561–3. doi:10.1080/00015550510035677
24. Barnadas MA, Gilaberte M, Pujol R, Agustí M, Gelpí C, Alomar A. Bullous pemphigoid in a patient with psoriasis during the course of PUVA therapy: study by ELISA test. *Int J Dermatol* (2006) 45:1089–92. doi:10.1111/j.1365-4632.2004.02517.x
25. Sugita K, Kabashima K, Nishio D, Hashimoto T, Tokura Y. Th2 cell fluctuation in association with reciprocal occurrence of bullous pemphigoid and psoriasis vulgaris. *J Eur Acad Dermatol Venereol* (2007) 21:569–70. doi:10.1111/j.1468-3083.2006.01966.x
26. Saraceno R, Citarella L, Spallone G, Chimenti S. A biological approach in a patient with psoriasis and bullous pemphigoid associated with losartan therapy. *Clin Exp Dermatol* (2008) 33:154–5. doi:10.1111/j.1365-2230.2007.02603.x
27. Kao CL, Krathen RA, Wolf JE Jr, Fuerst JF, Hsu S. Psoralen plus ultraviolet A-induced bullous pemphigoid. *J Drugs Dermatol* (2008) 7:695–6.
28. Takeichi S, Kubbo Y, Arase S, Hashimoto T, Ansai S. Brunsting-Perry type localized bullous pemphigoid, possibly induced by furosemide administration and sun exposure. *Eur J Dermatol* (2009) 19:500–3. doi:10.1684/ejd.2009.0715
29. Riyaz N, Nasir N, Bindu V, Sasidharanpillai S. Bullous pemphigoid induced by topical PUVASOL. *Indian J Dermatol Venereol Leprol* (2014) 80:363–4. doi:10.4103/0378-6323.136936
30. Özkesici B, Koç S, Akman-Karakaş A, Yılmaz E, Başsorgun İC, Uzun S. PUVA induced bullous pemphigoid in a patient with mycosis fungoides. *Case Rep Dermatol Med* (2017) 2017:6134752. doi:10.1155/2017/6134752
31. Asbrink E, Hovmark A. Clinical variations in bullous pemphigoid with respect to early symptoms. *Acta Derm Venereol* (1981) 61:417–21.
32. Brodell RT, Korman NJ. Stump pemphigoid. *Cutis* (1996) 57:245–6.
33. Massa MC, Freeark RJ, Kang JS. Localized bullous pemphigoid occurring in a surgical wound. *Dermatol Nurs* (1996) 8:101–3.
34. Freeman BD, Rubin BG. Bullous pemphigoid after prosthetic vascular graft placement. *Surgery* (1998) 124:112–3. doi:10.1016/S0039-6060(98)70085-6
35. Honl BA, Elston DM. Autoimmune bullous eruption localized to a breast reconstruction site: response to niacinamide. *Cutis* (1998) 62:85–6.
36. Anderson CK, Mowad CM, Goff ME, Pelle MT. Bullous pemphigoid arising in surgical wounds. *Br J Dermatol* (2001) 145:670–2. doi:10.1046/j.1365-2133.2001.04427.x
37. Yesudian PD, Dobson CM, Ahmad R, Azurdia RM. Trauma-induced bullous pemphigoid around venous access site in a haemodialysis patient. *Clin Exp Dermatol* (2002) 27:70–2. doi:10.1046/j.0307-6938.2001.00938.x
38. Korfitis C, Gregoriou S, Georgala S, Christofidou E, Danopoulou I. Trauma-induced bullous pemphigoid. *Indian J Dermatol Venereol Leprol* (2009) 75:617–9. doi:10.4103/0378-6323.57732
39. Sen BB, Ekiz Ö, Rifaioglu EN, Sen T, Atik E, Dogramaci AÇ. Localized bullous pemphigoid occurring on surgical scars. *Indian J Dermatol Venereol Leprol* (2013) 79:554. doi:10.4103/0378-6323.113111
40. Lo Schiavo A, Caccavale S, Alfano R, Gambardella A, Cozzi R. Bullous pemphigoid initially localized around the surgical wound of an arthroprothesis for coxarthrosis. *Int J Dermatol* (2014) 53:e289–90. doi:10.1111/ijd.12222
41. Zeng R, Chen H, Jiang Y, Li M. Bullous pemphigoid after femur fracture surgery: a mere coincidence? *Indian J Dermatol Venereol Leprol* (2014) 80:195. doi:10.4103/0378-6323.129438
42. Neville JA, Yosipovitch G. Flare of bullous pemphigoid in surgically treated skin. *Cutis* (2015) 75:169–70.
43. Garrido Colmenero C, García Durá E, Aneiros Fernández J, Arias Santiago S. Bullous pemphigoid on surgical scar. *Med Clin (Barc)* (2015) 144:e1. doi:10.1016/j.medcli.2014.05.011
44. Singh D, Swann A. Bullous pemphigoid after bilateral forefoot surgery. *Foot Ankle Spec* (2015) 8:68–72. doi:10.1177/1938640014546865
45. Murphy B, Walsh M, McKenna K. Bullous pemphigoid arising in lower leg vein graft incision site. *J Card Surg* (2016) 31:57–9. doi:10.1111/jocs.12668
46. Cecchi R, Paoli S, Giomi A. Peristomal bullous pemphigoid. *J Eur Acad Dermatol Venereol* (2004) 18:515–6. doi:10.1111/j.1468-3083.2004.00957.x
47. Torchia D, Caproni M, Ketabchi S, Antiga E, Fabbri P. Bullous pemphigoid initially localized around a urostomy. *Int J Dermatol* (2006) 45:1387–9. doi:10.1111/j.1365-4632.2006.03118.x
48. Nozu T, Mita H. Bullous pemphigoid and percutaneous endoscopic gastrostomy. *Intern Med* (2010) 49:971–5. doi:10.2169/internalmedicine.49.3346
49. Marzano AV, Vezzoli P, Colombo A, Serini SM, Crosti C, Berti E. Peristomal bullous pemphigoid. *J Dermatol* (2010) 37:840–2. doi:10.1111/j.1346-8138.2010.00851.x
50. Batalla A, Peón G, De la Torre C. Localized bullous pemphigoid at urostomy site. *Indian J Dermatol Venereol Leprol* (2011) 77:625. doi:10.4103/0378-6323.84067
51. Felton S, Al-Niaimi F, Lyon C. Peristomal and generalized bullous pemphigoid in patients with underlying inflammatory bowel disease: is plectin the missing link? *Ostomy Wound Manage* (2012) 58:34–8.
52. Jevtic A, Grigoris I. Bullous pemphigoid induced by a burn. *Australas J Dermatol* (1991) 32:69–70. doi:10.1111/j.1440-0960.1991.tb00065.x
53. Quartey-Papafio CM, Hudson PM. Bullous pemphigoid initially localized to sites of burns (scalds) in a patient on sulphasalazine for ulcerative colitis. *Clin Exp Dermatol* (1994) 19:281. doi:10.1111/j.1365-2230.1994.tb01192.x
54. Balato N, Ayala F, Patruno C, Ruocco V. Bullous pemphigoid induced by a thermal burn. *Int J Dermatol* (1994) 33:55–6. doi:10.1111/j.1365-4362.1994.tb01498.x
55. Vassileva S, Mateev G, Balabanova M, Tsankov N. Burn-induced bullous pemphigoid. *J Am Acad Dermatol* (1994) 30:1027–8. doi:10.1016/S0190-9622(09)80149-7
56. Wagner GH, Ive FA, Paraskevopoulos S. Bullous pemphigoid and burns: the unveiling of the attachment plaque? *Australas J Dermatol* (1995) 36:17–20. doi:10.1111/j.1440-0960.1995.tb00918.x
57. Xu HH, Xiao T, He CD, Jin GY, Wang YK, Gao XH, et al. Bullous pemphigoid triggered by a boiling water burn. *Eur J Dermatol* (2008) 18:466–7. doi:10.1684/ejd.2008.0449
58. Bachmeyer C, Cabanne-Hamy A, Moguelet P, Doizi S, Callard P. Bullous pemphigoid after boiling water burn. *South Med J* (2010) 103:1175–7. doi:10.1097/SMJ.0b013e3181efb58c
59. Neri I, Antonucci VA, Balestri R, Tengattini V, Iozzo I, Bardazzi F. Bullous pemphigoid appearing both on thermal burn scars and split-thickness skin graft donor sites. *J Dtsch Dermatol Ges* (2013) 11:675–6. doi:10.1111/ddg.12094
60. Damevska K, Gocev G, Nikolovska S. A case of burn-induced bullous pemphigoid. *J Burn Care Res* (2014) 35:e281–2. doi:10.1097/BCR.0b013e3182901124
61. Morita R, Oiso N, Ishii N, Tatebayashi M, Matsuda H, Hashimoto T, et al. Case of burn-associated bullous pemphigoid caused by anti-BP230 immunoglobulin G autoantibodies. *J Dermatol* (2015) 42:657–8. doi:10.1111/1346-8138.12848
62. Chen DM, Fairley JA. A bullous pemphigoid-like skin eruption after a chemical burn. *J Am Acad Dermatol* (1998) 38:337–40. doi:10.1016/S0190-9622(98)70578-X
63. McGrath J, Black M. Split skin grafting and bullous pemphigoid. *Clin Exp Dermatol* (1991) 16:72–3. doi:10.1111/j.1365-2230.1991.tb00306.x
64. Levin DL, Sadhwani A. Blistering on a squamous cell carcinoma graft site in a patient with bullous pemphigoid. *Cutis* (1994) 54:40.
65. Ghura HS, Johnston GA, Milligan A. Development of a bullous pemphigoid after split-skin grafting. *Br J Plast Surg* (2001) 54:447–9. doi:10.1054/bjps.2001.3601

66. Hafejee A, Coulson IH. Localized bullous pemphigoid 20 years after split skin grafting. *Clin Exp Dermatol* (2005) 30:187–8. doi:10.1111/j.1365-2230.2004.01689.x
67. Orvis AK, Ihnatsenka V, Hatch RL. Bullous lesions on a skin graft donor site. *J Am Board Fam Med* (2009) 22:89–92. doi:10.3122/jabfm.2009.01.080036
68. Sparrow GP, Moynahan EJ. Localized pemphigoid. *Br J Dermatol* (1976) 14:26–8.
69. Dahl MG, Cook LJ. Lesions induced by trauma in pemphigoid. *Br J Dermatol* (1979) 101:469–73. doi:10.1111/j.1365-2133.1979.tb00029.x
70. Macfarlane AW, Verbov JL. Trauma-induced bullous pemphigoid. *Clin Exp Dermatol* (1989) 14:245–9. doi:10.1111/j.1365-2230.1989.tb00944.x
71. Twine CP, Malik G, Street S, Williams IM. Bullous pemphigoid presenting as dry gangrene in a revascularized limb. *J Vasc Surg* (2010) 51:732–4. doi:10.1016/j.jvs.2009.10.110
72. Rakvit P, Kerr AC, Ibbotson SH. Localized bullous pemphigoid induced by photodynamic therapy. *Photodermatol Photoimmunol Photomed* (2011) 27:251–3. doi:10.1111/j.1600-0781.2011.00609.x
73. Ujiie H, Muramatsu K, Mushiroda T, Ozeki T, Miyoshi H, Iwata H, et al. HLA-DQB1*03:01 as a biomarker for genetic susceptibility to bullous pemphigoid induced by DPP-4 inhibitors. *J Invest Dermatol* (2017) (in press). doi:10.1016/j.jid.2017.11.023
74. Danno K, Takigawa M, Horio T. The alterations of keratinocyte surface and basement membrane markers by treatment with 8-methoxypsoralen plus long-wave ultraviolet light. *J Invest Dermatol* (1983) 80:172–4. doi:10.1111/1523-1747.ep12533415
75. Amber KT, Zikry J, Hertl M. A multi-hit hypothesis of bullous pemphigoid and associated neurological disease: is HLA-DQB1*03:01, a potential link between immune privileged antigen exposure and epitope spreading? *HLA* (2017) 89:127–34. doi:10.1111/tan.12960

Conflict of Interest Statement: The authors declare that the research was conducted in the absence of any commercial or financial relationships that could be construed as potential conflicts of interest.

frontiers in Immunology

ORIGINAL RESEARCH
published: 12 April 2018
doi: 10.3389/fimmu.2018.00451

A Shared Epitope of Collagen Type XI and Type II Is Recognized by Pathogenic Antibodies in Mice and Humans with Arthritis

Dongmei Tong[1,2,3], Erik Lönnblom[1], Anthony C. Y. Yau[1], Kutty Selva Nandakumar[1,3], Bibo Liang[1,2], Changrong Ge[1], Johan Viljanen[4], Lei Li[5], Mirela Bălan[6], Lars Klareskog[7], Andrei S. Chagin[5,8], Inger Gjertsson[9], Jan Kihlberg[4], Ming Zhao[2] and Rikard Holmdahl[1,3]**

[1] Department of Medical Biochemistry and Biophysics, Section for Medical Inflammation Research, Karolinska Institute, Stockholm, Sweden, [2] Department of Pathophysiology, Key Laboratory for Shock and Microcirculation Research of Guangdong, Southern Medical University, Guangzhou, China, [3] Medical Immunopharmacology Research, School of Pharmaceutical Sciences, Southern Medical University, Guangzhou, China, [4] Department of Chemistry—Biomedical Center, Section of Organic Chemistry, Uppsala University, Uppsala, Sweden, [5] Department of Physiology and Pharmacology, Karolinska Institute, Stockholm, Sweden, [6] Department of Medical Biochemistry and Biophysics, Section of Vascular Biology, Karolinska Institute, Stockholm, Sweden, [7] Rheumatology Unit, Department of Medicine, Karolinska Institute, Karolinska University Hospital, Stockholm, Sweden, [8] Institute for Regenerative Medicine, Sechenov First Moscow State Medical University, Moscow, Russia, [9] Department of Rheumatology and Inflammation Research, University of Gothenburg, Gothenburg, Sweden

Background: Collagen XI (CXI) is a heterotrimeric molecule with triple helical structure in which the α3(XI) chain is identical to the α1(II) chain of collagen II (CII), but with extensive posttranslational modifications. CXI molecules are intermingled in the cartilage collagen fibers, which are mainly composed of CII. One of the alpha chains in CXI is shared with CII and contains the immunodominant T cell epitope, but it is unclear whether there are shared B cell epitopes as the antibodies tend to recognize the triple helical structures.

Methods: Mice expressing the susceptible immune response gene A^q were immunized with CII or CXI. Serum antibody responses were measured, monoclonal antibodies were isolated and analyzed for specificity to CII, CXI, and triple helical collagen peptides using bead-based multiplex immunoassays, enzyme-linked immunosorbent assays, and Western blots. Arthritogenicity of the antibodies was investigated by passive transfer experiments.

Results: Immunization with CII or CXI leads to a strong T and B cell response, including a cross-reactive response to both collagen types. Immunization with CII leads to severe arthritis in mice, with a response toward CXI at the chronic stage, whereas CXI immunization induces very mild arthritis only. A series of monoclonal antibodies to CXI were isolated and of these, the L10D9 antibody bound to both CXI and CII equally strong, with a specific binding for the D3 epitope region of α3(XI) or α1(II) chain. The L10D9 antibody binds cartilage *in vivo* and induced severe arthritis. In contrast, the L5F3 antibody only showed weak binding and L7D8 antibody has no binding to cartilage and did not induce arthritis. The arthritogenic L10D9 antibody bound to an epitope shared with CII, the triple

OPEN ACCESS

Edited by:
Anne Cooke, University of Cambridge, United Kingdom

Reviewed by:
Irun R. Cohen, Weizmann Institute of Science, Israel
Peter M. Van Endert, Institut National de la Santé et de la Recherche Médicale (INSERM), France

***Correspondence:**
Ming Zhao
15602239057@163.com;
Rikard Holmdahl
rikard.holmdahl@ki.se

Specialty section:
This article was submitted to Immunological Tolerance and Regulation, a section of the journal Frontiers in Immunology

Received: *04 December 2017*
Accepted: *20 February 2018*
Published: *12 April 2018*

Citation:
Tong D, Lönnblom E, Yau ACY, Nandakumar KS, Liang B, Ge C, Viljanen J, Li L, Bălan M, Klareskog L, Chagin AS, Gjertsson I, Kihlberg J, Zhao M and Holmdahl R (2018) A Shared Epitope of Collagen Type XI and Type II Is Recognized by Pathogenic Antibodies in Mice and Humans with Arthritis. Front. Immunol. 9:451. doi: 10.3389/fimmu.2018.00451

helical D3 epitope. Antibody levels to the shared D3 epitope were elevated in the sera from mice with arthritis as well as in rheumatoid arthritis.

Conclusion: CXI is immunologically not exposed in healthy cartilage but contains T and B cell epitopes cross-reactive with CII, which could be activated in both mouse and human arthritis and could evoke an arthritogenic response.

Keywords: rheumatoid arthritis, arthritis, autoantibody, collagen XI, CII, cross-reactive

INTRODUCTION

Rheumatoid arthritis (RA) is a chronic inflammatory disease with a prevalence of around 0.5–1% in general population (1). B cells are likely to be important for arthritis progression as CD20+ B cell depletion treatment with rituximab improves the disease symptoms, especially in seropositive RA patients (2). Several mouse models that mimic RA are dependent on B cells and autoantibodies, for example, disease development in type II collagen-induced arthritis ($C^{II}IA$), was abrogated in B cell-deficient mice (3). Administration of monoclonal antibodies against either collagen II (CII), or other joint proteins, such as cartilage oligomeric matrix protein (4), can induce arthritis in naïve mice (5).

Collagen XI (CXI) is a minor component of articular cartilage, with the percentage ranging from 3 to 10% depending on the maturation stages (6), whereas CII constitutes 80–85% of the total cartilage. Both CXI and CII are triple helical molecules. CXI is a heterotrimer with three distinct α chains [α1(XI), α2(XI), α3(XI)], while CII is a homotrimer with three identical α chains [α1(II)]. Interestingly, α3(XI) is encoded by the same gene as α1(II), but with a higher degree of glycosylation modifications (7).

The collagen fibrillar network allows cartilage to entrap proteoglycans and provides tensile strength to the tissue; therefore, it is essential for normal cartilage development. Cartilage-specific fibrils contain a mixture of CII, CXI and CIX molecules. There are two different populations of fibrils in normal cartilage that could be distinguished according to their width (thin: 20 nm diameter, thick: 40 nm diameter). It has been shown that CXI molecules exist only in thin cartilage fibrils, which are constructed by a core of four micro-fibrils of which two are CII and the remaining two are CXI surrounded by a ring of 10 CII micro-fibrils (8). Cho/Cho mouse (autosomal recessive chondrodysplasia) having a mutation in the gene encoding for α1(XI) chain, and human Stickler/Marshall syndrome in which mutations in the genes encoding for α1(II), α1(XI), or α2(XI) were observed, have defect in the initiation of thin fibrils formation, and, therefore, develop abnormal cartilage and display osteochondrodysplasia phenotype (9–11).

Collagen XI molecules are suggested to be hidden within the cartilage fibrils, and thus most likely are not accessible to antibodies (8, 12). Nevertheless, antibody responses to both CXI and CII have been detected in sera from patients with established RA (13, 14). In the pristane-induced arthritis model (PIA), rats with a particular MHC allele exhibit antibody responses to CXI in both the acute and chronic phases of the disease; while the antibody responses to CII were detected only during the acute phase of the disease (13, 15). The anti-CXI antibody response could possibly be due to the sequence similarity between the two proteins and/or due to exposure of CXI because of the destruction of collagen fibrils in the peripheral joints during the later phase of arthritis. In fact, it has been shown that immunization of DA rats with homologous CXI leads to chronic and relapsing arthritis (15). However, in mice, conflicting results were observed on the pathogenicity of CXI though elevated antibody titers against CXI were observed (16, 17). The difference in the purity of the collagen preparations used in these studies might explain the observed variation in the results.

The importance of CXI in normal cartilage fibril formation, together with the structure and sequence similarity between CXI and CII led us to investigate the functional relevance of shared epitopes of CXI/CII both in mice and humans.

MATERIALS AND METHODS

Animals

DBA/1J, BQ.Cia9i, B10.RIII male, age-matched mice were used in current study. BQ.Cia9i congenic mice were generated by introgressing *NOD* gene fragment (170.9–173.4 Mbp) containing the cluster of *FcγR* genes on the B10.Q genetic background and are found to be highly susceptible to antibody initiated inflammation (18, 19). Similarly, B10.RIII is an MHC congenic strain with the $H2^r$ haplotype prone to antibody-induced arthritis (20). DA/OlaHsd rats were originated from Harlan Europe (The Netherlands) (21). All the animals were kept and bred in the Medical Inflammation Research animal facility, Karolinska Institute, which is specific pathogen free (Felasa II), and climate-controlled environment with a 14 h light/10 h dark cycles. All the animals were housed in intra-cage ventilated polystyrene cages containing wood shavings, fed standard rodent chow and *water ad libitum*. This study was carried out in accordance with the recommendations of N490/12, N35/16 (Stockholm ethical committee) and 86/609/EEC guidelines (European Community Council Directive). The protocols were approved by local animal welfare authorities.

Collagen Purification

Rat CII (rCII) and rat CXI (rCXI) were prepared from the Swarm rat chondrosarcoma grown in male DA rats by neutral salt extraction followed by salt precipitation and DEAE-cellulose chromatography (22, 23). Briefly, tumor tissue was homogenized and extracted with 1.0 M NaCl/50 mM Tris/pH 7.5 buffer. The polysaccharides and negatively charged proteins were removed and differential salt extraction procedure was used to separate different collagens, 0.9 M NaCl for CII and 1.2 M for CXI. The

bovine CXI (bCXI) was extracted from joint cartilage and further purified as described above. All the collagens were lyophilized, weighed, dissolved, and stored in 0.1 M acetic acid until used. The purity of the respective fractions was analyzed using SDS-PAGE.

Peptide Design and Synthesis

In order to identify the cross-reactive epitopes between α3(XI) and α1(II) in CXI antibodies, a library of human CII triple helical peptides as described previously was used (24). One subset of the CII peptides library was synthesized by GL Biochem, the 24 amino acids of interest (8 triplets) are flanked by 5 N-terminal and 5 C-terminal GPO repeats that help maintain its triple helical conformation. Of the C-terminal 9 amino acids of interest, all but the last peptide overlapping with the N-terminal 9 amino acids of the next peptide. Thus, each successive peptide sequence advances 15 amino acids along the triple helical sequence of human CII. All other triple helical peptides used in the present study were synthesized as covalently linked homotrimeric peptides with 5 N-terminal and 5 C-terminal GPO repeats. In these peptides, two of the α chains are carboxy-terminally linked to the amino groups of two consecutive lysine residues added to the sequence of the third chain (25). The cyclic peptides used as controls each have 15 amino acids derived from human CII. Two cysteine residues were added at both the terminal to achieve a cyclic structure. At the N-terminus of the peptide, we included biotin using the flexible linker aminohexanoic acid (Ahx). All the designed cyclic peptides were synthesized by WuXi Apptech (Wuxi, China).

T Cell Recall Assay

96-well culture plates were coated with antigens (bCXI, rCII, denatured bCXI, denatured rCII, GalCII259-273, or nCII259-273) in 100 µl culture medium (5% FCS, 10 mM HEPES, penicillin/streptomycin) at a concentration range of 0–20 µg/ml. Mouse splenocytes at a concentration of 5×10^5 cells/well in 50 µl volume were added to the culture plates coated with the antigen. T cell hybridomas HCQ3 and HCQ4, as described in detail previously (26), 5×10^4 cells/well in 50 µl volume, were added to the corresponding culture plates. IL-2 concentration in the supernatant was determined after 24 h (in the case of peptides) or 48 h (in the case of proteins).

Generation of CXI-Specific Monoclonal Antibodies

Anti-CXI monoclonal antibody-producing hybridomas were generated and characterized following the protocol described earlier (27). Briefly, 2 months old DBA/1J male mice were immunized intradermally at the base of the tail with 100 µg of bCXI dissolved in 0.1 M acetic acid and emulsified in an equal volume of complete Freund's adjuvant (CFA) (Difco, MI, USA) on day 0, followed by a booster with 50 µg of bCXI emulsified in incomplete Freund's adjuvant (IFA; Difco) on day 21. Three days after the booster dose, inguinal lymph cells were harvested and fused with NSO-bcl2 myeloma cells and cultured for 14 days in complete DMEM/HAT medium. Cells secreting anti-bCXI antibodies were selected using bCXI coated enzyme-linked immunosorbent assay (ELISA) plates, subcloned for five times by limiting dilution method and expanded for antibody production. Monoclonal antibodies were purified from cell culture supernatant using Gamma-bind plus affinity gel matrix (GammaBind Plus Sepharose; GE Healthcare, Uppsala, Sweden). Antibodies were eluted using 0.1 M glycine (pH 2.7) and neutralized with one-eighth volume of 1 M Tris–HCl (pH 9.0). The peak fractions were dialyzed three times against PBS (pH 7.0) extensively. Monoclonal antibodies were quantified spectrophotometrically at 280 nm. The antibody solutions were filter-sterilized using 0.2 µm syringe filters (Dynagard; Spectrum Laboratories, CA, USA) and stored at 4°C until used. Endotoxin content in the antibody solutions was found to be below the detection limit (less than 0.1 EU/mg) as analyzed using Limulus amebocyte lysate assay kit (Limulus Amebocyte Lysate, Lonza, USA).

Enzyme-Linked Immunosorbent Assays

Several monoclonal antibodies were generated from bCXI-immunized mice and their binding specificity was determined. Whole blood was collected from the mouse retro-orbital venous sinus on day 21 and day 70 after immunization with CII. 32 sera samples in total from each time point were measured for the anti-CII and anti-CXI antibody responses. 96-well flat-bottom ELISA plates (Nunc MaxiSorp; Denmark) were coated overnight with 5 µg/ml of purified rCXI, rCII, and bCXI, either native or denatured, or with 5 µg/ml synthetic peptides in PBS at 4°C. After the blockage with 3% non-fat milk in PBS at room temperature (RT) for 2 h, purified antibodies diluted according to a previously determined concentration and 1:1,000 diluted serum samples were incubated at RT for 2 h. The antibody titers were evaluated using HRP-conjugated anti-kappa-specific antibody (1:4,000, Southern Biotech) and ABTS (Roche) as detect system. For isotype specific assessment, biotinylated goat anti-mouse-IgM, -IgG1, -IgG2a, -IgG2b, or -IgG3 reagents (Southern Biotech) were used.

IL-2 Cytokine ELISA

96-well flat-bottom ELISA plates were coated overnight with 2 µg/ml of IL-2 antibody (Jes6-1A12) in PBS at 4°C. After the incubation of supernatant from T cell recall assay for 2 h at RT, the biotinylated IL-2 antibody (Jes6-5H4) was incubated for 1 h at RT. IL-2 titers were detected using europium-labeled streptavidin (DELFIA, 1:1,000 in assay buffer) on a Synergy 2 multi-mode plate reader (BioTek).

Bead-Based Multiplex Immunoassays

Autoantibody responses were analyzed by using the Luminex technology as described previously (28). Briefly, all the biotinylated peptides were captured on beads coated with NeutrAvidin (Thermo Fischer Scientific). Human serum samples were diluted 1:100 (v/v) and purified antibodies were prepared into a final concentration of 1 µg/ml in assay buffer (3% BSA, 5% milk powder, 0.1% ProClin300, 0.05% Tween 20, 100 µg/ml NeutrAvidin in PBS) and incubated for 1 h at RT on a shaker. Then, the samples were either transferred to a 384-well plate (Greiner Bio-One) containing the peptide-coated beads by a liquid handler (CyBi-SELMA, CyBio) or to a 96-well plate (Greiner Bio-One) by

manual pipetting. After incubation at RT on a shaker for 75 min, all the beads were washed with 0.05% Tween-20 in PBS (PBST) on a plate washer (EL406, Biotek or Bioplex Pro Wash station, Biorad), and then resuspended in a solution containing the secondary anti-human, anti-mouse, or anti-rat IgG Fcγ-PE (Jackson Immuno Research). After 40 min of incubation, the beads were washed with PBST and the fluorescence intensity was measured using FlexMap3D or Luminex 200 (Luminex Corp.) instrument. The median fluorescence intensity (MFI) was used to quantify the interactions of the antibody with the given peptides. For the comparison of responses to peptides in human and rat samples, the ratio value, calculated by dividing the MFI value for the peptide of interest by the median MFI value of five cyclic control peptides, was used.

Patients

In the present study, samples from a subset of previously described Epidemiological Investigation of RA (EIRA) cohort (29), consisting of 1,984 RA patients, included at disease onset and 400 age and sex-matched healthy controls, were used. RA was defined according to the American College of Rheumatology (ACR) 1987 criteria (30). This study was carried out in accordance with the recommendations of EIRA 96-174, EIRA II 2006/476-31/4, and 2007/718-32 guidelines with written informed consent from all subjects. The protocol was approved by the ethics committee at the Karolinska Institute and by Regional Stockholm ethics committee.

Induction and Evaluation of Arthritis (CIA, PIA, CAIA)

Collagen II-induced arthritis (C^{II}IA) or collagen XI-induced arthritis (C^{XI}IA) was induced by an intradermal injection of 100 μg of rCII or rCXI emulsified in an equal volume of CFA in DBA/1J mice, respectively. Followed with a booster, immunization of 50 μg of rCII or rCXI emulsified in IFA on day 21. 100 μg rCII emulsified in an equal volume of IFA or 100 μl of Pristane (2,6,10,14 tetramethylpentadecane, 95%, Acros Organics, Morris Plains, NJ, USA) was injected intradermally to induce C^{II}IA or PIA (21, 31) in 8–12 weeks old DA rats.

The J1 epitope (MPGERGAAGIAGPK)-specific antibody M2139 used in this study was produced as described earlier (32). The cocktail of two monoclonal antibodies was prepared by mixing equal concentrations of each of the sterile filtered antibody solution to achieve a final amount of 9 mg. Mice were injected with either 9 mg of M2139 + L10D9, M2139 + L5F3 or L10D9, or 4.5 mg of M2139 antibodies intravenously. All the mice received (25 μg/mouse) lipopolysaccharide from *Escherichia coli* O55: B5 (Sigma-Aldrich, Saint Louis, MO, USA) intraperitoneally on day 5 to enhance the disease incidence and severity.

Mice and rats were examined for arthritis development with the identity of the animals blinded for the investigator using an extended scoring protocol. Briefly, clinical arthritis is defined as swelling and redness in the joint and was scored as below: 1 point for each inflamed toe or knuckle, 5 points for an inflamed wrist or ankle, resulting in a maximum of 15 points per limb and a maximum of 60 points per animal (33).

Histology

To investigate the antibody binding with joints *in vivo* and *in vitro*, limbs from 2 days old neonatal BQ.Cia9i mice injected intraperitoneally with 100 μg biotinylated M2139, L10D9, L5F3, L7D8 antibodies, or PBS were collected and snap frozen, cryosectioned, whereas the paws from adult healthy or chronic C^{II}IA mice were harvested, fixed, decalcified, dehydrated, paraffin-embedded, and 7 μm thick sections were used. The sections from biotinylated antibodies injected mice were fixed in 4% paraformaldehyde for 5 min. The sections from naïve neonatal mice, and from paraffin-embedded joints, which underwent antigen retrieval, were subjected to 5 μg/ml biotinylated M2139, L10D9, L5F3, L7D8 antibodies, or PBS for 40 min in RT. After blocking with 3% H_2O_2 for 10 min, 5% BSA + 2% rat sera for 30 min, streptavidin for 15 min, biotin for 15 min, all the sections were incubated with ExtrAvidin-Peroxidase solution (Sigma-Aldrich, Saint Louis, MO, USA) for 30 min and developed with diaminobenzidine (DAB Kit; Dako, Copenhagen, Denmark) for 8–9 min (sections from biotinylated antibodies injected mice) or 3 min (sections from naïve neonatal, adult healthy, and chronic C^{II}IA mice).

For histological assessments, paws from the BQ.Cia9i and B10RIII mice used for CAIA experiments were dissected, fixed, decalcified, dehydrated, and then paraffin-embedded. Sections (7 μm) were stained with hematoxylin/eosin to observe joint morphology.

Immunofluorescence

Six-week-old BQ.Cia9i mice were injected with 1 mg of biotinylated M2139, L10D9, L5F3, L7D8 antibodies, or PBS intravenously. After 24 h, the nose was harvested, snap frozen, and kept in −80°C. Transversal snout sections (7 μm) were fixed in acetone on ice for 10 min, dried for 10 min, and hydrated in 1× PBS for 15 min. After blocking with 1× PBS containing 2% BSA + 0.1% Tween-20 for 45 min, the sections were incubated with streptavidin-conjugated Alexa Fluor 568 (Invitrogen, S11226, 1:300 diluted) for 60 min in RT and mounted using VECTASHIELD® Mounting Medium with DAPI (Vector, H-1200). The slides were dried for 15–30 min before scanning under a confocal microscope.

Statistical Analyses

Quantitative data are expressed as a mean ± SEM. Arthritis incidence was analyzed using Fisher's exact test, whereas the comparison of arthritis severity and serum antibody response between groups were performed using the non-parametric Mann–Whitney *U*-test. Pearson correlation test was used for analyzing the correlation of antibody response to arthritis disease severity. *p*-Values less than 0.05 were considered statistically significant.

RESULTS

Serum Antibody Response to CII and CXI in Mice

In order to understand the potential relationships between serum antibody profiles and arthritis development in C^{II}IA and C^{XI}IA,

we immunized the A^q-expressing DBA/1J mice with rCII or rCXI. Sera were collected on days 21 and 70. We observed severe arthritis with high frequency in C^{II}IA mice but only very mild disease with low frequency in C^{XI}IA mice (**Table 1**). Elevated serum antibody responses to CII and CXI were observed throughout the disease course in both C^{II}IA and C^{XI}IA mice, and the responses were increasing with time. Anti-CXI antibody response in C^{II}IA mice was higher than that in C^{XI}IA mice in the early stage (day 21: $p = 0.0009$), but not in the late stage (day 70: $p = 0.1393$) (**Figure 1**). No correlation could be observed between levels of the anti-CII/CXI antibody responses and disease severity (data not shown).

CXI Harbors the Same T Cell Glycosylated Epitope (Glycosylation at Position 264) as CII

To investigate whether CII and CXI harbor the same T cell epitope, T cell hybridomas HCQ3 and HCQ4, which are specific for glycosylated CII259-273 (GalCII259-273, glycosylation at position 264) and naked CII259-273 (nCII259-273, lysine at position 264) peptide, respectively, were used for T cell recall assay. HCQ3 showed a response to both native and denatured bCXI, but at a lower level compared to that of rCII and denatured rCII (**Figures 2A,B**). HCQ4 did not react to either native or denatured bCXI (**Figures 2C,D**). These data showed that CXI harbors the same posttranslationally modified epitope, which has glycosylation at position 264 as that of CII. The sequence alignment for T cell epitope between two different species was shown (Figure S2 in Supplementary Material).

TABLE 1 | Disease incidence and Max arthritis score of C^{II}IA and C^{XI}IA mice.

Immunogen	Strain	Gender	Age (weeks)	Incidence	Max arthritis score (mean ± SEM)
CII/CFA	DBA/1J	Male	10	7/8	20.13 ± 3.451
CXI/CFA	DBA/1J	Male	10	1/8	0.25 ± 0.25

C^{II}IA, collagen II-induced arthritis; C^{XI}IA, collagen XI-induced arthritis; CII, collagen II; CXI, collagen XI; CFA, complete Freund's adjuvant; IFA, incomplete Freund's adjuvant.

Generation and Characterization of Anti-CXI Monoclonal Antibodies

A series of 19 anti-CXI monoclonal antibodies were generated from DBA/1J mice immunized with bCXI protein. Antibodies with different isotypes and affinities to rCII, rCXI and bCXI were shown in the table (**Table 2**). L10D9 showed a strong binding to rCII, rCXI, bCXI, and their denatured forms, as revealed by ELISA (**Figure 3A**). L5F3 and L7D8 bound strongly to native rCXI and bCXI, but not their denatured forms. In contrast, a weak (L5F3) or no (L7D8) binding to CII was observed, indicating that these two clones bound specifically to CXI (**Figure 3A**).

To identify the potential binding of CXI antibodies to cross-reactive epitopes between α3(XI) and α1(II), we performed bead-based multiplex immunoassay using 198 triple helical CII peptides, including those with citrulline modified versions. L10D9 showed a unique binding to the triple helical peptides covering the D3 epitope of CII (34), both unmodified and modified forms, but neither the corresponding cyclic peptides covering the same region nor other CII peptides (**Figure 3B**) showed reactivity. The same specificity could also be confirmed using ELISA (**Figure 3B**). CIIC2, an antibody specific for the D3 epitope of CII, showed positive binding (**Figure 3B**). No such binding could be found for L5F3, L7D8, and other CXI specific antibodies in our current CII peptides library (data not shown).

In order to study which α chains of CXI are needed for the binding of the L10D9 antibody to the antigens, a heterotrimeric CXI_T_D3 peptide of 24 amino acid in length was synthesized. L10D9 bound specifically to this peptide, which indicated that only the α chain shared between CXI and CII [α3(XI)/α1(II)] was needed for binding of this antibody. The CII-specific CIIC2 antibody failed to bind to the CXI_T_D3 peptide indicating that more than one α chain from CII was needed for binding of this antibody (**Figure 3C**). The binding of L10D9 to α3(XI)/α1(II) was further confirmed by SDS-PAGE and Western blot. L10D9 showed unique binding to α3(XI) and α1(II), while the CII specific control antibody M2139 bound only to α1(II) (**Figure 3D**). L10D9, a CXI-responding antibody, cross-reacts to CII due to sequence identity (GPTGVTGPKGARGAQGPOGATGFO). The

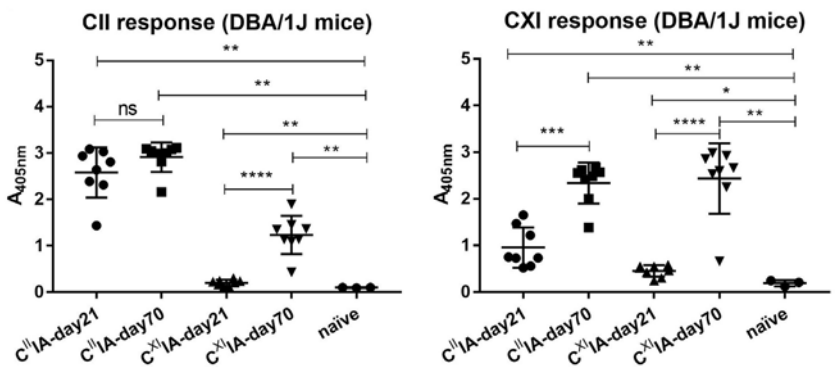

FIGURE 1 | Serum antibody response to native CII and CXI in C^{II}IA and C^{XI}IA mice. Serum antibody response to native CII (left panel) and CXI (right panel) protein on day 21 or day 70 were measured in C^{II}IA and C^{XI}IA DBA/1J mice using enzyme-linked immunosorbent assays (ELISA). Naïve mice sera samples were served as negative control. Mann–Whitney *U*-test was used for group comparison.

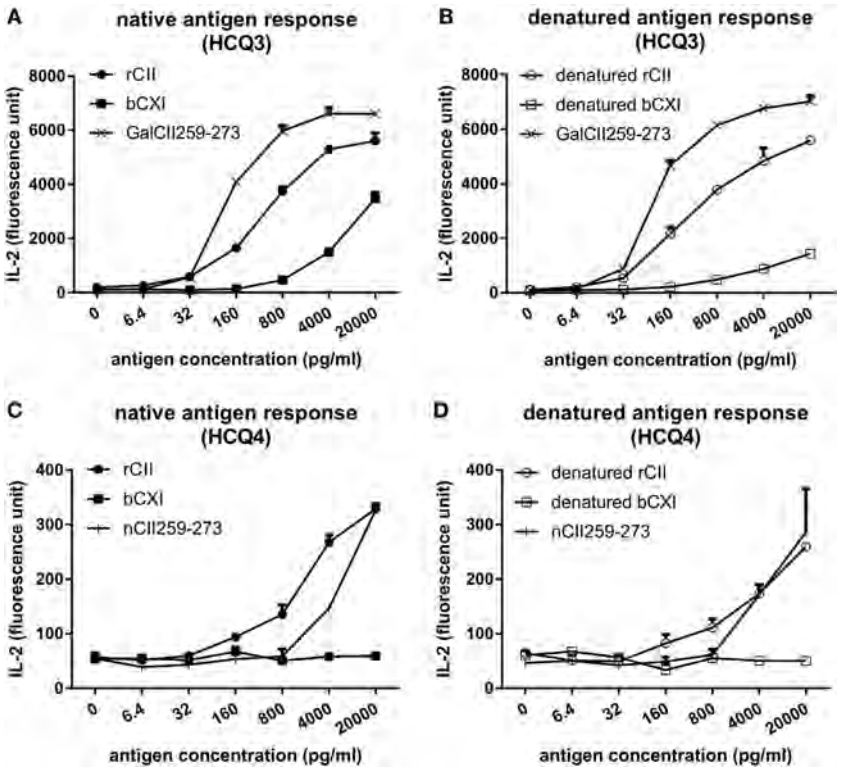

FIGURE 2 | T cell recall assay for CII and CXI. The response of HCQ3 and HCQ4 hybridoma to native **(A,C)** and denatured **(B,D)** collagens. The supernatant was collected and the IL-2 secretion was measured by cytokine enzyme-linked immunosorbent assay. Glycosylated CII259-273 peptide (GalCII259-273) and naked CII259-273 peptide (nCII259-273) were served as positive control peptides for HCQ3 and HCQ4 hybridoma, respectively. rCII, rat Collagen II; bCXI, bovine collagen XI.

TABLE 2 | The characteristics of 19 monoclonal CXI antibodies.

Clones	Isotype	bCXI	rCXI	rCII	Bind cartilage
L3C11	IgG1	+	+	+	P
L5F3	IgG2b	++	++	+	P
L10D5	IgG2b	++	++	+	P
L10D9	IgG2a	+++	+++	++++	P
L13G8	IgG2b	++	++	+	P
L1D7	IgG2b	++	–	–	N
L1D8	IgG2b	++	++	–	N
L2D9	IgG2a, 2b	+	–	–	N
L2G11	IgG2b	–	+	–	N
L3E2	IgG2b	+	+	–	N
L7A2	IgG2b	+	+	–	N
L7B6	IgG1	++	++	+	N
L7D8	IgG2a	++	++	+	N
L7H5	IgG2b	+++	+	–	N
L8F2	IgG1	++	++	+	N
L10B9	IgG2a	+++	–	–	N
L11C5	IgG1	+++	+++	+	N
L14E2	IgG1	+	+	–	N
L16G4	IgG1	+++	–	+	N

Scale for optical density (OD) values: – denotes <3 times SEM of negative control; + denotes >mean + 3SD of negative control; ++ denotes >0.5 OD; +++ denotes >1.0 OD; ++++ denotes >1.5 OD. P, positive binding to the cartilage; N, negative binding to the cartilage; rCXI, rat CXI.

CIID3 and CXID3 peptide sequences and the sequence alignments among four different species are shown in **Figure 3E** and Figure S2 in Supplementary Material.

D3 Epitope-Specific Antibody Binds Cartilage, While CXI Specific Antibodies Showed Negligible or Very Weak Binding

To test whether L10D9, L5F3, and L7D8 antibodies could bind to neonatal and adult cartilage *in vivo*, these antibodies were biotinylated and then injected intraperitoneally into neonatal or 6 weeks old BQ.Cia9i mice. The biotinylated M2139 antibody was used as a positive control. Joint tissues from the neonatal and snout tissues from the adult mice were obtained 24 h later after injection, and tissues were analyzed for antibody binding by immunohistochemistry (due to the difficulty of the sectioning for adult joints, we took snout tissue). The L10D9 antibody showed a similar staining pattern as the anti-CII antibody M2139, with specific binding along neonatal cartilage surface. L5F3 and L7D8 antibodies showed no clear and specific staining (**Figure 4A**, upper panel). In the adult tissue, the L10D9 antibody demonstrated strong staining along the cartilage surface. The CXI-specific antibody L5F3 showed a similar but weaker staining as compared to the anti-CII antibody, whereas the binding of the L7D8 antibody to the adult tissue was not detected (**Figure 4A**, bottom panel).

For the *in vitro* binding capacity of the L10D9 antibody to cartilage, paw sections from naïve neonatal BQ.Cia9i, adult mice with or without arthritis were incubated with biotinylated M2139, L10D9, L5F3, or L7D8 antibodies, followed by detection of antibodies binding to the sections. Both L10D9 and L5F3

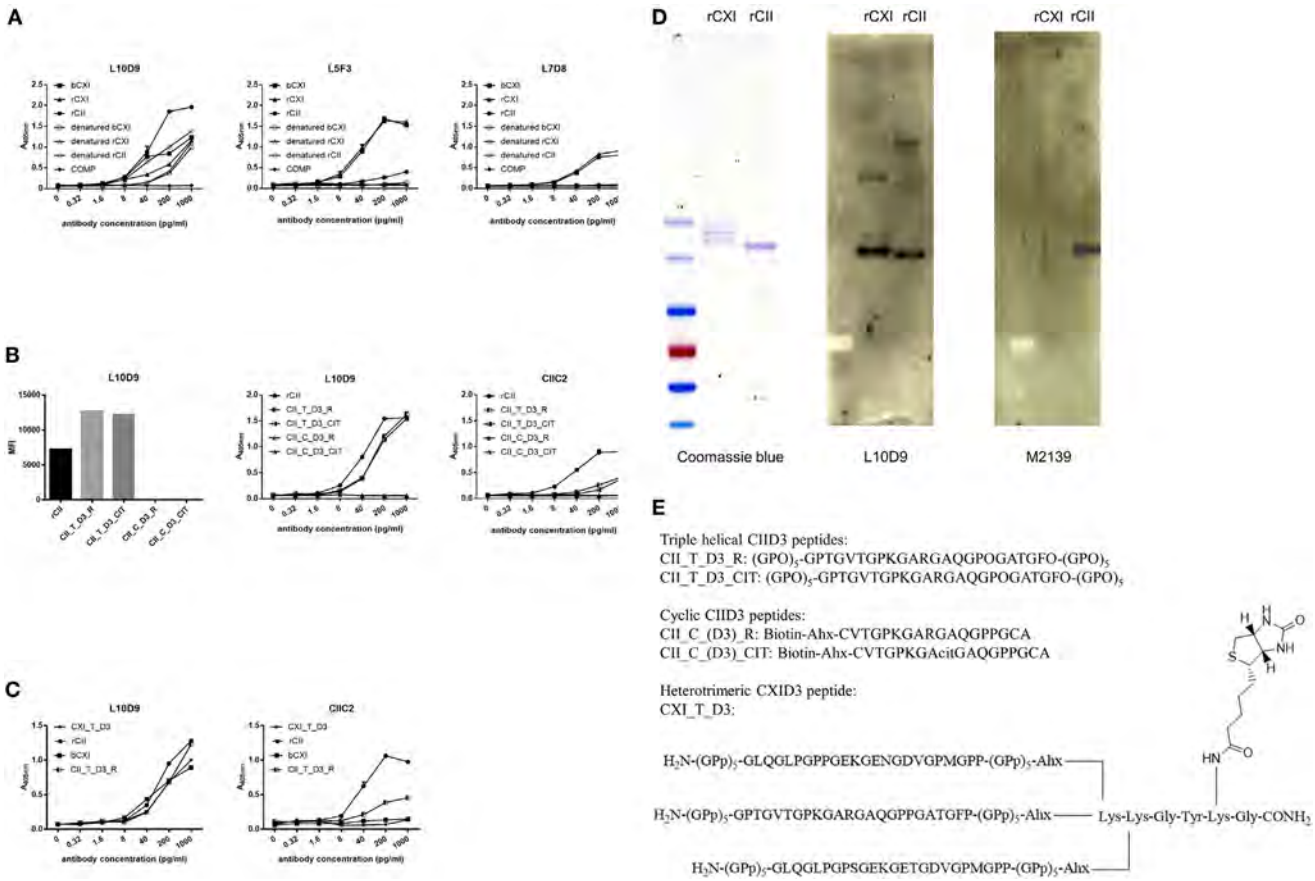

FIGURE 3 | L10D9 binds to CXI, cross-react with CII due to sequence similarity. **(A)** Kinetics of L10D9, L5F3, and L7D8 antibody response to bCXI, rCXI, rCII, and their denatured forms. Cartilage oligo matrix protein (COMP) was served as a negative control. Bead-based multiplex immunoassays [**(B)**, left panel] and enzyme-linked immunosorbent assays (ELISA) [**(B)**, middle and right panel] were used for the epitope mapping of L10D9. **(C)** The binding of L10D9 and CIIC2 to the heterotrimeric CXI_T_D3 peptide. **(D)** SDS-PAGE for rCXI and rCII (left panel). Western blotting for L10D9 (middle panel) and M2139 (right panel). **(E)** Sequence of the peptides involved in ELISA and bead-based multiplex immunoassays.

antibodies showed clear cartilage staining on the tissue sections from neonatal as well as adult healthy and sick mice, whereas L7D8 antibody binding was negative (**Figure 4B**).

L10D9 Induces and Enhances Acute Arthritis in Naïve Mice, but Not the CXI-Specific Antibody

To investigate the arthritogenicity of the antibodies, 8–17 weeks old BQ.Cia9i male mice were injected with 4.5 mg of M2139, 9 mg of L10D9, M2139 + L5F3, or M2139 + L10D9 antibody intravenously. A single injection of M2139 or L10D9 antibody induced very mild arthritis, while M2139 antibody combined with L10D9 antibody developed more severe disease compared to M2139 group ($p < 0.05$) (**Figure 5A**). The same finding is also seen in the B10RIII strain, suggesting that L10D9 has the capacity to induce mild arthritis by itself and a strong enhancing arthritis effect when combined together with the M2139 antibody (**Figure 5B**). No arthritis enhancing effect can be found for L5F3 antibody (**Figure 5C**). Representative histology pictures from each group show the infiltrating cells, glycosaminoglycan loss, and joint surface erosions (**Figure 5D**).

Elevated Antibody Response to the D3 Epitope in RA Patients and Arthritic Rodents

To investigate the value of D3 epitope response in a clinical setting and to serologically characterize the experimental rodent models; sera from humans, rats, and mice were measured for the response toward D3 epitope. We found that serum antibody response to D3 epitope was significantly elevated in RA patients' sera in the EIRA cohort compared to healthy controls ($p < 0.0001$). In particular, strong responses were found toward the citrullinated D3 variant (CII_T_D3_CIT) (**Figure 6A**, left and middle panel). We next investigated whether similar responses can be detected in murine models of arthritis. In rats, at day 23 after immunization with CII/IFA or Pristane, the anti-CII antibody response was most pronounced in those injected with Pristane followed by CII-immunized animals and, both types of immunization

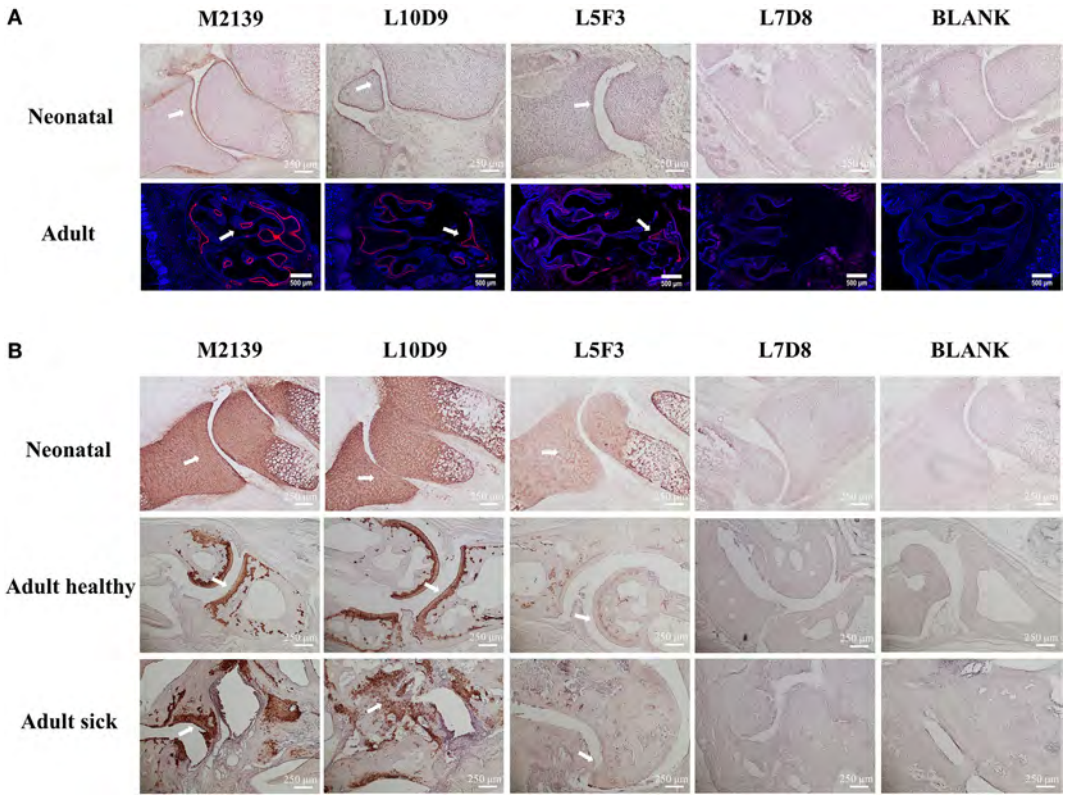

FIGURE 4 | L10D9 binds to cartilage both *in vivo* and *in vitro*. *In vivo* **(A)** and *in vitro* **(B)** histology staining of joint or transversal snout sections are shown. Positive binding to cartilage surfaces are marked by arrows.

mounted a CII_T_D3 specific responses that were significantly increased compared to naïve rats (**Figure 6A**, right panel). Similar findings were observed in C^{II}IA mice. Anti-D3 epitope response against CXI_T_D3, CII_T_D3_R (arginine version), and CII_T_D3_CIT (citrulline version) peptides can be found throughout the disease course, which increased as the disease progressed with time (**Figure 6B**).

To understand the value of the anti-D3 antibody response in disease development, we correlated D3 epitope specific antibody response to total arthritis score in C^{II}IA mice. Both the antibody response to CXI_T_D3 and to CII_T_D3_R was positively correlated with disease severity, but not the anti-CII_T_D3_CIT response (**Figure 6C**). We also observed increased antibody response to other major CII epitopes and the positive correlation between the antibody response to the C1 epitope and arthritis severity in C^{II}IA mice (Figures S1A,B in Supplementary Material).

DISCUSSION

Antibodies targeting cartilage is likely an important step toward arthritis development in both humans and experimental animals. Here, we have identified the structural requirements for an antibody mediated cross-reactive response to CII and CXI, which could explain why this response is highly arthritogenic. Collagen fibers in normal articular cartilage are mainly composed of CII together with the minor components CIX and CXI, in which CXI molecules are intermingled in the cartilage collagen fibers. CXI and CII molecules have similar triple helix structure, with three identical α chains for CII and three different α chains for CXI, in which α3(XI) is coded from the same gene as α1(II). Several studies indicate the potential arthritogenic and immunogenic effects of CXI in mice (16, 17). In our current study, we could only observe very mild disease with a low incidence of arthritis after immunization with CXI in mice, while in parallel, the C^{II}IA mice developed severe arthritis with high incidence. Elevated serum antibody response against CII and CXI could be found throughout the disease process in both C^{II}IA and C^{XI}IA mice, which increased with time. Both serum CII and CXI antibody responses were significantly higher in C^{II}IA compared to C^{XI}IA mice, except the anti-CXI antibody responses during the late stage of the disease. One possible explanation for the cross-reactive responses could be the common α chain between CII and CXI, the other could be due to the destruction of cartilage and subsequent exposure of CXI molecules during arthritis development. It is well known that injection of antibodies specific for CII after binding to cartilage *in vivo* can induce arthritis in rodents (32). High level of antibodies against CII could be the reason why C^{II}IA mice developed severe disease compared to C^{XI}IA mice, which had a much lower level of CII antibody titer. Although there was a high titer of CXI specific antibodies existing in C^{XI}IA mice, those antibodies could not contribute to the disease because the CXI molecules are not exposed for binding of antibodies *in vivo*. A perquisite for a

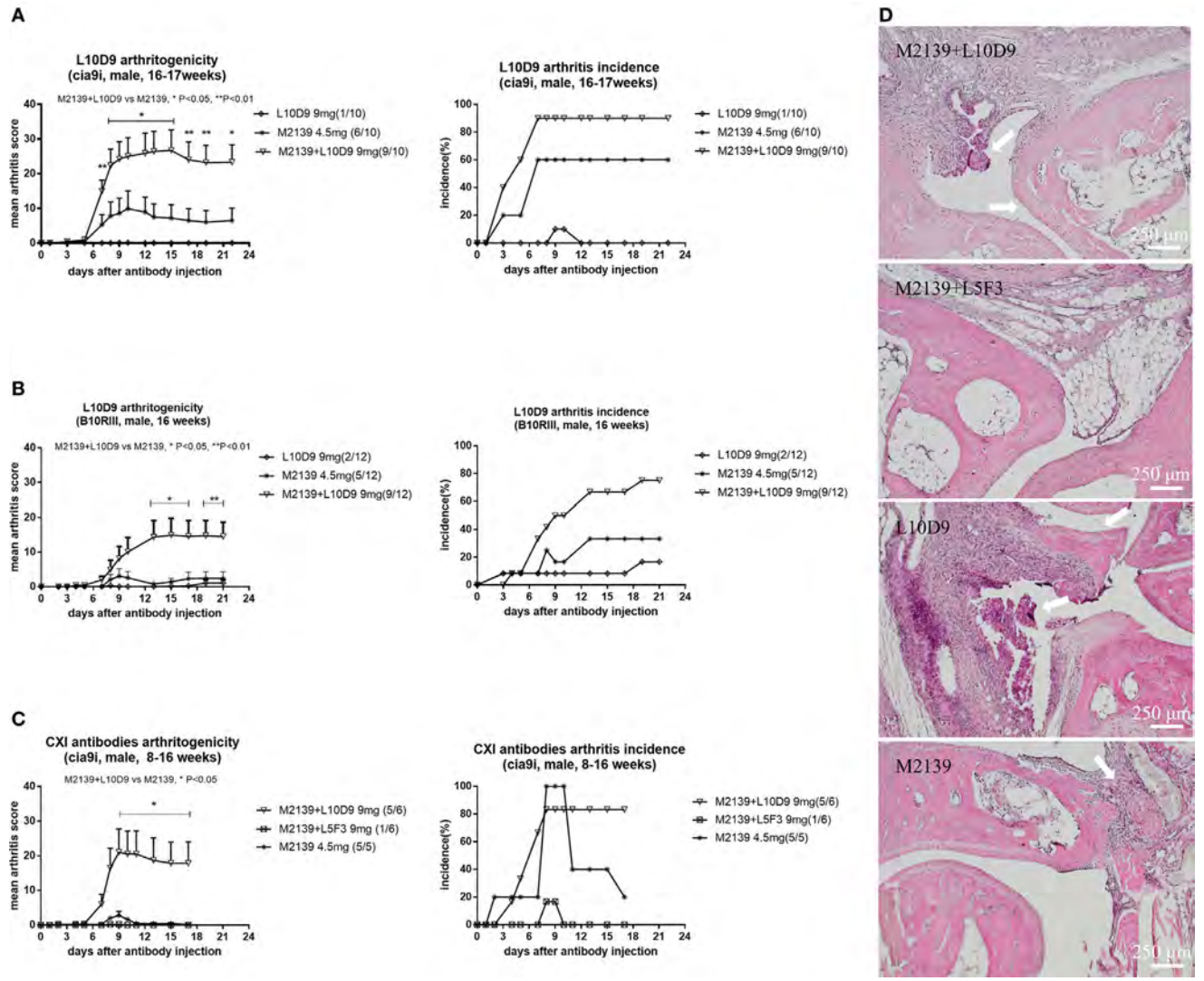

FIGURE 5 | L10D9 mediates arthritis in mice. Mean arthritis score and arthritis incidence in B10RIII strain **(B)** and BQ.Cia9i strain **(A,C)** are indicated. **(D)** Histology of joint sections. Results shown are representative pictures of each group. Infiltrating cells, glycosaminoglycan loss, and joint surface erosions are indicated with arrows. Statistics were determined by the Mann–Whitney *U*-test for daily mean arthritis score and Fisher's exact test for the disease incidence between groups.

strong immune response to CXI is that T cell could be specifically activated, and here, we could show that native CXI harbored the same glycosylated T cell epitope (GalCII259-273, glycosylation at position 264) as CII. Though the response to CXI by Gal-264-specific T cell hybridoma is significantly lower than to CII, this could be explained by the amount of the identical alpha chain containing the T cell epitope, as CII is a homotrimer whereas CXI only have one chain (α3) with the epitope. However, it can still be the difference in glycosylation pattern, in particular, with other forms of the lysine 264 side chain or glycosylation at the lysine 270 side chain, which is not addressed here. However, Gal-264, the most important glycosylation form for activation of T cells are present on CXI. The sequence similarity and shared T cell epitope is a prerequisite for the occurrence of high-affinity IgG cross-reactive antibodies after CII or CXI protein immunization.

We believe our most interesting finding is that we could isolate a CXI/CII cross-reactive autoantibody L10D9, from mice immunized with CXI, which could contribute to the development of arthritis. The L10D9 needed only one common α chain for successful binding, and it is possible that the alpha chains are partially flexed out from the triple helical structure in order to be accessible. This finding was further confirmed by Western blotting, showing that L10D9 only bound to the α3 chain of CXI and α1 chain of CII. The identified epitope is localized to an earlier defined CII epitope, denoted as D3. The L10D9 antibody also bound successfully to the synthesized heterotrimeric CXI_T_D3 peptide in which α3(XI) has the same sequence to α1(II) but not to the linear peptide with the same sequence as the CII_T_D3 triple helix peptide (data not shown). Thus, the epitope is most likely exposed by a structure formed by a

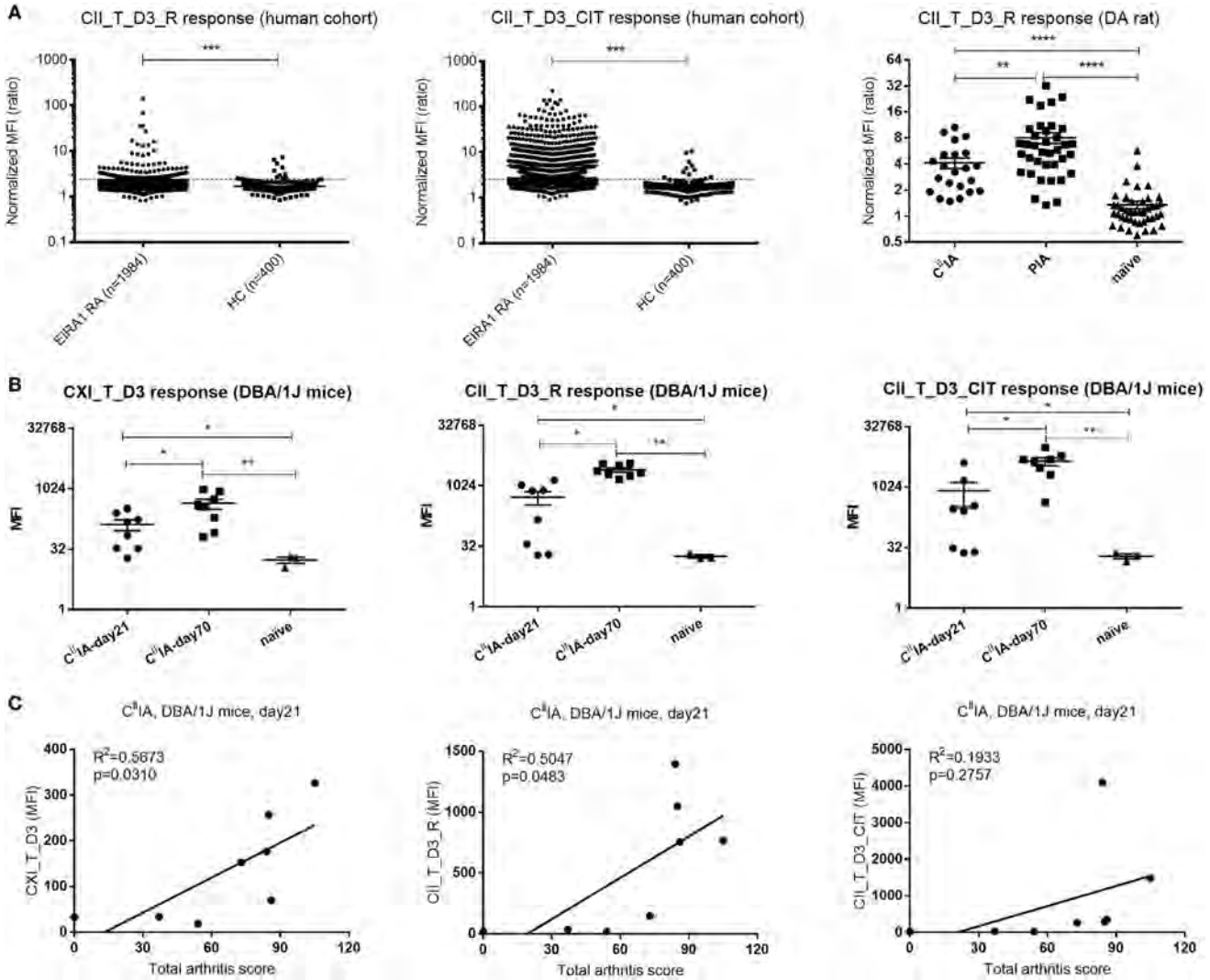

FIGURE 6 | The D3 epitope response in Epidemiological Investigation of RA (EIRA) cohort and arthritic rodents, and the correlation between D3 epitope response and arthritis severity in CIIIA mice. **(A)** IgG response of the (EIRA) cohort (rheumatoid arthritis: n = 1,984, HC: n = 142) to CII_T_D3_R and CII_T_D3_CIT (left and middle panel). The broken line indicates the cutoff (median + 5 × MAD) based on healthy controls. Anti-collagen antibody level against CII_T_D3_R peptide in CIIIA (n = 23), Pristane-induced arthritis model (n = 37), and naïve (n = 44) DA rats (right panel). Data are shown as normalized mean fluorescence intensity (MFI) ± SEM. **(B)** Anti-collagen antibody against CXI_T_D3, CII_T_D3_R and CII_T_D3_CIT in CIIIA DBA/1J mice. **(C)** Correlation between serum antibody response to CXI_T_D3, CII_T_D3_R, and CII_T_D3_CIT and total arthritis score in CIIIA mice. Statistics were determined by the Mann–Whitney U-test and Pearson correlation test for group comparison and correlation analysis, respectively.

partially unwound alpha chain from the triple helical structure. The L10D9 antibody bound as strongly as CII antibody to cartilage *in vivo* and *in vitro* whereas the CXI specific antibodies showed either much weaker or negligible staining. The weak staining could possibly be explained by the low level of cross-reactivity of L5F3 antibody to CII (see the ELISA result), and the absence of positive staining for the highly specific CXI antibody L7D8 further confirms that CXI molecules are not exposed in the joint tissue for binding. This likely also explains that the CXI specific antibodies could not induce arthritis. The situation could, however, be different in affected joints as it is then possible that more CXI molecules are exposed and accessible for both inducing not only a specific B cell response but also for targeting with antibodies at a later stage.

Importantly the L10D9 antibody is highly arthritogenic and is among the few antibodies that can actually induce arthritis by itself. Induction of arthritis by antibodies is clearly much more efficient if exposed to polyclonal or oligoclonal antibodies, but a few monoclonal antibodies seem to have the property to induce arthritis by themselves. Examples of these include the anti-CII antibody M2139, used in this study, the anti-citrulline protein antibody ACC1 that cross-reacts to CII (35) and the CXI-CII cross-reactive antibody L10D9 described in the current study. All of these antibodies seem to have the possibility to target a

single alpha chain within a triple helical structure, i.e., targeting a structure formed by a dynamically flexed out alpha chain from an unstable triple helical molecule and with the capacity to strongly bind to cartilage *in vivo*.

Furthermore, we detected antibodies targeting CII, CXI, or the triple helical D3 epitope during the development of arthritis in both experimental animal models and in RA patients. It is likely that such antibodies play a pathogenic role and could further perpetuate the disease during the chronic relapsing state of the disease.

ETHICS STATEMENT

The human study was carried out in accordance with the recommendations of EIRA 96-174, EIRA II 2006/476-31/4, and 2007/718-32 guidelines with written informed consent from all subjects. The protocol was approved by the ethics committee at the Karolinska Institutet and by Regional Stockholm ethics committee. The animal study was carried out in accordance with the recommendations of N490/12, N35/16 (Stockholm ethical committee) and 86/609/EEC guidelines (European Community Council Directive). The protocols were approved by local animal welfare authorities.

AUTHOR CONTRIBUTIONS

DT: designed the study, performed most of the experiments, data analysis, interpreted the data, and wrote the first draft of the manuscript. EL, BL, and AY: performed experiments, helped with data analysis interpretation, and manuscript writing. KN, CG, and IG: helped with experimental design and corrected manuscript. JV and JK: helped with triple helical peptide synthesis and analysis and corrected manuscript. LL, AC, and MB: helped with confocal analysis and corrected manuscript. LK: provided human cohort. RH: designed the study, data interpretation, manuscript writing, and supervised the project. All authors approved the final manuscript.

ACKNOWLEDGMENTS

The Swedish Strategic Science Foundation, Knut and Alice Wallenberg Foundation, Swedish Research Council, and the Pharmacy school of Southern Medical University supported this study. We acknowledge team grant from Guangdong province (201001Y04675344), matching grant from Dongguan city, and a grant (C1034211) from SMU, PR China. We would like to thank Carlos Palestro, Kristina Palestro, Evelina Wernersson, and Lu Li for the excellent animal care. We also thank Peter Nilsson and Burcu Ayoglu from Sci-life for the contribution of Luminex data; Emma Mondoc and Yi Jin for work with histology and confocal microscopy; Susanne Van Den Berg for CXI purification; Amit Saxena, Johan Bäcklund, Naru Zhang, Jianghong Zhong for T cell assays; Bingze Xu, Wenhua Zhu, Bruno Raposo, Daniëlle Vaartjes, Vilma Urbonaviciute, and Tenghao Zheng for their great help and suggestions.

SUPPLEMENTARY MATERIAL

The Supplementary Material for this article can be found online at https://www.frontiersin.org/articles/10.3389/fimmu.2018.00451/full#supplementary-material.

REFERENCES

1. Choy E. Understanding the dynamics: pathways involved in the pathogenesis of rheumatoid arthritis. *Rheumatology* (2012) 51:v3–11. doi:10.1093/rheumatology/kes113
2. Edwards JCW, Szczepański L, Szechiński J, Filipowicz-Sosnowska A, Emery P, Close DR, et al. Efficacy of B-cell-targeted therapy with rituximab in patients with rheumatoid arthritis. *N Engl J Med* (2004) 350:2572–81. doi:10.1056/NEJMoa032534
3. Svensson L, Jirholt J, Holmdahl R, Jansson L. B cell-deficient mice do not develop type II collagen-induced arthritis (CIA). *Clin Exp Immunol* (1998) 111:521–6. doi:10.1046/j.1365-2249.1998.00529.x
4. Geng H, Nandakumar KS, Pramhed A, Aspberg A, Mattsson R, Holmdahl R. Cartilage oligomeric matrix protein specific antibodies are pathogenic. *Arthritis Res Ther* (2012) 14:R191. doi:10.1186/ar4022
5. Nandakumar KS, Holmdahl R. Efficient promotion of collagen antibody induced arthritis (CAIA) using four monoclonal antibodies specific for the major epitopes recognized in both collagen induced arthritis and rheumatoid arthritis. *J Immunol Methods* (2005) 304:126–36. doi:10.1016/j.jim.2005.06.017
6. Eyre D. Collagen of articular cartilage. *Arthritis Res* (2002) 4:30–5. doi:10.1186/ar380
7. Furuto DK, Miller EJ. Different levels of glycosylation contribute to the heterogeneity of alpha 1(II) collagen chains derived from a transplantable rat chondrosarcoma. *Arch Biochem Biophys* (1983) 226:604–11. doi:10.1016/0003-9861(83)90329-6
8. Holmes DF, Kadler KE. The 10+4 microfibril structure of thin cartilage fibrils. *Proc Natl Acad Sci U S A* (2006) 103:17249–54. doi:10.1073/pnas.0608417103
9. Li Y, Lacerda DA, Warman ML, Beier DR, Yoshioka H, Ninomiya Y, et al. A fibrillar collagen gene, Col11a1, is essential for skeletal morphogenesis. *Cell* (1995) 80:423–30. doi:10.1016/0092-8674(95)90492-1
10. Körkkö J, Cohn DH, Ala-Kokko L, Krakow D, Prockop DJ. Widely distributed mutations in the COL2A1 gene produce achondrogenesis type II/hypochondrogenesis. *Am J Med Genet* (2000) 92:95–100. doi:10.1002/(SICI)1096-8628(20000515)92:2<95:AID-AJMG3>3.0.CO;2-9
11. Annunen S, Körkkö J, Czarny M, Warman ML, Brunner HG, Kääriäinen H, et al. Splicing mutations of 54-bp exons in the COL11A1 gene cause marshall syndrome, but other mutations cause overlapping marshall/stickler phenotypes. *Am J Hum Genet* (1999) 65:974–83. doi:10.1086/302585
12. Mendler M, Eich-Bender SG, Vaughan L, Winterhalter KH, Bruckner P. Cartilage contains mixed fibrils of collagen types II, IX, and XI. *J Cell Biol* (1989) 108:191–7. doi:10.1083/jcb.108.1.191
13. Tuncel J, Haag S, Carlsén S, Yau ACY, Lu S, Burkhardt H, et al. Class II major histocompatibility complex-associated response to type XI collagen regulates the development of chronic arthritis in rats. *Arthritis Rheum* (2012) 64:2537–47. doi:10.1002/art.34461
14. Charríre G, Hartmann DJ, Vignon E, Ronzíre MC, Herbage D, Ville G. Antibodies to types i, ii, ix, and xi collagen in the serum of patients with rheumatic diseases. *Arthritis Rheum* (1988) 31:325–32. doi:10.1002/art.1780310303
15. Lu SM, Carlsen S, Hansson AS, Holmdahl R. Immunization of rats with homologous type XI collagen leads to chronic and relapsing arthritis with different genetics and joint pathology than arthritis induced with homologous type II collagen. *J Autoimmun* (2002) 18:199–211. doi:10.1006/jaut.2001.0581
16. Cremer MA, Terato K, Seyer JM, Watson WC, O'Hagan GO, Townes AS, et al. Immunity to type XI collagen in mice. Evidence that the alpha3(XI) chain of type XI collagen and the alpha1(II) chain of type II collagen share

arthritogenic determinants and induce arthritis in DBA/1 mice. *J Immunol* (1991) 146:4130–7.
17. Boissier MC, Chiocchia G, Ronziere MC, Herbage D, Fournier C. Arthritogenicity of minor cartilage collagens (types IX and XI) in mice. *Arthritis Rheum* (1990) 33:1–8. doi:10.1002/art.1780330101
18. Lindqvist A-K, Johannesson M, Johansson ACM, Nandakumar KS, Blom AM, Holmdahl R. Backcross and partial advanced intercross analysis of nonobese diabetic gene-mediated effects on collagen-induced arthritis reveals an interactive effect by two major loci. *J Immunol* (2006) 177:3952–9. doi:10.4049/jimmunol.177.6.3952
19. Klaczkowska D, Ekman D, Holmdahl R, Nandakumar KS. Identification of arthritis promoting non-obese diabetic genes in the *Cia9* locus using different genetic strategies. *Ann Rheum Dis* (2012) 71:.1–.60. doi:10.1136/annrheumdis-2011-201236.23
20. Nandakumar KS, Holmdahl R. A genetic contamination in MHC-congenic mouse strains reveals a locus on chromosome 10 that determines autoimmunity and arthritis susceptibility. *Eur J Immunol* (2005) 35:1275–82. doi:10.1002/eji.200425925
21. Yau ACY, Lönnblom E, Zhong J, Holmdahl R. Influence of hydrocarbon oil structure on adjuvanticity and autoimmunity. *Sci Rep* (2017) 7:14998. doi:10.1038/s41598-017-15096-z
22. Smith BD, Martin GR, Miller EJ, Dorfman A, Swarm R. Nature of the collagen synthesized by a transplanted chondrosarcoma. *Arch Biochem Biophys* (1975) 166:181–6. doi:10.1016/0003-9861(75)90378-1
23. Miller EJ, Rhodes RK. Preparation and characterization of the different types of collagen. *Methods Enzymol* (1982) 82:33–64. doi:10.1016/0076-6879(82)82059-4
24. Ge C, Tong D, Liang B, Lönnblom E, Schneider N, Hagert C, et al. Anti-citrullinated protein antibodies cause arthritis by cross-reactivity to joint cartilage. *JCI Insight* (2017) 2:93688. doi:10.1172/jci.insight.93688
25. Fields GB. Synthesis and biological applications of collagen-model triple-helical peptides. *Org Biomol Chem* (2010) 8:1237. doi:10.1039/b920670a
26. Michaëlsson E, Malmström V, Reis S, Engström A, Burkhardt H, Holmdahl R. T cell recognition of carbohydrates on type II collagen. *J Exp Med* (1994) 180:745–9. doi:10.1084/jem.180.2.745
27. Holmdahl R, Rubin K, Klareskog L, Larsson E, Wigzell H. Characterization of the antibody response in mice with type II collagen-induced arthritis, using monoclonal anti-type II collagen antibodies. *Arthritis Rheum* (1986) 29:400–10. doi:10.1002/art.1780290314
28. Ayoglu B, Häggmark A, Khademi M, Olsson T, Uhlén M, Schwenk JM, et al. Autoantibody Profiling in Multiple Sclerosis Using Arrays of Human Protein Fragments. *Mol Cell Proteomics* (2013) 12:2657–72. doi:10.1074/mcp.M112.026757
29. Klareskog L, Stolt P, Lundberg K, Källberg H, Bengtsson C, Grunewald J, et al. A new model for an etiology of rheumatoid arthritis: smoking may trigger HLA-DR (shared epitope)-restricted immune reactions to autoantigens modified by citrullination. *Arthritis Rheum* (2006) 54:38–46. doi:10.1002/art.21575
30. Arnett FC, Edworthy SM, Bloch DA, Mcshane DJ, Fries JF, Cooper NS, et al. The American rheumatism association 1987 revised criteria for the classification of rheumatoid arthritis. *Arthritis Rheum* (1988) 31:315–24. doi:10.1002/art.1780310302
31. Tuncel J, Haag S, Hoffmann MH, Yau ACY, Hultqvist M, Olofsson P, et al. Animal models of rheumatoid arthritis (I): pristane-induced arthritis in the rat. *PLoS One* (2016) 11:e0155936. doi:10.1371/journal.pone.0155936
32. Nandakumar KS, Svensson L, Holmdahl R. Collagen type II-specific monoclonal antibody-induced arthritis in mice. *Am J Pathol* (2003) 163:1827–37. doi:10.1016/S0002-9440(10)63542-0
33. Holmdahl R, Carlsen S, Mikulowska A, Vestberg M, Brunsberg U, Hansson A, et al. Genetic analysis of mouse models for rheumatoid arthritis. In: Kenneth WA, editor. *Human Genome Methods*. New York: CRC Press (1998). p. 215–38.
34. Schulte S, Unger C, Mo JA, Wendler O, Bauer E, Frischholz S, et al. Arthritis-related B cell epitopes in collagen II are conformation-dependent and sterically privileged in accessible sites of cartilage collagen fibrils. *J Biol Chem* (1998) 273:1551–61. doi:10.1074/jbc.273.3.1551
35. Uysal H, Bockermann R, Nandakumar KS, Sehnert B, Bajtner E, Engström A, et al. Structure and pathogenicity of antibodies specific for citrullinated collagen type II in experimental arthritis. *J Exp Med* (2009) 206:449–62. doi:10.1084/jem.20081862

Conflict of Interest Statement: The authors declare that the research was conducted in the absence of any commercial or financial relationships that could be construed as a potential conflict of interest.

frontiers in Immunology

MINI REVIEW
published: 09 April 2018
doi: 10.3389/fimmu.2018.00680

Pathogenetic and Clinical Aspects of Anti-Neutrophil Cytoplasmic Autoantibody-Associated Vasculitides

Peter Lamprecht[1], Anja Kerstein[1], Sebastian Klapa[1], Susanne Schinke[1], Christian M. Karsten[2], Xinhua Yu[3,4], Marc Ehlers[5], Jörg T. Epplen[6,7], Konstanze Holl-Ulrich[8], Thorsten Wiech[9], Kathrin Kalies[10], Tanja Lange[1], Martin Laudien[11], Tamas Laskay[12], Timo Gemoll[13], Udo Schumacher[14], Sebastian Ullrich[14,15], Hauke Busch[16], Saleh Ibrahim[16], Nicole Fischer[17], Katrin Hasselbacher[18], Ralph Pries[18], Frank Petersen[4], Gesche Weppner[1], Rudolf Manz[2], Jens Y. Humrich[1], Relana Nieberding[1], Gabriela Riemekasten[1] and Antje Müller[1]*

[1] Department of Rheumatology and Clinical Immunology, University of Lübeck, Lübeck, Germany, [2] Institute for Systemic Inflammation Research, University of Lübeck, Lübeck, Germany, [3] Xiamen-Borstel Joint Laboratory of Autoimmunity, Medical College of Xiamen University, Xiamen, China, [4] Priority Area Asthma and Allergy, Research Center Borstel, Airway Research Center North (ARCN), German Center for Lung Research (DZL), Borstel, Germany, [5] Laboratories of Immunology and Antibody Glycan Analysis, Institute for Nutrition Medicine, University of Lübeck and University Medical Center Schleswig Holstein, Lübeck, Germany, [6] Department of Human Genetics, Ruhr-University, Bochum, Germany, [7] University of Witten/Herdecke, ZBAF, Witten, Germany, [8] Institute of Pathology, Cath. Mary's Hospital, Hamburg, Germany, [9] Institute of Pathology, University Hospital Hamburg-Eppendorf, Hamburg, Germany, [10] Institute of Anatomy, University of Lübeck, Lübeck, Germany, [11] Department of Otorhinolaryngology, Head and Neck Surgery, University of Kiel, Kiel, Germany, [12] Department for Infectious Diseases and Microbiology, University of Lübeck, Lübeck, Germany, [13] Department of Surgery, Section for Translational Surgical Oncology and Biobanking, University of Lübeck, University Medical Center Schleswig-Holstein, Lübeck, Germany, [14] Institute of Anatomy and Experimental Morphology, Center for Experimental Medicine, University Cancer Center, University Medical Center Hamburg-Eppendorf, Hamburg, Germany, [15] Medical Department 3, Gastroenterology/Rheumatology, Municipal Hospital Kiel, Kiel, Germany, [16] Lübeck Institute of Experimental Dermatology, University of Lübeck, Lübeck, Germany, [17] Institute of Medical Microbiology, Virology and Hygiene, University Medical Center Hamburg-Eppendorf, Hamburg, Germany, [18] Department of Otorhinolaryngology, University of Lübeck, Lübeck, Germany*

OPEN ACCESS

Edited by:
Falk Nimmerjahn, Friedrich-Alexander-Universität Erlangen-Nürnberg, Germany

Reviewed by:
Thomas Hellmark, Lund University, Sweden
Matthew Cook, Australian National University, Australia

***Correspondence:**
Peter Lamprecht
peter.lamprecht@uksh.de

Specialty section:
This article was submitted to Immunological Tolerance and Regulation, a section of the journal Frontiers in Immunology

Received: *30 November 2017*
Accepted: *20 March 2018*
Published: *09 April 2018*

Citation:
Lamprecht P, Kerstein A, Klapa S, Schinke S, Karsten CM, Yu X, Ehlers M, Epplen JT, Holl-Ulrich K, Wiech T, Kalies K, Lange T, Laudien M, Laskay T, Gemoll T, Schumacher U, Ullrich S, Busch H, Ibrahim S, Fischer N, Hasselbacher K, Pries R, Petersen F, Weppner G, Manz R, Humrich JY, Nieberding R, Riemekasten G and Müller A (2018) Pathogenetic and Clinical Aspects of Anti-Neutrophil Cytoplasmic Autoantibody-Associated Vasculitides. Front. Immunol. 9:680. doi: 10.3389/fimmu.2018.00680

Anti-neutrophil cytoplasmic autoantibodies (ANCA) targeting proteinase 3 (PR3) and myeloperoxidase expressed by innate immune cells (neutrophils and monocytes) are salient diagnostic and pathogenic features of small vessel vasculitis, comprising granulomatosis with polyangiitis (GPA), microscopic polyangiitis, and eosinophilic GPA. Genetic studies suggest that ANCA-associated vasculitides (AAV) constitute separate diseases, which share common immunological and pathological features, but are otherwise heterogeneous. The successful therapeutic use of anti-CD20 antibodies emphasizes the prominent role of ANCA and possibly other autoantibodies in the pathogenesis of AAV. However, to elucidate causal effects in AAV, a better understanding of the complex interplay leading to the emergence of B lymphocytes that produce pathogenic ANCA remains a challenge. Different scenarios seem possible; e.g., the break of tolerance induced by a shift from non-pathogenic toward pathogenic autoantigen epitopes in inflamed tissue. This review gives a brief overview on current knowledge about genetic and epigenetic factors, barrier dysfunction and chronic non-resolving inflammation, necro-inflammatory auto-amplification of cellular death and inflammation, altered autoantigen presentation, alternative complement pathway activation, alterations within peripheral and inflamed

tissue-residing T- and B-cell populations, ectopic lymphoid tissue neoformation, the characterization of PR3-specific T-cells, properties of ANCA, links between autoimmune disease and infection-triggered pathology, and animal models in AAV.

Keywords: anti-neutrophil cytoplasmic autoantibodies, anti-neutrophil cytoplasmic autoantibody vasculitides, microscopic polyangiitis, granulomatosis with polyangiitis, eosinophilic granulomatosis with polyangiitis

INTRODUCTION

Anti-neutrophil cytoplasmic autoantibody (ANCA)-associated vasculitides (AAV) are classified into three distinct diseases based on clinical and pathological features: granulomatosis with polyangiitis (GPA, formerly Wegener's granulomatosis), microscopic polyangiitis (MPA), and eosinophilic granulomatosis with polyangiitis (EGPA, Churg–Strauss syndrome). Etiology and pathogenesis of AAV are multifactorial (1, 2). The pathogenesis appears to be initiated by a combination of predisposing genetic and environmental factors, altered autoantigen presentation, ectopic lymphoid tissue neoformation, and imbalance of effector and regulatory B- and T-cells. Consequently, production of pathogenic autoantibodies originating from precursor natural autoantibodies results in ANCA-induced activation of neutrophils and monocytes with subsequent activation of the alternative complement pathway, vascular damage, and self-perpetuating non-resolving chronic inflammation (2–4). Herein, we briefly summarize current ideas, observations, and evidence on the pathogenesis of AAV.

CLINICAL MANIFESTATIONS

While each of the three AAV retains a unique clinical phenotype, many manifestations are shared among them owing to the systemic nature of the underlying small-vessel vasculitis, and, in GPA and EGPA, granulomatous inflammation. Thus, pulmonary–renal syndrome is the dominating clinical feature in GPA and MPA (5, 6). In EGPA, renal involvement is associated with positive ANCA-status (7, 8). Prodromes such as malaise, arthralgias, myalgias—and rhinitis and/or sinusitis in GPA and EGPA—often precede manifestations of the pulmonary–renal syndrome by weeks or months (5–7). Fulminant AAV is rare (9). EGPA patients typically have a long-standing history of asthma and allergic rhinitis (7, 10). Other organs frequently affected are peripheral and central nervous system, skin, gut, and heart (5–7). Laboratory findings show elevated markers of inflammation (3, 11). GPA is highly associated with proteinase 3 (PR3)-specific ANCA, whereas MPA and—less commonly—EGPA are associated with myeloperoxidase (MPO)-specific ANCA (12–14). The majority of AAV patients (approximately 80–90%) present with renal or other organ-threatening manifestations, i.e., generalized disease. Relapse is more common in GPA (15). Renal-limited AAV is less common. Fewer than 10% of patients have a localized phenotype restricted to the upper and/or lower respiratory tract or early-systemic phenotype without imminent organ failure with less frequently detected ANCA (5, 11, 12, 16, 17). Progression from localized to generalized GPA is rare (16).

Treatment is guided by severity of organ involvement and disease activity. Various cytotoxic immunosuppressants and the monoclonal anti-CD20 antibody rituximab are recommended for the induction and maintenance of remission (18, 19). While treatment options have improved the prognosis of AAV, therapy de-escalation still carries an immanent risk of relapse (20). Major causes of death are vasculitis and infections (21). Optimizing treatment strategies according to prognostic subsets, autoantibody- and autoantigen-targeted therapies, and therapeutic interference with chronic inflammation and break of tolerance will set the stage for individualized precision medicine, further improvement of outcomes, and eventually cure of AAV (20, 22, 23).

PATHOLOGY

ANCA-associated vasculitidies are systemic necrotizing small-vessel vasculitides, predominantly affecting intraparenchymal small arteries, arterioles, capillaries, venules, and less often medium-sized arteries and veins. In addition, patients with GPA and EGPA display extravascular inflammatory lesions with predilection for the upper and/or lower respiratory tract. Immunohistology discloses few or no immunoglobulin and C3 deposits at inflammatory sites. AAV are hence designated pauci-immune vasculitides (1, 24, 25). Swelling, necrosis, and detachment of endothelial cells are the earliest histomorphological alterations of necrotizing vasculitis. At the vessel wall, both marginating and transmigrating neutrophils undergo apoptosis and karyorrhexis (leukocytoclasia). In the kidney, degranulation of neutrophils induces rupture of glomerular basement membranes and necrosis of adjacent cells, followed by fibrin precipitation. Necrotic debris, fibrin, and proinflammatory factors spill into Bowman's space. Subsequently, monocytes accumulate and parietal (Bowman's) epithelial cells proliferate forming crescents. Neutrophils within glomerular lesions also display NETosis, i.e., cellular death characterized by the formation of neutrophil extracellular traps (NETs) (26). Proinflammatory cytokines, chemokines, and complement factors of the alternative pathway locate within inflammatory glomerular lesions. Later stages are characterized by growing influx of monocytes, macrophages, and T- and B-cells. Finally, fibrocellular accumulations progress to fibrotic (sclerotic) lesions. Chronic injury occur more frequently in MPA (27). Notably, renal outcome and risk of relapse correlate with the proportion of sclerotic glomeruli (28, 29) and inversely with the proportion of normal glomeruli (30). In GPA, early extravascular lesions are characterized by the accumulation of neutrophils forming microabscesses. In advanced lesions, geographic patterns of necrosis with peripheral accumulation of macrophages and giant cells are found. Concomitant cellular infiltrates eventually also contain dendritic cells, T- and B-cells,

and plasma cells (24, 25). Histopathological classification for extravascular granulomatous lesions in GPA has been proposed (31). Ectopic lymphatic structures have been found in both extravascular granulomatous lesions and glomerulonephritis (32, 33). In EGPA, extravascular and vascular lesions are characterized by eosinophilic infiltration (24, 25).

EPIDEMIOLOGY AND GENETIC BACKGROUND

A yearly incidence between 10 and 20 per million inhabitants and a prevalence of 120 and 140 per million inhabitants has been reported for AAV in Europe and the USA. Prevalence doubling during the last decade has been attributed to improved outcomes (34, 35). Recently, higher incidence of GPA than previously reported has been identified in a UK population (36). A cyclical pattern of occurrence is observed in GPA, but not MPA (37). By contrast, MPA has a higher prevalence than GPA in Japan and China (35). Familial cases are rare in AAV (38). While individual disease-associated alleles carry modest degrees of risk, multiple genetic factors of relatively small effect combine to convey susceptibility to chronic inflammation and autoimmunity (39). Notably, the HLA polymorphism shapes self-epitope specific regulatory T-cell (Treg) responses, thereby mediating protection or causation of autoimmunity (40). Among AAV, GPA displays a remarkable *HLA-DP* association ($p = 6.2 \times 10^{-89}$) (41). The *HLA-DPB1*0401* allele is closely linked to PR3-ANCA$^+$ GPA ($p = 1.2 \times 10^{-22}$) (42, 43). Reduced HLA-DP protein expression is observed in GPA patients with the associated *HLA-DP* allele (44). By contrast, MPO-ANCA$^+$ MPA is *HLA-DQ*-associated ($p = 2.1 \times 10^{-8}$) (41). Furthermore, GPA is associated with polymorphisms of α1-anti-trypsin and PR3 encoding genes (41). In EGPA, association with *HLA-DRB1*04* was reported, whereas *HLA-DR*13* is underrepresented (45). The *IL10.2* haplotype is associated with ANCA-negative EGPA and increased interleukin (IL)-10 production (46). By contrast, disease-associated PTPN22 *R620W* allele correlates with reduced IL-10 transcription in GPA and MPA (47, 48). Aberrant microRNA expression with dysregulation of genes involved in inflammation and autoimmunity has been reported for various autoimmune diseases (49). In AAV, miRNA expression patterns correlate with renal involvement and steroid doses (50, 51). Upregulated expression of miR-634 induces a proinflammatory phenotype of monocytes in PR3-ANCA$^+$ AVV (52). Furthermore, a GPA-specific miRNA expression pattern has been found in nasal tissue differentiating GPA from healthy and disease controls (53). These findings underscore a multifactorial process in which genetic and epigenetic factors play important roles in the genesis of AAV (54–57).

BARRIER DYSFUNCTION IN GPA AND EGPA

Granulomatosis with polyangiitis is known for its propensity toward necrotizing neutrophilic granulomatous inflammation of the respiratory tract (31). Accordingly, respiratory tract manifestations and flu-like symptoms represent the most frequent initial features and affect virtually all patients with GPA during follow-up in large cohorts (5, 58, 59). Moreover, the so-called "grumbling disease" related to persistent ENT disease activity is observed in many patients being otherwise in clinical remission and despite immunosuppressive treatment (17, 60). Asthma, ENT manifestations, and eosinophilic pulmonary infiltrates also represent the most frequent manifestations in EGPA (7, 61). The nasal mucosa displays a unique gene expression signature with differentially expressed transcripts of antimicrobial peptides, cytokines, extracellular matrix proteins, and molecules important for epithelial barrier integrity in GPA (62, 63). Ciliary motility is severely reduced (64). Chronic nasal carriage of *Staphylococcus aureus* is associated with endonasal activity and relapse in GPA and facilitated by decreased production of human beta-defensin-3 and anomalous cytokine expression pattern of nasal epithelial cells (65–68). Virulence genes, e.g., genes for pore-forming toxins such as leukocidins, may contribute to disease progression and/or relapse in PR3-ANCA$^+$ GPA (69). Sensitization to fungi resulting in allergic bronchopulmonary aspergillosis may play a role in the development of EGPA (70). Moreover, exposure to silica is associated with increased risk for AAV (71). Altogether, these findings suggest a link between respiratory barrier dysfunction, infection, and chronic inflammation in GPA and in EGPA (31).

CELL DEATH AND CHRONIC INFLAMMATION

Anti-neutrophil cytoplasmic autoantibody-induced pathogenesis is linked to neutrophil activation leading to vascular injury, generation of NETs, apoptosis, and necrosis (25). However, defects in the cell death machinery itself can trigger inflammation and autoimmunity in AAV in extravascular tissues. Dysregulation in neutrophil apoptosis and clearance of apoptotic cells was demonstrated *in vitro* and *in vivo* for GPA (72–74). Apoptotic cells displaying membrane-located PR3 contribute to non-resolving inflammation by disturbing proper clearance (efferocytosis) and subsequent proinflammatory polarization of macrophages (72). Prolonged survival of neutrophils lead to accumulation within inflamed tissue, demonstrated recently *in vivo* in a human transgenic PR3 mouse model (75). Without proper clearing, apoptotic neutrophils undergo secondary necrosis with subsequent release of proinflammatory cytokines, damage-associated molecular patterns (DAMPs), and potential autoantigens (76). Within necrotizing granulomatous inflammation of GPA, release of DAMPs such as high-mobility-group-protein B1 (HMGB1) and IL-33 perpetuate receptor-dependent local auto-amplificatory loops (77). HMGB1, also described as endogenous adjuvant (78), is expressed together with the autoantigen PR3 on the surface of apoptotic neutrophils, potentially contributing to the induction of a pathogenic autoimmune response (79). NETosis is linked to the pathogenesis of AAV by contributing to endothelial damage, stimulation of lymphocytes, and activation of the alternative complement cascade (80, 81). Furthermore, ANCA-induced NET formation has recently been shown to be controlled by caspase-independent form of regulated necrosis, namely necroptosis, in an MPA mouse model (82). Altogether, dysregulation in

the cell death machinery can lead to a necro-inflammatory auto-amplification loop (83), a relevant pathogenic feature in AAV and potential target for future treatment strategies.

ALTERNATIVE COMPLEMENT PATHWAY ACTIVATION

Evidence for involvement of the complement system in AAV comes from murine models of MPO-ANCA-induced glomerulonephritis and vasculitis, demonstrating activation of the alternative complement pathway and specifically C5 being essential for disease induction (84, 85). This has been confirmed by proteomic analysis of kidney biopsies (86). Moreover, in the murine model of MPO-ANCA vasculitis, liver-derived C5a is a key mediator (87). MPO- and PR3-ANCA-activated neutrophils elicit C5a release. Subsequent interaction of C5a with the C5a receptor 1 (C5aR1) may represent a proinflammatory amplification loop in AAV (88, 89). Consequently, elevated plasma and serum concentrations of C5a and C3a have been reported in active AAV, especially MPO-ANCA$^+$ AAV (90–92). Deposition of complement components is detected in human renal biopsies in AAV (93). Similarly, C5aR1 is expressed scarcely, whereas expression of C5aR2 is upregulated in MPO-ANCA$^+$ glomerulonephritis (92). Interestingly, the exact role of C5aR2 has not been clearly defined yet. In the context of AAV, human neutrophil-expressed C5aR2 interacting with C5a seem to play a proinflammatory role (94). However, in the murine model of MPO-ANCA-induced glomerulonephritis, blocking of C5aR1 with a small molecule antagonist (avacopan) is protective, whereas lack of C5aR2 lead to aggravated disease (95). The oral C5aR1-antagonist avacopan yields promising results as glucocorticoid-sparing agent in two randomized phase II clinical trials (NCT01363388 and NCT02222155) (96). In general, tissue expression and function of the anaphylatoxin receptors (C5aR1/2) are still poorly understood, specifically in humans (97). Therefore, it remains to be examined why results regarding tissue expression of C5aR1/2 in MPO-AAV and the function of C5aR2 differ between murine and human studies. Altogether, C5a can be regarded as one of the central players in the pathogenesis of AAV (98). Contribution of the corresponding C5aRs, however, needs to be further investigated.

ALTERATIONS OF EFFECTOR AND Tregs

Disruption of the balance between regulatory and effector T-cells and accumulation of effector T-cells in tissues with disease propagation favor chronic inflammation and autoimmunity (99). Alterations of the peripheral T-cell compartment have been reported in GPA such as the expansion of circulating effector memory T-cells (T_{EM}) including Th1-type CD4$^+$ and CD8$^+$ T-cell populations lacking costimulatory CD28 expression (CD28$^-$), Th17 and Th22 cells, IL-21-producing cells, and CD4$^+$CD8$^+$ double-positive cells. Conversely, the percentage of circulating naïve T-cells is decreased (4, 100–105). Depletion of circulating Vδ2 T-cells, mucosal-associated invariant T-cells, and innate lymphoid T-cell subsets have been observed (106, 107). Remission is associated with a shift toward circulating total Th2, Th9, and Treg populations in GPA (105). Notably, the cytokine profile of PR3-specific T-cells is skewed toward Th2-type, Th17, and Th22 cells independent of disease activity (102, 108, 109). PR3-specific T-cells are CCR7$^-$CD45RA$^-$ T_{EM} with either "intermediate" CD28$^+$CD27$^-$ or "early" CD28$^+$CD27$^+$ phenotype (4, 108, 109). They may express the costimulatory c-type lectin CD161 (**Figure 1**).

Percentages of total circulating T_{EM} decrease during active disease, suggestive of T_{EM} migration toward inflamed sites (101). Accordingly, CD28$^-$ T_{EM} are abundant in bronchoalveolar fluid, inflammatory lesions, and, during renal activity, in urine (100, 110, 111). In EGPA, the frequency of circulating total Th2 and Th17 cell populations is increased, whereas lower numbers of Treg are detected (112–114). Phenotype and function of Treg are

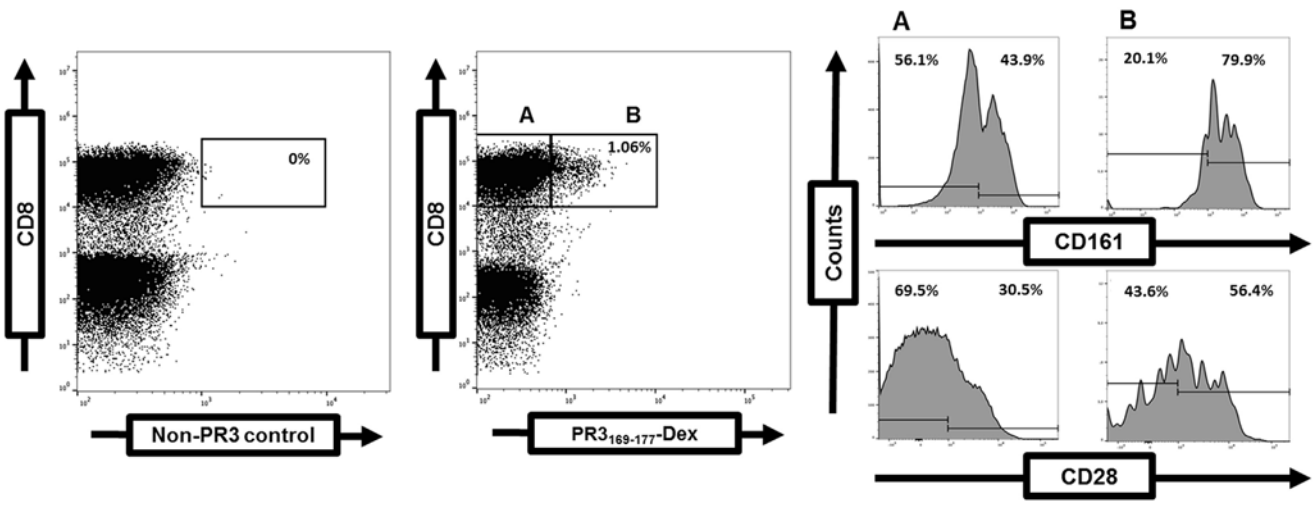

FIGURE 1 | Frequency and phenotype of proteinase 3 (PR3)-specific T-cells determined by flow cytometry. Detection of PR3-specific T-cells within the gated CD3$^+$CD8$^+$ T-cell population in a GPA-patient (right dot plot). A negative control (left dot plot). Costimulatory CD28 and CD161 expression on gated PR3-specific CD8$^+$ T-cells (A) in comparison to PR3-negative CD8$^+$ T-cells (B) (4).

altered and impaired, respectively, in AAV (115, 116). Expansion of circulating and tissue-resident $CD28^-$ T_{EM} lacking IL-2 production could favor Treg dysfunction in GPA (100). In line with an antigen-driven pathogenesis, oligoclonal T-cell proliferation has been reported in AAV previously (117, 118). Expansion of circulating $CD28^-$ T-cells has been attributed to latent cytomegalovirus (CMV) infection in GPA (119). However, concomitant cellular CMV- and Epstein–Barr virus (EBV)-infection rather than sole CMV or EBV infection is associated with expansion of $CD28^-$ T_{EM} (4). Transcriptome analysis suggests pathogen (*S. aureus*, EBV, and others) and inflammation (cytokine and chemokine)-driven alterations of the peripheral T-cell compartment linking autoimmune disease and infection-triggered pathology in GPA (4).

ANCA IMMUNOGLOBULINS

Myeloperoxidase- and PR3-ANCA are hallmarks of autoimmune vasculitis in AAV (Table S1 in Supplementary Material) (23, 120, 121). Functionally, numerous *in vitro* studies demonstrate IgG MPO- and PR3-ANCA interaction with neutrophils and monocytes. Interaction between circulating ANCA and neutrophils and monocytes causing their activation, PR3- and MPO-translocation to the cellular surface, microvascular adherence, vascular inflammation, and cell death is known as ANCA-cytokine-sequence theory (122). Notably, PR3- and MPO-ANCA display differences in neutrophil activation, e.g., respiratory burst (123, 124). In known or suspected AAV, the revised consensus on the use of ANCA testing now recommends high-quality immunoassays as primary screening method (13). Regarding IgG MPO-ANCA, epitope specificity determines pathogenicity, mainly by identifying an epitope of MPO (anti-$MPO_{447\text{-}459}$) that is exclusively linked to active MPA (125). IgG MPO-ANCA can be masked by a fragment of ceruloplasmin (125). Thus, true ANCA-negative vasculitis is considered as being less than 10% using contemporary ANCA tests (13, 121). In EGPA, IgA MPO-ANCA can occur together with IgG MPO-ANCA, but seem of less value as a biomarker (126). Of note, IgG, IgA, and IgM MPO-ANCA representing low-titer natural autoantibodies are found in healthy donors (126–128). With respect to PR3-ANCA, especially IgG isotypes (122), but IgA and IgM as well, have been linked to GPA. IgA PR3-ANCA are observed in about a quarter of GPA patients, being less prevalent in severe renal disease (129). Transient and recurring presence of IgM PR3-ANCA is reported in proportions of two large cohorts of patients with GPA or MPA and associated with a higher rate of alveolar hemorrhage (130). Similar to MPO-ANCA, IgG, IgA, and IgM PR3-ANCA are detected in healthy donors. However, the epitope specificity of natural ANCA in healthy donors differs from that of pathogenic ANCA in AAV (125, 127–129). Several studies indicate that ANCA and other autoantibodies present in AAV recognize targets apart from MPO and PR3 (Table S1 in Supplementary Material). Some of these studies though still lack confirmatory data or functional relevance.

ANCA GLYCOSYLATION

Altered Fc N-glycosylation patterns of IgG, differing between proinflammatory (agalactosylated) and antiinflammatory (galactosylated and sialylated) IgG antibodies (131), may contribute to the pathogenicity of IgG-ANCA and be a useful biomarker. Agalactosylation of total IgG has been associated with MPA, GPA, and EGPA (132). Instead, sialylation of IgG PR3-ANCA inversely correlates with disease activity and ROS production by neutrophils in GPA (133). Employing mass spectroscopy, reduced galactosylation and sialylation of IgG1 PR3-ANCA or total IgG was confirmed (134, 135). IgG-ANCA bind *via* their Fc part to FcγRIIa and FcγRIIIb, thereby co-operating with the antigen-binding site in neutrophil activation (136). Alteration of IgG-ANCA glycosylation attenuates experimental ANCA-induced glomerulonephritis (137).

ANIMAL MODELS OF ANCA-INDUCED VASCULITIS AND EXTRAVASCULAR GRANULOMATOSIS

While murine models demonstrated convincing evidence for MPO-ANCA-induced glomerulonephritis and vasculitis (138), it has proven extremely difficult to show pathogenicity of PR3-ANCA *in vivo* (139). Transfer of human hematopoietic stem cells and anti-PR3 antibodies in NOD-SCID-IL-$2R\gamma^{-/-}$ mice induced disease manifestations partially resembling systemic vasculitis (140), giving a hint of PR3-ANCA pathogenicity. A transgenic mouse model expressing human PR3 displays enhanced neutrophil survival and accumulation reflecting aspects of granulomatous inflammation in GPA (75). Besides active immunization and passive transfer of autoimmunity (141), transplantation of GPA tissue into immunodeficient mice provides evidence that fibroblasts induce nasal cartilage and bone destruction seen in GPA (142).

AUTOREACTIVE CIRCULATING AND LESIONAL B LYMPHOCYTES

Increased proportion of circulating matured B-cells recognizing PR3 in $PR3\text{-}ANCA^+$ AAV (143), presence of ectopic lymphoid structures and autoreactive B-cells in inflamed tissue of GPA (144, 145) and glomerulonephritis (32) provide a rationale for targeting B-cells. B-cell depletion proves to be an efficient therapy in AAV (146–148). Although IL-10-producing regulatory B-cells (Bregs) and $CD24^{high}$ $CD38^{high}$ Bregs, respectively, are reduced in AAV (149–151), their role in AAV remains to be further defined as such circulating cells are probably removed by B-cell-depleting therapies. Altogether, as possible scenario for ANCA-mediated pathogenesis, one could envision that B-cells producing natural autoantibodies which recognize PR3, MPO, or other antigens are selected in an inflamed microenvironment and mature with the help of autoantigen-specific T-cells. Subsequently, this could lead to the emergence and survival of pathogenic plasma cells (152) producing proinflammatory ANCA.

CONCLUSION

Much progress has been achieved in elucidating pathogenetic mechanisms in AAV, especially regarding the discovery of links

between genetic predispositions and ANCA as well as deciphering mostly deleterious functions of PR3- and MPO-ANCA by *in vitro* and in case of the latter by *in vivo* studies. Future research projects should, for instance, focus on investigating the role of microbes (bacteria and viruses) in the etiology of AAV. Altogether, a better understanding of the complex interplay between endogenous and exogenous factors contributing to pathogenic PR3- and MPO-ANCA may support the development of individualized therapies.

AUTHOR CONTRIBUTIONS

PL, AM, and AK substantially contributed to this review with regard to content and structure of the manuscript. All other authors listed have made direct and/or intellectual contribution to sections according to their area of expertise. All authors approved the manuscript for publication.

FUNDING

This work was supported by German Research Foundation grants EXC306 (HB and GR) and RTG1727 (AM, PL, and GR).

SUPPLEMENTARY MATERIAL

The Supplementary Material for this article can be found online at https://www.frontiersin.org/articles/10.3389/fimmu.2018.00680/full#supplementary-material.

REFERENCES

1. Jennette JC, Falk RJ, Bacon PA, Basu N, Cid MC, Ferrario F, et al. 2012 revised international Chapel Hill consensus conference nomenclature of vasculitides. *Arthritis Rheum* (2013) 65:1–11. doi:10.1002/art.37715
2. Jennette JC, Falk RJ, Gasim AH. Pathogenesis of antineutrophil cytoplasmic autoantibody vasculitis. *Curr Opin Nephrol Hypertens* (2011) 20:263–70. doi:10.1097/MNH.0b013e3283456731
3. Kerstein A, Holl-Ulrich K, Müller A, Riemekasten G, Lamprecht P. Granulomatose mit polyangiitis. *Dtsch Medizinische Wochenschrift* (2017) 142:24–31. doi:10.1055/s-0042-111610
4. Kerstein A, Schüler S, Cabral-Marques O, Fazio J, Häsler R, Müller A, et al. Environmental factor and inflammation-driven alteration of the total peripheral T-cell compartment in granulomatosis with polyangiitis. *J Autoimmun* (2017) 78:79–91. doi:10.1016/j.jaut.2016.12.004
5. Holle JU, Gross WL, Latza U, Nölle B, Ambrosch P, Heller M, et al. Improved outcome in 445 patients with Wegener's granulomatosis in a German vasculitis center over four decades. *Arthritis Rheum* (2011) 63:257–66. doi:10.1002/art.27763
6. Schirmer JH, Wright MN, Vonthein R, Herrmann K, Nölle B, Both M, et al. Clinical presentation and long-term outcome of 144 patients with microscopic polyangiitis in a monocentric German cohort. *Rheumatology (Oxford)* (2016) 55:71–9. doi:10.1093/rheumatology/kev286
7. Comarmond C, Pagnoux C, Khellaf M, Cordier J-F, Hamidou M, Viallard J-F, et al. Eosinophilic granulomatosis with polyangiitis (Churg-Strauss): clinical characteristics and long-term followup of the 383 patients enrolled in the French Vasculitis Study Group cohort. *Arthritis Rheum* (2013) 65:270–81. doi:10.1002/art.37721
8. Cottin V, Bel E, Bottero P, Dalhoff K, Humbert M, Lazor R, et al. Revisiting the systemic vasculitis in eosinophilic granulomatosis with polyangiitis (Churg-Strauss): a study of 157 patients by the Groupe d'Etudes et de Recherche sur les Maladies Orphelines Pulmonaires and the European respiratory society taskforce on eosinophilic granulomatosis with polyangiitis (Churg-Strauss). *Autoimmun Rev* (2017) 16:1–9. doi:10.1016/j.autrev.2016.09.018
9. Demiselle J, Auchabie J, Beloncle F, Gatault P, Grangé S, Du Cheyron D, et al. Patients with ANCA-associated vasculitis admitted to the intensive care unit with acute vasculitis manifestations: a retrospective and comparative multicentric study. *Ann Intensive Care* (2017) 7:39. doi:10.1186/s13613-017-0262-9
10. Gioffredi A, Maritati F, Oliva E, Buzio C. Eosinophilic granulomatosis with polyangiitis: an overview. *Front Immunol* (2014) 5:549. doi:10.3389/fimmu.2014.00549
11. Kallenberg CG. Antineutrophil cytoplasmic autoantibody-associated small-vessel vasculitis. *Curr Opin Rheumatol* (2007) 19:17–24. doi:10.1097/BOR.0b013e3280119842
12. Csernok E, Lamprecht P, Gross WL. Diagnostic significance of ANCA in vasculitis. *Nat Clin Pract Rheumatol* (2006) 2:174–5. doi:10.1038/ncprheum0159
13. Bossuyt X, Cohen Tervaert J-W, Arimura Y, Blockmans D, Flores-Suárez LF, Guillevin L, et al. Position paper: revised 2017 international consensus on testing of ANCAs in granulomatosis with polyangiitis and microscopic polyangiitis. *Nat Rev Rheumatol* (2017) 13(11):683–92. doi:10.1038/nrrheum.2017.140
14. Damoiseaux J, Csernok E, Rasmussen N, Moosig F, van Paassen P, Baslund B, et al. Detection of antineutrophil cytoplasmic antibodies (ANCAs): a multicentre European Vasculitis Study Group (EUVAS) evaluation of the value of indirect immunofluorescence (IIF) versus antigen-specific immunoassays. *Ann Rheum Dis* (2017) 76:647–53. doi:10.1136/annrheumdis-2016-209507
15. Specks U, Merkel PA, Seo P, Spiera R, Langford CA, Hoffman GS, et al. Efficacy of remission-induction regimens for ANCA-associated vasculitis. *N Engl J Med* (2013) 369:417–27. doi:10.1056/NEJMoa1213277
16. Holle JU, Gross WL, Holl-Ulrich K, Ambrosch P, Noelle B, Both M, et al. Prospective long-term follow-up of patients with localised Wegener's granulomatosis: does it occur as persistent disease stage? *Ann Rheum Dis* (2010) 69:1934–9. doi:10.1136/ard.2010.130203
17. Kallenberg CGM. Key advances in the clinical approach to ANCA-associated vasculitis. *Nat Rev Rheumatol* (2014) 10:484–93. doi:10.1038/nrrheum.2014.104
18. Yates M, Watts RA, Bajema IM, Cid MC, Crestani B, Hauser T, et al. EULAR/ERA-EDTA recommendations for the management of ANCA-associated vasculitis. *Ann Rheum Dis* (2016) 75:1583–94. doi:10.1136/annrheumdis-2016-209133
19. Schirmer JH, Aries PM, de Groot K, Hellmich B, Holle JU, Kneitz C, et al. S1-Leitlinie Diagnostik und Therapie der ANCA-assoziierten Vaskulitiden. *Z Rheumatol* (2017) 76:77–104. doi:10.1007/s00393-017-0394-1
20. Schinke S, Riemekasten G, Lamprecht P. [De-escalation of therapy in ANCA-associated vasculitides]. *Z Rheumatol* (2017) 76:15–20. doi:10.1007/s00393-016-0241-9
21. Flossmann O, Berden A, de Groot K, Hagen C, Harper L, Heijl C, et al. Long-term patient survival in ANCA-associated vasculitis. *Ann Rheum Dis* (2011) 70:488–94. doi:10.1136/ard.2010.137778
22. Guarino C, Hamon Y, Croix C, Lamort AS, Dallet-Choisy S, Marchand-Adam S, et al. Prolonged pharmacological inhibition of cathepsin C results in elimination of neutrophil serine proteases. *Biochem Pharmacol* (2017) 131:52–67. doi:10.1016/j.bcp.2017.02.009
23. van der Geest KSM, Brouwer E, Sanders J-S, Sandovici M, Bos NA, Boots AMH, et al. Towards precision medicine in ANCA-associated vasculitis. *Rheumatology* (2017):1–8. doi:10.1093/rheumatology/kex367
24. Holl-Ulrich K. [Histopathology of systemic vasculitis]. *Pathologe* (2010) 31:67–76. doi:10.1007/s00292-009-1156-x
25. Jennette JC, Falk RJ. Pathogenesis of antineutrophil cytoplasmic autoantibody-mediated disease. *Nat Rev Rheumatol* (2014) 10:463–73. doi:10.1038/nrrheum.2014.103
26. Kessenbrock K, Krumbholz M, Schönermarck U, Back W, Gross WL, Werb Z, et al. Netting neutrophils in autoimmune small-vessel vasculitis. *Nat Med* (2009) 15:623–5. doi:10.1038/nm.1959
27. Hauer HA, Bajema IM, Van Houwelingen HC, Ferrario F, Noël L-H, Waldherr R, et al. Renal histology in ANCA-associated vasculitis: differences between diagnostic and serologic subgroups. *Kidney Int* (2002) 61:80–9. doi:10.1046/j.1523-1755.2002.00089.x

28. Berden AE, Ferrario F, Hagen EC, Jayne DR, Jennette JC, Joh K, et al. Histopathologic classification of ANCA-associated glomerulonephritis. *J Am Soc Nephrol* (2010) 21:1628–36. doi:10.1681/ASN.2010050477
29. Göçeroğlu A, Berden AE, Fiocco M, Floßmann O, Westman KW, Ferrario F, et al. ANCA-associated glomerulonephritis: risk factors for renal relapse. *PLoS One* (2016) 11:e0165402. doi:10.1371/journal.pone.0165402
30. Hilhorst M, Wilde B, van Breda Vriesman P, van Paassen P, Cohen Tervaert JW, Limburg Renal Registry. Estimating renal survival using the ANCA-associated GN classification. *J Am Soc Nephrol* (2013) 24:1371–5. doi:10.1681/ASN.2012090912
31. Lamprecht P, Holl-Ulrich K, Gross WL. Granulomatosis with polyangiitis (Wegener's granulomatosis): pathogenesis. In: Ball GV, Fessler BJ, Bridges SL Jr, editors. *Oxford Textbook of Vasculitis*. 3rd ed. Oxford: Oxford University Press (2014). p. 385–400.
32. Steinmetz OM, Velden J, Kneissler U, Marx M, Klein A, Helmchen U, et al. Analysis and classification of B-cell infiltrates in lupus and ANCA-associated nephritis. *Kidney Int* (2008) 74:448–57. doi:10.1038/ki.2008.191
33. Mueller A, Brieske C, Schinke S, Csernok E, Gross WL, Hasselbacher K, et al. Plasma cells within granulomatous inflammation display signs pointing towards autoreactivity and destruction in granulomatosis with polyangiitis. *Arthritis Res Ther* (2014) 16:R55. doi:10.1186/ar4490
34. Herlyn K, Buckert F, Gross WL, Reinhold-Keller E. Doubled prevalence rates of ANCA-associated vasculitides and giant cell arteritis between 1994 and 2006 in northern Germany. *Rheumatology (Oxford)* (2014) 53:882–9. doi:10.1093/rheumatology/ket440
35. Pearce FA, Craven A, Merkel PA, Luqmani RA, Watts RA. Global ethnic and geographic differences in the clinical presentations of anti-neutrophil cytoplasm antibody-associated vasculitis. *Rheumatology (Oxford)* (2017) 56:1962–9. doi:10.1093/rheumatology/kex293
36. Pearce FA, Grainge MJ, Lanyon PC, Watts RA, Hubbard RB. The incidence, prevalence and mortality of granulomatosis with polyangiitis in the UK Clinical Practice Research Datalink. *Rheumatology (Oxford)* (2017) 56:589–96. doi:10.1093/rheumatology/kew413
37. Watts RA, Mooney J, Skinner J, Scott DGI, Macgregor AJ. The contrasting epidemiology of granulomatosis with polyangiitis (Wegener's) and microscopic polyangiitis. *Rheumatology (Oxford)* (2012) 51:926–31. doi:10.1093/rheumatology/ker454
38. Knudsen BB, Joergensen T, Munch-Jensen B. Wegener's granulomatosis in a family. A short report. *Scand J Rheumatol* (1988) 17:225–7. doi:10.3109/03009748809098787
39. Cho JH, Gregersen PK. Genomics and the multifactorial nature of human autoimmune disease. *N Engl J Med* (2011) 365:1612–23. doi:10.1056/NEJMra1100030
40. Ooi JD, Petersen J, Tan YH, Huynh M, Willett ZJ, Ramarathinam SH, et al. Dominant protection from HLA-linked autoimmunity by antigen-specific regulatory T cells. *Nature* (2017) 545:243–7. doi:10.1038/nature22329
41. Lyons PA, Rayner TF, Trivedi S, Holle JU, Watts RA, Jayne DRW, et al. Genetically distinct subsets within ANCA-associated vasculitis. *N Engl J Med* (2012) 367:214–23. doi:10.1056/NEJMoa1108735
42. Heckmann M, Holle JU, Arning L, Knaup S, Hellmich B, Nothnagel M, et al. The Wegener's granulomatosis quantitative trait locus on chromosome 6p21.3 as characterised by tagSNP genotyping. *Ann Rheum Dis* (2008) 67:972–9. doi:10.1136/ard.2007.077693
43. Hilhorst M, Arndt F, Joseph Kemna M, Wieczorek S, Donner Y, Wilde B, et al. HLA-DPB1 as a risk factor for relapse in antineutrophil cytoplasmic antibody-associated vasculitis: a cohort study. *Arthritis Rheumatol* (2016) 68:1721–30. doi:10.1002/art.39620
44. Merkel PA, Xie G, Monach PA, Ji X, Ciavatta DJ, Byun J, et al. Identification of functional and expression polymorphisms associated with risk for antineutrophil cytoplasmic autoantibody-associated vasculitis. *Arthritis Rheumatol* (2017) 69:1054–66. doi:10.1002/art.40034
45. Wieczorek S, Hellmich B, Gross WL, Epplen JT. Associations of Churg-Strauss syndrome with the HLA-DRB1 locus, and relationship to the genetics of antineutrophil cytoplasmic antibody-associated vasculitides: comment on the article by Vaglio et al. *Arthritis Rheum* (2008) 58:329–30. doi:10.1002/art.23209
46. Wieczorek S, Hellmich B, Arning L, Moosig F, Lamprecht P, Gross WL, et al. Functionally relevant variations of the interleukin-10 gene associated with antineutrophil cytoplasmic antibody-negative Churg-Strauss syndrome, but not with Wegener's granulomatosis. *Arthritis Rheum* (2008) 58:1839–48. doi:10.1002/art.23496
47. Jagiello P, Aries P, Arning L, Wagenleiter SEN, Csernok E, Hellmich B, et al. The PTPN22 620W allele is a risk factor for Wegener's granulomatosis. *Arthritis Rheum* (2005) 52:4039–43. doi:10.1002/art.21487
48. Cao Y, Yang J, Colby K, Hogan SL, Hu Y, Jennette CE, et al. High basal activity of the PTPN22 gain-of-function variant blunts leukocyte responsiveness negatively affecting IL-10 production in ANCA vasculitis. *PLoS One* (2012) 7:e42783. doi:10.1371/journal.pone.0042783
49. O'Connell RM, Rao DS, Chaudhuri AA, Baltimore D. Physiological and pathological roles for microRNAs in the immune system. *Nat Rev Immunol* (2010) 10:111–22. doi:10.1038/nri2708
50. Kurz T, Weiner M, Skoglund C, Basnet S, Eriksson P, Segelmark M. A myelopoiesis gene signature during remission in anti-neutrophil cytoplasm antibody-associated vasculitis does not predict relapses but seems to reflect ongoing prednisolone therapy. *Clin Exp Immunol* (2014) 175:215–26. doi:10.1111/cei.12236
51. Skoglund C, Carlsen AL, Weiner M, Kurz T, Hellmark T, Eriksson P, et al. Circulating microRNA expression pattern separates patients with anti-neutrophil cytoplasmic antibody associated vasculitis from healthy controls. *Clin Exp Rheumatol* (2015) 33:S–64–71.
52. Bertram A, Lovric S, Engel A, Beese M, Wyss K, Hertel B, et al. Circulating ADAM17 level reflects disease activity in proteinase-3 ANCA-associated vasculitis. *J Am Soc Nephrol* (2015) 26:2860–70. doi:10.1681/ASN.2014050477
53. Schinke S, Laudien M, Müller A, Gross WL, Häsler R. Disease-associated micro-RNA profiles in granulomatosis with polyangiitis nasal tissue indicate a regulatory network targeting pathophysiological processes. *Ann Rheum Dis* (2013) 71:477. doi:10.1136/annrheumdis-2012-eular.2967
54. Arning L, Holle JU, Harper L, Millar DS, Gross WL, Epplen JT, et al. Are there specific genetic risk factors for the different forms of ANCA-associated vasculitis? *Ann Rheum Dis* (2011) 70:707–8. doi:10.1136/ard.2010.130971
55. Wieczorek S, Holle JU, Cohen Tervaert JW, Harper L, Moosig F, Gross WL, et al. The SEM6A6 locus is not associated with granulomatosis with polyangiitis or other forms of antineutrophil cytoplasmic antibody-associated vasculitides in Europeans: comment on the article by Xie et al. *Arthritis Rheumatol* (2014) 66:1400–1. doi:10.1002/art.38367
56. Husmann CA, Holle JU, Moosig F, Mueller S, Wilde B, Cohen Tervaert JW, et al. Genetics of toll like receptor 9 in ANCA associated vasculitides. *Ann Rheum Dis* (2014) 73:890–6. doi:10.1136/annrheumdis-2012-202803
57. Ciavatta DJ, Yang J, Preston GA, Badhwar AK, Xiao H, Hewins P, et al. Epigenetic basis for aberrant upregulation of autoantigen genes in humans with ANCA vasculitis. *J Clin Invest* (2010) 120:3209–19. doi:10.1172/JCI40034DS1
58. Hoffman GS, Kerr GS, Leavitt RY, Hallahan CW, Lebovics RS, Travis WD, et al. Wegener granulomatosis: an analysis of 158 patients. *Ann Intern Med* (1992) 116:488–98. doi:10.7326/0003-4819-116-6-488
59. Reinhold-Keller E, Beuge N, Latza U, de Groot K, Rudert H, Nölle B, et al. An interdisciplinary approach to the care of patients with Wegener's granulomatosis: long-term outcome in 155 patients. *Arthritis Rheum* (2000) 43:1021–32. doi:10.1002/1529-0131(200005)43:5<1021:AID-ANR10>3.0.CO;2-J
60. Garske U, Haack A, Beltrán O, Flores-Suárez LF, Bremer JP, Lamprecht P, et al. Intra- and inter-rater reliability of endonasal activity estimation in granulomatosis with polyangiitis (Wegener's). *Clin Exp Rheumatol* (2012) 30:S22–8.
61. Petersen H, Götz P, Both M, Hey M, Ambrosch P, Bremer JP, et al. Manifestation of eosinophilic granulomatosis with polyangiitis in head and neck. *Rhinology* (2015) 53:277–85. doi:10.4193/Rhin14.074
62. Laudien M, Häsler R, Wohlers J, Böck J, Lipinski S, Bremer L, et al. Molecular signatures of a disturbed nasal barrier function in the primary tissue of Wegener's granulomatosis. *Mucosal Immunol* (2011) 4:564–73. doi:10.1038/mi.2011.9
63. Grayson PC, Steiling K, Platt M, Berman JS, Zhang X, Xiao J, et al. Defining the nasal transcriptome in granulomatosis with polyangiitis (Wegener's). *Arthritis Rheumatol* (2015) 67:2233–9. doi:10.1002/art.39185
64. Ullrich S, Gustke H, Lamprecht P, Gross WL, Schumacher U, Ambrosch P, et al. Severe impaired respiratory ciliary function in Wegener granulomatosis. *Ann Rheum Dis* (2009) 68:1067–71. doi:10.1136/ard.2008.096974

65. Stegeman CA, Tervaert JW, Sluiter WJ, Manson WL, de Jong PE, Kallenberg CG. Association of chronic nasal carriage of *Staphylococcus aureus* and higher relapse rates in Wegener granulomatosis. *Ann Intern Med* (1994) 120:12–7. doi:10.7326/0003-4819-120-1-199401010-00003
66. Laudien M, Gadola SD, Podschun R, Hedderich J, Paulsen J, Reinhold-Keller E, et al. Nasal carriage of *Staphylococcus aureus* and endonasal activity in Wegener's granulomatosis as compared to rheumatoid arthritis and chronic rhinosinusitis with nasal polyps. *Clin Exp Rheumatol* (2010) 28:51–5.
67. Hui Y, Wohlers J, Podschun R, Hedderich J, Lamprecht P, Ambrosch P, et al. Antimicrobial peptides in nasal secretion and mucosa with respect to *S. aureus* colonisation in Wegener's granulomatosis. *Clin Exp Rheumatol* (2011) 29:S49–56.
68. Wohlers J, Breucker K, Podschun R, Hedderich J, Lamprecht P, Ambrosch P, et al. Aberrant cytokine pattern of the nasal mucosa in granulomatosis with polyangiitis. *Arthritis Res Ther* (2012) 14:R203. doi:10.1186/ar4041
69. Glasner C, de Goffau MC, van Timmeren MM, Schulze ML, Jansen B, Tavakol M, et al. Genetic loci of *Staphylococcus aureus* associated with anti-neutrophil cytoplasmic autoantibody (ANCA)-associated vasculitides. *Sci Rep* (2017) 7:12211. doi:10.1038/s41598-017-12450-z
70. Ishiguro T, Takayanagi N, Takaku Y, Kagiyama N, Kurashima K, Sugita Y. Combined allergic bronchopulmonary aspergillosis and eosinophilic granulomatosis with polyangiitis: three cases and a review of the literature. *Intern Med* (2016) 55:793–7. doi:10.2169/internalmedicine.55.5431
71. Hogan SL, Cooper GS, Savitz DA, Nylander-French LA, Parks CG, Chin H, et al. Association of silica exposure with anti-neutrophil cytoplasmic autoantibody small-vessel vasculitis: a population-based, case-control study. *Clin J Am Soc Nephrol* (2007) 2:290–9. doi:10.2215/CJN.03501006
72. Millet A, Martin KR, Bonnefoy F, Saas P, Mocek J, Alkan M, et al. Proteinase 3 on apoptotic cells disrupts immune silencing in autoimmune vasculitis. *J Clin Invest* (2015) 125:4107–21. doi:10.1172/JCI78182
73. Abdgawad M, Pettersson Å, Gunnarsson L, Bengtsson AA, Geborek P, Nilsson L, et al. Decreased neutrophil apoptosis in quiescent ANCA-associated systemic vasculitis. *PLoS One* (2012) 7:e32439. doi:10.1371/journal.pone.0032439
74. Gabillet J, Millet A, Pederzoli-Ribeil M, Tacnet-Delorme P, Guillevin L, Mouthon L, et al. Proteinase 3, the autoantigen in granulomatosis with polyangiitis, associates with calreticulin on apoptotic neutrophils, impairs macrophage phagocytosis, and promotes inflammation. *J Immunol* (2012) 189:2574–83. doi:10.4049/jimmunol.1200600
75. Martin KR, Pederzoli-Ribeil M, Pacreau E, Burgener SS, Dahdah A, Candalh C, et al. Transgenic mice expressing human proteinase 3 exhibit sustained neutrophil-associated peritonitis. *J Immunol* (2017) 199:3914–24. doi:10.4049/jimmunol.1601522
76. Muñoz LE, Lauber K, Schiller M, Manfredi AA, Herrmann M. The role of defective clearance of apoptotic cells in systemic autoimmunity. *Nat Rev Rheumatol* (2010) 6:280–9. doi:10.1038/nrrheum.2010.46
77. Kerstein A, Erschig A, Müller A, Riemekasten G, Lamprecht P. Dangerous signaling in granulomatosis with polyangiitis – how alarmins perpetuate the granulomatous inflammation. *gms | 43. Kongress der Deutschen Gesellschaft für Rheumatologie, 29. Jahrestagung der Deutschen Gesellschaft für Orthopädische Rheumatologie, 25. Wissenschaftliche Jahrestagung der Gesellschaft für Kinder- und Jugendrheumatologie*. German Medical Science GMS Publishing House. ER.21 (2015). Available from: http://www.egms.de/static/de/meetings/dgrh2015/15dgrh075.shtml (Accessed: September 1, 2015).
78. Rovere-Querini P, Capobianco A, Scaffidi P, Valentinis B, Catalanotti F, Giazzon M, et al. HMGB1 is an endogenous immune adjuvant released by necrotic cells. *EMBO Rep* (2004) 5:825–30. doi:10.1038/sj.embor.7400205
79. Kerstein A, Müller A, Holl-Ulrich K, Lamprecht P. High-mobility group box 1 (HMGB1) as a link between the granulomatous inflammation and the induction of autoreactivity in granulomatosis with polyangiitis. *Nephron* (2015) 129(Suppl):205.
80. Lange C, Csernok E, Moosig F, Holle JU. Immune stimulatory effects of neutrophil extracellular traps in granulomatosis with polyangiitis. *Clin Exp Rheumatol* (2017) 35Suppl 103(1):33–9.
81. Söderberg D, Segelmark M. Neutrophil extracellular traps in ANCA-associated vasculitis. *Front Immunol* (2016) 7:256. doi:10.3389/fimmu.2016.00256
82. Schreiber A, Rousselle A, Becker JU, von Mässenhausen A, Linkermann A, Kettritz R. Necroptosis controls NET generation and mediates complement activation, endothelial damage, and autoimmune vasculitis. *Proc Natl Acad Sci U S A* (2017) 114:E9618–25. doi:10.1073/pnas.1708247114
83. Linkermann A, Stockwell BR, Krautwald S, Anders H-J. Regulated cell death and inflammation: an auto-amplification loop causes organ failure. *Nat Rev Immunol* (2014) 14:759–67. doi:10.1038/nri3743
84. Xiao H, Schreiber A, Heeringa P, Falk RJ, Jennette JC. Alternative complement pathway in the pathogenesis of disease mediated by anti-neutrophil cytoplasmic autoantibodies. *Am J Pathol* (2007) 170:52–64. doi:10.2353/ajpath.2007.060573
85. Huugen D, van Esch A, Xiao H, Peutz-Kootstra CJ, Buurman WA, Tervaert JWC, et al. Inhibition of complement factor C5 protects against anti-myeloperoxidase antibody-mediated glomerulonephritis in mice. *Kidney Int* (2007) 71:646–54. doi:10.1038/sj.ki.5002103
86. Sethi S, Zand L, De Vriese AS, Specks U, Vrana JA, Kanwar S, et al. Complement activation in pauci-immune necrotizing and crescentic glomerulonephritis: results of a proteomic analysis. *Nephrol Dial Transplant* (2017) 32:i139–45. doi:10.1093/ndt/gfw299
87. Freeley SJ, Popat RJ, Parmar K, Kolev M, Hunt BJ, Stover CM, et al. Experimentally-induced anti-myeloperoxidase vasculitis does not require properdin, MASP-2 or bone marrow-derived C5. *J Pathol* (2016) 240:61–71. doi:10.1002/path.4754
88. Schreiber A, Xiao H, Jennette JC, Schneider W, Luft FC, Kettritz R. C5a receptor mediates neutrophil activation and ANCA-induced glomerulonephritis. *J Am Soc Nephrol* (2009) 20:289–98. doi:10.1681/ASN.2008050497
89. Camous L, Roumenina L, Bigot S, Brachemi S, Frémeaux-Bacchi V, Lesavre P, et al. Complement alternative pathway acts as a positive feedback amplification of neutrophil activation. *Blood* (2011) 117:1340–9. doi:10.1182/blood-2010-05-283564
90. Gou S-J, Yuan J, Chen M, Yu F, Zhao M-H. Circulating complement activation in patients with anti-neutrophil cytoplasmic antibody-associated vasculitis. *Kidney Int* (2012) 83:129–37. doi:10.1038/ki.2012.313
91. Le Roux S, Pepper R, Dufay A, Néel M, Meffray E, Lamandé N, et al. Elevated soluble Flt1 inhibits endothelial repair in PR3-ANCA-associated vasculitis. *J Am Soc Nephrol* (2012) 23:155–64. doi:10.1681/ASN.2010080858
92. Yuan J, Gou S-J, Huang J, Hao J, Chen M, Zhao M-H. C5a and its receptors in human anti-neutrophil cytoplasmic antibody (ANCA)-associated vasculitis. *Arthritis Res Ther* (2012) 14:R140. doi:10.1186/ar3873
93. Hilhorst M, Van Paassen P, Van Rie H, Bijnens N, Heerings-Rewinkel P, Van Breda Vriesman P, et al. Complement in ANCA-associated glomerulonephritis. *Nephrol Dial Transplant* (2017) 32:1302–13. doi:10.1093/ndt/gfv288
94. Hao J, Wang C, Yuan J, Chen M, Zhao MH. A pro-inflammatory role of C5L2 in C5a-primed neutrophils for ANCA-induced activation. *PLoS One* (2013) 8:e66305. doi:10.1371/journal.pone.0066305
95. Xiao H, Dairaghi DJ, Powers JP, Ertl LS, Baumgart T, Wang Y, et al. C5a receptor (CD88) blockade protects against MPO-ANCA GN. *J Am Soc Nephrol* (2014) 25:225–31. doi:10.1681/ASN.2013020143
96. Jayne DRW, Bruchfeld AN, Harper L, Schaier M, Venning MC, Hamilton P, et al. Randomized trial of C5a receptor inhibitor avacopan in ANCA-associated vasculitis. *J Am Soc Nephrol* (2017) 28(9):2756–67. doi:10.1681/ASN.2016111179
97. Laumonnier Y, Karsten CM, Köhl J. Novel insights into the expression pattern of anaphylatoxin receptors in mice and men. *Mol Immunol* (2017) 89:44–58. doi:10.1016/j.molimm.2017.05.019
98. Chen M, Jayne DRW, Zhao M-H. Complement in ANCA-associated vasculitis: mechanisms and implications for management. *Nat Rev Nephrol* (2017) 13:359–67. doi:10.1038/nrneph.2017.37
99. Rosenblum MD, Remedios KA, Abbas AK. Mechanisms of human autoimmunity. *J Clin Invest* (2015) 125:1–6. doi:10.1172/JCI78088
100. Komocsi A, Lamprecht P, Csernok E, Mueller A, Holl-Ulrich K, Seitzer U, et al. Peripheral blood and granuloma CD4+CD28− T cells are a major source of interferon-γ and tumor necrosis factor-α in Wegener's granulomatosis. *Am J Pathol* (2002) 160:1717–24. doi:10.1016/S0002-9440(10)61118-2
101. Abdulahad WH, van der Geld YM, Stegeman CA, Kallenberg CGM. Persistent expansion of CD4+ effector memory T cells in Wegener's granulomatosis. *Kidney Int* (2006) 70:938–47. doi:10.1038/sj.ki.5001670
102. Abdulahad WH, Stegeman CA, Limburg PC, Kallenberg CGM. Skewed distribution of Th17 lymphocytes in patients with Wegener's granulomatosis in remission. *Arthritis Rheum* (2008) 58:2196–205. doi:10.1002/art.23557

103. Wilde B, Thewissen M, Damoiseaux J, Hilhorst M, van Paassen P, Witzke O, et al. Th17 expansion in granulomatosis with polyangiitis (Wegener's): the role of disease activity, immune regulation and therapy. *Arthritis Res Ther* (2012) 14:R227. doi:10.1186/ar4066
104. Abdulahad WH, Lepse N, Stegeman CA, Huitema MG, Doornbos-van der Meer B, Tadema H, et al. Increased frequency of circulating IL-21 producing Th-cells in patients with granulomatosis with polyangiitis (GPA). *Arthritis Res Ther* (2013) 15:R70. doi:10.1186/ar4247
105. Szczeklik W, Jakieła B, Wawrzycka-Adamczyk K, Sanak M, Hubalewska-Mazgaj M, Padjas A, et al. Skewing toward Treg and Th2 responses is a characteristic feature of sustained remission in ANCA-positive granulomatosis with polyangiitis. *Eur J Immunol* (2017) 47:724–33. doi:10.1002/eji.201646810
106. Fazio J, Quabius ES, Müller A, Adam-Klages S, Wesch D, Sebens S, et al. Vδ2 T cell deficiency in granulomatosis with polyangiitis (Wegener's granulomatosis). *Clin Immunol* (2013) 149:65–72. doi:10.1016/j.clim.2013.06.003
107. Braudeau C, Amouriaux K, Néel A, Herbreteau G, Salabert N, Rimbert M, et al. Persistent deficiency of circulating mucosal-associated invariant T (MAIT) cells in ANCA-associated vasculitis. *J Autoimmun* (2016) 70:73–9. doi:10.1016/j.jaut.2016.03.015
108. Fagin U, Csernok E, Müller A, Pitann S, Fazio J, Krause K, et al. Distinct proteinase 3-induced cytokine patterns in Wegener's granulomatosis, Churg-Strauss syndrome, and healthy controls. *Clin Exp Rheumatol* (2011) 29:S57–62.
109. Fagin U, Pitann S, Gross WL, Lamprecht P. Flow cytometric characterization of "early" and "late differentiated" T-cells including PR3-specific cells in granulomatosis with polyangiitis (Wegener's). *Cytometry B Clin Cytom* (2012) 82:173–5. doi:10.1002/cyto.b.21006
110. Lamprecht P. CD28 negative T cells are enriched in granulomatous lesions of the respiratory tract in Wegener's granulomatosis. *Thorax* (2001) 56:751–7. doi:10.1136/thorax.56.10.751
111. Abdulahad WH, Kallenberg CGM, Limburg PC, Stegeman CA. Urinary CD4+ effector memory T cells reflect renal disease activity in antineutrophil cytoplasmic antibody-associated vasculitis. *Arthritis Rheum* (2009) 60:2830–8. doi:10.1002/art.24747
112. Kiene M, Csernok E, Müller A, Metzler C, Trabandt A, Gross WL. Elevated interleukin-4 and interleukin-13 production by T cell lines from patients with Churg-Strauss syndrome. *Arthritis Rheum* (2001) 44:469–73. doi:10.1002/1529-0131(200102)44:2<469:AID-ANR66>3.0.CO;2-0
113. Tsurikisawa N, Saito H, Tsuburai T, Oshikata C, Ono E, Mitomi H, et al. Differences in regulatory T cells between Churg-Strauss syndrome and chronic eosinophilic pneumonia with asthma. *J Allergy Clin Immunol* (2008) 122:610–6. doi:10.1016/j.jaci.2008.05.040
114. Saito H, Tsurikisawa N, Tsuburai T, Oshikata C, Akiyama K. Cytokine production profile of CD4+ T cells from patients with active Churg-Strauss syndrome tends toward Th17. *Int Arch Allergy Immunol* (2009) 149(Suppl 1):61–5. doi:10.1159/000210656
115. Klapa S, Mueller A, Csernok E, Fagin U, Klenerman P, Holl-Ulrich K, et al. Lower numbers of FoxP3 and CCR4 co-expressing cells in an elevated subpopulation of CD4+CD25highregulatory T cells from Wegener's granulomatosis. *Clin Exp Rheumatol* (2010) 28:72–80.
116. Free ME, Bunch DO, McGregor JA, Jones BE, Berg EA, Hogan SL, et al. Patients with antineutrophil cytoplasmic antibody-associated vasculitis have defective Treg cell function exacerbated by the presence of a suppression-resistant effector cell population. *Arthritis Rheum* (2013) 65:1922–33. doi:10.1002/art.37959
117. Grunewald J, Halapi E, Wahlström J, Giscombe R, Nityanand S, Sanjeevi C, et al. T-cell expansions with conserved T-cell receptor beta chain motifs in the peripheral blood of HLA-DRB1*0401 positive patients with necrotizing vasculitis. *Blood* (1998) 92:3737–44.
118. Boita M, Guida G, Circosta P, Elia AR, Stella S, Heffler E, et al. The molecular and functional characterization of clonally expanded CD8+ TCR BV T cells in eosinophilic granulomatosis with polyangiitis (EGPA). *Clin Immunol* (2014) 152:152–63. doi:10.1016/j.clim.2014.03.001
119. Morgan MD, Pachnio A, Begum J, Roberts D, Rasmussen N, Neil DAH, et al. CD4+CD28− T cell expansion in granulomatosis with polyangiitis (Wegener's) is driven by latent cytomegalovirus infection and is associated with an increased risk of infection and mortality. *Arthritis Rheum* (2011) 63:2127–37. doi:10.1002/art.30366
120. Cornec D, Gall EC-L, Fervenza FC, Specks U. ANCA-associated vasculitis—clinical utility of using ANCA specificity to classify patients. *Nat Rev Rheumatol* (2016) 12:570–9. doi:10.1038/nrrheum.2016.123
121. Jennette JC, Nachman PH. ANCA glomerulonephritis and vasculitis. *Clin J Am Soc Nephrol* (2017) 12:1680–91. doi:10.2215/CJN.02500317
122. Csernok E. Anti-neutrophil cytoplasmic antibodies and pathogenesis of small vessel vasculitides. *Autoimmun Rev* (2003) 2:158–64. doi:10.1016/S1568-9972(03)00010-7
123. Franssen CF, Huitema MG, Muller Kobold AC, Oost-Kort WW, Limburg PC, Tiebosch A, et al. In vitro neutrophil activation by antibodies to proteinase 3 and myeloperoxidase from patients with crescentic glomerulonephritis. *J Am Soc Nephrol* (1999) 10:1506–15.
124. Harper L, Radford D, Plant T, Drayson M, Adu D, Savage COS. IgG from myeloperoxidase-antineutrophil cytoplasmic antibody-positive patients stimulates greater activation of primed neutrophils than IgG from proteinase 3-antineutrophil cytoplasmic antibody-positive patients. *Arthritis Rheum* (2001) 44:921–30. doi:10.1002/1529-0131(200104)44:4<921:AID-ANR149>3.0.CO;2-4
125. Roth AJ, Ooi JD, Hess JJ, van Timmeren MM, Berg EA, Poulton CE, et al. Epitope specificity determines pathogenicity and detectability in ANCA-associated vasculitis. *J Clin Invest* (2013) 123:1773–83. doi:10.1172/JCI65292
126. Oommen E, Hummel A, Allmannsberger L, Cuthbertson D, Carette S, Pagnoux C, et al. IgA antibodies to myeloperoxidase in patients with eosinophilic granulomatosis with polyangiitis (Churg-Strauss). *Clin Exp Rheumatol* (2017) 35:98–101. doi:10.1007/128
127. Finnern R, Bye JM, Dolman KM, Zhao MH, Short A, Marks JD, et al. Molecular characteristics of anti-self antibody fragments against neutrophil cytoplasmic antigens from human V gene phage display libraries. *Clin Exp Immunol* (1995) 102:566–74. doi:10.1111/j.1365-2249.1995.tb03854.x
128. Cui Z, Zhao M, Segelmark M, Hellmark T. Natural autoantibodies to myeloperoxidase, proteinase 3, and the glomerular basement membrane are present in normal individuals. *Kidney Int* (2010) 78:590–7. doi:10.1038/ki.2010.198
129. Kelley JM, Monach PA, Ji C, Zhou Y, Wu J, Tanaka S, et al. IgA and IgG antineutrophil cytoplasmic antibody engagement of Fc receptor genetic variants influences granulomatosis with polyangiitis. *Proc Natl Acad Sci U S A* (2011) 108:20736–41. doi:10.1073/pnas.1109227109
130. Clain JM, Hummel AM, Stone JH, Fervenza FC, Hoffman GS, Kallenberg CGM, et al. Immunoglobulin (Ig)M antibodies to proteinase 3 in granulomatosis with polyangiitis and microscopic polyangiitis. *Clin Exp Immunol* (2017) 188:174–81. doi:10.1111/cei.12925
131. Collin M, Ehlers M. The carbohydrate switch between pathogenic and immunosuppressive antigen-specific antibodies. *Exp Dermatol* (2013) 22:511–4. doi:10.1111/exd.12171
132. Holland M, Takada K, Okumoto T, Takahashi N, Kato K, Adu D, et al. Hypogalactosylation of serum IgG in patients with ANCA-associated systemic vasculitis. *Clin Exp Immunol* (2002) 129:183–90. doi:10.1046/j.1365-2249.2002.01864.x
133. Espy C, Morelle W, Kavian N, Grange P, Goulvestre C, Viallon V, et al. Sialylation levels of anti-proteinase 3 antibodies are associated with the activity of granulomatosis with polyangiitis (Wegener's). *Arthritis Rheum* (2011) 63:2105–15. doi:10.1002/art.30362
134. Wuhrer M, Stavenhagen K, Koeleman CAM, Selman MHJ, Harper L, Jacobs BC, et al. Skewed Fc glycosylation profiles of anti-proteinase 3 immunoglobulin G1 autoantibodies from granulomatosis with polyangiitis patients show low levels of bisection, galactosylation, and sialylation. *J Proteome Res* (2015) 14:1657–65. doi:10.1021/pr500780a
135. Kemna MJ, Plomp R, van Paassen P, Koeleman CAM, Jansen BC, Damoiseaux JGMC, et al. Galactosylation and sialylation levels of IgG predict relapse in patients with PR3-ANCA associated vasculitis. *EBioMedicine* (2017) 17:108–18. doi:10.1016/j.ebiom.2017.01.033
136. Kettritz R. How anti-neutrophil cytoplasmic autoantibodies activate neutrophils. *Clin Exp Immunol* (2012) 169:220–8. doi:10.1111/j.1365-2249.2012.04615.x
137. van Timmeren MM, van der Veen BS, Stegeman CA, Petersen AH, Hellmark T, Collin M, et al. IgG glycan hydrolysis attenuates ANCA-mediated glomerulonephritis. *J Am Soc Nephrol* (2010) 21:1103–14. doi:10.1681/ASN.2009090984

138. Xiao H, Heeringa P, Hu P, Liu Z, Zhao M, Aratani Y, et al. Antineutrophil cytoplasmic autoantibodies specific for myeloperoxidase cause glomerulonephritis and vasculitis in mice. *J Clin Invest* (2002) 110:955–63. doi:10.1172/JCI15918
139. Schreiber A, Eulenberg-Gustavus C, Bergmann A, Jerke U, Kettritz R. Lessons from a double-transgenic neutrophil approach to induce antiproteinase 3 antibody-mediated vasculitis in mice. *J Leukoc Biol* (2016) 100:1443–52. doi:10.1189/jlb.5A0116-037R
140. Little MA, Al-Ani B, Ren S, Al-Nuaimi H, Leite M, Alpers CE, et al. Anti-proteinase 3 anti-neutrophil cytoplasm autoantibodies recapitulate systemic vasculitis in mice with a humanized immune system. *PLoS One* (2012) 7:e28626. doi:10.1371/journal.pone.0028626
141. Petersen F, Yue X, Riemekasten G, Yu X. Dysregulated homeostasis of target tissues or autoantigens – a novel principle in autoimmunity. *Autoimmun Rev* (2017) 16:602–11. doi:10.1016/j.autrev.2017.04.006
142. Kesel N, Köhler D, Herich L, Laudien M, Holl-Ulrich K, Jüngel A, et al. Cartilage destruction in granulomatosis with polyangiitis (Wegener's granulomatosis) is mediated by human fibroblasts after transplantation into immunodeficient mice. *Am J Pathol* (2012) 180:2144–55. doi:10.1016/j.ajpath.2012.01.021
143. Cornec D, Berti A, Hummel A, Peikert T, Pers J-O, Specks U. Identification and phenotyping of circulating autoreactive proteinase 3-specific B cells in patients with PR3-ANCA associated vasculitis and healthy controls. *J Autoimmun* (2017) 84:122–31. doi:10.1016/j.jaut.2017.08.006
144. Voswinkel J, Mueller A, Kraemer JA, Lamprecht P, Herlyn K, Holl-Ulrich K, et al. B lymphocyte maturation in Wegener's granulomatosis: a comparative analysis of VH genes from endonasal lesions. *Ann Rheum Dis* (2006) 65:859–64. doi:10.1136/ard.2005.044909
145. Thurner L, Müller A, Cérutti M, Martin T, Pasquali J-L, Gross WL, et al. Wegener's granuloma harbors B lymphocytes with specificities against a proinflammatory transmembrane protein and a tetraspanin. *J Autoimmun* (2011) 36:87–90. doi:10.1016/j.jaut.2010.09.002
146. Unizony S, Villarreal M, Miloslavsky EM, Lu N, Merkel PA, Spiera R, et al. Clinical outcomes of treatment of anti-neutrophil cytoplasmic antibody (ANCA)-associated vasculitis based on ANCA type. *Ann Rheum Dis* (2016) 75:1166–9. doi:10.1136/annrheumdis-2015-208073
147. Koster MJ, Warrington KJ. Recent advances in understanding and treating vasculitis. *F1000Res* (2016) 5:1436. doi:10.12688/f1000research.8403.1
148. Cortazar FB, Pendergraft WF, Wenger J, Owens CT, Laliberte K, Niles JL. Effect of continuous B cell depletion with rituximab on pathogenic autoantibodies and total IgG levels in antineutrophil cytoplasmic antibody-associated vasculitis. *Arthritis Rheumatol* (2017) 69:1045–53. doi:10.1002/art.40032
149. Wilde B, Thewissen M, Damoiseaux J, Knippenberg S, Hilhorst M, van Paassen P, et al. Regulatory B cells in ANCA-associated vasculitis. *Ann Rheum Dis* (2013) 72:1416–9. doi:10.1136/annrheumdis-2012-202986
150. Lepse N, Abdulahad WH, Rutgers A, Kallenberg CGM, Stegeman CA, Heeringa P. Altered B cell balance, but unaffected B cell capacity to limit monocyte activation in anti-neutrophil cytoplasmic antibody-associated vasculitis in remission. *Rheumatology (Oxford)* (2014) 53(9):1683–92. doi:10.1093/rheumatology/keu149
151. Todd SK, Pepper RJ, Draibe J, Tanna A, Pusey CD, Mauri C, et al. Regulatory B cells are numerically but not functionally deficient in anti-neutrophil cytoplasm antibody-associated vasculitis. *Rheumatology (Oxford)* (2014) 53(9):1693–703. doi:10.1093/rheumatology/keu136
152. Tiburzy B, Kulkarni U, Hauser AE, Abram M, Manz RA. Plasma cells in immunopathology: concepts and therapeutic strategies. *Semin Immunopathol* (2014) 36:277–88. doi:10.1007/s00281-014-0426-8

Conflict of Interest Statement: The authors declare that the research was conducted in the absence of any commercial or financial relationships that could be construed as a potential conflict of interest.

frontiers in Immunology

PERSPECTIVE
published: 09 April 2018
doi: 10.3389/fimmu.2018.00695

Sparking Fire Under the Skin? Answers From the Association of Complement Genes With Pemphigus Foliaceus

*Valéria Bumiller-Bini[1], Gabriel Adelman Cipolla[1], Rodrigo Coutinho de Almeida[1†], Maria Luiza Petzl-Erler[1], Danillo Gardenal Augusto[1,2] and Angelica Beate Winter Boldt[1,3]**

[1] Laboratory of Human Molecular Genetics, Department of Genetics, Universidade Federal do Paraná, Curitiba, Brazil, [2] Departamento de Ciências Biológicas, Universidade Estadual de Santa Cruz, Ilhéus, Brazil, [3] Laboratory of Molecular Immunopathology, Department of Clinical Pathology, Hospital de Clínicas, Universidade Federal do Paraná, Curitiba, Brazil

OPEN ACCESS

Edited by:
Ralf J. Ludwig,
Universität zu Lübeck, Germany

Reviewed by:
Abhigyan Satyam,
Harvard Medical School,
United States
Hauke Busch,
Universität zu Lübeck, Germany

***Correspondence:**
Angelica Beate Winter Boldt
angelicaboldt@gmail.com

†Present address:
Rodrigo Coutinho de Almeida,
Molecular Epidemiology, Department of Biomedical Data Sciences, Leiden University Medical Center, Leiden, Netherlands

Specialty section:
This article was submitted to Immunological Tolerance and Regulation, a section of the journal Frontiers in Immunology

Received: 29 January 2018
Accepted: 21 March 2018
Published: 09 April 2018

Citation:
Bumiller-Bini V, Cipolla GA, de Almeida RC, Petzl-Erler ML, Augusto DG and Boldt ABW (2018) Sparking Fire Under the Skin? Answers From the Association of Complement Genes With Pemphigus Foliaceus. Front. Immunol. 9:695. doi: 10.3389/fimmu.2018.00695

Skin blisters of pemphigus foliaceus (PF) present concomitant deposition of autoantibodies and components of the complement system (CS), whose gene polymorphisms are associated with susceptibility to different autoimmune diseases. To investigate these in PF, we evaluated 992 single-nucleotide polymorphisms (SNPs) of 44 CS genes, genotyped through microarray hybridization in 229 PF patients and 194 controls. After excluding SNPs with minor allele frequency <1%, out of Hardy–Weinberg equilibrium in controls or in strong linkage disequilibrium ($r^2 \geq 0.8$), 201 SNPs remained for logistic regression. Polymorphisms of 11 genes were associated with PF. *MASP1* encodes a crucial serine protease of the lectin pathway (rs13094773: OR = 0.5, $p = 0.0316$; rs850309: OR = 0.23, $p = 0.03$; rs3864098: OR = 1.53, $p = 0.0383$; rs698104: OR = 1.52, $p = 0.0424$; rs72549154: OR = 0.55, $p = 0.0453$). *C9* (rs187875: OR = 1.46, $p = 0.0189$; rs700218: OR = 0.12, $p = 0.0471$) and *C8A* (rs11206934: OR = 4.02, $p = 0.0323$) encode proteins of the membrane attack complex (MAC) and *C5AR1* (rs10404456: OR = 1.43, $p = 0.0155$), a potent anaphylatoxin-receptor. Two encode complement regulators: MAC-blocking CD59 (rs1047581: OR = 0.62, $p = 0.0152$) and alternative pathway-blocking CFH (rs34388368: OR = 2.57, $p = 0.0195$). One encodes opsonin: *C3* (rs4807895: OR = 2.52, $p = 0.0239$), whereas four encode receptors for C3 fragments: *CR1* (haplotype with rs6656401: OR = 1.37, $p = 0.0382$), *CR2* (rs2182911: OR = 0.23, $p = 0.0263$), *ITGAM* (CR3, rs12928810: OR = 0.66, $p = 0.0435$), and *ITGAX* (CR4, rs11574637: OR = 0.63, $p = 0.0056$). Associations reinforced former findings, regarding differential gene expression, serum levels, C3, and MAC deposition on lesions. Deregulation of previously barely noticed processes, e.g., the lectin and alternative pathways and opsonization-mediated phagocytosis, also modulate PF susceptibility. The results open new crucial avenues for understanding disease etiology and may improve PF treatment through additional therapeutic targets.

Keywords: pemphigus foliaceus, complement, lectin pathway, acantholysis, membrane attack complex, alternative pathway, opsonin, complement receptors

INTRODUCTION

Pemphigus are blistering autoimmune diseases causing painful bullous lesions, resulting from keratinocyte detachment (acantholysis), through the loss of desmosomes (1). In pemphigus foliaceus (PF), they occur in the superficial granular layer, affecting the skin. Yet in pemphigus vulgaris (PV), they locate in suprabasal stratum, also damaging mucosa. Lesions' localization correlate with tissue distribution of the main antigens: desmoglein 1 (DSG1) in PF and DSG3 in PV (2). Non-lesional skin may present blisters in the subgranular spinous layer, when submitted to mechanical friction (Nikolsky's sign) (3). Epithelial PF lesions may be restricted to sun-exposed seborrheic trunk and head areas (localized form) or be ubiquitously distributed (generalized form) (4, 5).

PF—An Epidemiological and Etiopathological Puzzle

Pemphigus occurs sporadically around the world, with incidence of 0.75–5 cases/million per year (6, 7). Despite this, PF is the only autoimmune disease known to be endemic in certain regions, as South America and Tunisia (5, 8), but epidemiology is puzzling, exhibiting wide differences even in neighboring countries. Midwestern Brazilian Amerindian populations actually present prevalences as high as 3.04% (9, 10). There is no sexual disproportion for PF in Brazil; most patients are young (10–40 years old) and have affected relatives. In Colombia, PF affects male mine workers and post-menopausal women (11), whereas young women are predominantly affected in Tunisia (9 female:1 male) (8). Endemic and non-endemic PF are indistinguishable (12), with the exception of higher anti-DSG1 IgM and IgE serum levels in endemic PF (13–15).

The epidemiological puzzle adds to the lack of understanding regarding PF etiology, since postulated major causes differ among countries (11). Brazilian PF patients are usually rural low-wage workers (4), exposed to acantholysis-fostering factors such as UVB (16), thiol and other calcium-sequestering components (11). Most present frequent bites of black (Simuliidae) and sand flies (Phlebotominae), vectors of onchocerciasis and leishmaniasis, respectively. Bites were suggested to increase up to almost five times the susceptibility to PF (17, 18), and components of the fly saliva may trigger a cross-reaction against keratinocyte surface epitopes (19). Viral or bacterial etiology was also suggested (5, 11). Genetic susceptibility involves differential gene expression (20, 21), variants in genes encoding antigen-presenting molecules HLA-DR and HLA-DQ (22, 23) and their corresponding regulatory transcription factor CIITA (24). Several other associations with genes of the immune response have been reported (25–31).

Pemphigus foliaceus patients have higher serum immunoglobulin G (IgG) levels against desmocollins 1 and 2 and all four desmogleins (32). Most pathogenic antibodies, able to induce acantholysis *in vitro* and *in vivo* (33–35), are of the IgG4 subclass (36–38), directed against the DSG1 N-terminal ectodomains (39, 40). Anti-DSG1 IgG1 are common in asymptomatic individuals of endemic regions, but can be the only pathogenic antibodies in a subset of PF patients (19). In contrast to IgG4, they initiate the classical pathway of the complement system (CS). This agrees with the frequent concomitant deposition of antibodies and CS components in PF lesions (41–45). Administration of corticosteroids is crucial to achieve disease control in the acute stage. Due to numerous and severe side effects, pemphigus patients are in desperate need of new, specifically targeted therapeutic strategies to substitute common therapy [reviewed in Ref. (46)].

PF and Complement: A Controversial Issue

Complement includes more than 50 plasma and membrane-bound proteins working in the forefront of host defense, killing pathogens and altered cells, and connecting innate to adaptive immune responses. Classical activation begins with the recognition of IgG or IgM, molecules on microbial and apoptotic cells, and C-reactive protein (CRP) by the C1 complex (C1q complexed with serine proteases C1r and C1s). The alternative activation pathway unleashes by spontaneous proteolysis of component C3. The lectin pathway follows recognition of sugar moieties or acetylated residues by colectins (as mannose-binding lectin—MBL) or ficolins (FCNs), respectively, complexed with another set of serine proteases (MASP-1 and MASP-2) (47, 48). All pathways converge in the formation of C3 convertase, which produces opsonic fragments that enhance antigen clearance by phagocytosis. C3b opsonin may be incorporated in the C5 convertase, which leads to the release of C5a anaphylatoxins and to pores opening on target cells, by insertion of the membrane attack complex (C5b-9 complex or MAC). Recognition of CS fragments leads to phagocytosis or blockage of the cascade, which is constantly activated at low levels, being continuously controlled to avoid tissue damage. Far beyond these well-known roles, CS also accomplishes critical functions in regulating inflammation, nervous system development and maturation, coagulation and hemostasis (49, 50).

In a series of five 1980s articles, entitled "Complement fixation by pemphigus antibody," the Jordon's group chased the hypothesis that complement has an important role in PV blister formation (51–55). They were closely followed by others who argued the same for PF. Strong granular C3 deposition was repeatedly reported along the basement membrane zone and in intercellular spaces of the epidermal strata (41–45). C3 was also reported to colocalize with IgG1 deposits in the upper epidermis intercellular spaces, in intact as well as injured skin, with a trend for higher deposits in perilesional tissue (42, 43, 45, 56). In fact, C1q and C4 fragments (reported in one patient), and MAC deposits distinguish injured skin, since IgG4 also occurs abundantly in non-acantholytic tissue (42, 43). In cell culture, complement does not seem necessary for acantholysis, but enhances keratinocyte detachment (55, 57).

Serum levels of C3 and CRP (opsonins), Ba and C4d factors (indicative of activated alternative and classical/lectin pathways, respectively), are increased in PF patients with active disease (58–60). $CD4^+$ T cells of PF patients present upregulated *C1QA* gene expression, compared to controls (20). Protein levels and *C1QA* expression fall with therapeutic intervention (20, 59, 60). By contrast, anti-DSG1 IgG levels remain high during disease remission (61, 62). MASP-2 levels tend to decline in PF patients,

but MBL serum concentrations seem unaffected (63). In PV biopsies, MBL and FCN2, but not C1q nor FCN3, recognize antigens in the basal membrane zone and intercellular spaces of the epidermis (64).

Nevertheless, C5-deficient mice or complement-depleted mice (after inoculation with cobra venom factor) develop the disease when injected with non-endemic PF IgG4 or its F(ab′)2 fragments (65). Both models did not affect C3 upstream components of the classical and lectin pathways, meaning that any roles played by these initiator molecules in the acantholytic process were not appreciated. In addition, the abundant but non-pathogenic anti-DSG1 human IgG1 does not cross-react with murine epidermis (66). By contrast, anti-DSG3 autoantibodies of PF patients, with cutaneous disease only, induce PV-like lesions in mice (67). Conversely, anti-DSG1 autoantibodies of PV patients without superficial epithelial lesions induce PF-like lesions (68). Adding to this picture, *DSG* expression pattern greatly differs between human and mouse (69) and differences in the genetic background of mouse models, which may deliver completely different outcomes for cutaneous inflammation, were not accounted for (70). Thus, although the mouse model reproduces acantholysis, it cannot reproduce the natural history of the disease itself, and pathological mechanisms may be quite different. For example, murine lesions present apoptotic cells (71), an uncommon finding in human biopsies (3, 72–74), with one reported exception (75). These results undeniably places complement in the disease, but its possible roles are still an issue to be solved.

GENETIC ASSOCIATION BETWEEN COMPLEMENT GENES AND PF

In the late 90s, the observations from experimental models seemed to have settled the interest on the role of complement in pemphigus. Nevertheless, tissue damage and inflammation, through over-activation and/or deficiency of complement components, play a key role in many dermatological diseases (76). These host-offensive actions may be exacerbated by genetic variation (77), but the extensive polymorphism of complement components impairs the comprehension of their overall impact in any given disease. In addition to the great genetic variation, the pleiotropic effects observed for complement genes add another layer of complexity.

Knowing that genetic associations may reveal new elements that play pivotal roles in disease susceptibility, we intend to reignite this discussion with new results of a PF case–control study that encompass tag polymorphisms within CS genes (Table S1 in Supplementary Material). We analyzed 992 single-nucleotide polymorphisms (SNPs) distributed within 44 genes, out of a subset of 551,839 SNPs genotyped in 229 endemic PF patients and 194 controls, through microarray hybridization (CoreExome-24 v1.1 Illumina). Included patients presented confirmed clinical PF diagnosis, according to physical examination and immunohistochemistry results. Controls were individuals of the endemic region, with no diagnosis or familial history of autoimmune diseases and unrelated to the patients. This study was carried out in accordance with the recommendations of the guidelines of the Conselho Nacional de Ética em Pesquisa (CONEP) with written informed consent from all subjects. All subjects gave written informed consent in accordance with the Declaration of Helsinki. The protocol was approved by CONEP (number 505.988). The statistical analyses were done with PLINK v1.1.9 (78). After excluding those SNPs with minor allele frequencies >1%, genotypic distributions deviating from those expected by Hardy–Weinberg equilibrium in controls ($p < 0.05$) and high linkage disequilibrium ($r^2 \geq 0.8$), 201 SNPs remained for subsequent analyses. For haplotypic analysis, 35 additional SNPs with $r^2 > 0.8$ were included. Association analysis was carried out by binary logistic regression, using two principal components (PCA) as covariables, which efficiently eliminates spurious associations due to ethnical differences. Thus, significance level was set to $p = 0.05$. Rather than exhausting the debate, our purpose is to launch new hypotheses that could be further validated through functional studies, which will link the pathogenic role of the PF autoantibodies to CS underexplored arms.

THE LONG KNOWN VERSUS THE UNEXPECTED: COMPLEMENT IN PF

We found evidence of association with gene variants of almost all complement elements previously detected in the epidermis or with altered serum levels in PF patients (**Table 1**; **Figure 1**). Among them, homozygotes for the intronic *rs4807895*T* allele within the *C3* gene were more susceptible to the disease (OR = 2.52; $p = 0.0239$). C3 fragments have been consistently reported in PF lesions (41–45, 56, 79, 80) and necessarily result from the activation of proteolytic cascades that converge in its enzymatic cleavage. Given the lack of functional evidence for this association, we speculate that it could be partly explained by increased *C3* gene regulation. This would not only increase phagocytosis and MAC deposition, but also T cell-mediated skin inflammation, as reported in other autoimmune diseases (81, 82).

Among the pathways held responsible for generating C3 fragments, we found association with genetic variants within genes of the alternative and lectin pathways, but not with the classical pathway. This agrees with the almost complete absence of C1q in human biopsies (42, 64). It also argues against the traditional hypothesis that activation of the classical pathway by anti-DSG1 IgG1 would play an important role in PF (42, 52, 85). In fact, the most abundant pathogenic IgG subclass in pemphigus is IgG4, which is unable to activate complement (33, 34).

Regarding the alternative pathway, we found a surprising genetic association with factor H, its most important regulator. Homozygotes for *CFH rs34388368*T*, an intronic allele associated with higher *CFH* mRNA levels in the hypodermis (83), were more susceptible to PF (OR = 2.57; $p = 0.0195$). These results contradict the conception that uncontrolled complement activation would be one of the underlying causes of PF.

We also found association between PF and five *MASP1* polymorphisms, four of them associated with differential mRNA levels in sun-exposed skin and/or in the hypodermis (83). They can potentially interfere with alternative pre-mRNA splicing, which generates three *MASP1* products—the collectin/

TABLE 1 | Complement gene variants associated with PF.

Gene	SNP	eQTL	Direction	MAF (%)			Model	Contr	Pat	OR	95 % CI	*p*
				Ib	Contr	Pat						
C3	rs4807895	–	–	30.8	25.26	29.04	add	98/290	133/325	1.26	[0.93–1.72]	0.1377
19p13.3	*t>C*						**rec**	**9/185**	**23/206**	**2.52**	**[1.13–5.62]**	**0.0239**
	Intron 11						dom	89/105	110/119	1.14	[0.77–1.67]	0.5177
C5AR1	rs10404456	3.2×10^{-5}*a	Down	25.2	31.87	40.67	**add**	**123/263**	**183/267**	**1.43**	**[1.07–1.90]**	**0.0155**
19q13.32	*c>T*						rec	20/173	38/187	1.67	[0.93–3.00]	0.0836
	5′ UTR						**dom**	**103/90**	**145/80**	**1.55**	**[1.04–2.30]**	**0.0299**
C8A	rs11206934	–	–	22	17.62	19.38	add	68/318	88/366	1.15	[0.81–1.63]	0.4228
1p32.2	*T>c*						**rec**	**3/190**	**13/214**	**4.02**	**[1.12–14.3]**	**0.0323**
	Intron 10						dom	65/128	75/152	1.00	[0.66–1.51]	0.993
C9	rs700218	–	–	0.9	2.10	0.21	**add**	**8/380**	**1/457**	**0.12**	**[0.01–0.97]**	**0.0471**
5p13.1	*G>t*						rec	0/194	0/229	–	–	–
	Intron 1						**dom**	**8/186**	**1/228**	**0.12**	**[0.01–0.97]**	**0.0471**
	rs187875	6.5×10^{-6}b	Up	31.8	23.26	30	**add**	**87/287**	**132/308**	**1.46**	**[1.06–2.01]**	**0.0189**
	C>t						rec	10/177	23/197	2.13	[0.98–4.64]	0.0556
	Intron 6						dom	77/110	109/111	1.49	[1.00–2.23]	0.0509
CD59	rs1047581	7.3×10^{-9}a	Down	40.2	31.19	23.8	**add**	**121/267**	**109/349**	**0.72**	**[0.52–0.98]**	**0.0373**
11p13	*A>g*						rec	16/178	15/214	0.87	[0.41–1.83]	0.7166
	3′ UTR						**dom**	**105/89**	**94/135**	**0.62**	**[0.42–0.91]**	**0.0152**
CFH	rs34388368	7.1×10^{-7}b	Up	22.4	27.13	29.68	add	102/274	130/308	1.11	[0.81–1.50]	0.5185
1q31.3	*G>t*						**rec**	**9/179**	**25/194**	**2.57**	**[1.16–5.66]**	**0.0195**
	Intron 1						add	93/95	105/114	0.90	[0.61–1.34]	0.6075
CR2	rs2182911	–	–	18.2	19.85	18.72	add	77/311	85/369	0.93	[0.65–1.32]	0.6813
1q32.2	*c>T*						**rec**	**11/183**	**3/224**	**0.23**	**[0.06–0.84]**	**0.0263**
	Intron 19						dom	66/128	82/145	1.09	[0.73–1.64]	0.6644
ITGAM	rs12928810	–	–	25.9	23.7	19.56	add	91/293	88/362	0.74	[0.53–1.03]	0.0735
16p11.2	*G>a*						rec	76/150	12/213	0.84	[0.36–1.98]	0.693
	Intron 14						**dom**	**80/112**	**76/149**	**0.66**	**[0.44–0.99]**	**0.0435**
ITGAX	rs11574637	–	–	22.9	28.09	20	**add**	**109/279**	**90/360**	**0.63**	**[0.45–0.87]**	**0.0056**
16p11.2	*T>c*						rec	14/180	10/215	0.55	[0.23–-1.29]	0.1698
	Exon 4						**dom**	**95/99**	**80/145**	**0.57**	**[0.39–0.85]**	**0.0058**
MASP1	rs13094773	4.6×10^{-8}a	Down	35	34.9	30.22	add	134/250	136/314	0.82	[0.61–1.09]	0.1747
3q27.3	*A>g*						**rec**	**28/164**	**18/207**	**0.50**	**[0.27–0.94]**	**0.0316**
	Intron 1						dom	106/86	118/107	0.91	[0.62–1.35]	0.6479
	rs3864098	3.5×10^{-8}a	Up	15	17.53	22.22	add	68/320	102/356	1.34	[0.94–1.92]	0.1066
	T>c						rec	7/187	6/223	0.68	[0.22–2.09]	0.5043
	Intron 2						**dom**	**61/133**	**96/133**	**1.53**	**[1.02–2.29]**	**0.0383**
	rs698104	2.2×10^{-10}a	Up	14	20.62	26.86	add	80/308	123/335	1.36	[0.96–1.90]	0.0787
	t>C						rec	9/185	13/216	1.08	[0.44–2.62]	0.8698
	Intron 2						**dom**	**71/123**	**110/119**	**1.52**	**[1.01–2.26]**	**0.0424**
	rs850309	1.1×10^{-18}b	Up	19.2	20.68	21.78	add	79/303	98/352	1.06	[0.74–1.50]	0.7596
	A>g						**rec**	**10/181**	**3/222**	**0.23**	**[0.06–0.87]**	**0.03**
	Intron 3						dom	69/122	95/130	1.27	[0.85–1.90]	0.2357
	rs72549154	–	–	2.8	7.51	4.64	**add**	**29/357**	**21/431**	**0.55**	**[0.31–0.99]**	**0.0453**
	G>t						rec	3/190	0/226	–	–	–
	Exon 12						dom	26/167	21/205	0.60	[0.32–1.12]	0.1119

Logistic regression association tests were done with allele frequencies ("add"), frequency of homozygotes for the minor allele ("rec"—recessive model), and summed frequency of heterozygotes and homozygotes for the minor allele ("dom"—dominant model). The minor allele is given in lowercase.

In bold: significant results; SNP, single-nucleotide polymorphism; eQTL, expression quantitative trait loci (83).

[a]*In skin.*

[b]*In hypodermis, direction: increase or decrease of RNA expression in relation the MAF.*

MAF, minor allele frequency; Ib, Iberian population (84); Contr, controls; Pat, patients, Model, association tests; OR, odds ratio; CI, confidence interval; PF, pemphigus foliaceus. ENSEMBL 2018 http://www.ensembl.org/index.html, GTEx portal—https://www.gtexportal.org/home/.

ficolin-associated serine proteases 1 and 3 (MASP-1 and MASP-3) and the truncated non-catalytic MAp44 (also called MAp1, only expressed in cardiac tissue). These products play important roles in competitive activation and blockage of the lectin and alternative pathways, intracellular signaling, coagulation, and bradykinin/kinin systems (86). In our setting, homozygotes for

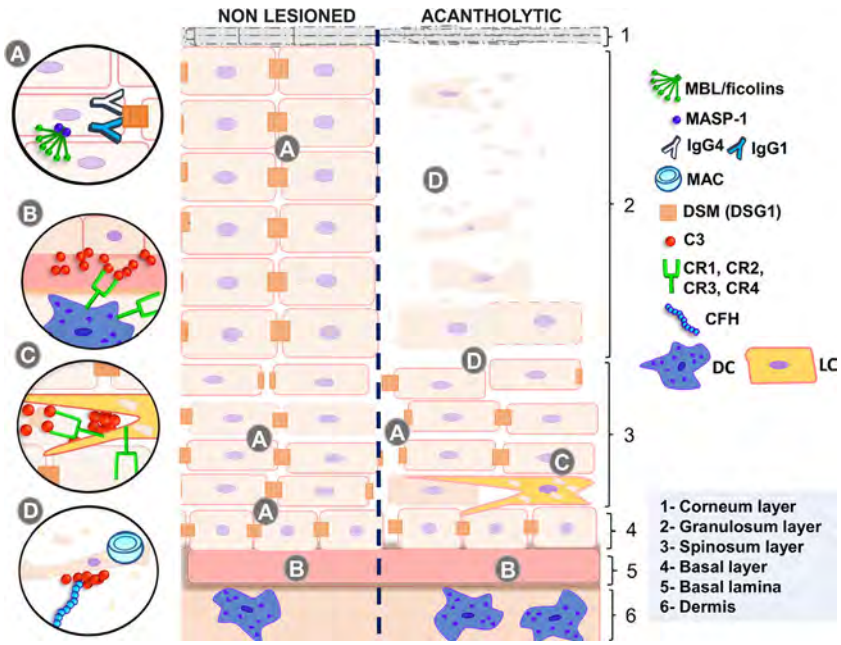

FIGURE 1 | Complement in non-lesioned and acantholytic PF lesions. **(A)** IgG1 and IgG4 autoantibodies binding to desmosomes causes shrinkage of keratinocytes, increasing intercellular spaces. This process is fostered by activation of the p38 MAPK signaling cascade, which may be unleashed by MASP-1, the serine protease associated with initiating molecules of the lectin pathway. **(B)** This is further accompanied by the release of antigens, most probably recognized by MBL or ficolins, leading to granular deposition of C3 fragments in the basal lamina. These deposits, as well as deposits of C3 fragments in the intercellular spaces, may also be caused by activation of the alternative pathway, inhibited by CFH. **(C)** Complement receptors recognize C3 fragments, leading to phagocytosis of autoantigens and increasing antigen presentation to T lymphocytes, thus feedbacking and diversifying autoantibody production. **(D)** Acantholytic lesions present formation of the membrane attack complex (blocked by CD59 expression), which may protect cells against apoptosis, if present in sublytic amounts. Active disease is also followed by increased C5a release, the latter recognized by C5A receptors in dendritic cells. MBL, mannose-binding lectin; MASP-1, mannose-binding lectin serine protease 1; MASP-2, mannose-binding lectin serine protease 2; MAC, membrane attack complex; IgG4, immunoglobulin 4; IgG1, immunoglobulin 1; DSM (DSG1), desmosome (desmoglein 1); C3, complement component 3; CR1, complement receptor type 1; CR2, complement receptor type 2; CR3, complement receptor type 3; CR4, complement receptor type 4; CFH, complement factor H; DC, dendritic cell; LC, Langerhans cell; PF, pemphigus foliaceus. Source: the author (2018).

*rs13094773*G* and *rs850309*G* (within an intronic region recognized by multiple regulatory proteins) (87) were more protected against PF (OR = 0.5; $p = 0.0316$ and OR = 0.23; $p = 0.03$, respectively). Yet individuals with intronic *rs3864098*C* (OR = 1.53; $p = 0.0383$) or *rs698104*T* (OR = 1.52; $p = 0.0424$) presented increased susceptibility to the disease. Of note, the *rs3864098*C* allele occurs in linkage disequilibrium with *rs710469*C*, an allele associated with lower MASP-3 levels in pre-admission critically ill children (88) (Table S2 in Supplementary Material). Finally, we found a protective association (OR = 0.55; $p = 0.0453$) with a missense variant affecting exclusively the serine protease domain of MASP-3 (*rs72549154*T* in exon 12, encoding p.Arg576Met). Heterozygotes for *rs72549154*T* present proportionally increased MASP-3 and decreased MASP-1 serum levels (89). Co-occurring *MASP1* alleles increase susceptibility to PF (not necessarily within the same haplotype): rs13094773**A* combined with rs3864098**C* (OR = 2.51 [95% CI = 1.26–4.97], $p = 0.0063$), rs13094773**A*, and rs698104**T* (OR = 2.37 [95% CI = 1.22–4.59], $p = 0.0074$) and between rs3864098**C* and rs698104**T* (OR = 1.67 [95% CI = 1.09–2.55], $p = 0.0141$). All the three variants are associated with higher MASP1 levels (83). Thus, it is conceivable that higher MASP-1 levels contribute to PF, while higher MASP-3 levels are protective. From the physiological point of view, altered MASP-1 levels would affect activation of the lectin pathway, which relies entirely on MASP-1 autoactivation (90). Additionally, MASP-1 activates MASP-3, which cleaves pro-factor D and launches the alternative complement cascade under non-inflammatory conditions (91). It further activates the p38 MAPK pathway in endothelial cells, which leads to IL-8 secretion and neutrophil recruitment (92, 93), both reported to occur in different forms of pemphigus (94–96). Most importantly, activation of the p38 MAPK signaling cascade causes acantholysis in keratinocytes and may be initiated by MASP-1 as well (97, 98).

Genetic variants of MAC components were also associated with PF. Homozygotes for the less common *C8A* allele *rs11206934*C* (OR = 4.02; $p = 0.0323$) in intron 10 and individuals with a *C9* haplotype harboring intronic variants consistently associated with increased gene expression in hypodermis and mucosa—*rs187875*T* (which disrupts a methylated CpG) (87) presented higher susceptibility to PF (Table S2 in Supplementary Material). By contrast, individuals with *rs700218*A* (intron 1 of *C9*) were more protected (OR = 0.12; $p = 0.0471$). We found no association with *C5* polymorphisms, as reported by others (who investigated only one SNP) (99). Nevertheless, individuals with the

*rs10404456*C* allele (located in the 5′ UTR of the *C5AR1* gene and associated with decreased mRNA levels in sun-exposed skin) (83) presented increased susceptibility to PF (OR = 1.43 $p = 0.0155$). This gene encodes the major receptor for C5a anaphylatoxin (49) and its deficiency has been rather associated with protection against several immune complex-mediated diseases, including epidermolysis bullosa acquisita (70, 100).

Keratinocytes may keep MAC formation at sublytic levels, eliciting pro-survival signal transduction, hence inhibiting apoptosis—instead of promoting cell destruction (101). This may be achieved by expressing low *CD59* levels, MAC's most important inhibitor. In fact, *rs1047581*G* in the 3′UTR region of the *CD59* gene, associated with reduced mRNA levels in sun-exposed skin (83), protected against PF (OR = 0.62; $p = 0.0152$). This result agrees with a recent study of our group, where the alternative allele of this same polymorphism occurs within a haplotype increasing *CD59* mRNA expression and PF susceptibility (32).

Among complement main roles, the removal of immune complexes and cellular debris is of critical importance for autoimmunity prevention (70). Within the context of the other associations, we suggest that protection may be explained by higher scavenging efficiency of acantholytic cell debris. Furthermore, we found associations with four opsonin-binding complement receptors (CR1-4, encoded by *CR1*, *CR2*, *ITGAM*, and *ITGAX*). Interestingly, we found a susceptibility association with a *CR1* haplotype that includes the major *rs6656401*G* allele (Table S2 in Supplementary Material), also associated with protection against Alzheimer's disease (102). The binding of CR2 to iC3b, C3dg, and C3d lowers the threshold for B cell activation (103) and homozygotes for *rs2182911*C* of the *CR2* gene were more protected against the disease (OR = 0.23; $p = 0.0263$). The products of *ITGAM* (CR3) and *ITGAX* (CR4) genes recognize iC3b (48). Individuals with the *rs12928810*A* (disrupts a CpG in intron 14 of *ITGAM*) or *rs11574637*C* (a missense variant—p.Phe180Leu—in exon 4 of *ITGAX*) were more resistant against PF (OR = 0.66; $p = 0.0435$ and OR = 0.63; $p = 0.0056$, respectively). Remarkably, the same *ITGAX* allele was associated with higher susceptibility to IgA nephropathy and systemic lupus erythematosus (104, 105). The *rs11574637*C* (*ITGAX*) and *rs4807895*T* (*C3*) combined are protective against PF (OR = 0.55 [95% CI = 0.32–0.95], $p = 0.0276$). The same occurs with the rs11574637**C* (*ITGAX*) and the rs12928810**A* (*ITGAM*) (OR = 0.59 [95% CI = 0.38–0.90], $p = 0.0115$). By contrast, individuals presenting both the rs10404456**C* (*C5AR1*) and rs12928810**G/G* (*ITGAM*) are more susceptible to PF (OR = 2.33 [95% CI = 1.27–4.28], $p = 0.0035$), as were those with rs10404456**C* (*C5AR1*) and rs11574637**T/T* (*ITGAX*) (OR = 2.64 [95% CI = 1.49–4.66], $p = 0.0006$). In a previous study of our group, the mRNA expression levels of *ITGAM* were increased in $CD4^+$ T cells of PF patients with generalized lesions, whereas *ITGAX* mRNA expression decreased after treatment (20).

PERSPECTIVES

Complement gene associations reinforced the findings of former studies, regarding the alternative pathway, C3 and MAC deposition on epidermal cells. Our results shed light on previously barely noticed processes, notably CS-mediated signaling, especially by MASP-1, and removal of opsonized elements, through complement receptors. The role of antigen-presenting phagocytes bearing CR1, CR2, CR3, and CR4, as dendritic and Langerhans cells, should be deeper investigated, since they probably exert crucial roles in the events preceding B cell activation and autoantibody production. Furthermore, lectin and alternative pathways, activated at low levels, are probably important to prevent the disease. Taken together, the results on these pathways lead us to suggest caution on the possible use of the two available complement-inhibiting drugs, able to prevent classical/lectin pathway initiation (C1INH) and MAC generation (Eculizumab), since complement activation appears desirable to PF prevention. Strong evidence for *MASP1* association, but not for *MASP2* or other genes of the lectin pathway, favor a pathogenic role carried out by MASP-1 in eliciting p38MAPK signaling and consequent DSG1 clustering on the keratinocyte cell membrane. Functional validation of the pathogenic roles exerted by this wide-reaching network of complement components will open new windows to understand PF etiology and development, hopefully improving therapeutic interventions.

ETHICS STATEMENT

This study was carried out in accordance with the recommendations of the guidelines of the Conselho Nacional de Ética em Pesquisa (CONEP) with written informed consent from all subjects. All subjects gave written informed consent in accordance with the Declaration of Helsinki. The protocol was approved by CONEP (number 505.988).

AUTHOR CONTRIBUTIONS

MP-E, AB, GC, RA, and DA contributed to conception of the work. AB and VB-B designed the study. MP-E provided the samples. DA performed microarray hybridization. VB-B and RA did the statistical analysis. VB-B, AB, and GC drafted the manuscript. All authors revised the work critically for intellectual content and approved the final version of the work.

ACKNOWLEDGMENTS

We gratefully acknowledge the patients for their participation in this study. We also thank the staff of the Laboratório de Genética Molecular Humana/UFPR for their assistance and helpful discussions. The Genotype-Tissue Expression (GTEx) Project was supported by the Common Fund of the Office of the Director of the National Institutes of Health, and by NCI, NHGRI, NHLBI, NIDA, NIMH, and NINDS. The data used for the analyses described in this manuscript were obtained from https://www.gtexportal.org on 16/01/2018.

FUNDING

This work was supported by grants of the following funding agencies: Fundação Araucária (FA protocol 39894.413.43926.1904/2013),

Conselho Nacional de Desenvolvimento Científico e Tecnológico (CNPq protocol 470483/2014-8), and Coordenação de Aperfeiçoamento de Pessoal de Nível Superior (a post-doc scholarship with bench rate for DA: CAPES protocol 400648/2014-8).

SUPPLEMENTARY MATERIAL

The Supplementary Material for this article can be found online at https://www.frontiersin.org/articles/10.3389/fimmu.2018.00695/full#supplementary-material.

REFERENCES

1. Amagai M, Stanley JR. Desmoglein as a target in skin disease and beyond. *J Invest Dermatol* (2012) 132:776–84. doi:10.1038/jid.2011.390
2. Spindler V, Drenckhahn D, Zillikens D, Waschke J. Pemphigus IgG causes skin splitting in the presence of both desmoglein 1 and desmoglein 3. *Am J Pathol* (2007) 171(3):906–16. doi:10.2353/ajpath.2007.070028
3. Sokol E, Kramer D, Diercks GFH, Kuipers J, Jonkman MF, Pas HH, et al. Large-scale electron microscopy maps of patient skin and mucosa provide insight into pathogenesis of blistering diseases. *J Invest Dermatol* (2015) 135(7):1763–70. doi:10.1038/jid.2015.109
4. Diaz LA, Sampaio SA, Rivitti EA, Martins CR, Cunha PR, Lombardi C, et al. Endemic pemphigus foliaceus (fogo selvagem): I. Clinical features and immunopathology. *J Am Acad Dermatol* (1989) 20(4):657–69. doi:10.1016/S0190-9622(89)70079-7
5. Castro RM, Roscoe JT, Sampaio SAP. Brazilian pemphigus foliaceus. *Clin Dermatol* (1983) 1(2):22–41. doi:10.1016/0738-081X(83)90021-4
6. Meyer N, Misery L. Geoepidemiologic considerations of auto-immune pemphigus. *Autoimmun Rev* (2010) 9(5):379–82. doi:10.1016/j.autrev.2009.10.009
7. Alpsoy E, Akman-Karakas A, Uzun S. Geographic variations in epidemiology of two autoimmune bullous diseases: pemphigus and bullous pemphigoid. *Arch Dermatol Res* (2015) 307(4):291–8. doi:10.1007/s00403-014-1531-1
8. Bastuji-Garin S, Souissi R, Blum L, Turki H, Nouira R, Jomaa B, et al. Comparative epidemiology of pemphigus in Tunisia and France: unusual incidence of pemphigus foliaceus in young Tunisian women. *J Invest Dermatol* (1995) 104(2):302–5. doi:10.1111/1523-1747.ep12612836
9. Friedman H, Campbell I, Rocha-Alvarez R, Ferrari I, Coimbra CE, Moraes JR, et al. Endemic pemphigus foliaceus (fogo selvagem) in native Americans from Brazil. *J Am Acad Dermatol* (1995) 32:949–56. doi:10.1016/0190-9622(95)91330-0
10. Hans-Filho G, dos Santos V, Katayama JH, Aoki V, Rivitti EA, Sampaio SAP, et al. An active focus of high prevalence of fogo selvagem on an Amerindian reservation in Brazil. *J Invest Dermatol* (1996) 107:68–75. doi:10.1111/1523-1747.ep12298213
11. Abréu-vélez AM, Messias-Reason IJ, Howard MS, Roselino A. Endemic pemphigus foliaceus over a century: part I. *N Am J Med Sci* (2010) 2(3):51–9.
12. Stanley JR, Klaus-Kovtun V, Sampaio SAP. Antigenic specificity of fogo selvagem autoantibodies is similar to North American pemphigus foliaceus and distinct from pemphigus vulgaris autoantibodies. *J Invest Dermatol* (1986) 87(2):197–201. doi:10.1111/1523-1747.ep12695334
13. Diaz LA, Prisayanh PS, Dasher DA, Li N, Evangelista F, Aoki V, et al. The IgM anti-desmoglein 1 response distinguishes Brazilian pemphigus foliaceus (fogo selvagem) from other forms of pemphigus. *J Invest Dermatol* (2008) 128(3):667–75. doi:10.1038/sj.jid.5701121
14. Qian Y, Prisayanh P, Andraca E, Qaqish BF, Aoki V, Hans-Filhio G, et al. IgE, IgM, and IgG4 anti-desmoglein 1 autoantibody profile in endemic pemphigus foliaceus (fogo selvagem). *J Invest Dermatol* (2011) 131(4):985–7. doi:10.1038/jid.2010.403
15. Qian Y, Jeong JS, Abdeladhim M, Valenzuela JG, Aoki V, Hans-Filhio G, et al. IgE anti-LJM11 sand fly salivary antigen may herald the onset of fogo selvagem in endemic Brazilian regions. *J Invest Dermatol* (2015) 135(3):913–5. doi:10.1038/jid.2014.430
16. Reis VM, Toledo RP, Lopez A, Diaz LA, Martins JE. UVB-induced acantholysis in endemic pemphigus foliaceus (fogo selvagem) and pemphigus vulgaris. *J Am Acad Dermatol* (2000) 42:571–6. doi:10.1016/S0190-9622(00)90167-1
17. Lombardi C, Borges PC, Chaul A, Sampaio SA, Rivitti EA, Friedman H, et al. Environmental risk factors in the endemic pemphigus foliaceus (fogo selvagem). *J Invest Dermatol* (1992) 98(6):847–50. doi:10.1111/1523-1747.ep12456932
18. Vernal S, Pepinelli M, Casanova C, Goulart TM, Kim O, De Paula NA, et al. Insights into the epidemiological link between biting flies and pemphigus foliaceus in Southeastern Brazil. *Acta Trop* (2017) 176:455–62. doi:10.1016/j.actatropica.2017.09.015
19. Qian Y, Jeong JS, Maldonado M, Valenzuela JG, Gomes R, Evangelista F, et al. Brazilian pemphigus foliaceus anti-desmoglein 1 autoantibodies cross-react with sand fly salivary LJM11 antigen. *J Immunol* (2012) 189(4):1535–9. doi:10.4049/jimmunol.1200842
20. Malheiros D, Panepucci RA, Roselino AM, Araújo AG, Zago MA, Petzl-Erler ML. Genome-wide gene expression profiling reveals unsuspected molecular alterations in pemphigus foliaceus. *Immunology* (2014) 143(3):381–95. doi:10.1111/imm.12315
21. Camargo CM, Augusto DG, Petzl-Erler M. Differential gene expression levels might explain association of LAIR2 polymorphisms with pemphigus. *Hum Genet* (2016) 135(2):233–44. doi:10.1007/s00439-015-1626-6
22. Petzl-Erler ML, Santamaria J. Are HLA class II genes controlling susceptibility and resistance to Brazilian pemphigus foliaceus (fogo selvagem)? *Tissue Antigens* (1989) 33(3):408–14. doi:10.1111/j.1399-0039.1989.tb01684.x
23. Pavoni DP, Roxo VMMS, Marquart Filho A, Petzl-Erler ML. Dissecting the associations of endemic pemphigus foliaceus (fogo selvagem) with HLA-DRB1 alleles and genotypes. *Genes Immun* (2003) 4(2):110–6. doi:10.1038/sj.gene.6363939
24. Piovezan BZ, Petzl-Erler ML. Both qualitative and quantitative genetic variation of MHC class II molecules may influence susceptibility to autoimmune diseases: the case of endemic pemphigus foliaceus. *Hum Immunol* (2013) 74(9):1134–40. doi:10.1016/j.humimm.2013.06.008
25. Pereira NF, Hansen JA, Lin MT, Roxo VMMS, Braun K, Petzl-Erler ML. Cytokine gene polymorphisms in endemic pemphigus foliaceus: a possible role for IL6 variants. *Cytokine* (2004) 28(6):233–41. doi:10.1016/j.cyto.2004.08.006
26. Malheiros D, Petzl-Erler ML. Individual and epistatic effects of genetic polymorphisms of B-cell co-stimulatory molecules on susceptibility to pemphigus foliaceus. *Genes Immun* (2009) 10(6):547–58. doi:10.1038/gene.2009.36
27. Dalla-Costa R, Pincerati MR, Beltrame MH, Malheiros D, Petzl-Erler ML. Polymorphisms in the 2q33 and 3q21 chromosome regions including T-cell coreceptor and ligand genes may influence susceptibility to pemphigus foliaceus. *Hum Immunol* (2010) 71(8):809–17. doi:10.1016/j.humimm.2010.04.001
28. Augusto DG, Lobo-Alves SC, Melo MF, Pereira NF, Petzl-Erler ML. Activating KIR and HLA Bw4 ligands are associated to decreased susceptibility to pemphigus foliaceus, an autoimmune blistering skin disease. *PLoS One* (2012) 7(7):e39991. doi:10.1371/journal.pone.0039991
29. Augusto DG, O'Connor GM, Lobo-Alves SC, Bass S, Martin MP, Carrington M, et al. Pemphigus is associated with KIR3DL2 expression levels and provides evidence that KIR3DL2 may bind HLA-A3 and A11 in vivo. *Eur J Immunol* (2015) 45(7):2052–60. doi:10.1002/eji.201445324
30. Cipolla GA, Park JK, de Oliveira LA, Lobo-Alves SC, de Almeida RC, Farias TDJ, et al. A 3′UTR polymorphism marks differential KLRG1 mRNA levels through disruption of a miR-584-5p binding site and associates with pemphigus foliaceus susceptibility. *Biochim Biophys Acta* (2016) 1859(10):1306–13. doi:10.1016/j.bbagrm.2016.07.006
31. Salviano-Silva A, Petzl-Erler ML, Boldt ABW. CD59 polymorphisms are associated with gene expression and different sexual susceptibility to pemphigus foliaceus. *Autoimmunity* (2017) 50(6):377–85. doi:10.1080/08916934.2017.1329830
32. Flores G, Culton DA, Prisayanh P, Qaqish BF, James K, Maldonado M, et al. IgG autoantibody response against keratinocyte cadherins in endemic pemphigus foliaceus (fogo selvagem). *J Invest Dermatol* (2012) 132(11):2573–80. doi:10.1038/jid.2012.232
33. Roscoe JT, Diaz L, Sampaio SAP, Castro RM, Labib RS, Takahashi Y, et al. Brazilian pemphigus foliaceus autoantibodies are pathogenic to BALB/c mice by passive transfer. *J Invest Dermatol* (1985) 85(6):538–41. doi:10.1111/1523-1747.ep12277362

34. Rock B, Martins CR, Theofilopoulos AN, Balderas RS, Anhalt GJ, Labib RS, et al. The pathogenic effect of IgG4 autoantibodies in endemic pemphigus foliaceus (fogo selvagem). *N Engl J Med* (1989) 320(22):1463–9. doi:10.1056/NEJM198906013202206
35. Rock B, Labib RS, Diaz LA. Monovalent Fab' immunoglobulin fragments from endemic pemphigus foliaceus autoantibodies reproduce the human disease in neonatal Balb/c mice. *J Clin Invest* (1990) 85:296–9. doi:10.1172/JCI114426
36. Warren SJ, Arteaga LA, Rivitti EA, Aoki V, Hans-Filho G, Qaqish BF, et al. The role of subclass switching in the pathogenesis of endemic pemphigus foliaceus. *J Invest Dermatol* (2003) 120(1):104–8. doi:10.1046/j.1523-1747.2003.12017.x
37. Qaqish BF, Prisayanh P, Qian Y, Andraca E, Li N, Aoki V, et al. Development of an IgG4-based classifier/predictor of endemic pemphigus foliaceus (fogo selvagem). *J Invest Dermatol* (2009) 129(1):110–8. doi:10.1038/jid.2008.189
38. Maldonado M, Diaz LA, Prisayanh P, Yang J, Qaqish BF, Aoki V, et al. Divergent specificity development of IgG1 and IgG4 autoantibodies in endemic pemphigus foliaceus (fogo selvagem). *Immunohorizons* (2017) 1(6):71–80. doi:10.4049/immunohorizons.1700029
39. Li N, Aoki V, Hans-Filho G, Rivitti EA, Diaz LA. The role of intramolecular epitope spreading in the pathogenesis of endemic pemphigus foliaceus (fogo selvagem). *J Exp Med* (2003) 197(11):1501–10. doi:10.1084/jem.20022031
40. Aoki V, Millikan RC, Rivitti EA, Hans-Filho G, Eaton DP, Warren SJP, et al. Environmental risk factors in endemic pemphigus foliaceus (fogo selvagem). *J Investig Dermatol Symp Proc* (2004) 9(1):34–40. doi:10.1111/1346-8138.12675
41. Messias-Reason IJ, von Kuster LC, Santamaria J, Kajdacsy-Balla A. Complement and antibody deposition in Brazilian pemphigus foliaceus and correlation of disease activity with circulating antibodies. *Arch Dermatol* (1988) 124(11):1664–8. doi:10.1001/archderm.1988.01670110024005
42. Kawana S, Geoghegan WD, Jordon RE, Nishiyanu S. Deposition of membrane attack complex of complement in pemphigus vulgaris and in pemphigus foliaceus skin. *J Invest Dermatol* (1989) 92(4):588–92. doi:10.1111/1523-1747.ep12709624
43. Pegas JR, dos Reis VMS. Direct immunofluorescence on uninvolved, lesional and perilesional skin in patients with endemic pemphigus foliaceus (fogo selvagem). *Med Sci Monit* (2004) 10(12):657–62.
44. Odo MEY, Rodrigues RML, Miyauchi L. Direct immunofluorescence in skin biopsy of Brazilian pemphigus foliaceus. *An Bras Dermatol* (1981) 56(2):1–5.
45. Hernandez C, Amagai M, Chan L. Pemphigus foliaceus: preferential binding of IgGl and C3 at the upper epidermis. *Br J Dermatol* (1997) 136:249–52. doi:10.1111/j.1365-2133.1997.tb14907.x
46. Grando SA. Pemphigus autoimmunity: hypotheses and realities. *Autoimmunity* (2012) 45(1):1–35. doi:10.3109/08916934.2011.606444
47. Beltrame MH, Catarino SJ, Goeldner I, Boldt ABW, Messias-Reason IJ. The lectin pathway of complement and rheumatic heart disease. *Front Pediatr* (2015) 2:148. doi:10.3389/fped.2014.00148
48. Holmskov U, Thiel S, Jensenius JC. Collectins and ficolins: humoral lectins of the innate immune defense. *Annu Rev Immunol* (2003) 21(1):547–78. doi:10.1146/annurev.immunol.21.120601.140954
49. Ricklin D, Hajishengallis G, Yang K, Lambris JD. Complement: a key system for immune surveillance and homeostasis. *Nat Immunol* (2010) 11(9):785–97. doi:10.1038/ni.1923
50. Gros P, Milder FJ, Janssen BJC. Complement driven by conformational changes. *Nat Rev Immunol* (2008) 8(1):48–58. doi:10.1038/nri2231
51. Kawana S, Janson M, Jordon RE. Complement fixation by pemphigus antibody. I. In vitro fixation to organ and tissue culture skin. *J Invest Dermatol* (1984) 48(5):506–10. doi:10.1111/1523-1747.ep12261058
52. Kawana S, Geoghegan WD, Jordon RE. Complement fixation by pemphigus antibody. II. Complement enhanced detachment of epidermal cells. *Clin Exp Immunol* (1985) 61(3):517–25.
53. Kawana S, Geoghegan WD, Jordon R. Complement fixation by pemphigus antibody. III. Altered epidermal cell membrane integrity mediated by pemphigus antibody and complement. *J Invest Dermatol* (1986) 86(1):29–33. doi:10.1111/1523-1747.ep12283762
54. Doubleday CW, Geoghegan WD, Jordon R. Complement fixation by pemphigus antibody. IV. Enhanced epidermal cell detachment in the absence of human plasminogen. *J Lab Clin Med* (1988) 111(1):28–34.
55. Xia P, Jordon RE, Geoghegan W. Complement fixation by pemphigus antibody. V. Assembly of the membrane attack complex on cultured human keratinocytes. *J Clin Invest* (1988) 82(6):1939–47. doi:10.1172/JCI113813
56. Hahn K, Kippes W, Amagai M, Rzany B, Bröcker EB, Zillikens D. Clinical aspects and immunopathology in 48 patients with pemphigus. *Hautarzt* (2000) 51(9):670–7. doi:10.1007/s001050051193
57. Hashimoto K, Shafran KM, Webber PS, Lazarus GS, Singer K. Anti-cell surface pemphigus autoantibody stimulates plasminogen activator activity of human epidermal cells – a mechanism for the loss of epidermal cohesion and blister formation. *J Exp Med* (1983) 157(1):259–72. doi:10.1084/jem.157.1.259
58. Ablin RJ. Levels of C'3 in the serum of patients with pemphigus. *J Invest Dermatol* (1971) 56(6):450–3. doi:10.1111/1523-1747.ep12261375
59. Messias-Reason IJ, Santamaria J, Ragiotto R, Doi EM, Kajdacsy-Balla A. Complement activation in Brazilian pemphigus foliaceus. *Clin Exp Dermatol* (1989) 14(1):51–5. doi:10.1111/j.1365-2230.1989.tb00883.x
60. Franquini J, Adad SJ, Murta AH, de Morais CA, Teixeira Vde P, Júnior VR. Tests of inflammatory activity in endemic pemphigus foliaceus. *Rev Soc Bras Med Trop* (1994) 27(1):25–9.
61. Harman KE, Seed PT, Gratian MJ, Bhogal BS, Challacombe SJ, Black MM. The severity of cutaneous and oral pemphigus is related to desmoglein 1 and 3 antibody levels. *Br J Dermatol* (2001) 144(4):775–80. doi:10.1046/j.1365-2133.2001.04132.x
62. Kwon EJ, Yamagami J, Nishikawa T, Amagai M. Anti-desmoglein IgG autoantibodies in patients with pemphigus in remission. *J Eur Acad Dermatol Venereol* (2008) 22(9):1070–5. doi:10.1111/j.1468-3083.2008.02715.x
63. Messias-Reason IJ, Bosco DG, Nisihara RM, Jakobsen LH, Petzl-Erler ML, Jensenius JC. Circulating levels of mannan-binding lectin (MBL) and MBL-associated serine protease 2 in endemic pemphigus foliaceus. *Clin Exp Dermatol* (2008) 33(4):495–7. doi:10.1111/j.1365-2230.2008.02743.x
64. Messias-Reason IJ, Nisihara RM, Mocelin V. Mannan-binding lectin and ficolin deposition in skin lesions of pemphigus. *Arch Dermatol Res* (2011) 303:521–5. doi:10.1007/s00403-011-1132-1
65. España A, Diaz LA, Mascaró JM, Giudice GJ, Fairley JA, Till GO, et al. Mechanisms of acantholysis in pemphigus foliaceus. *Clin Immunol Immunopathol* (1997) 85(1):83–9. doi:10.1006/clin.1997.4407
66. Hacker MK, Janson M, Fairley JA, Lin MS. Isotypes and antigenic profiles of pemphigus foliaceus and pemphigus vulgaris autoantibodies. *Clin Immunol* (2002) 105(1):64–74. doi:10.1006/clim.2002.5259
67. Arteaga LA, Prisayanh PS, Warren SJ, Liu Z, Diaz LA, Lin M-S. A subset of pemphigus foliaceus patients exhibits pathogenic autoantibodies against both desmoglein-1 and desmoglein-3. *J Invest Dermatol* (2002) 118(5):806–11. doi:10.1046/j.1523-1747.2002.01743.x
68. Ding X, Diaz LA, Fairley JA, Giudice GJ, Liu Z. The anti-desmoglein 1 autoantibodies in pemphigus vulgaris sera are pathogenic. *J Invest Dermatol* (1999) 112(5):739–43. doi:10.1046/j.1523-1747.1999.00585.x
69. Mahoney MG, Hu Y, Brennan D, Bazzi H, Christiano AM, Wahl JK. Delineation of diversified desmoglein distribution in stratified squamous epithelia: implications in diseases. *Exp Dermatol* (2006) 15(2):101–9. doi:10.1111/j.1600-0625.2006.00391.x
70. Karsten CM, Köhl J. The immunoglobulin, IgG Fc receptor and complement triangle in autoimmune diseases. *Immunobiology* (2012) 217:1067–79. doi:10.1016/j.imbio.2012.07.015
71. Li N, Zhao M, Wang J, Liu Z, Diaz LA. Involvement of the apoptotic mechanism in pemphigus foliaceus autoimmune injury of the skin. *J Immunol* (2009) 182(1):711–7. doi:10.4049/jimmunol.182.1.711
72. Janse IC, Wier VDG, Jonkman MF, Pas HH, Diercks GFH. No evidence of apoptotic cells in pemphigus acantholysis. *J Invest Dermatol* (2014) 134(7):2039–41. doi:10.1038/jid.2014.60
73. van der Wier G, Jonkman MF, Pas HH, Diercks GF. Ultrastructure of acantholysis in pemphigus foliaceus re-examined from the current perspective. *Br J Dermatol*. (2012) 167(6):1265–71. doi:10.1111/j.1365-2133.2012.11173.x
74. Zuccolotto I, Roselino AM, Ramalho LNZ, Zucoloto S. Apoptosis and p63 expression in the pathogenesis of bullous lesions of endemic pemphigus foliaceus. *Arch Dermatol Res* (2003) 295(7):284–6. doi:10.1007/s00403-003-0434-3
75. Rodrigues DBR, Pereira SAL, dos Reis MA, Adad SJ, Caixeta JE, Chiba AM, et al. In situ detection of inflammatory cytokines and apoptosis in

pemphigus foliaceus patients. *Arch Pathol Lab Med* (2009) 133(1):97–100. doi:10.1043/1543-2165-133.1.97
76. Palianus J, Meri S. Complement system in dermatological diseases – fire under the skin. *Front Med* (2015) 2:3. doi:10.3389/fmed.2015.00003
77. Ricklin D, Reis ES, Lambris JD. Complement in disease: a defence system turning offensive. *Nat Rev Nephrol* (2016) 12(7):383–401. doi:10.1038/nrneph.2016.70
78. Purcell S, Neale B, Todd-Brown K, Thomas L, Ferreira MAR, Bender D, et al. PLINK: a tool set for whole-genome association and population-based linkage analyses. *Am J Hum Genet* (2007) 81(3):559–75. doi:10.1086/519795
79. Amin MN, Islam AZMM. Clinical, histologic and immunologic features of pemphigus in Bangladesh. *Int J Dermatol* (2006) 45(11):1317–8. doi:10.1111/j.1365-4632.2006.02942.x
80. Júnior JVO, Maruta CW, Sousa JX, Santi CG, Valente NYS, Ichimura LMF, et al. Clinical and immunological profile of umbilical involvement in pemphigus vulgaris and pemphigus foliaceus. *Clin Exp Dermatol* (2013) 38(1):20–4. doi:10.1111/j.1365-2230.2012.04468.x
81. Schonthaler HB, Guinea-Viniegra J, Wculek SK, Ruppen I, Ximénez-Embún P, Guío-Carrión A, et al. S100A8-S100A9 protein complex mediates psoriasis by regulating the expression of complement factor C3. *Immunity* (2013) 39(6):1171–81. doi:10.1016/j.immuni.2013.11.011
82. Ma Q, Li D, Carreño R, Patenia R, Tsai KY, Xydes-Smith M, et al. Complement component C3 mediates Th1/Th17 polarization in human T cell activation and cutaneous graft-versus-host disease. *Bone Marrow Transplant* (2014) 49(7):972–6. doi:10.1038/bmt.2014.75
83. Consortium TG. The genotype-tissue expression (GTEx) project. *Nat Genet* (2013) 45(6):580–5. doi:10.1038/ng.2653
84. Zerbino DR, Achuthan P, Akanni W, Amode MR, Barrell D, Bhai J, et al. Ensembl 2018. *Nucleic Acids Res* (2018) 46:754–61. doi:10.1371/journal.pone.0051647
85. Nishikawa T, Kurihara S, Harada T, Sugawara M, Hatano H. Capability of complement fixation of pemphigus antibodies in vitro. *Arch Dermatol Res* (1977) 260:1–6. doi:10.1007/BF00558008
86. Boldt ABW, Boschmann SE, Catarino SJ, Andrade FA, Messias-Reason IJ. MASP1 and MASP2. In: Choi S, editor. *Encyclopedia of Signaling Molecules*. 2nd ed. Springer (2018). p. 2972–89. doi:10.1007/978-3-319-67199-4
87. Kent WJ, Sugnet CW, Furey TS, Roskin KM, Pringle TH, Zahler AM, et al. The human genome browser at UCSC. *Genome Res* (2002) 12(6):996–1006. doi:10.1101/gr.229102
88. Ingels C, Vanhorebeek I, Steffensen R, Derese I, Jensen L, Wouters PJ, et al. Lectin pathway of complement activation and relation with clinical complications in critically ill children. *Pediatr Res* (2014) 75(1):99–108. doi:10.1038/pr.2013.180
89. Ammitzboll CG, Steffensen R, Nielsen HJ, Thiel S, Stengaard-Pedersen K, Bogsted M, et al. Polymorphisms in the MASP1 gene are associated with serum levels of MASP-1, MASP-3, and MAp44. *PLoS Genet* (2013) 8(9):e73317. doi:10.1371/journal.pone.0073317
90. Degn SE, Jensen L, Hansen AG, Duman D, Tekin M, Jensenius JC, et al. Mannan-binding lectin-associated serine protease (MASP)-1 is crucial for lectin pathway activation in human serum, whereas neither MASP-1 nor MASP-3 is required for alternative pathway function. *J Immunol* (2012) 189(8):3957–69. doi:10.4049/jimmunol.1201736
91. Dobó J, Pál G, Cervenak L, Gál P. The emerging roles of mannose-binding lectin-associated serine proteases (MASPs) in the lectin pathway of complement and beyond. *Immunol Rev* (2016) 274(1):98–111. doi:10.1111/imr.12460
92. Jani PK, Kajdácsi E, Megyeri M, Dobó J, Doleschall Z, Futosi K, et al. MASP-1 induces a unique cytokine pattern in endothelial cells: a novel link between complement system and neutrophil granulocytes. *PLoS One* (2014) 9(1):e87104. doi:10.1371/journal.pone.0087104
93. Megyeri M, Mako V, Beinrohr L, Doleschall Z, Prohaszka Z, Cervenak L, et al. Complement protease MASP-1 activates human endothelial cells: PAR4 activation is a link between complement and endothelial function. *J Immunol* (2009) 183(5):3409–16. doi:10.4049/jimmunol.0900879
94. Lee SH, Hong WJ, Kim S. Analysis of serum cytokine profile in pemphigus. *Ann Dermatol* (2017) 29(4):438–45. doi:10.5021/ad.2017.29.4.438
95. Timóteo RP, Silva MV, Alves-Silva DA, Catarino JS, Alves FHC, Junior VR, et al. Cytokine and chemokines alterations in the endemic form of pemphigus foliaceus (fogo selvagem). *Front Immunol* (2017) 8:978. doi:10.3389/fimmu.2017.00978
96. Hoss DM, Shea CR, Grant-Kels J. Neutrophilic spongiosis in pemphigus. *Arch Dermatol* (1996) 132(3):315–8. doi:10.1001/archderm.132.3.315
97. Berkowitz P, Chua M, Liu Z, Diaz LA, Rubenstein DS. Autoantibodies in the autoimmune disease pemphigus foliaceus induce blistering via p38 mitogen-activated protein kinase-dependent signaling in the skin. *Am J Pathol* (2008) 173(6):1628–36. doi:10.2353/ajpath.2008.080391
98. Yoshida K, Ishii K, Shimizu A, Yokouchi M, Amagai M, Shiraishi K, et al. Non-pathogenic pemphigus foliaceus (PF) IgG acts synergistically with a directly pathogenic PF IgG to increase blistering by p38MAPK-dependent desmoglein 1 clustering. *J Dermatol Sci* (2017) 85(3):197–207. doi:10.1016/j.jdermsci.2016.12.010
99. Mejri K, Mbarek H, Kallel-Sellami M, Petit-Teixeira E, Zerzeri Y, Abida O, et al. TRAF1/C5 polymorphism is not associated with pemphigus. *Br J Dermatol* (2009) 160(6):1348–50. doi:10.1111/j.1365-2133.2009.09136.x
100. Karsten CM, Laumonnier Y, Eurich B, Ender F, Bröker K, Roy S, et al. Monitoring and cell-specific deletion of C5aR1 using a novel floxed GFP-C5aR1 reporter knock-in mouse. *J Immunol* (2015) 194:1841–55. doi:10.4049/jimmunol.1401401
101. Tegla CA, Cudrici C, Patel S, Trippe R, Rus V, Niculescu F, et al. Membrane attack by complement: the assembly and biology of terminal complement complexes. *Immunol Res* (2011) 51(1):45–60. doi:10.1007/s12026-011-8239-5
102. Shen N, Chen B, Jiang Y, Feng R, Liao M, Zhang L, et al. An updated analysis with 85,939 samples confirms the association between CR1 rs6656401 polymorphism and Alzheimer's disease. *Mol Neurobiol* (2015) 51(3):1017–23. doi:10.1007/s12035-014-8761-2
103. Hannan J. The structure-function relationships of complement receptor type 2 (CR2; CD21). *Curr Protein Pept Sci* (2016) 17(5):463–87. doi:10.2174/1389203717666151201192124
104. Kiryluk K, Li Y, Sanna-Cherchi S, Rohanizadegan M, Suzuki H, Eitner F, et al. Geographic differences in genetic susceptibility to IgA nephropathy: GWAS replication study and geospatial risk analysis. *PLoS Genet* (2012) 8(6):e1002765. doi:10.1371/journal.pgen.1002765
105. Hom G, Graham R, Modrek B, Taylor K, Ortmann W, Garnier S, et al. Association of systemic lupus erythematosus with C8orf13-BLK and ITGAM-ITGAX. *N Engl J Med* (2008) 358(9):900–9. doi:10.1056/NEJMoa0707865

Conflict of Interest Statement: The authors declare that the research was conducted in the absence of any commercial or financial relationships that could be construed as a potential conflict of interest.

The reviewer HB and handling Editor declared their shared affiliation.

frontiers in Immunology

REVIEW
published: 09 April 2018
doi: 10.3389/fimmu.2018.00689

Immunoglobulin E-Mediated Autoimmunity

Marcus Maurer, Sabine Altrichter, Oliver Schmetzer, Jörg Scheffel, Martin K. Church and Martin Metz*

Department of Dermatology and Allergy, Charité – Universitätsmedizin Berlin, Berlin, Germany

The study of autoimmunity mediated by immunoglobulin E (IgE) autoantibodies, which may be termed autoallergy, is in its infancy. It is now recognized that systemic lupus erythematosus, bullous pemphigoid (BP), and chronic urticaria, both spontaneous and inducible, are most likely to be mediated, at least in part, by IgE autoantibodies. The situation in other conditions, such as autoimmune uveitis, rheumatoid arthritis, hyperthyroid Graves' disease, autoimmune pancreatitis, and even asthma, is far less clear but evidence for autoallergy is accumulating. To be certain of an autoallergic mechanism, it is necessary to identify both IgE autoantibodies and their targets as has been done with the transmembrane protein BP180 and the intracellular protein BP230 in BP and IL-24 in chronic spontaneous urticaria. Also, IgE-targeted therapies, such as anti-IgE, must have been shown to be of benefit to patients as has been done with both of these conditions. This comprehensive review of the literature on IgE-mediated autoallergy focuses on three related questions. What do we know about the prevalence of IgE autoantibodies and their targets in different diseases? What do we know about the relevance of IgE autoantibodies in different diseases? What do we know about the cellular and molecular effects of IgE autoantibodies? In addition to providing answers to these questions, based on a broad review of the literature, we outline the current gaps of knowledge in our understanding of IgE autoantibodies and describe approaches to address them.

Keywords: immunoglobulin E-mediated autoimmunity, autoallergy, urticaria, bullous pemphigoid, immunoglobulin E-mechanisms

OPEN ACCESS

Edited by:
Ralf J. Ludwig,
Universität zu Lübeck, Germany

Reviewed by:
Mohey Eldin El Shikh,
Queen Mary University of London, United Kingdom
Reinhild Klein,
Universität Tübingen, Germany

****Correspondence:***
Martin K. Church
mkc@soton.ac.uk

Specialty section:
This article was submitted to Immunological Tolerance and Regulation, a section of the journal Frontiers in Immunology

Received: *02 February 2018*
Accepted: *20 March 2018*
Published: *09 April 2018*

Citation:
Maurer M, Altrichter S, Schmetzer O, Scheffel J, Church MK and Metz M (2018) Immunoglobulin E-Mediated Autoimmunity. Front. Immunol. 9:689. doi: 10.3389/fimmu.2018.00689

INTRODUCTION

Friend or Foe? This is the major question that the immune system must address in every individual from the time of conception, through the development of the fetus and the child, right into adulthood. But sometimes it gets this wrong and raises an inappropriate immunological response against self. Although there are several types of autoimmunity this review will address solely immunoglobulin E (IgE)-mediated autoimmunity. Because its mechanisms have much in common with classical allergy involving exogenous allergens, such as grass pollen or house dust mites, IgE-mediated autoimmunity is generally termed "autoallergy" and the target molecules of the response are called "autoallergens."

Although the presence of an allergic antibody has been postulated since the innovative serum transfer experiment of Prausnitz and Kustner in 1921 (1), it was not until 1967 that this antibody was characterized as IgE (2–4). IgE, which is the least abundant immunoglobulin isotype and found only in mammals, signals through 2 types of Fcε receptor, the high-affinity receptor, FcεRI, which is found primarily on mast cells and basophils, and the low-affinity receptor, FcεRII or CD23, a C-type

lectin, which is found on mature B cells, activated macrophages, eosinophils, follicular dendritic cells, and platelets. The primary role of IgE is held to be host defense, particularly initiating the expulsion of parasitic worms (helminths) and environmental substances, such as toxins, venoms, irritants, and xenobiotics.

Although IgE has a well-documented role in classical allergy to exogenous allergens, this review will address only IgE-mediated autoimmunity. It will focus on three related questions: what do we know about the prevalence of IgE autoantibodies and their targets in different diseases? What do we know about the relevance of IgE autoantibodies in different diseases? What do we know about the cellular and molecular effects of IgE autoantibodies? In addition to providing answers to these three questions, based on a comprehensive review of the literature, we outline the current gaps of knowledge in our understanding of IgE autoantibodies and describe approaches to address them.

WHAT DO WE KNOW ABOUT THE PREVALENCE OF IgE AUTOANTIBODIES AND THEIR TARGETS IN DIFFERENT CONDITIONS?

Within a decade of its discovery, reports began to incriminate IgE as a possible contributor to the pathogenesis of several chronic inflammatory disorders, such as rheumatoid arthritis (RA) (5–7), bullous pemphigoid (BP) (8, 9), atopic dermatitis (AD) (10), and systemic lupus erythematosus (SLE) (11, 12). More recently, IgE-mediated autoallergy has been suggested for other disorders including chronic spontaneous urticaria (CSU) (13, 14) and chronic inducible urticaria (CindU) (15). The conditions in which IgE autoantibodies have been detected, which are summarized in **Table 1**, will now be considered in more detail.

Atopic Dermatitis

Decades before the discovery of IgE, it was reported that human dander extract can elicit immediate-type skin reactions in patients with severe atopy and that this skin sensitivity could be passively transferred with serum (30–35). Many years later, the analysis of the presence of IgE autoantibodies in sera from patients with various manifestations of atopy and other autoimmune disorders indicated that IgE reactivity against a variety of autoantigens occurred most frequently in AD patients. IgE autoreactitvy has first been found and described in AD (36), where IgE autoantibodies are very frequent (23–91%) (19) and especially present in severely affected patients (37–39). IgE autoantibodies had been identified directed against Keratinocytes (40) and a broad variety of autoantigens (41), including, e.g., human protein manganese superoxide dismutase (38), thioredoxin (42), DFS70/LEDGF (43), and Hom s 1–5 (44, 45).

Interestingly, this phenomenon has already been seen in very young infants of less than 1 year where 15% of the children with atopic eczema mounted IgE autoreactivity and raised in the age group of 2–13 years with moderate to severe AE and total IgE serum levels higher 1,000 kU/L up to 80% (46).

TABLE 1 | Percentage of patients in which immunoglobulin E (IgE) autoantibodies have been detected in various diseases.

Disease	IgE against	Prevalence	Reference
Allergic rhinoconjunctivitis	Profilin		(16)
Asthma	n.a.	n.a.	(17, 18)
Atopic dermatitis	>140 IgE-binding self-antigens	23–91%	(19, 20)
Autoimmune pancreatitis	n.a.	n.a.	(21)
Bullous pemphigoid	BP 180 or 230	22–100%	(22)
Chronic spontaneous urticaria	Thyroidperoxidase (TPO), double stranded DNA (dsDNA), IL-24	0–80%	(23)
Graves disease	TPO, muscle autoantigens	67%	(24, 25)
Multiple sclerosis (MS)	Small myelin protein-derived peptides	n.a.	(26)
Pemphigus	Desmoglein1, Desmoglein 3, Lamininin-332 und LJM11	11–81%	(22)
Rheumatoid arthritis	ANA, anti-citrullinated protein?	60%	(27)
Systemic lupus erythematodes and lupus nephritis	dsDNA, Sm, SS-A/Ro, SS-B/La, APEX, MPG, CLIP4, ANA, RNP, nucleosome, specific IgE, acidic ribosomal P_2 protein	3.6–82%	(28)
Uveitis	Retinal S antigen	69%	(29)

n.a., not assessed.

Systemic Lupus Erythematosus

In SLE, several IgE autoantigens have been described (28, 47), and their occurrence is frequent. In a study of 92 SLE patients (48), 29 (32%) had antinuclear-IgE antibodies. No such antibodies were found in a parallel healthy control group. Sub-analysis of the IgE autoantibodies in the 29 positive patients showed reactions with nucleosomes (79.3%), double stranded DNA (dsDNA) (48.3%), SS-A/Ro (48.3%), SS-B/La (18.7%), Sm (48.3%), and RNP (62.1%). In a multicentre study of 196 SLE patients (49), more than 50% showed autoreactive IgE to one or more of the four common SLE nuclear autoantigens, dsDNA, SS-A/Ro, SS-B/La, and Sm. This figure rose to around 74% in patients with active disease where autoreactive IgE to dsDNA was most prevalent with an incidence of 63%. From these findings, Dema and colleagues (49) suggest that the presence of autoreactive IgE, and in particular dsDNA-specific IgE, in SLE, may be a reasonable clinical indicator of increased disease activity. This conclusion is supported by a study that showed that disease flares rates were higher in SLE patients with demonstrable circulating IgE-anti-dsDNA antibodies than in those without (50).

Because approximately half of SLE patients do not have demonstrable IgE antibodies to the common nuclear autoantigens, the prevalence of IgE autoantibodies to other autoallergens has been explored. One study showed high levels of IgE autoantibodies to APEX nuclease 1, *N*-methylpurine-DNA glycosylase and CAP-Gly domain-containing linker protein family member 4 in some SLE patients but not healthy controls. These autoantigens were unique in that they seemed specific targets of IgE autoantibodies but not autoantibodies of the IgG class (49). In another study, 31% of 90 SLE patients displayed IgE antibodies against human P 2 proteins, an antigen that has also been described to be

cross-reactive with other members of the ribosomal P 2 protein family, which are minor allergens in fungal allergy (51).

Finally and importantly, IgE to Ro/SSA, a ribonuclearprotein autoantigen has been suggested to be relevant for fetal loss by mothers with SLE (52). This is of special interest as IgG-anti-Ro/SSA antibodies are known to be associated with neonatal lupus (congenital heart block, neonatal transient skin rash, hematological and hepatic abnormalities). However, they are suggested not to negatively affect other gestational outcomes, and the general outcome of these pregnancies is good when managed by experienced multidisciplinary teams (53).

Bullous Pemphigoid

Bullous pemphigoid is an autoimmune blistering disease that mainly affects elderly patients. It is the most common pemphigoid disorder accounting for around 80% of all pemphigoid cases (28). IgG, IgA, and IgE autoantibodies are directed against two hemidesmosomal proteins, the transmembrane protein BP antigen 2 (BP180, type XVII collagen) and the intracellular BP antigen 1 (BP230) (22, 54, 55). Binding of autoantibodies leads to a complex inflammatory response involving complement activation, the infiltration of inflammatory cells, and the subsequent release of reactive oxygen species and distinct proteases that finally mediate subepidermal splitting (56).

Immunoglobulin E autoantibodies against BP180 target mainly the 16th non-collagenous domain (BP180 NC16A) (54, 57) although BP180 epitopes outside the NC16A domain have also been described to be recognized by IgE (58). That IgE-anti-BP180 is functional was demonstrated by the ability of serum from BP patients to sensitize mast cells and basophils for BP180-induced histamine release (59). The percentage of BP patients with IgE-anti-BP180 autoantibodies, shown in **Table 2**, varied substantially in the different reports. The reason in this variation is likely to be due to the different test systems used, i.e., ELISA or immunoblotting, and the use of diluted or undiluted patient sera.

Several studies were able to detect IgE autoantibodies against the intracellular BP230 autoantigen. Engineer et al. reported IgE-anti-BP230 without detection of BP180-specific IgE autoantibodies in 100% of six BP patients (67). In contrast, other studies revealed IgE-anti-BP230 and IgE-anti-BP180 autoantibodies in 67% of 67 sera (61) and 50% of 32 sera (68). IgE-anti-BP230 reactivity was associated with local eosinophil accumulation (61), with disease activity (69) and correlated with total IgE serum levels (68, 70).

TABLE 2 | Percentage of patients with bullous pemphigoid showing immunoglobulin E (IgE) reactivity to BP180.

Number of patients	Percentage with IgE-anti-BP180	Reference
37	22	(60)
67	30	(61)
117	40	(56)
44	41	(62)
18	55	(63)
31	61	(64)
56	71	(65)
43	77	(58)
18	83	(66)
10	100	(54)

Other Autoimmune Blistering Disorders

Pemphigus vulgaris (PV) is another severe autoimmune bullous skin disease and is primarily associated with IgG against desmoglein 3 (dsg3), a desmosomal adhesion protein. However, raised IgE in these patients has also been reported (71). Intercellular IgE deposits were detected in the epidermis of 37 patients with acute onset of the disease, and IgE-anti-dsg3 was detected more frequently in the sera of patients with acute onset, compared to chronic-active PV (72). Spaeth and colleagues reported dsg3-reactive IgE in the serum of 13% of 15 patients with acute onset, 11% of 18 patients with chronic-active, and none of 8 patients with remittent PV patients (73).

In mucus membrane pemphigoid, one of four patients showed IgE reactivity to the gamma2 subunit of laminin-332 (74). In endemic pemphigus foliaceus, IgE-anti-desmoglein 1 was found in 81% of 143 patients with fogo selvagem (75), and serum levels of IgE against LJM11, a major immunogenic component of sand fly salivary gland antigens, were significantly higher compared to controls (76).

In summary, reports in pemphigus are limited, but IgE reactivity seems to be more prevalent in the endemic form of pemphigus foliaceus than in PV.

Chronic Urticaria

An important role of IgE and FcεRI reactions was postulated in both CSU and CindU for several decades (77) before it was finally confirmed by the successful treatment of the disease with anti-IgE (omalizumab) (14, 15, 78). Although specific IgE against classical common allergens, i.e., aeroallergens and food allergens (79–82), or to less common allergens such as fungi (83, 84) can be detected in some patients with CSU, they are not regarded as pathophysiologically relevant for the development of the signs and symptoms of CSU (81, 85–87).

Perhaps the first evidence of autoreacitivitiy in CSU came with the clinical observation that CSU patients have high rates of thyroid diseases (88). Detailed analysis of CSU patients with thyroid pathology led to the detection of IgE anti-thyroidperoxidase (TPO) autoantibodies. Almost 20 years ago, Bar-Sela and coworkers reported the detection of IgE-anti-TPO in a female CSU patient who also had Hashimoto's thyroiditis (89). More recently, elevated levels of IgE-anti-TPO were reported in 61% of 478 CSU patients (13). However, other studies found only 13–17% of 23 patients (90) and 10% of 20 patients (91) to have IgE-anti-TPO, while a further study failed to find IgE-anti-TPO in 23 CU patients (92). The most likely explanation for these differences is the use of different assay systems, for example direct ELISA vs capture ELISA, and the interference of IgG autoantibodies against TPO (93). Functional relevance was suggested as flow cytometry analysis showed CD203c induction in a dose-dependent manner in basophils sensitized with serial additions of TPO in CU patients having high specific IgE to TPO (94).

Beside thyroid diseases, the prevalence of individual autoimmune diseases in chronic urticaria is increased in general (≥1% in most studies vs ≤1% in the general population). In a review,

the rates of comorbidity were ≥1% for insulin-dependent diabetes mellitus, RA, psoriasis, and celiac disease, ≥2% for Graves' disease, ≥3% for vitiligo, and ≥5% for pernicious anemia and Hashimoto's thyroiditis. Interestingly, >15% of CSU patients have a positive family history for autoimmune disease (95).

A recent review investigated also the correlation of chronic urticaria with other autoimmune diseases such as SLE. The prevalence of CSU and CSU-like rash in SLE was investigated from 42 independent studies. Comorbidity in adult patients reportedly ranged from 0 to 22% and 0.4 to 28%, respectively (urticarial vasculitis: 0–20%). In children with SLE, CSU was reported in 0–1.2% and CSU-like rash in 4.5–12% (urticarial vasculitis: 0–2.2%) (96). Specifically, significantly higher levels of IgE-anti-dsDNA, but not corresponding IgG levels, have also been found in a study of 85 chronic urticaria patients (97). Furthermore, basophils from 2 out of 9 of these patients exhibited degranulation in response to dsDNA, indicating functional relevance of these autoantibodies.

Beside these IgE antibodies that target antigens known in autoimmune diseases, patients with CSU can also develop IgE autoantibodies against probably disease-specific antigens. Schmetzer et al. found more than 200 IgE autoantigens in patients with CSU that were not found in healthy controls (98). Of the 31 IgE autoantigens detected in more than 70% of patients, 8 were soluble or membrane-bound and expressed in the skin and IgE autoantibodies to IL-24 were found in all patients with CSU. *In vitro* studies showed functional relevance, and clinically IgE-anti–IL-24 levels showed an association with disease activity. Detailed analysis of the remaining identified IgE targets had not been provided yet.

Other Diseases

In many diseases, single or few reports have indicated a presence or potential role of autoreactive IgE.

Autoimmune Uveitis

Beside IgG autoantibodies, in autoimmune uveitis specific IgE to retinal S antigen was positive in 69% of 32 patients. In contrast, patients suffering from bacterial uveitis, as well as the healthy controls were negative for autoantibodies to retinal S antigen (29). Furthermore, IgE, IgG, and IgA anti-Galectin-1 (Gal-1) antibodies were increased in sera from patients with autoimmune uveitis and toxoplasmic retinochoroiditis compared to healthy controls (99). Both, anti-Gal-1 IgE and IgG antibodies were associated with progressive disease and poor disease outcome.

Rheumatoid Arthritis

A role of IgE antibodies in RA was first suggested several decades ago (27, 100). Antinuclear antibodies of the IgE class were found in 60% of 20 RA patients with neutropenia, whereas only 16% of RA patients without neutropenia had IgE antibodies of similar specificity (27). Anti-citrullinated protein antibodies are suggested to be highly specific and predictive for RA. In a study from Schuerwegh and colleagues, evidence for IgE directed against citrullinated protein was proposed (101), but later the paper was retracted (102). In recent times, no valid studies regarding this topic have been published.

Multiple Sclerosis

A role of IgE antibodies in the disease was suggested, despite the fact that there was no association between MS and allergies (103). In a study from Mikol and colleagues in 26 MS patients, a total of 128 peptides showed some IgE reactivity (mean 4.9 per subject), compared to 59 among the 15 controls (mean 3.9 per subject) (26). A detailed analysis of short, unique myelin protein-derived peptides (SUMPPs) revealed that for several SUMPPs, MS patients had significantly more reactive IgE, whereas for other SUMPPs, there was no significant difference between MS subjects and controls. The authors speculated that IgE reactive against CNS target antigens may have diagnostic and pathogenic significance.

Hyperthyroid Graves' Disease

The presence of IgE autoantibodies in Grave's disease was first proposed 40 years ago (104). Elevation of serum IgE ≥ 170 U/mL was found in up to 36% of the patients (105–108), but not in another study (109). Furthermore, there was immunohistochemical evidence for IgE involvement in Graves' orbitopathy (110). Studies regarding specific IgE autoantibodies in thyroid disease showed IgE class TPO autoantibodies in 13 of 18 Graves' and in 12 of 17 Hashimoto patients (24) and muscle autoantigens in thyroid associated ophthalmopathy (25). Evidence for a functional relevance of these IgE autoantibodies was shown by Raikow and colleagues, who showed that serum IgE is elevated in connection with certain stages of rapid dysthyroid orbitopathy progression (111).

Autoimmune Pancreatitis

Elevated total IgE levels are frequent in patients with autoimmune pancreatitis (21, 112), and it was recently suggested that analysis of total IgE in serum might be useful in the differentiation between autoimmune pancreatitis and pancreatic carcinoma (113). Nevertheless, IgE specific targets remain currently unknown, although there may be cross-reactivity with environmental antigens, as patients with higher IgE levels and with allergic diseases were more likely to have onset in March, April, May, August, September, or October (21).

Asthma

Autoallergic mechanisms have been proposed in murine models of asthma (17, 114). In human asthma, approximately 50% of patients with non-allergic asthma react to intradermal injection of autologous serum, indicating the presence of circulating vasoactive factors and suggesting the possibility of an autoreactive mechanism (18). In one patient with corticosteroid-dependent asthma associated with aspirin sensitivity, the presence of circulating IgE antibodies against 55 and 68 kDa platelet antigens has been described (115). Overall, autoallergy in asthma has not been studied in detail in humans so far.

Allergic Rhinoconjunctivitis

There is very limited evidence for IgE autoreactivity in allergic rhinoconjunctivitis. IgE antibodies from allergic individuals that bind to natural and recombinant birch profilin also bind

to human profilin (16). Similar cross-reactivity was shown for human acidic ribosomal P2 protein in individuals sensitized to *Aspergillus fumigatus* P2 protein (116).

Diseases in Which IgE Autoantibodies Were Looked for but Not Found

In chronic rhinosinusitis with nasal polyps no IgE autoreactivity to epithelial antigens, or anti-IgE IgG, has been detected, despite extensive tests (117).

WHAT DO WE KNOW ABOUT THE RELEVANCE OF IgE AUTOANTIBODIES IN DIFFERENT DISEASES?

IgG-mediated autoimmune diseases occur in up to 9% of the population (118). Whether or not other immunoglobulin subtypes, including IgE, are critically involved in the pathogenesis of autoimmune diseases is largely unknown for most diseases. In contrast, polyreactive natural antibodies, which are not antigen-specific, can often detect self-antigens with low affinity. Most of these natural antibodies belong to the isotypes IgM, IgG_3, and IgA, and these unspecific antibodies, even if they can bind to self-antigens, are thought to be protective, rather than harmful (119, 120). There is also some published evidence for the existence of natural IgE antibodies against pancreatic cancer cells (121) and conserved biotinylated-enzyme molecules present in many organisms, such as *Anisakis simplex*, *Toxocara canis*, *Ascaris suum*, and *Culex quinquefasciatus* (122, 123). While there are currently no data available on the role and relevance of natural IgE antibodies and how they could affect disease activity, there is some published evidence for a role of antigen-specific IgE against self in different diseases. For some diseases, there is only a single report on the potential role for auto-IgE. As reviewed above, in PV, high concentrations of serum IgE autoantibodies have been detected, and a strong correlation between dsg3-reactive IgE has been observed in patients with acute disease onset, indicating a role for auto-IgE in pemphigus (72). In patients with MS, there are some data indicating that IgE against CNS target antigens may have a pathogenic significance, particularly if other peptide-specific, potentially blocking immunoglobulins are absent (26). In other autoimmune diseases or diseases in which autoimmunity is thought to play a role, some more information on the potential role of auto-IgE has been published.

Atopic Dermatitis

Although the pathogenesis of AD is still not completely understood, it is generally accepted that the underlying etiology is multifactorial, including environmental factors, impaired skin barrier function, and a hyper-immune activation (124). The role and relevance of autoimmunity in AD is as of yet unclear. In AD patients, many autoantigens can be detected, and IgE against self is highly prevalent (125, 126). Whether these auto-IgE antibodies indeed contribute to disease activity and severity or are merely bystanders cannot be concluded at present (125, 126). There is some evidence, however, that is suggestive of a pathogenic role for IgE against self in AD. Tang and colleagues have summarized this evidence and conclude that IgE autoreactivity is of importance in the pathogenesis of AD, especially because autoreactivity has been identified in various *in vitro* and direct clinical experiments across distinct study populations (19). Furthermore, significant associations between auto-IgE levels in AD patients and disease severity have been reported (37, 38), while a further two reports show a trend, but no significance for such a correlation (41, 46). In contrast, one investigation did not identify a correlation (39).

If auto-IgE is importantly involved in AD pathogenesis, treatment with anti-IgE antibodies should be able to improve symptoms. Because of the above mentioned investigations, omalizumab has been widely used in treatment refractory AD patients and many case reports and case series have been published. Two recent systematic reviews on the use of omalizumab in AD both come to the conclusion that anti-IgE treatment can be beneficial in the treatment of AD, but that larger clinical trials are missing to fully support this statement (127, 128).

Systemic Lupus Erythematosus

Autoreactive IgE against a number of different antigens has been reported in SLE (see respective section above). In many investigations, a close correlation between levels of auto-IgG and auto-IgE in the same patients has been shown, making it difficult to estimate the contribution of auto-IgE to the pathology of SLE (49, 51, 129, 130). However, Henault and colleagues reported that the concentration of IgE anti-dsDNA correlates with disease severity and is likely to contribute to disease pathology independent from IgG anti-dsDNA (129). Dema and colleagues similarly show an association of the levels of IgE against different autoantibodies with SLE, comparable to autoreactive IgG levels (49). The best prediction of disease activity was found to be the presence of both, dsDNA-specific IgE and IgG, possibly indicating a role for auto-IgE in SLE (49).

In a recent publication, Pan and colleagues have shown that SLE patients not only have high levels of IgE directed against various autoantigens but also strongly decreased numbers of circulating basophils, suggesting auto-IgE-dependent basophil activation in the blood (131). These authors also stated that basophils from SLE patients showed high rates of activation that closely correlated with SLE activity. How this correlates with disease mechanisms is not clear. Anti-IgE treatment has not been reported in SLE patients as of yet.

Bullous Pemphigoid

The largest body of evidence for a pathological role of autoreactive IgE in the literature can be found for BP. In those patients presenting with specific IgE directed against the autoantigen BP180, a correlation of auto-IgE and disease severity has been reported (56, 60, 63). Moreover, Freire and colleagues have shown that IgE-anti-BP180 cannot only be found in the serum of BP patients, but also in the skin, bound to the surface of tissue-resident mast cells (132). Furthermore, they show that patient-derived IgE-anti-BP180 complexes can activate basophils, indicating the functionality of these antibodies (132).

In a number of case reports and case series, excellent efficacy of treatment with omalizumab has been shown in BP patients (133–140). While these findings are highly suggestive of a

pathogenic role for auto-IgE in BP, controlled clinical trials with omalizumab in BP are necessary to prove the efficacy of anti-IgE treatment and thus of the relevance of auto-IgE in BP.

Chronic Urticaria

The evidence for a pathogenetic role of auto-IgE in chronic urticaria has been extensively discussed in a recent review (141). This paper concluded that there are still many aspects of the pathologic mechanisms of CSU that need to be resolved, but that it is becoming increasingly clear that there are at least two distinct pathways, type I (IgE-mediated) and type II (IgG-mediated) autoimmunity, both of which contribute to the pathogenesis of this complex disease.

Since then, further evidence for a role for auto-IgE in CSU has been presented by Schmetzer and colleagues. Overall, more than 200 autoantigens that are recognized by IgE have been detected in CSU patients, and in 80% of more than 1,000 CSU patients, IgE-anti-IL-24 was present (98). Furthermore, levels of IgE-anti-IL-24 in the serum correlated with CSU disease activity, and *ex vivo*, IL-24 was able to activate mast cells after pre-incubation with serum from IgE-anti-IL-24 positive patients, indicating a biological relevance for IgE-anti-IL-24 in CSU patients (98).

The clinical relevance of IgE in both CSU and CindU has been proven in numerous case reports and case series and in a number of randomized-controlled trials using the anti-IgE antibody omalizumab (142–145). In fact, the first multi-center placebo-controlled study of omalizumab in CSU, the XCUISITE trial, was done in CSU patients who had IgE-anti-TPO (146). In this trial, 70% of patients of omalizumab-treated patients, but only 5% of placebo-treated patients experienced complete protection from wheal development, and the onset of omalizumab effects was early after the initiation of treatment. This strongly argues that the rapid and profound neutralization of auto-IgE by omalizumab contributed to its effects and that these IgE autoantibodies play a role in the pathogenesis of CSU. Further support for this comes from a recent study that showed that serum reactivity predicts the time to response to omalizumab therapy in CSU patients (147), suggesting that patients with IgG autoantibody-mediated CSU show delayed responses, whereas patients with IgE-autoantibody-mediated CSU have fast onset of improvement. The exact mechanisms by which anti-IgE treatment leads to the resolution of symptoms in most CSU patients are, as of yet, unclear. Nonetheless, at least in a proportion of CSU patients, the massive reduction of autoantigen-specific IgE is likely to be the most relevant mechanism.

In CindU, there is also a strong indication for an important role of IgE against self. For example, anti-IgE treatment has been shown to be highly effective in CindU in numerous case reports and case series, as well as in two randomized-controlled trials (**Table 3**). Furthermore, a direct involvement of IgE in some patients with CindU has been shown by passive transfer experiments. In cold urticaria (148, 149) as well as in symptomatic dermographism (150) disease activity was, in some patients, transferable from patients to healthy subjects by intradermal injection of patient sera. In these investigations, IgE was identified to be the relevant serum factor (148–150).

TABLE 3 | Summary of chronic inducible urticaria patients showing a complete or partial response to omalizumab reported in case reports, case series, and clinical trials.

Condition	Total patients	No. of responders	Percentage responders
Symptomatic dermographism	58	43	74
Cold urticaria	51	39	76
Solar urticaria	47	34	72
Delayed pressure urticaria	32	29	91
Cholinergic urticaria	21	17	81
Heat urticaria	5	3	60
Vibratory angioedema	1	0	0
Aquagenic urticaria	1	1	100
Total	216	166	77

Data contained in this table were obtained from Ref. (145, 151–153).

WHAT DO WE KNOW ABOUT THE GENETIC BASIS OF IgE-MEDIATED AUTOALLERGY

In an effort to understand the genetic influence on autoallergic diseases, it is best to look first at well-analyzed diseases such as SLE, where autoreactive IgE has been known for four decades (27). The prevalence of SLE and the presence of new autoreactive IgE are remarkably dependent on sex and race being 2.3-fold higher in Black persons than in White persons and 10-fold higher in females than in males (154). The greater incidence in females may be partially explained by the observation that women treated with estrogen and progesterone have a 1.34 times higher risk of developing SLE flares as compared to placebo treated.

Autoreactive IgE has been assessed in two SLE patient cohorts, IgE targeting classical SLE antigens being found in 63.3% of patients of French origin but only 52.9% of the patients from the United States (49). Most prominent in this study was IgE-anti-dsDNA but also auto-IgE against other SLE antigens (Sm, SSA/Ro, SSB/La). Non-SLE IgE only antigens (APEX, MPG, CLIP4) were also found. This autoreactive IgE correlated highly significantly with disease activity (SLEDAI score) and reduced C3 or C4 levels suggesting that IgE facilitates the amplification of autoimmune inflammation (155).

Chronic spontaneous urticaria is another example of an auto-IgE-mediated disease, where a strong and complex genetic bias *via* multiple alleles exists. These include *C5AR1* (156), *FPRL1* (157), *FcvarepsilonR1beta* (158), *TGFbeta1* (159, 160), IgE (161), IL-13 (162), histamine *N*-methyltransferase (163), *PTPN-22* (164, 165), *CTLA-4* (166), and *ACE* (167).

In addition to the well-known loci linked to hypersensitivity and atopy, such as *PLA2G7*, *MS4A2*, *IL4R* (168), *IL-10* (169), *IL12RB1* (170), *STAT4/6, CTLA-4* (171), and *GATA3* (172), recent studies identified many new alleles which regulate IgE production independent of external stimuli. However, these are often single findings, and only a genome-wide screening could weigh these findings and determine their relation to atopy, IgE and auto-IgE. One genome-wide screening on alleles influencing total IgE level identified *FCER1A* polymorphisms as having most impact, followed by *RAD50* and *STAT6* as the lowest relation (173).

One genetic variant has been studied in detail which links elevated IgE concentrations to a polymorphism in the *IL21R* gene promoter (174). This −83T–C promoter polymorphism in the *IL21R* gene is linked to a changed response of IgE synthesis to IFN-gamma stimulation (175). If *IL-21* is knocked-out in murine models, IgE production after immunization is increased, while IgG subtypes are decreased in otherwise normal animals (176). In contrast, loss-of-function of the *IL-21R* gene in humans leads to a severe primary immune defect (177). The difference to the murine model is not surprising, given the low degree of homology of the IgE system between man and rodent.

In addition to this *IL-21* gene variant, environmental receptor encoding genes, such as *NOD1* have been linked to asthma (178). This opens a crucial new viewpoint on genetics where environmental stimuli are related to selected genotypes to explain the phenotype. Another example is the β2-adrenoreceptor gene promoter polymorphism that determines modulation of IgE production as a response to xenobiotics (β2-agonists and glucocorticoids) (179).

These examples demonstrate the vast complexity of the genetic regulation of IgE synthesis (180). With modern deep sequencing strategies there are more and more variants found which change the risk for asthma and atopy, and influence IgE level. Sequencing of the IL4 gene alone lead to 14 new, previously unrecognized polymorphisms in addition to only two known previously (181). There are no studies on auto-IgE and *HLA* polymorphisms. However, IgE is involved in antigen uptake *via* immune complexes and presentation *via* MHC class II to CD4 cells (44, 182, 183). Therefore, there is a high likelihood that HLA genotypes will be linked to auto-IgE, but the studies need to be done.

WHAT DO WE KNOW ABOUT THE CELLULAR AND MOLECULAR EFFECTS OF IgE AUTOANTIBODIES?

When looking on the effects of IgE autoantibodies, mast cells and basophils are usually the focus of attention as they express high levels of the high-affinity receptor for IgE (FcεRI). Antigen-dependent activation of mast cells and basophils *via* FcεRI is the cause of acute allergic reactions induced by the rapid release of preformed mediators from granules and subsequent liberation of *de novo* synthesized lipids, cytokines, and chemokines. Yet, mast cells and basophils are not the only cells that express FcεRI and, importantly, other receptors such as CD23 (FcεRII) and galectin-3 are capable of binding IgE and inducing cellular responses. Thus, mast cell and basophil activation may be only the tip of the iceberg when considering the biology of IgE autoantibodies and their contribution to diseases. In particular, the function of CD23 in IgE-dependent sensitization of the host to autoallergens, which in turn may further strengthen the production of autoreactive IgE might be of great importance in the development of autoallergies.

In general, all IgE, whether it is autoreactive or whether it recognizes exogenous antigens, can trigger the same cellular responses as there is no evidence yet that autoreactive IgE have special molecular characteristics that drive certain functions/responses such as, for instance, cytokinergic activity. However, certain activities are not necessarily triggered by autoreactive IgE such as the CD23-mediated transepithelial transport of IgE. Here, we will focus on IgE-binding receptors with regards to their contribution in autoallergy.

Effects of IgE/Autoantigen on FcεRI Signaling

The high-affinity receptor for IgE (FcεRI) consists of one IgE-binding α chain, which binds IgE with a very high affinity (10^{10} M^{-1}), but does not contain intracellular signaling motives, one transmembrane-spanning β chain, which crosses the plasma membrane four times and contains an immunoreceptor tyrosine-based activation motive (ITAM), and two identical γ chains each containing an ITAM (184). This αβγγ motive is mainly expressed by mast cells and basophils although expression has also been shown in airway smooth muscle cells and bronchial epithelial cells of asthmatic patients (185, 186). A αγγ version of this receptor can be expressed by a variety of other cells including subsets of dendritic cells and monocytes/macrophages (187–189), eosinophils (190), neutrophils (191), and platelets (192, 193). Because of its high affinity for IgE, the receptor is occupied by monomeric IgE. When cross-linked by a multivalent antigen, it triggers signaling cascades leading to the immediate degranulation in mast cells and basophils, i.e., the release of preformed mediators from intracellular granules and *de novo* synthesis of lipid mediators such as prostaglandins and leukotrienes as well as the production of cytokines and chemokines and the expression of various surface markers. These include chemokine receptors such as CCR7 on plasmacytoid dendritic cells (pDCs) (129) or the selectin CD62L on basophils (194) that facilitate the migration of activated cells to local lymph nodes, but also co-stimulatory molecules like CD83 and CD86 on pDCs. Moreover, autoreactive IgE activates pDCs more efficiently and further synergizes with IgG through co-engagement of activating FcγRIIa, even in concentrations several orders of magnitude below IgG concentrations and drive B cell expansion and plasma call differentiation (129, 130). FcεRI engagement by IgE and allergen also induces IL-16 in Langerhans cells, a chemoattractant for CD4+ T cells, dendritic cells, and eosinophils (195). Thus, autoreactive IgE may have the capacity to augment disease activity in autoimmunity.

Surface bound IgE has been shown to stabilize and enhance the surface expression of FcεRI on mast cells and basophils, thereby allowing cells to bind more IgE, which in turn may lower the threshold for antigen-induced cell activation (196). This amplification loop might be of particular importance in autoallergic patients who present with increased serum and tissue IgE levels. Consistently, treatment with antibodies directed against IgE does not only lower serum IgE levels but also FcεRI surface expression on dendritic cells, basophils, and mast cells (197–199). Moreover, FcεRI-bound IgE promotes mast cell survival and migration (200). Interestingly, certain IgEs even induce mast cell and basophil degranulation and cytokine release in an antigen-independent manner (201). Although the *in vivo* relevance of this "cytokinergic" activity

has not been demonstrated yet, it may have an impact in autoallergy. Cytokinergic IgE molecules associate with themselves and show an enhanced propensity to be polyreactive to various autoantigens (202, 203).

FcεRI-bound and antigen cross-linked IgE becomes internalized rapidly (129, 204). Thus, on the one hand, free serum IgE is cleared by dendritic cells and monocytes. On the other hand, when cross-linked, autoantigens become internalized and are capable of stimulating intracellular pattern recognition receptors such as TLRs. In pDCs, IgE autoantibodies directed against dsDNA become internalized and directed to phagolysosomes where TLR9 becomes activated to trigger the generation of inflammatory cytokines, such as INF-α, IL-6, IL-8, and TNF-α (129). Alternatively, internalized IgE/autoantigen is presented *via* MHC class-II by basophils, cutaneous Langerhans cells, or other dendritic cells in regional lymph nodes or local submucosal sites to naïve T cells to induce T_H2 cells (194, 196, 205, 206). In systemic lupus erythematosus (SLE), activation of basophils by autoreactive IgE can induce the upregulation of CD62L, MHC-II and the B cell-activating factor BAFF. Activated basophils then migrate into the secondary lymphoid organs, where they produce IL-4 and IL-6, thereby promoting a T_H2 environment with more IL-4 producing activated T cells and enhanced B cell proliferation with increased IgG_1 and IgE production (194). In addition, CD1c+ dendritic cells may have the capacity for cross-presentation of internalized antigen to induce cytotoxic CD8+ cells. However, this is strongly inhibited by IL-4-producing T_H2 cells (207). On monocytes, the engagement of FcεRI induces antibody-dependent cell-mediated cytotoxic activities of the cells rather than antibody-dependent cell-mediated phagocytic activities (ADCP), which are linked to the engagement of the low-affinity IgE receptor, CD23 (see below).

In BP, CSU and AD, the degranulation of mast cells and basophils contributes to disease manifestations. This, however, does not occur in systemic lupus erythematosus patients, who lack classical allergic manifestations. A possible mechanism for this is the co-engagement of inhibitory receptors such as FcγRIIb by autoreactive IgG in SLE (208). Moreover, cross-linking of FcεRI in monocytes and dendritic cells induces "late" anti-inflammatory IL-10, which can attenuate basophil and dendritic cell activation and suppresses monocyte phagocytic activity (209–211). Additionally, in monocytes, FcεRI engagement induces the upregulation of indoleamine 2,3-dioxygenase (IDO), which inhibits T cell proliferation and activates FOXP3+ regulatory T cells through the depletion of tryptophan (212).

A soluble version of FcεRI consisting of a single a-chain has been described (213). How sFcεRI is generated *in vivo* is not known so far. *In vitro* experiments suggest that it is generated during cellular FcεRI engagement. sFcεRI may bind to IgE with similar affinity as membrane-bound FcεRI and, therefore, might serve as a soluble regulator of free IgE and IgE-mediated cellular activation. Binding in a 1:1 ratio to IgE, it has the potential to prevent IgE from binding to the cellular receptor, and could negatively affect FceRI expression levels. *In vitro* and *in vivo* studies with sFcεRI show inhibitory properties on mast cell and basophil degranulation (214). Its impact in autoallergy, however, needs to be determined.

Effects of IgE/Autoantigen on CD23 (FcεRII) Signaling

Most studies on the effects of IgE-mediated responses focus on mast cells or basophils and FcεRI signaling, as they are responsible for the immediate allergic response. However, the so-called "low affinity" receptor for IgE, CD23, has important functions in positively or negatively regulating IgE synthesis as well as antigen presentation to T cells (215). It is expressed on various cells including epithelial cells, activated B and T cells, Langerhans cells, plasma cells, monocytes, and eosinophils (196). CD23 belongs to the family of C-type lectins, which are calcium-dependent carbohydrate binding structures and contain three lectin domains located on the C-terminal extracellular head of the molecule. Interestingly, binding of IgE to the head domains seems not to involve carbohydrate structures (216). Although the affinity of a single CD23 head for the IgE-Fc is comparably low, the combined interaction of all three heads with IgE results in an strong binding with an affinity (10^8–10^9 M^{-1}) that is comparable to that of FcεRI (215). Interestingly, CD23 is prone to shedding by disintegrin and metalloproteinase domain-containing protein 10 (ADAM10) resulting in various soluble forms (monomeric or trimeric with varying sizes), all of which are capable to bind IgE (214, 217) and are found in autoimmune diseases like SLE where auto-IgE has been described (218). Multiple ligands/interaction partners other than IgE have been described to interact with CD23 and are important for its function including the complement receptor 2, 3, and 4 (CD21; CD18/CD11b; CD18/CD11c), MHC-II, the receptor for vitronectin (αVβ3-integrin) and the αVβ5-integrin (215, 219). One important function of CD23 with regards to autoallergy is probably associated with the regulation of IgE production by B cells committed to IgE secretion. IgE-induced engagement of membrane CD23 induces a negative feedback while sCD23 (trimeric) through co-ligation of CD21 enhances IgE production (215). Moreover, CD23 bound IgE-antigen complexes can be presented to T cells *via* a process called facilitated antigen presentation (FAP). In FAP, the antigen-loaded IgE-CD23 gets internalized and loaded onto MHC-II molecules for presentation on the B-cells surface (219). A Th2 environment, as derived by activation of mast cells and basophils *via* FcεRII activation, may support this by increasing the expression of CD23 on B cells. Importantly, any activated B cell that expresses CD23, can present allergens to T cells independently of the specificity of the B cell receptor (BCR). By this, CD23-FAP can lead to epitope spreading, a process where the response to one epitope encountered by the BCR induces epitope-specific immunoglobulin production against the allergen internalized by CD23 (215). Epitope spreading can occur intra- or intermolecularly and is thought to be the driving cause for the development of polyspecific allergies to unrelated antigens. It is, therefore, of particular importance for the development of autoallergies. Antigen presentation via the CD23–MHC-II axis is as efficient as presentation of antigens by dendritic cells mediated by FcγRs and by far more efficient than BCR internalization (220). This is particularly dangerous when epitopes of an autoantigen and a pathogen are very similar

in sequence and/or conformation (molecular mimicry) and IgE against the pathogen (IgE_{PATH}) also binds to the autoantigen (221). Low-affinity IgE_{PATH}-autoantigen interactions can lead *via* FAP dependent epitope spreading to high affinity auto-IgE. For many autoimmune diseases, such as SLE and BP, where IgE autoantibodies have been identified, B cell epitope spreading has been recognized as an important contributor for disease development.

On monocytes and macrophages, engagement of CD23 induces nitric oxide synthase and proinflammatory cytokines and importantly mediates IgE-dependent phagocytosis of targeted cells suggesting a use for immunotherapy, for instance in cancer (188, 222). Interestingly, auto-IgE to tumor antigens can be found in tumor tissue as well as systematically, suggesting a tumor suppressive function of these IgE autoantibodies.

Effects of IgE/(Auto)Antigen on Galectin-3 Signaling

Galectin-3 is a secretory lectin containing a carbohydrate recognition domain connected to a non-lectin linker domain that associate to form a pentameric structure like IgM molecules. Galectin-3 is expressed by various immune cells including mast cells, basophils, neutrophils, monocytes, Langerhans cells, as well as T and B cells (196). It can be found in the nucleus, intracellular vesicles, or exosomes of expressing cells or gets secreted by a yet not fully characterized mechanism (223). Following secretion, it interacts with a large variety of cell surface and extracellular matrix proteins including IgE and FcεRI. Interestingly though, galectin-3 appears to have distinct binding capacities for IgE isoforms that are differentially glycosylated, although the consequence of this phenomenon in allergy and autoallergy is not clear (224). Because it is capable of binding to IgE and FcεRI, it can activate mast cells and other FcεRI-expressing and/or IgE-loaded cells in an IgE-dependent or independent manner and boost mast cell and basophil activation. In autoimmune diseases, galectin-3 is often increased in the serum and in tissues and may support auto-IgE-induced inflammation. However, most effects of galectin-3 on the immune system are independent of its ability to crosslink IgE and FcεRI. Its effects and relevance in autoallergy, therefore, need to be determined carefully (214, 225).

GAPS OF KNOWLEDGE, UNMET NEEDS, AND UNANSWERED QUESTIONS

Need for Improved Detection Methods

There are two different major drawbacks of the tests currently used to assess autoreactive IgE. First, different methods show a high variability and low reproducibility of IgE reactivity (226). This has been best demonstrated using the well characterized BP autoantigen BP180-NC16A. An improved ELISA method showed a significantly higher frequency of NC16A-specific IgE autoantibodies in the sera of BP patients than previously described (66). This study also demonstrated that most BP sera contain both, IgE and IgG class autoantibodies specific for NC16A and that IgG reactive to the same autoantigen as IgE can mask the detection of autoreactive IgE. This is the second major drawback of direct ELISA methods. This problem can be addressed by the use of indirect ELISA methods, where total IgE is first captured on the plate by anti-IgE and labeled autoantigen is used for detection (98). This approach, however, also has limitations. Saturation of the anti-IgE with non-autoreactive IgE in sera with very high total IgE concentrations can lead to the underestimation of autoallergen-specific IgE. Also, this method requires recombinant IgE to be able to calculate the specific IgE concentration in international units.

Yet unaddressed questions are the relevance of different conformational states of IgE, such as the bent-form, that may not be detectable by ELISA depending on which anti-IgE is used (227). Relevant cross-autoreactive IgE might also be prone to oligomerization due to stacking, which may hinder binding to capture antibodies.

Finally, autoreactive IgE may be preferentially captured in the tissue in patients with high FcεRI expression due to high IgE levels. Increased levels of IgE are frequently seen in patients with chronic urticaria and in atopic individuals (228, 229). *Vice versa*, as antigen reactivity encoded by the Fab-domain can change also the Fc part and, therefore, influence Fc receptor binding, some autoreactive IgEs might be over- or underrepresented in the non-cell bound IgE fraction due to changed FcεRI binding (230). Even assays detecting non-autoreactive IgE often fail to show a clinical relevance (231). The questions above need to be addressed for IgE in general, not only autoreactive IgE, in further studies, and improved methods need to be developed.

What Leads to the Development of Autoantibodies of the IgE Isotype?

There are several possible mechanisms that might lead to a preference of IgE isotype for autoantibodies. Most IgE autoantigens are phosphorylated molecules (97, 232, 233). It has been demonstrated that IgG autoantibodies in BP preferably recognize a phosphorylated epitope (232, 234). The importance of phosphorylation for the development of autoantibodies in general has been shown for myeloperoxidase-anti-neutrophil cytoplasmic IgG autoantibodies in a mouse model (235). However, further studies are needed to assess whether this is a general rule preferably for IgE autoantigens, or for all autoantigens.

IgE Cross-Reactivity Remains Largely Unexplained

In contrast to IgG and IgA, IgE has, in general, a much higher degree of cross-reactivity. This makes the determination of antigen-specific IgE difficult. As of now, very little is known about cross-reactivity of IgE autoantibodies. One study that performed site-directed mutagenesis of an allergenic peptide found that even after the mutation of all of the four residues that are mainly involved in IgE binding, the IgE still bound, albeit with a 100-fold reduced affinity (236). Furthermore, many studies have shown IgE cross-reactivity to structurally similar allergens, e.g., sensitization to the fungus *F. proliferatum* may lead to allergy to penicillin (237).

Usually, IgE cross-reactivity is explained by the recognition of carbohydrate-containing epitopes such as in cross-reactive IgEs against wheat/pollen or latex/hymenoptera proteins (238–241)

or between different pollen allergens (242–244). Hierarchies of cross-reactivity toward different pollen allergens have been established (245).

In latex–pollen–food allergy, a good example of non-carbohydrate based cross-reactivity, cross-reactive IgE binds to latex and maize (246) or other food allergens (247). The antigenic epitopes of these allergens are well characterized and show only a low degree of sequence homology. The cross-reactivity can only be explained by a similar charge distribution, which, in the case of IgG, does usually not lead to cross-reactive antibodies (248).

Other examples of IgE cross-reactivity include pollen–food allergy, such as apple–birch allergy or pollen–fruit allergy (249–253), dog–cat allergy (254, 255), poultry–meat allergy (256), fish–chicken allergy (257), birch–oak allergy (258), latex–hymenoptera allergy (239–241). IgE cross reactivity to latex and parasites like *Schistosoma* has also been described (259, 260). In mice sensitized to birch pollen that also developed anaphylactic reactions to apple, desensitization to birch pollen also provided protection from anaphylaxis to apple (261). Similar experiences have been reported in allergic patients, where tolerance induction against one allergen also reduced reactivity toward other allergens (262). While IgE cross-reactivity between classical allergens is much more common than previously thought (263), cross-reactivity between autoallergens needs to be investigated in future studies.

Unanswered Questions?

Many questions on IgE autoantibodies remain unanswered.

- Is IgE to self different from IgE to exogenous antigens in terms of its biochemical properties, its glycosylation, or its folding?
- Where is auto-IgE produced and what B cells are involved?
- Does the auto-IgE come from CD5+ B1 B cells of the marginal zone of the spleen (poorly negatively selected B cells that often produce autoantibodies) or from B cells that were previously allergen or pathogen reactive?
- Does the production of auto-IgE precede the onset of autoallergic signs and symptoms and when and why does it stop?

These and other questions are currently addressed by ongoing research. The answers that will come from these and future studies will help to better understand the biology and relevance of IgE autoantibodies in disease and to develop better approaches for the prevention and treatment of autoallergies.

AUTHOR CONTRIBUTIONS

All authors listed have made a substantial, direct, and intellectual contribution to the work and approved it for publication.

REFERENCES

1. Prausnitz C, Kustner H. Studien über die Ueberempfindlichkeit. *Zentralbl Bakteriol* (1921) 86:160–9.
2. Ishizaka K, Ishizaka T. Identification of gamma-E-antibodies as a carrier of reaginic activity. *J Immunol* (1967) 99(6):1187–98.
3. Johansson SG, Bennich H. Immunological studies of an atypical (myeloma) immunoglobulin. *Immunology* (1967) 13(4):381–94.
4. Johansson SG. The history of IgE: from discovery to 2010. *Curr Allergy Asthma Rep* (2011) 11(2):173–7. doi:10.1007/s11882-010-0174-3
5. Marcolongo R, Marsili C. [Determination of serum IgD and IgE levels in patients with rheumatoid arthritis]. *Reumatismo* (1972) 24(2):173–4.
6. Hunder GG, Gleich GJ. Immunoglobulin E (IgE) levels in serum and synovial fluid in rheumatoid arthritis. *Arthritis Rheum* (1974) 17(6):955–63. doi:10.1002/art.1780170606
7. Marcolongo R, Marsili C. Serum IgD and IgE in rheumatoid arthritis. *Z Immunitatsforsch Exp Klin Immunol* (1975) 148(4):285–90.
8. Arbesman CE, Wypych JI, Reisman RE, Beutner EH. IgE levels in sera of patients with pemphigus or bullous pemphigoid. *Arch Dermatol* (1974) 110(3):378–81. doi:10.1001/archderm.1974.01630090016003
9. Provost TT, Tomasi TB Jr. Immunopathology of bullous pemphigoid. Basement membrane deposition of IgE, alternate pathway components and fibrin. *Clin Exp Immunol* (1974) 18(2):193–200.
10. Ogawa M, Berger PA, McIntyre OR, Clendenning WE, Ishizaka K. IgE in atopic dermatitis. *Arch Dermatol* (1971) 103(6):575–80. doi:10.1001/archderm.1971.04000180001001
11. Igarashi R. [An immunohistochemical study of IgE in the skin of patients with systemic lupus erythematosus (author's transl)]. *Nihon Hifuka Gakkai Zasshi* (1975) 85(7):385–93.
12. Goldman JA, Klimek GA, Ali R. Allergy in systemic lupus erythematosus. IgE levels and reaginic phenomenon. *Arthritis Rheum* (1976) 19(4):669–76. doi:10.1002/1529-0131(197607/08)19:4<669::AID-ART1780190403>3.0.CO;2-E
13. Altrichter S, Peter HJ, Pisarevskaja D, Metz M, Martus P, Maurer M. IgE mediated autoallergy against thyroid peroxidase – a novel pathomechanism of chronic spontaneous urticaria? *PLoS One* (2011) 6(4):e14794. doi:10.1371/journal.pone.0014794
14. Chang TW, Chen C, Lin CJ, Metz M, Church MK, Maurer M. The potential pharmacologic mechanisms of omalizumab in patients with chronic spontaneous urticaria. *J Allergy Clin Immunol* (2015) 135(2):337–42. doi:10.1016/j.jaci.2014.04.036
15. Metz M, Ohanyan T, Church MK, Maurer M. Omalizumab is an effective and rapidly acting therapy in difficult-to-treat chronic urticaria: a retrospective clinical analysis. *J Dermatol Sci* (2014) 73(1):57–62. doi:10.1016/j.jdermsci.2013.08.011
16. Valenta R, Duchene M, Pettenburger K, Sillaber C, Valent P, Bettelheim P, et al. Identification of profilin as a novel pollen allergen; IgE autoreactivity in sensitized individuals. *Science* (1991) 253(5019):557–60. doi:10.1126/science.1857985
17. Garn H, Mittermann I, Valenta R, Renz H. Autosensitization as a pathomechanism in asthma. *Ann N Y Acad Sci* (2007) 1107:417–25. doi:10.1196/annals.1381.044
18. Tedeschi A, Asero R. Asthma and autoimmunity: a complex but intriguing relation. *Expert Rev Clin Immunol* (2008) 4(6):767–76. doi:10.1586/1744666X.4.6.767
19. Tang TS, Bieber T, Williams HC. Does "autoreactivity" play a role in atopic dermatitis? *J Allergy Clin Immunol* (2012) 129(5):1209–15.e2. doi:10.1016/j.jaci.2012.02.002
20. Valenta R, Seiberler S, Natter S, Mahler V, Mossabeb R, Ring J, et al. Autoallergy: a pathogenetic factor in atopic dermatitis? *J Allergy Clin Immunol* (2000) 105(3):432–7. doi:10.1067/mai.2000.104783
21. Zhang L, Guo L, Huang Y, Wang T, Shi X, Chang H, et al. Allergic diseases, immunoglobulin E, and autoimmune pancreatitis: a retrospective study of 22 patients. *Chin Med J (Engl)* (2014) 127(23):4104–9.
22. van Beek N, Schulze FS, Zillikens D, Schmidt E. IgE-mediated mechanisms in bullous pemphigoid and other autoimmune bullous diseases. *Expert Rev Clin Immunol* (2016) 12(3):267–77. doi:10.1586/1744666X.2016.1123092
23. Panaszek B, Pawlowicz R, Grzegrzolka J, Obojski A. Autoreactive IgE in chronic spontaneous/idiopathic urticaria and basophil/mastocyte priming phenomenon, as a feature of autoimmune nature of the syndrome. *Arch Immunol Ther Exp (Warsz)* (2017) 65(2):137–43. doi:10.1007/s00005-016-0417-7
24. Guo J, Rapoport B, McLachlan SM. Thyroid peroxidase autoantibodies of IgE class in thyroid autoimmunity. *Clin Immunol Immunopathol* (1997) 82(2):157–62. doi:10.1006/clin.1996.4297

25. Elisei R, Weightman D, Kendall-Taylor P, Vassart G, Ludgate M. Muscle autoantigens in thyroid associated ophthalmopathy: the limits of molecular genetics. *J Endocrinol Invest* (1993) 16(7):533–40. doi:10.1007/BF03348900
26. Mikol DD, Ditlow C, Usatin D, Biswas P, Kalbfleisch J, Milner A, et al. Serum IgE reactive against small myelin protein-derived peptides is increased in multiple sclerosis patients. *J Neuroimmunol* (2006) 180(1–2):40–9. doi:10.1016/j.jneuroim.2006.06.030
27. Permin H, Wiik A. The prevalence of IgE antinuclear antibodies in rheumatoid arthritis and systemic lupus erythematosus. *Acta Pathol Microbiol Scand C* (1978) 86C(5):245–9.
28. Sanjuan MA, Sagar D, Kolbeck R. Role of IgE in autoimmunity. *J Allergy Clin Immunol* (2016) 137(6):1651–61. doi:10.1016/j.jaci.2016.04.007
29. Muino JC, Juarez CP, Luna JD, Castro CC, Wolff EG, Ferrero M, et al. The importance of specific IgG and IgE autoantibodies to retinal S antigen, total serum IgE, and sCD23 levels in autoimmune and infectious uveitis. *J Clin Immunol* (1999) 19(4):215–22. doi:10.1023/A:1020516029883
30. Keller P. Beitrag zu den beziehungen von asthma und ekzem. *Arch Derm Syph Berl* (1924) 148:82–91. doi:10.1007/BF01827500
31. Storm van Leeuwen W, Bien Z, Varekamp H. Über die hautreaktion mit extrakten menschlicher kopfhautschuppen bei allergischen krankheiten. *Klin Wochenschr* (1926) 5:1023–5. doi:10.1007/BF01717944
32. Hampton SF, Cooke RA. The sensitivity of man to human dander, with particular reference to eczema (allergic dermatitis). *J Allergy* (1941) 13:63–76. doi:10.1016/S0021-8707(41)90008-4
33. Simon FA. Human dander: an important cause of infantile eczema. *JAMA* (1944) 125:350–9. doi:10.1001/jama.1944.02850230030008
34. Simon FA. On the allergen in human dander. *J Allergy* (1944) 15:338–45. doi:10.1016/S0021-8707(44)90143-7
35. Simon FA. The allergen of human dander present in skin of the general body surface. *J Invest Dermatol* (1947) 9(6):329–32. doi:10.1038/jid.1947.106
36. Valenta R, Maurer D, Steiner R, Seiberler S, Sperr WR, Valent P, et al. Immunoglobulin E response to human proteins in atopic patients. *J Invest Dermatol* (1996) 107(2):203–8. doi:10.1111/1523-1747.ep12329617
37. Szakos E, Lakos G, Aleksza M, Gyimesi E, Pall G, Fodor B, et al. Association between the occurrence of the anticardiolipin IgM and mite allergen-specific IgE antibodies in children with extrinsic type of atopic eczema/dermatitis syndrome. *Allergy* (2004) 59(2):164–7. doi:10.1046/j.1398-9995.2003.00367.x
38. Schmid-Grendelmeier P, Fluckiger S, Disch R, Trautmann A, Wuthrich B, Blaser K, et al. IgE-mediated and T cell-mediated autoimmunity against manganese superoxide dismutase in atopic dermatitis. *J Allergy Clin Immunol* (2005) 115(5):1068–75. doi:10.1016/j.jaci.2005.01.065
39. Higashi N, Niimi Y, Aoki M, Kawana S. Clinical features of antinuclear antibody-positive patients with atopic dermatitis. *J Nippon Med Sch* (2009) 76(6):300–7. doi:10.1272/jnms.76.300
40. Altrichter S, Kriehuber E, Moser J, Valenta R, Kopp T, Stingl G. Serum IgE autoantibodies target keratinocytes in patients with atopic dermatitis. *J Invest Dermatol* (2008) 128(9):2232–9. doi:10.1038/jid.2008.80
41. Zeller S, Rhyner C, Meyer N, Schmid-Grendelmeier P, Akdis CA, Crameri R. Exploring the repertoire of IgE-binding self-antigens associated with atopic eczema. *J Allergy Clin Immunol* (2009) 124(2): 278–85, 285.e1–7. doi:10.1016/j.jaci.2009.05.015
42. Balaji H, Heratizadeh A, Wichmann K, Niebuhr M, Crameri R, Scheynius A, et al. *Malassezia sympodialis* thioredoxin-specific T cells are highly cross-reactive to human thioredoxin in atopic dermatitis. *J Allergy Clin Immunol* (2011) 128(1):92–9.e4. doi:10.1016/j.jaci.2011.02.043
43. Watanabe K, Muro Y, Sugiura K, Tomita Y. IgE and IgG(4) autoantibodies against DFS70/LEDGF in atopic dermatitis. *Autoimmunity* (2011) 44(6):511–9. doi:10.3109/08916934.2010.549157
44. Natter S, Seiberler S, Hufnagl P, Binder BR, Hirschl AM, Ring J, et al. Isolation of cDNA clones coding for IgE autoantigens with serum IgE from atopic dermatitis patients. *FASEB J* (1998) 12(14):1559–69. doi:10.1096/fasebj.12.14.1559
45. Valenta R, Natter S, Seiberler S, Wichlas S, Maurer D, Hess M, et al. Molecular characterization of an autoallergen, Hom s 1, identified by serum IgE from atopic dermatitis patients. *J Invest Dermatol* (1998) 111(6):1178–83. doi:10.1046/j.1523-1747.1998.00413.x
46. Mothes N, Niggemann B, Jenneck C, Hagemann T, Weidinger S, Bieber T, et al. The cradle of IgE autoreactivity in atopic eczema lies in early infancy. *J Allergy Clin Immunol* (2005) 116(3):706–9. doi:10.1016/j.jaci.2005.06.025
47. Zhu H, Luo H, Yan M, Zuo X, Li QZ. Autoantigen microarray for high-throughput autoantibody profiling in systemic lupus erythematosus. *Genomics Proteomics Bioinformatics* (2015) 13(4):210–8. doi:10.1016/j.gpb.2015.09.001
48. Atta AM, Santiago MB, Guerra FG, Pereira MM, Sousa Atta ML. Autoimmune response of IgE antibodies to cellular self-antigens in systemic lupus erythematosus. *Int Arch Allergy Immunol* (2010) 152(4):401–6. doi:10.1159/000288293
49. Dema B, Pellefigues C, Hasni S, Gault N, Jiang C, Ricks TK, et al. Autoreactive IgE is prevalent in systemic lupus erythematosus and is associated with increased disease activity and nephritis. *PLoS One* (2014) 9(2):e90424. doi:10.1371/journal.pone.0090424
50. Hanaoka H, Okazaki Y, Satoh T, Kaneko Y, Yasuoka H, Seta N, et al. Circulating anti-double-stranded DNA antibody-secreting cells in patients with systemic lupus erythematosus: a novel biomarker for disease activity. *Lupus* (2012) 21(12):1284–93. doi:10.1177/0961203312453191
51. Rhyner C, Daigle I, Crameri R. Auto-reactive IgE responses to acidic ribosomal P(2) protein in systemic lupus erythematosus. *Allergy* (2011) 66(8):1127–9. doi:10.1111/j.1398-9995.2011.02581.x
52. Sekigawa I, Seta N, Yamada M, Iida N, Hashimoto H, Ogawa H. Possible importance of immunoglobulin E in foetal loss by mothers with anti-SSA antibody. *Scand J Rheumatol* (2004) 33(1):44–6. doi:10.1080/03009740310004658
53. Brucato A, Cimaz R, Caporali R, Ramoni V, Buyon J. Pregnancy outcomes in patients with autoimmune diseases and anti-Ro/SSA antibodies. *Clin Rev Allergy Immunol* (2011) 40(1):27–41. doi:10.1007/s12016-009-8190-6
54. Christophoridis S, Budinger L, Borradori L, Hunziker T, Merk HF, Hertl M. IgG, IgA and IgE autoantibodies against the ectodomain of BP180 in patients with bullous and cicatricial pemphigoid and linear IgA bullous dermatosis. *Br J Dermatol* (2000) 143(2):349–55. doi:10.1046/j.1365-2133.2000.03661.x
55. Thoma-Uszynski S, Uter W, Schwietzke S, Hofmann SC, Hunziker T, Bernard P, et al. BP230- and BP180-specific auto-antibodies in bullous pemphigoid. *J Invest Dermatol* (2004) 122(6):1413–22. doi:10.1111/j.0022-202X.2004.22603.x
56. van Beek N, Luttmann N, Huebner F, Recke A, Karl I, Schulze FS, et al. Correlation of serum levels of IgE autoantibodies against BP180 with bullous pemphigoid disease activity. *JAMA Dermatol* (2017) 153(1):30–8. doi:10.1001/jamadermatol.2016.3357
57. Hofmann S, Thoma-Uszynski S, Hunziker T, Bernard P, Koebnick C, Stauber A, et al. Severity and phenotype of bullous pemphigoid relate to autoantibody profile against the NH2- and COOH-terminal regions of the BP180 ectodomain. *J Invest Dermatol* (2002) 119(5):1065–73. doi:10.1046/j.1523-1747.2002.19529.x
58. Dresow SK, Sitaru C, Recke A, Oostingh GJ, Zillikens D, Gibbs BF. IgE autoantibodies against the intracellular domain of BP180. *Br J Dermatol* (2009) 160(2):429–32. doi:10.1111/j.1365-2133.2008.08858.x
59. Dimson OG, Giudice GJ, Fu CL, Van den Bergh F, Warren SJ, Janson MM, et al. Identification of a potential effector function for IgE autoantibodies in the organ-specific autoimmune disease bullous pemphigoid. *J Invest Dermatol* (2003) 120(5):784–8. doi:10.1046/j.1523-1747.2003.12146.x
60. Iwata Y, Komura K, Kodera M, Usuda T, Yokoyama Y, Hara T, et al. Correlation of IgE autoantibody to BP180 with a severe form of bullous pemphigoid. *Arch Dermatol* (2008) 144(1):41–8. doi:10.1001/archdermatol.2007.9
61. Ishiura N, Fujimoto M, Watanabe R, Nakashima H, Kuwano Y, Yazawa N, et al. Serum levels of IgE anti-BP180 and anti-BP230 autoantibodies in patients with bullous pemphigoid. *J Dermatol Sci* (2008) 49(2):153–61. doi:10.1016/j.jdermsci.2007.08.008
62. Yayli S, Pelivani N, Beltraminelli H, Wirthmuller U, Beleznay Z, Horn M, et al. Detection of linear IgE deposits in bullous pemphigoid and mucous membrane pemphigoid: a useful clue for diagnosis. *Br J Dermatol* (2011) 165(5):1133–7. doi:10.1111/j.1365-2133.2011.10481.x
63. Dopp R, Schmidt E, Chimanovitch I, Leverkus M, Brocker EB, Zillikens D. IgG4 and IgE are the major immunoglobulins targeting the NC16A domain of BP180 in bullous pemphigoid: serum levels of these immunoglobulins reflect disease activity. *J Am Acad Dermatol* (2000) 42(4):577–83. doi:10.1067/mjd.2000.103986
64. Pomponi D, Di Zenzo G, Zennaro D, Calabresi V, Eming R, Zuzzi S, et al. Detection of IgG and IgE reactivity to BP180 using the ISAC(R) microarray system. *Br J Dermatol* (2013) 168(6):1205–14. doi:10.1111/bjd.12161

65. Liu B, Zuo YG, Zhou XP, He CX, Li J, Tie D, et al. [Establishment of enzyme-linked immunosorbent assay in the detection of BP180NC16A-specific IgE and its significance in bullous pemphigoid]. *Zhonghua Yi Xue Za Zhi* (2013) 93(28):2244–7.
66. Messingham KA, Noe MH, Chapman MA, Giudice GJ, Fairley JA. A novel ELISA reveals high frequencies of BP180-specific IgE production in bullous pemphigoid. *J Immunol Methods* (2009) 346(1–2):18–25. doi:10.1016/j.jim.2009.04.013
67. Engineer L, Bhol K, Kumari S, Razzaque Ahmed A. Bullous pemphigoid: interaction of interleukin 5, anti-basement membrane zone antibodies and eosinophils. A preliminary observation. *Cytokine* (2001) 13(1):32–8. doi:10.1006/cyto.2000.0791
68. Fania L, Caldarola G, Muller R, Brandt O, Pellicano R, Feliciani C, et al. IgE recognition of bullous pemphigoid (BP)180 and BP230 in BP patients and elderly individuals with pruritic dermatoses. *Clin Immunol* (2012) 143(3):236–45. doi:10.1016/j.clim.2012.02.003
69. Cozzani E, Micalizzi C, Parodi A, Rebora A. Anti-230 kDa circulating IgE in bullous pemphigoid: relationship with disease activity. *Acta Derm Venereol* (1997) 77(3):236.
70. Ghohestani RF, Cozzani E, Delaporte E, Nicolas JF, Parodi A, Claudy A. IgE antibodies in sera from patients with bullous pemphigoid are autoantibodies preferentially directed against the 230-kDa epidermal antigen (BP230). *J Clin Immunol* (1998) 18(3):202–9. doi:10.1023/A:1020531005776
71. Bruns GR, Ablin RJ, Guinan PD. Serum immunoglobulin E in pemphigus. *J Invest Dermatol* (1978) 71(3):217–8. doi:10.1111/1523-1747.ep12547283
72. Nagel A, Lang A, Engel D, Podstawa E, Hunzelmann N, de Pita O, et al. Clinical activity of pemphigus vulgaris relates to IgE autoantibodies against desmoglein 3. *Clin Immunol* (2010) 134(3):320–30. doi:10.1016/j.clim.2009.11.006
73. Spaeth S, Riechers R, Borradori L, Zillikens D, Budinger L, Hertl M. IgG, IgA and IgE autoantibodies against the ectodomain of desmoglein 3 in active pemphigus vulgaris. *Br J Dermatol* (2001) 144(6):1183–8. doi:10.1046/j.1365-2133.2001.04228.x
74. Natsuga K, Nishie W, Shinkuma S, Moriuchi R, Shibata M, Nishimura M, et al. Circulating IgA and IgE autoantibodies in antilaminin-332 mucous membrane pemphigoid. *Br J Dermatol* (2010) 162(3):513–7. doi:10.1111/j.1365-2133.2009.09508.x
75. Qian Y, Prisayanh P, Andraca E, Qaqish BF, Aoki V, Hans-Filhio G, et al. IgE, IgM, and IgG4 anti-desmoglein 1 autoantibody profile in endemic pemphigus foliaceus (fogo selvagem). *J Invest Dermatol* (2011) 131(4):985–7. doi:10.1038/jid.2010.403
76. Qian Y, Jeong JS, Abdeladhim M, Valenzuela JG, Aoki V, Hans-Filhio G, et al. IgE anti-LJM11 sand fly salivary antigen may herald the onset of fogo selvagem in endemic Brazilian regions. *J Invest Dermatol* (2015) 135(3):913–5. doi:10.1038/jid.2014.430
77. Maurer M, Metz M, Magerl M, Siebenhaar F, Staubach P. [Autoreactive urticaria and autoimmune urticaria]. *Hautarzt* (2004) 55(4):350–6. doi:10.1007/s00105-004-0692-9
78. Maurer M, Rosen K, Hsieh HJ, Saini S, Grattan C, Gimenez-Arnau A, et al. Omalizumab for the treatment of chronic idiopathic or spontaneous urticaria. *N Engl J Med* (2013) 368(10):924–35. doi:10.1056/NEJMoa1215372
79. Caliskaner Z, Ozturk S, Turan M, Karaayvaz M. Skin test positivity to aeroallergens in the patients with chronic urticaria without allergic respiratory disease. *J Investig Allergol Clin Immunol* (2004) 14(1):50–4.
80. Kulthanan K, Jiamton S, Rutnin NO, Insawang M, Pinkaew S. Prevalence and relevance of the positivity of skin prick testing in patients with chronic urticaria. *J Dermatol* (2008) 35(6):330–5. doi:10.1111/j.1346-8138.2008.00477.x
81. Gecer E, Erdem T. Aeroallergen prick skin test and autologous serum skin test results in patients with chronic urticaria and their comparison. *Ann Dermatol* (2012) 24(4):472–4. doi:10.5021/ad.2012.24.4.472
82. Song Z, Zhai Z, Zhong H, Zhou Z, Chen W, Hao F. Evaluation of autologous serum skin test and skin prick test reactivity to house dust mite in patients with chronic spontaneous urticaria. *PLoS One* (2013) 8(5):e64142. doi:10.1371/journal.pone.0064142
83. Staubach P, Vonend A, Burow G, Metz M, Magerl M, Maurer M. Patients with chronic urticaria exhibit increased rates of sensitisation to *Candida albicans*, but not to common moulds. *Mycoses* (2009) 52(4):334–8. doi:10.1111/j.1439-0507.2008.01601.x
84. Zhang M, Liu F, Liu H, Shen Y, Kong Q, Sang H. Sensitization and cross-reactions of dermatophyte and *Candida albicans* allergens in patients with chronic urticaria. *Int J Dermatol* (2016) 55(10):1138–42. doi:10.1111/ijd.13162
85. Kulthanan K, Wachirakaphan C. Prevalence and clinical characteristics of chronic urticaria and positive skin prick testing to mites. *Acta Derm Venereol* (2008) 88(6):584–8. doi:10.2340/00015555-0546
86. Zuberbier T, Balke M, Worm M, Edenharter G, Maurer M. Epidemiology of urticaria: a representative cross-sectional population survey. *Clin Exp Dermatol* (2010) 35(8):869–73. doi:10.1111/j.1365-2230.2010.03840.x
87. Augey F, Gunera-Saad N, Bensaid B, Nosbaum A, Berard F, Nicolas JF. Chronic spontaneous urticaria is not an allergic disease. *Eur J Dermatol* (2011) 21(3):349–53. doi:10.1684/ejd.2011.1285
88. Kolkhir P, Metz M, Altrichter S, Maurer M. Comorbidity of chronic spontaneous urticaria and autoimmune thyroid diseases: a systematic review. *Allergy* (2017) 72(10):1440–60. doi:10.1111/all.13182
89. Bar-Sela S, Reshef T, Mekori YA. IgE antithyroid microsomal antibodies in a patient with chronic urticaria. *J Allergy Clin Immunol* (1999) 103(6):1216–7. doi:10.1016/S0091-6749(99)70204-6
90. Atta AM, Rodrigues MZ, Sousa CP, Medeiros Junior M, Sousa-Atta ML. Autoantibody production in chronic idiopathic urticaria is not associated with *Helicobacter pylori* infection. *Braz J Med Biol Res* (2004) 37(1):13–7. doi:10.1590/S0100-879X2004000100002
91. Concha LB, Chang CC, Szema AM, Dattwyler RJ, Carlson HE. IgE antithyroid antibodies in patients with Hashimoto's disease and chronic urticaria. *Allergy Asthma Proc* (2004) 25(5):293–6.
92. Tedeschi A, Lorini M, Asero R. Anti-thyroid peroxidase IgE in patients with chronic urticaria. *J Allergy Clin Immunol* (2001) 108(3):467–8. doi:10.1067/mai.2001.117792
93. Kadooka Y, Idota T, Gunji H, Shimatani M, Kawakami H, Dosako S, et al. A method for measuring specific IgE in sera by direct ELISA without interference by IgG competition or IgG autoantibodies to IgE. *Int Arch Allergy Immunol* (2000) 122(4):264–9. doi:10.1159/000024408
94. Shin YS, Suh DH, Yang EM, Ye YM, Park HS. Serum specific IgE to thyroid peroxidase activates basophils in aspirin intolerant urticaria. *J Korean Med Sci* (2015) 30(6):705–9. doi:10.3346/jkms.2015.30.6.705
95. Kolkhir P, Borzova E, Grattan C, Asero R, Pogorelov D, Maurer M. Autoimmune comorbidity in chronic spontaneous urticaria: a systematic review. *Autoimmun Rev* (2017) 16(12):1196–208. doi:10.1016/j.autrev.2017.10.003
96. Kolkhir P, Pogorelov D, Olisova O, Maurer M. Comorbidity and pathogenic links of chronic spontaneous urticaria and systemic lupus erythematosus – a systematic review. *Clin Exp Allergy* (2016) 46(2):275–87. doi:10.1111/cea.12673
97. Hatada Y, Kashiwakura J, Hayama K, Fujisawa D, Sasaki-Sakamoto T, Terui T, et al. Significantly high levels of anti-dsDNA immunoglobulin E in sera and the ability of dsDNA to induce the degranulation of basophils from chronic urticaria patients. *Int Arch Allergy Immunol* (2013) 161(Suppl 2):154–8. doi:10.1159/000350388
98. Schmetzer O, Lakin E, Topal FA, Preusse P, Freier D, Church MK, et al. IL-24 is a common and specific autoantigen of IgE in patients with chronic spontaneous urticaria. *J Allergy Clin Immunol* (2017). doi:10.1016/j.jaci.2017.10.035
99. Romero MD, Muino JC, Bianco GA, Ferrero M, Juarez CP, Luna JD, et al. Circulating anti-galectin-1 antibodies are associated with the severity of ocular disease in autoimmune and infectious uveitis. *Invest Ophthalmol Vis Sci* (2006) 47(4):1550–6. doi:10.1167/iovs.05-1234
100. Meretey K, Falus A, Erhardt CC, Maini RN. IgE and IgE-rheumatoid factors in circulating immune complexes in rheumatoid arthritis. *Ann Rheum Dis* (1982) 41(4):405–8. doi:10.1136/ard.41.4.405
101. Schuerwegh AJ, Ioan-Facsinay A, Dorjee AL, Roos J, Bajema IM, van der Voort EI, et al. Evidence for a functional role of IgE anticitrullinated protein antibodies in rheumatoid arthritis. *Proc Natl Acad Sci U S A* (2010) 107(6):2586–91. doi:10.1073/pnas.0913054107
102. Schuerwegh AJ, Ioan-Facsinay A, Dorjee AL, Roos J, Bajema IM, van der Voort EI, et al. Retraction for Schuerwegh et al., evidence for a functional role of IgE anticitrullinated protein antibodies in rheumatoid arthritis. *Proc Natl Acad Sci U S A* (2013) 110(50):20345. doi:10.1073/pnas.1320459110
103. Monteiro L, Souza-Machado A, Menezes C, Melo A. Association between allergies and multiple sclerosis: a systematic review and meta-analysis. *Acta Neurol Scand* (2011) 123(1):1–7. doi:10.1111/j.1600-0404.2010.01355.x

104. Matsui Y, Heiner DC, Beall GN. IgE and IgE autoantibodies in patients with autoimmune thyroid disorders and their relatives. *Proc Soc Exp Biol Med* (1978) 158(1):73–6. doi:10.3181/00379727-158-40142
105. Inoue M, Rakugi H, Nakamaru M, Masugi F, Ogihara T, Takai S. [Graves' disease with markedly elevated serum immunoglobulin E]. *Nihon Naibunpi Gakkai Zasshi* (1989) 65(11):1264–9.
106. Sayinalp S, Akalin S, Sayinalp N, Erbas T, Bayraktar M, Ozcebe OI, et al. Serum immunoglobulin E and soluble CD23 in patients with Graves' disease. *Horm Metab Res* (1996) 28(3):133–7. doi:10.1055/s-2007-979145
107. Sato A, Takemura Y, Yamada T, Ohtsuka H, Sakai H, Miyahara Y, et al. A possible role of immunoglobulin E in patients with hyperthyroid Graves' disease. *J Clin Endocrinol Metab* (1999) 84(10):3602–5. doi:10.1210/jcem.84.10.6038
108. Yamada T, Sato A, Komiya I, Nishimori T, Ito Y, Terao A, et al. An elevation of serum immunoglobulin E provides a new aspect of hyperthyroid Graves' disease. *J Clin Endocrinol Metab* (2000) 85(8):2775–8. doi:10.1210/jcem.85.8.6741
109. Latifi-Pupovci H, Gacaferri-Lumezi B, Lokaj-Berisha V. There is no elevation of immunoglobulin e levels in Albanian patients with autoimmune thyroid diseases. *J Thyroid Res* (2014) 2014:283709. doi:10.1155/2014/283709
110. Raikow RB, Dalbow MH, Kennerdell JS, Compher K, Machen L, Hiller W, et al. Immunohistochemical evidence for IgE involvement in Graves' orbitopathy. *Ophthalmology* (1990) 97(5):629–35. doi:10.1016/S0161-6420(90)32548-4
111. Raikow RB, Tyutyunikov A, Kennerdell JS, Kazim M, Dalbow MH, Scalise D. Correlation of serum immunoglobulin E elevations with clinical stages of dysthyroid orbitopathy. *Ophthalmology* (1992) 99(3):361–5. doi:10.1016/S0161-6420(92)31964-5
112. Hirano K, Tada M, Isayama H, Kawakubo K, Yagioka H, Sasaki T, et al. Clinical analysis of high serum IgE in autoimmune pancreatitis. *World J Gastroenterol* (2010) 16(41):5241–6. doi:10.3748/wjg.v16.i41.5241
113. van Toorenenbergen AW, van Heerde MJ, van Buuren HR. Potential value of serum total IgE for differentiation between autoimmune pancreatitis and pancreatic cancer. *Scand J Immunol* (2010) 72(5):444–8. doi:10.1111/j.1365-3083.2010.02453.x
114. Bunder R, Mittermann I, Herz U, Focke M, Wegmann M, Valenta R, et al. Induction of autoallergy with an environmental allergen mimicking a self protein in a murine model of experimental allergic asthma. *J Allergy Clin Immunol* (2004) 114(2):422–8. doi:10.1016/j.jaci.2004.05.029
115. Lassalle P, Joseph M, Ramon P, Dracon M, Tonnel AB, Capron A. Plasmapheresis in a patient with severe asthma associated with auto-antibodies to platelets. *Clin Exp Allergy* (1990) 20(6):707–12. doi:10.1111/j.1365-2222.1990.tb02712.x
116. Mayer C, Appenzeller U, Seelbach H, Achatz G, Oberkofler H, Breitenbach M, et al. Humoral and cell-mediated autoimmune reactions to human acidic ribosomal P2 protein in individuals sensitized to *Aspergillus fumigatus* P2 protein. *J Exp Med* (1999) 189(9):1507–12. doi:10.1084/jem.189.9.1507
117. De Schryver E, Calus L, Bonte H, Natalie R, Gould H, Donovan E, et al. The quest for autoreactive antibodies in nasal polyps. *J Allergy Clin Immunol* (2016) 138(3):893–895.e5. doi:10.1016/j.jaci.2016.03.040
118. Cooper GS, Bynum ML, Somers EC. Recent insights in the epidemiology of autoimmune diseases: improved prevalence estimates and understanding of clustering of diseases. *J Autoimmun* (2009) 33(3–4):197–207. doi:10.1016/j.jaut.2009.09.008
119. Panda S, Ding JL. Natural antibodies bridge innate and adaptive immunity. *J Immunol* (2015) 194(1):13–20. doi:10.4049/jimmunol.1400844
120. Kapsogeorgou EK, Tzioufas AG. Autoantibodies in autoimmune diseases: clinical and Critical evaluation. *Isr Med Assoc J* (2016) 18(9):519–24.
121. Fu SL, Pierre J, Smith-Norowitz TA, Hagler M, Bowne W, Pincus MR, et al. Immunoglobulin E antibodies from pancreatic cancer patients mediate antibody-dependent cell-mediated cytotoxicity against pancreatic cancer cells. *Clin Exp Immunol* (2008) 153(3):401–9. doi:10.1111/j.1365-2249.2008.03726.x
122. Das MK, Mishra A, Beuria MK, Dash AP. Human natural antibodies to *Culex quinquefasciatus*: age-dependent occurrence. *J Am Mosq Control Assoc* (1991) 7(2):319–21.
123. Lorenzo S, Iglesias R, Paniagua E, Ansotegui I, Alonso JM, Ubeira FM. Natural antibodies to nematode biotinyl-enzymes in human sera. *Med Microbiol Immunol* (2001) 189(4):177–83. doi:10.1007/s004300100065
124. Otsuka A, Nomura T, Rerknimitr P, Seidel JA, Honda T, Kabashima K. The interplay between genetic and environmental factors in the pathogenesis of atopic dermatitis. *Immunol Rev* (2017) 278(1):246–62. doi:10.1111/imr.12545
125. Cipriani F, Ricci G, Leoni MC, Capra L, Baviera G, Longo G, et al. Autoimmunity in atopic dermatitis: biomarker or simply epiphenomenon? *J Dermatol* (2014) 41(7):569–76. doi:10.1111/1346-8138.12464
126. Hradetzky S, Werfel T, Rosner LM. Autoallergy in atopic dermatitis. *Allergo J Int* (2015) 24(1):16–22. doi:10.1007/s40629-015-0037-5
127. Wang HH, Li YC, Huang YC. Efficacy of omalizumab in patients with atopic dermatitis: a systematic review and meta-analysis. *J Allergy Clin Immunol* (2016) 138(6):1719–22.e1. doi:10.1016/j.jaci.2016.05.038
128. Holm JG, Agner T, Sand C, Thomsen SF. Omalizumab for atopic dermatitis: case series and a systematic review of the literature. *Int J Dermatol* (2017) 56(1):18–26. doi:10.1111/ijd.13353
129. Henault J, Riggs JM, Karnell JL, Liarski VM, Li J, Shirinian L, et al. Self-reactive IgE exacerbates interferon responses associated with autoimmunity. *Nat Immunol* (2016) 17(2):196–203. doi:10.1038/ni.3326
130. Ettinger R, Karnell JL, Henault J, Panda SK, Riggs JM, Kolbeck R, et al. Pathogenic mechanisms of IgE-mediated inflammation in self-destructive autoimmune responses. *Autoimmunity* (2017) 50(1):25–36. doi:10.1080/08916934.2017.1280670
131. Pan Q, Gong L, Xiao H, Feng Y, Li L, Deng Z, et al. Basophil activation-dependent autoantibody and interleukin-17 production exacerbate systemic lupus erythematosus. *Front Immunol* (2017) 8:348. doi:10.3389/fimmu.2017.00348
132. Freire PC, Munoz CH, Stingl G. IgE autoreactivity in bullous pemphigoid: eosinophils and mast cells as major targets of pathogenic immune reactants. *Br J Dermatol* (2017) 177(6):1644–53. doi:10.1111/bjd.15924
133. Fairley JA, Baum CL, Brandt DS, Messingham KA. Pathogenicity of IgE in autoimmunity: successful treatment of bullous pemphigoid with omalizumab. *J Allergy Clin Immunol* (2009) 123(3):704–5. doi:10.1016/j.jaci.2008.11.035
134. Dufour C, Souillet AL, Chaneliere C, Jouen F, Bodemer C, Jullien D, et al. Successful management of severe infant bullous pemphigoid with omalizumab. *Br J Dermatol* (2012) 166(5):1140–2. doi:10.1111/j.1365-2133.2011.10748.x
135. London VA, Kim GH, Fairley JA, Woodley DT. Successful treatment of bullous pemphigoid with omalizumab. *Arch Dermatol* (2012) 148(11):1241–3. doi:10.1001/archdermatol.2012.1604
136. Yalcin AD, Genc GE, Celik B, Gumuslu S. Anti-IgE monoclonal antibody (omalizumab) is effective in treating bullous pemphigoid and its effects on soluble CD200. *Clin Lab* (2014) 60(3):523–4. doi:10.7754/Clin.Lab.2013.130642
137. Yu KK, Crew AB, Messingham KA, Fairley JA, Woodley DT. Omalizumab therapy for bullous pemphigoid. *J Am Acad Dermatol* (2014) 71(3):468–74. doi:10.1016/j.jaad.2014.04.053
138. Balakirski G, Alkhateeb A, Merk HF, Leverkus M, Megahed M. Successful treatment of bullous pemphigoid with omalizumab as corticosteroid-sparing agent: report of two cases and review of literature. *J Eur Acad Dermatol Venereol* (2016) 30(10):1778–82. doi:10.1111/jdv.13758
139. Gonul MZ, Keseroglu HO, Ergin C, Ozcan I, Erdem O. Bullous pemphigoid successfully treated with omalizumab. *Indian J Dermatol Venereol Leprol* (2016) 82(5):577–9. doi:10.4103/0378-6323.183628
140. Menzinger S, Kaya G, Schmidt E, Fontao L, Laffitte E. Biological and clinical response to omalizumab in a patient with bullous pemphigoid. *Acta Derm Venereol* (2017) 98(2):284–6. doi:10.2340/00015555-2845
141. Kolkhir P, Church MK, Weller K, Metz M, Schmetzer O, Maurer M. Autoimmune chronic spontaneous urticaria: what we know and what we do not know. *J Allergy Clin Immunol* (2017) 139(6):1772–81.e1. doi:10.1016/j.jaci.2016.08.050
142. Metz M, Maurer M. Omalizumab in chronic urticaria. *Curr Opin Allergy Clin Immunol* (2012) 12(4):406–11. doi:10.1097/ACI.0b013e328355365a
143. Urgert MC, van den Elzen MT, Knulst AC, Fedorowicz Z, van Zuuren EJ. Omalizumab in patients with chronic spontaneous urticaria: a systematic review and GRADE assessment. *Br J Dermatol* (2015) 173(2):404–15. doi:10.1111/bjd.13845
144. Zhao ZT, Ji CM, Yu WJ, Meng L, Hawro T, Wei JF, et al. Omalizumab for the treatment of chronic spontaneous urticaria: a meta-analysis of randomized clinical trials. *J Allergy Clin Immunol* (2016) 137(6):1742–50.e4. doi:10.1016/j.jaci.2015.12.1342
145. Maurer M, Metz M, Brehler R, Hillen U, Jakob T, Mahler V, et al. Omalizumab treatment in patients with chronic inducible urticaria: a systematic review of published evidence. *J Allergy Clin Immunol* (2017) 141(2):638–49. doi:10.1016/j.jaci.2017.06.032
146. Maurer M, Altrichter S, Bieber T, Biedermann T, Brautigam M, Seyfried S, et al. Efficacy and safety of omalizumab in patients with chronic urticaria

who exhibit IgE against thyroperoxidase. *J Allergy Clin Immunol* (2011) 128(1):202–9.e5. doi:10.1016/j.jaci.2011.04.038
147. Gericke J, Metz M, Ohanyan T, Weller K, Altrichter S, Skov PS, et al. Serum autoreactivity predicts time to response to omalizumab therapy in chronic spontaneous urticaria. *J Allergy Clin Immunol* (2017) 139(3):1059–61.e1. doi:10.1016/j.jaci.2016.07.047
148. Houser DD, Arbesman CE, Ito K, Wicher K. Cold urticaria. Immunologic studies. *Am J Med* (1970) 49(1):23–33.
149. Kaplan AP, Garofalo J, Sigler R, Hauber T. Idiopathic cold urticaria: in vitro demonstration of histamine release upon challenge of skin biopsies. *N Engl J Med* (1981) 305(18):1074–7. doi:10.1056/NEJM198110293051808
150. Newcomb RW, Nelson H. Dermographia mediated by immunoglobulin E. *Am J Med* (1973) 54(2):174–80. doi:10.1016/0002-9343(73)90221-0
151. Morgado-Carrasco D, Fusta-Novell X, Podlipnik S, Combalia A, Aguilera P. Clinical and photobiological response in eight patients with solar urticaria under treatment with omalizumab, and review of the literature. *Photodermatol Photoimmunol Photomed* (2017). doi:10.1111/phpp.12370
152. Rodriguez-Jimenez P, Chicharro P, Perez-Plaza A, de Argila D. Response to omalizumab in solar urticaria: report of 3 cases. *Actas Dermosifiliogr* (2017) 108(8):e53–5. doi:10.1016/j.ad.2016.08.011
153. Koumaki D, Seaton ED. Successful treatment of refractory cholinergic urticaria with omalizumab. *Int J Dermatol* (2018) 57(1):114. doi:10.1111/ijd.13808
154. Somers EC, Marder W, Cagnoli P, Lewis EE, DeGuire P, Gordon C, et al. Population-based incidence and prevalence of systemic lupus erythematosus: the michigan lupus epidemiology and surveillance program. *Arthritis Rheumatol* (2014) 66(2):369–78. doi:10.1002/art.38238
155. Dema B, Charles N, Pellefigues C, Ricks TK, Suzuki R, Jiang C, et al. Immunoglobulin E plays an immunoregulatory role in lupus. *J Exp Med* (2014) 211(11):2159–68. doi:10.1084/jem.20140066
156. Yan S, Chen W, Wen S, Zhu W, Guo A, Chen X, et al. Influence of component 5a receptor 1 (C5AR1) -1330T/G polymorphism on nonsedating H1-antihistamines therapy in Chinese patients with chronic spontaneous urticaria. *J Dermatol Sci* (2014) 76(3):240–5. doi:10.1016/j.jdermsci.2014.09.012
157. Yang EM, Kim SH, Kim NH, Park HS. The genetic association of the FPRL1 promoter polymorphism with chronic urticaria in a Korean population. *Ann Allergy Asthma Immunol* (2010) 105(1):96–7. doi:10.1016/j.anai.2010.05.003
158. Rasool R, Shera IA, Nissar S, Yousuf Q, Shah ZA. IgE FcvarepsilonR1beta polymorphism and risk of developing chronic spontaneous urticaria: a study in an ethnic Kashmiri population. *Allergol Immunopathol (Madr)* (2015) 43(3):243–8. doi:10.1016/j.aller.2014.04.001
159. Hosseini Farahabadi S, Tavakkol-Afshari J, Ganjali R, Rafatpanah H, Ghaffari J, Farid-Hosseini R. Association between the polymorphism of TGF-beta1 gene promoter (-509C>T) and idiopathic chronic urticaria. *Iran J Allergy Asthma Immunol* (2006) 5(3):109–13.
160. Park HJ, Ye YM, Hur GY, Kim SH, Park HS. Association between a TGFbeta1 promoter polymorphism and the phenotype of aspirin-intolerant chronic urticaria in a Korean population. *J Clin Pharm Ther* (2008) 33(6):691–7. doi:10.1111/j.1365-2710.2008.00957.x
161. Pan KY, Walls RS, Rajasekariah P, Sherritt M, Warlow RS. Polymorphism of IgE gene in chronic urticaria. *Immunol Cell Biol* (1996) 74(1):90–5. doi:10.1038/icb.1996.12
162. Palikhe NS, Kim SH, Choi GS, Ye YM, Park HS. No evidence of association between interleukin-13 gene polymorphism in aspirin intolerant chronic urticaria. *Allergy Asthma Immunol Res* (2009) 1(1):36–40. doi:10.4168/aair.2009.1.1.36
163. Kim SH, Kang YM, Kim SH, Cho BY, Ye YM, Hur GY, et al. Histamine N-methyltransferase 939A>G polymorphism affects mRNA stability in patients with acetylsalicylic acid-intolerant chronic urticaria. *Allergy* (2009) 64(2):213–21. doi:10.1111/j.1398-9995.2008.01795.x
164. Brzoza Z, Grzeszczak W, Trautsolt W, Moczulski D. Protein tyrosine phosphatase-22 (PTPN-22) polymorphism in the pathogenesis of chronic urticaria. *Allergy* (2011) 66(10):1392–3. doi:10.1111/j.1398-9995.2011.02651.x
165. Brzoza Z, Grzeszczak W, Rogala B, Trautsolt W, Moczulski D. PTPN22 polymorphism presumably plays a role in the genetic background of chronic spontaneous autoreactive urticaria. *Dermatology* (2012) 224(4):340–5. doi:10.1159/000339332
166. Brzoza Z, Grzeszczak W, Rogala B, Trautsolt W, Moczulski D. CTLA-4 polymorphism in the pathogenesis of chronic spontaneous autoreactive urticaria. *Allergol Immunopathol (Madr)* (2014) 42(3):241–4. doi:10.1016/j.aller.2013.01.008
167. Akcali C, Ozkur M, Erbagci Z, Benlier N, Aynacioglu AS. Association of insertion/deletion polymorphism of the angiotensin-converting enzyme gene with angio-oedema accompanying chronic urticaria but not chronic urticaria without angio-oedema or the autologous serum skin test response. *J Eur Acad Dermatol Venereol* (2008) 22(1):83–6. doi:10.1111/j.1468-3083.2007.02353.x
168. Bottini N, Borgiani P, Otsu A, Saccucci P, Stefanini L, Greco E, et al. IL-4 receptor alpha chain genetic polymorphism and total IgE levels in the English population: two-locus haplotypes are more informative than individual SNPs. *Clin Genet* (2002) 61(4):288–92. doi:10.1034/j.1399-0004.2002.610408.x
169. Shin HD, Park BL, Kim LH, Kim JS, Kim JW. Interleukin-10 haplotype associated with total serum IgE in atopic dermatitis patients. *Allergy* (2005) 60(9):1146–51. doi:10.1111/j.1398-9995.2005.00839.x
170. Takahashi N, Akahoshi M, Matsuda A, Ebe K, Inomata N, Obara K, et al. Association of the IL12RB1 promoter polymorphisms with increased risk of atopic dermatitis and other allergic phenotypes. *Hum Mol Genet* (2005) 14(21):3149–59. doi:10.1093/hmg/ddi347
171. Munthe-Kaas MC, Carlsen KH, Helms PJ, Gerritsen J, Whyte M, Feijen M, et al. CTLA-4 polymorphisms in allergy and asthma and the TH1/TH2 paradigm. *J Allergy Clin Immunol* (2004) 114(2):280–7. doi:10.1016/j.jaci.2004.03.050
172. Pykalainen M, Kinos R, Valkonen S, Rydman P, Kilpelainen M, Laitinen LA, et al. Association analysis of common variants of STAT6, GATA3, and STAT4 to asthma and high serum IgE phenotypes. *J Allergy Clin Immunol* (2005) 115(1):80–7. doi:10.1016/j.jaci.2004.10.006
173. Weidinger S, Gieger C, Rodriguez E, Baurecht H, Mempel M, Klopp N, et al. Genome-wide scan on total serum IgE levels identifies FCER1A as novel susceptibility locus. *PLoS Genet* (2008) 4(8):e1000166. doi:10.1371/journal.pgen.1000166
174. Hecker M, Bohnert A, Konig IR, Bein G, Hackstein H. Novel genetic variation of human interleukin-21 receptor is associated with elevated IgE levels in females. *Genes Immun* (2003) 4(3):228–33. doi:10.1038/sj.gene.6363954
175. Pene J, Guglielmi L, Gauchat JF, Harrer N, Woisetschlager M, Boulay V, et al. IFN-gamma-mediated inhibition of human IgE synthesis by IL-21 is associated with a polymorphism in the IL-21R gene. *J Immunol* (2006) 177(8):5006–13. doi:10.4049/jimmunol.177.8.5006
176. Ozaki K, Spolski R, Feng CG, Qi CF, Cheng J, Sher A, et al. A critical role for IL-21 in regulating immunoglobulin production. *Science* (2002) 298(5598):1630–4. doi:10.1126/science.1077002
177. Kotlarz D, Zietara N, Uzel G, Weidemann T, Braun CJ, Diestelhorst J, et al. Loss-of-function mutations in the IL-21 receptor gene cause a primary immunodeficiency syndrome. *J Exp Med* (2013) 210(3):433–43. doi:10.1084/jem.20111229
178. Hysi P, Kabesch M, Moffatt MF, Schedel M, Carr D, Zhang Y, et al. NOD1 variation, immunoglobulin E and asthma. *Hum Mol Genet* (2005) 14(7):935–41. doi:10.1093/hmg/ddi087
179. Chalubinski M, Grzegorczyk J, Grzelak A, Jarzebska M, Kowalski ML. The beta2-adrenoreceptor gene promoter polymorphisms may modulate beta2-agonist- and glucocorticoid-induced IgE synthesis. *Allergol Immunopathol (Madr)* (2014) 42(6):586–93. doi:10.1016/j.aller.2013.07.002
180. Pate MB, Smith JK, Chi DS, Krishnaswamy G. Regulation and dysregulation of immunoglobulin E: a molecular and clinical perspective. *Clin Mol Allergy* (2010) 8:3. doi:10.1186/1476-7961-8-3
181. Kabesch M, Tzotcheva I, Carr D, Hofler C, Weiland SK, Fritzsch C, et al. A complete screening of the IL4 gene: novel polymorphisms and their association with asthma and IgE in childhood. *J Allergy Clin Immunol* (2003) 112(5):893–8. doi:10.1016/j.jaci.2003.08.033
182. Maurer D, Fiebiger E, Reininger B, Ebner C, Petzelbauer P, Shi GP, et al. Fc epsilon receptor I on dendritic cells delivers IgE-bound multivalent antigens into a cathepsin S-dependent pathway of MHC class II presentation. *J Immunol* (1998) 161(6):2731–9.
183. Getahun A, Heyman B. IgG- and IgE-mediated antigen presentation on MHC class II. *Immunol Lett* (2004) 92(1–2):33–8. doi:10.1016/j.imlet.2003.09.015

184. Alvarez-Errico D, Lessmann E, Rivera J. Adapters in the organization of mast cell signaling. *Immunol Rev* (2009) 232(1):195–217. doi:10.1111/j.1600-065X.2009.00834.x
185. Campbell AM, Vachier I, Chanez P, Vignola AM, Lebel B, Kochan J, et al. Expression of the high-affinity receptor for IgE on bronchial epithelial cells of asthmatics. *Am J Respir Cell Mol Biol* (1998) 19(1):92–7. doi:10.1165/ajrcmb.19.1.2648
186. Redhu NS, Saleh A, Lee HC, Halayko AJ, Ziegler SF, Gounni AS. IgE induces transcriptional regulation of thymic stromal lymphopoietin in human airway smooth muscle cells. *J Allergy Clin Immunol* (2011) 128(4):892–6.e2. doi:10.1016/j.jaci.2011.06.045
187. Shibaki A. Fc epsilon RI on dendritic cells: a receptor, which links IgE mediated allergic reaction and T cell mediated cellular response. *J Dermatol Sci* (1998) 20(1):29–38. doi:10.1016/S0923-1811(99)00003-1
188. Karagiannis SN, Bracher MG, Beavil RL, Beavil AJ, Hunt J, McCloskey N, et al. Role of IgE receptors in IgE antibody-dependent cytotoxicity and phagocytosis of ovarian tumor cells by human monocytic cells. *Cancer Immunol Immunother* (2008) 57(2):247–63. doi:10.1007/s00262-007-0371-7
189. Shin JS, Greer AM. The role of FcepsilonRI expressed in dendritic cells and monocytes. *Cell Mol Life Sci* (2015) 72(12):2349–60. doi:10.1007/s00018-015-1870-x
190. Gounni AS, Lamkhioued B, Ochiai K, Tanaka Y, Delaporte E, Capron A, et al. High-affinity IgE receptor on eosinophils is involved in defence against parasites. *Nature* (1994) 367(6459):183–6. doi:10.1038/367183a0
191. Alphonse MP, Saffar AS, Shan L, HayGlass KT, Simons FE, Gounni AS. Regulation of the high affinity IgE receptor (Fc epsilonRI) in human neutrophils: role of seasonal allergen exposure and Th-2 cytokines. *PLoS One* (2008) 3(4):e1921. doi:10.1371/journal.pone.0001921
192. Joseph M, Gounni AS, Kusnierz JP, Vorng H, Sarfati M, Kinet JP, et al. Expression and functions of the high-affinity IgE receptor on human platelets and megakaryocyte precursors. *Eur J Immunol* (1997) 27(9):2212–8. doi:10.1002/eji.1830270914
193. Hasegawa S, Pawankar R, Suzuki K, Nakahata T, Furukawa S, Okumura K, et al. Functional expression of the high affinity receptor for IgE (FcepsilonRI) in human platelets and its' intracellular expression in human megakaryocytes. *Blood* (1999) 93(8):2543–51.
194. Charles N, Hardwick D, Daugas E, Illei GG, Rivera J. Basophils and the T helper 2 environment can promote the development of lupus nephritis. *Nat Med* (2010) 16(6):701–7. doi:10.1038/nm.2159
195. Reich K, Heine A, Hugo S, Blaschke V, Middel P, Kaser A, et al. Engagement of the Fc epsilon RI stimulates the production of IL-16 in langerhans cell-like dendritic cells. *J Immunol* (2001) 167(11):6321–9. doi:10.4049/jimmunol.167.11.6321
196. Galli SJ, Tsai M. IgE and mast cells in allergic disease. *Nat Med* (2012) 18(5):693–704. doi:10.1038/nm.2755
197. MacGlashan DW Jr, Bochner BS, Adelman DC, Jardieu PM, Togias A, McKenzie-White J, et al. Down-regulation of Fc(epsilon)RI expression on human basophils during in vivo treatment of atopic patients with anti-IgE antibody. *J Immunol* (1997) 158(3):1438–45.
198. Prussin C, Griffith DT, Boesel KM, Lin H, Foster B, Casale TB. Omalizumab treatment downregulates dendritic cell FcepsilonRI expression. *J Allergy Clin Immunol* (2003) 112(6):1147–54. doi:10.1016/j.jaci.2003.10.003
199. Metz M, Staubach P, Bauer A, Brehler R, Gericke J, Kangas M, et al. Clinical efficacy of omalizumab in chronic spontaneous urticaria is associated with a reduction of FcεRI-positive cells in the skin. *Theranostics* (2017) 7(5):1266–76. doi:10.7150/thno.18304
200. Kitaura J, Kinoshita T, Matsumoto M, Chung S, Kawakami Y, Leitges M, et al. IgE- and IgE+Ag-mediated mast cell migration in an autocrine/paracrine fashion. *Blood* (2005) 105(8):3222–9. doi:10.1182/blood-2004-11-4205
201. Kitaura J, Song J, Tsai M, Asai K, Maeda-Yamamoto M, Mocsai A, et al. Evidence that IgE molecules mediate a spectrum of effects on mast cell survival and activation via aggregation of the FcepsilonRI. *Proc Natl Acad Sci U S A* (2003) 100(22):12911–6. doi:10.1073/pnas.1735525100
202. Kashiwakura J, Okayama Y, Furue M, Kabashima K, Shimada S, Ra C, et al. Most highly cytokinergic IgEs have polyreactivity to autoantigens. *Allergy Asthma Immunol Res* (2012) 4(6):332–40. doi:10.4168/aair.2012.4.6.332
203. Bax HJ, Bowen H, Dodev TS, Sutton BJ, Gould HJ. Mechanism of the antigen-independent cytokinergic SPE-7 IgE activation of human mast cells in vitro. *Sci Rep* (2015) 5:9538. doi:10.1038/srep09538
204. Greer AM, Wu N, Putnam AL, Woodruff PG, Wolters P, Kinet JP, et al. Serum IgE clearance is facilitated by human FcepsilonRI internalization. *J Clin Invest* (2014) 124(3):1187–98. doi:10.1172/JCI68964
205. Perrigoue JG, Saenz SA, Siracusa MC, Allenspach EJ, Taylor BC, Giacomin PR, et al. MHC class II-dependent basophil-CD4+ T cell interactions promote T(H)2 cytokine-dependent immunity. *Nat Immunol* (2009) 10(7):697–705. doi:10.1038/ni.1740
206. Yoshimoto T, Yasuda K, Tanaka H, Nakahira M, Imai Y, Fujimori Y, et al. Basophils contribute to T(H)2-IgE responses in vivo via IL-4 production and presentation of peptide-MHC class II complexes to CD4+ T cells. *Nat Immunol* (2009) 10(7):706–12. doi:10.1038/ni.1737
207. Platzer B, Stout M, Fiebiger E. Functions of dendritic-cell-bound IgE in allergy. *Mol Immunol* (2015) 68(2 Pt A):116–9. doi:10.1016/j.molimm.2015.05.016
208. Bayry J. Lupus pathogenesis: role of IgE autoantibodies. *Cell Res* (2016) 26(3):271–2. doi:10.1038/cr.2016.12
209. Le T, Tversky J, Chichester KL, Bieneman AP, Huang SK, Wood RA, et al. Interferons modulate Fc epsilon RI-dependent production of autoregulatory IL-10 by circulating human monocytoid dendritic cells. *J Allergy Clin Immunol* (2009) 123(1):217–23. doi:10.1016/j.jaci.2008.09.013
210. Larson D, Hubner MP, Torrero MN, Morris CP, Brankin A, Swierczewski BE, et al. Chronic helminth infection reduces basophil responsiveness in an IL-10-dependent manner. *J Immunol* (2012) 188(9):4188–99. doi:10.4049/jimmunol.1101859
211. Pyle DM, Yang VS, Gruchalla RS, Farrar JD, Gill MA. IgE cross-linking critically impairs human monocyte function by blocking phagocytosis. *J Allergy Clin Immunol* (2013) 131(2):491–500.e1–5. doi:10.1016/j.jaci.2012.11.037
212. Mellor AL, Munn DH. IDO expression by dendritic cells: tolerance and tryptophan catabolism. *Nat Rev Immunol* (2004) 4(10):762–74. doi:10.1038/nri1457
213. Dehlink E, Platzer B, Baker AH, Larosa J, Pardo M, Dwyer P, et al. A soluble form of the high affinity IgE receptor, Fc-epsilon-RI, circulates in human serum. *PLoS One* (2011) 6(4):e19098. doi:10.1371/journal.pone.0019098
214. Platzer B, Ruiter F, van der Mee J, Fiebiger E. Soluble IgE receptors – elements of the IgE network. *Immunol Lett* (2011) 141(1):36–44. doi:10.1016/j.imlet.2011.08.004
215. Gould HJ, Sutton BJ. IgE in allergy and asthma today. *Nat Rev Immunol* (2008) 8(3):205–17. doi:10.1038/nri2273
216. Vercelli D, Helm B, Marsh P, Padlan E, Geha RS, Gould H. The B-cell binding site on human immunoglobulin E. *Nature* (1989) 338(6217):649–51. doi:10.1038/338649a0
217. Weskamp G, Ford JW, Sturgill J, Martin S, Docherty AJ, Swendeman S, et al. ADAM10 is a principal 'sheddase' of the low-affinity immunoglobulin E receptor CD23. *Nat Immunol* (2006) 7(12):1293–8. doi:10.1038/ni1399
218. Bansal A, Roberts T, Hay EM, Kay R, Pumphrey RS, Wilson PB. Soluble CD23 levels are elevated in the serum of patients with primary Sjogren's syndrome and systemic lupus erythematosus. *Clin Exp Immunol* (1992) 89(3):452–5. doi:10.1111/j.1365-2249.1992.tb06979.x
219. Acharya M, Borland G, Edkins AL, Maclellan LM, Matheson J, Ozanne BW, et al. CD23/FcepsilonRII: molecular multi-tasking. *Clin Exp Immunol* (2010) 162(1):12–23. doi:10.1111/j.1365-2249.2010.04210.x
220. Mudde GC, Bheekha R, Bruijnzeel-Koomen CA. Consequences of IgE/CD23-mediated antigen presentation in allergy. *Immunol Today* (1995) 16(8):380–3. doi:10.1016/0167-5699(95)80005-0
221. Cornaby C, Gibbons L, Mayhew V, Sloan CS, Welling A, Poole BD. B cell epitope spreading: mechanisms and contribution to autoimmune diseases. *Immunol Lett* (2015) 163(1):56–68. doi:10.1016/j.imlet.2014.11.001
222. Jensen-Jarolim E, Singer J. Why could passive Immunoglobulin E antibody therapy be safe in clinical oncology? *Clin Exp Allergy* (2011) 41(10):1337–40. doi:10.1111/j.1365-2222.2011.03764.x
223. Liu FT, Rabinovich GA. Galectins: regulators of acute and chronic inflammation. *Ann N Y Acad Sci* (2010) 1183:158–82. doi:10.1111/j.1749-6632.2009.05131.x
224. Robertson MW, Albrandt K, Keller D, Liu FT. Human IgE-binding protein: a soluble lectin exhibiting a highly conserved interspecies sequence and differential recognition of IgE glycoforms. *Biochemistry* (1990) 29(35):8093–100. doi:10.1021/bi00487a015
225. de Oliveira FL, Gatto M, Bassi N, Luisetto R, Ghirardello A, Punzi L, et al. Galectin-3 in autoimmunity and autoimmune diseases. *Exp Biol Med (Maywood)* (2015) 240(8):1019–28. doi:10.1177/1535370215593826

226. Sanz ML, Prieto I, Garcia BE, Oehling A. Diagnostic reliability considerations of specific IgE determination. *J Investig Allergol Clin Immunol* (1996) 6(3):152–61.
227. Drinkwater N, Cossins BP, Keeble AH, Wright M, Cain K, Hailu H, et al. Human immunoglobulin E flexes between acutely bent and extended conformations. *Nat Struct Mol Biol* (2014) 21(4):397–404. doi:10.1038/nsmb.2795
228. Maurer D, Fiebiger E, Reininger B, Wolff-Winiski B, Jouvin MH, Kilgus O, et al. Expression of functional high affinity immunoglobulin E receptors (Fc epsilon RI) on monocytes of atopic individuals. *J Exp Med* (1994) 179(2):745–50. doi:10.1084/jem.179.2.745
229. Yamaguchi M, Sayama K, Yano K, Lantz CS, Noben-Trauth N, Ra C, et al. IgE enhances Fc epsilon receptor I expression and IgE-dependent release of histamine and lipid mediators from human umbilical cord blood-derived mast cells: synergistic effect of IL-4 and IgE on human mast cell Fc epsilon receptor I expression and mediator release. *J Immunol* (1999) 162(9):5455–65.
230. Oda M, Kozono H, Morii H, Azuma T. Evidence of allosteric conformational changes in the antibody constant region upon antigen binding. *Int Immunol* (2003) 15(3):417–26. doi:10.1093/intimm/dxg036
231. Kochuyt AM. Sensitivity and specificity of food specific IgE and IgG determinations for the diagnosis of food allergy. *Acta Gastroenterol Belg* (2006) 69(1):43–8.
232. Zimina EP, Fritsch A, Schermer B, Bakulina AY, Bashkurov M, Benzing T, et al. Extracellular phosphorylation of collagen XVII by ecto-casein kinase 2 inhibits ectodomain shedding. *J Biol Chem* (2007) 282(31):22737–46. doi:10.1074/jbc.M701937200
233. Panneerselvam J, Shanker M, Jin J, Branch CD, Muralidharan R, Zhao YD, et al. Phosphorylation of interleukin (IL)-24 is required for mediating its anti-cancer activity. *Oncotarget* (2015) 6(18):16271–86. doi:10.18632/oncotarget.3977
234. Zimina EP, Hofmann SC, Fritsch A, Kern JS, Sitaru C, Bruckner-Tuderman L. Bullous pemphigoid autoantibodies preferentially recognize phosphoepitopes in collagen XVII. *J Invest Dermatol* (2008) 128(11):2736–9. doi:10.1038/jid.2008.132
235. Schreiber A, Rolle S, Peripelittchenko L, Rademann J, Schneider W, Luft FC, et al. Phosphoinositol 3-kinase-gamma mediates antineutrophil cytoplasmic autoantibody-induced glomerulonephritis. *Kidney Int* (2010) 77(2):118–28. doi:10.1038/ki.2009.420
236. Sircar G, Jana K, Dasgupta A, Saha S, Gupta Bhattacharya S. Epitope mapping of Rhi o 1 and generation of a hypoallergenic variant: a candidate molecule for fungal allergy vaccines. *J Biol Chem* (2016) 291(34):18016–29. doi:10.1074/jbc.M116.732032
237. Yeh CC, Tai HY, Chou H, Wu KG, Shen HD. Vacuolar serine protease is a major allergen of *Fusarium proliferatum* and an IgE-cross reactive pan-fungal allergen. *Allergy Asthma Immunol Res* (2016) 8(5):438–44. doi:10.4168/aair.2016.8.5.438
238. Donovan GR, Baldo BA. Crossreactivity of IgE antibodies from sera of subjects allergic to both ryegrass pollen and wheat endosperm proteins: evidence for common allergenic determinants. *Clin Exp Allergy* (1990) 20(5):501–9. doi:10.1111/j.1365-2222.1990.tb03142.x
239. Jappe U, Raulf-Heimsoth M, Hoffmann M, Burow G, Hubsch-Muller C, Enk A. In vitro hymenoptera venom allergy diagnosis: improved by screening for cross-reactive carbohydrate determinants and reciprocal inhibition. *Allergy* (2006) 61(10):1220–9. doi:10.1111/j.1398-9995.2006.01232.x
240. Mahler V, Gutgesell C, Valenta R, Fuchs T. Natural rubber latex and hymenoptera venoms share ImmunoglobinE-epitopes accounting for cross-reactive carbohydrate determinants. *Clin Exp Allergy* (2006) 36(11):1446–56. doi:10.1111/j.1365-2222.2006.02587.x
241. Carballada FJ, Gonzalez-Quintela A, Nunez-Orjales R, Vizcaino L, Boquete M. Double (honeybee and wasp) immunoglobulin E reactivity in patients allergic to hymenoptera venom: the role of cross-reactive carbohydrates and alcohol consumption. *J Investig Allergol Clin Immunol* (2010) 20(6):484–9.
242. Pham NH, Baldo BA. Allergenic relationship between taxonomically diverse pollens. *Clin Exp Allergy* (1995) 25(7):599–606. doi:10.1111/j.1365-2222.1995.tb01107.x
243. Twardosz A, Hayek B, Seiberler S, Vangelista L, Elfman L, Gronlund H, et al. Molecular characterization, expression in *Escherichia coli*, and epitope analysis of a two EF-hand calcium-binding birch pollen allergen, Bet v 4. *Biochem Biophys Res Commun* (1997) 239(1):197–204. doi:10.1006/bbrc.1997.6860
244. Oberhuber C, Ma Y, Wopfner N, Gadermaier G, Dedic A, Niggemann B, et al. Prevalence of IgE-binding to Art v 1, Art v 4 and Amb a 1 in mugwort-allergic patients. *Int Arch Allergy Immunol* (2008) 145(2):94–101. doi:10.1159/000108134
245. Tinghino R, Twardosz A, Barletta B, Puggioni EM, Iacovacci P, Butteroni C, et al. Molecular, structural, and immunologic relationships between different families of recombinant calcium-binding pollen allergens. *J Allergy Clin Immunol* (2002) 109(2):314–20. doi:10.1067/mai.2002.121528
246. Mares-Mejia I, Martinez-Caballero S, Garay-Canales C, Cano-Sanchez P, Torres-Larios A, Lara-Gonzalez S, et al. Structural insights into the IgE mediated responses induced by the allergens Hev b 8 and Zea m 12 in their dimeric forms. *Sci Rep* (2016) 6:32552. doi:10.1038/srep32552
247. Chelminska M, Specjalski K, Rozylo A, Kolakowska A, Jassem E. Differentiating of cross-reactions in patients with latex allergy with the use of ISAC test. *Postepy Dermatol Alergol* (2016) 33(2):120–7. doi:10.5114/ada.2016.59154
248. Aalberse RC, Crameri R. IgE-binding epitopes: a reappraisal. *Allergy* (2011) 66(10):1261–74. doi:10.1111/j.1398-9995.2011.02656.x
249. Fahlbusch B, Rudeschko O, Schumann C, Steurich F, Henzgen M, Schlenvoigt G, et al. Further characterization of IgE-binding antigens in kiwi, with particular emphasis on glycoprotein allergens. *J Investig Allergol Clin Immunol* (1998) 8(6):325–32.
250. Son DY, Scheurer S, Hoffmann A, Haustein D, Vieths S. Pollen-related food allergy: cloning and immunological analysis of isoforms and mutants of Mal d 1, the major apple allergen, and Bet v 1, the major birch pollen allergen. *Eur J Nutr* (1999) 38(4):201–15. doi:10.1007/s003940050063
251. Gavrovic-Jankulovic M, Cirkovic T, Burazer L, Vuckovic O, Jankov RM. IgE cross-reactivity between meadow fescue pollen and kiwi fruit in patients' sera with sensitivity to both extracts. *J Investig Allergol Clin Immunol* (2002) 12(4):279–86.
252. Cudowska B, Kaczmarski M, Restani P. Immunoblotting in the diagnosis of cross-reactivity in children allergic to birch. *Rocz Akad Med Bialymst* (2005) 50:268–73.
253. Iraneta SG, Seoane MA, Laucella SA, Apicella C, Alonso A, Duschak VG. Antigenicity and immunocrossreactivity of orange tree pollen and orange fruit allergenic extracts. *Int Arch Allergy Immunol* (2005) 137(4):265–72. doi:10.1159/000086419
254. Madhurantakam C, Nilsson OB, Uchtenhagen H, Konradsen J, Saarne T, Hogbom E, et al. Crystal structure of the dog lipocalin allergen Can f 2: implications for cross-reactivity to the cat allergen Fel d 4. *J Mol Biol* (2010) 401(1):68–83. doi:10.1016/j.jmb.2010.05.043
255. Apostolovic D, Sanchez-Vidaurre S, Waden K, Curin M, Grundstrom J, Gafvelin G, et al. The cat lipocalin Fel d 7 and its cross-reactivity with the dog lipocalin Can f 1. *Allergy* (2016) 71(10):1490–5. doi:10.1111/all.12955
256. Hemmer W, Klug C, Swoboda I. Update on the bird-egg syndrome and genuine poultry meat allergy. *Allergo J Int* (2016) 25:68–75. doi:10.1007/s40629-016-0108-2
257. Kuehn A, Codreanu-Morel F, Lehners-Weber C, Doyen V, Gomez-Andre SA, Bienvenu F, et al. Cross-reactivity to fish and chicken meat – a new clinical syndrome. *Allergy* (2016) 71(12):1772–81. doi:10.1111/all.12968
258. Jeong KY, Son M, Park JH, Park KH, Park HJ, Lee JH, et al. Cross-reactivity between oak and birch pollens in Korean tree pollinosis. *J Korean Med Sci* (2016) 31(8):1202–7. doi:10.3346/jkms.2016.31.8.1202
259. Doenhoff MJ, El-Faham M, Liddell S, Fuller HR, Stanley RG, Schramm G, et al. Cross-reactivity between *Schistosoma mansoni* antigens and the latex allergen Hev b 7: putative implication of cross-reactive carbohydrate determinants (CCDs). *PLoS One* (2016) 11(7):e0159542. doi:10.1371/journal.pone.0159542
260. Santiago Hda C, Nutman TB. Role in allergic diseases of immunological cross-reactivity between allergens and homologues of parasite proteins. *Crit Rev Immunol* (2016) 36(1):1–11. doi:10.1615/CritRevImmunol.2016016545

261. Utsch L, Logiantara A, Wallner M, Hofer H, van Ree R, van Rijt LS. Birch pollen immunotherapy inhibits anaphylaxis to the cross-reactive apple allergen Mal d 1 in mice. *Clin Exp Allergy* (2016) 46(11):1474–83. doi:10.1111/cea.12775
262. Geroldinger-Simic M, Kinaciyan T, Nagl B, Baumgartner-Durchschlag U, Huber H, Ebner C, et al. Oral exposure to Mal d 1 affects the immune response in patients with birch pollen allergy. *J Allergy Clin Immunol* (2013) 131(1):94–102. doi:10.1016/j.jaci.2012.06.039
263. Matricardi PM, Kleine-Tebbe J, Hoffmann HJ, Valenta R, Hilger C, Hofmaier S, et al. EAACI molecular allergology user's guide. *Pediatr Allergy Immunol* (2016) 27(Suppl 23):1–250. doi:10.1111/pai.12563

Conflict of Interest Statement: The authors declare that the research was conducted in the absence of any commercial or financial relationships that could be construed as a potential conflict of interest.

frontiers in Medicine

ORIGINAL RESEARCH
published: 09 April 2018
doi: 10.3389/fmed.2018.00088

Recognition and Relevance of Anti-DFS70 Autoantibodies in Routine Antinuclear Autoantibodies Testing at a Community Hospital

John B. Carter[1], Sara Carter[1], Sandra Saschenbrecker[2] and Bruce E. Goeckeritz[1]*

[1] Lexington Medical Center, West Columbia, SC, United States, [2] Institute for Experimental Immunology, Euroimmun AG, Luebeck, Germany

Antinuclear autoantibodies (ANA) displaying a dense fine speckled pattern (DFS, ICAP AC-2) on HEp-2 cells are frequently observed in clinical laboratory referrals, often associated with anti-DFS70 specificity. Anti-DFS70 positive patients rarely develop systemic autoimmune rheumatic disease (SARD), especially in the absence of clinical evidence or additional anti-extractable nuclear antigen (ENA) antibodies, prompting suggestions that an isolated DFS70-specific ENA may be an exclusionary finding for SARD. In this study, the frequency and diagnostic significance of anti-DFS70 autoantibodies was investigated in a community hospital cohort of patients undergoing routine ANA testing. ANA screening was performed by HEp-20-10-based indirect immunofluorescence, followed by ENA profiling using a multiparametric line immunoassay (LIA). Of 6,511 patient samples tested for ANA in 2016, the DFS pattern was identified in 1,758 (27.0%), 720 (41.0%) of which were anti-DFS70 positive by LIA. Of these, 526 (73.1%) revealed isolated anti-DFS70 reactivity, while 194 (26.9%) showed additional ENA specificities. Among 1,038 anti-DFS70 negative or borderline samples, 778 (75.0%) were ENA profile negative, while the remaining 260 (25.0%) showed a varied presence of other ENA specificities. Chart reviews of patients with an isolated anti-DFS70 ANA affirmed that ANA-related SARD is rare in the absence of clinical evidence or other ENA specificities, there being no case thus far identified. Rheumatoid arthritis patients occasionally had an isolated anti-DFS70 ANA and were positive for rheumatoid factor and anti-cyclic citrullinated peptide antibodies. In conclusion, the recognition of a DFS ANA pattern using a mitotic-rich HEp-2 substrate, followed by confirmation of anti-DFS70 specificity should be a routine ANA testing service. Use of an expanded ENA profile and clinical correlation is necessary to affirm the "isolation" of anti-DFS70 as the cause of an ANA. Recognition of isolated anti-DFS70 ANA enables reassurance of patients that SARD is unlikely, thus avoiding referral for more extensive testing. The presence of significant elevations of other ENAs may reflect SARD and warrants close clinical correlation and follow-up.

Keywords: antinuclear antibodies, autoantibody, autoimmunity, DFS70, LEDGFp75, systemic autoimmune rheumatic diseases

OPEN ACCESS

Edited by:
Ralf J. Ludwig,
Universität zu Lübeck, Germany

Reviewed by:
Constantinos Petrovas,
National Institutes of Health (NIH), United States
Sinisa Savic,
University of Leeds, United Kingdom

****Correspondence:***
John B. Carter
jbcarter@lexhealth.org

Specialty section:
This article was submitted to Rheumatology, a section of the journal Frontiers in Medicine

Received: *23 November 2017*
Accepted: *21 March 2018*
Published: *09 April 2018*

Citation:
Carter JB, Carter S, Saschenbrecker S and Goeckeritz BE (2018) Recognition and Relevance of Anti-DFS70 Autoantibodies in Routine Antinuclear Autoantibodies Testing at a Community Hospital. Front. Med. 5:88. doi: 10.3389/fmed.2018.00088

INTRODUCTION

The presence of antinuclear autoantibodies (ANA) is one of the key diagnostic criteria of systemic autoimmune rheumatic diseases (SARD), such as systemic lupus erythematosus (SLE), Sjögren's syndrome, systemic sclerosis, dermatomyositis/polymyositis (DM/PM), mixed connective tissue diseases, etc. (1, 2). Indirect immunofluorescence (IIF) using human epithelial (HEp-2) cells is

the recommended "gold standard" for ANA screening as this substrate provides a variety of more than 100 native autoantigens including proteins, DNA, and ribonucleoproteins (2–4).

The dense fine speckled (DFS) nuclear pattern is one of the most common IIF patterns in the ANA screening routine of clinical diagnostic laboratories, often occurring in very high titers. The autoantibodies producing this pattern target the DFS protein of 70 kDa (DFS70), which is identical to the lens epithelium-derived growth factor or transcription co-activator p75 (LEDGFp75). DFS70/LEDGFp75 confers cell protection by regulating transcription of stress-related genes and is relevant to the pathophysiology of AIDS, cancer, autoimmunity, and inflammatory conditions. Anti-DFS70 autoantibodies might play protective, pathogenic, or sensor roles (5–13). The International Consensus on ANA Patterns (ICAP) committee has recently classified the DFS pattern as "AC-2" competency level recognition pattern, defined by a dense and heterogeneous speckled staining in the nucleoplasm of interphase cells (sparing the nucleoli) and the metaphase chromosomal plate (14, 15). Recognition of this pattern on HEp-2 substrates is challenging as it can be confused with other nuclear patterns or may occur in the context of another clinically relevant ANA, and because IIF interpretation is dependent on technician expertise (16–19). Thus, a positive DFS IIF result has to be followed by a monospecific immunoassay (e.g., ELISA, CLIA, immunoblot, immunoadsorption) (20) to accurately confirm the presence of anti-DFS70 autoantibodies, as recommended in diagnostic algorithms (19, 21–26).

The clinical significance of anti-DFS70 autoantibodies is not clear due to the absence of disease specificity (9, 19, 22, 26–29). Regardless of the detection method, DFS ANA and/or anti-DFS70 antibodies have been detected at elevated frequency in apparently healthy individuals (0–21.6%) (13, 16, 30–43), but also in routine ANA screening cohorts (0.3–16.6%) (21, 22, 34, 36, 40, 41, 43–49), and various non-SARD inflammatory and neoplastic conditions (3.3–71.4%; e.g., Vogt–Harada syndrome, atopic dermatitis, psioriasis, interstitial cystitis, Hashimoto's thyroiditis, ocular diseases, chronic fatigue syndrome asthma, or prostate cancer) (13, 30–32, 34, 37, 40, 50–55). In contrast, they are rare in patients with SARD (0–28.6%) (13, 16, 33–35, 43, 45, 51, 52, 55–57), showing an overall frequency of only 2.8–4.5%, which is remarkably lower than in healthy individuals and control cohorts (19, 28). Anti-DFS70 reactivity in SARD is usually accompanied by additional SARD-related antibodies, while isolated anti-DFS70 reactivity in SARD reportedly amounts to only 0.5–0.7% (19, 28). Thus, antibodies to DFS70 are increasingly regarded as a negative predictive biomarker for excluding the diagnosis of SARD, particularly in the absence of clinically relevant ANA (16, 19, 23, 28, 33, 34, 53, 58–61). This is supported by studies reporting on healthy individuals with isolated anti-DFS70 reactivity who did not develop SARD within a follow-up of 3–4 years ("benign autoimmunity"), and by a likelihood ratio (LR+) for the absence of SARD of 10.9 ascribed to isolated reactivity to DFS70 (16, 42, 59).

A few recent surveys have examined the prevalence of DFS ANA in sera submitted for routine ANA screening, but only some of these used anti-DFS70 assays to confirm the antibodies' specificity in all or in just a subset of tested samples. Considering also the diverse composition of the screened cohorts as well as the differences in assays and IIF interpretation, the currently available data have to be interpreted with caution (19, 28). Thus, the objective of this retrospective study was to investigate the frequency of anti-DFS70 autoantibodies among consecutive sera referred for ANA testing in a community hospital laboratory, using HEp-20-10 IIF for antibody screening followed by a multiparametric line immunoassay (LIA) to confirm or disprove the presence of anti-DFS70 and/or other autoantibodies in all samples displaying a DFS ANA pattern. Chart review of medical records and clinical follow-up allowed for evaluation of associated clinical associations and diagnostic relevance.

MATERIALS AND METHODS

Patients and Serum Samples

We studied 6,511 serum samples from patients presenting at the Lexington Medical Center, a 400 bed acute-care community hospital with a strong rheumatology service, in West Columbia, SC, USA. These samples were collected for routine ANA testing, within a 1-year period. Individual and ethical approval was not mandatory for this study as patient data and samples were used anonymously to maintain confidentiality. Serological analyses were performed blinded to clinical data.

IIF Assay

ANA screening was performed using the IFA40: HEp-20-10 kit assay (Euroimmun, Luebeck, Germany). Testing and evaluation were carried out according to the manufacturer's instructions. In brief, microscope slides containing millimeter-sized biochips coated with HEp-20-10 cells were incubated with serial serum dilutions (starting with 1:40 in PBS-Tween) for 30 min at room temperature, washed with a flush of PBS-Tween, and immersed in PBS-Tween for 5 min. For detection of bound antibodies, fluorescein isothiocyanate-conjugated goat anti-human IgG was applied for 30 min at room temperature, followed by washing as described before. After embedding in mounting medium, the slides were cover-slipped and evaluated by two independent observers using fluorescence microscopy. Sera displaying ANA fluorescence patterns at a titer $\geq$1:40 were considered positive. All DFS ANA pattern results were reported as possibly DFS70-related, with extractable nuclear antigen (ENA) follow-up analysis recommended.

Immunoblot Assay

Specific profiling for anti-ENA autoantibodies was performed using the EUROLINE ANA profile 3 plus DFS70 (IgG) kit according to the manufacturer's instructions (Euroimmun). The blot strips contain 16 separate antigens, 11 of which are native purified proteins (nRNP/Sm, Sm, SS-A, SS-B, Scl-70, Jo-1, dsDNA, nucleosomes, histones, ribosomal P-protein, and AMA M2) and 5 of which are recombinant antigens (Ro-52, PM-Scl, CENP B, PCNA, and DFS70). The DFS70 antigen is a full-length recombinant protein (amino acids 1–530) expressed in mammalian cells. The EUROBlotOne system (Euroimmun) was used for automated processing of all incubation and washing steps. Buffer-soaked

blot strips were incubated with 1:101 diluted serum for 30 min at room temperature. After three washing cycles of 5 min each, binding of specific antibodies was detected by incubation with alkaline phosphatase-conjugated goat anti-human IgG for 30 min at room temperature. Subsequently, the strips were washed and then incubated with nitrobluetetrazoliumchloride/5-bromo-4-chloro-3-indolylphosphate (NBT/BCIP) for 10 min, followed by the addition of distilled water to stop the reaction. The incubated strips were automatically dried and photographed. Band intensities were evaluated by using the EUROLineScan software (Euroimmun). Signal intensities ≥15 were considered positive, 8–14 borderline, and ≤7 negative.

RESULTS

IIF Screening and ANA Differentiation

Among 6,511 serum samples tested for ANA in 2016, 5,339 (82.0%) were ANA positive by IIF at a titer ≥1:40 and 1,172 (18.0%) were negative (<1:40). A DFS, AC-2 IIF pattern was identified in 1,758 sera, corresponding to 27.0% of all samples tested, and 32.9% of ANA positive samples. Analysis of the DFS positive samples by LIA revealed the presence of anti-DFS70 autoantibodies in 720 (41.0%) of all DFS, AC-2 pattern ANAs. Among these, 526 (73.1%) had isolated anti-DFS70 reactivity, whereas the remaining 194 (26.9%) showed additional ENA specificities. 1,038 (59.0%) of the samples with a DFS IIF pattern were found anti-DFS70 negative (or borderline) by LIA, including 260 (25.0%) samples with a varied presence of other ENA specificities and 778 (75.0%) ENA profile negative samples (**Figure 1**). Thus, isolated anti-DFS70 reactivity was detectable in 29.9% of all DFS IIF positive samples, suggesting a low probability for the presence or development of SARD (**Figure 2**).

Diagnostic Relevance of Anti-DFS70 Positivity

Rheumatologist chart reviews of anti-DFS70 positive patients were performed to examine if the finding of isolated anti-DFS70 reactivity is useful as a rule-out for SARD. Thus far, no case of ANA-related SARD has been identified at our hospital among patients positive for isolated DFS70-specific autoantibodies. In contrast, the additional presence of other ENAs at a significant level has clinical relevance specific to those autoantibodies, as reflected by representative cases given in **Table 1**. Occasionally, we found rheumatoid arthritis patients with isolated anti-DFS70 ANA to be positive for rheumatoid factor and antibodies against cyclic citrullinated peptide (anti-CCP).

DISCUSSION

For many years, we noted a high number of samples containing often high-titer finely speckled ANAs but with a negative ENA profile. When a mitotic-rich HEp-2 cell substrate (HEp-20-10) became available, we realized that the majority of these finely speckled ANAs also showed a positive mitotic fluorescence, i.e., a mixed speckled/homogeneous pattern, later termed as "dense fine speckled," which was often associated with anti-DFS70 specificity. Despite the fact that the DFS IIF pattern has recently been classified for competent-level reporting by ICAP (AC-2 pattern) due to its negative association with SARD (14), it is still not widely recognized among commercial laboratories, and often reported as "speckled," "homogeneous," or even "negative," with no follow-up testing available. However, confirmatory tests are necessary in light of sustained concern that the recognition of the DFS pattern is challenging and prone to mistakes (18, 21, 22, 24, 25, 62). In this study, we examined the prevalence of anti-DFS70 autoantibodies and their association with ANA-related SARDs in a community hospital routine ANA referral cohort by using an expanded ENA profile for follow-up testing of samples with a DFS IIF pattern.

We observed the DFS IIF pattern in 27.0% of all samples submitted for ANA screening. Other groups reported the presence of this pattern in 0.3–16.6% of non-selected routine ANA cohorts, resulting in an overall frequency of about 7.7%, as indicated in **Table 2** (19, 21, 34, 36, 40, 41, 43–47, 49). Reasons for the wide range of positivity rates are speculative but may include heterogeneity in the composition of the studied ANA screening cohorts (e.g., gender, age, ethnicity, reasons for requesting ANA tests) as well as differences in the screening method and in defining an appropriate cut-off value (26). Of note, the analytical performance of HEp-2 IIF crucially depends on the quality of the substrate and assay, particularly with regard to the ratio of mitotic versus interphase cells, cell morphology, reproducibility, and dilution linearity. The HEp-20-10 substrate (a variant of the standard HEp-2 cell line with a 10-fold higher number of mitotic cells), as used in the present study, has been reported to facilitate the recognition, discrimination and titer estimation of ANA patterns (63).

Apart from the difficulties in recognizing the DFS IIF pattern, the high prevalence of anti-DFS70 autoantibodies in healthy individuals, lack of association with a particular disease group, and negative association with SARD necessitate the confirmation of anti-DFS70 reactivity (26). In the present study, 41.0% of samples with a DFS IIF pattern were confirmed to contain anti-DFS70 autoantibodies using the EUROLINE ANA Profile 3 plus DFS70. Bizzaro et al. reported for this LIA a sensitivity of 51.6% (specificity 96.6%) with respect to a presumptive DFS IIF pattern on HEp-2 cells, which was similar to other assays based on DFS70 truncated to the C-terminal major epitope region (CLIA, 43.5%; dot blot, 51.6%) (24, 64). In other surveys, the concordance rates between DFS IIF and specific anti-DFS70 assays (e.g., CLIA, ELISA, Westernblot) were highly divergent, ranging between 14% (17) and >90% (34, 44, 48). Our data are consistent with previous findings in that a subset of sera with a typical DFS IIF pattern does not show anti-DFS70 reactivity using a more specific method. Vice versa, samples with anti-DFS70 positivity by a monospecific assay may not clearly show a DFS IIF pattern (17, 56). Factors potentially contributing to these inconsistencies include: (1) Heterogeneity among the anti-DFS70 autoantibodies that cause a typical DFS pattern on HEp-2 cells but not all of which react with the antigenic substrate applied in the confirmatory assays. (2) Reactivity of the recombinant antigen is slightly affected by the procedure of antigen preparation, coating (loss of conformational epitope), and choice of the cut-off value. (3) A DFS-like ANA IIF

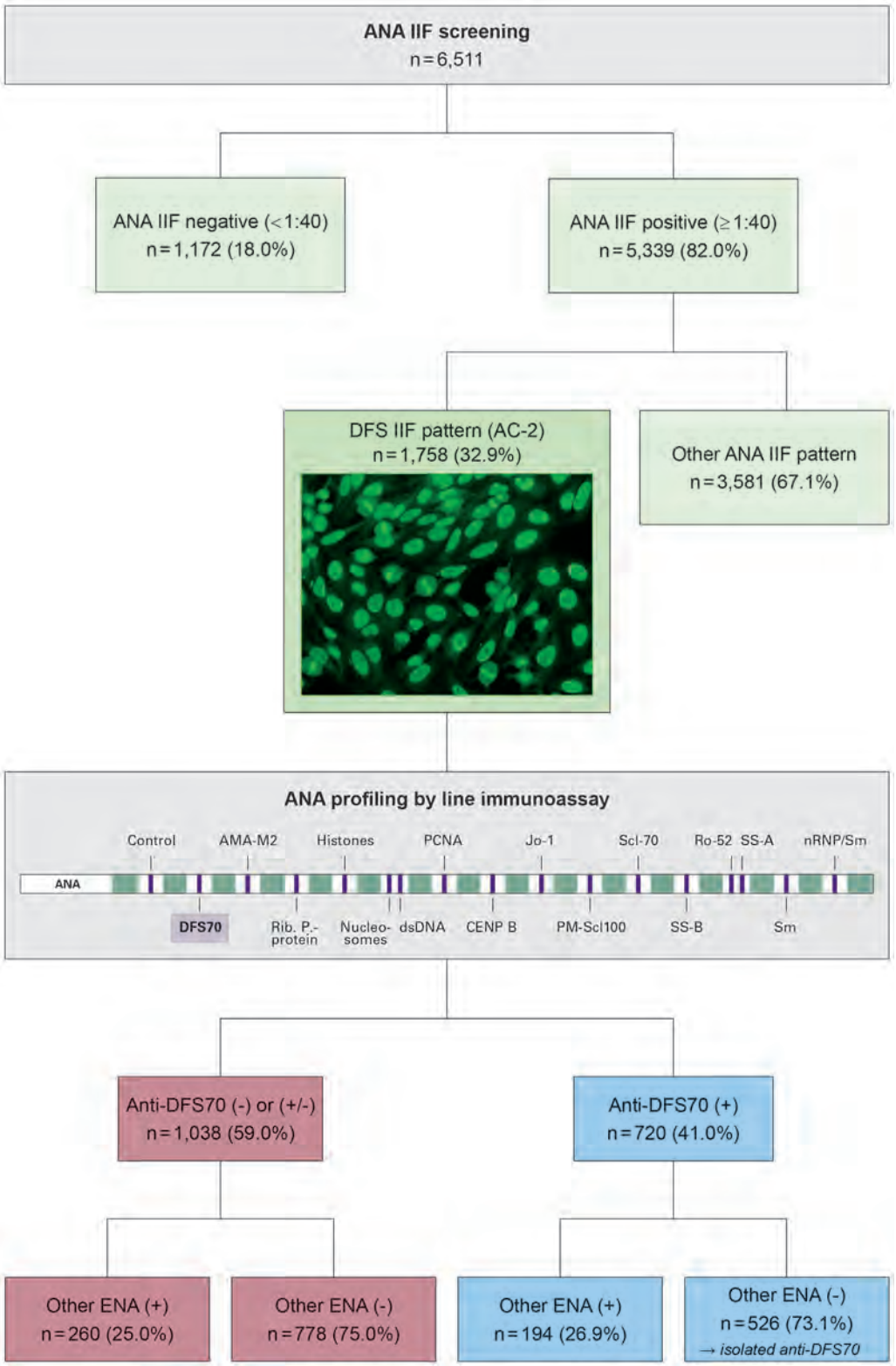

FIGURE 1 | Results of antinuclear autoantibody (ANA) testing in 6,511 patients samples, focusing on a subgroup of 1,758 samples with a dense fine speckled (DFS) pattern (AC-2) in indirect immunofluorescence (IIF). The DFS pattern is characterized by staining of dense fine speckles in interphase nuclei and strongly fluorescent mitotic chromosomes. Initial ANA screening was performed using IIF on HEp-20-10 cells. Samples showing a DFS IIF pattern were analyzed for specific autoantibody reactivity using a line immunoassay (LIA) containing 16 relevant antigens. Frequencies (percentage values in brackets) refer to the number of patients in the respective next higher subgroup. (+), positive; (±), borderline; (–), negative.

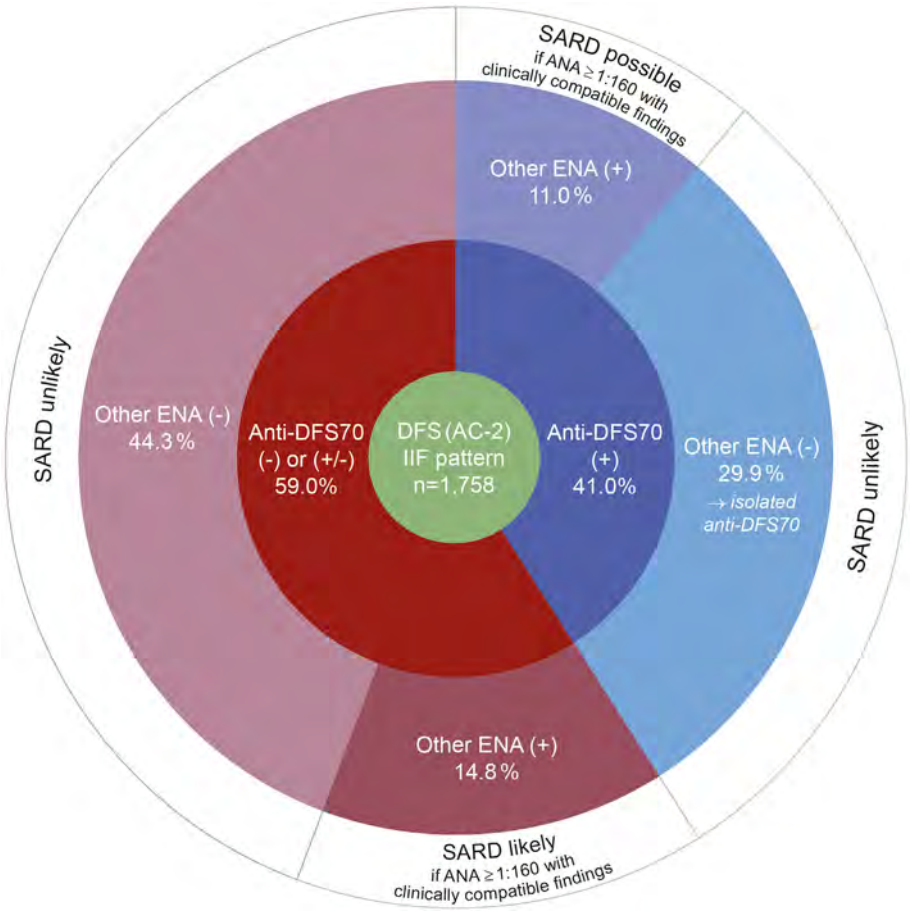

FIGURE 2 | Results of autoantibody profiling by line immunoassay in serum samples with a typical dense fine speckled (DFS) pattern (AC-2) in indirect immunofluorescence (IIF). Percentages for anti-DFS70 positive (blue) and negative (red) results by LIA refer to the total number DFS IIF positive cases (green). The likelihood for the presence or development of an associated systemic autoimmune rheumatic disease (SARD), in accordance with Conrad et al. (19), is indicated in the outermost circle (white). (+), positive; (±), borderline; (–), negative.

pattern may be produced by antibodies directed against nuclear antigen(s) other than DFS70, particularly interacting partners of this autoantigen or proteins sharing the same cellular localization, such as methyl CpG-binding protein 2 (MeCP2), pogo transposable element-derived protein with zinc finger (PogZ), c-Myc-interacting protein JPO2, or Cdc7-activator of S-phase kinase (Cdc7-ASK) (65–68). For example, MeCP2 was found to co-localize with DFS70 in the nucleus and to produce a DFS-like HEp-2 staining pattern, which is not affected by pre-adsorption of anti-DFS70 antibodies (24, 62).

According to a recent meta-analysis, the mean prevalence of isolated anti-DFS70 autoantibodies is only about 0.7% in SARD patients and that of anti-DFS70 accompanied by SARD-specific ENA is 3.8% (28). In contrast to this, isolated anti-DFS70 positivity is associated with a likelihood ratio (LR+) of 10.9 for the absence of SARD (59). Referring to the diagnostic algorithm recommended by Conrad et al. (19), 74.2% of our patients with a DFS IIF pattern can be classified as unlikely for the presence or development of SARD, either by the presence of isolated anti-DFS70 reactivity or by the absence of SARD-associated and DFS70-specific ENA (**Figure 2**). Gundin et al. reported that none of their patients with an isolated positive anti-DFS70 result developed SARD during a 10-year follow-up (60). Based on chart reviews, we also found no clinical evidence of active SARD in cases with isolated anti-DFS70 positivity. Rather, the additional presence of other ENA specificities at high levels has clinical relevance specific to those autoantibodies. While borderline elevations are not likely relevant for diagnostics, the presence of additional high-titer ENAs warrants close clinical correlation and follow-up. This observation conforms with the current classification of anti-DFS70 autoantibodies as a potential negative predictive biomarker of SARD in the absence of other clinically relevant ENA (16, 19, 23, 28, 33, 34, 53, 58–61). However, the presence of anti-DFS70 antibodies does not replace diligent ENA differentiation. If an ANA pattern is observed using IIF, elaborate monospecific ENA differentiation needs to be conducted in any case without exceptions, independently of whether antibodies against DFS70 are present or not. Only when no disease-relevant ENAs are detected after the specialized diagnostics, a positive DFS70 result can help

TABLE 1 | Characteristics of anti-DFS70 positive patients (aged between 26 and 69 years) with additional high-level autoantibodies (representative cases).

Patient ID	Clinical diagnosis	Autoantibodies against (specific results)
1	Uveitis	DFS70 (166), PM-Scl100 (86)
2	Systemic lupus erythematosus (SLE)	DFS70 (72), Histones (24), Chromatin (42), RNP (70), SS-A (74)
3	Raynaud's disease, polyarthralgias	DFS70 (118), Scl-70 (103)
4	SLE	DFS70 (170), DNA (45), CENP B (48)
5	Discoid lupus erythematosus, rheumatoid arthritis	DFS70 (202), CENP B (70)
6	Lupus, olfactory, visual and auditory hallucinations	DFS70 (170), Ro-52 (95), SS-A (84)
7	Sicca syndrome, Raynaud's disease, myalgia, and myositis	DFS70 (156), PM-Scl100 (27), RNP (18)
8	SLE with other organ involvement	DFS70 (110), Ro-52 (155), SS-A (110)
9	SLE	DFS70 (176), SS-B (22), Sm (23)
10	Sjögren's syndrome	DFS70 (169), SS-A (50)

Anti-DFS70, autoantibodies against the dense fine speckled protein of 70 kDa (identical to LEDGFp75, lens epithelium-derived growth factor or transcription co-activator p75).

to explain the observed IIF pattern. If confirmatory testing by means of a multiparametric assay ("multiplexing") (20) did not reveal a relevant antibody, the presence of other ENA cannot be ruled out and should be considered especially in patients with sustained suspicion of SARD. As discussed in a recent study (60), the number of follow-ups may be reduced to one or two per year in patients with a positive ANA IIF result but negative assays for both ENA and anti-DFS70. Through a reduction in the number of follow-up antibody testing and outpatient clinic visits, this contributes to substantially increased cost-efficiency (60), which conforms to our experience.

Due to increasing workload, some laboratories have switched their ANA screening to largely automated multiplex methods (69), with the option of using IIF as a second step. Because of the limited number of purified/recombinant antigens, multiplex assays focus on clinically significant ANAs, but also lack sensitivity compared to HEp-2 cells, leading to an estimated 35% of SARD patients with false negative screening results with respect to IIF (4). Accordingly, the American College of Rheumatology (ACR) and international committees recommend HEp-2 IIF as the standard screening method for ANA detection (2–4), reinforcing the outstanding potential of this technique. In cases of strong clinical suspicion and negative alternative methods, it is mandatory to perform IIF. This recommendation is followed in the present and earlier studies that include anti-DFS70 testing.

The diagnostic algorithm presented here conforms to several previously reported algorithms incorporating anti-DFS70 in that any sample revealing a (suspected) DFS ANA pattern in HEp-2 IIF screening should undergo confirmatory tests for anti-DFS70 and SARD-associated autoantibodies (**Figure 2**) (23, 26, 28, 60). Results are to be reported to the clinician with a comment on the diagnostic relevance of the serological result,

TABLE 2 | Frequency of DFS IIF (ICAP AC-2) and/or anti-DFS70 antibodies in unselected routine ANA screening cohorts, as determined in different studies.

Reference	ANA IIF	DFS IIF pattern		Anti-DFS70 reactivity			Detection method
	Positive/total	Positive/total	Positive/ANA positive	Positive/total	Positive/ANA positive	Positive/DFS IIF positive	
Dellavance (44)	13,641/30,728 (44.4%)	5,089/30,728 (16.6%)	5,089/13,641 (37.3%)	ND	ND	80/81 (98.8%)	WB
Bizzaro et al. (40)	ND	172/21,516 (0.8%)	ND	ND	ND	ND	–
Kang and Lee (45)	352/2,654 (13.3%)	101/2,654 (3.8%)	101/352 (28.7%)	ND	ND	ND	–
Pazini et al. (46)	790/2,788 (28.3%)	29/2,788 (1.0%)	29/790 (3.7%)	ND	ND	ND	–
Mahler et al. (34)	ND	53/3,263 (1.6%)	ND	53/3,263 (1.6%)	ND	53/53 (100%)	CLIA/ELISA
Bizzaro et al. (22)	ND	ND	ND	2/155 (1.3%)	ND	ND	CLIA
Marlet et al. (41)	ND	421/16,754 (2.5%)	ND	ND	ND	ND	–
Schmeling et al. (36)	55/200 (27.5%)[a]	ND	ND	9/200 (4.5%)[a]	9/55 (16.4%)[a]	ND	CLIA
Sener and Afsar (49)	1,302/5,800 (22.4%)	16/5,800 (0.3%)	16/1,302 (1.2%)	ND	ND	ND	–
Lee et al. (47)	ND	181/10,528 (1.7%)	ND	109/10,528 (1.0%)	ND	109/181 (60.2%)	ELISA
Mutlu et al. (21)	368/1,786 (20.6%)	90/1,786 (5.0%)	90/368 (24.5%)	ND	ND	62/74 (83.8%)	ELISA
Shovman et al. (43)	ND	ND	ND	13/85 (15.3%)	ND	ND	CLIA
Carter et al. (present study)	5,339/6,511 (82.0%)	1,758/6,511 (27.0%)	1,758/5,339 (32.9%)	720/6,511 (11.1%)	720/5,339 (13.5%)	720/1,758 (41.0%)	LIA
Total	21,847/50,467	7,910/102,328	7,083/21,792	906/20,742	729/5,394	1,024/2,147	
Overall frequency (95% CI)	43.3% (42.9–43.7%)	7.7% (7.6–7.9%)	32.5% (31.9–33.2%)	4.4% (4.1–4.7%)	13.5% (12.6–14.5%)	47.7% (45.6–49.8%)	
Range frequency (%)	13.3–82.0%	0.3–27.0%	1.2–37.3%	1.0–15.3%	13.5–16.4%	41.0–100%	

ANA, antinuclear autoantibodies; Anti-DFS70, autoantibodies against the dense fine speckled protein of 70 kDa (identical to LEDGFp75, lens epithelium-derived growth factor or transcription co-activator p75); CLIA, chemiluminescence immunoassay; DFS, dense fine speckled; ELISA, enzyme-linked immunosorbent assay; ICAP, International Consensus on ANA Patterns; IIF, indirect immunofluorescence; LIA, line immunoassay; ND, not determined; WB, Westernblot.

[a]*Pediatric cohort (≤18 years).*

pointing also on the significance of clinical findings and other laboratory tests.

In conclusion, DFS70 ANAs are common in a community hospital patient population. Recognition of the DFS IIF pattern using a mitotic-rich HEp-2 cell substrate, followed by confirmation of DFS70 specificity should be a routine ANA testing service. Use of an expanded ANA/ENA panel that includes a specific anti-DFS70 test, and close clinical correlation, is necessary to confirm the "isolation" of anti-DFS70 as the cause of an elevated ANA titer. Significant elevations of other ENAs in addition to anti-DFS70 may reflect SARD, and warrant close clinical correlation and follow-up testing. This testing enables reassurance of DFS70 ANA-positive patients who may otherwise be referred for extensive testing for autoimmune disease. An isolated DFS70 ANA does not "exclude" SARD, as that is largely a clinical diagnosis, supported by laboratory evidence. It is simply not a diagnostic point supportive of a SARD diagnosis. As many clinicians are not yet familiar with DFS70 ANAs, all related findings should be explained clearly in laboratory reports.

ETHICS STATEMENT

Individual and ethical approval was not mandatory for this study as patient data and samples were used anonymously to maintain confidentiality.

AUTHOR CONTRIBUTIONS

SC and JC designed and managed the study. BG was responsible for rheumatologic diagnostic assessment. SC and JC performed the laboratory analyses, with results interpretations and collated all data. JC provided medical staff consultation and advice regarding DFS70 ANA test results. JC, SC, SS and BG contributed to writing of the manuscript and approved the final version.

ACKNOWLEDGMENTS

The authors sincerely appreciate the technical expertise and experience of Donna Richardson, Anita Kelly, and Sara Blackmon in performance of this testing service.

REFERENCES

1. Solomon DH, Kavanaugh AJ, Schur PH. Evidence-based guidelines for the use of immunologic tests: antinuclear antibody testing. *Arthritis Rheum* (2002) 47:434–44. doi:10.1002/art.10561
2. Agmon-Levin N, Damoiseaux J, Kallenberg C, Sack U, Witte T, Herold M, et al. International recommendations for the assessment of autoantibodies to cellular antigens referred to as anti-nuclear antibodies. *Ann Rheum Dis* (2014) 73:17–23. doi:10.1136/annrheumdis-2013-203863
3. American College of Rheumatology. *Position Statement: Methodology of Testing for Antinuclear Antibodies*. Atlanta, GA: American College of Rheumatology (2015). Available from: https://www.rheumatology.org/Portals/0/Files/Methodology%20of%20Testing%20Antinuclear%20Antibodies%20Position%20Statement.pdf (Accessed: March 26, 2018).
4. Meroni PL, Schur PH. ANA screening: an old test with new recommendations. *Ann Rheum Dis* (2010) 69:1420–2. doi:10.1136/ard.2009.127100
5. Ge H, Si Y, Roeder RG. Isolation of cDNAs encoding novel transcription coactivators p52 and p75 reveals an alternate regulatory mechanism of transcriptional activation. *EMBO J* (1998) 17:6723–9. doi:10.1093/emboj/17.22.6723
6. Singh DP, Ohguro N, Chylack LT Jr, Shinohara T. Lens epithelium-derived growth factor: increased resistance to thermal and oxidative stresses. *Invest Ophthalmol Vis Sci* (1999) 40:1444–51.
7. Shinohara T, Singh DP, Fatma N. LEDGF, a survival factor, activates stress-related genes. *Prog Retin Eye Res* (2002) 21:341–58. doi:10.1016/S1350-9462(02)00007-1
8. Ganapathy V, Daniels T, Casiano CA. LEDGF/p75: a novel nuclear autoantigen at the crossroads of cell survival and apoptosis. *Autoimmun Rev* (2003) 2:290–7. doi:10.1016/S1568-9972(03)00063-6
9. Ochs RL, Mahler M, Basu A, Rios-Colon L, Sanchez TW, Andrade LE, et al. The significance of autoantibodies to DFS70/LEDGFp75 in health and disease: integrating basic science with clinical understanding. *Clin Exp Med* (2016) 16:273–93. doi:10.1007/s10238-015-0367-0
10. Basu A, Sanchez TW, Casiano CA. DFS70/LEDGFp75: an enigmatic autoantigen at the interface between autoimmunity, AIDS, and cancer. *Front Immunol* (2015) 6:116. doi:10.3389/fimmu.2015.00116
11. Debyser Z, Christ F, De Rijck J, Gijsbers R. Host factors for retroviral integration site selection. *Trends Biochem Sci* (2015) 40:108–16. doi:10.1016/j.tibs.2014.12.001
12. Basu A, Rojas H, Banerjee H, Cabrera IB, Perez KY, De Leon M, et al. Expression of the stress response oncoprotein LEDGF/p75 in human cancer: a study of 21 tumor types. *PLoS One* (2012) 7:e30132. doi:10.1371/journal.pone.0030132
13. Ochs RL, Muro Y, Si Y, Ge H, Chan EK, Tan EM. Autoantibodies to DFS 70 kd/transcription coactivator p75 in atopic dermatitis and other conditions. *J Allergy Clin Immunol* (2000) 105:1211–20. doi:10.1067/mai.2000.107039
14. Chan EK, Damoiseaux J, Carballo OG, Conrad K, de Melo CW, Francescantonio PL, et al. Report of the first international consensus on standardized nomenclature of antinuclear antibody HEp-2 cell patterns 2014-2015. *Front Immunol* (2015) 6:412. doi:10.3389/fimmu.2015.00412
15. Conrad K, Andrade LE, Chan EK, Mahler M, Meroni PL, Pruijn GJ, et al. From autoantibody research to standardized diagnostic assays in the management of human diseases – report of the 12th Dresden symposium on autoantibodies. *Lupus* (2016) 25:787–96. doi:10.1177/0961203316644337
16. Mariz HA, Sato EI, Barbosa SH, Rodrigues SH, Dellavance A, Andrade LE. Pattern on the antinuclear antibody-HEp-2 test is a critical parameter for discriminating antinuclear antibody-positive healthy individuals and patients with autoimmune rheumatic diseases. *Arthritis Rheum* (2011) 63:191–200. doi:10.1002/art.30084
17. Bizzaro N, Tonutti E, Villalta D. Recognizing the dense fine speckled/lens epithelium-derived growth factor/p75 pattern on HEP-2 cells: not an easy task! Comment on the article by Mariz et al. *Arthritis Rheum* (2011) 63:4036–7. doi:10.1002/art.30621
18. Bentow C, Fritzler MJ, Mummert E, Mahler M. Recognition of the dense fine speckled (DFS) pattern remains challenging: results from an international internet-based survey. *Auto Immun Highlights* (2016) 7:8. doi:10.1007/s13317-016-0081-2
19. Conrad K, Rober N, Andrade LE, Mahler M. The clinical relevance of anti-DFS70 autoantibodies. *Clin Rev Allergy Immunol* (2017) 52:202–16. doi:10.1007/s12016-016-8564-5
20. Ludwig RJ, Vanhoorelbeke K, Leypoldt F, Kaya Z, Bieber K, McLachlan SM, et al. Mechanisms of autoantibody-induced pathology. *Front Immunol* (2017) 8:603. doi:10.3389/fimmu.2017.00603
21. Mutlu E, Eyigor M, Mutlu D, Gultekin M. Confirmation of anti-DFS70 antibodies is needed in routine clinical samples with DFS staining pattern. *Cent Eur J Immunol* (2016) 41:6–11. doi:10.5114/ceji.2016.58812
22. Bizzaro N, Tonutti E, Tampoia M, Infantino M, Cucchiaro F, Pesente F, et al. Specific chemoluminescence and immunoasdorption tests for anti-DFS70 antibodies avoid false positive results by indirect immunofluorescence. *Clin Chim Acta* (2015) 451:271–7. doi:10.1016/j.cca.2015.10.008
23. Mahler M, Hanly JG, Fritzler MJ. Importance of the dense fine speckled pattern on HEp-2 cells and anti-DFS70 antibodies for the diagnosis of systemic autoimmune diseases. *Autoimmun Rev* (2012) 11:642–5. doi:10.1016/j.autrev.2011.11.005

24. Bizzaro N, Pesente F, Cucchiaro F, Infantino M, Tampoia M, Villalta D, et al. Anti-DFS70 antibodies detected by immunoblot methods: a reliable tool to confirm the dense fine speckles ANA pattern. *J Immunol Methods* (2016) 436:50–3. doi:10.1016/j.jim.2016.06.008
25. Bentow C, Rosenblum R, Correia P, Karayev E, Karayev D, Williams D, et al. Development and multi-center evaluation of a novel immunoadsorption method for anti-DFS70 antibodies. *Lupus* (2016) 25:897–904. doi:10.1177/0961203316641773
26. Malyavantham K, Suresh L. Analysis of DFS70 pattern and impact on ANA screening using a novel HEp-2 ELITE/DFS70 knockout substrate. *Auto Immun Highlights* (2017) 8:3. doi:10.1007/s13317-017-0091-8
27. Mierau R. Antinuclear antibodies without connective tissue disease: antibodies against LEDGF/DSF70. *Z Rheumatol* (2016) 75:372–80. doi:10.1007/s00393-016-0051-0
28. Seelig CA, Bauer O, Seelig HP. Autoantibodies against DFS70/LEDGF exclusion markers for systemic autoimmune rheumatic diseases (SARD). *Clin Lab* (2016) 62:499–517. doi:10.7754/Clin.Lab.2015.150905
29. Mahler M, Meroni PL, Andrade LE, Khamashta M, Bizzaro N, Casiano CA, et al. Towards a better understanding of the clinical association of anti-DFS70 autoantibodies. *Autoimmun Rev* (2016) 15:198–201. doi:10.1016/j.autrev.2015.11.006
30. Okamoto M, Ogawa Y, Watanabe A, Sugiura K, Shimomura Y, Aoki N, et al. Autoantibodies to DFS70/LEDGF are increased in alopecia areata patients. *J Autoimmun* (2004) 23:257–66. doi:10.1016/j.jaut.2004.07.004
31. Ayaki M, Ohoguro N, Azuma N, Majima Y, Yata K, Ibaraki N, et al. Detection of cytotoxic anti-LEDGF autoantibodies in atopic dermatitis. *Autoimmunity* (2002) 35:319–27. doi:10.1080/0891693021000003198
32. Yamada K, Senju S, Shinohara T, Nakatsura T, Murata Y, Ishihara M, et al. Humoral immune response directed against LEDGF in patients with VKH. *Immunol Lett* (2001) 78:161–8. doi:10.1016/S0165-2478(01)00243-7
33. Watanabe A, Kodera M, Sugiura K, Usuda T, Tan EM, Takasaki Y, et al. Anti-DFS70 antibodies in 597 healthy hospital workers. *Arthritis Rheum* (2004) 50:892–900. doi:10.1002/art.20096
34. Mahler M, Parker T, Peebles CL, Andrade LE, Swart A, Carbone Y, et al. Anti-DFS70/LEDGF antibodies are more prevalent in healthy individuals compared to patients with systemic autoimmune rheumatic diseases. *J Rheumatol* (2012) 39:2104–10. doi:10.3899/jrheum.120598
35. Vazquez-Del Mercado M, Gomez-Banuelos E, Navarro-Hernandez RE, Pizano-Martinez O, Saldana-Millan A, Chavarria-Avila E, et al. Detection of autoantibodies to DSF70/LEDGFp75 in Mexican Hispanics using multiple complementary assay platforms. *Auto Immun Highlights* (2017) 8:1. doi:10.1007/s13317-016-0089-7
36. Schmeling H, Mahler M, Levy DM, Moore K, Stevens AM, Wick J, et al. Autoantibodies to dense fine speckles in pediatric diseases and controls. *J Rheumatol* (2015) 42:2419–26. doi:10.3899/jrheum.150567
37. Chin MS, Caruso RC, Detrick B, Hooks JJ. Autoantibodies to p75/LEDGF, a cell survival factor, found in patients with atypical retinal degeneration. *J Autoimmun* (2006) 27:17–27. doi:10.1016/j.jaut.2006.04.002
38. Nilsson AC, Voss A, Lillevang ST. DFS70 autoantibodies are rare in healthy Danish individuals but may still serve as a diagnostic aid. *Scand J Immunol* (2015) 82:547–8. doi:10.1111/sji.12366
39. Goto N, Sugiura K, Ogawa Y, Watanabe A, Onouchi H, Tomita Y, et al. Anti-p80 coilin autoantibodies react with a conserved epitope and are associated with anti-DFS70/LEDGF autoantibodies. *J Autoimmun* (2006) 26:42–51. doi:10.1016/j.jaut.2005.09.001
40. Bizzaro N, Tonutti E, Visentini D, Alessio MG, Platzgummer S, Morozzi G, et al. Antibodies to the lens and cornea in anti-DFS70-positive subjects. *Ann N Y Acad Sci* (2007) 1107:174–83. doi:10.1196/annals.1381.019
41. Marlet J, Ankri A, Charuel JL, Ghillani-Dalbin P, Perret A, Martin-Toutain I, et al. Thrombophilia associated with anti-DFS70 autoantibodies. *PLoS One* (2015) 10:e0138671. doi:10.1371/journal.pone.0138671
42. Sperotto F, Seguso M, Gallo N, Plebani M, Zulian F. Anti-DFS70 antibodies in healthy schoolchildren: a follow-up analysis. *Autoimmun Rev* (2017) 16:210–1. doi:10.1016/j.autrev.2017.01.001
43. Shovman O, Gilburd B, Chayat C, Amital H, Langevitz P, Watad A, et al. Prevalence of anti-DFS70 antibodies in patients with and without systemic autoimmune rheumatic diseases. *Clin Exp Rheumatol* (2018) 36:121–6.
44. Dellavance A, Viana VS, Leon EP, Bonfa ES, Andrade LE, Leser PG. The clinical spectrum of antinuclear antibodies associated with the nuclear dense fine speckled immunofluorescence pattern. *J Rheumatol* (2005) 32:2144–9.
45. Kang SY, Lee WI. Clinical significance of dense fine speckled pattern in anti-nuclear antibody test using indirect immunofluorescence method. *Korean J Lab Med* (2009) 29:145–51. doi:10.3343/kjlm.2009.29.2.145
46. Pazini AM, Fleck J, dos Santos RS, Beck ST. Clinical relevance and frequency of cytoplasmic and nuclear dense fine speckled patterns observed in ANA-HEp-2. *Rev Bras Reumatol* (2010) 50:655–60. doi:10.1590/S0482-50042010000600006
47. Lee H, Kim Y, Han K, Oh EJ. Application of anti-DFS70 antibody and specific autoantibody test algorithms to patients with the dense fine speckled pattern on HEp-2 cells. *Scand J Rheumatol* (2016) 45:122–8. doi:10.3109/03009742.2015.1060260
48. Miyara M, Albesa R, Charuel JL, El AM, Fritzler MJ, Ghillani-Dalbin P, et al. Clinical phenotypes of patients with anti-DFS70/LEDGF antibodies in a routine ANA referral cohort. *Clin Dev Immunol* (2013) 2013:703759. doi:10.1155/2013/703759
49. Sener AG, Afsar I. Frequency of dense fine speckled pattern in immunofluorescence screening test. *Eur J Rheumatol* (2015) 2:103–5. doi:10.5152/eurjrheum.2015.0003
50. Daniels T, Zhang J, Gutierrez I, Elliot ML, Yamada B, Heeb MJ, et al. Antinuclear autoantibodies in prostate cancer: immunity to LEDGF/p75, a survival protein highly expressed in prostate tumors and cleaved during apoptosis. *Prostate* (2005) 62:14–26. doi:10.1002/pros.20112
51. Muro Y, Sugiura K, Morita Y, Tomita Y. High concomitance of disease marker autoantibodies in anti-DFS70/LEDGF autoantibody-positive patients with autoimmune rheumatic disease. *Lupus* (2008) 17:171–6. doi:10.1177/0961203307086311
52. Kuwabara N, Itoh Y, Igarshi T, Fukunaga Y. Autoantibodies to lens epithelium-derived growth factor/transcription co-activator P75 (LEDGF/P75) in children with chronic nonspecific complaints and with positive antinuclear antibodies. *Autoimmunity* (2009) 42:492–6. doi:10.1080/08916930902736663
53. Fabris M, Zago S, Tosolini R, Melli P, Bizzaro N, Tonutti E. Anti-DFS70 antibodies: a useful biomarker in a pediatric case with suspected autoimmune disease. *Pediatrics* (2014) 134:e1706–8. doi:10.1542/peds.2013-3914
54. Ochs RL, Stein TW Jr, Peebles CL, Gittes RF, Tan EM. Autoantibodies in interstitial cystitis. *J Urol* (1994) 151:587–92. doi:10.1016/S0022-5347(17)35023-1
55. Dai L, Li J, Ortega R, Qian W, Casiano CA, Zhang JY. Preferential autoimmune response in prostate cancer to cyclin B1 in a panel of tumor-associated antigens. *J Immunol Res* (2014) 2014:827827. doi:10.1155/2014/827827
56. Choi MY, Clarke AE, St PY, Hanly JG, Urowitz MB, Romero-Diaz J, et al. The prevalence and determinants of anti-DFS70 autoantibodies in an international inception cohort of systemic lupus erythematosus patients. *Lupus* (2017) 26(10):1051–9. doi:10.1177/0961203317692437
57. Muro Y, Sugiura K, Nakashima R, Mimori T, Akiyama M. Low prevalence of anti-DFS70/LEDGF antibodies in patients with dermatomyositis and other systemic autoimmune rheumatic diseases. *J Rheumatol* (2013) 40:92–3. doi:10.3899/jrheum.121168
58. Infantino M, Meacci F, Grossi V, Manfredi M, Li GF, Sarzi-Puttini P, et al. The clinical impact of anti-DFS70 antibodies in undifferentiated connective tissue disease: case reports and a review of the literature. *Immunol Res* (2017) 65:293–5. doi:10.1007/s12026-016-8836-4
59. Fitch-Rogalsky C, Steber W, Mahler M, Lupton T, Martin L, Barr SG, et al. Clinical and serological features of patients referred through a rheumatology triage system because of positive antinuclear antibodies. *PLoS One* (2014) 9:e93812. doi:10.1371/journal.pone.0093812
60. Gundin S, Irure-Ventura J, Asensio E, Ramos D, Mahler M, Martinez-Taboada V, et al. Measurement of anti-DFS70 antibodies in patients with ANA-associated autoimmune rheumatic diseases suspicion is cost-effective. *Auto Immun Highlights* (2016) 7:10. doi:10.1007/s13317-016-0082-1
61. Mahler M, Fritzler MJ. The clinical significance of the dense fine speckled immunofluorescence pattern on HEp-2 cells for the diagnosis of systemic autoimmune diseases. *Clin Dev Immunol* (2012) 2012:494356. doi:10.1155/2012/494356
62. Basu A, Woods-Burnham L, Ortiz G, Rios-Colon L, Figueroa J, Albesa R, et al. Specificity of antinuclear autoantibodies recognizing the dense fine speckled nuclear pattern: preferential targeting of DFS70/LEDGFp75 over its interacting partner MeCP2. *Clin Immunol* (2015) 161:241–50. doi:10.1016/j.clim.2015.07.014

63. Rohwäder E, Locke M, Fraune J, Fechner K. Diagnostic profile on the IFA 40: HEp-20-10 – an immunofluorescence test for reliable antinuclear antibody screening. *Expert Rev Mol Diagn* (2015) 15:451–62. doi:10.1586/14737159.2015.993612
64. Ogawa Y, Sugiura K, Watanabe A, Kunimatsu M, Mishima M, Tomita Y, et al. Autoantigenicity of DFS70 is restricted to the conformational epitope of C-terminal alpha-helical domain. *J Autoimmun* (2004) 23:221–31. doi:10.1016/j.jaut.2004.07.003
65. Leoh LS, van HB, De RJ, Filippova M, Rios-Colon L, Basu A, et al. The stress oncoprotein LEDGF/p75 interacts with the methyl CpG binding protein MeCP2 and influences its transcriptional activity. *Mol Cancer Res* (2012) 10:378–91. doi:10.1158/1541-7786.MCR-11-0314
66. Bartholomeeusen K, Christ F, Hendrix J, Rain JC, Emiliani S, Benarous R, et al. Lens epithelium-derived growth factor/p75 interacts with the transposase-derived DDE domain of PogZ. *J Biol Chem* (2009) 284:11467–77. doi:10.1074/jbc.M807781200
67. Maertens GN, Cherepanov P, Engelman A. Transcriptional co-activator p75 binds and tethers the Myc-interacting protein JPO2 to chromatin. *J Cell Sci* (2006) 119:2563–71. doi:10.1242/jcs.02995
68. Hughes S, Jenkins V, Dar MJ, Engelman A, Cherepanov P. Transcriptional co-activator LEDGF interacts with Cdc7-activator of S-phase kinase (ASK) and stimulates its enzymatic activity. *J Biol Chem* (2010) 285:541–54. doi:10.1074/jbc.M109.036491
69. Tozzoli R, Bonaguri C, Melegari A, Antico A, Bassetti D, Bizzaro N. Current state of diagnostic technologies in the autoimmunology laboratory. *Clin Chem Lab Med* (2013) 51:129–38. doi:10.1515/cclm-2012-0191

Conflict of Interest Statement: SS is an employee of Euroimmun AG, a company that develops and produces immunoassays for the detection of disease-associated antibodies. The other authors have nothing to disclose.

frontiers in Immunology

ORIGINAL RESEARCH
published: 05 April 2018
doi: 10.3389/fimmu.2018.00625

Anti-Thyroid Peroxidase Reactivity Is Heightened in Pemphigus Vulgaris and Is Driven by Human Leukocyte Antigen Status and the Absence of Desmoglein Reactivity

Kristina Seiffert-Sinha[1], Shahzaib Khan[1], Kristopher Attwood[2], John A. Gerlach[3] and Animesh A. Sinha[1]**

[1] Department of Dermatology, Jacobs School of Medicine and Biomedical Sciences, Buffalo, NY, United States, [2] Department of Biostatistics and Bioinformatics, Roswell Park Cancer Institute, Buffalo, NY, United States, [3] Biomedical Laboratory Diagnostics Program, Tissue Typing Laboratory, Michigan State University, East Lansing, MI, United States

Pemphigus vulgaris (PV) belongs to an autoimmune disease cluster that includes autoimmune thyroid disease (AITD), suggesting common mechanisms driving autoimmune susceptibility. Our group has shown that PV patients exhibit significant reactivity to AITD-related anti-thyroid peroxidase (anti-TPO), and anti-TPO antibodies affect signaling pathways in keratinocytes similar to anti-desmoglein (Dsg) 3 antibodies. To further assess the relevance of anti-TPO reactivity in PV, we analyzed anti-TPO levels in 280 PV and 167 healthy control serum samples across a comprehensive set of variable and static parameters of disease activity and etiopathogenesis. PV patients have significantly higher activity rates (A.R.s) for anti-TPO than healthy controls, but levels do not differ between phases of clinical activity and remission. Patients that carry both the PV-associated human leukocyte antigen (HLA) alleles DRB1*0402 and DQB1*0503, or DQB1*0503 alone show a low prevalence of anti-TPO (A.R. 9.5 and 4.8%, respectively), while patients that lack expression of these alleles or carry DRB1*0402 alone have a much higher prevalence of anti-TPO (A.R. 23.1 and 15.8%, respectively), suggesting that the absence of DQB1*0503 may predispose patients to the development of anti-TPO antibodies. Similarly, anti-Dsg1^{-}/3^{-} patients have a higher anti-TPO A.R. (26.9%) than anti-Dsg1^{-}/3^{+} (18.8%), anti-Dsg1^{+}/3^{-} (14.3%), and anti-Dsg1^{+}/3^{+} (3.9%) patients. Our data suggest that anti-TPO reactivity in PV is driven by genetic markers that may be in linkage disequilibrium with the established PV-susceptibility alleles and that this association drives the selection of a combination of anti-Dsg and anti-TPO antibodies, with anti-TPO filling the gap in active patients that do not carry the established PV-associated autoantibodies and/or are lacking the established PV-HLA-susceptibility alleles.

Keywords: pemphigus vulgaris, anti-thyroid peroxidase antibody, anti-thyroglobulin antibody, anti-desmoglein antibody, human leukocyte antigen

OPEN ACCESS

Edited by:
Ralf J. Ludwig,
University of Lübeck, Germany

Reviewed by:
Michael Kasperkiewicz,
University of Lübeck, Germany
Unni Samavedam,
University of Cincinnati, United States

****Correspondence:***
Kristina Seiffert-Sinha
krs2002@buffalo.edu;
Animesh A. Sinha
aasinha@buffalo.edu

Specialty section:
This article was submitted to Immunological Tolerance and Regulation, a section of the journal Frontiers in Immunology

Received: *12 January 2018*
Accepted: *13 March 2018*
Published: *05 April 2018*

Citation:
Seiffert-Sinha K, Khan S, Attwood K, Gerlach JA and Sinha AA (2018) Anti-Thyroid Peroxidase Reactivity Is Heightened in Pemphigus Vulgaris and Is Driven by Human Leukocyte Antigen Status and the Absence of Desmoglein Reactivity. Front. Immunol. 9:625. doi: 10.3389/fimmu.2018.00625

INTRODUCTION

It is well accepted that numerous autoimmune diseases can co-exist within individuals or certain families, a concept known as *autoimmune diathesis* (a broad genetic predisposition to develop autoimmune disease) (1, 2). Previous work from our lab and others has suggested that this is also

the case for pemphigus vulgaris (PV), a devastating autoimmune bullous skin disorder characterized by intraepidermal acantholysis and blister formation in skin and mucous membranes (3–10). Among the autoimmune diseases found in PV patients and/or their family members, autoimmune thyroid disease (AITD) is the most common, followed by rheumatoid arthritis (RA) and diabetes mellitus type I (4, 10, 11). These data indicate that PV belongs to an established autoimmune disease cluster comprised of AITD, RA and type I diabetes, suggesting the possibility of common genetic elements across clinically distinct diseases that might underlie autoimmune susceptibility (4, 8). Interestingly, a co-occurrence of autoantibodies associated with PV, AITD and RA has also been described in a large sampling of healthy control blood exhibiting ANA positivity with lupus erythematosus-associated staining patterns, further indicating a shared control of production of these autoantibodies (12).

Susceptibility to disease is complex, including (mostly unknown) genetic and environmental factors. Numerous studies have established a strong association between specific human leukocyte antigen (HLA) class II alleles, namely, DRB1*0402 and DQB1*0503, and increased risk for PV (13–15). It has been postulated that the specific binding pockets formed by these HLA molecules direct the preferential presentation of certain self-peptides and in turn inform production of specific autoantibodies (16). However, the broader impact of PV-associated HLA alleles in the development of the spectrum of PV-associated autoantibodies is not known.

Historically, PV has been linked to autoantibodies primarily targeting the desmosomal adhesion molecules desmoglein (Dsg) 3 and, in some cases, Dsg1, two members of the superfamily of cadherin molecules integral to intracellular adhesive junctions (17–19), where they act by steric hindrance and/or induction of intracellular signaling mechanisms (20). However, a growing body of literature suggests reactivities in PV against additional, non-desmoglein autoantigens, among them thyroid peroxidase (TPO) and muscarinic acetylcholine receptors (21, 22). Ongoing research in our lab revealed that PV patients exhibit significant reactivity to TPO (22), and that anti-thyroid peroxidase (anti-TPO) antibodies can induce keratinocyte dissociation *in vitro* and affect signaling pathways in keratinocytes similar to those seen after binding of anti-Dsg3 antibodies (Sajda et al., manuscript in preparation). This body of work clearly warrants further investigation into the role of thyroid-related autoantibodies in the PV patient population.

Although it has been reported that the AITD-related autoantibodies anti-TPO and anti-thyroglobulin (anti-Tg) are more prevalent in PV patients than the general population (3, 5, 6, 9, 23), thus far, levels of anti-thyroid antibodies have not been associated with static variables such as HLA status and sex or with dynamic clinical parameters including disease activity, morphology, and anti-desmoglein reactivity. Moreover, the link between specific HLA alleles and anti-thyroid autoantibody profiles in PV patients has not been investigated.

In this study, we aimed to address these gaps in knowledge as well as validate the findings in previous studies in a larger and ethnically different patient population. For this purpose, we measured anti-TPO and anti-Tg antibody levels in 280 serum samples from 225 North American PV patients and 167 serum samples from 148 healthy controls, and analyzed them across a comprehensive set of variable and static parameters of PV disease activity and etiopathogenesis.

We confirm in our North American study population that anti-thyroid antibodies are more prevalent in PV patients as compared with healthy controls. Furthermore, we find significant associations between anti-thyroid autoantibody reactivity, HLA status and anti-Dsg antibody profiles, thus providing insight into the complex interplay between HLA, autoantibody selection, and clinical outcomes.

MATERIALS AND METHODS

Patient Population

Two hundred twenty-five patients with a diagnosis of PV were enrolled in our database over a time span of more than 10 years from the dermatology outpatient clinics of Weill Medical College of Cornell University, Michigan State University and the University at Buffalo as well as annual meetings of International Pemphigus and Pemphigoid Foundation. The study was approved by the institutional review boards at Weill Cornell Medical College (IRB 0998-398), Michigan State University (IRB 05-1034), and the University at Buffalo (IRB 456887). The diagnosis of Pemphigus was based on clinical, histological, and/or serological criteria. All patients had a biopsy confirmed diagnosis of PV before enrollment in the study. Venous blood was drawn after obtaining written informed consent, and serum was separated and immediately stored at −80°C in our biorepository. Demographic information as well as information regarding disease activity, morphology, any reported comorbidities and family history was collected by a trained medical professional at the time of blood draw. Blood samples from 148 controls (both related and unrelated to pemphigus patients) were obtained as described earlier. Some of the patients and controls donated blood repeatedly. The maximum number of blood samples used in this study by any patient or control is 2, and the average number of samples per patients or controls is 1.14 and 1.13, respectively. The demographic information is summarized in **Table 1**.

Disease Activity

Phases of disease activity were defined by consensus guidelines (24). Briefly, patients were considered to be in the *active* phase of disease if three or more non-transient lesions were present for more than a week. Patients with absence of new or established lesions for more than 4 weeks were considered *remittent* while patients with transient lesions (lasting less than a week) were deemed *partially remittent* (25). For the analyses involving disease activity, *partially remittent* patients were excluded from the analysis, as they did not fit either of the two main activity categories.

Anti-TPO and Anti-Tg Enzyme-Linked Immunosorbent Assay (ELISA)

An ELISA for anti-TPO and anti-Tg antibodies was performed employing ELISA kits by GenWay Biotech (GWB-521202 and

TABLE 1 | Study population demographic data and human leukocyte antigen (HLA) association.

	PV	CR
# of Patients	225	148
# of Samples	280	167
Ethnicity		
% African American	3.6	9.5
% Hispanic	9.7	3.4
% Asian	9.7	18.4
% Caucasian (non-Jewish)	42.5	43.5
% Ashkenazi (Jewish)	30.1	20.4
% Other	4.4	4.8
Age at blood draw (years ± SD)	52.9 ± 14.4	46.0 ± 18.7
Age at onset (years ± SD)	45.1 ± 13.9	n/a
Male:female ratio (*n*)	1:1.92 (M = 77; F = 148)	1:1.55 (M = 90; F = 58)
% Active (*n*)	47.5 (133)	n/a
% Remittent (*n*)	36.07 (101)	n/a
% HLA$^+$ (*n*)	82.22 (185)	24.68
% HLA$^-$ (*n*)	14.66 (33)	75.32

*PV, pemphigus vulgaris; CR, healthy control; HLA$^+$, carriers of the PV-associated HLA-susceptibility alleles DRB1*0402 and/or DQB1*0503; HLA$^-$, carriers of any HLA allele except the PV-associated HLA-susceptibility alleles DRB1*0402 and/or DQB1*0503. Disease activity is determined as number of samples from patients in the active or remittent phase of disease out of 280 total samples (note: samples from patients with transient lesions only were not included in these analyses).*
HLA association was determined as number of patients carrying or lacking PV-associated HLA alleles out of the total number of 250 samples (note: DNA for HLA typing was not available in 7 cases).

GWB-521201, respectively) using 1:101 serum dilution as per the manufacturer's recommendations. Antibody positivity was defined as ELISA levels >35 AU/mL for anti-TPO antibodies and >10 AU/mL for anti-Tg antibodies.

Anti-Dsg3 and Anti-Dsg1 ELISA

The anti-Dsg ELISA was performed employing Dsg1 and Dsg3 ELISA kits (MBL Intl., RG-7593D) as per the manufacturer's guidelines using a 1:101 serum dilution. Serum samples with an anti-Dsg3 or anti-Dsg1 concentration of >150 U/ml were further diluted to avoid misinterpretation at the upper level of detectability for the ELISA kit. Antibody positivity for anti-Dsg1 and anti-Dsg3 was defined as ELISA levels >20 U/mL.

HLA Typing

High resolution HLA typing was performed by PCR amplification with sequence-specific primers at the Histocompatibility and Immunogenetics Laboratory at Michigan State University (26, 27) using commercially available kits (One lambda, Thermo Fisher Scientific). Patients with one or both of the PV-associated HLA alleles DRB1*0402 and DQB1*0503 were labeled as HLA-positive while those without either of these two alleles were labeled as HLA-negative.

Statistical Analysis

Patient demographics were reported as mean and SD for continuous data, and as frequencies and relative frequencies for categorical data.

The anti-TPO and anti-Tg antibody rates were modeled as a function of group (disease status, gender, HLA type, and anti-Dsg1/3 status) using a generalized estimating equations (GEE) logistic regression model. The GEE model takes into account the repeated measures collected on some patients. Estimates of the activity rates (A.R.s) and corresponding 95% confidence intervals are obtained from the fitted models. A.R.s represent the estimated percent positive in a given population based on multiple observations (i.e., taking into consideration that some patients were sampled more than once). The association between HLA and Dsg status was evaluated using Fisher's exact test. In a limited number of subjects, either DNA or serum was not available to perform all HLA typing and antibody determination, thus, the analyses listed reflect the number of patients in a given comparison where the required information was simultaneously accessible.

A descriptive cluster analysis of anti-TPO and anti-Tg antibody expression, Dsg1/3 status, and HLA type was performed using standard principle component methods. The overall variability explained by the optimal clustering model and the inter-cluster R^2 for each variable are obtained. Factor scores were obtained using the standardized scoring coefficients associated with the optimal clustering model. The clusters are displayed graphically using a tree diagram and using a scatter plot of the corresponding factor scores.

All analyses were conducted in SAS v9.4 (Cary, NC, USA) at a significance level of 0.05.

RESULTS

Correlation Between Reported History of AITD and Anti-Thyroid Antibody Profiles of PV Patients

We previously examined the self-reported co-existence of other autoimmune conditions in PV patients and found AITD to be the leading comorbidity in three independent studies (4, 8, 10). In this study, out of a total of 225 PV patients enrolled, 10.2% ($n = 23$) reported a personal history of AITD and 15.55% ($n = 35$) reported a history of thyroid disease in family members regardless of personal history of AITD. Among those with a self-reported positive personal history of AITD, 52.17% ($n = 12$) had detectable anti-thyroid autoantibodies (either anti-TPO or anti-Tg) in their sera, with nearly equal numbers of patients carrying either anti-TPO antibodies or anti-Tg antibodies (**Figure 1**). Of those who reported only a family history of thyroid disease (i.e., no personal history) ($n = 24$), only 16.66% ($n = 4$) had anti-TPO or anti-Tg antibodies in their sera (two patients carried anti-TPO antibodies only, one patient carried anti-Tg Abs only, and one carried both anti-TPO and anti-Tg antibodies). Among PV patients that did *not* report a history of thyroid disease ($n = 177$), 12.99% ($n = 23$) were found to still carry autoantibodies directed against either/or anti-TPO and anti-Tg, albeit with considerably lower levels of anti-Tg (3.95%, $n = 7$). These data indicate that while PV patients with a history of thyroid-related symptoms are substantially more likely to carry autoimmune thyroid-related autoantibodies than PV patients with no thyroid-related symptoms, this correlation is not strong. Conversely, a proportion of PV patients with no personal- or family history of AITD still carries AITD-related autoantibodies at levels similar to those observed in PV patients with a family history of AITD.

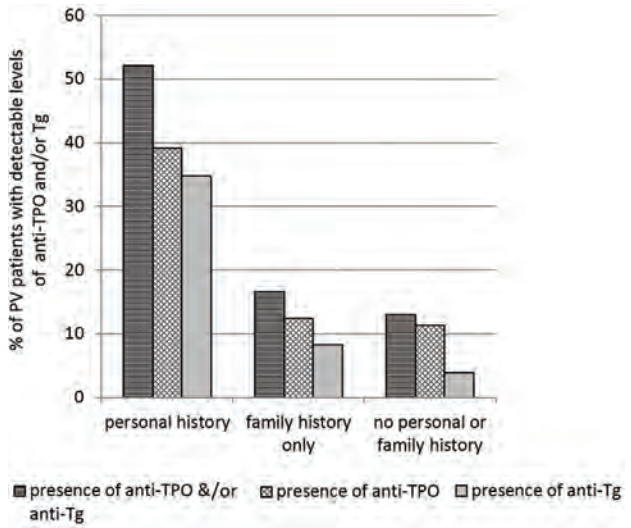

FIGURE 1 | Levels of anti-thyroid peroxidase (anti-TPO) and or anti-thyroglobulin (anti-Tg) by self-reported presence of personal or family history of autoimmune thyroid disease (AITD) in pemphigus vulgaris (PV) patients. Bars represent the percentage of PV patients that have detectable levels of anti-TPO or anti-Tg in subgroups divided by personal and family history of AITD.

Anti-Thyroid Antibodies Are Related to Disease Expression, but Not Disease Activity

To establish baseline and PV-related A.R.s in our study population, we determined levels of anti-TPO and anti-Tg reactivity in 225 PV patients compared with 148 healthy controls. We find that PV patients have a significantly higher prevalence of anti-TPO antibodies (A.R. 13.9%) than controls (A.R. 7.2%) (p-value = 0.042) (**Figure 2A**). Similarly, the prevalence of anti-Tg antibodies is significantly higher for PV patients (A.R. 6.8%) as compared with controls (A.R. 0.6%) (p-value < 0.001) (**Figure 2B**).

To establish a potential correlation between anti-thyroid antibodies and disease activity, we divided the patient cohort into active and remittent groups based on consensus guidelines (24). There were no statistically significant differences observed for either anti-TPO (**Figure 2C**) or anti-Tg antibodies (**Figure 2D**) between active (n = 133) and remittent (n = 101) patient samples (all p-values > 0.05), indicating that disease activity is not related to the levels of anti-thyroid autoantibodies.

Female PV Patients Have a Higher Prevalence of Anti-Thyroid Antibodies Than Male PV Patients

A female predominance has been reported for AITD (28). To explore potential differences in autoantibody production between genders, we analyzed serum samples from 148 female and 77 male patients. Female PV patients were found to be significantly more likely to carry anti-TPO antibodies than male patients (A.R. 19.4 vs. 3.3%, respectively, p-value > 0.001) (**Figure 3A**). A similar trend is seen for anti-Tg antibodies (A.R. 8.6% in females vs. 3.3% in males) where the difference in A.R.s trends toward statistical significance (p = 0.06) (**Figure 3B**). Likewise, in the control population, female controls (n = 90, 11.1%) were significantly more likely to carry anti-TPO than male controls (n = 58, 1.5%) (p-value = 0.019) (**Figure 3A**). However, the A.R. for anti-Tg in females (1.0%) does not differ significantly (p-value = 1.00) from that of males (0.0%) (**Figure 3B**). A significant (or trending toward significant) difference remains between female PV patients and female controls for anti-Tg and anti-TPO, respectively. Such a difference was not observed comparing male patients vs. male controls, potentially due to lower numbers of male samples.

PV Patients With Cutaneous Only Lesions Are More Likely to Display Anti-Thyroid Antibodies Compared With Other Morphological Subtypes

It has been suggested that disease morphology in PV patients is dictated by their anti-desmoglein antibody profile. The desmoglein-compensation hypothesis states that anti-Dsg3 antibodies are sufficient to induce mucosal lesions, while additional anti-Dsg1 antibodies are needed to induce cutaneous lesions (18, 29). To explore a possible relationship between lesion morphology and anti-thyroid antibodies, we compared anti-TPO and anti-Tg levels in PV patients with clearly documented lesional morphology classified into three subtypes: mucosal only, mucocutaneous, and cutaneous only. The prevalence of anti-TPO antibodies in patients with cutaneous only lesions (n = 25, A.R. 28.0%) is almost twice that observed in patients with mucosal only (n = 62, A.R. 14.5%) or mucocutaneous lesions (n = 34, A.R. 14.7%), although this difference does not reach statistical significance (p-value 0.409) (**Figure 4A**). On the other hand, a significant association is observed between anti-Tg antibody A.R. and morphology, where patients with cutaneous only lesions have significantly higher prevalence rates (A.R. 20%) than those with mucosal or mucocutaneous lesions (A.R. 8.1 and 0.0%, respectively) (p-value = 0.022) (**Figure 4B**).

"HLA-Negative" PV Patients Show a Higher Prevalence of Anti-Thyroid Antibodies Than "HLA-Positive" Patients

Many genetic studies in PV have confirmed the presence and etiopathogenetic role of two HLA alleles: DRB1*0402 and DQB1*0503 (13–15). To explore the extent to which HLA affects autoantibody production in PV patients, we subdivided our study population on the basis of presence or absence of one or both of the two PV-susceptibility alleles. We find that in the PV cohort there is a significant association between HLA type and anti-TPO antibody levels (p-value = 0.05): DRB1*0402$^-$/DQB1*0503$^-$ (HLA-negative) patients (n = 33) have the highest prevalence of anti-TPO (A.R. 23.1%) followed by DRB1*0402$^+$/DQB1*0503$^-$ patients (n = 117, A.R. 15.8%), DRB1*0402$^+$/DQB1*0503$^+$ patients (n = 19, A.R. 9.5%), and DRB1*0402$^-$/DQB1*0503$^+$ patients (n = 49, A.R. 4.8%) (**Figure 5A**), suggesting that the absence of DQB1*0503, regardless of the presence of

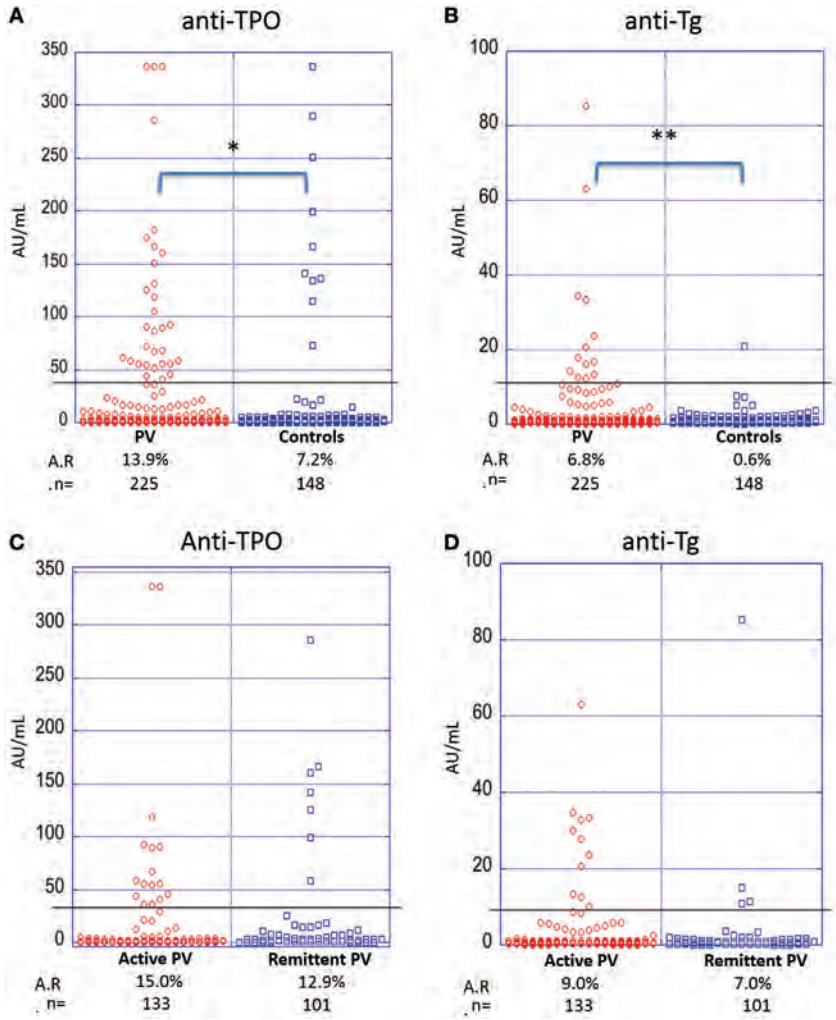

FIGURE 2 | Activity rates of anti-thyroid peroxidase (anti-TPO) and anti-thyroglobulin (anti-Tg) based on disease state and disease activity. Individual dots represent anti-TPO and anti-Tg levels (in AU/ml) in pemphigus vulgaris (PV) patients vs. controls **(A,B)** and active vs. remittent PV patients **(C,D)** for anti-TPO **(A,C)** and anti-Tg **(B,D)** antibodies (*$p < 0.05$ and **$p < 0.01$). Abbreviation: A.R., activity rate. Anti-TPO and anti-Tg antibody rates were modeled as a function of disease status and activity using a generalized estimating equations logistic regression model.

DRB1*0402, predisposes patient to the development of anti-TPO antibodies. No significant association is observed for anti-Tg antibody (p-value = 0.09); however, a similar trend is observed with DRB1*0402$^-$/DQB1*0503$^-$ patients having the highest prevalence of anti-Tg (A.R. 12.8%) followed by DRB1*0402$^+$/DQB1*0503$^-$ (A.R. 6.9%), DRB1*0402$^+$/DQB1*0503$^+$ (A.R. 4.8%), and DRB1*0402$^-$/DQB1*0503$^+$ patients (A.R. 1.6%) (**Figure 5B**).

To further explore the link between HLA haplotype and autoantibody prevalence in active PV patients (*note*: 125 of the 133 active patients in our study had both HLA typing data and anti-desmoglein levels), we visualized the presence or absence of anti-desmoglein and anti-thyroid autoantibodies in PV patients based on their HLA type. As expected, anti-Dsg3 is the predominant autoantibody in PV patients, regardless of their HLA type (**Figure 5C**). Interestingly, whereas DRB1*0402$^-$/DQB1*0503$^+$ patients have higher percentage positivity for anti-Dsg1 antibodies when compared with other HLA types, patients who do not express either of the two PV-susceptibility alleles, i.e., DRB1*0402$^-$/DQB1*0503$^-$ patients, have a higher likelihood of not bearing anti-Dsg3 or anti-Dsg1 antibodies, suggesting that non-desmoglein autoantibodies may fill this gap (**Figure 5C**). In addition, there is a significant association between HLA and Dsg status ($p = 0.023$), where HLA-double negative samples are much less likely to be Dsg-double positive. These data, taken together with the data on anti-TPO distribution based on HLA type, suggest that while anti-Dsg3 antibodies can be generated by a majority of PV patients regardless of HLA type; anti-TPO, and perhaps anti-Tg antibodies are preferably generated in PV patients that do not carry the classical PV-susceptibility alleles

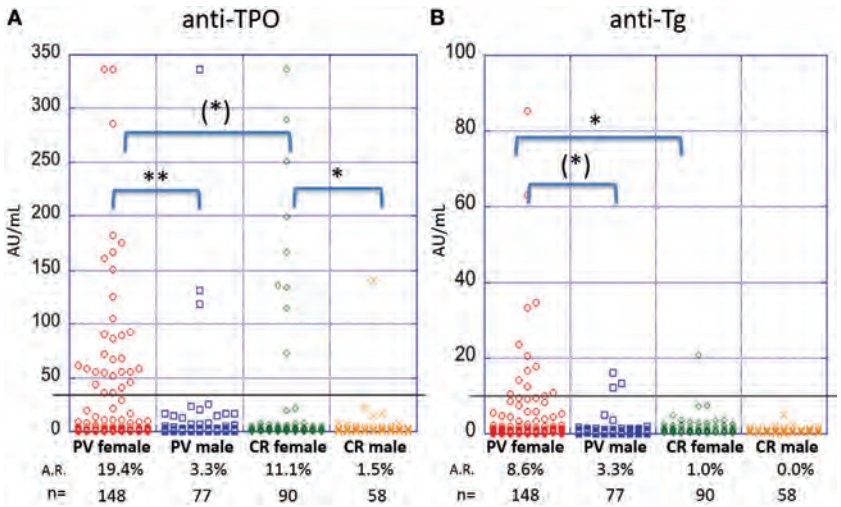

FIGURE 3 | Activity rates of anti-thyroid peroxidase (anti-TPO) and anti-thyroglobulin (anti-Tg) based on sex. Individual dots represent anti-TPO and anti-Tg levels (in AU/ml) in pemphigus vulgaris (PV) patients and controls, both female and male for **(A)** anti-TPO and **(B)** anti-Tg antibodies [(*)$p < 0.1$, *$p < 0.05$, and **$p < 0.01$]. Abbreviation: A.R., activity rate. Anti-TPO and anti-Tg antibody rates were modeled as a function of sex using a generalized estimating equations logistic regression model.

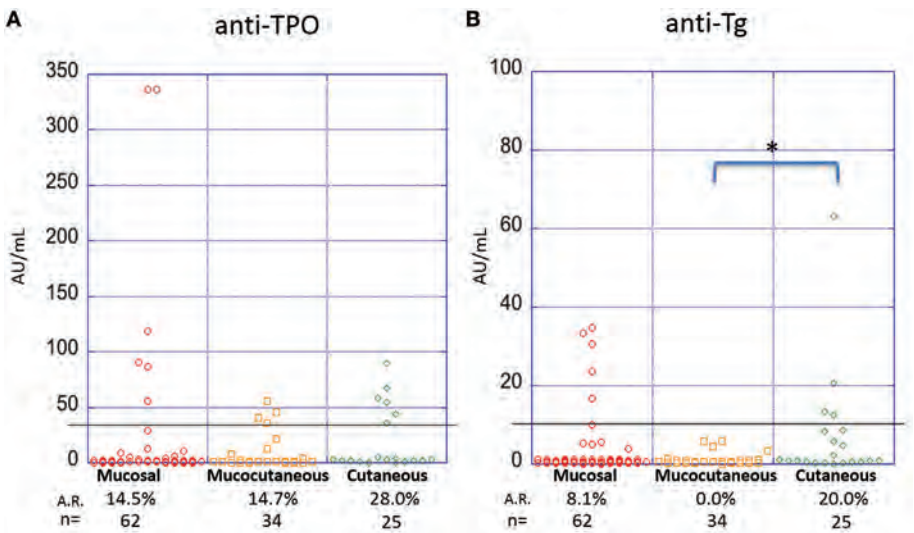

FIGURE 4 | Activity rates of anti-thyroid peroxidase (anti-TPO) and anti-thyroglobulin (anti-Tg) based on morphology. Individual dots represent anti-TPO and anti-Tg levels (in AU/ml) in pemphigus vulgaris patients subgrouped on the basis of lesion morphology for **(A)** anti-TPO and **(B)** anti-Tg antibodies (*$p < 0.05$). Abbreviation: A.R., activity rate. Anti-TPO and anti-Tg antibody rates were modeled as a function of disease morphology using a generalized estimating equations logistic regression model.

DRB1*0402 and DQB1*0503 and may be more relevant than anti-Dsg1 antibodies in this subpopulation.

Anti-Dsg1 and Anti-Dsg3 Negative Active PV Patients Have Higher Anti-Thyroid Activity

The pathogenic role of anti-desmoglein antibodies in PV is well established (17–19). To elucidate a potential association between anti-desmoglein and anti-thyroid autoantibodies, we again analyzed the autoantibody profiles of 133 PV patients with active lesions at the time of blood draw. We observed a significant association between the anti-TPO profiles and the absence or presence of anti-desmoglein antibodies (p-value 0.019), where anti-Dsg1$^-$/3$^-$ patients ($n = 26$) have a higher prevalence of anti-TPO antibodies (26.9%) than anti-Dsg1$^-$/3$^+$ patients ($n = 64$, 18.8%), anti-Dsg1$^+$/3$^-$ patients ($n = 7$, 14.3%), and anti-Dsg1$^+$/3$^+$ patients ($n = 36$, 3.9%) (**Figure 6A**).

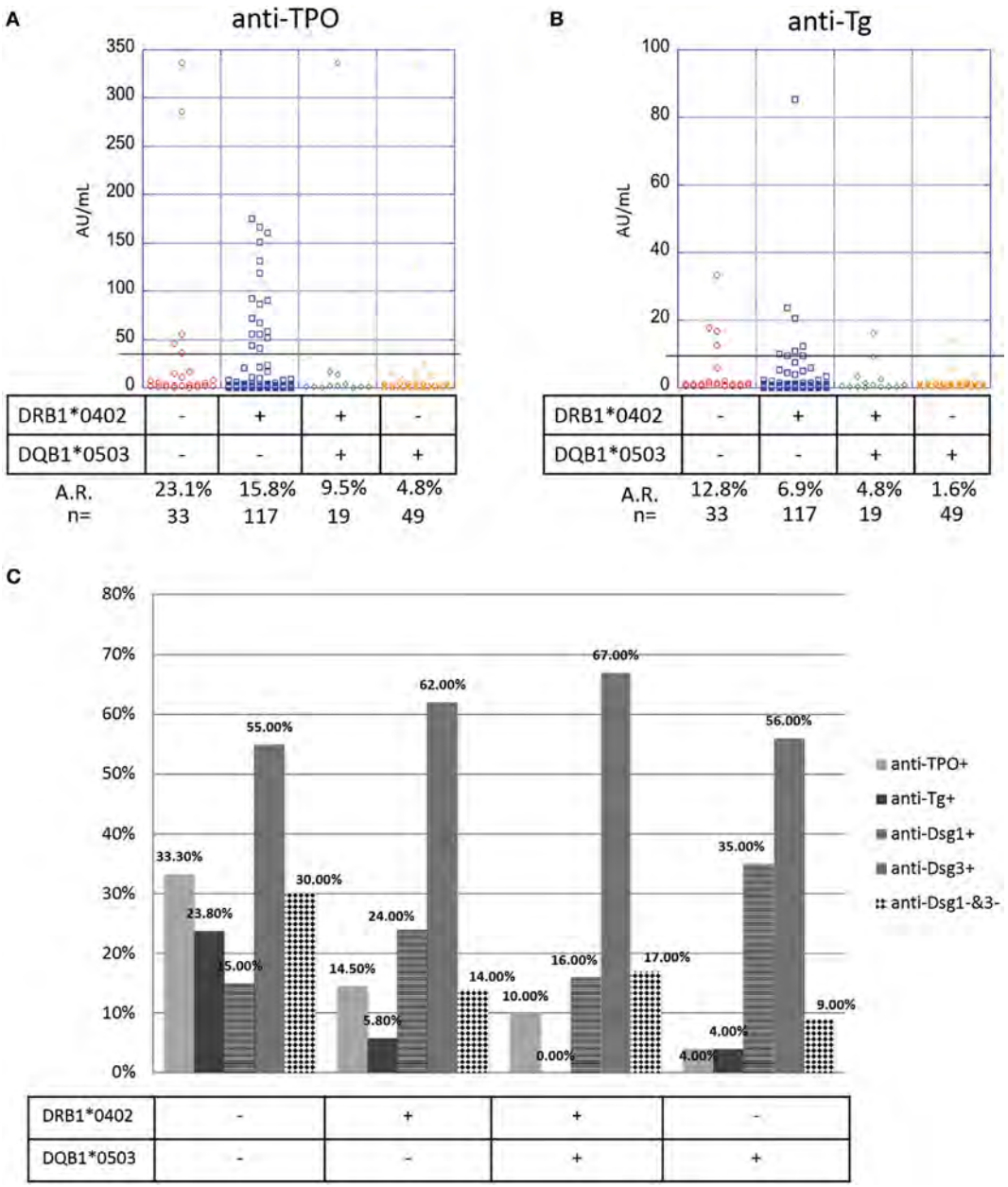

FIGURE 5 | Correlation of anti-thyroid peroxidase (anti-TPO), anti-thyroglobulin (anti-Tg), anti-Dsg3, and anti-Dsg1 levels and human leukocyte antigen (HLA) status. Levels of **(A)** anti-TPO and **(B)** anti-Tg antibodies in pemphigus vulgaris (PV) patients, subgrouped on the basis of presence or absence of PV-associated HLA susceptibility alleles. Individual dots represent anti-TPO and anti-Tg levels (in AU/ml). Anti-TPO and anti-Tg antibody rates were modeled as a function of absence or presence of the PV-associated HLA alleles DRB1*0402 and/or DQB1*0503 using a generalized estimating equations logistic regression model. **(C)** Percent positivity of anti-Dsg1, anti-Dsg3, anti-TPO, and anti-Tg in active PV patients, subgrouped based on the presence or absence of the two PV-associated HLA alleles DRB1*0402 and DQB1*0503. The association between HLA and Dsg status was evaluated using Fisher's exact test.

A similar trend is observed for anti-Tg antibody (p-value 0.032) with anti-Dsg1$^-$/3$^-$ patients having the highest prevalence (23.1%) followed by anti-Dsg1$^-$/3$^+$ patients (7.8%), anti-Dsg1$^+$/3$^+$ patients (2.8%), and anti-Dsg1$^+$/3$^-$ patients (0.0%) (**Figure 6B**), suggesting that the absence of both anti-desmoglein antibodies is correlated with the highest anti-thyroid activity, followed by the absence of anti-Dsg1 alone.

Interestingly, Dsg1$^-$/3$^-$ PV patients in active disease show significantly higher levels of anti-Tg (5.35 ± 8.71 AU/ml) than Dsg1$^-$/3$^-$ patients in remission (n = 44; 1.58 ± 3.08 AU/ml, p = 0.01). While anti-TPO levels were also higher in Dsg1$^-$/3$^-$ patients in active disease (30.71 ± 74.18 AU/ml) than remission (16.16 ± 34.08 AU/ml), this comparison did not reach significance (p = 0.28).

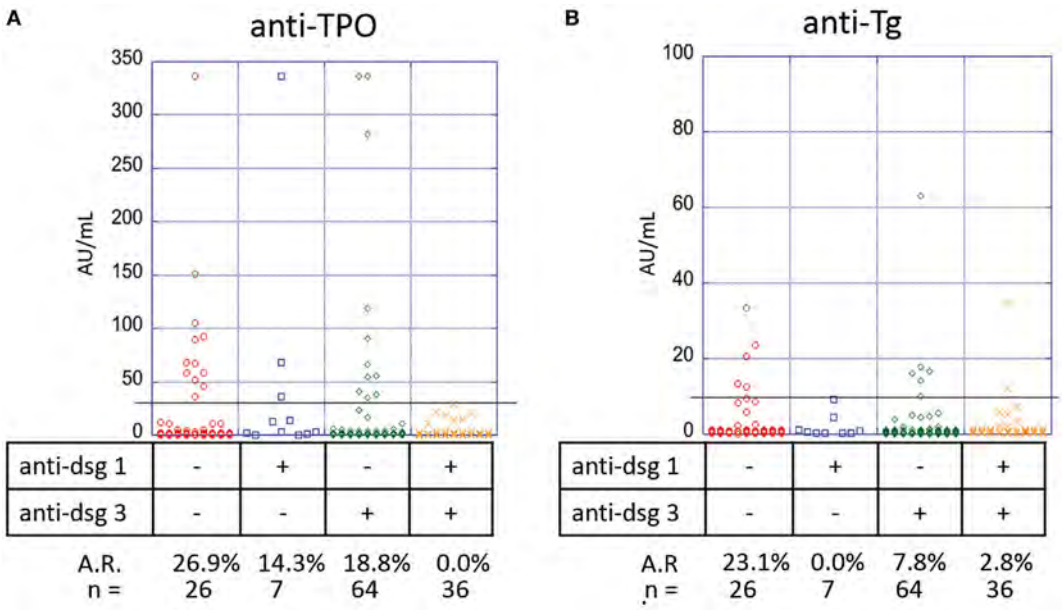

FIGURE 6 | Correlation of anti-thyroid peroxidase (anti-TPO), anti-thyroglobulin (anti-Tg), with anti-Dsg3/1 levels in pemphigus vulgaris (PV) patients with active lesions. Levels of **(A)** anti-TPO and **(B)** anti-Tg antibodies in PV patients, subgrouped on the basis of presence or absence of anti-Dsg3 and or anti-Dsg1 antibodies. Individual dots represent anti-TPO and anti-Tg levels (in AU/ml). Anti-TPO and anti-Tg antibody rates were modeled as a function of absence or presence of anti-Dsg3/1 serum antibodies using a generalized estimating equations logistic regression model.

Different Determinants of Disease Expression, Activity, and Phenotype Tend to Cluster Together

To assess further how and if the variables analyzed in our population relate to each other, principle component analysis was used to identify potential clustering of these variables. The analysis identified two distinct clusters (**Figure 7A**), which explain 48% of the variation. The first cluster includes presence of anti-TPO and anti-Tg antibodies, in the absence of DQB1*0503; while the second cluster is based on the association of anti-Dsg1, anti-Dsg3, and DRB1*0402 status. All variables show a much stronger positive correlation with their own cluster than the adjacent cluster (Table S1 in Supplementary Material), indicating that while the presence of DRB1*0402 may predispose patients to develop anti-Dsg3 and anti-Dsg1 antibodies, the absence of DQB1*0503 may predispose them to develop anti-TPO and anti-Tg antibodies.

To assess how theses clusters relate to the patient and control populations, factor scores were generated for each cluster using the corresponding standardized scoring coefficients. These factor scores were then plotted against one-another using a scatter plot, with the study sample cohorts represented by different colors (factor 1 = anti-TPO, anti-Tg, and absence of DQB1*0503; factor 2 = anti-Dsg1, anti-Dsg3, and presence of DRB1*0402). The resulting figure shows that PV patients have higher factor scores as compared with controls which tend to cluster toward low factor scores (**Figure 7B**, left), indicating that one or more variables are present in a given patient within the respective factor groups, but are lacking in the majority of controls. However, a minority of controls are positive for the PV-related factors. To further characterize the control population, we divided healthy controls into PV-related and PV-unrelated individuals. We found that related controls (first-, second-, or third-degree relation to a PV patient) have higher factor scores than unrelated controls (**Figure 7B**, right), which is particularly true for factor 2 that comprises of anti-Dsg1, anti-Dsg3 antibodies and presence of DRB1*0402. This finding is in line with previous work from our lab that found increased autoantibody levels, including those for anti-Dsg3 and anti-TPO, in PV patients and their relatives by multiplexed autoantigen array when compared with unrelated healthy controls (22).

DISCUSSION

Autoimmune thyroid disease is among the most commonly diagnosed autoimmune diseases in the general population. Various epidemiological studies have shown the prevalence of AITD to be 7–8% (28, 30, 31), with a reported female predominance of 9:1. The clinical manifestations of AITD may vary from hypothyroidism (Hashimoto's thyroiditis) to hyperthyroidism (Grave's disease). The diagnosis of AITD is made based on clinical findings, thyroid function abnormalities as well as the presence of either one of the anti-thyroid antibodies; anti-TPO, anti-Tg or anti-thyroid-stimulating hormone receptor antibodies.

Multiple previous studies from our group and others have reported a higher prevalence of AITD in patients with PV (4, 6–10). In fact, AITD is the most commonly self-reported autoimmune disease in PV patients and/or their first-degree relatives (4, 8). Similarly, levels of AITD-related antibodies, particularly anti-TPO, have been reported to be significantly elevated in PV patients when compared with controls in ethnically diverse populations in Argentina (9), Iran (3, 23), and Turkey (6), with

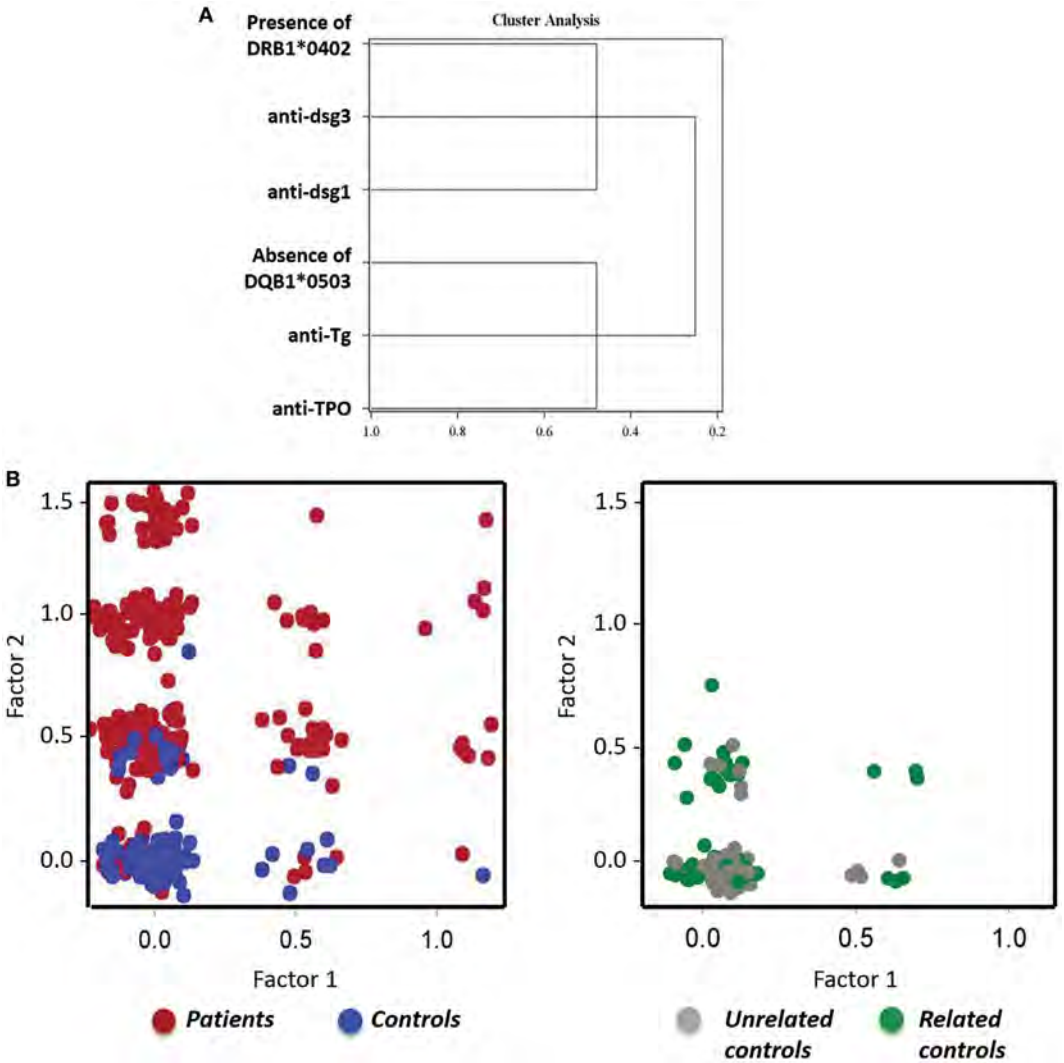

FIGURE 7 | Distinct clustering of anti-Dsg antibodies, anti-thyroid antibodies, and human leukocyte antigen (HLA). **(A)** A tree diagram visually demonstrates the structure and relationship of the clustering variables with anti-Dsg3, anti-Dsg1, and HLA DRB1*0402 in one cluster, and anti-thyroid peroxidase (anti-TPO), anti-thyroglobulin (anti-Tg), and DQB1*0503 a second, distinct cluster. **(B)** Scatter plot representation of pemphigus vulgaris (PV) patients and controls (left) and controls either related or unrelated to PV patients (right), with factor 1 (anti-TPO, anti-TG, and DRB1*0503) on the *x*-axis and factor 2 (anti-Dsg3, anti-Dsg1, and DQB1*0402) on the *y*-axis.

anti-TPO levels ranging from 16 to 40% in the patient population compared with only 6–12% in the healthy control population. Interestingly, numerous studies found that despite the presence of thyroid disease related autoantibodies, many patients were euthyroid clinically (3, 9). In our North American study population, 10.2% of patients reported a history of AITD compared with only 5.4% in the control population (data not shown; noteworthy, of the healthy controls with a personal history of AITD, all had a family history of autoimmune bullous disease, mainly PV), but a higher number of patients had serum reactivity to autoantibodies classically related to AITD (13.9% anti-TPO and 6.8% anti-Tg reactivity). As in previous studies, the self-reported history of AITD and the objectively determined anti-TPO/anti-Tg levels are not tightly correlated. In fact, only 52% of patients with a positive history of thyroid disease have detectable anti-TPO/anti-Tg levels. Conversely, 13% of patients without a personal or family history of AITD still carried detectable levels of anti-TPO/Tg, suggesting that these patients either have not been diagnosed with AITD, that these autoantibodies are non-pathogenic, or that they may be involved in processes unrelated to thyroid pathology. While the data on autoimmune thyroid conditions in PV patients in our study was self-reported and could not be independently verified by other imaging or clinical data, the rates of anti-TPO and anti-Tg levels from PV patients with a personal history of AITD are substantially higher compared with those with only a family history and those with no history (self or family). In future studies, it will be important to document objective measures of thyroid function such as thyroid-stimulating hormone, thyroxine

(T4), and triiodothyronine (T3) serum levels to assess the true overlap of thyroid disease and anti-thyroid autoantibody positivity in PV patients.

The overwhelming majority of patients with PV carry anti-desmoglein 3, and to a lesser extent, anti-Dsg1 antibodies; these antibodies have been shown to be sufficient to induce cell dissociation (*in vitro* and *in vivo*) (32). However, a subgroup of patients does develop lesions in the absence of anti-dsg antibodies [personal observation and Ref. (31)]. To date, it is unclear if autoantibodies with non-dsg specificities contribute to blister formation. However, ongoing work in our lab suggests this may be the case for anti-thyroid peroxidase (TPO) antibodies. Using high-throughput protein microarray technology, we found significant IgG reactivity in PV patients toward TPO, several muscarinic acetylcholine receptor subtypes, as well as the established PV-associated antigen desmoglein 3 (22). Furthermore, we observed that patient derived anti-TPO, similar to anti-desmoglein antibodies or patient derived PVIgG, can (i) activate p38MAPK, (ii) increase intracellular calcium and (iii) induce fragmentation of a keratinocyte monolayer (Sajda et al., manuscript in preparation). Likewise, the depletion of anti-TPO autoAbs inhibits the ability of patient purified IgG (PVIgG) to activate these pathways, suggesting a pathogenic role of anti-TPO antibodies in Pemphigus. In this context, it is interesting that anti-TPO and anti-Tg show the highest prevalence in patients that are anti-Dsg3 and anti-Dsg1 negative (A.R. 26.9 and 23.1%, respectively) and are negative or barely detectable in patients that are double-positive for anti-Dsg3 and anti-Dsg1, suggesting that anti-TPO antibodies may have a compensatory or additive function in the absence of the classical PV-related autoantobodies. Interestingly, we also observe a trend toward a higher prevalence of anti-TPO and anti-Tg antibodies in PV patients with the rare "cutaneous only" phenotype and a significant increase in anti-Tg in anti-Dsg1/3 double-negative patients in active disease vs. remission, suggesting that the "supporting role" anti-thyroid antibodies may play in disease pathogenesis is more pronounced in less common disease phenotypes.

A role for anti-TPO antibodies has been previously suggested in autoimmune conditions of non-thyroid origin other than PV, including type I diabetes mellitus (33, 34) and RA (35). Interestingly, we have found both DM type I and RA to be frequent autoimmune comorbidities in PV (4, 10). In fact, these diseases belong to a distinct autoimmune disease cluster along with PV and AITD (8), suggesting common genetic elements across clinically distinct diseases that might underlie autoimmune susceptibility. Autoimmune diseases are multifactorial in origin, with susceptibility controlled by genetic and environmental factors. Thus far, the strongest genetic associations for a wide range of autoimmune conditions, including PV, AITD, RA, and DM type 1, have been with variants in the HLA region (36). PV has a particularly strong associations with HLA with ~ 95% of North American patients carrying one of two HLA class II susceptibility alleles, DRB1*0402 and/or DQB1*0503 (13, 14, 37). Wucherpfennig et al. showed that autoaggressive T cells recognize a limited set of Dsg3 peptides presented by DRB1*0402, thus providing a compelling explanation for the observed association of disease expression and HLA haplotype in PV (16). To date, no such clear association has been found for DQB1*0503. Equally, it is not clear if and how other HLA alleles (non-DRB1*0402 or non-DQB1*0503) link with disease-relevant autoantibodies.

Our data indicate that patients who do not carry the prevalent PV-susceptibility HLA alleles DRB1*0402 and DQB1*0503 are more likely to have higher levels of anti-thyroid antibodies. Interestingly, many of these patients carry alleles in the HLA region that have been associated with thyroid autoimmunity (38, 39), such as DRB1*04, DQB1*0302, DQB1*0301 and DQA*0301 (40) (*data not shown*). Of note, HLA DRB1*0402 has been suggested to be in linkage disequilibrium with DQB1*0302, an allele that has been suggested as a disease causing allele for AITD (41), which may be one of the reasons for the significant overrepresentation of AITD-related autoantibodies in PV. Interestingly, current literature also suggests that DQB1*05 alleles are protective against development of AITD in pediatric DM type I patients (41), and, thus, it is not entirely surprising that we see the lowest levels of anti-TPO and anti-Tg antibodies in the presence of DQB1*0503 allele. Indeed, our cluster analysis reveals that the presence of DRB1*0402 may predispose patients to develop anti-Dsg3 and anti-Dsg1 antibodies, while the absence of DQB1*0503 may predispose them to develop anti-TPO and anti-Tg antibodies.

We did observe that female PV patients have higher antibody A.R.s than either male PV patients or controls. The discrepancy between female and male patients can likely be explained by higher prevalence of AITD in females in general, since there is no large difference in the relative female predominance in either PV patient or controls in our study. However, the exact mechanism behind the increased susceptibility of females to several autoimmune diseases, including pemphigus and AITD, remains to be established.

Taken together, our data support a role for non-desmoglein autoantibodies in PV, specifically anti-TPO antibodies. Our findings further suggest that anti-TPO reactivity in PV is driven by genetic markers that may be in linkage disequilibrium with the established PV-susceptibility alleles and that this association drives the selection of a combination of anti-Dsg and anti-TPO antibodies, with anti-TPO filling the gap in active patients that do not carry the established PV-associated autoantibodies and/or are lacking the established PV-HLA-susceptibility alleles. Understanding the genetic underpinnings and potential mechanistic interplay of anti-desmoglein and non-desmoglein autoantibodies relevant to disease pathogenesis and expression is crucial to improve both treatment and clinical decision making in autoimmune blistering conditions. Further studies are needed to determine both the potential functional correlates of anti-TPO and anti-Tg autoantibodies in the context of cell dissociation and whether the anti-TPO/anti-Tg antibodies detected in PV are similar or identical in specificity and affinity to those detected AITD.

ETHICS STATEMENT

This study was carried out in accordance with the recommendations of the Institutional Review Boards at Weill Cornell Medical College, Michigan State University, and the University at Buffalo with written informed consent from all subjects. All subjects gave

written informed consent in accordance with the Declaration of Helsinki. The protocol was approved by the review boards at Weill Cornell Medical College, Michigan State University and the University at Buffalo. No vulnerable populations were involved in this study.

AUTHOR CONTRIBUTIONS

KS-S and AS designed the study and enrolled the patients included in this study. KS-S and SK performed the experiments and analyzed the data. KS-S, SK, and AS wrote the manuscript. KA performed the statistical analysis of the final data set. JG provided high resolution HLA typing.

ACKNOWLEDGMENTS

The authors would like to thank Susan Forney of the Histocompatibility and Immunogenetics Laboratory, Michigan State University, East Lansing, MI, USA for her expert high resolution HLA typing and continued collaboration. They thank Birendra Kumar Sinha for continued guidance and support.

SUPPLEMENTARY MATERIAL

The Supplementary Material for this article can be found online at https://www.frontiersin.org/articles/10.3389/fimmu.2018.00625/full#supplementary-material.

REFERENCES

1. Grandhe NP, Dogra S, Kanwar AJ. Multiple autoimmune syndrome in a patient with pemphigus vulgaris. *Acta Derm Venereol* (2005) 85:91–2. doi:10.1080/00015550410021691
2. Ljubojevic S, Lipozenčić J. Autoimmune bullous diseases associations. *Clin Dermatol* (2012) 30:17–33. doi:10.1016/j.clindermatol.2011.03.006
3. Ansar A, Farshchian M, Farahnaki S. Thyroid autoimmunity in Iranian patients with pemphigus vulgaris. *J Eur Acad Dermatol Venereol* (2009) 23:719–20. doi:10.1111/j.1468-3083.2009.03172.x
4. Gupta VK, Kelbel TE, Nguyen D, Melonakos KC, Murrell DF, Xie Y, et al. A globally available internet-based patient survey of pemphigus vulgaris: epidemiology and disease characteristics. *Dermatol Clin* (2011) 29:393–404. doi:10.1016/j.det.2011.03.016
5. Iino Y, Hara H, Suda T, Okada T, Baba S, Suzuki H. Co-existence of pemphigus vulgaris and Hashimoto's thyroiditis. *Eur J Dermatol* (2005) 15:40–2.
6. Kavala M, Kural E, Kocaturk E, Zindanci I, Turkoglu Z, Can B. The evaluation of thyroid diseases in patients with pemphigus vulgaris. *ScientificWorldJournal* (2012) 2012:146897. doi:10.1100/2012/146897
7. Leshem YA, Katzenelson V, Yosipovitch G, David M, Mimouni D. Autoimmune diseases in patients with pemphigus and their first-degree relatives. *Int J Dermatol* (2011) 50:827–31. doi:10.1111/j.1365-4632.2010.04818.x
8. Parameswaran A, Attwood K, Sato R, Seiffert-Sinha K, Sinha AA. Identification of a new disease cluster of pemphigus vulgaris with autoimmune thyroid disease, rheumatoid arthritis and type I diabetes. *Br J Dermatol* (2015) 172:729–38. doi:10.1111/bjd.13433
9. Pitoia F, Moncet D, Glorio R, Graciela Diaz A, Rodriguez Costa G, Carbia S, et al. Prevalence of thyroid autoimmunity in patients with pemphigus vulgaris. *Medicina (B Aires)* (2005) 65:307–10.
10. Shah AA, Seiffert-Sinha K, Sirois D, Werth VP, Rengarajan B, Zrnchik W, et al. Development of a disease registry for autoimmune bullous diseases: initial analysis of the pemphigus vulgaris subset. *Acta Derm Venereol* (2015) 95:86–90. doi:10.2340/00015555-1854
11. Firooz A, Mazhar A, Ahmed AR. Prevalence of autoimmune diseases in the family members of patients with pemphigus vulgaris. *J Am Acad Dermatol* (1994) 31:434–7. doi:10.1016/S0190-9622(94)70206-3
12. Prussmann J, Prussmann W, Recke A, Rentzsch K, Juhl D, Henschler R, et al. Co-occurrence of autoantibodies in healthy blood donors. *Exp Dermatol* (2014) 23:519–21. doi:10.1111/exd.12445
13. Lee E, Lendas KA, Chow S, Pirani Y, Gordon D, Dionisio R, et al. Disease relevant HLA class II alleles isolated by genotypic, haplotypic, and sequence analysis in North American Caucasians with pemphigus vulgaris. *Hum Immunol* (2006) 67:125–39. doi:10.1016/j.humimm.2005.09.003
14. Sinha AA, Brautbar C, Szafer F, Friedmann A, Tzfoni E, Todd JA, et al. A newly characterized HLA DQ beta allele associated with pemphigus vulgaris. *Science* (1988) 239:1026–9. doi:10.1126/science.2894075
15. Todd JA, Acha-Orbea H, Bell JI, Chao N, Fronek Z, Jacob CO, et al. A molecular basis for MHC class II – associated autoimmunity. *Science* (1988) 240:1003–9. doi:10.1126/science.3368786
16. Wucherpfennig KW, Yu B, Bhol K, Monos DS, Argyris E, Karr RW, et al. Structural basis for major histocompatibility complex (MHC)-linked susceptibility to autoimmunity: charged residues of a single MHC binding pocket confer selective presentation of self-peptides in pemphigus vulgaris. *Proc Natl Acad Sci U S A* (1995) 92:11935–9. doi:10.1073/pnas.92.25.11935
17. Amagai M, Klaus-Kovtun V, Stanley JR. Autoantibodies against a novel epithelial cadherin in pemphigus vulgaris, a disease of cell adhesion. *Cell* (1991) 67:869–77. doi:10.1016/0092-8674(91)90360-B
18. Amagai M, Koch PJ, Nishikawa T, Stanley JR. Pemphigus vulgaris antigen (desmoglein 3) is localized in the lower epidermis, the site of blister formation in patients. *J Invest Dermatol* (1996) 106:351–5. doi:10.1111/1523-1747.ep12343081
19. Koch PJ, Mahoney MG, Ishikawa H, Pulkkinen L, Uitto J, Shultz L, et al. Targeted disruption of the pemphigus vulgaris antigen (desmoglein 3) gene in mice causes loss of keratinocyte cell adhesion with a phenotype similar to pemphigus vulgaris. *J Cell Biol* (1997) 137:1091–102. doi:10.1083/jcb.137.5.1091
20. Ludwig RJ, Vanhoorelbeke K, Leypoldt F, Kaya Z, Bieber K, McLachlan SM, et al. Mechanisms of autoantibody-induced pathology. *Front Immunol* (2017) 8:603. doi:10.3389/fimmu.2017.00603
21. Grando SA. Muscarinic receptor agonists and antagonists: effects on keratinocyte functions. *Handb Exp Pharmacol* (2012) 208:429–50. doi:10.1007/978-3-642-23274-9_18
22. Sajda T, Hazelton J, Patel M, Seiffert-Sinha K, Steinman L, Robinson W, et al. Multiplexed autoantigen microarrays identify HLA as a key driver of anti-desmoglein and -non-desmoglein reactivities in pemphigus. *Proc Natl Acad Sci U S A* (2016) 113(7):1859–64. doi:10.1073/pnas.1525448113
23. Daneshpazhooh M, Behjati J, Hashemi P, Shamohammadi S, Mortazavi H, Nazemi MJ, et al. Thyroid autoimmunity and pemphigus vulgaris: is there a significant association? *J Am Acad Dermatol* (2010) 62:349–51. doi:10.1016/j.jaad.2009.05.024
24. Murrell DF, Dick S, Ahmed AR, Amagia M, Barnadas MA, Borradori L, et al. Consensus statement on definitions of disease, end points, and therapeutic response for pemphigus. *J Am Acad Dermatol* (2008) 58:1043–6. doi:10.1016/j.jaad.2008.01.012
25. Naseer SY, Seiffert-Sinha K, Sinha AA. Detailed profiling of anti-desmoglein autoantibodies identifies anti-Dsg1 reactivity as a key driver of disease activity and clinical expression in pemphigus vulgaris. *Autoimmunity* (2015) 48:231–41. doi:10.3109/08916934.2014.976629
26. Bunce M, O'Neill CM, Barnardo MCNM, Krausa P, Browning MJ, Morris PJ, et al. Phototyping: comprehensive DNA typing for HLA-A, B, C, DRB1, DRB3, DRB4, DRB5 & DQB1 by PCR with 144 primer mixes utilizing sequence-specific primers (PCR-SSP). *Tissue Antigens* (1995) 46:355–67. doi:10.1111/j.1399-0039.1995.tb03127.x
27. Olerup O, Zetterquist H. HLA-DR typing by PCR amplification with sequence-specific primers (PCR-SSP) in 2 hours: an alternative to serological DR typing in clinical practice including donor-recipient matching in cadaveric transplantation. *Tissue Antigens* (1992) 39:225–35. doi:10.1111/j.1399-0039.1992.tb01940.x

28. Jacobson DL, Gange SJ, Rose NR, Graham NMH. Epidemiology and estimated population burden of selected autoimmune diseases in the United States. *Clin Immunol Immunopathol* (1997) 84:223–43. doi:10.1006/clin.1997.4412
29. Mahoney MG, Wang Z, Rothenberger K, Koch PJ, Amagai M, Stanley JR. Explanations for the clinical and microscopic localization of lesions in pemphigus foliaceus and vulgaris. *J Clin Invest* (1999) 103:461–8. doi:10.1172/JCI5252
30. Cooper GS, Bynum ML, Somers EC. Recent insights in the epidemiology of autoimmune diseases: improved prevalence estimates and understanding of clustering of diseases. *J Autoimmun* (2009) 33:197–207. doi:10.1016/j.jaut.2009.09.008
31. Yoshifuku A, Fujii K, Kawahira H, Katsue H, Baba A, Higashi Y, et al. Long-lasting localized pemphigus vulgaris without detectable serum autoantibodies against desmoglein 3 and desmoglein 1. *Indian J Dermatol* (2016) 61:427–9. doi:10.4103/0019-5154.185712
32. Kasperkiewicz M, Ellebrecht CT, Takahashi H, Yamagami J, Zillikens D, Payne AS, et al. Pemphigus. *Nat Rev Dis Primers* (2017) 3:17026. doi:10.1038/nrdp.2017.26
33. Abrams P, De Leeuw I, Vertommen J, Belgian Diabetes R. In new-onset insulin-dependent diabetic patients the presence of anti-thyroid peroxidase antibodies is associated with islet cell autoimmunity and the high risk haplotype HLA DQA1*0301-DQB1*0302. *Diabet Med* (1996) 13:415–9. doi:10.1002/(SICI)1096-9136(199605)13:5<415::AID-DIA96>3.0.CO;2-X
34. Kordonouri O, Meyer K, Egerer K, Hartmann R, Scheffler S, Burmester GR, et al. Prevalence of 20S proteasome, anti-nuclear and thyroid antibodies in young patients at onset of type 1 diabetes mellitus and the risk of autoimmune thyroiditis. *J Pediatr Endocrinol Metab* (2004) 17:975–81. doi:10.1515/JPEM.2004.17.7.975
35. Cardenas Roldan J, Amaya-Amaya J, Castellanos-de la Hoz J, Giraldo-Villamil J, Montoya-Ortiz G, Cruz-Tapias P, et al. Autoimmune thyroid disease in rheumatoid arthritis: a global perspective. *Arthritis* (2012) 2012:864907. doi:10.1155/2012/864907
36. Fernando MM, Stevens CR, Walsh EC, De Jager PL, Goyette P, Plenge RM, et al. Defining the role of the MHC in autoimmunity: a review and pooled analysis. *PLoS Genet* (2008) 4:e1000024. doi:10.1371/journal.pgen.1000024
37. Sinha AA. The genetics of pemphigus. *Dermatol Clin* (2011) 29:381–91, vii. doi:10.1016/j.det.2011.03.020
38. Badenhoop K, Schwarz G, Walfish PG, Drummond V, Usadel KH, Bottazzo GF. Susceptibility to thyroid autoimmune disease: molecular analysis of HLA-D region genes identifies new markers for goitrous Hashimoto's thyroiditis. *J Clin Endocrinol Metab* (1990) 71:1131–7. doi:10.1210/jcem-71-5-1131
39. Farid NR, Sampson L, Moens H, Barnard JM. The association of goitrous autoimmune thyroiditis with HLA-DR5*. *Tissue Antigens* (1981) 17:265–8. doi:10.1111/j.1399-0039.1981.tb00700.x
40. Tendon N, Zhang L, Weetman AP. HLA associations with Hashimoto's thyroiditis. *Clin Endocrinol* (1991) 34:383–6. doi:10.1111/j.1365-2265.1991.tb00309.x
41. Sumnik Z, Drevinek P, Snajderova M, Kolouskova S, Sedlakova P, Pechova M, et al. HLA-DQ polymorphisms modify the risk of thyroid autoimmunity in children with type 1 diabetes mellitus. *J Pediatr Endocrinol Metab* (2003) 16:851–8. doi:10.1515/JPEM.2003.16.6.851

Conflict of Interest Statement: The authors declare that the research was conducted in the absence of any commercial or financial relationships that could be construed as a potential conflict of interest.

The reviewer MK and handling Editor declared their shared affiliation.

frontiers in Immunology

MINI REVIEW
published: 29 March 2018
doi: 10.3389/fimmu.2018.00623

Autoantibodies to Chemokines and Cytokines Participate in the Regulation of Cancer and Autoimmunity

*Nathan Karin**

Department of Immunology, Faculty of Medicine, Technion – Israel Institute of Technology, Haifa, Israel

We have previously shown that predominant expression of key inflammatory cytokines and chemokines at autoimmune sites or tumor sites induces loss of B cells tolerance, resulting in autoantibody production against the dominant cytokine/chemokine that is largely expressed at these sites. These autoantibodies are high-affinity neutralizing antibodies. Based on animal models studies, we suggested that they participate in the regulation of cancer and autoimmunity, albeit at the level of their production cannot entirely prevent the development and progression of these diseases. We have, therefore, named this selective breakdown of tolerance as "Beneficial Autoimmunity." Despite its beneficial outcome, this process is likely to be stochastic and not directed by a deterministic mechanism, and is likely to be associated with the dominant expression of these inflammatory mediators at sites that are partially immune privileged. A recent study conducted on autoimmune regulator-deficient patients reported that in human this type of breakdown of B cell tolerance is T cell dependent. This explains, in part, why the response is highly restricted, and includes high-affinity antibodies. The current mini-review explores this subject from different complementary perspectives. It also discusses three optional translational aspects: amplification of autoantibody production as a therapeutic approach, development of autoantibody based diagnostic tools, and the use of B cells from donors that produce these autoantibodies for the development of high-affinity human monoclonal antibodies.

Keywords: autoantibodies, chemokines, cytokines, experimental autoimmune encephalomyelitis, type I diabetes, cancer, tolerance

OPEN ACCESS

Edited by:
Valentin A. Pavlov,
Northwell Health, United States

Reviewed by:
Rui Li,
University of Pennsylvania, United States
Dipyaman Ganguly,
Indian Institute of Chemical Biology (CSIR), India

***Correspondence:**
Nathan Karin
nkarin10@gmail.com

Specialty section:
This article was submitted to Inflammation, a section of the journal Frontiers in Immunology

Received: *04 January 2018*
Accepted: *13 March 2018*
Published: *29 March 2018*

Citation:
Karin N (2018) Autoantibodies to Chemokines and Cytokines Participate in the Regulation of Cancer and Autoimmunity. Front. Immunol. 9:623. doi: 10.3389/fimmu.2018.00623

INTRODUCTION

Autoantibodies to self-components are commonly associated with the development of autoimmunity, allergic diseases, and scleroderma (1–6). As opposed to these harmful antibodies, here we focus on those that are being produced during pathological conditions and are beneficial for the host. About 14 years ago, we have identified that along the course of rheumatoid arthritis (RA), the immune system produces neutralizing autoantibodies against tumor necrosis factor alpha (TNFα) (7), one of key drivers of the inflammatory process in this disease (8). Similar autoantibodies have also been observed in rodents after the induction of experimentally induced arthritis (i.e., adjuvant-induced arthritis), even before the onset of disease (7). In these rodents, amplification of this response by a targeted DNA vaccine encoding TNFα suppressed the experimental disease, whereas their elimination *via* induction of neonatal tolerance to TNFα aggravated the severity of disease (7). Collectively, this implies for a selective breakdown of B-cell tolerance that restrains

destructive autoimmunity. The relevance of such beneficial protective autoantibodies has recently been highlighted in a study focusing on breakdown of B-cell tolerance in APS1/APECED patients (9). These patients have a functional deficiency of the autoimmune regulator (AIRE) gene that is essential for the generation of central T cell tolerance to many self-antigens (10–12). The study showed that in the absence of central T cell tolerance the immune system promoted T-dependent high-affinity autoantibody production to key cytokines, and by so doing provokes resistance to autoimmunity (9). The disease in focus in this manuscript is type I diabetes (T1DM) and autoantibodies that are likely to affect the development of T1DM are produced against type-I interferons (9).

The current mini-review describes how we discovered this type of regulatory response long ago, and its relevance to cancer and autoimmunity. It also discusses the implications of these findings for therapy, diagnosis, and development of therapeutic human monoclonal antibodies.

THE DISCOVERY OF AUTOANTIBODY-BASED REGULATION OF AUTOIMMUNITY AND CANCER

Almost 20 years ago, we have applied the DNA vaccination technology to induce anti-chemokine autoantibody production and by so doing explore their differential role in the regulation of autoimmunity (13–16). The basic idea has been to inject rodents with CpG-enriched plasmid DNA encoding different chemokines or cytokines, and then to follow the effect of these vaccines on the generation of neutralizing autoantibodies to chemokines/cytokines and on the development and progression of the autoimmune condition. In continuing experiments, these autoantibodies were purified and their disease protective abilities were confirmed by adoptive transfer experiments (13–16). In one of these experiments, a CpG-enriched plasmid DNA vaccine encoding TNFα was administered just after the onset of experimental autoimmune encephalomyelitis (EAE), and surprisingly, its beneficial effect was very rapid (17). It should be noted that in contrast to EAE in multiple sclerosis, it is not clear whether TNFα suppresses or aggravates the disease (18, 19). Later, we learned that the generation of high antibody titer following administration of targeted DNA vaccines is very rapid because it amplifies an existing autoantibody response that by itself restrains the dynamics of these diseases (7). Finally, we have extended these experiments to cancer, showing that in these diseases anti-chemokine autoantibody production is apparent and could be amplified in a beneficial manner (20). The link between cancer and autoimmunity is that in both types of diseases some chemokines and cytokines are largely expressed at site that are partially segregated from the immune surveillance, as described below.

OUR WORKING HYPOTHESIS

Why are autoantibodies to inflammatory cytokines and chemokines being selectively produced in cancer and autoimmune diseases?

Immune privilege sites were originally believed to be associated with particular organs, which were believed to require superior protection from an excessive inflammatory activity that might cause direct damage to these organs. Key examples are as follows: the testes, brain, the anterior chamber of the eye, and the placenta. It is likely that in these areas the ability of regulatory T cells (T_{reg}) to restrain anti-self-immunity, under inflammatory conditions, is limited. This may explain, in part, the development of bystander autoimmunity following an inflammatory process within "classical" immune privileged sites (21). A newer and more comprehensive interpretation of immune privilege sites suggests that they can be acquired locally in many different tissues in response to self antigens (22). Aside of autoimmune sites this may also include tumor sites, and the tumor-draining lymph nodes (23). Our working hypothesis is that in these sites predominant expression of inflammatory cytokines or chemokines may lead to T-dependent breakdown of tolerance resulting in anti-inflammatory cytokines/chemokines autoantibody production (**Figure 1**).

Although it is tempting to speculate that the generation of these autoantibodies is deterministic, for the benefit of the host, it is more likely that their production is stochastic, and is due to the overexpression of gene products under inflammatory conditions at a site that is partially segregated from immune surveillance. Such conditions may give rise to a selective breakdown of immunological tolerance (24). As a stochastic process, it may also enable the production of autoantibodies that would be harmful to the host, such as anti-SR-A antibodies in systemic lupus erythematosus (25).

ANTI-TNF-α AUTOANTIBODIES IN RA AND PSORIASIS

Rheumatoid arthritis is a systemic autoimmune disease of the joints. Many pro-inflammatory cytokines, including TNFα, IL-1 chemokines, and growth factors, are expressed in diseased joints and have been associated with the development of the inflammatory process resulting in the degeneration of cartilage and erosion of juxta-articular bone (26, 27). In many studies, it has been shown that systemic administration of anti-TNFα antibody or soluble TNFα receptor fusion protein holds a beneficial effect for a major portion of the RA patients, implicating for the pivotal role of this cytokine in the pathogenesis of RA (28). Soluble levels of TNFα receptor showed positive correlation with disease activity in Inflammatory Bowel's disease (29). We identified the appearance of neutralizing autoantibodies to TNFα in the sera of RA patients, but not in sera of those developing osteoarthritis (7). Mapping of the target epitopes they bind revealed three epitopes on TNFα with very low cross reactivity to any known human protein (7). Thus, breakdown of tolerance to TNFα is highly selective and target specific.

Psoriasis is an inflammatory autoimmune disease of the skin. IL-17, TNFα, and IFNα are all key cytokines that promote the development and progression of disease (30–33). IL-17 and his receptor and TNFα are key targets for therapy in this disease (30–33). We could observe a significant titer of anti-TNFα and

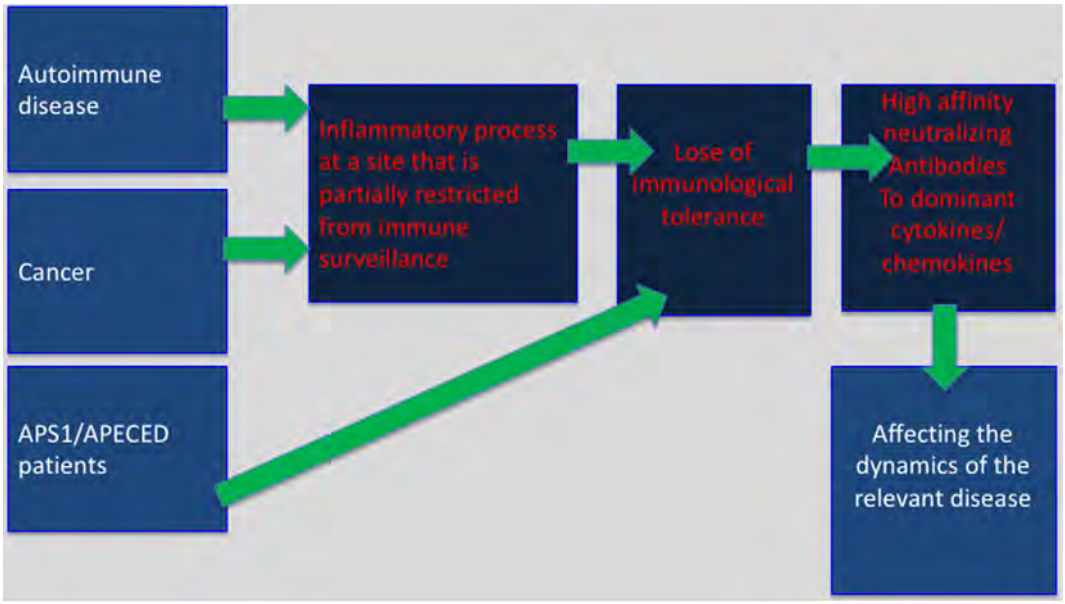

FIGURE 1 | Selective breakdown of B cell tolerance to key inflammatory cytokines/chemokines regulates cancer, autoimmunity and infectious diseases: selective breakdown of tolerance to chemokines and cytokines may result from the generation of an inflammatory process at sites that are partially restricted from immune surveillance (autoimmune sites, tumor sites) or as a results of a deficiency in central tolerance (APS1/APECES patients with autoimmune regulator deficiency). In both, it is believed that breakdown of B cell tolerance follows the breakdown of T cell tolerance. The data obtained from APS1/APECES patients strongly support this hypothesis.

IFN-α in patients with psoriasis compared to healthy subjects and patients with atopic dermatitis (34). These antibodies were found to be neutralizing antibodies. So were anti-TNFα antibodies in RA patients. We, therefore, think that they may possibly participate in the regulation of each disease; albeit in the low titer of their production cannot fully prevent its development and progression.

ANTI-CCL3 AUTOANTIBODIES IN TYPE I DIABETES

Type-1 diabetes mellitus (T1DM) is an organ-specific autoimmune disease resulted from the destruction of the insulin-secreting β-cells in the pancreatic islets of Langerhans (35). In this disease $CD4^+$ and $CD8^+$ T cells, macrophages and perhaps NK cells are required for β-cell destruction (36). The destruction of insulin-producing β-cells is likely to be directed by auto-reactive T cells that recognize several islet β-cells antigens. Among the well-characterized autoantibodies in this disease are as follows: anti-insulin Abs (CIAA), islet cell Abs (ICA), glutamic acid decarboxylase (GAD) 65 and 67 isotypes Abs, heat shock protein 60, and some uncharacterized β-cells antigens (37–39). Currently, the diagnosis of T1DM is based on measuring autoantibodies to GAD, ICA, ICA 512 (IA-2), and insulin (40–47). We have followed potential development of autoantibody titer to many different inflammatory cytokines and chemokines in the sera of T1DM patients and observed a significant autoantibody titer to a single dominant chemokine: CCL3 (48). Independently, Cameron et al. observed in NOD mice predominant expression of intra-pancreatic CCL3 in NOD mice, and along with this that CCR3 ko NOD mice display high resistance to T1DM (49). These results, together with ours may suggest that preferred expression of an inflammatory cytokine/chemokine at an autoimmune site that undergoes a destructive process may induce breakdown of tolerance and generation of autoantibodies to this predominant mediator, and that for anti-CCL3 it might be beneficial for the host.

ANTI-CCL2 AUTOANTIBODIES IN CANCER

The tumor microenvironment is the cellular environment in which the tumor exists. In addition to cancer cells, it includes different cells of either hematopoietic origin, or from mesenchymal origin, and also forms non-cellular components, all of which affect tumor development either due to a direct cross-talk with the tumor, or *via* affecting immune cells functions, within the TEM (50). Cells of the hematopoietic origin consists of cells that arise in the bone marrow and can be subdivided into cells of the lymphoid lineage, consisting of T cells, B cells, and natural killer cells, and those of the myeloid lineage, which includes macrophages, neutrophils, and myeloid-derived suppressor cells (MDSCs). Several studies, including ours, showed that the CCR2–CCL2 axis is critical for the mobilization from the BM to the blood, and later to the tumor site of tumor-associated macrophages to support it development and suppress anti-tumor immunity (20, 51–56). Very recently, we uncovered the mechanism by which "neutrophil like" polymorphonuclear MDSCs

are mobilized from the bone marrow to the blood to support tumor development (57). We have observed in patients suffering from cancer of the prostate the development of a significant antibody titer of neutralizing antibodies to the CC chemokine CCL2 (20). Similarly, in an immunocompetent model of the disease in mice these antibodies were also apparent, and the amplification of their level by a targeted DNA vaccine encoding CCL2 rapidly suppressed the development and progression of disease (20).

What do autoimmune sites and tumor sites have in common? Autoimmune sites, tumor sites, and the tumor-draining lymph nodes are partially immune previlaged, and in easch inflammatory cytokines/chemokins are largely expressed (23). Our working hypothesis is that in these sites predominant expression of inflammatory cytokines or chemokines may lead to T-dependent breakdown of tolerance resulting in anti-inflammatory cytokines/chemokines autoantibody production (**Figure 1**).

SUPPORTING EVIDENCE FOR T-DEPENDENT AUTOANTIBODY PRODUCTION FROM AIRE-DEFICIENT PATIENTS

Mapping of the target determinants to which anti-cytokine/chemokine autoantibodies are produced implicates for a highly restricted response (7). The antibodies that are being produced are mostly of the IgG isotype (IgG1 for human and IgG2a for mouse) (7). Together this implies for a possible T-dependent antibody production. Supporting evidence for T-dependent breakdown of tolerance resulting in neutralizing autoantibody production against cytokines that regulate autoimmunity came form a recent study that analyzes autoantibody production in APS1/APECED patients that due to genetic mutation do not express functional patients' loss of B cell tolerance that appears to be a T-dependent step (9). In the lack of T-dependent central B cell tolerance, these patients display very high-affinity, neutralizing autoantibodies, particularly against specific cytokines. Such antibodies were biologically active *in vitro* and *in vivo* (9). Clear association between the appearance of antibodies to type-1 interferons and T1DM could be observed (9). Based on our previous observations and these findings, we suggest a model in which the expression of inflammatory cytokines at sites that are partially segregated from immune surveillance would induce T-dependent loss of B cell tolerance and generation of neutralizing autoantibodies to these inflammatory mediators that are likely to participate in the regulation of cancer and autoimmunity (**Figure 1**).

Table 1 summarizes the appearance and role of the above anti-cytokine and anti-chemokine autoantibodies in autoimmunity, cancer, and infectious diseases.

THE TRANSLATIONAL ASPECTS OF THESE FINDINGS

We have shown in experimental models that autoantibody production to key inflammatory cytokines/chemokines that is developed during autoimmunity and cancer diseases could be amplified by specific targeted DNA plasmids, and that this could be beneficial for the host (7, 13, 17, 20). Thus, a potential direct therapeutic implication of these studies is the use of plasmid DNA vaccines encoding key inflammatory cytokines/chemokines to which patients display autoantibody response as method to amplify each response and by so doing suppress an ongoing disease. Even though at first glance this approach looks straightforward and promising it holds two major obstacles: the first refers to the ability of plasmid DNA vaccines in human to effectively induce immune response against the gene products they encode. Previous attempts to vaccinate against viruses using plasmid DNA vaccines, even though showed some promising results in animal models (58, 59) could not be successfully extended in human. The other obstacle is the limited ability to control this antibody response once being amplified.

Another translational aspect of these findings is their use for diagnosis of diseases, in particular early diagnosis. We observed in animal models that anti-cytokine/chemokine antibody response is initiated prior to the onset of the autoimmune condition (7). The relevance of these findings in human diseases has yet to be explored. A major limitation in this approach, however, is the specificity of this response. It is hard to believe that an anti-cytokine/chemokine antibody response would be entirely disease specific. A possible way to circumvent this obstacle could by integrating this biomarker with others that could be relevant for a given disease. For example, diagnosis of cancer of the prostate that would include combination of several biomarkers, none of which is highly selective and specific. The

TABLE 1 | The role of autoantibodies to cytokines and chemokines in the pathogenesis of autoimmune, cancer, and infectious diseases.

Autoantibodies	Disease	Suggested role in the regulation of disease	Reference
Anti-CCL2	Prostate cancer	Restrain by inhibiting CCR2+ tumor-associated macrophages accumulation at the tumor site	(20)
Anti-TNFα	Rheumatoid arthritis, Psoriasis	Restrain by blocking TNFα	(7, 34)
Anti-CCL3	Type-1 diabetes	Restrain by blocking CCL3	(48)
Anti-IFN-γ	Type-1 diabetes	Restrain by blocking IFN-γ	(9)
Anti-IFN-α	Psoriasis	Restrain by blocking IFN-α	(34)
Anti-IL-17	Chronic mucocutaneous candidiasis (CMC)	Aggravate by blocking IL-17	(61,62)
Anti-IL-22	CMC	Aggravate by blocking IL-22	(61)

The table summarizes data that are presented and discussed along the manuscript.

most abundant one is the measurement of increased level of blood prostate-specific antigen, but it also has its limitations (60). It is possible that including anti-CCL2 antibody titer, in combination with other biomarkers would assist the identification of high-risk subjects for the development of disease.

Finally, the third translational approach includes the use of B cells from patients that display a significant titer of high-affinity antibodies to given cytokines/chemokines as potential source for the development of human monoclonal antibodies for therapy.

AUTOANTIBODIES TO CYTOKINES AND INFECTIOUS DISEASES

Autoimmune regulator-deficient human and mice were studied for the appearance of autoantibodies to cytokines and chemokines, and if these antibodies may affect the development of infectious diseases. The most significant observations refer to the appearance of autoantibodies to IL-17 or IL-22 and increase susceptibility to chronic mucocutaneous candidiasis (CMC) (61, 62), as these cytokines have a major role in protecting against CMC.

CONCLUSION

In various cancer and autoimmune diseases, patients display selective breakdown of B cell tolerance that is likely to be T-dependent, and results in the generation of high-affinity antibody response to key inflammatory cytokines/chemokines that are predominantly expressed at the autoimmune/cancer site. Even though the underlying mechanism of tolerance breakdown is not fully understood; in some diseases, it is beneficial for the host. The translational implications of these findings may include novel therapeutics, diagnostic, and monoclonal antibodies development strategies.

AUTHOR CONTRIBUTIONS

The author confirms being the sole contributor of this work and approved it for publication.

FUNDING

This study was supported by the Israel Cancer Research Fund (ICRF), and by the Israel Science Foundation (ISF), Colleck Research Fund, and DKFZ-MOST grant.

REFERENCES

1. Gold M, Pul R, Bach JP, Stangel M, Dodel R. Pathogenic and physiological autoantibodies in the central nervous system. *Immunol Rev* (2012) 248(1): 68–86. doi:10.1111/j.1600-065X.2012.01128.x
2. Gabrielli A, Svegliati S, Moroncini G, Avvedimento EV. Pathogenic autoantibodies in systemic sclerosis. *Curr Opin Immunol* (2007) 19(6):640–5. doi:10.1016/j.coi.2007.11.004
3. Heissmeyer V, Ansel KM, Rao A. A plague of autoantibodies. *Nat Immunol* (2005) 6(7):642–4. doi:10.1038/ni1214
4. Fields ML, Erikson J. The regulation of lupus-associated autoantibodies: immunoglobulin transgenic models. *Curr Opin Immunol* (2003) 15(6):709–17. doi:10.1016/j.coi.2003.09.016
5. Schubert D, Schmidt M, Zaiss D, Jungblut PR, Kamradt T. Autoantibodies to GPI and creatine kinase in RA. *Nat Immunol* (2002) 3(5):411; author reply 2–3. doi:10.1038/ni0502-411a
6. Fiebiger E, Stingl G, Maurer D. Anti-IgE and anti-Fc epsilon RI autoantibodies in clinical allergy. *Curr Opin Immunol* (1996) 8(6):784–9. doi:10.1016/S0952-7915(96)80005-7
7. Wildbaum G, Nahir MA, Karin N. Beneficial autoimmunity to proinflammatory mediators restrains the consequences of self-destructive immunity. *Immunity* (2003) 19(5):679–88. doi:10.1016/S1074-7613(03)00291-7
8. Feldmann M, Brennan FM, Foxwell BM, Maini RN. The role of TNF alpha and IL-1 in rheumatoid arthritis. *Curr Dir Autoimmun* (2001) 3:188–99. doi:10.1159/000060522
9. Meyer S, Woodward M, Hertel C, Vlaicu P, Haque Y, Karner J, et al. AIRE-deficient patients harbor unique high-affinity disease-ameliorating autoantibodies. *Cell* (2016) 166(3):582–95. doi:10.1016/j.cell.2016.06.024
10. Mathis D, Benoist C. Back to central tolerance. *Immunity* (2004) 20(5):509–16. doi:10.1016/S1074-7613(04)00111-6
11. Mathis D, Benoist C. Aire. *Annu Rev Immunol* (2009) 27:287–312. doi:10.1146/annurev.immunol.25.022106.141532
12. Klein L, Kyewski B, Allen PM, Hogquist KA. Positive and negative selection of the T cell repertoire: what thymocytes see (and don't see). *Nat Rev Immunol* (2014) 14(6):377–91. doi:10.1038/nri3667
13. Youssef S, Maor G, Wildbaum G, Grabie N, Gour-Lavie A, Karin N. C-C chemokine-encoding DNA vaccines enhance breakdown of tolerance to their gene products and treat ongoing adjuvant arthritis. *J Clin Invest* (2000) 106(3):361–71. doi:10.1172/JCI9109
14. Wildbaum G, Westermann J, Maor G, Karin N. A targeted DNA vaccine encoding fas ligand defines its dual role in the regulation of experimental autoimmune encephalomyelitis. *J Clin Invest* (2000) 106(5):671–9. doi:10.1172/JCI8759
15. Youssef S, Wildbaum G, Karin N. Prevention of experimental autoimmune encephalomyelitis by MIP-1alpha and MCP-1 naked DNA vaccines. *J Autoimmun* (1999) 13(1):21–9. doi:10.1006/jaut.1999.0306
16. Youssef S, Wildbaum G, Maor G, Lanir N, Gour-Lavie A, Grabie N, et al. Long-lasting protective immunity to experimental autoimmune encephalomyelitis following vaccination with naked DNA encoding C-C chemokines. *J Immunol* (1998) 161(8):3870–9.
17. Wildbaum G, Karin N. Augmentation of natural immunity to a pro-inflammatory cytokine (TNF-alpha) by targeted DNA vaccine confers long-lasting resistance to experimental autoimmune encephalomyelitis. *Gene Ther* (1999) 6(6):1128–38. doi:10.1038/sj.gt.3300915
18. Raine CS. Multiple sclerosis: TNF revisited, with promise. *Nat Med* (1995) 1(3):211–4. doi:10.1038/nm0395-211
19. Sicotte NL, Voskuhl RR. Onset of multiple sclerosis associated with anti-TNF therapy. *Neurology* (2001) 57(10):1885–8. doi:10.1212/WNL.57.10.1885
20. Izhak L, Wildbaum G, Weinberg U, Shaked Y, Alami J, Dumont D, et al. Predominant expression of CCL2 at the tumor site of prostate cancer patients directs a selective loss of immunological tolerance to CCL2 that could be amplified in a beneficial manner. *J Immunol* (2010) 184(2):1092–101. doi:10.4049/jimmunol.0902725
21. Vanderlugt CL, Miller SD. Epitope spreading in immune-mediated diseases: implications for immunotherapy. *Nat Rev Immunol* (2002) 2(2):85–95. doi:10.1038/nri724
22. Cobbold SP, Adams E, Graca L, Daley S, Yates S, Paterson A, et al. Immune privilege induced by regulatory T cells in transplantation tolerance. *Immunol Rev* (2006) 213:239–55. doi:10.1111/j.1600-065X.2006.00428.x
23. Munn DH, Mellor AL. The tumor-draining lymph node as an immune-privileged site. *Immunol Rev* (2006) 213:146–58. doi:10.1111/j.1600-065X.2006.00444.x
24. Goodnow CC, Sprent J, de St Groth BF, Vinuesa CG. Cellular and genetic mechanisms of self tolerance and autoimmunity. *Nature* (2005) 435(7042):590–7. doi:10.1038/nature03724

25. Wermeling F, Chen Y, Pikkarainen T, Scheynius A, Winqvist O, Izui S, et al. Class A scavenger receptors regulate tolerance against apoptotic cells, and autoantibodies against these receptors are predictive of systemic lupus. *J Exp Med* (2007) 204(10):2259–65. doi:10.1084/jem.20070600
26. Feldmann M. Translating molecular insights in autoimmunity into effective therapy. *Annu Rev Immunol* (2009) 27:1–27. doi:10.1146/annurev-immunol-082708-100732
27. Feldmann M, Maini RN. Anti-TNF alpha therapy of rheumatoid arthritis: what have we learned? *Annu Rev Immunol* (2001) 19:163–96. doi:10.1146/annurev.immunol.19.1.163
28. Lipsky PE, van der Heijde DM, St Clair EW, Furst DE, Breedveld FC, Kalden JR, et al. Infliximab and methotrexate in the treatment of rheumatoid arthritis. Anti-Tumor Necrosis Factor Trial in Rheumatoid Arthritis with Concomitant Therapy Study Group. *N Engl J Med* (2000) 343(22):1594–602. doi:10.1056/NEJM200011303432202
29. Spoettl T, Hausmann M, Klebl F, Dirmeier A, Klump B, Hoffmann J, et al. Serum soluble TNF receptor I and II levels correlate with disease activity in IBD patients. *Inflamm Bowel Dis* (2007) 13(6):727–32. doi:10.1002/ibd.20107
30. Matos TR, O'Malley JT, Lowry EL, Hamm D, Kirsch IR, Robins HS, et al. Clinically resolved psoriatic lesions contain psoriasis-specific IL-17-producing alphabeta T cell clones. *J Clin Invest* (2017) 127(11):4031–41. doi:10.1172/JCI93396
31. Burkett PR, Kuchroo VK. IL-17 blockade in psoriasis. *Cell* (2016) 167(7):1669. doi:10.1016/j.cell.2016.11.044
32. Garber K. Anti-IL-17 mAbs herald new options in psoriasis. *Nat Biotechnol* (2012) 30(6):475–7. doi:10.1038/nbt0612-475
33. Sladden MJ, Mortimer NJ, Hutchinson PE. Extensive plaque psoriasis successfully treated with adalimumab (Humira). *Br J Dermatol* (2005) 152(5):1091–2. doi:10.1111/j.1365-2133.2005.06582.x
34. Bergman R, Ramon M, Wildbaum G, Avitan-Hersh E, Mayer E, Shemer A, et al. Psoriasis patients generate increased serum levels of autoantibodies to tumor necrosis factor-alpha and interferon-alpha. *J Dermatol Sci* (2009) 56(3):163–7. doi:10.1016/j.jdermsci.2009.08.006
35. Castano L, Eisenbarth GS. Type-I diabetes: a chronic autoimmune disease of human, mouse, and rat. *Annu Rev Immunol* (1990) 8:647–79. doi:10.1146/annurev.iy.08.040190.003243
36. Hutchings P, Rosen H, O'Reilly L, Simpson E, Gordon S, Cooke A. Transfer of diabetes in mice prevented by blockade of adhesion-promoting receptor on macrophages. *Nature* (1990) 348:639–42. doi:10.1038/348639a0
37. Kawasaki E, Takino H, Yano M, Uotani S, Matsumoto K, Takao Y, et al. Autoantibodies to glutamic acid decarboxylase in patients with IDDM and autoimmune thyroid disease. *Diabetes* (1994) 43(1):80–6. doi:10.2337/diab.43.1.80
38. Pleau JM, Fernandez-Saravia F, Esling A, Homo-Delarche F, Dardenne M. Prevention of autoimmune diabetes in nonobese diabetic female mice by treatment with recombinant glutamic acid decarboxylase (GAD 65). *Clin Immunol Immunopathol* (1995) 76(1 Pt 1):90–5. doi:10.1006/clin.1995.1092
39. Rudy G, Brusic V, Harrison LC, Lew AM. Sequence similarity between beta-cell autoantigens [letter]. *Immunol Today* (1995) 16(8):406–7.
40. Atkinson MA. The $64000 question in diabetes continues. *Lancet* (2000) 356(9223):4–6. doi:10.1016/S0140-6736(00)02421-1
41. Lohmann T, Hawa M, Leslie RD, Lane R, Picard J, Londei M. Immune reactivity to glutamic acid decarboxylase 65 in stiffman syndrome and type 1 diabetes mellitus. *Lancet* (2000) 356(9223):31–5. doi:10.1016/S0140-6736(00)02431-4
42. Scofield RH. Autoantibodies as predictors of disease. *Lancet* (2004) 363(9420):1544–6. doi:10.1016/S0140-6736(04)16154-0
43. Sellers E, Eisenbarth G, Young TK, Dean HJ. Diabetes-associated autoantibodies in aboriginal children. *Lancet* (2000) 355(9210):1156. doi:10.1016/S0140-6736(00)02067-5
44. Kaufman DL, Erlander MG, Claire-Salzler M, Atkinson MA, Maclaren NK, Tobin AJ. Autoimmunity to two forms of glutamine decarbosylase in insulin-dependent diabetes mellitus. *J Clin Invest* (1992) 89:283. doi:10.1172/JCI115573
45. Armstrong NW, Jones DB. Epitopes of GAD 65 in insulin-dependent diabetes mellitus. *Lancet* (1994) 344(8919):406–7. doi:10.1016/S0140-6736(94)91432-X
46. Atkinson MA, Bowman MA, Campbell L, Darrow BL, Kaufman DL, Maclaren NK. Cellular immunity to a determinant common to glutamate decarboxylase and coxsackie virus in insulin-dependent diabetes. *J Clin Invest* (1994) 94(5):2125–9. doi:10.1172/JCI117567
47. Schatz D, Krischer J, Horne G, Riley W, Spillar R, Silverstein J, et al. Islet cell antibodies predict insulin-dependent diabetes in United States school age children as powerfully as in unaffected relatives. *J Clin Invest* (1994) 93(6):2403–7. doi:10.1172/JCI117247
48. Shehadeh N, Pollack S, Wildbaum G, Zohar Y, Shafat I, Makhoul R, et al. Selective autoantibody production against CCL3 Is associated with human type 1 diabetes mellitus and serves as a novel biomarker for its diagnosis. *J Immunol* (2009) 182(12):8104–9. doi:10.4049/jimmunol.0803348
49. Cameron MJ, Arreaza GA, Grattan M, Meagher C, Sharif S, Burdick MD, et al. Differential expression of CC chemokines and the CCR5 receptor in the pancreas is associated with progression to type I diabetes. *J Immunol* (2000) 165(2):1102–10. doi:10.4049/jimmunol.165.2.1102
50. Pattabiraman DR, Weinberg RA. Tackling the cancer stem cells – what challenges do they pose? *Nat Rev Drug Discov* (2014) 13(7):497–512. doi:10.1038/nrd4253
51. Serbina NV, Pamer EG. Monocyte emigration from bone marrow during bacterial infection requires signals mediated by chemokine receptor CCR2. *Nat Immunol* (2006) 7(3):311–7. doi:10.1038/ni1309
52. Muller A, Homey B, Soto H, Ge N, Catron D, Buchanan ME, et al. Involvement of chemokine receptors in breast cancer metastasis. *Nature* (2001) 410(6824):50–6. doi:10.1038/35065016
53. Conti I, Rollins BJ. CCL2 (monocyte chemoattractant protein-1) and cancer. *Semin Cancer Biol* (2004) 14(3):149–54. doi:10.1016/j.semcancer.2003.10.009
54. Loberg RD, Day LL, Harwood J, Ying C, St John LN, Giles R, et al. CCL2 is a potent regulator of prostate cancer cell migration and proliferation. *Neoplasia* (2006) 8(7):578–86. doi:10.1593/neo.06280
55. Loberg RD, Ying C, Craig M, Day LL, Sargent E, Neeley C, et al. Targeting CCL2 with systemic delivery of neutralizing antibodies induces prostate cancer tumor regression in vivo. *Cancer Res* (2007) 67(19):9417–24. doi:10.1158/0008-5472.CAN-07-1286
56. Izhak L, Wildbaum G, Jung S, Stein A, Shaked Y, Karin N. Dissecting the autocrine and paracrine roles of the CCR2-CCL2 axis in tumor survival and angiogenesis. *PLoS One* (2012) 7(1):e28305. doi:10.1371/journal.pone.0028305
57. Hawila E, Razon H, Wildbaum G, Blattner C, Sapir Y, Shaked Y, et al. CCR5 directs the mobilization of CD11b(+)Gr1(+)Ly6C(low) polymorphonuclear myeloid cells from the bone marrow to the blood to support tumor development. *Cell Rep* (2017) 21(8):2212–22. doi:10.1016/j.celrep.2017.10.104
58. Sato Y, Roman M, Tighe H, Lee D, Corr M, Nguyen M, et al. Immunostimulatoey DNA sequinces necessery for effective intradermal gene immunization. *Science* (1996) 273:352–7. doi:10.1126/science.273.5273.352
59. Boyer JD, Ugen KE, Wang B, Agadjanyan M, Gilbert L, Bagarazzi ML, et al. Protection of chimpanzees from high-dose heterologous HIV-1 challenge by DNA vaccination [see comments]. *Nat Med* (1997) 3(5):526–32. doi:10.1038/nm0597-526
60. Thompson IM, Pauler DK, Goodman PJ, Tangen CM, Lucia MS, Parnes HL, et al. Prevalence of prostate cancer among men with a prostate-specific antigen level < or =4.0 ng per milliliter. *N Engl J Med* (2004) 350(22):2239–46. doi:10.1056/NEJMoa031918
61. Bichele R, Karner J, Truusalu K, Smidt I, Mandar R, Conti HR, et al. IL-22 neutralizing autoantibodies impair fungal clearance in murine oropharyngeal candidiasis model. *Eur J Immunol* (2018) 48(3):464–70. doi:10.1002/eji.201747209
62. Kisand K, Lilic D, Casanova JL, Peterson P, Meager A, Willcox N. Mucocutaneous candidiasis and autoimmunity against cytokines in APECED and thymoma patients: clinical and pathogenetic implications. *Eur J Immunol* (2011) 41(6):1517–27. doi:10.1002/eji.201041253

Conflict of Interest Statement: The author declares that the research was conducted in the absence of any commercial or financial relationships that could be construed as a potential conflict of interest.

frontiers in Immunology

MINI REVIEW
published: 28 March 2018
doi: 10.3389/fimmu.2018.00485

Atomic Force Microscopy Provides New Mechanistic Insights into the Pathogenesis of Pemphigus

*Franziska Vielmuth, Volker Spindler and Jens Waschke**

Institute of Anatomy, Faculty of Medicine, Ludwig-Maximilians-Universität München, Munich, Germany

Autoantibodies binding to the extracellular domains of desmoglein (Dsg) 3 and 1 are critical in the pathogenesis of pemphigus by mechanisms leading to impaired function of desmosomes and blister formation in the epidermis and mucous membranes. Desmosomes are highly organized protein complexes which provide strong intercellular adhesion. Desmosomal cadherins such as Dsgs, proteins of the cadherin superfamily which interact *via* their extracellular domains in Ca^{2+}-dependent manner, are the transmembrane adhesion molecules clustered within desmosomes. Investigations on pemphigus cover a wide range of experimental approaches including biophysical methods. Especially atomic force microscopy (AFM) has recently been applied increasingly because it allows the analysis of native materials such as cultured cells and tissues under near-physiological conditions. AFM provides information about the mechanical properties of the sample together with detailed interaction analyses of adhesion molecules. With AFM, it was recently demonstrated that autoantibodies directly inhibit Dsg interactions on the surface of living keratinocytes, a phenomenon which has long been considered the main mechanism causing loss of cell cohesion in pemphigus. In addition, AFM allows to study how signaling pathways altered in pemphigus control binding properties of Dsgs. More general, AFM and other biophysical studies recently revealed the importance of keratin filaments for regulation of Dsg binding and keratinocyte mechanical properties. In this mini-review, we reevaluate AFM studies in pemphigus and keratinocyte research, recapitulate what is known about the interaction mechanisms of desmosomal cadherins and discuss the advantages and limitations of AFM in these regards.

Keywords: atomic force microscopy, desmosome, pemphigus, desmosomal cadherin, cell adhesion

OPEN ACCESS

Edited by:
Ralf J. Ludwig,
University of Lübeck, Germany

Reviewed by:
Etienne Dague,
Centre national de la recherche scientifique (CNRS), France
Peter König,
University of Lübeck, Germany

****Correspondence:***
Jens Waschke
jens.waschke@med.unimuenchen.de

Specialty section:
This article was submitted to Immunological Tolerance and Regulation, a section of the journal Frontiers in Immunology

Received: *21 December 2017*
Accepted: *23 February 2018*
Published: *28 March 2018*

Citation:
Vielmuth F, Spindler V and Waschke J (2018) Atomic Force Microscopy Provides New Mechanistic Insights into the Pathogenesis of Pemphigus. Front. Immunol. 9:485. doi: 10.3389/fimmu.2018.00485

INTRODUCTION

Pemphigus with the two main forms pemphigus vulgaris (PV) and pemphigus foliaceus (PF) represents a group of autoimmune blistering skin diseases in which autoantibodies develop primarily against the desmosomal cadherins desmoglein (Dsg) 1 and 3. This leads to weakened keratinocyte cohesion by a vast and yet only partially understood set of mechanisms and in consequence causes intraepidermal splitting (1, 2). Patients suffer from painful blistering affecting skin and mucous membranes, including the risk of infections and nutritive problems (3, 4). A broad range of methods, including functional adhesion assays, molecular biology, and immunological approaches as well as animal models are used study pemphigus pathogenesis (2, 5). The investigation of some mechanisms underlying desmosome dysfunction, e.g., impaired desmosome turnover, requires complex

model systems such as passive IgG transfer in mouse models or ultrastructural analysis of human skin *ex vivo* (6). However, reductionist approaches such as atomic force microscopy (AFM) analysis of Dsg-binding properties and distribution either in cell-free models or 2D keratinocyte cultures yield important information about the effects of autoantibodies on the function of cell adhesion molecules. Moreover, these effects can be analyzed in concert with morphological alterations typical for pemphigus such as keratin filament retraction and changes in overall mechanical properties of keratinocytes. Insights in the mechanisms of desmosomal cadherin interactions and their regulation by intracellular signaling and plaque proteins may provide the molecular basis for targeted therapies in pemphigus. In the following, we will summarize the conclusions that could be drawn from studies utilizing AFM force spectroscopy and elasticity mapping to investigate pemphigus pathogenesis and outline strengths and weaknesses of this experimental approach.

PRINCIPLE OF CELL-FREE AND CELL SURFACE AFM MEASUREMENTS

Atomic force microscopy is used to construct topography maps based on the deflections of a flexible cantilever equipped with a sharp detection tip. Driven by highly accurate piezo steppers, the tip scans a freely definable region of interest while deflection of the cantilever is detected by the displacement of a laser beam on a photodiode (**Figure 1A**). This setup allows the measurement of virtually all kinds of materials. Being a non-optical imaging technique, the resolution is not limited by diffraction of light and reaches a spatial resolution down to 0.5–1 nm (7). Important for the field of basic biology, living cells, e.g., keratinocytes, can be imaged under near-physiological conditions (37°C, medium) without the necessity of fixation (8, 9). Depending on the imaging mode, mechanical properties such as elasticity of the sample can be acquired together with information about the surface topography (10, 11) (**Figure 1B**). The combination of AFM topography and elasticity mapping with force spectroscopy provides an additional set of data that can be extracted from the same scan (**Figure 1B**). In this approach, recombinant adhesion molecules, e.g., the extracellular domains of desmosomal cadherins, are coupled to the AFM tip (**Figures 1C,D**). The tip is repetitively lowered to and retracted from a given surface, e.g., a cell membrane. Scanning with these functionalized tips provides information about the binding partners of the respective molecule, their localization (e.g., position in the membrane) (**Figure 1B**), and a set of biophysical properties of single-molecule interactions, such as binding forces, lifetimes of the respective bonds, and step position (12, 13).

Several methods are established for protein functionalization of AFM cantilevers (14). However, usage of heterobifunctional PEG-linkers is often preferred because it allows coupling of the molecule of interest to the distal end of the linker and ensures a reproducible detection radius throughout the experiments (15). In addition, these linkers allow coupling with a broad range of molecules through amino groups (15). Thus, it is possible to coat full-length extracellular domains of desmosomal cadherins which has been done with his-tagged monomers (**Figure 1C**) (16) as well as with Fc-tagged dimers (**Figure 1D**) (17). The second setup was applied based on experiments using classical cadherins, in which cis-dimerization was thought to be crucial for proper adhesive function (18, 19). However, both approaches showed specific homophilic and heterophilic binding events (16, 20–22). Due to the freely moving linkers, the achievable resolution is reduced to around 50 nm (14) which is suitable for capturing desmosomal cadherin clusters at the surface of living keratinocytes. Importantly, AFM force spectroscopy can be combined with other imaging modalities. These range from conventional and superresolution fluorescence microscopy techniques to electron microscopy and may help to overcome technical limitations, such as non-specificity of adhesion measurements and low imaging speed (23, 24). Together, this highly flexible AFM-based multimodal imaging allows the simultaneous acquisition of a wide range of different parameters.

For characterization of binding properties of desmosomal cadherins often cell-free approaches are used in which recombinant proteins are immobilized not only on the scanning tip but also on the surface of, e.g., a silicon nitrite mica-sheet (25). This reductionist model allows unequivocal evaluation of binding partners and forces because the possible interaction partners are clearly defined (**Figure 1E**). By contrast, keratinocytes express several isoforms of desmosomal cadherins (**Figure 1F**) which hinders a clear identification of interaction partners. Moreover, cell monolayers are more complicated to handle because of the necessity of measurements under near-physiological conditions, including temperature control and application of media to avoid starving (8). The continuous reorganization and morphological changes of the monolayer limit lateral resolution and are challenging because of the time necessary for AFM measurements (14). On the other side, the increased complexity by application of living cells has numerous advantages and adds novel possibilities to characterize desmosomal adhesion. Changes of cell topography and mechanical properties can be monitored in response to manipulation of signaling pathways or genetic depletion of specific proteins (26–28). In addition, alterations in the localization of Dsg clusters at the surface of living keratinocytes, their mobility (20, 29), and the binding properties can be elucidated (20, 30). *Vice versa*, changes in cell behavior or intracellular signaling activity can be detected following AFM-based manipulation such as indentation of the membrane or severing of cytoskeletal components (31, 32).

AFM TO ELUCIDATE Dsg-BINDING PARTNERS AND TO STUDY THE EFFECTS OF AUTOANTIBODIES

Desmogleins and desmocollins have been shown to bind both in homophilic- and heterophilic fashion under cell-free conditions (17, 33, 34). By cell-free single-molecule AFM force spectroscopy using recombinant Fc-dimers of the entire extracellular domain, we found that Dsg1, Dsg2, Dsg3, and Dsc3 can interact homophilically. Importantly, these homophilic interactions were blocked by both EGTA treatment as

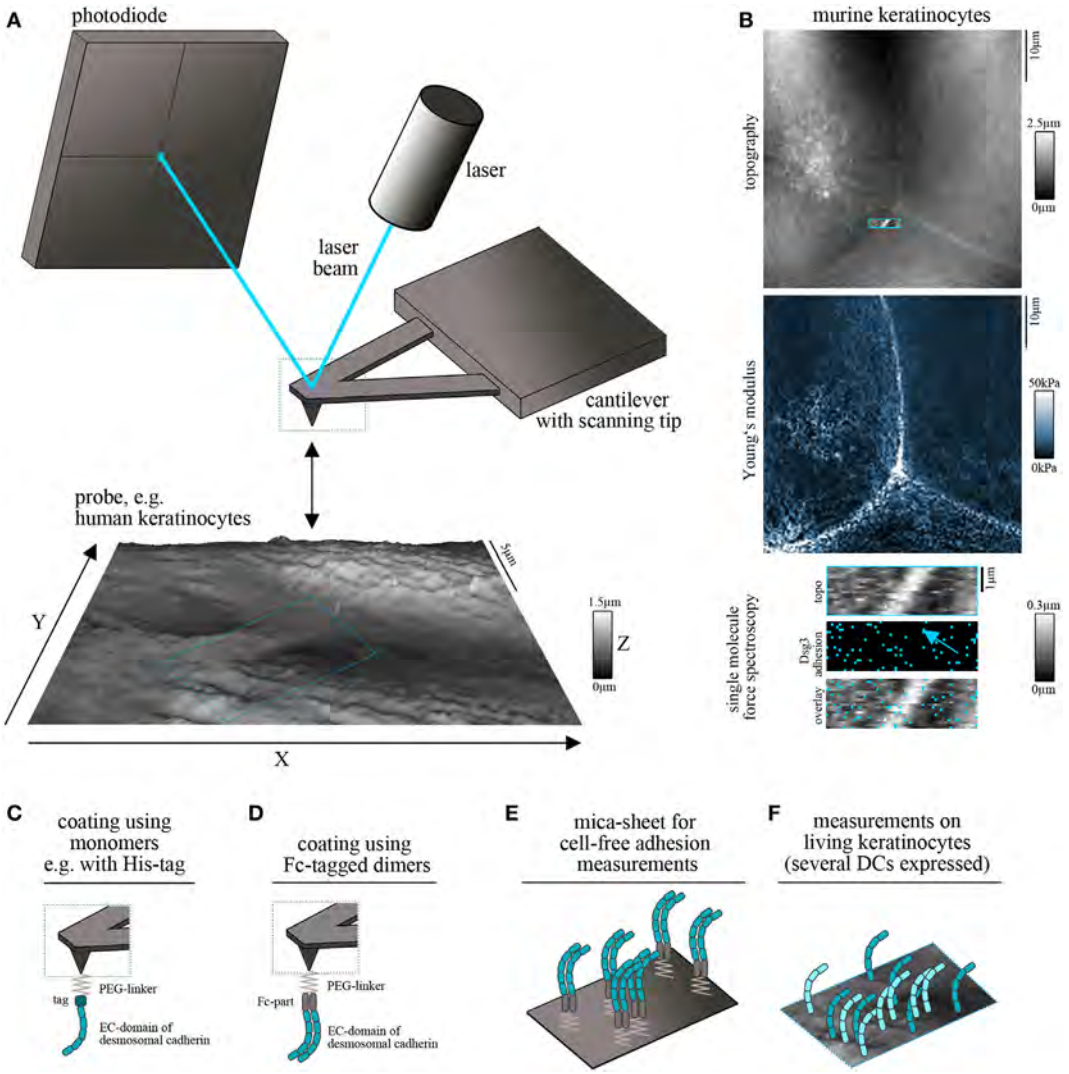

FIGURE 1 | Atomic force microscopy (AFM) setup for cadherin binding studies. **(A)** Schematic of an AFM setup. A flexible cantilever equipped with a sharp tip is repetitively lowered to and retracted from the surface of the probe. Deflection of the cantilever while contacting the surface is detected by a laser pointed on the cantilever and provides information about surface topography and mechanical properties. **(B)** Example for simultaneous measurement of topography (with elevated cell borders and filamental structures on the cell surface), elasticity (Young's modulus) and Dsg3 adhesion map (with each blue pixel represents on Dsg3-dependent binding event, arrow points on the cell border) on living murine keratinocytes. **(C,D)** To study single-molecule interaction tips can be functionalized with recombinant adhesion molecules using PEG-linkers. For desmosomal cadherins coating was conducted using full-length extracellular domains as either monomers **(C)** or Fc-tagged dimers **(D)**. **(E)** Probe setup for cell-free measurements on mica sheets coated with Fc-tagged dimers of desmosomal cadherin extracellular domains. **(F)** Probe setup for measurements on living keratinocytes. Cells express several desmosomal cadherin isoforms on their cell surface.

well as incubation with specific antibodies (16, 20, 21, 35, 36). As another indication for specific homophilic interactions, the bond rupture forces increased with the applied loading rate similar to classical cadherins (18, 37–39). Corresponding lifetimes were delineated at $\tau_0 \approx 0.17$ for Dsg1, $\tau_0 \approx 0.31$ for Dsg3, and $\tau_0 \approx 0.24$s for Dsc3 in cell-free AFM experiments and $\tau_0 \approx 0.31$ for Dsg3-dependent binding events on murine keratinocytes (20, 29, 35, 36) which were significantly lower than detected for classical cadherins (18, 37). Homophilic interactions of Dsc2 but not Dsg2 monomers were also observed recently (16). With regard to heterophilic interactions, binding of Dsg2 to Dsc2 and Dsg3 was observed by AFM as well as interactions between Dsg1 and Dsc3 (16, 20, 35). In a systematic approach, only heterophilic interactions of Dsgs and desmocollins were found by surface plasmon resonance measurements although homophilic interactions were observed when high concentrations of molecules were applied, which allowed to determine the crystal structure of two interacting Dsg2 molecules (40). The reasons for these in part contradictory *in vitro* findings are unclear yet. Nevertheless, in living keratinocytes, homophilic interactions appear to be a primary mode of interaction as revealed by extracellular cross-linking (41). In line with this, we detected primarily homophilic interactions of Dsg3 on the surface of living keratinocytes (20, 29).

Atomic force microscopy was further used to study the effects of pemphigus autoantibodies on Dsg binding. To be pathogenic and result in loss of cell cohesion, autoantibodies would either need to block Dsg interactions or lead to reorganization and internalization of Dsg molecules (**Figure 2A**). In the first concept, autoantibodies may sterically hinder interaction by preferentially targeting the adhesive EC1 domain of Dsgs or allosterically lead to conformational changes of the adhesive interface. These modes of interactions may be summarized as direct inhibition (**Figure 2A**). Release of Dsgs from desmosomes

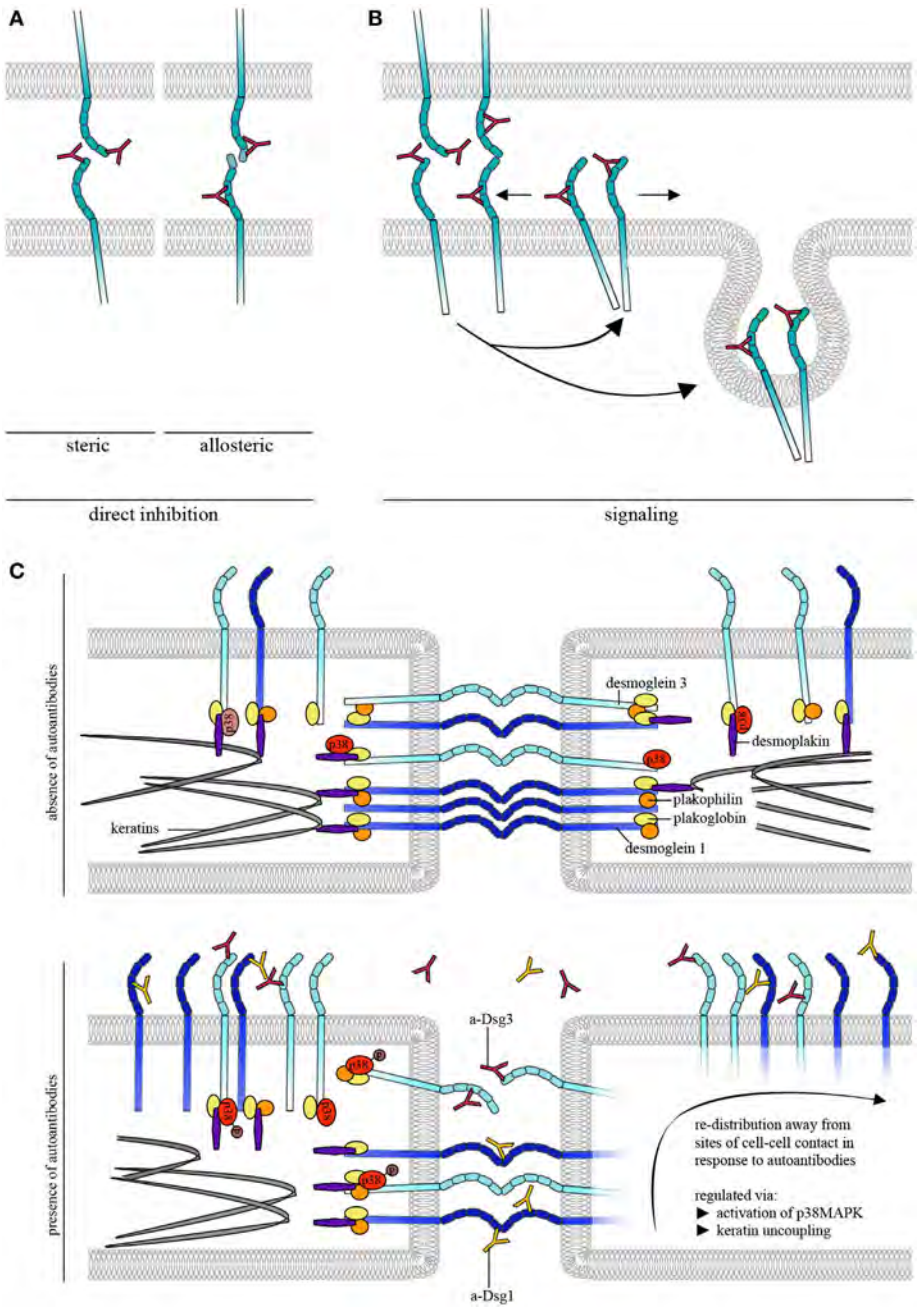

FIGURE 2 | Autoantibody effects on desmosomal cadherin binding properties. **(A)** To cause direct inhibition of desmoglein (Dsg)-binding autoantibodies may either sterically hinder desmosomal cadherin interaction by preferentially targeting the adhesive EC1 domain or allosterically lead to conformational changes, which also may involve the adhesive interface. **(B)** Autoantibodies induce intracellular signaling leading to reorganization and internalization of Dsg molecules. **(C)** Schematic of autoantibody effects on desmosomal cadherin distribution. For simplification, only Dsgs are shown. Under control conditions, Dsg3 is uniformly distributed over the cell surface whereas Dsg1 shows dense clustering along cell–cell contacts. Binding of pathogenic autoantibodies causes direct inhibition of Dsg3 but not of Dsg1 interactions. For both, Dsg1 and 3, binding of autoantibodies induces redistribution of binding events away from cell–cell contact sites, a process that is likely regulated through by keratin uncoupling and activation of p38MAPK.

and endocytosis would require additional cellular mechanisms and intracellular signaling (**Figure 2B**). For instance, it is possible that extradesmosomal molecules serve as scaffolds which, dependent on autoantibody binding modulate signaling pathways and, thus, influence the composition and turnover of desmosomes. We sought to apply pemphigus autoantibodies in cell-free AFM in order to demonstrate direct inhibition of Dsg binding which represented the most likely mechanism of antibody action (42). However, we were surprised that PF-IgG did not directly interfere with Dsg1 binding (17). Meanwhile, using various IgG fractions of both PF-IgG and PV-IgG, we were not able to detect direct inhibition of Dsg1 interaction, both in cell-free and in cell-based measurements (34, 43, 44). By contrast, in all experiments using PV-IgG or the monoclonal Dsg3-specific antibody AK23 derived from a pemphigus mouse model (45) direct inhibition of Dsg3 binding was demonstrated (26, 34, 43, 44, 46). Thus, these data do not rule out that some autoantibodies targeting Dsg1 may occur which also cause steric hindrance, especially since some antibodies isolated from patients by phage display have been shown to interact with both Dsg1 and Dsg3 (47). However, the amount of these appears to be low if present in IgG fractions of many patients.

Atomic force microscopy studies also showed that a Dsg-specific tandem peptide designed to cross-link interacting Dsgs was effective to abrogate PV-IgG- and AK23-induced loss of keratinocyte cohesion in culture and in living mice indicating that direct inhibition of Dsg3 binding contributes to blister formation (46, 48). However, since the peptide approach also abolished activation of pathogenic signaling pathways such as p38MAPK and pharmacologic inhibition of p38MAPK was effective to override autoantibody-induced loss of cell adhesion in the presence of autoantibodies directly inhibiting Dsg3 interaction, steric hindrance alone appears not to be sufficient to cause full loss of keratinocyte cohesion (26, 48). It has to be noted that a limitation of AFM interaction studies is that recombinant Dsg molecules attached to the AFM probe primarily will interact with extradesmosomal Dsg rather than Dsg1 and 3 in the core of desmosomes. This means that AFM studies cannot definitely prove that PV-IgG and AK23 are directly inhibiting the interaction of Dsg3 molecules inside of desmosomes. Nevertheless, because it was shown by immune-electron microscopy that the IgG-variant but not the IgM-variant of AK23 accessed the desmosomal core (49), it is likely that direct inhibition of Dsg3 binding in pemphigus also occurs in desmosomes and thereby contributes to desmosome dysfunction (6).

AFM TO QUANTIFY ALTERATIONS OF KERATINOCYTE ELASTICITY AND CYTOSKELETAL REORGANIZATION IN RESPONSE TO AUTOANTIBODIES

The cytoskeleton of eukaryotic cells comprises actin filaments, intermediate filaments, and microtubules. Keratin filaments, the intermediate filaments in cells of epithelial origin anchoring desmosomes, are pronouncedly affected in pemphigus. The so called "keratin retraction" describes the uncoupling of keratin filaments from desmosomes and the clustering around the nucleus. By AFM, keratin filaments can be visualized as stiff bundles underneath the membrane in the cell periphery inserting perpendicular to areas of cell–cell contact into desmosomes (26, 28). Interestingly, changes in the peripheral keratin network occur very rapidly within 1 h after autoantibody incubation and appear to even precede Dsg3 endocytosis, another hallmark of pemphigus (26, 50). Here, the first visible alteration is a reduced amount of keratin filaments in the basal part of the cell near areas of cell–cell contact, a region implicated in assembly of keratin filaments (51).[1] Furthermore, as demonstrated by AFM elasticity mapping and optical stretching, keratin filaments in contrast to the actin cytoskeleton are the main constituents responsible for keratinocyte stiffness (52–54). In line with these data and the observations that keratin filaments are rapidly altered upon application or pemphigus autoantibodies, elasticity changes in response to autoantibody binding were described (31). By probing the membrane above the nucleus, a rapid reduction in cellular stiffness was observed within minutes followed by an increase after several hours, the latter of which may be a result of keratin clustering around the nucleus. Nevertheless, it is unclear whether these changes are mainly a result of keratin reorganization or whether other mechanisms contribute, as these changes were related to FasL-dependent apoptotic signaling (31).

The actin cytoskeleton is also severely altered by autoantibody binding (55, 56). Strengthening of the cortical actin meshwork prevented autoantibody-induced loss of cell cohesion in keratinocytes, indicating a contribution of actin reorganization to epidermal blistering (57). In principle, the actin meshwork underneath the membrane is accessible for AFM-based imaging (58–60), albeit with reduced resolution compared to approaches involving a membrane "deroofing" step or inside-out measurements of membrane patches (61, 62). By AFM, the differentiation between the cortical actin and other cytoskeletal components is barely possible, especially because a cortical keratin filament meshwork may exist (63). Nevertheless, the observation that the delicate mesh pattern of the membrane of murine keratinocytes appears similar in cells with and without expression of keratin filaments indicates that these structures represent the cortical actin cytoskeleton (20). If and in which timeframe specific changes of the cortical actin cytoskeleton can be detected by AFM imaging remains to be elucidated.

STUDIES ON Dsg DISTRIBUTION PATTERNS AND BINDING PROPERTIES MODULATED BY PEMPHIGUS ANTIBODIES

In keratinocytes, Dsg3 and 1 are differentiation-dependently localized at sites of cell–cell junctions (64, 65). Interestingly, AFM

[1]Schlögl E, Radeva M, Vielmuth F, Schinner C, Waschke J, Spindler V. (under review). Keratin retraction and Dsg3 internalization independently contribute to autoantibody-induced cell dissociation in pemphigus vulgaris. Submitted to Immunology.

measurements showed that Dsg3 binding events are uniformly distributed on the surface of living keratinocytes (29) (**Figure 2C**). This could be related to Dsg3 molecules that are detectable away from junctions and referred to as extradesmosomal (30, 66, 67). Thus, molecules detected close to cell–cell junctions may be extradesmosomal, located in desmosomal precursors or located at the edge of the desmosomal core, as the "center" of the tightly packed desmosomes is most likely not accessible for the AFM scanning tip. Nevertheless, these molecules differ with regard to their binding properties. Molecules at cell–cell junctions reveal higher binding forces compared to molecules on the cell surface above the nucleus (29). By contrast, Dsg1 binding events are not distributed uniformly but rather show higher binding frequencies along cell–cell junctions, indicating that clustering of Dsgs differs between isoforms (44, **Figure 2C**). In this context, keratins not only regulate cell mechanics (53, 54) but also differentially regulate Dsg-binding properties. For example, keratins are crucial for maintenance of Dsg3 binding strength as well as for distribution of Dsg1 at cell junctions (20, 44).

Binding of pemphigus autoantibodies to the extracellular domains of Dsg1 and 3 on the surface of living keratinocytes was shown to induce altered clustering of the targeted molecules (68–70). Using AFM, redistribution of Dsg1 binding events away from cell junctions occurred after treatment with pemphigus IgG fractions containing a-Dsg1 antibodies which may explain the structural changes described above (44). Dsg1 redistribution seems to be dependent on uncoupling from the keratin filaments which is a common phenomenon after treatment with pathogenic autoantibodies and precedes reduction of Dsg1 binding strength (**Figure 2C**) (44, 48, 55). Due to direct inhibition of Dsg3 interaction, redistribution of Dsg3 molecules could not be evaluated after autoantibody treatment (26, 34). However, modulation of signaling pathways such as p38MAPK was used to mimic some effects of pemphigus autoantibodies on Dsg3 binding properties. p38MAPK is a central signaling molecule in pemphigus which is activated by binding of autoantibodies and was demonstrated to form a signaling complex containing Dsg3 and Dsc3 (71). Furthermore, activation of p38MAPK has been linked to keratin retraction and Dsg internalization whereas inhibition of p38MAPK prevented loss of intercellular adhesion (**Figure 2C**) (55, 66, 71–73). Interestingly, activation of p38MAPK led to keratin retraction and redistribution of Dsg1 and 3 binding events away from junctions indicating that p38MAPK signaling participates in the regulation of Dsg clustering (**Figure 2C**) (44). Furthermore, inhibition of p38MAPK prevented autoantibody-induced redistribution of Dsg1 binding events and restored Dsg3 binding strength under conditions where keratinocytes were depleted from keratins (20, 44) indicating that Dsg-binding properties are strongly dependent on p38MAPK. Taken together, AFM adds important information on molecule distribution and binding properties of Dsgs after autoantibody incubation.

CONCLUSION

Atomic force microscopy complements a broad range of methods in pemphigus research. Under cell-free conditions, AFM enables characterization of single-molecule desmocadherin interactions with and without the presence of pemphigus autoantibodies. When applied on living keratinocytes, this can be complemented by monitoring cytoskeletal alterations. So far, AFM is the only technique with which direct inhibition of Dsg interactions by pemphigus autoantibody binding was detected on the single-molecule level. Furthermore, it provides insights into alterations of keratinocyte properties. Although interaction partners on living cells cannot be completely identified and temporal resolution is low compared to other live-cell imaging approaches, investigation of Dsg mobility and redistribution in response to autoantibodies may add important information about the underlying mechanisms of loss of cell cohesion in pemphigus. Similarly, combination of Bio-AFM with high-resolution imaging techniques such as STED microscopy may elucidate whether alterations of Dsg binding properties in response to autoantibody binding maybe mediated by different association with signaling molecules and plaque proteins.

AUTHOR CONTRIBUTIONS

FV, VS, and JW designed the review, evaluated the literature, and wrote the manuscript.

ACKNOWLEDGMENTS

We thank the members of our group for fruitful discussion.

FUNDING

Supported by DFG FOR 2497 to JW.

REFERENCES

1. Kasperkiewicz M, Ellebrecht CT, Takahashi H, Yamagami J, Zillikens D, Payne AS, et al. Pemphigus. *Nat Rev Dis Primers* (2017) 3:17026. doi:10.1038/nrdp.2017.26
2. Spindler V, Eming R, Schmidt E, Amagai M, Grando S, Jonkman MF, et al. Mechanisms causing loss of keratinocyte cohesion in pemphigus. *J Invest Dermatol* (2018) 138(1):32–37. doi:10.1016/j.jid.2017.06.022
3. Kneisel A, Hertl M. Autoimmune Bullous skin diseases. Part 2: diagnosis and therapy. *J Dtsch Dermatol Ges* (2011) 9(11):927–47. doi:10.1111/j.1610-0387.2011.07809.x
4. Kneisel A, Hertl M. Autoimmune Bullous skin diseases. Part 1: clinical manifestations. *J Dtsch Dermatol Ges* (2011) 9(10):844–56; quiz 57. doi:10.1111/j.1610-0387.2011.07793.x
5. Pollmann R, Eming R. Research techniques made simple: mouse models of autoimmune blistering diseases. *J Invest Dermatol* (2017) 137(1):e1–6. doi:10.1016/j.jid.2016.11.003
6. Spindler V, Waschke J. Pemphigus – a disease of desmosome dysfunction caused by multiple mechanisms. *Front Immunol* (2018) 9:136. doi:10.3389/fimmu.2018.00136
7. Li M, Dang D, Xi N, Wang Y, Liu L. Nanoscale imaging and force probing of biomolecular systems using atomic force microscopy: from single molecules to living cells. *Nanoscale* (2017) 9(45):17643–66. doi:10.1039/c7nr07023c
8. Allison DP, Mortensen NP, Sullivan CJ, Doktycz MJ. Atomic force microscopy of biological samples. *Wiley Interdiscip Rev Nanomed Nanobiotechnol* (2010) 2(6):618–34. doi:10.1002/wnan.104
9. Parot P, Dufrene YF, Hinterdorfer P, Le Grimellec C, Navajas D, Pellequer JL, et al. Past, present and future of atomic force microscopy in life

sciences and medicine. *J Mol Recognit* (2007) 20(6):418–31. doi:10.1002/jmr.857
10. Alonso JL, Goldmann WH. Feeling the forces: atomic force microscopy in cell biology. *Life Sci* (2003) 72(23):2553–60. doi:10.1016/S0024-3205(03)00165-6
11. Zlatanova J, Lindsay SM, Leuba SH. Single molecule force spectroscopy in biology using the atomic force microscope. *Prog Biophys Mol Biol* (2000) 74(1–2):37–61. doi:10.1016/S0079-6107(00)00014-6
12. Muller DJ, Sapra KT, Scheuring S, Kedrov A, Frederix PL, Fotiadis D, et al. Single-molecule studies of membrane proteins. *Curr Opin Struct Biol* (2006) 16(4):489–95. doi:10.1016/j.sbi.2006.06.001
13. Sariisik E, Popov C, Muller JP, Docheva D, Clausen-Schaumann H, Benoit M. Decoding cytoskeleton-anchored and non-anchored receptors from single-cell adhesion force data. *Biophys J* (2015) 109(7):1330–3. doi:10.1016/j.bpj.2015.07.048
14. Chtcheglova LA, Hinterdorfer P. Simultaneous AFM topography and recognition imaging at the plasma membrane of mammalian cells. *Semin Cell Dev Biol* (2017). doi:10.1016/j.semcdb.2017.08.025
15. Ebner A, Wildling L, Kamruzzahan AS, Rankl C, Wruss J, Hahn CD, et al. A new, simple method for linking of antibodies to atomic force microscopy tips. *Bioconjug Chem* (2007) 18(4):1176–84. doi:10.1021/bc070030s
16. Lowndes M, Rakshit S, Shafraz O, Borghi N, Harmon R, Green K, et al. Different roles of cadherins in the assembly and structural integrity of the desmosome complex. *J Cell Sci* (2014) 127(Pt 10):2339–50. doi:10.1242/jcs.146316
17. Waschke J, Bruggeman P, Baumgartner W, Zillikens D, Drenckhahn D. Pemphigus foliaceus IgG causes dissociation of desmoglein 1-containing junctions without blocking desmoglein 1 transinteraction. *J Clin Invest* (2005) 115(11):3157–65. doi:10.1172/JCI23475
18. Baumgartner W, Hinterdorfer P, Ness W, Raab A, Vestweber D, Schindler H, et al. Cadherin interaction probed by atomic force microscopy. *Proc Natl Acad Sci U S A* (2000) 97(8):4005–10. doi:10.1073/pnas.070052697
19. Priest AV, Shafraz O, Sivasankar S. Biophysical basis of cadherin mediated cell-cell adhesion. *Exp Cell Res* (2017) 358(1):10–3. doi:10.1016/j.yexcr.2017.03.015
20. Vielmuth F, Wanuske MT, Radeva MY, Hiermaier M, Kugelmann D, Walter E, et al. Keratins regulate the adhesive properties of desmosomal cadherins through signaling. *J Invest Dermatol* (2018) 138(1):121–31. doi:10.1016/j.jid.2017.08.033
21. Schlegel N, Meir M, Heupel WM, Holthofer B, Leube RE, Waschke J. Desmoglein 2-mediated adhesion is required for intestinal epithelial barrier integrity. *Am J Physiol Gastrointest Liver Physiol* (2010) 298(5):G774–83. doi:10.1152/ajpgi.00239.2009
22. Dieding M, Debus JD, Kerkhoff R, Gaertner-Rommel A, Walhorn V, Milting H, et al. Arrhythmogenic cardiomyopathy related DSG2 mutations affect desmosomal cadherin binding kinetics. *Sci Rep* (2017) 7(1):13791. doi:10.1038/s41598-017-13737-x
23. Zhou L, Cai M, Tong T, Wang H. Progress in the correlative atomic force microscopy and optical microscopy. *Sensors (Basel)* (2017) 17(4):E938. doi:10.3390/s17040938
24. Hauser M, Wojcik M, Kim D, Mahmoudi M, Li W, Xu K. Correlative super-resolution microscopy: new dimensions and new opportunities. *Chem Rev* (2017) 117(11):7428–56. doi:10.1021/acs.chemrev.6b00604
25. Wagner P. Immobilization strategies for biological scanning probe microscopy. *FEBS Lett* (1998) 430(1–2):112–5. doi:10.1016/S0014-5793(98)00614-0
26. Vielmuth F, Waschke J, Spindler V. Loss of desmoglein binding is not sufficient for keratinocyte dissociation in pemphigus. *J Invest Dermatol* (2015) 135(12):3068–77. doi:10.1038/jid.2015.324
27. Fung CK, Seiffert-Sinha K, Lai KW, Yang R, Panyard D, Zhang J, et al. Investigation of human keratinocyte cell adhesion using atomic force microscopy. *Nanomedicine* (2010) 6(1):191–200. doi:10.1016/j.nano.2009.05.008
28. Fung CK, Xi N, Yang R, Seiffert-Sinha K, Lai KW, Sinha AA. Quantitative analysis of human keratinocyte cell elasticity using atomic force microscopy (AFM). *IEEE Trans Nanobioscience* (2011) 10(1):9–15. doi:10.1109/TNB.2011.2113397
29. Vielmuth F, Hartlieb E, Kugelmann D, Waschke J, Spindler V. Atomic force microscopy identifies regions of distinct desmoglein 3 adhesive properties on living keratinocytes. *Nanomedicine* (2015) 11(3):511–20. doi:10.1016/j.nano.2014.10.006
30. Waschke J, Spindler V. Desmosomes and extradesmosomal adhesive signaling contacts in pemphigus. *Med Res Rev* (2014) 34(6):1127–45. doi:10.1002/med.21310
31. Seiffert-Sinha K, Yang R, Fung CK, Lai KW, Patterson KC, Payne AS, et al. Nanorobotic investigation identifies novel visual, structural and functional correlates of autoimmune pathology in a blistering skin disease model. *PLoS One* (2014) 9(9):e106895. doi:10.1371/journal.pone.0106895
32. Muller DJ. AFM: a nanotool in membrane biology. *Biochemistry* (2008) 47(31):7986–98. doi:10.1021/bi800753x
33. Amagai M, Karpati S, Klaus-Kovtun V, Udey MC, Stanley JR. Extracellular domain of pemphigus vulgaris antigen (desmoglein 3) mediates weak homophilic adhesion. *J Invest Dermatol* (1994) 103(4):609–15. doi:10.1111/1523-1747.ep12397292
34. Heupel WM, Zillikens D, Drenckhahn D, Waschke J. Pemphigus vulgaris IgG directly inhibit desmoglein 3-mediated transinteraction. *J Immunol* (2008) 181(3):1825–34. doi:10.4049/jimmunol.181.3.1825
35. Spindler V, Heupel WM, Efthymiadis A, Schmidt E, Eming R, Rankl C, et al. Desmocollin 3-mediated binding is crucial for keratinocyte cohesion and is impaired in pemphigus. *J Biol Chem* (2009) 284(44):30556–64. doi:10.1074/jbc.M109.024810
36. Waschke J, Menendez-Castro C, Bruggeman P, Koob R, Amagai M, Gruber HJ, et al. Imaging and force spectroscopy on desmoglein 1 using atomic force microscopy reveal multivalent $Ca^{(2+)}$-dependent, low-affinity trans-interaction. *J Membr Biol* (2007) 216(2–3):83–92. doi:10.1007/s00232-007-9037-9
37. Baumgartner W, Golenhofen N, Grundhofer N, Wiegand J, Drenckhahn D. Ca^{2+} dependency of N-cadherin function probed by laser tweezer and atomic force microscopy. *J Neurosci* (2003) 23(35):11008–14.
38. Bell GI. Models for the specific adhesion of cells to cells. *Science* (1978) 200(4342):618–27. doi:10.1126/science.347575
39. Evans E, Ritchie K. Dynamic strength of molecular adhesion bonds. *Biophys J* (1997) 72(4):1541–55. doi:10.1016/S0006-3495(97)78802-7
40. Harrison OJ, Brasch J, Lasso G, Katsamba PS, Ahlsen G, Honig B, et al. Structural basis of adhesive binding by desmocollins and desmogleins. *Proc Natl Acad Sci U S A* (2016) 113(26):7160–5. doi:10.1073/pnas.1606272113
41. Nie Z, Merritt A, Rouhi-Parkouhi M, Tabernero L, Garrod D. Membrane-impermeable cross-linking provides evidence for homophilic, isoform-specific binding of desmosomal cadherins in epithelial cells. *J Biol Chem* (2011) 286(3):2143–54. doi:10.1074/jbc.M110.192245
42. Amagai M, Klaus-Kovtun V, Stanley JR. Autoantibodies against a novel epithelial cadherin in pemphigus vulgaris, a disease of cell adhesion. *Cell* (1991) 67(5):869–77. doi:10.1016/0092-8674(91)90360-B
43. Walter E, Vielmuth F, Rotkopf L, Sardy M, Horvath ON, Goebeler M, et al. Different signaling patterns contribute to loss of keratinocyte cohesion dependent on autoantibody profile in pemphigus. *Sci Rep* (2017) 7(1):3579. doi:10.1038/s41598-017-03697-7
44. Vielmuth F, Walter E, Fuchs M, Radeva M, Buechau F, Magin TM, et al. Keratins regulate p38MAPK-dependent desmoglein binding properties in pemphigus. *Front Immunol* (2018). doi:10.3389/fimmu.2018.00528
45. Tsunoda K, Ota T, Aoki M, Yamada T, Nagai T, Nakagawa T, et al. Induction of pemphigus phenotype by a mouse monoclonal antibody against the amino-terminal adhesive interface of desmoglein 3. *J Immunol* (2003) 170(4):2170–8. doi:10.4049/jimmunol.170.4.2170
46. Heupel WM, Muller T, Efthymiadis A, Schmidt E, Drenckhahn D, Waschke J. Peptides targeting the desmoglein 3 adhesive interface prevent autoantibody-induced acantholysis in pemphigus. *J Biol Chem* (2009) 284(13):8589–95. doi:10.1074/jbc.M808813200
47. Payne AS, Ishii K, Kacir S, Lin C, Li H, Hanakawa Y, et al. Genetic and functional characterization of human pemphigus vulgaris monoclonal autoantibodies isolated by phage display. *J Clin Invest* (2005) 115(4):888–99. doi:10.1172/JCI24185
48. Spindler V, Rotzer V, Dehner C, Kempf B, Gliem M, Radeva M, et al. Peptide-mediated desmoglein 3 crosslinking prevents pemphigus vulgaris autoantibody-induced skin blistering. *J Clin Invest* (2013) 123(2):800–11. doi:10.1172/JCI60139
49. Tsunoda K, Ota T, Saito M, Hata T, Shimizu A, Ishiko A, et al. Pathogenic relevance of IgG and IgM antibodies against desmoglein 3 in blister formation in pemphigus vulgaris. *Am J Pathol* (2011) 179(2):795–806. doi:10.1016/j.ajpath.2011.04.015
50. Jennings JM, Tucker DK, Kottke MD, Saito M, Delva E, Hanakawa Y, et al. Desmosome disassembly in response to pemphigus vulgaris IgG occurs in distinct phases and can be reversed by expression of exogenous Dsg3. *J Invest Dermatol* (2011) 131(3):706–18. doi:10.1038/jid.2010.389

51. Windoffer R, Beil M, Magin TM, Leube RE. Cytoskeleton in motion: the dynamics of keratin intermediate filaments in epithelia. *J Cell Biol* (2011) 194(5):669–78. doi:10.1083/jcb.201008095
52. Seltmann K, Fritsch AW, Kas JA, Magin TM. Keratins significantly contribute to cell stiffness and impact invasive behavior. *Proc Natl Acad Sci U S A* (2013) 110(46):18507–12. doi:10.1073/pnas.1310493110
53. Ramms L, Fabris G, Windoffer R, Schwarz N, Springer R, Zhou C, et al. Keratins as the main component for the mechanical integrity of keratinocytes. *Proc Natl Acad Sci U S A* (2013) 110(46):18513–8. doi:10.1073/pnas.1313491110
54. Broussard JA, Yang R, Huang C, Nathamgari SSP, Beese AM, Godsel LM, et al. The desmoplakin-intermediate filament linkage regulates cell mechanics. *Mol Biol Cell* (2017) 28(23):3156–64. doi:10.1091/mbc.E16-07-0520
55. Berkowitz P, Hu P, Liu Z, Diaz LA, Enghild JJ, Chua MP, et al. Desmosome signaling. Inhibition of p38MAPK prevents pemphigus vulgaris IgG-induced cytoskeleton reorganization. *J Biol Chem* (2005) 280(25):23778–84. doi:10.1074/jbc.M501365200
56. Waschke J, Spindler V, Bruggeman P, Zillikens D, Schmidt G, Drenckhahn D. Inhibition of Rho A activity causes pemphigus skin blistering. *J Cell Biol* (2006) 175(5):721–7. doi:10.1083/jcb.200605125
57. Gliem M, Heupel WM, Spindler V, Harms GS, Waschke J. Actin reorganization contributes to loss of cell adhesion in pemphigus vulgaris. *Am J Physiol Cell Physiol* (2010) 299(3):C606–13. doi:10.1152/ajpcell.00075.2010
58. Chtcheglova LA, Wildling L, Waschke J, Drenckhahn D, Hinterdorfer P. AFM functional imaging on vascular endothelial cells. *J Mol Recognit* (2010) 23(6):589–96. doi:10.1002/jmr.1052
59. Chtcheglova LA, Waschke J, Wildling L, Drenckhahn D, Hinterdorfer P. Nano-scale dynamic recognition imaging on vascular endothelial cells. *Biophys J* (2007) 93(2):L11–3. doi:10.1529/biophysj.107.109751
60. Curry N, Ghezali G, Kaminski Schierle GS, Rouach N, Kaminski CF. Correlative STED and atomic force microscopy on live astrocytes reveals plasticity of cytoskeletal structure and membrane physical properties during polarized migration. *Front Cell Neurosci* (2017) 11:104. doi:10.3389/fncel.2017.00104
61. Santacroce M, Orsini F, Perego C, Lenardi C, Castagna M, Mari SA, et al. Atomic force microscopy imaging of actin cortical cytoskeleton of *Xenopus laevis* oocyte. *J Microsc* (2006) 223(Pt1):57–65. doi:10.1111/j.1365-2818.2006.01596.x
62. Usukura E, Suzuki T, Furuike S, Soga N, Saita E, Hisabori T, et al. Torque generation and utilization in motor enzyme F0F1-ATP synthase: half-torque F1 with short-sized pushrod helix and reduced ATP synthesis by half-torque F0F1. *J Biol Chem* (2012) 287(3):1884–91. doi:10.1074/jbc.M111.305938
63. Quinlan RA, Schwarz N, Windoffer R, Richardson C, Hawkins T, Broussard JA, et al. A rim-and-spoke hypothesis to explain the biomechanical roles for cytoplasmic intermediate filament networks. *J Cell Sci* (2017) 130(20):3437–45. doi:10.1242/jcs.202168
64. Waschke J. The desmosome and pemphigus. *Histochem Cell Biol* (2008) 130(1):21–54. doi:10.1007/s00418-008-0420-0
65. Denning MF, Guy SG, Ellerbroek SM, Norvell SM, Kowalczyk AP, Green KJ. The expression of desmoglein isoforms in cultured human keratinocytes is regulated by calcium, serum, and protein kinase C. *Exp Cell Res* (1998) 239(1):50–9. doi:10.1006/excr.1997.3890
66. Rotzer V, Hartlieb E, Vielmuth F, Gliem M, Spindler V, Waschke J. E-cadherin and Src associate with extradesmosomal Dsg3 and modulate desmosome assembly and adhesion. *Cell Mol Life Sci* (2015) 72(24):4885–97. doi:10.1007/s00018-015-1977-0
67. Tsang SM, Brown L, Lin K, Liu L, Piper K, O'Toole EA, et al. Non-junctional human desmoglein 3 acts as an upstream regulator of Src in E-cadherin adhesion, a pathway possibly involved in the pathogenesis of pemphigus vulgaris. *J Pathol* (2012) 227(1):81–93. doi:10.1002/path.3982
68. Oktarina DA, van der Wier G, Diercks GF, Jonkman MF, Pas HH. IgG-induced clustering of desmogleins 1 and 3 in skin of patients with pemphigus fits with the desmoglein nonassembly depletion hypothesis. *Br J Dermatol* (2011) 165(3):552–62. doi:10.1111/j.1365-2133.2011.10463.x
69. Yoshida K, Ishii K, Shimizu A, Yokouchi M, Amagai M, Shiraishi K, et al. Non-pathogenic pemphigus foliaceus (PF) IgG acts synergistically with a directly pathogenic PF IgG to increase blistering by p38MAPK-dependent desmoglein 1 clustering. *J Dermatol Sci* (2017) 85(3):197–207. doi:10.1016/j.jdermsci.2016.12.010
70. Stahley SN, Warren MF, Feldman RJ, Swerlick RA, Mattheyses AL, Kowalczyk AP. Super-resolution microscopy reveals altered desmosomal protein organization in tissue from patients with pemphigus vulgaris. *J Invest Dermatol* (2016) 136(1):59–66. doi:10.1038/JID.2015.353
71. Rotzer V, Hartlieb E, Winkler J, Walter E, Schlipp A, Sardy M, et al. Desmoglein 3-dependent signaling regulates keratinocyte migration and wound healing. *J Invest Dermatol* (2016) 136(1):301–10. doi:10.1038/jid.2015.380
72. Berkowitz P, Hu P, Warren S, Liu Z, Diaz LA, Rubenstein DS. p38MAPK inhibition prevents disease in pemphigus vulgaris mice. *Proc Natl Acad Sci U S A* (2006) 103(34):12855–60. doi:10.1073/pnas.0602973103
73. Berkowitz P, Diaz LA, Hall RP, Rubenstein DS. Induction of p38MAPK and HSP27 phosphorylation in pemphigus patient skin. *J Invest Dermatol* (2008) 128(3):738–40. doi:10.1038/sj.jid.5701080

Conflict of Interest Statement: The authors declare that the research was conducted in the absence of any commercial or financial relationships that could be construed as a potential conflict of interest.

The reviewer PK and handling Editor declared their shared affiliation.

frontiers in Immunology

REVIEW
published: 27 March 2018
doi: 10.3389/fimmu.2018.00609

Autoantibodies in Autoimmune Liver Disease—Clinical and Diagnostic Relevance

Marcial Sebode[1†], Christina Weiler-Normann[1,2†], Timur Liwinski[1†] and Christoph Schramm[1,2]*

[1] 1st Department of Medicine, University Medical Centre Hamburg-Eppendorf, Hamburg, Germany, [2] Martin Zeitz Centre for Rare Diseases, University Medical Centre Hamburg-Eppendorf, Hamburg, Germany

Testing for liver-related autoantibodies should be included in the workup of patients with hepatitis or cholestasis of unknown origin. Although most of these autoantibodies are not disease specific, their determination is a prerequisite to diagnose autoimmune hepatitis (AIH) and primary biliary cholangitis (PBC), and they are components of the diagnostic scoring system in these diseases. In primary sclerosing cholangitis (PSC), on the other hand, autoantibodies are frequently present but play a minor role in establishing the diagnosis. In PSC, however, data on antibodies suggest a link between disease pathogenesis and the intestinal microbiota. This review will focus on practical aspects of antibody testing in the three major autoimmune liver diseases AIH, PBC, and PSC.

Keywords: autoimmune hepatitis, primary biliary cholangitis, primary sclerosing cholangitis, antinuclear antibodies, smooth muscle antibodies, antimitochondrial antibodies, soluble liver antigen/liver–pancreas antigen, serology

OPEN ACCESS

Edited by:
Ralf J. Ludwig, University of Lübeck, Germany

Reviewed by:
Urs Christen, Goethe University Frankfurt, Germany
Luis Eduardo Coelho Andrade, Federal University of São Paulo, Brazil

***Correspondence:**
Christoph Schramm
cschramm@uke.de

†These authors have contributed equally to this work.

Specialty section:
This article was submitted to Immunological Tolerance and Regulation, a section of the journal Frontiers in Immunology

Received: *29 January 2018*
Accepted: *12 March 2018*
Published: *27 March 2018*

Citation:
Sebode M, Weiler-Normann C, Liwinski T and Schramm C (2018) Autoantibodies in Autoimmune Liver Disease—Clinical and Diagnostic Relevance. Front. Immunol. 9:609. doi: 10.3389/fimmu.2018.00609

INTRODUCTION

Testing for liver-related autoantibodies should be included in the workup of patients with hepatitis or cholestasis of unknown origin. Although most of these autoantibodies are not disease specific, their determination is a prerequisite to diagnose autoimmune hepatitis (AIH) and primary biliary cholangitis (PBC), and they are components of the diagnostic scoring system in these diseases (1, 2) (**Table 1**). In primary sclerosing cholangitis (PSC), on the other hand, autoantibodies are frequently present but play a minor role in establishing the diagnosis, which is based on cholangiography. In PSC, however, data on antibodies suggest a link between disease pathogenesis and the intestinal microbiota (3).

Abbreviations: AIH, autoimmune hepatitis; AMA, antimitochondrial antibodies; ANA, antinuclear antibodies; ASGPR, asialoglycoprotein receptor; BEC, biliary epithelial cells; CD, cluster of differentiation; CYP, cytochrome P450; DILI, drug-induced liver injury; DNA, deoxyribonucleic acid; ds, double stranded; EASL, European Association for the Study of the Liver; ELISA, enzyme-linked immunosorbent assay; ERCP, endoscopic retrograde cholangiopancreatography; FTCD, formiminotransferase cyclodeaminase; FTSZ, filamenting temperature-sensitive mutant Z; GP, glycoprotein; HCC, hepatocellular carcinoma; HCV, viral hepatitis C; HLA, human leukocyte antigen; IAC, IgG4-associated cholangitis; IBD, inflammatory bowel disease; IFT, indirect immunofluorescence testing; IG, immunoglobulin; LC1, liver cytosol type 1; LKM, liver–kidney microsome; MRCP, magnetic-resonance cholangiography; p-ANCA, antineutrophil cytoplasmatic antibodies with a perinuclear staining pattern; PBC, primary biliary cholangitis; PDC-E2, pyruvate-dehydrogenase E2; PSC, primary sclerosing cholangitis; SEPSECS, *O*-phosphoseryl-tRNA:selenocysteine-tRNA synthase; SLA/LP, soluble liver antigen/liver–pancreas antigen; SLE, systemic lupus erythematodes; SMA, smooth muscle antibodies; SS, single stranded; TBB-5, beta-tubulin isoform 5; UGT, uridine glycuronosyl transferase; VGT, vascular/glomerular/tubular.

TABLE 1 | Autoantibodies in autoimmune liver diseases.

Antibody	Screening test	Confirmatory test	Positive in the following liver diseases	Recommended as initial screening for AILD	Prognostic value for AILD	Target antigen
ANA	SKL IFT	HEp-2 IFT (identification of a specific pattern) ELISA, WB (for selected nuclear antigens)	AIH1 PBC PSC HBV HCV DILI NAFLD	Yes	In PBC yes (only gp210)	In AIH: chromatin, histones, centromere, ds- and ss-DNA, cyclin A, ribonucleoproteins and other nuclear antigens In PBC: centromere, lamin-B-receptor, sp100, gp210
Anti-SMA/ anti-F-actin	SKL IFT	ELISA, WB IFT on fibroblasts (VSM47)	AIH1	Yes	Unclear	(Filamentous) actin, tubulin, or intermediate filaments
Anti-LKM-1	SKL IFT	ELISA, WB	AIH2 HCV	Yes	In AIH yes	CYP 2D6
Anti-SLA/LP	ELISA, WB		AIH1	Yes	Unclear	SepSecS
Anti-LC1	SKL IFT	WB Double immunodiffusion assay	AIH2 HCV	No	Unclear	FTCD
Anti-LKM-2	WB		Tielinic acid-induced DILI	No		CYP 2C9
Anti-LKM-3	WB	ELISA	AIH2 HCV HDV	No		UGTs
p-ANCA/p-ANNA	IFT on formaldehyde-fixed neutrophils	ELISA	AIH PSC HBV HCV	No	Unclear	Unclear, tubulin-beta chain?
Anti-ASGPR	ELISA, WB		AIH PBC HBV HCV	No	Unclear	ASGPR
AMA	SKL IFT	HEp-2 IFT ELISA, WB	PBC Variant syndromes Acute liver failure	Yes	No	Lipoylated domains of E3 binding protein, various epitopes of pyruvate-dehydrogenase complex, 2-oxo-acid dehydrogenase complex, branched chain 2-oxo-acid dehydrogenase complex
Anti-Kelch-like 12-antibodies, anti-hexokinase1-antibodies	ELISA, WB		PBC	Unclear	Unclear	Kelch like 12, hexokinase E1
Anti-GP2 IgA	IFT		PSC	No	In PSC yes	Glycoprotein 2

AIH, autoimmune hepatitis; AIH1 or 2, autoimmune hepatitis type 1 or 2; AILD, autoimmune liver diseases; AMA, antimitochondrial antibodies; ANA, antinuclear antibodies; ASGPR, asialoglycoprotein receptor; CYP, cytochrome P450; DILI, drug-induced liver injury; DNA, deoxyribonucleic acid; ds, double stranded; ELISA, enzyme-linked immunosorbent assay; FTCD, formiminotransferase cyclodeaminase; GP, glycoprotein; HBV, viral hepatitis B; HCV, viral hepatitis C; HDV, viral hepatitis D; HEp-2 IFT, indirect immunofluorescence testing on HEp-2 cells; IFT, indirect immunofluorescence testing; LC1, liver cytosol type 1; LKM, liver–kidney microsome; NAFLD, non-alcoholic fatty liver disease; SKL IFT, indirect immunofluorescence testing on rodent stomach, kidney, and liver tissue; p-ANCA, antineutrophil cytoplasmatic antibodies with a perinuclear staining pattern; PBC, primary biliary cholangitis; PSC, primary sclerosing cholangitis; SEPSECS, O-phosphoseryl-tRNA:selenocysteine-tRNA synthase; SLA/LP, soluble liver antigen/liver–pancreas antigen; SMA, smooth muscle antibodies; ss, single stranded; UGT, uridine glycuronosyl transferase; WB, western blot/immunoblot.

In Europe, screening for liver-related autoantibodies is traditionally conducted using indirect immunofluorescence testing (IFT) on rodent tissue slices (**Table 2**). Cutoff levels for titers included in diagnostic scores for AIH and PBC use IFT as a standard. In other parts of the world, solid-phase test systems are widely used and to date it is unclear, whether this results in altered sensitivity or specificity of the tests applied and how these findings can be translated into diagnostic scores. IFT has the advantage of not only assessing the titer of the autoantibodies but also the fluorescence pattern, which may provide additional information on the presence, e.g., of PBC-defining antinuclear antibodies (ANA). Therefore, fluorescence pattern of ANA should always be reported together with the antibody titer. It is important to note, however, that IFT is a subjective method that requires an experienced lab technician and that international standards for testing are currently lacking. Also, titers may differ between labs

TABLE 2 | Recommended serologic first line diagnostics for autoimmune liver diseases.

Test assay	Antibodies detected
SKL IFT	ANA Anti-SMA Anti-LKM AMA
HEp-2 IFT	ANA patterns indicative of antibodies to mitochondria (AMA), gp210, sp100, and centromere
ELISA or WB	Anti-SLA/LP

AMA, antimitochondrial antibodies; ANA, antinuclear antibodies; ELISA, enzyme-linked immunosorbent assay; GP, glycoprotein; HEp-2 IFT, indirect immunofluorescence testing on HEp-2 cells; LKM, liver–kidney microsome; SMA, smooth muscle antibodies; SKL IFT, indirect immunofluorescence testing on rodent stomach, kidney, and liver tissue; SLA/LP, soluble liver antigen/liver–pancreas antigen; WB, western blot/immunoblot.

due to different substrates used, and, therefore, the lab-specific reference values should be noted.

The following review will focus on practical aspects of antibody testing in the three major autoimmune liver diseases AIH, PBC, and PSC.

AUTOANTIBODIES IN AIH

Introduction

Diagnosis of AIH

Autoimmune hepatitis is a chronic inflammatory liver disease with unknown etiology (1, 4, 5). The diagnosis of AIH is based on a combination of typical findings, which are not disease specific and on the exclusion of other liver diseases, such as viral hepatitis (6–8). It is assumed that AIH is a T cell-mediated disease. However, there are hints at a relevant role for a humoral immune response in AIH pathogenesis: autoantibodies can frequently be detected, plasma cells are enriched in hepatic infiltrates and immunoglobulin G (IgG)/gammaglobulins serve as a diagnostic and disease activity markers. Nevertheless, the exact pathogenetic relevance of this humoral immune response for AIH is unclear and has not been investigated in detail (**Table 1**). The antigens that are targeted by autoantibodies in AIH have been identified in most cases. Still, it is uncertain whether these autoantigens play a relevant role for the induction or preservation of chronic liver inflammation in AIH.

The presence of AIH-related autoantibodies supports the diagnosis of AIH. However, most autoantibodies being associated with AIH have a relatively low disease specificity (**Table 1**). In the setting of acute or even chronic hepatitis of an etiology other than AIH, and even in healthy persons, liver autoantibodies can frequently be found. Besides, the presence of autoantibodies is not a prerequisite for the diagnosis of AIH: around 10–15% of patients present without known autoantibodies ("seronegative" AIH) or develop them during the course of disease after an acute onset.

Methods of Testing

As mentioned earlier, IFT on rodent kidney, liver, and stomach tissue and on HEp-2 cells is recommended as the standard method for the detection of liver autoantibodies (9). It is important to note that IFT testing is a subjective method and titers may vary depending on the laboratory performing the test. Antibody titers above 1:40 have a higher specificity for AIH, but it is unknown whether very high titers (e.g., >1:640) are associated with an even higher specificity. IFT enables the simultaneous analysis of most of the antibodies that are relevant for autoimmune liver diseases. HEp-2 cells with their prominent nuclei help to identify specific patterns of ANA. HEp-2 cells should not be used for initial screening for the presence of ANA since low titer antibodies can frequently be found in healthy subjects using these cells (10). Therefore, screening for ANA should be performed on rodent kidney, liver, and stomach tissue. In the case of positivity, the pattern of ANA should then be analysed on HEp-2 cells (9). The fluorescence pattern of ANA on HEp-2 cells provides additional diagnostic information: a pattern of multiple "nuclear dots" or a "nuclear rim" pattern suggest the presence of anti-sp100 or anti-gp210, respectively, and thereby hint at the diagnosis of PBC or a variant syndrome of AIH with features of PBC (see below section on autoantibodies in PBC). In Europe, there is consensus that solid-phase assays such as enzyme-linked immunosorbent assays (ELISA) or immunoblots should only be used to confirm the results of IFT, but not for initial screening of ANA. However, in the USA, ELISA are frequently used for screening purposes (4). For the diagnostic workup of autoimmune liver diseases, anti-soluble liver antigen/liver–pancreas antibodies (anti-SLA/LP) should already initially be tested for by ELISA or immunoblot since these autoantibodies cannot be detected by IFT and have high specificity for AIH.

Subclassification of AIH According to Autoantibody Pattern

Next to their diagnostic value, certain autoantibodies have been associated with a different clinical presentation and prognosis of AIH. These associations have led to the classification of type 1 and type 2 AIH. Type 1 AIH is the predominant type of AIH in adults and children and is defined by the presence of ANA and/or antismooth muscle antibodies (anti-SMA) (7). Anti-SMA (and especially anti-actin antibodies) have been associated with inflammatory activity of AIH in adult patients (11). However, these results still need to be validated. Type 2 AIH (about 5–10% of all AIH patients) is typically defined by anti-liver–kidney microsomal type 1 antibodies (anti-LKM-1) or, in rare cases, by anti-LKM-3 and/or anti-liver cytosol type 1 antibodies (anti-LC1) (12–14). Type 2 AIH presents at a younger age, often in childhood, and is associated with a more aggressive disease course than type 1 AIH (12, 15). It is still controversial whether the presence of anti-SLA/LP defines a third subgroup of AIH (type 3 AIH) with a potentially more aggressive clinical course or whether anti-SLA/LP-positive AIH patients experience a clinical course similar to type 1 AIH patients (16–19). In 5–10% of AIH patients, anti-SLA/LP are present in combination with ANA and/or anti-SMA. In up to 10% of AIH patients, anti-SLA/LP are the sole antibodies detected (20), a fact that mandates their testing for the diagnosis of AIH.

Special Considerations in Children

Antibody testing in pediatric patients demands special attention. Titers for most liver autoantibodies seem to correlate with age: in

children, lower titers (1:20 for ANA and anti-SMA and 1:10 for anti-LKM-1) can be diagnostic for AIH, whereas in adults, higher titers of ANA (1:80–1:160) can also be found in healthy individuals (9, 21). Therefore, the physician should be informed by the laboratory on any antibody titer that is detected and interpret the results according to patient's age.

Repeated Testing of Autoantibodies

Particularly in pediatric patients with autoimmune liver diseases, titers of liver-related autoantibodies can correlate with disease activity and response to treatment may be paralleled by reduction or even disappearance of antibody titers (21, 22). Thus, retesting of autoantibodies can be reasonable in children, as it can add information on the depth of remission achieved.

Retesting of autoantibodies for adult patients with AIH cannot be recommended in general, but can be helpful in special clinical settings. In cases of acute hepatitis and initially negative autoimmune serology, antibody testing should be repeated after 3–6 months since antibodies can appear during the course of disease. In adult patients, a variant syndrome of AIH with features of additional PBC can develop even several years after the diagnosis of classical AIH. Therefore, IFT should be repeated to screen for PBC-specific ANA or antimitochondrial antibodies (AMA) whenever cholestatic liver enzymes remain or become elevated or when symptoms suggestive of PBC develop in an AIH patient. Currently, regular retesting of autoantibodies in adult patients as a surrogate marker for inflammatory activity is not recommended.

Antinuclear Antibodies

Antinuclear antibodies were the first autoantibodies to be associated with AIH (23). However, they lack disease specificity. About 50–75% of AIH patients are ANA-positive (with or without anti-SMA) (24). ANA can also be detected in healthy persons or patients with other liver diseases such as fatty liver disease, drug-induced liver injury (DILI) disease, or viral hepatitis. The pattern of ANA in AIH often is speckled or homogenous. It is uncertain whether a distinct pattern of ANA has a higher specificity for AIH. ANA in AIH are directed against several antigens such as chromatin, histones, centromere, double-(ds) and single-(ss) stranded deoxyribonucleic acid (DNA), cyclin A, ribonucleoproteins or other nuclear antigens that have not yet been identified (25–29). A biochemical differentiation of these antigens is not recommended because they have not been associated with a certain clinical course or a higher diagnostic specificity for AIH. It is important to acknowledge that up to 20% of AIH patients may display anti-dsDNA antibodies. This may cause confusion with the diagnosis of systemic lupus erythematodes, which has to be ruled out in patients with respective clinical findings. In rare cases, both diseases may occur together (30).

Antismooth Muscle Antibodies

Similar to ANA, anti-SMA have been associated with AIH since the early days of the clinical definition of AIH. They are also not disease specific and can be detected in various liver diseases such as fatty liver disease (31, 32). Anti-SMA are present in about 50% of patients with type I AIH and can be the only detectable autoantibody. In IFT, anti-SMA react with the smooth muscles of the lamina propria and muscularis mucosae of the stomach or arterial walls of the liver. On kidney tissue, anti-SMA show different staining patterns: the vascular/glomerular and the vascular/glomerular/tubular (VGT) patterns are more specific for AIH than the vascular (V) pattern (9, 24). The VGT pattern can be confirmed by IFT performed on fibroblasts or vascular smooth muscle cells (VSM47) (33). On a molecular level, anti-SMA are a heterogeneous group of antibodies showing reactivity against actin, tubulin or intermediate filaments (34). Sera showing the VGT pattern react in 80% with filamentous actin (F-actin) (9, 33, 35). Actin is a ubiquitous contractile protein. The presence of anti-F-actin antibodies can be confirmed by solid-phase assays, such as ELISA (36). Anti-SMA showing reactivity against F-actin seem to be more specific for AIH, but can also be detected in other liver diseases (35, 37).

Anti-Liver–Kidney Microsomal Antibodies (Anti-LKM)

Anti-LKM-1, but also anti-LKM-3 are defining type 2 AIH (9). In IFT, anti-LKM stain, the cytoplasm of hepatocytes and the proximal, larger renal tubuli, but not parietal cells of the stomach (38). By contrast, AMA in PBC stain the mitochondria-rich, distal, smaller renal tubuli, and gastric parietal cells. ELISA tests are recommended to confirm positivity for anti-LKM in IFT (39). The autoantigen that is recognized by anti-LKM-1 in AIH is cytochrome P450 (CYP) 2D6 (40–44). Anti-LKM-1 are not AIH-specific and can also be found in patients with chronic viral hepatitis C (HCV) (45, 46). However, the epitopes that are targeted by anti-LKM-1 in HCV-infected patients differ from those in patients with AIH (47, 48). Anti-LKM-2 have been detected in cases of tielinic acid-induced DILI, a drug that has been withdrawn from the market (49). In contrast to anti-LKM-1, anti-LKM-2 target a different isoform of the cytochrome P 450, namely CYP 2C9. Anti-LKM-3 can be found in few patients with AIH, but also in HCV and viral hepatitis D. They recognize members of the uridine glycuronosyl transferases family 1 (26, 27, 50, 51).

Anti-Soluble Liver Antigen/Liver–Pancreas Antigen Antibodies (Anti-SLA/LP)

Anti-SLA/LP have the highest specificity for AIH among all AIH-related autoantibodies (9). However, they are present in only about 10–20% of patients. Due to their high specificity, anti-SLA/LP should be tested routinely when AIH is suspected or in any case of unclear elevation of liver enzymes. Anti-SLA/LP cannot be detected by IFT and need to be tested for by ELISA or Western blot (52). The cytosolic autoantigen targeted by anti-SLA/LP was described independently by different groups and has been characterized later on as *O*-phosphoseryl-tRNA:selenocysteine-tRNA synthase (SepSecS), a synthase (S) converting *O*-phosphoseryl-tRNA (Sep) to selenocysteinyl-tRNA (Sec) (20, 53–58). Anti-SLA/LP belong to the IgG1 subtype of immunoglobulins and recognize an immunodominant epitope at the carboxy terminus of the SepSecS protein (59). Interestingly, the epitopes of SepSecS recognized by anti-SLA/LP-antibodies overlap with CD4+ T cell epitopes. This points to a relevant pathogenetic role of SepSecS

for the subgroup of anti-SLA/LP-positive AIH patients (60). Anti-SLA/LP have been associated with the presence of a subtype of ANA (anti-Ro52) (61). Unexplained adverse pregnancy outcomes in AIH were highly associated with the presence anti-SLA/LP and anti-Ro52, potentially due to antibody-induced congenital heart block (62).

Other Antibodies Associated With AIH

Anti-Liver Cytosol Type 1 Antibodies (Anti-LC1)

Anti-LC1 antibodies directed against liver cytosol 1 (anti-LC1) target epitopes of the enzyme formiminotransferase cyclodeaminase (63). They are present in about 30% of type 2 AIH patients, alone or in combination with anti-LKM-1 (64, 65). In IFT, anti-LC1 stain hepatocytes but spare the centrilobular areas of the liver. By contrast, anti-LKM-1 stain hepatocytes throughout the liver lobule. When both antibodies are coexistent, anti-LKM-1 cover the spared areas of anti-LC1. Thereby, anti-LKM-1 can mask the presence of anti-LC1. Solid-phase assays help to identify anti-LC-1 (65). When anti-LC1 are the sole antibodies being detected, they strongly support the diagnosis of type 2 AIH. However, anti-LC1 are not AIH specific and can also be detected in patients with HCV (64).

Antineutrophil Cytoplasmatic Antibodies With a Perinuclear Staining Pattern (p-ANCA)

The presence of p-ANCA can support the diagnosis of AIH, especially in the absence of other autoantibodies (9). However, p-ANCA can also be detected in chronic viral hepatitis, inflammatory bowel disease (IBD), PSC or microscopic polyangiitis, and eosinophilic granulomatosis with polyangiitis (66–69). p-ANCA mainly react with myeloperoxidase. Atypical p-ANCA (p-ANNA), which are characterized by the retention of a perinuclear staining on formaldehyde-fixed neutrophils seem to be more specific for autoimmune liver diseases and IBD (9).

Anti-Asialoglycoprotein Receptor Antibodies (Anti-ASGPR)

Anti-ASGPR can be detected in 24–82% of AIH patients, depending on the diagnostic assay used (70). Anti-ASGPR target a liver-specific membrane receptor and seem to correlate with histological activity (70). However, anti-ASGPR are not disease specific and are also present in patients with chronic viral hepatitis or PBC.

AMA in Patients With AIH

Since IFT on the abovementioned rodent tissues allows the simultaneous detection of autoantibodies for different autoimmune liver diseases, PBC-specific AMA are occasionally detected during the diagnostic workup for AIH. In this case, a variant syndrome of AIH with features of PBC should be suspected, often indicated by persistent elevation of cholestatic liver enzymes after the AIH component has reached remission. In some rare cases, AMA develop during the course of classical AIH with a novel elevation of cholestatic liver enzymes (2). In other rare instances, AMA can be detected in AIH patients without any other laboratory or histological signs of concomitant PBC. It is unclear whether this is an epiphenomenon, whether these cases represent a subform of AIH or a very early stage of an AIH variant syndrome with additional PBC (71, 72). Additional treatment with UDCA should be decided upon on an individual basis. In acute AIH, AMA may be present as an unspecific sign of acute liver damage, and they usually disappear over time (73).

Pathogenetic Role of Autoantibodies in AIH

It is unclear whether autoantibodies substantially contribute to the pathogenesis of AIH (**Table 1**). Most knowledge on a potential pathogenetic role of autoantibodies in AIH derives from analyzes of anti-LKM. The cross-reaction of anti-LKM with homologous regions of CYP 2D6 and HCV hints at a viral infection being a possible trigger for type 2 AIH. Molecular mimicry has been proposed for several autoimmune diseases. However, it has not been convincingly shown that an acute viral infection is truly the disease initiating event for a substantial number of AIH patients. For type 2 AIH patients, an abnormal expression of CYP 2D6 as the respective autoantigen of anti-LKM has been detected on the surface of hepatocytes (74). It is unclear, how autoantibodies in other types of AIH are able to target intracellular antigens. The release of nuclear or cytosolic antigens due to hepatocyte damage has been proposed as one possible mechanism. Another area of uncertainty is the fact that almost all of the antigens addressed by antibodies in AIH are not exclusively expressed in the liver, such as CYP 2D6, which is also expressed, e.g., in the central nervous system. Also, the target antigen of anti-SLA/LP is expressed in liver, pancreas, lungs, kidneys, and activated lymphocytes, but anti-SLA/LP have only been associated with AIH (55, 57). Asialoglycoprotein receptor (ASGPR) is a hepatic C-type lectin expressed on the sinusoidal surface of hepatocytes physiologically and on the canalicular membrane of hepatocyctes under inflammatory conditions (70). A T cell-mediated immune reaction, overlapping in its targeted epitopes with the humoral immune response, has been identified for ASGPR, for CYP 2D6 (75, 76) and for SepSecS, the molecular target of anti-SLA/LP (60, 77).

AUTOANTIBODIES IN PBC

Introduction

Diagnosis of PBC

Primary biliary cholangitis is a chronic non-suppurative granulomatous inflammation of the small intrahepatic bile ducts (2). The first description of this disease dates back more than 100 years (78) and historically, PBC was often diagnosed only *postmortem* (79). Around 90% of all affected patients are female, and the vast majority (>90%) display autoantibodies. Clinically, PBC leads to elevation of cholestatic parameters and often a selective IgM elevation. In addition, many patients will have elevated cholesterol levels. Autoantibodies play a major role for the diagnosis of PBC: European Association for the Study of the Liver (EASL) recommends that in adult patients with chronic cholestasis and no likelihood of systemic disease, a diagnosis of PBC can be made based on elevated ALP and the presence of AMA at a titer of more

than 1:40. In the absence of AMA, PBC-specific ANA can serve to diagnose the disease (2) (**Table 1**).

Autoantibodies in PBC

Autoantibodies, and especially AMA, are a hallmark of the disease: The first tests for detection of AMA were developed in the 1960s (80) and facilitated diagnosis and timely treatment later on. The development not only of refined testing for AMA but also the addition of other PBC-defining autoantibodies to the repertoire has led to an increasing proportion of PBC patients displaying autoantibodies and likely also to earlier diagnosis. Today, even non-invasive testing for AMA seems feasible as a recently published approach to test AMA in saliva has demonstrated (81). It remains unclear whether these autoantibodies are pathogenetically relevant. There has been some debate about AMA being responsible for fatigue in PBC and trials to evaluate the effect of an anti-CD20 treatment are on the way (82). In patients with suspected PBC and negative AMA-testing, PBC-defining ANA should be sought (**Table 1**).

In all patients with unexplained chronic cholestasis or suspected PBC, autoantibody testing should be performed using IFT on rodent tissue and confirmation of fluorescence pattern using Hep-2 cells (see above) (2) Approximately 10% of PBC patients will not display AMA (2, 83). In these patients, diagnostic accuracy is improved by testing for PBC-specific nuclear autoantibodies, which will be present in approximately half of the AMA-negative patients (84). In addition, some of the nuclear antibodies have been associated with prognosis (see below); therefore, antibody pattern may in clinical practice help to risk stratify patients.

Antimitochondrial Antibodies

Antimitochondrial antibodies have initially been described in patients with PBC by Dame Sheila Sherlock (80). These antibodies are directed against the pyruvate-dehydrogenase E2 (PDC-E2) (85) subunit located in the inner mitochondrial membrane. In IFT, AMA lead to a typical cytoplasmic staining in rat liver and kidney slices, but they are often also visible on HEp-2 cells. The vast majority of PBC patients (exceeding 90%) (86) display these antibodies (87), and they may occasionally be found years preceding an elevation of liver enzymes (see below). Increasingly often, AMA are detected, e.g., due to rheumatological screens in patients with normal liver enzymes (88, 89), usually at lower titers than in patients with overt PBC (90). A considerable proportion of patients with positive AMA but no signs of PBC will likely develop symptomatic PBC at some time point and therefore these patients should be followed clinically and biochemically (91, 92). Current data and guidelines do not support treatment in AMA-positive persons without any elevated liver enzymes or signs of PBC (2, 83). Several subtypes of AMA have been identified (traditionally named M1–M9). In this historical classification, antibodies directed against M2, M4, M8, and M9 are associated with PBC. Nowadays, combined peptides covering these antigenic regions have been constructed (93) and are widely used in confirmatory solid-phase tests.

Antimitochondrial antibodies can be comprised of IgG, IgA (94), and IgM antibodies (95) or a combination thereof, whereby AMA of the IgG3 subtype and IgA directed against PDC-E2 have been associated with more severe disease (96). In a subgroup of patients, AMA seem to be solely comprised of IgM antibodies (REF). To date, it is unclear, whether testing systems should include the possibility to detect IgM antibodies.

AMA on IFT may be confused with other cytoplasmatic antibodies (e.g., cardiolipin antibodies), therefore, it is advisable to perform a confirmatory test using one of the ELISA or Western blot test systems, which include several of the known PDC epitopes.

Primary biliary cholangitis-specific autoantibodies should be sought in patients with chronic (>6 months) elevation of cholestatic liver enzymes. Of note, patients with acute liver damage of any kind or liver failure may also display AMA (73). These usually disappear with the resolution of the acute disease.

Anti-sp100 Antibodies

In patients without AMA and persisting suspicion of PBC, ANA should be sought by using IFT in HEp-2 cells. These antibodies will be present in around 30–50% of AMA-negative PBC patients and interestingly, have been described to be inversely correlated to the development of fibrosis (97). These ANA have so far have not been associated with any specific disease features. They are moderately specific for PBC and can rarely be detected in rheumatological diseases and in acute hepatitis of any origin (33, 98, 99). Anti-sp100 result in a typical pattern of "nuclear dots" in IFT on HEp-2-cells (100); a confirmatory test (ELISA and Western Blot) is available (101).

Anti-gp210 Antibodies and Anti-Lamin-B-Receptor Antibodies

A subgroup of patients with PBC may display anti-gp210 or, rarely, anti-lamin-B-receptor antibodies in addition to AMA or even exclusively. Anti-gp210 (102) and anti-lamin-B-receptor (103) result in a "nuclear rim" pattern on IFT using HEp-2 cells, where anti-lamin-B-receptor antibodies usually result in a smooth staining and the anti-gp210-antibody appears as discontinuous staining on IFT. For anti-gp210, a confirmatory test is widely available; confirmatory testing for anti-lamin-B-receptor is subject to specialized laboratories. These antibodies are present in around 20% PBC patients, and in around 30–50% of AMA-negative patients and are considered specific for PBC. In addition, an unfavorable course of PBC has been associated with the presence of anti-gp210 in several studies (99, 104, 105), and a higher incidence of hepatocellular carcinoma has been reported in this patient cohort (106). Therefore, patients with these antibodies may warrant special attention in disease surveillance (83).

Anti-Centromere Antibodies

Anti-centromere have been described in patients with systemic sclerosis but may occasionally occur in PBC patients without features of systemic sclerosis. Clinically, anti-centromere have been associated with increased portal hypertension in these patients (99) and a poor prognosis (107, 108). Anti-centromere have recently also been associated with the development of kidney disease in PBC patients (109).

Anti-Kelch-Like 12 Antibodies, Anti-Hexokinase1 Antibodies

Recently, two new autoantibodies, anti-Kelch-like 12 and anti-hexokinase1 have been described in PBC (110). So far, no clear associations with disease activity or clinical course have been established, and their prevalence in larger populations has yet to be established.

Antibodies Found in Patients With PBC and Additional Signs of AIH

Features of AIH may be present in 10–20% of patients who present with PBC. There are no generally accepted criteria to define these variant syndromes. In most patients, both diseases manifest simultaneously and in these patients, the Paris criteria have been established and endorsed by EASL to indicate additional AIH in a PBC patient (2, 111). AIH can be diagnosed if two of three criteria are present: (1) elevation of ALT levels >5 times upper limit the normal (ULN), (2) elevation of serum IgG levels >2 times ULN or positive anti-SMA, and (3) moderate to severe interface hepatitis on histology. In addition, the presence of anti-SLA/LP and anti-dsDNA may raise the suspicion of AIH in patients with PBC (112–114).

AUTOANTIBODIES IN PSC

Introduction

Diagnosis of PSC

Primary sclerosing cholangitis is a cholestatic liver disease of unknown origin that is characterized by progressive multifocal strictures of the extra- and/or intrahepatic bile ducts (115, 116). PSC is strongly associated with a unique phenotype of IBD, mostly presenting as a mild pancolitis (117). While the onset of PSC is often insidious, the natural course leads to liver cirrhosis, hepatobiliary malignancies, colon cancer, and episodes of superimposed bacterial cholangitis (118). This results in death or liver transplantation after a median time of approximately 15–20 years (119, 120). PSC is usually characterized by a cholestatic profile of liver enzymes with a leading elevation of alkaline phosphatase. The diagnosis is nowadays established by magnetic-resonance cholangiography, since invasive direct cholangiography using endoscopic retrograde cholangiopancreatography is associated with markedly more complications, although it may yield a slightly higher sensitivity with regard to small bile ducts and the extrahepatic duct (121). Liver biopsy is usually not required to establish the diagnosis (122), unless concurrent AIH or small-duct PSC is suspected (123).

Autoantibodies in PSC

Although various serum antibodies have been described in patients with PSC, immune serology in PSC is generally considered unspecific and therefore of limited value to establish the diagnosis (124, 125) (**Table 1**). The most prevalent serum antibodies in PSC are p-ANCA, which can be found in up to 93% of patients, followed by ANA (8–77%) and anti-SMA (0–83%) (126). However, p-ANCA are also frequently found in patients with ulcerative colitis without PSC, in patients with AIH and to a lesser extent in PBC (127, 128). Due to the lack of specificity, p-ANCA can support the diagnosis of PSC only in selected patients, mainly those lacking associated IBD.

Antineutrophil Cytoplasmic Antibodies With Perinuclear Staining Pattern (p-ANCA)

Usually, p-ANCA are demonstrated on IFT on alcohol-fixed human granulocytes. However, an experienced technician is required as evaluation of the staining patterns is challenging (129). The "atypical" pattern frequently found in sera of patients with PSC is characterized by broad inhomogeneous rim-like staining of the nuclear periphery and multiple intranuclear fluorescent foci. By contrast, "classical" p-ANCA with fine rim-like staining of the perinuclear cytoplasm are predominantly found in patients with microscopic polyangiitis (129).

The principal target antigen of p-ANCA is a matter of debate but is likely located within the cell nucleus rather than in the cytoplasm (130, 131). The most likely candidate antigen is beta-tubulin isoform 5 (TBB-5) (132). Interestingly, p-ANCA cross-react with FtsZ, which is considered an evolutionary ancestor of TBB-5 and is widely abundant in bacteria of the human intestine (132). This highlights that abnormal immune responses to commensal bacteria might be implied in the pathogenesis of PSC.

Both cytoplasmic ANCA (c-ANCA) and p-ANCA were also found in bile fluid of patients with PSC and correlated with several adverse clinical outcomes, which might further underline their pathogenetic significance (133).

The presence of p-ANCA in serum has been associated with unfavorable clinical outcomes in patients with PSC (134). However, this notion has been challenged by other authors (135). Recently, p-ANCA have been linked to a distinct clinical phenotype of PSC with p-ANCA-positive patients being younger at disease-onset and at lower risk of cholangiocarcinoma (68). Moreover, the genotypes of p-ANCA-positive patients more often comprised the strong PSC-risk alleles HLA-B*08 and DRB1*03 (68). In small-duct PSC, a more benign variant of "classical" PSC which presents with a normal cholangiogram, the prevalence, and clinical significance of p-ANCA is unclear (136).

Antibodies to Biliary Epithelial Cells (BEC)

Few studies found antibodies of different subtypes in sera of patients with PSC directed against BEC (137–140). Levels of IgA antibodies directed against BEC were correlated with adverse patient outcomes (140). Furthermore, it has been demonstrated that antibodies against BEC and bacterial lipopolysaccharides co-activate cytokine release by BEC and therefore induce biliary immune responses (139). This provides further evidence for the involvement of microbiota in the pathogenesis of PSC. Testing for anti-BEC antibodies has not been introduced into clinical practice.

Antibodies Found in Patients With PSC and Additional AIH

Additional features of AIH are found in approximately 5% of adult patients with PSC (141) but are prevalent in 35–65% of children

with PSC (142, 143). In children and adolescents, the primary manifestation of disease may be that of typical AIH, together with cholangiographic and histological changes of sclerosing cholangitis (also called autoimmune sclerosing cholangitis) (142). Testing patients with PSC for ANA, anti-SMA using IFT and for anti-SLA/LP using ELISA should be performed when additional AIH is suspected. Liver histology is mandatory to establish suspected AIH in patients with PSC, which will affect treatment decisions since AIH should be treated with immunosuppression (1, 125).

Antibodies Against Glycoprotein 2 (Anti-GP2)

Recently, IgA-class antibodies against glycoprotein 2 (anti-GP2 IgA), which were formerly linked to severe types of Crohn's disease (144), were detected in sera of patients with PSC at a prevalence of 46.7–71.5%. The presence of anti-GP2 IgA was strongly associated with large bile-duct involvement, development of cholangiocarcinoma, and increased mortality (3). Therefore, anti-GP2 might serve as a novel biomarker of risk stratification in patients with PSC. Moreover, evidence for the involvement of GP2 in immune responses of the intestinal mucosa to gut bacteria (145, 146) provides a further pathophysiological link to the recently discovered aberrant community structure of the gut microbiota in patients with PSC (147–149).

Other Antibodies: IgG4

IgG4-associated cholangitis (IAC) can display a cholangiographical pattern similar to PSC (150). Since patients with IAC usually benefit from treatment with corticosteroids, all patients with suspected PSC should be tested for elevated serum-IgG4 levels (124). However, 10–12% of patients with classical PSC might have increased levels of IgG4 as well (150). It is unclear to date, whether these patients represent a subgroup of PSC with a different clinical presentation or course of disease.

CONCLUSION

Testing for autoantibodies is required to diagnose AIH and PBC, and it may be helpful to diagnose selected patients with PSC. IFT on tissue sections and HEp-2 cells is the screening tool of choice in patients with suspected autoimmune liver disease. Immunofluorescence pattern on HEp-2 cells must be reported to correctly interpret obtained results. ELISA for anti-SLA/LP should be included in the diagnostic workup not to miss patients only presenting with these rather AIH-specific antibodies. Some of the autoantibodies may be associated with disease course, and emerging data on novel antibodies in PSC may help to elucidate the hitherto unknown pathogenesis of disease.

AUTHOR CONTRIBUTIONS

MS, CW-N, TL, and CS wrote the manuscript and reviewed the final version.

ACKNOWLEDGMENTS

MS, CW-N, and CS are supported by the DFG (SE 2665/1-1, SFB841 and KFO306). CS is supported by the Helmut and Hannelore Greve Foundation and the YAEL Foundation.

REFERENCES

1. European Association for the Study of the Liver. EASL clinical practice guidelines: autoimmune hepatitis. *J Heatol* (2015) 63:971–1004.
2. European Association for the Study of the Liver. EASL clinical practice guidelines: the diagnosis and management of patients with primary biliary cholangitis. *J Hepatol* (2017) 67:145–72. doi:10.1016/j.jhep.2017.03.022
3. Jendrek ST, Gotthardt D, Nitzsche T, Widmann L, Korf T, Michaels MA, et al. Anti-GP2 IgA autoantibodies are associated with poor survival and cholangiocarcinoma in primary sclerosing cholangitis. *Gut* (2017) 66:137–44. doi:10.1136/gutjnl-2016-311739
4. Manns MP, Czaja AJ, Gorham JD, Krawitt EL, Mieli-Vergani G, Vergani D, et al. Diagnosis and management of autoimmune hepatitis. *Hepatology* (2010) 51:2193–213. doi:10.1002/hep.23584
5. Manns MP, Lohse AW, Vergani D. Autoimmune hepatitis – update 2015. *J Hepatol* (2015) 62:100–11. doi:10.1016/j.jhep.2015.03.005
6. Johnson PJ, McFarlane IG. Meeting report: international autoimmune hepatitis group. *Hepatology* (1993) 18:998–1005. doi:10.1002/hep.1840180435
7. Alvarez F, Berg PA, Bianchi FB, Bianchi L, Burroughs AK, Cancado EL, et al. International autoimmune hepatitis group report: review of criteria for diagnosis of autoimmune hepatitis. *J Hepatol* (1999) 31:929–38. doi:10.1016/S0168-8278(99)80297-9
8. Hennes EM, Zeniya M, Czaja AJ, Parés A, Dalekos GN, Krawitt EL, et al. Simplified criteria for the diagnosis of autoimmune hepatitis. *Hepatology* (2008) 48:169–76. doi:10.1002/hep.22322
9. Vergani D, Alvarez F, Bianchi FB, Cançado EL, Mackay IR, Manns MP, et al. Liver autoimmune serology: a consensus statement from the committee for autoimmune serology of the international autoimmune hepatitis group. *J Hepatol* (2004) 41:677–83. doi:10.1016/j.jhep.2004.08.002
10. Tan EM, Feltkamp TE, Smolen JS, Butcher B, Dawkins R, Fritzler MJ, et al. Range of antinuclear antibodies in "healthy" individuals. *Arthritis Rheum* (1997) 40:1601–11. doi:10.1002/art.1780400909
11. Couto CA, Bittencourt PL, Porta G, Abrantes-Lemos CP, Carrilho FJ, Guardia BD, et al. Antismooth muscle and antiactin antibodies are indirect markers of histological and biochemical activity of autoimmune hepatitis. *Hepatology* (2014) 59:592–600. doi:10.1002/hep.26666
12. Homberg JC, Abuaf N, Bernard O, Islam S, Alvarez F, Khalil SH, et al. Chronic active hepatitis associated with antiliver/kidney microsome antibody type 1: a second type of "autoimmune" hepatitis. *Hepatology* (1987) 7:1333–9. doi:10.1002/hep.1840070626
13. Martini E, Abuaf N, Cavalli F, Durand V, Johanet C, Homberg JC. Antibody to liver cytosol (anti-LC1) in patients with autoimmune chronic active hepatitis type 2. *Hepatology* (1988) 8:1662–6. doi:10.1002/hep.1840080632
14. Durazzo M, Philipp T, Van Pelt FN, Lüttig B, Borghesio E, Michel G, et al. Heterogeneity of liver-kidney microsomal autoantibodies in chronic hepatitis C and D virus infection. *Gastroenterology* (1995) 108:455–62. doi:10.1016/0016-5085(95)90074-8
15. Gregorio GV, Portmann B, Reid F, Donaldson PT, Doherty DG, McCartney M, et al. Autoimmune hepatitis in childhood: a 20-year experience. *Hepatology* (1997) 25:541–7. doi:10.1002/hep.510250308
16. Kanzler S, Weidemann C, Gerken G, Löhr HF, Galle PR, Meyer zum Büschenfelde KH, et al. Clinical significance of autoantibodies to soluble liver antigen in autoimmune hepatitis. *J Hepatol* (1999) 31:635–40. doi:10.1016/S0168-8278(99)80342-0
17. Ballot E, Homberg JC, Johanet C. Antibodies to soluble liver antigen: an additional marker in type 1 auto-immune hepatitis. *J Hepatol* (2000) 33:208–15. doi:10.1016/S0168-8278(00)80361-X
18. Czaja AJ, Donaldson PT, Lohse AW. Antibodies to soluble liver antigen/liver pancreas and HLA risk factors for type 1 autoimmune hepatitis. *Am J Gastroenterol* (2002) 97:413–9. doi:10.1111/j.1572-0241.2002.05479.x

19. Kirstein MM, Metzler F, Geiger E, Heinrich E, Hallensleben M, Manns MP, et al. Prediction of short- and long-term outcome in patients with autoimmune hepatitis. *Hepatology* (2015) 62:1524–35. doi:10.1002/hep.27983
20. Manns M, Gerken G, Kyriatsoulis A, Staritz M, Meyer zum Buschenfelde KH. Characterisation of a new subgroup of autoimmune chronic active hepatitis by autoantibodies against a soluble liver antigen. *Lancet* (1987) 1:292–4. doi:10.1016/S0140-6736(87)92024-1
21. Mieli-Vergani G, Vergani D, Baumann U, Czubkowski P, Debray D, Dezsofi A, et al. Diagnosis and management of paediatric autoimmune liver disease: ESPGHAN hepatology committee position statement. *J Pediatr Gastroenterol Nutr* (2018) 66(2):345–60. doi:10.1097/MPG.0000000000001801
22. Gregorio GV, McFarlane B, Bracken P, Vergani D, Mieli-Vergani G. Organ and non-organ specific autoantibody titres and IgG levels as markers of disease activity: a longitudinal study in childhood autoimmune liver disease. *Autoimmunity* (2002) 35:515–9. doi:10.1080/0891693021000056721
23. Cowling DC, Mackay IR, Taft LI. Lupoid hepatitis. *Lancet* (1956) 271:1323–6.
24. Liberal R, Mieli-Vergani G, Vergani D. Clinical significance of autoantibodies in autoimmune hepatitis. *J Autoimmun* (2013) 46:17–24. doi:10.1016/j.jaut.2013.08.001
25. Czaja AJ, Nishioka M, Morshed SA, Hachiya T. Patterns of nuclear immunofluorescence and reactivities to recombinant nuclear antigens in autoimmune hepatitis. *Gastroenterology* (1994) 107:200–7. doi:10.1016/0016-5085(94)90078-7
26. Strassburg CP, Obermayer-Straub P, Alex B, Durazzo M, Rizzetto M, Tukey RH, et al. Autoantibodies against glucuronosyltransferases differ between viral hepatitis and autoimmune hepatitis. *Gastroenterology* (1996) 111:1576–86. doi:10.1016/S0016-5085(96)70020-3
27. Strassburg CP, Alex B, Zindy F, Gerken G, Lüttig B, Meyer zum Büschenfelde KH, et al. Identification of cyclin A as a molecular target of antinuclear antibodies (ANA) in hepatic and non-hepatic autoimmune diseases. *J Hepatol* (1996) 25:859–66. doi:10.1016/S0168-8278(96)80290-X
28. Czaja AJ, Morshed SA, Parveen S, Nishioka M. Antibodies to single-stranded and double-stranded DNA in antinuclear antibody-positive type 1-autoimmune hepatitis. *Hepatology* (1997) 26:567–72. doi:10.1002/hep.510260306
29. Parveen S, Morshed SA, Arima K, Nishioka M, Czaja AJ, Chow WC, et al. Antibodies to Ro/La, Cenp-B, and snRNPs antigens in autoimmune hepatitis of North America versus Asia: patterns of immunofluorescence, ELISA reactivities, and HLA association. *Dig Dis Sci* (1998) 43:1322–31. doi:10.1023/A:1018880429469
30. Beisel C, Weiler-Normann C, Teufel A, Lohse AW. Association of autoimmune hepatitis and systemic lupus erythematodes: a case series and review of the literature. *World J Gastroenterol* (2014) 20:12662–7. doi:10.3748/wjg.v20.i35.12662
31. Whittingham S, Irwin J, Mackay IR, Smalley M. Smooth muscle autoantibody in "autoimmune" hepatitis. *Gastroenterology* (1966) 51:499–505.
32. Cotler SJ, Kanji K, Keshavarzian A, Jensen DM, Jakate S. Prevalence and significance of autoantibodies in patients with non-alcoholic steatohepatitis. *J Clin Gastroenterol* (2004) 38:801–4. doi:10.1097/01.mcg.0000139072.38580.a0
33. Muratori P, Muratori L, Agostinelli D, Pappas G, Veronesi L, Granito A, et al. Smooth muscle antibodies and type 1 autoimmune hepatitis. *Autoimmunity* (2002) 35:497–500. doi:10.1080/0891693021000054066
34. Toh BH. Smooth muscle autoantibodies and autoantigens. *Clin Exp Immunol* (1979) 38:621–8.
35. Wiedmann KH, Melms A, Berg PA. Anti-actin antibodies of IgM and IgG class in chronic liver diseases detected by fluorometric immunoassay. *Liver* (1983) 3:369–76. doi:10.1111/j.1600-0676.1983.tb00890.x
36. Frenzel C, Herkel J, Lüth S, Galle PR, Schramm C, Lohse AW. Evaluation of F-actin ELISA for the diagnosis of autoimmune hepatitis. *Am J Gastroenterol* (2006) 101:2731–6. doi:10.1111/j.1572-0241.2006.00830.x
37. Liaskos C, Bogdanos DP, Davies ET, Dalekos GN. Diagnostic relevance of anti-filamentous actin antibodies in autoimmune hepatitis. *J Clin Pathol* (2007) 60:107–8. doi:10.1136/jcp.2006.039404
38. Czaja AJ, Manns MP, Homburger HA. Frequency and significance of antibodies to liver/kidney microsome type 1 in adults with chronic active hepatitis. *Gastroenterology* (1992) 103:1290–5. doi:10.1016/0016-5085(92)91518-9
39. Kerkar N, Ma Y, Davies ET, Cheeseman P, Mieli-Vergani G, Vergani D. Detection of liver kidney microsomal type 1 antibody using molecularly based immunoassays. *J Clin Pathol* (2002) 55:906–9. doi:10.1136/jcp.55.12.906
40. Gueguen M, Meunier-Rotival M, Bernard O, Alvarez F. Anti-liver kidney microsome antibody recognizes a cytochrome P450 from the IID subfamily. *J Exp Med* (1988) 168:801–6. doi:10.1084/jem.168.2.801
41. Manns MP, Johnson EF, Griffin KJ, Tan EM, Sullivan KF. Major antigen of liver kidney microsomal autoantibodies in idiopathic autoimmune hepatitis is cytochrome P450db1. *J Clin Invest* (1989) 83:1066–72. doi:10.1172/JCI113949
42. Zanger UM, Hauri HP, Loeper J, Homberg JC, Meyer UA. Antibodies against human cytochrome P-450db1 in autoimmune hepatitis type II. *Proc Natl Acad Sci U S A* (1988) 85:8256–60. doi:10.1073/pnas.85.21.8256
43. Manns MP, Griffin KJ, Sullivan KF, Johnson EF. LKM-1 autoantibodies recognize a short linear sequence in P450IID6, a cytochrome P-450 monooxygenase. *J Clin Invest* (1991) 88:1370–8. doi:10.1172/JCI115443
44. Yamamoto AM, Cresteil D, Boniface O, Clerc FF, Alvarez F. Identification and analysis of cytochrome P450IID6 antigenic sites recognized by anti-liver-kidney microsome type-1 antibodies (LKM1). *Eur J Immunol* (1993) 23:1105–11. doi:10.1002/eji.1830230519
45. Bortolotti F, Vajro P, Balli F, Giacchino R, Crivellaro C, Barbera C, et al. Non-organ specific autoantibodies in children with chronic hepatitis C. *J Hepatol* (1996) 25:614–20. doi:10.1016/S0168-8278(96)80228-5
46. Nishioka M, Morshed SA, Kono K, Himoto T, Parveen S, Arima K, et al. Frequency and significance of antibodies to P450IID6 protein in Japanese patients with chronic hepatitis C. *J Hepatol* (1997) 26:992–1000. doi:10.1016/S0168-8278(97)80107-9
47. Duclos-Vallee JC, Hajoui O, Yamamoto AM, Jacz-Aigrain E, Alvarez F. Conformational epitopes on CYP2D6 are recognized by liver/kidney microsomal antibodies. *Gastroenterology* (1995) 108:470–6. doi:10.1016/0016-5085(95)90076-4
48. Klein R, Zanger UM, Berg T, Hopf U, Berg PA. Overlapping but distinct specificities of anti-liver-kidney microsome antibodies in autoimmune hepatitis type II and hepatitis C revealed by recombinant native CYP2D6 and novel peptide epitopes. *Clin Exp Immunol* (1999) 118:290–7. doi:10.1046/j.1365-2249.1999.01027.x
49. Beaune P, Dansette PM, Mansuy D, Kiffel L, Finck M, Amar C, et al. Human anti-endoplasmic reticulum autoantibodies appearing in a drug-induced hepatitis are directed against a human liver cytochrome P-450 that hydroxylates the drug. *Proc Natl Acad Sci U S A* (1987) 84:551–5. doi:10.1073/pnas.84.2.551
50. Philipp T, Durazzo M, Trautwein C, Alex B, Straub P, Lamb JG, et al. Recognition of uridine diphosphate glucuronosyl transferases by LKM-3 antibodies in chronic hepatitis D. *Lancet* (1994) 344:578–81. doi:10.1016/S0140-6736(94)91966-6
51. Csepregi A, Nemesanszky E, Luettig B, Obermayer-Straub P, Manns MP. LKM3 autoantibodies in hepatitis C cirrhosis: a further phenomenon of the HCV-induced autoimmunity. *Am J Gastroenterol* (2001) 96:910–1. doi:10.1111/j.1572-0241.2001.03383.x
52. Baeres M, Herkel J, Czaja AJ, Wies I, Kanzler S, Cancado EL, et al. Establishment of standardised SLA/LP immunoassays: specificity for autoimmune hepatitis, worldwide occurrence, and clinical characteristics. *Gut* (2002) 51:259–64. doi:10.1136/gut.51.2.259
53. Berg PA, Stechemesser E, Strienz J. Hypergammaglobulinämische chronisch aktive Hepatitis mit Nachweis von Leber-Pankreas-spezifischen komplementbindenden Antikörpern. *Verh Dtsch Ges Inn Med* (1981) 87:921–8.
54. Gelpi C, Sontheimer EJ, Rodriguez-Sanchez JL. Autoantibodies against a serine tRNA-protein complex implicated in cotranslational selenocysteine insertion. *Proc Natl Acad Sci U S A* (1992) 89:9739–43. doi:10.1073/pnas.89.20.9739
55. Stechemesser E, Klein R, Berg PA. Characterization and clinical relevance of liver-pancreas antibodies in autoimmune hepatitis. *Hepatology* (1993) 18:1–9. doi:10.1002/hep.1840180102
56. Costa M, Rodriguez-Sanchez JL, Czaja AJ, Gelpi C. Isolation and characterization of cDNA encoding the antigenic protein of the human tRNP(Ser)Sec complex recognized by autoantibodies from patients withtype-1 autoimmune hepatitis. *Clin Exp Immunol* (2000) 121:364–74. doi:10.1046/j.1365-2249.2000.01280.x
57. Wies I, Brunner S, Henninger J, Herkel J, Kanzler S, Meyer zum Büschenfelde KH, et al. Identification of target antigen for SLA/LP autoantibodies in autoimmune hepatitis. *Lancet* (2000) 355:1510–5. doi:10.1016/S0140-6736(00)02166-8

58. Volkmann M, Martin L, Bäurle A, Heid H, Strassburg CP, Trautwein C, et al. Soluble liver antigen: isolation of a 35-kd recombinant protein (SLA-p35) specifically recognizing sera from patients with autoimmune hepatitis. *Hepatology* (2001) 33:591–6. doi:10.1053/jhep.2001.22218
59. Herkel J, Heidrich B, Nieraad N, Wies I, Rother M, Lohse AW. Fine specificity of autoantibodies to soluble liver antigen and liver/pancreas. *Hepatology* (2002) 35:403–8. doi:10.1053/jhep.2002.30699
60. Mix H, Weiler-Normann C, Thimme R, Ahlenstiel G, Shin EC, Herkel J, et al. Identification of CD4 T-cell epitopes in soluble liver antigen/liver pancreas autoantigen in autoimmune hepatitis. *Gastroenterology* (2008) 135:2107–18. doi:10.1053/j.gastro.2008.07.029
61. Zachou K, Gampeta S, Gatselis NK, Oikonomou K, Goulis J, Manoussakis MN, et al. Anti-SLA/LP alone or in combination with anti-Ro52 and fine specificity of anti-Ro52 antibodies in patients with autoimmune hepatitis. *Liver Int* (2015) 35:660–72. doi:10.1111/liv.12658
62. Schramm C, Herkel J, Beuers U, Kanzler S, Galle PR, Lohse AW. Pregnancy in autoimmune hepatitis: outcome and risk factors. *Am J Gastroenterol* (2006) 101:556–60. doi:10.1111/j.1572-0241.2006.00479.x
63. Lapierre P, Hajoui O, Homberg JC, Alvarez F. Formiminotransferase cyclodeaminase is an organ-specific autoantigen recognized by sera of patients with autoimmune hepatitis. *Gastroenterology* (1999) 116:643–9. doi:10.1016/S0016-5085(99)70186-1
64. Lenzi M, Manotti P, Muratori L, Cataleta M, Ballardini G, Cassani F, et al. Liver cytosolic 1 antigen-antibody system in type 2 autoimmune hepatitis and hepatitis C virus infection. *Gut* (1995) 36:749–54. doi:10.1136/gut.36.5.749
65. Muratori L, Cataleta M, Muratori P, Manotti P, Lenzi M, Cassani F, et al. Detection of anti-liver cytosol antibody type 1 (anti-LC1) by immunodiffusion, counterimmunoelectrophoresis and immunoblotting: comparison of different techniques. *J Immunol Methods* (1995) 187:259–64. doi:10.1016/0022-1759(95)00192-X
66. Dalekos GN, Tsianos EV. Anti-neutrophil antibodies in chronic viral hepatitis. *J Hepatol* (1994) 20:561. doi:10.1016/S0168-8278(05)80508-2
67. Papp M, Norman GL, Altorjay I, Lakatos PL. Utility of serological markers in inflammatory bowel diseases: gadget or magic? *World J Gastroenterol* (2007) 13:2028–36. doi:10.3748/wjg.v13.i14.2028
68. Hov JR, Boberg KM, Taraldsrud E, Vesterhus M, Boyadzhieva M, Solberg IC, et al. Antineutrophil antibodies define clinical and genetic subgroups in primary sclerosing cholangitis. *Liver Int* (2017) 37:458–65. doi:10.1111/liv.13238
69. Marzano AV, Raimondo MG, Berti E, Meroni PL, Ingegnoli F. Cutaneous manifestations of ANCA-associated small vessels vasculitis. *Clin Rev Allergy Immunol* (2017) 53:428–38. doi:10.1007/s12016-017-8616-5
70. Rigopoulou EI, Roggenbuck D, Smyk DS, Liaskos C, Mytilinaiou MG, Feist E, et al. Asialoglycoprotein receptor (ASGPR) as target autoantigen in liver autoimmunity: lost and found. *Autoimmun Rev* (2012) 12:260–9. doi:10.1016/j.autrev.2012.04.005
71. O'Brien C, Joshi S, Feld JJ, Guindi M, Dienes HP, Heathcote EJ. Long-term follow-up of antimitochondrial antibody-positive autoimmune hepatitis. *Hepatology* (2008) 48:550–6. doi:10.1002/hep.22380
72. Dinani AM, Fischer SE, Mosko J, Guindi M, Hirschfield GM. Patients with autoimmune hepatitis who have antimitochondrial antibodies need longterm follow-up to detect late development of primary biliary cirrhosis. *Clin Gastroenterol Hepatol* (2012) 10:682–4. doi:10.1016/j.cgh.2012.02.010
73. Leung PS, Rossaro L, Davis PA, Park O, Tanaka A, Kikuchi K, et al. Antimitochondrial antibodies in acute liver failure: implications for primary biliary cirrhosis. *Hepatology* (2007) 46:1436–42. doi:10.1002/hep.21828
74. Muratori L, Parola M, Ripalti A, Robino G, Muratori P, Bellomo G, et al. Liver/kidney microsomal antibody type 1 targets CYP2D6 on hepatocyte plasma membrane. *Gut* (2000) 46:553–61. doi:10.1136/gut.46.4.553
75. Ma Y, Bogdanos DP, Hussain MJ, Underhill J, Bansal S, Longhi MS, et al. Polyclonal T-cell responses to cytochrome P450IID6 are associated with disease activity in autoimmune hepatitis type 2. *Gastroenterology* (2006) 130:868–82. doi:10.1053/j.gastro.2005.12.020
76. Longhi MS, Hussain MJ, Bogdanos DP, Quaglia A, Mieli-Vergani G, Ma Y, et al. Cytochrome P450IID6-specific CD8 T cell immune responses mirror disease activity in autoimmune hepatitis type 2. *Hepatology* (2007) 46:472–84. doi:10.1002/hep.21658
77. Löhr H, Treichel U, Poralla T, Manns M, Meyer zum Büschenfelde KH, Fleischer B. The human hepatic asialoglycoprotein receptor is a target antigen for liver-infiltrating T cells in autoimmune chronic active hepatitis and primary biliary cirrhosis. *Hepatology* (1990) 12:1314–20. doi:10.1002/hep.1840120611
78. Hanot V. *Etude sur une Forme de Cirrhose Hypertrophique du Foie (Cirrhose Hypertrophique ave ictere chronique)*. Paris: J. B. Baillere et Fils (1876).
79. Heathcote EJ. Primary biliary cirrhosis: historical perspective. *Clin Liver Dis* (2003) 7:735–40. doi:10.1016/S1089-3261(03)00098-9
80. Walker JG, Doniach D, Roitt IM, Sherlock S. Serological tests in diagnosis of primary biliary cirrhosis. *Lancet* (1965) 1:827–31. doi:10.1016/S0140-6736(65)91372-3
81. Lu C, Hou X, Li M, Wang L, Zeng P, Jia H, et al. Detection of AMA-M2 in human saliva: potentials in diagnosis and monitoring of primary biliary cholangitis. *Sci Rep* (2017) 7:796. doi:10.1038/s41598-017-00906-1
82. Jopson L, Newton JL, Palmer J, Floudas A, Isaacs J, Qian J, et al. RITPBC: B-cell depleting therapy (rituximab) as a treatment for fatigue in primary biliary cirrhosis: study protocol for a randomised controlled trial. *BMJ Open* (2015) 5:e007985. doi:10.1136/bmjopen-2015-007985
83. Deutsche Gesellschaft für Gastroenterologie, Verdauungs- und Stoffwechselkrankheiten (DGVS) (federführend), Deutsche Gesellschaft für Innere Medizin (DGIM), Deutsche M. Crohn/Colitis ulcerosa Vereinigung (DCCV), Deutsche Leberhilfe EV; Deutsche Gesellschaft für Ultraschall in der Medizin (DEGUM), Deutsche Gesellschaft für Endoskopie und Bildgebende Verfahren (DGE-BV), et al. [Practice guideline autoimmune liver diseases – AWMF-Reg. No. 021-27]. *Z Gastroenterol* (2017) 55:1135–226. doi:10.1055/s-0043-120199
84. Muratori L, Granito A, Muratori P, Pappas G, Bianchi FB. Antimitochondrial antibodies and other antibodies in primary biliary cirrhosis: diagnostic and prognostic value. *Clin Liver Dis* (2008) 12:261–276; vii. doi:10.1016/j.cld.2008.02.009
85. Braun S, Berg C, Buck S, Gregor M, Klein R. Catalytic domain of PDC-E2 contains epitopes recognized by antimitochondrial antibodies in primary biliary cirrhosis. *World J Gastroenterol* (2010) 16:973–81. doi:10.3748/wjg.v16.i8.973
86. Muratori P, Muratori L, Gershwin ME, Czaja AJ, Pappas G, Maccariello S, et al. 'True' antimitochondrial antibody-negative primary biliary cirrhosis, low sensitivity of the routine assays, or both? *Clin Exp Immunol* (2004) 135:154–8. doi:10.1111/j.1365-2249.2004.02332.x
87. Agmon-Levin N, Shapira Y, Selmi C, Barzilai O, Ram M, Szyper-Kravitz M, et al. A comprehensive evaluation of serum autoantibodies in primary biliary cirrhosis. *J Autoimmun* (2010) 34:55–8. doi:10.1016/j.jaut.2009.08.009
88. Berg PA, Klein R, Lindenborn-Fotinos J, Kloppel W. ATPase-associated antigen (M2): marker antigen for serological diagnosis of primary biliary cirrhosis. *Lancet* (1982) 2:1423–6. doi:10.1016/S0140-6736(82)91327-7
89. Gershwin ME, Mackay IR, Sturgess A, Coppel RL. Identification and specificity of a cDNA encoding the 70 kd mitochondrial antigen recognized in primary biliary cirrhosis. *J Immunol* (1987) 138:3525–31.
90. Dellavance A, Cançado EL, Abrantes-Lemos CP, Harriz M, Marvulle V, Andrade LE. Humoral autoimmune response heterogeneity in the spectrum of primary biliary cirrhosis. *Hepatol Int* (2012) 7:775–84. doi:10.1007/s12072-012-9413-0
91. Metcalf JV, Mitchison HC, Palmer JM, Jones DE, Bassendine MF, James OF. Natural history of early primary biliary cirrhosis. *Lancet* (1996) 348:1399–402. doi:10.1016/S0140-6736(96)04410-8
92. Dahlqvist G, Gaouar F, Carrat F, Meurisse S, Chazouillères O, Poupon R, et al. Large-scale characterization study of patients with antimitochondrial antibodies but nonestablished primary biliary cholangitis. *Hepatology* (2017) 65(1):152–63. doi:10.1002/hep.28859
93. Moteki S, Leung PS, Coppel RL, Dickson ER, Kaplan MM, Munoz S, et al. Use of a designer triple expression hybrid clone for three different lipoyl domain for the detection of antimitochondrial autoantibodies. *Hepatology* (1996) 24:97–103. doi:10.1002/hep.510240117
94. Tanaka A, Nezu S, Uegaki S, Mikami M, Okuyama S, Kawamura N, et al. The clinical significance of IgA antimitochondrial antibodies in sera and saliva in primary biliary cirrhosis. *Ann N Y Acad Sci* (2007) 1107:259–70. doi:10.1196/annals.1381.028
95. Surh CD, Cooper AE, Coppel RL, Leung P, Ahmed A, Dickson R, et al. The predominance of IgG3 and IgM isotype antimitochondrial autoantibodies against recombinant fused mitochondrial polypeptide in patients

with primary biliary cirrhosis. *Hepatology* (1988) 8:290–5. doi:10.1002/hep.1840080217
96. Rigopoulou EI, Davies ET, Bogdanos DP, Liaskos C, Mytilinaiou M, Koukoulis GK, et al. Antimitochondrial antibodies of immunoglobulin G3 subclass are associated with a more severe disease course in primary biliary cirrhosis. *Liver Int* (2007) 27:1226–31. doi:10.1111/j.1478-3231.2007.01586.x
97. Tana MM, Shums Z, Milo J, Norman GL, Leung PS, Gershwin ME, et al. The significance of autoantibody changes over time in primary biliary cirrhosis. *Am J Clin Pathol* (2015) 144:601–6. doi:10.1309/AJCPQV4A7QAEEFEV
98. Invernizzi P, Selmi C, Ranftler C, Podda M, Wesierska-Gadek J. Antinuclear antibodies in primary biliary cirrhosis. *Semin Liver Dis* (2005) 25:298–310. doi:10.1055/s-2005-916321
99. Nakamura M, Kondo H, Mori T, Komori A, Matsuyama M, Ito M, et al. Anti-gp210 and anti-centromere antibodies are different risk factors for the progression of primary biliary cirrhosis. *Hepatology* (2007) 45:118–27. doi:10.1002/hep.21472
100. Szostecki C, Guldner HH, Netter HJ, Will H. Isolation and characterization of cDNA encoding a human nuclear antigen predominantly recognized by autoantibodies from patients with primary biliary cirrhosis. *J Immunol* (1990) 145:4338–47.
101. Bauer A, Habior A, Kraszewska E. Detection of anti-SP100 antibodies in primary biliary cirrhosis. Comparison of ELISA and immunofluorescence. *J Immunoassay Immunochem* (2013) 34:346–55. doi:10.1080/15321819.2012.741088
102. Courvalin JC, Lassoued K, Bartnik E, Blobel G, Wozniak RW. The 210-kD nuclear envelope polypeptide recognized by human autoantibodies in primary biliary cirrhosis is the major glycoprotein of the nuclear pore. *J Clin Invest* (1990) 86:279–85. doi:10.1172/JCI114696
103. Courvalin JC, Lassoued K, Worman HJ, Blobel G. Identification and characterization of autoantibodies against the nuclear envelope lamin B receptor from patients with primary biliary cirrhosis. *J Exp Med* (1990) 172:961–7. doi:10.1084/jem.172.3.961
104. Wesierska-Gadek J, Penner E, Battezzati PM, Selmi C, Zuin M, Hitchman E, et al. Correlation of initial autoantibody profile and clinical outcome in primary biliary cirrhosis. *Hepatology* (2006) 43:1135–44. doi:10.1002/hep.21172
105. Yang F, Yang Y, Wang Q, Wang Z, Miao Q, Xiao X, et al. The risk predictive values of UK-PBC and GLOBE scoring system in Chinese patients with primary biliary cholangitis: the additional effect of anti-gp210. *Aliment Pharmacol Ther* (2017) 45:733–43. doi:10.1111/apt.13927
106. Sfakianaki O, Koulentaki M, Tzardi M, Tsangaridou E, Theodoropoulos PA, Castanas E, et al. Peri-nuclear antibodies correlate with survival in Greek primary biliary cirrhosis patients. *World J Gastroenterol* (2010) 16:4938–43. doi:10.3748/wjg.v16.i39.4938
107. Liberal R, Grant CR, Sakkas L, Bizzaro N, Bogdanos DP. Diagnostic and clinical significance of anti-centromere antibodies in primary biliary cirrhosis. *Clin Res Hepatol Gastroenterol* (2013) 37:572–85. doi:10.1016/j.clinre.2013.04.005
108. Honda A, Ikegami T, Matsuzaki Y. Anti-gp210 and anti-centromere antibodies for the prediction of PBC patients with an incomplete biochemical response to UDCA and bezafibrate. *Hepatol Res* (2015) 45:827–8. doi:10.1111/hepr.12461
109. Mandai S, Kanda E, Arai Y, Hirasawa S, Hirai T, Aki S, et al. Anti-centromere antibody is an independent risk factor for chronic kidney disease in patients with primary biliary cirrhosis. *Clin Exp Nephrol* (2013) 17:405–10. doi:10.1007/s10157-012-0724-1
110. Norman GL, Yang CY, Ostendorff HP, Shums Z, Lim MJ, Wang J, et al. Anti-kelch-like 12 and anti-hexokinase 1: novel autoantibodies in primary biliary cirrhosis. *Liver Int* (2015) 35:642–51. doi:10.1111/liv.12690
111. Chazouilleres O, Wendum D, Serfaty L, Montembault S, Rosmorduc O, Poupon R. Primary biliary cirrhosis-autoimmune hepatitis overlap syndrome: clinical features and response to therapy. *Hepatology* (1998) 28:296–301. doi:10.1002/hep.510280203
112. Eyraud V, Chazouilleres O, Ballot E, Corpechot C, Poupon R, Johanet C. Significance of antibodies to soluble liver antigen/liver pancreas: a large French study. *Liver Int* (2009) 29:857–64. doi:10.1111/j.1478-3231.2009.01986.x
113. Kanzler S, Bozkurt S, Herkel J, Galle PR, Dienes HP, Lohse AW. Presence of SLA/LP autoantibodies in patients with primary biliary cirrhosis as a marker for secondary autoimmune hepatitis (overlap syndrome). *Dtsch Med Wochenschr* (2001) 126:450–6. doi:10.1055/s-2001-12906
114. Muratori P, Granito A, Pappas G, Pendino GM, Quarneti C, Cicola R, et al. The serological profile of the autoimmune hepatitis/primary biliary cirrhosis overlap syndrome. *Am J Gastroenterol* (2009) 104:1420–5. doi:10.1038/ajg.2009.126
115. Karlsen TH, Folseraas T, Thorburn D, Vesterhus M. Primary sclerosing cholangitis – a comprehensive review. *J Hepatol* (2017) 67:1298–323. doi:10.1016/j.jhep.2017.07.022
116. Warren KW, Athanassiades S, Monge JI. Primary sclerosing cholangitis – a study of forty-two cases. *Gut* (1966) 111:23–38.
117. Hirschfield GM, Karlsen TH, Lindor KD, Adams DH. Primary sclerosing cholangitis. *Lancet* (2013) 382:1587–99. doi:10.1016/S0140-6736(13)60096-3
118. Takakura WR, Tabibian JH, Bowlus CL. The evolution of natural history of primary sclerosing cholangitis. *Curr Opin Gastroenterol* (2017) 33:71–7. doi:10.1097/MOG.0000000000000333
119. Boonstra K, Weersma RK, van Erpecum KJ, Rauws EA, Spanier BWM, Poen AC, et al. Population-based epidemiology, malignancy risk, and outcome of primary sclerosing cholangitis. *Hepatology* (2013) 58:2045–55. doi:10.1002/hep.26565
120. Tischendorf JJW, Hecker H, Krüger M, Manns MP, Meier PN. Characterization, outcome, and prognosis in 273 patients with primary sclerosing cholangitis: a single center study. *Am J Gastroenterol* (2007) 102:107–14. doi:10.1111/j.1572-0241.2006.00872.x
121. Dave M, Elmunzer MBJ, Dwamena BA, Higgins PDR. Primary sclerosing cholangitis: meta-analysis of diagnostic performance of MR cholangiopancreatography. *Radiology* (2010) 256:387–96. doi:10.1148/radiol.10091953
122. Burak KW, Angulo P, Lindor KD. Is there a role for liver biopsy in primary sclerosing cholangitis? *Am J Gastroenterol* (2003) 98:1155–8. doi:10.1111/j.1572-0241.2003.07401.x
123. Lazaridis KN, LaRusso NF. Primary sclerosing cholangitis. *N Engl J Med* (2016) 375:1161–70. doi:10.1056/NEJMra1506330
124. Lindor KD, Kowdley KV, Edwyn Harrison M; American College of Gastroenterology. ACG clinical guideline: primary sclerosing cholangitis. *Am J Gastroenterol* (2015) 110:646–59. doi:10.1038/ajg.2015.112
125. European Association for the Study of the Liver. EASL clinical practice guidelines: management of cholestatic liver diseases. *J Hepatol* (2009) 51:237–67.
126. Hov JR, Boberg KM, Karlsen TH, Kozarek RA, Invernizzi P. Autoantibodies in primary sclerosing cholangitis. *World J Gastroenterol* (2008) 14:3781–91. doi:10.3748/wjg.14.3781
127. Roozendaal C, de Jong MA, van den Berg AP, van Wijk RT, Limburg PC, Kallenberg CG. Clinical significance of anti-neutrophil cytoplasmic autoimmune liver diseases antibodies (ANCA) in autoimmune liver diseases. *J Hepatol* (2000) 32:734–41. doi:10.1016/S0168-8278(00)80241-X
128. Terjung B, Herzog V, Worman HJ, Gestmann I, Bauer C, Sauerbruch T, et al. Atypical antineutrophil cytoplasmic antibodies with perinuclear fluorescence in chronic inflammatory bowel diseases and hepatobiliary disorders colocalize with nuclear lamina proteins. *Hepatology* (1998) 28:332–40. doi:10.1002/hep.510280207
129. Terjung B, Spengler U. Atypical p-ANCA in PSC and AIH: a hint toward a "leaky gut"? *Clin Rev Allergy Immunol* (2009) 36:40–51. doi:10.1007/s12016-008-8088-8
130. Terjung B, Spengler U, Sauerbruch T, Worman HJ. "Atypical p-ANCA" in IBD and hepatobiliary disorders react with a 50-kilodalton nuclear envelope protein of neutrophils and myeloid cell lines. *Gastroenterology* (2000) 119:310–22. doi:10.1053/gast.2000.9366
131. Terjung B, Worman HJ, Herzog V, Sauerbruch T, Spengler U. Differentiation of antineutrophil nuclear antibodies in inflammatory bowel and autoimmune liver diseases from antineutrophil cytoplasmic antibodies (p-ANCA) using immunofluorescence microscopy. *Clin Exp Immunol* (2001) 126:37–46. doi:10.1046/j.1365-2249.2001.01649.x
132. Terjung B, Sohne J, Lechtenberg B, Gottwein J, Muennich M, Herzog V, et al. p-ANCAs in autoimmune liver disorders recognise human beta-tubulin isotype 5 and cross-react with microbial protein FtsZ. *Gut* (2010) 59:808–16. doi:10.1136/gut.2008.157818
133. Lenzen H, Weismüller TJ, Negm AA, Wlecke J, Loges S, Strassburg CP, et al. Scandinavian journal of gastroenterology antineutrophil cytoplasmic antibodies in bile are associated with disease activity in primary sclerosing

cholangitis. *Scand J Gastroenterol* (2013) 48:1205–12. doi:10.3109/00365521.2013.825313
134. Pokorny CS, Norton ID, McCaughan GW, Selby WS. Anti-neutrophil cytoplasmic antibody: a prognostic indicator in primary sclerosing cholangitis. *J Gastroenterol Hepatol* (1994) 9:40–4. doi:10.1111/j.1440-1746.1994.tb01214.x
135. Lo SK, Fleming KA, Chapman RW. A 2-year follow-up study of anti-neutrophil antibody in primary sclerosing cholangitis: relationship to clinical activity, liver biochemistry and ursodeoxycholic acid treatment. *J Hepatol* (1994) 21:974–8. doi:10.1016/S0168-8278(05)80604-X
136. Tervaert J, van Hoek B, Koek G. Antineutrophil cytoplasmic antibodies in small-duct primary sclerosing cholangitis. *Gastroenterology* (2009) 136:364. doi:10.1053/j.gastro.2008.11.033
137. Xu B, Broome U, Ericzon BG, Sumitran-Holgersson S. High frequency of autoantibodies in patients with primary sclerosing cholangitis that bind biliary epithelial cells and induce expression of CD44 and production of interleukin 6. *Gut* (2002) 51:120–7. doi:10.1136/gut.51.1.120
138. Mandal A, Dasgupta A, Jeffers L, Squillante L, Hyder S, Reddy R, et al. Autoantibodies in sclerosing cholangitis against a shared peptide in biliary and colon epithelium. *Gastroenterology* (1994) 106:185–92. doi:10.1016/S0016-5085(94)95271-X
139. Karrar A, Broomé U, Södergren T, Jaksch M, Bergquist A, Björnstedt M, et al. Biliary epithelial cell antibodies link adaptive and innate immune responses in primary sclerosing cholangitis. *Gastroenterology* (2007) 132:1504–14. doi:10.1053/j.gastro.2007.01.039
140. Berglin L, Björkström NK, Bergquist A. Primary sclerosing cholangitis is associated with autoreactive IgA antibodies against biliary epithelial cells. *Scand J Gastroenterol* (2013) 48:719–28. doi:10.3109/00365521.2013.786131
141. Kaya M, Angulo P, Lindor KD. Overlap of autoimmune hepatitis and primary sclerosing cholangitis: an evaluation of a modified scoring system. *J Hepatol* (2000) 33:531–42. doi:10.1034/j.1600-0641.2000.033004537.x
142. Gregorio GV, Portmann B, Karani J, Harrison P, Donaldson PT, Vergani D, et al. Autoimmune hepatitis/sclerosing cholangitis overlap syndrome in childhood: a 16-year prospective study. *Hepatology* (2001) 33:544–53. doi:10.1053/jhep.2001.22131
143. Feldstein AE, Perrault J, El-Youssif M, Lindor KD, Freese DK, Angulo P. Primary sclerosing cholangitis in children: a long-term follow-up study. *Hepatology* (2003) 38:210–7. doi:10.1053/jhep.2003.50289
144. Papp M, Sipeki N, Tornai T, Altorjay I, Norman GL, Shums Z, et al. Rediscovery of the anti-pancreatic antibodies and evaluation of their prognostic value in a prospective clinical cohort of Crohn's patients: the importance of specific target antigens [GP2 and CUZD1]. *J Crohns Colitis* (2015) 9:659–68. doi:10.1093/ecco-jcc/jjv087
145. Yu S, Lowe AW. The pancreatic zymogen granule membrane protein, GP2, binds *Escherichia coli* type 1 fimbriae. *BMC Gastroenterol* (2009) 9:58. doi:10.1186/1471-230X-9-58
146. Hase K, Kawano K, Nochi T, Pontes GS, Fukuda S, Ebisawa M, et al. Uptake through glycoprotein 2 of FimH + bacteria by M cells initiates mucosal immune response. *Nature* (2009) 462:226–30. doi:10.1038/nature08529
147. Kummen M, Holm K, Anmarkrud JA, Nygård S, Vesterhus M, Høivik ML, et al. The gut microbial profile in patients with primary sclerosing cholangitis is distinct from patients with ulcerative colitis without biliary disease and healthy controls. *Gut* (2017) 66:611–9. doi:10.1136/gutjnl-2015-310500
148. Rühlemann MC, Heinsen F-A, Zenouzi R, Lieb W, Franke A, Schramm C. Faecal microbiota profiles as diagnostic biomarkers in primary sclerosing cholangitis. *Gut* (2017) 66:753–4. doi:10.1136/gutjnl-2016-312180
149. Sabino J, Vieira-Silva S, Machiels K, Joossens M, Falony G, Ballet V, et al. Primary sclerosing cholangitis is characterised by intestinal dysbiosis independent from IBD. *Gut* (2016) 65:1681–9. doi:10.1136/gutjnl-2015-311004
150. Mendes FD, Jorgensen R, Keach J, Katzmann JA, Smyrk T, Donlinger J, et al. Elevated serum IgG4 concentration in patients with primary sclerosing cholangitis. *Am J Gastroenterol* (2006) 101:2070–5. doi:10.1111/j.1572-0241.2006.00772.x

Conflict of Interest Statement: The authors declare that the research was conducted in the absence of any commercial or financial relationships that could be construed as a potential conflict of interest.

frontiers in Immunology

REVIEW
published: 26 March 2018
doi: 10.3389/fimmu.2018.00541

Autoantibodies Associated With Connective Tissue Diseases: What Meaning for Clinicians?

Kevin Didier[1], Loïs Bolko[2], Delphine Giusti[3,4], Segolene Toquet[5], Ailsa Robbins[1], Frank Antonicelli[3,6] and Amelie Servettaz[1,3]*

[1] Department of Internal Medicine, Infectious Diseases, and Clinical Immunology, Reims Teaching Hospitals, Robert Debré Hospital, Reims, France, [2] Rheumatology Department, Maison Blanche Hospital, Reims University Hospitals, Reims, France, [3] Laboratory of Dermatology, Faculty of Medicine, EA7319, University of Reims Champagne-Ardenne, Reims, France, [4] Laboratory of Immunology, Reims University Hospital, University of Reims Champagne-Ardenne, Reims, France, [5] Department of Internal Medicine, CHU de Reims, Reims, France, [6] Department of Biological Sciences, Immunology, UFR Odontology, University of Reims Champagne-Ardenne, Reims, France

OPEN ACCESS

Edited by:
Ralf J. Ludwig,
University of Lübeck, Germany

Reviewed by:
Kayo Masuko,
Sanno Medical Center, Japan
Maurizio Acampa,
Azienda Ospedaliera Universitaria Senese, Italy
Cheng-De Yang,
Ruijin Hospital, China

***Correspondence:**
Frank Antonicelli
frank.antonicelli@univ-reims.fr

Specialty section:
This article was submitted to Immunological Tolerance and Regulation, a section of the journal Frontiers in Immunology

Received: 15 January 2018
Accepted: 02 March 2018
Published: 26 March 2018

Citation:
Didier K, Bolko L, Giusti D, Toquet S, Robbins A, Antonicelli F and Servettaz A (2018) Autoantibodies Associated With Connective Tissue Diseases: What Meaning for Clinicians? Front. Immunol. 9:541. doi: 10.3389/fimmu.2018.00541

Connective tissue diseases (CTDs) such as systemic lupus erythematosus, systemic sclerosis, myositis, Sjögren's syndrome, and rheumatoid arthritis are systemic diseases which are often associated with a challenge in diagnosis. Autoantibodies (AAbs) can be detected in these diseases and help clinicians in their diagnosis. Actually, pathophysiology of these diseases is associated with the presence of antinuclear antibodies. In the last decades, many new antibodies were discovered, but their implication in pathogenesis of CTDs remains unclear. Furthermore, the classification of these AAbs is nowadays misused, as their targets can be localized outside of the nuclear compartment. Interestingly, in most cases, each antibody is associated with a specific phenotype in CTDs and therefore help in better defining either the disease subtypes or diseases activity and outcome. Because of recent progresses in their detection and in the comprehension of their pathogenesis implication in CTD-associated antibodies, clinicians should pay attention to the presence of these different AAbs to improve patient's management. In this review, we propose to focus on the different phenotypes and features associated with each autoantibody used in clinical practice in those CTDs.

Keywords: antibody, systemic lupus erythematosus, Sjögren's syndrome, systemic sclerosis, antisynthetase syndrome, dermatomyositis, necrotizing myopathy, rheumatoid arthritis

Abbreviations: AAb, autoantibody; ACPA, anti-citrullinated protein/peptide antibody; ACR, American College of Rheumatology; ANA, antinuclear antibody; anti-dsDNA, anti-double-stranded DNA; AQP4, aquaporin 4; APL, antiphospholipid; APS, antiphospholipid syndrome; ASS, antisynthetase syndrome; CCP, cyclic citrullinated peptide; CHB, congenital heart block; CN1a, cytosolic 5′-nucleotidase 1A; CTD, connective tissue disease; DM, dermatomyositis; dSSc, diffuse systemic sclerosis; EULAR, European League Against Rheumatism; GAPSS, global antiphospholipid score; HMGCR, 3-hydroxy-3-methylglutaryl-coenzyme A reductase; IBM, inclusion body myositis; IIF, indirect immunofluorescence; ILD, interstitial lung disease; lSSc, limited systemic sclerosis; MCTD, mixed connective tissue disease; MDA5, melanoma differentiation-associated gene 5; NM, necrotizing myopathy; NMO, neuromyelitis optica; NOR, nucleolus organizer region; NuRD, nucleosome remodeling histone deacetylase protein complex; NXP2, nuclear matrix protein 2; PAH, pulmonary arterial hypertension; PF, pulmonary fibrosis; RA, rheumatoid arthritis; RF, rheumatoid factor; SAE, small ubiquitin-like modifier activating enzyme; SLE, systemic lupus erythematosus; SLICC, Systemic Lupus International Collaborating Clinics; SRP, signal recognition particle; SS, Sjögren's syndrome; SSc, systemic sclerosis; TdP, torsade de pointes; TIF1-γ, transcription intermediary factor 1 gamma.

INTRODUCTION

Connective tissue diseases (CTDs) are autoimmune diseases characterized by the involvement of several organs and the presence of various autoantibodies (AAbs). Their implication in the pathogenesis of these CTD remains partly unclear; nevertheless, we know that some of these AAbs are directly involved in tissue damages whereas some are just markers of disease development.

During the last decades, many improvements were made in the comprehension of CTD pathogenesis, and a lot of new AAb were described. The presence of AAb can help the clinician in his approach to search an autoimmune disease (1), as sometimes the production of specific AAb precedes the symptoms and the diagnosis of the CTD (2, 3). Indeed, in most cases, those AAbs are detected in a specific CTD, making the diagnosis easier. Actually, most studies recently published focused on the clinical impact of AAb in different CTD and found that some AAbs are clearly associated with a specific phenotype in one type of CTD, allowing the clinician to adapt the follow-up of his patient and to predict some complications. However, relationship between AAb presence and disease diagnosis is not always that simple, as some other AAbs can be associated with more than one disease. Furthermore, differences can exist for the same kind of CTD according to the population studied, strengthening the fact that genetical factors in CTD pathogenesis are probably more important than we actually know. A potential explanation to these variations may be related to genetic and environmental factors, which may play a key role in these diseases predisposition and outcome.

Indeed, pathogenesis of CTD seems associated with the presence of AAb. However, many new AAbs were discovered, but their implication in pathogenesis of connective tissue diseases (CTDs) remains unclear. Many of these AAbs are antinuclear antibody (ANA). Nevertheless, the classification of ANA is nowadays misused, as their targets can be localized outside of the nuclear compartment (cytoplasmic, membrane, or extracellular), even if the term ANA is still currently used in clinic.

Because of the new improvements in their detection and comprehension of their pathological implication in CTDs-associated antibodies, clinicians should pay attention to the presence of the different AAbs to improve patient's management. In this review, we propose to focus on the different phenotypes and features associated with each AAb used in clinical practice in CTD clearly defined such as systemic lupus erythematosus (SLE), Sjögren's syndrome (SS), systemic sclerosis (SSc), myositis, and rheumatoid arthritis (RA). Especially, we will highlight the usefulness of their clinical determination.

AAb IN HEALTHY POPULATION AND IN NON-AUTOIMMUNE DISEASES

Biological autoimmunity is not always pathological and can be observed in healthy people. The highlighting of ANA in the general population is common and estimated between 5.92 and 30.8% (4–13) with a lower prevalence in the Chinese population (4) and a higher prevalence in the Afro-American population (13) (**Table 1**). In addition, ANAs are more commonly detected in women than in men (4–8, 10–14), and the prevalence of such ANA increases with aging, as it reaches up to 24% in subjects older than 85 years (14). ANAs are commonly detected by indirect immunofluorescence (IIF) on HEp2 cells, a human HELA-derivative cell line. Importantly, the relevance of a positive ANA test is directly linked to its titration. Thus, in a normal population, ANAs were found positive in 31.7% of individuals at 1/40 serum dilution, 13.3% at 1/80, 5.0% at 1/160, and 3.3% at 1/320 (15). The most accepted threshold is often the dilution 1/160 for first screening dilution (15–17). In complement to IIF assay, which is a very sensitive technic and can now be automated (18, 19), screening fluorescence enzyme or chemiluminescence immunoassays have been proposed in the last few years as detection assays. These multiparametric immunoassays allow simultaneous testing for 13–17 of commonest pathogenic autoantibody specificities in systemic autoimmune diseases [i.e., SSA-52kD, SSA-60kD, SSB, U1RNP (RNP 70,A,C), CENP-B, Scl70, Jo1, Fibrillarin, RNA polymerase III, ribosomal proteins, PM-Scl, PCNA, Mi2 proteins, Sm, dsDNA, and chromatin]. These screening immunoassays showed relatively good concordance with IIF (75–83%) and demonstrated similar or improved specificity and positive predictive value depending on the studies and the assays (20–24). However, due to the limited number of represented antigens in some screening assays and the better sensitivity of IIF, the American College of Rheumatology (ACR) ANA Task Force recommended that IIF should remain the gold standard for ANA testing (25).

In most healthy individuals with ANA, the antigenic target(s) remain(s) unknown with standard tests used to identify ANA

TABLE 1 | Presence of antinuclear antibody (ANA) in different populations considered as healthy people.

Reference	Population	Number	ANA positivity (%)	1/40 Nb (%)	1/80 Nb (%)	1/160 Nb (%)	1/320 Nb (%)	1/640 Nb (%)	1/1,280 Nb (%)	1/2,560 Nb (%)
Wang et al. (4)	Chinese	20,970	5.92	886 (4.23)	105 (0.50)	77 (0.37)	55 (0.26)	29 (0.14)	36 (0.17)	53 (0.25)
Minz et al. (5)	Indian	36,310	12.3	–	–	–	–	–	–	–
Selmi et al. (6)	Italian	2,690	18.1	–	–	–	–	–	–	–
Fernandez et al. (7)	Brazilian	500	22.6	73 (14.6)	23 (4.6)	10 (2.0)	1 (0.2)	–	2 (0.4)	2 (0.4)
Peene et al. (8)	Belgian	10,550	23.5	–	–	–	–	–	–	–
Hayashi et al. (10)	Japanese	2,181	25.9	–	–	–	–	–	–	–
Racoubian et al. (11)	Lebanese	10,814	26.4	–	2,162 (20.0)	–	400 (3.7)	183 (1.7)	119 (1.1)	–
Roberts-Thomson et al. (12)	Australian	20,205	28.3	–	–	–	–	–	–	–
Wandstrat et al. (13)	Afro-American	1,827	30.8	–	–	–	–	–	–	–

ANA positivity was defined as the first titer seen in this table for each study.

subtypes. Nevertheless, in a minority of cases, AAbs from healthy people recognize the same autoantigens as AAb from patients with autoimmune disease, especially anti-SSa in up to 3% and anti-DFS70 AAb (also called LEDGF for "lens epithelium-derived growth factor") (4, 10, 11). Anti-SSa AAbs are frequently detected in the sera from patients with SLE and SS, whereas anti-DFS70 AAbs have mostly been evidenced in healthy people, but also in the sera from patients with benign and common diseases such as atopic dermatitis (26–29). In general population, anti-Ro/SSa AAbs are associated with torsade de pointes (TdP) and arrhythmia, representing a clinically silent novel risk factor for TdP development *via* an autoimmune-mediated electrophysiological interference with the hERG channel (30).

Antinuclear antibody and other AAbs can also be observed in association with drugs (such as hydralazine and procainamide) or in non-autoimmune diseases associated with a process of tolerance breakdown such as infectious or lymphoproliferative diseases.

SYSTEMIC LUPUS ERYTHEMATOSUS-ASSOCIATED AAb

Systemic lupus erythematosus is a CTD with a great variability in its clinical presentation and its prognosis. Two main classification criteria are available, based on the presence of both clinical and immunological parameters [1997 ACR classification criteria and Systemic Lupus International Collaborating Clinics (SLICC) classification criteria (31, 32)]. The different AAbs associated with SLE and their main features are recapitulated in **Table 2**.

ANA in SLE

Antinuclear antibody is one of the immunological criteria present in the two SLE classifications criteria as an ANA titer detected by IIF on HEP2 cells >1/160 is observed in nearly all SLE patients [between 94 and 100% (33–35)]. The quantity of ANA progressively increases during the 3–5 years preceding SLE clinical expression and diagnosis (2). Consequently, ANA testing represents an essential screening tool because their negativity (titer less than 1/160) makes the diagnosis of SLE extremely unlikely (36). By contrast, their presence, even at higher titer is not SLE-specific as ANA can be produced in a lot of other circumstances such as other CTD, hematologic and hepatic diseases, virus infections, drugs uptake, and in healthy people as previously mentioned. In case of positivity, ANA antigen target(s) must be determined by additional tests with nuclear autoantigens.

Clinical Usefulness of ANA Testing

- In case of SLE suspicion given clinical symptoms
- Importantly, ANAs are useless in SLE follow-up as they remain positive whatever disease activity.

Antigen Targets of ANA in SLE

Anti-Double-Stranded DNA (Anti-dsDNA) AAb

Anti-double-stranded DNA AAbs are present in 43–92% of cases (37–39) with a specificity between 89 and 99% but with variable clinical sensitivities from 8 to 54% (40–46). The methods used for anti-dsDNA AAb detection are numerous, which explains the variability observed in terms of sensitivity. Anti-dsDNA AAbs are quite well identified by nuclear homogeneous IFI pattern (47), but their presence may also be evaluated by quantitative assays such as Farr radioimmunoassay (45), chemiluminescence immunoassay (42, 43), ELISA (46), and fluoro-enzyme immunoassay or by qualitative assays such as immunofluorescence test on *Crithidia luciliae* (CLIFT) (44, 46). For each method, performances will vary according to the manufacturer and the source of the dsDNA (synthetic or purified ds DNA from human or calf origin). Globally, ELISA methods to detect anti-dsDNA antibodies are highly sensitive, but are less specific for the diagnosis of SLE than the immunofluorescence test on CLIFT and the Farr assay as they also detect low-avidity antibodies (48).

Anti-double-stranded DNA AAb positivity is one criteria present in both ACR and SLICC classifications (49). As for the majority of AAb, the specificity of anti-dsDNA AAb in SLE is not of 100% [specificity between 96 and 99% according to the type of test and the published series (40, 41)]. Indeed, they can also be evidenced in the setting of infection, elevation of C reactive protein and in healthy individuals (50). In SLE, the serum level of this AAb is generally correlated with disease activity (51). Moreover, high level of such AAb and their association with anti-Sm antibodies (defined below) are associated with kidney involvement in patients with SLE (52, 53).

TABLE 2 | AAb associated with systemic lupus erythematosus (SLE).

AAb	Prevalence	Sensitivity	Specificity	Clinical features
Anti-dsDNA	43–92% (37–39)	8–54% (40–46)	89–99% (40–46)	Correlation with disease activity
Anti-nucleosome	59.8–61.9% (53–57)	52–61% (53–57)	87.5–95.7% (53–57)	Correlation with disease activity
Anti-Sm	15–55.5% (37–39, 61)	10–55% (62)	98–100% (62)	Most specific antibody in SLE often associated with anti-RNP AAb
Anti-histone	50–81% >90% in induced SLE (37, 71, 72)	–	–	Drug-induced SLE
Anti-C1q	4–60% (90–93)	28% (94–97)	92% (94–97)	Associated with glomerulonephritis
Anti-ribosomal P	12–60% (37, 103, 104)	36% (103, 104, 109)	97–100% (103, 104, 109)	Neuropsychiatric manifestations
Anti-Ro/SSa	36–64% (37, 38, 61, 75, 76)	–	–	Skin involvement+++ CHB
Anti-La/SSb	8–33.6% (37, 38, 61, 75, 76)	25.7% (85)	96.7% (85)	Skin involvement+++ CHB (less than anti-Ro AAb)
Anti-RNP	23.3–49% (37–39)	8–69% (62)	25–82% (62)	–

CHB, congenital heart block; anti-dsDNA, anti-double-stranded DNA; AAb, autoantibody.

Clinical Usefulness of Anti-dsDNA AAb Testing

- In case of SLE suspicion and ANA > 1/160
- In the follow-up of SLE patients when positive at time of diagnosis (the same test in the same laboratory should always be used in this setting).

Anti-Nucleosome AAb

The nucleosome is a basic unit of DNA packaging, implicated in the formation of repeating units of chromatin. The anti-nucleosome AAbs are detected in 59.8 and 61.9% of SLE patients' sera with a sensitivity between 52 and 61% (the highest sensitivity in SLE) and a specificity between 87.5 and 95.7% (54–57). Although, presenting the same nuclear homogenous pattern on Hep2 cells (47), they can be present in the absence of anti-dsDNA AAb and consequently may be helpful for clinicians at diagnosis. In SLE murine models, serum anti-nucleosome AAbs are produced before anti-dsDNA AAb (58). Consequently, the detection of these AAbs may be helpful to establish diagnosis. It is noteworthy that the level of anti-nucleosome AAb (especially IgG3 subtype) is correlated with SLE activity (59). The simultaneous presence of anti-dsDNA, anti-nucleosome, and anti-histone (defined below) AAb has been shown to be associated with severe kidney involvement (54, 60). However, such AAbs have also been detected in patients with mixed connective tissue disease (MCTD) and SSc (56).

Clinical Usefulness of Anti-Nucleosome AAb Testing

- In case of SLE suspicion and ANA > 1/160 and negative anti-dsDNA AAb
- In the follow-up of SLE patients when positive at time of diagnosis (the same test in the same laboratory should always be used in this setting)

Anti-Sm AAb

Sm proteins are linked to RNA in the nuclear compartment. Characterized by nuclear coarse speckled pattern on Hep2 cells (47), anti-Sm AAbs are present in 15–55.5% of SLE patients (37–39, 61). These AAbs have a low sensitivity (10–55%) but are very specific for SLE (98–100% according to the test used and to the studied population) and are therefore used in the classification criteria (31, 49, 62).

The main usefulness of anti-Sm AAb detection seems to be in the subset of patients with SLE but without anti-dsDNA AAb, for whom they are present in 14.8% of cases (63). The anti-Sm AAb highlighting in SLE seems to be associated with lupus nephritis (52, 64) and with a poorer prognosis if they are present at the onset of kidney disease (65) and with a higher clinical relevance if they are associated with anti-dsDNA AAb (52, 53). In this line, a recent study showed that the association of a low concentration of complement fraction C3 and signs of complement activity (CH50), together with a high rate of anti-Sm AAb is predictive of lupus nephritis (66). Furthermore, anti-Sm AAbs are mostly expressed in association with anti-RNP (see below) AAb (67). In contrast to anti-dsDNA and anti-nucleosome AAb, anti-Sm AAb level does not correlate with disease activity (68, 69).

Clinical Usefulness of Anti-Sm AAb Testing

- In case of SLE suspicion and ANA > 1/160 and negative anti-DNA AAb
- Not useful in the follow-up of SLE patients
- Association with lupus nephritis

Anti-Histone AAb

Histones are proteins strongly linked to DNA allowing its compaction, thus forming the nucleosome structure. AAb directed against histone are associated with nuclear homogenous pattern on Hep2 cells (47). In drug-induced SLE such as procainamide, hydralazine, and quinine (70), about 95% of these patients develop anti-histone AAb, whereas these AAbs are only detected in 50–81% of cases of primary SLE (37, 71, 72).

Generally, drug-induced SLE regresses with treatment interruption, and the production of anti-histone AAb decreases alongside the activity of the disease (70, 73, 74).

Clinical Usefulness of Anti-Histone AAb Testing

- In case of drug-induced SLE
- Decreased rate associated with regression of drug-induced SLE

Anti-Ro and Anti-La AAb

Anti-Ro (also called anti-SSa) and anti-La (also called anti-SSb) AAbs are often associated with SS but can also occur in SLE with a prevalence between 36 and 64% and between 8 and 33.6% for anti-Ro AAb and anti-La AAb, respectively (37, 38, 61, 75, 76). These antibodies are detected in sera about 3.6 years before SLE diagnosis (2) and commonly give a nuclear fine-speckled pattern on Hep2 cells (47).

In SLE, they are associated with skin (75, 77) and hematologic manifestations such as cytopenia (78). Furthermore, these AAbs are responsible for neonatal lupus by transplacental passage with cardiac, cutaneous, hematologic, hepatobiliary, and neurologic involvement (79). Neonatal lupus occurs in only 2% of female patients with anti-Ro/SSa or anti-La/SSb (80, 81). Maternal autoimmune disease associated with neonatal lupus development is not always SLE, since maternal SLE is responsible for only 15–50% of neonatal lupus cases (79, 82). AAbs directed against the subunit 52 kDa of Ro are associated with a higher risk of congenital heart block (CHB) (41). In more than 90% of neonatal lupus cases, AAb regress within 9 months (82) and only few infants will develop authentic SLE (80, 81). The risk of CHB in these infants may be prevented by maternal treatment with hydroxychloroquine during pregnancy (83, 84). The sensitivity of anti-SSb for SLE is lower than in SS, about 25% and the specificity about 97% (85).

Adult patients with anti-Ro/SSa-positive CTD show a high prevalence of QTc interval prolongation (86), with a direct correlation between anti-Ro52 kDa level and QTc duration (87). In fact, anti-Ro/SSa-positive patients have a particularly high risk of developing complex ventricular arrhythmias (88).

Clinical Usefulness of Anti-Ro and Anti-La AAb Testing

- In case of skin and hematologic manifestations
- Association with CHB

Anti-RNP AAb

Anti-RNP AAbs are found in serum from patients with MCTD. In SLE, these AAbs are detected in 23.3–49% of cases (37–39). These AAbs are frequently associated with nuclear coarse speckled pattern on Hep2 cells (47). Clinical sensitivity in SLE is between 8 and 69%, with a specificity between 25 and 82% (62). In contrast with other SLE AAb, anti-RNP AAbs are detected within the year preceding SLE diagnosis (2). However, up to now, correlation with SLE phenotype remains to be clarified.

Clinical Usefulness of Anti-RNP AAb Testing

- No specific phenotype in SLE
- Useless for follow-up

Non-Antinuclear AAb Frequently Observed in SLE

Anti-C1q AAb

Patients with genetic defect in C1q expression have an increased risk to develop a lupus-like disease (89). Anti-C1q AAbs are found in 4–60% of SLE patients, and their prevalence increase with aging (90–93).

High production of anti-C1q AAb is associated with membranoproliferative glomerulonephritis development with 28 and 92% of sensitivity and specificity, respectively (94–97).

These AAbs are detected 2–6 months before lupus nephritis onset (98–100). By contrast, the absence of anti-C1q AAb is associated with less kidney involvement during SLE course (101). These AAbs are also observed in hypocomplementemic urticarial vasculitis associated or not with SLE (also called McDuffie syndrome) (102).

Clinical Usefulness of Anti-C1q AAb Testing

- In case of lupus nephritis
- Also seen in hypocomplementemic urticarial vasculitis

Anti-Ribosomal P AAb

Substance P is a neuropeptide that acts as a neurotransmitter and a neuromodulator. Anti-ribosomal P AAb may be detected by very dense fine granular cytoplasmic pattern when testing for ANA on Hep2 cells (47). These AAbs are detected in 12–20% of SLE patients (37, 103, 104) and are associated with disease activity and with neuropsychiatric involvement (105–108). The specificity is between 97 and 100%, and the sensitivity is about 36% (103, 104, 109).

Clinical Usefulness of Anti-Ribosomal P AAb Testing

- In case of neuropsychiatric lupus
- Useless for follow-up

Antiphospholipid (APL) AAb

The antiphospholipid syndrome (APS) is observed in 29–46% of SLE patients (110). APS is defined by pregnancy morbidity (mainly fetal losses) and thromboses (arterial and/or venous) in association with the presence of at least one APL AAb [lupus anticoagulant, anticardiolipin (IgM or IgG), and anti-β2 glycoprotein I (IgM or IgG) AAb] on two or more occasions at least 12 weeks apart (111). Some non-thrombotic manifestations such as thrombocytopenia, livedo reticularis, renal microangiopathy, and myelitis can occur in APS but do not belong to classification criteria (112). In SLE, lupus anticoagulant and anticardiolipin are present, respectively, in about 40 and 30% of cases (with or without APS in the same proportion) (113, 114).

Patients having SLE with APS have a threefold higher risk than those without APL to develop a Libman–Sacks endocarditis (115, 116), an increased risk of vascular events (such as thrombosis) and death (113, 114, 117), and a higher risk to develop pulmonary hypertension (118). A global antiphospholipid score is currently developed in SLE to predict thrombotic risk (119).

Clinical Usefulness of Anti-APL AAb Testing

- In all SLE patients at diagnosis
- In all SLE patients regularly during the follow-up and in case of vascular thrombosis, and/or pregnancy morbidity

Anti-Aquaporin 4 (AQP4) AAb

Aquaporin 4 is the main water channel in the brain and is also responsible for glutamate and potassium regulation in the blood–brain barrier, synapses, and paranodes adjacent to the nodes of Ranvier. Anti-AQP4 AAb is well known to be specific to neuromyelitis optica (NMO), also called Devic's syndrome (120).

These AAbs can be detected in SLE and are associated with authentic NMO or atypical NMO (myelitis alone or optic neuritis alone) (121, 122). Anti-AQP4 AAb seem to be strongly associated with anti-Ro/SSa AAb and also, to a lesser extent, anti-dsDNA AAb (122, 123). Nevertheless, these AAbs can also be detected in SLE and persist for years without concurrent clinical or radiological NMO signs (124). These AAbs can be evidenced in the serum, but their detection in the cerebrospinal fluid from patients allows a higher sensitivity and specificity of the test (125).

Clinical Usefulness of Anti-AQP4 AAb Testing

- Useless for diagnosis
- Only if NMO signs

SJÖGREN'S SYNDROME-ASSOCIATED AAb

Sjögren's syndrome is a CTD affecting mainly women, and whose main feature is sicca syndrome. Various organs can be involved in severe forms. Classification criteria include both clinical and immunological parameters (126). Two different forms are observed: primary SS and secondary SS, which is associated with other CTD. The different AAbs observed in patients' sera and their main features are summarized in **Table 3**.

TABLE 3 | AAb associated with Sjögren's syndrome.

AAb	Prevalence	Sensitivity	Specificity	Features
Anti-Ro52	33–77.1% (130–134)	42% (130)	100% (130)	CHB++
Anti-Ro60	33–77.1% (130–134)	51% (130)	98% (130)	CHB
Anti-La/SSb	23–47.8% (130–134)	29% (130)	99% (130)	Doubt on pathogenicity
Anti-α-fodrin	98% (141–143)	40% (141–143)	80% (141–143)	–

CHB, congenital heart block; AAb, autoantibody.

ANA in SS

Antinuclear antibody prevalence is estimated between 41.9 and 64% in this disease (127–130). Nevertheless, important discrepancies are observed in the immunological presentation of these patients because the detection of AAb is not mandatory for diagnosis (126). Patients producing high level of ANA with anti-Ro/SSa and/or anti-La/SSb AAb display a more severe disease with various organ involvements.

Clinical Usefulness of ANA Testing

- Distribution disparity because of classification criteria of SS (immunologic criteria not always required in presence of sicca syndrome and histopathology)
- Importantly, ANAs are useless in SS follow-up.

Targets of ANA in SS

The two main antigens recognized by AAb in SS patients are the Ro/SSa (with two subunits, one of 52 kDa and one of 60 kDa) and the La/SSb antigens. The detection of either anti-Ro/SSa and/or anti-La/SSb AAb constitutes one of the classification criteria but their presence is not mandatory for diagnosis (126). These AAbs are evidenced 4–7 years before SS diagnosis (3, 130).

The sensitivity of anti-Ro52, anti-Ro60, and anti-La is estimated at about 42, 51, and 29%, respectively, whereas the specificity is estimated at about 100, 98, and 99%, respectively (130).

Anti-Ro/SSa AAbs are detected in 33–77.1% of primary SS, whereas anti-La/SSb AAbs are present in 23–47.8% of primary SS (130–134). Anti-Ro/SSa AAb can be observed without anti-La/SSb AAb in patients' sera, conversely anti-La/SSb alone are rarely evidenced (133). Of note, a recent study reported that the diagnosis of SS was unlikely in patients who had only anti-La/SSb AAb without any anti-Ro/SSa AAb (135).

Concerning disease features, patients displaying both anti-Ro/SSa and anti-La/SSb AAbs are more at risk to develop a non-Hodgkin lymphoma, whereas the absence of those AAbs seems to be associated with a better prognosis (136). In pregnant women, anti-Ro/SSa AAb can induce a high-degree atrioventricular block in fetus in 1–2% of pregnancies (137, 138). This conduction defect seems to be mainly due to anti-52 kDa Ro/SSa AAb (41, 139). Infants of mothers with SS represent 20–30% of neonatal lupus cases (79, 82). Except for cardiac involvement, neonatal lupus signs are completely solved in most of these infants at 9 months of life (82).

In primary SS, anti-Ro/SSa and anti-La/SSb AAbs are associated with earlier disease onset, longer disease duration, greater severity of glandular symptoms, and higher prevalence of extraglandular manifestations (140).

As described previously, adult patients with anti-Ro/SSa-positive CTD show a high prevalence of QTc interval prolongation (86), with a direct correlation between anti-Ro52 kDa level and QTc duration (87). These findings suggest that anti-Ro/SSa-positive patients may have a particularly high risk of developing life-threatening arrhythmias. In fact, anti-Ro/SSa-positive patients have a particularly high risk of developing complex ventricular arrhythmias (88).

Clinical Usefulness of Anti-Ro and Anti-La AAb Testing

- Association with disease severity (risk of non-Hodgkin lymphoma)
- Association with CHB (mostly anti-Ro52) and neonatal lupus by transplacental passage, necessity of screening test and cardiac fetal follow-up in pregnant women at risk
- Useless for follow-up

Non-Antinuclear AAb Observed in SS

Anti-Alpha-Fodrin AAb

Alpha-fodrin is an intracellular, actin-binding, organ-specific protein of the cytoskeleton. AAb directed against α-fodrin can be detected in SS in 98% of cases with a sensitivity of about 40% and a specificity of about 80% (141–143). This kind of AAb can also be detected in SLE patients' sera (141, 144).

These AAbs do not seem to be associated with disease activity or clinical manifestation (145). Anti-α-fodrin AAb could be useful in SS diagnosis when both anti-Ro/SSa and anti-La/SSb were not detected (146).

Clinical Usefulness Anti-α-Fodrin AAb Testing

- Useful for diagnosis in absence of anti-Ro/SSa and anti-La/SSb AAb
- Useless for follow-up

Anti-AQP4 AAb

As shown previously, anti-AQP4 AAbs are associated with NMO, also called Devic's syndrome (120) but can also be detected in SS in association with anti-Ro/SSa AAb in most of cases (122, 123). These AAbs in SS are associated with cranial/peripheral neuropathy, authentic NMO or atypical NMO (myelitis alone or optic neuritis alone) (121, 122). These AAbs can be evidenced both in the serum and in the cerebrospinal fluid (125).

Clinical Usefulness of Anti-AQP4 AAb Testing

- Useless for diagnosis
- Only if NMO signs

SYSTEMIC SCLEROSIS-ASSOCIATED AAb

Systemic sclerosis is a CTD characterized by fibrosis, vasculopathy, and autoimmunity. Clinical and immunological expressions of the disease are highly heterogeneous since a large

variety of organs can be involved, and various AAbs may be detected in the sera of patients with SSc. Some correlations have been observed between clinical expression and AAb type. In addition, some AAbs are listed in the European League Against Rheumatism (EULAR) classification criteria (147). The association of the different antibodies with the SSc variants is detailed in **Table 4**.

ANA in SSc

Antinuclear antibody prevalence is high in SSc, since about 95% of patients' sera display such AAb (148–150). Various nuclear proteins can be targeted in SSc. Topoisomerase I, centromeric proteins, and RNA polymerase III represent the three most frequent autoantigens recognized in SSc, but numerous other antigens can be identified. Surprisingly and unexplainedly, the production of two different AAbs by a single patient is exceptional (151).

Clinical Usefulness of ANA Testing

- In case of SSc suspicion given clinical symptoms, negative ANA in suspicion of SSc makes the diagnosis unlikely.
- Importantly, ANAs are useless in SSc follow-up as they remain positive whatever disease activity.

Targets of ANA in SSc

Anti-DNA Topoisomerase I AAb (Anti-Scl70 AAb)

Type I DNA topoisomerases are enzymes that cut one of the two strands of double-stranded-DNA, relax the strand and reanneal the strand. Anti-DNA topoisomerase I AAbs are detected in 30.1–41.2% of SSc sera (150, 152, 153) with a sensitivity estimated about 43% and a specificity about 90% (154). Classically, the associated immunofluorescence pattern on Hep2 cells is speckled and nucleolar (155, 156).

These AAbs are associated with diffuse systemic sclerosis (dSSc) and with a higher risk of pulmonary fibrosis (PF) (157, 158). Two studies reported that anti-Scl70 (a topoisomerase I protein) AAb levels were correlated with disease activity (159) and that negativation of their detection was associated with a better prognosis (160). Nevertheless, these results remain controversial, and their follow-up during disease evolution is not anymore recommended nowadays. Survival rate at 10 years after diagnosis in patients producing those AAbs is estimated at 66% (161).

Clinical Usefulness of Anti-Scl70 AAb Testing

- Association with diffuse SSc and PF
- Not recommended for follow-up nowadays

Anti-Centromere AAb

The centromere is a part of the chromosomal structure that links a pair of sister chromatids. Anti-centromere AAbs are detected in 28.2–36.9% of SSc patients (150, 152, 153) with a sensitivity estimated about 44% and a specificity about 93% (154).

These AAbs are associated with limited systemic sclerosis (lSSc) and with a higher risk to develop pulmonary arterial hypertension (PAH) (157, 158, 162). Survival rate at 10 years of patients with anti-centromere AAb, about 93%, is better the one those from patients with anti-Scl70 AAb (161).

Clinical Usefulness of Anti-Centromere AAb Testing

- Association with limited SSc with a good prognosis
- Association with PAH
- Useless for follow-up, not correlated with disease activity

TABLE 4 | AAb associated with systemic sclerosis (SSc).

AAb	Prevalence	Sensitivity	Specificity	Clinical features
Anti-Scl70/DNA topoisomerase I	30.1–41.2% (150, 152, 153)	43% (154)	90% (154)	Diffuse SSc PF
Anti-centromere	28.2–36.9% (150, 152, 153)	44% (154)	93% (154)	Limited SSc PAH
Anti-RNA polymerase III	3.8–19.4% (152, 153, 163, 164)	38% (154)	94% (154)	Diffuse SSc Scleroderma renal crisis
Anti-U1-RNP	4.8–4.9% (152, 153)	–	–	Limited SSc PAH Overlap with SLE or MCTD
Anti-U3-RNP	1.4–8% 16–18.5 in AA (152, 153, 181–183)	12% (154)	97% (154)	Diffuse SSc PAH
Anti-Pm/Scl	3.1–13% (150, 152, 173)	12.5% (154, 174)	98% (154, 174)	Limited SSc Overlap with myositis PF Digital ulcers
Anti-Ku	1.1–4.6% (150, 152, 176, 177)	–	–	Limited SSc Overlap with myositis
Anti-Th/To	0.2–3.4% (152, 153)	–	–	Limited SSc PAH
Anti-NOR90	6% (150)	–	–	Limited SSc PF

PAH, pulmonary arterial hypertension; AA, Afro-American population; SLE, systemic lupus erythematosus; MCTD, mixed connective tissue disease; PF, pulmonary fibrosis; AAb, autoantibody.

Anti-RNA Polymerase AAb

RNA polymerase III is used to transcribe DNA into small RNA. Characterized by fine-speckled nucleoplasmic stain with additional occasional bright dots on Hep2 cells (47), anti-RNA polymerase III AAbs are detected in 3.8–19.4% of SSc sera, depending on ethnic group (152, 153, 163, 164) with a sensitivity about 38% and a specificity about 94% (154).

These AAbs are associated with dSSc and with a higher risk of scleroderma renal crisis, gastric antral vascular ectasia (also called watermelon stomach), and cancer (mainly synchronous breast cancer) (157, 165–167). Patients with anti-RNA polymerase III have a higher Rodnan skin score (used for skin fibrosis graduation) than patients with other AAbs and also are more likely to be rapid progressor (167, 168). Survival rate at 10 years in patients producing these AAbs is low, about 30% (161).

Other polymerases can be targeted by self-reactive lymphocytes. Anti-RNA polymerase I AAb may also be produced by SSc patients, mainly in association with anti-RNA polymerase III AAb production. Of note, the detection of isolated anti-RNA polymerase I AAb is not associated with SSc (169). The presence of both anti-RNA polymerase I/III AAb is also associated with cancer and scleroderma renal crisis (170, 171). Furthermore, the concomitant production of anti-RNA polymerase II and III AAb seems to increase the risk of scleroderma renal crisis as compare to the production of anti-RNA polymerase III AAb alone (172).

Clinical Usefulness of Anti-RNA Polymerase AAb Testing

- Mostly concerning anti-RNA polymerase III AAb in clinical practice
- Association with risk of scleroderma renal crisis
- Cancer must be search (mostly breast cancer)
- Useless for follow-up, not correlated with disease activity

Anti-Pm/Scl AAb

Anti-Pm/Scl AAbs are detected in 3.1–13% of SSc patients (150, 152, 173) with a sensitivity about 12.5% and a specificity about 98% (154, 174). Anti-Pm/Scl AAbs are distinguished by homogeneous nucleolar pattern by IFI (47).

These AAbs are associated with lSSc, overlap syndrome with myositis, PF, and digital ulcers (157, 174, 175). By contrast, PAH is less frequent in patients producing those AAbs (174).

Clinical Usefulness of Anti-Pm/Scl AAb Testing

- Mostly seen in overlap syndrome with myositis
- Less likely to be associated with PAH
- Useless for follow-up, not correlated with disease activity

Anti-Ku AAb

Anti-Ku AAbs are detected in 1.1–4.6% of SSc sera (150, 152, 176, 177), frequently associated with nuclear fine-speckled pattern on Hep2 cells (47). They are associated with lSSc and with a higher risk of myositis and interstitial lung disease (ILD) (150, 157, 177), the absence of digital ulcers and telangiectasia (176).

Clinical Usefulness of Anti-Ku AAb Testing

- Rarely seen in practice
- Useless for follow-up, not correlated with disease activity

Anti-Th/To AAb

Anti-Th/To AAb can be detected in 0.2–3.4% of SSc patients (152, 153) with homogeneous nucleolar fluorescence such as anti-Pm/Scl AAb (47). These AAbs are associated with lSSc and a higher risk of PAH (157, 162). A recent long-term follow-up study evidenced that patients with anti-Th/To AAbs are more likely to develop pulmonary hypertension (PAH or pulmonary hypertension secondary to ILD) with a better prognosis and less joint involvement than other SSc patients with other AAbs (178).

Clinical Usefulness of Anti-Th/To AAb Testing

- Rarely seen in practice
- Association with pulmonary hypertension (PAH or pulmonary hypertension secondary to ILD)
- Useless for follow-up, not correlated with disease activity

Anti-RNP AAb

Anti-U1-RNP AAbs, distinguished by nuclear coarse speckled pattern by IFI (47), are found in 4.8–4.9% of SSc patients (152, 153). They are associated with lSSc and with a higher risk to develop PAH (157). Patients with anti-U1-RNP AAb-associated PAH seems to have a better prognosis than SSc related-PAH associated with other antibodies (179). The presence of this kind of AAb evokes an overlap syndrome with other autoimmune diseases, mostly SLE and MCTD (180).

Anti-U3-RNP AAbs (also called anti-fibrillarin AAb), distinguished by clumpy nucleolar pattern on Hep 2 cells (47), are globally detected in 1.4 and 8% of SSc cases, with important differences between the populations studied (150, 152, 153, 181–183) with a sensitivity about 12% and a specificity about 97% (154). However, these AAbs are more frequently detected in Afro-American people (16–18.5%) (183, 184). Fibrillarin is a component of several ribonucleoproteins including a nucleolar small nuclear ribonucleoprotein. These AAbs are frequently associated with rapidly progressive dSSc (with a Rodnan skin score lower than in other dSSc), muscular involvement, and a higher risk of PAH (182). The presence of anti-fibrillarin AAb in Afro-American population is associated with a higher risk of digital ulcers, pericarditis, and gastrointestinal involvement, but in contrast, with less pulmonary involvement (184).

Clinical Usefulness of Anti-RNP AAb Testing

- In practice, always ask for both U1 and U3-RNP AAb because of clinical differences
- Anti-U1-RNP AAb associated with PAH
- Anti-U3-RNP AAb frequent in Afro-American people and associated with diffuse SSc
- Useless for follow-up, not correlated with disease activity

Anti-Ro/SSa AAb

Anti-Ro/SSa AAbs, also evidenced in SLE and in the SS, are detected in 15–19% of SSc patients, especially AAb directed against the 52 kDa subunit (185). Conversely, anti-SSb AAbs are rarely observed in SSc.

Patients with anti-Ro/SSa AAb show a high prevalence of QTc interval prolongation correlated with anti-Ro52 kDa level and with a higher risk to develop complex ventricular arrhythmias (86–88).

Clinical Usefulness of Anti-Ro and Anti-La AAb Testing

- Not associated with clinical phenotype
- Useless for follow-up, not correlated with disease activity

Anti-NOR90 AAb

Nucleolus organizer regions (NORs) are chromosomal regions crucial for the formation of the nucleolus. Anti-NOR90 AAbs are directed against a 90 kDa component of NOR and are found in about 6% of SSc patients (150). These AAbs are associated with punctate nucleolar fluorescence on Hep2 cells (47). Anti-NOR90 AAbs seem to be associated with lSSc and PF (150). These AAbs can also be detected in patients with SLE, SS, and RA (186).

Clinical Usefulness of Anti-NOR90 AAb Testing

- Rarely seen in practice and not specific to SSc
- Useless for follow-up, not correlated with disease activity

Anti-Histone AAb

Anti-histone AAbs are evidenced in some SSc sera and seem to be associated with critical internal organ involvement such as cardiac, pulmonary, and renal involvement, and with a decreased survival rate (187, 188).

Clinical Usefulness of Anti-Histone AAb Testing

- Rarely seen in practice
- Useless for follow-up, not correlated with disease activity

Non-Antinuclear AAb Frequently Observed in SSc

Anti-Citrullinated Protein/Peptide AAb (ACPA)

These AAbs are commonly observed in patients with RA but can also be detected in 10% of SSc patients (189). In a recent meta-analysis, the presence of this kind of AAb in the setting of SSc was associated with dSSc, erosive arthritis, and PF (189).

Clinical Usefulness of ACPA Testing

- Association with erosive arthritis (means overlap syndrome with RA?)
- Useless for follow-up, not correlated with disease activity

MYOSITIS-ASSOCIATED AAb

Myositis are characterized by a high phenotypic heterogeneity ranging from isolated muscle involvement to various organs manifestations such as ILD, arthritis, or overlap syndrome with other autoimmune diseases. AAbs are currently evidenced in 60–80% of these patients (190, 191). AAbs observed in myositis can be divided in two different groups: myositis-specific AAb (mostly non-ANA) and AAb that can be also observed in other CTD. Four distinct forms of myositis with specific AAbs are currently recognized depending on their clinical and histological features: polymyositis [mainly the antisynthetase syndrome (ASS)], necrotizing myopathy (NM), dermatomyositis (DM), and inclusion body myositis (IBM) (192, 193). In all of these myositis manifestations, only one AAb is detectable in each patient (194). The different myositis-specific AAbs are recapitulated in **Table 5**.

TABLE 5 | AAb associated with myositis [antisynthetase syndrome (ASS), necrotizing myopathy (NM), dermatomyositis (DM), and inclusion body myositis (IBM)].

Kind of myositis	AAb	Prevalence	Clinical and therapeutical features
Anti-synthetase syndrome	Anti-Jo1	70% (194, 197)	Better prognosis More likely associated with myositis than ILD
	Anti-PL7	10% (194, 197)	Poor prognosis
	Anti-PL12	15% (194, 197)	More likely associated with ILD than myositis
	Anti-EJ Anti-OJ Anti-KS Anti-ZO Anti-HA	<2% (194, 197)	–
Necrotizing myopathy	Anti-HMGCR	12–34% (63% with statin history) (202, 205, 206)	Present in statin-associated myopathies Associated with cancer Correlated with disease activity Good response to immunosuppressive treatment (except for statin naïve patients)
	Anti-SRP	18–24% (202, 205)	Correlate with disease activity Associated with ILD Poor response to immunosuppressive treatment
Dermatomyositis	Anti-TIF1-γ	13–38% (212, 213)	Strongly associated with cancer
	Anti-NXP2	17% (212, 216)	Associated with cancer Calcinosis and muscle atrophy in juvenile DM
	Anti-MDA5	10% (40% Asian population) (219, 220)	Associated with severe ILD and skin ulcerations Correlate with disease activity Poor prognosis
	Anti-SAE	7–8% (225, 226)	Severe dysphagia
	Anti-Mi2	18–35% (228, 229)	Good response to immunosuppressive treatments
Inclusion body myositis	Anti-CN1a	30% (231)	Single AAb described in IBM up to now

ILD, interstitial lung disease; AAb, autoantibody.

Anti-Synthetase Syndrome-Associated AAb

Antisynthetase syndrome is characterized clinically by myositis, ILD, arthritis, Raynaud's phenomenon, mechanic's hands, fever, and immunologically by the presence of an anti-tRNA synthetase AAb (195). In contrast with other groups of myositis, no correlation with cancer was made in ASS. Amino-acyl-tRNA-synthetases are enzymes that attach the appropriate amino acid onto its tRNA.

The different AAbs describe up to now are the anti-Jo1, anti-PL7, anti-PL12, anti-EJ, anti-OJ, anti-KS, anti-Zo, and anti-Ha AAb. Such AAb, associated with cytoplasmic speckled or fine-speckled fluorescence (47), are detected in about 30% of ASS cases (196). Anti-Jo1 AAb is the most frequently evidenced in about 70% of ASS, followed by anti-PL12 AAb in 15%, anti-PL7 AAb in 10%, whereas other ASS-associated AAbs are observed in less than 2% of the cases (194, 197).

The phenotype and the survival rate depend on the protein targeted by the AAb. Anti-PL7 and anti-PL12 AAbs are mostly associated with ILD and with a worst outcome than anti-Jo1 AAb (198). A long-term follow-up study demonstrated that anti-Jo1 AAb-associated myositis preceded the development of ILD, whereas ILD started before anti-PL7 and PL12 AAb-associated myositis (199). Patients with anti-Jo1 AAb less frequently develop sclerodactyly and ILD but display more frequently myositis than patients producing other types of anti-tRNA synthetase AAb (194). Furthermore, the level of anti-Jo1 AAb seems to be modestly correlated with muscle (in particular serum creatine kinase) and joint activity (200).

Clinical Usefulness of ASS AAb Testing

- In cases of ASS, mostly anti-Jo1, anti-PL7, and PL12 are detected
- Development of myositis first in anti-Jo1 ASS, development of ILD first in anti-PL7 and PL12 ASS
- Useless for follow-up, not correlated with disease activity (except for anti-Jo1)

Necrotizing Myopathy-Associated AAb

Necrotizing myopathy is characterized by subacute proximal limb muscle weakness, strongly elevated creatine kinase levels, muscle fiber necrosis, and regeneration, phenomenon that can be observed on muscle biopsy specimens (201). The two main AAbs in NM are directed against the signal recognition particle (anti-SRP AAb) and the 3-hydroxy-3-methylglutaryl-coenzyme A reductase (anti-HMGCR AAb). These AAbs are present in about 60% of cases (202), and both probably play a pathogenic role in the disease (203, 204).

Anti-HMGCR AAb

The 3-hydroxy-3-methylglutaryl-coenzyme A reductase is the rate-limiting enzyme for cholesterol synthesis. The prevalence of anti-HMGCR AAb is of 12–34% (202, 205) and can reach up to 63% in patients with a past history of treatment by statin (206).

Necrotizing myopathy may be associated with cancer, especially when associated with anti-HMGCR AAb (202). Anti-HMGCR antibody serum level seems to be correlated with disease activity and with serum creatine kinase level (207). Generally, NM patients with anti-HMGCR AAb have a good response to immunosuppressive treatments but have a tendency to relapse (208). The presence of anti-HMGCR AAb in statin-naive patients is associated with a lower response to treatment (209).

Clinical Usefulness of Anti-HMGCR AAb Testing

- Strongly associated with NM with past history of statin treatment
- Cancer must be sought for in presence of one of these AAb
- Good response to immunosuppressive treatment
- Useful for follow-up, correlated with disease activity (and serum creatine kinase level)

Anti-SRP AAb

SRP is a complex of six proteins permitting the translocation of nascent proteins to the endoplasmic reticulum. The prevalence of anti-SRP AAb in NM is of 18–24% (202, 205). Like anti-HMGCR, the level of anti-SRP antibody is correlated with disease activity and with serum creatine kinase level (210). Anti-SRP AAbs share also with anti-HMGCR AAb a cytoplasmic dense fine granular pattern by IFI on HEP2 cells (47).

Patients with anti-SRP AAb seem to have more severe muscle weakness and ILD than patients with anti-HMGCR AAb (211). Finally, NM patients with anti-SRP AAb seem to have a reduced response to usual immunosuppressive treatments than other myopathies (208).

Clinical Usefulness of Anti-SRP AAb Testing

- Association with severe muscle weakness and ILD
- Poor response to immunosuppressive treatment
- Useful for follow-up, correlated with disease activity (and serum creatine kinase level)

Dermatomyositis-Associated AAb

Dermatomyositis is an inflammatory disease characterized by proximal muscle weakness and skin involvement. Muscle histology is typical with perifascicular atrophy, vasculopathy, and inflammatory infiltrations. In DM, five AAbs have been described. They are directed against transcription intermediary factor 1 gamma (anti-TIF1-γ AAb), nuclear matrix protein 2 (anti-NXP2 AAb), melanoma differentiation-associated gene 5 (anti-MDA5 AAb), and small ubiquitin-like modifier activating enzyme (anti-SAE AAb), while anti-Mi2 AAbs recognize the nucleosome remodeling histone deacetylase protein complex (NuRD).

Anti-TIF1-γ AAb

The TIF1-γ protein (also called TRIM 33 for Tripartite motif-containing 33) is a transcriptional corepressor that acts as a tumor suppressor protein. The anti-TIF1-γ AAb may be detected by nuclear fine-speckled fluorescence on Hep2 cells with a prevalence in DM of 13–38% (47, 212, 213).

The production of AAb directed against this protein is strongly associated with cancer occurrence with a sensitivity of 78%, a specificity of 89%, and positive and negative predictive values of 58 and 95%, respectively (212, 214). These patients are also more frequently diagnosed with dysphagia (215).

Clinical Usefulness of Anti-TIF1-γ AAb Testing

- Cancer must be sought for in presence of these AAb
- Useless for follow-up, not correlated with disease activity

Anti-NXP2 AAb

The prevalence of anti-NXP2 in DM is of 17% (212, 216). These AAbs are distinguished by multiple nuclear dots on the nucleoplasm of Hep2 cells by IFI (47). As for anti-TIF1-γ, anti-NXP2 AAb production is associated with a higher risk of cancer development (212). These AAbs are also associated with calcinosis and muscle atrophy, especially in juvenile DM (217, 218).

Clinical Usefulness of Anti-NXP2 AAb Testing

- Cancer must be sought for in presence of these AAbs
- Association with calcinosis, mostly in juvenile DM
- Useless for follow-up, not correlated with disease activity

Anti-MDA5 AAb

MDA5 is an RIG-I-like receptor functioning as a viral-sensing pattern recognition receptor. The prevalence of anti-MDA5 AAb in DM is of 10% (219) and seems to be higher (about 40%) in Asian population (220).

The presence of anti-MDA5 AAb is associated with a higher risk of developing an ILD (221). Subsequently, patients with this kind of AAb display poorer prognosis, with approximately 50% of death by respiratory failure within the first 6 months following diagnosis (222). Clinically, these patients also present with hand swelling, skin ulceration, panniculitis, and palmar papules (219). Serum level of AAb is correlated with disease activity, and it disappears with its remission (223, 224).

Clinical Usefulness of Anti-MDA5 AAb Testing

- Poor prognosis with respiratory failure
- Mostly, myositis not at the forefront
- Useful for follow-up, correlated with disease activity

Anti-SAE AAb

SAE is implicated in the nuclear-cytosolic transport and in the transcriptional regulation. The prevalence of anti-SAE AAb in DM is of 7–8% (225, 226) but, in contrast to the anti-MDA5 AAb, the anti-SAE AAbs are less common (about 2%) in the Asian population (227). Clinically, the presence of these AAbs is associated with severe dysphagia (226).

Clinical Usefulness of Anti-SAE AAb Testing

- Association with severe dysphagia
- Useless for follow-up, not correlated with disease activity

Anti-Mi2 AAb

Anti-Mi2 AAbs target NuRD, a nuclear proteic complex implicated in multiple transcriptional regulatory processes such as histone demethylation, histone deacetylation, and nucleosome mobilization. They are found in 18–35% of patients with DM (228, 229) and are associated with nuclear fine-speckled fluorescence by IFI on Hep2 cells (47).

Patients with anti-Mi2 AAb seem to have better response to immunosuppressive treatment (229).

Clinical Usefulness of Anti-Mi2 AAb Testing

- Not associated with a specific clinical phenotype
- Useless for follow-up, not correlated with disease activity

Inclusion Body Myositis-Associated AAb

Inclusion body myositis is a myopathy observed in middle-aged patients that leads to a progressive, asymmetric muscle weakness with swallowing troubles (230). Muscle biopsy evidences vacuolated muscle fibers, inflammatory infiltrates, and intracellular deposits of amyloid protein.

Recently, a novel AAb has been identified (231) in one-third of these IBM patients, which recognizes the cytosolic 5′-nucleotidase 1A (anti-CN1a). Nevertheless, these antibodies are also detected in SLE and in SS patients (232). Its presence or absence does not seem to affect disease prognosis nor evolution (233). This myopathy is poorly responsive to immunosuppressive treatment.

Clinical Usefulness of Anti-CN1a AAb Testing

- Single AAb described in IBM up to now
- Useless for follow-up, not correlated with disease activity

RHEUMATOÏD ARTHRITIS-ASSOCIATED AAb

Rheumatoid arthritis is the most common inflammatory rheumatoid disease with a world prevalence of approximatively 0.5–1% (234). The disease typically affects small and medium-sized joints symmetrically. The primary lesion is synovitis. Systemic involvement is often observed, with respiratory, cardiovascular, and hematopoietic systems being the more damaging lesioned sites.

Antinuclear AAb in RA

Antinuclear antibody is not the main type of AAb detected in RA but they are present in about 20% of cases (128). The ANA detection has no clinical relevance in RA but is useful for treatments. The highlighting of ANA under infliximab is associated with poorer response to treatment (developing antibody directed against infliximab) and a risk to develop induced lupus (235, 236).

Clinical Usefulness of ANA Testing

- Useless for diagnosis
- Useful in treatment to predict response and complications (induced lupus)

Non-Antinuclear AAb Frequently Observed in RA

The two main AAb associated with RA (recapitulated in **Table 6**) are chronologically rheumatoid factor (RF) and ACPA. Other AAbs [anti-CarP (237) and anti-NOR9 0 (186) AAb] are not available in routine practice nowadays. Two main classification criteria are available, based on the presence of both clinical and immunological parameters: the ACR 87 classification (238) and the 2010 classification criteria of the ACR/EULAR (239) collaborative initiative. RF or ACPA measurements between one and three times the upper limit of normal are designated "low"; higher measurements are designated "high." The high measurement increases the probability of positive diagnosis (238, 239). RA is typically divided into two subtypes designated "seropositive" and "seronegative" disease, with seropositivity being defined as the presence of AAb. The heritability of RA is currently estimated as 40–65% for seropositive RA, but lower (20%) for seronegative disease (240, 241).

TABLE 6 | AAb associated with rheumatoid arthritis.

AAb	Prevalence	Sensitivity	Specificity	Features
Rheumatoid factor	50–70% (243)	–	50–95% (245)	Associated with disease activity
ACPA	60–70% (249)	–	95% (243)	Associated with disease activity Erosive arthritis

ACPA, anti-citrullinated peptide AAb; AAb, autoantibody.
The term ACPA regroups anti-cyclic citrullinated peptide (anti-CCP) and also anti-non-cyclic citrullinated peptides AAb.

Rheumatoid Factor

Rheumatoid factor is the first well-known RA immunologic marker discover in 1957 (242) that targets the Fc part of human IgG. RFs are present in 50–70% (243) of patients at diagnosis, with little increase throughout disease course (234, 243). There is a correlation between RF titer and radiographic progression (244). The specificity of RF for RA diagnosis depends on clinical context: strong with an articular involvement and low without articular involvement (50–95%) (245).

Rheumatoid factor can also be found in healthy (elderly) individuals and patients with other autoimmune and infectious diseases (245). Despite this lack of specificity, the presence of RF was one of the seven diagnostic criteria for RA put forward by the ACR in 1987 and is also included in the ACR/EULAR 2010 classification criteria for RA.

Clinical Usefulness of RF Testing

- Useful for diagnosis
- Useful in follow-up to predict disease activity

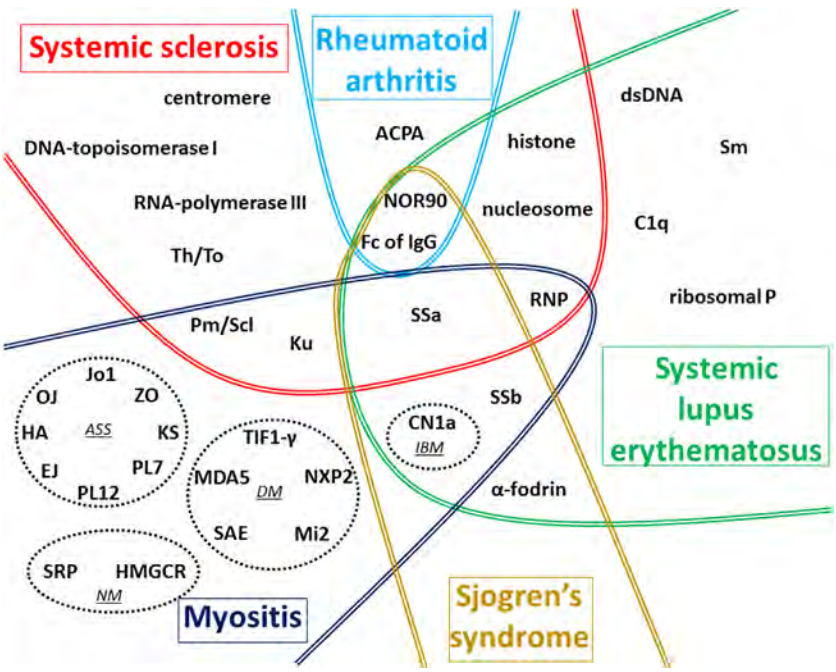

FIGURE 1 | Global vision of autoantigens targeted by autoantibody (AAb) according to the type of connective tissue diseases (CTDs). The main targets of AAb associated with the five CTDs detailed in this review are recapitulated on this figure. In myositis, four distinct forms associated with distinct AAbs are represented in dotted circles: antisynthetase syndrome (ASS), dermatomyositis (DM), necrotizing myopathy (NM), and inclusion body myositis (IBM). In systemic sclerosis (SSc), most AAbs are preferentially associated with one of the two cutaneous forms described: anti-centromere, anti-Th/To, anti-Pm/Scl, anti-Ku, and anti-U1-RNP AAbs are generally associated with limited form of SSc whereas anti-DNA-topoisomerase I, anti-RNA-polymerase III, and anti-U3-RNP AAbs are mostly associated with diffuse cutaneous SSc. The term ACPA regroups anti-cyclic citrullinated peptide and also anti-non-cyclic citrullinated peptides AAb. Fc of IgG corresponds to target of rheumatoid factor. Some AAbs are associated with more than one CTD as shown in the different overlap areas on the figure.

Anti-Citrullinated Protein/Peptide AAb

Citrullination is a process by which arginine residues in a given protein are post-translationally modified ("deiminated") in the presence of high calcium concentrations by an enzyme called PAD (peptidylarginine deiminase) (234, 246). In 1998, two AAbs present in serum samples from patients with RA that had already been described years earlier (antiperinuclear factor and anti-keratin antibodies) were found to share a common specificity for citrullinated filaggrin (247). First, a cyclic citrullinated peptide (CCP) was developed to improve antigen composition and antibody recognition. Then, new assays were developed to detect non-CCPs, and now the term anti-citrullinated protein/peptide AAb (ACPA) has thus replaced anti-cyclic citrullinated peptide (anti-CCP) AAb (248).

Using CCPs as antigens, ACPA are detected in 60–70% of RA patients (249). ACPA appear more specific for RA than RF. The specificity of ACPA is almost of 95% in RA (243). ACPA can also be detected in patients with SSc (189), psoriatic arthritis, SS, SLE, and MCTD (250).

ACPA are linked to erosive form of RA, and the likelihood of radiographic progression after 5 years is significantly greater among RA patients with ACPA (OR = 2.5) (251, 252). Moreover, detection of both RF and ACPA is associated with a more important radiographic progression and a poorer prognostic factor in patients with RA (252). ACPA can be detected in sera several years before clinical onset of arthritis (253). Recently, a new study showed that serological status (ACPA positivity) is a risk factor of serious infusion-related reactions in RA treated by non-TNF-targeted biologics (254).

Clinical Usefulness of Anti-ACPA Testing

- Useful for diagnosis
- Association with erosive arthritis
- Useful in follow-up to predict disease activity

CONCLUSION

Numerous AAbs can be evidenced in the sera of patients with CTD (**Figure 1**), and new autoantigens are regularly identified in this field of diseases. In the majority of cases, these AAbs are produced before clinical symptoms, but only a minority of these AAbs has been clearly demonstrated to be involved in the pathogenesis of these diseases. The understanding of the implication in pathogenesis of these AAbs still needs to be investigated, notably using animal models, to be able to find new therapeutic targets.

Evidence of these AAbs can help clinicians for disease diagnosis and is therefore frequently mentioned in international classification criteria. Moreover, since some AAbs are correlated with disease activity and/or specific organ involvement, their detection and in some cases their level follow-up can also be a helpful tool in the long-term management of patients with CTD. The final aim of such investigations would be to personalize medical care according to the CTD and AAb identified.

In conclusion, choice in the type of AAb tested should be carefully evaluated according to clinical context for each patient. Importantly, to properly handle the clinical usefulness of AAb detection, clinician should also be aware of both the advantages and the limits of the methods used to test AAb, to support the clinical evaluation, which remains the essential cornerstone for disease diagnosis and patients' management.

AUTHOR CONTRIBUTIONS

KD and AS designed the review. KD, LB, DG, ST, AR, FA, and AS wrote the manuscript. All the authors critically evaluated the data and approved the final version for publication.

REFERENCES

1. Bizzaro N, Tozzoli R, Shoenfeld Y. Are we at a stage to predict autoimmune rheumatic diseases? *Arthritis Rheum* (2007) 56(6):1736–44. doi:10.1002/art.22708
2. Arbuckle MR, McClain MT, Rubertone MV, Scofield RH, Dennis GJ, James JA, et al. Development of autoantibodies before the clinical onset of systemic lupus erythematosus. *N Engl J Med* (2003) 349(16):1526–33. doi:10.1056/NEJMoa021933
3. Jonsson R, Theander E, Sjöström B, Brokstad K, Henriksson G. Autoantibodies present before symptom onset in primary Sjögren syndrome. *JAMA* (2013) 310(17):1854–5. doi:10.1001/jama.2013.278448
4. Wang K-Y, Yang Y-H, Chuang Y-H, Chan P-J, Yu H-H, Lee J-H, et al. The initial manifestations and final diagnosis of patients with high and low titers of antinuclear antibodies after 6 months of follow-up. *J Microbiol Immunol Infect* (2011) 44(3):222–8. doi:10.1016/j.jmii.2011.01.019
5. Minz RW, Kumar Y, Anand S, Singh S, Bamberi P, Verma S, et al. Antinuclear antibody positive autoimmune disorders in North India: an appraisal. *Rheumatol Int* (2012) 32(9):2883–8. doi:10.1007/s00296-011-2134-1
6. Selmi C, Ceribelli A, Generali E, Scirè CA, Alborghetti F, Colloredo G, et al. Serum antinuclear and extractable nuclear antigen antibody prevalence and associated morbidity and mortality in the general population over 15 years. *Autoimmun Rev* (2016) 15(2):162–6. doi:10.1016/j.autrev.2015.10.007
7. Fernandez SAV, Lobo AZC, de Oliveira ZNP, Fukumori LMI, Prigo AM, Rivitti EA. Prevalence of antinuclear autoantibodies in the serum of normal blood dornors. *Rev Hosp Clin Fac Med Sao Paulo* (2003) 58(6):315–9. doi:10.1590/S0041-87812003000600005
8. Peene I, Meheus L, Veys EM, De Keyser F. Detection and identification of antinuclear antibodies (ANA) in a large and consecutive cohort of serum samples referred for ANA testing. *Ann Rheum Dis* (2001) 60(12):1131–6. doi:10.1136/ard.60.12.1131
9. Li Q-Z, Karp DR, Quan J, Branch VK, Zhou J, Lian Y, et al. Risk factors for ANA positivity in healthy persons. *Arthritis Res Ther* (2011) 13(2):R38. doi:10.1186/ar3271
10. Hayashi N, Koshiba M, Nishimura K, Sugiyama D, Nakamura T, Morinobu S, et al. Prevalence of disease-specific antinuclear antibodies in general population: estimates from annual physical examinations of residents of a small town over a 5-year period. *Mod Rheumatol* (2008) 18(2):153–60. doi:10.1007/s10165-008-0028-1
11. Racoubian E, Zubaid RM, Shareef MA, Almawi WY. Prevalence of antinuclear antibodies in healthy Lebanese subjects, 2008-2015: a cross-sectional study involving 10,814 subjects. *Rheumatol Int* (2016) 36(9):1231–6. doi:10.1007/s00296-016-3533-0
12. Roberts-Thomson PJ, Nikoloutsopoulos T, Cox S, Walker JG, Gordon TP. Antinuclear antibody testing in a regional immunopathology laboratory. *Immunol Cell Biol* (2003) 81(5):409–12. doi:10.1046/j.1440-1711.2003.01181.x
13. Wandstrat AE, Carr-Johnson F, Branch V, Gray H, Fairhurst A-M, Reimold A, et al. Autoantibody profiling to identify individuals at risk for systemic lupus erythematosus. *J Autoimmun* (2006) 27(3):153–60. doi:10.1016/j.jaut.2006.09.001

14. Nilsson B-O, Skogh T, Ernerudh J, Johansson B, Löfgren S, Wikby A, et al. Antinuclear antibodies in the oldest-old women and men. *J Autoimmun* (2006) 27(4):281–8. doi:10.1016/j.jaut.2006.10.002
15. Tan EM, Feltkamp TE, Smolen JS, Butcher B, Dawkins R, Fritzler MJ, et al. Range of antinuclear antibodies in "healthy" individuals. *Arthritis Rheum* (1997) 40(9):1601–11. doi:10.1002/art.1780400909
16. Hayashi N, Kawamoto T, Mukai M, Morinobu A, Koshiba M, Kondo S, et al. Detection of antinuclear antibodies by use of an enzyme immunoassay with nuclear HEp-2 cell extract and recombinant antigens: comparison with immunofluorescence assay in 307 patients. *Clin Chem* (2001) 47(9):1649–59.
17. Marin GG, Cardiel MH, Cornejo H, Viveros ME. Prevalence of antinuclear antibodies in 3 groups of healthy individuals: blood donors, hospital personnel, and relatives of patients with autoimmune diseases. *J Clin Rheumatol* (2009) 15(7):325–9. doi:10.1097/RHU.0b013e3181bb971b
18. Depincé-Berger AE, Moreau A, Bossy V, Genin C, Rinaudo M, Paul S. Comparison of screening dilution and automated reading for antinuclear antibody detection on HEP2 cells in the monitoring of connective tissue diseases. *J Clin Lab Anal* (2016) 30(5):471–8. doi:10.1002/jcla.21881
19. Bossuyt X, Cooreman S, De Baere H, Verschueren P, Westhovens R, Blockmans D, et al. Detection of antinuclear antibodies by automated indirect immunofluorescence analysis. *Clin Chim Acta* (2013) 415:101–6. doi:10.1016/j.cca.2012.09.021
20. Willems P, De Langhe E, Claessens J, Westhovens R, Van Hoeyveld E, Poesen K, et al. Screening for connective tissue disease-associated antibodies by automated immunoassay. *Clin Chem Lab Med* (2018). doi:10.1515/cclm-2017-0905
21. van der Pol P, Bakker-Jonges LE, Kuijpers JHSAM, Schreurs MWJ. Analytical and clinical comparison of two fully automated immunoassay systems for the detection of autoantibodies to extractable nuclear antigens. *Clin Chim Acta* (2018) 476:154–9. doi:10.1016/j.cca.2017.11.014
22. Robier C, Amouzadeh-Ghadikolai O, Stettin M, Reicht G. Comparison of the clinical utility of the Elia CTD Screen to indirect immunofluorescence on Hep-2 cells. *Clin Chem Lab Med* (2016) 54(8):1365–70. doi:10.1515/cclm-2015-1051
23. Op De Beéck K, Vermeersch P, Verschueren P, Westhovens R, Mariën G, Blockmans D, et al. Antinuclear antibody detection by automated multiplex immunoassay in untreated patients at the time of diagnosis. *Autoimmun Rev* (2012) 12(2):137–43. doi:10.1016/j.autrev.2012.02.013
24. Op De Beeck K, Vermeersch P, Verschueren P, Westhovens R, Mariën G, Blockmans D, et al. Detection of antinuclear antibodies by indirect immunofluorescence and by solid phase assay. *Autoimmun Rev* (2011) 10(12):801–8. doi:10.1016/j.autrev.2011.06.005
25. Meroni PL, Schur PH. ANA screening: an old test with new recommendations. *Ann Rheum Dis* (2010) 69(8):1420–2. doi:10.1136/ard.2009.127100
26. Ochs RL, Muro Y, Si Y, Ge H, Chan EK, Tan EM. Autoantibodies to DFS 70 kd/transcription coactivator p75 in atopic dermatitis and other conditions. *J Allergy Clin Immunol* (2000) 105(6 Pt 1):1211–20. doi:10.1067/mai.2000.107039
27. Watanabe A, Kodera M, Sugiura K, Usuda T, Tan EM, Takasaki Y, et al. Anti-DFS70 antibodies in 597 healthy hospital workers. *Arthritis Rheum* (2004) 50(3):892–900. doi:10.1002/art.20096
28. Mahler M, Parker T, Peebles CL, Andrade LE, Swart A, Carbone Y, et al. Anti-DFS70/LEDGF antibodies are more prevalent in healthy individuals compared to patients with systemic autoimmune rheumatic diseases. *J Rheumatol* (2012) 39(11):2104–10. doi:10.3899/jrheum.120598
29. Shovman O, Gilburd B, Chayat C, Amital H, Langevitz P, Watad A, et al. Prevalence of anti-DFS70 antibodies in patients with and without systemic autoimmune rheumatic diseases. *Clin Exp Rheumatol* (2018) 36(1):121–6.
30. Lazzerini PE, Yue Y, Srivastava U, Fabris F, Capecchi PL, Bertolozzi I, et al. Arrhythmogenicity of anti-Ro/SSA antibodies in patients with torsades de pointes. *Circ Arrhythm Electrophysiol* (2016) 9(4):e003419. doi:10.1161/CIRCEP.115.003419
31. Hochberg MC. Updating the American College of Rheumatology revised criteria for the classification of systemic lupus erythematosus. *Arthritis Rheum* (1997) 40(9):1725. doi:10.1002/art.1780400928
32. Petri M, Orbai A-M, Alarcón GS, Gordon C, Merrill JT, Fortin PR, et al. Derivation and validation of the systemic lupus international collaborating clinics classification criteria for systemic lupus erythematosus. *Arthritis Rheum* (2012) 64(8):2677–86. doi:10.1002/art.34473
33. Hochberg MC, Boyd RE, Ahearn JM, Arnett FC, Bias WB, Provost TT, et al. Systemic lupus erythematosus: a review of clinico-laboratory features and immunogenetic markers in 150 patients with emphasis on demographic subsets. *Medicine (Baltimore)* (1985) 64(5):285–95. doi:10.1097/00005792-198509000-00001
34. Koh WH, Fong KY, Boey ML, Feng PH. Systemic lupus erythematosus in 61 Oriental males. A study of clinical and laboratory manifestations. *Br J Rheumatol* (1994) 33(4):339–42. doi:10.1093/rheumatology/33.4.339
35. Ginsburg WW, Conn DL, Bunch TW, McDuffie FC. Comparison of clinical and serologic markers in systemic lupus erythematosus and overlap syndrome: a review of 247 patients. *J Rheumatol* (1983) 10(2):235–41.
36. Maddison PJ, Provost TT, Reichlin M. Serological findings in patients with "ANA-negative" systemic lupus erythematosus. *Medicine (Baltimore)* (1981) 60(2):87–94. doi:10.1097/00005792-198103000-00002
37. Boey ML, Peebles CL, Tsay G, Feng PH, Tan EM. Clinical and autoantibody correlations in Orientals with systemic lupus erythematosus. *Ann Rheum Dis* (1988) 47(11):918–23. doi:10.1136/ard.47.11.918
38. Ghedira I, Sakly W, Jeddi M. [Clinical and serological characteristics of systemic lupus erythematosus: 128 cases]. *Pathol Biol (Paris)* (2002) 50(1):18–24. doi:10.1016/S0369-8114(01)00262-0
39. Al-Maini MH, El-Ageb EM, Al-Wahaibi SS, Al-Farsi Y, Richens ER. Demographic, autoimmune, and clinical profiles of patients with systemic lupus erythematosus in Oman. *Rheumatol Int* (2003) 23(4):186–91. doi:10.1007/s00296-003-0303-6
40. Cortés-Hernández J, Ordi-Ros J, Labrador M, Buján S, Balada E, Segarra A, et al. Antihistone and anti-double-stranded deoxyribonucleic acid antibodies are associated with renal disease in systemic lupus erythematosus. *Am J Med* (2004) 116(3):165–73. doi:10.1016/j.amjmed.2003.08.034
41. Sawalha AH, Harley JB. Antinuclear autoantibodies in systemic lupus erythematosus. *Curr Opin Rheumatol* (2004) 16(5):534–40. doi:10.1097/01.bor.0000135452.62800.8f
42. Bentow C, Lakos G, Martis P, Wahl E, Garcia M, Viñas O, et al. International multi-center evaluation of a novel chemiluminescence assay for the detection of anti-dsDNA antibodies. *Lupus* (2016) 25(8):864–72. doi:10.1177/0961203316640917
43. Infantino M, Meacci F, Bentow C, Martis P, Benucci M, Afeltra A, et al. Clinical comparison of QUANTA Flash dsDNA chemiluminescent immunoassay with four current assays for the detection of anti-dsDNA autoantibodies. *J Immunol Res* (2015) 2015:902821. doi:10.1155/2015/902821
44. Zigon P, Lakota K, Cucnik S, Svec T, Ambrozic A, Sodin-Semrl S, et al. Comparison and evaluation of different methodologies and tests for detection of anti-dsDNA antibodies on 889 Slovenian patients' and blood donors' sera. *Croat Med J* (2011) 52(6):694–702. doi:10.3325/cmj.2011.52.694
45. Derksen RHWM, Bast EJEG, Strooisma T, Jacobs JWG. A comparison between the Farr radioimmunoassay and a new automated fluorescence immunoassay for the detection of antibodies against double stranded DNA in serum. *Ann Rheum Dis* (2002) 61(12):1099–102. doi:10.1136/ard.61.12.1099
46. Bizzaro N, Tozzoli R, Tonutti E, Piazza A, Manoni F, Ghirardello A, et al. Variability between methods to determine ANA, anti-dsDNA and anti-ENA autoantibodies: a collaborative study with the biomedical industry. *J Immunol Methods* (1998) 219(1–2):99–107. doi:10.1016/S0022-1759(98)00140-9
47. Chan EKL, Damoiseaux J, Carballo OG, Conrad K, de Melo Cruvinel W, Francescantonio PLC, et al. Report of the first international consensus on standardized nomenclature of antinuclear antibody HEp-2 cell patterns 2014-2015. *Front Immunol* (2015) 6:412. doi:10.3389/fimmu.2015.00412
48. Villalta D, Bizzaro N, Corazza D, Tozzoli R, Tonutti E. Evaluation of a new automated enzyme fluoroimmunoassay using recombinant plasmid dsDNA for the detection of anti-dsDNA antibodies in SLE. *J Clin Lab Anal* (2002) 16(5):227–32. doi:10.1002/jcla.10045
49. Tan EM, Cohen AS, Fries JF, Masi AT, McShane DJ, Rothfield NF, et al. The 1982 revised criteria for the classification of systemic lupus erythematosus. *Arthritis Rheum* (1982) 25(11):1271–7. doi:10.1002/art.1780251101
50. Albani S, Massa M, Viola S, Pellegrini G, Martini A. Antibody reactivity against single stranded DNA of various species in normal children and

in children with diffuse connective tissue diseases. *Autoimmunity* (1990) 8(1):77–80. doi:10.3109/08916939008998436
51. Schur PH, Sandson J. Immunologic factors and clinical activity in systemic lupus erythematosus. *N Engl J Med* (1968) 278(10):533–8. doi:10.1056/NEJM196803072781004
52. Alba P, Bento L, Cuadrado MJ, Karim Y, Tungekar MF, Abbs I, et al. Anti-dsDNA, anti-Sm antibodies, and the lupus anticoagulant: significant factors associated with lupus nephritis. *Ann Rheum Dis* (2003) 62(6):556–60. doi:10.1136/ard.62.6.556
53. Homma M, Mimori T, Takeda Y, Akama H, Yoshida T, Ogasawara T, et al. Autoantibodies to the Sm antigen: immunological approach to clinical aspects of systemic lupus erythematosus. *J Rheumatol Suppl* (1987) 14(Suppl 13):188–93.
54. Yang J, Xu Z, Sui M, Han J, Sun L, Jia X, et al. Co-positivity for anti-dsDNA, -nucleosome and -histone antibodies in lupus nephritis is indicative of high serum levels and severe nephropathy. *PLoS One* (2015) 10(10):e0140441. doi:10.1371/journal.pone.0140441
55. Sardeto GA, Simas LM, Skare TS, Nisihara RM, Utiyama SRR. Antinucleosome in systemic lupus erythematosus. A study in a Brazilian population. *Clin Rheumatol* (2012) 31(3):553–6. doi:10.1007/s10067-011-1889-9
56. Bizzaro N, Villalta D, Giavarina D, Tozzoli R. Are anti-nucleosome antibodies a better diagnostic marker than anti-dsDNA antibodies for systemic lupus erythematosus? A systematic review and a study of metanalysis. *Autoimmun Rev* (2012) 12(2):97–106. doi:10.1016/j.autrev.2012.07.002
57. Saisoong S, Eiam-Ong S, Hanvivatvong O. Correlations between antinucleosome antibodies and anti-double-stranded DNA antibodies, C3, C4, and clinical activity in lupus patients. *Clin Exp Rheumatol* (2006) 24(1):51–8.
58. Licht R, van Bruggen MC, Oppers-Walgreen B, Rijke TP, Berden JH. Plasma levels of nucleosomes and nucleosome-autoantibody complexes in murine lupus: effects of disease progression and lipopolyssacharide administration. *Arthritis Rheum* (2001) 44(6):1320–30. doi:10.1002/1529-0131(200106)44:6<1320::AID-ART224>3.0.CO;2-X
59. Amoura Z, Koutouzov S, Chabre H, Cacoub P, Amoura I, Musset L, et al. Presence of antinucleosome autoantibodies in a restricted set of connective tissue diseases: antinucleosome antibodies of the IgG3 subclass are markers of renal pathogenicity in systemic lupus erythematosus. *Arthritis Rheum* (2000) 43(1):76–84. doi:10.1002/1529-0131(200001)43:1<76::AID-ANR10>3.0.CO;2-I
60. Sui M, Sui M, Lin Q, Xu Z, Han X, Xie R, et al. Simultaneous positivity for anti-DNA, anti-nucleosome and anti-histone antibodies is a marker for more severe lupus nephritis. *J Clin Immunol* (2013) 33(2):378–87. doi:10.1007/s10875-012-9825-6
61. Wang CL, Ooi L, Wang F. Prevalence and clinical significance of antibodies to ribonucleoproteins in systemic lupus erythematosus in Malaysia. *Br J Rheumatol* (1996) 35(2):129–32. doi:10.1093/rheumatology/35.2.129
62. Benito-Garcia E, Schur PH, Lahita R; American College of Rheumatology Ad Hoc Committee on Immunologic Testing Guidelines. Guidelines for immunologic laboratory testing in the rheumatic diseases: anti-Sm and anti-RNP antibody tests. *Arthritis Rheum* (2004) 51(6):1030–44. doi:10.1002/art.20836
63. Flechsig A, Rose T, Barkhudarova F, Strauss R, Klotsche J, Dähnrich C, et al. What is the clinical significance of anti-Sm antibodies in systemic lupus erythematosus? A comparison with anti-dsDNA antibodies and C3. *Clin Exp Rheumatol* (2017) 35(4):598–606.
64. Jaekel HP, Klopsch T, Benkenstein B, Grobe N, Baldauf A, Schoessler W, et al. Reactivities to the Sm autoantigenic complex and the synthetic SmD1-aa83-119 peptide in systemic lupus erythematosus and other autoimmune diseases. *J Autoimmun* (2001) 17(4):347–54. doi:10.1006/jaut.2001.0545
65. Ahn SS, Yoo B-W, Song JJ, Park Y-B, Lee S-K, Lee S-W. Anti-Sm is associated with the early poor outcome of lupus nephritis. *Int J Rheum Dis* (2016) 19(9):897–902. doi:10.1111/1756-185X.12880
66. Ishizaki J, Saito K, Nawata M, Mizuno Y, Tokunaga M, Sawamukai N, et al. Low complements and high titre of anti-Sm antibody as predictors of histopathologically proven silent lupus nephritis without abnormal urinalysis in patients with systemic lupus erythematosus. *Rheumatology (Oxford)* (2015) 54(3):405–12. doi:10.1093/rheumatology/keu343
67. Habets WJ, Hoet MH, Sillekens PT, De Rooij DJ, Van de Putte LB, Van Venrooij WJ. Detection of autoantibodies in a quantitative immunoassay using recombinant ribonucleoprotein antigens. *Clin Exp Immunol* (1989) 76(2):172–7.
68. Gulko PS, Reveille JD, Koopman WJ, Burgard SL, Bartolucci AA, Alarcón GS. Survival impact of autoantibodies in systemic lupus erythematosus. *J Rheumatol* (1994) 21(2):224–8.
69. Kurien BT, Scofield RH. Autoantibody determination in the diagnosis of systemic lupus erythematosus. *Scand J Immunol* (2006) 64(3):227–35. doi:10.1111/j.1365-3083.2006.01819.x
70. Vedove CD, Del Giglio M, Schena D, Girolomoni G. Drug-induced lupus erythematosus. *Arch Dermatol Res* (2009) 301(1):99–105. doi:10.1007/s00403-008-0895-5
71. Rubin RL, Waga S. Antihistone antibodies in systemic lupus erythematosus. *J Rheumatol Suppl* (1987) 14(Suppl 13):118–26.
72. Sun X-Y, Shi J, Han L, Su Y, Li Z-G. Anti-histones antibodies in systemic lupus erythematosus: prevalence and frequency in neuropsychiatric lupus. *J Clin Lab Anal* (2008) 22(4):271–7. doi:10.1002/jcla.20248
73. van Rijthoven AW, Bijlsma JWJ, Canninga-van Dijk M, Derksen RHWM, van Roon JA. Onset of systemic lupus erythematosus after conversion of infliximab to adalimumab treatment in rheumatoid arthritis with a pre-existing anti-dsDNA antibody level. *Rheumatology (Oxford)* (2006) 45(10):1317–9. doi:10.1093/rheumatology/kel227
74. Gisondi P, Girolomoni G. Biologic therapies in psoriasis: a new therapeutic approach. *Autoimmun Rev* (2007) 6(8):515–9. doi:10.1016/j.autrev.2006.12.002
75. Harley JB, Scofield RH, Reichlin M. Anti-Ro in Sjögren's syndrome and systemic lupus erythematosus. *Rheum Dis Clin North Am* (1992) 18(2):337–58.
76. Tikly M, Burgin S, Mohanlal P, Bellingan A, George J. Autoantibodies in black South Africans with systemic lupus erythematosus: spectrum and clinical associations. *Clin Rheumatol* (1996) 15(3):261–5. doi:10.1007/BF02229704
77. Riemekasten G, Hahn BH. Key autoantigens in SLE. *Rheumatology (Oxford)* (2005) 44(8):975–82. doi:10.1093/rheumatology/keh688
78. Kurien BT, Newland J, Paczkowski C, Moore KL, Scofield RH. Association of neutropenia in systemic lupus erythematosus (SLE) with anti-Ro and binding of an immunologically cross-reactive neutrophil membrane antigen. *Clin Exp Immunol* (2000) 120(1):209–17. doi:10.1046/j.1365-2249.2000.01195.x
79. Vanoni F, Lava SAG, Fossali EF, Cavalli R, Simonetti GD, Bianchetti MG, et al. Neonatal systemic lupus erythematosus syndrome: a comprehensive review. *Clin Rev Allergy Immunol* (2017) 53(3):469–76. doi:10.1007/s12016-017-8653-0
80. Buyon JP, Clancy RM. Neonatal lupus: basic research and clinical perspectives. *Rheum Dis Clin North Am* (2005) 31(2):299–313,vii. doi:10.1016/j.rdc.2005.01.010
81. Lee LA. The clinical spectrum of neonatal lupus. *Arch Dermatol Res* (2009) 301(1):107–10. doi:10.1007/s00403-008-0896-4
82. Zuppa AA, Riccardi R, Frezza S, Gallini F, Luciano RMP, Alighieri G, et al. Neonatal lupus: follow-up in infants with anti-SSA/Ro antibodies and review of the literature. *Autoimmun Rev* (2017) 16(4):427–32. doi:10.1016/j.autrev.2017.02.010
83. Tunks RD, Clowse MEB, Miller SG, Brancazio LR, Barker PCA. Maternal autoantibody levels in congenital heart block and potential prophylaxis with antiinflammatory agents. *Am J Obstet Gynecol* (2013) 208(1):64.e1–7. doi:10.1016/j.ajog.2012.09.020
84. Izmirly PM, Costedoat-Chalumeau N, Pisoni CN, Khamashta MA, Kim MY, Saxena A, et al. Maternal use of hydroxychloroquine is associated with a reduced risk of recurrent anti-SSA/Ro-antibody-associated cardiac manifestations of neonatal lupus. *Circulation* (2012) 126(1):76–82. doi:10.1161/CIRCULATIONAHA.111.089268
85. Rao L, Liu G, Li C, Li Y, Wang Z, Zhou Z, et al. Specificity of anti-SSB as a diagnostic marker for the classification of systemic lupus erythematosus. *Exp Ther Med* (2013) 5(6):1710–4. doi:10.3892/etm.2013.1051
86. Lazzerini PE, Acampa M, Guideri F, Capecchi PL, Campanella V, Morozzi G, et al. Prolongation of the corrected QT interval in adult patients with anti-Ro/SSA-positive connective tissue diseases. *Arthritis Rheum* (2004) 50(4):1248–52. doi:10.1002/art.20130
87. Lazzerini PE, Capecchi PL, Acampa M, Morozzi G, Bellisai F, Bacarelli MR, et al. Anti-Ro/SSA-associated corrected QT interval prolongation in adults: the role of antibody level and specificity. *Arthritis Care Res* (2011) 63(10):1463–70. doi:10.1002/acr.20540
88. Lazzerini PE, Capecchi PL, Guideri F, Bellisai F, Selvi E, Acampa M, et al. Comparison of frequency of complex ventricular arrhythmias in patients

with positive versus negative anti-Ro/SSA and connective tissue disease. *Am J Cardiol* (2007) 100(6):1029–34. doi:10.1016/j.amjcard.2007.04.048
89. Pickering MC, Botto M, Taylor PR, Lachmann PJ, Walport MJ. Systemic lupus erythematosus, complement deficiency, and apoptosis. *Adv Immunol* (2000) 76:227–324. doi:10.1016/S0065-2776(01)76021-X
90. Siegert CE, Daha MR, Swaak AJ, van der Voort EA, Breedveld FC. The relationship between serum titers of autoantibodies to C1q and age in the general population and in patients with systemic lupus erythematosus. *Clin Immunol Immunopathol* (1993) 67(3 Pt 1):204–9. doi:10.1006/clin.1993.1066
91. Trendelenburg M, Lopez-Trascasa M, Potlukova E, Moll S, Regenass S, Frémeaux-Bacchi V, et al. High prevalence of anti-C1q antibodies in biopsy-proven active lupus nephritis. *Nephrol Dial Transplant* (2006) 21(11):3115–21. doi:10.1093/ndt/gfl436
92. Siegert CE, Daha MR, Halma C, van der Voort EA, Breedveld FC. IgG and IgA autoantibodies to C1q in systemic and renal diseases. *Clin Exp Rheumatol* (1992) 10(1):19–23.
93. Sinico RA, Radice A, Ikehata M, Giammarresi G, Corace C, Arrigo G, et al. Anti-C1q autoantibodies in lupus nephritis: prevalence and clinical significance. *Ann N Y Acad Sci* (2005) 1050:193–200. doi:10.1196/annals.1313.020
94. Siegert C, Daha M, Westedt ML, van der Voort E, Breedveld F. IgG autoantibodies against C1q are correlated with nephritis, hypocomplementemia, and dsDNA antibodies in systemic lupus erythematosus. *J Rheumatol* (1991) 18(2):230–4.
95. Gunnarsson I, Rönnelid J, Huang YH, Rogberg S, Nilsson B, Lundberg I, et al. Association between ongoing anti-C1q antibody production in peripheral blood and proliferative nephritis in patients with active systemic lupus erythematosus. *Br J Rheumatol* (1997) 36(1):32–7. doi:10.1093/rheumatology/36.1.32
96. Moroni G, Trendelenburg M, Del Papa N, Quaglini S, Raschi E, Panzeri P, et al. Anti-C1q antibodies may help in diagnosing a renal flare in lupus nephritis. *Am J Kidney Dis* (2001) 37(3):490–8. doi:10.1053/ajkd.2001.22071
97. Orbai A-M, Truedsson L, Sturfelt G, Nived O, Fang H, Alarcón GS, et al. Anti-C1q antibodies in systemic lupus erythematosus. *Lupus* (2015) 24(1):42–9. doi:10.1177/0961203314547791
98. Coremans IE, Spronk PE, Bootsma H, Daha MR, van der Voort EA, Kater L, et al. Changes in antibodies to C1q predict renal relapses in systemic lupus erythematosus. *Am J Kidney Dis* (1995) 26(4):595–601. doi:10.1016/0272-6386(95)90595-2
99. Siegert CE, Daha MR, Tseng CM, Coremans IE, van Es LA, Breedveld FC. Predictive value of IgG autoantibodies against C1q for nephritis in systemic lupus erythematosus. *Ann Rheum Dis* (1993) 52(12):851–6. doi:10.1136/ard.52.12.851
100. Siegert CE, Kazatchkine MD, Sjöholm A, Würzner R, Loos M, Daha MR. Autoantibodies against C1q: view on clinical relevance and pathogenic role. *Clin Exp Immunol* (1999) 116(1):4–8. doi:10.1046/j.1365-2249.1999.00867.x
101. Frémeaux-Bacchi V, Noël LH, Schifferli JA. No lupus nephritis in the absence of antiC1q autoantibodies? *Nephrol Dial Transplant* (2002) 17(12):2041–3. doi:10.1093/ndt/17.12.2041
102. Jachiet M, Flageul B, Deroux A, Le Quellec A, Maurier F, Cordoliani F, et al. The clinical spectrum and therapeutic management of hypocomplementemic urticarial vasculitis: data from a French nationwide study of fifty-seven patients. *Arthritis Rheumatol* (2015) 67(2):527–34. doi:10.1002/art.38956
103. Bonfa E, Elkon KB. Clinical and serologic associations of the antiribosomal P protein antibody. *Arthritis Rheum* (1986) 29(8):981–5. doi:10.1002/art.1780290806
104. Ghirardello A, Caponi L, Franceschini F, Zampieri S, Quinzanini M, Bendo R, et al. Diagnostic tests for antiribosomal p protein antibodies: a comparative evaluation of immunoblotting and ELISA assays. *J Autoimmun* (2002) 19(1–2):71–7. doi:10.1006/jaut.2002.0595
105. Borchers AT, Aoki CA, Naguwa SM, Keen CL, Shoenfeld Y, Gershwin ME. Neuropsychiatric features of systemic lupus erythematosus. *Autoimmun Rev* (2005) 4(6):329–44. doi:10.1016/j.autrev.2005.01.008
106. Eber T, Chapman J, Shoenfeld Y. Anti-ribosomal P-protein and its role in psychiatric manifestations of systemic lupus erythematosus: myth or reality? *Lupus* (2005) 14(8):571–5. doi:10.1191/0961203305lu2150rr
107. Sato T, Uchiumi T, Ozawa T, Kikuchi M, Nakano M, Kominami R, et al. Autoantibodies against ribosomal proteins found with high frequency in patients with systemic lupus erythematosus with active disease. *J Rheumatol* (1991) 18(11):1681–4.
108. Reichlin M. Autoantibodies to the ribosomal P proteins in systemic lupus erythematosus. *Clin Exp Med* (2006) 6(2):49–52. doi:10.1007/s10238-006-0094-7
109. Mei Y-J, Wang P, Jiang C, Wang T, Chen L-J, Li Z-J, et al. Clinical and serological associations of anti-ribosomal P0 protein antibodies in systemic lupus erythematosus. *Clin Rheumatol* (2018) 37(3):703–7. doi:10.1007/s10067-017-3886-0
110. Mok CC, Tang SSK, To CH, Petri M. Incidence and risk factors of thromboembolism in systemic lupus erythematosus: a comparison of three ethnic groups. *Arthritis Rheum* (2005) 52(9):2774–82. doi:10.1002/art.21224
111. Wilson WA, Gharavi AE, Koike T, Lockshin MD, Branch DW, Piette JC, et al. International consensus statement on preliminary classification criteria for definite antiphospholipid syndrome: report of an international workshop. *Arthritis Rheum* (1999) 42(7):1309–11. doi:10.1002/1529-0131(199907)42:7<1309::AID-ANR1>3.0.CO;2-F
112. Abreu MM, Danowski A, Wahl DG, Amigo M-C, Tektonidou M, Pacheco MS, et al. The relevance of "non-criteria" clinical manifestations of antiphospholipid syndrome: 14th international congress on antiphospholipid antibodies technical task force report on antiphospholipid syndrome clinical features. *Autoimmun Rev* (2015) 14(5):401–14. doi:10.1016/j.autrev.2015.01.002
113. Ruiz-Irastorza G, Egurbide M-V, Ugalde J, Aguirre C. High impact of antiphospholipid syndrome on irreversible organ damage and survival of patients with systemic lupus erythematosus. *Arch Intern Med* (2004) 164(1):77–82. doi:10.1001/archinte.164.1.77
114. Danowski A, de Azevedo MNL, de Souza Papi JA, Petri M. Determinants of risk for venous and arterial thrombosis in primary antiphospholipid syndrome and in antiphospholipid syndrome with systemic lupus erythematosus. *J Rheumatol* (2009) 36(6):1195–9. doi:10.3899/jrheum.081194
115. Lee JL, Naguwa SM, Cheema GS, Gershwin ME. Revisiting Libman-Sacks endocarditis: a historical review and update. *Clin Rev Allergy Immunol* (2009) 36(2–3):126–30. doi:10.1007/s12016-008-8113-y
116. Zuily S, Regnault V, Selton-Suty C, Eschwège V, Bruntz J-F, Bode-Dotto E, et al. Increased risk for heart valve disease associated with antiphospholipid antibodies in patients with systemic lupus erythematosus: meta-analysis of echocardiographic studies. *Circulation* (2011) 124(2):215–24. doi:10.1161/CIRCULATIONAHA.111.028522
117. Petri M. Detection of coronary artery disease and the role of traditional risk factors in the Hopkins Lupus Cohort. *Lupus* (2000) 9(3):170–5. doi:10.1191/096120300678828226
118. Zuily S, Domingues V, Suty-Selton C, Eschwège V, Bertoletti L, Chaouat A, et al. Antiphospholipid antibodies can identify lupus patients at risk of pulmonary hypertension: a systematic review and meta-analysis. *Autoimmun Rev* (2017) 16(6):576–86. doi:10.1016/j.autrev.2017.04.003
119. Sciascia S, Sanna G, Murru V, Roccatello D, Khamashta MA, Bertolaccini ML. GAPSS: the global anti-phospholipid syndrome score. *Rheumatology (Oxford)* (2013) 52(8):1397–403. doi:10.1093/rheumatology/kes388
120. Pereira WL, Reiche EMV, Kallaur AP, Kaimen-Maciel DR. Epidemiological, clinical, and immunological characteristics of neuromyelitis optica: a review. *J Neurol Sci* (2015) 355(1–2):7–17. doi:10.1016/j.jns.2015.05.034
121. Dellavance A, Alvarenga RR, Rodrigues SH, Kok F, de Souza AWS, Andrade LEC. Anti-aquaporin-4 antibodies in the context of assorted immune-mediated diseases. *Eur J Neurol* (2012) 19(2):248–52. doi:10.1111/j.1468-1331.2011.03479.x
122. Li H, Wang Y, Xu Q, Zhang A, Zhou H, Zhao S, et al. Features of anti-aquaporin 4 antibody-seropositive Chinese patients with neuromyelitis optica spectrum optic neuritis. *J Neurol* (2015) 262(10):2293–304. doi:10.1007/s00415-015-7844-y
123. Park J-H, Hwang J, Min J-H, Kim BJ, Kang E-S, Lee KH. Presence of anti-Ro/SSA antibody may be associated with anti-aquaporin-4 antibody positivity in neuromyelitis optica spectrum disorder. *J Neurol Sci* (2015) 348(1–2):132–5. doi:10.1016/j.jns.2014.11.020
124. Alexopoulos H, Kampylafka EI, Fouka P, Tatouli I, Akrivou S, Politis PK, et al. Anti-aquaporin-4 autoantibodies in systemic lupus erythematosus persist for years and induce astrocytic cytotoxicity but not CNS disease. *J Neuroimmunol* (2015) 289:8–11. doi:10.1016/j.jneuroim.2015.10.007

125. Long Y, Qiu W, Lu Z, Bao J, Wu A, Wang Y, et al. Aquaporin 4 antibodies in the cerebrospinal fluid are helpful in diagnosing Chinese patients with neuromyelitis optica. *Neuroimmunomodulation* (2012) 19(2):96–102. doi:10.1159/000330240
126. Shiboski CH, Shiboski SC, Seror R, Criswell LA, Labetoulle M, Lietman TM, et al. 2016 American College of Rheumatology/European League Against Rheumatism classification criteria for primary Sjögren's syndrome: a consensus and data-driven methodology involving three international patient cohorts. *Ann Rheum Dis* (2017) 76(1):9–16. doi:10.1136/annrheumdis-2016-210571
127. Mulli JC, Cruchaud A. Immunoreactivity to nuclear antigens in systemic lupus erythematosus with or without nephritis, and in other connective tissue diseases, with particular reference to the RNA-protein antigen. *Int Arch Allergy Appl Immunol* (1977) 53(3):279–89. doi:10.1159/000231763
128. Sulcebe G, Morcka K. Diagnostic and prognostic significance of different antinuclear antibodies in more than 1000 consecutive Albanian patients with rheumatic diseases. *Clin Exp Rheumatol* (1992) 10(3):255–61.
129. Schur PH, DeAngelis D, Jackson JM. Immunological detection of nucleic acids and antibodies to nucleic acids and nuclear antigens by counterimmunoelectrophoresis. *Clin Exp Immunol* (1974) 17(1):209–18.
130. Theander E, Jonsson R, Sjöström B, Brokstad K, Olsson P, Henriksson G. Prediction of Sjögren's syndrome years before diagnosis and identification of patients with early onset and severe disease course by autoantibody profiling. *Arthritis Rheumatol* (2015) 67(9):2427–36. doi:10.1002/art.39214
131. Skopouli FN, Dafni U, Ioannidis JP, Moutsopoulos HM. Clinical evolution, and morbidity and mortality of primary Sjögren's syndrome. *Semin Arthritis Rheum* (2000) 29(5):296–304. doi:10.1016/S0049-0172(00)80016-5
132. Zhao Y, Li Y, Wang L, Li X-F, Huang C-B, Wang G-C, et al. Primary Sjögren syndrome in Han Chinese: clinical and immunological characteristics of 483 patients. *Medicine (Baltimore)* (2015) 94(16):e667. doi:10.1097/MD.0000000000000667
133. Fauchais AL, Martel C, Gondran G, Lambert M, Launay D, Jauberteau MO, et al. Immunological profile in primary Sjögren syndrome: clinical significance, prognosis and long-term evolution to other auto-immune disease. *Autoimmun Rev* (2010) 9(9):595–9. doi:10.1016/j.autrev.2010.05.004
134. Nardi N, Brito-Zerón P, Ramos-Casals M, Aguiló S, Cervera R, Ingelmo M, et al. Circulating auto-antibodies against nuclear and non-nuclear antigens in primary Sjögren's syndrome: prevalence and clinical significance in 335 patients. *Clin Rheumatol* (2006) 25(3):341–6. doi:10.1007/s10067-005-0059-3
135. Baer AN, McAdams DeMarco M, Shiboski SC, Lam MY, Challacombe S, Daniels TE, et al. The SSB-positive/SSA-negative antibody profile is not associated with key phenotypic features of Sjögren's syndrome. *Ann Rheum Dis* (2015) 74(8):1557–61. doi:10.1136/annrheumdis-2014-206683
136. Quartuccio L, Baldini C, Bartoloni E, Priori R, Carubbi F, Corazza L, et al. Anti-SSA/SSB-negative Sjögren's syndrome shows a lower prevalence of lymphoproliferative manifestations, and a lower risk of lymphoma evolution. *Autoimmun Rev* (2015) 14(11):1019–22. doi:10.1016/j.autrev.2015.07.002
137. Ambrosi A, Sonesson S-E, Wahren-Herlenius M. Molecular mechanisms of congenital heart block. *Exp Cell Res* (2014) 325(1):2–9. doi:10.1016/j.yexcr.2014.01.003
138. Brucato A, Frassi M, Franceschini F, Cimaz R, Faden D, Pisoni MP, et al. Risk of congenital complete heart block in newborns of mothers with anti-Ro/SSA antibodies detected by counterimmunoelectrophoresis: a prospective study of 100 women. *Arthritis Rheum* (2001) 44(8):1832–5. doi:10.1002/1529-0131(200108)44:8<1832::AID-ART320>3.0.CO;2-C
139. Salomonsson S, Sonesson S-E, Ottosson L, Muhallab S, Olsson T, Sunnerhagen M, et al. Ro/SSA autoantibodies directly bind cardiomyocytes, disturb calcium homeostasis, and mediate congenital heart block. *J Exp Med* (2005) 201(1):11–7. doi:10.1084/jem.20041859
140. Bournia V-K, Vlachoyiannopoulos PG. Subgroups of Sjögren syndrome patients according to serological profiles. *J Autoimmun* (2012) 39(1–2):15–26. doi:10.1016/j.jaut.2012.03.001
141. Maruyama T, Saito I, Hayashi Y, Kompfner E, Fox RI, Burton DR, et al. Molecular analysis of the human autoantibody response to alpha-fodrin in Sjögren's syndrome reveals novel apoptosis-induced specificity. *Am J Pathol* (2004) 165(1):53–61. doi:10.1016/S0002-9440(10)63274-9
142. Qin Q, Wang H, Wang H-Z, Huang Y-L, Li H, Zhang W-W, et al. Diagnostic accuracy of anti-alpha-fodrin antibodies for primary Sjögren's syndrome. *Mod Rheumatol* (2014) 24(5):793–7. doi:10.3109/14397595.2013.865823
143. Hu Q, Wang D, Chen W. The accuracy of the anti-α-fodrin antibody test for diagnosis of Sjögren's syndrome: a meta-analysis. *Clin Biochem* (2013) 46(15):1372–6. doi:10.1016/j.clinbiochem.2013.04.020
144. Nordmark G, Rorsman F, Rönnblom L, Cajander S, Taussig MJ, Kämpe O, et al. Autoantibodies to alpha-fodrin in primary Sjögren's syndrome and SLE detected by an in vitro transcription and translation assay. *Clin Exp Rheumatol* (2003) 21(1):49–56.
145. Locht H, Pelck R, Manthorpe R. Diagnostic and prognostic significance of measuring antibodies to alpha-fodrin compared to anti-Ro-52, anti-Ro-60, and anti-La in primary Sjögren's syndrome. *J Rheumatol* (2008) 35(5):845–9.
146. Hernández-Molina G, Nuñez-Alvarez C, Avila-Casado C, Llorente L, Hernández-Hernández C, Calderillo ML, et al. Usefulness of IgA anti-α-fodrin antibodies in combination with rheumatoid factor and/or antinuclear antibodies as substitute immunological criterion in Sjögren syndrome with negative anti-SSA/SSB antibodies. *J Rheumatol* (2016) 43(10):1852–7. doi:10.3899/jrheum.151315
147. van den Hoogen F, Khanna D, Fransen J, Johnson SR, Baron M, Tyndall A, et al. 2013 classification criteria for systemic sclerosis: an American College of Rheumatology/European League against Rheumatism collaborative initiative. *Arthritis Rheum* (2013) 65(11):2737–47. doi:10.1002/art.38098
148. Salazar GA, Assassi S, Wigley F, Hummers L, Varga J, Hinchcliff M, et al. Antinuclear antibody-negative systemic sclerosis. *Semin Arthritis Rheum* (2015) 44(6):680–6. doi:10.1016/j.semarthrit.2014.11.006
149. Schneeberger D, Tyndall A, Kay J, Søndergaard KH, Carreira PE, Morgiel E, et al. Systemic sclerosis without antinuclear antibodies or Raynaud's phenomenon: a multicentre study in the prospective EULAR scleroderma trials and research (EUSTAR) database. *Rheumatology (Oxford)* (2013) 52(3):560–7. doi:10.1093/rheumatology/kes315
150. Liaskos C, Marou E, Simopoulou T, Barmakoudi M, Efthymiou G, Scheper T, et al. Disease-related autoantibody profile in patients with systemic sclerosis. *Autoimmunity* (2017) 50(7):414–21. doi:10.1080/08916934.2017.1357699
151. Heijnen IAFM, Foocharoen C, Bannert B, Carreira PE, Caporali R, Smith V, et al. Clinical significance of coexisting antitopoisomerase I and anti-centromere antibodies in patients with systemic sclerosis: a EUSTAR group-based study. *Clin Exp Rheumatol* (2013) 31(2 Suppl 76):96–102.
152. Mierau R, Moinzadeh P, Riemekasten G, Melchers I, Meurer M, Reichenberger F, et al. Frequency of disease-associated and other nuclear autoantibodies in patients of the German Network for Systemic Scleroderma: correlation with characteristic clinical features. *Arthritis Res Ther* (2011) 13(5):R172. doi:10.1186/ar3495
153. Hamaguchi Y, Hasegawa M, Fujimoto M, Matsushita T, Komura K, Kaji K, et al. The clinical relevance of serum antinuclear antibodies in Japanese patients with systemic sclerosis. *Br J Dermatol* (2008) 158(3):487–95. doi:10.1111/j.1365-2133.2007.08392.x
154. Reveille JD, Solomon DH; American College of Rheumatology Ad Hoc Committee of Immunologic Testing Guidelines. Evidence-based guidelines for the use of immunologic tests: anticentromere, Scl-70, and nucleolar antibodies. *Arthritis Rheum* (2003) 49(3):399–412. doi:10.1002/art.11113
155. Dellavance A, Gallindo C, Soares MG, da Silva NP, Mortara RA, Andrade LEC. Redefining the Scl-70 indirect immunofluorescence pattern: autoantibodies to DNA topoisomerase I yield a specific compound immunofluorescence pattern. *Rheumatology (Oxford)* (2009) 48(6):632–7. doi:10.1093/rheumatology/kep070
156. Jarzabek-Chorzelska M, Blaszczyk M, Jablonska S, Chorzelski T, Kumar V, Beutner EH. Scl 70 antibody – a specific marker of systemic sclerosis. *Br J Dermatol* (1986) 115(4):393–401. doi:10.1111/j.1365-2133.1986.tb06233.x
157. Graf SW, Hakendorf P, Lester S, Patterson K, Walker JG, Smith MD, et al. South Australian Scleroderma Register: autoantibodies as predictive biomarkers of phenotype and outcome. *Int J Rheum Dis* (2012) 15(1):102–9. doi:10.1111/j.1756-185X.2011.01688.x
158. Walker UA, Tyndall A, Czirják L, Denton C, Farge-Bancel D, Kowal-Bielecka O, et al. Clinical risk assessment of organ manifestations in systemic sclerosis: a report from the EULAR Scleroderma Trials and Research group database. *Ann Rheum Dis* (2007) 66(6):754–63. doi:10.1136/ard.2006.062901
159. Hu PQ, Fertig N, Medsger TA, Wright TM. Correlation of serum anti-DNA topoisomerase I antibody levels with disease severity and activity in systemic sclerosis. *Arthritis Rheum* (2003) 48(5):1363–73. doi:10.1002/art.10977
160. Kuwana M, Kaburaki J, Mimori T, Kawakami Y, Tojo T. Longitudinal analysis of autoantibody response to topoisomerase

I in systemic sclerosis. *Arthritis Rheum* (2000) 43(5):1074–84. doi:10.1002/1529-0131(200005)43:5<1074::AID-ANR18>3.0.CO;2-E
161. Kuwana M, Kaburaki J, Okano Y, Tojo T, Homma M. Clinical and prognostic associations based on serum antinuclear antibodies in Japanese patients with systemic sclerosis. *Arthritis Rheum* (1994) 37(1):75–83. doi:10.1002/art.1780370111
162. Mitri GM, Lucas M, Fertig N, Steen VD, Medsger TA. A comparison between anti-Th/To- and anticentromere antibody-positive systemic sclerosis patients with limited cutaneous involvement. *Arthritis Rheum* (2003) 48(1):203–9. doi:10.1002/art.10760
163. Santiago M, Baron M, Hudson M, Burlingame RW, Fritzler MJ. Antibodies to RNA polymerase III in systemic sclerosis detected by ELISA. *J Rheumatol* (2007) 34(7):1528–34.
164. Sobanski V, Dauchet L, Lefèvre G, Lambert M, Morell-Dubois S, Sy T, et al. Prevalence of anti-RNA polymerase III antibodies in systemic sclerosis: new data from a French cohort and a systematic review and meta-analysis. *Arthritis Rheumatol* (2014) 66(2):407–17. doi:10.1002/art.38219
165. Phan TG, Cass A, Gillin A, Trew P, Fertig N, Sturgess A. Anti-RNA polymerase III antibodies in the diagnosis of scleroderma renal crisis sine scleroderma. *J Rheumatol* (1999) 26(11):2489–92.
166. Moinzadeh P, Fonseca C, Hellmich M, Shah AA, Chighizola C, Denton CP, et al. Association of anti-RNA polymerase III autoantibodies and cancer in scleroderma. *Arthritis Res Ther* (2014) 16(1):R53. doi:10.1186/ar4486
167. Lazzaroni M-G, Cavazzana I, Colombo E, Dobrota R, Hernandez J, Hesselstrand R, et al. Malignancies in patients with anti-RNA polymerase III antibodies and systemic sclerosis: analysis of the EULAR scleroderma trials and research cohort and possible recommendations for screening. *J Rheumatol* (2017) 44(5):639–47. doi:10.3899/jrheum.160817
168. Herrick AL, Peytrignet S, Lunt M, Pan X, Hesselstrand R, Mouthon L, et al. Patterns and predictors of skin score change in early diffuse systemic sclerosis from the European Scleroderma Observational Study. *Ann Rheum Dis* (2018). doi:10.1136/annrheumdis-2017-211912
169. Ceribelli A, Krzyszczak ME, Li Y, Ross SJ, Chan JYF, Chan EKL, et al. Atypical clinical presentation of a subset of patients with anti-RNA polymerase III – non-scleroderma cases associated with dominant RNA polymerase I reactivity and nucleolar staining. *Arthritis Res Ther* (2011) 13(4):R119. doi:10.1186/ar3422
170. Shah AA, Rosen A, Hummers L, Wigley F, Casciola-Rosen L. Close temporal relationship between onset of cancer and scleroderma in patients with RNA polymerase I/III antibodies. *Arthritis Rheum* (2010) 62(9):2787–95. doi:10.1002/art.27549
171. Kuwana M, Kaburaki J, Mimori T, Tojo T, Homma M. Autoantibody reactive with three classes of RNA polymerases in sera from patients with systemic sclerosis. *J Clin Invest* (1993) 91(4):1399–404. doi:10.1172/JCI116343
172. Hamaguchi Y, Kodera M, Matsushita T, Hasegawa M, Inaba Y, Usuda T, et al. Clinical and immunologic predictors of scleroderma renal crisis in Japanese systemic sclerosis patients with anti-RNA polymerase III autoantibodies. *Arthritis Rheumatol* (2015) 67(4):1045–52. doi:10.1002/art.38994
173. Mahler M, Raijmakers R, Dähnrich C, Blüthner M, Fritzler MJ. Clinical evaluation of autoantibodies to a novel PM/Scl peptide antigen. *Arthritis Res Ther* (2005) 7(3):R704–13. doi:10.1186/ar1455
174. Hanke K, Brückner CS, Dähnrich C, Huscher D, Komorowski L, Meyer W, et al. Antibodies against PM/Scl-75 and PM/Scl-100 are independent markers for different subsets of systemic sclerosis patients. *Arthritis Res Ther* (2009) 11(1):R22. doi:10.1186/ar2614
175. Wodkowski M, Hudson M, Proudman S, Walker J, Stevens W, Nikpour M, et al. Clinical correlates of monospecific anti-PM75 and anti-PM100 antibodies in a tri-nation cohort of 1574 systemic sclerosis subjects. *Autoimmunity* (2015) 48(8):542–51. doi:10.3109/08916934.2015.1077231
176. Rozman B, Cucnik S, Sodin-Semrl S, Czirják L, Varjú C, Distler O, et al. Prevalence and clinical associations of anti-Ku antibodies in patients with systemic sclerosis: a European EUSTAR-initiated multi-centre case-control study. *Ann Rheum Dis* (2008) 67(9):1282–6. doi:10.1136/ard.2007.073981
177. Hoa S, Hudson M, Troyanov Y, Proudman S, Walker J, Stevens W, et al. Single-specificity anti-Ku antibodies in an international cohort of 2140 systemic sclerosis subjects: clinical associations. *Medicine (Baltimore)* (2016) 95(35):e4713. doi:10.1097/MD.0000000000004713
178. Charlton D, Laffoon M, Medsger TA, Domsic R. Long-term survival and follow-up of anti-Th/to antibody positive systemic sclerosis patients. *Arthritis Rheumatol* (2017) 69(Suppl 10):1–4426.
179. Sobanski V, Giovannelli J, Lynch BM, Schreiber BE, Nihtyanova SI, Harvey J, et al. Characteristics and survival of anti-U1 RNP antibody-positive patients with connective tissue disease-associated pulmonary arterial hypertension. *Arthritis Rheumatol* (2016) 68(2):484–93. doi:10.1002/art.39432
180. Ihn H, Yamane K, Yazawa N, Kubo M, Fujimoto M, Sato S, et al. Distribution and antigen specificity of anti-U1RNP antibodies in patients with systemic sclerosis. *Clin Exp Immunol* (1999) 117(2):383–7. doi:10.1046/j.1365-2249.1999.00961.x
181. Tormey VJ, Bunn CC, Denton CP, Black CM. Anti-fibrillarin antibodies in systemic sclerosis. *Rheumatology (Oxford)* (2001) 40(10):1157–62. doi:10.1093/rheumatology/40.10.1157
182. Aggarwal R, Lucas M, Fertig N, Oddis CV, Medsger TA. Anti-U3 RNP autoantibodies in systemic sclerosis. *Arthritis Rheum* (2009) 60(4):1112–8. doi:10.1002/art.24409
183. Arnett FC, Reveille JD, Goldstein R, Pollard KM, Leaird K, Smith EA, et al. Autoantibodies to fibrillarin in systemic sclerosis (scleroderma). An immunogenetic, serologic, and clinical analysis. *Arthritis Rheum* (1996) 39(7):1151–60. doi:10.1002/art.1780390712
184. Sharif R, Fritzler MJ, Mayes MD, Gonzalez EB, McNearney TA, Draeger H, et al. Anti-fibrillarin antibody in African American patients with systemic sclerosis: immunogenetics, clinical features, and survival analysis. *J Rheumatol* (2011) 38(8):1622–30. doi:10.3899/jrheum.110071
185. Schulte-Pelkum J, Fritzler M, Mahler M. Latest update on the Ro/SS-A autoantibody system. *Autoimmun Rev* (2009) 8(7):632–7. doi:10.1016/j.autrev.2009.02.010
186. Fujii T, Mimori T, Akizuki M. Detection of autoantibodies to nucleolar transcription factor NOR 90/hUBF in sera of patients with rheumatic diseases, by recombinant autoantigen-based assays. *Arthritis Rheum* (1996) 39(8):1313–8. doi:10.1002/art.1780390808
187. Morozzi G, Bellisai F, Fineschi I, Scaccia F, Pucci G, Simpatico A, et al. Prevalence of anti-histone antibodies, their clinical significance and correlation with other autoantibodies in a cohort of Italian scleroderma patients. *Auto Immun Highlights* (2011) 2(1):29–33. doi:10.1007/s13317-011-0015-y
188. Hesselstrand R, Scheja A, Shen GQ, Wiik A, Akesson A. The association of antinuclear antibodies with organ involvement and survival in systemic sclerosis. *Rheumatology (Oxford)* (2003) 42(4):534–40. doi:10.1093/rheumatology/keg170
189. Laustriat G, Ruyssen-Witrand A, Constantin A, Barnetche T, Adoue D, Cantagrel A, et al. Anti-citrullinated peptides antibodies in systemic sclerosis: meta-analysis of frequency and meaning. *Jt Bone Spine Rev Rhum* (2017) 85(2):147–53. doi:10.1016/j.jbspin.2017.11.006
190. Koenig M, Fritzler MJ, Targoff IN, Troyanov Y, Senécal J-L. Heterogeneity of autoantibodies in 100 patients with autoimmune myositis: insights into clinical features and outcomes. *Arthritis Res Ther* (2007) 9(4):R78. doi:10.1186/ar2276
191. Troyanov Y, Targoff IN, Tremblay J-L, Goulet J-R, Raymond Y, Senécal J-L. Novel classification of idiopathic inflammatory myopathies based on overlap syndrome features and autoantibodies: analysis of 100 French Canadian patients. *Medicine (Baltimore)* (2005) 84(4):231–49. doi:10.1097/01.md.0000173991.74008.b0
192. Hoogendijk JE, Amato AA, Lecky BR, Choy EH, Lundberg IE, Rose MR, et al. 119th ENMC international workshop: trial design in adult idiopathic inflammatory myopathies, with the exception of inclusion body myositis, 10-12 October 2003, Naarden, The Netherlands. *Neuromuscul Disord* (2004) 14(5):337–45. doi:10.1016/j.nmd.2004.02.006
193. Lloyd TE, Mammen AL, Amato AA, Weiss MD, Needham M, Greenberg SA. Evaluation and construction of diagnostic criteria for inclusion body myositis. *Neurology* (2014) 83(5):426–33. doi:10.1212/WNL.0000000000000642
194. Lega J-C, Fabien N, Reynaud Q, Durieu I, Durupt S, Dutertre M, et al. The clinical phenotype associated with myositis-specific and associated autoantibodies: a meta-analysis revisiting the so-called antisynthetase syndrome. *Autoimmun Rev* (2014) 13(9):883–91. doi:10.1016/j.autrev.2014.03.004
195. Connors GR, Christopher-Stine L, Oddis CV, Danoff SK. Interstitial lung disease associated with the idiopathic inflammatory myopathies: what progress has been made in the past 35 years? *Chest* (2010) 138(6):1464–74. doi:10.1378/chest.10-0180

196. Yoshifuji H, Fujii T, Kobayashi S, Imura Y, Fujita Y, Kawabata D, et al. Anti-aminoacyl-tRNA synthetase antibodies in clinical course prediction of interstitial lung disease complicated with idiopathic inflammatory myopathies. *Autoimmunity* (2006) 39(3):233–41. doi:10.1080/08916930600622884
197. Pinal-Fernandez I, Casal-Dominguez M, Huapaya JA, Albayda J, Paik JJ, Johnson C, et al. A longitudinal cohort study of the anti-synthetase syndrome: increased severity of interstitial lung disease in black patients and patients with anti-PL7 and anti-PL12 autoantibodies. *Rheumatology (Oxford)* (2017) 56(6):999–1007. doi:10.1093/rheumatology/kex021
198. Hervier B, Devilliers H, Stanciu R, Meyer A, Uzunhan Y, Masseau A, et al. Hierarchical cluster and survival analyses of antisynthetase syndrome: phenotype and outcome are correlated with anti-tRNA synthetase antibody specificity. *Autoimmun Rev* (2012) 12(2):210–7. doi:10.1016/j.autrev.2012.06.006
199. Marie I, Josse S, Decaux O, Dominique S, Diot E, Landron C, et al. Comparison of long-term outcome between anti-Jo1- and anti-PL7/PL12 positive patients with antisynthetase syndrome. *Autoimmun Rev* (2012) 11(10):739–45. doi:10.1016/j.autrev.2012.01.006
200. Stone KB, Oddis CV, Fertig N, Katsumata Y, Lucas M, Vogt M, et al. Anti-Jo-1 antibody levels correlate with disease activity in idiopathic inflammatory myopathy. *Arthritis Rheum* (2007) 56(9):3125–31. doi:10.1002/art.22865
201. Milone M. Diagnosis and management of immune-mediated myopathies. *Mayo Clin Proc* (2017) 92(5):826–37. doi:10.1016/j.mayocp.2016.12.025
202. Kassardjian CD, Lennon VA, Alfugham NB, Mahler M, Milone M. Clinical features and treatment outcomes of necrotizing autoimmune myopathy. *JAMA Neurol* (2015) 72(9):996–1003. doi:10.1001/jamaneurol.2015.1207
203. Arouche-Delaperche L, Allenbach Y, Amelin D, Preusse C, Mouly V, Mauhin W, et al. Pathogenic role of anti-signal recognition protein and anti-3-hydroxy-3-methylglutaryl-CoA reductase antibodies in necrotizing myopathies: myofiber atrophy and impairment of muscle regeneration in necrotizing autoimmune myopathies. *Ann Neurol* (2017) 81(4):538–48. doi:10.1002/ana.24902
204. Allenbach Y, Arouche-Delaperche L, Preusse C, Radbruch H, Butler-Browne G, Champtiaux N, et al. Necrosis in anti-SRP+ and anti-HMGCR+myopathies: role of autoantibodies and complement. *Neurology* (2018) 90(6):e507–17. doi:10.1212/WNL.0000000000004923
205. Watanabe Y, Uruha A, Suzuki S, Nakahara J, Hamanaka K, Takayama K, et al. Clinical features and prognosis in anti-SRP and anti-HMGCR necrotising myopathy. *J Neurol Neurosurg Psychiatry* (2016) 87(10):1038–44. doi:10.1136/jnnp-2016-313166
206. Christopher-Stine L, Casciola-Rosen LA, Hong G, Chung T, Corse AM, Mammen AL. A novel autoantibody recognizing 200-kd and 100-kd proteins is associated with an immune-mediated necrotizing myopathy. *Arthritis Rheum* (2010) 62(9):2757–66. doi:10.1002/art.27572
207. Werner JL, Christopher-Stine L, Ghazarian SR, Pak KS, Kus JE, Daya NR, et al. Antibody levels correlate with creatine kinase levels and strength in anti-3-hydroxy-3-methylglutaryl-coenzyme A reductase-associated autoimmune myopathy. *Arthritis Rheum* (2012) 64(12):4087–93. doi:10.1002/art.34673
208. Ashton C, Junckerstorff R, Bundell C, Hollingsworth P, Needham M. Treatment and outcomes in necrotising autoimmune myopathy: an Australian perspective. *Neuromuscul Disord* (2016) 26(11):734–40. doi:10.1016/j.nmd.2016.08.013
209. Mammen AL. Statin-associated autoimmune myopathy. *N Engl J Med* (2016) 374(7):664–9. doi:10.1056/NEJMra1515161
210. Benveniste O, Drouot L, Jouen F, Charuel J-L, Bloch-Queyrat C, Behin A, et al. Correlation of anti-signal recognition particle autoantibody levels with creatine kinase activity in patients with necrotizing myopathy. *Arthritis Rheum* (2011) 63(7):1961–71. doi:10.1002/art.30344
211. Pinal-Fernandez I, Parks C, Werner JL, Albayda J, Paik J, Danoff SK, et al. Longitudinal course of disease in a large cohort of myositis patients with autoantibodies recognizing the signal recognition particle. *Arthritis Care Res* (2017) 69(2):263–70. doi:10.1002/acr.22920
212. Fiorentino DF, Chung LS, Christopher-Stine L, Zaba L, Li S, Mammen AL, et al. Most patients with cancer-associated dermatomyositis have antibodies to nuclear matrix protein NXP-2 or transcription intermediary factor 1γ. *Arthritis Rheum* (2013) 65(11):2954–62. doi:10.1002/art.38093
213. Kaji K, Fujimoto M, Hasegawa M, Kondo M, Saito Y, Komura K, et al. Identification of a novel autoantibody reactive with 155 and 140 kDa nuclear proteins in patients with dermatomyositis: an association with malignancy. *Rheumatology (Oxford)* (2007) 46(1):25–8. doi:10.1093/rheumatology/kel161
214. Trallero-Araguás E, Rodrigo-Pendás JÁ, Selva-O'Callaghan A, Martínez-Gómez X, Bosch X, Labrador-Horrillo M, et al. Usefulness of anti-p155 autoantibody for diagnosing cancer-associated dermatomyositis: a systematic review and meta-analysis. *Arthritis Rheum* (2012) 64(2):523–32. doi:10.1002/art.33379
215. Mugii N, Hasegawa M, Matsushita T, Hamaguchi Y, Oohata S, Okita H, et al. Oropharyngeal dysphagia in dermatomyositis: associations with clinical and laboratory features including autoantibodies. *PLoS One* (2016) 11(5):e0154746. doi:10.1371/journal.pone.0154746
216. Ceribelli A, Fredi M, Taraborelli M, Cavazzana I, Franceschini F, Quinzanini M, et al. Anti-MJ/NXP-2 autoantibody specificity in a cohort of adult Italian patients with polymyositis/dermatomyositis. *Arthritis Res Ther* (2012) 14(2):R97. doi:10.1186/ar3822
217. Gunawardena H, Wedderburn LR, Chinoy H, Betteridge ZE, North J, Ollier WER, et al. Autoantibodies to a 140-kd protein in juvenile dermatomyositis are associated with calcinosis. *Arthritis Rheum* (2009) 60(6):1807–14. doi:10.1002/art.24547
218. Espada G, Maldonado Cocco JA, Fertig N, Oddis CV. Clinical and serologic characterization of an Argentine pediatric myositis cohort: identification of a novel autoantibody (anti-MJ) to a 142-kDa protein. *J Rheumatol* (2009) 36(11):2547–51. doi:10.3899/jrheum.090461
219. Fiorentino D, Chung L, Zwerner J, Rosen A, Casciola-Rosen L. The mucocutaneous and systemic phenotype of dermatomyositis patients with antibodies to MDA5 (CADM-140): a retrospective study. *J Am Acad Dermatol* (2011) 65(1):25–34. doi:10.1016/j.jaad.2010.09.016
220. Chen Z, Cao M, Plana MN, Liang J, Cai H, Kuwana M, et al. Utility of anti-melanoma differentiation-associated gene 5 antibody measurement in identifying patients with dermatomyositis and a high risk for developing rapidly progressive interstitial lung disease: a review of the literature and a meta-analysis. *Arthritis Care Res* (2013) 65(8):1316–24. doi:10.1002/acr.21985
221. Zhang L, Wu G, Gao D, Liu G, Pan L, Ni L, et al. Factors associated with interstitial lung disease in patients with polymyositis and dermatomyositis: a systematic review and meta-analysis. *PLoS One* (2016) 11(5):e0155381. doi:10.1371/journal.pone.0155381
222. Nakashima R, Imura Y, Kobayashi S, Yukawa N, Yoshifuji H, Nojima T, et al. The RIG-I-like receptor IFIH1/MDA5 is a dermatomyositis-specific autoantigen identified by the anti-CADM-140 antibody. *Rheumatology (Oxford)* (2010) 49(3):433–40. doi:10.1093/rheumatology/kep375
223. Muro Y, Sugiura K, Hoshino K, Akiyama M. Disappearance of anti-MDA-5 autoantibodies in clinically amyopathic DM/interstitial lung disease during disease remission. *Rheumatology (Oxford)* (2012) 51(5):800–4. doi:10.1093/rheumatology/ker408
224. Gono T, Sato S, Kawaguchi Y, Kuwana M, Hanaoka M, Katsumata Y, et al. Anti-MDA5 antibody, ferritin and IL-18 are useful for the evaluation of response to treatment in interstitial lung disease with anti-MDA5 antibody-positive dermatomyositis. *Rheumatology (Oxford)* (2012) 51(9):1563–70. doi:10.1093/rheumatology/kes102
225. Tarricone E, Ghirardello A, Rampudda M, Bassi N, Punzi L, Doria A. Anti-SAE antibodies in autoimmune myositis: identification by unlabelled protein immunoprecipitation in an Italian patient cohort. *J Immunol Methods* (2012) 384(1–2):128–34. doi:10.1016/j.jim.2012.07.019
226. Betteridge ZE, Gunawardena H, Chinoy H, North J, Ollier WER, Cooper RG, et al. Clinical and human leucocyte antigen class II haplotype associations of autoantibodies to small ubiquitin-like modifier enzyme, a dermatomyositis-specific autoantigen target, in UK Caucasian adult-onset myositis. *Ann Rheum Dis* (2009) 68(10):1621–5. doi:10.1136/ard.2008.097162
227. Muro Y, Sugiura K, Akiyama M. Low prevalence of anti-small ubiquitin-like modifier activating enzyme antibodies in dermatomyositis patients. *Autoimmunity* (2013) 46(4):279–84. doi:10.3109/08916934.2012.755958
228. Kang EH, Nakashima R, Mimori T, Kim J, Lee YJ, Lee EB, et al. Myositis autoantibodies in Korean patients with inflammatory myositis: anti-140-kDa polypeptide antibody is primarily associated with rapidly progressive interstitial lung disease independent of clinically amyopathic dermatomyositis. *BMC Musculoskelet Disord* (2010) 11:223. doi:10.1186/1471-2474-11-223

229. Petri MH, Satoh M, Martin-Marquez BT, Vargas-Ramírez R, Jara LJ, Saavedra MA, et al. Implications in the difference of anti-Mi-2 and -p155/140 autoantibody prevalence in two dermatomyositis cohorts from Mexico City and Guadalajara. *Arthritis Res Ther* (2013) 15(2):R48. doi:10.1186/ar4207
230. Schmidt K, Schmidt J. Inclusion body myositis: advancements in diagnosis, pathomechanisms, and treatment. *Curr Opin Rheumatol* (2017) 29(6):632–8. doi:10.1097/BOR.0000000000000436
231. Salajegheh M, Lam T, Greenberg SA. Autoantibodies against a 43 KDa muscle protein in inclusion body myositis. *PLoS One* (2011) 6(5):e20266. doi:10.1371/journal.pone.0020266
232. Herbert MK, Stammen-Vogelzangs J, Verbeek MM, Rietveld A, Lundberg IE, Chinoy H, et al. Disease specificity of autoantibodies to cytosolic 5′-nucleotidase 1A in sporadic inclusion body myositis versus known autoimmune diseases. *Ann Rheum Dis* (2016) 75(4):696–701. doi:10.1136/annrheumdis-2014-206691
233. Benveniste O, Stenzel W, Allenbach Y. Advances in serological diagnostics of inflammatory myopathies. *Curr Opin Neurol* (2016) 29(5):662–73. doi:10.1097/WCO.0000000000000376
234. Smolen JS, Aletaha D, McInnes IB. Rheumatoid arthritis. *Lancet Lond Engl* (2016) 388(10055):2023–38. doi:10.1016/S0140-6736(16)30173-8
235. Kapetanovic MC, Larsson L, Truedsson L, Sturfelt G, Saxne T, Geborek P. Predictors of infusion reactions during infliximab treatment in patients with arthritis. *Arthritis Res Ther* (2006) 8(4):R131. doi:10.1186/ar2020
236. Yukawa N, Fujii T, Kondo-Ishikawa S, Yoshifuji H, Kawabata D, Nojima T, et al. Correlation of antinuclear antibody and anti-double-stranded DNA antibody with clinical response to infliximab in patients with rheumatoid arthritis: a retrospective clinical study. *Arthritis Res Ther* (2011) 13(6):R213. doi:10.1186/ar3546
237. Othman MA, Ghazali WSW, Hamid WZWA, Wong KK, Yahya NK. Anti-carbamylated protein antibodies in rheumatoid arthritis patients and their association with rheumatoid factor. *Saudi Med J* (2017) 38(9):934–41. doi:10.15537/smj.2017.9.20841
238. Arnett FC, Edworthy SM, Bloch DA, McShane DJ, Fries JF, Cooper NS, et al. The American Rheumatism Association 1987 revised criteria for the classification of rheumatoid arthritis. *Arthritis Rheum* (1988) 31(3):315–24. doi:10.1002/art.1780310302
239. Aletaha D, Neogi T, Silman AJ, Funovits J, Felson DT, Bingham CO, et al. 2010 rheumatoid arthritis classification criteria: an American College of Rheumatology/European League Against Rheumatism collaborative initiative. *Arthritis Rheum* (2010) 62(9):2569–81. doi:10.1002/art.27584
240. Jiang X, Frisell T, Askling J, Karlson EW, Klareskog L, Alfredsson L, et al. To what extent is the familial risk of rheumatoid arthritis explained by established rheumatoid arthritis risk factors? *Arthritis Rheumatol* (2015) 67(2):352–62. doi:10.1002/art.38927
241. Frisell T, Hellgren K, Alfredsson L, Raychaudhuri S, Klareskog L, Askling J. Familial aggregation of arthritis-related diseases in seropositive and seronegative rheumatoid arthritis: a register-based case-control study in Sweden. *Ann Rheum Dis* (2016) 75(1):183–9. doi:10.1136/annrheumdis-2014-206133
242. Franklin EC, Holman HR, Muller-Eberhard HJ, Kunkel HG. An unusual protein component of high molecular weight in the serum of certain patients with rheumatoid arthritis. *J Exp Med* (1957) 105(5):425–38. doi:10.1084/jem.105.5.425
243. Taylor P, Gartemann J, Hsieh J, Creeden J. A systematic review of serum biomarkers anti-cyclic citrullinated Peptide and rheumatoid factor as tests for rheumatoid arthritis. *Autoimmune Dis* (2011) 2011:815038. doi:10.4061/2011/815038
244. Jónsson T, Thorsteinsson H, Arinbjarnarson S, Thorsteinsson J, Valdimarsson H. Clinical implications of IgA rheumatoid factor subclasses. *Ann Rheum Dis* (1995) 54(7):578–81. doi:10.1136/ard.54.7.578
245. Tan EM, Smolen JS. Historical observations contributing insights on etiopathogenesis of rheumatoid arthritis and role of rheumatoid factor. *J Exp Med* (2016) 213(10):1937–50. doi:10.1084/jem.20160792
246. Farid SS, Azizi G, Mirshafiey A. Anti-citrullinated protein antibodies and their clinical utility in rheumatoid arthritis. *Int J Rheum Dis* (2013) 16(4):379–86. doi:10.1111/1756-185X.12129
247. Young BJ, Mallya RK, Leslie RD, Clark CJ, Hamblin TJ. Anti-keratin antibodies in rheumatoid arthritis. *Br Med J* (1979) 2(6182):97–9. doi:10.1136/bmj.2.4670.97
248. Aggarwal R, Liao K, Nair R, Ringold S, Costenbader KH. Anti-citrullinated peptide antibody assays and their role in the diagnosis of rheumatoid arthritis. *Arthritis Rheum* (2009) 61(11):1472–83. doi:10.1002/art.24827
249. Schellekens GA, de Jong BA, van den Hoogen FH, van de Putte LB, van Venrooij WJ. Citrulline is an essential constituent of antigenic determinants recognized by rheumatoid arthritis-specific autoantibodies. *J Clin Invest* (1998) 101(1):273–81. doi:10.1172/JCI1316
250. Payet J, Goulvestre C, Bialé L, Avouac J, Wipff J, Job-Deslandre C, et al. Anticyclic citrullinated peptide antibodies in rheumatoid and nonrheumatoid rheumatic disorders: experience with 1162 patients. *J Rheumatol* (2014) 41(12):2395–402. doi:10.3899/jrheum.131375
251. Meyer O, Labarre C, Dougados M, Goupille P, Cantagrel A, Dubois A, et al. Anticitrullinated protein/peptide antibody assays in early rheumatoid arthritis for predicting five year radiographic damage. *Ann Rheum Dis* (2003) 62(2):120–6. doi:10.1136/ard.62.2.120
252. Syversen SW, Gaarder PI, Goll GL, Ødegård S, Haavardsholm EA, Mowinckel P, et al. High anti-cyclic citrullinated peptide levels and an algorithm of four variables predict radiographic progression in patients with rheumatoid arthritis: results from a 10-year longitudinal study. *Ann Rheum Dis* (2008) 67(2):212–7. doi:10.1136/ard.2006.068247
253. Nielen MMJ, van Schaardenburg D, Reesink HW, van de Stadt RJ, van der Horst-Bruinsma IE, de Koning MHMT, et al. Specific autoantibodies precede the symptoms of rheumatoid arthritis: a study of serial measurements in blood donors. *Arthritis Rheum* (2004) 50(2):380–6. doi:10.1002/art.20018
254. Salmon J-H, Perotin J-M, Morel J, Dramé M, Cantagrel A, Ziegler LE, et al. Serious infusion-related reaction after rituximab, abatacept and tocilizumab in rheumatoid arthritis: prospective registry data. *Rheumatology (Oxford)* (2018) 57(1):134–9. doi:10.1093/rheumatology/kex403

Conflict of Interest Statement: The authors declare that the research was conducted in the absence of any commercial or financial relationships that could be construed as a potential conflict of interest.

frontiers in Immunology

ORIGINAL RESEARCH
published: 22 March 2018
doi: 10.3389/fimmu.2018.00428

Autoantibodies in Serum of Systemic Scleroderma Patients: Peptide-Based Epitope Mapping Indicates Increased Binding to Cytoplasmic Domains of CXCR3

Andreas Recke[1,2], Ann-Katrin Regensburger[2†], Florian Weigold[3], Antje Müller[4], Harald Heidecke[5], Gabriele Marschner[4], Christoph M. Hammers[1], Ralf J. Ludwig[2] and Gabriela Riemekasten[4,6]*

[1] Department of Dermatology, University of Lübeck, Lübeck, Germany, [2] Lübeck Institute of Dermatological Research, University of Lübeck, Lübeck, Germany, [3] Department of Rheumatology and Clinical Immunology, Charité University Hospital, Berlin, Germany, [4] Department of Rheumatology, University of Lübeck, Lübeck, Germany, [5] CellTrend GmbH, Luckenwalde, Germany, [6] Priority Area Asthma & Allergy, Research Center Borstel, Airway Research Center North (ARCN), German Center for Lung Research (DZL), Borstel, Germany

OPEN ACCESS

Edited by:
Antony Basten,
Garvan Institute of Medical Research, Australia

Reviewed by:
Tom Paul Gordon,
Flinders Medical Centre, Australia
Stephen Paul Cobbold,
University of Oxford, United Kingdom

***Correspondence:**
Andreas Recke
andreas.recke@uksh.de

[†] This work contains parts of A-KRs thesis.

Specialty section:
This article was submitted to Immunological Tolerance and Regulation, a section of the journal Frontiers in Immunology

Received: 22 November 2017
Accepted: 16 February 2018
Published: 22 March 2018

Citation:
Recke A, Regensburger A-K, Weigold F, Müller A, Heidecke H, Marschner G, Hammers CM, Ludwig RJ and Riemekasten G (2018) Autoantibodies in Serum of Systemic Scleroderma Patients: Peptide-Based Epitope Mapping Indicates Increased Binding to Cytoplasmic Domains of CXCR3. Front. Immunol. 9:428. doi: 10.3389/fimmu.2018.00428

Systemic sclerosis (SSc) is a severe chronic autoimmune disease with high morbidity and mortality. Sera of patients with SSc contain a large variety of autoantibody (aab) reactivities. Among these are functionally active aab that bind to G protein-coupled receptors (GPCR) such as C-X-C motif chemokine receptor 3 (CXCR3) and 4 (CXCR4). Aab binding to the N-terminal portion of these two GPCRs have been shown to be associated with slower disease progression in SSc, especially deterioration of lung function. Aabs binding to GPCRs exhibit functional activities by stimulating or inhibiting GPCR signaling. The specific functional activity of aabs crucially depends on the epitopes they bind to. To identify the location of important epitopes on CXCR3 recognized by aabs from SSc patients, we applied an array of 36 overlapping 18-20mer peptides covering the entire CXCR3 sequence, comparing epitope specificity of SSc patient sera ($N = 32$, with positive reactivity with CXCR3) to healthy controls ($N = 30$). Binding of SSc patient and control sera to these peptides was determined by ELISA. Using a Bayesian model approach, we found increased binding of SSc patient sera to peptides corresponding to intracellular epitopes within CXCR3, while the binding signal to extracellular portions of CXCR3 was found to be reduced. Experimentally determined epitopes showed a good correspondence to those predicted by the *ABCpred* tool. To verify these results and to translate them into a novel diagnostic ELISA, we combined the peptides that represent SSc-associated epitopes into a single ELISA and evaluated its potential to discriminate SSc patients ($N = 31$) from normal healthy controls ($N = 47$). This ELISA had a sensitivity of 0.61 and a specificity of 0.85. Our data reveals that SSc sera preferentially bind intracellular epitopes of CXCR3, while an extracellular epitope in the N-terminal domain that appears to be target of aabs in healthy individuals is not bound by SSc sera. Based upon our results, we could devise a novel ELISA concept that may be helpful for monitoring of SSc patients.

Keywords: autoantibodies, CXCR3, peptide array, systemic sclerosis, G protein-coupled receptor

INTRODUCTION

Systemic sclerosis (SSc) is a severe chronic autoimmune disease with increased mortality, mainly due to affections of the lungs (1, 2). It is characterized by aa pathogenic triad of small vessel vasculopathy, dysregulation of the innate and adaptive immune system and generalized fibrosis of multiple organs (1, 3).

Sera of patients with SSc contain a large variety of autoantibodies (aab) such as anti-nuclear ab (ANA) directed against Scl-70, RNA polymerase 3, and centromere proteins (4). Recently, the presence of functionally active aab that bind to G protein-coupled receptors (GPCRs) such as angiotensin 1 receptor and endothelin A receptor, C-X-C motif chemokine receptor 3 (CXCR3), and 4 (CXCR4) has gained increasing interest (5–9). Interestingly, however, aab directed against GPCRs are found in both healthy individuals and SSc patients (9). Further, they appear to be important in glaucoma, cardiac diseases, preeclampsia, Alzheimer's disease, Sjögren's syndrome, renal diseases, renal transplantation, and some cases of metabolic syndrome (10–12). Interestingly, some of these anti-GPCR antibodies are not necessarily associated with clinical worsening of disease. For example, high concentrations of anti-CXCR3 aabs were found to predict a more benign clinical course of pulmonary disease in SSc (7), which is in contrast to anti-angiotensin and anti-endothelin receptor antibodies (13, 14). Of note, in the above mentioned study, an N-terminal extracellular domain fragment of CXCR3 was used to determine antibody binding (7).

CXCR3 is a GPCR that is expressed by activated naïve T cells, Th1-type $CD4^+$ T cells, effector $CD8^+$ T cells as well as by innate-type lymphocytes (15). It contains an extracellular N-terminus, seven transmembrane domains, and an intracellular C-terminal domain (16). CXCR3 features a series of rhodopsine-like motifs, which are shared among many GPCRs. The role of CXCR3 receptor in connective tissue diseases is supported by the finding that $CXCR3^+$ $CD4^+$ T cells are enriched in kidneys and urine of patients with systemic lupus erythematosus (17).

The functional activity of aab like those against CXCR3 is crucially dependent on their respective epitopes (9, 18–20). However, it is currently not known if anti-CXCR3 aabs target specific epitopes when comparing SSc patients to healthy controls. To address this knowledge gap, we applied a peptide array to screen a set of SSc patient sera in comparison to healthy controls.

MATERIALS AND METHODS

Patients and Controls

In this study, sera of patients with SSc ($N = 32$, **Table 1**) were compared to sera of healthy blood donors ($N = 65$). The age of SSc patients ranged from 38 to 76 years, with 15 female and 5 male subjects. The age of healthy blood donors ranged from 20 to 60 years, with a larger amount of male subjects. The diagnosis in SSc patients was established according to the ACR/EULAR classification criteria for SSc (1). In sera of all SSc patients, positive titers of anti-CXCR3 ab were detected (**Table 1**). Unselected healthy blood donor sera were obtained from the Institute of Transfusion Medicine at the University of Lübeck. All studies with human materials followed the ethical principles established by the Declaration of Helsinki and were approved by the local ethics committee (AZ16-199). All human participants gave their written informed consent.

TABLE 1 | Systemic sclerosis patient overview.

#	ID	SSc variant[1]	ENA[2]	CXCR3 Ab (U/ml)
1	51_SSC	limited	anti-Scl70	15.213
2	80_SSC	limited	anti-Scl70	3.775
3	88_SSC	diffuse with myositis overlap	anti-Ro52	5.156
4	96_SSC	diffuse	anti-Scl70	4.008
5	110_SSC	limited	anti-CENP-B	5.023
6	117_SSC	limited	anti-CENP-B	6.950
7	202_SSC	limited	anti-Scl70	15.399
8	215_SSC	diffuse	anti-Scl70	3.853
9	216_SSC	limited	anti-CENP-B	3.805
10	226_SSC	limited	anti-CENP-B	5.295
11	235_SSC	limited	anti-CENP-B	6.982
12	279_SSC	limited	anti-RNP/sm+ anti-Sm+ anti-PmScl75	7.984
13	313_SSC	diffuse	anti-Scl70	6.080
14	327_SSC	limited	anti-CENP-B	7.770
15	332_SSC	limited	anti-Scl70	4.350
16	335_SSC	diffuse	anti-Scl70	4.828
17	368_SSC	limited	anti-Scl70	4.299
18	373_SSC	limited	anti-CENP-B	4.084
19	383_SSC	diffuse	dense fine speckled pattern	8.065
20	384_SSC	limited	anti-Scl70	5.381
21	SKL011	limited	anti-CENP-B	6.577
22	SKL024	limited	anti-CENP-B	2.948
23	SKL028	diffuse	anti-Scl70	2.876
24	SKL033	diffuse	n.d.	12.163
25	SKL034	diffuse	anti-Scl70	6.542
26	SKL102	limited	anti-CENP-B	25.575
27	SKL103	UCTD	n.d.	18.678
28	SKL109	limited	anti-CENP-B	4.042
29	SKL111	MCTD	n.d.	13.025
30	SKL117	limited	anti-CENP-B	38.758
31	SKL157	limited	anti-CENP-B	11.802
32	SKL224	limited	anti-CENP-B	3.717

Limited or diffuse systemic sclerosis, undifferentiated connective tissue disease (UCTD), mixed connective tissue disease (MCTD).
Reactivity against specific extractable nuclear antigens (ENA). n.d., not differentiated.
All SSc patients were ANA-positive.

Human Anti-CXCR3 IgG ELISA

Anti-CXCR3 IgG aabs were measured by a commercially available sandwich ELISA kit from CellTrend GmbH (Luckenwalde, Berlin, Germany) (7). The antigen in this assay is a recombinant fragment comprising the N-terminal potion of CXCR3. Measurements were performed according to the manufacturer's instructions. The kit includes a standard to determine autoantibody concentrations (in U/ml).

Human CXCR3 Peptides

Thirty-six biotinylated 20mer peptides covering the entire sequence of CXCR3 (isoform 1, aa 1-368, UNIPROT accession ID P49682 (CXCR3_HUMAN), URL: www.uniprot.org, last accessed 9/25/2017) were synthesized by peptides & elephants (Henningsdorf, Germany), with overlaps of 10 aa to the

corresponding peptides upstream and downstream the protein sequence (**Table 2**). Peptides were delivered as lyophilized trifluoro-acetate salts and dissolved according to hydrophobicity and isoelectric point (pI) in NaOH, HCl, or DMF. Dissolved peptides were further diluted in phosphate-buffered saline (PBS), pH 7.2.

Peptide-Based ELISA

Biotinylated peptides were diluted in PBS (pH 7.2) containing 0.05% Tween-20 (PBS-T) to a concentration of 20 µg/ml and incubated for 1 h at room temperature with streptavidine-coated 96-well plates (Immobilizer Streptavidin F96 Clear; Thermo Fisher Scientific p/a Nunc, Langenselbold, Germany). For each well only one peptide was used. As positive control biotinylated anti-human IgG1 (Thermo Fisher Scientific, p/a Invitrogen, Carlsbad, CA, USA) was used, negative control wells were left empty. Each control and peptide was placed twice on a single 96-well plate, to allow for testing of two individual sera. We combined one SSc serum ($N = 32$) with one control serum ($N = 30$ of the 65) to aid comparability. After automatic washing of ELISA plates with an Columbus Pro plate washer (TECAN Group AG, Männedorf, Schweiz), plates were incubated for 1 h at room temperature on an orbital shaker containing 100 µl/well SSc patient or control sera diluted 1:100 in PBS-T. Subsequently, after another automatic washing step plates were incubated for 1 h at room temperature with a peroxidase-conjugated polyclonal anti-human IgG antibody (DAKO, Hamburg, Germany), diluted 1:1000 in PBS-T. 1-step™ Turbo-TMB-ELISA (Thermo Fisher Scientific, p/a Pierce Biotechnology, Rockford, USA) was used as chromogenic substrate with 0.5 M H_2SO_4 as stop solution. The optical density at 450 nm (OD450) was recorded by a VICTOR 3™ (PerkinElmer Inc., Waltham, MA, USA) reader.

Complete and annotated ELISA readout data used for this analysis is made available for public access (Supplementary Material).

TABLE 2 | Characteristics of peptide fragments of CXCR3.

#	Sequence[1]	Length	Residues[2]	MW[3]	Hydrophobicity[4]	pI[5]	Charge[6]
1	MVLEVSDHQVLNDAEVAALL	20	1–20	2392.3	0.72	3.74	−3.92
2	LNDAEVAALLENFSSSYDYG	20	11–30	2441.0	−0.13	3.30	−4.09
3	ENFSSSYDYGENESDSCCTS	20	21–40	2486.8	−1.26	3.23	−5.18
4	ENESDSCCTSPPCPQDFSLN	20	31–50	2435.7	−0.96	3.30	−4.23
5	PPCPQDFSLNFDRAFLPALY	20	41–60	2536.5	−0.06	4.11	−1.14
6	FDRAFLPALYSLLFLLGLLG	20	51–70	2464.9	1.50	6.33	−0.09
7	SLLFLLGLLGNGAVAAVLLS	20	61–80	2188.8	2.04	6.10	−0.09
8	NGAVAAVLLSRRTALSSTDT	20	71–90	2228.4	0.31	10.40	0.91
9	RRTALSSTDTFLLHLAVADT	20	81–100	2413.6	0.20	7.55	0.08
10	FLLHLAVADTLLVLTLPLWA	20	91–110	2446.1	1.82	5.29	−0.92
11	LLVLTLPLWAVDAAVQWVFG	20	101–120	2476.0	1.63	3.75	−1.09
12	VDAAVQWVFGSGLCKVAGAL	20	111–130	2215.7	1.16	6.16	−0.14
13	SGLCKVAGALFNINFYAGAL	20	121–140	2255.0	1.06	8.52	0.86
14	FNINFYAGALLLACISFDRY	20	131–150	2538.0	0.90	6.16	−0.14
15	LLACISFDRYLNIVHATQLY	20	141–160	2579.6	0.75	7.35	0.03
16	LNIVHATQLYRRGPPARVTL	20	151–170	2500.9	−0.11	12.20	3.07
17	RRGPPARVTLTCLAVWGLCL	20	161–180	2408.2	0.62	10.52	2.81
18	TCLAVWGLCLLFALPDFIFL	20	171–190	2501.5	2.07	3.75	−1.18
19	LFALPDFIFLSAHHDERLNA	20	181–200	2551.7	0.31	5.36	−1.75
20	SAHHDERLNATHCQYNFPQV	20	191–210	2592.7	−1.13	6.78	−0.64
21	THCQYNFPQVGRTALRVLQL	20	201–220	2571.2	−0.20	9.50	2.03
22	GRTALRVLQLVAGFLLPLLV	20	211–230	2375.3	1.50	12.50	1.91
23	VAGFLLPLLVMAYCYAHILA	20	221–240	2404.6	1.93	7.35	0.02
24	MAYCYAHILAVLLVSRGQRR	20	231–250	2546.0	0.51	10.13	3.02
25	VLLVSRGQRRLRAMRLVVVV	20	241–260	2545.8	0.85	13.10	4.91
26	LRAMRLVVVVVVAFALCWTP	20	251–270	2471.0	1.85	10.53	1.86
27	VVAFALCWTPYHLVVLVDIL	20	261–280	2497.5	1.92	5.29	−0.97
28	YHLVVLVDILMDLGALARNC	20	271–290	2454.4	1.21	5.41	−0.97
29	MDLGALARNCGRESRVDVAK	20	281–300	2388.1	−0.36	8.55	0.86
30	GRESRVDVAKSVTSGLGYMH	20	291–310	2374.9	−0.43	9.30	1.08
31	SVTSGLGYMHCCLNPLLYAF	20	301–320	2415.2	0.85	7.25	−0.02
32	CCLNPLLYAFVGVKFRERMW	20	311–330	2672.8	0.50	8.80	1.81
33	VGVKFRERMWMLLLRLGCPN	20	321–340	2644.2	0.25	11.38	2.86
34	MLLLRLGCPNQRGLQRQPSS	20	331–350	2492.9	−0.49	12.20	2.86
35	QRGLQRQPSSSRRDSSWSET	20	341–360	2574.1	−2.01	12.02	1.91
36	SRRDSSWSETSEASYSGL	18	351–368	2229.0	−1.27	4.43	−1.09

Sequence of peptides in one letter format. Each peptide listed is biotinylated at the N-terminus.
Residues are numbered according to Uniprot entry P49682 (CXCR3_HUMAN) isoform 1.
Molecular weight as determined by mass spectrometric quality report of manufacturer.
Hydrophobicity scores were calculated with the function hydrophobicity of R package peptides by the method of Kyte and Doolittle (21).
pI (isoelectric point) values were calculated with the function pI of R package peptides with the default EMBOSS method.
The peptide sum charge was calculated a pH 7.2 with the function charge of R packages peptides, with the method Stryer.

Mixed Peptide ELISA

Peptides 17, 24, 25, 33, and 34 were combined in PBS-T with a total concentration of 20 µg/ml and incubated with streptavidine-coated 96-well plates (Immobilizer Streptavidin F96 Clear; Thermo Fisher Scientific p/a Nunc, Langenselbold, Germany), as described above. All SSc patient sera, 16 healthy controls used for peptide mapping and 31 previously not used healthy controls were measured as duplicates. The experimental procedures for this assay were performed with exact timing, to ensure comparability of OD 450 nm values between plates.

In Silico Prediction of Epitopes

We used two different software approaches to predict continuous epitopes in the CXCR3 sequence. *Antigenic* from the *EMBOSS* package available online at http://www.bioinformatics.nl/cgi-bin/emboss/antigenic (last visited 2/9/2018) with a window size of 6 amino acids. *Antigenic* is based on sliding window averaging antigenicity scores of amino acids in the sequence of proteins. The other software, ABCpred, available at http://crdd.osdd.net/raghava/abcpred/ABC_submission.html (last visited 2/10/2018), is based upon a trained neural network that determines a score for subsequences of protein sequences in a sliding window approach. We used a window size of 20 amino acids and a minimum score of 0.8.

Statistical Analysis of Peptide-Mapping Data

For isolation of specific binding signals from peptide-mapping ELISA data, a mixed effects model was established using R open source statistical software (URL: http://www.r-project.org/, last visited 9/25/2017) together with the framework provided by R package *INLA* (URL: http://www.r-inla.org/, last visited 9/25/2017) (22–24). Peptide properties were calculated with R package *peptides*. 1.1 was determined and the normalized value $\hat{x} = (x-u)/(o-u)$ was calculated.

To normalize the ELISA signal x per plate, an upper limit $o = \max(x) \times 1.1$ and a lower limit $u = \min(x)/1.1$. The logit value of ELISA signals was calculated as $\text{logit}(x) = \ln\left(\hat{x}/1-\hat{x}\right)$. For sample runs with a variance below 25% quantile were not further processed.

To analyze the ELISA signals, a mixed effects model was set up using the INLA framework with logit(x) as the dependent variable and isoelectric point (pI) and hydrophobicity of peptides as fixed effects with the default vague prior distribution settings. As random effects, plate ID and serum ID were included with an *iid* model, and the peptide numbers with a special autoregressive model of order 1 (*ar1*). To separate the SSc autoantibody-binding signal, a simple *ar1* model was combined with a weighted *ar1* model. For SSc patients, the weighting factor was set to 1, for healthy controls it was set to 0. For all random effect models, the default vague prior distribution of the hyper-parameter was chosen.

A Bayesian analog of a p value (p_{Bayes}) was calculated as described (25, 26). Briefly, for a given posterior distribution of regression coefficients, the largest $\alpha \in [0;1]$ was determined such that the α highest-posterior density credibility interval does not contain the point 0. The p_{Bayes} was then calculated as $p_{\text{Bayes}} = (1-\alpha)$.

The R code and data set specifications are described in detail in the Supplementary Methods and Supplementary Information in Data Sheet S1 in Supplementary Material.

Statistical Analysis of Mixed-Peptide ELISA Data

Mixed peptide data were evaluated as raw OD450 data using R open source statistical software with additional packages *beeswarm* for visual representation of data (stacked scatter plots) and *ROCR* for receiver operator characteristic (ROC) analysis. The cut-off value was calculated by optimization of Matthew's correlation coefficient (MCC) (27). The MCC was calculated as:

$$\text{MCC} = \frac{\text{TP} \times \text{TN} - \text{FP} \times \text{FN}}{\sqrt{(\text{TP}+\text{FP})(\text{TP}+\text{FN})(\text{TN}+\text{FP})(\text{TN}+\text{FN})}}$$

with TP being the number of true positives, TN the number of true negatives, FP the number of false positives, and FN the number of false negatives.

For performance parameters sensitivity, specificity, positive likelihood ratio (LR)+, and negative LR−, 95% binomial confidence intervals (95% CI) were calculated using the Clopper–Pearson method.

RESULTS

Epitope Mapping Localizes Epitopes of Autoantibodies in SSc in Intracellular Regions of CXCR3

Aab recognizing an N-terminal extracellular fragment of CXCR3 ranging from 3.8 until 15.4 U/ml were detected by ELISA in sera of SSc patients (**Table 1**). A peptide array covering the whole aa sequence of CXCR3 (**Table 2**) was applied to determine epitopes of CXCR3 targeted by anti-CXCR3 contained in serum of patients with SSc and controls. The measurements were analyzed in comparison to those from sera of healthy control blood donors. Raw ELISA signal data of the peptide array is shown in Figure S1 in Supplementary Material.

Linear peptides, by design, do not have the same conformation as compared to a fully folded protein further stabilized by a cell membrane. This is a potential source of non-specific binding signal variation, which needs to be taken into account appropriately during data analysis. Additional variation is generated because sera of patients and healthy controls do not only contain ab directed against CXCR3, but a whole set of different antibodies that may bind non-specifically to the peptides.

To separate an SSc-specific binding signal from background noise, we used the Bayesian framework implemented by the *INLA* (Integrated Nested Laplace Approximation) package. Using this R package, we developed a model that incorporates the neighborhood structure, i.e., overlapping of peptides, employing autoregressive models. Non-specific binding of sera

and secondary detection antibody to the peptides was modeled by a simple autoregressive model (Figure S2 in Supplementary Material). SSc-specific binding was modeled by combining the autoregressive model with a *weighting* factor (**Figure 1**). The unspecific binding of serum samples and the inter-plate variability were included as additional random effects. Isoelectric point and hydrophobicity of each peptide were included as fixed effects. These additional random and fixed effects primarily served to remove noise from the SSc-specific binding signal (Figure S3 in Supplementary Material).

The result described in **Figure 1** was mapped for visualization to a serpentine model of CXCR3 (**Figure 2**). For comparison, the logit values of ELISA signals were analyzed peptide-wise with independent classical linear models (Figure S4 in Supplementary Material).

The regression analysis revealed a significant difference between healthy control and SSc patient binding signals for peptide 4 ($p_{\text{Bayes}} = 0.00879$), peptide 15 ($p_{\text{Bayes}} = 0.0225$), peptide 16 ($p_{\text{Bayes}} = 0.00684$), peptide 17 ($p_{\text{Bayes}} = 0.000977$), peptide 21 ($p_{\text{Bayes}} = 0.00488$), peptide 24 ($p_{\text{Bayes}} = 0.00293$), peptide 25 ($p_{\text{Bayes}} = 0.000977$), peptide 31 ($p_{\text{Bayes}} = 0.00879$), peptide 33 ($p_{\text{Bayes}} = 0.000977$), and peptide 34 ($p_{\text{Bayes}} = 0.000977$). When using a stricter threshold of $p < 0.00138 = 0.05/36$ to take multiple testing into account, peptides 17, 25, 33, and 34 remain as possible epitopes. In all of these peptides, the binding signal of SSc patients is higher than in healthy controls, except of peptides 4 and 15, which are located at the N-terminal extracellular rod domain. With the exception of peptide 21, all other peptides we identified are located intracellularly.

To compare the reactivity of SSc-abs on peptides with epitopes predicted by the primary structure of CXCR3, we used the EMBOSS *antigenic* software (**Figure 1**; Figures S2 and S4 in Supplementary Material). This software implements a method described by Kolaskar and Tongaonkar (28). However, there appears to be no true correspondence between predicted and the reactivity of SSc-abs.

In contrast to *antigenic*, the neural network-based *ABCpred* software detected epitopes on amino acid residues Y_{29}–L_{68}, L_{184}–C_{203}, V_{241}–V_{260}, G_{307}–R_{326}, and L_{332}–S_{351} (**Figure 1**; Figures S2 and S4 in Supplementary Material). From these epitopes, all

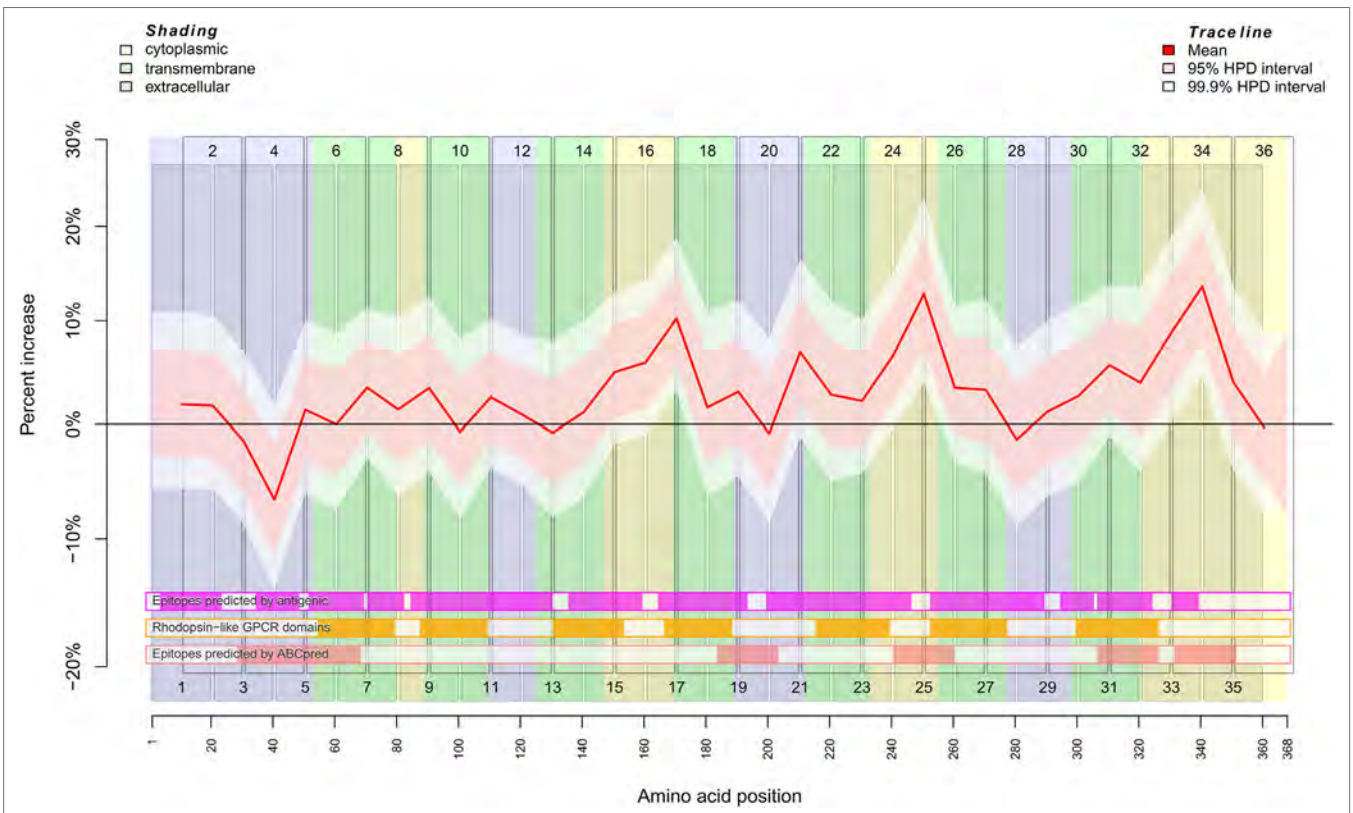

FIGURE 1 | Binding behavior of SSc patient and healthy control sera to individual peptides. Plot of the mean expectation value (red line) and 95 and 99.9% credibility bands (pink and white shading) of the SSc patient-specific ab-binding signal (percent increase). The *x* axis represents amino acid residues 1–368. The peptide localizations are indicated by staggered rectangles that include the peptide numbers. The percent increase indicates the increase or decrease of the binding signal in SSc patients in contrast to an averaged signal. If the 95% (99.9%) credibility interval of the percent increase does not include the zero value (black line), the corresponding peptide is regarded as an epitope that is significantly associated with SSc. By use of the *ar1* model, the percent increase, i.e., the binding signal estimator, for a peptide is influenced by the neighboring peptides. Other fixed and random effects of the statistical model are shown in Figures S2 and S3 in Supplementary Material. At the bottom, three heat maps indicate the position of putative epitopes predicted by *antigenic* (magenta hue), ABCpred (pink hue) and the presence of rhodopsine-like domains (orange hue). The background colors indicate the position of intracellular (yellow hue), transmembranous (green hue), or extracellular (blue hue) amino acid residues.

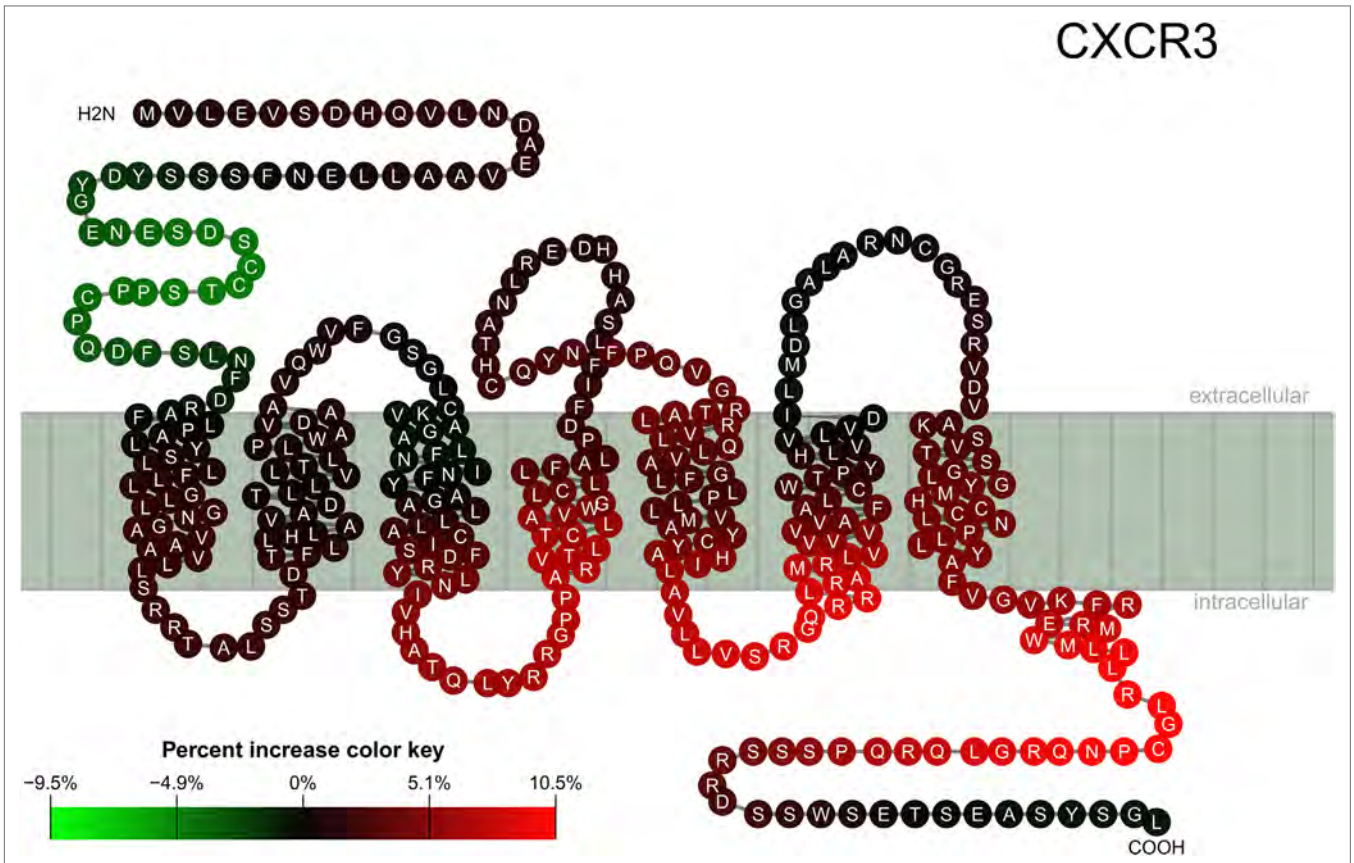

FIGURE 2 | Location of epitopes on the CXCR3 structure. Mapping of binding signal (compare **Figure 1**) of SSc patient sera to a serpentine model of CXCR3. Each pearl represents a single amino acid residue, the letter inside each pearl the amino acid in 1-letter code. The color of each pearl indicates the percent increase value of the SSc specific binding signal associated with the respective amino acid residue (color key).

except L_{184}–C_{203} corresponded to peptides we experimentally identified as possible epitopes that differ in the binding between SSc patients and healthy controls. Vice versa, peptides 17 and 21 which were identified by experiment do not correspond to any epitope detected by *ABCpred*. It may be noted that peptide 20 corresponding to *ABCpred* epitope L_{184}–C_{203} showed a peak in reactivity in the background signal (Figure S2 in Supplementary Material).

We further checked whether the reactivity of SSc-abs corresponds to conserved Rhodopsin-like GPCR domains (**Figure 1**; Figures S2 and S4 in Supplementary Material). These domains are mostly located in transmembrane regions of the protein. However, no difference in reactivity between SSc sera and healthy control sera was found in peptides that correspond to Rhodopsin-like GPCR domains.

A CXCR3 Peptide-Based ELISA Allows Discrimination of SSc and Healthy Control Sera

To verify the epitopes, we detected by the peptide array, we chose peptides 17, 24, 25, 33,and 34 that were positively correlated with SSc sera and combined them into one for coating of ELISA plates. This allowed us to compare 48 samples in duplicates a single microtiter plate. For inter-plate comparison, we used a set of samples as standard samples.

Using this ELISA design, we compared raw OD450 values from the 32 SSc patient sera with 16 of the healthy control sera and 31 additional healthy control sera from a new cohort (**Figure 3**, left panel). The OD450 values of SSc and healthy control sera differed significantly (Wilcoxon rank sum test $p = 4.52 \times 10^{-5}$). By ROC analysis (**Figure 3**, right panel), this corresponds to an area under curve (AUC) of 0.77, indicating a good classification ability. A cut-off for the OD450 value could be determined by optimizing Matthew's correlation coefficient to a value of 0.51. Using this cut-off, the sensitivity of this assay was 0.61 (95% CI: 0.42–0.78), with a specificity of 0.85 (95% CI: 0.72–0.94). This corresponds to a LR+ of 3.98 (95% CI: 2.06–9.28) and a LR− of 0.46 (95% CI: 0.27–0.68).

DISCUSSION

In this study, we were able to demonstrate that SSc patients' sera preferentially bind to intracellular epitopes on CXCR3. We furthermore could demonstrate that reactivity to extracellular epitopes is reduced or lost in SSc patients, compared to controls. This especially applies to in the N-terminal rod domain of

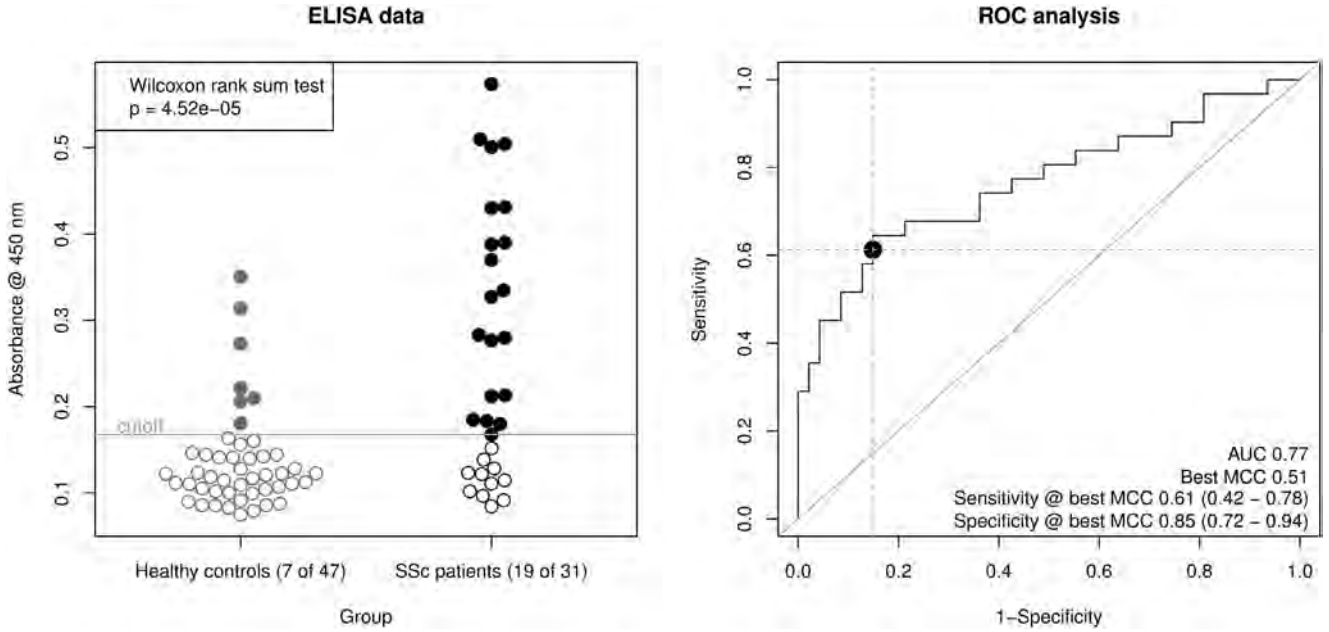

FIGURE 3 | Derivation of a mixed-peptide ELISA for the discrimination of SSc patients and healthy controls. Peptides 17, 24, 25, 33, and 34 were mixed for coating of ELISA plates. In total, 32 SSc patient sera and 47 healthy control sera were measured. Left panel, scatter plot of raw ELISA readout values (OD @ 450 nm) including a cut-off value optimized by maximization of Matthew's correlation coefficient. SSc patient showed a significantly higher ELISA signal than healthy control sera (Wilcoxon rank sum testing $p = 4.52 \times 10^{-5}$). Right panel, receiver operator characteristic (ROC) analysis of ELISA values. AUC (area under curve, 0.77) and best MCC (Matthew's correlation coefficient, 0.51) as well as Sensitivity (0.61) and Specificity (0.85) at the optimal cut-off are shown as performance indicators. The dot indicates the optimal cut-off position in the ROC curve.

CXCR3, where a previous study could show that reactivity to this domain is associated with a slower disease progression in SSc (7).

Aabs against GPCRs like CXCR3 have been shown to influence the signaling function of these receptors (5, 9). It is very likely that the epitopes on CXCR3 that are bound by aabs determine different functional and pathophysiological effects. In case of antibodies that bind to receptors the selection of target epitopes decides whether they exhibit activating, inhibiting, internalization-inducing or even neutral (i.e., no measurable) effects (9, 18–20). Peptide arrays provide a straightforward approach to locate linear epitopes recognized by aabs, using ELISA or dot bot methods (20, 29, 30). However, this approach has the drawback that peptides are more flexible in their tertiary structure and tend to bind abs with lower specificity than fully folded proteins. Therefore, a careful statistical evaluation is necessary to detect a specific binding signal (20). This study used an array of 20mer peptides with 10mer overlaps covering the full UNIPROT isoform 1 sequence of CXCR3 to identify linear epitopes bound by aabs in sera from SSc patients and healthy blood donors. The peptide array was employed to conduct a series of ELISA experiments. A highly standardized protocol was used, including anti-human IgG1 as positive process control and a balanced design that always combined sera of an SSc patient and a healthy donor on the same ELISA plate.

To isolate a specific autoantibody-binding signal, we used the Bayesian framework of the R package INLA to design a mixed effects model that separates an autoantibody-related binding signal from inter-experimental variation, variation due to physicochemical properties of individual peptides (hydrophobicity, isoelectric point) and non-specific patient or control serum properties (23, 24). A remarkable advantage of this framework is the possibility to incorporate the neighborhood structure into the model, i.e., the intuitive expectation that two 20mer peptides that have a 10mer overlap should yield a similar signal. Further, the framework provided by the package INLA enabled us to formulate a mathematically more sound model compared to the heuristic approach we used for previous peptide screening studies (20).

Using this mixed effects model, we observed an increased binding of ab from SSc patients to peptides representing intracellular domains of CXCR3, especially the C-terminal rod domain. In contrast, ab binding to the extracellular domains including the N-terminal rod domain appeared to be missing in SSc.

Interestingly, the epitopes we identified did not overlap with epitopes predicted by the *antigenic* software of the EMBOSS bioinformatics package. Only two of the epitopes predicted by *antigenic*, one within the N-terminal rod domain (corresponding to peptide 4) and one within the C-terminal intracellular rod domain (corresponding to peptide 34) appear to overlap. In contrast to *antigenic*, epitope prediction by *ABCpred* showed that 4 of 5 predicted epitope regions correspond to peptides with a binding significantly different between SSc patients and healthy controls. The one epitope predicted by *ABCpred* that showed no differential binding correspond to a peak in the background signal. Although the study is designed to detect epitopes with a reactivity that is different between SSc patients and healthy controls, this indicates that all epitopes predicted by *ABCpred* match our experimental data. The rhodopsin-like GPCR motifs

appear to be spared, which might be explained by their higher degree of conservation (31) compared to the other parts of the CXCR3 sequence.

An increased reactivity of abs against an N-terminal fragment of CXCR3 correlated with a more benign progression of lung fibrosis in SSc in an earlier study (7). Thus, we expected a decreased reactivity against linear epitopes within the N-terminal rod domain in our SSc study population, which could indeed be demonstrated with our peptide mapping approach.

To further validate the results from the peptide array, we designed a novel ELISA using a combination of peptides that were found to be associated with SSc. Differently from the peptide mapping approach, where only 2 samples could be processed per microtiter plate, this ELISA allowed to determine 48 samples in duplicates per plate. This allowed a better comparability between samples, as the plate-by-plate variation in ELISA methods is empirically relatively high. The readout of this ELISA allowed discriminating between SSc patient and healthy control sera with a considerably good performance, as expressed by a Matthew's correlation coefficient of 0.51 and an AUC of 0.77. Most of the healthy control sera used in this mixed peptide ELISA came from an independent cohort that has not been used for identification of epitopes.

We evaluated whether the results from the mixed-peptide ELISA differ between limited and diffuse variants of SSc, which was not the case. However, this novel ELISA concept might be promising for the development of diagnostic tools that allow a better prognosis on deterioration of lung function, pulmonary hypertension, or renal insufficiency and would therefore help to choose the optimal treatment for patients with SSc.

In contrast to extracellular epitopes, the biological relevance of intracellular epitopes—or antigens—is difficult to demonstrate, because they are in general not directly accessible by aabs. ANA, that are typical for collagenoses are directed against intracellular antigens. Although generally regarded as functionally irrelevant, some ANA like anti-Ro may even cross the placenta and cause neonatal lupus (32). It has to be noted here that anti-Ro aabs have been demonstrated to interact with an extracellular epitope of 5-hydroxytryptaminergic (5-HT4) receptor 4 (33), a GPCR like CXCR3. Besides intracellular antigens, intracellular domains of transmembrane proteins have been shown to be targets of aabs, like BP180 (34) and aquaporin-4 (35).

As an exception of the rule that intracellular antigens and epitopes are not accessible by abs, a certain type of aabs has been shown to be able to penetrate the cellular membrane and to bind subsequently to intracellular epitopes and trigger pathogenic mechanisms (36, 37). This observation led to the construction of TransMabs, ab that are designed to penetrate cell membranes using a short (17 aa) membrane translocation sequence (38). In case of anti-DNA mAbs, specific properties of the sequence of the heavy chain complementary-determining regions 2 and 3 appeared to be the prerequisite for their ability to penetrate the cell membrane (37). It may be possible, though challenging to demonstrate, that anti-GPCR aabs may have the ability to penetrate cell membranes and initiate important pathogenic mechanisms by binding to intracellular epitopes.

An interesting finding is the loss of autoreactivity to the N-terminal rod domain of CXCR3 in patients with SSc. Clinically, a lower titer of autoantibodies against the N-terminus of CXCR3 has been associated with a better prognosis of SSc, especially concerning deterioration of lung function (7). Furthermore, aabs against CXCR3 are not only found in SSc, but also in healthy individuals (9). Aabs against GPCRs have been demonstrated to be functionally active (5–9), and it might possible that this is of physiologic importance. Therefore, it appears to be rational to substitute the lacking aabs against CXCR3 and other GPCRs with intravenous immunoglobulins (IVIGs), although only limited evidence exists for a beneficial effect of IVIGs in SSc (39).

In conclusion, we were able to demonstrate that aabs against CXCR3 in SSc patient sera show a different binding pattern like healthy control sera, with increased binding to intracellular epitopes and loss of binding to the extracellular N-terminal rod domain. The results are supported by *in silico* prediction of linear epitopes on CXCR3. Based upon our results, we could devise a novel ELISA concept that may be helpful for monitoring of SSc patients.

ETHICS STATEMENT

All studies with human materials followed the ethical principles established by the Declaration of Helsinki and were approved by the local ethics committee (AZ16-199). All human participants gave their written informed consent.

AUTHOR CONTRIBUTIONS

AR designed research, recruited healthy control biomaterials, performed experiments, analyzed data, discussed results, and wrote the manuscript; A-KR performed experiments, analyzed data, discussed results, and wrote the manuscript; FW characterized SSc patients, has analyzed anti-CXCR3 ab in SSc patients, discussed results, and wrote the manuscript; AM recruited patient sera, discussed results, and wrote the manuscript; HH characterized SSc patients and analyzed anti-CXCR3 ab in SSc patients; GM recruited patient sera and kept a biobank; CH discussed results and wrote the manuscript; RL designed research, discussed results, and wrote the manuscript; GR designed research, recruited patient and healthy control biomaterials, discussed results, and wrote the manuscript.

ACKNOWLEDGMENTS

We thank everybody in the Department of Transfusion Medicine (University of Lübeck, Lübeck, Germany) involved in the collection of blood samples and all of the volunteers who donated blood for the experiments performed in this study. This work received infrastructural support from the Deutsche Forschungsgemeinschaft Cluster of Excellence Inflammation at Interfaces (Cluster 306/2), the project RI 1056 11/1-2, and from Research Training Group Grant 1727/1 (TP2) (to AR).

SUPPLEMENTARY MATERIAL

The Supplementary Material for this article can be found online at https://www.frontiersin.org/articles/10.3389/fimmu.2018.00428/full#supplementary-material.

REFERENCES

1. van den Hoogen F, Khanna D, Fransen J, Johnson SR, Baron M, Tyndall A, et al. 2013 classification criteria for systemic sclerosis: an American College of Rheumatology/European League against Rheumatism collaborative initiative. *Arthritis Rheum* (2013) 65:2737–47. doi:10.1002/art.38098
2. Ludwig RJ, Vanhoorelbeke K, Leypoldt F, Kaya Z, Bieber K, McLachlan SM, et al. Mechanisms of autoantibody-induced pathology. *Front Immunol* (2017) 8:603. doi:10.3389/fimmu.2017.00603
3. Varga J, Abraham D. Systemic sclerosis: a prototypic multisystem fibrotic disorder. *J Clin Invest* (2007) 117:557–67. doi:10.1172/JCI31139
4. Domsic RT. Scleroderma: the role of serum autoantibodies in defining specific clinical phenotypes and organ system involvement. *Curr Opin Rheumatol* (2014) 26:646–52. doi:10.1097/BOR.0000000000000113
5. Cabral-Marques O, Riemekasten G. Functional autoantibodies targeting G protein-coupled receptors in rheumatic diseases. *Nat Rev Rheumatol* (2017) 13:648–56. doi:10.1038/nrrheum.2017.134
6. Riemekasten G, Cabral-Marques O. Antibodies against angiotensin II type 1 receptor (AT1R) and endothelin receptor type A (ETAR) in systemic sclerosis (SSc)-response. *Autoimmun Rev* (2016) 15:935. doi:10.1016/j.autrev.2016.04.004
7. Weigold F, Günther J, Pfeiffenberger M, Cabral-Marques O, Siegert E, Dragun D, et al. *Antibodies against Chemokine Receptors CXCR3 and CXCR4 Predict Progressive Deterioration of Lung Function in Patients with Systemic Sclerosis* (2017).
8. Berger M, Steen VD. Role of anti-receptor autoantibodies in pathophysiology of scleroderma. *Autoimmun Rev* (2017) 16:1029–35. doi:10.1016/j.autrev.2017.07.019
9. Riemekasten G, Philippe A, Näther M, Slowinski T, Müller DN, Heidecke H, et al. Involvement of functional autoantibodies against vascular receptors in systemic sclerosis. *Ann Rheum Dis* (2011) 70:530–6. doi:10.1136/ard.2010.135772
10. Wallukat G, Schimke I. Agonistic autoantibodies directed against G-protein-coupled receptors and their relationship to cardiovascular diseases. *Semin Immunopathol* (2014) 36:351–63. doi:10.1007/s00281-014-0425-9
11. Dragun D, Müller DN, Bräsen JH, Fritsche L, Nieminen-Kelhä M, Dechend R, et al. Angiotensin II type 1-receptor activating antibodies in renal-allograft rejection. *N Engl J Med* (2005) 352:558–69. doi:10.1056/NEJMoa035717
12. Dragun D. The detection of antibodies to the angiotensin II-type 1 receptor in transplantation. *Methods Mol Biol* (2013) 1034:331–3. doi:10.1007/978-1-62703-493-7_19
13. Avouac J, Riemekasten G, Meune C, Ruiz B, Kahan A, Allanore Y. Autoantibodies against endothelin 1 type A receptor are strong predictors of digital ulcers in systemic sclerosis. *J Rheumatol* (2015) 42:1801–7. doi:10.3899/jrheum.150061
14. Becker MO, Kill A, Kutsche M, Guenther J, Rose A, Tabeling C, et al. Vascular receptor autoantibodies in pulmonary arterial hypertension associated with systemic sclerosis. *Am J Respir Crit Care Med* (2014) 190:808–17. doi:10.1164/rccm.201403-0442OC
15. Groom JR, Luster AD. CXCR3 ligands: redundant, collaborative and antagonistic functions. *Immunol Cell Biol* (2011) 89:207–15. doi:10.1038/icb.2010.158
16. Hutchings CJ, Koglin M, Marshall FH. Therapeutic antibodies directed at G protein-coupled receptors. *mAbs* (2010) 2:594–606. doi:10.4161/mabs.2.6.13420
17. Enghard P, Humrich JY, Rudolph B, Rosenberger S, Biesen R, Kuhn A, et al. CXCR3+CD4+ T cells are enriched in inflamed kidneys and urine and provide a new biomarker for acute nephritis flares in systemic lupus erythematosus patients. *Arthritis Rheum* (2009) 60:199–206. doi:10.1002/art.24136
18. Horn-Lohrens O, Tiemann M, Lange H, Kobarg J, Hafner M, Hansen H, et al. Shedding of the soluble form of CD30 from the Hodgkin-analogous cell line L540 is strongly inhibited by a new CD30-specific antibody (Ki-4). *Int J Cancer* (1995) 60:539–44. doi:10.1002/ijc.2910600419
19. Xia Y, Kellems RE. Angiotensin receptor agonistic autoantibodies and hypertension: preeclampsia and beyond. *Circ Res* (2013) 113:78–87. doi:10.1161/CIRCRESAHA.113.300752
20. Dworschak J, Recke A, Freitag M, Ludwig RJ, Langenhan J, Kreuzer OJ, et al. Mapping of B cell epitopes on desmoglein 3 in pemphigus vulgaris patients by the use of overlapping peptides. *J Dermatol Sci* (2012) 65:102–9. doi:10.1016/j.jdermsci.2011.11.012
21. Kyte J, Doolittle RF. A simple method for displaying the hydropathic character of a protein. *J Mol Biol* (1982) 157:105–32. doi:10.1016/0022-2836(82)90515-0
22. Team RDC. *R: A Language and Environment for Statistical Computing*. Vienna, Austria: Team RDC (2012).
23. Martins TG, Simpson D, Lindgren F, Rue H. Bayesian computing with INLA: new features. *Comput Stat Data Anal* (2013) 67:68–83. doi:10.1016/j.csda.2013.04.014
24. Rue H, Martino S, Chopin N. Approximate Bayesian inference for latent Gaussian models by using integrated nested Laplace approximations. *J R Stat Soc Ser B* (2009) 71:319–92. doi:10.1111/j.1467-9868.2008.00700.x
25. Recke A, Vidarsson G, Ludwig RJ, Freitag M, Möller S, Vonthein R, et al. Allelic and copy-number variations of FcγRs affect granulocyte function and susceptibility for autoimmune blistering diseases. *J Autoimmun* (2015) 61:36–44. doi:10.1016/j.jaut.2015.05.004
26. Koch K-R. *Einführung in die Bayes-Statistik*. Berlin; New York: Springer (2000).
27. Baldi P, Brunak S, Chauvin Y, Andersen CA, Nielsen H. Assessing the accuracy of prediction algorithms for classification: an overview. *Bioinforma Oxf Engl* (2000) 16:412–24.
28. Kolaskar AS, Tongaonkar PC. A semi-empirical method for prediction of antigenic determinants on protein antigens. *FEBS Lett* (1990) 276:172–4.
29. Forsström B, Bisławska Axnäs B, Rockberg J, Danielsson H, Bohlin A, Uhlen M. Dissecting antibodies with regards to linear and conformational epitopes. *PLoS One* (2015) 10:e0121673. doi:10.1371/journal.pone.0121673
30. Herrero-González JE, Mascaró JM, Herrero C, Dilling A, Zillikens D, Sitaru C. Autoantibodies from patients with BSLE inducing recruitment of leukocytes to the dermoepidermal junction and subepidermal splits in cryosections of human skin. *Arch Dermatol* (2006) 142:1513–6. doi:10.1001/archderm.142.11.1513
31. Rosenbaum DM, Rasmussen SGF, Kobilka BK. The structure and function of G-protein-coupled receptors. *Nature* (2009) 459:356–63. doi:10.1038/nature08144
32. Scofield RH. Autoantibodies as predictors of disease. *Lancet* (2004) 363:1544–6. doi:10.1016/S0140-6736(04)16154-0
33. Kamel R, Eftekhari P, Garcia S, Berthouze M, Berque-Bestel I, Peter J-C, et al. A high-affinity monoclonal antibody with functional activity against the 5-hydroxytryptaminergic (5-HT4) receptor. *Biochem Pharmacol* (2005) 70:1009–18. doi:10.1016/j.bcp.2005.07.005
34. Dresow SK, Sitaru C, Recke A, Oostingh GJ, Zillikens D, Gibbs BF. IgE autoantibodies against the intracellular domain of BP180. *Br J Dermatol* (2009) 160:429–32. doi:10.1111/j.1365-2133.2008.08858.x
35. Kampylafka EI, Routsias JG, Alexopoulos H, Dalakas MC, Moutsopoulos HM, Tzioufas AG. Fine specificity of antibodies against AQP4: epitope mapping reveals intracellular epitopes. *J Autoimmun* (2011) 36:221–7. doi:10.1016/j.jaut.2011.01.004
36. Alarcón-Segovia D, Llorente L, Ruíz-Argüelles A. The penetration of autoantibodies into cells may induce tolerance to self by apoptosis of autoreactive lymphocytes and cause autoimmune disease by dysregulation and/or cell damage. *J Autoimmun* (1996) 9:295–300. doi:10.1006/jaut.1996.0038
37. Avrameas A, Ternynck T, Nato F, Buttin G, Avrameas S. Polyreactive anti-DNA monoclonal antibodies and a derived peptide as vectors for the intracytoplasmic and intranuclear translocation of macromolecules. *Proc Natl Acad Sci U S A* (1998) 95:5601–6. doi:10.1073/pnas.95.10.5601
38. Muller S, Zhao Y, Brown TL, Morgan AC, Kohler H. TransMabs: cell-penetrating antibodies, the next generation. *Expert Opin Biol Ther* (2005) 5:237–41. doi:10.1517/14712598.5.2.237
39. Baleva M, Nikolov K. The role of intravenous immunoglobulin preparations in the treatment of systemic sclerosis. *Int J Rheumatol* (2011) 2011:1–4. doi:10.1155/2011/829751

Conflict of Interest Statement: The authors declare that the research was conducted in the absence of any commercial or financial relationships that could be construed as a potential conflict of interest.

frontiers in Immunology

ORIGINAL RESEARCH
published: 21 March 2018
doi: 10.3389/fimmu.2018.00570

Anti-Type VII Collagen Antibodies Are Identified in a Subpopulation of Bullous Pemphigoid Patients With Relapse

Delphine Giusti[1,2†], Grégory Gatouillat[1,2†], Sébastien Le Jan[1], Julie Plée[1,3], Philippe Bernard[1,3†], Frank Antonicelli[1,4†] and Bach-Nga Pham[1,2†]*

[1] Laboratory of Dermatology, Faculty of Medicine, University of Reims Champagne-Ardenne, Reims, France, [2] Laboratory of Immunology, Reims University Hospital, University of Reims Champagne-Ardenne, Reims, France, [3] Department of Dermatology, Reims University Hospital, University of Reims Champagne-Ardenne, Reims, France, [4] Department of Biological Sciences, Immunology, Faculty of Odontology, University of Reims Champagne-Ardenne, Reims, France

OPEN ACCESS

Edited by:
Ralf J. Ludwig,
University of Lübeck, Germany

Reviewed by:
Takashi Hashimoto,
Osaka City University, Japan
Jean Kanitakis,
Hospices Civils de Lyon, France
Hiroshi Koga,
Kurume University, Japan

***Correspondence:**
Frank Antonicelli
frank.antonicelli@univ-reims.fr

[†]These authors have contributed equally to this work.

Specialty section:
This article was submitted to Immunological Tolerance and Regulation, a section of the journal Frontiers in Immunology

Received: 12 January 2018
Accepted: 06 March 2018
Published: 21 March 2018

Citation:
Giusti D, Gatouillat G, Le Jan S, Plée J, Bernard P, Antonicelli F and Pham B-N (2018) Anti-Type VII Collagen Antibodies Are Identified in a Subpopulation of Bullous Pemphigoid Patients With Relapse. Front. Immunol. 9:570. doi: 10.3389/fimmu.2018.00570

Bullous pemphigoid (BP) is an autoimmune bullous skin disease characterized by anti-BP180 and anti-BP230 autoantibodies (AAbs). Mucous membrane involvement is an uncommon clinical feature of BP which may evoke epidermolysis bullosa acquisita, another skin autoimmune disease characterized by anti-type VII collagen AAbs. We therefore evaluated the presence of anti-type VII collagen AAbs in the serum of BP patients with and without mucosal lesions at time of diagnosis and under therapy. Anti-BP180, anti-BP230, and anti-type VII collagen AAbs were measured by ELISA in the serum of unselected patients fulfilling clinical and histo/immunopathological BP criteria at baseline ($n = 71$) and at time of relapse ($n = 24$). At baseline, anti-type VII collagen AAbs were detected in 2 out of 24 patients with BP presenting with mucosal involvement, but not in patients without mucosal lesions ($n = 47$). At the time of relapse, 10 out of 24 BP patients either displayed a significant induction or increase of concentrations of anti-type VII collagen AAbs ($P < 0.01$), independently of mucosal involvement. Those 10 relapsing BP patients were also characterized by a sustained high concentration of anti-BP180 AAb, whereas the serum anti-BP230 AAb concentrations did not vary in BP patients with relapse according to the presence of anti-type VII collagen AAbs. Thus, our study showed that anti-type VII collagen along with anti-BP180 AAbs detection stratified BP patients at time of relapse, illustrating a still dysregulated immune response that could reflect a potential epitope spreading mechanism in those BP patients.

Keywords: anti-type VII collagen antibodies, bullous pemphigoid, epitope spreading, mucous membrane involvement, relapse

INTRODUCTION

Bullous pemphigoid (BP) is the most common subepidermal autoimmune blistering skin disease that preferentially affects the elderly with various clinical manifestations. Clinically, BP patients typically present at diagnosis vesicles and tense clear blisters, which mainly occur on erythematous skin, together with erythematous or urticarial papules and plaques (1–4). BP is immunologically characterized by tissue-bound and circulating autoantibodies (AAbs) directed against either the

BP antigen 180 (BP180) or the BP antigen 230 (BP230) or even both, which are components of hemidesmosomes involved in the dermal–epidermal cohesion (2, 3, 5–9). Most of BP patients (82–94%) display in their serum AAb that bind to the NC16A domain of the transmembrane protein BP180 (3, 10–16). AAbs against other antigenic sites of BP180 are associated with the severity and the phenotype of BP. Depending on the detection assay used, the presence of AAb against both the BP180 N- and C-terminal of the ectodomain was found to be associated with the presence of mucosal lesions (12), or not (17). When presenting with mucosal involvement, BP may suggest the BP-like, inflammatory form of epidermolysis bullosa acquisita (EBA), another skin autoimmune disease characterized by AAb directed against type VII collagen, a protein of the basement membrane zone beneath the stratified squamous epithelia (8, 18–22). However, no study has investigated yet the presence of serum anti-type VII collagen AAb at time of diagnosis of BP patients with mucosal involvement and whether these AAb are associated with BP outcome.

Loss of immune self-tolerance eventually leads to the generation of AAb (22). Among the different AAb in BP, the pathogenicity was mainly attributed to those directed against the NC16A domain of BP180 (9, 10, 23, 24). Actually, high serum level of anti-BP180 NC16A AAb was correlated with disease activity at time of diagnosis and was shown as an independent risk factor for BP relapse after cessation of therapy (14, 15, 25–27). In addition, approximately 30% of the BP patients relapse during the first year of treatment (16, 28–31). For those latter BP patients, it was shown that the variations of serum IgG AAb directed toward the BP180 NC16A domain after 2 months of therapy may be useful to predict BP outcome (16, 32). However up to now, a comparison in BP patients of the AAb profile at time of relapse vs. baseline has been investigated neither with respect to mucosal involvement nor with respect to antibody directed against other epidermal basement membrane autoantigens such as the type VII collagen.

In this study, we investigated certain autoimmunity markers which result from the disturbance of self-tolerance in BP both at baseline with respect to mucous membrane involvement and at time of relapse. To that purpose, the presence of AAb against type VII collagen was evaluated at time of diagnosis both in the serum of BP patients with and without mucosal involvement. Furthermore, serum anti-type VII collagen AAb titer at baseline and at time of relapse was analyzed according to the initial clinical BP phenotype at baseline and compared with anti-BP180 and anti-BP230 AAb serum profiles.

MATERIALS AND METHODS

Patients

This retrospective study was conducted in the Dermatology Department of the University Hospital of Reims, belonging to the French Reference Center for Autoimmune Bullous Diseases. From January 2011 to July 2015, 71 consecutive patients with newly diagnosed BP were included in this study when they fulfilled the following criteria: (1) blistering skin dermatosis fulfilling at least three of four clinical criteria for BP (33) and (2) linear IgG and/or C3 deposits along the epidermal basement membrane zone by skin direct immunofluorescence microscopy of perilesional skin. Patients fulfilling less than three clinical criteria, were also included if they demonstrated high anti-BP180/230 titers and at least roof labeling by indirect immunofluorescence (IIF) on salt split skin (SSS). During a 1-year follow-up, the number and dates of potential relapses were recorded. Relapse was defined as the reappearance of at least three daily new blisters along with pruriginous, erythematous, or urticarial plaques (34). The disease activity was assessed at baseline using the Bullous Pemphigoid Disease Area Index (BPDAI) (34). Patients were separated into two groups and then analyzed according to the presence or the absence of mucosal involvement as recorded in the BPDAI evaluation.

AAbs Detection

For each patient, blood samples were collected in clot activator tubes. Sample collection was realized at the time of diagnosis in all BP patients, and at the time of relapse on therapy during the follow-up (mean time of 39 weeks after the beginning of treatment), or at an equivalent follow-up visit for patients with ongoing remission. All sera were stored at −20°C until analysis. The detection of serum anti-type VII collagen AAb was performed with a commercially available ELISA (MBL, Nagoya, Japan). This assay uses the NC1 and NC2 domains of type VII collagen as substrates (35). The 6 U/mL cutoff value recommended by the manufacturer was used. Anti-BP180-NC16A and anti-BP230 AAb were detected in serum samples using commercially available ELISA tests (MBL, Nagoya, Japan) (36, 37). ELISA values are expressed as Units per milliliter of serum with the cutoff value of 9 U/mL for both ELISAs as recommended by the manufacturer. Serum anti-basement membrane zone AAb were detected by IIF on monkey SSS, according to the manufacturer's instructions (Euroimmun, Lübeck, Germany).

Statistical Analysis

Quantitative variables were described as mean ± SD and qualitative data as number and percentage. Comparisons between groups were performed using Wilcoxon rank test, Fisher exact test or χ^2 test, as appropriate. A P-value <0.05 was considered statistically significant. All analyses were performed using Microsoft Excel and GraphPad Prism software.

RESULTS

Clinical and Immunological Characteristics of BP Patients According to Mucosal Involvement at Baseline

To investigate the potential implication of serum anti-type VII collagen AAb at the time of diagnosis and during follow-up on therapy in patients with BP, 71 patients were included in the study. Clinical and immunological characteristics of BP patients according to mucosal involvement at baseline are detailed in **Table 1**. Among the 71 BP patients, 47 (66%) had a typical clinical presentation and 24 (34%) also had mucous membrane involvement, i.e., blisters or erosions of the oral cavity in all 24 cases in addition with genital erosions in 1 case. We evidenced that the

presence of oral lesions was associated with higher total (**Table 1**, $P < 0.001$) and skin BPDAI scores ($P < 0.01$). We also found that anti-BP180 AAb were indifferently present in BP patients with or without mucosal lesions, with similar titers (**Table 1**), while the percentage of patients with positive anti-BP230 antibodies titer was lower in patients with mucosal involvement compared with patients without mucosal involvement (29 and 55%, respectively; $P < 0.05$). Further investigation of AAb expression in BP patients with and without mucosal involvement showed that, although not statistically significant, anti-type VII collagen AAb were only detected at diagnosis in the serum of patients presenting mucosal lesions (2/24 patients with mucosal involvement vs. 0/47 in patients without mucosal involvement, **Table 1**). In those two patients, the presence of high titers of serum anti-BP180 (66 and 109 U/mL) but low titers of anti-type VII collagen (13 and 8 U/mL) AAb confirmed the diagnosis of BP.

Clinical and Immunological Characteristics of BP Patients With Relapse

Of the 71 BP patients included in this study, 56 had both a complete clinical and biological follow-up of at least 1 year, including BPDAI scores and serum AAb detection every 2 months and also in case of relapse. At baseline, 24 out of those 56 BP patients experienced at least one relapse during this follow-up period. Both total and skin BPDAI scores tended to be higher for BP patients who relapsed than for BP patients who remained in clinical remission upon therapy (**Table 2**). Mucosal involvement at time of diagnosis was not more frequent in patients with later relapse than in BP patients with ongoing remission (46 and 31%, respectively; $P = 0.26$). For those 24 BP patients, the relapse occurred in a mean delay of 39 weeks after starting treatment, without any difference between patients with and without mucosal involvement at baseline (**Table 2**). At the time of relapse, the level of serum anti-type VII collagen AAb was higher compared with baseline values (mean value at relapse 7.8 U/mL vs. mean value at baseline 3.6 U/mL, $P < 0.01$) (**Figure 1A**). Such an increase was not observed in the serum of BP patients with ongoing remission when analyzed after a similar median duration of treatment (**Figure 1B**).

TABLE 1 | Clinical and immunological characteristics of BP patients at baseline.

	Total	Patients without mucosal involvement	Patients with mucosal involvement	*P* value
Patients no.	71	47	24	
Mean age ± SD (range), years	80.3 ± 10.1 (45 – 95)	82.6 ± 7.9 (53 – 95)	75.8 ± 12.6 (45 – 92)	0.05
Sex ratio (female/male)	1.7	2.1	1.2	0.25
Total BPDAI (mean ± SD)	46.0 ± 27.4	38.0 ± 22.9	61.3 ± 29.7	0.001
Skin BPDAI (mean ± SD)	44.8 ± 26.1	38.0 ± 22.9	57.9 ± 28.2	0.004
Relapse, patients no. (%)	24 (33.8)	13 (27.6)	11 (45.8)	0.12
Serum autoantibodies				
COL7 Ab				
Positive ELISA value, No (%)	2 (2.8)	0 (0.0)	2 (8.3)	0.11
Mean ± SD (U/mL)	2.6 ± 1.8	2.4 ± 1.3	3.1 ± 2.6	0.29
BP180 Ab				
Positive ELISA value, no. (%)	59 (83.1)	40 (85.1)	19 (79.2)	0.52
Mean ± SD (U/mL)	67.1 ± 50.0	65.8 ± 48.6	69.5 ± 56.2	0.80
BP230 Ab				
Positive ELISA value, no. (%)	33 (46.5)	26 (55.3)	7 (29.2)	0.046
Mean ± SD (U/mL)	26.2 ± 36.9	31.4 (39.7)	16.1 ± 28.8	0.10
IIF-SSS, no. (%)				
Roof labeling	47 (66.2)	33 (70.3)	14 (58.3)	
Roof and floor labeling	4 (5.6)	3 (6.4)	1 (4.2)	
Floor labeling	0 (0.0)	0 (0.0)	0 (0.0)	
Negative	20 (28.2)	11 (23.4)	9 (37.5)	

Clinical and immunological characteristics at baseline from the whole population and comparison of these characteristics between BP patients with and without mucosal involvement.

BPDAI, Bullous Pemphigoid Disease Area Index; COL7 Ab, anti-type VII collagen autoantibodies; BP180 Ab, anti-BP180 antibodies; BP230 Ab, anti-BP230 antibodies; IIF-SSS, indirect immunofluorescence on salt split skin; BP, bullous pemphigoid.

Anti-Type VII Collagen Antibody Positivity in a Subset of BP Patients at Time of Relapse

We then attempted to further characterize the subset of BP patients who relapsed during the follow-up. Serological analysis revealed that 10 (41%) of those 24 BP patients had increased serum levels of anti-type VII collagen AAb at time of relapse (mean value at time of relapse 15.4 U/mL) (**Figure 1C**), whereas the other relapsing patients did not (**Figure 1D**). Among those 10 BP patients with detectable serum anti-type VII collagen AAb at time of relapse, 6 had mucosal involvement at time of diagnosis. Other clinical features at baseline, including mean age, sex ratio, and BPDAI scores, were not different in patients with positive anti-type VII collagen at time of relapse from those who did not express this latter AAb (**Table 3**). Conversely, biological investigation of serum anti-BP180/230 AAb profiles between baseline and relapse highlighted that anti-BP180 ELISA scores remained elevated the 10 BP patients with concomitant positive anti-type VII collagen AAb, while they decreased in the subgroup of BP patients without anti-type VII collagen antibodies (**Figures 2A,C**). Such a difference in the serum AAb profiles was not observed when analyzing the variations in anti-BP230 antibody titers (**Figures 2B,D**).

TABLE 2 | Clinical characteristics of BP patients at baseline according to disease outcome.

	Ongoing remission	Relapse	*P* value
Patients no.	32	24	
Mean age ± SD (range), years	77.9 ± 10.3 (53 – 90)	80.8 ± 11.5 (45 – 95)	0.19
Sex ratio (female/male)	1.66	1.67	1.00
Total BPDAI (mean ± SD)	42.3 ± 28.8	54.4 ± 25.0	0.08
Skin BPDAI (mean ± SD)	40.3 ± 27.5	52.6 ± 24.9	0.06
Mucosal involvement, no. (%)	10 (31.2)	11 (45.8)	0.26

BPDAI, Bullous Pemphigoid Disease Area Index.

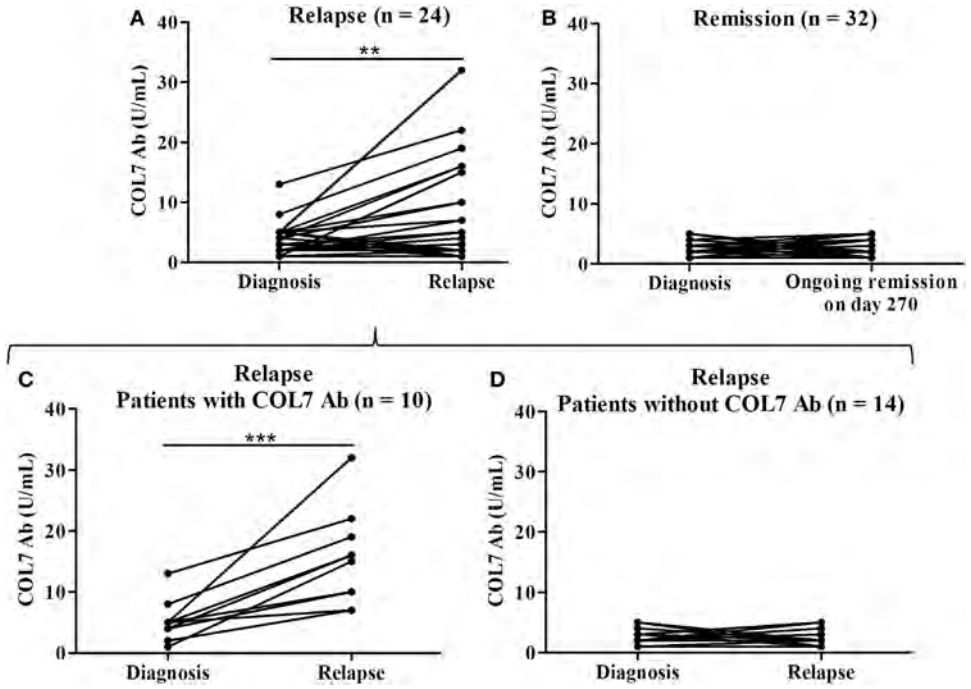

FIGURE 1 | Serum levels of anti-type VII collagen AAb (COL7 Ab) in patients with relapse ($n = 24$) (mean value at time of relapse 7.8 U/mL vs. mean value at baseline 3.6 U/mL) **(A)** and in patients with ongoing remission ($n = 32$) **(B)**. Mean delay between diagnosis and relapse was 270 days. Among the 24 patients with relapse, 10 patients were identified with positive ELISA score of anti-type VII collagen AAb at time of relapse (mean value at time of relapse 15.4 U/mL) **(C)** and 14 patients experienced relapse without presenting anti-type VII collagen AAb **(D)**. Comparison was made either between baseline and relapse or between baseline and day 270 for patients with ongoing remission (**$P < 0.01$, ***$P < 0.001$).

TABLE 3 | Clinical characteristics at baseline of BP patients who further relapsed under treatment.

	Patients with secondary appearance of COL7 Ab at relapse ($N = 10$)	Patients without secondary appearance COL7 Ab at relapse ($N = 14$)	*P* value
Mean age ± SD (range), years	79.8 ± 14.3 (45–95)	81.4 ± 9.6 (57.95)	1.00
Sex ratio (female/male)	2.5	1.3	0.52
Total BPDAI (mean ± SD)	57.3 ± 34.0	52.3 ± 17.0	0.72
Skin BPDAI (mean ± SD)	54.2 ± 32.4	51.5 ± 16.7	1.00
Mucosal involvement, no. (%)	6 (60.0)	5 (35.7)	0.24

The clinical characteristics at baseline of BP patients who further relapsed under treatment were analyzed according to the secondary appearance of anti-type VII collagen autoantibodies at relapse (COL7 Ab).
BPDAI, Bullous Pemphigoid Disease Area Index; BP, bullous pemphigoid.

DISCUSSION

The present study demonstrated that investigating both anti-BP180 and anti-type VII collagen antibodies serum concentrations was useful to exclude EBA diagnosis in BP patients with mucosal involvement at time of diagnosis. Furthermore, anti-type VII collagen AAb were identified in a subgroup of BP patients at time of relapse.

At diagnosis, anti-type VII collagen antibodies were detected only in 2 of 24 BP patients with oral involvement. However, high serum anti-BP180 titers compared to those of anti-type VII collagen antibodies advocated for a BP rather than an EBA for which the presence of serum anti-type VII collagen antibody remains the immunological hallmark at baseline (20, 35, 38). Although serum anti-type VII collagen antibodies were detected in the subgroup of BP patients with mucosal involvement, such a low frequency of antibody expression cannot be considered as a biological marker of mucosal subepidermal blistering in BP. Of note, this very low frequency of BP patients with serum anti-type VII collagen AAb and their low titers are in accordance with previous studies evaluating the performance of anti-type VII collagen antibody ELISA, in which 1–8% of patients with BP were positively tested (35, 39, 40). This is also in setting with the low prevalence of anti-type VII collagen antibodies in other autoimmune and autoinflammatory diseases, such as inflammatory bowel disease (16%) and pemphigus (9.5%), but also in healthy subjects (38). Furthermore, the low titer of anti-type VII collagen AAb in comparison with the high titer of anti-BP180 antibodies in our two patients with mucous membrane involvement, like in these other diseases, rather points out the production of anti-type VII collagen antibodies in BP as an epiphenomenon, as previously suggested (31). A possible diversification of the AAb response in BP could be related at least in part to disease severity, as BP patients with mucosal involvement had higher total and skin

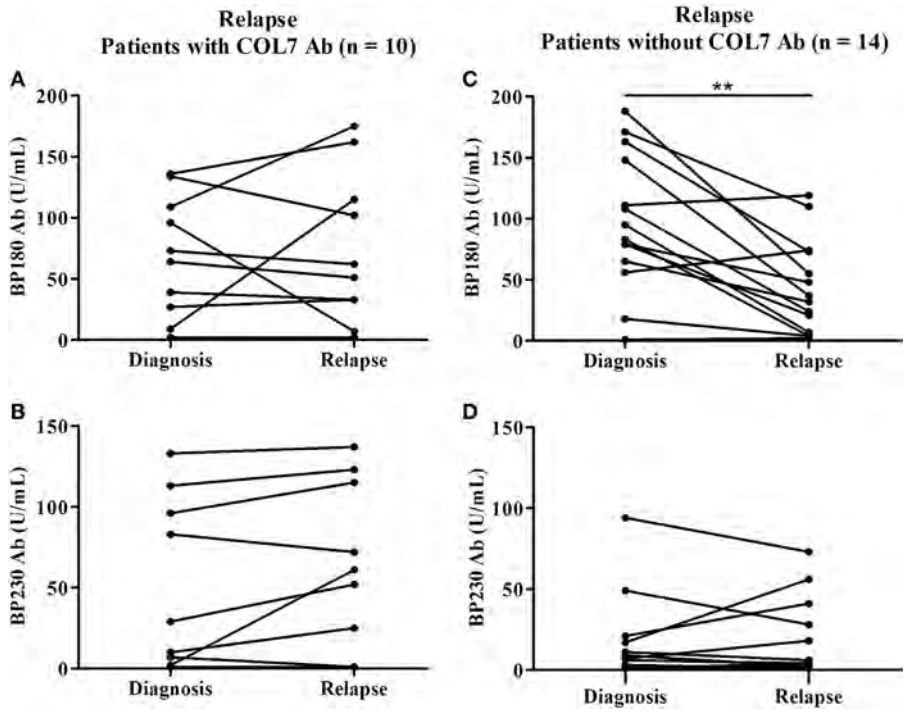

FIGURE 2 | Serum levels of anti-BP180 (BP180 Ab), anti-BP230 (BP230 Ab) autoantibodies (AAbs) in the relapsing patients (n = 24). Comparison was made between baseline and relapse either in patients with increased concentrations of anti-type VII collagen AAbs **(A,B)** or in patients without detectable anti-type VII collagen AAbs **(C,D)** (**P < 0.01).

BPDAI scores, especially the blisters/erosions activity score, as compared with the BPDAI score from patients with a typical form of BP (41).

Serum anti-type VII collagen antibodies were evidenced in about 40% of patients at the time of relapse and their titers were increasing. This is in line with a previous study which showed that the variation in the AAb profile, called epitope spreading, occurred as an early event in about 50% of BP patients (42). Our results complete our knowledge on BP-associated epitope spreading, by showing that the production of AAb against type VII collagen occurred in relapsing patients but not in patients with ongoing remission. This further illustrated that targets of immune responses in BP can be extended not only to other epitopes on the hemidesmosome protein (42, 43) but also to other proteins in their vicinity. The production of anti-type VII collagen AAb at time of relapse was not related to mucosal involvement at baseline, but to disease severity. Of note, it has been previously showed that the main predictive risk factor of relapse is the number of new daily blister at baseline (16). By contrast, the increase in the skin BPDAI score in BP patients with mucosal involvement was rather related to erosions than to blister formation. Thus, anti-type VII collagen production may result from situations in which tissue damage, induced by proteases activity linked to blister formation, causes the release and exposure of a previously encrypted antigen, thereby leading to a secondary autoimmune response against the newly exposed antigen as proposed for other autoimmune diseases (38, 39).

Noteworthy, serum anti-type VII collagen AAb was evidenced only in a subgroup of BP patients at the time of relapse. Then, the presence of anti-type VII collagen AAb may be an associated risk factor characterizing this subgroup of relapsing BP patients. Interestingly, this subgroup was also characterized by a high persistent titer of BP180 antibodies. Anti-BP180 antibody concentration has been correlated with BP disease activity (14, 15, 25, 26), and the decrease in anti-BP180 AAb levels after 2 months of treatment was lower in patients with further relapse in comparison with patients with ongoing remission (16). In the present study, if the serum level of anti-BP180 antibody remained elevated in all BP patients at time of relapse, we noticed that BP relapsing patients with serum anti-type VII collagen AAb displayed a sustained level of anti-BP180 antibody, suggesting that the immune response is still highly active in those patients. We also previously showed that the inflammatory response remained elevated in BP patients who relapsed during the first year of treatment. Especially, the production of IL-17, IL-23, CXCL10, and ECP also remained elevated after 2 months of treatment in the serum of relapsing BP patients (44–47). Then, one can hypothesize that the inflammatory response may also display a specific profile in this subgroup of BP patients with serum anti-type VII collagen AAb and high serum level of anti-BP180 at time of relapse. Of note, regulatory T (Treg) cells, a major regulatory system of autoimmunity, demonstrated plasticity and can convert to Th_{17} cells according to the cytokine environment (48). Accordingly, a previous study evidenced that Treg cells were upregulated (49),

whereas another study proposed a Treg cell downregulation in BP (50). Knowing that Treg activity and IL-17-producing cells may have opposite effects on autoimmunity (51, 52), an impaired Treg activity in an IL-17/IL-23 context (53, 54) could result in an imbalance between the pro-inflammatory and the regulatory cytokines levels which control the tolerance breakdown limit and therefore favors the production of anti-type VII collagen AAb and the sustained concentration of anti-BP180 AAb (47, 53, 55–57). In this line, it is worth to note that all of these inflammatory molecules promote matrix metalloproteinase MMP-9 and neutrophil elastase production and therefore participate to tissue degradation (44, 45, 53). Although further investigations are still needed to explain why some BP patients had circulating anti-type VII collagen AAb at time of relapse and not the other relapsing patients, our results support the hypothesis that chronic and dysregulated inflammation in line with persistent tissue damage and exposure of autoantigens may lead to tolerance breakdown and to autoimmunity.

In conclusion, we here showed the presence of AAb against the type VII collagen in the serum of relapsing BP patients who had a severe and difficult to treat disease. Actually, this is the first study demonstrating in those relapsing patients that the immune response is still dysregulated, probably due to prolonged epidermal/dermal damages which may sustain the immune tolerance breakdown process. Based on this observation, it will be interesting in a future prospective study to evaluate whether the autoimmune response spreads to other autoantigens identified in the subepidermal autoimmune-mediated blistering diseases such as the laminin-332 and the laminin gamma-1 chain (58, 59). Furthermore, it will also be of interest to determine whether the presence of serum anti-type VII collagen antibodies could be a predictive factor for relapse by analyzing the concentration of these AAbs at an earlier time point during the patients' follow-up in future prospective longitudinal studies. Finally, the pathogenicity of those anti-type VII collagen AAb in association with anti-BP180 NC16A AAb will also need to be investigated in animal models of BP (21, 60).

ETHICS STATEMENT

This study was carried out in accordance with the recommendations of the "Commission Nationale de l'Informatique et des libertés (CNIL)" and approved by the Ethic Committee of the University Hospital of Reims (institutional review board 14-04-2009). All subjects gave written informed consent in accordance with the Declaration of Helsinki.

AUTHOR CONTRIBUTIONS

DG and GG wrote the main manuscript text. DG, GG, and SJ conducted the experiments and statistical analyses. PB and JP participated to patients' care and clinical follow-up. FA, PB, and B-NP supervised this work and manuscript redaction. All the authors reviewed the article.

ACKNOWLEDGMENTS

We thank Dr Michael Maizières for his technical assistance during the study.

FUNDING

This study was supported by the French Department of Health's "Projet Hospitalier de Recherche Clinique (PHRC) Interregional" 2009, and by the university of Reims Champagne-Ardenne. The funding source had no role in the design and conduct of the study; collection, management, analysis, and interpretation of data; preparation, review, or approval of the manuscript; and decision to submit the manuscript for publication.

REFERENCES

1. Lever WF. Pemphigus. *Medicine* (1953) 32:1–123. doi:10.1097/00005792-195302000-00001
2. Schmidt E, Zillikens D. Pemphigoid diseases. *Lancet* (2013) 381:320–32. doi:10.1016/S0140-6736(12)61140-4
3. Bernard P, Antonicelli F. Bullous pemphigoid: a review of its diagnosis, associations and treatment. *Am J Clin Dermatol* (2017) 18(4):513–28. doi:10.1007/s40257-017-0264-2
4. Amber KT, Murrell DF, Schmidt E, Joly P, Borradori L. Autoimmune subepidermal bullous diseases of the skin and mucosae: clinical features, diagnosis, and management. *Clin Rev Allergy Immunol* (2018) 54(1):26–51. doi:10.1007/s12016-017-8633-4
5. Diaz LA, Ratrie H, Saunders WS, Futamura S, Squiquera HL, Anhalt GJ, et al. Isolation of a human epidermal cDNA corresponding to the 180-kD autoantigen recognized by bullous pemphigoid and herpes gestationis sera. Immunolocalization of this protein to the hemidesmosome. *J Clin Invest* (1990) 86:1088–94. doi:10.1172/JCI114812
6. Labib RS, Anhalt GJ, Patel HP, Mutasim DF, Diaz LA. Molecular heterogeneity of the bullous pemphigoid antigens as detected by immunoblotting. *J Immunol* (1986) 136:1231–5.
7. Stanley JR. Pemphigus and pemphigoid as paradigms of organ-specific, autoantibody-mediated diseases. *J Clin Invest* (1989) 83:1443–8. doi:10.1172/JCI114036
8. Goletz S, Zillikens D, Schmidt E. Structural proteins of the dermal-epidermal junction targeted by autoantibodies in pemphigoid diseases. *Exp Dermatol* (2017) 26:1154–62. doi:10.1111/exd.13446
9. Liu Y, Li L, Xia Y. BP180 is critical in the autoimmunity of bullous pemphigoid. *Front Immunol* (2017) 8:1752. doi:10.3389/fimmu.2017.01752
10. Giudice GJ, Emery DJ, Zelickson BD, Anhalt GJ, Liu Z, Diaz LA. Bullous pemphigoid and herpes gestationis autoantibodies recognize a common non-collagenous site on the BP180 ectodomain. *J Immunol* (1993) 151:5742–50.
11. Perriard J, Jaunin F, Favre B, Büdinger L, Hertl M, Saurat JH, et al. IgG autoantibodies from bullous pemphigoid (BP) patients bind antigenic sites on both the extracellular and the intracellular domains of the BP antigen 180. *J Invest Dermatol* (1999) 112:141–7. doi:10.1046/j.1523-1747.1999.00497.x
12. Hofmann S, Thoma-Uszynski S, Hunziker T, Bernard P, Koebnick C, Stauber A, et al. Severity and phenotype of bullous pemphigoid relate to autoantibody profile against the NH2- and COOH-terminal regions of the BP180 ectodomain. *J Invest Dermatol* (2002) 119:1065–73. doi:10.1046/j.1523-1747.2002.19529.x
13. Di Zenzo G, Thoma-Uszynski S, Fontao L, Calabresi V, Hofmann SC, Hellmark T, et al. Multicenter prospective study of the humoral autoimmune response in bullous pemphigoid. *Clin Immunol* (2008) 128:415–26. doi:10.1016/j.clim.2008.04.012
14. Roussel A, Benichou J, Randriamanantany ZA, Gilbert D, Drenovska K, Houivet E, et al. Enzyme-linked immunosorbent assay for the combination of

bullous pemphigoid antigens 1 and 2 in the diagnosis of bullous pemphigoid. *Arch Dermatol* (2011) 147:293–8. doi:10.1001/archdermatol.2011.21
15. Charneux J, Lorin J, Vitry F, Antonicelli F, Reguiai Z, Barbe C, et al. Usefulness of BP230 and BP180-NC16a enzyme-linked immunosorbent assays in the initial diagnosis of bullous pemphigoid: a retrospective study of 138 patients. *Arch Dermatol* (2011) 147:286–91. doi:10.1001/archdermatol.2011.23
16. Fichel F, Barbe C, Joly P, Bedane C, Vabres P, Truchetet F, et al. Clinical and immunologic factors associated with bullous pemphigoid relapse during the first year of treatment: a multicenter, prospective study. *JAMA Dermatol* (2014) 150:25–33. doi:10.1001/jamadermatol.2013.5757
17. Nakatani C, Muramatsu T, Shirai T. Immunoreactivity of bullous pemphigoid (BP) autoantibodies against the NC16A and C-terminal domains of the 180 kDa BP antigen (BP180): immunoblot analysis and enzyme-linked immunosorbent assay using BP180 recombinant proteins. *Br J Dermatol* (1998) 139:365–70. doi:10.1046/j.1365-2133.1998.02396.x
18. Chen M, Kim GH, Prakash L, Woodley DT. Epidermolysis bullosa acquisita: autoimmunity to anchoring fibril collagen. *Autoimmunity* (2012) 45:91–101. doi:10.3109/08916934.2011.606450
19. Kim JH, Kim YH, Kim S-C. Epidermolysis bullosa acquisita: a retrospective clinical analysis of 30 cases. *Acta Derm Venereol* (2011) 91:307–12. doi:10.2340/00015555-1065
20. Ludwig RJ. Clinical presentation, pathogenesis, diagnosis, and treatment of epidermolysis bullosa acquisita. *ISRN Dermatol* (2013) 2013:812029. doi:10.1155/2013/812029
21. Bieber K, Koga H, Nishie W. In vitro and in vivo models to investigate the pathomechanisms and novel treatments for pemphigoid diseases. *Exp Dermatol* (2017) 26:1163–70. doi:10.1111/exd.13415
22. Ludwig RJ, Vanhoorelbeke K, Leypoldt F, Kaya Z, Bieber K, McLachlan SM, et al. Mechanisms of autoantibody-induced pathology. *Front Immunol* (2017) 8:603. doi:10.3389/fimmu.2017.00603
23. Liu Z, Sui W, Zhao M, Li Z, Li N, Thresher R, et al. Subepidermal blistering induced by human autoantibodies to BP180 requires innate immune players in a humanized bullous pemphigoid mouse model. *J Autoimmun* (2008) 31:331–8. doi:10.1016/j.jaut.2008.08.009
24. Zillikens D, Rose PA, Balding SD, Liu Z, Olague-Marchan M, Diaz LA, et al. Tight clustering of extracellular BP180 epitopes recognized by bullous pemphigoid autoantibodies. *J Invest Dermatol* (1997) 109:573–9. doi:10.1111/1523-1747.ep12337492
25. Schmidt E, Obe K, Bröcker EB, Zillikens D. Serum levels of autoantibodies to BP180 correlate with disease activity in patients with bullous pemphigoid. *Arch Dermatol* (2000) 136:174–8. doi:10.1001/archderm.136.2.174
26. Haase C, Büdinger L, Borradori L, Yee C, Merk HF, Yancey K, et al. Detection of IgG autoantibodies in the sera of patients with bullous and gestational pemphigoid: ELISA studies utilizing a baculovirus-encoded form of bullous pemphigoid antigen 2. *J Invest Dermatol* (1998) 110:282–6. doi:10.1038/sj.jid.5602955
27. Bernard P, Reguiai Z, Tancrède-Bohin E, Cordel N, Plantin P, Pauwels C, et al. Risk factors for relapse in patients with bullous pemphigoid in clinical remission: a multicenter, prospective, cohort study. *Arch Dermatol* (2009) 145:537–42. doi:10.1001/archdermatol.2009.53
28. Joly P, Roujeau J-C, Benichou J, Delaporte E, D'Incan M, Dreno B, et al. A comparison of two regimens of topical corticosteroids in the treatment of patients with bullous pemphigoid: a multicenter randomized study. *J Invest Dermatol* (2009) 129:1681–7. doi:10.1038/jid.2008.412
29. Joly P, Roujeau J-C, Benichou J, Picard C, Dreno B, Delaporte E, et al. A comparison of oral and topical corticosteroids in patients with bullous pemphigoid. *N Engl J Med* (2002) 346:321–7. doi:10.1056/NEJMoa011592
30. Kyriakis KP, Paparizos VA, Panteleos DN, Tosca AD. Re-evaluation of the natural course of bullous pemphigoid. A prospective study. *Int J Dermatol* (1999) 38:909–13. doi:10.1046/j.1365-4362.1999.00754.x
31. Brulefert A, Le Jan S, Plée J, Durlach A, Bernard P, Antonicelli F, et al. Variation of the epidermal expression of glucocorticoid receptor-beta as potential predictive marker of bullous pemphigoid outcome. *Exp Dermatol* (2017) 26:1261–6. doi:10.1111/exd.13444
32. Cai SCS, Lim YL, Li W, Allen JC, Chua SH, Tan SH, et al. Anti-BP180 NC16A IgG titres as an indicator of disease activity and outcome in Asian patients with bullous pemphigoid. *Ann Acad Med Singapore* (2015) 44:119–26.
33. Vaillant L, Bernard P, Joly P, Prost C, Labeille B, Bedane C, et al. Evaluation of clinical criteria for diagnosis of bullous pemphigoid. French Bullous Study Group. *Arch Dermatol* (1998) 134:1075–80. doi:10.1001/archderm.134.9.1075
34. Murrell DF, Daniel BS, Joly P, Borradori L, Amagai M, Hashimoto T, et al. Definitions and outcome measures for bullous pemphigoid: recommendations by an international panel of experts. *J Am Acad Dermatol* (2012) 66:479–85. doi:10.1016/j.jaad.2011.06.032
35. Marzano AV, Cozzani E, Fanoni D, De Pità O, Vassallo C, Berti E, et al. Diagnosis and disease severity assessment of epidermolysis bullosa acquisita by ELISA for anti-type VII collagen autoantibodies: an Italian multicentre study. *Br J Dermatol* (2013) 168:80–4. doi:10.1111/bjd.12011
36. Kobayashi M, Amagai M, Kuroda-Kinoshita K, Hashimoto T, Shirakata Y, Hashimoto K, et al. BP180 ELISA using bacterial recombinant NC16a protein as a diagnostic and monitoring tool for bullous pemphigoid. *J Dermatol Sci* (2002) 30:224–32. doi:10.1016/S0923-1811(02)00109-3
37. Yoshida M, Hamada T, Amagai M, Hashimoto K, Uehara R, Yamaguchi K, et al. Enzyme-linked immunosorbent assay using bacterial recombinant proteins of human BP230 as a diagnostic tool for bullous pemphigoid. *J Dermatol Sci* (2006) 41:21–30. doi:10.1016/j.jdermsci.2005.11.002
38. Licarete E, Ganz S, Recknagel MJ, Di Zenzo G, Hashimoto T, Hertl M, et al. Prevalence of collagen VII-specific autoantibodies in patients with autoimmune and inflammatory diseases. *BMC Immunol* (2012) 13:16. doi:10.1186/1471-2172-13-16
39. Seta V, Aucouturier F, Bonnefoy J, Le Roux-Villet C, Pendaries V, Alexandre M, et al. Comparison of 3 type VII collagen (C7) assays for serologic diagnosis of epidermolysis bullosa acquisita (EBA). *J Am Acad Dermatol* (2016) 74:1166–72. doi:10.1016/j.jaad.2016.01.005
40. Schmidt T, Hoch M, Lotfi Jad SS, Solimani F, Di Zenzo G, Marzano AV, et al. Serological diagnostics in the detection of IgG autoantibodies against human collagen VII in epidermolysis bullosa acquisita – a multicenter analysis. *Br J Dermatol* (2017) 177(6):1683–92. doi:10.1111/bjd.15800
41. Clapé A, Muller C, Gatouillat G, Le Jan S, Barbe C, Pham BN, et al. Mucosal involvement in bullous pemphigoid is mostly associated with disease severity and to absence of anti-BP230 autoantibody. *Front Immunol* (2018) 9:479. doi:10.3389/fimmu.2018.00479
42. Di Zenzo G, Thoma-Uszynski S, Calabresi V, Fontao L, Hofmann SC, Lacour J-P, et al. Demonstration of epitope-spreading phenomena in bullous pemphigoid: results of a prospective multicenter study. *J Invest Dermatol* (2011) 131:2271–80. doi:10.1038/jid.2011.180
43. Chan LS, Vanderlugt CJ, Hashimoto T, Nishikawa T, Zone JJ, Black MM, et al. Epitope spreading: lessons from autoimmune skin diseases. *J Invest Dermatol* (1998) 110:103–9. doi:10.1046/j.1523-1747.1998.00107.x
44. Plée J, Le Jan S, Giustiniani J, Barbe C, Joly P, Bedane C, et al. Integrating longitudinal serum IL-17 and IL-23 follow-up, along with autoantibodies variation, contributes to predict bullous pemphigoid outcome. *Sci Rep* (2015) 5:18001. doi:10.1038/srep18001
45. Riani M, Le Jan S, Plée J, Durlach A, Le Naour R, Haegeman G, et al. Bullous pemphigoid outcome is associated with CXCL10-induced matrix metalloproteinase 9 secretion from monocytes and neutrophils but not lymphocytes. *J Allergy Clin Immunol* (2016) 139(3):863–72.e3. doi:10.1016/j.jaci.2016.08.012
46. Giusti D, Gatouillat G, Le Jan S, Plée J, Bernard P, Antonicelli F, et al. Eosinophil Cationic Protein (ECP), a predictive marker of bullous pemphigoid severity and outcome. *Sci Rep* (2017) 7:4833. doi:10.1038/s41598-017-04687-5
47. Giusti D, Le Jan S, Gatouillat G, Bernard P, Pham BN, Antonicelli F. Biomarkers related to bullous pemphigoid activity and outcome. *Exp Dermatol* (2017) 26(12):1240–7. doi:10.1111/exd.13459
48. Zhou X, Tang J, Cao H, Fan H, Li B. Tissue resident regulatory T cells: novel therapeutic targets for human disease. *Cell Mol Immunol* (2015) 12:543–52. doi:10.1038/cmi.2015.23
49. Gambichler T, Tsitlakidon A, Skrygan M, Höxtermann S, Susok L, Hessam S. T regulatory cells and other lymphocyte subsets in patients with bullous pemphigoid. *Clin Exp Dermatol* (2017) 42:632–7. doi:10.1111/ced.13135
50. Antiga E, Quaglino P, Volpi W, Pierini I, Del Bianco E, Bianchi B, et al. Regulatory T cells in skin lesions and blood of patients with bullous pemphigoid. *J Eur Acad Dermatol Venereol* (2014) 28:222–30. doi:10.1111/jdv.12091

51. Bieber K, Sun S, Witte M, Kasprick A, Beltsiou F, Behnen M, et al. Regulatory T cells suppress inflammation and blistering in pemphigoid diseases. *Front Immunol* (2017) 8:1628. doi:10.3389/fimmu.2017.01628
52. Schmidt T, Sitaru C, Amber K, Hertl M. BP180- and BP230-specific IgG autoantibodies in pruritic disorders of the elderly: a preclinical stage of bullous pemphigoid? *Br J Dermatol* (2014) 171:212–9. doi:10.1111/bjd.12936
53. Le Jan S, Plée J, Vallerand D, Dupont A, Delanez E, Durlach A, et al. Innate immune cell-produced IL-17 sustains inflammation in bullous pemphigoid. *J Invest Dermatol* (2014) 134:2908–17. doi:10.1038/jid.2014.263
54. Arakawa M, Dainichi T, Ishii N, Hamada T, Karashima T, Nakama T, et al. Lesional Th17 cells and regulatory T cells in bullous pemphigoid. *Exp Dermatol* (2011) 20:1022–4. doi:10.1111/j.1600-0625.2011.01378.x
55. D'Auria L, Cordiali Fei P, Ameglio F. Cytokines and bullous pemphigoid. *Eur Cytokine Netw* (1999) 10:123–34.
56. D'Auria L, Mussi A, Bonifati C, Mastroianni A, Giacalone B, Ameglio F. Increased serum IL-6, TNF-alpha and IL-10 levels in patients with bullous pemphigoid: relationships with disease activity. *J Eur Acad Dermatol Venereol* (1999) 12:11–5. doi:10.1111/j.1468-3083.1999.tb00801.x
57. Ameglio F, D'Auria L, Bonifati C, Ferraro C, Mastroianni A, Giacalone B. Cytokine pattern in blister fluid and serum of patients with bullous pemphigoid: relationships with disease intensity. *Br J Dermatol* (1998) 138:611–4. doi:10.1046/j.1365-2133.1998.02169.x
58. Bernard P, Antonicelli F, Bedane C, Joly P, Le Roux-Villet C, Duvert-Lehembre S, et al. Prevalence and clinical significance of anti-laminin 332 autoantibodies detected by a novel enzyme-linked immunosorbent assay in mucous membrane pemphigoid. *JAMA Dermatol* (2013) 149:533–40. doi:10.1001/jamadermatol.2013.1434
59. Commin M-H, Schmidt E, Duvert-Lehembre S, Lasek A, Morice C, Estival J-L, et al. Clinical and immunological features and outcome of anti-p200 pemphigoid. *Br J Dermatol* (2016) 175:776–81. doi:10.1111/bjd.14629
60. Antonicelli F, Ludwig RJ. New insights into pemphigoid diseases. *Exp Dermatol* (2017) 26:1151–3. doi:10.1111/exd.13469

Conflict of Interest Statement: The authors declare that the research was conducted in the absence of any commercial or financial relationships that could be construed as a potential conflict of interest.

frontiers in Immunology

ORIGINAL RESEARCH
published: 19 March 2018
doi: 10.3389/fimmu.2018.00528

Keratins Regulate p38MAPK-Dependent Desmoglein Binding Properties in Pemphigus

*Franziska Vielmuth[1], Elias Walter[1], Michael Fuchs[1], Mariya Y. Radeva[1], Fanny Buechau[2], Thomas M. Magin[2], Volker Spindler[1] and Jens Waschke[1]**

[1] Faculty of Medicine, Institute of Anatomy, Ludwig-Maximilians-Universität München, Munich, Germany, [2] Division of Cell and Developmental Biology, Institute of Biology, Sächsische Inkubator für Klinische Translation (SIKT), University of Leipzig, Leipzig, Germany

Keratins are crucial for the anchorage of desmosomes. Severe alterations of keratin organization and detachment of filaments from the desmosomal plaque occur in the autoimmune dermatoses pemphigus vulgaris and pemphigus foliaceus (PF), which are mainly caused by autoantibodies against desmoglein (Dsg) 1 and 3. Keratin alterations are a structural hallmark in pemphigus pathogenesis and correlate with loss of intercellular adhesion. However, the significance for autoantibody-induced loss of intercellular adhesion is largely unknown. In wild-type (wt) murine keratinocytes, pemphigus autoantibodies induced keratin filament retraction. Under the same conditions, we used murine keratinocytes lacking all keratin filaments (KtyII k.o.) as a model system to dissect the role of keratins in pemphigus. KtyII k.o. cells show compromised intercellular adhesion without antibody (Ab) treatment, which was not impaired further by pathogenic pemphigus autoantibodies. Nevertheless, direct activation of p38MAPK *via* anisomycin further decreased intercellular adhesion indicating that cell cohesion was not completely abrogated in the absence of keratins. Direct inhibition of Dsg3, but not of Dsg1, interaction *via* pathogenic autoantibodies as revealed by atomic force microscopy was detectable in both cell lines demonstrating that keratins are not required for this phenomenon. However, PF-IgG shifted Dsg1-binding events from cell borders toward the free cell surface in wt cells. This led to a distribution pattern of Dsg1-binding events similar to KtyII k.o. cells under resting conditions. In keratin-deficient keratinocytes, PF-IgG impaired Dsg1-binding strength, which was not different from wt cells under resting conditions. In addition, pathogenic autoantibodies were capable of activating p38MAPK in both KtyII wt and k.o. cells, the latter of which already displayed robust p38MAPK activation under resting conditions. Since inhibition of p38MAPK blocked autoantibody-induced loss of intercellular adhesion in wt cells and restored baseline cell cohesion in keratin-deficient cells, we conclude that p38MAPK signaling is (i) critical for regulation of cell adhesion, (ii) regulated by keratins, and (iii) targets both keratin-dependent and -independent mechanisms.

Keywords: desmosome, keratin, desmoglein, atomic force microscopy, p38MAPK

Abbreviations: AFM, atomic force microscopy; Dsg, desmoglein; EC, extracellular domain, PF, pemphigus foliaceus; PV, pemphigus vulgaris; NGS, normal goat serum; BSA, bovine serum albumin; PEG, polyethylenglycol; QI, quantitative imaging; FM, force mapping; FRAP, fluorescence recovery after photobleaching.

OPEN ACCESS

Edited by:
Ralf J. Ludwig, University of Lübeck, Germany

Reviewed by:
Marcel F. Jonkman, University Medical Center Groningen, Netherlands
Giovanni Di Zenzo, Istituto Dermopatico dell'Immacolata (IRCCS), Italy

****Correspondence:***
Jens Waschke
jens.waschke@med.uni-muenchen.de

Specialty section:
This article was submitted to Immunological Tolerance and Regulation, a section of the journal Frontiers in Immunology

Received: *30 November 2017*
Accepted: *28 February 2018*
Published: *19 March 2018*

Citation:
Vielmuth F, Walter E, Fuchs M, Radeva MY, Buechau F, Magin TM, Spindler V and Waschke J (2018) Keratins Regulate p38MAPK-Dependent Desmoglein Binding Properties in Pemphigus. Front. Immunol. 9:528. doi: 10.3389/fimmu.2018.00528

INTRODUCTION

Desmosomes are highly organized protein complexes required for proper intercellular adhesion especially in tissues which are constantly exposed to mechanical stress, such as the heart and the epidermis. They are composed of desmosomal cadherins which maintain the strong intercellular adhesion with their extracellular domains (EC), thus bridging the intercellular cleft, and plaque proteins connecting the desmosomal cadherins to the intermediate filament cytoskeleton (1–3).

Pemphigus is a life-threatening autoimmune dermatosis in which autoantibodies directed against the desmosomal cadherins desmoglein (Dsg) 1 and 3 lead to a flaccid blistering of the skin and mucous membranes (4, 5). On a morphological level, blistering occurs by separation of epidermal layers either suprabasal in pemphigus vulgaris (PV) or superficially in pemphigus foliaceus (PF) which represent the two main clinical manifestations of the disease (6). In PF, blisters are restricted to the skin and only Dsg1 autoantibodies occur. By contrast, in PV erosions additionally affect mucous membranes especially of the oral cavity. Blisters in PV are primarily caused by autoantibodies against both, Dsg1 and 3 (7). Thus, autoantibody profiles largely correlate with the clinical phenotype, a phenomenon which was proposed to be explained at least in part by autoantibody-specific cellular signaling patterns (8). In addition to signaling pathways which apparently are crucial for pemphigus pathogenesis (7, 9) direct inhibition of Dsg interactions by autoantibodies was described for Dsg3 but not for Dsg1 (10–12). Furthermore, the typical morphological hallmark of keratin filament retraction from cell borders is a common feature of all clinical phenotypes and can be detected in pemphigus models *in vitro* (13–16) as well as *ex vivo* and in patients' lesions (17–21). Keratins, the constituents of intermediate filaments in the epidermis, are crucial for proper desmosomal adhesion and retraction of the keratin cytoskeleton correlated with loss of intercellular adhesion induced by pemphigus autoantibodies (11, 22, 23). They, furthermore, account for the mechanical properties of keratinocytes (24) and are involved in the regulation of important signaling pathways for desmosomal adhesion, such as protein kinase C (PKC) and p38 mitogen-activated protein kinase (p38MAPK) both of which also regulate Dsg3-binding properties in a keratin-dependent fashion (22, 23, 25).

In these settings, the exact mechanism and contribution of alterations of the keratin cytoskeleton to loss of intercellular adhesion in pemphigus is not well characterized. Thus, we here use murine keratinocytes lacking all keratins to dissect the contribution of keratins in pemphigus pathogenesis. With this approach we demonstrate that keratins differentially regulate the binding properties of the two major antigens for autoantibodies in pemphigus, Dsg1 and 3. Moreover, we observed that p38MAPK underlies a keratin-mediated regulation, which is crucial for loss of intercellular adhesion in pemphigus.

MATERIALS AND METHODS

Cell Culture and Reagents

In this study, murine keratinocytes (KtyII) isolated from wild-type (KtyII wt) and keratin cluster II knockout (KtyII k.o.) were used. Cells were immortalized as described elsewhere in detail (22). Cells were grown in complete FAD media (0.05 mM $CaCl_2$) on collagen I-coated culture dishes (rat tail; BD). For all experiments, cells were grown to confluency before switching them to high Ca^{2+} (1.2 mM) for 48 h to induce proper differentiation and usage for experiments. For fluorescence recovery after photobleaching (FRAP) experiments, cells were transient transfected at 70% confluency with pEGFP-C1-*Dsg3* (kindly provided by Dr. Yasushi Hanakawa, Ehime University School of Medicine, Japan) using Lipofectamine 3000 (Invitrogen, Carlsbad, CA, USA) according to manufacturers' protocol. 24 h after transfection, cells were switched to high Ca^{2+} (1.2 mM) and grown for further 48 h before the experiments. Activity of p38MAPK was modulated using either p38 inhibitors SB202190 (Merck, Darmstadt, Germany) and SB203580 (Sigma Aldrich, Munich, Germany) (both 30 μM) or p38 activator anisomycin (60 μM) (Sigma Aldrich, Munich, Germany).

Purification of Recombinant Dsg Fc Constructs

Dsg1- and Dsg3-Fc constructs containing the full extracellular domain of the respective Dsg were stably expressed in Chinese hamster ovary cells (CHO-cells). Purification was performed as described elsewhere in detail (10). Briefly, transfected CHO-cells were grown to confluence, supernatants were collected and recombinant proteins were isolated using Protein A Agarose (Life Technologies). To test purity and specificity Coomassie staining and Western blotting using anti Dsg1-monoclonal antibody (mAb) (p124, Progen, Heidelberg, Germany) and anti Dsg3-mAb (clone5G11; Life Technologies) which both detect the extracellular domain of the respective Dsg were conducted (data not shown).

Purification of Patients IgG Fractions and Antibodies (Abs)

Serum of PV patients was provided by Enno Schmidt (Department of Dermatology, University of Lübeck). Sera were used with informed and written consent and under approval of the local ethic committee (number: AZ12-178). All patients had an active disease at the time of collection including lesions of the skin and the mucous membranes. ELISA scores are given in **Table 1**.

Purification of IgG fraction from pemphigus patients (PV-IgG) or healthy volunteer (control-IgG) was conducted as described elsewhere (10, 12, 26) using Protein A Agarose (Life Technologies). The pathogenic monoclonal Dsg3 Ab, AK23 (Biozol, Eching, Germany) was used at a concentration of 75 μg/ml.

TABLE 1 | ELISA score of pemphigus vulgaris (PV)-IgG fraction.

	Dsg1	Dsg3
PV1-IgG	1,207	3,906
PV2-IgG	212.27	181.440
Pemphigus foliaceus (PF)-IgG	215.34	8.2[a]

[a]*Beneath relevant threshold.*

Immunostaining

Murine keratinocytes were used 48 h after Ca^{2+} switch and 72 h after transfection for the FRAP and respective immunofluorescence experiments. Cells were fixed with freshly prepared 4% paraformaldehyde for 20 min, permeabilized with 1% Triton X-100 for 10 min and blocked with 10% normal goat serum/1% bovine serum albumin. Cytokeratin 14 mAb (LL002, Abcam, Cambridge, UK) was used as primary Ab. As secondary Ab Cy3-labeled goat anti-mouse Ab was used (Dianova, Hamburg, Germany). Furthermore, Alexa 488-phalloidin (Invitrogen, Carlsbad, CA, USA) and DAPI (Roche, Mannheim, Germany) were used to visualize the actin cytoskeleton and the nuclei respectively. Images were recorded using a Leica SP5 confocal microscopy with a 63× NA 1.4 PL APO objective controlled by LAS AF software (Leica, Mannheim, Germany). For some experiments, *z*-stacks were recorded, and pictures represent maximum intensity projections. For quantification of keratin retraction keratin 14 fluorescence intensity was measured at small areas in close proximity to the cell border and above the nucleus, and a ratio was calculated to quantify keratin filament retraction (Figure S1A in Supplementary Material).

Dispase-Based Keratinocytes Dissociation Assay

For dissociation assay, cells were grown in high Ca^{2+} medium for 48 h after confluence. Dispase assay was conducted as described in detail before (25, 27). Briefly, cells exposed to different conditions were removed from well bottom using a mixture of Dispase II (Sigma Aldrich) and 1% collagenase I (Thermo Fisher Scientific). After application of defined shear stress by pipetting the monolayers with a 1 ml pipette the resulting fragments were counted. The latter represent an inverse measure for intercellular adhesion.

Biotinylation Assay and Western Blotting

Cell surface biotinylation was conducted as described before (11, 25). In brief, cell monolayers were incubated with 0.25 mM of membrane-impermeable EZ-Link Sulfo-NHS-Biotin (Thermo Fisher Scientific, Waltham, MA, USA) on ice and rinsed in ice-cold PBS containing 100 mM glycin. Cells were lysed in PIPES buffer (50 mM NaCl, 10 mM PIPES, 3 mM $MgCl_2$, 1% Triton X-100, protease inhibitors) and centrifuged. Supernatants were collected, and pull-down of biotinylated molecules was carried out using NeutrAvidin (HighCapacity)-agarose (Thermo Fisher Scientific). Precipitated molecules were suspended in 3× Laemmli buffer with 50 mM dithiothreitol (AppliChem) and subjected to Western blotting.

For whole cell lysates SDS buffer (25 mmol/l HEPES, 2 mmol EDTA, 25 mmol/l NaF and 1% sodiumdodecylsulfate, and pH 7.4) was used. Western blotting was performed according to standard protocol (27).

Fluorescence Recovery After Photobleaching

For all FRAP experiments, KtyII cells were seeded in 8-well imaging chambers (Ibidi, Martinsried, Germany). Cells were transfected with pEGFP-C1-Dsg3 as described in cell culture section. FRAP experiments were conducted with the FRAP wizard software on a Leica SP5 confocal microscopy with a 63× NA 1.4 PL APO objective at 37°C as described before (25, 28). The Dsg3-GFP signal was bleached at cell border areas of two adjacent cells with the 488 nm line of an Argon laser at 100% transmission. Fluorescence recovery was monitored during the following 3 min and fluorescence intensities were analyzed. The immobile fraction was determined using the FRAP wizard.

Atomic Force Microscopy (AFM) Measurements

A NanoWizard® 3 AFM (JPK Instruments, Berlin, Germany) mounted on an inverted optical microscope (Carl Zeiss, Jena, Germany) was used throughout all experiments. The setup was described in detail before and allows the selection of the scanning areas by usage of an optical image acquired with a 63× objective (11, 25, 29). All measurements were accomplished at 37°C in cell culture medium containing 1.2 mM Ca^{2+}.

For all experiments pyramidal-shaped D-Tips of Si_3N_4 MLCT cantilevers (Bruker, Mannheim, Germany) with a nominal spring constant of 0.03 N/m and tip radius of 20 nm were functionalized with Dsg1- or 3-Fc constructs as described before (30). Briefly, a flexible heterobifunctional acetal-polyethylenglycol (synthetized by the Hermann Gruber Lab, Institute of Biophysics, Linz, Austria) was interspaced between the tip and the purified Fc construct whose concentration was adjusted to 0.15 mg/ml. For measurements on living murine keratinocytes a protocol which was recently developed in our group (29) was used. AFM was run in quantitative imaging (QI) mode for overview images or force mapping (FM) mode for measurement and characterization of Dsg binding properties. For the latter mode, a force map consisted of 1,200 pixels with each pixel representing one force–distance cycle that covered an area of 6 µm × 2 µm along cell borders or 4 µm × 2 µm above the nucleus. Settings of the respective modes can be found in **Table 2**.

Resulting force–distance curves were analyzed with regard to topography and adhesive properties of specific surface molecules (31).

For Ab experiments, the respective Abs were incubated solely on the cell to avoid binding to the scanning tip. After the incubation period, cells were extensively washed to remove unbound Abs and reprobed by AFM. For characterization of molecule distribution at the cell border areas a distribution coefficient was calculated as described before (32). Briefly, a ratio of number of binding events per area along the elevated cell borders (Figure S1B in Supplementary Material, green area) and in the surrounding cell surface (Figure S1B in Supplementary Material, red area) was

TABLE 2 | Atomic force microscopy settings.

Settings	Quantitative imaging mode	Force mapping mode
Setpoint	0.5 nN	0.5 nN
Z-length	1.5 µm	1.5 µm
Pulling speed	50 µm/s	10 µm/s
Resting contact time	–	0.1 s

calculated, in which values higher than 1 demonstrate increased localization of molecules along the cell borders.

Data Analysis and Statistics

For image processing, Adobe Photoshop CS5 (Adobe, Dublin, Ireland) was used. AFM images and data analysis of force–distance curves were done on JPK Data Processing Software (JPK Instruments). For further calculation of the analyzed AFM data with regard to unbinding forces, peak fitting, and step position Origin Pro 2016, 93G (Northampton, MA, USA) was used. In addition, Origin was utilized for comparison of data values with a paired Student's *t*-test (two sample groups) or one-way analysis of variance following Bonferroni correction (more than two groups), respectively. Error bars given in the figures are mean ± SD for all diagrams depicting unbinding forces ± SEM for all other experiments. Significance was presumed at a p-value < 0.05.

RESULTS

Keratin Deficiency Reduces Effect of Pathogenic Autoantibodies on Intercellular Adhesion

Keratin alterations are morphological hallmarks of pemphigus and correlate with loss of intercellular adhesion in human keratinocytes (11). Wild-type murine keratinocytes (KtyII wt) were used to test whether pathogenic autoantibodies are able to induce comparable changes of the keratin cytoskeleton in murine cells. Keratinocytes were treated either with control-IgG of healthy volunteers or with pathogenic autoantibodies for 24 h and subjected to immunostaining for keratin14 or keratinocyte dissociation assay, respectively (**Figures 1A,B**). We used AK23, a pathogenic monoclonal Ab derived from a PV mouse model, which is specific for Dsg3 (33), PF-IgG containing Ab against Dsg1 as well as PV-IgG with Abs against Dsg1 and 3 (**Table 1**). In control-IgG treated cells, the keratin cytoskeleton formed a dense network throughout the cells which is composed of delicate fibers and covers the cell periphery (**Figure 1A**). Actin was labeled to delineate the cell periphery and DAPI was included to stain nuclei (**Figure 1A**). By contrast, after treatment with all pathogenic autoantibodies keratin filament bundles were thicker and more irregular throughout and were retracted from some segments of cell borders (**Figure 1A**, arrows). Keratin retraction was quantified as described in materials and methods. In control-IgG treated cells, the coefficient was around 1 indicating a homogeneous distribution of the keratin network throughout the whole cell. The coefficient was significantly reduced after treatment with all pathogenic autoantibodies indicating a reduced fluorescent signal at cell border areas and thus confirms the occurrence of keratin retraction (**Figure 1B**).

To further dissect the role of keratins for loss of intercellular adhesion in pemphigus, KtyII k.o. cells were compared with wt monolayers in dissociation assays (Figure S1C in Supplementary Material). Under control conditions and after incubation with control-IgG, KtyII k.o. cells showed a significantly impaired intercellular adhesion compared with wt similar as shown before (22, 23, 25) (**Figure 1C**). Interestingly, treatment with AK23, PV-IgG or PF-IgG did not further compromise intercellular adhesion in KtyII k.o. cells whereas a significant reduction in wt cells was observed (**Figure 1C**). Given that anisomycin-mediated activation of p38MAPK as shown below (**Figure 4B**) was efficient to strongly reduce adhesion in keratin-deficient cells, these data indicate that keratins are important for the loss of intercellular adhesion in pemphigus.

Keratins Differentially Regulate Dsg-Binding Properties

Keratin filament alterations in response to autoantibodies were accompanied by depletion of Dsg3 from the cell membrane (8, 11). In a recent study, it was shown that keratins regulate Dsg3-binding properties through signaling (25). Thus, we next studied distribution, binding frequency, and binding strength of Dsg1 and Dsg3 by AFM in parallel. Dsgs can interact homo- and heterophilic (34–36). However, in our last studies by comparing parallel experiments under cell-free conditions and on living keratinocytes as well as by using isoform-specific inhibitory Abs, we predominantly detected homophilic interactions (25, 29, 32). A modified cantilever holder setup allowed the measurement at the same area with scanning tips functionalized with Dsg1 or Dsg3, respectively. First, topography overview images spanning an area of 50 µm × 30 µm were performed using QI mode (**Figures 1D,E**). In both cell lines, cell surfaces exhibited a reticular structure, and cell borders could be identified clearly by an elevated region (25) (**Figures 1D,E**, red arrows). Defined areas along cell borders were chosen for adhesion measurements (**Figures 1D,E**, red rectangles) and probed using FM mode with a pulling speed of 10 µm/s and a resting contact time of 0,1 s. Same areas along the cell border were chosen with both cantilevers after respective overview imaging to compare Dsg1 and 3 localization. In adhesion panels, each blue and green pixel represents a specific binding event of Dsg3 and Dsg1, respectively (**Figures 1D–F**). Evaluation of binding frequencies revealed a higher binding frequency for Dsg3 in keratin-deficient keratinocytes (**Figures 1D,G**) whereas the Dsg1-binding frequency was significantly reduced (**Figures 1E,H**). By contrast, binding forces of Dsg3 were reduced in KtyII k.o. cells as shown previously (25) (**Figures 1D,G**) whereas no difference in binding strength was observed for Dsg1 (**Figures 1E,H**). Finally, we analyzed the distribution of binding events using a distribution coefficient (see Material and Methods; Figure S1B in Supplementary Material) in which values >1 indicated higher binding frequency along the cell border. In accordance with former studies, Dsg3 shows a uniform distribution in both cell lines (25, 29) (**Figures 1D,F,G**). However, Dsg1-binding events were localized along cell borders (**Figures 1E,F,H**) in wt cells, whereas distribution was uniform in KtyII k.o. cells (**Figures 1E,F,H**) suggesting that keratins are important for proper localization of Dsg1 at cell junctions. Moreover, keratins differentially modulate Dsg binding properties.

Direct Inhibition of Dsg3 Single Molecule Interactions Occurs in Keratin-Deficient Keratinocytes

Direct inhibition of Dsg3 interactions is a well-characterized phenomenon in pemphigus which occurs fast after binding of

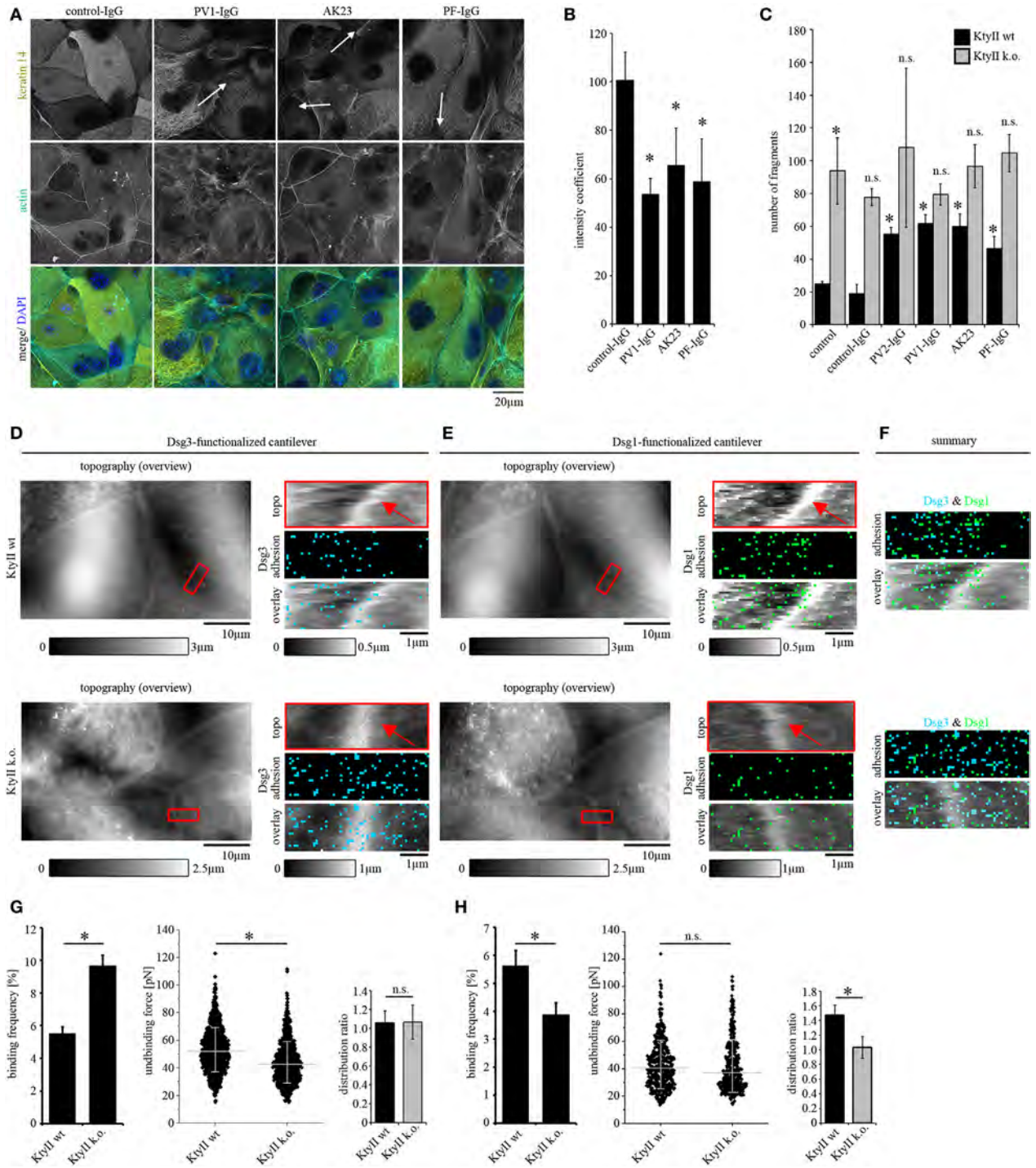

FIGURE 1 | Keratin retraction in murine keratinocytes and regulation of desmoglein binding properties through keratins. **(A)** Immunostaining of wild-type murine keratinocytes (KtyII wt) using keratin 14 monoclonal antibody and Alexa488-phalloidin for actin staining. Control-IgG treated keratinocytes show a dense keratin network throughout the whole cell whereas keratin filament retraction (arrows) and formation of thick filament bundles were detectable after treatment with pemphigus vulgaris (PV)-IgG, pemphigus foliaceus (PF)-IgG, and AK23. Pictures are representatives of $n > 4$. **(B)** Quantification of keratin retraction using an intensity coefficient confirms occurrence of keratin retraction in all autoantibody treated conditions. **(C)** Dissociation assay of KtyII wt and k.o. keratinocytes reveals that keratin-deficient keratinocytes show impaired intercellular adhesion. Treatment with pathogenic autoantibodies (PF-IgG, PV1- and PV2-IgG, and AK23) reduced intercellular adhesion in wild-type (wt) but not in KtyII k.o. cells. $n = 5$, $^*p > 0.05$ vs. wt control and wt control-IgG. **(D,E)** Atomic force microscopy adhesion measurements using Dsg3-Fc- or Dsg1-Fc-functionalized cantilevers on the same scanning area. In adhesion panels, each blue or green pixel represents a specific Dsg3- or Dsg1-binding event, respectively. **(F)** Merged panels of adhesion measurements reveal distinct clustering of Dsg1- and 3-binding events. **(G,H)** Analysis of binding frequency and unbinding forces of Dsg1 and 3 interactions. $n = 6$ from ≥3 independent coating procedures, 1,200 force–distance curves/adhesion maps ($^*p < 0.05$).

pathogenic autoantibodies but alone is not sufficient to cause complete loss of cell cohesion (5, 11, 26). To investigate the role of keratins for direct inhibition, we treated both cell lines with AK23 which is directed against the extracellular domain (EC) 1 of Dsg3 and was reported to interfere with Dsg3 interaction under cell-free conditions as well as in living keratinocytes (10, 11, 36). To avoid Ab binding to the AFM cantilever, AK23 was incubated on cells for 1 h in absence of cantilevers, washed extensively after incubation with fresh media to remove unbound Abs, and cells were reprobed. Doing so, small areas along the cell borders were chosen and measured before and after AK23 incubation. AK23 reduced Dsg3-binding frequency in both cell lines to a comparable extent suggesting that loss of keratins do not effect autoantibody-induced direct inhibition of Dsg3 interaction (**Figures 2A,B**). In line with this, distribution of the remaining binding events was not changed (**Figures 2A,B**).

Keratin Deficiency Accelerates Depletion of Dsg3

Next, we investigated depletion of Dsg3 which accompanied loss of intercellular adhesion and was linked to several signaling pathways such as p38MAPK in models of pemphigus (19, 37). As reported previously, keratin-deficient keratinocytes reveal a higher expression level of Dsg3 (25) (**Figure 2C**). Cells were treated with PV-IgG for 1 h and subjected to a surface

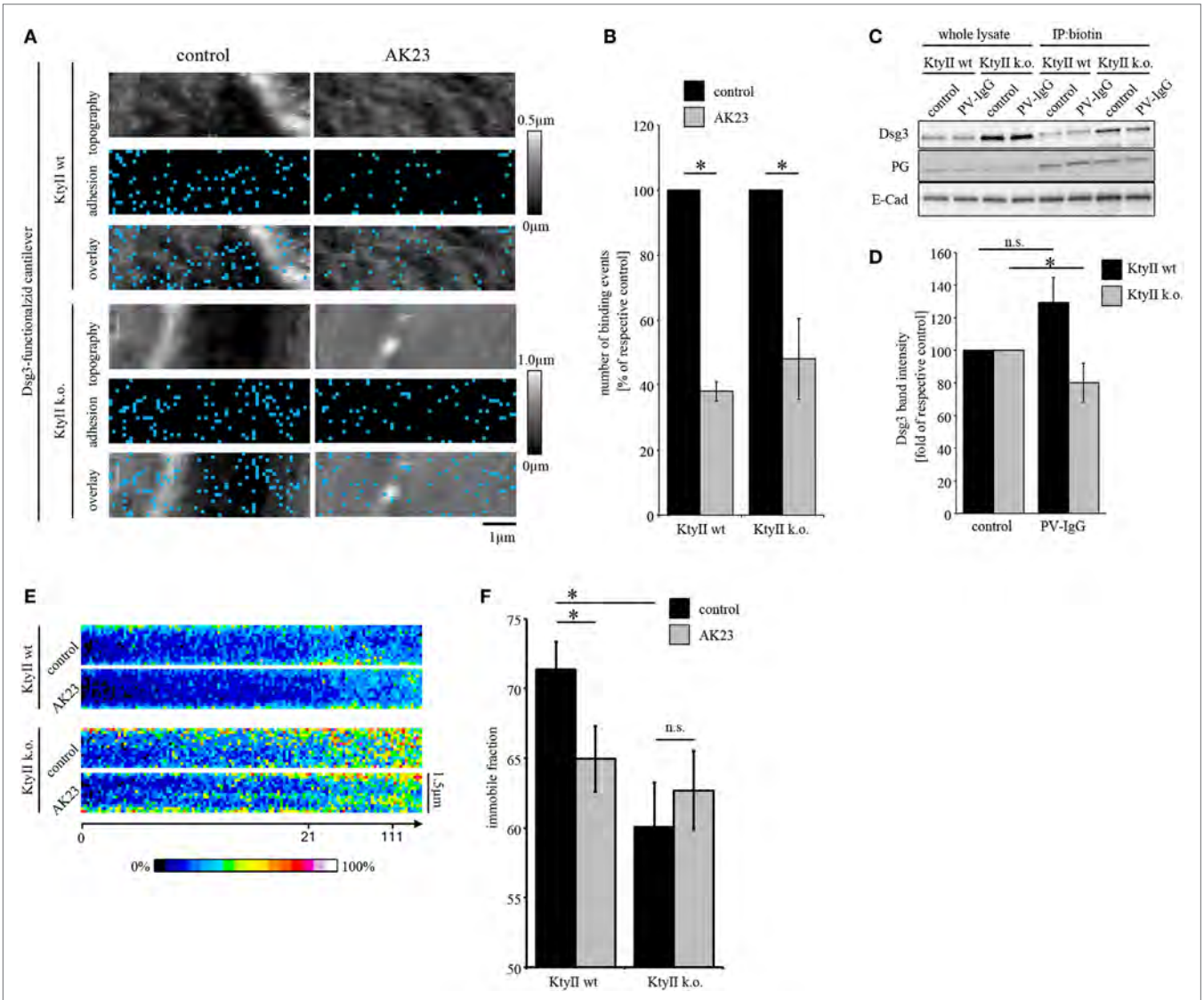

FIGURE 2 | Keratin-deficiency accelerates depletion of Dsg3. **(A,B)** Dsg3 adhesion measurements on KtyII wt and k.o. cells using AK23. Treatment of KtyII wt and k.o. cells with AK23 for 1 h reduced Dsg3 binding to comparable extent. $n = 6$ from ≥3 independent coating procedures, 1,200 force–distance curves/adhesion maps (*$p < 0.05$). **(C,D)** Cell surface biotinylation delineates depletion of Dsg3 in keratin-deficient keratinocytes after 1 h of pemphigus vulgaris (PV) 1-IgG treatment but not in wild-type keratinocytes. Representative of $n = 5$, *$p < 0.05$ vs. respective control. **(E)** Kymographs of fluorescence recovery after photobleaching experiments using Dsg3-eGFP-transfected KtyII wt and k.o. keratinocytes. **(F)** Immobile fractions of Dsg3-eGFP in KtyII wt and k.o. cells under basal conditions and after incubation with AK23 incubation for 1 h; $n = 7$, 5 cell borders/experiment; *$p < 0.05$.

biotinylation assay. In whole cell lysates, no reduction of Dsg3 levels was detectable in both cell lines (**Figure 2C**). However, in the surface membrane pool harvested *via* immunoprecipitation of biotin PV-IgG induced a significant depletion of Dsg3 in KtyII k.o. cells but not wt monolayers after 1 h of incubation (**Figures 2C,D**) indicating that the turnover of Dsgs is altered in keratin-deficient keratinocytes. This may be explained by enhanced mobility of Dsg3 when keratins are missing (25). Thus, we performed FRAP experiments on Dsg3-pEGFP-transfected KtyII cells using AK23. Indeed, KtyII k.o. cells revealed a reduced immobile fraction indicating higher mobility of Dsg3 molecules under basal conditions (**Figures 2E,F**). However, incubation of AK23 enhanced Dsg3 mobility in wt cells only suggesting that higher mobility resulted from keratin uncoupling (**Figures 2E,F**).

PF-IgG and PV-IgG Cause Redistribution of Dsg1-Binding Events and Subsequently Reduce Dsg1-Binding Strength

Under cell-free conditions, direct inhibition of Dsg interaction was observed for Dsg3 but not for Dsg1 (8, 10, 12). To test whether direct inhibition of Dsg1 occurs on living keratinocytes, we performed AFM adhesion measurements using PF-IgG. Small areas along cell borders and on the cell surface above the nucleus (Figure S2A in Supplementary Material) were chosen and probed in FM mode.

As outlined earlier, under control conditions Dsg1-binding events exhibited clusters along the cell borders in wt cells and uniform distribution in KtyII k.o. cells. In line with this, less Dsg1-binding events were detected on the cell surface of wt cells

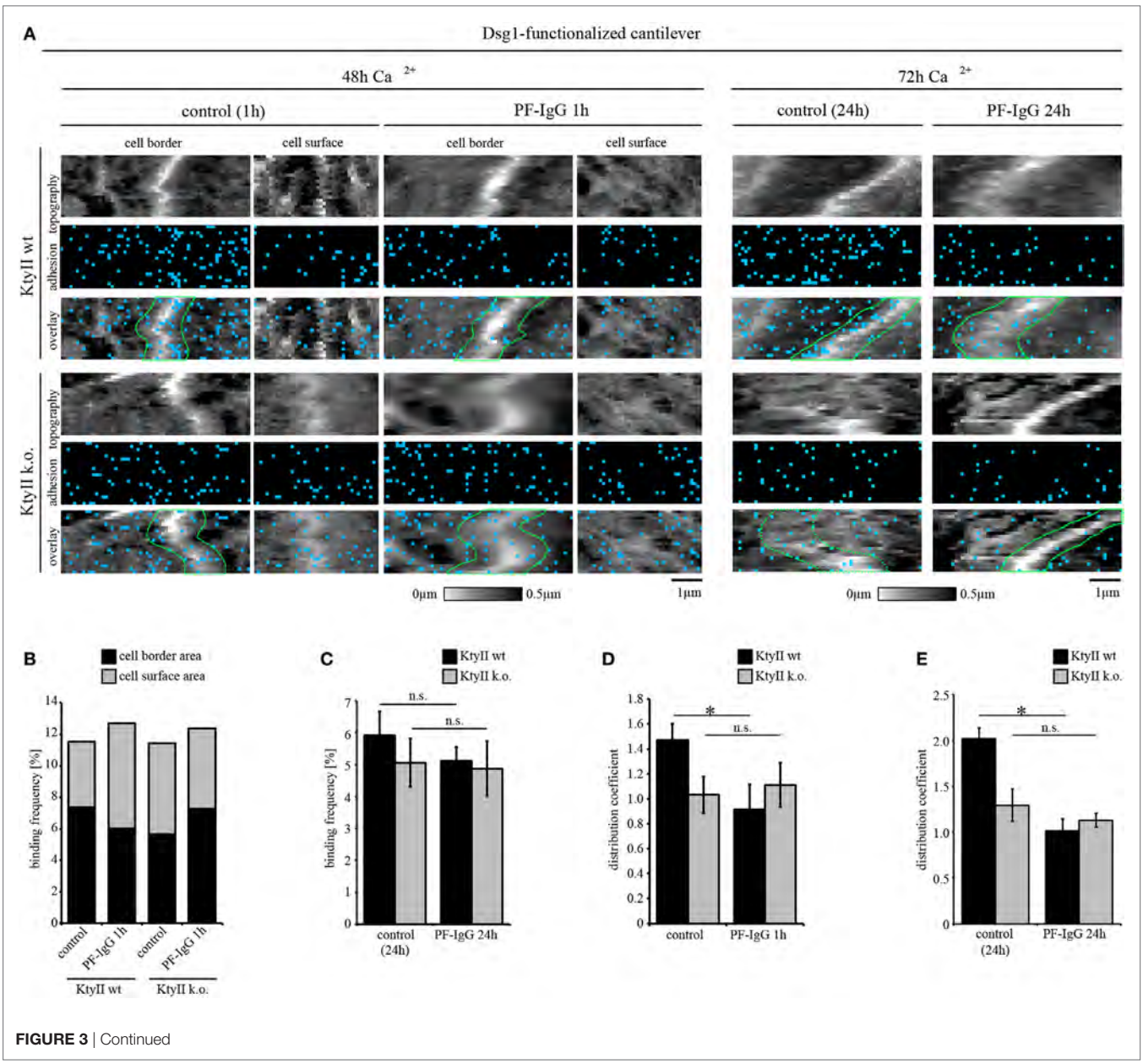

FIGURE 3 | Continued

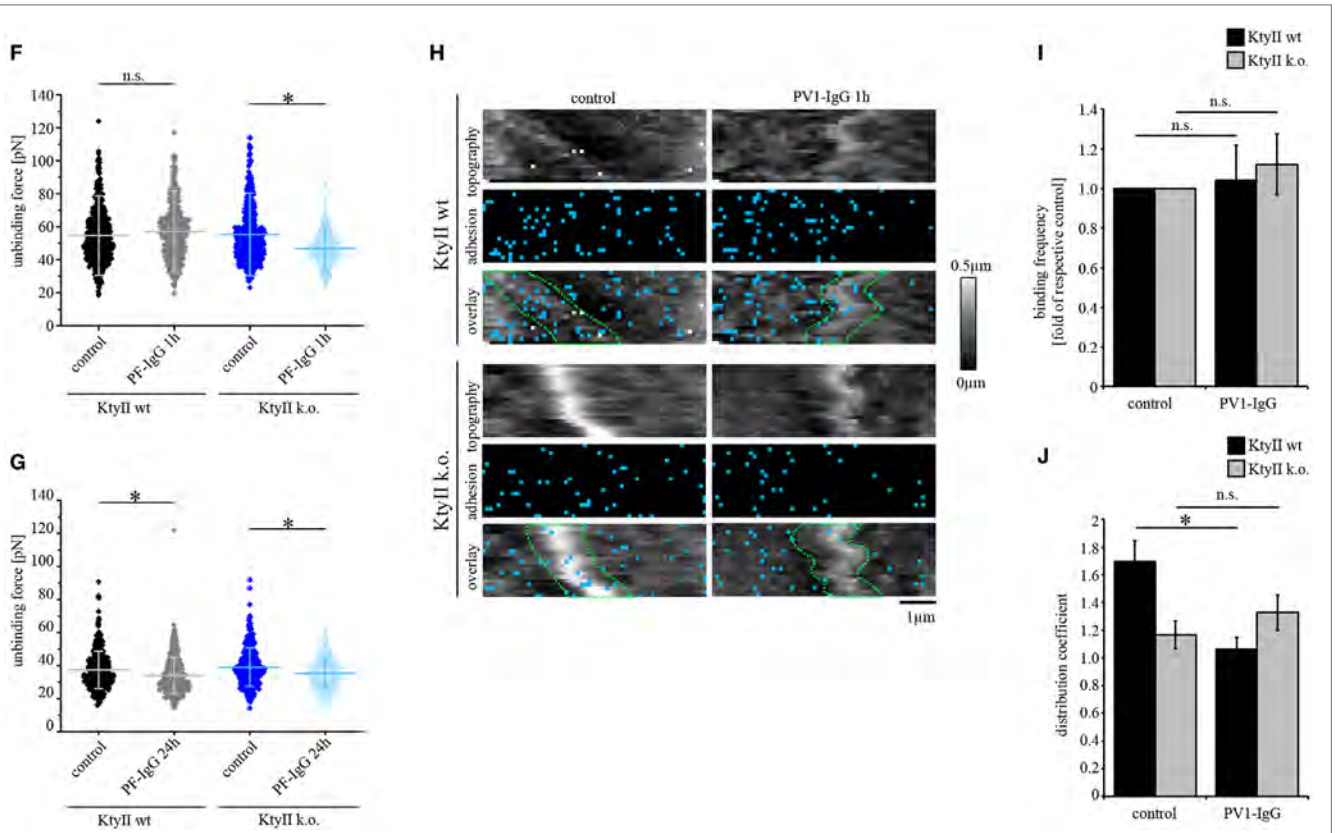

FIGURE 3 | aDsg1 antibodies (Abs) causes a keratin-dependent redistribution of Dsg1. **(A)** Atomic force microscopy (AFM) adhesion measurements using Dsg1-Fc-functionalized tips at small areas along cell borders and on the cell surface above the nucleus. Pemphigus foliaceus (PF)-IgG for 1 h and 24 h induced redistribution of Dsg1 from cell junctions in wild type. **(B)** Dsg1-binding frequencies under control condition and after 1 h of PF-IgG treatment show no direct inhibition of binding events. **(C)** 24 h of PF-IgG treatment slightly reduced Dsg1-binding frequency in KtyII wt and k.o. cells. **(D,E)** Distribution coefficient of Dsg1-binding events under control conditions and after 1 and 24 h of PF-IgG incubation. $n = 4$ from 3 independent coating procedures, 1,200 force–distance curves/adhesion map (*$p < 0.05$). **(F,G)** Unbinding forces of Dsg1-binding events under control conditions and after 1 or 24 h of PF-IgG incubation. $n = 4$ from 3 independent coating procedures, 1,200 force–distance curves/adhesion map (*$p < 0.05$). **(H)** AFM adhesion measurements using Dsg1-Fc functionalized tips in KtyII wt and k.o. cells under control conditions or after incubation with pemphigus vulgaris (PV) 1-IgG containing aDsg1 Abs for 1 h. **(I)** Dsg1-binding frequency did not change after 1 h of PV-IgG treatment in both cell lines. **(J)** Distribution of Dsg1-binding events was altered in KtyII wt but not in KtyII k.o. cells after PV1-IgG treatment. $n = 4$ from 3 independent coating procedures, 1,200 force–distance curves/adhesion map (*$p < 0.05$).

compared with cell borders whereas no difference in binding frequency was observed in KtyII k.o. (**Figures 3A,B**; Figure S2B in Supplementary Material). Interestingly, the sum of binding frequencies along cell borders and on the cell surface was similar in both lines (**Figures 3A,B**), indicating that attachment to desmosomes is crucial for the localization of Dsg1 at cell borders. To test the specificity of Dsg1-binding events, we used a monoclonal aDsg1, which was capable of blocking homophilic interactions under cell-free conditions (25, 36). Incubation of the Ab for 1 h on the cells in the absence of cantilevers revealed a significant reduction of binding frequency in both cell lines indicating that we measured specific Dsg1 interactions (Figures S2C,D in Supplementary Material).

Next, we tested whether PF-IgG can induce direct inhibition of Dsg1 binding. Interestingly, PF-IgG did not reduce Dsg1-binding frequency in both cell lines but led to a redistribution of Dsg1-binding events from cell borders in wt cells (**Figure 3A**, cell borders surrounded by dashed green lines, **Figures 3B,D**) as reflected by the distribution coefficient (**Figure 3D**). However, no shift was observed in keratin-deficient keratinocytes where Dsg1 was less localized at cell borders under resting conditions (**Figures 3A,B,D**) suggesting that keratin uncoupling may account for this phenomenon. By contrast, after PF-IgG treatment for 1 h Dsg1-binding strength was reduced in KtyII k.o. cells only (**Figure 3F**). Thus, we assumed a cascade in which redistribution of Dsg1-binding events occurs first, followed by a reduction of Dsg1-binding strength, both of which may contribute to loss of intercellular adhesion. To test this, we incubated wt and k.o. cells with PF-IgG for 24 h. Importantly, 72 h after Ca^{2+}-induction, we observed binding properties of Dsg1 similar to that after 48 h (**Figure 3A**). Incubation with PF-IgG for 24 h did not significantly alter Dsg1-binding frequency (**Figure 3C**). In agreement with the alterations described above, less Dsg1-binding events localized to cell borders after 24 h of PF-IgG treatment in wt cells (**Figure 3E**). By contrast, binding forces were reduced in both cell lines after 24 h of PF-IgG treatment (**Figure 3G**) indicating that relocalization of Dsg1 preceded alterations in Dsg1 adhesive strength.

We confirmed these results for aDsg1 Abs with PV-IgG in Dsg1 adhesion measurements. Similar to PF-IgG, incubation with PV-IgG for 1 h led to no reduction in binding frequency in both lines whereas a redistribution of Dsg1-binding events was present in wt cells only (**Figures 3H–J**). Thus, the distribution coefficient of Dsg1-binding events was comparable in wt and k.o. cells after treatment with both PF- and PV-IgG (**Figures 3D,E,J**).

p38MAPK Activation Induces Keratin Filament Retraction and Leads to Redistribution of Dsg1- and Dsg3-Binding Events

Activation of p38MAPK is a central signaling mechanism induced by pemphigus autoantibody binding and correlates with both, loss of intercellular adhesion and keratin filament retraction (13, 38, 39). Furthermore, inhibition of p38MAPK is capable of restoring intercellular adhesion and keratin filament alterations even under conditions in which direct inhibition of Dsg3 binding is present (11, 38). Furthermore, p38MAPK inhibition prevented Dsg3-binding force reduction in keratin-deficient keratinocytes which show an activation of p38MAPK already under basal conditions (25). Thus, we aimed to investigate how activation of p38MAPK affects Dsg binding properties. Since autoantibodies targeting Dsg3 induce direct inhibition and therefore do not allow characterization of binding properties by autoantibodies (8, 40), we followed a pharmacological approach more specific for p38MAPK and used anisomycin for 1 h to activate p38MAPK similar to previous studies (26). Anisomycin activated p38MAPK after 1 h of incubation both in KtyII k.o. and wt cells which was reduced by the p38MAPK

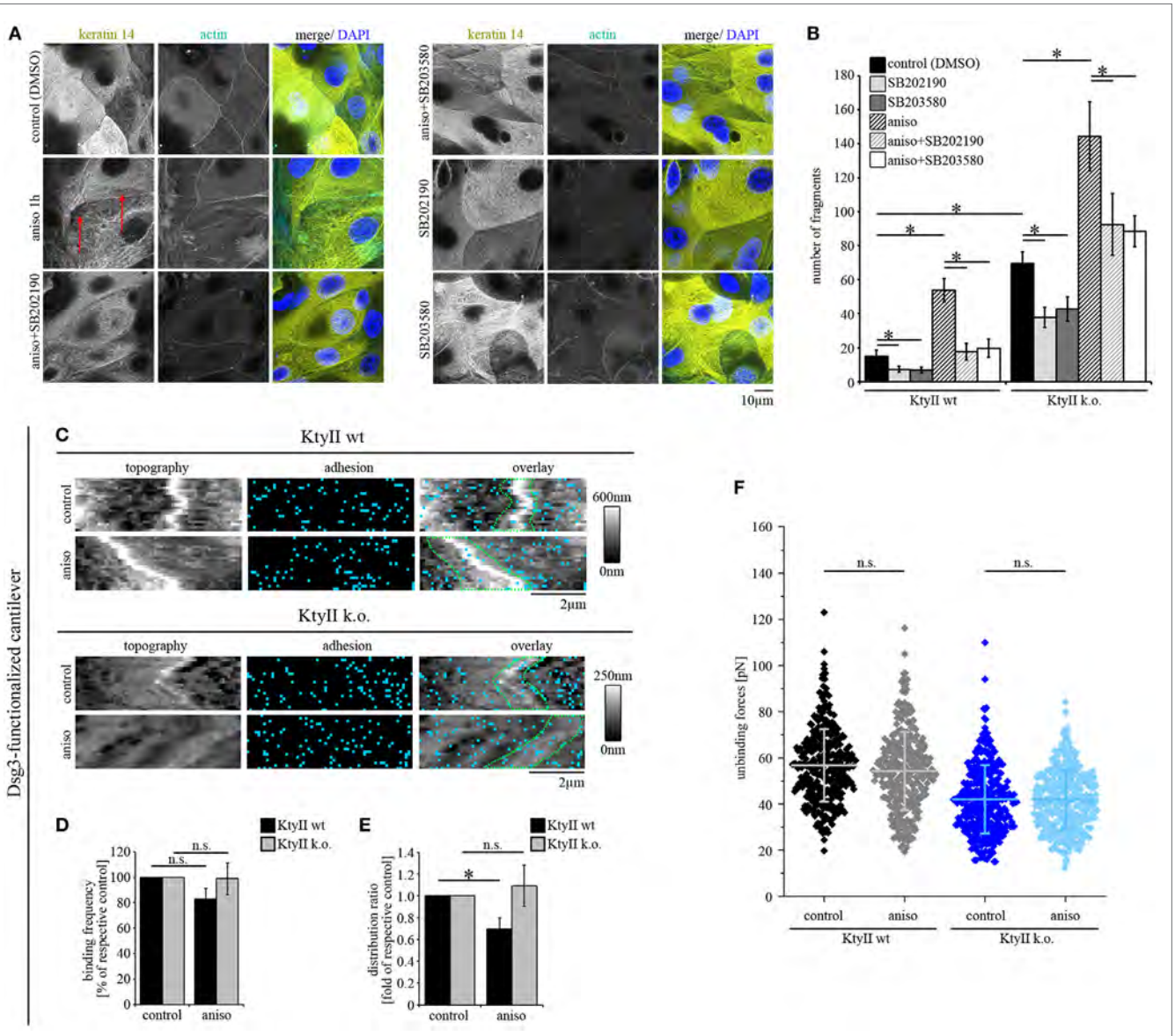

FIGURE 4 | Continued

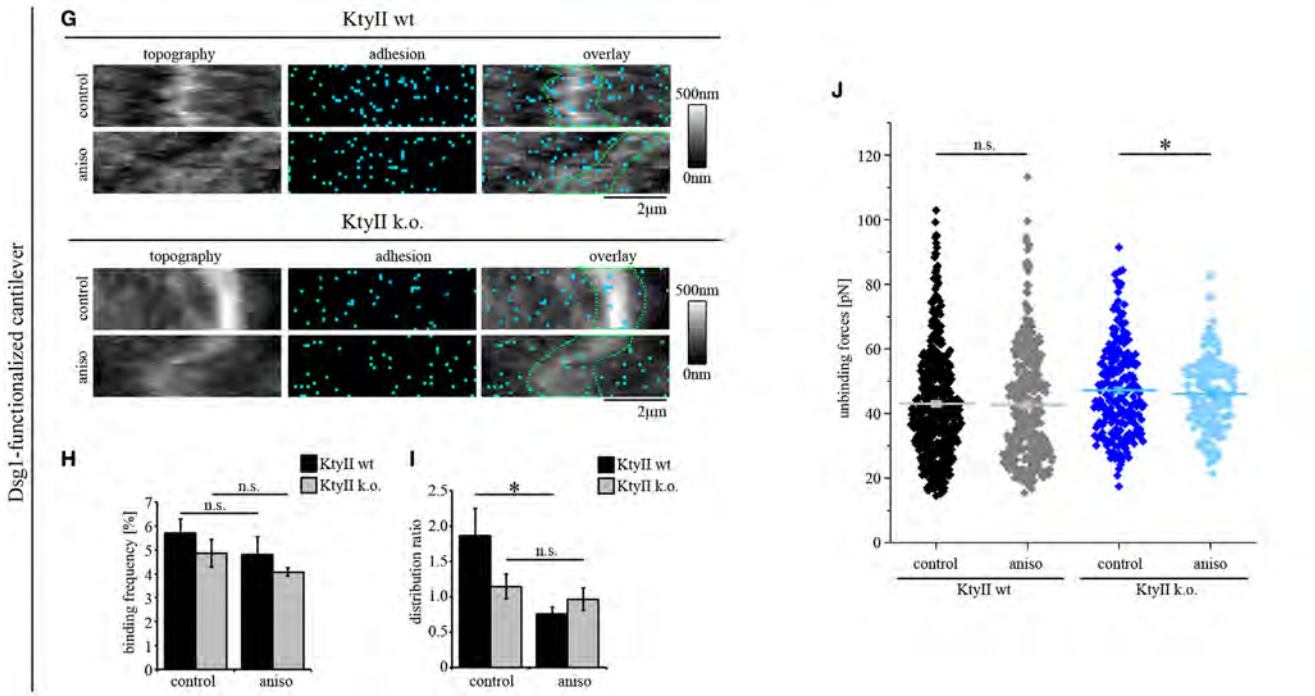

FIGURE 4 | p38MAPK activation induces redistribution of Dsg1- and Dsg3-binding events. **(A)** Immunostaining of keratin 14 and Alexa488-phalloidin staining of actin in KtyII wt after anisomycin treatment for 1 h revealed keratin filament retraction (red arrows), which was blocked by p38MAPK inhibitors SB202190 and SB203580 when preincubated for 1 h. Representative images from $n = 4$. **(B)** Dissociation assay after treatment with anisomycin alone or after preincubation with SB202190 or SB203580 in keratin-deficient keratinocytes compared with wild-type (wt) ($n > 4$, $^*p < 0.05$). **(C–E)** Dsg3 adhesion measurements show no change in binding frequency after anisomycin treatment but reveal a redistribution of binding events away from cell borders in KtyII wt but not in KtyII k.o. cells. **(F)** Unbinding forces of Dsg3 adhesion measurements were not significantly altered in both cell lines. $n = 4$ from 3 independent coating procedures, 1,200 force–distance curves/adhesion map ($^*p < 0.05$). **(G–I)** Dsg1 adhesion measurements revealed redistribution of binding events away from cell borders in KtyII wt but not in KtyII k.o. cells. **(J)** Unbinding forces of Dsg1 adhesion measurements were not significantly altered in wt but reduced in KtyII k.o. cells. $n = 4$ from 3 independent coating procedures, 1,200 force–distance curves/adhesion map ($^*p < 0.05$).

inhibitors SB202190 and SB203580 as revealed by Western blotting (Figure S3A in Supplementary Material). First, we performed immunostaining against keratin 14 to study anisomycin-mediated alterations of keratin filaments in wt cells (**Figure 4A**). Anisomycin induced keratin filament retraction and reorganization of filaments toward thick bundles similar as described earlier for experiments with pathogenic autoantibodies (**Figure 4A**, arrows, compare with **Figure 1**). To confirm that the alterations were induced by anisomycin *via* activation of p38MAPK, we used the p38MAPK inhibitors SB202190 and SB203580, which alone had no effect on the morphology of keratin filaments. Nevertheless, both inhibitors abrogated anisomycin-induced keratin filament alterations (**Figure 4A**). Next, we tested whether effects of p38MAPK on intercellular adhesion is dependent on keratin filaments using a dissociation assay. Interestingly, anisomycin induced a drastic loss of intercellular adhesion in both KtyII wt and k.o. cells (**Figure 4B**; Figure S3B in Supplementary Material), which was blocked by co-incubation with p38MAPK inhibitors SB202190 and SB203580. Interestingly, both inhibitors improved basal cell adhesion in wt and keratin-deficient keratinocytes (**Figure 4B**; Figure S3B in Supplementary Material).

Next, we performed AFM adhesion measurements for Dsg3 and Dsg1 to characterize the effects of p38MAPK activation on Dsg binding properties. Under control conditions Dsg3-binding events were distributed uniformly over the cell surface (**Figure 4C**). After incubation with anisomycin for 1 h, the overall binding frequency was not changed in both cell lines (**Figures 4C,D**), but the distribution of Dsg3 was altered in KtyII wt cells and the distribution coefficient indicated less binding events along cell borders (**Figures 4C,E**). By contrast, distribution was not changed in KtyII k.o. cells (**Figures 4C,E**). Moreover, aniosomycin did not affect Dsg3 unbinding force (**Figure 4F**). Next, we performed Dsg1 adhesion measurements. Activation of p38MAPK using anisomycin for 1 h led to a redistribution of Dsg1-binding events from the cell borders only in wt keratinocytes (**Figures 4G–I**). Furthermore, binding strength of Dsg1 interactions were slightly reduced in KtyII k.o., but not in wt cell after activation of p38MAPK using anisomycin (**Figure 4J**). Taken together these data indicate that p38MAPK regulates organization of Dsg binding events.

Effect of p38MAPK on Loss of Intercellular Adhesion Caused by Autoantibodies and Keratin Deficiency

Keratin-deficient keratinocytes show a robust activation of p38MAPK under untreated conditions (**Figure 5A**), which accounts for impaired Dsg3-binding forces on single molecule

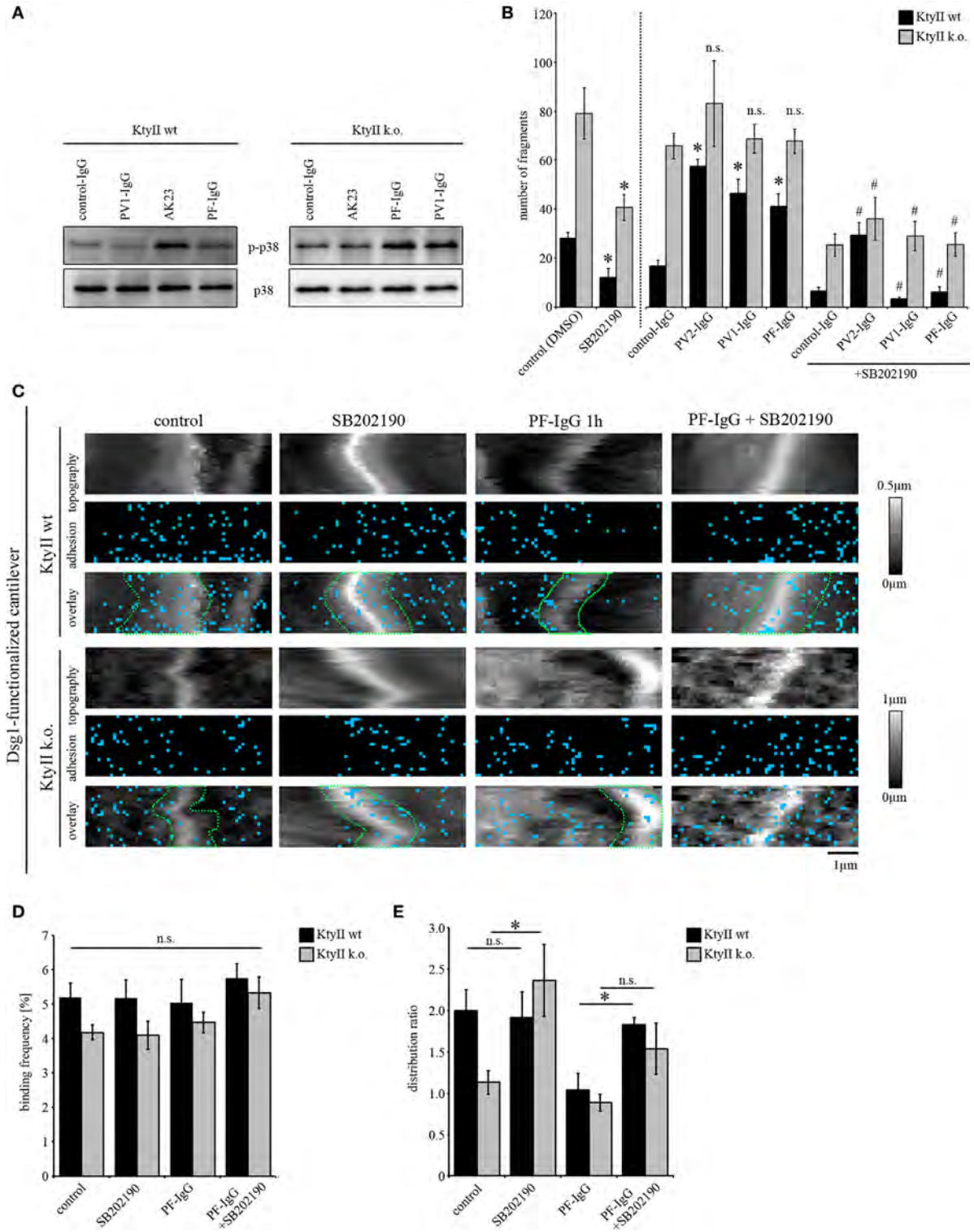

FIGURE 5 | p38MAPK inhibition restores loss of intercellular adhesion caused by autoantibodies and keratin deficiency. **(A)** Western blot showing activation of p38MAPK after treatment with AK23, pemphigus vulgaris (PV) 1-IgG and pemphigus foliaceus (PF)-IgG for 1 h. Representative of $n > 4$. **(B)** Dissociation assay of KtyII wt and k.o. cells after incubation with pathogenic autoantibodies alone or in combination with SB202190 for 24 h ($n > 5$). $^{*}p < 0.05$ vs. respective control (control panel for SB202190-treated cells and control-IgG for conditions treated with pathogenic autoantibodies); $^{\#}p < 0.05$ vs. respective condition treated with pathogenic autoantibodies alone. **(C–E)** Dsg1 adhesion measurements reveal a redistribution of binding events away from cell borders in KtyII wt but not in KtyII k.o. cells after 1 h PF-IgG. SB202190 preincubation for 1 h blocked PF-IgG-induced redistribution in KtyII wt cells and alone caused redistribution of Dsg1-binding events to cell borders in k.o. cells. Binding frequencies were not altered in all conditions. $n = 3$ from 3 independent coating procedures, 1,200 force–distance curves/adhesion map ($^{*}p < 0.05$).

level (25). On the other hand, pemphigus autoantibodies were not effective to induce additional loss of cell cohesion in KtyII k.o. cells. Thus, we investigated whether autoantibody-induced p38MAPK activation is dependent on expression of keratins. Interestingly, all autoantibodies induced an activation of p38MAPK after 1 h of incubation (**Figure 5A**) in both KtyII wt and k.o. cell lines indicating that mechanisms leading to an activation of p38MAPK after autoantibody binding are still present in keratin-deficient keratinocytes (**Figure 4A**). Thus, we wondered whether inhibition of p38MAPK would restore intercellular adhesion after autoantibody treatment in both cell lines. As efficiency of p38MAPK inhibition was similar for both inhibitors SB202190 and SB203580, we used SB202190 only for the further experiments (**Figure 5B**). As shown above, all Ab fractions caused loss of intercellular adhesion in KtyII wt but not in KtyII k.o. cells after 24 h of incubation (**Figure 5B**). SB202190 in KtyII wt cells blocked loss of cohesion after autoantibody treatment and in addition restored intercellular adhesion in keratin-deficient keratinocytes to levels of wt cells (**Figure 5B**).

Next, we probed the effect of p38MAPK inhibition on Dsg binding properties after autoantibody incubation by AFM. Since Dsg3-binding events cannot be characterized because of autoantibody-mediated direct inhibition (11) we here focused on Dsg1-binding properties. For AFM experiments, cells were treated either with SB202190 or PF-IgG alone or in a combination using a preincubation of SB202190 for 1 h followed by addition of PF-IgG for another 1 h. After treatment cells were extensively washed and reprobed using a cantilever functionalized with Dsg1. Again, PF-IgG alone caused redistribution of Dsg1-binding events away from the cell borders as outlined above whereas no change was observed in KtyII k.o. cells (**Figure 5C**). SB202190 alone did not change distribution or number of Dsg1-binding events in wt keratinocytes, but led to redistribution toward the cell borders in k.o. cells (**Figures 5C–E**). Furthermore, SB202190 abolished PF-IgG-induced redistribution in wt cells indicating that p38MAPK signaling participates in the relocalization of Dsg1 from cell junctions in pemphigus (**Figures 5C–E**). Taken together, the last set of data supports the notion that loss of cell cohesion caused by both autoantibodies and, keratin deficiency is mediated or at least modulated by p38MAPK and that relocalization of Dsg1 may be a primary mechanism to destabilize keratinocyte cohesion. Moreover, together with experiments using anisomycin described earlier, the data suggest that the targets of p38MAPK autoantibodies are to some extent not dependent on expression of keratins.

DISCUSSION

Taken together, the data presented demonstrate that keratins differentially regulate the binding properties of Dsg1 and 3, the two major antigens of pemphigus. Moreover, we observed that direct inhibition of Dsg3 but not of Dsg1-binding occurs on living keratinocytes treated with PV-IgG and PF-IgG. We found that p38MAPK signaling is crucial for loss of cell cohesion in response to both pemphigus autoantibodies as well as keratin deficiency. Importantly, PV-IgG and PF-IgG as well as direct p38MAPK activation induced redistribution of Dsg1-binding events away from cell borders in wt keratinocytes resulting in a Dsg1 distribution pattern similar to keratin-deficient keratinocytes. No temporal sequence and thus no causative relation between keratin retraction and Dsg redistribution as the underlying mechanism for loss of intercellular adhesion are provided by the data of the study. However, the data demonstrate that keratin deficiency induces activation of p38MAPK and that p38MAPK regulates Dsg distribution. This indicates that keratin uncoupling may account for loss of cell cohesion by redistribution of Dsg1. Thus, we propose the concept that as least in part loss of intercellular adhesion in pemphigus is mediated by keratin-dependent regulation of binding properties and distribution of desmosomal cadherins *via* p38MAPK.

Keratins Regulate Distribution and Binding Properties of Pemphigus Antigens Dsg1 and 3

Keratin filaments are crucial for mechanical properties and stability of keratinocytes (24, 41–43). Furthermore, they influence the turnover of desmosomal components (44) such as DP (45) and plakophilins (46, 47) and regulate desmosomal adhesion through signaling (22, 23, 48). Moreover, keratin filament retraction is a morphological hallmark in pemphigus pathogenesis and correlates with loss of intercellular adhesion, depletion of Dsgs from the cell membrane and is interconnected with several signaling pathways known to be crucial for pemphigus such as PKC and p38MAPK (11, 15, 25). Until now, no temporal sequence could be delineated for Dsg internalization and keratin retraction. Some studies indicate that keratin retraction does only occur when desmosomes are lost (17) whereas other studies implicate that Dsgs internalization and uncoupling from keratins are temporally closely related (Schlögl et al., this issue) or show that Dsgs which are not coupled to keratins get rapidly internalized after autoantibody treatment (49).

In the study presented here we show that keratins regulate the binding properties of Dsg1 and Dsg3, which are the major antigens in pemphigus (7, 50), and propose a new concept how keratins could directly influence desmosomal adhesion. It is conceivable that keratins by anchoring the desmosomal plaque modulate the binding properties of desmosomal cadherins which may account for the observation that retraction of keratin filaments from the desmosomal plaque after treatment with autoantibodies similar to deficiency of keratins impairs intercellular adhesion (13, 15, 22, 26). In line with this, it was reported that increased DP association to keratins strengthened intercellular adhesion and reduced autoantibody induces loss of intercellular adhesion in a pemphigus model (14, 45). With this respect, we observed the effect of keratins on desmosomal cadherin binding properties is different for Dsg isoforms. More Dsg3-binding events occurred in keratin-deficient keratinocytes whereas less interactions were detectable for Dsg1. For Dsg3, enhanced Dsg3 expression may reflect an insufficient compensatory mechanism because mRNA levels were elevated in keratin-deficient keratinocytes (25). Furthermore, it appears that keratins are not crucial for proper localization of Dsg3 at cell junctions (**Figure 2C**). By contrast, keratin expression was

crucial for proper localization of Dsg1 to cell junctions. As known for other desmosomal cadherins this may be explained by posttranslational modifications such as phosphorylation and palmitoylation leading to altered expression or membrane localization of the respective isoform (51, 52). However, also alterations in desmosomal turnover could account for this phenomenon (9, 23, 44). Interestingly, in pemphigus patients smaller desmosomes were reported for aDsg1 but not for aDsg3 antibodies, fitting to the observation that keratins differentially regulate Dsg distribution and binding properties (53). In addition, adhesive strength of Dsg3 but not of Dsg1 binding was altered by absence of keratins (**Figure 3**). Thus, additionally to reduced Dsg3-binding forces keratin-dependent clustering of Dsg1 may also be crucial for strong intercellular adhesion which is well established for classical cadherins (54, 55). Changes in binding forces maybe caused by missing anchorage of the molecules or by conformational changes induced by loss of keratin coupling (42, 56) or induced by signal pathways such as p38MAPK which were shown to restore Dsg3-binding force in keratin-deficient keratinocytes (25). Finally, Dsg3 depletion was accelerated in keratin-deficient keratinocytes, which could be caused by a higher molecule mobility found when keratins are missing. Beginning of depletion of Dsg3 molecules was not detectable before 1 h after incubation with PV-IgG in wt keratinocytes which is contradictory to other studies where depletion was already detectable after 30 min of autoantibody incubation (57, 58). However, these differences in our opinion can be explained by different model systems, methodical approach and several PV-IgG fractions used in the respective studies (51, 59–61). Changes in molecule mobility may depend on PKC signaling (22, 23, 25) and be accompanied with changes in clustering of the desmosomal molecules. Thus, clustering which conforms to the note that it is crucial for proper adhesive function (5, 62), could serve as an explanation for altered forces.

Mechanisms of Loss of Intercellular Adhesion in PF

Direct inhibition of Dsg interaction was thought to be the primary mechanism for loss of intercellular adhesion in pemphigus because autoantibodies predominantly target the EC1 domain (63). Indeed, direct inhibition of Dsg3 binding has been shown to occur after incubation with AK23 or with PV-IgG both under cell-free conditions as well as on the surface of living keratinocytes (8, 10, 11, 64). However, no direct inhibition of Dsg1 interactions was observed for both PV-IgG and PF-IgG, at least under cell-free conditions (8, 10, 12). Rather, signaling mechanisms were found to be crucial for loss of intercellular adhesion in response to pemphigus autoantibodies both in PV and PF (4, 7). Since several signaling pathways were found to be activated after binding of autoantibodies against Dsg1 and 3 such as p38MAPK, Erk, and Src (8, 37, 65–68), the molecular mechanism how PF-IgG impairs Dsg1 binding is not elucidated yet.

In this study, we demonstrate that keratins are crucial for proper localization of Dsg1 at cell junctions. Furthermore, we observed that PF-IgG led to a redistribution of Dsg1-binding events from cell junctions thereby inducing a distribution pattern similar to Dsg1 distribution of keratin-deficient keratinocytes. Together with the finding that PF-IgG similar to PV-IgG did not further impair keratinocyte cohesion in keratin-deficient cells, this suggests that uncoupling of keratin filaments from the desmosomal plaque maybe the underlying mechanism for both redistribution of Dsg1 and loss of keratinocyte cohesion. This is in line with an altered clustering of Dsg1 in pemphigus patients' lesions which was described using electron microscopy (17, 20). Furthermore, we observed Dsg1-binding forces were reduced after 1 h of PF-IgG treatment in keratin-deficient keratinocytes but not in wt cells whereas forces were reduced in the wt monolayers after 24 h as well, suggesting that redistribution of Dsg1 may precede reduction of Dsg1-binding forces. Thus, a possible sequence of events after PF-IgG binding is conceivable in which Dsg1 redistribution caused by uncoupling from keratins and subsequently impaired Dsg1-binding forces may account for loss of intercellular adhesion. Similarly, a sequence of distinct phases has been shown for treatment with PV-IgG before (49, 69, 70). Here, depletion of non-desmosomal Dsg3 with the first 2 h was followed by rearrangement of desmosomal components into linear arrays aligned with keratin filaments between 2 and 6 h. From these arrays, desmosomal components including Dsg3 were internalized within 6–24 h, which was paralleled by disassembly of desmosomes. Furthermore, uncoupling and redistribution of Dsg3 may also be explained by the concept of Dsg non-assembly depletion hypothesis (20). Direct inhibition of Dsg3 binding occurring as fast as within 15 min (11) may facilitate depletion of both non-desmosomal as well desmosomal Dsg3. Because within the first hour of autoantibody incubation we observed redistribution of Dsg1 from cell junctions, the data of this study are in line with the hypothesis that Dsg1 after treatment with PF-IgG is affected in comparable manner, however, in absence of direct inhibition of Dsg1 interaction.

Keratin-Dependent p38MAPK Signaling Contributes to Loss of Intercellular Adhesion in Pemphigus

Signaling pathways essentially contribute to the loss of intercellular adhesion in pemphigus (4, 7). As mentioned earlier, a broad spectrum of signaling mechanisms contribute to the loss of intercellular adhesion including PKC, Erk, Src, and p38MAPK (5). Especially, p38MAPK signaling is well characterized. Pemphigus autoantibodies induce activation of p38MAPK, and inhibition of this pathway is effective to inhibit both loss of intercellular adhesion and keratin filament alterations induced by pemphigus autoantibodies in cell culture (13, 38, 39, 71, 72). More recently, AK23- and PV-IgG-induced alterations of keratin insertion into desmosomes in human epidermis *ex vivo* as revealed by electron microscopy were shown to be dependent on p38MAPK (18). Furthermore, rapid disruption of the keratin cytoskeleton also induced p38MAPK activation whereas inhibition of p38MAPK abrogated pharmacological disruption of the keratin cytoskeleton (73–75) indicating that keratin reorganization and p38MAPK signaling are closely related.

Here, we observed that activation of p38MAPK both mediated by anisomycin as well as in response to pemphigus autoantibodies induced keratin filament retraction and led to a redistribution of

Dsg3-binding events away from the cell borders in wt but not in keratin-deficient keratinocytes. Similarly, pemphigus antibodies as well anisomycin activated p38MAPK in both wt and keratin-deficient cells, the latter of which displayed robust activation of p38MAPK under resting conditions (25). Interestingly, p38MAPK activation in response to AK23 and PV-IgG was stronger in keratin-deficient cells after 1 h when compared with wt cells. All these data indicate that keratins participate in the suppression of p38MAPK activity. By contrast, anisomycin was effective to further impair cell cohesion in keratin-deficient cells whereas AK23, PV-IgG, and PF-IgG were not. Since anisomycin-induced loss of cell adhesion was abrogated by two different inhibitors of p38MAPK, loss of adhesion appears not to be due to off-target effects. Rather, this discrepancy may be explained by the observation that anisomycin is stronger to activate p38MAPK compared with autoantibodies. Alternatively, it is possible that several p38MAPK pools are available in cells (76, 77) which when activated by anisomycin contribute to loss of cell cohesion, whereas p38MAPK activation in response to autoantibodies is restricted to the pool associated with desmosomal cadherins as shown for Dsg3 (26). Indeed, immunostaining revealed that in contrast to Src only a small portion of p38MAPK was confined to cell junctions (66). Nevertheless, inhibition of p38MAPK restored intercellular adhesion after pemphigus autoantibody treatment in wt and k.o. cells and rescued keratinocyte cohesion in keratin-deficient cells indicating that p38MAPK signaling is crucial for intercellular adhesion. This is in line with former studies which show that keratin filament alteration correlate with loss of intercellular adhesion in pemphigus (11, 13, 37). Moreover, these data demonstrate that the targets of p38MAPK are in part keratin dependent, as indicated by anisomycin-mediated keratin retraction which is similarly observed after treatment with autoantibodies. In addition, given the efficiency of p38MAPK inhibitors on cell cohesion in keratin-deficient cells, keratin-independent targets must also be involved. However, it has to be noted that no temporal sequence can be ascertained by the data provided. Taken together, the data show that p38MAPK activation in response to pemphigus autoantibodies is regulated *via* keratin filaments and is critical for loss of cell adhesion. This is at least in part mediated on the level of redistribution of Dsg1 and Dsg3 molecules from cell junctions.

ETHICS STATEMENT

The human sera used in this study were collected and used in accordance with the recommendations of ethic committee of University of Lübeck, AZ 12-178. Name of the indicated project: Autoantikörperreaktivität und Pathophysiologie bei blasenbildenden Autoimmundermatosen (Pemphigoid und Pemphigus).

AUTHOR CONTRIBUTIONS

FV, EW, MF, and MR performed experiments. FV, MR, and FB analyzed data. FV, TM, and VS discussed data and interpreted results. FV and JW designed the study and wrote the manuscript.

ACKNOWLEDGMENTS

We thank Andrea Wehmeyer, Sabine Mühlsimer, Kilian Skowranek, and Linda Jakobi for excellent technical assistance, Enno Schmidt (Department of Dermatology, University of Lübeck) for providing patients sera, and JPK Instruments for helpful discussion on the AFM data.

FUNDING

Supported by Friedrich-Baur-Stiftung 01/16 to FV and DFG SPP1782 and DFG FOR 2497 to JW.

SUPPLEMENTARY MATERIAL

The Supplementary Material for this article can be found online at https://www.frontiersin.org/articles/10.3389/fimmu.2018.00528/full#supplementary-material.

FIGURE S1 | Distribution coefficient to determine localization of desmoglein binding events. **(A)** For calculation of intensity coefficient areas in close proximity to the cell borders (red rectangle) and above the nuclei (green rectangle) were chosen, intensity was measured, and a coefficient was calculated in which values <1 indicate less keratin fluorescence signal at cell border areas, thus suggesting keratin retraction under these conditions. **(B)** For calculation of distribution coefficient, areas along the cell borders (green area) and on the cell surface (red area) were marked, and respective binding frequencies were defined by calculating a ratio of number of binding events per area. Distribution coefficient was calculated as a ratio from these. Binding frequencies in which values >1 announce increased clusters of the molecules along the cell borders. **(C)** Immunostaining of KtyII wt and KtyII k.o. cells show dense filamental structures throughout the whole cell in wild-type and confirm knockout in KtyII k.o. cells. Representative of $n = 4$.

FIGURE S2 | Dsg1-binding events in KtyII wt and k.o. cells. **(A)** Topography overview images of KtyII wt and k.o. cells. Small areas along the cell borders (green rectangles, 6 μm × 2 μm) and cell surfaces above the nucleus (red rectangles, 4 μm × 2 μm) were chosen for adhesion mapping presented in **Figure 3**. **(B)** Dsg1-binding frequency in KtyII wt and k.o. cells at cell border and cell surface areas under control conditions and after treatment with pemphigus foliaceus (PF)-IgG for 1 h. $n = 3$ from 3 independent coating procedures, 1,200 force–distance curves/adhesion map (*$p < 0.05$). **(C,D)** Dsg1 adhesion measurements at cell borders in KtyII wt and k.o. cells under control conditions and after treatment with aDsg1 monoclonal antibody (mAb) (p124). $n = 3$ from 3 independent coating procedures, 1,200 force–distance curves/adhesion map (*$p < 0.05$). **(E)** Immunostaining of keratin 14 in KtyII wt after anisomycin treatment in higher magnification for 1 h revealed keratin filament retraction. Representative images from $n = 4$.

FIGURE S3 | p38MAPK signaling is crucial for intercellular adhesion in KtyII wt and k.o. cells. **(A)** Western blot using SB202190 and SB203580 for 2 h to inhibit and anisomycin for 1 h to activate p38MAPK. KtyII k.o. cells show activation of p38MAPK under basal conditions compared with wild-type (wt) cells. Anisomycin drastically increased p38MAPK activation, which was partially blocked by SB202190 and SB203580. For co-incubation experiments, SB202190 and SB203580 were preincubated for 1 h before anisomycin was added for 1 h. **(B)** Pictures of dissociation assay from **Figure 4** confirmed impaired adhesion in keratin-deficient keratinocytes compared with wt. Activation of p38MAPK with anisomycin reduced intercellular adhesion whereas SB202190 or SB203580 improved intercellular adhesion in both cell lines ($n > 4$, *$p < 0.05$).

REFERENCES

1. Delva E, Tucker DK, Kowalczyk AP. The desmosome. *Cold Spring Harb Perspect Biol* (2009) 1(2):a002543. doi:10.1101/cshperspect.a002543
2. Garrod DR, Merritt AJ, Nie Z. Desmosomal adhesion: structural basis, molecular mechanism and regulation (review). *Mol Membr Biol* (2002) 19(2):81–94. doi:10.1080/09687680210132476
3. Waschke J. The desmosome and pemphigus. *Histochem Cell Biol* (2008) 130(1):21–54. doi:10.1007/s00418-008-0420-0
4. Kitajima Y. New insights into desmosome regulation and pemphigus blistering as a desmosome-remodeling disease. *Kaohsiung J Med Sci* (2013) 29(1):1–13. doi:10.1016/j.kjms.2012.08.001
5. Waschke J, Spindler V. Desmosomes and extradesmosomal adhesive signaling contacts in pemphigus. *Med Res Rev* (2014) 34(6):1127–45. doi:10.1002/med.21310
6. Kneisel A, Hertl M. Autoimmune bullous skin diseases. Part 1: clinical manifestations. *J Dtsch Dermatol Ges* (2011) 9(10):844–56; quiz 57. doi:10.1111/j.1610-0387.2011.07793.x
7. Spindler V, Eming R, Schmidt E, Amagai M, Grando S, Jonkman MF, et al. Mechanisms causing loss of keratinocyte cohesion in pemphigus. *J Invest Dermatol* (2018) 138(1):32–7. doi:10.1016/j.jid.2017.06.022
8. Walter E, Vielmuth F, Rotkopf L, Sardy M, Horvath ON, Goebeler M, et al. Different signaling patterns contribute to loss of keratinocyte cohesion dependent on autoantibody profile in pemphigus. *Sci Rep* (2017) 7(1):3579. doi:10.1038/s41598-017-03697-7
9. Spindler V, Waschke J. Pemphigus—a disease of desmosome dysfunction caused by multiple mechanisms. *Front Immunol* (2018) 9:136. doi:10.3389/fimmu.2018.00136
10. Heupel WM, Zillikens D, Drenckhahn D, Waschke J. Pemphigus vulgaris IgG directly inhibit desmoglein 3-mediated transinteraction. *J Immunol* (2008) 181(3):1825–34. doi:10.4049/jimmunol.181.3.1825
11. Vielmuth F, Waschke J, Spindler V. Loss of desmoglein binding is not sufficient for keratinocyte dissociation in pemphigus. *J Invest Dermatol* (2015) 135(12):3068–77. doi:10.1038/jid.2015.324
12. Waschke J, Bruggeman P, Baumgartner W, Zillikens D, Drenckhahn D. Pemphigus foliaceus IgG causes dissociation of desmoglein 1-containing junctions without blocking desmoglein 1 transinteraction. *J Clin Invest* (2005) 115(11):3157–65. doi:10.1172/JCI23475
13. Berkowitz P, Hu P, Liu Z, Diaz LA, Enghild JJ, Chua MP, et al. Desmosome signaling. Inhibition of p38MAPK prevents pemphigus vulgaris IgG-induced cytoskeleton reorganization. *J Biol Chem* (2005) 280(25):23778–84. doi:10.1074/jbc.M501365200
14. Dehner C, Rotzer V, Waschke J, Spindler V. A desmoplakin point mutation with enhanced keratin association ameliorates pemphigus vulgaris autoantibody-mediated loss of cell cohesion. *Am J Pathol* (2014) 184(9):2528–36. doi:10.1016/j.ajpath.2014.05.016
15. Muller EJ, Hunziker T, Suter MM. Keratin intermediate filament retraction is linked to plakoglobin-dependent signaling in pemphigus vulgaris. *J Am Acad Dermatol* (2007) 56(5):890–1; author reply 1–2. doi:10.1016/j.jaad.2006.10.989
16. Caldelari R, de Bruin A, Baumann D, Suter MM, Bierkamp C, Balmer V, et al. A central role for the armadillo protein plakoglobin in the autoimmune disease pemphigus vulgaris. *J Cell Biol* (2001) 153(4):823–34. doi:10.1083/jcb.153.4.823
17. Sokol E, Kramer D, Diercks GFH, Kuipers J, Jonkman MF, Pas HH, et al. Large-scale electron microscopy maps of patient skin and mucosa provide insight into pathogenesis of blistering diseases. *J Invest Dermatol* (2015) 135(7):1763–70. doi:10.1038/jid.2015.109
18. Egu DT, Walter E, Spindler V, Waschke J. Inhibition of p38MAPK signaling prevents epidermal blistering and alterations of desmosome structure induced by pemphigus autoantibodies in human epidermis. *Br J Dermatol* (2017) 177(6):1612–8. doi:10.1111/bjd.15721
19. Spindler V, Endlich A, Hartlieb E, Vielmuth F, Schmidt E, Waschke J. The extent of desmoglein 3 depletion in pemphigus vulgaris is dependent on Ca(2+)-induced differentiation: a role in suprabasal epidermal skin splitting? *Am J Pathol* (2011) 179(4):1905–16. doi:10.1016/j.ajpath.2011.06.043
20. Oktarina DA, van der Wier G, Diercks GF, Jonkman MF, Pas HH. IgG-induced clustering of desmogleins 1 and 3 in skin of patients with pemphigus fits with the desmoglein nonassembly depletion hypothesis. *Br J Dermatol* (2011) 165(3):552–62. doi:10.1111/j.1365-2133.2011.10463.x
21. Wilgram GF, Caulfield JB, Lever WF. An electron microscopic study of acantholysis in pemphigus vulgaris. *J Invest Dermatol* (1961) 36:373–82. doi:10.1038/jid.1961.58
22. Kroger C, Loschke F, Schwarz N, Windoffer R, Leube RE, Magin TM. Keratins control intercellular adhesion involving PKC-alpha-mediated desmoplakin phosphorylation. *J Cell Biol* (2013) 201(5):681–92. doi:10.1083/jcb.201208162
23. Loschke F, Homberg M, Magin TM. Keratin isotypes control desmosome stability and dynamics through PKCalpha. *J Invest Dermatol* (2015) 136:202–13. doi:10.1038/jid.2015.403
24. Ramms L, Fabris G, Windoffer R, Schwarz N, Springer R, Zhou C, et al. Keratins as the main component for the mechanical integrity of keratinocytes. *Proc Natl Acad Sci U S A* (2013) 110(46):18513–8. doi:10.1073/pnas.1313491110
25. Vielmuth F, Wanuske MT, Radeva MY, Hiermaier M, Kugelmann D, Walter E, et al. Keratins regulate the adhesive properties of desmosomal cadherins through signaling. *J Invest Dermatol* (2018) 138(1):121–31. doi:10.1016/j.jid.2017.08.033
26. Spindler V, Rotzer V, Dehner C, Kempf B, Gliem M, Radeva M, et al. Peptide-mediated desmoglein 3 crosslinking prevents pemphigus vulgaris autoantibody-induced skin blistering. *J Clin Invest* (2013) 123(2):800–11. doi:10.1172/JCI60139
27. Hartlieb E, Kempf B, Partilla M, Vigh B, Spindler V, Waschke J. Desmoglein 2 is less important than desmoglein 3 for keratinocyte cohesion. *PLoS One* (2013) 8(1):e53739. doi:10.1371/journal.pone.0053739
28. Rotzer V, Breit A, Waschke J, Spindler V. Adducin is required for desmosomal cohesion in keratinocytes. *J Biol Chem* (2014) 289(21):14925–40. doi:10.1074/jbc.M113.527127
29. Vielmuth F, Hartlieb E, Kugelmann D, Waschke J, Spindler V. Atomic force microscopy identifies regions of distinct desmoglein 3 adhesive properties on living keratinocytes. *Nanomedicine* (2015) 11(3):511–20. doi:10.1016/j.nano.2014.10.006
30. Ebner A, Wildling L, Kamruzzahan AS, Rankl C, Wruss J, Hahn CD, et al. A new, simple method for linking of antibodies to atomic force microscopy tips. *Bioconjug Chem* (2007) 18(4):1176–84. doi:10.1021/bc070030s
31. Carvalho FA, Santos NC. Atomic force microscopy-based force spectroscopy – biological and biomedical applications. *IUBMB Life* (2012) 64(6):465–72. doi:10.1002/iub.1037
32. Schinner C, Vielmuth F, Rotzer V, Hiermaier M, Radeva MY, Co TK, et al. Adrenergic signaling strengthens cardiac myocyte cohesion. *Circ Res* (2017) 120(8):1305–17. doi:10.1161/CIRCRESAHA.116.309631
33. Tsunoda K, Ota T, Aoki M, Yamada T, Nagai T, Nakagawa T, et al. Induction of pemphigus phenotype by a mouse monoclonal antibody against the amino-terminal adhesive interface of desmoglein 3. *J Immunol* (2003) 170(4):2170–8. doi:10.4049/jimmunol.170.4.2170
34. Nie Z, Merritt A, Rouhi-Parkouhi M, Tabernero L, Garrod D. Membrane-impermeable cross-linking provides evidence for homophilic, isoform-specific binding of desmosomal cadherins in epithelial cells. *J Biol Chem* (2011) 286(3):2143–54. doi:10.1074/jbc.M110.192245
35. Harrison OJ, Brasch J, Lasso G, Katsamba PS, Ahlsen G, Honig B, et al. Structural basis of adhesive binding by desmocollins and desmogleins. *Proc Natl Acad Sci U S A* (2016) 113(26):7160–5. doi:10.1073/pnas.1606272113
36. Spindler V, Heupel WM, Efthymiadis A, Schmidt E, Eming R, Rankl C, et al. Desmocollin 3-mediated binding is crucial for keratinocyte cohesion and is impaired in pemphigus. *J Biol Chem* (2009) 284(44):30556–64. doi:10.1074/jbc.M109.024810
37. Jolly PS, Berkowitz P, Bektas M, Lee HE, Chua M, Diaz LA, et al. p38MAPK signaling and desmoglein-3 internalization are linked events in pemphigus acantholysis. *J Biol Chem* (2010) 285(12):8936–41. doi:10.1074/jbc.M109.087999
38. Berkowitz P, Chua M, Liu Z, Diaz LA, Rubenstein DS. Autoantibodies in the autoimmune disease pemphigus foliaceus induce blistering via p38 mitogen-activated protein kinase-dependent signaling in the skin. *Am J Pathol* (2008) 173(6):1628–36. doi:10.2353/ajpath.2008.080391
39. Berkowitz P, Diaz LA, Hall RP, Rubenstein DS. Induction of p38MAPK and HSP27 phosphorylation in pemphigus patient skin. *J Invest Dermatol* (2008) 128(3):738–40. doi:10.1038/sj.jid.5701080

40. Spindler V, Waschke J. Desmosomal cadherins and signaling: lessons from autoimmune disease. *Cell Commun Adhes* (2014) 21(1):77–84. doi:10.3109/15419061.2013.877000
41. Osmani N, Labouesse M. Remodeling of keratin-coupled cell adhesion complexes. *Curr Opin Cell Biol* (2014) 32C:30–8. doi:10.1016/j.ceb.2014.10.004
42. Loschke F, Seltmann K, Bouameur JE, Magin TM. Regulation of keratin network organization. *Curr Opin Cell Biol* (2015) 32:56–64. doi:10.1016/j.ceb.2014.12.006
43. Seltmann K, Fritsch AW, Kas JA, Magin TM. Keratins significantly contribute to cell stiffness and impact invasive behavior. *Proc Natl Acad Sci U S A* (2013) 110(46):18507–12. doi:10.1073/pnas.1310493110
44. Nekrasova O, Green KJ. Desmosome assembly and dynamics. *Trends Cell Biol* (2013) 23(11):537–46. doi:10.1016/j.tcb.2013.06.004
45. Godsel LM, Hsieh SN, Amargo EV, Bass AE, Pascoe-McGillicuddy LT, Huen AC, et al. Desmoplakin assembly dynamics in four dimensions: multiple phases differentially regulated by intermediate filaments and actin. *J Cell Biol* (2005) 171(6):1045–59. doi:10.1083/jcb.200510038
46. Olivry T, Linder KE, Wang P, Bizikova P, Bernstein JA, Dunston SM, et al. Deficient plakophilin-1 expression due to a mutation in PKP1 causes ectodermal dysplasia-skin fragility syndrome in Chesapeake Bay retriever dogs. *PLoS One* (2012) 7(2):e32072. doi:10.1371/journal.pone.0032072
47. McGrath JA, McMillan JR, Shemanko CS, Runswick SK, Leigh IM, Lane EB, et al. Mutations in the plakophilin 1 gene result in ectodermal dysplasia/skin fragility syndrome. *Nat Genet* (1997) 17(2):240–4. doi:10.1038/ng1097-240
48. Bar J, Kumar V, Roth W, Schwarz N, Richter M, Leube RE, et al. Skin fragility and impaired desmosomal adhesion in mice lacking all keratins. *J Invest Dermatol* (2014) 134(4):1012–22. doi:10.1038/jid.2013.416
49. Calkins CC, Setzer SV, Jennings JM, Summers S, Tsunoda K, Amagai M, et al. Desmoglein endocytosis and desmosome disassembly are coordinated responses to pemphigus autoantibodies. *J Biol Chem* (2006) 281(11):7623–34. doi:10.1074/jbc.M512447200
50. Kitajima Y. 150 anniversary series: desmosomes and autoimmune disease, perspective of dynamic desmosome remodeling and its impairments in pemphigus. *Cell Commun Adhes* (2014) 21(6):269–80. doi:10.3109/15419061.2014.943397
51. Aoyama Y, Owada MK, Kitajima Y. A pathogenic autoantibody, pemphigus vulgaris-IgG, induces phosphorylation of desmoglein 3, and its dissociation from plakoglobin in cultured keratinocytes. *Eur J Immunol* (1999) 29(7):2233–40. doi:10.1002/(SICI)1521-4141(199907)29:07<2233::AID-IMMU2233>3.0.CO;2-4
52. Roberts BJ, Johnson KE, McGuinn KP, Saowapa J, Svoboda RA, Mahoney MG, et al. Palmitoylation of plakophilin is required for desmosome assembly. *J Cell Sci* (2014) 127(Pt 17):3782–93. doi:10.1242/jcs.149849
53. van der Wier G, Pas HH, Kramer D, Diercks GFH, Jonkman MF. Smaller desmosomes are seen in the skin of pemphigus patients with anti-desmoglein 1 antibodies but not in patients with anti-desmoglein 3 antibodies. *J Invest Dermatol* (2014) 134(8):2287–90. doi:10.1038/jid.2014.140
54. Brasch J, Harrison OJ, Honig B, Shapiro L. Thinking outside the cell: how cadherins drive adhesion. *Trends Cell Biol* (2012) 22(6):299–310. doi:10.1016/j.tcb.2012.03.004
55. Yap AS, Brieher WM, Pruschy M, Gumbiner BM. Lateral clustering of the adhesive ectodomain: a fundamental determinant of cadherin function. *Curr Biol* (1997) 7(5):308–15. doi:10.1016/S0960-9822(06)00154-0
56. Homberg M, Magin TM. Beyond expectations: novel insights into epidermal keratin function and regulation. *Int Rev Cell Mol Biol* (2014) 311:265–306. doi:10.1016/B978-0-12-800179-0.00007-6
57. Aoyama Y, Kitajima Y. Pemphigus vulgaris-IgG causes a rapid depletion of desmoglein 3 (Dsg3) from the Triton X-100 soluble pools, leading to the formation of Dsg3-depleted desmosomes in a human squamous carcinoma cell line, DJM-1 cells. *J Invest Dermatol* (1999) 112(1):67–71. doi:10.1046/j.1523-1747.1999.00463.x
58. Sato M, Aoyama Y, Kitajima Y. Assembly pathway of desmoglein 3 to desmosomes and its perturbation by pemphigus vulgaris-IgG in cultured keratinocytes, as revealed by time-lapsed labeling immunoelectron microscopy. *Lab Invest* (2000) 80(10):1583–92. doi:10.1038/labinvest.3780168
59. Saleh MA, Hashimoto R, Kase Y, Amagai M, Yamagami J. Low pathogenicity of anti-desmoglein 3 immunoglobulin G autoantibodies contributes to the atypical clinical phenotypes in pemphigus. *J Dermatol* (2015) 42(7):685–9. doi:10.1111/1346-8138.12888
60. Lo AS, Mao X, Mukherjee EM, Ellebrecht CT, Yu X, Posner MR, et al. Pathogenicity and epitope characteristics do not differ in IgG subclass-switched anti-desmoglein 3 IgG1 and IgG4 autoantibodies in pemphigus vulgaris. *PLoS One* (2016) 11(6):e0156800. doi:10.1371/journal.pone.0156800
61. Ishii K, Amagai M. In vitro pathogenicity assay for anti-desmoglein autoantibodies in pemphigus. *Methods Mol Biol* (2013) 961:219–25. doi:10.1007/978-1-62703-227-8_13
62. Stahley SN, Warren MF, Feldman RJ, Swerlick RA, Mattheyses AL, Kowalczyk AP. Super-resolution microscopy reveals altered desmosomal protein organization in tissue from patients with pemphigus vulgaris. *J Invest Dermatol* (2016) 136(1):59–66. doi:10.1038/JID.2015.353
63. Amagai M, Ahmed AR, Kitajima Y, Bystryn JC, Milner Y, Gniadecki R, et al. Are desmoglein autoantibodies essential for the immunopathogenesis of pemphigus vulgaris, or just "witnesses of disease"? *Exp Dermatol* (2006) 15(10):815–31. doi:10.1111/j.1600-0625.2006.00499_1.x
64. Heupel WM, Muller T, Efthymiadis A, Schmidt E, Drenckhahn D, Waschke J. Peptides targeting the desmoglein 3 adhesive interface prevent autoantibody-induced acantholysis in pemphigus. *J Biol Chem* (2009) 284(13):8589–95. doi:10.1074/jbc.M808813200
65. Rotzer V, Hartlieb E, Winkler J, Walter E, Schlipp A, Sardy M, et al. Desmoglein 3-dependent signaling regulates keratinocyte migration and wound healing. *J Invest Dermatol* (2016) 136(1):301–10. doi:10.1038/jid.2015.380
66. Rotzer V, Hartlieb E, Vielmuth F, Gliem M, Spindler V, Waschke J. E-cadherin and Src associate with extradesmosomal Dsg3 and modulate desmosome assembly and adhesion. *Cell Mol Life Sci* (2015) 72(24):4885–97. doi:10.1007/s00018-015-1977-0
67. Chernyavsky AI, Arredondo J, Kitajima Y, Sato-Nagai M, Grando SA. Desmoglein versus non-desmoglein signaling in pemphigus acantholysis: characterization of novel signaling pathways downstream of pemphigus vulgaris antigens. *J Biol Chem* (2007) 282(18):13804–12. doi:10.1074/jbc.M611365200
68. Tsang SM, Liu L, Teh MT, Wheeler A, Grose R, Hart IR, et al. Desmoglein 3, via an interaction with E-cadherin, is associated with activation of Src. *PLoS One* (2010) 5(12):e14211. doi:10.1371/journal.pone.0014211
69. Jennings JM, Tucker DK, Kottke MD, Saito M, Delva E, Hanakawa Y, et al. Desmosome disassembly in response to pemphigus vulgaris IgG occurs in distinct phases and can be reversed by expression of exogenous Dsg3. *J Invest Dermatol* (2011) 131(3):706–18. doi:10.1038/jid.2010.389
70. Yamamoto Y, Aoyama Y, Shu E, Tsunoda K, Amagai M, Kitajima Y. Anti-desmoglein 3 (Dsg3) monoclonal antibodies deplete desmosomes of Dsg3 and differ in their Dsg3-depleting activities related to pathogenicity. *J Biol Chem* (2007) 282(24):17866–76. doi:10.1074/jbc.M607963200
71. Berkowitz P, Hu P, Warren S, Liu Z, Diaz LA, Rubenstein DS. p38MAPK inhibition prevents disease in pemphigus vulgaris mice. *Proc Natl Acad Sci U S A* (2006) 103(34):12855–60. doi:10.1073/pnas.0602973103
72. Bektas M, Jolly PS, Berkowitz P, Amagai M, Rubenstein DS. A pathophysiologic role for epidermal growth factor receptor in pemphigus acantholysis. *J Biol Chem* (2013) 288(13):9447–56. doi:10.1074/jbc.M112.438010
73. Strnad P, Windoffer R, Leube RE. Induction of rapid and reversible cytokeratin filament network remodeling by inhibition of tyrosine phosphatases. *J Cell Sci* (2002) 115(Pt 21):4133–48. doi:10.1242/jcs.00096
74. Strnad P, Windoffer R, Leube RE. Light-induced resistance of the keratin network to the filament-disrupting tyrosine phosphatase inhibitor orthovanadate. *J Invest Dermatol* (2003) 120(2):198–203. doi:10.1046/j.1523-1747.2003.12038.x
75. Woll S, Windoffer R, Leube RE. p38 MAPK-dependent shaping of the keratin cytoskeleton in cultured cells. *J Cell Biol* (2007) 177(5):795–807. doi:10.1083/jcb.200703174
76. Mavropoulos A, Orfanidou T, Liaskos C, Smyk DS, Billinis C, Blank M, et al. p38 mitogen-activated protein kinase (p38 MAPK)-mediated autoimmunity: lessons to learn from ANCA vasculitis and pemphigus vulgaris. *Autoimmun Rev* (2013) 12(5):580–90. doi:10.1016/j.autrev.2012.10.019

77. Mavropoulos A, Orfanidou T, Liaskos C, Smyk DS, Spyrou V, Sakkas LI, et al. p38 MAPK signaling in pemphigus: implications for skin autoimmunity. *Autoimmune Dis* (2013) 2013:728529. doi:10.1155/2013/728529

Conflict of Interest Statement: The authors declare that the research was conducted in the absence of any commercial or financial relationships that could be construed as a potential conflict of interest.

frontiers in Immunology

ORIGINAL RESEARCH
published: 19 March 2018
doi: 10.3389/fimmu.2018.00559

Complement Factor H Inhibits Anti-Neutrophil Cytoplasmic Autoantibody-Induced Neutrophil Activation by Interacting With Neutrophils

Su-Fang Chen[1,2,3], Feng-Mei Wang[1,2,3], Zhi-Ying Li[1,2,3], Feng Yu[1,2,3], Min Chen[1,2,3] and Ming-Hui Zhao[1,2,3,4]*

[1] Renal Division, Department of Medicine, Peking University First Hospital, Institute of Nephrology, Peking University, Beijing, China, [2] Key Laboratory of Renal Disease, Ministry of Health of China, Beijing, China, [3] Key Laboratory of Chronic Kidney Disease Prevention and Treatment, Peking University, Ministry of Education, Beijing, China, [4] Peking-Tsinghua Center for Life Sciences, Beijing, China

OPEN ACCESS

Edited by:
Cordula M. Stover, University of Leicester, United Kingdom

Reviewed by:
Yebin Zhou, AbbVie, United States
Lubka T. Roumenina, INSERM UMRS 1138, Cordeliers Research Center, France

***Correspondence:**
Min Chen
chenmin74@sina.com

Specialty section:
This article was submitted to Molecular Innate Immunity, a section of the journal Frontiers in Immunology

Received: *19 January 2018*
Accepted: *06 March 2018*
Published: *19 March 2018*

Citation:
Chen S-F, Wang F-M, Li Z-Y, Yu F, Chen M and Zhao M-H (2018) Complement Factor H Inhibits Anti-Neutrophil Cytoplasmic Autoantibody-Induced Neutrophil Activation by Interacting With Neutrophils. Front. Immunol. 9:559. doi: 10.3389/fimmu.2018.00559

Our previous study demonstrated that plasma levels of complement factor H (FH) were inversely associated with the disease activity of patients with anti-neutrophil cytoplasmic autoantibody (ANCA)-associated vasculitis (AAV). In addition to serving as an inhibitor of the alternative complement pathway, there is increasing evidence demonstrating direct regulatory roles of FH on several cell types. Here, we investigated the role of FH in the process of ANCA-mediated activation of neutrophils and neutrophil–endothelium interaction. We demonstrated that FH bound to neutrophils by immunostaining and flow cytometry. Interestingly, ANCA-induced activation of neutrophils, including respiratory burst and degranulation, was inhibited by FH. Although FH enhanced neutrophils adhesion and migration toward human glomerular endothelial cells (hGEnCs), it inhibited ANCA-induced activation of neutrophils in the coculture system of hGEnCs and neutrophils. Moreover, the activation and injury of hGEnCs, reflected by the level of endothelin-1 in the supernatant of cocultures, was markedly reduced by FH. However, we found that FH from patients with active AAV exhibited a deficient ability in binding neutrophils and inhibiting ANCA-induced neutrophil activation in fluid phase and on endothelial cells, as compared with that from healthy controls. Therefore, our findings indicate a novel role of FH in inhibiting ANCA-induced neutrophil activation and protecting against glomerular endothelial injury. However, FH from patients with active AAV are deficient in their ability to bind neutrophils and inhibit neutrophil activation by ANCA. It further extends the current understanding of the pathogenesis of AAV, thus providing potential clues for intervention strategies.

Keywords: factor H, neutrophils, activation, anti-neutrophil cytoplasmic autoantibody, vasculitis

INTRODUCTION

Anti-neutrophil cytoplasmic autoantibody (ANCA)-associated vasculitis (AAV) is a group of potentially life-threatening autoimmune diseases, characterized by pauci-immune necrotizing vasculitis of small vessels and circulating autoantibodies targeting the cytoplasmic constituents of neutrophils, especially proteinase 3 (PR3) and myeloperoxidase (MPO) (1). It includes granulomatosis with

polyangiitis, microscopic polyangiitis, and eosinophilic granulomatosis with polyangiits (2). ANCA-induced neutrophil activation is crucial for the development of AAV. Using the mouse model of ANCA-associated crescentic glomerulonephritis induced by anti-MPO IgG, Xiao et al. demonstrated that ANCA and neutrophils are indispensable for the initiation of necrotizing crescentic glomerulonephritis (3, 4). *In vitro*, ANCAs are capable of inducing activation of primed neutrophils, resulting in respiratory burst and degranulation of neutrophils, which may directly participate in the development of vascular inflammation (5–8). Moreover, "endothelium–neutrophil interactions are essential to allow neutrophils to move toward inflammatory sites" and trigger an explosive activation of neutrophils by ANCA (9). In the past decade, accumulating evidence has demonstrated that activation of complement system *via* the alternative pathway is crucial for the development of AAV (10–15). Activation of neutrophils induced by ANCA results in releasing factors that trigger the activation of the alternative complement pathway and subsequently generating C5a (12). C5a further primes neutrophils for activation by ANCA (12, 16, 17), thus causing a self-amplification loop for ANCA-induced neutrophil activation.

Complement factor H (FH) is an abundant plasma glycoprotein that functions as a key regulator of the alternative complement activation by accelerating the decay of the C3 convertase (C3bBb) and by acting as a cofactor for factor I-mediated cleavage of C3b (18, 19). Our recent study found that plasma levels of FH were inversely associated with the disease activity and renal damage of AAV patients (20); and, an impaired complement regulatory activity of FH was found in AAV patients (21), indicating an important role of FH in the disease development. In addition to serving as an inhibitor of the alternative complement pathway, there is increasing evidence demonstrating direct regulatory roles of FH on several cell types. Mihlan et al. showed that FH inhibited the production of pro-inflammatory cytokines by activated macrophages during phagocytosis (22). As for neutrophils, "FH has been shown to bind to neutrophils *via* complement receptor type 3" (CR3; $\alpha_{M\beta2}$ integrin; CD11b/CD18) (23–25), and mediate adhesion and migration of neutrophils by serving as an adhesion molecule for neutrophils (24–26). Losse et al. further found that *Candida albicans*-bound FH facilitated neutrophil antimicrobial activity by enhancing the recognition of fungal (25). Given that CD11b/CD18, as the ligand for FH binding on neutrophils, plays an indispensable role in ANCA-mediated activation of neutrophils and leukocyte–endothelium interactions in the presence of anti-MPO antibodies (27, 28), we hypothesized that FH may participate in the process of ANCA-mediated activation of neutrophils and neutrophil–endothelium interaction, thus influencing the amplification loop between activation of neutrophils and the alternative complement pathway.

MATERIALS AND METHODS

Patients

Twelve patients who were newly diagnosed with active AAV in the Department of Nephrology, Peking University First Hospital from 2013 to 2014 were enrolled in this study. All these patients met the definition of AAV according to "the 2012 revised International Chapel Hill Consensus Conference Nomenclature of Vasculitides" (2). All the patients received plasma exchange therapy. Plasma samples of these patients were obtained at the beginning of the plasma exchange process prior to initiating the infusion of blood products and immunosuppressive therapy. Plasma samples were stored at −80°C in small aliquots until use. Four age-matched healthy blood donors were included as normal controls. Informed consent was obtained from each participant. The study was in compliance with the Declaration of Helsinki and was approved by the ethics committees of Peking University First Hospital.

Cells

Human neutrophils from healthy donors were isolated from anticoagulated peripheral blood by density gradient centrifugation using Polymorphprep and Lymphoprep (Nycomed, Oslo, Norway). Erythrocytes were lyzed by erythrocytes lyzing buffer (Tiangen Biotech, Beijing, China). Then, neutrophils were washed in Ca^{2+}/Mg^{2+} free Hanks balanced salt solution ($HBSS^{-/-}$) (Gibco, Grand Island, NY, USA) and prepared for further analysis.

Human glomerular endothelial cells (hGEnCs) (ScienCell Research Laboratories, San Diego, CA, USA) were grown at 37°C and 5% CO_2 in endothelial cell medium (ECM) (ScienCell Research Laboratories, San Diego, CA, USA) supplemented with 10% fetal bovine serum (FBS), 1% penicillin/streptomycin solution, and 1% endothelial cell growth factor, according to the manufacturer's instructions. All experiments were performed using hGEnCs at passages 3–5. For the synchronization of cell cycle, hGEnCs were kept in serum-free ECM without endothelial cell growth supplement for 12 h prior to experiments without bio coating.

Preparation of IgG

Anti-neutrophil cytoplasmic autoantibody-positive IgG was isolated from plasma of AAV patients with positive ANCA by affinity chromatography using a HiTrap Protein G HP column in an AKTA-FPLC system (GE Healthcare, Chicago, IL, USA) according to the methods described previously (29, 30).

Purification of FH From Plasma

Factor H was isolated from plasma of 12 patients with active AAV by three sequential chromatographic columns, consisting of L-lysine Sepharose 4B column, Resource Q column, and Superdex 200 high resolution HiLoad 16/600 column (GE Healthcare, Chicago, IL, USA), as described previously (21). FH from four age-matched healthy volunteers were also purified as normal controls. The purity of the final preparations of FH was determined to be comparable to commercial purified FH (Calbiochem, Darmstadt, Germany) by SDS-PAGE (see Figure S1 in Supplementary Material), which is consistent with previous studies (21, 31).

Binding of FH to Neutrophils

Binding of FH to neutrophils was analyzed by immunofluorescence staining and flow cytometry according to previously

described methods (25, 26), with some minor modifications. Briefly, neutrophils isolated from healthy blood donors were seeded on eight-well chamber slides in Roswell Park Memorial Institute (RPMI) 1640 supplemented with 0.5% FBS at a density of 10^5 cells/well and allowed to adhere for 1 h at 37°C. Then, neutrophils were incubated with 50 μg/ml FH or medium followed by fixed with 4% paraformaldehyde. After blocking, bound FH were detected using a goat polyclonal antibody directed against human FH (Calbiochem, Darmstadt, Germany) followed by Alexa Fluor 488-conjugated donkey anti-goat IgG (Molecular Probes-Invitrogen, Carlsbad, CA, USA). Normal goat IgG (Calbiochem, Darmstadt, Germany) was applied as the isotype control for the primary staining antibody. After washing, slides were mounted in fluorescence preserving medium fortified with 4′, 6-diamidino-2-phenylindole (ZSGB-BIO, Beijing, China). Immunofluorescence staining was visualized using a confocal microscope (Carl Zeiss, Germany).

For flow cytometry analysis, prepared neutrophils were suspended in "modified Hank's buffer (142 mM NaCl, 1 mM Na_2SO_4, 5 mM KCl, 1 mM NaH_2PO_4, 1 mM $MgCl_2$, 2.5 mM $CaCl_2$, 5 mM glucose, 10 mM HEPES; pH 7.4)" (26) containing 1% BSA to a concentration of 1×10^6 cells/ml. After blocking, cells were incubated with 100 μg/ml FH for 30 min at 30°C with gentle shaking. All further steps were performed in PBS containing 1% BSA at 4°C. After washing, a goat anti-human FH antibody was added for 30 min, followed by Alexa488-conjugated donkey anti-goat IgG for 30 min. Neutrophils were analyzed using a FACScan (Becton Dickinson, Heidelberg, Germany). Neutrophils were identified by forward/sideward scatter (FSC/SSC) and data were collected from 10,000 cells per sample.

Analysis of Activate CR3 (CD11b/CD18)

The expression level of active CR3 on neutrophils was detected according to previously described method (32), with some minor modifications. Briefly, prepared neutrophils were suspended in RPMI 1640 to a concentration of 2.5×10^6 cells/ml. Then 100 μg/ml FH, 5 ng/ml TNF-α (Sigma, St. Louis, MO, USA), or 1×10^{-8}M fMLP (Sigma, St. Louis, MO, USA) were added, respectively. Unstimulated cells incubated with medium were set as the blank controls. Thereafter, cells were incubated at 37°C for 30 min. After washing, cells were incubated with phycoerythrin-conjugated anti-CD11b monoclonal antibodies CBRM1/5 (eBioscience, San Diego, CA, USA) or isotype-matched control antibodies at 4°C for 30 min. Neutrophils were analyzed using a FACScan instrument. Neutrophils were gated by FSC and SSC, and 10,000 cells per sample were routinely collected for data analysis.

Adhesion Assays

To investigate the effect of FH on the interaction between neutrophils and endothelial cells, adhesion assays were performed. Endothelial monolayers were grown on wells of Costar 96-well black transparent-bottom plates (Corning Life Sciences, Corning, NY, USA) and pretreated with 50 μg/ml FH, human serum albumin (HSA), or medium for 1 h at 37°C. Prepared neutrophils were suspended in RPMI 1640 medium without serum to a concentration of 1×10^6 cells/ml and then stained with 5 μM Cell tracker green (Invitrogen) for 45 min at 37°C. After washing, neutrophils in serum-free ECM were primed with 2 ng/ml TNF-α and then added to the wells to adhere for 1 h at 37°C. In some experiments, TNF-α primed neutrophils were pre-incubated with 100 μg/ml FH or controls for 1 h at 37°C, followed by added to non-treated hGEnC monolayers. Non-adherent cells were removed by extensive washing. Adherent cells were reflected by fluorescence intensity (FI) of neutrophils measured by a fluorescence reader (TriStar Multimode Microplate Reader LB941, Berthold Technologies, Bad Wildbad, Germany) with filters of 495 nm (excitation) and 515 nm (emission).

Neutrophil Migration Assays

Neutrophil migration assays were performed using 24-well Costar transwell plates with 3 μm-pore polycarbonate membranes inserts (Corning Life Sciences, Corning, NY, USA) according to the previously described method (25, 26), with some modifications. Endothelial monolayers grown on the lower chamber were pre-incubated with 50 μg/ml FH, HSA, or serum-free ECM medium. Neutrophils were stained with 5 μM Cell tracker green for 45 min at 37°C. After washing, 10^6 neutrophils in serum-free ECM were added to the top chamber for 60 min at 37°C. "Then 25 mM EDTA was added to the lower chamber to release neutrophils adhering to the bottom of the membrane and the bottom of the well" (25). Migrated neutrophils were reflected by FI measured using a fluorescence reader with filters of 495 nm (excitation) and 515 nm (emission).

Measurement of Reactive Oxygen Species and Lactoferrin Released From Neutrophils

The generation of reactive oxygen species (ROS) by ANCA stimulated neutrophils was assessed using dihydrorhodamine (Sigma-Aldrich, St. Louis, MO, USA) as previously described (16). Neutrophils (2.5×10^6/ml) were pre-incubated with 5 μg/ml dihydrorhodamine in $HBSS^{-/-}$ for 30 min at 37°C. After washing, neutrophils were primed with 5 ng/ml TNF-α in modified Hank's buffer for 15 min, followed by incubation with 100 μg/ml FH or buffer for 30 min at 37°C. Then neutrophils were stimulated by ANCA-positive IgGs for 1 h. The reaction was stopped by centrifugation and suspension with 1 ml of ice-cold HBSS containing 1% BSA. Cells were analyzed using a FACScan. Neutrophils were gated by FSC and SSC, and 10,000 cells per sample were routinely collected for data analysis. The amount of generated reactive oxygen was represented by the mean fluorescence intensity (MFI).

To detect the generation of ROS by neutrophils cocultured with hGEnCs. Neutrophils pre-incubated with FH or HSA were added to endothelial monolayers grown on Costar 96-well black transparent-bottom plates and allowed to adhere for 1 h, followed by stimulation with ANCA-positive IgGs for 2 h. The fluorescence signal of the oxidized dihydrorhodamine was measured using a fluorescence reader with excitation and emission filter settings of 485 and 535 nm, respectively.

For detection of lactoferrin, which is considered as a biomarker of neutrophil degranulation, supernatants of neutrophils or cocultures were collected. Supernatant levels of lactoferrin were

tested by ELISA using a commercial kit following the instruction provided by the manufacturer (Abcam, Cambridge, MA, USA).

Evaluation of Endothelium Injury by Endothelin-1 (ET-1) Quantification

Endothelin-1 was considered as a biomarker of endothelial cell activation and injury (33), and neutrophils cannot release ET-1. Therefore, supernatants of the coculture system were collected for ET-1 measurement using a commercial ELISA kit (R&D Systems, Minneapolis, MN, USA), following the instruction provided by the manufacturer.

Mass Spectrometry Analysis of FH

Factor H purified from patients with active AAV and healthy controls, as well as commercially derived FH were further analyzed by mass spectrometry for detection of possible modifications. Samples were incubated in 8 M urea, 10 mM DTT in 50 mM ammonium bicarbonate (NH_4HCO_3) at 56°C for 40 min, followed by incubating in 55 mM iodoacetamide in 50 mM NH_4HCO_3 at room temperature for 1 h. The solution was then diluted with 50 mM NH_4HCO_3 to a final urea concentration of 2 M and digested with trypsin in 50 mM NH_4HCO_3 overnight at 37°C. The resulting peptides were centrifuged to dryness in vacuum. For LC-MS/MS analysis, the samples were re-dissolved in 0.2% formic acid and separated on a 75 μm × 15 cm capillary column packed with 4 μm C18 bulk material (InnosepBio, China) using an nLC 1000 system (Thermo Scientific, USA). Peptides were eluted in a linear gradient consisting of mobile phases A and B, which were 0.1% formic acid in water and 0.1% formic acid in acetonitrile, respectively. The elution system started with a linear gradient from 5% B to 30% B in 60 min, followed by 30% B to 75% B in the next 4 min, and maintained at 75% B for another 20 min. The eluted peptides were then sprayed directly into a Velos Pro Orbitrap Elite mass spectrometer (Thermo Scientific, USA) equipped with a nano-ESI source. The mass spectrometer was run in data-dependent mode with a full MS scan resolution of 120,000 in FT mode followed by collision-induced dissociation MS/MS scans of the 15 most abundant ions in the initial MS scan.

Database search were carried out using Mascot (version 2.3.02) for detecting variable modifications including Carbamidomethyl (Cys), Oxidation (Met/Cys), Nitration (Tyr), and Chlorination (Tyr). The mass tolerance was set to be ±10 ppm for peptide pass tolerance and ±0.6 Da for fragment mass tolerance.

Statistical Analysis

Quantitative data were presented as mean ± SD or median and interquartile range, according to the normality of data. The between-group differences in normally distributed quantitative parameters were assessed by *t* test or ANOVA as appropriate. The difference was considered statistically significant when the *P* values < 0.05. Analysis was performed with SPSS statistical software package (version 13.0, Chicago, IL, USA).

RESULTS

Clinical Data of Patients With Active AAV

Of the 12 patients with active AAV, seven were male and five were female, with an average age of 61.9 ± 8.4 (range 48–74) years at diagnosis. All the patients were ANCA positive, 10 patients were positive for MPO-ANCA and 2 were positive for PR3-ANCA. At the time of diagnosis, the level of serum creatinine was 634.9 ± 260.0 (range 254.2–1,118.0) μmol/l; the level of Birmingham Vasculitis Activity Scores was 20.8 ± 4.4 (range 12–29).

Binding of FH to Neutrophils

Previous studies reported that FH bound to neutrophils and influenced the activation of neutrophils upon certain stimulation (25, 26). Therefore, we analyzed the binding of FH to neutrophils. FH showed specific binding to human neutrophils by immunostaining and flow cytometry (**Figures 1A,B**), which is consistent with previous findings (23–26). FH purified from

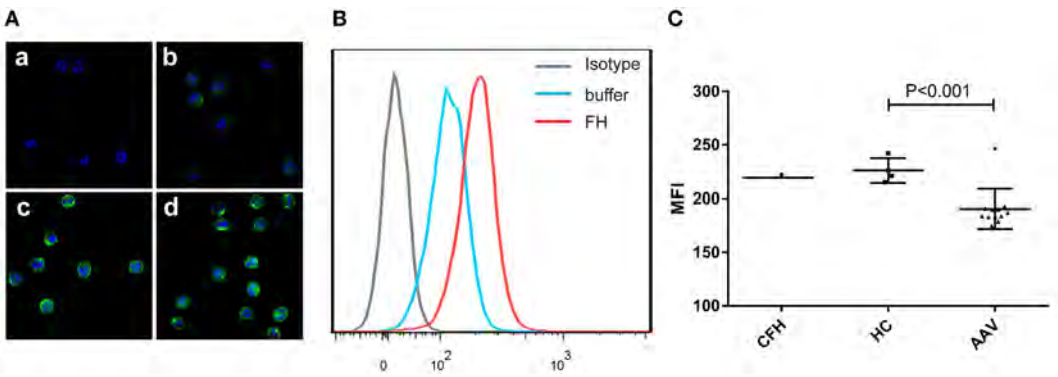

FIGURE 1 | Binding of factor H (FH) to human neutrophils. Neutrophils were incubated with FH or buffer, and bound FH was detected using goat anti-human FH antibody. Normal goat IgG was using as the relevant isotype control antibody. **(A)** Representative confocal images show binding of FH to the cell surface of neutrophils. [**(A)**, a] Isotype control; [**(A)**, b] negative control performed by incubating neutrophils with buffer only; [**(A)**, c,d] neutrophils were incubation with FH followed by detection using goat anti-human FH antibody. **(B)** Shown is a representative histogram out of three independent experiments performed by flow cytometry. **(C)** Flow cytometry analysis of binding of FH to neutrophils. FH purified from healthy controls exhibited similar binding activity to commercial FH, while FH from patients with active ANCA-associated vasculitis bound less efficiently to neutrophils.

healthy controls exhibited similar binding activity to commercially derived FH. However, FH from patients with active AAV bound less efficiently to neutrophils, as compared with that from normal controls (189.6 ± 15.8 vs. 226.0 ± 11.6, $P = 0.001$) (**Figure 1C**).

Binding of FH to Neutrophils Do Not Activate CR3

Previous studies demonstrated that CR3 ($\alpha_{M\beta2}$ integrin; CD11b/CD18) serves as a specific receptor for FH on neutrophils (24–26). Therefore, to investigate whether CR3 is activated with FH incubation, a monoclonal antibody (CBRM1/5) which specifically directs against the active domain of CD11b was used to detect the expression level of active CR3. Consistent with previous studies, a low-level activation of CR3 was observed at baseline, while priming neutrophils with TNF-α or fMLP significantly increased the expression of active CR3 (32, 34). Incubation of neutrophils with FH did not activate CR3. When incubating neutrophils with FH, the expression level of active CR3 on neutrophils was comparable to that of unstimulated cells (94.3 ± 1.5 vs. 95.0 ± 3.0, $P = 0.749$) (**Figure 2**).

FH Inhibits ANCA-Induced Respiratory Burst and Degranulation of Neutrophils

Anti-neutrophil cytoplasmic autoantibody-mediated activation of neutrophils plays a central role in the pathogenesis of AAV. Therefore, to further investigate whether FH influences ANCA-induced activation of neutrophils, human neutrophils were primed with TNF-α followed by activation with ANCA-positive IgGs. When neutrophils were pre-incubated with FH before stimulated by ANCA, the level of respiratory burst of neutrophils was significantly decreased, as determined by the MFI representing the intracellular development of ROS in neutrophils (132.4 ± 14.2 vs. 225.4 ± 31.4, $P < 0.001$). The level of ROS generation by neutrophils pre-incubated with FH was similar to that of neutrophils merely primed with TNF-α (**Figures 3A,B**). Degranulation of neutrophils was evaluated by measuring lactoferrin level in the supernatant of neutrophils in parallel. Consistently, pre-incubation of neutrophils with FH resulted in significantly less lactoferrin release from neutrophils upon activation by ANCA-positive IgGs (2,152.1 ± 459.1 ng/ml vs. 3,669.2 ± 487.1 ng/ml, $P < 0.001$) (**Figure 3C**).

Then we investigated the effect of FH from patients with AAV on ANCA-mediated activation of neutrophils. We found that FH from normal controls inhibited ANCA-induced activation of neutrophils, comparable to commercially derived FH. However, under the same condition, FH from active AAV patients could not effectively inhibit neutrophil activation upon ANCA stimulation, including ROS generation and lactoferrin degranulation, as compared with those from normal controls (199.1 ± 25.6 vs. 128.3 ± 8.8, $P < 0.001$; 4,055.6 ± 462.4 ng/ml vs. 2,639.6 ± 117.1 ng/ml, $P < 0.001$, respectively). The mean levels were similar to that of neutrophils not treated with FH prior to activation by ANCA (**Figures 3D,E**).

FH Enhances Neutrophils Adhesion and Migration Toward hGEnCs

Factor H was previously suggested as an adhesion molecule for human neutrophils (24), therefore we hypothesized that FH may facilitate the interaction between neutrophils and endothelial cells by interacting with glycosaminoglycans. To test this hypothesis, we performed adhesion and migration assays. We found that pre-incubation of TNF-α primed neutrophils with FH resulted in significantly increased number of neutrophils adhered to hGEnCs, as compared with pre-incubation with buffer or HSA ($38.1 \times 10^4 \pm 5.1 \times 10^4$ vs. $22.4 \times 10^4 \pm 4.7 \times 10^4$, $P < 0.001$; $38.1 \times 10^4 \pm 5.1 \times 10^4$ vs. $26.4 \times 10^4 \pm 4.1 \times 10^4$, $P < 0.001$, respectively). When endothelial cells were pretreated with FH before addition of primed neutrophils, adhesion of neutrophils were also enhanced ($50.6 \times 10^4 \pm 5.5 \times 10^4$ vs. $32.9 \times 10^4 \pm 10.0 \times 10^4$, $P = 0.009$; $50.6 \times 10^4 \pm 5.5 \times 10^4$ vs. $35.8 \times 10^4 \pm 7.1 \times 10^4$, $P = 0.006$, respectively) (**Figures 4A,B**). Consistently, pre-incubation of endothelial cells on the lower chamber of transwells with FH resulted in increased number of neutrophils migrated through the membrane inserts, as compared with HSA or medium (131.3 ± 6.7 vs. 115.5 ± 5.7%, $P = 0.011$; 131.3 ± 6.7 vs. 115.6 ± 6.1%, $P = 0.013$, respectively) (**Figure 4C**). Collectively, these data provides evidence to support the hypothesis that FH may facilitate the interaction between neutrophils and endothelial cells by serving as an adhesion molecule for neutrophils.

FH Inhibits ANCA-Induced Neutrophil Activation and Endothelial Injury in the Coculture System of hGEnCs and Neutrophils

One salient feature of AAV is massive endothelial injury, especially glomerular endothelial cells. It is mainly mediated by endothelium–neutrophil interactions and activation of neutrophils on endothelial cells by ANCA (9). Therefore, to assess whether enhanced adhesion mediated by FH would lead to functional effects on neutrophils, the generation of ROS, and the release of lactoferrin were measured in the coculture system of neutrophils and hGEnCs. However, we found that compared with neutrophils pre-incubated with buffer or HSA, FH-treated neutrophils showed less production of ROS ($21.6 \times 10^4 \pm 3.0 \times 10^4$ vs. $30.1 \times 10^4 \pm 1.1 \times 10^4$, $P < 0.001$; $21.6 \times 10^4 \pm 3.0 \times 10^4$ vs. $29.2 \times 10^4 \pm 3.2 \times 10^4$, $P < 0.001$, respectively) (**Figure 5A**), as represented by the FI of neutrophils cocultured with endothelial cells in each well of the black transparent-bottom plates. Consistently, the level of lactoferrin in the coculture supernatants was also decreased by pre-incubation of neutrophils with FH (2,933.6 ± 157.6 vs. 4,756.3 ± 180.7, $P < 0.001$; 2,933.6 ± 157.6 vs. 4,181.0 ± 368.2, $P < 0.001$, respectively), as compared with pre-incubation with buffer or HSA (**Figure 5B**). To assess whether the inhibition of neutrophil activation by FH also resulted in subsequent protection of endothelium injury, the level of ET-1, a biomarker of endothelial cell activation and injury, in the coculture supernatants was measured. It was found that FH bound on neutrophils obviously protected against endothelium injury induced by ANCA-mediated activation of neutrophils, whereas the control protein HSA had no effect (24.5 ± 1.5 vs. 35.1 ± 1.5,

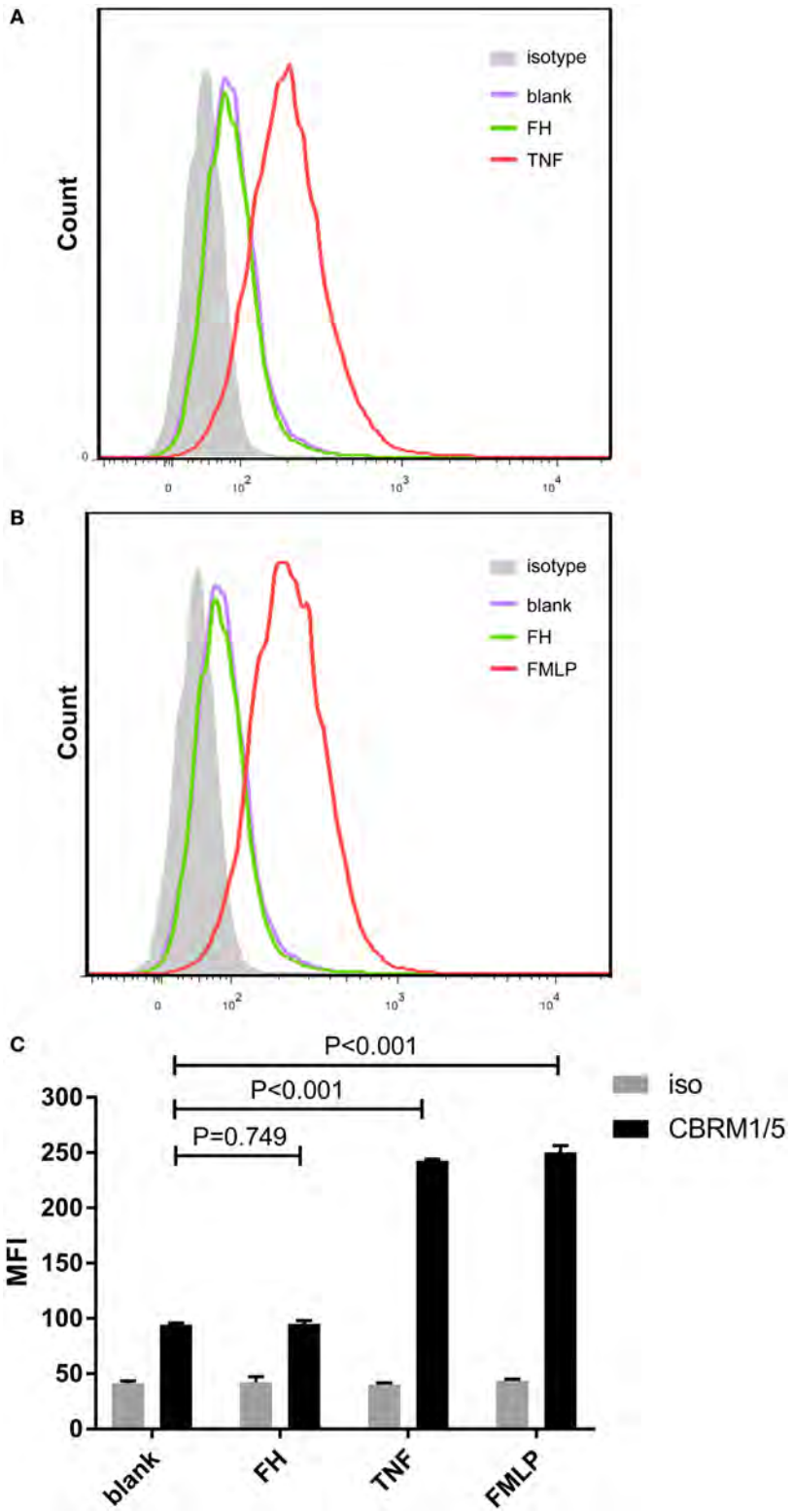

FIGURE 2 | Binding of factor H (FH) to neutrophils do not activate CR3 (CD11b/CD18). Activate CR3 on neutrophils were detected using phycoerythrin-conjugated anti-CD11b monoclonal antibodies CBRM1/5 after incubation with FH, TNF-α, or fMLP. Unstimulated cells incubated with medium were set as blank controls. **(A,B)** Representative histograms showing that priming neutrophils with TNF-α or fMLP-induced expression of activate CR3, while FH did not activate CR3. **(C)** Analysis of expression of activate CR3. The expression level of active CR3 on nuetrophils after incubation with FH was comparable to unstimulated neutrophils. The values represent mean ± SD derived from three independent experiments.

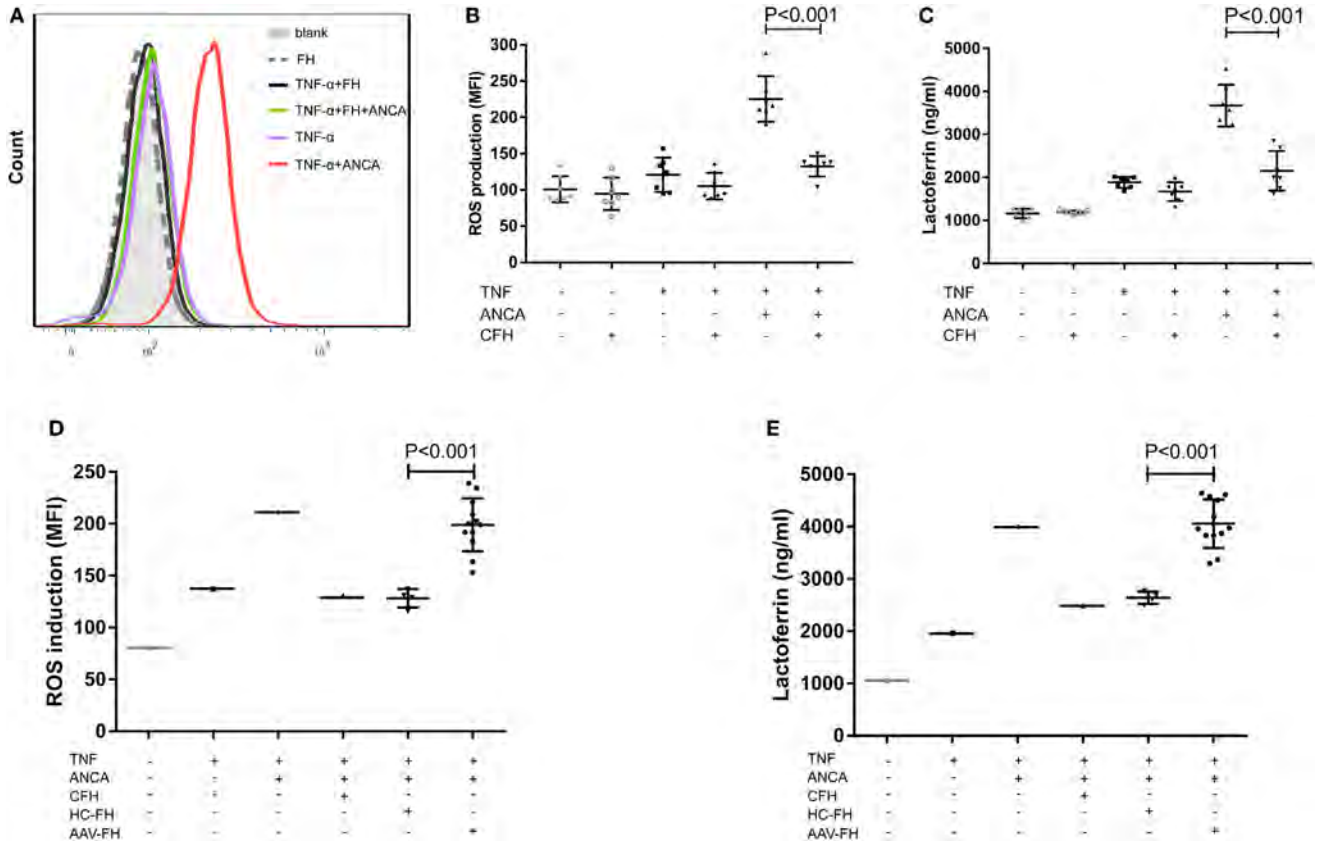

FIGURE 3 | Factor H (FH) inhibits anti-neutrophil cytoplasmic autoantibody (ANCA)-induced respiratory burst and degranulation of neutrophils. **(A,B)** Neutrophils were primed with TNF-α followed by activation with myeloperoxidase-ANCA positive IgGs or proteinase 3-ANCA positive IgGs. Pre-incubation of neutrophils with FH resulted in marked reduction of generation of reactive oxygen species (ROS). **(A)** Shown is a representative histogram out of seven independent experiments. **(B)** The bars and error bars represent mean ± SD of ROS production in seven independent experiments using ANCA-IgGs derived from different patients with ANCA-associated vasculitis (AAV). **(C)** Neutrophils pre-incubated with FH showed less degranulation of lactoferrin. The values represent mean ± SD derived from seven independent experiments. **(D,E)** FH from patients with active AAV exhibited deficient ability in inhibiting respiratory burst and degranulation of neutrophils activated by ANCA, as compared with FH from healthy controls. Shown is mean ± SD of ROS and lactoferrin production by neutrophils pre-incubated with FH from different patients or controls, respectively. Experiments were independently repeated three times.

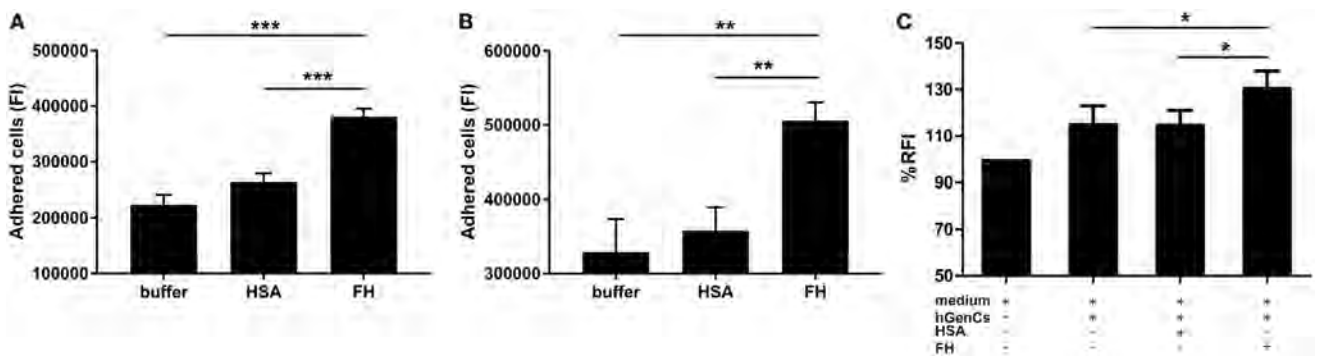

FIGURE 4 | Factor H (FH) enhances neutrophil adhesion and migration to hGEnCs. In all assays, neutrophils were stained with Cell tracker green. **(A)** TNF-α primed neutrophils pre-incubated with FH or controls were added to endothelial monolayers and allowed to adhere. Adherent cells were quantified by plate fluorimeter. **(B)** hGEnC monolayers were pretreated with FH or controls. TNF-α primed neutrophils were added and allowed to adhere. Adherent cells were quantified. Results are expressed as mean ± SD of fluorescence intensity (FI) values derived from five independent experiments. **(C)** hGEnC monolayers grown on the lower chamber of transwells were pre-incubated with FH, human serum albumin (HSA), or medium. TNF-α primed neutrophils were added to the upper wells. The migration of neutrophils through a membrane insert was quantified by measuring the fluorescence in the lower chamber. Transwells without cultivated hGEnCs were used as negative controls. The data were normalized after subtraction of negative controls and represent mean percentage values ± SD from five experiments performed with different cell donors (*$P < 0.05$; **$P < 0.01$; ***$P < 0.001$).

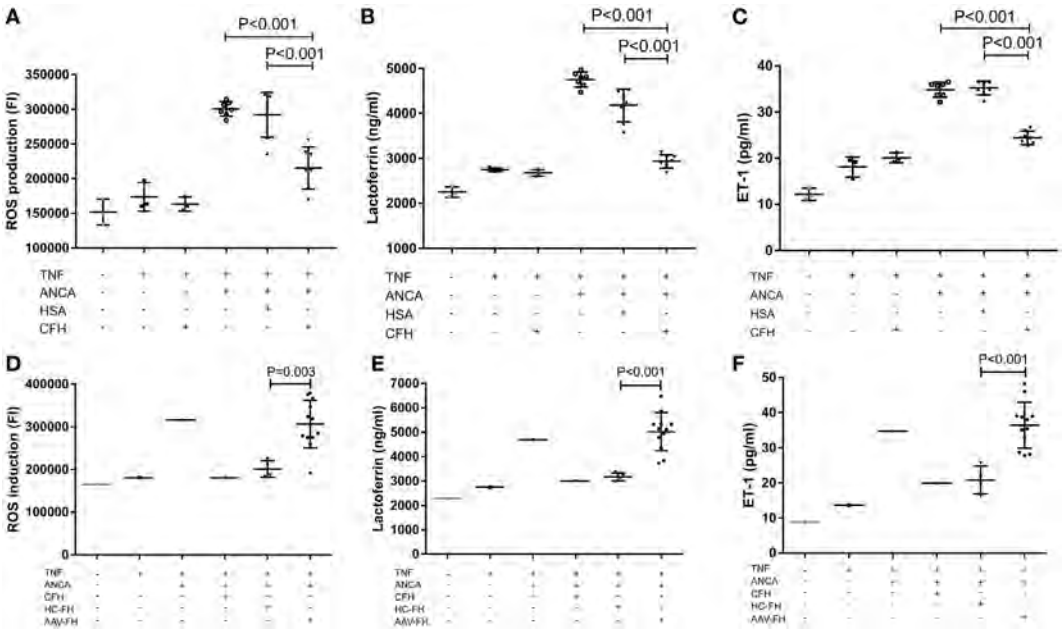

FIGURE 5 | Factor H (FH) inhibits anti-neutrophil cytoplasmic autoantibody (ANCA)-induced neutrophil activation and endothelial injury in the coculture system of hGEnCs and neutrophils. Neutrophils primed with TNF-α were allowed to adhere on endothelial monolayers and followed by activation with myeloperoxidase-ANCA positive IgGs or proteinase 3-ANCA positive IgGs. **(A)** Pre-incubation of neutrophils with FH resulted in less production of ROS in the cocultures of hGEnCs and neutrophils. The values represent mean ± SD of ROS production derived from three independent experiments using ANCA-IgGs from seven different patients with ANCA-associated vasculitis (AAV). **(B)** The level of lactoferrin in the coculture supernatants was decreased by pre-incubation of neutrophils with FH. Shown is mean ± SD of three independent experiments. **(C)** The levels of endothelin-1 (ET-1) in the supernatant of cocultures decreased significantly when pre-incubating neutrophils with FH. **(D,E)** FH from patients with active AAV exhibited deficient ability in inhibiting the production of ROS and degranulation of lactoferrin by neutrophils cocultured with hGEnCs in the presence of ANCA, as compared with FH from healthy controls. Shown is mean ± SD of ROS and lactoferrin production by neutrophils pre-incubated with FH from different patients or controls, respectively. Experiments were independently repeated three times. **(F)** Compared with neutrophils pre-incubated with FH from healthy controls, the level of ET-1 in the coculture supernatants was significantly higher when neutrophils were pretreated with FH from patients with active AAV.

$P < 0.001$) (**Figure 5C**). However, we found that compared with FH from healthy controls, FH from patients with active AAV exhibited a deficient ability in inhibiting ANCA-induced neutrophil activation on endothelial cells, including ROS production and degranulation of lactoferrin ($30.6 \times 10^4 \pm 5.6 \times 10^4$ vs. $20.1 \times 10^4 \pm 2.0 \times 10^4$, $P = 0.003$; 5,017.7 ± 779.0 vs. 3,171.5 ± 164.3, $P < 0.001$, respectively) (**Figures 5D,E**). In line with this finding, when neutrophils were pre-incubated with FH from patients with active AAV, the concentration of ET-1 in the coculture supernatants was significantly higher than those pre-incubated with FH from healthy controls (37.6 ± 6.4 vs. 20.8 ± 3.9, $P < 0.001$) (**Figure 5F**), indicating a deficient ability in protecting against endothelium injury mediated by ANCA-induced neutrophil activation. Collectively, these data indicates that FH is capable of inhibiting ANCA-induced neutrophil activation on endothelial cells and protecting against endothelial injury by interacting with neutrophils. However, FH from patients with active AAV exhibited a deficient protective ability.

Identification of FH Modifications by Mass Spectrometry

According to a recent published study, tyrosine nitration of FH, an oxidative posttranslational modification, potentiates the activation of monocytes that stimulated with lipid peroxidation by-products (35). Therefore, mass spectrometry was further performed to detect possible modifications of FH in patients with active AAV. Since nitration and chlorination of tyrosine residues could be induced by the MPO H_2O_2/Cl^- system during inflammatory processes (36), tyrosine nitration and chlorination were searched against the database. The position of the nitrated/chlorinated tyrosine was determined based on the theoretical nitrated/chlorinated peptide tandem mass spectrum with the highest Mascot score (35). A total of nine modification sites were specifically detected in six patients with active AAV as follows: four modifications at SCR2 of FH including two sites of tyrosine nitration and two tyrosine chlorination sites; two modifications at SCR6 including one site of tyrosine nitration and one tyrosine chlorination sites; and three modifications at SCR19 including two sites of tyrosine nitration and one tyrosine chlorination sites. The tyrosine residues of FH that are nitrated or chlorinated detected in patients with active AAV are summarized in **Figure 6A**. A piece of example tandem mass spectrum showing the nitration and chlorination of FH tyrosine residues is shown in **Figure 6B**. The result of FH modifications for each patient is listed in **Table 1**. None of the tyrosine nitration and chlorination sites was detected in FH from all the healthy controls.

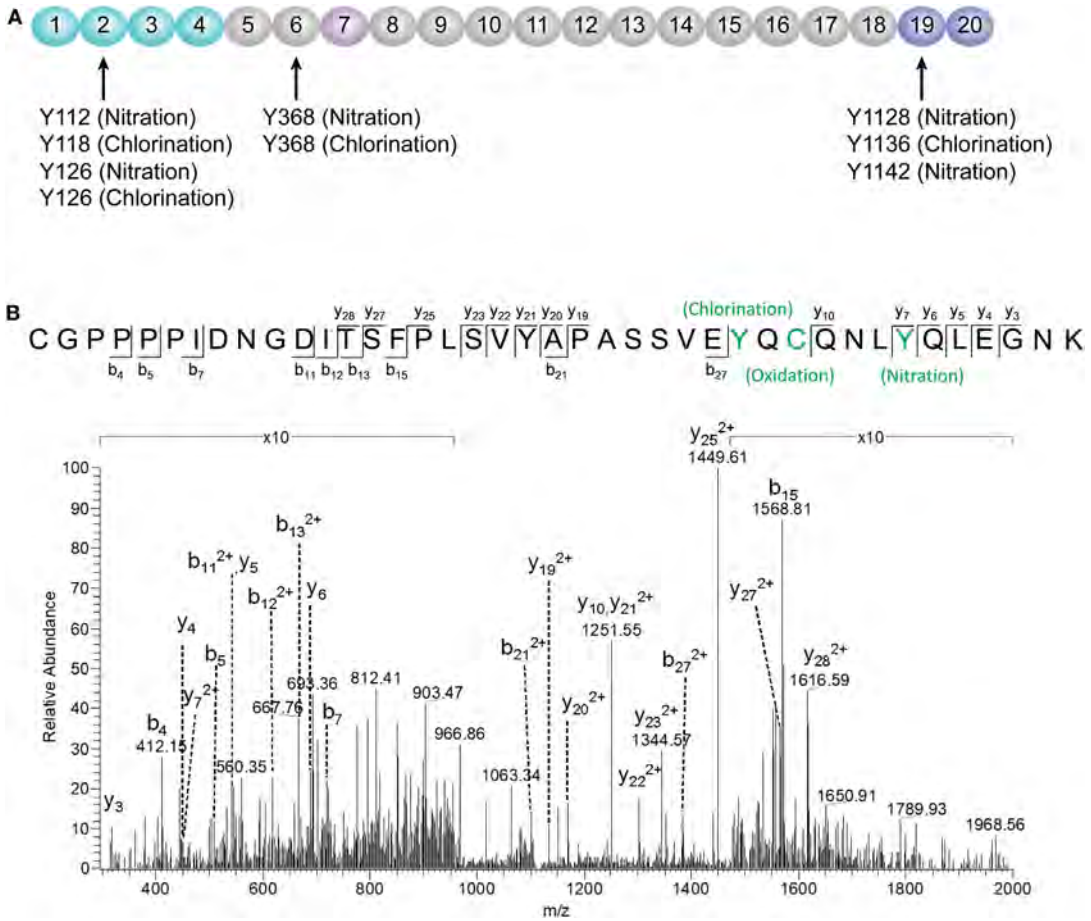

FIGURE 6 | Identification of factor H (FH) modifications by mass spectrometry analysis. **(A)** Summary of all tyrosine nitration and chlorination sites of FH identified in patients with active ANCA-associated vasculitis. The position of the nitrated/chlorinated tyrosine is determined based on the theoretical nitrated/chlorinated peptide tandem mass spectrum with the highest Mascot score. The amino acid sequence of FH is referred to the UniProt database. **(B)** A representative mass spectrogram showing the detection of chlorination of Y1136 and nitration of Y1142 located at SCR19 of FH.

TABLE 1 | Modification sites of factor H in patients with active ANCA-associated vasculitis detected by mass spectrometry.

P1	P2	P3	P4	P5	P6	P7	P8	P9	P10	P11	P12
Y1136 (chlorination)	None	None	Y368 (chlorination)	None	None	Y1128 (nitration)	None	Y112 (nitration)	None	Y368 (nitration)	Y118 (chlorination)
Y1142 (nitration)						Y1136 (chlorination)		Y126 (chlorination)		Y1136 (chlorination)	Y126 (nitration)
										Y1142 (nitration)	Y368 (chlorination)

DISCUSSION

Anti-neutrophil cytoplasmic autoantibody-induced neutrophil activation plays a crucial role in the development of AAV (3–8). Our current study showed that FH was capable of inhibiting respiratory burst and degranulation of neutrophils stimulated by ANCA. It extends our previous finding of FH in AAV (20, 21) and indicates a novel role of FH in the pathogenesis of AAV. A number of previous studies demonstrated that CR3 ($\alpha_{M\beta2}$ integrin; CD11b/CD18) serves as a specific receptor for FH on neutrophils (24–26). The $\alpha_{M\beta2}$ integrin has long been implicated in mediating interactions between neutrophils and various types of pathogens (37–40), as well as endothelial cells (28). Losse et al. showed that FH supported attachment and migration of neutrophils to *C. albicans* by interacting with the $\alpha_{M\beta2}$ integrin on neutrophils (25). Consistent with this finding, our current study showed that FH enhanced neutrophil adhesion and migration toward endothelial cells. This result provides evidence to support the hypothesis that FH may facilitate the neutrophils–endothelium interaction by serving as a bridge between neutrophils and

endothelial cells (24). Nevertheless, $\alpha_{M\beta2}$ integrin plays a critical role in the process of ANCA-induced activation of neutrophils (9). Interaction of $\alpha_{M\beta2}$ integrin with ICAM-3 expressed on adjacent neutrophils would increase homotypic aggregation of circulating neutrophils (41). And, interaction between $\alpha_{M\beta2}$ integrin and adhesion molecules on endothelial cells such as ICAM-1 facilitates activation of neutrophils in the presence of ANCA including respiratory burst and degranulation, and a substantial increase of ANCA antigen expression (9, 42). Moreover, engagement of $\alpha_{M\beta2}$ integrin together with TNF-α, triggers the clustering of FcγII receptors and the association with NADPH-oxidase components, which is crucial for ANCA-induced activation of neutrophils (27). Neutrophil activation induced by anti-PR3 or anti-MPO antibodies was strongly prevented by blocking $\alpha_{M\beta2}$ integrin (27). Therefore, we speculate that the current observation that FH inhibited ANCA-induced activation of neutrophils may result from the binding of FH to neutrophil $\alpha_{M\beta2}$ integrin. Ligation of FH on $\alpha_{M\beta2}$ integrin may obstruct some important downstream events of it in activating neutrophils. This hypothesis is supported by our findings that FH alone do not activate CR3 ($\alpha_{M\beta2}$ integrin; CD11b/CD18) on neutrophils, nor trigger activation of neutrophils. Consistent with our findings, FH was recently found to be capable of inhibiting phorbol 12-myristate 13-acetate induced release of neutrophil extracellular traps and ROS by neutrophils (26). However, Losse et al. demonstrated that when exposed to *C. albicans* yeasts, FH enhanced the generation of ROS and the release of the lactoferrin by human neutrophils, resulting in a more efficient killing of the fungal (25). It indicates that the effects of FH on neutrophil activation may be differential in different diseases. It also implicates that the FH effect may not be completely explained by the masking effect alone. Besides neutrophils, a recent study by Olivar et al. demonstrated that FH "is able to promote a distinctive tolerogenic and anti-inflammatory profile on monocyte-derived dendritic cells (MoDCs) challenged by a pro-inflammatory stimulus" (43). The anti-inflammatory effect of FH on monocyte/macrophage has also been reported previously (22, 35), while recently Calippe et al. reported a novel role of FH on mononuclear phagocytes (44). The authors showed that FH binding to mononuclear phagocytes inhibits the CD47-mediated homeostatic elimination of mononuclear phagocytes, resulting in non-resolving inflammation within the sub-retinal space, which may be involved in the pathogenesis of age-related macular degeneration (AMD). Collectively, these findings indicate that the effects of FH on different types of cells and in different diseases differ from each other. More importantly, it indicates that therapeutic manipulation of FH requires rigorous disease-specific target validation.

Another interesting finding in the current study is that FH from patients with active AAV exhibited a deficient ability in inhibiting ANCA-induced neutrophil activation in fluid phase and on endothelial cells. It potentially implicates an underlying mechanism for the overwhelming activation of neutrophils and destructive endothelium injury in AAV patients. Furthermore, excessive activation of neutrophils would result in more release of factors capable of activating the alternative complement pathway (12, 45, 46). In particular, according to our recent finding, MPO that released from neutrophils upon activation by ANCA, binds to FH and inhibits the complement regulatory activity of FH (47). Therefore, it indicates that FH deficiency may amplify the feedback loop between activation of neutrophils and the alternative complement pathway, thus contributing to the development of AAV. Interestingly, a recent study demonstrated that tyrosine nitration of FH, a type of oxidative posttranslational modification, occurred in patients with AMD (35). According to their finding, nitrated FH not only lost its cofactor activity for factor I-mediated cleavage of C3b but also significantly potentiated the activation of monocytes that stimulated with lipid peroxidation by-products (35). In the context of AAV, ANCA is capable of inducing the release of nitric oxide from human neutrophils (48). By reacting with superoxide, nitric oxide yields the production of oxidant peroxynitrite, an important mediator of nitration (49). Moreover, during inflammatory processes, nitration and chlorination of tyrosine residues could be induced by the MPO/H_2O_2/Cl^- system (36). In our current study, several tyrosine nitration and chlorination sites were identified in some patients with AAV, and most modification sites were located at SCR1–4 and SCR19–20 of FH. Interestingly, none of the tyrosine nitration and chlorination site was detected in FH from healthy controls and the two patients (patient 8 and 10) who exhibited relatively similar inhibitory effect on neutrophil activation to that from healthy controls. It implicates that nitration and chlorination of FH tyrosine residues may be relevant to the deficient activity of FH in binding neutrophils and inhibiting neutrophil activation, especially given that a main binding site for neutrophils within FH are located in SCR19–20, and a minor site may be present within SCR1–4 (25). In addition, we recently reported several genetic variations of FH in these patients with AAV, including the nonsynonymous variants Val62Ile and Tyr402His (21). The Val62 variant within the SCR1 domain of FH, which was associated with the risk of developing AMD and dense deposit disease (50, 51), showed less effective binding affinity to C3b and cofactor activity of FH compared with FH-Ile62 in previous studies (52–54). Whether it influences the interaction between FH and neutrophils is not clear. But considering that SCR1–4 of FH may serve as a binding site for neutrophils (25), we suspect that the Val62 of CFH might be in part related to the FH functional deficiency in inhibiting neutrophil activation. The Tyr402His variant of FH was found to be strongly associated the risk of AMD (55–57). Recently Calippe et al. showed that the risk variant His402 inhibited the homeostatic elimination of microglial cell, which may be related to a more effectively binding to CD11b, as compared with the non-risk variant Tyr402 (44). Whether it influences the binding of FH on neutrophils has not been elucidated. Limited by a relative small sample size, we are not able to find any firm association of this variant with the binding of FH to neutrophils; especially considering that FH used in the study were all purified from plasma, any modification that occurred in human blood may alter the results. Altogether, we suggest that the mechanism underlying FH deficiency in inhibiting neutrophil activation in AAV patients may be multifactorial. A proposed model of FH–neutrophil interaction in the pathogenesis of AAV has been illustrated in **Figure 7**. Nevertheless, these findings suggest a potential therapeutic role for FH in AAV, especially given

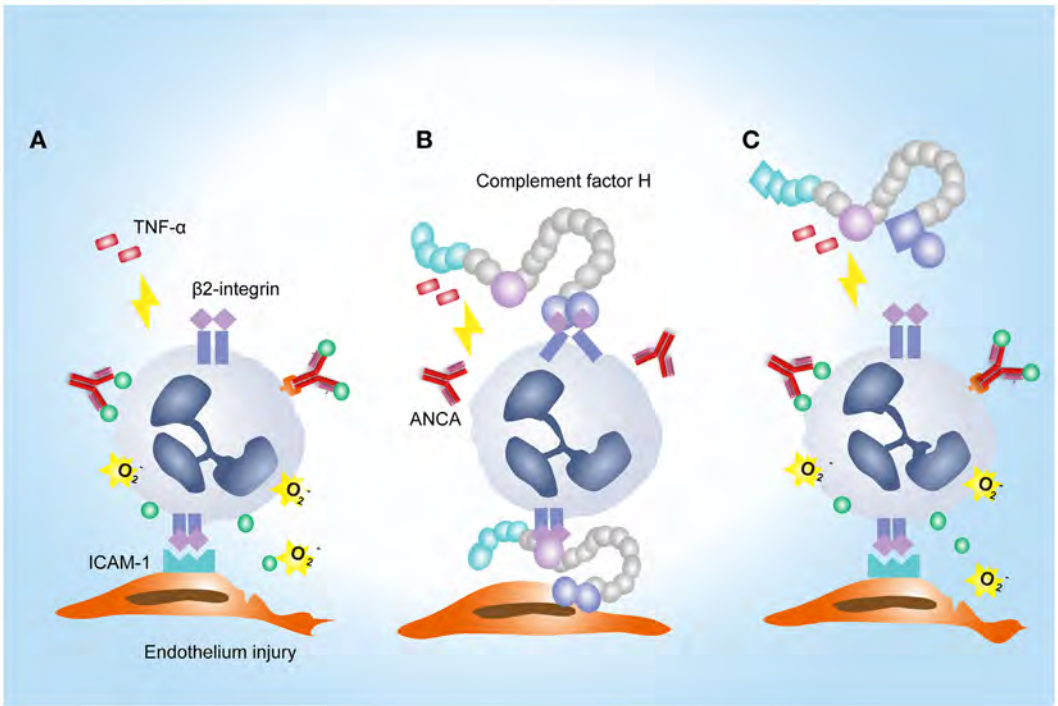

FIGURE 7 | A proposed model of factor H (FH)–neutrophil interaction in the pathogenesis of anti-neutrophil cytoplasmic autoantibody (ANCA)-associated vasculitis (AAV). **(A)** TNF/β2-integrin joint signals triggers explosive responses of neutrophils adherent to endothelial cells in the presence of ANCA, resulting in degranulation and oxidative burst of neutrophils. **(B)** Binding of FH on neutrophils through β2-integrin inhibits ANCA-induced activation of neutrophils. **(C)** In AAV, FH is deficient in binding neutrophils and inhibiting neutrophil activation by ANCA, which may be partly related to tyrosine nitration and chlorination of FH and genetic variations of FH.

that we recently found that the complement regulatory activity of FH is impaired in AAV patients (21).

In conclusion, FH inhibits ANCA-induced neutrophil activation and protects against glomerular endothelial injury by interacting with neutrophils. However, FH from patients with active AAV is deficient in the ability to bind neutrophils and inhibit neutrophil activation by ANCA. The current findings further extend the understanding of the pathogenesis of AAV, thus providing potential clues for intervention strategies.

ETHICS STATEMENT

Informed consent from each participant was obtained. The study was conducted in line with the Declaration of Helsinki and was approved by the ethics committees of Peking University First Hospital.

AUTHOR CONTRIBUTIONS

S-FC conducted the experiments, analyzed the data, and drafted the manuscript. F-MW contributed a part of methods used in the study. Z-YL provided reagents/materials/analysis tools and helped to revise the manuscript. FY participated in the design and guidance of the study and helped to revise the manuscript. M-HZ involved in its design, assisted with interpretation of data, and provided suggestion for revising the manuscript. MC conceived of the study, participated in the revision of the manuscript, and provided final approval of the version of the submitted manuscript. All authors read and approved the manuscript.

ACKNOWLEDGMENTS

This work was supported by a grant from the National Key Research and Development Program (No. 2016YFC0906102), two grants from the National Natural Science Fund (No. 81425008 and No. 81621092), and by the grant of University of Michigan Health System and Peking University Health Sciences Center Joint Institute for Translational and Clinical Research. We are very grateful to Wen Zhou from the Analysis and Test Center of Peking University, for technical assistance and data interpretation of the mass spectrometry analysis.

SUPPLEMENTARY MATERIAL

The Supplementary Material for this article can be found online at https://www.frontiersin.org/articles/10.3389/fimmu.2018.00559/full#supplementary-material.

REFERENCES

1. Falk RJ, Jennette JC. ANCA small-vessel vasculitis. *J Am Soc Nephrol* (1997) 8:314–22.
2. Jennette JC, Falk RJ, Bacon PA, Basu N, Cid MC, Ferrario F, et al. 2012 revised International Chapel Hill Consensus Conference Nomenclature of Vasculitides. *Arthritis Rheum* (2013) 65:1–11. doi:10.1002/art.37715
3. Xiao H, Heeringa P, Hu P, Liu Z, Zhao M, Aratani Y, et al. Antineutrophil cytoplasmic autoantibodies specific for myeloperoxidase cause glomerulonephritis and vasculitis in mice. *J Clin Invest* (2002) 110:955–63. doi:10.1172/JCI0215918
4. Xiao H, Heeringa P, Liu Z, Huugen D, Hu P, Maeda N, et al. The role of neutrophils in the induction of glomerulonephritis by anti-myeloperoxidase antibodies. *Am J Pathol* (2005) 167:39–45. doi:10.1016/S0002-9440(10)62951-3
5. Falk RJ, Terrell RS, Charles LA, Jennette JC. Anti-neutrophil cytoplasmic autoantibodies induce neutrophils to degranulate and produce oxygen radicals in vitro. *Proc Natl Acad Sci U S A* (1990) 87:4115–9. doi:10.1073/pnas.87.11.4115
6. Charles LA, Caldas ML, Falk RJ, Terrell RS, Jennette JC. Antibodies against granule proteins activate neutrophils in vitro. *J Leukoc Biol* (1991) 50:539–46. doi:10.1002/jlb.50.6.539
7. Keogan MT, Esnault VL, Green AJ, Lockwood CM, Brown DL. Activation of normal neutrophils by anti-neutrophil cytoplasm antibodies. *Clin Exp Immunol* (1992) 90:228–34. doi:10.1111/j.1365-2249.1992.tb07934.x
8. Mulder AH, Heeringa P, Brouwer E, Limburg PC, Kallenberg CG. Activation of granulocytes by anti-neutrophil cytoplasmic antibodies (ANCA): a Fc gamma RII-dependent process. *Clin Exp Immunol* (1994) 98:270–8. doi:10.1111/j.1365-2249.1994.tb06137.x
9. Halbwachs L, Lesavre P. Endothelium-neutrophil interactions in ANCA-associated diseases. *J Am Soc Nephrol* (2012) 23:1449–61. doi:10.1681/ASN.2012020119
10. Xiao H, Schreiber A, Heeringa P, Falk RJ, Jennette JC. Alternative complement pathway in the pathogenesis of disease mediated by anti-neutrophil cytoplasmic autoantibodies. *Am J Pathol* (2007) 170:52–64. doi:10.2353/ajpath.2007.060573
11. Huugen D, van Esch A, Xiao H, Peutz-Kootstra CJ, Buurman WA, Tervaert JW, et al. Inhibition of complement factor C5 protects against anti-myeloperoxidase antibody-mediated glomerulonephritis in mice. *Kidney Int* (2007) 71:646–54. doi:10.1038/sj.ki.5002103
12. Schreiber A, Xiao H, Jennette JC, Schneider W, Luft FC, Kettritz R. C5a receptor mediates neutrophil activation and ANCA-induced glomerulonephritis. *J Am Soc Nephrol* (2009) 20:289–98. doi:10.1681/ASN.2008050497
13. Gou SJ, Yuan J, Chen M, Yu F, Zhao MH. Circulating complement activation in patients with anti-neutrophil cytoplasmic antibody-associated vasculitis. *Kidney Int* (2013) 83:129–37. doi:10.1038/ki.2012.313
14. Gou SJ, Yuan J, Wang C, Zhao MH, Chen M. Alternative complement pathway activation products in urine and kidneys of patients with ANCA-associated GN. *Clin J Am Soc Nephrol* (2013) 8:1884–91. doi:10.2215/CJN.02790313
15. Xiao H, Dairaghi DJ, Powers JP, Ertl LS, Baumgart T, Wang Y, et al. C5a receptor (CD88) blockade protects against MPO-ANCA GN. *J Am Soc Nephrol* (2014) 25:225–31. doi:10.1681/ASN.2013020143
16. Hao J, Meng LQ, Xu PC, Chen M, Zhao MH. p38MAPK, ERK and PI3K signaling pathways are involved in C5a-primed neutrophils for ANCA-mediated activation. *PLoS One* (2012) 7:e38317. doi:10.1371/journal.pone.0038317
17. Hao J, Chen M, Zhao MH. Involvement of protein kinase C in C5a-primed neutrophils for ANCA-mediated activation. *Mol Immunol* (2013) 54:68–73. doi:10.1016/j.molimm.2012.10.041
18. Pangburn MK, Schreiber RD, Müller-Eberhard HJ. Human complement C3b inactivator: isolation, characterization, and demonstration of an absolute requirement for the serum protein beta1H for cleavage of C3b and C4b in solution. *J Exp Med* (1977) 146:257–70. doi:10.1084/jem.146.1.257
19. Weiler JM, Daha MR, Austen KF, Fearon DT. Control of the amplification convertase of complement by the plasma protein beta1H. *Proc Natl Acad Sci U S A* (1976) 73:3268–72. doi:10.1073/pnas.73.9.3268
20. Chen SF, Wang FM, Li ZY, Yu F, Zhao MH, Chen M. Plasma complement factor H is associated with disease activity of patients with ANCA-associated vasculitis. *Arthritis Res Ther* (2015) 17:129. doi:10.1186/s13075-015-0656-8
21. Chen SF, Wang FM, Li ZY, Yu F, Chen M, Zhao MH. The functional activities of complement factor H are impaired in patients with ANCA-positive vasculitis. *Clin Immunol* (2017) 175:41–50. doi:10.1016/j.clim.2016.11.013
22. Mihlan M, Stippa S, Józsi M, Zipfel PF. Monomeric CRP contributes to complement control in fluid phase and on cellular surfaces and increases phagocytosis by recruiting factor H. *Cell Death Differ* (2009) 16:1630–40. doi:10.1038/cdd.2009.103
23. Avery VM, Gordon DL. Characterization of factor H binding to human polymorphonuclear leukocytes. *J Immunol* (1993) 151:5545–53.
24. DiScipio RG, Daffern PJ, Schraufstätter IU, Sriramarao P. Human polymorphonuclear leukocytes adhere to complement factor H through an interaction that involves alphaMbeta2 (CD11b/CD18). *J Immunol* (1998) 160:4057–66.
25. Losse J, Zipfel PF, Józsi M. Factor H and factor H-related protein 1 bind to human neutrophils via complement receptor 3, mediate attachment to *Candida albicans*, and enhance neutrophil antimicrobial activity. *J Immunol* (2010) 184:912–21. doi:10.4049/jimmunol.0901702
26. Schneider AE, Sándor N, Kárpáti É, Józsi M. Complement factor H modulates the activation of human neutrophil granulocytes and the generation of neutrophil extracellular traps. *Mol Immunol* (2016) 72:37–48. doi:10.1016/j.molimm.2016.02.011
27. Reumaux D, Vossebeld PJ, Roos D, Verhoeven AJ. Effect of tumor necrosis factor-induced integrin activation on Fc gamma receptor II-mediated signal transduction: relevance for activation of neutrophils by anti-proteinase 3 or anti-myeloperoxidase antibodies. *Blood* (1995) 86:3189–95.
28. Nolan SL, Kalia N, Nash GB, Kamel D, Heeringa P, Savage CO. Mechanisms of ANCA-mediated leukocyte-endothelial cell interactions in vivo. *J Am Soc Nephrol* (2008) 19:973–84. doi:10.1681/ASN.2007111166
29. Choi M, Rolle S, Rane M, Haller H, Luft FC, Kettritz R. Extracellular signal-regulated kinase inhibition by statins inhibits neutrophil activation by ANCA. *Kidney Int* (2003) 63:96–106. doi:10.1046/j.1523-1755.2003.00718.x
30. Schreiber A, Rolle S, Peripelittchenko L, Rademann J, Schneider W, Luft FC, et al. Phosphoinositol 3-kinase-gamma mediates antineutrophil cytoplasmic autoantibody-induced glomerulonephritis. *Kidney Int* (2010) 77:118–28. doi:10.1038/ki.2009.420
31. Wang FM, Yu F, Zhao MH. A method of purifying intact complement factor H from human plasma. *Protein Expr Purif* (2013) 91:105–11. doi:10.1016/j.pep.2013.07.014
32. Zhou Y, Wu J, Kucik DF, White NB, Redden DT, Szalai AJ, et al. Multiple lupus-associated ITGAM variants alter Mac-1 functions on neutrophils. *Arthritis Rheum* (2013) 65:2907–16. doi:10.1002/art.38117
33. Szmitko PE, Wang CH, Weisel RD, de Almeida JR, Anderson TJ, Verma S. New markers of inflammation and endothelial cell activation: part I. *Circulation* (2003) 108:1917–23. doi:10.1161/01.CIR.0000089190.95415.9F
34. Bouaouina M, Blouin E, Halbwachs-Mecarelli L, Lesavre P, Rieu P. TNF-induced beta2 integrin activation involves Src kinases and a redox-regulated activation of p38 MAPK. *J Immunol* (2004) 173:1313–20. doi:10.4049/jimmunol.173.2.1313
35. Krilis M, Qi M, Madigan MC, Wong JWH, Abdelatti M, Guymer RH, et al. Nitration of tyrosines in complement factor H domains alters its immunological activity and mediates a pathogenic role in age related macular degeneration. *Oncotarget* (2017) 8:49016–32. doi:10.18632/oncotarget.14940
36. Eiserich JP, Hristova M, Cross CE, Jones AD, Freeman BA, Halliwell B, et al. Formation of nitric oxide-derived inflammatory oxidants by myeloperoxidase in neutrophils. *Nature* (1998) 391:393–7. doi:10.1038/34923
37. Forsyth CB, Mathews HL. Lymphocytes utilize CD11b/CD18 for adhesion to *Candida albicans*. *Cell Immunol* (1996) 170:91–100. doi:10.1006/cimm.1996.0138
38. Forsyth CB, Plow EF, Zhang L. Interaction of the fungal pathogen *Candida albicans* with integrin CD11b/CD18: recognition by the I domain is modulated by the lectin-like domain and the CD18 subunit. *J Immunol* (1998) 161:6198–205.
39. Agarwal V, Asmat TM, Luo S, Jensch I, Zipfel PF, Hammerschmidt S. Complement regulator factor H mediates a two-step uptake of *Streptococcus pneumoniae* by human cells. *J Biol Chem* (2010) 285:23486–95. doi:10.1074/jbc.M110.142703

40. Mobberley-Schuman PS, Weiss AA. Influence of CR3 (CD11b/CD18) expression on phagocytosis of *Bordetella pertussis* by human neutrophils. *Infect Immun* (2005) 73:7317–23. doi:10.1128/IAI.73.11.7317-7323.2005
41. Neelamegham S, Taylor AD, Shankaran H, Smith CW, Simon SI. Shear and time-dependent changes in Mac-1, LFA-1, and ICAM-3 binding regulate neutrophil homotypic adhesion. *J Immunol* (2000) 164:3798–805. doi:10.4049/jimmunol.164.7.3798
42. Brachemi S, Mambole A, Fakhouri F, Mouthon L, Guillevin L, Lesavre P, et al. Increased membrane expression of proteinase 3 during neutrophil adhesion in the presence of anti proteinase 3 antibodies. *J Am Soc Nephrol* (2007) 18:2330–9. doi:10.1681/ASN.2006121309
43. Olivar R, Luque A, Cárdenas-Brito S, Naranjo-Gómez M, Blom AM, Borràs FE, et al. The complement inhibitor factor H generates an anti-inflammatory and tolerogenic state in monocyte-derived dendritic cells. *J Immunol* (2016) 196:4274–90. doi:10.4049/jimmunol.1500455
44. Calippe B, Augustin S, Beguier F, Charles-Messance H, Poupel L, Conart JB, et al. Complement factor H inhibits CD47-mediated resolution of inflammation. *Immunity* (2017) 46:261–72. doi:10.1016/j.immuni.2017.01.006
45. Camous L, Roumenina L, Bigot S, Brachemi S, Frémeaux-Bacchi V, Lesavre P, et al. Complement alternative pathway acts as a positive feedback amplification of neutrophil activation. *Blood* (2011) 117:1340–9. doi:10.1182/blood-2010-05-283564
46. O'Flynn J, Dixon KO, Faber Krol MC, Daha MR, van Kooten C. Myeloperoxidase directs properdin-mediated complement activation. *J Innate Immun* (2014) 6:417–25. doi:10.1159/000356980
47. Chen SF, Wang FM, Li ZY, Yu F, Chen M, Zhao MH. Myeloperoxidase influences the complement regulatory activity of complement factor H. *Rheumatology (Oxford)* (2018). doi:10.1093/rheumatology/kex529
48. Tse WY, Williams J, Pall A, Wilkes M, Savage CO, Adu D. Antineutrophil cytoplasm antibody-induced neutrophil nitric oxide production is nitric oxide synthase independent. *Kidney Int* (2001) 59:593–600. doi:10.1046/j.1523-1755.2001.059002593.x
49. Radi R. Protein tyrosine nitration: biochemical mechanisms and structural basis of functional effects. *Acc Chem Res* (2013) 46:550–9. doi:10.1021/ar300234c
50. Hageman GS, Anderson DH, Johnson LV, Hancox LS, Taiber AJ, Hardisty LI, et al. A common haplotype in the complement regulatory gene factor H (HF1/CFH) predisposes individuals to age-related macular degeneration. *Proc Natl Acad Sci U S A* (2005) 102:7227–32. doi:10.1073/pnas.0501536102
51. Pickering MC, de Jorge EG, Martinez-Barricarte R, Recalde S, Garcia-Layana A, Rose KL, et al. Spontaneous hemolytic uremic syndrome triggered by complement factor H lacking surface recognition domains. *J Exp Med* (2007) 204:1249–56. doi:10.1084/jem.20070301
52. Tortajada A, Montes T, Martínez-Barricarte R, Morgan BP, Harris CL, de Córdoba SR. The disease-protective complement factor H allotypic variant Ile62 shows increased binding affinity for C3b and enhanced cofactor activity. *Hum Mol Genet* (2009) 18:3452–61. doi:10.1093/hmg/ddp289
53. Pechtl IC, Kavanagh D, McIntosh N, Harris CL, Barlow PN. Disease-associated N-terminal complement factor H mutations perturb cofactor and decay-accelerating activities. *J Biol Chem* (2011) 286:11082–90. doi:10.1074/jbc.M110.211839
54. Kerr H, Wong E, Makou E, Yang Y, Marchbank K, Kavanagh D, et al. Disease-linked mutations in factor H reveal pivotal role of cofactor activity in self-surface-selective regulation of complement activation. *J Biol Chem* (2017) 292:13345–60. doi:10.1074/jbc.M117.795088
55. Klein RJ, Zeiss C, Chew EY, Tsai JY, Sackler RS, Haynes C, et al. Complement factor H polymorphism in age-related macular degeneration. *Science* (2005) 308:385–9. doi:10.1126/science.1109557
56. Edwards AO, Ritter R III, Abel KJ, Manning A, Panhuysen C, Farrer LA. Complement factor H polymorphism and age-related macular degeneration. *Science* (2005) 308:421–4. doi:10.1126/science.1110189
57. Haines JL, Hauser MA, Schmidt S, Scott WK, Olson LM, Gallins P, et al. Complement factor H variant increases the risk of age-related macular degeneration. *Science* (2005) 308:419–21. doi:10.1126/science.1110359

Conflict of Interest Statement: The authors declare that the research was conducted in the absence of any commercial or financial relationships that could be construed as a potential conflict of interest.

frontiers in Immunology

ORIGINAL RESEARCH
published: 19 March 2018
doi: 10.3389/fimmu.2018.00555

Lineage-Specific Analysis of Syk Function in Autoantibody-Induced Arthritis

Tamás Németh[1,2], Krisztina Futosi[1,2], Kata Szilveszter[1,2], Olivér Vilinovszki[1], Levente Kiss-Pápai[1,2] and Attila Mócsai[1,2]**

[1] *Department of Physiology, Semmelweis University School of Medicine, Budapest, Hungary,* [2] *MTA-SE "Lendület" Inflammation Physiology Research Group of the Hungarian Academy of Sciences and Semmelweis University, Budapest, Hungary*

OPEN ACCESS

Edited by:
Ralf J. Ludwig, University of Lübeck, Germany

Reviewed by:
Katja Bieber, University of Lübeck, Germany
Marko Radic, University of Tennessee College of Medicine, United States
Aaron James Marshall, University of Manitoba, Canada

***Correspondence:**
Tamás Németh
nemeth.tamas@med.semmelweis-univ.hu;
Attila Mócsai
mocsai.attila@med.semmelweis-univ.hu

Specialty section:
This article was submitted to Immunological Tolerance and Regulation, a section of the journal Frontiers in Immunology

Received: *15 January 2018*
Accepted: *05 March 2018*
Published: *19 March 2018*

Citation:
Németh T, Futosi K, Szilveszter K, Vilinovszki O, Kiss-Pápai L and Mócsai A (2018) Lineage-Specific Analysis of Syk Function in Autoantibody-Induced Arthritis. Front. Immunol. 9:555. doi: 10.3389/fimmu.2018.00555

Autoantibody production and autoantibody-mediated inflammation are hallmarks of a number of autoimmune diseases. The K/BxN serum-transfer arthritis is one of the most widely used models of the effector phase of autoantibody-induced pathology. Several hematopoietic lineages including neutrophils, platelets, and mast cells have been proposed to contribute to inflammation and tissue damage in this model. We have previously shown that the Syk tyrosine kinase is critically involved in the development in K/BxN serum-transfer arthritis and bone marrow chimeric experiments indicated that Syk is likely involved in one or more hematopoietic lineages during the disease course. The aim of the present study was to further define the lineage(s) in which Syk expression is required for autoantibody-induced arthritis. To this end, K/BxN serum-transfer arthritis was tested in conditional mutant mice in which Syk was deleted in a lineage-specific manner from neutrophils, platelets, or mast cells. Combination of the MRP8-Cre, PF4-Cre, or Mcpt5-Cre transgene with floxed Syk alleles allowed efficient and selective deletion of Syk from neutrophils, platelets, or mast cells, respectively. This has also been confirmed by defective Syk-dependent *in vitro* functional responses of the respective cell types. *In vivo* studies revealed nearly complete defect of the development of K/BxN serum-transfer arthritis upon neutrophil-specific deletion of Syk. By contrast, Syk deletion from platelets or mast cells did not affect the development of K/BxN serum-transfer arthritis. Our results indicate that autoantibody-induced arthritis requires Syk expression in neutrophils, whereas, contrary to prior assumptions, Syk expression in platelets or mast cells is dispensable for disease development in this model.

Keywords: Syk, arthritis, neutrophils, platelets, mast cells

INTRODUCTION

A number of autoimmune diseases, including rheumatoid arthritis, systemic lupus erythematosus, small vessel vasculitis, or pemphigoid diseases, are characterized by production of autoantibodies against various autoantigens of the mammalian body (1). Those autoantibodies are thought to contribute to the autoimmune disease pathogenesis, either directly by engagement of their target autoantigens (activating or function-blocking autoantibodies), or by triggering an inflammatory reaction and concomitant tissue damage caused by the infiltrating inflammatory cells.

The K/BxN serum-transfer arthritis is one of the most widely used mouse model of autoantibody-induced tissue damage. This model is initiated by systemic injection of serum from so-called K/BxN mice in which the expression of a specific T-cell-receptor transgene on an autoimmunity-prone genetic background leads to the generation of high titers of autoantibodies against the ubiquitously expressed glucose 6-phosphate isomerase enzyme (2–5). Transferring those autoantibodies with the K/BxN serum to naive animals triggers robust inflammation of the distal joints and of other tissues. K/BxN serum-transfer arthritis is triggered by immune complex (IC) deposition and concomitant activation of Fcγ-receptors (5). A number of hematopoietic lineages are thought to be involved in the development of K/BxN serum-transfer arthritis. The role of neutrophils is indicated by the fact that antibody-mediated depletion (6) or genetic deletion (7, 8) of neutrophils prevents arthritis development in this model. Arthritis development was also reduced in mast cell-deficient $Kit^{W/W\text{-}v}$ mice (9) suggesting an important role of mast cells. In addition, platelets were proposed to be required for the development of K/BxN serum-transfer arthritis by releasing platelet-derived microparticles upon collagen-induced activation in the synovial tissue (10).

Syk is a nonreceptor tyrosine kinase primarily expressed in cells of the hematopoietic lineage (11). It mediates signaling by a number of cell surface receptors including B-cell-receptors (12, 13), Fcγ- and Fcε-receptors (14–18), β_2 and β_3 integrins (19–21), C-type lectins (11, 22), and other receptors coupled to immunoreceptor tyrosine-based activation motifs (ITAMs) (11, 23). Given its role in various hematopoietic lineages and signaling downstream of diverse cell surface receptors, Syk is indispensable for a number of *in vivo* processes including B-cell development (12, 13), various inflammatory disease processes (17, 24, 25), antifungal immunity (26), or lymph vessel development (27). Based on its central role in the immune system, Syk has been proposed as a therapeutic target in various autoimmune and inflammatory diseases (11, 28).

We have previously shown that Syk is critically involved in arthritis development in the autoantibody-induced K/BxN serum transfer model (25). Our additional studies indicated that Syk is involved in a pathway downstream of Fc-receptors and Src-family kinases (29) and activates further downstream processes through PLCγ2 (30) and CARD9 (31). However, it is at present incompletely understood in which lineage(s) Syk needs to be expressed for arthritis development in this model. Bone marrow chimeric experiments suggested the role for Syk in one or more hematopoietic lineages (25). Several lines of evidence suggest an important role for Syk in neutrophils (19, 31, 32). An important role for GpVI, an ITAM-coupled collagen receptor on platelets, for the development of K/BxN serum-transfer arthritis (10) suggested a role for Syk in platelets for disease development in this model (33). Finally, the proposed role of mast cells (9, 34) and the critical role for Syk in mast cell activation (14, 18) raised the possibility that Syk expression in mast cells contributes to development of K/BxN serum-transfer arthritis.

The above studies prompted us to perform lineage-specific deletion of Syk from neutrophils, platelets, and mast cells, and to test the effect of those mutations on the development of autoantibody-induced arthritis in the K/BxN serum-transfer model. Our results indicate an important role for Syk expression in neutrophils whereas, contrary to our expectations, Syk expression in platelets or mast cells appears to be dispensable for arthritis development in this model.

MATERIALS AND METHODS

Animals

Mice carrying a deleted *Syk* allele (Syk^{tm1Tyb}, referred to as Syk^{-}) (12) were kept in heterozygous form and used to obtain $Syk^{-/-}$ and control fetuses for fetal liver transplantation (19, 25). Lineage-specific deletion of *Syk* was achieved by crossing MRP8-Cre (35), PF4-Cre (36), or Mcpt5-Cre transgenic mice (37) with animals carrying a floxed Syk allele ($Syk^{tm1.2Tara}$, referred to as Syk^{flox}) (38) to obtain MRP8-Cre$^{+}Syk^{flox/flox}$, PF4-Cre$^{+}Syk^{flox/flox}$, and Mcpt5-Cre$^{+}Syk^{flox/flox}$ mice, referred to as $Syk^{\Delta PMN}$, $Syk^{\Delta PLT}$, and $Syk^{\Delta MC}$ animals, respectively. Mice carrying the KRN T-cell-receptor transgene (2) were maintained in heterozygous form by mating with C57BL/6 mice. All transgenic mice were backcrossed to the C57BL/6 genetic background for at least six generations. Genotyping was performed by allele-specific PCR.

Wild type (WT) control C57BL/6 mice were purchased from Charles River or the Hungarian National Institute of Oncology (Budapest, Hungary). NOD mice, as well as a congenic strain carrying the CD45.1 allele on the C57BL/6 genetic background (B6.SJL-$Ptprc^{a}$) were purchased from the Jackson Laboratory.

Mice were kept in individually sterile ventilated cages (Tecniplast) in a conventional facility. All animal experiments were approved by the Animal Experimentation Review Board of the Semmelweis University.

Bone marrow chimeras were generated by intravenous injection of unfractionated bone marrow or fetal liver cells into recipients carrying the CD45.1 allele on the C57BL/6 genetic background, which were lethally irradiated before by 11 Gy from a ^{137}Cs source using a Gamma-Service Medical (Leipzig, Germany) D1 irradiator. 4 weeks after transplantation, peripheral blood samples were stained for Ly6G and CD45.2 (Clones 1A8 and 104, respectively; both from BD Biosciences) and analyzed by a BD Biosciences FACSCalibur flow cytometer as previously described (see Figure S1A in Supplementary Material) (29).

K/BxN Serum-Transfer Arthritis

Mice carrying the KRN T-cell receptor transgene on the C57BL/6 genetic background were mated with NOD mice to obtain transgene-positive (arthritic) K/BxN and transgene-negative (non-arthritic) BxN mice (2, 30). The presence of the transgene was determined by allele-specific PCR and confirmed by phenotypic assessment. Blood was taken by retroorbital bleeding and sera from arthritic and control mice were pooled separately.

Arthritis was induced by a single intraperitoneal injection of 300 µl K/BxN (arthritic) or BxN (control) serum into intact mice or bone marrow chimeras, followed by daily assessment of arthritis severity for 2 weeks as described (30, 31, 39). Visible clinical signs were scored on a 0–10 scale by two investigators

blinded for the origin and treatment of the mice. Ankle thickness was measured by a spring-loaded caliper (Kroeplin).

Isolation and Activation of Neutrophils, Platelets, and Mast Cells

Mouse neutrophils were isolated from the bone marrow of the femurs and tibias of intact mice or chimeras by hypotonic lysis followed by Percoll (GE Healthcare) gradient centrifugation using sterile and endotoxin-free reagents as described (18, 31, 39). Cells were kept at room temperature in Ca^{2+}- and Mg^{2+}-free medium until use and prewarmed to 37°C prior to activation. Neutrophil assays were performed at 37°C in HBSS supplemented with 20 mM HEPES, pH 7.4. Adhesion-dependent superoxide release by neutrophils was followed by a cytochrome *c* reduction test from 100 µl aliquots of 4×10^6/ml cells plated on fibrinogen (Calbiochem) coated surfaces in the presence of 50 ng/ml murine TNF-α (PeproTech) as described (39).

Platelets were isolated from peripheral blood by mild centrifugation in the presence of heparin. For an *in vitro* aggregation assay (40), platelets were divided into two groups, one labeled with an anti-CD9-PE (Clone EM-04; Abcam) and the other one with an anti-CD9-APC (Clone eBioKMC8; eBioscience) antibody. The two differently labeled groups were mixed in equal volumes and were activated by 50 ng/ml Convulxin (Enzo Life Sciences) at 37°C while shaking at 700 rpm for 5 min. The reaction was stopped by BD FACS Lysing Solution (BD Biosciences). The samples were analyzed by flow cytometry, where platelets were identified according to their forward and side scatter characteristics. Aggregation was determined as the percentage of CD9-PE/CD9-APC double positive events (40).

Mast cells were cultured from the bone marrow in the presence of 5 ng/ml murine IL-3 and 20 ng/ml stem cell factor (both from PeproTech). The purity of the cultures was tested by an anti-FcεR antibody (Clone MAR-1; eBioscience) by flow cytometry. For *in vitro* activation, mast cells were first incubated with an anti-dinitrophenyl (DNP) IgE antibody (Clone SPE-7) at a final concentration of 0.5 µg/ml overnight at 37°C on fetal bovine serum (FBS)-coated plates, followed by the crosslinking of Fcε receptors by the addition of 100 ng/ml DNP-human serum albumin to the cell suspensions (both reagents from Sigma-Aldrich). After 30 min, the cells were washed and mast cells were kept in Dulbecco's Modified Eagle's Medium (DMEM; Sigma-Aldrich) overnight at 37°C on FBS-coated plates. The release of the inflammatory mediator MIP-1α was tested from the cell-free supernatants by a commercial ELISA kit (R&D Systems) according to the manufacturer's instructions. The absence of Syk did not have a major effect on neutrophil, platelet, or mast cell development and numbers (data not shown).

Biochemical Studies

For analysis of protein contents, neutrophils, platelets, and mast cells were lysed in 100 mM NaCl, 30 mM Na-HEPES (pH 7.4), 20 mM NaF, 1 mM Na-EGTA, 1% Triton X-100, 1 mM benzamidine, freshly supplemented with 0.1 U/ml Aprotinin, 1:100 Mammalian Protease Inhibitor Cocktail, 1:100 Phosphatase Inhibitor Cocktail 2, 1 mM PMSF, and 1 mM Na_3VO_4 (all from Sigma-Aldrich). After removal of insoluble material, lysates were boiled in sample buffer. Whole cell lysates were run on SDS-PAGE and immunoblotted using antibodies against Syk (Clone N19; Santa Cruz) or β-actin (Clone AC-74; Sigma-Aldrich) followed by peroxidase-labeled secondary antibodies (GE Healthcare). The signal was then developed using the ECL system (GE Healthcare) and exposed to X-ray film.

Presentation of the Data and Statistical Analysis

Experiments were performed the indicated number of times. Quantitative graphs and kinetic curves show mean and SEM from all independent *in vitro* experiments or from all individual mice from the indicated number of experiments. Statistical analyses were carried out by the STATISTICA software using two-way (factorial) ANOVA, with treatment and genotype being the two independent variables. In case of kinetic assays, area under the curve was used for statistical analysis. P values below 0.05 were considered statistically significant.

RESULTS

K/BxN Serum-Transfer Arthritis in $Syk^{-/-}$ Bone Marrow Chimeras

To test the role of Syk within hematopoietic lineage cells, we generated bone marrow chimeric mice by transplanting $Syk^{-/-}$ or WT control fetal liver cells into lethally irradiated recipients. As shown in **Figure 1A**, injection of arthritogenic K/BxN serum into WT control chimeras triggered robust inflammation of the ankle joints whereas no such response could be observed in $Syk^{-/-}$ bone marrow chimeras which carry Syk-deficient hematopoietic tissues. Quantitative kinetic analysis of the clinical scoring of arthritis (**Figure 1B**) or the ankle thickness (**Figure 1C**) revealed that $Syk^{-/-}$ bone marrow chimeras were completely protected from arthritis development in this model ($p = 3 \times 10^{-6}$ and $p = 1.3 \times 10^{-3}$, respectively). Those results confirmed our prior studies showing critical role for Syk in the hematopoietic compartment in K/BxN serum-transfer arthritis (25).

Syk Is Expressed in Neutrophils, Platelets, and Mast Cells

Prior studies suggested a role for neutrophils, platelets, and mast cells in K/BxN serum-transfer arthritis (6–10, 34), as well as the functional role for Syk in those cells (14, 16, 18–20). To confirm the presence of Syk in those lineages and its deletion from $Syk^{-/-}$ cells, we tested the expression of Syk in primary neutrophils and platelets, or bone marrow-derived mast cells, from WT and $Syk^{-/-}$ bone marrow chimeras. As shown in **Figure 1D**, Syk was present in all three cell types derived from WT but not $Syk^{-/-}$ bone marrow chimeras (see the entire blots in Figures S1B–D in Supplementary Material).

Efficacy and Specificity of Syk Deletion From Neutrophils, Platelets, and Mast Cells

To test the role of Syk in a linage-specific manner, we turned to Cre-lox-mediated lineage-specific conditional deletion of Syk. To this

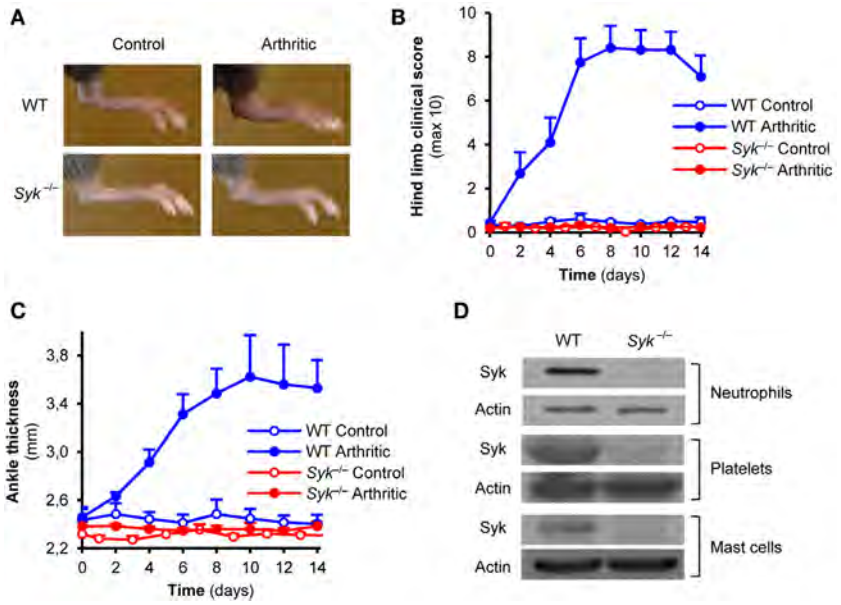

FIGURE 1 | Autoantibody-induced arthritis in Syk-deficient bone marrow chimeras. Wild type (WT) and $Syk^{-/-}$ bone marrow chimeras were injected with BxN (Control) or K/BxN (Arthritic) serum intraperitonally on day 0. Arthritis development was followed by photographing on day 7 **(A)**, clinical scoring of the hind limbs **(B)**, and ankle thickness measurement **(C)**. Panel **(D)** shows the absence of the Syk tyrosine kinase from whole cell lysates of $Syk^{-/-}$ neutrophils, platelets, and mast cells. Photos are representative of, and quantitative data show mean and SEM from, four control and four to five arthritic serum-treated individual mice per group from two independent experiments. Western blot images are representative of two to three independent experiments. See the text for actual *p* values.

end, we generated mice carrying the $Syk^{flox/flox}$ mutation along with a neutrophil-specific MRP8-Cre ($Syk^{\Delta PMN}$), the platelet-specific PF4-Cre ($Syk^{\Delta PLT}$), or the mast cell-specific Mcpt5-Cre ($Syk^{\Delta MC}$) transgenes. We then isolated neutrophils or platelets, and cultured bone marrow-derived mast cells, from those animals. As shown in **Figure 2A**, Syk expression was strongly reduced in $Syk^{\Delta PMN}$, but was not affected in $Syk^{\Delta PLT}$ or $Syk^{\Delta MC}$ neutrophils. Similarly, Syk was absent from $Syk^{\Delta PLT}$ but not from $Syk^{\Delta PMN}$ or $Syk^{\Delta MC}$ platelets (**Figure 2B**). Finally, Syk expression was abrogated in $Syk^{\Delta MC}$ but not in $Syk^{\Delta PMN}$ or $Syk^{\Delta PLT}$ mast cells (**Figure 2C**; see the entire blots in Figure S2 in Supplementary Material). Those results confirm both the efficacy and the specificity of the $Syk^{\Delta PMN}$, $Syk^{\Delta PLT}$, and $Syk^{\Delta MC}$ mutations.

Lineage-Specific Deletion of Syk Abrogates Functional Responses of Neutrophils, Platelets, and Mast Cells

To test the functional efficacy of lineage-specific Syk deletion, we also tested supposedly Syk-dependent functional responses of neutrophils, platelets, and mast cells. Superoxide release of neutrophils plated on a fibrinogen surface in the presence of a soluble TNF stimulus is mediated by β_2 integrins in a supposedly Syk-dependent manner (19). As shown in **Figure 3A**, this response was nearly completely blocked in neutrophils from $Syk^{\Delta PMN}$ animals ($p = 0.02$). Convulxin is a snake venom toxin activating the Fc-receptor-related collagen receptor GpVI on platelets in a Syk-dependent manner (40, 41). As shown in **Figure 3B**, convulxin induced aggregation of WT but not $Syk^{\Delta PLT}$ platelets ($p = 0.03$). Crosslinking of IgE bound to the surface of mast cells

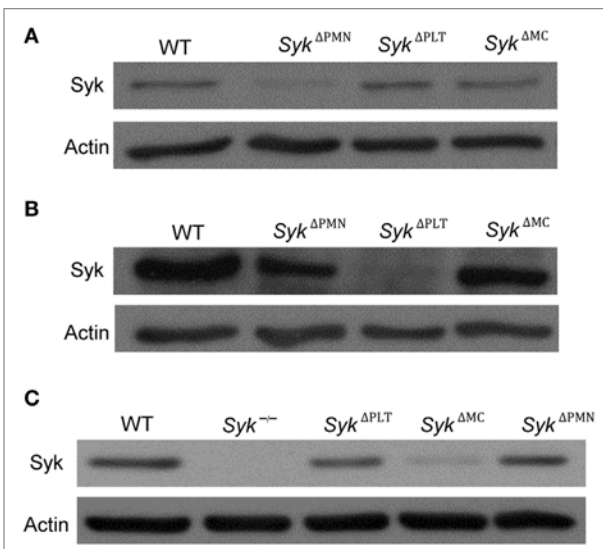

FIGURE 2 | The efficacy and specificity of lineage-specific Syk deletion from different cell types. The efficacy and specificity of lineage-specific deletion was tested by immunoblotting of whole cell lysates of neutrophils **(A)**, platelets **(B)**, and mast cells **(C)** derived from wild type (WT), $Syk^{\Delta PMN}$, $Syk^{\Delta PLT}$, or $Syk^{\Delta MC}$ mice or from $Syk^{-/-}$ bone marrow chimeras. Blots are representative of three independent experiments.

triggers release of various proinflammatory mediators through Fcε-receptors in a Syk-dependent manner (14). As shown in **Figure 3C**, MIP-1α release induced by IgE crosslinking of mast cells was abrogated by the $Syk^{\Delta MC}$ mutation ($p = 1.3 \times 10^{-4}$). Those

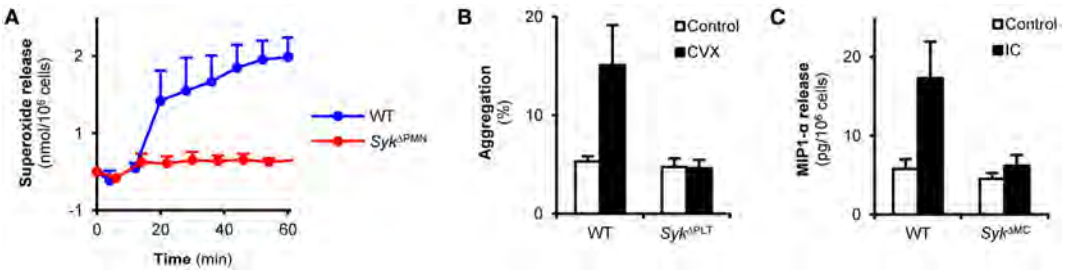

FIGURE 3 | Syk is indispensable for immunoreceptor tyrosine-based activation motif-mediated *in vitro* cellular responses of neutrophils, platelets, and mast cells. **(A)** Wild type (WT) or $Syk^{\Delta PMN}$ neutrophils were plated on fibrinogen-coated surfaces in the presence of TNF-α and their superoxide release was measured by a cytochrome *c* reduction test. Control data points were subtracted. **(B)** WT or $Syk^{\Delta PLT}$ platelets were isolated from peripheral blood, labeled by two different fluorochrome-conjugated CD9 antibodies and were activated by convulxin (CVX) for 5 min. Aggregation was measured as the percentage of CD9-PE/CD9-APC double positive events. **(C)** WT or $Syk^{\Delta MC}$ bone marrow-derived mast cells were incubated with anti-DNP IgE antibodies followed by an Fcε receptor crosslinking step with DNP-HSA. MIP-1α levels were determined from the cell-free supernatant by an ELISA assay. Kinetic curves and graphs represent mean and SEM from three **(A,C)** or six **(B)** samples from three **(A)** or two **(B,C)** independent experiments. See the text for actual *p* values. DNP, dinitrophenyl; HSA, human serum albumin, IC, immune complex.

results indicate that lineage-specific deletion of Syk from neutrophils, platelets, or mast cells leads to the expected functional consequences in those cells.

Neutrophil-Specific Deletion of Syk Abrogates Autoantibody-Induced Arthritis

We next tested the consequence of neutrophil-specific deletion of Syk on the development of K/BxN serum-transfer arthritis. As shown in **Figure 4A**, arthritogenic K/BxN serum triggered visible arthritis development in WT animals. However, no signs of arthritis could be observed in $Syk^{\Delta PMN}$ animals (**Figure 4A**). Quantitative kinetic analysis revealed that $Syk^{\Delta PMN}$ mice were nearly completely protected from development of clinical signs of arthritis (**Figure 4B**; $p = 1.5 \times 10^{-5}$) and arthritis-induced ankle swelling (**Figure 4C**; $p = 1.7 \times 10^{-3}$). Similar results could be observed when testing a larger cohort of bone marrow chimeras generated by transplanting WT or $Syk^{\Delta PMN}$ bone marrow cells into lethally irradiated WT recipients (**Figures 4D,E**; $p = 6.2 \times 10^{-7}$ and $p = 3.2 \times 10^{-6}$, respectively). Those results indicate a critical role for Syk expression within neutrophils for the development of autoantibody-induced arthritis *in vivo*.

Normal Arthritis Development Upon Platelet-Specific Deletion of Syk

Boilard et al. previously showed that genetic deletion of the Syk-coupled GpVI collagen receptor of platelets strongly reduced arthritis development in the K/BxN serum-transfer model (10), suggesting an important role for Syk expression in platelets in this model (33). To test this hypothesis experimentally, we tested K/BxN serum-transfer arthritis in $Syk^{\Delta PLT}$ mice in which Syk was deleted in a platelet-specific manner. Contrary to our expectations, platelet-specific Syk deletion did not affect the development of visual signs of arthritis in our model (**Figure 5A**). Quantitative kinetic analysis did not reveal any effect of the $Syk^{\Delta PLT}$ mutation on the clinical appearance (**Figure 5B**; $p = 0.51$) or on the ankle thickness increase (**Figure 5C**; $p = 0.76$) either. Similar results were obtained when using bone marrow chimeras generated by transplanting WT or $Syk^{\Delta PLT}$ bone marrow cells into lethally irradiated WT recipients (**Figures 5D,E**; $p = 0.49$ and $p = 0.9$, respectively). Those results, together with the lack of Syk (**Figure 2B**) and the defective Syk-dependent functional activation (**Figure 3B**) of $Syk^{\Delta PLT}$ platelets indicate that Syk expression in platelets is not required for the development of K/BxN serum-transfer arthritis.

Mast Cell-Specific Syk Deletion Does Not Affect Autoantibody-Induced Arthritis

Mast cells are one of the major targets of Syk function (14, 18) and they have also been proposed to participate in the development of K/BxN serum-transfer arthritis (9, 34). Therefore, we hypothesized that Syk expression in mast cells may be required for arthritis development in this model. To this end, we tested the development of K/BxN serum-transfer arthritis in $Syk^{\Delta MC}$ mice. As shown in **Figure 6A**, the $Syk^{\Delta MC}$ mutation did not affect the development of visible signs of arthritis in our model. Quantitative kinetic analysis did not reveal any inhibition of arthritis development either when scoring clinical signs of arthritis (**Figure 6B**; $p = 0.38$) or when measuring arthritis-induced increase of ankle thickness (**Figure 6C**; $p = 0.37$). By contrast, there was even a tendency of earlier arthritis development in the $Syk^{\Delta MC}$ animals (**Figures 6B,C**), raising the possibility of a negative role of Syk expressed in mast cells. Because of the radioresistance of mast cells, no bone marrow chimeras have been generated using $Syk^{\Delta MC}$ mice. The lack of inhibition of arthritis in $Syk^{\Delta MC}$ animals, together with the dramatic reduction of Syk expression (**Figure 2C**) and Syk-mediated functional responses (**Figure 3C**) in $Syk^{\Delta MC}$ mast cells indicates that Syk expression within mast cells is dispensable for arthritis development in the K/BxN serum-transfer model.

DISCUSSION

The Syk tyrosine kinase is critically involved in various inflammatory disease processes including the development of autoantibody-induced arthritis and dermatitis models (11, 17, 25). Given the wide expression of Syk in practically all hematopoietic lineages (11), understanding Syk function in a lineage-specific manner is of particular importance. Our results presented in this work indicate that of the three most prominent Syk-expressing lineages supposedly involved in the development of autoantibody-induced

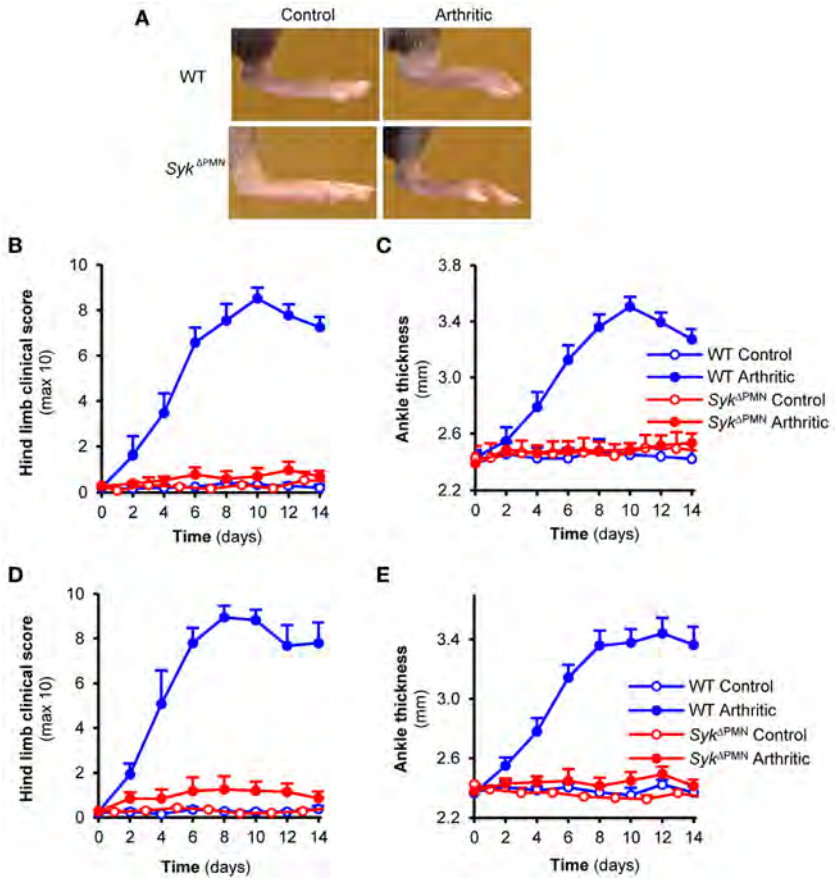

FIGURE 4 | Neutrophil-specific Syk deletion attenuates experimental arthritis. Wild type (WT) and *Syk*$^{\Delta PMN}$ intact animals **(A–C)** or bone marrow chimeras **(D,E)** were injected with BxN (Control) or K/BxN (Arthritic) serum intraperitonally on day 0. Arthritis development was followed by photographing **(A)**, clinical scoring of the hind limbs **(B,D)**, and ankle thickness measurement **(C,E)**. Quantitative data show mean and SEM from three control and five to six arthritic serum-treated individual mice per group from three independent experiments **(B,C)** or from five control and five to seven arthritic serum-treated mice per group from three independent experiments **(D,E)**. See the text for actual *p* values.

arthritis, Syk expression in neutrophils is critical, whereas that in platelets or mast cells is dispensable, for the development of K/BxN serum-transfer arthritis.

We and others have shown that Syk plays a critical role in various functional responses of neutrophils (16, 17, 19, 42, 43) without affecting neutrophil development (17, 19). Neutrophils have also been shown to be critical for the development of autoantibody-induced arthritis (6–8), likely at least in part through IgG IC-mediated activation of Fcγ-receptors expressed on the neutrophil cell surface (29), as well as by yet incompletely understood neutrophil-mediated initial vascular changes (8). Based on those studies, we hypothesized that Syk expression within neutrophils is critical for autoantibody-induced arthritis development. Our results confirmed that hypothesis, and they were also in line with prior studies from other groups (32) and our own analysis of neutrophil-specific deletion of the CARD9 adapter protein, a supposedly downstream effector of Syk (31). Though it is at present incompletely understood how Syk within neutrophils participates in autoantibody-induced arthritis development, our prior studies showing defective release of proinflammatory mediators by Syk-deficient neutrophils despite normal intrinsic migratory capacity of the cells (17, 19, 31) suggest that Syk, similar to Src-family kinases (29), participates in the amplification of neutrophil recruitment by neutrophil-derived proinflammatory mediators (44).

In contrast to our neutrophil-specific deletion studies, our platelet-specific deletion experiments did not support our hypothesis based on literature data. Though Syk is not required for platelet development (20), it plays a critical role in various platelet functions (11) including $\alpha_{IIb}\beta_3$ integrin-dependent platelet spreading (20), responses mediated by the hemITAM-coupled C-type lectin CLEC-2 (45), as well as signaling downstream of GpVI, an ITAM-coupled collagen-receptor of platelets (40, 41). GpVI is closely related to Fcα-receptors and it is directly associated with, and supposedly signals through, the ITAM-containing Fc-receptor γ-chain (FcRγ) (40, 41, 46–49). Platelets and, specifically, GpVI has been shown to play a critical role in the development of K/BxN serum-transfer arthritis (10), suggesting that Syk expression downstream of platelet GpVI is critically involved in arthritis development in this model (33). Our results of normal arthritis development upon platelet-specific deletion of Syk (**Figure 5**) despite practically complete lack of Syk from platelets

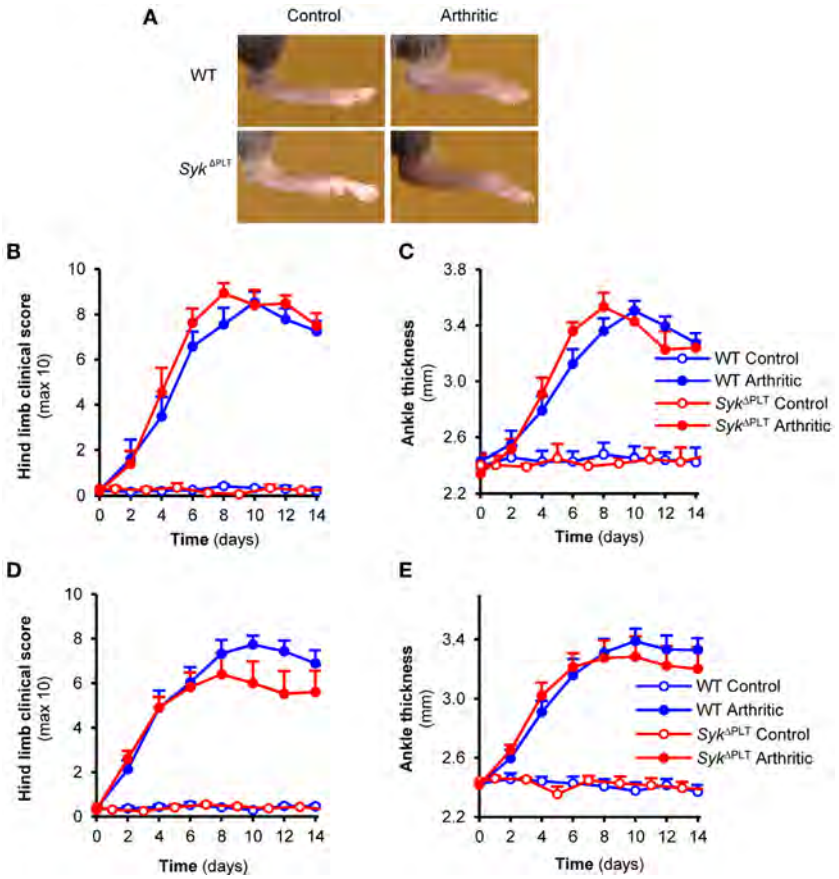

FIGURE 5 | Platelet-specific Syk deletion has no effect on autoantibody-induced arthritis. Wild type (WT) and *Syk*$^{\Delta PLT}$ intact animals **(A–C)** or bone marrow chimeras **(D,E)** were injected with BxN (Control) or K/BxN (Arthritic) serum intraperitonally on day 0. Arthritis development was followed by photographing **(A)**, clinical scoring of the hind limbs **(B,D)**, and ankle thickness measurement **(C,E)**. Quantitative data show mean and SEM from three control and five arthritic serum-treated individual mice per group from three independent experiments **(B,C)** or from six control and eight to nine arthritic serum-treated mice per group from three independent experiments **(D,E)**. See the text for actual *p* values.

(**Figure 2**) and completely defective GpVI-mediated *in vitro* platelet function (**Figure 3**) argues against that hypothesis. There are several possible explanations for those findings. Though GpVI is associated with the ITAM-containing FcRγ adapter, it may be able to bypass the ITAM-Syk pathway under certain conditions, using FcRγ as a chaperone required for cell surface expression but not as an ITAM-mediated signaling adaptor. Platelets have also been proposed to interact with fibroblast-like synoviocytes in a COX-1-dependent manner which is independent of platelet GpVI or FcRγ expression (50). This pathway may be able to compensate for the defective GpVI–FcRγ–Syk pathway upon platelet-specific Syk deletion. We also cannot exclude the possibility that GpVI needs to be expressed in a non-platelet lineage to support autoantibody-induced arthritis in mice. Finally, technical details such as a role for the small remaining Syk expression after Cre-mediated *Syk* deletion, or different experimental conditions may also account for the different conclusions drawn from our study and from those proposing a critical role for the platelet GpVI–FcRγ–Syk pathway in autoantibody-induced arthritis (10, 33). It should also be mentioned that our study focused on visible signs of arthritis and therefore we cannot exclude the possibility that Syk expression in platelets modulates the inflammation process by a mechanism not clearly visible by macroscopic inspection.

In the third part of our study, we tested the role of Syk in mast cells during autoantibody-induced arthritis. Syk has been shown to play a critical role in mast cell function without affecting mast cell survival (14, 18) and mast cells were proposed to be important players in autoantibody-induced arthritis development (9). Therefore, we hypothesized that Syk expression in mast cells may play a role in the development of K/BxN serum-transfer arthritis. Our results showing normal arthritis development in that model upon mast cell-specific Syk deletion (**Figure 6**) despite strongly reduced Syk expression (**Figure 2**) and defective Syk-mediated functional responses (**Figure 3**) in mast cells argue against that possibility. There are several possible explanations for those findings. Since the mechanism of how mast cells contribute to IgG autoantibody-induced disease pathogenesis is incompletely understood, it is possible that mast cells use a Syk-independent signal transduction pathway during K/BxN serum-transfer arthritis (e.g., when mast cells are not directly activated by the autoantibody-containing ICs, but rather indirectly through Syk-independent chemokine, cytokine, or PRR pathways). It

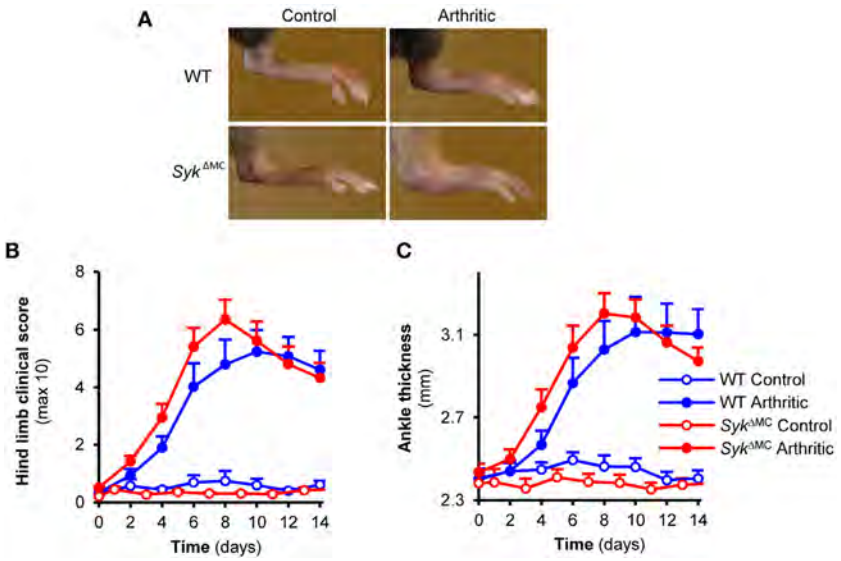

FIGURE 6 | Mast cell-specific Syk deletion does not affect the effector phase of experimental arthritis. Wild type (WT) and *Syk*$^{\Delta MC}$ animals were injected with BxN (Control) or K/BxN (Arthritic) serum intraperitonally on day 0. Arthritis development was followed by photographing **(A)**, clinical scoring of the hind limbs **(B)**, and ankle thickness measurement **(C)**. Quantitative data show mean and SEM from seven to nine control and twelve to thirteen arthritic serum-treated individual mice per group from four independent experiments. See the text for actual *p* values.

should also be mentioned that follow-up studies have questioned the critical role of mast cells in autoantibody-induced arthritis development (51, 52), pointing to difficulties of the interpretation of data obtained with different mast cell-deficient mouse strains. Indeed, our limited preliminary studies also suggested that the role of mast cells is highly dependent on the experimental conditions used for triggering autoantibody-induced arthritis in mice (Z. Jakus and A. M., unpublished observations). Finally, given that our experiments focused on visible signs of inflammation, we cannot exclude the possibility that Syk expression in mast cells may modulate arthritis development or the overall inflammation process in a manner not clearly visible by macroscopic assessment.

Besides neutrophils, platelets, and mast cells, Syk is also expressed in other lineages possibly involved in arthritis development. B-cells are one of the most prominent lineages requiring Syk function (12, 13). However, it is unlikely that Syk expressed in B-cells contributes to K/BxN serum-transfer arthritis since that model mimics the post-immunization effector phase of autoimmune arthritis and it develops normally even in the absence of B-cells in μMT-deficient or Rag-deficient mice (3). Macrophages have been proposed to be important players in the development of K/BxN serum-transfer arthritis (53). Unfortunately, currently available techniques do not allow the proper analysis of the *in vivo* relevance of Syk expression within macrophages because of the limited spectrum/specificity of the available macrophage-specific Cre-expressing mouse strains (54). We have previously shown that Syk is critically involved in osteoclast development and function (23). Though understanding the role of Syk in arthritis-induced bone erosions would be of clear importance, this question is beyond the scope of the present study focusing on the inflammatory aspect of autoantibody-induced disease processes.

Taken together, our results provide understanding of the role of Syk in autoantibody-induced arthritis at the cellular lineage level. Our findings indicate a critical role for Syk expression in neutrophils, but refute prior assumptions for the role of Syk in platelets and argue against a role for Syk expression in mast cells. Those results will strongly contribute to the understanding of the pathomechanism of autoantibody-mediated disease processes at the cellular and molecular level.

ETHICS STATEMENT

All animal experiments were approved by the Animal Experimentation Review Board of the Semmelweis University.

AUTHOR CONTRIBUTIONS

TN and AM conceived the study, designed the experiments, and wrote the manuscript. TN, KF, KS, OV, and LK-P performed the experiments. TN, KF, and AM analyzed and interpreted the data. AM supervised the project.

ACKNOWLEDGMENTS

We thank Edina Simon for expert technical assistance; Gábor Bánhegyi for access to equipment; Diane Mathis, Christophe Benoist, Victor Tybulewicz, Emmanuelle Passegue, Axel Roers, and Alexander Tarakhovsky for transgenic animals. This work was supported by the Lendület program of the Hungarian Academy of Sciences (LP2013-66/2013 to AM), the Hungarian National Research, Development and Innovation Office (NVKP_16-2016-1-0039 to AM), the Hungarian Ministry of National Economy (VEKOP-2.3.2-16-2016-00002 to AM), and the János Bolyai

Research Scholarships of the Hungarian Academy of Sciences (to TN and KF). AM was a recipient of a Wellcome Trust International Senior Research Fellowship (Grant No. 087782).

SUPPLEMENTARY MATERIAL

The Supplementary Material for this article can be found online at http://www.frontiersin.org/articles/10.3389/fimmu.2018.00555/full#supplementary-material.

FIGURE S1 | Flow cytometric analysis of bone marrow chimeras and Western blot images with more details. **(A)** Flow cytometric analysis of CD45.2-positive donor-derived neutrophils in the peripheral blood of wild type (WT) and *Syk*$^{\Delta PMN}$ bone marrow chimeras 4 weeks after bone marrow transplantation. **(B–D)** Detailed Western blot images showing the expression of Syk in neutrophil **(B)**, platelet **(C)**, or mast cell **(D)** lysates from **Figure 1D**.

FIGURE S2 | Detailed Western blot images showing the efficacy and specificity of lineage-specific Syk deletion in whole cell lysates of neutrophils **(A)**, platelets **(B)**, and mast cells **(C)** from **Figure 2**.

REFERENCES

1. Suurmond J, Diamond B. Autoantibodies in systemic autoimmune diseases: specificity and pathogenicity. *J Clin Invest* (2015) 125:2194–202. doi:10.1172/JCI78084
2. Kouskoff V, Korganow AS, Duchatelle V, Degott C, Benoist C, Mathis D. Organ-specific disease provoked by systemic autoimmunity. *Cell* (1996) 87:811–22. doi:10.1016/S0092-8674(00)81989-3
3. Korganow AS, Ji H, Mangialaio S, Duchatelle V, Pelanda R, Martin T, et al. From systemic T cell self-reactivity to organ-specific autoimmune disease via immunoglobulins. *Immunity* (1999) 10:451–61. doi:10.1016/S1074-7613(00)80045-X
4. Matsumoto I, Staub A, Benoist C, Mathis D. Arthritis provoked by linked T and B cell recognition of a glycolytic enzyme. *Science* (1999) 286:1732–5. doi:10.1126/science.286.5445.1732
5. Ji H, Ohmura K, Mahmood U, Lee DM, Hofhuis FM, Boackle SA, et al. Arthritis critically dependent on innate immune system players. *Immunity* (2002) 16:157–68. doi:10.1016/S1074-7613(02)00275-3
6. Wipke BT, Allen PM. Essential role of neutrophils in the initiation and progression of a murine model of rheumatoid arthritis. *J Immunol* (2001) 167:1601–8. doi:10.4049/jimmunol.167.3.1601
7. Jonsson H, Allen P, Peng SL. Inflammatory arthritis requires Foxo3a to prevent Fas ligand-induced neutrophil apoptosis. *Nat Med* (2005) 11:666–71. doi:10.1038/nm1248
8. Binstadt BA, Patel PR, Alencar H, Nigrovic PA, Lee DM, Mahmood U, et al. Particularities of the vasculature can promote the organ specificity of autoimmune attack. *Nat Immunol* (2006) 7:284–92. doi:10.1038/ni1306
9. Lee DM, Friend DS, Gurish MF, Benoist C, Mathis D, Brenner MB. Mast cells: a cellular link between autoantibodies and inflammatory arthritis. *Science* (2002) 297:1689–92. doi:10.1126/science.1073176
10. Boilard E, Nigrovic PA, Larabee K, Watts GF, Coblyn JS, Weinblatt ME, et al. Platelets amplify inflammation in arthritis via collagen-dependent microparticle production. *Science* (2010) 327:580–3. doi:10.1126/science.1181928
11. Mócsai A, Ruland J, Tybulewicz VL. The SYK tyrosine kinase: a crucial player in diverse biological functions. *Nat Rev Immunol* (2010) 10:387–402. doi:10.1038/nri2765
12. Turner M, Mee PJ, Costello PS, Williams O, Price AA, Duddy LP, et al. Perinatal lethality and blocked B-cell development in mice lacking the tyrosine kinase Syk. *Nature* (1995) 378:298–302. doi:10.1038/378298a0
13. Cheng AM, Rowley B, Pao W, Hayday A, Bolen JB, Pawson T. Syk tyrosine kinase required for mouse viability and B-cell development. *Nature* (1995) 378:303–6. doi:10.1038/378303a0
14. Costello PS, Turner M, Walters AE, Cunningham CN, Bauer PH, Downward J, et al. Critical role for the tyrosine kinase Syk in signalling through the high affinity IgE receptor of mast cells. *Oncogene* (1996) 13:2595–605.
15. Crowley MT, Costello PS, Fitzer-Attas CJ, Turner M, Meng F, Lowell C, et al. A critical role for Syk in signal transduction and phagocytosis mediated by Fcγ receptors on macrophages. *J Exp Med* (1997) 186:1027–39. doi:10.1084/jem.186.7.1027
16. Kiefer F, Brumell J, Al-Alawi N, Latour S, Cheng A, Veillette A, et al. The Syk protein tyrosine kinase is essential for Fcγ receptor signaling in macrophages and neutrophils. *Mol Cell Biol* (1998) 18:4209–20. doi:10.1128/MCB.18.7.4209
17. Németh T, Virtic O, Sitaru C, Mócsai A. The Syk tyrosine kinase is required for skin inflammation in an in vivo mouse model of epidermolysis bullosa acquisita. *J Invest Dermatol* (2017) 137:2131–9. doi:10.1016/j.jid.2017.05.017
18. Mócsai A, Zhang H, Jakus Z, Kitaura J, Kawakami T, Lowell CA. G-protein-coupled receptor signaling in Syk-deficient neutrophils and mast cells. *Blood* (2003) 101:4155–63. doi:10.1182/blood-2002-07-2346
19. Mócsai A, Zhou M, Meng F, Tybulewicz VL, Lowell CA. Syk is required for integrin signaling in neutrophils. *Immunity* (2002) 16:547–58. doi:10.1016/S1074-7613(02)00303-5
20. Obergfell A, Eto K, Mócsai A, Buensuceso C, Moores SL, Brugge JS, et al. Coordinate interactions of Csk, Src, and Syk kinases with αIIbβ3 initiate integrin signaling to the cytoskeleton. *J Cell Biol* (2002) 157:265–75. doi:10.1083/jcb.200112113
21. Jakus Z, Fodor S, Abram CL, Lowell CA, Mócsai A. Immunoreceptor-like signaling by β2 and β3 integrins. *Trends Cell Biol* (2007) 17:493–501. doi:10.1016/j.tcb.2007.09.001
22. Werninghaus K, Babiak A, Gross O, Holscher C, Dietrich H, Agger EM, et al. Adjuvanticity of a synthetic cord factor analogue for subunit Mycobacterium tuberculosis vaccination requires FcRγ-Syk-Card9-dependent innate immune activation. *J Exp Med* (2009) 206:89–97. doi:10.1084/jem.20081445
23. Mócsai A, Humphrey MB, Van Ziffle JA, Hu Y, Burghardt A, Spusta SC, et al. The immunomodulatory adapter proteins DAP12 and Fc receptor γ-chain (FcRγ) regulate development of functional osteoclasts through the Syk tyrosine kinase. *Proc Natl Acad Sci U S A* (2004) 101:6158–63. doi:10.1073/pnas.0401602101
24. Hirahashi J, Mekala D, Van Ziffle J, Xiao L, Saffaripour S, Wagner DD, et al. Mac-1 signaling via Src-family and Syk kinases results in elastase-dependent thrombohemorrhagic vasculopathy. *Immunity* (2006) 25:271–83. doi:10.1016/j.immuni.2006.05.014
25. Jakus Z, Simon E, Balázs B, Mócsai A. Genetic deficiency of Syk protects mice from autoantibody-induced arthritis. *Arthritis Rheum* (2010) 62:1899–910. doi:10.1002/art.27438
26. Gross O, Poeck H, Bscheider M, Dostert C, Hannesschlager N, Endres S, et al. Syk kinase signalling couples to the Nlrp3 inflammasome for anti-fungal host defence. *Nature* (2009) 459:433–6. doi:10.1038/nature07965
27. Abtahian F, Guerriero A, Sebzda E, Lu MM, Zhou R, Mócsai A, et al. Regulation of blood and lymphatic vascular separation by signaling proteins SLP-76 and Syk. *Science* (2003) 299:247–51. doi:10.1126/science.1079477
28. Geahlen RL. Getting Syk: spleen tyrosine kinase as a therapeutic target. *Trends Pharmacol Sci* (2014) 35:414–22. doi:10.1016/j.tips.2014.05.007
29. Kovács M, Németh T, Jakus Z, Sitaru C, Simon E, Futosi K, et al. The Src family kinases Hck, Fgr, and Lyn are critical for the generation of the in vivo inflammatory environment without a direct role in leukocyte recruitment. *J Exp Med* (2014) 211:1993–2011. doi:10.1084/jem.20132496
30. Jakus Z, Simon E, Frommhold D, Sperandio M, Mócsai A. Critical role of phospholipase Cγ2 in integrin and Fc receptor-mediated neutrophil functions and the effector phase of autoimmune arthritis. *J Exp Med* (2009) 206:577–93. doi:10.1084/jem.20081859
31. Németh T, Futosi K, Sitaru C, Ruland J, Mócsai A. Neutrophil-specific deletion of the CARD9 gene expression regulator suppresses autoantibody-induced inflammation in vivo. *Nat Commun* (2016) 7:11004. doi:10.1038/ncomms11004
32. Elliott ER, Van Ziffle JA, Scapini P, Sullivan BM, Locksley RM, Lowell CA. Deletion of Syk in neutrophils prevents immune complex arthritis. *J Immunol* (2011) 187:4319–30. doi:10.4049/jimmunol.1100341
33. Boilard E, Blanco P, Nigrovic PA. Platelets: active players in the pathogenesis of arthritis and SLE. *Nat Rev Rheumatol* (2012) 8:534–42. doi:10.1038/nrrheum.2012.118

34. Nigrovic PA, Binstadt BA, Monach PA, Johnsen A, Gurish M, Iwakura Y, et al. Mast cells contribute to initiation of autoantibody-mediated arthritis via IL-1. *Proc Natl Acad Sci U S A* (2007) 104:2325–30. doi:10.1073/pnas.0610852103
35. Passegue E, Wagner EF, Weissman IL. JunB deficiency leads to a myeloproliferative disorder arising from hematopoietic stem cells. *Cell* (2004) 119: 431–43. doi:10.1016/j.cell.2004.10.010
36. Tiedt R, Schomber T, Hao-Shen H, Skoda RC. Pf4-Cre transgenic mice allow the generation of lineage-restricted gene knockouts for studying megakaryocyte and platelet function in vivo. *Blood* (2007) 109:1503–6. doi:10.1182/blood-2006-04-020362
37. Scholten J, Hartmann K, Gerbaulet A, Krieg T, Muller W, Testa G, et al. Mast cell-specific Cre/loxP-mediated recombination in vivo. *Transgenic Res* (2008) 17:307–15. doi:10.1007/s11248-007-9153-4
38. Saijo K, Schmedt C, Su IH, Karasuyama H, Lowell CA, Reth M, et al. Essential role of Src-family protein tyrosine kinases in NF-κB activation during B cell development. *Nat Immunol* (2003) 4:274–9. doi:10.1038/ni893
39. Németh T, Futosi K, Hably C, Brouns MR, Jakob SM, Kovács M, et al. Neutrophil functions and autoimmune arthritis in the absence of p190RhoGAP: generation and analysis of a novel null mutation in mice. *J Immunol* (2010) 185:3064–75. doi:10.4049/jimmunol.0904163
40. Meinders M, Hoogenboezem M, Scheenstra MR, De Cuyper IM, Papadopoulos P, Németh T, et al. Repercussion of megakaryocyte-specific Gata1 loss on megakaryopoiesis and the hematopoietic precursor compartment. *PLoS One* (2016) 11:e0154342. doi:10.1371/journal.pone.0154342
41. Watson SP, Herbert JM, Pollitt AY. GPVI and CLEC-2 in hemostasis and vascular integrity. *J Thromb Haemost* (2010) 8:1456–67. doi:10.1111/j.1538-7836.2010.03875.x
42. Schymeinsky J, Sindrilaru A, Frommhold D, Sperandio M, Gerstl R, Then C, et al. The Vav binding site of the non-receptor tyrosine kinase Syk at Tyr 348 is critical for β2 integrin (CD11/CD18)-mediated neutrophil migration. *Blood* (2006) 108:3919–27. doi:10.1182/blood-2005-12-030387
43. Frommhold D, Mannigel I, Schymeinsky J, Mócsai A, Poeschl J, Walzog B, et al. Spleen tyrosine kinase Syk is critical for sustained leukocyte adhesion during inflammation in vivo. *BMC Immunol* (2007) 8:31. doi:10.1186/1471-2172-8-31
44. Németh T, Mócsai A. Feedback amplification of neutrophil function. *Trends Immunol* (2016) 37:412–24. doi:10.1016/j.it.2016.04.002
45. Suzuki-Inoue K, Fuller GL, Garcia A, Eble JA, Pohlmann S, Inoue O, et al. A novel Syk-dependent mechanism of platelet activation by the C-type lectin receptor CLEC-2. *Blood* (2006) 107:542–9. doi:10.1182/blood-2005-05-1994
46. Gibbins JM, Okuma M, Farndale R, Barnes M, Watson SP. Glycoprotein VI is the collagen receptor in platelets which underlies tyrosine phosphorylation of the Fc receptor γ-chain. *FEBS Lett* (1997) 413:255–9. doi:10.1016/S0014-5793(97)00926-5
47. Tsuji M, Ezumi Y, Arai M, Takayama H. A novel association of Fc receptor γ-chain with glycoprotein VI and their co-expression as a collagen receptor in human platelets. *J Biol Chem* (1997) 272:23528–31. doi:10.1074/jbc.272.38.23528
48. Clemetson JM, Polgar J, Magnenat E, Wells TN, Clemetson KJ. The platelet collagen receptor glycoprotein VI is a member of the immunoglobulin superfamily closely related to FcαR and the natural killer receptors. *J Biol Chem* (1999) 274:29019–24. doi:10.1074/jbc.274.41.29019
49. Kasirer-Friede A, Kahn ML, Shattil SJ. Platelet integrins and immunoreceptors. *Immunol Rev* (2007) 218:247–64. doi:10.1111/j.1600-065X.2007.00532.x
50. Boilard E, Larabee K, Shnayder R, Jacobs K, Farndale RW, Ware J, et al. Platelets participate in synovitis via Cox-1-dependent synthesis of prostacyclin independently of microparticle generation. *J Immunol* (2011) 186:4361–6. doi:10.4049/jimmunol.1002857
51. Zhou JS, Xing W, Friend DS, Austen KF, Katz HR. Mast cell deficiency in KitW-sh mice does not impair antibody-mediated arthritis. *J Exp Med* (2007) 204:2797–802. doi:10.1084/jem.20071391
52. Feyerabend TB, Weiser A, Tietz A, Stassen M, Harris N, Kopf M, et al. Cre-mediated cell ablation contests mast cell contribution in models of antibody- and T cell-mediated autoimmunity. *Immunity* (2011) 35:832–44. doi:10.1016/j.immuni.2011.09.015
53. Solomon S, Rajasekaran N, Jeisy-Walder E, Snapper SB, Illges H. A crucial role for macrophages in the pathology of K/BxN serum-induced arthritis. *Eur J Immunol* (2005) 35:3064–73. doi:10.1002/eji.200526167
54. Abram CL, Roberge GL, Hu Y, Lowell CA. Comparative analysis of the efficiency and specificity of myeloid-Cre deleting strains using ROSA-EYFP reporter mice. *J Immunol Methods* (2014) 408:89–100. doi:10.1016/j.jim.2014.05.009

Conflict of Interest Statement: The authors declare that the research was conducted in the absence of any commercial or financial relationships that could be construed as a potential conflict of interest.

The reviewer KB and handling editor declared their shared affiliation.

frontiers in Immunology

HYPOTHESIS AND THEORY
published: 19 March 2018
doi: 10.3389/fimmu.2018.00553

Novel Concepts of Altered Immunoglobulin G Galactosylation in Autoimmune Diseases

*Gillian Dekkers[1,2], Theo Rispens[2] and Gestur Vidarsson[1]**

[1] Sanquin Research and Landsteiner Laboratory, Department of Experimental Immunohematology, Academic Medical Centre, University of Amsterdam, Amsterdam, Netherlands, [2] Sanquin Research and Landsteiner Laboratory, Department of Immunopathology, Academic Medical Centre, University of Amsterdam, Amsterdam, Netherlands

The composition of the conserved N297 glycan in immunoglobulin G (IgG) has been shown to affect antibody effector functions *via* C1q of the complement system and Fc gamma receptors (FcγR) on immune cells. Changes in the general levels of IgG-glycoforms, such as lowered total IgG galactosylation observed in many autoimmune diseases have been associated with elevated disease severity. Agalactosylated IgG has therefore been regarded and classified by many as pro-inflammatory. However, and somewhat counterintuitively, agalactosylation has been shown by several groups to decrease affinity for FcγRIII and decrease C1q binding and downstream activation, which seems at odds with this proposed pro-inflammatory nature. In this review, we discuss these circumstances where altered IgG galactosylation/glycosylation is found. We propose a novel model based on these observations and current biochemical evidence, where the levels of IgG galactosylation found in the total bulk IgG affect the threshold required to achieve immune activation by autoantibodies through either C1q or FcγR. Although this model needs experimental verification, it is supported by several clinical observations and reconciles apparent discrepancies in the literature, and suggests a general mechanism in IgG-mediated autoimmune diseases.

Keywords: autoimmunity, immune regulation, immunoglobulin G glycosylation, galactosylation, Fc gamma receptor, complement, antibody effector functions

OPEN ACCESS

Edited by:
Joanna Davies, San Diego Biomedical Research Institute, United States

Reviewed by:
Mattias Collin, Lund University, Sweden
Christian Marcel Karsten, University of Lübeck, Germany
Yannic Christoph Bartsch, Universitätsklinikum Schleswig-Holstein, Germany

****Correspondence:***
Gestur Vidarsson
g.vidarsson@sanquin.nl

Specialty section:
This article was submitted to Immunological Tolerance and Regulation, a section of the journal Frontiers in Immunology

Received: *15 January 2018*
Accepted: *05 March 2018*
Published: *19 March 2018*

Citation:
Dekkers G, Rispens T and Vidarsson G (2018) Novel Concepts of Altered Immunoglobulin G Galactosylation in Autoimmune Diseases. Front. Immunol. 9:553. doi: 10.3389/fimmu.2018.00553

INTRODUCTION

Antibodies are crucial sentinels of the immune system, generated by B cells that sense incoming foreign antigens by their membrane-bound immunoglobulins or B cell receptor (BCR). With each B cell carrying a unique BCR, collectively they are able to respond to virtually any invading substance, let alone a complex pathogen (1). Once recognizing their cognate antigen, each B cell becomes activated and can class switch from the initial IgM and IgD type of BCR, to immunoglobulin G (IgG), IgA, or IgE (2). After maturation to plasmablasts and plasma cells, the B cells start to secrete the acquired BCR in the form of soluble immunoglobulin where it can mount humoral immune responses from complement activation (IgM and IgG) or cellular responses through myeloid and NK cells *via* Fc-receptors (all immunoglobulin types). In plasma, IgG is the most abundant immunoglobulin type found and consists of four subclasses, IgG1, IgG2, IgG3, and IgG4 in order of decreasing abundance. Since the first structures of IgG were solved, it became apparent that these structures are glycoproteins, with a conserved N-linked Fc-glycan attached to the asparagine found at position 297, situated in the constant region of the heavy chain domains (3) (**Figure 1**). However, it

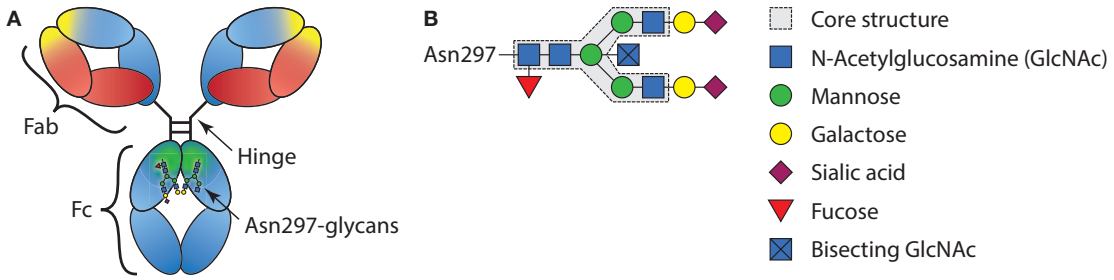

FIGURE 1 | Schematic representation of immunoglobulin G (IgG) structure and glycan composition. **(A)** Schematic representation of antibody with heavy chains and light chains, respectively, in blue and red, with general Y shaped structure. The Fab, Fc, and hinge domains are indicated. Within the Fab domains, the antigen-binding domain is indicated in yellow and within the Fc, the region where the FcγRs and C1q bind is indicated in green. **(B)** Schematic representation of IgG-Fc-N297-glycan with the different sugar groups and their respective positions.

remained enigmatic if, and then how, this rather flexible structure affects the function of IgG. In recent years, these aspects have become ever more clear, although fundamental discrepancies between clinical and experimental observations seem to prevail. These observations and possible resolutions will be discussed further below.

MECHANISM OF GLYCOSYLATION

Most membrane surface proteins and secreted proteins found in plasma are glycosylated. Glycan synthesis starts at the endoplasmic reticulum (ER) when a lipid-linked precursor oligosaccharide is synthesized (**Figure 2**) (4). In the ER lumen, this precursor is transferred to the Asn site of the protein at accessible residues containing the Asn-X-Ser/Thr motif, where X is any amino acid except proline. Further processing of the glycan then takes place in the ER and Golgi apparatus, which includes trimming and remodeling of the glycan. The cell type-specific spatial and temporal organization of glycosidases and glycosyltransferase expression in ER and Golgi apparatus regulate the final composition of the glycans (4–6). For IgG, assembly of heavy and light chains takes place early in the ER (6). After initial trimming of glucose and mannose groups by the glucosidases and ER mannosidase I in the ER, the whole complex is transported to the *cis*-Golgi (6). The diversity of the glycans derives from several factors; involvement of many different enzymes and substrates in different compartments, variable modification of glycan core structure to bi-, tri-, and tetra-antennary, competition between enzymes for substrates and acceptors, accessibility of the enzymes to the glycan, incomplete processing, and other posttranslational modifications on the same protein (6). For the IgG N-glycans, we know they assemble in a bi-antennary glycan with a core structure of mannose and *N*-acetylglucosamine groups and variable extension of galactose, sialic acid, fucose, and bisecting *N*-acetylglucosamine (bisection) (**Figure 1B**).

Extracellularly, glycosyltransferases and glycosidases are present in circulation, mainly editing the terminal sialic acid groups on glycans (7). This has been proven to be a functional mechanism in the sialylation of IgG, found in a study where mice with ST6GalT1-deficient B-cells did contain sialylated IgG. This occurs through liver-derived ST6galT1 and platelet-derived CMP-sialic acid as sugar donor, which are present in the circulation (7). Although sialylation of IgG seems to be affected also in plasma, we have observed several immune responses against both red blood cell (RBC) and platelet antigens formed after transfusion or pregnancy, can have markedly different sialylation than total IgG in the same patient (8–11), suggesting that B cells can also have a significant influence on the IgG sialylation in humans. This is supported by mouse work, where they show *in vivo* that overexpression or knockout of sialyltransferase in B-cells attenuates IgG sialylation and disease activity in collagen-induced arthritis (12).

IgG-Fc GLYCOSYLATION IN HUMANS AND IN AUTOIMMUNITY

When analyzing normal IgG repertoire in normal human serum it is found that the overall total glycosylation pattern is, although heterogeneous, generally quite constant, with high fucosylation (96%), low bisection (8%), intermediate galactosylation (40%), and low sialylation (4%) (13). Age and gender are two factors that were found to be correlated with the overall IgG glycosylation patterns. The main variations consist of a decrease in average galactosylation and sialylation and slight increase in bisection associated with higher age (13). The degree of fucosylation is almost 100% shortly after birth (when maternal antibodies have dissipated), after which levels of IgG fucosylation gradually reach ~96% around 20 years of age (14). Infection status, BMI, and epigenetic influences also seem to alter total IgG glycosylation (15–17).

Glycosylation patterns of total IgG have also been observed to temporarily change during certain conditions. During pregnancy, in particular, the degree of galactosylation and sialylation increases, with additional minor decrease in bisection while fucosylation remains stable (18, 19). Furthermore, in autoimmune diseases, changes in total IgG have been detected in, for example, rheumatoid arthritis (RA) (20, 21), inflammatory bowel disease (22), multiple sclerosis (23), myasthenic gravis (24), ankylosing spondylitis, primary Sjögren's syndrome, psoriatic arthritis (25), and systemic lupus erythematosus (SLE) (26). In all these diseases, a lower degree of total IgG galactosylation is

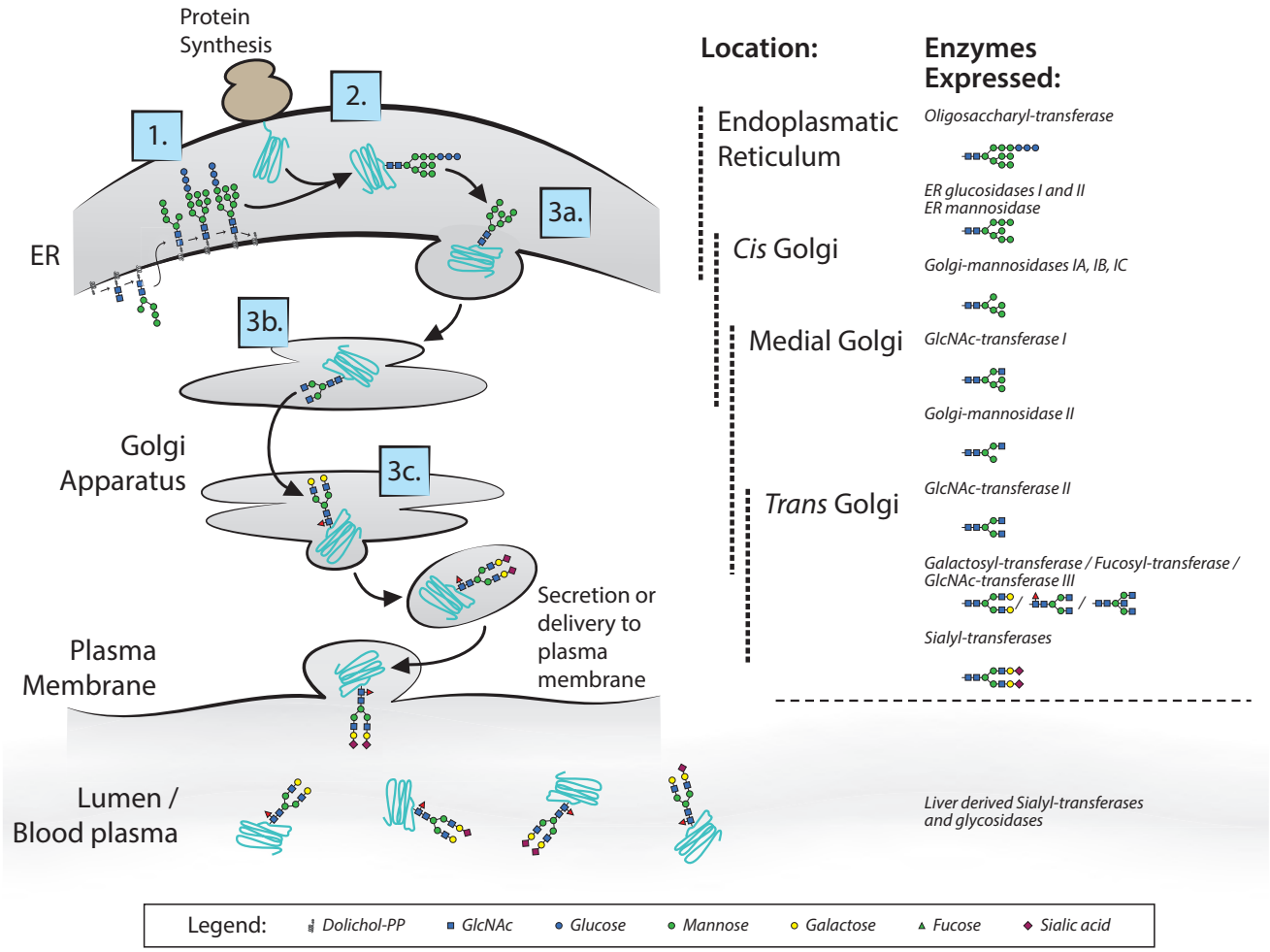

FIGURE 2 | N-glycan biosynthesis. Overview of the N-glycan biosynthesis pathways in the cell and in circulation as also occurs for immunoglobulin G glycosylation (4). In the left panel, the different cell compartments are illustrated with the different steps of synthesis indicated: 1. synthesis of lipid-linked precursor oligosaccharide, 2. *En Bloc* transfer to protein, 3. processing; 3a. initial trimming of sugar residues, 3b. trimming and modification of branch structure, 3c. addition of terminal sugar residues. In the right panel, the different involved glycosidases and glycosyltransferases listed at the position in the endoplasmic reticulum and Golgi apparatus where they proposed to be expressed. Extracellularly, glycosyltransferases and glycosidases are present in circulation, mainly editing the terminal sialic acid groups on glycans.

associated with disease progression and flare (20–28). However, the relevance of galactosylation of total IgG, which by definition are not causing the disease, on the disease severity is unknown. In inflammatory autoimmune disorders, such as RA and SLE, IgG autoantibodies presumably play a role in initiating or perpetuating the inflammatory condition (29, 30). In particular in RA, several types of autoantibodies have been identified that target a range of subtle chemical modifications of autologous proteins, including anti-citrullinated protein antibodies (ACPA) and anti-carbamylated protein antibodies—which may be referred to collectively as anti-modified protein response (31). The exact role of the autoantibodies in these diseases has not been fully elucidated as yet, although certain passive transfer mouse models suggest a pathogenic role for ACPAs (32). To our knowledge, the IgG Fc glycosylation patterns have only been determined for disease-associated autoantibodies of a few antigen-specific IgG, including ACPAs and anti-RBC autoantibodies (11, 33–37). In all these diseases, fucosylation is not lowered, even increased for ACPA in RA (11, 33, 34). Several studies suggest similarly low, but variable, levels of galactosylation in the antigen-specific IgG as found in the total IgG (11, 34, 35, 38). However, in two studies, differential changes in glycosylation patterns have been observed between total IgG and specific IgG1 (11, 34), observed in PR3-ACPA and anti-RBC autoantibodies. In both these studies, the galactosylation was variable between the patients, with total IgG galactosylation often diverging from antigen-specific IgG galactosylation. The PR3-ANCA IgG1 antibodies also showed a particularly stable and relatively high galactosylation during relapse, while the total IgG galactosylation was lowered (34). Importantly, this may be a relevant phenomenon that may affect the disease outcome, most likely due to elevated FcγRIIIa and/or FcγRIIIb occupancy which is likely to affect effector functions, as will be discussed in detail in the following sections of this review.

THE IMPORTANCE OF IgG-Fc GLYCOSYLATION FOR FcγR-MEDIATED EFFECTOR FUNCTIONS

Immunoglobulin G binds with the Fc region to FcγRs. These immune receptors are expressed on myeloid and NK cells of the immune system. Humans express five different FcγR, which can occur in several allotypic variants (39) (**Figure 3**). Of these five variants, FcγRIa, FcγRIIa, and FcγRIIIa contain an immunoreceptor tyrosine activation motif (ITAM), FcγRIIb an immunoreceptor tyrosine inhibitory motif (ITIM), and FcγRIIIb which is GPI-linked, contains no intracellular signaling domain (40). Binding of IgG to these receptors followed by clustering of the intracellular domains induces an ITAM-mediated signal transduction which can be counteracted by inclusion of the ITIM-containing FcγRIIb, if present (41).

Structurally, the glycan opens up the Fc-portion of IgG and keeps the two CH2 domains at a distance from each other, allowing for interactions with not only FcγR but also C1q that both require similar residues in the IgG for binding (42–44). In addition to the fact that the glycan has been found to show direct, but minor, interactions with the protein backbone of FcγR (43), the IgG Fc-glycan also interacts with a glycan found only in human FcγRIIIa and FcγRIIIb (45, 46) thereby affecting binding affinity of IgG to those receptors. If, and then how, the exact glycan composition—thus not only the mere presence of a glycan—affects binding to the other FcγR or C1q has remained unknown until recently, as discussed further below. The final secreted IgG eventually protects us by opsonizing incoming pathogens. These are then recognized by FcγR, the first component of the complement system (C1q), or both. This can trigger multiple effector functions, such as complement deposition and lysis (47), but also FcγR- and or complement-mediated phagocytosis by myeloid cells (monocytes, macrophages, or neutrophils), trogocytosis (where myeloid cells rupture the membrane of target cells), or FcγR-mediated antibody-dependent cellular cytotoxicity (ADCC) through NK or myeloid cells. These effector functions are currently utilized and have been improved upon by protein and glycan-engineering for many current and future therapeutic antibody approaches. However, these effector functions are also triggered in various allo- and autoimmune diseases (48).

In humans, we know FcγRIIIa is an important activating FcγR, and of all FcγRs, its affinity for IgG is most influenced by changes in IgG Fc glycosylation. It has been known for over a decade that afucosylation increases affinity of IgG1 to FcγRIIIa and FcγRIIIb (49, 50), and later confirmed for other IgG subclasses (51, 52). Earlier studies have hinted at the possibility that galactosylation may also affect binding to FcγRIIIa in a positive way (53–56), and sialylation in a negative fashion (56–59), but the effect of the other glycans had not been extensively studied. We have recently confirmed that for IgG1 additional galactosylation increases the affinity for FcγRIIIa and FcγRIIIb, but only for afucosylated IgG1 (60), which is found in 6% of IgG1 at the glycopeptide level (13, 61, 62). An overview of the effect of glycovariation on the affinity for FcγRs is displayed in **Figure 4**. The degree of galactosylation of IgG ranges roughly from 20 to 60% on total IgG and similarly for afucosylated IgG (13, 61, 62). The apparent affinity increases by approximately twofold between afucosylated IgG1 with either 20 vs 70% galactosylation, which corresponds to ~20× or 40× increased affinity compared to fucosylated IgG1, respectively (60).

For bisection and sialylation, we found only small effects on binding to FcγRIII. Additional sialylation of the galactosylated, afucosylated IgG1 caused a slight or no decrease in affinity (56–60). Variation in bisection did not appear to have any effect in the experiments conducted up until now, except for potentially strengthening the negative effect of sialylation on FcγRIIIa and FcγRIIIb-binding (60).

In recent years, it has become apparent that during viral infections of HIV and dengue fever, antigen-specific IgG may contain decreased levels of Fc fucosylation (63, 64). For HIV, this was observed especially for those patients who had a longer disease free survival, the so-called elite controllers, and this correlated with the degree of antibody-mediated cellular viral inhibition (ADCVI) of the patient's serum. In dengue, a higher degree of afucosylation was more often found in patients with antibody-dependent enhancement of disease (64). For these infections, and possibly more viral infections, the enhanced affinity for FcγRIIIa of the afucosylated antigen-specific IgG indeed enhances ADCC and ADCVI of the virus and virus infected cells (65). For HIV, this rationalizes the better clinical outcome for the patients who have more antigen-specific

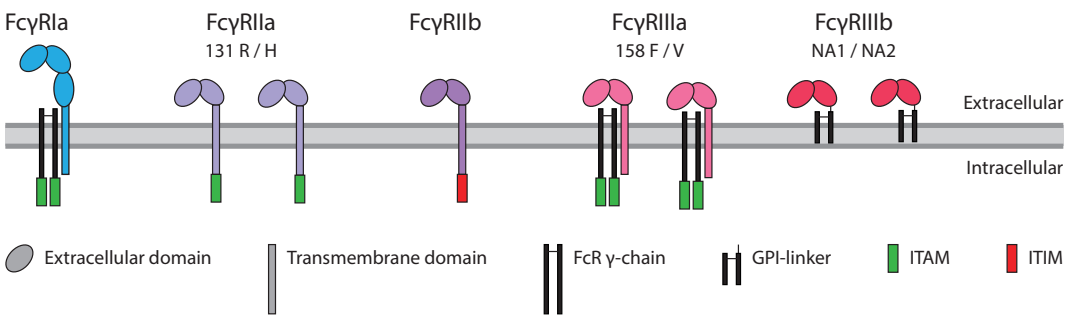

FIGURE 3 | Human FcγR family. The family of human FcγR in with allotypes indicated. Green box: immunoreceptor tyrosine activation motif (ITAM), red box: immunoreceptor tyrosine inhibitory motif (ITIM).

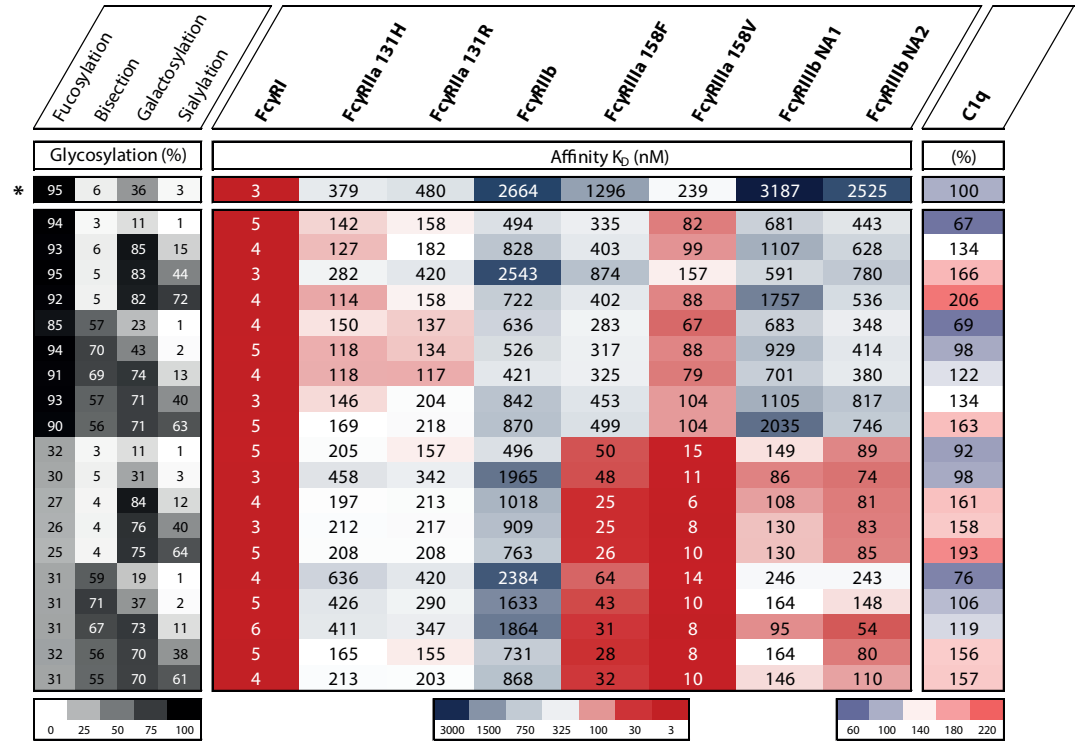

*												
95	6	36	3	3	379	480	2664	1296	239	3187	2525	100
94	3	11	1	5	142	158	494	335	82	681	443	67
93	6	85	15	4	127	182	828	403	99	1107	628	134
95	5	83	44	3	282	420	2543	874	157	591	780	166
92	5	82	72	4	114	158	722	402	88	1757	536	206
85	57	23	1	4	150	137	636	283	67	683	348	69
94	70	43	2	5	118	134	526	317	88	929	414	98
91	69	74	13	4	118	117	421	325	79	701	380	122
93	57	71	40	3	146	204	842	453	104	1105	817	134
90	56	71	63	5	169	218	870	499	104	2035	746	163
32	3	11	1	5	205	157	496	50	15	149	89	92
30	5	31	3	3	458	342	1965	48	11	86	74	98
27	4	84	12	4	197	213	1018	25	6	108	81	161
26	4	76	40	3	212	217	909	25	8	130	83	158
25	4	75	64	5	208	208	763	26	10	130	85	193
31	59	19	1	4	636	420	2384	64	14	246	243	76
31	71	37	2	5	426	290	1633	43	10	164	148	106
31	67	73	11	6	411	347	1864	31	8	95	54	119
32	56	70	38	5	165	155	731	28	8	164	80	156
31	55	70	61	4	213	203	868	32	10	146	110	157

FIGURE 4 | The effect of IgG1 glycovariation and receptor affinity. Heat map displaying various glycoengineered IgG1 and their monomeric affinity in K_D (nanomolar) for the FcγRs as determined by SPR and relative affinity for C1q as determined by ELISA, data adopted from Dekkers et al. (60). Heat map legends are displayed below. The degree of glycosylation of indicated glycan end groups is colored from white (low) to black (high), the affinity to FcγRs is colored from dark blue (high K_D, low affinity) *via* white to dark red (low K_D, high affinity), the relative affinity for C1q is colored from light blue (low affinity) *via* white to pink (high affinity). *Indicates the normally produced, unmodified IgG1 glycoform which is not glycoengineered.

antibodies with low fucose, but for dengue, the stronger side effects have negative side effects.

Interestingly, the changes in antibody fucosylation and galactosylation of antigen-specific IgGs are also found in alloimmune settings. Examples of this are after blood transfusion, fetal neonatal immune thrombocytopenia (FNAIT) and hemolytic disease of the fetus or newborn (HDFN) (8–10, 66, 67). Both these latter diseases are in a pregnancy setting where the fetus is positive while the mother herself is negative for a paternal antigen on platelets or RBCs, respectively, for FNAIT or HDFN, and thus makes antibodies against the blood cells of the child upon exposure. This can lead to complications and is dangerous for the health of the child and hence it is important to diagnose correctly and timely and also treat accordingly (68).

We have recently shown that glycosylation status of these antibodies matters for pathogenicity (8, 66, 69). The lower degree of fucosylation, in particular, and also increased galactosylation of these antibodies correlate with enhanced disease severity (8–10, 66, 69). The effector mechanism of these antibodies is thought to take place *via* FcγR-bearing cells in the liver and spleen of the fetus, which target the RBC or platelets (70). Previous work has already suggested that FcγRIIIa is the main receptor involved in both RBC and platelet clearance because patients are more likely to carry the high-affinity FcγRIIIa allele (70, 71), now further supported by the observation that IgG with glycosylation patterns that target them to FcγRIIIa with higher affinity also seem to correlate with enhanced disease severity in these diseases (8–10, 66).

As mentioned above, altered glycosylation has been detected and described for many autoimmune diseases (20, 26, 28). This can be either in the total IgG of a patient (i.e., all IgG specificities and not directly related to the disease entity itself) (20–26) or in the IgG specific for the disease (11, 33–37). Most often, a decrease in total IgG Fc-galactosylation has been found and associated with disease progression or severity (5, 20, 22, 26). By contrast, total IgG Fc galactosylation increases during pregnancy, which is clearly associated with disease remission in RA (18, 72–74). It has been shown that FcγRs are important for RA and other autoimmune diseases but axillary involvement of complement is very likely (75, 76). These associations have almost exclusively brought about the hypothesis that agalactosylated IgGs are pro-inflammatory, while highly galactosylated and sialylated IgGs are anti-inflammatory. This anti-inflammatory nature of IgG has been shown in mice not only to stem from binding of hypersialylated IgG to SIGN-R1 (in humans DC-SIGN) (77, 78) but also to the structural homolog and previously identified low affinity IgE-receptor CD23 (77–79). Structural changes in sialylated IgG do not seem to support this model (80–82), and work with sialic-acid enriched IVIg by other groups does not support this notion (83–87). Using detailed glycoengineered IgG (60), we also find

no binding of any glycoform to the human receptors (Temming et al. manuscript in preparation). For galactosylation, the exact role of IgG galactosylation and its influence on disease activity also needs to be further elucidated. Importantly, recent affinity data seem at odds with the widespread notion that agalactosylated IgG are pro-inflammatory, given the weaker binding of agalactosylated and afucosylated IgG to FcγRIIIa in comparison to galactosylated, afucosylated IgG as described above. In addition, highly galactosylated IgG has also been associated with enhanced anti-inflammatory properties when present in immune complexes, as it apparently promotes the association of FcγRIIb with Dectin-1 (88).

However, an often overlooked aspect of FcγR binding and subsequent activation through IgG-containing immune complexes or IgG-opsonized cells, is the fact that this occurs in the presence of high concentrations of monomeric (total) IgG in circulation. At these high concentrations (around 10 mg/mL or 60–70 μM, or 7 mg/mL or 40–50 μM of IgG1), exceeding the K_D for binding of the most common glycoforms of IgG1 to, e.g., FcγRIIa or FcγRIIIa by at least two orders of magnitude (39), most Fc receptors will be bound to monomeric IgG (i.e., a degree of saturation of ca. 98% or more). This is even higher for the high-affinity FcγRIa, which is saturated to an even higher degree, and with less displacement. Upon encounter of, e.g., an FcγR-bearing cell with an opsonized cell providing higher-avidity interactions, the monomeric IgG occupying the FcγR may quickly dissociate and binding of the opsonized cell will take place. How efficient this occurs will depend on the nature of the monomeric IgG (subclass and affinity); which will be strongly influenced by the relative levels of the different Fc glycovariants, but only for FcγRIIIa and FcγRIIIb.

The most important glycosylation changes affecting this are again fucosylation and galactosylation. As explained above, we and others have observed that afucosylated, highly galactosylated IgG has a higher affinity for FcγRIIIa and FcγRIIIb. These changes are reflected not only in the activity of NK cell to mediate ADCC *via* FcγRIIIa (53, 55, 60, 89) but also on how irrelevant antibodies, which may bind as monomeric entity to these FcγR, can inhibit the ADCC of specific antibodies (52). This may be relevant, e.g., in the context of RA, where during disease remission, the bulk of antibodies have a normal galactose percentage while during a flare the bulk of antibodies is lowered in galactose, including the afucosylated fraction. Of note, given the ca. 20-fold stronger binding of afucosylated IgG for FcγRIII (49, 60, 90), approximately 50% of IgGs bound to FcγRIII are expected to be afucosylated (given that the concentration of the latter is ca. 20-fold lower). Therefore, comparing a theoretical transition from a flare to remission, an elevated portion of receptor-bound monomeric IgG can be expected to consist of afucosylated, galactosylated IgG with a 2- to 3-fold higher affinity compared to afucosylated, agalactosylated IgG during remission. Under these conditions, immune complexes, in case of autoantibodies almost exclusively fucosylated judging from the current knowledge on ACPA and anti-RBC autoantibodies (11, 34, 38), are expected to have less capacity to displace these higher-affinity IgG from the FcγR. How strong this effect is, will particularly depend on the relative shifts in galactosylation profiles of the total IgG, although galactosylation changes in the autoantibodies themselves may also affect this balance (54–56). Theoretically, immune-complexes therefore have less tendency to cause crosslinking and immune activation if the bulk of IgG show relative elevated IgG-Fc galactosylation, and hence have diminished capacity to cause disease (**Figure 5**). Overall, the altered glycosylation profiles of autoantibodies may result in altered FcγR-binding and activation, but this may be attenuated by altered glycosylation profiles of non-specific total IgG. We should, of course, realize that all these autoimmune diseases are characterized by multifactorial components, ultimately resulting in disease onset and progression. For RA, this includes the acquirement of multiple disease factors, such as infiltration of immune cells into the joint, ACPA, anti-hinge antibodies, rheumatoid factor (IgM based), increased TNF levels, and complement discussed below (75, 91).

THE IMPORTANCE OF IgG-Fc GLYCOSYLATION FOR COMPLEMENT-MEDIATED FUNCTIONS

Fc glycosylation—the presence of the Fc glycan—is important for classical complement activation, has been known already for a long time (42, 92). In RA, the complement system has been suggested to play an important part of the pathological features, and so have changes in IgG Fc glycosylation are in the galactose end groups (18, 20, 93). The same seems true for many other autoimmune disease where lowered IgG-Fc galactosylation of total IgG correlates with disease severity (5, 11, 20, 22, 26). One study proposed that activation of complement by these agalactosylated IgG species involves specific recognition by the mannose-binding lectin and activation through the lectin pathway of complement activation (94). However, to our knowledge, these results have never been verified. In contrary, we have recently found that IgG agalactosylation—irrespective of all other glycan end groups—does not induce activation of complement *via* the lectin pathway, confirming various other studies on this subject (60, 95, 96). This seems to leave the classical pathway as the main route for enhanced disease activity possibly affected by IgG-Fc glycan variations, by binding of antibody (complexes) to C1q, although deviations from this are likely to exist depending on the disease etiology.

Having established that low galactosylation of total IgG seems to correlate with enhanced disease activity in several autoimmune diseases where complement seem to play an important role (5, 11, 20, 22, 26), has led to the suggestion that agaloctosylated IgG is pro-inflammatory with enhanced complement activity. In contrary, several publications seem now to suggest the opposite to be true. While a few studies found that fucosylation does not affect complement-mediated activity (49, 51, 60), two recent studies suggest that galactosylation of human IgG positively affects C1q binding and downstream activation (60, 97, 98). In our recent study where we screened 20 different and highly defined IgG glycovariants for C1q binding and activation, we found that galactosylation primarily enhanced C1q binding and increased CDC and that additional sialylation increases this effect on the classical complement activation

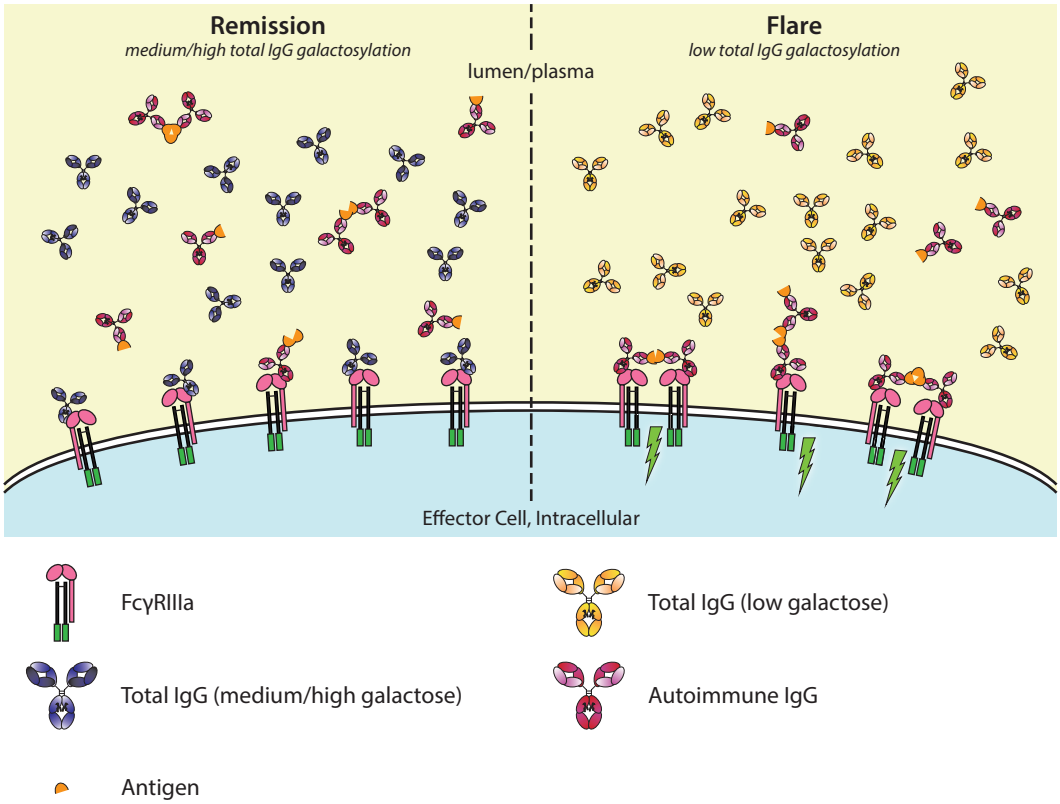

FIGURE 5 | Galactosylation of total immunoglobulin G (IgG) affects IgG-occupation of FcγRIIIa, affecting activation thresholds and flares in autoimmunity. In autoimmune diseases, such as rheumatoid arthritis, disease severity is negatively correlated with the degree of galactosylation. Galactosylation of IgG is important for binding to FcγRIIIa, where—in combination with afucosylation—a higher degree of IgG-Fc galactosylation increases the affinity. Only ~6% of normal serum IgGs is afucosylated. During remission (left), the total IgG galactosylation is relatively high, which prevents autoantibodies to engage the FcγRs. During a flare of disease (right), the total IgG galactosylation is low, which reduces the overall binding affinity of total IgG to FcγRIII, and therefore lowers the threshold for FcγR-activation by allowing more easy access by pathogenic autoantibodies, causing immune activation (green lightning bolt).

pathway. Bisection showed no affect in any combination with fucose, galactose, or sialylation (60) (**Figure 4**). Similarly, Quast et al. (97) showed that increased galactosylation enhances C1q binding and CDC in antibody models, where CDC is the main effector function. However, in their model, the addition of sialic acid hampered this enhanced effect (97). The difference in effector function might depend on the nature of the antigen, effector cells, and/or target cells. This is plausible as hexamerization of IgG on the surface of the target is likely needed for proper binding and activation of C1q, and the propensity of different antibodies/antigens to do this may vary as they take on different molecular configurations (99, 100). Much more research on this mechanism is, however, required as we do not know how the specificity of the IgG influences this effect or whether these changes are also relevant in a setting where IgG is already enhanced for CDC by protein engineering (101, 102).

It may seem counterintuitive that agalactosylated IgG has been associated with higher pathogenicity while new studies with glycoengineered IgG shows it to have lower potential to activate C1q compared to galactosylated IgG. A possible explanation may be similar to that what we propose for FcγRs (**Figure 6**). During remission, total IgG galactosylation is relatively high, while during a flare of the autoimmune disease the total IgG galactosylation is relatively low. In the latter case, the threshold for activation of C1q might be lowered due to lower steady-state occupancy by the low-galactosylated IgG. If so, then this could allow for relatively increase in activation of complement by pathogenic IgG complexed by its cognate autoantigen.

Although the binding affinity of monomeric to IgG has been estimated to be very low, i.e., in the 20–100 μM range (103–106), we again have to take into account the exceptionally high concentration of IgG in serum, making this model plausible. Considering IgG1, present at concentrations around 40–50 μM, this translates to ca. 30–70% saturation of C1q. However, care should be taken as measurements of the affinity of monomeric IgG binding to C1q might have been influenced by the presence of trace amounts of aggregates, resulting in an overestimation of the deduced affinities.

Furthermore, we do not know how well these biochemical principles translate into the *in vivo* setting. This could be experimentally determined, but needs high concentrations of both IgG and C1q as the monomeric affinity is generally very low. However, it is important to keep in mind that we do not yet

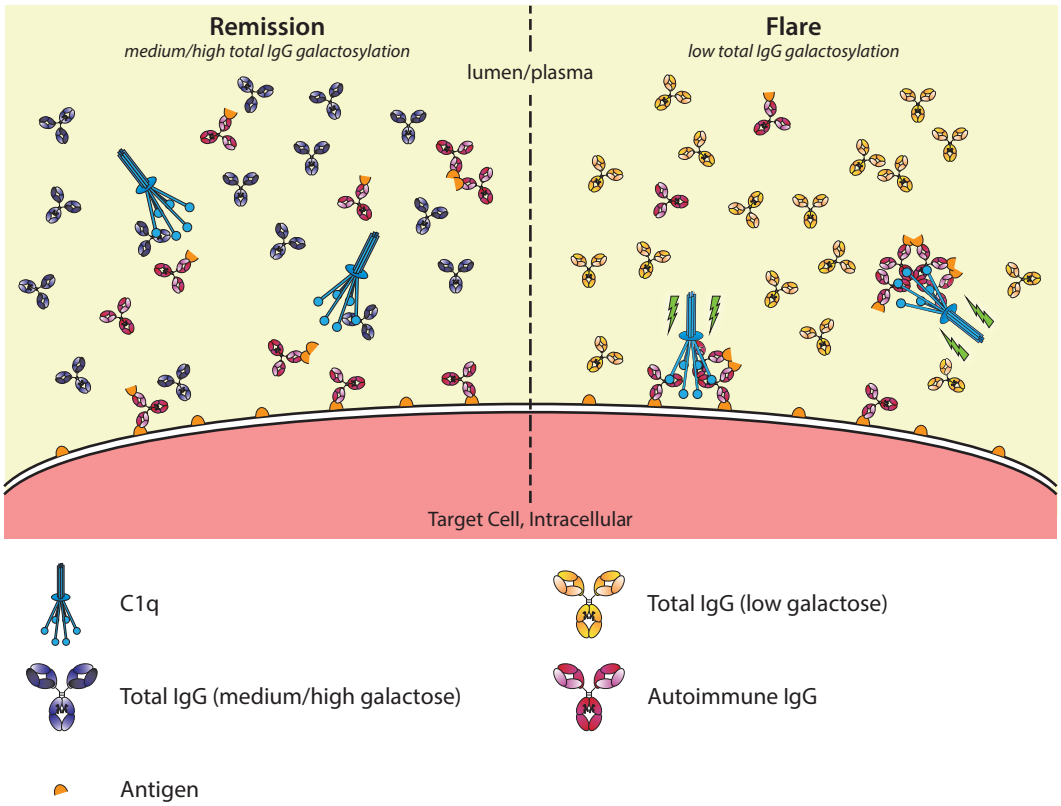

FIGURE 6 | Galactosylation of total immunoglobulin G (IgG) affects C1q occupation and activation in autoimmune remission and flare. In autoimmune diseases, such as rheumatoid arthritis, disease severity is negatively correlated with the degree of galactosylation found in total IgG. Galactosylation of IgG is important for binding to C1q, where a higher degree of IgG Fc galactosylation—and sialylation—increases the affinity. Additionally, C1q requires multimerization/hexamers of IgG for proper activation. During remission (left), C1q-autoantibody engagement might be prevented by preferential interaction with aspecific highly galactosylated IgG, which is abundantly present. During a flare (right), the total IgG galactosylation is low, which reduces the overall threshold of C1q binding, allowing for relatively better binding of pathogenic IgG/immune complexes, allowing activation of the classical complement pathway (green lightning bolt).

know whether the observed changes in IgG galactosylation in, for example, RA are truly causative of disease flares or a response to the flares. Efforts to investigate the causative association should be undertaken.

CONCLUSION

All in all, it was shown that glycan alterations found in IgG seem to be driven by the type of response and have functional consequences. The knowledge that afucosylation imposes better effector functions has already been put to use to enhance the function of therapeutic antibodies used in cancer treatment (107, 108). Additional glycoengineering of the galactose end groups could thus even further improve the functionality of these antibodies. These changes do occur naturally in humans as they are formed in certain immune reactions resulting in stronger humoral immune responses (9, 63, 64, 66, 69). For autoimmune mediated diseases, where changes in galactosylation in both the bulk and the pathogenic antibodies are frequently found, glycosylation changes effects both of binding to FcγR and C1q, which in turn affects their downstream activation. Based on the current evidence, the glycan changes in the bulk of endogenous IgG have the opposite effect on what is observed for antigen-specific IgG. Skewing toward lowered levels of galactose of the bulk IgG lowers its potential to efficiently block both FcγR, but also potentially C1q, giving more room for activation by existing pathogenic IgG-complexes. Eventually, it might be possible to monitor the glycosylation status, especially degree of galactosylation, of the total or disease-specific antibodies in autoimmune diseases. This could help to predict or detect an upcoming flare in autoimmune diseases, enabling intervention early after, or even before symptoms to set in.

AUTHOR CONTRIBUTIONS

GD composed and made the figures. GD, TR, and GV wrote and edited the manuscript.

FUNDING

This study was supported by Sanquin Product and Process Development Plasma Products, 12-001, Gestur Vidarsson.

REFERENCES

1. Hoehn KB, Fowler A, Lunter G, Pybus OG. The diversity and molecular evolution of B-cell receptors during infection. *Mol Biol Evol* (2016) 33:1147–57. doi:10.1093/molbev/msw015
2. Vidarsson G, Dekkers G, Rispens T. IgG subclasses and allotypes: from structure to effector functions. *Front Immunol* (2014) 5:520. doi:10.3389/fimmu.2014.00520
3. Huber R, Deisenhofer J, Colman PM, Matsushima M, Palm W. Crystallographic structure studies of an IgG molecule and an Fc fragment. *Nature* (1976) 264:415–20. doi:10.1038/264415a0
4. Taylor ME, Drickamer K. *Introduction to Glycobiology*. 3rd ed. New York, NY: Oxford University Press Inc. (2011).
5. Maverakis E, Kim K, Shimoda M, Gershwin ME, Patel F, Wilken R, et al. Glycans in the immune system and The Altered Glycan Theory of Autoimmunity: a critical review. *J Autoimmun* (2015) 57:1–13. doi:10.1016/j.jaut.2014.12.002
6. Hristodorov D, Fischer R, Linden L. With or without sugar? (A)glycosylation of therapeutic antibodies. *Mol Biotechnol* (2013) 54:1056–68. doi:10.1007/s12033-012-9612-x
7. Jones MB, Oswald DM, Joshi S, Whiteheart SW, Orlando R, Cobb BA. B-cell-independent sialylation of IgG. *Proc Natl Acad Sci U S A* (2016) 113:7207–12. doi:10.1073/pnas.1523968113
8. Kapur R, Kustiawan I, Vestrheim A, Koeleman CAM, Visser R, Einarsdottir HK, et al. A prominent lack of IgG1-Fc fucosylation of platelet alloantibodies in pregnancy. *Blood* (2014) 123:471–80. doi:10.1182/blood-2013-09-527978
9. Sonneveld ME, Natunen S, Sainio S, Koeleman CAM, Holst S, Dekkers G, et al. Glycosylation pattern of anti-platelet IgG is stable during pregnancy and predicts clinical outcome in alloimmune thrombocytopenia. *Br J Haematol* (2016) 174:310–20. doi:10.1111/bjh.14053
10. Sonneveld ME, Koelewijn J, de Haas M, Admiraal J, Plomp R, Koeleman CAM, et al. Antigen specificity determines anti-red blood cell IgG-Fc alloantibody glycosylation and thereby severity of haemolytic disease of the fetus and newborn. *Br J Haematol* (2017) 176:651–60. doi:10.1111/bjh.14438
11. Sonneveld ME, de Haas M, Koeleman C, de Haan N, Zeerleder SS, Ligthart PC, et al. Patients with IgG1-anti-red blood cell autoantibodies show aberrant Fc-glycosylation. *Sci Rep* (2017) 7:8187. doi:10.1038/s41598-017-08654-y
12. Ohmi Y, Ise W, Harazono A, Takakura D, Fukuyama H, Baba Y, et al. Sialylation converts arthritogenic IgG into inhibitors of collagen-induced arthritis. *Nat Commun* (2016) 7:11205. doi:10.1038/ncomms11205
13. Baković MP, Selman MHJ, Hoffmann M, Rudan I, Campbell H, Deelder AM, et al. High-throughput IgG Fc N-glycosylation profiling by mass spectrometry of glycopeptides. *J Proteome Res* (2013) 12:821–31. doi:10.1021/pr300887z
14. de Haan N, Reiding KR, Driessen G, van der Burg M, Wuhrer M. Changes in healthy human IgG Fc-glycosylation after birth and during early childhood. *J Proteome Res* (2016) 15:1853–61. doi:10.1021/acs.jproteome.6b00038
15. Menni C, Keser T, Mangino M, Bell JT, Erte I, Akmačić I, et al. Glycosylation of immunoglobulin g: role of genetic and epigenetic influences. *PLoS One* (2013) 8:e82558. doi:10.1371/journal.pone.0082558
16. Nikolac Perkovic M, Pucic Bakovic M, Kristic J, Novokmet M, Huffman JE, Vitart V, et al. The association between galactosylation of immunoglobulin G and body mass index. *Prog Neuropsychopharmacol Biol Psychiatry* (2014) 48:20–5. doi:10.1016/j.pnpbp.2013.08.014
17. Pucić M, Knezević A, Vidic J, Adamczyk B, Novokmet M, Polasek O, et al. High throughput isolation and glycosylation analysis of IgG-variability and heritability of the IgG glycome in three isolated human populations. *Mol Cell Proteomics* (2011) 10:M111.010090. doi:10.1074/mcp.M111.010090
18. Bondt A, Selman MHJ, Deelder AM, Hazes JMW, Willemsen SP, Wuhrer M, et al. Association between galactosylation of immunoglobulin G and improvement of rheumatoid arthritis during pregnancy is independent of sialylation. *J Proteome Res* (2013) 12:4522–31. doi:10.1021/pr400589m
19. Bondt A, Rombouts Y, Selman MHJ, Hensbergen PJ, Reiding KR, Hazes JMW, et al. Immunoglobulin G (IgG) Fab glycosylation analysis using a new mass spectrometric high-throughput profiling method reveals pregnancy-associated changes. *Mol Cell Proteomics* (2014) 13:3029–39. doi:10.1074/mcp.M114.039537
20. Parekh RB, Dwek RA, Sutton BJ, Fernandes DL, Leung A, Stanworth D, et al. Association of rheumatoid arthritis and primary osteoarthritis with changes in the glycosylation pattern of total serum IgG. *Nature* (1985) 316:452–7. doi:10.1038/316452a0
21. Ercan A, Cui J, Chatterton DEW, Deane KD, Hazen MM, Brintnell W, et al. Aberrant IgG galactosylation precedes disease onset, correlates with disease activity, and is prevalent in autoantibodies in rheumatoid arthritis. *Arthritis Rheum* (2010) 62:2239–48. doi:10.1002/art.27533
22. Trbojević Akmačić I, Ventham NT, Theodoratou E, Vučković F, Kennedy NA, Krištić J, et al. Inflammatory bowel disease associates with proinflammatory potential of the immunoglobulin G glycome. *Inflamm Bowel Dis* (2015) 21:1237–47. doi:10.1097/MIB.0000000000000372
23. Wuhrer M, Selman MHJ, McDonnell LA, Kümpfel T, Derfuss T, Khademi M, et al. Pro-inflammatory pattern of IgG1 Fc glycosylation in multiple sclerosis cerebrospinal fluid. *J Neuroinflammation* (2015) 12:235. doi:10.1186/s12974-015-0450-1
24. Selman MHJ, Niks EH, Titulaer MJ, Verschuuren JJGM, Wuhrer M, Deelder AM. IgG fc N-glycosylation changes in Lambert-Eaton myasthenic syndrome and myasthenia gravis. *J Proteome Res* (2011) 10:143–52. doi:10.1021/pr1004373
25. Watson M, Rudd PM, Bland M, Dwek RA, Axford JS. Sugar printing rheumatic diseases: a potential method for disease differentiation using immunoglobulin G oligosaccharides. *Arthritis Rheum* (1999) 42:1682–90. doi:10.1002/1529-0131(199908)42:8<1682:AID-ANR17>3.0.CO;2-X
26. Vučković F, Krištić J, Gudelj I, Teruel M, Keser T, Pezer M, et al. Association of systemic lupus erythematosus with decreased immunosuppressive potential of the IgG glycome. *Arthritis Rheumatol* (2015) 67:2978–89. doi:10.1002/art.39273
27. Förger F, Ostensen M. Is IgG galactosylation the relevant factor for pregnancy-induced remission of rheumatoid arthritis? *Arthritis Res Ther* (2010) 12:108. doi:10.1186/ar2919
28. Biermann MHC, Griffante G, Podolska MJ, Boeltz S, Stürmer J, Muñoz LE, et al. Sweet but dangerous – the role of immunoglobulin G glycosylation in autoimmunity and inflammation. *Lupus* (2016) 25:934–42. doi:10.1177/0961203316640368
29. Bax M, Huizinga TWJ, Toes REM. The pathogenic potential of autoreactive antibodies in rheumatoid arthritis. *Semin Immunopathol* (2014) 36:313–25. doi:10.1007/s00281-014-0429-5
30. Conigliaro P, Chimenti MS, Triggianese P, Sunzini F, Novelli L, Perricone C, et al. Autoantibodies in inflammatory arthritis. *Autoimmun Rev* (2016) 15:673–83. doi:10.1016/j.autrev.2016.03.003
31. Trouw LA, Rispens T, Toes REM. Beyond citrullination: other post-translational protein modifications in rheumatoid arthritis. *Nat Rev Rheumatol* (2017) 13:331–9. doi:10.1038/nrrheum.2017.15
32. Kuhn KA, Kulik L, Tomooka B, Braschler KJ, Arend WP, Robinson WH, et al. Antibodies against citrullinated proteins enhance tissue injury in experimental autoimmune arthritis. *J Clin Invest* (2006) 116:961–73. doi:10.1172/JCI25422
33. Rombouts Y, Ewing E, van de Stadt LA, Selman MHJ, Trouw LA, Deelder AM, et al. Anti-citrullinated protein antibodies acquire a pro-inflammatory Fc glycosylation phenotype prior to the onset of rheumatoid arthritis. *Ann Rheum Dis* (2015) 74:234–41. doi:10.1136/annrheumdis-2013-203565
34. Kemna MJ, Plomp R, van Paassen P, Koeleman CAM, Jansen BC, Damoiseaux JGMC, et al. Galactosylation and sialylation levels of IgG predict relapse in patients with PR3-ANCA associated vasculitis. *EBioMedicine* (2017) 17:108–18. doi:10.1016/j.ebiom.2017.01.033
35. Scherer HU, van der Woude D, Ioan-Facsinay A, el Bannoudi H, Trouw LA, Wang J, et al. Glycan profiling of anti-citrullinated protein antibodies isolated from human serum and synovial fluid. *Arthritis Rheum* (2010) 62:1620–9. doi:10.1002/art.27414
36. Magorivska I, Muñoz LE, Janko C, Dumych T, Rech J, Schett G, et al. Sialylation of anti-histone immunoglobulin G autoantibodies determines their capabilities to participate in the clearance of late apoptotic cells. *Clin Exp Immunol* (2016) 184:110–7. doi:10.1111/cei.12744
37. Fickentscher C, Magorivska I, Janko C, Biermann M, Bilyy R, Nalli C, et al. The pathogenicity of anti-β2GP1-IgG autoantibodies depends on Fc glycosylation. *J Immunol Res* (2015) 2015:638129. doi:10.1155/2015/638129

38. Rombouts Y, Willemze A, van Beers JJBC, Shi J, Kerkman PF, van Toorn L, et al. Extensive glycosylation of ACPA-IgG variable domains modulates binding to citrullinated antigens in rheumatoid arthritis. *Ann Rheum Dis* (2016) 75:578–85. doi:10.1136/annrheumdis-2014-206598
39. Bruhns P, Iannascoli B, England P, Mancardi DA, Fernandez N, Jorieux S, et al. Specificity and affinity of human Fcgamma receptors and their polymorphic variants for human IgG subclasses. *Blood* (2009) 113:3716–25. doi:10.1182/blood-2008-09-179754
40. Powell MS, Hogarth PM. Fc receptors. *Adv Exp Med Biol* (2008) 640:22–34. doi:10.1007/978-0-387-09789-3_3
41. Getahun A, Cambier JC. Of ITIMs, ITAMs, and ITAMis: revisiting immunoglobulin Fc receptor signaling. *Immunol Rev* (2015) 268:66–73. doi:10.1111/imr.12336
42. Duncan AR, Winter G. The binding site for C1q on IgG. *Nature* (1988) 332:738–40. doi:10.1038/332738a0
43. Sondermann P, Huber R, Oosthuizen V, Jacob U. The 3.2-A crystal structure of the human IgG1 Fc fragment-Fc gammaRIII complex. *Nature* (2000) 406:267–73. doi:10.1038/35018508
44. Ramsland PA, Farrugia W, Bradford TM, Sardjono CT, Esparon S, Trist HM, et al. Structural basis for Fc gammaRIIa recognition of human IgG and formation of inflammatory signaling complexes. *J Immunol* (2011) 187:3208–17. doi:10.4049/jimmunol.1101467
45. Ferrara C, Stuart F, Sondermann P, Brünker P, Umaña P. The carbohydrate at FcgammaRIIIa Asn-162. An element required for high affinity binding to non-fucosylated IgG glycoforms. *J Biol Chem* (2006) 281:5032–6. doi:10.1074/jbc.M510171200
46. Ferrara C, Grau S, Jäger C, Sondermann P, Brünker P, Waldhauer I, et al. Unique carbohydrate-carbohydrate interactions are required for high affinity binding between FcgammaRIII and antibodies lacking core fucose. *Proc Natl Acad Sci U S A* (2011) 108:12669–74. doi:10.1073/pnas.1108455108
47. Merle NS, Church SE, Fremeaux-Bacchi V, Roumenina LT. Complement system part I – molecular mechanisms of activation and regulation. *Front Immunol* (2015) 6:262. doi:10.3389/fimmu.2015.00262
48. Dijstelbloem HM, van de Winkel JG, Kallenberg CGM. Inflammation in autoimmunity: receptors for IgG revisited. *Trends Immunol* (2001) 22:510–6. doi:10.1016/S1471-4906(01)02014-2
49. Shields RL, Lai J, Keck R, O'Connell LY, Hong K, Meng YG, et al. Lack of fucose on human IgG1 N-linked oligosaccharide improves binding to human Fcgamma RIII and antibody-dependent cellular toxicity. *J Biol Chem* (2002) 277:26733–40. doi:10.1074/jbc.M202069200
50. Shinkawa T, Nakamura K, Yamane N, Shoji-Hosaka E, Kanda Y, Sakurada M, et al. The absence of fucose but not the presence of galactose or bisecting N-acetylglucosamine of human IgG1 complex-type oligosaccharides shows the critical role of enhancing antibody-dependent cellular cytotoxicity. *J Biol Chem* (2003) 278:3466–73. doi:10.1074/jbc.M210665200
51. Niwa R, Natsume A, Uehara A, Wakitani M, Iida S, Uchida K, et al. IgG subclass-independent improvement of antibody-dependent cellular cytotoxicity by fucose removal from Asn297-linked oligosaccharides. *J Immunol Methods* (2005) 306:151–60. doi:10.1016/j.jim.2005.08.009
52. Bruggeman CW, Dekkers G, Bentlage AEH, Treffers LW, Nagelkerke SQ, Lissenberg-Thunnissen S, et al. Enhanced effector functions due to antibody defucosylation depend on the effector cell Fcγ receptor profile. *J Immunol* (2017) 199:204–11. doi:10.4049/jimmunol.1700116
53. Houde D, Peng Y, Berkowitz SA, Engen JR. Post-translational modifications differentially affect IgG1 conformation and receptor binding. *Mol Cell Proteomics* (2010) 9:1716–28. doi:10.1074/mcp.M900540-MCP200
54. Dashivets T, Thomann M, Rueger P, Knaupp A, Buchner J, Schlothauer T. Multi-angle effector function analysis of human monoclonal IgG glycovariants. *PLoS One* (2015) 10:e0143520. doi:10.1371/journal.pone.0143520
55. Thomann M, Schlothauer T, Dashivets T, Malik S, Avenal C, Bulau P, et al. In vitro glycoengineering of IgG1 and its effect on Fc receptor binding and ADCC activity. *PLoS One* (2015) 10:e0134949. doi:10.1371/journal.pone.0134949
56. Subedi GP, Barb AW. The immunoglobulin G1 N-glycan composition affects binding to each low affinity Fc γ receptor. *MAbs* (2016) 8:1512–24. doi:10.1080/19420862.2016.1218586
57. Kaneko Y, Nimmerjahn F, Ravetch JV. Anti-inflammatory activity of immunoglobulin G resulting from Fc sialylation. *Science* (2006) 313:670–3. doi:10.1126/science.1129594
58. Li T, DiLillo DJ, Bournazos S, Giddens JP, Ravetch JV, Wang L-X. Modulating IgG effector function by Fc glycan engineering. *Proc Natl Acad Sci U S A* (2017) 114:3485–90. doi:10.1073/pnas.1702173114
59. Scallon BJ, Tam SH, McCarthy SG, Cai AN, Raju TS. Higher levels of sialylated Fc glycans in immunoglobulin G molecules can adversely impact functionality. *Mol Immunol* (2007) 44:1524–34. doi:10.1016/j.molimm.2006.09.005
60. Dekkers G, Treffers L, Plomp R, Bentlage AEH, de Boer M, Koeleman CAM, et al. Decoding the human immunoglobulin G-glycan repertoire reveals a spectrum of Fc-receptor- and complement-mediated-effector activities. *Front Immunol* (2017) 8:877. doi:10.3389/fimmu.2017.00877
61. Fokkink WJR, Falck D, Santbergen TCM, Huizinga R, Wuhrer M, Jacobs BC. Comparison of Fc N-glycosylation of pharmaceutical products of Intravenous Immunoglobulin G. *PLoS One* (2015) 10:e0139828. doi:10.1371/journal.pone.0139828
62. Huhn C, Selman MHJ, Ruhaak LR, Deelder AM, Wuhrer M. IgG glycosylation analysis. *Proteomics* (2009) 9:882–913. doi:10.1002/pmic.200800715
63. Ackerman ME, Crispin M, Yu X, Baruah K, Boesch AW, Harvey DJ, et al. Natural variation in Fc glycosylation of HIV-specific antibodies impacts antiviral activity. *J Clin Invest* (2013) 123:2183–92. doi:10.1172/JCI65708
64. Wang TT, Sewatanon J, Memoli MJ, Wrammert J, Bournazos S, Bhaumik SK, et al. IgG antibodies to dengue enhanced for FcγRIIIA binding determine disease severity. *Science* (2017) 355:395–8. doi:10.1126/science.aai8128
65. Moldt B, Shibata-Koyama M, Rakasz EG, Schultz N, Kanda Y, Dunlop DC, et al. A nonfucosylated variant of the anti-HIV-1 monoclonal antibody b12 has enhanced FcγRIIIa-mediated antiviral activity in vitro but does not improve protection against mucosal SHIV challenge in macaques. *J Virol* (2012) 86:6189–96. doi:10.1128/JVI.00491-12
66. Kapur R, Della Valle L, Sonneveld M, Hipgrave Ederveen A, Visser R, Ligthart P, et al. Low anti-RhD IgG-Fc-fucosylation in pregnancy: a new variable predicting severity in haemolytic disease of the fetus and newborn. *Br J Haematol* (2014) 166:936–45. doi:10.1111/bjh.12965
67. Kapur R, Della Valle L, Verhagen OJHM, Hipgrave Ederveen A, Ligthart P, de Haas M, et al. Prophylactic anti-D preparations display variable decreases in Fc-fucosylation of anti-D. *Transfusion* (2015) 55:553–62. doi:10.1111/trf.12880
68. Urbaniak SJ, Greiss MA. RhD haemolytic disease of the fetus and the newborn. *Blood Rev* (2000) 14:44–61. doi:10.1054/blre.1999.0123
69. Wuhrer M, Porcelijn L, Kapur R, Koeleman CAM, Deelder A, de Haas M, et al. Regulated glycosylation patterns of IgG during alloimmune responses against human platelet antigens. *J Proteome Res* (2009) 8:450–6. doi:10.1021/pr800651j
70. Stegmann TC, Veldhuisen B, Nagelkerke SQ, Winkelhorst D, Schonewille H, Verduin EP, et al. RhIg-prophylaxis is not influenced by FCGR2/3 polymorphisms involved in red blood cell clearance. *Blood* (2017) 129:1045–8. doi:10.1182/blood-2016-05-716365
71. Breunis WB, van Mirre E, Bruin M, Geissler J, de Boer M, Peters M, et al. Copy number variation of the activating FCGR2C gene predisposes to idiopathic thrombocytopenic purpura. *Blood* (2008) 111:1029–38. doi:10.1182/blood-2007-03-079913
72. Ruhaak LR, Uh H-W, Deelder AM, Dolhain REJM, Wuhrer M. Total plasma N-glycome changes during pregnancy. *J Proteome Res* (2014) 13:1657–68. doi:10.1021/pr401128j
73. Rook GA, Steele J, Brealey R, Whyte A, Isenberg D, Sumar N, et al. Changes in IgG glycoform levels are associated with remission of arthritis during pregnancy. *J Autoimmun* (1991) 4:779–94. doi:10.1016/0896-8411(91)90173-A
74. van de Geijn FE, Wuhrer M, Selman MH, Willemsen SP, de Man YA, Deelder AM, et al. Immunoglobulin G galactosylation and sialylation are associated with pregnancy-induced improvement of rheumatoid arthritis and the postpartum flare: results from a large prospective cohort study. *Arthritis Res Ther* (2009) 11:R193. doi:10.1186/ar2892
75. el Bannoudi H, Ioan-Facsinay A, Toes REM. Bridging autoantibodies and arthritis: the role of Fc receptors. *Curr Top Microbiol Immunol* (2014) 382:303–19. doi:10.1007/978-3-319-07911-0_14
76. Thabet MM, Huizinga TWJ, Marques RB, Stoeken-Rijsbergen G, Bakker AM, Kurreeman FA, et al. Contribution of Fcgamma receptor IIIA gene 158V/F polymorphism and copy number variation to the risk of ACPA-positive

rheumatoid arthritis. *Ann Rheum Dis* (2009) 68:1775–80. doi:10.1136/ard.2008.099309
77. Anthony RM, Nimmerjahn F, Ashline DJ, Reinhold VN, Paulson JC, Ravetch JV. Recapitulation of IVIG anti-inflammatory activity with a recombinant IgG Fc. *Science* (2008) 320:373–6. doi:10.1126/science.1154315
78. Anthony RM, Kobayashi T, Wermeling F, Ravetch JV. Intravenous gammaglobulin suppresses inflammation through a novel T(H)2 pathway. *Nature* (2011) 475:110–3. doi:10.1038/nature10134
79. Sondermann P, Pincetic A, Maamary J, Lammens K, Ravetch JV. General mechanism for modulating immunoglobulin effector function. *Proc Natl Acad Sci U S A* (2013) 110:9868–72. doi:10.1073/pnas.1307864110
80. Yu X, Vasiljevic S, Mitchell DA, Crispin M, Scanlan CN. Dissecting the molecular mechanism of IVIg therapy: the interaction between serum IgG and DC-SIGN is independent of antibody glycoform or Fc domain. *J Mol Biol* (2013) 425:1253–8. doi:10.1016/j.jmb.2013.02.006
81. Crispin M, Yu X, Bowden TA. Crystal structure of sialylated IgG Fc: implications for the mechanism of intravenous immunoglobulin therapy. *Proc Natl Acad Sci U S A* (2013) 110:E3544–6. doi:10.1073/pnas.1310657110
82. Ahmed AA, Giddens J, Pincetic A, Lomino JV, Ravetch JV, Wang L-X, et al. Structural characterization of anti-inflammatory immunoglobulin G Fc proteins. *J Mol Biol* (2014) 426:3166–79. doi:10.1016/j.jmb.2014.07.006
83. Campbell IK, Miescher S, Branch DR, Mott PJ, Lazarus AH, Han D, et al. Therapeutic effect of IVIG on inflammatory arthritis in mice is dependent on the Fc portion and independent of sialylation or basophils. *J Immunol* (2014) 192:5031–8. doi:10.4049/jimmunol.1301611
84. Leontyev D, Katsman Y, Ma X-Z, Miescher S, Käsermann F, Branch DR. Sialylation-independent mechanism involved in the amelioration of murine immune thrombocytopenia using intravenous gammaglobulin. *Transfusion* (2012) 52:1799–805. doi:10.1111/j.1537-2995.2011.03517.x
85. Guhr T, Bloem J, Derksen NIL, Wuhrer M, Koenderman AHL, Aalberse RC, et al. Enrichment of sialylated IgG by lectin fractionation does not enhance the efficacy of immunoglobulin G in a murine model of immune thrombocytopenia. *PLoS One* (2011) 6:e21246. doi:10.1371/journal.pone.0021246
86. Bayry J, Bansal K, Kazatchkine MD, Kaveri SV. DC-SIGN and alpha2,6-sialylated IgG Fc interaction is dispensable for the anti-inflammatory activity of IVIg on human dendritic cells. *Proc Natl Acad Sci U S A* (2009) 106:E24; author reply E25. doi:10.1073/pnas.0900016106
87. Tjon ASW, van Gent R, Jaadar H, Martin van Hagen P, Mancham S, van der Laan LJW, et al. Intravenous immunoglobulin treatment in humans suppresses dendritic cell function via stimulation of IL-4 and IL-13 production. *J Immunol* (2014) 192:5625–34. doi:10.4049/jimmunol.1301260
88. Karsten CM, Pandey MK, Figge J, Kilchenstein R, Taylor PR, Rosas M, et al. Anti-inflammatory activity of IgG1 mediated by Fc galactosylation and association of FcγRIIB and dectin-1. *Nat Med* (2012) 18:1401–6. doi:10.1038/nm.2862
89. Thomann M, Reckermann K, Reusch D, Prasser J, Tejada ML. Fc-galactosylation modulates antibody-dependent cellular cytotoxicity of therapeutic antibodies. *Mol Immunol* (2016) 73:69–75. doi:10.1016/j.molimm.2016.03.002
90. Okazaki A, Shoji-Hosaka E, Nakamura K, Wakitani M, Uchida K, Kakita S, et al. Fucose depletion from human IgG1 oligosaccharide enhances binding enthalpy and association rate between IgG1 and FcgammaRIIIa. *J Mol Biol* (2004) 336:1239–49. doi:10.1016/j.jmb.2004.01.007
91. Colafrancesco S, Agmon-Levin N, Perricone C, Shoenfeld Y. Unraveling the soul of autoimmune diseases: pathogenesis, diagnosis and treatment adding dowels to the puzzle. *Immunol Res* (2013) 56:200–5. doi:10.1007/s12026-013-8429-4
92. Jefferis R. Recombinant antibody therapeutics: the impact of glycosylation on mechanisms of action. *Trends Pharmacol Sci* (2009) 30:356–62. doi:10.1016/j.tips.2009.04.007
93. Trouw LA, Pickering MC, Blom AM. The complement system as a potential therapeutic target in rheumatic disease. *Nat Rev Rheumatol* (2017) 13:538–47. doi:10.1038/nrrheum.2017.125
94. Malhotra R, Wormald MR, Rudd PM, Fischer PB, Dwek RA, Sim RB. Glycosylation changes of IgG associated with rheumatoid arthritis can activate complement via the mannose-binding protein. *Nat Med* (1995) 1:237–43. doi:10.1038/nm0395-237
95. van de Geijn FE, de Man YA, Wuhrer M, Willemsen SP, Deelder AM, Hazes JMW, et al. Mannose-binding lectin does not explain the course and outcome of pregnancy in rheumatoid arthritis. *Arthritis Res Ther* (2011) 13:R10. doi:10.1186/ar3231
96. Nimmerjahn F, Anthony RM, Ravetch JV. Agalactosylated IgG antibodies depend on cellular Fc receptors for in vivo activity. *Proc Natl Acad Sci U S A* (2007) 104:8433–7. doi:10.1073/pnas.0702936104
97. Quast I, Keller CW, Maurer MA, Giddens JP, Tackenberg B, Wang LX, et al. Sialylation of IgG Fc domain impairs complement-dependent cytotoxicity. *J Clin Invest* (2015) 125:4160–70. doi:10.1172/JCI82695
98. Peschke B, Keller CW, Weber P, Quast I, Lünemann JD. Fc-galactosylation of human immunoglobulin gamma isotypes improves C1q binding and enhances complement-dependent cytotoxicity. *Front Immunol* (2017) 8:646. doi:10.3389/fimmu.2017.00646
99. Diebolder CA, Beurskens FJ, de Jong RN, Koning RI, Strumane K, Lindorfer MA, et al. Complement is activated by IgG hexamers assembled at the cell surface. *Science* (2014) 343:1260–3. doi:10.1126/science.1248943
100. Teeling JL, Mackus WJM, Wiegman LJJM, van den Brakel JHN, Beers SA, French RR, et al. The biological activity of human CD20 monoclonal antibodies is linked to unique epitopes on CD20. *J Immunol* (2006) 177:362–71. doi:10.4049/jimmunol.177.1.362
101. Kellner C, Derer S, Valerius T, Peipp M. Boosting ADCC and CDC activity by Fc engineering and evaluation of antibody effector functions. *Methods* (2014) 65:105–13. doi:10.1016/j.ymeth.2013.06.036
102. de Jong RN, Beurskens FJ, Verploegen S, Strumane K, van Kampen MD, Voorhorst M, et al. A novel platform for the potentiation of therapeutic antibodies based on antigen-dependent formation of IgG hexamers at the cell surface. *PLoS Biol* (2016) 14:e1002344. doi:10.1371/journal.pbio.1002344
103. Schumaker VN, Calcott MA, Spiegelberg HL, Müller-Eberhard HJ. Ultracentifuge studies of the binding of IgG of different subclasses to the Clq subunit of the first component of complement. *Biochemistry* (1976) 15:5175–81. doi:10.1021/bi00668a035
104. Painter RH, Foster DB, Gardner B, Hughes-Jones NC. Functional affinity constants of subfragments of immunoglobulin G for Clq. *Mol Immunol* (1982) 19:127–31. doi:10.1016/0161-5890(82)90254-1
105. Sledge CR, Bing DH. Binding properties of the human complement protein Clq. *J Biol Chem* (1973) 248:2818–23.
106. Hughes-Jones NC. Functional affinity constants of the reaction between 125I-labelled C1q and C1q binders and their use in the measurement of plasma C1q concentrations. *Immunology* (1977) 32:191–8.
107. Malphettes L, Freyvert Y, Chang J, Liu P-Q, Chan E, Miller JC, et al. Highly efficient deletion of FUT8 in CHO cell lines using zinc-finger nucleases yields cells that produce completely nonfucosylated antibodies. *Biotechnol Bioeng* (2010) 106:774–83. doi:10.1002/bit.22751
108. Beck A, Reichert JM. Marketing approval of mogamulizumab: a triumph for glyco-engineering. *MAbs* (2012) 4:419–25. doi:10.4161/mabs.20996

Conflict of Interest Statement: Sanquin Research conducts Academic research in the field of immno- and hematology. It operates within "Stichting Sanquin Bloedvoorziening," a not for profit organization that manages the supply-chain of blood and blood products in the Netherlands. The authors declare no competing interests.

frontiers in Immunology

ORIGINAL RESEARCH
published: 16 March 2018
doi: 10.3389/fimmu.2018.00535

Specific Inhibition of Complement Activation Significantly Ameliorates Autoimmune Blistering Disease in Mice

Sidonia Mihai[1,2], Misa Hirose[1], Yi Wang[3], Joshua M. Thurman[4], V. Michael Holers[4], B. Paul Morgan[5], Jörg Köhl[6,7], Detlef Zillikens[1], Ralf J. Ludwig[1] and Falk Nimmerjahn[2]*

[1]Lübeck Institute of Experimental Dermatology and Department of Dermatology, University of Lübeck, Lübeck, Germany, [2]Institute of Genetics, Department of Biology, University of Erlangen-Nuremberg, Erlangen, Germany, [3]Alexion Pharmaceuticals, Cheshire, CT, United States, [4]Departments of Medicine and Immunology, University of Colorado Health Sciences Center, Denver, CO, United States, [5]Systems Immunity Research Institute, School of Medicine, Cardiff University, Cardiff, United Kingdom, [6]Institute for Systemic Inflammation Research, University of Lübeck, Lübeck, Germany, [7]Division of Immunobiology, Cincinnati Children's Hospital Medical Center and University of Cincinnati, College of Medicine, Cincinnati, OH, United States

OPEN ACCESS

Edited by:
Heiko Mühl,
Goethe University Frankfurt, Germany

Reviewed by:
Zhi Liu,
University of North Carolina at Chapel Hill, United States
Steven L. Spitalnik,
Columbia University, United States
Carlo Pincelli,
University of Modena and Reggio Emilia, Italy

***Correspondence:**
Sidonia Mihai
sidonia.mihai@uk-erlangen.de

Specialty section:
This article was submitted to Inflammation, a section of the journal Frontiers in Immunology

Received: 28 November 2017
Accepted: 02 March 2018
Published: 16 March 2018

Citation:
Mihai S, Hirose M, Wang Y, Thurman JM, Holers VM, Morgan BP, Köhl J, Zillikens D, Ludwig RJ and Nimmerjahn F (2018) Specific Inhibition of Complement Activation Significantly Ameliorates Autoimmune Blistering Disease in Mice. Front. Immunol. 9:535. doi: 10.3389/fimmu.2018.00535

Epidermolysis bullosa acquisita (EBA) is an antibody-mediated blistering skin disease associated with tissue-bound and circulating autoantibodies to type VII collagen (COL7). Transfer of antibodies against COL7 into mice results in a subepidermal blistering phenotype, strictly depending on the complement component C5. Further, activation predominantly by the alternative pathway is required to induce experimental EBA, as blistering was delayed and significantly ameliorated only in factor $B^{-/-}$ mice. However, C5 deficiency not only blocked the activation of terminal complement components and assembly of the membrane attack complex (MAC) but also eliminated the formation of C5a. Therefore, in the present study, we first aimed to elucidate which molecules downstream of C5 are relevant for blister formation in this EBA model and could be subsequently pharmaceutically targeted. For this purpose, we injected mice deficient in C5a receptor 1 (C5aR1) or C6 with antibodies to murine COL7. Importantly, *C5ar1*$^{-/-}$ mice were significantly protected from experimental EBA, demonstrating that C5a–C5aR1 interactions are critical intermediates linking pathogenic antibodies to tissue damage in this experimental model of EBA. By contrast, *C6*$^{-/-}$ mice developed widespread blistering disease, suggesting that MAC is dispensable for blister formation in this model. In further experiments, we tested the therapeutic potential of inhibitors of complement components which were identified to play a key role in this experimental model. Complement components C5, factor B (fB), and C5aR1 were specifically targeted using complement inhibitors both prophylactically and in mice that had already developed disease. All complement inhibitors led to a significant improvement of the blistering phenotype when injected shortly before anti-COL7 antibodies. To simulate a therapeutic intervention, anti-fB treatment was first administered in full-blown EBA (day 5) and induced significant

Abbreviations: COL7, type VII collagen; EBA, epidermolysis bullosa acquisita; C5aR, C5a receptor; MAC, membrane attack complex; fB, factor B; PD, pemphigoid diseases; IF, immunofluorescence; FcγR, Fc gamma receptor.

amelioration only in the final phase of disease evolution, suggesting that early intervention in disease development may be necessary to achieve higher efficacy. Anti-C5 treatment in incipient EBA (day 2) significantly ameliorated disease during the whole experiment. This finding is therapeutically relevant, since the humanized anti-C5 antibody eculizumab is already successfully used in patients. In conclusion, in this study, we have identified promising candidate molecules for complement-directed therapeutic intervention in EBA and similar autoantibody-mediated diseases.

Keywords: autoantibodies, complement, complement inhibition, immunotherapy, autoimmune diseases

INTRODUCTION

Pemphigoid diseases (PD), such as bullous pemphigoid (BP) and epidermolysis bullosa acquisita (EBA) are prototypical, antibody-mediated autoimmune diseases of the skin. They are clinically characterized by (muco)-cutaneous inflammation and blistering and caused by autoantibodies against structural proteins of the skin (1–3). Tissue-bound and circulating antibodies in EBA are directed against the noncollagenous domain 1 of type VII collagen (COL7). The pathogenic relevance of antibodies to COL7 was demonstrated through multiple lines of experimental evidence: (1) EBA autoantibodies recruit and activate leukocytes *ex vivo* and induce dermal–epidermal separation in cryosections of human skin (4, 5). (2) Passive transfer of antibodies to COL7 (6, 7) and immunization with recombinant COL7 (8) in mice results in a blistering phenotype closely resembling human EBA.

In recent years, use of animal models has significantly contributed to the understanding of PD pathogenesis. Three major checkpoints lead to PD: first, loss of tolerance to PD antigens leads to the CD4- and neutrophil-dependent generation of antigen-specific plasma cells. Second, autoantibodies are released into the circulation, where the half-life of IgG autoantibodies is controlled by the neonatal Fc receptor. Third, in the effector phase, autoantibodies bind to their target antigens located in the skin, which leads to the formation of a pro-inflammatory milieu allowing an ICAM-1- and CD18-dependent extravasation of myeloid effector cells into the skin. Within the skin, myeloid cells bind to the immune complexes *via* specific Fc gamma receptors (FcγRs), become activated, and release reactive oxygen species and proteases, which ultimately facilitate inflammation and blistering (9, 10).

Intriguingly, activation of the complement system has emerged as a key requirement to mediate inflammation and blistering in PD. Specifically, in antibody transfer models of BP and EBA, mice lacking the complement component C5 failed to develop clinically significant experimental PD (6, 11, 12). Upstream of C5, complement activation by both classical and alternative pathway is required to induce clinical manifestations. Interestingly, induction of experimental BP mainly depended on classical complement activation, whereas the alternative pathway predominantly drives inflammation in experimental EBA. Regarding the lectin-pathway, MBL-null mice developed a blistering phenotype similar to the wild-type control animals in experimental EBA, while no data has been published in this context relating to BP (13, 14).

C5 is cleaved by the C5 convertase into C5a and C5b fragments. "When C5b associates with C6 and C7, the complex inserts into cell membranes and interacts with C8, inducing the binding of several units of C9 to form a lytic pore, the terminal membrane complex (C5b-9, also known as the membrane attack complex, MAC). Many pathogens are protected from MAC-mediated lysis through their cell wall architecture or by employing evading strategies that interfere with MAC assembly. However, even sublytic amounts of MAC or partial complexes such as C5b-8 drive nonlethal signaling events. Pro-inflammatory signaling and phagocytosis are essential for complement-mediated defense. During activation and amplification, C5a is constantly released and triggers strong pro-inflammatory signaling mainly through its corresponding G-protein-coupled receptor C5a receptor 1 (C5aR1, CD88), guiding neutrophils, monocytes, and macrophages toward sites of complement activation" [reviewed in Ref. (15)]. C5a also binds to the more recently discovered seven transmembrane receptor C5aR2 (C5L2, GPR77), which is uncoupled from G proteins (16). However, the exact biologic function of this C5aR is not yet fully determined. Depending on the experimental setting it exerts either decoy, regulatory or even pro-inflammatory functions (15, 17). Its role on EBA development has not been explored. We recently showed that C5aR1-deficient mice are almost completely protected from inflammation and blistering in antibody transfer-induced EBA (18). It was, however, so far unclear whether the membrane attack complex (MAC) also contributes to skin blistering in EBA, and if pharmacological targeting of complement can ameliorate the EBA effector phase. Current evidence suggests that generation of C5a and the formation of MAC are both essential for triggering pro-inflammatory responses in disease models like collagen-antibody-induced arthritis (19) and renal ischemia/reperfusion injury (20, 21). This lack of clarity may be particularly relevant to the use of the C5 antibody eculizumab in PD (22). To address these knowledge gaps, we here systematically evaluated the contribution of complement components downstream of C5 and evaluated the therapeutic potential of targeting the implicated complement proteins in both preventive and therapeutic settings.

MATERIALS AND METHODS

Mice

C5ar1$^{-/-}$ mice ($n = 10$) backcrossed to BALB/c mice were acquired from The Jackson Laboratory. *C6*$^{-/-}$ mice ($n = 6$) backcrossed to C57BL/6J mice were kindly provided by Prof. B. Paul Morgan,

Cardiff University, UK. The *C6*$^{-/-}$ C57BL/6J mice were derived from a *C6*$^{-/-}$ C3H/He mouse strain lacking functional C6 (23). Age-matched female BALB/c and C57BL/6J mice were purchased from Charles River (Sulzfeld, Germany). Female mice, at 6–8 weeks of age, on the BALB/c background ($n = 4$/group), obtained from Charles River (Sulzfeld, Germany) were used for all complement-blocking experiments. Anesthesia in mice was induced by inhalation of isoflurane or intraperitoneal administration of a mixture of ketamine (100 µg/g) and xylazine (15 µg/g). The experiments were approved by the local authorities of the Animal Care and Use Committee (6/v/08) and performed by certified personnel.

Affinity-Purification of Antibodies

Total IgG from rabbits immunized with murine COL7c was purified by affinity chromatography using protein G affinity as previously reported and reviewed (6, 24). Before use in preclinical models, reactivity of IgG fractions was analyzed by immunofluorescence (IF) microscopy on murine skin.

EBA Induction

Passive transfer studies followed published protocols with minor modifications (6). Briefly, mice received six injections of 10 mg rabbit IgG every second day, over a period of 12 days. Skin affected by blisters and/or erosions was quantified as a percentage of the total mouse body surface area, as extensively described in Ref. (24). The evaluation of the affected body area was not performed by blinded observers. At the end of the experiment (day 12), mice were sacrificed and skin biopsies were taken for examination by histopathology and IF microscopy (to detect tissue-bound IgG and complement C3 deposits), as described (6). Deposition of murine C5 was detected by incubation of cryosections of perilesional skin with a monoclonal antibody

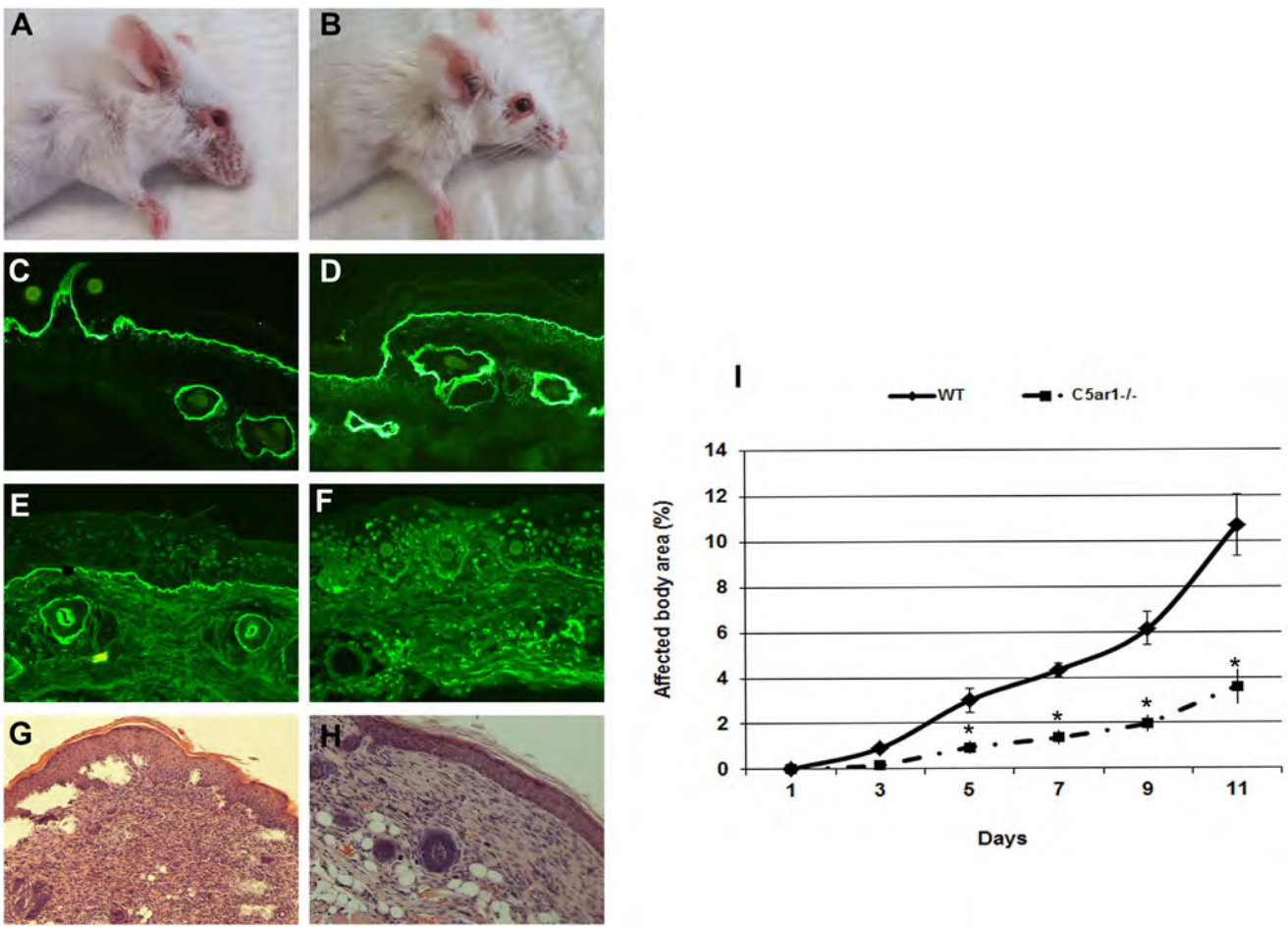

FIGURE 1 | C5a receptor 1 (C5aR1)-deficient mice are protected from blister induction in experimental epidermolysis bullosa acquisita. Representative day 12 clinical pictures showing extensive skin lesions, including blisters, erosions, partly covered by crusts on the ear and front leg, and alopecia of snout and around the eyes in a control mouse **(A)**, in contrast to a C5aR1-deficient mouse receiving the same dose of anti-type VII collagen (COL7) IgG **(B)**. Immunofluorescence analysis revealed linear deposition of rabbit IgG **(C,D)** at the dermal–epidermal junction in all mice injected with anti-COL7. Deposition of murine C5 was strong in the skin of the control mouse **(E)** and weak or absent in the skin of the C5aR1-deficient mouse **(F)**. Histological analysis of lesional murine skin revealed subepidermal cleavage and a neutrophil-rich inflammatory infiltrate in the skin of the control mouse **(G)** and to a lesser extent, in the **(H)** skin of the C5aR1-deficient mouse defiecient mouse. Affected body area of C5aR1-deficient mice vs control mice is represented as mean ± SEM. *$p < 0.05$ represents significant difference of disease activity between the two groups **(I).** These data were obtained from two independent experiments ($n = 5$/group/experiment).

specific to murine C5 (BB5.1) (25) and, finally, with a FITC-labeled antibody specific to mouse IgG (DAKO, Glostrup, Denmark), as described (6).

Complement Inhibition

The alternative pathway of complement activation was inhibited by a monoclonal antibody to murine factor B (fB) (clone 1379) (26). For prophylactic application, mice were pre-injected intraperitoneally (ip) daily with 2 mg anti-fB or control mouse polyclonal IgG, and, subsequently, with 10 mg of purified anti-COL7 IgG, subcutaneously, every second day, for 12 days. For the therapeutic approach, mice were treated with six injections of 10 mg anti-COL7 IgG. Starting with day 5, when cutaneous lesions were clearly visible in both groups, mice were additionally injected ip daily with anti-fB or control mouse IgG. For C5-inhibition, a monoclonal antibody to murine C5 (clone BB5.1) was used (25). In a first approach, mice were pre-injected ip twice a week with 40 mg/kg of anti-C5 mAb or an isotype control (HFN7.1), and, subsequently, with 10 mg anti-COL7 IgG, every second day, for 12 days. For the therapeutic approach, mice were injected with six doses of pathogenic rabbit IgG. 24 h after the first anti-COL7 IgG injection and then twice a week (on days 4, 7, and 10) mice were additionally injected with anti-murine C5 or an isotype control. C5aR1 was pharmacologically targeted using a C5aR1/2 antagonist A8Δ71–73 (C5aRA) (27). Mice were injected subcutaneously with 10 mg anti-COL7 IgG, every second day, for 12 days. One group of mice was pretreated daily with 10^{-5}M C5aRA, intravenously for the first 5 days and ip for the rest of the experiment.

Statistical Analysis

Differences in disease severity were calculated using the Mann–Whitney *U*-test. Means are presented ±SEM; $p < 0.05$ was considered statistically significant.

RESULTS

C5aR1-Deficient Mice Are Protected From Induction of Experimental EBA

The anaphylatoxin C5a is a powerful chemoattractant for neutrophils, mast cells, and monocytes, and it exerts many of its biologic functions exclusively by activation of C5aR1 (17). Leukocyte recruitment to the dermal–epidermal junction by antibodies and release of inflammatory mediators are prerequisites for blister induction in this animal model (28). To study the C5a–C5aR1 interactions, *C5ar1*$^{-/-}$ and control mice were injected with rabbit antibodies to murine COL7 to induce experimental EBA. C5aR1-deficient mice were significantly protected from blister induction (**Figure 1**), confirming that C5a–C5aR1 interactions are critical intermediates linking pathogenic antibodies to tissue damage in this experimental model of EBA.

C6-Deficient Mice Are Susceptible to Induction of Experimental EBA

In the skin of EBA patients, deposition of different complement components, including MAC, are found with an incidence ranging from 40 to 100%. In addition, direct IF microscopy of perilesional skin showed linear deposits of MAC at the dermal–epidermal junction of mice injected with antibodies to murine COL7 (6). C6 is the

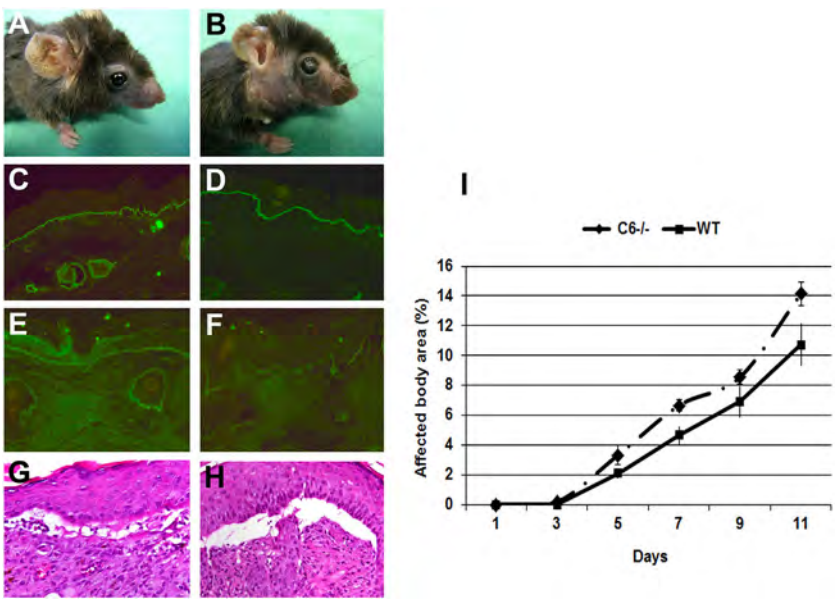

FIGURE 2 | C6-deficient mice are susceptible to inflammation and blistering in experimental epidermolysis bullosa acquisita. Skin lesions, including blisters and erosions covered by crusts on the ear and front leg, and alopecia of the snout and around eyes developed in both **(A)** C6-sufficient and **(B)** C6-deficient mice (day 12). Immunofluorescence analysis of perilesional skin revealed deposition of rabbit IgG **(C,D)** and murine C3 **(E,F)** at the dermal–epidermal junction of both C6-sufficient and C6-deficient mice. Histological analysis of lesional skin revealed extensive dermal–epidermal separation in both C6-sufficient **(G)** and C6-deficient mice **(H)**. Affected body area of C6-deficient mice vs control mice is represented as mean ± SEM **(I)**. These data were obtained from a single experiment (n = 6/group).

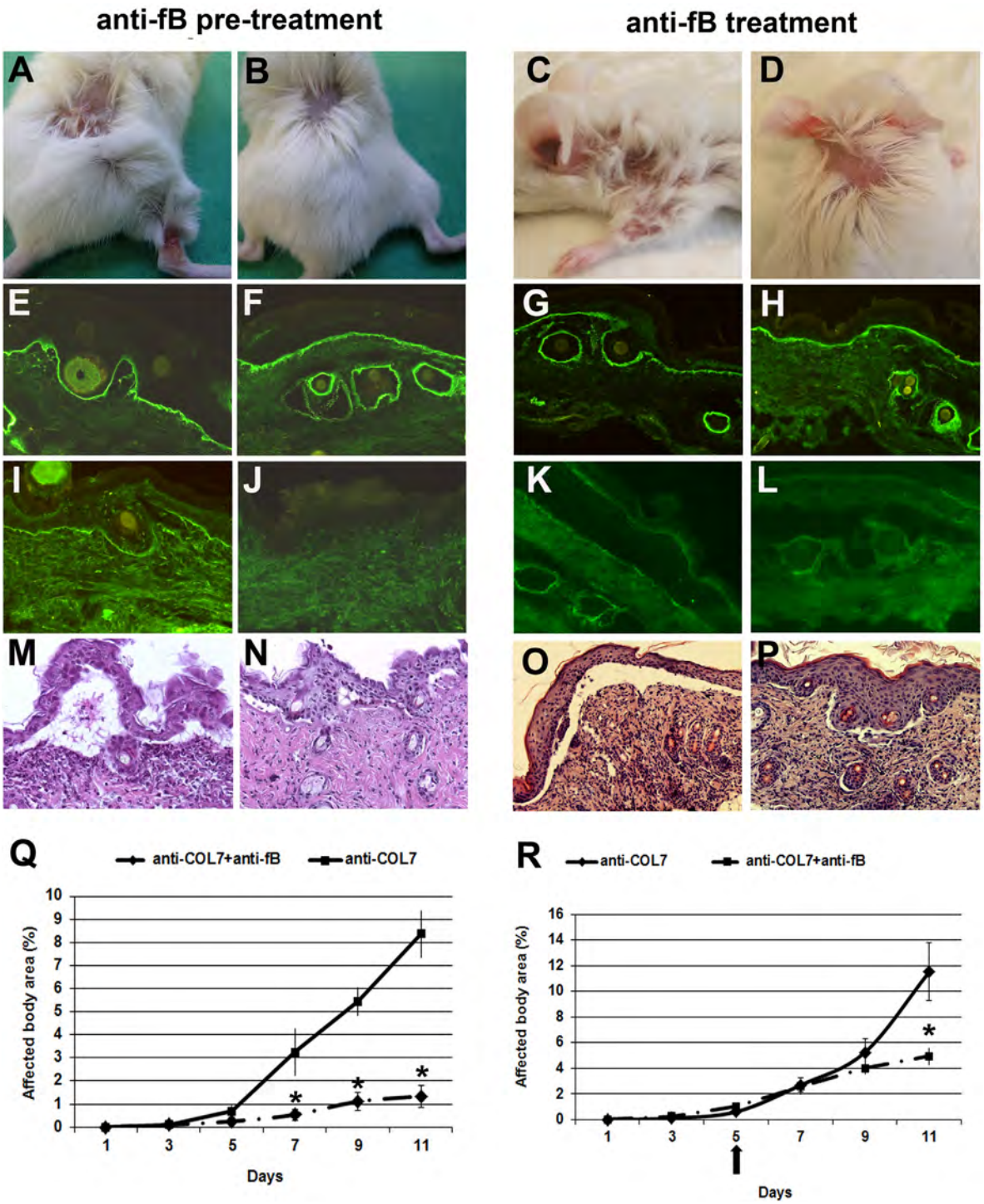

FIGURE 3 | Mice pretreated with a monoclonal Ab to murine factor B (fB) develop a significantly less severe blistering phenotype. BALB/c mice were pretreated with anti-fB (left), followed by injection of anti-type VII collagen (COL7) IgG, and evaluated for skin lesions. To test for a potential therapeutic relevance, mice were injected with anti-fB in incipient disease (right). Erosions covered by crusts on the back and leg of a BALB/c mouse injected with rabbit IgG against murine COL7 **(A,C)**. Less intensive lesions (alopecia) in a **(B,D)** BALB/c mouse challenged with the same dose of pathogenic IgG and a mAb to murine fB. Direct immunofluorescenc analysis of mouse skin revealed deposition of rabbit IgG in mice injected with pathogenic rabbit IgG and **(E,G)** control murine IgG or **(F,H)** anti-murine fB. Deposits of mouse C5 along the dermal–epidermal junction were strong in the skin of the **(I,K)** BALB/c mouse injected with pathogenic rabbit IgG and control murine IgG and absent in the skin of the **(J,L)** BALB/c mouse treated with antibodies to COL7and anti-murine fB. Histological analysis revealed extensive dermal–epidermal separation and inflammatory infiltrates, consisting mainly of neutrophils, in the skin of the control mice **(M,O)** and, to a lesser extent, in the skin of the treated mice **(N,P)**. Affected body area of anti-fB treated vs control mice is represented as mean ± SEM. $^*p < 0.05$ represents significant difference of disease activity between the two groups **(Q,R)**. The arrow indicates the beginning of anti-fB treatment. These data were obtained from a single experiment ($n = 4$/group).

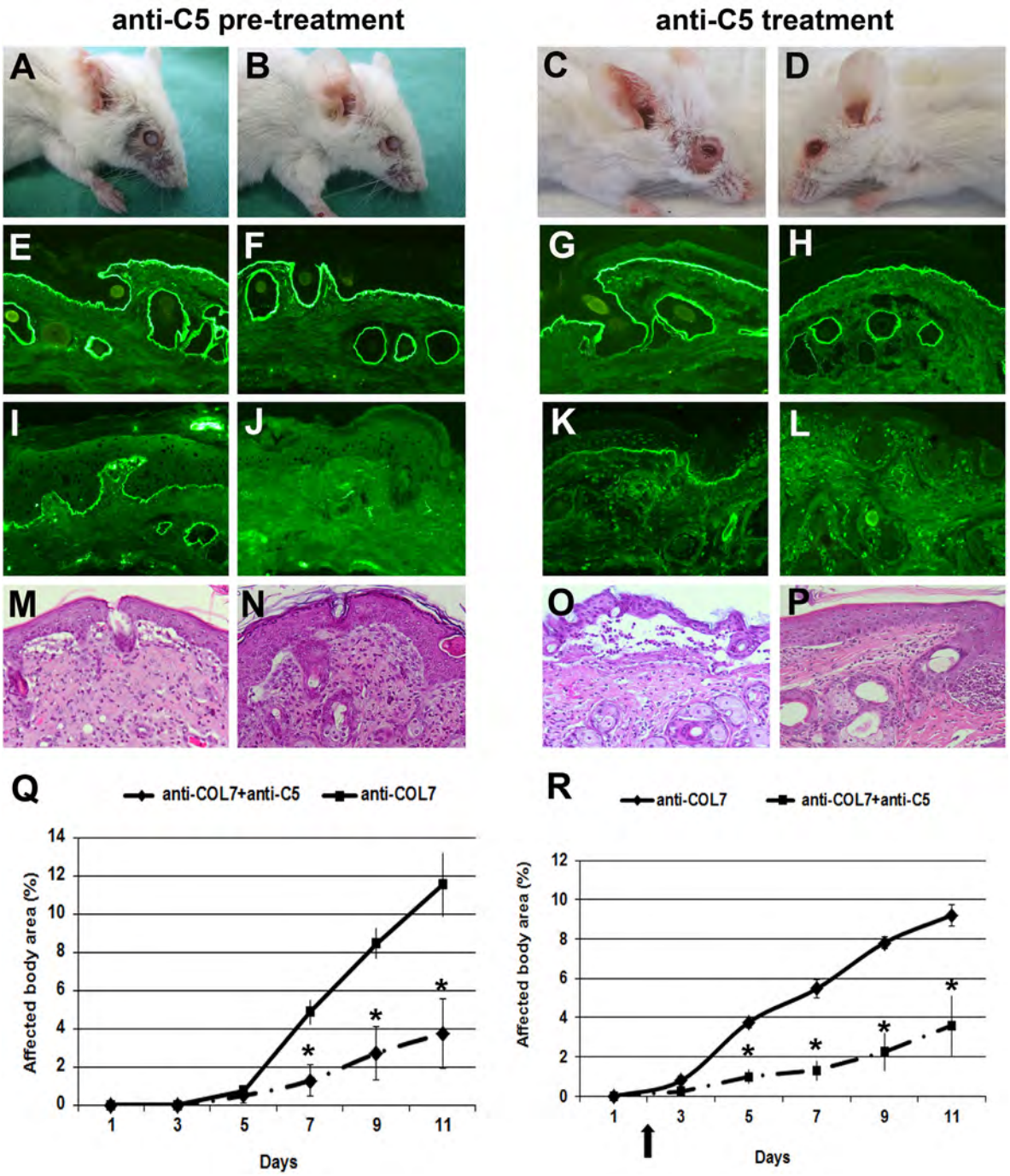

FIGURE 4 | Anti-C5 treatment significantly ameliorates blistering in epidermolysis bullosa acquisita. BALB/c mice were pretreated with anti-C5 (left), followed by injection of anti-type VII collagen (COL7), and evaluated for skin lesions. Alternatively, to test for a potential therapeutic relevance, mice were injected with anti-C5 in incipient disease (right). Injection of rabbit anti-COL7 IgG resulted in extensive skin lesions, including blisters, erosions, partly covered by crusts on the ear and front leg, and alopecia around the eyes in a BALB/c mouse treated with the mock antibody **(A,C)**. A BALB/c mouse receiving the same dose of pathogenic IgG and the anti-murine C5 mAb **(B,D)** showed less extensive lesions. Direct immunofluorescenc analysis revealed linear deposition of rabbit IgG **(E, F, G, H)** at the dermal–epidermal junction in all mice injected with antibodies to COL7. Deposition of murine C5 was strong in the skin of the control mouse **(I,K)** and weak or absent in the skin of the mouse treated with anti-murine C5 antibody **(J,L)**. Histological analysis of lesional murine skin revealed subepidermal cleavage and a neutrophil-rich inflammatory infiltrate in skin of the **(M,O)** BALB/c mouse injected with the mock antibody, and to a lesser extent, in skin of the **(N,P)** BALB/c mouse receiving antibodies to COL7and the blocking anti-C5 antibody. Affected body area of anti-murine C5 treated vs control mice is represented as mean ± SEM. $^*p < 0.05$ represents significant difference of disease activity between the two groups **(Q, R)**. The arrow indicates the beginning of anti-C5 treatment. These data were obtained from a single experiment (n = 4/group).

first among terminal complement components that associates with C5b to initiate the assembly of MAC. To study the implication of complement in tissue destruction *via* C5b-9, mice deficient in C6 and wild-type mice were injected with rabbit antibodies to murine COL7. Both C6-deficient and control mice developed widespread blistering disease (**Figure 2**), to a similar extent, indicating that MAC is dispensable for blister formation in this model.

Therapeutic Complement Inhibition in Experimental EBA

In further experiments, we aimed to evaluate the efficiency of novel therapeutic approaches using complement inhibitors. To test their prophylactic potential, mice were pretreated with complement inhibitors and, subsequently, injected with rabbit antibodies to murine COL7. To test for a potential therapeutic relevance of complement inhibition, mice were injected with complement inhibitors in incipient disease.

Mice Pretreated With a Monoclonal Antibody to Murine Factor B Develop Less Severe Blistering

We have previously demonstrated that fB-deficient mice are significantly protected from blistering when injected with pathogenic antibodies to murine COL7 (14). To pharmacologically inhibit the alternative pathway of complement activation in this model, we used a blocking mAb to murine fB (clone 1379). In previous studies, this antibody prevented antiphospholipid antibody-induced fetal loss in a murine model dependent upon activation of the alternative complement pathway (26). In a first set of experiments, BALB/c mice were pre-injected with anti-fB or control antibody, and, subsequently, with anti-COL7 IgG. Mice pretreated with anti-fB, in contrast to control mice, developed significantly less severe blistering throughout the whole experiment (**Figure 3**).

As the prophylactic application of anti-fB impaired induction of blistering, we next tested the potential therapeutic relevance of this antibody. To address this, experimental EBA was induced in BALB/c mice by repetitive applications of anti-COL7 IgG. On day 5 of the experiment, when cutaneous lesions were clearly visible, one group of mice was additionally injected with anti-fB, while the other group was injected with similar amounts of control mouse IgG. Anti-fB treatment in incipient EBA-induced significant amelioration of disease progression (**Figure 3**). This identifies fB as an additional target of therapy in inflammatory PD.

Anti-C5 Significantly Ameliorates Blister Formation in Mice

We previously showed that C5-deficient mice are (almost completely) resistant to blister induction by transfer of anti-COL7 IgG (6, 12). To test the prophylactic and therapeutic effects of C5-inhibition, we used a blocking mAb to murine C5 (clone BB5.1) (29). In a first approach, BALB/c mice were pre-injected with anti-C5 or an isotype control (HFN7.1), and, subsequently, with anti-COL7 IgG. In line with the experiments using C5-deficient mice (6), mice treated with anti-C5 developed

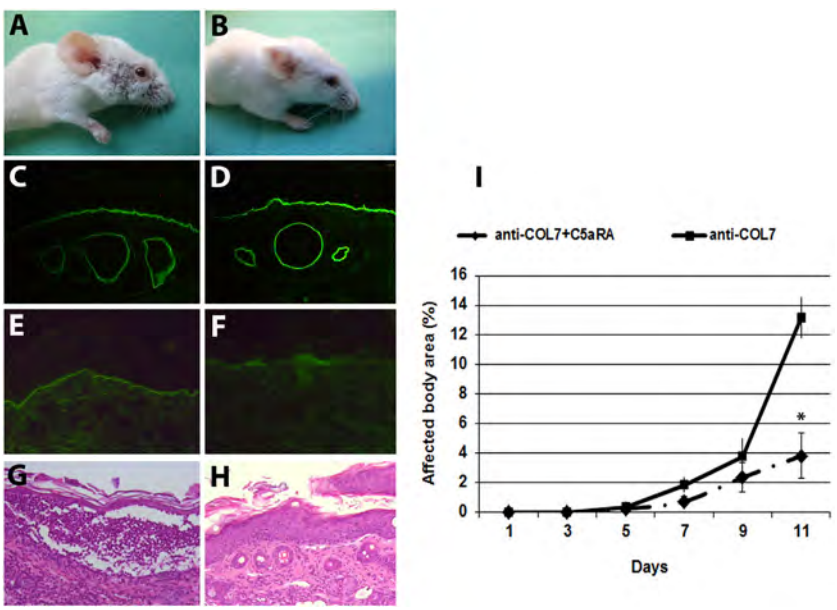

FIGURE 5 | Mice pretreated with a C5a receptor (C5aR) antagonist develop less severe blistering. Skin lesions, including blisters and erosions covered by crusts on the ear, snout, front leg, and around eyes developed in a control mouse injected with pathogenic IgG **(A)**. A BALB/c mouse pretreated with a C5aR antagonist and subsequently challenged with the same dose of antibodies to type VII collagen (COL7) showed less extensive skin lesions **(B)**. Immunofluorescenc analysis of perilesional skin revealed deposition of rabbit IgG at the dermal–epidermal junction of both mice groups **(C,D)**. Deposits of mouse C5 along the dermal–epidermal junction were weak in the skin of the pretreated **(F)** vs non-treated mouse **(E)**. Subepidermal cleavage and neutrophil infiltration was extensive in the skin of control mice **(G)** and less present in the skin of treated mice **(H)**, as revealed by histopathology. Affected body area of C5aRA treated vs control mice is represented as mean ± SEM. $^*p < 0.05$ represents significant difference of disease activity between the two groups **(I)**. These data were obtained from a single experiment ($n = 4$/group).

significantly less blistering disease, during the whole observation period (**Figure 4**).

In a next set of experiments, we evaluated the potential therapeutic relevance of C5-inhibition. Based on the results obtained with anti-fB, we here initiated treatment at day 2 to evaluate if early treatment may have a more pronounced effect on inflammation and blistering in experimental EBA. Anti-C5 treatment in incipient EBA successfully and significantly ameliorated disease during the entire observation period (**Figure 4**).

C5aR1 Inhibition Leads to a Significant Improvement of the Blistering Phenotype at the End of the Observation Period

As the experiments using C5aR1-deficient mice demonstrated that C5a–C5aR1 interactions are critical for blister formation in this model, we pharmacologically targeted the C5aR1 signaling using a C5aRA (27). BALB/c mice were injected with anti-COL7 IgG for EBA induction. One group of mice was pretreated with the C5aRA and showed a less severe blistering phenotype compared to control mice (**Figure 5**). These findings identify C5aR1 as a potential drug candidate for EBA treatment.

DISCUSSION

While the importance of C5 and mechanisms leading to C5 cleavage in driving blistering and inflammation in PD are well established, relatively little was known regarding which complement components downstream of C5 cleavage are involved in this process. We here close this knowledge gap, confirming a major role of the C5a/C5aR1 axis and excluding a significant contribution of the MAC in the effector phase of EBA. The insights into the contribution of complement components in EBA were then translated into assessment of treatment in pre-clinical disease models. Specifically, antibodies against fB or C5 prevented onset of blistering and ameliorated disease progression in already established EBA.

Our data also add to the understanding of the complex contribution of the complement system in the pathogenesis of blistering and inflammation in EBA. First, we highlight the predominant role of the C5a/C5aR1 axis, by demonstrating a pronounced amelioration of the blistering phenotype in antibody transfer-induced EBA in mice lacking the C5aR1. These insights into C5a/C5aR1 pathophysiology also shape out current understanding of EBA pathogenesis: the binding of the autoantibodies to COL7 initiates blistering in EBA; one of the immediate subsequent events is the activation of complement, which in antibody transfer-induced EBA occurs within 24 h after anti-COL7 IgG injection (30). Complement activation thus precedes the onset of blistering. Taking into account the effects of C5a on myeloid cells, i.e., induction of migration and activation (31), it is likely that C5a facilitates myeloid cell extravasation into the skin. Furthermore, "C5a can act as a general regulator of Fcgamma receptor (FcγR) expression and the C5aR1 signaling cascade seems to be important for this regulation, suggesting a hierarchical relationship between the two receptors: C5a attracts FcγR-bearing leucocytes, and C5aR transcriptionally regulates expression of inhibitory and activating FcγRs on macrophages to lower the threshold of immune complex activation. Recent studies also suggest the importance of direct cross-talk between C5aR1 and human FcγRs for progression of inflammatory disease, thus highlighting new aspects of this complex interaction" [reviewed in Ref. (32)]. Moreover, the recently discovered negative feedback loop in the C5aR-FcγR cross-talk *via* dectin-1 (18) and galactosylated IgG1 Abs (33) may have an impact on the development of glycoengineered intravenous immunoglobulins (IVIG) analogous to the IVIG preparations administered in autoimmune diseases as an anti-inflammatory therapy (34). However, complement activation significantly, but not exclusively contributes to the formation of this pro-inflammatory milieu and other pro-inflammatory mediators, such as GM-CSF (35) or IL-1β (36), could compensate for the lack of complement-mediated myeloid cell recruitment into the skin. This assumption is further supported by the observation of the occurrence of blistering in the absence of complement activation in (albeit few) outbred mice after immunization with COL7 for EBA induction (37).

Second, our data exclude a significant contribution of the MAC in the induction of inflammation and blistering in EBA. Previously, deposits of human IgG, murine C3, and the MAC were detected in the skin of mice injected with IgG antibodies purified from a patient with severe EBA (38). Furthermore, IgG antibodies from BP patients were able to fix all terminal complement components (C5–C9) resulting in MAC assembly *in vitro* (39). Hence, a contribution of the MAC to pathogenesis of blistering in PD may well have been assumed. Noteworthy, C6-deficient mice are unable to generate functional MAC but can still form C5a. Therefore, our data do not exclude the possibility that MAC might contribute to the skin damage, but support the critical role of the C5a/C5aR1 axis, suggesting that skin inflammation due to leukocyte recruitment and activation by C5a is sufficient to induce blistering.

Since a number of complement-targeting compounds are either in clinical trials or already licensed, our findings can be translated into clinical practice in a relatively timely fashion. More specifically, the humanized anti-C5 antibody (eculizumab) is widely used to treat atypical hemolytic uremic syndrome and paroxysmal nocturnal hemoglobinuria (22). In addition, eculizumab was shown to be safe and well-tolerated in a phase 1 trial in patients with systemic lupus erythematosus (40). These encouraging data suggest that anti-C5 therapy, as well as inhibition of the C5a–C5aR1-axis, could prevent complement-mediated injury in human EBA, and attenuate skin inflammation due to decreased leukocyte recruitment and activation by C5a. In support of this view, the C5aR1 antagonist CCX168 (ChemoCentryx) showed a significant therapeutic effect in a phase 2 study of anti-neutrophil cytoplasmatic antibody-associated renal vasculitis (34). Regarding inhibition of fB, a fragment of the anti-fB antibody 1379 (TA106) is currently available at Taligen Therapeutics/Alexion Pharmaceuticals, but no development intentions have been declared yet (34). Another inhibitor of the alternative pathway, an mAb against factor D, lampalizumab (Roche), has been very recently shown to reduce geographic atrophy progression secondary to age-related macular degeneration (41). Yet, based on our findings of a superior response to preventive vs therapeutic

fB inhibition, we envision that complement-targeting treatments may be best employed to maintain the therapeutic response after achieving clinical remission. Furthermore, an alternative mode of drug application involving complement-targeting topical therapy could be potentially very appealing to prevent disease progression in PD. Hence, daily topical application of a purinergic P2X receptor antagonist inhibited complement deposition and choroidal neovascularization in experimental age-related macular degeneration (42).

A serious drawback of (prolonged) C5-directed treatment is the high risk of infections. Deficiency of the terminal complement proteins (C5–C9) is associated with meningococcal infections, and all patients treated with eculizumab are vaccinated against *Neisseria meningitidis*. The selective blockade of either fB or the C5a/C5aR1-axis, which may even be tailored to each individual patient's needs, is likely to have less side effects than blockade of C5. In addition, especially in BP, where activation of C5 predominantly depends on the classical pathway (13), selective blockade of the classical pathway through C1s inhibition (43), might prove useful for PD treatment.

Different models of EBA are available to mimic the clinical situation in patients, explore disease progression and develop new therapeutic approaches. The use of the antibody transfer model closely resembles the clinical situation and enables the examination of the effector phase of EBA. Testing therapeutic drugs or investigating the pathogenesis of EBA is easily performed because the clinical symptoms are visible within days after the IgG transfer (24). However, antibody transfer models are not suitable for the evaluation of long-term therapeutic effects (24). Recent data brought evidence for a xenogeneic immune reaction to rabbit anti-mouse COL7 IgG, a confounding effect that may contribute to immune complex-driven inflammation and tissue damage in this model, especially at later time points. Therefore, evaluation of results within the first 2 weeks after pathogenic antibody injection is recommended (44). Complex immunization-induced models are more suitable for the investigation of all aspects of autoimmune blistering diseases, including long-term therapeutic intervention (24). In the immunization-induced model of EBA, injection of mice with the immunodominant NC1 domain of COL7 leads to anti-COL7 autoantibody-production in most mice strains, whereas development of subepidermal blistering is restricted to certain strains. Furthermore, comparison of the autoantibody response in EBA-susceptible and -resistant mice showed an association of clinical disease with formation of complement-fixing (IgG2) anti-COL7 antibodies (8). Hence, we emphasize that complement-blocking therapy may ameliorate disease progression in the EBA immunization-induced model. However, due to the dependency on complement-fixing antibodies, activation by the classical pathway might be more relevant in the immunization-model. Thus, selective blockade of the classical pathway might prove more useful than fB inhibition. Similar to the antibody transfer model, anti-C5 therapy, as well as inhibition of the C5a–C5aR1-axis, would probably efficiently ameliorate complement-mediated injury in immunization-induced EBA and attenuate skin inflammation due to decreased leukocyte recruitment and activation by C5a. However, overwhelming the natural tolerance against skin proteins remains challenging in immunization models. In addition, the effects of adjuvants during immunization remain largely unknown (24).

In conclusion, our study identified promising candidate molecules for complement-directed therapeutic concepts in EBA. Novel therapeutic agents are required in autoimmune disease, as treatment strategies of most antibody-mediated diseases, including EBA, are unspecific and resume to prolonged administration of systemic corticosteroids and additional immunosuppressants, being frequently associated with severe side effects, including death (45). At this point, the clinically available anti-C5 antibody eculizumab is the most promising candidate for clinical trials in EBA.

ETHICS STATEMENT

This study was carried out in accordance with the recommendations of European Community rules for animal care. The protocol was approved by the Ministry for Energy, Agriculture, the Environment and Rural Areas, Kiel, Schleswig-Holstein and the Government of Middle Franconia, Germany.

AUTHOR CONTRIBUTIONS

SM, DZ, and FN conceived and designed the research studies. SM and MH performed experiments, collected, assembled, and interpreted data. YW, JMT, VMH, BPM, JK, and RJL provided reagents, performed data analysis and interpretation. SM, RJL, and FN wrote the manuscript. All authors contributed to editing, reviewed and approved the final manuscript.

FUNDING

This work was supported by grants MI1314/1-1 (to SM) and SFB1181-A07 (to FN) from the German Research Foundation, NIH R01 AR51749 (to VMH) and E24-2008 (to SM) from the University of Lübeck. In addition, we received infrastructural support from the German Research Foundation through EXC 306/2 Inflammation at Interfaces and CRU 303/1 Pemphigoid Diseases (to RJL, JK, and DZ).

REFERENCES

1. Schmidt E, Zillikens D. Pemphigoid diseases. *Lancet* (2013) 381:320–32. doi:10.1016/S0140-6736(12)61140-4
2. Ludwig RJ, Kalies K, Kohl J, Zillikens D, Schmidt E. Emerging treatments for pemphigoid diseases. *Trends Mol Med* (2013) 19:501–12. doi:10.1016/j.molmed.2013.06.003
3. Ludwig RJ, Vanhoorelbeke K, Leypoldt F, Kaya Z, Bieber K, McLachlan SM, et al. Mechanisms of autoantibody-induced pathology. *Front Immunol* (2017) 8:603. doi:10.3389/fimmu.2017.00603
4. Shimanovich I, Mihai S, Oostingh GJ, Ilenchuk TT, Brocker EB, Opdenakker G, et al. Granulocyte-derived elastase and gelatinase B are required for dermal-epidermal separation induced by autoantibodies from patients with epidermolysis bullosa acquisita and bullous pemphigoid. *J Pathol* (2004) 204:519–27. doi:10.1002/path.1674
5. Sitaru C, Kromminga A, Hashimoto T, Brocker EB, Zillikens D. Autoantibodies to type VII collagen mediate Fcgamma-dependent neutrophil activation and induce dermal-epidermal separation in cryosections of human skin. *Am J Pathol* (2002) 161:301–11. doi:10.1016/S0002-9440(10)64182-X

6. Sitaru C, Mihai S, Otto C, Chiriac MT, Hausser I, Dotterweich B, et al. Induction of dermal-epidermal separation in mice by passive transfer of antibodies specific to type VII collagen. *J Clin Invest* (2005) 115:870–8. doi:10.1172/JCI200521386
7. Woodley DT, Ram R, Doostan A, Bandyopadhyay P, Huang Y, Remington J, et al. Induction of epidermolysis bullosa acquisita in mice by passive transfer of autoantibodies from patients. *J Invest Dermatol* (2006) 126:1323–30. doi:10.1038/sj.jid.5700254
8. Sitaru C, Chiriac MT, Mihai S, Buning J, Gebert A, Ishiko A, et al. Induction of complement-fixing autoantibodies against type VII collagen results in subepidermal blistering in mice. *J Immunol* (2006) 177:3461–8. doi:10.4049/jimmunol.177.5.3461
9. Kasperkiewicz M, Sadik CD, Bieber K, Ibrahim SM, Manz RA, Schmidt E, et al. Epidermolysis bullosa acquisita: from pathophysiology to novel therapeutic options. *J Invest Dermatol* (2016) 136:24–33. doi:10.1038/JID.2015.356
10. Heimbach L, Li N, Diaz A, Liu Z. Experimental animal models of bullous pemphigoid. *G Ital Dermatol Venereol* (2009) 144:423–31.
11. Liu Z, Giudice GJ, Swartz SJ, Fairley JA, Till GO, Troy JL, et al. The role of complement in experimental bullous pemphigoid. *J Clin Invest* (1995) 95:1539–44. doi:10.1172/JCI117826
12. Iwata H, Witte M, Samavedam UK, Gupta Y, Shimizu A, Ishiko A, et al. Radiosensitive hematopoietic cells determine the extent of skin inflammation in experimental epidermolysis bullosa acquisita. *J Immunol* (2015) 195:1945–54. doi:10.4049/jimmunol.1501003
13. Nelson KC, Zhao M, Schroeder PR, Li N, Wetsel RA, Diaz LA, et al. Role of different pathways of the complement cascade in experimental bullous pemphigoid. *J Clin Invest* (2006) 116:2892–900. doi:10.1172/JCI17891
14. Mihai S, Chiriac MT, Takahashi K, Thurman JM, Holers VM, Zillikens D, et al. The alternative pathway of complement activation is critical for blister induction in experimental epidermolysis bullosa acquisita. *J Immunol* (2007) 178:6514–21. doi:10.4049/jimmunol.178.10.6514
15. Ricklin D, Hajishengallis G, Yang K, Lambris JD. Complement: a key system for immune surveillance and homeostasis. *Nat Immunol* (2010) 11:785–97. doi:10.1038/ni.1923
16. Li R, Coulthard LG, Wu MC, Taylor SM, Woodruff TM. C5L2: a controversial receptor of complement anaphylatoxin, C5a. *FASEB J* (2013) 27:855–64. doi:10.1096/fj.12-220509
17. Klos A, Tenner AJ, Johswich KO, Ager RR, Reis ES, Kohl J. The role of the anaphylatoxins in health and disease. *Mol Immunol* (2009) 46:2753–66. doi:10.1016/j.molimm.2009.04.027
18. Karsten CM, Pandey MK, Figge J, Kilchenstein R, Taylor PR, Rosas M, et al. Anti-inflammatory activity of IgG1 mediated by Fc galactosylation and association of FcgammaRIIB and dectin-1. *Nat Med* (2012) 18:1401–6. doi:10.1038/nm.2862
19. Banda NK, Hyatt S, Antonioli AH, White JT, Glogowska M, Takahashi K, et al. Role of C3a receptors, C5a receptors, and complement protein C6 deficiency in collagen antibody-induced arthritis in mice. *J Immunol* (2012) 188:1469–78. doi:10.4049/jimmunol.1102310
20. de Vries B, Kohl J, Leclercq WK, Wolfs TG, van Bijnen AA, Heeringa P, et al. Complement factor C5a mediates renal ischemia-reperfusion injury independent from neutrophils. *J Immunol* (2003) 170:3883–9. doi:10.4049/jimmunol.170.7.3883
21. Zhou W, Farrar CA, Abe K, Pratt JR, Marsh JE, Wang Y, et al. Predominant role for C5b-9 in renal ischemia/reperfusion injury. *J Clin Invest* (2000) 105:1363–71. doi:10.1172/JCI8621
22. Hillmen P, Young NS, Schubert J, Brodsky RA, Socie G, Muus P, et al. The complement inhibitor eculizumab in paroxysmal nocturnal hemoglobinuria. *N Engl J Med* (2006) 355:1233–43. doi:10.1056/NEJMoa061648
23. Orren A, Wallace ME, Horbart MJ, Lachmann PJ. C6 polymorphism and C6 deficiency in site strains of the mutation-prone Peru-Coppock mice. *Complemment Inflamm* (1989) 6:295–6.
24. Bieber K, Koga H, Nishie W. In vitro and in vivo models to investigate the pathomechanisms and novel treatments for pemphigoid diseases. *Exp Dermatol* (2017) 26(12):1163–70. doi:10.1111/exd.13415
25. Frei Y, Lambris JD, Stockinger B. Generation of a monoclonal antibody to mouse C5 application in an ELISA assay for detection of anti-C5 antibodies. *Mol Cell Probes* (1987) 1:141–9. doi:10.1016/0890-8508(87)90022-3
26. Thurman JM, Kraus DM, Girardi G, Hourcade D, Kang HJ, Royer PA, et al. A novel inhibitor of the alternative complement pathway prevents antiphospholipid antibody-induced pregnancy loss in mice. *Mol Immunol* (2005) 42:87–97. doi:10.1016/j.molimm.2004.07.043
27. Otto M, Hawlisch H, Monk PN, Muller M, Klos A, Karp CL, et al. C5a mutants are potent antagonists of the C5a receptor (CD88) and of C5L2: position 69 is the locus that determines agonism or antagonism. *J Biol Chem* (2004) 279:142–51. doi:10.1074/jbc.M310078200
28. Chiriac MT, Roesler J, Sindrilaru A, Scharffetter-Kochanek K, Zillikens D, Sitaru C. NADPH oxidase is required for neutrophil-dependent autoantibody-induced tissue damage. *J Pathol* (2007) 212:56–65. doi:10.1002/path.2157
29. Wang Y, Rollins SA, Madri JA, Matis LA. Anti-C5 monoclonal antibody therapy prevents collagen-induced arthritis and ameliorates established disease. *Proc Natl Acad Sci U S A* (1995) 92:8955–9. doi:10.1073/pnas.92.19.8955
30. Ishii N, Recke A, Mihai S, Hirose M, Hashimoto T, Zillikens D, et al. Autoantibody-induced intestinal inflammation and weight loss in experimental epidermolysis bullosa acquisita. *J Pathol* (2011) 224:234–44. doi:10.1002/path.2857
31. Tonnesen MG, Smedly LA, Henson PM. Neutrophil-endothelial cell interactions. Modulation of neutrophil adhesiveness induced by complement fragments C5a and C5a des arg and formyl-methionyl-leucyl-phenylalanine in vitro. *J Clin Invest* (1984) 74:1581–92. doi:10.1172/JCI111574
32. Mihai S, Nimmerjahn F. The role of Fc receptors and complement in autoimmunity. *Autoimmun Rev* (2013) 12:657–60. doi:10.1016/j.autrev.2012.10.008
33. Schwab I, Mihai S, Seeling M, Kasperkiewicz M, Ludwig RJ, Nimmerjahn F. Broad requirement for terminal sialic acid residues and FcgammaRIIB for the preventive and therapeutic activity of intravenous immunoglobulins in vivo. *Eur J Immunol* (2014) 44:1444–53. doi:10.1002/eji.201344230
34. Ricklin D, Lambris JD. Complement in immune and inflammatory disorders: therapeutic interventions. *J Immunol* (2013) 190:3839–47. doi:10.4049/jimmunol.1203200
35. Samavedam UK, Iwata H, Muller S, Schulze FS, Recke A, Schmidt E, et al. GM-CSF modulates autoantibody production and skin blistering in experimental epidermolysis bullosa acquisita. *J Immunol* (2014) 192:559–71. doi:10.4049/jimmunol.1301556
36. Sadeghi H, Lockmann A, Hund AC, Samavedam UK, Pipi E, Vafia K, et al. Caspase-1-independent IL-1 release mediates blister formation in autoantibody-induced tissue injury through modulation of endothelial adhesion molecules. *J Immunol* (2015) 194:3656–63. doi:10.4049/jimmunol.1402688
37. Ludwig RJ, Muller S, Marques A, Recke A, Schmidt E, Zillikens D, et al. Identification of quantitative trait loci in experimental epidermolysis bullosa acquisita. *J Invest Dermatol* (2012) 132:1409–15. doi:10.1038/jid.2011.466
38. Borradori L, Caldwell JB, Briggaman RA, Burr CE, Gammon WR, James WD, et al. Passive transfer of autoantibodies from a patient with mutilating epidermolysis bullosa acquisita induces specific alterations in the skin of neonatal mice. *Arch Dermatol* (1995) 131:590–5. doi:10.1001/archderm.131.5.590
39. Jordon RE, Xia P, Geoghegan WD. Bullous pemphigoid autoantibodies reactive with intracellular basal keratinocyte antigens: studies of subclass distribution and complement activation. *J Clin Immunol* (1992) 12:163–9. doi:10.1007/BF00918084
40. Barilla-Labarca ML, Toder K, Furie R. Targeting the complement system in systemic lupus erythematosus and other diseases. *Clin Immunol* (2013) 148:313–21. doi:10.1016/j.clim.2013.02.014
41. Yaspan BL, Williams DF, Holz FG, Regillo CD, Li Z, Dressen A, et al. Targeting factor D of the alternative complement pathway reduces geographic atrophy progression secondary to age-related macular degeneration. *Sci Transl Med* (2017) 9(395):eaaf1443. doi:10.1126/scitranslmed.eaaf1443
42. Birke K, Lipo E, Birke MT, Kumar-Singh R. Topical application of PPADS inhibits complement activation and choroidal neovascularization in a model of age-related macular degeneration. *PLoS One* (2013) 8:e76766. doi:10.1371/journal.pone.0076766
43. Kasprick A, Holtsche MM, Rose EL, Hussain S, Schmidt E, Petersen F, et al. The anti-C1s antibody TNT003 prevents complement activation in the skin induced by bullous pemphigoid autoantibodies. *J Invest Dermatol* (2018) 138(2):458–61. doi:10.1016/j.jid.2017.08.030
44. Niebuhr M, Kasperkiewicz M, Maass S, Hauenschild E, Bieber K, Ludwig RJ, et al. Evidence for a contributory role of a xenogeneic immune response in experimental epidermolysis bullosa acquisita. *Exp Dermatol* (2017) 26:1207–13. doi:10.1111/exd.13439

45. Joly P, Roujeau JC, Benichou J, Picard C, Dreno B, Delaporte E, et al. A comparison of oral and topical corticosteroids in patients with bullous pemphigoid. *N Engl J Med* (2002) 346:321–7. doi:10.1056/NEJMoa011592

Conflict of Interest Statement: The authors declare a potential conflict of interest and state it below. RJL has received funding from True North Therapeutics, a manufacturer of the C1s antibody TNT003. VMH and JMT receive royalties from Alexion Therapeutics.

frontiers in Immunology

ORIGINAL RESEARCH
published: 15 March 2018
doi: 10.3389/fimmu.2018.00488

Tissue Destruction in Bullous Pemphigoid Can Be Complement Independent and May Be Mitigated by C5aR2

*Christian M. Karsten[1†], Tina Beckmann[2†], Maike M. Holtsche[3], Jenny Tillmann[1], Sabrina Tofern[2], Franziska S. Schulze[2], Eva Nina Heppe[2], Ralf J. Ludwig[2], Detlef Zillikens[3], Inke R. König[4], Jörg Köhl[1,5] and Enno Schmidt[2,3]**

[1] Institute of Systemic Inflammation, University of Lübeck, Lübeck, Germany, [2] Lübeck Institute of Experimental Dermatology (LIED), University of Lübeck, Lübeck, Germany, [3] Department of Dermatology, University of Lübeck, Lübeck, Germany, [4] Institute of Medical Biometry and Statistics, University of Lübeck, Lübeck, Germany, [5] Division of Immunobiology, Cincinnati Children's Hospital and College of Medicine, University of Cincinnati, Cincinnati, OH, United States

OPEN ACCESS

Edited by:
Massimo Gadina, National Institute of Arthritis and Musculoskeletal and Skin Diseases, United States

Reviewed by:
Takashi Hashimoto, Osaka City University Graduate School of Medicine, Japan
Gang Wang, Fourth Military Medical University, China

***Correspondence:**
Enno Schmidt
enno.schmidt@uksh.de

†These authors have contributed equally to this work.

Specialty section:
This article was submitted to Inflammation, a section of the journal Frontiers in Immunology

Received: *16 January 2018*
Accepted: *23 February 2018*
Published: *15 March 2018*

Citation:
Karsten CM, Beckmann T, Holtsche MM, Tillmann J, Tofern S, Schulze FS, Heppe EN, Ludwig RJ, Zillikens D, König IR, Köhl J and Schmidt E (2018) Tissue Destruction in Bullous Pemphigoid Can Be Complement Independent and May Be Mitigated by C5aR2. Front. Immunol. 9:488. doi: 10.3389/fimmu.2018.00488

Bullous pemphigoid (BP), the most frequent autoimmune bullous disorder, is a paradigmatic autoantibody-mediated disease associated with autoantibodies against BP180 (type XVII collagen, Col17). Several animal models have been developed that reflect important clinical and immunological features of human BP. Complement activation has been described as a prerequisite for blister formation, however, the recent finding that skin lesions can be induced by anti-Col17 $F(ab')_2$ fragments indicates complement-independent mechanisms to contribute to blister formation in BP. Here, *C5*$^{-/-}$ mice injected with anti-Col17 IgG showed a reduction of skin lesions by about 50% associated with significantly less skin-infiltrating neutrophils compared to wild-type mice. Reduction of skin lesions and neutrophil infiltration was seen independently of the employed anti-Col17 IgG dose. Further, *C5ar1*$^{-/-}$ mice were protected from disease development, whereas the extent of skin lesions was increased in *C5ar2*$^{-/-}$ animals. Pharmacological inhibition of C5a receptor 1 (C5aR1) by PMX53 led to reduced disease activity when applied in a prophylactic setting. In contrast, PMX-53 treatment had no effect when first skin lesions had already developed. While C5aR1 was critically involved in neutrophil migration *in vitro*, its role for Col17-anti-Col17 IgG immune complex-mediated release of reactive oxygen species from neutrophils was less pronounced. Our data demonstrate that complement-dependent and -independent mechanisms coexist in anti-Col17-autoantibody-mediated tissue destruction. C5aR1 and C5aR2 seem to play opposing roles in this process with C5aR1 exerting its primary effect in recruiting inflammatory cells to the skin during the early phase of the disease. Further studies are required to fully understand the role of C5aR2 in autoantibody-mediated skin inflammation.

Keywords: autoantibody, dermal–epidermal junction, BP180, type XVII collagen, skin, treatment

INTRODUCTION

Type XVII collagen (Col17), also termed BP180, is a component of the dermal–epidermal junction (DEJ) and target antigen in various subepidermal blistering autoimmune disorders, the most frequent being bullous pemphigoid (BP) (1–4). The majority of BP sera reacts with epitopes clustered within the 16th non-collagenous (NC16A) domain of Col17 (5). Due to the relatively low homology between human NC16A and the corresponding murine NC15A domain, direct evidence for the

functional relevance of antihuman (h)Col17 was only successful after Nishie et al. had expressed *hCOL17* in mice (6, 7). Before, the passive transfer of rabbit antibodies generated against murine and hamster Col17 in neonatal animals had resulted in a subepidermal blistering phenotype mimicking important immunopathological signs of human BP (8, 9).

The neonatal mouse model based on the passive transfer of rabbit antimurine collagen type XVII (anti-mCol17) IgG has vigorously been explored by the group of Liu and Diaz that highlighted the pathogenic importance of, e.g., complement activation, inflammatory cells such as neutrophils, mast cells, and macrophages, and the release of proteolytic enzymes at the DEJ in this model [(8), reviewed in Ref. (10)]. Of note, complement activation appeared to be pivotal in this model as shown by several lines of evidence: *C5*- and *C4*-deficient ($^{-/-}$) mice were completely protected against the pathogenic effect of anti-mCol17 IgG, and pharmacological inhibition of C1q as well as complement depletion by cobra venom prevented skin lesions in the neonatal mouse model of BP (11, 12). Furthermore, in this model, factor B ($CFB)^{-/-}$ mice developed delayed and less intense blistering and the C5a receptor 1 (C5aR1) on mast cells was shown to be critical for the formation of skin lesions (12, 13). In addition, mutated non-C1q-binding anti-hCol17 IgG1 was not capable to induce BP lesions in neonatal *COL17*-humanized mice (14). More recently, however, in neonatal mice, the injection of $F(ab')_2$ fragments of BP patients' IgG and rabbit anti-hCOL17 IgG resulted in skin fragility questioning the impact of complement activation for lesion formation in BP (15).

To further clarify the role of complement activation in the pathogenesis of BP and to explore the potential therapeutic use of complement inhibitors that are increasingly being developed (16), we made use of a recently established passive transfer model of BP in adult mice (17). In this model, the injection of rabbit IgG generated against the murine homolog (amino acids 497–573) of the immunodominant human NC16A domain of BP180 in adult C57BL/6 or Balb/c mice on days 2, 4, 6, 8, and 10 triggered an inflammatory reaction that mimicked major characteristics of the human disease including (i) complement-fixing IgG along the DEJ, (ii) spontaneous erythema and erosions arising from day 4, (iii) subepidermal blisters by histopathology, and (iv) lesional infiltration of neutrophils and eosinophils. Furthermore, skin lesions develop over some days and thus, this model is suitable to study anti-inflammatory mediators in a quasitherapeutic setting, i.e., in mice with already established skin lesions (17).

Here, the extent of BP skin lesions was markedly reduced in $C5^{-/-}$ mice as compared to wild-type mice and pathogenicity was mediated by C5aR1, while C5aR2 was protective. Pharmacological inhibition of C5aR1 as well as *in vitro* analyses indicated that complement activation may exert its major pathophysiological impact in the early phase of the disease through the regulation of neutrophil accumulation in the skin.

MATERIALS AND METHODS

Mice

C57BL/6J, Balb/c, $Fcer^{-/-}$ mice (B6;129P2-$Fcer^{tm1Rav}$/J), $C5ar1^{-/-}$ (on C57BL/6 background), and $C5ar2^{-/-}$ mice (for *in vivo* experiments on Balb/c background, for *in vitro* experiments on C57BL/6 background) were bred and housed at 12 h light–dark cycle at the experimental animal facility in the University of Lübeck. $C5^{-/-}$ mice (B10.D2-Hc^0 $H2^d$ $H2\text{-}T18^c$/oSnJ) and the corresponding wild-type controls (B10.D2-Hc^1 $H2^d$ $H2\text{-}T18^c$/nSnJ) were obtained from Jackson Laboratories (Bar Harbor, ME, USA). All injections and bleedings were performed on eight to twelve-week old mice narcotized by intraperitoneal (i.p.) injection of a mixture of ketamine (100 µg/g) and xylazine (15 µg/g).

Animal experiments were approved by the Animal Care and Use Committee of Schleswig-Holstein (Kiel, Germany; 21-2/11, 40-3/15) and performed by certified personnel.

Generation and Characterization of Rabbit Antibodies to mCol17

The extracellular portion of the 15th non-collagenous domain (NC15A) of mCol17 covering the stretch directly adjacent to the transmembrane domain (amino acids 497–573) was expressed as glutathione-*S*-transferase (GST) fusion protein and purified by affinity chromatography as previously described (18). Pathogenic anti-mCol17 IgG was generated in New Zealand white rabbits as reported (17, 19). Normal rabbit serum was obtained from CCPro (Oberdorla, Germany).

EndoS Preparation and IgG Hydrolysis *In Vitro*

Pretreatment of rabbit IgG was performed as previously described (20, 21). One milligram of rabbit anti-mCOL17 IgG was incubated with 5 µg recombinant GST-EndoS in PBS for 16 h at 37°C followed by affinity removal of GST-EndoS by serial passages over Glutathione-Sepharose 4B columns (GE Healthcare, Uppsala, Sweden). IgG hydrolysis was verified by SDS-PAGE and lectin blot analyses as previously described (21).

Passive Transfer Mouse Model

Affinity-purified rabbit anti-mCol17 IgG and normal rabbit IgG, respectively, was injected subcutaneously into the neck of mice every second day over a period of 12 days at individual doses of 7.5 or 10 mg/ml IgG unless stated otherwise. At the time of IgG injections, mice were weighed and examined for their general condition and evidence of cutaneous lesions (i.e., erythema, blisters, erosions, and crusts). Cutaneous lesions were scored as involvement of the skin surface as previously described (17, 22). At day 12, all mice were sacrificed, blood was taken, and both lesional and perilesional biopsies were taken for histopathological analysis (stored in 4% buffered formalin) and direct IFM (stored at −80°C), respectively. C5a receptor antagonist PMX53 was provided by Dr. Trent Woodruff (University of Queensland, Brisbane, Australia). 20 µg of PMX53 per mouse were daily injected i.p. from days 0 to 11 and from days 4 to 11, respectively.

Immunofluorescence Microscopy and Histopathology

Tissue-bound autoantibodies and complement deposits were detected by direct IF microscopy of frozen sections using FITC-conjugated rabbit antimouse IgG (1:100; Dako, Hamburg,

Germany), FITC-conjugated murine antimouse C3 (1:50; Cappel, MP Biomedicals, Solon, OH, USA), and murine antimouse C5 antibody (1:100; Cell Sciences, Canton, MA, USA) detected by FITC-labeled rabbit antimouse IgG (1:100; Dako). Staining was evaluated using a Keyence BZ-9000 microscope (Keyence, Neu-Isenburg, Germany) and quantified using ImageJ (http://rsbweb.nih.gov/ij/) software. Formalin-fixed skin samples were processed into paraffin blocks. Four micrometer sections were stained with hematoxylin and eosin according to standard protocols.

Neutrophil-Specific Myeloperoxidase (MPO) Activity

Myeloperoxidase activity, corresponding to the total granulocyte infiltration, was assessed in homogenized ear-specimens as described in previous protocols (23). MPO content was expressed as units of MPO activity per milligram of protein. Protein concentrations were determined by a dye binding assay (Thermo Scientific, Rockford, IL, USA) using bovine serum albumin as a standard.

Neutrophil Preparation

Mouse neutrophils were purified as previously described (24). Briefly, bone marrow cells from femurs and tibiae were flushed, red blood cells lysed with hypotonic NaCl and cells were separated by 62.5% Percoll® (GE Healthcare, Uppsala, Sweden) gradient. For higher purity of neutrophils, T- and B-cells were depleted by MACS separation with anti-CD3ε and anti-CD19 antibodies (Miltenyi Biotech, Bergisch Gladbach, Germany). Purity of neutrophils was consistently >90% as determined by FACS analysis.

Reactive Oxygen Species (ROS) Release Assay

In this assay, intra- and extracellular ROS of neutrophils was measured using luminol-amplified chemiluminescence after incubation with immune complexes and various controls, respectively, as described previously (25, 26). In brief, 96-well plates were coated with 20 mg/ml of mCol17 NC15A overnight. After blocking with PBS containing 1% BSA and 0.05% Tween-20 (PBS-T), 1 mg/ml rabbit anti-mCol17 IgG was incubated for 1 h at 37°C. After washing with PBS-T untreated or heat-inactivated (30 min, 56°C) mouse serum or recombinant C5a (R&D Systems Inc., Minneapolis, MN, USA) diluted in 100 µl of chemiluminescence medium were added to the immune complexes. 100 µl of cell suspension (2×10^6/ml) containing 60 µg/ml of luminol (5-amino-2,3-dihydro-1,4-phthalazindione; Sigma Aldrich, Hamburg, Germany) was given to each well and generation of ROS was determined in a microplate luminometer (Wallac 1420 VICTOR TM, Perkin Elmer, Waltham, MA, USA). Chemiluminescence data were expressed as relative light units. Data are derived from at least two independent experiments performed in quadruplicates.

Migration Assay

Chemotaxis of bone-marrow-derived cells was performed as described previously (27). Briefly, bone-marrow neutrophils were collected as described above and then resuspended in chemotaxis medium (HBSS containing 2% BSA) at a density of 5×10^6 cells/ml. As a chemoattractant, we used C5a (12.5 nM; Hycult, Uden, Netherlands), which was diluted in chemotaxis medium. The chemoattractant was placed in the bottom wells of a modified Boyden chamber (Neuro Probe, Gaithersburg, MD, USA) and overlaid with a 3 µm polycarbonate membrane. Then, 50 µl of the cell suspension were placed in the top wells of the assembled Boyden chamber and incubated at 37°C in 5% CO_2 for 30 min. Subsequently, the membranes were removed and the cells on the bottom of the membrane stained with Diff-Quick (Merck, Darmstadt, Germany). The numbers of migrated cells for each well were counted in five different high-power fields and the number of cells per mm^2 was calculated by computer-assisted light microscopy. Results are expressed as the mean value of triplicate samples of at least two independent set of experiments.

Statistical Analysis

Sigma plot 11.0 (Systat Software Inc., Chicago, IL, USA) and R version 3.4.0 (April 21, 2017) (http://www.r-project.org/) were used to perform statistical analyses. *p*-Values were determined by Mann–Whitney *U*-tests for comparisons between two independent groups, Kruskal–Wallis tests for comparisons between more than two independent groups, nd non-parametric analyses of variance for comparisons including different time points. For the latter, we employed the R package nparLD (28).

RESULTS

Complement Deposition at the DEJ Does Not Correlate with Disease Activity in Experimental BP

Adult mice lacking the activating γ-chain of the Fc receptor (*Fcer*$^{-/-}$; $n = 5$), the FcγRIV (*Fcgr4*$^{-/-}$, $n = 5$), and the FcγRIIB (*Fcgr2*$^{-/-}$, $n = 5$), respectively, as well as wild-type C57BL/6J animals ($n = 5$) were injected with rabbit anti-Col17 IgG and EndoS-treated Col17-specific IgG ($n = 5$), respectively. EndoS, an endoglycosidase that specifically hydrolyzes the N-linked glycan on IgG heavy chains (20, 29), reduces the binding to activating FcγR, and increases the binding to the inhibiting FcγRIIB (20, 29). Disease activity was greatly reduced in *Fcer*$^{-/-}$ and *Fcgr4*$^{-/-}$ mice as well as in mice injected with EndoS-pretreated anti-Col17 IgG, whereas *Fcgr2*$^{-/-}$mice showed significantly more skin lesions compared to wild-type animals as shown previously (17). MPO activity determined in extracts of an entire ear reflected disease activity and was significantly higher in *Fcgr2*$^{-/-}$ mice ($p < 0.001$) and significantly lower in *Fcgr4*$^{-/-}$ mice ($p < 0.01$) compared to wild-type animals (**Figure 1**). Of note, the intensity of bound anti-C3 and anti-C5 IgG at the DEJ as detected by direct IF microscopy of perilesional skin biopsies taken at day 12 was not different compared to wild-type animals (*Fcer*$^{-/-}$, $p = 0.69$, $p = 0.22$; *Fcgr4*$^{-/-}$, $p = 0.73$, $p = 0.56$; *Fcgr2*$^{-/-}$, $p = 0.90$, $p = 0.63$; EndoS-pretreated IgG, $p = 0.92$, $p = 0.26$; **Figure 1**).

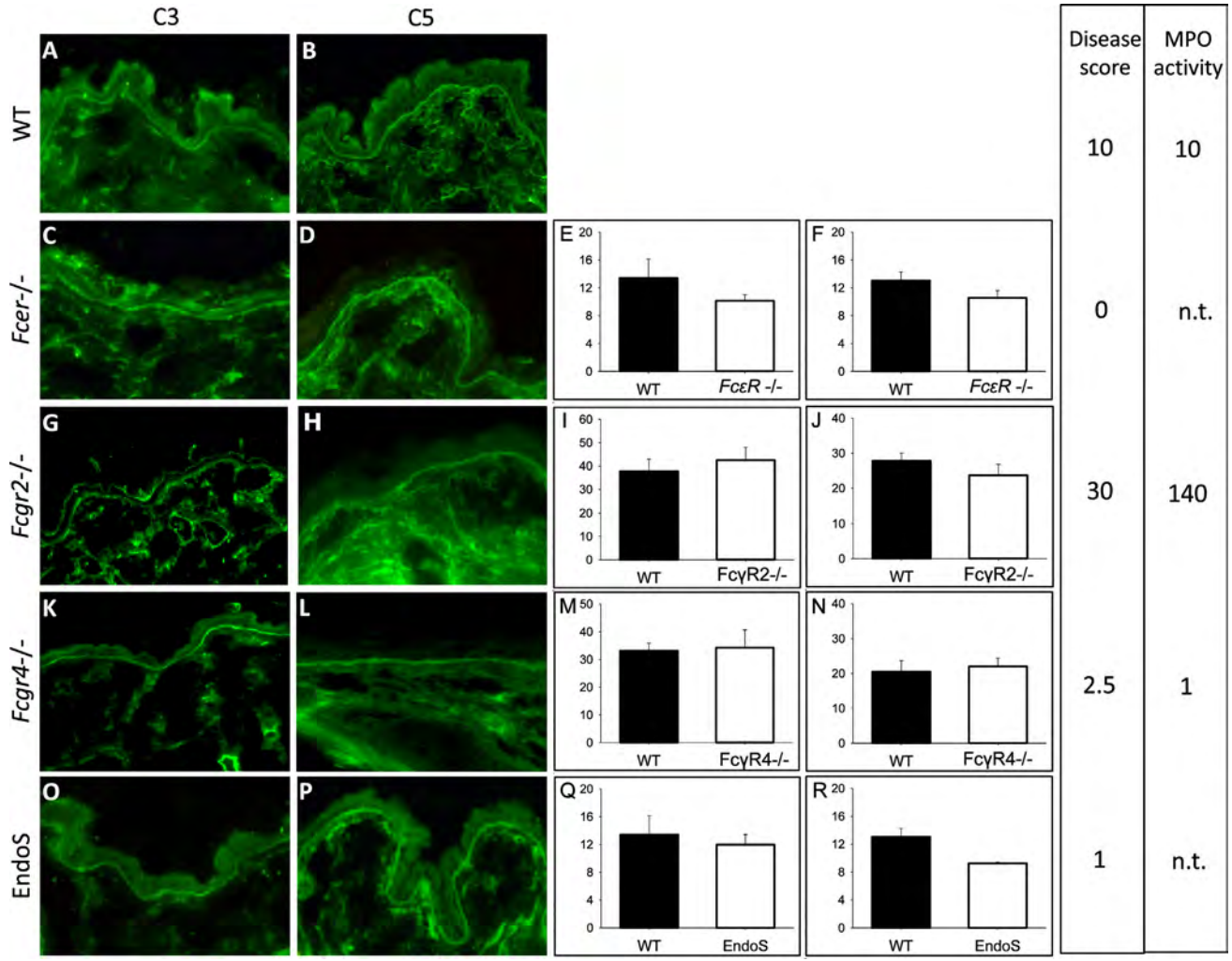

FIGURE 1 | Complement activation at the dermal–epidermal junction (DEJ) is not related to the extent of clinical disease in experimental bullous pemphigoid. The intensity of C3 **(E,I,M,Q)** and C5 deposition **(F,J,N,R)** at the DEJ did not differ between wild-type (WT; **A,B**) mice, mice deficient of the FcRγ [*Fcer*$^{-/-}$; **(C,D)**], FcγRIIB [*Fcgr2b*$^{-/-}$; **(G,H)**], FcγRIV [*Fcgr4*$^{-/-}$; **(K,L)**], and EndoS-treated animals **(O,P)** as quantified using Image J software. Furthermore, the amount of complement deposition was not reflected by the extent of skin lesions/disease score and the myeloperoxidase (MPO) activity determined in ear skin. Data for disease activity were assembled from different experiments with five mice in each group done at different time points (17). A and B are representative pictures selected from one of the experiments. For direct comparison, disease activity and MPO activity are indicated in arbitrary units related to the mean clinical score and MPO activity in WT animals in each experiment set to 10. n.t., not tested.

Complement Activation Is Important, but Not a Prerequisite for the Development of Skin Lesions

C5$^{-/-}$ and corresponding wild-type mice were injected six times with 5, 10, and 15 mg of pathogenic anti-Col17 IgG, respectively (each group, $n = 5$). All mice developed cutaneous BP lesions. Disease activity in *C5*$^{-/-}$ mice was reduced to between 36 and 54% compared to corresponding wild-type animals independent of the injected IgG concentration (30 mg IgG, $p = 0.004$; 60 mg IgG, $p = 0.013$; 90 mg IgG, $p \leq 0.001$; **Figure 2**). While the disease activity was clearly dependent on the amount of injected anti-Col17 IgG ($p = 0.025$; **Figures 2A,B**), the extent of disease reduction in *C5*$^{-/-}$ mice in relation to wild-type animals was independent of the anti-Col17 IgG dose (**Figures 2A,B**). The MPO reactivity, corresponding to the magnitude of myeloid cell infiltration, in the ears was notably higher in wild-type compared to *C5*$^{-/-}$mice ($p < 0.001$; **Figure 2J**). In contrast, no difference in the linear deposits of IgG at the DEJ by direct IF microscopy of perilesional biopsies taken at day 12 was seen between wild-type and *C5*$^{-/-}$ mice ($p = 0.413$; **Figures 2G,I**).

C5aR1 Mediates the Pathogenic Effect of Anti-Col17 IgG-Induced C5 while C5aR2 Is Protective

C5ar1$^{-/-}$ ($n = 10$) and *C5ar2*$^{-/-}$ mice ($n = 15$) as well as the corresponding wild-type animals ($n = 10$ and $n = 18$) were injected six times with 5 mg of pathogenic anti-Col17 IgG in two independent experiments. *C5ar1*$^{-/-}$ mice developed less disease compared

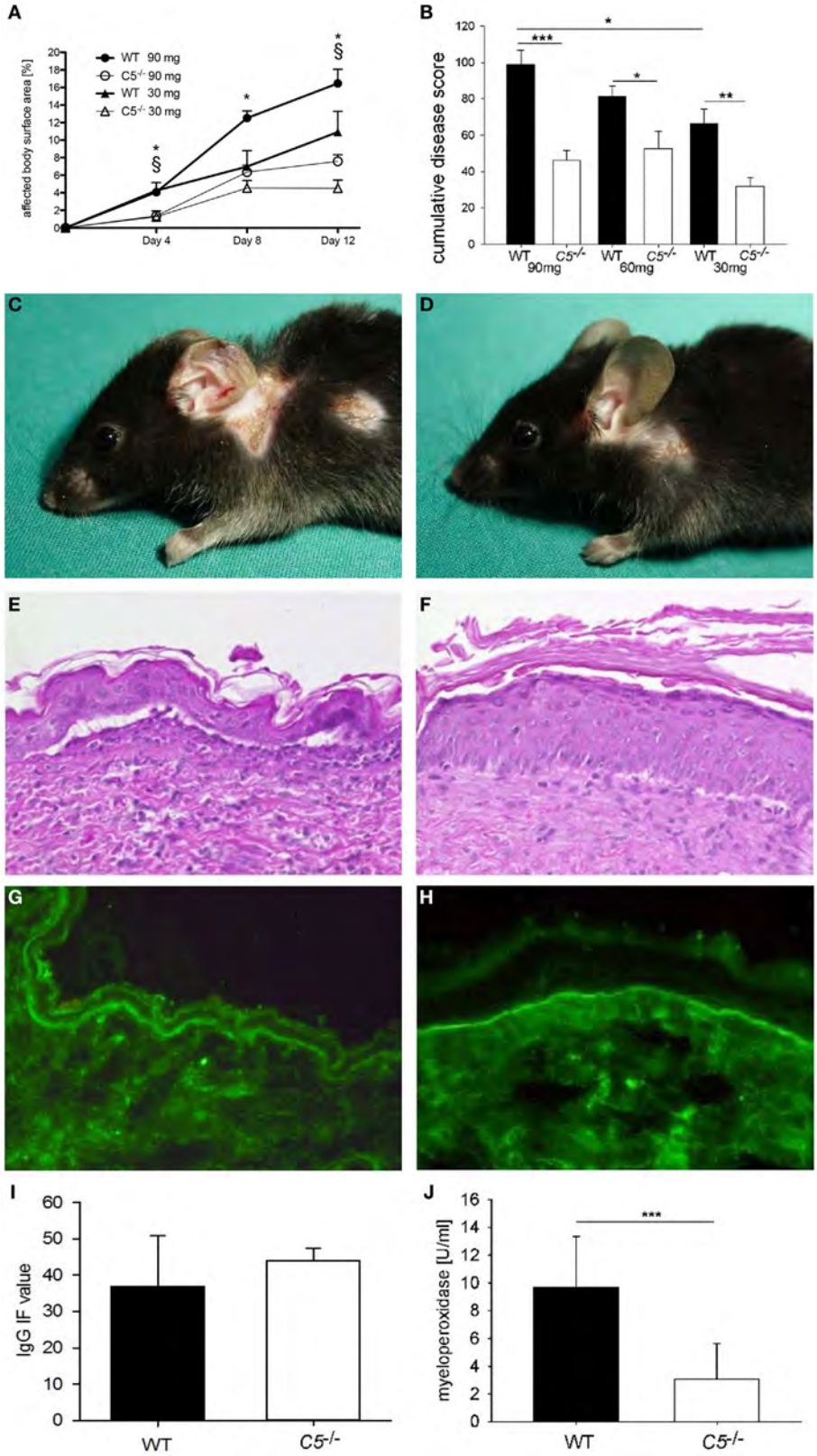

FIGURE 2 | Continued

FIGURE 2 | Anti-mCol17 IgG induces cutaneous disease in complement five-deficient ($C5^{-/-}$) mice. $C5^{-/-}$ ($n = 5$) and wild-type (WT; $n = 5$) mice were injected with three different doses of anti-mCol17 IgG (six times 5 mg, six times 10 mg, and six times 15 mg) every second day. Disease activity was measured as percentage of affected body surface area on days 4, 8, and 12 **(A)**. The overall clinical activity of all mice in each group was derived from the area under the curve of the affected body surface and expressed as cumulative score. The cumulative score of $C5^{-/-}$ was about half compared to WT mice independent of the injected amount of anti-Col17 IgG **(B)**. Infiltration of neutrophils in lesional ear skin as reflected by myeloperoxidase activity **(J)** was significantly reduced in $C5^{-/-}$ compared to WT animals. In contrast, deposits of IgG at the dermal–epidermal junction did not differ between WT and $C5^{-/-}$ mice **(I)**. Representative pictures of clinical lesions **(C,D)**, lesional histopathology **(E,F)**, and IgG deposits by direct immunofluorescence microscopy **(G,H)** are shown in WT **(C,E,G)** and $C5^{-/-}$ mice **(D,F,H)**. $^{*}p < 0.05$, 90 mg groups; $^{\S}p < 0.05$, 30 mg groups **(A)**. $^{*}p < 0.05$; $^{**}p < 0.01$; $^{***}p < 0.001$ **(B,J)**.

to wild-type mice. Differences were detected between the two groups when the whole observation period was considered ($p = 0.001$) as well as individually on days 4 ($p < 0.001$) and 12 ($p = 0.007$; **Figures 3A–E**). The difference between the two groups increased over time (p for interaction = 0.005). In contrast, in $C5ar2^{-/-}$ mice, more skin lesions developed as compared to wild-type mice (whole observation period, $p = 0.004$) as well as on days 4 ($p = 0.018$), 8 ($p = 0.033$), and 12 ($p = 0.046$; **Figures 3F–J**). The difference between the two groups also increased over time (p for interaction = 0.017). The mean infiltration of neutrophils as determined by MPO activity in the right ears appeared to be lower in $C5ar1^{-/-}$ mice (although statistical significance was not reached with $p = 0.052$) but not in $C5ar2^{-/-}$animals compared to wild-type mice ($p = 0.178$; **Figures 3K,L**).

Pharmacological Inhibition of C5aR Reduces Skin Lesions in a Prophylactic but Not in a Therapeutic Approach

To assess the potential of C5aR1 as a new therapeutic target in BP, C57Bl/6 mice were injected six times with 5 mg of anti-Col17 IgG and received daily injections of 200 µg of the C5aR1 antagonist PMX53 (days 0–11; $n = 11$) and PBS ($n = 13$), respectively (prophylactic setting). In the PMX53-injected mice, skin lesions, disease and MPO activity in the right ears were less increased compared to control mice (although statistical significance was not reached with $p = 0.082$ and $p = 0.068$; **Figures 4A,C**). In a quasitherapeutic approach, daily injections of PMX53 at individual doses of 200 µg were given at day 4, when first skin lesions had already developed, and continued until day 11. In this setting, disease activity and neutrophil infiltration did not differ between PMX53-injected and control mice over time ($p = 0.952$, $p = 0.720$; **Figures 4B,D**).

Complement Is Not a Main Driver of Immune Complex-Mediated ROS Release from Neutrophils

The role of complement as a mediator of ROS release from neutrophils in response to immune complexes of recombinant mCol17 NC15A and anti-mCol17 IgG was explored by the use of a previously described *in vitro* assay (25, 26). In the first set of experiments, immune complexes were incubated in the presence of normal mouse serum and heat inactivated mouse serum, respectively, before mouse neutrophils were added. While the ROS release increased in response to the addition of normal mouse serum at different dilutions ($p < 0.001$), no difference in ROS release was observed between incubation with normal mouse serum and heat inactivated serum ($p = 0.229$, $p = 548$, $p = 0.345$; **Figure 5A**).

In the next set of experiments, we tested the involvement of C5aR1 and C5aR2 in driving the ROS release using neutrophils from wild-type, $C5ar1^{-/-}$, and $C5ar2^{-/-}$ mice. While clear differences were seen between immune complexes and antigen alone using wild-type, $C5ar1^{-/-}$, and $C5ar2^{-/-}$ neutrophils ($p = 0.020$, $p = 0.005$, and $p = 0.008$), no statistical difference was observed between the ROS release of wild-type neutrophils and neutrophils from $C5ar1^{-/-}$ and $C5ar2^{-/-}$ mice ($p = 0.655$, $p = 0.554$; **Figure 5B**). In contrast, when neutrophils from $Fcer^{-/-}$ mice that lack the activating γ-chain of the Fc receptor were used, the ROS release was nearly abrogated compared to the use of wild-type neutrophils ($p < 0.001$; **Figure 5C**).

The Migration of $C5ar1^{-/-}$ but Not $C5ar2^{-/-}$ Neutrophils Is Greatly Impaired

To test the hypothesis that neutrophil chemotaxis can be mediated by C5aRs *in vitro*, migration of wild-type neutrophils and neutrophils from $C5ar1^{-/-}$ and $C5ar2^{-/-}$ mice toward C5a was quantified using a modified Boyden chamber. $C5ar1^{-/-}$ neutrophils showed a significantly lower migration potential compared to wild-type cells ($p < 0.001$; **Figure 5D**). In contrast, no difference was seen between the migration of wild-type and $C5ar2^{-/-}$ neutrophils ($p = 0.901$; **Figure 5D**).

DISCUSSION

Complement can be activated by three pathways, the classical, the alternative, and the lectin pathway (30, 31). Activation of the complement system by any of the three pathways leads to activation of C3 and subsequently, to activation of C5 to form C5a and C5b. C5a is crucially involved in the host defense, immune surveillance, and tissue homeostasis (32, 33). However, C5a can also be the driver in autoimmune (34, 35) and other inflammatory diseases (36). Strong and prolonged activation of C5a leads to downregulation of immune responses in leukocytes, but has opposing effects in other cell types (37). This controversial function of C5a is often explained by the differential expression of the two C5aRs, C5aR1 and C5aR2. While signaling through C5aR1 is well characterized and reported to induce chemotaxis, mediate interaction with toll-like receptors, and regulate FcγR expression (30, 31, 38, 39), the functional properties of C5aR2 are still elusive, and both anti- and proinflammatory responses have been reported (37, 40–46).

In BP, like in various other autoantibody-mediated diseases including anti-neutrophil cytoplasmatic autoantibody-associated

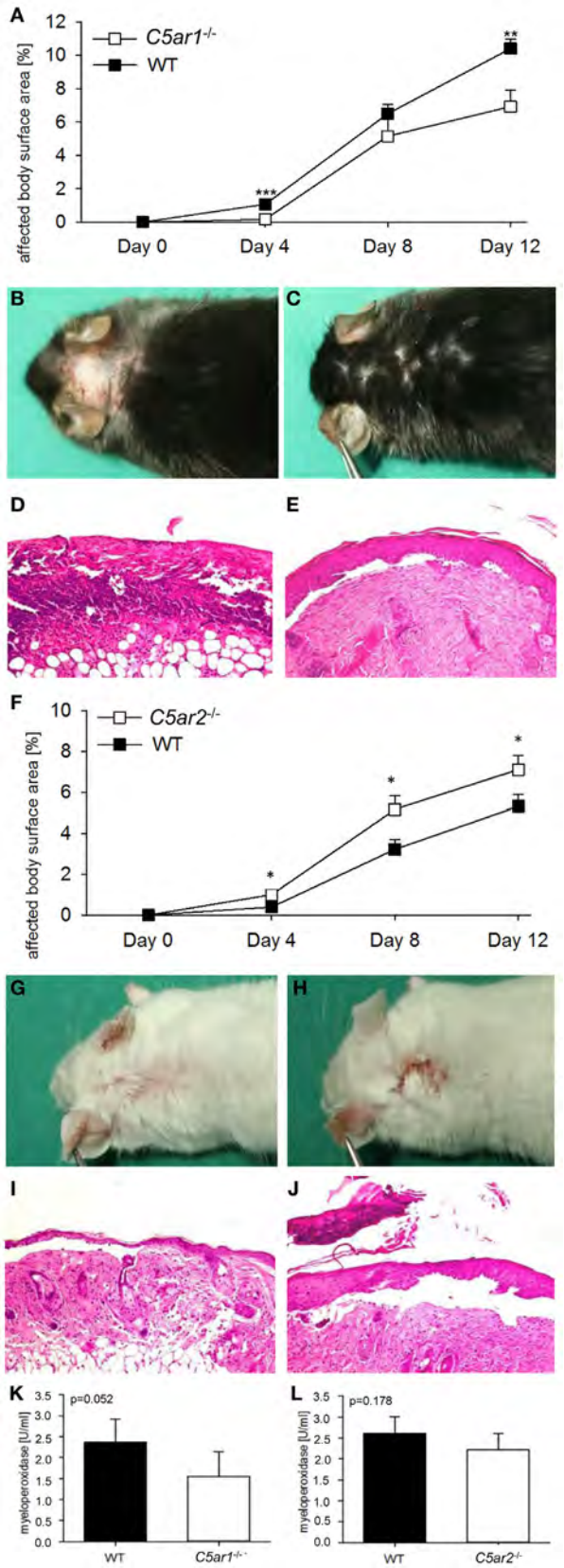

FIGURE 3 | Continued

FIGURE 3 | C5a receptor 1 (C5aR1) mediates tissue destruction by anti-mCol17 IgG, while C5aR2 is protective. Injection of anti-mCol17 IgG in *C5ar1*-deficient (*C5ar1*$^{-/-}$) mice ($n = 10$) resulted in significantly less bullous pemphigoid skin lesions compared to wild-type (WT) mice [$n = 10$; **(A)**]. In contrast, injection of anti-mCol17 IgG in *C5ar2*$^{-/-}$ mice ($n = 15$) led to a higher disease activity compared to WT mice [$n = 18$; **(F)**]. Representative pictures of clinical **(B,C,G,H)** and histopathological lesions **(D,E,I,J)** are shown in *C5ar1*$^{-/-}$ **(C,E)**, *C5ar2*$^{-/-}$ **(H,D)**, and WT mice **(B,D,G,I)**. Infiltration of neutrophils in skin lesions, as reflected by myeloperoxidase activity, was reduced in *C5ar1*$^{-/-}$ compared to WT animals [$p = 0.052$, **(K)**] and unchanged in *C5ar2*$^{-/-}$ mice **(L)**. $^{*}p < 0.05$; $^{**}p < 0.01$; $^{***}p < 0.001$.

vasculitides, systemic lupus erythematosus, rheumatoid arthritis, antiglomerular basement membrane disease, epidermolysis bullosa acquisita, and antilaminin 332 mucous membrane pemphigoid, complement activation is regarded as pivotal for lesion formation (11–14, 19, 34, 47–51). The traditional view derived from the neonatal mouse model of BP that complement activation is required for lesion formation has recently been challenged by the observation that F(ab′)$_2$ fragments of anti-hCol17 IgG also induced BP-like skin lesions in neonatal *COL17*-humanized mice (15). Complement-independent pathogenic effects of anti-Col17 antibodies have also been demonstrated *in vitro* when treatment of cultured keratinocytes with anti-Col17 antibodies led to the secretion of IL-6 and IL-8 as well as reduced cell surface expression of Col17 followed by weakened attachment of keratinocytes (52–54).

We have recently established a novel experimental model of BP in adult mice that overcame some of the shortcomings of the neonatal models, e.g., lesions develop spontaneously over some days without the application of friction (17). Importantly, in contrast to the neonatal mouse models, the novel adult mouse model was shown to be suitable to analyze the potential of anti-inflammatory agents in a quasi-therapeutic setting, i.e., in mice with already established skin lesions (17).

The two aims of the current study were therefore to clarify the pathophysiological role of complement activation by the use of the recently established BP model in adult mice and explore the therapeutic potential of complement inhibition for BP. The therapeutic potential of C5aR1 targeting is of particular relevance given the growing list of complement inhibitors that are in phase II and III clinical trials (16) and the urgent need for more specific and safe treatment options in BP. So far, long-term use of superpotent topical or oral corticosteroids is the therapeutic backbone of BP, often supplemented with potentially steroid-sparing agents such as azathioprine, methotrexate, dapsone, or doxycycline (55–58).

In previous experiments, we have shown that mice lacking the FcγR (*Fcer*$^{-/-}$) were completely protected from the development of cutaneous disease after injection of anti-Col17, while skin lesions were significantly more extended in *Fcgr2b*$^{-/-}$ animals (17). Identical findings were also made in an adult antibody transfer-induced model of inflammatory epidermolysis bullosa acquisita (24). When wild-type mice were injected with anti-Col17 IgG pretreated with EndoS, an endoglycosidase that specifically hydrolyzes the N-linked glycan on IgG heavy chains, only few skin lesions occurred (21, 29). Hydrolysis of IgG glycan has previously been shown to reduce the binding to activating FcγRs and thus the proinflammatory effect of autoantibodies (21). When we

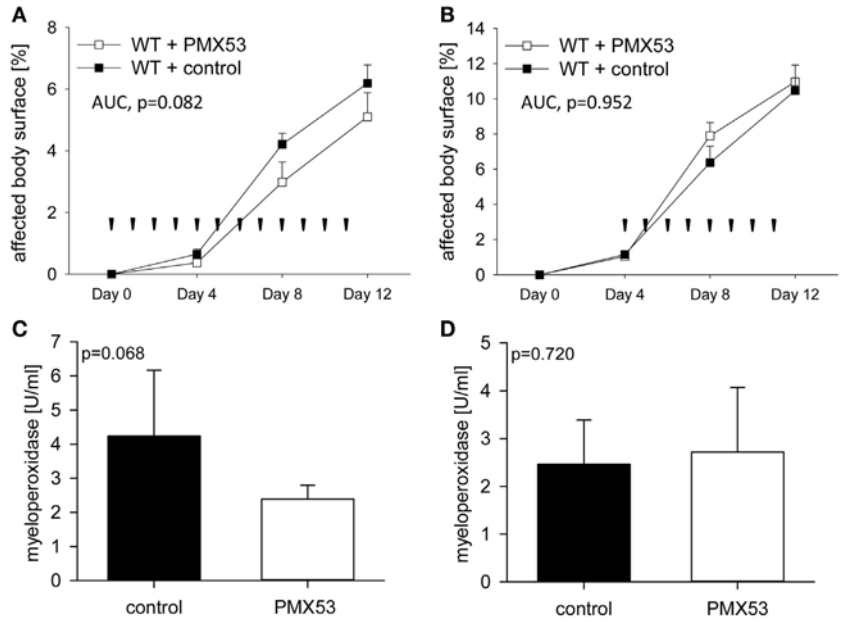

FIGURE 4 | Pharmacological inhibition of C5a receptor 1 (C5aR1) reduces clinical disease in experimental bullous pemphigoid (BP) only in a prophylactic approach but not when skin lesions have already developed. When C57BL/6 mice were injected daily with the C5aR1 inhibitor PMX53 (n = 11) and PBS (n = 13), respectively, in parallel with injection of anti-mCol17 IgG on days 0, 2, 4, 6, 8, and 10, less BP lesions were observed in PMX53-treated mice **(A)**. In contrast, when PMX53 and PBS injections were started on day 4, the extent of clinical disease did not differ between the PMX53-injected and the control mice **(B)**. Arrow heads indicate injections of PMX53 and PBS, respectively. Infiltration of neutrophils in skin lesions, as reflected by myeloperoxidase activity, was reduced in the prophylactic **(C)** but not in the therapeutic approach **(D)**.

here quantified the intensity of C3 and C5 deposition at the DEJ at the end of the experiment on day 12, no differences between wild-type animals and mice deficient for the FcγR, FcγRIV, and FcγRIIB, respectively, and mice injected with EndoS-pretreated anti-Col17 IgG were seen. In contrast, in the same mice, significant differences in both extent of skin lesions (17) and MPO activity in ear skin, which paralleled disease activity, were seen.

A somehow similar observation was made in pemphigus, an autoimmune blistering disease characterized by autoantibodies against structural components of the desmosome, desmoglein 1 and 3 (59, 60). In pemphigus, complement deposits in the skin/epithelium is found in almost all patients, however, complement activation is not required for lesion formation (61). Our observations that complement activation at the DEJ appeared to be unrelated to the extent of clinical disease prompted us to further explore the role of complement in this novel model of experimental BP.

We then asked the question whether complement activation is a prerequisite for the induction of clinical disease in this model. When *C5*$^{-/-}$ mice were injected with different amounts of anti-Col17 IgG, the extent of skin lesions decreased by about 50% compared to wild-type animals. Of note, the impact of C5 was independent of the anti-Col17 IgG dose. This finding is in contrast to previous findings in experimental neonatal BP in which *C5*$^{-/-}$ mice were completely resistant to the pathogenic effect of anti-Col17 IgG (11). In fact, with *C4*$^{-/-}$ and anti-C1q-antibody-injected mice being completely protected and factor B (*CFB*)$^{-/-}$ mice being partly protected, both the classical and, to a lesser extent, the alternative pathway were shown to be crucial in this model (12). The importance of the classical complement pathway was also elegantly demonstrated in the *Col17*-humanized neonatal mouse model. Neonatal *Col17*$^{m-/-,h+}$ mice injected with a monoclonal anti-human Col17 IgG1 antibody that was mutated at the C1q binding site developed less pathogenic activity compared to the unmutated antihuman Col17 IgG1-injected animals (14).

More recently, similar to our model, complement-independent pathogenic effects of anti-Col17 IgG were shown in neonatal *Col17*-humanized mice when F(ab′)$_2$ fragments of anti-hCol17 IgG and anti-hCol17 IgG4, which do not activate complement at the DEJ, induced skin blistering (15, 62). In line, BP patients with predominant IgG autoantibodies and no C3 deposition at the DEJ have been described, and in 15–20% of BP patients, no C3 deposits along the DEJ can be detected (63, 64).

In subsequent experiments, we dissected the role of the two C5aRs downstream of C5 in the pathogenesis of BP and addressed the question at what stage of the disease complement activation may be important. Using knock-out mice and a specific inhibitor, we found that C5aR1 mediated the pathogenic effect of C5a, while C5aR2 appeared to protect from BP skin lesions. This is line with previous reports suggesting an anti-inflammatory role for C5aR2 counter-regulating pro-inflammatory properties of C5aR1 (42, 43). Given that the effect of C5-deficiency was more pronounced than that of C5R1-deciciency may suggest that in addition to C5aR1 and C5aR2, the membrane attack complex may exert pro-inflammatory effects. Indeed, sublytic amounts

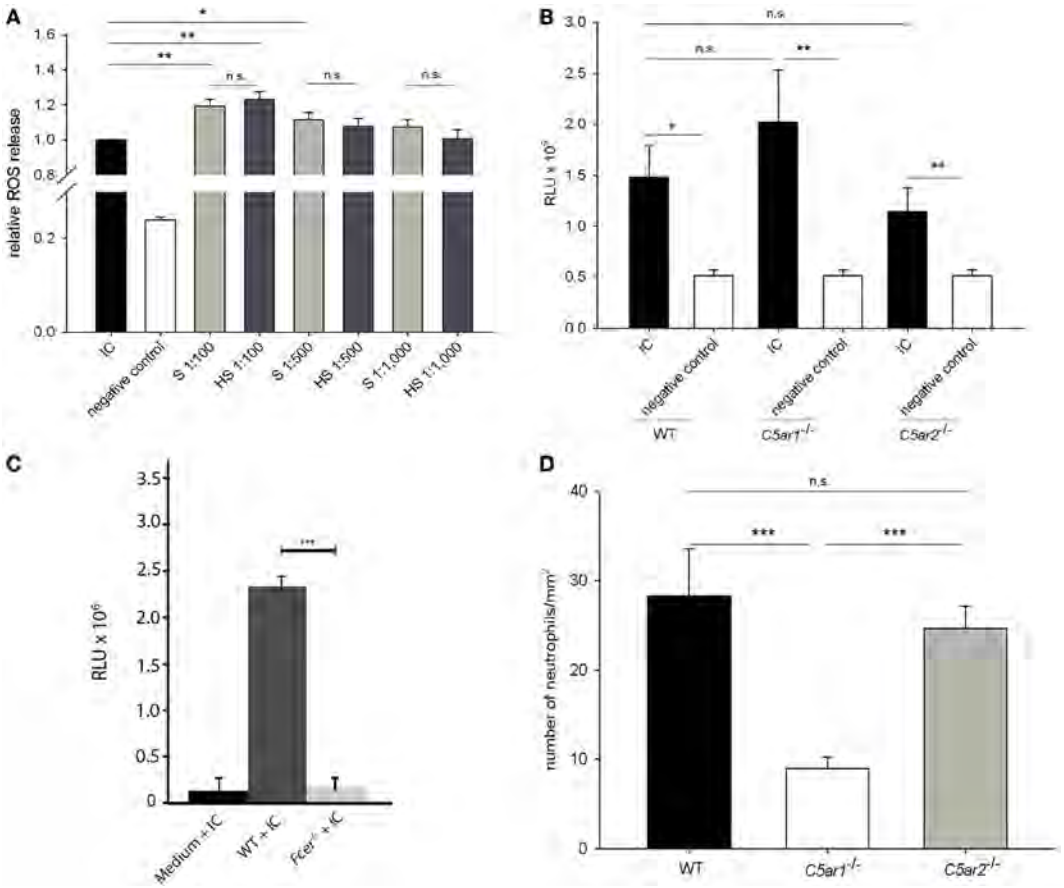

FIGURE 5 | While complement activation is not the main driver of immune complex-mediated release of reactive oxygen species (ROS) from mouse neutrophils, C5a is a strong chemoattractant for neutrophils. Neutrophils isolated from the bone marrow of C57Bl/6 mice were incubated with immune complexes of mCol17 and anti-mCol17 IgG. Addition of serum (S) and heat-inactivated serum (HS), respectively, led to significantly higher ROS releases compared to stimulation with immune complexes alone, while no difference between incubation with S and HS was seen **(A)**. When neutrophils from C57BL/6 wild-type (WT), *C5ar1*$^{-/-}$, and *C5ar2*$^{-/-}$ mice were incubated with immune complexes, a significantly higher ROS release was seen compared to incubation with the collagen alone. No differences were observed between the ROS release of wild-type, *C5ar1*$^{-/-}$, and *C5ar2*$^{-/-}$ neutrophils in response to immune complexes **(B)**. In contrast, in neutrophils that lack the activating γ-chain of the Fc receptor (*Fcer*$^{-/-}$) the ROS release was greatly reduced compared to WT cells **(C)**. Migration of bone marrow-derived neutrophils from *C5ar1*$^{-/-}$ mice toward recombinant C5a was significantly lower compared to neutrophils from both C57BL/6 WT and *C5ar2*$^{-/-}$ mice. No difference was seen between the migration of *C5ar2*$^{-/-}$ and WT neutrophils. Depicted is the number of migrated cells per mm^2 as calculated from the evaluation of ten high-power fields. PBS-treated cells served as control (not shown). Means of triplicate samples are shown **(D)**. n.s., not significant; *$p < 0.05$; **$p < 0.01$; ***$p < 0.001$.

can activate the NLRP3 inflammasome (65), a mechanism that may also apply to the activation of effector cells in BP.

When we addressed the second aim of our study, i.e., the pharmacological inhibition of C5aR1, we observed reduced skin lesions after the prophylactic application of the C5aR1 inhibitor PMX53. However, this effect was weaker than that obtained with *C5ar1*$^{-/-}$ mice. This discrepancy may be explained by an insufficient dosing or an incomplete silencing of C5aR1 by PMX. When PMX was applied in a quasi-therapeutic setting, i.e., when first skin lesions had already developed, no effect on both skin lesions and neutrophil infiltration in the dermis was seen. Combined with our results in the first set of experiments that had revealed strong complement activation along the DEJ during the course of the disease (at day 12) irrespective of the disease severity, we hypothesized that complement activation in the skin may be relevant in the early disease phase, while in established disease, complement-mediated tissue destruction may be redundant.

This hypothesis was addressed applying neutrophils, the main effector cell of tissue destruction in experimental murine BP, in two *in vitro* models. The migration assay toward C5a reflects an early disease time point when C5a is released in close vicinity of the DEJ following the attachment of anti-Col17 IgG to Col17. The ROS release assay mimics a later time point when leukocytes have already attached along the DEJ. While migration was drastically reduced in *C5ar1*$^{-/-}$ neutrophils, no difference in the ROS release of wild-type leukocytes between stimulation with serum and heat-inactivated serum was seen. Furthermore, no significant differences in the ROS release of wild-type and *C5ar1*$^{-/-}$ and *C5ar2*$^{-/-}$ neutrophils were observed. In contrast, the ROS release was nearly abrogated in neutrophils from mice that lack the activating γ-chain of the Fc receptor compared to

wild-type neutrophils. These results suggest that complement activation may be of particular importance in the early phase of the disease when neutrophils are attracted to the DEJ. In fact, C5a may lead to an increased expression of adhesion molecules on endothelial cells and neutrophils and can delay apoptosis (31, 66). Due to logistical constrains, cells from *C5ar2*$^{-/-}$ mice on a C57BL/6 background were used for the *in vitro* studies. Since in previous experiments with the antibody transfer-induced mouse model of BP both wild-type and *Fcgr1*$^{-/-}$ mice on a Balb/c background developed the same extent of clinical disease compared to animals on a C57BL/6 background (17), we believe that no principle differences between *C5ar2*$^{-/-}$ mice on a C57BL/6 and Balb/c background in our *in vitro* studies could be expected.

Neutrophils have been identified as drivers of tissue destruction in the different mouse models of BP (6–8, 11, 18). The view that C5aR1 is important during the early phase of the disease is supported by the observation that C5aR expression on mast cells, a cell resident in the dermis, is essential for blister formation (13). Once the skin inflammation has fully developed, release of ROS and proteases from neutrophils and macrophages may become independent of complement and may be mainly mediated *via* FcγRs. This hypothesis is corroborated by previous findings in *C4*$^{-/-}$ neonatal mice, that, although completely resistant against the pathogenic effect of anti-Col17 IgG, developed clinical blisters after injection of the neutrophil attractant IL-8 or neutrophils in the skin (12). The mechanism underlying the C5aR2-mediated anti-inflammatory effect in experimental BP requires further investigations. Two peptides with C5aR2-agonistic effect have recently been identified (37) and will facilitate this endeavor.

ETHICS STATEMENT

Animal experiments were approved by the Animal Care and Use Committee of Schleswig-Holstein (Kiel, Germany; 21-2/11, 40-3/15) and performed by certified personnel.

AUTHOR CONTRIBUTIONS

TB, MH, JT, ST, FSS, and EH have performed the experiments and analyzed the data. RL, DZ, JK, CK, and ES have designed the work and interpreted the data. FS and ST generated the figures. IK has interpreted the data and performed the statistical analyses. CK and ES have, in addition, overseen the experimental work and written the manuscript. All authors have approved the final version of the manuscript.

ACKNOWLEDGMENTS

We thank Rebecca Cames for excellent technical assistance. We are grateful to Dr. Trent Woodruff, University of Queensland, Brisbane, Australia, for providing PMX53.

FUNDING

This work was supported by grants from the Excellence Cluster "Inflammation at Interfaces" (EXC306/2), the University of Lübeck, the Research Training Group 1727 Modulation of Autoimmunity (GRK1727/1), and the Clinical Research Unit 303 Pemphigoid Diseases.

REFERENCES

1. Langan SM, Smeeth L, Hubbard R, Fleming KM, Smith CJ, West J. Bullous pemphigoid and pemphigus vulgaris – incidence and mortality in the UK: population based cohort study. *BMJ* (2008) 337:a180. doi:10.1136/bmj.a180
2. Joly P, Baricault S, Sparsa A, Bernard P, Bedane C, Duvert-Lehembre S, et al. Incidence and mortality of bullous pemphigoid in France. *J Invest Dermatol* (2012) 132(8):1998–2004. doi:10.1038/jid.2012.35
3. Schmidt E, Zillikens D. Pemphigoid diseases. *Lancet* (2013) 381(9863):320–32. doi:10.1016/S0140-6736(12)61140-4
4. Hubner F, Recke A, Zillikens D, Linder R, Schmidt E. Prevalence and age distribution of pemphigus and pemphigoid diseases in Germany. *J Invest Dermatol* (2016) 136(12):2495–8. doi:10.1016/j.jid.2016.07.013
5. Zillikens D, Rose PA, Balding SD, Liu Z, Olague-Marchan M, Diaz LA, et al. Tight clustering of extracellular BP180 epitopes recognized by bullous pemphigoid autoantibodies. *J Invest Dermatol* (1997) 109(4):573–9. doi:10.1111/1523-1747.ep12337492
6. Nishie W, Sawamura D, Goto M, Ito K, Shibaki A, McMillan JR, et al. Humanization of autoantigen. *Nat Med* (2007) 13(3):378–83. doi:10.1038/nm1496
7. Ujiie H, Shibaki A, Nishie W, Sawamura D, Wang G, Tateishi Y, et al. A novel active mouse model for bullous pemphigoid targeting humanized pathogenic antigen. *J Immunol* (2010) 184(4):2166–74. doi:10.4049/jimmunol.0903101
8. Liu Z, Diaz LA, Troy JL, Taylor AF, Emery DJ, Fairley JA, et al. A passive transfer model of the organ-specific autoimmune disease, bullous pemphigoid, using antibodies generated against the hemidesmosomal antigen, BP180. *J Clin Invest* (1993) 92(5):2480–8. doi:10.1172/JCI116856
9. Yamamoto K, Inoue N, Masuda R, Fujimori A, Saito T, Imajoh-Ohmi S, et al. Cloning of hamster type XVII collagen cDNA, and pathogenesis of anti-type XVII collagen antibody and complement in hamster bullous pemphigoid. *J Invest Dermatol* (2002) 118(3):485–92. doi:10.1046/j.0022-202x.2001.01683.x
10. Leighty L, Li N, Diaz LA, Liu Z. Experimental models for the autoimmune and inflammatory blistering disease, bullous pemphigoid. *Arch Dermatol Res* (2007) 299(9):417–22. doi:10.1007/s00403-007-0790-5
11. Liu Z, Giudice GJ, Swartz SJ, Fairley JA, Till GO, Troy JL, et al. The role of complement in experimental bullous pemphigoid. *J Clin Invest* (1995) 95(4):1539–44. doi:10.1172/JCI117826
12. Nelson KC, Zhao M, Schroeder PR, Li N, Wetsel RA, Diaz LA, et al. Role of different pathways of the complement cascade in experimental bullous pemphigoid. *J Clin Invest* (2006) 116(11):2892–900. doi:10.1172/JCI17891
13. Heimbach L, Li Z, Berkowitz P, Zhao M, Li N, Rubenstein DS, et al. The C5a receptor on mast cells is critical for the autoimmune skin-blistering disease bullous pemphigoid. *J Biol Chem* (2011) 286(17):15003–9. doi:10.1074/jbc.M111.221036
14. Li Q, Ujiie H, Shibaki A, Wang G, Moriuchi R, Qiao HJ, et al. Human IgG1 monoclonal antibody against human collagen 17 noncollagenous 16A domain induces blisters via complement activation in experimental bullous pemphigoid model. *J Immunol* (2010) 185(12):7746–55. doi:10.4049/jimmunol.1000667
15. Natsuga K, Nishie W, Shinkuma S, Ujiie H, Nishimura M, Sawamura D, et al. Antibodies to pathogenic epitopes on type XVII collagen cause skin fragility in a complement-dependent and -independent manner. *J Immunol* (2012) 188(11):5792–9. doi:10.4049/jimmunol.1003402
16. Morgan BP, Harris CL. Complement, a target for therapy in inflammatory and degenerative diseases. *Nat Rev Drug Discov* (2015) 14(12):857–77. doi:10.1038/nrd4657
17. Schulze FS, Beckmann T, Nimmerjahn F, Ishiko A, Collin M, Kohl J, et al. Fcgamma receptors III and IV mediate tissue destruction in a novel adult

mouse model of bullous pemphigoid. *Am J Pathol* (2014) 184(8):2185–96. doi:10.1016/j.ajpath.2014.05.007
18. Hirose M, Recke A, Beckmann T, Shimizu A, Ishiko A, Bieber K, et al. Repetitive immunization breaks tolerance to type XVII collagen and leads to bullous pemphigoid in mice. *J Immunol* (2011) 187(3):1176–83. doi:10.4049/jimmunol.1100596
19. Sitaru C, Mihai S, Otto C, Chiriac MT, Hausser I, Dotterweich B, et al. Induction of dermal-epidermal separation in mice by passive transfer of antibodies specific to type VII collagen. *J Clin Invest* (2005) 115(4):870–8. doi:10.1172/JCI200521386
20. Collin M, Olsen A. EndoS, a novel secreted protein from *Streptococcus pyogenes* with endoglycosidase activity on human IgG. *EMBO J* (2001) 20(12): 3046–55. doi:10.1093/emboj/20.12.3046
21. Hirose M, Vafia K, Kalies K, Groth S, Westermann J, Zillikens D, et al. Enzymatic autoantibody glycan hydrolysis alleviates autoimmunity against type VII collagen. *J Autoimmun* (2012) 39(4):304–14. doi:10.1016/j.jaut.2012.04.002
22. Bieber K, Koga H, Nishie W. In vitro and in vivo models to investigate the pathomechanisms and novel treatments for pemphigoid diseases. *Exp Dermatol* (2017) 26(12):1163–70. doi:10.1111/exd.13415
23. Hammers CM, Bieber K, Kalies K, Banczyk D, Ellebrecht CT, Ibrahim SM, et al. Complement-fixing anti-type VII collagen antibodies are induced in Th1-polarized lymph nodes of epidermolysis bullosa acquisita-susceptible mice. *J Immunol* (2011) 187(10):5043–50. doi:10.4049/jimmunol.1100796
24. Kasperkiewicz M, Nimmerjahn F, Wende S, Hirose M, Iwata H, Jonkman MF, et al. Genetic identification and functional validation of FcgammaRIV as key molecule in autoantibody-induced tissue injury. *J Pathol* (2012) 228(1):8–19. doi:10.1002/path.4023
25. Yu X, Holdorf K, Kasper B, Zillikens D, Ludwig RJ, Petersen F. FcgammaRIIA and FcgammaRIIIB are required for autoantibody-induced tissue damage in experimental human models of bullous pemphigoid. *J Invest Dermatol* (2010) 130(12):2841–4. doi:10.1038/jid.2010.230
26. Recke A, Vidarsson G, Ludwig RJ, Freitag M, Moller S, Vonthein R, et al. Allelic and copy-number variations of FcgammaRs affect granulocyte function and susceptibility for autoimmune blistering diseases. *J Autoimmun* (2015) 61:36–44. doi:10.1016/j.jaut.2015.05.004
27. Karsten CM, Laumonnier Y, Kohl J. Functional analysis of C5a effector responses in vitro and in vivo. *Methods Mol Biol* (2014) 1100:291–304. doi:10.1007/978-1-62703-724-2_23
28. Noguchi K, Gel YR, Brunner E, Konietschke F. nparLD: an R software package for the nonparametric analysis of longitudinal data in factorial experiments. *J Stat Softw* (2012) 50(12):1–23. doi:10.18637/jss.v050.i12
29. Collin M, Shannon O, Bjorck L. IgG glycan hydrolysis by a bacterial enzyme as a therapy against autoimmune conditions. *Proc Natl Acad Sci U S A* (2008) 105(11):4265–70. doi:10.1073/pnas.0711271105
30. Ricklin D, Hajishengallis G, Yang K, Lambris JD. Complement: a key system for immune surveillance and homeostasis. *Nat Immunol* (2010) 11(9): 785–97. doi:10.1038/ni.1923
31. Verschoor A, Karsten CM, Broadley SP, Laumonnier Y, Kohl J. Old dogs-new tricks: immunoregulatory properties of C3 and C5 cleavage fragments. *Immunol Rev* (2016) 274(1):112–26. doi:10.1111/imr.12473
32. Guo RF, Riedemann NC, Ward PA. Role of C5a-C5aR interaction in sepsis. *Shock* (2004) 21(1):1–7. doi:10.1097/01.shk.0000105502.75189.5e
33. Guo RF, Ward PA. Role of C5a in inflammatory responses. *Annu Rev Immunol* (2005) 23:821–52. doi:10.1146/annurev.immunol.23.021704.115835
34. Karsten CM, Pandey MK, Figge J, Kilchenstein R, Taylor PR, Rosas M, et al. Anti-inflammatory activity of IgG1 mediated by Fc galactosylation and association of FcgammaRIIB and dectin-1. *Nat Med* (2012) 18(9):1401–6. doi:10.1038/nm.2862
35. Ludwig RJ, Vanhoorelbeke K, Leypoldt F, Kaya Z, Bieber K, McLachlan SM, et al. Mechanisms of autoantibody-induced pathology. *Front Immunol* (2017) 8:603. doi:10.3389/fimmu.2017.00603
36. Fonseca MI, Ager RR, Chu SH, Yazan O, Sanderson SD, LaFerla FM, et al. Treatment with a C5aR antagonist decreases pathology and enhances behavioral performance in murine models of Alzheimer's disease. *J Immunol* (2009) 183(2):1375–83. doi:10.4049/jimmunol.0901005
37. Croker DE, Monk PN, Halai R, Kaeslin G, Schofield Z, Wu MC, et al. Discovery of functionally selective C5aR2 ligands: novel modulators of C5a signalling. *Immunol Cell Biol* (2016) 94(8):787–95. doi:10.1038/icb.2016.43
38. Kolev M, Le Friec G, Kemper C. Complement – tapping into new sites and effector systems. *Nat Rev Immunol* (2014) 14(12):811–20. doi:10.1038/nri3761
39. Hawlisch H, Belkaid Y, Baelder R, Hildeman D, Gerard C, Kohl J. C5a negatively regulates toll-like receptor 4-induced immune responses. *Immunity* (2005) 22(4):415–26. doi:10.1016/j.immuni.2005.02.006
40. Gerard NP, Lu B, Liu P, Craig S, Fujiwara Y, Okinaga S, et al. An anti-inflammatory function for the complement anaphylatoxin C5a-binding protein, C5L2. *J Biol Chem* (2005) 280(48):39677–80. doi:10.1074/jbc.C500287200
41. Rittirsch D, Flierl MA, Nadeau BA, Day DE, Huber-Lang M, Mackay CR, et al. Functional roles for C5a receptors in sepsis. *Nat Med* (2008) 14(5):551–7. doi:10.1038/nm1753
42. Scola AM, Johswich KO, Morgan BP, Klos A, Monk PN. The human complement fragment receptor, C5L2, is a recycling decoy receptor. *Mol Immunol* (2009) 46(6):1149–62. doi:10.1016/j.molimm.2008.11.001
43. Bamberg CE, Mackay CR, Lee H, Zahra D, Jackson J, Lim YS, et al. The C5a receptor (C5aR) C5L2 is a modulator of C5aR-mediated signal transduction. *J Biol Chem* (2010) 285(10):7633–44. doi:10.1074/jbc.M109.092106
44. Zhang X, Schmudde I, Laumonnier Y, Pandey MK, Clark JR, Konig P, et al. A critical role for C5L2 in the pathogenesis of experimental allergic asthma. *J Immunol* (2010) 185(11):6741–52. doi:10.4049/jimmunol.1000892
45. Kemper C. Targeting the dark horse of complement: the first generation of functionally selective C5aR2 ligands. *Immunol Cell Biol* (2016) 94(8):717–8. doi:10.1038/icb.2016.62
46. Karsten CM, Wiese AV, Mey F, Figge J, Woodruff TM, Reuter T, et al. Monitoring C5aR2 expression using a floxed tdTomato-C5aR2 knock-in mouse. *J Immunol* (2017) 199(9):3234–48. doi:10.4049/jimmunol.1700710
47. Mihai S, Chiriac MT, Takahashi K, Thurman JM, Holers VM, Zillikens D, et al. The alternative pathway of complement activation is critical for blister induction in experimental epidermolysis bullosa acquisita. *J Immunol* (2007) 178(10):6514–21. doi:10.4049/jimmunol.178.10.6514
48. Chen M, Daha MR, Kallenberg CG. The complement system in systemic autoimmune disease. *J Autoimmun* (2010) 34(3):J276–86. doi:10.1016/j.jaut.2009.11.014
49. Chen M, Jayne DRW, Zhao MH. Complement in ANCA-associated vasculitis: mechanisms and implications for management. *Nat Rev Nephrol* (2017) 13(6):359–67. doi:10.1038/nrneph.2017.37
50. Heppe EN, Tofern S, Schulze FS, Ishiko A, Shimizu A, Sina C, et al. Experimental laminin 332 mucous membrane pemphigoid critically involves C5aR1 and reflects clinical and immunopathological characteristics of the human disease. *J Invest Dermatol* (2017) 137(8):1709–18. doi:10.1016/j.jid.2017.03.037
51. Trouw LA, Pickering MC, Blom AM. The complement system as a potential therapeutic target in rheumatic disease. *Nat Rev Rheumatol* (2017) 13(9):538–47. doi:10.1038/nrrheum.2017.125
52. Schmidt E, Reimer S, Kruse N, Jainta S, Brocker EB, Marinkovich MP, et al. Autoantibodies to BP180 associated with bullous pemphigoid release interleukin-6 and interleukin-8 from cultured human keratinocytes. *J Invest Dermatol* (2000) 115(5):842–8. doi:10.1046/j.1523-1747.2000.00141.x
53. Iwata H, Kamio N, Aoyama Y, Yamamoto Y, Hirako Y, Owaribe K, et al. IgG from patients with bullous pemphigoid depletes cultured keratinocytes of the 180-kDa bullous pemphigoid antigen (type XVII collagen) and weakens cell attachment. *J Invest Dermatol* (2009) 129(4):919–26. doi:10.1038/jid.2008.305
54. Messingham KN, Srikantha R, DeGueme AM, Fairley JA. FcR-independent effects of IgE and IgG autoantibodies in bullous pemphigoid. *J Immunol* (2011) 187(1):553–60. doi:10.4049/jimmunol.1001753
55. Joly P, Roujeau JC, Benichou J, Picard C, Dreno B, Delaporte E, et al. A comparison of oral and topical corticosteroids in patients with bullous pemphigoid. *N Engl J Med* (2002) 346(5):321–7. doi:10.1056/NEJMoa011592
56. Feliciani C, Joly P, Jonkman MF, Zambruno G, Zillikens D, Ioannides D, et al. Management of bullous pemphigoid: the European dermatology forum consensus in collaboration with the European academy of dermatology and venereology. *Br J Dermatol* (2015) 172(4):867–77. doi:10.1111/bjd.13717
57. Sticherling M, Franke A, Aberer E, Glaser R, Hertl M, Pfeiffer C, et al. An open, multicenter, randomized clinical study in patients with bullous pemphigoid comparing methylprednisolone and azathioprine with methylprednisolone and dapsone. *Br J Dermatol* (2017) 177(5):1299–305. doi:10.1111/bjd.15649
58. Williams HC, Wojnarowska F, Kirtschig G, Mason J, Godec TR, Schmidt E, et al. Doxycycline versus prednisolone as an initial treatment strategy for bullous pemphigoid: a pragmatic, non-inferiority, randomised controlled trial. *Lancet* (2017) 389(10079):1630–8. doi:10.1016/S0140-6736(17)30560-3

59. Kasperkiewicz M, Ellebrecht CT, Takahashi H, Yamagami J, Zillikens D, Payne AS, et al. Pemphigus. *Nat Rev Dis Primers* (2017) 3:17026. doi:10.1038/nrdp.2017.26
60. Schmidt E. Rituximab as first-line treatment of pemphigus. *Lancet* (2017) 389(10083):1956–8. doi:10.1016/S0140-6736(17)30787-0
61. Anhalt GJ, Till GO, Diaz LA, Labib RS, Patel HP, Eaglstein NF. Defining the role of complement in experimental pemphigus vulgaris in mice. *J Immunol* (1986) 137(9):2835–40.
62. Ujiie H, Sasaoka T, Izumi K, Nishie W, Shinkuma S, Natsuga K, et al. Bullous pemphigoid autoantibodies directly induce blister formation without complement activation. *J Immunol* (2014) 193(9):4415–28. doi:10.4049/jimmunol.1400095
63. Dainichi T, Nishie W, Yamagami Y, Sonobe H, Ujiie H, Kaku Y, et al. Bullous pemphigoid suggestive of complement-independent blister formation with anti-BP180 IgG4 autoantibodies. *Br J Dermatol* (2016) 175(1):187–90. doi:10.1111/bjd.14411
64. Romeijn TR, Jonkman MF, Knoppers C, Pas HH, Diercks GF. Complement in bullous pemphigoid: results from a large observational study. *Br J Dermatol* (2017) 176(2):517–9. doi:10.1111/bjd.14822
65. Triantafilou K, Hughes TR, Triantafilou M, Morgan BP. The complement membrane attack complex triggers intracellular Ca2+ fluxes leading to NLRP3 inflammasome activation. *J Cell Sci* (2013) 126(Pt 13):2903–13. doi:10.1242/jcs.124388
66. Laudes IJ, Chu JC, Huber-Lang M, Guo RF, Riedemann NC, Sarma JV, et al. Expression and function of C5a receptor in mouse microvascular endothelial cells. *J Immunol* (2002) 169(10):5962–70. doi:10.4049/jimmunol.169.10.5962

Conflict of Interest Statement: The authors declare that the research was conducted in the absence of any commercial or financial relationships that could be construed as a potential conflict of interest.

frontiers in Immunology

ORIGINAL RESEARCH
published: 15 March 2018
doi: 10.3389/fimmu.2018.00373

Trib1 Is Overexpressed in Systemic Lupus Erythematosus, While It Regulates Immunoglobulin Production in Murine B Cells

*Léa Simoni[1], Virginia Delgado[1], Julie Ruer-Laventie[1], Delphine Bouis[1], Anne Soley[1,2], Vincent Heyer[3], Isabelle Robert[3,4,5,6], Vincent Gies[1,2,7], Thierry Martin[1,2,7], Anne-Sophie Korganow[1,2,7], Bernardo Reina San Martin[3,4,5,6] and Pauline Soulas-Sprauel[1,2,7,8]**

[1] CNRS UPR 3572 "Immunopathology and Therapeutic Chemistry"/Laboratory of Excellence Medalis, Institute of Molecular and Cellular Biology (IBMC), Strasbourg, France, [2] UFR Médecine, Université de Strasbourg, Strasbourg, France, [3] Institut de Génétique et de Biologie Moléculaire et Cellulaire (IGBMC), Illkirch, France, [4] Institut National de la Santé et de la Recherche Médicale (INSERM), U964, Illkirch, France, [5] Centre National de la Recherche Scientifique (CNRS), UMR7104, Illkirch, France, [6] Université de Strasbourg, Illkirch, France, [7] Department of Clinical Immunology and Internal Medicine, National Reference Center for Autoimmune Diseases, Hôpitaux Universitaires de Strasbourg, Strasbourg, France, [8] UFR Sciences pharmaceutiques, Université de Strasbourg, Illkirch-Graffenstaden, France

OPEN ACCESS

Edited by:
Ignacio Sanz, Emory University, United States

Reviewed by:
Lee Ann Garrett-Sinha, University at Buffalo, United States
Laura Mandik-Nayak, Lankenau Institute for Medical Research, United States

***Correspondence:**
Pauline Soulas-Sprauel
pauline.soulas@ibmc-cnrs.unistra.fr

Specialty section:
This article was submitted to B Cell Biology, a section of the journal Frontiers in Immunology

Received: *16 October 2017*
Accepted: *09 February 2018*
Published: *15 March 2018*

Citation:
Simoni L, Delgado V, Ruer-Laventie J, Bouis D, Soley A, Heyer V, Robert I, Gies V, Martin T, Korganow A-S, San Martin BR and Soulas-Sprauel P (2018) Trib1 Is Overexpressed in Systemic Lupus Erythematosus, While It Regulates Immunoglobulin Production in Murine B Cells. Front. Immunol. 9:373. doi: 10.3389/fimmu.2018.00373

Systemic lupus erythematosus (SLE) is a severe and heterogeneous autoimmune disease with a complex genetic etiology, characterized by the production of various pathogenic autoantibodies, which participate in end-organ damages. The majority of human SLE occurs in adults as a polygenic disease, and clinical flares interspersed with silent phases of various lengths characterize the usual evolution of the disease in time. Trying to understand the mechanism of the different phenotypic traits of the disease, and considering the central role of B cells in SLE, we previously performed a detailed wide analysis of gene expression variation in B cells from quiescent SLE patients. This analysis pointed out an overexpression of *TRIB1*. TRIB1 is a pseudokinase that has been implicated in the development of leukemia and also metabolic disorders. It is hypothesized that Trib1 plays an adapter or scaffold function in signaling pathways, notably in MAPK pathways. Therefore, we planned to understand the functional significance of *TRIB1* overexpression in B cells in SLE. We produced a new knock-in model with B-cell-specific overexpression of *Trib1*. We showed that overexpression of *Trib1* specifically in B cells does not impact B cell development nor induce any development of SLE symptoms in the mice. By contrast, Trib1 has a negative regulatory function on the production of immunoglobulins, notably IgG1, but also on the production of autoantibodies in an induced model. We observed a decrease of Erk activation in BCR-stimulated *Trib1* overexpressing B cells. Finally, we searched for Trib1 partners in B cells by proteomic analysis in order to explore the regulatory function of Trib1 in B cells. Interestingly, we find an interaction between Trib1 and CD72, a negative regulator of B cells whose deficiency in mice leads to the development of autoimmunity. In conclusion, the overexpression of *Trib1* could be one of the molecular pathways implicated in the negative regulation of B cells during SLE.

Keywords: lupus, B cells, Trib1, mouse model, Ig secretion, negative regulator

INTRODUCTION

Systemic lupus erythematosus (SLE) is a severe and heterogeneous systemic autoimmune disease, mostly affecting women. Patients produce various pathogenic autoantibodies such as antinuclear antibodies (anti double-stranded DNA, anti-chromatin…), which participate in end-organ damages by a variety of mechanisms, notably *via* immune complex-mediated inflammation leading to glomerulonephritis and vasculitis, for example. The majority of human SLE occurs in adult and the usual evolution of the disease in time is characterized by clinical flares interspersed with silent phases of various lengths (1, 2). To date, we have no molecular explanation to the establishment and the maintenance of these clinically silent phases.

Several lines of evidence indicate that B cells are essential to the disease process and could present intrinsic abnormalities (3, 4): (1) B cells produce the autoantibodies; (2) in murine spontaneous models of SLE, B cells are activated before the disease onset, and in humans, autoantibodies are detectable long before the first symptoms (5); (3) murine models of SLE mice devoid of mature B cells no longer develop lupus phenotype (6); (4) it seems that the important role of B cells in lupus could also implicate their function of antigen presentation to CD4 T cells, and/or cytokine secretion (7). Intrinsic B cell abnormalities are illustrated by the fact that (NZBXNZW)F1 B-lineage cells present an enhanced *in vitro* responsiveness to accessory cell-derived signals (8). Most importantly, the disease can be transferred in mice by B cells: immunodeficient SCID mice populated with pre-B cells from (NZBXNZW)F1 mice, but not those populated with pre-B cells from non-autoimmune mice, develop many of the autoimmune symptoms present in (NZBXNZW)F1 mice, suggesting that genetic defects responsible for the development of SLE disease in (NZBXNZW)F1 mice are intrinsic to their B cells (9).

Considering the central role of B cells in SLE, in a previous work, we performed a genome-wide transcriptome analysis of B cells in lupus patients using microarrays, focusing on the remission phase of the disease, in order to avoid gene expression variations linked to B cell activation which accompanies lupus flares (10). We notably identified an underexpression of *CARABIN*, and then defined Carabin as a new regulator of B cell function by functional genomics in new transgenic mouse models (11). In addition, we described an overexpression of *FKBP11*, which leads in mice to B cell tolerance breakdown and initiates plasma cell differentiation, two features of lupus B cells (12).

Our transcriptome analysis also pointed out an overexpression of *TRIB1* in B cells in quiescent SLE patients. Trib1 belongs to the tribbles family of proteins. The *tribbles* gene was first identified in Drosophila (13). In mammals, tribbles family of proteins is composed of three members: Trib1, Trib2, and Trib3, all pseudokinases, whose amino acids sequence is very highly conserved between human and mice. Despite high degrees of similarity between human tribbles protein sequences, Trib1, Trib2, and Trib3 show distinct patterns of expression in human tissues and cellular functions, and are linked to different diseases. Trib1 has been notably linked to the development of human myeloid leukemia and to the negative regulation of lipid metabolism and the development of metabolic disorders (14, 15). It is hypothesized that tribbles play an adapter or scaffold function in signaling pathways, notably in MAPKs pathways (13, 16). Indeed, Trib1 interacts with MEK-1 (upstream activator of ERK) and MKK4 (upstream activator of JNK). Overexpression of Trib1 in HeLa and in murine bone marrow (BM) cells enhances the extent and rate of ERK phosphorylation (17, 18) and inhibits AP1 activity, leading notably to a repression of IL8 promoter (17). But it seems that the expression of tribbles is regulated in a cell-dependent manner, thus contributing to the cell-type specificity of MAPK responses (14). Trib1, as the other tribbles proteins, targets protein substrates to the proteasome and controls their E3 ligase-dependent ubiquitination (16). Trib1 is a serine/threonine pseudokinase containing a N-terminal PEST domain, and a central pseudokinase domain, which could position and regulate potential substrates targeting for ubiquitination. The C-terminal domain of Trib1 contains a MAPKK/MEK regulatory motif, which was shown to bind to MEK1 in some cell types, and an ubiquitin E3 ligase-targeting motif, which binds to COP1 (16). Trib1 is highly expressed in BM, peripheral blood leukocytes (with the highest expression in the myeloid compartment), thyroid gland, and pancreas (16, 17). In immune system, Trib1 is known to be critical for the development of M2 macrophages (19) and to interact with Foxp3 in regulatory T cells (20). However, its role in B cells is totally unknown.

After having confirmed *TRIB1* overexpression in B cells in an additional cohort group of quiescent SLE patients, we planned to understand the functional significance of *TRIB1* overexpression in B cells in human SLE. For this purpose, we generated a new knock-in (KI) model with B-cell-specific overexpression of *Trib1*. We showed that overexpression of *Trib1* specifically in B cells does not impact B cell development nor induce any development of SLE symptoms in the mice. By contrast, Trib1 has a negative regulatory function on production of immunoglobulins, notably IgG1, but also on the production of autoantibodies. Finally, we searched for Trib1 partners in B cells by proteomic analysis in order to decipher the mechanisms of regulatory function of Trib1 in B cells. We notably described for the first time in B cells the interaction between Trib1 and COP1, and with CD72, a negative regulator of B cells whose deficiency in mice leads to the development of autoimmunity. In conclusion, the overexpression of *Trib1* could be one of the molecular pathways implicated in the negative regulation of B cells during SLE.

MATERIALS AND METHODS

Patients

The first cohort comprised 17 patients and 9 age- and sex-matched healthy controls. SLE patients fulfilling at least four diagnostic criteria according to the American College of Rheumatology (21) were prospectively included, provided that they were in a quiescent phase of the disease (with a SLEDAI score less than 4) and were receiving minimal treatment [no immunosuppressive drugs and less than 10 mg of prednisone per day if they needed steroids (4 patients)]. 10 patients were treated with hydroxychloroquine. Purified $CD19^+$ B cells from 17 patients blood sample ("cohort 1") and 9 age- and sex-matched controls were subjected to a pangenomic transcriptome analysis (Affymetrix GeneChip human genome U133 plus 2.0) (10). For the second cohort of patients

("cohort 2"), 4 quiescent patients (3 females and 1 male) aging from 25 to 32 years old with the diagnosis of SLE were selected. Only patients with no treatment, or hydroxychloroquine, or steroids less than 20 mg per day and without immunosuppressive treatments in the previous 6 months, at the time of diagnosis, were included. Patients were compared to healthy age- and sex-matched individuals. Mature naive B cells ($CD3^-CD19^+CD27^-IgM^+CD24^{low}CD38^{low}$) were sorted (FACSAria II, BD Biosciences) and cell viability was assessed with DAPI (Sigma-Aldrich), before extraction of RNA for quantitative real-time RT-PCR analysis.

This study was approved by the ethics committee of the "Hôpitaux Universitaires de Strasbourg" and patients gave their written informed consent.

Mice

Total RNA was extracted from C57BL/6 total splenocytes using RNeasy Kit (Qiagen). cDNA synthesis was done using High Capacity Reverse Transcription Kit (Applied Biosystems). The coding sequence of mTrib1 (1118 pb, NM144549.4) was amplified from cDNA using the following primers: Forward 5′-ATGCGGGTCGGTCCCGTGCG-3′ and Reverse 5′-CTAGCAGAAGAAGGAACTTATGTCACTG-3′. The PCR conditions were as follows: 94°C for 5 min; 35 cycles at 94°C for 30 s, 58°C for 30 s, and 72°C for 1 min. The PCR product was firstly cloned in the pCR2.1 TA cloning vector (Invitrogen) then two Asc1 restriction sites were added by PCR using the following primers: Forward 5′AAGGCGCGCCGCGCAGATCCAGGGATTTACAAAGCCGGGGCCGCTCCGGCCAGGGCCGCGATGCGGGTCGGTCCC-3′ and Reverse 5′-AAAGGCGCGCCCTAGCAGAAGAAGGA-3′. The PCR conditions were as follows: 94°C for 5 min; 30 cycles at 94°C for 30 s, 60°C for 30 s, and 72°C for 45 s. After a digestion step with AscI (Biolabs), the PCR product was cloned into the CTV Vector (Addgene) (22, 23). The Trib1-ROSA KI mutant mouse line was established at the MCI/ICS (Mouse Clinical Institute—Institut Clinique de la Souris, Illkirch, France[1]). The linearized construct was electroporated in C57BL/6N mouse embryonic stem (ES) cells (ICS proprietary line). After G418 selection, targeted clones were identified by long-range PCR and further confirmed by Southern blot with an internal (Neo) probe and a 5′ external probe. Two positive ES clones were validated by karyotype spreading and microinjected into BALB/C blastocysts. Resulting male chimeras were bred with wild-type C57BL/6N females. Germline transmission was achieved in the first litter. The presence of the transgene in the mice was assessed by a PCR performed on tail DNA, using the following primers: Forward 5′-ACGACCAAGTGACAGCAATG-3′ and Reverse 5′-CTCGACCAGTTTAGTTACCC-3′. Trib1-ROSA Mb1Cre mice were obtained by crossing Trib1-ROSA KI mice with Mb1Cre Mice (24) that will allow *Trib1* overexpression specifically in B cells from the pro-B cell stage. The presence of the Mb1Cre transgene was assessed by a PCR performed on tail DNA, using the following primers: Forward 5′ ACCTCTGATGAAGTCAGGAAGAAC-3′ and Reverse 5′-GCAGATGTCCTTCACTCTGATTCT-3′. All animal experiments were performed with the approval of the "Direction départementale des services vétérinaires" (Strasbourg, France) and protocols were approved by the ethics committee ("Comité d'éthique en matière d'Experimentation Animale de Strasbourg," CREMEAS, approval number AL/02/15/09/11 and AL/31/38/02/13).

[1]http://www.ics-mci.fr/en/.

Quantitative Real-time RT-PCR Analysis

RNA was prepared with RNeasy Kit (Qiagen) and cDNA was obtained with High Capacity Reverse Transcription Kit (Applied Biosystems). For RNA isolated from patients' cells, a preamplification of 10 ng of cDNA was performed, with TaqMan® PreAmp Master Mix Kit (Applied Biosystems) on a T100™ Thermal cycler (Biorad). Quantitative real-time PCR was performed on 10 ng cDNA using Taqman Universal Mastermix (Applied Biosystems) and Assays-on-Demand probes (Applied Biosystems) (Hprt1: Mm01318743_m1, Trib1: Mm00457875_m1, Pax5: Mm00435501_m1, Blimp1: Mm01187285_m1, total Xbp1: Mm00457357_m1, Bach2: Mm00464379_m1, Bcl-6: Mm00477633_m1, Irf4: Mm00516431_m1, Aicda: Mm00507771_m1, HPRT1: Hs01003267_m1, ACTB: Hs99999903_m1, GAPDH: Hs99999905_m1, TRIB1: Hs00179769_m1). Each sample was amplified in triplicate in a StepOnePlus real-time PCR machine (Applied Biosystems). Relative expression levels were calculated with the StepOne v2.1 software (Applied Biosystems), using the comparative cycle threshold method, and normalized to the endogenous control *Hprt1, Gapdh* and/or *Beta-actin*.

Flow Cytometry Analysis

Analyses of GFP expression, of cell phenotype, and class-switch recombination were performed on splenic, lymph nodes (LNs), thymic, and BM lymphoid populations by four-color fluorescence analysis according to standard protocols. The following antibodies were used: PE, PerCP, Cy5 or APC anti-mouse B220, CD3, CD4, CD8, CD19, CD21, CD23, CD5, CD86, I-A/I-E, CD44, IgM, IgG1, IgG3, and CD138 (all from BD Biosciences). Propidium iodide was used for discrimination of live and dead cells. For proliferation analysis, cells were permeabilized after extracellular staining and fixed with the cytofix/cytoperm permeabilization kit (BD Biosciences), then stained with the PerCP Cy5.5 anti-Ki67 antibody (BD Biosciences). For intracellular IgG1 staining, membrane B220 staining was performed along with a saturation step using goat anti-mouse IgG (5 µg/mL, Jackson Immunoresearch) for 30 min at 4°C. After a washing step, cells were fixed with 100 µL of fixation buffer from Fixation/Permeabilization kit (eBioscience) during 20 min at room temperature, in the dark. Cells were then permeabilized with the permeabilization buffer from Fixation/Permeabilization kit (eBioscience) and incubated for 30 min at room temperature in the dark with anti-mouse IgG1 (PE, Southern Biotech) and washed before acquisition by a cytometer. For all stainings, cells were analyzed using the FACS Calibur (BD Biosciences). The data were analyzed with FlowJo software (Treestar).

Mice Immunization

3-month-old mice were injected intraperitoneally at days 0, 7, and 14 with, respectively, 50, 25, and 25 µg of LPS from *S. typhimurium* (Sigma) diluted in PBS; at days 0, 10, and 20 with 100 µg of

Ovalbumin (OVA) (Sigma) associated with 250 μg of alum hydroxide; or at days 0 and 23 with, respectively, 100 and 10 μg of NP-KLH (Biosearch technology) associated with 250 μg of alum hydroxide.

Antibody Detection by ELISA

Total IgG, IgG1, IgG2b, IgG3, or IgM levels were measured in serum from 3- or 6-month-old mice, and in supernatant after 3 days of stimulation, as previously described (12). Anti-dsDNA autoantibodies were measured as previously described (12). Anti-OVA and anti-NP-specific antibodies were measured as previously described (11).

Cell Preparation and Culture

To evaluate *Trib1* overexpression within the different cell compartments, splenic mature CD43$^-$ B cells, CD43$^+$ splenocytes and splenic T cells were purified, using B-cell isolation kit (anti-CD43 (Ly-48) microbeads, Miltenyi Biotech) and Dynabeads Untouched Mouse T cells kit (Invitrogen) according to the supplier's protocols. To study the activation of splenic mature B cells *in vitro*, total splenocytes were plated at 1.10^6 cells/ml in a culture medium composed of RPMI-1640 (Lonza) containing 10% (v/v) FCS (PAN), 50 mM β-Mercaptoethanol (Gibco), 1% Penicillin/Streptomycin (Gibco), 10 mM HEPES (Lonza), and 1 mM Sodium Pyruvate (Lonza). Cells were stimulated with a combination of LPS (10 μg/mL, Sigma) and IL-4 (10 ng/mL, Sigma), or a combination of IL-4 (5 ng/mL, Sigma), IL-21 (10 ng/mL, Sigma), and anti-CD40 (10 μg/mL, BD Biosciences), or with agonists of TLR1/2 (250 ng/mL, PAM3CSK4, Invivogen), or TLR7 (1 μg/mL, Imiquimod, Invivogen) or TLR9 (5 μM, ODN2395, Invivogen). In some experiments, purified splenic mature B cells (CD43$^-$) were plated at 1.10^6 cells/ml and were stimulated for 3 or 4 days with a combination of LPS (10 μg/mL, Sigma) and IL-4 (10 ng/mL, Sigma) or with LPS only (10 μg/mL, Sigma) using the same culture medium described above for total splenic cells. For the analysis of IgG secretion after blockade of protein transport, GolgiStop™ (BD Biosciences), containing monensin, was added in the appropriate wells directly into the medium (final dilution of GolgiStop™: 1:1,000), 8 h before the acquisition with the cytometer.

To evaluate the activation of signaling pathways by immunoblot analysis, splenic sorted mature B cells were stimulated with F(ab′)$_2$ goat anti-mouse IgM antibody at 10 μg/mL (Jackson Immunoresearch).

Trib1-Flag Expression

Flag-tagged Trib1 and Flag-tagged GFP (negative control) were cloned using standard molecular biology into the pMX-PIE and the pQCXIP retroviral vectors respectively, then were used to establish stably expressing CH12F3 (CH12) cell lines (25) as described previously (26, 27).

Immunoblot Analysis

Immunoprecipitation (IP) products or protein extracts were loaded on a bisacrylamide gel. Primary antibodies and dilutions were as follows: rabbit anti-phospho Erk (Cell signaling, 1:1,000), rabbit anti-Total Erk (Cell signaling, 1:1,000), anti-phospho Syk (Cell signaling, 1:500), anti-Total Syk (Cell signaling, 1:1,000), mouse anti-phospho IkB (Cell signaling, 1:1,000), rabbit anti-Total IkB (Cell signaling, 1:1,000), mouse anti-Flag-M2 (Sigma, 1/1,000 or 1:20,000), anti-COP1 (Bethyl, 1:1,000), anti-CD72 (Santa Cruz Biotechnology, 1:1,000). The secondary antibodies and dilution were as follows: donkey anti-rabbit IgG (GE Healthcare, 1:10,000), mouse anti-rabbit light chain (Abcam, 1:20,000). The ratio phospho-p42/Total-p42 for one sample corresponds with the ratio between the values of phospho-Erk and total-Erk band density for that sample. The density of each band was measured with ImageJ software.

Anti-Flag IP and Mass Spectrometry Analysis

Cytoplasmic extracts from CH12-Trib1 and control cell lines were prepared using standard techniques. 20 mg of clarified extracts was taken into IP buffer [IP-300: 20 mM Tris, pH 7.9, 20% glycerol, 300 mM KCl, 0.125 mM EGTA, 0.25 mM EDTA, 1 mM DTT, 0.5 mM PMSF, 1× protease inhibitor cocktail (Roche), 100 U/ml Benzonase (EMD), 0.025% NP-40], and precleared with protein G-agarose beads and mouse IgG (GE Healthcare) for 1 h at 4°C. 40 μL of Flag M2 agarose beads were added (50% slurry; Sigma-Aldrich) and incubated overnight at 4°C. Proteins were eluted three times with 40 μL of Flag peptide (0.2 mg/mL; 30 min at 4°C). Eluted proteins were submitted to identification by mass spectrometry as previously described (27). Proteomics data are available in Table S2 in Supplementary Material.

Statistical Analysis

Statistical significance was calculated with a two-tailed Mann and Whitney test using Prism software (GraphPad). All data were presented as mean ± SD.

RESULTS

Overexpression of TRIB1 in B Cells in SLE Patients

We previously analyzed a pangenomic transcriptome of purified CD19$^+$ peripheral B cells in patients with inactive SLE in comparison to B cells from age- and sex-matched controls (10). We pointed out a 2.8-times overexpression of *TRIB1* in all patients ($p = 0.049$) (**Figure 1A**). The overexpression of *TRIB1* was much higher (mean of 5.6-fold over healthy controls) in a subgroup of five patients (**Figure 1A**) displaying a similar and distinct gene expression pattern with many genes implicated in the unfolded protein response. This subgroup of five patients was not different from the other patients of the same cohort (cohort 1), considering their clinical or phenotypical characteristics (10). TRIB1 overexpression was validated by quantitative real-time RT-PCR in a second cohort of SLE patients versus controls (**Figure 1B**).

Generation of B Cell-Specific Trib1 KI Conditional Mice

As the role of Trib1 in B cells and in autoimmunity has never been described, we decided to investigate in detail the possible role of TRIB1 overexpression in B cell function and in the promotion of SLE. Therefore, we developed a functional genomic study in mice, by the generation of B cell-specific Trib1 KI conditional mice. We inserted the coding sequence for murine

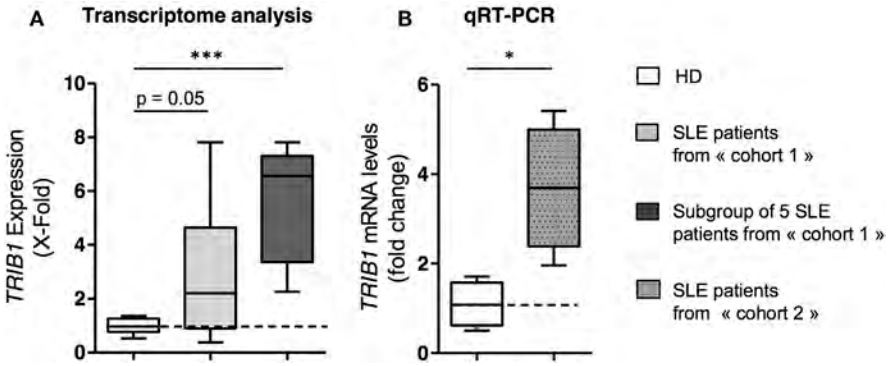

FIGURE 1 | *TRIB1* is overexpressed in B cells from quiescent systemic lupus erythematosus (SLE) patients. **(A)** *TRIB1* mRNA expression levels in transcriptome analysis of purified mature B cells from 17 SLE quiescent patients (light gray) and from a subgroup of 5 patients (dark gray) compared to 9 age- and sex-matched healthy donors (HD). X-fold represents the $2exp^{(Pi-Tmean)}$ value for the patients, where *Pi* is the value of the TRIB1 probe set signal for a given patient, and *T mean* the mean value of signals for the same probe set for the HD ($T_{mean} = 8.005$). **(B)** Quantitative real-time RT-PCR analysis of *TRIB1* mRNA expression performed on purified B cells from HDs ($n = 4$) and quiescent SLE patients ($n = 4$). Relative expression levels were calculated with the comparative Ct method using the mean of the Ct between *HPRT1*, *ACTB*, and *GAPDH* for normalization. Each bar represents the level of *TRIB1* mRNA relative to HD controls (Error bars, SD; $^*p < 0.05$, $^{***}p < 0.001$, Mann and Whitney test).

trib1, preceded by the synthetic CAG promoter and a loxP-flanked Neo-STOP cassette, into the ubiquitously expressed ROSA26 locus in the genome of C57BL/6 mice. We used the CTV vector designed by Xiao et al. in Rajewsky's lab (22). A frt-flanked IRES-EGFP cassette, which is placed between the cloning site for *trib1* insertion and the polyadenylation signal (pA), allows the detection of cells in which excision of Neo-STOP cassette has been efficient and, therefore, constitutes a good reporter for *Trib1* overexpression (**Figure 2A**). The mice obtained by this strategy were named Trib1-ROSA mice. These Trib1-ROSA mice were used as controls in all experiments. Then, we developed a B cell-specific Trib1 KI model, by crossing Trib1-ROSA mice with Mb1 Cre animals. The *mb-1* gene encodes the BCR Ig-α subunit (CD79a), and is expressed from the very early pro-B cell stage in BM (24). The mice, overexpressing *Trib1* specifically in B cell lineage, will be thereafter named Trib1-ROSA Mb1Cre.

We first evaluated the specificity of *trib1* overexpression in B cells in Trib1-ROSA Mb1Cre mice. We detected a six-times overexpression of *Trib1* mRNA in sorted splenic mature B cells in Trib1-ROSA Mb1Cre mice, compared to control mice, by quantitative real-time RT-PCR. The overexpression was not seen in the rest of splenic cells, neither in sorted splenic T cells (**Figure 2B**). We also analyzed the expression of GFP, reporter for Trib1 overexpression, in different lymphoid organs by flow cytometry. The average percentage of GFP^+ cells was very high in $B220^+IgM^+$ B cells in spleen and LNs of Trib1-ROSA Mb1Cre mice (98.0 and 95.0%, respectively), compared to control mice (1.4 and 2.3%, respectively), with almost no GFP expression in splenic $CD3^+$ T cells (5.8 and 3.5% in Trib1-ROSA Mb1Cre and control mice, respectively) (**Figures 2C,D**). These results show that the deletion of the STOP cassette was very efficient and specific of the B cell lineage in Trib1-ROSA Mb1Cre mice. Finally, about 70% of BM $B220^+$ cells express GFP, compared to about 1% in control mice (**Figures 2C,D**). This could be explained in part by the fact that, during B cell development in BM, B220 is expressed earlier (at Hardy's fraction A, i.e., pre-proB stage) than Ig-α (Hardy's fraction B, i.e., proB cell stage) (28). In conclusion, as expected with the Mb1Cre model, *Trib1* is specifically overexpressed in B cell lineage in Trib1-ROSA Mb1Cre mice.

B Cell Phenotype in Mice Overexpressing *Trib1* in B Cells

We next assessed the development of B cells in primary and secondary lymphoid organs in Trib1-ROSA Mb1Cre mice, by flow cytometry analysis. The proportions of the different subsets of B cells in BM, spleen, and LNs were not different between Trib1-ROSA Mb1Cre and Trib1-ROSA control mice, showing that *Trib1* overexpression in B cells does not have any impact on their development (**Table 1**). We detected in the spleen and LNs two distinct populations of GFP positive B cells in Trib1-ROSA Mb1Cre mice (**Figure 2D**). However, the proportions of MZ, T1, T2, and follicular B cells were not different between splenic GFP^+ and GFP^{high} populations. Of note, as expected, *Trib1* overexpression in B cells did not impact neither T cell development (Table S1 in Supplementary Material), nor the expression of activation markers CD44 and CD69 after stimulation with anti-CD3 and anti-CD28 antibodies for 72 h *in vitro* (data not shown). Because SLE is often associated with B cell hyperactivity (2), we analyzed the expression of activation markers (CD86, MHC II, CD44) on B cells in spleen and LNs. The results showed that *Trib1* overexpression in B cells does not increase basal activation of B cells in secondary lymphoid organs (Figure S1 in Supplementary Material). In addition, the expression of CD86 expression on splenic B cells was not different between Trib1-ROSA Mb1Cre and Trib1-ROSA mice, after *in vitro* stimulation with various TLR agonists (Figure S2 in Supplementary Material).

A majority of SLE patients and lupus murine models develop a hypergammaglobulinemia (2, 29). The level of serum IgM was comparable between the two groups of mice, and the levels of IgG was even decreased in Trib1-ROSA Mb1Cre mice compared

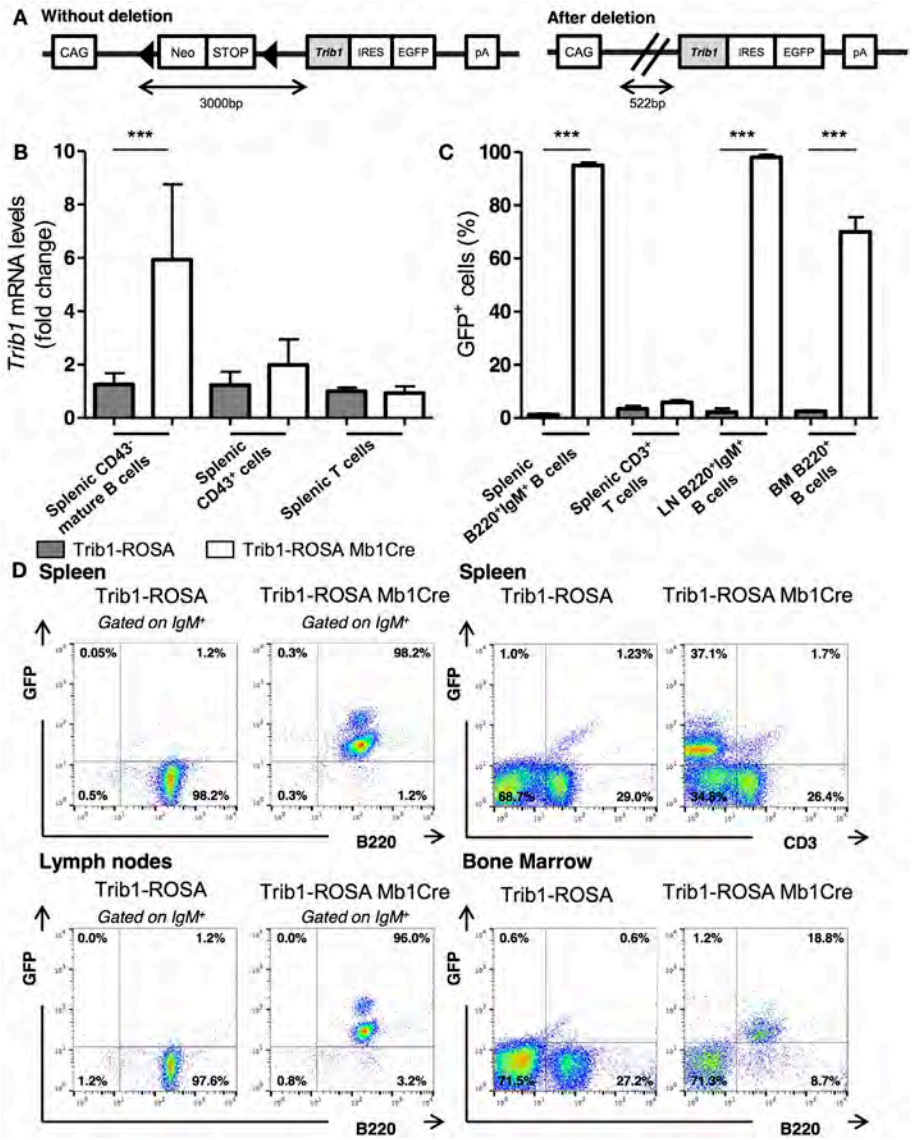

FIGURE 2 | Generation of Trib1-ROSA mice and validation of *Trib1* overexpression and GFP expression in Trib1-ROSA Mb1Cre mice. **(A)** Simplified representation of Trib1-ROSA construct. **(B)** Quantitative real-time RT-PCR analysis of *Trib1* mRNA expression performed on sorted splenic CD43⁻ mature B cells ($n = 9$), splenic CD43⁺ cells ($n = 9$) and splenic T cells ($n = 3$), from 3-month-old Trib1-ROSA and Trib1-ROSA Mb1Cre mice. Each sample was normalized to the endogenous control *Hprt1*. Each bar represents the level of *Trib1* mRNA relative to control mice. **(C)** Percentages of GFP⁺ cells analyzed by flow cytometry **(D)** within B cell or T cell compartment from spleen [B220⁺IgM⁺ B cells ($n = 9$), CD3⁺ T cells ($n = 4$)], LN [B220⁺IgM⁺ B cells ($n = 9$)], and BM [B220⁺ B cells ($n = 9$)] of Trib1-ROSA and Trib1-ROSA Mb1Cre mice (Error bars, SD; ***$p < 0.001$, Mann and Whitney test).

to Trib1-ROSA mice, although the difference was not statistically significant (**Figure 3A**). When IgG subclasses were quantified in serum, we noticed that the most decreased IgG subclass was IgG1 (186 µg/mL in Trib1-ROSA Mb1Cre versus 263.5 µg/mL in control mice) (**Figure 3A**). The production of antigen-specific antibodies was decreased after immunization with a T-dependent antigen (OVA) in Trib1-ROSA Mb1Cre mice compared to control mice, at day 20 for IgM and at day 30 for IgM and IgG, and the decrease was statistically significant for IgM (**Figure 3B**).

In conclusion, *Trib1* overexpression in B cells does not have any impact on the development of B cells, nor on their activation status, but seems to have a slight negative impact on immunoglobulin production.

B-Cell-Specific Trib1 Overexpressing Mice Do Not Develop Any Sign of Lupus

Trib1-ROSA Mb1Cre mice were analyzed to evaluate the development of lupus symptoms. They do not develop any proteinuria, even at old age (18 months) (data not shown). We quantified the basal level of serum anti-dsDNA IgM autoantibodies, one of the hallmarks of SLE disease, by ELISA. At a young age (3-month-old), Trib1-ROSA Mb1Cre and Trib1-ROSA produce

TABLE 1 | Flow cytometry analysis of B cell subsets from bone marrow (BM), spleen, and lymph nodes (LN) does not show any defect in B-cell development and differentiation in Trib1-ROSA Mb1Cre mice.

	Trib1-ROSA ($n = 9$)	Trib1-ROSA Mb1Cre ($n = 9$)
BM		
Pro-pre B	8.3 ± 2.2%	8.0 ± 2.9%
Immature	1.9 ± 1.0%	1.7 ± 0.7%
Transitional	1.4 ± 0.7%	0.8 ± 0.4%
Mature	1.8 ± 1.0%	1.5 ± 0.6%
Spleen		
Total cellularity	*66.6 10^6 ± 2.0.10^7*	*60.7 10^6 ± 1.9.10^7*
Total splenic B cells	39.2 ± 12.7%	46.0 ± 10.3%
	25.4 10^6 ± 10.1 10^6	*28.2 10^6 ± 12.0 10^6*
Fo	29.9 ± 11.2%	34.1 ± 5.1%
	17.1 10^6 ± 6.0 10^6	*20.6 10^6 ± 6.8 10^6*
MZ	1.3 ± 0.5%	2.5 ± 2.5%
	0.9 10^6 ± 0.6 10^6	*1.8 10^6 ± 2.4 10^6*
T1	10.8 ± 4.1%	10.3 ± 1.8%
	6.4 10^6 ± 2.1 10^6	*6.4 10^6 ± 2.8 10^6*
T2	7.3 ± 2.9%	6.4 ± 1.8%
	4.2 10^6 ± 1.9 10^6	*3.9 10^6 ± 1.8 10^6*
PB	1.1 ± 1.0%	1.1 ± 1.0%
	0.74 10^6 ± 0.68 10^6	*0.67 10^6 ± 0.68 10^6*
B1 cells	0.8 ± 0.7%	0.7 ± 0.4%
	0.43 10^6 ± 0.37 10^6	*0.9 10^6 ± 0.8 10^6*
LN		
Total cellularity	*6.3 10^6 ± 4.2 10^6*	*5.1 10^6 ± 3.0 10^6*
Total LN B cells	28.1 ± 11.4%	28.0 ± 4.0%
	2.2 10^6 ± 1.8 10^6	*1.5 10^6 ± 1.1 10^6*
PB	1.7 ± 0.7%	1.9 ± 0.3%
	0.09 10^6 ± 0.06 10^6	*0.11 10^6 ± 0.05 10^6*

BM: Pro-Pre B ($B220^+IgM^-$); Immature ($B220^{int}IgM^+$); Transitional ($B220^{int}IgM^{high}$); Mature ($B220^{high}IgM^+$). Spleen/LN: Fo: Follicular ($B220^+IgM^+CD23^+CD21^{low}$); MZ: Marginal Zone ($B220^+IgM^+CD23^-CD21^{high}$); T1: Transitional 1 ($B220^+IgM^+CD23^-CD21^-$); T2: Transitional 2 ($B220^+IgM^+CD23^+CD21^{high}$); PB: Plasmablast ($B220^+CD138^{low}$); B1 cells ($CD19^+B220^+CD5^+$). italic: absolute numbers.

the same amount of anti-dsDNA IgM, whereas at 6 months, Trib1-ROSA Mb1Cre mice produce even less autoantibodies than control mice (**Figure 4A**). At 3 months, as mice from C57BL/6 genetic background do not produce high titers of autoantibodies, we boosted the production of anti-dsDNA autoantibodies by an injection of LPS. The injection of LPS mimics a bacterial infection and induces a polyclonal activation of B cells, including autoreactive B cells producing natural autoantibodies. LPS from *Salmonella typhimurium* was chosen because it was shown to induce a high production of anti-DNA antibodies in young C57BL/6 and in (NZB × NZW)F1 mice (30). Mice were injected at days 0, 14, and 28, and the production of anti-dsDNA IgM was quantified at day 28 by ELISA. The injection of LPS induced an increase of anti-dsDNA IgM production both in Trib1-ROSA Mb1Cre and in Trib1-ROSA control mice compared to PBS-injected mice (**Figure 4B**). However, B-cell-specific *Trib1* overexpressing mice produce less anti-dsDNA IgM than control mice, and the difference was statistically significant. In conclusion, the overexpression of *Trib1* in B cells does not induce the development of SLE. On the contrary, it could have a regulatory function on anti-dsDNA antibody production, considering the results obtained *in vivo* in an induced model of autoantibody production.

Trib1 Overexpression in B Cells Negatively Regulates Ig Production

In order to better understand the impact of *Trib1* overexpression on Ig (and notably IgG1) production, we stimulated total splenocytes and splenic sorted B cells with various stimuli, including a combination of LPS and IL-4, known to induce the class-switching of B cells into IgG1-producing cells, and with several TLR agonists (TLR7, TLR9, and TLR1/2) known to play a role in lupus physiopathology in both lupus mouse models and patients (31). We stimulated total splenocytes from Trib1-ROSA Mb1Cre and Trib1-ROSA control mice during 72 h with TLR agonists or with a combination of LPS and IL-4 and quantified the production of total IgG and IgG1 in supernatants by ELISA. All tested stimuli induced a decrease of IgG and IgG1 secretion in culture supernatants from Trib1-ROSA Mb1Cre splenocytes, compared to Trib1-ROSA splenocytes. The decrease in IgG production was notably statistically significant after TLR1/2 and TLR7 agonists stimulation (**Figures 5A,B**). The stimulation of total splenocytes with LPS (TLR4 agonist) alone led to a non-statistically significant decrease of IgG secretion in Trib1-ROSA Mb1Cre mice, compared to Trib1-ROSA mice (data not shown), however, LPS in combination with IL-4 induced a statistically significant decrease of both IgG and IgG1 secretion (**Figures 5A,B**). In both cases, IgM secretion was not affected (data not shown). Importantly, this defect of IgG/IgG1 secretion was intrinsic to B cells, because the stimulation of sorted splenic mature B cells only, with LPS and IL-4, led also to a decrease of IgG1 production (**Figure 5C**). We also tested a stimulation protocol that better mimics T cell help: the stimulation of total splenocytes with anti-CD40, IL-4, and IL-21 induced a non-statistically significant decrease of IgG secretion in Trib1-ROSA Mb1Cre mice, compared to Trib1-ROSA mice (**Figure 5D**), and IgM secretion was marginally affected (data not shown).

Then we analyzed the potential mechanisms leading to Ig production defect in *Trib1* overexpressing B cells. As mentioned earlier, this deficiency could not be attributed to a defect in B cell activation process, considering the equal/similar expression of activation markers after stimulation *in vitro* (Figure S2 in Supplementary Material). An increase of B cell mortality or a decrease of B cell proliferation could be responsible for the phenotype. However, there was no difference between the two groups of mice in the percentages of dead cells (Figures S3A,B in Supplementary Material) nor in the percentage of proliferating ($B220^+Ki67^+$) B cells after stimulation *in vitro* (Figures S3C,D in Supplementary Material). We also analyzed the plasma cell (PC) differentiation process. We tested two known models of *in vitro* plasmablast differentiation, i.e., stimulation of B cells with LPS and with LPS/IL-4, then we quantified the percentage of $B220^{low}CD138^+$ plasmablasts by flow cytometry. Our results showed no difference between the two groups of mice (Figures S4A,B in Supplementary Material). In addition, we analyzed the expression of plasma cell differentiation program genes (repressed genes, such as *Pax5*, *Bach2*, *Bcl-6*, *Aicda*; induced genes, such as *Blimp1*, *Xbp1*, and *Irf4*) by quantitative real-time RT-PCR analysis. Considering the results, *Trib1* overexpression does not interfere with PC differentiation genetic program (Figures S4C,D in Supplementary Material). Finally, a defect of class-switching

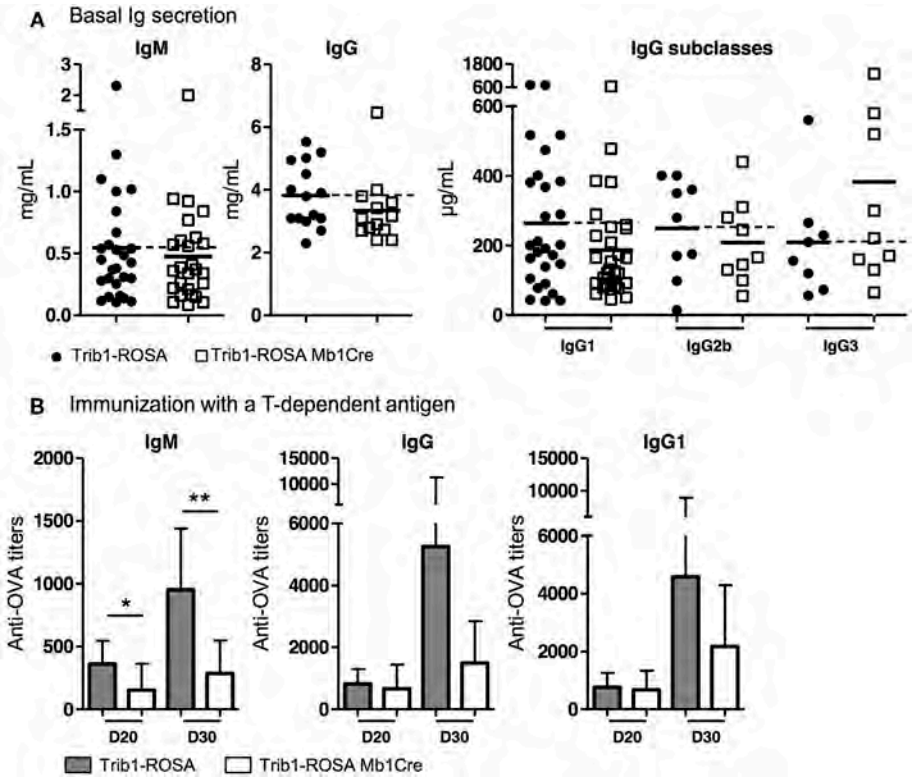

FIGURE 3 | Ig production in Trib1-ROSA Mb1Cre compared to Trib1-ROSA control mice, at basal level and after immunization with a T-dependent antigen. **(A)** Sera from 6-month-old Trib1-ROSA and Trib1-ROSA Mb1Cre mice were collected and total IgM and IgG, IgG1, IgG2b, and IgG3 concentrations were determined by ELISA. Each dot represents the result for one animal. **(B)** Trib1-ROSA mice ($n = 7$) and Trib1-ROSA Mb1Cre mice ($n = 6$) were immunized with ovalbumin (OVA) associated with alum hydroxide at days 0, 10, and 20. Serum was collected at days 20 and 30, then anti-OVA IgM, IgG, and IgG1 titers were measured by ELISA (*$p < 0.05$, **$p < 0.001$, Mann and Whitney test).

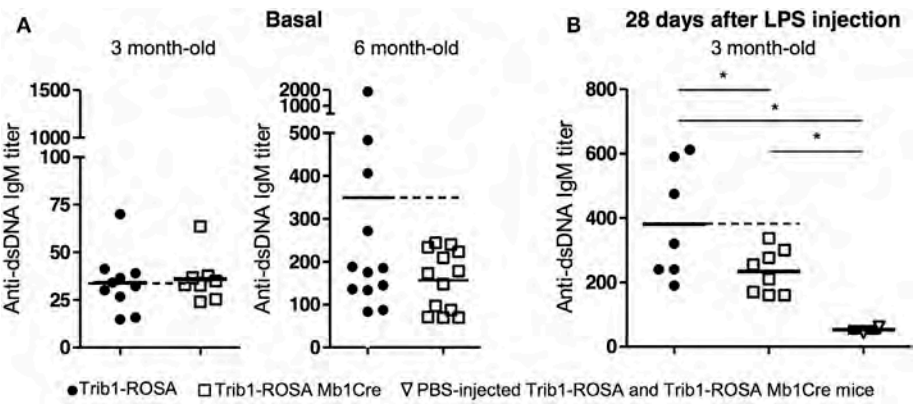

FIGURE 4 | *Trib1* overexpression in B cells induces a decrease of autoantibody production in a LPS-induced lupus mouse model. **(A)** Sera from 3-month-old and 6-month-old Trib1-ROSA and Trib1-ROSA Mb1Cre mice were collected and basal anti-dsDNA IgM autoantibody titers were determined by ELISA. **(B)** 3-month-old Trib1-ROSA and Trib1-ROSA Mb1Cre mice were injected with PBS or LPS (at days 0, 7, and 14) and bleeded every week until day 28. The titers of anti-dsDNA IgM at day 28 were measured by ELISA. Because results were not different between PBS-injected Trib1-ROSA and Trib1-ROSA Mb1Cre mice, these mice were pooled on the PBS-injected control group. Each dot represents the result for one animal (*$p < 0.05$, Mann and Whitney test).

could lead to a decrease of Ig secretion by *Trib1* overexpressing B cells. We stimulated total splenocytes with LPS and IL-4 (for IgG1 class-switching) and with LPS (for IgG3) and quantified the MFI for surface Ig expression and the percentages of $IgG1^+$ or $IgG3^+B220^+$ cells by flow cytometry. We did not detect any difference between *Trib1* overexpressing and control B cells (Figures

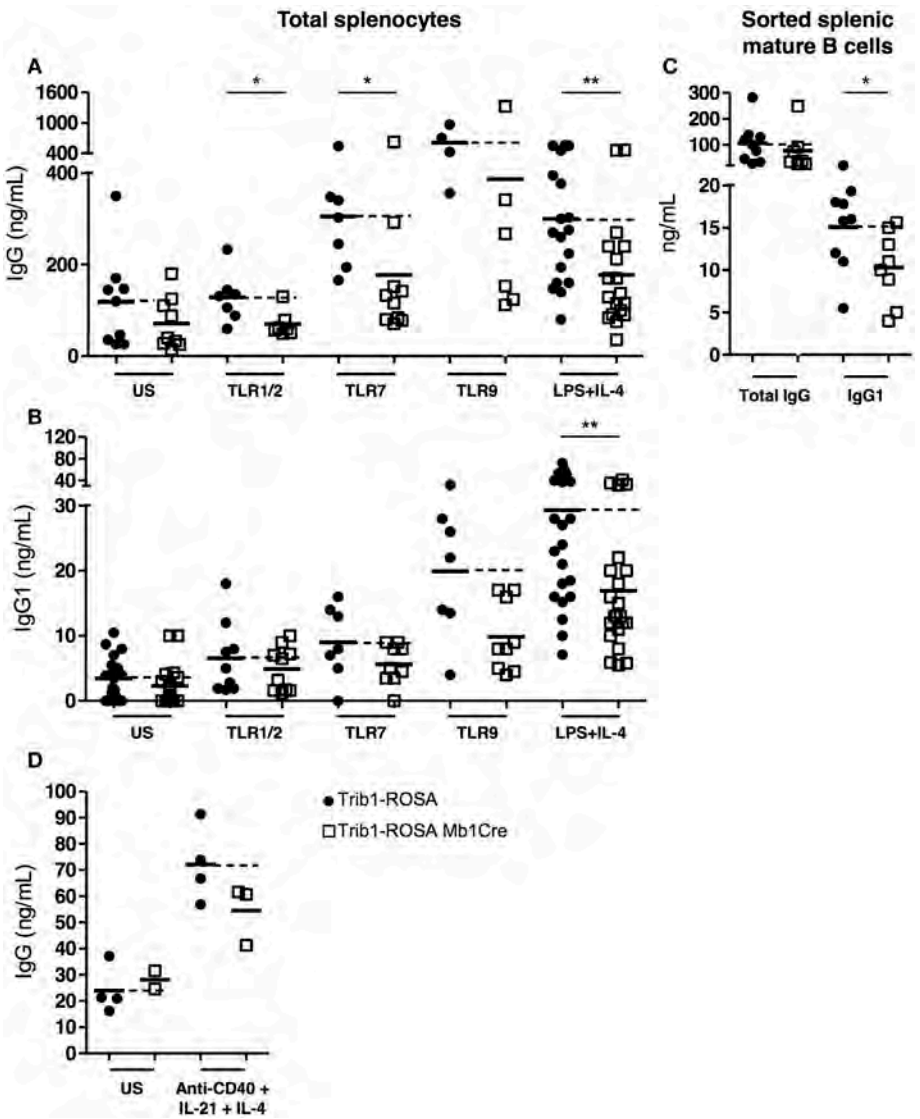

FIGURE 5 | *Trib1* overexpression in B cells negatively regulates Ig production *in vitro*. **(A,B)** Total splenocytes were collected from Trib1-ROSA and Trib1-ROSA Mb1Cre mice and stimulated with TLR ligands or a combination of LPS (TLR4 ligand) and IL-4 during 72 h *in vitro*. The concentration of total IgG **(A)** and IgG1 **(B)** in the supernatant was measured by ELISA. **(C)** Splenic mature B cells were purified from Trib1-ROSA and Trib1-ROSA Mb1Cre mice and stimulated *in vitro* with a combination of LPS and IL-4. The concentration of total IgG and IgG1 in the supernatant was measured by ELISA. **(D)** Total splenocytes from Trib1-ROSA and Trib1-ROSA Mb1Cre mice were stimulated with anti-CD40, IL-4, and IL-21 during 72 h *in vitro*. The concentration of total IgG in the supernatant was measured by ELISA. Each dot represents the result for one animal (US: unstimulated) (*$p < 0.05$, **$p < 0.001$, Mann and Whitney test).

S5A–C in Supplementary Material). The blockade of protein transport with GolgiStop™, containing monensin, in the culture of splenocytes with LPS and IL-4, showed a decrease of intracellular IgG1 positive B cells and of intracellular IgG1 MFI in B cells, in Trib1-ROSA Mb1Cre compared to control mice (**Figure 6**). In conclusion, *Trib1* overexpression in B cells negatively regulates the Ig secretory capacity.

Trib1 Interacts with CD72 and Its Overexpression Affects Erk Signaling

In order to find hypotheses on the mechanisms of B cell phenotype due to *Trib1* overexpression, and considering the role of Trib1 in MAPK signaling (13, 16), we analyzed Erk signaling in splenic sorted mature B cells from Trib1-ROSA-Mb1 and control mice, after stimulation with anti-IgM antibody, by Western Blot. Indeed, Erk-dependent pathway is one of the major MAPK pathways activated in B cells after BCR engagement. The phosphorylation of Erk was decreased in B cells from Trib1-ROSA-Mb1 mice, compared to control mice, and the difference was statistically significant at 2 min of stimulation (**Figure 7**). Proximal BCR signaling Syk pathway was not affected (data not shown). The defect in Erk pathway in *Trib1* overexpressing B cells probably does not explain the phenotype of these cells on its own. Therefore, we determined the partners of Trib1 in B cells in order to have

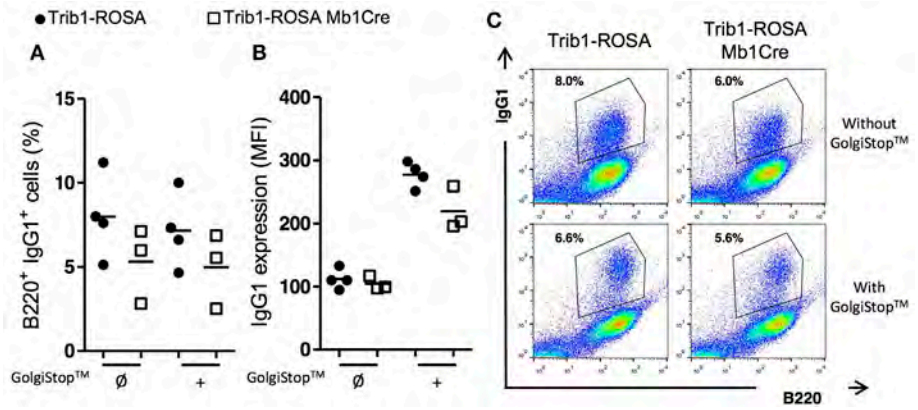

FIGURE 6 | Trib1 overexpression in B cells induces a reduction in the production of secreted form of IgG1. Total splenocytes from Trib1-ROSA and Trib1-ROSA Mb1Cre mice were stimulated with LPS/IL-4 for 72 h *in vitro* [with (+) or without (Ø) the addition of a protein transport inhibitor "GolgiStop™" for the last 8 h of culture], then stained for intracytoplasmic IgG1 after a step of membrane Ig blocking using an anti-murine IgG antibody, a step of fixation and permeabilization, and finally were analyzed by flow cytometry. **(A)** Percentage of B220+ B cells stained for intracellular IgG1. **(B)** MFI of intracellular IgG1 staining on B220+ B cells. **(C)** A representative sample of each condition is shown. Each dot represents the result for one animal.

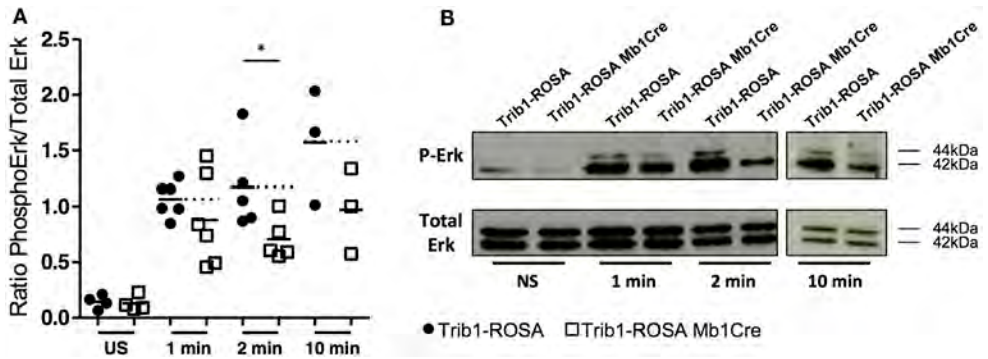

FIGURE 7 | *Trib1* overexpression in B cells induces a decrease of Erk phosphorylation after BCR engagement. Purified mature splenic B cells (CD43−) from Trib1-ROSA and Trib1-ROSA Mb1Cre mice were stimulated with anti-IgM (10 µg/mL) for the indicated time. Cell lysates were analyzed by western blot using anti-phospho Erk antibody (P-Erk). Total Erk was used as a loading control. The ratio of phospho-p42/Total p42 was calculated for each condition and represented in **(A)**. Each dot is representative of one mouse. Representative immunoblots of the indicated stimulation timepoints are presented in **(B)**. (US: unstimulated) (*$p < 0.05$, Mann and Whitney test).

a better insight of Trib1 function in these cells. We transduced a murine B cell line (CH12) with a retrovirus encoding a Flag-mTrib1 and IRES-GFP reporter (CH12-Trib1) or only a Flag-GFP as a control (CH12-GFP). To identify cytoplasmic partners of Trib1, we performed Flag IP followed by SDS-PAGE and mass spectrometry identification.

Mass spectrometry analysis of 5 independent experiments revealed a list of 236 proteins specifically enriched in CH12-TRIB1 cells. Proteins were ranked according to the number of experiments in which they were identified, and their confidence score. We kept those proteins identified in at least three out of the five experiments (**Table 2**). These proteins were classified into the following groups: proteins implicated in ubiquitination process, regulators of signal transduction, regulators of protein production, and secretion and chaperone proteins (**Table 2**). Among the previously identified and best characterized partner of Trib1, COP1 (13, 32), we found additional proteins, including notably CD72 (**Table 2**). CD72 is a very interesting candidate because it is a well-known negative B cell regulator. The association between Trib1, COP1, and CD72 was verified by co-IP and Western Blot (**Figure 8**). Several partners of Trib1 are linked to the regulation of signal transduction (for example Spre1, Stk40, and Ppm1b) (**Table 2**; Figure S6 in Supplementary Material). Interestingly, Spre1 has been described as a negative regulator of Erk pathway (33, 34). Further experiments will be needed to understand the potential implication of these partners in the negative regulatory function of Trib1 in B cells.

DISCUSSION

We identified an overexpression of *TRIB1* in human SLE B cells during clinically inactive disease by transcriptome analysis (10). This overexpression was confirmed in a second cohort of SLE quiescent patients, by real-time qRT-PCR. This led us to study the

TABLE 2 | Proteins implicated in protein ubiquitination, signal transduction, protein production secretion are found as Trib1 partners in CH12 B cell line.

Accession number	Full name	Function	*n*	Score
Protein ubiquitination				
COP1	E3 Ubiquitin-protein ligase COP1	Ubiquitin ligase	5	112
MALT1	Isoform 2 of mucosa-associated lymphoid tissue lymphoma translocation protein 1	Ubiquitin ligase—involved in BCL-10-induced NF-κB pathway activation	3	16
Signalization and signal transduction				
Stk40	Serine/threonine-protein kinase 40	Serine/threonine kinase, negative regulator of NF-κB pathway, and p53-induced gene transcription	5	45
St38L	Serine/threonine-protein kinase 38-like	Kinase—involved in signal transduction regulation	4	45
MARCS	Myristoylated alanine-rich C-kinase substrate	Protein kinase C substrate	4	19
LAP2	Isoform 2 of Protein LAP2	HER2 adaptor—Inhibitor of NOD2-dependant NF-κB pathway and pro-inflammatory cytokine secretion	3	71
PPM1B	Isoform Beta-2 of protein phosphatase 1B	Associated to IKKB dephosphorylation and inactivation (NF-κB pathway)	3	23
CALM	Calmoduline	Implicated in calcium flux	3	21
FLII	Protein flightless-1 homolog	Involved in estrogen-induced signaling	3	18
CD72	B-cell differentiation antigen CD72	Negative regulator of B cells	3	16
SPRE1	Sprouty-related, EVH1 domain-containing protein 1	MAPK pathway regulator	3	15
JAK3	Tyrosine-protein kinase JAK3	Kinase involved in cytokine production pathway, cell development, differentiation, and proliferation	3	10
TR19L	Tumor necrosis factor receptor superfamily member 19 L	Involved in NF-κB pathway activation	3	8
Protein production and secretion				
Eif4b	Eukaryotic translation initiation factor 4B	Required for mRNA binding to ribosome	3	39
EPN4	Clathrin interactor 1	Associated to clathrin vesicles transport from Trans-Golgi to endosomes	3	30
RS6	40S ribosomal protein S6	Ribosomal protein	3	15
RS18	40S ribosomal protein S18	Ribosomal protein	3	13
STX7	Syntaxin-7	Implicated in protein traffic from early endosomes to plasma membrane	3	13
RS19	*40S ribosomal protein S19*	Ribosomal protein	3	7
Chaperone protein				
HS90B	Heat shock protein HSP 90-beta	Chaperone protein	4	37
HS90A	Heat shock protein HSP 90-alpha	Chaperone protein	4	29
CDC37	Hsp90 co-chaperone Cdc37	Chaperone protein	3	14
Others				
RNF219	RING Finger protein 219	Zinc finger protein	5	122

Mass spectrometry analysis was performed on immunoprecipitation product (n_{total} = 5). In each subgroup defining their main function, the proteins are ranked according to the number of experiments in which they were found as Trib1 partners (column « n ») and their confidence score. (Accession numbers are coming from Swissprot Database).

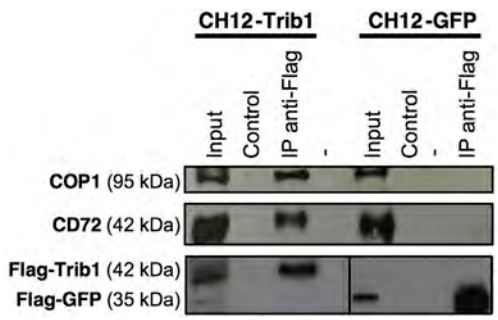

FIGURE 8 | Trib1 interacts with COP1 and CD72 in B cells. CH12 cells were transfected with pMX-PIE/Flag-tagged Trib1 or GFP. The samples were immunoprecipitated with an anti-Flag antibody to precipitate both Flag-tagged proteins from cell cytoplasmic lysates (IP anti-Flag) or with total mouse serum (Control). The result is representative of at least three independent experiments. Note: considering the differences in Flag protein expression in CH12-Trib1 and CH12-GFP cells, two different dilutions of anti-Flag antibody were used for the bottom left part (1:1,000) and the bottom right part (1:20,000). (Input, total protein lysate; -, empty well).

consequences of *Trib1* overexpression on B cell phenotype and on the development of SLE in a new murine transgenic model. For this purpose, we developed a B-cell-specific Trib1 KI conditional model, by an insertion of murine *Trib1* coding sequence, preceded by a floxed STOP cassette, into ROSA locus. We detected a six-times overexpression of *Trib1* in splenic mature B cells in this model, thanks to an efficient deletion of the STOP cassette by the Cre recombinase under the control of Mb1 promoter. Therefore, the level of *Trib1* overexpression in this model was close to the one detected in B cells from quiescent SLE patients in our transcriptome analysis or in the second cohort of patients. Because the overexpression of *Trib1* begins at very early stage in B cell lineage in BM, we checked if *Trib1* overexpression in our model could have an impact on B cell development. Our results showed that this was not the case. Altogether, these characteristics made this new mouse model suitable for this study.

Trib1-ROSA-Mb1 mice did not display any symptom of lupus disease: activation status of B cells is normal, and we did not detect any feature of renal disease. On the contrary, we showed that *Trib1* overexpression specifically in B cells had a negative

impact on autoantibody production, notably after induction of anti-dsDNA antibody production with injection of LPS, mimicking an infectious event. Moreover, *Trib1* overexpression in B cells negatively regulated Ig production, *in vivo* at basal level or after immunization notably with a T-dependent antigen, and also after *in vitro* stimulation. The most impacted Ig subtype was IgG1. However, the effect does not seem to be specific of IgG1. Because class switching into IgG subclasses is notably guided by specific stimuli (as LPS and IL-4 in murine B cells, for IgG1) (35), one could hypothesize that the degree of engagement of Trib1 in this negative regulation depends on the signaling pathways activated in B cells and, therefore, on the receptor engaged at the surface of the cells. Our results showed that the defect in Ig production was neither the consequence of an activation defect of B cells, nor an increase of mortality or a decrease of viability, nor a defect in class switching and plasma cell differentiation program. However, we detected a decrease of the percentage of intracellular IgG1 positive B cells and of intracellular IgG1 MFI in B cells in Trib1-ROSA Mb1Cre compared to control mice after stimulation with LPS and IL-4. In conclusion, it seems that the decrease in Ig levels was mostly the consequence of a defect in Ig secretory capacity. Interestingly, the analysis of *Trib1* expression in the different B cell subpopulations has been done in C57BL/6 mice (corresponding to background of our Trib1 transgenic model),[2] and in humans notably for B cells and plasma cells[3] and shows that *Trib1* is highly expressed in plasmablasts and in plasma cells, thereby arguing for an important function of Trib1 in Ig production.

We searched for Trib1 partners in murine B cells, in order to understand the immunosuppressive role of Trib1. After IP of Trib1 in CH12 B cell line and mass spectrometry identification, we selected a short list of Trib1 partners that could potentially be implicated in signal transduction and protein production and secretion. Among these partners, COP1 E3 ubiquitin ligase was already identified as a partner of Trib1 in different cell types (13, 19, 32), but never in B cells. It was notably shown in myeloid cells that COP1, via Trib1, targets C/EBPα for degradation by the proteasome (32). In mammals, C/EBPα is an important transcription factor controlling myeloid differentiation (13). According to this function, it is almost exclusively expressed in myeloid cells[4]; therefore, this could explain why we did not identify it as a partner of Trib1 in B cells. We confirmed the association of COP1 with Trib1 in CH12 cells by IP and Western-Blot analysis. It is known that COP1 binding to Trib1 is essential to target protein substrates for degradation (13). Further experiments should explore in details the role of COP1 in the degradation of proteins implicated in Ig synthesis and secretion in B cells. Moreover, we pointed out JAK3 as a Trib1 partner in B cells. JAK3 is a kinase associated with different cytokine receptors, notably IL-4 receptor, therefore giving one explanation for the phenotype of Trib1 overexpressing B cells after stimulation with LPS and IL-4.

The regulation of several signaling pathways was a frequent characteristic of the partners we identified for Trib1 in B cells (**Table 2**). Trib1 has been mostly described in the literature as a regulator of MAPK signaling, in different cell types. In HeLa cells, BM and myeloid leukemia cells, Trib1 was shown to interact, *via* its C-terminus domain, with MEK-1, and to be responsible for a hyperphosphorylation of Erk (13, 17). In other cell types, as muscular cells, Trib1 overexpression does not have any impact on Erk phosphorylation (36). Generally speaking, Tribbles proteins seem to act either as activators or inhibitors of MAPK pathways (17). We showed here that, in murine B cells, Trib1 overexpression seems to decrease Erk phosphorylation. This could be linked to the defect in Ig production and secretion observed in Trib1-ROSA-Mb1 mice. Among the partners, we identified for Trib1 in B cells, Spred1 is a suppressor of Ras signaling, notably in innate lymphoid cells (34). Therefore, Trib1, *via* the recruitment of Spred1, could negatively regulate Erk signaling in B cells. The immunosuppressive role of Trib1 in B cells probably also implicate other partners. We identified CD72 as another cofactor of Trib1 in B cells. CD72 is a negative regulator of B cells (37). It is a very interesting candidate because the production of immunoglobulin is increased in CD72-deficient mice (38), and a decreased expression of CD72 was associated with an increased surface IgG on B cells and to a severe disease in patients with lupus nephritis (39), arguing for a negative role of CD72 on immunoglobulin production. Moreover, the expression of the "b" isoform of CD72 which is the one expressed in C57BL/6 mice (and, therefore, in the mice analyzed in our study) and in CH12 cells (40), in MRL.CD72^b/lpr congenic mice, is protective against the development of the lupus disease (41, 42). In addition, CD72 downregulates BCR signaling, and notably NF-κB and Erk (43–45). Our preliminary experiments showed that NF-κB signaling was not affected in *Trib1* overexpressing B cells after stimulation of the BCR pathway (with anti-IgM antibody). However, it could be interesting to see if it is also the case when CD72 and BCR pathways are synergistically activated.

In conclusion, we described a new role of Trib1 as a negative regulator of B cells. Despite the polygenic nature of lupus disease in humans, one feature of B cells from quiescent SLE patients, i.e., Trib1 overexpression, in mice, is sufficient on its own to have an immunosuppressive effect on B cells. It would be interesting to see the effect of B cell-specific *Trib1* overexpression on the development of the disease in an SLE murine model. Moreover, there is no molecular explanation for the phenotype of SLE patients during silent phases of the disease, or for the maintenance of the clinically silent phases (46). As such, the overexpression of TRIB1 in B cells could constitute one of these protective molecular pathways. It would be interesting in the future to analyze the overexpression of *TRIB1* in B cells in a prospective way, in order to study the correlation between *TRIB1* expression and the quiescent or active nature of the disease in the same patient.

ETHICS STATEMENT

This study was carried out in accordance with the recommendations of the ethics committee of the "Hôpitaux Universitaires de Strasbourg" with written informed consent from all subjects. All subjects gave written informed consent in accordance with the Declaration of

[2] https://www.immgen.org.
[3] http://amazonia.transcriptome.eu.
[4] http://immgen.org.

Helsinki. The protocol was approved by the ethics committee of the "Hôpitaux de Strasbourg" (Strasbourg, France). This study was carried out in accordance with the recommendations of "Direction départementale des services vétérinaires" (Strasbourg, France). Protocols were approved by the ethics committee ("Comité d'éthique en matière d'Experimentation Animale de Strasbourg," CREMEAS, approval number AL/02/15/09/11 and AL/31/38/02/13).

AUTHOR CONTRIBUTIONS

LS, VD, JR-L, TM, A-SK, BRSM, and PS-S designed the research. LS, VD, JR-L, AS, VH, IR, VG, and DB performed the research. LS, VD, JR-L, VH, VG, TM, A-SK, BRSM, and PS-S. analyzed the data. LS, VD, IR, A-SK, BRSM, and PS-S wrote the paper.

ACKNOWLEDGMENTS

We thank Pr M. Reth for providing us the Mb1-Cre transgenic mice. We thank M. Duval, D. Lamon, D. Bock, I. Ghazouani, and K. Sablon for excellent animal care. We thank F. Gros for scientific discussions.

FUNDING

This work was supported by grants from Strasbourg University (UdS), Centre National de la Recherche Scientifique (CNRS), Arthritis Courtin foundation, by the Agence Nationale de la Recherche (ANR-13-JSV3-0007-01, LEDsGO; and ANR-11-EQPX-022), and by EU-funded (ERDF) project INTERREG V "RARENET." LS, JR-L, and DB were supported by the Ministère de la Recherche et de la Technologie. JR-L was supported by Arthritis Courtin foundation. VD was supported by Initiative of Excellence (IdEx), Strasbourg University, France.

SUPPLEMENTARY MATERIAL

The Supplementary Material for this article can be found online at http://www.frontiersin.org/articles/10.3389/fimmu.2018.00373/full#supplementary-material.

TABLE S1 | T cell subpopulations from Trib1-ROSA and Trib1-ROSA Mb1Cre were analyzed by flow cytometry.

TABLE S2 | Proteomics raw data.

REFERENCES

1. Tsokos GC. Systemic lupus erythematosus. *N Engl J Med* (2011) 365(22): 2110–21. doi:10.1056/NEJMra1100359
2. Moulton VR, Suarez-Fueyo A, Meidan E, Li H, Mizui M, Tsokos GC. Pathogenesis of human systemic lupus erythematosus: a cellular perspective. *Trends Mol Med* (2017) 23(7):615–35. doi:10.1016/j.molmed.2017.05.006
3. Mandik-Nayak L, Ridge N, Fields M, Park AY, Erikson J. Role of B cells in systemic lupus erythematosus and rheumatoid arthritis. *Curr Opin Immunol* (2008) 20(6):639–45. doi:10.1016/j.coi.2008.08.003
4. Nashi E, Wang Y, Diamond B. The role of B cells in lupus pathogenesis. *Int J Biochem Cell Biol* (2010) 42(4):543–50. doi:10.1016/j.biocel.2009.10.011
5. Arbuckle MR, McClain MT, Rubertone MV, Scofield RH, Dennis GJ, James JA, et al. Development of autoantibodies before the clinical onset of systemic lupus erythematosus. *N Engl J Med* (2003) 349(16):1526–33. doi:10.1056/NEJMoa021933
6. Steinberg EB, Santoro TJ, Chused TM, Smathers PA, Steinberg AD. Studies of congenic MRL-Ipr/Ipr.xid mice. *J Immunol* (1983) 131(6):2789–95.
7. Chan OT, Hannum LG, Haberman AM, Madaio MP, Shlomchik MJ. A novel mouse with B cells but lacking serum antibody reveals an antibody-independent role for B cells in murine lupus. *J Exp Med* (1999) 189(10): 1639–48. doi:10.1084/jem.189.10.1639
8. Prud'homme GJ, Balderas RS, Dixon FJ, Theofilopoulos AN. B cell dependence on and response to accessory signals in murine lupus strains. *J Exp Med* (1983) 157(6):1815–27. doi:10.1084/jem.157.6.1815
9. Reininger L, Winkler TH, Kalberer CP, Jourdan M, Melchers F, Rolink AG. Intrinsic B cell defects in NZB and NZW mice contribute to systemic lupus erythematosus in (NZB x NZW)F1 mice. *J Exp Med* (1996) 184(3):853–61. doi:10.1084/jem.184.3.853
10. Garaud JC, Schickel JN, Blaison G, Knapp AM, Dembele D, Ruer-Laventie J, et al. B cell signature during inactive systemic lupus is heterogeneous: toward a biological dissection of lupus. *PLoS One* (2011) 6(8):e23900. doi:10.1371/journal.pone.0023900
11. Schickel JN, Pasquali JL, Soley A, Knapp AM, Decossas M, Kern A, et al. Carabin deficiency in B cells increases BCR-TLR9 costimulation-induced autoimmunity. *EMBO Mol Med* (2012) 4(12):1261–75. doi:10.1002/emmm.201201595
12. Ruer-Laventie J, Simoni L, Schickel JN, Soley A, Duval M, Knapp AM, et al. Overexpression of Fkbp11, a feature of lupus B cells, leads to B cell tolerance breakdown and initiates plasma cell differentiation. *Immun Inflamm Dis* (2015) 3(3):265–79. doi:10.1002/iid3.65
13. Yokoyama T, Nakamura T. Tribbles in disease: signaling pathways important for cellular function and neoplastic transformation. *Cancer Sci* (2011) 102(6):1115–22. doi:10.1111/j.1349-7006.2011.01914.x
14. Sung HY, Francis SE, Crossman DC, Kiss-Toth E. Regulation of expression and signalling modulator function of mammalian tribbles is cell-type specific. *Immunol Lett* (2006) 104(1–2):171–7. doi:10.1016/j.imlet.2005.11.010
15. Dedhia PH, Keeshan K, Uljon S, Xu L, Vega ME, Shestova O, et al. Differential ability of Tribbles family members to promote degradation of C/EBPalpha and induce acute myelogenous leukemia. *Blood* (2010) 116(8):1321–8. doi:10.1182/blood-2009-07-229450
16. Eyers PA, Keeshan K, Kannan N. Tribbles in the 21st century: the evolving roles of tribbles pseudokinases in biology and disease. *Trends Cell Biol* (2017) 27(4):284–98. doi:10.1016/j.tcb.2016.11.002
17. Kiss-Toth E, Bagstaff SM, Sung HY, Jozsa V, Dempsey C, Caunt JC, et al. Human tribbles, a protein family controlling mitogen-activated protein kinase cascades. *J Biol Chem* (2004) 279(41):42703–8. doi:10.1074/jbc.M407732200
18. Yokoyama T, Kanno Y, Yamazaki Y, Takahara T, Miyata S, Nakamura T. Trib1 links the MEK1/ERK pathway in myeloid leukemogenesis. *Blood* (2010) 116(15):2768–75. doi:10.1182/blood-2009-10-246264
19. Satoh T, Kidoya H, Naito H, Yamamoto M, Takemura N, Nakagawa K, et al. Critical role of Trib1 in differentiation of tissue-resident M2-like macrophages. *Nature* (2013) 495(7442):524–8. doi:10.1038/nature11930
20. Dugast E, Kiss-Toth E, Docherty L, Danger R, Chesneau M, Pichard V, et al. Identification of tribbles-1 as a novel binding partner of Foxp3 in regulatory T cells. *J Biol Chem* (2013) 288(14):10051–60. doi:10.1074/jbc.M112.448654
21. Hochberg MC. Updating the American College of Rheumatology revised criteria for the classification of systemic lupus erythematosus. *Arthritis Rheum* (1997) 40(9):1725. doi:10.1002/art.1780400928
22. Xiao C, Calado DP, Galler G, Thai TH, Patterson HC, Wang J, et al. MiR-150 controls B cell differentiation by targeting the transcription factor c-Myb. *Cell* (2007) 131(1):146–59. doi:10.1016/j.cell.2007.07.021
23. Xiao C, Srinivasan L, Calado DP, Patterson HC, Zhang B, Wang J, et al. Lymphoproliferative disease and autoimmunity in mice with increased miR-17-92 expression in lymphocytes. *Nat Immunol* (2008) 9(4):405–14. doi:10.1038/ni1575
24. Hobeika E, Thiemann S, Storch B, Jumaa H, Nielsen PJ, Pelanda R, et al. Testing gene function early in the B cell lineage in mb1-cre mice. *Proc Natl Acad Sci U S A* (2006) 103(37):13789–94. doi:10.1073/pnas.0605944103
25. Nakamura M, Kondo S, Sugai M, Nazarea M, Imamura S, Honjo T. High frequency class switching of an IgM+ B lymphoma clone CH12F3 to IgA+ cells. *Int Immunol* (1996) 8(2):193–201. doi:10.1093/intimm/8.2.193

26. Barreto V, Reina-San-Martin B, Ramiro AR, McBride KM, Nussenzweig MC. C-terminal deletion of AID uncouples class switch recombination from somatic hypermutation and gene conversion. *Mol Cell* (2003) 12(2):501–8. doi:10.1016/S1097-2765(03)00309-5
27. Jeevan-Raj BP, Robert I, Heyer V, Page A, Wang JH, Cammas F, et al. Epigenetic tethering of AID to the donor switch region during immunoglobulin class switch recombination. *J Exp Med* (2011) 208(8):1649–60. doi:10.1084/jem.20110118
28. Hardy RR, Hayakawa K. B cell development pathways. *Annu Rev Immunol* (2001) 19:595–621. doi:10.1146/annurev.immunol.19.1.595
29. Perry D, Sang A, Yin Y, Zheng YY, Morel L. Murine models of systemic lupus erythematosus. *J Biomed Biotechnol* (2011) 2011:271694. doi:10.1155/2011/271694
30. Fournie GJ, Lambert PH, Meischer PA. Release of DNA in circulating blood and induction of anti-DNA antibodies after injection of bacterial lipopolysaccharides. *J Exp Med* (1974) 140(5):1189–206. doi:10.1084/jem.140.5.1189
31. Ma K, Li J, Fang Y, Lu L. Roles of B cell-intrinsic TLR signals in systemic lupus erythematosus. *Int J Mol Sci* (2015) 16(6):13084–105. doi:10.3390/ijms160613084
32. Yoshida A, Kato JY, Nakamae I, Yoneda-Kato N. COP1 targets C/EBPalpha for degradation and induces acute myeloid leukemia via Trib1. *Blood* (2013) 122(10):1750–60. doi:10.1182/blood-2012-12-476101
33. Wakioka T, Sasaki A, Kato R, Shouda T, Matsumoto A, Miyoshi K, et al. Spred is a sprouty-related suppressor of Ras signalling. *Nature* (2001) 412(6847):647–51. doi:10.1038/35088082
34. Suzuki M, Morita R, Hirata Y, Shichita T, Yoshimura A. Spred1, a suppressor of the Ras-ERK pathway, negatively regulates expansion and function of group 2 innate lymphoid cells. *J Immunol* (2015) 195(3):1273–81. doi:10.4049/jimmunol.1500531
35. Pan-Hammarstrom Q, Zhao Y, Hammarstrom L. Class switch recombination: a comparison between mouse and human. *Adv Immunol* (2007) 93:1–61. doi:10.1016/S0065-2776(06)93001-6
36. Sung HY, Guan H, Czibula A, King AR, Eder K, Heath E, et al. Human tribbles-1 controls proliferation and chemotaxis of smooth muscle cells via MAPK signaling pathways. *J Biol Chem* (2007) 282(25):18379–87. doi:10.1074/jbc.M610792200
37. Parnes JR, Pan C. CD72, a negative regulator of B-cell responsiveness. *Immunol Rev* (2000) 176:75–85. doi:10.1034/j.1600-065X.2000.00608.x
38. Pan C, Baumgarth N, Parnes JR. CD72-deficient mice reveal nonredundant roles of CD72 in B cell development and activation. *Immunity* (1999) 11(4):495–506. doi:10.1016/S1074-7613(00)80124-7
39. Nakano S, Morimoto S, Suzuki J, Mitsuo A, Nakiri Y, Katagiri A, et al. Down-regulation of CD72 and increased surface IgG on B cells in patients with lupus nephritis. *Autoimmunity* (2007) 40(1):9–15. doi:10.1080/08916930601118890
40. Robinson WH, Ying H, Miceli MC, Parnes JR. Extensive polymorphism in the extracellular domain of the mouse B cell differentiation antigen Lyb-2/CD72. *J Immunol* (1992) 149(3):880–6.
41. Xu M, Hou R, Sato-Hayashizaki A, Man R, Zhu C, Wakabayashi C, et al. Cd72(c) is a modifier gene that regulates Fas(lpr)-induced autoimmune disease. *J Immunol* (2013) 190(11):5436–45. doi:10.4049/jimmunol.1203576
42. Oishi H, Tsubaki T, Miyazaki T, Ono M, Nose M, Takahashi S. A bacterial artificial chromosome transgene with polymorphic Cd72 inhibits the development of glomerulonephritis and vasculitis in MRL-Faslpr lupus mice. *J Immunol* (2013) 190(5):2129–37. doi:10.4049/jimmunol.1202196
43. Li DH, Tung JW, Tarner IH, Snow AL, Yukinari T, Ngernmaneepothong R, et al. CD72 down-modulates BCR-induced signal transduction and diminishes survival in primary mature B lymphocytes. *J Immunol* (2006) 176(9):5321–8. doi:10.4049/jimmunol.176.9.5321
44. Li DH, Winslow MM, Cao TM, Chen AH, Davis CR, Mellins ED, et al. Modulation of peripheral B cell tolerance by CD72 in a murine model. *Arthritis Rheum* (2008) 58(10):3192–204. doi:10.1002/art.23812
45. Adachi T, Wakabayashi C, Nakayama T, Yakura H, Tsubata T. CD72 negatively regulates signaling through the antigen receptor of B cells. *J Immunol* (2000) 164(3):1223–9. doi:10.4049/jimmunol.164.3.1223
46. Liu CC, Kao AH, Manzi S, Ahearn JM. Biomarkers in systemic lupus erythematosus: challenges and prospects for the future. *Ther Adv Musculoskelet Dis* (2013) 5(4):210–33. doi:10.1177/1759720X13485503

Conflict of Interest Statement: The authors declare that the research was conducted in the absence of any commercial or financial relationships that could be construed as a potential conflict of interest.

frontiers in Immunology

ORIGINAL RESEARCH
published: 13 March 2018
doi: 10.3389/fimmu.2018.00479

Mucosal Involvement in Bullous Pemphigoid Is Mostly Associated with Disease Severity and to Absence of Anti-BP230 Autoantibody

Ariane Clapé[1,2,3], Céline Muller[1], Grégory Gatouillat[1,3], Sébastien Le Jan[1], Coralie Barbe[4], Bach-Nga Pham[1,3†], Frank Antonicelli[1,5†] and Philippe Bernard[1,2†]*

[1] Laboratory of Dermatology, Faculty of Medicine, EA7319, University of Reims Champagne-Ardenne, Reims, France, [2] Department of Dermatology, Reims University Hospital, University of Reims Champagne-Ardenne, Reims, France, [3] Laboratory of Immunology, Reims University Hospital, University of Reims Champagne-Ardenne, Reims, France, [4] Clinical Research Unit, Reims University Hospital, Reims, France, [5] Department of Biological Sciences, Immunology, UFR Odontology, University of Reims Champagne-Ardenne, Reims, France

OPEN ACCESS

Edited by:
Ralf J. Ludwig, University of Lübeck, Germany

Reviewed by:
Hiroshi Koga, Kurume University School of Medicine, Japan
Takashi Hashimoto, Osaka City University Graduate School of Medicine, Japan

***Correspondence:**
Frank Antonicelli
frank.antonicelli@reims-reims.fr

†These authors have contributed equally to this work.

Specialty section:
This article was submitted to Immunological Tolerance and Regulation, a section of the journal Frontiers in Immunology

Received: *12 January 2018*
Accepted: *22 February 2018*
Published: *13 March 2018*

Citation:
Clapé A, Muller C, Gatouillat G, Le Jan S, Barbe C, Pham B-N, Antonicelli F and Bernard P (2018) Mucosal Involvement in Bullous Pemphigoid Is Mostly Associated with Disease Severity and to Absence of Anti-BP230 Autoantibody. Front. Immunol. 9:479. doi: 10.3389/fimmu.2018.00479

Bullous pemphigoid (BP) is the most common autoimmune bullous disease and typically affects the elderly. Binding of specific autoantibodies to BP180/230 hemidesmosomal components induces an inflammatory response leading to skin blister formation. Unusual manifestations of BP include additional mucous membrane involvement, without pathophysiological knowledge associated to the formation of these lesions. We here performed a prospective study on series of consecutive BP patients with (n = 77) and without (n = 18) mucosal involvements at baseline to further investigate why some BP patients display mucosal lesion and other not. Analysis of disease activity showed that BP patients with mucosal involvement displayed a higher total BP Disease Area Index (BPDAI) score (P = 0.008), but also higher skin and blister/erosion BPDAI scores (P = 0.02 and P = 0.001, respectively). By contrast, the erythema/urticaria BPDAI score was identical between the two groups of patients. The erythema/urticaria BPDAI score, but not the blister/erosion BPDAI score, was correlated with the serum concentration of anti-BP180 NC16A autoantibodies in patients with mucosal involvement. In multivariate analysis, the absence of anti-BP230 autoantibody was the only factor independently associated with mucosal involvement (OR 7.8; 95% CI, 3.1–19.6) (P < 0.0001). Analysis of the distribution of BP patients according to BPDAI scores revealed a shift toward higher blister/erosion BPDAI scores for BP patients with mucosal involvement. This study indicates that mucosal lesions are clinically mainly related to disease severity and immunologically to the absence of anti-BP230 antibodies.

Keywords: bullous pemphigoid, BP Disease Area Index, mucosal involvement, anti-BP230, autoantibodies

INTRODUCTION

Bullous pemphigoid (BP) is an autoimmune skin disease characterized by the binding of autoantibodies directed against two hemidesmosal proteins of the dermal–epidermal junction, namely BP180 and BP230 (1–6). The disease typically presents in the elderly with a generalized pruritic blistering eruption (7–9), which results from an inflammatory associated disruption of the dermal–epidermal junction induced by the binding of autoantibodies onto their targets. Clinical criteria for typical skin eruption of BP include the absence of associated external mucous membrane (almost exclusively oral) involvement, the absence of skin atrophy, and the absence

of head and neck predominant involvement (10). However, clinical presentation of BP can be polymorphic, notably during the early, pre-bullous stage of the disease or in atypical variants, in which full-blown bullous lesions may be absent (11, 12). Beside, blisters and erosions arising on mucosal membranes, mainly within the oral cavity, may be observed in up to 20% of BP patients (6, 11–13), without identified pathophysiologic mechanism(s) associated with their development.

Despite the interest of the research community in always better understanding BP pathophysiology, no study demonstrated whether mucosal involvement occurred as a consequence of BP extent and severity or whether skin and mucosal lesions occurred concomitantly. Recently a clinical activity score named BP Disease Area Index (BPDAI) was proposed as an international consensus to evaluate both the disease extent and the location and type of skin lesions (9). The BPDAI also has the advantage to measure separate scores for skin and mucous membrane activity. Besides, the skin BPDAI score also evaluates separately the ultimate skin lesions, i.e., blisters/erosions, and the early, pre-bullous inflammatory skin lesions, i.e., urticaria/erythema, and their extent as well as the residual damages. Thus, such specific clinical score may be useful to better characterize those BP patients with associated mucosal involvement and improve their monitoring.

Immunological and biological investigations in BP brought strong evidence that autoantibodies to BP180 are pathogenic and play a key role in subepidermal blister formation (14–20). Biopsy specimens from BP lesional skin exhibit dense inflammatory infiltration of eosinophils, basophils, neutrophils, lymphocytes, and mast cells in the dermis (1, 11, 13, 21, 22). Inflammatory cells infiltration and activation release cytokines and proteases that may create an auto-amplification loop reported to induce dermal–epidermal separation (23–27). However, variations in this pathophysiological process are still missing to explain why some BP patients will exhibit mucosal involvement and other not. In this matter, a more precise clinical characterization of BP patients with mucosal involvement may help to point out variations in the autoimmune and inflammatory responses in this particular BP subset.

We here performed a prospective study on series of consecutive BP patients with and without mucosal involvement. To further understand why some BP patients display mucosal blisters or erosions and other not, we compared the total BPDAI and its different components with other clinical and immunological parameters of disease activity at baseline, including the number of daily new blisters and the anti-BP180 and anti-BP230 autoantibody titers.

MATERIALS AND METHODS

Study Patients and Design

A prospective, single-center study was conducted in the Dermatology Department of the Reims University Hospital (French Referral Center for Autoimmune Bullous Diseases) between September 2013 and July 2017. The investigation was conducted under the approval of the Ethic Committee of the University Hospital of Reims (CNIL authorization DR-2013-320), and all of the subjects gave their informed and written consent before participating in the study in accordance with the Helsinki Declaration. Consecutive patients with newly diagnosed BP were included in this prospective study. Patients were diagnosed as having BP using the following criteria: clinical features typical of BP with the presence of at least three of four well-established criteria according to Vaillant et al. (10); subepidermal blister on skin biopsy, and deposits of IgG and/or C3 in a linear pattern along the epidermal basement membrane zone by direct immunofluorescence. Non-inclusion criteria were administration of a specific BP treatment for more than 2 days, pregnancy and expected survival after BP diagnosis shorter than 3 months.

Clinical Data Collection

Clinical data recorded at baseline were gender, age, number of daily new blisters (determined over a 3-day period), and BPDAI. BPDAI was calculated according to the International Pemphigoid Committee recommendations (9). At baseline, BPDAI was recorded. The total BPDAI computes two scores: total BPDAI activity and total BPDAI damage. The total BPDAI activity score is the arithmetic sum of the three subcomponents—cutaneous blisters/erosions, cutaneous urticaria/erythema, and mucosal blisters/erosions. The total BPDAI damage score is the arithmetic sum of the items rated regionally for damage caused by more permanent features such as post-inflammatory hyperpigmentation, scarring, and other. BPDAI also takes into account lesion number and size thresholds and skin lesions are rated based on the regions affected. Scores can range from 0 to 360 for BPDAI total activity (maximum 240 for total skin activity and 120 for mucosal activity) and 0 to 12 for BPDAI damage, with higher scores indicating greater disease activity or damage. On the basis of previous literature (28), severe BP at baseline was defined as a total BPDAI score $\geq$56. BP patients who did not fulfill these criteria were classified as having moderate BP.

Anti-BP180 and Anti-BP230 Autoantibody Detection

Anti-BP180 and anti-BP230 autoantibodies were detected in serum and in blister fluids (BFs) using specific commercially available enzyme-linked immunosorbent assays (ELISAs) following the manufacturer's instructions (MBL, Nagoya, Japan). Anti-BP180 and anti-BP230 antibodies' detection was routinely performed on classically used dilution with no further dilution when titers were high. ELISA values were expressed as units per milliliters of serum (U/mL), and the 9 U/mL cut-off value recommended by the manufacturer was used in both anti-BP180 and anti-BP230 ELISAs (29–32).

Statistical Analysis

Quantitative variables were described as mean $\pm$ SD and qualitative data as number and percentage. Kolmogorov–Smirnov test was performed to compare BP population distribution. The Kolmogorov–Smirnov test works by comparing the cumulative distribution of the two data sets and computes a P value that depends on the largest discrepancy between distributions. In contrast to Mann–Whitney test that is mostly sensitive

to changes in the median, the Kolmogorov–Smirnov test is sensitive to changes in the shape, spread, or median of the two distributions. Chi² tests were used for comparison between qualitative variables and nonparametric, Mann–Whitney tests for comparison between quantitative values. Owing to absence of normal distribution, comparisons between groups were performed using Spearman's correlation coefficient to explore the relationship between continuous variables (BPDAI with immunological parameters, immunological parameters in serum with those in BF). A P value <0.05 was considered statistically significant. Multivariate analyses were then performed using stepwise logistic regressions, with enter and removal limits set at 0.20 and factors significant at $P = 0.20$ included.

RESULTS

Patient Characteristics

A total of 97 patients with newly diagnosed BP were included in this study, 79 had typical clinical manifestations of BP and 18 presented with mucosal lesions in additional to skin blisters or erosions. In those BP patients with mucosal involvement, indirect immunofluorescence on salt-split skin was either positive with labeling of the epidermal side of the cleavage or negative. Using the same technique, two patients with positive immunolabeling on the dermal side only were subsequently excluded from the group with typical clinical BP presentation.

The clinical characteristics of those 77 patients with typical BP features (81%, 51 women and 26 men) and of the 18 BP patients with mucosal involvement (19%, 11 women and 7 men) are shown in **Table 1**. In the 18 BP patients with unconventional mucosal involvement, oral mucosal lesions were observed in 17 cases and anogenital mucosae lesions in 1 case. Among the 17 patients with oral lesions, 1 patient also displayed anogenital mucosae involvement, and another 1 had concomitant pharyngeal mucosa lesions. In those 18 BP patients, neither conjunctival nor nasal mucosa involvement was observed. Occurrence of mucosal lesions was correlated neither with the gender ($P = 0.78$) nor with the age ($P = 0.24$) of patients.

Skin Disease Activity and Mucosal Involvement

At the time of diagnosis, the number of patients with at least 10 daily new blisters was significantly higher in BP patients with mucosal involvement ($P = 0.02$) compared with patients with typical BP (**Table 1**), whereas the number of daily new blisters only tended to be higher in BP patients with mucosal involvement ($P = 0.07$).

Total BPDAI mean score was 39.6 ± 27 at baseline in the whole BP population (**Table 1**). Based on a cut-off BPDAI value of 56 (see Materials and Methods), the percentage of BP patients with a severe disease was significantly lower in BP patients without mucosal involvement (20.8%) as compared to those with mucosal involvement (44.4%) (**Table 1**; $P = 0.04$). Deeper analysis showed that compared with BP patients with a typical disease, BP patients with mucosal involvement displayed a higher total BPDAI score (**Table 1**; $P = 0.008$), but also higher skin BPDAI and blister/erosion BPDAI scores (**Table 1**; $P = 0.021$ and $P = 0.001$, respectively). By contrast, the erythema/urticaria BPDAI score was not different between those two groups of patients (**Table 1**; $P = 0.91$).

Analysis of the whole BP population distribution according to BPDAI score revealed that most patients had a mild to moderate disease and that the higher the BPDAI was, the lower the number of BP patients was (**Figure 1A**). Such a distribution was also observed for BP patients without mucosal involvement (**Figure 1B**), but was significantly different in BP patients with mucosal involvement ($D = 0.6154$; $P = 0.008$). Indeed, BP patients with mucosal involvement were evenly distributed from moderate to severe disease (**Figure 1C**). To further understand these discrepancies, the same analysis was then performed using the separate skin activity. The relative distribution according to the erythema/urticaria BPDAI score of BP patients without mucosal involvement superposed with the one of BP patients with mucosal involvement ($D = 0.1667$; $P = 0.991$) (**Figure 2A**). Analysis of the distribution according to the blisters/erosions BPDAI revealed a high percentage of patients with mucosal involvement when the BPDAI values

TABLE 1 | Clinical characteristics of patients with BP according to mucosal involvement.

	All BP patients	Patients without mucosal involvement	Patients with mucosal involvement	*P* value
Number of patients (*n*)	95	77	18	NA
Sex ratio (F/M)	1.88	1.96	1.57	0.68
Age, mean ± SD	81.7 ± 9.3	82.4 ± 8.9	78.7 ± 10.6	0.18
Patients with at least 10 daily new blisters,[a] *n* (%)	45 (47.4)	32 (41.6)	13 (72.2)	0.02
Number of daily new blisters,[a] mean ± SD	19.3 ± 29.8	17.6 ± 27.1	26.5 ± 39.4	0.07
BPDAI global score, mean ± SD	39.6 ± 27	35.8 ± 25.1	56.1 ± 29.2	0.008
Activity of total skin involvement, mean ± SD	38.1 ± 26	35.1 ± 25	51.0 ± 26.8	0.021
Blisters/erosions, mean ± SD	24.9 ± 17.6	22.1 ± 16.4	36.9 ± 17.6	0.001
Erythema/urticaria, mean ± SD	13.2 ± 13.6	13 ± 13.3	14.1 ± 15.1	0.91
Activity of mucosal involvement, mean ± SD	0.8 ± 2.4	0	4.0 ± 4.2	NA
Damage, mean ± SD	0.8 ± 2	0.7 ± 1.8	1.1 ± 2.6	0.78
Patients with severe disease according BPDAI,[b] *n* (%)	24 (25)	16 (20.8)	8 (44.4)	0.04

Subsets of BP patients with or without mucosal involvement were compared and P-value was obtained using Chi² tests for comparison between qualitative variables and nonparametric, Mann–Whitney tests for comparison between quantitative values.

[a]*Determined over a 3-day period.*

[b]*Determined by BPDAI global score ≥56.*

NA, not applicable; BP, bullous pemphigoid; BPDAI, BP Disease Area Index.

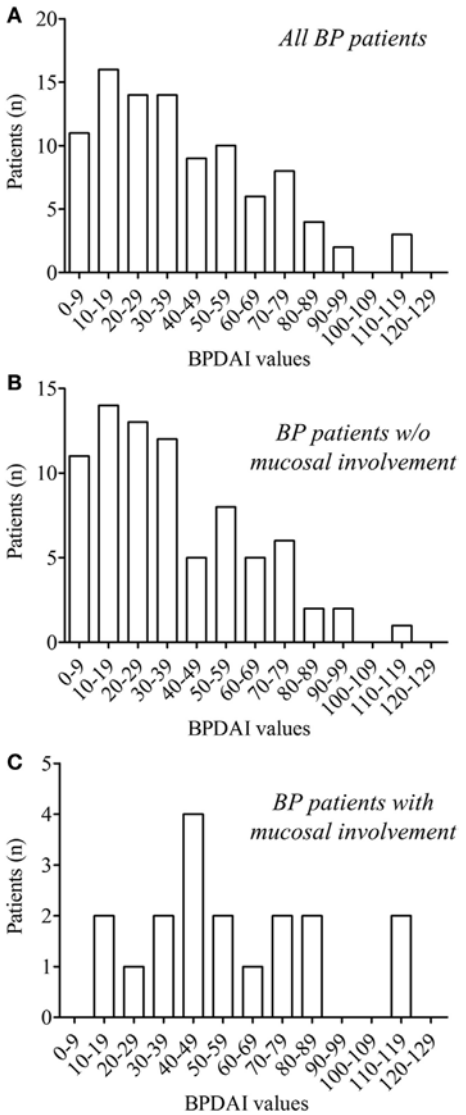

FIGURE 1 | Distribution of the whole bullous pemphigoid (BP) patients ($n = 95$) **(A)** and of BP patients without ($n = 77$) **(B)** and with ($n = 18$) **(C)** mucosal involvement according to total BP Disease Area Index (BPDAI) values at the time of diagnosis. In the whole BP group and in the subgroup of BP without mucosal involvement, the number of BP included decrease when the values of the BPDAI increased, whereas BP patients with mucosal involvement were evenly distributed. Comparison of the cumulative distribution by the Kolmogorov–Smirnov test showed significant difference between BP patients with **(C)** and without **(B)** mucosal involvement ($D = 0.6154$; $P = 0.008$).

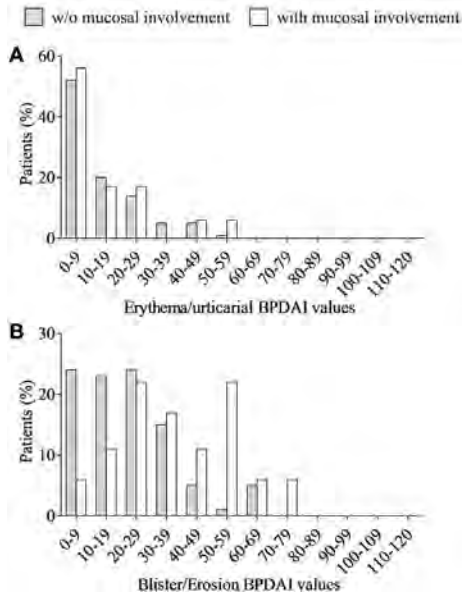

FIGURE 2 | Distribution of both bullous pemphigoid (BP) patients with (white column) and without (gray column) mucosal involvement according to erythema/urticaria BP Disease Area Index (BPDAI) values **(A)** and blisters/erosions BPDAI values **(B)** at the time of diagnosis. No statistical differences were observed between the distributions of these two BP groups according to the Kolmogorov–Smirnov test, although a clear different distribution could be visualized within the low (0–19) and within the high (50–79) values of the blisters/erosions BPDAI values **(B)**.

increased and a low percentage of those patients when the BPDAI values were low ($D = 0.33$; $P = 0.433$) (**Figure 2B**).

Immunological Profiles and Mucosal Involvement

In the aim to analyze the clinical features through the BPDAI scores with regards to the autoimmune response, we first measured anti-BP180 and anti-BP230 autoantibody concentrations in the BF of patients with BP. Anti-BP180 and anti-BP230 antibodies were detected in the BF of 32 (86.5%) and 16 (43.2%) patients with a mean titer of 79.4 ± 51.2 and 31.2 ± 40.3 U/mL, respectively (**Table 2A**). Subgroup analysis of BP patients with and without mucosal involvement showed no significant difference both within the number of BP patients who produced these antibodies and within the mean BF titer related to each antibody. We then investigated whether serum autoantibody concentrations reflected those measured in the BF of the same patients to seek a relationship between BPDAI scores and autoantibody production in the whole BP patients included. Anti-BP180 and anti-BP230 antibodies titers within the BF were highly and significantly correlated with those measured in the serum ($r = 0.78$ and $r = 0.73$; $P < 0.0001$, respectively) (**Table 2B**). Such a correlation was also found for the anti-BP180 antibody titers within the two subsets of patients with or without mucosal involvement ($r = 0.74$ and $r = 0.89$; $P < 0.0001$ and $P = 0.01$, respectively) (**Table 2B**). Anti-BP230 antibody titers in BF from typical BP patients were highly and significantly correlated with those measured in the serum of these patients ($r = 0.74$; $P < 0.0001$), whereas only a high tendency was found for BP patients with mucosal involvement ($r = 0.75$; $P = 0.07$) (**Table 2B**).

Anti-BP180 antibodies were found in the serum of 77 patients (81.9%) with a mean titer of 63.9 ± 50.8 U/mL (**Table 3**). Subgroup analysis of BP patients with and without mucosal involvement showed no significant difference both within the number of BP patients who produced anti-BP180 antibodies and within the mean serum titer for this autoantibody (**Table 3**). In BP patients

TABLE 2 | Blister fluid (BF) immunological characteristics (A) and correlation between serum and BF autoantibody titers (B) in patients with BP according to mucosal involvement.

	All BP patients	Patients without mucosal involvement	Patients with mucosal involvement	*P* value
(A)				
Number of patients (*n*)[a]	37	30	7	NA
BF anti-BP180 NC16A				
Number of patients with titer ≥9 U/mL, *n* (%)	32 (86.5)	26 (86.7)	6 (85.7)	0.95
Mean value ± SD (U/mL)	79.4 ± 51.2	78.5 ± 51.8	83.5 ± 52.2	0.66
BF anti-BP230				
Number of patients with titer ≥9 U/mL, *n* (%)	16 (43.2)	14 (46.7)	2 (28.7)	0.38
Mean value ± SD (U/mL)	31.2 ± 40.3	34.2 ± 41.5	18.2 ± 34.2	0.65
(B)				
Number of patients[a]	37	30	7	
Anti-BP180 NC16A	$r = 0.78$	$r = 0.74$	$r = 0.89$	
	$P < 0.0001$	$P < 0.0001$	$P = 0.01$	
Anti-BP230	$r = 0.73$	$r = 0.74$	$r = 0.75$	
	$P < 0.0001$	$P < 0.0001$	$P = 0.07$	

Subsets of BP patients with or without mucosal involvement were compared and P-value was calculated using Chi² tests for comparison between qualitative variables and nonparametric, Mann–Whitney tests for comparison between quantitative values. Spearman's correlation coefficient was used to explore the relationship between immunological parameters in serum with those in BF.

[a]Patient for whom BF and serum anti-BP180 NC16A and anti-BP230 ELISA values were available.

NA, not applicable; BP, bullous pemphigoid; ELISA, enzyme-linked immunosorbent assay.

TABLE 3 | Serum immunological characteristics of patients with BP according to mucosal involvement.

	All BP patients	Patients without mucosal involvement	Patients with mucosal involvement	*P* value
Serum anti-BP180 NC16A				
Number of patients (*n*)[a]	94	76	18	NA
Number of patients with titer ≥9 U/mL, *n* (%)	77 (81.9)	62 (81.6)	15 (83.3)	0.86
Mean value ± SD (U/mL)	63.9 ± 50.8	62 ± 50.1	71.9 ± 54.4	0.53
Serum anti-BP230				
Number of patients (*n*)[b]	93	75	18	NA
Number of patients with titer ≥9 U/mL, *n* (%)	44 (47.3)	39 (52)	5 (27.8)	0.06
Mean value ± SD (U/mL)	29.1 ± 37	32.2 ± 37.8	16.2 ± 30.9	0.07

Subsets of BP patients with or without mucosal involvement were compared and P-value was obtained using Chi² tests for comparison between qualitative variables and nonparametric, Mann–Whitney tests for comparison between quantitative values.

[a]Patients for whom serum anti-BP180 ELISA values were available.

[b]Patients for whom serum anti-BP230 ELISA values were available.

NA, not applicable; BP, bullous pemphigoid; ELISA, enzyme-linked immunosorbent assay.

without mucosal involvement at baseline, serum anti-BP180 ELISA values were significantly correlated with all BPDAI scores except mucosal BPDAI, i.e., total, skin, blister/erosion, and erythema/urticaria BPDAI scores ($P < 0.0001$, **Figures 3A–D**, **Table 4A**). In BP patients with mucosal involvement at baseline, anti-BP180 ELISA values were only correlated with the erythema/urticaria BPDAI score ($P = 0.03$). Within this subgroup of BP patients, only a correlation tendency was observed with the total BPDAI score ($P = 0.09$) and the skin BPDAI score ($P = 0.06$), whereas no correlation could be drawn with the blister/erosion BPDAI score ($P = 0.30$) (**Figures 3E–H**, **Table 4A**). Finally, no correlation was found between the mucous membrane part of BPDAI score and the anti-BP180-NC16A ELISA values.

Anti-BP230 antibodies were found in the serum of 44 BP patients (47.3%) with a mean titer of 29.1 ± 37 U/mL (**Table 3**). Interestingly, 39 BP patients without mucosal involvement (52%) but only 5 among BP patients with mucosal involvement (27.8%) had a positive anti-BP230 ELISA value ($P = 0.06$). Such a difference tendency was also observed when analyzing the anti-BP230 mean titer (32.2 ± 37.8 and 16.2 ± 30.9 U/mL; $P = 0.07$, respectively) (**Table 3**). At baseline, anti-BP230 antibody serum concentrations were correlated with none of the BPDAI scores within these two groups (**Table 4B**).

Factors Associated with Mucosal Involvement in BP

In univariate analysis, clinical features associated with mucosal involvement at baseline were a number of daily new blisters >10 ($P = 0.02$), a higher total, skin and blister/erosion BPDAI ($P = 0.004$, $P = 0.02$, $P = 0.001$, respectively), and a severe disease according BPDAI ($P = 0.04$). The absence of anti-BP230 autoantibody also showed a tendency of association with a mucosal involvement ($P = 0.08$). By contrast, univariate analysis revealed no relationship between anti-BP180 autoantibody serum concentration and mucosal involvement. In multivariate

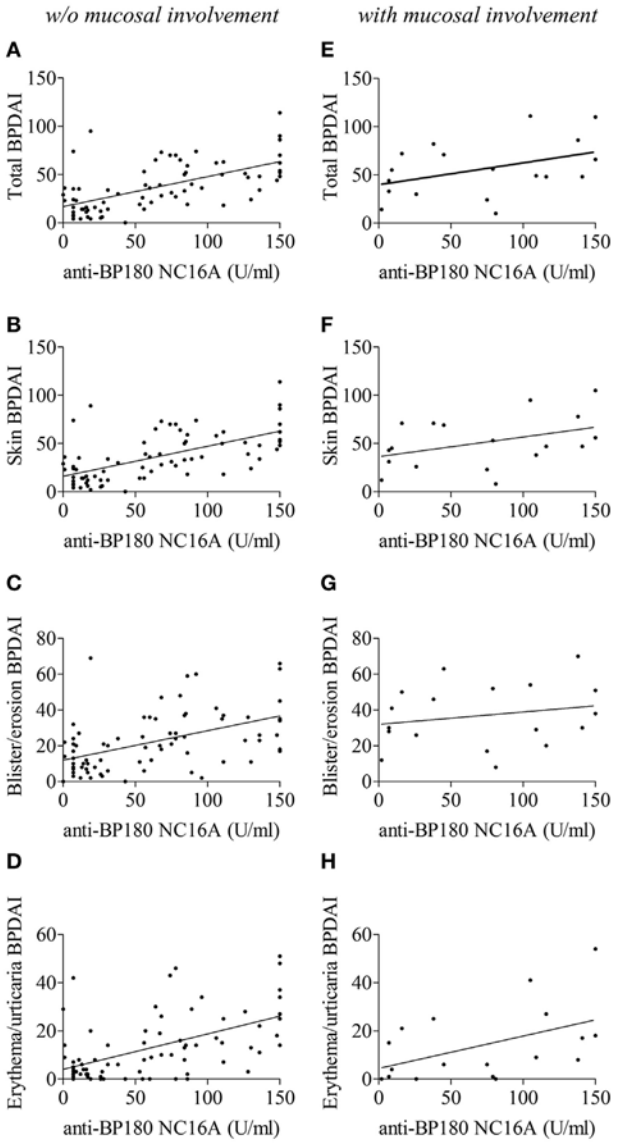

FIGURE 3 | Correlation of serum anti-BP180 NC16A titers with total BP Disease Area Index (BPDAI) **(A,E)**, total skin BPDAI **(B,F)**, blister/erosion BPDAI **(C,G)**, and erythema/urticaria BPDAI **(D,H)** scores in bullous pemphigoid patients without **(A–D)** or with **(E–H)** mucosal involvement. The correlation coefficients and statistical significances were calculated according to Spearman's correlation test and are summarized in **Table 4**.

analysis, the absence of serum anti-BP230 autoantibody was the only factor independently associated with mucosal involvement (OR 7.8; 95% CI, 3.1–19.6) ($P < 0.0001$).

DISCUSSION

This study is the first one to compare at baseline the clinical characteristics by means of the BPDAI score along with the concentrations of anti-BP180 and anti-BP230 antibodies in BP patients with and without mucosal involvement. Analysis of separate and independent BPDAI sub-scores highlighted that skin lesions, more specifically blisters, and erosions were more substantial in patients with mucosal involvement than in typical BP. Such clinical characteristics were associated with the absence of anti-BP230 autoantibody in the serum of BP patients with mucosal involvement. Furthermore, we showed that mucosal lesions are clinically mainly related to disease severity, but not only. Altogether, our results suggest that compared to the classical pathophysiological processes previously defined in BP (12, 16, 17, 24, 33–36), specific immunological mechanisms should be triggered to end with mucosal lesions.

In BP patients with mucosal involvement, skin and mucosal lesions are likely to concomitantly occur during the disease process. Although our results showed that mucosal involvement in BP was associated with disease severity, we also observed mucosal involvement in BP patient with mild disease. Actually, there was a broad distribution of total BPDAI score among BP patients with mucosal involvement, but the percentage of patients with mucosal involvement increased along with the BPDAI values (**Figure 1C**). This suggests that mucous membrane involvement in patients with mild BP is not just a consequence of the extent or severity of the disease, and therefore that some BP patients are more prone to develop mucosal lesions than others. Thus, we can speculate that specific biological/immunological mechanisms responsible for these lesions are activated in those BP patients. This further raised the question of the event on which a break of tolerance outside of the skin tissue could originate. Occurrence of mucosal lesions in some patients with BP recalls the variation in the number of sites involved in patients with mucous membrane pemphigoid (37). Previous study suggested that regulatory T (T_{reg}) cells play an indispensable role in maintaining self-tolerance in BP leading to an increase in autoreactive Th_2, Th_1, and B cells that can recognize different domains of BP180 (38–40). The role of T_{reg} cells in pemphigoid diseases was further demonstrated by mean of mice models (41). Although T_{reg} cells account for less than 10% of peripheral CD4+ T cells, recent studies have reported that tissue resident T_{reg} cells can even control non-immunological processes. Both T_{reg} types demonstrated plasticity and can convert to Th_{17} cells according to the cytokine environment (42). In this line, we and other groups demonstrated the presence of cytokines such as IL-1, IL-6, IL-23, TGFβ, etc, in BP skin lesions. We also demonstrated that the cytokines panel more likely originated from BP epiphenomenon that still remained to be elucidated (26). Such variations could account for variations in a deficit in T_{reg} cells and favor the development of tissue damages. In turn, skin remodeling could impact on both the number and the T_{reg} homing at different levels of the skin compartments. Although aging has been associated with a loss of central immune tolerance in elderly patients as in BP (43), further investigations are now required to determine the events specifically responsible for the mucosal involvement in patients with BP, especially of the oral cavity.

Although the analysis of skin BPDAI highlighted an increase in the blisters/erosions activity in BP patients with mucosal involvement, serum titers of autoantibodies directed against BP180-NC16A, the dominant autoantigen in BP, were not different between patients with and without mucosal involvement. Of note, Hofmann et al. showed that the presence of

TABLE 4 | Correlation between BPDAI scores and serum anti-BP180 (A) or anti-BP230 (B) antibody titers in BP patients according to mucosal involvement.

	All BP patients	Patients without mucosal involvement	Patients with mucosal involvement
(A)			
Number of patients (*n*)[a]	94	76	18
Total BPDAI	$r = 0.57$	$r = 0.62$	$r = 0.42$
	$P < 0.0001$	$P < 0.0001$	$P = 0.09$
Total skin BPDAI	$r = 0.58$	$r = 0.63$	$r = 0.46$
	$P < 0.0001$	$P < 0.0001$	$P = 0.06$
Skin BPDAI: blisters/erosions	$r = 0.46$	$r = 0.52$	$r = 0.26$
	$P < 0.0001$	$P < 0.0001$	$P = 0.30$
Skin BPDAI: erythema/urticaria	$r = 0.52$	$r = 0.53$	$r = 0.52$
	$P < 0.0001$	$P < 0.0001$	$P = 0.03$
Mucosal BPDAI	$r = 0.07$	NA	$r = 0.15$
	$P = 0.48$	NA	$P = 0.55$
(B)			
Number of patients (*n*)[b]	93	75	18
Total BPDAI	$r = -0.01$	$r = 0.05$	$r = 0.04$
	$P = 0.93$	$P = 0.69$	$P = 0.89$
Total skin BPDAI	$r = 0.001$	$r = 0.06$	$r = 0.02$
	$P = 0.99$	$P = 0.63$	$P = 0.94$
Skin BPDAI: blisters/erosions	$r = 0.03$	$r = 0.11$	$r = -0.05$
	$P = 0.76$	$P = 0.33$	$P = 0.86$
Skin BPDAI: erythema/urticaria	$r = 0.01$	$r = -0.01$	$r = 0.21$
	$P = 0.89$	$P = 0.9$	$P = 0.41$
Mucosal BPDAI	$r = -0.20$	NA	$r = -0.26$
	$P = 0.06$	NA	$P = 0.31$

Spearman's correlation coefficient was used to explore the relationship between BPDAI score and serum autoantibody titers.

[a]*Patients for whom serum anti-BP180 ELISA values were available.*

[b]*Patients for whom serum anti-BP230 ELISA values were available.*

NA, not applicable; BP, bullous pemphigoid; BPDAI, BP Disease Area Index; ELISA, enzyme-linked immunosorbent assay.

autoantibodies against both the BP180 N- and C-terminal of the ectodomain was associated with the presence of mucosal lesions (44). Then, Di Zenzo et al. (21) and Mariotti et al. (45) found that autoantibody reactivity against three extracellular epitopes of BP180 (NC16A, AA 1,080–1,107 and AA 1,331–1,404) appeared to be related to the presence of both skin and mucosal involvement in BP patients. By contrast, in our study, the uni- and multivariate analysis highlighted that the absence of anti-BP230 antibody was the only factor independently associated with mucosal involvement in BP. This unconventional result could imply that the immune response may be shifted toward other autoantibodies in those BP patients with mucosal involvement which could be related to a lower threshold of tolerance breakdown in line with a reduced level of T_{reg} cells or of T_{reg} homing as mentioned above. Based on a recent publication (20), we can hypothesize that the loss of immune tolerance curbs both the innate and the adaptive immune responses, which leads to the release of a specific panel of proteases associated with blister formation and tissue remodeling, and subsequently to a shift of the epitope targeted as compared with the classical pathophysiological mechanisms associated with BP. Altogether, this could be reflected by a reduced activity of the adaptive immune response toward the hemidesmosomal proteins of the basal keratinocyte layer and an increased activity toward the antigenic cryptic domains of molecules involved in the anchoring of those basal keratinocyte to the basal membrane structure. To address those mechanisms, it would be relevant to compare in future prospective studies the number and the activity of T_{reg} in biopsy specimens from either skin or mucosa BP lesions with others samples collected from patients with inflammatory non-autoimmune diseases.

The presence of other autoantibodies may interfere with the classical pathophysiological process of BP (12, 16, 17, 24, 33–36, 46). In BP patients without mucosal involvement, the serum concentration of anti-BP180 NC16A autoantibodies was well correlated with both the skin erythema/urticaria and the blisters/erosions BPDAI scores, which is in line with the fact that anti-BP180 autoantibody binding onto their target induced an inflammatory response leading to blister formation (14–18). By contrast, the correlation between anti-BP180 autoantibody titer and the skin blisters/erosions BPDAI score was not evidenced for BP patients with mucosal involvement. Of note, the BPDAI investigated the presence of both blisters and erosions. Thus, considering that the number of daily new blisters only displayed a higher tendency in BP patients with mucosal involvement, the highly significant difference in the BPDAI scores associated to blisters and erosions lesions may be related to the presence of erosions rather than to new blisters. This implies that the mechanisms leading to skin blisters/erosions and maybe to mucosal involvement too, rely on either different or additional trigger than anti-BP180-NC16A autoantibodies in BP patients with mucosal lesion. It was proposed that differential epitope recognition of BP180 could be associated with distinct clinical severity (5). However, additional studies are necessary to define the panel of autoantibodies associated with BP with mucosal lesions, to decipher the pathogenic role of these autoantibodies as well the immunologic mechanisms associated to their production.

Several limitations of the study are to be acknowledged, mainly its relatively limited number of BP patients with mucosal involvement. However, the prospective collection of clinical data including BPDAI assessment allowed a good evaluation of the percentage of BP patients with mucosal involvement, which was very close to results from previous large series of BP patients (5, 6, 21, 32, 44, 45) and from a recent retrospective study performed in our dermatology department (manuscript under consideration). Another weakness is the lack of investigations regarding biopsy specimens or BFs from oral mucous membrane for pathophysiological purpose. Unfortunately, recent intact oral blisters were rare and too transient for an effective, systematic sampling. To avoid biases, our present results were based on clinical or biological data which could systematically be collected in all consecutive patients. Although we observed that mucosal involvement also occurred in patients with mild or moderate disease, we here showed that mucosal involvement was more frequent in patients with severe BP according to the BPDAI score. Actually, in those severe BP patients, mucosal involvement could represent a severity criterion but not a clinical atypia. Considering all elements discussed above, further investigations should help defining the pathophysiological particularities of severe BP patients with

mucosal involvement. Finally, in patients with moderate or minimal BP disease, other diagnoses could be considered, including anti-P200 pemphigoid and epidermolysis bullosa acquisita, which was very unlikely in our present series since indirect immunofluorescence on salt-split skin was either positive with labeling of the epidermal side of the cleavage or negative. The latter BP patients may represent an interesting subset of patients to identify in future studies the specific mechanisms responsible for mucous membrane lesions with the ultimate goal to propose innovative targeted therapy to preserve the quality of life for those elderly fragile patients.

ETHICS STATEMENT

This study was carried out in accordance with the recommendations of the "Commission Nationale de l'Informatique et des libertés (CNIL, authorization DR-2013-320)" and approved by the Ethic Committee of the University Hospital of Reims. All subjects gave written informed consent in accordance with the Declaration of Helsinki.

AUTHOR CONTRIBUTIONS

FA, PB, and B-NP designed the study. AC, CM, GG, SJ, and CB performed experiments and analyzed clinical and biological data. AC, FA, and PB wrote the manuscript. All authors critically evaluated the data and approved the final version for publication.

ACKNOWLEDGMENTS

We thank Maizières M., Ph.D., for technical support during the study.

FUNDING

This work was supported by the French Department of Health's "Projet Hospitalier de Recherche Clinique (PHRC) Interregional" 2012, and by the university of Reims Champagne-Ardenne. The funding source had no role in the design and conduct of the study, collection, management, analysis, and interpretation of data.

REFERENCES

1. Bernard P, Antonicelli F. Bullous pemphigoid: a review of its diagnosis, associations and treatment. *Am J Clin Dermatol* (2017) 18(4):513–28. doi:10.1007/s40257-017-0264-2
2. Stanley JR, Tanaka T, Mueller S, Klaus-Kovtun V, Roop D. Isolation of complementary DNA for bullous pemphigoid antigen by use of patients' autoantibodies. *J Clin Invest* (1988) 82(6):1864–70. doi:10.1172/JCI113803
3. Giudice GJ, Emery DJ, Diaz LA. Cloning and primary structural analysis of the bullous pemphigoid autoantigen BP180. *J Invest Dermatol* (1992) 99(3):243–50. doi:10.1111/1523-1747.ep12616580
4. Zillikens D, Rose PA, Balding SD, Liu Z, Olague-Marchan M, Diaz LA, et al. Tight clustering of extracellular BP180 epitopes recognized by bullous pemphigoid autoantibodies. *J Invest Dermatol* (1997) 109(4):573–9. doi:10.1111/1523-1747.ep12337492
5. Thoma-Uszynski S, Uter W, Schwietzke S, Schuler G, Borradori L, Hertl M. Autoreactive T and B cells from bullous pemphigoid (BP) patients recognize epitopes clustered in distinct regions of BP180 and BP230. *J Immunol* (2006) 176(3):2015–23. doi:10.4049/jimmunol.176.3.2015
6. Di Zenzo G, Thoma-Uszynski S, Fontao L, Calabresi V, Hofmann SC, Hellmark T, et al. Multicenter prospective study of the humoral autoimmune response in bullous pemphigoid. *Clin Immunol* (2008) 128(3):415–26. doi:10.1016/j.clim.2008.04.012
7. Joly P, Baricault S, Sparsa A, Bernard P, Bédane C, Duvert-Lehembre S, et al. Incidence and mortality of bullous pemphigoid in France. *J Invest Dermatol* (2012) 132(8):1998–2004. doi:10.1038/jid.2012.35
8. Bernard P, Vaillant L, Labeille B, Bedane C, Arbeille B, Denoeux JP, et al. Incidence and distribution of subepidermal autoimmune bullous skin diseases in three French regions. Bullous Diseases French Study Group. *Arch Dermatol* (1995) 131(1):48–52. doi:10.1001/archderm.1995.01690130050009
9. Murrell DF, Daniel BS, Joly P, Borradori L, Amagai M, Hashimoto T, et al. Definitions and outcome measures for bullous pemphigoid: recommendations by an international panel of experts. *J Am Acad Dermatol* (2012) 66(3):479–85. doi:10.1016/j.jaad.2011.06.032
10. Vaillant L, Bernard P, Joly P, Prost C, Labeille B, Bedane C, et al. Evaluation of clinical criteria for diagnosis of bullous pemphigoid. French Bullous Study Group. *Arch Dermatol* (1998) 134(9):1075–80. doi:10.1001/archderm.134.9.1075
11. Korman N. Bullous pemphigoid. *J Am Acad Dermatol* (1987) 16(5 Pt 1):907–24. doi:10.1016/S0190-9622(87)70115-7
12. Di Zenzo G, Marazza G, Borradori L. Bullous pemphigoid: physiopathology, clinical features and management. *Adv Dermatol* (2007) 23:257–88. doi:10.1016/j.yadr.2007.07.013
13. Schmidt E, Zillikens D. Pemphigoid diseases. *Lancet* (2013) 381(9863):320–32. doi:10.1016/S0140-6736(12)61140-4
14. Gammon WR, Merritt CC, Lewis DM, Sams WM, Carlo JR, Wheeler CE. An in vitro model of immune complex-mediated basement membrane zone separation caused by pemphigoid antibodies, leukocytes, and complement. *J Invest Dermatol* (1982) 78(4):285–90. doi:10.1111/1523-1747.ep12507222
15. Sitaru C, Schmidt E, Petermann S, Munteanu LS, Bröcker E-B, Zillikens D. Autoantibodies to bullous pemphigoid antigen 180 induce dermal-epidermal separation in cryosections of human skin. *J Invest Dermatol* (2002) 118(4):664–71. doi:10.1046/j.1523-1747.2002.01720.x
16. Liu Z, Diaz LA, Troy JL, Taylor AF, Emery DJ, Fairley JA, et al. A passive transfer model of the organ-specific autoimmune disease, bullous pemphigoid, using antibodies generated against the hemidesmosomal antigen, BP180. *J Clin Invest* (1993) 92(5):2480–8. doi:10.1172/JCI116856
17. Nishie W, Sawamura D, Goto M, Ito K, Shibaki A, McMillan JR, et al. Humanization of autoantigen. *Nat Med* (2007) 13(3):378–83. doi:10.1038/nm1496
18. Ujiie H, Shibaki A, Nishie W, Sawamura D, Wang G, Tateishi Y, et al. A novel active mouse model for bullous pemphigoid targeting humanized pathogenic antigen. *J Immunol* (2010) 184(4):2166–74. doi:10.4049/jimmunol.0903101
19. Ludwig RJ, Vanhoorelbeke K, Leypoldt F, Kaya Z, Bieber K, McLachlan SM, et al. Mechanisms of autoantibody-induced pathology. *Front Immunol* (2017) 8:603. doi:10.3389/fimmu.2017.00603
20. Bieber K, Koga H, Nishie W. In vitro and in vivo models to investigate the pathomechanisms and novel treatments for pemphigoid diseases. *Exp Dermatol* (2017) 26(12):1163–70. doi:10.1111/exd.13415
21. Di Zenzo G, Grosso F, Terracina M, Mariotti F, De Pità O, Owaribe K, et al. Characterization of the anti-BP180 autoantibody reactivity profile and epitope mapping in bullous pemphigoid patients. *J Invest Dermatol* (2004) 122(1):103–10. doi:10.1046/j.0022-202X.2003.22126.x
22. Schmidt E, della Torre R, Borradori L. Clinical features and practical diagnosis of bullous pemphigoid. *Immunol Allergy Clin North Am* (2012) 32(2):217–232, v. doi:10.1016/j.iac.2012.04.002
23. Niimi Y, Pawankar R, Kawana S. Increased expression of matrix metalloproteinase-2, matrix metalloproteinase-9 and matrix metalloproteinase-13 in lesional skin of bullous pemphigoid. *Int Arch Allergy Immunol* (2006) 139(2):104–13. doi:10.1159/000090385
24. Verraes S, Hornebeck W, Polette M, Borradori L, Bernard P. Respective contribution of neutrophil elastase and matrix metalloproteinase 9 in the degradation of BP180 (type XVII collagen) in human bullous pemphigoid. *J Invest Dermatol* (2001) 117(5):1091–6. doi:10.1046/j.0022-202x.2001.01521.x

25. Le Jan S, Plée J, Vallerand D, Dupont A, Delanez E, Durlach A, et al. Innate immune cell-produced IL-17 sustains inflammation in bullous pemphigoid. *J Invest Dermatol* (2014) 134(12):2908–17. doi:10.1038/jid.2014.263
26. Plée J, Le Jan S, Giustiniani J, Barbe C, Joly P, Bedane C, et al. Integrating longitudinal serum IL-17 and IL-23 follow-up, along with autoantibodies variation, contributes to predict bullous pemphigoid outcome. *Sci Rep* (2015) 5:18001. doi:10.1038/srep18001
27. Giusti D, Gatouillat G, Le Jan S, Plée J, Bernard P, Antonicelli F, et al. Eosinophil cationic protein (ECP), a predictive marker of bullous pemphigoid severity and outcome. *Sci Rep* (2017) 7(1):4833. doi:10.1038/s41598-017-04687-5
28. Lévy-Sitbon C, Barbe C, Plee J, Goeldel A-L, Antonicelli F, Reguiaï Z, et al. Assessment of bullous pemphigoid disease area index during treatment: a prospective study of 30 patients. *Dermatology* (2014) 229(2):116–22. doi:10.1159/000362717
29. Kobayashi M, Amagai M, Kuroda-Kinoshita K, Hashimoto T, Shirakata Y, Hashimoto K, et al. BP180 ELISA using bacterial recombinant NC16a protein as a diagnostic and monitoring tool for bullous pemphigoid. *J Dermatol Sci* (2002) 30(3):224–32. doi:10.1016/S0923-1811(02)00109-3
30. Tsuji-Abe Y, Akiyama M, Yamanaka Y, Kikuchi T, Sato-Matsumura KC, Shimizu H. Correlation of clinical severity and ELISA indices for the NC16A domain of BP180 measured using BP180 ELISA kit in bullous pemphigoid. *J Dermatol Sci* (2005) 37(3):145–9. doi:10.1016/j.jdermsci.2004.10.007
31. Yoshida M, Hamada T, Amagai M, Hashimoto K, Uehara R, Yamaguchi K, et al. Enzyme-linked immunosorbent assay using bacterial recombinant proteins of human BP230 as a diagnostic tool for bullous pemphigoid. *J Dermatol Sci* (2006) 41(1):21–30. doi:10.1016/j.jdermsci.2005.11.002
32. Charneux J, Lorin J, Vitry F, Antonicelli F, Reguiai Z, Barbe C, et al. Usefulness of BP230 and BP180-NC16a enzyme-linked immunosorbent assays in the initial diagnosis of bullous pemphigoid: a retrospective study of 138 patients. *Arch Dermatol* (2011) 147(3):286–91. doi:10.1001/archdermatol.2011.23
33. Hirose M, Recke A, Beckmann T, Shimizu A, Ishiko A, Bieber K, et al. Repetitive immunization breaks tolerance to type XVII collagen and leads to bullous pemphigoid in mice. *J Immunol* (2011) 187(3):1176–83. doi:10.4049/jimmunol.1100596
34. Schulze FS, Beckmann T, Nimmerjahn F, Ishiko A, Collin M, Köhl J, et al. Fcγ receptors III and IV mediate tissue destruction in a novel adult mouse model of bullous pemphigoid. *Am J Pathol* (2014) 184(8):2185–96. doi:10.1016/j.ajpath.2014.05.007
35. Kasperkiewicz M, Zillikens D. The pathophysiology of bullous pemphigoid. *Clin Rev Allergy Immunol* (2007) 33(1–2):67–77. doi:10.1007/s12016-007-0030-y
36. Kasperkiewicz M, Zillikens D, Schmidt E. Pemphigoid diseases: pathogenesis, diagnosis, and treatment. *Autoimmunity* (2012) 45(1):55–70. doi:10.3109/08916934.2011.606447
37. Zehou O, Raynaud J-J, Le Roux-Villet C, Alexandre M, Airinei G, Pascal F, et al. Oesophageal involvement in 26 consecutive patients with mucous membrane pemphigoid. *Br J Dermatol* (2017) 177(4):1074–85. doi:10.1111/bjd.15592
38. Antiga E, Quaglino P, Volpi W, Pierini I, Del Bianco E, Bianchi B, et al. Regulatory T cells in skin lesions and blood of patients with bullous pemphigoid. *J Eur Acad Dermatol Venereol* (2014) 28(2):222–30. doi:10.1111/jdv.12091
39. Quaglino P, Antiga E, Comessatti A, Caproni M, Nardò T, Ponti R, et al. Circulating CD4+ CD25brightFOXP3+ regulatory T-cells are significantly reduced in bullous pemphigoid patients. *Arch Dermatol Res* (2012) 304(8):639–45. doi:10.1007/s00403-012-1213-9
40. Liu Y, Li L, Xia Y. BP180 is critical in the autoimmunity of bullous pemphigoid. *Front Immunol* (2017) 8:1752. doi:10.3389/fimmu.2017.01752
41. Bieber K, Sun S, Witte M, Kasprick A, Beltsiou F, Behnen M, et al. Regulatory T cells suppress inflammation and blistering in pemphigoid diseases. *Front Immunol* (2017) 8:1628. doi:10.3389/fimmu.2017.01628
42. Zhou X, Tang J, Cao H, Fan H, Li B. Tissue resident regulatory T cells: novel therapeutic targets for human disease. *Cell Mol Immunol* (2015) 12(5):543–52. doi:10.1038/cmi.2015.23
43. Dorshkind K, Montecino-Rodriguez E, Signer RAJ. The ageing immune system: is it ever too old to become young again? *Nat Rev Immunol* (2009) 9(1):57–62. doi:10.1038/nri2471
44. Hofmann SC, Thoma-Uszynski S, Stauber A, Schuler G, Hertl M, Hunziker T, et al. Severity and phenotype of bullous pemphigoid relate to autoantibody profile against the NH2- and COOH-terminal regions of the BP180 ectodomain. *J Invest Dermatol* (2002) 119(5):1065–73. doi:10.1046/j.1523-1747.2002.19529.x
45. Mariotti F, Grosso F, Terracina M, Ruffelli M, Cordiali-Fei P, Sera F, et al. Development of a novel ELISA system for detection of anti-BP180 IgG and characterization of autoantibody profile in bullous pemphigoid patients. *Br J Dermatol* (2004) 151(5):1004–10. doi:10.1111/j.1365-2133.2004.06245.x
46. Goletz S, Zillikens D, Schmidt E. Structural proteins of the dermal-epidermal junction targeted by autoantibodies in pemphigoid diseases. *Exp Dermatol* (2017) 26(12):1154–62. doi:10.1111/exd.13446

Conflict of Interest Statement: The authors declare that the research was conducted in the absence of any commercial or financial relationships that could be construed as a potential conflict of interest.

frontiers in Immunology

REVIEW
published: 08 March 2018
doi: 10.3389/fimmu.2018.00478

Our Environment Shapes Us: The Importance of Environment and Sex Differences in Regulation of Autoantibody Production

*Michael Edwards, Rujuan Dai and S. Ansar Ahmed**

Department of Biomedical Sciences and Pathobiology, Virginia-Maryland College of Veterinary Medicine, Virginia Tech, Blacksburg, VA, United States

Consequential differences exist between the male and female immune systems' ability to respond to pathogens, environmental insults or self-antigens, and subsequent effects on immunoregulation. In general, females when compared with their male counterparts, respond to pathogenic stimuli and vaccines more robustly, with heightened production of antibodies, pro-inflammatory cytokines, and chemokines. While the precise reasons for sex differences in immune response to different stimuli are not yet well understood, females are more resistant to infectious diseases and much more likely to develop autoimmune diseases. Intrinsic (i.e., *sex hormones, sex chromosomes, etc.*) and extrinsic (*microbiome composition, external triggers, and immune modulators*) factors appear to impact the overall outcome of immune responses between sexes. Evidence suggests that interactions between environmental contaminants [e.g., endocrine disrupting chemicals (EDCs)] and host leukocytes affect the ability of the immune system to mount a response to exogenous and endogenous insults, and/or return to normal activity following clearance of the threat. Inherently, males and females have differential immune response to external triggers. In this review, we describe how environmental chemicals, including EDCs, may have sex differential influence on the outcome of immune responses through alterations in epigenetic status (such as modulation of microRNA expression, gene methylation, or histone modification status), direct and indirect activation of the estrogen receptors to drive hormonal effects, and differential modulation of microbial sensing and composition of host microbiota. Taken together, an intriguing question develops as to how an individual's environment directly and indirectly contributes to an altered immune response, dysregulation of autoantibody production, and influence autoimmune disease development. Few studies exist utilizing well-controlled cohorts of both sexes to explore the sex differences in response to EDC exposure and the effects on autoimmune disease development. Translational studies incorporating multiple environmental factors in animal models of autoimmune disease are necessary to determine the interrelationships that occur between potential etiopathological factors. The presence or absence of autoantibodies is not a reliable predictor of disease. Therefore, future studies should incorporate all the susceptibility/influencing factors, coupled with individual genomics, epigenomics, and proteomics, to develop a model that better predicts, diagnoses, and treats autoimmune diseases in a personalized-medicine fashion.

Keywords: sex hormones, lupus, microbiota, endocrine disrupting chemicals, DNA methylation, epigenetics

OPEN ACCESS

Edited by:
Ralf J. Ludwig, University of Lübeck, Germany

Reviewed by:
Ayanabha Chakraborti, University of Alabama at Birmingham, United States
Jun-ichi Kira, Kyushu University, Japan
Maja Wallberg, University of Cambridge, United Kingdom

***Correspondence:**
S. Ansar Ahmed
ansrahmd@vt.edu

Specialty section:
This article was submitted to Immunological Tolerance and Regulation, a section of the journal Frontiers in Immunology

Received: *15 December 2017*
Accepted: *22 February 2018*
Published: *08 March 2018*

Citation:
Edwards M, Dai R and Ahmed SA (2018) Our Environment Shapes Us: The Importance of Environment and Sex Differences in Regulation of Autoantibody Production. Front. Immunol. 9:478. doi: 10.3389/fimmu.2018.00478

INTRODUCTION

The incidence of autoimmune and allergic diseases has been increasing for multiple decades (1, 2). Despite intensive studies in many laboratories, the etiology of autoimmune diseases is not well understood. It is nevertheless clear that there is no single genetic factor that solely determines the susceptibility to autoimmune diseases. Rather, susceptibility to autoimmune diseases appears to involve complex interactions of genetic, epigenetic, hormonal, and environmental factors. Many (but not all) autoimmune diseases preferentially demonstrate a female dominant susceptibility bias. The high female to male incidence ratios in autoimmune diseases such as autoimmune thyroiditis, systemic lupus erythematosus (SLE), and Sjögren's syndrome in both humans and relevant animal models have been widely reported (3–8). Interestingly, even those diseases that did not show a strong female bias of susceptibility in the past, such as multiple sclerosis (MS), now appear to tilt toward female predisposition. Patients diagnosed with MS were initially reported to have close to a 1:1 female:male ratio in the 1950s (9). This ratio increased to 2:1 in the 1980s (10), and further to 3:1 in recent reports (11). While the precise reasons for sex differences are not known, the potential contribution of changes in environmental factors remains an intriguing possibility. The implication of non-genetic factors (e.g., epigenetic and environmental factors) is also evident in studies that reported the concordance rate of monozygotic twins manifesting autoimmune diseases is only between 20 and 35% (12–15). Further evidence for an environmental component driving autoimmune pathology exists with the Gullah population in South Carolina who are genetically very similar to members of their ancestral home of Sierra Leone. In a recent report, while the SLE disease prevalence (as measured by serum antinuclear antibodies) in the Gullah population is similar to their African counterparts, notably, the African cohort had higher levels of circulating anti-Smith and anti-cardiolipin autoantibodies, as well as increased numbers of seropositive individuals to multiple viral infections (16). This suggests that in genetically very similar populations, environmental factors can promote autoantibody production. The potential contribution of differences in exposure to environmental chemicals between these two population groups cannot be discounted. Interestingly, human SLE patients with pet dogs are more likely to have dogs that also suffer from SLE (17). This finding supports the claim that a transmissible or common environmental agent, or agents, may be present that increased the risk for SLE development within the human and canine populations. Even in genetically susceptible inbred mice that spontaneously develop autoimmune diseases, such as lupus, differences in the outcome or severity of the diseases has been noted among various laboratories (18–24). This supports non-genetic environmental factors influence on autoimmune disease.

It is now recognized that sex differences in the immune system cannot be solely attributable to differences in sex chromosomes and sex hormones (6, 7, 25). Direct comparisons among various studies exploring the specific mechanisms underlying the observed female bias in many autoimmune disorders are difficult due to differences in study methodology, population cohorts, and various extrinsic factors unable to be controlled for in human populations. Nevertheless, when the data are explored as a whole, the consequence of these variations can be mitigated and trends can be identified regarding sex-based differences in multiple systems.

In general, normal healthy males are thought to have immune systems that maintain tolerance, while the female immune system is susceptible to break in immune tolerance as evidenced by higher production of autoantibodies (26–28). Sex chromosomes contribute genetic differences, with multiple genes involved in immune system responses present on the X-chromosome, including genes for FoxP3 and toll-like receptors (TLRs) 7 and 8. These genes can be differentially expressed in males and females due to incomplete X-chromosome inactivation in the females, leading to potentially increased gene expression in females (29). Steroidal sex hormone levels vary between sexes, with female predominant estrogens promoting B cell survival and contributing to exacerbation of multiple autoimmune diseases, and androgens exerting immune regulatory effects to prevent, suppress, or delay autoimmunity (30, 31). Endocrine disrupting chemicals (EDCs) act through multiple mechanisms, displaying both estrogenic and anti-estrogenic properties, reducing androgen production, and influencing epigenetic regulation (28, 32). It is now prudent to incorporate environmental influences (e.g., EDCs) in studying the development of autoimmune diseases, which will provide a more comprehensive understanding of mechanisms of autoimmune diseases (33). Assessed individually, these various factors may not be able to induce autoimmunity sufficiently. However, when multiple internal and environmental factors interact, these may cause the loss of tolerance, the production of autoantibodies, and drive autoimmune disease pathogenesis (**Figure 1**). This review will focus on how sex differences identified in genetics, epigenetics, hormonal responses, and response to microbial stimuli influence immune tolerance dysregulation and autoantibody production, with an emphasis on the contributing effects of EDCs on immunological functions.

Abbreviations: AID, activation-induced cytidine deaminase; AIRE, autoimmune regulator; AR, androgen receptor; BAFF, B-cell-activating factor; BPA, bisphenol-A; CLRs, C-type lectin receptors; CMV, cytomegalovirus; DHT, dihydrotestosterone; DNMT, DNA methyltransferase; EBV, Epstein–Barr virus; EDC, endocrine disrupting chemicals; ER, estrogen receptor; GPR, G protein-coupled estrogen receptor; HDAC, histone deacetylase; HEV-hepatitis E virus; IFN, interferon; LPS, lipopolysaccharide; MAMPs, microbial-associated molecular patterns; miRNA, microRNA; MRL/lpr, MRL/MpJ-Faslpr/J; MS, multiple sclerosis; NLR, NOD-like receptor; NZB/W_{F1}, New Zealand Black/White F1 progeny; NOD mice, non-obese diabetic mice; PBMCs, peripheral blood mononuclear cells; pDCs, plasmacytoid dendritic cells; PPAR, peroxisome proliferator-activated receptor; RLRs, RIG-I-like receptors; SCFA, short chain fatty acid; SLE, systemic lupus erythematosus; T1DM, type-1 diabetes mellitus; TLR, toll-like receptor.

SEX DIFFERENCES IN GENETICS AND AUTOIMMUNITY

Female cells are genetically the same as male cells in all chromosomes except the sex-specific X and Y chromosomes. To compensate for gene copy differences, female cells, other than egg cells, undergo X-chromosome inactivation, thereby permanently

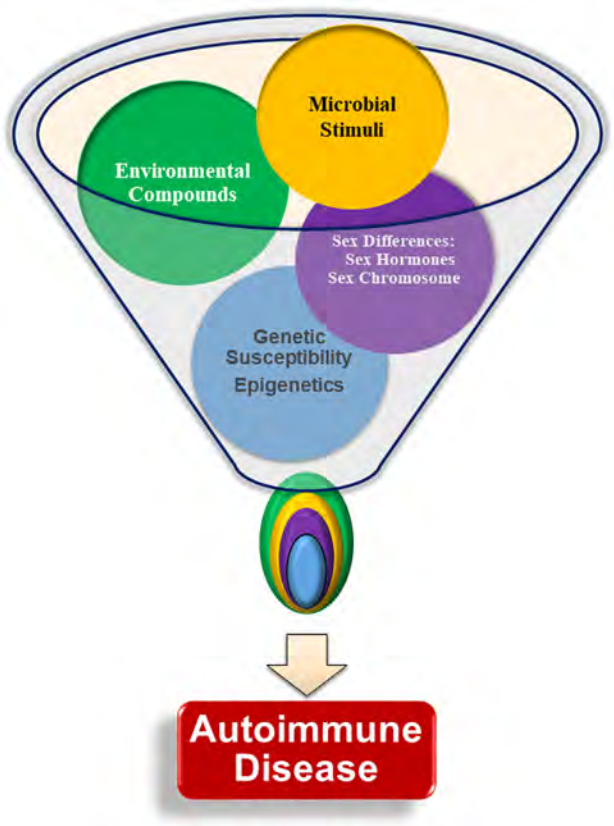

FIGURE 1 | Interactions of multiple factors are required for the development of autoimmunity. Genetic susceptibility, sex chromosomes, sex hormones, infections and microbial stimuli, and environmental factors are all thought to contribute to autoimmune pathogenesis and lead to autoantibody production. There is little evidence that any one particular factor is able to initiate autoimmunity without input from another factor. The specific relationships and interplay among each of the various factors, such as the relative importance of one factor compared with the others, age at, or duration of, exposure, is not yet understood.

silencing one copy of the X chromosome. This process may be incomplete in some individuals, leading to overexpression of genes present on the X-chromosome. Abnormalities in chromosome numbers may exist, such as in Klinefelter syndrome, where males have one or more extra X chromosomes. Notably, men with Klinefelter syndrome are predicted to have a similar risk of SLE to that of females, and a 14-fold increase in SLE risk compared with healthy males (34). It is conceivable that in the context of incomplete X-chromosome inactivation, females could have alterations in the expression of X-chromosome linked genes that promote inflammation and subsequent autoimmunity, such as TLR7/8.

Many autosomal genes are differentially expressed in males and females. The transcription factor vestigial-like family 3 (VGLL3) was recently found to be upregulated in female tissues, such as ovaries, the uterus, adipose tissue, and smooth muscle. *VGLL3* is located on chromosome 3, and it is unknown at this time what contributes to this sexual differential expression pattern. This transcription factor contributes to the differential expression of hundreds of genes between sexes. Genes of interest regulated

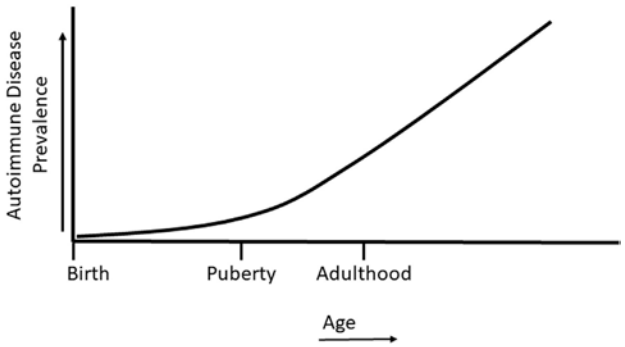

FIGURE 2 | Autoimmune disease prevalence in relation to life stage. Autoimmune diseases can develop during childhood, but most autoimmune diseases develop following the onset of puberty and in later life.

by VGLL3 include *BAFF*, *ITGAM*, *IL-7*, *ICAM-1*, *MMP9*, and *ETS1*. These female biased genes are associated with known autoimmunity susceptibility loci and inflammatory processes, and the increased expression of these genes appears independent of sex hormone regulation (35). Furthermore, it is also possible that other newly identified and unknown transcription factors are contributing to the sex bias gene expression and autoimmune disease susceptibility.

SEX HORMONES AND ENVIRONMENTAL EDC REGULATION OF IMMUNITY AND AUTOIMMUNITY

Sex differences in sex steroid hormone levels and regulation on the immune system of normal and autoimmune individuals have been extensively studied (7, 36–40). While the sex differential effects on immunity and autoimmunity cannot be solely attributable to sex hormone profiles, sex steroid hormones do have a major impact on various aspects of the immune system, including their contribution to cell differentiation, cytokine profiles, epigenetic alterations, and autoimmune disease (36, 38–44). The case for the role of sex hormones in autoimmune diseases can be further made by the fact that a majority of autoimmune diseases are manifested after sexual maturity, at a time when sex hormone levels are elevated and differential biological responses of sex-hormone regulated genes are evident (**Figure 2**). Interestingly, it is not yet understood why women are at a higher risk of developing autoimmune diseases such as SLE, rheumatoid arthritis, Graves' disease, and thyroiditis following menopause (45). EDCs are able to exert agonistic or antagonistic roles on normal physiological sex hormone actions, enhancing or mitigating hormonal effects on immune cells (25, 46–48). As with many endocrine components, sex hormones and EDCs exert differential effects, not only due to dosage but also in temporally dependent and context-specific manners.

Exposure to EDCs is nearly impossible to avoid in current societies. These compounds can be present in drinking water, cosmetic products, paper products, food and beverage containers, many forms of plastics, and the food we eat (32). The route

and dosage of exposure are important considerations when determining the effect EDCs will have on various aspects of health and physiology. Many EDCs have been determined to be able to elicit bi-phasic dose responses, with evidence that very low EDC concentrations can exert a positive effect, while at higher concentrations they may have opposite effects, and *vice versa*. Currently, controversy exists regarding evaluation of internal concentrations, metabolites, and daily exposure levels of EDCs (49).

Little consensus has been reached regarding when, where, and how EDCs disrupt endocrine homeostasis in exposed individuals. One vital issue that impairs our understanding of the mechanisms and overall influence of EDCs on health is the potential lag between exposure and development of clinical signs, such as reproductive disorders. In humans, the lag period may be years or decades before sexual maturity and fertility can be tested (50). Much of the current data on EDC functions and effects are targeting alterations in reproductive systems. Due to the wide variety of compounds and exposure routes, this review will only address how well-studied models of EDCs, such as bisphenol-A (BPA) and phytoestrogens, may affect the immune system.

Estrogen, Natural, and Environmental

The effects of estrogen on immune cell populations and functions have been extensively studied and reviewed (6, 36–40). We will highlight the important aspects of estrogen's actions that promote or inhibit autoantibody production. Estrogens are able to exert effects on multiple immune cell phenotypes through activating either estrogen receptors (ERs)-mediated genomic signaling or G protein-coupled estrogen receptor 1 (GPR30/GPER1)-coupled non-genomic signaling pathways (30). Following ligand binding, ERα and/or ERβ binds to the estrogen response element (ERE), which drives transcriptional regulation, particularly Pax5, BSAP, HOXC4/HoxC4, and activation-induced cytidine deaminase (AID) genes in B cells, promoting B cell maturation and survival. Estrogen activated GPR30 signals through P38/ERK MAPK and PI3 kinase pathways, driving B cell activation and rearrangement of the Ig heavy and light chain, as well as activating NF-κB (30). Furthermore, sex hormones and hormone metabolites can also induce their effects on target cells (such as cells of the immune system) in sex-hormone receptor independent mechanisms (51, 52). Activated ERs can bind to other transcription factors (such as NF-κB) to mediate cell signaling for regulating gene expression. In addition, ERs can be activated independent of ligand binding (53, 54). Therefore, it is conceivable that, in females, direct and indirect activation of ERs by external triggers, such as endocrine disruptors, can potentially have differential effects compared with males.

In most instances, estrogen enhances both cell-mediated and humoral immunity. Studies in peroxisome proliferator-activated receptor (PPAR) knockout mice show that T follicular helper cell responses, important for antibody production, were upregulated in female but not in male CD4-PPARγ^{KO} mice, in part due to estrogen (55). In regards to B cells and antibody production, estrogen drives B cell maturation, immunoglobulin class switch recombination, and somatic hypermutation in germinal centers, promotes B cell survival, and enhances antibody production (30, 56, 57). Directly, estrogen regulates gene transcription through ERs binding to ERE sites. Indirectly, estrogen promotes B cell survival through increased B-cell-activating factor (BAFF) production. In mouse models, BAFF gene expression is upregulated by estrogens and interferon (IFN) stimulation both at the mRNA and protein levels through a mechanism involving ERα, IRF5, or STAT1. Treatment of the mouse macrophage cell line RAW264.7 with IFNα, IFNγ, or estrogen induced p202, which correlated with increased BAFF production, contributing to sex differences (58). In humans, under normal physiological conditions, no detectable differences are found between male and female BAFF levels. However, following estradiol treatment, both sexes had an increase in BAFF production, with the increase in females being much more profound (59). Thus, in the presence of estrogen, B cell survival, and maturation is enhanced through multiple mechanisms, potentially increasing the ability of autoreactive B cells to break tolerance and drive autoantibody production (**Figure 3**).

BALB/c transgenic mice treated with estrogen had increased Bcl-2 production that allowed naïve B cells to break tolerance induction and drive anti-dsDNA autoantibody production (60). Anti-cardiolipin autoantibody was shown to be enhanced in orchiectomized male and normal female B6 mice treated with 17β-estradiol, but replacement of dihydrotestosterone (DHT) in castrated males had no effect, and intact males had lower levels of circulating autoantibodies than females (43). Autoreactive B cell pools are created predominantly in females, and ER signal-mediated activation of DCs was found to modulate T and B cell responses (61–63). Enhanced B cell survival through estrogen's various actions promotes self-reactive B cell escape from negative selection in the bone marrow, and progression of autoantibody production (64, 65). Therefore, it is conceivable that the lower levels of circulating E2 in males, in combination with higher levels of androgens, allows for better regulation and removal of autoreactive B cell populations before autoimmunity onset.

Evolutionarily, the female immune system is biologically equipped to robustly respond to infectious threats to protect the young dependent offspring and in the larger sense aiding in the survival of species. With the passage of time in the relatively recent era, introduction of new chemicals and emerging and re-emerging infections now pose unique challenges to the primed female immune system. It can be argued that initially the female immune system had biologically been exposed to natural estrogens. With the advent of, and exposure to, EDCs, the female immune system may be exposed to "surges or overloads" of endocrine compounds with competing endocrine effects, thus increasing the chance for deviation of immune modulation by hormones. Whether these new threats have contributed to increased autoimmune diseases is an open question that warrants investigation.

The ability of EDCs to influence the immune system subsets and alter disease susceptibility is poorly understood at this time. BPA has multiple estrogenic-like functions that alter T cell subset, B cell function, and dendritic cell activity, inducing abnormal immune signaling and disrupting ER and PPAR signaling, thus, altering target gene transcription. In mice, BPA induced splenocyte proliferation and shifted the cytokine profile from Th2- to Th1-mediated cytokines, enhancing autoimmunity (32). For example, BPA has been associated with the development of

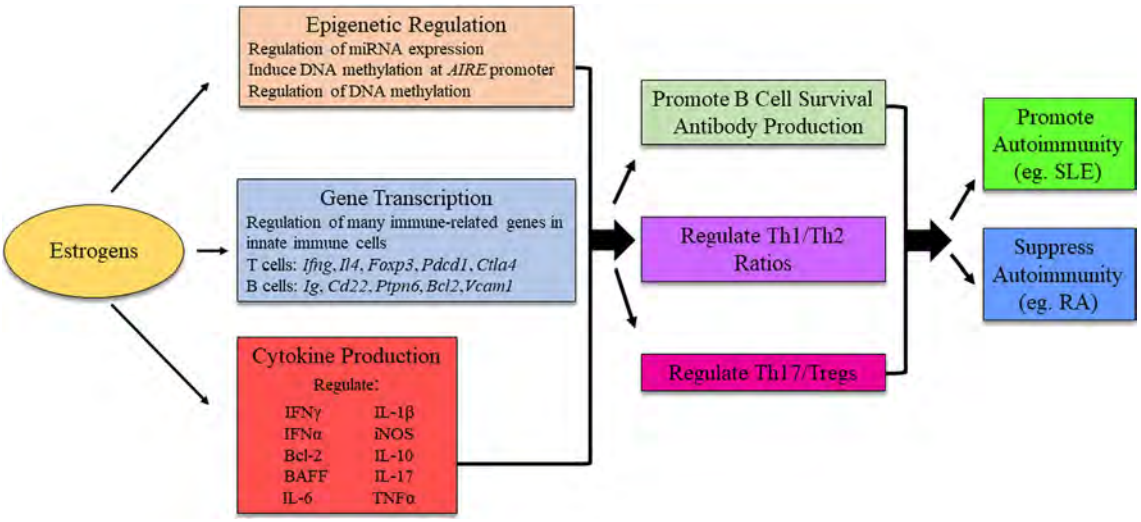

FIGURE 3 | Possible mechanism for estrogens to influence immunity and autoimmune disease development. The exact mechanism for estrogenic influence on autoimmune disease development is likely disease- and context-dependent, and research is ongoing to identify distinct pathways in which estrogen is able to exert its effects. The figure illustrates potential molecular mechanisms of estrogen regulation. *AIRE*, autoimmune regulator.

type 1 diabetes mellitus (T1DM) in non-obese diabetic (NOD) mice, a mouse model of insulitis and leukocytic infiltration of pancreatic islets leading to type 1 diabetes mellitus (66–68). Human studies have also associated EDCs with the development of organ-specific autoimmune diseases mediated by autoreactive T cells. For example, serum BPA levels correlated with increased antithyroperoxidase in human patients of Hashimoto's thyroiditis, and estrogens regulate miR-21, which may drive inflammation in polymyositis (69, 70). Exaggerated T cell activation and polar Th1/Th2 shifts are due in part to increased antigen-specific IFNγ following BPA exposure (71). In this way, BPA shows an antagonistic effect to physiological estrogen responses. BPA can affect the MAPK and STAT pathways, disrupting the normal prevention of autoreactive T cell proliferation and survival (72). IFN-associated mechanisms modulated by BPA have been shown to influence SLE pathogenesis (73). Interestingly, prenatally BPA exposed mice showed an increase in IL-4 and IFNγ. However, mice exposed after reaching adulthood showed increases in IL-4, IL-10, and IL-13, but not IFNγ. In both cases, Tregs were reduced (74). This disparity shows that the effects of EDCs are strongly dependent on age at exposure.

Bisphenol-A has been shown repeatedly to increase immunoglobulin production in B cells. B1 cells have been associated with Sjögren's syndrome and rheumatoid arthritis patients (75–77), and in mouse models of SLE have been shown to be more sensitive to EDC's modulatory effects than B2 cells (78). B1 cells increased production of anti-dsDNA autoantibody, enhanced IgG deposition and glomerulonephritis and overall worsened SLE signs following BPA implantation (79). MRL/*lpr* mice fed diets that contained phytoestrogen compounds diadzin and genistin had higher levels of IgG and complement component C3 deposition in glomeruli, along with altered immune cell infiltration into glomeruli compared with mice fed a diet devoid of estrogenic components (23). The majority of evidence supports that exposure to EDCs enhances autoantibody production and autoimmunity in mouse models of disease.

The complex immunological effects of EDCs can also display immune-suppressive effects. In people under 18 years of age, circulating BPA levels were negatively associated with anti-cytomegalovirus (CMV) antibody titers, suggesting that some EDCs may attenuate antiviral immunity (80). Short-term BPA exposure in New Zealand Black/White F1 progeny (NZB/W_{F1}) mice suppressed autoimmunity, reduced albuminuria, and extended the disease-free period, through modulation of IFNγ (81). Thus, when determining the impact of EDC exposure on disease states, it is vital to view data in the context of dosage, exposure length, age, and infection status, due to the wide range of effects that may be altered by EDC exposure.

To date, less is known regarding the role EDC exposure has on androgens, and androgen receptors (ARs) compared with EDC effects on ERs. EDCs may act in a manner that primarily disrupts the balance between androgen and estrogenic signals, altering the endogenous ratio of testosterone, DHT, and 17β-estradiol synthesis (28). Urinary BPA concentration was inversely correlated to free androgen index in males (82) with evidence that BPA can potentially interfere with androgen production and function (83–85). EDCs did not affect functions of normal ARs, though it is possible that in certain disease states, such as prostate cancer, EDCs could influence patient therapy through mutant ARs (86, 87). Much work needs to be done to evaluate the differential effects that EDCs have on the various immune pathways important in disease management, tolerance, and autoantibody production in a sex-dependent context. It is possible that the actions exerted by various EDCs on androgens may reduce the immunoregulatory efficacy and tip the delicate balance toward promotion of autoimmunity.

Nevertheless, much work needs to be done to definitively understand the effects of endocrine disruptors on autoimmunity.

Distinct sex-based responses to EDC exposure may contribute to dysregulation of the immune system to varying degrees in a disease-specific manner (**Figure 4**). Significant effort is still required to identify and molecularly characterize the impact of various environmental triggers, especially ubiquitous environmental contaminants, on the regulatory mechanisms of host immune systems.

Androgens

The effects of DHT and testosterone in mammalian species have been shown to be primarily immunosuppressive (31, 88–91). ARs are expressed in lymphoid and non-lymphoid cells of the thymus and bone marrow. However, they have not been found in peripheral lymphocytes (92). This suggests that while androgens may not have a direct effect on lymphocyte function, they are important in developmental stages of T and B lymphocytes. Thymic epithelial cells and bone marrow stromal cells also act as mediators of androgen's effects on immature lymphocytes (92). AR levels were not altered in the thymus following castration and were present on $CD3^+CD4^+$ and $CD3^+CD8^+$ thymic cells, with the highest level found on $CD3^{lo}CD8^+$ immature lymphocytes. ARs were also present in both cortical and medullary regions of the thymus following castration (92). The effects of castration extend to B cell development, leading to increased immature B cell populations in the bone marrow, as well as increased splenic B cells and enhanced antibody and autoantibody production in mice. Androgen replacement reversed the changes in the bone marrow, but did not affect splenic B cells (93).

In general, there is good evidence that androgens downregulate immune system response in both normal and autoimmune individuals (**Figure 5**). Gonadectomized male mice, compared with intact females, had increased responses to, and reduced infection by, protozoans and fungi (31, 88–90). Androgens have been shown to suppress various autoimmune disorders including lupus and autoimmune thyroiditis (94, 95). Androgen deprivation led to increased T cell numbers (96). Inhibition of IL-12-induced STAT4 phosphorylation occurs through the AR binding to Ptpn1 conserved region, inhibiting IL-12 signaling in $CD4^+$ T cells, and suppressing Th1 differentiation (97). Androgens reduce IFNγ production through decreased PPARγ (98). Suppressive effects are also exerted on B cell antibody production by androgens (99). In psoriatic arthritis patients, testosterone appears to exert a protective effect. Higher serum BAFF concentrations are associated with increased disease activity, while serum BAFF concentrations negatively correlate with circulating levels of testosterone (100). Therefore, it is possible that androgens can regulate the immune responses of a genetically autoimmune susceptible individual to favor the maintenance of homeostasis (**Figure 5**).

SEX DIFFERENCE IN STRESS RESPONSE AND AUTOIMMUNITY

Associations have long been suspected between stressor events in a patient's past and development of autoimmune diseases, such as SLE, MS, RA, and T1DM. Lack of evidence-based and prospective studies contribute to the skepticism that stressful life events are major etiopathological factors to consider in autoimmune disease development. Nevertheless, these events cannot be discounted, as stress responses can directly and indirectly influence immune responses. Sexual dimorphism exists in the hypothalamus–pituitary–adrenal (HPA) axis, a major component of the physiological stress response (101). Stress primarily acts upon the immune system through release of glucocorticoids, leading to alterations in cytokine production. In general, glucocorticoids inhibit the production of pro-inflammatory cytokines, such as IL-6, TNFα, and IFNα, whereas IL-4 and IL-10 are unaffected (102). Glucocorticoids are also able to inhibit the activation, proliferation, and differentiation of many cell types (103–106).

Fetal exposure to glucocorticoids can potentially impact a person's HPA axis, either directly or indirectly; an effect to which

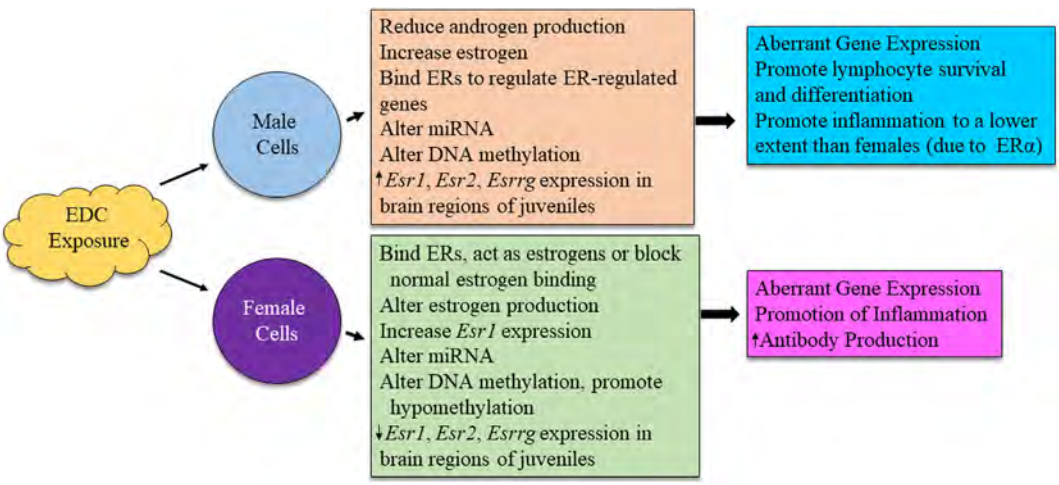

FIGURE 4 | Possible mechanism for sex differences in environmental EDC exposure on immune function. The exact mechanism for immune system alterations due to EDC exposure in each sex is not yet well understood. Here, we propose possible mechanisms in which EDCs may exert sex-specific influence on immune cell functions.

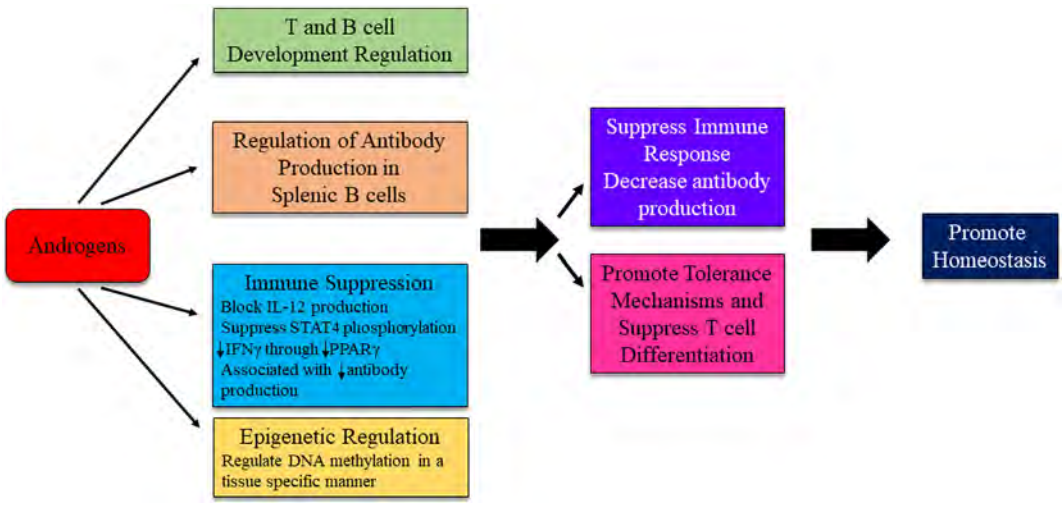

FIGURE 5 | Possible mechanism for androgens to influence immunity and autoimmune disease development. The exact mechanism for androgenic influence on autoimmune disease development is likely disease and context dependent. Potential mechanisms of androgen regulation are depicted. Research is ongoing to identify distinct pathways in which androgens are able to exert effects on immune system regulation.

female offspring are particularly vulnerable. Females exposed to a "prenatal stressor" had higher HPA reactivity than similarly exposed male offspring (107). Sex differences in cortisol response have been found in multiple life stages. Boys younger than 8 years of age had higher cortisol response than females of the same age. From 8 to 18 years of age, females have higher cortisol reactivity than males, an effect that is reversed in adulthood (107–112). Men have a more robust acute HPA response when compared with women, as determined by cortisol levels and sympathetic nervous system evaluation (113, 114). Men had higher glucocorticoid sensitivity and reduction in lipopolysaccharide (LPS)-stimulated cytokine production, whereas women had a decreased glucocorticoid sensitivity and increased LPS-stimulated cytokine production following a stress challenge (115). The type of stressor is also important when evaluating sexual dimorphism, as women had greater levels of cortisol in response to a social rejection challenge, while males had higher levels of cortisol in response to an achievement stimulus (116). Stress is able to alter plasma estradiol levels (117, 118) and estrogens have been shown to dampen the HPA and sympathetic nervous system response in certain studies (113, 119). However, other studies report a higher female HPA response independent of circulating gonadal hormone levels, suggesting either an innate difference in HPA mechanisms of action or an early developmental difference in response to sex hormone exposure (120).

A recent meta-analysis of 14 retrospective case–control studies supports major psychosocial stress as a risk factor for autoimmune disease development (121). This associated risk remained independent of the autoimmune disease reported. Appropriate controls in human studies exploring the role of stressors on autoimmune disease are difficult to determine, as the etiology of autoimmune diseases are still not well characterized. Most human retrospective studies rely on patient recall of stressful events that occur relatively close to disease diagnosis. It is possible that immune dysregulation and autoantibody production occur many years before the appearance of clinical signs. This would suggest that a stressor event that happens temporally close to the time of diagnosis would be a disease exacerbator, rather than an etiological factor. Consideration must also be given to the potential that the recrudescence of a latent virus or alteration in microbiota composition induced by a stressful event may be a driving factor in autoimmune disease development. Due to experimental limitations on human subjects, and the species differences in HPA axis response, these questions remain difficult to address, though the use of humanized rodent models may help to mitigate these limitations.

SEX DIFFERENCES IN EPIGENETIC REGULATION AND AUTOIMMUNITY

Recent studies highlight the importance of epigenetic regulation in biological systems development and function. Abnormal epigenetic regulation, such as microRNA (miRNA) dysregulation and DNA hypomethylation, has been implicated in autoimmune diseases (122–128). Epigenetic mechanisms are important contributors to the balance between functional gene expression and regulation. These pathways, such as those that drive specific gene DNA methylation status, are dynamic processes and may potentially be altered in response to environmental cues and contaminants.

Hormones Influence Epigenetic Regulation

Recent studies have suggested that sex hormones regulate immunity and autoimmunity through epigenetic mechanisms (**Figures 3** and **5**). miRNAs is a class of small non-coding RNAs that has emerged as a key epigenetic regulator of immune system functions

in the last two decades (129). We have reported that estrogen regulated a set of miRNA in the splenic cells of normal B6 mice, of which, miR-146a and miR-223 were further validated to contribute to enhanced inflammation in splenocytes from estrogen-treated mice (130). Many estrogen-regulated miRNAs, such as miR-17-92, miR-125, miR-181a, miR-155, and miR-150, have been implicated in the regulation of B cell development and antibody production by targeting different genes such as Bim, C-Myc, Lin28, Pu.1, and AID (129, 131, 132). This suggests that estrogen may regulate B cell functions and antibody production *via* miRNA regulation. We recently reported that select lupus-associated miRNAs were differentially expressed in male and female NZB/W_{F1} mice and that estrogen promoted the expression of these lupus-associated miRNAs in orchidectomized male NZB/W_{F1} mice. Estrogen conferred a female expression pattern of miRNAs on the male NZB/W_{F1} mice, contributing to the female bias of lupus (36). Estrogen regulation of miRNA expression and the underlying mechanism has been further reviewed in more detail in our previous publication (5).

Increasing evidence indicates that sex influences the DNA methylome, which contributes to the sex differences in organ development, function, and susceptibility to specific diseases. Estrogen regulation of DNA methylation is suggested by the finding of the positive correlation between ER-positive status and promoter hypermethylation in breast tumors (133, 134). Estrogen has been reported to upregulate DNA methyltransferase (DNMT)3b expression in Ishikawa endometrial adenocarcinoma cells to facilitate malignant transformation of endometrial cancer cells (135). However, the inhibitory effect of estrogen on DNA methylation has also been observed in prostate cancer cell lines, which was mediated by the activation of ERβ, suggesting the importance of context on estrogen's actions (136). There are limited data with regard to estrogen regulation of DNA methylation in immune cells. Autoimmune regulator (*AIRE*) is a negative regulator of autoimmunity, which is differentially expressed in the male and female thymus and contributes to the gender difference of autoimmune diseases (39). A recent study revealed that estrogen downregulated *AIRE* expression by inducing DNA methylation at the promoter, contributing to the female bias of autoimmune diseases (39). Nevertheless, the detailed mechanism of estrogen-mediated promotion of DNA methylation at the *AIRE* promoter remains to be clarified in future studies.

DNA methylation plays an essential role in regulation of sexual dimorphism of brain function during early development. It has been shown that females display higher DNMTs activity and hypermethylation in the highly sexually dimorphic preoptic area at postnatal day 1. Treatment with the testosterone metabolite estradiol significantly reduced global methylation at the preoptic area, leading to brain masculinization (137). Yolk testosterone was positively correlated with methylation levels of the ERα promoter in the diencephalon (138). The AR can both prevent DNA methylation through binding of the AR to the promoter of a gene of interest and promote DNA methylation through interaction of the AR with a suppressor, silencing expression of the gene of interest and eventual DNA methylation. AR function is associated with distinct DNA methylation patterns in genital tissues (139). Interestingly, the DNA methylation analysis of human blood revealed that there was a tendency of higher methylation levels in healthy males when compared with healthy females (140). Although the mechanism was unknown, we observed a reduction of global DNA methylation in splenocytes from estrogen-treated B6 mice when compared with placebo-controls. Given that DNA hypomethylation plays an important role in autoimmune diseases, such as lupus, it is significant to understand whether the gender difference in DNA methylation in immune cells contributes to the female bias of autoimmune disease directly and whether estrogen plays a role in the sexual dimorphism of DNA methylation in immune cells. It is noteworthy that sex hormones may regulate DNA methylation differentially in the context of different tissues, developmental stages, and pathological conditions. It should also be considered that the effect of estrogen on the global methylation level and the methylation of specific gene loci in defined subsets of cells of the immune system may be different.

EDCs Influence Epigenetic Regulation

An individual's ability to respond to an immunological stimulus can be modified generations before that individual is even conceived, primarily through the trans-generational effect of EDC exposure on epigenetic regulation of immune system development (141–143). After conception, maternal exposure to EDCs can also lead to alterations in the fetal epigenome, potentially leading to aberrant development of multiple body systems in the developing fetus (49). Following birth, that individual will continue to encounter EDCs through various sources and routes of exposure including, but not limited to, drinking water, cosmetics and personal hygiene products, handling of food containers and consumption of the stored contaminated food, medications, and pesticides (144–146). Exposure to these myriad EDCs can potentially alter an individual's epigenome throughout all stages of life, influencing the body's development and overall response to stimuli.

Endocrine disrupting chemicals have been shown to be involved in the three known forms of epigenetic regulation: miRNA production, DNA methylation, and histone modification. BPA is commonly used as a model EDC to investigate mechanisms by which estrogenic EDCs are able to modulate cellular functions. To date, most studies have focused on BPA's ability to alter non-lymphoid tissue epigenetics. Dose and sex-specific changes were noted in ER gene expression, DNMT1 and DNMT3a expression, and DNA methylation status of the ERα gene *Esr1* in various areas of the brains of BALB/c mice exposed *in utero* to BPA. Male mice had increased *Esr1, Esr2, Esrrg, DNMT1*, and *DNMT3a* expression in the hypothalamus at low- and mid-range doses of BPA, but reduced expression at high doses, while the females showed the reverse effect. Female mice showed hypomethylation on multiple exons of the *Esr1* gene when exposed *in utero* (141). BPA exposure by pre-pubescent girls in Egypt led to evidence of hypomethylation of CpG-islands on the X-chromosome and reduced methylation levels in multiple genes associated with immune function (147). Overall, exposure to estrogenic EDCs, such as BPA, is associated with hypomethylation. $CD4^+$ T cells have been shown to be hypomethylated in human SLE patients compared with healthy control (148). Therefore, it is possible that the reduced methylation associated with exposure to EDCs

contributes to the hypomethylation of $CD4^+$ T cells seen in SLE and systemic sclerosis patients, promoting aberrant gene expression in these cells, contributing to disease pathology.

Estrogenic environmental agent exposure can lead to aberrant miRNA expression profiles. BPA and DDT are able to alter the miRNA expression in a similar manner to estrogen. Increases have been seen in miR-21 and miR-146a. BPA was shown to decrease miR-134 (149–152). Lupus-prone MRL/*lpr* mice fed a chow-based diet containing phytoestrogens had increased expression of multiple miRNA and higher levels of global DNA methylation following LPS stimulation in splenic leukocytes along with increased DNMT1 expression (23). While the precise mechanism for this paradoxical finding is not yet known, it is possible that in select immune cell subsets, DNA methylation was reduced, or that the increased DNA methylation status suppressed immunoregulatory pathways, contributing to the enhanced disease phenotype seen in these mice. We are further investigating these findings. Long-term BPA exposure enhanced the expression and function of histone deacetylase 2 in adult mice, specifically in the hippocampus (153). Currently, there are no known effects of epigenetic regulation by BPA specifically on immune cell subsets. Further investigation is warranted into mechanisms by which estrogenic EDCs can alter the epigenome in immune cell subsets and promote tolerance dysregulation and antibody production.

AUTOIMMUNITY AND MICROBIAL AGENTS

Observational relationships between infections and autoimmune diseases have long been recognized. Infections have been reported in a number of autoimmune diseases that either preceded overt expression of autoimmune disease or noted concurrently. Associations have been made between human CMV and Epstein–Barr virus (EBV) and autoantibody production in SLE patients, EBV and *Mycoplasma arthritidis* in RA patients, and multiple viruses, including hepatitis E virus, in type I diabetes mellitus (154–158). In most associations, antigenic mimicry is thought to be the mechanism that drives autoantibody production. It is evident that for the majority of vaccinations and viral pathogens, females mount a much stronger antibody response, suggesting that if subsets of female B cells were to break central and peripheral tolerance, that these abnormal B cells would drive higher autoantibody production than male autoreactive B cells. In the same manner as gene associations, it is very difficult to link a single infection, or multiple infections, with causation of autoimmune diseases. Alterations in commensal gut microbiota composition have been found in multiple mouse models of SLE as well as human SLE patients (22, 159). Breaks in the mucosal barrier during stressful events or during the female reproductive cycle may expose the immune system to both infectious and commensal microbes (160). As the role of infectious agents potentially contributing to autoimmunity has been well documented to date, this review will focus on recent evidence linking sex differences in response to microbial stimulation, commensal microbiota, and environmental factors that may influence autoantibody production in susceptible individuals.

Sex Differences and Microbiota

The host microbiota, which has repeatedly been shown to influence immune phenotype, is dependent on multiple host factors, including age, diet, sex hormones, antibiotic usage, host genetics, obesity status, and various lifestyle choices. Early host–microbe interactions during childhood development can have long term and profound consequences on adult health through immune system "training" and induction of tolerance (161). Males and females have distinct microbial profiles, seen both in humans and mouse models of disease (162, 163). Gnotobiotic male and female C57BL/6 mice were administered the colonic contents of a human male. Upon analysis, the female mice had higher diversity as assessed by Shannon Diversity index, and a separate profile, whereas the male mice more closely resembled the donor profile. Forty-six distinct operational taxonomic units (OTUs) were different between the sexes, with 33 OTUs being overrepresented in the female fecal microbiota (162). Sex differences in microbial profiles were observed in multiple strains of mice. Gonadectomy with or without hormone replacement revealed further evidence of hormone effects on sex differences in mouse gut microbiota (164). In humans, the microbiota of males had reduced representation of *Bacteroides* at a BMI > 33, and the level of these microbes was reduced with increasing BMI. Post-menopausal females did not show an alteration in *Bacteroides* associated with BMI (165). An early critical window for microbial alteration of disease was shown for T1DM development in non-obese diabetic mice (NOD mice). Genetically similar mice housed in separate facilities eventually led to differing rates of T1DM development resulting in NOD^{low} and NOD^{high} communities. Co-housing or oral gavage of fecal contents from the NOD^{high} mice to NOD^{low} weanlings did not alter T1DM incidence. However, the offspring of the co-housed NOD^{low} mice did have increased T1DM incidence, suggesting that a window exists either *in utero* or before weaning where alterations of the microbiota result in disease development later in life (24). The importance of differing environmental, housing, and laboratory conditions on animal models of disease phenotypes is evident in this study. It is plausible that male and female epithelial and immune cells respond in a differential manner to microbial recognition during the formative periods in infancy and early childhood, and this differential response contributes to the distinct differences found in microbial composition in adulthood. It follows that if male and female cells inherently respond differently to microbial recognition during development, then exposure to EDCs during this important time period could drastically alter the microbial composition, thereby exerting long-term consequences on adult health from childhood exposures. Further investigation is vital to determine the role EDCs play in the development of microbial composition and resultant functional alterations in childhood and adulthood.

Communication between the host and commensal microbes occurs through multiple pathways, which are not yet well understood. Recognition of microbial-associated molecular patterns (MAMPs), production of soluble mediators, and interactions within the microbiota–gut–brain axis are thought to be the predominant methods of host–microbe communication. Resident immune cells at mucosal sites are able to recognize MAMPs and promote inflammation or induce regulation through Foxp3-positive T cell

populations (166–168). Cytokines, metabolites, hormones, mucus, and anti-microbial peptides are all mediators produced by the host in response to the presence of microbes, while microbes release short chain fatty acids, polysaccharide A, formyl peptides, and D-glyceo-β-D-mannoheptose-1,7-bisphosphate (HBP), all of which can modulate the host response and microenvironment (169). It is currently understood that a two-way communication channel exists between the gut microbiota and the central nervous system. Microbes exert effects on the vagal afferents and enteric nervous system, and resultant stress responses act through the HPA axis to drive or dampen cortisol secretion. Cortisol acts both locally and systemically on immune cells, promoting the secretion of various cytokines and chemokines, which in turn alters gut permeability and intestinal barrier function. These actions alter the microbial composition within the gut (170, 171). Thus, complex mechanisms of communication between the host and microbiota, which is dependent on specific microbial composition, may promote either tolerance or inflammation, both locally and systemically in a context-dependent manner.

In the context of autoimmune disease, Markle et al. investigated the sex differences in microbiota in a mouse model of autoimmune T1DM. Transfer of the male microbiota to female mice led to systemic alterations in sex hormone levels and protection of female mice against development of T1DM (163). This protective effect conferred by the transfer of male microbiota to female mice was dependent on AR activity. Blockage of AR activity by the AR antagonist flutamide, attenuated the protection from insulitis, autoantibody production, metabolome changes, and the capacity of T cell transfer to confer autoimmune disease in NOD SCID mice. Bacteria are able to metabolize sex hormones, thereby regulating the balance between active and inactive hormones, and potentially modulating hormone function (172). Probiotics were shown to enhance antibody response to vaccines, potentially affecting the efficacy of oral vaccinations due to gut microbiota (173, 174). We and colleagues showed that in a mouse model of SLE, *Lactobacillus* spp. was inversely associated with disease severity. Supplementation with *Lactobacillus* spp. led to reduced IL-6 production, suppression of IgG2a production and glomerular deposition, and increased IL-10 in circulation along with increased Treg populations and decreased Th17 subsets. *Lactobacillus* was also associated with reduced renal pathology. These protective effects were seen in female and castrated male MRL/*lpr* mice, but not in intact MRL/*lpr* mice, suggesting that some microbial effects act in a sex-hormone dependent manner (22). Sex-based differences in microbiota and effects on disease development or progression in the context of sex-biased autoimmune diseases are summarized in **Table 1**.

Sex Differences, Pathogen Sensing, and TLR7/8/9

Microbial signals are recognized through multiple pattern-recognition receptors, including TLRs, NOD-like receptors, C-type lectin receptors, and RIG-I-like receptors that are present in varying levels between cell subsets. Males and females tend to be exposed to the same pathogens and inflammatory triggers. However, the responses and outcomes to these exposures can be vastly different between sexes. One key sex difference in pathogen and inflammatory trigger sensing comes from the different levels of receptor expression. There are multiple immune-related genes, including TLR7, TLR8, FOXP3, CD40L, and CD13 that are present on the X-chromosome (177). It is possible that incomplete X chromosome inactivation can lead to increased numbers of $FoxP3^+$ cells. Interestingly, while the number of $FoxP3^+$ cells increased, the mean fluorescent intensity of FoxP3 was decreased and functional ability of these cells to regulate immune responses

TABLE 1 | Sex-based differences in microbiota and autoimmune disease development.

Autoimmune disorder	Animal models	Microbiota phenotype	Outcome	Reference
Systemic lupus erythematosus (SLE)	MRL-lpr mice	Elevated *Lachnospiraceae* sp.	Associated with more severe glomerulonephritis	(23)
SLE	MRL-lpr mice	Administration of *Lactobacillus*	Reduced proteinuria and renal pathology, serum IgG2a, IL-10, and IgA in castrated males, not intact males	(22)
			Decreased circulating luteinizing hormone	
SLE	MRL-lpr mice	Female MRL-lpr have elevated *Lachnospiraceae* and reduced *Lactobacillus* compared to controls, males showed no difference from controls	Accelerated disease in females compared with males	(21)
Type-1 diabetes mellitus (T1DM)	NOD mice	Male microbiota and gavage of male microbiota to female mice	Reduce T1DM in association with functional androgen receptor	(163)
		Germ-free conditions	Attenuated sex differences in cumulative T1D (%)	
T1DM	NOD mice	Segmented filamentous bacteria monocolonized Specific pathogen free conditions and colonization with segmented filamentous bacteria	Protected males but not females Increased blood testosterone levels in males compared to germ free	(175)
Rheumatoid arthritis	HLA-DRB1 0401, 0402 mice	0401 *Clostridium*-like bacterium dominant, loss of age, and sex differences in microbiota	More susceptible to disease	(176)
		0402 *Porphyromonadaceae* and *Bifidobacteria* dominant, retain sex- and age-based microbiota differences	Resistant to disease	

was suppressed (178). There is a potential for increased levels of TLR7 and 8 expression due to incomplete inactivation of the X-chromosome in females. The balance among TLR7, 8, and 9 has been shown to be vital to disease development in mouse models of SLE. TLR7 and 8 sense single-stranded RNA, and TLR9 binds to specific unmethylated CpG DNA motifs. Mice with increased levels of TLR7, or loss of TLR9, had enhanced autoantibody production and diseases severity, with TLR9 suppressing the autoantibody production induced by TLR7 (179). Male mice had higher levels of TLR4, circulating LPS-binding protein, and increased expression of CD14 on macrophages than female mice following LPS stimulation *in vivo*. These changes were seen at the protein level, while mRNA expression was unchanged between sexes (180, 181). Therefore, the potential differences in ability of male and female cells to recognize microbial or self stimuli may contribute to the observed differential responses.

Sex differences are also observed in how immune cells respond internally following ligand binding to receptors. Female Kuppfer cells produce IL-6 in a MyD88-dependent pathway, while male cells produce IL-6 in a MyD88-independent pathway (182). The ligation of CD200–CD200R is important in the suppression of TLR7 response to pathogens and control of IFNα production (183). Release of this inhibition through the knockout of the CD200 gene in mice enhanced sex differences in TLR7 and

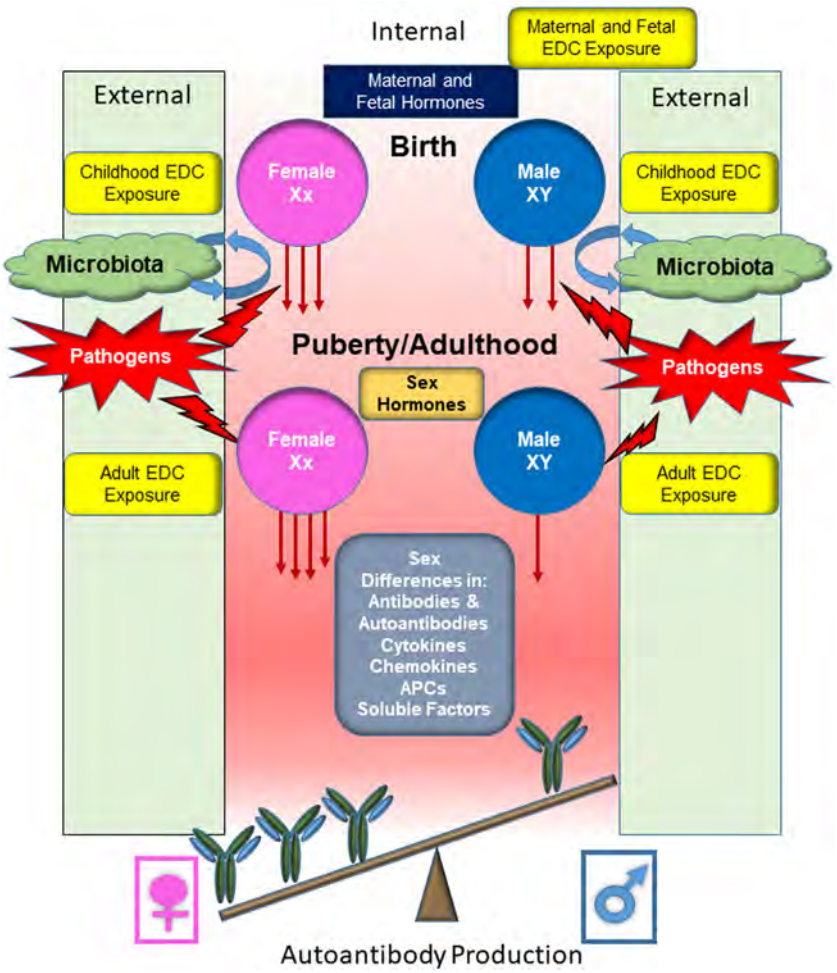

FIGURE 6 | Overview of the responses by male and female B cells to external stimuli and subsequent production of autoantibodies. Before conception, the maternal systems are augmented in various ways, including exposure to endocrine disrupting chemicals (EDCs). Following conception, the fetus is subjected to EDC exposure through continued maternal exposure. Fetal and maternal hormones contribute to immune system development. Following parturition, an infant becomes exposed to microbial organisms and the establishment of commensal microbial population begins, being influenced by both endogenous and exogenous factors before stabilization. The microbiota composition will influence the developing immune system and promote recognition of pathogens and support the development of tolerance mechanisms. Juveniles continue to be exposed to EDCs and pathogenic microbes will be encountered, further stimulating the immune system. At puberty, cells become exposed to higher levels of female or male sex hormones, altering immune cell function and signaling pathways. During adulthood, immune cells continue to be exposed to EDCs and microbial stimuli, both commensal and pathogenic. Sex differential levels of cytokines, chemokines, hormones, and other soluble factors make up the microenvironment that the immune cells are exposed to, further promoting or inhibiting immune cell activation and response. The female cells, which may be primed due to sex differences and environmental contributing factors, generally respond more robustly to the same immunological stimulus compared with male cells. This more robust response likely contributes to the female biased dominance in many autoimmune diseases.

outcomes of viral infection. In HIV-1 infection, female plasmacytoid dendritic cells produced higher levels of IFNα after TLR7 stimulation than males and also had enhanced expression levels of all 13 IFNα subtypes and IFNβ following stimulation of TLR7 on peripheral blood mononuclear cells (PBMCs) (183). Caution must be taken when evaluating changes in expression levels and correlating that to immune responses, as PBMCs from human SLE patients showed increased expression of TLR9 mRNA and proteins compared with healthy controls. However, the function of TLR9 was impaired in SLE PBMCs leading to reduced IFNα following stimulation (184). Therefore, it is plausible that female cells may be more sensitive to PAMPs, and following receptor binding, internal signaling differences may enhance inflammatory responses compared with male cells.

CONCLUSION AND FUTURE DIRECTIONS

Biological differences exist in immunological responses to stimuli between males and females, and this likely contributes to the sex difference in the loss of immunological tolerance and production of autoantibodies. These differences manifest in a complex network of intrinsic differences in the ability of immune cells to recognize a stimulus, respond, and return to homeostasis. Female and male cells could have differential cell signaling and outcomes to environmental contaminants exposure, concurrent disease or pathogen exposure, commensal populations, age, sex hormone fluctuations, and other environmental influences. While this biological end point generally protects females from infectious diseases, it predisposes genetically susceptible individuals to chronic inflammatory conditions and development of autoimmunity compared with their male counterparts. Our understanding of environmental interactions with sex-specific characteristics remains incomplete, with evidence that sex-specific therapies or preventive measures may exist. Sex-based differences have been seen in response to treatment with methylprednisolone and rituximab (a monoclonal antibody against CD20) (185, 186). Sex disparities in clinical presentation, progression, and outcome of autoimmune diseases exist, suggesting that separation of sex-based groups in the evaluation of treatment strategies may help to appropriately tailor multiple treatment modalities in the future (187, 188). Environmental exposures may also influence an individual's response to medication, highlighting the importance of considering a patient's environment when determining the best possible treatment regimen. Further investigation into the precise mechanism of how environmental chemical exposure alters distinct ligand–receptor signaling cascades in specific immune cell subsets is vital for better understanding the extent to which these ubiquitous chemicals can modify human and animal physiology. The exploration into associations between commensal microbial dysregulation and host disease susceptibility, or severity, must also take into account, to the best extent possible, the environment to which that particular individual has been exposed. Microbial metabolism of EDCs may exert protection or promote exacerbation of certain disease processes depending on resultant metabolites and bioavailability.

Given that multi-factors are likely required for the induction of autoimmune diseases, a different approach is needed to understand sex differences in susceptibility to these chronic conditions. Biologically, male and female cells of the immune system are differentially exposed to sex hormones and sex hormone-regulated proteins (other unidentified internal regulators) and manifest inherent genetic differences in sex chromosomes. Thus, the cells of the innate and adaptive immune system could be molecularly primed differently between sexes. It is therefore conceivable that male and female cells will differently perceive the binding of their receptor to the same ligand. In females, exposure to these triggers may have adverse effects. Following external triggers, the female immune system may be more prone to dysregulation (e.g., break in immune tolerance) and have augmented induction of autoantibodies and cytokines/chemokines that have been associated with autoimmune diseases. We further postulate that in genetically susceptible individuals, sex differences, both intrinsic and in response to environmental contaminants, such as estrogenic EDCs, contribute to female bias of immune tolerance dysregulation and drive autoantibody production and subsequent pathology (**Figure 6**). Understanding the complex interactions among differences in sex hormones, a wide range of chemicals, genetic variations, infections, and environmental triggers and deriving conclusions about impacts on pathogenesis will likely require the utilization of complex computational models. With the progression of individualized medicine, these environmental exposures will likely prove unique to various lifestyles and geographical locations.

AUTHOR CONTRIBUTIONS

All authors listed have made a substantial, direct, and intellectual contribution to the work and approved it for publication.

FUNDING

Preparation of this publication was supported by the Virginia-Maryland College of Veterinary Medicine (VMCVM) Intramural Research Competition (IRC) Grant (grant number 175185); Interdepartmental funds to SAA, and by the National Institutes of Health T32 training grant (grant number 5T32OD010430-09). The publication fee for this article is supported by Virginia Tech's Open Access Subvention Fund. The content is solely the responsibility of the authors and does not necessarily represent the official view of the National Institutes of Health or VMCVM.

REFERENCES

1. Bach JF. The effect of infections on susceptibility to autoimmune and allergic diseases. *N Engl J Med* (2002) 347(12):911–20. doi:10.1056/NEJMra020100
2. Lerner A, Matthias T. Rheumatoid arthritis-celiac disease relationship: joints get that gut feeling. *Autoimmun Rev* (2015) 14(11):1038–47. doi:10.1016/j.autrev.2015.07.007
3. Karpuzoglu E, Ahmed SA. Estrogen regulation of nitric oxide and inducible nitric oxide synthase (iNOS) in immune cells: implications for immunity, autoimmune diseases, and apoptosis. *Nitric Oxide* (2006) 15(3):177–86. doi:10.1016/j.niox.2006.03.009
4. Karpuzoglu E, Fenaux JB, Phillips RA, Lengi AJ, Elvinger F, Ansar Ahmed S. Estrogen up-regulates inducible nitric oxide synthase, nitric oxide, and cyclooxygenase-2 in splenocytes activated with T cell stimulants: role of

interferon-gamma. *Endocrinology* (2006) 147(2):662–71. doi:10.1210/en.2005-0829
5. Dai R, Ahmed SA. Sexual dimorphism of miRNA expression: a new perspective in understanding the sex bias of autoimmune diseases. *Ther Clin Risk Manag* (2014) 10:151–63. doi:10.2147/TCRM.S33517
6. Khan D, Ansar Ahmed S. The immune system is a natural target for estrogen action: opposing effects of estrogen in two prototypical autoimmune diseases. *Front Immunol* (2016) 6:635. doi:10.3389/fimmu.2015.00635
7. Khan D, Dai R, Ansar Ahmed S. Sex differences and estrogen regulation of miRNAs in lupus, a prototypical autoimmune disease. *Cell Immunol* (2015) 294(2):70–9. doi:10.1016/j.cellimm.2015.01.004
8. Calemine JB, Gogal RM Jr, Lengi A, Sponenberg P, Ahmed SA. Immunomodulation by diethylstilbestrol is dose and gender related: effects on thymocyte apoptosis and mitogen-induced proliferation. *Toxicology* (2002) 178(2):101–18. doi:10.1016/S0300-483X(02)00201-9
9. Buckley OE. Introduction. In: Miner RW, editor. *The Status of Multiple Sclerosis. Ann NY Acad Sci.* (1954). p. 541–720.
10. Confavreux C, Aimard G, Devic M. Course and prognosis of multiple sclerosis assessed by the computerized data processing of 349 patients. *Brain* (1980) 103(2):281–300. doi:10.1093/brain/103.2.281
11. Ramagopalan SV, Goldacre R, Skingsley A, Conlon C, Goldacre MJ. Associations between selected immune-mediated diseases and tuberculosis: record-linkage studies. *BMC Med* (2013) 11:97. doi:10.1186/1741-7015-11-97
12. Gregersen PK. Discordance for autoimmunity in monozygotic twins. Are "identical" twins really identical? *Arthritis Rheum* (1993) 36(9):1185–92. doi:10.1002/art.1780360902
13. Bogdanos DP, Smyk DS, Rigopoulou EI, Mytilinaiou MG, Heneghan MA, Selmi C, et al. Twin studies in autoimmune disease: genetics, gender and environment. *J Autoimmun* (2012) 38(2–3):J156–69. doi:10.1016/j.jaut.2011.11.003
14. Generali E, Ceribelli A, Stazi MA, Selmi C. Lessons learned from twins in autoimmune and chronic inflammatory diseases. *J Autoimmun* (2017) 83:51–61. doi:10.1016/j.jaut.2017.04.005
15. Castillo-Fernandez JE, Spector TD, Bell JT. Epigenetics of discordant monozygotic twins: implications for disease. *Genome Med* (2014) 6(7):60. doi:10.1186/s13073-014-0060-z
16. Gilkeson G, James J, Kamen D, Knackstedt T, Maggi D, Meyer A, et al. The United States to Africa lupus prevalence gradient revisited. *Lupus* (2011) 20(10):1095–103. doi:10.1177/0961203311404915
17. Chiou SHLJ, Lin SL, Chen DY, Tsai NY, Kuan CY, Lin TY, et al. Pet dogs owner by lupus patients are at a higher risk of developing lupus. *Lupus* (2004) 13(6):442–9. doi:10.1191/0961203303lu1039oa
18. van Blokland SC, van Helden-Meeuwsen CG, Wierenga-Wolf AF, Drexhage HA, Hooijkaas H, van de Merwe JP, et al. Two different types of sialoadenitis in the NOD- and MRL/lpr mouse models for Sjogren's syndrome: a differential role for dendritic cells in the initiation of sialoadenitis? *Lab Invest* (2000) 80(4):575–85. doi:10.1038/labinvest.3780062
19. Mannoor K, Matejuk A, Xu Y, Beardall M, Chen C. Expression of natural autoantibodies in MRL-lpr mice protects from lupus nephritis and improves survival. *J Immunol* (2012) 188(8):3628–38. doi:10.4049/jimmunol.1102859
20. Keil A, Hall SR, Korner M, Herrmann M, Schmid RA, Frese S. Suppression of lupus nephritis and skin lesions in MRL/lpr mice by administration of the topoisomerase I inhibitor irinotecan. *Arthritis Res Ther* (2016) 18(1):243. doi:10.1186/s13075-016-1144-5
21. Zhang HLX, Sparks JB, Luo XM. Dynamics of gut microbiota in autoimmune lupus. *Appl Environ Microbiol* (2014) 80(24):7551–60. doi:10.1128/AEM.02676-14
22. Mu Q, Zhang H, Liao X, Lin K, Liu H, Edwards MR, et al. Control of lupus nephritis by changes of gut microbiota. *Microbiome* (2017) 5(1):73. doi:10.1186/s40168-017-0300-8
23. Edwards MR, Dai R, Heid B, Cecere TE, Khan D, Mu Q, et al. Commercial rodent diets differentially regulate autoimmune glomerulonephritis, epigenetics and microbiota in MRL/lpr mice. *Int Immunol* (2017) 29(6):263–76. doi:10.1093/intimm/dxx033
24. De Riva A, Wallberg M, Ronchi F, Coulson R, Sage A, Thorne L, et al. Regulation of type 1 diabetes development and B-cell activation in nonobese diabetic mice by early life exposure to a diabetogenic environment. *PLoS One* (2017) 12(8):e0181964. doi:10.1371/journal.pone.0181964
25. Khan D, Ahmed SA. Epigenetic regulation of non-lymphoid cells by bisphenol A, a model endocrine disrupter: potential implications for immunoregulation. *Front Endocrinol* (2015) 6:91. doi:10.3389/fendo.2015.00091
26. Whitacre CC. Sex differences in autoimmune disease. *Nat Immunol* (2001) 2(9):777–80. doi:10.1038/ni0901-777
27. Fish EN. The X-files in immunity: sex-based differences predispose immune responses. *Nat Rev Immunol* (2008) 8(9):737–44. doi:10.1038/nri2394
28. Pellegrini M, Bulzomi P, Lecis M, Leone S, Campesi I, Franconi F, et al. Endocrine disruptors differently influence estrogen receptor beta and androgen receptor in male and female rat VSMC. *J Cell Physiol* (2014) 229(8):1061–8. doi:10.1002/jcp.24530
29. Wang J, Syrett CM, Kramer MC, Basu A, Atchison ML, Anguera MC. Unusual maintenance of X chromosome inactivation predisposes female lymphocytes for increased expression from the inactive X. *Proc Natl Acad Sci U S A* (2016) 113(14):E2029–38. doi:10.1073/pnas.1520113113
30. Asaba J, Bandyopadhyay M, Kindy M, Dasgupta S. Estrogen receptor signal in regulation of B cell activation during diverse immune responses. *Int J Biochem Cell Biol* (2015) 68:42–7. doi:10.1016/j.biocel.2015.08.012
31. Olsen NJ, Kovacs WJ. Gonadal steroids and immunity. *Endocr Rev* (1996) 17(4):369–84. doi:10.1210/edrv-17-4-369
32. Rogers JA, Metz L, Yong VW. Review: endocrine disrupting chemicals and immune responses: a focus on bisphenol-A and its potential mechanisms. *Mol Immunol* (2013) 53(4):421–30. doi:10.1016/j.molimm.2012.09.013
33. Mallampalli MP, Davies E, Wood D, Robertson H, Polato F, Carter CL. Role of environment and sex differences in the development of autoimmune diseases: a roundtable meeting report. *J Womens Health (Larchmt)* (2013) 22(7):578–86. doi:10.1089/jwh.2013.4462
34. Scofield RH, Bruner GR, Namjou B, Kimberly RP, Ramsey-Goldman R, Petri M, et al. Klinefelter's syndrome (47,XXY) in male systemic lupus erythematosus patients: support for the notion of a gene-dose effect from the X chromosome. *Arthritis Rheum* (2008) 58(8):2511–7. doi:10.1002/art.23701
35. Liang Y, Tsoi LC, Xing X, Beamer MA, Swindell WR, Sarkar MK, et al. A gene network regulated by the transcription factor VGLL3 as a promoter of sex-biased autoimmune diseases. *Nat Immunol* (2017) 18(2):152–60. doi:10.1038/ni.3643
36. Dai R, McReynolds S, Leroith T, Heid B, Liang Z, Ahmed SA. Sex differences in the expression of lupus-associated miRNAs in splenocytes from lupus-prone NZB/WF1 mice. *Biol Sex Differ* (2013) 4(1):19. doi:10.1186/2042-6410-4-19
37. Dai R, Cowan C, Heid B, Khan D, Liang Z, Pham CT, et al. Neutrophils and neutrophil serine proteases are increased in the spleens of estrogen-treated C57BL/6 mice and several strains of spontaneous lupus-prone mice. *PLoS One* (2017) 12(2):e0172105. doi:10.1371/journal.pone.0172105
38. Priyanka HP, Krishnan HC, Singh RV, Hima L, Thyagarajan S. Estrogen modulates in vitro T cell responses in a concentration- and receptor-dependent manner: effects on intracellular molecular targets and antioxidant enzymes. *Mol Immunol* (2013) 56(4):328–39. doi:10.1016/j.molimm.2013.05.226
39. Dragin N, Bismuth J, Cizeron-Clairac G, Biferi MG, Berthault C, Serraf A, et al. Estrogen-mediated downregulation of AIRE influences sexual dimorphism in autoimmune diseases. *J Clin Invest* (2016) 126(4):1525–37. doi:10.1172/JCI81894
40. Dragin N, Nancy P, Villegas J, Roussin R, Panse RL, Berrih-Aknin S. Balance between estrogens and proinflammatory cytokines regulates chemokine production involved in thymic germinal center formation. *Sci Rep* (2017) 7(1):7970. doi:10.1038/s41598-017-08631-5
41. Khan D, Dai R, Karpuzoglu E, Ahmed SA. Estrogen increases, whereas IL-27 and IFN-gamma decrease, splenocyte IL-17 production in WT mice. *Eur J Immunol* (2010) 40(9):2549–56. doi:10.1002/eji.201040303
42. Li J, McMurray RW. Effects of cyclic versus sustained estrogen administration on peripheral immune functions in ovariectomized mice. *Am J Reprod Immunol* (2010) 63(4):274–81. doi:10.1111/j.1600-0897.2009.00784.x
43. Ahmed SA, Verthelyi D. Antibodies to cardiolipin in normal C57BL/6J mice: induction by estrogen but not dihydrotestosterone. *J Autoimmun* (1993) 6(3):265–79. doi:10.1006/jaut.1993.1023
44. Rubtsova K, Marrack P, Rubtsov AV. Sexual dimorphism in autoimmunity. *J Clin Invest* (2015) 125(6):2187–93. doi:10.1172/JCI78082
45. Ramos-Casals M, Garcia-Carrasco M, Brito MP, Lopez-Soto A, Font J. Autoimmunity and geriatrics: clinical significance of autoimmune manifestations in the elderly. *Lupus* (2003) 12(5):341–55. doi:10.1191/0961203303lu383ed

46. Chakhtoura M, Sriram U, Heayn M, Wonsidler J, Doyle C, Dinnall JA, et al. Bisphenol A does not mimic estrogen in the promotion of the in vitro response of murine dendritic cells to toll-like receptor ligands. *Mediators Inflamm* (2017) 2017:2034348. doi:10.1155/2017/2034348
47. Ahmed SA. The immune system as a potential target for environmental estrogens (endocrine disrupters): a new emerging field. *Toxicology* (2000) 150(1–3):191–206. doi:10.1016/S0300-483X(00)00259-6
48. Ahmed SA, Hissong BD, Verthelyi D, Donner K, Becker K, Karpuzoglu-Sahin E. Gender and risk of autoimmune diseases: possible role of estrogenic compounds. *Environ Health Perspect* (1999) 107(Suppl 5):681–6. doi:10.2307/3434327
49. Schug TT, Janesick A, Blumberg B, Heindel JJ. Endocrine disrupting chemicals and disease susceptibility. *J Steroid Biochem Mol Biol* (2011) 127(3–5):204–15. doi:10.1016/j.jsbmb.2011.08.007
50. Diamanti-Kandarakis E, Bourguignon JP, Giudice LC, Hauser R, Prins GS, Soto AM, et al. Endocrine-disrupting chemicals: an Endocrine Society scientific statement. *Endocr Rev* (2009) 30(4):293–342. doi:10.1210/er.2009-0002
51. Yue W, Wang JP, Li Y, Fan P, Liu G, Zhang N, et al. Effects of estrogen on breast cancer development: role of estrogen receptor independent mechanisms. *Int J Cancer* (2010) 127(8):1748–57. doi:10.1002/ijc.25207
52. Yue W, Yager JD, Wang JP, Jupe ER, Santen RJ. Estrogen receptor-dependent and independent mechanisms of breast cancer carcinogenesis. *Steroids* (2013) 78(2):161–70. doi:10.1016/j.steroids.2012.11.001
53. El-Tanani MK, Green CD. Two separate mechanisms for ligand-independent activation of the estrogen receptor. *Mol Endocrinol* (1997) 11(7):928–37. doi:10.1210/mend.11.7.9939
54. Maggi A. Liganded and unliganded activation of estrogen receptor and hormone replacement therapies. *Biochim Biophys Acta* (2011) 1812(8):1054–60. doi:10.1016/j.bbadis.2011.05.001
55. Park HJ, Park HS, Lee JU, Bothwell AL, Choi JM. Gender-specific differences in PPARgamma regulation of follicular helper T cell responses with estrogen. *Sci Rep* (2016) 6:28495. doi:10.1038/srep28495
56. Straub RH. The complex role of estrogens in inflammation. *Endocr Rev* (2007) 28(5):521–74. doi:10.1210/er.2007-0001
57. Herblot S, Aplan PD, Hoang T. Gradient of E2A activity in B-cell development. *Mol Cell Biol* (2002) 22(3):886–900. doi:10.1128/MCB.22.3.886-900.2002
58. Panchanathan R, Choubey D. Murine BAFF expression is up-regulated by estrogen and interferons: implications for sex bias in the development of autoimmunity. *Mol Immunol* (2013) 53(1–2):15–23. doi:10.1016/j.molimm.2012.06.013
59. Drehmer MN, Suterio DG, Muniz YC, de Souza IR, Lofgren SE. BAFF expression is modulated by female hormones in human immune cells. *Biochem Genet* (2016) 54(5):722–30. doi:10.1007/s10528-016-9752-y
60. Bynoe MS, Grimaldi CM, Diamond B. Estrogen up-regulates Bcl-2 and blocks tolerance induction of naive B cells. *Proc Natl Acad Sci U S A* (2000) 97(6):2703–8. doi:10.1073/pnas.040577497
61. Seillet C, Rouquie N, Foulon E, Douin-Echinard V, Krust A, Chambon P, et al. Estradiol promotes functional responses in inflammatory and steady-state dendritic cells through differential requirement for activation function-1 of estrogen receptor alpha. *J Immunol* (2013) 190(11):5459–70. doi:10.4049/jimmunol.1203312
62. Carreras E, Turner S, Frank MB, Knowlton N, Osban J, Centola M, et al. Estrogen receptor signaling promotes dendritic cell differentiation by increasing expression of the transcription factor IRF4. *Blood* (2010) 115(2):238–46. doi:10.1182/blood-2009-08-236935
63. Kovats S. Estrogen receptors regulate an inflammatory pathway of dendritic cell differentiation: mechanisms and implications for immunity. *Horm Behav* (2012) 62(3):254–62. doi:10.1016/j.yhbeh.2012.04.011
64. Grimaldi CM, Jeganathan V, Diamond B. Hormonal regulation of B cell development: 17 beta-estradiol impairs negative selection of high-affinity DNA-reactive B cells at more than one developmental checkpoint. *J Immunol* (2006) 176(5):2703–10. doi:10.4049/jimmunol.176.5.2703
65. Grimaldi CM. Sex and systemic lupus erythematosus: the role of the sex hormones estrogen and prolactin on the regulation of autoreactive B cells. *Curr Opin Rheumatol* (2006) 18(5):456–61. doi:10.1097/01.bor.0000240354.37927.dd
66. Bodin J, Kocbach Bolling A, Wendt A, Eliasson L, Becher R, Kuper F, et al. Exposure to bisphenol A, but not phthalates, increases spontaneous diabetes type 1 development in NOD mice. *Toxicol Rep* (2015) 2:99–110. doi:10.1016/j.toxrep.2015.02.010
67. Bodin J, Bolling AK, Samuelsen M, Becher R, Lovik M, Nygaard UC. Long-term bisphenol A exposure accelerates insulitis development in diabetes-prone NOD mice. *Immunopharmacol Immunotoxicol* (2013) 35(3):349–58. doi:10.3109/08923973.2013.772195
68. Bodin J, Bolling AK, Becher R, Kuper F, Lovik M, Nygaard UC. Transmaternal bisphenol A exposure accelerates diabetes type 1 development in NOD mice. *Toxicol Sci* (2014) 137(2):311–23. doi:10.1093/toxsci/kft242
69. Chailurkit LO, Aekplakorn W, Ongphiphadhanakul B. The association of serum bisphenol A with thyroid autoimmunity. *Int J Environ Res Public Health* (2016) 13(11):E1153. doi:10.3390/ijerph13111153
70. Yan W, Chen C, Chen H. Estrogen downregulates miR-21 expression and induces inflammatory infiltration of macrophages in polymyositis: role of CXCL10. *Mol Neurobiol* (2017) 54(3):1631–41. doi:10.1007/s12035-016-9769-6
71. Goto M, Takano-Ishikawa Y, Ono H, Yoshida M, Yamaki K, Shinmoto H. Orally administered bisphenol A disturbed antigen specific immunoresponses in the naive condition. *Biosci Biotechnol Biochem* (2007) 71(9):2136–43. doi:10.1271/bbb.70004
72. Wildner G, Kaufmann U. What causes relapses of autoimmune diseases? The etiological role of autoreactive T cells. *Autoimmun Rev* (2013) 12(11):1070–5. doi:10.1016/j.autrev.2013.04.001
73. Pollard KM, Cauvi DM, Toomey CB, Morris KV, Kono DH. Interferon-gamma and systemic autoimmunity. *Discov Med* (2013) 16(87):123–31.
74. Yan H, Takamoto M, Sugane K. Exposure to bisphenol A prenatally or in adulthood promotes T(H)2 cytokine production associated with reduction of CD4CD25 regulatory T cells. *Environ Health Perspect* (2008) 116(4):514–9. doi:10.1289/ehp.10829
75. Dauphinee M, Tovar Z, Talal N. B cells expressing CD5 are increased in Sjogren's syndrome. *Arthritis Rheum* (1988) 31(5):642–7. doi:10.1002/art.1780310509
76. Plater-Zyberk C, Lam K, Kennedy TD, Maini RN, Janossy G. Increased representation of a subpopulation of early B cells in the peripheral blood of patients with rheumatoid arthritis. *Adv Exp Med Biol* (1985) 186:957–61.
77. Plater-Zyberk C, Maini RN, Lam K, Kennedy TD, Janossy G. A rheumatoid arthritis B cell subset expresses a phenotype similar to that in chronic lymphocytic leukemia. *Arthritis Rheum* (1985) 28(9):971–6. doi:10.1002/art.1780280903
78. Ishikawa S. Possible roles of B1 cells and environmental estrogens (endocrine disruptors) in the development of autoimmune diseases. *Allergol Int* (2005) 54(4):499–505. doi:10.2332/allergolint.54.499
79. Yurino H, Ishikawa S, Sato T, Akadegawa K, Ito T, Ueha S, et al. Endocrine disruptors (environmental estrogens) enhance autoantibody production by B1 cells. *Toxicol Sci* (2004) 81(1):139–47. doi:10.1093/toxsci/kfh179
80. Clayton EM, Todd M, Dowd JB, Aiello AE. The impact of bisphenol A and triclosan on immune parameters in the U.S. population, NHANES 2003–2006. *Environ Health Perspect* (2011) 119(3):390–6. doi:10.1289/ehp.1002883
81. Sawai C, Anderson K, Walser-Kuntz D. Effect of bisphenol A on murine immune function: modulation of interferon-gamma, IgG2a, and disease symptoms in NZB X NZW F1 mice. *Environ Health Perspect* (2003) 111(16):1883–7. doi:10.1289/ehp.6359
82. Mendiola J, Jorgensen N, Andersson AM, Calafat AM, Ye X, Redmon JB, et al. Are environmental levels of bisphenol a associated with reproductive function in fertile men? *Environ Health Perspect* (2010) 118(9):1286–91. doi:10.1289/ehp.1002037
83. Akingbemi BT, Sottas CM, Koulova AI, Klinefelter GR, Hardy MP. Inhibition of testicular steroidogenesis by the xenoestrogen bisphenol A is associated with reduced pituitary luteinizing hormone secretion and decreased steroidogenic enzyme gene expression in rat Leydig cells. *Endocrinology* (2004) 145(2):592–603. doi:10.1210/en.2003-1174
84. Lee HJ, Chattopadhyay S, Gong EY, Ahn RS, Lee K. Antiandrogenic effects of bisphenol A and nonylphenol on the function of androgen receptor. *Toxicol Sci* (2003) 75(1):40–6. doi:10.1093/toxsci/kfg150
85. Paris F, Servant N, Terouanne B, Sultan C. Evaluation of androgenic bioactivity in human serum by recombinant cell line: preliminary results. *Mol Cell Endocrinol* (2002) 198(1–2):123–9. doi:10.1016/S0303-7207(02)00375-1
86. Wetherill YB, Fisher NL, Staubach A, Danielsen M, de Vere White RW, Knudsen KE. Xenoestrogen action in prostate cancer: pleiotropic effects dependent on androgen receptor status. *Cancer Res* (2005) 65(1):54–65.

87. Luccio-Camelo DC, Prins GS. Disruption of androgen receptor signaling in males by environmental chemicals. *J Steroid Biochem Mol Biol* (2011) 127(1–2):74–82. doi:10.1016/j.jsbmb.2011.04.004
88. Alexander J. Sex differences and cross-immunity in DBA/2 mice infected with *L. mexicana* and *L. major*. *Parasitology* (1988) 96(Pt 2):297–302. doi:10.1017/S0031182000058303
89. Kamis AB, Ahmad RA, Badrul-Munir MZ. Worm burden and leukocyte response in *Angiostrongylus malaysiensis*-infected rats: the influence of testosterone. *Parasitol Res* (1992) 78(5):388–91. doi:10.1007/BF00931693
90. Kittas C, Henry L. Effect of gonadectomy and oestrogen administration on the response of lymph-node post-capillary venules to infection with *Toxoplasma gondii*. *J Pathol* (1979) 127(3):129–36. doi:10.1002/path.1711270305
91. Foo YZ, Nakagawa S, Rhodes G, Simmons LW. The effects of sex hormones on immune function: a meta-analysis. *Biol Rev Camb Philos Soc* (2017) 92(1):551–71. doi:10.1111/brv.12243
92. Olsen NJ, Kovacs WJ. Effects of androgens on T and B lymphocyte development. *Immunol Res* (2001) 23(2–3):281–8. doi:10.1385/IR:23:2-3:281
93. Viselli SM, Reese KR, Fan J, Kovacs WJ, Olsen NJ. Androgens alter B cell development in normal male mice. *Cell Immunol* (1997) 182(2):99–104. doi:10.1006/cimm.1997.1227
94. Roubinian JR, Talal N, Greenspan JS, Goodman JR, Siiteri PK. Effect of castration and sex hormone treatment on survival, anti-nucleic acid antibodies, and glomerulonephritis in NZB/NZW F1 mice. *J Exp Med* (1978) 147(6):1568–83. doi:10.1084/jem.147.6.1568
95. Ahmed SA, Penhale WJ. The influence of testosterone on the development of autoimmune thyroiditis in thymectomized and irradiated rats. *Clin Exp Immunol* (1982) 48(2):367–74.
96. Roden AC, Moser MT, Tri SD, Mercader M, Kuntz SM, Dong H, et al. Augmentation of T cell levels and responses induced by androgen deprivation. *J Immunol* (2004) 173(10):6098–108. doi:10.4049/jimmunol.173.10.6098
97. Kissick HT, Sanda MG, Dunn LK, Pellegrini KL, On ST, Noel JK, et al. Androgens alter T-cell immunity by inhibiting T-helper 1 differentiation. *Proc Natl Acad Sci U S A* (2014) 111(27):9887–92. doi:10.1073/pnas.1402468111
98. Zhang MA, Rego D, Moshkova M, Kebir H, Chruscinski A, Nguyen H, et al. Peroxisome proliferator-activated receptor (PPAR)alpha and -gamma regulate IFNgamma and IL-17A production by human T cells in a sex-specific way. *Proc Natl Acad Sci U S A* (2012) 109(24):9505–10. doi:10.1073/pnas.1118458109
99. Furman D, Hejblum BP, Simon N, Jojic V, Dekker CL, Thiebaut R, et al. Systems analysis of sex differences reveals an immunosuppressive role for testosterone in the response to influenza vaccination. *Proc Natl Acad Sci U S A* (2014) 111(2):869–74. doi:10.1073/pnas.1321060111
100. Pongratz G, Straub RH, Scholmerich J, Fleck M, Harle P. Serum BAFF strongly correlates with PsA activity in male patients only – is there a role for sex hormones? *Clin Exp Rheumatol* (2010) 28(6):813–9.
101. Stojanovich L. Stress and autoimmunity. *Autoimmun Rev* (2010) 9(5):A271–6. doi:10.1016/j.autrev.2009.11.014
102. Homo-Delarche F, Fitzpatrick F, Christeff N, Nunez EA, Bach JF, Dardenne M. Sex steroids, glucocorticoids, stress and autoimmunity. *J Steroid Biochem Mol Biol* (1991) 40(4–6):619–37. doi:10.1016/0960-0760(91)90285-D
103. Bateman A, Singh A, Kral T, Solomon S. The immune-hypothalamic-pituitary-adrenal axis. *Endocr Rev* (1989) 10(1):92–112. doi:10.1210/edrv-10-1-92
104. Mcgregor AM. Immunoendocrine interactions and autoimmunity. *N Engl J Med* (1990) 322(24):1739–41. doi:10.1056/Nejm199006143222409
105. Cupps TR, Fauci AS. Corticosteroid-mediated immunoregulation in man. *Immunol Rev* (1982) 65:133–55. doi:10.1111/j.1600-065X.1982.tb00431.x
106. Homodelarche F. Glucocorticoids, lymphokines and the cell response. *Int Congr Ser* (1988) 799:349–54.
107. Gifford RM, Reynolds RM. Sex differences in early-life programming of the hypothalamic-pituitary-adrenal axis in humans. *Early Hum Dev* (2017) 114:7–10. doi:10.1016/j.earlhumdev.2017.09.011
108. Carpenter T, Grecian SM, Reynolds RM. Sex differences in early-life programming of the hypothalamic-pituitary-adrenal axis in humans suggest increased vulnerability in females: a systematic review. *J Dev Orig Health Dis* (2017) 8(2):244–55. doi:10.1017/S204017441600074X
109. Hollanders JJ, van der Voorn B, Rotteveel J, Finken MJJ. Is HPA axis reactivity in childhood gender-specific? A systematic review. *Biol Sex Differ* (2017) 8(1):23. doi:10.1186/s13293-017-0144-8
110. Hodyl NA, Wyper H, Osei-Kumah A, Scott N, Murphy VE, Gibson P, et al. Sex-specific associations between cortisol and birth weight in pregnancies complicated by asthma are not due to differential glucocorticoid receptor expression. *Thorax* (2010) 65(8):677–83. doi:10.1136/thx.2009.123091
111. van der Voorn B, Hollanders JJ, Ket JCF, Rotteveel J, Finken MJJ. Gender-specific differences in hypothalamus-pituitary-adrenal axis activity during childhood: a systematic review and meta-analysis. *Biol Sex Differ* (2017) 8:3. doi:10.1186/s13293-016-0123-5
112. Stark MJ, Wright IM, Clifton VL. Sex-specific alterations in placental 11beta-hydroxysteroid dehydrogenase 2 activity and early postnatal clinical course following antenatal betamethasone. *Am J Physiol Regul Integr Comp Physiol* (2009) 297(2):R510–4. doi:10.1152/ajpregu.00175.2009
113. Kajantie E, Phillips DI. The effects of sex and hormonal status on the physiological response to acute psychosocial stress. *Psychoneuroendocrinology* (2006) 31(2):151–78. doi:10.1016/j.psyneuen.2005.07.002
114. Kudielka BM, Kirschbaum C. Sex differences in HPA axis responses to stress: a review. *Biol Psychol* (2005) 69(1):113–32. doi:10.1016/j.biopsycho.2004.11.009
115. Rohleder N, Schommer NC, Hellhammer DH, Engel R, Kirschbaum C. Sex differences in glucocorticoid sensitivity of proinflammatory cytokine production after psychosocial stress. *Psychosom Med* (2001) 63(6):966–72. doi:10.1097/00006842-200111000-00016
116. Stroud LR, Salovey P, Epel ES. Sex differences in stress responses: social rejection versus achievement stress. *Biol Psychiatry* (2002) 52(4):318–27. doi:10.1016/S0006-3223(02)01333-1
117. Galea LA, McEwen BS, Tanapat P, Deak T, Spencer RL, Dhabhar FS. Sex differences in dendritic atrophy of CA3 pyramidal neurons in response to chronic restraint stress. *Neuroscience* (1997) 81(3):689–97. doi:10.1016/S0306-4522(97)00233-9
118. Shors TJ, Pickett J, Wood G, Paczynski M. Acute stress persistently enhances estrogen levels in the female rat. *Stress* (1999) 3(2):163–71. doi:10.3109/10253899909001120
119. Goldstein JM, Jerram M, Poldrack R, Ahern T, Kennedy DN, Seidman LJ, et al. Hormonal cycle modulates arousal circuitry in women using functional magnetic resonance imaging. *J Neurosci* (2005) 25(40):9309–16. doi:10.1523/JNEUROSCI.2239-05.2005
120. Patchev VK, Almeida OF. Gender specificity in the neural regulation of the response to stress: new leads from classical paradigms. *Mol Neurobiol* (1998) 16(1):63–77. doi:10.1007/BF02740603
121. Porcelli B, Pozza A, Bizzaro N, Fagiolini A, Costantini MC, Terzuoli L, et al. Association between stressful life events and autoimmune diseases: a systematic review and meta-analysis of retrospective case-control studies. *Autoimmun Rev* (2016) 15(4):325–34. doi:10.1016/j.autrev.2015.12.005
122. Lu Q, Wu A, Tesmer L, Ray D, Yousif N, Richardson B. Demethylation of CD40LG on the inactive X in T cells from women with lupus. *J Immunol* (2007) 179(9):6352–8. doi:10.4049/jimmunol.179.9.6352
123. Zhang Z, Zhang R. Epigenetics in autoimmune diseases: pathogenesis and prospects for therapy. *Autoimmun Rev* (2015) 14(10):854–63. doi:10.1016/j.autrev.2015.05.008
124. Lian X, Xiao R, Hu X, Kanekura T, Jiang H, Li Y, et al. DNA demethylation of CD40l in CD4+ T cells from women with systemic sclerosis: a possible explanation for female susceptibility. *Arthritis Rheum* (2012) 64(7):2338–45. doi:10.1002/art.34376
125. Liao J, Liang G, Xie S, Zhao H, Zuo X, Li F, et al. CD40L demethylation in CD4(+) T cells from women with rheumatoid arthritis. *Clin Immunol* (2012) 145(1):13–8. doi:10.1016/j.clim.2012.07.006
126. Moore CS, Rao VT, Durafourt BA, Bedell BJ, Ludwin SK, Bar-Or A, et al. miR-155 as a multiple sclerosis-relevant regulator of myeloid cell polarization. *Ann Neurol* (2013) 74(5):709–20. doi:10.1002/ana.23967
127. Pauley KM, Stewart CM, Gauna AE, Dupre LC, Kuklani R, Chan AL, et al. Altered miR-146a expression in Sjogren's syndrome and its functional role in innate immunity. *Eur J Immunol* (2011) 41(7):2029–39. doi:10.1002/eji.201040757
128. Stanczyk J, Pedrioli DM, Brentano F, Sanchez-Pernaute O, Kolling C, Gay RE, et al. Altered expression of microRNA in synovial fibroblasts and

synovial tissue in rheumatoid arthritis. *Arthritis Rheum* (2008) 58(4):1001–9. doi:10.1002/art.23386
129. Dai R, Lu R, Ahmed SA. The upregulation of genomic imprinted DLK1-Dio3 miRNAs in murine lupus is associated with global DNA hypomethylation. *PLoS One* (2016) 11(4):e0153509. doi:10.1371/journal.pone.0153509
130. Dai R, Phillips RA, Zhang Y, Khan D, Crasta O, Ahmed SA. Suppression of LPS-induced Interferon-gamma and nitric oxide in splenic lymphocytes by select estrogen-regulated microRNAs: a novel mechanism of immune modulation. *Blood* (2008) 112(12):4591–7. doi:10.1182/blood-2008-04-152488
131. Li J, Wan Y, Ji Q, Fang Y, Wu Y. The role of microRNAs in B-cell development and function. *Cell Mol Immunol* (2013) 10(2):107–12. doi:10.1038/cmi.2012.62
132. Klinge CM. miRNAs regulated by estrogens, tamoxifen, and endocrine disruptors and their downstream gene targets. *Mol Cell Endocrinol* (2015) 418(Pt 3):273–97. doi:10.1016/j.mce.2015.01.035
133. Li L, Lee KM, Han W, Choi JY, Lee JY, Kang GH, et al. Estrogen and progesterone receptor status affect genome-wide DNA methylation profile in breast cancer. *Hum Mol Genet* (2010) 19(21):4273–7. doi:10.1093/hmg/ddq351
134. Benevolenskaya EV, Islam AB, Ahsan H, Kibriya MG, Jasmine F, Wolff B, et al. DNA methylation and hormone receptor status in breast cancer. *Clin Epigen* (2016) 8:17. doi:10.1186/s13148-016-0184-7
135. Cui M, Wen Z, Yang Z, Chen J, Wang F. Estrogen regulates DNA methyltransferase 3B expression in Ishikawa endometrial adenocarcinoma cells. *Mol Biol Rep* (2009) 36(8):2201–7. doi:10.1007/s11033-008-9435-9
136. Adjakly M, Ngollo M, Lebert A, Dagdemir A, Penault-Llorca F, Boiteux JP, et al. Comparative effects of soy phytoestrogens and 17beta-estradiol on DNA methylation of a panel of 24 genes in prostate cancer cell lines. *Nutr Cancer* (2014) 66(3):474–82. doi:10.1080/01635581.2014.884236
137. Nugent BM, Wright CL, Shetty AC, Hodes GE, Lenz KM, Mahurkar A, et al. Brain feminization requires active repression of masculinization via DNA methylation. *Nat Neurosci* (2015) 18(5):690–7. doi:10.1038/nn.3988
138. Bentz AB, Sirman AE, Wada H, Navara KJ, Hood WR. Relationship between maternal environment and DNA methylation patterns of estrogen receptor alpha in wild Eastern Bluebird (*Sialia sialis*) nestlings: a pilot study. *Ecol Evol* (2016) 6(14):4741–52. doi:10.1002/ece3.2162
139. Ammerpohl O, Bens S, Appari M, Werner R, Korn B, Drop SL, et al. Androgen receptor function links human sexual dimorphism to DNA methylation. *PLoS One* (2013) 8(9):e73288. doi:10.1371/journal.pone.0073288
140. El-Maarri O, Becker T, Junen J, Manzoor SS, Diaz-Lacava A, Schwaab R, et al. Gender specific differences in levels of DNA methylation at selected loci from human total blood: a tendency toward higher methylation levels in males. *Hum Genet* (2007) 122(5):505–14. doi:10.1007/s00439-007-0430-3
141. Kundakovic M, Gudsnuk K, Franks B, Madrid J, Miller RL, Perera FP, et al. Sex-specific epigenetic disruption and behavioral changes following low-dose in utero bisphenol A exposure. *Proc Natl Acad Sci U S A* (2013) 110(24):9956–61. doi:10.1073/pnas.1214056110
142. Cruz G, Foster W, Paredes A, Yi KD, Uzumcu M. Long-term effects of early-life exposure to environmental oestrogens on ovarian function: role of epigenetics. *J Neuroendocrinol* (2014) 26(9):613–24. doi:10.1111/jne.12181
143. Mileva G, Baker SL, Konkle AT, Bielajew C. Bisphenol-A: epigenetic reprogramming and effects on reproduction and behavior. *Int J Environ Res Public Health* (2014) 11(7):7537–61. doi:10.3390/ijerph110707537
144. Kavlock RJ, Daston GP, DeRosa C, Fenner-Crisp P, Gray LE, Kaattari S, et al. Research needs for the risk assessment of health and environmental effects of endocrine disruptors: a report of the U.S. EPA-sponsored workshop. *Environ Health Perspect* (1996) 104(Suppl 4):715–40. doi:10.2307/3432708
145. Agay-Shay K, Martinez D, Valvi D, Garcia-Esteban R, Basagana X, Robinson O, et al. Exposure to endocrine-disrupting chemicals during pregnancy and weight at 7 years of age: a multi-pollutant approach. *Environ Health Perspect* (2015) 123(10):1030–7. doi:10.1289/ehp.1409049
146. Combarnous Y. Endocrine disruptor compounds (EDCs) and agriculture: the case of pesticides. *C R Biol* (2017) 340(9–10):406–9. doi:10.1016/j.crvi.2017.07.009
147. Kim JH, Rozek LS, Soliman AS, Sartor MA, Hablas A, Seifeldin IA, et al. Bisphenol A-associated epigenomic changes in prepubescent girls: a cross-sectional study in Gharbiah, Egypt. *Environ Health* (2013) 12:33. doi:10.1186/1476-069X-12-33
148. Lei W, Luo Y, Lei W, Luo Y, Yan K, Zhao S, et al. Abnormal DNA methylation in CD4+ T cells from patients with systemic lupus erythematosus, systemic sclerosis, and dermatomyositis. *Scand J Rheumatol* (2009) 38(5):369–74. doi:10.1080/03009740902758875
149. Veiga-Lopez A, Luense LJ, Christenson LK, Padmanabhan V. Developmental programming: gestational bisphenol-A treatment alters trajectory of fetal ovarian gene expression. *Endocrinology* (2013) 154(5):1873–84. doi:10.1210/en.2012-2129
150. Kovanecz I, Gelfand R, Masouminia M, Gharib S, Segura D, Vernet D, et al. Oral Bisphenol A (BPA) given to rats at moderate doses is associated with erectile dysfunction, cavernosal lipofibrosis and alterations of global gene transcription. *Int J Impot Res* (2014) 26(2):67–75. doi:10.1038/ijir.2013.37
151. Tilghman SL, Bratton MR, Segar HC, Martin EC, Rhodes LV, Li M, et al. Endocrine disruptor regulation of microRNA expression in breast carcinoma cells. *PLoS One* (2012) 7(3):e32754. doi:10.1371/journal.pone.0032754
152. Avissar-Whiting M, Veiga KR, Uhl KM, Maccani MA, Gagne LA, Moen EL, et al. Bisphenol A exposure leads to specific microRNA alterations in placental cells. *Reprod Toxicol* (2010) 29(4):401–6. doi:10.1016/j.reprotox.2010.04.004
153. Kumar D, Thakur MK. Effect of perinatal exposure to bisphenol-A on DNA methylation and histone acetylation in cerebral cortex and hippocampus of postnatal male mice. *J Toxicol Sci* (2017) 42(3):281–9. doi:10.2131/jts.42.281
154. Hsieh AH, Jhou YJ, Liang CT, Chang M, Wang SL. Fragment of tegument protein pp65 of human cytomegalovirus induces autoantibodies in BALB/c mice. *Arthritis Res Ther* (2011) 13(5):R162. doi:10.1186/ar3481
155. Cole BC, Ahmed E, Araneo BA, Shelby J, Kamerath C, Wei S, et al. Immunomodulation in vivo by the *Mycoplasma arthritidis* superantigen, MAM. *Clin Infect Dis* (1993) 17(Suppl 1):S163–9. doi:10.1093/clinids/17.Supplement_1.S163
156. Cole BC, Griffiths MM. Triggering and exacerbation of autoimmune arthritis by the *Mycoplasma arthritidis* superantigen MAM. *Arthritis Rheum* (1993) 36(7):994–1002. doi:10.1002/art.1780360717
157. Schwab JH, Brown RR, Anderle SK, Schlievert PM. Superantigen can reactivate bacterial cell wall-induced arthritis. *J Immunol* (1993) 150(9):4151–9.
158. Christen U, Bender C, von Herrath MG. Infection as a cause of type 1 diabetes? *Curr Opin Rheumatol* (2012) 24(4):417–23. doi:10.1097/BOR.0b013e3283533719
159. Luo XM, Edwards MR, Mu Q, Yu Y, Vieson MD, Reilly CM, et al. Gut microbiota in human systemic lupus erythematosus and a mouse model of lupus. *Appl Environ Microbiol* (2018) 84(4). doi:10.1128/AEM.02288-17
160. Tiniakou E, Costenbader KH, Kriegel MA. Sex-specific environmental influences on the development of autoimmune diseases. *Clin Immunol* (2013) 149(2):182–91. doi:10.1016/j.clim.2013.02.011
161. Kollmann TR, Levy O, Montgomery RR, Goriely S. Innate immune function by toll-like receptors: distinct responses in newborns and the elderly. *Immunity* (2012) 37(5):771–83. doi:10.1016/j.immuni.2012.10.014
162. Wang J, Roderiquez G, Norcross MA. Control of adaptive immune responses by *Staphylococcus aureus* through IL-10, PD-L1, and TLR2. *Sci Rep* (2012) 2:606. doi:10.1038/srep00606
163. Markle JG, Frank DN, Mortin-Toth S, Robertson CE, Feazel LM, Rolle-Kampczyk U, et al. Sex differences in the gut microbiome drive hormone-dependent regulation of autoimmunity. *Science* (2013) 339(6123):1084–8. doi:10.1126/science.1233521
164. Org E, Mehrabian M, Parks BW, Shipkova P, Liu X, Drake TA, et al. Sex differences and hormonal effects on gut microbiota composition in mice. *Gut Microbes* (2016) 7(4):313–22. doi:10.1080/19490976.2016.1203502
165. Haro C, Rangel-Zuniga OA, Alcala-Diaz JF, Gomez-Delgado F, Perez-Martinez P, Delgado-Lista J, et al. Intestinal microbiota is influenced by gender and body mass index. *PLoS One* (2016) 11(5):e0154090. doi:10.1371/journal.pone.0154090
166. Sudo N, Sawamura S, Tanaka K, Aiba Y, Kubo C, Koga Y. The requirement of intestinal bacterial flora for the development of an IgE production system fully susceptible to oral tolerance induction. *J Immunol* (1997) 159(4):1739–45.
167. Wannemuehler MJ, Kiyono H, Babb JL, Michalek SM, McGhee JR. Lipopolysaccharide (LPS) regulation of the immune response: LPS converts germfree mice to sensitivity to oral tolerance induction. *J Immunol* (1982) 129(3):959–65.
168. Weiner HL, da Cunha AP, Quintana F, Wu H. Oral tolerance. *Immunol Rev* (2011) 241(1):241–59. doi:10.1111/j.1600-065X.2011.01017.x
169. Walsh CJ, Guinane CM, O'Toole PW, Cotter PD. Beneficial modulation of the gut microbiota. *FEBS Lett* (2014) 588(22):4120–30. doi:10.1016/j.febslet.2014.03.035

170. Cryan JF, Dinan TG. Mind-altering microorganisms: the impact of the gut microbiota on brain and behaviour. *Nat Rev Neurosci* (2012) 13(10):701–12. doi:10.1038/nrn3346
171. Grenham S, Clarke G, Cryan JF, Dinan TG. Brain-gut-microbe communication in health and disease. *Front Physiol* (2011) 2:94. doi:10.3389/fphys.2011.00094
172. Garcia-Gomez E, Gonzalez-Pedrajo B, Camacho-Arroyo I. Role of sex steroid hormones in bacterial-host interactions. *Biomed Res Int* (2013) 2013:928290. doi:10.1155/2013/928290
173. Brotman RM, Ravel J, Bavoil PM, Gravitt PE, Ghanem KG. Microbiome, sex hormones, and immune responses in the reproductive tract: challenges for vaccine development against sexually transmitted infections. *Vaccine* (2014) 32(14):1543–52. doi:10.1016/j.vaccine.2013.10.010
174. Ferreira RB, Antunes LC, Finlay BB. Should the human microbiome be considered when developing vaccines? *PLoS Pathog* (2010) 6(11):e1001190. doi:10.1371/journal.ppat.1001190
175. Yurkovetskiy L, Burrows M, Khan AA, Graham L, Volchkov P, Becker L, et al. Gender bias in autoimmunity is influenced by microbiota. *Immunity* (2013) 39(2):400–12. doi:10.1016/j.immuni.2013.08.013
176. Gomez A, Luckey D, Yeoman CJ, Marietta EV, Berg Miller ME, Murray JA, et al. Loss of sex and age driven differences in the gut microbiome characterize arthritis-susceptible 0401 mice but not arthritis-resistant 0402 mice. *PLoS One* (2012) 7(4):e36095. doi:10.1371/journal.pone.0036095
177. van Lunzen J, Altfeld M. Sex differences in infectious diseases-common but neglected. *J Infect Dis* (2014) 209(Suppl 3):S79–80. doi:10.1093/infdis/jiu159
178. Broen JC, Wolvers-Tettero IL, Geurts-van Bon L, Vonk MC, Coenen MJ, Lafyatis R, et al. Skewed X chromosomal inactivation impacts T regulatory cell function in systemic sclerosis. *Ann Rheum Dis* (2010) 69(12):2213–6. doi:10.1136/ard.2010.129999
179. Nickerson KM, Christensen SR, Shupe J, Kashgarian M, Kim D, Elkon K, et al. TLR9 regulates TLR7- and MyD88-dependent autoantibody production and disease in a murine model of lupus. *J Immunol* (2010) 184(4):1840–8. doi:10.4049/jimmunol.0902592
180. Marriott I, Bost KL, Huet-Hudson YM. Sexual dimorphism in expression of receptors for bacterial lipopolysaccharides in murine macrophages: a possible mechanism for gender-based differences in endotoxic shock susceptibility. *J Reprod Immunol* (2006) 71(1):12–27. doi:10.1016/j.jri.2006.01.004
181. Marriott I, Huet-Hudson YM. Sexual dimorphism in innate immune responses to infectious organisms. *Immunol Res* (2006) 34(3):177–92. doi:10.1385/IR:34:3:177
182. Zheng R, Pan G, Thobe BM, Choudhry MA, Matsutani T, Samy TS, et al. MyD88 and Src are differentially regulated in Kupffer cells of males and proestrus females following hypoxia. *Mol Med* (2006) 12(4–6):65–73. doi:10.2119/2006-00037.Zheng
183. Karnam G, Rygiel TP, Raaben M, Grinwis GC, Coenjaerts FE, Ressing ME, et al. CD200 receptor controls sex-specific TLR7 responses to viral infection. *PLoS Pathog* (2012) 8(5):e1002710. doi:10.1371/journal.ppat.1002710
184. Mortezagholi S, Babaloo Z, Rahimzadeh P, Namdari H, Ghaedi M, Gharibdoost F, et al. Evaluation of TLR9 expression on PBMCs and CpG ODN-TLR9 ligation on IFN-alpha production in SLE patients. *Immunopharmacol Immunotoxicol* (2017) 39(1):11–8. doi:10.1080/08923973.2016.1263859
185. Lew KH, Ludwig EA, Milad MA, Donovan K, Middleton E Jr, Ferry JJ, et al. Gender-based effects on methylprednisolone pharmacokinetics and pharmacodynamics. *Clin Pharmacol Ther* (1993) 54(4):402–14. doi:10.1038/clpt.1993.167
186. Nabhan C, Zhou X, Day BM, Dawson K, Zelenetz AD, Friedberg JW, et al. Disease, treatment, and outcome differences between men and women with follicular lymphoma in the United States. *Am J Hematol* (2016) 91(8):770–5. doi:10.1002/ajh.24401
187. Yacoub Wasef SZ. Gender differences in systemic lupus erythematosus. *Gend Med* (2004) 1(1):12–7. doi:10.1016/S1550-8579(04)80006-8
188. Schwartzman-Morris J, Putterman C. Gender differences in the pathogenesis and outcome of lupus and of lupus nephritis. *Clin Dev Immunol* (2012) 2012:604892. doi:10.1155/2012/604892

Conflict of Interest Statement: The authors declare that the research was conducted in the absence of any commercial or financial relationships that could be construed as a potential conflict of interest.

frontiers in Immunology

MINI REVIEW
published: 06 March 2018
doi: 10.3389/fimmu.2018.00439

Interrelation of Diet, Gut Microbiome, and Autoantibody Production

Ioanna Petta[1,2†], Judith Fraussen[2†], Veerle Somers[2] and Markus Kleinewietfeld[1,2*]*

[1] VIB Laboratory of Translational Immunomodulation, Center for Inflammation Research, Hasselt University, Diepenbeek, Belgium, [2] Biomedical Research Institute, Hasselt University, and School of Life Sciences, Transnationale Universiteit Limburg, Hasselt, Belgium

B cells possess a predominant role in adaptive immune responses *via* antibody-dependent and -independent functions. The microbiome of the gastrointestinal tract is currently being intensively investigated due to its profound impact on various immune responses, including B cell maturation, activation, and IgA antibody responses. Recent findings have demonstrated the interplay between dietary components, gut microbiome, and autoantibody production. "Western" dietary patterns, such as high fat and high salt diets, can induce alterations in the gut microbiome that in turn affects IgA responses and the production of autoantibodies. This could contribute to multiple pathologies including autoimmune and inflammatory diseases. Here, we summarize current knowledge on the influence of various dietary components on B cell function and (auto)antibody production in relation to the gut microbiota, with a particular focus on the gut–brain axis in the pathogenesis of multiple sclerosis.

Keywords: B cells, autoantibodies, diet, microbiome, multiple sclerosis, experimental autoimmune encephalomyelitis

OPEN ACCESS

Edited by:
Ralf J. Ludwig, University of Lübeck, Germany

Reviewed by:
Anne L. Astier, UMR5282 Centre de Physiopathologie de Toulouse Purpan (CPTP), France
Michael Kogut, Agricultural Research Service (USDA), United States

***Correspondence:**
Veerle Somers
veerle.somers@uhasselt.be;
Markus Kleinewietfeld
markus.kleinewietfeld@uhasselt.vib.be

†These authors have contributed equally to this work.

Specialty section:
This article was submitted to Immunological Tolerance and Regulation, a section of the journal Frontiers in Immunology

Received: *22 December 2017*
Accepted: *19 February 2018*
Published: *06 March 2018*

Citation:
Petta I, Fraussen J, Somers V and Kleinewietfeld M (2018) Interrelation of Diet, Gut Microbiome, and Autoantibody Production. Front. Immunol. 9:439. doi: 10.3389/fimmu.2018.00439

INTRODUCTION

B cells are involved in humoral and cell-mediated immunity. They secrete antibodies following differentiation into plasma cells, produce cytokines, and regulate T cell responses *via* antigen presentation and costimulation (1–3). B cells develop in the bone marrow from hematopoietic stem cells to immature B cells that further mature in the periphery into transitional and mature naïve B cells (4). Following activation, short-lived plasma cells are generated that produce low-affinity immunoglobulin (Ig)M antibodies for a few days (4). A fraction of the responding B cells undergoes a germinal center response, which results in the generation of memory B cells and long-lived Ig class-switched plasma cells that produce high-affinity IgG, IgA, or IgE antibodies.

Autoantibodies can originate from autoreactive B cells that escape tolerance mechanisms following molecular mimicry of infectious antigens with autoantigens, bystander activation, novel autoantigen presentation, or recognition of circulating autoantigens. They can clear target cells *via* antibody-dependent cell-mediated cytotoxicity or complement activation (5, 6). In addition, B cells are highly effective antigen-presenting cells, effectively activating antigen-specific $CD4^+$ T helper (Th) cells (2, 7). Depending on the cytokine profile, B cells can stimulate pro- and anti-inflammatory immune responses (8–10).

The humoral immune response in the gastrointestinal tract is mediated by IgA^+ memory B cells and IgA-producing plasma cells in the gut-associated lymphoid tissue (GALT). The protective and nutrient-rich environment of the gastrointestinal tract accommodates an extremely dense and diverse bacterial community (11) that in turn provides metabolic advantages and serves as a natural defense against colonization with pathogens (12, 13). Commensal bacteria act as critical stimuli,

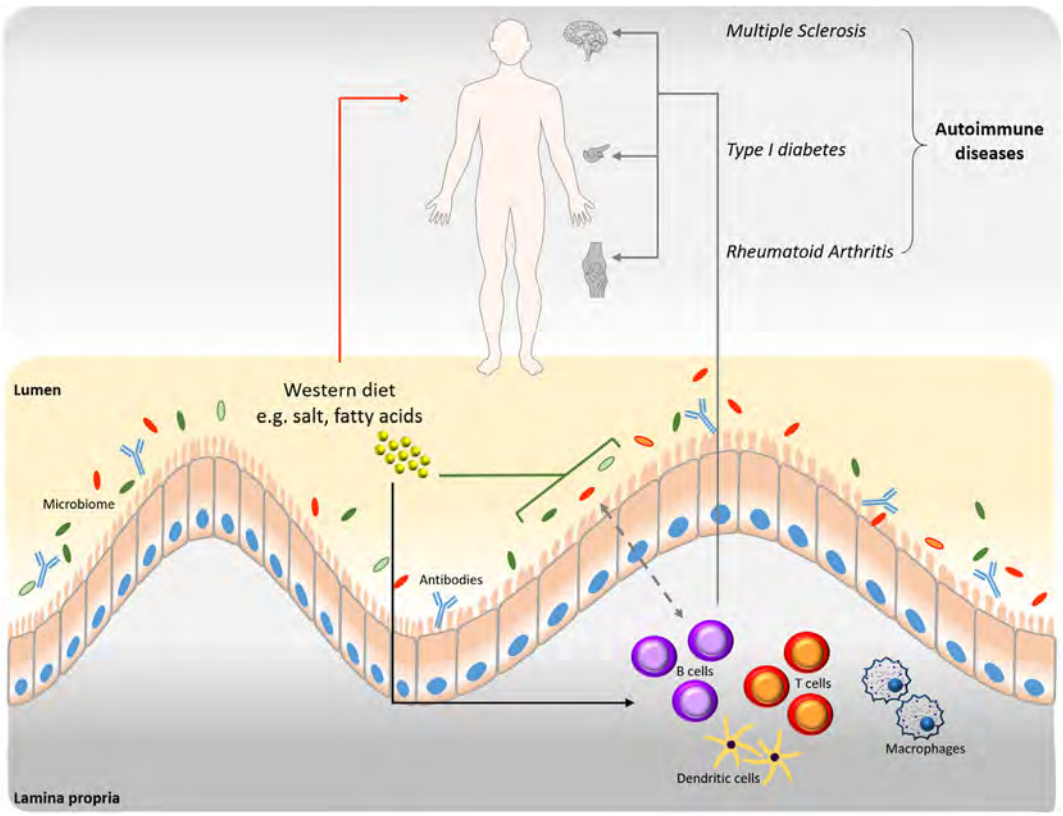

FIGURE 1 | Interrelation among B cells, microbiome, and diet in disease progression. Western type nutritional patterns influence the composition of the intestinal microbiome (green line). Alterations of the gut microbiome induced by nutrient components impact homeostasis and the onset of various diseases (red arrow). Western diet dietary components influence B cell function and production of autoantibodies (black arrow), which are involved in disease progression (gray arrows). The connection between B cells and microbiome is bidirectional (dashed gray arrow). B cell-derived antibodies modulate the intestinal microbiome and *vice versa*.

playing an important role for the maturation of the GALT and further induce IgA production by B cells (14). Class switching to IgA-producing plasma cells occurs in the Peyer's patches and lamina propria, following T cell-dependent or -independent mechanisms (15). The secreted IgA (SIgA) into the gut provides a first-line defense against pathogens mainly by blocking toxins and pathogens from adhering to the intestinal epithelium at the earliest steps of the infection process (16).

In this review, we describe the interrelation of dietary components, microbiome and B cell function with a focus on the production of (auto)antibodies. Special emphasis is placed on multiple sclerosis (MS) and its animal model experimental autoimmune encephalomyelitis (EAE).

DIETARY INFLUENCES ON B CELL HOMEOSTASIS AND FUNCTION

Modern nutritional patterns, collectively termed "Western-diet," are characterized by high energy density, animal protein, total and saturated fats, sugars and salt but low levels of plant-derived fibers. This "Western-diet" has a profound influence on the prevalence of autoantibodies, although changes in antibody-independent B cell functions have been reported as well. Additionally, a "Western-diet" may influence the balanced composition of the gut microbiome leading to perturbed immune responses, including effects on B cell production, activity, and maturation (17, 18) (**Figure 1**).

Effects of a high-fat diet (HFD) on B cell function have mostly been studied in diet-induced obesity models. Here, B cells contribute to pro-inflammatory reactions in the adipose tissue mediating insulin insensitivity and diminished glucose clearance. More specifically, B cells secrete pathogenic IgG antibodies and pro-inflammatory cytokines, which could interfere with macrophage polarization, $CD4^+$ T cell function, such as regulatory T cell inhibition or Th17 cell polarization, and $CD8^+$ T cell activation (19, 20). Reduced systemic antibody production has been demonstrated following influenza infection and/or *ex vivo* stimulation in a HFD-induced obesity mouse model and in obese individuals (21–23). Underlying mechanisms could involve effects on the responding plasma cells and molecular deregulation. Yet, autoreactive and pro-inflammatory antibodies were increased in obese humans and HFD-fed mice (20, 24, 25), probably through CD40 ligand (CD40L) signaling. CD40L has been shown to induce inflammatory cytokine production in adipose cells *in vitro* and *in vivo* (26, 27). The increased natural autoreactive IgM antibodies under HFD formed an immune complex

with apoptosis inhibitor of macrophage, which promoted IgG autoantibody production (28). Increased B cell frequencies and IgG levels were found in mouse obese white adipose tissue and obese humans, who additionally demonstrated a positive correlation between IgM levels and body mass index (21). Furthermore, obese humans displayed reduced IL-10$^+$ regulatory B cell levels in subcutaneous adipose tissue, which could contribute to the occurrence of autoantibodies (29). Mouse models further indicated diverse roles for different B cell subtypes in obesity-associated pro-inflammatory responses (20, 29–31). Thus, B cells might play a crucial role in secondary inflammation following obesity and constitute a potential therapeutic target in diet-induced obesity.

High-fat diet also induces changes in the gut microbiota that are related to the development of obesity and diabetes. Obesity is associated with a decreased intestinal abundance of *Bacteroidetes* and an increased proportion of *Firmicutes*, both in mice and humans (32–34). It has been shown that germ-free (GF) mice may be protected against diet-induced obesity and the mechanism possibly involves the fasting-induced adipose factor (Fiaf) in the intestinal epithelium and the AMP-activated protein kinase in skeletal muscle and liver (35). In addition, colonization of GF mice with microbiota harvested from conventionally raised animals resulted in a 60% increase in body fat content and insulin resistance (36). However, more research is necessary to unravel the link between HFD-mediated alterations of gut microbiota and B cell function or autoantibody production.

Another factor associated with "Western-diet" is the high salt content in processed foods and so-called "fast foods." High salt diets have been shown to exert profound effects on animal models of autoimmunity by affecting Th cell populations and macrophages promoting a pro-inflammatory environment (37, 38). However, if high salt also affects B cells is less well understood. Hybridoma cells under hyperosmotic stress exert suppressed cell growth but enhanced specific antibody production (39–41). Increased differentiation of Th17 and follicular helper T (Tfh) cells was demonstrated following a high salt diet in EAE and a lupus mouse model (42, 43). Tfh cells are involved in the selection of high-affinity B cells during the germinal center response. The mechanism involved in the high salt-mediated Th17 activation is dependent on nuclear factor of activated T cells 5 (NFAT5), p38/MAPK, and the serum/glucocorticoid-regulated kinase 1 (SGK1). SGK1 expression is induced upon salt treatment and its activation depends on p38/MAPK. Silencing of SGK1 reverts the effect of salt on IL-17 levels. To exclude the possibility that high osmolarity mediates the enhanced Th17 pro-inflammatory profile, mannitol and $MgCl_2$ were tested along and proved to have only a slight effect (42). Furthermore, high salt conditions result in cellular osmotic stress that is regulated *via* the guanine nucleotide exchange factor Brx-induced expression of NFAT5 (44). Interestingly, Brx was shown to be necessary for B cell differentiation in high salt conditions *via* NFAT5-mediated production of B cell activating factor (BAFF) that regulates splenic B cell differentiation and Ig production. A recent study described the correlation between salt intake and gut microbiome changes in EAE. More specifically, salt intake decreased the population of *Lactobacillus murinus*, while supplementation of *L. murinus* reduced the salt-induced EAE clinical scores and Th17 cell frequencies (45).

By contrast, dietary supplementation with $n-3$ polyunsaturated fatty acids (PUFAs) derived from fish oils could impact B cell function and suppress pro-inflammatory responses (46). Results from mouse models for obesity, colitis, peritonitis, and systemic lupus erythematosus indicated that dietary administration of fish oil containing n-3 PUFAs elevated splenic B cell numbers, increased B cell cytokine and IgM production while reducing autoantibodies (47–51). Monthly consumption of fish oil by postpartum women led to lower levels of anti-thyroid autoantibodies (52). In individuals at risk for rheumatoid arthritis, the use of n-3 PUFA food supplements and n-3 PUFA levels in red blood cell membranes were inversely associated with anti-cyclic citrullinated peptide and rheumatoid factor positivity (53, 54). Specialized pro-resolving lipid mediators (SPMs) that are endogenously synthesized from n-3 and n-6 PUFAs play a role in suppressing adipose tissue inflammation. In obese humans, selected SPMs were declined in adipose tissue (55). 17-hydroxydosahexaenoic acid (17-HDHA), DHA and resolving D1 stimulated increased Ig production in humans or mice with diet-induced obesity (21, 56). Furthermore, DHA and eicosapentaenoic acid (EPA) induced differential effects on B cell cytokine production and on distinct B cell subtypes that correlated with increased natural serum IgM and cecal IgA in murine obesity (57). Opposed to this, lipoxin A4 decreased (antigen-specific) IgM and IgG production and inhibited memory B cell function in an ovalbumin immunized mouse model (58). Thus, $n-3$ PUFAs and their derived SPMs can have profound effects on B cell function. More research is needed to clarify the differential effects associated with different types of PUFAs and to mechanistically link the effects to inflammation in obesity. Of note, in MS, EPA and DHA had no beneficial effects on disease activity (OFAMS study) (59).

Furthermore, a diet rich in short-chain fatty acids (SCFAs) could positively impact gut microbiota and inflammatory processes (37). The microbiome converts non-digestible carbohydrates (dietary fibers) to SCFAs, including acetate, butyrate, and propionate, which reduce the risk of inflammatory diseases, type 2 diabetes, obesity, heart disease, and other conditions (60). Non-obese diabetic mice on a diet rich in acetate were characterized by decreased IL-12-producing marginal zone B cells, a B cell subtype linked to the disruption of immune tolerance, in the spleen and the Payer's patches that additionally showed decreased expression of major histocompatibility complex I and CD86 (61). At the transcriptional level, changes were detected in genes associated with B cell costimulation, antigen presentation, proliferation, and differentiation. Thus, SCFAs and in particular acetate could affect the ability of B cells to expand autoreactive T cells *in vivo* and the development of type 1 diabetes. Butyrate was also suggested to protect against the development of anti-islet cell autoantibodies involved in type 1 diabetes (62). Early introduction of a non-milk diet in infants increased the risk for autoantibody production by reduced butyrate production and was associated with high *Bacteroides* levels. A milk-based diet resulted in a competitive advantage of acetogens compared to sulfate reducing bacteria, thereby leading to increased butyrate production *via* co-fermentation of acetate.

Dietary components such as gluten (63, 64), selenium (65), and iodine [reviewed in Ref. (66)] have been shown to increase

autoantibody production. Additionally, impaired protein intake alters IgA responses, attenuating the protective efficacy of vaccination against cholera and *Salmonella enterica* serovar Typhimurium in mice (67). On the contrary, a cocoa-rich diet decreases autoantibody production and confers beneficial immune function (68–72).

CROSS-TALK BETWEEN MICROBIOME AND B CELLS

Studies in various animal models of impaired microbial control [including GF, antibiotic-treated mice, mice with restricted flora and activation-induced cytidine deaminase knockout ($AID^{-/-}$) mice], but also in humans, have demonstrated that gastrointestinal bacteria participate in B cell differentiation, maturation, and activation (73–76). A proof-of-principle study in Pakistani infants living in impoverished areas showed an accelerated maturation of the salivary IgA system compared with healthy Swedish infants (77). In contrast, in Swedish infants, the gut microbiota took longer to establish and was characterized by a lower diversity (78–80). B cell maturation in Swedish infants was shaped by the intestinal bacterial colonization pattern, mainly by *Escherichia coli* and *Bifidobacteria* (74).

On the other hand, intestinal IgA can influence the gut microbiota composition. Natural and specific IgA antibodies in breast milk were capable of binding commensal bacteria and might be involved in establishing the newborn's microbiome (81). High-affinity IgA, generated *via* T cell-dependent mechanisms, was essential in mice for the protection from invasive commensal species, such as segmented filamentous bacteria (SFB), and from true pathogens, such as *Salmonella typhimurium* and *Enterobacter cloacae* (82). Of note, SFB increased IgA^+ B cells *in vivo* (83, 84). Moreover, SIgA promoted the establishment of host–microbial relationships by modulating bacterial epitopes and modifying bacterial metabolism, as demonstrated by the downregulation of bacterial genes involved in the metabolism of oxidative products, i.e., *Bacteroides thetaiotaomicron* (85). An alternative mechanism proposed a mouse monoclonal IgA which was reactive against multiple commensal but not beneficial bacteria by specific recognition of an epitope in serine hydroxymethyltransferase, a bacterial metabolic enzyme (86). Oral administration of this IgA antibody *in vivo* effectively prevented the development of colitis in several mouse models (86, 87).

Probiotics, live microbial food ingredients, have been demonstrated to affect B cell function by stimulating systemic and mucosal IgA production in humans (88, 89). More specifically, probiotic strains such as *Bifidobacterium lactis* and *Saccharomyces boulardii* enhanced IgA production through alteration of the gut mucosa cytokine milieu in preterm infants and mice, respectively (90, 91). Probiotic bacteria can induce TGF-β, IL-10, and IL-6 expression by epithelial cells, which potentiate IgA production through B cell maturation and class switching to IgA (92, 93). Finally, probiotics augment the expression of polymeric Ig receptors on the basolateral surface of intestinal epithelial cells enhancing IgA transcytosis into the gut lumen (94). Not only supplementation of preterm infants with *B. lactis* but also administration of *Lactobacillus casei* in mice resulted in increased IgA-producing cells (95, 96). Pretreatment of mice with the *Bifidobacterium* species *B. bifidum and B. infantis* increased gut mucosal pathogen-specific IgA antibody titers and reduced illness after challenge with rotavirus (97, 98). Similar results were described in infant rabbits and gnotobiotic pigs, pinpointing the effects of several commensals on IgA production (99, 100). Dietary components, shown to directly affect microbiome composition with subsequent influence on human's immunity and health, include proteins, fats, carbohydrates, and polyphenols. Data from clinical studies prove that plant-derived proteins, non-digestible carbohydrates (prebiotics), and restricted fat consumption and polyphenols increase the intestinal numbers of beneficial bacteria such as *Bifodobacterium* and *Lactobacillus*. Interestingly, contrary to animal-derived proteins that can lead to inflammatory bowel disease and cardiovascular diseases, plant-derived proteins increase SCFAs and regulatory T cells, counteracting inflammatory responses (101).

Therefore, a "Western-diet" lacking components of high nutrient value such as probiotics may negatively modulate immune responses, thereby leading to decreased immune tolerance as well as disease and infection progression.

INTERPLAY OF B CELLS AND MICROBIOME IN MS

B cells are important players in MS pathogenesis *via* antibody-dependent and -independent mechanisms (1). Bidirectional trafficking of B cells has been demonstrated between the periphery and CNS, where they could locally produce (auto)antibodies (102). IgA antibodies, that mediate humoral immunity in the gastrointestinal tract, have been described to play a role in MS as well. Increased serum IgA antibodies directed against myelin basic protein (MBP), myelin oligodendrocyte glycoprotein (MOG), plant and human aquaporins, and S100B have been described in MS (103, 104). Anti-MBP IgA antibodies were able to catalyze MBP hydrolysis, which could contribute to demyelination (105). Intrathecal IgG, IgA, and IgM synthesis correlated with the presence of anti-MBP or anti-proteolipid protein-secreting cells (106). Interestingly, IgA antibodies were found to be associated with a progressive disease course (103). More specifically, cerebrospinal fluid (CSF) IgA synthesis was correlated with the yearly disease progression rate in primary progressive MS (107). In addition, IgA antibodies directed against gliadin, gluten, and casein were increased in MS patients (108). In the CNS, IgA was reported as a major component of immune responses in MS with IgA^+ plasma cells showing signs of clonal expansion, intraclonal diversification, and anti-axonal reactivity (109–111). An important correlation was found between CSF levels of chemokine C-X-C motif ligand (CXCL)13 and the extent of intrathecal IgA synthesis (112).

In addition, mounting evidence highlights the implication of the gut environment in MS onset and progression. Recently, microbiome analysis indicated altered levels of several commensals in MS patients (113–115). Possible mechanisms employed by microbiota to induce MS could potentially include low-grade

microbial translocation such as peptidoglycan, a bacterial cell wall component, from the gut to the CNS (115, 116). Additionally, gut microbiota can lead to disruption of the blood–brain barrier (117), microglia activation (118), limited astrocyte pathogenicity (119), and expression of myelinating genes (120). Interestingly, microbiota transplantation of MS patients to GF mice resulted in more severe EAE symptoms and reduced IL-10$^+$ regulatory T cells compared to mice transplanted with selected healthy human microbiomes (113, 121). Commensal microbiota is necessary for disease development in spontaneous and actively induced EAE models (122, 123). MOG-immunized GF mice showed reduced anti-MOG antibodies that could be increased by colonization with microbiota from MS-affected twins. Furthermore, GF housing conditions resulted in impaired B cell recruitment to brain-draining lymph nodes and reduced MOG-specific IgG2a antibodies in spontaneously developing EAE (121). In line with this, an antibiotic mixture orally administered before EAE induction impaired EAE development due to increased regulatory T cells in the mesenteric and cervical lymph nodes and increased IL-10-producing CD5$^+$ B cells in cervical lymph nodes (124). The induced B cells were able to reduce EAE severity when adoptively transferred into naïve recipient mice by causing a shift from a Th1/Th17 toward a Th2 cytokine profile (125). Thus, antibiotic treatment stimulated both regulatory T and B cells, which both contributed to the protection against EAE.

In addition, dietary interventions have been tested in EAE models. A prophylactic diet of 66% caloric restriction protected Lewis rats from developing EAE as evident by reduced splenic CD8$^+$ T cells and B cells, lymphoid and thymic CD4$^+$ T cells and B cells, and IFN-γ production (126). Other dietary interventions that demonstrated efficacy in reducing EAE symptoms are SCFAs, low fat diets, and zinc aspartate (127). However, currently no information is available on the effects of these dietary components on B cell function or autoantibody production. Moreover, some vitamins, i.e., A, E, and D are important immune regulators and have been shown to limit EAE progression (116). Of note, vitamin D, which is mainly produced by sun exposure but is also contained in food such as salmon, beef meet, and egg yolks, has been shown to decrease EAE manifestations *in vivo*. Administration of 1,25-dihydroxyvitamin D_3 to mice, the active form of vitamin D, prevented EAE development and significantly reduced serum anti-MBP antibody production (128). In MS patients, different dietary interventions have been studied although mostly unsuccessful or causality could not be demonstrated (116). However, preliminary data from a recent study indicated that a fasting mimicking diet or chronic ketogenic diet could be safe, feasible, and potentially effective in MS treatment (129).

CONCLUSION

Increasing evidence is being gathered for the interplay between diet, microbiome, and autoantibody production. Deregulation of this system could contribute to different pathologies, including MS. A "Western-diet" consisting among others of high fat and high salt content has been associated with increased autoantibody production, obesity, inflammatory disorders, and autoimmune diseases. Gut bacteria have been shown to modulate B cell differentiation, maturation, and activation with a profound influence on IgA responses (**Figure 1**). Dietary interventions and the use of probiotics could restore immune deregulation that is seen in case of diet-induced microbiome alterations. They thus may represent valuable tools for improving the treatment of inflammatory and autoimmune disorders. However, more research is needed to clarify the mechanisms underlying the effects of dietary components on autoantibody production and its relation to disease development in order to obtain a more efficient and preventive treatment line. In MS patients, IgA antibodies against several autoantigens have been described. Additionally, a disturbed microbiome has been observed in MS patients and animal studies have supported a possible link between the microbiome and the disease. However, the exact role of diet and the microbiome in B cell-mediated pathology in MS, along with the respective mechanisms, remain to be determined.

AUTHOR CONTRIBUTIONS

IP, JF, VS, and MK wrote the manuscript. All authors approved the work for publication.

FUNDING

MK was supported by the European Research Council (ERC) under the European Union's Horizon 2020 research and innovation program (640116), by a SALK-grant from the government of Flanders, Belgium, and by an Odysseus grant of the Research Foundation Flanders, Belgium (FWO). JF is a postdoctoral fellow of the FWO.

REFERENCES

1. Claes N, Fraussen J, Stinissen P, Hupperts R, Somers V. B cells are multifunctional players in multiple sclerosis pathogenesis: insights from therapeutic interventions. *Front Immunol* (2015) 6:642. doi:10.3389/fimmu.2015.00642
2. Fraussen J, Claes N, Van Wijmeersch B, van Horssen J, Stinissen P, Hupperts R, et al. B cells of multiple sclerosis patients induce autoreactive proinflammatory T cell responses. *Clin Immunol* (2016) 173:124–32. doi:10.1016/j.clim.2016.10.001
3. Rajewsky K. Clonal selection and learning in the antibody system. *Nature* (1996) 381(6585):751–8. doi:10.1038/381751a0
4. Pieper K, Grimbacher B, Eibel H. B-cell biology and development. *J Allergy Clin Immunol* (2013) 131(4):959–71. doi:10.1016/j.jaci.2013.01.046
5. Bhakdi S, Tranum-Jensen J. Complement lysis: a hole is a hole. *Immunol Today* (1991) 12(9):318–20. doi:10.1016/0167-5699(91)90007-G
6. Esser AF. Big MAC attack: complement proteins cause leaky patches. *Immunol Today* (1991) 12(9):316–8. doi:10.1016/0167-5699(91)90006-F
7. Lanzavecchia A. Antigen-specific interaction between T and B cells. *Nature* (1985) 314(6011):537–9. doi:10.1038/314537a0
8. Bar-Or A, Fawaz L, Fan B, Darlington PJ, Rieger A, Ghorayeb C, et al. Abnormal B-cell cytokine responses a trigger of T-cell-mediated disease in MS? *Ann Neurol* (2010) 67(4):452–61. doi:10.1002/ana.21939
9. Fillatreau S, Sweenie CH, McGeachy MJ, Gray D, Anderton SM. B cells regulate autoimmunity by provision of IL-10. *Nat Immunol* (2002) 3(10):944–50. doi:10.1038/ni833

10. Shen P, Roch T, Lampropoulou V, O'Connor RA, Stervbo U, Hilgenberg E, et al. IL-35-producing B cells are critical regulators of immunity during autoimmune and infectious diseases. *Nature* (2014) 507(7492):366–70. doi:10.1038/nature12979
11. Sonnenburg JL, Angenent LT, Gordon JI. Getting a grip on things: how do communities of bacterial symbionts become established in our intestine? *Nat Immunol* (2004) 5(6):569–73. doi:10.1038/ni1079
12. O'Hara AM, Shanahan F. The gut flora as a forgotten organ. *EMBO Rep* (2006) 7(7):688–93. doi:10.1038/sj.embor.7400731
13. Turnbaugh PJ, Ley RE, Hamady M, Fraser-Liggett CM, Knight R, Gordon JI. The human microbiome project. *Nature* (2007) 449(7164): 804–10. doi:10.1038/nature06244
14. Round JL, Mazmanian SK. The gut microbiota shapes intestinal immune responses during health and disease. *Nat Rev Immunol* (2009) 9(5):313–23. doi:10.1038/nri2515
15. Suzuki K, Ha SA, Tsuji M, Fagarasan S. Intestinal IgA synthesis: a primitive form of adaptive immunity that regulates microbial communities in the gut. *Semin Immunol* (2007) 19(2):127–35. doi:10.1016/j.smim.2006.10.001
16. Helander A, Miller CL, Myers KS, Neutra MR, Nibert ML. Protective immunoglobulin A and G antibodies bind to overlapping intersubunit epitopes in the head domain of type 1 reovirus adhesin sigma1. *J Virol* (2004) 78(19):10695–705. doi:10.1128/JVI.78.19.10695-10705.2004
17. Shaikh SR, Haas KM, Beck MA, Teague H. The effects of diet-induced obesity on B cell function. *Clin Exp Immunol* (2015) 179(1):90–9. doi:10.1111/cei.12444
18. Conlon MA, Bird AR. The impact of diet and lifestyle on gut microbiota and human health. *Nutrients* (2014) 7(1):17–44. doi:10.3390/nu7010017
19. DeFuria J, Belkina AC, Jagannathan-Bogdan M, Snyder-Cappione J, Carr JD, Nersesova YR, et al. B cells promote inflammation in obesity and type 2 diabetes through regulation of T-cell function and an inflammatory cytokine profile. *Proc Natl Acad Sci U S A* (2013) 110(13):5133–8. doi:10.1073/pnas.1215840110
20. Winer DA, Winer S, Shen L, Wadia PP, Yantha J, Paltser G, et al. B cells promote insulin resistance through modulation of T cells and production of pathogenic IgG antibodies. *Nat Med* (2011) 17(5):610–7. doi:10.1038/nm.2353
21. Kosaraju R, Guesdon W, Crouch MJ, Teague HL, Sullivan EM, Karlsson EA, et al. B cell activity is impaired in human and mouse obesity and is responsive to an essential fatty acid upon murine influenza infection. *J Immunol* (2017) 198(12):4738–52. doi:10.4049/jimmunol.1601031
22. Milner JJ, Sheridan PA, Karlsson EA, Schultz-Cherry S, Shi Q, Beck MA. Diet-induced obese mice exhibit altered heterologous immunity during a secondary 2009 pandemic H1N1 infection. *J Immunol* (2013) 191(5):2474–85. doi:10.4049/jimmunol.1202429
23. Sheridan PA, Paich HA, Handy J, Karlsson EA, Hudgens MG, Sammon AB, et al. Obesity is associated with impaired immune response to influenza vaccination in humans. *Int J Obes (Lond)* (2012) 36(8):1072–7. doi:10.1038/ijo.2011.208
24. Marzullo P, Minocci A, Tagliaferri MA, Guzzaloni G, Di Blasio A, De Medici C, et al. Investigations of thyroid hormones and antibodies in obesity: leptin levels are associated with thyroid autoimmunity independent of bioanthropometric, hormonal, and weight-related determinants. *J Clin Endocrinol Metab* (2010) 95(8):3965–72. doi:10.1210/jc.2009-2798
25. Rosenbloom AL. Obesity, insulin resistance, beta-cell autoimmunity, and the changing clinical epidemiology of childhood diabetes. *Diabetes Care* (2003) 26(10):2954–6. doi:10.2337/diacare.26.10.2954
26. Wolf D, Jehle F, Ortiz Rodriguez A, Dufner B, Hoppe N, Colberg C, et al. CD40L deficiency attenuates diet-induced adipose tissue inflammation by impairing immune cell accumulation and production of pathogenic IgG-antibodies. *PLoS One* (2012) 7(3):e33026. doi:10.1371/journal.pone.0033026
27. Missiou A, Wolf D, Platzer I, Ernst S, Walter C, Rudolf P, et al. CD40L induces inflammation and adipogenesis in adipose cells – a potential link between metabolic and cardiovascular disease. *Thromb Haemost* (2010) 103(4):788–96. doi:10.1160/TH09-07-0463
28. Arai S, Maehara N, Iwamura Y, Honda S, Nakashima K, Kai T, et al. Obesity-associated autoantibody production requires AIM to retain the immunoglobulin M immune complex on follicular dendritic cells. *Cell Rep* (2013) 3(4):1187–98. doi:10.1016/j.celrep.2013.03.006
29. Nishimura S, Manabe I, Takaki S, Nagasaki M, Otsu M, Yamashita H, et al. Adipose natural regulatory B cells negatively control adipose tissue inflammation. *Cell Metab* (2013) S1550–4131(13):00386. doi:10.1016/j.cmet.2013.09.017
30. van Dam AD, van Beek L, Pronk ACM, van den Berg SM, Van den Bossche J, de Winther MPJ, et al. IgG is elevated in obese white adipose tissue but does not induce glucose intolerance via Fcgamma-receptor or complement. *Int J Obes (Lond)* (2017) 42(2):260–9. doi:10.1038/ijo.2017.209
31. Nus M, Sage AP, Lu Y, Masters L, Lam BYH, Newland S, et al. Marginal zone B cells control the response of follicular helper T cells to a high-cholesterol diet. *Nat Med* (2017) 23(5):601–10. doi:10.1038/nm.4315
32. Ley RE, Backhed F, Turnbaugh P, Lozupone CA, Knight RD, Gordon JI. Obesity alters gut microbial ecology. *Proc Natl Acad Sci U S A* (2005) 102(31):11070–5. doi:10.1073/pnas.0504978102
33. Turnbaugh PJ, Backhed F, Fulton L, Gordon JI. Diet-induced obesity is linked to marked but reversible alterations in the mouse distal gut microbiome. *Cell Host Microbe* (2008) 3(4):213–23. doi:10.1016/j.chom.2008.02.015
34. Turnbaugh PJ, Ley RE, Mahowald MA, Magrini V, Mardis ER, Gordon JI. An obesity-associated gut microbiome with increased capacity for energy harvest. *Nature* (2006) 444(7122):1027–31. doi:10.1038/nature05414
35. Backhed F, Manchester JK, Semenkovich CF, Gordon JI. Mechanisms underlying the resistance to diet-induced obesity in germ-free mice. *Proc Natl Acad Sci U S A* (2007) 104(3):979–84. doi:10.1073/pnas.0605374104
36. Backhed F, Ding H, Wang T, Hooper LV, Koh GY, Nagy A, et al. The gut microbiota as an environmental factor that regulates fat storage. *Proc Natl Acad Sci U S A* (2004) 101(44):15718–23. doi:10.1073/pnas.0407076101
37. Jorg S, Grohme DA, Erzler M, Binsfeld M, Haghikia A, Muller DN, et al. Environmental factors in autoimmune diseases and their role in multiple sclerosis. *Cell Mol Life Sci* (2016) 73(24):4611–22. doi:10.1007/s00018-016-2311-1
38. Manzel A, Muller DN, Hafler DA, Erdman SE, Linker RA, Kleinewietfeld M. Role of "Western diet" in inflammatory autoimmune diseases. *Curr Allergy Asthma Rep* (2014) 14(1):404. doi:10.1007/s11882-013-0404-6
39. Bibila TA, Ranucci CS, Glazomitsky K, Buckland BC, Aunins JG. Monoclonal antibody process development using medium concentrates. *Biotechnol Prog* (1994) 10(1):87–96. doi:10.1021/bp00025a011
40. Reddy S, Bauer KD, Miller WM. Determination of antibody content in live versus dead hybridoma cells: analysis of antibody production in osmotically stressed cultures. *Biotechnol Bioeng* (1992) 40(8):947–64. doi:10.1002/bit.260400811
41. Soo Ryu J, Min Lee G. Effect of hypoosmotic stress on hybridoma cell growth and antibody production. *Biotechnol Bioeng* (1997) 55(3):565–70. doi:10.1002/(SICI)1097-0290(19970805)55:3<565::AID-BIT14>3.0.CO;2-F
42. Kleinewietfeld M, Manzel A, Titze J, Kvakan H, Yosef N, Linker RA, et al. Sodium chloride drives autoimmune disease by the induction of pathogenic TH17 cells. *Nature* (2013) 496(7446):518–22. doi:10.1038/nature11868
43. Wu H, Huang X, Qiu H, Zhao M, Liao W, Yuan S, et al. High salt promotes autoimmunity by TET2-induced DNA demethylation and driving the differentiation of Tfh cells. *Sci Rep* (2016) 6:28065. doi:10.1038/srep28065
44. Kino T, Takatori H, Manoli I, Wang Y, Tiulpakov A, Blackman MR, et al. Brx mediates the response of lymphocytes to osmotic stress through the activation of NFAT5. *Sci Signal* (2009) 2(57):ra5. doi:10.1126/scisignal.2000081
45. Wilck N, Matus MG, Kearney SM, Olesen SW, Forslund K, Bartolomaeus H, et al. Salt-responsive gut commensal modulates TH17 axis and disease. *Nature* (2017) 551(7682):585–9. doi:10.1038/nature24628
46. Kim J, Li Y, Watkins BA. Fat to treat fat: emerging relationship between dietary PUFA, endocannabinoids, and obesity. *Prostaglandins Other Lipid Mediat* (2013) 10(4–105):32–41. doi:10.1016/j.prostaglandins.2012.11.005
47. Gurzell EA, Teague H, Harris M, Clinthorne J, Shaikh SR, Fenton JI. DHA-enriched fish oil targets B cell lipid microdomains and enhances ex vivo and in vivo B cell function. *J Leukoc Biol* (2013) 93(4):463–70. doi:10.1189/jlb.0812394
48. Pestka JJ, Vines LL, Bates MA, He K, Langohr I. Comparative effects of n-3, n-6 and n-9 unsaturated fatty acid-rich diet consumption on lupus nephritis, autoantibody production and CD4+ T cell-related gene responses in the autoimmune NZBWF1 mouse. *PLoS One* (2014) 9(6):e100255. doi:10.1371/journal.pone.0100255
49. Rockett BD, Salameh M, Carraway K, Morrison K, Shaikh SR. n-3 PUFA improves fatty acid composition, prevents palmitate-induced apoptosis,

and differentially modifies B cell cytokine secretion in vitro and ex vivo. *J Lipid Res* (2010) 51(6):1284–97. doi:10.1194/jlr.M000851
50. Teague H, Fhaner CJ, Harris M, Duriancik DM, Reid GE, Shaikh SR. n-3 PUFAs enhance the frequency of murine B-cell subsets and restore the impairment of antibody production to a T-independent antigen in obesity. *J Lipid Res* (2013) 54(11):3130–8. doi:10.1194/jlr.M042457
51. Tomasdottir V, Thorleifsdottir S, Vikingsson A, Hardardottir I, Freysdottir J. Dietary omega-3 fatty acids enhance the B1 but not the B2 cell immune response in mice with antigen-induced peritonitis. *J Nutr Biochem* (2014) 25(2):111–7. doi:10.1016/j.jnutbio.2013.09.010
52. Benvenga S, Vigo MT, Metro D, Granese R, Vita R, Le Donne M. Type of fish consumed and thyroid autoimmunity in pregnancy and postpartum. *Endocrine* (2016) 52(1):120–9. doi:10.1007/s12020-015-0698-3
53. Gan RW, Demoruelle MK, Deane KD, Weisman MH, Buckner JH, Gregersen PK, et al. Omega-3 fatty acids are associated with a lower prevalence of autoantibodies in shared epitope-positive subjects at risk for rheumatoid arthritis. *Ann Rheum Dis* (2017) 76(1):147–52. doi:10.1136/annrheumdis-2016-209154
54. Gan RW, Young KA, Zerbe GO, Demoruelle MK, Weisman MH, Buckner JH, et al. Lower omega-3 fatty acids are associated with the presence of anti-cyclic citrullinated peptide autoantibodies in a population at risk for future rheumatoid arthritis: a nested case-control study. *Rheumatology (Oxford)* (2016) 55(2):367–76. doi:10.1093/rheumatology/kev266
55. Claria J, Dalli J, Yacoubian S, Gao F, Serhan CN. Resolvin D1 and resolvin D2 govern local inflammatory tone in obese fat. *J Immunol* (2012) 189(5): 2597–605. doi:10.4049/jimmunol.1201272
56. Ramon S, Gao F, Serhan CN, Phipps RP. Specialized proresolving mediators enhance human B cell differentiation to antibody-secreting cells. *J Immunol* (2012) 189(2):1036–42. doi:10.4049/jimmunol.1103483
57. Teague H, Harris M, Fenton J, Lallemand P, Shewchuk BM, Shaikh SR. Eicosapentaenoic and docosahexaenoic acid ethyl esters differentially enhance B-cell activity in murine obesity. *J Lipid Res* (2014) 55(7):1420–33. doi:10.1194/jlr.M049809
58. Ramon S, Bancos S, Serhan CN, Phipps RP. Lipoxin A(4) modulates adaptive immunity by decreasing memory B-cell responses via an ALX/FPR2-dependent mechanism. *Eur J Immunol* (2014) 44(2):357–69. doi:10.1002/eji.201343316
59. Torkildsen O, Wergeland S, Bakke S, Beiske AG, Bjerve KS, Hovdal H, et al. omega-3 fatty acid treatment in multiple sclerosis (OFAMS Study): a randomized, double-blind, placebo-controlled trial. *Arch Neurol* (2012) 69(8):1044–51. doi:10.1001/archneurol.2012.283
60. Rios-Covian D, Ruas-Madiedo P, Margolles A, Gueimonde M, de Los Reyes-Gavilan CG, Salazar N. Intestinal short chain fatty acids and their link with diet and human health. *Front Microbiol* (2016) 7:185. doi:10.3389/fmicb.2016.00185
61. Marino E, Richards JL, McLeod KH, Stanley D, Yap YA, Knight J, et al. Gut microbial metabolites limit the frequency of autoimmune T cells and protect against type 1 diabetes. *Nat Immunol* (2017) 18(5):552–62. doi:10.1038/ni.3713
62. Endesfelder D, Engel M, Davis-Richardson AG, Ardissone AN, Achenbach P, Hummel S, et al. Towards a functional hypothesis relating anti-islet cell autoimmunity to the dietary impact on microbial communities and butyrate production. *Microbiome* (2016) 4:17. doi:10.1186/s40168-016-0163-4
63. Kumar J, Kumar M, Pandey R, Chauhan NS. Physiopathology and management of gluten-induced celiac disease. *J Food Sci* (2017) 82(2):270–7. doi:10.1111/1750-3841.13612
64. Lebwohl B, Sanders DS, Green PHR. Coeliac disease. *Lancet* (2017) 391(10115):70–81. doi:10.1016/S0140-6736(17)31796-8
65. McLachlan SM, Aliesky H, Banuelos B, Que Hee SS, Rapoport B. Variable effects of dietary selenium in mice that spontaneously develop a spectrum of thyroid autoantibodies. *Endocrinology* (2017) 158(11):3754–64. doi:10.1210/en.2017-00275
66. Burek CL, Talor MV. Environmental triggers of autoimmune thyroiditis. *J Autoimmun* (2009) 33(3–4):183–9. doi:10.1016/j.jaut.2009.09.001
67. Rho S, Kim H, Shim SH, Lee SY, Kim MJ, Yang BG, et al. Protein energy malnutrition alters mucosal IgA responses and reduces mucosal vaccine efficacy in mice. *Immunol Lett* (2017) 190:247–56. doi:10.1016/j.imlet.2017.08.025
68. Abril-Gil M, Massot-Cladera M, Perez-Cano FJ, Castellote C, Franch A, Castell M. A diet enriched with cocoa prevents IgE synthesis in a rat allergy model. *Pharmacol Res* (2012) 65(6):603–8. doi:10.1016/j.phrs.2012.02.001
69. Abril-Gil M, Perez-Cano FJ, Franch A, Castell M. Effect of a cocoa-enriched diet on immune response and anaphylaxis in a food allergy model in Brown Norway rats. *J Nutr Biochem* (2016) 27:317–26. doi:10.1016/j.jnutbio.2015.09.022
70. Camps-Bossacoma M, Massot-Cladera M, Abril-Gil M, Franch A, Perez-Cano FJ, Castell M. Cocoa diet and antibody immune response in preclinical studies. *Front Nutr* (2017) 4:28. doi:10.3389/fnut.2017.00028
71. Perez-Berezo T, Ramiro-Puig E, Perez-Cano FJ, Castellote C, Permanyer J, Franch A, et al. Influence of a cocoa-enriched diet on specific immune response in ovalbumin-sensitized rats. *Mol Nutr Food Res* (2009) 53(3): 389–97. doi:10.1002/mnfr.200700396
72. Ramos-Romero S, Perez-Cano FJ, Castellote C, Castell M, Franch A. Effect of cocoa-enriched diets on lymphocytes involved in adjuvant arthritis in rats. *Br J Nutr* (2012) 107(3):378–87. doi:10.1017/S0007114511003035
73. Fagarasan S, Muramatsu M, Suzuki K, Nagaoka H, Hiai H, Honjo T. Critical roles of activation-induced cytidine deaminase in the homeostasis of gut flora. *Science* (2002) 298(5597):1424–7. doi:10.1126/science.1077336
74. Lundell AC, Bjornsson V, Ljung A, Ceder M, Johansen S, Lindhagen G, et al. Infant B cell memory differentiation and early gut bacterial colonization. *J Immunol* (2012) 188(9):4315–22. doi:10.4049/jimmunol.1103223
75. Ouwehand A, Isolauri E, Salminen S. The role of the intestinal microflora for the development of the immune system in early childhood. *Eur J Nutr* (2002) 41(Suppl 1):I32–7. doi:10.1007/s00394-002-1105-4
76. Wei B, Su TT, Dalwadi H, Stephan RP, Fujiwara D, Huang TT, et al. Resident enteric microbiota and CD8+ T cells shape the abundance of marginal zone B cells. *Eur J Immunol* (2008) 38(12):3411–25. doi:10.1002/eji.200838432
77. Mellander L, Carlsson B, Jalil F, Soderstrom T, Hanson LA. Secretory IgA antibody response against *Escherichia coli* antigens in infants in relation to exposure. *J Pediatr* (1985) 107(3):430–3. doi:10.1016/S0022-3476(85)80528-X
78. Adlerberth I, Carlsson B, de Man P, Jalil F, Khan SR, Larsson P, et al. Intestinal colonization with Enterobacteriaceae in Pakistani and Swedish hospital-delivered infants. *Acta Paediatr Scand* (1991) 80(6–7):602–10. doi:10.1111/j.1651-2227.1991.tb11917.x
79. Adlerberth I, Wold AE. Establishment of the gut microbiota in Western infants. *Acta Paediatr* (2009) 98(2):229–38. doi:10.1111/j.1651-2227.2008.01060.x
80. Nowrouzian F, Hesselmar B, Saalman R, Strannegard IL, Aberg N, Wold AE, et al. *Escherichia coli* in infants' intestinal microflora: colonization rate, strain turnover, and virulence gene carriage. *Pediatr Res* (2003) 54(1):8–14. doi:10.1203/01.PDR.0000069843.20655.EE
81. Sekirov I, Russell SL, Antunes LC, Finlay BB. Gut microbiota in health and disease. *Physiol Rev* (2010) 90(3):859–904. doi:10.1152/physrev.00045.2009
82. Harris NL, Spoerri I, Schopfer JF, Nembrini C, Merky P, Massacand J, et al. Mechanisms of neonatal mucosal antibody protection. *J Immunol* (2006) 177(9):6256–62. doi:10.4049/jimmunol.177.9.6256
83. Glenn JD, Mowry EM. Emerging concepts on the gut microbiome and multiple sclerosis. *J Interferon Cytokine Res* (2016) 36(6):347–57. doi:10.1089/jir.2015.0177
84. Wekerle H, Berer K, Krishnamoorthy G. Remote control-triggering of brain autoimmune disease in the gut. *Curr Opin Immunol* (2013) 25(6):683–9. doi:10.1016/j.coi.2013.09.009
85. Peterson DA, McNulty NP, Guruge JL, Gordon JI. IgA response to symbiotic bacteria as a mediator of gut homeostasis. *Cell Host Microbe* (2007) 2(5):328–39. doi:10.1016/j.chom.2007.09.013
86. Okai S, Usui F, Ohta M, Mori H, Kurokawa K, Matsumoto S, et al. Intestinal IgA as a modulator of the gut microbiota. *Gut Microbes* (2017) 8(5):486–92. doi:10.1080/19490976.2017.1310357
87. Okai S, Usui F, Yokota S, Hori IY, Hasegawa M, Nakamura T, et al. High-affinity monoclonal IgA regulates gut microbiota and prevents colitis in mice. *Nat Microbiol* (2016) 1(9):16103. doi:10.1038/nmicrobiol.2016.103
88. Fukushima Y, Kawata Y, Hara H, Terada A, Mitsuoka T. Effect of a probiotic formula on intestinal immunoglobulin A production in healthy children. *Int J Food Microbiol* (1998) 42(1–2):39–44. doi:10.1016/S0168-1605(98)00056-7
89. Kaila M, Isolauri E, Soppi E, Virtanen E, Laine S, Arvilommi H. Enhancement of the circulating antibody secreting cell response in human diarrhea by a human *Lactobacillus* strain. *Pediatr Res* (1992) 32(2):141–4. doi:10.1203/00006450-199208000-00002
90. Mohan R, Koebnick C, Schildt J, Mueller M, Radke M, Blaut M. Effects of *Bifidobacterium lactis* Bb12 supplementation on body weight, fecal pH,

acetate, lactate, calprotectin, and IgA in preterm infants. *Pediatr Res* (2008) 64(4):418–22. doi:10.1203/PDR.0b013e318181b7fa
91. Rodrigues AC, Cara DC, Fretez SH, Cunha FQ, Vieira EC, Nicoli JR, et al. *Saccharomyces boulardii* stimulates sIgA production and the phagocytic system of gnotobiotic mice. *J Appl Microbiol* (2000) 89(3):404–14. doi:10.1046/j.1365-2672.2000.01128.x
92. He B, Xu W, Santini PA, Polydorides AD, Chiu A, Estrella J, et al. Intestinal bacteria trigger T cell-independent immunoglobulin A(2) class switching by inducing epithelial-cell secretion of the cytokine APRIL. *Immunity* (2007) 26(6):812–26. doi:10.1016/j.immuni.2007.04.014
93. Shang L, Fukata M, Thirunarayanan N, Martin AP, Arnaboldi P, Maussang D, et al. Toll-like receptor signaling in small intestinal epithelium promotes B-cell recruitment and IgA production in lamina propria. *Gastroenterology* (2008) 135(2):529–38. doi:10.1053/j.gastro.2008.04.020
94. Resendiz-Albor AA, Reina-Garfias H, Rojas-Hernandez S, Jarillo-Luna A, Rivera-Aguilar V, Miliar-Garcia A, et al. Regionalization of pIgR expression in the mucosa of mouse small intestine. *Immunol Lett* (2010) 128(1):59–67. doi:10.1016/j.imlet.2009.11.005
95. Galdeano CM, Perdigon G. The probiotic bacterium *Lactobacillus casei* induces activation of the gut mucosal immune system through innate immunity. *Clin Vaccine Immunol* (2006) 13(2):219–26. doi:10.1128/CVI.13.2.219-226.2006
96. Holscher HD, Faust KL, Czerkies LA, Litov R, Ziegler EE, Lessin H, et al. Effects of prebiotic-containing infant formula on gastrointestinal tolerance and fecal microbiota in a randomized controlled trial. *JPEN J Parenter Enteral Nutr* (2012) 36(1 Suppl):95S–105S. doi:10.1177/0148607111430087
97. Qiao H, Duffy LC, Griffiths E, Dryja D, Leavens A, Rossman J, et al. Immune responses in rhesus rotavirus-challenged BALB/c mice treated with *Bifidobacteria* and prebiotic supplements. *Pediatr Res* (2002) 51(6):750–5. doi:10.1203/00006450-200206000-00015
98. Shu Q, Gill HS. A dietary probiotic (*Bifidobacterium lactis* HN019) reduces the severity of *Escherichia coli* O157:H7 infection in mice. *Med Microbiol Immunol* (2001) 189(3):147–52. doi:10.1007/s430-001-8021-9
99. Ogawa M, Shimizu K, Nomoto K, Takahashi M, Watanuki M, Tanaka R, et al. Protective effect of *Lactobacillus casei* strain Shirota on Shiga toxin-producing *Escherichia coli* O157:H7 infection in infant rabbits. *Infect Immun* (2001) 69(2):1101–8. doi:10.1128/IAI.69.2.1101-1108.2001
100. Zhang W, Azevedo MS, Gonzalez AM, Saif LJ, Van Nguyen T, Wen K, et al. Influence of probiotic lactobacilli colonization on neonatal B cell responses in a gnotobiotic pig model of human rotavirus infection and disease. *Vet Immunol Immunopathol* (2008) 122(1–2):175–81. doi:10.1016/j.vetimm.2007.10.003
101. Singh RK, Chang HW, Yan D, Lee KM, Ucmak D, Wong K, et al. Influence of diet on the gut microbiome and implications for human health. *J Transl Med* (2017) 15(1):73. doi:10.1186/s12967-017-1175-y
102. Stern JN, Yaari G, Vander Heiden JA, Church G, Donahue WF, Hintzen RQ, et al. B cells populating the multiple sclerosis brain mature in the draining cervical lymph nodes. *Sci Transl Med* (2014) 6(248):248ra107. doi:10.1126/scitranslmed.3008879
103. Egg R, Reindl M, Deisenhammer F, Linington C, Berger T. Anti-MOG and anti-MBP antibody subclasses in multiple sclerosis. *Mult Scler* (2001) 7(5):285–9. doi:10.1191/135245801681137979
104. Vojdani A, Mukherjee PS, Berookhim J, Kharrazian D. Detection of antibodies against human and plant aquaporins in patients with multiple sclerosis. *Autoimmune Dis* (2015) 2015:905208. doi:10.1155/2015/905208
105. Polosukhina DI, Buneva VN, Doronin BM, Tyshkevich OB, Boiko AN, Gusev EI, et al. Hydrolysis of myelin basic protein by IgM and IgA antibodies from the sera of patients with multiple sclerosis. *Med Sci Monit* (2005) 11(8):BR266–72.
106. Sellebjerg F, Christiansen M, Garred P. MBP, anti-MBP and anti-PLP antibodies, and intrathecal complement activation in multiple sclerosis. *Mult Scler* (1998) 4(3):127–31. doi:10.1191/135245898678909475
107. Abdelhak A, Hottenrott T, Mayer C, Hintereder G, Zettl UK, Stich O, et al. CSF profile in primary progressive multiple sclerosis: re-exploring the basics. *PLoS One* (2017) 12(8):e0182647. doi:10.1371/journal.pone.0182647
108. Reichelt KL, Jensen D. IgA antibodies against gliadin and gluten in multiple sclerosis. *Acta Neurol Scand* (2004) 110(4):239–41. doi:10.1111/j.1600-0404.2004.00303.x
109. Link H, Muller R. Immunoglobulins in multiple sclerosis and infections of the nervous system. *Arch Neurol* (1971) 25(4):326–44. doi:10.1001/archneur.1971.00490040052007
110. Olsson JE, Link H. Immunoglobulin abnormalities in multiple sclerosis. Relation to clinical parameters: exacerbations and remissions. *Arch Neurol* (1973) 28(6):392–9. doi:10.1001/archneur.1973.00490240052009
111. Zhang Y, Da RR, Hilgenberg LG, Tourtellotte WW, Sobel RA, Smith MA, et al. Clonal expansion of IgA-positive plasma cells and axon-reactive antibodies in MS lesions. *J Neuroimmunol* (2005) 167(1–2):120–30. doi:10.1016/j.jneuroim.2005.05.006
112. Kowarik MC, Cepok S, Sellner J, Grummel V, Weber MS, Korn T, et al. CXCL13 is the major determinant for B cell recruitment to the CSF during neuroinflammation. *J Neuroinflammation* (2012) 9:93. doi:10.1186/1742-2094-9-93
113. Cekanaviciute E, Yoo BB, Runia TF, Debelius JW, Singh S, Nelson CA, et al. Gut bacteria from multiple sclerosis patients modulate human T cells and exacerbate symptoms in mouse models. *Proc Natl Acad Sci U S A* (2017) 114(40):10713–8. doi:10.1073/pnas.1711235114
114. Jangi S, Gandhi R, Cox LM, Li N, von Glehn F, Yan R, et al. Alterations of the human gut microbiome in multiple sclerosis. *Nat Commun* (2016) 7:12015. doi:10.1038/ncomms12015
115. Mirza A, Mao-Draayer Y. The gut microbiome and microbial translocation in multiple sclerosis. *Clin Immunol* (2017) 183:213–24. doi:10.1016/j.clim.2017.03.001
116. van den Hoogen WJ, Laman JD, t Hart BA. Modulation of multiple sclerosis and its animal model experimental autoimmune encephalomyelitis by food and gut microbiota. *Front Immunol* (2017) 8:1081. doi:10.3389/fimmu.2017.01081
117. Braniste V, Al-Asmakh M, Kowal C, Anuar F, Abbaspour A, Toth M, et al. The gut microbiota influences blood-brain barrier permeability in mice. *Sci Transl Med* (2014) 6(263):263ra158. doi:10.1126/scitranslmed.3009759
118. Erny D, Hrabe de Angelis AL, Jaitin D, Wieghofer P, Staszewski O, David E, et al. Host microbiota constantly control maturation and function of microglia in the CNS. *Nat Neurosci* (2015) 18(7):965–77. doi:10.1038/nn.4030
119. Rothhammer V, Mascanfroni ID, Bunse L, Takenaka MC, Kenison JE, Mayo L, et al. Type I interferons and microbial metabolites of tryptophan modulate astrocyte activity and central nervous system inflammation via the aryl hydrocarbon receptor. *Nat Med* (2016) 22(6):586–97. doi:10.1038/nm.4106
120. Hoban AE, Stilling RM, Ryan FJ, Shanahan F, Dinan TG, Claesson MJ, et al. Regulation of prefrontal cortex myelination by the microbiota. *Transl Psychiatry* (2016) 6:e774. doi:10.1038/tp.2016.42
121. Berer K, Gerdes LA, Cekanaviciute E, Jia X, Xiao L, Xia Z, et al. Gut microbiota from multiple sclerosis patients enables spontaneous autoimmune encephalomyelitis in mice. *Proc Natl Acad Sci U S A* (2017) 114(40):10719–24. doi:10.1073/pnas.1711233114
122. Le Berre L, Rousse J, Gourraud PA, Imbert-Marcille BM, Salama A, Evanno G, et al. Decrease of blood anti-alpha1,3 galactose Abs levels in multiple sclerosis (MS) and clinically isolated syndrome (CIS) patients. *Clin Immunol* (2017) 180:128–35. doi:10.1016/j.clim.2017.05.006
123. Lee YK, Menezes JS, Umesaki Y, Mazmanian SK. Proinflammatory T-cell responses to gut microbiota promote experimental autoimmune encephalomyelitis. *Proc Natl Acad Sci U S A* (2011) 108(Suppl 1):4615–22. doi:10.1073/pnas.1000082107
124. Ochoa-Reparaz J, Mielcarz DW, Ditrio LE, Burroughs AR, Foureau DM, Haque-Begum S, et al. Role of gut commensal microflora in the development of experimental autoimmune encephalomyelitis. *J Immunol* (2009) 183(10):6041–50. doi:10.4049/jimmunol.0900747
125. Ochoa-Reparaz J, Mielcarz DW, Haque-Begum S, Kasper LH. Induction of a regulatory B cell population in experimental allergic encephalomyelitis by alteration of the gut commensal microflora. *Gut Microbes* (2010) 1(2):103–8. doi:10.4161/gmic.1.2.11515
126. Esquifino AI, Cano P, Jimenez-Ortega V, Fernandez-Mateos MP, Cardinali DP. Immune response after experimental allergic encephalomyelitis in rats subjected to calorie restriction. *J Neuroinflammation* (2007) 4:6. doi:10.1186/1742-2094-4-6

127. Haghikia A, Jorg S, Duscha A, Berg J, Manzel A, Waschbisch A, et al. Dietary fatty acids directly impact central nervous system autoimmunity via the small intestine. *Immunity* (2015) 43(4):817–29. doi:10.1016/j.immuni.2015.09.007
128. Lemire JM, Archer DC. 1,25-dihydroxyvitamin D3 prevents the in vivo induction of murine experimental autoimmune encephalomyelitis. *J Clin Invest* (1991) 87(3):1103–7. doi:10.1172/JCI115072
129. Choi IY, Piccio L, Childress P, Bollman B, Ghosh A, Brandhorst S, et al. A diet mimicking fasting promotes regeneration and reduces autoimmunity and multiple sclerosis symptoms. *Cell Rep* (2016) 15(10):2136–46. doi:10.1016/j.celrep.2016.05.009

Conflict of Interest Statement: The authors declare the absence of any commercial or financial relationships that could be construed as a potential conflict of interest.

frontiers in Immunology

REVIEW
published: 05 March 2018
doi: 10.3389/fimmu.2018.00427

Plasma Cell Differentiation Pathways in Systemic Lupus Erythematosus

Susan Malkiel[1†], Ashley N. Barlev[1,2†], Yemil Atisha-Fregoso[1,3†], Jolien Suurmond[1‡] and Betty Diamond[1‡]*

[1] Center of Autoimmune Musculoskeletal and Hematopoietic Diseases, The Feinstein Institute for Medical Research, Northwell Health, Manhasset, NY, United States, [2] Donald and Barbara Zucker School of Medicine at Hofstra/Northwell, Hempstead, NY, United States, [3] Tecnologico de Monterrey, Monterrey, Mexico

Plasma cells (PCs) are responsible for the production of protective antibodies against infectious agents but they also produce pathogenic antibodies in autoimmune diseases, such as systemic lupus erythematosus (SLE). Traditionally, high affinity IgG autoantibodies are thought to arise through germinal center (GC) responses. However, class switching and somatic hypermutation can occur in extrafollicular (EF) locations, and this pathway has also been implicated in SLE. The pathway from which PCs originate may determine several characteristics, such as PC lifespan and sensitivity to therapeutics. Although both GC and EF responses have been implicated in SLE, we hypothesize that one of these pathways dominates in each individual patient and genetic risk factors may drive this predominance. While it will be important to distinguish polymorphisms that contribute to a GC-driven or EF B cell response to develop targeted treatments, the challenge will be not only to identify the differentiation pathway but the molecular mechanisms involved. In B cells, this task is complicated by the cross-talk between the B cell receptor, toll-like receptors (TLR), and cytokine signaling molecules, which contribute to both GC and EF responses. While risk variants that affect the function of dendritic cells and T follicular helper cells are likely to primarily influence GC responses, it will be important to discover whether some risk variants in the interferon and TLR pathways preferentially influence EF responses. Identifying the pathways of autoreactive PC differentiation in SLE may help us to understand patient heterogeneity and thereby guide precision therapy.

Keywords: systemic lupus erythematosus, autoantibodies, B cells, plasma cells, tolerance

OPEN ACCESS

Edited by:
Ralf J. Ludwig, University of Lübeck, Germany

Reviewed by:
Rudolf Armin Manz, University of Lübeck, Germany
Giovanni Di Zenzo, Istituto Dermopatico dell'Immacolata (IRCCS), Italy

****Correspondence:***
Jolien Suurmond
jsuurmond@northwell.edu

[†]These authors contributed equally to this work.

[‡]These authors share senior authorship.

Specialty section:
This article was submitted to Immunological Tolerance and Regulation, a section of the journal Frontiers in Immunology

Received: *11 January 2018*
Accepted: *16 February 2018*
Published: *05 March 2018*

Citation:
Malkiel S, Barlev AN, Atisha-Fregoso Y, Suurmond J and Diamond B (2018) Plasma Cell Differentiation Pathways in Systemic Lupus Erythematosus. Front. Immunol. 9:427. doi: 10.3389/fimmu.2018.00427

INTRODUCTION

Systemic lupus erythematosus (SLE) is a systemic autoimmune disease characterized by the production of pathogenic autoantibodies that target a variety of nuclear self-antigens, some of which cross-react with tissue antigens. These autoantibodies cause tissue inflammation and lead to organ damage in the kidneys, skin, and more. Presence of IgG ANA is a diagnostic feature

Abbreviations: AID, activation-induced cytidine deaminase; BCR, B cell receptor; BM, bone marrow; CSR, class switch recombination; DC, dendritic cell; EF, extrafollicular; FDC, follicular dendritic cell; FO, follicular; GC, germinal center; ICOS, inducible T-cell costimulator; IFN, interferon; MHC, major histocompatibility complex; MZ, marginal zone; PB, plasmablast; PBMC, peripheral blood mononuclear cell; PC, plasma cell; pDC, plasmacytoid dendritic cell; SHM, somatic hypermutation; SLE, systemic lupus erythematosus; Tfh, T follicular helper; TLR, Toll-like receptor.

for SLE and other systemic autoimmune diseases, and these antibodies have an important role in disease pathogenesis (1, 2). In contrast, IgM ANA are considered to be protective against autoimmunity. They can be present in healthy individuals and assist in the non-inflammatory clearance of cellular debris and inhibit responses induced by IgG ANA (3–5). Other isotypes include IgA and IgE, but the pathogenicity of these isotypes has been less well studied.

Antibodies are secreted by plasma cells (PCs), which arise as a terminal differentiation step from B cells. Most of our knowledge of immune tolerance to nuclear antigens, and the break of tolerance in SLE patients, is derived from studies with B cell receptor (BCR)-transgenic mice and single cell studies in humans, where self-reactivity is usually censored in developing B cells prior to their achieving immunocompetence (6, 7). Autoreactive cells that escape these mechanisms often become anergic (8–10), a process that mitigates against these cells giving rise to high affinity IgG autoantibody-producing PCs.

Plasma cells can arise through two pathways: through activation of B cells and direct differentiation in extrafollicular (EF) foci or through a germinal center (GC) response. Although traditionally pathogenic high affinity autoantibodies have been associated with the GC response, recent insights have implicated the EF pathway in SLE as well. We hypothesize that both pathways can contribute to production of SLE autoantibodies. Understanding the regulation of each pathway and how genetic risk alleles may preferentially target one or the other of these pathways will be the focus of this review.

Different subtypes of PCs have been described, including plasmablasts (PB), pre-PC, early PC, short-lived PC, and long-lived PC. These terms are sometimes used interchangeably or not clearly defined. The confusion in part derives from the original paradigm that the EF pathway only results in short-lived proliferating PBs, whereas the GC pathway was thought to result only in long-lived quiescent PCs (11). However, lifespan and proliferation can operate independently from each other, such that there are short-lived PCs which are not proliferating, and long-lived PCs from GC origin can proliferate prior to becoming quiescent (12–14). In addition, PC differentiation is a continuum where expression of canonical B cell markers [B220, CD19, major histocompatibility complex (MHC) class II] is gradually lost and PC markers (such as Blimp-1, CD138, secreted Ig) are gradually upregulated (14). It is therefore difficult to define specific PC subsets based on the expression of these markers. Here, we define PCs as antibody secreting cells and we will only mention specific PC subsets if these have been clearly verified. Definitions used in this review are PBs, if proliferation has been verified; short-lived plasma cells, if a short lifespan of <7 days has been shown; or long-lived PC, if a long lifespan of >28 days has been demonstrated.

T-INDEPENDENT B CELL ACTIVATION AND PC DIFFERENTIATION

The B cell lineage consists of several subsets and cells diverge early in development. Each of these naive cell subsets can give rise to PCs, but they each preferentially respond to specific types of antigen. Antigens can activate B cells in a T-independent or T-dependent manner. T-independent responses do not require cognate T cell help. T-independent activation therefore leads to plasma cell differentiation in the absence of GCs. There are two types of T-independent antigens that can induce activation of B cells; TI-1 antigens can activate B cells through coengagement of Toll-like receptors (TLR), such as LPS or other bacterial polysaccharides, whereas TI-2 antigens lead to extensive crosslinking of the BCR, such as polymeric protein antigens or repeated structural motifs (15). In TI-2 responses, competition for antigen enhances the activation and expansion of high-affinity cells, while antigen affinity is less important in TI-1 responses (16).

Although TI-1 and TI-2 antigens have been considered to induce T cell-independent responses, it is now clear that this distinction is not absolute: TI-2 and possibly TI-1 antigens can induce a transient GC (17), and the TI-2 serum antibody responses, in particular IgG, can still be T cell-dependent, even if the antigen cannot directly trigger T cells through MHC class II (18). It has therefore been proposed that the characteristics of the antigen is not the leading determinant of the response, but rather the B cell subset and the ancillary cell types involved determine the nature of the response (19).

In addition to the strength of the initial stimulus through the BCR and cognate and non-cognate T cell interactions, B cell activation is also modified by the presence of other potent stimuli. Pattern recognition receptors, such as TLRs, interact with damage-associated molecular patterns or highly conserved microbial structures present in bacteria or virus. Included among these are both dsDNA (CpG enriched) and RNA. Many TLRs signal through MyD88, and MyD88-deficient mice have diminished antibody responses, both early and late after immunization (20–23). Simultaneous engagement of the BCR and TLRs has a synergistic effect on signaling and subsequent B cell activation (24).

Cytokines, such as type I interferon (IFN), IL-6, and BAFF, can activate B cells and enhance both T-independent and T-dependent activation (25–27). BAFF has three recognized receptors, and one of them, TACI, signals through MyD88 (28), the same adaptor used by TLR7 and TLR9. Antigen-presenting cells, such as dendritic cell (DC) and macrophages, induce CD40-independent PC differentiation through secretion of cytokines such as BAFF and APRIL (26).

Two processes that alter the antibody response are somatic hypermutation (SHM) and class switch recombination (CSR), both of which are mediated by the enzyme activation-induced cytidine deaminase (AID) (29). These processes can change antigen recognition by the BCR (SHM) or change the isotype that is expressed (CSR), and are usually associated with GC responses (discussed below). Although T-independent responses are usually associated with the IgM isotype, CSR can occur in certain infections and does not require cognate T–B interactions (30). CSR can be driven by MyD88 signaling or cytokines such as BAFF, APRIL, IFN-gamma, and IL-21 (20, 23, 31, 32).

B-1 Cells

B-1 cells represent a distinct population of B cells that arises during fetal development (33, 34). They are mainly found in the

peritoneal and pleural cavities of mice and are rare in lymphoid organs and blood (**Figure 1**) (35). B-1 cells generally express germline-encoded, polyreactive IgM and IgA antibodies with limited V-gene segment usage, and are activated by T-independent antigens, such as LPS (TI-1) or multivalent antigens (TI-2) (36–38). In mice, B-1 cells can be further divided into B-1a and B-1b according to the expression of CD5 (CD5+ or CD5−, respectively). B-1a cells have been proposed as a major source of natural autoantibodies (37–40). These low-affinity polyreactive antibodies can be secreted spontaneously and are important in the clearance of apoptotic debris. They also contribute to protection against pathogens such as *Streptococcus pneumoniae* and influenza (41, 42). B-1b cells respond primarily to T-independent antigens (TI-1 and TI-2) and generate IgM memory cells, which contribute to protection against reinfection with *Borrelia hermsii*, *S. pneumoniae*, and Salmonella (19, 41, 43–45).

B-1 cells are poor at forming GCs (46); however, class-switched, somatically mutated B-1 antibodies showing evidence of antigen selection have been isolated from humans (47). Although elevated numbers of B-1 cells are present in some lupus-prone mouse strains (36, 48), there is not a clear association with SLE (49, 50).

Marginal Zone (MZ) B Cells

Marginal zone and follicular (FO) B cells differentiate from transitional B cells and both can participate in T-dependent and T-independent immune responses. MZ B cells are located in the MZ of the spleen, where they can serve as a first line of defense to T-independent and blood-borne antigens, such as lipopolysaccharide from bacteria (51). They are characterized by high responsiveness to TLR activation, as well as a preactivated state with high expression of complement receptors and costimulatory molecules. Due to these characteristics, they are known for their ability to quickly differentiate into PCs in response to T-independent antigens (51–53). MZ B cells do not require cognate T cell help, as soluble factors such as cytokines and costimulation derived from DCs, neutrophils, iNKT cells, and T cells, can also lead to their activation, CSR, and differentiation into PCs (28, 31, 54, 55).

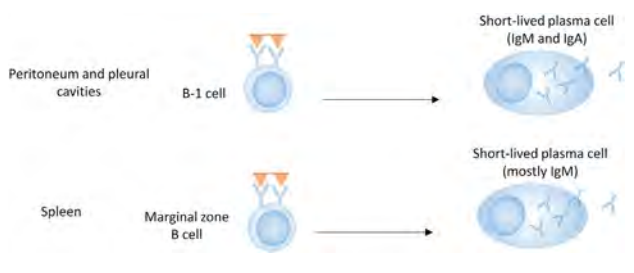

FIGURE 1 | B cell subsets in T-independent plasma cell development. B-1 cells in the peritoneal and pleural cavities can produce antibodies of the IgM and IgA isotype, either spontaneously (B-1a) or in response to T-independent antigens (B-1a and B-1b). Marginal zone B cells produce mostly IgM in response to T-independent antigens.

FO B Cells

Follicular B cells are migratory cells that move between lymph nodes, splenic follicles and the circulation until they interact with antigen. While MZ B cells are specialized in the response to T-independent antigen, they can also transport these antigens to the follicles and transfer such antigens to FO B cells (56, 57). However, compared to MZ B cells which become blasts within 24 h of mitogen activation, FO B cells do not show blast formation in response to mitogen, due to their requirement for cognate T cell help, and therefore the contribution of FO B cells in T-independent responses is probably limited (51).

T-CELL-DEPENDENT ACTIVATION OF B CELLS

Although there are models where T-independent responses can contribute to lupus in mice (58, 59), the majority of studies in lupus-prone mice and SLE patients suggest that T-dependent responses are the main driver of the disease. Therefore, we will focus on T cell-dependent responses for the remainder of this review. Here, we will first discuss the initial activation of B cells in a T-dependent response, including the cell fate decisions into either the EF or the GC pathway, followed by a discussion of the PC differentiation pathways after they diverge.

T-dependent responses are thought to be dominated by FO B cells, although MZ B cells can migrate to the T–B border, activate T cells, and enter a GC (60–63). Although it is unclear how much they contribute to class-switched GC-derived antibody responses, MZ B cells can certainly contribute to T-dependent EF responses (**Figure 2**) (64, 65). MZ B cells can also capture and deliver blood borne antigens to the follicles, thereby enhancing T-dependent FO responses (66). This indicates that although MZ B cells do not require cognate T cell interactions for their differentiation into PCs, they can still participate in T-dependent responses (**Figure 2**).

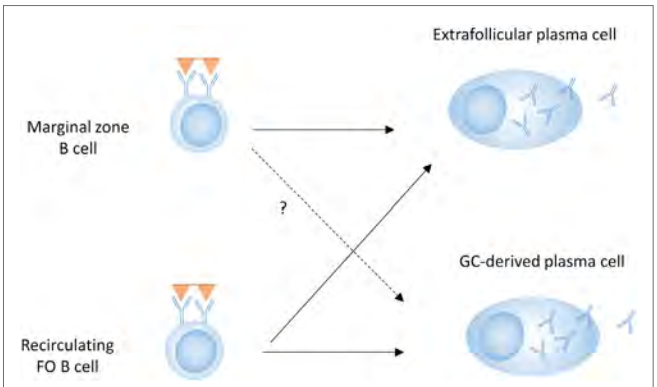

FIGURE 2 | B cell subsets in T-dependent plasma cell (PC) development. Both marginal zone B cells and follicular (FO) B cells can contribute to the extrafollicular (EF) PC response, whereas the germinal center (GC) response and subsequent PC differentiation is predominantly driven by FO B cells.

Recirculating FO B cells are activated by antigen in peripheral tissues or in lymphoid tissue where they encounter soluble antigen or antigen arrayed on follicular dendritic cells (FDCs). Activated B cells upregulate chemotactic factors (CCR7, EBI2) that favor their migration to the B–T border in the lymph nodes or spleen (67, 68). At the same time, CD4+ T cells are activated by DCs in the T cell zone, and these activated T cells will also migrate to the B–T cell border. The differentiation of Th cells [Th1, Th2, Th17, T follicular helper cells (Tfh)] is determined by T cell–DC interactions and is driven by the engagement of pattern recognition receptors by pathogens- or damage-associated molecules (69). At the T–B border, cognate interactions between antigen-specific B and T cells drives initial proliferation, and some B cells will undergo immunoglobulin CSR under the influence of T cell-derived cytokines (60, 70–73).

After activation, B cells can diverge into EF PCs and GC B cells. While it is well known which transcription factors drive the differentiation into GC B cells versus EF PCs, whether there is direct competition between EF and GC differentiation has not been fully demonstrated. Since B cells can proliferate at the T–B border prior to making cell-fate decisions, it is possible that the distinction between cells with the same high affinity that enter an EF or a GC pathway is partly stochastic and that the same B cell clone can be found in both pathways (74, 75).

Under non-competitive conditions, low-, medium-, or high-affinity B cells can all seed a GC, whereas the low-affinity cells are unable to generate an EF antibody response (76), due to failure to expand low-affinity EF PCs rather than a lack of initiation of PC differentiation (75). In contrast, under competitive conditions, low-affinity cells compete with high affinity cells and are unable to expand or enter a GC response (77). The advantage of high affinity B cells in each response can be at least partly explained by the degree of T cell help that is received, as high affinity B cells stimulated with antigen express higher amounts of MHC class II in the membrane, and are able to present more peptide to T cells, establishing a more effective immunological synapse (77), which can affect both EF and GC responses.

Although TLR activation during T-independent responses clearly increases the magnitude of the EF response, TLR ligation in T-dependent responses can enhance both the GC response and the EF response (22), in a B cell-extrinsic or -intrinsic manner (78).

PC DIFFERENTIATION

PC Differentiation in EF Responses

As EF PCs can provide an initial wave of secreted antibodies during the first week of an infection, these cells are an important part of the initial antibody response against pathogens (11). During expansion at the T–B border, those cells destined to become EF PCs will upregulate Blimp-1, CD138, and CXCR4 (79). Differentiation of EF PCs is driven by T–B interactions with a specific subset of Th cells that resembles Tfh cells but is located in EF areas. These Th cells are dependent on Bcl-6 and Stat3, and their interaction with B cells is mediated through CD40-CD40L and inducible T-cell costimulator (ICOS)–ICOSL interactions as well as cytokines, such as IL-21 (75, 79, 80). These interactions lead to heavy chain CSR as well as initiation of PC differentiation (**Figure 4**).

Under the influence of CXCR4, EF PCs migrate to the red pulp, where they can further proliferate and differentiate in EF foci. Proliferation is driven by BCR signaling, as cells with high affinity BCRs have increased proliferation and decreased apoptosis compared to cells with low affinity BCRs (75). Cofactors, such as CD19 and other molecules that enhance BCR signaling, can enhance EF proliferation. Lyn, an inhibitory molecule in the BCR signaling pathway, can diminish proliferation while in fact driving terminal PC differentiation (16). After the proliferative stage, PBs will differentiate further into PCs, characterized by higher expression of Blimp-1, further loss of MHC class II and costimulatory molecules. However, as discussed below, many EF PBs are short-lived and die prior to full differentiation into PCs (75). Some, however, complete their PC differentiation, after which they can survive in specialized niches in the spleen or bone marrow (BM) (12, 14).

Recent evidence suggests that several characteristics previously attributed to GC responses can also occur in EF responses. This includes the formation of memory B cells, CSR, SHM, and induction of long-lived PCs (discussed below). Whereas the previous understanding was that memory B cells are generated only in the GC, memory cells initially appear in blood before GC formation (81), and Bcl-6-deficient mice, which are unable to form GCs, generate memory cells (82). Most of these are non-mutated and IgM + memory cells, suggesting an EF origin at least for some memory cells. Although CSR and a low degree of SHM occur during early B–T interactions at the T–B border, continued AID expression and affinity maturation in EF sites has been observed (83).

GC Responses

Germinal centers are areas of T-dependent B cell development in spleen, tonsils, lymph nodes, and Peyers' patches. FDCs are important for normal splenic architecture and B cell development, as well as for maintaining the structure and function of the GC (84). Importantly, they capture antigen in immune complexes and retain the antigen in native form. Antigens are presented by FDCs on the cell surface (85). Several sequential events are involved in the formation of the GC. At the T–B border, B cell and T cell encounter with antigen stimulates formation of a GC (86), and migration from the T–B border into the follicle is mediated by CXCR5 (87). B cells receiving more T-help are more prone to differentiate into GC B cells (88, 89), and T cells differentiate into Tfh under the influence of B cell costimulatory molecules, including OX40L and CD80, which are essential for the maturation of Tfh cells (90, 91). The transcription factor Bcl-6 is required for the development of both GC B cells and Tfh cells (92). Tfh cells are specialized T helper cells that are involved in the selection and survival of B cells in the GC. The canonical costimulatory signal involved in the B–T cell interaction in the GC is CD40–CD40L (93, 94), but other signals such as ICOS–ICOSL, and IL-21 produced by Tfh cells are also required (95, 96).

The structure of the GC, with a light zone and a dark zone, aligns with the processes of SHM, affinity maturation, and selection (**Figure 5**). B cells in the light zone are referred to as

centrocytes. They interact with FDCs through antigen and with Tfh cells through MHC–peptide interactions (97). Those B cells which make stronger interactions with Tfh cells, due to an increased T cell receptor peptide–MHC interaction, are positively selected and enter the dark zone where their proliferation is greater (98, 99). As more antigen is added, the population of B cells with BCRs that bind antigen sufficiently to induce positive selection increases (99). Positive selection in the light zone is important as it leads to GC B cells with the greatest affinity for antigen. Interactions between Tfh cells, antigen, and B cells in the light zone determine the extent of proliferation in the dark zone (99). Fewer cells move from the light zone to the dark zone than from the dark zone to the light zone indicating that selection occurs in the light zone (99, 100).

The dark zone is the location where the most active proliferation of GC B cells takes place, as all GC B cells that are in G2 or M phase are in the dark zone; however, S phase cells are present in both the light zone and dark zone (100). Proliferation can occur under the influence of mTORC1 kinase, which activates the metabolic program that permits proliferation of B cells in the dark zone (98). After positive selection in the light zone and while undergoing proliferation in the dark zone, SHM occurs to effect a process called affinity maturation. During this process, point mutations occur in the BCR which affect its affinity for antigen. When the B cell returns to the light zone, the B cells that have undergone mutations to enhance affinity for the antigen are preferentially selected (101). A stronger interaction with Tfh cells in the light zone allows the B cell to undergo more rounds of proliferation in the dark zone. Therefore, each time the cell divides and more mutations are acquired, more affinity maturation can occur for B cells that were most positively selected for in the light zone (99).

Negative selection also occurs in the GC. B cells with weak affinity for antigens in the GC, or autoreactive B cells recognizing ubiquitously expressed self-antigens are eliminated (102, 103). Proposed mechanisms for the negative selection of these B cells are Fas-mediated apoptosis of cells that fail to bind antigen, failure to receive continuing T cell help, or the activity of T follicular regulatory cells (Tfr) (102). A recent study, however, suggests that negative selection primarily occurs in cells with an unproductive BCR as a consequence of SHM rather than in cells with lower affinity (104).

PC Differentiation in the GC

Both memory B cells and PCs arise from the GC, and many studies have examined the factors that determine if a given B cell will become a memory B cell or a PC. High affinity GC B cells become PCs, while lower affinity GC B cells become memory B cells (105–107). The initiation of PC differentiation in the light zone requires strong affinity for antigen; further differentiation in the dark zone requires help from Tfh cells (108). Light zone B cells become memory B cells early in the GC reaction, while PCs are formed later (105, 109). Preventing apoptosis in the GC allows for lower affinity B cells to become memory B cells but does not change the development of PCs, further suggesting that selection of B cells into the PC population is dependent on high affinity for antigen (106).

Certain cytokines favor the development of PCs. Among them, IL-21 is the most potent inducer of PC differentiation from memory and naive B cells (110, 111). This cytokine is produced by Tfh cells in the GC and activates the JAK1/3 STAT3 pathway. IL-21-deficient mice are unable to generate fully functional GCs. Without IL-21 or Tfh cells, PC formation is disrupted, affinity maturation does not occur, and the population of memory B cells is expanded (91, 96, 110).

Toll-like receptor ligands also enhance GC responses through both DCs and B cells (21, 78, 112). Whereas soluble TLR ligands can enhance GC responses through an effect on DCs, an antigen that can trigger both endosomal TLRs and BCRs can enhance the IgG antibody response in a B cell-intrinsic manner (21). This probably reflects the requirement for BCR-mediated uptake of ligands for endosomal TLRs in this process, and explains why some studies reported no effect of TLR signaling on GC responses induced with LPS (113, 114). B cell-intrinsic MyD88 signaling specifically enhances the formation of GC B cells, affinity maturation, and CSR in response to the TLR-9 ligand CpG coupled to the hapten NP, without affecting the number of PCs. In contrast, MyD88 signaling in DCs contributes to PC differentiation without affecting affinity maturation (78).

Different transcription factors are involved in the differentiation of PCs and memory B cells. Bach2 is reported to be important for selection of GC B cells into memory B cells; in the light zone, B cells with lower affinity for antigen have higher expression of Bach2, probably due to a lower degree of T cell help in those cells (105, 115). In addition to Bach2, ABF-1 leads to memory B cell differentiation and prevents PC differentiation (116). The transcription factors Blimp-1, XBP-1, and IRF4 are all involved in PC differentiation (117–119). Blimp-1 leads to decreased expression of genes involved in B cell signaling pathways including Pax5, which in turn leads to increased expression of Blimp-1 and XBP-1. This feed-forward mechanism is needed for PC differentiation (120, 121). Whereas Blimp-1 is required for PC differentiation, XBP-1 is more specifically needed for the unfolded protein response that is required for the production of high amounts of immunoglobulin in PCs (122).

It has been recently reported that PC differentiation is initiated in light zone B cells after which they migrate to the dark zone to further differentiate (108). Together with simulation data, this suggests that PCs exit the GC through the dark zone (123). Similar to the EF response, GC-derived PCs are characterized by a proliferative PB stage. Proliferating PBs have been reported in the dark zone of the GC, as well as the T–B border directly adjacent to the GC (123, 124), and their proliferation decreases as they migrate further from the GC, and is completely lost as they reach the medulla of the lymph node or the splenic red pulp (124). This suggests that proliferation of GC-derived PBs occurs during their transit out of the GC, at distinct locations from EF PBs, which proliferate in EF foci mainly in the red pulp of the spleen or the medulla of the LN. Some GC-derived PCs migrate to the red pulp in the spleen or the medullary cords in the lymph nodes, and others migrate through the blood to the BM (14, 81). Their exit out of the secondary lymphoid organs occurs prior to completion of their differentiation, as circulating PBs that arise in

GC responses in humans show signs of recent proliferation such as expression of Ki67 (14, 125).

PC Survival

Two studies in the late 1990s showed the existence of long-lived PCs, disputing previous thinking that PCs were short-lived (126, 127). A more recent study showed that 10 years after vaccination, long-lived PCs were still present in the BM, despite memory B cell depletion (128). Another study shows the survival of these long lived PCs despite CD19 directed CAR T cell therapy (129). These PCs have become a challenge in treatment of SLE, as they are often not eliminated by traditional therapies (130, 131). Although most evidence suggests that selection of PCs into the long-lived PC pool is dependent on extrinsic factors (132, 133), there is some evidence that B cell-intrinsic factors are also involved (134, 135). Identification of intrinsic factors leading to long-lived PC survival could represent therapeutic targets for SLE and other autoimmune diseases.

Plasma cell survival depends on cytokines secreted by stromal cells and eosinophils in the BM (136, 137), but they can also survive in the spleen or other organs, particularly under inflammatory conditions. PCs can survive anywhere as long as sufficient survival factors are present (138), but niches have the capacity to support only a limited number of PCs (132). Two related factors important for survival of PCs are BAFF and APRIL, which act through binding to TACI and BCMA (139–141). Both cytokines are anti-apoptotic and increase PC survival (140). A study in autoimmune thrombocytopenia suggests that an increase in BAFF caused by B cell depletion promotes differentiation of short-lived PCs into long lived PCs in the spleen (142, 143). Other molecules which can enhance survival of PCs are IL-6, VCAM-1, CXCR4, and CD28 (11, 136, 144).

CD93, a C1q receptor on B cells, is needed for the survival of PCs in the BM and is expressed only by a subset of PCs in mice (145). Induction of CD93 expression may, therefore, be an example of a B cell-intrinsic factor that contributes to PC survival.

Despite the traditional paradigm mentioned above, there are descriptions of long-lived PCs in T-independent responses, T cell-deficient, and GC-deficient mice, with survival up to at least 100 days (12, 132, 146, 147). In addition, PCs exit the GC as PBs, and require a survival niche for full differentiation. As many of them fail to find the appropriate niche, not all GC-derived PCs are long-lived (12). As far as we know now, transcription factors that drive PC differentiation in each response are similar, and it is not clear if all PCs have the potential to become long-lived or whether some are selected, preferentially in the GC, to become long-lived, and whether this is accompanied by altered expression of key survival molecules and transcription factors that drive this distinction.

TOLERANCE

Tolerance in EF Responses

As autoimmunity has been traditionally thought to arise through the GC, tolerance checkpoints in EF responses have not been extensively studied. Whereas the fast rate of the EF response is needed for adequate responses against pathogens, it also limits the time window for tolerance checkpoints. Therefore, it is likely that autoreactive B cells can be activated during EF responses, either through direct activation by self-antigen in an inflammatory milieu, cross-reactivity with foreign antigen, or through TLR ligands or cytokines (148). However, even if autoreactive PCs are generated in EF responses, they are mostly short-lived limiting the inflammation and tissue damage that is induced by autoantibodies. Therefore, the transient nature of the EF response may itself be a tolerance mechanism.

In addition to the short-lived nature of the response, tolerance in EF responses can be maintained through the balance between IgM and other (more pathogenic) isotypes. As most EF PBs secrete IgM, even though some CSR can occur, the balance between IgG and IgM that is generated in EF responses may result in prevention of autoimmunity, through downregulating myeloid cell activation in a LAIR-1 dependent fashion and minimizing local inflammation (3, 5, 149). In addition, sialylation of IgG antibodies, which occurs in T-independent responses can also contribute to tolerance, as these antibodies have lower pathogenicity, at least in the context of rheumatoid arthritis [(150), p. 296; (151), p. 429].

T cell help during initial activation might play a role in tolerance in EF foci, where class-switched EF responses can occur through cytokines secreted by bystander T cells or non-T cells. Since there is no requirement for cognate T cell help, the T cell repertoire is unlikely to restrict autoreactivity in the EF response.

Tolerance in GC Responses

Although the mechanisms of central tolerance preclude many autoreactive B cells from entering GCs, self-reactive B cells developing in the BM can bypass tolerance mechanisms. This may occur if they are reactive to monovalent antigen, if their affinity for antigen is below a certain threshold, or if they are present in an inflammatory milieu (152, 153). Therefore, it is normal to have circulating autoreactive mature (naive) B cells (154).

Importantly, however, mechanisms of peripheral tolerance are also in place to further eliminate autoreactivity. Mature self-reactive B cells can be thwarted from entering the follicle and be induced to become anergic (155). Still, some self-reactive B cells are able to enter the follicle. Evidence also suggests that autoreactive B cells that were initially excluded from the follicle can later be recruited into the GC, at which point these cells undergo SHM which may remove autoreactivity (156, 157), but can also lead to enhanced self-reactivity (153, 158). One important tolerance mechanism is the short lifespan of these B cells without mitogenic stimulation. Thus, only in an inflammatory milieu are these cells likely to access a GC response.

B cells that acquire autoreactivity in the GC must be eliminated or prevented from becoming PCs. In the GC itself, several tolerance mechanisms have been described, including apoptosis and receptor editing. However, a recent study showed that autoreactive GC B cells are not strongly selected to undergo apoptosis, perhaps because so many autoreactive B cells are cross-reactive with an eliciting antigen (104, 159–163). It is conceivable that these tolerance mechanisms are initiated by lack of cognate T cell

help. As described, T-cell help is needed for positive selection of B cells into PCs in the GC, and without this help, self-reactive PCs will not develop (100, 102, 152, 153). Thus, although self-reactive memory B cells can develop, the requirement for Tfh cells and FDCs that recognize or present the autoantigen makes it more difficult for non-cross-reactive autoreactive PCs to develop. T cells recognizing foreign antigen may be able to stimulate autoreactive GC B cells, if the BCR crossreacts with the eliciting antigen or an antigen present in a multimolecular complex with the eliciting antigen.

As IgG + memory B cells in healthy individuals have a much higher frequency of self-reactivity than IgG + PCs (164), an additional tolerance checkpoint must exist that prevents the differentiation of autoreactive PCs in addition to a tolerance checkpoint in GC B cells (**Figure 3**). Interestingly, switched PCs maintain expression of MHC class II and the antigen presentation machinery required for cognate T cell interactions at least until they are no longer proliferating, suggesting that this stage of PC differentiation may represent a T cell-dependent tolerance checkpoint (165). Although this has not been extensively studied, Th cells are required for the completion of GC-derived PC differentiation (103), and PCs can undergo cognate T cell interactions after their migration out of the GC at the T–B border (165). This suggests that a lack of T cell help may prevent the terminal differentiation of autoreactive PCs or that autoreactive B cells committed to becoming PCs are more susceptible to apoptosis or receptor editing than B cells committed to a memory pathway.

PC DIFFERENTIATION IN SLE

EF PC Differentiation in SLE

Because there are no definite markers that discriminate PCs based on their pathway of differentiation, it is hard to establish the pathway through which they were derived, especially in humans where access to lymphoid organs is limited. In addition, most studies discriminating EF responses from GC responses use acute immunization models, and it is not clear if all the paradigms that have been proposed for the distinction between EF and GC responses apply in the chronic immune activation present in autoimmune conditions. Although EF PC differentiation in autoimmunity has not been emphasized, recent studies indicate this pathway may have a specific role in autoimmunity (125, 166, 167). MRL/lpr mice exhibit EF PC generation, although they have increased formation of spontaneous GCs as well (166, 168, 169). In humans, recent research supports that a large proportion of the PCs in some SLE patients are clonally related to naive cells, suggesting an EF origin (125). Here, we propose mechanisms which can lead to enhanced EF responses in SLE (**Figure 4**).

Expansion of MZ B Cells

Marginal zone B cells are expanded in several lupus-prone mouse strains. In humans, the characterization of MZ B cells is much more complicated [reviewed in Ref. (13)], and it is unclear if SLE patients also have an expansion of this population. However, the high BAFF levels often present in SLE patients would support MZ expansion. Mice overexpressing BAFF develop an SLE-like phenotype that is characterized by a high titer of class-switched autoantibodies and PCs, in a T cell-independent manner (59). A preference for autoreactive B cells to differentiate into MZ B cells compared to FO B cells has been described in mice (170–173), and MZ B cells can differentiate directly into IgG + PCs in EF responses (174, 175). Therefore, development of serum autoantibodies in some lupus-prone mice has been attributed to MZ expansion and activation, although some studies have challenged this paradigm (176–180).

Enhanced TLR Signaling

Another mechanism by which EF PC responses in SLE may be altered is through enhanced TLR signaling. MyD88-deficient MRL/lpr mice develop lower autoantibody titers and are

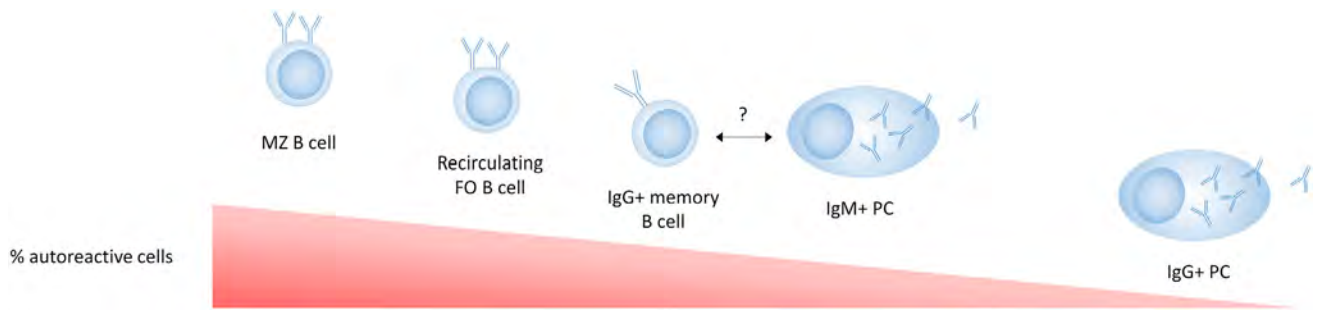

FIGURE 3 | Tolerance in mature cell subsets in healthy individuals. B-1 cells are not shown in this figure as their relative autoreactivity compared to the other subsets is not exactly known. Marginal zone (MZ) B cells are enriched for autoreactive B cell receptors (BCRs) (polyreactive or antinuclear) compared to follicular B cells. IgG + memory B cells have a lower frequency of autoreactivity compared to naive B cells, suggesting a tolerance checkpoint in the germinal center. The autoreactivity in IgM plasma cells (PCs) has not been directly reported, but the fact that IgM autoantibodies are commonly found in healthy individuals and have an anti-inflammatory role, suggests that some autoreactive IgM + PCs are present and more common than autoreactive IgG + PCs. The low frequency of autoreactive BCRs in IgG + PCs compared to IgG + memory B cells suggests an additional strong tolerance checkpoint that prevents the development of serum IgG autoantibodies.

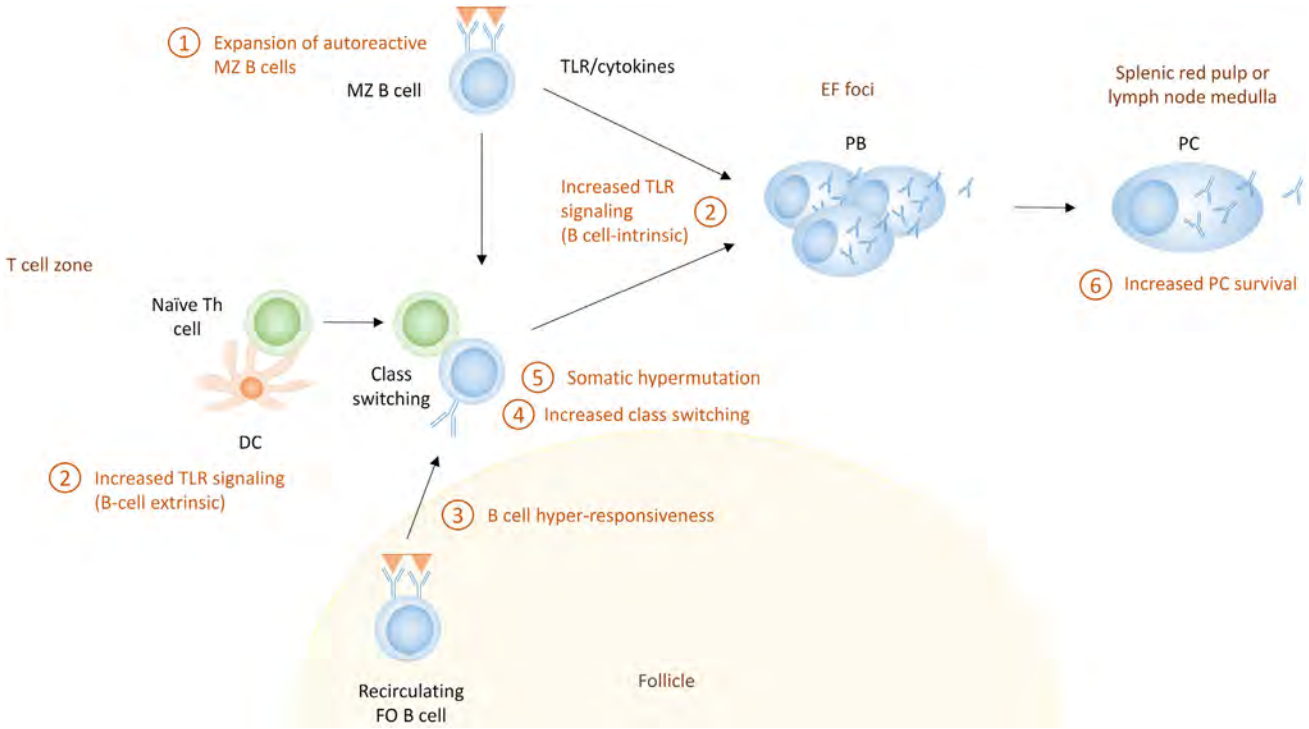

FIGURE 4 | The extrafollicular (EF) pathway for the generation of autoreactive plasma cells (PCs) in systemic lupus erythematosus. Shown here are the potential mechanisms that can contribute to enhanced extrafollicular PC responses. These include (1) expansion of marginal zone (MZ) B cells, which often exhibit autoreactive receptors; (2) increased Toll-like receptor (TLR) signaling, which can directly activate B cells (B cell-intrinsic) or can enhance Th responses through their effect on dendritic cells (B cell-extrinsic); (3) B cell hyperresponsiveness, which can affect the activation of follicular B cells; (4) increased class switch recombination which can lead to more pathogenic IgG autoantibodies; (5) somatic hypermutation which can lead to affinity maturation of autoreactive PCs; and (6) increased PC survival.

protected from disease (181, 182), suggesting a role for TLRs in EF responses in MRL/lpr mice. Although TLR-7 or -9 deficiency each diminished the production of specific types of autoantibodies in MRL/lpr mice, only TLR-7 deficiency diminished lymphocyte activation, IgG production, and kidney disease (183, 184). This suggests that although each receptor can enhance EF responses, only TLR-7 induces the production of pathogenic antibodies, or permits the inflammatory response needed to cause disease.

Besides a B cell-intrinsic role of TLR signaling, B cell extrinsic TLR signaling can also enhance T–B interactions through the increased activation of DCs (185). Enhanced T–B interactions in this situation have the potential to enhance T-dependent PC differentiation in both EF and GC pathways. B cells as well as myeloid cells from SLE patients have increased expression of TLRs, and SLE patients may have increased proinflammatory responses to TLR ligands (186), which can contribute to stronger T-independent and T-dependent EF responses.

B Cell Hyperresponsiveness

A well-known feature of SLE is B cell hyperresponsiveness, which causes increased signaling upon BCR ligation by antigen (187, 188). The increased signaling can derive from increased activity of signaling molecules in the BCR pathway (many of which are genetic risk factors for SLE; discussed below) (189), or through a synergy between BCR triggering and other signaling pathways, such as TLR, BAFF, and type I IFN, which can each lower the threshold for B cell activation through the BCR and contribute to the activation of B cells (59, 190, 191). Type I IFN is necessary for a complete response after BCR/TLR7 stimulation, and increments in type I IFN can overcome tolerance that normally occurs after repetitive stimulation of TLRs (192). The fact that high affinity B cells are more prone to expansion at the EF PB stage (75, 76) suggests that the increased BCR signaling that occurs in SLE may preferentially stimulate EF responses.

Increased CSR

Increased CSR in EF responses is another feature of SLE that may contribute to enhanced pathogenicity of EF PCs, in particular if the balance between protective IgM and pathogenic IgG is altered. Increased CSR has been described both in lupus-prone mouse models as well as SLE patients (193). In particular, a special subset of EF T cells in the MRL/lpr mice has been described to contribute to the expansion of class switched IgG + EF PCs. These EF T cells are dependent on Bcl-6, Stat3, and ICOS, and they mediate IgG CSR through CD40–CD40L interactions and IL-21 (167, 168). A similar subset of T cells has been described in EF responses in

non-autoimmune mice, although there they localized at the T–B border, and it is not clear if they migrate to EF foci as well (80). EF Th cells express CXCR4, as opposed to Tfh cells which express CXCR5 (or both) (194, 195). While the EF Th cell subset is present in MRL/lpr mice which have a dominant EF phenotype, mice with a more pronounced GC pathway, such as NZB/W, have a more mixed T cell phenotype (168). IgG CSR in MRL/lpr mice, as well as in graft versus host-mediated autoimmunity, is almost completely dependent on ICOS, as ICOS-deficiency leads to lower expression of CXCR4, as well as diminished secretion of IL-21 (167, 168). T-independent factors can also increase EF CSR in SLE. In AM14 rheumatoid factor transgenic MRL/lpr mice, T cells are required for the spontaneous production of rheumatoid factor, but not when B cells are exposed to chromatin immune complexes which will trigger both the BCR and TLR (196).

Increased CSR has been described in circulating PBs of SLE patients, and at least some of these have low mutation rates, suggestive of an EF origin (125). However, all EF-derived PBs need not have low mutation rates. Factors that increase CSR in EF PCs in mice, such as IL-21, are increased in SLE patients (197), and factors that mediate T-independent CSR, such as TLR signaling and the myeloid-derived cytokine BAFF, are also increased in SLE (198). It is therefore conceivable that SLE patients can exhibit increased CSR in EF responses.

Increased SHM

Besides the increased CSR in EF PCs in MRL/lpr mice, SHM has also been shown to occur in EF foci, probably under the influence of EF Th cells. However, SHM can also occur in response to chromatin immune complexes in a T-independent manner (166, 168, 196, 199). This SHM potentially leads to affinity maturation (although probably to a lesser extent than in the GC) in autoreactive EF PCs, but no mechanism has been described for antigen selection and affinity maturation in EF responses.

GC Responses in SLE

Germinal center responses are well known to be increased in lupus-prone mice, and SLE patients have increased numbers of circulating pre-GC B cells, switched memory B cells and Tfh cells, suggestive of enhanced GC responses (169, 200, 201). Given that IgG anti-DNA autoantibodies which are considered to be pathogenic in SLE show evidence of SHM (202), the production of autoreactive PCs by SHM of nonautoreactive naive B cells within the GC has been considered an important contributor to the development of SLE in both mice (203) and humans (204). The following mechanisms can contribute to GC-derived autoreactive PCs (**Figure 5**).

Loss of FO Exclusion

In normal conditions, autoreactive naive B cells undergo anergy that leads to FO exclusion and prevents their recruitment into GC responses. However, in SLE, these B cells are able to enter the GC, and continue their differentiation into PCs (155, 205).

B Cell Hyperresponsiveness

As discussed above, B cell hyperresponsiveness can enhance EF responses and may also potentiate GC responses (206). Hyperresponsiveness could lead to increased positive selection

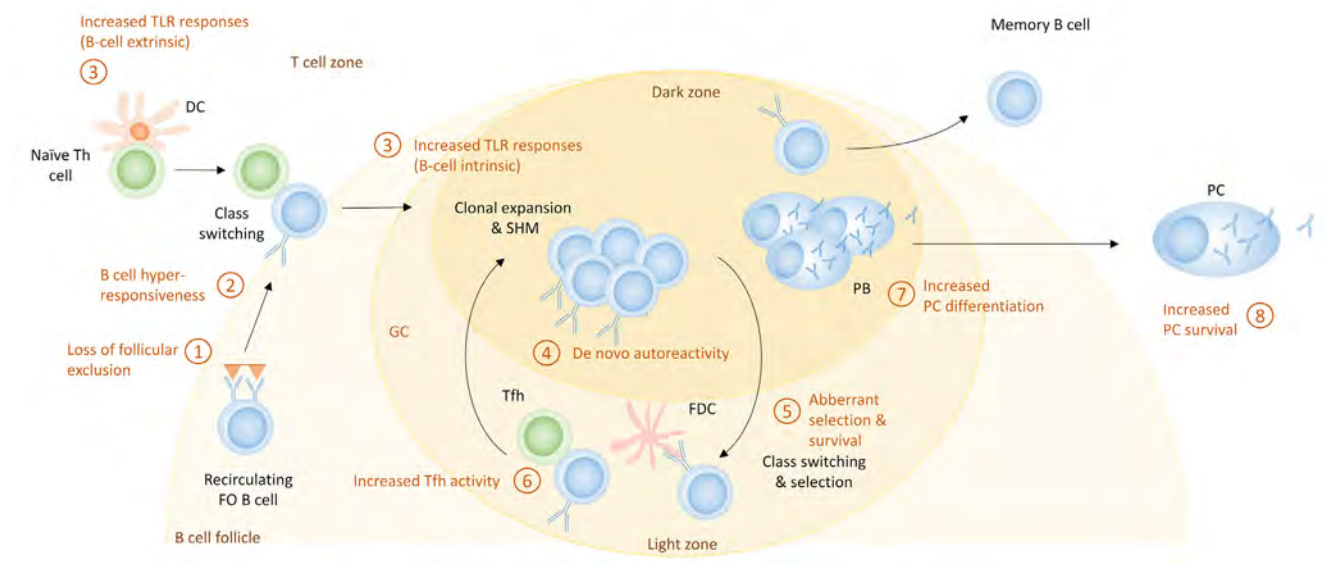

FIGURE 5 | The germinal center (GC) pathway for the generation of autoreactive plasma cells (PCs) in systemic lupus erythematosus. Shown here are the potential mechanisms that can contribute to enhanced PC differentiation during GC responses. These include (1) loss of follicular exclusion, which can lead to recruitment of autoreactive B cells into GC responses; (2) B cell hyperresponsiveness which can affect the activation of follicular B cells; (3) increased Toll-like receptor (TLR) signaling, which can affect initial activation of B cells as well as the GC response itself; (4) *de novo* autoreactivity, generated through somatic hypermutation (SHM) and leading to the generation of autoreactive GC B cells from non-autoreactive precursors; (5) aberrant selection and survival, which can diminish tolerance mechanisms; (6) increased T follicular helper (Tfh) activity, which can increase the extent of GC responses as well as PC differentiation; (7) cell fate decisions that increase PC differentiation; and (8) increased PC survival.

in the light zone and subsequent proliferation in the dark zone, thereby amplifying GC responses (207).

Increased TLR Responses

Toll-like receptors, which are involved in the EF pathway, also have a role in the GC response. Loss of MyD88 causes a loss of GC formation; interestingly, this alteration may be attributed to the function of TLR-7 and not TLR-9 (208, 209). Increased function of TLR-7 causes an increment in spontaneous GC formation and an autoimmunity phenotype (208). B cell-intrinsic MyD88 signaling specifically enhances GC responses when antigen and TLR ligand are coupled; self-antigen that can trigger both TLRs and the BCR will presumably have the same ability. It was recently demonstrated that FDCs, which are crucial for the maintenance of GCs and FO architecture, express type I IFN through a TLR-7 pathway upon internalizing complement-opsonized self-immune complexes through the complement receptor CD21 in the 564Igi RNP-specific lupus mouse model; this pathway is important for spontaneous GC formation and production of isotype-switched autoantibodies (210). 564Igi BM chimeras in which the recipient FDCs were TLR-7-deficient exhibited less autoimmunity. As many SLE antigens can activate TLRs (1, 190, 191), these represent potent pathways to amplify GC responses.

De Novo Autoreactivity

Although loss of FO exclusion can lead to recruitment of autoreactive naive cells into GC reactions, SHM of nonautoreactive B cells can lead to *de novo* autoreactivity in GC B cells (202, 211). Whether these cells are able to differentiate into PCs has not been reported, but most pathogenic antibodies in SLE show signs of SHM, and *de novo* autoreactivity explains a large fraction of the autoreactive IgG + memory cells in SLE patients (204, 212). These studies suggest that GC B cells retain autoreactivity generated through SHM.

Aberrant Selection and Survival of GC B Cells

Another mechanism for the generation of autoreactive PCs in the GC is increased survival of GC B cells. It has been shown that SLE patients have increased levels of BAFF (213). While BAFF has a large role in the EF pathway of differentiation of PCs, it also expands the Tfh cell population and promotes formation of GC and survival of B cells. This could be a contributing factor in allowing the breach of B cell tolerance seen in SLE patients (214, 215). As a result of increased BAFF, naive B cells with moderate affinity that would normally undergo apoptosis, may be rescued and enter a GC response.

Increased Tfh Activity

Another mechanism that leads to the development of autoreactive PCs in the GC is increased Tfh activity (216). One cytokine important for the development of autoreactive PCs is IL-21, a cytokine produced by Tfh cells (72). The number of Tfh cells as well as the level of IL-21 has been shown to be increased in lupus-prone mice and SLE patients (217, 218). IL-21 increases IgG PC number (72, 217), and Tfh cells can alter selection and allow the differentiation of autoreactive B cells into autoreactive antibody secreting PCs (219). In lupus-prone mice, OX40L expression by B cells contributes to the autoimmune phenotype, presumably through its effect on Tfh cells (90, 220).

Increased PC Differentiation

B cell hyperresponsiveness may also increase the generation of PCs in SLE by directing more B cells to undergo PC differentiation. SLE patients often have increased numbers of circulating PBs; in one study this inversely correlates with the number of CD27 + memory cells, suggesting a preferred differentiation pathway (221). Lupus-prone mice, including the ones that have a GC phenotype, have vast increases in their PC numbers, which exceeds the expansion of the memory compartment. This suggests that there may be preferential output of PCs from the GC in SLE.

Increased Survival of PCs

Another possible mechanism for increased autoantibody titers is increased survival of PCs (**Figures 2** and **3**), which might occur if excess survival factors are present. Increased expression of the cytokines BAFF, APRIL, and IL-6 is present in lupus-prone mice (222, 223), suggesting that these cytokines can support enhanced PC survival. Although in healthy mice a limited number of PCs can survive in BM and spleen, these organs in lupus-prone mice gain additional capacity and exhibit an increased number of PCs (224). Both lupus-prone mice and SLE patients often exhibit hypergammaglobulinemia (225, 226), which may also be caused by an increased capacity to support PC survival in SLE patients. As both EF and GC-derived PCs can either stay in the spleen or stay in the lymph nodes or migrate to the BM, these factors will probably affect both types of PCs. In addition, several lupus-prone mouse strains have increased levels of CXCL12 in their inflamed kidneys, which may allow recruitment of PCs to this organ (226–228).

GENETIC RISK ALLELES

Whereas both EF and GC pathways can lead to autoantibody production, we propose that genetic factors may cause a dominance of either of these pathways in individual patients. Approximately one hundred risk loci have been associated with SLE, and genes within these loci have been broadly cast into categories involving DNA degradation and clearance of apoptotic/cellular debris, innate immunity, including TLR and IFN signaling, and adaptive immunity (229). Some overlap or fall outside these categories, and others are undefined. Most variants are in non-coding regions that may alter expression levels that can determine the magnitude of a response in a cell-lineage and stage-specific manner. Several risk genes have been described to alter B cell selection, activation, differentiation and/or survival in a B cell-intrinsic fashion, including LYN, BLK, BANK1, PTPN22, TNFAIP3, TNIP1, CSK, and FCGR2B (189, 230). Although it is known that these risk alleles alter B cell signaling, their effect on PC differentiation has not been

TABLE 1 | The role of genes with risk alleles in EF and GC responses.

Gene	Function of gene	Function of risk allele	Potential role in EF	Potential role in GC	Reference
HLA class II genes	Antigen presentation	Presentation of self-specific T cell epitopes	May increase T-dependent EF responses	Expansion of Tfh, GC responses and PC differentiation	(103, 231, 232)
TNFS4 (OX40L)	Costimulatory molecule on many cell types primarily interacting with OX40 on activated T cells promoting T cell functions, cytokine and Ab production, and PC generation	Most likely a response eQTL, as DNA heterozygous for the 5′ rs2205860 SNP had enhanced binding to NF-κB; no significant differences in basal expression in EBV-transformed cells or primary cells	Required for T cell-dependent EF Ab response driven by MZ DCs	Supports Tfh maturation in mice (B cell-intrinsic) and in humans (expression on myeloid APCs)	(64, 90, 220, 233, 234)
CD80	T cell costimulation through CD28, CTLA-4, PD-L1	Unknown	Little effect on Ab production by short-lived plasmablasts (in CD80−/− mice)	Increased maturation of Tfh and generation of long-lived PC	(91)
LYN	Src-family kinase that phosphorylates both activating and inhibitory receptors in B cells and myeloid cells. Its role in activating ITAMs is probably redundant with other Src family kinases, therefore its role in inhibitory receptors seems most crucial	Unknown SLE patients have decreased expression of Lyn in B cells	Lyn−/− mice have EF PC differentiation without GCs in some studies	Lyn−/− mice have spontaneous GCs in some studies	(187, 235, 236)
BLK	Src-family kinase that phosphorylates both activating and inhibitory receptors in B cells	Decreased expression in B cells, increased B cell activation	Increased TI IgG antibody responses in Blk+/− mice, with no effect on IgM	Increased numbers of switched memory cells in risk carriers suggests more active GC responses, but TD antibody responses in Blk+/− or −/− mice not affected	(237–240)
BANK1	Signaling molecule involved in BCR- and CD40-mediated signaling in B cells, positively regulates Ca^{2+} release in B cells, negatively regulates CD40-mediated signaling	Differential expression of two splice variants, but functional consequences unknown	Normal antibody responses to TI antigen, but the IgM response in TD responses was increased, possibly due to increased survival of EF PCs	Normal IgG antibody responses to TD antigen suggesting that there is no major influence on switched TD responses, although there is a slight increase in spontaneous IgG2a in Bank1−/− mice	(241–243)
PTPN22 (Lyp)	Protein tyrosine phosphatase that has inhibitory function in B and T cell signaling	Risk allele has increased inhibitory function, causing decreased B cell activation, proliferation and signaling leading to impaired central B cell tolerance as well as impaired T cell responses	Impaired central tolerance; unclear if PTPN22 affects EF responses; deficiency of PEP (mouse ortholog) in mice did not alter spontaneous IgM and IgG3 levels, suggesting no effect on extrafollicular antibody production	Lower frequency of memory cells in risk allele carriers suggests that it may inhibit GC responses consistent with increased GCs and serum IgG in PEP−/− mice	(206, 244–247)
TNFAIP3 (A20)	Negative regulator of NF-κB signaling in response to TLR, TNF, and CD40 signaling in B cells and other immune cells	Reduced expression in EBV transformed cells with one risk variant and reduced anti-inflammatory activity in transfected HEK cells with another risk variant	B cell-specific A20 deficiency in mice leads to alterations in the MZ compartment and consistently enhanced IgM production (spontaneous, as well as TD and TI immunizations), but no difference in IgG3	B cell specific A20 deficiency in mice leads to elevated numbers of GC B cells, and spontaneous IgG2 levels in old mice which deposited in kidneys; however, inconsistent effects on TD IgG production upon immunization in different studies	(248–253)

(*Continued*)

TABLE 1 | Continued

Gene	Function of gene	Function of risk allele	Potential role in EF	Potential role in GC	Reference
TNIP1	Ubiquitin-binding protein with diverse targets; interaction with TNFAIP3 negatively regulates NF-κB; also known to repress PPARs, which may increase B cell activity	Reduced expression in EBV-transformed B cells from H1 and H2 risk haplotypes; H1 contains coding SNP near a nuclear export sequence	Mutation of polyubiquitin binding site increased formation of EF PCs	Mutation of polyubiquitin-binding site induced spontaneous GC, increased TFH, CSR, and production of autoreactive Abs thru TLR-mediated NF-κB pathway	(254, 255)
CSK	Tyrosine kinase protein that phosphorylates Src family kinases leading to their inactivation. Src family kinases can act on both activating and inhibitory receptors in B and T cells	Increased expression in B cells, increased B cell activation (Lyn phosphorylation, Ca^{2+} mobilization), expansion of transitional B cells	Unknown, but increased signaling may enhance PC differentiation	Csk is low in memory cells but its function in GC responses is not known	(256)
FCGR2B	Inhibitory receptor for IgG on B cells and other immune cells	Impairment of receptor mobility, lipid rafts and inhibitory signaling	Enhanced antibody production upon TI immunization, although not observed in all studies	Enhanced GC responses in FCGR2B−/− mice. Spontaneous GC B cells have increased self-reactivity, but the checkpoint to PCs is still intact in FCGR2B−/− mice, so uncertain if autoreactive PCs in these mice are GC-derived	(150, 257–262)
IRF5	Production of type I IFN in response to TLR ligands, macrophage polarization, enhanced PC differentiation	Increased expression and activation in monocytes from SLE patients with the risk allele	IRF5−/− mice have decreased IgG1 responses upon TI immunization and have decreased PC numbers in MRL/lpr mice, suggesting that increased expression of IRF5 may enhance EF responses	IRF5−/− mice have diminished GC-derived antibodies, suggesting the IRF5 risk allele may enhance GC PC differentiation	(263–267)
STAT4	Transcription factor critical for myeloid and lymphocyte functions; major responder to IL-12; role in IFN-α signaling	Increased expression in PBMCs correlated with SNPs rs3821236, rs3024866 (both in the same haplotype block) and rs7574865 but not with other SNPs	STAT4−/− had no effect on antibody titers or pathology in EF model (MRL/lpr)	Regulates Tfh through Bcl-6 and T-bet in T cells; indirectly upregulates T-bet in B cells, which facilitates spontaneous GC; STAT4−/− reduced autoantibody production and glomerulonephritis in B6.TC model (Sle1,2,3 congenic)	(268–270)
BACH2	Transcriptional repressor that promotes CSR/SHM and is required for memory B cell differentiation	No expression differences associated with rs597325 in primary blood cell types	Deficiency increases IgM PC differentiation *in vitro*	Bach2 can enhance memory B cell differentiation while blocking plasma cell differentiation	(105, 271–273)
PRDM1 (Blimp-1)	Transcription factor required for PC differentiation/transcription factor that alters DC function	Decreased expression of Blimp-1 in DCs leading to increased cytokine production (unknown function of risk allele in PCs)	Unknown	Expansion of Tfh and increased GC responses in DC-Blimp-1-deficient mice	(274, 275)
IRF8	Transcription factor that inhibits PC differentiation together with PU.1 and distribution into FO or MZ compartments	Increased expression in EBV-transformed cells	Increased IRF8 expression presumably would decrease PC differentiation	Increased function of IRF8 could lead to enhanced GC responses, through regulation of Bcl-6, AID, and MDM2	(276–278)
IKZF3 (Aiolos)	Transcription factor involved in lymphocyte development and function; important in B cell maturation and activation	Unknown	Deficiency impairs the MZ B cell compartment but not the generation of short-lived PCs following immunization	Deficiency induces spontaneous GCs and production of autoantibodies; deficiency prevents generation of high-affinity BM PCs following immunization	(279–281)

(*Continued*)

TABLE 1 | Continued

Gene	Function of gene	Function of risk allele	Potential role in EF	Potential role in GC	Reference
ETS1	Transcription factor important for lymphocyte development and differentiation; it is also involved in maintaining B cell tolerance through anergy maintenance	Reduced expression of Ets1 in EBV-transformed cells and PBMCs	Increased EF PC responses in Ets1−/−	Loss of anergy may increase participation of autoreactive B cells in GC reactions	(282–285)
FASL	Apoptosis of immune cells through engagement of Fas	Increased surface expression on circulating fibrocytes	Based on studies in MRL/lpr mice, increased expression of FasL would be expected to decrease EF PC responses	Fas/FasL interactions are important for apoptosis in GC, thereby potentially affecting survival and selection of autoreactive GC B cells	(286, 287)
TLR7	Activation of immune cells by RNA viruses or self-antigen	Increased expression in PBMCs	EF PCs in AM14 Tg MRL/lpr mice are driven by TLR-7	GC responses are driven by B cell-intrinsic TLR7 in B6 and B6.Sle1b mice and FDCs in 564Igi RNP-specific lupus model	(184, 208, 210, 288, 289)
SLC15A4	Lysosomal amino-acid transporter required for endosomal TLR signaling and IFN1 production	One risk variant is associated with reduced expression in monocytes	SLC15a4 mutant mice, which are unable to produce IFN1, have reduced anti-chromatin IgG and IgM in B6/lpr mice, but have otherwise normal T-dependent and independent responses	T-dependent IgG2a/c OVA responses are decreased in SLC15a4−/− mice, but not in SLC15a4 mutant mice. IgG autoantibodies in pristane-induced lupus aC15a4 deficiency, suggesting that reduced expression in risk allele carriers may block GC-derived PCs	(290–293)

The categories "potential role in EF or GC" are speculative and based on our understanding of the literature included in the reference column.

extensively investigated, and most of our understanding of the role of these genes in EF and GC responses derives from mouse models. Other risk alleles are involved in B–T cell interactions, memory or PC differentiation, and IFN/TLR signaling. For many of these, the functional consequence of the risk allele has not been determined. However, it is reasonable to ask whether these risk alleles may alter EF or GC responses.

Table 1 shows risk alleles that can alter B cell responses and subsequently PC differentiation. These risk alleles can function in a B cell-intrinsic or -extrinsic manner. We propose that some risk alleles, such as TLR7, FAS, IRF5, TNFAIP3, and TNIP1, can modify both EF and GC responses.

Certain risk alleles, such as HLA class II genes, FCGR2B, STAT4, CD80, IRF8, and PRDM1, most likely drive GC responses, whereas other risk alleles, such as ETS1, LYN, BACH2, and BLK, may preferentially drive EF responses in SLE, although this pathway has not been extensively explored. Further understanding of the exact role of each risk allele in plasma cell differentiation pathways may enhance our insight into patient heterogeneity.

CONCLUSION

In this review, we have described the PC differentiation pathways which can contribute to the development of autoantibody production in SLE. Whereas both EF and GC pathways may be active in the same patient, we propose that certain genetic risk alleles contribute to the dominance of one of these pathways. The dominant PC differentiation pathway, determined by the composite of risk alleles, may contribute to patient heterogeneity and to response to therapy. Although it is likely that different therapeutics alter each pathway to a different extent, there is to our knowledge not enough understanding of the molecular pathways in each response nor is there clear evidence which therapeutics target which pathway. These pathways are not as distinct as we thought, nor can the pathway taken by a PC be easily distinguished with current knowledge. A more thorough analysis of these pathways, their role in SLE, and the contribution of genetic risk alleles to each pathway may provide us with distinct targets to allow precision therapy.

AUTHOR CONTRIBUTIONS

SM, AB, and YA-F contributed to writing the manuscript. JS and BD contributed to the concept, reviewing, and writing of the manuscript.

FUNDING

JS received financial support from American Autoimmune Related Disease Association. This work was further supported by NIH 1P01 AI073693 and Lupus Research Institute.

REFERENCES

1. Suurmond J, Diamond B. Autoantibodies in systemic autoimmune diseases: specificity and pathogenicity. *J Clin Invest* (2015) 125(6):2194–202. doi:10.1172/JCI78084
2. Tan EM, Cohen AS, Fries JF, Masi AT, McShane DJ, Rothfield NF, et al. The 1982 revised criteria for the classification of systemic lupus erythematosus. *Arthritis Rheum* (1982) 25(11):1271–7. doi:10.1002/art.1780251101
3. Vas J, Gronwall C, Marshak-Rothstein A, Silverman GJ. Natural antibody to apoptotic cell membranes inhibits the proinflammatory properties of lupus autoantibody immune complexes. *Arthritis Rheum* (2012) 64(10):3388–98. doi:10.1002/art.34537
4. Li QZ, Xie C, Wu T, Mackay M, Aranow C, Putterman C, et al. Identification of autoantibody clusters that best predict lupus disease activity using glomerular proteome arrays. *J Clin Invest* (2005) 115(12):3428–39. doi:10.1172/JCI23587
5. Mannoor K, Matejuk A, Xu Y, Beardall M, Chen C. Expression of natural autoantibodies in MRL-lpr mice protects from lupus nephritis and improves survival. *J Immunol* (2012) 188(8):3628–38. doi:10.4049/jimmunol.1102859
6. Nemazee D, Buerki K. Clonal deletion of autoreactive B lymphocytes in bone marrow chimeras. *Proc Natl Acad Sci U S A* (1989) 86(20):8039–43. doi:10.1073/pnas.86.20.8039
7. Wardemann H, Yurasov S, Schaefer A, Young JW, Meffre E, Nussenzweig MC. Predominant autoantibody production by early human B cell precursors. *Science* (2003) 301(5638):1374–7. doi:10.1126/science.1086907
8. Pewzner-Jung Y, Friedmann D, Sonoda E, Jung S, Rajewsky K, Eilat D. B cell deletion, anergy, and receptor editing in "knock in" mice targeted with a germline-encoded or somatically mutated anti-DNA heavy chain. *J Immunol* (1998) 161(9):4634–45.
9. Mandik-Nayak L, Bui A, Noorchashm H, Eaton A, Erikson J. Regulation of anti-double-stranded DNA B cells in nonautoimmune mice: localization to the T-B interface of the splenic follicle. *J Exp Med* (1997) 186(8):1257–67. doi:10.1084/jem.186.8.1257
10. Pugh-Bernard AE, Silverman GJ, Cappione AJ, Villano ME, Ryan DH, Insel RA, et al. Regulation of inherently autoreactive VH4-34 B cells in the maintenance of human B cell tolerance. *J Clin Invest* (2001) 108(7):1061–70. doi:10.1172/JCI12462
11. Nutt SL, Hodgkin PD, Tarlinton DM, Corcoran LM. The generation of antibody-secreting plasma cells. *Nat Rev Immunol* (2015) 15(3):160–71. doi:10.1038/nri3795
12. Chernova I, Jones DD, Wilmore JR, Bortnick A, Yucel M, Hershberg U, et al. Lasting antibody responses are mediated by a combination of newly formed and established bone marrow plasma cells drawn from clonally distinct precursors. *J Immunol* (2014) 193(10):4971–9. doi:10.4049/jimmunol.1401264
13. Sanz I, Wei C, Lee FE, Anolik J. Phenotypic and functional heterogeneity of human memory B cells. *Semin Immunol* (2008) 20(1):67–82. doi:10.1016/j.smim.2007.12.006
14. Kallies A, Hasbold J, Tarlinton DM, Dietrich W, Corcoran LM, Hodgkin PD, et al. Plasma cell ontogeny defined by quantitative changes in blimp-1 expression. *J Exp Med* (2004) 200(8):967–77. doi:10.1084/jem.20040973
15. Jeurissen A, Ceuppens JL, Bossuyt X. T lymphocyte dependence of the antibody response to 'T lymphocyte independent type 2' antigens. *Immunology* (2004) 111(1):1–7. doi:10.1111/j.1365-2567.2004.01775.x
16. Shih TA, Roederer M, Nussenzweig MC. Role of antigen receptor affinity in T cell-independent antibody responses in vivo. *Nat Immunol* (2002) 3(4):399–406. doi:10.1038/ni776
17. Lentz VM, Manser T. Cutting edge: germinal centers can be induced in the absence of T cells. *J Immunol* (2001) 167(1):15–20. doi:10.4049/jimmunol.167.1.15
18. Mongini PK, Stein KE, Paul WE. T cell regulation of IgG subclass antibody production in response to T-independent antigens. *J Exp Med* (1981) 153(1):1–12. doi:10.1084/jem.153.1.1
19. Vinuesa CG, Chang PP. Innate B cell helpers reveal novel types of antibody responses. *Nat Immunol* (2013) 14(2):119–26. doi:10.1038/ni.2511
20. Khan AQ, Chen Q, Wu ZQ, Paton JC, Snapper CM. Both innate immunity and type 1 humoral immunity to *Streptococcus pneumoniae* are mediated by MyD88 but differ in their relative levels of dependence on toll-like receptor 2. *Infect Immun* (2005) 73(1):298–307. doi:10.1128/IAI.73.1.298-307.2005
21. Hou B, Saudan P, Ott G, Wheeler ML, Ji M, Kuzmich L, et al. Selective utilization of toll-like receptor and MyD88 signaling in B cells for enhancement of the antiviral germinal center response. *Immunity* (2011) 34(3):375–84. doi:10.1016/j.immuni.2011.01.011
22. Guay HM, Andreyeva TA, Garcea RL, Welsh RM, Szomolanyi-Tsuda E. MyD88 is required for the formation of long-term humoral immunity to virus infection. *J Immunol* (2007) 178(8):5124–31. doi:10.4049/jimmunol.178.8.5124
23. Raval FM, Mishra R, Garcea RL, Welsh RM, Szomolanyi-Tsuda E. Long-lasting T cell-independent IgG responses require MyD88-mediated pathways and are maintained by high levels of virus persistence. *MBio* (2013) 4(6):e812–3. doi:10.1128/mBio.00812-13
24. Leadbetter EA, Rifkin IR, Hohlbaum AM, Beaudette BC, Shlomchik MJ, Marshak-Rothstein A. Chromatin-IgG complexes activate B cells by dual engagement of IgM and toll-like receptors. *Nature* (2002) 416(6881):603–7. doi:10.1038/416603a
25. Jego G, Palucka AK, Blanck JP, Chalouni C, Pascual V, Banchereau J. Plasmacytoid dendritic cells induce plasma cell differentiation through type I interferon and interleukin 6. *Immunity* (2003) 19(2):225–34. doi:10.1016/S1074-7613(03)00208-5
26. Litinskiy MB, Nardelli B, Hilbert DM, He B, Schaffer A, Casali P, et al. DCs induce CD40-independent immunoglobulin class switching through BLyS and APRIL. *Nat Immunol* (2002) 3(9):822–9. doi:10.1038/ni829
27. Moore PA, Belvedere O, Orr A, Pieri K, LaFleur DW, Feng P, et al. BLyS: member of the tumor necrosis factor family and B lymphocyte stimulator. *Science* (1999) 285(5425):260–3. doi:10.1126/science.285.5425.260
28. He B, Santamaria R, Xu W, Cols M, Chen K, Puga I, et al. The transmembrane activator TACI triggers immunoglobulin class switching by activating B cells through the adaptor MyD88. *Nat Immunol* (2010) 11(9):836–45. doi:10.1038/ni.1914
29. Stavnezer J, Guikema JE, Schrader CE. Mechanism and regulation of class switch recombination. *Annu Rev Immunol* (2008) 26:261–92. doi:10.1146/annurev.immunol.26.021607.090248
30. Rothaeusler K, Baumgarth N. B-cell fate decisions following influenza virus infection. *Eur J Immunol* (2010) 40(2):366–77. doi:10.1002/eji.200939798
31. Puga I, Cols M, Barra CM, He B, Cassis L, Gentile M, et al. B cell-helper neutrophils stimulate the diversification and production of immunoglobulin in the marginal zone of the spleen. *Nat Immunol* (2011) 13(2):170–80. doi:10.1038/ni.2194
32. Pone EJ, Zhang J, Mai T, White CA, Li G, Sakakura JK, et al. BCR-signalling synergizes with TLR-signalling for induction of AID and immunoglobulin class-switching through the non-canonical NF-kappaB pathway. *Nat Commun* (2012) 3:767. doi:10.1038/ncomms1769
33. Herzenberg LA, Stall AM, Lalor PA, Sidman C, Moore WA, Parks DR. The Ly-1 B cell lineage. *Immunol Rev* (1986) 93:81–102.
34. Hardy RR, Carmack CE, Li YS, Hayakawa K. Distinctive developmental origins and specificities of murine CD5+ B cells. *Immunol Rev* (1994) 137:91–118.
35. Baumgarth N. The double life of a B-1 cell: self-reactivity selects for protective effector functions. *Nat Rev Immunol* (2011) 11(1):34–46. doi:10.1038/nri2901
36. Hardy RR, Hayakawa K. CD5 B cells, a fetal B cell lineage. *Adv Immunol* (1994) 55:297–339.
37. Kasaian MT, Casali P. Autoimmunity-prone B-1 (CD5 B) cells, natural antibodies and self recognition. *Auto immunity* (1993) 15(4):315–29. doi:10.3109/08916939309115755
38. Hayakawa K, Hardy RR, Honda M, Herzenberg LA, Steinberg AD. Ly-1 B cells: functionally distinct lymphocytes that secrete IgM autoantibodies. *Proc Natl Acad Sci U S A* (1984) 81(8):2494–8. doi:10.1073/pnas.81.8.2494
39. Griffin DO, Holodick NE, Rothstein TL. Human B1 cells in umbilical cord and adult peripheral blood express the novel phenotype CD20+ CD27+ CD43+ CD70. *J Exp Med* (2011) 208(1):67–80. doi:10.1084/jem.20101499
40. Conger JD, Sage HJ, Corley RB. Correlation of antibody multireactivity with variable region primary structure among murine anti-erythrocyte autoantibodies. *Eur J Immunol* (1992) 22(3):783–90. doi:10.1002/eji.1830220323
41. Sindhava VJ, Bondada S. Multiple regulatory mechanisms control B-1 B cell activation. *Front Immunol* (2012) 3:372. doi:10.3389/fimmu.2012.00372
42. Cole LE, Yang Y, Elkins KL, Fernandez ET, Qureshi N, Shlomchik MJ, et al. Antigen-specific B-1a antibodies induced by *Francisella tularensis* LPS

provide long-term protection against *F. tularensis* LVS challenge. *Proc Natl Acad Sci U S A* (2009) 106(11):4343–8. doi:10.1073/pnas.0813411106
43. Berland R, Wortis HH. Origins and functions of B-1 cells with notes on the role of CD5. *Annu Rev Immunol* (2002) 20:253–300. doi:10.1146/annurev.immunol.20.100301.064833
44. Haas KM, Poe JC, Steeber DA, Tedder TF. B-1a and B-1b cells exhibit distinct developmental requirements and have unique functional roles in innate and adaptive immunity to S. pneumoniae. *Immunity* (2005) 23(1):7–18. doi:10.1016/j.immuni.2005.04.011
45. Alugupalli KR, Leong JM, Woodland RT, Muramatsu M, Honjo T, Gerstein RM. B1b lymphocytes confer T cell-independent long-lasting immunity. *Immunity* (2004) 21(3):379–90. doi:10.1016/j.immuni.2004.06.019
46. Linton PJ, Lo D, Lai L, Thorbecke GJ, Klinman NR. Among naive precursor cell subpopulations only progenitors of memory B cells originate germinal centers. *Eur J Immunol* (1992) 22(5):1293–7.
47. Mantovani L, Wilder RL, Casali P. Human rheumatoid B-1a (CD5+ B) cells make somatically hypermutated high affinity IgM rheumatoid factors. *J Immunol* (1993) 151(1):473–88.
48. Murakami M, Yoshioka H, Shirai T, Tsubata T, Honjo T. Prevention of autoimmune symptoms in autoimmune-prone mice by elimination of B-1 cells. *Int Immunol* (1995) 7(5):877–82. doi:10.1093/intimm/7.5.877
49. Casali P, Notkins AL. Probing the human B-cell repertoire with EBV: polyreactive antibodies and CD5+ B lymphocytes. *Annu Rev Immunol* (1989) 7:513–35. doi:10.1146/annurev.iy.07.040189.002501
50. Suzuki N, Sakane T, Engleman EG. Anti-DNA antibody production by CD5+ and CD5- B cells of patients with systemic lupus erythematosus. *J Clin Invest* (1990) 85(1):238–47.
51. Martin F, Oliver AM, Kearney JF. Marginal zone and B1 B cells unite in the early response against T-independent blood-borne particulate antigens. *Immunity* (2001) 14(5):617–29. doi:10.1016/S1074-7613(01)00129-7
52. Genestier L, Taillardet M, Mondiere P, Gheit H, Bella C, Defrance T. TLR agonists selectively promote terminal plasma cell differentiation of B cell subsets specialized in thymus-independent responses. *J Immunol* (2007) 178(12):7779–86. doi:10.4049/jimmunol.178.12.7779
53. Oliver AM, Martin F, Gartland GL, Carter RH, Kearney JF. Marginal zone B cells exhibit unique activation, proliferative and immunoglobulin secretory responses. *Eur J Immunol* (1997) 27(9):2366–74. doi:10.1002/eji.1830270935
54. Balazs M, Martin F, Zhou T, Kearney J. Blood dendritic cells interact with splenic marginal zone B cells to initiate T-independent immune responses. *Immunity* (2002) 17(3):341–52. doi:10.1016/S1074-7613(02)00389-8
55. Bialecki E, Paget C, Fontaine J, Capron M, Trottein F, Faveeuw C. Role of marginal zone B lymphocytes in invariant NKT cell activation. *J Immunol* (2009) 182(10):6105–13. doi:10.4049/jimmunol.0802273
56. van den Eertwegh AJ, Laman JD, Schellekens MM, Boersma WJ, Claassen E. Complement-mediated follicular localization of T-independent type-2 antigens: the role of marginal zone macrophages revisited. *Eur J Immunol* (1992) 22(3):719–26. doi:10.1002/eji.1830220315
57. Liu YJ, Zhang J, Lane PJ, Chan EY, MacLennan IC. Sites of specific B cell activation in primary and secondary responses to T cell-dependent and T cell-independent antigens. *Eur J Immunol* (1991) 21(12):2951–62. doi:10.1002/eji.1830211209
58. Pao LI, Lam KP, Henderson JM, Kutok JL, Alimzhanov M, Nitschke L, et al. B cell-specific deletion of protein-tyrosine phosphatase Shp1 promotes B-1a cell development and causes systemic autoimmunity. *Immunity* (2007) 27(1):35–48. doi:10.1016/j.immuni.2007.04.016
59. Groom JR, Fletcher CA, Walters SN, Grey ST, Watt SV, Sweet MJ, et al. BAFF and MyD88 signals promote a lupuslike disease independent of T cells. *J Exp Med* (2007) 204(8):1959–71. doi:10.1084/jem.20062567
60. MacLennan IC, Toellner KM, Cunningham AF, Serre K, Sze DM, Zuniga E, et al. Extrafollicular antibody responses. *Immunol Rev* (2003) 194:8–18. doi:10.1034/j.1600-065X.2003.00058.x
61. Song H, Cerny J. Functional heterogeneity of marginal zone B cells revealed by their ability to generate both early antibody-forming cells and germinal centers with hypermutation and memory in response to a T-dependent antigen. *J Exp Med* (2003) 198(12):1923–35. doi:10.1084/jem.20031498
62. Oliver AM, Martin F, Kearney JF. IgMhighCD21high lymphocytes enriched in the splenic marginal zone generate effector cells more rapidly than the bulk of follicular B cells. *J Immunol* (1999) 162(12):7198–207.
63. Attanavanich K, Kearney JF. Marginal zone, but not follicular B cells, are potent activators of naive CD4 T cells. *J Immunol* (2004) 172(2):803–11. doi:10.4049/jimmunol.172.2.803
64. Chappell CP, Draves KE, Giltiay NV, Clark EA. Extrafollicular B cell activation by marginal zone dendritic cells drives T cell-dependent antibody responses. *J Exp Med* (2012) 209(10):1825–40. doi:10.1084/jem.20120774
65. Rubtsov A, Strauch P, Digiacomo A, Hu J, Pelanda R, Torres RM. Lsc regulates marginal-zone B cell migration and adhesion and is required for the IgM T-dependent antibody response. *Immunity* (2005) 23(5):527–38. doi:10.1016/j.immuni.2005.09.018
66. Cinamon G, Zachariah MA, Lam OM, Foss FW Jr, Cyster JG. Follicular shuttling of marginal zone B cells facilitates antigen transport. *Nat Immunol* (2008) 9(1):54–62. doi:10.1038/ni1542
67. Reif K, Ekland EH, Ohl L, Nakano H, Lipp M, Forster R, et al. Balanced responsiveness to chemoattractants from adjacent zones determines B-cell position. *Nature* (2002) 416(6876):94–9. doi:10.1038/416094a
68. Pereira JP, Kelly LM, Xu Y, Cyster JG. EBI2 mediates B cell segregation between the outer and centre follicle. *Nature* (2009) 460(7259):1122–6. doi:10.1038/nature08226
69. Toellner KM, Luther SA, Sze DM, Choy RK, Taylor DR, MacLennan IC, et al. T helper 1 (Th1) and Th2 characteristics start to develop during T cell priming and are associated with an immediate ability to induce immunoglobulin class switching. *J Exp Med* (1998) 187(8):1193–204. doi:10.1084/jem.187.8.1193
70. Rousset F, Garcia E, Defrance T, Peronne C, Vezzio N, Hsu DH, et al. Interleukin 10 is a potent growth and differentiation factor for activated human B lymphocytes. *Proc Natl Acad Sci U S A* (1992) 89(5):1890–3. doi:10.1073/pnas.89.5.1890
71. Lundgren M, Persson U, Larsson P, Magnusson C, Smith CI, Hammarstrom L, et al. Interleukin 4 induces synthesis of IgE and IgG4 in human B cells. *Eur J Immunol* (1989) 19(7):1311–5. doi:10.1002/eji.1830190724
72. Bryant VL, Ma CS, Avery DT, Li Y, Good KL, Corcoran LM, et al. Cytokine-mediated regulation of human B cell differentiation into Ig-secreting cells: predominant role of IL-21 produced by CXCR5+ T follicular helper cells. *J Immunol* (2007) 179(12):8180–90. doi:10.4049/jimmunol.179.12.8180
73. Avery DT, Deenick EK, Ma CS, Suryani S, Simpson N, Chew GY, et al. B cell-intrinsic signaling through IL-21 receptor and STAT3 is required for establishing long-lived antibody responses in humans. *J Exp Med* (2010) 207(1):155–71. doi:10.1084/jem.20091706
74. Jacob J, Kelsoe G. In situ studies of the primary immune response to (4-hydroxy-3-nitrophenyl)acetyl. II. A common clonal origin for periarteriolar lymphoid sheath-associated foci and germinal centers. *J Exp Med* (1992) 176(3):679–87. doi:10.1084/jem.176.3.679
75. Chan TD, Gatto D, Wood K, Camidge T, Basten A, Brink R. Antigen affinity controls rapid T-dependent antibody production by driving the expansion rather than the differentiation or extrafollicular migration of early plasmablasts. *J Immunol* (2009) 183(5):3139–49. doi:10.4049/jimmunol.0901690
76. Phan TG, Paus D, Chan TD, Turner ML, Nutt SL, Basten A, et al. High affinity germinal center B cells are actively selected into the plasma cell compartment. *J Exp Med* (2006) 203(11):2419–24. doi:10.1084/jem.20061254
77. Schwickert TA, Victora GD, Fooksman DR, Kamphorst AO, Mugnier MR, Gitlin AD, et al. A dynamic T cell-limited checkpoint regulates affinity-dependent B cell entry into the germinal center. *J Exp Med* (2011) 208(6):1243–52. doi:10.1084/jem.20102477
78. Rookhuizen DC, DeFranco AL. Toll-like receptor 9 signaling acts on multiple elements of the germinal center to enhance antibody responses. *Proc Natl Acad Sci U S A* (2014) 111(31):E3224–33. doi:10.1073/pnas.1323985111
79. Garcia De Vinuesa C, Gulbranson-Judge A, Khan M, O'Leary P, Cascalho M, Wabl M, et al. Dendritic cells associated with plasmablast survival. *Eur J Immunol* (1999) 29(11):3712–21. doi:10.1002/(SICI)1521-4141(199911)29:11<3712::AID-IMMU3712>3.0.CO;2-P
80. Lee SK, Rigby RJ, Zotos D, Tsai LM, Kawamoto S, Marshall JL, et al. B cell priming for extrafollicular antibody responses requires Bcl-6 expression by T cells. *J Exp Med* (2011) 208(7):1377–88. doi:10.1084/jem.20102065
81. Blink EJ, Light A, Kallies A, Nutt SL, Hodgkin PD, Tarlinton DM. Early appearance of germinal center-derived memory B cells and plasma cells in blood after primary immunization. *J Exp Med* (2005) 201(4):545. doi:10.1084/jem.20042060

82. Toyama H, Okada S, Hatano M, Takahashi Y, Takeda N, Ichii H, et al. Memory B cells without somatic hypermutation are generated from Bcl6-deficient B cells. *Immunity* (2002) 17(3):329–39. doi:10.1016/S1074-7613(02)00387-4
83. Di Niro R, Lee SJ, Vander Heiden JA, Elsner RA, Trivedi N, Bannock JM, et al. Salmonella infection drives promiscuous B cell activation followed by extrafollicular affinity maturation. *Immunity* (2015) 43(1):120–31. doi:10.1016/j.immuni.2015.06.013
84. Wang X, Cho B, Suzuki K, Xu Y, Green JA, An J, et al. Follicular dendritic cells help establish follicle identity and promote B cell retention in germinal centers. *J Exp Med* (2011) 208(12):2497–510. doi:10.1084/jem.20111449
85. Heesters BA, Chatterjee P, Kim YA, Gonzalez SF, Kuligowski MP, Kirchhausen T, et al. Endocytosis and recycling of immune complexes by follicular dendritic cells enhances B cell antigen binding and activation. *Immunity* (2013) 38(6):1164–75. doi:10.1016/j.immuni.2013.02.023
86. Gatto D, Brink R. The germinal center reaction. *J Allergy Clin Immunol* (2010) 126(5):898–907. doi:10.1016/j.jaci.2010.09.007
87. Legler DF, Loetscher M, Roos RS, Clark-Lewis I, Baggiolini M, Moser B. B cell-attracting chemokine 1, a human CXC chemokine expressed in lymphoid tissues, selectively attracts B lymphocytes via BLR1/CXCR5. *J Exp Med* (1998) 187(4):655–60. doi:10.1084/jem.187.4.655
88. Allen CD, Okada T, Tang HL, Cyster JG. Imaging of germinal center selection events during affinity maturation. *Science* (2007) 315(5811):528–31. doi:10.1126/science.1136736
89. Qi H, Cannons JL, Klauschen F, Schwartzberg PL, Germain RN. SAP-controlled T-B cell interactions underlie germinal centre formation. *Nature* (2008) 455(7214):764–9. doi:10.1038/nature07345
90. Cortini A, Ellinghaus U, Malik TH, Cunninghame Graham DS, Botto M, Vyse TJ. B cell OX40L supports T follicular helper cell development and contributes to SLE pathogenesis. *Ann Rheum Dis* (2017) 76(12):2095–103. doi:10.1136/annrheumdis-2017-211499
91. Good-Jacobson KL, Song E, Anderson S, Sharpe AH, Shlomchik MJ. CD80 expression on B cells regulates murine T follicular helper development, germinal center B cell survival, and plasma cell generation. *J Immunol* (2012) 188(9):4217–25. doi:10.4049/jimmunol.1102885
92. Kitano M, Moriyama S, Ando Y, Hikida M, Mori Y, Kurosaki T, et al. Bcl6 protein expression shapes pre-germinal center B cell dynamics and follicular helper T cell heterogeneity. *Immunity* (2011) 34(6):961–72. doi:10.1016/j.immuni.2011.03.025
93. Noelle RJ, Ledbetter JA, Aruffo A. CD40 and its ligand, an essential ligand-receptor pair for thymus-dependent B-cell activation. *Immunol Today* (1992) 13(11):431–3.
94. Allen RC, Armitage RJ, Conley ME, Rosenblatt H, Jenkins NA, Copeland NG, et al. CD40 ligand gene defects responsible for X-linked hyper-IgM syndrome. *Science* (1993) 259(5097):990–3. doi:10.1126/science.7679801
95. Taylor JJ, Pape KA, Jenkins MK. A germinal center-independent pathway generates unswitched memory B cells early in the primary response. *J Exp Med* (2012) 209(3):597–606. doi:10.1084/jem.20111696
96. Linterman MA, Beaton L, Yu D, Ramiscal RR, Srivastava M, Hogan JJ, et al. IL-21 acts directly on B cells to regulate Bcl-6 expression and germinal center responses. *J Exp Med* (2010) 207(2):353–63. doi:10.1084/jem.20091738
97. El Shikh ME, El Sayed RM, Sukumar S, Szakal AK, Tew JG. Activation of B cells by antigens on follicular dendritic cells. *Trends Immunol* (2010) 31(6):205–11. doi:10.1016/j.it.2010.03.002
98. Ersching J, Efeyan A, Mesin L, Jacobsen JT, Pasqual G, Grabiner BC, et al. Germinal center selection and affinity maturation require dynamic regulation of mTORC1 kinase. *Immunity* (2017) 46(6):1045–58e6. doi:10.1016/j.immuni.2017.06.005
99. Gitlin AD, Shulman Z, Nussenzweig MC. Clonal selection in the germinal centre by regulated proliferation and hypermutation. *Nature* (2014) 509(7502):637–40. doi:10.1038/nature13300
100. Victora GD, Schwickert TA, Fooksman DR, Kamphorst AO, Meyer-Hermann M, Dustin ML, et al. Germinal center dynamics revealed by multiphoton microscopy with a photoactivatable fluorescent reporter. *Cell* (2010) 143(4):592–605. doi:10.1016/j.cell.2010.10.032
101. Klein U, Dalla-Favera R. Germinal centres: role in B-cell physiology and malignancy. *Nat Rev Immunol* (2008) 8(1):22–33. doi:10.1038/nri2217
102. Hao Z, Duncan GS, Seagal J, Su YW, Hong C, Haight J, et al. Fas receptor expression in germinal-center B cells is essential for T and B lymphocyte homeostasis. *Immunity* (2008) 29(4):615–27. doi:10.1016/j.immuni.2008.07.016
103. Chan TD, Wood K, Hermes JR, Butt D, Jolly CJ, Basten A, et al. Elimination of germinal-center-derived self-reactive B cells is governed by the location and concentration of self-antigen. *Immunity* (2012) 37(5):893–904. doi:10.1016/j.immuni.2012.07.017
104. Mayer CT, Gazumyan A, Kara EE, Gitlin AD, Golijanin J, Viant C, et al. The microanatomic segregation of selection by apoptosis in the germinal center. *Science* (2017) 358(6360):eaao2602. doi:10.1126/science.aao2602
105. Shinnakasu R, Inoue T, Kometani K, Moriyama S, Adachi Y, Nakayama M, et al. Regulated selection of germinal-center cells into the memory B cell compartment. *Nat Immunol* (2016) 17(7):861–9. doi:10.1038/ni.3460
106. Smith KG, Light A, O'Reilly LA, Ang SM, Strasser A, Tarlinton D. Bcl-2 transgene expression inhibits apoptosis in the germinal center and reveals differences in the selection of memory B cells and bone marrow antibody-forming cells. *J Exp Med* (2000) 191(3):475–84. doi:10.1084/jem.191.3.475
107. Smith KG, Light A, Nossal GJ, Tarlinton DM. The extent of affinity maturation differs between the memory and antibody-forming cell compartments in the primary immune response. *EMBO J* (1997) 16(11):2996–3006. doi:10.1093/emboj/16.11.2996
108. Krautler NJ, Suan D, Butt D, Bourne K, Hermes JR, Chan TD, et al. Differentiation of germinal center B cells into plasma cells is initiated by high-affinity antigen and completed by Tfh cells. *J Exp Med* (2017) 214(5):1259–67. doi:10.1084/jem.20161533
109. Weisel FJ, Zuccarino-Catania GV, Chikina M, Shlomchik MJ. A temporal switch in the germinal center determines differential output of memory B and plasma cells. *Immunity* (2016) 44(1):116–30. doi:10.1016/j.immuni.2015.12.004
110. Zotos D, Coquet JM, Zhang Y, Light A, D'Costa K, Kallies A, et al. IL-21 regulates germinal center B cell differentiation and proliferation through a B cell-intrinsic mechanism. *J Exp Med* (2010) 207(2):365–78. doi:10.1084/jem.20091777
111. Moens L, Tangye SG. Cytokine-mediated regulation of plasma cell generation: IL-21 takes center stage. *Front Immunol* (2014) 5:65. doi:10.3389/fimmu.2014.00065
112. Kasturi SP, Skountzou I, Albrecht RA, Koutsonanos D, Hua T, Nakaya HI, et al. Programming the magnitude and persistence of antibody responses with innate immunity. *Nature* (2011) 470(7335):543–7. doi:10.1038/nature09737
113. Gavin AL, Hoebe K, Duong B, Ota T, Martin C, Beutler B, et al. Adjuvant-enhanced antibody responses in the absence of toll-like receptor signaling. *Science* (2006) 314(5807):1936–8. doi:10.1126/science.1135299
114. Meyer-Bahlburg A, Khim S, Rawlings DJ. B cell intrinsic TLR signals amplify but are not required for humoral immunity. *J Exp Med* (2007) 204(13):3095–101. doi:10.1084/jem.20071250
115. Suan D, Sundling C, Brink R. Plasma cell and memory B cell differentiation from the germinal center. *Curr Opin Immunol* (2017) 45:97–102. doi:10.1016/j.coi.2017.03.006
116. Chiu YK, Lin IY, Su ST, Wang KH, Yang SY, Tsai DY, et al. Transcription factor ABF-1 suppresses plasma cell differentiation but facilitates memory B cell formation. *J Immunol* (2014) 193(5):2207–17. doi:10.4049/jimmunol.1400411
117. Reimold AM, Iwakoshi NN, Manis J, Vallabhajosyula P, Szomolanyi-Tsuda E, Gravallese EM, et al. Plasma cell differentiation requires the transcription factor XBP-1. *Nature* (2001) 412(6844):300–7. doi:10.1038/35085509
118. Minnich M, Tagoh H, Bonelt P, Axelsson E, Fischer M, Cebolla B, et al. Multifunctional role of the transcription factor Blimp-1 in coordinating plasma cell differentiation. *Nat Immunol* (2016) 17(3):331–43. doi:10.1038/ni.3349
119. Sciammas R, Shaffer AL, Schatz JH, Zhao H, Staudt LM, Singh H. Graded expression of interferon regulatory factor-4 coordinates isotype switching with plasma cell differentiation. *Immunity* (2006) 25(2):225–36. doi:10.1016/j.immuni.2006.07.009
120. Nera KP, Kohonen P, Narvi E, Peippo A, Mustonen L, Terho P, et al. Loss of Pax5 promotes plasma cell differentiation. *Immunity* (2006) 24(3):283–93. doi:10.1016/j.immuni.2006.02.003
121. Shaffer AL, Lin KI, Kuo TC, Yu X, Hurt EM, Rosenwald A, et al. Blimp-1 orchestrates plasma cell differentiation by extinguishing the mature B cell

gene expression program. *Immunity* (2002) 17(1):51–62. doi:10.1016/S1074-7613(02)00335-7
122. Shaffer AL, Shapiro-Shelef M, Iwakoshi NN, Lee AH, Qian SB, Zhao H, et al. XBP1, downstream of Blimp-1, expands the secretory apparatus and other organelles, and increases protein synthesis in plasma cell differentiation. *Immunity* (2004) 21(1):81–93. doi:10.1016/j.immuni.2004.06.010
123. Meyer-Hermann M, Mohr E, Pelletier N, Zhang Y, Victora GD, Toellner KM. A theory of germinal center B cell selection, division, and exit. *Cell Rep* (2012) 2(1):162–74. doi:10.1016/j.celrep.2012.05.010
124. Mohr E, Serre K, Manz RA, Cunningham AF, Khan M, Hardie DL, et al. Dendritic cells and monocyte/macrophages that create the IL-6/APRIL-rich lymph node microenvironments where plasmablasts mature. *J Immunol* (2009) 182(4):2113–23. doi:10.4049/jimmunol.0802771
125. Tipton CM, Fucile CF, Darce J, Chida A, Ichikawa T, Gregoretti I, et al. Diversity, cellular origin and autoreactivity of antibody-secreting cell population expansions in acute systemic lupus erythematosus. *Nat Immunol* (2015) 16(7):755–65. doi:10.1038/ni.3175
126. Slifka MK, Antia R, Whitmire JK, Ahmed R. Humoral immunity due to long-lived plasma cells. *Immunity* (1998) 8(3):363–72. doi:10.1016/S1074-7613(00)80541-5
127. Manz RA, Thiel A, Radbruch A. Lifetime of plasma cells in the bone marrow. *Nature* (1997) 388(6638):133–4. doi:10.1038/40540
128. Hammarlund E, Thomas A, Amanna IJ, Holden LA, Slayden OD, Park B, et al. Plasma cell survival in the absence of B cell memory. *Nat Commun* (2017) 8(1):1781. doi:10.1038/s41467-017-01901-w
129. Bhoj VG, Arhontoulis D, Wertheim G, Capobianchi J, Callahan CA, Ellebrecht CT, et al. Persistence of long-lived plasma cells and humoral immunity in individuals responding to CD19-directed CAR T-cell therapy. *Blood* (2016) 128(3):360–70. doi:10.1182/blood-2016-01-694356
130. Hiepe F, Radbruch A. Plasma cells as an innovative target in autoimmune disease with renal manifestations. *Nat Rev Nephrol* (2016) 12(4):232–40. doi:10.1038/nrneph.2016.20
131. Taddeo A, Khodadadi L, Voigt C, Mumtaz IM, Cheng Q, Moser K, et al. Long-lived plasma cells are early and constantly generated in New Zealand Black/New Zealand White F1 mice and their therapeutic depletion requires a combined targeting of autoreactive plasma cells and their precursors. *Arthritis Res Ther* (2015) 17:39. doi:10.1186/s13075-015-0551-3
132. Sze DM, Toellner KM, Garcia de Vinuesa C, Taylor DR, MacLennan IC. Intrinsic constraint on plasmablast growth and extrinsic limits of plasma cell survival. *J Exp Med* (2000) 192(6):813–21. doi:10.1084/jem.192.6.813
133. Minges Wols HA, Ippolito JA, Yu Z, Palmer JL, White FA, Le PT, et al. The effects of microenvironment and internal programming on plasma cell survival. *Int Immunol* (2007) 19(7):837–46. doi:10.1093/intimm/dxm051
134. Kometani K, Kurosaki T. Differentiation and maintenance of long-lived plasma cells. *Curr Opin Immunol* (2015) 33:64–9. doi:10.1016/j.coi.2015.01.017
135. Tarte K, Zhan F, De Vos J, Klein B, Shaughnessy J Jr. Gene expression profiling of plasma cells and plasmablasts: toward a better understanding of the late stages of B-cell differentiation. *Blood* (2003) 102(2):592–600. doi:10.1182/blood-2002-10-3161
136. Tokoyoda K, Egawa T, Sugiyama T, Choi BI, Nagasawa T. Cellular niches controlling B lymphocyte behavior within bone marrow during development. *Immunity* (2004) 20(6):707–18. doi:10.1016/j.immuni.2004.05.001
137. Chu VT, Frohlich A, Steinhauser G, Scheel T, Roch T, Fillatreau S, et al. Eosinophils are required for the maintenance of plasma cells in the bone marrow. *Nat Immunol* (2011) 12(2):151–9. doi:10.1038/ni.1981
138. Wilmore JR, Allman D. Here, there, and anywhere? Arguments for and against the physical plasma cell survival niche. *J Immunol* (2017) 199(3):839–45. doi:10.4049/jimmunol.1700461
139. Belnoue E, Pihlgren M, McGaha TL, Tougne C, Rochat AF, Bossen C, et al. APRIL is critical for plasmablast survival in the bone marrow and poorly expressed by early-life bone marrow stromal cells. *Blood* (2008) 111(5):2755–64. doi:10.1182/blood-2007-09-110858
140. Benson MJ, Dillon SR, Castigli E, Geha RS, Xu S, Lam KP, et al. Cutting edge: the dependence of plasma cells and independence of memory B cells on BAFF and APRIL. *J Immunol* (2008) 180(6):3655–9. doi:10.4049/jimmunol.180.6.3655
141. O'Connor BP, Raman VS, Erickson LD, Cook WJ, Weaver LK, Ahonen C, et al. BCMA is essential for the survival of long-lived bone marrow plasma cells. *J Exp Med* (2004) 199(1):91–8. doi:10.1084/jem.20031330
142. Mahevas M, Michel M, Weill JC, Reynaud CA. Long-lived plasma cells in autoimmunity: lessons from B-cell depleting therapy. *Front Immunol* (2013) 4:494. doi:10.3389/fimmu.2013.00494
143. Mahevas M, Patin P, Huetz F, Descatoire M, Cagnard N, Bole-Feysot C, et al. B cell depletion in immune thrombocytopenia reveals splenic long-lived plasma cells. *J Clin Invest* (2013) 123(1):432–42. doi:10.1172/JCI65689
144. Rozanski CH, Arens R, Carlson LM, Nair J, Boise LH, Chanan-Khan AA, et al. Sustained antibody responses depend on CD28 function in bone marrow-resident plasma cells. *J Exp Med* (2011) 208(7):1435–46. doi:10.1084/jem.20110040
145. Chevrier S, Genton C, Kallies A, Karnowski A, Otten LA, Malissen B, et al. CD93 is required for maintenance of antibody secretion and persistence of plasma cells in the bone marrow niche. *Proc Natl Acad Sci U S A* (2009) 106(10):3895–900. doi:10.1073/pnas.0809736106
146. Hsu MC, Toellner KM, Vinuesa CG, Maclennan IC. B cell clones that sustain long-term plasmablast growth in T-independent extrafollicular antibody responses. *Proc Natl Acad Sci U S A* (2006) 103(15):5905–10. doi:10.1073/pnas.0601502103
147. Bortnick A, Chernova I, Quinn WJ III, Mugnier M, Cancro MP, Allman D. Long-lived bone marrow plasma cells are induced early in response to T cell-independent or T cell-dependent antigens. *J Immunol* (2012) 188(11):5389–96. doi:10.4049/jimmunol.1102808
148. Sanderson NS, Zimmermann M, Eilinger L, Gubser C, Schaeren-Wiemers N, Lindberg RL, et al. Cocapture of cognate and bystander antigens can activate autoreactive B cells. *Proc Natl Acad Sci U S A* (2017) 114(4):734–9. doi:10.1073/pnas.1614472114
149. Son M, Santiago-Schwarz F, Al-Abed Y, Diamond B. C1q limits dendritic cell differentiation and activation by engaging LAIR-1. *Proc Natl Acad Sci U S A* (2012) 109(46):E3160–7. doi:10.1073/pnas.1212753109
150. Hess C, Winkler A, Lorenz AK, Holecska V, Blanchard V, Eiglmeier S, et al. T cell-independent B cell activation induces immunosuppressive sialylated IgG antibodies. *J Clin Invest* (2013) 123(9):3788–96. doi:10.1172/JCI65938
151. Pfeifle R, Rothe T, Ipseiz N, Scherer HU, Culemann S, Harre U, et al. Regulation of autoantibody activity by the IL-23-TH17 axis determines the onset of autoimmune disease. *Nat Immunol* (2017) 18(1):104–13. doi:10.1038/ni.3579
152. Klinman NR. The "clonal selection hypothesis" and current concepts of B cell tolerance. *Immunity* (1996) 5(3):189–95. doi:10.1016/S1074-7613(00)80314-3
153. Linton PJ, Rudie A, Klinman NR. Tolerance susceptibility of newly generating memory B cells. *J Immunol* (1991) 146(12):4099–104.
154. Malkiel S, Jeganathan V, Wolfson S, Manjarrez Orduno N, Marasco E, Aranow C, et al. Checkpoints for autoreactive B cells in the peripheral blood of lupus patients assessed by flow cytometry. *Arthritis Rheumatol* (2016) 68(9):2210–20. doi:10.1002/art.39710
155. Cappione A III, Anolik JH, Pugh-Bernard A, Barnard J, Dutcher P, Silverman G, et al. Germinal center exclusion of autoreactive B cells is defective in human systemic lupus erythematosus. *J Clin Invest* (2005) 115(11):3205–16. doi:10.1172/JCI24179
156. Sabouri Z, Schofield P, Horikawa K, Spierings E, Kipling D, Randall KL, et al. Redemption of autoantibodies on anergic B cells by variable-region glycosylation and mutation away from self-reactivity. *Proc Natl Acad Sci U S A* (2014) 111(25):E2567–75. doi:10.1073/pnas.1406974111
157. Reed JH, Jackson J, Christ D, Goodnow CC. Clonal redemption of autoantibodies by somatic hypermutation away from self-reactivity during human immunization. *J Exp Med* (2016) 213(7):1255–65. doi:10.1084/jem.20151978
158. Ait-Azzouzene D, Kono DH, Gonzalez-Quintial R, McHeyzer-Williams LJ, Lim M, Wickramarachchi D, et al. Deletion of IgG-switched autoreactive B cells and defects in Fas(lpr) lupus mice. *J Immunol* (2010) 185(2):1015–27. doi:10.4049/jimmunol.1000698
159. Rice JS, Newman J, Wang C, Michael DJ, Diamond B. Receptor editing in peripheral B cell tolerance. *Proc Natl Acad Sci U S A* (2005) 102(5):1608–13. doi:10.1073/pnas.0409217102
160. Hande S, Notidis E, Manser T. Bcl-2 obstructs negative selection of autoreactive, hypermutated antibody V regions during memory B cell development. *Immunity* (1998) 8(2):189–98. doi:10.1016/S1074-7613(00)80471-9

161. Notidis E, Heltemes L, Manser T. Dominant, hierarchical induction of peripheral tolerance during foreign antigen-driven B cell development. *Immunity* (2002) 17(3):317–27. doi:10.1016/S1074-7613(02)00392-8
162. Pulendran B, Kannourakis G, Nouri S, Smith KG, Nossal GJ. Soluble antigen can cause enhanced apoptosis of germinal-centre B cells. *Nature* (1995) 375(6529): 331–4. doi:10.1038/375331a0
163. Wang YH, Diamond B. B cell receptor revision diminishes the autoreactive B cell response after antigen activation in mice. *J Clin Invest* (2008) 118(8): 2896–907. doi:10.1172/JCI35618
164. Scheid JF, Mouquet H, Kofer J, Yurasov S, Nussenzweig MC, Wardemann H. Differential regulation of self-reactivity discriminates between IgG+ human circulating memory B cells and bone marrow plasma cells. *Proc Natl Acad Sci U S A* (2011) 108(44):18044–8. doi:10.1073/pnas.1113395108
165. Pelletier N, McHeyzer-Williams LJ, Wong KA, Urich E, Fazilleau N, McHeyzer-Williams MG. Plasma cells negatively regulate the follicular helper T cell program. *Nat Immunol* (2010) 11(12):1110–8. doi:10.1038/ni.1954
166. William J, Euler C, Christensen S, Shlomchik MJ. Evolution of autoantibody responses via somatic hypermutation outside of germinal centers. *Science* (2002) 297(5589):2066–70. doi:10.1126/science.1073924
167. Deng R, Hurtz C, Song Q, Yue C, Xiao G, Yu H, et al. Extrafollicular CD4+ T-B interactions are sufficient for inducing autoimmune-like chronic graft-versus-host disease. *Nat Commun* (2017) 8(1):978. doi:10.1038/s41467-017-00880-2
168. Odegard JM, Marks BR, DiPlacido LD, Poholek AC, Kono DH, Dong C, et al. ICOS-dependent extrafollicular helper T cells elicit IgG production via IL-21 in systemic autoimmunity. *J Exp Med* (2008) 205(12):2873–86. doi:10.1084/jem.20080840
169. Luzina IG, Atamas SP, Storrer CE, daSilva LC, Kelsoe G, Papadimitriou JC, et al. Spontaneous formation of germinal centers in autoimmune mice. *J Leukoc Biol* (2001) 70(4):578–84. doi:10.1189/jlb.70.4.578
170. Li Y, Li H, Weigert M. Autoreactive B cells in the marginal zone that express dual receptors. *J Exp Med* (2002) 195(2):181–8. doi:10.1084/jem.20011453
171. Julien S, Soulas P, Garaud JC, Martin T, Pasquali JL. B cell positive selection by soluble self-antigen. *J Immunol* (2002) 169(8):4198–204. doi:10.4049/jimmunol.169.8.4198
172. Cariappa A, Tang M, Parng C, Nebelitskiy E, Carroll M, Georgopoulos K, et al. The follicular versus marginal zone B lymphocyte cell fate decision is regulated by Aiolos, Btk, and CD21. *Immunity* (2001) 14(5):603–15. doi:10.1016/S1074-7613(01)00135-2
173. Martin F, Kearney JF. Positive selection from newly formed to marginal zone B cells depends on the rate of clonal production, CD19, and btk. *Immunity* (2000) 12(1):39–49. doi:10.1016/S1074-7613(00)80157-0
174. Cerutti A, Cols M, Puga I. Marginal zone B cells: virtues of innate-like antibody-producing lymphocytes. *Nat Rev Immunol* (2013) 13(2):118–32. doi:10.1038/nri3383
175. Phan TG, Gardam S, Basten A, Brink R. Altered migration, recruitment, and somatic hypermutation in the early response of marginal zone B cells to T cell-dependent antigen. *J Immunol* (2005) 174(8):4567–78. doi:10.4049/jimmunol.174.8.4567
176. Zhou Z, Niu H, Zheng YY, Morel L. Autoreactive marginal zone B cells enter the follicles and interact with CD4+ T cells in lupus-prone mice. *BMC Immunol* (2011) 12:7. doi:10.1186/1471-2172-12-7
177. Grimaldi CM, Michael DJ, Diamond B. Cutting edge: expansion and activation of a population of autoreactive marginal zone B cells in a model of estrogen-induced lupus. *J Immunol* (2001) 167(4):1886–90. doi:10.4049/jimmunol.167.4.1886
178. Wither JE, Loh C, Lajoie G, Heinrichs S, Cai YC, Bonventi G, et al. Colocalization of expansion of the splenic marginal zone population with abnormal B cell activation and autoantibody production in B6 mice with an introgressed New Zealand Black chromosome 13 interval. *J Immunol* (2005) 175(7):4309–19. doi:10.4049/jimmunol.175.7.4309
179. Atencio S, Amano H, Izui S, Kotzin BL. Separation of the New Zealand Black genetic contribution to lupus from New Zealand Black determined expansions of marginal zone B and B1a cells. *J Immunol* (2004) 172(7):4159–66. doi:10.4049/jimmunol.172.7.4159
180. Amano H, Amano E, Moll T, Marinkovic D, Ibnou-Zekri N, Martinez-Soria E, et al. The Yaa mutation promoting murine lupus causes defective development of marginal zone B cells. *J Immunol* (2003) 170(5):2293–301. doi:10.4049/jimmunol.170.5.2293
181. Nickerson KM, Christensen SR, Shupe J, Kashgarian M, Kim D, Elkon K, et al. TLR9 regulates TLR7- and MyD88-dependent autoantibody production and disease in a murine model of lupus. *J Immunol* (2010) 184(4): 1840–8. doi:10.4049/jimmunol.0902592
182. Teichmann LL, Schenten D, Medzhitov R, Kashgarian M, Shlomchik MJ. Signals via the adaptor MyD88 in B cells and DCs make distinct and synergistic contributions to immune activation and tissue damage in lupus. *Immunity* (2013) 38(3):528–40. doi:10.1016/j.immuni.2012.11.017
183. Christensen SR, Kashgarian M, Alexopoulou L, Flavell RA, Akira S, Shlomchik MJ. Toll-like receptor 9 controls anti-DNA autoantibody production in murine lupus. *J Exp Med* (2005) 202(2):321–31. doi:10.1084/jem.20050338
184. Christensen SR, Shupe J, Nickerson K, Kashgarian M, Flavell RA, Shlomchik MJ. Toll-like receptor 7 and TLR9 dictate autoantibody specificity and have opposing inflammatory and regulatory roles in a murine model of lupus. *Immunity* (2006) 25(3):417–28. doi:10.1016/j.immuni.2006.07.013
185. Teichmann LL, Ols ML, Kashgarian M, Reizis B, Kaplan DH, Shlomchik MJ. Dendritic cells in lupus are not required for activation of T and B cells but promote their expansion, resulting in tissue damage. *Immunity* (2010) 33(6): 967–78. doi:10.1016/j.immuni.2010.11.025
186. Wong CK, Wong PT, Tam LS, Li EK, Chen DP, Lam CW. Activation profile of toll-like receptors of peripheral blood lymphocytes in patients with systemic lupus erythematosus. *Clin Exp Immunol* (2010) 159(1):11–22. doi:10.1111/j.1365-2249.2009.04036.x
187. Flores-Borja F, Kabouridis PS, Jury EC, Isenberg DA, Mageed RA. Decreased Lyn expression and translocation to lipid raft signaling domains in B lymphocytes from patients with systemic lupus erythematosus. *Arthritis Rheum* (2005) 52(12):3955–65. doi:10.1002/art.21416
188. Pritchard NR, Cutler AJ, Uribe S, Chadban SJ, Morley BJ, Smith KG. Autoimmune-prone mice share a promoter haplotype associated with reduced expression and function of the Fc receptor FcgammaRII. *Curr Biol* (2000) 10(4):227–30. doi:10.1016/S0960-9822(00)00344-4
189. Suurmond J, Calise J, Malkiel S, Diamond B. DNA-reactive B cells in lupus. *Curr Opin Immunol* (2016) 43:1–7. doi:10.1016/j.coi.2016.07.002
190. Chaturvedi A, Dorward D, Pierce SK. The B cell receptor governs the subcellular location of toll-like receptor 9 leading to hyperresponses to DNA-containing antigens. *Immunity* (2008) 28(6):799–809. doi:10.1016/j.immuni.2008.03.019
191. Lau CM, Broughton C, Tabor AS, Akira S, Flavell RA, Mamula MJ, et al. RNA-associated autoantigens activate B cells by combined B cell antigen receptor/toll-like receptor 7 engagement. *J Exp Med* (2005) 202(9):1171–7. doi:10.1084/jem.20050630
192. Poovassery JS, Bishop GA. Type I IFN receptor and the B cell antigen receptor regulate TLR7 responses via distinct molecular mechanisms. *J Immunol* (2012) 189(4):1757–64. doi:10.4049/jimmunol.1200624
193. Boes M, Schmidt T, Linkemann K, Beaudette BC, Marshak-Rothstein A, Chen J. Accelerated development of IgG autoantibodies and autoimmune disease in the absence of secreted IgM. *Proc Natl Acad Sci U S A* (2000) 97(3):1184–9. doi:10.1073/pnas.97.3.1184
194. Haynes NM, Allen CD, Lesley R, Ansel KM, Killeen N, Cyster JG. Role of CXCR5 and CCR7 in follicular Th cell positioning and appearance of a programmed cell death gene-1high germinal center-associated subpopulation. *J Immunol* (2007) 179(8):5099–108. doi:10.4049/jimmunol.179.8.5099
195. Elsner RA, Ernst DN, Baumgarth N. Single and coexpression of CXCR4 and CXCR5 identifies CD4 T helper cells in distinct lymph node niches during influenza virus infection. *J Virol* (2012) 86(13):7146–57. doi:10.1128/JVI.06904-11
196. Herlands RA, Christensen SR, Sweet RA, Hershberg U, Shlomchik MJ. T cell-independent and toll-like receptor-dependent antigen-driven activation of autoreactive B cells. *Immunity* (2008) 29(2):249–60. doi:10.1016/j.immuni.2008.06.009
197. Wang L, Zhao P, Ma L, Shan Y, Jiang Z, Wang J, et al. Increased interleukin 21 and follicular helper T-like cells and reduced interleukin 10+ B cells in patients with new-onset systemic lupus erythematosus. *J Rheumatol* (2014) 41(9):1781–92. doi:10.3899/jrheum.131025
198. He B, Qiao X, Cerutti A. CpG DNA induces IgG class switch DNA recombination by activating human B cells through an innate pathway that requires TLR9 and cooperates with IL-10. *J Immunol* (2004) 173(7):4479–91. doi:10.4049/jimmunol.173.7.4479

199. Sweet RA, Christensen SR, Harris ML, Shupe J, Sutherland JL, Shlomchik MJ. A new site-directed transgenic rheumatoid factor mouse model demonstrates extrafollicular class switch and plasmablast formation. *Autoimmunity* (2010) 43(8):607–18. doi:10.3109/08916930903567500
200. Arce E, Jackson DG, Gill MA, Bennett LB, Banchereau J, Pascual V. Increased frequency of pre-germinal center B cells and plasma cell precursors in the blood of children with systemic lupus erythematosus. *J Immunol* (2001) 167(4):2361–9. doi:10.4049/jimmunol.167.4.2361
201. Zhang X, Lindwall E, Gauthier C, Lyman J, Spencer N, Alarakhia A, et al. Circulating CXCR5+CD4+helper T cells in systemic lupus erythematosus patients share phenotypic properties with germinal center follicular helper T cells and promote antibody production. *Lupus* (2015) 24(9):909–17. doi:10.1177/0961203314567750
202. Brink R. The imperfect control of self-reactive germinal center B cells. *Curr Opin Immunol* (2014) 28:97–101. doi:10.1016/j.coi.2014.03.001
203. Guo W, Smith D, Aviszus K, Detanico T, Heiser RA, Wysocki LJ. Somatic hypermutation as a generator of antinuclear antibodies in a murine model of systemic autoimmunity. *J Exp Med* (2010) 207(10):2225–37. doi:10.1084/jem.20092712
204. Mietzner B, Tsuiji M, Scheid J, Velinzon K, Tiller T, Abraham K, et al. Autoreactive IgG memory antibodies in patients with systemic lupus erythematosus arise from nonreactive and polyreactive precursors. *Proc Natl Acad Sci U S A* (2008) 105(28):9727–32. doi:10.1073/pnas.0803644105
205. Paul E, Nelde A, Verschoor A, Carroll MC. Follicular exclusion of autoreactive B cells requires FcgammaRIIb. *Int Immunol* (2007) 19(4):365–73. doi:10.1093/intimm/dxm002
206. Dai X, James RG, Habib T, Singh S, Jackson S, Khim S, et al. A disease-associated PTPN22 variant promotes systemic autoimmunity in murine models. *J Clin Invest* (2013) 123(5):2024–36. doi:10.1172/JCI66963
207. Nowosad CR, Spillane KM, Tolar P. Germinal center B cells recognize antigen through a specialized immune synapse architecture. *Nat Immunol* (2016) 17(7):870–7. doi:10.1038/ni.3458
208. Walsh ER, Pisitkun P, Voynova E, Deane JA, Scott BL, Caspi RR, et al. Dual signaling by innate and adaptive immune receptors is required for TLR7-induced B-cell-mediated autoimmunity. *Proc Natl Acad Sci U S A* (2012) 109(40):16276–81. doi:10.1073/pnas.1209372109
209. Jackson SW, Scharping NE, Kolhatkar NS, Khim S, Schwartz MA, Li QZ, et al. Opposing impact of B cell-intrinsic TLR7 and TLR9 signals on autoantibody repertoire and systemic inflammation. *J Immunol* (2014) 192(10):4525–32. doi:10.4049/jimmunol.1400098
210. Das A, Heesters BA, Bialas A, O'Flynn J, Rifkin IR, Ochando J, et al. Follicular dendritic cell activation by TLR Ligands promotes autoreactive B cell responses. *Immunity* (2017) 46(1):106–19. doi:10.1016/j.immuni.2016.12.014
211. Woods M, Zou YR, Davidson A. Defects in germinal center selection in SLE. *Front Immunol* (2015) 6:425. doi:10.3389/fimmu.2015.00425
212. Diamond B, Scharff MD. Somatic mutation of the T15 heavy chain gives rise to an antibody with autoantibody specificity. *Proc Natl Acad Sci U S A* (1984) 81(18):5841–4. doi:10.1073/pnas.81.18.5841
213. Zhang J, Roschke V, Baker KP, Wang Z, Alarcon GS, Fessler BJ, et al. Cutting edge: a role for B lymphocyte stimulator in systemic lupus erythematosus. *J Immunol* (2001) 166(1):6–10. doi:10.4049/jimmunol.166.1.6
214. Coquery CM, Loo WM, Wade NS, Bederman AG, Tung KS, Lewis JE, et al. BAFF regulates follicular helper t cells and affects their accumulation and interferon-gamma production in autoimmunity. *Arthritis Rheumatol* (2015) 67(3):773–84. doi:10.1002/art.38950
215. Mackay F, Woodcock SA, Lawton P, Ambrose C, Baetscher M, Schneider P, et al. Mice transgenic for BAFF develop lymphocytic disorders along with autoimmune manifestations. *J Exp Med* (1999) 190(11):1697–710. doi:10.1084/jem.190.11.1697
216. Simpson N, Gatenby PA, Wilson A, Malik S, Fulcher DA, Tangye SG, et al. Expansion of circulating T cells resembling follicular helper T cells is a fixed phenotype that identifies a subset of severe systemic lupus erythematosus. *Arthritis Rheum* (2010) 62(1):234–44. doi:10.1002/art.25032
217. Nakou M, Papadimitraki ED, Fanouriakis A, Bertsias GK, Choulaki C, Goulidaki N, et al. Interleukin-21 is increased in active systemic lupus erythematosus patients and contributes to the generation of plasma B cells. *Clin Exp Rheumatol* (2013) 31(2):172–9.
218. Wong CK, Wong PT, Tam LS, Li EK, Chen DP, Lam CW. Elevated production of B cell chemokine CXCL13 is correlated with systemic lupus erythematosus disease activity. *J Clin Immunol* (2010) 30(1):45–52. doi:10.1007/s10875-009-9325-5
219. Linterman MA, Rigby RJ, Wong RK, Yu D, Brink R, Cannons JL, et al. Follicular helper T cells are required for systemic autoimmunity. *J Exp Med* (2009) 206(3):561–76. doi:10.1084/jem.20081886
220. Jacquemin C, Schmitt N, Contin-Bordes C, Liu Y, Narayanan P, Seneschal J, et al. OX40 ligand contributes to human lupus pathogenesis by promoting T follicular helper response. *Immunity* (2015) 42(6):1159–70. doi:10.1016/j.immuni.2015.05.012
221. Luo J, Niu X, Liu H, Zhang M, Chen M, Deng S. Up-regulation of transcription factor Blimp1 in systemic lupus erythematosus. *Mol Immunol* (2013) 56(4):574–82. doi:10.1016/j.molimm.2013.05.241
222. Guimaraes PM, Scavuzzi BM, Stadtlober NP, Franchi Santos L, Lozovoy MAB, Iriyoda TMV, et al. Cytokines in systemic lupus erythematosus: far beyond Th1/Th2 dualism lupus: cytokine profiles. *Immunol Cell Biol* (2017) 95(9):824–31. doi:10.1038/icb.2017.53
223. Salazar-Camarena DC, Ortiz-Lazareno PC, Cruz A, Oregon-Romero E, Machado-Contreras JR, Munoz-Valle JF, et al. Association of BAFF, APRIL serum levels, BAFF-R, TACI and BCMA expression on peripheral B-cell subsets with clinical manifestations in systemic lupus erythematosus. *Lupus* (2016) 25(6):582–92. doi:10.1177/0961203315608254
224. Hoyer BF, Moser K, Hauser AE, Peddinghaus A, Voigt C, Eilat D, et al. Short-lived plasmablasts and long-lived plasma cells contribute to chronic humoral autoimmunity in NZB/W mice. *J Exp Med* (2004) 199(11):1577–84. doi:10.1084/jem.20040168
225. Lo MS, Zurakowski D, Son MB, Sundel RP. Hypergammaglobulinemia in the pediatric population as a marker for underlying autoimmune disease: a retrospective cohort study. *Pediatr Rheumatol Online J* (2013) 11(1):42. doi:10.1186/1546-0096-11-42
226. Cassese G, Lindenau S, de Boer B, Arce S, Hauser A, Riemekasten G, et al. Inflamed kidneys of NZB/W mice are a major site for the homeostasis of plasma cells. *Eur J Immunol* (2001) 31(9):2726–32. doi:10.1002/1521-4141(200109)31:9<2726::AID-IMMU2726>3.0.CO;2-H
227. Starke C, Frey S, Wellmann U, Urbonaviciute V, Herrmann M, Amann K, et al. High frequency of autoantibody-secreting cells and long-lived plasma cells within inflamed kidneys of NZB/W F1 lupus mice. *Eur J Immunol* (2011) 41(7):2107–12. doi:10.1002/eji.201041315
228. Wang A, Fairhurst AM, Tus K, Subramanian S, Liu Y, Lin F, et al. CXCR4/CXCL12 hyperexpression plays a pivotal role in the pathogenesis of lupus. *J Immunol* (2009) 182(7):4448–58. doi:10.4049/jimmunol.0801920
229. Deng Y, Tsao BP. Updates in lupus genetics. *Curr Rheumatol Rep* (2017) 19(11):68. doi:10.1007/s11926-017-0695-z
230. Vaughn SE, Kottyan LC, Munroe ME, Harley JB. Genetic susceptibility to lupus: the biological basis of genetic risk found in B cell signaling pathways. *J Leukoc Biol* (2012) 92(3):577–91. doi:10.1189/jlb.0212095
231. Teruel M, Alarcon-Riquelme ME. The genetic basis of systemic lupus erythematosus: what are the risk factors and what have we learned. *J Autoimmun* (2016) 74:161–75. doi:10.1016/j.jaut.2016.08.001
232. Ghodke-Puranik Y, Niewold TB. Immunogenetics of systemic lupus erythematosus: a comprehensive review. *J Autoimmun* (2015) 64:125–36. doi:10.1016/j.jaut.2015.08.004
233. Zhou XJ, Cheng FJ, Qi YY, Zhao MH, Zhang H. A replication study from Chinese supports association between lupus-risk allele in TNFSF4 and renal disorder. *Biomed Res Int* (2013) 2013:597921. doi:10.1155/2013/597921
234. Manku H, Langefeld CD, Guerra SG, Malik TH, Alarcon-Riquelme M, Anaya JM, et al. Trans-ancestral studies fine map the SLE-susceptibility locus TNFSF4. *PLoS Genet* (2013) 9(7):e1003554. doi:10.1371/journal.pgen.1003554
235. Lamagna C, Hu Y, DeFranco AL, Lowell CA. B cell-specific loss of Lyn kinase leads to autoimmunity. *J Immunol* (2014) 192(3):919–28. doi:10.4049/jimmunol.1301979
236. Hua Z, Gross AJ, Lamagna C, Ramos-Hernandez N, Scapini P, Ji M, et al. Requirement for MyD88 signaling in B cells and dendritic cells for germinal center anti-nuclear antibody production in Lyn-deficient mice. *J Immunol* (2014) 192(3):875–85. doi:10.4049/jimmunol.1300683
237. Simpfendorfer KR, Olsson LM, Manjarrez Orduno N, Khalili H, Simeone AM, Katz MS, et al. The autoimmunity-associated BLK haplotype exhibits cis-regulatory effects on mRNA and protein expression that are prominently

observed in B cells early in development. *Hum Mol Genet* (2012) 21(17): 3918–25. doi:10.1093/hmg/dds220
238. Simpfendorfer KR, Armstead BE, Shih A, Li W, Curran M, Manjarrez-Orduno N, et al. Autoimmune disease-associated haplotypes of BLK exhibit lowered thresholds for B cell activation and expansion of Ig class-switched B cells. *Arthritis Rheumatol* (2015) 67(11):2866–76. doi:10.1002/art.39301
239. Samuelson EM, Laird RM, Maue AC, Rochford R, Hayes SM. Blk haploinsufficiency impairs the development, but enhances the functional responses, of MZ B cells. *Immunol Cell Biol* (2012) 90(6):620–9. doi:10.1038/icb.2011.76
240. Texido G, Su IH, Mecklenbrauker I, Saijo K, Malek SN, Desiderio S, et al. The B-cell-specific Src-family kinase Blk is dispensable for B-cell development and activation. *Mol Cell Biol* (2000) 20(4):1227–33. doi:10.1128/MCB.20.4.1227-1233.2000
241. Kozyrev SV, Abelson AK, Wojcik J, Zaghlool A, Linga Reddy MV, Sanchez E, et al. Functional variants in the B-cell gene BANK1 are associated with systemic lupus erythematosus. *Nat Genet* (2008) 40(2):211–6. doi:10.1038/ng.79
242. Yokoyama K, Su Ih IH, Tezuka T, Yasuda T, Mikoshiba K, Tarakhovsky A, et al. BANK regulates BCR-induced calcium mobilization by promoting tyrosine phosphorylation of IP(3) receptor. *EMBO J* (2002) 21(1–2):83–92. doi:10.1093/emboj/21.1.83
243. Aiba Y, Yamazaki T, Okada T, Gotoh K, Sanjo H, Ogata M, et al. BANK negatively regulates Akt activation and subsequent B cell responses. *Immunity* (2006) 24(3):259–68. doi:10.1016/j.immuni.2006.01.002
244. Rieck M, Arechiga A, Onengut-Gumuscu S, Greenbaum C, Concannon P, Buckner JH. Genetic variation in PTPN22 corresponds to altered function of T and B lymphocytes. *J Immunol* (2007) 179(7):4704–10. doi:10.4049/jimmunol.179.7.4704
245. Hasegawa K, Martin F, Huang G, Tumas D, Diehl L, Chan AC. PEST domain-enriched tyrosine phosphatase (PEP) regulation of effector/memory T cells. *Science* (2004) 303(5658):685–9. doi:10.1126/science.1092138
246. Schickel JN, Kuhny M, Baldo A, Bannock JM, Massad C, Wang H, et al. PTPN22 inhibition resets defective human central B cell tolerance. *Sci Immunol* (2016) 1(1):aaf7153. doi:10.1126/sciimmunol.aaf7153
247. Vang T, Congia M, Macis MD, Musumeci L, Orru V, Zavattari P, et al. Autoimmune-associated lymphoid tyrosine phosphatase is a gain-of-function variant. *Nat Genet* (2005) 37(12):1317–9. doi:10.1038/ng1673
248. Graham RR, Cotsapas C, Davies L, Hackett R, Lessard CJ, Leon JM, et al. Genetic variants near TNFAIP3 on 6q23 are associated with systemic lupus erythematosus. *Nat Genet* (2008) 40(9):1059–61. doi:10.1038/ng.200
249. Musone SL, Taylor KE, Lu TT, Nititham J, Ferreira RC, Ortmann W, et al. Multiple polymorphisms in the TNFAIP3 region are independently associated with systemic lupus erythematosus. *Nat Genet* (2008) 40(9):1062–4. doi:10.1038/ng.202
250. Adrianto I, Wen F, Templeton A, Wiley G, King JB, Lessard CJ, et al. Association of a functional variant downstream of TNFAIP3 with systemic lupus erythematosus. *Nat Genet* (2011) 43(3):253–8. doi:10.1038/ng.766
251. Tavares RM, Turer EE, Liu CL, Advincula R, Scapini P, Rhee L, et al. The ubiquitin modifying enzyme A20 restricts B cell survival and prevents autoimmunity. *Immunity* (2010) 33(2):181–91. doi:10.1016/j.immuni.2010.07.017
252. Chu Y, Vahl JC, Kumar D, Heger K, Bertossi A, Wojtowicz E, et al. B cells lacking the tumor suppressor TNFAIP3/A20 display impaired differentiation and hyperactivation and cause inflammation and autoimmunity in aged mice. *Blood* (2011) 117(7):2227–36. doi:10.1182/blood-2010-09-306019
253. Hovelmeyer N, Reissig S, Xuan NT, Adams-Quack P, Lukas D, Nikolaev A, et al. A20 deficiency in B cells enhances B-cell proliferation and results in the development of autoantibodies. *Eur J Immunol* (2011) 41(3):595–601. doi:10.1002/eji.201041313
254. Adrianto I, Wang S, Wiley GB, Lessard CJ, Kelly JA, Adler AJ, et al. Association of two independent functional risk haplotypes in TNIP1 with systemic lupus erythematosus. *Arthritis Rheum* (2012) 64(11):3695–705. doi:10.1002/art.34642
255. Nanda SK, Venigalla RK, Ordureau A, Patterson-Kane JC, Powell DW, Toth R, et al. Polyubiquitin binding to ABIN1 is required to prevent autoimmunity. *J Exp Med* (2011) 208(6):1215–28. doi:10.1084/jem.20102177
256. Manjarrez-Orduno N, Marasco E, Chung SA, Katz MS, Kiridly JF, Simpfendorfer KR, et al. CSK regulatory polymorphism is associated with systemic lupus erythematosus and influences B-cell signaling and activation. *Nat Genet* (2012) 44(11):1227–30. doi:10.1038/ng.2439
257. Floto RA, Clatworthy MR, Heilbronn KR, Rosner DR, MacAry PA, Rankin A, et al. Loss of function of a lupus-associated FcgammaRIIb polymorphism through exclusion from lipid rafts. *Nat Med* (2005) 11(10):1056–8. doi:10.1038/nm1288
258. Blank MC, Stefanescu RN, Masuda E, Marti F, King PD, Redecha PB, et al. Decreased transcription of the human FCGR2B gene mediated by the -343 G/C promoter polymorphism and association with systemic lupus erythematosus. *Hum Genet* (2005) 117(2–3):220–7. doi:10.1007/s00439-005-1302-3
259. Kono H, Kyogoku C, Suzuki T, Tsuchiya N, Honda H, Yamamoto K, et al. FcgammaRIIB Ile232Thr transmembrane polymorphism associated with human systemic lupus erythematosus decreases affinity to lipid rafts and attenuates inhibitory effects on B cell receptor signaling. *Hum Mol Genet* (2005) 14(19):2881–92. doi:10.1093/hmg/ddi320
260. Tiller T, Kofer J, Kreschel C, Busse CE, Riebel S, Wickert S, et al. Development of self-reactive germinal center B cells and plasma cells in autoimmune Fc gammaRIIB-deficient mice. *J Exp Med* (2010) 207(12):2767–78. doi:10.1084/jem.20100171
261. Takai T, Ono M, Hikida M, Ohmori H, Ravetch JV. Augmented humoral and anaphylactic responses in Fc gamma RII-deficient mice. *Nature* (1996) 379(6563):346–9. doi:10.1038/379346a0
262. Xiang Z, Cutler AJ, Brownlie RJ, Fairfax K, Lawlor KE, Severinson E, et al. FcgammaRIIb controls bone marrow plasma cell persistence and apoptosis. *Nat Immunol* (2007) 8(4):419–29. doi:10.1038/ni1440
263. Niewold TB, Kelly JA, Flesch MH, Espinoza LR, Harley JB, Crow MK. Association of the IRF5 risk haplotype with high serum interferon-alpha activity in systemic lupus erythematosus patients. *Arthritis Rheum* (2008) 58(8):2481–7. doi:10.1002/art.23613
264. Feng D, Stone RC, Eloranta ML, Sangster-Guity N, Nordmark G, Sigurdsson S, et al. Genetic variants and disease-associated factors contribute to enhanced interferon regulatory factor 5 expression in blood cells of patients with systemic lupus erythematosus. *Arthritis Rheum* (2010) 62(2):562–73. doi:10.1002/art.27223
265. Purtha WE, Swiecki M, Colonna M, Diamond MS, Bhattacharya D. Spontaneous mutation of the Dock2 gene in Irf5-/- mice complicates interpretation of type I interferon production and antibody responses. *Proc Natl Acad Sci U S A* (2012) 109(15):E898–904. doi:10.1073/pnas.1118155109
266. Yasuda K, Watkins AA, Kochar GS, Wilson GE, Laskow B, Richez C, et al. Interferon regulatory factor-5 deficiency ameliorates disease severity in the MRL/lpr mouse model of lupus in the absence of a mutation in DOCK2. *PLoS One* (2014) 9(7):e103478. doi:10.1371/journal.pone.0103478
267. Thackray LB, Shrestha B, Richner JM, Miner JJ, Pinto AK, Lazear HM, et al. Interferon regulatory factor 5-dependent immune responses in the draining lymph node protect against West Nile virus infection. *J Virol* (2014) 88(19):11007–21. doi:10.1128/JVI.01545-14
268. Abelson AK, Delgado-Vega AM, Kozyrev SV, Sanchez E, Velazquez-Cruz R, Eriksson N, et al. STAT4 associates with systemic lupus erythematosus through two independent effects that correlate with gene expression and act additively with IRF5 to increase risk. *Ann Rheum Dis* (2009) 68(11):1746–53. doi:10.1136/ard.2008.097642
269. Liang Y, Pan HF, Ye DQ. Therapeutic potential of STAT4 in autoimmunity. *Expert Opin Ther Targets* (2014) 18(8):945–60. doi:10.1517/14728222.2014.920325
270. Xu Z, Duan B, Croker BP, Morel L. STAT4 deficiency reduces autoantibody production and glomerulonephritis in a mouse model of lupus. *Clin Immunol* (2006) 120(2):189–98. doi:10.1016/j.clim.2006.03.009
271. Muto A, Ochiai K, Kimura Y, Itoh-Nakadai A, Calame KL, Ikebe D, et al. Bach2 represses plasma cell gene regulatory network in B cells to promote antibody class switch. *EMBO J* (2010) 29(23):4048–61. doi:10.1038/emboj.2010.257
272. Morris DL, Sheng Y, Zhang Y, Wang YF, Zhu Z, Tombleson P, et al. Genome-wide association meta-analysis in Chinese and European individuals identifies ten new loci associated with systemic lupus erythematosus. *Nat Genet* (2016) 48(8):940–6. doi:10.1038/ng.3603
273. Hipp N, Symington H, Pastoret C, Caron G, Monvoisin C, Tarte K, et al. IL-2 imprints human naive B cell fate towards plasma cell through ERK/

ELK1-mediated BACH2 repression. *Nat Commun* (2017) 8(1):1443. doi:10.1038/s41467-017-01475-7
274. Kim SJ, Gregersen PK, Diamond B. Regulation of dendritic cell activation by microRNA let-7c and BLIMP1. *J Clin Invest* (2013) 123(2):823–33. doi:10.1172/JCI64712
275. Kim SJ, Schatzle S, Ahmed SS, Haap W, Jang SH, Gregersen PK, et al. Increased cathepsin S in Prdm1-/- dendritic cells alters the TFH cell repertoire and contributes to lupus. *Nat Immunol* (2017) 18(9):1016–24. doi:10.1038/ni.3793
276. Cunninghame Graham DS, Morris DL, Bhangale TR, Criswell LA, Syvanen AC, Ronnblom L, et al. Association of NCF2, IKZF1, IRF8, IFIH1, and TYK2 with systemic lupus erythematosus. *PLoS Genet* (2011) 7(10):e1002341. doi:10.1371/journal.pgen.1002341
277. Carotta S, Willis SN, Hasbold J, Inouye M, Pang SH, Emslie D, et al. The transcription factors IRF8 and PU.1 negatively regulate plasma cell differentiation. *J Exp Med* (2014) 211(11):2169–81. doi:10.1084/jem.20140425
278. Lee CH, Melchers M, Wang H, Torrey TA, Slota R, Qi CF, et al. Regulation of the germinal center gene program by interferon (IFN) regulatory factor 8/IFN consensus sequence-binding protein. *J Exp Med* (2006) 203(1):63–72. doi:10.1084/jem.20051450
279. Cai X, Huang W, Liu X, Wang L, Jiang Y. Association of novel polymorphisms in TMEM39A gene with systemic lupus erythematosus in a Chinese Han population. *BMC Med Genet* (2017) 18(1):43. doi:10.1186/s12881-017-0405-8
280. Cortes M, Georgopoulos K. Aiolos is required for the generation of high affinity bone marrow plasma cells responsible for long-term immunity. *J Exp Med* (2004) 199(2):209–19. doi:10.1084/jem.20031571
281. Wang JH, Avitahl N, Cariappa A, Friedrich C, Ikeda T, Renold A, et al. Aiolos regulates B cell activation and maturation to effector state. *Immunity* (1998) 9(4):543–53. doi:10.1016/S1074-7613(00)80637-8
282. Russell L, John S, Cullen J, Luo W, Shlomchik MJ, Garrett-Sinha LA. Requirement for transcription factor Ets1 in B cell tolerance to self-antigens. *J Immunol* (2015) 195(8):3574–83. doi:10.4049/jimmunol.1500776
283. John SA, Clements JL, Russell LM, Garrett-Sinha LA. Ets-1 regulates plasma cell differentiation by interfering with the activity of the transcription factor Blimp-1. *J Biol Chem* (2008) 283(2):951–62. doi:10.1074/jbc.M705262200
284. Lu X, Zoller EE, Weirauch MT, Wu Z, Namjou B, Williams AH, et al. Lupus risk variant increases pSTAT1 binding and decreases ETS1 expression. *Am J Hum Genet* (2015) 96(5):731–9. doi:10.1016/j.ajhg.2015.03.002
285. Yang W, Shen N, Ye DQ, Liu Q, Zhang Y, Qian XX, et al. Genome-wide association study in Asian populations identifies variants in ETS1 and WDFY4 associated with systemic lupus erythematosus. *PLoS Genet* (2010) 6(2):e1000841. doi:10.1371/journal.pgen.1000841
286. Ols ML, Cullen JL, Turqueti-Neves A, Giles J, Shlomchik MJ. Dendritic cells regulate extrafollicular autoreactive B cells via T cells expressing Fas and Fas ligand. *Immunity* (2016) 45(5):1052–65. doi:10.1016/j.immuni.2016.10.005
287. Wu J, Metz C, Xu X, Abe R, Gibson AW, Edberg JC, et al. A novel polymorphic CAAT/enhancer-binding protein beta element in the FasL gene promoter alters Fas ligand expression: a candidate background gene in African American systemic lupus erythematosus patients. *J Immunol* (2003) 170(1):132–8. doi:10.4049/jimmunol.170.1.132
288. Shen N, Fu Q, Deng Y, Qian X, Zhao J, Kaufman KM, et al. Sex-specific association of X-linked toll-like receptor 7 (TLR7) with male systemic lupus erythematosus. *Proc Natl Acad Sci U S A* (2010) 107(36):15838–43. doi:10.1073/pnas.1001337107
289. Soni C, Wong EB, Domeier PP, Khan TN, Satoh T, Akira S, et al. B cell-intrinsic TLR7 signaling is essential for the development of spontaneous germinal centers. *J Immunol* (2014) 193(9):4400–14. doi:10.4049/jimmunol.1401720
290. Blasius AL, Arnold CN, Georgel P, Rutschmann S, Xia Y, Lin P, et al. Slc15a4, AP-3, and Hermansky-Pudlak syndrome proteins are required for toll-like receptor signaling in plasmacytoid dendritic cells. *Proc Natl Acad Sci U S A* (2010) 107(46):19973–8. doi:10.1073/pnas.1014051107
291. Sasawatari S, Okamura T, Kasumi E, Tanaka-Furuyama K, Yanobu-Takanashi R, Shirasawa S, et al. The solute carrier family 15A4 regulates TLR9 and NOD1 functions in the innate immune system and promotes colitis in mice. *Gastroenterology* (2011) 140(5):1513–25. doi:10.1053/j.gastro.2011.01.041
292. Kobayashi T, Shimabukuro-Demoto S, Yoshida-Sugitani R, Furuyama-Tanaka K, Karyu H, Sugiura Y, et al. The histidine transporter SLC15A4 coordinates mTOR-dependent inflammatory responses and pathogenic antibody production. *Immunity* (2014) 41(3):375–88. doi:10.1016/j.immuni.2014.08.011
293. Baccala R, Gonzalez-Quintial R, Blasius AL, Rimann I, Ozato K, Kono DH, et al. Essential requirement for IRF8 and SLC15A4 implicates plasmacytoid dendritic cells in the pathogenesis of lupus. *Proc Natl Acad Sci U S A* (2013) 110(8):2940–5. doi:10.1073/pnas.1222798110

Conflict of Interest Statement: The authors declare that the research was conducted in the absence of any commercial or financial relationships that could be construed as a potential conflict of interest.

The reviewer RM and handling editor declared their shared affiliation.

frontiers in Immunology

CLINICAL TRIAL
published: 02 March 2018
doi: 10.3389/fimmu.2018.00336

Omega-3 Fatty Acid Supplementation Improves Endothelial Function in Primary Antiphospholipid Syndrome: A Small-Scale Randomized Double-Blind Placebo-Controlled Trial

*Sheylla M. Felau[1], Lucas P. Sales[1], Marina Y. Solis[1], Ana Paula Hayashi[1], Hamilton Roschel[1], Ana Lúcia Sá-Pinto[1], Danieli Castro Oliveira De Andrade[1], Keyla Y. Katayama[2], Maria Claudia Irigoyen[2], Fernanda Consolim-Colombo[2], Eloisa Bonfa[1], Bruno Gualano[1] and Fabiana B. Benatti[1,3]**

[1] Applied Physiology and Nutrition Research Group, Laboratory of Assessment and Conditioning in Rheumatology, Faculdade de Medicina FMUSP, Universidade de Sao Paulo, Sao Paulo, Brazil, [2] Heart Institute (InCor), Faculdade de Medicina FMUSP, Universidade de Sao Paulo, Sao Paulo, Brazil, [3] School of Applied Sciences, Universidade Estadual de Campinas (UNICAMP), Limeira, Brazil

OPEN ACCESS

Edited by:
Niccolo Terrando,
Duke University, United States

Reviewed by:
Jesmond Dalli,
Queen Mary University of London, United Kingdom
Joan Clària,
Hospital Clínic de Barcelona, Spain

***Correspondence:**
Fabiana B. Benatti
fabenatti@usp.br

Specialty section:
This article was submitted to Inflammation, a section of the journal Frontiers in Immunology

Received: 30 November 2017
Accepted: 06 February 2018
Published: 02 March 2018

Citation:
Felau SM, Sales LP, Solis MY, Hayashi AP, Roschel H, Sá-Pinto AL, Andrade DCOD, Katayama KY, Irigoyen MC, Consolim-Colombo F, Bonfa E, Gualano B and Benatti FB (2018) Omega-3 Fatty Acid Supplementation Improves Endothelial Function in Primary Antiphospholipid Syndrome: A Small-Scale Randomized Double-Blind Placebo-Controlled Trial. Front. Immunol. 9:336. doi: 10.3389/fimmu.2018.00336

Endothelial cells are thought to play a central role in the pathogenesis of antiphospholipid syndrome (APS). Omega-3 polyunsaturated fatty acid (n-3 PUFA) supplementation has been shown to improve endothelial function in a number of diseases; thus, it could be of high clinical relevance in APS. The aim of this study was to evaluate the efficacy of n-3 PUFA supplementation on endothelial function (primary outcome) of patients with primary APS (PAPS). A 16-week randomized clinical trial was conducted with 22 adult women with PAPS. Patients were randomly assigned (1:1) to receive placebo (PL, $n = 11$) or n-3 PUFA (ω-3, $n = 11$) supplementation. Before (pre) and after (post) 16 weeks of the intervention, patients were assessed for endothelial function (peripheral artery tonometry) (primary outcome). Patients were also assessed for systemic markers of endothelial cell activation, inflammatory markers, dietary intake, international normalized ratio (INR), and adverse effects. At post, ω-3 group presented significant increases in endothelial function estimates reactive hyperemia index (RHI) and logarithmic transformation of RHI (LnRHI) when compared with PL (+13 vs. −12%, $p = 0.06$, ES = 0.9; and +23 vs. −22%, $p = 0.02$, ES = 1.0). No changes were observed for e-selectin, vascular adhesion molecule-1, and fibrinogen levels ($p > 0.05$). In addition, ω-3 group showed decreased circulating levels of interleukin-10 (−4 vs. +45%, $p = 0.04$, ES = −0.9) and tumor necrosis factor (−13 vs. +0.3%, $p = 0.04$, ES = −0.95) and a tendency toward a lower intercellular adhesion molecule-1 response (+3 vs. +48%, $p = 0.1$, ES = −0.7) at post when compared with PL. No changes in dietary intake, INR, or self-reported adverse effects were observed. In conclusion, 16 weeks of n-3 PUFA supplementation improved endothelial function in patients with well-controlled PAPS. These results support a role of n-3 PUFA supplementation as an adjuvant therapy in APS. Registered at http://ClinicalTrials.gov as NCT01956188.

Keywords: antiphospholipid syndrome, n-3 PUFA, endothelial function, coagulation, inflammation

INTRODUCTION

Antiphospholipid syndrome (APS) is a systemic autoimmune disease characterized by recurrent thrombotic episodes and/or obstetric morbidities and persistent serum antiphospholipid antibodies (aPL). APS can be classified as primary or secondary if concurrent with another autoimmune disease, tumor, or hematologic disorder (1). Despite adequate anticoagulant treatment, primary APS (PAPS) is significantly associated with high morbidity and mortality from vascular thrombotic events (2) and an increased risk of cardiovascular diseases (CVDs) (3).

Previous studies propose that endothelial cells play a central role in the pathogenesis of APS (4). aPLs have been shown to bind to endothelial cell beta-2 glycoprotein I (β2GPI) receptors leading to endothelial malfunction and formation of thrombosis (5). Evidence exists that patients with APS show an impaired endothelial function when compared with their healthy peers (6, 7). Although not fully elucidated, potential underlying mechanisms include aPL-mediated endothelial cell activation due to increases in the production and release of adhesion-cell molecules and pro-inflammatory cytokines (4, 8), particularly tumor necrosis factor (TNF) and interleukin (IL)-1β (8, 9). Endothelial dysfunction is the earliest detectable stage predisposing to the formation of atherosclerotic lesions and cardiovascular events (10). Thus, strategies capable of minimizing endothelial dysfunction may be of high clinical relevance in APS.

Supplementation of marine-derived omega-3 polyunsaturated fatty acids (n-3 PUFA), eicosapentaenoic acid (EPA), and docosahexanoic acid (DHA) (≥2.0 g/day) has been shown to have antiatherogenic and antithrombotic properties *via* improvements in endothelial function in type 2 diabetes mellitus (T2D) and dyslipidemia (11–14), which are conditions associated with accelerated atherosclerosis and an increased CVD risk (15, 16). Supplementation of marine n-3 PUFA may also be beneficial in autoimmune rheumatic diseases, since the intake of 3 g/day of EPA and DHA has been shown to improve clinical features, disease activity, and endothelial function in systemic lupus erythematosus (SLE) patients (17). However, no studies have assessed the potential beneficial effects of n-3 PUFA supplementation in APS.

The aim of the present study was to evaluate the efficacy of n-3 PUFA supplementation on endothelial function (primary outcome) in patients with PAPS. Secondary outcomes were systemic inflammation and lipid profile.

METHODS

Experimental Design

A 16-week randomized clinical trial was conducted between May 2014 and November 2016 in São Paulo, SP, Brazil (registered at http://ClinicalTrials.gov as NCT01956188). This manuscript is reported according to the CONSORT guidelines and approved by the Ethics Committee for Analysis of Research Projects of the General Hospital, School of Medicine, University of São Paulo, affiliated to the National Committee for Ethics in Research of Brazil. Patients were randomly assigned (1:1) to receive either placebo (PL, $n = 11$) or n-3 PUFA (ω-3, $n = 11$) supplementation according to a computer-generated treatment sequence in a double-blind design. Before (pre) and after (post) 16 weeks of intervention, patients were assessed for endothelial function using peripheral artery tonometry (primary outcome). Patients were also assessed for systemic markers of endothelial cell activation [intercellular adhesion molecule-1 (ICAM-1), vascular adhesion molecule-1 (VCAM-1), e-selectin, and fibrinogen], systemic inflammatory markers [C-reactive protein (CRP), IL-6, IL-10, TNF, IL-1ra, and IL-1β], lipid profile, dietary intake, international normalized ratio (INR), and self-reported adverse effects. At pre, patients were also assessed for physical activity level (using the short version of the International Physical Activity Questionnaire) for characterization purposes (18). Blood collection and endothelial function assessments were performed on the same day. Patients were instructed to maintain habitual physical activity and food intake throughout the study.

Patients

Patients were recruited from the outpatient APS clinic of the Rheumatology Division, School of Medicine, University of São Paulo. Sample consisted of 22 adult women (aged 27–45 years) diagnosed with PAPS according to the international criteria (1). Exclusion criteria were as follows: age >45 years; body mass index (BMI) ≥35 kg/m^2; secondary APS; menopause or amenorrhea; pregnancy or lactation; prednisone current use or in the 3 months before entering the study; previous n-3 PUFA supplementation; chronic use of anti-inflammatory drugs; hemorrhagic or thrombotic episode in the 6 months before entering the study; untreated thyroid dysfunction; uncontrolled hypertension; T2DM; treatment with statins, fibrate, insulin, or insulin sensitizers; tobacco use; acute renal failure, hepatic, cardiac, and pulmonary involvement. This study was approved by the Ethics Committee for Analysis of Research Projects of the General Hospital, School of Medicine, University of São Paulo, affiliated to the National Committee for Ethics in Research of Brazil. All subjects signed the informed consent prior to participation.

Supplementation Protocol and Blinding Procedure

The ω-3 group received 1.8 g of EPA and 1.3 g of DHA as re-esterified triglycerides contained in five capsules (three capsules of HiOmega-3 + two capsules of Omega-3 DHA 500, Naturalis®, São Paulo, SP, Brazil) which were consumed once per day. EPA and DHA contained in the capsules were extracted from whole fish oil. The same dose and proportion of EPA and DHA has been shown to beneficially impact endothelial function in patients with T2D (11), chronic heart failure (19), and SLE patients (17). PL group received the exact same amount of capsules per day, similar in size, shape, and color, containing soy oil. Supplement packages were coded so that neither patients nor investigators were aware of the content until completion of analyses. Compliance to supplementation was monitored weekly.

Endothelial Function Estimates

Endothelial function was assessed *via* peripheral artery tonometry using the EndoPAT-2000 device (Caesarea, Israel).

This is a reactive hyperemia peripheral arterial plethysmography which measures the vascular endothelial response to temporary vascular deprivation in the arm by measuring blood volume in the finger. To that end, a probe was applied to a finger in each hand, whereas an inflatable blood pressure cuff was applied to one upper arm. A baseline measurement of finger volumes was recorded for 5 min. Then, the arm cuff was inflated to either 60 mm Hg above systemic systolic blood pressure or 200 mm Hg (whichever was higher) for 5 min. When the cuff was deflated, changes in finger blood volume were recorded from each finger for another 4 min. In healthy subjects, the period of circulatory deprivation in an arm is followed by a marked vasodilatation in the ipsilateral finger 90–120 s after cuff deflation which is due to a local release of NO and prostaglandins as a response to shear stress and/or tissue hypoxia. Differences between the pre- and post-occlusion finger blood volume in each hand are used to calculate the reactive hyperemia index (RHI), which is a measure of the endothelial response to occlusion and reactive hyperemia corrected for systemic effects on the basis of volume changes in the contralateral finger. The augmentation index (AI), an estimate of vascular stiffness, is also automatically calculated, as well as the logarithmic transformation of RHI (LnRHI). Patients were instructed to refrain from physical exercise, alcohol, and caffeine intake 24 h prior to the test. Moreover, they consumed a standardized meal 1 h prior to testing.

Blood Analysis

Blood samples were collected after a 10-h overnight fast. Endothelial function markers (ICAM-1, VCAM-1, and e-selectin) and inflammatory cytokines (IL-10, IL-6, IL-1-β, IL-1-ra, and TNF) were measured *via* immunoassays using multiplex human panels according to the manufacturer's procedures (Milliplex®, USA). Serum levels of fibrinogen were determined using the Clauss method, whereas serum levels of CRP were measured using the immunoturbidimetry method (Cobas 8000). Plasma levels of blood cholesterol, high-density lipoprotein (HDL)-cholesterol, and triglycerides were assessed *via* colorimetric enzymatic methods (CELM, Brazil). From these, very-low lipoprotein-cholesterol (VLDL-cholesterol) (VLDL-cholesterol = triglycerides/5) and low-density lipoprotein (LDL) cholesterol [LDL-cholesterol = total cholesterol − (HDL-cholesterol + VLDL-cholesterol)] levels were calculated. Prothrombin time was measured in an automated coagulometer (3000 IL) with the use of bovine thromboplastin and was expressed as INR.

Dietary Intake

Dietary intake was assessed using three 24-h dietary recalls undertaken on separate days (2 weekdays and 1 weekend day) using a visual aid photo album of real foods. Energy and macronutrient intake were analyzed by Avanutri software (Rio de Janeiro, Brazil). n-3 PUFA intake was estimated based on the content of DHA, EPA, and α-linoleic acid (ALA) of foods according to the United States Department of Agriculture National Nutrient Database for Standard Reference available at https://ndb.nal.usda.gov/ndb/search/list.

Statistical Analysis

To minimize the impact of inter-individual variability, all values were converted into delta scores (i.e., post–pre-values) and thereafter tested by a mixed model, having pre-values from all dependent variables as covariates. Tukey *post hoc* was used for multiple comparisons. Baseline data were compared using Fisher's exact tests and unpaired Student's *t*-tests. Fisher's exact tests were also used to compare adherence to supplementation, whereas McNemar's test and Fisher's exact tests were used to compare within- and between-group proportion changes in lipid profile. Cohen's *d* was used to determine between-group effect sizes (ES) for dependent variables (20). Data are presented as mean (standard deviation), difference between delta changes, and 95% confidence interval (95% CI) unless otherwise stated. The significance level was set at $p \leq 0.05$, with a trend toward significance being accepted at $p \leq 0.1$.

Post hoc power analyses were performed with the assistance of the G-Power® software (version 3.1.2), which demonstrated a power of 65 and 73% at an alpha level of 5% to detect significant differences in RHI and LnRHI between PL and ω-3 with ES of 0.9 and 1.0.

RESULTS

Patients and Adherence to the Supplementation Protocol

Two-hundred and thirty-six patients were screened for participation and 71 met the inclusion criteria. Thirty-five agreed to take part in the study and were randomly assigned to either the ω-3 ($n = 18$) or PL ($n = 17$) group. Five patients withdrew from the study for personal reasons, three patients became pregnant, one patient entered menopause, one patient was diagnosed with another autoimmune disease, and three patients experienced disease complications not related to APS. Thus, the 22 patients who completed the study were analyzed (ω-3 = 11, PL = 11) (**Figure 1**). We chose a "per protocol" approach instead of an intention-to-treat (ITT) protocol as the primary research goal of our study was to determine the potential efficacy of n-3 PUFA supplementation and not its effectiveness (21). In this context, ITT analysis has been regarded as more susceptible to type II error (22, 23), as the treatment effect may be diluted due to dropouts (23). Importantly, baseline comparisons using Fisher's exact tests and unpaired *t*-tests analyses of those lost to follow-up and those retained in each group did not show any dropout bias (data not shown).

Due to technical issues, two patients (one from each group) were not assessed for endothelial function. **Table 1** shows the demographic characteristics at baseline. No between-group differences were observed at baseline for any of the parameters. Adherence to supplementation protocol was 83% in ω-3 and 88% in PL ($p = 0.2$, between-group comparison).

Endothelial Function

Following the intervention, ω-3 presented significant increases in LnRHI (+23 vs. −22%, $p = 0.02$, ES = 1.0) and a tendency toward increases in RHI (+13 vs. −12%, $p = 0.06$, ES = 0.9)

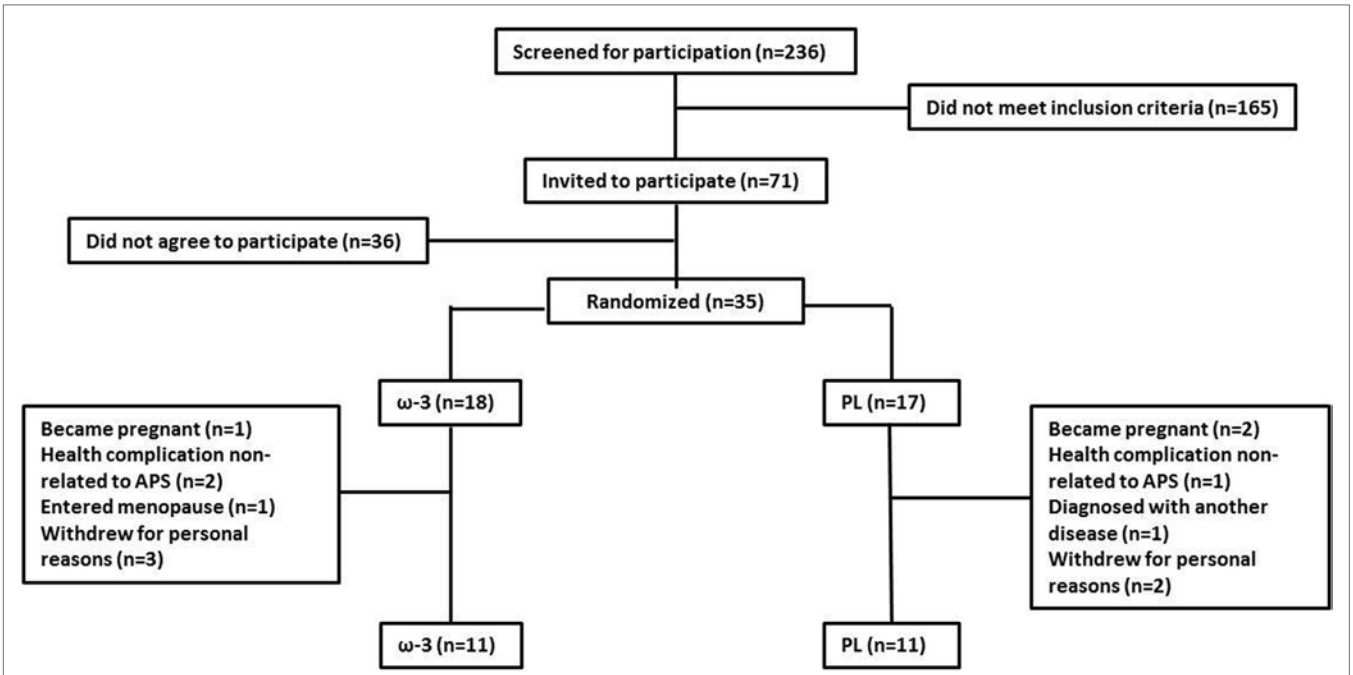

FIGURE 1 | Flow diagram of patients. Symbol abbreviation: APS, antiphospholipid syndrome.

TABLE 1 | Demographic and current clinical and treatment data in ω-3 and PL.

	PL ($n = 11$)	ω-3 ($n = 11$)	p
Age (years)	37.6 ± 6.5	34.8 ± 4.5	0.29
BMI (kg/m^2)	28.8 ± 4.3	29.8 ± 4.3	0.55
Disease duration (years)	8.4 ± 5.8	10.0 ± 5.1	0.52
Previous thrombotic event [no. (%)]	8 (72.7)	10 (90.9)	0.59
Previous obstetric morbidity [no. (%)]	6 (54.5)	7 (63.6)	1.0
Anti-cardiolipin antibody positivity [no. (%)]	9 (81.8)	5 (45.4)	0.18
Lupic anticoagulant antibody positivity [no. (%)]	7 (63.6)	11 (100)	0.1
Anti-beta-2 glycoprotein I antibody positivity [no. (%)]	3 (27.3)	2 (18.2)	1.0
Triple antiphospholipid antibody positivity [no. (%)]	2 (18.2)	1 (9.1)	1.0
Arterial hypertension [no. (%)]	1 (9.1)	3 (27.3)	0.59
Drug intake			
Oral contraceptives (progestogen) [no. (%)]	5 (45.4)	4 (36.4)	1.0
Glucocorticoid [no. (%)]	0 (0)	0 (0)	1.0
Hydroxychloroquine [no. (%)]	4 (36.4)	5 (54.5)	1.0
Acetylsalicylic acid [no. (%)]	2 (18.2)	2 (18.2)	1.0
Anticoagulant drugs [no. (%)]	9 (81.8)	9 (81.8)	1.0
Physical activity level			
Low [no. (%)]	2 (18.2)	4 (36.4)	0.63
Moderate [no. (%)]	4 (36.4)	4 (36.4)	1.0
High [no. (%)]	5 (45.4)	3 (27.3)	0.65

Data expressed as mean ± SD or number of patients (percentage) and level of significance (p) calculated using unpaired Student's t-test or Fisher exact test. BMI, body mass index.

when compared with PL. Previous studies have shown between- and within-day coefficient variation (CV) ranging from 11 to 22% in PAT-derived measures of endothelial function (24–26). Thus, it is noteworthy that out of the 10 patients in ω-3, 6 patients showed increases and 2 patients showed decreases in endothelial function estimates above the previously reported CVs (> + 30% in RHI and > + 50% in LnRHI), whereas two patients showed no change. By contrast, out of the 10 patients in PL, 5 patients showed decreases in endothelial function estimates above the previously reported CVs (>25% in RHI and >30% in LnRHI), whereas 5 showed no change (**Table 2**; **Figure 2**). By contrast, no significant differences between ω-3 and PL were observed in AI (+27 vs. +16%, $p = 0.5$, ES = 0.2) (**Figure 2**; **Table 2**) and circulating levels of fibrinogen (−23 vs. −13%, $p = 0.7$, ES = −0.1), e-selectin (−6 vs. −5%, $p = 0.7$, ES = −0.03), and VCAM-1 (+8 vs. +20%, $p = 0.3$, ES = −0.3). ω-3 showed a tendency toward reduced ICAM-1 levels (+3 vs. +48%, $p = 0.1$, ES = −0.7) when compared with PL (**Table 2**).

Inflammatory Profile

After the intervention, no significant differences between ω-3 and PL were observed in circulating levels of CRP (−51 vs. −45%, $p = 0.9$, ES = −0.3), IL-6 (−23 vs. −13%, $p = 0.9$, ES = −0.4), IL-1ra (−33 vs. −58%, $p = 0.5$, ES = 0.04), and IL-1β (−22 vs. +12%, $p = 0.2$, ES = −0.7). By contrast, ω-3 showed decreased circulating levels of IL-10 (−4 vs. +45%, $p = 0.001$, ES = −0.9) and TNF (−14 vs. +0.3%, $p = 0.04$, ES = −0.95) when compared with PL (**Table 2**).

Lipid Profile

Following the intervention, ω-3, when compared with PL, showed increases in total cholesterol (+6 vs. −2%, $p = 0.07$, ES = 0.7) and LDL-cholesterol (+11 vs. −0.3%, $p = 0.02$, ES = 0.8). It is notable that before the intervention, only one patient in PL and three

TABLE 2 | Endothelial function, inflammatory parameters, and lipid profile before and after the intervention in ω-3 and PL.

	PL (n = 11)			ω-3 (n = 11)			PL vs. ω-3		
	Pre	Post	Δ (95% CI)	Pre	Post	Δ (95% CI)	Δ difference (95% CI)	p	ES
Inflammatory markers									
C-reactive protein (mg/l)	3.6 ± 3.7	2.0 ± 1.0	−1.7 (−2.4 to −1.0)	4.4 ± 3.5	2.2 ± 1.8	−1.7 (−2.3 to −0.9)	−0.06 (−1.02 to 0.91)	0.9	−0.3
IL-6 (pg/ml)	0.84 ± 0.51	0.73 ± 0.46	−0.14 (−0.39 to 0.11)	1.32 ± 0.95	1.02 ± 0.61	−0.16 (−0.39 to 0.07)	0.02 (−0.32 to 0.36)	0.9	−0.4
IL-10 (pg/ml)	1.70 ± 0.57	2.17 ± 1.21	0.69 (0.40 to 0.99)	2.18 ± 1.74	2.10 ± 1.68	−0.07 (−0.35 to 0.20)	0.77 (0.37 to 1.17)	0.001	−0.9
TNF (pg/ml)	2.15 ± 1.00	2.16 ± 0.90	−0.01 (−0.19 to 0.17)	2.43 ± 0.84	2.10 ± 0.75	−0.30 (−0.49 to −0.10)	0.29 (0.01 to 0.56)	0.04	−0.95
IL-1-ra (pg/ml)	49.3 ± 64.3	20.6 ± 12.3	−22.3 (−44.8 to 0.2)	48.7 ± 55.9	32.8 ± 44.5	−11.6 (−34.1 to 10.9)	−10.7 (−42.5 to 21.1)	0.5	0.04
IL-1β (pg/ml)	0.90 ± 0.49	1.01 ± 0.60	0.08 (−0.22 to 0.38)	1.19 ± 0.68	0.92 ± 0.54	−0.18 (−0.49 to 0.11)	0.27 (−0.15 to 0.69)	0.2	−0.7
Lipid profile									
Triglycerides (mg/dl)	99.8 ± 27.8	81.5 ± 25.3	−23.0 (−37.8 to −8.2)	113.3 ± 62.2	91.0 ± 19.1	−16.5 (−30.3 to −2.7)	−6.5 (−26.7 to 13.7)	0.5	−0.06
LDL-chol (mg/dl)	104.4 ± 23.2	104.1 ± 26.9	−0.3 (−8.0 to 7.4)	107.7 ± 29.8	119.6 ± 21.9	12.4 (4.7 to 20.1)	−12.7 (−23.6 to −1.8)	0.02	0.85
HDL-chol (mg/dl)	45.9 ± 7.5	44.8 ± 7.9	−1.1 (−6.5 to 4.3)	46.0 ± 9.1	49.1 ± 13.2	3.1 (−2.3 to 8.5)	−4.2 (−11.9 to 3.5)	0.3	0.45
LDL/HDL ratio	2.35 ± 0.73	2.38 ± 0.71	0.0 (−0.3 to 0.3)	2.44 ± 0.83	2.62 ± 0.94	0.2 (−0.1 to 0.5)	−0.17 (−0.61 to 0.27)	0.4	0.32
Total cholesterol (mg/dl)	169.7 ± 24.5	165.8 ± 31.5	−4.3 (−16.8 to 8.3)	176.5 ± 34.8	186.2 ± 27.0	11.4 (−1.1 to 24.0)	−15.7 (−33.5 to 2.1)	0.07	0.67
Markers of endothelial cell activation									
Fibrinogen (mg/dl)	357 ± 71	310 ± 60	−98 (−155 to −43)	396 ± 134	307 ± 65	−85 (−145 to −24)	−14 (−96 to 69)	0.7	−0.11
e-selectin (ng/ml)	108 ± 46	103 ± 45	−1.0 (−23.7 to 21.6)	93 ± 39	88 ± 41	−6.6 (−28.3 to 15.0)	5.6 (−25.7 to 36.9)	0.7	−0.03
ICAM-1 (ng/ml)	635 ± 488	940 ± 608	274 (35 to 513)	712 ± 584	695 ± 457	29 (−199 to 256)	245 (−85 to 576)	0.1	−0.68
VCAM-1 (ng/ml)	657 ± 253	792 ± 339	112 (−41 to 265)	583 ± 276	631 ± 184	12 (−132 to 157)	99 (−111 to 309)	0.3	−0.25
Safety									
INR	2.0 ± 0.8	1.7 ± 0.7	−0.3 (−0.8 to 0.3)	2.3 ± 0.7	2.1 ± 0.7	−0.1 (−0.6 to 0.4)	−0.16 (−0.92 to 0.59)	0.7	−0.17
Endothelial function estimates									
RHI	2.08 ± 0.34	1.83 ± 0.53	−0.28 (−0.56 to −0.01)	1.80 ± 0.42	2.03 ± 0.36	0.08 (−0.18 to 0.34)	−0.37 (−0.7 to 0.01)	0.06	0.9
LnRHI	0.72 ± 0.16	0.56 ± 0.31	−0.19 (−0.34 to −0.05)	0.56 0.24	0.69 ± 0.17	0.05 (−0.09 to 0.18)	−0.24 (−0.44 to −0.04)	0.02	1.0
AI	−1.8 ± 14.1	−2.1 ± 13.7	−1.4 (−9.1 to 6.4)	7.7 ± 14.2	9.8 ± 20.0	3.4 (−4.1 to 11.6)	−4.7 (−16.0 to 6.5)	0.5	0.21

Data expressed as mean ± SD. Delta change (Δ) and 95% confidence interval (95% CI), estimated difference between delta changes (Δ difference) and 95% CI, and level of significance (p) calculated using a mixed model adjusted by pre-values: effect size (ES).

IL, interleukin; TNF, tumor necrosis factor; LDL, low-density lipoprotein; HDL, high-density lipoprotein; INR, international normalized ratio; ICAM-1, intercellular adhesion molecule-1; VCAM-1, vascular adhesion molecule-1; INR, international normalized ratio; RHI, reactive hyperemia index; LnRHI, reactive hyperemia index after natural log transformation; AI, augmentation index.

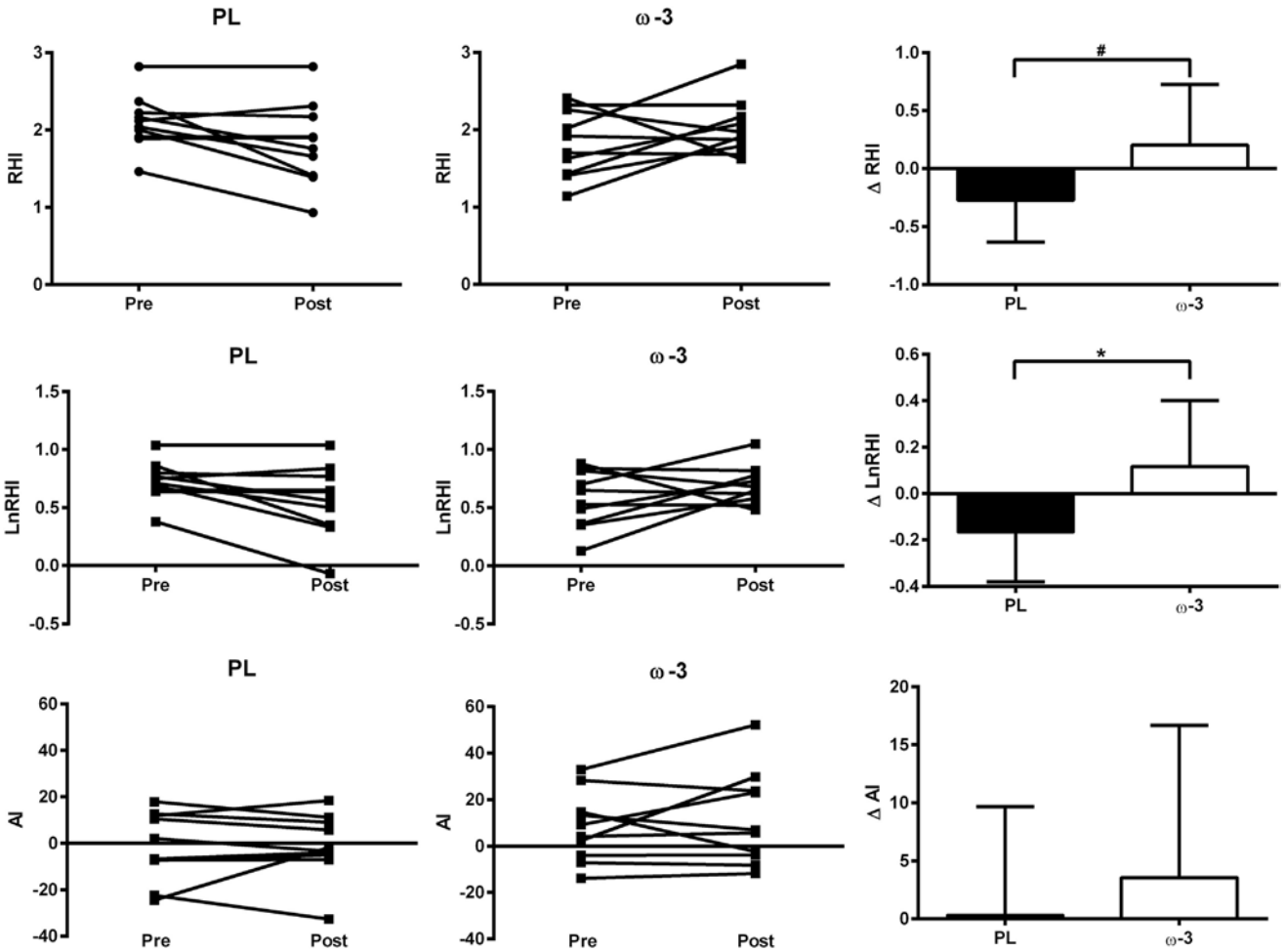

FIGURE 2 | Individual data at pre and post and absolute change (data expressed as mean and standard deviation) in endothelial function estimates RHI, LnRHI, and AI in ω-3 and PL. Differences between delta changes were calculated using a mixed model adjusted by pre-values. *means $p < 0.05$, ω-3 vs. PL; #means $p = 0.06$, ω-3 vs. PL. Symbol abbreviation: RHI, reactive hyperemia index; LnRHI, reactive hyperemia index after natural log transformation; AI, augmentation index.

patients in ω-3 presented borderline levels of total cholesterol (>200 and <239 mg/dl), whereas one patient in PL and two patients in ω-3 presented borderline levels of LDL-cholesterol (>120 and <159 mg/dl). After the intervention, two patients in PL and four patients in ω-3 presented borderline levels of total cholesterol, whereas two patients in PL and four patients in ω-3 presented borderline levels of LDL-cholesterol. Importantly, these changes were not different within or between groups ($p > 0.05$). None of the patients presented high levels of total cholesterol (>240 mg/dl) or LDL-cholesterol (>159 mg/dl) (27) at any time. Moreover, no significant differences were observed between ω-3 and PL in HDL-cholesterol (+7 vs. −2%, $p = 0.3$, ES = 0.5), LDL-cholesterol/HDL-cholesterol ratio (+7 vs. +1%, $p = 0.4$, ES = 0.3), and triglycerides (−20 vs. −18%, $p = 0.5$, ES = −0.06).

Dietary Intake

There were no significant differences for total energy, macronutrient, EPA, DHA, and ALA intake (without accounting for supplementation) between groups ($p > 0.05$ for all variables, **Table 3**).

Adverse Effects

There were no differences between ω-3 and PL in INR (−13.5 vs. −11.5%, $p = 0.7$, ES = 0.17) (**Table 2**). Importantly, all patients were within targeted INR before and after the intervention. There were no self-reported adverse events throughout the trial.

DISCUSSION

To the best of our knowledge, this is the first study to assess the safety and efficacy of n-3 PUFA supplementation in APS. Our main findings are that 16 weeks of n-3 PUFA supplementation was safe and improved endothelial function of patients with well-controlled PAPS.

Endothelial dysfunction mediated by aPLs has been associated with an increased risk of thrombosis, accelerated atherosclerosis, myocardial infarction, and stroke in patients with APS (5).

TABLE 3 | Dietary intake before and after the intervention in ω-3 and PL.

	PL (n = 11)			ω-3 (n = 11)			PL vs. ω-3		
	Pre	Post	Δ (95% CI)	Pre	Post	Δ (95% CI)	Δ difference (95% CI)	p	ES
Total energy (kcal)	1,567 ± 272	1,528 ± 665	−146 (−820 to 528)	1,738 ± 370	1,771 ± 406	62 (−476 to 599)	−208 (−1,071 to 654)	0.6	0.12
Protein (g)	61.1 ± 20.6	80.1 ± 33.5	0.1 (−31.9 to 32.0)	80.7 ± 23.8	77.1 ± 17.6	5.7 (−19.0 to 30.5)	−5.7 (−46.1 to 34.8)	0.8	−0.6
Protein (%)	15.2 ± 4.2	21.7 ± 7.6	−2.0 (−5.6 to 9.6)	19.1 ± 3.3	18.1 ± 4.6	1.2 (−5.0 to 7.4)	0.8 (−8.9 to 10.6)	0.8	−0.8
Carbohydrate (g)	223.0 ± 31.5	190.9 ± 94.1	−32.4 (−115.6 to 50.7)	219.5 ± 63.5	229.9 ± 62.4	6.8 (−63.3 to 77.0)	−39.2 (−148.1 to 69.5)	0.4	−0.5
Carbohydrate (%)	58.2 ± 7.0	48.2 ± 6.2	−4.2 (−11.8 to 3.4)	50.1 ± 7.5	51.6 ± 4.6	−1.4 (−7.4 to 4.5)	−2.8 (−12.4 to 6.9)	0.5	0.9
Fat (g)	47.8 ± 16.5	49.2 ± 19.4	−5.8 (−29.7 to 18.1)	59.7 ± 17.3	60.3 ± 16.6	6.2 (−13.1 to 25.6)	−12.1 (−42.9 to 18.7)	0.4	0.07
Fat (%)	26.6 ± 4.8	30.1 ± 4.5	−2.0 (−11.0 to 6.9)	35.7 ± 18.5	30.3 ± 4.5	−1.4 (−6.6 to 3.7)	−0.6 (−10.9 to 9.8)	0.9	−0.5
EPA (mg)[a]	8.0 ± 0.8	6.7 ± 5.0	−0.3 (−1.0 to 1.0)	9.5 ± 5.4	8.0 ± 6.7	−3.0 (−7.2 to 0.5)	3.0 (−6.9 to 13.1)	0.5	−0.4
DHA (mg)[a]	21.3 ± 22.0	11.3 ± 13.6	−12.6 (−26.5 to 1.1)	25.9 ± 21.9	13.7 ± 16.2	−13.2 (−24.8 to 1.6)	0.6 (−17.5 to 18.6)	0.9	−0.2
ALA (mg)	326 ± 476	290 ± 304	−74 (−299 to 151)	481 ± 263	473 ± 244	79 (−113 to 271)	−153 (−448 to 143)	0.3	0.2

Data expressed as mean ± SD. Delta change (Δ) and 95% confidence interval (95% CI), estimated difference between delta changes (Δ difference) and 95% CI, and level of significance (p) calculated using a mixed model adjusted by pre-values: effect size (ES).

EPA, eicosapentaenoic acid; DHA, docosahexanoic acid; ALA, α-linoleic acid.

[a]*Values without accounting for supplementation.*

Thus, strategies capable of minimizing this burden may be valuable in the management of this disease.

In this study, we showed that 16 weeks of n-3 PUFA supplementation (3 g of EPA and DHA/day) led to improvements in endothelial function estimates in PAPS patients. Although mean improvements may be considered modest, half of the patients in ω-3 showed improvements in endothelial function estimates above the previously reported CVs (>30% change in RHI), whereas half of the patients in PL showed decreases in endothelial function estimates above the previously reported CVs (>25% change in RHI) (**Figure 2**). Importantly, this was observed in patients with similar physical activity levels and no changes in food intake, including n-3 PUFA intake, throughout the intervention, which are important confounding factors. It is worth noting that increases in RHI similar to those observed in the present study have been reported in response to pharmacological (anti-inflammatory drugs) (28) and nonpharmacological treatments (antioxidant-rich foods and physical exercise) (29–32) in previous studies. Thus, the beneficial effects of n-3 PUFA supplementation on endothelial function in our APS patients may be considered clinically relevant.

Our results corroborate the beneficial effects of marine-derived n-3 PUFA supplementation on endothelial function in patients with conditions associated with accelerated atherosclerosis, such as T2D, dyslipidemia, and obesity (11, 12, 14, 33). The exact mechanisms underlying this effect remain elusive. Nonetheless, the incorporation of n-3 PUFAS into cell membrane phospholipids seems to play a fundamental role as it modulates a number of cellular functions, including signal transduction, protein and membrane trafficking, and ion channel kinetics, which could beneficially impact endothelial function (34).

In this regard, marine n-3 PUFA supplementation has been shown to increase endothelial nitric oxide synthesis (eNOS) *via* increased translocation of eNOS from cell membrane caveolin to the cytosol, leading to eNOS system activation and vasodilation (35, 36). Another possibility is that the anti-inflammatory effect of marine n-3 PUFA could positively affect endothelial function (37). This may occur *via* a lower incorporation of n-6 PUFA on cell membranes (due to a higher n-3 PUFA incorporation) (38, 39), ensuing a lower production of pro-inflammatory eicosanoids (e.g., two-series prostaglandins and four-series leukotrienes) (40). Moreover, EPA and DHA are precursors for not only less potent pro-inflammatory eicosanoids but also to anti-inflammatory and inflammation-resolving lipid mediators, namely resolvins, protectins, and maresins (the latter two being derived from DHA only) (41). These lipid mediators have been shown to reduce the infiltration of neutrophils to inflamed sites, activate macrophage phagocytosis of apoptotic cells, and reduce the production of the classic pro-inflammatory cytokines TNF and IL-1β (42–44). Finally, n-3 PUFA may also exert its anti-inflammatory effect *via* binding to the G-protein coupled cell membrane receptor 120 (GPR120) on macrophages, which inhibits the activation of nuclear factor kappa B ($NF_{\kappa}B$), a well-known transcription factor involved in the upregulation of genes encoding pro-inflammatory cytokines (45). These anti-inflammatory effects of n-3 PUFA supplementation are thought to lead to a lower production of endothelial adhesion molecules and leukocyte–endothelial interaction (46), which are critical to the initiation of vascular inflammation, thus positively affecting endothelial function.

We observed a tendency toward a reduced ICAM-1 response to n-3 PUFA supplementation when compared with placebo controls. This is in concert with a meta-analysis showing that n-3 PUFA supplementation reduces ICAM-1, but not VCAM-1 or e-selectin, in healthy and dyslipidemic individuals (47). VCAM-1 and e-selectin are expressed in endothelial cells upon cytokine activation, whereas ICAM-1 is expressed also in a number of immune cells (monocytes, macrophages, and lymphocytes). Based on this, the authors have suggested that n-3 PUFA selectively suppresses monocytes, rather than endothelial cells, leading to lower circulating levels of ICAM-1, but not the other markers of endothelial activation, which is corroborated by our data.

The selective suppression of monocytes, which leads to the downregulation of inflammatory cytokine secretion from these cells, may also explain the well-known anti-inflammatory effects of n-3 PUFA supplementation (48). Supplementation of ≥3 g/day of EPA and DHA has been shown to lead to reductions in TNF-circulating levels in T2D (49) and decreased TNF and IL-1β production by endotoxin-stimulated mononuclear cells of

healthy individuals (50). This is in line with our current results of decreased levels of TNF in response to n-3 PUFA supplementation when compared with placebo. Notably, we also observed significant reductions in IL-10 levels in response to n-3 PUFA supplementation. Because IL-10 is a classic anti-inflammatory cytokine (51), this could be interpreted as detrimental. However, it is likely that the modest decrease in the pro-inflammatory cytokine TNF may have led to a downregulation of IL-10 secretion in a homeostatic manner, which may have contributed to the improvements in endothelial function in response to n-3 PUFA supplementation when compared with placebo.

Similar to previous findings (52), we observed modestly increased levels of total cholesterol and LDL-cholesterol in ω-3 after the intervention when compared with those in PL. However, the proportion of patients moving from desirable to borderline levels of total cholesterol and LDL-cholesterol was the same between groups. Moreover, the nonsignificant increase in HDL in response to n-3 PUFA supplementation led to an unchanged LDL-cholesterol/HDL-cholesterol ratio, a superior predictor of CVD risk than total cholesterol and LDL-cholesterol levels (53), which argues against a harmful effect. Finally, previous studies have demonstrated that n-3 PUFA-induced increase in LDL-cholesterol derives from an increase in large buoyant non-atherogenic LDL particles rather than that in small dense atherogenic LDL particles (54) due to a reduction in VLDL-cholesterol production which enhances the rate of conversion of VLDL-cholesterol to LDL-cholesterol particles (52).

Another safety concern was that n-3 PUFA supplementation could impair prothrombin time in APS patients. However, we did not observe any changes in INR in ω-3 in response to supplementation, and all patients remained within their targeted INR throughout the study, which suggests that n-3 PUFA supplementation in these patients does not seem to predispose to hemorrhagic episodes. Moreover, there were no self-reported adverse effects throughout the intervention. Altogether, these results attest to the safety of up to 4 months n-3 PUFA supplementation (3 g/day) in patients with well-controlled PAPS.

This study was not without limitations. This was a relatively small-scale study, likely with limited power to detect modest albeit potentially clinically relevant changes in secondary outcomes. Moreover, we cannot generalize our findings to APS patients with different disease severity, drug regimens, and comorbidities. In fact, our patients had well-controlled disease, as none of them had presented with hemorrhagic or thrombotic episodes in the year before entering nor during the study, and none of the patients had T2D, a condition associated with endothelial dysfunction and accelerated atherosclerosis (15). This rigid internal control to eliminate potential confoundable conditions, which could introduce interpretation bias, may partially explain the modest improvements in endothelial function observed in this study, as a ceiling effect may have occurred. In this regard, we cannot rule out the possibility that patients with a more severe disease or associated metabolic diseases might respond differently to the supplementation of n-3 PUFA, with greater improvements in systemic inflammatory markers and in endothelial function. Finally, this was a short-term study whose primary end point is a surrogate marker for endothelial function and, thus, CVD risk. Long-term follow-up studies with higher sample sizes and statistical power are warranted in order to evaluate if the observed changes in endothelial function will effectively lead to significant improvements in CVD morbidity and mortality and clinical features of the disease and to attest the safety of n-3 PUFA in APS.

In conclusion, our findings suggest that 16 weeks of n-3 PUFA supplementation was safe and led to improvements in endothelial function in patients with well-controlled PAPS. These results support the role of n-3 PUFA supplementation as an adjuvant therapy in APS focused on reducing an important cardiovascular risk factor.

ETHICS STATEMENT

Clinical trial registered at http://ClinicalTrials.gov as NCT 01956188. This manuscript is reported according to the CONSORT guidelines.

AUTHOR CONTRIBUTIONS

SF and FB conceived the study, analyzed and interpreted the data, and drafted the manuscript. SF, LS, MS, AH, BG, EB, AS-P, DA, KK, and MI acquired data. HR analyzed the data. All authors revised and approved the final version of the manuscript and are, thus, accountable for its content.

FUNDING

The authors thank Conselho Nacional de Desenvolvimento Tecnologico and FAPESP (2017/02546-1; 2014/06911-8) for the financial support.

REFERENCES

1. Miyakis S, Lockshin MD, Atsumi T, Branch DW, Brey RL, Cervera R, et al. International consensus statement on an update of the classification criteria for definite antiphospholipid syndrome (APS). *J Thromb Haemost* (2006) 4(2):295–306. doi:10.1111/j.1538-7836.2006.01753.x
2. Espinosa G, Cervera R. Antiphospholipid syndrome: frequency, main causes and risk factors of mortality. *Nat Rev Rheumatol* (2010) 6(5):296–300. doi:10.1038/nrrheum.2010.47
3. Soltesz P, Szekanecz Z, Kiss E, Shoenfeld Y. Cardiac manifestations in antiphospholipid syndrome. *Autoimmun Rev* (2007) 6(6):379–86. doi:10.1016/j.autrev.2007.01.003
4. Corban MT, Duarte-Garcia A, McBane RD, Matteson EL, Lerman LO, Lerman A. Antiphospholipid syndrome: role of vascular endothelial cells and implications for risk stratification and targeted therapeutics. *J Am Coll Cardiol* (2017) 69(18):2317–30. doi:10.1016/j.jacc.2017.02.058
5. Mineo C. Inhibition of nitric oxide and antiphospholipid antibody-mediated thrombosis. *Curr Rheumatol Rep* (2013) 15(5):324. doi:10.1007/s11926-013-0324-4
6. Stalc M, Poredos P, Peternel P, Tomsic M, Sebestjen M, Kveder T. Endothelial function is impaired in patients with primary antiphospholipid syndrome. *Thromb Res* (2006) 118(4):455–61. doi:10.1016/j.thromres.2005.09.005
7. Der H, Kerekes G, Veres K, Szodoray P, Toth J, Lakos G, et al. Impaired endothelial function and increased carotid intima-media thickness in association with elevated von Willebrand antigen level in primary antiphospholipid syndrome. *Lupus* (2007) 16(7):497–503. doi:10.1177/0961203307080224
8. Swadzba J, Iwaniec T, Musial J. Increased level of tumor necrosis factor-alpha in patients with antiphospholipid syndrome: marker not only of

inflammation but also of the prothrombotic state. *Rheumatol Int* (2011) 31(3):307–13. doi:10.1007/s00296-009-1314-8
9. Del Papa N, Raschi E, Catelli L, Khamashta MA, Ichikawa K, Tincani A, et al. Endothelial cells as a target for antiphospholipid antibodies: role of anti-beta 2 glycoprotein I antibodies. *Am J Reprod Immunol* (1997) 38(3):212–7. doi:10.1111/j.1600-0897.1997.tb00301.x
10. Gimbrone MA Jr, Garcia-Cardena G. Vascular endothelium, hemodynamics, and the pathobiology of atherosclerosis. *Cardiovasc Pathol* (2013) 22(1):9–15. doi:10.1016/j.carpath.2012.06.006
11. McVeigh GE, Brennan GM, Cohn JN, Finkelstein SM, Hayes RJ, Johnston GD. Fish oil improves arterial compliance in non-insulin-dependent diabetes mellitus. *Arterioscler Thromb* (1994) 14(9):1425–9. doi:10.1161/01.ATV.14.9.1425
12. Goodfellow J, Bellamy MF, Ramsey MW, Jones CJ, Lewis MJ. Dietary supplementation with marine omega-3 fatty acids improve systemic large artery endothelial function in subjects with hypercholesterolemia. *J Am Coll Cardiol* (2000) 35(2):265–70. doi:10.1016/S0735-1097(99)00548-3
13. Nestel P, Shige H, Pomeroy S, Cehun M, Abbey M, Raederstorff D. The n-3 fatty acids eicosapentaenoic acid and docosahexaenoic acid increase systemic arterial compliance in humans. *Am J Clin Nutr* (2002) 76(2):326–30. doi:10.1093/ajcn/76.2.326
14. Stirban A, Nandrean S, Gotting C, Tamler R, Pop A, Negrean M, et al. Effects of n-3 fatty acids on macro- and microvascular function in subjects with type 2 diabetes mellitus. *Am J Clin Nutr* (2010) 91(3):808–13. doi:10.3945/ajcn.2009.28374
15. Creager MA, Luscher TF, Cosentino F, Beckman JA. Diabetes and vascular disease: pathophysiology, clinical consequences, and medical therapy: part I. *Circulation* (2003) 108(12):1527–32. doi:10.1161/01.CIR.0000091257.27563.32
16. Cavieres V, Valdes K, Moreno B, Moore-Carrasco R, Gonzalez DR. Vascular hypercontractility and endothelial dysfunction before development of atherosclerosis in moderate dyslipidemia: role for nitric oxide and interleukin-6. *Am J Cardiovasc Dis* (2014) 4(3):114–22.
17. Wright SA, O'Prey FM, McHenry MT, Leahey WJ, Devine AB, Duffy EM, et al. A randomised interventional trial of omega-3-polyunsaturated fatty acids on endothelial function and disease activity in systemic lupus erythematosus. *Ann Rheum Dis* (2008) 67(6):841–8. doi:10.1136/ard.2007.077156
18. Craig CL, Marshall AL, Sjostrom M, Bauman AE, Booth ML, Ainsworth BE, et al. International physical activity questionnaire: 12-country reliability and validity. *Med Sci Sports Exerc* (2003) 35(8):1381–95. doi:10.1249/01.MSS.0000078924.61453.FB
19. Morgan DR, Dixon LJ, Hanratty CG, El-Sherbeeny N, Hamilton PB, McGrath LT, et al. Effects of dietary omega-3 fatty acid supplementation on endothelium-dependent vasodilation in patients with chronic heart failure. *Am J Cardiol* (2006) 97(4):547–51. doi:10.1016/j.amjcard.2005.08.075
20. Cohen J. *Statistical Power Analysis for the Behavioral Sciences*. Hillsdale, USA: Lawrence Erlbaum Associates (1998).
21. Victora CG, Habicht JP, Bryce J. Evidence-based public health: moving beyond randomized trials. *Am J Public Health* (2004) 94(3):400–5. doi:10.2105/AJPH.94.3.400
22. Hollis S, Campbell F. What is meant by intention to treat analysis? Survey of published randomised controlled trials. *BMJ* (1999) 319(7211):670–4. doi:10.1136/bmj.319.7211.670
23. Fergusson D, Aaron SD, Guyatt G, Hebert P. Post-randomisation exclusions: the intention to treat principle and excluding patients from analysis. *BMJ* (2002) 325(7365):652–4. doi:10.1136/bmj.325.7365.652
24. Haller MJ, Stein J, Shuster J, Theriaque D, Silverstein J, Schatz DA, et al. Peripheral artery tonometry demonstrates altered endothelial function in children with type 1 diabetes. *Pediatr Diabetes* (2007) 8(4):193–8. doi:10.1111/j.1399-5448.2007.00246.x
25. McCrea CE, Skulas-Ray AC, Chow M, West SG. Test–retest reliability of pulse amplitude tonometry measures of vascular endothelial function: implications for clinical trial design. *Vasc Med* (2012) 17(1):29–36. doi:10.1177/1358863X11433188
26. Onkelinx S, Cornelissen V, Goetschalckx K, Thomaes T, Verhamme P, Vanhees L. Reproducibility of different methods to measure the endothelial function. *Vasc Med* (2012) 17(2):79–84. doi:10.1177/1358863X12436708
27. Stone NJ, Robinson JG, Lichtenstein AH, Bairey Merz CN, Blum CB, Eckel RH, et al. 2013 ACC/AHA guideline on the treatment of blood cholesterol to reduce atherosclerotic cardiovascular risk in adults: a report of the American College of Cardiology/American Heart Association Task Force on Practice Guidelines. *J Am Coll Cardiol* (2014) 63(25 Pt B):2889–934. doi:10.1016/j.jacc.2013.11.002
28. Tabit CE, Holbrook M, Shenouda SM, Dohadwala MM, Widlansky ME, Frame AA, et al. Effect of sulfasalazine on inflammation and endothelial function in patients with established coronary artery disease. *Vasc Med* (2012) 17(2):101–7. doi:10.1177/1358863X12440117
29. Bonetti PO, Barsness GW, Keelan PC, Schnell TI, Pumper GM, Kuvin JT, et al. Enhanced external counterpulsation improves endothelial function in patients with symptomatic coronary artery disease. *J Am Coll Cardiol* (2003) 41(10):1761–8. doi:10.1016/S0735-1097(03)82170-8
30. Kwak JH, Paik JK, Kim HI, Kim OY, Shin DY, Kim HJ, et al. Dietary treatment with rice containing resistant starch improves markers of endothelial function with reduction of postprandial blood glucose and oxidative stress in patients with prediabetes or newly diagnosed type 2 diabetes. *Atherosclerosis* (2012) 224(2):457–64. doi:10.1016/j.atherosclerosis.2012.08.003
31. Flammer AJ, Martin EA, Gossl M, Widmer RJ, Lennon RJ, Sexton JA, et al. Polyphenol-rich cranberry juice has a neutral effect on endothelial function but decreases the fraction of osteocalcin-expressing endothelial progenitor cells. *Eur J Nutr* (2013) 52(1):289–96. doi:10.1007/s00394-012-0334-4
32. Widmer RJ, Freund MA, Flammer AJ, Sexton J, Lennon R, Romani A, et al. Beneficial effects of polyphenol-rich olive oil in patients with early atherosclerosis. *Eur J Nutr* (2013) 52(3):1223–31. doi:10.1007/s00394-012-0433-2
33. Dangardt F, Osika W, Chen Y, Nilsson U, Gan LM, Gronowitz E, et al. Omega-3 fatty acid supplementation improves vascular function and reduces inflammation in obese adolescents. *Atherosclerosis* (2010) 212(2):580–5. doi:10.1016/j.atherosclerosis.2010.06.046
34. Mozaffarian D, Wu JH. Omega-3 fatty acids and cardiovascular disease: effects on risk factors, molecular pathways, and clinical events. *J Am Coll Cardiol* (2011) 58(20):2047–67. doi:10.1016/j.jacc.2011.06.063
35. Okuda Y, Kawashima K, Sawada T, Tsurumaru K, Asano M, Suzuki S, et al. Eicosapentaenoic acid enhances nitric oxide production by cultured human endothelial cells. *Biochem Biophys Res Commun* (1997) 232(2):487–91. doi:10.1006/bbrc.1997.6328
36. Omura M, Kobayashi S, Mizukami Y, Mogami K, Todoroki-Ikeda N, Miyake T, et al. Eicosapentaenoic acid (EPA) induces Ca(2+)-independent activation and translocation of endothelial nitric oxide synthase and endothelium-dependent vasorelaxation. *FEBS Lett* (2001) 487(3):361–6. doi:10.1016/S0014-5793(00)02351-6
37. Yagi S, Fukuda D, Aihara KI, Akaike M, Shimabukuro M, Sata M. n-3 polyunsaturated fatty acids: promising nutrients for preventing cardiovascular disease. *J Atheroscler Thromb* (2017) 24(10):999–1010. doi:10.5551/jat.RV17013
38. Park Y, Lee A, Shim SC, Lee JH, Choe JY, Ahn H, et al. Effect of n-3 polyunsaturated fatty acid supplementation in patients with rheumatoid arthritis: a 16-week randomized, double-blind, placebo-controlled, parallel-design multicenter study in Korea. *J Nutr Biochem* (2013) 24(7):1367–72. doi:10.1016/j.jnutbio.2012.11.004
39. Widenhorn-Muller K, Schwanda S, Scholz E, Spitzer M, Bode H. Effect of supplementation with long-chain omega-3 polyunsaturated fatty acids on behavior and cognition in children with attention deficit/hyperactivity disorder (ADHD): a randomized placebo-controlled intervention trial. *Prostaglandins Leukot Essent Fatty Acids* (2014) 91(1–2):49–60. doi:10.1016/j.plefa.2014.04.004
40. Rees D, Miles EA, Banerjee T, Wells SJ, Roynette CE, Wahle KW, et al. Dose-related effects of eicosapentaenoic acid on innate immune function in healthy humans: a comparison of young and older men. *Am J Clin Nutr* (2006) 83(2):331–42. doi:10.1093/ajcn/83.2.331
41. Mas E, Croft KD, Zahra P, Barden A, Mori TA. Resolvins D1, D2, and other mediators of self-limited resolution of inflammation in human blood following n-3 fatty acid supplementation. *Clin Chem* (2012) 58(10):1476–84. doi:10.1373/clinchem.2012.190199
42. Serhan CN, Clish CB, Brannon J, Colgan SP, Chiang N, Gronert K. Novel functional sets of lipid-derived mediators with antiinflammatory actions generated from omega-3 fatty acids *via* cyclooxygenase 2-nonsteroidal antiinflammatory drugs and transcellular processing. *J Exp Med* (2000) 192(8):1197–204. doi:10.1084/jem.192.8.1197
43. Serhan CN, Hong S, Gronert K, Colgan SP, Devchand PR, Mirick G, et al. Resolvins: a family of bioactive products of omega-3 fatty acid transformation

circuits initiated by aspirin treatment that counter proinflammation signals. *J Exp Med* (2002) 196(8):1025–37. doi:10.1084/jem.20020760
44. Schwab JM, Chiang N, Arita M, Serhan CN. Resolvin E1 and protectin D1 activate inflammation-resolution programmes. *Nature* (2007) 447(7146):869–74. doi:10.1038/nature05877
45. Kumar A, Takada Y, Boriek AM, Aggarwal BB. Nuclear factor-kappaB: its role in health and disease. *J Mol Med (Berl)* (2004) 82(7):434–48. doi:10.1007/s00109-004-0555-y
46. Robinson JG, Stone NJ. Antiatherosclerotic and antithrombotic effects of omega-3 fatty acids. *Am J Cardiol* (2006) 98(4A):39i–49i. doi:10.1016/j.amjcard.2005.12.026
47. Yang Y, Lu N, Chen D, Meng L, Zheng Y, Hui R. Effects of n-3 PUFA supplementation on plasma soluble adhesion molecules: a meta-analysis of randomized controlled trials. *Am J Clin Nutr* (2012) 95(4):972–80. doi:10.3945/ajcn.111.025924
48. Calder PC. n-3 polyunsaturated fatty acids, inflammation, and inflammatory diseases. *Am J Clin Nutr* (2006) 83(6 Suppl):1505S–19S. doi:10.1093/ajcn/83.6.1505S
49. Mori TA, Dunstan DW, Burke V, Croft KD, Rivera JH, Beilin LJ, et al. Effect of dietary fish and exercise training on urinary F2-isoprostane excretion in non-insulin-dependent diabetic patients. *Metabolism* (1999) 48(11):1402–8. doi:10.1016/S0026-0495(99)90150-6
50. Kelley DS, Taylor PC, Nelson GJ, Schmidt PC, Ferretti A, Erickson KL, et al. Docosahexaenoic acid ingestion inhibits natural killer cell activity and production of inflammatory mediators in young healthy men. *Lipids* (1999) 34(4):317–24. doi:10.1007/s11745-999-0369-5
51. Mosser DM, Zhang X. Interleukin-10: new perspectives on an old cytokine. *Immunol Rev* (2008) 226:205–18. doi:10.1111/j.1600-065X.2008.00706.x
52. Oscarsson J, Hurt-Camejo E. Omega-3 fatty acids eicosapentaenoic acid and docosahexaenoic acid and their mechanisms of action on apolipoprotein B-containing lipoproteins in humans: a review. *Lipids Health Dis* (2017) 16(1):149. doi:10.1186/s12944-017-0541-3
53. Kathiresan S, Otvos JD, Sullivan LM, Keyes MJ, Schaefer EJ, Wilson PW, et al. Increased small low-density lipoprotein particle number: a prominent feature of the metabolic syndrome in the Framingham Heart Study. *Circulation* (2006) 113(1):20–9. doi:10.1161/CIRCULATIONAHA.105.567107
54. Davidson MH. Omega-3 fatty acids: new insights into the pharmacology and biology of docosahexaenoic acid, docosapentaenoic acid, and eicosapentaenoic acid. *Curr Opin Lipidol* (2013) 24(6):467–74. doi:10.1097/MOL.0000000000000019

Conflict of Interest Statement: The authors declare that the research was conducted in the absence of any commercial or financial relationships that could be construed as a potential conflict of interest.

frontiers in Immunology

REVIEW
published: 01 March 2018
doi: 10.3389/fimmu.2018.00407

The Autoimmune Skin Disease Bullous Pemphigoid: The Role of Mast Cells in Autoantibody-Induced Tissue Injury

*Hui Fang[1], Yang Zhang[2,3], Ning Li[2], Gang Wang[1] and Zhi Liu[2,4,5]**

[1] Department of Dermatology, Xijing Hospital, Fourth Military Medical University, Xi'an, China, [2] Department of Dermatology, School of Medicine, University of North Carolina at Chapel Hill, Chapel Hill, NC, United States, [3] Department of Dermatology, The Second Hospital, School of Medicine, Xi'an Jiaotong University, Xi'an, China, [4] Department of Microbiology and Immunology, School of Medicine, University of North Carolina at Chapel Hill, Chapel Hill, NC, United States, [5] Lineberger Comprehensive Cancer Center, University of North Carolina at Chapel Hill, Chapel Hill, NC, United States

Bullous pemphigoid (BP) is an autoimmune and inflammatory skin disease associated with subepidermal blistering and autoantibodies directed against the hemidesmosomal components BP180 and BP230. Animal models of BP were developed by passively transferring anti-BP180 IgG into mice, which recapitulates the key features of human BP. By using these *in vivo* model systems, key cellular and molecular events leading to the BP disease phenotype are identified, including binding of pathogenic IgG to its target, complement activation of the classical pathway, mast cell degranulation, and infiltration and activation of neutrophils. Proteinases released by infiltrating neutrophils cleave BP180 and other hemidesmosome-associated proteins, causing DEJ separation. Mast cells and mast cell-derived mediators including inflammatory cytokines and proteases are increased in lesional skin and blister fluids of BP. BP animal model evidence also implicates mast cells in the pathogenesis of BP. However, recent studies questioned the pathogenic role of mast cells in autoimmune diseases such as multiple sclerosis, rheumatoid arthritis, and epidermolysis bullosa acquisita. This review highlights the current knowledge on BP pathophysiology with a focus on a potential role for mast cells in BP and mast cell-related critical issues needing to be addressed in the future.

Keywords: autoantibodies, bullous pemphigoid, hemidesmosome, mast cells, skin autoimmunity

OPEN ACCESS

Edited by:
Falk Nimmerjahn, University of Erlangen-Nuremberg, Germany

Reviewed by:
Kempuraj Duraisamy, University of Missouri, United States
Frank Petersen, Forschungszentrum Borstel (LG), Germany

***Correspondence:**
Zhi Liu
zhi_liu@med.unc.edu

Specialty section:
This article was submitted to Immunological Tolerance and Regulation, a section of the journal Frontiers in Immunology

Received: *29 November 2017*
Accepted: *14 February 2018*
Published: *01 March 2018*

Citation:
Fang H, Zhang Y, Li N, Wang G and Liu Z (2018) The Autoimmune Skin Disease Bullous Pemphigoid: The Role of Mast Cells in Autoantibody-Induced Tissue Injury. Front. Immunol. 9:407. doi: 10.3389/fimmu.2018.00407

MAST CELLS (MCs) AND MC RECEPTORS

Mast cells are derived from hematopoietic progenitor cells and have been considered as a central player in functional interaction between innate and adaptive immunity. MCs are initially located in the blood vessel and the lymphatic system before homing to tissues, where they acquire their final effector characteristics (1). There are at least two subpopulations of murine MCs based on the composition of chymases and tryptases within their granules. While $MC_{T\ cell}$s are the prominent MC type within the mucosa of the respiratory and gastrointestinal tracts, MC_{TC} cells are localized within connective tissues including the dermis, submucosa of the conjunctivae, gastrointestinal tract, heart, and perivascular tissues (2). The maturation of MCs in the tissue mainly relies on stem cell factor (SCF) expressed on the homing tissue, which is the ligand of KIT (1).

Mast cells express KIT (CD117) and FcεRI on their surface, which are the receptors of SCF and IgE, respectively. MCs also express other cell surface receptors, including IgG receptors (FcγRIII, FcγRIIa, and FcγRI), C3a and C5a receptors (C5aRs), Toll-like receptors, and receptors for many cytokines/chemokines (3). These receptors mediate activation of MCs. Upon activation, MCs release their mediators to the homing sites, which act in host defense and various pathological conditions (4). Mediators produced by MCs are divided into two categories: preformed and newly synthesized (5). Many mediators are preformed and stored in granules, such as histamine, serine proteases (tryptase and chymase), and TNF-α (6). Upon activation of MCs, these preformed mediators are released into the extracellular environment within minutes (7–9).

After the initial activation, the synthesized bioactive metabolites of arachidonic acid, prostaglandins, leukotrienes (LTs), and cytokines/chemokines will be released into the affected tissue sites rapidly. The second release of granules will amplify the immediate hypersensitivity reaction through the interaction with local cells and infiltrating immune cells (4).

MCs IN NON-SKIN AUTOIMMUNE DISEASES MULTIPLE SCLEROSIS (MS) AND RHEUMATOID ARTHRITIS

Mast cells have been considered as key effector cells in many immune activities, especially IgE-associated immune responses, including host defense to parasites, allergic diseases, chronic inflammatory disorders (10, 11), and cancer (12, 13). MCs have also been implicated in autoimmune diseases (14–19), such as MS, rheumatoid arthritis (RA), and the autoimmune skin blistering diseases bullous pemphigoid (BP) and epidermolysis bullosa acquisita (EBA).

Multiple sclerosis is an autoimmune disease of the central nervous system characterized by chronic inflammation and progressive demyelination (20). MCs and activated MCs are present in the target tissues of MS patients and correlated with disease severity (21–24). The animal model of MS, experimental autoimmune encephalomyelitis (EAE), can be induced by active immunization of susceptible mouse strains with myelin components such as myelin basic protein and myelin oligodendrocyte glycoprotein (MOG) (25). RA is an autoimmune disease of the joints characterized by chronic inflammation and cartilage destruction (26). Increased MCs and MC-derived inflammatory mediators are found in the inflamed joints of RA patients (27–29). K/BxN mouse serum contains autoantibodies against the glucose-6-phosphate isomerase and, when passively transferred to mice, induces experimental RA (30).

ROLE OF MCs IN EXPERIMENTAL MS AND RHEUMATOID ARTHRITIS

Mast cell-deficient mice have been widely used to determine the role of MCs in various physiological and pathological conditions, including autoimmune diseases. Whether MCs actively participate in the pathogenesis of MS and RA has been extensively debated recently due to controversial results obtained from different MC-deficient mouse strains. For a more comprehensive and in-depth review, please refer to the studies by Yu et al. and Rivellese et al. (15, 31). In MOG-induced EAE, MC-deficient $Kit^{W/W\text{-}v}$ mice (caused by Kit mutations) developed a significantly reduced disease, and reconstitution of MC-deficient $Kit^{W/W\text{-}v}$ mice with wild-type bone marrow-derived MCs restored the disease (32). Similarly, MC-deficient $Kit^{W/W\text{-}v}$ mice were protected from K/BxN serum-induced RA (33). K/BxN serum also failed to induce RA in $Mgf^{Sl/Sl\text{-}d}$ mice, another MC-deficient strain caused by mutations in the gene encoding the Kit ligand SCF (33). Since MC deficiency by Kit or SCF mutations also caused a variety of immunological abnormalities, new Kit-independent MC-specific deletion mouse strains were developed recently. It turned out that MCs were not required in the development of EAE and serum-induced RA (34).

BP: CLINICAL AND IMMUNOHISTOLOGICAL FEATURES

Bullous pemphigoid is an autoimmune subepidermal blistering disease induced by autoantibodies against the two components of the hemidesmosome, BP180 and BP230. BP is the most common autoimmune blistering disease and most prevalent in the elderly. BP typically presents with tense, mostly clear blisters, and erythema, frequently in conjunction with urticarial plaques (35). Blisters occur on either a normal or a erythematous base, containing serous or serosanguinous fluid (36). The disease has a symmetric distribution, and the predilection sites include the lower abdomen, flexor surfaces of the limbs, groin, and axillae (37). In almost all patients, severe pruritus is present. About 10–20% of patients show mucosal involvement, with the oral mucosa being the most common mucosal site (38, 39). Two prospective studies showed that up to 20% of patients with BP have no obvious blistering at the time of diagnosis (38–40).

Histopathologically, hematoxylin and eosin staining of early bulla in BP reveals subepidermal blistering with dense inflammatory infiltrate consisting predominantly of eosinophils, but also lymphocytes, neutrophils, and MCs. Eosinophils are seen within the blister and in the edematous papillary dermis (41). In the early non-bullous phase, subepidermal clefts and eosinophilic spongiosis (epidermal spongiosis with eosinophils within the epidermis) can be found (41). Therefore, BP is an autoimmune and inflammatory disease (**Figure 1**). Direct immunofluorescence staining exhibits linear deposition of IgG and/or complement components (C3 and/or C5) at the dermal–epidermal junction. IgG deposition sometimes is combined with weaker linear IgA or IgE staining. To identify circulating autoantibodies to the DEJ, indirect immunofluorescence (IIF) with normal human skin as the substrate is usually examined. Artificial blisters can be induced by incubating the skin specimen with 1 M NaCl solution. Since BP180 and BP230 are on the epidermal side of the artificial blisters, autoantibodies from BP patients are known to react with the epidermal side of the blisters (42). In contrast, autoantibodies from other autoimmune blistering diseases, including EBA

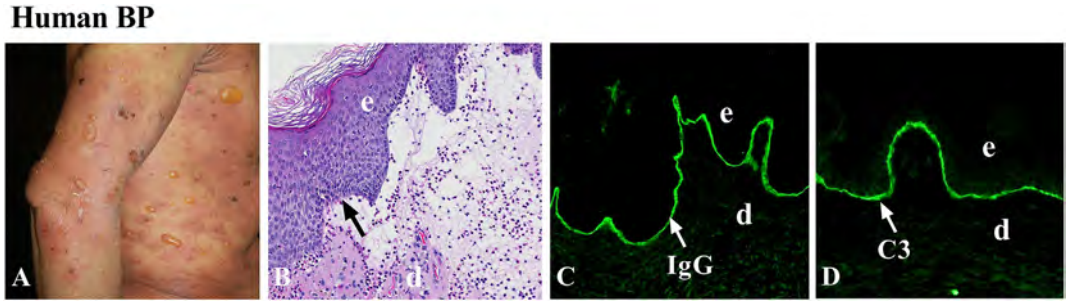

FIGURE 1 | Human bullous pemphigoid (BP). **(A)** Large, tense bullae, and erythematous patches seen in BP patient. **(B)** Histology reveals dermal–epidermal junction separation with inflammatory cell infiltration. Immunofluorescence shows linear deposition of IgG **(C)** and complement C3 **(D)** at the basement membrane zone (BMZ). d, dermis; e, epidermis. Arrow, the BMZ. Original magnification, 100× for panels **(B–D)**.

and anti-laminin γ1 pemphigoid, react with the dermal side of the artificial blisters (35). Thus, IIF with the salt-split skin as a substrate is helpful in distinguishing BP from other autoimmune blistering disorders.

BP AUTOANTIGENS

Bullous pemphigoid autoantibodies target two hemidesmosomal components BP180 (BPAG2) and BP230 (BPAG1), which are involved in dermal–epidermal cohesion (43–45). BP180 is a type II transmembrane glycoprotein with a globular cytoplasmic domain and a large extracellular region containing 15 collagenous and 16 non-collagenous (NC1-16) domains. The 16th non-collagenous (NC16A) domain is the immunodominant region in BP (46). Anti-NC16A IgG autoantibodies are detected in more than 90% of BP patients (47) and have been shown to be pathogenic in skin organ culture system and in animal models of BP (48–50) (see below). BP230 is a 230-kDa intracellular component of the hemidesmosomal plaque and belongs to the plakin family of proteins. Anti-BP230 autoantibodies are detected in nearly 60% of BP patients (51). In addition to IgG reactivity, anti-BP180/BP230 IgE autoantibodies are present in serum samples from most patients (47, 52, 53).

GENETICS OF BP

Genetic, environmental, and stochastic factors contribute to susceptibility to most autoimmune diseases. The human MHC encodes many glycoproteins that include the HLA class I and class II molecules, which provide a pivotal role in the recognition of antigenic peptides by T cells. A lot of polymorphisms of HLA-II class alleles have been identified in several populations of patients with BP (54–58). These polymorphisms HLA class II alleles occur likely due to changes in the charge of the active binding site on the HLA molecules for binding of autoantigenic peptides. A common HLA class II allele, HLA-DQB1*03:01, is positively associated with BP in multiple populations (54, 55, 58) and also appears to be associated with distinct clinical pemphigoid variants (59–61). In addition, the activation of BP180-autoreactive T cells from a cohort of BP patients with HLA-DQB1*03:01 was found to be restricted by this BP-associated HLA class II allele (55).

T CELL RESPONSE IN BP

CD4+ T helper (Th) cells are thought to participate in early disease development and perpetuation of autoantibody-mediated autoimmune blistering diseases. Th cells, upon proper costimulation, are activated and produce and secrete distinct cytokines that stimulate B cells. This Th–B cell interaction thus fosters plasma cell development and autoantibody production (62). In BP, autoreactive CD4+ T lymphocytes recognize unique epitopes within the extracellular region of BP180 (63). The majority of BP patients examined have both Th1 and Th2 responses against the BP180 ectodomain (55, 64). BP180-reactive Th cells and IgG autoantibodies recognized similar or identical epitopes clustered in distinct regions of the BP180 ectodomain and BP230 (49, 62, 65). Li et al. found that follicular T helper (Tfh) cells and IL-21 were crucial for the secretion of antibodies against BP180NC16A domain in T cell/B cell co-culture system, indicating that these Tfh cells may be involved in the pathogenesis of BP (66).

MCs IN HUMAN BP

In 1978, Wintroub et al. found that increased MCs and increased degranulation of MCs at the BP lesional sites are the earliest events in BP lesion formation (67). The evolution of clinical BP lesions is associated with a sequence of histopathologic events, starting with MC alternation and proceeding to immune cell infiltration first with lymphocytes followed by eosinophils and basophils. Electron and light microscopy revealed that MCs are mainly present in the papillary dermis adjacent to the dermal–epidermal junction and demonstrate a unique, focal, irregular loss of granule contents (68).

Various inflammatory mediators have been found in lesional/perilesional skin, blister fluids, and/or blood of patients with BP, including C5a, histamine, LTs, and many cytokines/chemokines (e.g., IL-1, IL-2, IL-5, IL-6, IL-8, TNF-α, eotaxins, and IFN-γ) (69–75). These mediators can recruit and directly activate MCs and leukocytes. Moreover, MCs can

influence biological responses through the production of multifunctional cytokines and enzymes (76–78). Evidence suggests that metalloproteinase (MMP9 in particular), leukotrienes (LT), heparin and platelet activating factor (PAF) derived from MCs also play a role in the inflammatory process during blister formation (67). Tryptase is a specific proteolytic enzyme synthesized and stored in MCs and released by MCs when activated by various stimulating factors. Tryptase, therefore, is considered a reliable marker for the presence of MCs (79). A previous study showed that tryptase levels in BP blister fluid were increased compared with the respective sera and significantly correlated with several cytokines/chemokines (IL-3, IL-4, IL-5, IL-6, IL-7, IL-8, and RANTES), VEGF, and sICAM-1. Most importantly, the blister fluid tryptase levels were also positively correlated with titers of autoantibodies against basement membrane zone antigens (80), which relates to the severity of the disease. Increased levels of cytokines (including IL-1β, IL-5, IL-6, IL-10, IL-15, and TNF-α) and chemokines (such as CCL2, CCL5, CCL11, CCL13, and CCL18, and IL-8) were identified in serum samples and blister fluids of patients with BP, and some of these mediators parallel disease activity (81). Bieber et al. investigated serum parameters related to activation of different inflammatory cells and found higher serum concentrations of MCs tryptase during ongoing disease. The serum levels of MCs tryptase significantly decreased at the time of clinical remission of the patients. In addition, serum concentrations of MCs tryptase were significantly associated with levels of circulating anti-BP180 autoantibodies (82). These data suggested that increased concentrations of MCs tryptase in BP blister fluids and/or serum partly correlate with cytokines, autoantibodies, and clinical disease severity in BP patients.

BP180-specific IgG autoantibodies are the most abundant immunoglobulin isotype; however, IgE autoantibodies with the same or similar epitope specificity are also present in about 70–90% of BP patients (83, 84). It has been speculated that IgE autoantibody–mediated activation of MCs in the skin may be involved in the development of certain clinical symptoms typical of BP, such as urticarial plaques, dermal edema, and eosinophilic inflammation. Dimson et al. found IgE-coated MCs in the perilesional skin of the BP patients, and BP180 peptides were co-localized on these MCs, suggesting that BP180-specific IgE that bind to the surface of MCs through IgE receptors, when interacting with BP180 peptides, result in MC degranulation. Moreover, basophils obtained from untreated BP patients stimulated with recombinant BP180NC16A released significantly higher histamine compared to NC16-stimulated basophils from normal control or from treated BP patients (83). In addition, Freire et al. reported that IgE co-localized with MCs in the perilesional skin of BP patients, and IgE-BP180 complexes could activate MCs *via* the high-affinity IgE receptor (FcεRI), conceivably triggering MC degranulation-mediated events resulting in tissue inflammation (85).

Omalizumab is a recombinant humanized monoclonal antibody that inhibits the binding of IgE to FcεRI on the surface of MCs and basophils. Patients with BP treated with omalizumab showed reduced disease severity including decreased itching and blister count, reduced urticarial plaques, and reduced eosinophilic inflammation (86, 87). Together, these clinical research and clinical trial data suggest that IgE autoantibodies in BP patients are involved in BP development likely through FcεRI-induced degranulation of MCs and basophils. However, pathogenic anti-BP180 IgE autoantibodies could also act on eosinophils in BP tissue injury since eosinophils express IgE receptors and are predominant infiltrating immune cells in BP (41).

ANIMAL MODELS OF BP

Bullous pemphigoid autoantibodies were thought to be responsible for blister formation in BP; however, passive transfer of IgG autoantibodies from BP patients could not induce a BP-like disease in animals (88, 89). It turned out that BP autoantibodies reacting with NC16A domain that harbors immunodominant and potentially pathogenic epitopes fail to cross-react with mouse BP180; therefore, BP IgG autoantibodies cannot be tested for pathogenicity in a conventional passive transfer mouse model. In 1993, Liu et al. (90) subcloned a segment of the murine BP180 protein homologous with the human BP180 NC16A (mBP180 NC14A), generated rabbit polyclonal antibodies against mBP180 NC14A, and administrated the purified rabbit anti-mBP180 IgG intradermally or intraperitoneally into neonatal BALB/c mice. This experimental BP model reproduced all of the key clinical, histological, and immunopathological features of BP, including deposition of rabbit anti-mBP180 IgG and mouse complement C3 at dermal–epidermal junction, infiltration of inflammatory cells, and subepidermal blistering (90) (**Figure 2**). Anti-BP180 IgG-induced BP blistering required complement activation and neutrophil recruitment (91, 92). Subsequently, BP serum-purified IgG autoantibodies against BP180 or NC16A domain were also demonstrated to be pathogenic in BP180 humanized mouse models (93, 94).

BP180-specific IgE autoantibodies purified from serum of BP patients when passively transferred into human skin grafted onto athymic nude mice induced skin lesions that recapitulated the initial phase of disease. The features of the early phase of the disease are characterized by increased plaques and MC degranulation in comparison with injection of normal control human IgE (95). Lesional skin of the anti-BP180 IgE-injected mice also exhibited infiltration of neutrophils and eosinophils (95). However, it remains to be determined whether the pathogenic activity of anti-BP180 IgE depends on eosinophils, MCs, or both.

ROLE OF MCs IN EXPERIMENTAL BP

To determine whether MCs were involved in experimental BP, Chen et al. (19) demonstrated that wild-type MC-sufficient mice administrated intradermally with pathogenic anti-mBP180 IgG developed BP disease with extensive MC degranulation in the upper dermis, which preceded infiltration of neutrophils and subsequent dermal–epidermal separation. In contrast, MC-deficient $Kit^{W/W\text{-}v}$ and $Mgf^{Sl/Sl\text{-}d}$ mice failed to develop BP (19). Moreover, these MC-deficient mice reconstituted with wild-type bone marrow-derived MCs, and polymorphonuclear leukocytes from these MC-deficient mice or by intradermal injection of IL-8 (a neutrophil chemoattractant) became susceptible to experimental

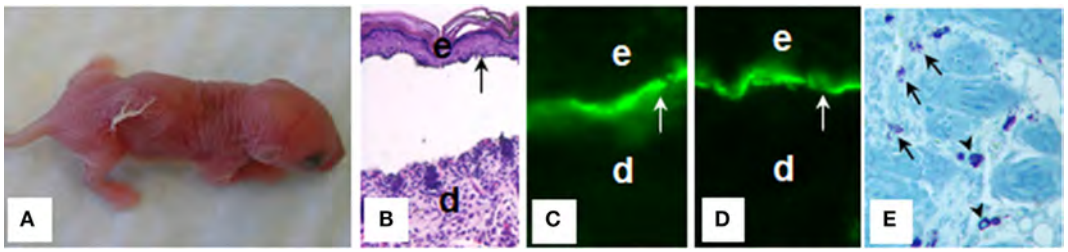

FIGURE 2 | Mouse bullous pemphigoid. The anti-BP180 IgG induce extensive blistering disease in neonatal B6 mice clinically **(A)** and histologically **(B)**. The skin of these animals shows linear deposition of anti-BP180 IgG **(C)** and murine C3 **(D)** at the BMZ, as determined by direct IF. Toluidine blue staining shows resting and degranulating mast cells in the dermis **(E)**. d, dermis; e, epidermis; v, vesicle; arrow, the BMZ. Original magnification, 200× for panels **(B–D)**, 400× for panel **(E)**. **(E)** Arrows for degranulating mast cells, and arrow heads for normal resting mast cells.

BP (19). Blocking MC degranulation by treating MC-sufficient mice with an MC degranulation inhibitor also significantly reduced disease phenotype (19).

To determine the functional relationship between MCs and neutrophils, Chen et al. found that anti-BP180 antibody-induced neutrophil infiltration depends mainly on MCs in experimental BP (19). Without MCs, $Kit^{W/W\text{-}v}$ and $Mgf^{Sl/Sl\text{-}d}$ mice injected with pathogenic IgG show about 70% reduction of infiltrating neutrophils in the skin (96). Further examination of the experimental BP model also implicated macrophages in anti-BP180 IgG-triggered neutrophil infiltration in mice, and that macrophage-mediated neutrophil infiltration depends on MC activation (96). The findings that neutrophil recruitment is not completely impaired in MC-deficient mice in experimental BP suggest that at least two neutrophil recruitment pathways could exist: MC-dependent and MC-independent (96). Nevertheless, these data suggest a major role of MCs in infiltration of neutrophils into the dermis in this animal model setting.

Mast cells express surface receptors that directly bind the cleaved products of the activated complement cascade (97). Skin MCs express the C5aR (98), and upon the molecular interaction of C5a and C5aR, MCs degranulate, releasing several pro-inflammatory cytokines including TNF-α, IL-1, IL-6, and GM-CSF (99). Moreover, human C3a and C5a could degranulate MCs *in vitro* to release histamine and tryptase. Heimbach et al. (100) demonstrated that interaction of C5a–C5aR on MCs activated the p38 MAPK pathway that trigger MC degranulation and subsequent tissue injury and blister formation.

Mast cells store proteases in large quantities in the secretory granules, and these fully functional enzymes are a major class of inflammatory mediators (101, 102). Human cutaneous MCs contain a single chymase, and mouse MC protease-4 (mMCP-4) has been generally recognized as the likely homolog of the human chymase (103–105). Importantly, mMCP-4 can activate MMP-9, a key proteolytic enzyme for tissue injury in experimental BP (106). Interestingly, $mMCP\text{-}4^{-/-}$ mice are resistant to anti-BP180 IgG-induced experimental BP (107). In experimental BP, mMCP-4 activates MMP-9 and directly cleaves BP180. mMCP-4, MMP-9, and other proteolytic enzymes work together to degrade BP180 and other hemidesmosomal proteins and proteins in extracellular matrix of the BMZ (107), leading to clinical and histological BP-like blistering.

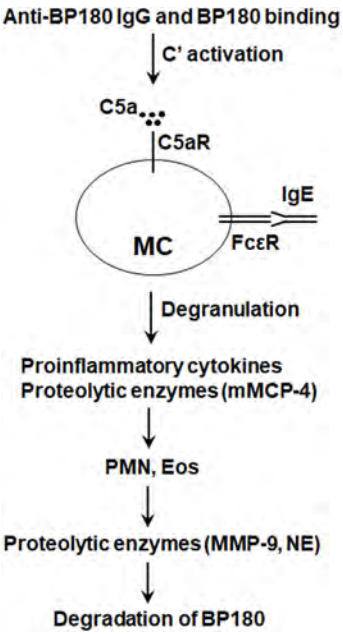

FIGURE 3 | Proposed role of mast cells (MCs) in bullous pemphigoid (BP). Anti-BP180 IgG binding to BP180 on the surface of basal keratinocytes activates the complement (C), generating C5a. C5a acts on C5a receptor (C5aR) to cause MCs to degranulate and release pro-inflammatory cytokines/chemokines (e.g., TNFα) and proteolytic enzymes including mouse MC protease-4 (mMCP-4). Anti-BP180 IgE could also activate MCs. The released pro-inflammatory mediators interact with local cells to recruit neutrophils (PMN) and eosinophils (Eos). Infiltrating PMN and Eos, upon activation through interactions between immobilized anti-BP180 IgG/IgE and FcγR/FcεR, release neutrophil elastase (NE), MMP-9, and other proteolytic enzymes. mMCP-4 activates MMP-9 and also directly cleaves BP180 and other BP180-associated proteins in concert with MMP-9 and NE, resulting in subepidermal blistering.

Taken together, results of these studies using MC-deficient and C5aR and mMCP-4 knockout mice implicate a pathogenic role of MCs in BP (**Figure 3**). However, since the studies on the role of MCs in anti-BP180 IgG-induced experimental BP have been performed only in MC-deficient $Kit^{W/W\text{-}v}$ and $Mgf^{Sl/Sl\text{-}d}$ mice, KIT-independent MC-specific deletion mouse strains need to be tested to confirm or clarify the involvement of MCs in experimental BP.

ROLE OF MCs IN EPIDERMAL BULLOSA ACQUISITA (EBA)

Epidermal bullosa acquisita is another autoimmune subepidermal blistering skin disease caused by autoantibodies against collagen VII (108). Experimental EBA can be induced by passive transfer of anticollagen VII IgG (109, 110). Immunopathogenically, experimental EBA shares many key features with experimental BP such as their dependency on complement, C5a-C5aR signaling, and neutrophils (109, 111). However, anticollagen VII IgG causes similar disease severity in both wild-type control and MC-deficient $Kit^{W/W\text{-}v}$ mice (112). KIT-independent MC-specific deletion mice are also not protected from experimental EBA (112). These studies demonstrate that MCs do not contribute to experimental EBA, further emphasizing a need to revisit the role of MCs in experimental BP using KIT-independent MC-specific deletion strains.

CONCLUDING REMARKS

We presented several lines of BP animal model evidence, together with clinical observations, implicating that MCs are likely to be involved in the immunopathogenesis of BP. The role of MCs in experimental BP, however, was investigated exclusively in KIT-dependent MC-deficient mice. Based on the observed discrepancies in different MC-deficient models of EAE, RA, and EBA, it is necessary to perform anti-BP180 IgG-induced BP studies in KIT-independent MC-specific deletion strains to clarify whether MCs play a role in BP.

Bullous pemphigoid patients also have anti-BP180 IgE autoantibodies, which are involved in tissue injury (95); therefore, a potential role of MCs in anti-BP180 IgE-induced BP should be determined in both KIT-dependent and KIT-independent MC-deficient strains. Future studies could also investigate whether and how MCs interact with anti-BP180 IgG, anti-BP180 IgE, and eosinophils during disease development. Giving the fact that MCs have a variety of immunomodulatory activities (14), MC contribution to BP could be multifaceted. Advanced tools need to be developed to clarify and fully appreciate the contribution of MCs to BP and help uncover new therapeutic targets for this potentially fatal skin autoimmune disease.

AUTHOR CONTRIBUTIONS

HF, YZ, NL, GW, and ZL wrote the manuscript; HF, YZ, and NL prepared the figures.

ACKNOWLEDGMENTS

We thank our colleagues and collaborator for their support. We apologize for not mentioning and citing some related studies due to space limitations. This work was supported by the National Institutes of Health (grants R01 AI40768 and R01 AR070276 to ZL) and National Natural Science Foundation of China (no. 81220108016 to GW).

REFERENCES

1. Stone KD, Prussin C, Metcalfe DD. IgE, mast cells, basophils, and eosinophils. *J Allergy Clin Immunol* (2010) 125(2 Suppl 2):S73–80. doi:10.1016/j.jaci.2009.11.017
2. Maurer M. Urticaria and angioedema. *Chem Immunol Allergy* (2014) 100:101–4. doi:10.1159/000358614
3. Sayed BA, Christy A, Quirion MR, Brown MA. The master switch: the role of mast cells in autoimmunity and tolerance. *Annu Rev Immunol* (2008) 26:705–39. doi:10.1146/annurev.immunol.26.021607.090320
4. Rivera J, Fierro NA, Olivera A, Suzuki R. New insights on mast cell activation via the high affinity receptor for IgE. *Adv Immunol* (2008) 98:85–120. doi:10.1016/S0065-2776(08)00403-3
5. Arthur G, Bradding P. New developments in mast cell biology: clinical implications. *Chest* (2016) 150(3):680–93. doi:10.1016/j.chest.2016.06.009
6. Young JD, Liu CC, Butler G, Cohn ZA, Galli SJ. Identification, purification, and characterization of a mast cell-associated cytolytic factor related to tumor necrosis factor. *Proc Natl Acad Sci U S A* (1987) 84(24):9175–9. doi:10.1073/pnas.84.24.9175
7. Kalesnikoff J, Galli SJ. New developments in mast cell biology. *Nat Immunol* (2008) 9(11):1215–23. doi:10.1038/ni.f.216
8. Nakae S, Suto H, Iikura M, Kakurai M, Sedgwick JD, Tsai M, et al. Mast cells enhance T cell activation: importance of mast cell costimulatory molecules and secreted TNF. *J Immunol* (2006) 176(4):2238–48. doi:10.4049/jimmunol.176.4.2238
9. Harmon B, Chylek LA, Liu Y, Mitra ED, Mahajan A, Saada EA, et al. Timescale separation of positive and negative signaling creates history-dependent responses to IgE receptor stimulation. *Sci Rep* (2017) 7(1):15586. doi:10.1038/s41598-017-15568-2
10. Muto Y, Wang Z, Vanderberghe M, Two A, Gallo RL, Di Nardo A. Mast cells are key mediators of cathelicidin-initiated skin inflammation in rosacea. *J Invest Dermatol* (2014) 134(11):2728–36. doi:10.1038/jid.2014.222
11. Kovanen PT. Mast cells and degradation of pericellular and extracellular matrices: potential contributions to erosion, rupture and intraplaque haemorrhage of atherosclerotic plaques. *Biochem Soc Trans* (2007) 35(Pt 5):857–61. doi:10.1042/BST0350857
12. Gounaris E, Erdman SE, Restaino C, Gurish MF, Friend DS, Gounari F, et al. Mast cells are an essential hematopoietic component for polyp development. *Proc Natl Acad Sci U S A* (2007) 104(50):19977–82. doi:10.1073/pnas.0704620104
13. Wasiuk A, de Vries VC, Hartmann K, Roers A, Noelle RJ. Mast cells as regulators of adaptive immunity to tumours. *Clin Exp Immunol* (2009) 155(2):140–6. doi:10.1111/j.1365-2249.2008.03840.x
14. Galli SJ, Grimbaldeston M, Tsai M. Immunomodulatory mast cells: negative, as well as positive, regulators of immunity. *Nat Rev Immunol* (2008) 8(6):478–86. doi:10.1038/nri2327
15. Yu X, Kasprick A, Petersen F. Revisiting the role of mast cells in autoimmunity. *Autoimmun Rev* (2015) 14(9):751–9. doi:10.1016/j.autrev.2015.04.008
16. Steinman L. Multiple sclerosis: a two-stage disease. *Nat Immunol* (2001) 2(9):762–4. doi:10.1038/ni0901-762
17. Brown MA, Tanzola MB, Robbie-Ryan M. Mechanisms underlying mast cell influence on EAE disease course. *Mol Immunol* (2002) 38(16–18):1373–8. doi:10.1016/S0161-5890(02)00091-3
18. Ji H, Ohmura K, Mahmood U, Lee DM, Hofhuis FMA, Boackle SA, et al. Arthritis critically dependent on innate immune system players. *Immunity* (2002) 16(2):157–68. doi:10.1016/S1074-7613(02)00275-3
19. Chen R, Ning G, Zhao ML, Fleming MG, Diaz LA, Werb Z, et al. Mast cells play a key role in neutrophil recruitment in experimental bullous pemphigoid. *J Clin Invest* (2001) 108(8):1151–8. doi:10.1172/JCI11494
20. McFarland HF, Martin R. Multiple sclerosis: a complicated picture of autoimmunity. *Nat Immunol* (2007) 8(9):913–9. doi:10.1038/ni1507
21. Couturier N, Zappulla JP, Lauwers-Cances V, Uro-Coste E, Delisle MB, Clanet M, et al. Mast cell transcripts are increased within and outside multiple sclerosis lesions. *J Neuroimmunol* (2008) 195(1–2):176–85. doi:10.1016/j.jneuroim.2008.01.017
22. Kruger PG, Bo L, Myhr KM, Karlsen AE, Taule A, Nyland HI, et al. Mast cells and multiple sclerosis: a light and electron microscopic study of mast cells in multiple sclerosis emphasizing staining procedures. *Acta Neurol Scand* (1990) 81(1):31–6. doi:10.1111/j.1600-0404.1990.tb00927.x

23. Toms R, Weiner HL, Johnson D. Identification of IgE-positive cells and mast cells in frozen sections of multiple sclerosis brains. *J Neuroimmunol* (1990) 30(2–3):169–77. doi:10.1016/0165-5728(90)90101-R
24. Rozniecki JJ, Hauser SL, Stein M, Lincoln R, Theoharides TC. Elevated mast cell tryptase in cerebrospinal fluid of multiple sclerosis patients. *Ann Neurol* (1995) 37(1):63–6. doi:10.1002/ana.410370112
25. Rangachari M, Kuchroo VK. Using EAE to better understand principles of immune function and autoimmune pathology. *J Autoimmun* (2013) 45:31–9. doi:10.1016/j.jaut.2013.06.008
26. Aletaha D, Neogi T, Silman AJ, Funovits J, Felson DT, Bingham CO III, et al. 2010 rheumatoid arthritis classification criteria: an American college of rheumatology/European league against rheumatism collaborative initiative. *Arthritis Rheum* (2010) 62(9):2569–81. doi:10.1002/art.27584
27. Bridges AJ, Malone DG, Jicinsky J, Chen M, Ory P, Engber W, et al. Human synovial mast cell involvement in rheumatoid arthritis and osteoarthritis. Relationship to disease type, clinical activity, and antirheumatic therapy. *Arthritis Rheum* (1991) 34(9):1116–24. doi:10.1002/art.1780340907
28. Gotis-Graham I, Smith MD, Parker A, McNeil HP. Synovial mast cell responses during clinical improvement in early rheumatoid arthritis. *Ann Rheum Dis* (1998) 57(11):664–71. doi:10.1136/ard.57.11.664
29. Nakano S, Mishiro T, Takahara S, Yokoi H, Hamada D, Yukata K, et al. Distinct expression of mast cell tryptase and protease activated receptor-2 in synovia of rheumatoid arthritis and osteoarthritis. *Clin Rheumatol* (2007) 26(8): 1284–92. doi:10.1007/s10067-006-0495-8
30. Kouskoff V, Korganow AS, Duchatelle V, Degott C, Benoist C, Mathis D. Organ-specific disease provoked by systemic autoimmunity. *Cell* (1996) 87(5):811–22. doi:10.1016/S0092-8674(00)81989-3
31. Rivellese F, Nerviani A, Rossi FW, Marone G, Matucci-Cerinic M, de Paulis A, et al. Mast cells in rheumatoid arthritis: friends or foes? *Autoimmun Rev* (2017) 16(6):557–63. doi:10.1016/j.autrev.2017.04.001
32. Secor VH, Secor WE, Gutekunst CA, Brown MA. Mast cells are essential for early onset and severe disease in a murine model of multiple sclerosis. *J Exp Med* (2000) 191(5):813–22. doi:10.1084/jem.191.5.813
33. Lee DM, Friend DS, Gurish MF, Benoist C, Mathis D, Brenner MB. Mast cells: a cellular link between autoantibodies and inflammatory arthritis. *Science* (2002) 297(5587):1689–92. doi:10.1126/science.1073176
34. Feyerabend TB, Weiser A, Tietz A, Stassen M, Harris N, Kopf M, et al. Cre-mediated cell ablation contests mast cell contribution in models of antibody- and T cell-mediated autoimmunity. *Immunity* (2011) 35(5):832–44. doi:10.1016/j.immuni.2011.09.015
35. Schmidt E, Zillikens D. Pemphigoid diseases. *Lancet* (2013) 381(9863):320–32. doi:10.1016/S0140-6736(12)61140-4
36. Amber KT, Murrell DF, Schmidt E, Joly P, Borradori L. Autoimmune subepidermal bullous diseases of the skin and mucosae: clinical features, diagnosis, and management. *Clin Rev Allergy Immunol* (2017) 54(1):26–51. doi:10.1007/s12016-017-8633-4
37. Walsh SRA, Hogg D, Mydlarski PR. Bullous pemphigoid: from bench to bedside. *Drugs* (2005) 65(7):905–26. doi:10.2165/00003495-200565070-00002
38. Di Zenzo G, Della Torre R, Zambruno G, Borradori L. Bullous pemphigoid: from the clinic to the bench. *Clin Dermatol* (2012) 30(1):3–16. doi:10.1016/j.clindermatol.2011.03.005
39. della Torre R, Combescure C, Cortes B, Marazza G, Beltraminelli H, Naldi L, et al. Clinical presentation and diagnostic delay in bullous pemphigoid: a prospective nationwide cohort. *Br J Dermatol* (2012) 167(5):1111–7. doi:10.1111/j.1365-2133.2012.11108.x
40. Joly P, Baricault S, Sparsa A, Bernard P, Bedane C, Duvert-Lehembre S, et al. Incidence and mortality of bullous pemphigoid in France. *J Invest Dermatol* (2012) 132(8):1998–2004. doi:10.1038/jid.2012.35
41. Kneisel A, Hertl M. Autoimmune bullous skin diseases. Part 2: diagnosis and therapy. *J Dtsch Dermatol Ges* (2011) 9(11):927–47. doi:10.1111/j.1610-0387.2011.07809.x
42. Nishie W. Update on the pathogenesis of bullous pemphigoid: an autoantibody-mediated blistering disease targeting collagen XVII. *J Dermatol Sci* (2014) 73(3):179–86. doi:10.1016/j.jdermsci.2013.12.001
43. Stanley JR, Hawley-Nelson P, Yuspa SH, Shevach EM, Katz SI. Characterization of bullous pemphigoid antigen: a unique basement membrane protein of stratified squamous epithelia. *Cell* (1981) 24(3):897–903. doi:10.1016/0092-8674(81)90115-X
44. Labib RS, Anhalt GJ, Patel HP, Mutasim DF, Diaz LA. Molecular heterogeneity of the bullous pemphigoid antigens as detected by immunoblotting. *J Immunol* (1986) 136(4):1231–5.
45. Diaz LA, Ratrie H III, Saunders WS, Futamura S, Squiquera HL, Anhalt GJ, et al. Isolation of a human epidermal cDNA corresponding to the 180-kD autoantigen recognized by bullous pemphigoid and herpes gestationis sera. Immunolocalization of this protein to the hemidesmosome. *J Clin Invest* (1990) 86(4):1088–94. doi:10.1172/JCI114812
46. Giudice GJ, Emery DJ, Zelickson BD, Anhalt GJ, Liu Z, Diaz LA. Bullous pemphigoid and herpes gestationis autoantibodies recognize a common non-collagenous site on the BP180 ectodomain. *J Immunol* (1993) 151(10):5742–50. doi:10.1016/0923-1811(93)90940-Q
47. Ishiura N, Fujimoto M, Watanabe R, Nakashima H, Kuwano Y, Yazawa N, et al. Serum levels of IgE anti-BP180 and anti-BP230 autoantibodies in patients with bullous pemphigoid. *J Dermatol Sci* (2008) 49(2):153–61. doi:10.1016/j.jdermsci.2007.08.008
48. Perriard J, Jaunin F, Favre B, Budinger L, Hertl M, Saurat JH, et al. IgG autoantibodies from bullous pemphigoid (BP) patients bind antigenic sites on both the extracellular and the intracellular domains of the BP antigen 180. *J Invest Dermatol* (1999) 112(2):141–7. doi:10.1046/j.1523-1747.1999.00497.x
49. Hofmann S, Thoma-Uszynski S, Hunziker T, Bernard P, Koebnick C, Stauber A, et al. Severity and phenotype of bullous pemphigoid relate to autoantibody profile against the NH2- and COOH-terminal regions of the BP180 ectodomain. *J Invest Dermatol* (2002) 119(5):1065–73. doi:10.1046/j.1523-1747.2002.19529.x
50. Di Zenzo G, Thoma-Uszynski S, Fontao L, Calabresi V, Hofmann SC, Hellmark T, et al. Multicenter prospective study of the humoral autoimmune response in bullous pemphigoid. *Clin Immunol* (2008) 128(3):415–26. doi:10.1016/j.clim.2008.04.012
51. Kromminga A, Sitaru C, Hagel C, Herzog S, Zillikens D. Development of an ELISA for the detection of autoantibodies to BP230. *Clin Immunol* (2004) 111(1):146–52. doi:10.1016/j.clim.2003.12.007
52. Messingham KN, Srikantha R, DeGueme AM, Fairley JA. FcR-independent effects of IgE and IgG autoantibodies in bullous pemphigoid. *J Immunol* (2011) 187(1):553–60. doi:10.4049/jimmunol.1001753
53. Delaporte E, Dubost-Brama A, Ghohestani R, Nicolas JF, Neyrinck JL, Bergoend H, et al. IgE autoantibodies directed against the major bullous pemphigoid antigen in patients with a severe form of pemphigoid. *J Immunol* (1996) 157(8):3642–7.
54. Banfield CC, Wojnarowska F, Allen J, George S, Venning VA, Welsh KI. The association of HLA-DQ7 with bullous pemphigoid is restricted to men. *Br J Dermatol* (1998) 138(6):1085–90. doi:10.1046/j.1365-2133.1998.02350.x
55. Budinger L, Borradori L, Yee C, Eming R, Ferencik S, Grosse-Wilde H, et al. Identification and characterization of autoreactive T cell responses to bullous pemphigoid antigen 2 in patients and healthy controls. *J Clin Invest* (1998) 102(12):2082–9. doi:10.1172/JCI3335
56. Okazaki A, Miyagawa S, Yamashina Y, Kitamura W, Shirai T. Polymorphisms of HLA-DR and -DQ genes in Japanese patients with bullous pemphigoid. *J Dermatol* (2000) 27(3):149–56. doi:10.1111/j.1346-8138.2000.tb02141.x
57. Gao XH, Winsey S, Li G, Barnardo M, Zhu XJ, Chen HD, et al. HLA-DR and DQ polymorphisms in bullous pemphigoid from northern China. *Clin Exp Dermatol* (2002) 27(4):319–21. doi:10.1046/j.1365-2230.2002.01037.x
58. Esmaili N, Mortazavi H, Chams-Davatchi C, Daneshpazhooh M, Damavandi MR, Aryanian Z, et al. Association between HLA-DQB1*03:01 and bullous pemphigoid in Iranian patients. *Iran J Immunol* (2013) 10(1):1–9.
59. Delgado JC, Turbay D, Yunis EJ, Yunis JJ, Morton ED, Bhol K, et al. A common major histocompatibility complex class II allele HLA-DQB1* 0301 is present in clinical variants of pemphigoid. *Proc Natl Acad Sci U S A* (1996) 93(16):8569–71. doi:10.1073/pnas.93.16.8569
60. Chan LS, Hammerberg C, Cooper KD. Significantly increased occurrence of HLA-DQB1*0301 allele in patients with ocular cicatricial pemphigoid. *J Invest Dermatol* (1997) 108(2):129–32. doi:10.1111/1523-1747.ep12332352
61. Setterfield J, Theron J, Vaughan RW, Welsh KI, Mallon E, Wojnarowska F, et al. Mucous membrane pemphigoid: HLA-DQB1*0301 is associated with all clinical sites of involvement and may be linked to antibasement membrane IgG production. *Br J Dermatol* (2001) 145(3):406–14. doi:10.1046/j.1365-2133.2001.04380.x
62. Thoma-Uszynski S, Uter W, Schwietzke S, Schuler G, Borradori L, Hertl M. Autoreactive T and B cells from bullous pemphigoid (BP) patients recognize

epitopes clustered in distinct regions of BP180 and BP230. *J Immunol* (2006) 176(3):2015–23. doi:10.4049/jimmunol.176.3.2015
63. Hertl M, Eming R, Veldman C. T cell control in autoimmune bullous skin disorders. *J Clin Invest* (2006) 116(5):1159–66. doi:10.1172/JCI28547
64. Lin MS, Fu CL, Giudice GJ, Olague-Marchan M, Lazaro AM, Stastny P, et al. Epitopes targeted by bullous pemphigoid T lymphocytes and autoantibodies map to the same sites on the bullous pemphigoid 180 ectodomain. *J Invest Dermatol* (2000) 115(6):955–61. doi:10.1046/j.1523-1747.2000.00153.x
65. Thoma-Uszynski S, Uter W, Schwietzke S, Hofmann SC, Hunziker T, Bernard P, et al. BP230- and BP180-specific auto-antibodies in bullous pemphigoid. *J Invest Dermatol* (2004) 122(6):1413–22. doi:10.1111/j.0022-202X.2004.22603.x
66. Li Q, Liu Z, Dang E, Jin L, He Z, Yang L, et al. Follicular helper T cells (Tfh) and IL-21 involvement in the pathogenesis of bullous pemphigoid. *PLoS One* (2013) 8(7):e68145. doi:10.1371/journal.pone.0068145
67. Wintroub BU, Mihm MCJ, Goetzl EJ, Soter NA, Austen KF. Morphologic and functional evidence for release of mast-cell products in bullous pemphigoid. *N Engl J Med* (1978) 298(8):417–21. doi:10.1056/NEJM197802232980803
68. Dvorak AM, Mihm MCJ, Osage JE, Kwan TH, Austen KF, Wintroub BU. Bullous pemphigoid, an ultrastructural study of the inflammatory response: eosinophil, basophil and mast cell granule changes in multiple biopsies from one patient. *J Invest Dermatol* (1982) 78(2):91–101. doi:10.1111/1523-1747.ep12505711
69. Baba T, Sonozaki H, Seki K, Uchiyama M, Ikesawa Y, Toriisu M. An eosinophil chemotactic factor present in blister fluids of bullous pemphigoid patients. *J Immunol* (1976) 116(1):112–6.
70. Endo H, Iwamoto I, Fujita M, Okamoto S, Yoshida S. Increased immunoreactive interleukin-5 levels in blister fluids of bullous pemphigoid. *Arch Dermatol Res* (1992) 284(5):312–4. doi:10.1007/BF00372588
71. Takiguchi Y, Kamiyama O, Saito E, Nagao S, Kaneko F, Minagawa T. Cell-mediated immune reaction in the mechanism of blister formation in bullous pemphigoid. *Dermatologica* (1989) 179(Suppl):137. doi:10.1159/000248478
72. Katayama I, Doi T, Nishioka K. High histamine level in the blister fluid of bullous pemphigoid. *Arch Dermatol Res* (1984) 276(2):126–7. doi:10.1007/BF00511070
73. Kawana S, Ueno A, Nishiyama S. Increased levels of immunoreactive leukotriene B4 in blister fluids of bullous pemphigoid patients and effects of a selective 5-lipoxygenase inhibitor on experimental skin lesions. *Acta Derm Venereol* (1990) 70(4):281–5.
74. Schmidt E, Ambach A, Bastian B, Brocker EB, Zillikens D. Elevated levels of interleukin-8 in blister fluid of bullous pemphigoid compared with suction blisters of healthy control subjects. *J Am Acad Dermatol* (1996) 34(2 Pt 1): 310–2. doi:10.1016/S0190-9622(96)80146-0
75. Grando SA, Glukhenky BT, Drannik GN, Epshtein EV, Kostromin AP, Korostash TA. Mediators of inflammation in blister fluids from patients with pemphigus vulgaris and bullous pemphigoid. *Arch Dermatol* (1989) 125(7):925–30. doi:10.1001/archderm.125.7.925
76. Galli SJ. New concepts about the mast cell. *N Engl J Med* (1993) 328(4):257–65. doi:10.1056/NEJM199301283280408
77. Galli SJ, Gordon JR, Wershil BK. Cytokine production by mast cells and basophils. *Curr Opin Immunol* (1991) 3(6):865–72. doi:10.1016/S0952-7915(05)80005-6
78. Zebrowska A, Wagrowska-Danilewicz M, Danilewicz M, Stasikowska-Kanicka O, Kulczycka-Siennicka L, Wozniacka A, et al. Mediators of mast cells in bullous pemphigoid and dermatitis herpetiformis. *Mediators Inflamm* (2014) 2014:936545. doi:10.1155/2014/936545
79. Castells MC, Irani AM, Schwartz LB. Evaluation of human peripheral blood leukocytes for mast cell tryptase. *J Immunol* (1987) 138(7):2184–9.
80. D'Auria L, Pietravalle M, Cordiali-Fei P, Ameglio F. Increased tryptase and myeloperoxidase levels in blister fluids of patients with bullous pemphigoid: correlations with cytokines, adhesion molecules and anti-basement membrane zone antibodies. *Exp Dermatol* (2000) 9(2):131–7. doi:10.1034/j.1600-0625.2000.009002131.x
81. Kasperkiewicz M, Zillikens D, Schmidt E. Pemphigoid diseases: pathogenesis, diagnosis, and treatment. *Autoimmunity* (2012) 45(1):55–70. doi:10.3109/08916934.2011.606447
82. Bieber K, Ernst AL, Tukaj S, Holtsche MM, Schmidt E, Zillikens D, et al. Analysis of serum markers of cellular immune activation in patients with bullous pemphigoid. *Exp Dermatol* (2017) 26(12):1248–52. doi:10.1111/exd.13382
83. Dimson OG, Giudice GJ, Fu CL, Van den Bergh F, Warren SJ, Janson MM, et al. Identification of a potential effector function for IgE autoantibodies in the organ-specific autoimmune disease bullous pemphigoid. *J Invest Dermatol* (2003) 120(5):784–8. doi:10.1046/j.1523-1747.2003.12146.x
84. Messingham KAN, Holahan HM, Fairley JA. Unraveling the significance of IgE autoantibodies in organ-specific autoimmunity: lessons learned from bullous pemphigoid. *Immunol Res* (2014) 59(1–3):273–8. doi:10.1007/s12026-014-8547-7
85. Freire PC, Munoz CH, Stingl G. IgE auto-reactivity in bullous pemphigoid: eosinophils and mast cells as major targets of pathogenic immune reactants. *Br J Dermatol* (2017) 177(6):1644–53. doi:10.1111/bjd.15924
86. Fairley JA, Baum CL, Brandt DS, Messingham KAN. Pathogenicity of IgE in autoimmunity: successful treatment of bullous pemphigoid with omalizumab. *J Allergy Clin Immunol* (2009) 123(3):704–5. doi:10.1016/j.jaci.2008.11.035
87. Yu KK, Crew AB, Messingham KAN, Fairley JA, Woodley DT. Omalizumab therapy for bullous pemphigoid. *J Am Acad Dermatol* (2014) 71(3):468–74. doi:10.1016/j.jaad.2014.04.053
88. Anhalt GJ, Diaz LA. Animal models for bullous pemphigoid. *Clin Dermatol* (1987) 5(1):117–25. doi:10.1016/0738-081X(87)90056-3
89. Sams WMJ, Gleich GJ. Failure to transfer bullous pemphigoid with serum from patients. *Proc Soc Exp Biol Med* (1971) 136(4):1027–31. doi:10.3181/00379727-136-35421
90. Liu Z, Diaz LA, Troy JL, Taylor AF, Emery DJ, Fairley JA, et al. A passive transfer model of the organ-specific autoimmune disease, bullous pemphigoid, using antibodies generated against the hemidesmosomal antigen, BP180. *J Clin Invest* (1993) 92(5):2480–8. doi:10.1172/JCI116856
91. Liu Z, Giudice GJ, Swartz SJ, Fairley JA, Till GO, Troy JL, et al. The role of complement in experimental bullous pemphigoid. *J Clin Invest* (1995) 95(4):1539–44. doi:10.1172/JCI117826
92. Liu Z, Giudice GJ, Zhou X, Swartz SJ, Troy JL, Fairley JA, et al. A major role for neutrophils in experimental bullous pemphigoid. *J Clin Invest* (1997) 100(5):1256–63. doi:10.1172/JCI119639
93. Nishie W, Sawamura D, Goto M, Ito K, Shibaki A, McMillan JR, et al. Humanization of autoantigen. *Nat Med* (2007) 13(3):378–83. doi:10.1038/nm1496
94. Liu Z, Sui W, Zhao M, Li Z, Li N, Thresher R, et al. Subepidermal blistering induced by human autoantibodies to BP180 requires innate immune players in a humanized bullous pemphigoid mouse model. *J Autoimmun* (2008) 31(4):331–8. doi:10.1016/j.jaut.2008.08.009
95. Fairley JA, Burnett CT, Fu CL, Larson DL, Fleming MG, Giudice GJ. A pathogenic role for IgE in autoimmunity: bullous pemphigoid IgE reproduces the early phase of lesion development in human skin grafted to nu/nu mice. *J Invest Dermatol* (2007) 127(11):2605–11. doi:10.1038/sj.jid.5700958
96. Chen R, Fairley JA, Zhao ML, Giudice GJ, Zillikens D, Diaz LA, et al. Macrophages, but not T and B lymphocytes, are critical for subepidermal blister formation in experimental bullous pemphigoid: macrophage-mediated neutrophil infiltration depends on mast cell activation. *J Immunol* (2002) 169(7):3987–92. doi:10.4049/jimmunol.169.7.3987
97. Brown MA, Hatfield JK. Mast cells are important modifiers of autoimmune disease: with so much evidence, why is there still controversy? *Front Immunol* (2012) 3:147. doi:10.3389/fimmu.2012.00147
98. Fureder W, Agis H, Willheim M, Bankl HC, Maier U, Kishi K, et al. Differential expression of complement receptors on human basophils and mast cells. Evidence for mast cell heterogeneity and CD88/C5aR expression on skin mast cells. *J Immunol* (1995) 155(6):3152–60.
99. Marshall JS. Mast-cell responses to pathogens. *Nat Rev Immunol* (2004) 4(10):787–99. doi:10.1038/nri1460
100. Heimbach L, Li Z, Berkowitz P, Zhao M, Li N, Rubenstein DS, et al. The C5a receptor on mast cells is critical for the autoimmune skin-blistering disease bullous pemphigoid. *J Biol Chem* (2011) 286(17):15003–9. doi:10.1074/jbc.M111.221036
101. Schwartz LB, Irani AM, Roller K, Castells MC, Schechter NM. Quantitation of histamine, tryptase, and chymase in dispersed human T and TC mast cells. *J Immunol* (1987) 138(8):2611–5.
102. Schwartz LB, Lewis RA, Austen KF. Tryptase from human pulmonary mast cells. Purification and characterization. *J Biol Chem* (1981) 256(22):11939–43.
103. Reynolds DS, Stevens RL, Lane WS, Carr MH, Austen KF, Serafin WE. Different mouse mast cell populations express various combinations of at

least six distinct mast cell serine proteases. *Proc Natl Acad Sci U S A* (1990) 87(8):3230–4. doi:10.1073/pnas.87.8.3230
104. Tchougounova E, Pejler G, Abrink M. The chymase, mouse mast cell protease 4, constitutes the major chymotrypsin-like activity in peritoneum and ear tissue. A role for mouse mast cell protease 4 in thrombin regulation and fibronectin turnover. *J Exp Med* (2003) 198(3):423–31. doi:10.1084/jem.20030671
105. Andersson MK, Karlson U, Hellman L. The extended cleavage specificity of the rodent beta-chymases rMCP-1 and mMCP-4 reveal major functional similarities to the human mast cell chymase. *Mol Immunol* (2008) 45(3):766–75. doi:10.1016/j.molimm.2007.06.360
106. Tchougounova E, Lundequist A, Fajardo I, Winberg JO, Abrink M, Pejler G. A key role for mast cell chymase in the activation of pro-matrix metalloprotease-9 and pro-matrix metalloprotease-2. *J Biol Chem* (2005) 280(10):9291–6. doi:10.1074/jbc.M410396200
107. Lin L, Bankaitis E, Heimbach L, Li N, Abrink M, Pejler G, et al. Dual targets for mouse mast cell protease-4 in mediating tissue damage in experimental bullous pemphigoid. *J Biol Chem* (2011) 286(43):37358–67. doi:10.1074/jbc.M111.272401
108. Chen M, Kim GH, Prakash L, Woodley DT. Epidermolysis bullosa acquisita: autoimmunity to anchoring fibril collagen. *Autoimmunity* (2012) 45(1): 91–101. doi:10.3109/08916934.2011.606450
109. Sitaru C, Mihai S, Otto C, Chiriac MT, Hausser I, Dotterweich B, et al. Induction of dermal-epidermal separation in mice by passive transfer of antibodies specific to type VII collagen. *J Clin Invest* (2005) 115(4):870–8. doi:10.1172/JCI21386
110. Woodley DT, Ram R, Doostan A, Bandyopadhyay P, Huang Y, Remington J, et al. Induction of epidermolysis bullosa acquisita in mice by passive transfer of autoantibodies from patients. *J Invest Dermatol* (2006) 126(6):1323–30. doi:10.1038/sj.jid.5700254
111. Mihai S, Chiriac MT, Takahashi K, Thurman JM, Holers VM, Zillikens D, et al. The alternative pathway of complement activation is critical for blister induction in experimental epidermolysis bullosa acquisita. *J Immunol* (2007) 178(10):6514–21. doi:10.4049/jimmunol.178.10.6514
112. Kasprick A, Yu X, Scholten J, Hartmann K, Pas HH, Zillikens D, et al. Conditional depletion of mast cells has no impact on the severity of experimental epidermolysis bullosa acquisita. *Eur J Immunol* (2015) 45(5):1462–70. doi:10.1002/eji.201444769

Conflict of Interest Statement: The authors declare that the research was conducted in the absence of any commercial or financial relationships that could be construed as a potential conflict of interest.

frontiers in Immunology

MINI REVIEW
published: 28 February 2018
doi: 10.3389/fimmu.2018.00386

The Role of Mast Cells in Autoimmune Bullous Dermatoses

*Xinhua Yu[1,2], Anika Kasprick[3], Karin Hartmann[4] and Frank Petersen[1,2]**

[1] Priority Area Asthma and Allergy, Research Center Borstel, Borstel, Germany, [2] Airway Research Center North (ARCN), German Center for Lung Research (DZL), Borstel, Germany, [3] Lübeck Institute of Experimental Dermatology, University of Lübeck, Lübeck, Germany, [4] Department of Dermatology, University of Lübeck, Lübeck, Germany

Skin mast cells (MCs), a resident immune cell type with broad regulatory capacity, play an important role in sensing danger signals as well as in the control of the local immune response. It is conceivable to expect that skin MCs regulate autoimmune response and are thus involved in autoimmune diseases in the skin, e.g., autoimmune bullous dermatoses (AIBD). Therefore, exploring the role of MCs in AIBD will improve our understanding of the disease pathogenesis and the search for novel therapeutic targets. Previously, in clinical studies with AIBD, particularly bullous pemphigoid, patients' samples have demonstrated that MCs are likely involved in the development of the diseases. However, using MC-deficient mice, studies with mouse models of AIBD have obtained inconclusive or even discrepant results. Therefore, it is necessary to clarify the observed discrepancies and to elucidate the role of MCs in AIBD. Here, in this review, we aim to clarify discrepant findings and finally elucidate the role of MCs in AIBD by summarizing and discussing the findings in both clinical and experimental studies.

Keywords: mast cells, autoimmune bullous dermatoses, mouse models, autoantibodies, pathogenesis

OPEN ACCESS

Edited by:
Falk Nimmerjahn, University of Erlangen-Nuremberg, Germany

Reviewed by:
Maja Wallberg, University of Cambridge, United Kingdom
Yisong Wan, University of North Carolina at Chapel Hill, United States

***Correspondence:**
Frank Petersen
fpetersen@fz-borstel.de

Specialty section:
This article was submitted to Immunological Tolerance and Regulation, a section of the journal Frontiers in Immunology

Received: *29 November 2017*
Accepted: *12 February 2018*
Published: *28 February 2018*

Citation:
Yu X, Kasprick A, Hartmann K and Petersen F (2018) The Role of Mast Cells in Autoimmune Bullous Dermatoses. Front. Immunol. 9:386. doi: 10.3389/fimmu.2018.00386

INTRODUCTION

Autoimmune bullous dermatoses (AIBD) are a group of autoimmune disorder affecting structure proteins in the skin which either mediate cell–cell or cell–matrix adhesion (1). Autoantibodies directed against these proteins impair the adhesion resulting in skin split formation and thus in a loss of the barrier integrity (1). Based on the location of split formation, AIBD can be categorized into two subgroups, pemphigus and pemphigoid disorders. Pemphigus diseases are intraepidermal blistering diseases caused by autoantibodies against adhesion molecules of the epidermis, such as desmoglein 1, desmoglein 3, envoplakin, and periplakin (1). In contrast to pemphigus, pemphigoid diseases are featured by subepidermal split formation (2).

Mast cells (MCs) originate from precursors of the hematopoietic lineage in the bone marrow (3). After homing to their target tissues, the precursors develop into mature MCs, a process regulated by various factors, including adhesion molecules and several cytokines. Among these, stem cell factor (SCF), a ligand of KIT, represents the most important one (4). MCs are distributed throughout almost all tissues and reside in proximity to nerves, blood, and lymphatic vessels (5). Besides the most prominent high-affinity receptor for IgE (FcεRI), MCs also express a plethora of other receptors, e.g., complement receptors, FcγR, and toll-like receptors enabling a response toward diverse stimuli (5, 6). Upon activation, MCs release a wide spectrum of products, including immediately secreted mediators like histamine and proteases, rapidly synthesized bioactive metabolites derived from arachidonic acid, such as prostaglandins and leukotrienes, and newly synthesized molecules *via* upregulated gene expression in response to stimulation, including most cytokines

and chemokines (5). Their wide tissue distribution and broad activating capacity designates MCs as major immune cells at the body interface regulating both innate and adaptive immunity (7, 8). These properties give rise to the question whether MCs have the ability to regulate immune responses against autoantigens and in skin autoimmune diseases like AIBD. This idea has been substantiated by clinical observations in which MC activation has been shown in some AIBD, and experimentally by employing MC-deficient mice in animal models of AIBD. In this mini-review article, we summarize and discuss clinical and experimental findings to clarify the role of MCs in these diseases.

MCs IN HUMAN AIBD

The first evidence indicating a role of MCs in AIBD can be traced back to 1978, when Wintroub et al. investigated bullous pemphigoid (BP) (9), the most common autoimmune blistering disease characterized by autoantibodies against the autoantigens BP180 (also named type XVII collagen, COL17) and BP230 (10). Besides autoantibodies and complement deposition at the basement-membrane zone, they observed a progressive MC degranulation and subsequent eosinophil infiltration in affected skin of BP patients (9). This MC degranulation was associated with elevated levels of MC-derived mediators and proteases, including eosinophil chemotactic factor, in bullous fluid suggesting for the first time a role of MCs in the pathogenesis of BP (9). Later, Dvorak et al. confirmed this hypothesis by investigating histological changes of clinical lesions in a BP patient during pathogenesis (11). They found that the clinical lesions were featured by a sequence of histopathologic events starting with MC degranulation and proceeding to infiltration of lymphocytes and later on eosinophils and basophils. The notion of a role of MC in BP was further strengthened when Delaporte et al. discovered that most patients express IgE autoantibodies which specifically activate MCs and eosinophils (12). In 2007, Fairley transferred total IgE isolated from BP patients or healthy controls into immune-deficient mice engrafted with human skin. Twenty-four hours after IgE injection, mice receiving BP IgE, but not control IgE, showed erythematous elevated plaques, MC activation, and dermal infiltrates of inflammatory cells. Furthermore, dermal-epidermal separation, a key clinical feature of BP, was also observed in recipient mice when a high dose of patient-derived IgE was transferred (13). This evidence from humanized mice demonstrates that IgE autoantibodies in BP patients are able to promote disease manifestation, further supporting a potential role of MCs in the pathogenesis of BP.

Besides BP, an involvement of MCs was also suggested in a range of other AIBD. For example, increased numbers of MCs have been detected in the skin of pemphigus vulgaris (PV) patients (14), in the conjunctiva of patients with ocular cicatricial pemphigoid (a subtype of MMP) (15), and in the lesional bullous skin of patients with linear IgA disease (LAD) (16). Moreover, activation of MCs has also been observed in some AIBD, including LAD (16), epidermolysis bullosa acquisita (EBA) (17), and PV (18). In addition, the presence of high concentrations of Dgs3-reactive IgE and intercellular IgE deposits in PV patients in the acute onset of the disease also indicates an involvement of MCs in PV (19).

MCs IN MOUSE MODELS OF AIBD

Experimental Models of Autoimmune Blistering Diseases

Animal models have been established for different AIBD, such as BP, EBA, and PV *via* diverse strategies namely immunization with autoantigen, transfer of autoantibodies or autoreactive lymphocytes, and genetic modification (20). These animal models have been extensively used for investigation of disease pathogenesis (20), including the role of MCs. Here, we highlight those animal models which have been used for studying the role of MCs in AIBD (17, 21).

In 1993, Liu and his colleagues for the first time established an antibody transfer-induced mouse model for BP. By immunizing rabbits with a segment of murine COL17A homologous to the human COL17A autoantibody reactive domain, the authors generated rabbit anti-murine COL17A IgG antibodies and injected them intradermally into neonatal mice. The recipient mice developed an inflammatory blistering disease at the injection site in 2 days, providing an acute and local antibody transfer-induced model of BP. Similarly, a local antibody transfer-induced mouse model of EBA can be established, when the rabbit anti-murine COL7 IgG are transferred into mice *via* intradermal injection. In this experimental setting, IgG are injected intradermally into the base of the ear of adult mice, and the mice develop skin symptoms at the injection site within 48 h after the antibody application (17, 22). Thus, these experimental settings present acute and local antibody transfer-induced mouse models of BP and EBA.

A systemic and more chronic type of EBA can be induced in mice by repeated subcutaneous injection of rabbit anti-murine COL7 IgG directed against the pathogenic epitope of the disease (23). 4 days after the antibody injection, first disease symptoms manifest in the skin of susceptible mice, including inflammatory cell infiltration and dermal–epidermal separation. Using a similar approach, Schulze et al. established a chronic and systemic antibody transfer-induced mouse model of BP by transfer of rabbit anti-murine COL17 IgG (24).

All antibody transfer-induced mouse models for BP and EBA are characterized by infiltration of inflammatory cells into the skin, antibody, and complement deposition, and dermal–epidermal separation, representing the hallmarks of the inflammatory type of human AIBDs and make these models ideal tools to investigate the role of MCs in these diseases.

MC-Deficient Mouse Strains

MC-deficient mouse strains are indispensable tools for investigating the role of MCs. So far, many MC-deficient strains have been reported, and those strains can be categorized into two groups according to the principle of the MC deficiency. The first group comprises KIT-dependent MC-deficient mice like WBB6F1-Kit$^{W/W\text{-}v}$, WCB6F1-Mgf$^{Sl/Sl\text{-}d}$, and C57BL/6-Kit$^{W\text{-}sh}$ mice. These mouse strains with an impaired Kit signaling due to genetic mutations affecting Kit signaling pathway. The KIT pathway is essential for the maturation and survival of MCs (4, 25). As a consequence, functional mutation within genes involved in the KIT receptor signaling could lead to the deficiency of MCs (26). However, since KIT is also expressed on many other cell

types, the KIT receptor signaling deficient strains demonstrate diverse abnormalities depending on the type of genetic defects (26). The second group contains KIT-independent MC-deficient mice which are selectively deficient in MCs independent of Kit mutations, and thus without altering other parts of the immune system, such as *Cpa3*$^{Cre/+}$ knock-in mice, Mcpt5^{Cre} transgenic mice, and Mas-TRECK mice. Among those MC-deficient mouse strains, WBB6F1-Kit$^{W/W-v}$, WCB6F1-Mgf$^{Sl/Sl-d}$, C57BL/6-Kit^{W-sh}, and Mcpt5^{Cre} transgenic mice have been used for examining the involvement of MCs in the development and progression of AIBD. An overview on the four MC-deficient mouse lines and their phenotypes are summarized in **Table 1**.

WBB6F1-Kit$^{W/W-v}$ Mice

The "white spotting" (*W*) locus is named after the pigment deficiency which is a result of mutations in the *Kit* gene affecting the function of melanocytes. The WBB6F1-Kit$^{W/W-v}$ mice are the hybrid form of WB/Re and C57BL/6 strains and carry two different types of mutations in the *W* locus, namely *W* and *W-v*. The *W* mutation, a point mutation altering a splicing site in the transcript, causes a loss of the transmembrane domain and thus hinders/impairs the cell surface expression of KIT (27). In contrast, *W-v*, a missense mutation within the KIT tyrosine kinase domain, considerably reduces the kinase activity (28). Consequently, the development of MCs in WBB6F1-Kit$^{W/W-v}$ mice is dramatically impaired resulting in less than 1% MCs compared to the MC-sufficient littermate controls (29). However, KIT-deficiency impairs many cell types and results e.g., in decreased numbers of neutrophils, basophils, platelets, intraepithelial TcRγδ lymphocytes, and some other KIT-associated abnormalities (29).

WCB6F1-Mgf$^{Sl/Sl-d}$ Mice

WCB6F1-Mgf$^{Sl/Sl-d}$ mice carry two loss of function mutations, Steel (*Sl*) and Steel-Dicke (*Sl-d*) in the *Scf* gene encoding the ligand of KIT (30). The *Sl* mutation contains DNA rearrangements which lead to dysregulation of expression of the *Scf* gene (31), while the *Sl-d* mutation encodes the SCF molecule lacking the transmembrane and cytoplasmic domain (32). Combination of the two mutations dramatically impairs the production or function of SCF, and thus leading to the deficiency in the KIT signaling. As a consequence, WCB6F1-Mgf$^{Sl/Sl-d}$ mice show a similar pattern of abnormalities to that of WBB6F1-Kit$^{W/W-v}$ mice (30–32) (**Table 1**).

C57BL/6-Kit^{W-sh} Mice

The *W-sh* mutation leading to MC deficiency is an inversion located in the regulatory region upstream of the transcription start site of the *W* locus (26), affecting the expression but not changing the function of the protein. Different to Kit$^{W/W-v}$ mice, Kit^{W-sh} mice are fertile and do not develop anemia, but are characterized by a proinflammatory phenotype including splenomegaly, thrombocytosis, and increased numbers of neutrophils and basophils.

Mcpt5^{Cre} iDTR Mice

Mast cell protease 5 (MCPT5) is a protease exclusively expressed in connective tissue MCs (CTMCs), such as peritoneal and skin MCs. In 2008, Scholten et al. generated a Mcpt5^{Cre} transgenic mouse line expressing Cre under the control of the *Mcpt5* promoter (33). Mating this transgenic strain to other mouse lines carrying loxP-flanked genes, allows the creation of mouse lines with gene deficiency in a CTMC-specific manner. By taking this advantage, Dudeck and colleagues generated Mcpt5^{Cre} iDTR mice by crossing Mcpt5^{Cre} with iDTR mice (34), which express a simian diphtheria toxin receptor (DTR) in loxP-flanked stop element deleted cells. In this manner, generated Mcpt5^{Cre} iDTR mice express the DTR exclusively on CTMCs, namely peritoneal and skin MCs, which are selectively ablated by the injection of diphtheria toxin (34). This inducible MC-deficient strain develops

TABLE 1 | Summary of mast cell (MC)-deficient mouse strains investigated in animal models of autoimmune bullous dermatoses (AIBD).

		Kit$^{W/W-v}$	Mgf$^{Sl/Sl-d}$	Kit^{W-sh}	Mcpt5^{Cre}
Abnormalities in immune system	MC deficiency	Yes	Yes	Yes	Yes[a]
	Splenomegaly	No	No	Yes	No
	Neutrophils	Decreased	–	Increased	Increased
	Basophils	Decreased	–	Increased	–
	TcRγδ intraepithelial lymphocytes	Reduced	–	Normal	Normal
	Thrombocytosis	No	No	Yes	No
Kit signaling associated abnormalities	KIT receptor signaling	Reduced	Reduced	Reduced	Not affected
	Lack of pigment	Yes	Yes	Yes	No
	Bile reflux	Yes	Yes	Yes	No
	Lack of interstitial cells of Cajal	Yes	–	Yes	No
Other abnormalities	Sterile	Yes	Yes	No	No
	Anemic	Yes	Yes	No	No
	Stomach papillomas and ulcers	Yes	Yes	No	No
	Idiopathic dermatitis	Yes	Yes	No	No
	Cardiac hypertrophy	No	–	Yes	No
Reference		(27–29)	(30–32)	(26)	(33, 34)

–, not known.

[a]*Deficiency in connective tissue MCs.*

no abnormalities in the cellular composition of spleen, blood, skin, and bone marrow (34), presenting a selective MC-deficient mouse model.

Disease Development of Experimental AIBD in MC-Deficient Mice

Initial findings in experimental AIBD like the induction of MC degranulation after local transfer of antibodies in BP and EBA or the blockade of disease symptoms by the MC stabilizer cromolyn (17, 21) draw a high interest on the role of MC in autoantibody-mediated diseases. Consequently, pathogenesis of antibody transfer-induced AIBDs was evaluated in four different MC-deficient mouse strains. Major results were summarized in **Table 2**.

Antibody Transfer-Induced BP in MC-Deficient Mice

In 2001, Chen et al. investigated for the first time MC-deficient mice in a local antibody transfer-induced mouse model of BP (21). In this study, rabbit anti-murine COL17 IgG was injected intradermally into neonatal $Kit^{W/W\text{-}v}$ and $Mgf^{Sl/Sl\text{-}d}$ mice as well as their MC-sufficient littermate controls. As expected, the MC-sufficient littermate controls developed an inflammatory skin-blistering disease, while both, $Kit^{W/W\text{-}v}$ and $Mgf^{Sl/Sl\text{-}d}$ mice, were entirely protected against the disease suggesting an indispensable role of MCs in this experimental system. Due to the numerous KIT-dependent side-effects, MC-specific effects have to be proven by further experiments, e.g., MC reconstitution in MC-deficient strains (35). Chen and colleagues could show that reconstitution of $Kit^{W/W\text{-}v}$ mice with bone marrow-derived MCs restored the disease confirming the essential role of MCs in this model (21). Furthermore, they found that MC activation is essential for the recruitment of neutrophils which themselves are the final executors of tissue damage (21, 36). In subsequent work, the same group could provide some information concerning the molecular mechanisms involved in MC activation in experimental BP. In 2011, they reported that $Kit^{W/W\text{-}v}$ mice reconstituted with C5a receptor (C5aR)-sufficient, but not C5aR-deficient MCs were susceptible to experimental BP suggesting the C5aR on MCs is critical for the development of the disease (37). Using a similar approach, they demonstrated that the role of MCs in experimental BP is also critically dependent on the MC-derived chymase MCPT4 which activates MMP9 and cleaves COL17 (38).

Taken together, the above studies employing the neonatal mouse model of antibody transfer induced BP suggesting that C5a-mediated MC activation and consequent release of MCPT4 from MCs is critical for recruitment of neutrophils from blood to the skin, and thus indicating that MCs are indispensable for the development of BP.

Antibody Transfer-Induced EBA in MC-Deficient Mice

Antibody transfer-induced models of BP and EBA share many clinical and histological features. Moreover, they are also comparable in pathogenesis, in terms of essential role of Fc receptors, C5a-C5aR signaling, and neutrophils (23, 39). Therefore, it is reasonable to hypothesize that MCs play an essential role in experimental EBA.

To verify this hypothesis, our group employed three different MC-deficient mouse strains to study the role of MCs in experimental EBA induced by transfer of rabbit anti-murine COL7 IgG (17). Surprisingly, when $Kit^{W/W\text{-}v}$ mice were used, a strain which has also been studied in BP, MC-deficient mice developed disease symptoms comparable to MC-sufficient littermate controls (17). This suggests that MCs are not required for antibody transfer-induced EBA which is in sharp contrast to their essential role in experimental BP. Moreover, repetition of this experiment in $Kit^{W\text{-}sh}$ mice, a further KIT-dependent MC knockout, revealed that disease developed in this strain with significant increased severity as compared to the MC-sufficient littermate controls (17). Although this increased susceptibility of $Kit^{W\text{-}sh}$ mice might not be due to a protective effect of MC, but more to a general proinflammatory abnormality present in this strain, these results suggest that MCs are not required for the disease manifestation in experimental EBA. Consequently, to avoid the interference from KIT signaling deficiency related other abnormalities, we investigated experimental EBA in $Mcpt5^{Cre}$ iDTR mice, where MC ablation was induced by treatment with diphtheria toxin. In this

TABLE 2 | Summary of development of experimental autoimmune bullous dermatoses (AIBD) in mast cell (MC)-deficient mouse strains.

		Antibody transfer-induced bullous pemphigoid		Antibody transfer-induced epidermolysis bullosa acquisita	
		Local model	**Systemic model**	**Local model**	**Systemic model**
Mice		Neonatal mice	Adult mice	Adult mice	Adult mice
Activation of mast cells (MCs)[a]		Yes	–	Yes	–
Disease development in MC-deficient mice[b]	$Kit^{W/W\text{-}v}$	protected	–	–	susceptible, severity comparable to littermates
	$Mgf^{Sl/Sl\text{-}d}$	Protected	–	–	–
	$Kit^{W\text{-}sh}$	–	–	–	Susceptible, severity increased to littermates
	$Mcpt5^{Cre}$ iDTR	–	–	Susceptible, severity comparable to littermates	Susceptible, severity comparable to littermates
Reference		(21, 37, 38)	–	(17)	(17)

[a] *Evaluated in the skin lesion of wildtype mice.*

[b] *As compared with corresponding MC-sufficient control mice.*

–, not evaluated.

KIT-independent model, MC-deficient mice were susceptible to experimental disease and developed symptoms indistinguishable from those in the corresponding MC-sufficient controls. These findings derived from systemic antibody transfer-induced EBA could be reproduced in a local model induced by injection of rabbit anti-murine COL7 IgG into the base of the ear. Mcpt5^{Cre} iDTR mice pretreated with DT also developed skin lesion at the injection site comparable to those of the MC-sufficient controls.

Taken together, these results provide strong evidence that in contrast to experimental BP, MCs are dispensable for antibody transfer-induced EBA (17).

CONCLUSION AND PERSPECTIVES

So far, investigations on the role of MCs have been limited to mouse models of BP and EBA and data on other AIBD are still missing. Given the similarities in clinical and pathological features between antibody transfer-induced BP and EBA, the discrepancy in the role of MCs between the two models is unexpected, but of high interest. In the last section, we will try to discuss this discrepancy and attempt to clarify the role of MCs in AIBD.

The discrepancy in the role of MCs between experimental BP and EBA may have many reasons. First of all, mice investigated in the two experimental AIBD were different; while the local model of BP was induced in neonatal mice, both local and systemic models of EBA were established in adult animals (17, 21). Since, neonatal and adult mice are different in their immune system (40, 41), this difference could also affect the role of MCs in the models. To verify this possibility, models of antibody transfer-induced BP in which adult mice are used should be employed. Second, since the role of MCs in experimental BP has been only investigated in Kit$^{W/W\text{-}v}$ and Mgf$^{Sl/Sl\text{-}d}$ mice, two strains characterized by a decreased expression of neutrophils, neutropenia, might contribute to the disease resistance as indicated for models of antibody-induced arthritis (42). This problem can be solved by investigating KIT-independent MC-deficient mice in antibody transfer-induced BP. Finally, the differences between COL17 and COL7, autoantigens of BP and EBA, respectively, might also contribute to diverging roles of MCs in both diseases.

Results derived from the different mouse models of AIBD do not provide a conclusive result on the role of MCs, more experiments need to be performed to address this issue. While it appears to be quite clear that antibody-induced EBA proceeds independently of MC, the role of these cells in corresponding models of BP needs to be reevaluated in adult KIT-independent MC-deficient mice. However, it is important to notice that each mouse model reflects only parts of the complicate entire pathogenesis of human autoimmune disease. Thus, antibody transfer-induced models mimic specifically the effector phase of inflammatory BP and EBA, and are unable to evaluate the role of MCs in the proceeding afferent phase of diseases. Since, there is evidence that MCs play a role in regulating adaptive immune responses (43), animal models mimicking both, the afferent and effector phases of AIBD, need to be used for such investigation. Furthermore, the transferred antibodies in the experimental models of BP and EBA belong to the class of IgG, and, therefore, can represent only IgG-mediated disease manifestation. Since, there is evidence that IgE autoantibodies might play a pathogenic role in BP, an animal model in which pathogenic IgE alone or in combination with IgG is transferred could address this potential key aspect in the difference between BP and EBA.

AUTHOR CONTRIBUTIONS

XY and FP were involved in drafting the manuscript. AK and KH were involved in correction and revision of the manuscript.

FUNDING

This work was supported by the Deutsche Forschungsgemeinschaft, German Center for Lung Research (DZL), and Research Training Group GRK1727 Modulation of Autoimmunity.

REFERENCES

1. Schmidt E, Zillikens D. Modern diagnosis of autoimmune blistering skin diseases. *Autoimmun Rev* (2010) 10(2):84–9. doi:10.1016/j.autrev.2010.08.007
2. Schmidt E, Zillikens D. Pemphigoid diseases. *Lancet* (2013) 381(9863):320–32. doi:10.1016/S0140-6736(12)61140-4
3. Chen CC, Grimbaldeston MA, Tsai M, Weissman IL, Galli SJ. Identification of mast cell progenitors in adult mice. *Proc Natl Acad Sci USA* (2005) 102(32):11408–13. doi:10.1073/pnas.0504197102
4. Kitamura Y, Oboki K, Ito A. Molecular mechanisms of mast cell development. *Immunol Allergy Clin North Am* (2006) 26(3):387–405. doi:10.1016/j.iac.2006.05.004
5. Galli SJ, Tsai M. Mast cells: versatile regulators of inflammation, tissue remodeling, host defense and homeostasis. *J Dermatol Sci* (2008) 49(1):7–19. doi:10.1016/j.jdermsci.2007.09.009
6. Galli SJ, Grimbaldeston M, Tsai M. Immunomodulatory mast cells: negative, as well as positive, regulators of immunity. *Nat Rev Immunol* (2008) 8(6):478–86. doi:10.1038/nri2327
7. Galli SJ, Nakae S. Mast cells to the defense. *Nat Immunol* (2003) 4(12):1160–2. doi:10.1038/ni1203-1160
8. Tsai M, Grimbaldeston M, Galli SJ. Mast cells and immunoregulation/immunomodulation. *Adv Exp Med Biol* (2011) 716:186–211. doi:10.1007/978-1-4419-9533-9_11
9. Wintroub BU, Mihm MC Jr, Goetzl EJ, Soter NA, Austen KF. Morphologic and functional evidence for release of mast-cell products in bullous pemphigoid. *N Engl J Med* (1978) 298(8):417–21. doi:10.1056/NEJM197802232980803
10. Kasperkiewicz M, Zillikens D. The pathophysiology of bullous pemphigoid. *Clin Rev Allergy Immunol* (2007) 33(1–2):67–77. doi:10.1007/s12016-007-0030-y
11. Dvorak AM, Mihm MC Jr., Osage JE, Kwan TH, Austen KF, Wintroub BU. Bullous pemphigoid, an ultrastructural study of the inflammatory response: eosinophil, basophil and mast cell granule changes in multiple biopsies from one patient. *J Invest Dermatol* (1982) 78(2):91–101. doi:10.1111/1523-1747.ep12505711
12. Delaporte E, Dubost-Brama A, Ghohestani R, Nicolas JF, Neyrinck JL, Bergoend H, et al. IgE autoantibodies directed against the major bullous pemphigoid antigen in patients with a severe form of pemphigoid. *J Immunol* (1996) 157(8):3642–7.
13. Fairley JA, Burnett CT, Fu CL, Larson DL, Fleming MG, Giudice GJ. A pathogenic role for IgE in autoimmunity: bullous pemphigoid IgE reproduces the early phase of lesion development in human skin grafted to nu/nu mice. *J Invest Dermatol* (2007) 127(11):2605–11. doi:10.1038/sj.jid.5700958
14. Levi-Schaffer F, Klapholz L, Kupietzky A, Weinrauch L, Shalit M, Okon E. Increased numbers of mast cells in pemphigus vulgaris skin lesions. A histochemical study. *Acta Derm Venereol* (1991) 71(3):269–71.

15. Yao L, Baltatzis S, Zafirakis P, Livir-Rallatos C, Voudouri A, Markomichelakis N, et al. Human mast cell subtypes in conjunctiva of patients with atopic keratoconjunctivitis, ocular cicatricial pemphigoid and Stevens-Johnson syndrome. *Ocul Immunol Inflamm* (2003) 11(3):211–22. doi:10.1076/ocii.11.3.211.17353
16. Caproni M, Rolfo S, Bernacchi E, Bianchi B, Brazzini B, Fabbri P. The role of lymphocytes, granulocytes, mast cells and their related cytokines in lesional skin of linear IgA bullous dermatosis. *Br J Dermatol* (1999) 140(6):1072–8. doi:10.1046/j.1365-2133.1999.02904.x
17. Kasprick A, Yu X, Scholten J, Hartmann K, Pas HH, Zillikens D, et al. Conditional depletion of mast cells has no impact on the severity of experimental epidermolysis bullosa acquisita. *Eur J Immunol* (2015) 45(5):1462–70. doi:10.1002/eji.201444769
18. Ghaly NR, Roshdy OA, Nassar SA, Hamad SM, El-Shafei AM. Role of mast cells and T-lymphocytes in pemphigus vulgaris: significance of CD44 and the c-kit gene product (CD117). *East Mediterr Health J* (2005) 11(5–6):1009–17.
19. Nagel A, Lang A, Engel D, Podstawa E, Hunzelmann N, de PO, et al. Clinical activity of pemphigus vulgaris relates to IgE autoantibodies against desmoglein 3. *Clin Immunol* (2010) 134(3):320–30. doi:10.1016/j.clim.2009.11.006
20. Iwata H, Bieber K, Hirose M, Ludwig RJ. Animal models to investigate pathomechanisms and evaluate novel treatments for autoimmune bullous dermatoses. *Curr Pharm Des* (2015) 21(18):2422–39. doi:10.2174/1381612821666150316122502
21. Chen R, Ning G, Zhao ML, Fleming MG, Diaz LA, Werb Z, et al. Mast cells play a key role in neutrophil recruitment in experimental bullous pemphigoid. *J Clin Invest* (2001) 108(8):1151–8. doi:10.1172/JCI11494
22. Deng F, Chen Y, Zheng J, Huang Q, Cao X, Zillikens D, et al. CD11b-deficient mice exhibit an increased severity in the late phase of antibody transfer-induced experimental epidermolysis bullosa acquisita. *Exp Dermatol* (2017) 26(12):1175–8. doi:10.1111/exd.13434
23. Sitaru C, Mihai S, Otto C, Chiriac MT, Hausser I, Dotterweich B, et al. Induction of dermal-epidermal separation in mice by passive transfer of antibodies specific to type VII collagen. *J Clin Invest* (2005) 115(4):870–8. doi:10.1172/JCI200521386
24. Schulze FS, Beckmann T, Nimmerjahn F, Ishiko A, Collin M, Kohl J, et al. Fcgamma receptors III and IV mediate tissue destruction in a novel adult mouse model of bullous pemphigoid. *Am J Pathol* (2014) 184(8):2185–96. doi:10.1016/j.ajpath.2014.05.007
25. Gilfillan AM, Rivera J. The tyrosine kinase network regulating mast cell activation. *Immunol Rev* (2009) 228(1):149–69. doi:10.1111/j.1600-065X.2008.00742.x
26. Grimbaldeston MA, Chen CC, Piliponsky AM, Tsai M, Tam SY, Galli SJ. Mast cell-deficient W-sash c-kit mutant Kit W-sh/W-sh mice as a model for investigating mast cell biology in vivo. *Am J Pathol* (2005) 167(3):835–48. doi:10.1016/S0002-9440(10)62055-X
27. Hayashi S, Kunisada T, Ogawa M, Yamaguchi K, Nishikawa S. Exon skipping by mutation of an authentic splice site of c-kit gene in W/W mouse. *Nucleic Acids Res* (1991) 19(6):1267–71. doi:10.1093/nar/19.6.1267
28. Nocka K, Tan JC, Chiu E, Chu TY, Ray P, Traktman P, et al. Molecular bases of dominant negative and loss of function mutations at the murine c-kit/white spotting locus: W37, Wv, W41 and W. *EMBO J* (1990) 9(6):1805–13.
29. Kitamura Y, Go S, Hatanaka K. Decrease of mast cells in W/Wv mice and their increase by bone marrow transplantation. *Blood* (1978) 52(2):447–52.
30. Copeland NG, Gilbert DJ, Cho BC, Donovan PJ, Jenkins NA, Cosman D, et al. Mast cell growth factor maps near the steel locus on mouse chromosome 10 and is deleted in a number of steel alleles. *Cell* (1990) 63(1):175–83. doi:10.1016/0092-8674(90)90298-S
31. Bedell MA, Brannan CI, Evans EP, Copeland NG, Jenkins NA, Donovan PJ. DNA rearrangements located over 100 kb 5' of the Steel (Sl)-coding region in Steel-panda and Steel-contrasted mice deregulate Sl expression and cause female sterility by disrupting ovarian follicle development. *Genes Dev* (1995) 9(4):455–70. doi:10.1101/gad.9.4.455
32. Brannan CI, Lyman SD, Williams DE, Eisenman J, Anderson DM, Cosman D, et al. Steel-Dickie mutation encodes a c-kit ligand lacking transmembrane and cytoplasmic domains. *Proc Natl Acad Sci U S A* (1991) 88(11):4671–4. doi:10.1073/pnas.88.11.4671
33. Scholten J, Hartmann K, Gerbaulet A, Krieg T, Muller W, Testa G, et al. Mast cell-specific Cre/loxP-mediated recombination in vivo. *Transgenic Res* (2008) 17(2):307–15. doi:10.1007/s11248-007-9153-4
34. Dudeck A, Dudeck J, Scholten J, Petzold A, Surianarayanan S, Kohler A, et al. Mast cells are key promoters of contact allergy that mediate the adjuvant effects of haptens. *Immunity* (2011) 34(6):973–84. doi:10.1016/j.immuni.2011.03.028
35. Galli SJ, Tsai M, Gordon JR, Geissler EN, Wershil BK. Analyzing mast cell development and function using mice carrying mutations at W/c-kit or Sl/MGF (SCF) loci. *Ann N Y Acad Sci* (1992) 664:69–88. doi:10.1111/j.1749-6632.1992.tb39750.x
36. Liu Z, Giudice GJ, Zhou X, Swartz SJ, Troy JL, Fairley JA, et al. A major role for neutrophils in experimental bullous pemphigoid. *J Clin Invest* (1997) 100(5):1256–63. doi:10.1172/JCI119639
37. Heimbach L, Li Z, Berkowitz P, Zhao M, Li N, Rubenstein DS, et al. The C5a receptor on mast cells is critical for the autoimmune skin-blistering disease bullous pemphigoid. *J Biol Chem* (2011) 286(17):15003–9. doi:10.1074/jbc.M111.221036
38. Lin L, Bankaitis E, Heimbach L, Li N, Abrink M, Pejler G, et al. Dual targets for mouse mast cell protease-4 in mediating tissue damage in experimental bullous pemphigoid. *J Biol Chem* (2011) 286(43):37358–67. doi:10.1074/jbc.M111.272401
39. Mihai S, Chiriac MT, Takahashi K, Thurman JM, Holers VM, Zillikens D, et al. The alternative pathway of complement activation is critical for blister induction in experimental epidermolysis bullosa acquisita. *J Immunol* (2007) 178(10):6514–21. doi:10.4049/jimmunol.178.10.6514
40. Kovarik J, Siegrist CA. Immunity in early life. *Immunol Today* (1998) 19(4):150–2. doi:10.1016/S0167-5699(97)01230-9
41. Rodewald HR, Dessing M, Dvorak AM, Galli SJ. Identification of a committed precursor for the mast cell lineage. *Science* (1996) 271(5250):818–22. doi:10.1126/science.271.5250.818
42. Zhou JS, Xing W, Friend DS, Austen KF, Katz HR. Mast cell deficiency in Kit(W-sh) mice does not impair antibody-mediated arthritis. *J Exp Med* (2007) 204(12):2797–802. doi:10.1084/jem.20071391
43. Brown MA, Sayed BA, Christy A. Mast cells and the adaptive immune response. *J Clin Immunol* (2008) 28(6):671–6. doi:10.1007/s10875-008-9247-7

Conflict of Interest Statement: The authors declare that the research was conducted in the absence of any commercial or financial relationships that could be construed as a potential conflict of interest.

frontiers in Immunology

ORIGINAL RESEARCH
published: 26 February 2018
doi: 10.3389/fimmu.2018.00370

Soluble Fas Ligand Is Essential for Blister Formation in Pemphigus

*Roberta Lotti[1], En Shu[1], Tiziana Petrachi[1], Alessandra Marconi[1], Elisabetta Palazzo[1], Marika Quadri[1], Ann Lin[2], Lorraine A. O'Reilly[2,3] and Carlo Pincelli[1]**

[1] Laboratory of Cutaneous Biology, Department of Surgical, Medical, Dental and Morphological Sciences, University of Modena and Reggio Emilia, Modena, Italy, [2] Molecular Genetics of Cancer Division, The Walter and Eliza Hall Institute of Medical Research, Parkville, VIC, Australia, [3] Department of Medical Biology, The University of Melbourne, Parkville, VIC, Australia

Pemphigus is a blistering disease characterized by pemphigus autoantibodies (PVIgG) directed mostly against desmogleins (Dsgs), resulting in the loss of keratinocyte adhesion (acantholysis). Yet, the mechanisms underlying blister formation remain to be clarified. We have shown previously that anti-Fas ligand (FasL) antibody (Ab) prevents PVIgG-induced caspase-8 activation and Dsg cleavage in human keratinocytes, and that sera from pemphigus patients contain abnormally increased levels of FasL. Here, we demonstrate that recombinant FasL induces the activation of caspases prior to Dsg degradation, and anti-FasL Ab prevents acantholysis in cultured keratinocytes. Moreover, the silencing of FasL reduces PVIgG-induced caspase-8 activation and Dsg3 cleavage. Following injection of PVIgG into mice, FasL is upregulated at 1–3 h and is followed by caspase-8-mediated keratinocyte apoptosis, before blister formation. The administration of anti-FasL Ab after PVIgG injection blocks blister formation in mice. Furthermore, we injected PVIgG into two different gene-targeted mutant mice that selectively lack either secreted soluble FasL (sFasL), *FasL*$^{\Delta s/\Delta s}$ mice, or the membrane-bound form of FasL (mFasL), *FasL*$^{\Delta m/\Delta m}$ mice. After PVIgG treatment, blisters are only visible in *FasL*$^{\Delta m/\Delta m}$ animals, lacking mFasL, but still producing sFasL, similar to wild-type (C57BL/6) animals. By contrast, a significant decrease in the relative acantholytic area is observed in the *FasL*$^{\Delta s/\Delta s}$ animals. These results demonstrate that soluble FasL plays a crucial role in the mechanisms of blister formation, and blockade of FasL could be an effective therapeutic approach for pemphigus.

Keywords: pemphigus, Fas ligand, apoptosis, keratinocytes, autoantibodies, cell adhesion, mouse model

OPEN ACCESS

Edited by:
Takayuki Yoshimoto, Tokyo Medical University, Japan

Reviewed by:
Pedro A. Reche, Complutense University of Madrid, Spain
Hiroshi Koga, Kurume University School of Medicine, Japan

***Correspondence:**
Carlo Pincelli
carlo.pincelli@unimore.it

Specialty section:
This article was submitted to Inflammation, a section of the journal Frontiers in Immunology

Received: *15 December 2017*
Accepted: *09 February 2018*
Published: *26 February 2018*

Citation:
Lotti R, Shu E, Petrachi T, Marconi A, Palazzo E, Quadri M, Lin A, O'Reilly LA and Pincelli C (2018) Soluble Fas Ligand Is Essential for Blister Formation in Pemphigus. Front. Immunol. 9:370. doi: 10.3389/fimmu.2018.00370

INTRODUCTION

Pemphigus is a rare and potentially lethal autoimmune skin disease, characterized by the loss of keratinocyte adhesion at the level of desmosomes, a phenomenon known as acantholysis. This results in the formation of flaccid blisters and/or erosions in both skin and mucous membranes (1). Pathogenic autoantibodies [pemphigus autoantibodies (PVIgG)] in sera from pemphigus patients target predominantly molecular components of the desmosomes, such as desmoglein (Dsg)3 [pemphigus vulgaris (PV)] and Dsg1 [pemphigus foliaceous (PF)] [reviewed by Stanley and Amagai (2)]. Although autoantibodies play an essential role in the pathogenesis of pemphigus (3), the mechanisms leading to the formation of the blisters remain largely unknown (4, 5). Several lines of evidence indicate that apoptosis is involved in the pathological mechanisms of pemphigus [reviewed by Grando et al., (6)]. In particular, cleaved caspase-8 and -3 are detected in pemphigus lesions, and caspase-8-positive cells express Fas ligand (FasL)/Fas binding (7, 8).

Fas Ligand is a transmembrane protein (mFasL) that can be proteolytically cleaved to generate its soluble form of 26 kDa (sFasL) (9). Both forms of FasL can bind to their receptor, Fas, also known as CD95 or Apo1. The membrane-bound form triggers the extrinsic apoptotic pathway through the activation of caspase-8 (10), while the soluble form appears to have both apoptotic and pro-inflammatory activities in immune cells (11, 12). In healthy skin, FasL is localized in the basal layer and in the first suprabasal layers of the epidermis, homogeneously distributed within the cytoplasm, in association with intermediate filaments (13). PVIgG upregulate FasL at the mRNA and protein level in human keratinocytes (14). We have shown previously that anti-FasL antibodies (Ab) prevent PVIgG-induced caspase-8 activation and Dsg cleavage in human keratinocytes (6) and that sera from pemphigus patients contain abnormally increased levels of FasL (15).

In this study, we demonstrate that the inhibition of FasL prevents apoptosis and acantholysis *in vitro*, and anti-FasL Ab blocks blister formation *in vivo*. Finally, using two mutant mice selectively lacking the sFasL or mFasL, we provide evidence that sFasL plays a critical role in blister formation in pemphigus.

MATERIALS AND METHODS

Pemphigus Samples

Biopsies (4-mm punch) from lesional and perilesional pemphigus skin as well as from normal skin of healthy volunteers were obtained from the Institute of Dermatology, at the University of Modena and Reggio Emilia. Samples were embedded in OCT and frozen at −20°C. In all patients, diagnosis was based on (1) typical skin and/or mucous membrane lesions, (2) detection of circulating autoantibodies by indirect immunofluorescence on monkey esophagus (a titer of 1:320), and (3) reactivity to Dsgs in patients' sera by ELISA (MBL International Corp., Nagoya, Japan). Sera were collected from patients with PV, mucocutaneous pemphigus, and PF and pooled for IgG purification (Dsg1: 106.2 U/ml; Dsg3: 158.2 U/ml). Sera were also collected from healthy volunteers (Dsg1: 2.6 U/ml; Dsg3: 3.2 U/ml).

IgG Purification

Pemphigus autoantibodies and normal human IgG (NIgG) were purified by affinity binding on a HiTrapProtein G HP column (GE Healthcare Bio-Science, Piscataway, NJ, USA). Sera were pooled and diluted (1:10) in 20 mM phosphate buffer (pH 7) and loaded on the column. Bound IgG was eluted with 0.1 M glycine/HCl (pH 2.7) and immediately neutralized by Tris 1 M (pH 9). Purified IgGs were dialyzed extensively against phosphate-buffered saline (PBS) (pH 7.4), concentrated by ultrafiltration (Amicon, Beverly, MA, USA), filter-sterilized, and stored at +4°C until use. Protein concentration was determined by Bradford assay using protein Standard I (BioRad, Hercules, CA, USA).

Cell Cultures

Normal human keratinocytes were obtained from foreskin and cultured as described previously (16). Briefly, normal human keratinocytes were amplified on mitomycin C (Sigma-Aldrich, St Louis, MO, USA)-treated 3T3 cells and cultivated in Dulbecco's modified Eagle's medium and Ham's F12 medium. Subconfluent secondary cultures for experiments were plated in a defined serum-free medium (KGM, Lonza Walkersville Inc., Walkersville, MD, USA). When cells were confluent, Ca^{2+} concentration was increased to 1.8 mM for 24 h, to induce keratinocyte differentiation, before the addition of any stimulus. Either human recombinant soluble FasL (rFasL) (0.1, 10, or 50 ng/ml, Sigma) or PVIgG and NIgG (1.5 mg/ml) were diluted in keratinocyte basal medium (Lonza) plus 1.8 mM Ca^{2+} and cycloheximide (Sigma) 1 μg/ml, and incubated for a further 72 h. For *in vitro* inhibitory experiments, keratinocyte cultures were pretreated with either 1 or 15 μg/ml of purified mouse anti-human FasL monoclonal Ab (NOK-2; BD Biosciences Pharmingen, San Diego, CA, USA) for 1 h, which was also added when medium was provided with NIgG, PVIgG, or rFasL.

Passive Transfer Pemphigus Mouse Model

Neonatal C57BL/6NCrl mice (1–2 days old with body weight of approximately 1.3 g) were used for IgG passive transfer experiments [modified from Ref. (17)]. C57BL/6NCrl adult mice were obtained from Charles River (Calco, Italy) and maintained at the Laboratory Animal Facility, University of Modena and Reggio Emilia (Modena). Briefly, 5 mg/g/bw of purified PVIgG or NIgG in a total volume of maximum 50 μl was administered to neonatal mice by a single subcutaneous (s.c.) injection in the dorsal area. Twenty hours after IgG injection, animals were sacrificed and samples were collected. $FasL^{\Delta m/\Delta m}$ and $FasL^{\Delta s/\Delta s}$ animals were generated as described by O'Reilly et al. (12) and maintained at the Walter and Eliza Hall Institute of Medical Research (Melbourne) Animal Facility. FasL-mutant mice and their WT littermates were treated as described above. Direct immunofluorescence with anti-human IgG (Dako, Glostrup, Denmark) was used to demonstrate PVIgG deposition at the skin level. For time course studies, animals ($n = 5$) were sacrificed at various time points post IgG injection (0, 1, 3, 6, 9, 12, 18, and 24 h). Skin samples of each animal were harvested for hematoxylin and eosin (H&E) staining, TUNEL assay, and Western blotting. For inhibitory experiments, mice were injected s.c. with 40 μg/mouse of purified hamster anti-mouse CD178 (FasL) monoclonal Ab (MFL3; BD Pharmingen, San Jose, CA, USA) in the same dorsal area of PVIgG or NIgG (for control) injection, either 1, 2, or 3 h after IgG administration. As negative control, we used purified hamster IgG1, κ-Isotype control (40 μg/mouse; BD Pharmingen).

Ethics Statements

For human samples, this study was carried out in accordance with the recommendations of the Ethic Committee of the IDI-IRCCS (Istituto Dermatopatico dell'Immacolata, Rome) with written informed consent from all subjects. All subjects gave written informed consent in accordance with the Declaration of Helsinki. The protocol was approved by the Ethic Committee of the IDI-IRCCS (Istituto Dermatopatico dell'Immacolata, Rome).

For WT C57BL/6 mice procedures, this study was carried out in accordance with the recommendations of the Ethical Committee of the University of Modena and Reggio Emilia and was in accordance with the Italian Institute of Health guidelines.

The protocol was approved by the Italian Institute of Health. Animal studies conducted on FasL-mutant mice at the Walter and Eliza Hall Institute were approved by the Institute's Animal Ethics Committee.

Immunohistochemistry

Cryosections (4 μm) of skin from healthy donor and from pemphigus patients were methanol-fixed and rehydrated in PBS. The staining was performed using the UltraVision LP Detection System AP Polymer & Fast Red Chromogen assay (Thermo Fisher Scientific), according to the manufacturer's instructions. Briefly, slides were treated with Ultra V Block, and samples were incubated with mouse anti-CD95/Fas Ab (UB2; Immunotech, Marseille, France) for 1 h at room temperature. After washes in PBS, Primary Antibody Enhancer (Thermo Fisher Scientific) was added for 20 min at room temperature, followed by incubation with AP Polymer anti-mouse/rabbit IgG for 30 min at room temperature. Slides were stained with Fast Red using Naphthol Phosphate as substrate. Samples were analyzed under a conventional optical microscope (Zeiss Axioskope 40).

FasL siRNA Keratinocyte Transfection

About 8×10^4 cells/well were plated on six-well plates in penicillin/streptomycin-free medium. After 24 h, normal human keratinocytes were transfected with 40 nM FasL siRNA (siGenome SMARTpool) or scrambled RNAi, as control (Dharmacon Inc., Lafayette, CO, USA), combined with Lipofectamine 2000 and Opti-MEM (both from Invitrogen Corporation, Carlsbad, CA, USA), according to manufacturer's indications. Cells were transfected twice and used for PVIgG experiments. FasL protein levels were detected by Western blotting, as described below.

Western Blotting

Cells were washed with PBS and lysed on ice in RIPA buffer (pH 7.5) containing protease inhibitors (Complete Mini Tablets, Roche). Total protein of 40 μg was analyzed on polyacrylamide gels and blotted onto nitrocellulose membranes. Blots were blocked for 2 h in a blocking buffer (5% nonfat milk in PBS/0.2% Tween20, Sigma) and incubated overnight at 4°C with the following primary Ab: anti-Dsg3 (5H10; Santa Cruz Biotechnology), anti-caspase-8 (Ab-3; Calbiochem, Darmstadt, Germany), anti-FasL (Abcam, Cambridge, UK), or anti-β-actin Ab (AC-15; Sigma). Membranes were washed in PBS/Tween, incubated with HRP-conjugated goat anti-mouse Ab (Biorad) for 45 min at room temperature, washed, and developed using the ECL chemiluminescent detection system (Amersham Biosciences UK Limited, Little Chalfont Buckinghamshire, UK). Mouse skin proteins were extracted by homogenization in SDS buffer (62.5 mM Tris-HCl pH 6.8, 2% SDS, and 10% glycerol). Proteins were separated by SDS-PAGE and transferred onto nitrocellulose membranes. Blots were blocked with 5% nonfat dry milk in TBS/0.1% Tween 20 for 1 h, then incubated overnight at 4°C with the primary rabbit polyclonal Ab mouse-specific anti-caspase-8 (Cell Signaling Technology, Danvers, MA, USA), anti-caspase-3 (Cell Signaling Technology), anti-FasL (Abcam, Cambridge, UK), or anti-β-actin Ab (AC-15; Sigma). Subsequently, membranes were incubated with the appropriate HRP-conjugated secondary Ab (Biorad) and developed, as described above. The band intensity was quantitatively determined using Image J software.

Immunofluorescence

For double cell staining, keratinocyte cultures were washed in PBS, fixed in 4% paraformaldehyde for 20 min, and air-dried. After rehydration in PBS, cells were permeabilized for 2 min with 0.1% Triton X-100, treated for 5 min with 50 mM NH_4Cl, and incubated with 1% bovine serum albumin for 20 min. Cells were then incubated at room temperature for 45 min with mouse monoclonal anti-Dsg3 Ab (5H10, Santa Cruz Biotechnology Inc., Santa Cruz, CA, USA) and for 45 min with Alexa Fluor 488 anti-mouse (Invitrogen). Keratinocytes were washed in PBS/Tween, labeled with rabbit polyclonal anti-caspase-3 active Ab (R&D Systems Inc., Minneapolis, MN, USA) for 45 min and with Alexa Fluor 546 anti-rabbit IgG (Invitrogen) for 45 min. For visualization of nuclei, 4',6-diamidino-2-phenylindole (DAPI) (1 μg/ml, Sigma) was used. Fluorescent specimens were analyzed by a Confocal Scanning Laser Microscopy (Leica TCS SP2). For mouse-tissue staining, paraffin-embedded tissue sections (4 μm) of skin from NIgG and PVIgG-treated mice were paraffin dewaxed, rehydrated, and antigen retrieved (citrate buffer, Thermo Fisher Scientific Inc., Fremont, CA, USA). Sections were incubated for 1 h with anti-active/cleaved caspase-8 (Novus Biologicals, Littleton, CO, USA) and for 45 min with Alexa Fluor 546 anti-rabbit IgG Ab (Invitrogen). For visualization of nuclei, 4',6-DAPI (1 μg/ml, Sigma) was used. Fluorescent specimens were analyzed by a Confocal Scanning Laser Microscopy (Leica TCS SP2).

Dispase-Based Dissociation Assay

Normal human keratinocytes were seeded onto 12-well plates, cultured, and treated at confluency, as described above. After washing with PBS twice, cells were incubated with dispase II (>2.4 U/ml; Roche) for 30 min to release cells as monolayers. Released monolayers were carefully washed with PBS twice and subjected to mechanical stress by pipetting with a 1-ml pipetman. Fragments were fixed with 4% formaldehyde and stained with 1% Rhodamine B (Sigma). For each single well, the particle number was counted and dissociation scores were calculated using the number of fragmented cell sheets (N) using the following formula: dissociation score = $[(\text{N-NNIgG})/(\text{NPVIgG-NNIgG})] \times 100$.

Measurement of the Relative Acantholytic Area

The extent of epidermal acantholysis was measured microscopically by H&E staining. Samples were analyzed using a conventional optical microscope (Zeiss Axioskope 40). Five random microscopic fields per sample were captured at 200× magnification. AxioVision AC imaging software was used to acquire sample images. ImageJ software was used to count the number of pixels corresponding to the length of each cleft corresponding to the areas of the epidermis in which suprabasal cell detachment spreads along more than four adjacent basal cells. The percentage of the acantholytic area was calculated as the mean of different fields. All samples were reported as a ratio against PVIgG

treatment or WT animals (in FasL-mutant mice experiments), to which a value of 1 was assigned.

Caspase Assay

Normal human keratinocytes were grown in a multi-96 well black plate and treated with FasL (50 ng/ml). The rate of caspase-3 and -7 activation was measured simultaneously with the fluorimetric Apo-ONE Homogeneous Caspase-3/7 Assay (Promega Corporation, Madison, WI, USA), according to the manufacturer's instructions. Briefly, Apo-ONE Caspase-3/7 reagent mixture, containing the profluorescent substrate Z-DEVD-Rhodamine 110 and lysis/permeabilization buffer, was added to each well, gently mixed, and incubated in the dark for 2 h at room temperature. After incubation, the amount of fluorescent product, which is proportional to the amount of caspase-3/7 cleavage, was measured with a FLUOstar Galaxy fluorimeter (BMG Labtech, Germany), using an excitation wavelength of 499 nm and an emission of 521 nm. Living cell number was quantified by MTT assay in a duplicate transparent plate, by incubating in MTT solution (Sigma) for 4 h at 37°C. The formazan dye produced after DMSO solubilization was evaluated by a multiwell scanning spectrophotometer at 540 nm. The final RFLU/O.D. caspase assay results were normalized in relation to MTT values from the same experiment.

TUNEL Assay

Mouse skin samples were fixed in 4% buffered formalin and embedded in paraffin. Paraffin sections were processed for TUNEL assay using the "*In situ* cell death detection kit" (Roche Diagnostics, Basel, Switzerland), according to the manufacturer's instructions. Briefly, following dewaxing and rehydration, sections were treated with proteinase K (20 µg/ml; Roche) for 30 min at room temperature and incubated with a reaction mixture containing TdT and fluorescence-conjugated dUTP for 1 h at 37°C. The labeled DNA was examined by a Confocal Scanning Laser Microscopy (Leica TCS SP2 with AOBS).

Statistical Analysis

Data are presented as mean ± SEM or as ratios with group differences, obtained from three to five different experiments. Prism Software (Graph Pad Software V7.0) was used to perform statistical analysis. A two-tailed unpaired Student's *t*-test was used for statistical comparisons between two groups, while one-way ANOVA was used for multiple comparisons (as indicated in figure legends). A value of $P < 0.05$ or less was assumed to indicate a statistically significant difference in the compared parameters.

RESULTS

FasL Induces Apoptosis and Acantholysis in Human Keratinocytes

Since PVIgG have been shown to induce the co-aggregation of FasL and Fas receptor with caspase-8 in death–inducing-signaling complex (7), we first analyzed the expression of Fas in pemphigus skin. While in normal epidermis, Fas expression is confined to the surface of all basal cells, in pemphigus lesions, Fas is also found in the suprabasal layers, even before cell detachment (**Figure 1A**). Given that PVIgG upregulate caspase-8 and caspases can cleave several adhesion molecules, including Dsgs (18, 19), we investigated the effect of recombinant soluble FasL (rFasL) on apoptosis and Dsg3. rFasL induces the cleavage of Dsg3 in a dose-dependent manner (Figure S1 in Supplementary Material) with the appearance of a cleaved 80 kD band after 12 h (**Figures 1B,C**), generated by the first degradation of the Dsg3 intracellular tail. In addition, rFasL induces the activation of caspase-8 commencing at 2 h (**Figures 1B,C**), followed by the activation of caspase-3/7 at 4–6 h (**Figure 1D**). An additional Dsg3 cleavage band at 45 kDa is progressively generated (**Figures 1B,C**), indicating further Dsg degradation induced by caspases. By confocal microscopy, cleaved (active) caspase-3-expressing cells (red) start to appear from 6 h when Dsg expression (green) is still intact. The increase in cleaved caspase-3-positive cells is associated with a reduction in Dsg expression and a progressive cell-to-cell detachment (**Figure 1E**, arrows). These findings suggest that the final step of the apoptotic process (e.g., activation of the executioner caspase-3) occurs in the presence of Dsg3 and before cell detachment.

To further evaluate the role of FasL in pemphigus, we performed the cell dissociation assay, a well-established dispase-based method to measure keratinocyte acantholysis *in vitro* (20). The addition of anti-FasL Ab clearly protects keratinocytes against acantholysis induced by PVIgG treatment, in a dose-dependent fashion (**Figure 2A**). Dissociation scoring shows a statistically significant reduction of cell sheet fragmentation in the presence of anti-FasL (**Figure 2B**). These data indicate that FasL is relevant to cell-to-cell detachment *in vitro*. In addition, the silencing of FasL using siRNA diminishes Dsg3 cleavage and the activation of caspase-8 induced by PVIgG (**Figures 2C,D**). The finding was further confirmed by immunofluorescence and indicated that blocking FasL by siRNA inhibits Dsg (green) the degradation and the activation of caspase-3 (red, **Figure 2E**). Taken together, these findings show that FasL plays a critical role in mediating PVIgG-induced apoptosis and acantholysis *in vitro*.

Anti-FasL Ab Blocks Blister Formation *In Vivo*

To confirm the role of FasL in the pathological mechanisms of pemphigus *in vivo*, we s.c. injected neonatal C57BL/6N mice with purified pathogenic PVIgG or NIgG. Twenty hours later, the intraepidermal blister and the deposition of autoantibodies at the floor and the roof of the cleft (Figure S2A in Supplementary Material) recapitulate the immuno-histologic alterations of pemphigus in humans. In addition, we detected the activated form of caspase-3 in the skin of PVIgG-treated mice but not those injected with NIgG, as shown by the appearance of the cleaved form of caspase-3 (Figure S2B in Supplementary Material). Our findings indicate that PVIgG can activate the apoptotic process *in vivo*. In particular, PVIgG can induce the upregulation of FasL protein in mouse epidermis starting at 1 h and caspase-8 activation at 6 h post injection, respectively (**Figure 3A**). While blisters, as measured by the relative acantholytic areas, were observed at 12 h (**Figure 3B**), TUNEL-positive epidermal cells were already detected from 9 h after PVIgG treatment (**Figure 3C**). These

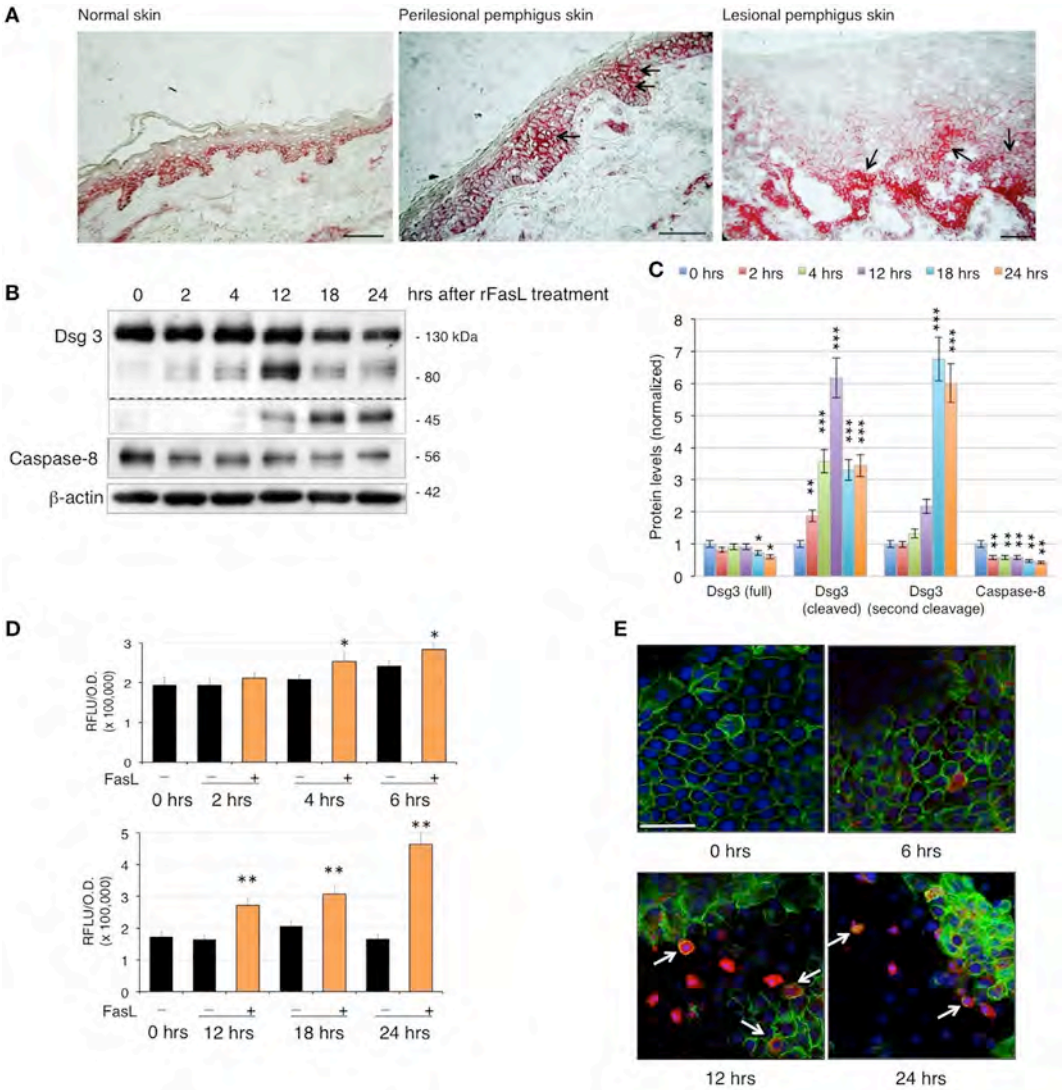

FIGURE 1 | Fas ligand (FasL)-induced apoptosis precedes acantholysis in human keratinocytes: **(A)** Fas is upregulated in pemphigus skin before cell detachment. Cryosections from normal human skin, perilesional, and lesional pemphigus skin were methanol-fixed and stained with anti-Fas antibody (arrows), scale bar: 100 µm. **(B–E)** rFasL induces desmoglein (Dsg)3 cleavage through caspases activation in a time-dependent manner. Differentiated keratinocyte monolayers were treated with 50 ng/ml of recombinant soluble FasL (rFasL) for different time points. Cell lysates were **(B)** immunoblotted and **(C)** protein amounts were quantified (means ± SEM; $^{*}P < 0.05$; $^{**}P < 0.01$; $^{***}P < 0.001$ per Student's *t*-test vs cntrl; $n = 5$ independent experiments). Dsg3 (full), 130 kDa; Dsg3 (cleaved), 80 kDa; Dsg3 (second cleavage), 45 kDa. **(D)** Caspase-3/7 activity was measured at each time point in the presence (+, orange bars) or absence (–, black bars) of rFasL (see Materials and Materials). Statistical analysis was performed comparing rFasL-treated samples with its cntrl (–, diluent) at each time point (means ± SEM; $^{*}P < 0.05$; $^{**}P < 0.01$ per Student's *t*-test, compared with diluent; $n = 3$–5 independent experiments). **(E)** A representative immunofluorescence image shows Dsg3 (green) and active caspase-3 (red) expression in keratinocytes treated with rFasL at the indicated time points. Nuclei are shown in blue (4',6-diamidino-2-phenylindole). Scale bar = 70 µm.

results demonstrate that pathogenic autoantibodies first induce the release of FasL, followed by the appearance of apoptotic epidermal cells, which in turn precedes the onset of blisters *in vivo*.

To further define the role of FasL *in vivo*, mice were injected with PVIgG alone or in combination with a FasL-blocking Ab (40 µg/mouse). Control mice that received PVIgG alone developed skin lesions 20 h after injection. By contrast, when anti-FasL Ab was administered 1 or 2 h after PVIgG injection, blisters were still visible but of lesser magnitude. Further, when anti-FasL Ab was administered 3 h after PVIgG injection, no blister formation was observed (**Figure 3D**), indicating that blocking FasL prevents acantholysis *in vivo*. The protective effect of anti-FasL Ab against acantholysis was confirmed by measuring the relative acantholytic areas in multiple fields from all skin specimens. The relative acantholytic area was significantly decreased when anti-FasL Ab was given 1 h after PVIgG, almost undetectable at 2 h and not measurable in mice treated with PVIgG followed by the administration of anti-FasL Ab, 3 h later (**Figure 3E**). Moreover, the percentage of TUNEL-positive cells was significantly higher in the epidermis from mice treated with PVIgG alone, compared

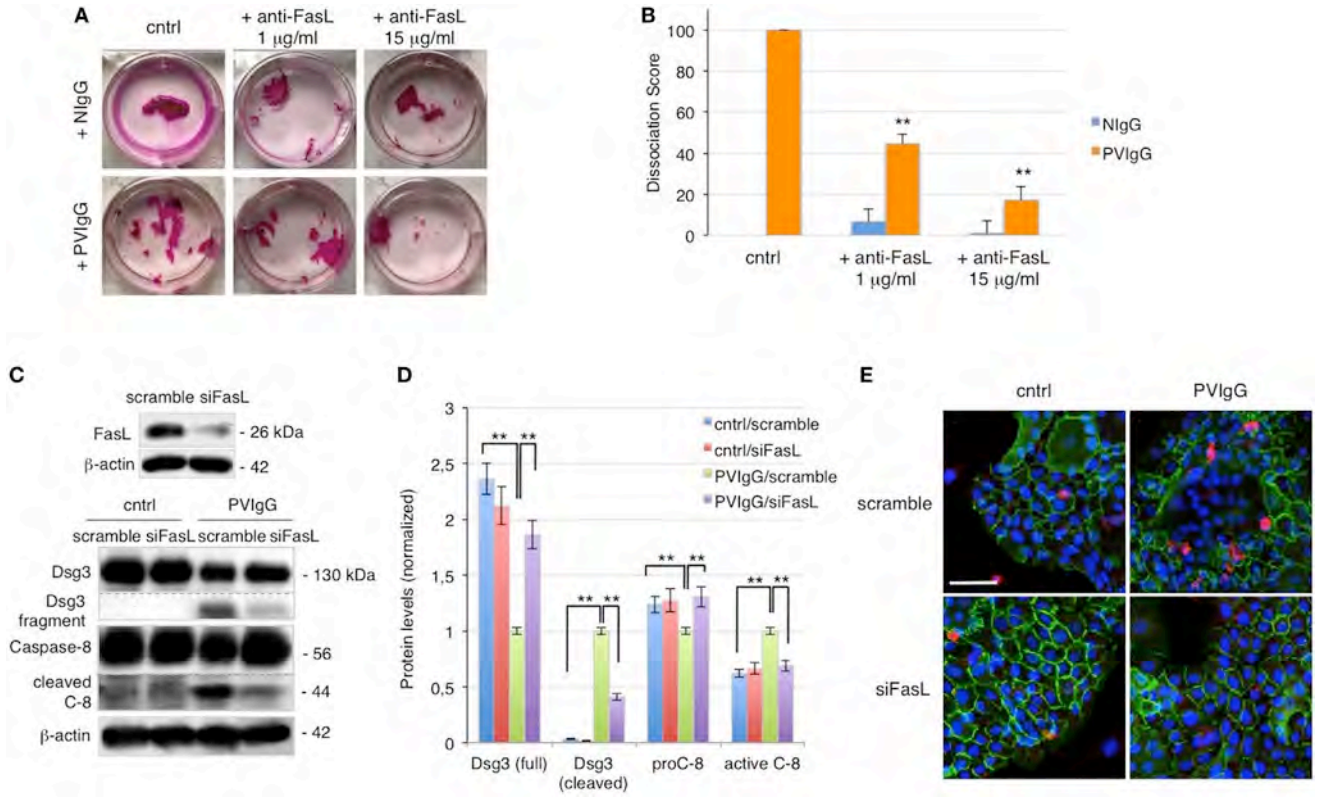

FIGURE 2 | Keratinocyte-derived Fas ligand (FasL) induces desmoglein (Dsg)3, cleavage, and caspase activation. **(A,B)** Anti-FasL antibody (Ab) prevents keratinocyte acantholysis. Keratinocytes were cultured with purified normal human IgG (NIgG) or pemphigus autoantibodies (PVIgG) in the presence or absence of anti-FasL Ab (1 or 15 μg/ml), and dispase-based dissociation assay was performed. **(A)** Representative images of cell sheet fragmentation. **(B)** Quantification obtained by counting the number of fragments of cell sheets and represented as dissociation score (means ± SEM; $^{**}P < 0.01$ per one-way ANOVA versus PVIgG; $n = 5$ independent experiments). **(C–E)** FasL silenced keratinocytes are protected from PVIgG-induced acantholysis and apoptosis. FasL or scrambled siRNA transfected keratinocytes were treated with PVIgG or diluent (cntrl), and levels of Dsg3 and caspase-8 were assessed by immunoblot **(C)** and measured by relative protein quantification **(D)**. **(E)** Immunofluorescence showing Dsg3 (green) and active caspase-3 (red) expression in keratinocytes. Scale bar = 70 μm.

to mice treated with anti-FasL Ab at 1 or 2 h after PVIgG. No TUNEL-positive cells were detected in the epidermis of mice that received anti-FasL Ab, 3 h after PVIgG (**Figure 3F**). Mice were subsequently treated with decreasing amounts of anti-FasL Ab which inhibited blister formation in a dose-dependent manner, as measured by the relative acantholytic area (**Figure 3G**).

Soluble FasL Is Required for Blister Formation in Pemphigus

To definitely assess the role of FasL in the mechanisms underlying pemphigus, we injected PVIgG into two different gene-targeted mutant mice that selectively lack either the secreted soluble FasL (sFasL), $FasL^{\Delta s/\Delta s}$ mice, or the membrane-bound FasL (mFasL), $FasL^{\Delta m/\Delta m}$ mice (12). Twenty hours after PVIgG treatment, despite the deposition of human IgG at the inter-keratinocyte level (**Figure 4A**), no acantholysis was detected in $FasL^{\Delta s/\Delta s}$ animals, as determined by the histological examination of H&E-stained sections (**Figure 4B**) and the measurement of the relative acantholytic areas (**Figure 4C**). By contrast, blisters were clearly visible in PVIgG-treated $FasL^{\Delta m/\Delta m}$ animals, lacking mFasL and in wild-type (WT) (C57BL/6) mice (**Figure 4B**). The magnitude of the acantholytic areas was significantly decreased (not detectable) in $FasL^{\Delta s/\Delta s}$ animals, as compared to that in control and $FasL^{\Delta m/\Delta m}$ mice (**Figure 4C**). Moreover, TUNEL-positive cells were statistically increased only in the skin of PVIgG-treated WT and $FasL^{\Delta m/\Delta m}$, but not in $FasL^{\Delta s/\Delta s}$ animals (**Figure 4D**). Finally, PVIgG injection failed to induce the activation of caspase-8 only in $FasL^{\Delta s/\Delta s}$ animals (**Figure 4E**).

DISCUSSION

Pemphigus is caused by autoantibodies targeting keratinocyte surface antigens. PVIgG binding to these proteins has long been considered to directly induce blister formation (21). Yet, it has now become clear that additional mechanisms following Ab binding contribute to skin blistering in pemphigus. A number of studies have provided evidence that reduced desmosomal adhesion and splitting follow changes in desmosomal structure and Dsg depletion (5). Moreover, several signaling pathways downstream of Ab binding, including p38 mitogen-activated protein kinase, EGFR, c-Myc, etc., have been shown to be involved in the loss of keratinocyte adhesion in pemphigus (22). In this context, the role of apoptosis has been the subject of much controversy. *In vitro* studies claim that apoptosis is not a prerequisite for skin

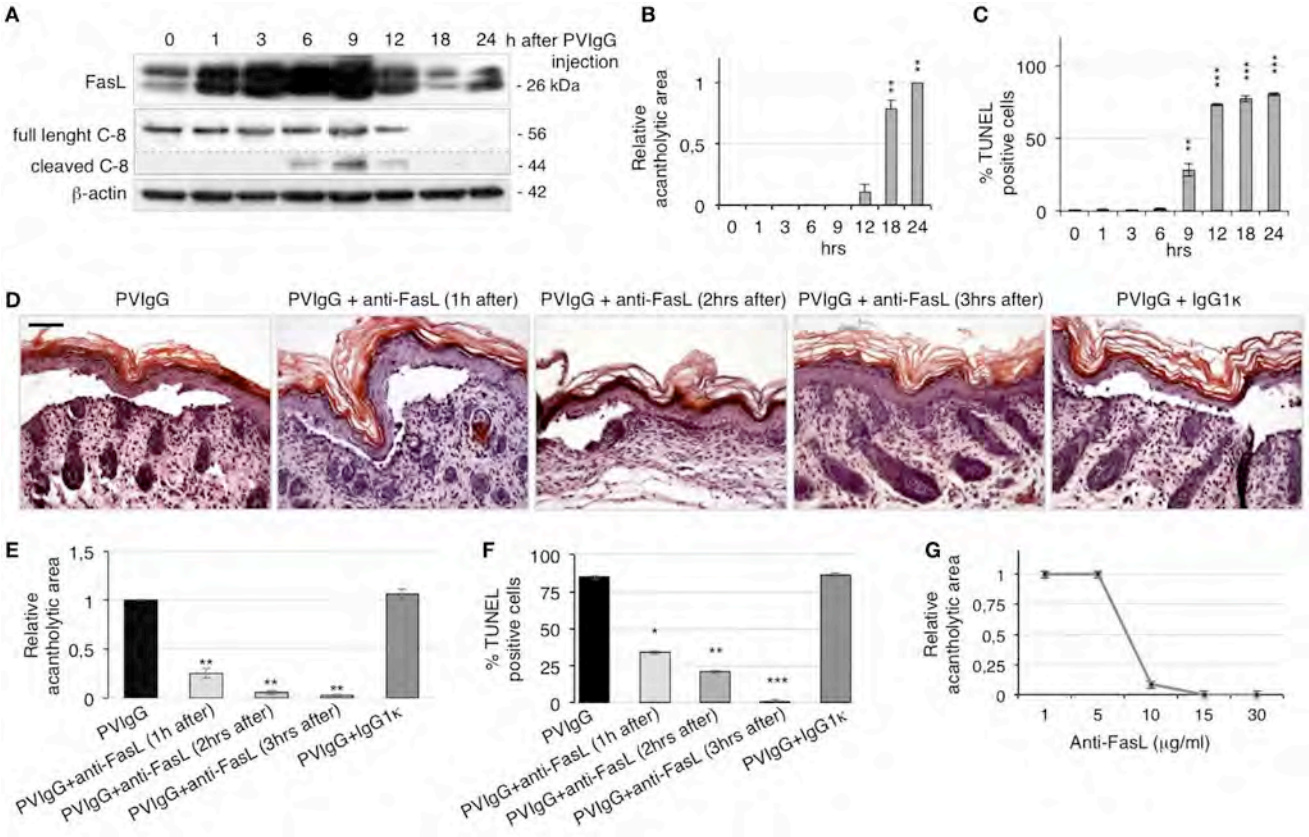

FIGURE 3 | Anti-Fas ligand (FasL) antibody (Ab) inhibits blister formation in pemphigus *in vivo*. **(A–C)** Neonatal mice were injected with pemphigus autoantibodies (PVIgG), sacrificed at various time points, and analyzed for the presence of FasL, acantholysis, and apoptosis activation. **(A)** FasL protein expression and caspase-8 activation in mouse skin extracts. **(B)** Relative acantholytic areas and **(C)** the percentage of TUNEL-positive cells in mouse skin. Each time point was compared to 0 h for statistical analysis (means ± SEM; $^{**}P < 0.01$; $^{***}P < 0.001$ per one-way ANOVA; $n = 5$ animals/each time point). **(D–F)** Neonatal mice were injected with normal human IgG (NIgG) or PVIgG, treated with anti-FasL Ab at the indicated time points and sacrificed at 20 h post PVIgG injection. IgG1κ was used as an isotype control for the anti-FasL Ab. **(D)** Hematoxylin and eosin staining of the neonatal mouse skin. Scale bar = 100 μm. **(E)** Relative acantholytic areas in mouse skin and **(F)** the percentage of TUNEL-positive cells in mouse skin (means ± SEM; $^{*}P < 0.05$; $^{**}P < 0.01$; $^{***}P < 0.001$ per Student's *t*-test, compared with PVIgG; $n = 5$ animals/each treatment). **(G)** Mice were treated with PVIgG and, 3 h later, with decreasing doses of anti-FasL Ab. Relative acantholysis areas were measured in at least three different fields ($n = 5$ animals/each treatment).

blistering but can contribute to the acantholytic process (23). By contrast, apoptotic cells are detected before blister formation, and the inhibition of caspase 3/7 prevents intraepidermal blistering in a murine pemphigus model (24). Most importantly, ST18 overexpression in pemphigus skin (25) confers a significant risk for the disease by both upregulating apoptosis and disrupting keratinocyte adhesion (26).

Our results clearly indicate a critical role of the Fas/FasL-induced extrinsic apoptotic pathway in the pathogenesis of pemphigus, consistent with previous studies showing the expression and the activation of Fas and FasL in acantholytic cells (7, 8). Specifically, we show for the first time that Fas/FasL system is operational before blister formation. Upon binding to pemphigus antigens, the Fas/FasL system leads to the activation of apoptosis and acantholysis. Moreover, we provide evidence that apoptosis precedes acantholysis, as Fas overexpression, caspase activation, and the appearance of TUNEL-positive cells occur before cell detachment *in vivo*.

Pemphigus autoantibodies upregulate FasL at the mRNA and protein level in human keratinocytes *in vitro* (14). Here, we report that the exposure to PVIgG results in the rapid release of soluble FasL *in vivo*. Deposits of FasL are present in association with intermediate filaments in keratinocytes (13). Because keratins control intercellular adhesion (27) and their retraction is associated with signaling pathways in pemphigus (28), we speculate that PVIgG-induced keratin uncoupling from the desmosomal complex may contribute to the rapid mobilization and release of FasL, resulting in the upregulation of FasL in the intercellular milieu. Altogether, our results demonstrate that pathogenic autoantibodies first induce the release of FasL, followed by the appearance of apoptotic epidermal cells, which in turn precedes the onset of blisters *in vivo*.

The addition of an anti-FasL-neutralizing Ab blocks blister formation in mice at 1–3 h after PVIgG injection. This is consistent with the timing of FasL upregulation in the epidermis, strongly indicating that anti-FasL blocks its target when it is locally released from keratinocytes, upon PVIgG stimulation.

Because mice lacking soluble FasL fail to develop blister upon PVIgG injection, we conclude that sFasL is responsible for

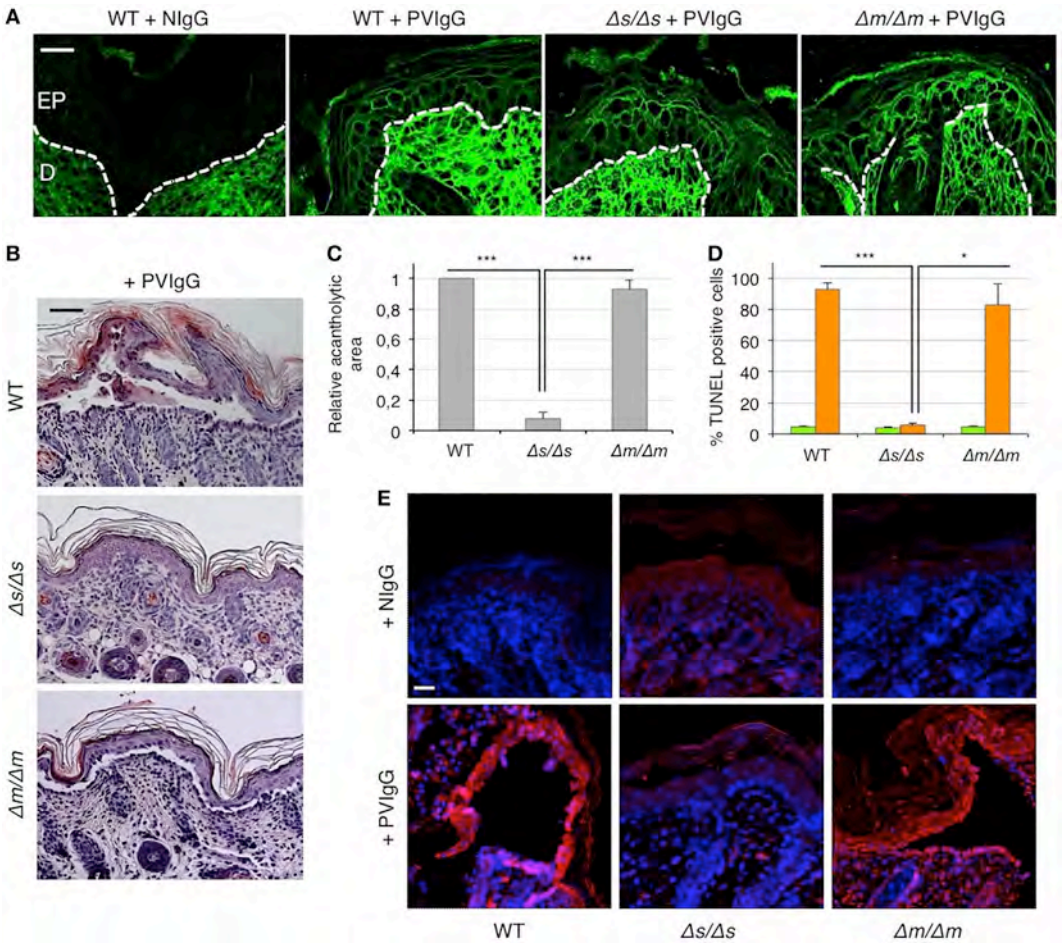

FIGURE 4 | Blister formation is blocked in mice selectively lacking soluble Fas ligand (FasL). Wild-type (WT), FasL$^{\Delta s/\Delta s}$, and FasL$^{\Delta m/\Delta m}$ mice were each injected with either normal human IgG (NIgG) or with pemphigus autoantibodies (PVIgG) and sacrificed at 20 h after injection. FasL$^{\Delta s/\Delta s}$: mice selectively lacking the soluble FasL; FasL$^{\Delta m/\Delta m}$: mice selectively lacking the membrane-bound FasL. **(A)** Representative images of PVIgG binding at the inter-keratinocyte level in the indicated mouse strains. Direct immunofluorescence: mouse skin specimens were challenged against fluorescein-conjugated human IgG. EP, Epidermis; D, dermis. Scale bar = 100 µm. NIgG (normal IgG) used as a negative control. **(B)** Representative hematoxylin and eosin staining of mouse skin. Scale bar = 75 µm. **(C)** Relative acantholytic areas in mouse skin (means ± SEM; ***$P < 0.001$ per one-way ANOVA; $n = 10$–11 mice/strain). **(D)** The percentage of TUNEL-positive cells in mouse skin treated either with NIgG (green bars) or with PVIgG (orange bars) (means ± SEM; *$P < 0.05$; ***$P < 0.001$ per one-way ANOVA; $n = 10$–11 mice/strain). **(E)** A representative immunofluorescence image showing active caspase-8 (red) expression at the skin level of NIgG or PVIgG-treated mice. Nuclei are shown in blue (DAPI). Scale bar = 100 µm.

acantholysis *in vivo*. The data presented here strongly indicate sFasL activation of caspase-8 and subsequent activation of caspase-3 as the main mechanism accounting for Dsg cleavage and blister formation in pemphigus. However, soluble FasL does not only trigger the extrinsic apoptotic pathway but also exert a number of pro-inflammatory activities (29, 30), which may be involved in pathological mechanisms of pemphigus. Whether these inflammatory responses could contribute to the development of blister remains to be determined.

Previous studies have attempted to prevent blister formation by pretreating mice with various signal transduction inhibitors, before PVIgG injection (31, 32). By contrast, in the present study, anti-FasL Ab blocks blister formation by acting after PVIgG injection, thus functioning in a system that is closely analogous to human disease. Currently, pemphigus therapy consists of the chronic administration of steroids and other immunosuppressors, which often results in severe side effects with a high fatality incidence. Blocking FasL-induced blister formation provides a relevant proof of concept that may lead to the development of new drugs to ameliorate pemphigus, possibly replacing the use of broad immunosuppressive agents.

AUTHOR CONTRIBUTIONS

RL, AM, and CP designed the studies; RL, ES, and TP conducted *in vivo* experiments on WT animals; AL and LO conducted *in vivo* experiments on FasL-mutant mice; RL, MQ, and EP conducted *in vitro* experiments; RL and AM analyzed data; RL, LO, and CP wrote the manuscript.

ACKNOWLEDGMENTS

We thank G. Cianchini and G. Di Zenzo (IDI-IRCSS, Rome, Italy) for providing sera from pemphigus patients. We thank L. E. French (Zurich University Hospital, Zurich, Switzerland) and A. Strasser (WEHI, VIC, Australia) for the critical reading of the manuscript.

FUNDING

This work was supported by a grant from the Italian Ministry of Instruction, University and Research PRIN 20077FPJ22_001. ES was supported by the Japan Health Sciences Foundation. This work was further supported by a Cancer Australia and Cancer Council New South Wales project grant #1047672 (LO), the Victorian State Government (OIS grant), and the Leukemia and Lymphoma Society (SCOR grant #7413 and #7001-13, LO).

SUPPLEMENTARY MATERIAL

The Supplementary Material for this article can be found online at http://www.frontiersin.org/articles/10.3389/fimmu.2018.00370/full#supplementary-material.

REFERENCES

1. Kasperkiewicz M, Ellebrecht CT, Takahashi H, Yamagami J, Zillikens D, Payne AS, et al. Pemphigus. *Nat Rev Dis Primers* (2017) 3:17026. doi:10.1038/nrdp.2017.26
2. Stanley JR, Amagai M. Pemphigus, bullous impetigo, and the staphylococcal scalded-skin syndrome. *N Engl J Med* (2006) 355(17):1800–10. doi:10.1056/NEJMra061111
3. Amagai M, Tsunoda K, Suzuki H, Nishifuji K, Koyasu S, Nishikawa T. Use of autoantigen-knockout mice in developing an active autoimmune disease model for pemphigus. *J Clin Invest* (2000) 105(5):625–31. doi:10.1172/JCI8748
4. Amagai M, Ahmed AR, Kitajima Y, Bystryn JC, Milner Y, Gniadecki R, et al. Are desmoglein autoantibodies essential for the immunopathogenesis of pemphigus vulgaris, or just "witnesses of disease"? *Exp Dermatol* (2006) 10:815–31. doi:10.1111/j.1600-0625.2006.00499_1.x
5. Vielmuth F, Waschke J, Spindler V. Loss of desmoglein binding is not sufficient for keratinocyte dissociation in pemphigus. *J Invest Dermatol* (2015) 135(12):3068–77. doi:10.1038/jid.2015.324
6. Grando SA, Bystryn JC, Chernyavsky AI, Frusić-Zlotkin M, Gniadecki R, Lotti R, et al. Apoptolysis: a novel mechanism of skin blistering in pemphigus vulgaris linking the apoptotic pathways to basal cell shrinkage and suprabasal acantholysis. *Exp Dermatol* (2009) 18(9):764–70. doi:10.1111/j.1600-0625.2009.00934.x
7. Wang X, Brégégère F, Frusić-Zlotkin M, Feinmesser M, Michel B, Milner Y. Possible apoptotic mechanism in epidermal cell acantholysis induced by pemphigus vulgaris autoimmunoglobulins. *Apoptosis* (2004) 9(2):131–43. doi:10.1023/B:APPT.0000018795.05766.1f
8. Frusic-Zlotkin M, Pergamentz R, Michel B, David M, Mimouni D, Brégégère F, et al. The interaction of pemphigus autoimmunoglobulins with epidermal cells: activation of the Fas apoptotic pathway and the use of caspase activity for pathogenicity tests of pemphigus patients. *Ann N Y Acad Sci* (2005) 1050:371–9. doi:10.1196/annals.1313.040
9. Tanaka M, Suda T, Takahashi T, Nagata S. Expression of the functional soluble form of human Fas ligand in activated lymphocytes. *EMBO J* (1995) 14(6):1129–35.
10. Schneider P, Tschopp J. Apoptosis induced by death receptors. *Pharm Acta Helv* (2000) 74(2–3):281–6. doi:10.1016/S0031-6865(99)00038-2
11. Holler N, Tardivel A, Kovacsovics-Bankowski M, Hertig S, Gaide O, Martinon F, et al. Two adjacent trimeric Fas ligands are required for Fas signaling and formation of a death-inducing signaling complex. *Mol Cell Biol* (2003) 23(4):1428–40. doi:10.1128/MCB.23.4.1428-1440.2003
12. O'Reilly LA, Tai L, Lee L, Kruse EA, Grabow S, Fairlie WD, et al. Membrane-bound Fas ligand only is essential for Fas-induced apoptosis. *Nature* (2009) 461(7264):659–63. doi:10.1038/nature08402
13. Viard-Leveugle I, Bullani RR, Meda P, Micheau O, Limat A, Saurat JH, et al. Intracellular localization of keratinocyte Fas ligand explains lack of cytolytic activity under physiological conditions. *J Biol Chem* (2003) 278(18):16183–8. doi:10.1074/jbc.M212188200
14. Arredondo J, Chernyavsky AI, Karaouni A, Grando SA. Novel mechanisms of target cell death and survival and of therapeutic action of IVIg in pemphigus. *Am J Pathol* (2005) 167(6):1531–44. doi:10.1016/S0002-9440(10)61239-4
15. Puviani M, Marconi A, Cozzani E, Pincelli C. Fas ligand in pemphigus sera induces keratinocyte apoptosis through the activation of caspase-8. *J Invest Dermatol* (2003) 120(1):164–7. doi:10.1046/j.1523-1747.2003.12014.x
16. Pincelli C, Haake AR, Benassi L, Grassilli E, Magnoni C, Ottani D, et al. Autocrine nerve growth factor protects human keratinocytes from apoptosis through its high affinity receptor (TRK): a role for BCL-2. *J Invest Dermatol* (1997) 109(6):757–64. doi:10.1111/1523-1747.ep12340768
17. Takahashi Y, Patel HP, Labib RS, Diaz LA, Anhalt GJ. Experimentally induced pemphigus vulgaris in neonatal BALB/c mice: a time-course study of clinical, immunologic, ultrastructural, and cytochemical changes. *J Invest Dermatol* (1985) 84(1):41–6. doi:10.1111/1523-1747.ep12274679
18. Weiske J, Schöneberg T, Schröder W, Hatzfeld M, Tauber R, Huber O. The fate of desmosomal proteins in apoptotic cells. *J Biol Chem* (2001) 276(44):41175–81. doi:10.1074/jbc.M105769200
19. Dusek RL, Getsios S, Chen F, Park JK, Amargo EV, Cryns VL, et al. The differentiation-dependent desmosomal cadherin desmoglein 1 is a novel caspase-3 target that regulates apoptosis in keratinocytes. *J Biol Chem* (2006) 281(6):3614–24. doi:10.1074/jbc.M508258200
20. Ishii K, Harada R, Matsuo I, Shirakata Y, Hashimoto K, Amagai M. *In vitro* keratinocyte dissociation assay for evaluation of the pathogenicity of anti-desmoglein 3 IgG autoantibodies in pemphigus vulgaris. *J Invest Dermatol* (2005) 124(5):939–46. doi:10.1111/j.0022-202X.2005.23714.x
21. Heupel WM, Zillikens D, Drenckhahn D, Waschke J. Pemphigus vulgaris IgG directly inhibit desmoglein 3-mediated transinteraction. *J Immunol* (2008) 181(3):1825–34. doi:10.4049/jimmunol.181.3.1825
22. Spindler V, Eming R, Schmidt E, Amagai M, Grando S, Jonkman MF, et al. Mechanisms causing loss of keratinocyte cohesion in pemphigus. *J Invest Dermatol* (2018) 138(1):32–7. doi:10.1016/j.jid.2017.06.022
23. Schmidt E, Gutberlet J, Siegmund D, Berg D, Wajant H, Waschke J. Apoptosis is not required for acantholysis in pemphigus vulgaris. *Am J Physiol Cell Physiol* (2009) 296(1):C162–72. doi:10.1152/ajpcell.00161.2008
24. Li N, Zhao M, Wang J, Liu Z, Diaz LA. Involvement of the apoptotic mechanism in pemphigus foliaceous autoimmune injury of the skin. *J Immunol* (2009) 182(1):711–7. doi:10.4049/jimmunol.182.1.711
25. Sarig O, Bercovici S, Zoller L, Goldberg I, Indelman M, Nahum S, et al. Population-specific association between a polymorphic variant in ST18, encoding a pro-apoptotic molecule, and pemphigus vulgaris. *J Invest Dermatol* (2012) 132(7):1798–805. doi:10.1038/jid.2012.46
26. Vodo D, Sarig O, Geller S, Ben-Asher E, Olender T, Bochner R, et al. Identification of a functional risk variant for pemphigus vulgaris in the ST18 gene. *PLoS Genet* (2016) 12(5):e1006008. doi:10.1371/journal.pgen.1006008
27. Kröger C, Loschke F, Schwarz N, Windoffer R, Leube RE, Magin TM. Keratins control intercellular adhesion involving PKC-α-mediated desmoplakin phosphorylation. *J Cell Biol* (2013) 201(5):681–92. doi:10.1083/jcb.201208162
28. Dehner C, Rötzer V, Waschke J, Spindler V. A desmoplakin point mutation with enhanced keratin association ameliorates pemphigus vulgaris autoantibody-mediated loss of cell cohesion. *Am J Pathol* (2014) 184(9):2528–36. doi:10.1016/j.ajpath.2014.05.016

29. Peter ME, Budd RC, Desbarats J, Hedrick SM, Hueber AO, Newell MK, et al. The CD95 receptor: apoptosis revisited. *Cell* (2007) 129(3):447–50. doi:10.1016/j.cell.2007.04.031
30. Man SM, Kanneganti TD. Converging roles of caspases in inflammasome activation, cell death and innate immunity. *Nat Rev Immunol* (2016) 16(1): 7–21. doi:10.1038/nri.2015.7
31. Sánchez-Carpintero I, España A, Pelacho B, López Moratalla N, Rubenstein DS, Diaz LA, et al. *In vivo* blockade of pemphigus vulgaris acantholysis by inhibition of intracellular signal transduction cascades. *Br J Dermatol* (2004) 151(3):565–70. doi:10.1111/j.1365-2133.2004.06147.x
32. Berkowitz P, Hu P, Warren S, Liu Z, Diaz LA, Rubenstein DS. p38MAPK inhibition prevents disease in pemphigus vulgaris mice. *Proc Natl Acad Sci U S A* (2006) 103(34):12855–60. doi:10.1073/pnas.0602973103

Conflict of Interest Statement: CP and AM are cofounders of PinCell s.r.l., a start-up company involved in drug development for pemphigus. They are coinventors on a patent that includes some data presented in this work (WO2010066914A3). Other authors declare no competing financial interests.

frontiers in Immunology

MINI REVIEW
published: 19 February 2018
doi: 10.3389/fimmu.2018.00254

Targeting IgE Antibodies by Immunoadsorption in Atopic Dermatitis

Michael Kasperkiewicz[1], Enno Schmidt[1,2], Ralf J. Ludwig[1,2] and Detlef Zillikens[1,2]*

[1] Department of Dermatology, University of Lübeck, Lübeck, Germany, [2] Lübeck Institute of Experimental Dermatology, University of Lübeck, Lübeck, Germany

One major hallmark of atopic dermatitis (AD) is the elevated level of total serum IgE, which has been reported to be partly of the autoreactive type in a subset of patients. Immunoadsorption (IA) has been successfully applied in various classical autoantibody-mediated diseases such as pemphigus. Recent reports proposed the use of IA also for patients with severe AD and high total serum IgE levels. In this mini-review, we summarize the current knowledge about this novel treatment approach for AD and briefly discuss the so far incompletely known role of autoreactive IgE as potential target of IA therapy in this common inflammatory skin disorder.

Keywords: atopic dermatitis, autoantibody, IgE, immunoadsorption, inflammation

OPEN ACCESS

Edited by:
Rachel R. Caspi, National Institutes of Health (NIH), United States

Reviewed by:
David Voehringer, University of Erlangen-Nuremberg, Germany
Alessandro Fiocchi, Bambino Gesù Ospedale Pediatrico (IRCCS), Italy

****Correspondence:***
Michael Kasperkiewicz
michael.kasperkiewicz@uksh.de

Specialty section:
This article was submitted to Immunological Tolerance and Regulation, a section of the journal Frontiers in Immunology

Received: *16 November 2017*
Accepted: *29 January 2018*
Published: *19 February 2018*

Citation:
Kasperkiewicz M, Schmidt E, Ludwig RJ and Zillikens D (2018) Targeting IgE Antibodies by Immunoadsorption in Atopic Dermatitis. Front. Immunol. 9:254. doi: 10.3389/fimmu.2018.00254

INTRODUCTION

Atopic dermatitis (AD) is a chronic or chronically relapsing, eczematous, pruritic skin disease affecting 2–20% of the general population, which can considerably affect the patient's quality of life. It is often associated with type I allergic diseases, including food allergy, asthma, and allergic rhinitis (1).

The pathophysiology of AD is complex and involves the interplay of genetic, immunological, and environmental factors. Both skin barrier dysfunction due to decreased filaggrin expression and a biphasic T cell-mediated immune reaction driven by a Th2 phenotype in childhood and acute disease phase that is shifted toward a Th1 signal in the chronic stage are considered to play important roles in the disease process. One major hallmark of the disease is the elevated level of total serum IgE in approximately 80% of AD patients. In fact, AD patients mount IgE antibody responses to various environmental allergens and autoantigens, which will be discussed later in this review (1).

The drug therapy of AD consists of topical emollients for barrier dysfunction and topical corticosteroids and calcineurin inhibitors for skin inflammation, as well as, in severe cases, systemic anti-inflammatory agents such as cyclosporine A. However, these conventional treatments may not show uniform efficacy and can be limited by severe side effects. Thus, several new targeting therapies, including the newly approved promising IL-4 receptor α chain antagonist dupilumab, have emerged (1).

Clinical benefit has been also achieved through sequestering of free IgE by the anti-IgE monoclonal antibody omalizumab in AD patients with poor response to traditional therapy, although some controversial results have been reported. Effects of this treatment seem to depend on baseline total serum IgE levels as less favorable clinical responses were associated with concentrations of more that 700 kU/L compared with lower levels. This observation is based on a recent systematic review and meta-analysis of 103 AD patients from 13 studies, which overall revealed that 43% of these patients

could achieve an excellent clinical response after omalizumab treatment, while 27% showed satisfying results and 30% had irrelevant clinical changes or deterioration (2). Restricted clinical efficacy in some cases may be related to insufficient IgE neutralization by omalizumab, for which the recommended dosing table is limited to 150–1,200 mg/month (2, 3).

In the recent years, immunoadsorption (IA) has evolved as an alternative anti-IgE treatment for patients with severe AD displaying high total serum IgE (4–9). In addition, it has been reported that IA can increase the threshold of IgE immunoreactivity to different food allergens and thus reduce the risk of anaphylaxis in multiple food allergy (10, 11). Most recently, a pilot study indicated that IA may also be used to treat patients with allergic asthma (12). While much more experience with this treatment exists in classical autoantibody-mediated diseases such as pemphigus (13), application of IA in AD is limited to only a few centers so far. The active principle of most available adsorber types is the non-specific removal of the different immunoglobulins from the patient's circulation (13), although an IgE-specific adsorber column has more recently become available (5, 8–12).

This mini-review summarizes the current knowledge about IA in AD and briefly discusses the role of autoreactive IgE as potential target of IA therapy in this inflammatory skin disease.

IA in AD

IA Protocols

To date, six studies on the use of IA in 2–50 patients per case series with severe AD and high total serum IgE levels have been published (summarized in **Table 1**) (4–9). The first IA treatment protocol for AD has been introduced by our group in 2011. In this pilot study, patients with treatment-refractory AD and total serum IgE levels >4,500 kU/L were treated with a total of 10 IA on days 1–5 (week 1) and days 29–33 (week 5) by using adsorption columns that contained polyclonal sheep antihuman immunoglobulin antibodies binding the different human immunoglobulins with similar affinity (referred to as panimmunoglobulin IA) (4). The same treatment protocol was used in our two following studies, with the major difference that the adsorber consisted of monoclonal mouse antihuman IgE (referred to as IgE-selective IA) (5, 9). Three other independent studies used panimmunoglobulin IA in patients with severe AD and high total serum IgE applying (i) 1–5 cycles of 5 consecutive aphereses at monthly intervals (6), (ii) 1 cycle of 2–4 consecutive aphereses followed by omalizumab every 2 weeks for 24 weeks (7), and (iii) 3 cycles of 3–4 consecutive aphereses at weeks 1, 3, and 8 (8). Some patients of the latter study were treated with IgE-selective IA (8). In all studies except for the trial combining IA with omalizumab (7), the patients' preceding topical and systemic treatments for AD were continued during IA therapy and modified as needed (4–6, 8, 9).

Effects on the Clinical Course

During a follow-up time of 3–18 months, the published studies uniformly revealed a satisfactory initial linear decrease of the disease severity [measured by Scoring Atopic Dermatitis (SCORAD) or Eczema Area and Severity Index] as early as within the first 3 weeks after initiation of IA regardless of the IA treatment protocol used (4–9). Results from our three reports indicate that IA treatment resulted in continuous and stable SCORAD improvements of up to approximately 60% for at least 3–6 months (4, 5, 9), although some minor re-increases in the SCORAD (being still lower than before initiation of IA) were observed in patients treated by IgE-selective IA during the second half of the observation period (5, 9). In the study by Reich et al., clinical effects remained widely stable until 6 months of follow-up with no major differences in clinical efficacy between panimmunoglobulin IA- and IgE-selective IA-treated patients (8). Combined use of IA and omalizumab resulted in a steady decrease of the SCORAD throughout the 6-month treatment period, whereas a reverse trend was observed during treatment-free follow-up of another 6 months (7). No additional benefit with regard to further SCORAD improvement was observed in one study when more than three monthly cycles of five consecutive panimmunoglobulin IA were applied, although one patient who completed five IA cycles exhibited a long lasting clinical benefit over 12 months (6).

Of note, the studies demonstrated that IA was associated with disease amelioration in patients' refractory to multiple conventional treatments including cyclosporine A, which could be partly reduced or discontinued after IA (4–6, 8, 9).

Effects on Circulating IgE and Other Serum Parameters

Results from our three reports revealed that serum IgE levels were effectively reduced by a mean of more than 90% with each IA cycle regardless of the specificity of the adsorber (4, 5, 9). Similar IgE reductions were observed in the other three studies ranging from an average of approximately 60–90% depending on the length of the IA cycle (6–8). In contrast to panimmunoglobulin IA, however, which reduced other immunoglobulin isotypes to a similar degree (4, 8), serum concentrations of IgM, IgA, and IgG were decreased by only less than half using IgE-selective IA (5, 8, 9). The concomitant decrease of immunoglobulins other than IgE by the IgE-selective adsorber is considered to be non-specific and explained by IA-related elution and dilution procedures (5, 8, 9). Effects of IgE-selective and –non-selective IA on peripheral levels of IgE and other immunoglobulins were transient since immunoglobulin levels started to rise again following each IA procedure and precycle values remained widely similar over time (4–6, 8, 9). Thus, considering the generally steady decrease of the disease activity following IA, total serum IgE levels only incompletely paralleled the clinical course of the patients. By contrast, a different observation was made by the combinatory use of IA and omalizumab. After initial reduction in total circulating IgE by IA, free serum IgE levels continued to fall during omalizumab treatment [in parallel with SCORAD improvement and reduction in serum levels of the biomarker thymus and activation regulated chemokine (TARC)] and started to increase again (in parallel with SCORAD worsening and increase of TARC) during follow-up after anti-IgE therapy was discontinued (7).

TABLE 1 | Summary of published studies relating to IA and AD.

Reference	Patient characteristics	IA protocol	Concomitant therapy	Follow-up time after IA start (months)	Main clinical outcomes	Main laboratory outcomes	Side effects
Kasperkiewicz et al. (4)	12 patients, 3 females, and 9 males; 24–66 (mean 42) years; SCORAD 55–98 (mean 78.6); total serum IgE 4,666–86, 119 (mean 22,034) kU/L	2 cycles of 5 consecutive panimmunoglobulin IA (TheraSorb-Ig®, Miltenyi Biotec) at weeks 1 and 5	Topical corticosteroids/ calcineurin inhibitors, oral antihistamines, and cyclosporine A	3	Mean SCORAD improvement by 38% (week 3), 46% (week 5), 56% (week 9), and 59% (week 13); parallel improvement of EASI	Temporal mean serum IgE reduction by >90% per IA cycle (similarly for IgG/IgM/IgA); sustained reduction of skin-bound IgE as well as histologic alterations (hyperkeratosis, spongiosis, acanthosis, and dermal infiltrate)	Central venous catheter-related *Staphylococcus aureus* septicemia ($n = 1$)
Kasperkiewicz et al. (5)	2 male patients; 40–60 years; SCORAD 66 and 77 (mean 71.5); total serum IgE 17,020 and 46,540, (mean 31,780) kU/L, respectively	2 cycles of 5 consecutive IgE-selective IA (TheraSorb-IgE®, Miltenyi Biotec) at weeks 1 and 5	Topical corticosteroids/ calcineurin inhibitors, oral antihistamines, and cyclosporine A	6	Mean SCORAD improvement by 33% (week 3), 37% (week 5), 54% (week 9), 53% (week 13), 55% (week 17), and 49% (week 25)	Temporal mean serum IgE reduction by >90% per IA cycle (36–49% for IgG/IgM/IgA)	None
Daeschlein et al. (6)	7 patients, 2 females and 5 males; 17–61 (mean 35.3) years; SCORAD 21.3–77 (mean 52); total serum IgE 724–28,500 (mean 11,015) kU/L	1–5 cycles of 5 consecutive panimmunoglobulin IA (TheraSorb-Ig flex®, Miltenyi Biotec) at monthly intervals	Topical corticosteroids/ calcineurin inhibitors, oral antihistamines, cyclosporine A	12–18	Mean SCORAD improvement by 25.1% (after 1. IA cycle), 27.9% (after 2. IA cycle), 37.6% (after 3. IA cycle), 24.1% (after 4. IA cycle), and 11.1% (after 5. IA cycle)	Temporal mean serum IgE reduction by 74–80% per IA cycle	Drop of blood pressure ($n = 2$)
Zink et al. (7)	10 patients, 2 females and 8 males; 26–65 (mean 43.7) years; SCORAD 50.2–74.6 (mean 59.9); total serum IgE 3,728–69,872 (mean 18,094) kU/L	1 cycle of 2–4 consecutive panimmunoglobulin IA (TheraSorb-Ig flex®, Miltenyi Biotec) followed by omalizumab every 2 weeks for 24 weeks	Topical corticosteroids	12	Mean SCORAD improvement by 27% (week 3), 40% (week 13), 55% (week 25), and 19% (re-increased; week 49); parallel improvement and re-increase of VAS subjective severity score	Mean serum IgE reduction by 58–86% after 2–4 IA, respectively; serum IgE and TARC levels decreased continuously during omalizumab therapy and re-increased during treatment-free follow-up	IA-related: dizziness ($n = 1$) and fatigue ($n = 2$); omalizumab-related: headache ($n = 1$), abdominal pain ($n = 1$), axillary lymph node swelling ($n = 1$), and elevation of liver enzymes ($n = 3$)
Reich et al. (8)	50 patients, 20 females and 30 males; 21–75 (mean 45.6) years; mean EASI and SCORAD 21.3 and 40.5, respectively; median total serum IgE 6,700 k	3 cycles of 3–4 consecutive panimmunoglobulin IA ($n = 24$; TheraSorb-Ig flex®, Miltenyi Biotec) or IgE-selective IA ($n = 26$; TheraSorb-IgE®, Miltenyi Biotec) at weeks 1, 3, and 8	Topical and systemic corticosteroids, topical calcineurin inhibitors, cyclosporine A, methotrexate, and mycophenolate mofetil	8	Median EASI improvement by 39 and 47% (week 6), 52 and 45% (week 12), and 61 and 60% (week 32) in the panimmunoglobulin and IgE-selective IA group, respectively; parallel improvement of SCORAD, POEM, and DLQI	Temporal median serum IgE reduction by 85 and 90% per IA cycle in the panimmunoglobulin and IgE-selective IA group (85 and 20% for IgG), respectively	Panimmunoglobulin IA group only: herpes labialis ($n = 2$), herpes keratitis ($n = 1$), bacterial conjunctivitis ($n = 1$), bacterial sinusitis ($n = 1$), air embolism during central venous catheter placement ($n = 1$), cubital vein thrombophlebitis ($n = 1$), and generalized cutaneous allergic drug reaction ($n = 1$)
Kasperkiewicz et al. (9)	10 patients, 3 females and 7 males; 18–70 (mean 40.3) years; SCORAD 61.5–81 (mean 67.5); total IgE 931–21,510 (mean 5,377) kU/L	2 cycles of 5 consecutive IgE-selective IA (TheraSorb-IgE®; Miltenyi Biotec) at weeks 1 and 5	Topical and systemic corticosteroids, topical calcineurin inhibitors, oral antihistamines	6	Mean SCORAD improvement by 19% (week 3), 29% (week 5), 43% (week 9), 21% (week 13), 25% (week 17), and 29% (week 25)	Temporal mean serum IgE reduction by > 90% per IA cycle (35–43% for IgG/IgM/IgA)	Central venous catheter-related *S. aureus* septicemia ($n = 1$), fatigue ($n = 1$), and edema of hands and feet ($n = 1$)

AD, atopic dermatitis; DLQI, Dermatology Life Quality Index; EASI, Eczema Area and Severity Index; IA, immunoadsorption; POEM, Patient-Oriented Eczema Measure; SCORAD, Scoring Atopic Dermatitis; TARC, thymus and activation regulated chemokine; VAS, Visual Analog Scale.

Effects on Skin-bound IgE and Other Skin Parameters

In contrast to the abovementioned kinetics of circulating IgE, a continuous reduction of the amount of skin-bound IgE was observed by immunohistochemistry in our initial IA pilot study (4). It can be hypothesized that a redistribution of tissue-bound IgE from inflammatory skin sites into the intravascular compartment occurs, which may at least partly explain the rebound phenomenon of serum IgE levels following IA. In addition, repetitive skin biopsies after IA revealed a steady decrease in skin infiltration by antigen-presenting cells and T cell as well as improvement of altered epidermal morphology including hyperkeratosis, spongiosis, and acanthosis (4). In this context, it is worth noting that omalizumab has been previously shown to inhibit antigen processing and presentation to T cells by downregulating the expression of the high-affinity IgE receptor FcepsilonRI on dendritic cells (14). Thus, impairment of IgE-mediated antigen exposure in the skin could represent a possible mechanism of action of IA contributing to disease amelioration in AD patients.

Safety

IA in patients with AD, who usually have an increased genetic susceptibility to skin infections by pathogens such as *Staphylococcus aureus* and *Herpes simplex* virus (1), is generally well tolerated (4–9). The selective IgE adsorber has been developed to decrease the potential higher risk of infections due to the parallel considerable reduction of protective immunoglobulins as it occurs with panimmunoglobulin IA. In fact, in the study by Reich et al., infectious adverse events, including bacterial conjunctivitis/sinusitis and herpes labialis/keratitis, were observed in AD patients treated by panimmunoglobulin IA but not IgE-selective IA (8). By contrast, however, we reported two cases of *S. aureus* septicemia, one occurring after panimmunoglobulin IA and the other following IgE-selective IA, both performed by a central venous catheter (4, 9). Thus, IgE-selective IA using peripheral venous access seems most preferable, although further studies are needed to better define the safety profile of this treatment in AD patients.

Autoreactive IgE as Potential Target of IA in AD

With the help of Th2 cytokines, activated B cells undergo production of IgE antibodies, which have been reported to be partly of the autoreactive type in AD (15–18). More than 140 autoantigens triggering IgE autoantibodies in AD patients have been reported (16), some of them potentially binding to cell membrane and intracellular structures of cultured human keratinocytes (15). IgE autoantibodies can either be specific for autoantigens (Homs 1–5, antinuclear antibodies, DSF70, and p80-coilin) or cross-react with environmental allergens due to their high homology with self-antigens (manganese superoxide dismutase, thioredoxin, profilin, and acidic ribosomal P2 protein) (18). In fact, a systematic review involving 1,253 AD patients and 1,391 control subjects found autoreactivity in up to 91% compared with 0–12%, respectively, although it remains widely unknown whether this is a cause or consequence of skin inflammation in AD (17).

It has been hypothesized that scratching-induced tissue damage can lead to the release of autoantigens that bind to IgE autoantibodies. This may consecutively result in immediate-type hypersensitivity reactions as well as T cell activation and cytokine secretion through IgE cross-linking on the cell surface and IgE-mediated autoantigen presentation, respectively (18). In contrast to other IgE-driven diseases, such as bullous pemphigoid (19), however, it is less known whether autoreactive IgE in AD patients are truly pathogenic or only represent a bystander epiphenomenon.

Pathogenicity of IgE-mediated autoreactivity in AD is supported by the following reported evidence: (i) IgE autoantibodies are not present in other allergic diseases, such as allergic asthma or allergic rhinoconjunctivitis, which are characterized by increased total IgE levels (17); (ii) existence of pro-inflammatory cytokine-producing autoreactive T cells specific for autoantigens [e.g., α-NAC (Homs 2)] for which autoreactivity has been described on the humoral level (20, 21); (iii) disease severity in AD patients is higher in autoreactive patients than in non-autoreactive ones (15, 17); (iv) SCORAD values and serum TARC levels correlate with IgE autoantibodies to human manganese superoxide dismutase and DSF70, respectively (22, 23); and (v) cyclosporine A-induced improvement of skin symptoms in AD patients is accompanied by reduction in IgE autoreactivity (but not IgE antibodies to exogenous allergens), with a reverse trend without treatment; clinical improvement precedes decrease of IgE autoreactivity, potentially suggesting reduced tissue injury-driven exposure of self-antigens to autoreactive B cells in these patients (24, 25).

Therefore, it is tempting to speculate that disease amelioration by IA in some AD patients may also, at least in part, be attributed to a decrease of IgE autoreactivity.

CONCLUSION

Clinical evidence suggests that IA seems to be an effective treatment option for patients severely affected by AD with highly elevated IgE serum levels. IA is associated with temporal and sustained reduction of circulating and skin-bound IgE, but the exact mechanisms underlying the clinical response in AD patients remain to be elucidated (4–9). Although the role of IgE in AD is still a matter of debate, these findings favor a pathogenic potential of IgE antibodies in this disorder. Future studies should explore whether a particular subset of AD patients who have circulating autoreactive IgE antibodies may especially benefit from this type of direct antibody depletion therapy.

AUTHOR CONTRIBUTIONS

MK wrote the paper with the help of ES, RL, and DZ.

FUNDING

This work was supported by infrastructural funding provided by Deutsche Forschungsgemeinschaft Excellence Cluster Inflammation at Interfaces (EXC 306/2).

REFERENCES

1. Weidinger S, Novak N. Atopic dermatitis. *Lancet* (2016) 387:1109–22. doi:10.1016/S0140-6736(15)00149-X
2. Wang HH, Li YC, Huang YC. Efficacy of omalizumab in patients with atopic dermatitis: a systematic review and meta-analysis. *J Allergy Clin Immunol* (2016) 138:1719–22. doi:10.1016/j.jaci.2016.05.038
3. Kornmann O, Watz H, Fuhr R, Krug N, Erpenbeck VJ, Kaiser G. Omalizumab in patients with allergic (IgE-mediated) asthma and IgE/bodyweight combinations above those in the initially approved dosing table. *Pulm Pharmacol Ther* (2014) 28:149–53. doi:10.1016/j.pupt.2014.03.003
4. Kasperkiewicz M, Schmidt E, Frambach Y, Rose C, Meier M, Nitschke M, et al. Improvement of treatment-refractory atopic dermatitis by immunoadsorption: a pilot study. *J Allergy Clin Immunol* (2011) 127:267–70. doi:10.1016/j.jaci.2010.07.042
5. Kasperkiewicz M, Süfke S, Schmidt E, Zillikens D. IgE-specific immunoadsorption for treatment of recalcitrant atopic dermatitis. *JAMA Dermatol* (2014) 150:1350–1. doi:10.1001/jamadermatol.2014.2082
6. Daeschlein G, Scholz S, Lutze S, Eming R, Arnold A, Haase H, et al. Repetitive immunoadsorption cycles for treatment of severe atopic dermatitis. *Ther Apher Dial* (2015) 19:279–87. doi:10.1111/1744-9987.12267
7. Zink A, Gensbaur A, Zirbs M, Seifert F, Suarez IL, Mourantchanian V, et al. Targeting IgE in severe atopic dermatitis with a combination of immunoadsorption and omalizumab. *Acta Derm Venereol* (2016) 96:72–6. doi:10.2340/00015555-2165
8. Reich K, Deinzer J, Fiege AK, von Gruben V, Sack AL, Thraen A, et al. Panimmunoglobulin and IgE-selective extracorporeal immunoadsorption in patients with severe atopic dermatitis. *J Allergy Clin Immunol* (2016) 137:1882–4. doi:10.1016/j.jaci.2016.01.016
9. Kasperkiewicz M, Mook SC, Knuth-Rehr D, Vorobyev A, Ludwig RJ, Zillikens D, et al. IgE-selective immunoadsorption for severe atopic dermatitis. *Front Med* (2018) 5:27. doi:10.3389/fmed.2018.00027
10. Dahdah L, Ceccarelli S, Amednola S, Campagnano P, Cancrini C, Mazzina O. IgE immunoadsorption knocks down the risk of food-related anaphylaxis. *Pediatrics* (2015) 136:e1617–20. doi:10.1542/peds.2015-1757
11. Dahdah L, Leone G, Artesani M, Raccardi C, Mazzina O. Apheresis in food allergies. *Curr Opin Allergy Clin Immunol* (2017) 17:227–31. doi:10.1097/ACI.0000000000000366
12. Lupinek C, Derfler K, Lee S, Prikoszovich T, Movadat O, Wollmann E, et al. Extracorporeal IgE immunoadsorption in allergic asthma: safety and efficacy. *EBioMedicine* (2017) 17:119–33. doi:10.1016/j.ebiom.2017.02.007
13. Meyersburg D, Schmidt E, Kasperkiewicz M, Zillikens D. Immunoadsorption in dermatology. *Ther Apher Dial* (2012) 16:311–20. doi:10.1111/j.1744-9987.2012.01075.x
14. Prussin C, Griffith DT, Boesel KM, Lin H, Foster B, Casale TB. Omalizumab treatment downregulates dendritic cell FcepsilonRI expression. *J Allergy Clin Immunol* (2003) 112:1147–54. doi:10.1016/j.jaci.2003.10.003
15. Altrichter S, Kriehuber E, Moser J, Valenta R, Kopp T, Stingl G. Serum IgE autoantibodies target keratinocytes in patients with atopic dermatitis. *J Invest Dermatol* (2008) 128:2232–9. doi:10.1038/jid.2008.80
16. Zeller S, Rhyner C, Meyer N, Schmid-Grendelmeier P, Akdis CA, Crameri R. Exploring the repertoire of IgE-binding self-antigens associated with atopic eczema. *J Allergy Clin Immunol* (2009) 124: 278–85, 285.e1–7. doi:10.1016/j.jaci.2009.05.015
17. Tang TS, Bieber T, Williams HC. Does "autoreactivity" play a role in atopic dermatitis? *J Allergy Clin Immunol* (2012) 129: 1209–15.e2. doi:10.1016/j.jaci.2012.02.002
18. Hradetzky S, Werfel T, Rösner LM. Autoallergy in atopic dermatitis. *Allergo J Int* (2015) 24:16–22. doi:10.1007/s40629-015-0037-5
19. van Beek N, Schulze FS, Zillikens D, Schmidt E. IgE-mediated mechanisms in bullous pemphigoid and other autoimmune bullous diseases. *Expert Rev Clin Immunol* (2016) 12:267–77. doi:10.1586/1744666X.2016.1123092
20. Heratizadeh A, Mittermann I, Balaji H, Wichmann K, Niebuhr M, Valenta R, et al. The role of T-cell reactivity towards the autoantigen α-NAC in atopic dermatitis. *Br J Dermatol* (2011) 164:316–24. doi:10.1111/j.1365-2133.2010.10090.x
21. Roesner LM, Heratizadeh A, Wieschowski S, Mittermann I, Valenta R, Eiz-Vesper B, et al. α-NAC-specific autoreactive CD8+ T cells in atopic dermatitis are of an effector memory type and secrete IL-4 and IFN-γ. *J Immunol* (2016) 196:3245–52. doi:10.4049/jimmunol.1500351
22. Schmid-Grendelmeier P, Flückiger S, Disch R, Trautmann A, Wüthrich B, Blaser K, et al. IgE-mediated and T cell-mediated autoimmunity against manganese superoxide dismutase in atopic dermatitis. *J Allergy Clin Immunol* (2005) 115:1068–75. doi:10.1016/j.jaci.2005.01.065
23. Watanabe K, Muro Y, Sugiura K, Tomita Y. IgE and IgG(4) autoantibodies against DFS70/LEDGF in atopic dermatitis. *Autoimmunity* (2011) 44:511–9. doi:10.3109/08916934.2010.549157
24. Kinaciyan T, Natter S, Kraft D, Stingl G, Valenta R. IgE autoantibodies monitored in a patient with atopic dermatitis under cyclosporin A treatment reflect tissue damage. *J Allergy Clin Immunol* (2002) 109:717–9. doi:10.1067/mai.2002.123303
25. Lucae S, Schmid-Grendelmeier P, Wüthrich B, Kraft D, Valenta R, Linhart B. IgE responses to exogenous and endogenous allergens in atopic dermatitis patients under long-term systemic cyclosporine A treatment. *Allergy* (2016) 71:115–8. doi:10.1111/all.12711

Conflict of Interest Statement: All authors have a research cooperation with Miltenyi Biotec. The authors declare that the research was conducted in the absence of any commercial or financial relationships that could be construed as a potential conflict of interest.

frontiers in Immunology

ORIGINAL RESEARCH
published: 19 February 2018
doi: 10.3389/fimmu.2018.00248

Effectiveness and Safety of Rituximab in Recalcitrant Pemphigoid Diseases

Aniek Lamberts, H. Ilona Euverman, Jorrit B. Terra, Marcel F. Jonkman and Barbara Horváth*

Center for Blistering Diseases, Department of Dermatology, University Medical Center Groningen, University of Groningen, Groningen, Netherlands

Introduction: Rituximab (RTX) is a monoclonal antibody targeting CD20, a transmembrane protein expressed on B cells, causing B cell depletion. RTX has shown great efficacy in studies of pemphigus vulgaris, but data of pemphigoid diseases are limited.

Objective: To assess the effectiveness and safety of RTX in pemphigoid diseases.

Methods: The medical records of 28 patients with pemphigoid diseases that were treated with RTX were reviewed retrospectively. Early and late endpoints, defined according to international consensus, were disease control (DC), partial remission (PR), complete remission (CR), and relapses. Safety was measured by reported adverse events.

Results: Patients with bullous pemphigoid (n = 8), mucous membrane pemphigoid (n = 14), epidermolysis bullosa acquisita (n = 5), and linear IgA disease (n = 1) were included. Treatment with 500 mg RTX (n = 6) or 1,000 mg RTX (n = 22) was administered on days 1 and 15. Eight patients received additional 500 mg RTX at months 6 and 12. Overall, DC was achieved in 67.9%, PR in 57.1%, and CR in 21.4% of the cases. During follow-up, 66.7% patients relapsed. Repeated treatment with RTX led to remission (PR or CR) in 85.7% of the retreated cases. No significant difference in response between pemphigoid subtypes was found. IgA-dominant cases (n = 5) achieved less DC (20 vs. 81.3%; p = 0.007), less PR (20 vs. 62.5%; p = 0.149), and less CR (0 vs. 18.8%; p = 0.549) compared to IgG-dominant cases (n = 16). Five severe adverse events and three deaths were reported. One death was possibly related to RTX and one death was disease related.

Conclusion: RTX can be effective in recalcitrant IgG-dominant pemphigoid diseases, however not in those where IgA is dominant.

Keywords: pemphigoid diseases, autoimmune bullous diseases, rituximab, IgA, mucous membrane pemphigoid, linear IgA disease, epidermolysis bullosa acquisita, case series

OPEN ACCESS

Edited by:
Qizhi Tang,
University of California, San Francisco, United States

Reviewed by:
Robert Gniadecki,
University of Alberta, Canada
Philippe Musette,
Centre Hospitalier Universitaire (CHU) de Rouen, France

****Correspondence:***
Aniek Lamberts
m.a.lamberts@umcg.nl

Specialty section:
This article was submitted to Immunological Tolerance and Regulation, a section of the journal Frontiers in Immunology

Received: *30 November 2017*
Accepted: *29 January 2018*
Published: *19 February 2018*

Citation:
Lamberts A, Euverman HI, Terra JB, Jonkman MF and Horváth B (2018) Effectiveness and Safety of Rituximab in Recalcitrant Pemphigoid Diseases. Front. Immunol. 9:248. doi: 10.3389/fimmu.2018.00248

Abbreviations: RTX, rituximab; BMZ, basement membrane zone; BP, bullous pemphigoid; MMP, mucous membrane pemphigoid; EBA, epidermolysis bullosa acquisita; LAD, linear IgA disease; RA, rheumatoid arthritis; DIF, direct immunofluorescence microscopy; IIF, indirect immunofluorescence microscopy; SSS, salt-split skin; DC, disease control; PR, partial remission; CR, complete remission; HIVIg, human intravenous immunoglobulin; MTX, methotrexate; AZA, azathioprine; cyclo, cyclophosphamide; MMF, mycophenolate mofetil; IV, intravenous.

INTRODUCTION

Pemphigoid diseases are a heterogeneous group of autoantibody-mediated subepidermal blistering diseases (1). IgG, IgA, or IgM autoantibodies target distinct antigens located in the basement membrane zone (BMZ) inducing different pemphigoid subtypes. Cutaneous pemphigoid is the subgroup of pemphigoid diseases that predominantly affect the skin (1, 2). Pemphigoid, be it non-bullous or bullous (BP), is the most prevalent disease within this subgroup and mainly presents at older age (3). Mucous membrane pemphigoid (MMP) opposes cutaneous pemphigoid in the spectrum of pemphigoid diseases, and is characterized by primary involvement of the mucosa (2, 4). Beside the classification based on body localization, pemphigoid diseases may be classified based on targeted auto-antigens, such as 180 kDa BP antigen (BP180) and the 230 kDa BP antigen (BP230) in pemphigoid, laminin-332 in anti-laminin-332 MMP, the p200 protein in anti-p200 pemphigoid (anti-laminin γ1 pemphigoid), and type VII collagen in epidermolysis bullosa acquisita (EBA) (2). Last, classification may be based on predominant class of autoantibodies IgG or IgA. Pemphigoid diseases with the exclusive IgA involvement are named linear IgA disease (LAD), regardless of the targeted antigen or clinical presentation (5). IgA-mediated pemphigoid diseases are difficult to treat if dapsone is contraindicated, and mostly show high resistance to usual immunosuppressants (6).

The 2014 European consensus guideline for the management of BP recommends transcutaneous systemic clobetasol therapy as initial treatment (7, 8). The alternative is oral systemic prednisolone therapy (0.5–1.0 mg/kg/day), which was associated with adverse events and higher mortality (8, 9). Recently, doxycycline was found to be non-inferior to and safer than prednisolone for short-term blister control (10), although the statistical margins were wide (11). As third-line rituximab (RTX) is recommended in cases in which conventional immunosuppressive drugs were not effective, were contraindicated, or showed unacceptable side effects (8, 12, 13).

Rituximab is a chimeric monoclonal antibody targeting CD20, a transmembrane protein expressed by all B cells in the pre-plasma cell lineage (14). Binding of RTX to CD20 leads to B cell depletion in the peripheral circulation by various mechanisms (15). RTX is registered for treatment of B cell lymphoma's, rheumatoid arthritis (RA), and granulomatosis with polyangiitis (15, 16). Recently, RTX was shown to be effective as first-line therapy in pemphigus (17). However, the position of RTX on the therapeutically ladder of pemphigoid diseases is unknown. Data regarding the effectiveness and safety of RTX in pemphigoid diseases are limited and are mainly of retrospective nature (18–26). Furthermore, it is unclear which treatment regime is most beneficial and which factors might be predictive for treatment response (27, 28). Therefore, the aim of our study was to retrospectively analyze our daily practice experience with RTX in pemphigoid diseases by evaluating the effectiveness and safety, and to identify clinical or serological factors that might be associated with treatment response.

MATERIALS AND METHODS

All patients with pemphigoid diseases treated with RTX between 2010 and September 2017 at the Center for Blistering Diseases at the University Medical Center Groningen were included in the study. Pemphigoid diseases were diagnosed based on the following criteria: linear depositions of IgG, IgA, IgM, or C3c along the BMZ by direct immunofluorescence microscopy (DIF) and/or positive indirect immunofluorescence microscopy (IIF) on monkey esophagus (MO) or salt-split skin (SSS), in combination with clinical presentation, histopathological findings, or other immunoserological tests compatible with the diagnosis of a pemphigoid disease. Patients with a linear u-serrated immunodeposition pattern seen by DIF were diagnosed with EBA. Patients with exclusive involvement of IgA were diagnosed with LAD.

Patients charts were reviewed retrospectively by the first (Aniek Lamberts) and second (H. Ilona Euverman) authors. Response outcomes were defined according to international consensus and measured by the early endpoint disease control (DC), and the late endpoints partial remission (PR), complete remission (CR), and the number of relapses (29, 30). Safety was measured by reported adverse events. Discrepancies in the assessment by Aniek Lamberts and H. Ilona Euverman were resolved through discussion with the other authors (Barbara Horváth and Marcel F. Jonkman).

Treatment Regimes

There were two treatment protocols administered. In the period of 2010–2012, patients were treated with RTX 500 mg at days 1 and 15 (low-dose RA protocol), since this dose was effective in pemphigus patients (Horvath et al. 2011) (31, 32). Additional 500 mg RTX at month 6 and/or 12 was only administered on indication (33). From 2012 the protocol was adjusted to 1,000 mg RTX at days 1 and 15 (high-dose RA protocol—published in 2011) (28). Since 2014, patients standardly received additional 500 mg RTX at months 6 and 12, and if indicated at month 18. Patients that relapsed within 1 year after the last RTX infusion received re-treatment with a single infusion of 500 mg RTX. Relapsed patients beyond 1 year after the last RTX infusion were retreated with a new cycle of 1,000 mg RTX at days 1 and 15.

Statistical Analysis

The Kolmogorov–Smirnov test was used to test for normal distributions. Correlations between bivariate outcome measures were analyzed with Fisher's exact test. Comparing means of non-normally distributed data was done with the Mann–Whitney *U* test. Statistical significance was defined by a p-value <0.05. Statistical analyses were performed in IBM SPSS statistics version 23.

RESULTS

Patient Population

A total of 28 patients were included. The patient characteristics are listed in **Table 1**. The mean delay in diagnosis was 10.5 months in BP (range 1–19), 24.3 months in MMP (range 4–60), and 19.0 months in EBA patients (range 3–47). One MMP outlier with an exceptional long delay in diagnosis of 285 months was not taken into account. This patient showed severe laryngeal, oral, genital, and ocular (foster stage 4) involvement. The mean time between diagnosis and RTX treatment was longer for BP

TABLE 1 | Demographics of pemphigoid patients treated with RTX.

Mean age at first cycle RTX	BP ($n = 8$)[a]	67.13 years	SD 9.4, range 53–78
	MMP ($n = 14$) Ocular involvement ($n = 7$)[b] Oral involvement ($n = 11$) Laryngeal involvement ($n = 4$) Genital involvement ($n = 2$)	64.9 years	SD 12.3, range 45–84
	EBA, all inflammatory subtype ($n = 5$) LAD ($n = 1$) Total ($n = 28$)	54.0 years 48.0 years 63.0 years	SD 22.8, range 25–87 – SD 14.3, range 25–87
Dominant Ig in DIF and IIF on SSS	IgG dominant IgA dominant IgM dominant IgG/IgA equally dominant	16 patients 5 patients 1 patient 6 patients	
Gender	Male Female	13 (46.4%) 15 (53.6%)	
First cycle of 2 × 500 mg	 Additional cycle 2 × 1,000 mg Additional cycle 2 × 500 mg	6 patients 3 patients 1 patient	
First cycle of 2 × 1,000 mg	 Additional cycle 2 × 1,000 mg Additional cycle 2 × 500 mg	22 patients[c] 1 patients 1 patient	
Additional gifts of RTX	500 mg at M6 and/or M12 500 mg at M6 and M12	15 patients[d] 8 patients	
Mean total follow-up time (first RTX cycle till last contact)		30.3 months	SD 23.0, range 2–79

RTX, rituximab; BP, bullous pemphigoid; MMP, mucous membrane pemphigoid; EBA, epidermolysis bullosa acquisita; LAD, linear IgA disease; Ig, immunoglobulin; DIF, direct immunofluorescence microscopy; IIF, indirect immunofluorescence microscopy; SSS, salt-split skin; M6, month 6; M12, month 12.

[a]*All patients with pemphigoid presented with the BP.*

[b]*Two patients had exclusive ocular involvement, also known as pure ocular MMP.*

[c]*One patient only received 1 × 1,000 mg due to the development of pneumocystis pneumonia.*

[d]*Five patients only received 500 mg RTX at M6, two patients only received 500 mg RTX at M12.*

patients (64.3 months; range 1–272), EBA (29.1 months; range 0.5–84), and LAD patients (49.0 months) compared to MMP (13.8 months; range 2–63). Prior to RTX, all patients received one or more immunosuppressants (Table S1 in Supplementary Material) with suboptimal effect or with unacceptable side effects. Therefore, RTX was administered as last resort in several cases. Six patients received low-dose RTX (500 mg) and 22 patients high-dose RTX (1,000 mg), of which eight patients also received repeated RTX doses (500 mg) at months 6 and 12. In all patients RTX was added to pre-existing treatment with a local steroid and/or one or two systemic drugs (Table S1 in Supplementary Material).

Effectiveness of First Course of RTX

DC was achieved in 19 of 28 patients (67.9%) at a mean time of 14.5 weeks (range 1–36; SD 9.1). Remission (partial or complete) was achieved by 57.1% ($n = 16$) of the treatment resistant pemphigoid cases (**Figures 1** and **2**). PR was achieved by 16 patients (57.1%) at a mean time of 34.2 weeks (range 9–71; SD 18.1). Six of 28 patients (21.4%) also achieved CR at a mean time of 59.2 weeks (range 24–85; SD 22.1). **Figures 3** and **4** display a flowchart and bar chart of the achieved early and late endpoints during follow-up. A complete overview of the outcome measurements of all included patients can be found in Table S1 in Supplementary Material.

We analyzed whether early administration of RTX was more beneficial. We compared the mean time between onset of symptoms and RTX treatment of patients with PR or CR (52.2 months; $n = 16$) and patients without PR or CR (64.9 months; $n = 12$). No significant difference was found [Mann–Whitney test ($p = 0.642$)].

Comparison of Treatment Regimes

Significantly more patients achieved DC with 1,000 mg RTX at days 1 and 15 (85.0%) compared to 500 mg RTX (33.3%; $p = 0.028$). Furthermore, patients more often achieved PR (63.6 vs. 16.7%; $p = 0.057$) and CR (27.3 vs. 0%; $p = 0.289$). Relapses were seen in both two cases receiving 500 mg RTX and 12 out of 19 cases (63.2%) with 1,000 mg RTX ($p = 0.533$).

Patients receiving repeated RTX infusions ($n = 8$) achieved DC (100 vs. 63.2%; $p = 0.134$) and PR (87.5 vs. 45.0%; $p = 0.088$) more frequently than patients without additional RTX infusions. A similar number of patients achieved CR (25.0 vs. 20%; $p = 1.000$). The relapse rate in the group with the additional gifts was lower (50.0 vs. 76.9%; $p = 0.346$), and the mean time until relapse was longer [81.3 weeks (range 32–170; SD 62.3) vs. 69.0 weeks (range 12–238; SD 66.6); $p = 0.572$].

Response in the Different Pemphigoid Subtypes

Mucous membrane pemphigoid patients showed the most benefit of RTX with DC in 85.7%, PR in 64.3%, and CR in 28.6% patients. During follow-up, 75% of the MMP patients relapsed. BP patients

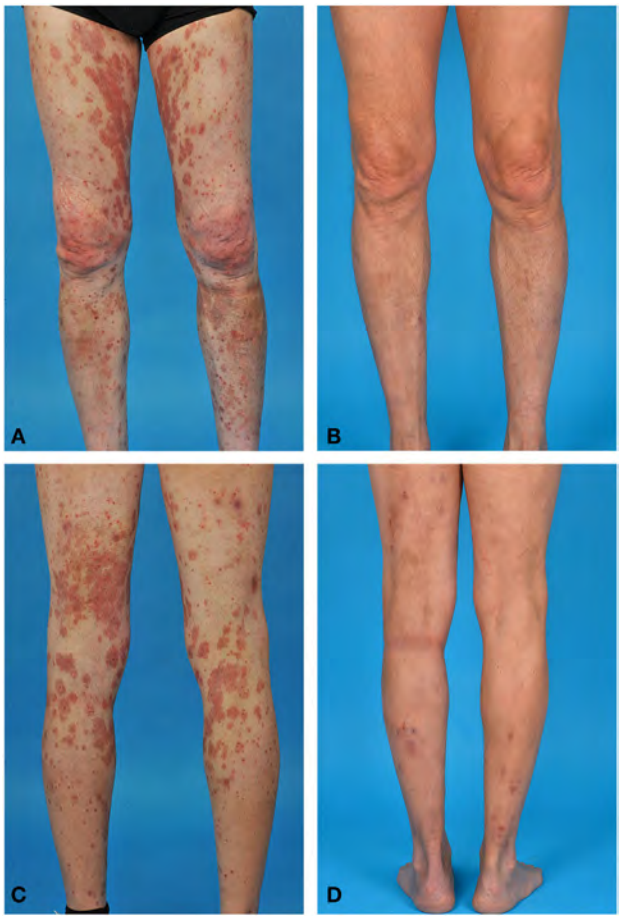

FIGURE 1 | Bullous pemphigoid in a 69-year-old male. **(A,C)** Erythematous plaques and papules on both legs before rituximab (RTX) treatment. **(B,D)** Remission with minimal therapy after RTX treatment.

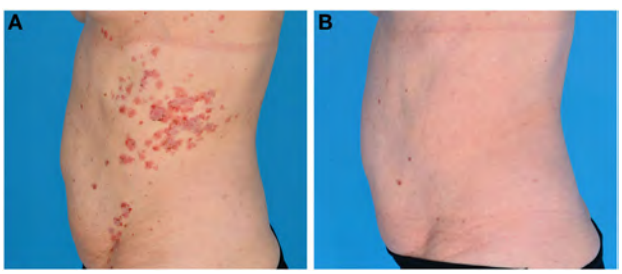

FIGURE 2 | Epidermolysis bullosa acquisita (EBA) in a 59-year-old female. **(A)** Nummular erythematous plaques, papules and circinate configurated crustae, vesicles, and bullae on the trunk, before rituximab (RTX) treatment. **(B)** Remission off therapy after RTX treatment.

achieved DC in 83.3%, PR in 62.5%, and CR in 12.5% with a relapse rate of 71.4%. In EBA patients, DC was found in 40%, PR in 40%, and CR in 20% without relapse. The patient with LAD was unresponsive to RTX treatment. No significant difference was found in the effectiveness of RTX between the different pemphigoid subtypes by Fisher's exact test.

Immunological Findings

The dominant immunoglobulin class prior to RTX treatment assessed by staining intensity in DIF and IIF on SSS was IgG in the majority of the cases (57.1%; $n = 16$), IgA in 17.9% ($n = 5$), and IgM in 3.6% ($n = 1$). Equal intensity of IgA and IgG staining was observed in 21.4% ($n = 6$) of the cases. IgA-dominant pemphigoid cases ($n = 5$) showed significantly less DC (20 vs. 81.3%; $p = 0.007$) compared to IgG-dominant cases ($n = 16$). The proportion of patients achieving PR (20 vs. 62.5%; $p = 0.149$) and CR (0 vs. 18.8%; $p = 0.549$) did not differ significantly; however, it showed a clear trend of ineffectiveness of RTX in IgA-dominant cases. Post treatment analysis was not performed.

Deposition of C3c along the BMZ was seen in 67.9% ($n = 19$) of DIF biopsies. No differences in effectiveness of RTX were found between patients with or without complement depositions.

Relapses

Fourteen of 21 patients (66.7%) relapsed after a mean time of 72.5 weeks (range 12–238; SD 63.2). Four of 14 relapsed patients showed B cell repopulation; in one case repopulation preceded relapse and in three cases repopulation was objectified after the relapse. Five of 14 relapsed patients showed maintained B cell depletion and in five patients B cells were not followed up. Seven of 14 relapsed patients were retreated with RTX, which led to PR or CR in six out of seven patients (85.7%).

Safety

Table 2 provides an overview of reported adverse events and deaths after RTX treatment. One patient died 4 months after RTX infusion due to sepsis which led to multi-organ failure. This death was interpreted as possibly related to RTX, since neutropenia (possibly RTX induced late onset neutropenia) might have contributed to a higher infection risk. All cases that reported grade 3 or grade 4 adverse events fully recovered. Five infusion reactions were observed in three patients during RTX administration: dyspnea with chest pain, tired feeling of the legs, and dizziness plus a burning sensation in the groins. All infusions could be successfully continued at lower infusion rate. One patient was accidently shortly infused with RTX subcutaneously, causing temporary pain and swelling of the arm.

B Cell Depletion

B cells were undetectable in the peripheral blood within 2 weeks in all patients after a single RTX infusion. In 13 patients, B cell levels remained undetectable during a mean follow-up time of 77.5 weeks (range 24–269; SD 64.6). All 13 patients received repeated RTX infusions at months 6, 12, or both. Repopulation of B cells was seen in six patients after a mean time of 95.2 weeks (range 36–250; sd 82.4). B cell levels were not followed up in nine patients. B cell levels showed no clear relation with response to RTX. All data on B cell levels should be interpreted with caution, since B cells were not measured at standard time points in our study population.

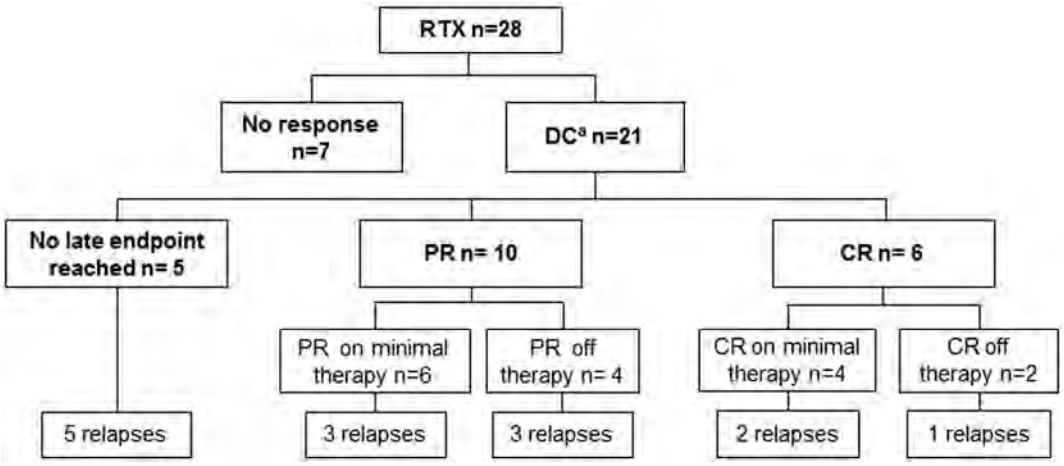

FIGURE 3 | Flowchart of the effectiveness of RTX in pemphigoid patients, showing the highest endpoint reached after the first RTX cycle. RTX, rituximab; DC, disease control; PR, partial remission; CR, complete remission. [a]Two patients already achieved DC before RTX was administered.

FIGURE 4 | Bar chart showing the achieved endpoints and repeated treatment of RTX of each individual pemphigoid patient. Bars represent patients until the end of follow-up. The pemphigoid subtypes are indicated on the *y*-axis and the *x*-axis displays time in years. RTX, rituximab; BP, bullous pemphigoid; MMP, mucous membrane pemphigoid; EBA, epidermolysis bullosa acquisita; LAD, linear IgA disease.

TABLE 2 | Adverse events and deaths reported in pemphigoid patients treated with rituximab (RTX).

		GRADE[a]	Concomitant immunosuppressive drugs
Reported adverse events			
Patient 1	Erysipelas right arm	3	Prednisolone 30 mg/day
	Herpes simplex labialis (confirmed HSV-1)	2	Prednisolone 30 mg/day
Patient 2,3	Upper respiratory infection probably viral (not confirmed)	1	Patient 2: prednisolone 10 mg/day Patient 3: none
Patient 4	PCP twice (no prophylaxis) - after first gift of 1,000 mg RTX	4	Prednisolone 60 mg/day + cyclophosphamide 150 mg/day
	- after second cycle of 2 × 1,000 mg RTX	4	Prednisolone 20 mg/day
Patient 5	Urticaria e.c.i., self-limiting	1	Prednisolone 15 mg/day
Patient 6	Flare-up of concomitant psoriasis	2	Prednisolone 10 mg/day + dapsone 100 mg/day
Patient 7	Polyarthritis and fever, possibly caused by serum sickness (not confirmed)	3	Prednisolone 7.5 mg/day
Patient 8	Diarrhea and loss of consciousness, followed by hospitalization	3	Prednisolone 40 mg/day
Patient 9	Generalized pain e.c.i., self-limiting	2	Prednisolone 35 mg/day
	Urinary tract infection (female)	2	Prednisolone 35 mg/day
Patient 10	Upper respiratory infection probably viral (not confirmed)	2	Prednisolone 5 mg/day + cyclophosphamide 50 mg/day
	Urinary tract infection (male)	2	Prednisolone 5 mg/day + cyclophosphamide 50 mg/day
Patient 11	Myalgia e.c.i., self-limiting	1	Prednisolone 5 mg/day
Deaths that occurred after RTX administration			
Male, 78 years old, BP			Cognitive and physical decline. Exact cause of death unknown
Female, 73 years old, BP			Sepsis due to neglected urinary tract infection and neutropenia/leukopenia (possibly late onset neutropenia due to RTX), multi-organ failure eventually led to death
Female, 87 years old, EBA			Active disease with severe mucosal involvement, weight loss and physical decline, exact cause of death unknown (possibly disease related)

RTX, rituximab; HSV-1, Herpes Simplex Virus type 1; PCP, pneumocystis pneumonia; e.c.i., e causa ingnota (of unknown cause); BP, bullous pemphigoid; MMP, mucous membrane pemphigoid; EBA, epidermolysis bullosa acquisita; LAD, linear IgA disease.

[a]*Adverse events were graded according to the Common Terminology Criteria for Adverse Events v4.0 (CTCAE) (34).*

DISCUSSION

Our study showed partial or CR with RTX in 57.1% of the cases with a pemphigoid disease, that previously failed on a variety of immunosuppressants. RTX was most beneficial in refractory MMP and BP patients with partial or CR in 64.3 and 62.5% of the cases. Interestingly, IgA-dominant pemphigoid diseases responded poorly on RTX.

Only two other studies described RTX treatment of MMP patients ($n = 14$; 11 cases with isolated ocular involvement) according to the RA protocol and showed PR or CR in all cases (19, 20). Both studies reported high relapse rates (83.3 and 100%); however, repeated treatment led to remission in all cases. These findings are in accordance with our observed relapse rate (66.7%) and remission rate after repeated RTX treatment (85.7%).

Previous studies on RTX therapy in MMP and BP reported either mixed responses with serious infectious adverse events and death (24–26), or high remission rates with limited non-serious adverse events (18–23). Studies on RTX in combination with immunoadsorption (protein A) or human intravenous immunoglobulin found high response rates in ocular MMP, resistant EBA, and recalcitrant BP (35–38). Interestingly, our study showed lower remission rates compared to most reports in the literature; DC in 100% (21) , PR and/or CR in 66% (24), 86% (25), 88% (26), 92% (18), and 100% (23) . These differences in the results can be explained by the clinical heterogeneity of the previous studies, caused by using different RTX regimes (21, 22, 24–26), by assessing different populations (multiple pemphigoid subtypes in a tertiary referral center in our study, MMP patients in most studies) (19–21, 26, 36) , or by using different definitions for the outcome measurements (19, 22, 23, 39). Studies prior to the pemphigoid consensus of 2012 either used definitions of the pemphigus consensus of 2008, in which minimal adjuvant therapy was less well defined, or other definitions for treatment response (19, 22, 23, 39).

An important result is the observation of significantly more DC ($p = 0.028$), and more PR ($p = 0.057$) and CR ($p = 0.289$) in patients treated with a high dosage regime compared to a low dosage regime. Moreover, we noticed a beneficial effect of repeated RTX infusions with less relapses.

A major finding of our study is that four out of five (80%) IgA-dominant pemphigoid diseases were completely unresponsive to RTX treatment. Previously, He et al. demonstrated persistent IgA-secreting plasma cells in a MMP patient not responding to RTX treatment (40). They speculated that plasma cells could be

derived from a tissue resident memory B cell population that is resistant to anti-CD20 therapy. Mei et al. described the continuous presence of IgA + plasma cells in the peripheral circulation and the gastrointestinal mucosa of RA patients during successful B cell depletion by RTX (41). Further characterization of the circulating plasma cells revealed a mucosal phenotype, indicating that their precursor B cells are mucosal resident, and not depleted by RTX. All these findings could explain the unresponsiveness in our IgA-dominant cases.

Fourteen adverse events were reported in 11 (39.3%) pemphigoid cases treated with RTX. The majority of adverse events were infectious ($n = 8$). Five adverse event were severe (grade 3 of 4), and one reported death was possibly related to RTX. Noteworthy is one disease-related death in an older EBA patient, demonstrating that pemphigoid diseases can be life-threatening in therapy resistant cases and underlining the urgent need for effective treatment options. Our safety data is comparable with the reports of Maley et al. and Cho et al. who found adverse events in 33 and 31% of the MMP patients treated with RTX (18, 21). Yet, both studies observed a significantly higher adverse event rate in patients treated with conventional therapies (48 and 53%). Other studies have reported less adverse events compared to our data (23, 35–37). This might be explained by the frequent use of concomitant immunosuppressive drugs in our population with high disease severity, causing a high risk of infection.

Pemphigoid diseases appear to respond less on RTX than pemphigus, despite successful B cell depletion in the peripheral circulation in both diseases (17, 32). Furthermore, our data also showed that it takes almost 4 months (mean time till DC is 14.4 weeks) until RTX has effect, whereas in pemphigus effect is noticed within 2 months (DC at 4.0–9.3 weeks) (42–46). Possibly, B cell depletion stops pathogenic autoantibody production in both diseases, though other ongoing pathophysiological mechanisms that are not interrupted by B cell depletion might play a more substantial role in the pathogenesis of pemphigoid (27, 47). Nevertheless, PR and CR in responding pemphigoid disease patients was reached after the same time or slightly later than in pemphigus patients (32, 45, 46).

The greatest limitation of this study is its retrospective nature, which led to incomplete and/or missing data, such as objective disease scores (BPDAI and MMPDAI), and laboratory measurements of B cells and pathogenic autoantibodies at standard time points. Furthermore, a major limitation is the small sample size, especially when comparing the different pemphigoid subtypes, and the heterogeneity of our study population. The use of concomitant immunosuppressants in almost all patients (Table S1 in Supplementary Material) did not allow us to draw conclusions regarding RTX monotherapy. Nonetheless, the immunosuppressants alone did not succeed to establish DC or remission prior to RTX treatment. Moreover, the use of co-medication in severe pemphigoid diseases does reflect upon our daily practice. Lastly, it is important to emphasize that consensus late endpoints PR and CR imply to define two contrasting outcomes, but in clinical setting the difference can be minimal (one insignificant lesion once weekly vs. no lesions); therefore, patients on PR and CR might be equally satisfied with treatment result. Prospective studies with a greater sample size are needed to provide a higher level of evidence on the effectiveness of RTX in pemphigoid diseases.

In conclusion, this study demonstrated that RTX was effective in 57.1% of recalcitrant pemphigoid diseases and that the high dose regime of twice 1,000 mg was more effective than the low dose. Although relapse rates were high (66.7%), repeated RTX therapy led to remission in the majority of the relapsed cases (85.7%). An important finding is that most pemphigoid patients with IgA-dominant disease showed poor response to RTX. This finding suggests that RTX can be eliminated from the clinicians' arsenal when encountering IgA-dominant pemphigoid patients; however, future studies are required for confirmation. RTX showed to be relatively safe. Prospective comparative studies are needed to further determine the position of RTX in the therapeutic algorithm for pemphigoid diseases.

AUTHOR CONTRIBUTIONS

All authors contributed to the design of the work. AL and HIE performed the data acquisition. AL performed the data analysis and all authors contributed to the interpretation of the data. Drafting the work was done by AL. All authors revised the work critically for important intellectual content and all finally approved the version to be published.

SUPPLEMENTARY MATERIAL

The Supplementary Material for this article can be found online at http://www.frontiersin.org/articles/10.3389/fimmu.2018.00248/full#supplementary-material.

REFERENCES

1. Schmidt E, Zillikens D. Pemphigoid diseases. *Lancet* (2013) 381(9863):320–32. doi:10.1016/S0140-6736(12)61140-4
2. Amber KT, Murrell DF, Schmidt E, Joly P, Borradori L. Autoimmune subepidermal bullous diseases of the skin and mucosae: clinical features, diagnosis, and management. *Clin Rev Allergy Immunol* (2018) 54:26–51. doi:10.1007/s12016-017-8633-4
3. Joly P, Baricault S, Sparsa A, Bernard P, Bédane C, Duvert-Lehembre S, et al. Incidence and mortality of bullous pemphigoid in France. *J Invest Dermatol* (2012) 132(8):1998–2004. doi:10.1038/jid.2012.35
4. Chan LS, Ahmed AR, Anhalt GJ, Bernauer W, Cooper KD, Elder MJ, et al. The first international consensus on mucous membrane pemphigoid: definition, diagnostic criteria, pathogenic factors, medical treatment, and prognostic indicators. *Arch Dermatol* (2002) 138(3):370–9. doi:10.1001/archderm.138.3.370
5. Guide SV, Marinkovich MP. Linear IgA bullous dermatosis. *Clin Dermatol* (2001) 19(6):719–27. doi:10.1016/S0738-081X(00)00185-1
6. Gottlieb J, Ingen-Housz-Oro S, Alexandre M, Grootenboer-Mignot S, Aucouturier F, Sbidian E, et al. Idiopathic linear IgA bullous dermatosis: prognostic factors based on a case series of 72 adults. *Br J Dermatol* (2017) 177(1):212–22. doi:10.1111/bjd.15244
7. Feliciani C, Joly P, Jonkman MF, Zambruno G, Zillikens D, Ioannides D, et al. Management of bullous pemphigoid: the European dermatology forum consensus in collaboration with the European academy of dermatology and venereology. *Br J Dermatol* (2015) 172(4):867–77. doi:10.1111/bjd.13717

8. Joly P, Roujeau JC, Benichou J, Picard C, Dreno B, Delaporte E, et al. A comparison of oral and topical corticosteroids in patients with bullous pemphigoid. *N Engl J Med* (2002) 346(5):321–7. doi:10.1056/NEJMoa011592
9. Kirtschig G, Middleton P, Bennett C, Murrell DF, Wojnarowska F, Khumalo NP. Interventions for bullous pemphigoid. *Cochrane Database Syst Rev* (2010) 10:CD002292. doi:10.1002/14651858.CD002292.pub3
10. Williams HC, Wojnarowska F, Kirtschig G, Mason J, Godec TR, Schmidt E, et al. Doxycycline versus prednisolone as an initial treatment strategy for bullous pemphigoid: a pragmatic, non-inferiority, randomised controlled trial. *Lancet* (2017) 389(10079):1630–8. doi:10.1016/S0140-6736(17)30560-3
11. Grantham HJ, Stocken DD, Reynolds NJ. Doxycycline: a first-line treatment for bullous pemphigoid? *Lancet* (2017) 389(10079):1586–8. doi:10.1016/S0140-6736(17)30549-4
12. Kalinska-Bienias A, Lukowska-Smorawska K, Jagielski P, Kowalewski C, Wozniak K. Mortality in bullous pemphigoid and prognostic factors in 1st and 3rd year of follow-up in specialized centre in Poland. *Arch Dermatol Res* (2017) 309(9):709–19. doi:10.1007/s00403-017-1772-x
13. Sadik CD, Zillikens D. Current treatments and developments in pemphigoid diseases as paradigm diseases for autoantibody-driven, organ-specific autoimmune diseases. *Semin Hematol* (2016) 53(Suppl 1):S51–3. doi:10.1053/j.seminhematol.2016.04.015
14. Reff ME, Carner K, Chambers KS, Chinn PC, Leonard JE, Raab R, et al. Depletion of B cells in vivo by a chimeric mouse human monoclonal antibody to CD20. *Blood* (1994) 83(2):435–45.
15. Gurcan HM, Keskin DB, Stern JN, Nitzberg MA, Shekhani H, Ahmed AR. A review of the current use of rituximab in autoimmune diseases. *Int Immunopharmacol* (2009) 9(1):10–25. doi:10.1016/j.intimp.2008.10.004
16. Pescovitz MD. Rituximab, an anti-cd20 monoclonal antibody: history and mechanism of action. *Am J Transplant* (2006) 6(5 Pt 1):859–66. doi:10.1111/j.1600-6143.2006.01288.x
17. Joly P, Maho-Vaillant M, Prost-Squarcioni C, Hebert V, Houivet E, Calbo S, et al. First-line rituximab combined with short-term prednisone versus prednisone alone for the treatment of pemphigus (ritux 3): a prospective, multicentre, parallel-group, open-label randomised trial. *Lancet* (2017) 389(10083):2031–40. doi:10.1016/S0140-6736(17)30070-3
18. Cho YT, Chu CY, Wang LF. First-line combination therapy with rituximab and corticosteroids provides a high complete remission rate in moderate-to-severe bullous pemphigoid. *Br J Dermatol* (2015) 173(1):302–4. doi:10.1111/bjd.13633
19. Rubsam A, Stefaniak R, Worm M, Pleyer U. Rituximab preserves vision in ocular mucous membrane pemphigoid. *Expert Opin Biol Ther* (2015) 15(7):927–33. doi:10.1517/14712598.2015.1046833
20. Heelan K, Walsh S, Shear NH. Treatment of mucous membrane pemphigoid with rituximab. *J Am Acad Dermatol* (2013) 69(2):310–1. doi:10.1016/j.jaad.2013.01.046
21. Maley A, Warren M, Haberman I, Swerlick R, Kharod-Dholakia B, Feldman R. Rituximab combined with conventional therapy versus conventional therapy alone for the treatment of mucous membrane pemphigoid (MMP). *J Am Acad Dermatol* (2016) 74(5):835–40. doi:10.1016/j.jaad.2016.01.020
22. Shetty S, Ahmed AR. Critical analysis of the use of rituximab in mucous membrane pemphigoid: a review of the literature. *J Am Acad Dermatol* (2013) 68(3):499–506. doi:10.1016/j.jaad.2012.10.018
23. Kasperkiewicz M, Shimanovich I, Ludwig RJ, Rose C, Zillikens D, Schmidt E. Rituximab for treatment-refractory pemphigus and pemphigoid: a case series of 17 patients. *J Am Acad Dermatol* (2011) 65(3):552–8. doi:10.1016/j.jaad.2010.07.032
24. Schmidt E, Seitz CS, Benoit S, Brocker EB, Goebeler M. Rituximab in autoimmune bullous diseases: mixed responses and adverse effects. *Br J Dermatol* (2007) 156(2):352–6. doi:10.1111/j.1365-2133.2006.07646.x
25. Lourari S, Herve C, Doffoel-Hantz V, Meyer N, Bulai-Livideanu C, Viraben R, et al. Bullous and mucous membrane pemphigoid show a mixed response to rituximab: experience in seven patients. *J Eur Acad Dermatol Venereol* (2011) 25(10):1238–40. doi:10.1111/j.1468-3083.2010.03889.x
26. Le Roux-Villet C, Prost-Squarcioni C, Alexandre M, Caux F, Pascal F, Doan S, et al. Rituximab for patients with refractory mucous membrane pemphigoid. *Arch Dermatol* (2011) 147(7):843–9. doi:10.1001/archdermatol.2011.54
27. Sitaru C, Thiel J. The need for markers and predictors of rituximab treatment resistance. *Exp Dermatol* (2014) 23(4):236–7. doi:10.1111/exd.12331
28. Buch MH, Smolen JS, Betteridge N, Breedveld FC, Burmester G, Dörner T, et al. Updated consensus statement on the use of rituximab in patients with rheumatoid arthritis. *Ann Rheum Dis* (2011) 70(6):909–20. doi:10.1136/ard.2010.144998
29. Murrell DF, Marinovic B, Caux F, Prost C, Ahmed R, Wozniak K, et al. Definitions and outcome measures for mucous membrane pemphigoid: recommendations of an international panel of experts. *J Am Acad Dermatol* (2015) 72(1):168–74. doi:10.1016/j.jaad.2014.08.024
30. Murrell DF, Daniel BS, Joly P, Borradori L, Amagai M, Hashimoto T, et al. Definitions and outcome measures for bullous pemphigoid: recommendations by an international panel of experts. *J Am Acad Dermatol* (2012) 66(3):479–85. doi:10.1016/j.jaad.2011.06.032
31. Smolen JS, Keystone EC, Emery P, Breedveld FC, Betteridge N, Burmester GR, et al. Consensus statement on the use of rituximab in patients with rheumatoid arthritis. *Ann Rheum Dis* (2007) 66(2):143–50. doi:10.1136/ard.2006.061002
32. Horvath B, Huizinga J, Pas HH, Mulder AB, Jonkman MF. Low-dose rituximab is effective in pemphigus. *Br J Dermatol* (2012) 166(2):405–12. doi:10.1111/j.1365-2133.2011.10663.x
33. Cianchini G, Lupi F, Masini C, Corona R, Puddu P, De Pita O. Therapy with rituximab for autoimmune pemphigus: results from a single-center observational study on 42 cases with long-term follow-up. *J Am Acad Dermatol* (2012) 67(4):617–22. doi:10.1016/j.jaad.2011.11.007
34. National Cancer Institute. *Common Terminology Criteria for Adverse Events v4.0*. NCI, NIH, DHHS. NIH publication # 09-7473. (2009)
35. Kolesnik M, Becker E, Reinhold D, Ambach A, Heim MU, Gollnick H, et al. Treatment of severe autoimmune blistering skin diseases with combination of protein A immunoadsorption and rituximab: a protocol without initial high dose or pulse steroid medication. *J Eur Acad Dermatol Venereol* (2014) 28(6):771–80. doi:10.1111/jdv.12175
36. Foster CS, Chang PY, Ahmed AR. Combination of rituximab and intravenous immunoglobulin for recalcitrant ocular cicatricial pemphigoid: a preliminary report. *Ophthalmology* (2010) 117(5):861–9. doi:10.1016/j.ophtha.2009.09.049
37. Ahmed AR, Shetty S, Kaveri S, Spigelman ZS. Treatment of recalcitrant bullous pemphigoid (BP) with a novel protocol: a retrospective study with a 6-year follow-up. *J Am Acad Dermatol* (2016) 74(4):700.e–8.e. doi:10.1016/j.jaad.2015.11.030
38. Oktem A, Akay BN, Boyvat A, Kundakci N, Erdem C, Bostancı S, et al. Long-term results of rituximab-intravenous immunoglobulin combination therapy in patients with epidermolysis bullosa acquisita resistant to conventional therapy. *J Dermatolog Treat* (2017) 28(1):50–4. doi:10.1080/09546634.2016.1179711
39. Murrell DF, Dick S, Ahmed AR, Amagai M, Barnadas MA, Borradori L, et al. Consensus statement on definitions of disease, end points, and therapeutic response for pemphigus. *J Am Acad Dermatol* (2008) 58(6):1043–6. doi:10.1016/j.jaad.2008.01.012
40. He Y, Shimoda M, Ono Y, Villalobos IB, Mitra A, Konia T, et al. Persistence of autoreactive IgA-secreting B cells despite multiple immunosuppressive medications including rituximab. *JAMA Dermatol* (2015) 151(6):646–50. doi:10.1001/jamadermatol.2015.59
41. Mei HE, Frölich D, Giesecke C, Loddenkemper C, Reiter K, Schmidt S, et al. Steady-state generation of mucosal IgA+ plasmablasts is not abrogated by B-cell depletion therapy with rituximab. *Blood* (2010) 116(24):5181–90. doi:10.1182/blood-2010-01-266536
42. Sharma VK, Bhari N, Gupta S, Sahni K, Khanna N, Ramam M, et al. Clinical efficacy of rituximab in the treatment of pemphigus: a retrospective study. *Indian J Dermatol Venereol Leprol* (2016) 82(4):389–94. doi:10.4103/0378-6323.174379
43. Bhattacharjee R, De D, Handa S, Minz RW, Saikia B, Joshi N. Assessment of the effects of rituximab monotherapy on different subsets of circulating T-regulatory cells and clinical disease severity in severe pemphigus vulgaris. *Dermatology* (2016) 232(5):572–7. doi:10.1159/000448031
44. Leshem YA, David M, Hodak E, Waitman DA, Vardy D, Israeli M, et al. A prospective study on clinical response and cell-mediated immunity of pemphigus patients treated with rituximab. *Arch Dermatol Res* (2014) 306(1):67–74. doi:10.1007/s00403-013-1355-4
45. Kim JH, Kim YH, Kim MR, Kim SC. Clinical efficacy of different doses of rituximab in the treatment of pemphigus: a retrospective study of 27 patients. *Br J Dermatol* (2011) 165(3):646–51. doi:10.1111/j.1365-2133.2011.10411.x

46. Wang HH, Liu CW, Li YC, Huang YC. Efficacy of rituximab for pemphigus: a systematic review and meta-analysis of different regimens. *Acta Derm Venereol* (2015) 95(8):928–32. doi:10.2340/00015555-2116
47. Hammers CM, Stanley JR. Mechanisms of disease: pemphigus and bullous pemphigoid. *Annu Rev Pathol* (2016) 11:175–97. doi:10.1146/annurev-pathol-012615-044313

Conflict of Interest Statement: MJ received a grant from Castle Creek and honoraria from Roche/Genentech. The authors declare that the research was conducted in the absence of any commercial or financial relationships that could be construed as a potential conflict of interest.

frontiers in Immunology

REVIEW
published: 16 February 2018
doi: 10.3389/fimmu.2018.00163

Autoantibodies in Autoimmune Hepatitis: Can Epitopes Tell Us about the Etiology of the Disease?

Urs Christen and Edith Hintermann*

Pharmazentrum Frankfurt/ZAFES, Goethe University Hospital, Frankfurt am Main, Germany

Autoimmune hepatitis (AIH), primary biliary cholangitis (PBC), and primary sclerosing cholangitis (PSC) are serious autoimmune liver diseases that are characterized by a progressive destruction of the liver parenchyma and/or the hepatic bile ducts and the development of chronic fibrosis. Left untreated autoimmune liver diseases are often life-threatening, and patients require a liver transplantation to survive. Thus, an early and reliable diagnosis is paramount for the initiation of a proper therapy with immunosuppressive and/or anticholelithic drugs. Besides the analysis of liver biopsies and serum markers indicating liver damage, the screening for specific autoantibodies is an indispensable tool for the diagnosis of autoimmune liver diseases. Such liver autoantigen-specific antibodies might be involved in the disease pathogenesis, and their epitope specificity may give some insight into the etiology of the disease. Here, we will mainly focus on the generation and specificity of autoantibodies in AIH patients. In addition, we will review data from animal models that aim toward a better understanding of the origins and pathogenicity of such autoantibodies.

Keywords: LKM-1, cytochrome P450 2D6 epitopes, epitope mapping, epitope spreading, molecular mimicry, diagnostic antibodies, pathogenic antibodies

OPEN ACCESS

Edited by:
Ralf J. Ludwig, University of Lübeck, Germany

Reviewed by:
Weici Zhang, University of California, Davis, United States
Reinhild Klein, Universität Tübingen, Germany
Frank Tacke, Uniklinik RWTH Aachen, Germany

****Correspondence:***
Urs Christen
christen@med.uni-frankfurt.de

Specialty section:
This article was submitted to Immunological Tolerance and Regulation, a section of the journal Frontiers in Immunology

Received: *29 November 2017*
Accepted: *18 January 2018*
Published: *16 February 2018*

Citation:
Christen U and Hintermann E (2018) Autoantibodies in Autoimmune Hepatitis: Can Epitopes Tell Us about the Etiology of the Disease? Front. Immunol. 9:163. doi: 10.3389/fimmu.2018.00163

INTRODUCTION: AUTOIMMUNE LIVER DISEASES

There are three major autoimmune diseases that target the liver. These autoimmune liver diseases affect either the liver parenchyma like in autoimmune hepatitis (AIH) or the bile ducts like in primary biliary cholangitis (PBC) and PSC. They all have in common that an aggressive autoimmune reaction results in destruction of liver tissue, which may subsequently ensue the development of severe hepatic fibrosis.

Abbreviations: AIH, autoimmune hepatitis; PBC, primary biliary cholangitis; PSC, primary sclerosing cholangitis; AMA, anti-mitochondrial antibodies; BEC, biliary epithelial cells; MMF, mycophenolate mofetil; PDC-E2, E2-subunits of the pyruvate dehydrogenase complex; BCOADC-E2, branched chain 2-oxo acid dehydrogenase; OGDC-E2, 2-oxo-glutarate dehydrogenase; UDCA, ursodeoxycholic acid; OCA, obeticholic acid; IBD, inflammatory bowel disease; FXR, farnesoid X receptor; PPAR, peroxisome proliferator-activated receptor; IAC, immunoglobulin G4-associated cholangitis; pANCA, perinuclear anti-neutrophil cytoplasmic antibodies; pANNA, peripheral antinuclear neutrophil antibodies; OS, overlap syndromes; AP, alkaline phosphatase; GGT, γ-glutamyl transpeptidase; ALT, alanine aminotransferase; IgG, immunoglobulin G; AIH-1, AIH-2, and AIH-3, type 1, type 2, and type 3 AIH, respectively; ANA, antinuclear antibodies; SMA, anti-smooth muscle antibodies; SLA, soluble liver antigen; ACA, anti-centromer antibodies; SSc, systemic sclerosis; NAFLD, non-alcoholic fatty liver disease; NASH, non-alcoholic steatohepatitis; LKM-1, type 1 liver/kidney microsomal antibodies; LKM-3, type 3 liver/kidney microsomal antibodies; CYP2D6, cytochrome P450 2D6; CYP2E1, cytochrome P450 2E1; LC-1, liver cytosol type 1 antibodies; FTCD, formiminotransferase cyclodeaminase; LSP, liver-specific membrane lipoprotein; ASGPR, asialoglycoprotein receptor; NOD, non-obese diabetic; aa, amino acid; Ad-2D6, adenovirus encoding human CYP2D6; ICP4, infected cell protein 4; HSV-1, herpes simplex virus 1; HCV, hepatitis C virus; HIV, human immunodeficiency virus; HHV-5, human cytomegalovirus; HHV-8, Karposi's sacrcoma associated herpes virus; TFA-adduct, trifluoroacteylated protein adduct; HCFC, hydrochlorofluorocarbons.

Autoimmune hepatitis is an often life-threatening disease characterized by the progressive destruction of the parenchyma and the development of chronic fibrosis (1–5). AIH occurs in children and adults of all ages, has a female predominance (sex ratio, 3.6:1), and affects different ethnic groups with an overall prevalence of 10–20 cases per million persons in Northern Europe and the United States (6–8). The disease is primarily associated with the presence of HLA class I B8 and HLA class II DR3, DR4, and DR52a (9–11). The histological hallmark of AIH is the presence of interface hepatitis, characterized by piecemeal necrosis affecting patches of hepatocytes (3, 12). In addition, according to the revised and simplified scoring system of the International AIH Group (IAIHG) (13), one of the core diagnostic criteria of AIH and its subtypes is the presence of specific antibodies to particular liver autoantigens (see below). Besides antibodies and histology, the IAIHG scoring system also considers hypergammaglobulinemia and the absence of viral markers (13). The current standard therapy of AIH is a glucocorticoid treatment with prednisone or prednisolone alone or in combination with azathioprine (14). However, recently alternative treatments have been successfully introduced, in particular for patients suffering from AIH relapses after corticosteroid withdrawal. The next generation glucocorticoid budesonide (15) as well as the calcineurin inhibitors cyclosporine A and tacrolimus potentially could improve the outcome of AIH (16, 17). Interestingly, the combination treatment budesonide/azathioprine resulted in fewer side effects than the conventional prednisone/azathioprine therapy in AIH patients without cirrhosis (15). However, the clinical guidelines of the European Association for the Study of the Liver (EASL) does not recommend using budesonide in patients with cirrhosis or peri-hepatic shunting, since the lack of efficient first-pass hepatic clearing of budesonide might result in undesired side effects (14). In addition, the immunosuppressant mycophenolate mofetil (MMF), a cytostatic drug that reversibly inhibits the purine biosynthesis, has been demonstrated to be safe and effective as first-line or rescue therapy in inducing and maintaining remission (18). EASL clinical practice guidelines suggest using MMF mainly as a second-line therapy in cases of azathioprine intolerance (14). Unfortunately, during standard therapy, adults rarely achieve resolution of their laboratory and liver tissue abnormalities in less than 12 months, and withdrawal of therapy after 2 years leads to relapse in 85% of cases (6). Moreover, these long-term therapies carry the risk of significant steroid-specific and azathioprine-related side effects.

PBC, formerly known as primary biliary cirrhosis, has recently been renamed to primary biliary cholangitis due to a lack of consistent cirrhosis in a large proportion of patients (19). It has an incidence ranging from 0.3 to 5.8 in 100,000 and has clear female dominance (F:M 9:1) (20). PBC is an autoimmune liver disease characterized by a chronic cholestasis, destruction of the intrahepatic small bile ducts, and the presence of anti-mitochondrial antibodies (AMA) in over 95% of patients (21–23). The target structure is cholangiocytes/biliary epithelial cells (BEC) that are attacked by an aggressive autoimmune response occurring due to a loss of tolerance against several liver autoantigens, including the E2-subunits of the pyruvate dehydrogenase complex (PDC-E2), branched chain 2-oxo acid dehydrogenase, and 2-oxo-glutarate dehydrogenase (22). It has been shown that AMA contribute to the pathogenesis of PBC by increasing macrophage-derived TNFα production resulting in enhanced apoptosis of BEC (24). Besides AMA, particular antinuclear antibodies (ANA) specific for the nuclear body-associated protein sp100 or the nuclear pore membrane protein gp120 are present in more than 50% of PBC patients (25). Although alternative treatments are being evaluated, current therapy is still largely restricted to the administration of ursodeoxycholic acid (UDCA) (26). However, almost 40% of patients are unresponsive to UDCA treatment (27). Recently, obeticholic acid in combination with UDCA has been approved as the first new drug in almost 20 years for treatment of PBC, especially of patient refractory to UDCA single treatment (28, 29). Alternative unlicensed drugs include the corticosteroid budesonide as well as fibric acid derivatives, which act *via* activation of peroxisome proliferator-activated receptors (PPARs). However, there is yet no clear evidence that a therapy with budesonide or fibrates alone or in combination with UDCA is superior to UDCA monotherapy (30).

Finally, PSC is a chronic cholangiopathy characterized by progressive inflammation of the bile duct region resulting in the development of biliary fibrosis, which can advance to cirrhosis and hepatobiliary malignancy (31). PSC has an annual incidence of approximately 1 in 100,000 (32), is typically diagnosed between 30 and 40 years of age, and has a male predominance (M:F 2:1). Most PSC patients display damage of the large bile ducts (90–95%) with characteristic strictures and dilatations of the biliary tree as well as onion skin fibrosis surrounding the damaged ducts. About 20% of patients show small bile duct damage that progresses to large duct disease over a period of 10 years (33). Strikingly, approximately 70–80% of PSC patients also present with inflammatory bowel disease (IBD) and are associated with a higher risk for malignancies (34). Patients with PSC do not generate AMA, but a significant proportion of patients generate "atypical" perinuclear anti-neutrophil cytoplasmic antibodies (pANCA). However, such antibodies are not considered for diagnostic purposes (35). Patients suffering from PSC have a higher risk for hepatobiliary malignancies, but even among PSCpatients with cirrhosis the risk for developing a hepatocellular carcinoma is low (36). In contrast to PBC, the administration of UDCA is controversial for the therapy of PSC. A meta-analysis of several clinical trials revealed no beneficial role of UDCA in slowing the progression of PSC (37). Alternative treatments including the UDCA derivative NorUDCA and agonists to several nuclear receptors, such as farnesoid X receptor and PPAR, are under current investigation in preclinical models (31). Besides PBC and PSC, immunoglobulin G4-associated cholangitis (IAC) is another biliary disease that presents with biochemical and cholangiographic features that are very similar to those found in patients with PSC (38). IAC is characterized by elevated serum immunoglobulin G4 (IgG4) levels and marked infiltration of liver and bile ducts by IgG4-positive plasma cells and contrary to PSC, IAC is not associated with IBD (38). The EASL clinical practice guidelines suggest a corticosteroid as an initial treatment followed by azathioprine in patients with proximal and intrahepatic stenoses and/or relapses during/after corticosteroid therapy.

In addition to the three major autoimmune liver diseases, several overlap syndromes (OS) have been described. According to IAIHG, patients are classified as having an OS if they display overlapping features within the spectrum of AIH and PBC or AIH and PSC (39). OS are not rare occurrences, since a considerable proportion of AIH patients also exhibit features of PBC (7–13%), PSC (6–11%), or a cholestatic syndrome with additional diagnostic features, such as specific antibodies (5–11%) (40). For diagnosis of the AIH-PBC OS the so-called "Paris criteria" have been suggested (41). They include PBC criteria, such as elevated serum levels exceeding the upper limit of normal values by at least a factor 2 for alkaline phosphatase (AP) and a factor of 5 for γ-glutamyl transpeptidase (GGT), presence of AMA, and a liver biopsy showing bile duct lesions. On the AIH side, the criteria comprise serum levels of alanine aminotransferase (ALT) that are elevated by at least five times the upper limit of normal values, serum levels of immunoglobulin G (IgG) that are at least two times higher than the upper limit of normal values, presence of AIH-typical autoantibodies, and a liver biopsy showing interface hepatitis with moderate or severe periportal or periseptical lymphocytic piecemeal necrosis (41). These criteria have been verified in a larger study with 134 PBC, AIH, or AIH-PBC OS patients confirming a high level of sensitivity and specificity for the detection of an AIH-PBC OS (42). AIH-PSC OS is histologically characterized by the presence of an interface hepatitis with or without the presence of plasma cells, portal edema or fibrosis, ductopenia, ductal distortion, ductular proliferation, cholate stasis or, in some patients, obliterative fibrous cholangitis (40). By cholangiography, focal strictures and dilatations of the biliary tree characteristic for PSC are often found in patients with diagnosed AIH, resulting in diagnosis of AIH-PSC OS instead (40). In addition, the criteria for AIH-PSC OS include elevated levels of AST/ALT, γ-globulin, IgG, AP, GGT as well as the absence of AMA that would point toward PBC (40).

AUTOANTIBODIES IN AIH

Historically, three types of AIH have been classified upon the presence of specific autoantibodies. In type 1 AIH (AIH-1) ANA and/or SMA are typical, whereas type 1 liver/kidney microsomal antibodies (LKM-1) have been considered as the hallmark of type 2 AIH (AIH-2). In addition, the term type 3 AIH (AIH-3) has been used to classify patients with antibodies directed against soluble liver antigen (SLA) (3, 6, 12, 43). However, recently such a classification has been questioned since patients with AIH-1 and AIH-2 share the same clinical phenotype (44). Due to the observed change of the autoantibody profile from one subtype to another in some patients over time, AIH-2 might as well constitute an early form of AIH appearing in younger patients who later during disease convert to a AIH-1. In addition, AIH-3 is considered obsolete since anti-SLA autoantibodies are often present together with other antibodies that point toward AIH-1 (45). In this review, we will adhere to the traditional classification into AIH-1 and AIH-2. Possibly the most complex group of autoantibodies are the ANA. In patients with AIH-1 the target structure of ANA in the nucleus is the entire chromatin, including DNA, centromers, histones, sn-RNPs, and cyclin A (46, 47), whereas in PBC ANA are more specifically reacting to histones and centromers, respectively. Anti-centromer antibodies (ACA) are found in up to 30% of PBC patients, who mostly also suffer from systemic sclerosis (SSc) for which ACA are considered as a diagnostic marker (48). Approximately 80% of patients with a PBC/SSc overlap syndrome carry ACA (48, 49). However, ANA are also found in patients with drug-induced hepatitis, chronic hepatitis B or C, as well as in patients with non-alcoholic fatty liver disease (NAFLD) (50). There is not much known about how NAFLD is influencing AIH, but many patients with non-alcoholic steatohepatitis also manifested signs of AIH, including interface hepatitis and ANA generation (51). Interestingly, experimental AIH is exacerbated in mice with NAFLD (52). The precise target molecules for many ANA have not yet been identified. Thus, the actual pattern of nuclear staining is important for diagnosis and the mere presence of any ANA may be compatible with AIH-1 but is not considered a *bona fide* diagnostic marker. To achieve diagnostic value, a detailed analysis of the staining patterns and a consideration of the actual ANA titers is required (50). Similarly, SMA recognizing filamentous actin are valid as diagnostic antibodies for AIH-1 if evaluated carefully. Like ANA, SMA can be detected in other liver diseases with an autoimmune or viral background, but the titers are normally higher in AIH-1. In addition, the staining pattern of SMA on rat kidney sections is mainly focused on tubular and glomerular structures (53). More detailed information on staining patterns of ANA and SMA including images of immunocytochemistry and immunohistochemistry is available in recent review articles by Liberal et al. (50) and Muratori et al. (53).

In patients with AIH-2, the target for anti-LKM-1 antibodies has been identified as the 2D6 isoform of the large cytochrome P450 enzyme family [cytochrome P450 2D6 (CYP2D6)] (54, 55). Anti-LKM-1 antibodies are considered diagnostic, if a hepatitis C virus (HCV) infection can be excluded, since reactivity to CYP2D6 has also been found in chronic hepatitis C patients (see Molecular Mimicry and Epitope Spreading) (56–58). Besides CYP2D6, two additional targets recognized by LKM-1 antibodies have been identified as ERp57 and carboxylesterase 1 (CES1) (59). Although ANA, SMA, or LKM-1 are the most frequent autoantibodies generated in patients with AIH, some patients have no detectable or only marginal titers. However, they may carry other autoantibodies such as peripheral antinuclear neutrophil antibodies that have also been termed "atypical" pANCA since they recognize in contrast to "typical" pANCA beta-tubulin isotype 5, rather than myeloperoxidase (60). Further autoantibodies include anti-SLA and anti-liver and pancreas antigen (LP) antibodies both recognizing UGA suppressor tRNA-associated protein (61), liver cytosol type 1 antibodies (LC-1) specific for formiminotransferase cyclodeaminase (FTCD) or type 3 liver/kidney microsomal antibodies (LKM-3) recognizing family 1 UDP glucuronosyltransferases (3). Like LKM-1, LC-1 antibodies are considered *bona fide* diagnostic markers for AIH-2, whereas LKM-3 have only a minor significance in AIH diagnosis, since they have also been detected in a fraction of patients with hepatitis D (62, 63) and have only a low sensitivity (3, 53). LKM-2 antibodies recognizing cytochrome P450 2C9 have been reported in some patients with AIH-1 or AIH-2 but are predominantly

associated with drug-induced hepatitis induced by tienilic acid (64, 65). Furthermore, anti-liver-specific membrane lipoprotein (LSP) antibodies and, reacting to asialoglycoprotein receptor (ASGPR), which is highly expressed at the surface of hepatocytes, are present in up to 88% of patients (66) and may be used as a general marker compatible with AIH-1 or AIH-2, but not as a diagnostic tool, since they are found also in patients with other liver diseases, such as chronic hepatitis B and C, alcoholic liver disease, and PBC (67). Anti-liver membrane antibodies, which show also reactivity to ASGPR are less well defined and are rarely used. Recently, the reactivity to ASGPR in sera of patients with different autoimmune liver diseases has been investigated using an improved ELISA (68). It has been found that 29.1 and 16.7% of patients with AIH-1 and AIH-2, respectively, carry autoantibodies against ASGPR. However, using the same method such autoantibodies have also been found in patients with PSC or hepatitis C (68).

There is a plethora of commercial kits for autoantibody detection available, some of which use obsolete or outdated autoantibody and/or target antigen nomenclature. Thus, it is important to keep in mind that the conventional markers for AIH-1 are ANA and SMA, whereas LKM-1 are the hallmark autoantibodies used for diagnosis of AIH-2. A summary of autoantibodies in AIH is displayed in **Table 1**. Besides serving as disease markers or even as *bona fide* diagnostics tools autoantibodies might also be involved in the pathogenesis of AIH. Interestingly, the presence of anti-SLA antibodies has been associated with a more severe phenotype of AIH (69). Thus, one possibility would be that anti-SLA antibodies might actively enhance the hepatocellular damage. However, such additional autoantibodies might also originate as result of enhanced hepatocellular destruction as the associated release and presentation of critical amounts of additional liver autoantigens can drive the expansion of SLA-specific B cells. Quite a while ago, it has been found that the titers of LSP antibodies reacting to ASGPR correlated with the severity of AIH (70). However, again a higher titer might just be the result of an exacerbated state of disease, rather than an indication of a pathogenic nature of the antibody. In addition, LSP antibodies are not specific for AIH.

Mechanistically, antibodies might be involved in the pathogenesis of AIH by decorating hepatocytes and thereby induce complement-mediated cell lysis. Indeed, antibodies have been detected at the surface of hepatocytes isolated from liver biopsies (71). Interestingly, CYP2D6, one of the main target autoantigen of LKM-1 antibodies, has been initially found to be expressed at the surface of rat hepatocytes and therefore might have been indeed an excellent target for LKM-1 antibodies (72). However, subsequent more detailed studies could not confirm this finding (73, 74). The observations that cellular infiltrations detected in interface hepatitis are dominated by CD4, rather than CD8 T cells or other lymphoid cells (75) and that most serum autoantibodies are of the IgG isotype (76) might indicate that CD4 T cells execute an essential helper function in the pathogenesis of AIH. In summary, so far there is no firm evidence for the presence of pathogenic autoantibodies in AIH. In animal models, the presence of autoantibodies to liver autoantigens FTCD or CYP2D6 is not sufficient to induce AIH-like disease (77, 78). Thereby, an immunization of mice with recombinant CYP2D6 resulted in the generation of anti-CYP2D6 antibodies, but no substantial T cell response in the liver and no clinical features of AIH (77). In addition, transfer of total IgG isolated from mice with AIH-like disease and high titers of anti-CYP2D6 antibodies (>1/10,000) did not induce AIH-like disease in naïve recipient mice (Holdener and Christen, unpublished data). Furthermore, Hardtke-Wolenski et al. recently demonstrated that the genetic background does not play a role in the generation of autoantibodies to CYP2D6 or FTCD but is important for the development of AIH. Administration of FTCD encoded by a liver-specific virus resulted in AIH-like disease in the autoimmunity-prone non-obese diabetic mice, but not in normal Balb/c, C57BL/6, or FVB/N mice (78). Further, they found that the generation of autoantibodies was required, but not sufficient, for the development of AIH (78). In summary, although there is no firm proof for a direct pathogenic effect, it is likely that autoantibodies are more than just clinical markers and contribute at least partially to the chronic inflammation of the liver.

TABLE 1 | Autoantibodies in autoimmune hepatitis.

	Autoantibody	Target structure/molecule	Diagnostic value
Type 1 AIH (AIH-1)	Antinuclear antibodies	Chromatin	Yes, after detailed analysis of staining pattern in immunocytochemistry
	Anti-smooth muscle antibodies	Filamentous actin; tubular and glomerular specificity in kidney	Yes, after detailed analysis of staining pattern in immunocytochemistry
	Soluble liver antigen/LP	UGA suppressor tRNA-associated protein	Associated with severe phenotype
	Type 2 liver/kidney microsomal antibodies	Cytochrome P450 2C9	No, more associated with drug-induced hepatitis
	Peripheral antinuclear neutrophil antibodies	Beta-tubulin isotype 5	Compatible with AIH-1
Type 2 AIH (AIH-2)	Type 1 liver/kidney microsomal antibodies	Cytochrome P450 2D6	Yes, if hepatitis C virus is excluded
	Type 2 liver/kidney microsomal antibodies	Cytochrome P450 2C9	No, more associated with drug-induced hepatitis
	Type 3 liver/kidney microsomal antibodies	Family 1 UDP-glucuronosyltransferases	Yes, but low sensitivity
	Liver cytosol type 1 antibodies	Formiminotransferase cyclodeaminase	Yes
	Liver-specific membrane lipoprotein	Asialoglycoprotein receptor	Compatible with AIH-2

CYP2D6 EPITOPES

The major autoantigen in AIH-2, CYP2D6, is the best characterized autoantigen in AIH. Extensive epitope mapping has been performed in patients as well as in mouse models (**Figure 1**). Early after the identification of CYP2D6 as the target of LKM-1 antibodies, an immunodominant B-cell epitope has been mapped to a region spanning amino acids 254–271 (aa254–271). This epitope has been recognized by sera of the majority of patients with AIH-2, ranging from 62 to 100%, depending on the individual study (79–84). Besides this immunodominant epitope, several other regions of CYP2D6 have been identified as molecular targets for LKM-1 antibodies in various proportions of patients' sera, including the sequential regions spanning aa321–351, aa373–389, and aa410–429 (82); aa196–218 (85); aa193–212, aa238–257, aa268–287, and aa478–497 (86); aa55–63, aa139–147, aa203–211, aa239–aa247, and aa379–aa429 (84), aa284–391, aa412–429, as well as conformational epitopes located in the region of aa1–146 (87) and aa321–379 (88). The majority of these epitopes is located at the surface of the CYP2D6 molecule and is therefore easily accessible to autoantibodies (84).

The CYP2D6 molecule is also recognized by CD4 and CD8 T cells if properly presented by MHC I or II. Such autoreactive CYP2D6-specific CD4 and CD8 T cells have been found in the blood and the liver of patients with AIH-2 (89, 90). By testing the proliferative T cell response to 61 overlapping peptides covering the entire CYP2D6 molecule, a polyclonal reactivity to seven regions has been found in HLA *DRB1*07* and four regions in non-*DRB1*07* patients (**Figure 1**) (91). Furthermore, by using HLA-A2–CYP2D6–peptide tetramers, CYP2D6-specific CD8 T cells producing high levels of IFNγ have been found in AIH-2 patients. Whereby IFNγ production and cytotoxicity were higher at the time of diagnosis than after beginning of immunosuppressive treatment, and the frequency of CYP2D6-specific CD8 T cells correlated well with the severity of the disease (92).

MOLECULAR MIMICRY AND EPITOPE SPREADING

One possibility of how the reactivity of autoantibodies might give insight into the initiation and/or propagation of AIH is a concept known as "molecular mimicry" (93–96). Thereby, a similarity between a pathogen component and a self-antigen would cause the pathogen-specific antibodies and/or T cells to attack the similar self-antigen as well [see Ref. (97) for a detailed review on molecular mimicry]. Pathogen infections might play a role as drivers of an autoimmune process on several other levels, including causing direct damage to hepatocytes and triggering a strong inflammatory response in the liver (98). However, evidence for such triggering pathogen infections is hard to find, since the pathogen itself might have disappeared at the time of diagnosis (hit-and-run event) and only susceptible individuals develop autoimmune manifestations. In addition, more than just one trigger might be necessary to induce an autoimmune disease, and it has been demonstrated that some pathogens might even prevent autoimmunity by either deleting autoaggressive lymphocytes (99) or by inducing counteracting suppressive mechanisms, i.e., regulatory T cells (100).

Another factor that hampers the detection of a possible structural similarity between pathogen and self-antigen is a mechanism termed "epitope spreading" or "determinant spreading" (101). Thereby, the initial immune response (antibodies and/or T cells), which is directed against the initiating epitope, would spread intramolecularly to other epitopes of the same self-antigen and in some instances even intermolecularly to other self-antigens. Since the initiating epitope might not necessarily

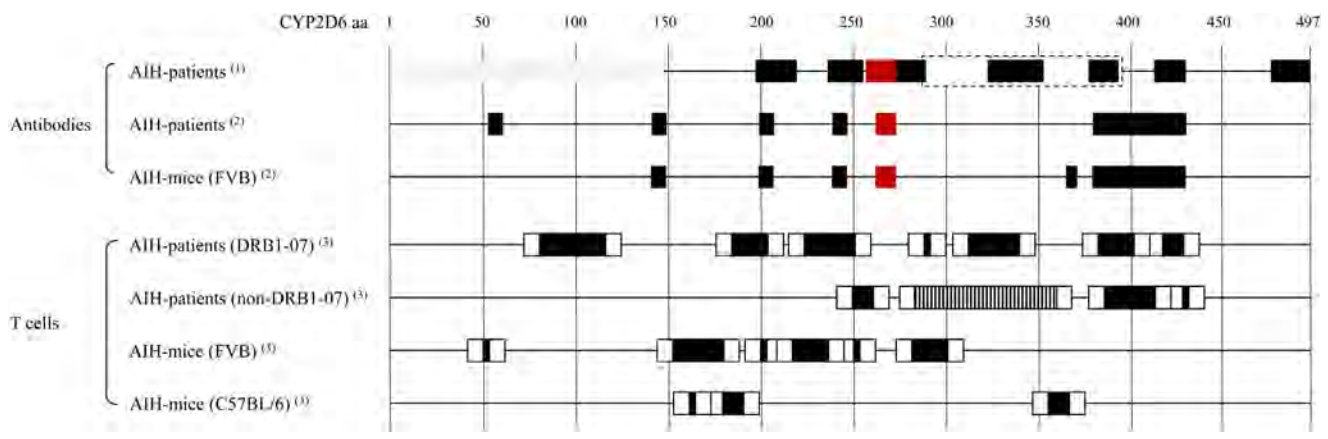

FIGURE 1 | Cytochrome P450 2D6 (CYP2D6)-specific antibody and T cell epitopes: B cell/antibody and T cell epitopes detected in patients with type 1 AIH (AIH-1) and in the CYP2D6 mouse model. Note that B cell/antibody epitopes are similar in patients and mice, whereas due to differences in the MHC, the T cell epitopes are different. Red boxes: immunodominant epitope recognized by high titer autoantibodies in most of autoimmune hepatitis (AIH) patients. Gray boxes: conformational epitopes (87, 88). Dashed box: large epitope with no further subdivision, possibly dominated by the indicated smaller epitopes within (87). T cell epitope mapping has been performed using staggered, overlapping 20-mer peptides covering the entire CYP2D6 protein, therefore the epitope sequences have been divided into a core (back boxes) and peripheral (white boxes) region. Vertical striped box: several overlapping epitopes (91). (1) Collective data from Ref. (82, 73, 79–80, 85–88). (2) Patient and mouse data from the same epitope mapping assay (84). (3) Data from epitope mapping using the same set of staggered 20-mer CYP2D6 peptides (77, 91).

be the final immunodominant one, the specificity of the patients' autoantibodies and/or T cells might be strongest to a late epitope appearing as result of spreading and not to the initiating epitope at time of diagnosis. A possible scenario for an involvement of molecular mimicry as well as epitope spreading is displayed in **Figure 2**.

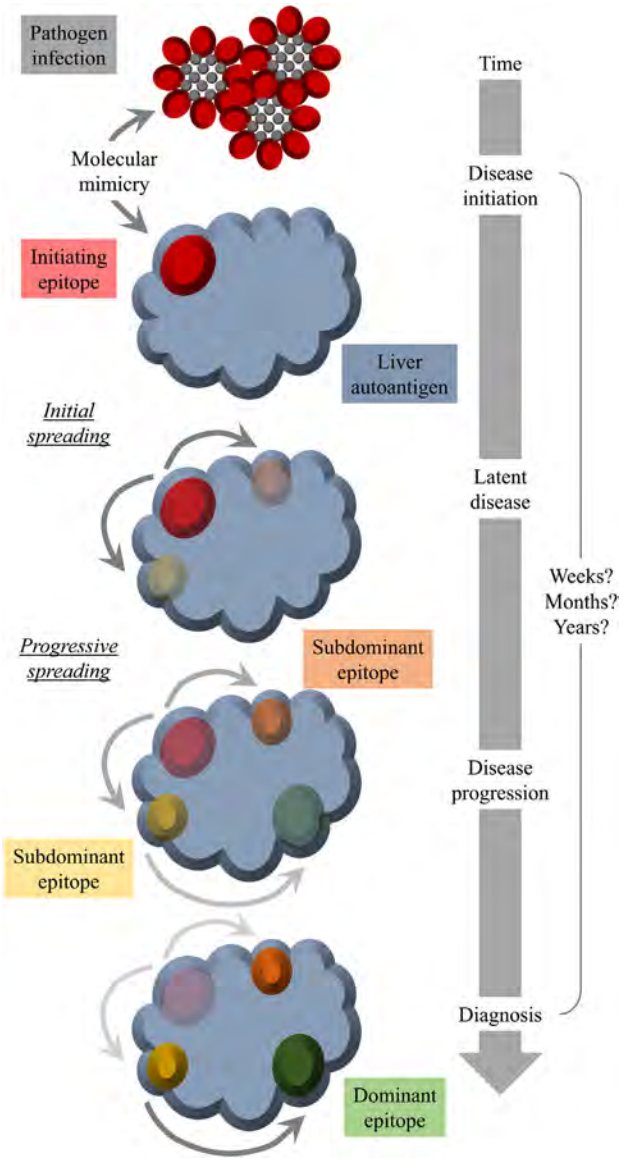

FIGURE 2 | Molecular mimicry and epitope spreading: hypothetical scenario for environmental triggering factors as inducers of autoimmune disease. Infection of the host by a pathogen that shares a structural similarity with a host molecule (molecular mimicry) occurs long before diagnosis. The initial epitope recognized by specific antibodies functions as an origin of intramolecular epitope spreading occurring as result of somatic hypermutations in B cells and the subsequent dynamic antibody response. Thereby, the reactivity to the initiating epitope might be lost over time leaving behind immunodominant epitopes that have nothing in common with the pathogen structure that was responsible for the initiation of the autoreactivity. Thus, at the time of diagnosis, there is no obvious link to an infection with a pathogen that mimics a host component.

Unfortunately, such a scenario is difficult to demonstrate in patients, since processes of molecular mimicry and epitope spreading might have long passed at the time of diagnosis. In PBC and in other autoimmune diseases, including type 1 diabetes, multiple sclerosis, rheumatoid arthritis, and autoimmune Addison's disease, the development of autoantibodies may precede the clinical onset of disease by 10 years or even more (102). Indeed, epitope mapping with sera collected from AIH patients over more than a decade after diagnosis revealed a very stable epitope specificity (84). This indicates that in most patients only a steady state rather than a dynamically developing immune specificity can be observed. Therefore, we have developed an inducible mouse model for AIH using adenovirus encoded human CYP2D6 (Ad-2D6) as a trigger. Infection of wild-type C57BL/6 or FVB mice with Ad-2D6 results in the breakdown of tolerance to the mouse Cyp homologs that are similar, but not identical, to the human CYP2D6 (83, 103). Such Ad-2D6-infected mice develop AIH-like disease characterized by cellular infiltrations with an interface hepatitis-like pattern, hepatic fibrosis, and the generation of CYP2D6-specific autoantibodies (83) and T cells (77). Several animal models for AIH have been developed in the past [see Ref. (104) for a detailed review on current models]. However, the presence of a clearly defined target autoantigen and the possibility of being able to initiate the autoimmune response/disease at a defined time allow the use of the CYP2D6 model to perform a detailed study of the CYP2D6-specific immune response over time. Thus, the hypothesis that a pathogen infection might be involved in the etiology of AIH can be evaluated.

We found that Ad-2D6-infected mice first develop antibodies reactive to the region around the CYP2D6 sequence DPAQPPRD (aa263–270), indicating that this region might be involved in the initiation of the CYP2D6-specific immune response (84). At later times after infection, the antibody reactivity spreads to other epitopes, which are predominantly located at the surface of the CYP2D6 molecule (84). A similar predominance of surface epitopes has also been previously reported using sera of patients with AIH-2 (105). Importantly, even 8 weeks after infection, the highest titers of anti-CYP2D6 antibodies were determined for the initiating DPAQPPRD (aa263–270) epitope (84). Thus, in the mouse model the initiating epitope remains immunodominant over time. Interestingly, this epitope is also immunodominant in patients with AIH-2 (**Figure 2**). This stands in contrast to T cell epitopes, which are found to be dissimilar in patients and mice (77, 91). Naturally, the difference in MHC molecules able to present critical CYP2D6 peptides predominantly accounts for this divergence (**Figure 1**).

Several of the identified linear CYP2D6 B cell epitopes share sequence homologies to human pathogens. Already at the time of identification of the immunodominant CYP2D6 epitope DPAQPPRD (aa263–270), a shared sequence homology with the infected cell protein 4 of herpes simplex virus 1 (HSV-1) has been reported (81). Since this immunodominant region has been also detected by LKM-1 antibodies of (depending on the study) up to 100% of AIH patients (79) and has been identified as the initiating and immunodominant region in the CYP2D6 mouse (84) HSV-1 infection might indeed be involved in the etiology

of AIH. Unfortunately, no epidemiological evidence supports such an association between AIH and HSV-1 infection. By contrast, there is epidemiological evidence for an association between HCV infection and the development of AIH-2 (106, 107). In addition, LKM-1 antibodies have been detected in up to 10% of patients with a chronic HCV infection (56–58). Interestingly, *vice versa* antibodies to HCV have been found in a large proportion of AIH-2 patients, which suggests that AIH patients might have experienced HCV infection in the past (108, 109). In fact, it has been demonstrated that antibodies specific for the HCV proteins NS3 and NS5a cross-react to a specific conformational epitope on CYP2D6 spanning aa254–288 (110), which contains the immunodominant epitope DPAQPPRD (aa263–270). Further screening of the NCBI GenBank revealed additional sequence homologies to the immunodominant CYP2D6 epitope by the envelope glycoprotein E1 of HCV and by proteins of the human immunodeficiency virus (HIV) (84). Several sequence homologies of subdominant CYP2D6 epitopes that have appeared later as the initiating epitope have been found to various human pathogens, including HCV, HIV, rabies virus, human cytomegalovirus, Karposi's sacrcoma associated herpes virus, and *Legionella pneumophila*, and with several *Mycobacterium*, *Burkholdria*, and *Brucella* species (84).

Another triggering factor for autoimmune liver diseases might be protein adduct formation by reactive drug metabolites. The best documented case of drug-induced hepatotoxicity with an autoimmune component is halothane hepatitis (111–113). Upon oxidative, cytochrome P450 2E1 (CYP2E1)-dependent metabolism of the anesthetic agent halothane, trifluoroacteylated protein adducts (TFA-adducts) are formed, which act as neoantigens. Susceptible patients generate TFA-adduct-specific antibodies and T cells and develop a fulminant hepatitis. Several such neoantigens have been identified and include CYP2E1 as well as CYP2D6 (113). Interestingly, TFA-adduct-specific antibodies generated in patients and in experimental animals cross-react with the lipoic acid moiety of the E2-subunits of the 2-oxoacid dehydrogenase family enyzmes, including PDC-E2, which constitute the major autoantigens in PBC (114, 115). Furthermore, CES1, which has been identified as additional target autoantigen recognized by LKM-1 antibodies is also a target antigen in halothane hepatitis (116). However, sera of patients with AIH or halothane hepatitis react to different epitopes (59). The anesthetic agent halothane has been withdrawn from the market in the early 1990s; however, the closely related general anesthetic isoflurane is still in use. Protein modifications similar to TFA-adducts are also formed upon anesthesia with modern isoflurane derivatives, such as desflurane. In addition, some hydrochlorofluorocarbons (HCFC), which are frequently used as foam blowing agents, refrigerants, and propellants, are metabolized in a similar way, giving raise to TFA-adducts as well (117). Although cases of isoflurane (118), desflurane (119), and HCFC hepatitis (120) have been reported, there is yet no firm proof that drug-adduct formation and the subsequent generation of drug-adduct-specific antibodies contribute to the development of AIH or another autoimmune liver disease.

CONCLUSION

The diagnosis of autoimmune liver diseases is difficult and relies on histological analysis of liver biopsies as well as systematic serology, including the presence of specific autoantibodies and distinct enzymatic makers that indicate the nature of the liver damage. Thus, a detailed characterization of autoantibody pattern and titer is indispensable for the diagnosis of AIH, as well as other autoimmune liver diseases, such as PBC and PSC. In fact, with proper analysis of immunofluorescent staining patterns and autoantibody titer a serologic reactivity is found in more than 95% of AIH patients (121). In AIH, some autoantibodies correlate with the severity of the disease, but there is no firm proof that such autoantibodies are pathogenic *per se*. In general, there is still desperate need for more knowledge on the etiology and immunopathogenesis of AIH to develop novel therapeutic interventions. AIH therapy still largely relies on a corticosteroid and/or cytostatic drug regimen and since autoimmune diseases are a lifelong burden, such chronic therapies are often associated with long-term side effects. Novel animal models (104) might provide a basis to identify crucial inflammatory factors that drive the disease pathogenesis and/or contribute to its chronicity.

AUTHOR CONTRIBUTIONS

All authors listed have made a substantial, direct, and intellectual contribution to the work and approved it for publication.

FUNDING

This research project was funded by the University Hospital Frankfurt, Frankfurt am Main, Germany and grants of the German Research Foundation (DFG) to UC and EH.

REFERENCES

1. Czaja AJ. Diagnosis and management of autoimmune hepatitis. *Clin Liver Dis* (2015) 19(1):57–79. doi:10.1016/j.cld.2014.09.004
2. Liberal R, Grant CR, Mieli-Vergani G, Vergani D. Autoimmune hepatitis: a comprehensive review. *J Autoimmun* (2013) 41:126–39. doi:10.1016/j.jaut.2012.11.002
3. Vierling JM. Diagnosis and treatment of autoimmune hepatitis. *Curr Gastroenterol Rep* (2012) 14(1):25–36. doi:10.1007/s11894-011-0236-2
4. Lohse AW, Wiegard C. Diagnostic criteria for autoimmune hepatitis. *Best Pract Res Clin Gastroenterol* (2011) 25(6):665–71. doi:10.1016/j.bpg.2011.10.004
5. Manns MP, Lohse AW, Vergani D. Autoimmune hepatitis – update 2015. *J Hepatol* (2015) 62(1 Suppl):S100–11. doi:10.1016/j.jhep.2015.03.005
6. Manns MP, Czaja AJ, Gorham JD, Krawitt EL, Mieli-Vergani G, Vergani D, et al. Diagnosis and management of autoimmune hepatitis. *Hepatology* (2010) 51(6):2193–213. doi:10.1002/hep.23584
7. Boberg KM. Prevalence and epidemiology of autoimmune hepatitis. *Clin Liver Dis* (2002) 6(3):635–47. doi:10.1016/S1089-3261(02)00021-1
8. Czaja AJ. Autoimmune hepatitis-approach to diagnosis. *MedGenMed* (2006) 8(2):55.
9. Donaldson PT, Doherty DG, Hayllar KM, McFarlane IG, Johnson PJ, Williams R. Susceptibility to autoimmune chronic active hepatitis: human

leukocyte antigens DR4 and A1-B8-DR3 are independent risk factors. *Hepatology* (1991) 13(4):701–6. doi:10.1002/hep.1840130415
10. Doherty DG, Donaldson PT, Underhill JA, Farrant JM, Duthie A, Mieli-Vergani G, et al. Allelic sequence variation in the HLA class II genes and proteins in patients with autoimmune hepatitis. *Hepatology* (1994) 19(3):609–15. doi:10.1002/hep.1840190311
11. Czaja AJ, Carpenter HA, Santrach PJ, Moore SB. Significance of HLA DR4 in type 1 autoimmune hepatitis. *Gastroenterology* (1993) 105(5):1502–7. doi:10.1016/0016-5085(93)90157-8
12. Czaja AJ. Challenges in the diagnosis and management of autoimmune hepatitis. *Can J Gastroenterol* (2013) 27(9):531–9. doi:10.1155/2013/981086
13. Hennes EM, Zeniya M, Czaja AJ, Pares A, Dalekos GN, Krawitt EL, et al. Simplified criteria for the diagnosis of autoimmune hepatitis. *Hepatology* (2008) 48(1):169–76. doi:10.1002/hep.22322
14. European Association for the Study of the Liver. EASL clinical practice guidelines: autoimmune hepatitis. *J Hepatol* (2015) 63(4):971–1004. doi:10.1016/j.jhep.2015.06.030
15. Manns MP, Woynarowski M, Kreisel W, Lurie Y, Rust C, Zuckerman E, et al. Budesonide induces remission more effectively than prednisone in a controlled trial of patients with autoimmune hepatitis. *Gastroenterology* (2010) 139(4):1198–206. doi:10.1053/j.gastro.2010.06.046
16. Strassburg CP, Manns MP. Therapy of autoimmune hepatitis. *Best Pract Res Clin Gastroenterol* (2011) 25(6):673–87. doi:10.1016/j.bpg.2011.08.003
17. Czaja AJ. Advances in the current treatment of autoimmune hepatitis. *Dig Dis Sci* (2012) 57(8):1996–2010. doi:10.1007/s10620-012-2151-2
18. Zachou K, Gatselis N, Papadamou G, Rigopoulou EI, Dalekos GN. Mycophenolate for the treatment of autoimmune hepatitis: prospective assessment of its efficacy and safety for induction and maintenance of remission in a large cohort of treatment-naive patients. *J Hepatol* (2011) 55(3):636–46. doi:10.1016/j.jhep.2010.12.032
19. Beuers U, Gershwin ME, Gish RG, Invernizzi P, Jones DE, Lindor K, et al. Changing nomenclature for PBC: from 'cirrhosis' to 'cholangitis'. *Hepatology* (2015) 62(5):1620–2. doi:10.1002/hep.28140
20. Boonstra K, Beuers U, Ponsioen CY. Epidemiology of primary sclerosing cholangitis and primary biliary cirrhosis: a systematic review. *J Hepatol* (2012) 56(5):1181–8. doi:10.1016/j.jhep.2011.10.025
21. Oertelt S, Rieger R, Selmi C, Invernizzi P, Ansari AA, Coppel RL, et al. A sensitive bead assay for antimitochondrial antibodies: chipping away at AMA-negative primary biliary cirrhosis. *Hepatology* (2007) 45(3):659–65. doi:10.1002/hep.21583
22. Hirschfield GM, Gershwin ME. The immunobiology and pathophysiology of primary biliary cirrhosis. *Annu Rev Pathol* (2013) 8:303–30. doi:10.1146/annurev-pathol-020712-164014
23. Katsumi T, Tomita K, Leung PS, Yang GX, Gershwin ME, Ueno Y. Animal models of primary biliary cirrhosis. *Clin Rev Allergy Immunol* (2015) 48(2–3):142–53. doi:10.1007/s12016-015-8482-y
24. Lleo A, Bowlus CL, Yang GX, Invernizzi P, Podda M, Van de Water J, et al. Biliary apotopes and anti-mitochondrial antibodies activate innate immune responses in primary biliary cirrhosis. *Hepatology* (2010) 52(3):987–98. doi:10.1002/hep.23783
25. Worman HJ, Courvalin JC. Antinuclear antibodies specific for primary biliary cirrhosis. *Autoimmun Rev* (2003) 2(4):211–7. doi:10.1016/S1568-9972(03)00013-2
26. Floreani A, Sun Y, Zou ZS, Li B, Cazzagon N, Bowlus CL, et al. Proposed therapies in primary biliary cholangitis. *Expert Rev Gastroenterol Hepatol* (2016) 10(3):371–82. doi:10.1586/17474124.2016.1121810
27. Tanaka A, Gershwin ME. Finding the cure for primary biliary cholangitis – still waiting. *Liver Int* (2017) 37(4):500–2. doi:10.1111/liv.13344
28. Nevens F, Andreone P, Mazzella G, Strasser SI, Bowlus C, Invernizzi P, et al. A placebo-controlled trial of obeticholic acid in primary biliary cholangitis. *N Engl J Med* (2016) 375(7):631–43. doi:10.1056/NEJMoa1509840
29. Chascsa D, Carey EJ, Lindor KD. Old and new treatments for primary biliary cholangitis. *Liver Int* (2017) 37(4):490–9. doi:10.1111/liv.13294
30. European Association for the Study of the Liver. EASL clinical practice guidelines: the diagnosis and management of patients with primary biliary cholangitis. *J Hepatol* (2017) 67(1):145–72. doi:10.1016/j.jhep.2017.03.022
31. Halilbasic E, Fuchs C, Hofer H, Paumgartner G, Trauner M. Therapy of primary sclerosing cholangitis – today and tomorrow. *Dig Dis* (2015) 33(Suppl 2):149–63. doi:10.1159/000440827
32. Molodecky NA, Kareemi H, Parab R, Barkema HW, Quan H, Myers RP, et al. Incidence of primary sclerosing cholangitis: a systematic review and meta-analysis. *Hepatology* (2011) 53(5):1590–9. doi:10.1002/hep.24247
33. Bjornsson E, Olsson R, Bergquist A, Lindgren S, Braden B, Chapman RW, et al. The natural history of small-duct primary sclerosing cholangitis. *Gastroenterology* (2008) 134(4):975–80. doi:10.1053/j.gastro.2008.01.042
34. Rizvi S, Eaton JE, Gores GJ. Primary sclerosing cholangitis as a premalignant biliary tract disease: surveillance and management. *Clin Gastroenterol Hepatol* (2015) 13(12):2152–65. doi:10.1016/j.cgh.2015.05.035
35. Weismuller TJ, Wedemeyer J, Kubicka S, Strassburg CP, Manns MP. The challenges in primary sclerosing cholangitis – aetiopathogenesis, autoimmunity, management and malignancy. *J Hepatol* (2008) 48(Suppl 1):S38–57. doi:10.1016/j.jhep.2008.01.020
36. Zenouzi R, Weismuller TJ, Hubener P, Schulze K, Bubenheim M, Pannicke N, et al. Low risk of hepatocellular carcinoma in patients with primary sclerosing cholangitis with cirrhosis. *Clin Gastroenterol Hepatol* (2014) 12(10):1733–8. doi:10.1016/j.cgh.2014.02.008
37. Triantos CK, Koukias NM, Nikolopoulou VN, Burroughs AK. Meta-analysis: ursodeoxycholic acid for primary sclerosing cholangitis. *Aliment Pharmacol Ther* (2011) 34(8):901–10. doi:10.1111/j.1365-2036.2011.04822.x
38. Ghazale A, Chari ST, Zhang L, Smyrk TC, Takahashi N, Levy MJ, et al. Immunoglobulin G4-associated cholangitis: clinical profile and response to therapy. *Gastroenterology* (2008) 134(3):706–15. doi:10.1053/j.gastro.2007.12.009
39. Boberg KM, Chapman RW, Hirschfield GM, Lohse AW, Manns MP, Schrumpf E, et al. Overlap syndromes: the International Autoimmune Hepatitis Group (IAIHG) position statement on a controversial issue. *J Hepatol* (2011) 54(2):374–85. doi:10.1016/j.jhep.2010.09.002
40. Czaja AJ. Diagnosis and management of the overlap syndromes of autoimmune hepatitis. *Can J Gastroenterol* (2013) 27(7):417–23. doi:10.1155/2013/981086
41. Chazouilleres O, Wendum D, Serfaty L, Montembault S, Rosmorduc O, Poupon R. Primary biliary cirrhosis-autoimmune hepatitis overlap syndrome: clinical features and response to therapy. *Hepatology* (1998) 28(2):296–301. doi:10.1002/hep.510280203
42. Kuiper EM, Zondervan PE, van Buuren HR. Paris criteria are effective in diagnosis of primary biliary cirrhosis and autoimmune hepatitis overlap syndrome. *Clin Gastroenterol Hepatol* (2010) 8(6):530–4. doi:10.1016/j.cgh.2010.03.004
43. Krawitt EL. Autoimmune hepatitis. *N Engl J Med* (2006) 354(1):54–66. doi:10.1056/NEJMra050408
44. Muratori P, Lalanne C, Fabbri A, Cassani F, Lenzi M, Muratori L. Type 1 and type 2 autoimmune hepatitis in adults share the same clinical phenotype. *Aliment Pharmacol Ther* (2015) 41(12):1281–7. doi:10.1111/apt.13210
45. Kanzler S, Weidemann C, Gerken G, Lohr HF, Galle PR, Meyer zum Buschenfelde KH, et al. Clinical significance of autoantibodies to soluble liver antigen in autoimmune hepatitis. *J Hepatol* (1999) 31(4):635–40. doi:10.1016/S0168-8278(99)80342-0
46. Czaja AJ, Nishioka M, Morshed SA, Hachiya T. Patterns of nuclear immunofluorescence and reactivities to recombinant nuclear antigens in autoimmune hepatitis. *Gastroenterology* (1994) 107(1):200–7. doi:10.1016/0016-5085(94)90078-7
47. Strassburg CP, Alex B, Zindy F, Gerken G, Luttig B, Meyer zum Buschenfelde KH, et al. Identification of cyclin A as a molecular target of antinuclear antibodies (ANA) in hepatic and non-hepatic autoimmune diseases. *J Hepatol* (1996) 25(6):859–66. doi:10.1016/S0168-8278(96)80290-X
48. Liberal R, Grant CR, Sakkas L, Bizzaro N, Bogdanos DP. Diagnostic and clinical significance of anti-centromere antibodies in primary biliary cirrhosis. *Clin Res Hepatol Gastroenterol* (2013) 37(6):572–85. doi:10.1016/j.clinre.2013.04.005
49. Rigamonti C, Shand LM, Feudjo M, Bunn CC, Black CM, Denton CP, et al. Clinical features and prognosis of primary biliary cirrhosis associated with systemic sclerosis. *Gut* (2006) 55(3):388–94. doi:10.1136/gut.2005.075002
50. Liberal R, Mieli-Vergani G, Vergani D. Clinical significance of autoantibodies in autoimmune hepatitis. *J Autoimmun* (2013) 46:17–24. doi:10.1016/j.jaut.2013.08.001
51. Tsuneyama K, Baba H, Kikuchi K, Nishida T, Nomoto K, Hayashi S, et al. Autoimmune features in metabolic liver disease: a single-center experience

and review of the literature. *Clin Rev Allergy Immunol* (2013) 45(1):143–8. doi:10.1007/s12016-013-8383-x
52. Muller P, Messmer M, Bayer M, Pfeilschifter JM, Hintermann E, Christen U. Non-alcoholic fatty liver disease (NAFLD) potentiates autoimmune hepatitis in the CYP2D6 mouse model. *J Autoimmun* (2016) 69:51–8. doi:10.1016/j.jaut.2016.02.007
53. Muratori P, Lenzi M, Cassani F, Lalanne C, Muratori L. Diagnostic approach to autoimmune hepatitis. *Expert Rev Clin Immunol* (2017) 13(8):769–79. doi:10.1080/1744666X.2017.1327355
54. Manns MP, Johnson EF, Griffin KJ, Tan EM, Sullivan KF. Major antigen of liver kidney microsomal autoantibodies in idiopathic autoimmune hepatitis is cytochrome P450db1. *J Clin Invest* (1989) 83(3):1066–72. doi:10.1172/JCI113949
55. Zanger UM, Hauri HP, Loeper J, Homberg JC, Meyer UA. Antibodies against human cytochrome P-450db1 in autoimmune hepatitis type II. *Proc Natl Acad Sci U S A* (1988) 85(21):8256–60. doi:10.1073/pnas.85.21.8256
56. Zachou K, Rigopoulou E, Dalekos GN. Autoantibodies and autoantigens in autoimmune hepatitis: important tools in clinical practice and to study pathogenesis of the disease. *J Autoimmune Dis* (2004) 1(1):2. doi:10.1186/1740-2557-1-2
57. Strassburg CP, Vogel A, Manns MP. Autoimmunity and hepatitis C. *Autoimmun Rev* (2003) 2(6):322–31. doi:10.1016/S1568-9972(03)00036-3
58. Ferri S, Muratori L, Lenzi M, Granito A, Bianchi FB, Vergani D. HCV and autoimmunity. *Curr Pharm Des* (2008) 14(17):1678–85. doi:10.2174/138161208784746824
59. Komurasaki R, Imaoka S, Tada N, Okada K, Nishiguchi S, Funae Y. LKM-1 sera from autoimmune hepatitis patients that recognize ERp57, carboxylesterase 1 and CYP2D6. *Drug Metab Pharmacokinet* (2010) 25(1):84–92. doi:10.2133/dmpk.25.84
60. Terjung B, Spengler U, Sauerbruch T, Worman HJ. "Atypical p-ANCA" in IBD and hepatobiliary disorders react with a 50-kilodalton nuclear envelope protein of neutrophils and myeloid cell lines. *Gastroenterology* (2000) 119(2):310–22. doi:10.1053/gast.2000.9366
61. Wies I, Brunner S, Henninger J, Herkel J, Kanzler S, Meyer zum Buschenfelde KH, et al. Identification of target antigen for SLA/LP autoantibodies in autoimmune hepatitis. *Lancet* (2000) 355(9214):1510–5. doi:10.1016/S0140-6736(00)02166-8
62. Philipp T, Durazzo M, Trautwein C, Alex B, Straub P, Lamb JG, et al. Recognition of uridine diphosphate glucuronosyl transferases by LKM-3 antibodies in chronic hepatitis D. *Lancet* (1994) 344(8922):578–81. doi:10.1016/S0140-6736(94)91966-6
63. Strassburg CP, Obermayer-Straub P, Alex B, Durazzo M, Rizzetto M, Tukey RH, et al. Autoantibodies against glucuronosyltransferases differ between viral hepatitis and autoimmune hepatitis. *Gastroenterology* (1996) 111(6):1576–86. doi:10.1016/S0016-5085(96)70020-3
64. Obermayer-Straub P, Strassburg CP, Manns MP. Target proteins in human autoimmunity: cytochromes P450 and UDP-glucuronosyltransferases. *Can J Gastroenterol* (2000) 14(5):429–39. doi:10.1155/2000/910107
65. Mizutani T, Shinoda M, Tanaka Y, Kuno T, Hattori A, Usui T, et al. Autoantibodies against CYP2D6 and other drug-metabolizing enzymes in autoimmune hepatitis type 2. *Drug Metab Rev* (2005) 37(1):235–52. doi:10.1081/DMR-200028798
66. Poralla T, Treichel U, Lohr H, Fleischer B. The asialoglycoprotein receptor as target structure in autoimmune liver diseases. *Semin Liver Dis* (1991) 11(3):215–22. doi:10.1055/s-2008-1040439
67. Manns MP, Strassburg CP. Autoimmune hepatitis: clinical challenges. *Gastroenterology* (2001) 120(6):1502–17. doi:10.1053/gast.2001.24227
68. Villalta D, Mytilinaiou MG, Elsner M, Hentschel C, Cuccato J, Somma V, et al. Autoantibodies to asialoglycoprotein receptor (ASGPR) in patients with autoimmune liver diseases. *Clin Chim Acta* (2015) 450:1–5. doi:10.1016/j.cca.2015.07.021
69. Ma Y, Okamoto M, Thomas MG, Bogdanos DP, Lopes AR, Portmann B, et al. Antibodies to conformational epitopes of soluble liver antigen define a severe form of autoimmune liver disease. *Hepatology* (2002) 35(3):658–64. doi:10.1053/jhep.2002.32092
70. McFarlane BM, McSorley CG, Vergani D, McFarlane IG, Williams R. Serum autoantibodies reacting with the hepatic asialoglycoprotein receptor protein (hepatic lectin) in acute and chronic liver disorders. *J Hepatol* (1986) 3(2):196–205. doi:10.1016/S0168-8278(86)80026-5
71. Vergani D, Mieli-Vergani G, Mondelli M, Portmann B, Eddleston AL. Immunoglobulin on the surface of isolated hepatocytes is associated with antibody-dependent cell-mediated cytotoxicity and liver damage. *Liver* (1987) 7(6):307–15. doi:10.1111/j.1600-0676.1987.tb00361.x
72. Loeper J, Descatoire V, Maurice M, Beaune P, Feldmann G, Larrey D, et al. Presence of functional cytochrome P-450 on isolated rat hepatocyte plasma membrane. *Hepatology* (1990) 11(5):850–8. doi:10.1002/hep.1840110521
73. Yamamoto AM, Mura C, De Lemos-Chiarandini C, Krishnamoorthy R, Alvarez F. Cytochrome P450IID6 recognized by LKM1 antibody is not exposed on the surface of hepatocytes. *Clin Exp Immunol* (1993) 92(3):381–90. doi:10.1111/j.1365-2249.1993.tb03409.x
74. Trautwein C, Gerken G, Lohr H, Meyer zum Buschenfelde KH, Manns M. Lack of surface expression for the B-cell autoepitope of cytochrome P450 IID6 evidenced by flow cytometry. *Z Gastroenterol* (1993) 31(4):225–30.
75. Senaldi G, Portmann B, Mowat AP, Mieli-Vergani G, Vergani D. Immunohistochemical features of the portal tract mononuclear cell infiltrate in chronic aggressive hepatitis. *Arch Dis Child* (1992) 67(12):1447–53. doi:10.1136/adc.67.12.1447
76. Liberal R, Longhi MS, Mieli-Vergani G, Vergani D. Pathogenesis of autoimmune hepatitis. *Best Pract Res Clin Gastroenterol* (2011) 25(6):653–64. doi:10.1016/j.bpg.2011.09.009
77. Ehser J, Holdener M, Christen S, Bayer M, Pfeilschifter JM, Hintermann E, et al. Molecular mimicry rather than identity breaks T-cell tolerance in the CYP2D6 mouse model for human autoimmune hepatitis. *J Autoimmun* (2013) 42:39–49. doi:10.1016/j.jaut.2012.11.001
78. Hardtke-Wolenski M, Dywicki J, Fischer K, Hapke M, Sievers M, Schlue J, et al. The influence of genetic predisposition and autoimmune hepatitis inducing antigens in disease development. *J Autoimmun* (2017) 78:39–45. doi:10.1016/j.jaut.2016.12.001
79. Gueguen M, Boniface O, Bernard O, Clerc F, Cartwright T, Alvarez F. Identification of the main epitope on human cytochrome P450 IID6 recognized by anti-liver kidney microsome antibody. *J Autoimmun* (1991) 4(4):607–15. doi:10.1016/0896-8411(91)90180-K
80. Kitazawa E, Igarashi T, Kawaguchi N, Matsushima H, Kawashima Y, Hankins RW, et al. Differences in anti-LKM-1 autoantibody immunoreactivity to CYP2D6 antigenic sites between hepatitis C virus-negative and -positive patients. *J Autoimmun* (2001) 17(3):243–9. doi:10.1006/jaut.2001.0565
81. Manns MP, Griffin KJ, Sullivan KF, Johnson EF. LKM-1 autoantibodies recognize a short linear sequence in P450IID6, a cytochrome P-450 monooxygenase. *J Clin Invest* (1991) 88(4):1370–8. doi:10.1172/JCI115443
82. Yamamoto AM, Cresteil D, Boniface O, Clerc FF, Alvarez F. Identification and analysis of cytochrome P450IID6 antigenic sites recognized by anti-liver-kidney microsome type-1 antibodies (LKM1). *Eur J Immunol* (1993) 23(5):1105–11. doi:10.1002/eji.1830230519
83. Holdener M, Hintermann E, Bayer M, Rhode A, Rodrigo E, Hintereder G, et al. Breaking tolerance to the natural human liver autoantigen cytochrome P450 2D6 by virus infection. *J Exp Med* (2008) 205(6):1409–22. doi:10.1084/jem.20071859
84. Hintermann E, Holdener M, Bayer M, Loges S, Pfeilschifter JM, Granier C, et al. Epitope spreading of the anti-CYP2D6 antibody response in patients with autoimmune hepatitis and in the CYP2D6 mouse model. *J Autoimmun* (2011) 37(3):242–53. doi:10.1016/j.jaut.2011.06.005
85. Klein R, Zanger UM, Berg T, Hopf U, Berg PA. Overlapping but distinct specificities of anti-liver-kidney microsome antibodies in autoimmune hepatitis type II and hepatitis C revealed by recombinant native CYP2D6 and novel peptide epitopes. *Clin Exp Immunol* (1999) 118(2):290–7. doi:10.1046/j.1365-2249.1999.01027.x
86. Kerkar N, Choudhuri K, Ma Y, Mahmoud A, Bogdanos DP, Muratori L, et al. Cytochrome P4502D6(193-212): a new immunodominant epitope and target of virus/self cross-reactivity in liver kidney microsomal autoantibody type 1-positive liver disease. *J Immunol* (2003) 170(3):1481–9. doi:10.4049/jimmunol.170.3.1481
87. Imaoka S, Obata N, Hiroi T, Osada-Oka M, Hara R, Nishiguchi S, et al. A new epitope of CYP2D6 recognized by liver kidney microsomal autoantibody from Japanese patients with autoimmune hepatitis. *Biol Pharm Bull* (2005) 28(12):2240–3. doi:10.1248/bpb.28.2240
88. Sugimura T, Obermayer-Straub P, Kayser A, Braun S, Loges S, Alex B, et al. A major CYP2D6 autoepitope in autoimmune hepatitis type 2 and

chronic hepatitis C is a three-dimensional structure homologous to other cytochrome P450 autoantigens. *Autoimmunity* (2002) 35(8):501–13. doi:10.1080/0891693021000069556
89. Lohr H, Manns M, Kyriatsoulis A, Lohse AW, Trautwein C, Meyer zum Buschenfelde KH, et al. Clonal analysis of liver-infiltrating T cells in patients with LKM-1 antibody-positive autoimmune chronic active hepatitis. *Clin Exp Immunol* (1991) 84(2):297–302. doi:10.1111/j.1365-2249.1991.tb08164.x
90. Lohr HF, Schlaak JF, Lohse AW, Bocher WO, Arenz M, Gerken G, et al. Autoreactive CD4+ LKM-specific and anticlonotypic T-cell responses in LKM-1 antibody-positive autoimmune hepatitis. *Hepatology* (1996) 24(6):1416–21. doi:10.1002/hep.510240619
91. Ma Y, Bogdanos DP, Hussain MJ, Underhill J, Bansal S, Longhi MS, et al. Polyclonal T-cell responses to cytochrome P450IID6 are associated with disease activity in autoimmune hepatitis type 2. *Gastroenterology* (2006) 130(3):868–82. doi:10.1053/j.gastro.2005.12.020
92. Longhi MS, Hussain MJ, Bogdanos DP, Quaglia A, Mieli-Vergani G, Ma Y, et al. Cytochrome P450IID6-specific CD8 T cell immune responses mirror disease activity in autoimmune hepatitis type 2. *Hepatology* (2007) 46(2): 472–84. doi:10.1002/hep.21658
93. Damian RT. Common antigens between adult *Schistosoma mansoni* and the laboratory mouse. *J Parasitol* (1967) 53(1):60–4. doi:10.2307/3276622
94. Oldstone MBA. Molecular mimicry as a mechanism for the cause and as a probe uncovering etiologic agent(s) of autoimmune disease. *Curr Top Microbiol Immunol* (1989) 145:127–36.
95. Christen U, von Herrath MG. Induction, acceleration or prevention of autoimmunity by molecular mimicry. *Mol Immunol* (2004) 40(14–15):1113–20. doi:10.1016/j.molimm.2003.11.014
96. Christen U, Hintermann E, Holdener M, von Herrath MG. Viral triggers for autoimmunity: is the 'glass of molecular mimicry' half full or half empty? *J Autoimmun* (2010) 34(1):38–44. doi:10.1016/j.jaut.2009.08.001
97. Christen U. Molecular mimiry. In: Shoenfeld Y, Meroni PL, Gershwin ME, editors. *Autoantibodies*. Waltham, MA, USA: Elsevier (2014). p. 35–42.
98. Christen U. Pathogen infection and autoimmunity. *Int Rev Immunol* (2014) 33(4):261–5. doi:10.3109/08830185.2014.921162
99. Christen U, Benke D, Wolfe T, Rodrigo E, Rhode A, Hughes AC, et al. Cure of prediabetic mice by viral infections involves lymphocyte recruitment along an IP-10 gradient. *J Clin Invest* (2004) 113(1):74–84. doi:10.1172/JCI17005
100. Filippi CM, Estes EA, Oldham JE, von Herrath MG. Immunoregulatory mechanisms triggered by viral infections protect from type 1 diabetes in mice. *J Clin Invest* (2009) 119(6):1515–23. doi:10.1172/JCI38503
101. Lehmann PV, Forsthuber T, Miller A, Sercarz EE. Spreading of T-cell autoimmunity to cyptic determinants of an autoantigen. *Nature* (1992) 358:155–7. doi:10.1038/358155a0
102. Ma WT, Chang C, Gershwin ME, Lian ZX. Development of autoantibodies precedes clinical manifestations of autoimmune diseases: a comprehensive review. *J Autoimmun* (2017) 83:95–112. doi:10.1016/j.jaut.2017.07.003
103. Hintermann E, Ehser J, Christen U. The CYP2D6 animal model: how to induce autoimmune hepatitis in mice. *J Vis Exp* (2012) 60:e3644. doi:10.3791/3644
104. Christen U, Hintermann E. An update on animal models of autoimmune hepatitis: are we there yet? *Curr Pharm Des* (2015) 21(18):2391–400. doi:10.2174/1381612821666150316121319
105. Ma Y, Thomas MG, Okamoto M, Bogdanos DP, Nagl S, Kerkar N, et al. Key residues of a major cytochrome P4502D6 epitope are located on the surface of the molecule. *J Immunol* (2002) 169(1):277–85. doi:10.4049/jimmunol.169.1.277
106. Lenzi M, Ballardini G, Fusconi M, Cassani F, Selleri L, Volta U, et al. Type 2 autoimmune hepatitis and hepatitis C virus infection. *Lancet* (1990) 335(8684):258–9. doi:10.1016/0140-6736(90)90070-L
107. Miyakawa H, Kitazawa E, Kikuchi K, Fujikawa H, Kawaguchi N, Abe K, et al. Immunoreactivity to various human cytochrome P450 proteins of sera from patients with autoimmune hepatitis, chronic hepatitis B, and chronic hepatitis C. *Autoimmunity* (2001) 33(1):23–32. doi:10.3109/08916930108994106
108. Lunel F, Abuaf N, Frangeul L, Grippon P, Perrin M, Le Coz Y, et al. Liver/kidney microsome antibody type 1 and hepatitis C virus infection. *Hepatology* (1992) 16(3):630–6. doi:10.1002/hep.1840160304
109. Michel G, Ritter A, Gerken G, Meyer zum Buschenfelde KH, Decker R, Manns MP. Anti-GOR and hepatitis C virus in autoimmune liver diseases. *Lancet* (1992) 339(8788):267–9. doi:10.1016/0140-6736(92)91332-3
110. Marceau G, Lapierre P, Beland K, Soudeyns H, Alvarez F. LKM1 autoantibodies in chronic hepatitis C infection: a case of molecular mimicry? *Hepatology* (2005) 42(3):675–82. doi:10.1002/hep.20816
111. Pohl LR, Kenna JG, Satoh H, Christ D, Martin JL. Neoantigens associated with halothane hepatitis. *Drug Metab Rev* (1989) 20(2–4):203–17. doi:10.3109/03602538909103537
112. Gut J, Christen U, Huwyler J. Mechanisms of halothane toxicity: novel insights. *Pharmacol Ther* (1993) 58(2):133–55. doi:10.1016/0163-7258(93)90047-H
113. Neuberger J. Halothane hepatitis. *Eur J Gastroenterol Hepatol* (1998) 10(8):631–3.
114. Christen U, Jeno P, Gut J. Halothane metabolism: the dihydrolipoamide acetyltransferase subunit of the pyruvate dehydrogenase complex molecularly mimics trifluoroacetyl-protein adducts. *Biochemistry* (1993) 32(6):1492–9. doi:10.1021/bi00057a013
115. Christen U, Quinn J, Yeaman SJ, Kenna JG, Clarke JB, Gandolfi AJ, et al. Identification of the dihydrolipoamide acetyltransferase subunit of the human pyruvate dehydrogenase complex as an autoantigen in halothane hepatitis. Molecular mimicry of trifluoroacetyl-lysine by lipoic acid. *Eur J Biochem* (1994) 223(3):1035–47. doi:10.1111/j.1432-1033.1994.tb19082.x
116. Smith GC, Kenna JG, Harrison DJ, Tew D, Wolf CR. Autoantibodies to hepatic microsomal carboxylesterase in halothane hepatitis. *Lancet* (1993) 342(8877):963–4. doi:10.1016/0140-6736(93)92005-E
117. Huwyler J, Aeschlimann D, Christen U, Gut J. The kidney as a novel target tissue for protein adduct formation associated with metabolism of halothane and the candidate chlorofluorocarbon replacement 2,2-dichloro-1,1,1-trifluoroethane. *Eur J Biochem* (1992) 207(1):229–38. doi:10.1111/j.1432-1033.1992.tb17042.x
118. Njoku DB, Shrestha S, Soloway R, Duray PR, Tsokos M, Abu-Asab MS, et al. Subcellular localization of trifluoroacetylated liver proteins in association with hepatitis following isoflurane. *Anesthesiology* (2002) 96(3):757–61. doi:10.1097/00000542-200203000-00036
119. Anderson JS, Rose NR, Martin JL, Eger EI, Njoku DB. Desflurane hepatitis associated with hapten and autoantigen-specific IgG4 antibodies. *Anesth Analg* (2007) 104(6):1452–3. doi:10.1213/01.ane.0000263275.10081.47
120. Hoet P, Graf ML, Bourdi M, Pohl LR, Duray PH, Chen W, et al. Epidemic of liver disease caused by hydrochlorofluorocarbons used as ozone-sparing substitutes of chlorofluorocarbons. *Lancet* (1997) 350(9077):556–9. doi:10.1016/S0140-6736(97)03094-8
121. Terziroli Beretta-Piccoli B, Mieli-Vergani G, Vergani D. Serology in autoimmune hepatitis: a clinical-practice approach. *Eur J Intern Med* (2017). doi:10.1016/j.ejim.2017.10.006

Conflict of Interest Statement: The authors declare that the research was conducted in the absence of any commercial or financial relationships that could be construed as a potential conflict of interest.

frontiers in Immunology

ORIGINAL RESEARCH
published: 15 February 2018
doi: 10.3389/fimmu.2018.00249

Whole-Genome Expression Profiling in Skin Reveals SYK As a Key Regulator of Inflammation in Experimental Epidermolysis Bullosa Acquisita

Unni K. Samavedam[1†‡], Nina Mitschker[1†], Anika Kasprick[2], Katja Bieber[2], Enno Schmidt[1,2], Tamás Laskay[3], Andreas Recke[1,2], S. Goletz[2], Gestur Vidarsson[4], Franziska S. Schulze[2], Mikko Armbrust[2], Katharina Schulze Dieckhoff[2], Hendri H. Pas[5], Marcel F. Jonkman[5], Kathrin Kalies[6], Detlef Zillikens[1,2], Yask Gupta[1], Saleh M. Ibrahim[1] and Ralf J. Ludwig[1,2]*

[1] Department of Dermatology, University of Lübeck, Lübeck, Germany, [2] Lübeck Institute of Experimental Dermatology, University of Lübeck, Lübeck, Germany, [3] Institute for Medical Microbiology and Hygiene, University of Lübeck, Lübeck, Germany, [4] Department of Experimental Hematology, Sanquin Research Institute, Amsterdam, Netherlands, [5] Center for Blistering Diseases, Department of Dermatology, University Medical Center Groningen, University of Groningen, Groningen, Netherlands, [6] Institute of Anatomy, University of Lübeck, Lübeck, Germany

Because of the morbidity and limited therapeutic options of autoimmune diseases, there is a high, and thus far, unmet medical need for development of novel treatments. Pemphigoid diseases, such as epidermolysis bullosa acquisita (EBA), are prototypical autoimmune diseases that are caused by autoantibodies targeting structural proteins of the skin, leading to inflammation, mediated by myeloid cells. To identify novel treatment targets, we performed cutaneous genome-wide mRNA expression profiling in 190 outbred mice after EBA induction. Comparison of genome-wide mRNA expression profiles in diseased and healthy mice, and construction of a co-expression network identified *Sykb* (spleen tyrosine kinase, SYK) as a major hub gene. Aligned, pharmacological SYK inhibition protected mice from experimental EBA. Using lineage-specific SYK-deficient mice, we identified SYK expression on myeloid cells to be required to induce EBA. Within the predicted co-expression network, interactions of *Sykb* with several partners (e.g., *Tlr13*, *Jdp2*, and *Nfkbid*) were validated by curated databases. Additionally, novel gene interaction partners of SYK were experimentally validated. Collectively, our results identify SYK expression in myeloid cells as a requirement to promote inflammation in autoantibody-driven pathologies. This should encourage exploitation of SYK and SYK-regulated genes as potential therapeutic targets for EBA and potentially other autoantibody-mediated diseases.

Keywords: skin, autoimmunity, spleen tyrosine kinase, signal transduction, animal models, treatment, pemphigoid, epidermolysis bullosa acquisita

OPEN ACCESS

Edited by:
Anne Fletcher,
Monash University, Australia

Reviewed by:
Frank Antonicelli,
Université de Reims Champagne-Ardenne, France
Huanfa Yi,
Jilin University, China

***Correspondence:**
Ralf J. Ludwig
ralf.ludwig@uksh.de

[†]These authors have contributed equally to this work.

[‡]Present address:
Unni K. Samavedam,
Division of Immunobiology, Cincinnati Children's Hospital Medical Center, Cincinnati, OH, United States

Specialty section:
This article was submitted to Immunological Tolerance and Regulation, a section of the journal Frontiers in Immunology

Received: *17 October 2017*
Accepted: *29 January 2018*
Published: *15 February 2018*

Citation:
Samavedam UK, Mitschker N, Kasprick A, Bieber K, Schmidt E, Laskay T, Recke A, Goletz S, Vidarsson G, Schulze FS, Armbrust M, Schulze Dieckhoff K, Pas HH, Jonkman MF, Kalies K, Zillikens D, Gupta Y, Ibrahim SM and Ludwig RJ (2018) Whole-Genome Expression Profiling in Skin Reveals SYK As a Key Regulator of Inflammation in Experimental Epidermolysis Bullosa Acquisita. Front. Immunol. 9:249. doi: 10.3389/fimmu.2018.00249

INTRODUCTION

In pemphigoid disease (PD), autoantibodies against defined structural proteins of the skin cause inflammation and subsequently subepidermal blistering (1, 2). During the last years, animal models of the PD epidermolysis bullosa acquisita (EBA) shaped our current understanding of the disease pathogenesis (3). In EBA, autoantibody-induced inflammation and subepidermal blistering are

initiated by binding of autoantibodies to their target antigen [type VII collagen (COL7)]. Subsequently, the complement cascade is activated (4–6). This and cytokine release permit a CD18/ICAM1-dependent extravasation of Gr-1$^+$ myeloid cells (7, 8). Within the skin, binding of myeloid cells to the immune complexes (ICs) located at the dermal–epidermal junction (DEJ) through specific Fc gamma receptors (FcγR) is unequivocally required to induce clinically manifest disease (9). The engagement of FcγR to skin-bound ICs triggers intracellular signaling, involving PI3K beta, AKT, p38 MAPK, ERK, Src family kinases, PDE4, CARD9, and RORα (10–15); ultimately leading to the release of reactive oxygen species (ROS) and proteases that facilitate inflammation and subepidermal blistering (7, 16).

To obtain further insights into EBA pathogenesis and to define novel treatment targets, we determined the whole-genome expression profile of 190 outbred mice of an advanced intercross line (17) after EBA induction. Of the identified hub genes, we functionally validated the spleen tyrosine kinase (*Sykb*, SYK). SYK is a non-receptor cytoplasmic enzyme that is mainly expressed in hematopoietic cells, which is essential in regulating cellular responses to extracellular antigens or antigen-immunoglobulin complexes (18, 19). As an important example, SYK acts downstream of activating FcγR and has thus emerged as a drug target for antibody-induced diseases, such as rheumatoid arthritis, where autoantibody-induced inflammation depends on FcγR. Yet, we recently described anti-inflammatory properties of SYK, triggered by binding of highly galactosylated ICs to FcγRIIB and dectin-1 to block the pro-inflammatory signaling triggered by G-protein coupled, membrane-bound receptors, exemplified by the C5aR1. The inhibition of signaling downstream of the C5aR1 was mediated by tyrosine phosphorylation of the ITAM-like motif downstream of dectin-1 and transient phosphorylation of SYK (6). Thus, inhibition of SYK may have either anti- or pro-inflammatory effects.

Hence, to address the functional role of the identified hub gene *Sykb* in experimental EBA, we performed an in-depth functional analysis using a variety of *in vitro* and *in vivo* model systems. Ultimately, we also verified the predicted gene network of the *Sykb* hub gene, leading to the identification of novel *Sykb*-interacting genes.

MATERIALS AND METHODS

Experiments with Human Biomaterials

Foreskin and blood collections from healthy volunteers and patients were performed after written informed consent was obtained. All experiments with human samples were approved by the ethical committee of the Medical Faculty of the University of Lübeck and were performed in accordance with the Declaration of Helsinki. Skin biopsies from bullous pemphigoid (BP) patients for RNA expression profiling were obtained from five patients. The diagnosis was based on clinical presentation, detection of linear IgG and/or C3 deposits along the DEJ in perilesional skin biopsies by direct IF microscopy, and the detection of circulating anti-NC16A IgG by ELISA. Biopsies for RNA expression profiling were obtained from perilesional skin biopsies. Biopsies from corresponding, non-affected body sites served as controls. We included four female and one male BP patient. The mean age was 87 years (range 83–90 years). RNA expression profiling was performed using the Human Gene 1.0ST (Affymetrix, Santa Clara, CA, USA). The complete dataset is currently under analysis. Herein, we focused the analysis on *SKY* and contrasted the expression levels of perilesional versus control skin. The data (CEL files) were processed using R oligo package. The data were corrected for background, and RMA normalization was performed. The normalized gene expression for *SYK* was used for accessing statistical significance.

Animal Experiments and Immunization-Induced Murine EBA

C57Bl/6 (B6) mice were obtained from Charles River Laboratories (Sulzfeld, Germany). Mice expressing the cre gene on LysM [B6.129P2-Lyz2tm1(cre)Ifo/J], CD2 [B6.Cg-Tg(CD2-cre)4Kio/J], and SYK-loxP-flanked (B6.129P2-Syktm1.2Tara/J) strains were obtained from the Jackson Laboratory (Bar Harbor, ME, USA) and were crossed to obtain cell lineage-specific Syk deletions. Mice were housed under specific pathogen-free conditions and provided standard mouse chow and acidified drinking water *ad libitum*. Animal experiments were approved by local authorities of the Animal Care and Use Committee (Kiel, Germany) and performed by certified personnel. Skin specimens from mice with immunization-induced EBA were obtained for unbiased mRNA expression profiling (see below) from a previously published study (17) using mice of an autoimmune-prone intercross outbred line (AIL mice). In brief, in order to generate a genetically diverse mouse line, EBA-susceptible (MRL/MpJ) and -resistant mice (NZM2410/J, Cast, and BXD2J), and the offspring of each generation were intercrossed for several generations. Genetic diversity of this so termed four-way, autoimmune-prone intercross mouse line, is reflected by the different morphological traits, including weight, tail length, or fur color. For the induction of experimental EBA, mice of the fourth generation were used.

Generation of Microarray Data (miRNAs/Genes) and Bioinformatics Analysis

To monitor gene expression in the skin samples derived from AIL mice, total RNA was extracted from ears and hybridized to the Affymetrix Mouse Gene 1.0 ST Array (Affymetrix, Santa Clara, CA, USA). Raw data were processed using the "oligo" R package. The RMA method incorporated in the R package was used for normalization of probe intensities for all samples (20). The limma R package was used to assess differentially expressed genes between the EBA and wild-type mice. *p*-Values were corrected for multiple testing using Bonferroni correction. For gene expression profiling, low intensity probes were omitted to avoid putative false-positive signals and to lower the barrier for correction of multiple testing; these probes were filtered out using the median-based method as implemented in the function "expressionBasedfilter" from the R DCGL package (21). Additionally, genes that did not show significant variations (p-value < 0.05) across the samples were filtered using the function "varianceBasedfilter"

in the same package. This function reduces the data to the most variable genes, which are presumably critical for the phenotype.

Ab Initio Gene and Network Predictions

For *ab initio* prediction, genes were clustered based on their co-expression profiles across different samples. The standard weighted correlation network (WGCNA) analysis procedure was used for cluster or module detection (22). A weighted adjacency matrix of pair-wise connection strengths (correlation coefficients of gene expression levels) was constructed using the soft-threshold approach with a scale-independent topological power $\beta = 6$ (mRNA). Scale-free topology is a network whose degree of distribution follows a power law. For each probe, the connectivity was defined as the sum of all connection strengths with all others. Probes were aggregated into modules by hierarchical clustering and refined with the dynamic cut tree algorithm (23). Pearson correlation coefficient was determined for each phenotype-module pair. The representative module expression profiles or module eigengene values are the first principal component of the gene expression profiles within a module. The correlation between the module eigengene and the sample trait of interest yields the eigengene significance as assessed by a correlation test. Modules were assigned different colors, with gray assigned to traits that could not be clustered in any other module. Additionally, partial least squares (PLS) regression was used to filter out false-positive interactions among the genes in each module (24). Briefly, PLS measures associations between each pair of genes under the influence of all other genes present in the dataset. Thus, it assigns the weight or numerical measurement for each edge/interaction for each pair of genes. The statistical significance of these edges is calculated using an empirical Bayes technique that uses a false discovery rate to assess significance (25). The DAVID web software was used for pathway and gene ontology analysis (26). The software is based on the modified Fisher's exact test and performs gene ontology analyses for the group of genes based on metabolic pathways, cellular components, and biological functions. Briefly, DAVID has pre-defined database in which various sets of genes are assigned to ontology terms such as metabolic pathways, cellular compartments, and biological processes. DAVID provides a list of genes. Thereafter, DAVID calculates how many genes in the list are associated with a specific ontology term. The significance of the ontology term for these genes is calculated by the modified Fisher's exact test. *p*-Values obtained for each ontology term are corrected for multiple testing using Bonferroni corrections.

IC-Induced Activation of Polymorphonuclear Leukocytes (PMNs)

Anti-coagulated (EDTA) blood collected from healthy blood donors was used for PMN isolation. Inhibition of ROS release in presence of BAY 61-3606 or PRT062607 (Selleckchem, Munich, Germany) was measured from IC- or C5a-activated PMNs using published protocols (27, 28).

IC-Induced Neutrophil Activation

Peripheral heparinized blood was collected by venipuncture from healthy adult volunteers. Neutrophils were isolated as described previously using Percoll gradient centrifugation (29). Plate-bound immobilized immune complexes (iICs) were formed using a human serum albumin (HSA) antigen and a rabbit polyclonal anti-HSA-IgG1 antibody as described (30). Neutrophil activation was assayed by ROS release as described earlier.

Determination of Cell Surface Marker Expression

Activation of PMN in the presence of BAY61-3606 was assayed using flow cytometry following established protocols (11, 31).

Measurement of PMN-Dependent Dermal–Epidermal Separation

Ex vivo induction of dermal–epidermal separation was performed as previously described (32). In brief, cryosections of human neonatal foreskin were incubated with recombinant anti-COL7 antibodies (32). After washing, slides were incubated for 2 h at 37°C with PMN, isolated by dextran sedimentation of freshly collected, heparinized blood from healthy volunteers. Here, sections were treated with either solvent or BAY61-3606 at the indicated concentrations. After fixation in 4% formaldehyde, slides were stained by H&E and examined by light microscopy for the presence of split formation within the DEJ zone. An observer unaware of the sections treatment has performed the later step. The degree of dermal–epidermal separation is expressed in relation to the length of the entire DEJ zone of each section. A detailed, step-by-step protocol for this assay has recently been published (33).

Evaluation of PMN Viability

The viability of PMN in presence of BAY61-3606 was assayed using the FITC Annexin V Apoptosis Detection Kit II following the protocol provided by the manufacturer (BD Pharmigen™, Heidelberg, Germany). PMNs treated with UV light for 20 min served as positive control.

Activation of Neutrophils by iICs and Western Blotting Analysis

Neutrophils (5×10^6 in 1 ml of RPMI 1640 containing 10% heat-inactivated FCS) were pre-incubated in presence or absence of 250 ng/ml of the Syk BAY 61-3606 (medchemexpress, Princeton, NJ, USA) inhibitor for 20 min at 37°C. Subsequently, cells were added to wells coated with HSA-anti-HSA iIC and incubated for 15 min at 37°C. Following iIC stimulation, whole-cell lysates were prepared using TCA as previously described (34). Western blotting analysis was performed using Abs against human phospho-Akt (Thr308), phospho-p44/42 MAPK (ERK1/2 and Thr202/Tyr204), phospho-p38 MAPK (Thr180/Tyr182), and β-actin (all from Cell Signaling Technology) and probed with HRP-conjugated anti-rabbit or anti-mouse IgG (New England Biolabs, Beverly, MA, USA).

Anti-COL7 IgG Transfer-Induced Murine EBA and Treatment Protocol

To induce experimental EBA, mice were injected on alternating days with anti-COL7 IgG according to established protocols (35).

In brief, New Zealand white rabbits were s.c. immunized with 250 mg murine von Willebrand factor A-like domain 2 protein that was suspended in CFA. The animals were boosted three times (at 13-day intervals) with the same protein preparation in IFA, and immune sera were characterized using immunofluorescent (IF) microscopy on cryosections of murine skin. IgG from immune and normal rabbit sera was purified using protein G affinity. Immune rabbit IgG or normal rabbit IgG (5 mg/injection) was injected s.c. into adult mice every second day for a total of six injections. Some mice were treated with BAY61-3606 dissolved in water. Mice were treated twice-daily p.o. with either solvent or BAY61-3606 at a dose of 25 or 50 mg/kg body weight. Treatments were initiated 1 day prior to the first anti-COL7 IgG injection, applied daily, and maintained until day 11. Clinical disease manifestation (expressed as the percentage of body surface area covered by EBA skin lesions) was determined 4, 8, and 12 days after the initial anti-COL7 IgG injection. From these data, the area under the curve (AUC) was used to calculate overall EBA severity.

Immunofluorescence Microscopy

Biopsies of non-lesional skin were obtained 2 days after the last IgG injection, and IgG and C3 deposits were detected by direct immunofluorescence (IF) microscopy. The sections were probed with 100-fold diluted fluorescein isothiocyanate (FITC)-labeled antibodies specific to rabbit IgG (Dako, Glostrup, Denmark and Abcam plc, Cambridge, UK) and FITC-labeled anti-murine C3 (MP Biomedicals, Solon, OH, USA).

Flow Cytometry

For FACS analysis, healthy and lesional skin (both from corresponding anatomical sites) or blood was taken from mice after induction of experimental EBA. Single cell solutions from and blood were erythrocyte lysed with RB cell lysis buffer (Miltenyi). The skin samples were cut into small pieces and digested with 345 mg/ml liberase (Roche) in RPMI for 30 min/37°C. Single cells were stained for the following surface markers using standard FACS procedures: CD45-VioGreen (clone: 30F11), CD3-VioBlue (clone: 17A2), Ly6C-FITC (clone: 1G7.G10), as well as Ly6G-APC Vio770 (clone: 1A8) and for blood CD19-APC (clone: 6D5), all from Miltenyi. For the subsequent intracellular staining, the cells were fixed in fixation buffer (BioLegend) and permeabilized using the Intracellular Staining Perm Wash Buffer (BioLegend) following the manufacturer's protocol. Intracellular staining was performed with SYK-PE (clone: 4D10.2). Cells were first gated for scatter (SSC-A/FSC-A) and singlets (FSC-H/FSC-A). The $CD45^+$ gates were further analyzed for double-positive staining of SYK with the appropriate cell markers. Measurements were performed at the Miltenyi MacsQuant10, and data were analyzed with the MACSQuantify™ Software (version 2.8).

RT-PCR

For gene expression analysis, TaqMan gene expression assays were purchased for the following transcripts: Plaur Mm01149438_m1, formyl peptide receptor 1 (Fpr1) Mm00442803_s1, CD3001b Mm01701741_m1, and *Gapdh* Mm99999915_g1 (Thermo Fisher Scientific, Waltham, MA, USA). RNA isolation, reverse transcription, and real-time RT-PCR were performed as described (36). All data were normalized to *Gapdh*.

Western Blot Analysis

Sections of frozen skin tissue (20 µm × 20 µm, either skin from immunization-induced EBA or corresponding healthy skin sections from Titermax™-injected controls) were scraped using a 30 G syringe in 100 µl RIPA buffer and the protein concentration was measured using BCA protein assay following manufacturer's protocols (Thermo Fisher Scientific). 15 µg protein were mixed in 5× Laemmli buffer and heated for 5 min at 95°C. Samples were separated by 10% SDS-PAGE and transferred to Immobilon-P membrane (Millipore, Bedford, MA, USA). The membrane was blocked for 1 h with TBS containing 0.1% Tween 20 and 5% skim milk or 5% BSA and incubated for overnight (4°C) with the primary antibody (either SYK, clone D3Z1E (XP) or Rabbit mAb (Cell Signaling Technology, Danvers, MA, USA)) diluted in blocking buffer following the manufacturer's instructions. Then the membrane was washed three times for 5 min with TBS containing 0.1% Tween 20 and incubated with peroxidase-conjugated anti-rabbit secondary antibodies (Dako Deutschland GmbH, Hamburg, Germany) for 1 h at room temperature. After a washing step, the membrane was incubated for 1 min with ECL reagent (GE Healthcare Europe GmbH, Freiburg, Germany) and exposed to film. For reprobing with GAPDH antibody (Cell Signaling Technology), the membrane was washed twice in PBS, stripped for 10 min/37°C with stripping buffer (GE Healthcare Europe GmbH), and washed three times for 5 min with TBS at room temperature. The relative SYK expression was calculated using ImageJ 1.51f (NIH, USA), and after background subtraction, the relative mean density of SYK/GAPDH was calculated.

Histopathology

Skin sections from corresponding anatomical sites were obtained 2 days after the last IgG injection and prepared for examination by histopathology as described. The dermal neutrophil cell infiltrate was assessed semi-quantitatively using a score ranging from 0 to 3 indicating no, mild, moderate, or severe infiltration, respectively (37).

Statistical Analysis

Unless otherwise noted, data were presented as mean ± SD. For comparisons of two groups, *t*-test or Mann–Whitney Rank Sum test was used when appropriate. For comparisons of more than two groups, ANOVA was used. For equally distributed data, one-way ANOVA followed by Bonferroni *t*-test for multiple comparisons was used; if the data were non-parametric, ANOVA on ranks (Kruskal–Wallis) was applied followed by Bonferroni *t*-test for multiple comparisons. In all tests, $p < 0.05$ was considered significant. All statistical analyses were performed using SigmaPlot 13.0 (Systat Software, Erkrath, Germany). The number of replicates for each experiment is detailed at the respective table/figure legends.

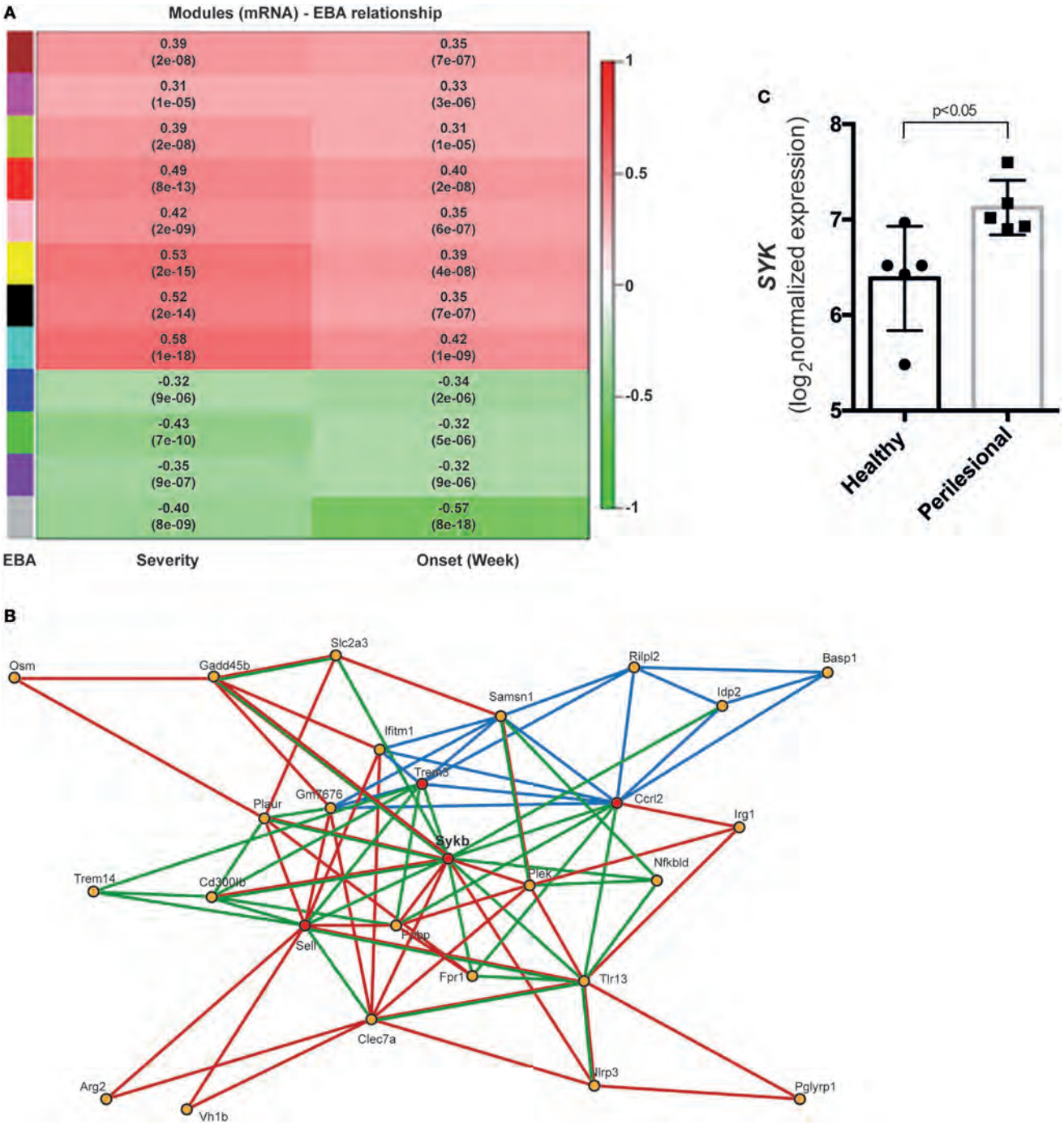

FIGURE 1 | Differential co-expression of cutaneous mRNA expression levels in mice with experimental epidermolysis bullosa acquisita (EBA) identifies SYK as a major hub gene candidate. **(A)** We applied hierarchical clustering to cluster gene profiles and the dynamic cut tree method to combine branches and define co-expressed groups (modules) from the expression data. We found 12 modules and assigned them different colors, with gray used for genes that could not be assigned to any other module. To identify disease-related modules, we correlated module eigenvalues to the disease score for EBA severity and onset. Bar on the left corresponds to modules, and bar on the right displays the range for Pearson correlation (from −1 to 1). Data are derived from 68 mice with experimental EBA and 122 mice that remained healthy after type VII collagen immunization (17). **(B)** This image shows the gene network of the yellow module. Red lines display the interaction information from STRING database. Green lines display predicted interactions using domain interaction information. Dark blue lines represent PLSR-based interactions. Red circles indicate hub genes. **(C)** In patients with bullous pemphigoid, which shares a lot of similarity with the inflammatory EBA variant (2), we observed an increased SYK expression in perilesional, as compared to non-affected skin of corresponding anatomical sites.

RESULTS

Cutaneous mRNA Expression Profiling Identifies SYK As One of the Major Differently Expressed Hub Genes in Experimental EBA

From mice of the outbred mouse line, 68 had clinically manifest EBA, while the remaining 122 mice were clinically healthy. Collectively, 1,038 mRNA probes were differentially expressed (adjusted $p < 0.05$, Bonferroni corrected). Of these, in samples from mice with clinically manifest EBA, 425 probes were downregulated and 613 were upregulated (Tables S1 and S2 in Supplementary Material). Next, a gene co-expression network of differentially expressed genes was constructed. Of the identified 12 modules, 8 showed a positive correlation, while 4 negatively correlated with the EBA phenotype (**Figure 1A**). In the yellow module ($r = 0.53$, p-value = 2e−15, **Figure 1B**), 86 interactions among the genes were validated by different statistical and database approaches (DOMINE, STRING, IPA databases, and PLS regression). Furthermore, four hub genes (degree of interaction > 10) were identified: *Sykb*, *Ccrl2*, *Sell*, and *Trem3*.

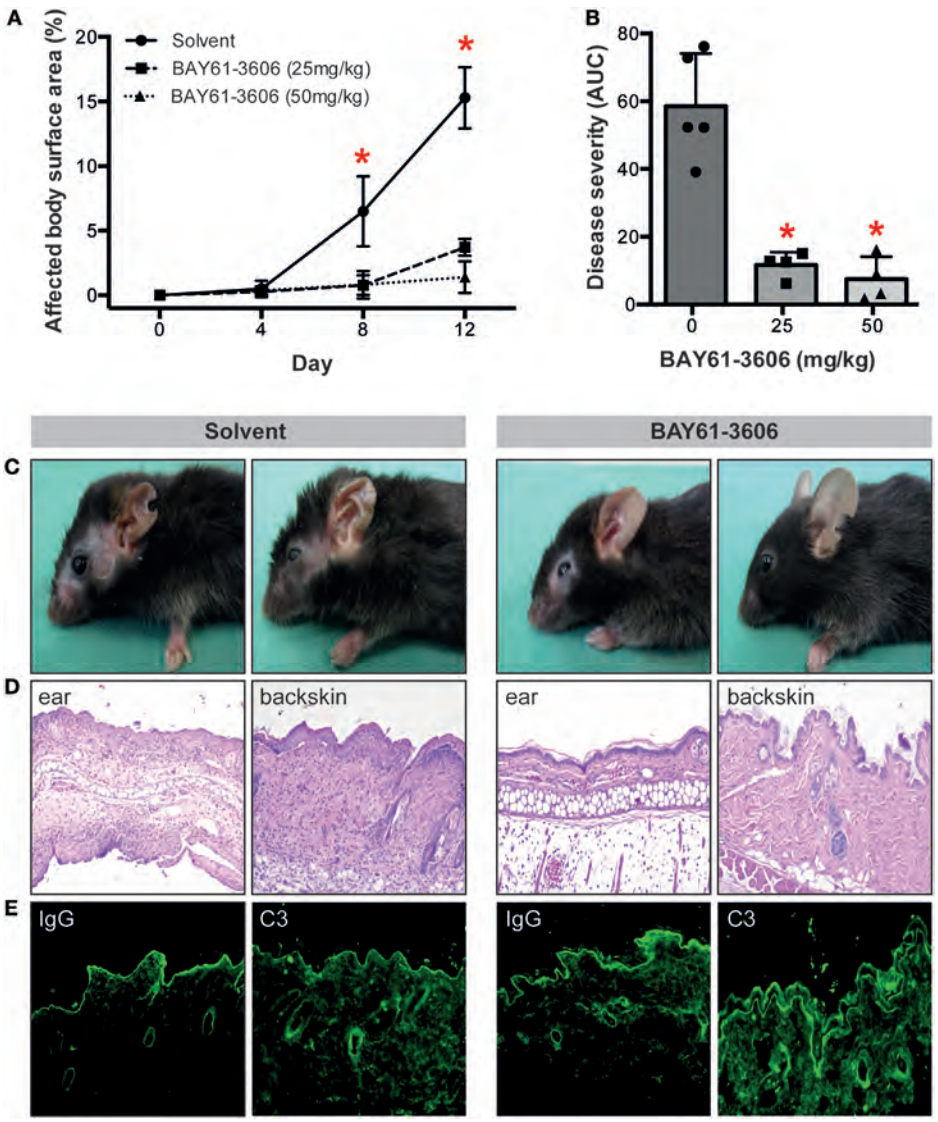

FIGURE 2 | The SYK inhibitor BAY61-3606 protects mice from inflammation in antibody transfer-induced epidermolysis bullosa acquisita (EBA). **(A)** Treatment of mice with the SYK inhibitor BAY61-3606 almost completely protected them from induction of experimentally induced EBA by transfer of anti-type VII collagen IgG. Graph shows the mean (SD) body surface area affected by EBA skin lesions. **(B)** Overall disease activity was calculated as area under the curve (AUC) derived from individual mice in each of the treatment groups. Here, the mean (SD) of the AUC is shown. Individual dots represent disease severity (AUC) of individual mice (*$p < 0.05$, ANOVA with a Bonferroni post-test, $n = 4$–5 mice/group). Representative **(C)** clinical images of mice at day 12 of the experiment, **(D)** H&E-stained skin sections at 100× original magnification and **(E)** direct immunofluorescent microscopy staining for IgG and C3 from perilesional skin from solvent (left)- and BAY61-3606 (right)-treated animals (50 mg/kg dose) at 100× original magnification. For panels **(C,D)**, data are based on five solvent and four (per concentration) BAY61-3606 treated animals.

We focused on the yellow module, specifically, *Sykb* because it has emerged as a therapeutic target in autoimmune diseases (38), and we observed an increased expression of *SYK* mRNA in perilesional skin of BP patients (**Figure 1C**). Our interest in SYK was further provoked by the contrasting effects of its blockade in mouse models and clinical trials in arthritis (39, 40).

Pharmacological SYK Blockade Dose-Dependently and Almost Completely Impairs Induction of Experimental EBA in Mice Induced by Transfer of Anti-COL7 IgG

To validate the importance of SYK in EBA pathogenesis *in vivo*, we induced EBA in mice by anti-COL7 IgG transfer in the absence or presence of the SYK inhibitor BAY61-3606. Pharmacological blockade of SYK almost completely prevented the EBA-inducing activity of anti-COL7 IgG (**Figures 2A–C**). Consistent with the clinical observations, a reduction of dermal infiltration was observed in BAY61-3606-treated animals compared to the corresponding anatomical sites in controls (**Figure 2D**). These changes were independent of alterations in IgG or C3 deposition along the DEJ (**Figure 2E**).

Induction of Anti-COL7 IgG-Induced EBA Requires SYK Expression in Cells of Myeloid, but Not Lymphoid Linage

We next aimed to identify the cellular source of SYK. Because SYK is mainly expressed in hematopoietic cells (18), we focused on these. We first evaluated the cellular composition within the dermal infiltrate of experimental EBA, and simultaneously determined if lymphoid and/or myeloid cells within the infiltrate express SYK. Comparison of lesional versus non-lesional skin of mice injected with anti-COL7 IgG at the end of the experiment showed a significant increase in cell numbers, while the proportion of most leukocytes within the dermis remained constant, the amount of Ly6G$^+$ cells, which are key effector cells in experimental EBA, increased significantly (**Figure 3A**). In line with previous observations (41), all CD45$^+$ cells expressed SYK, which, in addition, showed an identical proportional expression level in lesional and non-lesional skin (**Figures 3B,C**).

A

	Lesional skin	Non-lesional skin
Cell count	3.6 ± 1.9 x 10^6 / 100mg *	1.2 ± 1.1 x 10^6 / 100mg
CD45 / singlets (%)	68.1 ± 7.8	67.4 ± 5.2
CD3/CD45(%)	51.8 ± 18.1	35.8 ± 15.3
Ly6G/CD45 (%)	25.6 ± 11.3 *	7.4 ± 0.7
Ly6C/CD45 (%)	7.1 ± 2.3	6.9 ± 2.8

B

SYK+ (%)	Blood	Lesional skin	Non-lesional skin
CD45	98.3 ± 1.4	89.9 ± 4.6	88.9 ± 1.5
CD3	95.7 ± 2.7	75.5 ± 12.9	75.3 ± 6.3
CD19	99.5 ± 0.4	n.d.	n.d.
Ly6G	99.6 ± 0.2	82.7 ± 16.6	85.7 ± 3.1
Ly6C	99.0 ± 0.6	86.9 ± 3.6	88.6 ± 4.0

C

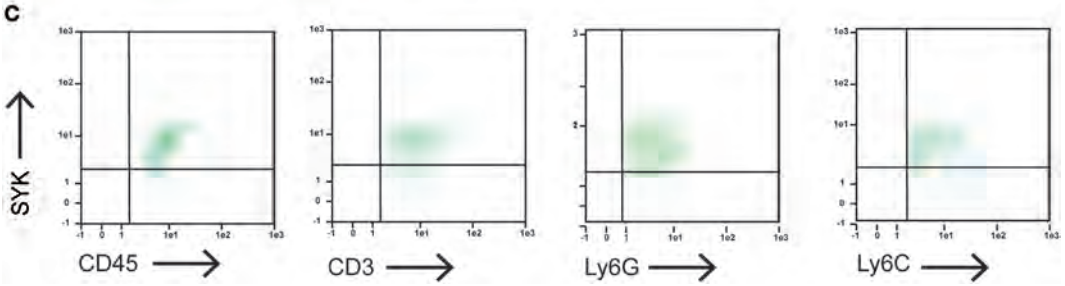

FIGURE 3 | Expression of CD45$^+$ cells is increased, while proportional expression of SYK in leukocytes remains constant in lesional versus non-lesional skin in mice with experimental epidermolysis bullosa acquisita (EBA). **(A)** Specimen from lesional and non-lesional skin of mice injected with anti-type VII collagen IgG were analyzed for quality and quantity of dermal leukocyte infiltration. Yield of cells was higher from lesional skin compared to non-lesional skin from corresponding sites. Regarding the relative distribution of all leukocytes (CD45$^+$) or subsets, we observed a difference regarding neutrophils (CD45$^+$/Ly6G$^+$; $^*p < 0.05$, *t*-test). Hence, the relative distribution of the dermal infiltrate remains constant, while the absolute number of CD45$^+$ cell increases in the skin of mice with experimental EBA. CD19$^+$ cells were not observed in the skin samples (not shown). **(B)** Separately, expression of SYK was evaluated in CD45$^+$ cells obtained from lesional and non-lesional skin. Relative expression of SYK in CD45$^+$, CD45$^+$/CD3$^+$, CD45$^+$/Ly6G$^+$, and CD45$^+$/Ly6C$^+$ was identical in both groups. CD45$^+$ cells from blood were used as positive control. **(C)** Representative FACS stainings from lesional skin, gated on CD45$^+$/singlet cells. All data are based on four to five samples per group.

To evaluate the functional impact of SYK expression on cells from the myeloid and lymphoid linage, floxed SYK mice were crossed with either LysM-Cre or CD2-Cre mice to selectively deplete SYK from myeloid or lymphoid cells. Notably, $SYK^{fl/fl}$ LysM-Cre mice were completely protected from EBA induction by anti-COL7 IgG transfer (**Figures 4A–C**); while transfer of anti-COL7 IgG-induced experimental EBA in $SYK^{fl/fl}$ CD2-Cre mice comparable to controls (**Figures 5A–C**). Changes in $SYK^{fl/fl}$ LysM-Cre mice were independent of changes in IgG or C3 deposition along the DEJ. Overall, this indicated that SYK expression in myeloid cells is an absolute requirement for induction of experimental EBA.

The SYK Inhibitor BAY61-3606 Dose-Dependently Blocks IC-Induced PMN Activation

To further validate the contribution of SYK to IC-induced neutrophil activation, we stimulated neutrophils or PMNs with IgG IC in presence of different concentrations of different SYK

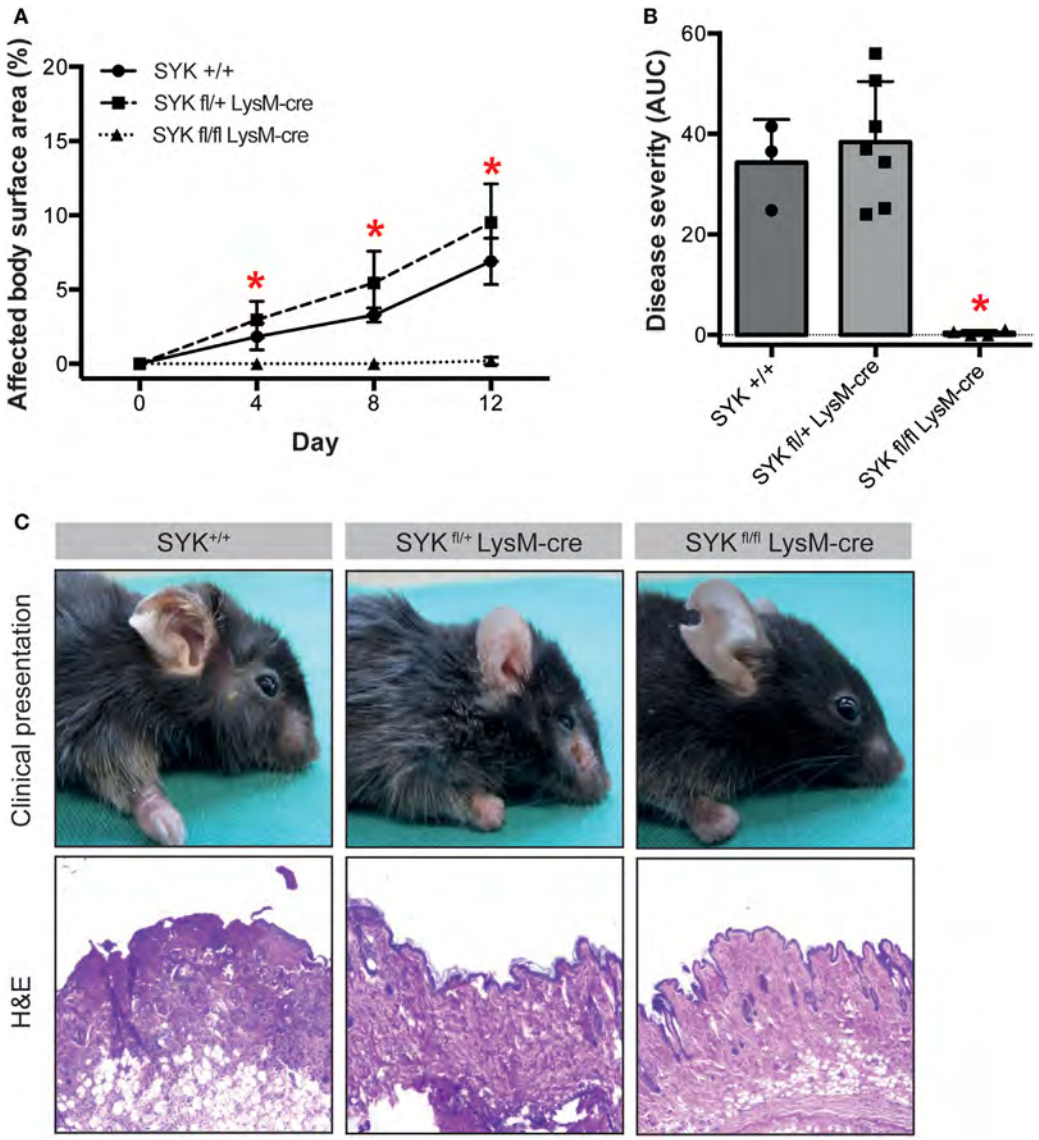

FIGURE 4 | $SYK^{fl/fl}$ LysM-Cre mice are completely protected from induction of antibody transfer-induced epidermolysis bullosa acquisita (EBA). **(A)** Mean (SD) of affected body surface area after repetitive injections of anti-type VII collagen IgG into indicated mouse strains over the 12-day observation period (n = 3–7/strain). SYK wild type (+/+) and mice with only one SYK allele in their myeloid cells ($SYK^{fl/+}$ LysM-cre) developed clinically manifested skin lesions, whereas mice deficient for SYK in myeloid cells ($SYK^{fl/fl}$ LysM-cre) were completely protected from induction of EBA (*$p < 0.05$, ANOVA with Bonferroni post-test). **(B)** The cumulative disease severity [area under the curve (AUC)] confirms complete protection of the $SYK^{fl/fl}$ LysM-cre mice (*$p < 0.05$, ANOVA with a Bonferroni post-test). Individual dots correspond to the AUCs of single mice. **(C)** Representative clinical images and H&E-stained sections from the back skin of indicated mouse strains (100× original magnification). All images shown are from day 12 of the experiment.

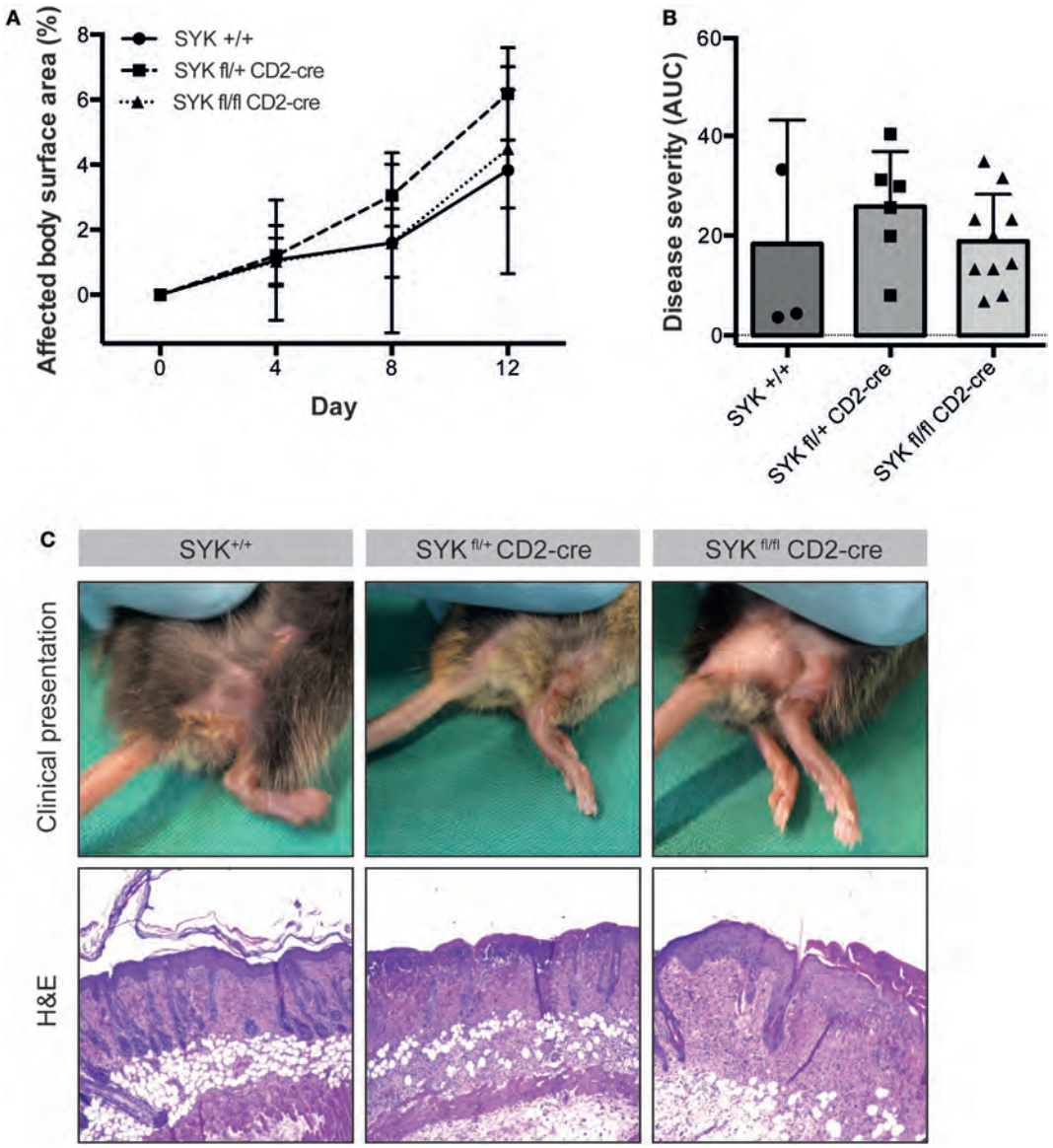

FIGURE 5 | SYK$^{fl/fl}$ CD2-Cre mice develop blistering in antibody transfer-induced epidermolysis bullosa acquisita (EBA). **(A)** Mean (SD) of the affected body surface area after repetitive injections of anti-type VII collagen IgG into the indicated mouse strains over the 12-day observation period (n = 3–9/strain). In contrast to the SYK$^{fl/fl}$ LysM-cre mice, mice with the specific deletion of SYK in lymphoid cells were completely susceptible to EBA induction. **(B)** The cumulative disease severity [expressed as the area under the curve (AUC)] calculated from the graphs in panel **(A)** is shown. The individual dots correspond to the AUCs of individual mice. **(C)** Representative clinical images and H&E-stained sections from the back skin of the indicated mouse strains (100× original magnification). All images shown are from day 12 of the experiment.

inhibitors (BAY61-3606 or PRT062607). BAY61-3606 dose-dependently reduced IgG IC-triggered release of ROS from PMNs (**Figures 6A,B**). Consistent with this finding, PRT062607 significantly reduced IgG IC-triggered ROS (not shown). In some PD, i.e., EBA, anti-COL7 IgA is the only identified Ig class in approximately 30% of patients (42). Furthermore, anti-COL7 IgA induces PMN activation and subepidermal blistering *in vitro* (27, 43). We thus assessed whether SYK blockade can also modulate ROS release from IgA IC-activated PMNs. Compared to IgG-IC-activated PMNs, we observed an almost identical level of inhibition (**Figures 6C,D**). In line, BAY61-3606 also ablates ROS-dependent dermal–epidermal separation in cryosections of human skin incubated with anti-COL7 IgG and PMNs (**Figures 6E–H**). Regarding other neutrophil responses, inhibition of SYK normalized activation-triggered CD66b expression, but had no effect on L-selectin sheading (**Figures 6I–L**). These effects of BAY61-3606 were achieved at non-toxic concentrations (**Figures 6M–P**).

BAY61-3606 Ablates Signaling Events in IC-Activated PMN

Regarding the mechanisms downstream of SYK, we extended our previous findings that the IC-induced activation of PMNs

leads to the phosphorylation of ERK, AKT, and p38 (11). By adding BAY61-3606 to IC-activated PMNs, we show that SYK blockade leads to a reduction in the phosphorylation of ERK, AKT, and p38 in IC-activated PMNs (**Figure 7**). We next aimed to obtain novel insights into the pathways controlled by SYK. For this, PMNs were activated with ICs in the presence or absence of BAY61-3606, and expression levels of nine randomly genes from the predicted gene network controlled by SYK (**Figure 1B**) were evaluated. Two novel SYK-interacting genes, *Plaur* and *Fpr1*, were validated (**Figure 8A**). The latter is downregulated after the inhibition of SYK in IC-activated PMNs, while *Plaur* expression increased if SYK was inhibited. Furthermore, within the predicted co-expression network, several interacting partners of SKY were validated by curated databases (not shown); examples include *Plek*, *Ppbp*, *Clec7a*, and *Nlrp3*, which were predicted by the STRING database. Furthermore, the expression of *Sykb*, *Plaur*, and *Fpr1* were determined in skin specimen from mice with and without experimental EBA. In line with the data shown in **Figure 1**, an increased expression of *Sykb* was noted in mice with experimental EBA. Similar differences among healthy and disease mice were observed for *Plaur* and *Fpr1* (**Figure 8B**). RT-PCR data were confirmed using western blotting, detecting SYK (**Figures 8C,D**) almost exclusively in skin affected by EBA skin lesions.

DISCUSSION

In an unbiased approach using whole-genome expression profiling, aiming to pinpoint novel therapeutic targets for the treatment of EBA and other PD, we identified *Sykb* as a hub gene in mice with experimental EBA. Based on this morphological observation, we hypothesized that inhibition of SYK may have

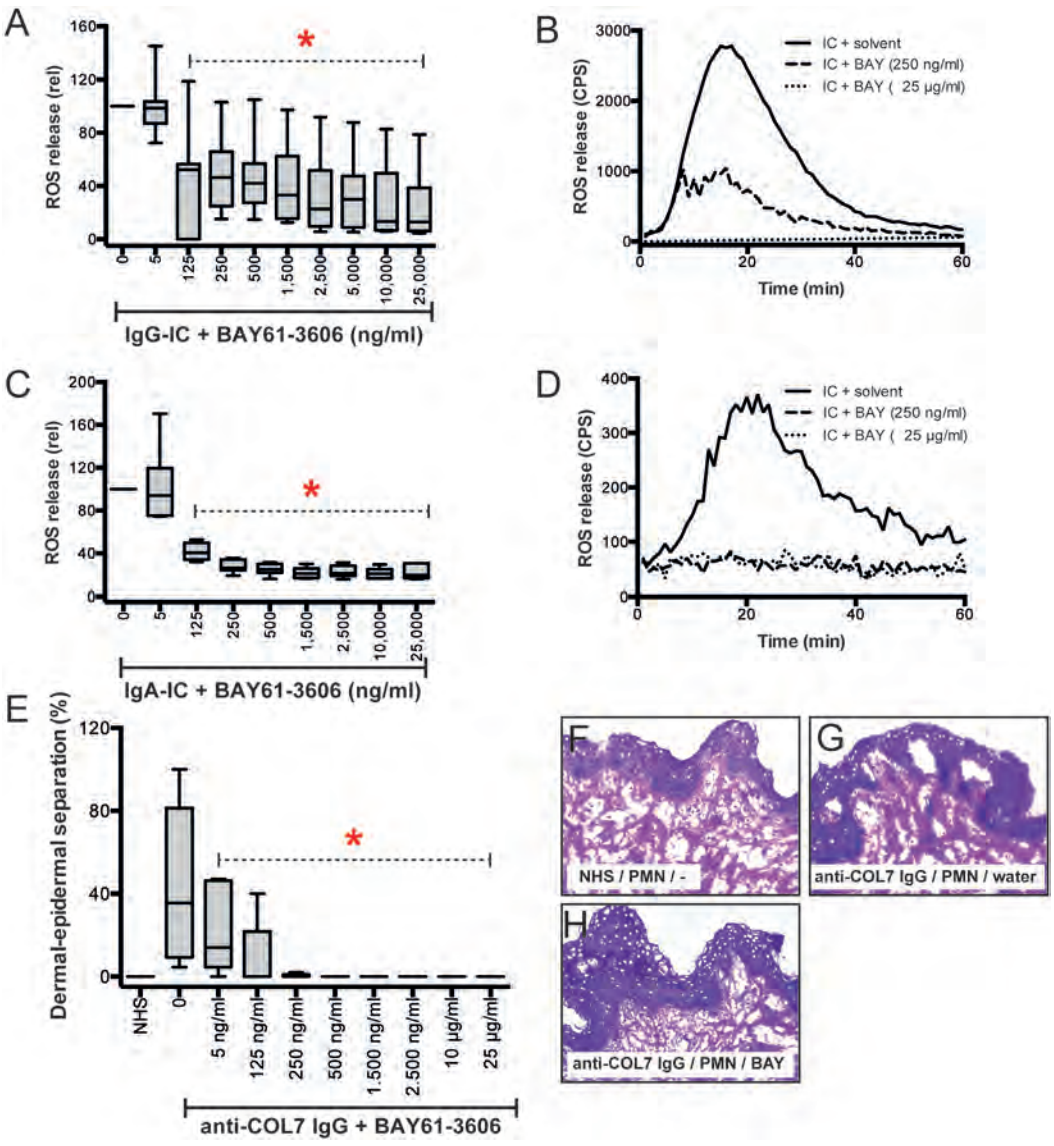

FIGURE 6 | Continued

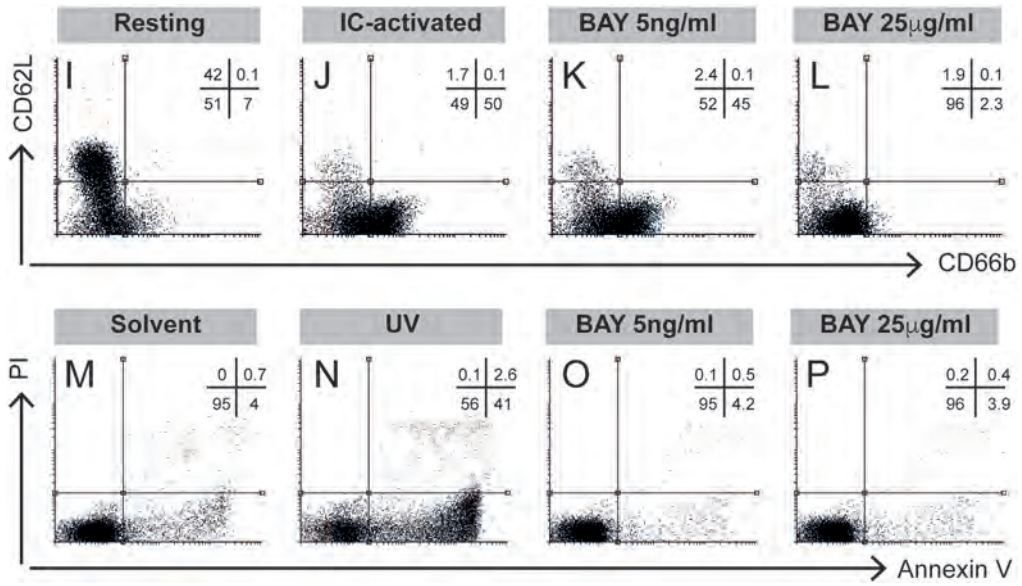

FIGURE 6 | Pharmacological inhibition of SYK blocks immune complex (IC)-induced activation of polymorphonuclear leukocytes (PMNs) *in vitro* and *ex vivo*. **(A)** Human PMNs were activated using IgG-ICs, and their activation was determined by measuring the release of reactive oxygen species (ROS). The data (n = 11–30/group) were normalized to IC-activated PMNs in the presence of solvent (water) and are displayed as the median (black line), the 27/75 percentiles (box), and the 5/95 percentiles (error bars). BAY61-3606 reduced the release of ROS from IC-activated PMNs in a dose-dependent manner (ANOVA on Ranks with Dunn's post-test). **(B)** Representative ROS release expressed as counts per second (CPS) over the 60-min experimental period. **(C)** Human PMNs were activated using IgA-ICs, and their activation was determined by measuring the release of ROS. The data (n = 6/group) were normalized to the IC-activated PMNs in the presence of solvent (water) and are displayed as the median (black line), the 27/75 percentiles (box), and the 5/95 percentiles (error bars). BAY61-3606 reduced the release of ROS from IC-activated PMNs in a dose-dependent manner (ANOVA on Ranks with Dunn's post-test). **(D)** Representative ROS release expressed as CPS over the 60 min experiment. **(E)** BAY61-3606 also ablates dermal–epidermal separation in cryosections of human skin incubated with anti-type VII collagen (COL7) IgG and PMNs. The data are presented as the mean (boxes) and STD (error bars) and are based on five experiments per group. To calculate whether the effects of BAY61-3606 were significant, ANOVA with Ranks and Dunn's post-test was used. **(F–H)** Representative images of the cryosection assay at a 200× original magnification showing **(F)** no dermal–epidermal separation in the sections incubated with normal human serum (NHS) and PMNs, **(G)** no dermal–epidermal separation in the sections incubated with anti-COL7 IgG, and **(H)** no dermal–epidermal separation in the sections incubated with anti-COL7 IgG, PMNs, and 25 mg/ml BAY61-3606. **(I–L)** Representative experiments evaluating the expression of CD66b (x-axis) and L-selectin (CD62L, y-axis) in immune complex-stimulated PMNs. **(I)** CD66b and CD62L expression in resting PMNs show low expression of CD66b and high expression of CD62L. Data are based on five experiments per group. **(J)** By contrast, IC activation leads to L-selectin shedding and increased CD66b expression. **(K)** Low concentrations of BAY61-3606 had no impact on the IC-induced changes in PMN surface molecule expression. **(L)** Higher compound concentrations normalized CD66b expression, but had no effect on L-selectin sheading. **(M–P)** These effects of BAY61-3606 were achieved at non-toxic concentrations, as evaluated by annexin V/propidium iodine staining. Representative results from **(M)** solvent- (water), **(N)** UV-irradiated- (positive control), and **(O,P)** BAY-61-3606-treated activated PMNs.

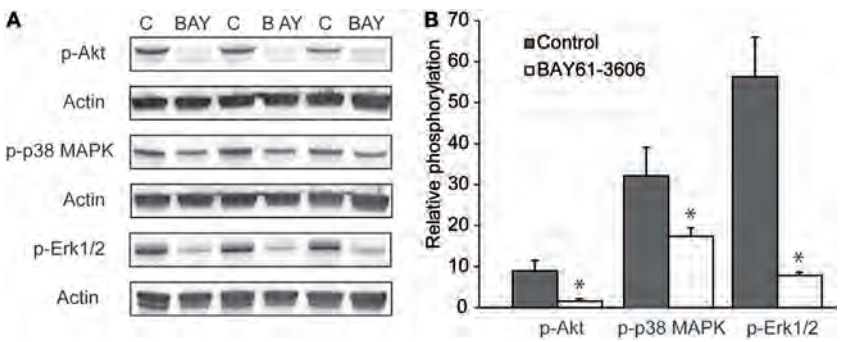

FIGURE 7 | Pharmacological inhibition of SYK ablates signaling events in immune complex-activated polymorphonuclear leukocyte (PMN). **(A)** Representative blots from immune complex-activated PMN ("C") or activated PMNs treated with BAY61-3606 ("BAY") from three blood donors. **(B)** Image analysis showed that BAY61-3606 ablated pAkt phosphorylation and significantly reduced p38 and Erk phosphorylation. The data are presented as the mean (boxes) and STD (error bars) and are based on three experiments per group (*$p < 0.05$, t-test).

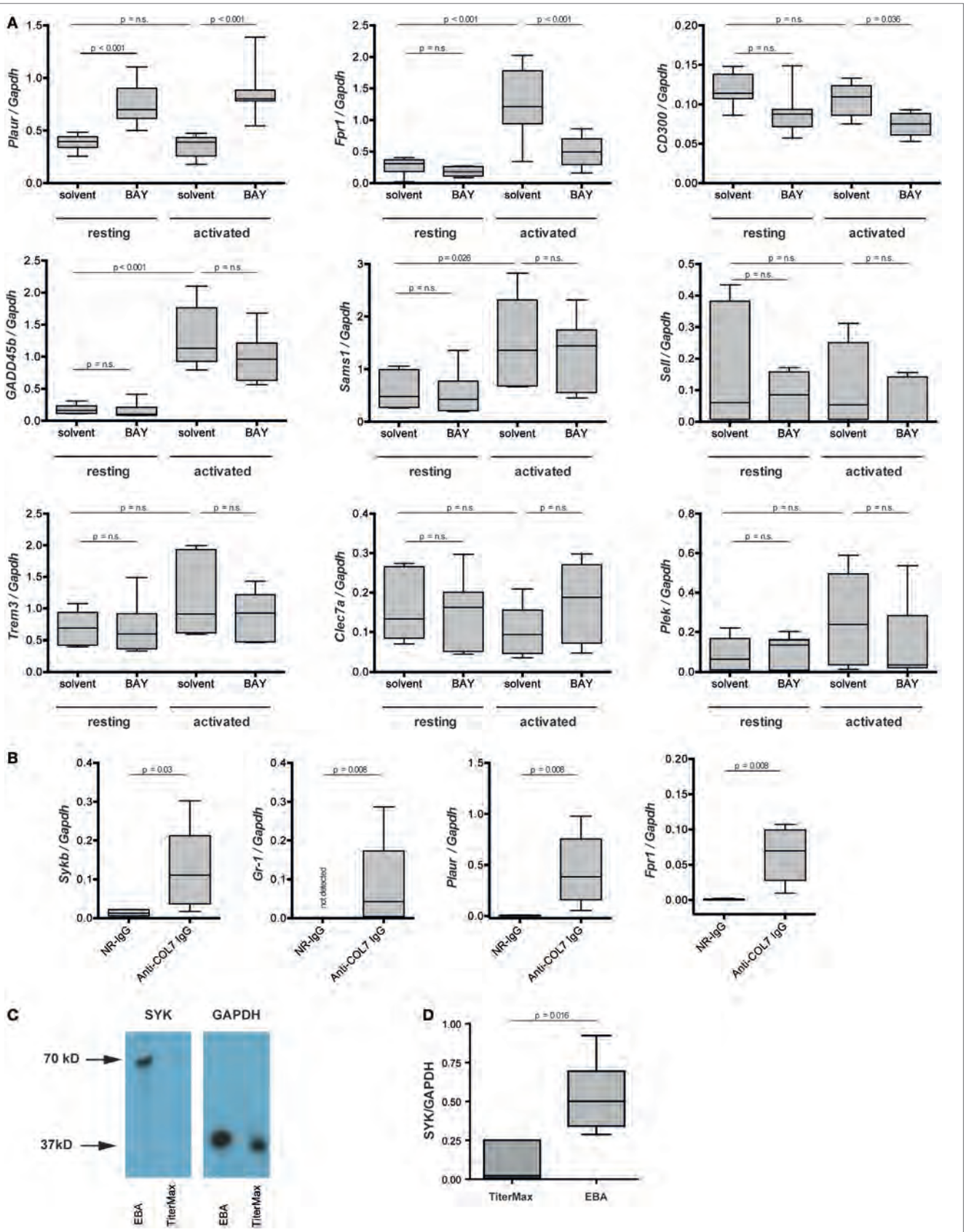

FIGURE 8 | Continued

FIGURE 8 | *Plaur* and formyl peptide receptor 1 (*Fpr1*) are regulated by SYK in immune complex-activated murine neutrophils. **(A)** Neutrophils were activated by immune complexes in absence or presence of BAY-61-3606 (BAY). Solvent and resting cells served as controls. Plots represent the expression of indicated gene in relation to *Gapdh*. Because of the non-parametric distribution, data are presented as median (centered vertical line), 25/75-percentile (boxes), and the 5/95-percentile (bars). Data are based on 8–10 samples per group. Statistical analysis was performed using ANOVA Ranks with the Student–Newman–Keuls post-test. **(B)** mRNA expression of *Sykb*, *Gr-1*, *Plaur*, and *Fpr1* were determined in the skin of healthy mice (NR-IgG) and mice with experimental epidermolysis bullosa acquisita (EBA) (anti-type VII collagen IgG). For expression analysis, skin specimens from corresponding areas were obtained. Myeloid cell infiltration, mirrored by an increase in *Gr-1* expression, was accompanied by an increased expression of *Sykp*, *Plaur*, and *Fpr1*. Data are based on five mice per group. Statistical calculations were performed using Rank Sum test. **(C)** Western blot analysis of SYK and GAPDH expression in the same samples of immunization-induced EBA and normal mouse skin. SYK expression could, in most cases, be detected only in lesional skin—with very few SYK expression in healthy skin. The graph shows the relative amount of the mean gray value (MD) of the SYK bands per GAPDH bands. Here representative blots are shown. **(D)** Quantitative analysis of the Western blots from five mice per group (*t*-test).

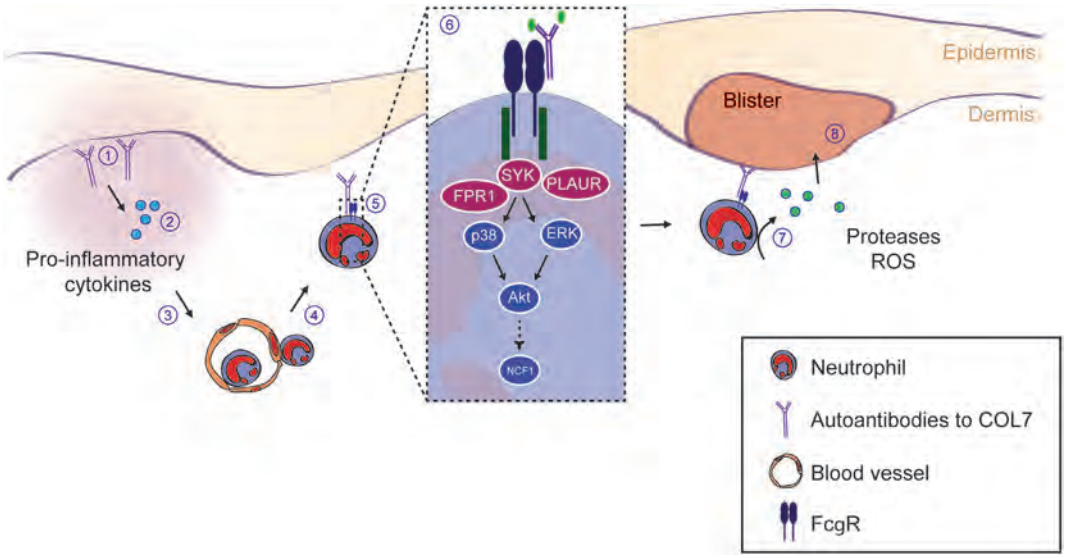

FIGURE 9 | SYK and downstream kinases are essential to drive inflammation and blistering in experimental epidermolysis bullosa acquisita (EBA). This schematic summarizes the current understanding of the events leading to blistering in experimental EBA. (1) The initial event is the binding of the IgG and/or IgA autoantibodies directed against type VII collagen (COL7). (2) Thereafter, anaphylatoxins are generated by activation of the complement cascade. Furthermore, several cytokines lipid mediators are released, which collectedly leads (3) to the activation of endothelial cells and allows the (4) CD18/ICAM-1-dependent extravasation of Gr-1$^+$ myeloid cells into the skin. (5) Within the skin, myeloid cells bind to the skin-bound immune complexes *via* specific activating Fc gamma receptors (FcγR). (6) FcγR binding triggers an intracellular signaling cascade involving SYK, p38, ERK, and Akt, ultimately leading to the activation of the NCF1 gene, which is part of the NADPH oxidase complex and generates reactive oxygen species (ROS). Within this pathway, we show an absolute requirement of SYK for blister induction in EBA. Blockade of downstream kinases (i.e., p38, Akt, or individual Src family kinases) only partially reduces the blistering phenotype, indicating that SYK activation is in the center stage of EBA pathogenesis. (7) Ultimately, this intracellular signaling process leads to the release of ROS and proteases from the myeloid cells, which (8) mediates blistering. Image modified from Ludwig et al. (2).

either anti- or pro-inflammatory effects. In support of the first assumption, SYK acts downstream of activating FcγR (44), which is essential to mediate inflammation in PD (9, 45) and other autoantibody-mediated diseases (46). By contrast, we recently identified an inhibitory signaling cascade, triggered by binding of highly galactosylated ICs to FcγRIIB and dectin-1 to block the pro-inflammatory signaling triggered by C5aR1. Inhibition of signaling downstream of C5aR1 was mediated by tyrosine phosphorylation of the ITAM-like motif downstream of dectin-1 and transient phosphorylation of SYK (6). Our results clearly document that SYK expression by myeloid, but not lymphoid, cells is an absolute requirement for induction of inflammation in antibody transfer-induced EBA, which has also been recently demonstrated elsewhere (47). In this paper, the authors also demonstrated a complete lack of skin lesion in SKY-deficient mice, which were generated by injection of bone marrow cells of *Syk*^{tm1Tyb} mice into lethally irradiated CD45.1$^+$ recipient wild-type mice. Hence, also herein, SKY expression on radiosensitive (hematopoietic) cells has convincingly been demonstrated. By use of myeloid- and lymphoid cell-specific SYK-deficient mice, we are here able to link the SYK-dependency to the myeloid cell lineage (**Figures 4** and **5**). This is in line with the *in vitro* observations made here (**Figure 6**) and by Németh et al. who also demonstrated a complete unresponsiveness of neutrophils from SYK-deficient mice to stimulation with ICs (47). In experimental EBA, myeloid and T cells have been demonstrated to mediate skin inflammation and blistering (7, 48), while mast cells were activated, but not required for clinical disease induction (49). Based on the findings presented here, myeloid, but not T cell expressed SYK mediates EBA pathogenesis. Of these, both neutrophils and monocytes/

macrophages, which have been recently been demonstrated to contribute to EBA pathogenesis (50), are the two most likely cell types expressing SYK and contributing to EBA pathogenesis.

The almost complete absence of dermal myeloid cell infiltration after genetic or pharmacologic SYK inhibition is, at first glance, puzzling, because ablation of Syk does not greatly impair the migration properties of neutrophils (51). Furthermore, similar observations were made in mice lacking FcγR IV expression (9). We therefore hypothesize that when myeloid cells become activated by ICs located at the DEJ, they not only mediate blistering, but also release numerous mediators that in turn trigger an amplification of myeloid cell recruitment into the skin. So far, this has not been formerly demonstrated for EBA. In experimental BP, neutrophil elastase degrades collagens, leading to the formation of chemotactic peptides, which sustains the influx of neutrophils into the skin (52).

We next aimed to validate the predicted *Sykb*-gene network (**Figure 1B**). Within the predicted co-expression network, several interacting partners of SKY (e.g., *Cd300b*, *Tlr13*, *Jdp2*, and *Nfkbid*) were validated by curated databases (not shown). In addition, two novel *Sykb*-interacting genes, *Plaur* and *Fpr1*, were validated. *Plaur* (plasminogen activator, urokinase receptor) is expressed in conjunction with the C3-receptor on the surface of neutrophils (53). The function of *Plaur* has been linked to neutrophil migration (54, 55). *Fpr1* is expressed on activated neutrophils and promotes further activation upon ligand binding (56).

Our finding adds to the current view of mechanisms leading to tissue damage in EBA (2), which is initiated and triggered by the binding of IgG/A autoantibodies to COL7. This initial binding leads to increased concentrations of potent chemoattractants such as C5a (57) and leukotriene B4 (58), which lead to a CD18/ICAM-1-dependent influx of myeloid cells into the skin (7, 8). In the skin, myeloid cells bind to the tissue-deposited ICs in an FcγRIV-dependent fashion (9). This engagement of FcγR to ICs triggers intracellular signaling, involving SYK, PI3Kβ and δ, AKT, p38 MAPK, ERK, Src family kinases, CARD9, and RORα (10–14, Koga et al., submitted[1]). Of note, we here demonstrate that ERK, AKT, and p38 act downstream of SYK, which is (at least) required for ROS release and degranulation (**Figure 6**). The two newly identified interacting genes of *Sykb*, namely *Fpr1* and *Plaur*, most likely also act downstream of *Sykb*, but this awaits experimental confirmation. Collectively, myeloid cell activation leads to cytokine release, which sustains further neutrophil recruitment (8, 50, 59) and, through release of ROS and proteases, induces subepidermal blistering (7, 16). This concept of autoantibody-mediated tissue damage in EBA is graphically summarized in **Figure 9**.

Collectively, these insights into EBA pathogenesis were driven by an unbiased expression profiling approach and identified myeloid SYK as a central player in driving inflammation in a prototypical autoantibody-induced disease. Furthermore, we recognized and experimentally validated novel gene interaction partners of SYK, specifically *Fpr1* and *Plaur*. This should encourage the exploitation of SYK and SYK-regulated genes as potential therapeutic targets for EBA, as well as diseases with autoantibody-driven pathology.

ETHICS STATEMENT

Foreskin and blood collections from healthy volunteers and patients were performed after written informed consent was obtained. All experiments with human samples were approved by the ethical committee of the Medical Faculty of the University of Lübeck (reference numbers: 09-140, 04-061, 04-144, 05-056) and were performed in accordance with the Declaration of Helsinki.

AUTHOR CONTRIBUTIONS

US, NM, AK, KB, ES, TL, AR, SG, GV, FS, MA, KD, HP, MJ, KK, DZ, and SI performed experiments, YG performed statistical analysis, US and RL designed the study. All authors critically evaluated the data, wrote the manuscript, and approved the final version for publication.

ACKNOWLEDGMENTS

We thank Claudia Kauderer and Astrid Fischer for their excellent technical support.

FUNDING

This work was supported by the Excellence Cluster "Inflammation at Interfaces" (EXC 306/2), the Research Training Group "Modulation of Autoimmunity" (GRK 1727/1 and 2), grants SA2849/1-1, LU 877/8-1, and DFG LU 877/9-1, and the Clinical Research Unit "Pemphigoid Diseases—Molecular Pathways and their Therapeutic Potential" (KFO303/1, project LU 877/12-1) from the Deutsche Forschungsgemeinschaft.

SUPPLEMENTARY MATERIAL

The Supplementary Material for this article can be found online at http://www.frontiersin.org/articles/10.3389/fimmu.2018.00249/full#supplementary-material.

[1]Koga H, Kasprick A, Lopez R, et al. Therapeutic effect of a novel PI3Kδ inhibitor in experimental epidermolysis bullosa acquisita. *Front Immunol* (2017).

REFERENCES

1. Schmidt E, Zillikens D. Pemphigoid diseases. *Lancet* (2013) 381:320–32. doi:10.1016/S0140-6736(12)61140-4
2. Ludwig RJ, Vanhoorelbeke K, Leypoldt F, Kaya Z, Bieber K, McLachlan SM, et al. Mechanisms of autoantibody-induced pathology. *Front Immunol* (2017) 8:603. doi:10.3389/fimmu.2017.00603
3. Kasperkiewicz M, Sadik CD, Bieber K, Ibrahim SM, Manz RA, Schmidt E, et al. Epidermolysis bullosa acquisita: from pathophysiology to novel therapeutic options. *J Invest Dermatol* (2016) 136:24–33. doi:10.1038/JID.2015.356
4. Sitaru C, Mihai S, Otto C, Chiriac MT, Hausser I, Dotterweich B, et al. Induction of dermal-epidermal separation in mice by passive transfer of antibodies specific to type VII collagen. *J Clin Invest* (2005) 115:870–8. doi:10.1172/JCI21386
5. Mihai S, Chiriac MT, Takahashi K, Thurman JM, Holers VM, Zillikens D, et al. The alternative pathway in complement activation is critical for blister induction in experimental epidermolysis bullosa acquisita. *J Immunol* (2007) 178:6514–21. doi:10.4049/jimmunol.178.10.6514

6. Karsten CM, Pandey MK, Figge J, Kilchenstein R, Taylor PR, Rosas M, et al. Anti-inflammatory activity of IgG1 mediated by Fc galactosylation and association of FcgammaRIIB and dectin-1. *Nat Med* (2012) 18:1401–6. doi:10.1038/nm.2862
7. Chiriac MT, Roesler J, Sindrilaru A, Scharffetter-Kochanek K, Zillikens D, Sitaru C. NADPH oxidase is required for neutrophil-dependent autoantibody-induced tissue damage. *J Pathol* (2007) 212:56–65. doi:10.1002/path.2157
8. Sadeghi H, Lockmann A, Hund AC, Samavedam UK, Pipi E, Vafia K, et al. Caspase-1-independent IL-1 release mediates blister formation in autoantibody-induced tissue injury through modulation of endothelial adhesion molecules. *J Immunol* (2015) 194:3656–63. doi:10.4049/jimmunol.1402688
9. Kasperkiewicz M, Nimmerjahn F, Wende S, Hirose M, Iwata H, Jonkman MF, et al. Genetic identification and functional validation of FcγRIV as key molecule in autoantibody-induced tissue injury. *J Pathol* (2012) 228:8–19. doi:10.1002/path.4023
10. Kulkarni S, Sitaru C, Jakus Z, Anderson KE, Damoulakis G, Davidson K, et al. Essential role for PI3Kβ in neutrophil activation by immune complexes. *Sci Signal* (2011) 4:ra23. doi:10.1126/scisignal.2001617
11. Hellberg L, Samavedam UK, Holdorf K, Hänsel M, Recke A, Beckmann T, et al. Methylprednisolone blocks autoantibody-induced tissue damage in experimental models of bullous pemphigoid and epidermolysis bullosa acquisita through inhibition of neutrophil activation. *J Invest Dermatol* (2013) 133:2390–9. doi:10.1038/jid.2013.91
12. Sadeghi H, Gupta Y, Möller S, Samavedam UK, Behnen M, Kasprick A, et al. The retinoid-related orphan receptor alpha is essential for the end-stage effector phase of experimental epidermolysis bullosa acquisita. *J Pathol* (2015) 237:111–22. doi:10.1002/path.4556
13. Kovács M, Németh T, Jakus Z, Sitaru C, Simon E, Futosi K, et al. The Src family kinases Hck, Fgr, and Lyn are critical for the generation of the in vivo inflammatory environment without a direct role in leukocyte recruitment. *J Exp Med* (2014) 211:1993–2011. doi:10.1084/jem.20132496
14. Németh T, Futosi K, Sitaru C, Ruland J, Mócsai A. Neutrophil-specific deletion of the CARD9 gene expression regulator suppresses autoantibody-induced inflammation in vivo. *Nat Commun* (2016) 7:11004. doi:10.1038/ncomms11004
15. Koga H, Recke A, Vidarsson G, Pas HH, Jonkman MF, Hashimoto T, et al. PDE4 inhibition as potential treatment of epidermolysis bullosa acquisita. *J Invest Dermatol* (2016) 136:2211–20. doi:10.1016/j.jid.2016.06.619
16. Shimanovich I, Mihai S, Oostingh GJ, Ilenchuk TT, Bröcker EB, Opdenakker G, et al. Granulocyte-derived elastase and gelatinase B are required for dermal-epidermal separation induced by autoantibodies from patients with epidermolysis bullosa acquisita and bullous pemphigoid. *J Pathol* (2004) 204:519–27. doi:10.1002/path.1674
17. Ludwig RJ, Müller S, Marques Ad, Recke A, Schmidt E, Zillikens D, et al. Identification of quantitative trait loci in experimental epidermolysis bullosa acquisita. *J Invest Dermatol* (2012) 132:1409–15. doi:10.1038/jid.2011.466
18. Geahlen RL. Getting Syk: spleen tyrosine kinase as a therapeutic target. *Trends Pharmacol Sci* (2014) 35:414–22. doi:10.1016/j.tips.2014.05.007
19. GeneCards. *SYK Gene*. (2015). Available from: http://www.genecards.org/cgi-bin/carddisp.pl?gene=SYK
20. Carvalho BS, Irizarry RA. A framework for oligonucleotide microarray preprocessing. *Bioinformatics* (2010) 26:2363–7. doi:10.1093/bioinformatics/btq431
21. Chen Z, McGee M, Liu Q, Kong YM, Huang X, Yang JY, et al. Identifying differentially expressed genes based on probe level data for GeneChip arrays. *Int J Comput Biol Drug Des* (2010) 3:237–57. doi:10.1504/IJCBDD.2010.038028
22. Langfelder P, Zhang B, Horvath S. Defining clusters from a hierarchical cluster tree: the dynamic tree cut package for R. *Bioinformatics* (2008) 24:719–20. doi:10.1093/bioinformatics/btm563
23. Langfelder P, Horvath S. WGCNA: an R package for weighted correlation network analysis. *BMC Bioinformatics* (2008) 9:559. doi:10.1186/1471-2105-9-559
24. Pihur V, Datta S, Datta S. Reconstruction of genetic association networks from microarray data: a partial least squares approach. *Bioinformatics* (2008) 24:561–8. doi:10.1093/bioinformatics/btm640
25. Efron B. Large-scale simultaneous hypothesis testing: the choice of a null hypothesis. *J Am Stat Assoc* (2004) 99:96–104. doi:10.1198/016214504000000089
26. Huang DW, Sherman BT, Tan Q, Collins JR, Alvord WG, Roayaei J, et al. The DAVID gene functional classification tool: a novel biological module-centric algorithm to functionally analyze large gene lists. *Genome Biol* (2007) 8:R183. doi:10.1186/gb-2007-8-9-r183
27. Recke A, Trog LM, Pas HH, Vorobyev A, Abadpour A, Jonkman MF, et al. Recombinant human IgA1 and IgA2 autoantibodies to type VII collagen induce subepidermal blistering ex vivo. *J Immunol* (2014) 193:1600–8. doi:10.4049/jimmunol.1400160
28. Kemmer A, Bieber K, Abadpour A, Yu X, Mitschker N, Roth S, et al. A recombinant fusion protein derived from dog hookworm inhibits autoantibody-induced dermal-epidermal separation ex vivo. *Exp Dermatol* (2015) 24:872–8. doi:10.1111/exd.12804
29. Aga E, Katschinski DM, van Zandbergen G, Laufs H, Hansen B, Müller K, et al. Inhibition of the spontaneous apoptosis of neutrophil granulocytes by the intracellular parasite *Leishmania major*. *J Immunol* (2002) 169:898–905. doi:10.4049/jimmunol.169.2.898
30. Behnen M, Leschczyk C, Moller S, Batel T, Klinger M, Solbach W, et al. Immobilized immune complexes induce neutrophil extracellular trap release by human neutrophil granulocytes via FcgammaRIIIB and Mac-1. *J Immunol* (2014) 193:1954–65. doi:10.4049/jimmunol.1400478
31. Müller S, Behnen M, Bieber K, Möller S, Hellberg L, Witte M, et al. Dimethylfumarate impairs neutrophil functions. *J Invest Dermatol* (2016) 136:117–26. doi:10.1038/JID.2015.361
32. Recke A, Sitaru C, Vidarsson G, Evensen M, Chiriac MT, Ludwig RJ, et al. Pathogenicity of IgG subclass autoantibodies to type VII collagen: induction of dermal-epidermal separation. *J Autoimmun* (2010) 34:435–44. doi:10.1016/j.jaut.2009.11.003
33. Bieber K, Koga H, Nishie W. In vitro and in vivo models to investigate the pathomechanisms and novel treatments for pemphigoid diseases. *Exp Dermatol* (2017) 26:1163–70. doi:10.1111/exd.13415
34. Yamamoto N, Takeshita K, Shichijo M, Kokubo T, Sato M, Nakashima K, et al. The orally available spleen tyrosine kinase inhibitor 2-[7-(3,4-dimethoxyphenyl)-imidazo[1,2-c]pyrimidin-5-ylamino]nicotinamide dihydrochloride (BAY 61-3606) blocks antigen-induced airway inflammation in rodents. *J Pharmacol Exp Ther* (2003) 306:1174–81. doi:10.1124/jpet.103.052316
35. Iwata H, Witte M, Samavedam UK, Gupta Y, Shimizu A, Ishiko A, et al. Radiosensitive hematopoietic cells determine the extent of skin inflammation in experimental epidermolysis bullosa acquisita. *J Immunol* (2015) 195:1945–54. doi:10.4049/jimmunol.1501003
36. Kalies K, Blessenohl M, Nietsch J, Westermann J. T cell zones of lymphoid organs constitutively express Th1 cytokine mRNA: specific changes during the early phase of an immune response. *J Immunol* (2006) 176:741–9. doi:10.4049/jimmunol.176.2.741
37. Ludwig RJ, Zollner TM, Santoso S, Hardt K, Gille J, Baatz H, et al. Junctional adhesion molecules (JAM)-B and -C contribute to leukocyte extravasation to the skin and mediate cutaneous inflammation. *J Invest Dermatol* (2005) 125:969–76. doi:10.1111/j.0022-202X.2005.23912.x
38. Patterson H, Nibbs R, McInnes I, Siebert S. Protein kinase inhibitors in the treatment of inflammatory and autoimmune diseases. *Clin Exp Immunol* (2014) 176:1–10. doi:10.1111/cei.12248
39. Genovese MC, Kavanaugh A, Weinblatt ME, Peterfy C, DiCarlo J, White ML, et al. An oral Syk kinase inhibitor in the treatment of rheumatoid arthritis: a three-month randomized, placebo-controlled, phase II study in patients with active rheumatoid arthritis that did not respond to biologic agents. *Arthritis Rheum* (2011) 63:337–45. doi:10.1002/art.30114
40. Jakus Z, Simon E, Balázs B, Mócsai A. Genetic deficiency of Syk protects mice from autoantibody-induced arthritis. *Arthritis Rheum* (2010) 62:1899–910. doi:10.1002/art.27438
41. Mocsai A, Ruland J, Tybulewicz VL. The SYK tyrosine kinase: a crucial player in diverse biological functions. *Nat Rev Immunol* (2010) 10:387–402. doi:10.1038/nri2765
42. Buijsrogge JJ, Diercks GF, Pas HH, Jonkman MF. The many faces of epidermolysis bullosa acquisita after serration pattern analysis by direct immunofluorescence microscopy. *Br J Dermatol* (2011) 165:92–8. doi:10.1111/j.1365-2133.2011.10346.x
43. van der Steen LP, Bakema JE, Sesarman A, Florea F, Tuk CW, Kirtschig G, et al. Blocking Fcalpha receptor I on granulocytes prevents tissue damage

induced by IgA autoantibodies. *J Immunol* (2012) 189:1594–601. doi:10.4049/jimmunol.1101763
44. Kleinau S, Martinsson P, Heyman B. Induction and suppression of collagen-induced arthritis is dependent on distinct Fcgamma receptors. *J Exp Med* (2000) 191:1611–6. doi:10.1084/jem.191.9.1611
45. Zhao M, Trimbeger ME, Li N, Diaz LA, Shapiro SD, Liu Z. Role of FcRs in animal model of autoimmune bullous pemphigoid. *J Immunol* (2006) 177:3398–405. doi:10.4049/jimmunol.177.5.3398
46. Corr M, Crain B. The role of FcgammaR signaling in the K/B x N serum transfer model of arthritis. *J Immunol* (2002) 169:6604–9. doi:10.4049/jimmunol.169.11.6604
47. Németh T, Virtic O, Sitaru C, Mócsai A. The Syk tyrosine kinase is required for skin inflammation in an in vivo mouse model of epidermolysis bullosa acquisita. *J Invest Dermatol* (2017) 137:2131–9. doi:10.1016/j.jid.2017.05.017
48. Bieber K, Witte M, Sun S, Hundt JE, Kalies K, Dräger S, et al. T cells mediate autoantibody-induced cutaneous inflammation and blistering in epidermolysis bullosa acquisita. *Sci Rep* (2016) 6:38357. doi:10.1038/srep38357
49. Kasprick A, Yu X, Scholten J, Hartmann K, Pas HH, Zillikens D, et al. Conditional depletion of mast cells has no impact on the severity of experimental epidermolysis bullosa acquisita. *Eur J Immunol* (2015) 45:1462–70. doi:10.1002/eji.201444769
50. Hirose M, Kasprick K, Beltisou F, Dieckhoff Schulze K, Schulze FS, Samavedam UK, et al. Reduced skin blistering in experimental epidermolysis bullosa acquisita after anti-TNF treatment. *Mol Med* (2017). doi:10.2119/molmed.2015.00206
51. Futosi K, Mócsai A. Tyrosine kinase signaling pathways in neutrophils. *Immunol Rev* (2016) 273:121–39. doi:10.1111/imr.12455
52. Lin L, Betsuyaku T, Heimbach L, Li N, Rubenstein D, Shapiro SD, et al. Neutrophil elastase cleaves the murine hemidesmosomal protein BP180/type XVII collagen and generates degradation products that modulate experimental bullous pemphigoid. *Matrix Biol* (2012) 31:38–44. doi:10.1016/j.matbio.2011.09.003
53. Xue W, Kindzelskii AL, Todd RF, Petty HR. Physical association of complement receptor type 3 and urokinase-type plasminogen activator receptor in neutrophil membranes. *J Immunol* (1994) 152:4630–40.
54. Pliyev BK, Antonova OA, Menshikov M. Participation of the urokinase-type plasminogen activator receptor (uPAR) in neutrophil transendothelial migration. *Mol Immunol* (2011) 48:1168–77. doi:10.1016/j.molimm.2011.02.011
55. Renckens R, Roelofs JJ, Florquin S, van der Poll T. Urokinase-type plasminogen activator receptor plays a role in neutrophil migration during lipopolysaccharide-induced peritoneal inflammation but not during *Escherichia coli*-induced peritonitis. *J Infect Dis* (2006) 193:522–30. doi:10.1086/499601
56. Dorward DA, Lucas CD, Chapman GB, Haslett C, Dhaliwal K, Rossi AG. The role of formylated peptides and formyl peptide receptor 1 in governing neutrophil function during acute inflammation. *Am J Pathol* (2015) 185:1172–84. doi:10.1016/j.ajpath.2015.01.020
57. Kasprick A, Holtsche MM, Rose EL, Hussain S, Schmidt E, Petersen F, et al. The anti-C1s antibody TNT003 prevents complement activation in the skin induced by bullous pemphigoid autoantibodies. *J Invest Dermatol* (2018) 138:458–61. doi:10.1016/j.jid.2017.08.030
58. Sezin T, Krajewski M, Wutkowski A, Mousavi S, Chakievska L, Bieber K, et al. The leukotriene B4 and its receptor BLT1 act as critical drivers of neutrophil recruitment in murine bullous pemphigoid-like epidermolysis bullosa acquisita. *J Invest Dermatol* (2017) 137:1104–13. doi:10.1016/j.jid.2016.12.021
59. Hirose M, Brandolini L, Zimmer D, et al. The allosteric CXCR1/2 inhibitor DF2156A improves experimental epidermolysis bullosa acquisita. *J Genet Syndr Gene Ther* (2013). doi:10.4172/2157-7412.S3-005

Conflict of Interest Statement: The authors declare that the research was conducted in the absence of any commercial or financial relationships that could be construed as a potential conflict of interest.

frontiers in Immunology

ORIGINAL RESEARCH
published: 12 February 2018
doi: 10.3389/fimmu.2018.00145

Agonistic Autoantibodies to the β2-Adrenergic Receptor Involved in the Pathogenesis of Open-Angle Glaucoma

Anselm Jünemann[1†], Bettina Hohberger[2†], Jürgen Rech[3], Ahmed Sheriff[3], Qin Fu[4,5], Ursula Schlötzer-Schrehardt[2], Reinhard Edmund Voll[6], Sabine Bartel[5], Hubert Kalbacher[7], Johan Hoebeke[8], Robert Rejdak[9], Folkert Horn[2], Gerd Wallukat[5†], Rudolf Kunze[10†] and Martin Herrmann[3†]*

[1] Department of Ophthalmology, University of Rostock, Rostock, Germany, [2] Department of Ophthalmology, Friedrich-Alexander-University of Erlangen-Nürnberg, Erlangen, Germany, [3] Department of Internal Medicine III, Institute of Clinical Immunology and Rheumatology, University of Erlangen-Nürnberg, Erlangen, Germany, [4] Department of Pharmacology, Tongji Medical College, Huazhong University of Science and Technology, Wuhan, China, [5] Max Delbrück Center for Molecular Medicine, Berlin, Germany, [6] IZKF Research Group 2, Nikolaus-Fiebiger-Center of Molecular Medicine, University of Erlangen-Nürnberg, Erlangen, Germany, [7] IFIB - Institute of Biochemistry, University of Tübingen, Tübingen, Germany, [8] C.N.R.S. UPR 9021 «Chimie et Immunologie Thérapeutiques», Strasbourg, France, [9] Department of General Ophthalmology, Medical University of Lublin, Lublin, Poland, [10] Science Office, Berlin-Buch, Campus Max Delbrück Center for Molecular Medicine, Berlin, Germany

OPEN ACCESS

Edited by:
Robert Weissert,
University of Regensburg, Germany

Reviewed by:
Jennifer Maynard,
University of Texas at Austin, United States
Reinhild Klein,
Universität Tübingen, Germany

***Correspondence:**
Bettina Hohberger
bettina.hohberger@uk-erlangen.de

[†]These authors have contributed equally to this work.

Specialty section:
This article was submitted to Multiple Sclerosis and Neuroimmunology, a section of the journal Frontiers in Immunology

Received: 24 August 2017
Accepted: 17 January 2018
Published: 12 February 2018

Citation:
Jünemann A, Hohberger B, Rech J, Sheriff A, Fu Q, Schlötzer-Schrehardt U, Voll RE, Bartel S, Kalbacher H, Hoebeke J, Rejdak R, Horn F, Wallukat G, Kunze R and Herrmann M (2018) Agonistic Autoantibodies to the β2-Adrenergic Receptor Involved in the Pathogenesis of Open-Angle Glaucoma. Front. Immunol. 9:145. doi: 10.3389/fimmu.2018.00145

Glaucoma is a frequent ocular disease that may lead to blindness. Primary open-angle glaucoma (POAG) and ocular hypertension (OHT) are common diseases with increased intraocular pressure (IOP), which are mainly responsible for these disorders. Their pathogenesis is widely unknown. We screened the sera of patients with POAG and OHT for the prevalence of autoantibodies (AAb) against G protein-coupled receptors (GPCRs) in comparison to controls. Employing frequency modulation of spontaneously contracting neonatal rat cardiomyocytes *in vitro*, agonistic GPCR AAb were to be detected in roughly 75% of the patients with POAG and OHT, however, not in controls. Using inhibitory peptides the AAb' target was identified as β2 adrenergic receptor (β2AR). The AAb interact with the second extracellular loop of β2AR. The peptides 181–187 and 186–192 were identified as binding sites of the AAb within the extracellular loop II. The binding of the AAb to β2ARs was verified by surface-plasmon-resonance analysis. The isotype of the AAb was (immunoglobulin) IgG3. In an additional pilot principal-of-proof study, including four patients with POAG, the removal of the AAb against the β2AR and other immunoglobulins G by immunoadsorption resulted in a transient reduction of IOP. These findings might indicate a possible role of agonistic AAb directed against β2ARs in the dynamics of aqueous humor and might support a contribution of adaptive autoimmunity in the etiopathogenesis of POAG and OHT.

Keywords: autoantibodies, glaucoma, ocular hypertension, β2-adrenergic receptor, agonistic, immunoadsorption

INTRODUCTION

Glaucoma is one of the leading causes of blindness in the world. Over 67 million people are affected by glaucoma (1, 2). Elevated intraocular pressure (IOP) is the major risk factor for glaucoma. Primary open-angle glaucoma (POAG) is now defined as a progressive disease of retinal ganglion cells characterized by structural change in the optic disk and by typical, slowly progressive loss of

function. The most common form of the group of glaucomatous diseases is POAG with about 80%. Ocular hypertension (OHT) is characterized by elevated IOP without optic nerve degeneration. One to 2% of patients with OHT per year convert to POAG.

The pathogenesis of the optic nerve damage in POAG is complex and associated with increased IOP, neurotoxicity and apoptosis (3, 4), changes of the extracellular matrix (5, 6), activation of glia cells (7), an interrupted transport of neutrophins (8), oxidative stress (9, 10), and hypoxia due to ocular and systemic vascular dysregulation (9). There are also reports of glaucoma-associated degenerative processes of the central visual pathways in the brain (11). Thus, new targets for therapeutic intervention, such as improving ocular blood flow and direct neuroprotection of retinal ganglion cells, are under investigation.

Since elevated IOP is the primary risk factor for the development and progression of glaucoma, the lowering of the IOP is the primary goal of all treatment strategies (12). Many studies have shown that IOP reduction can slow the progression of glaucoma (13–17) and delay or even prevent the onset of retinal ganglion cell loss. Lowering the IOP by 1 mmHg prevents progressive visual field loss by 10% (18). Conservative [e.g., β2-adrenergic receptor (β2AR) blocker] and surgical therapeutic options are offered to achieve IOP lowering. The β2AR blocker Timolol reduces the IOP in humans (19) by suppressing the rate of aqueous humor formation (20, 21) by 30–50% (20–26). The relative potency of the β2-adrenergic blocker Timolol is higher than that of the β1-adrenergic receptor blocker Betaxolol (27), indicating the prominent role of β2ARs in the formation of aqueous humor and/or regulation of its flow.

Trabecular meshwork and ciliary body express β2ARs (28, 29), regulating the aqueous humor system in the eye and consequently influencing IOP. Thus, β2AR plays a key role in the regulation of both aqueous humor production and outflow. In addition, β2AR is also expressed in human optic nerve and in microvessels (30, 31). β2ARs are members of the G protein-coupled receptors (GPCR) family, comprised of more than 600 genes (32, 33). They have seven membrane spanning domains, three intra- and extracellular loops, an extracellular N-terminus, and an intracellular C-terminal tail. Most of the GPCR form homodimers upon ligand activation. It has been shown that functional autoantibodies (AAbs), directed against GPCR, are associated with various human diseases. The first AAb against a GPCR was described for the β2AR in patients with allergic asthma in 1980 (34). Several groups identified agonistic AAb against the β1-adrenergic receptor in Chagas' disease (35, 36), dilated cardiomyopathy (37–39), ischemic cardiomyopathy (40), and myocarditis (41). β2- and α1-AAb were seen in Alzheimer's and vascular dementia (42). β1-, β2-, and α1-AAb were shown to be increased in patients with preeclampsia (43). α1-AAb were also detected in primary and malignant hypertension (44).

We hypothesize that AAb against GPCR might be involved in the pathogenesis of glaucomatous disease by influencing the dynamics of aqueous humor.

To study the hypothesis that circulating immunoglobulins of patients with glaucoma activate GPCRs, isolated rat cardiomyocytes were employed as target cell. Frequency modulation of spontaneously beating neonatal cardiomyocytes is highly efficient to investigate such targets (1–3, 37, 45). The rat cardiomyocytes contain a spectrum of relevant GPCRs, e.g., β1-, β2-, α-ARs, and Angiotensin-1 receptor, which display a high homology to their corresponding human receptors. The homology of the amino acids between the human and the rat second extracellular loop is 88%; however, the homology in the estimated binding site of the AAbs in this extracellular loop is 100%. The cells were exposed to IgG prepared from controls or patients with glaucoma and OHT. To verify the specificity of the effects, the heart cells were treated with receptor-specific agonists in the presence or absence of receptor-specific antagonists and compared with the AAb-mediated responses. In screening studies using respective agonists and blocking agents an interaction of the glaucoma-associated IgG with the β1AR, α-AR, or with AT1-receptor system has been excluded (not shown). Based on these findings, the potential importance of β2AR-directed antibodies associated with glaucoma was analyzed in more detail. These findings were the basis for the following experiments. Investigations of the target loop as well as the target epitope of the GPCR and the IgG isotype of the AAb were added. Surface plasmon resonance analysis confirmed the receptor specificity of the agonistic β2AR AAb.

In order to draw a bow between the molecular findings and clinical data, correlation analyses of the patients' clinical parameter with the β2AR AAb were done. Finally, a pilot proof-of-principal study was performed in four glaucoma patients using an extracorporal immunoadsorption (IA) for removal of AABs against β2AR and other immunoglobulins G in order to monitor a potentially transient or permanent change of IOP.

MATERIALS AND METHODS

Patients

Patients with POAG and patients with OHT were recruited from the Department of Ophthalmology of the University of Erlangen-Nürnberg (Friedrich-Alexander-Universität Erlangen-Nürnberg (FAU)). The control groups were from the Max Delbrück Centre of Molecular Medicine Berlin (MDC) and from the University of Erlangen-Nürnberg [normal healthy donors (NHD) and cataract patients].

All controls and patients were thoroughly examined by slit lamp inspection, applanation tonometry, funduscopy, gonioscopy, perimetry, and papillometry. In addition, a 24 h IOP curve was measured in all glaucoma patients (6 determinations: 7:00 a.m., 12:00 a.m., 5:00 p.m., 9:00 p.m., 12:00 p.m., and 7:00 a.m.). Papillometric evaluations of the patients were based on 15-color photographs and subsequent planimetry (Zeiss Morphomat 30) of the area of the optic disk and the neuroretinal rim area (46). Criteria for all glaucoma diagnoses were an open anterior chamber angle and glaucomatous changes of the optic nerve head including an unusually small neuroretinal rim area in relation to the optic disk size and higher vertical cup-to-disk ratios than horizontal ratios (45). All subjects underwent visual field testing with standard white-on-white perimetry using a computerized static projection perimeter (Octopus 500, Interzeag, Schlieren, Switzerland; program G1, 3 phases). Subjects with more than 12% false-positive or false-negative responses were not included

in this study. A glaucomatous visual field was defined as an white-on-white visual field with (a) at least three adjacent test points having a deviation of equal to or greater than 5 dB and with one test point with a deviation greater than 10 dB lower than normal, (b) at least two adjacent test points with a deviation equal to or greater than 10 dB, (c) at least three adjacent test points with a deviation equal to or greater than 5 dB abutting the nasal horizontal meridian, or (d) a mean visual field defect of more than 2.6 dB. Exclusion criteria were all eye diseases other than glaucoma, OHT or cataract, respectively. The clinical characteristics of controls (cataract and NHD) and patients can be found in **Tables 1** and **2**. For the patients, antiglaucomatous therapy and general diseases are given in **Tables 3** and **4**.

The study followed the tenets of the declaration of Helsinki for research. Written informed consent to use serum samples for research purposes was obtained from each participants of the study. The institutional review board of the University Hospital Erlangen approved the protocols.

POAG Patients

The patients of the glaucoma group were referred by ophthalmologists for further diagnosis and follow-up of glaucoma. The POAG group included 39 patients with POAG, characterized by IOP measurements higher than 21 mmHg. All POAG patients had glaucomatous optic disk damage and pathological cumulative perimetric defect curves, i.e., local and/or diffuse visual field loss in white-on-white perimetry.

OHT Patients

The OHT group included 9 patients with elevated IOP (24 mmHg at least in one eye) showing normal optic disk and normal retinal nerve fiber layer. Computerized visual field examinations with white-on-white perimetry (Octopus program G1) were normal.

Control Group

This group included eight patients referred by ophthalmologists for cataract surgery. Slit-lamp inspection, tonometry, fundoscopy, and papillometry were normal in control subjects. In addition, nine NHD were included.

Methods

Cardiomyocyte Bioassay—Isolation and Culture of Cardiac Myocytes

Primary cultures of cardiac myocytes were prepared from ventricle of 1- to 2-day-old Sprague-Dawley rats as described previously (37). Briefly, the myocardial cells were dispersed by digestion with a 0.25% solution of crude porcine trypsin (Serva,

TABLE 1 | Clinical characteristics of patients with primary open-angle glaucoma (POAG) and ocular hypertension (OHT).

	POAG	OHT
Number	39	9
Age (years)	71.18 ± 8.8 (48–86)	51.0 ± 7.7 (42–68)
Gender	12 m (31%), 17 f (69%)	5 m (56%), 4 f (44%)
Glaucoma history (years)	15.2 ± 11.1 (1–39)	6.8 ± 3.9 (3–14)
IOPmax (mmHg) OD	34,2 ± 12,7 (20–67)	28.7 ± 3.7 (23–35)
IOPmax (mmHg) OS	33.0 ± 12.2 (19–67)	26.9 ± 4.1 (22–35)
IOPact (mmHg) OD	17.8 ± 6.8 (10–38)	15.7 ± 3.9 (9–21)
IOPact (mmHg) OS	17.5 ± 5.7 (9–42)	17.4 ± 3.7 (13–22)
MD (dB) OD	10.8 ± 7.9 (−4.3 to 25.0)	−0.13 ± 0.96 (−1.5 to 1.5)
MD (dB) OS	11.9 ± 7.9 (−0.7 to 28.6)	0.25 ± 1.1 (−1.4 to 1.8)
CLV (dB^2) OD	42.2 ± 32.1 (4.0–112.7)	3.15 ± 1.42 (1.5–5.8)
CLV (dB^2) OS	40.7 ± 26.1 (1.7–124.0)	3.1 ± 1.7 (1.8–6.8)
Visual acuity OD	0.59 ± 0.3 (0.002–1.2)	1.0 ± 0.1 (1.0–1.2)
Visual acuity OS	0.59 ± 0.3 (0.004–1.0)	1.1 ± 0.1 (0.8–1.2)

Values are given as mean ± SD (range).
IOPmax, maximal intraocular pressure; IOPact, actual intraocular pressure; MD, mean defect; CLV, corrected loss variance; OD, right eye; OS, left eye; m, male; f, female.

TABLE 2 | Clinical characteristics of control group.

	Cataract patients	Normal healthy donors
Number	8	9
Age (years)	71.0 ± 10.7 (55–83)	44.6 ± 15.4 (22–65)
Gender	3 m (37%), 5 f (63%)	1 m (11%), 8 f (89%)
IOPact (mmHg) OD	13.3 ± 2.5 (10–17)	
IOPact (mmHg) OS	13.6 ± 3.4 (10–21)	
Visual acuity OD	0.47 ± 0.3 (0.002–1.0)	
Visual acuity OS	0.59 ± 0.3 (0.002–1.0)	

IOPact, actual intraocular pressure; OD = right eye. OS, left eye; m, male, f, female.

TABLE 3 | Glaucoma therapy of patients with primary open-angle glaucoma (POAG) and ocular hypertension (OHT).

Therapy	POAG (*n*)	OHT (*n*)
Antiglaucomatous medication	10	7
Glaucoma surgery without medication	6	0
Glaucoma surgery with medication	23	0
Number of antiglaucomatous medication		
0	3	2
1	13	4
2	5	3
3	11	0
4	4	0
Antiglaucomatous medication		
Betablockers	23	1
Prostaglandins	21	7
CAI	19	1
A2-agonists	7	1
Pilocarpine	4	0

CAI, carboanhydrase inhibitor.

TABLE 4 | General diseases of patients with primary open-angle glaucoma (POAG) and ocular hypertension (OHT).

	POAG	OHT
Diabetes	9 (23%)	0
Arterial hypertension	20 (51%)	3
Heart insufficiency	2 (5%)	0
Coronary heart disease	5 (13%)	0
Myocardial infarction	2 (5%)	0
Cardiac arrhythmia	3 (8%)	0
Stroke	3 (8%)	0
Immunological disease	4 (10%)	0
Rheumatoid arthritis	1	
Muscle rheumatism	1	
Psoriasis	1	
Raynaud's phenomenon	1	
Thyroid disease	7 (18%)	0

Germany) and were suspended in a SM20-I medium (Biochrom, Germany), containing 10% heat-inactivated neonatal calf serum (Gibco, Germany), streptomycin (HEFA Pharma; Germany), penicillin (Heyl, Germany), hydrocortisone (Merck, Germany), glutamine (Serva, Germany), and fluorodeoxyuridine (Serva, Germany), the latter to prevent proliferation of non-muscle cells. The cardiomyocytes were plated at a field density of 160,000 cells/cm^2. Twenty-four hours after seeding, the culture medium was renewed and the cells were cultured for 3–4 days at 37°C before stimulation. The medium was replaced with fresh culture solution 2 h before being used in experiments. Seven to 10 selected cells or synchronously contracting cell clusters per flask were counted for 15 s on a heated stage of an inverted microscope at 37°C. The basal contraction rate of the spontaneously beating cardiomyocytes was measured to be 162 ± 4 min under these conditions. If not noted otherwise, the cardiomyocytes were incubated with immunoglobulin fractions derived from sera of healthy persons and patients for 60 min in a dilution of 1:40. The immunoglobulins were added in excess (in 50 µl: 0.4–0.5 mg IgG fraction; this volume was added to 2 ml culture medium/flask). The agonistic and antagonistic drugs for the β2AR, peptides, etc. were added to the heart cells singly or cumulatively as indicated. β2AR activation was induced by the β2AR agonist clenbuterol (Sigma, Germany, concentration of 1 µM) and inhibited by the specific β2AR blocker ICI118.551 (Sigma, Germany, concentrations of 0.1–0.3 µM) applied 5 min before. Then, IgG-containing fractions of the sera from glaucoma patients were added to cardiomyocytes in a standard dilution. The effect of the IgG fractions was antagonized by ICI118.551. Performance and in-house validation and reproducibility of the bioassay were tested previously (47).

Preparation of the Serum Immunoglobulin Fractions

The immunoglobulin fractions were prepared from sera by direct ammonium sulfate precipitation (final concentration of 40%). After overnight incubation at 4°C the precipitates were centrifuged at 4,000 × *g* for 30 min, and the pellets were dissolved in dialysis buffer (154 mmol/l NaCl, 10 mmol/l Na_2HPO_4/NaH_2PO_4, pH 7.2). The procedure of precipitating (50% final concentration of ammonium sulfate for a removal of small biological active compounds such as catecholamines or peptides), washing, and dissolving was repeated twice. Prior to the assays all samples were extensively dialyzed against phosphate-buffered saline at 4°C for 3 days. The buffer was changed twice daily. After ammonium sulfate precipitation a concentration of 800–900 mg protein per milliliter was measured. Fifty microliters of this protein amount were inserted for analyses. The immunoglobulin fractions were stored at −20°C until use.

Affinity Purification of AAb

IgG preparations of patients with POAG and OHT were affinity purified using the biotinylated peptide biotin-AINCYANETCCD corresponding to the second extracellular loop of the β2AR. One milliliter of IgG was treated with 300 µl of the peptide (100 µg/ml) for 1 h. The peptide–antibody complex was incubated with streptavidin-coated magnetic particles (Roche, Germany) for 30 min. The separation was performed with a magnetic separator (Dynal, Germany). The particles were washed five times with PBS. The antibodies were eluted with 3 M KSCN in two 0.5 ml steps. The antibody solution was dialyzed against PBS for 48 h at 4°C.

Identification of the Target Loop of AAb against β2AR

β2AR-derived peptides identical to the extracellular loops I, II, or III were employed to identify the loop that interacts with the immunoglobulins isolated from the sera of patients with glaucoma. The following peptides were selected:

loop I (HILMKMWTFGNFWCEFWT)
loop II (HWYRATHQEAINCYANETCCDFFTNQ)
loop III (VIQDNLIRKEV).

The synthetic loop peptides were added in excess (0.5 µg in 50 µl) to 50 µl of the immunoglobulin fraction. The mixtures were shaken and incubated at room temperature for 1 h. The samples were then added to neonatal rat cardiomyocytes cultured in 2 ml of medium to a final IgG dilution of 1:40. Sixty minutes after addition of the peptide/immunoglobulin mixture the beating rate was monitored for 15 s.

Epitope Screening on Extracellular Loop II of β2AR

To identify the epitopes of the second extracellular loop of β2AR, mapping studies with small overlapping synthetic peptides were performed. The interacting sites between specific regions within the second extracellular loop and the IgG from glaucoma patients were screened with the following peptides:

HWYRAT (AS172–177),
ATHQEAI (AS176–182),
AINCYAN (AS181–187),
ANETCCD (AS186–192),
DFFTNQ (AS192–197).

The epitope analysis was performed similar as the loop screening.

IgG Subclass Analysis of the AAb against β2AR

To determine the IgG subclass of glaucoma-associated AAb against β2AR, IgGs from selected patients were treated with murine monoclonal anti-human IgG1, 2, 3, and 4 antibodies (SEROTEC, Germany). According to previous experiments (data not shown here), 3 µl of these antibodies were added to 50 µl of the IgG preparations. After 1 h at RT the samples were treated with 3 µl of a polyclonal anti-mouse Fc antibodies for 1 h to increase the complex. The samples were centrifuged at 10,000 × *g* and the supernatants were used in the cardiomyocyte bioassay at a dilution of 1:40.

Surface Plasmon Resonance

Binding of the AAb to the β2AR fragments was verified and quantified by surface-plasmon-resonance analysis (BIAcore). The IgG fractions of patients or controls were passed over biotinylated peptides loaded on a streptavidin-biosensor (BIAcore3000) at a flow rate of 5 µl/min. As β2AR-derived loop II peptide H19C (biotinyl-LC-HWYRATHQEAINCYANETC) was used. A biotinylated unrelated peptide served as control and its sensorgrams were subtracted from the specific signals. The initial linear association phase slope under conditions of high density of ligand is

directly correlated with the molar concentration of the binding molecules.

Pilot Proof-of-Principal Study on IA for the Treatment of Patients with POAG

In a pilot proof-of-principal study IA was performed in four patients with POAG to prospectively study safety and pressure-reducing efficacy of IA by unspecific removal of IgG and thereby the reduction of agonistic AAbs. The study followed the tenets of the declaration of Helsinki for research and was approved by the local Ethics Committee (3483; ClinicalTrials.gov Identifier NCT00494923). All subjects signed an informed consent form before participating in any part of the study. Data of a follow-up of at least half a year are presented. Levels of AAb and immunoglobulins as well as IOP were monitored before IA (visit 0: with local antiglaucomatous eye drops; visit 1: with systemic antiglaucomatous medication, yet without local antiglaucomatous eye drops), during IA as well as randomly 2 weeks, 2, 4, and 6 months after IA. At each visit, the IOP was measured six times a day (7:00 a.m., 12:00 p.m., 5:00 p.m., 9:00 p.m., 12:00 a.m., 7:00 a.m. of the following day). Mean IOP was calculated for each patient for statistical analysis.

Patients

The clinical characteristics of the patients are displayed in **Table 5**. All four patients suffered from POAG and were on maximal combination therapy with antiglaucomatous eye drops without any surgical procedure in the past. Only in the first patient, the left eye was excluded from the statistical analysis since he had undergone trabeculectomy in the past. Inclusion criteria were the failure of the current therapy to control IOP and the refusal of surgical procedures. Two female and two male Caucasian patients aged between 52 and 71 years were included. Systemic diseases of the patients were:

patient 1 nephrectomy because of cancer in 1995,
patient 2 arterial hypertension,
patient 3 asthma bronchiale, hyperthyreosis,
patient 4 spine arthrosis, cyste of the hip, tinnitus.

Immunoadsorption

All four patients underwent one treatment cycle of five consecutive days from Monday to Friday. Two Globaffin® adsorbers (double-columns system, columns for re-use; Fresenius Medical Care Affina GmbH) were used (48). Each adsorber contains 60 ml of a matrix based on sepharose CL-4B, suspended in sodium citrate buffer (10 mM; pH 4.0). One adsorber contains at least 250 mg of PGAM146 peptide covalently bound to Sepharose. The full synthetic peptide PGAM146 is a ligand for IgGs and binds them independent of the antigen specificity. The synthetic peptide PGAM-146 mimics a protein A ligand. In Globaffin the peptide is used as ligand to bind immunoglobulins from human plasma. The high affinity to all immunoglobulins (esp. IgG) or immunocomplexes that contain this Fc-part makes the peptide to a potential ligand for the removal of these substances. The peptide ligand is immobilized to cross linked agarose (Sepharose CL-4B). During treatment, the columns were regenerated with special buffer solutions (15 g/l glycine-hydrochloric acid, pH 2.8 and 8 g/l NaCl, 0.2 g/l KCL, 3.6 g/l $Na_2HPO_4 \times 12\ H_2O$ (phosphate-buffered saline, PBS) solution). After termination of the treatment, the Globaffin® adsorbers were preserved using bacteriostatic and toxic buffers [0.4 g/l polyhexamethylene-biguanide (PHMB), 0.3 g/l tryptophan, 3.3 g/l sodium citrate dihydrate, 5.4 g/l sodium acetate trihydrate, 2.9 g/l sodium monohydrogen phosphate × 12 H_20, 0.26 g/l potassium dihydrogen phosphate, pH 7.0 (PHMB-Trp) solution]. For preservation, each adsorber was rinsed with at least 350 ml of preservation buffer [0.1 g/l sodium azide (PBS, 0.1%)]. Afterward, the adsorbers were stored at 2–10°C until the next treatment cycle. Extracorporal plasma separation was performed by centrifugation (Cobe Spectra®) while the running parameters, such as column volume, loading volume (250 ml/cycle), desorption and regeneration volume, speed of processing, and numbers of cycles, were fixed and controlled by the Adasorb® device (medicap, Ulrichstein). Prior to connecting the patient

TABLE 5 | Pilot proof-of-principal study: demographic data of the four glaucoma patients.

Patient	Age (years)	Race	Sex	Diagnosis	Perimetric mean defect before IA (dB)		Glaucoma history (years)	*R*× before	*R*× in the end
					RA	LA			
1	71	Caucasian	M	OAG	11.7	17.0	12	Dorzolamid 2× Timolol 0.5% 2× Travoprost 1×	none
2	52	Caucasian	F	OAG	–0.9	0.0	6	Brimonidin 2× Timolol 0.5% 2× Latanoprost 2×	Dorzolamid 2× Timolol 0.5% 2× Latanoprost 1×
3	56	Caucasian	F	OAG	6.8	8.0	5	Dorzolamid 2× Timolol 0.5% 2×	Dorzolamid 1× Timolol 0.5% 1×
4	57	Caucasian	M	OAG	–2.8	0.1	9	Clonidin 4× Dorzolamid 2× Timolol 0.5% 2× Latanoprost 1×	none

to the system, the adsorber was washed with 2 l of 0.9% NaCl solution. During treatment, the plasma was alternately passed through the adsorbers. One adsorber served for the removal of immunoglobulins, the second was simultaneously regenerated by a glycin buffer. The amount of plasma to be treated (plasma volume, PV) was calculated before the treatment [females: PV (ml) = $a \times 9.03 + b \times 24.13 - 766$; males: PV (ml) = $a \times 19.9 + b \times 13.1 - 2{,}000$ (a = body height in cm; b = body weight in kg)].

Procedure of IA

Before the procedure, a 1250 IE heparin i.v. bolus was given. Access to circulation was provided *via* the cubital vein. Peripheral blood was drawn, anti-coagulated, and separated into plasma and blood cells. Extracorporal anti-coagulation was achieved by sodium citrate (ACD-A, 2.2%; 1:15–1:20 v/v to blood). The plasma was pumped through an adsorber column (Globaffin®) regulated by the Adasorb® device. The separated plasma was perfused through the columns at a flow rate between 11 and 28 ml/min; one cycle contained 250 ml plasma. The treated plasma was subsequently remixed with the other blood components and reinfused. During one cycle of treatment, the twofold volume of the individually calculated plasma volume was cleared by the adsorber.

Statistical Analysis

Student's *t*-test was used to compare variables between the groups. Values of $P < 0.05$ are significant. Continuous data are presented as medians (with ranges). We performed comparisons between groups with use of Fisher's exact test for categorical values and the Mann–Whitney *U* test for continuous variables. In addition, statistical analysis was done using four-field analysis.

RESULTS

Sera of Patients with POAG and OHT Contain AAb Stimulating Rat Cardiomyocytes

Immunoglobulin-enriched fractions of sera of patients with POAG, OHT, cataract, and of healthy donors (NHD) were analyzed for AAbs against GPCRs. We calculated the cutoff as mean of the beating rate in normals added to three times of the SD. As shown in **Figure 1**, the beat rate of cardiomyocytes was increased by the immunoglobulin fractions in POAG, OHT, yet not in cataract and NHD. 73% of the POAG patients and 78% of the OHT patients showed increased beat rates of the cardiomyocytes, whereas 0% of the cataract and NHD yielded an increased beat rate. This indicates the presence of agonistic AAb in patients with POAG and OHT. To identify the specific target(s) and IgG fraction of these AAb receptor-specific analyses were performed.

Immunoglobulins from POAG and OHT *Patients Interact* with the β2AR

The positive chronotropic responses of the AAb from patients with POAG and OHT were analyzed for their receptor specificity using respective antagonists. The action of AAb on the cardiomyocytes was blunted by ICI118.551 and the β1/β2 adrenergic antagonist propranolol (**Figure 2**), but not by bisoprolol (β1AR antagonist) or losartan (AT1 antagonist; not shown). The β2AR-specific agonist clenbuterol enhanced the cardiomyocyte beat rate of all samples, indicating functionality of the detection system (not shown).

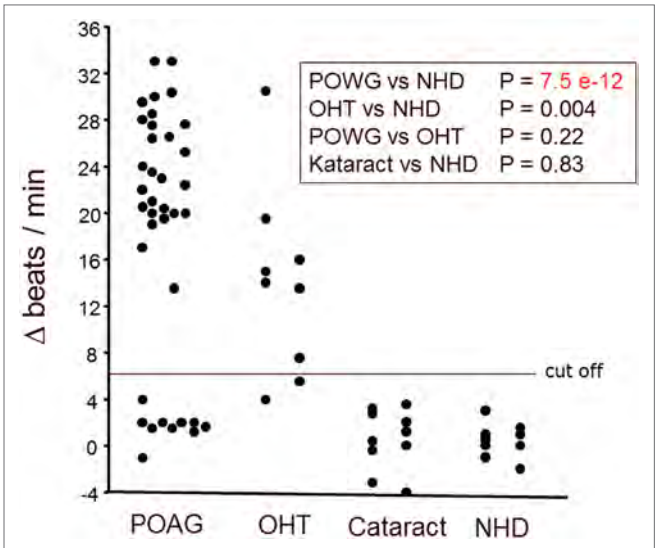

FIGURE 1 | Antibodies stimulating rat cardiomyocytes in sera of patients with POAG and OHT. Immunoglobulin-enriched serum fractions were added to cardiomyocyte cultures in a 1:20 dilution and incubated for 60 min at 37°C. The data are displayed as the changes of the beats/min. Each point represents 6–10 separate single-cell check points in a culture flask. Repeated measurements of the effects with different cell cultures prepared on different days resulted in almost identical data. The differences between patients with POAG or OHT versus healthy controls were highly significant. Primary open-angle glaucoma (POAG, $n = 37$); ocular hypertension (OHT, $n = 9$); cataract ($n = 10$); healthy donors (NHD, $n = 10$).

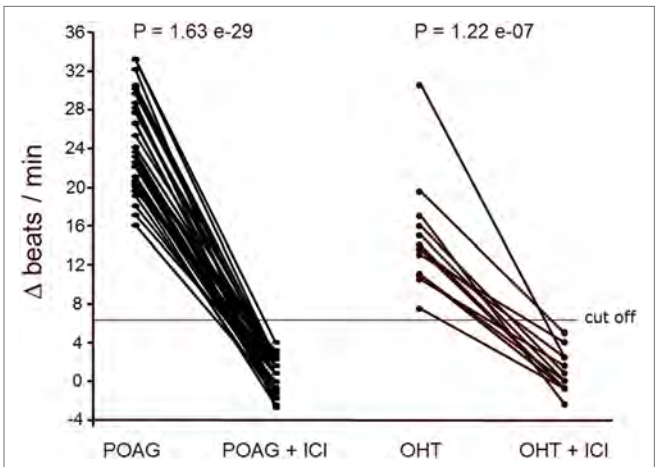

FIGURE 2 | β2-adrenergic receptor (β2AR) agonistic autoantibodies (AAbs) in patients with primary open-angle glaucoma (POAG) or ocular hypertension (OHT). The neonatal cardiomyocytes were incubated with the immunoglobulin fractions from POAG ($n = 33$) and OHT ($n = 14$) patients as described in **Figure 1**. The agonistic effect of the AAbs was blocked by the β2AR antagonist ICI118551 (ICI; 0.1 μM). ICI (0.1 μM) did not affect the basal beating rate of the cardiomyocytes.

Reportedly, agonistic AAb against the β1 adrenoceptor or monoclonal antibodies against the second extracellular loop of the β2 adrenoceptor did not desensitize the corresponding receptors within 4 to 6 h (49). Therefore, we analyzed the long term effect of the β2 AAb prepared from patients with POAG. The AAb did not induce desensitization of the β2AR within 5 h. ICI118.551 normalized the beating rate of the cardiomyocytes. A successive washing procedure removed ICI118.551 and the AAbs. When the washed cells were stimulated with the β2 agonist clenbuterol, a maximal response to this agonist was to be observed (**Figure 3A**). On the other hand, clenbuterol desensitized the receptor mediated signal cascade and decreased the beating rate of the cardiomyocytes. After washing out the agonist and a further stimulation with clenbuterol, we observed an increase of the beating rate by only 30% of the response obtained in the first stimulation with clenbuterol. We conclude that, in contrast to clenbuterol (**Figure 3B**), AAb did not desensitized the β2AR mediated signal cascade.

The β2 AAb Recognize Two Peptide Epitopes of the Second Extracellular Loop II of the β2AR

The binding of the AAb to distinct extracellular loops of β2AR was characterized in the presence of loop-specific synthetic peptides. As presented in **Figure 4** only the loop II peptide neutralized the agonistic activity. This indicates that the second extracellular loop of β2AR is the target of the AAb in the sera of patients with glaucoma.

To identify the epitopes of the AAbs, we pretreated the AAb with short overlapping peptides corresponding to the second extracellular loop of the β2AR. For these studies five synthetic

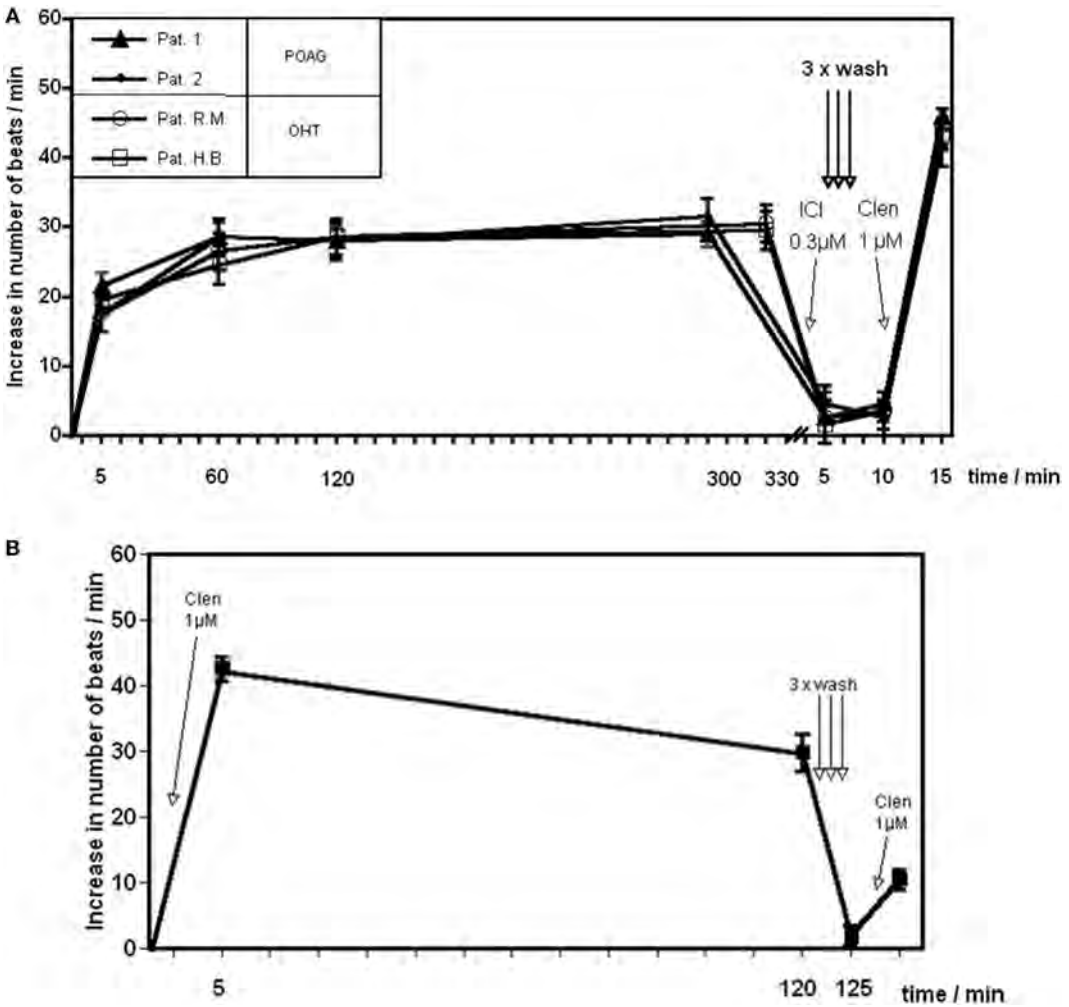

FIGURE 3 | Time response curve of β2 adrenergic agonists. Effect of **(A)** the agonistic autoantibody (AAb) prepared from patients with primary open-angle glaucoma (POAG) or ocular hypertension (OHT) on spontaneously beating rat cardiomyocytes and **(B)** clenbuterol (Clen). Clenbuterol induced a desensitization of the β adrenergic response within 2 h. After 2 h, clenbuterol was washed out and restimulation with clenbuterol resulted in approximately 30% of the initial stimulation **(B)**. β2-adrenergic receptor AAb showed no desensitization for at least 5 h **(A)**. Before washing, the antibodies were removed from the receptors by ICI118551. After washing, the cells react to a clenbuterol stimulation with a maximal response (n = 10 for each point of measurement).

oligopeptides were prepared covering the loop II amino acid 172–197. Only the loop II-borne peptides AINCYAN (181–187) and ANETCCD (186–192) abolished the agonistic activity of the AAb from five representative patients with POAG (**Figure 5**) and, thus, represent the dominant epitope of the β2AR.

Affinity Purified AAb of POAG and OHT Patients Induce Agonistic Effects in a Dose-Dependent Manner

Affinity purified AAb against the β2AR exert a dose-dependent positive chronotropic effect on cultured spontaneously beating rat cardiomyocytes. The maximal response for the POAG and OHT was observed at a dilution of the antibodies of 1:200 and 1:100, respectively.

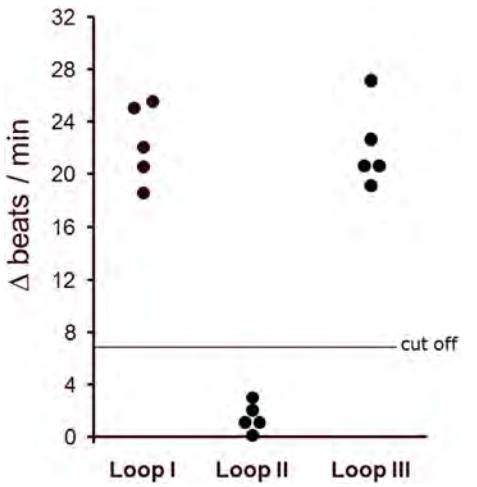

FIGURE 4 | The agonistic anti-β2AR autoantibodies (AAbs) of patients with primary open-angle glaucoma (POAG) recognized the second extracellular loop of the β2-adrenergic receptor. The antibody preparations from patients with POAG ($n = 5$) were pretreated with loop-specific peptides corresponding to the extracellular loops I–III. The antibody–peptide complexes were added to the cardiomyocytes to measure remaining agonistic capabilities. The final AAb dilution was 1:40. The data are presented as the increase in beats/min versus baseline beating rates.

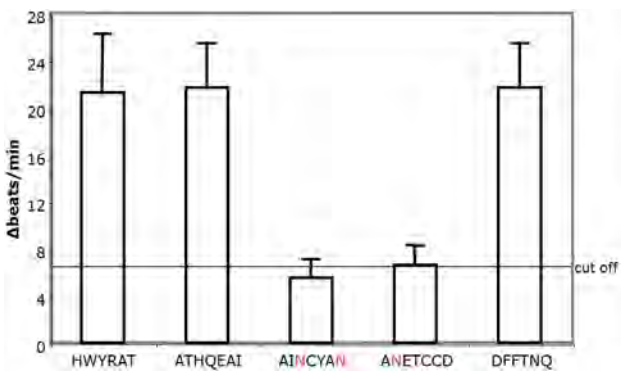

FIGURE 5 | The agonistic anti-β2AR autoantibodies (AAbs) of patients with primary open-angle glaucoma (POAG) recognize the epitopes AINCYAN and ANETCCD of loop II. The procedure to detect epitope-specific responses of immunoglobulins isolated from POAG patients is similar to the one used in the studies for loop analyses. The final AAb dilution was 1:40. Data are displayed as individual measurements of five independent patients with POAG.

Surface Plasmon Resonance Analysis Confirmed the Receptor Specificity of the Agonistic AAb

Surface plasmon resonance allows to determine direct physico-chemical interactions between macromolecules. Analyzing the IgG fractions of sera from patients with glaucoma we observed a significant binding activity to a loop II peptide from the β2AR (**Table 6**). We subjected the values to a statistical four-field analysis. The Fisher-test revealed a significance of $p = 0.01282$, a relative risk (CI) of 0.37721 (0.37093–0.84993), a sensitivity of 0.35 and a specificity of 0.0066. Therefore, the AAb from the sera of patients with glaucoma display a higher affinity for the loop II of the β2AR than those of controls.

The *Agonistic* β2AR AAb in the *Sera* of *Patients* with POAG Are of the IgG3 *Isotype*

To define the nature of the molecules in immunoglobulin-enriched fractions, which increased beating rates of cardiomyocytes, we used antibodies against immunoglobulins IgG and IgM (**Figure 6**). Only anti-IgG significantly prevented the agonistic activity. We next analyzed the IgG subclass of the agonist-like β2AR AAb with antibodies specifically depleting certain IgG subclasses (**Figure 7**). Only IgG3-precipitating antibodies eliminated the agonistic activity. Therefore, most of the agonistic AAb are of the IgG3 isotype.

Clinical Parameters in Correlation to AAbs

We analyzed the clinical parameters of the patients with respect to treatment for glaucoma, IOP, and general diseases including

TABLE 6 | Surface plasmon resonance analysis of binding of IgG fractions to the biotinylated H19C peptide (biotinyl-LC-HWYRATHQEAINCYANETC) derived from loop II of the β2AR.

Proband	Initial association phase slope on H19C peptide
1	0.441
2	0.0579
3	−2.98E−03
4	0.102
5	0.0439
6	0.0572
7	−0.0544
8	0.333
9	−0.0224
10	0.0955
11	0.102
12	0.176
13	0.413
14	0.326
15	0.11
16	0.396
17	0.115
18	0.356

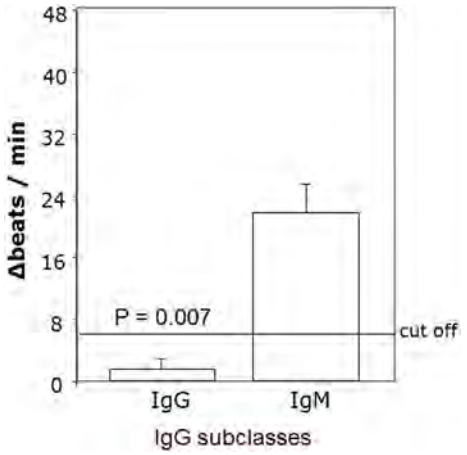

FIGURE 6 | Agonistic anti-β2AR IgG autoantibodies in patients with primary open-angle glaucoma. The neutralization of IgG from the immunoglobulin-enriched fraction lead to the loss of the stimulatory potential. Antibodies against IgM had no effect. The β2 receptor agonist clenbuterol served as positive control (not shown).

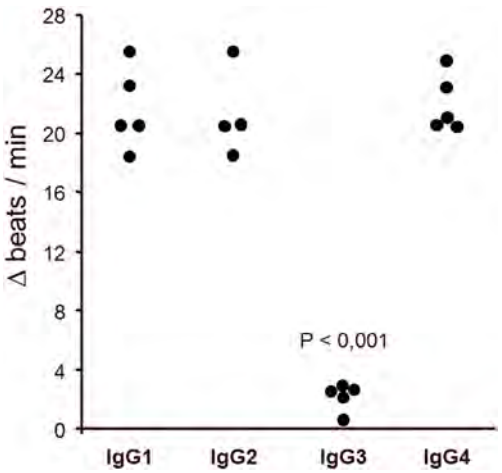

FIGURE 7 | IgG3 subclass of the agonistic anti-β2-adrenergic receptor autoantibodies in patients with primary open-angle glaucoma. The neutralization of IgG3 from the immunoglobulin-enriched fraction leads to the loss of the stimulatory potential. Antibodies against IgG1, 2, and 4 had no effect. The β2 receptor agonist clenbuterol served as positive control (not shown).

cardiovascular disease and diabetes (**Tables 3** and **4**). We could not detect any correlation of these parameters between AAb positive POAG and OHT patients with NHD or AAb negative patients (data not shown).

Pilot Proof-of-Principal Study on IA for Patients with POAG

The IA was well tolerated in all patients—no adverse events were to be observed. Specifically, no change in visual acuity, visual field, and intraocular flare measured by laser flare cell meter was detected (not shown). The levels of the AAb before and after IA are shown in **Table 7**. The IOP course is presented in **Table 8** for each patient. Time course of IOP and levels of AAbs during IA are shown in **Figure 8**.

The individual IOP course of each patient was as follows.

Patient 1 (Male, 71 Years Old)

Mean IOP before immune adsorption of the first patient showed a reduction only during the first days of IA (**Figure 8A**. The IOP dropped from 15.6 ± 1.8 mmHg to 15.1 ± 03 mmHg (3.2%) during the first day and raised to 23.9 ± 1.9 mmHg during the last day of IA. Because of the advanced stage of glaucoma, trabeculectomy was performed 4 weeks after IA.

Patient 2 (Female, 52 Years Old)

In the second patient largest reduction of IOP was found 2 months after IA (visit 4) (**Figure 8B**). IOP dropped about 27.8% at the right eye (OD) and 32.1% at the left eye (OS) if compared to IOP at visit 1. At visit 7 (12 months after IA) mean IOP was still decreased by about 21.9% at the right eye and 12.5% at the left eye in comparison to visit 1.

Patient 3 (Female, 56 Years Old)

Largest drop of IOP was found in the third patient (**Figure 8C**). At visit 4, the reduction of IOP was 11% for the right eye and 46.3% for the left eye with additional two topical medications. Without topical medications, IOP reduction was found to be 12.5% at the left eye, yet IOP increase of about 11% at the right eye (visit 2, 2 weeks after IA) compared to IOP at visit 1.

Patient 4 (Male, 57 Years Old)

The fourth patient showed the lowest IOP measurement (without topical medication) at the end of the observation period (without medication visit 7) (**Figure 8D**). One month after IA, IOP was equal to IOP before IA (without medication, visit 1) with an increase of mean IOP up to 23.5 ± 4.6 mmHg at the right eye and 23.5 ± 4.0 mmHg at the left eye (6 months after IA, visit 6). In comparison to visit 0 (three medications), no topical medication was necessary at the end of the observation period.

Taking together, in all patients, AAb and other IgGs were washed out almost completely by IA, resulting in autoantibody concentrations below the detection limit at the end of treatment. In two patients (1 and 3) AAb remained undetectable during the 6 months follow-up period. The two other patients showed detectable AAb-levels 4 months after IA. The reduction of total IgG and IgG3 levels ranged from 88 to 95 and from 64 to 80%, respectively. Four weeks after IA total IgG and IgG3 concentrations reached normal values.

DISCUSSION

In the present study, we describe formerly unknown circulating AAb in patients with glaucoma (50). We screened patient sera for antibodies that activate a GPCR expressed by cardiomyocytes and detected AAb against the β2AR employing specific inhibitory peptides. These agonistic AAb induced a dose-dependent stimulation and their effects were blocked by the selective antagonist

TABLE 7 | AABs, IgG (mg/dl), and IgG3 (mg/dl) before and after immunoadsorption (IA).

		Before IA	End of IA	After IA			
				2 weeks	2 months	4 months	6 months
1	AAB	5.8	0	−0.25	−0.25		−0.38
	IgG	1,190	134	469	859		1,000
	IgG3	51.8	16.3	32.5	38.1		42.2
Date of examination		(25.09)	(29.09.)	(06.10)	(09.11)		(16.05 of following year)
2	AAB	4.63	0.75	0	−0.88	6.0	7.67
	IgG	1,500	122			1520	1,410
	IgG3	44.8	15.1			37.1	47.6
Date of examination		(13.11)	(17.11)			(07.02 of following year)	(22.06 of following year)
3	AAB	7.25				0.67	0.33
	IgG	1,370	178	574	914	1240	
	IgG3	49.1	17.9	31.8	59.1		
Date of examination		(07.05)	(11.05)	(25.05)	(20.06)	(21.08)	
4	AAB	3.83			−0.17	3.17	
	IgG	1,150	92.0	773	1030		1,020
	IgG3	54.2	15.9	61.4			91.3
Date of examination		(04.08.)	(08.08)	(25.08)	(14.10)		(17.02 of following year)

ICI118.551, and neutralized by peptides corresponding to the second extracellular loop of the β2AR (AS 181–192).

Autoantibody can be detected by several methods: (1) enzyme-linked immunosorbent assay detects the patient's antigen bound AAb by a specific (to human IgG) animal sourced and enzyme (peroxidase or alkalic phosphatase) labeled antibody; (2) fluorescence (microscopy) detects AAb as (1), but the detection of the AAb is fluorescence labeled (e.g., fluorescein isothiocyanate, FITC); (3) radioimmunoassay detects AAb as (1), however, the detection of the AAb is radio labeled (e.g., iodine); (4) bioassay (with spontaneous beating neonatal rat cardiomyocytes) measures the increase in the beating rate, induced by added IgG (fraction from human serum) due to the binding of AAb to the corresponding receptor (here: β2-AR). The detection methods (1)–(4) measure the AAb indirectly, however method (4) additionally directly. As the detected signal extent of the bioassay is proportional to the AAb bound to the surface fixed target, we decided to choose the cardiomyocyte bioassay for the detection of the AAb. Next to the detection of the AAbs, this method enables functional analyses.

The AAb found in glaucoma patients are of the IgG3 subclass. The antibodies that trigger effector functions, and that are most likely to be involved in immunoregulatory activity, are IgG3 and IgG1 (51). In addition, it is known that IgG3 is involved in antibody-dependent cellular cytotoxicity (52). Complement activation is most effective with IgG3 and, to a lesser extent, with IgG1, IgG2, and IgG4. Usually, complement binding and activation leads to destruction of the target structure. The plasma concentration of IgG3 is low, and its half-life is shorter than that of any of the other IgG-subclasses. Further investigations are necessary to elucidate whether complement activation and cell death are involved in the pathogenesis of glaucomatous diseases.

Recent studies support the hypothesis that glaucoma-associated neurodegenerative processes are partially caused by immune-mediated mechanisms (53–56). These studies report complex AAb repertoires in patients with glaucoma which were directed against retinal and optical nerve antigens. Such autoantibody reactivities were shown in optical nerve extracts from bovine eyes. The later findings are of interest in respect to ocular pressure-dependent and independent autoimmune responses. With regard to AAb-mediated immunoreactions, these pathomechanisms seem to be driven by inflammation.

The β2AR is one of the best investigated GPCR. The modulation of cardiac contractility is also mediated by β2AR, and its activation might have chronic effects on cellular metabolism, on cell growth, or on excitability (57). This receptor seems to be involved in allergic asthma, several cardiomyopathies, such as Chagas' disease, and cardiac electrical disturbances (58–60). However, whereas the AAb in the case of Chagas disease were functionally active in cardiomyocytes, β2-AAb from asthmatic patients react in the opposite way. Respective loop analyses explained these findings; in the Chagas-related cardiac disorders the loop II was identified to be the target of AAbs, whereas in the asthmatic disease the loop III was recognized. Thus, it was concluded that the various extracellular loops of the β-AR are functionally linked to distinct antibody-mediated responses.

Several years ago, the effect of monoclonal antibodies directed against the second extracellular loop of the beta2 adrenoceptor was investigated. Interestingly, similar results were detected as seen with the AAbs prepared from the sera of glaucoma patients (61). The agonist-like effect of this mAB (6H8) was blocked by the specific β2-adrenergic antagonist ICI118.551 and a peptide HWYRATHQEAINCYANETC corresponding to the second extracellular loop of the β2-adrenoceptor. The β1-adrenoceptor antagonist bisoprolol was without influence. The AAb were directed against loop II and recognized the overlapping epitopes AINCYAN and ANETCCD. Considering that the peptide corresponding to the second extracellular loop and the short overlapping peptides cannot form the correct conformation of the extracellular loop, the anti-β2 receptor antibodies were pretreated with the peptides corresponding to the first, second or third extracellular loop for 1 h. Under these conditions, only

TABLE 8 | Intraocular pressure (IOP) before and after immunoadsorption (IA)—Visit 0: less than 3 months before IA under maximal combination therapy.

Patient		Before IA						After IA									
		Visit 0		Visit 1		2 weeks		1 month		2 months		4 months		6 months		12 months	
		IOP	Med	IOP	Med	IOP	Med	IOP	Med	IOP	Med	IOP	Med	IOP	Med	IOP	Med
1	OD	21.7 ± 4.0 (17–26, 9)	3	18.4 ± 2.8 (13–21, 8)	0	27.0 ± 6.5 (20–37, 17)	2	TE									
2	OD	20.0 ± 2.0 (17–23, 6)	3	23.3 ± 3.7 (17–33, 16)	0	22.4 ± 3.9 (17–29, 12)	2	23.8 ± 4.5 (19–30, 11)	2	16.8 ± 1.9 (15–20, 5)	3	18.2 ± 2.3 (15–22, 7)	3	23.8 ± 4.5 (19–30, 11)	3	18.2 ± 2.3 (15–22, 7)	3
	OS	26.0 ± 4.5 (21–33, 12)	3	29.7 ± 4.6 (22–40, 18)	0	23.0 ± 4.4 (19–30, 11)	2	21.2 ± 3.8 (16–26, 10)	2	20.2 ± 2.3 (18–24, 6)	3	26.0 ± 3.0 (22–31, 9)	3	21.2 ± 3.8 (16–26, 10)	3	26.0 ± 3.0 (22–31, 9)	3
3	OD	17.4 ± 3.7 (12–24, 12)	2	15.5 ± 5.2 (10–23, 13)	0	17.2 ± 6.9 (12–31, 19)	0	14.3 ± 3.5 (10–19, 9)	2	13.8 ± 0.4 (12–14, 1)	2	13.2 ± 1.6 (12–16, 4)	2	14.8 ± 3.4 (12–19, 7)	2	13.8 ± 2.4 (12–16, 4)	2
	OS	23.9 ± 7.9 (16–40, 24)	2	25.5 ± 8.4 (16–42, 26)	0	22.3 ± 14.6 (14–52, 38)	0	14.7 ± 3.6 (10–19, 9)	2	13.7 ± 0.8 (12–16, 2)	2	15.2 ± 1.8 (12–17, 5)	2	22.5 ± 6.8 (16–32, 16)	2	15.5 ± 2.4 (12–19, 7)	2
4	OD	17.6 ± 3.3 (11–25, 14)	4	20.4 ± 2.8 (18–24, 6)	0	21.5 ± 5.4 (14–30, 16)	0	20.7 ± 5.3 (15–26, 11)	0	21.5 ± 5.4 (14–29, 15)	0	23.5 ± 4.6 (17–28, 11)	0	23.5 ± 4.6 (17–28, 11)	0	19 ± 1.8 (17–22, 5)	0
	OS	17.4 ± 2.9 (12–23, 11)	4	21.0 ± 2.5 (18–24, 6)	0	22.4 ± 4.3 (17–30, 13)	0	21.2 ± 4.7 (16–26, 10)	0	22.8 ± 4.5 (16–29, 13)	0	23.7 ± 4.1 (20–28, 8)	0	23.5 ± 4.0 (20–28, 8)	0	19.7 ± 4.0 (15–26, 11)	0

Visit 1: two days before IA with systemic medications (acetazolamide), yet without topical medications. Mean ± SD (minimum–maximum, range) of 24 h IOP curve are presented.

the peptide that corresponds to the second extracellular loop was able to neutralize the AAb activity. The peptides of the first and third extracellular loops were without effect. Similar results we observed also for the short overlapping peptides with an amino acid sequence of 5–6 amino acids. In these experiments, the sequence (AINCYANETCCD) was able to neutralize the AAb action. Therefore, it is assumed that this sequence represents the epitope of the AAb on the second extracellular loop. Plasmon resonance and affinity purification confirmed the direct interaction of the AAb with loop II of the β2AR. The agonistic β2AR antibodies described here are good mechanistic candidates that might induce and maintain an elevated IOP as a critical step in the development of glaucomatous diseases.

In this study, we present first *in vivo* data of four patients with POAG that underwent IA in a pilot proof-of- principal study: glaucoma therapy is considered to be effective when IOP reduction is 20% from wash out baseline (62). Even not all patients in a study group must show a substantial IOP decrease of 20%, in cases when representative parts of the patients display even more than 20% IOP reduction. Thus, an IOP decrease could be observed in 3 of 4 patients after IA: patients 2 and 3 showed an IOP decrease of 27.8% (OD)/32.1% (OS) and 11% (OD)/46.3% (OS) using equal number of topical antiglaucomatous eye drops. An IOP decrease of 2.9% (OD) and 6.2% (OS) could be observed 12 months after IA in patient 4. As it is known that each single millimeter of mercury increases glaucoma progression rate about 12–13% (18) even the IOP decrease in this patient is important and enables winning sighted lifetime. The IOP of patient 4 is considered to be even lower after IA as the number of local antiglaucomatous eye drops decreased from 4 to 0, thus, measured IOP values under no local therapy can be seen as a lowered IOP after IA with even higher IOP under quadruple therapy before IA. Summarizing, immunoadsorption seemed to lower IOP or even number of antiglaucomatous therapy. Possibly, the decrease of IOP could even be larger, if β2AR AAbs are blocked specifically. Because IA is a non-specific method for adsorbing AAbs and other IgGs, several other AAb were removed in addition to the agonistic β2AR AAb. As known for other autoimmune diseases, AAb relapse. This effect was also seen in our patients. Detection of β2AR AAbs went along with an IOP increase (patients 2 and 4). The delay in the decrease of IOP might be possibly due to a re-sensitization of the β2AR in the absence of stimulating AAbs. In addition, the therapy was well tolerated and no adverse effects were observed.

The most important target of glaucoma treatment is elevated IOP. A large body of evidence has established the importance of the reduction of the IOP in the medical management of glaucomatous diseases (13–17, 63). The pathogenic damage of the optic nerve in POAG is not well understood. It is supposed to be associated with increased IOP, glutamate toxicity (64), interrupted transport of neutrophins (8), apoptosis (4, 65), extracellular matrix changes (5, 6), and hypoxia due to ocular and systemic vascular dysregulation (66).

The aqueous humor dynamic plays the major role in the regulation of IOP. Four factors maintain the steady-state IOP of the healthy eye. These are flow of aqueous humor, resistance to outflow, episcleral venous pressure (67), and uveoscleral outflow (68).

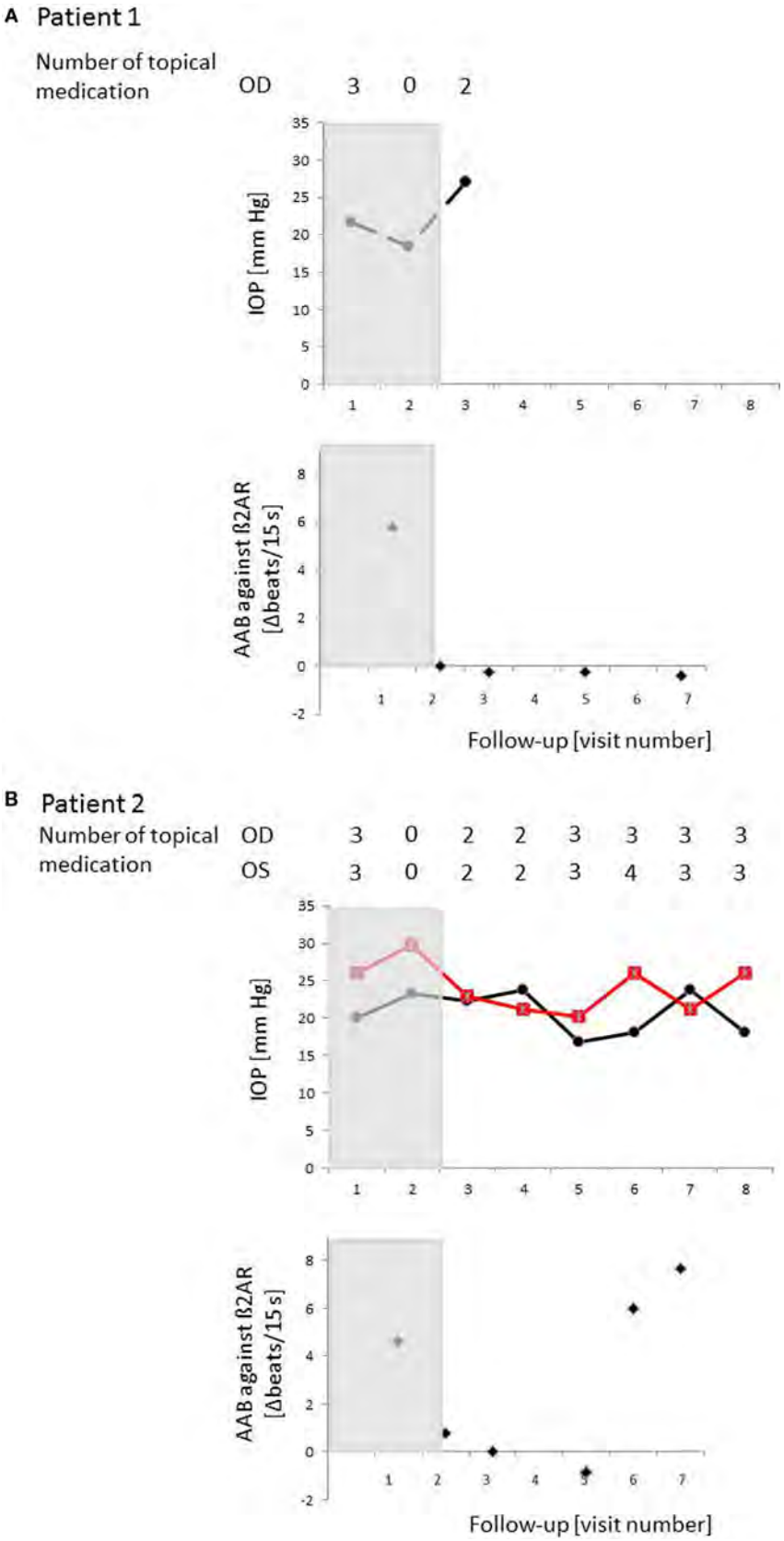

FIGURE 8 | Continued

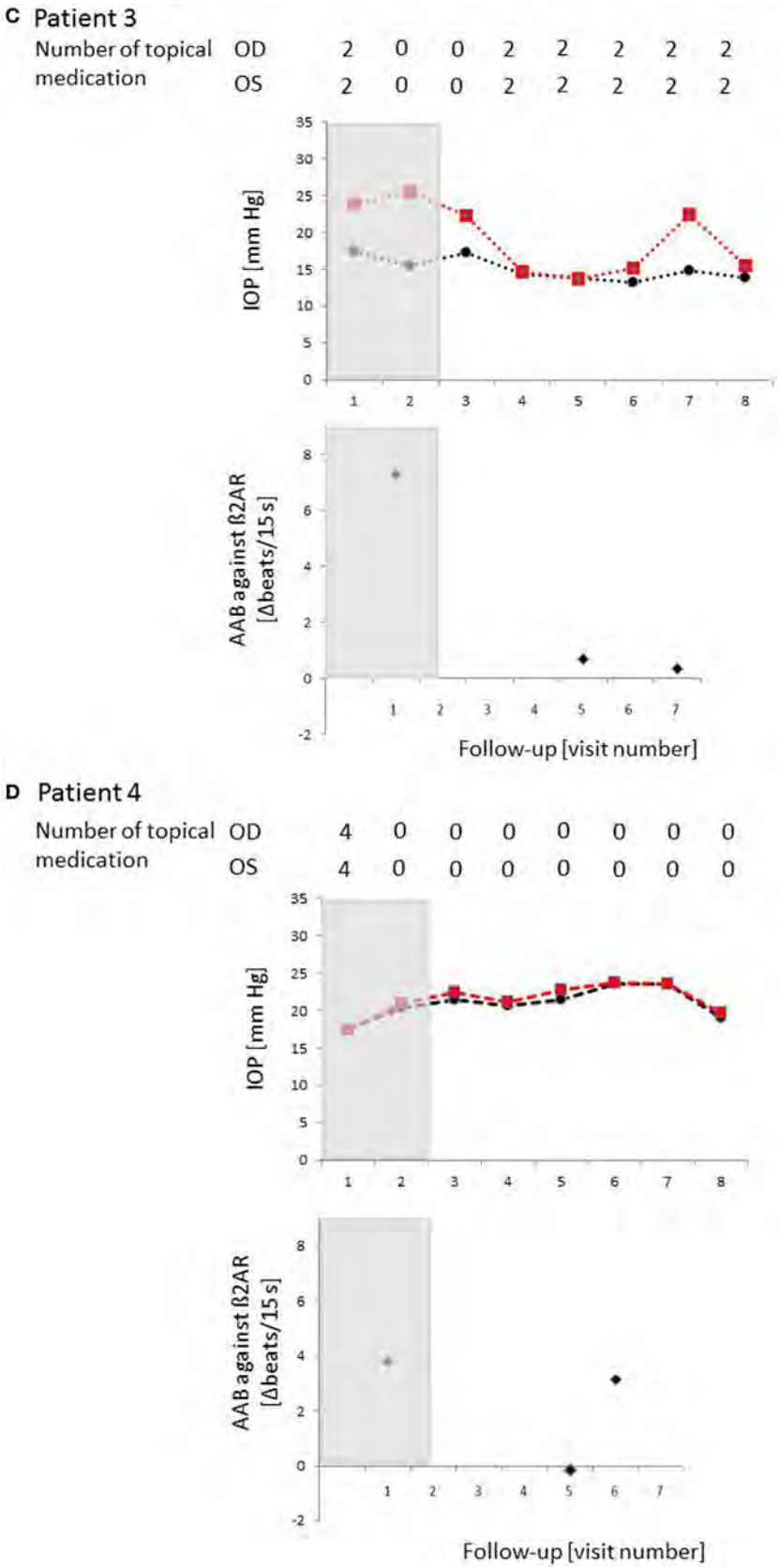

FIGURE 8 | Continued

FIGURE 8 | Time course of IOP, levels of autoantibodies (AAbs) and number of local antiglaucomatous eye drops during immunoadsorption (IA) for the patient with primary open-angle glaucoma (POAG). Patient 1/2/3/4 (A)/(B)/(C)/(D): a decrease in IOP under reduced number of local antiglaucomatous therapy was to be observed in all patients, going along with a decrease of the AAb. Intraocular pressure (IOP) increased, when AAbs relapsed after the IA; OD, right eye (black); OS, left eye (red); grayish area, data before IA; visit 1, IOP graph: less than 3 months before immunoadsorption under maximal combination therapy, AAB against β2AR graphs: before immunoadsorption; visit 2 – IOP graph: two days before immunoadsorption with system medications (acetazolamide), yet without topical medications, AAB against β2AR graphs: at the end of immunoadsorption; IOP/AAB against β2AR graphs: visit 3–2 weeks after immunoadsorption; visit 4–1 month after immunoadsorption; visit 5–2 months after immunoadsorption; visit 6–4 months after immunoadsorption; visit 7–6 months after immunoadsorption; visit 8–12 months after immunoadsorption.

The IOP reflects the balance between in- and outflow of aqueous humor. A major strategy in medical treatment of glaucoma is the reduction of inflow and, thereby, normalization of IOP. Understanding the mechanisms and regulation of inflow is, thus, of undoubted clinical relevance. Several mechanisms underlying increased inflow have been identified, however, the integration and regulation of these mechanisms is still elusive (69). The balance of in- and outflow of aqueous humor is modulated by the local β2AR activity and may be chronically influenced by agonistic AAbs.

Usually, night-time aqueous flows are approximately half of those observed at daytime in active humans (70–72). The ability of aqueous flow stimulation by epinephrine during night-time shows a low basal β-adrenergic stimulation during the night (23). Patients with POAG form in average 15% more aqueous humor/24 h than control subjects of the same age. This is due to a significantly higher aqueous flow in the night in comparison to control subjects (73). Thus, a β-adrenergic overdrive precludes the downregulation of the aqueous flow during the night. This observation is underlined by the lack of receptor desensitization by agonistic AAb displayed in **Figure 3**. Usually, β2AR agonists such as clenbuterol desensitize the receptor within 1–2 h (**Figure 3B**). By contrast, the β2AR AAb do not desensitize the β2AR *in vitro* for at least 5 h. This chronic β2-adrenergic stimulation may explain the higher aqueous flow and the elevation of the IOP in patients with POAG. Alteration of the circadian rhythm of IOP in POAG can be explained by the presence of AAb. The lack of tachyphylaxia was also observed for agonistic antibodies against anti-β1AR-, anti-α1AR-, anti-AT1-, and anti-muscarinic M2 receptor in several cardiovascular diseases (74, 75).

The AAb might also play a modulatory role in the aqueous outflow. Putney et al. (76) found an increase of cell volume of trabecular meshwork cells *via* Na^+-K^+-Cl^- cotransporters in glaucoma leading to a reduced outflow. As β-adrenergic stimulation results in an activation of Na^+-K^+-Cl^- cotransporters, agonistic AAb might also contribute to reduced outflow facility.

An "organ specificity" for the AAb against the β2AR can be assumed as patients of glaucoma suffered not of other diseases, which can be caused by these AAb (e.g., allergic asthma). It can be hypothesized that the chemical surrounding has to be changed before the autoantibodies can act specifically. Previous data showed that the βAR is not accessible for the AAb under adequate oxygen conditions. However, the βAR seemed to be unmasked, if ischemia occurred (77, 78). This could be a potential reason as glaucoma is hypothesized to be a disorder with local ischemia (79).

The data presented here offer another insight into eye disorders associated with high IOP. The newly identified AAb against the β2AR were exclusively found in the sera of patients with POAG and OHT but neither in those with cataract, nor in controls. Based on these observations, we suggest that these AAbs are not only immunological markers with a high incidence in POAG and OHT, but might also be pathomechanistically relevant β2AR activating molecules. The common, broadly successful therapy with β2AR antagonists further supports the idea that AAb-mediated mechanisms might be of pathogenic importance. In addition to their effect on IOP, the AAb might also have a direct effect on retinal ganglion cells as β-adrenoreceptor antagonists showed neuroprotective properties (80).

CONCLUSION

In patients with POAG and OHT, however, not in controls, agonistic AAb directed to β2AR were detected. These AAb interacted with the second extracellular loop of β2AR (peptides 181–187 and 186–192), thus functionally different links to distinct antibody-mediated responses are assumed. Data of our clinical pilot proof-of-principal study might suggest that a reduction of total IgG, including AABs against β2AR (IgG3 isotype) by IA, transiently decreases IOP. These findings might indicate a possible role of these AAb in the dynamics of aqueous humor and might support a contribution of adaptive autoimmunity in the etiopathogenesis of POAG and OHT. A specific blocking of AABs against β2AR might be of interest for further studies.

ETHICS STATEMENT

The study followed the tenets of the declaration of Helsinki for research. Written informed consent to use serum samples for research purposes was obtained from each participants of the study. The institutional review board of the University Hospital Erlangen approved the protocols (3483; ClinicalTrials.gov Identifier NCT00494923).

AUTHOR CONTRIBUTIONS

RK, MH, and GW had the idea and planned the study; GW, QF, and SB performed the laboratory work; AJ, JR, and RV planned and performed the clinical trial; HK did the synthetic work; JH did laboratory work; AS and BH performed data acquisition and statistical analysis; RR was involved in the analysis and revised the manuscript, FH was involved in the analysis, BH was responsible for the draft of the manuscript. US-S interpreted results and edited the manuscript. All authors have no financial interest in any topic regarding the present study and approved the final version of the manuscript.

ACKNOWLEDGMENTS

We thank Karin Karczewski (MDC, Berlin) for excellent technical assistance and Dr. med. Sabine Froese-Duill (Celle) for helpful discussions about the pathomechanism of glaucoma.

FUNDING

Globaffin was kindly provided by Fresenius Medical Care Deutschland GmbH, Bad Homburg, Germany. This work was supported by "Freundeskreis of the MDC, Berlin," "Deutsche Forschungsgemeinschaft" SFB643 (project B5), SFB539 ("glaucoma including Pseudoexfoliation syndrome"), by the Interdisciplinary Center for Clinical Research (IZKF) (project number A4 and N2) at the University Hospital of the Friedrich-Alexander-Universität Erlangen-Nürnberg (FAU), by the European Commissions [E.U. (QLK3-CT-2002-02017_APOCLEAR)], by the Lupus Erythemathodes Selbsthilfegemeinschaft e.V., by the responsif GmbH Erlangen, and the University of Erlangen's ELAN program, and by the Doktor Robert Pfleger Foundation, Bamberg.

REFERENCES

1. Quigley HA. Number of people with glaucoma worldwide. *Br J Ophthalmol* (1996) 80:389–93. doi:10.1136/bjo.80.5.389
2. Quigley HA, Broman AT. The number of people with glaucoma worldwide in 2010 and 2020. *Br J Ophthalmol* (2006) 90:262–7. doi:10.1136/bjo.2005.081224
3. Sucher NJ, Lipton SA, Dreyer EB. Molecular basis of glutamate toxicity in retinal ganglion cells. *Vision Res* (1997) 37:3483–93. doi:10.1016/S0042-6989(97)00047-3
4. Moore P, El-Sherbeny A, Roon P, Schoenlein PV, Ganapathy V, Smith SB. Apoptotic cell death in the mouse retinal ganglion cell layer is induced in vivo by the excitatory amino acid homocysteine. *Exp Eye Res* (2001) 73:45–57. doi:10.1006/exer.2001.1009
5. Yuan L, Neufeld AH. Activated microglia in the human glaucomatous optic nerve head. *J Neurosci Res* (2001) 64:523–32. doi:10.1002/jnr.1104
6. Kirwan RP, Leonard MO, Murphy M, Clark AF, O'brien CJ. Transforming growth factor-beta-regulated gene transcription and protein expression in human GFAP-negative lamina cribrosa cells. *Glia* (2005) 52:309–24. doi:10.1002/glia.20247
7. Varela HJ, Hernandez MR. Astrocyte responses in human optic nerve head with primary open-angle glaucoma. *J Glaucoma* (1997) 6:303–13. doi:10.1097/00061198-199710000-00007
8. Quigley HA. Ganglion cell death in glaucoma: pathology recapitulates ontogeny. *Aust N Z J Ophthalmol* (1995) 23:85–91. doi:10.1111/j.1442-9071.1995.tb00135.x
9. Osborne NN. Pathogenesis of ganglion "cell death" in glaucoma and neuroprotection: focus on ganglion cell axonal mitochondria. *Prog Brain Res* (2008) 173:339–52. doi:10.1016/S0079-6123(08)01124-2
10. Kong GY, Van Bergen NJ, Trounce IA, Crowston JG. Mitochondrial dysfunction and glaucoma. *J Glaucoma* (2009) 18:93–100. doi:10.1097/IJG.0b013e318181284f
11. Gupta N, Ang LC, Noël de Tilly L, Bidaisee L, Yücel YH. Human glaucoma and neural degeneration in intracranial optic nerve, lateral geniculate nucleus, and visual cortex. *Br J Ophthalmol* (2006) 90:674–8. doi:10.1136/bjo.2005.086769
12. Distelhorst JS, Hughes GM. Open-angle glaucoma. *Am Fam Physician* (2003) 67:1937–44.
13. The effectiveness of intraocular pressure reduction in the treatment of normal-tension glaucoma. Collaborative normal-tension glaucoma study group. *Am J Ophthalmol* (1998) 126:498–505. doi:10.1016/S0002-9394(98)00272-4
14. Van Veldhuisen PC, Ederer F, Gaasterland DE, Sullivan EK, Beck A, Prum BE, et al. The Advanced Glaucoma Intervention Study (AGIS): 7. the relationship between control of intraocular pressure and visual field deterioration. *Am J Ophthalmol* (2000) 130:429–40. doi:10.1016/S0002-9394(00)00538-9
15. Lichter PR, Musch DC, Gillespie BW, Guire KE, Janz NK, Wren PA, et al. Interim clinical outcomes in the collaborative initial glaucoma treatment study comparing initial treatment randomized to medications or surgery. *Ophthalmology* (2001) 108:1943–53. doi:10.1016/S0161-6420(01)00873-9
16. Heijl A, Leske MC, Bengtsson B, Hyman L, Bengtsson B, Hussein M, et al. Reduction of intraocular pressure and glaucoma progression: results from the early manifest glaucoma trial. *Arch Ophthalmol* (2002) 120:1268–79. doi:10.1001/archopht.120.10.1268
17. Kass MA, Heuer DK, Higginbotham EJ, Johnson CA, Keltner JL, Miller JP, et al. The ocular hypertension treatment study – a randomized trial determines that topical ocular hypotensive medication delays or prevents the onset of primary open-angle glaucoma. *Arch Ophthalmol* (2002) 120:701–13. doi:10.1001/archopht.120.6.701
18. Leske MC, Heijl A, Hussein M, Bengtsson B, Hyman L, Komaroff E, et al. Factors for glaucoma progression and the effect of treatment: the early manifest glaucoma trial. *Arch Ophthalmol* (2003) 121:48–56. doi:10.1001/archopht.121.1.48
19. Katz IM, Hubbard WA, Getson AJ, Gould AL. Intraocular pressure decrease in normal volunteers following timolol ophthalmic solution. *Invest Ophthalmol* (1976) 15:489–92.
20. Coakes RL, Brubaker RF. The mechanism of timolol in lowering intraocular pressure. In the normal eye. *Arch Ophthalmol* (1978) 96:2045–8. doi:10.1001/archopht.1978.03910060433007
21. Yablonski ME, Zimmerman TJ, Waltman SR, Becker B. A fluorophotometric study of the effect of topical timolol on aqueous humor dynamics. *Exp Eye Res* (1978) 27:135–42. doi:10.1016/0014-4835(78)90083-0
22. Dailey RA, Brubaker RF, Bourne WM. The effects of timolol maleate and acetazolamide on the rate of aqueous formation in normal human subjects. *Am J Ophthalmol* (1982) 93:232–7. doi:10.1016/0002-9394(82)90419-6
23. Topper JE, Brubaker RF. Effects of timolol, epinephrine, and acetazolamide on aqueous flow during sleep. *Invest Ophthalmol Vis Sci* (1985) 26:1315–9.
24. Mccannel CA, Heinrich SR, Brubaker RF. Acetazolamide but not timolol lowers aqueous-humor flow in sleeping humans. *Graefes Arch Clin Exp Ophthalmol* (1992) 230:518–20. doi:10.1007/BF00181771
25. Wayman L, Larsson LI, Maus T, Alm A, Brubaker R. Comparison of dorzolamide and timolol as suppressors of aqueous humor flow in humans. *Arch Ophthalmol* (1997) 115:1368–71. doi:10.1001/archopht.1997.01100160538002
26. Larsson LI. Aqueous humor flow in normal human eyes treated with brimonidine and timolol, alone and in combination. *Arch Ophthalmol* (2001) 119:492–5. doi:10.1001/archopht.119.4.492
27. Gaul GR, Will NJ, Brubaker RF. Comparison of a noncardioselective beta-adrenoceptor blocker and a cardioselective blocker in reducing aqueous flow in humans. *Arch Ophthalmol* (1989) 107:1308–11. doi:10.1001/archopht.1989.01070020378039
28. Wax MB, Molinoff PB. Distribution and properties of beta-adrenergic receptors in human iris-ciliary body. *Invest Ophthalmol Vis Sci* (1987) 28:420–30.
29. Crider JY, Sharif NA. Adenylyl cyclase activity mediated by beta-adrenoceptors in immortalized human trabecular meshwork and non-pigmented ciliary epithelial cells. *J Ocul Pharmacol Ther* (2002) 18:221–30. doi:10.1089/108076802760116142
30. Mantyh PW, Rogers SD, Allen CJ, Catton MD, Ghilardi JR, Levin LA, et al. Beta 2-adrenergic receptors are expressed by glia in vivo in the normal and injured central nervous system in the rat, rabbit, and human. *J Neurosci* (1995) 15:152–64.
31. Feher LZ, Kalman J, Puskas LG, Gyulveszi G, Kitajka K, Penke B, et al. Impact of haloperidol and risperidone on gene expression profile in the rat cortex. *Neurochem Int* (2005) 47:271–80. doi:10.1016/j.neuint.2005.04.020
32. Lander ES, Linton LM, Birren B, Nusbaum C, Zody MC, Baldwin J, et al. Initial sequencing and analysis of the human genome. *Nature* (2001) 409:860–921. doi:10.1038/35057062
33. Venter JC, Adams MD, Myers EW, Li PW, Mural RJ, Sutton GG, et al. The sequence of the human genome. *Science* (2001) 291:1304–51. doi:10.1126/science.1058040

34. Venter JC, Fraser CM, Harrison LC. Autoantibodies to beta 2-adrenergic receptors: a possible cause of adrenergic hyporesponsiveness in allergic rhinitis and asthma. *Science* (1980) 207:1361–3. doi:10.1126/science.6153472
35. Borda E, Pascual J, Cossio P, Delavega M, Arana R, Sterinborda L. A Circulating IgG in Chagas-disease which binds to beta-adrenoceptors of myocardium and modulates their activity. *Clin Exp Immunol* (1984) 57:679–86.
36. Labovsky V, Smulski CR, Gomez K, Levy G, Levin MJ. Anti-beta 1-adrenergic receptor autoantibodies in patients with chronic Chagas heart disease. *Clin Exp Immunol* (2007) 148:440–9. doi:10.1111/j.1365-2249.2007.03381.x
37. Wallukat G, Wollenberger A. Effects of the serum gamma globulin fraction of patients with allergic asthma and dilated cardiomyopathy on chronotropic beta adrenoceptor function in cultured neonatal rat heart myocytes. *Biomed Biochim Acta* (1987) 46:S634–9.
38. Wallukat G, Nissen E, Morwinski R, Muller J. Autoantibodies against the beta- and muscarinic receptors in cardiomyopathy. *Herz* (2000) 25:261–6. doi:10.1007/s000590050017
39. Jahns R, Boivin V, Hein L, Triebel S, Angermann CE, Ertl G, et al. Direct evidence for a beta 1-adrenergic receptor-directed autoimmune attack as a cause of idiopathic dilated cardiomyopathy. *J Clin Invest* (2004) 113:1419–29. doi:10.1172/JCI200420149
40. Zhang L, Hu D, Shi X, Li J, Zeng W, Xu L, et al. [Autoantibodies against the myocardium beta 1-adrenergic and M2-muscarinic receptors in patients with heart failure]. *Zhonghua Nei Ke Za Zhi* (2001) 40:445–7.
41. Wallukat G, Morwinski M, Kowal K, Forster A, Boewer V, Wollenberger A. Autoantibodies against the beta-adrenergic receptor in human myocarditis and dilated cardiomyopathy: beta-adrenergic agonism without desensitization. *Eur Heart J* (1991) 12(Suppl D):178–81. doi:10.1093/eurheartj/12.suppl_D.178
42. Karczewski P, Hempel P, Kunze R, Bimmler M. Agonistic autoantibodies to the alpha(1)-adrenergic receptor and the beta(2)-adrenergic receptor in Alzheimer's and vascular dementia. *Scand J Immunol* (2012) 75:524–30. doi:10.1111/j.1365-3083.2012.02684.x
43. Wallukat G, Homuth V, Fischer T, Lindschau C, Horstkamp B, Jupner A, et al. Patients with preeclampsia develop agonistic autoantibodies against the angiotensin AT1 receptor. *J Clin Invest* (1999) 103:945–52. doi:10.1172/JCI4106
44. Luther HP, Homuth V, Wallukat G. Alpha 1-adrenergic receptor antibodies in patients with primary hypertension. *Hypertension* (1997) 29:678–82. doi:10.1161/01.HYP.29.2.678
45. Jonas JB, Budde WM, Panda-Jonas S. Ophthalmoscopic evaluation of the optic nerve head. *Surv Ophthalmol* (1999) 43:293–320. doi:10.1016/S0039-6257(98)00049-6
46. Jonas JB, Gusek GC, Naumann GO. Optic disc morphometry in chronic primary open-angle glaucoma. II. Correlation of the intrapapillary morphometric data to visual field indices. *Graefes Arch Clin Exp Ophthalmol* (1988) 226:531–8. doi:10.1007/BF02169200
47. Wenzel K, Schulze-Rothe S, Haberland A, Muller J, Wallukat G, Davideit H. Performance and in-house validation of a bioassay for the determination of beta1-autoantibodies found in patients with cardiomyopathy. *Heliyon* (2017) 3:e00362. doi:10.1016/j.heliyon.2017.e00362
48. Ronspeck W, Brinckmann R, Egner R, Gebauer F, Winkler D, Jekow P, et al. Peptide based adsorbers for therapeutic immunoadsorption. *Ther Apher Dial* (2003) 7:91–7. doi:10.1046/j.1526-0968.2003.00017.x
49. Wallukat G, Muller J, Podlowski S, Nissen E, Morwinski R, Hetzer R. Agonist-like beta-adrenoceptor antibodies in heart failure. *Am J Cardiol* (1999) 83:75H–9H. doi:10.1016/S0002-9149(99)00265-9
50. Junemann AG, Herrmann M, Sheriff A, Stergiopoulos P, Schlotzer–Schrehardt U, Kruse FE, et al. Agonistic autoantibodies against beta2-adrenergic receptors in ocular hypertension and primary open-angle glaucoma. *Invest Ophthalmol Vis Sci* (2006) 47:3384.
51. Bruggemann M, Williams GT, Bindon CI, Clark MR, Walker MR, Jefferis R, et al. Comparison of the effector functions of human immunoglobulins using a matched set of chimeric antibodies. *J Exp Med* (1987) 166:1351–61. doi:10.1084/jem.166.5.1351
52. Tebo AE, Kremsner PG, Luty AJ. *Plasmodium falciparum*: a major role for IgG3 in antibody-dependent monocyte-mediated cellular inhibition of parasite growth in vitro. *Exp Parasitol* (2001) 98:20–8. doi:10.1006/expr.2001.4619
53. Grus FH, Joachim SC, Hoffmann EM, Pfeiffer N. Complex autoantibody repertoires in patients with glaucoma. *Mol Vis* (2004) 10:132–7.
54. Joachim SC, Pfeiffer N, Grus FH. Autoantibodies in patients with glaucoma: a comparison of IgG serum antibodies against retinal, optic nerve, and optic nerve head antigens. *Graefes Arch Clin Exp Ophthalmol* (2005) 243:817–23. doi:10.1007/s00417-004-1094-5
55. Joachim SC, Reichelt J, Berneiser S, Pfeiffer N, Grus FH. Sera of glaucoma patients show autoantibodies against myelin basic protein and complex autoantibody profiles against human optic nerve antigens. *Graefes Arch Clin Exp Ophthalmol* (2008) 246:573–80. doi:10.1007/s00417-007-0737-8
56. Reichelt J, Joachim SC, Pfeiffer N, Grus FH. Analysis of autoantibodies against human retinal antigens in sera of patients with glaucoma and ocular hypertension. *Curr Eye Res* (2008) 33:253–61. doi:10.1080/02713680701871157
57. Xiao RP, Avdonin P, Zhou YY, Cheng H, Akhter SA, Eschenhagen T, et al. Coupling of beta2-adrenoceptor to Gi proteins and its physiological relevance in murine cardiac myocytes. *Circ Res* (1999) 84:43–52. doi:10.1161/01.RES.84.1.43
58. Sterin-Borda L, Perez Leiros C, Wald M, Cremaschi G, Borda E. Antibodies to beta 1 and beta 2 adrenoreceptors in Chagas' disease. *Clin Exp Immunol* (1988) 74:349–54.
59. Chiale PA, Rosenbaum MB, Elizari MV, Hjalmarson A, Magnusson Y, Wallukat G, et al. High prevalence of antibodies against beta 1- and beta 2-adrenoceptors in patients with primary electrical cardiac abnormalities. *J Am Coll Cardiol* (1995) 26:864–9. doi:10.1016/0735-1097(95)00262-2
60. Elies R, Ferrari I, Wallukat G, Lebesgue D, Chiale P, Elizari M, et al. Structural and functional analysis of the B cell epitopes recognized by anti-receptor autoantibodies in patients with Chagas' disease. *J Immunol* (1996) 157:4203–11.
61. Lebesgue D, Wallukat G, Mijares A, Granier C, Argibay J, Hoebeke J. An agonist-like monoclonal antibody against the human beta(2)-adrenoceptor. *Eur J Pharmacol* (1998) 348:123–33. doi:10.1016/S0014-2999(98)00136-8
62. Caprioli J, Kim JH, Friedman DS, Kiang T, Moster MR, Parrish RK II, et al. Special commentary: supporting innovation for safe and effective minimally invasive glaucoma surgery: summary of a joint meeting of the American Glaucoma Society and the Food and Drug Administration, Washington, DC, February 26, 2014. *Ophthalmology* (2015) 122:1795–801. doi:10.1016/j.ophtha.2015.02.029
63. Sambhara D, Aref AA. Glaucoma management: relative value and place in therapy of available drug treatments. *Ther Adv Chronic Dis* (2014) 5:30–43. doi:10.1177/2040622313511286
64. Vorwerk CK, Lipton SA, Zurakowski D, Hyman BT, Sabel BA, Dreyer EB. Chronic low-dose glutamate is toxic to retinal ganglion cells - toxicity blocked by memantine. *Invest Ophthalmol Vis Sci* (1996) 37:1618–24.
65. Kerrigan LA, Zack DJ, Quigley HA, Smith SD, Pease ME. TUNEL-positive ganglion cells in human primary open-angle glaucoma. *Arch Ophthalmol* (1997) 115:1031–5. doi:10.1001/archopht.1997.01100160201010
66. Fuchsjager-Mayrl G, Wally B, Georgopoulos M, Rainer G, Kircher K, Buehl W, et al. Ocular blood flow and systemic blood pressure in patients with primary open-angle glaucoma and ocular hypertension. *Invest Ophthalmol Vis Sci* (2004) 45:834–9. doi:10.1167/iovs.03-0461
67. Goldmann H. [Out-flow pressure, minute volume and resistance of the anterior chamber flow in man]. *Doc Ophthalmol* (1951) 5-6:278–356. doi:10.1007/BF00143664
68. Bill A. The aqueous humor drainage mechanism in the cynomolgus monkey (*Macaca irus*) with evidence for unconventional routes. *Invest Ophthalmol* (1965) 4:911–9.
69. Civan MM, Macknight AD. The ins and outs of aqueous humour secretion. *Exp Eye Res* (2004) 78:625–31. doi:10.1016/j.exer.2003.09.021
70. Ericson LA. Twenty-four hourly variations in the inflow of the aqueous humour. *Acta Ophthalmol (Copenh)* (1958) 36:381. doi:10.1111/j.1755-3768.1958.tb00806.x
71. Ericson LA. Twenty-four hourly variations of the aqueous flow; examinations with perilimbal suction cup. *Acta Ophthalmol Suppl* (1958) 37:1–95.
72. Reiss GR, Lee DA, Topper JE, Brubaker RF. Aqueous-humor flow during sleep. *Invest Ophthalmol Vis Sci* (1984) 25:776–8.
73. Larsson LI, Rettig ES, Brubaker RF. Aqueous flow in open-angle glaucoma. *Arch Ophthalmol* (1995) 113:283–6. doi:10.1001/archopht.1995.01100030037018
74. Magnusson Y, Wallukat G, Waagstein F, Hjalmarson A, Hoebeke J. Autoimmunity in idiopathic dilated cardiomyopathy. Characterization of antibodies against the beta 1-adrenoceptor with positive chronotropic effect. *Circulation* (1994) 89:2760–7. doi:10.1161/01.CIR.89.6.2760

75. Wallukat G, Fu ML, Magnusson Y, Hjalmarson A, Hoebeke J, Wollenberger A. Agonistic effects of anti-peptide antibodies and autoantibodies directed against adrenergic and cholinergic receptors: absence of desensitization. *Blood Press Suppl* (1996) 3:31–6.
76. Putney LK, Vibat CR, O'donnell ME. Intracellular Cl regulates Na-K-Cl cotransport activity in human trabecular meshwork cells. *Am J Physiol* (1999) 277:C373–83. doi:10.1152/ajpcell.1999.277.3.C373
77. Wallukat G, Nemecz G, Farkas T, Kuehn H, Wollenberger A. Modulation of the beta-adrenergic response in cultured rat heart cells. I. Beta-adrenergic supersensitivity is induced by lactate via a phospholipase A2 and 15-lipoxygenase involving pathway. *Mol Cell Biochem* (1991) 102:35–47.
78. Wallukat G, Wollenberger A. Supersensitivity to beta-adrenoceptor stimulation evoked in cultured neonatal rat heart myocytes by L(+)-lactate and pyruvate. *J Auton Pharmacol* (1993) 13:1–14. doi:10.1111/j.1474-8673.1993.tb00394.x
79. Evangelho K, Mogilevskaya M, Losada-Barragan M, Vargas-Sanchez JK. Pathophysiology of primary open-angle glaucoma from a neuroinflammatory and neurotoxicity perspective: a review of the literature. *Int Ophthalmol* (2017) 37:1–14. doi:10.1007/s10792-017-0795-9
80. Wood JP, Schmidt KG, Melena J, Chidlow G, Allmeier H, Osborne NN. The beta-adrenoceptor antagonists metipranolol and timolol are retinal neuroprotectants: comparison with betaxolol. *Exp Eye Res* (2003) 76:505–16. doi:10.1016/S0014-4835(02)00335-4

Conflict of Interest Statement: (1) Patent: EP 1832600 A1 (2) RK is working for Fresenius Medical Care GmbH.

The reviewer RK declared a shared affiliation, with no collaboration, with one of the authors, HK, to the handling editor.

frontiers in Medicine

ORIGINAL RESEARCH
published: 12 February 2018
doi: 10.3389/fmed.2018.00027

IgE-Selective Immunoadsorption for Severe Atopic Dermatitis

Michael Kasperkiewicz[1], Sophie-Charlotte Mook[1], Diana Knuth-Rehr[1], Artem Vorobyev[1,2], Ralf J. Ludwig[1,2], Detlef Zillikens[1,2], Philip Muck[3] and Enno Schmidt[1,2]*

[1] Department of Dermatology, University of Lübeck, Lübeck, Germany, [2] Lübeck Institute of Experimental Dermatology, University of Lübeck, Lübeck, Germany, [3] Department of Internal Medicine, University of Lübeck, Lübeck, Germany

Introduction: Recent reports proposed the application of immunoadsorption (IA) for patients with recalcitrant atopic dermatitis (AD) and high-serum IgE levels. However, experience with this novel treatment approach, especially with the newly available IgE-specific adsorber, is limited and recommendation for its use in clinical practice awaits evidence from more studies.

Materials and methods: Patients with severe AD (SCORAD ≥ 60) and total serum IgE levels ≥750 kU/L were included in this study. The treatment protocol consisted of two cycles of five consecutive treatments with IgE-selective IA 3 weeks apart.

Results: Ten patients were enrolled and four patients completed the study. The mean SCORAD was significantly improved by up to 43% within a few weeks and until the end of a 6-month follow-up period, with 50% of patients achieving an at least 50% individual reduction of the baseline SCORAD. Each IA cycle induced a temporal average decrement of total serum levels of IgE, IgM, IgA, and IgG by 92, 43, 38, and 35%, respectively. Except for one case of *Staphylococcus aureus* septicemia, no major adverse events occurred.

Conclusion: Although limited by a considerable withdrawal rate, our observations strengthen our and other recent results further suggesting that IgE-selective IA is an effective treatment option for patients severely affected by AD with highly elevated IgE levels.

Keywords: atopic dermatitis, IgE, immunoadsorption, immunoglobulin, SCORAD

OPEN ACCESS

Edited by:
Mette Søndergaard Deleuran, Aarhus University Hospital, Denmark

Reviewed by:
Rene De Waal Malefyt, Merck, United States
Giampiero Girolomoni, University of Verona, Italy

****Correspondence:***
Michael Kasperkiewicz
michael.kasperkiewicz@uk-sh.de

Specialty section:
This article was submitted to Dermatology, a section of the journal Frontiers in Medicine

Received: *24 October 2017*
Accepted: *26 January 2018*
Published: *12 February 2018*

Citation:
Kasperkiewicz M, Mook S-C, Knuth-Rehr D, Vorobyev A, Ludwig RJ, Zillikens D, Muck P and Schmidt E (2018) IgE-Selective Immunoadsorption for Severe Atopic Dermatitis. Front. Med. 5:27. doi: 10.3389/fmed.2018.00027

INTRODUCTION

Atopic dermatitis (AD) is characterized by pruritic, eczematous skin lesions, and is commonly associated with elevated serum IgE levels. AD can considerably impact the patient's quality of life and is one of the most frequent chronic inflammatory cutaneous disorders. For patients who are severely affected by the disease, conventional immunosuppressive treatments may not show uniform efficacy and can be limited by severe side effects (1).

Although the role of IgE in the pathophysiology of AD is not fully understood, sequestering free IgE by the anti-IgE monoclonal antibody omalizumab showed some clinical benefit in AD patients with poor response to traditional therapy (2). However, studies of this treatment have yielded controversial results. A recent systematic review and meta-analysis of the efficacy of omalizumab in 103 AD patients from 13 studies revealed that serum IgE concentrations of >700 kU/L were associated with less-favorable clinical responses compared with lower levels (2). The limited effect of omalizumab in AD patients with high total IgE serum levels may be related to insufficient IgE

neutralization by omalizumab. The recommended dosing table for omalizumab is limited to 150–1,200 mg/month, according to total IgE concentrations within a range between 30 and 1,500 kU/L (3).

While adjuvant immunoadsorption (IA) has been introduced in dermatology by its successful application in patients with severe and/or refractory pemphigus (4), its use in AD is still limited to individual centers. We and others, however, have recently demonstrated that IA may represent an alternative IgE depletion method in patients with very high IgE concentrations leading to normalization of cutaneous inflammation parameters and clinical improvement of AD (5–9). While panimmunoglobulin IA was initially employed, an IgE-specific adsorber column has more recently become available (6, 9). Since experience with this novel treatment approach in AD is limited and recommendation for its use in clinical practice will require more clinical data, we employed IgE-selective IA in a further series of patients with severe AD and considerably elevated serum IgE levels. For this group of patients, there still remains a large unmet medical need for powerful new treatment options.

MATERIALS AND METHODS

Patients

In this study, 10 patients (seven males and three females, mean age 40.3 ± 18.7, range 18–70 years) with severe AD [mean SCORAD (SCORing AD index) 67.5 ± 5.4, range 61.5–81] and greatly elevated serum IgE levels (mean 5,377.7 ± 6,775.3 kU/L, range 931–21,510 kU/L) were enrolled at the Department of Dermatology of the University of Lübeck. The inclusion criteria were as follows: (1) severe AD, i.e., SCORAD ≥ 60, requiring systemic immunosuppressive treatment, (2) total serum IgE level ≥750 kU/L, and (3) ≥18 years of age. The exclusion criteria were as follows: (1) known hypersensitivity or allergy to materials used in the adsorber columns, (2) no possibility of an adequate anticoagulation (e.g., multiple allergies to various anticoagulants), (3) bleeding disorders including hypo- and hypercoagulabilities, (4) severe cardiovascular disease (cardiac failure, NYHA III and IV), (5) severe systemic infections extending beyond skin, (6) serum IgG level <250 mg/dL, (7) severe immunodeficiency (e.g., AIDS), (8) treatment with an angiotensin-converting enzyme inhibitor that could not be omitted 72 h before IA, and (9) pregnancy. The majority of patients had previously not adequately responded to or had side effects from treatment with systemic corticosteroids and/or cyclosporine A. Written informed consent was obtained from all patients before participation in this study, which was approved by the ethics committee of the University of Lübeck and followed the Declaration of Helsinki.

Treatment

Two cycles of five IA sessions on days 1 to 5 (week 1) and days 29 to 33 (week 5) were performed as described previously (5, 6), except for one patient in whom the second cycle was split into two parts (2 × IA and 3 × IA 2 weeks apart) because of an adverse event. In each IA, plasma was separated using a blood cell separation technique (Life-18 Apheresis Unit; Miltenyi Biotec, Bergisch Glattbach, Germany) followed by alternate application of two patient plasma volumes to two adsorption columns (30–35 cycles of approximately 8,000 mL separated plasma) containing monoclonal mouse anti-human IgE (TheraSorb®-IgE; Miltenyi Biotec).

In half of the patients, a peripheral venous catheter was used, and in the other half, central venous access was required due to difficult peripheral veins. Patients receiving a central venous catheter were instructed to prophylactically apply topical fusidic acid to the neck area for 3 days before each IA cycle. Previous topical [corticosteroids ($n = 9$ patients in total; class I: $n = 1$, class II: $n = 1$, class III: $n = 1$, class IV: $n = 3$, class V: $n = 2$, class VII: $n = 3$), calcineurin inhibitors ($n = 1$; tacrolimus)] and/or systemic treatments [antihistamines ($n = 5$ patients in total; cetirizine 10–20 mg/day: $n = 3$, hydroxyzine 25 mg/day: $n = 3$, desloratadine 20 mg/day: $n = 1$, loratadine 20 mg/day: $n = 1$), corticosteroids ($n = 1$; prednisolone 10 mg/day), cyclosporine A ($n = 0$)] were initially continued without change of frequency and/or dosage and were subsequently allowed to be modified as needed.

Clinical and Laboratory Examinations

Patients were prospectively assessed by dermatologists both as inpatients (on the days when IA was performed) and outpatients at the Department of Dermatology of the University of Lübeck. During a follow-up period of up to 6 months following IA (weeks 1, 3, 5, 9, 13, 17, and 25), the SCORAD index was applied to evaluate the clinical course of the patients. Additionally, the use of concomitant therapy for AD and adverse events were documented. Total levels of serum IgE, IgG, IgM, and IgA were measured before and after IA using the UniCAP system (Phadia; IgE) and the BN Prospec Nephelometer system (Siemens; IgG, IgM, and IgA) (5).

Statistical Analyses

Data are presented as means ± SD (SCORAD) and box-and-whisker plots (serum immunoglobulins). Repeated measurements of SCORAD were compared with baseline values using one-way ANOVA, with $P < 0.05$ considered statistically significant.

RESULTS

Clinical Course

Of the 10 patients enrolled, two patients withdrew from the study due to an adverse event (central venous catheter-associated *Staphylococcus aureus* septicemia and pain related to intravenous catheter insertion, respectively) during the first IA cycle. Two other patients dropped out because of a coping/compliance problem and absence from follow-up examinations in week 5, but were included in the analysis. Other adverse events included fatigue in one patient necessitating to split the second IA cycle into two parts and edema formation of the hands and feet in another patient. Otherwise, IA was relatively well tolerated.

The mean initial SCORAD (68.3 ± 5.7) improved significantly by 19% at week 3 (to a mean score of 54.5 ± 9.9; $p < 0.05$), by 29% at week 5 (to a mean score of 48.0 ± 10.7; $p < 0.001$), by 43% at week 9 (to a mean score of 38.9 ± 18.5; $p < 0.001$), by 21% at week 13 (to a mean score of 54.0 ± 8.0 $p < 0.05$), by 25% at week 17

(to a mean score of 50.6 ± 14.2; $p < 0.01$), and by 29% at week 25 (to a mean score of 48.2 ± 13.1; $p < 0.01$), with individual maximal SCORAD reductions ranging from 15 to 80% and a SCORAD50 response (i.e., an at least 50% reduction of the baseline SCORAD) in 50% of patients. A slight increase in the mean SCORAD was observed in week 13, although by this time and later, only 3–4 patients could be analyzed as the remainder had dropped out or was additionally lost to follow-up (**Table 1**; **Figures 1** and **2**).

There were generally no major changes in the use of the previously prescribed topical and systemic medications during the study, except for one patient in whom cyclosporine A (250 mg/day) was reinitiated because of worsening of the disease in week 17.

Serum Immunoglobulin Levels

Each IA cycle induced an average decrement of total IgE levels by 92%. Less substantial reductions in IgM, IgA, and IgG were found, with means of 43, 38, and 35%, respectively. Levels of all immunoglobulins were lowered only transiently and reached similar precycle values again (**Figure 3**).

TABLE 1 | Individual SCORAD values of the analyzed study patients.

Pat. no.	Week 1 (1. IA cycle)	Week 3	Week 5 (2. IA cycle)	Week 9	Week 13	Week 17	Week 25
1	69.5	61.0	65.5	58.5	61.5	61.5	61.5
2	66.5	40.2	35.2	26.0	–	–	43.5
3	68.0	62.5	53.0	44.4	45.5	34.5	32.0
4	64.5	61.2	56.1	–	55.0	56.0	56.0
5	69.0	–	39.0	14.0	–	–	–
6	67.0	–	54.6	–	–	–	–
7	61.5	–	43.3	–	–	–	–
8	81.0	48.0	38.0	52.0	–	–	–

IA, immunoadsorption.

DISCUSSION

We recently reported a successful response of a series of treatment-refractory AD patients with excessively high-serum IgE levels to panimmunoglobulin IA and two such patients to IgE-selective IA (5, 6). Using the same treatment protocol of two cycles of five apheresis sessions as in these previous case series, this new study with a further cohort of patients with severe AD and greatly elevated IgE levels extends our knowledge regarding the efficacy of IgE-specific IA. Although somewhat lower mean SCORAD reductions were observed compared with our two preceding reports (e.g., by 19% and 33–38% at week 3 and by 21% and 53–59% at week 13, respectively) (5, 6), the observed clinical improvements were still constantly significant at all examination time points including the last follow-up week 25 compared with baseline.

Recently, an independent head-to-head comparison trial of three cycles of a total of 10 IA sessions of either panimmunoglobulin IA or IgE-selective IA applied over a 2-month period in patients with severe AD with excessive IgE levels revealed that there are no major differences in the positive clinical response between the two different IA treatment groups (9).

Like in our two previous studies (5, 6), serum IgE levels were effectively but transiently reduced by a mean of more than 90% with each IA cycle. In contrast to panimmunoglobulin IA which decreased all other immunoglobulin isotypes to a similar degree (5), serum concentrations of IgM, IgA, and IgG were found to be reduced by only less than half with the IgE-selective adsorber.

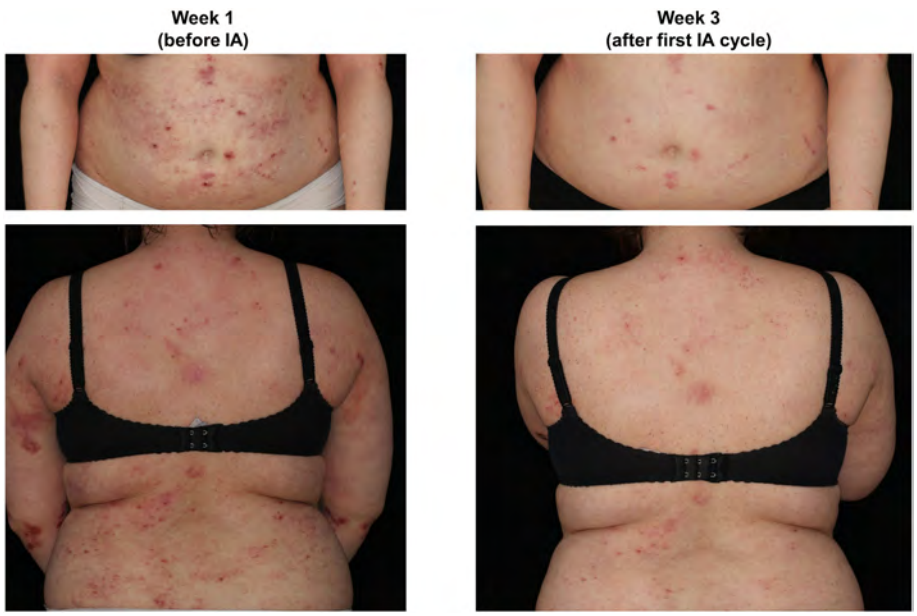

FIGURE 1 | Representative presentation of a study patient before (week 1) and after immunoadsorption (IA) (week 3).

This latter finding is considered to be nonspecific and has been attributed to IA-related elution and dilution procedures as reported before (6, 9).

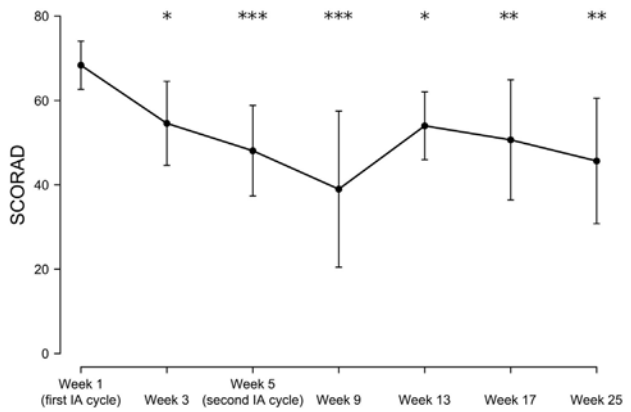

FIGURE 2 | Time-dependent mean SCORAD changes following immunoadsorption (IA). n = 3–8 patients (8, 5, 8, 5, 3, 3, and 4 patients at week 1, 3, 5, 9, 13, 17, and 25, respectively). $^{*}P < 0.05$, $^{**}P < 0.01$, and $^{***}P < 0.001$.

Correlation between serum IgE levels and AD severity has been suggested, but study results are partly conflicting (10, 11). A recent study combining panimmunoglobulin IA for 2–4 days with subsequent biweekly omalizumab treatment for 6 months showed that after initial reduction in total serum IgE levels by IA, free IgE levels continued to fall during omalizumab administration and began to increase again during treatment-free follow-up. In addition, in parallel with free IgE levels, an improvement in AD was found during the treatment period, with aggravation during follow-up (8). On the other hand, we and others showed that a prolonged decrease of the SCORAD is not hampered by the commonly seen reincrease in serum IgE that occurs within a relatively short time after IA (5–7, 9). Since in our initial study, an IA-induced continuous reduction of the amount of skin-bound IgE was observed, which correlated with histoimmunological and clinical improvements (5), we speculate that this indirect effect rather than a sole impact of IA on circulating IgE contributes to amelioration of AD. In fact, omalizumab has been previously shown to interfere with antigen processing and presentation to T cells by downregulating IgE-Fcε receptor I expression on dendritic cells (12). Nevertheless, the role of circulating and tissue-bound IgE in the pathogenesis and disease activity of AD as well as the detailed mechanistic

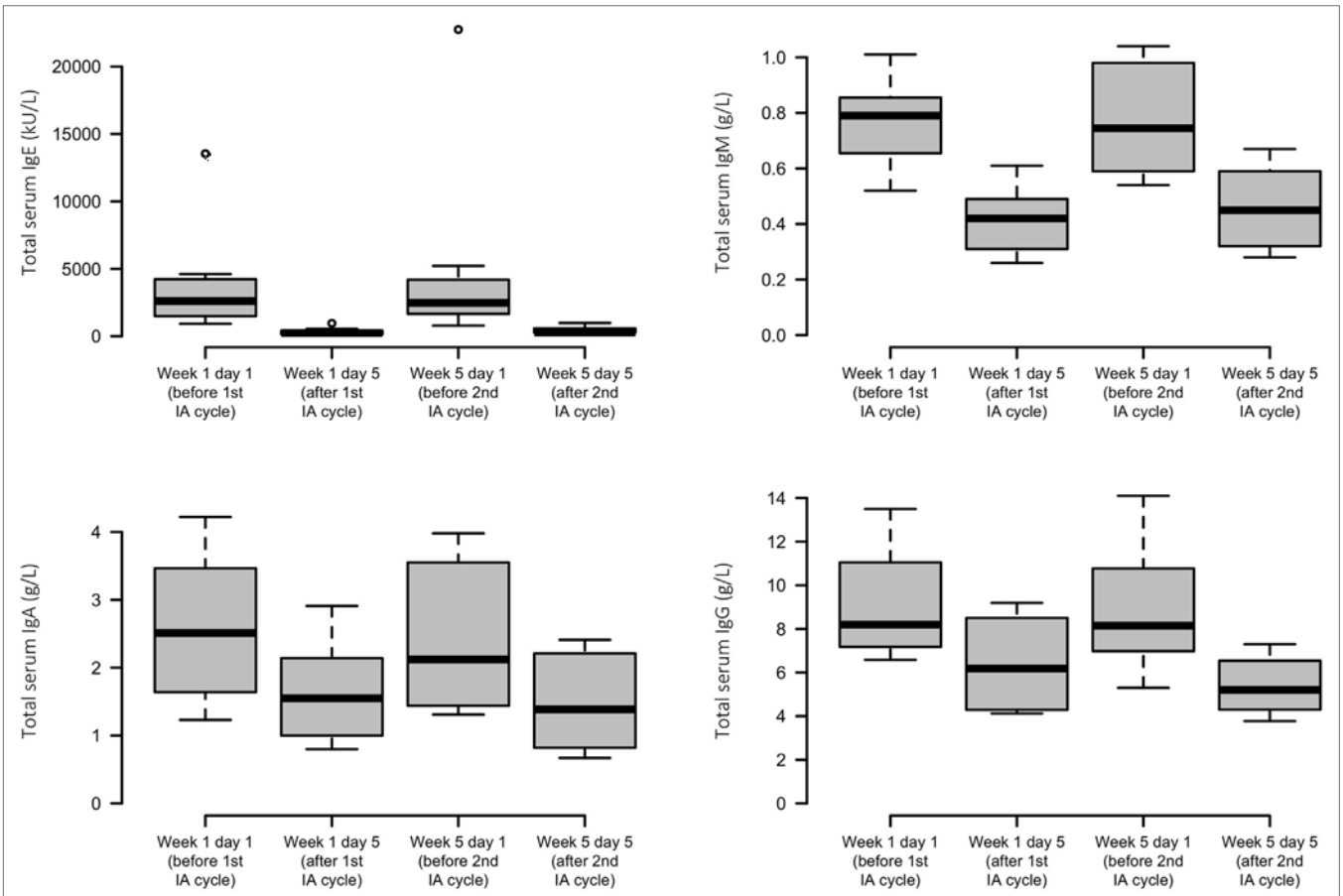

FIGURE 3 | Effects of immunoadsorption (IA) on serum immunoglobulin levels. Box plots of peripheral IgE, IgM, IgA, and IgG levels of the study patients before and after each IA cycle; n = 6–8 patients (varying by time point and analyte).

interaction of IA with IgE-associated processes in this disease remain in need of further elucidation.

It also remains to be clarified which kind of IA protocol is best suited for AD patients and how long they can ultimately benefit from this treatment. The published trials so far using different IA protocols with follow-up times ranging from 3 to 18 months uniformly revealed a satisfactory initial linear response after treatment (5–9). Results from this current study and our former two reports indicate that IA treatment results in continuous and stable clinical improvements of at least 3–6 months (5, 6), although some minor reincreases in the SCORAD were observed during the second half of the extended observation timeframe (from 3 months in the panimmunglobulin IA trial up to 6 months) in this and our previous IgE-selective IA case series (6). However, this slight worsening in the mean disease severity observed in the current investigation, which was still significantly lower than before initiation of IA, could be at least partly explained by a potential bias due to the relatively high proportion of patients who dropped out or were additionally lost to follow-up during this time period. In fact, the considerable withdrawal rate, the observation that concomitant AD treatment was basically not reduced or discontinued during the study, and the lack of an appropriate control group represent major limitations in judging the effects of adjuvant IA in this patient cohort.

In the study by Reich et al. (9), clinical effects remained stable until 6 months of follow-up in the IgE-selective IA group and slightly reincreased toward the last visit in the panimmunoglobulin arm. As mentioned before, the IA-omalizumab combinatory study revealed a steady decrease in the SCORAD throughout the 6-month treatment period, whereas a reverse trend was observed during follow-up of another 6 months (8). Finally, a study that investigated the efficacy of 1–5 series of panimmunoglobulin IA, each consisting of five consecutive treatments performed on a monthly regimen, revealed no additional benefit with regard to further SCORAD improvement when more than three series were applied. However, one of the patients of this study who completed five IA series exhibited a long lasting clinical benefit over 12 months (7).

A shortcoming of panimmunoglobulin IA is the patient's potential risk of infections because of the parallel reduction of protective immunoglobulins. In fact, in the study directly comparing unspecific with specific IA in AD, infectious adverse events were limited to the panimmunoglobulin group and comprised herpes labialis/keratitis and bacterial conjunctivitis/sinusitis (9). In contrast, however, a central venous catheter-related *S. aureus* septicemia was observed in both our previous and current study using the nonselective and selective adsorber, respectively (5). Thus, even with IgE-specific IA, a thorough risk-benefit assessment is advised especially for patients in whom a peripheral venous access is not possible, considering that AD is strongly associated with increased susceptibility to skin infections by this bacterial pathogen.

In conclusion, our observations strengthen our and other recent results further suggesting that IgE-selective IA is an effective treatment option for patients severely affected by AD with highly elevated IgE levels. However, given the limitations of this study, including the relatively small number of patients, these results should certainly be considered suggestive rather than definite. In fact, considering that IA has only recently been introduced and that it represents a so far restrictedly used new treatment method for AD, information on efficacy and safety currently still relies on low-level evidence case series. Nevertheless, collection of available data even from these small studies, including the current one, may be important for future meta-analyses or systematic reviews to generate better estimates of the treatment outcomes and may also serve as basis for a potential randomized controlled trial. Thus, future investigations are required to better characterize, among others, the long-term effects and cost–benefit (approximately 6,000 euro for a reusable TheraSorb®-IgE adsorber column pair allowing for up to 10 treatment sessions) of IA in AD, for which more optimized treatment protocols still need to be defined.

ETHICS STATEMENT

This study was carried out in accordance with the recommendations of the ethics committee of the University of Lübeck with written informed consent from all subjects. All subjects gave written informed consent in accordance with the Declaration of Helsinki. The protocol was approved by the ethics committee of the University of Lübeck.

AUTHOR CONTRIBUTIONS

MK, RL, DZ, and ES contributed to the conception and design of study and analyzed the data. MK, S-CM, DK-R, and PM contributed to the data acquisition. MK, S-CM, DK-R, AV, RL, DZ, PM, and ES interpreted the data, drafted the manuscript, approved the final version of the manuscript, and agreed to be accountable to all aspects of this work. MK, S-CM, DK-R, AV, RL, DZ, PM, and ES approved the final version of the manuscript.

FUNDING

This work was supported by infrastructural funding provided by Deutsche Forschungsgemeinschaft Excellence Cluster Inflammation at Interfaces (EXC 306/2).

REFERENCES

1. Weidinger S, Novak N. Atopic dermatitis. *Lancet* (2016) 387:1109–22. doi:10.1016/S0140-6736(15)00149-X
2. Wang HH, Li YC, Huang YC. Efficacy of omalizumab in patients with atopic dermatitis: a systematic review and meta-analysis. *J Allergy Clin Immunol* (2016) 138:1719–22. doi:10.1016/j.jaci.2016.05.038
3. Kornmann O, Watz H, Fuhr R, Krug N, Erpenbeck VJ, Kaiser G. Omalizumab in patients with allergic (IgE-mediated) asthma and IgE/bodyweight combinations above those in the initially approved dosing table. *Pulm Pharmacol Ther* (2014) 28:149–53. doi:10.1016/j.pupt.2014.03.003
4. Meyersburg D, Schmidt E, Kasperkiewicz M, Zillikens D. Immunoadsorption in dermatology. *Ther Apher Dial* (2012) 16:311–20. doi:10.1111/j.1744-9987.2012.01075.x

5. Kasperkiewicz M, Schmidt E, Frambach Y, Rose C, Meier M, Nitschke M, et al. Improvement of treatment-refractory atopic dermatitis by immunoadsorption: a pilot study. *J Allergy Clin Immunol* (2011) 127:267–70. doi:10.1016/j.jaci.2010.07.042
6. Kasperkiewicz M, Süfke S, Schmidt E, Zillikens D. IgE-specific immunoadsorption for treatment of recalcitrant atopic dermatitis. *JAMA Dermatol* (2014) 150:1350–1. doi:10.1001/jamadermatol.2014.2082
7. Daeschlein G, Scholz S, Lutze S, Eming R, Arnold A, Haase H, et al. Repetitive immunoadsorption cycles for treatment of severe atopic dermatitis. *Ther Apher Dial* (2015) 19:279–87. doi:10.1111/1744-9987.12267
8. Zink A, Gensbaur A, Zirbs M, Seifert F, Suarez IL, Mourantchanian V, et al. Targeting IgE in severe atopic dermatitis with a combination of immunoadsorption and omalizumab. *Acta Derm Venereol* (2016) 96:72–6. doi:10.2340/00015555-2165
9. Reich K, Deinzer J, Fiege AK, von Gruben V, Sack AL, Thraen A, et al. Panimmunoglobulin and IgE-selective extracorporeal immunoadsorption in patients with severe atopic dermatitis. *J Allergy Clin Immunol* (2016) 137:1882–4. doi:10.1016/j.jaci.2016.01.016
10. Laske N, Niggemann B. Does the severity of atopic dermatitis correlate with serum IgE levels? *Pediatr Allergy Immunol* (2004) 15:86–8. doi:10.1046/j.0905-6157.2003.00106.x
11. Murat-Susić S, Lipozencić J, Zizić V, Husar K, Marinović B. Serum eosinophil cationic protein in children with atopic dermatitis. *Int J Dermatol* (2006) 45:1156–60. doi:10.1111/j.1365-4632.2006.02865.x
12. Prussin C, Griffith DT, Boesel KM, Lin H, Foster B, Casale TB. Omalizumab treatment downregulates dendritic cell FcepsilonRI expression. *J Allergy Clin Immunol* (2003) 112:1147–54. doi:10.1016/j.jaci.2003.10.003

Conflict of Interest Statement: The authors declare that the research was conducted in the absence of any commercial or financial relationships that could be construed as a potential conflict of interest.

frontiers in Immunology

REVIEW
published: 12 February 2018
doi: 10.3389/fimmu.2018.00097

A New Classification System for IgG4 Autoantibodies

*Inga Koneczny**

Institute of Neurology, Medical University of Vienna, Vienna, Austria

IgG4 autoimmune diseases are characterized by the presence of antigen-specific autoantibodies of the IgG4 subclass and contain well-characterized diseases such as muscle-specific kinase myasthenia gravis, pemphigus, and thrombotic thrombocytopenic purpura. In recent years, several new diseases were identified, and by now 14 antigens targeted by IgG4 autoantibodies have been described. The IgG4 subclass is considered immunologically inert and functionally monovalent due to structural differences compared to other IgG subclasses. IgG4 usually arises after chronic exposure to antigen and competes with other antibody species, thus "blocking" their pathogenic effector mechanisms. Accordingly, in the context of IgG4 autoimmunity, the pathogenicity of IgG4 is associated with blocking of enzymatic activity or protein–protein interactions of the target antigen. Pathogenicity of IgG4 autoantibodies has not yet been systematically analyzed in IgG4 autoimmune diseases. Here, we establish a modified classification system based on Witebsky's postulates to determine IgG4 pathogenicity in IgG4 autoimmune diseases, review characteristics and pathogenic mechanisms of IgG4 in these disorders, and also investigate the contribution of other antibody entities to pathophysiology by additional mechanisms. As a result, three classes of IgG4 autoimmune diseases emerge: class I where IgG4 pathogenicity is validated by the use of subclass-specific autoantibodies in animal models and/or *in vitro* models of pathogenicity; class II where IgG4 pathogenicity is highly suspected but lack validation by the use of subclass specific antibodies in *in vitro* models of pathogenicity or animal models; and class III with insufficient data or a pathogenic mechanism associated with multivalent antigen binding. Five out of the 14 IgG4 antigens were validated as class I, five as class II, and four as class III. Antibodies of other IgG subclasses or immunoglobulin classes were present in several diseases and could contribute additional pathogenic mechanisms.

Keywords: IgG4 autoimmunity, IgG4, autoimmunity, neuronal autoantibodies, muscle-specific kinase myasthenia gravis, thrombotic thrombocytopenic purpura, pemphigus, IgG4-related disease

OPEN ACCESS

Edited by:
Ralf J. Ludwig,
University of Lübeck, Germany

Reviewed by:
Jun-ichi Kira,
Kyushu University, Japan
Lars Komorowski,
Institute of Experimental Immunology Affiliated to Euroimmun AG, Germany

***Correspondence:**
Inga Koneczny
inga.koneczny@gmail.com

Specialty section:
This article was submitted to Immunological Tolerance and Regulation, a section of the journal Frontiers in Immunology

Received: *16 November 2017*
Accepted: *12 January 2018*
Published: *12 February 2018*

Citation:
Koneczny I (2018) A New Classification System for IgG4 Autoantibodies.. Front. Immunol. 9:97. doi: 10.3389/fimmu.2018.00097

INTRODUCTION

Autoantibodies are key pathogenic players in a wide range of autoimmune diseases. Immunoglobulins (Ig) of IgG or IgM class that bind either to cell surface-expressed or extracellular matrix antigens induce organ-specific damage in type II hypersensitivity diseases. More systemic autoimmune diseases are classified as type III hypersensitivity diseases and are characterized by circulating IgG and

Abbreviations: ADAMTS13, disintegrin and metalloproteinase with thrombospondin motifs 13; CIDP, chronic inflammatory demyelinating polyneuropathy; CNTN1, contactin 1; Caspr1,2, contactin associated protein1,2; Dsg1,3, desmoglein 1, 3; DPPX, dipeptidyl peptidase-like protein 6; FAE, Fab-arm exchange; GSH, glutathione; Iglon5, IgLON family member 5; Lgi1, leucine-rich, glioma-inactivated 1; Lrp4, low-density lipoprotein receptor-related protein 4; MBL, mannose-binding lectin; MuSK, muscle-specific kinase; MG, myasthenia gravis; PLA2R, phospholipase A2 receptor; THSD7A, thrombospondin type-1 domain-containing 7A; TTP, thrombotic thrombocytopenic purpura; vWF, von Willebrand factor.

IgM as well as IgA that binds soluble antigen and forms immune complexes. Antibody-mediated autoimmune diseases include many different pathogenic mechanisms [reviewed in detail by Ref. (1)]. Among these are complement activation, recruitment of immune cells *via* Fc receptors (leading to antibody-dependent cellular cytotoxicity, opsonization, phagocytosis, and overall immune-mediated damage and inflammation), cross-linking of antigen that leads to immune complex formation or endocytosis of transmembrane antigen, or the direct modulation of antigen function. With the exception of the latter, these mechanisms rely on antibody class and subclass, particularly on the sequence and structure of the constant regions. Single amino acids in the constant region of IgG4 are responsible for structural differences that render it unable to exert most of the known pathogenic functions of antibodies. Despite their immunological inertness, several well-described autoimmune diseases are caused by IgG4 subclass autoantibodies, such as pemphigus, muscle-specific kinase (MuSK) myasthenia gravis (MG), and thrombotic thrombocytopenic purpura (TTP), and in recent years the number of potential IgG4 autoimmune diseases has rapidly grown. By now, 14 autoantigens are known that are targeted by IgG4 subclass autoantibodies; these antigens are found throughout the body (**Table 1**), with more than half being located in the central and peripheral nervous system. Whether all of the newly described IgG4 autoantibodies are pathogenic at all, if so by what mechanism, and if they are the sole pathogenic entity in their disease are essential questions that have been addressed to variable extent in the different fields. Here, we review what is known about IgG4 autoantibodies within the scope of IgG4 autoimmunity and attempt to analyze and classify proposed IgG4 autoimmune diseases based on a set of modified Witebsky postulates to validate IgG4 pathogenicity.

IgG4: FROM STRUCTURE TO FUNCTION

IgG4 Structure

IgG is the predominant antibody class and one of the most abundant glycoproteins in the human plasma with concentrations of approximately 7–15 g/L. In humans, four subclasses are known, IgG1, 2, 3 and 4, which are named in descending order of frequency (136). IgG4 is the least common IgG subclass, comprising only 5% of total IgG (137, 138). It is important to keep in mind that there is a different distribution in mice which are often used as animal models for pathogenicity, here the IgG1 subclass is the non-complement fixing subclass equivalent to IgG4, and in addition there are complement fixing IgG2a, IgG2b, and IgG3 subclasses (139–141). Also, there is different capability of human IgG to bind to rodent complement or Fc receptors, which needs to be considered in passive transfer models, e.g., by additional transfer of human complement (142).

The four human IgG subclasses share a similar structure with over 90% sequence homology. IgGs are heterotetramers, consisting of two heavy (50 kDa) and two light chains (25 kDa) of either κ or λ type. The heavy chain consists of three constant domains (C_H) that mediate the antibody effector functions, a hinge region between C_H1 and C_H2, and one N-terminal variable domain (V_H), which recognizes antigen. Similarly, the light chain is comprised of one variable (V_L) antigen binding and one constant (C_L) region. The V_H contains three complementarity-determining regions (CDR 1–3). These three CDRs, and particularly the CDR3, are hypervariable to allow for improved and highly specific binding of antigen. Increased mutation rates at this genetic locus indicate antigen-driven somatic mutations.

Disulfide bridges connect the light and heavy chains to form half-antibodies (HL), and two HL are joined together by covalent and non-covalent interactions between the heavy chains to form a whole antibody (H_2L_2). The heavy chains are mainly connected by disulfide bridges in the hinge region, which vary in numbers between the IgG subclasses. IgG1 and IgG4 have two disulfide bridges in the hinge region, while IgG2 has four and IgG3 11 (143–145). The disulfide bonds that connect heavy and light chains also vary between subclasses, in IgG1 they connect the n-term of the C_L domain with the c-term of the C_H1 domain, while in IgG2–4 the c-term of the C_L domain is connected to the n-term of the C_H1 region.

Upon enzymatic digestion with papain, antibodies are divided into three fragments, one Fc fragment ("Fragment crystallized"), consisting of the C_H2–C_H3 of both heavy chains including the hinge, and two Fab fragments ("Fragment, antigen binding"), consisting of the C_H1, V_H, C_L, and V_L. The corresponding regions in the intact antibody are thus named "Fab" or "Fc" region [**Figure 1A**, reviewed by Ref. (146)]. Particularly interesting in IgG4 is the hinge and Fc region; while there is a high degree of homology between the IgG subclasses, there are single amino acid differences that have immediate consequences for IgG4 structure and effector function.

Functional Characteristics of IgG4: Immunological Inertness and Fab-Arm Exchange (FAE)

Single amino acid changes in the C_H2 region (exchange of a proline for a serine at position 331, "P331S") prevent binding of the protein C1q (148, 149), the initial binding molecule of the classic complement cascade, and together with further changes (single amino acid replacements of L234F, P331S, and A327G) also cause a reduced binding to activating Fcγ receptors, but not to the inhibitory FcγRIIb (150–155). The exchange of a proline for a serine in the IgG4 hinge region at position 228 compared to IgG1 (P228S) leads to greater stereometric flexibility. This flexibility allows disulfide bridges in the hinge to additionally form within the same heavy chain ("intra-chain" disulfide bonds) instead connecting the two heavy chains ("inter-chain" disulfide bonds). Under reducing conditions, these states are dynamic and in equilibrium [**Figure 1A** (156–158)]. Together with reduced non-covalent interactions between the heavy chains in the C_H3 region caused by an arginine instead of lysine (R409K) (159, 160), the two HL can dissociate (161–163) and recombine with other HL, in a process termed FAE [**Figure 1B** (161, 164–166)]. The resulting antibodies are bispecific and can cross-link two different

TABLE 1 | Classification of IgG4 autoimmune diseases.

Disease	Antigen	Epitope	Other antibodies	Antibody binding to affected organ	Pathogenic mechanism of IgG4	Active immunization or passive transfer model	Biopsy/imaging finding	Other pathogenic mechanisms	References
Class I diseases									
MuSK-MG	MuSK	Ig-like domain 1,2, CARD domain	10% IgG1, 2	Neuromuscular junction	Yes. Block of MuSK–Lrp4 and reduced AChR clustering, block of MuSK–ColQ interaction	Yes, passive transfer of serum and IgG4, active immunization	Pre- and postsynaptic abnormalities at the NMJ	IgG1/2? MuSK endocytosis? Block of retrograde signaling?	(2–28)
CIDP	CNTN1	Ig-like domains (protein core, glycosylation independent)	IgG2, 3	Paranodal axoglial junctions of motoneurons	Yes. Block of contactin/Caspr and NF155 interaction, paranode dismantling	Yes, passive transfer of IgG4	Nerve: transverse band loss and paranodal loop detachment	N/A	(29–35)
Pemphigus foliaceus Pemphigus vulgaris	Dsg1 Dsg3	N-terminal EC1 and EC2 domains, others	IgG1, 2, 3, IgA	Keratinocytes mostly in superficial layers of the skin Keratinocytes mostly in basal/ parabasal layers of the skin	Yes. Block of cell adhesion, cell sheet dissociation in cultured human keratinocytes, and human skin explants. Pathogenicity was reduced after depletion of IgG4	Yes, several different models, e.g., passive transfer of cloned patient abs (IgG4). Also passive transfer from pregnant women to the fetus	Antibodies in circulation, patient skin and mucosal keratinocytes	IgG1, Dsg clustering and endocytosis, and keratinocyte signaling	(36–57)
Thrombotic thrombocytopenic purpura	ADAMTS13	5 small solvent-exposed loops in the spacer domain, others	IgG1, 2, 3, IgM, IgA	IgG in blood circulation (ADAMTS13 is a secreted protease)	Yes. Cloned IgG4 blocked ADAMTS13 protease activity which leads to von Willebrand Factor (vWF) accumulation and microthrombosis	Yes, transfection with recombinant anti-ADAMTS13 scFv cloned from patients, passive transfer of mAbs to baboons	IgG4 levels associated with relapse, circulating antigen/ antibody complexes, some patients have exclusively IgG4	Yes. IgG1 cloned from patients also blocked ADAMTS13 activity. IgG, IgM: other mechanisms may include complement activation and clearing of ADAMTS13 from the circulation	(58–69)
Class II diseases									
Encephalitis, Morvan's syndrome	Lgi1	Leucine-rich repeat and EPTP repeat domains	IgG1, 2	Synaptic cleft of CNS neurons, hippocampal neurons	Unclear. Serum: block of Lgi1–ADAM22 interaction and reduction of AMPA receptors *in vitro*, excitation of hippocampal CA3 pyramidal cells *ex vivo*	N/A	Brain atrophy in encephalitis-associated regions	CD8+ T cells, complement activation	(70–78)
CIDP, AIDP	Neurofascin 155	Fibronectin type III domains (FN3, FN4), N-glycosylated	IgG1,2, 3, IgM, and IgA	Central and peripheral paranodes	No. Suspected: block of NF155–CNTN1–CASPR1 interaction	N/A	Sural nerve: paranodal demyelination	N/A	(32, 79–85)
CNS and PNS disorders	CASPR2	N-Terminal discoidin and laminin γ1 modules of Caspr2 (glycosylation independent)	IgG1 in 12–63%	Juxtaparanodal region of myelinated axons, hippocampal GABAergic interneurons	No. Suspected: serum could affect Gephyrin clustering by blocking TAG1–Caspr2 interaction	N/A	IgG depositions in brain biopsy of 1 patient (but also complement)	Complement depositions and immune cell infiltrates in brain biopsy in 1 patient	(86–96)

(*Continued*)

TABLE 1 | Continued

Disease	Antigen	Epitope	Other antibodies	Antibody binding to affected organ	Pathogenic mechanism of IgG4	Active immunization or passive transfer model	Biopsy/imaging finding	Other pathogenic mechanisms	References
Membranous nephropathy	PLA2R	Conformational epitope in tertiary structure of CysR domain, some also in CTLD1 and CTLD7	IgG1,3	Podocytes (kidney)	No. Suspected: atypical complement activation *via* the lectin pathway by IgG4 (serum/biopsies/purified IgG4, data not published). Block of podocyte adhesion to collagen IV?	No, due to technical challenges: PLA2R is not expressed in rodent podocytes	PLA2R-IgG in patient kidney biopsies	IgG1/3, classical complement activation	(97–109)
Membranous nephropathy	THSD7A	N/A, conformational epitope	IgG1,3	Podocytes (kidney)	Unclear, possibly a functional block of cell adhesion or altered signal transduction. Changes in architecture in cultured podocyte cells induced by IgG. Detachment and apoptosis of THSD7A overexpressing HEK293 cells	Yes, passive transfer of purified human or rabbit anti-THSD7A to mice, absence of complement deposition, altered podocyte architecture, increased stress fiber formation, activation of signaling at focal adhesions	Renal biopsy: IgG4 staining	IgG1/3? Complement staining (C5b-9)	(110–118)
Class III diseases									
Goodpasture syndrome	Type IV collagen	Alpha 3 chain of NCI domain	IgG1, 2, 3 (in few patients)	Glomerular basement membrane (kidney), lungs not tested	N/A	N/A	IgG deposition in glomerular basement membrane (kidney biopsy)	N/A	(119–123)
CIDP	CASPR1	N/A	IgG1	Paranodes (murine teased fibers)	N/A	N/A	Axonal degeneration		(35, 124)
DPPX encephalitis	DPPX	Extra- and intra-cellular domains (DPPX-L/S/X)	IgG1,2	Somatodendritic and perisynaptic neuronal surface, hippocampus, small intestine	No. Modulation/loss of DPPX and Kv4.2 by total IgG likely by IgG1/2. Hyperexcitation of enteric neurons.		Cerebrospinal (CSF) pleocytosis, increased IgG index or oligoclonal bands, and abnormal brain MRI	Modulation/loss of DPPX and Kv4.2 by total IgG likely by IgG1/2. Hyperexcitation of enteric neurons	(125–129)
Iglon5 parasomnia	Iglon5	Ig-like domain 2 (non-glycosylated)	IgG1, 2	Rat brain neuropil	N/A	N/A	Brainstem, hypothalamus: neuronal loss, deposits of hyperphosphorylated tau	IgG1 induces endocytosis of Iglon5	(130–135)

ADAMTS13, disintegrin and metalloproteinase with thrombospondin motifs 13; Caspr, contactin-associated protein; CIDP, chronic inflammatory demyelinating polyradiculoneuropathy; CNTN1, contactin 1; DPPX, dipeptidyl peptidase-like protein 6; Dsg1, desmoglein 1; Dsg3, desmoglein 3; Ig, immunoglobulin; Iglon5, IgLON family member 5; Lgi1, leucine-rich, glioma-inactivated 1; Lrp4, low-density lipoprotein receptor-related protein 4; MUSK, muscle-specific kinase; PLA2R, phospholipase A2 receptor; scFv, single chain variable region fragments; THSD7A, thrombospondin type-1 domain-containing 7A; vWF, von Willebrand factor.

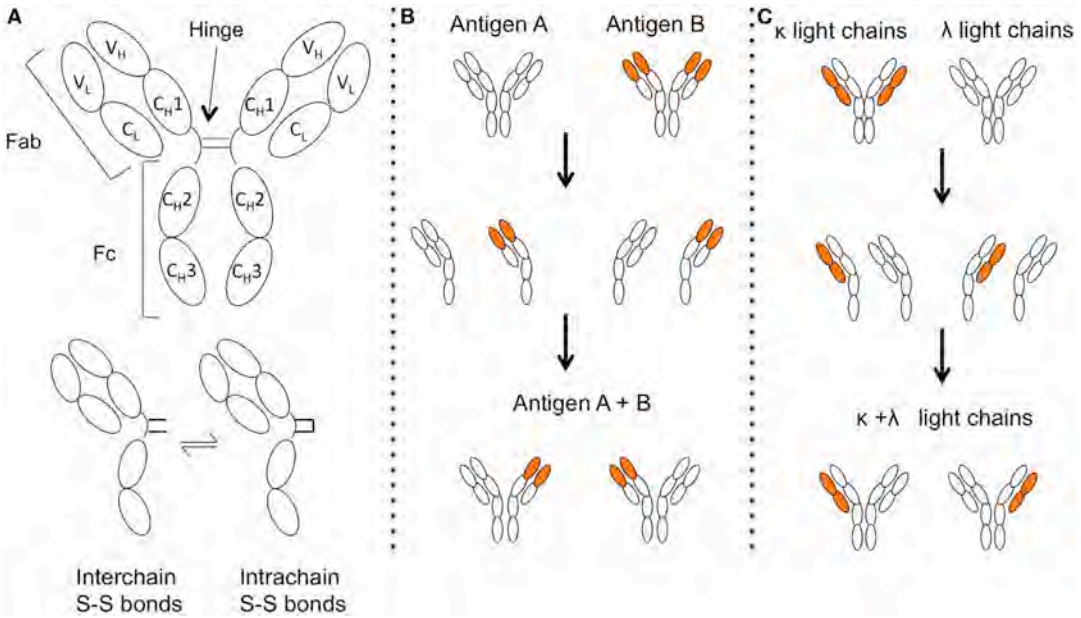

FIGURE 1 | The structure of IgG4 allows for Fab-arm exchange (FAE). **(A)** Structure of IgG4. One single amino acid change in the IgG4 hinge allows for greater structural flexibility and two different hinge isomers, with either interchain disulfide bonds that connect the two different heavy chains, or intrachain disulfide bridges within the same heavy chains. Under reducing conditions, the two isoforms are in a dynamic equilibrium. Figure adapted from Ref. (147). **(B)** When the two half-antibodies (HL) are not connected by interchain disulfide bonds they can then split up. HL of different idiotypes recombine randomly, resulting in antibodies that recognize two different antigens and are bispecific. **(C)** Antibodies are produced with light chains of either κ or λ type. Upon FAE, antibodies with both κ and λ light chains can be generated.

antigens instead of two antigens of the same kind [**Figure 1B** (166, 167)]. As a consequence, IgG4 is not able to activate the classic complement pathway or activate immune cells as discussed in the part of the protective role of IgG4 in immunity. The following reviews are suggested for further reading on IgG4 structure (147, 168–170).

FAE: Regulation and Kinetics

Fab-arm exchange seems to occur spontaneously in the body, since antibodies that are bispecific for two different allergens can be found in allergy patients (166). Here, endogenous IgG4 was able to cross-link two different allergens suggesting that an exchange between two distinct allergen-specific IgG4 molecules (birch and cat allergen) had taken place. FAE also occurred between human IgG and therapeutic, humanized antibodies (natalizumab) given as therapy to patients; here, the therapeutic antibodies exchanged half-molecules *in vivo* with endogenous IgG4 (171, 172). Bi-specific IgG4 was also detected in healthy probands, as IgG4 possessing both a λ and a κ light chain simultaneously was found in their serum [**Figure 1C** (173)]. FAE is inducible *in vitro* using reducing agents, such as glutathione (GSH) at concentrations of 1 mM and less (166, 171, 174–176). It is not known if and how FAE is regulated, or where it occurs in the body. The concentrations of GSH in human serum are too low to allow for efficient FAE, but other yet unidentified compartments in the body might provide the required GSH concentrations, e.g., human red blood cells, as they contain approximately 1 mM GSH (177).

In vitro-induced FAE occurs rapidly, in less than an hour (167), but *in vivo* it could take hours to days. The therapeutic monoclonal anti-integrin antibody natalizumab was found to exchange Fab arms in patients with endogenous IgG4 (172), with quantitative data obtained by injection of natalizumab into rats demonstrated an exchange half-life of less than 6 h (178). Human IgG4 has a metabolic half-life of around 21 days (179). Calculations led by Peter Molenaar based on these findings using first-order kinetics suggest that up to 99% of IgG4 should be bispecific in the body (17). There is further evidence: in IgG4 the κ light chain is more commonly used with a 3:1 κ: λ ratio. After FAE, IgG4 can harbor a κ and a λ light chain simultaneously (**Figure 1C**). The chance of a κ-half molecule to exchange with another κ-half-molecule is, therefore, more likely than the exchange with a λ-half-molecule, leading to a "silent" bispecificity hidden in the κ/κ and λ/λ fractions (173). The exchange is thought to be random. Calculating recombination probabilities using a Punnet square and assuming a 100% exchange rate, we expect a ratio of 9:6:1 (κ/κ:κ/λ:λ/λ). That means 37.5% of IgG4 would be κ/λ bispecific, which is close to the values measured in one study with healthy individuals (173). Taken together, it suggests that the majority of IgG4 in the human body is bispecific under normal circumstances. Despite the reduced avidity of IgG4, autoantibody binding can be demonstrated in tissue- and cell-based assays *in vitro*, e.g (3, 72, 88, 99)., perhaps due to the high affinity of the antibody with a Kd that can be in the picomolar range (180). Bispecificity also has functional consequences, as bispecific IgG4 is unable to divalently bind and cross-link one single species of antigen.

IgG4 Fc–Fc Interactions

The Fc region of IgG4 is also able to directly interact with IgG by Fc–Fc interactions, but only if the binding partner is immobilized on a solid phase (181–183). The relevance of this interaction is not understood, but notably occurs in rheumatoid arthritis, IgG4-related disease (IgG4-RLD), and membranous nephropathy (MN), the latter being proposed as an IgG4 autoimmune disease (184–186). It is possible that IgG4 containing immune complexes could form by this mechanism; these would not otherwise form by divalent binding and cross-linking due to the bispecificity of the antibody (163). Modifications of the Fc region of IgG4 induced the formation of artificial hexameric complexes *via* non-covalent interactions that were able to bind C1q and activate the classical complement pathway (187). Whether this is relevant for pathophysiology of IgG4 is unclear.

IgG4 Has a Protective Role in Immunity

IgG4 and IgE are usually produced in response to chronic exposure to antigens (188). The production of IgE and IgG4 is stimulated by T_h2 cytokines IL-4 and IL-13. Furthermore, the additional presence of IL-10 is thought to tip the balance toward IgG4 production and IgE inhibition (189–192). In addition, secretion of IL-10 by regulatory T cells was also found to induce IgG4 rather than IgG1 production (193) and a majority of isolated IL-10-producing regulatory B cells produced IgG4 in contrast to other B-cell subsets (194). These findings link IgG4 with anti-inflammatory tolerance mechanisms [discussed in more detail here (147)]. At present, most literature reveals that IgG4 has an anti-inflammatory function. It has been shown that its levels only rise slowly after chronic exposure to antigen (195–197) or after allergy immunotherapy (198). Thereafter, IgG4 seems to protect against antibodies of other IgG subclasses by competition for antigen without exerting an effector function, thus blocking the epitope to prevent the harmful effect of other antibody classes or subclasses [**Figure 2** (196–204)]. It has also been shown that passive transfer of IgG4 derived from hyperimmune beekeepers is clinically protective in allergy patients (205, 206) and protects mice from the effects of lethal africanized honey bee venom (207). Similarly, IgG4 subclass autoantibodies against the AChR protect against the pathogenic effects of IgG1 of the same idiotype in rhesus monkeys (166). The immunological inertness and the anti-inflammatory effect of IgG4 make it an unlikely subclass in the context of autoimmunity (**Figure 2**). In many cases [although there are exceptions (49)], antigen cross-linking and endocytosis in the context of autoimmunity rely on divalent binding [**Figure 2** (208–213)], which IgG4 cannot do (2, 3, 166). IgG4 does not form immune complexes that would stimulate antigen-presenting cells and mount an immune response nor does it activate the classical complement system (166, 170, 214). Furthermore, IgG4 inhibits immune precipitation by IgG1 antibodies (163, 200). Only pathogenic mechanisms that are independent of Fc effector functions can be exerted by IgG4, e.g., a block of protein–protein interaction or a direct activation or

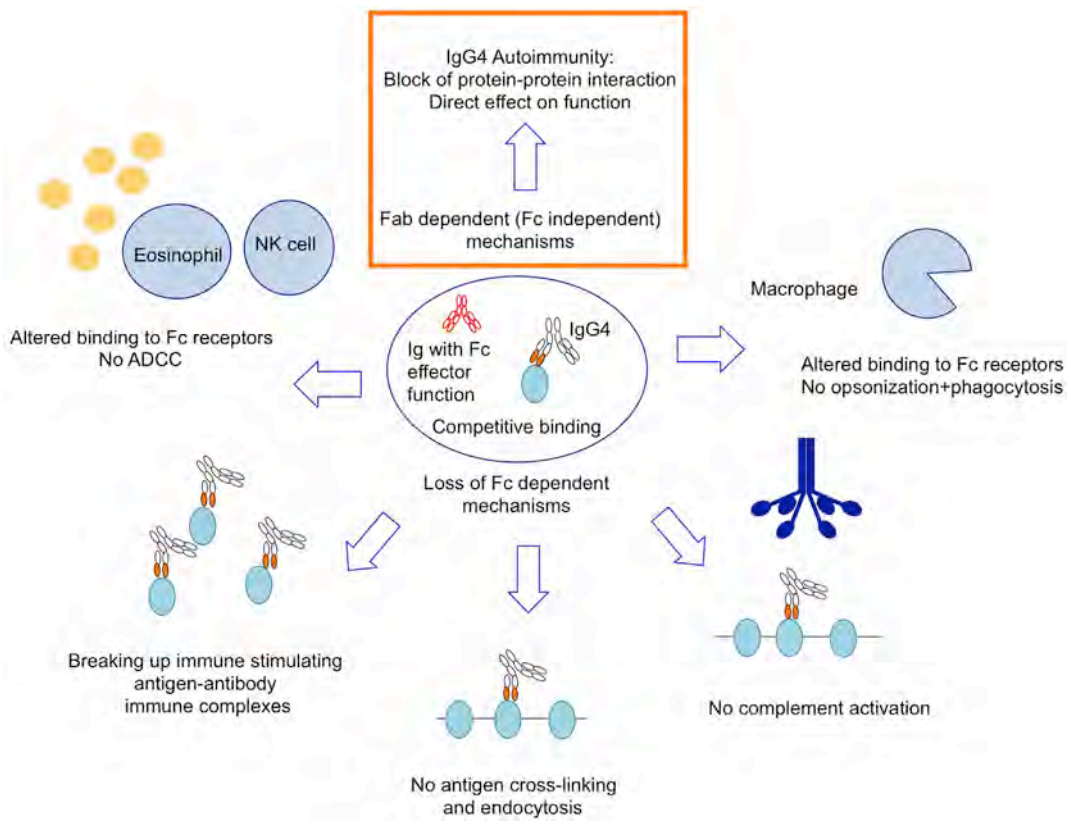

FIGURE 2 | IgG4 autoantibodies rely on pathogenic mechanisms that are independent of Fc effector function or multivalent binding.

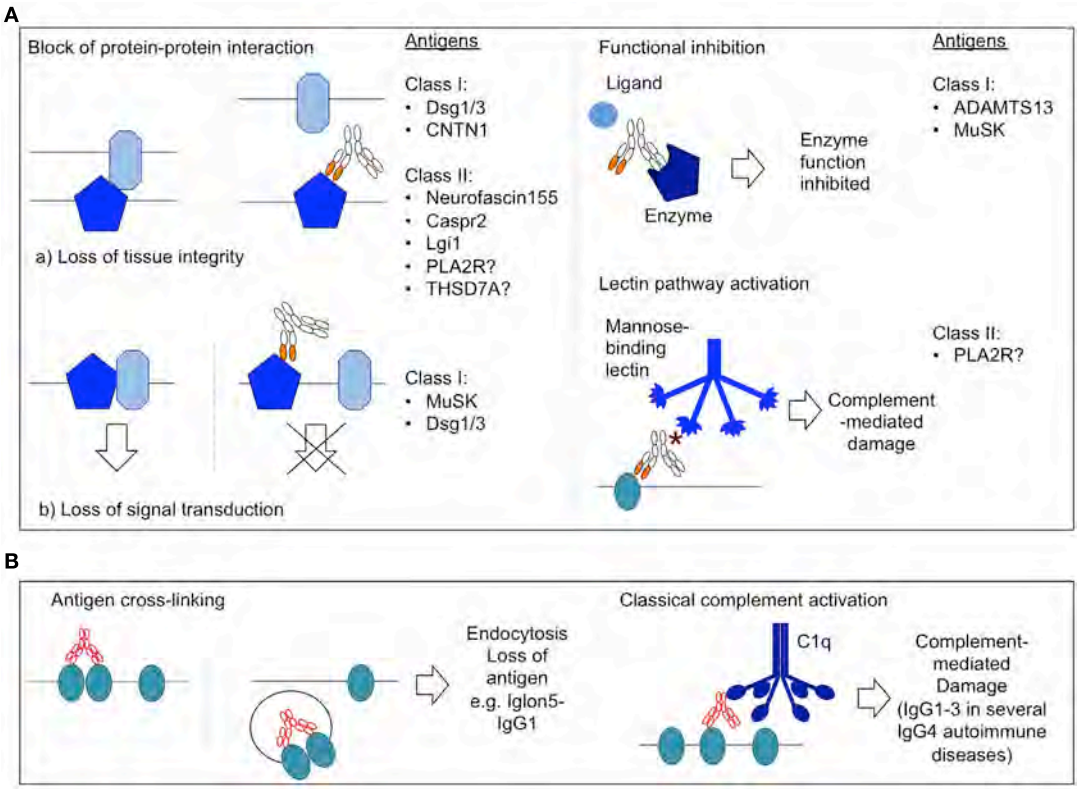

FIGURE 3 | Selected pathogenic mechanisms of IgG autoantibodies. **(A)** Pathogenic mechanisms of IgG4 autoantibodies. * = hypogalactosylated glycan side chain of IgG4. **(B)** Selected pathogenic mechanisms of IgG1–3 autoantibodies.

inactivation of enzymes or receptors by competitive or allosteric binding (**Figure 3A**).

DEFINITION AND VALIDATION OF IgG4 AUTOIMMUNE DISEASES

Autoantibodies are in general considered pathogenic when they bind an extracellular antigen in the target organ, e.g., the extracellular portion of a transmembrane antigen, and have a direct pathogenic effect, either directly on the target antigen (e.g., by induction of endocytosis or blocking of antigen function) or on the whole organ by recruitment and activation of complement or immune cells that attack the tissue (1, 215). Antibodies against intracellular antigens are not considered to be pathogenic as they are generally inaccessible (215), although they can be valuable biomarkers (216). IgG4 subclass autoantibodies are certainly unexpected culprits in autoimmunity. Particularly, as IgG4 can arise during an immune-dampening response to pathogenic antibodies of other classes and subclasses, candidate diseases should be carefully investigated to determine the pathogenic status of autoreactive IgG4. Using a modification of the postulates by Witebsky, Rose and Bona, and taking into account remarks by Naparstek and Plotz (215, 217, 218), the individual IgG4 autoantibodies in IgG4 autoimmunity were tested to validate the status of IgG4 autoimmunity.

Several aspects should be considered to define IgG4 autoimmunity:

(A) Indicators for antibody-mediated autoimmunity
   1. Autoantibodies with specificity for an extracellular antigen are present in the affected organ.
   2. A pathogenic mechanism for antibodies is demonstrated *in vitro*.
   3. The autoimmune disease can be reproduced in experimental animals by passive transfer of patient serum or purified abs or active immunization with antigen.
   4. Clinical cues for autoimmunity are present such as HLA association, genetic clustering of other autoimmune diseases in the family, and the clinical improvement of the patients after therapies that reduce autoantibody levels, such as plasma exchange or B-cell depletion therapy.

(B) Specific indicators for IgG4 pathogenicity
   1. Autoantibodies of IgG4 subclass against extracellular antigen are present.
   2. A pathogenic mechanism for IgG4 can be demonstrated *in vitro*. IgG4 could be purified from patient serum, and the purity of isolated IgG4 should be validated; ideally also the IgG4-depleted IgG1–3 fraction should be used as a control group to ensure the effects derived from IgG4. Alternatively, cloned patient antibodies

from IgG4+ B-cells could be used, although these may not be representative of the whole autoimmune B-cell population.

3. Reproduction of disease in animals by passive transfer of purified IgG4 from patients, monoclonal IgG or single chain variable region fragments (scFv) cloned from IgG4+ B-cells of patients.

The 14 proposed IgG4 autoantibodies and their associated diseases were evaluated according to these aspects (**Table 1**). With particular focus on the pathogenicity of IgG4 autoantibodies, three classes emerged with different levels of evidence and also with different likeliness of IgG4 pathogenicity. *Class I diseases* fulfill two or three postulates of IgG4 pathogenicity (B.1–3), here the pathogenicity of IgG4 autoantibodies could be proven by passive transfer of patient IgG4, or an IgG4 pathogenic mechanism was demonstrated *in vitro* (in most cases this is was a blocking effect). *Class II diseases* fulfill one postulate for IgG4 pathogenicity (B.1), but there exists substantial circumstantial evidence that would be in line with pathogenicity of IgG4. Examples would be if IgG4 levels correlated with disease severity or the presence of a known pathogenic mechanism that relies on functional blocking. *Class III diseases* still fulfill one postulate of IgG4 pathogenicity (B.1) but have the least supportive evidence for IgG4 pathogenicity, either because the pathogenic mechanism relies on divalent binding or is unknown. At this point, a conclusion regarding IgG4 pathogenicity cannot be drawn for class II and III diseases, and more studies are required to validate pathogenicity of their IgG4 autoantibodies.

Class I Diseases

One of the best-studied IgG4-mediated diseases is pemphigus. Here, autoantibodies bind to transmembrane proteins of keratinocytes, which leads to loss of cell–cell adhesion and blistering of the skin (acantholysis). The antigenic targets define different subforms of disease. In pemphigus foliaceus, the antigenic target is desmoglein 1 (Dsg1), which is expressed at high concentrations in the superficial layers of the epidermis; in pemphigus vulgaris, the mucosal-dominant type antibodies target desmoglein 3 (Dsg3) in basal and parabasal layers of the skin. Patients with pemphigus vulgaris of the mucocutaneous type have antibodies against both Dsg1 and Dsg3 (38, 39). Anti-Dsg autoantibodies are predominantly IgG4 (36, 37). They bind to extracellular epitopes and disrupt cell–cell adhesion, as seen *in vitro* where they induced cell sheet dissociation of cultured human keratinocytes (57, 219) and human skin explants (51). Additionally, the disease could be reproduced by passive transfer of monoclonal patient-derived antibodies that were of IgG4 subclass (42, 43). This means that pathogenicity of IgG4 could be demonstrated in the absence of patient antibodies of other IgG subclasses. Also, depletion of IgG4 reduced pathogenicity of patient serum in one study (220). Nevertheless, this does not mean that IgG4 is the exclusive pathogenic entity, and one study demonstrated that cloned patient IgG1 against Dsg3 was as pathogenic as IgG4 (221). The role of other IgG subclasses in IgG4 autoimmunity is discussed below in more detail. There are in fact several different disease models to investigate pathophysiology of pemphigus by passive or adoptive transfer [reviewed by Ref. (52)]. Maternal antibodies can also transfer to the fetus and cause neonatal pemphigus (54). Antibodies to Dsg1/3 may also affect signal transduction pathways that affect cytoskeleton rearrangement and modulate cell adhesion in keratinocytes, and several targets have been proposed (51, 222–228). Indeed, the MAPK signaling was suggested as potential therapeutic target in pemphigus (225), which can in part modulate the disruption of cell adhesion caused by pathogenic pemphigus autoantibodies (229).

Muscle-specific kinase MG is an autoimmune disease of the neuromuscular synapse hallmarked by fatigable muscle weakness. The autoantibodies target MuSK, a protein at the neuromuscular junction. Approximately 90% of the antibodies are of IgG4 subclass (3, 16), and the pathogenic mechanism of MuSK IgG4 is known and can be demonstrated *in vitro* with purified IgG4 (2, 3). Notably, the pathogenic effect was exclusive for IgG4 subclass antibodies. Passive transfer of purified IgG4 reproduced the disease in experimental animals (4), as did active immunization of complement-deficient mice (5). There is also evidence for a genetic predisposition in these patients (14, 15). Binding of antibodies to MuSK similarly affects its function as tyrosine kinase and organizer of neuromuscular junction development and maintenance. As the binding of the agrin coreceptor low-density lipoprotein receptor-related protein 4 (Lrp4) to MuSK is blocked by MuSK-IgG4 (2, 3), MuSK autophosphorylation in response to agrin is inhibited (2), which impairs its ability not only to induce clustering of the AChR (3, 27) but also to maintain the preexisting clusters (3). This leads to reduced densities of the AChR at the synapse and reduced efficiency of neuromuscular transmission, thus causing fatigable muscle weakness. A recent study demonstrated that inhibiting MuSK dephosphorylation counteracted the effects of MuSK antibodies *in vitro*, which would be an interesting new therapeutic strategy (230). Interestingly, the MuSK antibodies also modify the cross talk between motoneuron and muscle, as presynaptic abnormalities were observed in patients and passive transfer animal models, and led to a reduced quantal release of acetylcholine neurotransmitter into the synaptic cleft (5, 21, 22, 26, 231). The affected retrograde signaling pathway is not known, but as Lrp4 may be part of a retrograde signaling pathway (232, 233), it is very likely that the Lrp4–MuSK interaction plays a role, perhaps by anchoring Lrp4 at the synapse.

Disintegrin and metalloproteinase with thrombospondin motifs 13 (ADAMTS13) is a protease in the blood circulation that cleaves von Willebrand factor (vWF). In TTP, antibodies against the spacer domain of ADAMTS13 inhibit proteolysis of vWF (60, 234), which leads to accumulation of vWF, binding to platelets and causing microthrombosis. Since the inhibitory antibodies recognize the spacer domain that is also required for binding to vWF, the functional block could be due to blocked protein–protein interaction. IgG4 (but also IgG1) antibodies cloned from TTP patients by EBV immortalization demonstrated pathogenicity *in vitro* in assays measuring ADAMTS13 activity (69). Also, several patient-derived scFv were shown to be pathogenic when expressed in mice, albeit the original subclass of the patient antibodies is unknown (59). There is also additional circumstantial evidence that pathogenic antibodies of IgG4 subclass exist in TTP

as IgG4 levels are associated with relapse and some patients have exclusively IgG4 autoantibodies (235).

Contactin 1 (CNTN1), together with contactin-associated protein 1 (Caspr1), is expressed on the axonal surface and together they bind to neurofascin 155 on the surface of oligodendroglia (236–239). They are cell adhesion molecules at the axoglial junction of myelin sheaths that are important for efficient nerve impulse propagation along myelinated axons. Antibodies against CNTN1 of IgG4 and IgG1 subclass are present in chronic inflammatory demyelinating polyradiculoneuropathy (CIDP) (29, 34, 35, 124) and were proven to be pathogenic. Autoantibodies recognize CNTN1 in the paranodal axoglial junctions of motoneurons and block interaction of neurofascin 155 with CNTN1 in the CNTN1/Caspr1 complex (30). This leads to transverse band loss and paranodal loop detachment in the peripheral nerves. Pathogenicity of IgG4 was proven by passive transfer of purified IgG4 to Lewis rats (31) with loss of paranodal clusters that contain CNTN1, Caspr1, and neurofascin 155 and impaired motor nerve conduction.

Class II Diseases

Membranous nephropathy, a cause of proteinuria and nephrotic syndrome, is hallmarked by immune deposits containing IgG [predominantly IgG4 antibodies to the phospholipase A2 receptor (PLA2R) in primary MN], autoantigens such as PLA2R, and complement beneath the basal surface of podocytes in the kidney. PLA2R-IgG4 was proposed to have a unique mechanism of complement activation *via* the lectin pathway (98, 99, 103, 108, 109). This activation is hypothesized to derive from galactose-deficient side chains in PLA2R-IgG4 (97, 98) that might recruit mannose-binding lectin (MBL), which is also seen in rheumatoid arthritis (240) and IgA nephropathy (241). MBL binding leads to the activation of the lectin pathway and formation of the membrane-attack complex (103). Preliminary data by Beck and Salant from experiments with purified IgG4 from patients with primary MN showed that more of the IgG4 glycan chains lacked terminal galactose residues than did the IgG4 from control subjects and demonstrated increased binding of MBL to PLA2R-IgG4 (108). Additional evidence comes from a more recent study, where MBL deposition in glomeruli correlated with IgG4 positivity in biopsies from Japanese MN patients (109). A recent study by the group of Andreas Kistler demonstrated hypogalactosylated glycan side chains for IgG4, IgG induced complement-mediated injury to PLA2R-expressing podocytes *in vitro* and its prevention by MASP inhibitors, which adds further evidence to this unusual mechanism (poster presentation at the 2017 American Society of Nephrology meeting). However, both the Kistler and the Ma studies have not yet been published in peer-reviewed journals and need further investigation. IgG4-mediated activation of the lectin pathway may not be the only pathogenic mechanism, as one patient with characteristic PLA2R-IgG4-positive MN was deficient for MBL but revealed complement activation *via* the alternative pathway (242), and a small fraction of patients is negative for PLA2R-IgG4 (243). Additionally, a monoclonal IgG3 kappa with specificity for PLA2R was able to cause MN in the native kidney and the allograft *via* the classical pathway (244). An additional blocking mechanism was proposed since antibodies against PLA2R in MN were found to block adhesion of podocytes to collagen IV (245). In another study, PLA2R, however, was not found to bind collagen IV or I in general (106, 246). Furthermore, attempts to reproduce the disease in rodents by passive transfer have been unsuccessful, since the podocytes of rodent glomeruli do not express PLA2R [summarized by Ref. (247)]. Therefore, further studies are required to validate this finding and pinpoint the mechanism to IgG4.

Thrombospondin type-1 domain-containing 7A is expressed in glomeruli in the kidney and is another antibody targeted in MN (110, 113, 114, 118). Histologically, a thickening of the glomerular basement membrane with IgG and complement deposition can be observed. Anti-THSD7A antibodies were predominantly IgG4 (but also IgG1) (110, 116) and *in vitro* were shown to affect cytoskeletal architecture with the formation of stress fibers in cultured primary murine podocyte cells and could also induce detachment of THSD7A overexpressing HEK293 cells (111). Passive transfer of patient serum to mice led to proteinuria with late complement activation, but transient proteinuria in the absence of complement involvement was induced after passive transfer of THSD7A affinity-purified patient antibodies (111). Passive transfer of anti-THSD7A antibodies generated in rabbits could reproduce disease independent of complement activation (112). Taken together, there is evidence that THSD7A antibodies affect podocyte attachment, perhaps by a (reversible) blocking effect, but also that complement activation *via* C1q or lectin-binding pathway as a second pathogenic mechanism plays a role.

In three different neurological disorders with IgG4 subclass antibodies, targeting leucine-rich, glioma-inactivated 1 (Lgi1), contactin-associated protein 2 (Caspr2), and Neurofascin155, respectively, a pathogenic mechanism has been suggested that is based on the block of protein–protein interaction (70, 80, 87, 93, 248). The predominant mechanism of IgG4 antibodies in class 1 IgG4 autoimmune diseases was found to be a blocking mechanism, which may also be associated with a subclass switch to IgG4. It should be kept in mind that a blocking mechanism is not *per se* restricted to the IgG4 subclass [e.g., Ref. (69)], although it is more commonly associated with IgG4 autoimmunity. In detail, Lgi1 is expressed at the synaptic cleft of CNS neurons and in hippocampal neurons in culture, like CASPR2, it is part of the voltage-gated potassium channel complex, and antibodies against Lgi1 are associated with limbic encephalitis (72, 77, 93, 249). Here, serum from patients with Lgi1 encephalitis led to a block of Lgi1–ADAM22 interaction *in vitro*, which caused reduced AMPA receptors and excitation of hippocampal CA3 pyramidal cells *ex vivo* (70). These effects were not yet proven to be IgG4 specific. Caspr2 is expressed in the peripheral and central nervous system, particularly in the juxtaparanodal region of myelinated axons and in hippocampal GABAergic interneurons, and autoantibodies are associated with different clinical syndromes (88, 91, 250–252). It is suspected that the antibodies block the interaction between Caspr2 and TAG-1 and affect inhibitory interneuron function, thus leading to hyperexcitability (87). Importantly, many patients harbor not only IgG4 subclass antibodies against Caspr2 or Lgi1 but also IgG1 and IgG2 (88). Antibodies to neurofascin 155 are thought to have a similar effect to antibodies against CNTN1, with a block of CNTN1/Caspr1–neurofascin 155 interaction affecting

paranodal structure and causing peripheral neuropathies (30, 79, 81, 84).

Class III Diseases

IgLON family member 5 (Iglon5) is a CNS antigen and is targeted by autoantibodies in Iglon5 parasomnia, which is a severe autoimmune disease characterized by abnormal sleep behavior. Here, a population of pathogenic IgG1autoantibodies induced endocytosis of Iglon5 (134) (discussed in more detail below). It was demonstrated that purified Iglon5-IgG4 as well as digested Fab fragments did not induce this mechanism. It cannot be excluded that Iglon5-IgG4 antibodies have an additional pathogenic mechanism, but at this moment there is no indication that they are pathogenic at all.

Similarly, in the case of dipeptidyl peptidase-like protein 6 (DPPX) antibodies, the described pathogenic mechanism is the loss of DPPX and associated Kv4.2 from the cell surface, perhaps by antigenic modulation, which would require divalent binding and cross-linking of antigen. Unless an additional pathogenic mechanism is found for DPPX-IgG4, or alternatively, it is demonstrated that the loss of DPPX and Kv4.2 results from a mechanism that does not rely on divalent binding, it is not likely that DPPX encephalitis is an IgG4 autoimmune disease.

Only one patient has been described with IgG4 subclass antibodies against Caspr1 [a second one if antibodies against complexed CNTN1/Caspr1 are considered (35, 124)], and at this point not enough data are available to estimate pathogenicity of IgG4. There are also insufficient data available regarding pathogenicity of IgG4 subclass anti-collagen type IV (alpha3NC1 domain) antibodies in Goodpasture syndrome, the most convincing circumstantial evidence being temporal occurrence and reoccurrence of IgG4 autoantibodies and lung hemorrhage (119).

In summary, the pathogenicity of IgG4 in most IgG4 autoimmune diseases has not been proven yet. A key experiment could be the isolation of IgG4 subclass antibodies from patient serum or plasmapheresis material, followed by passive transfer to a suitable animal model, or to use purified IgG4 in already established *in vitro* models of pathogenicity.

PROPERTIES OF IgG4 AND IgG4 AUTOIMMUNE DISEASES

One key pathogenic mechanism in antibody-mediated autoimmunity, especially in the peripheral and central nervous system, is the divalent binding, cross-linking, and endocytosis of antigen, as seen with antibodies against AChR, GlyR, NMDAR, and Iglon5 [**Figure 3B** (134, 208–210, 253)]. The effect is usually lost when using Fab fragments instead of whole IgG1, which underlines the relevance for multivalent binding. A possibility how IgG4 autoantibodies could remain pathogenic by cross-linking and endocytosis would be the loss of FAE, as then monospecific IgG4 could still cross-link and internalize antigen. An example could be the presence of point mutations or sequence variants in the IgG4 hinge or the C_H3 region that would remove its ability to undergo FAE. This possibility was investigated in several IgG4-associated diseases. In IgG4-RLD, sequencing showed that the FAE abolishing variant K409 was not present (254), and a recent study demonstrated high levels of bispecific IgG4 in IgG4-RLD (255). Similarly, IgG4 autoantibodies in rheumatoid arthritis were found to be bispecific (256), and recently we were able to demonstrate the same for an example of IgG4 autoimmunity, as a large proportion of patient-derived MuSK autoantibodies were bispecific as well (17). These are only a few publications yet, and more studies are needed to validate the findings in additional IgG4-associated diseases. Until then, there is no indication that impaired FAE affects IgG4 in IgG4-associated disorders, which suggests that pathogenic mechanisms of IgG4 autoantibodies do not rely on divalent binding. Notably, the authors of the IgG4-RLD study suggest increased levels of FAE as a new biomarker. As IgG4-RLD is also associated with elevated levels of IgG4, and up to 99% of IgG4 are probably bispecific, it would be interesting to test a correlation between IgG4 concentrations and κ/λ bispecific IgG4. Enrichment of κ/λ IgG within the total IgG4 population (compared to κ/κ and λ/λ antibodies) could indicate a change in light chain usage.

Blocking as a Main Pathogenic Mechanism of IgG4

Blocking mechanisms are independent of the Fc domain and as such are the main effector mechanisms for IgG4 autoantibodies (**Figure 3A**). The binding of antibody to antigen can cause the inappropriate activation or blocking of enzymes or receptors. As examples, blocking antibodies of IgG1–3 subclass prevent binding of the neurotransmitter acetylcholine to the acetylcholine receptor in AChR MG (257–259), blocking antibodies against thyroxin peroxidase reduce production of thyroid-stimulating hormone (TSH) thus causing hypothyroidism (260), while stimulating antibodies against the TSH receptor are associated with hyperthyroidism (261). Functional blocking as a pathogenic mechanism is found in not only the IgG4 autoimmune diseases TTP and MuSK MG but also pemphigus (2, 52, 60, 234).

Block of protein–protein interaction is overall considered a main pathogenic mechanism for IgG4 and was demonstrated in several class I and II IgG4 autoimmune diseases (**Figure 3A**). The consequence of such a block could be the block of a signal transduction pathway (MuSK, Dsg1/3) or the loss of tissue integrity (e.g., Dsg1/3, Caspr1, and CNTN1). Most IgG4 autoantibodies were found to block protein–protein interaction.

Complement Activation

Another key mechanism of IgG1–3 autoantibodies is the recruitment of C1q protein and activation of the classical complement pathway, which leads to complement mediated damage, e.g., by antibodies against AChR or aquaporin 4 [**Figure 3B** (262–265)]. IgG4 does not bind C1q, but intriguingly, complement activation by the lectin pathway may emerge as a novel mechanism of IgG4 autoantibodies, as it is found in PLA2R-IgG4 with hypogalactosylated glycan side chains [**Figure 3A** (98, 99, 103, 108, 109)].

IgG4 Autoimmune Diseases

IgG4 pathogenic mechanisms translate to a range of different disorders that are clinically very diverse. An excellent introduction to the different IgG4 autoimmune diseases can be found here (266). A selection of disease specific reviews is found here

(9, 52, 80, 106, 235, 267–271). A good response to B-cell depletion therapy and plasmapheresis has been reported in several IgG4 autoimmune diseases (6–13, 32, 78, 272–274).

Contribution of Other Antibody Classes and Subclasses

As IgG4 levels usually increase after repeated or strong exposure to antigen, a high level of IgG4 may coexist with (smaller quantities of) pathogenic antibody of other class or subclass (e.g., IgE or IgG1) and could have clinical implications for treatment decisions. Specifically, after the evaluation and classification of the proposed IgG4 autoimmune diseases, it emerged that in most cases several different antibody classes and/or subclasses are present in patient serum (**Table 1**), with varying degree of potential pathogenicity. Of note, IgG4 concentrations could potentially be overestimated depending on the choice of secondary antibody (16), and cross-reactivity between secondary antibodies against IgG4 and IgG2 is also known to occur. A correlation between overall antibody titer and antigen-specific IgG4 titer would increase confidence in the quantification data (3).

Furthermore, pathogenic mechanisms were described for serum or IgG from patients with IgG4 autoimmunity that are likely not caused by IgG4 subclass antibodies as they depend on divalent binding or Fc effector function (**Figure 3B**, endocytosis of antigen and complement activation) or have been demonstrated using purified or cloned patient IgG1–3 [e.g., Dsg3-IgG1 (221), ADAMTS13-IgG1 (69), Lgi1-IgG3 (275), MuSK-IgG1–3 (3), or Iglon5-IgG1 (134)]. Indications for complement activation were found in several disorders (**Table 1**).

Particularly interesting are Iglon5 autoantibodies in which an irreversible internalization of Iglon5 was shown. Here, a clear pathogenic mechanism of IgG1, depending on divalent binding (134), was shown. Iglon family members are glucosylphosphatidylinositol-anchored proteins that have a role in membrane stabilization. Iglon5 parasomnia also has an unusual association with tauopathy (130, 276, 277) linking autoimmunity to neurodegenerative diseases. Combined, these findings led to the current hypothesis that Iglon5-IgG1 antibodies, by antigenic modulation of Iglon5, cause a destabilization of the cytoskeleton. This may affect microtubule stability and hyperphosphorylation of associated tau protein that could lead to the observed tauopathy (276). Whether IgG4 subclass antibodies to Iglon5 are pathogenic at all is unclear, thus making it a class III IgG4 autoimmune disease.

Similarly, DPPX antibodies cause a reversible loss of cell surface-expressed DPPX and Kv4.2, thus leading to hyperexcitation of neurons (127). This requires divalent binding and cross-linking of antigens. As IgG4 is mostly bispecific [also in the context of IgG4 autoimmune diseases (17)], it is likely that DPPX-IgG4 is not able to divalently bind and cross-link DPPX. While the precise mechanism for downregulation of cell-surface-expressed antigen has not yet been demonstrated, it is likely that this is a function of IgG1–3 that causes internalization by divalent binding and cross-linking of antigen. This possibility could be explored by a modification of the experiment using purified IgG subclasses and Fab fragments.

Notably, 10% of MuSK antibodies are of IgG1 and IgG2 (and very little IgG3) subclass and were pathogenic *in vitro* (3). MuSK IgG1–3 pathogenicity *in vivo* could not yet be demonstrated, but can also not yet be excluded, as passive transfer experiments were impaired by the low concentration of MuSK antibodies in the IgG1–3 fraction that were below detection limit in the experimental animals (4). The exact mechanism of pathogenicity for MuSK IgG1–3 is unknown. MuSK-IgG1–3 were able to affect MuSK function in a cellular model of the muscle and neuromuscular synapse, the C2C12 mouse myotubes. Agrin stimulation leads to MuSK activation and clustering of AChRs, which can be quantified. MuSK antibodies impaired this mechanism and led to reduced clustering of AChRs, and while it is thought that MuSK-IgG4 induce this phenomenon by blocking MuSK–Lrp4 interaction (2, 3), it is unclear how MuSK IgG1–3 affected the AChR clustering as they do not interfere with Lrp4–MuSK interaction. Interestingly, MuSK antibodies (both IgG4 and IgG1–3) also disrupted preexisting AChR clusters that were induced by overexpression of Dok7 in C2C12 myotubes [(3) Koneczny/Vincent et al. unpublished data] independent of agrin signaling, which was also found using autoantibodies against Lrp4 derived from an active immunization mouse model (278). An earlier study suggested that Lrp4 is required to make MuSK susceptible to Dok7-induced activation and induction of AChR clustering, presumably with a role for AChR prepatterning before innervation (279). MuSK IgG1–3 could also have an effect on Lrp4, though it is not clear how, or MuSK antibodies may affect Dok7-mediated MuSK activation, perhaps by altering MuSK conformation, MuSK kinase activity and/or preventing binding of Dok7 to MuSK, as observed in CMS with a MuSK mutation (280). It would be interesting to study whether MuSK-IgG1–3 antibodies affect MuSK–Dok7 interaction.

Another potential mechanism of MuSK IgG1–3 is the induction of MuSK endocytosis, which is also suggested to be part of the normal response of MuSK to agrin stimulation (281–283). One study demonstrated that serum from MuSK patients led to the internalization of MuSK in mouse muscle cells using time-lapse microscopy and confocal microscopy (28). Two different studies could not reproduce these findings using different approaches (2, 3). However, different patients were tested in these studies, and only a few patients were investigated for endocytosis in all three studies, which is important, as there could be variability in the pathogenic mechanisms in the overall MuSK MG population. In addition, there were technical limitations in the later studies [including my own, as discussed there (3)], hence it is still very possible that MuSK IgG1–3 induce MuSK endocytosis. Further studies are indicated using purified MuSK IgG1–3, MuSK expressed in muscle cells (as transient expression in non-muscle cell environment could affect MuSK endocytosis), and perhaps more appropriate methodology.

In TTP, antibodies of IgG, IgM, and IgA class are present; these may convey pathogenicity by the accelerated clearance of ADAMTS13 from the circulation (234, 284). The functional block of ADAMTS13 activity was not restricted to the IgG4 subclass and could also be induced by IgG1 (69). Therefore, the pathogenic mechanism is not linked to the antibody subclass, but rather the

epitope, as only antibodies that recognize the spacer domain are associated with an inhibitory role (234).

In patients with MN with anti-PLA2R abs, a subclass switch from IgG1 to IgG4 was reported over the course of the disease, with an inverse correlation with C1q involvement (285). It is thus clear that in the initial stage of the disease, IgG1 contributes to pathogenicity by activation of the classical complement pathway (100), which may then at later stages of the disease be replenished or replaced by IgG4 that may be protective, inert, or pathogenic (99).

In pemphigus, IgG1 antibodies against Dsg1 or 3 are present and they may also contribute to the blocking mechanism (221). Additional pathogenic mechanisms in pemphigus were proposed as desmosome disassembly by clustering and endocytosis of Dsg and stimulation of signaling pathways that modulate keratinocyte cell adhesion (50, 51). It is thought that multivalent polyclonal Dsg antibodies can cross-link and endocytose Dsg, which leads to Dsg depletion from desmosomes and failed cell adhesion (44–48). However, also monovalent pathogenic anti-Dsg3 antibodies led to a depletion of Dsg3, which suggests that this could also be a mechanism of potentially bispecific (and thus monovalent) Dsg3-IgG4 (49).

Taken together, the presence of more than one pathogenic entity in IgG4 autoimmune diseases is quite possible and makes sense, if we consider that a rise of antigen-specific IgG4 in theory could have been an attempt of the immune system to dampen an inappropriate answer to the antigen by a different antibody species. This could also have clinical consequences, as monitoring of different Ig class/IgG subclass-specific autoantibodies may provide a deeper understanding of the autoimmune response, the individual antibody levels or a ratio thereof could be useful as biomarkers for disease progression or the selection of appropriate therapy.

Presence of Multiple Antibodies in Individual Cases

Two case reports describe the co-occurrence of MuSK MG or TTP with IgG4-RLD (286, 287), which brought up the interesting question whether these diseases might be related. The term IgG4 autoimmunity is relatively new and was introduced in 2015 (266). IgG4-RLD [which is also a relatively new term (288)] is at this point considered as a separate clinical entity. IgG4-related disease is not discussed extensively here, an excellent review is suggested for further reading (289) and also a review with focus on IgG4 in IgG4-related disease (290). Due to the rareness of the IgG4 subclass and its involvement in pathology, the possibility exists that IgG4-RLD and IgG4 autoimmunity could be part of the same spectrum. Both diseases are associated with IgG4, and both have a favorable clinical response to B-cell depletion therapy with rituximab (6, 32, 78, 272–274, 289). However, IgG4-RLD is defined by the formation of tumefactive lesions in target organs, which is not normally described in IgG4 autoimmunity, and by IgG4+ plasma cell infiltrates and increased serum IgG4 levels. Normal IgG4 concentrations are variable, but are thought to comprise 5% of total IgG (137, 138). As mean IgG concentrations vary between 7 and 15 g/L with a mean around 10 g/L, IgG4 concentrations are expected to be around 0.5 g/L (but can rise up to 100-fold in immune responses). IgG4 concentrations above 1.35 g/L are considered as a diagnostic marker for IgG4-RLD (291). In IgG4 autoimmunity, few studies have looked at serum IgG4 levels, but in one study total serum IgG4 was found to be elevated in a small fraction of pemphigus patients (220), which is notable, but only occurred in a minority of patients: three of 27 pemphigus vulgaris patients and three of 16 pemphigus foliaceus patients had IgG4 concentrations above the threshold of 1.35 g/L (or 135 mg/dL). In addition, the total IgG concentrations were reduced in these patients, likely a consequence of immunosuppressive treatment [pemphigus is routinely treated with immunosuppression (292)]. Perhaps the immunosuppressive treatment in combination with an on-going IgG4 autoimmune disease also increased relative IgG4 levels, which would be interesting to study in any IgG4 autoimmune disease using patient serum before and after treatment.

A key characteristic in IgG4 autoimmunity is the presence of antigen-specific autoantibodies of IgG4 subclass with direct pathogenic function. In IgG4-RLD, the role of IgG4 is not well understood, but it is thought that IgG4 may have a blocking, anti-inflammatory function. There is indirect evidence for an antigen-driven pathogenicity, namely the presence of oligoclonal bands in the CSF of patients and the presence of oligoclonal expansions of somatically hypermutated IgG4+ B-cell clones, but these were not associated with any known autoantigen (293–296). Only a few antigen-specific autoantibodies have been described that are also not consistently found in the disease, and the pathogenicity of these autoantibodies is not known (297, 298). Experiments with purified antibodies from patients with a pancreatic form of IgG4-RLD showed that IgG4 blocked pathogenic effects of IgG1 in a passive transfer animal model (299), and a recent study identified Annexin A11 as an antigenic target in some patients with autoimmune pancreatitis. The study findings also suggest that the pathogenic entity may be IgG1 and that IgG4 may be upregulated as an anti-inflammatory measure that blocks pathogenic IgG1 (300). More studies are needed to validate this finding, also for other subtypes of IgG4-RLD. However, the relatively clear pathogenic role of IgG4 in IgG4 autoimmunity and the potentially protective role of IgG4 in IgG4-RLD make it as a consequence not very likely that these disorders are (closely) related.

ETIOLOGY OF IgG4 AUTOIMMUNITY

The etiology of most autoimmune diseases and thus of most IgG4-mediated autoimmune diseases is not known, but there are a few interesting observations that could give a clue to potential factors and mechanisms that may contribute to immunopathogenesis.

Environmental Antigens

In Europe, MuSK MG frequency correlates with geographical latitude (301), with few cases in northern countries but higher prevalence in the south. This pattern is shared by another IgG4 autoimmune disease, pemphigus (302, 303). The distribution might be coincidental, as epidemiology data of MG in the rest of the northern hemisphere do not reflect the same pattern. Or it could indicate an environmental and/or genetic factor, for example, different availability of an environmental antigen, or different

climates with different exposure levels to parasites/helminths in the past could have influenced the type 1 hypersensitivity immune answer including the intensity of the IgG4 response. However, the most striking example for environmental antigen-induced autoimmunity comes from fogo selvagem, which is an endemic form of pemphigus that is found mainly in rural areas of Brazil, but also in Colombia and Tunisia (303, 304). Here, an association between insect bites and autoimmunity has been found. The bite of the sand fly (*Lutzomyia longipalpis*) exposes the patient to salivary proteins, specifically LJM11, against which most humans then develop antibodies. While LJM11 itself is a non-pathogenic environmental antigen, mounting an immune response against it is thought to be protective against parasites (specifically *Leishmania major*) that are also transmitted by the bite of the sand fly (305). Unfortunately, the responding antibodies against the non-pathogenic environmental antigen can also cross-react with self-antigen desmoglein 1 (Dsg1) in individuals with genetic predisposition (306, 307). The initial subclinical antibody response is thought to contain IgE, IgG1, and IgM (308–310), then a switch to IgG4 subclass occurs, probably associated with an intramolecular epitope spreading event (311) that is associated with disease onset (312, 313). Etiology of autoimmune diseases is rarely as well documented as in the fascinating case of fogo selvagem. It would be interesting to study if a similar mechanism could be at hand in other IgG4-mediated diseases. A test for antigen-specific IgE in IgG4-associated diseases could give first indications if this was the case. Indeed, a potential link to allergy recently emerged for a different IgG4-associated disease, IgG4-RLD. An association of IgG4-RLD with a history of allergy was already suspected (314), then a polyclonal response to multiple non-infectious environmental antigens was discovered (315) and a rise in IgE and eosinophil levels was found to predict relapse and to have potential use as diagnostic and prognostic biomarkers (316).

Infection

Several different (potential) IgG4 autoimmune diseases may have a link to infection, generally thought to be conveyed by molecular mimicry, where antibodies against pathogens cross-react against self-antigen. The autoreactive B-cells in pemphigus showed a shared VH1–46 gene usage, and these were associated with few somatic mutations, which suggests that naïve B-cells that use VH1–46 genes are prone to react against Dsg3 (55). VH1–46 B cells are also associated with an increased reaction toward rotavirus capsid protein VP6 and may thus confer a protection toward infection, highlighting the potential for rare cross-reactive clones to trigger the onset of pemphigus autoimmunity (317, 318). In one of two known CIDP patient with Caspr1-IgG4, disease onset was 10 days after preceding virus infection (common cold) (124). Patients with DPPX encephalitis usually experience severe prodromal symptoms of diarrhea and weight loss (median 20 kg), sometimes accompanied by headache or mood disorder, then within a few months the patients develop a range of neurological symptoms (125, 127, 128). DPPX is strongly expressed in not only the myenteric plexus, a mesh of neurons in the gastrointestinal tract, but also the hippocampus, cerebellum, and striatum. The curious shift in symptoms is reminiscent of a gastrointestinal infection that leads to the mounting of an autoimmune attack against the myenteric plexus *via* molecular mimicry or bystander attack mechanisms, as seen, e.g., in *Campylobacter jejuni* infection that causes the Guillain–Barré syndrome [reviewed, e.g., by Ref. (319)]. So far, no pathogen was found to be associated with the prodromal symptoms in DPPX-encephalitis, and it is also possible that this shift may have different causality, but it is an intriguing possibility to keep in mind.

In case of PLA2R antibody-positive MN, infection and molecular mimicry were proposed to potentially contribute to immunopathogenesis, as there is partial homology between PLA2R peptides and bacterial cell wall enzymes of Clostridium species (101, 320, 321). A link between infection and Goodpasture's disease with antibodies against non-collagenous domain 1 of α3 chain of type IV collagen was also described (322, 323). One case of TTP was associated with Epstein–Barr virus reactivation (324), another case disease onset was associated with an influenza A infection (325) and another with dengue virus infection (326).

Vaccination

There are a few cases of TTP onset or relapse after vaccination (327–329). This is interesting, as a related disease, immune thrombocytopenic purpura, which has antibodies against platelets, is also associated with vaccination (330).

Malignancy

Overexpression of antigen by tumors can trigger an autoimmune response. THSD7A-positive MN is associated with malignancy, as THSD7A itself may also play a role in certain cancers (331) and specifically two cases were described, one with gallbladder carcinoma, one with endometrial cancer, where THSD7A was overexpressed in the tumor and taken up by follicular dendritic cells in a regional lymph node (106, 113, 115, 116).

Summary and Conclusion

In recent years, many IgG4 autoantibodies were discovered, particularly against neuronal targets. By now, 14 different antigen targets have been described and suggested to play a causative role in "IgG4 autoimmunity" (266). Using a modified version of the Witebsky postulates to identify IgG4 autoimmune diseases with proven pathogenicity of IgG4 autoantibodies, the diseases were classified into three categories: class I with proven pathogenicity of IgG4 autoantibodies (including TTP with ADAMTS13 antibodies, pemphigus vulgaris with anti-Dsg3 antibodies, pemphigus foliaceus with anti-Dsg1 antibodies, MuSK MG and CIDP with anti-CNTN1 antibodies), class II where pathogenicity of IgG4 is highly suspected (anti-Lgi1- and Caspr2-associated encephalitis/Morvan's syndrome, CIDP with anti-neurofascin155 antibodies, and MN with anti-PLA2R or anti-THSD7A antibodies), and finally class III with diseases where IgG4 pathogenicity has not been studied extensively yet (anti-Caspr1-associated CIDP and Goodpasture syndrome with IgG4 antibodies against Collagen IV alpha3NCI) or that have a main pathogenic mechanism that relies on divalent binding, cross-linking and endocytosis of antigen (Iglon5 parasomnia and anti-DPPX encephalitis). Class II and III diseases require further investigation to determine the pathogenicity of IgG4, ideally by passive transfer experiments with purified patient IgG4. Evaluation of the diseases suggests that IgG4 is

mainly pathogenic by blocking protein–protein interaction, but that in many cases non-IgG4 autoantibodies are present that may contribute to pathogenicity by other mechanisms, in many cases activation of classical complement is suspected. This may have clinical consequences for treatment decisions. The possibility of an association between IgG4 autoimmunity and IgG4-RLD was discussed but found unlikely.

AUTHOR CONTRIBUTIONS

The author confirms being the sole contributor of this work and approved it for publication.

ACKNOWLEDGMENTS

I would like to express my deepest gratitude to Jan Bauer, Laurence Beck, Aimee Payne, Mårten Segelmark, Donald Siegel, and Angela Vincent (in alphabetical order) for their helpful suggestions and/or scientific advice. Especially helpful was the thorough review of the manuscript by Jan Bauer, Laurence Beck, and Aimee Payne, which has greatly improved its quality. Furthermore, I want to thank Theo Rispens that I could base **Figure 1A** partly on one of his previously published figures. IK was funded by an Erwin-Schrödinger fellowship by the Austrian Science Fund (FWF): Project number J3545-B13.

REFERENCES

1. Ludwig RJ, Vanhoorelbeke K, Leypoldt F, Kaya Z, Bieber K, McLachlan SM, et al. Mechanisms of autoantibody-induced pathology. *Front Immunol* (2017) 8:603. doi:10.3389/fimmu.2017.00603
2. Huijbers MG, Zhang W, Klooster R, Niks EH, Friese MB, Straasheijm KR, et al. MuSK IgG4 autoantibodies cause myasthenia gravis by inhibiting binding between MuSK and Lrp4. *Proc Natl Acad Sci U S A* (2013) 110(51):20783–8. doi:10.1073/pnas.1313944110
3. Koneczny I, Cossins J, Waters P, Beeson D, Vincent A. MuSK myasthenia gravis IgG4 disrupts the interaction of LRP4 with MuSK but both IgG4 and IgG1-3 can disperse preformed agrin-independent AChR clusters. *PLoS One* (2013) 8(11):e80695. doi:10.1371/journal.pone.0080695
4. Klooster R, Plomp JJ, Huijbers MG, Niks EH, Straasheijm KR, Detmers FJ, et al. Muscle-specific kinase myasthenia gravis IgG4 autoantibodies cause severe neuromuscular junction dysfunction in mice. *Brain* (2012) 135(Pt 4):1081–101. doi:10.1093/brain/aws025
5. Mori S, Kubo S, Akiyoshi T, Yamada S, Miyazaki T, Hotta H, et al. Antibodies against muscle-specific kinase impair both presynaptic and postsynaptic functions in a murine model of myasthenia gravis. *Am J Pathol* (2012) 180(2):798–810. doi:10.1016/j.ajpath.2011.10.031
6. Hehir MK, Hobson-Webb LD, Benatar M, Barnett C, Silvestri NJ, Howard JF Jr, et al. Rituximab as treatment for anti-MuSK myasthenia gravis: multicenter blinded prospective review. *Neurology* (2017) 89(10):1069–77. doi:10.1212/WNL.0000000000004341
7. Keung B, Robeson KR, Dicapua DB, Rosen JB, O'Connor KC, Goldstein JM, et al. Long-term benefit of rituximab in MuSK autoantibody myasthenia gravis patients. *J Neurol Neurosurg Psychiatry* (2013) 84(12):1407–9. doi:10.1136/jnnp-2012-303664
8. Diaz-Manera J, Martinez-Hernandez E, Querol L, Klooster R, Rojas-Garcia R, Suarez-Calvet X, et al. Long-lasting treatment effect of rituximab in MuSK myasthenia. *Neurology* (2012) 78(3):189–93. doi:10.1212/WNL.0b013e3182407982
9. Evoli A, Padua L. Diagnosis and therapy of myasthenia gravis with antibodies to muscle-specific kinase. *Autoimmun Rev* (2013) 12(9):931–5. doi:10.1016/j.autrev.2013.03.004
10. Nowak RJ, DiCapua DB, Zebardast N, Goldstein JM. Response of patients with refractory myasthenia gravis to rituximab: a retrospective study. *Ther Adv Neurol Disord* (2011) 4(5):259–66. doi:10.1177/1756285611411503
11. Thakre M, Inshasi J, Marashi M. Rituximab in refractory MuSK antibody myasthenia gravis. *J Neurol* (2007) 254(7):968–9. doi:10.1007/s00415-006-0442-2
12. Hain B, Jordan K, Deschauer M, Zierz S. Successful treatment of MuSK antibody-positive myasthenia gravis with rituximab. *Muscle Nerve* (2006) 33(4):575–80. doi:10.1002/mus.20479
13. Evoli A, Bianchi MR, Riso R, Minicuci GM, Batocchi AP, Servidei S, et al. Response to therapy in myasthenia gravis with anti-MuSK antibodies. *Ann N Y Acad Sci* (2008) 1132:76–83. doi:10.1196/annals.1405.012
14. Niks EH, Kuks JB, Roep BO, Haasnoot GW, Verduijn W, Ballieux BE, et al. Strong association of MuSK antibody-positive myasthenia gravis and HLA-DR14-DQ5. *Neurology* (2006) 66(11):1772–4. doi:10.1212/01.wnl.0000218159.79769.5c
15. Bartoccioni E, Scuderi F, Augugliaro A, Chiatamone Ranieri S, Sauchelli D, Alboino P, et al. HLA class II allele analysis in MuSK-positive myasthenia gravis suggests a role for DQ5. *Neurology* (2009) 72(2):195–7. doi:10.1212/01.wnl.0000339103.08830.86
16. McConville J, Farrugia ME, Beeson D, Kishore U, Metcalfe R, Newsom-Davis J, et al. Detection and characterization of MuSK antibodies in seronegative myasthenia gravis. *Ann Neurol* (2004) 55(4):580–4. doi:10.1002/ana.20061
17. Koneczny I, Stevens JA, De Rosa A, Huda S, Huijbers MG, Saxena A, et al. IgG4 autoantibodies against muscle-specific kinase undergo Fab-arm exchange in myasthenia gravis patients. *J Autoimmun* (2017) 77:104–15. doi:10.1016/j.jaut.2016.11.005
18. Otsuka K, Ito M, Ohkawara B, Masuda A, Kawakami Y, Sahashi K, et al. Collagen Q and anti-MuSK autoantibody competitively suppress agrin/LRP4/MuSK signaling. *Sci Rep* (2015) 5:13928. doi:10.1038/srep13928
19. Mori S, Yamada S, Kubo S, Chen J, Matsuda S, Shudou M, et al. Divalent and monovalent autoantibodies cause dysfunction of MuSK by distinct mechanisms in a rabbit model of myasthenia gravis. *J Neuroimmunol* (2012) 244(1–2):1–7. doi:10.1016/j.jneuroim.2011.12.005
20. Shigemoto K, Kubo S, Maruyama N, Hato N, Yamada H, Jie C, et al. Induction of myasthenia by immunization against muscle-specific kinase. *J Clin Invest* (2006) 116(4):1016–24. doi:10.1172/JCI21545
21. Morsch M, Reddel SW, Ghazanfari N, Toyka KV, Phillips WD. Muscle specific kinase autoantibodies cause synaptic failure through progressive wastage of postsynaptic acetylcholine receptors. *Exp Neurol* (2012) 237(2):286–95. doi:10.1016/j.expneurol.2012.06.034
22. Selcen D, Fukuda T, Shen XM, Engel AG. Are MuSK antibodies the primary cause of myasthenic symptoms? *Neurology* (2004) 62(11):1945–50. doi:10.1212/01.WNL.0000128048.23930.1D
23. Shiraishi H, Motomura M, Yoshimura T, Fukudome T, Fukuda T, Nakao Y, et al. Acetylcholine receptors loss and postsynaptic damage in MuSK antibody-positive myasthenia gravis. *Ann Neurol* (2005) 57(2):289–93. doi:10.1002/ana.20341
24. Farrugia ME, Kennett RP, Newsom-Davis J, Hilton-Jones D, Vincent A. Single-fiber electromyography in limb and facial muscles in muscle-specific kinase antibody and acetylcholine receptor antibody myasthenia gravis. *Muscle Nerve* (2006) 33(4):568–70. doi:10.1002/mus.20491
25. Cole RN, Reddel SW, Gervasio OL, Phillips WD. Anti-MuSK patient antibodies disrupt the mouse neuromuscular junction. *Ann Neurol* (2008) 63(6):782–9. doi:10.1002/ana.21371
26. Viegas S, Jacobson L, Waters P, Cossins J, Jacob S, Leite MI, et al. Passive and active immunization models of MuSK-Ab positive myasthenia: electrophysiological evidence for pre and postsynaptic defects. *Exp Neurol* (2012) 234(2):506–12. doi:10.1016/j.expneurol.2012.01.025
27. Hoch W, McConville J, Helms S, Newsom-Davis J, Melms A, Vincent A. Auto-antibodies to the receptor tyrosine kinase MuSK in patients with myasthenia gravis without acetylcholine receptor antibodies. *Nat Med* (2001) 7(3):365–8. doi:10.1038/85520
28. Cole RN, Ghazanfari N, Ngo ST, Gervasio OL, Reddel SW, Phillips WD. Patient autoantibodies deplete postsynaptic muscle-specific kinase leading to disassembly of the ACh receptor scaffold and myasthenia gravis in mice. *J Physiol* (2010) 588(Pt 17):3217–29. doi:10.1113/jphysiol.2010.190298

29. Miura Y, Devaux JJ, Fukami Y, Manso C, Belghazi M, Wong AH, et al. Contactin 1 IgG4 associates to chronic inflammatory demyelinating polyneuropathy with sensory ataxia. *Brain* (2015) 138(Pt 6):1484–91. doi:10.1093/brain/awv054
30. Labasque M, Hivert B, Nogales-Gadea G, Querol L, Illa I, Faivre-Sarrailh C. Specific contactin N-glycans are implicated in neurofascin binding and autoimmune targeting in peripheral neuropathies. *J Biol Chem* (2014) 289(11):7907–18. doi:10.1074/jbc.M113.528489
31. Manso C, Querol L, Mekaouche M, Illa I, Devaux JJ. Contactin-1 IgG4 antibodies cause paranode dismantling and conduction defects. *Brain* (2016) 139(Pt 6):1700–12. doi:10.1093/brain/aww062
32. Querol L, Rojas-Garcia R, Diaz-Manera J, Barcena J, Pardo J, Ortega-Moreno A, et al. Rituximab in treatment-resistant CIDP with antibodies against paranodal proteins. *Neurol Neuroimmunol Neuroinflamm* (2015) 2(5):e149. doi:10.1212/NXI.0000000000000149
33. Mathey EK, Garg N, Park SB, Nguyen T, Baker S, Yuki N, et al. Autoantibody responses to nodal and paranodal antigens in chronic inflammatory neuropathies. *J Neuroimmunol* (2017) 309:41–6. doi:10.1016/j.jneuroim.2017.05.002
34. Doppler K, Appeltshauser L, Wilhelmi K, Villmann C, Dib-Hajj SD, Waxman SG, et al. Destruction of paranodal architecture in inflammatory neuropathy with anti-contactin-1 autoantibodies. *J Neurol Neurosurg Psychiatry* (2015) 86(7):720–8. doi:10.1136/jnnp-2014-309916
35. Querol L, Nogales-Gadea G, Rojas-Garcia R, Martinez-Hernandez E, Diaz-Manera J, Suarez-Calvet X, et al. Antibodies to contactin-1 in chronic inflammatory demyelinating polyneuropathy. *Ann Neurol* (2013) 73(3):370–80. doi:10.1002/ana.23794
36. Futei Y, Amagai M, Ishii K, Kuroda-Kinoshita K, Ohya K, Nishikawa T. Predominant IgG4 subclass in autoantibodies of pemphigus vulgaris and foliaceus. *J Dermatol Sci* (2001) 26(1):55–61. doi:10.1016/S0923-1811(00)00158-4
37. Rock B, Martins CR, Theofilopoulos AN, Balderas RS, Anhalt GJ, Labib RS, et al. The pathogenic effect of IgG4 autoantibodies in endemic pemphigus foliaceus (fogo selvagem). *N Engl J Med* (1989) 320(22):1463–9. doi:10.1056/NEJM198906013202206
38. Stanley JR, Amagai M. Pemphigus, bullous impetigo, and the staphylococcal scalded-skin syndrome. *N Engl J Med* (2006) 355(17):1800–10. doi:10.1056/NEJMra061111
39. Amagai M. Desmoglein as a target in autoimmunity and infection. *J Am Acad Dermatol* (2003) 48(2):244–52. doi:10.1067/mjd.2003.7
40. Boggon TJ, Murray J, Chappuis-Flament S, Wong E, Gumbiner BM, Shapiro L. C-cadherin ectodomain structure and implications for cell adhesion mechanisms. *Science* (2002) 296(5571):1308–13. doi:10.1126/science.1071559
41. Harrison OJ, Brasch J, Lasso G, Katsamba PS, Ahlsen G, Honig B, et al. Structural basis of adhesive binding by desmocollins and desmogleins. *Proc Natl Acad Sci U S A* (2016) 113(26):7160–5. doi:10.1073/pnas.1606272113
42. Tsunoda K, Ota T, Aoki M, Yamada T, Nagai T, Nakagawa T, et al. Induction of pemphigus phenotype by a mouse monoclonal antibody against the amino-terminal adhesive interface of desmoglein 3. *J Immunol* (2003) 170(4):2170–8. doi:10.4049/jimmunol.170.4.2170
43. Di Zenzo G, Di Lullo G, Corti D, Calabresi V, Sinistro A, Vanzetta F, et al. Pemphigus autoantibodies generated through somatic mutations target the desmoglein-3 cis-interface. *J Clin Invest* (2012) 122(10):3781–90. doi:10.1172/JCI64413
44. Oktarina DA, van der Wier G, Diercks GF, Jonkman MF, Pas HH. IgG-induced clustering of desmogleins 1 and 3 in skin of patients with pemphigus fits with the desmoglein nonassembly depletion hypothesis. *Br J Dermatol* (2011) 165(3):552–62. doi:10.1111/j.1365-2133.2011.10463.x
45. van der Wier G, Pas HH, Kramer D, Diercks GFH, Jonkman MF. Smaller desmosomes are seen in the skin of pemphigus patients with anti-desmoglein 1 antibodies but not in patients with anti-desmoglein 3 antibodies. *J Invest Dermatol* (2014) 134(8):2287–90. doi:10.1038/jid.2014.140
46. Aoyama Y, Kitajima Y. Pemphigus vulgaris-IgG causes a rapid depletion of desmoglein 3 (Dsg3) from the Triton X-100 soluble pools, leading to the formation of Dsg3-depleted desmosomes in a human squamous carcinoma cell line, DJM-1 cells. *J Invest Dermatol* (1999) 112(1):67–71. doi:10.1046/j.1523-1747.1999.00463.x
47. Jennings JM, Tucker DK, Kottke MD, Saito M, Delva E, Hanakawa Y, et al. Desmosome disassembly in response to pemphigus vulgaris IgG occurs in distinct phases and can be reversed by expression of exogenous Dsg3. *J Invest Dermatol* (2011) 131(3):706–18. doi:10.1038/jid.2010.389
48. Stahley SN, Saito M, Faundez V, Koval M, Mattheyses AL, Kowalczyk AP. Desmosome assembly and disassembly are membrane raft-dependent. *PLoS One* (2014) 9(1):e87809. doi:10.1371/journal.pone.0087809
49. Mao X, Choi EJ, Payne AS. Disruption of desmosome assembly by monovalent human pemphigus vulgaris monoclonal antibodies. *J Invest Dermatol* (2009) 129(4):908–18. doi:10.1038/jid.2008.339
50. Calkins CC, Setzer SV, Jennings JM, Summers S, Tsunoda K, Amagai M, et al. Desmoglein endocytosis and desmosome disassembly are coordinated responses to pemphigus autoantibodies. *J Biol Chem* (2006) 281(11):7623–34. doi:10.1074/jbc.M512447200
51. Saito M, Stahley SN, Caughman CY, Mao X, Tucker DK, Payne AS, et al. Signaling dependent and independent mechanisms in pemphigus vulgaris blister formation. *PLoS One* (2012) 7(12):e50696. doi:10.1371/journal.pone.0050696
52. Kasperkiewicz M, Ellebrecht CT, Takahashi H, Yamagami J, Zillikens D, Payne AS, et al. Pemphigus. *Nat Rev Dis Primers* (2017) 3:17026. doi:10.1038/nrdp.2017.26
53. Yamagami J, Payne AS, Kacir S, Ishii K, Siegel DL, Stanley JR. Homologous regions of autoantibody heavy chain complementarity-determining region 3 (H-CDR3) in patients with pemphigus cause pathogenicity. *J Clin Invest* (2010) 120(11):4111–7. doi:10.1172/JCI44425
54. Zhao CY, Chiang YZ, Murrell DF. Neonatal autoimmune blistering disease: a systematic review. *Pediatr Dermatol* (2016) 33(4):367–74. doi:10.1111/pde.12859
55. Cho MJ, Lo AS, Mao X, Nagler AR, Ellebrecht CT, Mukherjee EM, et al. Shared VH1-46 gene usage by pemphigus vulgaris autoantibodies indicates common humoral immune responses among patients. *Nat Commun* (2014) 5:4167. doi:10.1038/ncomms5167
56. Joly P, Maho-Vaillant M, Prost-Squarcioni C, Hebert V, Houivet E, Calbo S, et al. First-line rituximab combined with short-term prednisone versus prednisone alone for the treatment of pemphigus (Ritux 3): a prospective, multicentre, parallel-group, open-label randomised trial. *Lancet* (2017) 389(10083):2031–40. doi:10.1016/S0140-6736(17)30070-3
57. Payne AS, Ishii K, Kacir S, Lin C, Li H, Hanakawa Y, et al. Genetic and functional characterization of human pemphigus vulgaris monoclonal autoantibodies isolated by phage display. *J Clin Invest* (2005) 115(4):888–99. doi:10.1172/JCI24185
58. Casina VC, Hu W, Mao JH, Lu RN, Hanby HA, Pickens B, et al. High-resolution epitope mapping by HX MS reveals the pathogenic mechanism and a possible therapy for autoimmune TTP syndrome. *Proc Natl Acad Sci U S A* (2015) 112(31):9620–5. doi:10.1073/pnas.1512561112
59. Ostertag EM, Bdeir K, Kacir S, Thiboutot M, Gulendran G, Yunk L, et al. ADAMTS13 autoantibodies cloned from patients with acquired thrombotic thrombocytopenic purpura: 2. Pathogenicity in an animal model. *Transfusion* (2016) 56(7):1775–85. doi:10.1111/trf.13583
60. Tsai HM, Lian EC. Antibodies to von Willebrand factor-cleaving protease in acute thrombotic thrombocytopenic purpura. *N Engl J Med* (1998) 339(22):1585–94. doi:10.1056/NEJM199811263392203
61. Ostertag EM, Kacir S, Thiboutot M, Gulendran G, Zheng XL, Cines DB, et al. ADAMTS13 autoantibodies cloned from patients with acquired thrombotic thrombocytopenic purpura: 1. Structural and functional characterization in vitro. *Transfusion* (2016) 56(7):1763–74. doi:10.1111/trf.13584
62. Ferrari S, Mudde GC, Rieger M, Veyradier A, Kremer Hovinga JA, Scheiflinger F. IgG subclass distribution of anti-ADAMTS13 antibodies in patients with acquired thrombotic thrombocytopenic purpura. *J Thromb Haemost* (2009) 7(10):1703–10. doi:10.1111/j.1538-7836.2009.03568.x
63. Nakao H, Ishiguro A, Ikoma N, Nishi K, Su C, Nakadate H, et al. Acquired idiopathic thrombotic thrombocytopenic purpura successfully treated with intravenous immunoglobulin and glucocorticoid: a case report. *Medicine (Baltimore)* (2017) 96(14):e6547. doi:10.1097/MD.0000000000006547
64. Coppo P, Busson M, Veyradier A, Wynckel A, Poullin P, Azoulay E, et al. HLA-DRB1*11: a strong risk factor for acquired severe ADAMTS13 deficiency-related idiopathic thrombotic thrombocytopenic purpura in Caucasians. *J Thromb Haemost* (2010) 8(4):856–9. doi:10.1111/j.1538-7836.2010.03772.x
65. Sinkovits G, Szilagyi A, Farkas P, Inotai D, Szilvasi A, Tordai A, et al. The role of human leukocyte antigen DRB1-DQB1 haplotypes in the susceptibility to acquired idiopathic thrombotic thrombocytopenic purpura. *Hum Immunol* (2017) 78(2):80–7. doi:10.1016/j.humimm.2016.11.005

66. Ferrari S, Palavra K, Gruber B, Kremer Hovinga JA, Knobl P, Caron C, et al. Persistence of circulating ADAMTS13-specific immune complexes in patients with acquired thrombotic thrombocytopenic purpura. *Haematologica* (2014) 99(4):779–87. doi:10.3324/haematol.2013.094151
67. Feys HB, Roodt J, Vandeputte N, Pareyn I, Lamprecht S, van Rensburg WJ, et al. Thrombotic thrombocytopenic purpura directly linked with ADAMTS13 inhibition in the baboon (*Papio ursinus*). *Blood* (2010) 116(12):2005–10. doi:10.1182/blood-2010-04-280479
68. Luken BM, Turenhout EA, Hulstein JJ, Van Mourik JA, Fijnheer R, Voorberg J. The spacer domain of ADAMTS13 contains a major binding site for antibodies in patients with thrombotic thrombocytopenic purpura. *Thromb Haemost* (2005) 93(2):267–74. doi:10.1160/TH04-05-0301
69. Schaller M, Vogel M, Kentouche K, Lammle B, Kremer Hovinga JA. The splenic autoimmune response to ADAMTS13 in thrombotic thrombocytopenic purpura contains recurrent antigen-binding CDR3 motifs. *Blood* (2014) 124(23):3469–79. doi:10.1182/blood-2014-04-561142
70. Ohkawa T, Fukata Y, Yamasaki M, Miyazaki T, Yokoi N, Takashima H, et al. Autoantibodies to epilepsy-related LGI1 in limbic encephalitis neutralize LGI1-ADAM22 interaction and reduce synaptic AMPA receptors. *J Neurosci* (2013) 33(46):18161–74. doi:10.1523/JNEUROSCI.3506-13.2013
71. Irani SR, Pettingill P, Kleopa KA, Schiza N, Waters P, Mazia C, et al. Morvan syndrome: clinical and serological observations in 29 cases. *Ann Neurol* (2012) 72(2):241–55. doi:10.1002/ana.23577
72. Arino H, Armangue T, Petit-Pedrol M, Sabater L, Martinez-Hernandez E, Hara M, et al. Anti-LGI1-associated cognitive impairment: presentation and long-term outcome. *Neurology* (2016) 87(8):759–65. doi:10.1212/WNL.0000000000003009
73. Bien CG, Vincent A, Barnett MH, Becker AJ, Blumcke I, Graus F, et al. Immunopathology of autoantibody-associated encephalitides: clues for pathogenesis. *Brain* (2012) 135(Pt 5):1622–38. doi:10.1093/brain/aws082
74. Lalic T, Pettingill P, Vincent A, Capogna M. Human limbic encephalitis serum enhances hippocampal mossy fiber-CA3 pyramidal cell synaptic transmission. *Epilepsia* (2011) 52(1):121–31. doi:10.1111/j.1528-1167.2010.02756.x
75. van Sonderen A, Roelen DL, Stoop JA, Verdijk RM, Haasnoot GW, Thijs RD, et al. Anti-LGI1 encephalitis is strongly associated with HLA-DR7 and HLA-DRB4. *Ann Neurol* (2017) 81(2):193–8. doi:10.1002/ana.24858
76. Kim TJ, Lee ST, Moon J, Sunwoo JS, Byun JI, Lim JA, et al. Anti-LGI1 encephalitis is associated with unique HLA subtypes. *Ann Neurol* (2017) 81(2):183–92. doi:10.1002/ana.24860
77. van Sonderen A, Thijs RD, Coenders EC, Jiskoot LC, Sanchez E, de Bruijn MA, et al. Anti-LGI1 encephalitis: clinical syndrome and long-term follow-up. *Neurology* (2016) 87(14):1449–56. doi:10.1212/WNL.0000000000003173
78. Irani SR, Gelfand JM, Bettcher BM, Singhal NS, Geschwind MD. Effect of rituximab in patients with leucine-rich, glioma-inactivated 1 antibody-associated encephalopathy. *JAMA Neurol* (2014) 71(7):896–900. doi:10.1001/jamaneurol.2014.463
79. Ng JK, Malotka J, Kawakami N, Derfuss T, Khademi M, Olsson T, et al. Neurofascin as a target for autoantibodies in peripheral neuropathies. *Neurology* (2012) 79(23):2241–8. doi:10.1212/WNL.0b013e31827689ad
80. Querol L, Devaux J, Rojas-Garcia R, Illa I. Autoantibodies in chronic inflammatory neuropathies: diagnostic and therapeutic implications. *Nat Rev Neurol* (2017) 13(9):533–47. doi:10.1038/nrneurol.2017.84
81. Devaux JJ, Miura Y, Fukami Y, Inoue T, Manso C, Belghazi M, et al. Neurofascin-155 IgG4 in chronic inflammatory demyelinating polyneuropathy. *Neurology* (2016) 86(9):800–7. doi:10.1212/WNL.0000000000002418
82. Shimizu M, Koda T, Nakatsuji Y, Ogata H, Kira JI, Mochizuki H. A case of anti-neurofascin 155 antibody-positive combined central and peripheral demyelination successfully treated with plasma exchange. *Rinsho Shinkeigaku* (2017) 57(1):41–4. doi:10.5692/clinicalneurol.cn-000964
83. Querol L, Nogales-Gadea G, Rojas-Garcia R, Diaz-Manera J, Pardo J, Ortega-Moreno A, et al. Neurofascin IgG4 antibodies in CIDP associate with disabling tremor and poor response to IVIg. *Neurology* (2014) 82(10):879–86. doi:10.1212/WNL.0000000000000205
84. Kadoya M, Kaida K, Koike H, Takazaki H, Ogata H, Moriguchi K, et al. IgG4 anti-neurofascin155 antibodies in chronic inflammatory demyelinating polyradiculoneuropathy: clinical significance and diagnostic utility of a conventional assay. *J Neuroimmunol* (2016) 301:16–22. doi:10.1016/j.jneuroim.2016.10.013
85. Ogata H, Yamasaki R, Hiwatashi A, Oka N, Kawamura N, Matsuse D, et al. Characterization of IgG4 anti-neurofascin 155 antibody-positive polyneuropathy. *Ann Clin Transl Neurol* (2015) 2(10):960–71. doi:10.1002/acn3.248
86. Olsen AL, Lai Y, Dalmau J, Scherer SS, Lancaster E. Caspr2 autoantibodies target multiple epitopes. *Neurol Neuroimmunol Neuroinflmm* (2015) 2(4):e127. doi:10.1212/NXI.0000000000000127
87. Pinatel D, Hivert B, Boucraut J, Saint-Martin M, Rogemond V, Zoupi L, et al. Inhibitory axons are targeted in hippocampal cell culture by anti-Caspr2 autoantibodies associated with limbic encephalitis. *Front Cell Neurosci* (2015) 9:265. doi:10.3389/fncel.2015.00265
88. van Sonderen A, Arino H, Petit-Pedrol M, Leypoldt F, Kortvelyessy P, Wandinger KP, et al. The clinical spectrum of Caspr2 antibody-associated disease. *Neurology* (2016) 87(5):521–8. doi:10.1212/WNL.0000000000002917
89. Kortvelyessy P, Bauer J, Stoppel CM, Bruck W, Gerth I, Vielhaber S, et al. Complement-associated neuronal loss in a patient with CASPR2 antibody-associated encephalitis. *Neurol Neuroimmunol Neuroinflamm* (2015) 2(2):e75. doi:10.1212/NXI.0000000000000075
90. Sunwoo JS, Lee ST, Byun JI, Moon J, Shin JW, Jeong DE, et al. Clinical manifestations of patients with CASPR2 antibodies. *J Neuroimmunol* (2015) 281:17–22. doi:10.1016/j.jneuroim.2015.03.005
91. Lancaster E, Huijbers MG, Bar V, Boronat A, Wong A, Martinez-Hernandez E, et al. Investigations of caspr2, an autoantigen of encephalitis and neuromyotonia. *Ann Neurol* (2011) 69(2):303–11. doi:10.1002/ana.22297
92. Bien CG, Mirzadjanova Z, Baumgartner C, Onugoren MD, Grunwald T, Holtkamp M, et al. Anti-contactin-associated protein-2 encephalitis: relevance of antibody titres, presentation and outcome. *Eur J Neurol* (2017) 24(1):175–86. doi:10.1111/ene.13180
93. Irani SR, Alexander S, Waters P, Kleopa KA, Pettingill P, Zuliani L, et al. Antibodies to Kv1 potassium channel-complex proteins leucine-rich, glioma inactivated 1 protein and contactin-associated protein-2 in limbic encephalitis, Morvan's syndrome and acquired neuromyotonia. *Brain* (2010) 133(9):2734–48. doi:10.1093/brain/awq213
94. Brimberg L, Mader S, Jeganathan V, Berlin R, Coleman TR, Gregersen PK, et al. Caspr2-reactive antibody cloned from a mother of an ASD child mediates an ASD-like phenotype in mice. *Mol Psychiatry* (2016) 21(12):1663–71. doi:10.1038/mp.2016.165
95. Sundal C, Vedeler C, Miletic H, Andersen O. Morvan syndrome with Caspr2 antibodies. Clinical and autopsy report. *J Neurol Sci* (2017) 372:453–5. doi:10.1016/j.jns.2016.10.046
96. Balint B, Regula JU, Jarius S, Wildemann B. Caspr2 antibodies in limbic encephalitis with cerebellar ataxia, dyskinesias and myoclonus. *J Neurol Sci* (2013) 327(1–2):73–4. doi:10.1016/j.jns.2013.01.040
97. Beck LH Jr, Salant DJ. Membranous nephropathy: from models to man. *J Clin Invest* (2014) 124(6):2307–14. doi:10.1172/JCI72270
98. Yang Y, Wang C, Jin L, He F, Li C, Gao Q, et al. IgG4 anti-phospholipase A2 receptor might activate lectin and alternative complement pathway meanwhile in idiopathic membranous nephropathy: an inspiration from a cross-sectional study. *Immunol Res* (2016) 64(4):919–30. doi:10.1007/s12026-016-8790-1
99. Segawa Y, Hisano S, Matsushita M, Fujita T, Hirose S, Takeshita M, et al. IgG subclasses and complement pathway in segmental and global membranous nephropathy. *Pediatr Nephrol* (2010) 25(6):1091–9. doi:10.1007/s00467-009-1439-8
100. Kanigicherla D, Gummadova J, McKenzie EA, Roberts SA, Harris S, Nikam M, et al. Anti-PLA2R antibodies measured by ELISA predict long-term outcome in a prevalent population of patients with idiopathic membranous nephropathy. *Kidney Int* (2013) 83(5):940–8. doi:10.1038/ki.2012.486
101. Fresquet M, Jowitt TA, Gummadova J, Collins R, O'Cualain R, McKenzie EA, et al. Identification of a major epitope recognized by PLA2R autoantibodies in primary membranous nephropathy. *J Am Soc Nephrol* (2015) 26(2):302–13. doi:10.1681/ASN.2014050502
102. Kao L, Lam V, Waldman M, Glassock RJ, Zhu Q. Identification of the immunodominant epitope region in phospholipase A2 receptor-mediating autoantibody binding in idiopathic membranous nephropathy. *J Am Soc Nephrol* (2015) 26(2):291–301. doi:10.1681/ASN.2013121315
103. Lhotta K, Wurzner R, Konig P. Glomerular deposition of mannose-binding lectin in human glomerulonephritis. *Nephrol Dial Transplant* (1999) 14(4):881–6. doi:10.1093/ndt/14.4.881

104. Lv J, Hou W, Zhou X, Liu G, Zhou F, Zhao N, et al. Interaction between PLA2R1 and HLA-DQA1 variants associates with anti-PLA2R antibodies and membranous nephropathy. *J Am Soc Nephrol* (2013) 24(8):1323–9. doi:10.1681/ASN.2012080771
105. Muller-Deile J, Schiffer L, Hiss M, Haller H, Schiffer M. A new rescue regimen with plasma exchange and rituximab in high-risk membranous glomerulonephritis. *Eur J Clin Invest* (2015) 45(12):1260–9. doi:10.1111/eci.12545
106. Beck LH Jr. PLA2R and THSD7A: disparate paths to the same disease? *J Am Soc Nephrol* (2017) 28(9):2579–89. doi:10.1681/ASN.2017020178
107. Borza DB. Alternative pathway dysregulation and the conundrum of complement activation by IgG4 immune complexes in membranous nephropathy. *Front Immunol* (2016) 7:157. doi:10.3389/fimmu.2016.00157
108. Ma H, Beck LJ, Salant D. Membranous nephropathy-associated anti-phospholipase A2 receptor IgG4 autoantibodies activate the lectin complement pathway (abstract). *J Am Soc Nephrol* (2011) 22:62A.
109. Hayashi N, Okada K, Matsui Y, Fujimoto K, Adachi H, Yamaya H, et al. Glomerular mannose-binding lectin deposition in intrinsic antigen-related membranous nephropathy. *Nephrol Dial Transplant* (2017). doi:10.1093/ndt/gfx235
110. Tomas NM, Beck LH Jr, Meyer-Schwesinger C, Seitz-Polski B, Ma H, Zahner G, et al. Thrombospondin type-1 domain-containing 7A in idiopathic membranous nephropathy. *N Engl J Med* (2014) 371(24):2277–87. doi:10.1056/NEJMoa1409354
111. Tomas NM, Hoxha E, Reinicke AT, Fester L, Helmchen U, Gerth J, et al. Autoantibodies against thrombospondin type 1 domain-containing 7A induce membranous nephropathy. *J Clin Invest* (2016) 126(7):2519–32. doi:10.1172/JCI85265
112. Tomas NM, Meyer-Schwesinger C, von Spiegel H, Kotb AM, Zahner G, Hoxha E, et al. A heterologous model of thrombospondin type 1 domain-containing 7A-associated membranous nephropathy. *J Am Soc Nephrol* (2017) 28(11):3262–77. doi:10.1681/ASN.2017010030
113. Kronbichler A, Oh J, Meijers B, Mayer G, Shin JI. Recent progress in deciphering the etiopathogenesis of primary membranous nephropathy. *Biomed Res Int* (2017) 2017:1936372. doi:10.1155/2017/1936372
114. Iwakura T, Ohashi N, Kato A, Baba S, Yasuda H. Prevalence of enhanced granular expression of thrombospondin type-1 domain-containing 7A in the glomeruli of Japanese patients with idiopathic membranous nephropathy. *PLoS One* (2015) 10(9):e0138841. doi:10.1371/journal.pone.0138841
115. Hoxha E, Beck LH Jr, Wiech T, Tomas NM, Probst C, Mindorf S, et al. An indirect immunofluorescence method facilitates detection of thrombospondin type 1 domain-containing 7A-specific antibodies in membranous nephropathy. *J Am Soc Nephrol* (2017) 28(2):520–31. doi:10.1681/ASN.2016010050
116. Hoxha E, Wiech T, Stahl PR, Zahner G, Tomas NM, Meyer-Schwesinger C, et al. A mechanism for cancer-associated membranous nephropathy. *N Engl J Med* (2016) 374(20):1995–6. doi:10.1056/NEJMc1511702
117. Iwakura T, Fujigaki Y, Katahashi N, Sato T, Ishigaki S, Tsuji N, et al. Membranous nephropathy with an enhanced granular expression of thrombospondin type-1 domain-containing 7A in a pregnant woman. *Intern Med* (2016) 55(18):2663–8. doi:10.2169/internalmedicine.55.6726
118. Wang J, Cui Z, Lu J, Probst C, Zhang YM, Wang X, et al. Circulating antibodies against thrombospondin type-I domain-containing 7A in chinese patients with idiopathic membranous nephropathy. *Clin J Am Soc Nephrol* (2017) 12(10):1642–51. doi:10.2215/CJN.01460217
119. Ohlsson S, Herlitz H, Lundberg S, Selga D, Molne J, Wieslander J, et al. Circulating anti-glomerular basement membrane antibodies with predominance of subclass IgG4 and false-negative immunoassay test results in anti-glomerular basement membrane disease. *Am J Kidney Dis* (2014) 63(2):289–93. doi:10.1053/j.ajkd.2013.08.032
120. Cui Z, Zhao MH, Singh AK, Wang HY. Antiglomerular basement membrane disease with normal renal function. *Kidney Int* (2007) 72(11):1403–8. doi:10.1038/sj.ki.5002525
121. Nasr SH, Collins AB, Alexander MP, Schraith DF, Herrera Hernandez L, Fidler ME, et al. The clinicopathologic characteristics and outcome of atypical anti-glomerular basement membrane nephritis. *Kidney Int* (2016) 89(4):897–908. doi:10.1016/j.kint.2016.02.001
122. Qu Z, Cui Z, Liu G, Zhao MH. The distribution of IgG subclass deposition on renal tissues from patients with anti-glomerular basement membrane disease. *BMC Immunol* (2013) 14:19. doi:10.1186/1471-2172-14-19
123. Rosales IA, Colvin RB. Glomerular disease with idiopathic linear immunoglobulin deposition: a rose by any other name would be atypical. *Kidney Int* (2016) 89(4):750–2. doi:10.1016/j.kint.2016.01.018
124. Doppler K, Appeltshauser L, Villmann C, Martin C, Peles E, Kramer HH, et al. Auto-antibodies to contactin-associated protein 1 (Caspr) in two patients with painful inflammatory neuropathy. *Brain* (2016) 139(Pt 10):2617–30. doi:10.1093/brain/aww189
125. Hara M, Arino H, Petit-Pedrol M, Sabater L, Titulaer MJ, Martinez-Hernandez E, et al. DPPX antibody-associated encephalitis: main syndrome and antibody effects. *Neurology* (2017) 88(14):1340–8. doi:10.1212/WNL.0000000000003796
126. Doherty L, Gold D, Solnes L, Probasco J, Venkatesan A. Anti-DPPX encephalitis: prominent nystagmus reflected by extraocular muscle FDG-PET avidity. *Neurol Neuroimmunol Neuroinflamm* (2017) 4(4):e361. doi:10.1212/NXI.0000000000000361
127. Piepgras J, Holtje M, Michel K, Li Q, Otto C, Drenckhahn C, et al. Anti-DPPX encephalitis: pathogenic effects of antibodies on gut and brain neurons. *Neurology* (2015) 85(10):890–7. doi:10.1212/WNL.0000000000001907
128. Boronat A, Gelfand JM, Gresa-Arribas N, Jeong HY, Walsh M, Roberts K, et al. Encephalitis and antibodies to dipeptidyl-peptidase-like protein-6, a subunit of Kv4.2 potassium channels. *Ann Neurol* (2013) 73(1):120–8. doi:10.1002/ana.23756
129. Tobin WO, Lennon VA, Komorowski L, Probst C, Clardy SL, Aksamit AJ, et al. DPPX potassium channel antibody: frequency, clinical accompaniments, and outcomes in 20 patients. *Neurology* (2014) 83(20):1797–803. doi:10.1212/WNL.0000000000000991
130. Sabater L, Gaig C, Gelpi E, Bataller L, Lewerenz J, Torres-Vega E, et al. A novel non-rapid-eye movement and rapid-eye-movement parasomnia with sleep breathing disorder associated with antibodies to IgLON5: a case series, characterisation of the antigen, and post-mortem study. *Lancet Neurol* (2014) 13(6):575–86. doi:10.1016/S1474-4422(14)70051-1
131. Honorat JA, Komorowski L, Josephs KA, Fechner K, St Louis EK, Hinson SR, et al. IgLON5 antibody: neurological accompaniments and outcomes in 20 patients. *Neurol Neuroimmunol Neuroinflamm* (2017) 4(5):e385. doi:10.1212/NXI.0000000000000385
132. Haitao R, Yingmai Y, Yan H, Fei H, Xia L, Honglin H, et al. Chorea and parkinsonism associated with autoantibodies to IgLON5 and responsive to immunotherapy. *J Neuroimmunol* (2016) 300:9–10. doi:10.1016/j.jneuroim.2016.09.012
133. Bonello M, Jacob A, Ellul MA, Barker E, Parker R, Jefferson S, et al. IgLON5 disease responsive to immunotherapy. *Neurolo Neuroimmunol Neuroinflamm* (2017) 4(5):e383. doi:10.1212/NXI.0000000000000383
134. Sabater L, Planaguma J, Dalmau J, Graus F. Cellular investigations with human antibodies associated with the anti-IgLON5 syndrome. *J Neuroinflammation* (2016) 13(1):226. doi:10.1186/s12974-016-0689-1
135. Hogl B, Heidbreder A, Santamaria J, Graus F, Poewe W. IgLON5 autoimmunity and abnormal behaviours during sleep. *Lancet* (2015) 385(9977):1590. doi:10.1016/S0140-6736(15)60445-7
136. Schur PH. IgG subclasses. A historical perspective. *Monogr Allergy* (1988) 23:1–11.
137. French M. Serum IgG subclasses in normal adults. *Monogr Allergy* (1986) 19:100–7.
138. Aucouturier P, Danon F, Daveau M, Guillou B, Sabbah A, Besson J, et al. Measurement of serum IgG4 levels by a competitive immunoenzymatic assay with monoclonal antibodies. *J Immunol Methods* (1984) 74(1):151–62. doi:10.1016/0022-1759(84)90376-4
139. Briles DE, Claflin JL, Schroer K, Forman C. Mouse Igg3 antibodies are highly protective against infection with *Streptococcus pneumoniae*. *Nature* (1981) 294(5836):88–90. doi:10.1038/294088a0
140. Ey PL, Russell-Jones GJ, Jenkin CR. Isotypes of mouse IgG – I. Evidence for 'non-complement-fixing' IgG1 antibodies and characterization of their capacity to interfere with IgG2 sensitization of target red blood cells for lysis by complement. *Mol Immunol* (1980) 17(6):699–710. doi:10.1016/0161-5890(80)90139-X
141. Germann T, Bongartz M, Dlugonska H, Hess H, Schmitt E, Kolbe L, et al. Interleukin-12 profoundly up-regulates the synthesis of antigen-specific complement-fixing IgG2a, IgG2b and IgG3 antibody subclasses in vivo. *Eur J Immunol* (1995) 25(3):823–9. doi:10.1002/eji.1830250329

142. Saadoun S, Waters P, Bell BA, Vincent A, Verkman AS, Papadopoulos MC. Intra-cerebral injection of neuromyelitis optica immunoglobulin G and human complement produces neuromyelitis optica lesions in mice. *Brain* (2010) 133(Pt 2):349–61. doi:10.1093/brain/awp309
143. Pinck JR, Milstein C. Disulphide bridges of a human immunoglobulin G protein. *Nature* (1967) 216(5118):941–2. doi:10.1038/216941a0
144. Frangione B, Milstein C. Disulphide bridges of immunoglobulin G-1 heavy chains. *Nature* (1967) 216(5118):939–41. doi:10.1038/216939b0
145. Frangione B, Milstein C, Pink JR. Structural studies of immunoglobulin G. *Nature* (1969) 221(5176):145–8. doi:10.1038/221145a0
146. Schroeder HW Jr, Cavacini L. Structure and function of immunoglobulins. *J Allergy Clin Immunol* (2010) 125(2 Suppl 2):S41–52. doi:10.1016/j.jaci.2009.09.046
147. Lighaam LC, Rispens T. The immunobiology of immunoglobulin G4. *Semin Liver Dis* (2016) 36(3):200–15. doi:10.1055/s-0036-1584322
148. Lu Y, Harding SE, Michaelsen TE, Longman E, Davis KG, Ortega A, et al. Solution conformation of wild-type and mutant IgG3 and IgG4 immunoglobulins using crystallohydrodynamics: possible implications for complement activation. *Biophys J* (2007) 93(11):3733–44. doi:10.1529/biophysj.107.108993
149. Abe Y, Gor J, Bracewell DG, Perkins SJ, Dalby PA. Masking of the Fc region in human IgG4 by constrained X-ray scattering modelling: implications for antibody function and therapy. *Biochem J* (2010) 432(1):101–11. doi:10.1042/BJ20100641
150. Tao MH, Smith RI, Morrison SL. Structural features of human immunoglobulin G that determine isotype-specific differences in complement activation. *J Exp Med* (1993) 178(2):661–7. doi:10.1084/jem.178.2.661
151. Brekke OH, Michaelsen TE, Aase A, Sandin RH, Sandlie I. Human IgG isotype-specific amino acid residues affecting complement-mediated cell lysis and phagocytosis. *Eur J Immunol* (1994) 24(10):2542–7. doi:10.1002/eji.1830241042
152. Canfield SM, Morrison SL. The binding affinity of human IgG for its high affinity Fc receptor is determined by multiple amino acids in the CH2 domain and is modulated by the hinge region. *J Exp Med* (1991) 173(6):1483–91. doi:10.1084/jem.173.6.1483
153. Sondermann P, Huber R, Oosthuizen V, Jacob U. The 3.2-A crystal structure of the human IgG1 Fc fragment-Fc gammaRIII complex. *Nature* (2000) 406(6793):267–73. doi:10.1038/35018508
154. Shields RL, Namenuk AK, Hong K, Meng YG, Rae J, Briggs J, et al. High resolution mapping of the binding site on human IgG1 for Fc gamma RI, Fc gamma RII, Fc gamma RIII, and FcRn and design of IgG1 variants with improved binding to the Fc gamma R. *J Biol Chem* (2001) 276(9):6591–604. doi:10.1074/jbc.M009483200
155. Radaev S, Motyka S, Fridman WH, Sautes-Fridman C, Sun PD. The structure of a human type III Fcgamma receptor in complex with Fc. *J Biol Chem* (2001) 276(19):16469–77. doi:10.1074/jbc.M100350200
156. Schuurman J, Perdok GJ, Gorter AD, Aalberse RC. The inter-heavy chain disulfide bonds of IgG4 are in equilibrium with intra-chain disulfide bonds. *Mol Immunol* (2001) 38(1):1–8. doi:10.1016/S0161-5890(01)00050-5
157. Bloom JW, Madanat MS, Marriott D, Wong T, Chan SY. Intrachain disulfide bond in the core hinge region of human IgG4. *Protein Sci* (1997) 6(2):407–15. doi:10.1002/pro.5560060217
158. Angal S, King DJ, Bodmer MW, Turner A, Lawson AD, Roberts G, et al. A single amino acid substitution abolishes the heterogeneity of chimeric mouse/human (IgG4) antibody. *Mol Immunol* (1993) 30(1):105–8. doi:10.1016/0161-5890(93)90432-B
159. Davies AM, Rispens T, den Bleker TH, McDonnell JM, Gould HJ, Aalberse RC, et al. Crystal structure of the human IgG4 C(H)3 dimer reveals the role of Arg409 in the mechanism of Fab-arm exchange. *Mol Immunol* (2013) 54(1):1–7. doi:10.1016/j.molimm.2012.10.029
160. Labrijn AF, Rispens T, Meesters J, Rose RJ, den Bleker TH, Loverix S, et al. Species-specific determinants in the IgG CH3 domain enable Fab-arm exchange by affecting the noncovalent CH3-CH3 interaction strength. *J Immunol* (2011) 187(6):3238–46. doi:10.4049/jimmunol.1003336
161. King DJ, Adair JR, Angal S, Low DC, Proudfoot KA, Lloyd JC, et al. Expression, purification and characterization of a mouse-human chimeric antibody and chimeric Fab' fragment. *Biochem J* (1992) 281(Pt 2):317–23. doi:10.1042/bj2810317
162. Margni RA, Binaghi RA. Nonprecipitating asymmetric antibodies. *Annu Rev Immunol* (1988) 6:535–54. doi:10.1146/annurev.iy.06.040188.002535
163. van der Zee JS, van Swieten P, Aalberse RC. Serologic aspects of IgG4 antibodies. II. IgG4 antibodies form small, nonprecipitating immune complexes due to functional monovalency. *J Immunol* (1986) 137(11):3566–71.
164. Petersen JG, Dorrington KJ. An in vitro system for studying the kinetics of interchain disulfide bond formation in immunoglobulin G. *J Biol Chem* (1974) 249(17):5633–41.
165. Colcher D, Milenic D, Roselli M, Raubitschek A, Yarranton G, King D, et al. Characterization and biodistribution of recombinant and recombinant/chimeric constructs of monoclonal antibody B72.3. *Cancer Res* (1989) 49(7):1738–45.
166. van der Neut Kolfschoten M, Schuurman J, Losen M, Bleeker WK, Martinez-Martinez P, Vermeulen E, et al. Anti-inflammatory activity of human IgG4 antibodies by dynamic Fab arm exchange. *Science* (2007) 317(5844):1554–7. doi:10.1126/science.1144603
167. Rispens T, Davies AM, Ooijevaar-de Heer P, Absalah S, Bende O, Sutton BJ, et al. Dynamics of inter-heavy chain interactions in human immunoglobulin G (IgG) subclasses studied by kinetic Fab arm exchange. *J Biol Chem* (2014) 289(9):6098–109. doi:10.1074/jbc.M113.541813
168. Vidarsson G, Dekkers G, Rispens T. IgG subclasses and allotypes: from structure to effector functions. *Front Immunol* (2014) 5:520. doi:10.3389/fimmu.2014.00520
169. Nirula A, Glaser SM, Kalled SL, Taylor FR. What is IgG4? A review of the biology of a unique immunoglobulin subtype. *Curr Opin Rheumatol* (2011) 23(1):119–24. doi:10.1097/BOR.0b013e3283412fd4
170. Aalberse RC, Stapel SO, Schuurman J, Rispens T. Immunoglobulin G4: an odd antibody. *Clin Exp Allergy* (2009) 39(4):469–77. doi:10.1111/j.1365-2222.2009.03207.x
171. Hansen K, Ruttekolk IR, Glauner H, Becker F, Brock R, Hannus S. The in vitro biological activity of the HLA-DR-binding clinical IgG4 antibody 1D09C3 is a consequence of the disruption of cell aggregates and can be abrogated by Fab arm exchange. *Mol Immunol* (2009) 46(16):3269–77. doi:10.1016/j.molimm.2009.07.031
172. Labrijn AF, Buijsse AO, van den Bremer ET, Verwilligen AY, Bleeker WK, Thorpe SJ, et al. Therapeutic IgG4 antibodies engage in Fab-arm exchange with endogenous human IgG4 in vivo. *Nat Biotechnol* (2009) 27(8):767–71. doi:10.1038/nbt.1553
173. Young E, Lock E, Ward DG, Cook A, Harding S, Wallis GL. Estimation of polyclonal IgG4 hybrids in normal human serum. *Immunology* (2014) 142(3):406–13. doi:10.1111/imm.12265
174. Rispens T, Ooijevaar-de Heer P, Bende O, Aalberse RC. Mechanism of immunoglobulin G4 Fab-arm exchange. *J Am Chem Soc* (2011) 133(26):10302–11. doi:10.1021/ja203638y
175. Stubenrauch K, Wessels U, Regula JT, Kettenberger H, Schleypen J, Kohnert U. Impact of molecular processing in the hinge region of therapeutic IgG4 antibodies on disposition profiles in cynomolgus monkeys. *Drug Metab Dispos* (2010) 38(1):84–91. doi:10.1124/dmd.109.029751
176. Rispens T, den Bleker TH, Aalberse RC. Hybrid IgG4/IgG4 Fc antibodies form upon 'Fab-arm' exchange as demonstrated by SDS-PAGE or size-exclusion chromatography. *Mol Immunol* (2010) 47(7–8):1592–4. doi:10.1016/j.molimm.2010.02.021
177. Jones DP, Liang Y. Measuring the poise of thiol/disulfide couples in vivo. *Free Radic Biol Med* (2009) 47(10):1329–38. doi:10.1016/j.freeradbiomed.2009.08.021
178. Shapiro RI, Plavina T, Schlain BR, Pepinsky RB, Garber EA, Jarpe M, et al. Development and validation of immunoassays to quantify the half-antibody exchange of an IgG4 antibody, natalizumab (Tysabri(R)) with endogenous IgG4. *J Pharm Biomed Anal* (2011) 55(1):168–75. doi:10.1016/j.jpba.2011.01.006
179. Bonilla FA. Pharmacokinetics of immunoglobulin administered via intravenous or subcutaneous routes. *Immunol Allergy Clin North Am* (2008) 28(4):803–19, ix. doi:10.1016/j.iac.2008.06.006
180. Koneczny I. *Potential Mechanisms in MuSK Myasthenia Gravis [Dissertation]*. Oxford: Oxford University (2014).
181. Rispens T, Ooievaar-De Heer P, Vermeulen E, Schuurman J, van der Neut Kolfschoten M, Aalberse RC. Human IgG4 binds to IgG4 and

conformationally altered IgG1 via Fc-Fc interactions. *J Immunol* (2009) 182(7):4275–81. doi:10.4049/jimmunol.0804338
182. Zack DJ, Stempniak M, Wong AL, Weisbart RH. Localization of an Fc-binding reactivity to the constant region of human IgG4. Implications for the pathogenesis of rheumatoid arthritis. *J Immunol* (1995) 155(10):5057–63.
183. Kawa S, Kitahara K, Hamano H, Ozaki Y, Arakura N, Yoshizawa K, et al. A novel immunoglobulin-immunoglobulin interaction in autoimmunity. *PLoS One* (2008) 3(2):e1637. doi:10.1371/journal.pone.0001637
184. Cohen PL, Cheek RL, Hadler JA, Yount WJ, Eisenberg RA. The subclass distribution of human IgG rheumatoid factor. *J Immunol* (1987) 139(5):1466–71.
185. Detlefsen S, Brasen JH, Zamboni G, Capelli P, Kloppel G. Deposition of complement C3c, immunoglobulin (Ig)G4 and IgG at the basement membrane of pancreatic ducts and acini in autoimmune pancreatitis. *Histopathology* (2010) 57(6):825–35. doi:10.1111/j.1365-2559.2010.03717.x
186. Ma H, Sandor DG, Beck LH Jr. The role of complement in membranous nephropathy. *Semin Nephrol* (2013) 33(6):531–42. doi:10.1016/j.semnephrol.2013.08.004
187. Diebolder CA, Beurskens FJ, de Jong RN, Koning RI, Strumane K, Lindorfer MA, et al. Complement is activated by IgG hexamers assembled at the cell surface. *Science* (2014) 343(6176):1260–3. doi:10.1126/science.1248943
188. Lichtenstein LM, Holtzman NA, Burnett LS. A quantitative in vitro study of the chromatographic distribution and immunoglobulin characteristics of human blocking antibody. *J Immunol* (1968) 101(2):317–24.
189. Punnonen J, Aversa G, Cocks BG, McKenzie AN, Menon S, Zurawski G, et al. Interleukin 13 induces interleukin 4-independent IgG4 and IgE synthesis and CD23 expression by human B cells. *Proc Natl Acad Sci U S A* (1993) 90(8):3730–4. doi:10.1073/pnas.90.8.3730
190. Meiler F, Zumkehr J, Klunker S, Ruckert B, Akdis CA, Akdis M. In vivo switch to IL-10-secreting T regulatory cells in high dose allergen exposure. *J Exp Med* (2008) 205(12):2887–98. doi:10.1084/jem.20080193
191. Meiler F, Klunker S, Zimmermann M, Akdis CA, Akdis M. Distinct regulation of IgE, IgG4 and IgA by T regulatory cells and toll-like receptors. *Allergy* (2008) 63(11):1455–63. doi:10.1111/j.1398-9995.2008.01774.x
192. Jeannin P, Lecoanet S, Delneste Y, Gauchat JF, Bonnefoy JY. IgE versus IgG4 production can be differentially regulated by IL-10. *J Immunol* (1998) 160(7):3555–61.
193. Satoguina JS, Weyand E, Larbi J, Hoerauf A. T regulatory-1 cells induce IgG4 production by B cells: role of IL-10. *J Immunol* (2005) 174(8):4718–26. doi:10.4049/jimmunol.174.8.4718
194. van de Veen W, Stanic B, Yaman G, Wawrzyniak M, Sollner S, Akdis DG, et al. IgG4 production is confined to human IL-10-producing regulatory B cells that suppress antigen-specific immune responses. *J Allergy Clin Immunol* (2013) 131(4):1204–12. doi:10.1016/j.jaci.2013.01.014
195. Aalberse RC, van der Gaag R, van Leeuwen J. Serologic aspects of IgG4 antibodies. I. Prolonged immunization results in an IgG4-restricted response. *J Immunol* (1983) 130(2):722–6.
196. Nakagawa T, Miyamoto T. The role of IgG4 as blocking antibodies in asthmatics and in bee keepers. *Int Arch Allergy Appl Immunol* (1985) 77(1–2):204–5. doi:10.1159/000233787
197. Platts-Mills T, Vaughan J, Squillace S, Woodfolk J, Sporik R. Sensitisation, asthma, and a modified Th2 response in children exposed to cat allergen: a population-based cross-sectional study. *Lancet* (2001) 357(9258):752–6. doi:10.1016/S0140-6736(00)04168-4
198. James LK, Bowen H, Calvert RA, Dodev TS, Shamji MH, Beavil AJ, et al. Allergen specificity of IgG(4)-expressing B cells in patients with grass pollen allergy undergoing immunotherapy. *J Allergy Clin Immunol* (2012) 130(3):663–70.e3. doi:10.1016/j.jaci.2012.04.006
199. Van der Zee S, Aalberse RC. IgG4 and hyposensitization. *N Engl Reg Allergy Proc* (1987) 8(6):389–91. doi:10.2500/108854187778999667
200. van der Zee JS, van Swieten P, Aalberse RC. Inhibition of complement activation by IgG4 antibodies. *Clin Exp Immunol* (1986) 64(2):415–22.
201. Margni RA, Perdigon G, Abatangelo C, Gentile T, Binaghi RA. Immunobiological behaviour of rabbit precipitating and non-precipitating (co-precipitating) antibodies. *Immunology* (1980) 41(3):681–6.
202. van Toorenenbergen AW, Aalberse RC. IgG4 and release of histamine from human peripheral blood leukocytes. *Int Arch Allergy Appl Immunol* (1982) 67(2):117–22. doi:10.1159/000233000
203. Aalberse RC, Dieges PH, Knul-Bretlova V, Vooren P, Aalbers M, van Leeuwen J. IgG4 as a blocking antibody. *Clin Rev Allergy* (1983) 1(2):289–302.
204. Santos AF, James LK, Bahnson HT, Shamji MH, Couto-Francisco NC, Islam S, et al. IgG4 inhibits peanut-induced basophil and mast cell activation in peanut-tolerant children sensitized to peanut major allergens. *J Allergy Clin Immunol* (2015) 135(5):1249–56. doi:10.1016/j.jaci.2015.01.012
205. Kemeny DM, MacKenzie-Mills M, Harries MG, Youlten LJ, Lessof MH. Antibodies to purified bee venom proteins and peptides. II. A detailed study of changes in IgE and IgG antibodies to individual bee venom antigens. *J Allergy Clin Immunol* (1983) 72(4):376–85. doi:10.1016/0091-6749(83)90503-1
206. Kemeny DM, McKenzie-Mills M, Harries MG, Youlten LJ, Lessof MH. Changes in the levels of anti-phospholipase A2 and hyaluronidase antibodies during bee venom immunotherapy. *Monogr Allergy* (1983) 18:150–2.
207. Schumacher MJ, Egen NB, Tanner D. Neutralization of bee venom lethality by immune serum antibodies. *Am J Trop Med Hyg* (1996) 55(2):197–201. doi:10.4269/ajtmh.1996.55.197
208. Drachman DB, Angus CW, Adams RN, Michelson JD, Hoffman GJ. Myasthenic antibodies cross-link acetylcholine receptors to accelerate degradation. *N Engl J Med* (1978) 298(20):1116–22. doi:10.1056/NEJM197805182982004
209. Heinemann S, Bevan S, Kullberg R, Lindstrom J, Rice J. Modulation of acetylcholine receptor by antibody against the receptor. *Proc Natl Acad Sci U S A* (1977) 74(7):3090–4. doi:10.1073/pnas.74.7.3090
210. Hughes EG, Peng X, Gleichman AJ, Lai M, Zhou L, Tsou R, et al. Cellular and synaptic mechanisms of anti-NMDA receptor encephalitis. *J Neurosci* (2010) 30(17):5866–75. doi:10.1523/JNEUROSCI.0167-10.2010
211. Moscato EH, Peng X, Jain A, Parsons TD, Dalmau J, Balice-Gordon RJ. Acute mechanisms underlying antibody effects in anti-N-methyl-D-aspartate receptor encephalitis. *Ann Neurol* (2014) 76(1):108–19. doi:10.1002/ana.24195
212. Lai M, Hughes EG, Peng X, Zhou L, Gleichman AJ, Shu H, et al. AMPA receptor antibodies in limbic encephalitis alter synaptic receptor location. *Ann Neurol* (2009) 65(4):424–34. doi:10.1002/ana.21589
213. Peng X, Hughes EG, Moscato EH, Parsons TD, Dalmau J, Balice-Gordon RJ. Cellular plasticity induced by anti-alpha-amino-3-hydroxy-5-methyl-4-isoxazolepropionic acid (AMPA) receptor encephalitis antibodies. *Ann Neurol* (2015) 77(3):381–98. doi:10.1002/ana.24293
214. Collins AM, Davies JM. Enhanced cell-binding by allergen multimers: how complex is it? *Immunol Cell Biol* (2013) 91(2):115–7. doi:10.1038/icb.2013.5
215. Naparstek Y, Plotz PH. The role of autoantibodies in autoimmune disease. *Annu Rev Immunol* (1993) 11:79–104. doi:10.1146/annurev.iy.11.040193.000455
216. Skeie GO, Aarli JA, Gilhus NE. Titin and ryanodine receptor antibodies in myasthenia gravis. *Acta Neurol Scand Suppl* (2006) 183:19–23. doi:10.1111/j.1600-0404.2006.00608.x
217. Witebsky E, Rose NR, Terplan K, Paine JR, Egan RW. Chronic thyroiditis and autoimmunization. *J Am Med Assoc* (1957) 164(13):1439–47. doi:10.1001/jama.1957.02980130015004
218. Rose NR, Bona C. Defining criteria for autoimmune diseases (Witebsky's postulates revisited). *Immunol Today* (1993) 14(9):426–30. doi:10.1016/0167-5699(93)90244-F
219. Ishii K, Harada R, Matsuo I, Shirakata Y, Hashimoto K, Amagai M. In vitro keratinocyte dissociation assay for evaluation of the pathogenicity of anti-desmoglein 3 IgG autoantibodies in pemphigus vulgaris. *J Invest Dermatol* (2005) 124(5):939–46. doi:10.1111/j.0022-202X.2005.23714.x
220. Funakoshi T, Lunardon L, Ellebrecht CT, Nagler AR, O'Leary CE, Payne AS. Enrichment of total serum IgG4 in patients with pemphigus. *Br J Dermatol* (2012) 167(6):1245–53. doi:10.1111/j.1365-2133.2012.11144.x
221. Lo AS, Mao X, Mukherjee EM, Ellebrecht CT, Yu X, Posner MR, et al. Pathogenicity and epitope characteristics do not differ in IgG subclass-switched anti-desmoglein 3 IgG1 and IgG4 autoantibodies in pemphigus vulgaris. *PLoS One* (2016) 11(6):e0156800. doi:10.1371/journal.pone.0156800
222. Waschke J, Spindler V, Bruggeman P, Zillikens D, Schmidt G, Drenckhahn D. Inhibition of Rho A activity causes pemphigus skin blistering. *J Cell Biol* (2006) 175(5):721–7. doi:10.1083/jcb.200605125
223. Li N, Zhao M, Wang J, Liu Z, Diaz LA. Involvement of the apoptotic mechanism in pemphigus foliaceus autoimmune injury of the skin. *J Immunol* (2009) 182(1):711–7. doi:10.4049/jimmunol.182.1.711

224. Cipolla GA, Park JK, Lavker RM, Petzl-Erler ML. Crosstalk between signaling pathways in pemphigus: a role for endoplasmic reticulum stress in p38 mitogen-activated protein kinase activation? *Front Immunol* (2017) 8:1022. doi:10.3389/fimmu.2017.01022
225. Egu DT, Walter E, Spindler V, Waschke J. Inhibition of p38MAPK signaling prevents epidermal blistering and alterations of desmosome structure induced by pemphigus autoantibodies in human epidermis. *Br J Dermatol* (2017) 177(6):1612–8. doi:10.1111/bjd.15721
226. Mavropoulos A, Orfanidou T, Liaskos C, Smyk DS, Spyrou V, Sakkas LI, et al. p38 MAPK signaling in pemphigus: implications for skin autoimmunity. *Autoimmune Dis* (2013) 2013:728529. doi:10.1155/2013/728529
227. Spindler V, Vielmuth F, Schmidt E, Rubenstein DS, Waschke J. Protective endogenous cyclic adenosine 5'-monophosphate signaling triggered by pemphigus autoantibodies. *J Immunol* (2010) 185(11):6831–8. doi:10.4049/jimmunol.1002675
228. Walter E, Vielmuth F, Rotkopf L, Sardy M, Horvath ON, Goebeler M, et al. Different signaling patterns contribute to loss of keratinocyte cohesion dependent on autoantibody profile in pemphigus. *Sci Rep* (2017) 7(1):3579. doi:10.1038/s41598-017-03697-7
229. Spindler V, Eming R, Schmidt E, Amagai M, Grando S, Jonkman MF, et al. Mechanisms causing loss of keratinocyte cohesion in pemphigus. *J Invest Dermatol* (2017) 138(1):32–7. doi:10.1016/j.jid.2017.06.022
230. Huda S, Cao M, De Rosa A, Woodhall M, Cossins J, Maestri M, et al. Inhibition of the tyrosine phosphatase Shp2 alleviates the pathogenic effects of MuSK antibodies in vitro. *Neuromuscul Dis* (2007) 27:S36. doi:10.1016/S0960-8966(17)30325-5
231. Niks EH, Kuks JB, Wokke JH, Veldman H, Bakker E, Verschuuren JJ, et al. Pre- and postsynaptic neuromuscular junction abnormalities in musk myasthenia. *Muscle Nerve* (2010) 42(2):283–8. doi:10.1002/mus.21642
232. Yumoto N, Kim N, Burden SJ. Lrp4 is a retrograde signal for presynaptic differentiation at neuromuscular synapses. *Nature* (2012) 489(7416):438–42. doi:10.1038/nature11348
233. Wu H, Lu Y, Shen C, Patel N, Gan L, Xiong WC, et al. Distinct roles of muscle and motoneuron LRP4 in neuromuscular junction formation. *Neuron* (2012) 75(1):94–107. doi:10.1016/j.neuron.2012.04.033
234. Thomas MR, de Groot R, Scully MA, Crawley JT. Pathogenicity of anti-ADAMTS13 autoantibodies in acquired thrombotic thrombocytopenic purpura. *EBioMedicine* (2015) 2(8):942–52. doi:10.1016/j.ebiom.2015.06.007
235. Kremer Hovinga JA, Coppo P, Lammle B, Moake JL, Miyata T, Vanhoorelbeke K. Thrombotic thrombocytopenic purpura. *Nat Rev Dis Primers* (2017) 3:17020. doi:10.1038/nrdp.2017.20
236. Faivre-Sarrailh C, Devaux JJ. Neuro-glial interactions at the nodes of Ranvier: implication in health and diseases. *Front Cell Neurosci* (2013) 7:196. doi:10.3389/fncel.2013.00196
237. Peles E, Nativ M, Lustig M, Grumet M, Schilling J, Martinez R, et al. Identification of a novel contactin-associated transmembrane receptor with multiple domains implicated in protein-protein interactions. *EMBO J* (1997) 16(5):978–88. doi:10.1093/emboj/16.5.978
238. Rios JC, Melendez-Vasquez CV, Einheber S, Lustig M, Grumet M, Hemperly J, et al. Contactin-associated protein (Caspr) and contactin form a complex that is targeted to the paranodal junctions during myelination. *J Neurosci* (2000) 20(22):8354–64.
239. Charles P, Tait S, Faivre-Sarrailh C, Barbin G, Gunn-Moore F, Denisenko-Nehrbass N, et al. Neurofascin is a glial receptor for the paranodin/Caspr-contactin axonal complex at the axoglial junction. *Curr Biol* (2002) 12(3):217–20. doi:10.1016/S0960-9822(01)00680-7
240. Malhotra R, Wormald MR, Rudd PM, Fischer PB, Dwek RA, Sim RB. Glycosylation changes of IgG associated with rheumatoid arthritis can activate complement via the mannose-binding protein. *Nat Med* (1995) 1(3):237–43. doi:10.1038/nm0395-237
241. Roos A, Bouwman LH, van Gijlswijk-Janssen DJ, Faber-Krol MC, Stahl GL, Daha MR. Human IgA activates the complement system via the mannan-binding lectin pathway. *J Immunol* (2001) 167(5):2861–8. doi:10.4049/jimmunol.167.5.2861
242. Bally S, Debiec H, Ponard D, Dijoud F, Rendu J, Faure J, et al. Phospholipase A2 receptor-related membranous nephropathy and mannan-binding lectin deficiency. *J Am Soc Nephrol* (2016) 27(12):3539–44. doi:10.1681/ASN.2015101155
243. Hofstra JM, Debiec H, Short CD, Pelle T, Kleta R, Mathieson PW, et al. Antiphospholipase A2 receptor antibody titer and subclass in idiopathic membranous nephropathy. *J Am Soc Nephrol* (2012) 23(10):1735–43. doi:10.1681/ASN.2012030242
244. Debiec H, Hanoy M, Francois A, Guerrot D, Ferlicot S, Johanet C, et al. Recurrent membranous nephropathy in an allograft caused by IgG3kappa targeting the PLA2 receptor. *J Am Soc Nephrol* (2012) 23(12):1949–54. doi:10.1681/ASN.2012060577
245. Skoberne A, Behnert A, Teng B, Fritzler MJ, Schiffer L, Pajek J, et al. Serum with phospholipase A2 receptor autoantibodies interferes with podocyte adhesion to collagen. *Eur J Clin Invest* (2014) 44(8):753–65. doi:10.1111/eci.12292
246. Jurgensen HJ, Johansson K, Madsen DH, Porse A, Melander MC, Sorensen KR, et al. Complex determinants in specific members of the mannose receptor family govern collagen endocytosis. *J Biol Chem* (2014) 289(11):7935–47. doi:10.1074/jbc.M113.512780
247. Foster MH. Optimizing the translational value of animal models of glomerulonephritis: insights from recent murine prototypes. *Am J Physiol Ren Physiol* (2016) 311(3):F487–95. doi:10.1152/ajprenal.00275.2016
248. Lai M, Huijbers MG, Lancaster E, Graus F, Bataller L, Balice-Gordon R, et al. Investigation of LGI1 as the antigen in limbic encephalitis previously attributed to potassium channels: a case series. *Lancet Neurol* (2010) 9(8):776–85. doi:10.1016/S1474-4422(10)70137-X
249. Irani SR, Michell AW, Lang B, Pettingill P, Waters P, Johnson MR, et al. Faciobrachial dystonic seizures precede Lgi1 antibody limbic encephalitis. *Ann Neurol* (2011) 69(5):892–900. doi:10.1002/ana.22307
250. van Sonderen A, Petit-Pedrol M, Dalmau J, Titulaer MJ. The value of LGI1, Caspr2 and voltage-gated potassium channel antibodies in encephalitis. *Nat Rev Neurol* (2017) 13(5):290–301. doi:10.1038/nrneurol.2017.43
251. Vincent A, Irani SR. Caspr2 antibodies in patients with thymomas. *J Thorac Oncol* (2010) 5(10 Suppl 4):S277–80. doi:10.1097/JTO.0b013e3181f23f04
252. Vale TC, Pedroso JL, Dutra LA, Azevedo L, Filho LH, Prado LB, et al. Morvan syndrome as a paraneoplastic disorder of thymoma with anti-CASPR2 antibodies. *Lancet* (2017) 389(10076):1367–8. doi:10.1016/S0140-6736(16)31459-3
253. Carvajal-Gonzalez A, Leite MI, Waters P, Woodhall M, Coutinho E, Balint B, et al. Glycine receptor antibodies in PERM and related syndromes: characteristics, clinical features and outcomes. *Brain* (2014) 137(Pt 8):2178–92. doi:10.1093/brain/awu142
254. Ahmad M, Mahajan VS, Mattoo H, Stone JH, Pillai S. Individuals with IgG4-related disease do not have an increased frequency of the K409 variant of IgG4 that compromises Fab-arm exchange. *J Rheumatol* (2014) 41(1):185–7. doi:10.3899/jrheum.131017
255. Hao M, Li W, Yi L, Yu S, Fan G, Lu T, et al. Hybrid kappa\lambda antibody is a new serological marker to diagnose autoimmune pancreatitis and differentiate it from pancreatic cancer. *Sci Rep* (2016) 6:27415. doi:10.1038/srep27415
256. Yi L, Hao M, Lu T, Lin G, Chen L, Gao M, et al. Increased kappa/lambda hybrid antibody in serum is a novel biomarker related to disease activity and inflammation in rheumatoid arthritis. *Mediators Inflamm* (2016) 2016:2953072. doi:10.1155/2016/2953072
257. Howard FM Jr, Lennon VA, Finley J, Matsumoto J, Elveback LR. Clinical correlations of antibodies that bind, block, or modulate human acetylcholine receptors in myasthenia gravis. *Ann N Y Acad Sci* (1987) 505:526–38. doi:10.1111/j.1749-6632.1987.tb51321.x
258. Shibuya N, Mori K, Nakazawa Y. Serum factor blocks neuromuscular transmission in myasthenia gravis: electrophysiologic study with intracellular microelectrodes. *Neurology* (1978) 28(8):804–11. doi:10.1212/WNL.28.8.804
259. Vincent A, Li Z, Hart A, Barrett-Jolley R, Yamamoto T, Burges J, et al. Seronegative myasthenia gravis. Evidence for plasma factor(s) interfering with acetylcholine receptor function. *Ann N Y Acad Sci* (1993) 681:529–38. doi:10.1111/j.1749-6632.1993.tb22936.x
260. Rapoport B, Chazenbalk GD, Jaume JC, McLachlan SM. The thyrotropin (TSH) receptor: interaction with TSH and autoantibodies. *Endocr Rev* (1998) 19(6):673–716. doi:10.1210/edrv.19.6.0352
261. Drexhage HA, Bottazzo GF, Bitensky L, Chayen J, Doniach D. Thyroid growth-blocking antibodies in primary myxoedema. *Nature* (1981) 289(5798):594–6. doi:10.1038/289594a0

262. Engel AG, Lambert EH, Howard FM. Immune complexes (IgG and C3) at the motor end-plate in myasthenia gravis: ultrastructural and light microscopic localization and electrophysiologic correlations. *Mayo Clin Proc* (1977) 52(5):267–80.
263. Sahashi K, Engel AG, Lambert EH, Howard FM Jr. Ultrastructural localization of the terminal and lytic ninth complement component (C9) at the motor end-plate in myasthenia gravis. *J Neuropathol Exp Neurol* (1980) 39(2):160–72. doi:10.1097/00005072-198003000-00005
264. Lennon VA, Lambert EH. Monoclonal autoantibodies to acetylcholine receptors: evidence for a dominant idiotype and requirement of complement for pathogenicity. *Ann N Y Acad Sci* (1981) 377:77–96. doi:10.111 1/j.1749-6632.1981.tb33725.x
265. Misu T, Hoftberger R, Fujihara K, Wimmer I, Takai Y, Nishiyama S, et al. Presence of six different lesion types suggests diverse mechanisms of tissue injury in neuromyelitis optica. *Acta Neuropathol* (2013) 125(6):815–27. doi:10.1007/s00401-013-1116-7
266. Huijbers MG, Querol LA, Niks EH, Plomp JJ, van der Maarel SM, Graus F, et al. The expanding field of IgG4-mediated neurological autoimmune disorders. *Eur J Neurol* (2015) 22(8):1151–61. doi:10.1111/ene.12758
267. Binks SNM, Klein CJ, Waters P, Pittock SJ, Irani SR. LGI1, CASPR2 and related antibodies: a molecular evolution of the phenotypes. *J Neurol Neurosurg Psychiatry* (2017). doi:10.1136/jnnp-2017-315720
268. Phillips WD, Vincent A. Pathogenesis of myasthenia gravis: update on disease types, models, and mechanisms. *F1000Res* (2016) 5(F1000 Faculty Rev):1513. doi:10.12688/f1000research.8206.1
269. Dalmau J, Geis C, Graus F. Autoantibodies to synaptic receptors and neuronal cell surface proteins in autoimmune diseases of the central nervous system. *Physiol Rev* (2017) 97(2):839–87. doi:10.1152/physrev.00010.2016
270. Alenzi FQ, Salem ML, Alenazi FA, Wyse RK. Cellular and molecular aspects of Goodpasture syndrome. *Iran J Kidney Dis* (2012) 6(1):1–8.
271. Aoki V, Rivitti EA, Diaz LA; Cooperative Group on Fogo Selvagem Research. Update on fogo selvagem, an endemic form of pemphigus foliaceus. *J Dermatol* (2015) 42(1):18–26. doi:10.1111/1346-8138.12675
272. Anandan V, Jameela WA, Sowmiya R, Kumar MMS, Lavanya P. Rituximab: a magic bullet for pemphigus. *J Clin Diagn Res* (2017) 11(4):WC01–6. doi:10.7860/JCDR/2017/21868.9717
273. Schmidt E. Rituximab as first-line treatment of pemphigus. *Lancet* (2017) 389(10083):1956–8. doi:10.1016/S0140-6736(17)30787-0
274. Kanwar AJ, Vinay K, Sawatkar GU, Dogra S, Minz RW, Shear NH, et al. Clinical and immunological outcomes of high- and low-dose rituximab treatments in patients with pemphigus: a randomized, comparative, observer-blinded study. *Br J Dermatol* (2014) 170(6):1341–9. doi:10.1111/bjd.12972
275. Appeltshauser L, Weishaupt A, Sommer C, Doppler K. Complement deposition induced by binding of anti-contactin-1 auto-antibodies is modified by immunoglobulins. *Exp Neurol* (2017) 287(Pt 1):84–90. doi:10.1016/j.expneurol.2016.10.006
276. Gelpi E, Hoftberger R, Graus F, Ling H, Holton JL, Dawson T, et al. Neuropathological criteria of anti-IgLON5-related tauopathy. *Acta Neuropathol* (2016) 132(4):531–43. doi:10.1007/s00401-016-1591-8
277. Cagnin A, Mariotto S, Fiorini M, Gaule M, Bonetto N, Tagliapietra M, et al. Microglial and neuronal TDP-43 pathology in anti-IgLON5-related tauopathy. *J Alzheimers Dis* (2017) 59(1):13–20. doi:10.3233/JAD-170189
278. Mori S, Motohashi N, Takashima R, Kishi M, Nishimune H, Shigemoto K. Immunization of mice with LRP4 induces myasthenia similar to MuSK-associated myasthenia gravis. *Exp Neurol* (2017) 297:158–67. doi:10.1016/j.expneurol.2017.08.006
279. Tezuka T, Inoue A, Hoshi T, Weatherbee SD, Burgess RW, Ueta R, et al. The MuSK activator agrin has a separate role essential for postnatal maintenance of neuromuscular synapses. *Proc Natl Acad Sci U S A* (2014) 111(46):16556–61. doi:10.1073/pnas.1408409111
280. Maselli RA, Arredondo J, Cagney O, Ng JJ, Anderson JA, Williams C, et al. Mutations in MUSK causing congenital myasthenic syndrome impair MuSK-Dok-7 interaction. *Hum Mol Genet* (2010) 19(12):2370–9. doi:10.1093/hmg/ddq110
281. Zhu D, Yang Z, Luo Z, Luo S, Xiong WC, Mei L. Muscle-specific receptor tyrosine kinase endocytosis in acetylcholine receptor clustering in response to agrin. *J Neurosci* (2008) 28(7):1688–96. doi:10.1523/JNEUROSCI.4130-07.2008
282. Luiskandl S, Woller B, Schlauf M, Schmid JA, Herbst R. Endosomal trafficking of the receptor tyrosine kinase MuSK proceeds via clathrin-dependent pathways, Arf6 and actin. *FEBS J* (2013) 280(14):3281–97. doi:10.1111/febs.12309
283. Woller B, Luiskandl S, Popovic M, Prieler BE, Ikonge G, Mutzl M, et al. Rin-like, a novel regulator of endocytosis, acts as guanine nucleotide exchange factor for Rab5a and Rab22. *Biochim Biophys Acta* (2011) 1813(6):1198–210. doi:10.1016/j.bbamcr.2011.03.005
284. Scheiflinger F, Knobl P, Trattner B, Plaimauer B, Mohr G, Dockal M, et al. Nonneutralizing IgM and IgG antibodies to von Willebrand factor-cleaving protease (ADAMTS-13) in a patient with thrombotic thrombocytopenic purpura. *Blood* (2003) 102(9):3241–3. doi:10.1182/blood-2003-05-1616
285. Huang CC, Lehman A, Albawardi A, Satoskar A, Brodsky S, Nadasdy G, et al. IgG subclass staining in renal biopsies with membranous glomerulonephritis indicates subclass switch during disease progression. *Mod Pathol* (2013) 26(6):799–805. doi:10.1038/modpathol.2012.237
286. Raibagkar P, Ferry JA, Stone JH. Is MuSK myasthenia gravis linked to IgG4-related disease? *J Neuroimmunol* (2017) 305:82–3. doi:10.1016/j.jneuroim.2017.02.004
287. Saeki T, Ito T, Youkou A, Ishiguro H, Sato N, Yamazaki H, et al. Thrombotic thrombocytopenic purpura in IgG4-related disease with severe deficiency of ADAMTS-13 activity and IgG4 autoantibody against ADAMTS-13. *Arthritis Care Res (Hoboken)* (2011) 63(8):1209–12. doi:10.1002/acr.20484
288. Stone JH, Khosroshahi A, Deshpande V, Chan JK, Heathcote JG, Aalberse R, et al. Recommendations for the nomenclature of IgG4-related disease and its individual organ system manifestations. *Arthritis Rheum* (2012) 64(10):3061–7. doi:10.1002/art.34593
289. Bozzalla Cassione E, Stone JH. IgG4-related disease. *Curr Opin Rheumatol* (2017) 29(3):223–7. doi:10.1097/BOR.0000000000000383
290. Trampert DC, Hubers LM, van de Graaf SFJ, Beuers U. On the role of IgG4 in inflammatory conditions: lessons for IgG4-related disease. *Biochim Biophys Acta* (2017). doi:10.1016/j.bbadis.2017.07.038
291. Umehara H, Okazaki K, Kawano M, Mimori T, Chiba T. How to diagnose IgG4-related disease. *Ann Rheum Dis* (2017) 76(11):e46. doi:10.1136/annrheumdis-2017-211330
292. Hertl M, Jedlickova H, Karpati S, Marinovic B, Uzun S, Yayli S, et al. Pemphigus. S2 Guideline for diagnosis and treatment – guided by the European Dermatology Forum (EDF) in cooperation with the European Academy of Dermatology and Venereology (EADV). *J Eur Acad Dermatol Venereol* (2015) 29(3):405–14. doi:10.1111/jdv.12772
293. Mattoo H, Mahajan VS, Della-Torre E, Sekigami Y, Carruthers M, Wallace ZS, et al. De novo oligoclonal expansions of circulating plasmablasts in active and relapsing IgG4-related disease. *J Allergy Clin Immunol* (2014) 134(3):679–87. doi:10.1016/j.jaci.2014.03.034
294. Della Torre E, Bozzolo EP, Passerini G, Doglioni C, Sabbadini MG. IgG4-related pachymeningitis: evidence of intrathecal IgG4 on cerebrospinal fluid analysis. *Ann Intern Med* (2012) 156(5):401–3. doi:10.7326/0003-4819-156-5-201203060-00025
295. Maillette de Buy Wenniger LJ, Doorenspleet ME, Klarenbeek PL, Verheij J, Baas F, Elferink RP, et al. Immunoglobulin G4+ clones identified by next-generation sequencing dominate the B cell receptor repertoire in immunoglobulin G4 associated cholangitis. *Hepatology* (2013) 57(6):2390–8. doi:10.1002/hep.26232
296. Doorenspleet ME, Hubers LM, Culver EL, Maillette de Buy Wenniger LJ, Klarenbeek PL, Chapman RW, et al. Immunoglobulin G4(+) B-cell receptor clones distinguish immunoglobulin G 4-related disease from primary sclerosing cholangitis and biliary/pancreatic malignancies. *Hepatology* (2016) 64(2):501–7. doi:10.1002/hep.28568
297. Lohr JM, Faissner R, Koczan D, Bewerunge P, Bassi C, Brors B, et al. Autoantibodies against the exocrine pancreas in autoimmune pancreatitis: gene and protein expression profiling and immunoassays identify pancreatic enzymes as a major target of the inflammatory process. *Am J Gastroenterol* (2010) 105(9):2060–71. doi:10.1038/ajg.2010.141
298. Asada M, Nishio A, Uchida K, Kido M, Ueno S, Uza N, et al. Identification of a novel autoantibody against pancreatic secretory trypsin inhibitor in patients with autoimmune pancreatitis. *Pancreas* (2006) 33(1):20–6. doi:10.1097/01.mpa.0000226881.48204.fd

299. Shiokawa M, Kodama Y, Kuriyama K, Yoshimura K, Tomono T, Morita T, et al. Pathogenicity of IgG in patients with IgG4-related disease. *Gut* (2016) 65(8):1322–32. doi:10.1136/gutjnl-2015-310336
300. Hubers LM, Vos H, Schuurman AR, Erken R, Oude Elferink RP, Burgering B, et al. Annexin A11 is targeted by IgG4 and IgG1 autoantibodies in IgG4-related disease. *Gut* (2017). doi:10.1136/gutjnl-2017-314548
301. Vincent A, Leite MI, Farrugia ME, Jacob S, Viegas S, Shiraishi H, et al. Myasthenia gravis seronegative for acetylcholine receptor antibodies. *Ann N Y Acad Sci* (2008) 1132:84–92. doi:10.1196/annals.1405.020
302. Tron F, Gilbert D, Mouquet H, Joly P, Drouot L, Makni S, et al. Genetic factors in pemphigus. *J Autoimmun* (2005) 24(4):319–28. doi:10.1016/j.jaut.2005.03.006
303. Meyer N, Misery L. Geoepidemiologic considerations of auto-immune pemphigus. *Autoimmun Rev* (2010) 9(5):A379–82. doi:10.1016/j.autrev.2009.10.009
304. Warren SJ, Lin MS, Giudice GJ, Hoffmann RG, Hans-Filho G, Aoki V, et al. The prevalence of antibodies against desmoglein 1 in endemic pemphigus foliaceus in Brazil. Cooperative Group on Fogo Selvagem Research. *N Engl J Med* (2000) 343(1):23–30. doi:10.1056/NEJM200007063430104
305. Gomes R, Oliveira F, Teixeira C, Meneses C, Gilmore DC, Elnaiem DE, et al. Immunity to sand fly salivary protein LJM11 modulates host response to vector-transmitted leishmania conferring ulcer-free protection. *J Invest Dermatol* (2012) 132(12):2735–43. doi:10.1038/jid.2012.205
306. Qian Y, Jeong JS, Maldonado M, Valenzuela JG, Gomes R, Teixeira C, et al. Cutting edge: Brazilian pemphigus foliaceus anti-desmoglein 1 autoantibodies cross-react with sand fly salivary LJM11 antigen. *J Immunol* (2012) 189(4):1535–9. doi:10.4049/jimmunol.1200842
307. Qian Y, Jeong JS, Ye J, Dang B, Abdeladhim M, Aoki V, et al. Overlapping IgG4 responses to self- and environmental antigens in endemic pemphigus foliaceus. *J Immunol* (2016) 196(5):2041–50. doi:10.4049/jimmunol.1502233
308. Diaz LA, Prisayanh PS, Dasher DA, Li N, Evangelista F, Aoki V, et al. The IgM anti-desmoglein 1 response distinguishes Brazilian pemphigus foliaceus (fogo selvagem) from other forms of pemphigus. *J Invest Dermatol* (2008) 128(3):667–75. doi:10.1038/sj.jid.5701121
309. Qian Y, Jeong JS, Abdeladhim M, Valenzuela JG, Aoki V, Hans-Filhio G, et al. IgE anti-LJM11 sand fly salivary antigen may herald the onset of fogo selvagem in endemic Brazilian regions. *J Invest Dermatol* (2015) 135(3):913–5. doi:10.1038/jid.2014.430
310. Qian Y, Prisayanh P, Andraca E, Qaqish BF, Aoki V, Hans-Filhio G, et al. IgE, IgM, and IgG4 anti-desmoglein 1 autoantibody profile in endemic pemphigus foliaceus (fogo selvagem). *J Invest Dermatol* (2011) 131(4):985–7. doi:10.1038/jid.2010.403
311. Li N, Aoki V, Hans-Filho G, Rivitti EA, Diaz LA. The role of intramolecular epitope spreading in the pathogenesis of endemic pemphigus foliaceus (fogo selvagem). *J Exp Med* (2003) 197(11):1501–10. doi:10.1084/jem.20022031
312. Qaqish BF, Prisayanh P, Qian Y, Andraca E, Li N, Aoki V, et al. Development of an IgG4-based predictor of endemic pemphigus foliaceus (fogo selvagem). *J Invest Dermatol* (2009) 129(1):110–8. doi:10.1038/jid.2008.189
313. Warren SJ, Arteaga LA, Rivitti EA, Aoki V, Hans-Filho G, Qaqish BF, et al. The role of subclass switching in the pathogenesis of endemic pemphigus foliaceus. *J Invest Dermatol* (2003) 120(1):104–8. doi:10.1046/j.1523-1747.2003.12017.x
314. Kamisawa T, Anjiki H, Egawa N, Kubota N. Allergic manifestations in autoimmune pancreatitis. *Eur J Gastroenterol Hepatol* (2009) 21(10):1136–9. doi:10.1097/MEG.0b013e3283297417
315. Culver EL, Vermeulen E, Makuch M, van Leeuwen A, Sadler R, Cargill T, et al. Increased IgG4 responses to multiple food and animal antigens indicate a polyclonal expansion and differentiation of pre-existing B cells in IgG4-related disease. *Ann Rheum Dis* (2015) 74(5):944–7. doi:10.1136/annrheumdis-2014-206405
316. Culver EL, Sadler R, Bateman AC, Makuch M, Cargill T, Ferry B, et al. Increases in IgE, eosinophils, and mast cells can be used in diagnosis and to predict relapse of IgG4-related disease. *Clin Gastroenterol Hepatol* (2017) 15(9):1444–52.e6 doi:10.1016/j.cgh.2017.02.007
317. Tian C, Luskin GK, Dischert KM, Higginbotham JN, Shepherd BE, Crowe JE Jr. Immunodominance of the VH1-46 antibody gene segment in the primary repertoire of human rotavirus-specific B cells is reduced in the memory compartment through somatic mutation of nondominant clones. *J Immunol* (2008) 180(5):3279–88. doi:10.4049/jimmunol.180.5.3279
318. Cho MJ, Ellebrecht CT, Hammers CM, Mukherjee EM, Sapparapu G, Boudreaux CE, et al. Determinants of VH1-46 cross-reactivity to pemphigus vulgaris autoantigen desmoglein 3 and rotavirus antigen VP6. *J Immunol* (2016) 197(4):1065–73. doi:10.4049/jimmunol.1600567
319. Phongsisay V. The immunobiology of *Campylobacter jejuni*: innate immunity and autoimmune diseases. *Immunobiology* (2016) 221(4):535–43. doi:10.1016/j.imbio.2015.12.005
320. Beck LH Jr. The dominant humoral epitope in phospholipase A2 receptor-1: presentation matters when serving up a slice of pi. *J Am Soc Nephrol* (2015) 26(2):237–9. doi:10.1681/ASN.2014090877
321. Stanescu HC, Arcos-Burgos M, Medlar A, Bockenhauer D, Kottgen A, Dragomirescu L, et al. Risk HLA-DQA1 and PLA(2)R1 alleles in idiopathic membranous nephropathy. *N Engl J Med* (2011) 364(7):616–26. doi:10.1056/NEJMoa1009742
322. Jia XY, Cui Z, Yang R, Hu SY, Zhao MH. Antibodies against linear epitopes on the Goodpasture autoantigen and kidney injury. *Clin J Am Soc Nephrol* (2012) 7(6):926–33. doi:10.2215/CJN.09930911
323. Li JN, Jia X, Wang Y, Xie C, Jiang T, Cui Z, et al. Plasma from patients with anti-glomerular basement membrane disease could recognize microbial peptides. *PLoS One* (2017) 12(4):e0174553. doi:10.1371/journal.pone.0174553
324. Oka S, Nohgawa M. EB virus reactivation triggers thrombotic thrombocytopenic purpura in a healthy adult. *Leuk Res Rep* (2017) 8:1–3. doi:10.1016/j.lrr.2017.06.001
325. Kosugi N, Tsurutani Y, Isonishi A, Hori Y, Matsumoto M, Fujimura Y. Influenza A infection triggers thrombotic thrombocytopenic purpura by producing the anti-ADAMTS13 IgG inhibitor. *Intern Med* (2010) 49(7):689–93. doi:10.2169/internalmedicine.49.2957
326. Rossi FC, Angerami RN, de Paula EV, Orsi FL, Shang D, del Guercio VM, et al. A novel association of acquired ADAMTS13 inhibitor and acute dengue virus infection. *Transfusion* (2010) 50(1):208–12. doi:10.1111/j.1537-2995.2009.02391.x
327. Kojima Y, Ohashi H, Nakamura T, Nakamura H, Yamamoto H, Miyata Y, et al. Acute thrombotic thrombocytopenic purpura after pneumococcal vaccination. *Blood Coagul Fibrinolysis* (2014) 25(5):512–4. doi:10.1097/MBC.0000000000000058
328. Hermann R, Pfeil A, Busch M, Kettner C, Kretzschmar D, Hansch A, et al. [Very severe thrombotic thrombocytopenic purpura (TTP) after H1N1 vaccination]. *Med Klin* (2010) 105(9):663–8. doi:10.1007/s00063-010-1107-6
329. Brodin-Sartorius A, Guebre-Egziabher F, Fouque D, Cozon G, Villar E, Laville M, et al. Recurrent idiopathic thrombotic thrombocytopenic purpura: a role for vaccination in disease relapse? *Am J Kidney Dis* (2006) 48(3):e31–4. doi:10.1053/j.ajkd.2006.04.090
330. Perricone C, Ceccarelli F, Nesher G, Borella E, Odeh Q, Conti F, et al. Immune thrombocytopenic purpura (ITP) associated with vaccinations: a review of reported cases. *Immunol Res* (2014) 60(2–3):226–35. doi:10.1007/s12026-014-8597-x
331. Hou Z, Abudureheman A, Wang L, Hasim A, Ainiwaer J, Zhang H, et al. Expression, prognosis and functional role of Thsd7a in esophageal squamous cell carcinoma of Kazakh patients, Xinjiang. *Oncotarget* (2017) 8(36):60539–57. doi:10.18632/oncotarget.16966

Conflict of Interest Statement: The author declares that the research was conducted in the absence of any commercial or financial relationships that could be construed as a potential conflict of interest.

frontiers in Immunology

PERSPECTIVE
published: 01 February 2018
doi: 10.3389/fimmu.2018.00136

Pemphigus—A Disease of Desmosome Dysfunction Caused by Multiple Mechanisms

Volker Spindler[1]* *and Jens Waschke*[2]*

[1] Department of Biomedicine, University of Basel, Basel, Switzerland, [2] Faculty of Medicine, Ludwig-Maximilians-Universität (LMU) Munich, Munich, Germany

Pemphigus is a severe autoimmune-blistering disease of the skin and mucous membranes caused by autoantibodies reducing desmosomal adhesion between epithelial cells. Autoantibodies against the desmosomal cadherins desmogleins (Dsgs) 1 and 3 as well as desmocollin 3 were shown to be pathogenic, whereas the role of other antibodies is unclear. Dsg3 interactions can be directly reduced by specific autoantibodies. Autoantibodies also alter the activity of signaling pathways, some of which regulate cell cohesion under baseline conditions and alter the turnover of desmosomal components. These pathways include Ca^{2+}, p38MAPK, PKC, Src, EGFR/Erk, and several others. In this review, we delineate the mechanisms relevant for pemphigus pathogenesis based on the histology and the ultrastructure of patients' lesions. We then dissect the mechanisms which can explain the ultrastructural hallmarks detectable in pemphigus patient skin. Finally, we reevaluate the concept that the spectrum of mechanisms, which induce desmosome dysfunction upon binding of pemphigus autoantibodies, finally defines the clinical phenotype.

Keywords: pemphigus, autoantibodies, cell adhesion, desmosomes, keratinocytes

OPEN ACCESS

Edited by:
Ralf J. Ludwig, University of Lübeck, Germany

Reviewed by:
Robert Gniadecki, University of Alberta, Canada
Hendri H. Pas, University Medical Center Groningen, Netherlands

***Correspondence:**
Volker Spindler
volker.spindler@unibas.ch;
Jens Waschke
jens.waschke@med.uni-muenchen.de

Specialty section:
This article was submitted to Immunological Tolerance and Regulation, a section of the journal Frontiers in Immunology

Received: *29 November 2017*
Accepted: *16 January 2018*
Published: *01 February 2018*

Citation:
Spindler V and Waschke J (2018) Pemphigus—A Disease of Desmosome Dysfunction Caused by Multiple Mechanisms. Front. Immunol. 9:136. doi: 10.3389/fimmu.2018.00136

INTRODUCTION

Pemphigus is a severe autoimmune-blistering skin disease caused by autoantibodies primarily targeting the desmosomal adhesion molecules desmogleins (Dsgs) 1 and 3 (1), which are required for the firm intercellular adhesion of keratinocytes. Autoantibodies targeting Dsg3 are found during the mucosal-dominant phase in pemphigus vulgaris (mPV) which is frequently followed by a mucocutaneous phase (mcPV) with additional epidermal blistering and characterized by the presence of both anti-Dsg3 and anti-Dsg1 antibodies. By contrast, in pemphigus foliaceus (PF), flaccid blisters are found in the skin only, and their formation is associated with the occurrence of anti-Dsg1 autoantibodies. Autoantibodies against other desmosomal cadherins such as desmocollin (Dsc) 3 are rarely detectable in PV or PF but can be pathogenic (2–5). The pathogenicity of autoantibodies against a range of non-desmosomal autoantibodies that are often present in patients' sera in addition to anti-Dsg antibodies is unclear (6). We here focus on the mechanisms causing skin blistering in response to autoantibodies against Dsg1 and Dsg3. In addition to suppressing autoimmunity, which is the current basis for disease management (1), we believe that novel targeted therapeutic strategies are necessary to stabilize desmosomes in situations when autoantibodies are present. It is essential to better understand the regulation of desmosomal adhesion, and we aim to provide perspectives for future research by reevaluating the mechanisms leading to desmosome dysfunction, loss of keratinocyte cohesion, and blistering.

HISTOLOGY AND ULTRASTRUCTURE OF PATIENT'S LESIONS HIGHLIGHT RELEVANT MECHANISMS

Cultured keratinocytes or mouse models can only partially reproduce the situation in patients. We believe that for the identification of relevant mechanisms in pemphigus pathogenesis, the careful evaluation of patients' lesions is the gold standard. On the histological level, skin blistering in PV occurs by suprabasal splitting (**Figure 1**), whereas PF is characterized by superficial lesions restricted to granular or upper spinous layers of the epidermis (1). Although exceptions occur, PF splitting is usually found in the upper half of the epidermis, whereas PV affects the lower half. At least in some parts of typical PV but not PF lesions, the histological hallmark of a "tomb-stone appearance" of keratinocytes in the blister bottom can be detected (7, 8).

By immunostaining, the clustering of Dsg3 together with autoantibodies has been detected in the mucosal and skin lesions in mcPV but also in unaffected epidermis in the mucosal-dominant type (mPV) in the absence of ultrastructural alterations of desmosomes (9, 10). By contrast, Dsg1 clustering was found in mcPV skin and PF epidermis only, i.e., when antibodies against Dsg1 were present (9, 10) (**Figure 1**). Since Dsg3 clustering was shown to be the structural correlate of Dsg3 depletion (11), these data indicate that the depletion of Dsg3 alone may be a primary mechanism in mucosal eroding but alone is not sufficient to cause epidermal blistering. Nevertheless, Dsg3 depletion may drastically worsen desmosome destabilization in the epidermis which is suggested by the fact that glucocorticoids rapidly improve the clinical phenotype (1) at least in part *via* Stat3-induced Dsg3 transcription increase (12).

On the ultrastructural level, smaller desmosomes were found only in conditions when patients presented with antibodies against Dsg1 such as in mcPV and PF but not in mPV (9, 10, 13, 14), suggesting that Dsg1 targeting is critical and may interfere with desmosome assembly or cause dismantling of existing desmosomes (**Figure 1**). Besides a reduced size, a general loss of desmosomes is present under all conditions where blistering occurred. Electron microscopy revealed the formation of double-membrane structures in PV and PF containing desmosomes with reduced size and altered morphology which may be the correlate for the depletion of extradesmosomal Dsg molecules and the uptake of entire desmosomes (13). Similarly, interdesmosomal widening, which is the first ultrastructural sign to be detected in pemphigus lesions, may be caused by the endocytosis of extradesmosomal Dsg1 rather than of Dsg3 (13, 15). This alone appears not to be sufficient for blister formation since it was detected also in the unaffected deep epidermis and the mucosa of PF patients but not in mPV with intact Dsg1 distribution.

Split desmosomes both with and without attached keratin filaments were detected by electron microscopy and SIM on the keratinocyte surface facing blisters in PF and mcPV (13, 14). Desmosome splitting can be induced by mechanical stress (14) and may be the ultrastructural correlate for the direct inhibition of Dsg binding. Since split desmosomes in this study were of reduced size, altered desmosome structure appears to be required, suggesting an additional role of impaired desmosome assembly or the depletion of desmosomal Dsg. The final hallmark described early for both PV and PF by electron microscopy is keratin retraction (16, 17) (**Figure 1**). Recently, keratin filament retraction was observed only when desmosomes were completely absent (13). This can be interpreted in the way that keratin filaments are not the cause but rather the consequence of desmosomal loss or the changes are temporally tightly correlated.

Apoptosis is not a major mechanism because cells displaying signs of apoptotic cell death are absent or sparse in PV and PF skin lesions and therefore cannot explain acantholysis of a significant epidermal area (13, 18, 19).

AUTOANTIBODY-TRIGGERED MECHANISMS IMPAIRING DESMOSOME TURNOVER

As outlined earlier, split desmosomes, reduced desmosome numbers and size, and keratin retraction are ultrastructural hallmarks in pemphigus skin. Reduced desmosome size or numbers cannot be explained by the direct interference of pemphigus autoantibodies with Dsg binding but rather are a consequence of the altered turnover of desmosomal proteins. These changes are likely steered by intracellular-signaling pathways, which are modulated in response to autoantibody binding and represent potential pharmacologic targets. In principal, reduced desmosome size and numbers can result either from interference with desmosome assembly or from the enhanced disassembly of desmosomes. Available data suggest that in pemphigus, both mechanisms contribute to impaired desmosome turnover, shifting the balance toward an overall reduction of desmosomal components (20).

Desmosome assembly is tightly interwoven with adherens junction formation and appears to proceed in distinct steps (21) (**Figure 2**, left panel). Desmosomal cadherins are initially transported to the cell membrane in a microtubule- and kinesin-dependent process (22), which, in case of Dsg2, is enhanced by its palmitoylation (23). The precise mechanisms are unclear but once membrane-localized, desmosomal cadherins appear to cluster in an intermediate junction with E-cadherin, β-catenin, and plakoglobin and probably segregate to form desmosomes clusters later on (24, 25). Plakophilins (Pkps) are essential as they are required to assemble keratin-anchored DP pools in the cortical regions of the cell (26, 27). Pkp3 was shown to participate in transferring DP clusters to the membrane and to stabilize desmosomal cadherins in a Rap1-dependent manner (28). In addition, cortical actin and actin-binding proteins such as adducins and RhoA signaling are necessary for full desmosome assembly (29–31). Desmosomal molecules localize to lipid rafts and the raft-associated proteins Flotillin-1 and -2 (32, 33). In line with this, interference with lipid raft composition prevents both desmosomal assembly and disassembly, suggesting these lipid-enriched membrane domains to be hot spots for desmosome turnover. Compared to the assembly, the disassembly of desmosomes under physiologic conditions is poorly understood, which may be related to the relative chemical inaccessibility and the stability of maturated desmosomes (34).

Pemphigus autoantibodies interfere with desmosome turnover by enhancing the internalization of desmosomal components (**Figure 2**, right panel). However, a clear separation of mechanisms

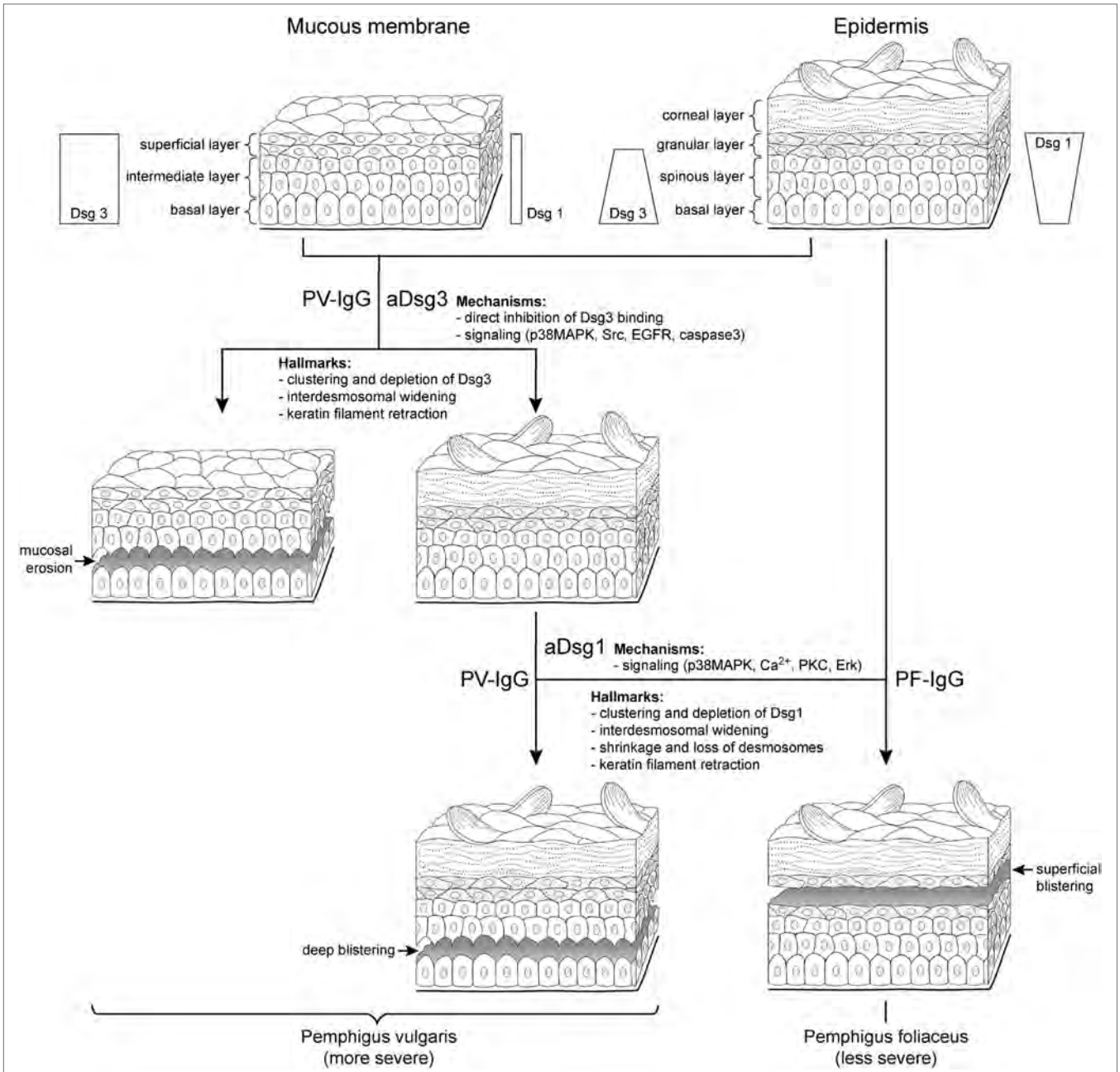

FIGURE 1 | Clinical phenotypes correlate with autoantibody profiles and mechanisms causing desmosome dysfunction. It is well established that clinical phenotypes of pemphigus largely correlate with autoantibody profiles but the underlying mechanisms are not clear. In pemphigus vulgaris (PV) (left), mucosal erosions often precede epidermal blistering. During the mucosal-dominant phase, autoantibodies (PV-IgG) primarily against desmoglein (aDsg3) are pathogenic, which is the most abundant Dsg isoform in the mucosal epithelium. The occurrence of antibodies targeting Dsg1 (aDsg1), which is strongly expressed in the superficial epidermis compared to Dsg3, usually correlates with skin blistering, affecting the deep epidermis right above the basal layer. By contrast, in pemphigus foliaceus (PF), autoantibodies (PF-IgG) primarily against Dsg1 (aDsg1) cause superficial epidermal blistering. The different phenotypes are characterized by structural hallmarks in patients' lesions, and the mechanisms causing desmosome dysfunction in response to autoantibody binding appear to be different for aDsg1 and aDsg3. Please note that the distribution of Dsg1 and Dsg3 in the epidermis is indicated for all layers except the for corneal layer.

specifically affecting either the assembly or the disassembly pathway in most cases is not possible. It is conceivable that autoantibodies reach Dsgs located in extradesmosomal membrane pools more easily than those densely packed in a mature desmosome. In line with this scenario, the non-desmosomal pool of Dsg3 is the first to be depleted (35, 36). Consequently, the reduced availability of supply molecules leads to the destabilization of desmosomes and in the longer run may favor the depletion of desmosome-localized, now more easily accessible molecules. Thus, the reduced desmosome assembly route in pemphigus is at

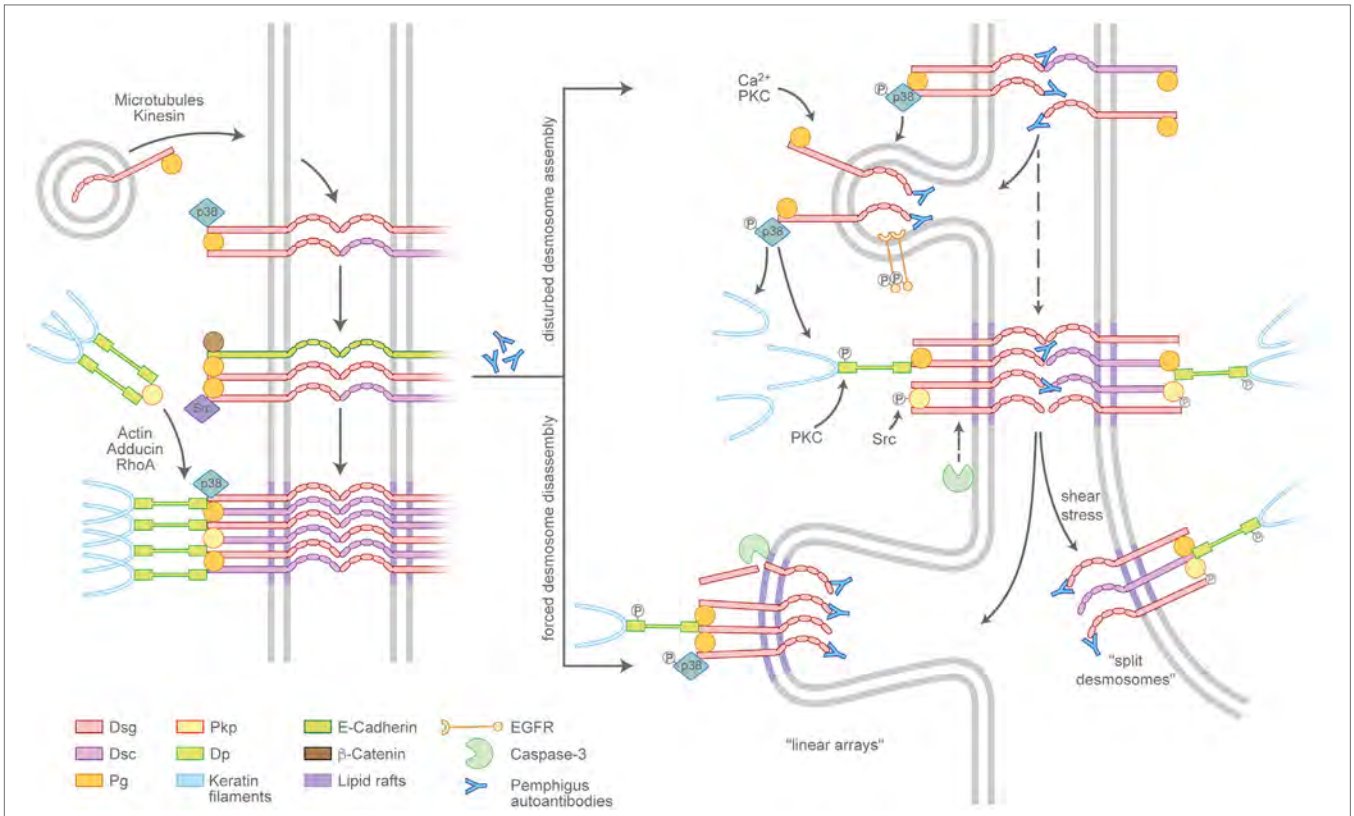

FIGURE 2 | Pemphigus autoantibodies interfere with desmosome turnover. Left panel: a simplified view of the assembly pathway of desmosomes. Desmosomal cadherins and the plaque components desmoplakin (DP), plakophilins (Pkps), as well as the keratins are transported to the plasma membrane by distinct routes and may involve an intermediate complex containing adherens junction proteins. Right panel: Pemphigus autoantibodies interfere with the assembly of nascent desmosomes and promote the disassembly of existing desmosomes. The modulation of desmosome turnover is tied to changes of intracellular-signaling cascades which, for instance, lead to the phosphorylation or cleavage of desmosomal components. Linear arrays represent zones of desmosome disassembly. Split desmosomes may occur if the already-weakened desmosomes are exposed to shear stress.

least in part a result of internalized extradesmosomal molecules, summarized as "desmoglein nonassembly depletion hypothesis" (9, 37). However, the situation apparently is more complex than a simple disbalance in supply and demand. Importantly, especially the extradesmosomal molecules are considered to serve as signaling scaffolds (38, 39). As an example, it was shown that a complex of Dsg3 and Pg binds p38MAPK and suppresses its activity (40, 41). Upon the loss of Dsg3 interaction, e.g., by steric hindrance through pemphigus autoantibodies, this suppressive function is abolished and p38MAPK is activated. Indeed, p38MAPK signaling was shown to promote Dsg3 internalization (42) as well as keratin retraction (41, 43), suggesting that p38MAPK is a central signaling molecule in desmosome turnover. *Vice versa*, keratin filaments were shown to influence both desmosome stability and Dsg3-binding characteristics in a signaling-dependent manner. Under physiologic conditions, the keratin-dependent suppression of p38MAPK signaling increases Dsg3-binding strength, whereas the suppression of PKC signaling through the adapter protein Rack-1 prevents DP phosphorylation, stabilizes Dsg3 in the desmosome (44, 45), and, together with Pkp1 (46), promotes a hyperadhesive state. These functions appear to be disturbed by autoantibody-induced keratin retraction (Vielmuth et al., Frontiers Immunol, this issue). Furthermore, Pkp3 is phosphorylated in response to autoantibody binding in an Src-dependent manner (47), which may be connected to Src being present in the intermediate E-cadherin/Dsg3 complex (25). Together, these data suggest a feed-forward loop from extradesmosomal complexes to desmosomes that, at least in part through interference with keratin-dependent signaling, destabilizes desmosome composition and function. As the precise mechanisms are unclear, it is possible that keratins affect both the assembly and the disassembly pathways of desmosomes.

The occurrence of desmosome disassembly can be concluded from observations that Dsg3 together with PV-IgG is excluded from desmosomes and internalized (48). This is supported by observations that IgG autoantibodies can access Dsgs in native desmosomes (49). Clusters of desmosomal molecules localizing in arrays perpendicular to the cell–cell border may represent sites of internalization of single desmosomal components or the entire complexes (50). These may correspond to the "double-membrane structures" that are visible in patients' skin and are thought to be regions of internalization for partially dismantled desmosomes (13). Although all desmosomal proteins eventually are internalized, the degradation pathways of specific components are not uniform. Dsg3 as well as Pg colocalize with markers for endosomes and lysosomes, whereas DP and presumably other

plaque proteins use different, yet unknown, routes (35, 42). Lipid rafts are thought to be important for desmosome disassembly, as the impairment of raft composition prevents the depletion at least of Dsg3 and reduces loss of cell cohesion (32) (Schlögl et al., this issue). In addition, the cleavage of Dsg3 by caspase-3 independent from apoptosis was observed and may promote internalization (51–53), the latter of which was shown to require EGFR signaling (54).

Split desmosomes are rarely detectable in keratinocyte cultures incubated with pemphigus antibodies in the absence of mechanical stress (55) but are enhanced when cultures are subjected to mechanical strain as well as in human skin models and in patients' skin (14, 56). Furthermore, split desmosomes appear typically severely altered with reduced plaque sizes and aberrant keratin insertion. This may indicate that desmosome splitting occurs secondary to changes in desmosome composition. Collectively, interference with desmosome turnover can largely explain the ultrastructural hallmarks of pemphigus patients' lesions.

DESMOSOME DYSFUNCTION DEFINES THE CLINICAL PHENOTYPE OF PEMPHIGUS

All mechanisms described earlier finally lead to desmosome dysfunction, which impair keratinocyte cohesion. However, the functional interplay of the different mechanisms is not well understood at present. It is also unclear why epidermal splitting affects the deep epidermis in PV, whereas PF blisters are restricted to superficial epidermal layers (**Figure 1**). Besides homophilic adhesion, Dsgs were shown to undergo heterophilic interactions both with other Dsg isoforms and Dscs, respectively (5, 45, 57, 58). Moreover, the genetic deletion of Dsc3 causes a PV phenotype with suprabasal blistering in mice (59). On the other hand, the forced overexpression of Dsg2, a Dsg isoform not present in the adult human epidermis except hair follicles, which is upregulated in PV lesions, can compensate for the loss of Dsg1 in a PF mouse model (60, 61). Therefore, it is likely that all desmosomal cadherins (i.e., Dsg1–4, Dsc1–3) contribute to keratinocyte cohesion and epidermal integrity in a layer-specific manner.

In the mucosa, Dsg3 is the predominant desmosomal cadherin, and in the superficial epidermis Dsg1 is strongly expressed, whereas other isoforms of desmosomal cadherins are largely absent except of Dsc1 (**Figure 1**) (8). The cadherin distribution pattern can well explain the clinical phenotype of mPV and PF because the loss of function of the target molecules cannot be outbalanced by relevant amounts of other desmosomal cadherins (1). However, the Dsg compensation theory falls short in mcPV, because if Dsg1 and Dsg3 would specifically compensate for each other, the whole epidermis or at least the lower epidermis should disintegrate completely when considering that autoantibodies entering the epidermis from the dermis may be concentrated most in the first few layers of cells. Rather, epidermal splitting typically occurs right at the suprabasal level, i.e., between the basal keratinocytes and the first layer of the spinous layer cells where in intact epidermis as well as in PV lesions, Dsg1 and Dsg3 are expressed (8). This favors the hypothesis that different mechanisms contribute to desmosome dysfunction in a layer-specific manner.

The direct inhibition of Dsg3 binding by PV-IgG has been described under cell-free conditions as well as on the surface of living keratinocytes; however, it was ineffective to induce the complete loss of cell cohesion (62–64). By contrast, the interference of anti-Dsg1 autoantibodies with Dsg1 binding was detectable neither in cell-free AFM experiments (63, 65, 66) nor in studies with intact keratinocytes (Vielmuth 2018, Frontiers Immun, this issue). This suggests that the mechanisms underlying the loss of keratinocyte cohesion in pemphigus are autoantibody-specific. In this respect, it was reported recently that autoantibody profiles in pemphigus correlate with signaling patterns which makes it intriguing to speculate that specific signaling patterns may be defining the clinical phenotype (65). It has been reported that p38MAPK and Src can be activated by PV-IgG containing antibodies against Dsg3 as well as by AK23 which is Dsg3-specific (**Figure 1**). In addition, EGFR and caspase-3 activation in response to AK23 and PV-IgG was shown in mouse models (53, 54, 67). By contrast, the increase of intracellular Ca^{2+} as well as Erk activation was induced only by PV-IgG and PF-IgG containing Dsg1 autoantibodies, which was paralleled by p38MAPK activation (65). In this line of thoughts, the direct inhibition of Dsg3 binding together with the signaling of p38MAPK, Src, EGFR, and caspase-3 would be sufficient to cause mucosal erosions (**Figure 1**), whereas additional mechanisms such as Ca^{2+}, which has been shown to be associated with PKC activation in keratinocytes treated with pemphigus antibodies (68, 69), as well as Erk would be required for epidermal blistering. If so, it could be postulated that one function of Dsg and Dsc isoforms expressed in the epidermis but not in the mucosa may be to further strengthen keratinocyte cohesion by regulating signaling pathway which control desmosome turnover and function.

For most of the pathways described earlier, it was shown that modulation is sufficient to largely reduce skin blistering in mice (6). However, mice differ from humans with respect to epidermal Dsg expression patterns. Moreover, the genetic deletion of Dsg3 or the inactivation of Dsg3 *via* incubation with AK23 is sufficient to cause skin blisters in mice (41, 70). This is different to the situation in mPV where the skin is usually not affected and indicates that Dsg3 is more critical for epidermal integrity in mice compared to humans. Therefore, to prevent misinterpretations, studies including ultrastructural analyses of human skin are required in addition to mouse models. Indeed, studies in human skin *ex vivo* indicate that the significance of p38MAPK for blister formation may be different in PV and PF. When using PV-IgG, the inhibition of p38MAPK was sufficient to abrogate blistering (11, 56) but not when PF-IgG was applied (71). On the other hand, it was shown that p38MAPK in response to PV-IgG and PF-IgG is involved in the reduction of desmosome length (56, 71). However, since the shortening of desmosomes and interdesmosomal widening were detectable also in the absence of blistering following treatment with AK23, this indicates that p38MAPK-mediated reduction of desmosome length and interdesmosomal widening may not be sufficient to cause skin blistering. Rather, the complete loss of desmosomes appears to be required (56) for

which other mechanisms such as Ca^{2+}, PKC, or Erk may be necessary to induce superficial epidermal blistering in PF (**Figure 1**). However, when bolstered by the direct inhibition of Dsg3 binding and Src activation, the panel of mechanisms causing desmosome dysfunction may be sufficient to cause suprabasal splitting as seen in mcPV. Taken together, it is likely that the clinical phenotype in pemphigus is caused by a complex set of mechanisms causing desmosome dysfunction.

AUTHOR CONTRIBUTIONS

VS and JW conceived the perspective and wrote the manuscript.

FUNDING

The study was supported by the Deutsche Forschungsgemeinschaft (DFG SP1300/1-3 to VS and FOR2497 to JW).

REFERENCES

1. Kasperkiewicz M, Ellebrecht CT, Takahashi H, Yamagami J, Zillikens D, Payne AS, et al. Pemphigus. *Nat Rev Dis Primers* (2017) 3:17026. doi:10.1038/nrdp.2017.26
2. Mindorf S, Dettmann IM, Krüger S, Fuhrmann T, Rentzsch K, Karl I, et al. Routine detection of serum antidesmocollin autoantibodies is only useful in patients with atypical pemphigus. *Exp Dermatol* (2017) 26(12):1267–70. doi:10.1111/exd.13409
3. Mao X, Nagler AR, Farber SA, Choi EJ, Jackson LH, Leiferman KM, et al. Autoimmunity to desmocollin 3 in pemphigus vulgaris. *Am J Pathol* (2010) 177:2724–30. doi:10.2353/ajpath.2010.100483
4. Rafei D, Müller R, Ishii N, Llamazares M, Hashimoto T, Hertl M, et al. IgG Autoantibodies against desmocollin 3 in pemphigus sera induce loss of keratinocyte adhesion. *Am J Pathol* (2011) 178:718–23. doi:10.1016/j.ajpath.2010.10.016
5. Spindler V, Heupel W-M, Efthymiadis A, Schmidt E, Eming R, Rankl C, et al. Desmocollin 3-mediated binding is crucial for keratinocyte cohesion and is impaired in pemphigus. *J Biol Chem* (2009) 284:30556–64. doi:10.1074/jbc.M109.024810
6. Spindler V, Eming R, Schmidt E, Amagai M, Grando S, Jonkman MF, et al. Mechanisms causing loss of keratinocyte cohesion in pemphigus. *J Invest Dermatol* (2017) 138(1):32–7. doi:10.1016/j.jid.2017.06.022
7. Ohata C, Ishii N, Furumura M. Locations of acantholysis in pemphigus vulgaris and pemphigus foliaceus. *J Cutan Pathol* (2014) 41:880–9. doi:10.1111/cup.12384
8. Waschke J. The desmosome and pemphigus. *Histochem Cell Biol* (2008) 130:21–54. doi:10.1007/s00418-008-0420-0
9. Oktarina DAM, van der Wier G, Diercks GFH, Jonkman MF, Pas HH. IgG-induced clustering of desmogleins 1 and 3 in skin of patients with pemphigus fits with the desmoglein nonassembly depletion hypothesis. *Br J Dermatol* (2011) 165:552–62. doi:10.1111/j.1365-2133.2011.10463.x
10. van der Wier G, Pas HH, Kramer D, Diercks GFH, Jonkman MF. Smaller desmosomes are seen in the skin of pemphigus patients with anti-desmoglein 1 antibodies but not in patients with anti-desmoglein 3 antibodies. *J Invest Dermatol* (2014) 134:2287–90. doi:10.1038/jid.2014.140
11. Saito M, Stahley SN, Caughman CY, Mao X, Tucker DK, Payne AS, et al. Signaling dependent and independent mechanisms in pemphigus vulgaris blister formation. *PLoS One* (2012) 7:e50696. doi:10.1371/journal.pone.0050696
12. Mao X, Cho MJT, Ellebrecht CT, Mukherjee EM, Payne AS. Stat3 regulates desmoglein 3 transcription in epithelial keratinocytes. *JCI Insight* (2017) 2:92253. doi:10.1172/jci.insight.92253
13. Sokol E, Kramer D, Diercks GF, Kuipers J, Jonkman MF, Pas HH, et al. Large-scale electron microscopy maps of patient skin and mucosa provide insight into pathogenesis of blistering diseases. *J Invest Dermatol* (2015) 135:1763–70. doi:10.1038/jid.2015.109
14. Stahley SN, Warren MF, Feldman RJ, Swerlick RA, Mattheyses AL, Kowalczyk AP. Super-resolution microscopy reveals altered desmosomal protein organization in tissue from patients with pemphigus vulgaris. *J Invest Dermatol* (2016) 136:59–66. doi:10.1038/JID.2015.353
15. van der Wier G, Jonkman MF, Pas HH, Diercks GF. Ultrastructure of acantholysis in pemphigus foliaceus re-examined from the current perspective. *Br J Dermatol* (2012) 167:1265–71. doi:10.1111/j.1365-2133.2012.11173.x
16. Wilgram GF, Caulfield JB, Lever WF. An electron microscopic study of acantholysis in pemphigus vulgaris. *J Invest Dermatol* (1961) 36:373–82. doi:10.1038/jid.1961.58
17. Wilgram GF, Caulfield JB, Madgic EB. An electron microscopic study of acantholysis and dyskeratosis in pemphigus foliaceus: with a special note on peculiar intracytoplasmic bodies. *J Invest Dermatol* (1964) 43:287–99. doi:10.1038/jid.1964.159
18. Janse IC, van der Wier G, Jonkman MF, Pas HH, Diercks GFH. No evidence of apoptotic cells in pemphigus acantholysis. *J Invest Dermatol* (2014) 134:2039–41. doi:10.1038/jid.2014.60
19. Schmidt E, Waschke J. Apoptosis in pemphigus. *Autoimmun Rev* (2009) 8:533–7. doi:10.1016/j.autrev.2009.01.011
20. Kitajima Y. 150(th) anniversary series: desmosomes and autoimmune disease, perspective of dynamic desmosome remodeling and its impairments in pemphigus. *Cell Commun Adhes* (2014) 21:269–80. doi:10.3109/15419061.2014.943397
21. Nekrasova O, Green KJ. Desmosome assembly and dynamics. *Trends Cell Biol* (2013) 23:537–46. doi:10.1016/j.tcb.2013.06.004
22. Nekrasova OE, Amargo EV, Smith WO, Chen J, Kreitzer GE, Green KJ. Desmosomal cadherins utilize distinct kinesins for assembly into desmosomes. *J Cell Biol* (2011) 195:1185–203. doi:10.1083/jcb.201106057
23. Roberts BJ, Svoboda RA, Overmiller AM, Lewis JD, Kowalczyk AP, Mahoney MG, et al. Palmitoylation of desmoglein 2 is a regulator of assembly dynamics and protein turnover. *J Biol Chem* (2016) 291:24857–65. doi:10.1074/jbc.M116.739458
24. Hatzfeld M, Keil R, Magin TM. Desmosomes and intermediate filaments: their consequences for tissue mechanics. *Cold Spring Harb Perspect Biol* (2017) 9:a029157. doi:10.1101/cshperspect.a029157
25. Rotzer V, Hartlieb E, Vielmuth F, Gliem M, Spindler V, Waschke J. E-cadherin and Src associate with extradesmosomal Dsg3 and modulate desmosome assembly and adhesion. *Cell Mol Life Sci* (2015) 72:4885–97. doi:10.1007/s00018-015-1977-0
26. Bass-Zubek AE, Hobbs RP, Amargo EV, Garcia NJ, Hsieh SN, Chen X, et al. Plakophilin 2: a critical scaffold for PKCα that regulates intercellular junction assembly. *J Cell Biol* (2008) 181:605–13. doi:10.1083/jcb.200712133
27. Godsel LM, Hsieh SN, Amargo EV, Bass AE, Pascoe-McGillicuddy LT, Huen AC, et al. Desmoplakin assembly dynamics in four dimensions. *J Cell Biol* (2005) 171:1045–59. doi:10.1083/jcb.200510038
28. Todorovic V, Koetsier JL, Godsel LM, Green KJ. Plakophilin 3 mediates Rap1-dependent desmosome assembly and adherens junction maturation. *Mol Biol Cell* (2014) 25:3749–64. doi:10.1091/mbc.E14-05-0968
29. Godsel LM, Dubash AD, Bass-Zubek AE, Amargo EV, Klessner JL, Hobbs RP, et al. Plakophilin 2 couples actomyosin remodeling to desmosomal plaque assembly *via* RhoA. *Mol Biol Cell* (2010) 21:2844–59. doi:10.1091/mbc.E10-02-0131
30. Pasdar M, Li Z. Disorganization of microfilaments and intermediate filaments interferes with the assembly and stability of desmosomes in MDCK epithelial cells. *Cell Motil Cytoskeleton* (1993) 26:163–80. doi:10.1002/cm.970260207
31. Rötzer V, Breit A, Waschke J, Spindler V. Adducin is required for desmosomal cohesion in keratinocytes. *J Biol Chem* (2014) 289:14925–40. doi:10.1074/jbc.M113.527127
32. Stahley SN, Saito M, Faundez V, Koval M, Mattheyses AL, Kowalczyk AP. Desmosome assembly and disassembly are membrane raft-dependent. *PLoS One* (2014) 9:e87809. doi:10.1371/journal.pone.0087809

33. Vollner F, Ali J, Kurrle N, Exner Y, Eming R, Hertl M, et al. Loss of flotillin expression results in weakened desmosomal adhesion and pemphigus vulgaris-like localisation of desmoglein-3 in human keratinocytes. *Sci Rep* (2016) 6:28820. doi:10.1038/srep28820
34. Windoffer R, Borchert-Stuhltrager M, Leube RE. Desmosomes: interconnected calcium-dependent structures of remarkable stability with significant integral membrane protein turnover. *J Cell Sci* (2002) 115:1717–32.
35. Calkins CC, Setzer SV, Jennings JM, Summers S, Tsunoda K, Amagai M, et al. Desmoglein endocytosis and desmosome disassembly are coordinated responses to pemphigus autoantibodies. *J Biol Chem* (2006) 281:7623–34. doi:10.1074/jbc.M512447200
36. Yamamoto Y, Aoyama Y, Shu E, Tsunoda K, Amagai M, Kitajima Y. Anti-desmoglein 3 (Dsg3) monoclonal antibodies deplete desmosomes of Dsg3 and differ in their Dsg3-depleting activities related to pathogenicity. *J Biol Chem* (2007) 282:17866–76. doi:10.1074/jbc.M607963200
37. Kitajima Y. New insights into desmosome regulation and pemphigus blistering as a desmosome-remodeling disease. *Kaohsiung J Med Sci* (2013) 29:1–13. doi:10.1016/j.kjms.2012.08.001
38. Müller EJ, Williamson L, Kolly C, Suter MM. Outside-in signaling through integrins and cadherins: a central mechanism to control epidermal growth and differentiation? *J Invest Dermatol* (2008) 128:501–16. doi:10.1038/sj.jid.5701248
39. Waschke J, Spindler V. Desmosomes and extradesmosomal adhesive signaling contacts in pemphigus. *Med Res Rev* (2014) 34:1127–45. doi:10.1002/med.21310
40. Spindler V, Dehner C, Hubner S, Waschke J. Plakoglobin but not desmoplakin regulates keratinocyte cohesion *via* modulation of p38MAPK signaling. *J Invest Dermatol* (2014) 134:1655–64. doi:10.1038/jid.2014.21
41. Spindler V, Rotzer V, Dehner C, Kempf B, Gliem M, Radeva M, et al. Peptide-mediated desmoglein 3 crosslinking prevents pemphigus vulgaris autoantibody-induced skin blistering. *J Clin Invest* (2013) 123:800–11. doi:10.1172/JCI60139
42. Jolly PS, Berkowitz P, Bektas M, Lee H-E, Chua M, Diaz LA, et al. p38MAPK signaling and desmoglein-3 internalization are linked events in pemphigus acantholysis. *J Biol Chem* (2010) 285:8936–41. doi:10.1074/jbc.M109.087999
43. Berkowitz P, Hu P, Liu Z, Diaz LA, Enghild JJ, Chua MP, et al. Desmosome signaling. Inhibition of p38MAPK prevents pemphigus vulgaris IgG-induced cytoskeleton reorganization. *J Biol Chem* (2005) 280:23778–84. doi:10.1074/jbc.M501365200
44. Dehner C, Rotzer V, Waschke J, Spindler V. A desmoplakin point mutation with enhanced keratin association ameliorates pemphigus vulgaris autoantibody-mediated loss of cell cohesion. *Am J Pathol* (2014) 184:2528–36. doi:10.1016/j.ajpath.2014.05.016
45. Vielmuth F, Wanuske MT, Radeva MY, Hiermaier M, Kugelmann D, Walter E, et al. Keratins regulate the adhesive properties of desmosomal cadherins through signaling. *J Invest Dermatol* (2017) 138(1):121–31. doi:10.1016/j.jid.2017.08.033
46. Tucker DK, Stahley SN, Kowalczyk AP. Plakophilin-1 protects keratinocytes from pemphigus vulgaris IgG by forming calcium-independent desmosomes. *J Invest Dermatol* (2014) 134:1033–43. doi:10.1038/jid.2013.401
47. Cirillo N, AlShwaimi E, McCullough M, Prime SS. Pemphigus vulgaris autoimmune globulin induces Src-dependent tyrosine-phosphorylation of plakophilin 3 and its detachment from desmoglein 3. *Autoimmunity* (2014) 47:134–40. doi:10.3109/08916934.2013.866100
48. Aoyama Y, Nagai M, Kitajima Y. Binding of pemphigus vulgaris IgG to antigens in desmosome core domains excludes immune complexes rather than directly splitting desmosomes. *Br J Dermatol* (2010) 162:1049–55. doi:10.1111/j.1365-2133.2010.09672.x
49. Shimizu A, Ishiko A, Ota T, Tsunoda K, Amagai M, Nishikawa T. IgG Binds to desmoglein 3 in desmosomes and causes a desmosomal split without keratin retraction in a pemphigus mouse model. *J Invest Dermatol* (2004) 122:1145–53. doi:10.1111/j.0022-202X.2004.22426.x
50. Jennings JM, Tucker DK, Kottke MD, Saito M, Delva E, Hanakawa Y, et al. Desmosome disassembly in response to pemphigus vulgaris IgG occurs in distinct phases and can be reversed by expression of exogenous Dsg3. *J Invest Dermatol* (2011) 131:706–18. doi:10.1038/jid.2010.389
51. Cirillo N, Campisi G, Gombos F, Perillo L, Femiano F, Lanza A. Cleavage of desmoglein 3 can explain its depletion from keratinocytes in pemphigus vulgaris. *Exp Dermatol* (2008) 17:858–63. doi:10.1111/j.1600-0625.2008.00719.x
52. Hariton WVJ, Galichet A, Vanden Berghe T, Overmiller AM, Mahoney MG, Declercq W, et al. Feasibility study for clinical application of caspase-3 inhibitors in pemphigus vulgaris. *Exp Dermatol* (2017) 26(12):1274–7. doi:10.1111/exd.13458
53. Luyet C, Schulze K, Sayar BS, Howald D, Muller EJ, Galichet A. Preclinical studies identify non-apoptotic low-level caspase-3 as therapeutic target in pemphigus vulgaris. *PLoS One* (2015) 10:e0119809. doi:10.1371/journal.pone.0119809
54. Bektas M, Jolly PS, Berkowitz P, Amagai M, Rubenstein DS. A pathophysiologic role for epidermal growth factor receptor in pemphigus acantholysis. *J Biol Chem* (2013) 288:9447–56. doi:10.1074/jbc.M112.438010
55. Mao X, Choi EJ, Payne AS. Disruption of desmosome assembly by monovalent human pemphigus vulgaris monoclonal antibodies. *J Invest Dermatol* (2009) 129:908–18. doi:10.1038/jid.2008.339
56. Egu DT, Walter E, Spindler V, Waschke J. Inhibition of p38MAPK signalling prevents epidermal blistering and alterations of desmosome structure induced by pemphigus autoantibodies in human epidermis. *Br J Dermatol* (2017) 177(6):1612–8. doi:10.1111/bjd.15721
57. Harrison OJ, Brasch J, Lasso G, Katsamba PS, Ahlsen G, Honig B, et al. Structural basis of adhesive binding by desmocollins and desmogleins. *Proc Natl Acad Sci U S A* (2016) 113:7160–5. doi:10.1073/pnas.1606272113
58. Nie Z, Merritt A, Rouhi-Parkouhi M, Tabernero L, Garrod D. Membrane-impermeable cross-linking provides evidence for homophilic, isoform-specific binding of desmosomal cadherins in epithelial cells. *J Biol Chem* (2011) 286:2143–54. doi:10.1074/jbc.M110.192245
59. Chen J, Den Z, Koch PJ. Loss of desmocollin 3 in mice leads to epidermal blistering. *J Cell Sci* (2008) 121:2844–9. doi:10.1242/jcs.031518
60. Brennan D, Hu Y, Medhat W, Dowling A, Mahoney MG. Superficial dsg2 expression limits epidermal blister formation mediated by pemphigus foliaceus antibodies and exfoliative toxins. *Dermatol Res Pract* (2010) 2010:410278. doi:10.1155/2010/410278
61. Hartlieb E, Kempf B, Partilla M, Vigh B, Spindler V, Waschke J. Desmoglein 2 is less important than desmoglein 3 for keratinocyte cohesion. *PLoS One* (2013) 8:e53739. doi:10.1371/journal.pone.0053739
62. Heupel W-M, Müller T, Efthymiadis A, Schmidt E, Drenckhahn D, Waschke J. Peptides targeting the desmoglein 3 adhesive interface prevent autoantibody-induced acantholysis in pemphigus. *J Biol Chem* (2009) 284:8589–95. doi:10.1074/jbc.M808813200
63. Heupel WM, Zillikens D, Drenckhahn D, Waschke J. Pemphigus vulgaris IgG directly inhibit desmoglein 3-mediated transinteraction. *J Immunol* (2008) 181:1825–34. doi:10.4049/jimmunol.181.3.1825
64. Vielmuth F, Waschke J, Spindler V. Loss of desmoglein binding is not sufficient for keratinocyte dissociation in pemphigus. *J Invest Dermatol* (2015) 135:3068–77. doi:10.1038/jid.2015.324
65. Walter E, Vielmuth F, Rotkopf L, Sardy M, Horvath ON, Goebeler M, et al. Different signaling patterns contribute to loss of keratinocyte cohesion dependent on autoantibody profile in pemphigus. *Sci Rep* (2017) 7:3579. doi:10.1038/s41598-017-03697-7
66. Waschke J, Bruggeman P, Baumgartner W, Zillikens D, Drenckhahn D. Pemphigus foliaceus IgG causes dissociation of desmoglein 1-containing junctions without blocking desmoglein 1 transinteraction. *J Clin Invest* (2005) 115:3157–65. doi:10.1172/JCI23475
67. Sayar BS, Ruegg S, Schmidt E, Sibilia M, Siffert M, Suter MM, et al. EGFR inhibitors erlotinib and lapatinib ameliorate epidermal blistering in pemphigus vulgaris in a non-linear, V-shaped relationship. *Exp Dermatol* (2014) 23:33–8. doi:10.1111/exd.12290
68. Osada K, Seishima M, Kitajima Y. Pemphigus IgG activates and translocates protein kinase C from the cytosol to the particulate/cytoskeleton fractions in human keratinocytes. *J Invest Dermatol* (1997) 108:482–7. doi:10.1111/1523-1747.ep12289726
69. Seishima M, Esaki C, Osada K, Mori S, Hashimoto T, Kitajima Y. Pemphigus IgG, but not bullous pemphigoid IgG, causes a transient increase in intracellular calcium and inositol 1,4,5-triphosphate in DJM-1 cells, a squamous cell

carcinoma line. *J Invest Dermatol* (1995) 104:33–7. doi:10.1111/1523-1747.ep12613469

70. Rotzer V, Hartlieb E, Winkler J, Walter E, Schlipp A, Sardy M, et al. Desmoglein 3-dependent signaling regulates keratinocyte migration and wound healing. *J Invest Dermatol* (2016) 136:301–10. doi:10.1038/JID.2015.380
71. Yoshida K, Ishii K, Shimizu A, Yokouchi M, Amagai M, Shiraishi K, et al. Non-pathogenic pemphigus foliaceus (PF) IgG acts synergistically with a directly pathogenic PF IgG to increase blistering by p38MAPK-dependent desmoglein 1 clustering. *J Dermatol Sci* (2017) 85:197–207. doi:10.1016/j.jdermsci.2016.12.010

Conflict of Interest Statement: The authors declare that the research was conducted in the absence of any commercial or financial relationships that could be construed as a potential conflict of interest.

frontiers in Immunology

MINI REVIEW
published: 25 January 2018
doi: 10.3389/fimmu.2018.00066

Autoantibodies in Chronic Obstructive Pulmonary Disease

*Lifang Wen[1], Susanne Krauss-Etschmann[2,3], Frank Petersen[2] and Xinhua Yu[1,2]**

[1] Xiamen-Borstel Joint Laboratory of Autoimmunity, Medical College of Xiamen University, Xiamen, China, [2] Priority Area Asthma and Allergy, Research Center Borstel, Airway Research Center North (ARCN), German Center for Lung Research (DZL), Borstel, Germany, [3] Institute of Experimental Medicine, Christian-Albrechts-University of Kiel, Kiel, Germany

Chronic obstructive pulmonary disease (COPD), the fourth leading cause of death worldwide, is characterized by irreversible airflow limitation based on obstructive bronchiolitis, emphysema, and chronic pulmonary inflammation. Inhaled toxic gases and particles, e.g., cigarette smoke, are major etiologic factors for COPD, while the pathogenesis of the disease is only partially understood. Over the past decade, an increasing body of evidence has been accumulated for a link between COPD and autoimmunity. Studies with clinical samples have demonstrated that autoantibodies are present in sera of COPD patients and some of these antibodies correlate with specific disease phenotypes. Furthermore, evidence from animal models of COPD has shown that autoimmunity against pulmonary antigens occur during disease development and is capable of mediating COPD-like symptoms. The idea that autoimmunity could contribute to the development of COPD provides a new angle to understand the pathogenesis of the disease. In this review article, we provide an advanced overview in this field and critically discuss the role of autoantibodies in the pathogenesis of COPD.

Keywords: autoimmunity, autoantibodies, chronic obstructive pulmonary disease, biomarkers, emphysema, experimental models, pathogenesis

OPEN ACCESS

Edited by:
Falk Nimmerjahn, University of Erlangen-Nuremberg, Germany

Reviewed by:
Simon Fillatreau, Deutsches Rheuma-Forschungszentrum (DRFZ), Germany
Dunja Bruder, Universitätsklinikum Magdeburg, Germany

***Correspondence:**
Xinhua Yu
xinhuayu@fz-borstel.de

Specialty section:
This article was submitted to Immunological Tolerance and Regulation, a section of the journal Frontiers in Immunology

Received: *23 October 2017*
Accepted: *10 January 2018*
Published: *25 January 2018*

Citation:
Wen L, Krauss-Etschmann S, Petersen F and Yu X (2018) Autoantibodies in Chronic Obstructive Pulmonary Disease. Front. Immunol. 9:66. doi: 10.3389/fimmu.2018.00066

INTRODUCTION

Chronic obstructive pulmonary disease (COPD) is a major public health problem affecting more than 200 million people worldwide and leading to millions of death annually (1). COPD patients suffer from a progressive and not fully reversible airflow limitation. Pathologically, COPD is characterized by persistent pulmonary inflammation, obstruction of the small airways (obstructive bronchiolitis) and structural changes of the airways (emphysema) (2). It is widely accepted that COPD is triggered by inhaled toxic gases and particles. However, the pathogenesis of COPD remains largely unclear (2, 3).

Cigarette smoking (CS) is the major etiologic and risk factor for COPD (4, 5), and smoking cessation is beneficial for patients in terms of lung function (6). However, smoke cessation does not attenuate the pulmonary inflammation once COPD is established in patients (7, 8). The persistence of the pulmonary inflammation after smoking cessation and the presence of well-organized lymphoid follicles around small airways and lung parenchyma of COPD patients (9–11) implicate that there are memory adaptive immune responses to non-cigarette antigens, such as autoantigens, commensal microbiota, and infectious pathogens (8, 12, 13). Among these candidates, autoantigens are of specific interest because both clinical and experimental evidence suggest that CS is capable of triggering autoimmunity. Thus, the exploration of the contribution of autoimmune responses

to the development of COPD could provide a new angle for understanding the pathogenesis of this disease.

In 2002, Cosio et al. proposed a novel concept that COPD could be considered as an autoimmune disease triggered by smoking (14). In 2007, Lee et al. reported that emphysema is characterized by the presence of humoral and cellular autoimmune responses against elastin, an extracellular protein important for lung integrity (12), for the first time showing evidence for a role of autoimmunity in COPD pathogenesis. Thereafter, many efforts have been made to determine the role of autoimmunity in the development of COPD by the use of clinical samples and animal models. In this review article, we aim to summarize recent advances in this field, discuss the contribution of autoimmunity to COPD, and outline prospects for future research. Since the role of self-reactive T cells in COPD has been reviewed elsewhere (14–16), we focus here on autoantibodies in COPD and its animal models.

AUTOANTIBODIES IN COPD PATIENTS

Presence of Autoantibodies in COPD

According to their targets, studies investigating the presence of autoantibodies in COPD can be roughly categorized into two groups, those addressing autoantibodies against undefined and those addressing defined antigens (**Table 1**).

The first group consists of studies in which autoantibodies against undefined autoantigens, such as tissues or cells were investigated. Given that the majority of autoantigens in COPD is probably unknown, determination of autoantibodies against lung tissue or its major cell types, e.g., epithelial or endothelial cells provides a proof-of-principle evidence for the presence of autoantibodies in this disease. In 2008, Feghali-Bostwick and colleagues detected IgG deposition within alveolar septa and small airway walls by immunohistochemical staining in six out of six of patients with severe COPD, but in none of six controls (17) indicating for the first time that anti-tissue antibodies are present in COPD patients. Such anti-tissue antibodies in COPD were also described in another study using indirect immunohistochemical staining in which Packard et al. showed that IgG from COPD patients have a higher binding capability to non-smoker lung tissue section than IgG from healthy smokers (18). In addition, anti-tissue antibodies in COPD could also be detected using rodent tissues as antigen (19) confirming the presence of anti-tissue antibodies.

Aside from studying anti-tissue autoantibodies, Feghali-Bostwick et al. went on to investigate autoantibodies more specifically directed against epithelial and endothelial cells (17). Their results showed that the prevalence of autoantibodies against epithelial cells, including both hepatoma (HEp-2) cell and primary pulmonary artery epithelial cells, is significantly higher in COPD patients as compared with smoker or non-smoker (17). In addition, 50% of the COPD patients are also characterized by autoantibodies against primary pulmonary artery endothelial cells (17). This study shows for the first time the presence of anti-epithelial and anti-endothelial autoantibodies in COPD patients. By using a cell-based enzyme-linked immunosorbent assay with human umbilical vein endothelial cells (HUVECs) as coated antigen, two independent research groups confirmed the presence of anti-endothelial IgG in COPD patients (20, 21). Recently, the presence of anti-epithelial IgG has also been shown in a study using human bronchial epithelial cells as target (22). Taken together, these studies demonstrate convincingly that autoantibodies against lung tissue as well as pulmonary epithelial and endothelial cells are detectable in patients with COPD.

In the second group of studies, autoantibodies against defined antigens suspected to be present in or functionally related to the disease were investigated. This group includes extracellular matrix (ECM) proteins, cellular proteins from pulmonary cells, neo-autoantigens, immune molecules, and autoantigens in common autoimmune diseases.

The main function of cellular matrix proteins is to maintain the structure and integrity of the lung. Since degradation of matrix proteins is a hallmark of emphysema, these proteins are promising candidates for autoantigens in COPD. As mentioned earlier, autoantibodies against elastin have been detected in emphysema patients, showing for the first time the presence of autoantibodies in COPD (12). However, beside one exception (18), all following studies failed to confirm levels of anti-elastin antibodies in COPD patients surmounting those of healthy controls (23–26). Moreover, results from two independent groups showed that levels of anti-elastin antibodies are even lower in COPD patients than in healthy controls (27, 28). Beside elastin, collagens have been also extensively investigated as candidate autoantigens for COPD. Using an autoantigen array with 70 proteins, Packard and colleagues showed that levels of autoantibodies reactive to a broad spectrum of self-antigens are significantly higher in COPD patients involving emphysema than in healthy controls, including autoantibodies against collagen I, collagen II, and collagen IV (18). However, similar to the findings for anti-elastase antibodies, these results were not confirmed by other groups (12, 23, 25), keeping this issue under debate. Moreover, autoantibodies against aggrecan, another ECM protein, have been detected in patients with COPD (18).

In addition to ECM proteins, cellular proteins from pulmonary cells have also been regarded as potential autoantigens in COPD. Using immunoblotting assays with lysates prepared from alveolar cells as targets, Kuo et al. showed that autoantibodies against multiple cellular antigens are more frequently present in sera of COPD patients than in controls (29). Among those antigens, a 45-kDa cellular protein was identified as cytokeratin 18 (CK-18), an intermediate filament protein located in the intracytoplasmic cytoskeleton of epithelial tissue. Although this interesting finding has not been observed in a report based on a small number of samples (25), it has been confirmed in a recent study where 228 COPD patients and 136 controls were included (30). Here, Xiong et al. could show that the levels of circulating IgG, IgA, and IgM autoantibodies against CK-18 are elevated in COPD patients as compared with healthy controls (30). Furthermore, they also demonstrated that COPD patient express autoantibodies against another intermediate filament protein, CK-19, suggesting another cellular autoantigen for the diseases (30).

Neo-autoantigens are antigens expressed under specific pathophysiological conditions and are not ubiquitously in our body (31). Well-known neo-autoantigens in autoimmune diseases

TABLE 1 | Summary of autoantibodies in COPD.

Autoantigen			Method	COPD vs control	Association with disease parameters	Reference
Tissues and cells	Tissue	Rodent tissue	IIF	Increased	ATS/ERS stage and DLCO	(19)
		Human lung tissue	DIH	Increased	–	(17)
		Human lung tissue	IIH	Increased	Emphysema	(18)
	Epithelial	HEp-2 cells	IIF	Increased	No	(17)
		primary PAEpC	IIF	Increased	–	(17)
		HBEC	IIF	Increased	GOLD stages	(22)
	Endothelial	primary PAEdC	IIF	Increased	–	(17)
		HUVEC	ELISA	Increased	No	(20)
		HUVEC	ELISA	Increased	–	(21)
Defined autoantigens	ECM proteins	Elastin	ELISA	Increased	–	(12)
			PA	Increased	–	(18)
			ELISA	No difference	–	(25)
			ELISA	No difference	–	(23)
			ELISA	No difference	–	(26)
			ELISA	No difference	–	(24)
			ELISA	Decreased	Emphysema and GOLD stage	(27)
			ELISA	Decreased	–	(28)
		Collagen I	PA	Increased	–	(18)
			ELISA	No difference	–	(23)
			ELISA	No difference	–	(12)
			ELISA	Decreased	–	(25)
		Collagen II	PA	Increased	Emphysema	(18)
			ELISA	No difference	–	(25)
		Collagen IV	PA	Increased	–	(18)
			ELISA	No difference	–	(25)
		Aggrecan	PA	Increased	Emphysema	(18)
	Alveolar cellular proteins	Cytokeratin 18	WB	Increased	FEV1(L) and FEV1 (% predicted)	(29)
			ELISA	Increased	GOLD stage	(30)
			ELISA	No difference	–	(25)
		Cytokeratin 19	ELISA	Increased	GOLD stage	(30)
	Immune molecules	Soluble CD80	ELISA, WB	Increased	GOLD stage	(38)
		αB-crystallin	ELISA	Increased	No association	(37)
		β2-Microglobulin	PA	Increased	–	(18)
	Neo-autoantigen	CCP	ELISA	Increased	No association	(35)
			ELISA	No difference	–	(33)
			ELISA	No difference	–	(34)
			ELISA	No difference	–	(28)
		CFFCP	ELISA	Increased	No association	(34)
		MCV	ELISA	No difference	No association	(28)
		CMP	ELISA	Increased	FEV1 (% predicted) and GOLD stages	(21)
	Autoantigens in common autoimmune disease	Nuclear	IIF	Increased	No association	(19)
			IIF	Increased	No association	(39)
			IIF	No difference	–	(33)
			IIF	No difference	–	(26)
		Cardiolipin, CENP-B, cytochrome *C*, DGPs, H1, H2A, H2B, histone, JO-1, La/SS-B, LC1, PL-12, PL-7, Ro52 (SSA), thyroglobulin, topoisomerase, snRNP-68, U1-snRNP-BB, and U1-snRNP-A	PA	Increase	Emphysema	(18)

HEp-2 cells, hepatoma cell; primary PAEpC, primary pulmonary airway epithelial cells; HBEC, human bronchial epithelial cell; primary PAEdC, primary pulmonary artery endothelial cells; HUVEC, human umbilical vein endothelial cell; IIF, indirect immunofluorescence, DIH, direct immunohistochemistry; IIH, indirect immunohistochemistry; ELISA, enzyme-linked immunosorbent assay; WB, western blot; PA, protein array; ECM, extracellular matrix proteins; CCP, citrullinated peptides; CFFCP, chimeric citrullinated peptides of human fibrin and filaggrin; MCV, mutated citrullinated vimentin; DGPs, deamidated gliadin peptides; CMP, carbonyl-modified proteins; COPD, chronic obstructive pulmonary disease; ATS/ERS, American Thoracic Society/European Respiratory Society.

such as rheumatoid arthritis (RA) are citrullinated peptides or proteins which are generated by a posttranslational modification process occurring under certain inflammatory conditions (32). Results from several studies using different citrullinated peptides or proteins as antigens have shown that the frequencies of sera with anti-citrullinated protein antibody (ACPA) are very low in both COPD patients and healthy controls and without significant difference between these two groups (33–35). When the concentrations of ACPA are used for comparison, levels of anti-cyclic citrullinated peptide antibodies (CCP2) have been shown to

be higher in sera of COPD patients than controls in one study (35), which was not confirmed by three other groups (28, 33, 34). Carbonyl-modified proteins (CMP) represent another type of neo-autoantigen, which are investigated in COPD. Oxidants, a major constituent of cigarette smoke, can cause the formation of carbonyl adducts on proteins *in vivo* (36), making it conceivable that autoantibodies against CMP are generated in COPD patients. To verify this hypothesis, Kirkham et al. determined levels of autoantibodies against CMP in the sera of COPD patients and controls. They found that antibody titers against carbonyl-modified self-protein were significantly increased in patients with COPD as compared with controls (21) showing the presence of such autoantibodies.

Apart from molecules from cells residing in the lung, some molecules from immune cells have also been shown to act as autoantigens in COPD. In 2012, Cherneva and colleagues reported that concentrations of autoantibodies against αB-crystallin (HspB5), a marker of innate immune activation, were increased in patients with COPD (37). Notably, according to this study, those autoantibodies are also present in inflammatory lung diseases suggesting that they are not COPD specific. Very recently, Luo et al. investigated autoantibodies against a soluble form of CD80 (sCD80), a co-stimulatory molecule for T cell activation, in sera of patients with COPD (38). They found that serum levels of anti-sCD80 were higher in patients with COPD than in controls and were positively correlated to inflammatory cytokines, e.g., IL-6 and IL-8 (38). Another immune molecule, β2-microglobulin that is a component of MHC class I molecules, has also been identified as an autoantigen in COPD (18).

Finally, autoantigens that have already been described in some common autoimmune diseases have also been investigated in COPD. For example, using indirect immunofluorescence staining, two independent groups have demonstrated that antinuclear antibodies are more prevalent in patients with COPD than healthy controls (19, 39). Although this difference has not been found in two other studies using the same detection method (26, 33), a study using protein arrays carrying 70 different antigens has confirmed that sera of patients with emphysema have autoantibodies reactive to many common nuclear antigens (18). In this study, the reactivity of sera derived from patients suffering from systemic lupus erythematosus (SLE) and RA was analyzed in comparison. Interestingly, emphysema-associated COPD was characterized by a lower autoantibody reactivity than SLE, but a higher than RA (18), suggesting COPD is indeed associated with a substantial level of autoimmunity.

Taken together, a number of previous studies have demonstrated that autoantibodies are present in patients with COPD. However, their determination and visualization appear to be autoantigen and method depending.

Does the Presence of Autoantibodies Correlate with Clinical Parameters in COPD?

Aside from demonstrating the mere presence of autoantibodies, their potential correlation with disease parameters is important for their clinical relevance as biomarkers and could provide further evidence for a role of autoantibodies in COPD. Therefore, some studies with well characterized patients investigated the correlation between autoantibodies and clinical parameters of COPD.

By comparing subgroups of COPD patients categorized by clinical parameters, Nunez and colleagues demonstrated that the prevalence of anti-tissue antibodies are significantly different among patients groups with various disease severity as indicated by American Thoracic Society/European Respiratory Society (ATS/ERS) stage or diffusing capacity of carbon monoxide (DLCO). Patients with more severe disease showed higher prevalence of anti-tissue antibodies (19), suggesting an association between the presence of anti-tissue antibodies and an increased disease severity. In another study, Packard and colleagues described that sera from COPD patients with emphysema showed a higher anti-tissue antibody reactivity than sera from COPD patients without emphysema, suggesting an association of this autoantibody with emphysematous disease.

Recently, an association between severity of COPD and anti-epithelial antibodies has been demonstrated by Cheng et al. (22). They found that the prevalence of both anti-epithelial IgG and IgA are elevated in patients with severe disease (GOLD stage III or IV) as compared with patients with milder symptoms (GOLD stage I or II) (22). However, the association of anti-epithelial antibodies with disease severity has not been observed in a study with a rather small number of patients (17). Based on these inconsistent results from current studies, it remains unclear whether anti-epithelial antibodies are indeed associated with severity of COPD.

The correlation with clinical parameters of COPD has also been shown for autoantibodies directed against some defined antigens. For example, in Packard's study, they found that serum levels of autoantibodies against many antigens are significantly higher than in COPD patients without emphysema (18). Disease severity is also reported to be associated with autoantibodies against several other antigens. In 2010, Kuo et al. reported that levels of autoantibodies against CK-18 were inversely correlated with lung function parameters (29). This correlation is confirmed by investigations of Xiong et al. who showed that circulating levels of both anti-CK-18 and anti-CK-19 autoantibodies correlate significantly with the severity of the disease (30). Besides anti-CK-18 and anti-CK-19, two other autoantibodies have been reported to correlate with disease severity in COPD. While the presence of anti-sCD80 antibodies was shown to be associated with a high GOLD stage (38), autoantibodies against CMP correlated with a high GOLD stage and were inversely correlated with lung function parameters (21).

Notably, anti-elastin antibodies are also associated with disease parameters, but in contrast to all autoantibodies mentioned earlier, in the opposite direction where a lower antibody titer was associated with more severe disease and emphysema (27).

AUTOANTIBODIES IN ANIMAL MODELS OF COPD

Animal models are powerful research tools for investigating the pathogenesis of human diseases. For COPD, such models have

been established in many species, including mice, rat, dog, monkey, and guinea pig (40). In consistence with findings in COPD patients, evidence from animal models also supports a role of autoantibodies in the pathogenesis of COPD, especially in those with emphysema (**Table 2**).

In 2010, Brandsma and colleagues reported that chronic CS-exposure leads to the pulmonary inflammation and production of autoantibodies against multiple ECM components in mice (41). To further explore the role of autoantibodies against ECM in this mouse model, the authors immunized mice with a mixture of lung ECM. As expected, mice immunized with ECM produced high levels of autoantibodies against different ECM components. In addition, the immunization alone increased the number of macrophage in the lung tissue suggesting a proinflammatory role of autoimmunity against ECM (41). Unfortunately, emphysema, which is associated with autoantibodies in human COPD, was not observed in their model disabling the evaluation of a potential association between autoimmunity against ECM and emphysema development (41). Very recently, a study investigating CS-induced rat model of COPD shed some new light on this field (42). In this study, Hu et al. reported that CS-exposed rats produce higher levels of autoantibodies against β2-adrenergic receptors (β2-ARs) than control rats (42). Moreover, autoantibodies against β2-ARs are associated with severity of CS-induced emphysema suggesting that the autoimmunity might be involved in the formation of emphysema. To confirm this notion, the authors immunized rats with the peptide of the second extracellular loop of β2-ARs which contains an epitope recognized by agnostic autoantibodies against β2-ARs (42, 43). Rat immunized with the β2-ARs peptide produces autoantibodies against β2-ARs and development of emphysema, confirming the role of autoimmunity against β2-ARs in pathogenesis of COPD-like disease (42). Therefore, evidence from CS-induced animal models demonstrates that CS-exposure triggers autoimmunity against multiple autoantigens in the lung and such autoimmunity contribute to COPD-like symptoms.

Beside CS-expose induced approaches, models induced by active immunization also provide evidence for a role of autoimmunity in the pathogenesis of COPD. In 2005, Taraseviciene-Stewart and colleagues reported a new animal model for COPD in rats (44). Rats immunized with HUVECs raised antibodies against HUVECs and developed emphysema. Interestingly, adoptive transfer of either serum or CD4+ T cells from the HUVECs-immunized rat into naive immunocompetent rats induced subsequent emphysema (44). These results suggest an autoimmune-driven mechanism beneath the disease manifestation in experimental COPD which involves both autoreactive T cells and autoantibodies.

TABLE 2 | Autoantibodies in animal models of COPD.

Animal models	Disease symptoms	Autoantibodies	Reference
CS-exposed mice	Pulmonary inflammation with macrophages and B cells	Anti-ECM	(41)
ECM-immunized mice	Pulmonary inflammation with macrophages	Anti-ECM	(41)
CS-exposed rat	emphysema	Anti- β2-AR	(42)
β2-AR immunized rat	Emphysema	Anti- β2-AR	(42)
HUVEC-immunized rat	Emphysema	Anti-HUVEC	(44)
IgG transfer-induced rat	Emphysema	Anti-HUVEC	(44)

CS, cigarette smoking; ECM, extracellular matrix, β2-AR, β2-adrenergic receptor; HUVEC, human umbilical vein endothelial cell; COPD, chronic obstructive pulmonary disease.

CONCLUSION AND PERSPECTIVES

In summary, the abovementioned clinical and experimental studies provide some evidence for the role of autoantibodies in COPD. First, autoantibodies are present in both COPD patients and in corresponding animal models, particularly those involving emphysema. This notion is supported by the finding that severe COPD with emphysema is associated with HLA II alleles which is associated with most autoimmune diseases (45). Second, correlation between autoantibodies and disease severity has been described but appears not to be consistent among different studies. Third, autoantibodies in animal models of COPD are capable of inducing a COPD-like disease phenotype. Those evidence, alone with the fact that COPD patients are characterized by increased numbers of B cells, plasma cells, and B cell-rich lymphoid follicles that correlate directly with disease severity (11, 46), support a role of autoantibodies in the development of COPD. Besides humoral autoimmunity, it is important to mention that cellular autoimmunity might also contribute to COPD pathogenesis. As aforementioned, human autoreactive CD8+ and CD4+ T cells have been suggested to contribute to COPD (14–16). In addition, transfer of CD4+ T cells from the HUVECs-immunized rat is able to induce emphysema, supporting a role of autoreactive CD4+ T cells in experimental COPD (44).

With immunodeficient mice which lack both T- and B-cells, the role of adaptive immunity in experimental COPD can be explored. In 2010, Motz et al. reported that transfer of T cells from CS-exposed mice, but not T cells from fresh air-exposed mice, into Rag2−/− mice led to the development of pulmonary inflammation and emphysema in the recipient mice (47), suggesting that adaptive immune responses are capable to mediate COPD-like symptoms. However, by directly exposing immunodeficient mice to CS, two research groups have demonstrated that immunodeficient mice develop comparable COPD-like disease as wild-type controls mice (48, 49), indicating that adaptive immune responses are not required for CS-induced COPD in mice. Since autoimmunity is a part of adaptive immune responses, the abovementioned experimental evidence suggests that autoimmunity is potentially pathogenic but dispensable for CS-induced COPD in animals. However, since human differ from animals in many aspects, findings from animal models might not sufficiently reflect human diseases. Therefore, whether autoimmunity is a pathogenic or an indispensable event in the development of COPD remains elucidative.

In conclusion, previous studies have suggested a potential role of autoimmunity in COPD and its animal models, opening a new field for exploring the pathogenesis of the diseases. Further investigations in this field will not only help for understanding the pathogenesis of COPD but also help for both diagnostic and treatment of the disease.

AUTHOR CONTRIBUTIONS

LW was involved in search and identification of relevant literatures. XY and LW were involved in drafting the manuscript. SK-E and FP critically read the manuscript and contributed with significant revision.

FUNDING

This work was supported by the Deutsche Forschungsgemeinschaft, German Center for Lung Research (DZL) and Research Training Group GRK1727 *Modulation of Autoimmunity*, as well as by the National Natural Science Foundation of China (No.81371325).

REFERENCES

1. Mannino DM. COPD: epidemiology, prevalence, morbidity and mortality, and disease heterogeneity. *Chest* (2002) 121(5 Suppl):121S–6S. doi:10.1378/chest.121.5_suppl.121S
2. Hogg JC, Timens W. The pathology of chronic obstructive pulmonary disease. *Annu Rev Pathol* (2009) 4:435–59. doi:10.1146/annurev.pathol.4.110807.092145
3. Tuder RM, Petrache I. Pathogenesis of chronic obstructive pulmonary disease. *J Clin Invest* (2012) 122(8):2749–55. doi:10.1172/JCI60324
4. Brusselle GG, Joos GF, Bracke KR. New insights into the immunology of chronic obstructive pulmonary disease. *Lancet* (2011) 378(9795):1015–26. doi:10.1016/S0140-6736(11)60988-4
5. Caramori G, Casolari P, Barczyk A, Durham AL, Di SA, Adcock I. COPD immunopathology. *Semin Immunopathol* (2016) 38(4):497–515. doi:10.1007/s00281-016-0561-5
6. Kohansal R, Martinez-Camblor P, Agusti A, Buist AS, Mannino DM, Soriano JB. The natural history of chronic airflow obstruction revisited: an analysis of the Framingham offspring cohort. *Am J Respir Crit Care Med* (2009) 180(1):3–10. doi:10.1164/rccm.200901-0047OC
7. Gamble E, Grootendorst DC, Hattotuwa K, O'Shaughnessy T, Ram FS, Qiu Y, et al. Airway mucosal inflammation in COPD is similar in smokers and ex-smokers: a pooled analysis. *Eur Respir J* (2007) 30(3):467–71. doi:10.1183/09031936.00013006
8. Rutgers SR, Postma DS, ten Hacken NH, Kauffman HF, van Der Mark TW, Koeter GH, et al. Ongoing airway inflammation in patients with COPD who do not currently smoke. *Thorax* (2000) 55(1):12–8. doi:10.1136/thorax.55.1.12
9. Brusselle GG, Demoor T, Bracke KR, Brandsma CA, Timens W. Lymphoid follicles in (very) severe COPD: beneficial or harmful? *Eur Respir J* (2009) 34(1):219–30. doi:10.1183/09031936.00150208
10. Hogg JC, Chu F, Utokaparch S, Woods R, Elliott WM, Buzatu L, et al. The nature of small-airway obstruction in chronic obstructive pulmonary disease. *N Engl J Med* (2004) 350(26):2645–53. doi:10.1056/NEJMoa032158
11. Seys LJ, Verhamme FM, Schinwald A, Hammad H, Cunoosamy DM, Bantsimba-Malanda C, et al. Role of B cell-activating factor in chronic obstructive pulmonary disease. *Am J Respir Crit Care Med* (2015) 192(6):706–18. doi:10.1164/rccm.201501-0103OC
12. Lee SH, Goswami S, Grudo A, Song LZ, Bandi V, Goodnight-White S, et al. Antielastin autoimmunity in tobacco smoking-induced emphysema. *Nat Med* (2007) 13(5):567–9. doi:10.1038/nm1583
13. Sze MA, Dimitriu PA, Suzuki M, McDonough JE, Campbell JD, Brothers JF, et al. Host response to the lung microbiome in chronic obstructive pulmonary disease. *Am J Respir Crit Care Med* (2015) 192(4):438–45. doi:10.1164/rccm.201502-0223OC
14. Cosio MG, Majo J, Cosio MG. Inflammation of the airways and lung parenchyma in COPD: role of T cells. *Chest* (2002) 121(5 Suppl):160S–5S. doi:10.1378/chest.121.5_suppl.160S
15. Cosio MG, Saetta M, Agusti A. Immunologic aspects of chronic obstructive pulmonary disease. *N Engl J Med* (2009) 360(23):2445–54. doi:10.1056/NEJMra0804752
16. Kheradmand F, Shan M, Xu C, Corry DB. Autoimmunity in chronic obstructive pulmonary disease: clinical and experimental evidence. *Expert Rev Clin Immunol* (2012) 8(3):285–92. doi:10.1586/eci.12.7
17. Feghali-Bostwick CA, Gadgil AS, Otterbein LE, Pilewski JM, Stoner MW, Csizmadia E, et al. Autoantibodies in patients with chronic obstructive pulmonary disease. *Am J Respir Crit Care Med* (2008) 177(2):156–63. doi:10.1164/rccm.200701-014OC
18. Packard TA, Li QZ, Cosgrove GP, Bowler RP, Cambier JC. COPD is associated with production of autoantibodies to a broad spectrum of self-antigens, correlative with disease phenotype. *Immunol Res* (2013) 55(1–3):48–57. doi:10.1007/s12026-012-8347-x
19. Nunez B, Sauleda J, Anto JM, Julia MR, Orozco M, Monso E, et al. Anti-tissue antibodies are related to lung function in chronic obstructive pulmonary disease. *Am J Respir Crit Care Med* (2011) 183(8):1025–31. doi:10.1164/rccm.201001-0029OC
20. Karayama M, Inui N, Suda T, Nakamura Y, Nakamura H, Chida K. Antiendothelial cell antibodies in patients with COPD. *Chest* (2010) 138(6):1303–8. doi:10.1378/chest.10-0863
21. Kirkham PA, Caramori G, Casolari P, Papi AA, Edwards M, Shamji B, et al. Oxidative stress-induced antibodies to carbonyl-modified protein correlate with severity of chronic obstructive pulmonary disease. *Am J Respir Crit Care Med* (2011) 184(7):796–802. doi:10.1164/rccm.201010-1605OC
22. Cheng G, Zhang N, Wang Y, Rui J, Yin X, Cui T. Antibodies of IgG, IgA and IgM against human bronchial epithelial cell in patients with chronic obstructive pulmonary disease. *Clin Lab* (2016) 62(6):1101–8. doi:10.7754/Clin.Lab.2015.151020
23. Brandsma CA, Kerstjens HA, Geerlings M, Kerkhof M, Hylkema MN, Postma DS, et al. The search for autoantibodies against elastin, collagen and decorin in COPD. *Eur Respir J* (2011) 37(5):1289–92. doi:10.1183/09031936.00116710
24. Cottin V, Fabien N, Khouatra C, Moreira A, Cordier JF. Anti-elastin autoantibodies are not present in combined pulmonary fibrosis and emphysema. *Eur Respir J* (2009) 33(1):219–21. doi:10.1183/09031936.00140208
25. Daffa NI, Tighe PJ, Corne JM, Fairclough LC, Todd I. Natural and disease-specific autoantibodies in chronic obstructive pulmonary disease. *Clin Exp Immunol* (2015) 180(1):155–63. doi:10.1111/cei.12565
26. Greene CM, Low TB, O'Neill SJ, McElvaney NG. Anti-proline-glycine-proline or antielastin autoantibodies are not evident in chronic inflammatory lung disease. *Am J Respir Crit Care Med* (2010) 181(1):31–5. doi:10.1164/rccm.200904-0545OC
27. Rinaldi M, Lehouck A, Heulens N, Lavend'homme R, Carlier V, Saint-Remy JM, et al. Antielastin B-cell and T-cell immunity in patients with chronic obstructive pulmonary disease. *Thorax* (2012) 67(8):694–700. doi:10.1136/thoraxjnl-2011-200690
28. Wood AM, de PP, Buckley CD, Ahmad A, Stockley RA. Smoke exposure as a determinant of autoantibody titre in alpha(1)-antitrypsin deficiency and COPD. *Eur Respir J* (2011) 37(1):32–8. doi:10.1183/09031936.00033710
29. Kuo YB, Chang CA, Wu YK, Hsieh MJ, Tsai CH, Chen KT, et al. Identification and clinical association of anti-cytokeratin 18 autoantibody in COPD. *Immunol Lett* (2010) 128(2):131–6. doi:10.1016/j.imlet.2009.12.017
30. Xiong Y, Gao S, Luo G, Cheng G, Huang W, Jiang R, et al. Increased circulating autoantibodies levels of IgG, IgA, IgM against cytokeratin 18 and cytokeratin 19 in chronic obstructive pulmonary disease. *Arch Med Res* (2017) 48(1):79–87. doi:10.1016/j.arcmed.2017.01.007
31. Rosen A, Casciola-Rosen L. Autoantigens in systemic autoimmunity: critical partner in pathogenesis. *J Intern Med* (2009) 265(6):625–31. doi:10.1111/j.1365-2796.2009.02102.x

32. Darrah E, Andrade F. Rheumatoid arthritis and citrullination. *Curr Opin Rheumatol* (2018) 30(1):72–8. doi:10.1097/BOR.0000000000000452
33. Newkirk MM, Mitchell S, Procino M, Li Z, Cosio M, Mazur W, et al. Chronic smoke exposure induces rheumatoid factor and anti-heat shock protein 70 autoantibodies in susceptible mice and humans with lung disease. *Eur J Immunol* (2012) 42(4):1051–61. doi:10.1002/eji.201141856
34. Ruiz-Esquide V, Gomara MJ, Peinado VI, Gomez Puerta JA, Barbera JA, Canete JD, et al. Anti-citrullinated peptide antibodies in the serum of heavy smokers without rheumatoid arthritis. A differential effect of chronic obstructive pulmonary disease? *Clin Rheumatol* (2012) 31(7):1047–50. doi:10.1007/s10067-012-1971-y
35. Sigari N, Moghimi N, Shahraki FS, Mohammadi S, Roshani D. Anti-cyclic citrullinated peptide (CCP) antibody in patients with wood-smoke-induced chronic obstructive pulmonary disease (COPD) without rheumatoid arthritis. *Rheumatol Int* (2015) 35(1):85–91. doi:10.1007/s00296-014-3083-2
36. le-Donne I, Aldini G, Carini M, Colombo R, Rossi R, Milzani A. Protein carbonylation, cellular dysfunction, and disease progression. *J Cell Mol Med* (2006) 10(2):389–406. doi:10.1111/j.1582-4934.2006.tb00407.x
37. Cherneva RV, Georgiev OB, Petrova DS, Trifonova NL, Stamenova M, Ivanova V, et al. The role of small heat-shock protein alphaB-crystalline (HspB5) in COPD pathogenesis. *Int J Chron Obstruct Pulmon Dis* (2012) 7:633–40. doi:10.2147/COPD.S34929
38. Luo XM, Liu XY, Tang JH, Yang W, Ni ZH, Chen QG, et al. Autoantibodies against CD80 in patients with COPD. *Clin Transl Immunology* (2016) 5(10):e103. doi:10.1038/cti.2016.57
39. Bonarius HP, Brandsma CA, Kerstjens HA, Koerts JA, Kerkhof M, Nizankowska-Mogilnicka E, et al. Antinuclear autoantibodies are more prevalent in COPD in association with low body mass index but not with smoking history. *Thorax* (2011) 66(2):101–7. doi:10.1136/thx.2009.134171
40. Ghorani V, Boskabady MH, Khazdair MR, Kianmeher M. Experimental animal models for COPD: a methodological review. *Tob Induc Dis* (2017) 15:25. doi:10.1186/s12971-017-0130-2
41. Brandsma CA, Timens W, Geerlings M, Jekel H, Postma DS, Hylkema MN, et al. Induction of autoantibodies against lung matrix proteins and smoke-induced inflammation in mice. *BMC Pulm Med* (2010) 10:64. doi:10.1186/1471-2466-10-64
42. Hu JY, Liu BB, Du YP, Zhang Y, Zhang YW, Zhang YY, et al. Increased circulating beta2-adrenergic receptor autoantibodies are associated with smoking-related emphysema. *Sci Rep* (2017) 7:43962. doi:10.1038/srep43962
43. Kohr D, Singh P, Tschernatsch M, Kaps M, Pouokam E, Diener M, et al. Autoimmunity against the beta2 adrenergic receptor and muscarinic-2 receptor in complex regional pain syndrome. *Pain* (2011) 152(12):2690–700. doi:10.1016/j.pain.2011.06.012
44. Taraseviciene-Stewart L, Scerbavicius R, Choe KH, Moore M, Sullivan A, Nicolls MR, et al. An animal model of autoimmune emphysema. *Am J Respir Crit Care Med* (2005) 171(7):734–42. doi:10.1164/rccm.200409-1275OC
45. Faner R, Nunez B, Sauleda J, Garcia-Aymerich J, Pons J, Crespi C, et al. HLA distribution in COPD patients. *COPD* (2013) 10(2):138–46. doi:10.3109/15412555.2012.729621
46. Polverino F, Seys LJ, Bracke KR, Owen CA. B cells in chronic obstructive pulmonary disease: moving to center stage. *Am J Physiol Lung Cell Mol Physiol* (2016) 311(4):L687–95. doi:10.1152/ajplung.00304.2016
47. Motz GT, Eppert BL, Wesselkamper SC, Flury JL, Borchers MT. Chronic cigarette smoke exposure generates pathogenic T cells capable of driving COPD-like disease in Rag2-/- mice. *Am J Respir Crit Care Med* (2010) 181(11):1223–33. doi:10.1164/rccm.200910-1485OC
48. Botelho FM, Gaschler GJ, Kianpour S, Zavitz CC, Trimble NJ, Nikota JK, et al. Innate immune processes are sufficient for driving cigarette smoke-induced inflammation in mice. *Am J Respir Cell Mol Biol* (2010) 42(4):394–403. doi:10.1165/rcmb.2008-0301OC
49. D'hulst AI, Maes T, Bracke KR, Demedts IK, Tournoy KG, Joos GF, et al. Cigarette smoke-induced pulmonary emphysema in scid-mice. Is the acquired immune system required? *Respir Res* (2005) 6:147. doi:10.1186/1465-9921-6-147

Conflict of Interest Statement: The authors declare that the research was conducted in the absence of any commercial or financial relationships that could be construed as a potential conflict of interest.

frontiers in Immunology

ORIGINAL RESEARCH
published: 17 January 2018
doi: 10.3389/fimmu.2017.01992

Gene Expression Analysis Reveals Novel Shared Gene Signatures and Candidate Molecular Mechanisms between Pemphigus and Systemic Lupus Erythematosus in CD4+ T Cells

Tanya Sezin[1†], Artem Vorobyev[2†], Christian D. Sadik[1], Detlef Zillikens[1,2], Yask Gupta[2†] and Ralf J. Ludwig[1,2†]*

[1] Department of Dermatology, University of Lübeck, Lübeck, Germany, [2] Lübeck Institute of Experimental Dermatology (LIED), University of Lübeck, Lübeck, Germany

OPEN ACCESS

Edited by:
Herman Waldmann,
University of Oxford, United Kingdom

Reviewed by:
Huanfa Yi,
Jilin University, China
Anne Fletcher,
Monash University, Australia

***Correspondence:**
Tanya Sezin
tanya.sezin@uksh.de

†These authors have contributed equally to this work.

Specialty section:
This article was submitted to Immunological Tolerance and Regulation, a section of the journal Frontiers in Immunology

Received: 30 August 2017
Accepted: 22 December 2017
Published: 17 January 2018

Citation:
Sezin T, Vorobyev A, Sadik CD, Zillikens D, Gupta Y and Ludwig RJ (2018) Gene Expression Analysis Reveals Novel Shared Gene Signatures and Candidate Molecular Mechanisms between Pemphigus and Systemic Lupus Erythematosus in CD4+ T Cells. Front. Immunol. 8:1992. doi: 10.3389/fimmu.2017.01992

Pemphigus and systemic lupus erythematosus (SLE) are severe potentially life-threatening autoimmune diseases. They are classified as B-cell-mediated autoimmune diseases, both depending on autoreactive CD4+ T lymphocytes to modulate the autoimmune B-cell response. Despite the reported association of pemphigus and SLE, the molecular mechanisms underlying their comorbidity remain unknown. Weighted gene co-expression network analysis (WGCNA) of publicly available microarray datasets of CD4+ T cells was performed, to identify shared gene expression signatures and putative overlapping biological molecular mechanisms between pemphigus and SLE. Using WGCNA, we identified 3,280 genes co-expressed genes and 14 co-expressed gene clusters, from which one was significantly upregulated for both diseases. The pathways associated with this module include type-1 interferon gamma and defense response to viruses. Network-based meta-analysis identified RSAD2 to be the most highly ranked hub gene. By associating the modular genes with genome-wide association studies (GWASs) for pemphigus and SLE, we characterized IRF8 and STAT1 as key regulatory genes. Collectively, in this *in silico* study, we identify novel candidate genetic markers and pathways in CD4+ T cells that are shared between pemphigus and SLE, which in turn may facilitate the identification of novel therapeutic targets in these diseases.

Keywords: autoimmunity, gene expression analysis, weighted gene co-expression analysis, pemphigus, systemic lupus erythematosus, CD4+ T cells

INTRODUCTION

Pemphigus is a rare autoimmune bullous dermatosis, clinically characterized by intraepidermal blistering of the skin and/or mucous membranes. Immunologically, pemphigus is characterized by autoantibodies directed against desmosomal and non-desmosomal adhesion molecules expressed in the skin and mucosa. Binding of the pathogenic autoantibodies in the skin leads to dissociation of adjacent keratinocytes and formation of blisters. Based on the clinical presentation and the specificity of the anti-desmoglein (Dsg) autoantibodies, pemphigus is classified into two main forms, pemphigus

vulgaris (PV), with autoantibodies targeting Dsg3, and in some cases also Dsg1, and pemphigus foliaceus (PF), with autoantibodies targeting Dsg1 (1). The association of pemphigus with connective tissue diseases such as systemic lupus erythematosus (SLE) has been previously noted on a case report/case series basis (2, 3). In line, pemphigus autoantibodies and antinuclear autoantibodies, one immunological hallmark of SLE (4), coexist in healthy blood donors (5). However, the molecular mechanism remains unknown. The co-occurrence of pemphigus and SLE can suggest a common network of multifunctional genes and pathways. Alternatively, it can be altogether serendipitous. Due to the complexity of such a system, weighted gene co-expression network analysis (WGCNA) can serve as a comprehensive tool for identifying gene clusters of correlating and connected shared genes (6, 7). This approach has been previously successfully applied in various biological contexts to identify regulatory genes and networks associated with multiple disease phenotypes (8–11).

Systemic lupus erythematosus and pemphigus are characterized by the production of autoantibodies and traditionally classified as B-cell-mediated autoimmune diseases. Compelling evidence has, however, shown that autoreactive helper-T lymphocytes are crucial in pathogenicity of both diseases by regulating B cells response and promoting autoantibodies production (12–15). Thus, studying gene expression networks within the $CD4^+$ T-cell population is not only essential for understanding the underlying pathophysiology but also for identifying predictive biomarkers and establishment of novel therapeutic targets for these diseases.

Using publically available gene expression data from NCBI GEO database, we investigated gene co-expression networks of $CD4^+$ T cells obtained from pemphigus (PV as well as PF) and SLE patients (16). Our analysis revealed 14 distinct modules containing 3,280 co-expressed genes between the two diseases. Two out of 14 modules were found significantly upregulated: one in PF and SLE, and the other in PV. We further identified biological pathways such as "type I interferon signaling pathway" and "defense response to virus" using KEGG database, to be enriched in disease-associated modules. To the best of our knowledge, this is the first study applying a systems biology approach to identify shared molecular mechanisms between pemphigus and SLE.

MATERIALS AND METHODS

Data Collection

All the data for the analysis were collected by searching expression databases such as NCBI GEO and Array Express for $CD4^+$ T cells for pemphigus and SLE (17, 18). The datasets from other tissues or cell type were discarded. Also, the datasets, which did not have raw data files, were discarded from the downstream analysis. Two datasets, one for pemphigus (GSE53873) and one for SLE (GDS4185), were included in this study. The covariate information available for the patients is summarized in Table S1 in Supplementary Material. Altogether 46 samples (4 PV, 15 PF, 13 SLE, and 14 healthy controls) were used in the analysis.

To avoid a potential bias that could be introduced by obtaining two separate microarray datasets, the deposited gene expression data were directly used for batch normalization. The expression profiles were log2 transformed and batch normalization was done using "sva" and "combat" functions in SVA R package (19). The effect of normalization was investigated by principal component analysis using the R-based "prcomp" function. Since batch normalization still produced biased results (**Figure 1**), the raw files were preprocessed again and an additional normalization

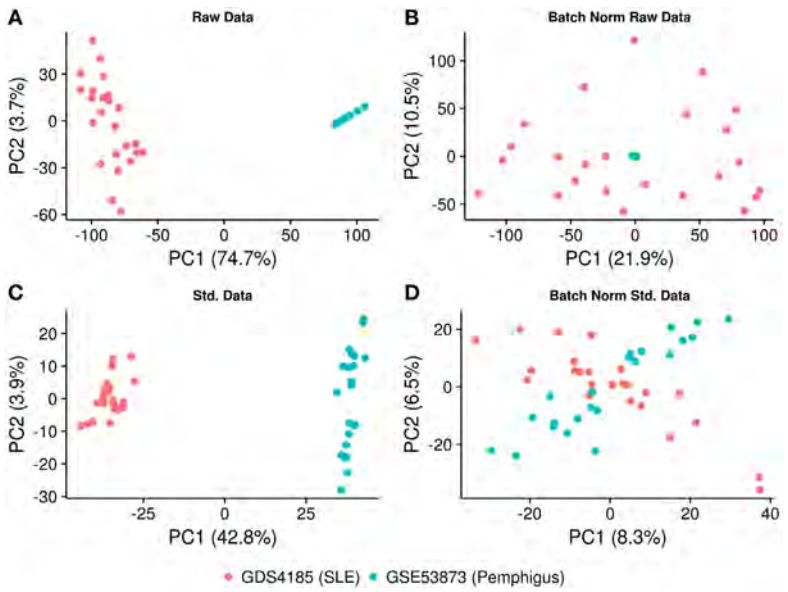

FIGURE 1 | PCA plot illustrating the normalization procedure. **(A)** PCA plot showing clustering of the samples based on the gene expression profiling, before and **(B)** after batch correction on raw data. **(C)** PCA plot showing clustering of the samples after using identical background correction and normalization methods, before and **(D)** after batch correction. The *X*- and *Y*-axes represent the first and the second principal components and the associated percentage of variation.

step was performed. In detail, raw gene expression profiles were deduced from text files (Codelink array) using Codelink R package (20). Using the same package, first, the background was corrected with the "normexp" method and then normalized by the "cyclicloess" method. For Affymetrix data, raw gene expression for each sample was derived using R Affy package (21). The background correction was performed by "backgroundCorrect (method = 'normexp')" and cyclic normalization was performed on log2 expression values using limma R package (22). All the probes from each of the microarray platforms were filtered out for significant low expression/variation ($P < 0.05$) using the "varianceBasedfilter" function from DCGL R package (23). The remaining probes were mapped to Ensembl gene identifiers and probes' expression was collapsed to gene-level expression using "collapseRows" function with default parameters in WGCNA R package (24). Consequently, batch normalization and statistical analysis were performed on the overlapping genes between two platforms using "combat" and PCA analyses, respectively (25). The data were further investigated for the presence of confounding effects such as clinical form of the disease (generalized vs. localized) and treatment group (predisnome vs. untreated) for pemphigus dataset (GSE53873) using anosim function with 999 permutations in vegan R package (26).

Co-Expression Networks

Co-expression modules were generated using WGCNA R package. A signed weighted adjacency matrix of pair-wise connection strengths (bicor correlation) was constructed using the soft-threshold approach with a scale-independent topological power $\beta = 6$. For a gene, the connectivity was defined as the sum of all connection strengths with all other genes. Genes were aggregated into modules by hierarchical clustering and refined by the dynamic tree cut algorithm. Thereafter, module eigenvalues were calculated. The eigenvalue is the first principal component of the gene expression profile within a module, representing average module expression profile (27). The statistical significance ($P < 0.05$) of module eigenvalues among the groups was accessed by Kruskal–Wallis test. Modular hub gene candidates were identified by correlating the gene expression with its module eigenvalues ("chooseTopHubInEachModule" function in WGCNA). To generate the causal network within a module, the C3NET R package was used (28). The algorithm uses mutual information theory to construct gene networks from gene expression data. The final network was generated using "c3net" function with default setting. A gene–gene interaction was considered to be significant if $\alpha < 0.05$.

Functional Characterization of a Module

To investigate known gene–gene interactions, we used the INMEX web server (29). All genes within a specific module were queried, and a minimum network connecting all genes within this module was obtained. The hub gene candidates from this analysis were defined by their degree of interactions. Gene ontology terms, enriched KEGG pathways, and transcription factor binding sites for each module were obtained using David web server. Thereafter, all the mapped genes and reported genes to the disease-associated loci were selected from genome-wide association study (GWAS) catalog. The selected genes and modular genes were connected to each other based on known gene–gene interactions (INMEX web server). Only the direct interactions between the modular genes and GWAS genes were considered. Gene–gene interactions were visualized using Cytoscape software and figures were generated using R programing language. Intermediate gene conversions and data formatting were done using Perl programing language (30).

RESULTS

Data Selection and Normalization

Microarray data were obtained for peripheral $CD4^+$ T-cell samples from 19 pemphigus patients (4 PV; 15 PF), 13 SLE patients, and 14 healthy controls from NCBI GEO and EBI Array Express (GSE53873; GDS4185). Altogether, our dataset included 46 samples derived from Codelink and Affymetrix arrays. Only datasets comprising raw files were included in the downstream meta-analysis. Therefore, we excluded samples GSE4588 and GSM260948 from our analysis.

To implement the co-expression network analysis, we standardized and batch-normalized the datasets. We collected common probes across the two chip-arrays. The CodeLink Human Whole Genome Bioarray from GE Healthcare consisted of 54,359 probes, while the Affymetrix Human Genome U133A array consisted of 22,283 probes. We converted these probes to ensemble gene identifiers using ensemble biomart and found that 12,980 genes were common between the two platforms. Consequently, the datasets were merged based on the expression of common genes and "combat" and "sva" (SVA R package) functions were applied to remove the batch effect. Our results show that while the Affymetrix samples were distributed uniformly among the principal components, the data generated from the CodeLink array still clustered together (**Figures 1A,B**), suggesting that the dataset was not properly normalized and required further optimization. To further optimize the datasets, we used the "normexp" method for background correction and "cyclicloess" on log2 transformed values. Additionally, each dataset was separately filtered for low expressing/varying probes, as well as multiple probes were collapsed for each gene. Briefly, 18,038 probes representing 12,980 genes were identified in the CodeLink dataset. These probes were filtered for low variation and collapsed to generate 5,646 gene expression profiles. Similarly, the Affymetrix gene chip consisted of 20,366 probes representing 12,980 genes. These probes were filtered and collapsed, resulting in 6,073 gene expression profiles. Overall, the overlap between the two datasets consisted of 3,280 gene expression profiles, which were further used in the downstream analysis. After applying the batch effect normalization "combat" algorithm, we observed that the samples were distributed among first principal component with only 8.3% variation explained by the first component (**Figures 1C,D**). We also analyzed confounding effects by stratifying the dataset for different covariates. We found no significant differences for covariate generalized vs. localized ($P = 0.402$) and prednisone treated vs. untreated ($P = 0.596$) for pemphigus samples. No covariate information was available for SLE samples (Figure S1 in Supplementary Material).

Detection of Co-Expression Modules Related to Pemphigus and SLE

Next, we set out to identify system-level similarity between pemphigus and SLE. Therefore, we applied WGCNA, aiming to identify gene modules that are co-expressed between pemphigus and SLE samples, and that are likely to be involved in common pathways. The major advantage of using such an approach is that it alleviates the multiple-testing problem that is inherent to microarray datasets. Using WGCNA, we identified 14 modules of co-expressed genes for 3,280 highly expressed and varying gene expression profiles, which are represented by different color codes (**Figure 2**; Figure S1, Data Sheet 1 in Supplementary Material). Two out of 14 modules showed differences between control and disease samples. The module "magenta" was significantly upregulated for both PF ($P = 0.005$) and SLE ($P = 0.016$) in comparison to healthy controls, and the module "salmon" was specifically upregulated only in PV ($P = 0.034$) (**Figure 2**).

Biological Pathways in the PF- and SLE-Associated Module "Magenta"

Module "magenta" consisted of 74 genes and, compared with controls, was significantly upregulated in PF and SLE. To investigate different known mechanisms associated with this module, we performed gene ontology analysis using DAVID database (31). We found that this module was, among others, enriched in biological processes such as "type I interferon signaling pathway" (P.adj = 6.4E−11), "defense response to virus" (P.adj = 2.7E−10), and "cytokine-mediated signaling pathway" (P.adj = 1.3E−7) (**Table 1**). This module was also enriched in KEGG pathways, including "measles" (P.adj = 2.3E−4), "influenza A" (P.adj = 2.7E−4), and "herpes simplex infection" (P.adj = 1.3E−3). On the basis of statistical module membership and eigengenes value, we identified s-adenosyl methionine domain containing 2 (RSAD2) gene as the most highly ranked hub gene for this module. To identify subnetworks and statistical interactions within the modules we used the "c3net" algorithm. The "c3net" algorithm investigates the direct physical interaction for gene expression data, further providing putative mechanisms within a module and characterizing its key regulating genes (9). We found 2'-5'-oligoadenylate synthetase 1 (OAS1), MX dynamin-like GTPase 1 (MX1), interferon-induced protein with tetratricopeptide repeats 3 (IFIT3), and spermatogenesis-associated serine-rich 2 like (SPATS2L) genes as master regulator genes of the module (degree ≥ 5) (**Figure 3**). Moreover, to further explore known gene–gene interactions among the genes in "magenta" module, we used the INMEX web server (32). We were specifically interested in examining "minimum interaction networks." In this type of networks, a minimum number of genes are required to connect all the nodes to a given set of genes. Using this approach, we further derived additional regulators such as junction plakoglobin (JUP), B-cell CLL/lymphoma 2 (BCL2), ISG15 ubiquitin-like modifier (ISG15), STAT1, S-phase kinase-associated protein 2 (SKP2), and eukaryotic translation initiation factor 2 alpha kinase 2 (EIF2AK2) (Figure S2 in Supplementary Material).

Biological Pathways in the PV-Associated Module "Salmon"

Although the sample size for PV samples was small ($n = 4$), we identified a distinct module that, compared with controls, was significantly upregulated in PV, namely the "salmon" module ($P = 0.034$). The "salmon" module comprises 39 genes (**Table 1**) and was enriched in the following biological processes: "blood coagulation" (P.adj = 1.4E−1) and the KEGG pathway "platelet activation" (P.adj = 1.8E−1). Using statistical module eigengenes, we identified platelet glycoprotein IX (GP9) as a hub gene of this

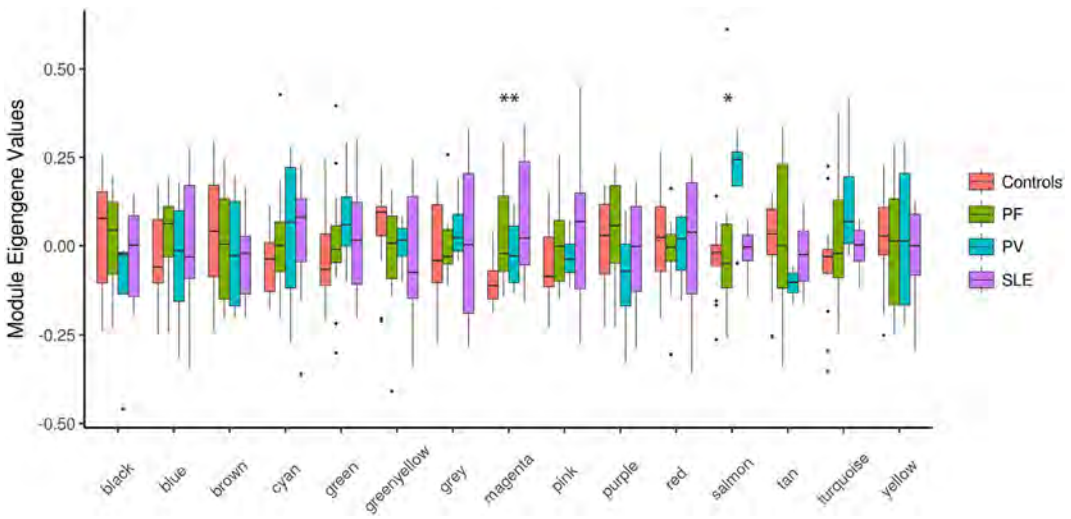

FIGURE 2 | Boxplots of eigengene values across modules. Boxplots depicting different identified modules on the *X*-axis and the corresponding module eigengene values for each group of samples on the *Y*-axis. The significance among the groups was calculated using Kruskal–Wallis test. *$P < 0.05$; **$P < 0.01$. PF, pemphigus foliaceus; PV, pemphigus vulgaris; SLE, systemic lupus erythematosus.

TABLE 1 | Gene ontology and enriched KEGG pathways for "magenta" and "salmon" modules.

Module	Category	Term	*P*-value	Benjamini
Magenta	UP_KEYWORDS	Antiviral defense	1.18273E−16	1.84297E−14
	UP_KEYWORDS	Immunity	1.22704E−13	1.01824E−11
	GOTERM_BP_DIRECT	GO:0060337~type-I interferon signaling pathway	9.37804E−14	6.3981E−11
	UP_KEYWORDS	Innate immunity	3.82091E−12	2.11426E−10
	GOTERM_BP_DIRECT	GO:0051607~defense response to virus	7.83394E−13	2.6713E−10
	GOTERM_BP_DIRECT	GO:0045071~negative regulation of viral genome replication	1.21675E−10	2.76607E−08
	GOTERM_BP_DIRECT	GO:0009615~response to virus	2.90413E−10	4.95154E−08
	GOTERM_BP_DIRECT	GO:0019221~cytokine-mediated signaling pathway	9.178E−10	1.25188E−07
	KEGG_PATHWAY	hsa05162:Measles	4.89228E−06	0.00022502
	KEGG_PATHWAY	hsa05164:Influenza A	2.9062E−06	0.000267335
	KEGG_PATHWAY	hsa05168:Herpes simplex infection	4.20496E−05	0.001288717
	GOTERM_MF_DIRECT	GO:0003725~double-stranded RNA binding	6.2164E−05	0.009466294
	GOTERM_BP_DIRECT	GO:0060333~interferon-gamma-mediated signaling pathway	0.000216281	0.024286767
Salmon	GOTERM_BP_DIRECT	GO:0030041~actin filament polymerization	0.000889415	0.183621158
	GOTERM_BP_DIRECT	GO:0007596~blood coagulation	0.001317229	0.139518478
	KEGG_PATHWAY	hsa04611:Platelet activation	0.003518509	0.179124611

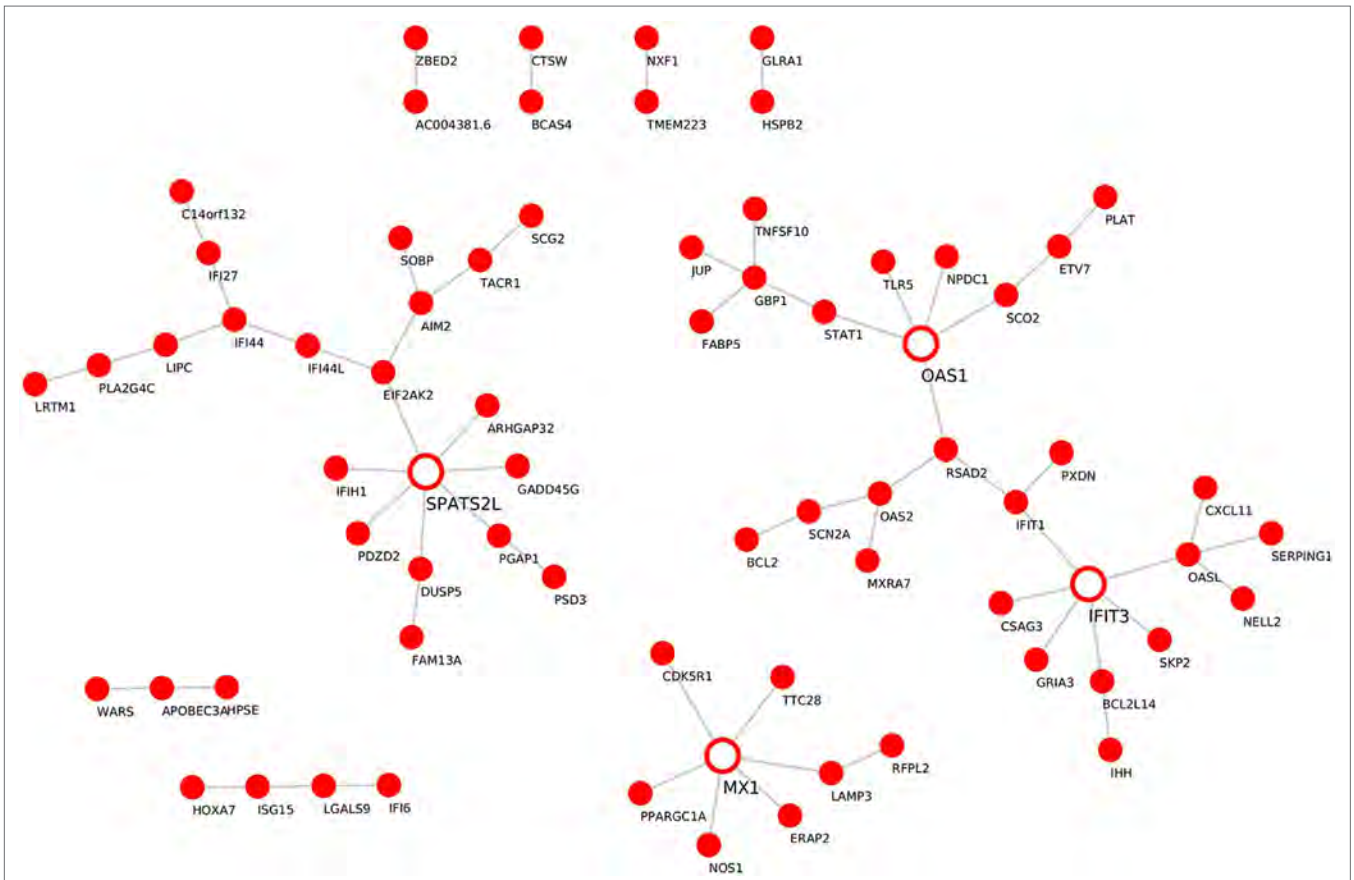

FIGURE 3 | Gene–gene interaction network for the "magenta" module. *De novo* network generated by C3NET algorithm for the "magenta" module. The figure shows statistically significant ($\alpha < 0.05$) edges predicted by the algorithm. Fully colored nodes represent the "magenta" module-associated genes. Empty nodes represent the regulatory genes (degree ≥ 5).

module. Additionally, using the "c3net" algorithm, we identified pro-platelet basic protein (PPBP), G protein subunit gamma 11 (GNG11), and thrombospondin 1 (THBS1) genes as key regulators of the "salmon" module (degree ≥ 4) (**Figure 4**). In addition, while using the INMEX server we identified protein kinase cAMP-dependent type-II regulatory subunit beta (PRKAR2B), Src homology 2 domain-containing-transforming protein 3 (SHC3), tensin 1 (TNS1), PPBP, and GNG11 as regulatory genes

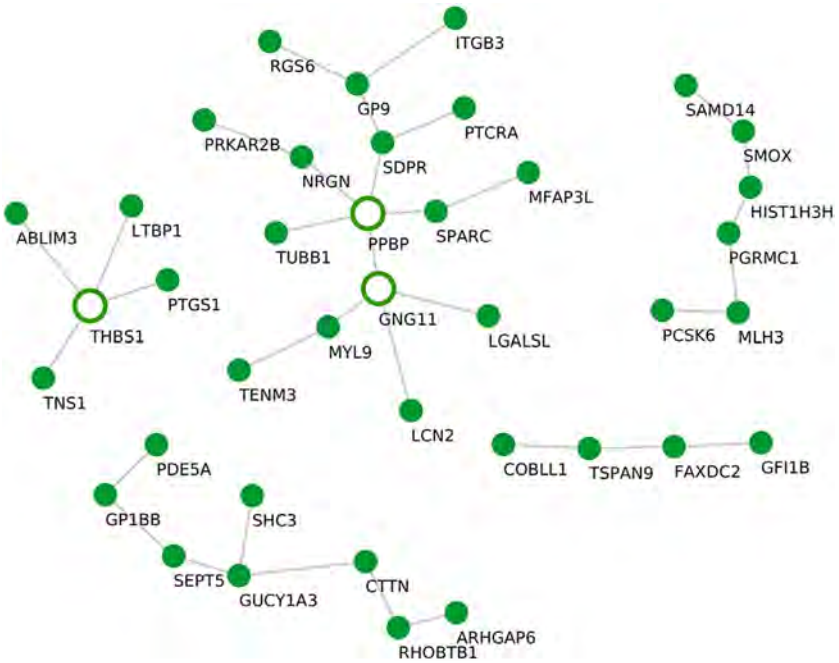

FIGURE 4 | Gene–gene interaction network for the "salmon" module. *De novo* network generated by C3NET algorithm for the "salmon" module. The figure shows statistically significant ($\alpha < 0.05$) edges predicted by the algorithm. Fully colored nodes represent the "salmon" module-associated genes. Empty nodes represent the regulatory genes (degree ≥ 4).

(Figure S3 in Supplementary Material). Interestingly, both PPBP and GNG11 genes coincided with the list of the aforementioned C3NET-derived key regulatory genes.

Cross-Linking SLE and Pemphigus GWA Studies with Clusters of Co-Expressed Genes in the "Magenta" and the "Salmon" Modules

While multiple GWA studies had been undertaken in a continuous effort to identify SLE susceptibility genes, only one GWA study was previously conducted in pemphigus, namely in PV (33, 34). In contrast to GWA studies that normally investigate the causal genes for a disease phenotype, gene expression profiles indicate the downstream effector phase. In the present work, we investigated direct interactions between previously reported susceptibility genes in SLE and pemphigus GWA studies and genes comprising the "magenta" and "salmon" modules, which were identified herein. We found the SLE-susceptible gene interferon regulatory factor 8 (IRF8) to have the largest number of direct interactions with "magenta" module-associated genes (**Figure 5**). The IRF8 gene interacted with genes encoding for interferon-induced protein with tetratricopeptide repeats 1 (IFIT1), interferon-induced guanylate-binding protein 1 (GBP1), 2'-5'-oligoadenylate synthetase 2 (OAS2), 2'-5'-oligoadenylate synthetase-like (OASL), and signal transducer and activator of transcription 1 (STAT1). Both IRF5 and STAT1 SLE GWAS genes directly interacted with IRF8 and with the other 4 "magenta" module-associated genes such as interferon induced with helicase C domain 1 (IFIH1), IFIT1, GBP1, OASL, OAS2, and EIF2AK2 (**Figure 5**). Polymorphism in the gene ST18 has been previously found in a PV GWA study. However, we could not identify direct interactions between ST18 and genes associated with the "salmon" module. To further establish a putative association of ST18 to other genes in the "salmon" module, we performed the transcriptional factor binding sites enrichment analysis (39 "salmon" genes and the ST18 gene). We observed that 34 out of the 40 analyzed genes are regulated by the nuclear hormone peroxisome proliferator activated receptor γ (PPAR-γ; P. adj = 8.3E−3) and 25 out of 40 genes are regulated by growth factor independent 1 transcriptional repressor (GFI1; P.adj = 8.3E−3).

DISCUSSION

The pathogenesis of most autoimmune disorders is still largely unknown. Environmental triggers in genetically susceptible individuals, as well as molecular mimicry mechanisms, may only partially account for this phenomenon (35). The co-occurrence of autoimmune diseases has been previously documented and aided in our understanding of autoimmunity (36).

Pemphigus and SLE are well-characterized autoimmune diseases that were previously reported to coexist in the same patient (37). Even though each of these two autoimmune diseases affects distinct organs and systems, the comorbidity of both diseases suggests an existence of fundamental common pathophysiological mechanisms. As we were interested in systems level similarity between the diseases rather than characterizing individual gene signatures, we used WGCNA to study pemphigus and SLE. Using this analytical approach, we identify modules across

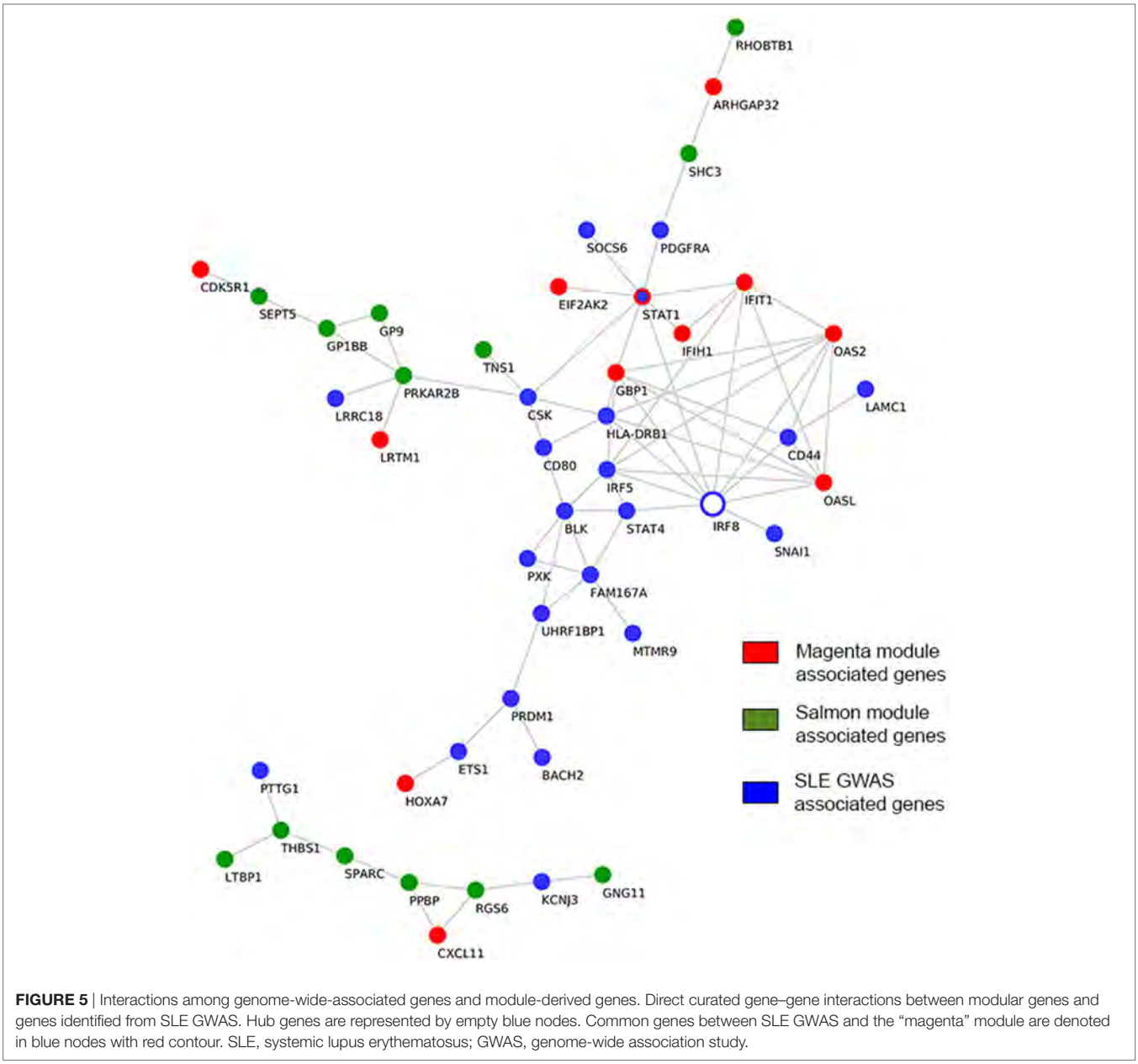

FIGURE 5 | Interactions among genome-wide-associated genes and module-derived genes. Direct curated gene–gene interactions between modular genes and genes identified from SLE GWAS. Hub genes are represented by empty blue nodes. Common genes between SLE GWAS and the "magenta" module are denoted in blue nodes with red contour. SLE, systemic lupus erythematosus; GWAS, genome-wide association study.

microarray datasets obtained from CD4$^+$ T cells in pemphigus and SLE patients. In this study, we further demonstrate that gene expression data processed by two different batch correction algorithms remains biased and can lead to false positive estimations. Therefore, to standardize and remove batch effects from both datasets, we used "normexp," "cyclicloess," and "combat" algorithms. Using this strategy, we could compensate for the potential bias introduced by obtaining two distinct microarray datasets (**Figure 1**).

Our network analysis revealed two co-expression modules (denoted as "magenta" and "salmon") that were significantly associated with PF and SLE, or PV only, respectively (**Figure 2**). Identification of the "magenta" module suggests common underlying mechanisms for pemphigus and SLE and identifies key regulatory genes for both diseases in CD4$^+$ T cells. In terms of functional relevance, based on DAVID and KEGG ontology analyses, the "magenta" module is enriched in genes corresponding to type-I interferon (IFN) signaling and viral infection including herpes simplex, measles, and influenza viruses. Although type-I interferons were initially described and termed for their ability to "interfere" with viral replication, their role as immune modulators of both innate and adaptive immunity is now widely established (38). Moreover, a role for viruses in an induction of autoimmune diseases through several potential mechanisms, such as epitope spreading, molecular mimicry, cryptic antigens, and bystander activation, was also previously reported (39). The role of viral infection in the etiopathogenesis of SLE, the so-called "viral hypothesis," has been extensively studied (40–42). SLE

patients may present severe systemic viral infections primarily associated with Epstein-Bar virus (EBV), cytomegalovirus, and herpes simplex virus (HSV). With respect to pemphigus, in 1974, Krain et al. first reported the association between HSV and PV (43); meanwhile, several additional case reports were published examining this association (44–46). A more recent study by Kurata and colleagues demonstrated high levels of HSV DNA in the saliva of PV patients at the earliest stage of the disease without a history of herpetic infection, thus suggesting the presence of cases of pemphigus induced by herpesviruses (47).

In our work, on the basis of statistical module membership and its eigengene value, we identified RSAD2 gene as the hub gene of the "magenta" module. Notably, by examining the expression levels of RSAD2 gene in our datasets we could demonstrate its significant upregulation in PF ($P = 0.005$) and SLE ($P = 0.007$) in comparison to healthy controls (Figure S4A in Supplementary Material). To confirm, the expression of the RSAD2 gene is encoding for interferon-inducible viperin protein, which inhibits viral replication and facilitates T-cell receptor-mediated GATA3 activation, and optimal Th2 cytokine production through modulation of NFKB1 and JUNB activities. As a result, viperin-deficient mice show impaired Th2 cell development (48). Interestingly, transcripts for RSAD2 were found to be upregulated in SLE $CD3^+$ $CD4^+$ cells, as well as SLE $CD19^+$ B cells, and SLE $CD33^+$ myeloid cells in comparison to similar cellular subsets isolated from healthy controls (49). Although it has been previously demonstrated that Th2 cells exert broad activity in blister formation in pemphigus, the association of RSAD2 with pemphigus is unknown. To examine the relevance of Th2 response in pemphigus and SLE, a set of 44 genes associated with Th2 differentiation were downloaded from the PathCards Pathway Unification Database from the Weizmann Institute of Science, and examined for their fold change expression in our disease datasets (PV, PF, and SLE) in comparison to healthy controls (Figure S4B in Supplementary Material). Our findings confirm that the fold change expression of Th2-associated genes was positively correlated between SLE and PF ($P = 0.01$, $\rho = 0.36$) and between SLE vs. PV ($P = 1.087\text{E}{-}05$ $\rho = 0.62$), suggesting that the Th2 response is skewed in a similar pattern between SLE and pemphigus. While investigating subnetworks within the "magenta" module (using the "c3net" algorithm), we identified OAS1, MX1, IFIT3, and SPATS2L genes as master regulators (**Figure 3**). Additional regulatory genes such as JUP, BCL2, ISG15, STAT1, SKP2, and EIF2AK2 were identified using known gene–gene interactions database (INMEX) (Figure S2 in Supplementary Material). Transcripts of 7 out of the 11 identified genes (i.e., RSAD2, OAS1, MX1, IFIT3, ISG15, STAT1, and EIF2AK2) were previously shown to be upregulated in SLE $CD3^+$ $CD4^+$ cells (49). Consistent with a previous study that examined possible related signaling pathways shared in the pathogenesis of several systemic autoimmune diseases (SAID) such as dermatomyositis, polymyositis, rheumatoid arthritis, and SLE, a subset of five viral-related differentially expressed genes (i.e., RSAD2, IFIT3, ISG15, STAT1, and EIF2AK) was detected in peripheral blood of SAID probands and their unaffected twins (50). Additionally, other genes that were identified in our study, including BCL2, OAS1, MX1, and SKP2 have been previously associated with various autoimmune diseases (51–54). Therefore, our findings further suggest that these common IFN signature genes are shared across multiple autoimmune diseases including pemphigus and SLE.

Here, we identified a PV-specific associated module. The "salmon" module consisted of 39 genes and was enriched in genes involved in blood coagulation and platelet activation. Based on the eigenegene value, the gene GP9 was identified as the hub gene of the "salmon" module. GP9 encodes a small-membrane glycoprotein that is part of the GPIb-V-IX complex that mediates platelet adhesion to blood vessels and promotes hemostasis. Thus, mutations in the GP9 protein lead to a coagulation disorder, also known as the Bernard–Soulier syndrome, characterized by thrombocytopenia. Of note, although this is a first report suggesting a role for GP9 in PV, a previous study by Hunziker et al. identified platelet-derived factors to enhance pemphigus acantholysis in skin organ cultures (55). Moreover, another study by Mizutani et al. found increased expression of the coagulation factor on keratinocytes, which shield blisters in PV (56). In line with this observation, using the "c3net" algorithm, we identified an additional list of platelet-associated genes i.e., PPBP, GNG11, and THSB1, as key regulators of the "salmon" module (**Figure 4**). Furthermore, by examining known gene–gene interactions, we could identify PPBP, GNG11, as well as another group of platelet-function-associated genes such as PRKAR2B, SHC3, and TNS1 (Figure S3 in Supplementary Material) as additional regulators of this module.

Further in our analysis, we associated the genes found in the "magenta" and "salmon" modules with known susceptibility markers of PV and SLE, which had been formerly identified by GWASs. GWASs are applied to identify genetic variants that are associated with a disease trait. However, the identification of loci harboring the susceptible genes does not fully reveal the molecular mechanisms that are at play to yield the observed phenotype. Therefore, linking these susceptibility genes with the module-associated genes may identify pathways that control the disease phenotype and provide potential therapeutic targets for intervention. By cross-linking susceptibility genes derived from SLE GWAS with clusters of co-expressed genes in "magenta" module, we found IRF8 to directly interact with the largest number of interferon-induced genes present in the "magenta" module including IFIT1, GBP1, OAS2, OASL, and STAT1 (**Figure 5**). Interestingly, STAT1 was identified both as an SLE susceptibility gene and as a key regulator gene of the "magenta" module. Therefore, based on our analysis, we predict IRF8 to have pharmacological relevance, as previously described (57). With regard to PV, we did not identify direct interactions between the known GWAS gene, ST18, and the 39 "salmon" module-associated genes. To circumvent this finding, we additionally performed a transcriptional factor binding sites enrichment analysis for the 40 genes. We found that the majority of the genes are regulated by the transcription factors PPAR-γ and GFI1 that have been previously described for their role in Th2 cell development (58, 59). Moreover, PPAR-γ has been suggested as a pharmacological target for PV (60).

Altogether, our work reveals conserved molecular mechanisms and pathways between pemphigus and SLE and identifies novel gene candidates that could be used as biomarkers or as potential targets for therapeutic intervention.

AUTHOR CONTRIBUTIONS

TS, AV, YG, and RL designed the study, interpreted the data, and wrote the manuscript. All authors contributed equally to this work. YG downloaded and analyzed the data. CS and DZ discussed the results and contributed to the writing of the manuscript.

ACKNOWLEDGMENTS

We thank Prof. SM Ibrahim (*Lübecker Institut für Experimentelle Dermatologie (LIED)*, Lübeck, Germany) for critical discussion and assistance in preparation of the manuscript.

FUNDING

This study was supported by the *Deutsche Forschungsgemeinschaft* through the training programs "Modulation of Autoimmunity" (grant number GRK 1727/1) and "Genes, Environment and Inflammation" (grant number GRK 1743/1).

SUPPLEMENTARY MATERIAL

The Supplementary Material for this article can be found online at http://www.frontiersin.org/articles/10.3389/fimmu.2017.01992/full#supplementary-material.

REFERENCES

1. Hammers CM, Stanley JR. Mechanisms of disease: pemphigus and bullous pemphigoid. *Annu Rev Pathol* (2016) 11:175–97. doi:10.1146/annurev-pathol-012615-044313
2. Malik M, Ahmed AR. Concurrence of systemic lupus erythematosus and pemphigus: coincidence or correlation? *Dermatol Basel Switz* (2007) 214:231–9. doi:10.1159/000099588
3. Calebotta A, Cirocco A, Giansante E, Reyes O. Systemic lupus erythematosus and pemphigus vulgaris: association or coincidence. *Lupus* (2004) 13:951–3. doi:10.1191/0961203304lu1073cr
4. Rahman A, Isenberg DA. Systemic lupus erythematosus. *N Engl J Med* (2008) 358:929–39. doi:10.1056/NEJMra071297
5. Prüßmann J, Prüßmann W, Recke A, Rentzsch K, Juhl D, Henschler R, et al. Co-occurrence of autoantibodies in healthy blood donors. *Exp Dermatol* (2014) 23:519–21. doi:10.1111/exd.12445
6. Holtman IR, Raj DD, Miller JA, Schaafsma W, Yin Z, Brouwer N, et al. Induction of a common microglia gene expression signature by aging and neurodegenerative conditions: a co-expression meta-analysis. *Acta Neuropathol Commun* (2015) 3:31. doi:10.1186/s40478-015-0203-5
7. Granlund Av, Flatberg A, Østvik AE, Drozdov I, Gustafsson BI, Kidd M, et al. Whole genome gene expression meta-analysis of inflammatory bowel disease colon mucosa demonstrates lack of major differences between Crohn's disease and ulcerative colitis. *PLoS One* (2013) 8(2):e56818. doi:10.1371/journal.pone.0056818
8. Cárdenas-Roldán J, Rojas-Villarraga A, Anaya J-M. How do autoimmune diseases cluster in families? A systematic review and meta-analysis. *BMC Med* (2013) 11:73. doi:10.1186/1741-7015-11-73
9. Troy NM, Hollams EM, Holt PG, Bosco A. Differential gene network analysis for the identification of asthma-associated therapeutic targets in allergen-specific T-helper memory responses. *BMC Med Genomics* (2016) 9:9. doi:10.1186/s12920-016-0171-z
10. Zhao H, Cai W, Su S, Zhi D, Lu J, Liu S. Screening genes crucial for pediatric pilocytic astrocytoma using weighted gene coexpression network analysis combined with methylation data analysis. *Cancer Gene Ther* (2014) 21:448–55. doi:10.1038/cgt.2014.49
11. Ring KL, An MC, Zhang N, O'Brien RN, Ramos EM, Gao F, et al. Genomic analysis reveals disruption of striatal neuronal development and therapeutic targets in human Huntington's disease neural stem cells. *Stem Cell Reports* (2015) 5:1023–38. doi:10.1016/j.stemcr.2015.11.005
12. Nishifuji K, Amagai M, Kuwana M, Iwasaki T, Nishikawa T. Detection of antigen-specific B cells in patients with pemphigus vulgaris by enzyme-linked immunospot assay: requirement of T cell collaboration for autoantibody production. *J Invest Dermatol* (2000) 114:88–94. doi:10.1046/j.1523-1747.2000.00840.x
13. Takahashi H, Kouno M, Nagao K, Wada N, Hata T, Nishimoto S, et al. Desmoglein 3-specific CD4+ T cells induce pemphigus vulgaris and interface dermatitis in mice. *J Clin Invest* (2011) 121:3677–88. doi:10.1172/JCI57379
14. Mak A, Kow NY. The pathology of T cells in systemic lupus erythematosus. *J Immunol Res* (2014) 2014:e419029. doi:10.1155/2014/419029
15. Konya C, Paz Z, Tsokos GC. The role of T cells in systemic lupus erythematosus: an update. *Curr Opin Rheumatol* (2014) 26:493–501. doi:10.1097/BOR.0000000000000082
16. Barrett T, Wilhite SE, Ledoux P, Evangelista C, Kim IF, Tomashevsky M, et al. NCBI GEO: archive for functional genomics data sets––update. *Nucleic Acids Res* (2013) 41:D991–5. doi:10.1093/nar/gks1193
17. Jeffries MA, Dozmorov M, Tang Y, Merrill JT, Wren JD, Sawalha AH. Genome-wide DNA methylation patterns in CD4+ T cells from patients with systemic lupus erythematosus. *Epigenetics* (2011) 6:593–601. doi:10.4161/epi.6.5.15374
18. Malheiros D, Panepucci RA, Roselino AM, Araújo AG, Zago MA, Petzl-Erler ML. Genome-wide gene expression profiling reveals unsuspected molecular alterations in pemphigus foliaceus. *Immunology* (2014) 143:381–95. doi:10.1111/imm.12315
19. Leek JT, Johnson WE, Parker HS, Jaffe AE, Storey JD. The sva package for removing batch effects and other unwanted variation in high-throughput experiments. *Bioinformatics* (2012) 28:882–3. doi:10.1093/bioinformatics/bts034
20. Diez D, Alvarez R, Dopazo A. Codelink: an R package for analysis of GE healthcare gene expression bioarrays. *Bioinforma Oxf Engl* (2007) 23:1168–9. doi:10.1093/bioinformatics/btm072
21. Gautier L, Cope L, Bolstad BM, Irizarry RA. affy—analysis of Affymetrix GeneChip data at the probe level. *Bioinforma Oxf Engl* (2004) 20:307–15. doi:10.1093/bioinformatics/btg405
22. Ritchie ME, Phipson B, Wu D, Hu Y, Law CW, Shi W, et al. limma powers differential expression analyses for RNA-sequencing and microarray studies. *Nucleic Acids Res* (2015) 43(7):e47. doi:10.1093/nar/gkv007
23. Liu BH, Yu H, Tu K, Li C, Li YX, Li YY. DCGL: an R package for identifying differentially coexpressed genes and links from gene expression microarray data. *Bioinformatics* (2010) 26:2637–8. doi:10.1093/bioinformatics/btq471
24. Miller JA, Cai C, Langfelder P, Geschwind DH, Kurian SM, Salomon DR, et al. Strategies for aggregating gene expression data: the collapseRows R function. *BMC Bioinformatics* (2011) 12:322. doi:10.1186/1471-2105-12-322
25. Johnson WE, Li C, Rabinovic A. Adjusting batch effects in microarray expression data using empirical Bayes methods. *Biostat Oxf Engl* (2007) 8:118–27. doi:10.1093/biostatistics/kxj037
26. Dixon P. VEGAN, a package of R functions for community ecology. *J Veg Sci* (2003) 14:927–30. doi:10.1111/j.1654-1103.2003.tb02228.x
27. Langfelder P, Horvath S. Eigengene networks for studying the relationships between co-expression modules. *BMC Syst Biol* (2007) 1:54. doi:10.1186/1752-0509-1-54
28. Altay G, Emmert-Streib F. Inferring the conservative causal core of gene regulatory networks. *BMC Syst Biol* (2010) 4:132. doi:10.1186/1752-0509-4-132
29. Xia J, Fjell CD, Mayer ML, Pena OM, Wishart DS, Hancock REW. INMEX—a web-based tool for integrative meta-analysis of expression data. *Nucleic Acids Res* (2013) 41:W63–70. doi:10.1093/nar/gkt338
30. Thornton-Wells TA, Johnson KB. Perl Programming for biologists. *J Am Med Inform Assoc* (2004) 11:173. doi:10.1197/jamia.M1457
31. Dennis G Jr, Sherman BT, Hosack DA, Yang J, Gao W, Lane HC, et al. DAVID: database for annotation, visualization, and integrated discovery. *Genome Biol* (2003) 4:3. doi:10.1186/gb-2003-4-5-p3

32. Xia J, Benner MJ, Hancock REW. Network Analyst––integrative approaches for protein-protein interaction network analysis and visual exploration. *Nucleic Acids Res* (2014) 42:W167–74. doi:10.1093/nar/gku443
33. Sarig O, Bercovici S, Zoller L, Goldberg I, Indelman M, Nahum S, et al. Population-specific association between a polymorphic variant in ST18, encoding a pro-apoptotic molecule, and pemphigus vulgaris. *J Invest Dermatol* (2012) 132:1798–805. doi:10.1038/jid.2012.46
34. Vodo D, Sarig O, Geller S, Ben-Asher E, Olender T, Bochner R, et al. Identification of a functional risk variant for pemphigus vulgaris in the ST18 gene. *PLoS Genet* (2016) 12:e1006008. doi:10.1371/journal.pgen.1006008
35. Manolio TA, Collins FS, Cox NJ, Goldstein DB, Hindorff LA, Hunter DJ, et al. Finding the missing heritability of complex diseases. *Nature* (2009) 461:747–53. doi:10.1038/nature08494
36. Cojocaru M, Cojocaru IM, Silosi I. Multiple autoimmune syndrome. *Maedica (Buchar)* (2010) 5:132–4.
37. Sawamura S, Kajihara I, Makino K, Makino T, Fukushima S, Jinnin M, et al. Systemic lupus erythematosus associated with myasthenia gravis, pemphigus foliaceus and chronic thyroiditis after thymectomy. *Australas J Dermatol* (2016) 58(3):e120–2. doi:10.1111/ajd.12510
38. Theofilopoulos AN, Baccala R, Beutler B, Kono DH. Type I interferons (alpha/beta) in immunity and autoimmunity. *Annu Rev Immunol* (2005) 23:307–36. doi:10.1146/annurev.immunol.23.021704.115843
39. Olson JK, Croxford JL, Miller SD. Virus-induced autoimmunity: potential role of viruses in initiation, perpetuation, and progression of T-cell-mediated autoimmune disease. *Viral Immunol* (2001) 14:227–50. doi:10.1089/088282401753266756
40. Phillips PE. The virus hypothesis in systemic lupus erythematosus. *Ann Intern Med* (1975) 83:709–15. doi:10.7326/0003-4819-83-5-709
41. Denman AM. Systemic lupus erythematosus—is a viral aetiology a credible hypothesis? *J Infect* (2000) 40:229–33. doi:10.1053/jinf.2000.0670
42. Ramos-Casals M. Viruses and lupus: the viral hypothesis. *Lupus* (2008) 17:163–5. doi:10.1177/0961203307086268
43. Krain LS. Pemphigus. Epidemiologic and survival characteristics of 59 patients, 1955-1973. *Arch Dermatol* (1974) 110:862–5. doi:10.1001/archderm.1974.01630120012002
44. Marzano AV, Tourlaki A, Merlo V, Spinelli D, Venegoni L, Crosti C. Herpes simplex virus infection and pemphigus. *Int J Immunopathol Pharmacol* (2009) 22:781–6. doi:10.1177/039463200902200324
45. Senger P, Sinha AA. Exploring the link between herpes viruses and pemphigus vulgaris: literature review and commentary. *Eur J Dermatol* (2012) 22:728–35. doi:10.1684/ejd.2012.1836
46. Takahashi I, Kobayashi TK, Suzuki H, Nakamura S, Tezuka F. Coexistence of pemphigus vulgaris and herpes simplex virus infection in oral mucosa diagnosed by cytology, immunohistochemistry, and polymerase chain reaction. *Diagn Cytopathol* (1998) 19:446–50. doi:10.1002/(SICI)1097-0339(199812)19:6<446::AID-DC8>3.0.CO;2-2
47. Kurata M, Mizukawa Y, Aoyama Y, Shiohara T. Herpes simplex virus reactivation as a trigger of mucous lesions in pemphigus vulgaris. *Br J Dermatol* (2014) 171:554–60. doi:10.1111/bjd.12961
48. Seo J-Y, Yaneva R, Cresswell P. Viperin: a multifunctional, interferon-inducible protein that regulates virus replication. *Cell Host Microbe* (2011) 10:534–9. doi:10.1016/j.chom.2011.11.004
49. Becker AM, Dao KH, Han BK, Kornu R, Lakhanpal S, Mobley AB, et al. SLE peripheral blood B cell, T cell and myeloid cell transcriptomes display unique profiles and each subset contributes to the interferon signature. *PLoS One* (2013) 8:e67003. doi:10.1371/journal.pone.0067003
50. Gan L, O'Hanlon TP, Lai Z, Fannin R, Weller ML, Rider LG, et al. Gene expression profiles from disease discordant twins suggest shared antiviral pathways and viral exposures among multiple systemic autoimmune diseases. *PLoS One* (2015) 10(11):e0142486. doi:10.1371/journal.pone.0142486
51. Tischner D, Woess C, Ottina E, Villunger A. Bcl-2-regulated cell death signalling in the prevention of autoimmunity. *Cell Death Dis* (2010) 1:e48. doi:10.1038/cddis.2010.27
52. Choi UY, Kang J-S, Hwang YS, Kim Y-J. Oligoadenylate synthase-like (OASL) proteins: dual functions and associations with diseases. *Exp Mol Med* (2015) 47:e144. doi:10.1038/emm.2014.110
53. Ferreira RC, Guo H, Coulson RM, Smyth DJ, Pekalski ML, Burren OS, et al. A type I interferon transcriptional signature precedes autoimmunity in children genetically at risk for type 1 diabetes. *Diabetes* (2014) 63:2538–50. doi:10.2337/db13-1777
54. Wang D, Qin H, Du W, Shen YW, Lee WH, Riggs AD, et al. Inhibition of S-phase kinase-associated protein 2 (Skp2) reprograms and converts diabetogenic T cells to Foxp3+ regulatory T cells. *Proc Natl Acad Sci U S A* (2012) 109:9493–8. doi:10.1073/pnas.1207293109
55. Hunziker T, Nydegger UE, Lerch PG, Vassalli JD. Platelet-derived factors enhance pemphigus acantholysis in skin organ cultures. *Clin Exp Immunol* (1986) 64:442–9.
56. Mizutani H, Ohyanagi S, Nouchi N, Inachi S, Shimizu M. Tissue factor and thrombomodulin expression on keratinocytes as coagulation/anti-coagulation cofactor and differentiation marker. *Australas J Dermatol* (1996) 37(Suppl):1. doi:10.1111/j.1440-0960.1996.tb01085.x
57. Chrabot BS, Kariuki SN, Zervou MI, Feng X, Arrington J, Jolly M, et al. Genetic variation near IRF8 is associated with serologic and cytokine profiles in systemic lupus erythematosus and multiple sclerosis. *Genes Immun* (2013) 14:471–8. doi:10.1038/gene.2013.42
58. Choi J-M, Bothwell ALM. The nuclear receptor PPARs as important regulators of T-cell functions and autoimmune diseases. *Mol Cells* (2012) 33:217–22. doi:10.1007/s10059-012-2297-y
59. Zhu J, Jankovic D, Grinberg A, Guo L, Paul WE. Gfi-1 plays an important role in IL-2-mediated Th2 cell expansion. *Proc Natl Acad Sci U S A* (2006) 103:18214–9. doi:10.1073/pnas.0608981103
60. McCarthy FP, Delany AC, Kenny LC, Walsh SK. PPAR-γ––a possible drug target for complicated pregnancies. *Br J Pharmacol* (2013) 168:1074–85. doi:10.1111/bph.12069

Conflict of Interest Statement: The authors declare that the research was conducted in the absence of any commercial or financial relationships that could be construed as a potential conflict of interest.

frontiers in Immunology

REVIEW
published: 20 December 2017
doi: 10.3389/fimmu.2017.01845

Thyroid Autoantibodies Display both "Original Antigenic Sin" and Epitope Spreading

Sandra M. McLachlan and Basil Rapoport*

Thyroid Autoimmune Disease Unit, Cedars-Sinai Medical Center, UCLA School of Medicine, Los Angeles, CA, United States

Evidence for original antigenic sin in spontaneous thyroid autoimmunity is revealed by autoantibody interactions with immunodominant regions on thyroid autoantigens, thyroglobulin (Tg), thyroid peroxidase (TPO), and the thyrotropin receptor (TSHR) A-subunit. In contrast, antibodies induced by immunization of rabbits or mice recognize diverse epitopes. Recognition of immunodominant regions persists despite fluctuations in autoantibody levels following treatment or over time. The enhancement of spontaneously arising pathogenic TSHR antibodies in transgenic human thyrotropin receptor/NOD.$H2^{h4}$ mice by injecting a non-pathogenic form of TSHR A-subunit protein also provides evidence for original antigenic sin. From other studies, antigen presentation by B cells, not dendritic cells, is likely responsible for original antigenic sin. Recognition of restricted epitopes on the large glycosylated thyroid autoantigens (60-kDa A-subunit, 100-kDa TPO, and 600-kDa Tg) facilitates exploring the amino acid locations in the immunodominant regions. Epitope spreading has also been revealed by autoantibodies in thyroid autoimmunity. In humans, and in mice that spontaneously develop autoimmunity to all three thyroid autoantigens, autoantibodies develop first to Tg and later to TPO and the TSHR A-subunit. The pattern of intermolecular epitope spreading is related in part to the thyroidal content of Tg, TPO and TSHR A-subunit and to the molecular sizes of these proteins. Importantly, the epitope spreading pattern provides a rationale for future antigen-specific manipulation to block the development of all thyroid autoantibodies by inducing tolerance to Tg, first in the autoantigen cascade. Because of its abundance, Tg may be the autoantigen of choice to explore antigen-specific treatment, preventing the development of pathogenic TSHR antibodies.

Keywords: thyroid autoantibodies, intermolecular and intramolecular epitope spreading, immunodominant region, original antigenic sin, thyroglobulin, thyroid peroxidase, thyrotropin receptor

OPEN ACCESS

Edited by:
Ralf J. Ludwig,
University of Lübeck, Germany

Reviewed by:
Yaron Tomer,
Albert Einstein College of Medicine, United States
Yi-chi Kong,
Wayne State University School of Medicine, United States

****Correspondence:***
Sandra M. McLachlan
mclachlans@cshs.org

Specialty section:
This article was submitted to Immunological Tolerance and Regulation, a section of the journal Frontiers in Immunology

Received: *10 October 2017*
Accepted: *06 December 2017*
Published: *20 December 2017*

Citation:
McLachlan SM and Rapoport B (2017) Thyroid Autoantibodies Display both "Original Antigenic Sin" and Epitope Spreading. Front. Immunol. 8:1845. doi: 10.3389/fimmu.2017.01845

INTRODUCTION

The concept of "original antigenic sin" arose from findings in humans and mice infected with influenza virus (1, 2) and in mice responding to Chlamydia proteins (3). For example, in sequential immunization of mice with two antigenically related but different strains of influenza A virus, antibodies induced by the second infection reacted more strongly with the primary than with the secondary virus (1). Similarly, humans infected with a novel influenza virus expanded antibodies against a viral strain of a previous infection and failed to develop antibody responses to epitopes on the new viral strain (4). Unlike in viral infections, the presently held authoritative opinion is that autoimmunity involves the converse of the "doctrine" of original antigenic sin, thereby facilitating "an unforseen

platform for immune therapy" (5). In this review, we present contrary evidence supporting the concept of an original antigenic sin component occurring for autoantibodies in thyroid autoimmunity and perhaps for other autoantibody-mediated diseases.

A phenomenon interlinked with original antigenic sin is epitope spreading, a well-recognized feature of some autoimmune conditions such as type 1 diabetes mellitus and multiple sclerosis, as well as for the animal models of these diseases, namely NOD mice and experimental autoimmune encephalomyelitis (EAE). Spreading can involve increasing the number of epitopes recognized on the same autoantigen (intramolecular) and subsequent recognition of additional autoantigens (intermolecular) over time. An example of intermolecular spreading, in EAE, SWX mice immunized with myelin proteolipid protein (PLP) develop the (as expected) T cell reactivity to determinants on PLP and to determinants on myelin basic protein and myelin oligodendrocyte glycoprotein (6). Similarly, in type 1 diabetes that develops spontaneously in NOD mice, T cell recognition of islet autoantigens spreads from proinsulin to other islet autoantigens such as islet-specific glucose-6-phosphatase catalytic subunit-related protein (IGRP) [for example, Ref. (7, 8)].

Thyroid autoimmune disease, Hashimoto's thyroiditis, and Graves' disease are the most common organ-specific autoimmune diseases affecting humans, far more common than type 1 diabetes mellitus and multiple sclerosis. In particular, approximately 1% of the population will develop Graves' disease in their lifetime and ~15% of adult females have autoimmune thyroiditis, although usually subclinical (9, 10). Animal models (induced and spontaneous) are available that provide insight into thyroid autoimmunity in humans. Three thyroid-specific autoantigens are targeted by the immune system: abundant soluble thyroglobulin (Tg), the much less abundant membrane-bound protein thyroid peroxidase (TPO), and the thyrotropin receptor (TSHR) [reviewed in Ref. (11)]. Although the great majority of Hashimoto patients have autoantibodies to TPO and many have Tg autoantibodies, hypothyroid patients with seronegative Hashimoto's disease have been reported (12).

Whether autoantibodies to TPO and Tg play a role in thyroid cell destruction is unclear, but they are excellent markers of the immune response to the thyroid. Moreover, B cells are increasingly recognized as powerful antigen-presenting cells by means of their membrane-bound antibodies that capture small amount of antigen for processing and presentation to T cells [for example, Ref. (13)]. TPO autoantibody-mediated and -modulated presentation to T cells has been reported (14, 15). Also, the enhancing or suppressing effects of Tg antibodies on the processing of a pathogenic T cell epitope on Tg have been described (16). Importantly, the successful treatment of Graves' ophthalmopathy patients with a monoclonal antibody to B cells (ritixumab) was suggested to involve antibody presentation by B cells (17). Turning to responses to the TSHR, stimulating TSHR autoantibodies are the direct cause of hyperthyroidism in Graves' disease [reviewed in Ref. (18)] and blocking TSHR autoantibodies are responsible for hypothyroidism in rare patients [for example, Ref. (19)].

Here, we examine evidence involving thyroid autoantibodies for both *intramolecular* original antigenic sin and *intermolecular* epitope spreading in autoimmune thyroid disease. Our findings have important implications for understanding disease pathogenesis and for developing novel antigen-specific therapeutic approaches to control the development of thyroid autoantibodies and thereby prevent thyroid autoimmunity rather than treating the clinical disease.

AUTOANTIBODY RECOGNITION IN HUMANS OF AN IMMUNODOMINANT REGION (IDR)—A REFLECTION OF ORIGINAL ANTIGENIC SIN

Antibody Recognition of an IDR on Tg and TPO

It has long been recognized that antibodies induced experimentally to Tg interact with multiple, widely diverse epitopes on the large (600 kDa) dimeric Tg molecule, whereas human Tg autoantibodies interact with a restricted number of epitopes (**Figure 1**) (20–23). Similar observations have been made for TPO (24, 25). Panels of human monoclonal TPO and Tg autoantibodies isolated from combinatorial immunoglobulin libraries and expressed as recombinant Fab confirmed restricted epitope recognition [for example (26, 27)]. Recombinant Fab provided the tools to characterize the IDRs on TPO and Tg recognized by antibodies in patients and some euthyroid controls with subclinical disease (**Table 1**). Characterization of the epitopes recognized by TPO and Tg autoantibodies has also been performed by competition assays using mouse monoclonal antibodies generated (for example) to Tg polypeptides (28), to purified TPO (25), or to TPO peptides (25, 29).

It should be emphasized that binding by the majority of patients' autoantibodies to TPO is decreased following protein denaturation (47, 48), demonstrating that most TPO autoantibodies interact with epitopes on conformationally intact protein. However, some studies have shown interaction between serum autoantibodies and reduced and denatured TPO [for example, Ref. (49, 50)], suggesting that not all TPO epitopes are conformational. Further, several linear epitopes (51, 52) and polypeptide fragments (53–56) are recognized by some patients' TPO autoantibodies. Similarly, Tg autoantibodies predominantly recognize native protein [for example, Ref. (57)]. However, recognition of peptide fragments by some Tg autoantibodies has been reported [for example, Ref. (38, 58)].

In this review, because of their dominance in the patient repertoire, we will focus on autoantibodies to TPO and Tg that interact with conformational epitopes.

Autoantibody Recognition of TPO and Tg Is Stable over Time

TPOAb epitopic "fingerprints" of the IDR are stable over time, that is *without* intramolecular epitope spreading, for example, in families in which the proband has juvenile Hashimoto's thyroiditis (30), women who develop postpartum thyroiditis (35), and for TgAb in most patients on iodine supplementation (39) (**Table 1**). Similarly, after iodine-131 treatment in Graves' disease, there was no evidence of TgAb intramolecular antibody spreading (44). There is some evidence that TPOAb epitopic patterns are inherited in families (36, 37).

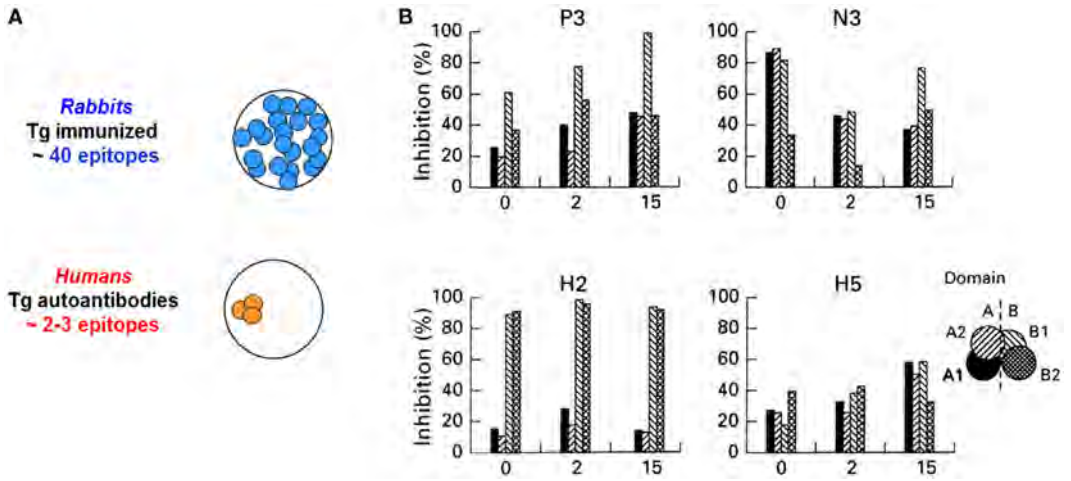

FIGURE 1 | **(A)** Diverse antibody epitopic recognition in rabbits immunized with human thyroglobulin (Tg) versus restricted antibody recognition by human Tg autoantibodies in humans. Schematic illustration of the concept described in Ref. (20–23). **(B)** Recognition of thyroid peroxidase autoantibody epitopes ("fingerprints") is stable over 15 years. The inset provides the key to the A and B domains (and subdomains) recognized by autoantibodies in the sera. Adapted from Ref. (30).

TABLE 1 | Recognition of an autoantibody immunodominant region (IDR) on thyroglobulin and thyroid peroxidase (TPO) in spontaneous thyroid autoimmunity (humans and a mouse model) versus thyroid antibodies induced in rabbits or mice that are either restricted or not restricted to an IDR.

	Thyroid autoAb	Recognition	Reference
Humans (spontaneous)			
AITD	TPOAb	IDR	(31–33)
Normal, elderly women	TPOAb	IDR	(34)
Postpartum thyroiditis	TPOAb	IDR, stable over time	(35)
Juvenile HT; Amish HT	TPOAb	IDR, stable over time	(30, 36)
HT twins	TPOAb	IDR, stable over time	(37)
Thyroiditis; also after I_2	TgAb	IDR	(27, 38–41)
Differentiated thyroid cancer	TgAb	IDR	(42)
Subacute thyroiditis	TgAb	IDR-B	(43)
GD treated with ^{131}Iodine	TgAb	IDR	(44)
Mice (spontaneous)			
Thyrotropin receptor (hTSHR)/ NOD.*H2*^{h4} injected with TSHR A-subunit	TSHR-Ab: pathogenic	Expanded by "inactive" antigen	(45)
Mice rabbits (induced)			
AKR/J-mice TPO fibroblasts	TPOAb	IDR	(46)
AKR/J-mice TPO + complete Freund's adjuvant (CFA)	TPOAb	Not restricted	(46)
Rabbits Tg + CFA	TgAb	Not restricted	(20)

TSHR Autoantibody Recognition

Changes are rare in the epitopes recognized by TSHR antibodies, namely thyroid-stimulating antibodies (TSAbs), which are responsible for hyperthyroidism in Graves' disease, and TSH-blocking antibodies (TBAbs), which cause hypothyroidism. In rare patients, TSHRAb switching from TSAb to TBAb (or vice versa) has been observed [reviewed in Ref. (59)]. The derivation of monoclonal TSAb and TBAb from one blood sample of an unusual patient who alternated between hyperthyroidism and hypothyroidism (60) demonstrated that the contrasting serum biological activities were due to two distinct antibodies.

IDR Recognition by TPOAb Induced in Mice

It is of interest that injecting mice with TPO expressed together with MHC class II on a fibroblast line induced TPOAb that resembled autoantibodies from Hashimoto or Graves' patients in terms of a high affinity for TPO and recognition of an IDR (46). In the same mouse strain, conventional immunization with TPO protein and adjuvant induced antibodies with lower affinity that recognized diverse epitopes on TPO (**Table 1**).

Other Autoantibody Recognition of an IDR

Autoantibodies interact with epitopes in an IDR in other autoantibody-mediated diseases [reviewed in Ref. (61)]. For example, in myasthenia gravis, autoantibodies to the acetylcholine receptor are restricted to a major IDR on the α1 subunit (62). Similarly, in the skin blistering diseases such as pemphigus vulgaris and pemphigus foliaceous, autoantibodies interact with an IDR on desmoglein (63).

Overall, the stability of human thyroid autoantibody recognition of an IDR is suggestive of "original antigenic sin." It is possible that this concept may also apply to other human autoantibodies directed to an IDR on their respective autoantigens.

EVIDENCE FOR ORIGINAL ANTIGENIC SIN IN A MOUSE MODEL OF THYROID AUTOIMMUNITY

In mice *induced* to develop Graves' disease by immunization with an adenovirus encoding the TSHR A-subunit gene,

pretreatment with a non-pathogenic (or "inactive") form of TSHR A-subunit protein attenuated hyperthyroidism by diverting pathogenic TSHR antibodies to a non-functional variety (64). Subsequently, pathogenic TSHR antibody diversion was attempted using the same approach in a mouse model that *spontaneously* develops pathogenic TSHR autoantibodies, human thyrotropin receptor (hTSHR)/NOD.$H2^{h4}$ mice with the human TSHR A-subunit transgene targeted to the thyroid (65). Unexpectedly, in an example of original antigenic sin, rather than attenuating the pre-existing pathogenic TSHRAb level, injecting "inactive" TSHR A-subunit protein into hTSHR/NOD.$H2^{h4}$ mice enhanced the levels of pathogenic TSH-binding inhibition and TSAbs, as well as increasing the levels of non-pathogenic antibodies detected by ELISA (45). This effect was TSHR specific as spontaneously occurring autoantibodies to Tg and TPO were unaffected.

In hTSHR/NOD.$H2^{h4}$ mice, the original antigenic sin is the initial selection of B cells for the transgenically expressed TSHR protein, namely precursors specific for both non-functional antibodies (detectable only by ELISA) as well as pathogenic TSHR antibodies (detectable only in functional assays) (**Figure 2**). B cells with affinity for self antigens (like the transgenic hTSHR) are tolerized by a number of mechanisms including receptor editing and anergy (functional unresponsiveness) rather than deletion as for self-reactive T cells (66). By using transgenic hen egg lysozyme-specific transgenic mouse models, it was demonstrated that self-reactive B cells were not eliminated when this antigen was expressed by thyroid cells (67). Similarly, in the spontaneous hTSHR/NOD.$H2^{h4}$ model, two types of precursor B cells for pathogenic and non-pathogenic TSHRAb remain in the repertoire and both can be expanded by the "cross-reacting" antigen, the non-pathogenic TSHR A-subunit protein.

MECHANISMS AND IMPLICATIONS OF ORIGINAL ANTIGENIC SIN IN THYROID AUTOIMMUNITY

Mechanisms of Original Antigenic Sin

The mechanisms responsible for original antigenic sin are not fully understood. However, because of the problems caused for vaccination against novel viral strains, approaches have been used to overcome original antigenic sin. These studies provide insight into the basis for this phenomenon, at least from the perspective of T cell epitopes.

One approach involves eliciting cross-reactive responses by immunization with multiple peptide variants (68) or injecting yeasts carrying diverse virus-like particles (69). It has also been suggested that, at least for CD8+ T cell responses, original antigen sin can be overcome by treatment with neutralizing interleukin 10 together with linked T cell epitopes (70). A different strategy involves immunization with adjuvants (such as *Bordetella pertussis* toxin) that activate dendritic cells (71). The latter approach is of interest in the context of comments by Kim et al. (4) concerning viral antibodies, namely that antigen presentation by B cells favors the activation of memory B cells specific for the first virus rather than naive B cells specific for the subsequent cross-reacting virus. Finally, a simple mechanistic explanation proposes that original antigenic sin occurs because regulatory T cells induced by the first antigen decrease the amount of the second antigen on dendritic cells that activate naive B cells (72).

Implications of Original Antigenic Sin in Thyroid Autoimmunity

The most likely explanation for original antigenic sin in thyroid autoantibodies appears to involve antigen presentation by B cells

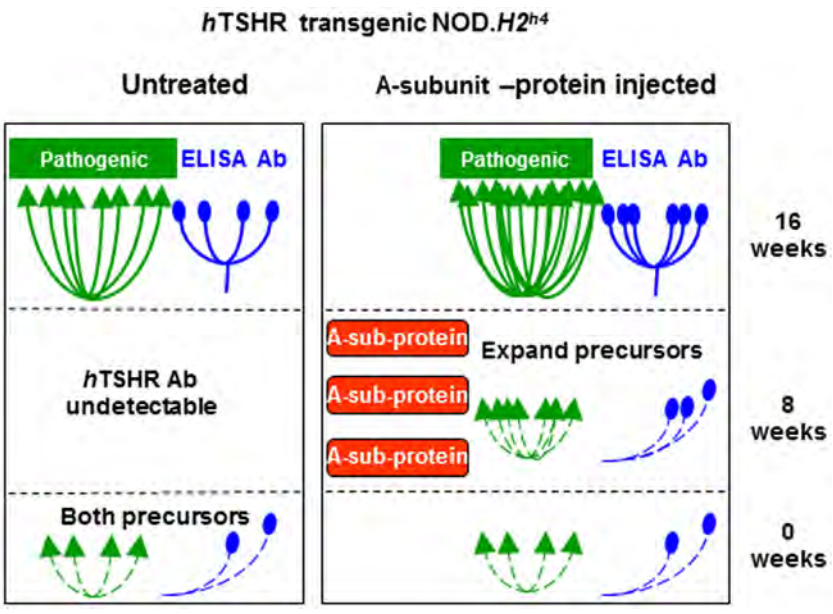

FIGURE 2 | "Original antigenic sin" observed in human thyrotropin receptor (hTSHR)/NOD.$H2^{h4}$ mice injected with an inappropriate form of thyrotropin receptor A-subunit or saline (as control). See text for explanation. Adapted with permission from Ref. (45).

or (in the case of TPO) thyroid cells, rather than dendritic cells. It should be noted that a restricted antibody response focused on the TPO IDR (as in humans) occurs in AKR/J-mice injected with cells expressing human TPO but not in mice of the same strain immunized with human TPO protein and adjuvant (46). The restricted response is likely related to the much lower concentration of cell-associated TPO than TPO injected with adjuvant. Because of their efficiency as specific antigen-presenting cells [for example, Ref. (13)], B cells are likely the antigen-presenting cells in spontaneously arising autoantibodies to Tg and the TSHR A-subunit. *Via* their specific immunoglobulin receptors, B cells may also capture conformationally intact thyroid autoantigens, a critical factor for the induction of pathogenic TSHR antibodies [reviewed in Ref. (73)].

In addition to suggesting the likely cells involved in autoantigen presentation, IDR recognition simplifies what would otherwise be a gargantuan task, namely exploring the regions recognized by autoantibodies on large, glycosylated thyroid autoantigens:

(i) Tg, the largest thyroid autoantigen comprising a homodimer of 300 kDa molecules, poses a major challenge. Iodination of Tg alters recognition by human autoantibodies (74), possibly by denaturing the antigen. However, epitope mapping using Tg fragments (fusion proteins or digestion products) suggests that some Tg autoantibody epitopes are located in the central region (75) or at the *C*-terminal end of the molecule (76, 77).

(ii) TPO is a homodimer (each 110 kDa) inserted in the plasma membrane, and TPO autoantibodies are directed against the ectodomain. The TPO epitope of an human autoantibody (expressed as a recombinant Fab) was identified using footprinting technology (78). In addition, progress has been made in delineating the amino acids targeted by other autoantibodies [for example, Ref. (79–81)]. However, definitive mapping of autoantibodies epitopes will require crystallization of a TPO monoclonal autoantibody with TPO protein.

(iii) The TSHR, like TPO, is also membrane bound but pathogenic TSHR autoantibodies (as in Graves' disease) are induced spontaneously to the heavily glycosylated TSHR A-subunit (~60 kDa) shed after cleavage of the membrane-bound receptor [reviewed in Ref. (73)]. Amino acid residues involved in the binding sites of TSAb were initially explored using chimeric TSHR-luteinizing hormone receptors together with mutagenesis [for example, Ref. (82)]. More recently, the epitopes for monoclonal human (M22) and a monoclonal human TBAb (K1-70) have been determined by co-crystalizing each antibody with the major portion of the TSHR A-subunit (83, 84).

TABLE 2 | Thyroid antibodies: induced or spontaneous intermolecular or intramolecular antigenic spreading.

Strains/disease	Treatment	First Ab	Second Ab	Reference
Induced—intermolecular spreading				
Rabbit	Tg peptide + CFA	Peptide Ab	hTgAb, mTgAb	(85)
Rabbit	Tg/Tg peptide + CFA	TgAb	TPOAb, TgPOAb	(86)
HLA-DR3	hTSHR-DNA	hTSHR Ab	mTg	(89)
BALB/c hTSHR A-Subunit (Lo-expressor)	Anti-CD25, hTSHR A-subunit-adenovirus	hTSHR Ab	mTg, mTPO	(90)
Spontaneous—intermolecular spreading				
NOD.$H2^{h4}$ mice	No Tx; time	TgAb	TPOAb	(91)
Juvenile HT	No Tx; time	TgAb	TPOAb	(91)
HT	No Tx; time	TgAb	TPOAb	(92)
GD	No Tx; time	TgAb, TPOAb	TSHRAb	(92)
Hyper to hypo		TSAb	TBAb	(93, 94)
Hypo to hyper	L-T4	TBAb	TSAb	(95, 96)
Spontaneous—intramolecular spreading				
HT	Iodine prophylaxis	TgAb	TgAb-B epitope	(97)

CFA, complete Freund's adjuvant; h, human; m, mouse; HT, Hashimoto thyroiditis; hTSHR, human thyrotropin receptor; GD, Graves' disease; TBAb, TSH-blocking antibody; Tg, thyroglobulin; TSAb, thyroid-stimulating antibody.

EPITOPE SPREADING OF THYROID AUTOANTIBODIES

Intermolecular Spreading

Induced and spontaneous intermolecular spreading for thyroid autoantibodies has been demonstrated for thyroid autoimmunity (**Table 2**). For example, rabbits immunized with human Tg and complete Freund's adjuvant develop antibodies to Tg, as expected, as well as antibodies to TPO and antibodies that bind to both Tg and TPO (85, 86). It should be noted that searching for previously postulated bispecific human autoantibodies that recognize both Tg and TPO ("TgPO antibodies") [for example, Ref. (87)] in a phage display immunoglobulin gene combinatorial, constructed from thyroid-infiltrating B cells of a patient with library serum TgPO-like autoantibody activity, led to multiple antibodies specific for *either* Tg or TPO but none had TgPOAb activity (88).

Returning to intermolecular epitope spreading, transgenic HLA-DR3 mice immunized with hTSHR DNA develop TSHR antibodies and, in a few mice, mild thyroiditis in association with antibodies to Tg (89). Transgenic BALB/c mice expressing low intrathyroidal levels of the human TSHR A-subunit, depleted of regulatory T cells (CD25 positive) before immunization with human TSHR-A-subunit adenovirus, developed TSHR antibodies and (unexpectedly) TgAb- and TPOAb-associated with massive thyroiditis and hypothyroidism (90). Incidentally, anti-CD25-treated BALB/c mice transplanted with TUBO tumor cells developed antitumor responses together with antithyroid immunity (98).

Of particular interest are observations of *spontaneous* antibody epitope spreading. NOD.$H2^{h4}$ mice develop thyroid autoimmunity, a process that is enhanced by iodide in the drinking water. The first autoantibodies to appear are directed against Tg (99–101), and subsequently, TPO antibodies appear (91). A similar pattern was observed in siblings of probands with juvenile Hashimoto thyroiditis (91). Moreover, TSHR antibodies develop spontaneously in NOD.$H2^{h4}$ mice transgenically expressing the human TSHR A-subunit (65).

Combining published data from published studies (45, 102) studies, the development of autoantibodies in female hTSHR/

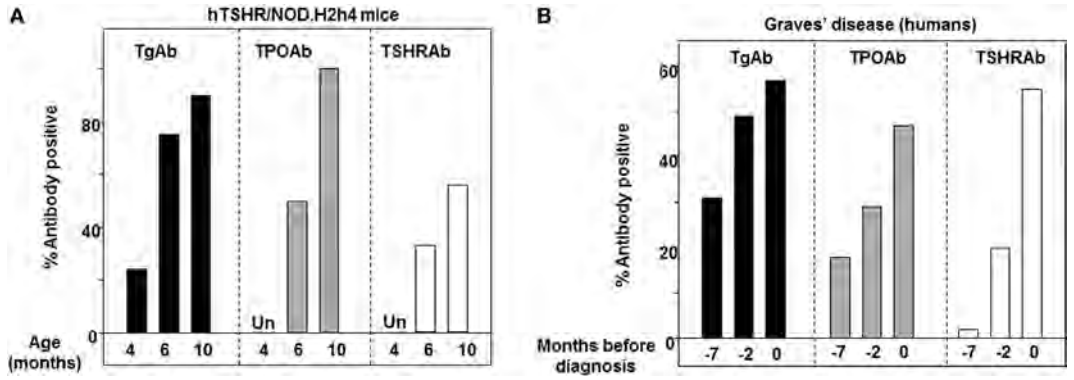

FIGURE 3 | Intermolecular antigenic spreading from thyroglobulin (Tg) to thyrotropin receptor (TPO) and the thyrotropin receptor (TSHR). **(A)** Percentage of human thyrotropin receptor (hTSHR)/NOD.$H2^{h4}$ female mice positive for TgAb, TPOAb, and TSHRAb (TSHR binding inhibition) aged 4, 6, and 10 months. **(B)** Prediagnostic TgAb, TPOAb, and TSHRAb levels (7, 2, and 0 years) in patients with Graves' disease [data plotted from Ref. (92)].

NOD.$H2^{h4}$ mice permits comparing the appearance of thyroid autoantibodies over time: TgAbs are present in some 4-month-old mice, and TSHRAb and TPOAb are detectable after the age of 6 months, and all three thyroid autoantibodies were present in more mice after 10 months (**Figure 3A**). Turning to humans, in a study of prediagnostic markers in Graves' patients, TPOAb and TgAb were detectable several years before TSHR antibodies (92). Importantly, although in humans the maximum percentage of positive TgAb and TPOAb in humans did not approach 100% as in NOD.$H2^{h4}$ mice, the time sequence of antibody reactivity to Tg, TPO, and the TSHR in transgenic NOD.$H2^{h4}$ mice (**Figure 3A**) resembles that in humans (**Figure 3B**).

Intramolecular Spreading

There is less extensive evidence for intramolecular thyroid autoantibody epitope spreading (**Table 2**): Latrofa and colleagues demonstrated that iodine prophylaxis revealed recognition of a previously cryptic TgAb epitope, but this phenomenon may involve the iodination of Tg, thereby generating a neo-antigen (97). In addition, as already mentioned, there are rare examples of TSHR antibody switching from TBAb to TSAb associated with thyroxine therapy, or the reverse, namely TBAb to switching to TSAb [reviewed in Ref. (59)]. As would be expected for antibodies with differing functional effects, the epitopes on the TSHR ectodomain recognized by TSAb and TBAb are different (103, 104), although they interact with closely overlapping portions of the amino terminus of the TSHR A-subunit (105).

The apparent antibody epitope spreading in maternally transferred TSHR antibodies from initial TBAb to TSAb is due to progressive dilution of the high titer TBAb overpowering the lower concentrations of TSAb as human IgG is metabolized [reviewed in Ref. (59)].

IMPLICATIONS OF EPITOPE SPREADING FOR THYROID AUTOIMMUNITY

The phenomenon of epitope spreading provides important background information on thyroid autoantigen recognition. In particular, epitope spreading appears to be related to the amount and the size of each thyroid autoantigen, being greatest for Tg and less for both TPO and the TSHR A-subunit in the thyroid as well as in the thymus (**Figure 4**) [reviewed in Ref. (11)]. In part, epitope spreading involves the greater availability of peptides available to stimulate T cells and protein to stimulate B cells from the abundant, large Tg molecule compared with the more limited amount and smaller molecular size of TPO and even fewer peptides from the TSHR A-subunit [reviewed in Ref. (11)]. Central tolerance also plays a role, with responses regulated by intrathymic expression of antigens like the highly expressed transgenic human TSHR A-subunit (106).

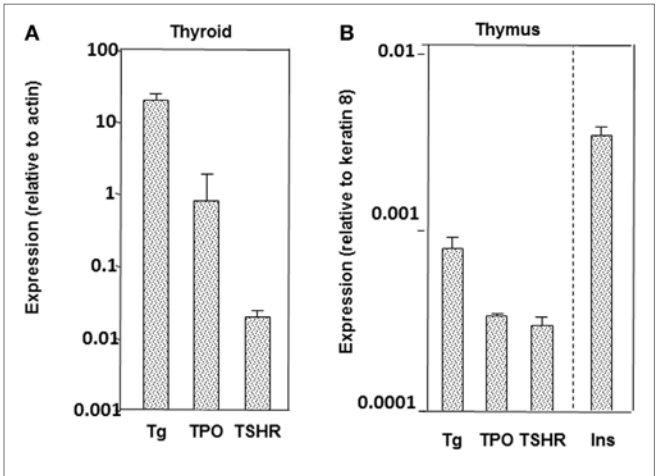

FIGURE 4 | Relative expression of thyroglobulin (Tg), thyrotropin receptor (TPO), and the thyrotropin receptor (TSHR) in thyroid **(A)** and thymus **(B)** in mice (BALB/c strain). For the thymus, data are included for insulin, which is highly expressed in the thymus. Adapted with permission from the data in Ref. (107).

Knowledge of the autoantigen "cascade" suggests approaches for antigen-specific treatment. For example, in NOD mice, responses against islet antigens are prevented by inducing tolerance against proinsulin but not against IGRP (8), an autoantigen

recognized later in the "cascade." In the same way, it is possible that successful induction of tolerance against Tg in NOD.$H2^{h4}$ mice could prevent the subsequent breakdown in tolerance to TPO (91) and perhaps even to the TSHR in hTSHR/NOD.$H2^{h4}$ mice (65). In a mouse model of experimentally induced thyroiditis, increasing the circulating level of Tg strengthened self-tolerance and reduced the extent of experimental thyroiditis [reviewed in Ref. (108)]. These findings suggest that increasing Tg levels could possibly regulate autoimmunity to Tg in the hTSHR/NOD.$H2^{h4}$ strain. However, as we previously reported, an antigen-specific approach used successfully in an induced model may not be directly applicable to a spontaneous model (45). Consequently, it may be necessary to test multiple modes of Tg presentation to downregulate the cascade of autoimmune responses to Tg, TPO, and the TSHR in hTSHR/NOD.$H2^{h4}$ mice.

CONCLUSION

The evidence for intermolecular epitope spreading in thyroid autoimmunity is focused on autoantibodies, unlike the emphasis on T cell epitope spreading in multiple sclerosis and IDDM type 1 (or their animal models EAE and NOD mice). Unlike multiple sclerosis or EAE, original antigenic sin appears to be characteristic of thyroid autoimmunity as reflected by the recognition of an autoantibody IDR in humans and in the response of transgenic hTSHR/NOD.$H2^{h4}$ mice to injection with inappropriate TSHR antigen. This difference likely reflects the importance of T cell immunity in EAE/MS versus autoantibodies in thyroid autoimmunity, particularly Graves' disease for which stimulatory autoantibodies to the TSHR are the direct cause.

Finally, the pattern observed for intermolecular epitope spreading provides the rationale for antigen-specific manipulation to block thyroid autoantibody development by inducing tolerance to the first autoantigen in the antigen cascade, namely Tg. Because of its abundance, Tg may be the autoantigen of choice to explore antigen-specific treatment to block the development of pathogenic TSHR antibodies.

AUTHOR CONTRIBUTIONS

SM and BR contributed to the concept, writing, and preparation of figures for this review.

FUNDING

National Institutes of Health Grants DK 54684 (SM) and previously funded National Institutes of Health Grants 19289 (BR) and 36182 (BR).

REFERENCES

1. Virelizier JL, Allison AC, Schild GC. Antibody responses to antigenic determinants of influenza virus hemagglutinin. II. Original antigenic sin: a bone marrow-derived lymphocyte memory phenomenon modulated by thymus-derived lymphocytes. *J Exp Med* (1974) 140(6):1571–8. doi:10.1084/jem.140.6.1571
2. Webster RG, Kasel JA, Couch RB, Laver WG. Influenza virus subunit vaccines. II. Immunogenicity and original antigenic sin in humans. *J Infect Dis* (1976) 134(1):48–58. doi:10.1093/infdis/134.1.48
3. Berry JD, Peeling RW, Brunham RC. Analysis of the original antigenic sin antibody response to the major outer membrane protein of *Chlamydia trachomatis*. *J Infect Dis* (1999) 179(1):180–6. doi:10.1086/314538
4. Kim JH, Skountzou I, Compans R, Jacob J. Original antigenic sin responses to influenza viruses. *J Immunol* (2009) 183(5):3294–301. doi:10.4049/jimmunol.0900398
5. Steinman L. Absence of "original antigenic sin" in autoimmunity provides an unforeseen platform for immune therapy. *J Exp Med* (1999) 189(7):1021–4. doi:10.1084/jem.189.7.1021
6. Tuohy VK, Yu M, Yin L, Kawczak JA, Kinkel RP. Spontaneous regression of primary autoreactivity during chronic progression of experimental autoimmune encephalomyelitis and multiple sclerosis. *J Exp Med* (1999) 189(7):1033–42. doi:10.1084/jem.189.7.1033
7. Prasad S, Kohm AP, McMahon JS, Luo X, Miller SD. Pathogenesis of NOD diabetes is initiated by reactivity to the insulin B chain 9-23 epitope and involves functional epitope spreading. *J Autoimmun* (2012) 39(4):347–53. doi:10.1016/j.jaut.2012.04.005
8. Krishnamurthy B, Dudek NL, McKenzie MD, Purcell AW, Brooks AG, Gellert S, et al. Responses against islet antigens in NOD mice are prevented by tolerance to proinsulin but not IGRP. *J Clin Invest* (2006) 116(12):3258–65. doi:10.1172/JCI29602
9. Vanderpump MPJ, Tunbridge WMG, French JM, Appleton D, Bates D, Clark F, et al. The incidence of thyroid disorders in the community: a twenty-year follow-up of the Whickham survey. *Clin Endocrinol* (1995) 43:55–68. doi:10.1111/j.1365-2265.1995.tb01894.x
10. Hollowell JG, Staehling NW, Flanders WD, Hannon WH, Gunter EW, Spencer CA, et al. Serum TSH, T(4), and thyroid antibodies in the United States population (1988 to 1994): National Health and Nutrition Examination Survey (NHANES III). *J Clin Endocrinol Metab* (2002) 87(2):489–99. doi:10.1210/jcem.87.2.8182
11. McLachlan SM, Rapoport B. Breaking tolerance to thyroid antigens: changing concepts in thyroid autoimmunity. *Endocr Rev* (2014) 35(1):59–105. doi:10.1210/er.2013-1055
12. Rotondi M, de Martinis L, Coperchini F, Pignatti P, Pirali B, Ghilotti S, et al. Serum negative autoimmune thyroiditis displays a milder clinical picture compared with classic Hashimoto's thyroiditis. *Eur J Endocrinol* (2014) 171(1):31–6. doi:10.1530/EJE-14-0147
13. Lanzavecchia A. Antigen-specific interaction between T and B cells. *Nature* (1985) 314:537–9. doi:10.1038/314537a0
14. Guo J, Quaratino S, Jaume JC, Costante G, Londei M, McLachlan SM, et al. Autoantibody-mediated capture and presentation of autoantigen to T cells via the Fc epsilon receptor by a recombinant human autoantibody Fab converted to IgE. *J Immunol Methods* (1996) 195:81–92. doi:10.1016/0022-1759(96)00091-9
15. Quaratino S, Osman M, Ruf J, McLachlan SM, Rapoport B, Londei M. Human autoantibodies modulate the T cell epitope repertoire but fail to unmask a pathogenic cryptic epitope. *J Immunol* (2005) 174:557–63. doi:10.4049/jimmunol.174.1.557
16. Dai Y, Carayanniotis KA, Eliades P, Lymberi P, Shepherd P, Kong Y, et al. Enhancing or suppressive effects of antibodies on processing of a pathogenic T cell epitope in thyroglobulin. *J Immunol* (1999) 162(12):6987–92.
17. Salvi M, Vannucchi G, Curro N, Campi I, Covelli D, Dazzi D, et al. Efficacy of B-cell targeted therapy with rituximab in patients with active moderate to severe Graves' orbitopathy: a randomized controlled study. *J Clin Endocrinol Metab* (2015) 100(2):422–31. doi:10.1210/jc.2014-3014
18. Rapoport B, McLachlan SM. The thyrotropin receptor in Graves' disease. *Thyroid* (2007) 17(10):911–22. doi:10.1089/thy.2007.0170
19. Endo K, Kasagi K, Konishi J, Ikekubo K, Tatsuyo O, Takeda Y, et al. Detection and properties of TSH-binding inhibitor immunoglobulins in patients with Graves' disease and Hashimoto's thyroiditis. *J Clin Endocrinol Metab* (1978) 46:734–9. doi:10.1210/jcem-46-5-734
20. Roitt IM, Campbell PN, Doniach D. The nature of the thyroid auto-antibodies present in patients with Hashimoto's thyroiditis (lymhpadenoid goitre). *Biochem J* (1958) 69:248–57. doi:10.1042/bj0690248
21. Shulman S, Witebsky E. Studies on organ specificity. IX. Biophysical and immunochemical studies on human thyroid autoantibody. *J Immunol* (1960) 85:559–67.

22. Nye L, Pontes de Carvalho LC, Roitt IM. Restrictions in the response to autologous thyroglobulin in the human. *Clin Exp Immunol* (1980) 41:252–63.
23. Male DK, Champion BR, Pryce G, Matthews H, Shepherd P. Antigenic determinants of human thyroglobulin differentiated using antigen fragments. *Immunology* (1985) 54:419–26.
24. Ruf J, Toubert M, Czarnocka B, Durand-Gorde J, Ferrand M, Carayon P. Relationship between immunological structure and biochemical properties of human thyroid peroxidase. *Endocrinology* (1989) 125:1211–8. doi:10.1210/endo-125-3-1211
25. Czarnocka B, Pastuszko D, Carayon P, Ruf J, Gardas A. Majority of thyroid peroxidase in patients with autoimmune thyroid disease are directed to a single TPO domain. *Autoimmunity* (1996) 23:145–54. doi:10.3109/08916939608995338
26. Guo J, Wang Y, Jaume JC, Rapoport B, McLachlan SM. Rarity of autoantibodies to a major autoantigen, thyroid peroxidase, that interact with denatured antigen or with epitopes outside the immunodominant region. *Clin Exp Immunol* (1999) 117:19–29. doi:10.1046/j.1365-2249.1999.00934.x
27. Latrofa F, Phillips M, Rapoport B, McLachlan SM. Human monoclonal thyroglobulin autoantibodies: epitopes and immunoglobulin genes. *J Clin Endocrinol Metab* (2004) 89(10):5116–23. doi:10.1210/jc.2003-032173
28. Malthiery Y, Henry M, Zanelli E. Epitope mapping of human thyroglobulin reveals a central immunodominant region. *FEBS Lett* (1991) 279(2):190–2. doi:10.1016/0014-5793(91)80146-T
29. Gora M, Gardas A, Wiktorowicz W, Hobby P, Watson PF, Weetman AP, et al. Evaluation of conformational epitopes on thyroid peroxidase by antipeptide antibody binding and mutagenesis. *Clin Exp Immunol* (2004) 136(1):137–44. doi:10.1111/j.1365-2249.2004.02422.x
30. Jaume JC, Burek CL, Hoffman WH, Rose N, McLachlan SM, Rapoport B. Thyroid peroxidase autoantibody epitopic 'fingerprints' in juvenile Hashimoto's thyroiditis: evidence for conservation over time and in families. *Clin Exp Immunol* (1996) 104:115–23. doi:10.1046/j.1365-2249.1996.d01-659.x
31. Chazenbalk GD, Portolano S, Russo D, Hutchison JS, Rapoport B, McLachlan SM. Human organ-specific autoimmune disease: molecular cloning and expression of an autoantibody gene repertoire for a major autoantigen reveals an antigenic dominant region and restricted immunoglobulin gene usage in the target organ. *J Clin Invest* (1993) 92:62–74. doi:10.1172/JCI116600
32. Czarnocka B, Janota-Bzowski M, McIntosh RS, Asghar MS, Watson PF, Kemp EH, et al. Immunoglobulin G kappa anti-thyroid peroxidase antibodies in Hashimoto's thyroiditis: epitope mapping analysis. *J Clin Endocrinol Metab* (1997) 82:2639–44. doi:10.1210/jcem.82.8.4124
33. Bresson D, Cerutti M, Devauchelle G, Pugniere M, Roquet F, Bes C, et al. Localization of the discontinuous immunodominant region recognized by human anti-thyroperoxidase autoantibodies in autoimmune thyroid diseases. *J Biol Chem* (2003) 278(11):9560–9. doi:10.1074/jbc.M211930200
34. Jaume JC, Costante G, Nishikawa T, Phillips DIW, Rapoport B, McLachlan SM. Thyroid peroxidase autoantibody fingerprints in hypothyroid and euthyroid individuals. I. Cross-sectional study in elderly women. *J Clin Endocrinol Metab* (1995) 80:994–9. doi:10.1210/jc.80.3.994
35. Jaume JC, Parkes AB, Lazarus JH, Hall R, Costante G, McLachlan SM, et al. Thyroid peroxidase autoantibody fingerprints. II. A longitudinal study in postpartum thyroiditis. *J Clin Endocrinol Metab* (1995) 80:1000–5. doi:10.1210/jc.80.3.1000
36. Jaume JC, Guo J, Pauls DL, Zakarija M, McKenzie JM, Egeland JA, et al. Evidence for genetic transmission of thyroid peroxidase autoantibody epitopic "fingerprints". *J Clin Endocrinol Metab* (1999) 84(4):1424–31. doi:10.1210/jc.84.4.1424
37. Brix TH, Hegedus L, Gardas A, Banga JP, Nielsen CH. Monozygotic twin pairs discordant for Hashimoto's thyroiditis share a high proportion of thyroid peroxidase autoantibodies to the immunodominant region A. Further evidence for genetic transmission of epitopic "fingerprints". *Autoimmunity* (2011) 44(3):188–94. doi:10.3109/08916934.2010.518575
38. Henry M, Zanelli E, Piechaczyk M, Pau B, Malthiery Y. A major human thyroglobulin epitope defined with monoclonal antibodies is mainly recognized by human autoantibodies. *Eur J Immunol* (1992) 22(2):315–9. doi:10.1002/eji.1830220205
39. Okosieme OE, Premawardhana LD, Jayasinghe A, Kaluarachi WN, Parkes AB, Smyth PP, et al. Thyroglobulin autoantibodies in iodized subjects: relationship between epitope specificities and longitudinal antibody activity. *Thyroid* (2005) 15(9):1067–72. doi:10.1089/thy.2005.15.1067
40. Estienne V, McIntosh RS, Ruf J, Asghar MS, Watson PF, Carayon P, et al. Comparative mapping of cloned human and murine antithyroglobulin antibodies: recognition by human antibodies of an immunodominant region. *Thyroid* (1998) 8(8):643–6. doi:10.1089/thy.1998.8.643
41. Okosieme OE, Premawardhana LD, Jayasinghe A, de Silva DG, Smyth PP, Parkes AB, et al. Thyroglobulin epitope recognition in a post iodine-supplemented Sri Lankan population. *Clin Endocrinol (Oxf)* (2003) 59(2):190–7. doi:10.1046/j.1365-2265.2003.01819.x
42. Okosieme OE, Evans C, Moss L, Parkes AB, Premawardhana LD, Lazarus JH. Thyroglobulin antibodies in serum of patients with differentiated thyroid cancer: relationship between epitope specificities and thyroglobulin recovery. *Clin Chem* (2005) 51(4):729–34. doi:10.1373/clinchem.2004.044511
43. Latrofa F, Ricci D, Montanelli L, Altea MA, Pucci A, Pinchera A, et al. Thyroglobulin autoantibodies of patients with subacute thyroiditis are restricted to a major B cell epitope. *J Endocrinol Invest* (2012) 35(8):712–4. doi:10.1007/BF03345804
44. Latrofa F, Ricci D, Montanelli L, Piaggi P, Mazzi B, Bianchi F, et al. Thyroglobulin autoantibodies switch to immunoglobulin (Ig)G1 and IgG3 subclasses and preserve their restricted epitope pattern after 131I treatment for Graves' hyperthyroidism: the activity of autoimmune disease influences subclass distribution but not epitope pattern of autoantibodies. *Clin Exp Immunol* (2014) 178(3):438–46. doi:10.1111/cei.12438
45. Rapoport B, Banuelos B, Aliesky HA, Hartwig Trier N, McLachlan SM. Critical differences between induced and spontaneous mouse models of Graves' disease with implications for antigen-specific immunotherapy in humans. *J Immunol* (2016) 197:4560–8. doi:10.4049/jimmunol.1601393
46. Jaume JC, Guo J, Wang Y, Rapoport B, McLachlan SM. Cellular thyroid peroxidase (TPO), unlike purified TPO and adjuvant, induces antibodies in mice that resemble autoantibodies in human autoimmune thyroid disease. *J Clin Endocrinol Metab* (1999) 84(5):1651–7. doi:10.1210/jcem.84.5.5666
47. Nakajima Y, Howells RD, Pegg C, Davies Jones E, Rees Smith B. Structure activity analysis of microsomal antigen/thyroid peroxidase. *Mol Cell Endocrinol* (1987) 53:15–23. doi:10.1016/0303-72078790187-0
48. Gardas A, Domek H. The effect of sulphydryl reagents on the human thyroid microsomal antigen. *J Endocrinol Invest* (1988) 11:385–8. doi:10.1007/BF03349061
49. Hamada N, Jaeduck N, Portmann L, Ito K, DeGroot LJ. Antibodies against denatured and reduced thyroid microsomal antigen in autoimmune thyroid disease. *J Clin Endocrinol Metab* (1987) 64:230–8. doi:10.1210/jcem-64-2-230
50. Bermann M, Magee M, Koenig RJ, Kaplan MM, Maastricht J, Johnson J, et al. Differential autoantibody responses to thyroid peroxidase in patients with Graves' disease and Hashimoto's thyroiditis. *J Clin Endocrinol Metab* (1993) 77:1098–101. doi:10.1210/jcem.77.4.8408460
51. Finke R, Seto P, Ruf J, Carayon P, Rapoport B. Determination at the molecular level of a B-cell epitope on thyroid peroxidase likely to be associated with autoimmune thyroid disease. *J Clin Endocrinol Metab* (1991) 73:919–21. doi:10.1210/jcem-73-4-919
52. Libert F, Ludgate M, Dinsart C, Vassart G. Thyroperoxidase, but not the thyrotropin receptor, contains sequential epitopes recognized by autoantibodies in recombinant peptides expressed in the pUEX vector. *J Clin Endocrinol Metab* (1991) 73:857–60. doi:10.1210/jcem-73-4-857
53. Banga JP, Barnett PS, Ewins DL, Page M, McGregor AM. Mapping of autoantigenic epitopes on recombinant thyroid peroxidase fragments using the polymerase chain reaction. *Autoimmunity* (1990) 6:257–68. doi:10.3109/08916939008998418
54. Maastricht J, Koenig RJ, Kaplan MM, Arscott P, Thompson N, Baker JR Jr. Identification of localized autoantibody epitopes in thyroid peroxidase. *J Clin Endocrinol Metab* (1992) 75:121–6. doi:10.1210/jc.75.1.121
55. Zanelli E, Henry M, Malthiery Y. Use of recombinant epitopes to study the heterogeneous nature of the autoantibodies against thyroid peroxidase in autoimmune thyroid disease. *Clin Exp Immunol* (1992) 87:80–6. doi:10.1111/j.1365-2249.1992.tb06417.x
56. Arscott PL, Koenig RJ, Kaplan MM, Glick GD, Baker JR Jr. Unique autoantibody epitopes in an immunodominant region of thyroid peroxidase. *J Biol Chem* (1996) 271:4966–73. doi:10.1074/jbc.271.9.4966
57. Shimojo N, Saito K, Kohno Y, Sasaki N, Tarutani O, Nakajima H. Antigenic determinants on thyroglobulin: comparison of the reactivities of different thyroglobulin preparations with serum antibodies and T cells of patients with

chronic thyroiditis. *J Clin Endocrinol Metab* (1988) 66(4):689–95. doi:10.1210/jcem-66-4-689
58. Caturegli P, Mariotti S, Kuppers RC, Burek CL, Pinchera A, Rose NR. Epitopes on thyroglobulin: a study of patients with thyroid disease. *Autoimmunity* (1994) 18:41–9. doi:10.3109/08916939409014678
59. McLachlan SM, Rapoport B. Thyrotropin-blocking autoantibodies and thyroid-stimulating autoantibodies: potential mechanisms involved in the pendulum swinging from hypothyroidism to hyperthyroidism or vice versa. *Thyroid* (2013) 23(1):14–24. doi:10.1089/thy.2012.0374
60. Evans M, Sanders J, Tagami T, Sanders P, Young S, Roberts E, et al. Monoclonal autoantibodies to the TSH receptor, one with stimulating activity and one with blocking activity, obtained from the same blood sample. *Clin Endocrinol (Oxf)* (2010) 73(3):404–12. doi:10.1111/j.1365-2265.2010.03831.x
61. Ludwig RJ, Vanhoorelbeke K, Leypoldt F, Kaya Z, Bieber K, McLachlan SM, et al. Mechanisms of autoantibody-induced pathology. *Front Immunol* (2017) 8:603. doi:10.3389/fimmu.2017.00603
62. Luo J, Taylor P, Losen M, De Baets MH, Shelton GD, Lindstrom J. Main immunogenic region structure promotes binding of conformation-dependent myasthenia gravis autoantibodies, nicotinic acetylcholine receptor conformation maturation, and agonist sensitivity. *J Neurosci* (2009) 29(44):13898–908. doi:10.1523/JNEUROSCI.2833-09.2009
63. Sekiguchi M, Futei Y, Fujii Y, Iwasaki T, Nishikawa T, Amagai M. Dominant autoimmune epitopes recognized by pemphigus antibodies map to the N-terminal adhesive region of desmogleins. *J Immunol* (2001) 167(9):5439–48. doi:10.4049/jimmunol.167.9.5439
64. Misharin AV, Nagayama Y, Aliesky H, Mizutori Y, Rapoport B, McLachlan SM. Attenuation of induced hyperthyroidism in mice by pretreatment with thyrotropin receptor protein: deviation of thyroid-stimulating antibody to non-functional antibodies. *Endocrinology* (2009) 150(8):3944–52. doi:10.1210/en.2009-0181
65. Rapoport B, Aliesky HA, Banuelos B, Chen CR, McLachlan SM. A unique mouse strain that develops spontaneous, iodine-accelerated, pathogenic antibodies to the human thyrotrophin receptor. *J Immunol* (2015) 194(9):4154–61. doi:10.4049/jimmunol.1500126
66. Zikherman J, Parameswaran R, Weiss A. Endogenous antigen tunes the responsiveness of naive B cells but not T cells. *Nature* (2012) 489(7414):160–4. doi:10.1038/nature11311
67. Akkaraju S, Canaan K, Goodnow CC. Self-reactive B cells are not eliminated or inactivated by autoantigen expressed on thyroid epithelial cells. *J Exp Med* (1997) 186(12):2005–12. doi:10.1084/jem.186.12.2005
68. Anderson DE, Carlos MP, Nguyen L, Torres JV. Overcoming original (antigenic) sin. *Clin Immunol* (2001) 101(2):152–7. doi:10.1006/clim.2001.5114
69. Garcia-Quintanilla A. Overcoming viral escape with vaccines that generate and display antigen diversity in vivo. *Virol J* (2007) 4:125. doi:10.1186/1743-422X-4-125
70. Liu XS, Dyer J, Leggatt GR, Fernando GJ, Zhong J, Thomas R, et al. Overcoming original antigenic sin to generate new CD8 T cell IFN-gamma responses in an antigen-experienced host. *J Immunol* (2006) 177(5):2873–9. doi:10.4049/jimmunol.177.5.2873
71. Kim JH, Davis WG, Sambhara S, Jacob J. Strategies to alleviate original antigenic sin responses to influenza viruses. *Proc Natl Acad Sci U S A* (2012) 109(34):13751–6. doi:10.1073/pnas.0912458109
72. Ndifon W. A simple mechanistic explanation for original antigenic sin and its alleviation by adjuvants. *J R Soc Interface* (2015) 12(112):ii:20150627. doi:10.1098/rsif.2015.0627
73. Rapoport B, McLachlan SM. TSH receptor cleavage into subunits and shedding of the A-subunit; a molecular and clinical perspective. *Endocr Rev* (2016) 37:114–34. doi:10.1210/er.2015-1098
74. Saboori AM, Rose NR, Bresler HS, Vladut-Talor M, Burek CL. Iodination of human thyroglobulin (Tg) alters its immunoreactivity. I. Iodination alters multiple epitopes of human Tg. *Clin Exp Immunol* (1998) 113(2):297–302. doi:10.1046/j.1365-2249.1998.00643.x
75. Henry M, Malthiery Y, Zanelli E, Charvet B. Epitope mapping of human thyroglobulin. Heterogeneous recognition by thyroid pathologic sera. *J Immunol* (1990) 145(11):3692–8.
76. Saboori AM, Rose NR, Yuhasz SC, Amzel LM, Burek CL. Peptides of human thyroglobulin reactive with sera of patients with autoimmune thyroid disease. *J Immunol* (1999) 163(11):6244–50.
77. Duthoit C, Estienne V, Delom F, Durand-Gorde JM, Mallet B, Carayon P, et al. Production of immunoreactive thyroglobulin C-terminal fragments during thyroid hormone synthesis. *Endocrinology* (2000) 141(7):2518–25. doi:10.1210/endo.141.7.7573
78. Guo J, Yan X-M, McLachlan SM, Rapoport B. Search for the autoantibody immunodominant region on thyroid peroxidase: epitopic footprinting with a human monoclonal autoantibody locates a facet on the native antigen containing a highly conformational epitope. *J Immunol* (2001) 166:1327–33. doi:10.4049/jimmunol.166.2.1327
79. Guo J, McLachlan SM, Rapoport B. Localization of the thyroid peroxidase autoantibody immunodominant region to a junctional region containing portions of the domains homologous to complement control protein and myeloperoxidase. *J Biol Chem* (2002) 277(43):40189–95. doi:10.1074/jbc.M205524200
80. Bresson D, Pugniere M, Roquet F, Rebuffat SA, Guyen B, Cerutti M, et al. Directed mutagenesis in region 713-720 of human thyroperoxidase assigns 713KFPED717 residues as being involved in the B domain of the discontinuous immunodominant region recognized by human autoantibodies. *J Biol Chem* (2004) 279(37):39058–67. doi:10.1074/jbc.M403897200
81. Le SN, Porebski BT, McCoey J, Fodor J, Riley B, Godlewska M, et al. Modelling of thyroid peroxidase reveals insights into its enzyme function and autoantigenicity. *PLoS One* (2015) 10(12):e0142615. doi:10.1371/journal.pone.0142615
82. Nagayama Y, Wadsworth HL, Russo D, Chazenbalk GD, Rapoport B. Binding domains of stimulatory and inhibitory thyrotropin (TSH) receptor autoantibodies determined with chimeric TSH- lutropin/chorionic gonadotropin receptors. *J Clin Invest* (1991) 88:336–40. doi:10.1172/JCI115297
83. Sanders J, Chirgadze DY, Sanders P, Baker S, Sullivan A, Bhardwaja A, et al. Crystal structure of the TSH receptor in complex with a thyroid-stimulating autoantibody. *Thyroid* (2007) 17(5):395–410. doi:10.1089/thy.2007.0041
84. Sanders P, Young S, Sanders J, Kabelis K, Baker S, Sullivan A, et al. Crystal structure of the TSH receptor (TSHR) bound to a blocking-type TSHR autoantibody. *J Mol Endocrinol* (2011) 46(2):81–99. doi:10.1530/JME-10-0127
85. Thrasyvoulides A, Lymberi P. Evidence for intramolecular B-cell epitope spreading during experimental immunization with an immunogenic thyroglobulin peptide. *Clin Exp Immunol* (2003) 132(3):401–7. doi:10.1046/j.1365-2249.2003.02162.x
86. Thrasyvoulides A, Lymberi P. Antibodies cross-reacting with thyroglobulin and thyroid peroxidase are induced by immunization of rabbits with an immunogenic thyroglobulin 20mer peptide. *Clin Exp Immunol* (2004) 138(3):423–9. doi:10.1111/j.1365-2249.2004.02657.x
87. Estienne V, Duthoit C, Costanzo VD, Lejeune PJ, Rotondi M, Kornfeld S, et al. Multicenter study on TGPO autoantibody prevalence in various thyroid and non-thyroid diseases; relationships with thyroglobulin and thyroperoxidase autoantibody parameters. *Eur J Endocrinol* (1999) 141(6):563–9. doi:10.1530/eje.0.1410563
88. Latrofa F, Pichurin P, Guo J, Rapoport B, McLachlan SM. Thyroglobulin-thyroperoxidase autoantibodies are polyreactive, not bispecific: analysis using human monoclonal autoantibodies. *J Clin Endocrinol Metab* (2003) 88(1):371–8. doi:10.1210/jc.2002-021073
89. Flynn JC, Rao PV, Gora M, Alsharabi G, Wei W, Giraldo AA, et al. Graves' hyperthyroidism and thyroiditis in HLA-DRB1*0301 (DR3) transgenic mice after immunization with thyrotropin receptor DNA. *Clin Exp Immunol* (2004) 135(1):35–40. doi:10.1111/j.1365-2249.2004.02333.x
90. McLachlan SM, Nagayama Y, Pichurin PN, Mizutori Y, Chen CR, Misharin A, et al. The link between Graves' disease and Hashimoto's thyroiditis: a role for regulatory T cells. *Endocrinology* (2007) 148(12):5724–33. doi:10.1210/en.2007-1024
91. Chen CR, Hamidi S, Braley-Mullen H, Nagayama Y, Bresee C, Aliesky HA, et al. Antibodies to thyroid peroxidase arise spontaneously with age in NOD.H-2h4 mice and appear after thyroglobulin antibodies. *Endocrinology* (2010) 151(9):4583–93. doi:10.1210/en.2010-0321
92. Hutfless S, Matos P, Talor MV, Caturegli P, Rose NR. Significance of prediagnostic thyroid antibodies in women with autoimmune thyroid disease. *J Clin Endocrinol Metab* (2011) 96(9):E1466–71. doi:10.1210/jc.2011-0228
93. Tamai H, Kasagi K, Takaichi Y, Takamatsu J, Komaki G, Matsubayashi S, et al. Development of spontaneous hypothyroidism in patients with Graves' disease treated with antithyroidal drugs: clinical, immunological,

and histological findings in 26 patients. *J Clin Endocrinol Metab* (1989) 69(1):49–53. doi:10.1210/jcem-69-1-49
94. Shigemasa C, Mitani Y, Taniguch T, Adachi T, Ueta Y, Urabe K, et al. Three patients who spontaneously developed persistent hypothyroidism during or following treatment with antithyroid drugs for Graves' hyperthyroidism. *Arch Int Med* (1990) 150:1105–9. doi:10.1001/archinte.150.5.1105
95. Takasu N, Yamada T, Sato A, Nakagawa M, Komiya I, Nagasawa Y, et al. Graves' disease following hypothyroidism due to Hashimoto's disease: studies of eight cases. *Clin Endocrinol (Oxf)* (1990) 33(6):687–98. doi:10.1111/j.1365-2265.1990.tb03906.x
96. Kamath C, Young S, Kabelis K, Sanders J, Adlan MA, Furmaniak J, et al. Thyrotrophin receptor antibody characteristics in a woman with long-standing Hashimoto's who developed Graves' disease and pretibial myxoedema. *Clin Endocrinol (Oxf)* (2012) 77(3):465–70. doi:10.1111/j.1365-2265.2012.04397.x
97. Latrofa F, Fiore E, Rago T, Antonangeli L, Montanelli L, Ricci D, et al. Iodine contributes to thyroid autoimmunity in humans by unmasking a cryptic epitope on thyroglobulin. *J Clin Endocrinol Metab* (2013) 98(11):E1768–74. doi:10.1210/jc.2013-2912
98. Jacob JB, Kong YC, Nalbantoglu I, Snower DP, Wei WZ. Tumor regression following DNA vaccination and regulatory T cell depletion in neu transgenic mice leads to an increased risk for autoimmunity. *J Immunol* (2009) 182(9):5873–81. doi:10.4049/jimmunol.0804074
99. Rasooly L, Burek CL, Rose NR. Iodine-induced autoimmune thyroiditis in NOD-H2h4 mice. *Clin Immunol Immunopathol* (1996) 81:287–92. doi:10.1006/clin.1996.0191
100. Braley-Mullen H, Sharp GC, Medling B, Tang H. Spontaneous autoimmune thyroiditis in NOD.H-2h4 mice. *J Autoimmun* (1999) 12(3):157–65. doi:10.1006/jaut.1999.0272
101. Hutchings PR, Verma S, Phillips JM, Harach SZ, Howlett S, Cooke A. Both CD4(+) T cells and CD8(+) T cells are required for iodine accelerated thyroiditis in NOD mice. *Cell Immunol* (1999) 192(2):113–21. doi:10.1006/cimm.1998.1446
102. McLachlan SM, Aliesky H, Banuelos B, Que Hee SS, Rapoport B. Variable effects of dietary selenium in mice that spontaneously develop a spectrum of thyroid autoantibodies. *Endocrinology* (2017) 158(11):3754–64. doi:10.1210/en.2017-00275
103. Schwarz-Lauer L, Chazenbalk G, McLachlan SM, Ochi Y, Nagayama Y, Rapoport B. Evidence for a simplified view of autoantibody interactions with the TSH receptor. *Thyroid* (2002) 12(2):115–20. doi:10.1089/105072502753522347
104. Chazenbalk GD, Pichurin P, Chen CR, Latrofa F, Johnstone AP, McLachlan SM, et al. Thyroid-stimulating autoantibodies in Graves disease preferentially recognize the free A subunit, not the thyrotropin holoreceptor. *J Clin Invest* (2002) 110(2):209–17. doi:10.1172/JCI0215745
105. Furmaniak J, Sanders J, Rees SB. Blocking type TSH receptor antibodies. *Auto Immun Highlights* (2013) 4(1):11–26. doi:10.1007/s13317-012-0028-1
106. McLachlan SM, Aliesky HA, Banuelos B, Lesage S, Collin R, Rapoport B. High-level intrathymic thyrotrophin receptor expression in thyroiditis-prone mice protects against the spontaneous generation of pathogenic thyrotrophin receptor autoantibodies. *Clin Exp Immunol* (2017) 188(2):243–53. doi:10.1111/cei.12928
107. Misharin AV, Rapoport B, McLachlan SM. Thyroid antigens, not central tolerance, control responses to immunization in BALB/c versus C57BL/6 mice. *Thyroid* (2009) 19(5):503–9. doi:10.1089/thy.2008.0420
108. Kong YM, Brown NK, Morris GP, Flynn JC. The essential role of circulating thyroglobulin in maintaining dominance of natural regulatory T cell function to prevent autoimmune thyroiditis. *Horm Metab Res* (2015) 47(10):711–20. doi:10.1055/s-0035-1548872

Conflict of Interest Statement: The authors declare that the research was conducted in the absence of any commercial or financial relationships that could be construed as a potential conflict of interest.

The handling editor declared a past co-authorship with author SM.

frontiers in Immunology

ORIGINAL RESEARCH
published: 20 December 2017
doi: 10.3389/fimmu.2017.01816

Both Systemic and Intra-articular Immunization with Citrullinated Peptides Are Needed to Induce Arthritis in the Macaque

Samuel Bitoun[1,2], Pierre Roques[2], Thibaut Larcher[3], Gaétane Nocturne[1], Che Serguera[4], Pascale Chrétien[5], Guy Serre[6], Roger Le Grand[2] and Xavier Mariette[1,2]**

[1] Rheumatology Department, Université Paris-Sud, AP-HP, Hôpitaux Universitaires Paris-Sud, INSERM U1184, Le Kremlin Bicêtre, France, [2] Immunology of Viral Infections and Autoimmune Diseases, IDMIT Infrastructure CEA, Université Paris-Sud, INSERM U1184, Fontenay-Aux-Roses, France, [3] INRA UMR703 Veterinary School of Nantes, Nantes, France, [4] Modélisation des Biothérapies MIRCen, CEA/INSERM US27, Fontenay-Aux-Roses, France, [5] Immunology Department AP-HP, Hôpitaux Universitaires Paris-Sud, Le Kremlin Bicêtre, France, [6] "Epithelial Differentiation and Rheumatoid Autoimmunity" Unit, INSERM U1056, Université de Toulouse, Toulouse, France

OPEN ACCESS

Edited by:
Lisa Mullen,
Brighton and Sussex Medical School, United Kingdom

Reviewed by:
Ralf J. Ludwig,
University of Lübeck, Germany
Mary A. Markiewicz,
University of Kansas Medical Center, United States

***Correspondence:**
Samuel Bitoun
samuelbitoun@yahoo.fr;
Xavier Mariette
xavier.mariette@aphp.fr

Specialty section:
This article was submitted to Inflammation, a section of the journal Frontiers in Immunology

Received: 06 October 2017
Accepted: 01 December 2017
Published: 20 December 2017

Citation:
Bitoun S, Roques P, Larcher T, Nocturne G, Serguera C, Chrétien P, Serre G, Grand RL and Mariette X (2017) Both Systemic and Intra-articular Immunization with Citrullinated Peptides Are Needed to Induce Arthritis in the Macaque. Front. Immunol. 8:1816. doi: 10.3389/fimmu.2017.01816

Objectives: Anti-citrullinated peptides antibodies (ACPAs) have high specificity for the diagnosis of rheumatoid arthritis (RA), but their role in the pathophysiology is not fully established. The main genetic risk factor for RA, the shared epitope in major histocompatibility complex class II, is associated with ACPAs. Among certain non-human primates, 8% carry the shared epitope called H6 haplotype, and being similar to humans, are ideal candidates to study the role of ACPAs in RA. The goal of this study was to develop a macaque model of RA based on immunization against citrullinated peptides to generate an ACPA-mediated model of arthritis.

Methods: Cynomolgus macaques were immunized with four citrullinated peptides from vimentin, fibrinogen, and aggrecan, known to induce T-cell response in RA patients, and received an intra-articular (IA) boost with the same four citrullinated peptides pooled.

Results: In the macaque, the T-cell response was specific to citrullinated peptides. Antibodies generated in response to immunization were cross-reactive between the citrulline and arginine peptides. The presence of the H6 haplotype did not affect the magnitude of the immune response. Since no clinical response was observed, macaques received an IA boost with the same four peptides pooled and incomplete Freund's adjuvant, which led to a prolonged neutrophil-rich mono-arthritis, preferentially in H6-positive animals. Conversely, animals boosted with incomplete Freund's adjuvant alone presented only transient mono-arthritis.

Conclusion: This two-hit model of prolonged mono-arthritis mimics what could happen in RA. Despite the limited number of joints with disease in the macaque model, the model appears unique to study the events occurring during the preclinical phase of RA, from immunization against citrullinated peptides to the clinical appearance of disease.

Keywords: rheumatoid arthritis, ACPA, neutrophils, citrulline, shared epitope, macaque

INTRODUCTION

Rheumatoid arthritis (RA) is a debilitating disease that affects the joints and causes severe handicap. Posttranslational modification of arginine to citrulline residues occurs in a wide range of proteins during various inflammatory processes and might trigger an immune response against citrullinated epitopes generating autoantibodies (1). In RA, antibodies against citrullinated peptides (ACPAs) are frequent (75% of patients) and specific to the disease (up to 98% diagnosis specificity). This very high specificity for RA has led to the inclusion of ACPAs in the latest disease diagnostic criteria from the American College of Rheumatology/European League Against Rheumatism (ACR/EULAR 2010) (2).

The current paradox is that despite the high diagnostic value of ACPAs, their implication in the pathophysiology of RA is not fully established. For instance, in transgenic mice expressing the human major histocompatibility complex (MHC) class II shared epitope, arthritides have been induced with citrullinated peptides (3), but these results have been poorly reproduced and remain controversial (4). In humans, the shared epitope confers increased risk of RA and was also thought to increase ACPA level. The link has been suggested to rely on the increased affinity of some citrullinated peptides for the human leukocyte antigen (HLA) molecule as compared with the native unmodified peptides (5).

In a species of macaque, *Macaca fascicularis*, 8% naturally carry a version of the shared epitope. Previous macaque models of RA relied only on collagen immunization (6), which usually led to rapid severe joint destruction mimicking acute arthritis (7), which is far from the mechanism of RA pathogenesis in humans.

The purpose of this study was to set up an experimental macaque model of RA closer to the human disease than the currently available mouse models. Macaques carrying the shared epitope were immunized with different citrullinated peptides for presentation to T cells by the MHC molecule expressed in these animals. This model led to robust anti-citrullinated peptide T-cell and B-cell responses. A second-hit intra-articular (IA) injection of citrullinated peptides induced chronic articular inflammation only in previously immunized animals.

MATERIALS AND METHODS

Study Design

Ten animals were used in this study. We immunized four H6 animals (carrying the shared epitope) with citrullinated peptides ($n = 2$) or native arginine peptides ($n = 2$) and two non-H6 animals were immunized with citrullinated peptides. Four control animals were used: two without systemic immunization and two with intradermal immunization with recombinant human myelin oligodendrocyte glycoprotein (rhMOG). A summary of the design is in Table S1 in Supplementary Material.

Animals

Adult captive-bred 3- to 5-year-old female cynomolgus macaques (*M. fascicularis*) were used. The study was approved by the regional animal care and ethics committee (Comité Régional d'Ethique sur l'Expérimentation Animale Île de France Sud, Fontenay-Aux-Roses, France; decision #A13_026). The CEA Institute was approved as compliant with ETS123 recommendations for animal breeding (European Union Directive 2010/63/EU, September 22, 2010) and with Standards for Human Care and Use of Laboratory Animals (Animal Welfare Assurance, OLAW no. #A5826-01). The study was also approved by the French department of education and research (MENESR; study no. 02769.01) as defined in French law "décret 2013-118 from 2013 Feb 1st." At the end of each study, sedated animals were euthanized by intravenous injection of a lethal dose of pentobarbital.

Genotyping

Cynomolgus macaques (*M. fascicularis*) from Mauritius have a well-characterized genetic background and limited MHC diversity because of their isolation. Microsatellite analysis revealed six common haplotypes (H1–6) of MHC class II (8). The H6 genotype in the DRB1 region shares the same amino acid sequence as the 70–74 sequence of the human shared epitope DRB1 04-04 (QRRAA) (Table S2 in Supplementary Material). H6 animals were identified by a DNA microsatellite technique as described in Ref. (9). Presence of the shared epitope was confirmed after whole-blood RNA extraction with two specifically designed RT-PCR primers and probes followed by sequencing (Table S3 in Supplementary Material). Thus, the amino acid sequence on the macaque *Mafa* class II DRB alleles in positions 11 and 70–74 could be precisely identified.

Peptide Selection

Several proteins identified as targets of ACPAs include fibrinogen, vimentin, aggrecan, and enolase. Certain peptides from these proteins can induce a citrulline-specific T-cell response in patients with RA who carry the shared epitope (5, 10–12). We chose four peptides that are presented by DRB1 04-04 (5). These peptides originating from vimentin 59-71 (Vim59), vimentin 66-78 (Vim66) fibrinogen alpha chain 79-91 (Fg79), and aggrecan 89-103 (Agg89) (Table S4 in Supplementary Material) were synthesized in native or citrullinated form, the arginyl substituted by citrullyl residues (Genscript, Piscataway, NJ, USA).

Immunization

Monkeys were immunized intradermally, each peptide injected individually, at 500 µg/peptide. Peptides were adjuvated with CpG and Montanide® (kindly provided by Seppic, Puteaux, France) and injected in the back of the animals every 2 weeks for a total of four injections.

Immune Response

Peripheral blood mononuclear cells (PBMCs) were collected, and the T-cell response was assessed by comparing treatment with the pool of four citrullinated peptides used for immunization of animals to that of native peptides. T-cell response against citrullinated peptides and against arginine peptides was assessed using a macaque anti-interferon-gamma (IFNγ) Enzyme Linked Immunospot (ELISPOT) kit (Mabtech, Nacka Strand, Sweden). In total, 200 000 cells were exposed to a pool of 2 µg/mL of each peptide for 18 h. Positive controls were phorbol myristate acetate and ionomycin. Negative controls (cells with medium only)

were subtracted from the sample for each animal. Positive spots were defined as 40 wide with 20 intensity using an AID EliSpot reader (Autoimmun Diagnostika, Strassberg, Germany). B-cell response against citrullinated peptides and arginine peptides was assessed using an in-house-designed ELISA (13). Briefly, peptides were passively coated overnight. After washing, blocking was performed for 1 h at 4°C with 2% bovine serum albumin (BSA). After washing, serum diluted in 2% BSA was incubated for 1 h at 4°C. Goat anti-monkey IgG (BioRad, Watford, UK) was then added to wells and revealed using 3,3′,5,5′;-tetramethylbenzidine (Lifetech, Villebon Sur Yvette, France). Results are displayed as ratio of optical densities to the preimmunization state for each animal. Ratios >2 were considered positive. Cytokine analysis was performed on plasma collected in heparin lithium tubes using a non-human primate 23-cytokine multiplex assay (Millipore, Guyancourt, France, Table S5 in Supplementary Material).

IA Injection

Animals were injected in the right knee with the citrullinated peptides Vim59, Vim66, Fg79, and Agg89 with or without incomplete Freund's adjuvant (IFA) (Sigma-Aldrich, Saint-Quentin-Fallavier, France). Control animals were injected with IFA alone. Other control animals previously immunized with rhMOG (1–125) were injected intra-articularly with rhMOG + IFA. See experimental procedure in Method S6 in Supplementary Material.

Measurement of Clinical and Inflammatory Response

Clinical inflammation was scored from 0 to 4. Systemic inflammation was measured by plasma C-reactive protein (CRP) level. Blood counting was performed at each blood sampling using an HMX Hematology analyzer (Beckman Coulter, Villepinte, France).

Histology

Tissue samples were fixed in 4% formalin, embedded in paraffin wax or 2-hydroxyethyl(glycol)methacrylate, then transversally cut into 5-µm thick sections. Sections were stained by a routine hematoxylin–eosin–safranin staining method. All samples were evaluated by a skilled pathologist in a double-blind manner, and all lesions were systematically recorded. Serial additional sections of the knee joint were stained with safranin O/fast green for better observation of osteochondral structures (Histalim, Toulouse, France).

Statistics

When applicable, data were compared by non-parametric tests, and continuous values were compared by Mann–Whitney tests with GraphPad Prism 7. $P < 0.05$ was considered statistically significant.

RESULTS

Citrullinated Peptide Immunization Leads to a Citrulline-Specific Non-H6-Restricted T-Cell Response

At 4 and 13 weeks' postimmunization, T-cell response to the pool of citrullinated peptides was greater for animals immunized with the citrullinated peptides (4/4 animals) than arginine peptides (0/2 animals) (**Figure 1A**). Likewise, T-cell response to the pool of arginine peptides was greater for animals immunized with the arginine version of the peptides (2/2 animals) than the citrulline version (1/4 animals) (**Figure 1A**). Therefore, after intradermal immunization, the T-cell response was rather citrulline- or arginine-specific depending on the type of peptides used for immunization. Analysis of responses to individual peptides showed a high response to citrullinated Vim59 and native Agg89, whereas all animals showed low or no response to citrullinated or native Fg79-91 (data not shown). Of note, the magnitude of the T-cell response was similar for H6 and non-H6 carriers (**Figure 1B**). Thus, H6 and non-H6 animals immunized with citrullinated peptides were pooled in the following experiments.

B-Cell Response to Citrullinated Peptides Is Largely Cross-reactive

Serum antibody response against the four immunizing peptides was monitored individually during and after the immunization phase using ELISA. As for the T-cell response, the B-cell response, animals immunized with the citrulline or native version of the peptides were compared. All animals displayed a strong IgG response as compared with the preimmunization state (**Figure 2**). This response appeared between 4 and 6 weeks after the first immunization. For Vim59, the antibody response was systematically stronger against the citrullinated peptide than its arginine version (**Figure 2A**). However, the response was not exclusively dependent on citrullination because animals immunized with arginine peptides also showed a response against the citrullinated form (**Figures 2A–C**). In general, and contrary to the T-cell response, the B-cell response showed a high degree of cross-reactivity between antibodies against the citrullinated and the native peptide form, whatever the peptide used for immunization. Cross-reactivity was confirmed using an ELISA competition assay—preincubation with arginine or citrulline peptides inhibited anti-citrullinated response in a similar fashion (Figure S7 in Supplementary Material). Of note, all animals had a low or no response to citrullinated or native Fg79. Similar to the T-cell response, the presence of the shared epitope did not affect the B-cell response against the citrullinated or native version of peptides overall (Figure S8 in Supplementary Material).

IA Boost of Citrullinated Peptides Induces Mono-Arthritis in Animals Immunized against Citrullinated Peptides

During this first systemic immunization phase, despite a significant T- and B-cell response, no clinical manifestations of arthritis were noted. Because in humans, ACPA positivity can be asymptomatic for years before the occurrence of arthritis, second hits may be required to induce arthritis in immunized humans or animals. As a second hit, we chose unilateral injection of citrullinated peptides in the right knee 30 weeks after initial immunization. Five of the six animals previously immunized with citrullinated ($n = 3$) or arginine ($n = 2$) peptides were available for this second step. IA injection of citrullinated peptides without IFA did not

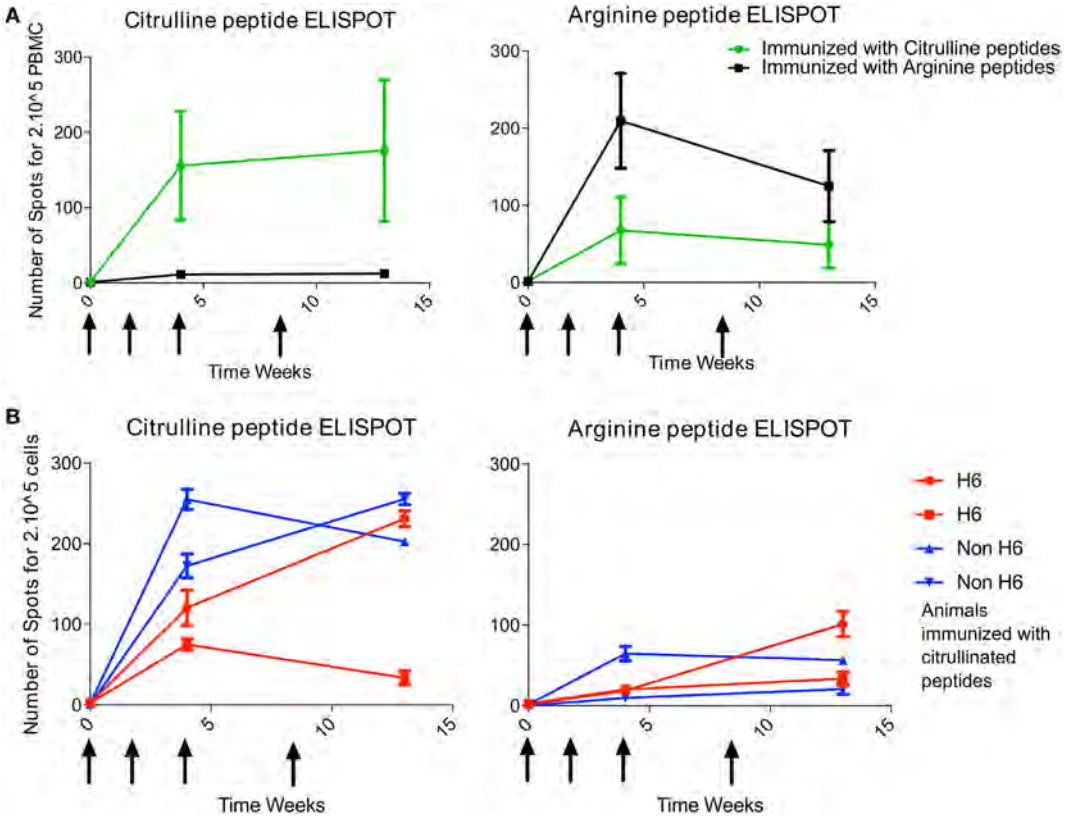

FIGURE 1 | T-cell response to immunization is citrulline dependent. Animals were immunized at weeks 0, 2, 4, and 8 (arrows) with pooled citrulline ($n = 4$) or arginine ($n = 2$) peptides: Vim59 and 66, Fg79, and Agg89. **(A)** Antigen-specific T-cell response of PBMCs was assessed by interferon-gamma (IFNγ) ELISPOT directed against the pool of the same citrullinated or arginine peptides. Data are mean ± SD values for individual animals (performed in triplicate). **(B)** H6 ($n = 2$) and non-H6 ($n = 2$) macaques were immunized with pooled Vim59 and 66, Fg79, and Agg89 peptides at weeks 0, 2, 4, and 8 (arrows). Antigen-specific T-cell response of PBMCs was assessed by IFNγ ELISPOT directed against the pool of the same citrullinated or arginine peptides. Data are mean ± SD for individual animals (performed in triplicate). PBMC, peripheral blood mononuclear cell; ELISPOT, Enzyme Linked Immunospot.

induce clinical signs or local immune response. Then, previously immunized animals were unilaterally injected in the right knee with IFA alone ($n = 2$) or citrullinated peptides + IFA ($n = 3$). IFA alone led to a 4-day unilateral knee swelling. Conversely, with IA injection of citrullinated peptides + IFA, two of three animals showed a 7-week unilateral swelling with joint effusion (**Figures 3A,B**). No other joint was clinically involved. This prolonged mono-arthritis resulted from both previous systemic immunization with citrullinated peptides and knee injection of citrullinated peptides + IFA. Indeed, the same knee injection of citrullinated peptides in two non-immunized animals led to a 4-day transient swelling similar to IFA injection alone.

To study the peptide specificity, IA injection of rhMOG + IFA in two animals previously immunized with rhMOG induced only mild transient swelling for 4 days, similar to that with IFA alone (**Figure 3A**). Finally, IA immunization with arginine peptides + IFA in a systemically citrullinated primed animal did not yield prolonged swelling. Therefore, only specific and citrullinated antigens could induce prolonged arthritis in an animal immunized against this antigen.

Among the three animals with an IA boost with citrullinated peptides, the two showing prolonged mono-arthritis were H6-positive and the one showing only a short episode of inflammation was not.

IA Boost with Citrullinated Peptides Induces a High Systemic Immune Response

The T-cell response was striking with IA boost with citrullinated peptides + IFA versus IFA alone (3/3 vs 0/2 animals) (**Figure 4A**). The magnitude of the response after IA boost was two to six times higher than after the intradermal prime, and three boosts with similar quantities of peptides and after late intradermal boost (**Figure 4B**). This response retained a degree of specificity to citrullinated peptides, with a higher response against these citrullinated peptides versus the pool of arginine peptides. Control animals receiving IA IFA alone showed no response. The B-cell response, which was high before the IA boost, was increased in one of the three animals receiving an IA boost with citrullinated peptides + IFA and in none of the others (**Figure 4C**).

The striking immune activation after the IA boost with citrullinated peptides + IFA but not IFA alone suggests that the prolonged articular swelling was due to an immune response against

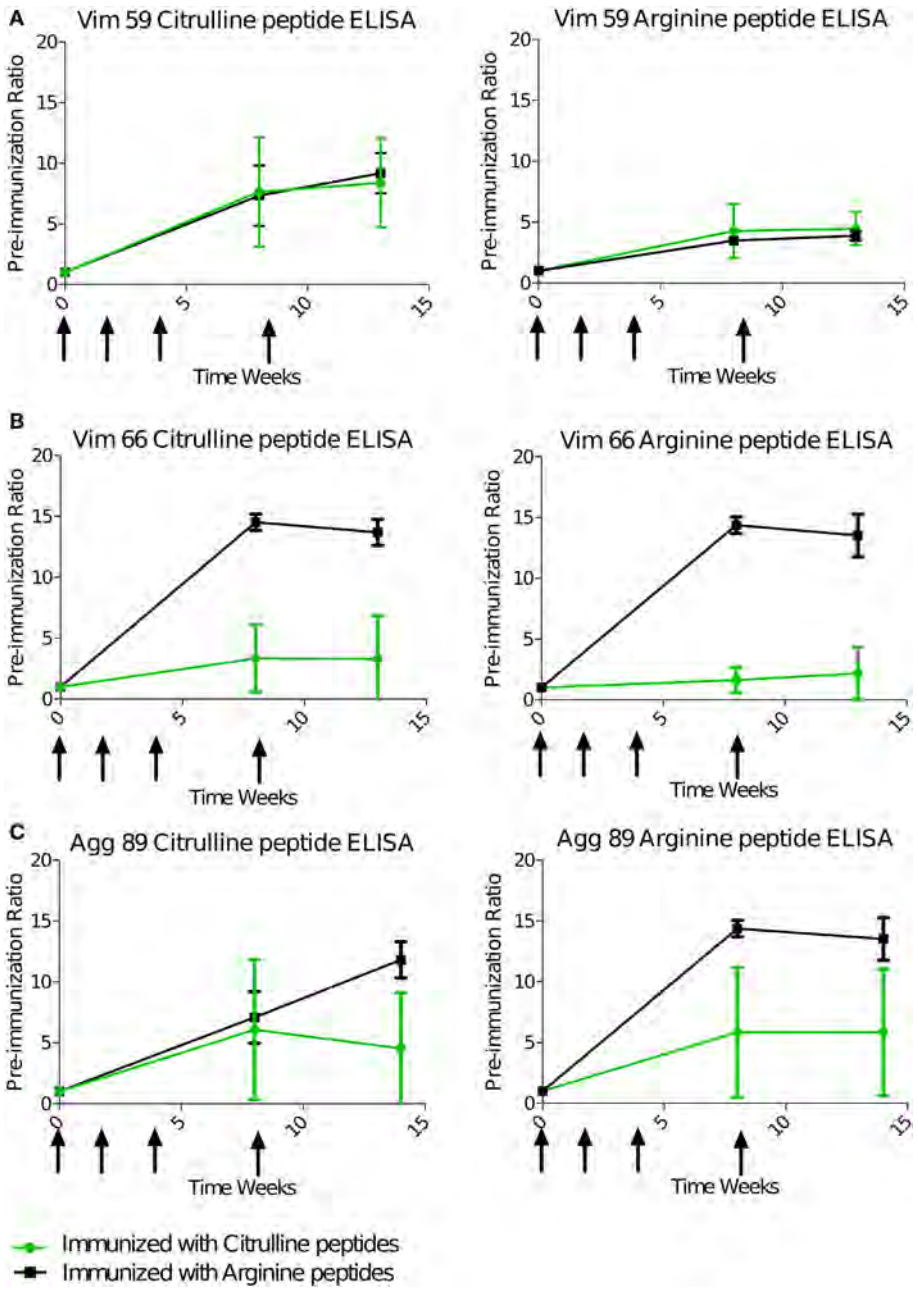

FIGURE 2 | B-cell response is cross-reactive to citrulline and arginine. Animals were immunized with pooled citrulline ($n = 4$) or arginine ($n = 2$), Vim59 and 66, Fg79, and Agg89 peptides at weeks 0, 2, 4, and 8 (arrows). Antibody levels in the serum were assessed by ELISA directed against Vim59 **(A)**, Vim66 **(B)**, and Agg89 **(C)** with cit (left) or arginine (right) except for Fg79 (no response). Data are mean ± SD ratio to the preimmunization state. cit, citrullinated.

the citrullinated peptides, whereas the transient swelling was due to a non-specific inflammatory response to IFA.

This finding is further emphasized by the level of systemic inflammation measured by CRP level in serum at day 1 after the boost. CRP level was higher for animals that received an IA boost with citrullinated peptides + IFA than IFA alone (3/3 animals > 100 mg/mL vs 2/2 animals < 60 mg/mL). rhMOG + IFA or citrullinated peptides + IFA, without a previous prime; all displayed significantly lower levels of CRP (**Figure 5A**).

This increase in CRP level occurred at the same time (day 1) as a reduced lymphocyte count and an increased neutrophil cell count in blood (**Figure 5B**). Among a panel of 23 analyzed cytokines (Table S5 in Supplementary Material), a significant increase in ratio of circulating cytokines on day 1 to the pre-IA injection level was limited to proinflammatory and angiogenic cytokines [interleukin (IL)-6, IL-1B, IL1-RA, and VEGF] and granulocyte-stimulating chemokines (GM-CSF and MIP1A) in animals that received an IA boost with citrullinated peptides + IFA versus IFA alone (**Figure 5C**).

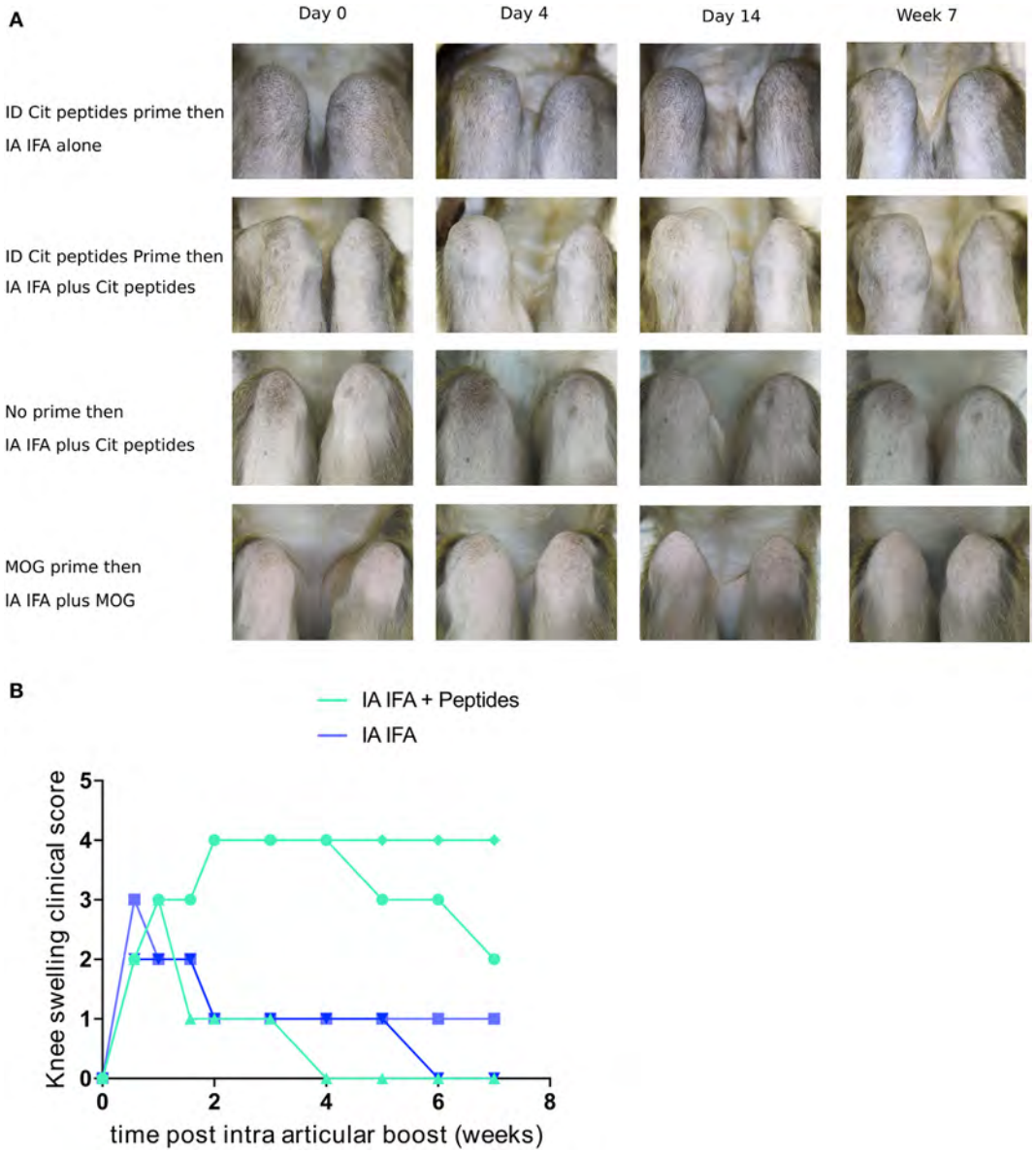

FIGURE 3 | IA boost with citrullinated peptides leads to prolonged articular swelling. **(A)** Animals previously immunized with citrullinated peptides were boosted with IFA alone or citrullinated peptides + IFA in the right knee (upper two panels). Other control groups were (1) naïve animals injected with citrullinated peptides + IFA and (2) rhMOG-primed animals boosted intra-articularly with rhMOG + IFA (lower two panels). Weekly clinical monitoring of both knees is summarized with key time points. Photographs show 90° flexed right knees on the left side of the pictures. **(B)** Semi-quantitative longitudinal clinical evaluation of knee swelling for each animal with previous prime. Comparison between IFA alone and IA with citrullinated peptides + IFA. IFA, incomplete Freund's adjuvant; IA, intra-articular; cit, citrullinated; rhMOG, recombinant human myelin oligodendrocyte glycoprotein.

IA Boost with Citrullinated Peptides Induces Mono-Arthritis

Articular swelling was confirmed by taping effusion liquid. During the first phase of aspecific swelling that appeared in most animals, low cellularity with a predominance of granulocytes occurred (**Figure 5D** left panel). At later times (7–14 days postinjection), animals with prolonged swelling upon IFA + peptide injection presented high cellularity (**Figure 5D** middle and right panel).

Histological analysis of the synovial tissue of the injected knee performed at euthanasia 15 weeks after articular challenge revealed different types of lesions in the injected knee without any clear differences between an IA boost with citrullinated peptides + IFA or IFA alone: unspecific adjuvant-related granulomas (**Figure 6A**), diffuse mononuclear-cell and granulocyte infiltration of the synovial layer (**Figure 6B**) with lymphocyte infiltration foci (**Figure 6C**), and synovial proliferation (**Figures 6D,E**) without any bone or cartilage

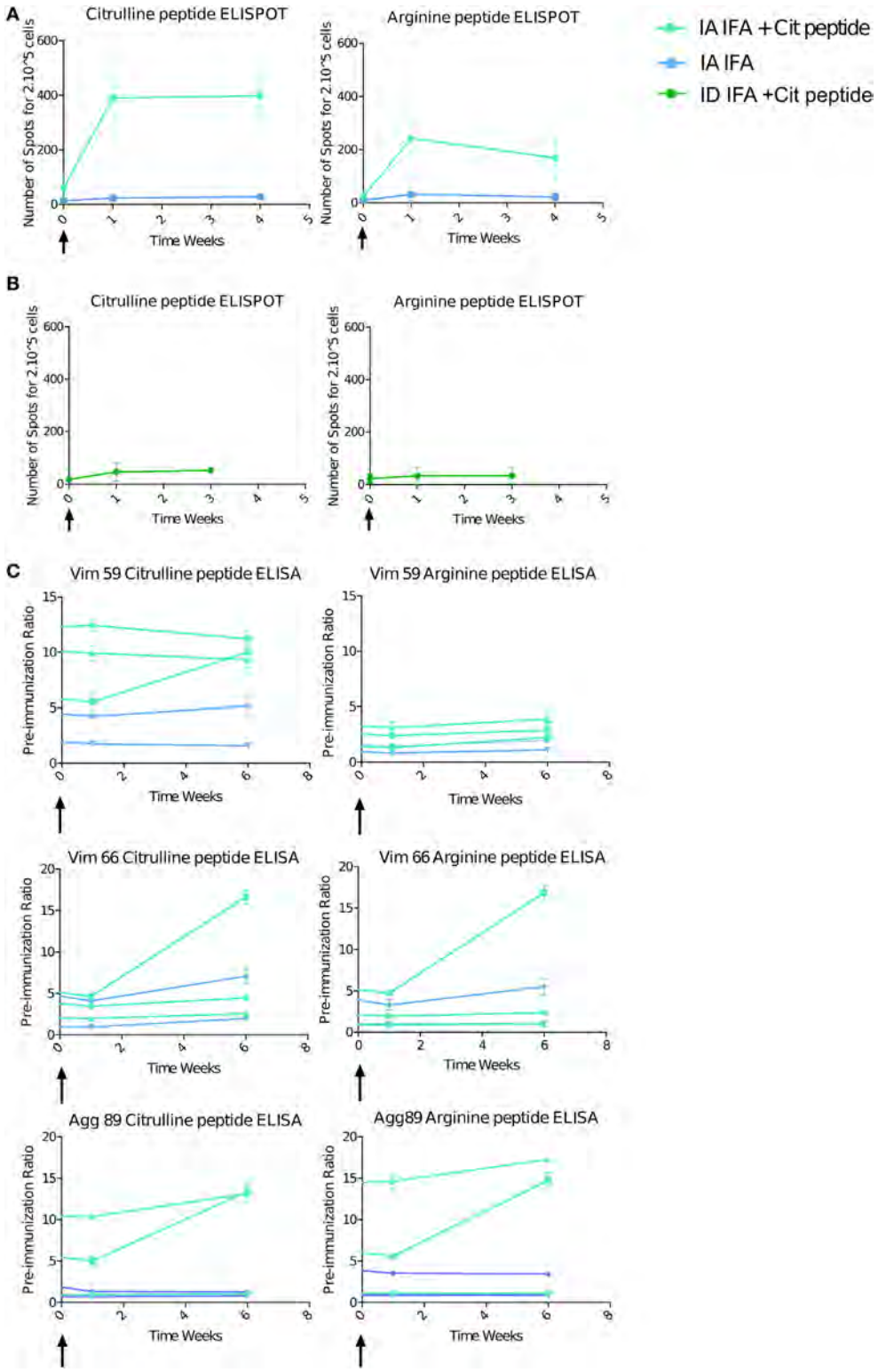

FIGURE 4 | Intra-articular (IA) boost with citrullinated peptides and incomplete Freund's adjuvant (IFA) induces a strong immune response. At 30 weeks' post-initial prime, animals received an IA boost with pooled citrullinated Vim59 and 66, Fg79, and Agg89 plus IFA ($n = 3$) or IFA alone ($n = 2$). **(A)** T-cell response assessed by interferon-gamma (IFNγ) Enzyme Linked Immunospot (ELISPOT) against the pooled citrullinated or arginine pool of peptide. Data are mean ± SD values for individual animals (performed in triplicate). **(B)** At 34 weeks' postimmunization, two animals were intradermally boosted with the same citrullinated peptide pool, and response was assessed by IFNγ ELISPOT. **(C)** ELISA of B-cell response against Vim59 and 66, Fg79 and Agg89 in their citrullinated and arginine form. Data are mean ± SD values for individual animals (performed in triplicate). The time scale is shown as time post-IA injection.

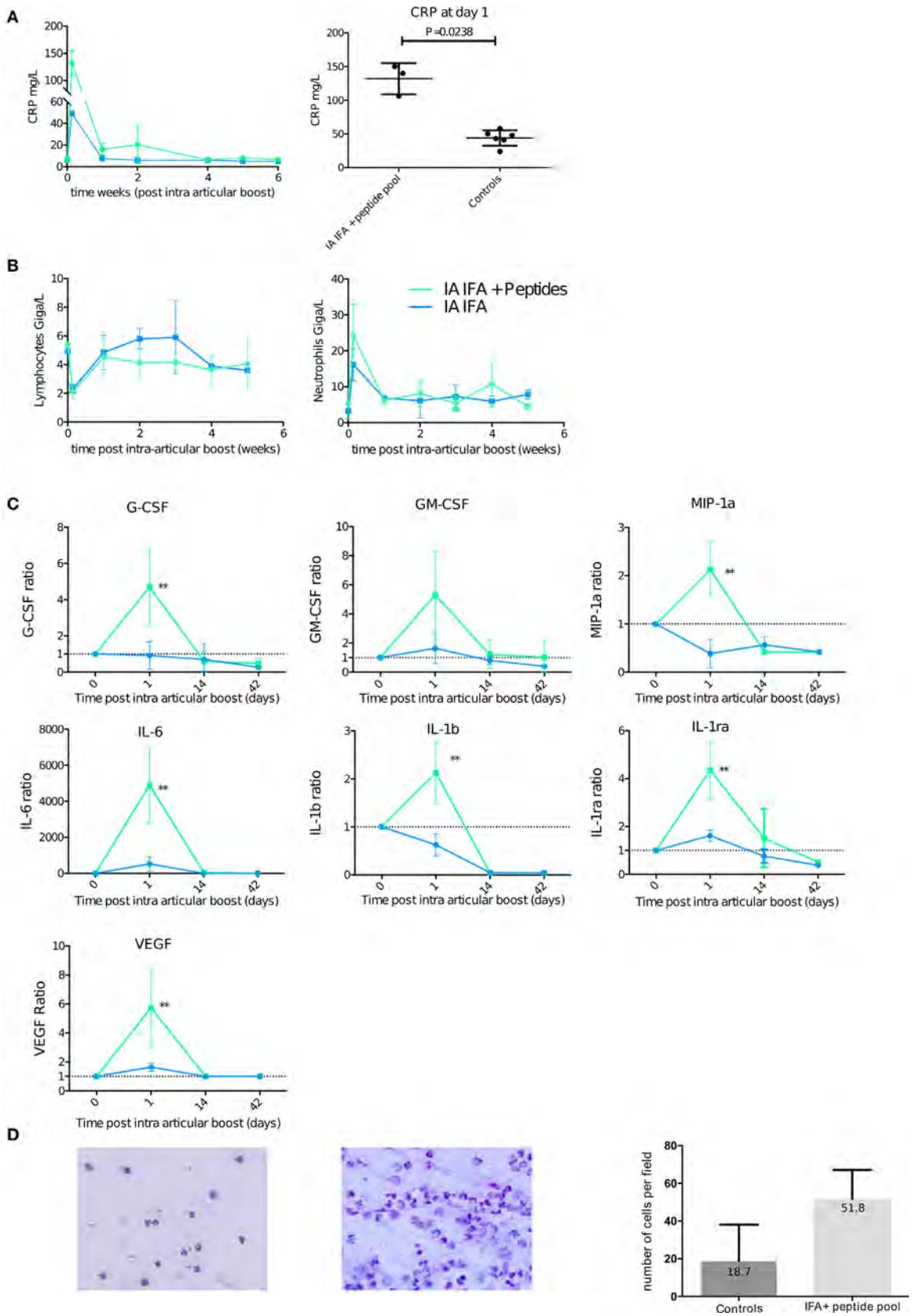

FIGURE 5 | Continued

FIGURE 5 | Intra-articular (IA) boost leads to systemic inflammation favoring neutrophilic joint effusion. At 30 weeks post-initial prime, animals received an IA boost with pooled citrullinated Vim59 and 66, Fg79, and Agg89 plus incomplete Freund's adjuvant (IFA) ($n = 3$) or IFA alone ($n = 2$) as a control. **(A)** Left panel: Plasma C-reactive protein (CRP) level with citrullinated peptides + IFA and IFA alone. Right panel: Plasma CRP level for citrullinated peptides + IFA and all controls at day 1 post-IA boost (Mann–Whitney test). **(B)** Complete blood counts of lymphocyte and neutrophils after IA boost with citrullinated peptides + IFA and IFA alone. **(C)** Non-human primate multiplex 23-cytokine array after IA boost with citrullinated peptides + IFA and IFA alone. Data are ratio of levels to the pre-IA injection level. $^{**}P < 0.001$ Mann–Whitney test. **(D)** Synovial fluid smears stained with May-Grünwald Giemsa showing typical cellular counts of transient swelling with IFA alone 4 days post-IA injection (left panel) and citrullinated peptides + IFA 14 days post-IA boost (middle panel). 20× magnification. Quantification of at least five high power fields of synovial fluid smears comparing animals with transient swelling on IFA injection (controls) and those who received citrullinated peptides + IFA and presented prolonged swelling. Data are mean ± SD.

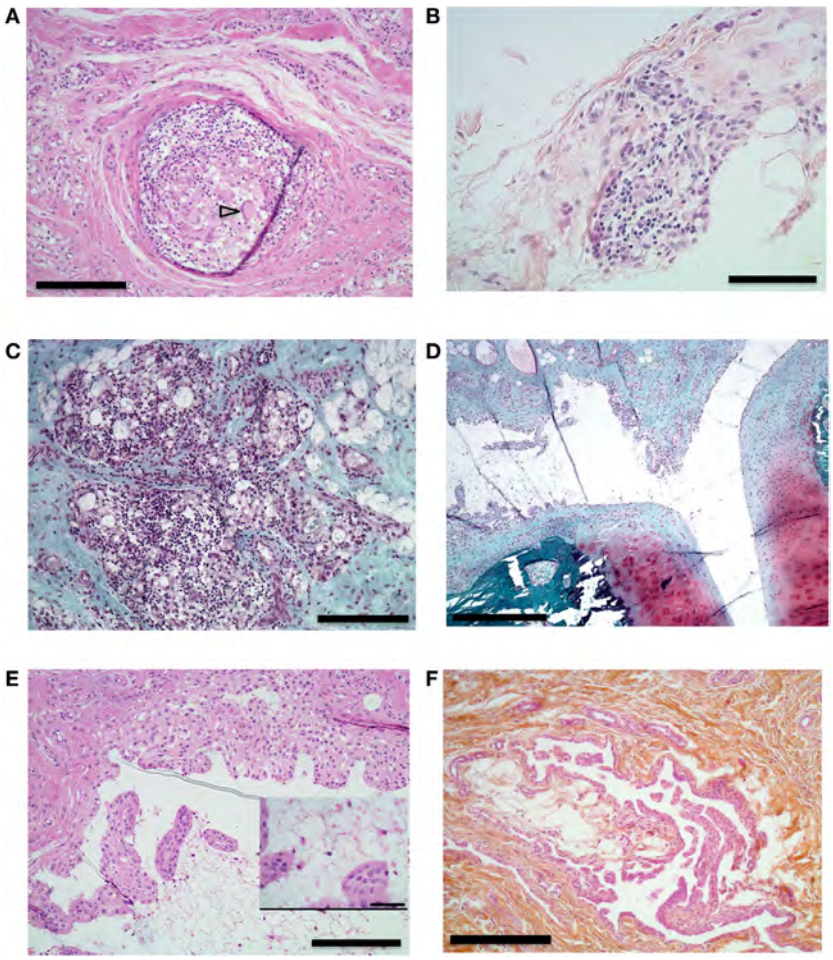

FIGURE 6 | Histological analysis of synovial proliferation. Sections with hematoxylin eosin **(A,B,E,F)** or safranin O and Fast Green **(C,D)** stain. **(A)** Synovial membrane of knee of an animal that received intra-articular (IA) injection containing incomplete Freund's adjuvant (IFA). Arrowhead shows multinucleated gigantic cell. 10× magnification, bar 200 µm. **(B)** Synovial membrane of right knee of an animal that received IA boost with citrullinated peptides + IFA and presented prolonged swelling. 20× magnification, bar 100 µm. **(C)** Knee synovial membrane. 10× magnification, bar 200 µm. **(D)** Knee synovial membrane, bone, and cartilage of the same animal. 4× magnification, bar 500 µm. **(E)** Right knee synovial membrane of an animal that received an IA boost with citrullinated peptides + IFA and presented prolonged swelling. Insert shows fibrin and leukocyte in the synovial cleft. 10× magnification, bar: 200 µm, insert bar 50 µm. **(F)** Section of metacarpophalangeal joint synovial membrane of an animal without clinically identified manifestation on these joints. 10× magnification bar 200 µm.

lesions (**Figure 6D**). Finally, systematic sampling of metacarpophalangeal and metatarsophalangeal joints revealed synovial proliferation in two animals with citrullinated peptides + IFA injection (**Figure 6F**): the animal that died prematurely and thus did not receive the IA boost and an animal with prolonged knee swelling after IA boost with citrullinated peptides + IFA. These last histological lesions were present despite the absence of clinical swelling in these joints.

DISCUSSION

In this study, we show that intradermal immunization followed by an IA boost with citrullinated peptides can induce a prolonged local synovitis in macaques. This persistent mono-arthritis was restricted to animals previously primed intradermally with a pool of four citrullinated peptides (Vim59-71, Vim66-78, Fg79-91, and Agg89-103). Our model displays many aspects of RA including clinical swelling and pertinent biological modifications with the limitation of a mono-articular disease. Synovial effusion parallels the human disease as it shows high neutrophil predominance.

This study shows clear evidence that the T-cell response against injected peptides is specific to citrullinated peptides. By contrast, the B-cell response to the peptides was largely cross-reactive between citrullinated and native peptides. Citrullinated peptides that react with specific T cells in RA patients may not be able to induce a citrulline-specific B-cell response in macaques. Of note, these peptides present only one posttranslational modification from arginine to citrulline. The cross-reactivity of the B-cell response could simply result from reactivity to epitopes independent of arginine/citrulline and shared by each form of the peptides. However, even in human disease, cross-reactivity of the B-cell response between citrullinated and arginine peptides has been frequently described. In the natural history of the disease, antibodies to some citrullinated peptides can be preceded by antibodies against the arginine counterpart (14, 15). This is also true in mice, because immunization with alpha-enolase induces arthritis with the citrullinated or native forms of the protein (16). Our model forces the generation of antibodies to citrullinated peptides as compared with the natural history of the disease and might need other stimuli to select the clones directed to citrullinated epitopes. Interestingly, in human RA, the clinical signs could appear only after maturation of the B-cell response by epitope spreading against different targets of citrullinated peptides resulting from somatic mutations (17). This maturation might be accompanied by the disappearance of the response to native peptides. The absence of maturation of ACPAs in our model could explain the absence of clinical signs in the first phase of the study before the IA boost.

We based our model on the identity of the H6 genotype of the macaques with one of the human shared epitopes—HLA DRB 01*01 for the 70–74 amino acids (QRRAA). However, comparison of the B- and T-cell response to the peptides did not show a clear effect of the H6 haplotype on the magnitude of the immune response to citrullinated peptides measured as specific antibody titers or specific IFNγ ELISPOT response, respectively. This could be considered surprising given what is usually admitted that there is a better presentation of citrullinated peptides by the shared epitope However, this assumption based on only two studies (3, 5) is still debated. Another study (18) that systematically analyzed T-cell reactivity to peptides derived from the whole alpha and beta chains of fibrinogen in RA patients did not confirm these results and showed that depending on the peptide, the citrullinated form can be more, equally or less reactive than its arginine counterpart. Finally, since we did not use anti-MHC blocking antibodies to block the reaction, we cannot eliminate the possibility that the IFN production we found could have been secreted by T cells not activated through MHC or by other PBMC like NK cells.

Moreover, a recent study of twins showed that bearing the shared epitope most likely favors declaring clinical signs of ACPA-positive RA [odds ratio (OR) 5.65 (95% CI 3.03–10.52)] rather than developing asymptomatic ACPAs alone [OR 1.85 (1.41–2.42)] (19). Among the three animals in our study with an IA boost of citrullinated peptides, only the two H6-positive animals showed prolonged articular swelling. Another explanation for the absence of the H6-carriage effect is that recent literature has highlighted the importance of the presence of the valine in the 11th position (20) with a relative influence of the 70–74 amino acids. The H6 haplotype displays a phenylalanine rather than a valine in the 11th position. Moreover, heterozygous carriage of the shared epitope (as for our animals) only moderately increases the risk of ACPAs [OR 1.85 (1.42–2.42)] as compared with homozygous carriers [OR 3.74 (2.7–5.18)] (19). Finally, interpretations about the effect of the H6 carriage must remain cautious because we only studied two H6 and two non-H6 animals injected with citrullinated peptides. A larger number of animals in each group would be needed to confirm these results, but studies on macaque are not easy to conduct.

One of the most interesting results of our study is the requirement of a multistep process to induce clinical symptoms, in favor of the second-hit hypothesis (21). The IA injection of the citrullinated peptides that had been used for the intradermic prime was chosen as a second hit. Surprisingly, the T-cell response induced by the IA boost was markedly more efficient than an intradermal boost. A similar strong systemic response has been described in staphylococcal septic arthritis (22, 23). However, a simple articular injection of peptides without previous immunization was inefficient to induce clinical signs. The requirement of adjuvant IFA suggests that transient local inflammation is necessary to trigger a prolonged effect linked to a specific immune response. With this IA boost strategy, long-term mono-arthritis developed in two of the three animals injected with citrullinated peptides + IFA. This clinical manifestation displayed many features of the human disease, including swelling and articular effusion, but limited to a single joint. Even if IFA was required, the role of a specific response against anti-citrullinated peptides was demonstrated by (1) an extended duration of arthritis as compared with the transient inflammation induced by IFA alone, (2) the requirement for a previous intradermic immunization with citrullinated peptides, and (3) the absence of prolonged arthritis in animals previously intradermally immunized with rhMOG protein and receiving an IA boost with rhMOG + IFA. These findings suggest that the citrullinated proteins may be a tissue-specific articular target on the RA joint inflammation and need to be locally present to perpetuate the clinical response. Indeed, fibrinogen (24), vimentin (25), and aggrecan (10) but not rhMOG are present in the joint and are citrullinated in the presence of inflammation, which perpetuates the immune response and possibly the clinical manifestation. Antigen specificity and not non-specific Arthus phenomenon or immune complexes seem involved here because the same course of immunization with rhMOG did not induce arthritis.

The main limitation of the current model is its restriction to clinical mono-arthritis despite a specific T-cell response associated with a strong systemic immune response after IA injection. However, histological analysis showed synovial tissue proliferation in joints distant from the knee, which suggests initiation of diffuse joint inflammation similar to human RA. The systemic inflammation, assessed by increased blood neutrophil count and serum CRP level, does not seem sufficient to cause clinically relevant joint inflammation in other non-injected joints. Neutrophils, which are probably implicated in the pathophysiology of RA (26), were present in the affected joint of our model. Such an acute inflammation leading to neutrophil extracellular trap (NET) or NETosis, could enhance citrullination of local proteins, making them targets for ACPAs and permitting the formation of ACPA immune complexes, responsible for the perpetuation of local inflammation (27, 28). To improve this model, an objective could be to initiate joint inflammation using viral infection to favor migration of neutrophils to other joints. IL-8 could be a good candidate for this spread because it attracts neutrophils and was found released by patient-derived osteoclasts (29). However, despite the absence of clinical polyarthritis, we observed elevated blood neutrophil count in the two animals with long-term mono-arthritis. As discussed previously, the absence of maturation of the ACPAs could, at least, be part of the explanation. Nevertheless, the histological examination of metacarpophalangeal and metatarsophalangeal joints in two animals immunized with citrullinated peptides displayed a synovial proliferation very similar to what is observed in human RA. This histological abnormality was not clinically detectable. Ultrasonography would thus be required for the follow-up of the animals in further experiments.

CONCLUSION

Immunization of macaques with citrullinated peptides followed by an IA boost with the same citrullinated peptides plus IFA induced prolonged mono-arthritis. The presence of the shared epitope did not restrict the T-cell response against citrullinated peptides but seemed to favor the prolonged swelling after the IA boost. This two-step model of prolonged mono-arthritis mimics what could happen in human RA except that the animals develop mono-arthritis and not polyarthritis. Further use of systemic viral infection and a neutrophil chemoattractant might lead to a polyarticular disease. Nevertheless, this model appears interesting to study the events occurring during the preclinical phase of RA from immunization against citrullinated peptides to development of the clinical disease.

ETHICS STATEMENT

This study was carried out in accordance with the recommendations of "European Union Directive 2010/63/EU, 2010." The protocol was approved by the "Comité Régional d'Ethique sur l'Expérimentation Animale Île de France Sud, Fontenay-Aux-Roses, France."

AUTHOR CONTRIBUTIONS

SB, PR, TL, GN, CS, PC, GS, RG, and XM made substantial contributions to study conception and design, and analysis and interpretation of data and gave final approval of the article. SB, PR, TL, PC, and CS made substantial contributions to acquisition of data. SB, PR, CS, GS, RG, and XM drafted the article for important intellectual content.

FUNDING

This work was supported by French government "Programme d'Investissements d'Avenir" under [Grant number ANR-11-INBS-0008] funding the Infectious Disease Models and Innovative Therapies (IDMIT, Fontenay-aux-Roses, France) infrastructure; and two Ph.D. grants from Société Française de Rhumatologie and INSERM. The authors warmly thank the IDMIT infrastructure staff for excellent technical assistance. The IDMIT infrastructure and its FlowCyTech facility are supported by the French government "Programme d'Investissements d'Avenir" (PIA), under grants ANR-11-INBS-0008 and ANR-10-EQPX-02-01, respectively.

SUPPLEMENTARY MATERIAL

The Supplementary Material for this article can be found online at http://www.frontiersin.org/articles/10.3389/fimmu.2017.01816/full#supplementary-material.

REFERENCES

1. Ludwig RJ, Vanhoorelbeke K, Leypoldt F, Kaya Z, Bieber K, McLachlan SM, et al. Mechanisms of autoantibody-induced pathology. *Front Immunol* (2017) 8:603. doi:10.3389/fimmu.2017.00603
2. Aletaha D, Neogi T, Silman AJ, Funovits J, Felson DT, Bingham CO, et al. 2010 Rheumatoid arthritis classification criteria: an American College of Rheumatology/European League Against Rheumatism collaborative initiative. *Arthritis Rheum* (2010) 62:2569–81. doi:10.1002/art.27584
3. Hill JA, Bell DA, Brintnell W, Yue D, Wehrli B, Jevnikar AM, et al. Arthritis induced by posttranslationally modified (citrullinated) fibrinogen in DR4-IE transgenic mice. *J Exp Med* (2008) 205:967–79. doi:10.1084/jem.20072051
4. Cantaert T, Teitsma C, Tak PP, Baeten D. Presence and role of anti-citrullinated protein antibodies in experimental arthritis models. *Arthritis Rheum* (2012) 65:939–48. doi:10.1002/art.37839
5. Scally SW, Petersen J, Law SC, Dudek NL, Nel HJ, Loh KL, et al. A molecular basis for the association of the HLA-DRB1 locus, citrullination, and rheumatoid arthritis. *J Exp Med* (2013) 210:2569–82. doi:10.1084/jem.20131241
6. Bakker NP, van Erck MG, Botman CA, Jonker M, 't Hart BA. Collagen-induced arthritis in an outbred group of rhesus monkeys comprising responder and nonresponder animals. Relationship between the course of arthritis and collagen-specific immunity. *Arthritis Rheum* (1991) 34:616–24. doi:10.1002/art.1780340514

7. Yoo TJ, Kim SY, Stuart JM, Floyd RA, Olson GA, Cremer MA, et al. Induction of arthritis in monkeys by immunization with type II collagen. *J Exp Med* (1988) 168:777–82. doi:10.1084/jem.168.2.777
8. O'Connor SL, Blasky AJ, Pendley CJ, Becker EA, Wiseman RW, Karl JA, et al. Comprehensive characterization of MHC class II haplotypes in Mauritian cynomolgus macaques. *Immunogenetics* (2007) 59:449–62. doi:10.1007/s00251-007-0209-7
9. Blancher A, Tisseyre P, Dutaur M, Apoil P-A, Maurer C, Quesniaux V, et al. Study of cynomolgus monkey (*Macaca fascicularis*) MhcDRB (Mafa-DRB) polymorphism in two populations. *Immunogenetics* (2006) 58:269–82. doi:10.1007/s00251-006-0102-9
10. von Delwig A, Locke J, Robinson JH, Ng W-F. Response of Th17 cells to a citrullinated arthritogenic aggrecan peptide in patients with rheumatoid arthritis. *Arthritis Rheum* (2010) 62:143–9. doi:10.1002/art.25064
11. Snir O, Rieck M, Gebe JA, Yue BB, Rawlings CA, Nepom G, et al. Identification and functional characterization of T cells reactive to citrullinated vimentin in HLA-DRB1*0401-positive humanized mice and rheumatoid arthritis patients. *Arthritis Rheum* (2011) 63:2873–83. doi:10.1002/art.30445
12. Law SC, Street S, Yu C-HA, Capini C, Ramnoruth S, Nel HJ, et al. T-cell autoreactivity to citrullinated autoantigenic peptides in rheumatoid arthritis patients carrying HLA-DRB1 shared epitope alleles. *Arthritis Res Ther* (2012) 14:R118. doi:10.1186/ar3848
13. Sebbag M, Moinard N, Auger I, Clavel C, Arnaud J, Nogueira L, et al. Epitopes of human fibrin recognized by the rheumatoid arthritis-specific autoantibodies to citrullinated proteins. *Eur J Immunol* (2006) 36:2250–63. doi:10.1002/eji.200535790
14. Brink M, Hansson M, Rönnelid J, Klareskog L, Rantapää Dahlqvist S. The autoantibody repertoire in periodontitis: a role in the induction of autoimmunity to citrullinated proteins in rheumatoid arthritis? Antibodies against uncitrullinated peptides seem to occur prior to the antibodies to the corresponding citrullinated peptides. *Ann Rheum Dis* (2014) 73:e46. doi:10.1136/annrheumdis-2014-205498
15. de Pablo P, Dietrich T, Chapple ILC, Milward M, Buckley CD, Venables PJ. The autoantibody repertoire in periodontitis: a role in the induction of autoimmunity to citrullinated proteins in rheumatoid arthritis? Antibodies against uncitrullinated peptides seem to occur prior to the antibodies to the corresponding citrullinated peptides. *Ann Rheum Dis* (2014) 73:e47. doi:10.1136/annrheumdis-2014-205519
16. Kinloch AJ, Alzabin S, Brintnell W, Wilson E, Barra L, Wegner N, et al. Immunization with *Porphyromonas gingivalis* enolase induces autoimmunity to mammalian α-enolase and arthritis in DR4-IE-transgenic mice. *Arthritis Rheum* (2011) 63:3818–23. doi:10.1002/art.30639
17. Amara K, Steen J, Murray F, Morbach H, Fernandez-Rodriguez BM, Joshua V, et al. Monoclonal IgG antibodies generated from joint-derived B cells of RA patients have a strong bias toward citrullinated autoantigen recognition. *J Exp Med* (2013) 210:445–55. doi:10.1084/jem.20121486
18. Auger I, Sebbag M, Vincent C, Balandraud N, Guis S, Nogueira L, et al. Influence of HLA-DR genes on the production of rheumatoid arthritis-specific autoantibodies to citrullinated fibrinogen. *Arthritis Rheum* (2005) 52:3424–32. doi:10.1002/art.21391
19. Hensvold AH, Magnusson PKE, Joshua V, Hansson M, Israelsson L, Ferreira R, et al. Environmental and genetic factors in the development of anticitrullinated protein antibodies (ACPAs) and ACPA-positive rheumatoid arthritis: an epidemiological investigation in twins. *Ann Rheum Dis* (2015) 74:375–80. doi:10.1136/annrheumdis-2013-203947
20. Viatte S, Plant D, Han B, Fu B, Yarwood A, Thomson W, et al. Association of HLA-DRB1 haplotypes with rheumatoid arthritis severity, mortality, and treatment response. *JAMA* (2015) 313:1645–56. doi:10.1001/jama.2015.3435
21. Catrina AI, Joshua V, Klareskog L, Malmström V. Mechanisms involved in triggering rheumatoid arthritis. *Immunol Rev* (2016) 269:162–74. doi:10.1111/imr.12379
22. Deng GM, Nilsson IM, Verdrengh M, Collins LV, Tarkowski A. Intra-articularly localized bacterial DNA containing CpG motifs induces arthritis. *Nat Med* (1999) 5:702–5. doi:10.1038/9554
23. Tarkowski A. Infectious arthritis. *Best Pract Res Clin Rheumatol* (2006) 20:1029–44. doi:10.1016/j.berh.2006.08.001
24. Masson-Bessière C, Sebbag M, Girbal-Neuhauser E, Nogueira L, Vincent C, Senshu T, et al. The major synovial targets of the rheumatoid arthritis-specific antifilaggrin autoantibodies are deiminated forms of the alpha- and beta-chains of fibrin. *J Immunol* (2001) 166:4177–84. doi:10.4049/jimmunol.166.6.4177
25. Snir O, Widhe M, Hermansson M, von Spee C, Lindberg J, Hensen S, et al. Antibodies to several citrullinated antigens are enriched in the joints of rheumatoid arthritis patients. *Arthritis Rheum* (2010) 62:44–52. doi:10.1002/art.25036
26. Grayson PC, Schauer C, Herrmann M, Kaplan MJ. Review: neutrophils as invigorated targets in rheumatic diseases. *Arthritis Rheumatol* (2016) 68:2071–82. doi:10.1002/art.39745
27. Khandpur R, Carmona-Rivera C, Vivekanandan-Giri A, Gizinski A, Yalavarthi S, Knight JS, et al. NETs are a source of citrullinated autoantigens and stimulate inflammatory responses in rheumatoid arthritis. *Sci Transl Med* (2013) 5:178ra40. doi:10.1126/scitranslmed.3005580
28. Clavel C, Nogueira L, Laurent L, Iobagiu C, Vincent C, Sebbag M, et al. Induction of macrophage secretion of tumor necrosis factor alpha through Fcgamma receptor IIa engagement by rheumatoid arthritis-specific autoantibodies to citrullinated proteins complexed with fibrinogen. *Arthritis Rheum* (2008) 58:678–88. doi:10.1002/art.23284
29. Krishnamurthy A, Joshua V, Haj Hensvold A, Jin T, Sun M, Vivar N, et al. Identification of a novel chemokine-dependent molecular mechanism underlying rheumatoid arthritis-associated autoantibody-mediated bone loss. *Ann Rheum Dis* (2016) 75:721–9. doi:10.1136/annrheumdis-2015-208093

Conflict of Interest Statement: The authors declare that the research was conducted in the absence of any commercial or financial relationships that could be construed as a potential conflict of interest.

frontiers in Immunology

REVIEW
published: 12 December 2017
doi: 10.3389/fimmu.2017.01791

The CD40–CD40L Dyad in Experimental Autoimmune Encephalomyelitis and Multiple Sclerosis

Suzanne A. B. M. Aarts[1†], *Tom T. P. Seijkens*[1,2†], *Koos J. F. van Dorst*[3], *Christine D. Dijkstra*[4], *Gijs Kooij*[4†] *and Esther Lutgens*[1,2*†]

[1] *Department of Medical Biochemistry, Subdivision of Experimental Vascular Biology, Academic Medical Center, University of Amsterdam, Amsterdam, Netherlands,* [2] *Institute for Cardiovascular Prevention (IPEK), Ludwig Maximilians University (LMU), Munich, Germany,* [3] *Medical Faculty, VU University Medical Center, Amsterdam, Netherlands,* [4] *Department of Molecular Cell Biology and Immunology, Neuroscience Campus Amsterdam, VU University Medical Center, Amsterdam, Netherlands*

OPEN ACCESS

Edited by:
David Cameron Wraith, University of Birmingham, United Kingdom

Reviewed by:
Cris S. Constantinescu, University of Nottingham, United Kingdom
Thomas Korn, Technische Universität München, Germany

***Correspondence:**
Esther Lutgens
e.lutgens@amc.uva.nl, esther.lutgens@med.uni-muenchen.de

[†]*These authors have contributed equally to this work.*

Specialty section:
This article was submitted to Multiple Sclerosis and Neuroimmunology, a section of the journal Frontiers in Immunology

Received: *06 September 2017*
Accepted: *29 November 2017*
Published: *12 December 2017*

Citation:
Aarts SABM, Seijkens TTP, van Dorst KJF, Dijkstra CD, Kooij G and Lutgens E (2017) The CD40–CD40L Dyad in Experimental Autoimmune Encephalomyelitis and Multiple Sclerosis. Front. Immunol. 8:1791. doi: 10.3389/fimmu.2017.01791

The CD40–CD40L dyad is an immune checkpoint regulator that promotes both innate and adaptive immune responses and has therefore an essential role in the development of inflammatory diseases, including multiple sclerosis (MS). In MS, CD40 and CD40L are expressed on immune cells present in blood and lymphoid organs, affected resident central nervous system (CNS) cells, and inflammatory cells that have infiltrated the CNS. CD40–CD40L interactions fuel the inflammatory response underlying MS, and both genetic deficiency and antibody-mediated inhibition of the CD40–CD40L dyad reduce disease severity in experimental autoimmune encephalomyelitis (EAE). Both proteins are therefore attractive therapeutic candidates to modulate aberrant inflammatory responses in MS. Here, we discuss the genetic, experimental and clinical studies on the role of CD40 and CD40L interactions in EAE and MS and we explore novel approaches to therapeutically target this dyad to combat neuroinflammatory diseases.

Keywords: CD40, CD40L, multiple sclerosis, experimental autoimmune encephalomyelitis, inflammation, tumor necrosis factor receptor-associated factors

INTRODUCTION

Multiple sclerosis (MS), a chronic inflammatory, demyelinating disease of the central nervous system (CNS), affects approximately 2.5 million people worldwide and is the most common cause of non-traumatic neurological disability in young adults (1). MS can be subdivided in different disease courses, including relapsing remitting MS (RRMS), secondary progressive MS (SPMS), and primary progressive MS (PPMS) (2). At disease onset, 85% of the patients have RRMS, which is characterized by acute attacks (relapses) followed by a period of partial or full recovery (remission) of the symptoms. Approximately 50% of these patients will subsequently develop SPMS. Although the etiology of MS is unknown, the disease is characterized by dynamic inflammatory lesions, consisting of activated T cells, B cells, macrophages and CNS-resident cells that eventually cause severe CNS tissue damage resulting in neurological deficits (3–6). Glucocorticoids are commonly used to inhibit the inflammatory response causing relapses. Although these drugs promote a faster recovery, there are no long-term neuroprotective effects (7, 8). In RRMS, reduced frequency of relapses and inhibition of disease progression is observed upon treatment with disease modifying drugs, including interferons,

glatiramer acetate, sphingosine-1-phosphate receptor modulators and monoclonal antibodies directed against α4-integrin (natalizumab), CD52 (alemtuzumab), CD25 (daclizumab), and CD20 (ocrelizumab, ofatumumab) (7). These agents successfully extended the treatment strategies for RRMS, but disease modifying drugs lacked efficacy in progressive MS and may have potentially severe adverse effects including cytopenias, infectious diseases, and progressive multifocal leukoencephalopathy (9–12). Identification of additional therapeutic targets, especially for progressive MS, is therefore a widely recognized scientific goal with great clinical implications.

CD40 is a membrane-bound costimulatory protein and is a member of the tumor necrosis factor receptor (TNFR) family. CD40 is constitutively expressed by B cells and dendritic cells, but upon cell activation the protein is broadly expressed on hematopoietic cells, including T cells, monocytes and macrophages, but also on non-hematopoietic cells, such as endothelial cells (ECs) and CNS resident cells. The classical ligand for CD40 is the tumor necrosis factor (TNF) family member CD40 ligand (CD40L), which is expressed on both T cells and platelets. During inflammation CD40L is also expressed on B cells, dendritic cells, monocytes, macrophages, EC, and CNS resident cells, amongst others. CD40-mediated signaling depends on adaptor molecules, the TNF-receptor-associated factors (TRAFs) that bind to the cytoplasmic tail of CD40 and can activate multiple signaling cascades dependent on the TRAF family member that binds and the cell-type that is activated. The CD40 cytoplasmic domain has a proximal TRAF-6 binding site and a more distal TRAF-2/3/5 binding site (13). The CD40–CD40L dyad is an immune checkpoint regulator that promotes both humoral and cellular immune responses by regulating the inflammatory phenotype of immune and non-immune cells. Genetic and antibody-mediated inhibition of CD40 or CD40L successfully reduced disease burden in experimental models of atherosclerosis, Crohn's disease, psoriasis, rheumatoid arthritis (RA), and experimental autoimmune encephalomyelitis (EAE) (14).

Experimental studies identified the CD40–CD40L dyad as a potent therapeutic target in MS (15–21). A pilot study with anti-CD40L mAb IDEC-131 in MS patients was successful, which led to the launch of a phase II trial. Unfortunately, this trial was halted after a case of severe thromboembolism in an IDEC-131 trial in Crohn's disease patients (22). Clinical applicability of antibody-mediated blockage of CD40 is compromised by the risk of severe immunosuppression. Interestingly, recent insights in the downstream CD40 signaling pathways identified novel possibilities to inhibit the CD40–CD40L dyad without these side effects (13, 23).

In this review, we discuss genetic, experimental, and clinical studies on the role of CD40 and CD40L in the neuroinflammatory response underlying MS and we explore novel strategies that may eventually overcome the current limitations of antagonizing the CD40–CD40L dyad in MS.

EXPRESSION OF CD40L DURING MS

Our knowledge on the expression of CD40L and CD40 in MS is based on postmortal human studies and on reports from studying EAE, a widely used animal model of MS. In this model, neuroinflammation is initiated by T cells. However, for demyelination monocyte-derived macrophages, opsonizing antibodies and complement have been shown to play an essential role (24).

T Cells

In order to initiate a proper T cell-mediated immune response, cell–cell interactions between T cells and antigen-presenting cells (APCs), such as B cells, macrophages, and dendritic cells are required. Three distinct signals are needed for T cell activation: binding of the T cell receptor with the MHC class II complex on APCs is the first signal, the second signal is generated by costimulatory molecules, and the third signal originates from cytokines. CD40L expressing T cells can activate resting APCs *via* interaction with their CD40 receptors. Upon activation the APCs will upregulate cytokine receptors and other costimulatory molecules (25).

Both $CD4^+$ and $CD8^+$ T cells are abundantly present in MS lesions. During immune activation, both T cell subsets can express CD40L, however, in MS CD40L expression is only detected on $CD4^+$ T cells, and not $CD8^+$ T cells (26). CD40L is not detected in the healthy CNS, nor in the CNS of patients with other neurodegenerative disorders like Alzheimer's Disease (15), suggesting that infiltrated $CD40L^+$ T cells are the driver of CD40-mediated inflammation in MS. Infiltrated $CD40L^+$ T cells induce activation of the various CD40-expressing cells (27) (**Figure 1A**). Likewise, in murine relapsing-remitting EAE, CD40L-expressing T cells infiltrate the CNS as early as day 4 postimmunization, and the number of $CD40L^+$ T cells increased in the acute phase and peaked during remission, indeed suggesting that CD40L drives the initial phases of neuroinflammation (28).

Soluble CD40L (sCD40L)

Besides membrane-bound CD40L, CD40L also exists as a soluble protein: sCD40L, which is mainly derived from activated platelets (95%) and T cells (5%) (29, 30). After cleavage from the platelet surface, sCD40L remains trimeric and can bind to integrin $\alpha_{IIb}\beta_3$ on platelets or the CD40 receptor, which induces the expression of inflammatory mediators, such adhesion molecules, tissue factor, and chemokines (30).

Multiple population studies have demonstrated that serum sCD40L concentrations were increased in MS patients with active disease compared to healthy controls (5.65 ± 2.87 vs. 0.14 ± 0.12 ng/mL, $p < 0.001$) or patients with inactive MS (5.65 ± 2.87 vs. 0.64 ± 0.30 ng/mL, $p < 0.001$) (31, 32). A similar increase of sCD40L was detected in the CSF of MS patients compared to patients suffering from other inflammatory or neurological diseases (38.5 vs. 4.8 pg/mL, $p < 0.002$; SD not mentioned in the manuscript) (33). Although serum sCD40L concentrations, but not CSF sCD40L concentrations, positively correlated (Kendall tau-$b = 0.29$, $p = 0.044$) with the CSF/serum albumin ratio ("Qalb"), an indicator of blood-brain barrier permeability (33), it is currently unknown whether sCD40L directly contributes to BBB breakdown. Interestingly, serum concentrations of sCD40L decreased upon treatment with Glatiramer acetate (copaxone) (34), IFN-β (35), or natalizumab (36), suggesting that sCD40L can be used as a biomarker to monitor the effectiveness of these therapies.

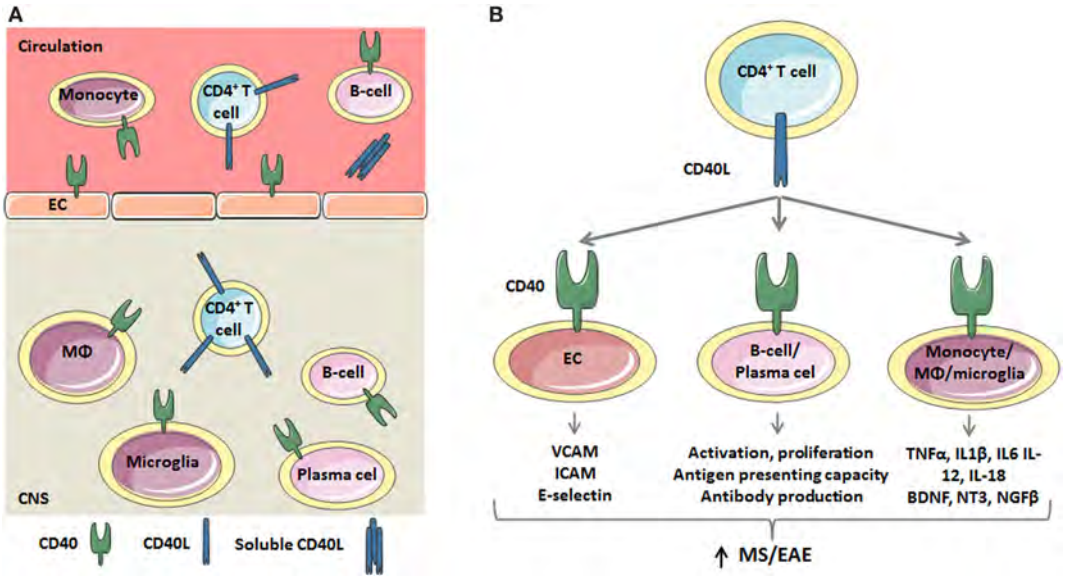

FIGURE 1 | The critical role of the CD40 ligand (CD40L)–CD40 dyad in the inflammatory response underlying multiple sclerosis (MS)/experimental autoimmune encephalomyelitis (EAE). **(A)** During MS/EAE, the number of $CD40L^+CD4^+$ T cells in the peripheral blood and central nervous system (CNS) increases. Besides a membrane bound form, CD40L also exists as soluble trimer, which is mainly derived from platelets. CD40L interacts with CD40 on endothelial cells (ECs) and circulating monocytes and B cells. Within the CNS, T cells activate $CD40^+$ macrophages, microglia, B cells, and plasma cells. **(B)** CD40L-mediated activation of CD40 on EC results in the expression of adhesion molecules, including VCAM, ICAM, and E-selectin, which promotes the recruitment of inflammatory cells to the CNS. CD40L also induces B cell activation, characterized by CD69 expression, and proliferation. Furthermore, the antigen presenting capacity of B cells is improved as a result of increased MHC class II, CD54, CD80, and CD86 expression. CD40L also promotes the secretion of proinflammatory cytokines by circulating monocytes and macrophages and microglia in the CNS. Thus, the CD40L–CD40 dyad critically regulates both adaptive and innate immune responses.

In contrast to these results, a large cohort study with 833 MS patients showed decreased levels of sCD40L in patients with inactive MS compared to healthy individuals (86.3 ± 9.3 vs. 54.3 ± 5.4 pg/mL, $p < 0.001$) (37). Several factors may contribute to these conflicting findings, including the use of antiplatelet drugs, such as cyclooxygenase inhibitors or adenosine diphosphate receptor inhibitors, which limit the release of sCD40L from activated platelets (29). Importantly, the use of these agents has not been reported in the population studies. In addition, a circadian rhythm in serum sCD40L levels has been observed in patient suffering from myocardial infarction, sCD40L levels were 41.5% higher in samples obtained at 9 p.m. compared to samples drawn at 2 a.m., possibly due to diurnal fluctuations in proteinase levels (38). Whether a similar circadian rhythm is present in MS patients is currently unknown. Finally, differences in blood sample handling may affect serum sCD40L levels, as low temperatures limit the *ex vivo* release of sCD40L from platelets (29). Carefully monitoring of these factors in future studies is required to fully elucidate the role of sCD40L in MS.

EXPRESSION OF CD40 DURING MS

Macrophages and Microglia

Autopsy studies in MS patients revealed that monocytes, macrophages and activated microglia are the main cell types expressing CD40 in the CNS (15). Microglia in a resting state show low or no CD40 expression, while ~45% of the activated microglia and ~73% of recruited peripheral macrophages express CD40 during EAE (39). Macrophages form a functionally heterogeneous population, with proinflammatory M1 macrophages and anti-inflammatory M2 macrophages representing the extremes of a spectrum that is present *in vivo* (40). CD40 is an M1 marker for perivascular macrophages, activated microglia and myelin-loaded macrophages in MS lesions and its expression is associated with the coexpression of other M1-markers, such as CD86, CD64, and CD32. CD40L-induced activation of these cells results in the secretion of M1-associated cytokines and chemokines, including interleukin (IL)-1, IL-6, IL-12, IL-18, and TNF-α (41–43), which fuels the ongoing inflammation in the CNS (**Figure 1B**) (44–47). However, 70% of the $CD40^+$ cells also express M2 markers, including CD163 and CD206, suggesting that a mixed M1/M2 phenotype exists in MS lesions (48). The abundant expression of CD40 on mononuclear cells in perivascular infiltrates was also found in the brain of marmoset monkeys (*Callithrix jacchus*) with acute EAE (24). In murine relapsing-remitting EAE, CD40 expressing cells infiltrate the CNS as early as day 4 postimmunization and the numbers of $CD40^+$ cells peaked in the acute and relapsing phases of the disease and decreased during remission (28). The amount of CD40 present in the CNS correlated with the expression of the inflammatory cytokines IL-12, IFN-γ, and TNF-α (28). Correspondingly, in the mouse spinal cord CD40 was abundantly expressed by monocytes and monocyte-derived macrophages (17). The expression of CD40 in the CNS found in mice and marmoset monkeys suggests that there is HLA class

II-restricted antigen presentation, and that effector functions of CD40 expressing macrophages are triggered by CD40L-expressing activated $CD4^+$ T cells (17, 24). *In vitro*, interactions between T cells and macrophages can stimulate the production of proinflammatory cytokines, nitric oxide, and matrix metalloproteinases, which are all components that play a role in the immunopathogenesis of MS and other chronic inflammatory diseases (17).

B Cells

In order to initiate a humoral immune response, CD40L present on activated $CD4^+$ T cells needs to interact with the CD40 receptor on antigen activated B cells. During this response, high titers of isotype-switched, high affinity antibodies are generated by the B cells and germinal centers (GCs) are formed (49, 50). Furthermore, CD40–CD40L signaling between follicular helper $CD4^+$ T cells (T_{FH}) and GC B cells is required for the formation of memory B cells, antibody-secreting plasma cells and the maintenance of GC (51, 52). The number of circulating $CD40^+CD20^+$ B cells did not differ between MS patients and controls; however, the density of CD40 on these cells was increased, which may have several effects on B cell function (53). First, CD40 activation on both naïve ($CD19^+CD27^-$) B cells and memory ($CD19^+CD27^+$) B cells results in the activation of these cells, characterized by CD69 expression (54). Second, the proliferative response of both naïve and memory B cells is increased upon CD40 activation (55). Third, the antigen presenting capacity of B cells was also affected as upon ligation of CD40 by CD40L, B cells from MS patients exhibited increased expression of MHC class I and II, CD54, CD80 and CD86, which promoted the activation and proliferation of T cells, especially $CD4^+$ T cells. These $CD4^+$ T cells subsequently induced the proliferation of CNS-antigen specific $CD8^+$ T cells, at least *in vitro* (54, 56).

NF-κB and MAPKs (P38, ERK, and JNK) are essential components of signaling pathways downstream of CD40 binding in B cells. Following CD40 stimulation, memory and naive B cells from MS patients showed a significantly higher level of NF-κB activation, reflected by increased levels phosphorylated p65, compared with healthy controls (57). Treatment with glatiramer acetate (Copaxone) reduced the phosphorylation of p65 in B cells of RRMS patients to levels observed in healthy individuals. These results suggest that reducing CD40-mediated activation of the canonical NFkB pathways may be a common mechanism by which some existing treatments limit inflammation in MS (57).

In recent years, a novel subset of regulatory B cells, which secrete anti-inflammatory cytokines such as IL-10 and TGF-β, has been described (58). CD40-induced activation of these cells reduced inflammation and disease severity in a murine model of systemic lupus erythematosus in an IL-10-dependent manner (59). However, Michel et al. reported that both the frequency and function of regulatory B cells was not affected in MS patients, specifically, CD40L-induced cytokine secretion was unaffected, suggesting that a similar mechanism is not present in MS (60).

The clinical success of B cell depleting therapies implicates an important role for these cells in the pathogenesis of MS. Indeed, ectopic B cell follicles have been detected in the meninges of patients with progressive MS, immunoglobulin depositions are present in MS lesions and oligoclonal immunoglobulins are detected in the CSF of 90% of the patients (61). Although the pathologic effect of these autoantibodies is incompletely understood, several autoantigens have been detected, including MOG, neurofascin, sperm-associated antigen 16 (SPAG16), contactin-2 and inward-Rectifying Potassium Channel (KIR4.1) (62). Interestingly, the CD40–CD40L dyad has a critical role in B cell biology, as it regulates antibody production, immunoglobulin isotype switching and B cell follicle formation, accordingly, antibody-mediated inhibition of CD40 reduced anti-MOG antibody production in non-human primates subjected to EAE (20). Whether CD40 signaling plays a relevant role in the generation of autoantibodies in the context of MS is currently unknown.

CD40 Expression on T Cells

CD40 expression is mostly described on APCs, but $CD4^+$ and $CD8^+$ T cells can also express low levels of CD40 mRNA that increase after activation. Effector T cells deficient for CD40 have poor capacity to proliferate, and antigen stimulated cytokine secretion during the primary immune response and in the memory phase is as low as that of naive T cells. Priming with $CD4^+$ T cells did not increase the proliferation and cytokine secretion capacity of CD40-deficient T cells, demonstrating that CD4 help to $CD8^+$ T cells requires interactions with CD40 expressed by $CD8^+$ T cells (63). The role of $CD8^+$ T cells in MS and EAE is not completely understood and is rather controversial with evidence for both a pathogenic and a regulatory function (64). The role of $CD4^+$ T cells expressing CD40 ($CD40^+CD4^+$ T cells) in EAE is recently investigated. $CD40^+CD4^+$ T cells are found in lesions in the CNS and stimulate a more severe EAE disease development than conventional $CD4^+$ T cells (65). Adoptive $CD40^+CD4^+$ T cell transfer from EAE-induced donors transfers EAE without further *in vitro* expansion and without requirement of an EAE inducing procedure to the recipient animals. Coinjection of the $CD40^+CD4^+$ donor T cells with CFA in the recipient animals results in a more severe disease outcome (65), indicating that in addition to the specific T cell response to CNS antigen, a general activation of the immune system is necessary to induce severe disease. Moreover, this suggests that any event leading to $CD40^+CD4^+$ T cell expansion might result in susceptible individuals.

Endothelial Cells

In addition to immune cells, 25% of brain EC constitutively express CD40 *in situ* and *in vitro* and the expression is further increased by inflammatory stimuli (48, 66–68). Activation of endothelial CD40 by CD40L induces the expression of the adhesion molecules E-selectin, VCAM-1, and ICAM-1 (**Figure 1B**), which facilitates the migration of monocytes and $CD4^+$ T and $CD8^+$ T cells into the CNS. Brain ECs also induce T cell activation and proliferation *via* MHC-II-dependent antigen presentation and CD40-mediated costimulation (66). Thus, CD40–CD40L-mediated interactions between EC and immune cells promote CNS inflammation by facilitating transmigration of leukocytes across the BBB and subsequently inducing T cell activation and proliferation (67).

Resident CNS Cells

CD40 is also expressed on other resident CNS cell types like astrocytes and neurons. Astrocyte CD40 induces the secretion of proinflammatory cytokines and chemokines, which trigger an autocrine activation of these cells that aggravate EAE (69). CD40 is constitutively expressed on neurons (70). CD40L-induced activation of primary cultured neuronal cells results in activation of p44/42 MAPK signaling pathways, and increases neurofilament expression, a marker of neuronal differentiation. In addition, CD40 has a critical role in neuronal survival as neuronal cell injury induced by serum withdrawal can be rescued by CD40 ligation in wild-type neurons, but injury could not be reduced by CD40 ligation in CD40-deficient neurons. These *in vitro* findings are further supported by observations in aged *Cd40*$^{-/-}$ mice. Examination of the brain of CD40-deficient mice showed that at older age (16 months) CD40 deficiency results in decreased neurofilament expression, neuronal dysmorphology, reduced brain weights, and increased TUNEL reaction, indicating increased presence of apoptotic cells (70). Additionally, phenotypic analysis of *Cd40*$^{-/-}$ mice showed that CD40 regulates growth from excitatory and inhibitory neuron dendrites (71). In conclusion, neuronal CD40 has an important role in neuronal development, maintenance, and survival.

Expression of CD40–CD40L on Circulating Immune Cells in MS

In addition to the local alterations in the CNS discussed above, the systemic immune system is also affected in MS (1). The expression of CD40 and CD40L on peripheral blood monocytes, especially the CD16$^+$ proinflammatory subset, is increased in MS patients, reflecting the higher activation status of these cells (53, 72–74). Besides inflammatory cytokines, monocytes also produce protective anti-inflammatory mediators upon CD40L-induced activation such as the neurotrophins BDNF, NT3, and NGFβ (39). Interestingly, this protective response is reduced in monocytes from MS patients, but restored upon IFNβ treatment (75–77).

Circulating CD40L$^+$ CD4$^+$ T cells and CD40L$^+$ CD8$^+$ T cells are also more abundant in MS patients compared to healthy controls (53, 78). Upon *in vitro* CD3-induced reactivation, CD4$^+$ T cells from MS patients expressed more CD40L and produced increased levels of inflammatory mediators, compared to T cells from healthy controls, suggesting that CD40L is especially expressed by activated proinflammatory T cells (79). Interestingly, IFNβ reversed the increased expression of CD40L on CD4$^+$ T cells (53, 80).

Taken together, during neuroinflammation, CD40L$^+$ CD4$^+$ T cells infiltrate the CNS and activate CD40$^+$ monocytes, macrophages, B cells, ECs, and other CNS resident cells, which propagates the ongoing inflammatory response and aggravates lesion development (**Figures 1A,B**). Consequently, two strategies can be applied to therapeutically target the CD40–CD40L dyad in MS; (1) inhibition of CD40 on resident and immune cells; (2) inhibition of CD40L on T cells. While the role of CD40L-induced activation of CD40$^+$ cells in immunity and inflammation is well known, only limited data exist on the reciprocal activation of CD40L$^+$ cells. The intracellular domain of CD40L does not contain any signaling motifs, however upon activation its transmembrane domain associates with lipid rafts, thereby inducing AKT and p38 MAPKs pathways and the subsequent production of IL-2, based on *in vitro* experiments (81). Additionally, this may promote IL-4, IL-10, TNF-α, and IFN-γ production (82). However, the pathophysiological relevance of the reciprocal activation of CD40L$^+$ cells in MS or other inflammatory diseases has not been explored and requires further attention as it may result in the identification of novel therapeutic targets.

CD40 SINGLE-NUCLEOTIDE POLYMORPHISMS (SNPs) AND MS

Genome-wide association studies have identified a correlation between SNPs in immune related loci, including the CD40 locus, and the incidence of MS (83). In particular, the SNP rs1883832C- > T in the CD40 gene was associated with an increased risk for MS. Compared to rs1883832CC individuals, heterozygous rs1883832CT and homozygous rs1883832TT individuals had a 1.5-fold and 2.5-fold increased risk for MS, respectively (84). Counterintuitively, the high-risk allele was associated with a 45.5% decreased expression of CD40 mRNA in an *in vitro* translation/transcription system (85, 86). A second CD40 SNP (rs6074022T- > C) was also associated with a minor decrease in the expression of CD40 mRNA in whole blood RNA from MS patients (87–89). Thus, at least two high risk SNPs are associated with a decreased expression of CD40, which seems contradictory and requires further attention, as *in vivo* studies have established the proinflammatory role of CD40 in neuroinflammation, as discussed below. In RA and Graves' disease CD40 rs1883832 is associated with reduced CD40 expression and disease protection. These findings are in line with the role of CD40 as a costimulator in T cell activation supporting the autoimmune inflammatory process (86). How to explain the increased risk for MS upon decreased CD40 mRNA expression is so far unclear. Until now, no polymorphisms of the CD40L gene have been associated with MS (84).

PROMISING THERAPEUTIC POTENTIAL OF THE CD40L–CD40 DYAD FOR EAE AND MS

Several EAE studies in mice and non-human primates showed that the CD40–CD40L signaling pathway is an interesting target to reduce incidence and severity of neuroinflammation. Combination therapies can even further increase treatment efficiency. A discussion of this research is described here.

Genetic Deficiency of CD40 or CD40L in Mouse EAE

Both CD40- and CD40L-knock-out mice do not develop EAE after immunization. CD40–CD40L interactions are required for the B7.1 and B7.2 expression on APCs, essential for T cell activation. Lack of costimulation through B7.1 and B7.2 may result in a reduction of secondary signaling and prevention of T cell activation, possibly responsible for protection of CD40L-deficient mice

from EAE (16). Experiments with *Cd40*$^{-/-}$ mice showed that in the absence of CD40, T cells both enter the CNS and induce disease. This suggests that activated T cell trans-migration through the endothelial BBB does not require CD40 (90). However, CD40 is necessary for Th1 cell activation as in the presence of CD40, there is an earlier entrance of Th1 cells into the CNS and more severe induction of disease (90). CD40 on peripheral hematopoietic cells is known to be pivotal to the development of autoimmunity (25). By using bone marrow (BM) chimeric mice, Becher et al. showed that lack of expression of CD40 on CNS-resident microglia also diminishes EAE severity and reduces the amount of leukocyte infiltration into the CNS (91). Reduced microglial expression of CD40 did not affect peripheral T cell priming or recall responses. Encephalitogenic T cells could not elicit the expression of chemokines in a CNS environment in which parenchymal microglia were CD40 depleted. So, outside of the systemic immune compartment CD40 increases organ-specific autoimmunity and within the CNS CD40 expressing cells regulate the EAE development in BM chimeric mice (91).

Antibody-Mediated Inhibition of CD40L in Mouse EAE

Treatment of EAE-induced mice with an antagonistic anti-CD40L mAb (MR1) during disease induction (days 0–4) completely prevented development of disease (15). Treatment during days 4–8 and days 7–11 after induction reduced disease burden by 80 and 67%, respectively (15). Antibody treatment inhibited CNS inflammatory processes, as the number and size of CNS infiltrates of animals treated with anti-CD40L antibodies during EAE induction were strongly reduced compared to animals treated with an irrelevant antibody (17). Besides treatment at disease induction, EAE disease development and CNS inflammation were also blocked effectively by anti-CD40L antibody treatment of animals at the peak of acute disease and by treatment during remission (18). Interestingly, transient anti-CD40L blockade at the peak of the acute phase of R-EAE in SJL mice reduced clinical relapses by 80%, and in mice that did develop a relapse, the duration and severity was reduced as compared to control antibody treated animals (19). Short-term (4 days) treatment with anti-CD40L during EAE induction could prevent clinical disease and did not affect the long-term Th1/Th2 balance (92).

Mechanism of Disease Reduction upon Anti-CD40L Treatment

Myelin-specific T cells in anti-CD40L-treated mice subjected to EAE secreted little IFNγ but exhibited strongly enhanced levels of IL-4, compared to control treated mice (**Figure 2A**). Anti-CD40L mAb did not result in systemic tolerance of encephalitogenic T cells (93) nor caused expansion of myelin-specific T cells. However, treatment with anti-CD40L antibody at the peak of acute disease or during remission inhibited Th1 differentiation and effector function. While T cell proliferation and secretion of the cytokines IL-2, IL-4, IL-5, and IL-10 were normal (18), antibody treatment strongly impaired IFN-γ production, delayed-type hypersensitivity responses against myelin peptide, and encephalitogenic effector cell activation (18, 93). Treatment with anti-CD40L antibody also reduced clinical disease expression in adoptive recipients of encephalitogenic T cells, suggesting involvement of CD40–CD40L interactions in their effector ability to activate CNS macrophages/microglia (18).

CD40–CD40L interactions between APCs and T cells results in IL-12 secretion, an essential cytokine for Th1 responses and EAE induction. This has led to the hypothesis that the protective effects of CD40L blockade in EAE can be overcome by IL-12 administration. Mice cotreated with exogenous IL-12 and the anti-CD40L antibody developed severe EAE and anti-IL-12 antibody treatment protected mice from EAE (94). However, the protein IL-12 consists of a p35 and a p40 subunit, the IL-12p40 subunit is shared by other cytokines. *Il-12p40*$^{-/-}$ mice are protected against EAE, but *Il-12p35*$^{-/-}$ mice develop severe EAE, verifying that the p40 subunit, and not IL-12 is critical for the development of EAE (95). IL-23, another cytokine containing the p40 subunit, has later been shown to play a critical role in the EAE disease development instead of IL-12 (96, 97). Whether the beneficial effect of CD40 blockade in EAE is mediated through reduced levels of IL-23 is not yet investigated, and the role of CD40–CD40L interactions in IL-23 secretion is still unclear.

To investigate whether the mechanism of EAE inhibition by anti-CD40L mAb depends on its Fc effector interactions, Nagelkerken et al. compared an anti-CD40L mAb (produced in mammalian cells) with its a-glycosylated counterpart, which has strongly reduced FcγR binding and impaired complement binding activity. They found that both forms of the Ab have similar ability to inhibit clinical signs of EAE (98). Therefore, in the context of EAE, FcR interactions do not play a crucial role in the protective effect of anti-CD40L mAb (98). Activation of microglial cells is a multistep process and microglial cell CD40 expression facilitates EAE disease development. Activation of microglial cells at the onset of EAE is a process independent of CD40, and their activation is characterized by increased expression of CD45 and MHC class II. However, at the peak of disease, complete activation of microglial cells is dependent on their CD40 expression (39). These results show that in order to facilitate the progression of EAE clinical disease activation of microglial cells in the CNS is needed (39).

Anti-CD40 and CD40L Antibody Treatment in EAE in Non-Human Primates

As treatment of EAE-induced mice with anti-CD40L mAb effectively blocked clinical disease progression and CNS inflammation (15, 17, 18), CD40L–CD40 interaction inhibiting experiments were extrapolated to non-human primate models of EAE. Anti-CD40 mAb showed beneficial activities in a EAE model in non-human primates when administered early in disease development (20) or after the onset of neuroinflammation (21). Inhibition of CD40–CD40L interactions was tested in marmoset monkeys with anti-human CD40 mAb (ch5D12), a chimeric antagonist. Severe clinical signs of EAE were observed in all placebo-treated monkeys, whereas in the ch5D12-treated group the animals did not develop disease symptoms at all. Postmortem analysis of the CNS showed that ch5D12 treatment resulted in a reduced lesion load (20). The same model was used to test the anti-human

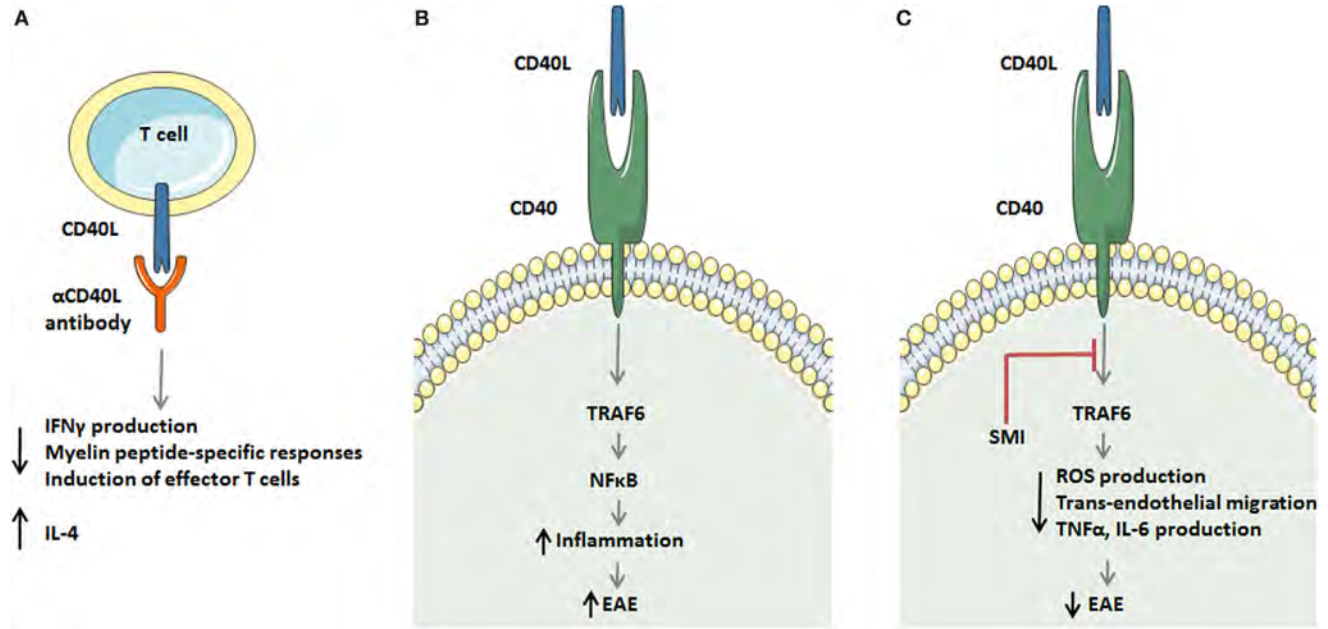

FIGURE 2 | Strategies to target the CD40 ligand (CD40L)–CD40L dyad in experimental autoimmune encephalomyelitis (EAE). **(A)** Antagonistic CD40L antibodies limit detrimental T cell responses in multiple sclerosis (MS) by decreasing IFNγ production, reducing myelin peptide-specific delayed-type hypersensitivity responses, and limiting in effector T cell formation. In addition, antibody treatment enhances the production of the Th2 cytokine interleukin (IL)-4. **(B,C)** A novel strategy to target the CD40L–CD40 axis in monocytes and macrophages during EAE. The CD40L–CD40–TRAF6 axis activates the transcription factor NF-κB, which subsequently induces an inflammatory monocyte/macrophage phenotype that aggravates EAE. Small molecule-mediated inhibition of the CD40–TRAF6 interaction reduces ROS, TNFα, and IL6 production by macrophages and limits transendothelial migration of monocytes, thereby improving EAE in mice and rats.

CD40 monoclonal antibody in its parent murine form (mu5D12). mu5D12 mAb treatment interfered with development of clinical symptoms, even when mu5D12 mAb was given several weeks after T cell priming. *In vivo* localization shows that in addition to entering the secondary lymphoid organs, the mu5D12 mAb also enters the perivascular spaces of the CNS and to a smaller extent penetrates in the brain parenchyma. Therefore, anti-CD40 can inhibit activation of primary and secondary antigen-specific T cells and B cells in both the secondary lymphoid organs and CNS lesions. The activity in secondary lymphoid organs is important since pathogenic T cells are continuously activated in the periphery during established EAE (21). Supporting this data, serial MRI demonstrated that ch5D12 treatment prevented the expansion of existing white matter lesions (99).

Combination Therapy of CD40–CD40L Blockade and Other Disease Modifying Agents

Blocking CD40–CD40L has been proven to be effective in reducing EAE, as described above. Disruption of CD40–CD40L interaction blocks activation of autoantigen-specific T cells and decreased leukocyte infiltration into the CNS. Therefore, it would be interesting to restore self-tolerance by enhancing Tregs in addition to the inhibition of the proinflammatory mechanisms. To achieve this, we should block multiple costimulatory dyads simultaneously to further increase the efficiency of the treatment. In the oncology field it has already been shown that immune checkpoint inhibitor combination therapy results in better outcomes compared to the use of a single immune checkpoint inhibitor, an example is the combination of nivolumab (anti-PD-1) and ipilimumab (anti-CTLA-4) (100).

Inflammatory cytokine production by astrocytes is induced upon activation by the CD40–CD40L interaction in a mast cell coculture. These cytokines re-activate astrocytes leading to increased release of cytokines that contribute to aggravating EAE development. Pretreatment with a combination of anti-CD40 antibody and the Rac inhibitor 8-hydroxydeoxyguanosine (8-oxo-dG) decreased the EAE induced TNFR1 expression and colocalization of TNFR1 and astrocytes in the brain. This combination therapy was able to decrease the clinical scores further than one of the treatments alone (69). Moreover, analysis of EAE brain tissues show that anti-CD40 Ab and 8-oxo-dG treatment enhanced the number of Treg cells, increased OX40 expression, and increased production of cytokines associated with Treg cells and their suppressive function (101).

Treatment of EAE with a combination of the CD40L antagonistic MR1 antibody and CTLA4Ig, blocking the CD28-B7 interaction, provides additive protection in mice compared to single treatment, particularly in case of delayed administration. After treatment with the Anti-CD40L and CTLA4Ig combination mononuclear cell infiltrates were absent in the CNS, and in lymph nodes combination treatment is associated with a strong reduction in proliferation of primed T cells. According to these results, CD28 and CD40L might deliver different costimulatory signals for complete T cell activation, although there probably is

an additional regulatory role for CD40L–CD40 interaction on B7 expression. Blocking both the CD40–CD40L and the CD28-B7 pathways *in vivo* possibly results in better suppression of pathogenic immune responses (102).

Simultaneous knock-down of CD40 and the p19 subunit of IL-23 expression on bone marrow-derived DCs (BMDCs) by injection of double-transduced $CD40^+p19LV^-$ BMDCs in EAE mice resulted in reduced clinical scores, significant decreased production of IL-17 and an increase in IL-10 compared with EAE mice treated with control lentiviral vector-DCs-(p19LV-DCs and CD40LV-DCs) (103). These studies show that combination therapies including blocking of CD40–CD40L interactions and an additional blockade can, by different mechanisms, more efficiently reduce EAE disease severity than anti-CD40L Ab or anti-CD40 Ab treatment alone.

Anti-CD40L Treatment in Clinical Trials

The experimental studies in rodents and primates highlighted the therapeutic potential of CD40–CD40L targeting strategies in MS and (15–21) paved the way for clinical studies. Anti-CD40L mAb IDEC-131 treatment was found to be successful in a phase I clinical trial with 15 MS patients, in this trial no relapses were observed in the complete cohort for at least 6 months. After this pilot, a phase II clinical trial with 46 MS patients was initiated in 2002. However, due to a severe case of thromboembolism in a similar trial with anti-CD40L mAb in Crohn's disease patients (22), these trials were halted. The thromboembolic complications were caused by disruption of CD40L-$\alpha_{IIb}\beta_3$ interactions between platelets in arterial thrombi (13, 104, 105). For this reason, but also because of potential immunosuppressive adverse effects of antibody-mediated inhibition of CD40–CD40L, alternative strategies are required to exploit the therapeutic potential of CD40–CD40L inhibition in MS.

NOVEL STRATEGIES TO TARGET THE CD40–CD40L DYAD

One approach to reduce side-effects in treatment of EAE is specific delivery of drugs to CD40L positive T cells. Based on CD40L crystal structure and molecular docking studies, Ding et al. designed a CD40L specific peptide ligand (A25). The peptide A25 was conjugated on the surface of liposomes and capable of facilitating specific liposomal drug delivery to $CD40L^+$ cells. $CD40L^+$ cell ratios in EAE mice were significantly reduced by the A25 modified liposome loaded with methotrexate (MTX), a cytostatic drug, resulting in markedly reduced clinical scores (106).

Based on our recent findings, we propose that more specific downstream inhibition of the CD40L–CD40 dyad may be another approach to overcome the current limitations. Using mice specifically lacking CD40-TRAF6 or CD40-TRAF2/3/5 interactions, we showed that only CD40-TRAF6-deficient mice had a skewing in the immune response toward an anti-inflammatory profile and were protected against atherosclerosis (107). Based on these results, we developed small molecule inhibitors (SMIs) that efficiently and specifically block CD40-TRAF6 interactions and leave CD40-TRAF2/3/5 interactions intact (108). These SMIs are able to reduce peritonitis, sepsis, obesity-associated adipose tissue inflammation, and diabetes (108–111). Using an *in vitro* model for (neuro-) inflammation, we were able to show that SMI 6877002 skews the phenotype of human monocytes toward a less inflammatory profile with reduced monocyte trans-endothelial migration capacity across brain ECs *in vitro* (23). Furthermore, upon SMI treatment EAE disease severity was reduced in Lewis rats, but not mice. However, in both models the SMI-treated animals had reduced levels of CNS-infiltrated monocyte-derived macrophages, but not T cells (23). The experiments with SMI 6877002 in EAE illustrate the therapeutic potential of CD40-TRAF6 targeting strategies (**Figures 2B,C**), with the ability to reduce monocyte recruitment and macrophage activation in the CNS and this approach could potentially be used as a cotreatment to ameliorate MS.

CONCLUSION AND FUTURE DIRECTIONS

This review emphasizes that besides the classical adaptive immunity-related CD40L–CD40 signaling, this dyad has an essential role in the establishment and pathogenesis of MS in multiple ways. In particular, CD40 and CD40L are widely expressed on both resident and CNS-infiltrated cells in MS lesions and CD40 gene SNPs associate with MS incidence. There are several treatments available for RRMS, but additional therapeutic targets are still necessary, especially for progressive MS. Progressive MS is characterized more by nerve degeneration rather than inflammation. Monocyte-derived macrophages play an essential role in demyelination. In MS patients increased expression of CD40 on peripheral monocytes, and high expression of CD40 on myelin-loaded macrophages in MS lesions was observed. Using EAE as a model for MS, inhibition of the CD40–CD40L dyad has found to be an effective strategy to reduce the onset and development of EAE in rodent and primates. However, treatment with anti-CD40/CD40L mAb resulted in unforeseen thromboembolic side effects in human clinical trials, and bears the risk of immune suppression, which hampered further development of this strategy. Nevertheless, novel insights regarding treatment with combinations of immune checkpoint regulators, the use of nanoparticles, and the pivotal CD40L–CD40–TRAF signaling pathway in inflammatory diseases have revived the therapeutic potential of the CD40–CD40L dyad. These novel approaches are examples that the current limitations of long-term CD40 and CD40L inhibition in MS and other inflammatory diseases can be overcome. CD40–CD40L plays an important role in the pathogenesis of MS and research has proven that this dyad is an important therapeutic target for treatment of MS.

AUTHOR CONTRIBUTIONS

The study presented here was carried out in collaboration among all authors. All authors read and approved the final manuscript.

FUNDING

This work was supported by the MS Research Foundation [13-809MS]; the Netherlands CardioVascular Research Initiative for the GENIUS project [CVON2011-19]; the Netherlands Organization for Scientific Research [NWO VICI grant to EL]; The European Research Council [ERC Consolidator grant to EL]; and the Deutsche Forschungsgemeinschaft [SFB 1054 and SFB1123 to EL]. Amsterdam Cardiovascular Sciences [MD/PhD grant to TS].

REFERENCES

1. Hemmer B, Kerschensteiner M, Korn T. Role of the innate and adaptive immune responses in the course of multiple sclerosis. *Lancet Neurol* (2015) 14(4):406–19. doi:10.1016/S1474-4422(14)70305-9
2. Lublin FD, Reingold SC, Cohen JA, Cutter GR, Sorensen PS, Thompson AJ, et al. Defining the clinical course of multiple sclerosis: the 2013 revisions. *Neurology* (2014) 83(3):278–86. doi:10.1212/WNL.0000000000000560
3. Peterson JW, Trapp BD. Neuropathobiology of multiple sclerosis. *Neurol Clin* (2005) 23(1):107–29. doi:10.1016/j.ncl.2004.09.008
4. Frohman EM, Racke MK, Raine CS. Multiple sclerosis – the plaque and its pathogenesis. *N Engl J Med* (2006) 354(9):942–55. doi:10.1056/NEJMra052130
5. Stys PK, Zamponi GW, van Minnen J, Geurts JJG. Will the real multiple sclerosis please stand up? *Nat Rev Neurosci* (2012) 13(7):507–14. doi:10.1038/nrn3275
6. Milo R, Miller A. Revised diagnostic criteria of multiple sclerosis. *Autoimmun Rev* (2014) 13(4–5):518–24. doi:10.1016/j.autrev.2014.01.012
7. Dargahi N, Katsara M, Tselios T, Androutsou ME, de Courten M, Matsoukas J, et al. Multiple sclerosis: immunopathology and treatment update. *Brain Sci* (2017) 7(7):78. doi:10.3390/brainsci7070078
8. Galea I, Ward-Abel N, Heesen C. Relapse in multiple sclerosis. *BMJ* (2015) 350:h1765. doi:10.1136/bmj.h1765
9. Lorscheider J, Jokubaitis VG, Spelman T, Izquierdo G, Lugaresi A, Havrdova E, et al. Anti-inflammatory disease-modifying treatment and short-term disability progression in SPMS. *Neurology* (2017) 89(10):1050–9. doi:10.1212/WNL.0000000000004330
10. Shirani A, Okuda DT, Stuve O. Therapeutic advances and future prospects in progressive forms of multiple sclerosis. *Neurotherapeutics* (2016) 13(1):58–69. doi:10.1007/s13311-015-0409-z
11. Soelberg Sorensen P. Safety concerns and risk management of multiple sclerosis therapies. *Acta Neurol Scand* (2017) 136(3):168–86. doi:10.1111/ane.12712
12. Winkelmann A, Loebermann M, Reisinger EC, Hartung HP, Zettl UK. Disease-modifying therapies and infectious risks in multiple sclerosis. *Nat Rev Neurol* (2016) 12(4):217–33. doi:10.1038/nrneurol.2016.21
13. Engel D, Seijkens T, Poggi M, Sanati M, Thevissen L, Beckers L, et al. The immunobiology of CD154–CD40–TRAF interactions in atherosclerosis. *Semin Immunol* (2009) 21(5):308–12. doi:10.1016/j.smim.2009.06.004
14. Peters AL, Stunz LL, Bishop GA. CD40 and autoimmunity: the dark side of a great activator. *Semin Immunol* (2009) 21(5):293–300. doi:10.1016/j.smim.2009.05.012
15. Gerritse K, Laman JD, Noelle RJ, Aruffo A, Ledbetter JA, Boersma WJ, et al. CD40-CD40 ligand interactions in experimental allergic encephalomyelitis and multiple sclerosis. *Proc Natl Acad Sci U S A* (1996) 93(6):2499–504. doi:10.1073/pnas.93.6.2499
16. Grewal I, Foellmer H, Grewal K, Xu J, Hardardottir F, Baron J, et al. Requirement for CD40 ligand in costimulation induction, T cell activation, and experimental allergic encephalomyelitis. *Science* (1996) 273(5283):1864–7. doi:10.1126/science.273.5283.1864
17. Laman J, Maassen C, Schellekens M, Visser L, Kap M, de Jong E, et al. Therapy with antibodies against CD40L (CD154) and CD44-variant isoforms reduces experimental autoimmune encephalomyelitis induced by a proteolipid protein peptide. *Mult Scler* (1998) 4(3):147–53. doi:10.1177/135245859800400312
18. Howard LM, Miga AJ, Vanderlugt CL, Canto MCD, Laman JD, Noelle RJ, et al. Mechanisms of immunotherapeutic intervention by anti-CD40L (CD154) antibody in an animal model of multiple sclerosis. *J Clin Invest* (1999) 103(2):281–90. doi:10.1172/JCI5388
19. Howard LM, Dal Canto MC, Miller SD. Transient anti-CD154-mediated immunotherapy of ongoing relapsing experimental autoimmune encephalomyelitis induces long-term inhibition of disease relapses. *J Neuroimmunol* (2002) 129(1–2):58–65. doi:10.1016/S0165-5728(02)00175-3
20. Boon L, Brok HPM, Bauer J, Ortiz-Buijsse A, Schellekens MM, Ramdien-Murli S, et al. Prevention of experimental autoimmune encephalomyelitis in the common marmoset (*Callithrix jacchus*) using a chimeric antagonist monoclonal antibody against human CD40 Is associated with altered B cell responses. *J Immunol* (2001) 167(5):2942–9. doi:10.4049/jimmunol.167.5.2942
21. Laman J, 't Hart B, Brok H, Meurs M, Schellekens M, Kasran A, et al. Protection of marmoset monkeys against EAE by treatment with a murine antibody blocking CD40 (mu5D12). *Eur J Immunol* (2002) 32(8):2218–28. doi:10.1002/1521-4141(200208)32:8<2218::AID-IMMU2218>3.0.CO;2-0
22. Couzin J. Drug discovery. Magnificent obsession. *Science* (2005) 307(5716):1712–5. doi:10.1126/science.307.5716.1712
23. Aarts S, Seijkens TTP, Kusters PJH, van der Pol SMA, Zarzycka B, Heijnen P, et al. Inhibition of CD40-TRAF6 interactions by the small molecule inhibitor 6877002 reduces neuroinflammation. *J Neuroinflammation* (2017) 14(1):105. doi:10.1186/s12974-017-0875-9
24. Laman J, van Meurs M, Schellekens M, de Boer M, Melchers B, Massacesi L, et al. Expression of accessory molecules and cytokines in acute EAE in marmoset monkeys (*Callithrix jacchus*). *J Neuroimmunol* (1998) 86(1):30–45. doi:10.1016/S0165-5728(98)00024-1
25. Grewal IS, Flavell RA. CD40 and CD154 in cell-mediated immunity. *Annu Rev Immunol* (1998) 16:111–35. doi:10.1146/annurev.immunol.16.1.111
26. Mackey MF, Barth RJ Jr, Noelle RJ. The role of CD40/CD154 interactions in the priming, differentiation, and effector function of helper and cytotoxic T cells. *J Leukoc Biol* (1998) 63(4):418–28.
27. Dittel BN. CD4 T cells: balancing the coming and going of autoimmune-mediated inflammation in the CNS. *Brain Behav Immun* (2008) 22(4):421–30. doi:10.1016/j.bbi.2007.11.010
28. Issazadeh S, Navikas V, Schaub M, Sayegh M, Khoury S. Kinetics of expression of costimulatory molecules and their ligands in murine relapsing experimental autoimmune encephalomyelitis in vivo. *J Immunol* (1998) 161(3):1104–12.
29. Seijkens T, Kusters P, Engel D, Lutgens E. CD40-CD40L: linking pancreatic, adipose tissue and vascular inflammation in type 2 diabetes and its complications. *Diab Vasc Dis Res* (2013) 10(2):115–22. doi:10.1177/1479164112455817
30. Andre P, Nannizzi-Alaimo L, Prasad SK, Phillips DR. Platelet-derived CD40L: the switch-hitting player of cardiovascular disease. *Circulation* (2002) 106(8):896–9. doi:10.1161/01.CIR.0000028962.04520.01
31. Sanchooli J, Ramroodi N, Sanadgol N, Sarabandi V, Ravan H, Rad RS. Relationship between metalloproteinase 2 and 9 concentrations and soluble CD154 expression in Iranian patients with multiple sclerosis. *Kaohsiung J Med Sci* (2014) 30(5):235–42. doi:10.1016/j.kjms.2013.12.008
32. Zabaleta M, Marino R, Borges J, Camargo B, Ordaz P, De Sanctis JB, et al. Activity profile in multiple sclerosis: an integrative approach. A preliminary report. *Mult Scler* (2002) 8(4):343–9. doi:10.1191/1352458502ms803oa
33. Masuda H, Mori M, Uchida T, Uzawa A, Ohtani R, Kuwabara S. Soluble CD40 ligand contributes to blood-brain barrier breakdown and central nervous system inflammation in multiple sclerosis and neuromyelitis optica spectrum disorder. *J Neuroimmunol* (2017) 305:102–7. doi:10.1016/j.jneuroim.2017.01.024
34. Carrieri PB, Carbone F, Perna F, Bruzzese D, La Rocca C, Galgani M, et al. Longitudinal assessment of immuno-metabolic parameters in multiple sclerosis patients during treatment with glatiramer acetate. *Metabolism* (2015) 64:1112–21. doi:10.1016/j.metabol.2015.05.001
35. Guerrero-Garcia J, Rojas-Mayorquin AE, Valle Y, Padilla-Gutierrez JR, Castaneda-Moreno VA, Mireles-Ramirez MA, et al. Decreased serum levels of sCD40L and IL-31 correlate in treated patients with relapsing-remitting multiple sclerosis. *Immunobiology* (2017) 223(1):135–41. doi:10.1016/j.imbio.2017.10.001

36. Balasa RI, Mihaela S, Voidazan S, Barcutean LI, Bajko Z, Hutanu A, et al. Natalizumab changes the peripheral profile of the Th17 panel in MS patients: new mechanisms of action. *CNS Neurol Disord Drug Targets* (2017) 16. doi:10.2174/1871527316666170807130632
37. Martins TB, Rose JW, Jaskowski TD, Wilson AR, Husebye D, Seraj HS, et al. Analysis of proinflammatory and anti-inflammatory cytokine serum concentrations in patients with multiple sclerosis by using a multiplexed immunoassay. *Am J Clin Pathol* (2011) 136(5):696–704. doi:10.1309/AJCP7UBK8IBVMVNR
38. Dominguez-Rodriguez A, Abreu-Gonzalez P, Garcia-Gonzalez MJ, Kaski JC. Diurnal variation of soluble CD40 ligand in patients with acute coronary syndrome. Soluble CD40 ligand and diurnal variation. *Thromb Res* (2009) 123(4):617–21. doi:10.1016/j.thromres.2008.05.006
39. Ponomarev ED, Shriver LP, Dittel BN. CD40 expression by microglial cells is required for their completion of a two-step activation process during central nervous system autoimmune inflammation. *J Immunol* (2006) 176(3):1402–10. doi:10.4049/jimmunol.176.3.1402
40. Vogel DY, Heijnen PD, Breur M, de Vries HE, Tool AT, Amor S, et al. Macrophages migrate in an activation-dependent manner to chemokines involved in neuroinflammation. *J Neuroinflammation* (2014) 11:23. doi:10.1186/1742-2094-11-23
41. Jensen J, Krakauer M, Sellebjerg F. Increased T cell expression of CD154 (CD40-ligand) in multiple sclerosis. *Eur J Neurol* (2001) 8(4):321–8. doi:10.1046/j.1468-1331.2001.00232.x
42. de Goer de Herve MG, Delfraissy JF, Taoufik Y. Following direct CD40 activation, human primary microglial cells produce IL-12 p40 but not bioactive IL-12 p70. *Cytokine* (2001) 14(2):88–96. doi:10.1006/cyto.2000.0855
43. D'Aversa TG, Weidenheim KM, Berman JW. CD40-CD40L interactions induce chemokine expression by human microglia: implications for human immunodeficiency virus encephalitis and multiple sclerosis. *Am J Pathol* (2002) 160(2):559–67. doi:10.1016/S0002-9440(10)64875-4
44. Sanders P, De Keyser J. Janus faces of microglia in multiple sclerosis. *Brain Res Rev* (2007) 54(2):274–85. doi:10.1016/j.brainresrev.2007.03.001
45. Aloisi F. Immune function of microglia. *Glia* (2001) 36(2):165–79. doi:10.1002/glia.1106
46. Wesemann DR, Dong Y, O'Keefe GM, Nguyen VT, Benveniste EN. Suppressor of cytokine signaling 1 inhibits cytokine induction of CD40 expression in macrophages. *J Immunol* (2002) 169(5):2354–60. doi:10.4049/jimmunol.169.5.2354
47. Karni A, Koldzic DN, Bharanidharan P, Khoury SJ, Weiner HL. IL-18 is linked to raised IFN-gamma in multiple sclerosis and is induced by activated CD4(+) T cells via CD40-CD40 ligand interactions. *J Neuroimmunol* (2002) 125(1–2):134–40. doi:10.1016/S0165-5728(02)00018-8
48. Vogel DY, Vereyken EJ, Glim JE, Heijnen PD, Moeton M, van der Valk P, et al. Macrophages in inflammatory multiple sclerosis lesions have an intermediate activation status. *J Neuroinflammation* (2013) 10:35. doi:10.1186/1742-2094-10-35
49. Elgueta R, Benson MJ, de Vries VC, Wasiuk A, Guo Y, Noelle RJ. Molecular mechanism and function of CD40/CD40L engagement in the immune system. *Immunol Rev* (2009) 229(1):152–72. doi:10.1111/j.1600-065X.2009.00782.x
50. De Silva NS, Klein U. Dynamics of B cells in germinal centres. *Nat Rev Immunol* (2015) 15(3):137–48. doi:10.1038/nri3804
51. Crotty S. Follicular helper CD4 T cells (TFH). *Annu Rev Immunol* (2011) 29:621–63. doi:10.1146/annurev-immunol-031210-101400
52. Jacob N, Stohl W. Autoantibody-dependent and autoantibody-independent roles for B cells in systemic lupus erythematosus: past, present, and future. *Autoimmunity* (2010) 43(1):84–97. doi:10.3109/08916930903374600
53. Teleshova N, Bao W, Kivisakk P, Ozenci V, Mustafa M, Link H. Elevated CD40 ligand expressing blood T-cell levels in multiple sclerosis are reversed by interferon-beta treatment. *Scand J Immunol* (2000) 51(3):312–20. doi:10.1046/j.1365-3083.2000.00688.x
54. Harp CT, Lovett-Racke AE, Racke MK, Frohman EM, Monson NL. Impact of myelin-specific antigen presenting B cells on T cell activation in multiple sclerosis. *Clin Immunol* (2008) 128(3):382–91. doi:10.1016/j.clim.2008.05.002
55. Ireland SJ, Blazek M, Harp CT, Greenberg B, Frohman EM, Davis LS, et al. Antibody-independent B cell effector functions in relapsing remitting multiple sclerosis: clues to increased inflammatory and reduced regulatory B cell capacity. *Autoimmunity* (2012) 45(5):400–14. doi:10.3109/08916934.2012.665529
56. Arbour N, Lapointe R, Saikali P, McCrea E, Regen T, Antel JP. A new clinically relevant approach to expand myelin specific T cells. *J Immunol Methods* (2006) 310(1–2):53–61. doi:10.1016/j.jim.2005.12.009
57. Chen D, Ireland SJ, Remington G, Alvarez E, Racke MK, Greenberg B, et al. CD40-mediated NF-kappaB activation in B cells is increased in multiple sclerosis and modulated by therapeutics. *J Immunol* (2016) 197(11):4257–65. doi:10.4049/jimmunol.1600782
58. Rincon-Arevalo H, Sanchez-Parra CC, Castano D, Yassin L, Vasquez G. Regulatory B cells and mechanisms. *Int Rev Immunol* (2016) 35(2):156–76. doi:10.3109/08830185.2015.1015719
59. Blair PA, Chavez-Rueda KA, Evans JG, Shlomchik MJ, Eddaoudi A, Isenberg DA, et al. Selective targeting of B cells with agonistic anti-CD40 is an efficacious strategy for the generation of induced regulatory T2-like B cells and for the suppression of lupus in MRL/lpr mice. *J Immunol* (2009) 182(6):3492–502. doi:10.4049/jimmunol.0803052
60. Michel L, Chesneau M, Manceau P, Genty A, Garcia A, Salou M, et al. Unaltered regulatory B-cell frequency and function in patients with multiple sclerosis. *Clin Immunol* (2014) 155(2):198–208. doi:10.1016/j.clim.2014.09.011
61. Fraussen J, de Bock L, Somers V. B cells and antibodies in progressive multiple sclerosis: contribution to neurodegeneration and progression. *Autoimmun Rev* (2016) 15(9):896–9. doi:10.1016/j.autrev.2016.07.008
62. Probstel AK, Sanderson NS, Derfuss T. B cells and autoantibodies in multiple sclerosis. *Int J Mol Sci* (2015) 16(7):16576–92. doi:10.3390/ijms160716576
63. Bourgeois C, Rocha B, Tanchot C. A role for CD40 expression on CD8+ T cells in the generation of CD8+ T cell memory. *Science* (2002) 297(5589):2060–3. doi:10.1126/science.1072615
64. Sinha S, Boyden AW, Itani FR, Crawford MP, Karandikar NJ. CD8(+) T-cells as immune regulators of multiple sclerosis. *Front Immunol* (2015) 6:619. doi:10.3389/fimmu.2015.00619
65. Vaitaitis GM, Yussman MG, Waid DM, Wagner DH Jr. Th40 cells (CD4+CD40+ Tcells) drive a more severe form of experimental autoimmune encephalomyelitis than conventional CD4 T cells. *PLoS One* (2017) 12(2):e0172037. doi:10.1371/journal.pone.0172037
66. Wheway J, Obeid S, Couraud PO, Combes V, Grau GE. The brain microvascular endothelium supports T cell proliferation and has potential for alloantigen presentation. *PLoS One* (2013) 8(1):e52586. doi:10.1371/journal.pone.0052586
67. Omari KM, Dorovini-Zis K. CD40 expressed by human brain endothelial cells regulates CD4+ T cell adhesion to endothelium. *J Neuroimmunol* (2003) 134(1–2):166–78. doi:10.1016/S0165-5728(02)00423-X
68. Peferoen LA, Vogel DY, Ummenthum K, Breur M, Heijnen PD, Gerritsen WH, et al. Activation status of human microglia is dependent on lesion formation stage and remyelination in multiple sclerosis. *J Neuropathol Exp Neurol* (2015) 74(1):48–63. doi:10.1097/NEN.0000000000000149
69. Kim DY, Hong GU, Ro JY. Signal pathways in astrocytes activated by cross-talk between of astrocytes and mast cells through CD40-CD40L. *J Neuroinflammation* (2011) 8:25. doi:10.1186/1742-2094-8-25
70. Tan J, Town T, Mori T, Obregon D, Wu Y, DelleDonne A, et al. CD40 is expressed and functional on neuronal cells. *EMBO J* (2002) 21(4):643–52. doi:10.1093/emboj/21.4.643
71. Carriba P, Davies AM. CD40 is a major regulator of dendrite growth from developing excitatory and inhibitory neurons. *Elife* (2017) 6:e30442. doi:10.7554/eLife.30442
72. Chuluundorj D, Harding SA, Abernethy D, La Flamme AC. Expansion and preferential activation of the CD14(+)CD16(+) monocyte subset during multiple sclerosis. *Immunol Cell Biol* (2014) 92(6):509–17. doi:10.1038/icb.2014.15
73. Sofo V, Salmeri FM, Di Bella P, Sessa E, D'Aleo G, Trimarchi G, et al. Short communication: impairment of membrane markers on peripheral blood mononuclear cells and imbalance of cytokine secretion in the pathogenesis of multiple sclerosis active phases. *J Interferon Cytokine Res* (2005) 25(11):661–5. doi:10.1089/jir.2005.25.661
74. Huang WX, Huang P, Hillert J. Systemic upregulation of CD40 and CD40 ligand mRNA expression in multiple sclerosis. *Mult Scler* (2000) 6(2):61–5. doi:10.1191/135245800678827509
75. Urshansky N, Mausner-Fainberg K, Auriel E, Regev K, Farhum F, Karni A. Dysregulated neurotrophin mRNA production by immune cells of patients with relapsing remitting multiple sclerosis. *J Neurol Sci* (2010) 295(1–2):31–7. doi:10.1016/j.jns.2010.05.019

76. Azoulay D, Urshansky N, Karni A. Low and dysregulated BDNF secretion from immune cells of MS patients is related to reduced neuroprotection. *J Neuroimmunol* (2008) 195(1–2):186–93. doi:10.1016/j.jneuroim.2008.01.010
77. Azoulay D, Mausner-Fainberg K, Urshansky N, Fahoum F, Karni A. Interferon-beta therapy up-regulates BDNF secretion from PBMCs of MS patients through a CD40-dependent mechanism. *J Neuroimmunol* (2009) 211(1–2):114–9. doi:10.1016/j.jneuroim.2009.04.004
78. Kosmaczewska A, Bilinska M, Ciszak L, Noga L, Pawlak E, Szteblich A, et al. Different patterns of activation markers expression and CD4+ T-cell responses to ex vivo stimulation in patients with clinically quiescent multiple sclerosis (MS). *J Neuroimmunol* (2007) 189(1–2):137–46. doi:10.1016/j.jneuroim.2007.06.021
79. Balashov KE, Smith DR, Khoury SJ, Hafler DA, Weiner HL. Increased interleukin 12 production in progressive multiple sclerosis: induction by activated CD4+ T cells via CD40 ligand. *Proc Natl Acad Sci U S A* (1997) 94(2):599–603. doi:10.1073/pnas.94.2.599
80. Filion LG, Matusevicius D, Graziani-Bowering GM, Kumar A, Freedman MS. Monocyte-derived IL12, CD86 (B7-2) and CD40L expression in relapsing and progressive multiple sclerosis. *Clin Immunol* (2003) 106(2):127–38. doi:10.1016/S1521-6616(02)00028-1
81. Benslimane N, Hassan GS, Yacoub D, Mourad W. Requirement of transmembrane domain for CD154 association to lipid rafts and subsequent biological events. *PLoS One* (2012) 7(8):e43070. doi:10.1371/journal.pone.0043070
82. Blair PJ, Riley JL, Harlan DM, Abe R, Tadaki DK, Hoffmann SC, et al. CD40 ligand (CD154) triggers a short-term CD4(+) T cell activation response that results in secretion of immunomodulatory cytokines and apoptosis. *J Exp Med* (2000) 191(4):651–60. doi:10.1084/jem.191.4.651
83. International Multiple Sclerosis Genetics Consortium (IMSGC), Beecham AH, Patsopoulos NA, Xifara DK, Davis MF, Kemppinen A, et al. Analysis of immune-related loci identifies 48 new susceptibility variants for multiple sclerosis. *Nat Genet* (2013) 45(11):1353–60. doi:10.1038/ng.2770
84. Wagner M, Wisniewski A, Bilinska M, Pokryszko-Dragan A, Cyrul M, Kusnierczyk P, et al. Investigation of gene–gene interactions between CD40 and CD40L in Polish multiple sclerosis patients. *Hum Immunol* (2014) 75(8):796–801. doi:10.1016/j.humimm.2014.05.013
85. Jacobson EM, Concepcion E, Oashi T, Tomer Y. A Graves' disease-associated Kozak sequence single-nucleotide polymorphism enhances the efficiency of CD40 gene translation: a case for translational pathophysiology. *Endocrinology* (2005) 146(6):2684–91. doi:10.1210/en.2004-1617
86. Field J, Shahijanian F, Schibeci S, Johnson L, Gresle M, Laverick L, et al. The MS risk allele of CD40 is associated with reduced cell-membrane bound expression in antigen presenting cells: implications for gene function. *PLoS One* (2015) 10(6):e0127080. doi:10.1371/journal.pone.0127080
87. Gonsky R, Deem R, Kakuta Y, McGovern DP, Targan S. Tu1926 functional characterization of the CD40 IBD risk SNP rs6074022: integrated Gwas, eQTL, and mQTL defines IBD patient subgroups with altered pathobiology and distinct natural history of disease. *Gastroenterology* (2014) 146(5):S–874. doi:10.1016/S0016-5085(14)63180-2
88. Gandhi KS, McKay FC, Cox M, Riveros C, Armstrong N, Heard RN, et al. The multiple sclerosis whole blood mRNA transcriptome and genetic associations indicate dysregulation of specific T cell pathways in pathogenesis. *Hum Mol Genet* (2010) 19(11):2134–43. doi:10.1093/hmg/ddq090
89. Sokolova EA, Malkova NA, Korobko DS, Rozhdestvenskii AS, Kakulya AV, Khanokh EV, et al. Association of SNPs of CD40 gene with multiple sclerosis in Russians. *PLoS One* (2013) 8(4):e61032. doi:10.1371/journal.pone.0061032
90. Abromson-Leeman S, Maverakis E, Bronson R, Dorf ME. CD40-mediated activation of T cells accelerates, but is not required for, encephalitogenic potential of myelin basic protein-recognizing T cells in a model of progressive experimental autoimmune encephalomyelitis. *Eur J Immunol* (2001) 31(2):527–38. doi:10.1002/1521-4141(200102)31:2<527::AID-IMMU527>3.0.CO;2-D
91. Becher B, Durell BG, Miga AV, Hickey WF, Noelle RJ. The clinical course of experimental autoimmune encephalomyelitis and inflammation is controlled by the expression of CD40 within the central nervous system. *J Exp Med* (2001) 193(8):967–74. doi:10.1084/jem.193.8.967
92. Howard LM, Ostrovidov S, Smith CE, Dal Canto MC, Miller SD. Normal Th1 development following long-term therapeutic blockade of CD154-CD40 in experimental autoimmune encephalomyelitis. *J Clin Invest* (2002) 109(2):233–41. doi:10.1172/JCI0214374
93. Samoilova E, Horton J, Zhang H, Chen Y. CD40L blockade prevents autoimmune encephalomyelitis and hampers TH1 but not TH2 pathway of T cell differentiation. *J Mol Med* (1997) 75(8):603–8. doi:10.1007/s001090050145
94. Constantinescu CS, Hilliard B, Wysocka M, Ventura ES, Bhopale MK, Trinchieri G, et al. IL-12 reverses the suppressive effect of the CD40 ligand blockade on experimental autoimmune encephalomyelitis (EAE). *J Neurol Sci* (1999) 171(1):60–4. doi:10.1016/S0022-510X(99)00249-X
95. Becher B, Durell BG, Noelle RJ. Experimental autoimmune encephalitis and inflammation in the absence of interleukin-12. *J Clin Invest* (2002) 110(4):493–7. doi:10.1172/JCI0215751
96. Becher B, Durell BG, Noelle RJ. IL-23 produced by CNS-resident cells controls T cell encephalitogenicity during the effector phase of experimental autoimmune encephalomyelitis. *J Clin Invest* (2003) 112(8):1186–91. doi:10.1172/JCI200319079
97. Cua DJ, Sherlock J, Chen Y, Murphy CA, Joyce B, Seymour B, et al. Interleukin-23 rather than interleukin-12 is the critical cytokine for autoimmune inflammation of the brain. *Nature* (2003) 421(6924):744–8. doi:10.1038/nature01355
98. Nagelkerken L, Haspels I, van Rijs W, Blauw B, Ferrant JL, Hess DM, et al. FcR interactions do not play a major role in inhibition of experimental autoimmune encephalomyelitis by anti-CD154 monoclonal antibodies. *J Immunol* (2004) 173(2):993–9. doi:10.4049/jimmunol.173.2.993
99. 't Hart BA, Blezer ELA, Brok HPM, Boon L, de Boer M, Bauer J, et al. Treatment with chimeric anti-human CD40 antibody suppresses MRI-detectable inflammation and enlargement of pre-existing brain lesions in common marmosets affected by MOG-induced EAE. *J Neuroimmunol* (2005) 163(1–2):31–9. doi:10.1016/j.jneuroim.2005.02.005
100. Larkin J, Chiarion-Sileni V, Gonzalez R, Grob JJ, Cowey CL, Lao CD, et al. Combined nivolumab and ipilimumab or monotherapy in untreated melanoma. *N Engl J Med* (2015) 373(1):23–34. doi:10.1056/NEJMoa1504030
101. Hong GU, Kim NG, Jeoung D, Ro JY. Anti-CD40 Ab- or 8-oxo-dG-enhanced Treg cells reduce development of experimental autoimmune encephalomyelitis via down-regulating migration and activation of mast cells. *J Neuroimmunol* (2013) 260(1–2):60–73. doi:10.1016/j.jneuroim.2013.04.002
102. Schaub M, Issazadeh S, Stadlbauer T, Peach R, Sayegh M, Khoury S. Costimulatory signal blockade in murine relapsing experimental autoimmune encephalomyelitis. *J Neuroimmunol* (1999) 96(2):158–66. doi:10.1016/S0165-5728(99)00022-3
103. Kalantari T, Karimi MH, Ciric B, Yan Y, Rostami A, Kamali-Sarvestani E. Tolerogenic dendritic cells produced by lentiviral-mediated CD40- and interleukin-23p19-specific shRNA can ameliorate experimental autoimmune encephalomyelitis by suppressing T helper type 17 cells. *Clin Exp Immunol* (2014) 176(2):180–9. doi:10.1111/cei.12266
104. Andre P, Prasad KS, Denis CV, He M, Papalia JM, Hynes RO, et al. CD40L stabilizes arterial thrombi by a beta3 integrin-dependent mechanism. *Nat Med* (2002) 8(3):247–52. doi:10.1038/nm0302-247
105. Kawai T, Andrews D, Colvin RB, Sachs DH, Cosimi AB. Thromboembolic complications after treatment with monoclonal antibody against CD40 ligand. *Nat Med* (2000) 6(2):114. doi:10.1038/72162
106. Ding Q, Si X, Liu D, Peng J, Tang H, Sun W, et al. Targeting and liposomal drug delivery to CD40L expressing T cells for treatment of autoimmune diseases. *J Control Release* (2015) 207(0):86–92. doi:10.1016/j.jconrel.2015.03.035
107. Lutgens E, Lievens D, Beckers L, Wijnands E, Soehnlein O, Zernecke A, et al. Deficient CD40-TRAF6 signaling in leukocytes prevents atherosclerosis by skewing the immune response toward an antiinflammatory profile. *J Exp Med* (2010) 207(2):391–404. doi:10.1084/jem.20091293
108. van den Berg SM, Seijkens TT, Kusters PJ, Zarzycka B, Beckers L, den Toom M, et al. Blocking CD40-TRAF6 interactions by small-molecule inhibitor 6860766 ameliorates the complications of diet-induced obesity in mice. *Int J Obes (Lond)* (2015) 39(5):782–90. doi:10.1038/ijo.2014.198
109. Chatzigeorgiou A, Seijkens T, Zarzycka B, Engel D, Poggi M, van den Berg S, et al. Blocking CD40-TRAF6 signaling is a therapeutic target in obesity-associated insulin resistance. *Proc Natl Acad Sci U S A* (2014) 111(7):2686–91. doi:10.1073/pnas.1400419111
110. Zarzycka B, Seijkens T, Nabuurs SB, Ritschel T, Grommes J, Soehnlein O, et al. Discovery of small molecule CD40-TRAF6 inhibitors. *J Chem Inf Model* (2015) 55(2):294–307. doi:10.1021/ci500631e
111. Steven S, Dib M, Hausding M, Kashani F, Oelze M, Kröller-Schön S, et al. CD40L controls obesity-associated vascular inflammation, oxidative stress,

and endothelial dysfunction in high fat diet-treated and db/db mice. *Cardiovasc Res* (2017). doi:10.1093/cvr/cvx197

Conflict of Interest Statement: The authors declare that the research was conducted in the absence of any commercial or financial relationships that could be construed as a potential conflict of interest.

frontiers in Immunology

REVIEW
published: 08 December 2017
doi: 10.3389/fimmu.2017.01752

BP180 Is Critical in the Autoimmunity of Bullous Pemphigoid

Yale Liu[1†], Liang Li[2†] and Yumin Xia[1]*

[1] Department of Dermatology, The Second Affiliated Hospital, School of Medicine, Xi'an Jiaotong University, Xi'an, China, [2] National-Local Joint Engineering Research Center of Biodiagnostics and Biotherapy, The Second Affiliated Hospital, School of Medicine, Xi'an Jiaotong University, Xi'an, China

Bullous pemphigoid (BP) is by far the most common autoimmune blistering dermatosis that mainly occurs in the elderly. The BP180 is a transmembrane glycoprotein, which is highly immunodominant in BP. The structure and location of BP180 indicate that it is a significant autoantigen and plays a key role in blister formation. Autoantibodies from BP patients react with BP180, which leads to its degradation and this has been regarded as the central event in BP pathogenesis. The consequent blister formation involves the activation of complement-dependent or -independent signals, as well as inflammatory pathways induced by BP180/anti-BP180 autoantibody interaction. As a multi-epitope molecule, BP180 can cause dermal–epidermal separation *via* combining each epitope with specific immunoglobulin, which also facilitates blister formation. In addition, some inflammatory factors can directly deplete BP180, thereby leading to fragility of the dermal–epidermal junction and blister formation. This review summarizes recent investigations on the role of BP180 in BP pathogenesis to determine the potential targets for the treatment of patients with BP.

Keywords: BP180, bullous pemphigoid, autoantibody, dermal–epidermal junction, cytokine

OPEN ACCESS

Edited by:
Piotr Trzonkowski, Gdańsk Medical University, Poland

Reviewed by:
Frank Antonicelli, University of Reims Champagne-Ardenne, France
Angelo Valerio Marzano, Università degli Studi di Milano, Italy

***Correspondence:**
Yumin Xia
xiayumin1202@163.com

†These authors have contributed equally to this work.

Specialty section:
This article was submitted to Immunological Tolerance and Regulation, a section of the journal Frontiers in Immunology

Received: *17 October 2017*
Accepted: *24 November 2017*
Published: *08 December 2017*

Citation:
Liu Y, Li L and Xia Y (2017) BP180 Is Critical in the Autoimmunity of Bullous Pemphigoid. Front. Immunol. 8:1752. doi: 10.3389/fimmu.2017.01752

INTRODUCTION

Bullous pemphigoid (BP), by far the most common autoimmune blistering disease, is induced by autoantibodies against the structural components of the dermal–epidermal junction (DEJ) (1). In most cases, the disease develops cryptically (2). The suggested causes of BP include silicosis (3), psoralen and ultraviolet A therapy (4), infections (5), physical or chemical insults (6–8), certain fruits (9), and medications (10, 11). However, the validation of these factors in the pathogenesis of BP remains be established. BP mainly affects the older age group of both sexes, or those 70 years old and above, but it can also affect infants, children, and adolescents (1, 12). This disease mainly involves the skin but occasionally the eyes, mouth, and genitals (1, 2). The cutaneous manifestations of BP are polymorphic and can be classified into three groups, namely classical BP, non-bullous cutaneous pemphigoid, and various rare variants (13, 14). Classical BP is clinically characterized by large (1–3 cm), tense, serous, or hemorrhagic blisters that appear on erythematous, urticarial, or eczematous lesions and even on apparently normal skin (1, 13). The biopsied lesions exhibit subepidermal splitting or blisters, which is the hallmark of BP, with dense inflammatory infiltration of eosinophils, basophils, neutrophils, lymphocytes, and mast cells in the dermis (1). Immunofluorescence analysis is necessary for the diagnosis of BP (15). Direct immunofluorescence is the most sensitive method for BP diagnosis, in which the lesion shows linear deposition of immunoglobulin G (IgG), C3 complement, and even IgE at the DEJ (16–18). Indirect immunofluorescence using the patient's sera and a substrate, especially salt-split skin, reveals a linear deposition of IgG along the roof of the artificial split (18).

One typical serologic characteristic of BP is the presence of circulating autoantibodies, which are mostly against BP180 (collagen XVII) and BP230 (15, 19, 20). BP180 is a 180 kDa transmembrane

glycoprotein with a 16th non-collagenous (NC16A) domain, which is the immunodominant part in BP (14). BP230 is an intracellular constituent of the hemidesmosomal plaque and belongs to the spectraplakin family (20, 21). The autoantibodies reported in BP include IgG and IgE (1, 22). Usually, IgG autoantibodies to BP180 are the ones first to be detected, and then IgG autoantibodies to BP230 subsequently appear (23). IgE antibodies to BP230 can also be detected in the blood of BP patients (24). Given the existence of autoantibodies, there have been commercially available enzyme-linked immunosorbent assay (ELISA) kits that target BP180 and BP230 antibodies for BP auxiliary diagnosis (25, 26).

Due to the age group involved and the application of more sensitive and specific diagnostic assay systems, the reported BP morbidity has increased (14, 19, 27, 28). Moreover, for disease-specific factors, due to the concomitant occurrence of neurodegenerative disorders, use of higher doses of oral corticosteroids, and the propensity to malignancies and venous thromboembolism, BP mortality showed an increasing trend as well (19, 29–36). These findings suggested the contributory role of activation of blood coagulation in the pathogenesis of BP (35, 36). Presently, topical or systematic corticosteroids, with or without immunosuppressive agents, are still the mainstays for BP treatment (1, 14, 37, 38). Intravenous Ig has also been introduced as an alternative therapy for BP (39–41), however, its effectiveness is still questionable (42, 43). Therefore, it is of highly importance to discover new targets to reduce BP morbidity and mortality. Recently, increasing evidences show that autoimmune responses to BP180 are important in the initiation and evolution of BP (44). The binding of autoantibodies to BP180 is a central step for blister formation. Moreover, BP180 is associated with severe and extensive lesions that require higher dose of steroids, which is a key risk factor for death (14, 28, 45). The serum level of anti-BP180 NC16A autoantibody correlates with the more active and severe disease, as well as poorer prognosis (33, 46). We, thus, consider BP180 as the most important culprit in the pathogenesis of BP and focused this review on recently updated knowledge on BP180 and its autoantibodies in BP.

THE BASIC STRUCTURE OF BP180

BP180 is a type II transmembrane protein with a cytosolic NH2 terminal and an extracellular COOH domain (47). The N-terminal domain, transmembranous stretch, and extracellular C-terminus have 466, 23, and 1,008 amino acids (aa) in length, respectively (48). The ectodomain contains 15 collagenous subdomains (COL1–COL15) interspersed by 16 non-collagenous sequences (NC1–NC16). The NC16A domain, a juxtamembranous linker region, appears to be biologically important, as it serves as the nucleus for the formation of a collagen-like triple helix (49, 50). The extracellular domain contains coiled-coil structures, which are physiologically shed from the cell surface by a disintegrin metalloproteinase (ADAM) (50). The ectodomain forms a loop structure as it spans the lamina lucida, extends to lamina densa, and then kinks back into the lamina lucida (49). BP180 contains multiple binding sites for hemidesmosome proteins, including the extracellular domains of integrin α6 and laminin-332 (laminin-5) and the cytoplasmic domains of integrin β4, plectin, and BP230 (20). The structure and location of BP180 indicate that it acts as a core anchor protein that connects the intracellular and extracellular hemidesmosomal proteins and plays a key role in the pathogenesis of BP.

THE EPITOPE PROFILES OF BP180

Previous studies mainly focused on extracellular NC16A domain (aa residues 490–562), which is the main target of BP autoantibodies. The NC16A domain has seven antigenic sites, including NC16A1, NC16A1-3, NC16A1-5, NC16A2, NC16A2.5, NC16A3, and NC16A3-4 (51–53) (**Figure 1**). Among these sites, NC16A2 and NC16A2.5 are the major antigenic sites, which can be targeted by all IgG and IgE antibodies. However, recent studies have described additional autoantibody-binding domains of BP180, such as the intracellular domain (ICD) and ectodomain (44, 54). The ICD (aa 1–452) has five target sites, namely ICD A, ICD B, ICD C, ICD D, and ICD A-D, and a central region (aa 112–199) (**Figure 1**). A previously published study reported that out of 18 sera of BP patients, 16 reacted with recombinant ICDs and that most of the antibodies bind to the central portion (55). A great number of sera combined with at least one of the ICD regions. With regard to ectodomain, it has been reported that 7.8–47% of BP sera recognized the C-terminal regions of the ectodomain (54, 56). Further mapping identified the six regions outside of NC16A that were recognized by the sera of the patients: aa 809–1106, aa 1080–1107, aa 1280–1315, aa 1331–1404, aa 1365–1413, and aa 1048–1465 (11, 52, 54, 57). aa 809–1106 and aa 1080–1107 were at the midportion, whereas aa 1331–1404 and aa 1365–1413 were at the COOH-terminal (**Figure 1**). Other epitopes embracing more than one domain, such as aa 467–567, aa 490–812, and aa 490–1497, were also reported (11, 52). It has been suggested that the pattern of epitope recognition may influence the course of the disease (23). Therefore, the recognition of target regions within BP180 is substantial in understanding the disease initiation and clinical characteristics of BP.

THE SOURCE OF AUTOANTIBODIES TO BP180

The etiology of BP is complex, but the presence of autoantibodies was widely accepted as the *sine qua non* of the condition. Anti-BP180 autoantibodies also exist in healthy people, even though these antibodies are conformationally different from pathogenic ones; however, only those bound to skin basement membrane can induce BP—suggesting that autoantibodies in the healthy may not be pathological *per se* (58, 59). The autoantibodies may assume function of surveillance and self-tolerance (60). In pathologic conditions, self-tolerance of the autoantibodies is dysfunctional, thus leading to the production of a higher-level of autoantibodies that bind to skin basement membrane and give rise to the occurrence of BP. The development of BP suggests that there is a threshold or checkpoint in terms of autoantibody generation (61). It remains unclear why immune tolerance to BP180 is dysfunctional in some individuals. Previous study

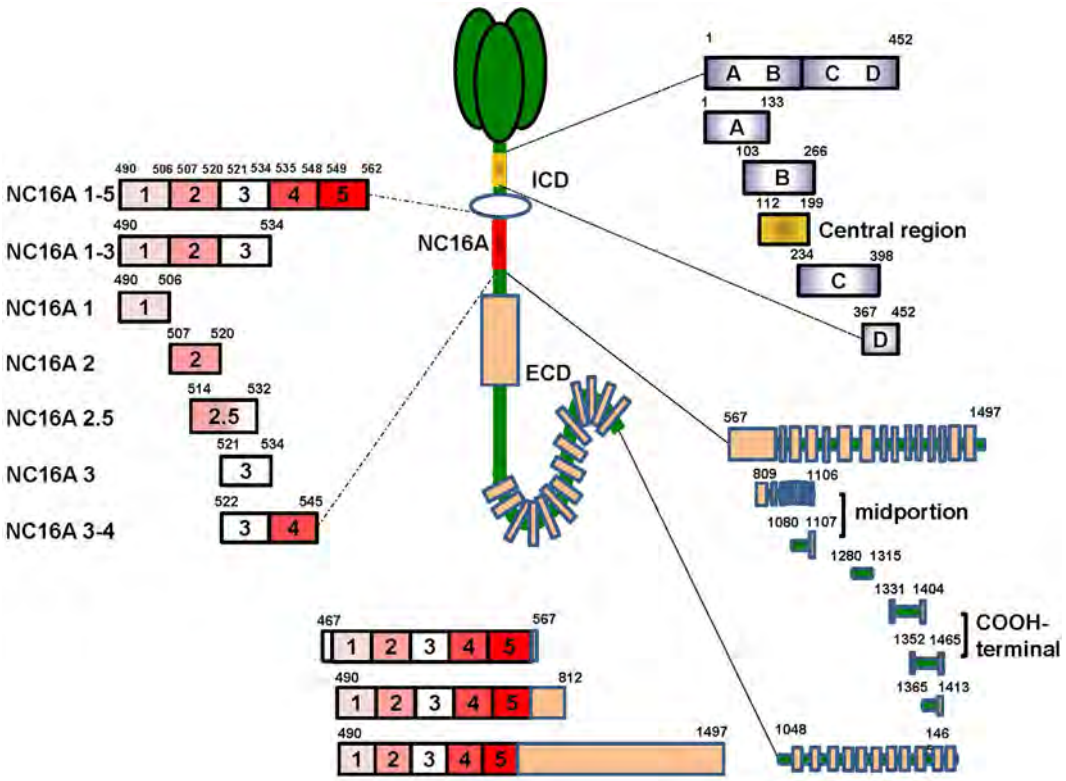

FIGURE 1 | The target sites of the BP180 molecule. BP180 is a multi-epitope protein with three major domains-the intracellular domain (ICD), the NC16A domain and the ectodomain outside NC16A domain. The ICD include five target sites, including aa 1–452, aa 1–133, aa 103–266, aa 234–398, aa 36–452 and a central region aa 112–199. The NC6A domain contain seven targeted sites, that is, NC16A1-5, 1-3, 1, 2, 2.5, 3, 3-4. The ectodomain domain also have eight functional sites, namely aa 567–1497, aa 809–1106, aa 1080–1107, aa 1280–1315, aa 1331–1404, aa 1352–1465, aa 1365–1413, and aa 1048–1465. Additionally, there are also target sites crossing more than one domain, such as aa 46–567, aa 490–812, and aa 490–1497.

suggests that CD4+ CD25+ Foxp3+ regulatory T (Treg) cells play an indispensable role in maintaining self-tolerance and in suppressing excessive production of autoantibodies deleterious to the host (62–65).

The reduction of CD4+ CD25+ Foxp3+ Treg cells in BP, as induced by triggers that are variants of pre-existing genetic factors, such as HLA-BQB1*0301, CYP2D6, MT-ATP8, and so on, leads to the breakage of self-tolerance, followed by the increase in autoreactive Th2, Th1, and B cells that can recognize different domains of BP180 mediated by epitope spreading to produce different autoantibodies (14, 44, 59, 65–69). The pathogens can exacerbate the process by sensitizing B cells *via* binding to toll-like receptors. The autoreactive T cells can interact with autoreactive B cells *via* combinations of CD40L–CD40, B-cell activating factor–transmembrane activator and CAML interactor (TACI)/B-cell maturation antigen, and proliferation-inducing ligand–TACI to further break peripheral tolerance and induce Ig production and class switching (70–74) (**Figure 2**). Moreover, the reactivity of T and B cells that target the NH2-terminal portion of the BP180 ectodomain is associated with severe BP, whereas the crosstalk of T and B cells targeting the central portion of BP180 is more frequently recognized in limited BP (75). The exploration in gene therapy might provide clues to retrieve Treg-mediated tolerance and to hinder the production of autoantibodies in skin-grafted animals (76).

AUTOANTIBODIES TARGETING NC16A OF BP180

Previously, most studies pointed out that the NC16A might be the major pathogenic epitope in BP (47, 74). ELISA analysis using recombinant BP180 NC16A demonstrated that 22–100% of BP sera reacted to BP180 NC16A peptides and that autoantibodies targeting NC16A domain are associated with tense blisters, severe urticarial erythema, extensive lesions, and elevated eosinophils (45, 77). Therefore, there is a variety of autoantibody types that act on this domain and mediate various pathogenesis.

Anti-NC16A IgG

Anti-NC16A IgG is associated with BP-affected areas and with the occurrence of erosions and blisters in BP (46). High titers of anti-BP180 NC16A IgG at the time of therapy cessation represented the main factor in the prediction of risk of relapse in BP (78). Passive transfer of rabbit antimurine IgG antibodies against BP180 can lead to the development of BP-like skin phenotype, in

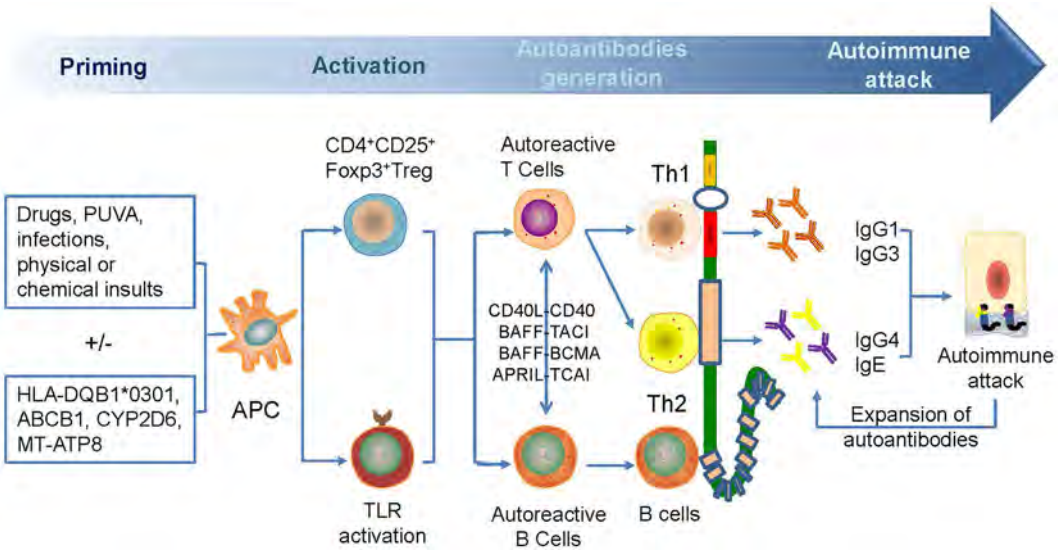

FIGURE 2 | A possible mechanism for the generation of anti-BP180 autoantibodies. Antibodies are generated for the breakage of self-tolerance which is caused by drugs, psoralen, and ultraviolet A therapy, infections, physical, or chemical insults. Autoactivated Th1 and Th2 and B cell can target different domains of BP180, leading to the generation of anti-BP180 autoantibodies *via* epitope spreading and Ig class-switch. Such autoantibodies could be present in the serum for a long time before occurrence of clinical features. Attacked BP180 can be a source of new antigens to initiate the further expansion of autoantibodies and acceleration of disease.

which the mechanisms involved are complement activation, mast cell degradation, neutrophil infiltration, production of reactive oxygen species and proteases, and BP180 degradation (14, 79); and these mechanisms suggest a complement-dependent inflammatory pathway in BP development. The pathways induced by antimurine BP180 NC16A domain is further verified in studies using mast cell-deficient (80), C5-null (16), C4-null, alternative pathway component factor B-deficient (28, 81), membrane CD46 upregulated (82), Fab-IgG-deficient (83), and FcγR-deficient (84) mice. All these studies were able to identify the complement-dependent inflammatory pathway of anti-BP180 NC16A IgG (**Figure 3A**).

There are complement-independent mechanisms that account for the induction of BP by anti-NC16A IgG. Nearly one-fifth of BP cases may develop blisters in a complement-independent manner mainly through BP internalization (16) Immunofluorescence microscopy revealed that BP180 content in BP lesions is reduced by approximately 40% (85). As demonstrated by vibration assay *in vitro*, keratinocytes stimulated with anti-NC16A IgG demonstrated BP180 internalization and significant decrease in cell-plate adhesion (86). Further supporting data stem from an *in vivo* study using neonatal C3-deficient BP180-humanized mice without complement activation (87). The effects are attributed to the internalization of BP180/anti-BP180 complex via a macropinocytic pathway, which involves ICD phosphorylation by protein kinase C and potential degradation of BP180 through a ubiquitin/proteasome pathway (85, 88, 89). As BP-IgG-induced BP180 internalization is insufficient to induce blister formation, various inflammatory responses mediated by FcγR-independent and FcγR-dependent pathways must be involved, which further lead to a BP-specific split (85). At least interleukin (IL)-6 and IL-8, which are induced by autoantibodies, participate in the inflammatory responses (28, 90) In addition, neutrophils partly recruited by IL-8 are also essential for blister formation (91) (**Figure 3B**). These studies emphasized the complement-independent inflammatory pathway of anti-BP180 NC16A IgG.

However, the role of complements in BP pathogenesis, as mediated by anti-BP180 NC16A IgG autoantibodies, is still controversial. Negative C3 deposition along the epidermal basement membrane zone was found in 16.9% of BP lesions (16). Antihuman BP180 NC16A IgG4, which has low ability to bind to the Fc receptor and fixing complement, can induce dermal–epidermal separation in *in vitro* cryosection assays and blister formation in patients (89, 92). IgG4 autoantibodies are also the major IgG subclasses of autoantibodies found in more than 54.4% of BP patients, and it is parallel with the disease severity (93). An *in vitro* study found that anti-NC16A IgG4 might prevent the induction of BP blistering by competitively inhibiting the binding of IgG1 and IgG3 autoantibodies to the NC16A region and by blocking IgG1- and IgG3-induced complement fixation and neutrophil infiltration (94). Another study reported that anti-NC16A IgG4 has a protective role in BP (94). However, the provided C5a complement could successfully induce BP through anti-NC16A IgG4 (94). The revealed discrepancies may be explained by the different research methods used in the studies, as well as the complexity of BP, or by the possibility that the protective role of IgG4 autoantibodies in BP is due to the competitive blockade of IgG1 and IgG3 autoantibodies, which in turn gives rise to the suppression of complement-dependent blister formation. However, the "IgG4-dominant complement-independent BP" cannot be excluded. When the abovementioned studies are summarized, as well as the findings of complement fixation at basement

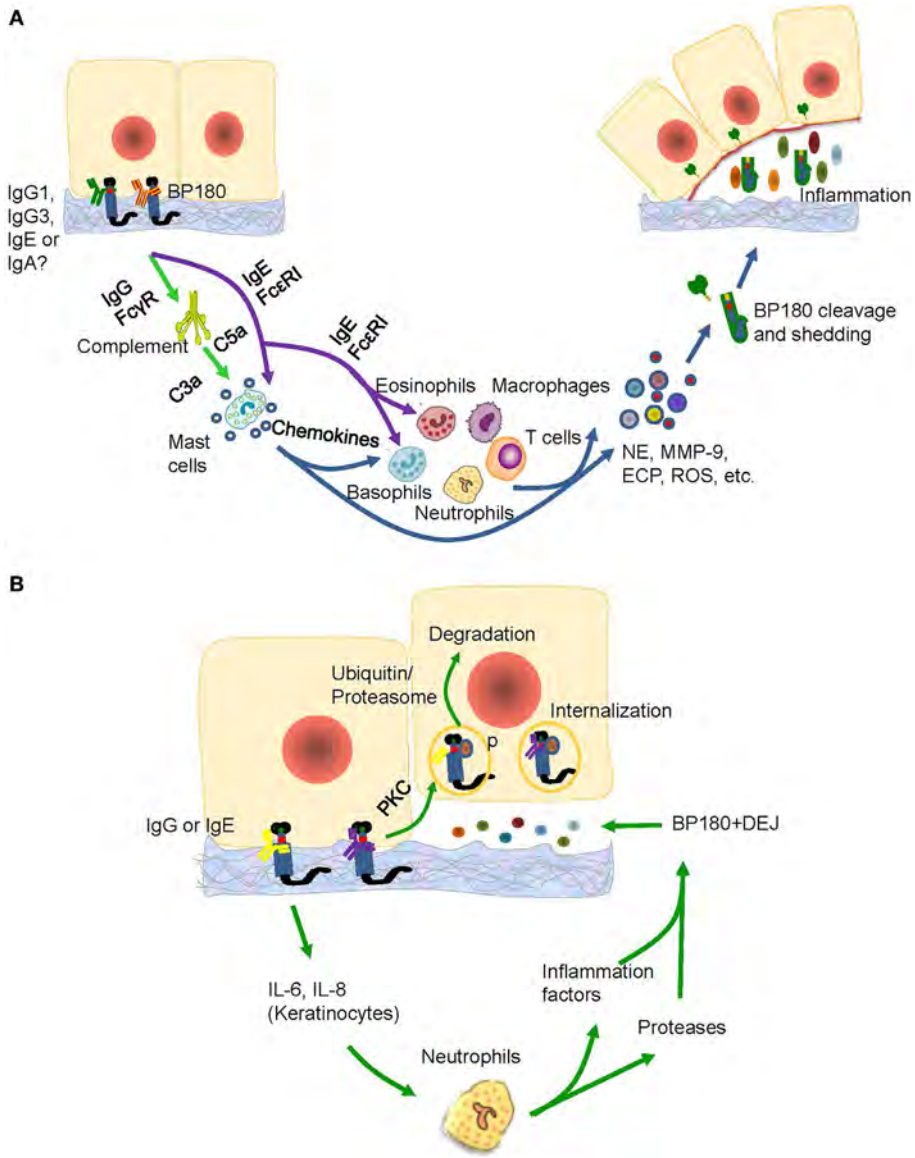

FIGURE 3 | The possible pathogenic mechanism of the anti-BP180 NC16A autoantibodies. **(A)** The IgG1, IgG3, IgE, or IgA anti-BP180 NC16A autoantibodies-mediated pathways for blister formation in bullous pemphigoid (BP). The binding of IgG1, IgG3 with NC16A activates complements *via* FcγR followed by mast cell degradation and neutrophilic, eosinophilic, basophilic, and macrophage infiltration, which lead to the degradation of BP180 by releasing inflammatory factors and proteases. While the IgE anti-BP180 NC16A autoantibodies activate infiltration of mast cell, eosinophils, and basophils *via* FcεRI. **(B)** The immunoglobulin G (IgG) or IgE-mediated pathways for blister formation in BP. On the one hand, the binding of IgG or IgE with NC16A domain activates the protein kinase C followed by BP180 phosphorylation and degradation, which leads to the reduced adhesion. The binding, on the other hand, causes the release of interleukin (IL)-6 and IL-8 by keratinocytes, which prompts recruitment of neutrophils, release of inflammatory factors and neutrophil elastase (NE), and blister formation.

membrane in BP patients, we can conclude that complement amplifies blister formation by inducing inflammation (16, 51, 95).

Anti-NC16A IgE

In addition to the IgG autoantibodies, 22–100% BP patients also produce IgE autoantibodies against BP180 NC16A (24, 46, 96, 97). The level of anti-NC16A IgE is correlated with disease activity (24, 46), occurrence of urticarial lesions and erythema (46, 98, 99), higher prednisolone dosage, longer duration before remission, and more intensive therapies (100). Immunofluorescence revealed the deposition of IgE autoantibodies along the DEJ in up to 41% of BP patients (101). Moreover, the early pathological changes in BP, including urticaria, eosinophil infiltration, and spontaneous blistering, can only be observed in models that utilized IgE autoantibodies from patient sera or recombinant monoclonal IgE antibodies specific for BP180 (102). These observations indicate that IgE autoantibodies may also be involved in the pathogenesis of BP and correlate with certain distinct clinical features. Furthermore, epitope mapping studies have demonstrated that

these IgE autoantibodies preferably target the NC16A domain of the BP180 protein as IgG (46, 53, 103).

Injecting purified anti-BP180 NC16A IgE autoantibodies into human skin grafted on nu/nu mice can induce histologic dermal–epidermal separation, as well as erythematous and urticarial plaques; and the mechanisms of these processes include mast cell infiltration and degranulation and influx of eosinophils, lymphocytes, and neutrophils (104). An *in vitro* investigation showed that the injection of IgE into the dermis of a human cryosection model led to histologic separation at the DEJ through the binding of FcεRI on mast cell surface, which triggered mast cell degranulation, subsequent eosinophil infiltration, and direct activation of eosinophils and basophils mediated by high-affinity FcεRI (95, 105, 106). Interestingly, the amount of circulating eosinophils is correlated with the levels of both NC16A-specific IgG and IgE in BP sera (106). These results provide indirect evidence that anti-BP180 NC16A IgE autoantibodies contribute to BP-like damage and to certain distinct clinical features by triggering mast cell degranulation and basophil histamine release that is FcεRI dependent (106, 107) (**Figure 3A**). The successful use of omalizumab in preventing the interaction of IgE with FcεRI in BP patients further verifies the FcεRI-dependent pathways (108, 109). However, recent studies also revealed that IgE autoantibodies from BP patients could be internalized into cultured human keratinocytes or skin tissues where they stimulate production of IL-6 and IL-8 and lead to the depletion of hemidesmosomes, as observed through BP IgG autoantibodies and as the effect of anti-NC16A IgG on keratinocytes *in vitro* (110–112) (**Figure 3B**). These studies suggest that the direct function of anti-BP180 NC16A IgE autoantibodies is to promote inflammation and fragility of the DEJ in BP. Further studies utilizing IgE monoclonal antibody are necessary to explore the mechanisms underlying NC16A-specific IgE autoantibody-mediated tissue damage in BP (113).

Anti-NC16A IgA

An increasing number of studies reported the potential role of anti-BP180 IgA, aside from anti-NC16A IgG and IgE, in BP pathogenesis (52, 107, 114, 115). Comparable to IgG and IgE, IgA autoantibodies mainly target the NC16A domain (106). Anti-BP180 NC16A IgA can be found in sera of 20–65% of BP patients (51, 113); and it can also be detected in the saliva of 36%, parotid gland of 44%, and in sera of 28% of mucous membrane pemphigoid patients (114). Moreover, IgA basement membrane zone deposition has been reported in 13% of BP patients (17, 116). However, investigation that mechanistically elucidates the functions of IgA autoantibodies in BP are still lacking. Epitope spreading or antibody class switching are likely to be involved in the pathogenesis of BP, as there is a determined clinical association between BP and linear IgA bullous disease (LAD) (114, 117). Recent studies reported that there is a linear IgA deposition in basement membrane zone, which is dapsone-responsive and characterized by a flexural distribution of intensely pruritic subepidermal bullae, thus suggesting that IgA might be associated with specific clinical features of BP or that BP may have comparable or overlapping pathomechanisms with LAD (118, 119). Like LAD, the anti-BP180 IgA autoantibodies directly act on NC16A domain, leading to the release of inflammatory factors and neutrophils, degranulation of neutrophils and mast cells, and release of proteolytic enzymes—all of which are similar to the effects of IgG and IgE (118) (**Figure 3A**). In fact, most serum samples from LAD and BP patients contain both IgA and IgG antibodies against BP180 (114, 120, 121). Thus, the two diseases could be regarded as different ends of a continuous spectrum of autoimmune responses to BP180 in subepidermal blistering diseases (119). Further studies using cell and animal models are needed to comprehensively unveil the pathogenic role of anti-BP180 NC16A IgA autoantibodies.

AUTOANTIBODIES TARGETING ICD AND ECTODOMAIN OF BP180

Recent studies reported that 59–82% of BP sera can recognize the ICD of BP180, while 7.8–49% of BP sera are reactive against the ectodomain of BP180 (54, 77, 122, 123). All autoantibodies, including IgG, IgE, and IgA, can target ICD; however, these autoantibodies bind to different sites (55, 114, 122, 123). The autoantibodies can penetrate live cells, reach their intracellular targets, and alter cellular functions (124) (**Figure 4**). The central region of BP180 ICD harbors binding sites that are critical for the interaction of BP180 with β4 subunit of the α6β4 integrin, which is vital for the incorporation of the protein into the hemidesmosome (49). Thus, it implicates that autoantibodies against BP180 ICD impair the interaction of BP180 with other molecular constituents of the hemidesmosome. Otherwise, the damaged basal keratinocyte induced by the binding of autoantibodies to BP180 ectodomain leads to the exposure of the ICD to the immune system, which is referred to as "epitope spreading" (125) (**Figure 4**).

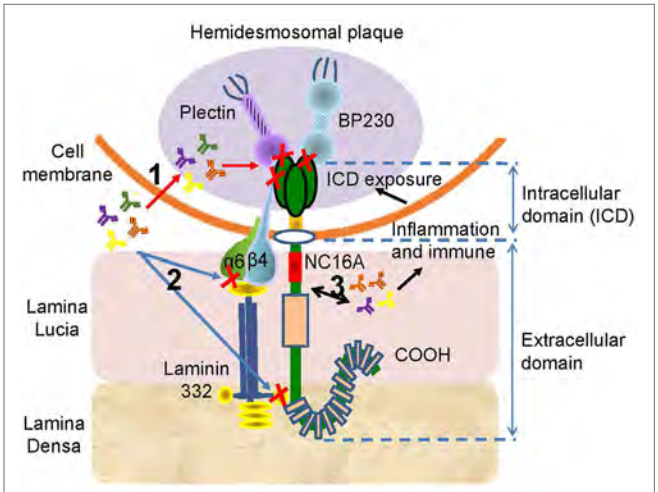

FIGURE 4 | The potential pathogenesis of the anti-BP180 autoantibodies targeting the intracellular domain (ICD) or the ectodomain outside the NC16A. There are three possible mechanism associated the autoantibodies with ICD or ectodomain. (1) The autoantibodies penetrate cells, reach the ICD, and inhibit the interaction of BP180 with plectin, BP230, or β4. (2) The binding of autoantibodies with ectodomain interferes the interplay of BP180, α6, β4, and laminin-332. (3) The interaction between autoantibodies and ectodomain induces inflammatory and immune responses, which lead to the exposure of the ICD, initiating the effect of autoantibodies on ICD.

In addition, the COOH-terminal region of the BP180 ectodomain is shown to be recognized by 47% of BP sera (56). IgG, IgE, and IgA autoantibodies can all bind to the terminal region (52, 54, 103, 122). The presence of autoantibodies against N- or C-terminal portions of the BP180 ectodomain is associated with the mucosal lesions in BP patients (56, 126). In addition, there are existing autoantibodies against the midportion of BP180; and these are associated with the occurrence of hemiplegia, clinical presentation of lack of erythema around the bullae, and histopathologic eosinophil infiltration inside and around subepidermal bullae (57). Other studies revealed that high levels of autoantibodies against C-terminal portions are associated with older age, administration of dipeptidyl peptidase-4 inhibitors before BP onset, and a positive response to moderate doses of oral prednisolone (11, 123). However, there is also a report refuting the association of autoantibodies with dipeptidyl peptidase-4 inhibitors (127). As BP180 extends from the cytoplasm of the basal keratinocyte to the lamina densa, it is presumed that the autoantibodies against this region might be responsible for the scarring phenotype observed in cicatricial pemphigoid patients (56) (**Figure 4**). The development of novel ELISA kits to detect the autoantibodies against the ectodomain, or even ICD, is beneficial in diagnosing BP without NC16A domain (56, 128).

More novel animal models have been recently constructed, thus making it possible to determine the role of different domains. One of the animal models is the ΔNC14A mice, which have BP180 NC14A replaced with the homologous human BP180 NC16A epitope cluster region (129). BP lesion develops in these ΔNC14A mice after passive transfer of BP IgG (129). The NC14A region can also be genetically deleted in C57BL/6 mice, which then have less amount of BP180 in skin but have normal ectodomain shedding (130). They spontaneously produce IgG and IgA autoantibodies against BP180 and present eosinophilic infiltrations, as well as the clinical features of pruritus and crusted erosions (130). Hence, the ΔNC14A mice may be an ideal experimental model for investigating the early clinical changes in BP. However, in the absence of NC16A domain, it is impossible to explore the detailed functions of anti-NC16A autoantibodies. It is also presumed that the pruritus and eosinophils are associated with the ectodomain. Therefore, the ΔNC14A mice may be utilized as a model for the exploration of autoantibodies acting on the ICD or on the ectodomain. However, the mechanisms involved remain to be confirmed. Another animal model is the COL17-humanized mice, which can express human BP180, and it is suitable for the analysis of the pathogenesis of BP in humans (131). The spontaneous production of high titers of anti-BP180 antibodies in blisters and erosions on erythematous skin lesions makes the observation of dynamic immune reactions possible. The pathogenicity of autoantibodies against ICD and ectodomain of BP180 remains unclear, and further studies are warranted. The development of novel ELISA system to detect such autoantibodies is necessary (77).

IgM AUTOANTIBODIES IN BP

An IgM-mediated BP has been recently reported (132, 133). Direct immunofluorescence microscopy showed that linear deposition of IgM can be found at the DEJ of 6–22% of BP patients (17, 134, 135). However, the target of IgM autoantibodies is unknown, and immunoblotting with recombinant protein of BP180 C-terminal domain showed multiple non-specific bands (136). IgM is mainly associated with BP caused by lupus erythematosus (132); however, it is rarely associated with BP due to infections (137), macroglobulinemia (136, 138), and surgical factors (139). The presence of IgM autoantibodies seems to not influence the course or outcome of the disease; and the role of IgM autoantibodies in the pathophysiology of BP remains elusive.

THE CLEAVAGE AND DEPLETION OF BP180

Followed by various autoantibody-mediated inflammatory responses, the BP180 cleavage and depletion have been proposed as the terminal effect that causes reduced adhesion and blister formation. *In vitro*, the cleavage and shedding of BP180 ectodomain is an event related to detachment, migration, proliferation, differentiation, and wound healing of keratinocytes (50, 140–144). Generally, the cleaved ectodomain does not generate pathogenic epitopes. However, excessive cleavage, shedding, or depletion can lead to reduced adhesion and blister formation.

Bullous pemphigoid autoantibody-induced infiltration of mast cells, eosinophils, and neutrophils can lead to the production of various inflammatory factors and proteases that contribute to the induction of blister formation. Increased levels of IL-1β, IL-2, IL-4, IL-5, IL-6, IL-8, IL-10, IL-13, IL-17, IL-22, IL-23, IL-31, IL-36, interferon-γ, tumor necrosis factor (TNF)-α, transforming growth factor-β, RANTES (regulated on activation, normal T cell expressed and secreted), monocyte chemotactic protein 1, interferon gamma-induced protein 10, and C-C chemokine ligand (CCL) 17 have been detected in skin lesions, serum, or blister fluid of BP patients (14, 19, 97, 145–150). In addition, C-C chemokine receptor 3 ligands, such as CCL 11, CCL13, CCL18, CCL26, and CCL28, have been shown to be increased in skin and/or sera of BP patients (43, 146, 151, 152). Increased levels of CCL1, CCL2, and chemokine C-X-C motif ligand-10 were detected in sera of BP patients (153, 154). Moreover, increasing data revealed their functional involvements in BP (97, 149, 151, 153, 155–158) (**Figure 5A**). The proteases produced by inflammatory cells are functionally involved as well (79, 159) (**Figure 5B**). The inflammatory cells can release mast cell protease (MCP)-4, matrix metalloproteinase (MMP)-9, neutrophil elastase (NE), plasmin, and eosinophil cationic protein (ECP), which cleave and degrade BP180, thus leading to dermal–epidermal separation and blister formation (20, 149, 157, 160–164) Pathogenic anti-BP180 IgG failed to induce subepidermal blistering in mice that were deficient in either NE or MMP-9 (89). MMP-9 can regulate NE activity by inactivating α1-proteinase inhibitor (α1-PI) (159). Furthermore, α1-PI serves as a chemoattractant for neutrophils once it is cleaved and exacerbates tissue damage (165). MMP-9 can also cleave BP180 into small tripeptides Pro-Gly-Pro, which significantly enhance neutrophil chemotaxis and NE release (149). These infiltrated cells also release IL-17, which significantly upregulates the production of MMP-9 and elastase in

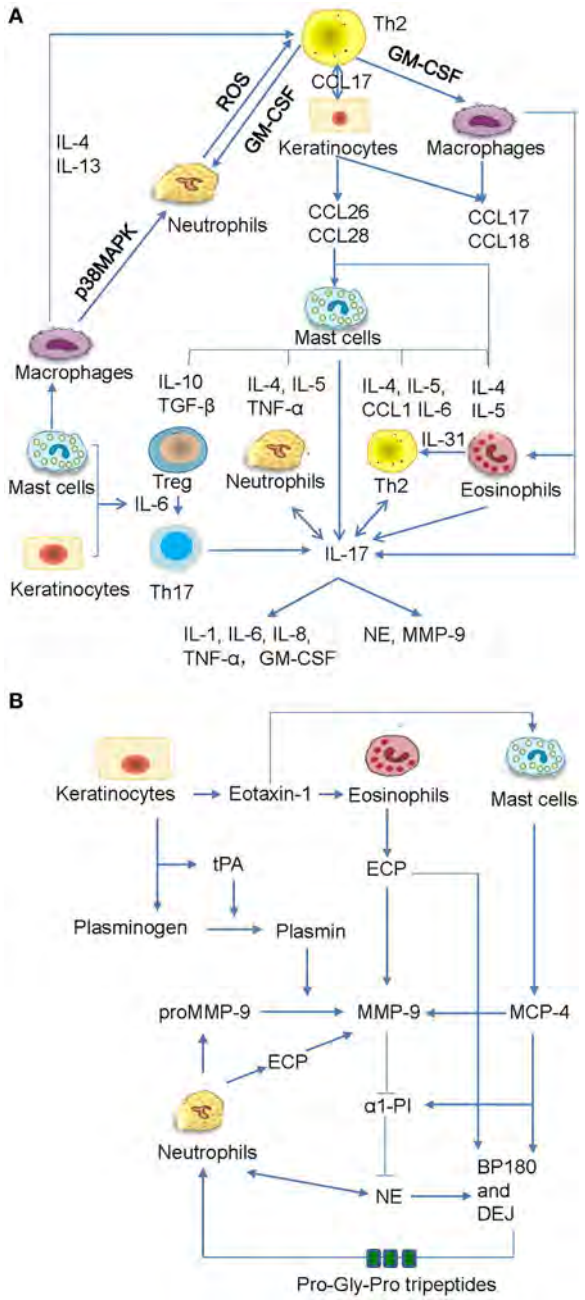

FIGURE 5 | The crosstalk networks of the inflammatory cells and the proteases. **(A)** The autoactive Th2 cells secrete type II cytokines, which act on macrophages, keratinocytes, and fibroblasts and induce the chemotaxis of mast cells. The mast cells produce various cytokines and chemokines, which act on the regulatory T (Treg) cells, neutrophils, Th2, eosinophils, and macrophages. All these inflammatory cells can release interleukin (IL)-17, which not only act on neutrophils and Th2 but also prompt inflammatory response and proteases release. **(B)** The keratinocytes synthesize tissue plasmogen activator (tPA), which activates plasmin followed by the activation of matrix metalloproteinase (MMP)-9. The eosinophil cationic protein (ECP) and mast cell protease (MCP)-4 can also activate MMP-9. MMP-9 inhibits production of α1-proteinase inhibitor (α1-PI) while promote generation of neutrophil elastase (NE). All these proteases act on BP180 and dermal–epidermal junction (DEJ). The cleaved BP180 can release pro-gly-pro tripeptides and attract neutrophils.

neutrophils (149, 166). The released IL-17 could, in turn, stimulate neutrophils to produce more IL-17 and form an amplified loop (167) (**Figure 5A**). Therefore, inflammatory factors and proteases induced by inflammatory cells play key roles in the cleavage and depletion of BP180, and targeting these inflammatory networks may be a promising therapeutic strategy in the treatment of BP.

However, BP180 cleavage may also occur in the absence of anti-BP180 autoantibodies (140). Such physiological cleavage is mediated by ADAMs (140). Our study further reveals that TNF-like weak inducer of apoptosis (TWEAK), which is a multifaceted cytokine that participates in various skin inflammatory responses, can exacerbate the BP180 reduction and keratinocyte adhesion (19). Moreover, the effect of TWEAK on BP180 cleavage involves the activation of extracellular signal-regulated kinase and nuclear factor-κB pathways as well as the downstream ADAMs, in which ADAM 8, 9, 10, 15, and 17 have been suggested to participate in BP180 cleavage or BP development (19, 168, 169). We also found high expression of MMP-9, ADAM9, ADAM10, and ADAM17 in BP lesions and in keratinocytes upon TWEAK/Fn14 activation (19). The upregulation of MMP-9 and ADAM10 is responsible for the shedding of membrane CD46, which further enhances BP180 NC16A IgG-mediated complement activation and blister formation (82). Therefore, the role of TWEAK in BP development can be mainly ascribed to the abnormally high expression of ADAMs and other proteases. By considering the absence or insignificant expression of TWEAK in noninvolved skin, we conclude that TWEAK likely plays a secondary inflammatory role rather than being a primary participant (19, 170). Further investigations are required to establish the clear-cut function of TWEAK in BP.

POTENTIAL THERAPEUTIC TARGETS

Considerable progress made by recent studies updated our understanding of BP pathogenesis. The availability of novel BP animal models provides important tools to further gain insights on the pathophysiology of the autoimmune disease. However, there is a limited progress regarding BP therapy. As BP180 is a molecule with multiple epitopes, a better insight on the mechanisms of immune responses induced by binding of autoantibodies to BP180 on different epitopes is crucial for the design of novel and more specific therapeutic strategies for this life-threatening autoimmune disorder (**Table 1**).

The Recovery of Immune Tolerance

Targeting immune tolerance is a coveted approach for the treatment of various autoimmune diseases, as current treatment options often involve non-specific immunosuppression. BP is closely associated with the disturbance of self-tolerance, in which the reduction in Treg cells plays a key role. Therefore, the increase in Treg cells will help to recover immune tolerance and prevent BP development. Previously, recombinant IL-10 has been used to increase circulating Treg cells and to lower CD4+ T cells (171). The use of low-dose recombinant IL-2 could also induce significant expansion of Treg cells *in vivo* and preferentially restore Treg cells (172). Low-dose IL-2-induced Treg cell proliferation is subsequently followed by increased programmed cell death 1 (PD-1) expression (173). PD-1 inhibitor causes BP eruptions, thus

TABLE 1 | Potential treatment targets for bullous pemphigoid (BP).

Categories	Targets	Drugs or methods	Potential effects	Reference
Immune tolerance	Regulatory T (Treg) cells	Interleukin (IL)-10	Increasing Treg cells	(171)
		Low-dose IL-2	Inducing significant Treg cells expansion	(172, 173)
		Oxymatrine	Upregulating FOXP3 Treg cells and reducing the production of tumor necrosis factor-α and IL-17A	(174)
	BP180 NC16A	Gene gun delivery of NC16a-encoding DNA	Inducting tolerance of BP180	(175)
	BP180	Lactic-co-glycolic acid nanoparticles	Inducing antigen-specific T cell tolerance	(176)
B cells	CD20	Rituximab	Reducing all subclasses of immunoglobulin G (IgG) anti-BP180 autoantibodies	(102, 177)
		Rituximab and intravenous immunoglobulin	Producing a prolonged and sustained remission in patients with active and recalcitrant BP	(39, 178)
		Calcineurin inhibitors	Suppressing naive B cells	(179)
T cells	CD25	Anti-CD25 antibodies	Targeting IL-2 receptor on activated T cells	(180)
	Calcineurin	Calcineurin inhibitors	Inhibiting nuclear factor of activated T cells and blocking T-cell-dependent production of IgG	(181)
	CD4+ T cells	IL-10	Lowering the number of circulating CD4+ T cells	(171)
Co-stimulators	BAFF–APRIL	Tabaluma (anti-BAFF)	Neutralizing autoreactive and memory B cells	(182)
		Anti-APRIL	Anti-proliferation and reducing autoantibodies production	(183, 184)
	CD40–CD40L	Anti-CD40	Regulating both innate and adaptive immunity and the activation of antigen-specific T cells	(185)
Autoantibodies	IgG	SM101	A soluble FcγR that competes with the interaction of IgG with membrane FcγRs	(186)
	IgE	Omalizumab	Inhibiting IgE binding to FcεRI	(108)
	Autoantibodies	Immunoadsorption	Declining the serum autoantibody levels	(187, 188)

APRIL, a proliferation-inducing ligand; BAFF, B-cell activating factor.

suggesting the value of targeting PD-1 upregulation in BP treatment (102, 189). Oxymatrine, a monosomic alkaloid extracted from the Chinese herb *Sophora flavescens* Ait, can upregulate FOXP3+ Treg cells and reduce the production of TNF-α and IL-17A, thus aiding in the recovery of immune tolerance (174). Previously, nanotechnology is therapeutically used to inhibit the detrimental immune responses in autoimmunity through its direct immunosuppressive effect on antigen-presenting cells B and T cells, or indirectly by delivering compounds that result in immunotolerance (190). Gene gun delivery of NC16A-encoding DNA on gold particles results in Treg cell-mediated tolerance to BP180 (175). Antigen-coupled biodegradable poly (lactic-co-glycolic acid) nanoparticles have been used to induce antigen-specific T cell tolerance, which is a promising method that targets organ-specific BP (176). All aforementioned methods could improve immune tolerance and block the potential production of autoantibodies.

Therapeutic Prevention of Excessive Antibody Production

Targeting the effector B and T cells to prevent the production of "pathogenic" autoantibodies may be a promising method in BP treatment. Rituximab used for depleting CD20+ B cells can reduce all subclasses of anti-BP180 IgG antibodies and has shown efficacy in case reports of patients with refractory BP (39, 177, 178). Autoreactive T cells are also associated with IgG autoantibodies production. Targeting autoreactive T cells using anti-CD25 antibodies and calcineurin inhibitors could modulate immune responses (181, 191). Anti-CD25 antibodies bind to high-affinity heterotrimeric IL-2 receptor on activated T cells, block the IL-2/IL-2 receptor signaling, and inhibit the propagation of T cell activation, thereby limiting the damaging effects of further T cell recruitment in autoimmune diseases (180). Calcineurin can dephosphorylate and inhibit nuclear factors of activated T cells and regulate T-cell activation and differentiation (181). The inhibition of nuclear factors of activated T cells may directly suppress skin injuries by blocking T-cell-dependent production of IgG, as IgG deposition is central to the development of bullae in BP. Additionally, the interaction between T and B cells needs co-stimulatory factors. Hence, targeting co-stimulatory molecules using special monoclonal antibodies could also disrupt the interaction of T and B cells and block the synthesis of autoantibodies (182–185, 192). For pathogen-induced BP, the suppression of dendritic cell-mediated autoimmunity or toll-like receptor antagonist is also practicable (193, 194).

Neutralization of Pathogenic Antibodies

Immunoglobulin G autoantibodies are the main pathogenetic antibodies that act on FcγR to induce blister production. SM101, a soluble FcγR, competes with the interaction of IgG and membrane FcγRs and prevents the development of BP (186). Omalizumab, which targets IgE autoantibodies, can neutralize the activity of IgE in BP and control the disease activity (108). Furthermore, therapies targeting IgE–mast cells–eosinophils/

basophils interaction may also demonstrate promising results in the treatment of BP (112). Moreover, immunoadsorption with high-affinity matrices that selectively bind to human IgG and IgE provides an alternative way of removing autoantibodies (187, 195).

Prospective

Despite the complexity and diversity of the dermatosis, there is still hope for BP patients. Novel promising agents targeting different mechanisms of BP development are necessary. In addition, a multifactorial animal model for BP is warranted as well, and it should mimic not only the presence of specific pathogenic autoantibodies but also the additional triggers, such as environmental factors, medications, comorbid conditions, and infections, in disease initiation. Furthermore, future investigations are required as there may be the presence of unidentified antigenic epitopes that are indispensable for disease development.

CONCLUSION

Bullous pemphigoid has been regarded as a well-characterized, organ-specific, mainly anti-BP180 autoantibody-mediated blistering skin disorder. Both IgG and IgE play vital roles in BP development *via* complement-dependent or -independent inflammatory pathways. However, the roles of IgA and IgM are still uncertain, and further investigation is needed. Knowledge of the BP180 target sites and of the interaction between BP180 and anti-BP180 autoantibodies is pivotal for the exploration of novel and more specific therapeutic methods so as to reduce BP morbidity and mortality. The translation of bench findings into bedside strategies for the treatment of this complex disease still remains to be a challenge. Although BP180-based therapy appears not to be close at hand yet, a better understanding of the role of BP180 would further approximate that to practice.

AUTHOR CONTRIBUTIONS

YL and YX conceived this paper. YL and LL wrote this manuscript. All the authors read and approved the final manuscript.

FUNDING

This study was supported by the National Natural Science Foundation of China (Projects No.81472876 and No.81630081) and the Natural Science Foundation of Shaanxi Province (No.2017ZDJC-06).

REFERENCES

1. Schmidt E, Zillikens D. Pemphigoid diseases. *Lancet* (2013) 381:320–32. doi:10.1016/s0140-6736(12)61140-4
2. Rosenbach M, Wanat KA, Lynm C. Bullous pemphigoid. *JAMA Dermatol* (2013) 149:382. doi:10.1001/jamadermatol.2013.112
3. Zhu T, Ma DL, Zeng YP, Song L, Li L. Bullous pemphigoid associated with silicosis. *J Eur Acad Dermatol Venereol* (2017). doi:10.1111/jdv.14419
4. Caca-Biljanovska N, Arsovska-Bezhoska I, V'Lckova-Laskoska M. PUVA-induced bullous pemphigoid in psoriasis. *Acta Dermatovenerologica Croatica* (2016) 24:214–7.
5. Sagi L, Baum S, Agmon-Levin N, Sherer Y, Katz BS, Barzilai O, et al. Autoimmune bullous diseases the spectrum of infectious agent antibodies and review of the literature. *Autoimmun Rev* (2011) 10:527–35. doi:10.1016/j.autrev.2011.04.003
6. Wang HE, Wells JM, Rizk DV. Bullous lesions after use of a commercial therapeutic hypothermia temperature management system: a possible burn injury? *Ther Hypothermia Temp Manag* (2013) 3:147–50. doi:10.1089/ther.2013.0013
7. Shon W, Wada DA, Kalaaji AN. Radiation-induced pemphigus or pemphigoid disease in 3 patients with distinct underlying malignancies. *Cutis* (2016) 97:219–22.
8. Annabestani Z, Mohseni S, Torkaman G, Nasirpoor F, Larijani B, Mohajeri-Tehrani MR. Electrical stimulation-induced bullous formation in a pemphigoid diabetic patient: a case report. *Int J Diabetes Dev Ctries* (2015) 35:55–7. doi:10.1007/s13410-014-0212-0
9. Belcher MD, Kaddour-Djebbar I, Bollag WB, Davis LS. The proteolytic effect of bromelain on bullous pemphigoid antigen-2. *J Am Acad Dermatol* (2016) 75:838–40. doi:10.1016/j.jaad.2016.05.025
10. Kanahara SM, Agrawal A. Drug-induced bullous pemphigoid. *J Gen Intern Med* (2016) 31:1393–4. doi:10.1007/s11606-016-3679-1
11. Sakai A, Shimomura Y, Ansai O, Saito Y, Tomii K, Tsuchida Y, et al. Linagliptin-associated bullous pemphigoid that was most likely caused by IgG autoantibodies against the midportion of BP180. *Br J Dermatol* (2017) 176:541–3. doi:10.1111/bjd.15111
12. Zhao CY, Murrell DF. Blistering diseases in neonates. *Curr Opin Pediatr* (2016) 28:500–6. doi:10.1097/mop.0000000000000381
13. Cozzani E, Gasparini G, Burlando M, Drago F, Parodi A. Atypical presentations of bullous pemphigoid: clinical and immunopathological aspects. *Autoimmun Rev* (2015) 14:438–45. doi:10.1016/j.autrev.2015.01.006
14. Bagci IS, Horvath ON, Ruzicka T, Sardy M. Bullous pemphigoid. *Autoimmun Rev* (2017) 16:445–55. doi:10.1016/j.autrev.2017.03.010
15. Bernard P, Antonicelli F. Bullous pemphigoid: a review of its diagnosis, associations and treatment. *Am J Clin Dermatol* (2017) 18:513–28. doi:10.1007/s40257-017-0264-2
16. Romeijn TR, Jonkman MF, Knoppers C, Pas HH, Diercks GF. Complement in bullous pemphigoid: results from a large observational study. *Br J Dermatol* (2017) 176:517–9. doi:10.1111/bjd.14822
17. Moriuchi R, Nishie W, Ujiie H, Natsuga K, Shimizu H. In vivo analysis of IgE autoantibodies in bullous pemphigoid: a study of 100 cases. *J Dermatol Sci* (2015) 78:21–5. doi:10.1016/j.jdermsci.2015.01.013
18. Sardy M, Kostaki D, Varga R, Peris K, Ruzicka T. Comparative study of direct and indirect immunofluorescence and of bullous pemphigoid 180 and 230 enzyme-linked immunosorbent assays for diagnosis of bullous pemphigoid. *J Am Acad Dermatol* (2013) 69:748–53. doi:10.1016/j.jaad.2013.07.009
19. Liu Y, Peng L, Li L, Liu C, Hu X, Xiao S, et al. TWEAK/Fn14 activation contributes to the pathogenesis of bullous pemphigoid. *J Invest Dermatol* (2017) 137(7):1512–22. doi:10.1016/j.jid.2017.03.019
20. Furue M, Kadono T. Bullous pemphigoid: what's ahead? *J Dermatol* (2016) 43:237–40. doi:10.1111/1346-8138.13207
21. Ali A, Hu L, Zhao F, Qiu W, Wang P, Ma X, et al. BPAG1, a distinctive role in skin and neurological diseases. *Semin Cell Dev Biol* (2017) 69:34–9. doi:10.1016/j.semcdb.2017.06.005
22. Osawa M, Ueda-Hayakawa I, Isei T, Yoshimura K, Fukuda S, Hashimoto T, et al. A case of childhood bullous pemphigoid with IgG and IgA autoantibodies to various domains of BP180. *J Am Acad Dermatol* (2014) 70:e129–31. doi:10.1016/j.jaad.2013.06.006
23. Di Zenzo G, Thoma-Uszynski S, Calabresi V, Fontao L, Hofmann SC, Lacour JP, et al. Demonstration of epitope-spreading phenomena in bullous pemphigoid: results of a prospective multicenter study. *J Invest Dermatol* (2011) 131:2271–80. doi:10.1038/jid.2011.180
24. Hashimoto T, Ohzono A, Teye K, Numata S, Hiroyasu S, Tsuruta D, et al. Detection of IgE autoantibodies to BP180 and BP230 and their relationship to clinical features in bullous pemphigoid. *Br J Dermatol* (2011) 177:141–51. doi:10.1111/bjd.15114
25. Keller JJ, Kittridge AL, Debanne SM, Korman NJ. Evaluation of ELISA testing for BP180 and BP230 as a diagnostic modality for bullous pemphigoid:

a clinical experience. *Arch Dermatol Res* (2016) 308:269–72. doi:10.1007/s00403-016-1631-1
26. van Beek N, Dahnrich C, Johannsen N, Lemcke S, Goletz S, Hubner F, et al. Prospective studies on the routine use of a novel multivariant enzyme-linked immunosorbent assay for the diagnosis of autoimmune bullous diseases. *J Am Acad Dermatol* (2017) 76:889–94.e5. doi:10.1016/j.jaad.2016.11.002
27. Tampoia M, Giavarina D, Di Giorgio C, Bizzaro N. Diagnostic accuracy of enzyme-linked immunosorbent assays (ELISA) to detect anti-skin autoantibodies in autoimmune blistering skin diseases: a systematic review and meta-analysis. *Autoimmun Rev* (2012) 12:121–6. doi:10.1016/j.autrev.2012.07.006
28. Nishie W. Update on the pathogenesis of bullous pemphigoid: an autoantibody-mediated blistering disease targeting collagen XVII. *J Dermatol Sci* (2014) 73:179–86. doi:10.1016/j.jdermsci.2013.12.001
29. Barrick BJ, Lohse CM, Lehman JS. Specific causes of death in patients with bullous pemphigoid as measured by death certificate data: a retrospective cohort study. *Int J Dermatol* (2015) 54:56–61. doi:10.1111/ijd.12243
30. Atzmony L, Mimouni I, Reiter O, Leshem YA, Taha O, Gdalevich M, et al. Association of bullous pemphigoid with malignancy: a systematic review and meta-analysis. *J Am Acad Dermatol* (2017) 77:691–9. doi:10.1016/j.jaad.2017.05.006
31. Lai YC, Yew YW, Lambert WC. Bullous pemphigoid and its association with neurological diseases: a systematic review and meta-analysis. *J Eur Acad Dermatol Venereol* (2016) 30:2007–15. doi:10.1111/jdv.13660
32. Cugno M, Marzano AV, Bucciarelli P, Balice Y, Cianchini G, Quaglino P, et al. Increased risk of venous thromboembolism in patients with bullous pemphigoid. The INVENTEP (INcidence of VENous ThromboEmbolism in bullous Pemphigoid) study. *J Thromb Haemost* (2016) 115:193–9. doi:10.1160/th15-04-0309
33. Liu YD, Wang YH, Ye YC, Zhao WL, Li L. Prognostic factors for mortality in patients with bullous pemphigoid: a meta-analysis. *Arch Dermatol Res* (2017) 309:335–47. doi:10.1007/s00403-017-1736-1
34. Li J, Zuo YG, Zheng HY. Mortality of bullous pemphigoid in China. *JAMA Dermatol* (2013) 149:106–8. doi:10.1001/archdermatol.2012.2994
35. Marzano AV, Tedeschi A, Berti E, Fanoni D, Crosti C, Cugno M. Activation of coagulation in bullous pemphigoid and other eosinophil-related inflammatory skin diseases. *Clin Exp Immunol* (2011) 165:44–50. doi:10.1111/j.1365-2249.2011.04391.x
36. Marzano AV, Tedeschi A, Fanoni D, Bonanni E, Venegoni L, Berti E, et al. Activation of blood coagulation in bullous pemphigoid: role of eosinophils, and local and systemic implications. *Br J Dermatol* (2009) 160:266–72. doi:10.1111/j.1365-2133.2008.08880.x
37. Grantham HJ, Stocken DD, Reynolds NJ. Doxycycline: a first-line treatment for bullous pemphigoid? *Lancet* (2017) 389:1586–8. doi:10.1016/s0140-6736(17)30549-4
38. Williams HC, Wojnarowska F, Kirtschig G, Mason J, Godec TR, Schmidt E, et al. Doxycycline versus prednisolone as an initial treatment strategy for bullous pemphigoid: a pragmatic, non-inferiority, randomised controlled trial. *Lancet* (2017) 389:1630–8. doi:10.1016/s0140-6736(17)30560-3
39. Ahmed AR, Shetty S, Kaveri S, Spigelman ZS. Treatment of recalcitrant bullous pemphigoid (BP) with a novel protocol: a retrospective study with a 6-year follow-up. *J Am Acad Dermatol* (2016) 74:700–8.e3. doi:10.1016/j.jaad.2015.11.030
40. Tuchinda P, Ritchie S, Gaspari AA. Bullous pemphigoid treated with intravenous immunoglobulin. *Cutis* (2014) 93:264–8.
41. Amagai M, Ikeda S, Hashimoto T, Mizuashi M, Fujisawa A, Ihn H, et al. A randomized double-blind trial of intravenous immunoglobulin for bullous pemphigoid. *J Dermatol Sci* (2017) 85:77–84. doi:10.1016/j.jdermsci.2016.11.003
42. von Gunten S, Shoenfeld Y, Blank M, Branch DR, Vassilev T, Kasermann F, et al. IVIG pluripotency and the concept of Fc-sialylation: challenges to the scientist. *Nat Rev Immunol* (2014) 14:349. doi:10.1038/nri3401-c1
43. Ruocco E, Wolf R, Caccavale S, Brancaccio G, Ruocco V, Lo Schiavo A. Bullous pemphigoid: associations and management guidelines: facts and controversies. *Clin Dermatol* (2013) 31:400–12. doi:10.1016/j.clindermatol.2013.01.007
44. Pickford WJ, Gudi V, Haggart AM, Lewis BJ, Herriot R, Barker RN, et al. T cell participation in autoreactivity to NC16a epitopes in bullous pemphigoid. *Clin Exp Immunol* (2015) 180:189–200. doi:10.1111/cei.12566
45. Kalowska M, Ciepiela O, Kowalewski C, Demkow U, Schwartz RA, Wozniak K. Enzyme-linked immunoassay index for anti-NC16a IgG and IgE auto-antibodies correlates with severity and activity of bullous pemphigoid. *Acta Derm Venereol* (2016) 96:191–6. doi:10.2340/00015555-2101
46. van Beek N, Luttmann N, Huebner F, Recke A, Karl I, Schulze FS, et al. Correlation of serum levels of IgE autoantibodies against BP180 with bullous pemphigoid disease activity. *JAMA Dermatol* (2017) 153:30–8. doi:10.1001/jamadermatol.2016.3357
47. Wada M, Nishie W, Ujiie H, Izumi K, Iwata H, Natsuga K, et al. Epitope-dependent pathogenicity of antibodies targeting a major bullous pemphigoid autoantigen collagen XVII/BP180. *J Invest Dermatol* (2016) 136:938–46. doi:10.1016/j.jid.2015.11.030
48. Wei W, He HL, Chen CY, Zhao Y, Jiang HL, Liu WT, et al. Whole exome sequencing implicates PTCH1 and COL17A1 genes in ossification of the posterior longitudinal ligament of the cervical spine in Chinese patients. *Genet Mol Res* (2014) 13:1794–804. doi:10.4238/2014.March.17.7
49. Walko G, Castanon MJ, Wiche G. Molecular architecture and function of the hemidesmosome. *Cell Tissue Res* (2015) 360:529–44. doi:10.1007/s00441-015-2216-6
50. Nishie W, Jackow J, Hofmann SC, Franzke CW, Bruckner-Tuderman L. Coiled coils ensure the physiological ectodomain shedding of collagen XVII. *J Biol Chem* (2012) 287:29940–8. doi:10.1074/jbc.M112.345454
51. Natsuga K, Nishie W, Shinkuma S, Ujiie H, Nishimura M, Sawamura D, et al. Antibodies to pathogenic epitopes on type XVII collagen cause skin fragility in a complement-dependent and -independent manner. *J Immunol* (2012) 188:5792–9. doi:10.4049/jimmunol.1003402
52. Horvath B, Niedermeier A, Podstawa E, Muller R, Hunzelmann N, Karpati S, et al. IgA autoantibodies in the pemphigoids and linear IgA bullous dermatosis. *Exp Dermatol* (2010) 19:648–53. doi:10.1111/j.1600-0625.2010.01080.x
53. Dopp R, Schmidt E, Chimanovitch I, Leverkus M, Brocker EB, Zillikens D. IgG4 and IgE are the major immunoglobulins targeting the NC16A domain of BP180 in Bullous pemphigoid: serum levels of these immunoglobulins reflect disease activity. *J Am Acad Dermatol* (2000) 42:577–83. doi:10.1067/mjd.2000.103986
54. Fairley JA, Bream M, Fullenkamp C, Syrbu S, Chen M, Messingham KN. Missing the target: characterization of bullous pemphigoid patients who are negative using the BP180 enzyme-linked immunosorbant assay. *J Am Acad Dermatol* (2013) 68:395–403. doi:10.1016/j.jaad.2012.09.012
55. Dresow SK, Sitaru C, Recke A, Oostingh GJ, Zillikens D, Gibbs BF. IgE autoantibodies against the intracellular domain of BP180. *Br J Dermatol* (2009) 160:429–32. doi:10.1111/j.1365-2133.2008.08858.x
56. Hofmann S, Thoma-Uszynski S, Hunziker T, Bernard P, Koebnick C, Stauber A, et al. Severity and phenotype of bullous pemphigoid relate to autoantibody profile against the NH2- and COOH-terminal regions of the BP180 ectodomain. *J Invest Dermatol* (2002) 119:1065–73. doi:10.1046/j.1523-1747.2002.19529.x
57. Tsuruta D, Nishikawa T, Yamagami J, Hashimoto T. Unilateral bullous pemphigoid without erythema and eosinophil infiltration in a hemiplegic patient. *J Dermatol* (2012) 39:787–9. doi:10.1111/j.1346-8138.2012.01562.x
58. Wieland CN, Comfere NI, Gibson LE, Weaver AL, Krause PK, Murray JA. Anti-bullous pemphigoid 180 and 230 antibodies in a sample of unaffected subjects. *Arch Dermatol* (2010) 146:21–5. doi:10.1001/archdermatol.2009.331
59. Xu L, Robinson N, Miller SD, Chan LS. Characterization of BALB/c mice B lymphocyte autoimmune responses to skin basement membrane component type XVII collagen, the target antigen of autoimmune skin disease bullous pemphigoid. *Immunol Lett* (2001) 77:105–11. doi:10.1016/S0165-2478(01)00212-7
60. Madi A, Bransburg-Zabary S, Maayan-Metzger A, Dar G, Ben-Jacob E, Cohen IR. Tumor-associated and disease-associated autoantibody repertoires in healthy colostrum and maternal and newborn cord sera. *J Immunol* (2015) 194:5272–81. doi:10.4049/jimmunol.1402771
61. Olsen NJ, Karp DR. Autoantibodies and SLE: the threshold for disease. *Nat Rev Rheumatol* (2014) 10:181–6. doi:10.1038/nrrheum.2013.184
62. Yang S, Fujikado N, Kolodin D, Benoist C, Mathis D. Immune tolerance. Regulatory T cells generated early in life play a distinct role in maintaining self-tolerance. *Science* (2015) 348:589–94. doi:10.1126/science.aaa7017
63. Kalekar LA, Schmiel SE, Nandiwada SL, Lam WY, Barsness LO, Zhang N, et al. CD4(+) T cell anergy prevents autoimmunity and generates regulatory T cell precursors. *Nat Immunol* (2016) 17:304–14. doi:10.1038/ni.3331

64. Baruch K, Rosenzweig N, Kertser A, Deczkowska A, Sharif AM, Spinrad A, et al. Breaking immune tolerance by targeting Foxp3(+) regulatory T cells mitigates Alzheimer's disease pathology. *Nat Commun* (2015) 6:7967. doi:10.1038/ncomms8967
65. Antiga E, Quaglino P, Volpi W, Pierini I, Del Bianco E, Bianchi B, et al. Regulatory T cells in skin lesions and blood of patients with bullous pemphigoid. *J Eur Acad Dermatol Venereol* (2014) 28:222–30. doi:10.1111/jdv.12091
66. Rychlik-Sych M, Baranska M, Wojtczak A, Skretkowicz J, Zebrowska A, Waszczykowska E. The impact of the CYP2D6 gene polymorphism on the risk of pemphigoid. *Int J Dermatol* (2015) 54:1396–401. doi:10.1111/ijd.12967
67. Zakka LR, Reche P, Ahmed AR. Role of MHC Class II genes in the pathogenesis of pemphigoid. *Autoimmun Rev* (2011) 11:40–7. doi:10.1016/j.autrev.2011.07.002
68. Quaglino P, Antiga E, Comessatti A, Caproni M, Nardo T, Ponti R, et al. Circulating CD4+ CD25brightFOXP3+ regulatory T-cells are significantly reduced in bullous pemphigoid patients. *Arch Dermatol Res* (2012) 304:639–45. doi:10.1007/s00403-012-1213-9
69. Lo Schiavo A, Ruocco E, Brancaccio G, Caccavale S, Ruocco V, Wolf R. Bullous pemphigoid: etiology, pathogenesis, and inducing factors: facts and controversies. *Clin Dermatol* (2013) 31:391–9. doi:10.1016/j.clindermatol.2013.01.006
70. Qian H, Kusuhara M, Li X, Tsuruta D, Tsuchisaka A, Ishii N, et al. B-cell activating factor detected on both naive and memory B cells in bullous pemphigoid. *Exp Dermatol* (2014) 23:596–605. doi:10.1111/exd.12421
71. Watanabe R, Fujimoto M, Yazawa N, Nakashima H, Asashima N, Kuwano Y, et al. Increased serum levels of a proliferation-inducing ligand in patients with bullous pemphigoid. *J Dermatol Sci* (2007) 46:53–60. doi:10.1016/j.jdermsci.2006.12.008
72. Wong HK, Bechtel MA. Blistering insights into the pathogenesis of bullous pemphigoid. *Clin Immunol* (2012) 142:101–4. doi:10.1016/j.clim.2011.12.003
73. Vincent FB, Saulep-Easton D, Figgett WA, Fairfax KA, Mackay F. The BAFF/APRIL system: emerging functions beyond B cell biology and autoimmunity. *Cytokine Growth Factor Rev* (2013) 24:203–15. doi:10.1016/j.cytogfr.2013.04.003
74. Ujiie H, Shibaki A, Nishie W, Shinkuma S, Moriuchi R, Qiao H, et al. Noncollagenous 16A domain of type XVII collagen-reactive CD4+ T cells play a pivotal role in the development of active disease in experimental bullous pemphigoid model. *Clin Immunol* (2012) 142:167–75. doi:10.1016/j.clim.2011.10.002
75. Thoma-Uszynski S, Uter W, Schwietzke S, Schuler G, Borradori L, Hertl M. Autoreactive T and B cells from bullous pemphigoid (BP) patients recognize epitopes clustered in distinct regions of BP180 and BP230. *J Immunol* (2006) 176:2015–23. doi:10.4049/jimmunol.176.3.2015
76. Lin MS, Fu CL, Giudice GJ, Olague-Marchan M, Lazaro AM, Stastny P, et al. Epitopes targeted by bullous pemphigoid T lymphocytes and autoantibodies map to the same sites on the bullous pemphigoid 180 ectodomain. *J Invest Dermatol* (2000) 115:955–61. doi:10.1046/j.1523-1747.2000.00153.x
77. Izumi K, Nishie W, Mai Y, Wada M, Natsuga K, Ujiie H, et al. Autoantibody profile differentiates between inflammatory and noninflammatory bullous pemphigoid. *J Invest Dermatol* (2016) 136:2201–10. doi:10.1016/j.jid.2016.06.622
78. Fichel F, Barbe C, Joly P, Bedane C, Vabres P, Truchetet F, et al. Clinical and immunologic factors associated with bullous pemphigoid relapse during the first year of treatment: a multicenter, prospective study. *JAMA Dermatol* (2014) 150:25–33. doi:10.1001/jamadermatol.2013.5757
79. de Graauw E, Sitaru C, Horn M, Borradori L, Yousefi S, Simon HU, et al. Evidence for a role of eosinophils in blister formation in bullous pemphigoid. *Allergy* (2017) 72:1105–13. doi:10.1111/all.13131
80. Yu X, Kasprick A, Petersen F. Revisiting the role of mast cells in autoimmunity. *Autoimmun Rev* (2015) 14:751–9. doi:10.1016/j.autrev.2015.04.008
81. Nelson KC, Zhao M, Schroeder PR, Li N, Wetsel RA, Diaz LA, et al. Role of different pathways of the complement cascade in experimental bullous pemphigoid. *J Clin Invest* (2006) 116:2892–900. doi:10.1172/jci17891
82. Qiao P, Dang E, Cao T, Fang H, Zhang J, Qiao H, et al. Dysregulation of mCD46 and sCD46 contribute to the pathogenesis of bullous pemphigoid. *Sci Rep* (2017) 7:145. doi:10.1038/s41598-017-00235-3
83. Wang G, Ujiie H, Shibaki A, Nishie W, Tateishi Y, Kikuchi K, et al. Blockade of autoantibody-initiated tissue damage by using recombinant fab antibody fragments against pathogenic autoantigen. *Am J Pathol* (2010) 176:914–25. doi:10.2353/ajpath.2010.090744
84. Schulze FS, Beckmann T, Nimmerjahn F, Ishiko A, Collin M, Kohl J, et al. Fcgamma receptors III and IV mediate tissue destruction in a novel adult mouse model of bullous pemphigoid. *Am J Pathol* (2014) 184:2185–96. doi:10.1016/j.ajpath.2014.05.007
85. Hiroyasu S, Ozawa T, Kobayashi H, Ishii M, Aoyama Y, Kitajima Y, et al. Bullous pemphigoid IgG induces BP180 internalization via a macropinocytic pathway. *Am J Pathol* (2013) 182:828–40. doi:10.1016/j.ajpath.2012.11.029
86. Iwata H, Kitajima Y. Bullous pemphigoid: role of complement and mechanisms for blister formation within the lamina lucida. *Exp Dermatol* (2013) 22:381–5. doi:10.1111/exd.12146
87. Ujiie H, Sasaoka T, Izumi K, Nishie W, Shinkuma S, Natsuga K, et al. Bullous pemphigoid autoantibodies directly induce blister formation without complement activation. *J Immunol* (2014) 193:4415–28. doi:10.4049/jimmunol.1400095
88. Iwata H, Kamaguchi M, Ujiie H, Nishimura M, Izumi K, Natsuga K, et al. Macropinocytosis of type XVII collagen induced by bullous pemphigoid IgG is regulated via protein kinase C. *Lab Invest* (2016) 96:1301–10. doi:10.1038/labinvest.2016.108
89. Dainichi T, Chow Z, Kabashima K. IgG4, complement, and the mechanisms of blister formation in pemphigus and bullous pemphigoid. *J Dermatol Sci* (2017) 88:265–70. doi:10.1016/j.jdermsci.2017.07.012
90. Tukaj S, Gruner D, Tukaj C, Zillikens D, Kasperkiewicz M. Calcitriol exerts anti-inflammatory effects in keratinocytes treated with autoantibodies from a patient with bullous pemphigoid. *J Eur Acad Dermatol Venereol* (2016) 30:288–92. doi:10.1111/jdv.12929
91. Van den Bergh F, Eliason SL, Burmeister BT, Giudice GJ. Collagen XVII (BP180) modulates keratinocyte expression of the proinflammatory chemokine, IL-8. *Exp Dermatol* (2012) 21:605–11. doi:10.1111/j.1600-0625.2012.01529.x
92. Dainichi T, Nishie W, Yamagami Y, Sonobe H, Ujiie H, Kaku Y, et al. Bullous pemphigoid suggestive of complement-independent blister formation with anti-BP180 IgG4 autoantibodies. *Br J Dermatol* (2016) 175:187–90. doi:10.1111/bjd.14411
93. Zhou XP, Liu B, Xu Q, Yang Y, He CX, Zuo YG, et al. Serum levels of immunoglobulins G1 and G4 targeting the non-collagenous 16A domain of BP180 reflect bullous pemphigoid activity and predict bad prognosis. *J Dermatol* (2016) 43:141–8. doi:10.1111/1346-8138.13051
94. Zuo Y, Evangelista F, Culton D, Guilabert A, Lin L, Li N, et al. IgG4 autoantibodies are inhibitory in the autoimmune disease bullous pemphigoid. *J Autoimmun* (2016) 73:111–9. doi:10.1016/j.jaut.2016.06.019
95. Hammers CM, Stanley JR. Mechanisms of disease: pemphigus and bullous pemphigoid. *Annu Rev Pathol* (2016) 11:175–97. doi:10.1146/annurev-pathol-012615-044313
96. Bing L, Xiping Z, Li L, Jun P, Yi-Xia W, Min Y, et al. Levels of anti-BP180 NC16A IgE do not correlate with severity of disease in the early stages of bullous pemphigoid. *Arch Dermatol Res* (2015) 307:849–54. doi:10.1007/s00403-015-1598-3
97. Salz M, Haeberle S, Hoffmann J, Enk AH, Hadaschik EN. Elevated IL-31 serum levels in bullous pemphigoid patients correlate with eosinophil numbers and are associated with BP180-IgE. *J Dermatol Sci* (2017) 87:309–11. doi:10.1016/j.jdermsci.2017.07.019
98. Cho YT, Liao SL, Wang LF, Chu CY. High serum anti-BP180 IgE levels correlate to prominent urticarial lesions in patients with bullous pemphigoid. *J Dermatol Sci* (2016) 83:78–80. doi:10.1016/j.jdermsci.2016.03.009
99. Kamiya K, Aoyama Y, Noda K, Miyake T, Yamaguchi M, Hamada T, et al. Possible correlation of IgE autoantibody to BP180 with disease activity in bullous pemphigoid. *J Dermatol Sci* (2015) 78:77–9. doi:10.1016/j.jdermsci.2015.02.009
100. Iwata Y, Komura K, Kodera M, Usuda T, Yokoyama Y, Hara T, et al. Correlation of IgE autoantibody to BP180 with a severe form of bullous pemphigoid. *Arch Dermatol* (2008) 144:41–8. doi:10.1001/archdermatol.2007.9
101. Yayli S, Pelivani N, Beltraminelli H, Wirthmuller U, Beleznay Z, Horn M, et al. Detection of linear IgE deposits in bullous pemphigoid and mucous membrane pemphigoid: a useful clue for diagnosis. *Br J Dermatol* (2011) 165:1133–7. doi:10.1111/j.1365-2133.2011.10481.x

102. Sowerby L, Dewan AK, Granter S, Gandhi L, LeBoeuf NR. Rituximab treatment of nivolumab-induced bullous pemphigoid. *JAMA Dermatol* (2017) 153:603–5. doi:10.1001/jamadermatol.2017.0091
103. Fairley JA, Fu CL, Giudice GJ. Mapping the binding sites of anti-BP180 immunoglobulin E autoantibodies in bullous pemphigoid. *J Invest Dermatol* (2005) 125:467–72. doi:10.1111/j.0022-202X.2005.23853.x
104. Fairley JA, Burnett CT, Fu CL, Larson DL, Fleming MG, Giudice GJ. A pathogenic role for IgE in autoimmunity: bullous pemphigoid IgE reproduces the early phase of lesion development in human skin grafted to nu/nu mice. *J Invest Dermatol* (2007) 127:2605–11. doi:10.1038/sj.jid.5700958
105. Messingham KN, Wang JW, Holahan HM, Srikantha R, Aust SC, Fairley JA. Eosinophil localization to the basement membrane zone is autoantibody- and complement-dependent in a human cryosection model of bullous pemphigoid. *Exp Dermatol* (2016) 25:50–5. doi:10.1111/exd.12883
106. Messingham KN, Holahan HM, Frydman AS, Fullenkamp C, Srikantha R, Fairley JA. Human eosinophils express the high affinity IgE receptor, FcepsilonRI, in bullous pemphigoid. *PLoS One* (2014) 9:e107725. doi:10.1371/journal.pone.0107725
107. van Beek N, Schulze FS, Zillikens D, Schmidt E. IgE-mediated mechanisms in bullous pemphigoid and other autoimmune bullous diseases. *Expert Rev Clin Immunol* (2016) 12:267–77. doi:10.1586/1744666x.2016.1123092
108. Yu KK, Crew AB, Messingham KA, Fairley JA, Woodley DT. Omalizumab therapy for bullous pemphigoid. *J Am Acad Dermatol* (2014) 71:468–74. doi:10.1016/j.jaad.2014.04.053
109. Balakirski G, Alkhateeb A, Merk HF, Leverkus M, Megahed M. Successful treatment of bullous pemphigoid with omalizumab as corticosteroid-sparing agent: report of two cases and review of literature. *J Eur Acad Dermatol Venereol* (2016) 30:1778–82. doi:10.1111/jdv.13758
110. Messingham KN, Srikantha R, DeGueme AM, Fairley JA. FcR-independent effects of IgE and IgG autoantibodies in bullous pemphigoid. *J Immunol* (2011) 187:553–60. doi:10.4049/jimmunol.1001753
111. Iwata H, Kamio N, Aoyama Y, Yamamoto Y, Hirako Y, Owaribe K, et al. IgG from patients with bullous pemphigoid depletes cultured keratinocytes of the 180-kDa bullous pemphigoid antigen (type XVII collagen) and weakens cell attachment. *J Invest Dermatol* (2009) 129:919–26. doi:10.1038/jid.2008.305
112. Messingham KA, Holahan HM, Fairley JA. Unraveling the significance of IgE autoantibodies in organ-specific autoimmunity: lessons learned from bullous pemphigoid. *Immunol Res* (2014) 59:273–8. doi:10.1007/s12026-014-8547-7
113. Messingham KA, Onoh A, Vanderah EM, Giudice GJ, Fairley JA. Functional characterization of an IgE-class monoclonal antibody specific for the bullous pemphigoid autoantigen, BP180. *Hybridoma* (2005) 2012(31):111–7. doi:10.1089/hyb.2011.0102
114. Kromminga A, Scheckenbach C, Georgi M, Hagel C, Arndt R, Christophers E, et al. Patients with bullous pemphigoid and linear IgA disease show a dual IgA and IgG autoimmune response to BP180. *J Autoimmun* (2000) 15:293–300. doi:10.1006/jaut.2000.0437
115. Ali S, Kelly C, Challacombe SJ, Donaldson AN, Dart JK, Gleeson M, et al. Salivary IgA and IgG antibodies to bullous pemphigoid 180 noncollagenous domain 16a as diagnostic biomarkers in mucous membrane pemphigoid. *Br J Dermatol* (2016) 174:1022–9. doi:10.1111/bjd.14351
116. Miyamoto S, Chikazu D, Yasuda T, Enomoto A, Oh-i T, Hirako Y, et al. A case of oral mucous membrane pemphigoid with IgG antibodies to integrin alpha6beta4. *Br J Dermatol* (2014) 171:1555–7. doi:10.1111/bjd.13113
117. Matsui K, Makino T, Takegami Y, Murayama S, Seki Y, Ishii N, et al. Bullous pemphigoid with IgG anti-LAD-1 antibodies. *Eur J Dermatol* (2014) 24:275–6. doi:10.1684/ejd.2014.2322
118. Fortuna G, Marinkovich MP. Linear immunoglobulin A bullous dermatosis. *Clin Dermatol* (2012) 30:38–50. doi:10.1016/j.clindermatol.2011.03.008
119. Zillikens D, Herzele K, Georgi M, Schmidt E, Chimanovitch I, Schumann H, et al. Autoantibodies in a subgroup of patients with linear IgA disease react with the NC16A domain of BP1801. *J Invest Dermatol* (1999) 113:947–53. doi:10.1046/j.1523-1747.1999.00808.x
120. Christophoridis S, Budinger L, Borradori L, Hunziker T, Merk HF, Hertl M. IgG, IgA and IgE autoantibodies against the ectodomain of BP180 in patients with bullous and cicatricial pemphigoid and linear IgA bullous dermatosis. *Br J Dermatol* (2000) 143:349–55. doi:10.1046/j.1365-2133.2000.03661.x
121. Viglizzo G, Cozzani E, Nozza P, Occella C, Parodi A. A case of linear IgA disease in a child with IgA and IgG circulating antibodies directed to BPAg2. *Int J Dermatol* (2007) 46:1302–4. doi:10.1111/j.1365-4632.2007.03317.x
122. Perriard J, Jaunin F, Favre B, Budinger L, Hertl M, Saurat JH, et al. IgG autoantibodies from bullous pemphigoid (BP) patients bind antigenic sites on both the extracellular and the intracellular domains of the BP antigen 180. *J Invest Dermatol* (1999) 112:141–7. doi:10.1046/j.1523-1747.1999.00497.x
123. Laffitte E, Skaria M, Jaunin F, Tamm K, Saurat JH, Favre B, et al. Autoantibodies to the extracellular and intracellular domain of bullous pemphigoid 180, the putative key autoantigen in bullous pemphigoid, belong predominantly to the IgG1 and IgG4 subclasses. *Br J Dermatol* (2001) 144:760–8. doi:10.1046/j.1365-2133.2001.04130.x
124. Alarcon-Segovia D, Llorente L, Ruiz-Arguelles A. The penetration of autoantibodies into cells may induce tolerance to self by apoptosis of autoreactive lymphocytes and cause autoimmune disease by dysregulation and/or cell damage. *J Autoimmun* (1996) 9:295–300. doi:10.1006/jaut.1996.0038
125. Schmidt E, Skrobek C, Kromminga A, Hashimoto T, Messer G, Brocker EB, et al. Cicatricial pemphigoid: IgA and IgG autoantibodies target epitopes on both intra- and extracellular domains of bullous pemphigoid antigen 180. *Br J Dermatol* (2001) 145:778–83. doi:10.1046/j.1365-2133.2001.04471.x
126. Nakatani C, Muramatsu T, Shirai T. Immunoreactivity of bullous pemphigoid (BP) autoantibodies against the NC16A and C-terminal domains of the 180 kDa BP antigen (BP180): immunoblot analysis and enzyme-linked immunosorbent assay using BP180 recombinant proteins. *Br J Dermatol* (1998) 139:365–70. doi:10.1046/j.1365-2133.1998.02396.x
127. Tan CW, Pang Y, Sim B, Thirumoorthy T, Pang SM, Lee HY. The association between drugs and bullous pemphigoid. *Br J Dermatol* (2017) 176:549–51. doi:10.1111/bjd.15195
128. Mariotti F, Grosso F, Terracina M, Ruffelli M, Cordiali-Fei P, Sera F, et al. Development of a novel ELISA system for detection of anti-BP180 IgG and characterization of autoantibody profile in bullous pemphigoid patients. *Br J Dermatol* (2004) 151:1004–10. doi:10.1111/j.1365-2133.2004.06245.x
129. Liu Z, Sui W, Zhao M, Li Z, Li N, Thresher R, et al. Subepidermal blistering induced by human autoantibodies to BP180 requires innate immune players in a humanized bullous pemphigoid mouse model. *J Autoimmun* (2008) 31:331–8. doi:10.1016/j.jaut.2008.08.009
130. Hurskainen T, Kokkonen N, Sormunen R, Jackow J, Loffek S, Soininen R, et al. Deletion of the major bullous pemphigoid epitope region of collagen XVII induces blistering, autoimmunization, and itching in mice. *J Invest Dermatol* (2015) 135:1303–10. doi:10.1038/jid.2014.443
131. Ujiie H, Shibaki A, Nishie W, Sawamura D, Wang G, Tateishi Y, et al. A novel active mouse model for bullous pemphigoid targeting humanized pathogenic antigen. *J Immunol* (2010) 184:2166–74. doi:10.4049/jimmunol.0903101
132. Tazudeen N, Au S, Pewitt J, Tu E, Aronson IK. IgM ocular cicatricial pemphigoid: a unique insight into the immune system. *Dermatol Online J* (2015) 21.
133. Hashimoto T, Tsuruta D, Koga H, Fukuda S, Ohyama B, Komai A, et al. Summary of results of serological tests and diagnoses for 4774 cases of various autoimmune bullous diseases consulted to Kurume University. *Br J Dermatol* (2016) 175:953–65. doi:10.1111/bjd.14692
134. Glauser S, Rutz M, Cazzaniga S, Hegyi I, Borradori L, Beltraminelli H. Diagnostic value of immunohistochemistry on formalin-fixed, paraffin-embedded skin biopsy specimens for bullous pemphigoid. *Br J Dermatol* (2016) 175:988–93. doi:10.1111/bjd.14686
135. Arbache ST, Nogueira TG, Delgado L, Miyamoto D, Aoki V. Immunofluorescence testing in the diagnosis of autoimmune blistering diseases: overview of 10-year experience. *An Bras Dermatol* (2014) 89:885–9. doi:10.1590/abd1806-4841.20143221
136. Maki N, Demitsu T, Umemoto N, Nagashima K, Nakamura T, Kakurai M, et al. Possible paraneoplastic syndrome case of bullous pemphigoid with immunoglobulin G anti-BP180 C-terminal domain antibodies associated with psoriasis and primary macroglobulinemia. *J Dermatol* (2016) 43:571–4. doi:10.1111/1346-8138.13170
137. Baroero L, Coppo P, Bertolino L, Maccario S, Savino F. Three case reports of post immunization and post viral bullous pemphigoid: looking for the right trigger. *BMC Pediatr* (2017) 17:60. doi:10.1186/s12887-017-0813-0
138. Chattopadhyay M, Rytina E, Dada M, Bhogal BS, Groves R, Handfield-Jones S. Immunobullous dermatosis associated with Waldenstrom macroglobulinaemia treated with rituximab. *Clin Exp Dermatol* (2013) 38:866–9. doi:10.1111/ced.12166

139. Anderson CK, Mowad CM, Goff ME, Pelle MT. Bullous pemphigoid arising in surgical wounds. *Br J Dermatol* (2001) 145:670–2. doi:10.1046/j.1365-2133.2001.04427.x
140. Franzke CW, Tasanen K, Schacke H, Zhou Z, Tryggvason K, Mauch C, et al. Transmembrane collagen XVII, an epithelial adhesion protein, is shed from the cell surface by ADAMs. *EMBO J* (2002) 21:5026–35. doi:10.1093/emboj/cdf532
141. Powell AM, Sakuma-Oyama Y, Oyama N, Black MM. Collagen XVII/BP180: a collagenous transmembrane protein and component of the dermoepidermal anchoring complex. *Clin Exp Dermatol* (2005) 30:682–7. doi:10.1111/j.1365-2230.2005.01937.x
142. Jackow J, Loffek S, Nystrom A, Bruckner-Tuderman L, Franzke CW. Collagen XVII shedding suppresses re-epithelialization by directing keratinocyte migration and dampening mTOR signaling. *J Invest Dermatol* (2016) 136:1031–41. doi:10.1016/j.jid.2016.01.012
143. Jackow J, Schlosser A, Sormunen R, Nystrom A, Sitaru C, Tasanen K, et al. Generation of a functional non-shedding collagen XVII mouse model: relevance of collagen XVII shedding in wound healing. *J Invest Dermatol* (2016) 136:516–25. doi:10.1016/j.jid.2015.10.060
144. Nishie W, Natsuga K, Iwata H, Izumi K, Ujiie H, Toyonaga E, et al. Context-dependent regulation of collagen XVII ectodomain shedding in skin. *Am J Pathol* (2015) 185:1361–71. doi:10.1016/j.ajpath.2015.01.012
145. Kabuto M, Fujimoto N, Takahashi T, Tanaka T. Decreased level of interleukin-10-producing B cells in patients with pemphigus but not in patients with pemphigoid. *Br J Dermatol* (2017) 176:1204–12. doi:10.1111/bjd.15113
146. Bieber K, Ernst AL, Tukaj S, Holtsche MM, Schmidt E, Zillikens D, et al. Analysis of serum markers of cellular immune activation in patients with bullous pemphigoid. *Exp Dermatol* (2017). doi:10.1111/exd.13382
147. Zebrowska A, Wagrowska-Danilewicz M, Danilewicz M, Stasikowska-Kanicka O, Cynkier A, Sysa-Jedrzejowska A, et al. IL-17 expression in dermatitis herpetiformis and bullous pemphigoid. *Mediators Inflamm* (2017) 2013:967987. doi:10.1155/2013/967987
148. Zebrowska A, Wozniacka A, Juczynska K, Ociepa K, Waszczykowska E, Szymczak I, et al. Correlation between IL36alpha and IL17 and activity of the disease in selected autoimmune blistering diseases. *Mediators Inflamm* (2017) 2017:8980534. doi:10.1155/2017/8980534
149. Le Jan S, Plee J, Vallerand D, Dupont A, Delanez E, Durlach A, et al. Innate immune cell-produced IL-17 sustains inflammation in bullous pemphigoid. *J Invest Dermatol* (2014) 134:2908–17. doi:10.1038/jid.2014.263
150. Nin-Asai R, Muro Y, Sekiya A, Sugiura K, Akiyama M. Serum thymus and activation-regulated chemokine (TARC/CCL17) levels reflect the disease activity in a patient with bullous pemphigoid. *J Eur Acad Dermatol Venereol* (2016) 30:327–8. doi:10.1111/jdv.12719
151. Kagami S, Kai H, Kakinuma T, Miyagaki T, Kamata M, Sugaya M, et al. High levels of CCL26 in blister fluid and sera of patients with bullous pemphigoid. *J Invest Dermatol* (2012) 132:249–51. doi:10.1038/jid.2011.251
152. Engmann J, Rudrich U, Behrens G, Papakonstantinou E, Gehring M, Kapp A, et al. Increased activity and apoptosis of eosinophils in blister fluids, skin and peripheral blood of patients with bullous pemphigoid. *Acta Derm Venereol* (2017) 97:464–71. doi:10.2340/00015555-2581
153. Riani M, Le Jan S, Plee J, Durlach A, Le Naour R, Haegeman G, et al. Bullous pemphigoid outcome is associated with CXCL10-induced matrix metalloproteinase 9 secretion from monocytes and neutrophils but not lymphocytes. *J Allergy Clin Immunol* (2017) 139:863–72.e3. doi:10.1016/j.jaci.2016.08.012
154. Frossi B, Mion F, Tripodo C, Colombo MP, Pucillo CE. Rheostatic functions of mast cells in the control of innate and adaptive immune responses. *Trends Immunol* (2017) 138:648–56. doi:10.1016/j.it.2017.04.001
155. Gunther C, Wozel G, Meurer M, Pfeiffer C. Up-regulation of CCL11 and CCL26 is associated with activated eosinophils in bullous pemphigoid. *Clin Exp Immunol* (2011) 166:145–53. doi:10.1111/j.1365-2249.2011.04464.x
156. Miossec P, Kolls JK. Targeting IL-17 and TH17 cells in chronic inflammation. *Nat Rev Drug Discov* (2012) 11:763–76. doi:10.1038/nrd3794
157. Xu Y, Chen G. Mast cell and autoimmune diseases. *Mediators Inflamm* (2015) 2015:246126. doi:10.1155/2015/246126
158. Furudate S, Fujimura T, Kambayashi Y, Kakizaki A, Aiba S. Comparison of CD163+ CD206+ M2 macrophages in the lesional skin of bullous pemphigoid and pemphigus vulgaris: the possible pathogenesis of bullous pemphigoid. *Dermatology* (2014) 229:369–78. doi:10.1159/000365946
159. Koepke J, Dresel M, Schmid S, Greulich T, Beutel B, Schmeck B, et al. Therapy with plasma purified alpha1-antitrypsin (Prolastin(R)) induces time-dependent changes in plasma levels of MMP-9 and MPO. *PLoS One* (2015) 10:e0117497. doi:10.1371/journal.pone.0117497
160. Lin L, Bankaitis E, Heimbach L, Li N, Abrink M, Pejler G, et al. Dual targets for mouse mast cell protease-4 in mediating tissue damage in experimental bullous pemphigoid. *J Biol Chem* (2011) 286:37358–67. doi:10.1074/jbc.M111.272401
161. Lin L, Betsuyaku T, Heimbach L, Li N, Rubenstein D, Shapiro SD, et al. Neutrophil elastase cleaves the murine hemidesmosomal protein BP180/type XVII collagen and generates degradation products that modulate experimental bullous pemphigoid. *Matrix Biol* (2012) 31:38–44. doi:10.1016/j.matbio.2011.09.003
162. Diny NL, Rose NR, Cihakova D. Eosinophils in autoimmune diseases. *Front Immunol* (2017) 8:484. doi:10.3389/fimmu.2017.00484
163. Simon D, Borradori L, Simon HU. Eosinophils as putative therapeutic targets in bullous pemphigoid. *Exp Dermatol* (2017). doi:10.1111/exd.13416
164. Tedeschi A, Marzano AV, Lorini M, Balice Y, Cugno M. Eosinophil cationic protein levels parallel coagulation activation in the blister fluid of patients with bullous pemphigoid. *J Eur Acad Dermatol Venereol* (2015) 29:813–7. doi:10.1111/jdv.12464
165. Bergin DA, Reeves EP, Hurley K, Wolfe R, Jameel R, Fitzgerald S, et al. The circulating proteinase inhibitor alpha-1 antitrypsin regulates neutrophil degranulation and autoimmunity. *Sci Transl Med* (2014) 6:217ra1. doi:10.1126/scitranslmed.3007116
166. Plee J, Le Jan S, Giustiniani J, Barbe C, Joly P, Bedane C, et al. Integrating longitudinal serum IL-17 and IL-23 follow-up, along with autoantibodies variation, contributes to predict bullous pemphigoid outcome. *Sci Rep* (2015) 5:18001. doi:10.1038/srep18001
167. Taylor PR, Roy S, Leal SM Jr, Sun Y, Howell SJ, Cobb BA, et al. Activation of neutrophils by autocrine IL-17A-IL-17RC interactions during fungal infection is regulated by IL-6, IL-23, RORgammat and dectin-2. *Nat Immunol* (2014) 15:143–51. doi:10.1038/ni.2797
168. Liu Q, Xiao S, Xia Y. TWEAK/Fn14 activation participates in skin inflammation. *Mediators Inflamm* (2017) 2017:6746870. doi:10.1155/2017/6746870
169. Liu Y, Xu M, Min X, Wu K, Zhang T, Li K, et al. TWEAK/Fn14 activation participates in Ro52-mediated photosensitization in cutaneous lupus erythematosus. *Front Immunol* (2017) 8:651. doi:10.3389/fimmu.2017.00651
170. Peternel S, Manestar-Blazic T, Brajac I, Prpic-Massari L, Kastelan M. Expression of TWEAK in normal human skin, dermatitis and epidermal neoplasms: association with proliferation and differentiation of keratinocytes. *J Cutan Pathol* (2011) 38:780–9. doi:10.1111/j.1600-0560.2011.01762.x
171. Harmon A, Cornelius D, Amaral L, Paige A, Herse F, Ibrahim T, et al. IL-10 supplementation increases Tregs and decreases hypertension in the RUPP rat model of preeclampsia. *Hypertens Pregnancy* (2015) 34:291–306. doi:10.3109/10641955.2015.1032054
172. Kim N, Jeon Y-W, Nam Y-S, Lim J-Y, Im K-I, Lee E-S, et al. Therapeutic potential of low-dose IL-2 in a chronic GVHD patient by in vivo expansion of regulatory T cells. *Cytokine* (2016) 78:22–6. doi:10.1016/j.cyto.2015.11.020
173. Asano T, Meguri Y, Yoshioka T, Kishi Y, Iwamoto M, Nakamura M, et al. PD-1 modulates regulatory T-cell homeostasis during low-dose interleukin-2 therapy. *Blood* (2017) 129:2186–97. doi:10.1182/blood-2016-09-741629
174. Ma A, Yang Y, Wang Q, Wang Y, Wen J, Zhang Y. Antiinflammatory effects of oxymatrine on rheumatoid arthritis in rats via regulating the imbalance between Treg and Th17 cells. *Mol Med Rep* (2017) 15:3615–22. doi:10.3892/mmr.2017.6484
175. Ettinger M, Peckl-Schmid D, Gruber C, Laimer M, Thalhamer J, Hintner H, et al. Transcutaneous gene gun delivery of hNC16A Induces BPAG2-specific tolerance. *J Invest Dermatol* (2012) 132:1665–71. doi:10.1038/jid.2012.19
176. Hunter Z, McCarthy DP, Yap WT, Harp CT, Getts DR, Shea LD, et al. A biodegradable nanoparticle platform for the induction of antigen-specific immune tolerance for treatment of autoimmune disease. *ACS Nano* (2014) 8:2148–60. doi:10.1021/nn405033r
177. Ronaghy A, Streilein RD, Hall RP III. Rituximab decreases without preference all subclasses of IgG anti-BP180 autoantibodies in refractory bullous pemphigoid (BP). *J Dermatol Sci* (2014) 74:93–4. doi:10.1016/j.jdermsci.2013.11.014

178. Nguyen T, Ahmed AR. Positive clinical outcome in a patient with recalcitrant bullous pemphigoid treated with rituximab and intravenous immunoglobulin. *Clin Exp Dermatol* (2017) 42:516–9. doi:10.1111/ced.13092
179. De Bruyne R, Bogaert D, De Ruyck N, Lambrecht BN, Van Winckel M, Gevaert P, et al. Calcineurin inhibitors dampen humoral immunity by acting directly on naive B cells. *Clin Exp Immunol* (2015) 180:542–50. doi:10.1111/cei.12604
180. Flynn MJ, Hartley JA. The emerging role of anti-CD25 directed therapies as both immune modulators and targeted agents in cancer. *Br J Haematol* (2017) 179:20–35. doi:10.1111/bjh.14770
181. Deng GM, Tsokos GC. Pathogenesis and targeted treatment of skin injury in SLE. *Nat Rev Rheumatol* (2015) 11:663–9. doi:10.1038/nrrheum.2015.106
182. Genovese MC, Fleischmann RM, Greenwald M, Satterwhite J, Veenhuizen M, Xie L, et al. Tabalumab, an anti-BAFF monoclonal antibody, in patients with active rheumatoid arthritis with an inadequate response to TNF inhibitors. *Ann Rheum Dis* (2013) 72:1461–8. doi:10.1136/annrheumdis-2012-202775
183. Gao Q, Li Q, Xue Z, Wu P, Yang X. In vitro and in vivo evaluation of a humanized anti-APRIL antibody. *Curr Mol Med* (2013) 13:464–5. doi:10.2174/156652413805076867
184. Kim YG, Alvarez M, Suzuki H, Hirose S, Izui S, Tomino Y, et al. Pathogenic role of a proliferation-inducing ligand (APRIL) in murine IgA nephropathy. *PLoS One* (2015) 10:e0137044. doi:10.1371/journal.pone.0137044
185. Björck P, Filbert E, Yang X, Trifan OC. A humanized anti-CD40 antibody with strong immune-modulatory activities capable of tumor eradication. *Cancer Res* (2016) 76:5004. doi:10.1158/1538-7445.AM2016-5004
186. Sondermann P. The FcγR/IgG interaction as target for the treatment of autoimmune diseases. *J Clin Immunol* (2016) 36:95–9. doi:10.1007/s10875-016-0272-7
187. Biesenbach P, Kain R, Derfler K, Perkmann T, Soleiman A, Benharkou A, et al. Long-term outcome of anti-glomerular basement membrane antibody disease treated with immunoadsorption. *PLoS One* (2014) 9:e103568. doi:10.1371/journal.pone.0103568
188. Kasperkiewicz M, Schulze F, Meier M, van Beek N, Nitschke M, Zillikens D, et al. Treatment of bullous pemphigoid with adjuvant immunoadsorption: a case series. *J Am Acad Dermatol* (2014) 71:1018–20. doi:10.1016/j.jaad.2014.06.014
189. Le Naour S, Peuvrel L, Saint-Jean M, Dreno B, Quereux G. Three new cases of bullous pemphigoid during anti-PD-1 antibody therapy. *J Eur Acad Dermatol Venereol* (2017). doi:10.1111/jdv.14579
190. Smith DM, Simon JK, Baker JR Jr. Applications of nanotechnology for immunology. *Nat Rev Immunol* (2013) 13:592–605. doi:10.1038/nri3488
191. Huss DJ, Pellerin AF, Collette BP, Kannan AK, Peng L, Datta A, et al. Anti-CD25 monoclonal antibody Fc variants differentially impact regulatory T cells and immune homeostasis. *Immunology* (2016) 148:276–86. doi:10.1111/imm.12609
192. Kinnear G, Jones ND, Wood KJ. Costimulation blockade: current perspectives and implications for therapy. *Transplantation* (2013) 95:527–35. doi:10.1097/TP.0b013e31826d4672
193. Quintana FJ, Yeste A, Mascanfroni ID. Role and therapeutic value of dendritic cells in central nervous system autoimmunity. *Cell Death Differ* (2015) 22:215–24. doi:10.1038/cdd.2014.125
194. Mbongue J, Nicholas D, Firek A, Langridge W. The role of dendritic cells in tissue-specific autoimmunity. *J Immunol Res* (2014) 2014:857143. doi:10.1155/2014/857143
195. Huang J, Song G, Yin Z, He W, Zhang L, Kong W, et al. Rapid reduction of antibodies and improvement of disease activity by immunoadsorption in Chinese patients with severe systemic lupus erythematosus. *Clin Rheumatol* (2016) 35:2211–8. doi:10.1007/s10067-016-3354-2

Conflict of Interest Statement: The authors declare that the research was conducted in the absence of any commercial or financial relationships that could be construed as a potential conflict of interest.

frontiers in Immunology

ORIGINAL RESEARCH
published: 04 December 2017
doi: 10.3389/fimmu.2017.01723

The Role of Estrogen Membrane Receptor (G Protein-Coupled Estrogen Receptor 1) in Skin Inflammation Induced by Systemic Lupus Erythematosus Serum IgG

*Zhenming Cai[1], Changhao Xie[1], Wei Qiao[1], Xibin Fei[1], Xuanxuan Guo[1], Huicheng Liu[1], Xiaoyan Li[1], Xiang Fang[1], Guangqiong Xu[1], Hui Dou[1] and Guo-Min Deng[1,2,3]**

[1] Key Laboratory of Antibody Techniques of Ministry of Health, Nanjing Medical University, Nanjing, China, [2] State Key Laboratory of Reproductive Medicine, Nanjing Medical University, Nanjing, China, [3] First Affiliated Hospital, Nanjing Medical University, Nanjing, China

Skin injury is the second most common clinical manifestation in patients with systemic lupus erythematosus (SLE). Estrogen may affect the onset and development of SLE through its receptor. In this study, we investigated the role of estrogen membrane receptor G protein-coupled estrogen receptor 1 (GPER1) in skin injury of SLE. We found that skin injury induced by SLE serum was more severe in female mice and required monocytes. Estrogen promoted activation of monocytes induced by lupus IgG through the membrane receptor GPER1 which was located in lipid rafts. Blockade of GPER1 and lipid rafts reduced skin inflammation induced by SLE serum. The results we obtained suggest that GPER1 plays an important role in the pathogenesis of skin inflammation induced by lupus IgG and might be a therapeutic target in skin lesions of patients with SLE.

Keywords: estrogen, systemic lupus erythematosus, IgG, skin inflammation, G protein-coupled estrogen receptor 1

OPEN ACCESS

Edited by:
Fulvio D'Acquisto, Queen Mary University of London, United Kingdom

Reviewed by:
Luz Pamela Blanco, National Institutes of Health (NIH), United States
Caroline Jefferies, Cedars-Sinai Medical Center, United States

****Correspondence:***
Guo-Min Deng
gmdeng@njmu.edu.cn

Specialty section:
This article was submitted to Inflammation, a section of the journal Frontiers in Immunology

Received: *27 June 2017*
Accepted: *21 November 2017*
Published: *04 December 2017*

Citation:
Cai Z, Xie C, Qiao W, Fei X, Guo X, Liu H, Li X, Fang X, Xu G, Dou H and Deng G-M (2017) The Role of Estrogen Membrane Receptor (G Protein-Coupled Estrogen Receptor 1) in Skin Inflammation Induced by Systemic Lupus Erythematosus Serum IgG. Front. Immunol. 8:1723. doi: 10.3389/fimmu.2017.01723

INTRODUCTION

Systemic lupus erythematosus (SLE) is a chronic autoimmune disease characterized by high levels of autoantibodies and multi-organ tissue damage (including the kidney, skin, lungs, brain, and heart) (1, 2). The prevalence of SLE in population ranges from 20 to 150 cases per 100,000, with up to 90% affecting women of childbearing age (3, 4). The female-to-male ratio in prepuberty is 3:1, and this ratio increases to 10:1 during the reproductive age and decreases again to 8:1 after menopause (5). In SLE patients, serum estrogen levels are much higher than in healthy subjects and correlated with disease severity (6, 7). Using of exogenous estrogen could increase the risk of SLE development in healthy women and exacerbate the disease in SLE patients and mouse models (8–10). It was reported that in (NZB × NZW)F1 mice, lupus development was strongly influenced by gender, and lupus incidence was higher, and survival time was reduced in female mice compared with males (11). In addition, exogenous estrogens also could accelerate lupus development and autoantibody production in male and female (NZB × NZW)F1 mice (12, 13). These data suggest that estrogen may have an important role in the onset and development of SLE.

Estrogens have important influences on several immune functions (14). It has been shown that female sex hormones could affect T cell function and antibody production in B cells. Estrogens are a class of sex steroid hormones that were synthesized from cholesterol. Three forms of physiological estrogens exist in female animals: estrone (E1), estradiol (E2, or 17-β estradiol), and estriol (E3). E2 is the staple product of this process and the most potent estrogen during the childbearing age

(15). Estrogen binds two types of receptors, which were named nuclear receptors (ERα and ERβ) and cell membrane receptors [G protein-coupled estrogen receptor 1 (GPER1) and ER-X], to trigger direct and indirect responses within the cell (16). ERα and ERβ which belong to the superfamily of nuclear receptors are soluble receptors that shuttle between the cytoplasm and the nucleus (17). After binding estrogen-responsive elements (EREs) and recruiting co-regulatory and chromatin remodeling proteins, ERα or ERβ regulates transcription of target genes (18). GPR30 which is now named GPER1 is a seven transmembrane-domain G protein-coupled receptor. As an integral membrane estrogen receptor, GPER1 can elicit rapid estrogen-responsive signaling independent of ERα and ERβ (19).

It has been shown that mortality and glomerulonephritis severity were significantly decreased in ERα-deficient female (NZB × NZW)F1 mice (20), and ERα activation has an immunostimulatory role in murine lupus, whereas ERβ activation performs mild immunosuppressive effects (21). In human studies, it has been found that polymorphisms of ERα but not ERβ may be associated with susceptibility or development of SLE (22, 23). These data suggest that ERα plays a main role in mediating the effects of estrogens in SLE. However, the role of estrogen membrane receptor GPER1 in the onset and development of SLE remains unclear.

In the patients with SLE, skin injury is the second most common clinical manifestation (24). However, the role of estrogen in the development of skin inflammation is not well known. In this study, we investigated the role and mechanism of estrogen in the development of skin inflammation in SLE. We found that estrogen could promote the development of skin injury induced by SLE serum through GPER1 and that lipid rafts serve an important function in the regulatory effect of GPER1 in skin inflammation induced by SLE IgG.

MATERIALS AND METHODS

Information of SLE Patients

A total of 398 SLE patients hospitalized in The First Affiliated Hospital of Bengbu Medical College between January 2010 and December 2011 were recruited. All patients fulfilled at least four of the American College of Rheumatology criteria for SLE (25). The local ethics committee approved the protocol and written informed consents were obtained.

Mice and Reagents

The Csf-1-deficient mice were purchased from The Jackson Laboratory, and C57BL/6 mice were purchased from Nanjing University. All mice were housed in the animal facility of Nanjing Medical University.

Sera of SLE patients were collected from The First Affiliated Hospital of Nanjing Medical University. We adopt the criteria of the American College of Rheumatology as the classification of SLE. All patients had SLE disease-activity index scores ranging from 0 to 20.

Protein G agarose was purchased from Millipore. FITC-conjugated CTB, methyl-β-cyclodextrin (MβCD) and β-estradiol 6-(*O*-carboxy-methyl)oxime: BSA (E2-BSA) were purchased from Sigma-Aldrich. G15 was purchased from TOCRIS bioscience. ICI 182,780 (Fulvestrant), a specific antagonist of nuclear estrogen receptors, was purchased from Santa Cruz Biotechnology.

Anti-CD11b, TNF-α, and MCP-1 antibodies were purchased from Abcam. Anti-phospho-NF-kB p65 rabbit mAb, NF-κB p65 rabbit mAb, and GAPDH rabbit mAb antibodies were purchased from Cell Signaling Technology. Anti-CD3, CD20, GPER1, and CD64 antibodies were purchased from Santa Cruz Biotechnology.

Injection Protocol

Systemic lupus erythematosus serum (100 μl) or SLE IgG (50 μg/100 μl) was injected intradermally in the back of the neck of treated mice and PBS (100 μl) was used as control. MβCD (1 mg/mouse, in a volume of 100 μl) or G15 (2 μg/mouse, in a volume of 100 μl) were intraperitoneally injected three times a week for 2 weeks before SLE serum injection. Control mice received the same volume of the PBS.

Histopathological and Immunohistochemical Examination of Skin Lesions

Histopathological examination of skin tissue was performed as described earlier (26). After routine fixation and paraffin embedding, tissue sections from skin were cut and stained with H&E. The slides were coded and evaluated in a blinded manner. Skin inflammation severity was scored as described before (26).

After deparaffinization and Ag retrieval, the skin tissues were stained with antibodies to CD3, CD11b, CD20, α-NAE, MCP-1, and TNF-α followed by incubation with biotinylated secondary antibodies, avidin–biotin–peroxidase complexes, and 3-amino-9-ethyl-carbazole-containing H_2O_2. All sections were counterstained with Mayer's hematoxylin (26).

Monocyte Differentiation into Dendritic Cells (DCs)

Mononuclear cells isolated from spleens of C57BL/6 mice were incubated in 24-well plates at 37°C for 3 h and then monocytes were obtained after removing suspended lymphocytes. Monocytes were cultured in DMEM medium with 5% FBS, on 37°C, and 5% CO_2. Monocytes were stimulated with SLE serum or SLE IgG for 3 and 48 h. Then, we examined the differentiation of monocytes into DCs by light microscopy. RAW264.7 cells were cultured in DMEM medium with 5% FBS, on 37°C, and 5% CO_2.

Measurement of MCP-1 and TNF-α

The levels of MCP-1 and TNF-α in supernatants were determined by using a mouse MCP-1 Flex cytokine kit, mouse TNF-α Flex cytokine kit and cytometric bead array according to the manufacturer's instructions (BD Biosciences).

Western Blotting and Coimmunoprecipitation

Raw264.7 cells were lysed in RIPA buffer, and the supernatants of homogenates were subjected to SDS-PAGE. Blotted onto

polyvinylidene difluoride (PVDF) membranes and stained for p-NF-κB p65/NF-κB p65 and GAPDH.

Raw264.7 cells were lysed in RIPA buffer, and homogenates were incubated with protein G beads pre-absorbed with anti-CD64 antibody. Pre- and post-CD64-immunoprecipitated supernatants and anti-CD64 beads were subjected to SDS-PAGE, blotted onto PVDF membranes, and stained for GPER1.

Immunofluorescent Staining

After fixing with 3% paraformaldehyde in PBS and cytospuning onto slides, monocytes were permeabilized with 0.05% Triton X-100 for 5 min at room temperature and blocked with PBS containing 10% normal goat serum for 1 h. Then, the cells were incubated with primary antibodies (CD64 or GPER1) in 0.5% BSA at room temperature for 45 min. The cells were washed after incubating with a secondary antibody and FITC-conjugated CTB for 45 min; the slides were washed three times by PBS. After staining the nuclei with DAPI for 5 min, the slides were mounted with a coverslip using Fluoromount-G, and cells were observed using a Zeiss LSM 510 META confocal microscope (26).

Statistics

Statistical evaluations of skin inflammation severity, levels of MCP-1 and TNF-α were performed using Student's *t*-test. $P < 0.05$ was considered statistically significant.

RESULTS

Estrogen Is Involved in the Pathogenesis of SLE

Because females have high estrogen levels, we investigated female SLE patients to determine the role of estrogen in the pathogenesis of SLE. We investigated 398 SLE patients and found that 374 (94.0%) of the patients were females and 279 (83.7%) were in the childbearing age (18–45 years) (**Table 1**). These data suggest that estrogen may play a role in the pathogenesis of SLE.

To further investigate whether estrogen regulates SLE-related organ and tissue damage, we used an animal model in which SLE serum is administered to induce skin inflammation (26). We injected SLE serum intradermally in female and male C57BL/6 mice. Histopathological examination demonstrated that resulting skin lesions were more severe in female mice than in males (**Figure 1A**). These data suggest that female mice are more susceptible to SLE serum-induced skin inflammation and estrogen may be involved in the pathogenesis of skin inflammation in SLE.

TABLE 1 | The demographics of systemic lupus erythematosus patients.

Sex		
	Female	Male
	374	24
Age (years)		
Median	34.5 ± 13.4	31.8 ± 13.9
Range	10–69	13–76
<18	23 (6.1%)	2
18–45	313 (83.7%)	20
>45	38 (10.2%)	2

We also use serum from healthy volunteer as negative controls and we did not find skin inflammation induced by healthy volunteer and PBS (Figure S1 in Supplementary Material).

Monocytes Contribute to the Development of SLE Serum-Induced Skin Inflammation

Because estrogen may regulate the severity of SLE serum-induced skin inflammation, we investigated the role of its immune cell targets in this regulatory effect. Immunohistochemical staining demonstrated that there were abundant $CD11b^+$ cells but very few $CD3^+$, $CD20^+$, and $\alpha\text{-NAE}^+$ cells in skin lesions (**Figure 1B**). These data indicate that monocytes/macrophages may play an important role in the development of SLE serum-induced skin inflammation. Previous work has shown that monocytes/macrophages, but not lymphocytes, were important in the development of this inflammation (26). To further verify the role of monocytes/macrophages in SLE serum-induced skin inflammation, we tried to induce skin inflammation in $Csf\text{-}1^{-/-}$ mice lacking mature monocytes. Compared to wild-type mice, we found that the severity and incidence of skin inflammation decreased significantly in $Csf\text{-}1^{-/-}$ mice (**Figure 1C**). In addition, the expression of MCP-1 and TNF-α was increased in skin lesions of mice (**Figure 1D**). These data suggest that monocytes may play an important role in the development of SLE serum-induced skin inflammation.

Lipid Rafts Have an Important Regulatory Role in the Activity of Monocytes Triggered by SLE IgG

Lipid rafts are sphingolipid- and cholesterol-rich domains of the plasma membrane that contain various signaling and transport proteins (27). These domains contribute significantly to the pathogenesis of organ and tissue damage in lupus-prone mice (28). Based on this information, we next investigated whether SLE serum triggered lipid raft aggregation on monocytes. We found that clustering of lipid rafts developed on monocytes 3 and 48 h after SLE serum treatment (**Figure 2A**). These data suggest that SLE serum-induced lipid raft clustering on monocytes.

Because SLE serum can induce differentiation of monocytes into DCs (26), we next investigated whether depletion of lipid rafts using MβCD would affect this differentiation. We found that lipid raft depletion inhibited both SLE serum-induced and SLE IgG-induced monocyte differentiation into DCs (**Figures 2B,C**). These data indicate that lipid rafts have an important role in monocyte differentiation into DCs.

To understand how lipid rafts regulate the effects of SLE IgG which is major contributor in SLE serum-induced skin inflammation, we assessed whether they contained Fcγ receptors (FcγRs) which are IgG receptors (29). First, we analyzed the expression of FcγRI (CD64) in skin lesions induced by SLE serum and found a large amount of $CD64^+$ cells (**Figure 2D**). Then, we analyzed whether lipid rafts contain CD64. We observed colocalization of CD64 and lipid rafts in monocytes treated with SLE IgG and this colocalization was abolished by MβCD treatment (**Figure 2E**).

To further characterize the regulatory role of lipid rafts in the expression of intracellular signaling molecules induced by SLE

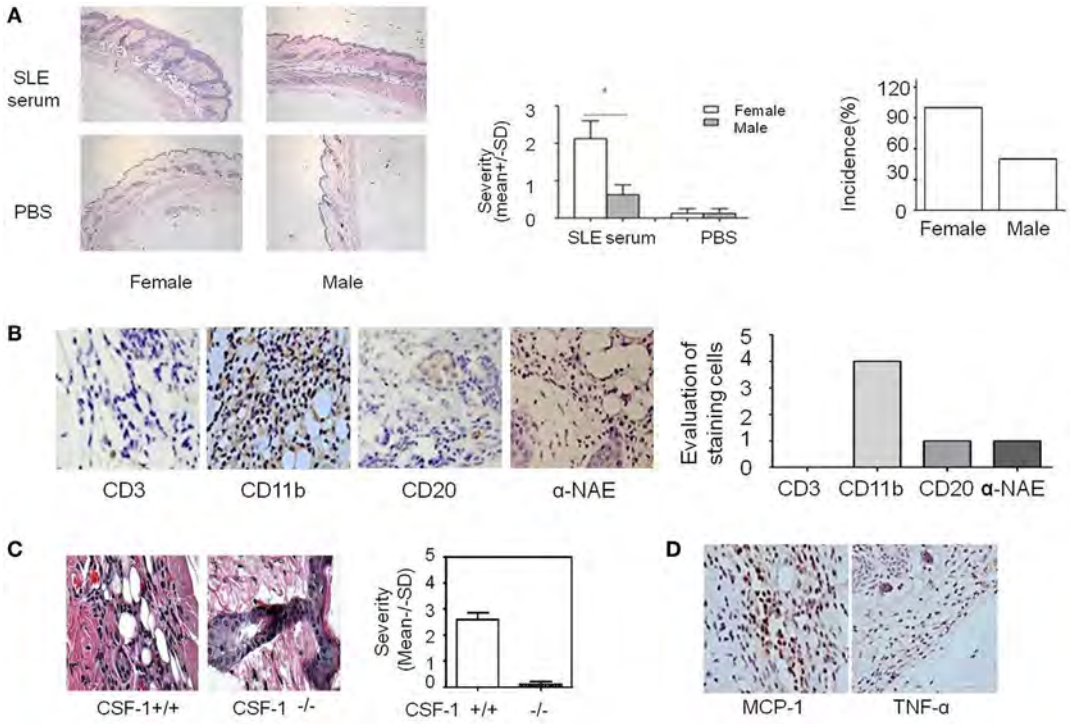

FIGURE 1 | Analysis of systemic lupus erythematosus (SLE) serum-induced skin inflammation in mice and the role of monocytes in this progress. **(A)** Representative histopathological photomicrograph of the severity and incidence of skin inflammation in female and male C57BL/6 mice sacrificed 3 days after intradermal inoculation of serum (100 μl) from SLE patients (n = 8 per group). H&E, original magnification 20×. **(B)** Immunohistochemical staining for CD3, CD11b, CD20, and α-NAE expression in skin lesions of C57BL/6 mice 3 days after intradermal inoculation of serum (100 μl) from SLE patients (the scoring system: 0, no positive cells; 1, 1–5 positive cells; 2, 6–10 positive cells; 3, 10–20 positive cells; 4, >20 positive cells in a field). **(C)** Severity and picture of SLE serum-induced skin inflammation in female Csf-1$^{-/-}$ mice and wild-type mice (n = 5 per group) 3 days after intradermal inoculation of serum (100 μl) from SLE patients. **(D)** Immunohistochemical staining for MCP-1 and TNF-α expression in skin lesions of C57BL/6 mice 3 days after intradermal inoculation of SLE serum. *P < 0.05.

IgG, we analyzed the expression of p-NF-κB p65/NF-κB p65 in Raw264.7 cells. We found that SLE IgG increased levels of p-NF-κB p65, MCP-1, and TNF-α in supernatants of Raw264.7 cells (**Figures 2F–H**). Conversely, MβCD decreased the expression of p-NF-κB p65, MCP-1, and TNF-α. These results indicate that lipid rafts are important in the expression of inflammatory and intracellular signaling molecules in monocytes triggered by SLE IgG.

E2 Promotes Activation of SLE IgG-Induced Monocytes *via* the Membrane Receptor GPER1

Estrogens exert their functions by binding nuclear receptors (ERα and ERβ) that act as ligand-dependent transcription factors or by binding membrane-bound receptors (GPR30 and ER-X) that initiate signal transduction pathways (16). Although several studies have shown that ERα plays a major role in mediating the effects of estrogens in SLE (20, 21), there are no data to describe the role of the estrogen cell membrane receptor GPER1 (also called GPR30) in SLE. To determine the role of GPER1 in SLE, we used E2-BSA, an activator specifically bound to GPER1.

First, we investigated whether monocytes express GPER1. We found a number of GPER1$^+$ cells in the skin lesions induced by SLE serum (**Figure 3A**). We also saw GPER1 expression in monocytes from C57BL/6 mice and Raw264.7 cells by western blotting, and there was no significant difference of GPER1 expression between female and male mice (**Figure 3B**). Next, we determined whether E2-BSA regulates the activity of monocytes triggered by SLE IgG. We observed that SLE IgG or SLE IgG with E2-BSA could induce monocyte differentiation into DCs but not E2-BSA alone (**Figure 3C**). There were no significant differences between cells treated with SLE IgG or SLE IgG with E2-BSA. These data indicate that E2-BSA alone did not enhance SLE IgG-induced monocyte differentiation into DCs.

To investigate the effect of E2-BSA on expression of intracellular signaling molecules induced by SLE IgG, we analyzed the expression of p-NF-κB p65/NF-κB p65 in Raw264.7 cells treated with SLE IgG in the presence or absence of E2-BSA. We found that E2-BSA increased levels of p-NF-κB p65 induced by SLE IgG compared with the cells treated with SLE IgG only (**Figure 3D**). We also measured the levels of MCP-1 and TNF-α in supernatants of Raw264.7 cells treated with SLE IgG in presence or absence of E2-BSA for 24 h and found that E2-BSA increased levels of MCP-1 and TNF-α triggered by SLE IgG (**Figure 3E**). To further confirm the effect of estrogen membrane receptor on SLE IgG, we used G15, a specific antagonist of GPER1 (30). We found that G15 abolished the effect of E2-BSA on expression of p-NF-κB

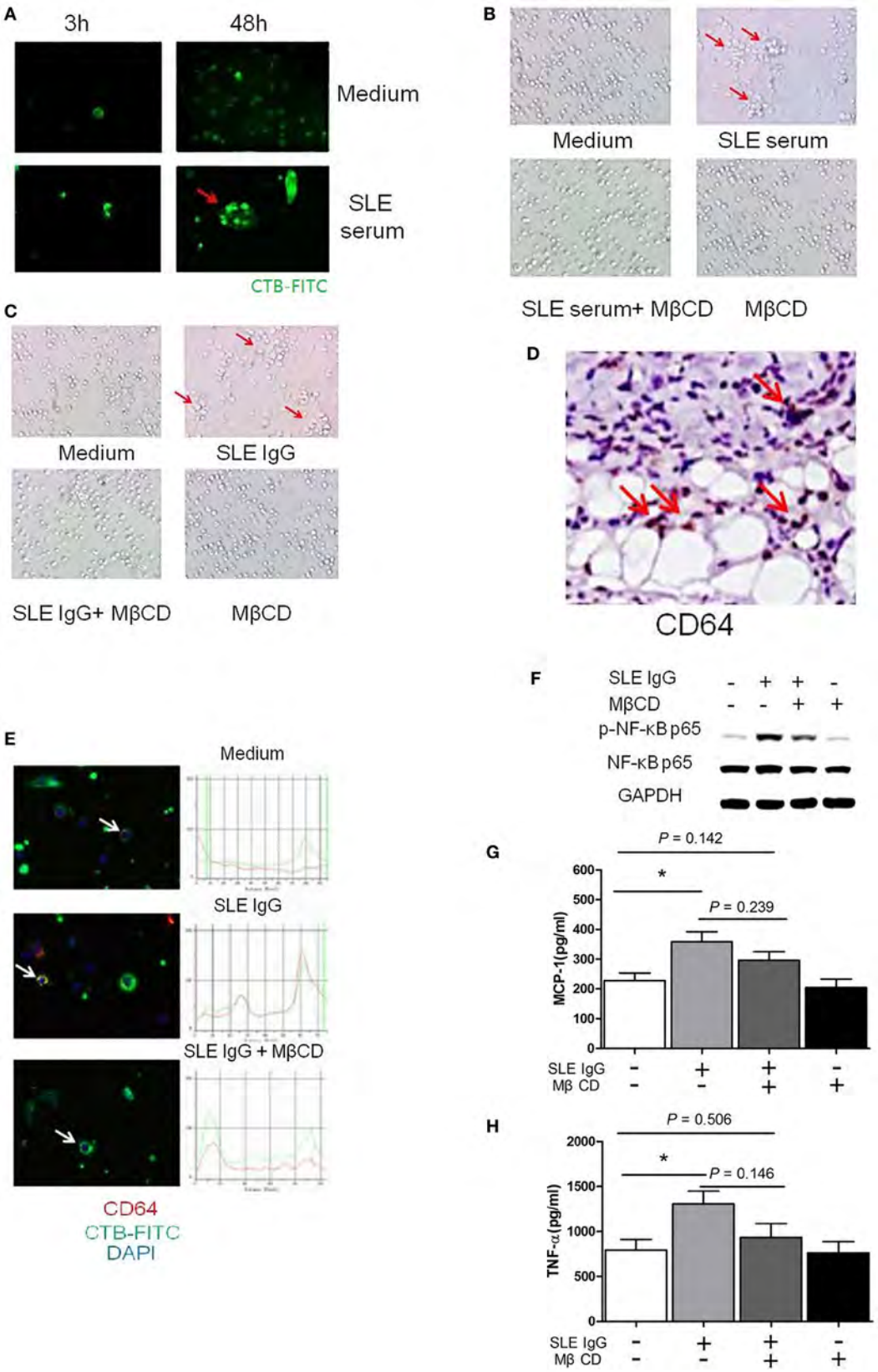

FIGURE 2 | Continued

FIGURE 2 | Continued
Lipid rafts are important in the process of systemic lupus erythematosus (SLE) IgG-induced differentiation of monocytes into dendritic cells (DCs). **(A)** Confocal microscopy analysis of lipid raft clustering using FITC-conjugated CTB in monocytes cultured with SLE serum or medium control for 3 and 48 h. The arrows represent typical clustered lipid rafts. **(B,C)** Representative photographs of monocytes cultured with SLE serum with or without methyl-β-cyclodextrin (MβCD) for 48 h **(B)** or SLE IgG with or without MβCD for 48 h **(C)**. Original magnification 20× and the arrows represent typical differentiation of monocytes into DCs. **(D)** Immunohistochemical staining for CD64 (FcγRI) expression in skin lesions of C57BL/6 mice 3 days after intradermal inoculation of SLE serum. The arrows represent $CD64^+$ cells. **(E)** Confocal microscopy analysis of colocalization of CD64 and lipid rafts in monocytes cultured with medium control, SLE IgG, SLE IgG, and MβCD for 3 h. The arrows represent the cells which were analyzed. **(F)** Western blot analysis of expression of p-NF-κB p65/NF-κB p65 and GAPDH in Raw264.7 cells treated with medium control, SLE IgG, SLE IgG + MβCD, or MβCD for 30 min. **(G,H)** CBA-measured levels of MCP-1 or TNFα in supernatants of Raw264.7 cells treated with medium control, SLE IgG, SLE IgG + MβCD, or MβCD for 24 h. $^*P < 0.05$.

p65 (**Figure 3F**) and expression of MCP-1 and TNF-α triggered by SLE IgG (**Figure 3G**).

To further determine whether estrogen nuclear receptors regulate activation of NF-κB p65 triggered by SLE IgG, we blocked the effect of ERα and ERβ by using ICI 182,780 (Fulvestrant), a specific antagonist of nuclear estrogen receptors. We found that blockade of estrogen nuclear receptors did not inhibit the effect of E2-BSA on activation of NF-κB p65 triggered by SLE IgG (Figure S2A in Supplementary Material).

In addition, we further investigated the effects of estrogen and G15 on activation of NF-κB p65 triggered by SLE IgG. We found that E2, E2-BSA, or G15 did not directly activate NF-κB p65; E2-BSA enhanced but G15 decreased activation of NF-κB p65 triggered by SLE IgG; E2 did not affect levels of p-NF-κB p65 induced by SLE IgG (Figure S2B in Supplementary Material). These results indicate that estrogen membrane receptor not nuclear receptors promote activation of NF-κB p65 triggered by SLE IgG.

To determine whether GPER1 activation enhances skin inflammation induced by SLE serum, we treated mice with intradermal injection of SLE serum in the presence or absence of E2-BSA. As shown in Figure S3 in Supplementary Material, E2-BSA alone did not induce skin inflammation, but enhanced the skin inflammation induced by SLE serum. These data suggest that activated membrane receptor of estrogen may promote skin inflammation induced by SLE serum.

E2 Promotes Activation of SLE IgG-Induced Monocytes through Lipid Rafts

E2 promotes SLE IgG-induced monocyte activation and cytokine production *via* GPER1 but the mechanism was still unknown. We hypothesized that GPER1 might bind to CD64 to promote this process. We used coimmunoprecipitation to identify the relationship between GPER1 and CD64. As shown in **Figure 4A**, we did not find direct binding of GPER1 and CD64.

Because GPER1 and CD64 are membrane receptors and we have shown that CD64 localized in clustered lipid rafts in SLE serum-treated monocytes, we investigated whether clustered lipid rafts contain GPER1 and CD64. We found that GPER1 and CD64 colocalized with clustered lipid rafts in SLE serum-treated monocytes (**Figure 4B**). These results indicate that lipid rafts serve as platforms for the interaction between GPER1 and CD64. To confirm this point, we used MβCD to inhibit the lipid raft clustering in Raw264.7 cells treated with SLE IgG in the presence or absence of E2-BSA. We found that MβCD decreased levels of p-NF-κB p65 trigged by SLE IgG with E2-BSA (**Figure 4C**). We also found that MβCD inhibited the effect of E2-BSA on SLE IgG-induced expression of MCP-1 and TNF-α (**Figures 4D,E**). These results indicated that E2 promoted SLE IgG-induced monocyte activation through lipid rafts.

Inhibition of GPER1 and Lipid Rafts Reduced SLE Serum-Induced Skin Inflammation

We have shown that G15 and MβCD could inhibit SLE IgG-induced monocyte activation and cytokine production. Here, we investigated the effect of G15 and MβCD in SLE serum-induced skin inflammation. We found that the severity of SLE serum-induced skin inflammation was significantly decreased in the mice treated with G15 (**Figure 4F**) and mice treated with MβCD (**Figure 4G**). In addition, we analyzed the serum E2 levels of female mice treated with MβCD or G15. There was no significant difference between the control mice (PBS treated) and MβCD or G15 treated mice (data not shown). These data indicate that inhibition of GPER1 and lipid rafts reduced SLE serum-induced skin inflammation.

DISCUSSION

Our study demonstrates that there is a higher incidence of SLE and more severe skin inflammation induced by SLE serum in female mice. We showed that monocytes are important in the development of SLE serum-induced skin inflammation and estrogen may enhance the activity of monocytes and SLE serum-induced skin inflammation through the membrane receptor GPER1. We also showed that lipid rafts exert an important role in estrogen mediating effects through GPER1.

Although the pathogenesis of SLE remains unclear, several lines of evidence suggest that SLE may be caused by immunological abnormalities including loss of B cell tolerance, abnormal interactions between T and B cell signaling, hyperactivity of immune cells, production of pathogenic autoantibodies, and defective clearance of auto-antigens and immune complexes (1, 31). The factor enhancing these abnormalities may promote pathological progression of SLE.

The observed female prevalence is highest after puberty. In (NZB × NZW) F1 (NZB/w F1) mice, the disease is more serious and has an earlier onset and higher mortality rate in females (32). This evidence suggests that estrogen may be involved in the onset and development of SLE. In this study, we examined 398 SLE patients and found that the female-to-male ratio was 15.5:1

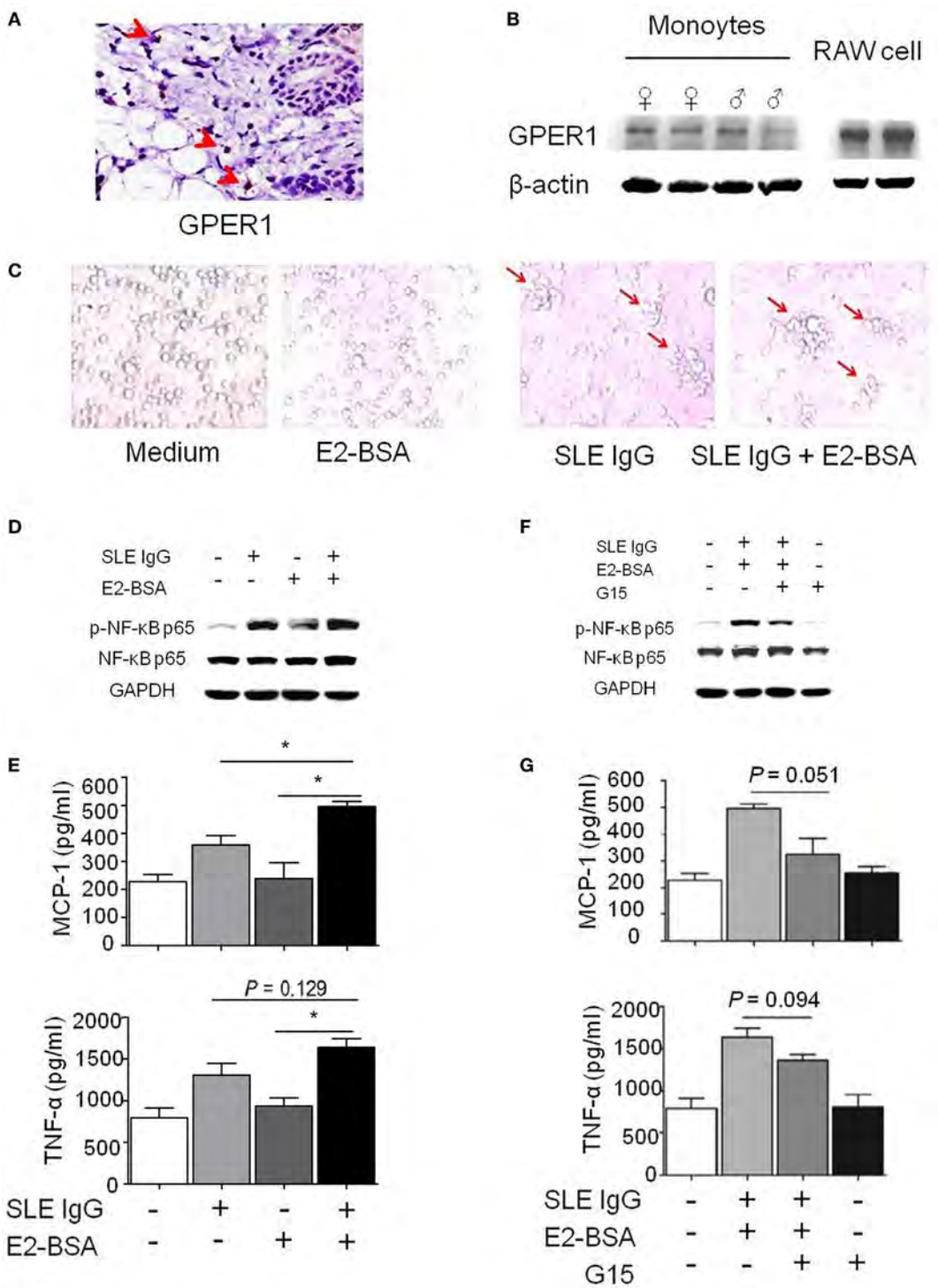

FIGURE 3 | E2 promotes activation of systemic lupus erythematosus (SLE) IgG-induced monocytes *via* the membrane receptor G protein-coupled estrogen receptor 1 (GPER1). **(A)** Immunohistochemical staining for GPER1 expression in skin lesions of C57BL/6 mice 3 days after intradermal inoculation of SLE serum. The arrows represent GPER1$^+$ cells. **(B)** Western blot-measured GPER1 expression in Raw264.7 cells and monocytes from C57BL/6 mice. **(C)** Representative photographs of monocytes cultured with medium control, E2-BSA, SLE IgG, or SLE IgG + E2-BSA for 48 h. Monocytes were isolated from spleen of C57BL/6 mice. Original magnification 20× and the arrows represent typical differentiation of monocytes into dendritic cells. **(D)** Western blot-measured levels of p-NF-κB p65/NF-κB p65 in Raw264.7 cells treated with medium control, SLE IgG, E2-BSA, or SLE IgG + E2-BSA for 30 min. **(E)** CBA-measured levels MCP-1 or TNF-α in supernatants of Raw264.7 cells treated with medium control, SLE IgG, E2-BSA, or SLE IgG + E2-BSA for 24 h. *$P < 0.05$. **(F)** Western blot-measured levels of p-NF-κB p65/NF-κB p65 in Raw264.7 cells treated with medium control, SLE IgG + E2-BSA, SLE IgG + E2-BSA + G15, or G15 for 30 min. **(G)** CBA-measured levels of MCP-1 or TNF-α in supernatants of Raw264.7 cells treated with medium control, SLE IgG + E2-BSA, SLE IgG + E2-BSA + G15, or G15 for 24 h.

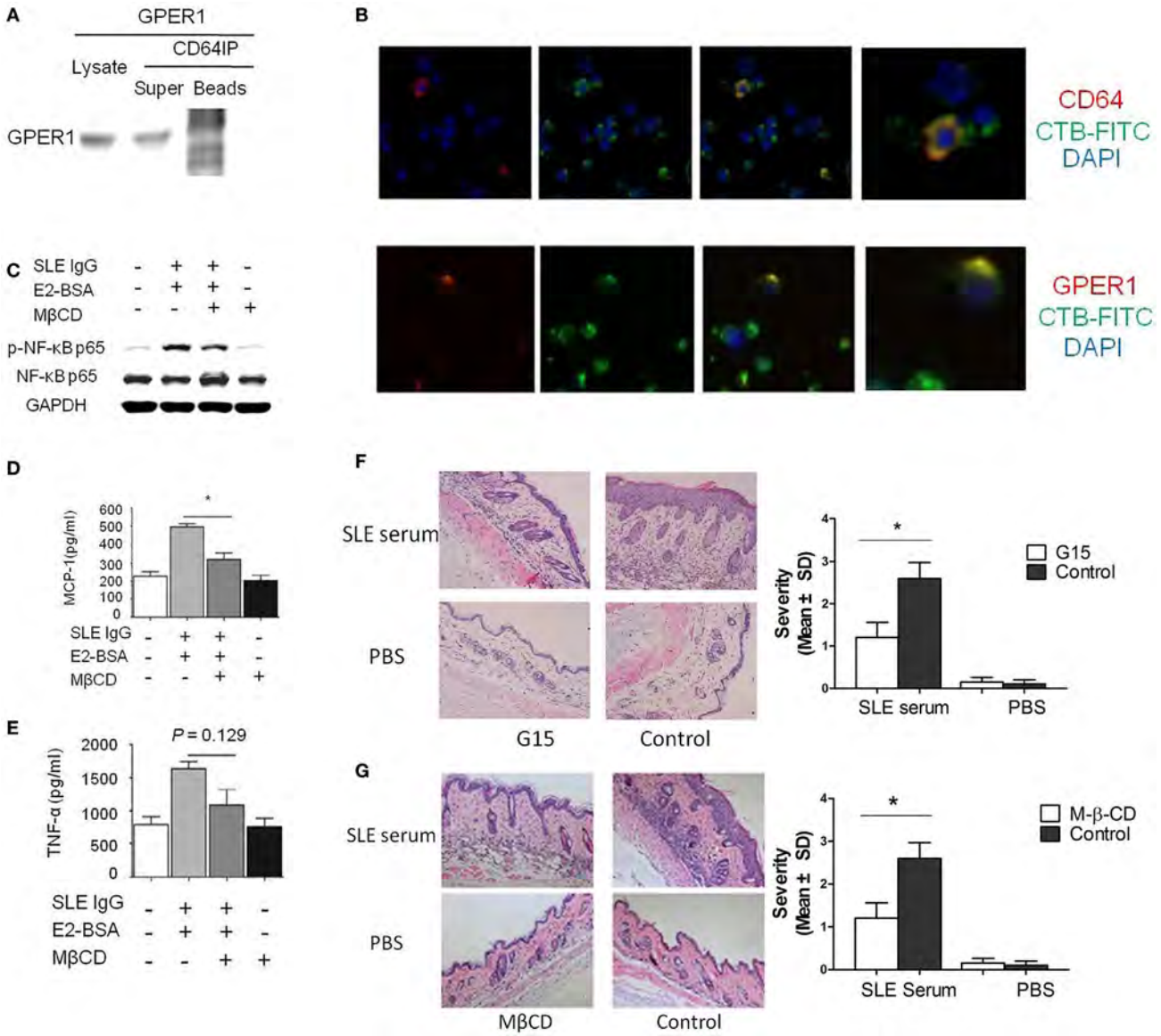

FIGURE 4 | E2 promotes activation of systemic lupus erythematosus (SLE) IgG-induced monocytes and skin inflammation through lipid rafts. **(A)** Relationship of G protein-coupled estrogen receptor 1 (GPER1) and CD64 measured by western blot and immunoprecipitation in Raw264.7 cells. **(B)** Immunofluorescent staining of GPER1 and lipid rafts or CD64 and lipid rafts on monocytes treated with SLE IgG. **(C)** Western blot-measured levels of p-NF-κB p65/NF-κB p65 in Raw264.7 cells treated with medium, SLE IgG + E2-BSA, SLE IgG + E2-BSA + methyl-β-cyclodextrin (MβCD), or MβCD for 30 min. **(D,E)** CBA-measured levels of MCP-1 **(D)** or TNF-α **(E)** in supernatants of Raw264.7 cells treated with medium, SLE IgG + E2-BSA, SLE IgG + E2-BSA + MβCD, or MβCD for 24 h. **(F)** Histopathological photomicrograph and severity of skin inflammation in female C57BL/6 mice treated with or without G15 and sacrificed 3 days after intradermal inoculation of SLE serum. G15 at dose of 2 μg was administered intraperitoneally three times a week for 2 weeks ($n = 10$ per group). **(G)** Histopathological photomicrograph and severity of skin inflammation in female C57BL/6 mice treated with or without MβCD (1 mg/mouse three times a week, i.p., for 2 weeks) sacrificed 3 days after intradermal inoculation of serum (100 μl) from a SLE patient ($n = 8$ per group). H&E, original magnification 20×. *$P < 0.05$.

and that 279 patients (83.7%) were in their reproductive age (18–45 years). Female mice had more serious skin lesions induced by SLE serum than males. Our data indicate that estrogen may play an important role in the development of SLE serum-induced skin inflammation.

We have previously reported that monocytes play a crucial role in the development of SLE serum-induced skin inflammation and that SLE serum IgG can induce monocyte differentiation into DCs (26). In this study, we confirmed our previous results. In addition, we found out that SLE IgG increased the levels of signaling molecules of cell activation (p-NF-κB p65) and inflammatory cytokines (MCP-1 and TNF-α) produced in monocytes. And we also found that FcγRs, which are widely expressed on cells throughout the hematopoietic system (33), were expressed on

monocytes and that FcγRI (CD64) was expressed in skin lesions induced by SLE serum.

It has been shown that estrogens could modulate lymphoid cell growth and differentiation, activation and proliferation, cytokine secretion, and antibody production (14). Estrogens have been demonstrated to promote the pathological progression of SLE by inhibiting activation-induced apoptosis of SLE T cells through downregulating the Fas-L expression (34) and enhancing autoantibody levels in autoimmune diseases (35). Estrogens can also stimulate the production of IL-1, IL-4, IL-6, and IL-10 in macrophages and T cells (36). Estrogen exerts its effects by binding two types of receptors: nuclear receptors and cell membrane receptors (16). After binding EREs and recruiting coregulatory and chromatin remodeling proteins, ERα or ERβ could regulate the transcription of target genes (18). GPER1 is an integral membrane estrogen receptor that can trigger rapid estrogen-responsive signaling independent of ERα and ERβ (19). Our study indicates that GPER1 also plays an important role in skin injury of SLE. E2-BSA, which specifically binds to GPER1, increased the activation of monocytes and the production of inflammatory cytokines induced by SLE IgG and these effects were inhibited by G15, a specific GPER1 antagonist. On the other hand, a specific antagonist of nuclear estrogen receptors (ICI 182,780) did not inhibit the effect of E2-BSA on expression of p-NF-κB p65 induced by SLE IgG. In addition, we found that E2-BSA augmented skin inflammation induced by SLE serum and blockade of GPER1 reduced skin inflammation induced by SLE serum. These results indicate that estrogen promotes the monocyte activation induced by SLE IgG and skin inflammation induced by SLE serum through the membrane receptor GPER1 but not nuclear receptors.

Systemic lupus erythematosus IgG exerts its effect by binding FcγR on cell membrane. Our study supports that GPER1 regulates the effect of FcγR through lipid rafts. Lipid rafts which contain various signaling and transport proteins are sphingolipid- and cholesterol-rich domains of the plasma membrane (27). It has been reported that lipid rafts regulate the pathogenesis of organ and tissue damage in lupus-prone mice (28), play an important role in mediating the transport of substrates across the plasma membrane (27, 37, 38). In this study, we found that SLE IgG triggered lipid raft aggregation in monocytes and MβCD could inhibit the clustering of lipid rafts and monocyte differentiation into DCs. MβCD also inhibited monocyte activation and inflammatory cytokine production induced by SLE IgG. In addition, we demonstrated that aggregated lipid rafts contained CD64 and GPER1.

Our study suggests that the membrane estrogen receptor GPER1 is involved in the pathological progression of SLE and that estrogen may promote skin injury introduced by SLE serum through membrane receptor GPER1. Furthermore, lipid rafts play an important regulatory role in the effect of estrogen on the pathological progression of SLE through GPER1.

ETHICS STATEMENT

This study was carried out in accordance with the recommendations of "IACUC of Nanjing Medical University" with written informed consent from all subjects. All subjects gave written informed consent in accordance with the Declaration of Helsinki. The protocol was approved by the "IACUC of Nanjing Medical University." For statements involving animal subjects, please use: this study was carried out in accordance with the recommendations of "IACUC of guidelines, Nanjing Medical University of committee." The protocol was approved by the "Nanjing Medical University of committee."

AUTHOR CONTRIBUTIONS

ZC, CX, and G-MD conceived the idea and designed the research. ZC, XL, WQ, XG, HL, XF, XF, and G-MD initiated the study and drafted the manuscript; ZC and CX conducted the experiments; ZC, XL, CX, and G-MD analyzed the results. All the authors reviewed and approved the manuscript.

ACKNOWLEDGMENTS

The authors would like to thank the participating patients and Doctor Muhammad Haidar Zaman for revising the manuscript.

FUNDING

This work was partly supported by the National Natural Science Foundation of China (G-MD, Grant Number: 81472111) and the Postdoctoral Science Foundation of Jiangsu (ZC, Grant Numbers: DG220D5145 and 1402160C). This work was also supported in part by a grant of the Research Initiating Fund of Nanjing Medical University (KY101RC071203).

SUPPLEMENTARY MATERIAL

The Supplementary Material for this article can be found online at http://www.frontiersin.org/article/10.3389/fimmu.2017.01723/full#supplementary-material.

FIGURE S1 | Skin inflammation induced by PBS, healthy serum, and systemic lupus erythematosus (SLE) serum. Histopathological photomicrograph **(A)** and severity of skin inflammation **(B)** in female C57BL/6 mice treated with PBS, healthy serum, and SLE serum (100 μl) in female C57BL/6 mice ($n = 5$ per group). H&E, original magnification 20×. $^{**}P < 0.01$.

FIGURE S2 | Different effects of estrogen receptors on activation of NF-κB triggered by systemic lupus erythematosus (SLE) IgG. **(A)** Western blot detected activation of NF-κB in RAW cells treated with SLE IgG, SLE IgG + E2-BSA, SLE IgG + E2-BSA + ICI, SLE IgG + ICI, and ICI alone. ICI is a specific inhibitor of estrogen nuclear receptors. **(B)** Western blot detected activation of NF-κB in RAW cells treated with SLE IgG, E2, E2-BSA, SLE IgG + E2, SLE IgG + E2-BSA, G15, SLE IgG + G15, and SLE IgG + E2-BSA + G15. G15 is a specific inhibitor of estrogen membrane receptor G protein-coupled estrogen receptor 1. Band densities of p-NF-κB p65 were quantified with densitometric analysis using ImageJ and normalized to the negative control treated with medium.

FIGURE S3 | Effect of estrogen membrane receptor G protein-coupled estrogen receptor 1 (GPER1) on skin inflammation induced by systemic lupus erythematosus (SLE) serum. Histopathological photomicrograph **(A)** and severity of skin inflammation **(B)** in female C57BL/6 mice with intradermal injection of SLE serum (25 μl) in the presence or absence of GPER1 activator (E2-BSA, 250 nM) ($n = 8$ per group) and intraperitoneal injection of E2-BSA (250 nM). H&E, original magnification 20×. $^{*}P < 0.05$.

REFERENCES

1. Tsokos GC. Systemic lupus erythematosus. *N Engl J Med* (2011) 365:2110–21. doi:10.1056/NEJMra1100359
2. Rahman A, Isenberg DA. Systemic lupus erythematosus. *N Engl J Med* (2008) 358:929–39. doi:10.1056/NEJMra071297
3. Chakravarty EF, Bush TM, Manzi S, Clarke AE, Ward MM. Prevalence of adult systemic lupus erythematosus in California and Pennsylvania in 2000: estimates obtained using hospitalization data. *Arthritis Rheum* (2007) 56:2092–4. doi:10.1002/art.22641
4. Pons-Estel GJ, Alarcon GS, Scofield L, Reinlib L, Cooper GS. Understanding the epidemiology and progression of systemic lupus erythematosus. *Semin Arthritis Rheum* (2010) 39:257–68. doi:10.1016/j.semarthrit.2008.10.007
5. Kassi E, Moutsatsou P. Estrogen receptor signaling and its relationship to cytokines in systemic lupus erythematosus. *J Biomed Biotechnol* (2010) 2010:317452. doi:10.1155/2010/317452
6. Lahita RG, Bradlow L, Fishman J, Kunkel HG. Estrogen metabolism in systemic lupus erythematosus: patients and family members. *Arthritis Rheum* (1982) 25:843–6. doi:10.1002/art.1780250726
7. Folomeev M, Dougados M, Beaune J, Kouyoumdjian JC, Nahoul K, Amor B, et al. Plasma sex hormones and aromatase activity in tissues of patients with systemic lupus erythematosus. *Lupus* (1992) 1:191–5. doi:10.1177/096120339200100312
8. Garovich M, Agudelo C, Pisko E. Oral contraceptives and systemic lupus erythematosus. *Arthritis Rheum* (1980) 23:1396–8. doi:10.1002/art.1780231213
9. Carlsten H, Nilsson N, Jonsson R, Backman K, Holmdahl R, Tarkowski A. Estrogen accelerates immune complex glomerulonephritis but ameliorates T cell-mediated vasculitis and sialadenitis in autoimmune MRL lpr/lpr mice. *Cell Immunol* (1992) 144:190–202. doi:10.1016/0008-8749(92)90236-I
10. Lang TJ. Estrogen as an immunomodulator. *Clin Immunol* (2004) 113:224–30. doi:10.1016/j.clim.2004.05.011
11. Andrews BS, Eisenberg RA, Theofilopoulos AN, Izui S, Wilson CB, McConahey PJ, et al. Spontaneous murine lupus-like syndromes. Clinical and immunopathological manifestations in several strains. *J Exp Med* (1978) 148:1198–215. doi:10.1084/jem.148.5.1198
12. Walker SE, Bole GG Jr. Influence of natural and synthetic estrogens on the course of autoimmune disease in the NZB-NZW mouse. *Arthritis Rheum* (1973) 16:231–9. doi:10.1002/art.1780160215
13. Roubinian J, Talal N, Siiteri PK, Sadakian JA. Sex hormone modulation of autoimmunity in NZB/NZW mice. *Arthritis Rheum* (1979) 22:1162–9. doi:10.1002/art.1780221102
14. Kolkova Z, Casslen V, Henic E, Ahmadi S, Ehinger A, Jirstrom K, et al. The G protein-coupled estrogen receptor 1 (GPER/GPR30) does not predict survival in patients with ovarian cancer. *J Ovarian Res* (2012) 5:9. doi:10.1186/1757-2215-5-9
15. Cui J, Shen Y, Li R. Estrogen synthesis and signaling pathways during aging: from periphery to brain. *Trends Mol Med* (2013) 19:197–209. doi:10.1016/j.molmed.2012.12.007
16. Levin ER. Plasma membrane estrogen receptors. *Trends Endocrinol Metab* (2009) 20:477–82. doi:10.1016/j.tem.2009.06.009
17. Edwards DP. Regulation of signal transduction pathways by estrogen and progesterone. *Annu Rev Physiol* (2005) 67:335–76. doi:10.1146/annurev.physiol.67.040403.120151
18. Heldring N, Pike A, Andersson S, Matthews J, Cheng G, Hartman J, et al. Estrogen receptors: how do they signal and what are their targets. *Physiol Rev* (2007) 87:905–31. doi:10.1152/physrev.00026.2006
19. Thomas P, Pang Y, Filardo EJ, Dong J. Identity of an estrogen membrane receptor coupled to a G protein in human breast cancer cells. *Endocrinology* (2005) 146:624–32. doi:10.1210/en.2004-1064
20. Bynote KK, Hackenberg JM, Korach KS, Lubahn DB, Lane PH, Gould KA. Estrogen receptor-alpha deficiency attenuates autoimmune disease in (NZB x NZW)F1 mice. *Genes Immun* (2008) 9:137–52. doi:10.1038/sj.gene.6364458
21. Li J, McMurray RW. Effects of estrogen receptor subtype-selective agonists on autoimmune disease in lupus-prone NZB/NZW F1 mouse model. *Clin Immunol* (2007) 123:219–26. doi:10.1016/j.clim.2007.01.008
22. Lee YJ, Shin KS, Kang SW, Lee CK, Yoo B, Cha HS, et al. Association of the oestrogen receptor alpha gene polymorphisms with disease onset in systemic lupus erythematosus. *Ann Rheum Dis* (2004) 63:1244–9. doi:10.1136/ard.2003.012583
23. Johansson M, Arlestig L, Moller B, Smedby T, Rantapaa-Dahlqvist S. Oestrogen receptor {alpha} gene polymorphisms in systemic lupus erythematosus. *Ann Rheum Dis* (2005) 64:1611–7. doi:10.1136/ard.2004.032425
24. Wang C, Dehghani B, Magrisso IJ, Rick EA, Bonhomme E, Cody DB, et al. GPR30 contributes to estrogen-induced thymic atrophy. *Mol Endocrinol* (2008) 22:636–48. doi:10.1210/me.2007-0359
25. Kastenberger I, Schwarzer C. GPER1 (GPR30) knockout mice display reduced anxiety and altered stress response in a sex and paradigm dependent manner. *Horm Behav* (2014) 66:628–36. doi:10.1016/j.yhbeh.2014.09.001
26. Deng GM, Liu LN, Kyttaris VC, Tsokos GC. Lupus serum IgG induces skin inflammation through the TNFR1 signaling pathway. *J Immunol* (2010) 184:7154–61. doi:10.4049/jimmunol.0902514
27. Michel V, Bakovic M. Lipid rafts in health and disease. *Biol Cell* (2007) 99:129–40. doi:10.1042/BC20060051
28. Deng GM, Tsokos GC. Cholera toxin B accelerates disease progression in lupus-prone mice by promoting lipid raft aggregation. *J Immunol* (2008) 181:4019–26. doi:10.4049/jimmunol.181.6.4019
29. Hogarth PM, Pietersz GA. Fc receptor-targeted therapies for the treatment of inflammation, cancer and beyond. *Nat Rev Drug Discov* (2012) 11:311–31. doi:10.1038/nrd2909
30. Dennis MK, Burai R, Ramesh C, Petrie WK, Alcon SN, Nayak TK, et al. In vivo effects of a GPR30 antagonist. *Nat Chem Biol* (2009) 5:421–7. doi:10.1038/nchembio.168
31. Zhang J, Jacobi AM, Wang T, Berlin R, Volpe BT, Diamond B. Polyreactive autoantibodies in systemic lupus erythematosus have pathogenic potential. *J Autoimmun* (2009) 33:270–4. doi:10.1016/j.jaut.2009.03.011
32. Theofilopoulos AN, Dixon FJ. Murine models of systemic lupus erythematosus. *Adv Immunol* (1985) 37:269–390. doi:10.1016/S0065-2776(08)60342-9
33. Nimmerjahn F, Ravetch JV. Fc gamma receptors as regulators of immune responses. *Nat Rev Immunol* (2008) 8:34–47. doi:10.1038/nri2206
34. Kim WU, Min SY, Hwang SH, Yoo SA, Kim KJ, Cho CS. Effect of oestrogen on T cell apoptosis in patients with systemic lupus erythematosus. *Clin Exp Immunol* (2010) 161:453–8. doi:10.1111/j.1365-2249.2010.04194.x
35. Verthelyi DI, Ahmed SA. Estrogen increases the number of plasma cells and enhances their autoantibody production in nonautoimmune C57BL/6 mice. *Cell Immunol* (1998) 189:125–34. doi:10.1006/cimm.1998.1372
36. Gonzalez DA, Diaz BB, Perez MDR, Hernandez AG, Chico BND, de Leon AC. Sex hormones and autoimmunity. *Immunol Lett* (2010) 133:6–13. doi:10.1016/j.imlet.2010.07.001
37. Lingwood D, Simons K. Lipid rafts as a membrane-organizing principle. *Science* (2010) 327:46–50. doi:10.1126/science.1174621
38. Simons K, Gerl MJ. Revitalizing membrane rafts: new tools and insights. *Nat Rev Mol Cell Biol* (2010) 11:688–99. doi:10.1038/nrm2977

Conflict of Interest Statement: The authors declare that the research was conducted in the absence of any commercial or financial relationships that could be construed as a potential conflict of interest.

frontiers in Immunology

CORRECTION
published: 31 July 2018
doi: 10.3389/fimmu.2018.01732

Corrigendum: The Role of Estrogen Membrane Receptor (G Protein-Coupled Estrogen Receptor 1) in Skin Inflammation Induced by Systemic Lupus Erythematosus Serum IgG

*Zhenming Cai[1], Changhao Xie[1], Wei Qiao[1], Xibin Fei[1], Xuanxuan Guo[1], Huicheng Liu[1], Xiaoyan Li[1], Xiang Fang[1], Guangqiong Xu[1], Hui Dou[1] and Guo-Min Deng[1,2,3]**

[1] Key Laboratory of Antibody Techniques of Ministry of Health, Nanjing Medical University, Nanjing, China, [2] State Key Laboratory of Reproductive Medicine, Nanjing Medical University, Nanjing, China, [3] First Affiliated Hospital, Nanjing Medical University, Nanjing, China

Keywords: estrogen, systemic lupus erythematosus, IgG, skin inflammation, G protein-coupled estrogen receptor 1

OPEN ACCESS

Approved by:
Frontiers in Immunology Editorial Office, Frontiers Media SA, Switzerland

****Correspondence:***
Guo-Min Deng
gmdeng@njmu.edu.cn

Specialty section:
This article was submitted to Inflammation, a section of the journal Frontiers in Immunology

Received: *08 July 2018*
Accepted: *12 July 2018*
Published: *31 July 2018*

Citation:
Cai Z, Xie C, Qiao W, Fei X, Guo X, Liu H, Li X, Fang X, Xu G, Dou H and Deng G-M (2018) Corrigendum: The Role of Estrogen Membrane Receptor (G Protein-Coupled Estrogen Receptor 1) in Skin Inflammation Induced by Systemic Lupus Erythematosus Serum IgG. Front. Immunol. 9:1732. doi: 10.3389/fimmu.2018.01732

A corrigendum on

The Role of Estrogen Membrane Receptor (G Protein-Coupled Estrogen Receptor 1) in Skin Inflammation Induced by Systemic Lupus Erythematosus Serum IgG
by Cai Z, Xie C, Qiao W, Fei X, Guo X, Liu H, et al. Front Immunol (2017) 8:1723. doi: 10.3389/fimmu.2017.01723

Yacong Guo was included as an author in the published article. At his request, this author is being removed, and this does not change the scientific conclusions of the article in any way.

The original article has been updated.

Conflict of Interest Statement: The authors declare that the research was conducted in the absence of any commercial or financial relationships that could be construed as a potential conflict of interest.

frontiers in Immunology

ORIGINAL RESEARCH
published: 27 November 2017
doi: 10.3389/fimmu.2017.01669

Anti-idiotypic Antibodies against BP-IgG Prevent Type XVII Collagen Depletion

Mayumi Kamaguchi[1,2], Hiroaki Iwata[1], Yuiko Mori[1], Ellen Toyonaga[1], Hideyuki Ujiie[1], Yoshimasa Kitagawa[2] and Hiroshi Shimizu[1]*

[1] Department of Dermatology, Hokkaido University Graduate School of Medicine, Sapporo, Japan, [2] Department of Oral Diagnosis and Medicine, Graduate School of Dental Medicine, Hokkaido University, Sapporo, Japan

Bullous pemphigoid (BP) mainly targets type XVII collagen (COL17). Intravenous immunoglobulin (IVIg) is used to treat numerous autoimmune diseases, including BP. The major mechanism of action for IVIG is thought to be its immunomodulatory effect. However, little is known about the precise mechanisms of IVIg in BP. We investigate the cellular effects of IVIg, toward treatments for BP. Keratinocytes were treated with IgG from BP patients (BP-IgG) and with IVIg, and then the COL17 expression was detected by Western blotting. Cell adhesion and *ex vivo* dermal–epidermal separation were also investigated for the condition with BP-IgG and IVIg. BP-IgG targeting the non-collagenous 16A domain induces the depletion of COL17 in cultured keratinocytes (DJM-1 cells). The COL17 levels in DJM-1 cells were decreased by 50% after 4 h of BP-IgG stimulation as determined by Western blotting. By contrast, BP-IgG with IVIg was found to result in 70–90% increases in COL17 and to restore adhesion to the plate. Interestingly, IVIg significantly inhibited the binding of BP-IgG to the COL17-enzyme-linked immunosorbent assay plate, and this was due to anti-idiotypic antibodies against BP-IgG. When anti-idiotypic antibodies against BP-IgG in 0.02% of IVIg were depleted from IVIg, those antibodies did not exhibit inhibitory effects on COL17 depletion. When cryosections of human skin were incubated with BP-IgG in the presence of leukocytes, dermal–epidermal separation was observed. BP-IgG treatment with IVIg or anti-idiotypic antibodies did not induce such separation. These findings strongly suggest the presence of anti-idiotypic antibodies against anti-COL17 IgG in IVIg. This mechanism of IVIg could be a target for therapies against BP.

Keywords: bullous pemphigoid, type XVII collagen, intravenous immunoglobulin, idiotypic antibody, depletion, autoantibody

OPEN ACCESS

Edited by:
Falk Nimmerjahn, University of Erlangen-Nuremberg, Germany

Reviewed by:
Bruce David Mazer, The Research Institute of the McGill University Health Center, Canada
Jan Lunemann, University of Zurich, Switzerland

****Correspondence:***
Hiroaki Iwata
hiroaki.iwata@med.hokudai.ac.jp

Specialty section:
This article was submitted to Immunological Tolerance and Regulation, a section of the journal Frontiers in Immunology

Received: *29 August 2017*
Accepted: *14 November 2017*
Published: *27 November 2017*

Citation:
Kamaguchi M, Iwata H, Mori Y, Toyonaga E, Ujiie H, Kitagawa Y and Shimizu H (2017) Anti-idiotypic Antibodies against BP-IgG Prevent Type XVII Collagen Depletion. Front. Immunol. 8:1669. doi: 10.3389/fimmu.2017.01669

INTRODUCTION

The first uses of intravenous immunoglobulin (IVIg) were in immunodeficient individuals and individuals with severe infections. IVIg is currently used to treat numerous autoimmune diseases, including rheumatoid arthritis, systemic lupus erythematosus, and autoimmune blistering diseases (AIBDs) (1). Controlled studies of IVIg as a treatment for pemphigus and pemphigoid patients found IVIg to be a safe, effective treatment (2, 3). Furthermore, several case reports have

Abbreviations: IVIg, intravenous immunoglobulin; AIBD, autoimmune blistering disease; EBA, epidermolysis bullosa acquisita; BP, bullous pemphigoid; COL17, type XVII collagen; NC16A, the non-collagenous 16A domain; RT, room temperature; BSA, bovine serum albumin; FcRn, neonatal Fc receptor; ELISA, enzyme-linked immunosorbent assay.

described the use of IVIg to treat AIBDs such as pemphigoid and epidermolysis bullosa acquisita (EBA) (4–6). Although various modes of action for IVIg have been proposed in AIBDs, the mechanisms behind its effect are still not fully understood (7, 8). The major mechanism of action for IVIg in AIBDs is thought to be its immunomodulatory effect (1, 9–11). In addition, anti-idiotypic antibodies against pathogenic antibodies have been reported in autoimmune disorders (1, 12). Although there are many autoimmune disorders, anti-idiotypic antibodies against autoantibodies have been proved in only several autoimmune disorders (13–18).

Bullous pemphigoid (BP) is the most common AIBD (19). Two autoantigens, type XVII collagen (COL17, also called BP180) and BP230, which form a hemidesmosome, are targeted in BP, and COL17 is particularly relevant to the pathogenesis (19). Antibody-induced tissue damage is a major pathology in autoantibody-mediated autoimmune diseases (20). The activation of complements and/or inflammatory cells, including neutrophils and eosinophils, is crucial to the development of clinical phenotypes in animal models (21–23). In addition, molecular or cellular mechanisms have been proposed. IgG from BP patients (BP-IgG) targeting the non-collagenous 16A (NC16A) domain of COL17 induces the depletion of COL17 in cultured keratinocytes (24). It is thought that the shortage of COL17 causes an insufficiency of hemidesmosomes during remodeling that eventually results in weak cell adhesion to the basement membrane (25).

Regarding treatments for BP patients, it has been reported recently that IVIg provides therapeutic benefits to BP patients (3). A randomized, double-blind, placebo-controlled clinical study concluded that IVIg has therapeutic benefits for patients with BP who are resistant to systemic steroid therapy. The inhibition of autoantibody production and inflammatory cascades are major strategies in BP treatment. Prednisolone is thought to have dual effects and is commonly used. In most BP treatments, the targets are immune cells, including neutrophils and antigen-specific B cells and/or T cells. However, little is known about the effects of IVIg in keratinocytes expressing the autoantigens. This study focused on the cellular effects of IVIg, for the treatment of BP.

MATERIALS AND METHODS

BP Patients and Total IgG Purification

The BP patients fulfilled both inclusion criteria: (i) clinical blistering or erosions on the skin and (ii) circulating autoantibodies against COL17 as detected by BP180-NC16A enzyme-linked immunosorbent assay (ELISA)/CLEIA (MBL, Nagoya, Japan). BP-IgG was purified from plasma obtained by apheresis in a severe BP patient. Total IgG was purified using a protein G affinity column according to the manufacturer's instructions (GE Healthcare, Amersham, UK). In accordance with the Hokkaido University Hospital bylaws and standard operating procedures approved by the Hokkaido University Hospital Review Board, we obtained patient consent for experimental procedures to be performed at Hokkaido University Hospital. A full review and approval by an ethics committee were not required, according to local guidelines. The studies were conducted in accordance with the Helsinki guidelines.

Anti-COL17 NC16A IgG Purification

Anti-COL17 NC16A IgG was purified from total IgG using a protein G affinity column by means of the HiTrap HNS-activated HP column according to the manufacturer's instructions (GE Healthcare). Briefly, GST fusion COL17 NC16A was produced as previously described (26). The recombinant protein was coupled with the HiTrap NHS-activated HP column. The titer of anti-COL17-specific IgG was measured by indirect immunofluorescent staining. Indirect immunofluorescent staining using anti-COL17-specific IgG (concentration 0.1 mg/ml) demonstrated titers greater than 1:32,000.

Treatment Agents

Two different IVIgs (Nihon Pharmaceutical Co., Ltd., Tokyo, Japan, and Baxter International Inc., Deerfield, IL, USA; diluted with PBS) were purchased and used for this study. The concentrations of each agent for the treatment are given in Section "Results" and the figure legends.

Depletion of Anti-idiotypic Antibodies

To deplete anti-idiotypic antibodies against anti-COL17 NC16A IgG, anti-COL17 NC16A IgG was coupled to a HiTrap NHS-activated HP column according to the manufacturer's instructions (GE Healthcare). IVIg was passed through the column to remove anti-idiotypic antibodies, and then flow-through fractions (the "IVIg-depleted" sample) and the elution fraction (the "idiotype" sample) were used for the depletion assay. To evaluate the depletion efficacy, 96-well microtiter plates (Maxisorp; Nunc, Roskilde, Denmark) were coated with purified anti-COL17 NC16A IgG (500 ng/well), normal human IgG and PBS. Nonspecific binding was reduced by blocking with protein-free blocking buffer (Thermo Fisher Scientific, Rockford, IL, USA) at room temperature (RT) for 1 h. Plates were subsequently incubated with biotin-conjugated IVIg (1 mg/ml). IVIg was conjugated with biotin using a biotin labeling kit according to the manufacturer's instructions (Dojindo, Kumamoto, Japan). Finally, plates were incubated with HRP-conjugated streptavidin (Thermo Fisher Scientific) for IgG subclasses at RT for 0.5 h.

Cell Culture

DJM-1 cells isolated from human skin squamous cell carcinoma (27) were cultured in DMEM. To investigate the depletion of COL17, cells were cultured to approximately 40% confluence (24). DJM-1 cells were pretreated with agents for 1 h, and then BP-IgG (concentration 1 mg/ml) was added to the culture media for 4-h incubation. In some experiments, DJM-1 cells were treated with BP-IgG for 4 h followed by IVIg for 1 h.

Western Blotting

For Western blot analysis of whole-cell lysates, cells were lysed in RIPA buffer (Thermo Fisher Scientific) containing a protease inhibitor cocktail (Sigma Aldrich), and the lysates were

centrifuged. Each fraction was subjected to SDS–PAGE in 6% polyacrylamide gel. The gels were transferred onto nitrocellulose membranes. Blotting was performed using rabbit anti-COL17 (1:2,000 dilution) (26), rabbit anti-β-tubulin (Abcam, Tokyo, Japan, 1:20,000 dilution), and anti-integrin α6 (Santa Cruz, Dallas, TX, USA, 1:500 dilution) as the primary antibodies, followed by incubation with HRP-conjugated goat anti-rabbit or anti-mouse IgG (Life Technologies, 1:5,000 dilution). Signals were visualized with Clarity Western ECL Substrate (Bio-Rad Laboratories, Hercules, CA, USA).

Enzyme-Linked Immunosorbent Assay

BP180-NC16A ELISA was performed according to the manufacturer's instructions with minor modifications (MBL). Briefly, the ELISA plate was incubated with 100 µl of IVIg (5 mg/ml), bovine serum albumin (BSA, 5 mg/ml), or PBS. Subsequently, the plate was incubated with 1 mg/ml BP-IgG with/without PBS washing. The ELISA index value was calculated according to the manufacturer's instructions. ELISA using sera from BP patients and healthy volunteers was performed without washing the plate after IVIg incubation.

Cell Adhesion Test

BP-IgG stimulation leads to reductions in COL17 amount and in cell adhesion to the culture plate (24). Cells were placed on a vortex mixer for 20 min after BP-IgG stimulation with/without IVIg pretreatment. The adhesion of DJM-1 cells to the bottom of the culture plate was assayed by determining the number of adherent cells after vibration. After PBS washing, cells that remained on the bottom of the culture plate were treated with 0.25% trypsin for 5 min at 37°C. The released cells were counted using a blood cell counter under a microscope.

Ex Vivo Dermal–Epidermal Separation Assay (Cryosection Assay)

Ex vivo autoantibody-induced, neutrophil-dependent dermal–epidermal separation was performed as described (28, 29). Briefly, 5-µm cryosections from normal human skin were incubated with BP-IgG (2 mg/ml) in the presence or absence of 5 mg/ml IVIg at 37°C for 1 h. After washing with PBS, the slides were covered with a second slide that was taped at each end to form a chamber. Subsequently, 10^7 cells/ml of freshly isolated normal human leukocyte suspension was injected into the chamber and incubated at 37°C for 5 h. Sections were subsequently stained with H&E. We tested the experiments using two different blood donors.

Statistical Analyses

Statistical calculations were performed using SigmaPlot (Version 12.0, Systat Software, Chicago, IL, USA). To compare the parameters in the COL17-depletion assay and COL17-ELISA, one-way ANOVA test was used. A comparison of the COL17-ELISA using patient sera with/without IVIg was performed using the Wilcoxon signed-rank test. A p-value of <0.05 was considered statistically significant. The graphs present the median ± SD.

RESULTS

IVIg Prevents COL17 Depletion of Keratinocytes Induced by BP-IgG

When DJM-1 cells are treated with BP-IgG, the amount of COL17 is decreased as determined by Western blotting (COL17-depletion assay) (24). In this study, we examined the effects of IVIg by means of a COL17-depletion assay. For a COL17-depletion assay, 40% confluent cells were incubated with BP-IgG (concentration: 1 mg/ml) for 4 h. The amount of COL17 relative to β-tubulin was determined by Western blotting. DJM-1 cells were treated with BP-IgG before (the pretreatment sample) or after (the posttreatment sample) the addition of serially diluted IVIg. BP-IgG without IVIg induced an approximately 50–60% reduction of COL17 in DJM-1 cells. By contrast, BP-IgG pretreated with 5 mg/ml IVIg restored the amount of COL17 by 70–90% ($p < 0.05$, **Figure 1A**). IVIg posttreatment after 4 h of BP-IgG stimulation did not influence COL17 depletion (**Figure 1B**). Given that IVIg has direct effects on keratinocytes, such as on caspase expression (30), we incubated BP-IgG with IVIg in advance and then added them to the culture medium together (simultaneous sample). The COL17 depletion was restored similar to that in **Figure 1A** (**Figure 1C**). The amount of integrin α6, which is a transmembrane protein that is a hemidesmosomal component, was unchanged (**Figure 1D**). The same concentration (5 mg/ml) of BSA and normal human IgG did not influence the amount of COL17 under any conditions (**Figure 1D**).

The highest concentration of IVIg (5 mg/ml) was designed based on the estimated serum concentration with standard daily IVIg treatment (0.4 g/kg/day) (3).

IVIg Restores the Loss of Cell Adhesion That Is Induced by BP-IgG

Furthermore, cell adhesion was found to be reduced by approximately 60% under BP-IgG stimulation (**Figure 2**). Pretreatment with IVIg restored cell adhesion. Cells remaining in the culture plate were significantly increased with 5 mg/ml IVIg pretreatment ($p < 0.05$, **Figure 2**). Pretreatment with 5 mg/ml IVIg restored adhesion by 90% compared with normal IgG stimulation.

IVIg Prevents BP-IgG Binding to COL17

We subsequently investigated the mechanism of action of IVIg in this COL17-depletion assay. The titer of BP-IgG used for the COL17-depletion assay was measured with IVIg (5 mg/ml), BSA (5 mg/ml) or PBS by ELISA. ELISA plates were preincubated with either IVIg or BSA, and BP-IgG was subsequently added. To rule out the possibility of IVIg masking the antigen, the ELISA plate was washed with PBS after IVIg pretreatment, and then BP-IgG was added. Interestingly, 5 mg/ml IVIg (without washing) significantly inhibited the binding of BP-IgG to the ELISA plate ($p < 0.05$, **Figure 3A**). IVIg pretreatment (without washing) reduced the average titer by 30% compared with PBS pretreatment (**Figure 3A**, black bar). This inhibition was not observed using IVIg (with washing) or the same concentration of BSA. These results suggest that IVIg impairs BP-IgG's ability to bind to COL17, in which IVIg may function as an anti-idiotypic

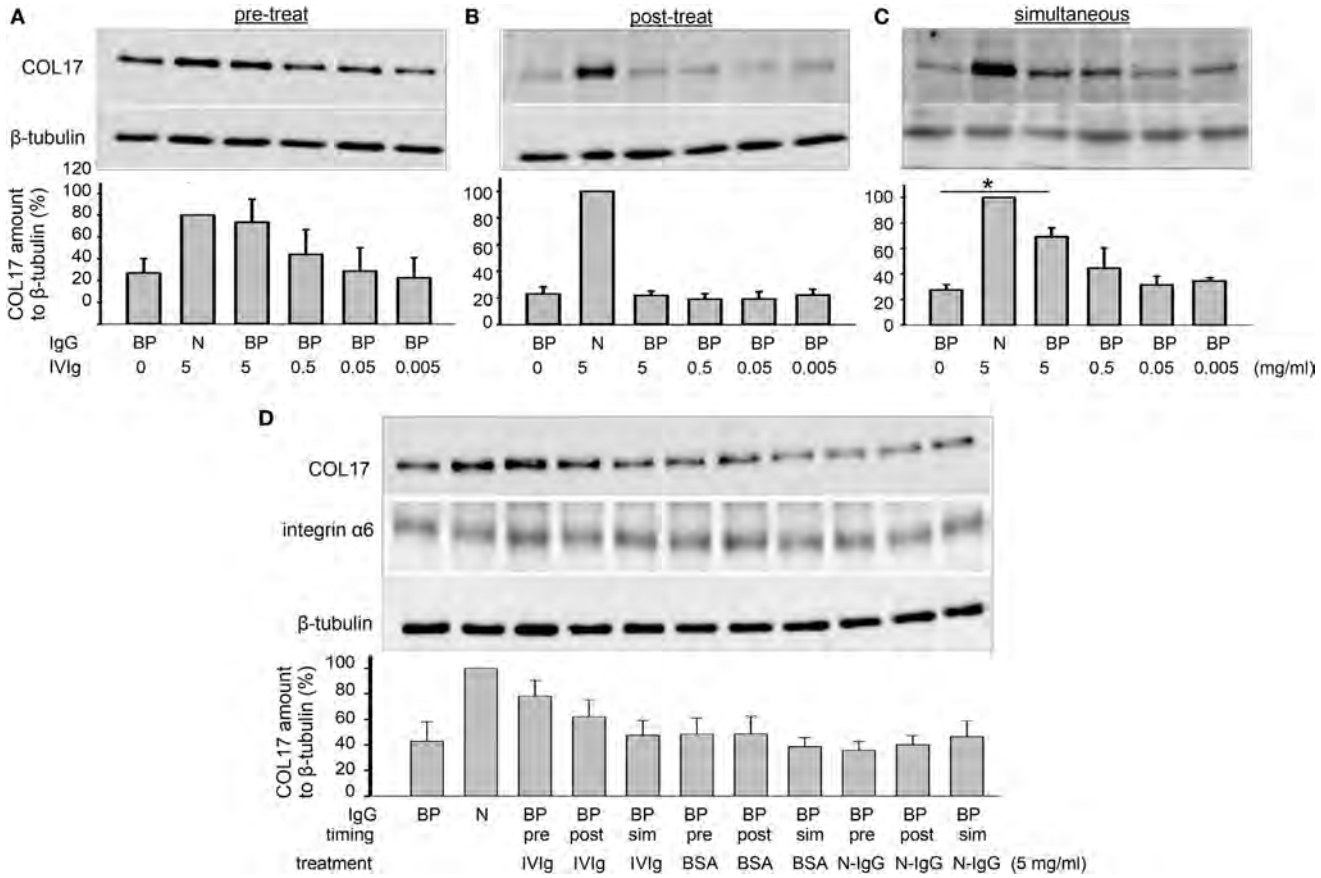

FIGURE 1 | Intravenous immunoglobulin (IVIg) prevents BP-IgG-induced type XVII collagen (COL17) depletion. DJM-1 cells (40% confluency) were treated with 1.0 mg/ml BP-IgG. Western blotting using total cell lysate was performed for anti-COL17. **(A)** DJM-1 cells were treated with IVIg (5–0.5–0.05–0.005 mg/ml) for 1 h followed by BP-IgG for 4 h (pretreatment). **(B)** DJM-1 cells were treated with BP-IgG for 4 h followed by IVIg for 1 h (posttreatment). **(C)** BP-IgG and IVIg were incubated in advance, and then added to the culture medium together (simultaneous). **(D)** DJM-1 cells were treated with appropriate controls. The amount of integrin α6, which is a transmembrane protein and a hemidesmosome component, was not changed. The representative Western blot is presented. Each experiment was performed at least three times, with $p < 0.05$. BP, BP-IgG; N, normal human IgG.

antibody. To confirm our results, samples from 10 BP patients were evaluated in the same manner. The serum titers for all 10 patients were found to be reduced by approximately 40% in the presence of IVIg (without washing) ($p < 0.05$, **Figure 3B**).

IVIg Contains Anti-idiotypic Antibodies against Anti-COL17 IgG

Next, to confirm that anti-idiotypic antibodies were actually present in the IVIg, we performed experiments to identify them directly. Anti-idiotypic antibodies in the IVIg were depleted by anti-COL17 NC16A IgG (IVIg, IVIg depleted, and idiotype fractions, **Figure 4A**). IVIg contained approximately 0.02% of anti-idiotypic antibodies against COL17 IgG (**Figure 4B**). The depletion efficiency was more than 90% (**Figure 4C**). The titers of BP-IgG were measured in the presence of IVIg (IVIg 5 mg/ml and idiotype 2.6 μg/ml) and normal IgG (5 mg/ml). The titers were found to be decreased in the setting of BP-IgG with IVIg and idiotype, but not BP-IgG with IVIg depleted (**Figure 4D**). Next, a COL17-depletion assay was performed using IVIg (5 mg/ml) and anti-idiotypic antibodies (2.6 μg/ml). IVIg depleted did not show blocking effects on COL17-depletion (**Figure 4E**). Furthermore, adhesion was also tested using IVIg and anti-idiotypic antibodies. IVIg depleted did not restore the adhesive strength compared with IVIg and idiotype (**Figure 4F**).

IVIg Mitigates BP-IgG-Induced Dermal–Epidermal Separation on Cryosections

According to our results, the therapeutic effects of IVIg potentially involve anti-idiotypic antibodies. We next examined the blocking effects of IVIg using an *ex vivo* assay, demonstrating the dermal–epidermal separation induced by BP-IgG in the presence of leukocytes (28, 29). In case of BP-IgG with PBS, dermal–epidermal separation was observed 5 h after incubation with normal human leukocytes (**Figure 5**, upper left). Next, we added IVIg, BSA and normal human IgG and incubated them with BP-IgG on the cryosections for 1 h, followed by incubation with normal human leukocytes for 5 h. IVIg depleted (5 mg/ml, upper right) and normal human IgG (5 mg/ml, lower middle) did not block

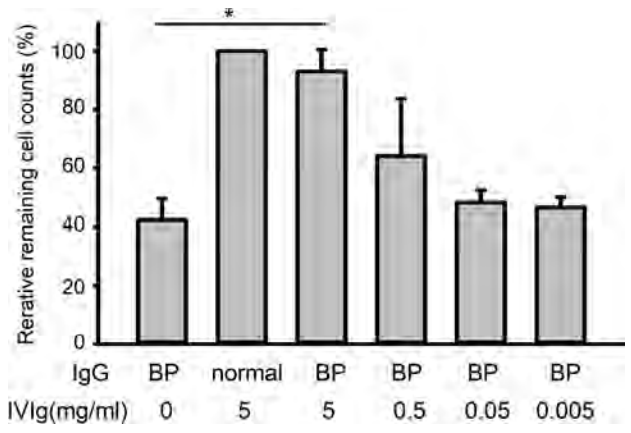

FIGURE 2 | Intravenous immunoglobulin (IVIg) restores the loss of cell adhesion induced by BP-IgG. DJM-1 cells were treated with 1.0 mg/ml BP-IgG. Culture plates were placed on a vortex for 20 min. After PBS washing, cells that remained on the bottom of the culture plate were counted using a blood cell counter under a microscope. The experiment was performed three times, with $p < 0.05$.

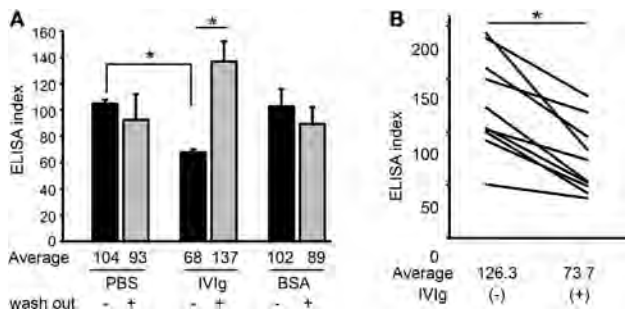

FIGURE 3 | Intravenous immunoglobulin (IVIg) prevents BP-IgG from binding to type XVII collagen (COL17). **(A)** BP-IgG titers were measured using a COL17-non-collagenous 16A enzyme-linked immunosorbent assay (ELISA) in the presence of IVIg and bovine serum albumin (BSA). The ELISA plates were washed with PBS after IVIg pretreatment to remove IVIg. Each experiment was performed four times. **(B)** The ELISA indexes of 10 BP patients' sera were measured with/without IVIg. Each experiment was performed three times, with $p < 0.05$.

the dermal–epidermal separations. By contrast, IVIg (5 mg/ml, upper middle) and the idiotype (2.6 μg/ml, lower left) protected the dermal–epidermal separation.

The Results Were Reproduced Using a Different Company's Product

There is great concern about differences arising from differences in IVIg lots or in companies. Therefore, we tested an IVIg from the different company. An IVIg product from this different company was found to prevent the COL17 depletion of keratinocytes induced by BP-IgG (**Figure 6A**). Furthermore, we found the same blocking effects of IVIg using an *ex vivo* assay (**Figure 6B**).

DISCUSSION

Intravenous immunoglobulin therapy is currently applied in autoimmune diseases, and various mechanisms of action for IVIg are involved. Previous clinical studies concluded that IVIg therapy for AIBD is a safe, effective strategy (2, 3, 31–34). The modes of action of IVIg are divided into two major mechanisms (1). One mechanism involves the F(ab)2 fragment, which is responsible for antigen recognition. The other mechanism involves the Fc fragment, which contributes to effector cell activation. Anti-idiotypic antibodies work *via* the F(ab)2 fragment, which neutralize the pathogenic antibodies in several autoimmune disorders (1, 12). However, until now, there have been no reports on anti-idiotypic antibodies in BP. According to our COL17-depletion results, we expected IVIg to contain anti-idiotypic antibodies against BP-IgG and to prevent BP-IgG binding to autoantigen COL17. We clearly demonstrated the presence of very small amounts of anti-idiotypic antibodies against anti-COL17 IgG (0.02%) in IVIg. Even very small amounts of anti-idiotypic antibodies can prevent COL17 depletion. In addition, after the depletion of anti-idiotypic antibodies from IVIg, the ability of IVIg to block COL17 depletion was not observed. IVIg is purified from serum pooled from healthy volunteers; therefore, the IVIg used in this study may have contained anti-idiotypic antibodies to BP-IgG by chance. However, we ruled this out by reconfirming similar results using IVIg from a different company.

Although there are several lines of clinical evidence, the precise mechanisms of IVIg have yet to be fully elucidated in AIBD. Li et al. reported that IVIg therapy inhibited an experimental model of AIBD by accelerating the degradation of pathogenic IgG (9). This inhibitory effect of IVIg in experimental BP was completely dependent on the neonatal Fc receptor (FcRn) *via* the Fc fragment. FcRn is associated with the half-life of IgG, and IgG recycled *via* FcRn increases that half-life (1). In an experimental model of EBA, IVIg exhibited therapeutic effects similar to those seen in systemic steroid therapy (10). In this EBA model, the disease was associated with neutrophil activation *via* the Fc gamma receptor (FcgR) IV (35). Interestingly, IVIg treatment was found to reduce circulating autoantibodies and to modulate FcgRIV expression on neutrophils (10). FcgR modulation on neutrophils is also mediated by the Fc fragment of IVIg (1).

Systemic prednisolone is the most common and the most recommended therapy for BP (19, 36, 37). Long-term prednisolone administration is associated with several risks, such as diabetes mellitus, infections, and osteoporosis. By contrast, IVIg is a safe, useful treatment for severe or high-risk cases, e.g., immunocompromised individuals or those with chronic viral infections, because it is less immunosuppressive. Although anti-idiotypic antibodies have been reported in several autoimmune disorders, a disease-specific therapy using anti-idiotypic antibodies has not been established. One major difficulty is that patients have polyclonal autoantibodies. Therefore, it is harder to neutralize polyclonal antibodies than it is in molecular-targeted therapies, such as anti-epidermal growth factor receptor therapy. BP may be a disease for which anti-idiotypic therapies have potential. The pathogenesis of BP-IgG has been clearly proved using animal models (38, 39). Autoantibodies from more than 80% BP patients

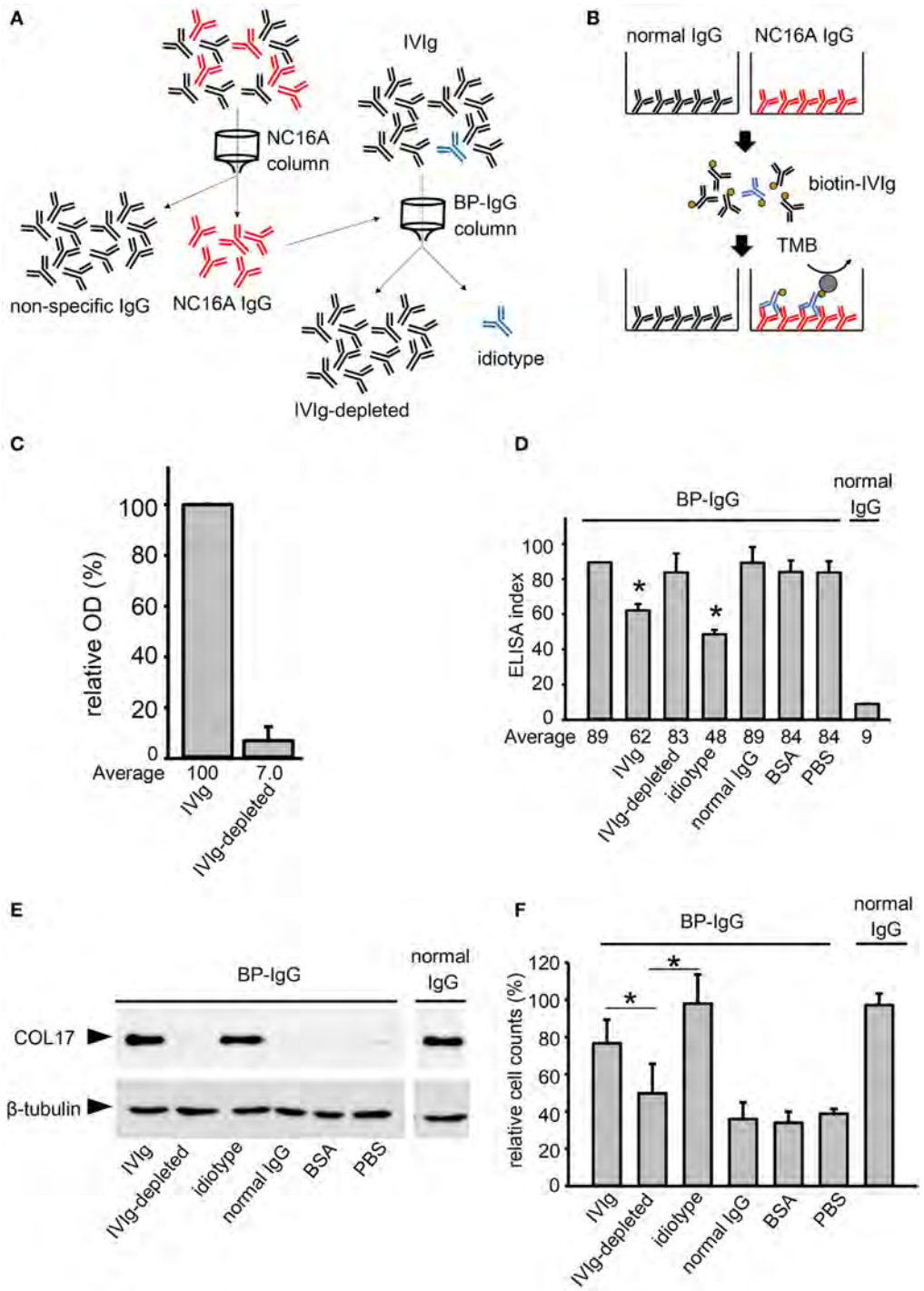

FIGURE 4 | Intravenous immunoglobulin (IVIg) contains anti-idiotypic antibodies against anti-type XVII collagen (COL17) IgG. **(A)** To deplete idiotypic antibodies, anti-COL17 non-collagenous 16A (NC16A) IgG was purified. Next, anti-COL17 NC16A IgG was coupled to a column. IVIg was passed through the column, and then the flow-through fraction (IVIg depleted) and the elution fraction (idiotype) were corrected. **(B)** To evaluate the depletion efficacy, 96-well microtiter plates were coated with anti-COL17 NC16A IgG and normal human IgG (500 ng/well). The plates were incubated with biotin-conjugated IVIg (1 mg/ml; idiotype sample: 0.1 mg/ml). Finally, the plates were incubated with HRP-conjugated streptavidin. The depletion efficacy was calculated as follows: $\frac{(\text{IVIg-depleted OD to anti-COL17 NC16A IgG}) - (\text{IVIg OD to normal IgG})}{(\text{IVIg OD to anti-COL17 NC16A}) - (\text{IVIg OD to normal IgG})} \times 100$. **(C)** To calculate the depletion efficacy, the relative OD score of biotin-conjugated IVIg (5 mg/ml) against anti-COL17 NC16A IgG was determined. Using IVIg samples, the following were performed: **(D)** COL17 NC16A ELISA, **(E)** COL17-depletion assay, and **(F)** cell adhesion test. Bovine serum albumin (BSA) and normal human IgG at the same concentrations were used as controls. Data are based on duplicate samples, and each experiment was performed three times, with $p < 0.05$.

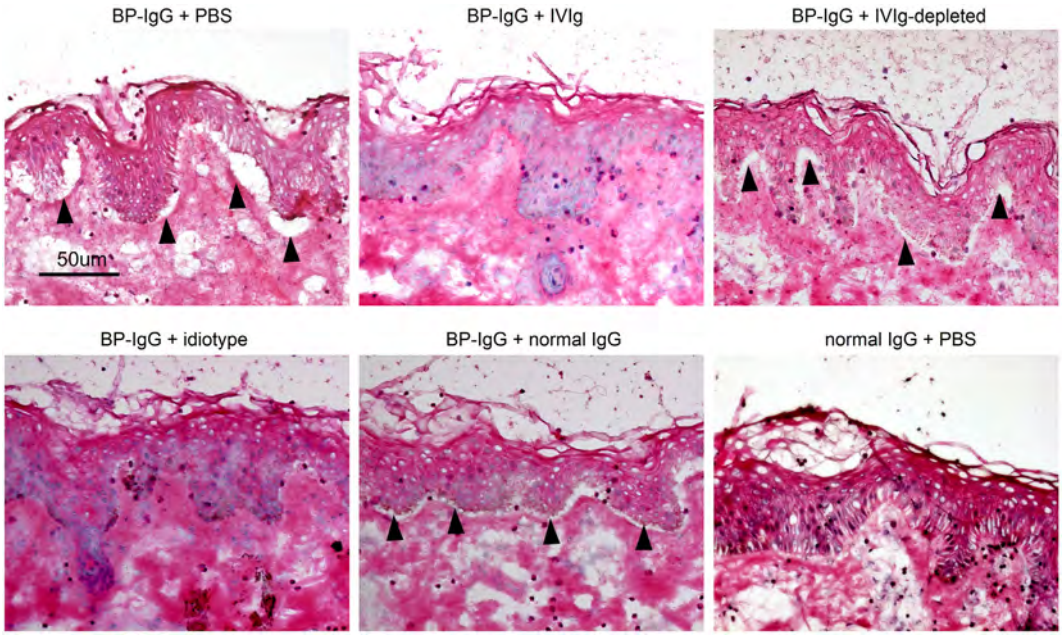

FIGURE 5 | Intravenous immunoglobulin (IVIg) prevents dermal–epidermal separation *ex vivo*. Cryosections of human skin were incubated with BP-IgG in the presence of IVIg (5 mg/ml, idiotype 2.6 μg/ml) and normal human IgG (5 mg/ml) for 1 h. After washing with PBS, sections were incubated with freshly isolated human leukocytes (1×10^7 cells/ml) for 5 h. Arrows indicate dermal–epidermal separation. Each experiment was performed three times. Representative results for each setting are presented.

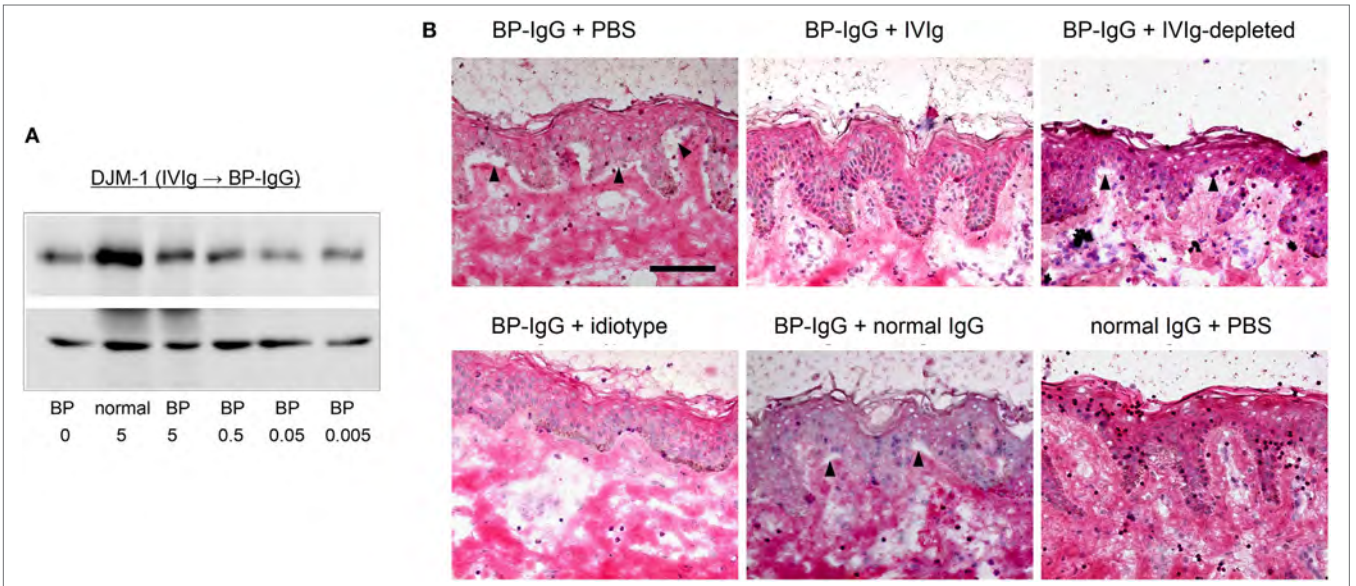

FIGURE 6 | A different company's intravenous immunoglobulin (IVIg) reproduces the results. Using IVIg from a different company, the type XVII collagen (COL17)-depletion assay and *ex vivo* assay were performed. **(A)** COL17-depletion assay using IVIg from a different company (pretreatment). **(B)** *Ex vivo* assay using IVIg from a different company.

target to N-terminal 72 amino acids of the COL17-NC16A domain (40, 41). Furthermore, a precise epitope mapping study showed that 14 amino acids within the NC16A domain are recognized by 50–60% of BP sera (42). These indicate that BP-IgG may be less variable than other autoimmune disorders and may be neutralized effectively by anti-idiotypic antibodies. In conclusion, we demonstrated the effects of IVIg in preventing COL17 depletion induced by BP-IgG due to anti-idiotypic antibodies. This study is the first to demonstrate the presence of anti-idiotypic antibodies against anti-COL17 IgG in IVIg. Disease-specific

therapies using anti-idiotypic antibodies may have potential as treatments for BP.

ETHICS STATEMENT

In accordance with the Hokkaido University Hospital bylaws and standard operating procedures approved by the Hokkaido University Hospital Review Board, we obtained patient consent for experimental procedures to be performed at Hokkaido University Hospital. The studies were conducted in accordance with the Helsinki guidelines.

AUTHOR CONTRIBUTIONS

YM, MK, ET, and HI performed the experiments. HI, HU, YK, and HS designed the experiments. HI wrote the manuscript, and all the coauthors had final approval of the submission.

ACKNOWLEDGMENTS

The authors wish to sincerely thank Ms. Mika Tanabe for her technical assistance. This work was supported in part by a JSPS Grant-in-Aid for Young Scientists (B) (26860861 to HI).

REFERENCES

1. Schwab I, Nimmerjahn F. Intravenous immunoglobulin therapy: how does IgG modulate the immune system? *Nat Rev Immunol* (2013) 13(3):176–89. doi:10.1038/nri3401
2. Amagai M, Ikeda S, Shimizu H, Iizuka H, Hanada K, Aiba S, et al. A randomized double-blind trial of intravenous immunoglobulin for pemphigus. *J Am Acad Dermatol* (2009) 60(4):595–603. doi:10.1016/j.jaad.2008.09.052
3. Amagai M, Ikeda S, Hashimoto T, Mizuashi M, Fujisawa A, Ihn H, et al. A randomized double-blind trial of intravenous immunoglobulin for bullous pemphigoid. *J Dermatol Sci* (2017) 85(2):77–84. doi:10.1016/j.jdermsci.2016.11.003
4. Segura S, Iranzo P, Martínez-de Pablo I, Mascaró JM Jr, Alsina M, Herrero J, et al. High-dose intravenous immunoglobulins for the treatment of autoimmune mucocutaneous blistering diseases: evaluation of its use in 19 cases. *J Am Acad Dermatol* (2007) 56(6):960–7. doi:10.1016/j.jaad.2006.06.029
5. Harman KE, Black MM. High-dose intravenous immune globulin for the treatment of autoimmune blistering diseases: an evaluation of its use in 14 cases. *Br J Dermatol* (1999) 140(5):865–74. doi:10.1046/j.1365-2133.1999.02817.x
6. Jolles S. A review of high-dose intravenous immunoglobulin (hdIVIg) in the treatment of the autoimmune blistering disorders. *Clin Exp Dermatol* (2001) 26(2):127–31. doi:10.1046/j.1365-2230.2001.00779.x
7. Ishii N, Hashimoto T, Zillikens D, Ludwig RJ. High-dose intravenous immunoglobulin (IVIG) therapy in autoimmune skin blistering diseases. *Clin Rev Allergy Immunol* (2010) 38(2–3):186–95. doi:10.1007/s12016-009-8153-y
8. Czernik A, Toosi S, Bystryn JC, Grando SA. Intravenous immunoglobulin in the treatment of autoimmune bullous dermatoses: an update. *Autoimmunity* (2012) 45(1):111–8. doi:10.3109/08916934.2011.606452
9. Li N, Zhao M, Hilario-Vargas J, Prisayanh P, Warren S, Diaz LA, et al. Complete FcRn dependence for intravenous Ig therapy in autoimmune skin blistering diseases. *J Clin Invest* (2005) 115(12):3440–50. doi:10.1172/JCI24394
10. Hirose M, Tiburzy B, Ishii N, Pipi E, Wende S, Rentz E, et al. Effects of intravenous immunoglobulins on mice with experimental epidermolysis bullosa acquisita. *J Invest Dermatol* (2015) 135(3):768–75. doi:10.1038/jid.2014.453
11. Nagelkerke SQ, Kuijpers TW. Immunomodulation by IVIg and the role of Fc-gamma receptors: classic mechanisms of action after all? *Front Immunol* (2015) 5:674. doi:10.3389/fimmu.2014.00674
12. Kazatchkine MD, Kaveri SV. Immunomodulation of autoimmune and inflammatory diseases with intravenous immune globulin. *N Engl J Med* (2001) 345(10):747–55. doi:10.1056/NEJMra993360
13. Tandon N, Jayne DR, McGregor AM, Weetman AP. Analysis of anti-idiotypic antibodies against anti-microsomal antibodies in patients with thyroid autoimmunity. *J Autoimmun* (1992) 5(5):557–70. doi:10.1016/0896-8411(92)90153-H
14. Rossi F, Jayne DR, Lockwood CM, Kazatchkine MD. Anti-idiotypes against anti-neutrophil cytoplasmic antigen autoantibodies in normal human polyspecific IgG for therapeutic use and in the remission sera of patients with systemic vasculitis. *Clin Exp Immunol* (1991) 83(2):298–303. doi:10.1111/j.1365-2249.1991.tb05631.x
15. Mimouni D, Blank M, Payne AS, Anhalt GJ, Avivi C, Barshack I, et al. Efficacy of intravenous immunoglobulin (IVIG) affinity-purified anti-desmoglein anti-idiotypic antibodies in the treatment of an experimental model of pemphigus vulgaris. *Clin Exp Immunol* (2010) 162(3):543–9. doi:10.1111/j.1365-2249.2010.04265.x
16. Evans MJ, Suenaga R, Abdou NI. Detection and purification of antiidiotypic antibody against anti-DNA in intravenous immune globulin. *J Clin Immunol* (1991) 11(5):291–5. doi:10.1007/BF00918187
17. Blank M, Anafi L, Zandman-Goddard G, Krause I, Goldman S, Shalev E, et al. The efficacy of specific IVIG anti-idiotypic antibodies in antiphospholipid syndrome (APS): trophoblast invasiveness and APS animal model. *Int Immunol* (2007) 19(7):857–65. doi:10.1093/intimm/dxm052
18. Shoenfeld Y, Rauova L, Gilburd B, Kvapil F, Goldberg I, Kopolovic J, et al. Efficacy of IVIG affinity-purified anti-double-stranded DNA anti-idiotypic antibodies in the treatment of an experimental murine model of systemic lupus erythematosus. *Int Immunol* (2002) 14(11):1303–11. doi:10.1093/intimm/dxf099
19. Schmidt E, Zillikens D. Pemphigoid diseases. *Lancet* (2013) 381(9863):320–32. doi:10.1016/S0140-6736(12)61140-4
20. Ludwig RJ, Vanhoorelbeke K, Leypoldt F, Kaya Z, Bieber K, McLachlan SM, et al. Mechanisms of autoantibody-induced pathology. *Front Immunol* (2017) 8(May):603. doi:10.3389/fimmu.2017.00603
21. Liu Z, Giudice GJ, Swartz SJ, Fairley JA, Till GO, Troy JL, et al. The role of complement in experimental bullous pemphigoid. *J Clin Invest* (1995) 95(4):1539–44. doi:10.1172/JCI117826
22. Liu Z, Shapiro SD, Zhou X, Twining SS, Senior RM, Giudice GJ, et al. A critical role for neutrophil elastase in experimental bullous pemphigoid. *J Clin Invest* (2000) 105(1):113–23. doi:10.1172/JCI3693
23. Diny NL, Rose NR, Čiháková D. Eosinophils in autoimmune diseases. *Front Immunol* (2017) 8:484. doi:10.3389/fimmu.2017.00484
24. Iwata H, Kamio N, Aoyama Y, Yamamoto Y, Hirako Y, Owaribe K, et al. IgG from patients with bullous pemphigoid depletes cultured keratinocytes of the 180-kDa bullous pemphigoid antigen (type XVII collagen) and weakens cell attachment. *J Invest Dermatol* (2009) 129(4):919–26. doi:10.1038/jid.2008.305
25. Iwata H, Kitajima Y. Bullous pemphigoid: role of complement and mechanisms for blister formation within the lamina lucida. *Exp Dermatol* (2013) 22(6):381–5. doi:10.1111/exd.12146
26. Natsuga K, Nishie W, Shinkuma S, Ujiie H, Nishimura M, Sawamura D, et al. Antibodies to pathogenic epitopes on type XVII collagen cause skin fragility in a complement-dependent and -independent manner. *J Immunol* (2012) 188(11):5792–9. doi:10.4049/jimmunol.1003402
27. Kitajima Y, Inoue S, Yaoita H. Effects of pemphigus antibody on the regeneration of cell-cell contact in keratinocyte cultures grown in low to normal Ca++ concentration. *J Invest Dermatol* (1987) 89(2):167–71. doi:10.1111/1523-1747.ep12470554
28. Sitaru C, Schmidt E, Petermann S, Munteanu LS, Bröcker EB, Zillikens D. Autoantibodies to bullous pemphigoid antigen 180 induce dermal-epidermal separation in cryosections of human skin. *J Invest Dermatol* (2002) 118(4):664–71. doi:10.1046/j.1523-1747.2002.01720.x
29. Sitaru C. Experimental models of epidermolysis bullosa acquisita. *Exp Dermatol* (2007) 16(6):520–31. doi:10.1111/j.1600-0625.2007.00564.x
30. Arredondo J, Chernyavsky AI, Karaouni A, Grando SA. Novel mechanisms of target cell death and survival and of therapeutic action of IVIg in

pemphigus. *Am J Pathol* (2005) 167(6):1531–44. doi:10.1016/S0002-9440(10)61239-4
31. Sami N, Ali S, Bhol KC, Ahmed AR. Influence of intravenous immunoglobulin therapy on autoantibody titres to BP Ag1 and BP Ag2 in patients with bullous pemphigoid. *J Eur Acad Dermatol Venereol* (2003) 17(6):641–5. doi:10.1046/j.1468-3083.2003.00714.x
32. Arnold DF, Burton J, Shine B, Wojnarowska F, Misbah SA. An 'n-of-1' placebo-controlled crossover trial of intravenous immunoglobulin as adjuvant therapy in refractory pemphigus vulgaris. *Br J Dermatol* (2009) 160(5):1098–102. doi:10.1111/j.1365-2133.2009.09034.x
33. Ahmed AR, Gürcan HM. Treatment of epidermolysis bullosa acquisita with intravenous immunoglobulin in patients non-responsive to conventional therapy: clinical outcome and post-treatment long-term follow-up. *J Eur Acad Dermatol Venereol* (2012) 26(9):1074–83. doi:10.1111/j.1468-3083.2011.04205.x
34. Gaitanis G, Alexis I, Pelidou SH, Gazi IF, Kyritsis AP, Elisaf MS, et al. High-dose intravenous immunoglobulin in the treatment of adult patients with bullous pemphigoid. *Eur J Dermatol* (2012) 22(3):363–9. doi:10.1684/ejd.2012.1717
35. Kasperkiewicz M, Nimmerjahn F, Wende S, Hirose M, Iwata H, Jonkman MF, et al. Genetic identification and functional validation of FcγRIV as key molecule in autoantibody-induced tissue injury. *J Pathol* (2012) 228(1):8–19. doi:10.1002/path.4023
36. Kirtschig G, Middleton P, Bennett C, Murrell DF, Wojnarowska F, Khumalo NP, et al. Interventions for bullous pemphigoid. In: Kirtschig G, editor. *Cochrane Database of Systematic Reviews*. Chichester, UK: John Wiley & Sons, Ltd. (2010). CD002292 p.
37. Bernard P, Antonicelli F. Bullous pemphigoid: a review of its diagnosis, associations and treatment. *Am J Clin Dermatol* (2017) 18(4):513–28. doi:10.1007/s40257-017-0264-2
38. Nishie W, Sawamura D, Goto M, Ito K, Shibaki A, McMillan JR, et al. Humanization of autoantigen. *Nat Med* (2007) 13(3):378–83. doi:10.1038/nm1496
39. Liu Z, Sui W, Zhao M, Li Z, Li N, Thresher R, et al. Subepidermal blistering induced by human autoantibodies to BP180 requires innate immune players in a humanized bullous pemphigoid mouse model. *J Autoimmun* (2008) 31(4):331–8. doi:10.1016/j.jaut.2008.08.009
40. Schmidt E, Obe K, Bröcker EB, Zillikens D. Serum levels of autoantibodies to BP180 correlate with disease activity in patients with bullous pemphigoid. *Arch Dermatol* (2000) 136(2):174–8. doi:10.1001/archderm.136.2.174
41. Kobayashi M, Amagai M, Kuroda-Kinoshita K, Hashimoto T, Shirakata Y, Hashimoto K, et al. BP180 ELISA using bacterial recombinant NC16a protein as a diagnostic and monitoring tool for bullous pemphigoid. *J Dermatol Sci* (2002) 30(3):224–32. doi:10.1016/S0923-1811(02)00109-3
42. Zillikens D, Rose PA, Balding SD, Liu Z, Olague-Marchan M, Diaz LA, et al. Tight clustering of extracellular BP180 epitopes recognized by bullous pemphigoid autoantibodies. *J Invest Dermatol* (1997) 109(4):573–9. doi:10.1111/1523-1747.ep12337492

Conflict of Interest Statement: The authors declare that the research was conducted in the absence of any commercial or financial relationships that could be construed as a potential conflict of interest.

frontiers in Immunology

ORIGINAL RESEARCH
published: 24 November 2017
doi: 10.3389/fimmu.2017.01628

Regulatory T Cells Suppress Inflammation and Blistering in Pemphigoid Diseases

Katja Bieber[1]‡, Shijie Sun[1†‡], Mareike Witte[2], Anika Kasprick[1], Foteini Beltsiou[1], Martina Behnen[3], Tamás Laskay[3], Franziska S. Schulze[1], Elena Pipi[1], Niklas Reichhelm[1], René Pagel[4], Detlef Zillikens[2], Enno Schmidt[1,2], Tim Sparwasser[5], Kathrin Kalies[4] and Ralf J. Ludwig[1,2]*

[1] Lübeck Institute of Experimental Dermatology, University of Lübeck, Lübeck, Germany, [2] Department of Dermatology, University of Lübeck, Lübeck, Germany, [3] Department for Infectious Diseases and Microbiology, University of Lübeck, Lübeck, Germany, [4] Institute of Anatomy, University of Lübeck, Lübeck, Germany, [5] Institute for Experimental Infection Research, TWINCORE, Centre for Experimental and Clinical Infection Research, A Joint Venture between the Helmholtz Centre for Infection Research and the Hannover Medical School, Hanover, Germany

OPEN ACCESS

Edited by:
Kjetil Taskén,
University of Oslo, Norway

Reviewed by:
Zlatko Kopecki,
University of South Australia, Australia
Hajo Haase,
Technische Universität Berlin, Germany
Johan Van Der Vlag,
Radboud University Nijmegen, Netherlands

***Correspondence:**
Katja Bieber
katja.bieber@uksh.de

†Present address:
Shijie Sun,
Department of Immunology, Dalian Medical University, Dalian, China

‡These authors have contributed equally contributed to this work.

Specialty section:
This article was submitted to T Cell Biology, a section of the journal Frontiers in Immunology

Received: 03 May 2017
Accepted: 09 November 2017
Published: 24 November 2017

Citation:
Bieber K, Sun S, Witte M, Kasprick A, Beltsiou F, Behnen M, Laskay T, Schulze FS, Pipi E, Reichhelm N, Pagel R, Zillikens D, Schmidt E, Sparwasser T, Kalies K and Ludwig RJ (2017) Regulatory T Cells Suppress Inflammation and Blistering in Pemphigoid Diseases. Front. Immunol. 8:1628. doi: 10.3389/fimmu.2017.01628

Regulatory T cells (Tregs) are well known for their modulatory functions in adaptive immunity. Through regulation of T cell functions, Tregs have also been demonstrated to indirectly curb myeloid cell-driven inflammation. However, direct effects of Tregs on myeloid cell functions are insufficiently characterized, especially in the context of myeloid cell-mediated diseases, such as pemphigoid diseases (PDs). PDs are caused by autoantibodies targeting structural proteins of the skin. Autoantibody binding triggers myeloid cell activation through specific activation of Fc gamma receptors, leading to skin inflammation and subepidermal blistering. Here, we used mouse models to address the potential contribution of Tregs to PD pathogenesis *in vivo*. Depletion of Tregs induced excessive inflammation and blistering both clinically and histologically in two different PD mouse models. Of note, in the skin of Treg-depleted mice with PD, we detected increased expression of different cytokines, including Th2-specific *IL-4*, *IL-10*, and *IL-13* as well as pro-inflammatory Th1 cytokine *IFN-γ* and the T cell chemoattractant *CXCL-9*. We next aimed to determine whether Tregs alter the migratory behavior of myeloid cells, dampen immune complex (IC)-induced myeloid cell activation, or both. *In vitro* experiments demonstrated that co-incubation of IC-activated myeloid cells with Tregs had no impact on the release of reactive oxygen species (ROS) but downregulated β2 integrin expression. Hence, Tregs mitigate PD by altering the migratory capabilities of myeloid cells rather than their release of ROS. Modulating cytokine expression by administering an excess of IL-10 or blocking IFN-γ may be used in clinical translation of these findings.

Keywords: regulatory T cells, autoimmunity, skin, pemphigoid disease, neutrophil activation, Th1, Th2

INTRODUCTION

Regulatory T cells (Tregs) are of major importance in modulating host responses to tumors and infections and in inhibiting the development of autoimmunity and allergies mostly through regulating adaptive immune functions. The effects of Tregs on adaptive immune functions are well characterized (1). Evidence also supports the notion that Tregs can indirectly, through the modulation of antigen-specific T cells, dampen myeloid cell-driven immune responses (2). However, if and how Tregs can directly modulate myeloid cell-dependent inflammation has been less studied. The

role of Tregs in skin inflammation has previously been shown. The percentage of Tregs in skin infiltrate is considerable since in humans, 5–20% of resident T cells in the skin are Tregs (3), and in mice, the percentage is even higher (60–80%) (4). Thus, the skin, an outermost organ constantly exposed to external insults, appears to serve as a major site for the immunosuppressive action of Tregs. Reducing the number of Tregs in neonatal mice leads to the development of a scurfy-like disease in "depletion of regulatory T cell" (DEREG) mice. By contrast, the depletion of Tregs in adult mice is not sufficient to induce clinical symptoms (5), but Treg-deficient scurfy mice bear an autoimmune phenotype (6).

Further studies have attempted to unravel the mechanism by which Tregs modulate neutrophil functions. In a mouse melanoma model, Tregs limit neutrophil accumulation and survival. This effect is associated with decreased expression of the neutrophil chemoattractants CXCL1 and CXCL2, which promote the survival of inoculated tumor cells (7). Further *in vitro* coculture assays using LPS-stimulated human Tregs and neutrophils showed a decrease in CD62L shedding after 45 min of incubation and a decrease in IL-6, IL-8, and TNF-α production after 18 h of incubation. Neutrophil death was accelerated doubly in the presence of Tregs that had been stimulated with LPS (8). Currently, there is a knowledge gap concerning the influence of Tregs on immune complex (IC)-stimulated inflammation.

Prototypical IC-dependent diseases are pemphigoid diseases (PDs). Here, skin inflammation and subepidermal blistering are caused by autoantibodies directed against structural proteins. However, in most PDs, autoantibody binding alone is not sufficient to cause clinical disease manifestation. For the latter, myeloid cells are a prerequisite. By activating specific Fc gamma receptors, myeloid cells bind to skin-bound ICs, get activated and ultimately release reactive oxygen species (ROS) and proteases, leading to inflammation and blistering (9–12). The involvement of macrophages/monocytes was shown in *ex vivo* assays of human skin (13), but not *in vivo*. Regarding cell types besides myeloid cells, mast cells are required to induce the PD bullous pemphigoid [BP, mediated by autoantibodies against type XVII collagen (COL17)] (14), while in the PD epidermolysis bullosa acquisita [EBA, mediated by autoantibodies against type VII collagen (COL7)], mast cells were activated, but dispensable for inflammation and blistering (15). Of note, in these antibody transfer-induced models of PD, a role of natural killer T (NKT) cells and γδ T cells was recently shown; both cell types are able to increase CD18 expression and CD62L shedding in neutrophils, thereby contributing to a more inflammatory phenotype by releasing TNFα (16). The involvement of other T cells in the effector phase of PDs has not been shown yet. Interestingly, in BP patients, alterations in the T cell compartment have been noted. Specifically, compared with healthy controls or patients with pemphigus, BP patients had lower Treg numbers in the skin and circulation, while Th17 cells were found more frequently in the skin of these patients (17, 18). PD animal models allow distinguishing between effects of these cells on tolerance loss or autoantibody production and events leading to skin inflammation and blistering (19). For this reason, we used antibody transfer-induced disease models for the investigation of the role of Tregs during IC-induced inflammation.

MATERIALS AND METHODS

Mice

C57BL/6J mice were obtained from Charles River Laboratories (Sulzfeld, Germany). FoxP3$^{DTR\text{-}eGFP}$ (DEREG) mice were kindly provided by Tim Sparwasser, Hannover, Germany (5). Heterozygous DEREG mice were set up for mating with wild-type littermates. Gender-matched littermates aged 8–12 weeks were used for the experiments. The mice were fed with standardized mouse chow and acidified drinking water *ad libitum*. All clinical examinations, biopsies and bleedings were performed under anesthesia using intraperitoneal (i.p.) administration of a mixture of ketamine (100 mg/g, Sigma-Aldrich, Taufkirchen, Germany) and xylazine (15 mg/g, Sigma-Aldrich). All animal experiments were conducted according to the European Community rules for animal care, approved by the respective governmental administration [V242.29833/2016(49-4/16), V245-46582/2015(78-5/12), V312-7224.122-5(30-2/13)], Ministry for Energy, Agriculture, the Environment and Rural Areas and performed by certified personnel.

Generation of Anti-Mouse COL7 and Anti-COL17 IgG

Total rabbit anti-mouse COL7 IgG and rabbit anti-mouse COL17 IgG were prepared as previously described (16, 20). Rabbits were immunized with recombinant proteins of the non-collagenous (NC)-1 domain of murine COL7 or the extracellular portion of murine COL17 (NC15A), which were supplied commercially (Eurogentec, Seraing, Belgium). IgG from immune and normal rabbit sera was purified by affinity chromatography using protein G. The reactivity of all IgG fractions was analyzed by immunofluorescence microscopy of murine skin.

Induction of Experimental EBA and BP in DEREG Mice

Antibody transfer-induced studies for the induction of experimental EBA and BP followed published protocols with minor modifications (16, 20). To induce Treg depletion, mice were treated with 1 µg diphtheria toxin (DT, Sigma-Aldrich)/100 µl PBS/mouse on days 1, 2, 5, 8, and 11 after initial IgG injections. For *experimental EBA induction*, mice received a total of four i.p. injections of 1 mg rabbit anti-mCOL7 IgG on days 0, 3, 6, and 9 (in total 4 mg rabbit anti-mCOL7 IgG). For *experimental BP induction*, mice received a total of six i.p. injections of 5 mg rabbit anti-mCOL17 IgG on days 0, 2, 4, 6, 8, and 10 (in total 30 mg rabbit anti-mCOL17 IgG). Different body parts were individually scored by the appearance of crust, erythema, lesions and/or alopecia by blinded personal. Control animals were injected with a total of four i.p. injections of 1 mg normal rabbit IgG on days 0, 3, 6, and 9 (in total 4 mg IgG). The total body score is a composite of 2.5% per ear, snout and oral mucosa; 0.5% per eye; 9% for head and neck (excluding eyes, ears, oral mucosa, and snout); 5% per front limb; 10% per hind limb and tail; and 40% for the remaining trunk (21). Blood and tissue samples were collected on days 5 and 12. Serum was collected from the blood samples by centrifugation and was analyzed for cytokine release using the LEGENDplex™ Mouse Inflammation Panel (BioLegend) as

described by the manufacturer's protocol. Tissue samples were snap frozen in liquid nitrogen for the analysis of mRNA and for immunostainings.

All experiments were repeated with a minimum of two independent experiments using different batches of purified IgG.

Immunofluorescence, Immunohistochemistry, and Histological Studies

Direct *immunofluorescence* microscopy was performed to detect rabbit IgG and murine C3 in experimental PD as described (16, 20). Briefly, frozen sections were prepared from tissue biopsies and incubated with FITC-labeled goat anti-rabbit IgG antibody (Dako Deutschland GmbH, Hamburg, Germany). For *histology*, skin samples were fixed in 3.7% paraformaldehyde. The 8-µm-thick sections from paraffin-embedded tissues were stained with hematoxylin and eosin (H&E) according to standard protocols. For *immunohistochemistry*, paraffin sections from lesional skin were stained for T cells and granulocytes as previously described (16). Briefly, mAbs against CD4 (BD Biosciences, Heidelberg, Germany) and Gr-1 (BD Biosciences) were used as primary antibodies, and biotin rabbit anti-rat IgG (Dako) was used as the secondary Ab, followed by detection with ExtrAvidin® alkaline phosphatase (Sigma-Aldrich). Alkaline phosphate activity was visualized with Fast Blue (BB Salt, Sigma-Aldrich). Samples were stained by hematoxylin according to standard protocols.

Flow Cytometry

For FACS analysis, the following antibodies were used: Vio-Green; Brilliant Violet 421™; FITC-, Alexa 647-, PE-, allophycocyanin (APC)-, or APC-Vio770-conjugated anti-mouse CD4 (clone L3T4, or RM4-5); Gr-1 (clone RB6-8C5); CD45 (clone 30F11); CD18 (clone M18/2); CD62L (clone MEL-14); CD11b (clone M1/70); CD25 (clone PC61); Ly6G (clone 1A8); Foxp3 (clone MF23); or appropriate isotype control antibodies (eBioscience *via* Thermo Fisher Scientific, Dreieich, Germany, Miltenyi Biotec, Bergisch-Gladbach, Germany or BD). After erythrocyte lysis cell suspensions were blocked with anti-mouse CD16/CD32 mAb before staining, and dead cells were excluded from the analysis using propidium iodide (PI). Briefly, for the staining of CD45/Gr-1/CD11b and CD45/CD4 cells, blocked single cell suspensions from spleen and blood of mice suffering from experimental PD were first gated for singlets (FSC-H compared with FSC-A) and leukocytes (SSC-A compared with FSC-A). The leukocyte gates were further analyzed for their uptake of PI to differentiate between live and dead cells and for their expression of CD45, thus, selecting only the live, healthy leukocyte population. To further analyze the purity of isolated Tregs and PMNs for *in vitro* analysis, cells were stained with CD4/Foxp3/CD25 or Ly6G/CD45/PI, respectively. For PMNs, the purity and viability was ≥90%; for Tregs, the purity was 80%. To determine the activation status of PMNs after treatment w/o ICs and Tregs, the cells were stained with CD45/CD62L/CD18/Ly6G/PI. All stainings were performed using standard protocols for cell surface staining, except for CD4/Foxp3/CD25, where intranuclear staining was performed using FOXP3 Fix/Perm Buffer (BioLegend, San Diego, CA, USA) and BD Perm/Wash™ buffer following manufacturer protocols. FACS analysis was performed using Miltenyi MacsQuant10 or FACSCalibur with MACSQuantify™ (version 2.8) or BD CellQuest Pro (version 5.1) software.

Assessment of Neutrophil Activation by Analysis of Cell Surface Markers and Cytokine Release

PMNs were isolated from the femurs and tibias of healthy C57BL/6J mice as described in detail elsewhere (16). Tregs were isolated from the spleen of the same animal using a $CD4^+CD25^+$ Regulatory T Cell Isolation Kit, mouse (Miltenyi) following the manufacturer's protocol. The enrichment of cells was determined by FACS. In total, 2×10^5 PMNs/100 µl were stimulated with ICs formed by 10 µg/ml mCOL7 and 2 µg/ml rabbit anti-mCOL7 IgG as described elsewhere (22) for 60 min at 37°C. Isolated Tregs were then cocultured with the IC-stimulated PMNs for an additional 4.5 h in a ratio of 1:4 (5×10^4 Tregs/2×10^5 PMN/200 µl). To evaluate the activation status, cells were stained for flow cytometry analysis using CD18-FITC, CD62L-PE-Vio770, Ly6G-APC-Vio770, and CD45-VioGreen (Miltenyi) following standard procedures. Dead cells were excluded using PI.

Assessment of Neutrophil Activation by ROS

Neutrophil activation was assessed by determining IC-induced ROS release using a previously published protocol (16). Isolated murine neutrophils (2×10^5 cells/100 µl) were preincubated w/ isolated murine Tregs (5×10^4 cells/200 µl), for 1 h at 37°C (without ICs), followed by incubation on a 96-well plate (Lumitrac 600, Greiner Bio-One, Frickenhausen, Germany) coated with ICs formed by 10 µg/ml mCOL7 and 2 µg/ml rabbit anti-mCOL7 IgG. ROS release was analyzed using luminol (Sigma-Aldrich) (22). Each plate was analyzed for 99 repeats using a plate reader (GloMax®-Multi Detection System, Promega GmbH, Mannheim, Germany); the values are expressed as relative luminescence units.

Assessment of Neutrophil Activation by NETosis

Neutrophil activation was assessed by determining neutrophil extracellular trap (NET) formation using a previously published protocol (16, 23). Blood collection was conducted with the understanding and written consent of each participant and was approved by the Ethical Committee of the Medical Faculty of the University of Lübeck (09-140). Isolated human neutrophils (2×10^5 cells) were either stimulated with 20 nM PMA or with ICs formed by 10 µg/ml mCOL7 and 2 µg/ml rabbit anti-mCOL7 IgG. The stimulation was performed w/o isolated human Tregs (5×10^4 cells) on a 96-well FLUOTRAC™ 600 plate (Greiner Bio-One) in 10 mM HEPES-buffered medium. NET formation was analyzed for 7 h (IC) or 4 h (PMA) every 5 min at 37°C by using Tecan infinite M200 Pro reader and Tecan i-control 1.7 Software. CO_2 control was achieved during the assay by the use of a Tecan gas module. For statistical analysis, the area under the curve was calculated.

RNA Extraction, Reverse Transcription, and Real-time Quantitative PCR

For gene expression analysis in skin sections, 10 cryo-sections (12 µm) were prepared and used for RNA isolation, reverse transcription, and real-time RT-PCR as previously described (24). Briefly, total RNA was isolated according the manufacturer's protocol (innuPrep RNA Mini Kit, Analytic Jena AG). After reverse transcription, the cDNA was added to either qPCR Master Mix Plus or qPCR Master Mix SYBR Green Plus (Thermo Fisher Scientific Inc., Waltham, USA) and amplified using an SDS ABI 7900 system (Applied Biosystems, Darmstadt, Germany). The amount of cDNA copies was normalized to the housekeeping gene GAPDH using the 2^ΔCT method.

Primer sequences and concentrations of the analyzed genes were previously published (24, 25) or depicted below: *Ccr5* (for: 5′-CCC ACT CTA CTC CCT GGT ATT C-3′; rev: 5′-GCA GGA AGA GCA GGT CAG AG-3′; 0.5 µM each), *Ccr7* (for: 5′-TGG TGG TGG CTC TCC TTG-3′; rev: 5′-GGC CTT AAA GTT CCG CAC ATC-3′; 0.5 µM each), *Cd11c* (for: 5′-CCA CTG TCT GCC TTC ATA TTC-3′; rev: 5′-GAC GGC CAT GGT CTA GAG-3′; 0.5 µM each), Cd19 (for: 5′-GAA AAT GCA GAT GAG GAG CTG G-3′; rev: 5′-GCT GCA TAG AGG ATC CCT CTC-3′; probe: 5′-CAA CCA GTT GGC AGG ATG ATG GAC TTC CT-3′), *Cd3* (for: 5′-ATA GGA AGG CCA AGG CCA AG-3′; rev: 5′-TCA GGC CAG AAT ACA GGT C-3′; probe: 5′-CCA GAC TAT GAG CCC ATC CGC AAA GG-3′), *Cxcl-1/KC* (for: 5′-CAG ACC ATG GCT GGG ATT C-3′; rev: 5′-GAA CCA AGG GAG CTT CAG-3′; probe: 5′-CCT CGC GAC CAT TCT TGA GTG TGG CTA TGA C-3′), *Cxcl-10/IP-10* (for: 5′-GAG GGC CAT AGG GAA GCT TG-3′; rev: 5′-CGG ATT CAG ACA TCT CTG CTC-3′; probe: 5′-CAT CGT GGC AAT GAT CTC AAC ACG TGG-3′), *Cxcl-2/MIP-2* (for: 5′-AGT GAA CTG CGC TGT CAA TG-3′; rev: 5′-GCT TCA GGG TCA AGG CAA AC-3′; 0.125 µM each), *Cxcl-9/MIG* (for: 5′-TTG GGC ATC ATC TTC CTG GAG-3′; rev: 5′-GCA GGA GCA TCG TGC ATT C-3′; probe: 5′-CTT ATC ACT AGG GTT CCT CGA ACT CCA CAC-3′), *Gapdh* (for: 5′-GAC GGC CGC ATC TTC TTG T-3′; rev: 5′-CAC ACC GAC CTT CAC CAT TTT-3′; probe: 5′-CAG TGC CAG CCT CGT CCC GTA GA-3′), Gr-1 (for: 5′-GCG TTG CTC TGG AGA TAG AAG-3′; rev: 5′-CTT CAC GTT GAC AGC ATT ACC-3′; 0.25 µM each), *Ifn-g* (for: 5′-GCA AGG CGA AAA AGG ATG C-3′; rev: 5′-GAC CAC TCG GAT GAG CTC ATT G-3′; probe: 5′-TGC CAA GTT TGA GGT CAA CAA CCC ACA G-3′), *Il-10* (for: 5′-TCC CTG GGT GAG AAG CTG AAG-3′; rev: 5′-CAC CTG CTC CAC TGC CTT G-3′; probe: 5′-CTG AGG CGC TGT CAT CGA TTT CTC CC-3′), *Il-13* (for: 5′-GGA GCT TAT TGA GGA GCT GAG-3′; rev: 5′-CAG GGA ATC CAG GGC TAC AC-3′; probe: 5′-CAT CAC ACA AGA CCA GAC TCC CCT GTG C-3′), *Il-17a* (for: 5′-TCA GAC TAC CTC AAC CGT TCC-3′; rev: 5′-CTT TCC CTC CGC ATT GAC AC-3′; probe: 5′-CAC CCT GGA CTC TCC ACC GCA ATG AAG-3′), *Il-33* (for: 5′-GTG ATC AAT GTT GAC GAC TCT GG-3′; rev: 5′-GGG ACT CAT GTT CAC CAT CAG-3′; 0.5 µM each), *Il-4* (for: 5′-GAG ACT CTT TCG GGC TTT TCG-3′; rev: 5′-AGG CTT TCC AGG AAG TCT TTC AG-3′; probe: 5′-CCT GGA TTC ATC GAT AAG CTG CAC CAT G-3′), *Itgam/Mac-1* (for: 5′-CTT CAC GGC TTC AGA GAT GAC-3′; rev: 5′-CTG AAC AGG GAT CCA GAA GAC-3′; 0.5 µM each), *Tnf-a* (for: 5′-CCC TCA CAC TCA GAT CAT CTT CTC-3′; rev: 5′-TGG CTC AGC CAC TCC AG-3′; probe: 5′-CTG TAG CCC ACG TCG TAG CAA ACC AC-3′).

Statistical Analysis

The data were analyzed using SigmaPlot, version 12 (Systat Software Inc., Chicago, IL, USA). Applied tests and confidence intervals are indicated in the respective text and figure legends. A p-value < 0.05 was considered statistically significant.

RESULTS

Depletion of Tregs Induces Excessive Disease Progression during PD

To investigate the impact of Tregs on skin inflammation and blistering in PDs, we assessed the impact on Treg depletion in antibody transfer models of BP (20) and EBA (26). In brief, experimental PD was induced by repetitive injections of rabbit anti-mouse COL7 (**Figure 1A**) or anti-mouse COL17 IgG (**Figure 2A**) in wild-type or DEREG mice (5), which were both injected with DT. Subsequently, clinical disease manifestation, expressed as body surface area affected by PD skin lesions, was assessed as the primary endpoint.

In antibody transfer-induced EBA, Treg depletion in DEREG mice led to a significant (more than twofold) increase in skin inflammation and blistering (**Figure 1B,C**), accompanied by an increase in leukocyte dermal infiltration, while IgG binding and C3 deposition at the dermal-epidermal junction were not affected (**Figure 1D**) compared with DT injected wild-type controls. In the dermal infiltrate, we could detect large numbers of Gr-1-positive cells (neutrophils and macrophages) and CD4-positive cells (**Figure 1D**). To verify whether these cell types are influenced by Treg depletion, we analyzed them in the spleens of DEREG and wild-type mice after 12 days of experimental EBA (**Figure 1E**). Here, in DEREG mice, the percentages of CD4 T cells and Gr-1^{int}/CD11b neutrophils are significantly increased, but the number of Gr-1^{hi}/CD11b macrophages is stable. These data implicate an effect of Treg depletion on CD4 T cells and neutrophils that will be investigated in more detail. Importantly, an injection of the same amount of normal rabbit IgG into DT-treated DEREG mice was not sufficient to induce a skin blistering phenotype, but an increase of Gr-1-positive cells in the dermis was detectable (Figure S1 in Supplementary Material). To control the depletory effect of the DT treatment on DEREG mice, we examined the number of Foxp3/CD25-positive CD4 T cells and showed that the depletion is valid throughout the whole experimental procedure in blood and spleen. The number of Tregs is reduced by half (**Figure 1F**).

Corresponding observations were made in antibody transfer-induced BP (**Figure 2**). Again, the depletion of Tregs in DEREG mice led to significant aggravation of skin inflammation and blistering (**Figures 2A–C**) and an increase in leukocyte dermal infiltration (**Figure 2D**), while IgG binding and C3 deposition (**Figure 2D**) at the dermal-epidermal junction were not affected. Taken together, we

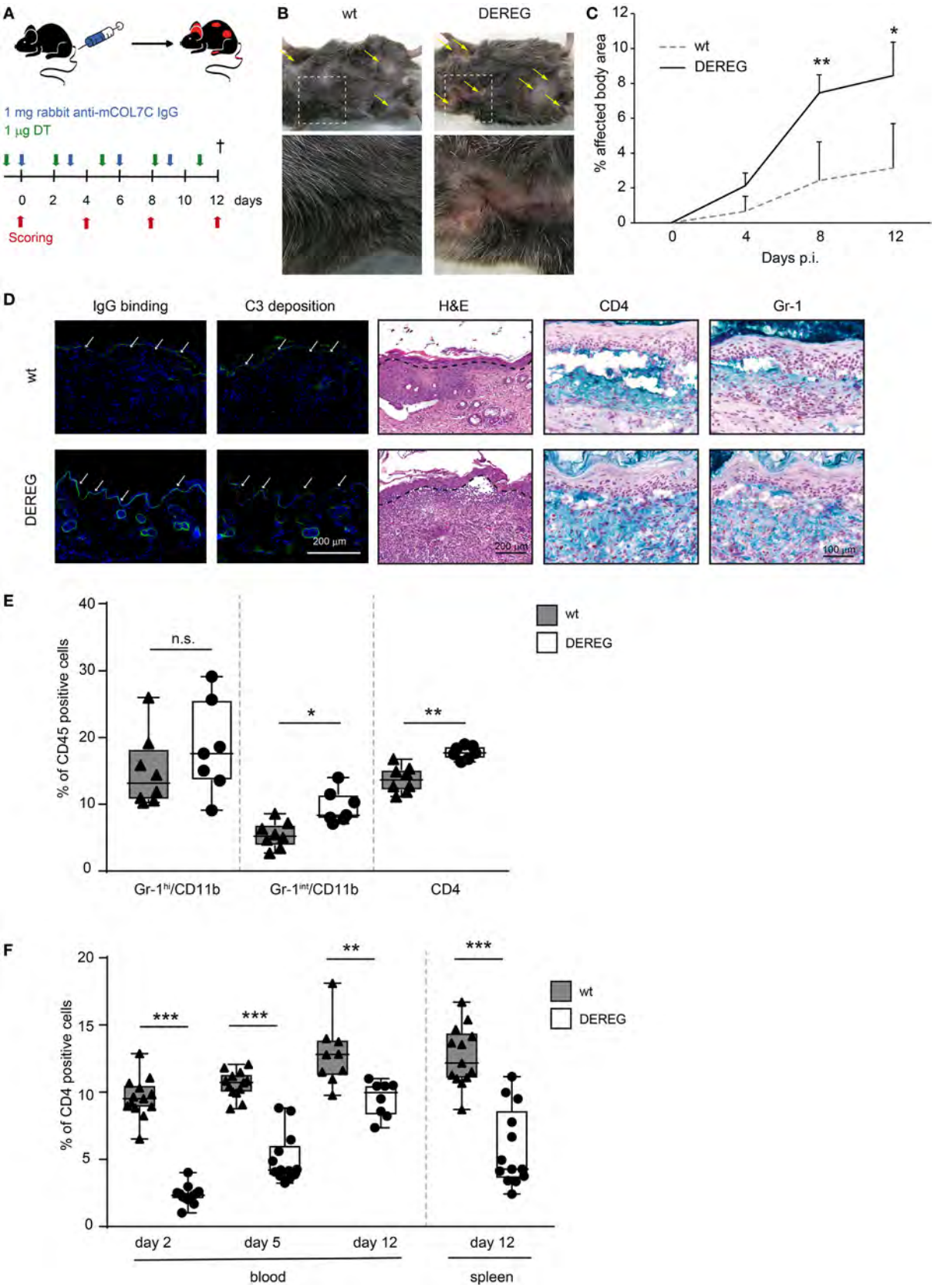

FIGURE 1 | Continued

FIGURE 1 | Continued
Depletion of regulatory T cells (Tregs) increases disease progression in experimental epidermolysis bullosa acquisita (EBA). **(A)** EBA was induced by repetitive injections of 4× 1 mg rabbit anti-mouse COL7 in wild-type or depletion of regulatory T cell (DEREG) mice, which were injected with diphtheria toxin (DT). **(B,C)** Treg depletion in DEREG mice led to a significant (more than twofold) increase in skin inflammation and blistering over a period of 12 days. Panel **(B)** shows representative clinical images obtained on day 12 of the experiment. Panel **(C)** displays the development of the affected body surface area over the 12-day observation period. **(D)** Mice after 12 days of experimental EBA were analyzed for IgG binding, C3 deposition, leukocyte dermal infiltration, and presence of CD4-positive T cells and Gr-1-positive cells (neutrophils and macrophages): staining with an anti-rabbit IgG-FITC antibody or anti-rabbit C3-FITC antibody respective showed no differences in IgG and C3 deposition at the DEJ. Histology (hematoxylin and eosin staining) indicated stronger inflammation in the epidermis and more split formation at the DEJ of DEREG ear sections; the DEJ is marked by a dotted line. Both wild-type and DEREG mice had strong infiltrates of CD4 T cells and Gr-1 (Fast Blue)-positive cells. **(E)** The amount of different CD45-positive populations (Gr-1^{hi}/CD11b^{pos} macrophages, Gr-1^{int}/CD11b^{pos} neutrophils, and CD4^{pos} T cells) was evaluated from lysed spleens at day 12 of experimental EBA or blood from days 2, 5, and 12. DEREG mice have increased numbers of CD4 T cells and Gr-1^{int}/CD11b^{pos} neutrophils. **(F)** The efficacy of Treg depletion after DT treatment was evaluated from the same time points. DEREG mice have significantly reduced numbers of Foxp3-positive cells. **(C,E,F)** Mann–Whitney *U*-test with a Bonferroni *post hoc* test (**$p < 0.01$, ***$p < 0.001$): **(C)** the mean (+SD), $n = 8$/group **(E,F)**. The data are presented as medians (black line), 25th/75th percentiles (boxes), and max/min values (error bars); the dots represent actual results for each sample.

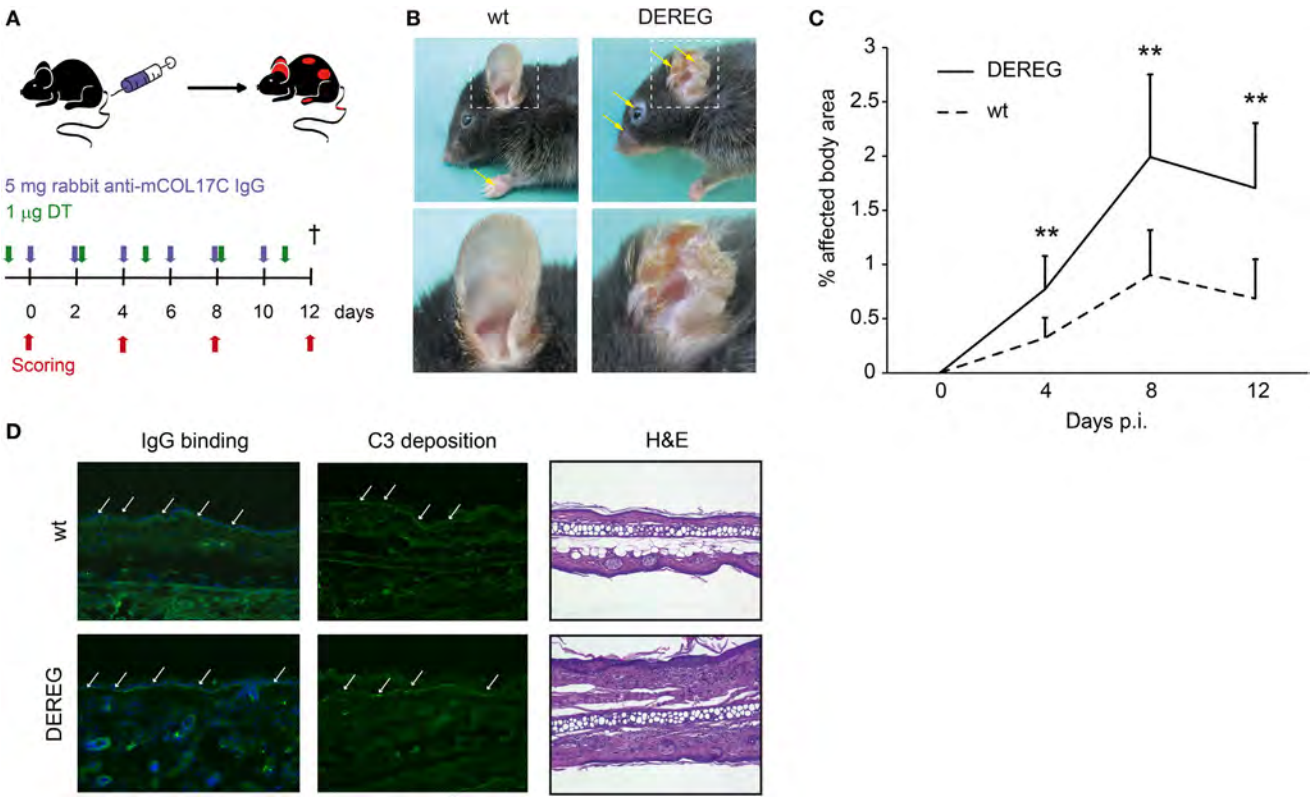

FIGURE 2 | Depletion of regulatory T cells (Tregs) increases disease progression in experimental BP. **(A)** BP was induced by repetitive injections of 6× 5 mg rabbit anti-mouse COL17 in wild-type or DEREG mice, which were injected with diphtheria toxin (DT). **(B,C)** Treg depletion in DE REG mice led to a significant increase in disease progression. Panel **(B)** shows representative clinical images obtained on day 12 of the experiment. Panel **(C)** displays the development of the affected body surface area over the 12-day observation period. **(D)** Staining with anti-rabbit IgG-FITC antibody showed no differences in IgG deposition at the DEJ. Histology (hematoxylin and eosin staining) indicated increased inflammation in the epidermis of DEREG ear sections. **(C)** Mann–Whitney *U*-test (**$p < 0.01$): the mean (+SD), $n = 9$/group.

demonstrate the crucial role of Tregs in dampening (auto) antibody-induced, myeloid cell-driven skin inflammation and blistering.

Depletion of Tregs Induces a Pro-inflammatory Cytokine Milieu in Skin and Serum during PD

In principle, Tregs could modulate myeloid-driven skin inflammation by two mechanisms that are not mutually exclusive. First, Tregs could alter the migratory behavior of myeloid cells. Second, Tregs might dampen IC-induced myeloid cell activation. Both myeloid migration and activation are essential for inflammation and blistering in PD (12). To address the first possibility, chemokine and cytokine expression in lesional skin of wild-type or DEREG mice after experimental BP and EBA was evaluated (for comparison to healthy skin see Table S1 in Supplementary Material). Interestingly, the expression of innate cytokines, such as *TNF,* known as prominent cytokines in PD skin lesions (13, 27),

did only slightly differ between wild-type and DEREG mice and was not significant in BP skin lesions (**Tables 1** and **2**). Of note, the Th2 cytokines *IL-4*, *IL-10*, and *IL-13* were significantly higher expressed in lesional DEREG skin (**Tables 1** and **2**). The presence of these Th2 cytokines would implicate a rather anti-inflammatory cytokine milieu. By contrast, the expression of the inflammatory Th1 cytokine *IFN-γ* and the chemokine *CXCL-9* was evaluated in DEREG lesions. Therefore, the increased dermal infiltrate observed in DEREG mice after PD induction is most likely driven by *IFN-γ* and *CXCL-9* (28, 29), whereas the anti-inflammatory properties of the other differentially expressed cytokines, especially *IL-10* (30), are not sufficient to prevent blistering. The ratio of Th2-specific *IL-10* to Th1-specific *IFN-γ* is significantly shifted to a more Th1-specific phenotype in DEREG mice in EBA and BP (**Figure 3**). In accordance with this finding, we evaluated pro-inflammatory cytokine expression in the serum of wild-type or DEREG mice after 12 days of PD; here, the most prominent cytokine is IFN-γ, which is released in DEREG mice but nearly undetectable in wild-type mice in experimental EBA and BP (**Tables 3** and **4**). In addition, in experimental BP IL-1β that is slightly reduced. By contrast, IL-10 shows no significant change in the serum, which is in line with the assumption that the increased expression of anti-inflammatory cytokines in the skin is ineffective.

TABLE 1 | Analysis of mRNA in skin biopsies of wt or depletion of regulatory T cell (DEREG) mice after experimental epidermolysis bullosa acquisita.

mRNA	wt	DEREG	*p*-Value
Cd3	0.00041 ± 0.00045	0.00207 ± 0.00297	0.027
Cd19	0.00000 ± 0.00000	0.00000 ± 0.00000	> 0.999
Gr-1	0.01769 ± 0.01580	0.03129 ± 0.03653	0.626
Cd11c	0.03212 ± 0.02166	0.03428 ± 0.02354	0.912
Mac-1	0.28203 ± 0.27184	0.40627 ± 0.31225	0.353
Il-10	0.00055 ± 0.00102	0.00115 ± 0.00088	0.033
Tnf-α	0.01174 ± 0.01139	0.01492 ± 0.01259	0.033
Il-17A	0.00270 ± 0.00680	0.00240 ± 0.00343	0.436
Ifn-γ	0.00001 ± 0.00001	0.00011 ± 0.00005	0.001
Il-4	0.00017 ± 0.00016	0.00104 ± 0.00108	0.001
Il-33	0.39346 ± 0.39972	0.31200 ± 0.38451	0.393
Cxcl-2/MIP-2	2.95181 ± 2.44523	2.76091 ± 3.20865	0.9182
CCR5	0.15055 ± 0.13897	0.26642 ± 0.29714	0.594
CCR7	0.01631 ± 0.02362	0.02631 ± 0.04100	0.620
Il-13	0.00004 ± 0.00004	0.00026 ± 0.00034	0.009
Cxcl-1/KC	0.01131 ± 0.01117	0.04612 ± 0.06437	0.075
Cxcl-9/MIG	0.01325 ± 0.03193	0.02061 ± 0.01402	0.013
Cxcl-10/IP-10	0.01403 ± 0.03168	0.00873 ± 0.00451	0.393

DEREG and wild- type (wt) mice were injected with 4× 1 mg rabbit anti-mCOL7 IgG, and lesional skin (of comparable disease index) was taken for mRNA extraction. Analysis of mRNA by qRT-PCR for the indicated markers was done relative to the housekeeping gene GAPDH using the $2^{\Delta CT}$ method. Mann–Whitney U-test, mean (±SD), n = 9/group. Significant differences in gene expression are indicated in gray.

TABLE 2 | Analysis of mRNA in skin biopsies of wt or depletion of regulatory T cell (DEREG) mice after experimental pemphigoid disease.

mRNA	wt	DEREG	*p*-Value
Cd3	0.00216 ± 0.00368	0.00490 ± 0.00389	0.123
Cd19	0.00003 ± 0.00007	0.00001 ± 0.00001	0.283
Gr-1	0.00104 ± 0.00106	0.00156 ± 0.00201	0.483
Cd11c	0.03002 ± 0.02234	0.03024 ± 0.01847	0.981
Mac-1	0.08454 ± 0.05235	0.15347 ± 0.10119	0.072
Il-10	0.00066 ± 0.00044	0.00131 ± 0.00082	0.039
Tnf-α	0.00593 ± 0.00428	0.00895 ± 0.00759	0.288
Il-17A	0.00000 ± 0.00001	0.00001 ± 0.00001	0.413
Ifn-γ	0.00006 ± 0.00006	0.00017 ± 0.00010	0.008
Il-4	0.00048 ± 0.00034	0.00214 ± 0.00184	0.011
Il-33	0.26453 ± 0.19083	0.18644 ± 0.10926	0.276
CXCL-2/MIP-2	0.99754 ± 0.91675	0.97397 ± 1.15808	0.960
Ccr5	0.17625 ± 0.20268	0.26582 ± 0.20309	0.337
Ccr7	0.01070 ± 0.00833	0.00983 ± 0.00708	0.804
Il-13	0.00012 ± 0.00008	0.00027 ± 0.00015	0.014
Cxcl-1/KC	0.00397 ± 0.00531	0.00360 ± 0.00291	0.849
Cxcl-9/MIG	0.01409 ± 0.01044	0.04539 ± 0.03481	0.014
Cxcl-10/IP-10	0.01556 ± 0.01446	0.01280 ± 0.00842	0.608

DEREG and wild-type (wt) mice were injected with 6× 5 mg rabbit anti-mCOL17 IgG at days 0, 2, 4, 6, 8, and 10, and lesional skin (of comparable disease index) was taken for mRNA extraction. Analysis of mRNA by qRT-PCR for the indicated markers was done relative to the housekeeping gene GAPDH using the $2^{\Delta CT}$ method. Mann–Whitney U-test, mean (±SD), n = 10/group. Significant differences in gene expression are indicated in gray.

Coculture of Tregs with PMNs Changes the Surface Expression of Integrins after IC Stimulation

To investigate a potential direct effect of Tregs on PMN function in more detail, we performed *in vitro* assays and stimulated PMNs with ICs consisting of COL7/anti-COL7 in the presence or absence of Tregs (**Figure 4**). Whereas the expression of β2 integrin (CD18) is strongly reduced by Tregs (**Figure 4A**), the shedding of CD62L in Ly6G-positive neutrophils is unchanged (**Figure 4B**). This finding is in accordance with previous data that clearly show the importance of CD18 in experimental PD (31). An effect on the survival of PMNs in the observed time period could not be detected (**Figure 4C**). In contrast to the effects on the cell surface marker expression, Tregs do not influence the IC-induced ROS release of PMNs after 1 h preincubation of both cell types (**Figures 5A,B**) and had no effect on the production of NETs, which are released during a programmed cell death, the so-called NETosis induced by IC or PMA (**Figures 5C–E**).

DISCUSSION

Regulatory T cells are essential for establishing and maintaining self-tolerance and inhibiting immune responses to innocuous environmental antigens. Imbalances and dysfunction in Tregs lead to a variety of immune-mediated diseases because deficits in Treg function contribute to the development of autoimmune diseases and pathological tissue damage, whereas an overabundance of Tregs can promote chronic infection and tumorigenesis (4). To determine by what mechanism Tregs can contribute to the development of PDs, we used antibody transfer-induced models of experimental EBA and BP. By using DEREG mice, we depleted Tregs in these models and observed a twofold increase in clinical disease severity. Analysis of skin and serum of these mice, along with *in vitro* coculture experiments, revealed a dual mechanism by which Tregs can influence IC-induced inflammation in the

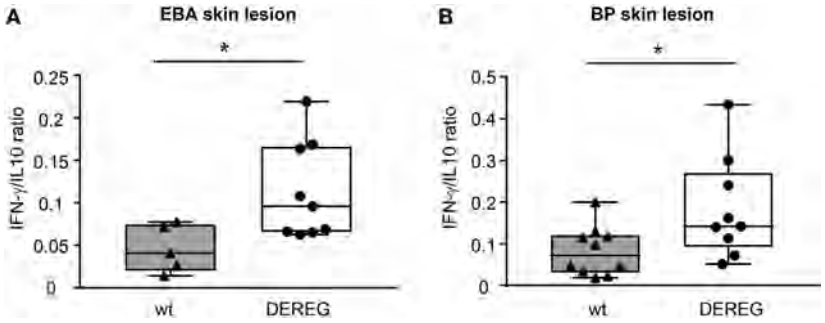

FIGURE 3 | Depletion of regulatory T cells increases Th1/Th2 ratio in depletion of regulatory T cell (DEREG) mice. **(A)** Epidermolysis bullosa acquisita (EBA) was induced by repetitive injections of 4× 1 mg rabbit anti-mouse COL7 in wild-type (wt) or DEREG mice, which were injected with diphtheria toxin (DT). The mRNA expression ratio of Th1-specific *IFN-γ* to Th2-specific *IL-10* is significantly shifted to a more Th1-specific phenotype in the skin. **(B)** BP was induced by repetitive injections of 6× 5 mg rabbit anti-mouse COL17 in wild-type or DEREG mice, which were injected with DT. Mann–Whitney *U*-test (*$p < 0.05$), $n = 8$–9/group.

TABLE 3 | Analysis of inflammatory cytokines in serum of wt or depletion of regulatory T cell (DEREG) mice after experimental epidermolysis bullosa acquisita.

Cytokine	wt	DEREG	*p*-Value
IL-1α	32.50 ± 23.97	25.53 ± 14.97	0.734
IL-23	97.29 ± 86.81	160.32 ± 143.70	0.379
IFN-γ	4.74 ± 4.07	11.32 ± 6.63	0.010
TNF-α	8.60 ± 7.45	12.36 ± 6.17	0.179
IFN-β	327.43 ± 257.70	381.63 ± 289.79	0.878
GM-CSF	67.56 ± 42.99	83.90 ± 41.87	0.403
CCL2/MCP-1	26.80 ± 27.20	46.06 ± 25.70	0.079
IL-1β	36.08 ± 31.64	44.12 ± 28.47	0.516
IL-10	102.49 ± 84.85	135.66 ± 120.32	0.647
IL-12p70	1.31 ± 2.71	4.30 ± 5.76	0.189
IL-6	36.66 ± 25.52	44.77 ± 30.62	0.600
IL-27	544.88 ± 370.61	594.16 ± 383.73	0.830
IL-17A	28.84 ± 16.32	43.14 ± 30.56	0.225

DEREG and wild-type (wt) mice were injected with rabbit anti-mCOL7 IgG, and serum was taken for LEGENDplex™ cytokine analysis. Values are indicated as picograms per milliliter serum. Mann–Whitney U-test, mean (±SD), n ≥ 8/group. Outliners were excluded from analysis. Significant differences in cytokine concentrations are indicated in gray.

TABLE 4 | Analysis of inflammatory cytokines in serum of wt or depletion of regulatory T cell (DEREG) mice after experimental pemphigoid disease.

Cytokine	wt	DEREG	*p*-Value
IL-1α	5.48 ± 5.81	10.48 ± 8.83	0.076
IL-23	7.52 ± 8.86	7.79 ± 13.84	0.479
IFN-γ	0.02 ± 0.07	1.27 ± 1.11	0.001
TNF-α	2.42 ± 3.57	8.03 ± 18.69	0.182
IFN-β	44.89 ± 45.57	85.42 ± 110.01	0.148
GM-CSF	10.37 ± 15.39	8.21 ± 11.06	0.362
CCL2/MCP-1	0.42 ± 0.73	0.23 ± 0.53	0.258
IL-1β	1.66 ± 2.77	0.00 ± 0.00	0.037
IL-10	12.83 ± 13.90	9.65 ± 14.54	0.311
IL-12p70	0.42 ± 0.73	0.23 ± 0.53	0.258
IL-6	3.44 ± 4.72	152.56 ± 476.70	0.168
IL-27	20.21 ± 15.36	13.68 ± 18.04	0.197
IL-17A	1.38 ± 1.53	0.48 ± 0.83	0.060

DEREG and wild-type (wt) mice were injected with 6× 5 mg rabbit anti-mCOL17 IgG at days 0, 2, 4, 6, 8, and 10, and serum was taken for LEGENDplex™ cytokine analysis. Values are indicated as picograms per milliliter serum. Mann–Whitney U-test, mean (±SD), n = 10/group. Significant differences in cytokine concentrations are indicated in gray.

skin (**Figure 6**). First, the mRNA expression of anti-inflammatory *IL-10*- and Th2-specific cytokines, such as *IL-13*, *IL-4*, and *IL-10*, is increased in the skin. These data are in accordance with the scurfy mouse phenotype, where the main effector cells are IL-6-, IL-10-, and IL-4-positive CD4 T cells (32). Under pathological conditions in the skin, these cells can contribute to allergic reactions and atopic dermatitis (33–36). Interestingly, no correlation with autoimmunity has been described thus far, indicating a possible insufficient counter mechanism, as described for IL-6 (19), where Tregs may self-inhibit their function in antibody-induced inflammation. Therefore, the anti-inflammatory properties of the other differentially expressed cytokines, especially IL-10 (30), are not sufficient to prevent blistering. Second, in addition to the fact that Th2 cytokines are increasingly expressed in the skin, the *IFN-γ* is strongly upregulated in the skin. IFN-γ, is secreted predominantly by T cells and natural killer (NK) cells (37) and, to a lesser extent, by other cell types such as macrophages, dendritic cells (DC) and B cells (38). It has been described, that during innate immune responses IFN-γ is produced by NK and NKT cells as well as macrophages and DCs whereas in adaptive immunity it is produced by $CD8^+$ cells and Th1 cells (39). IFN-γ was linked to autoimmunity as upregulation is found in patients with different autoimmune diseases like systemic lupus erythematosus, Sjögren's syndrome, polymyositis, dermatomyositis, and systemic sclerosis (39, 40). Fontolizumab, a humanized monoclonal antibody against IFN-γ, was well tolerated and showed some efficacy in patients with Crohn's disease (41, 42). In this context, we could show that upregulation of *IFN-γ* in the skin, accompanied by an increase of IFN-γ in the serum after blocking Treg could be an important mechanism by which Treg normally contribute to the inhibition of immune responses. Together with the fact that inhibition of Treg led to an increase of the T cell chemoattractant *CXCL-9* in the skin this could subsequently increase the number of neutrophils in the blood and the amount of infiltrating cells into the inflamed skin.

In addition to the effect on T cells, the absence of Tregs in DEREG mice also directly affect the number of neutrophils within the dermal infiltrate in PDs. Direct interaction of Tregs with neutrophils also blocks CD18 expression on neutrophils, indicating that an increase in CD18 after Treg depletion could

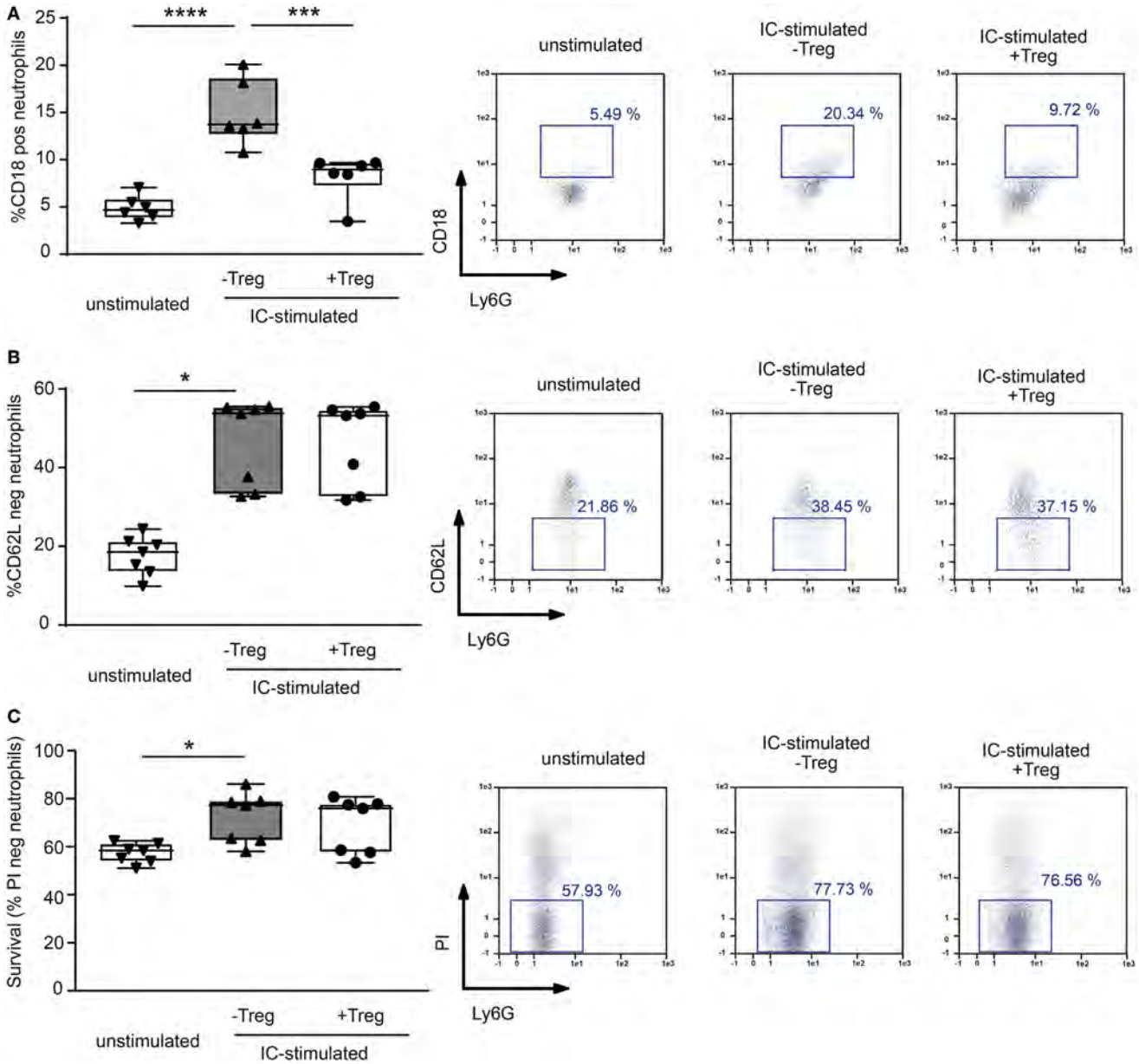

FIGURE 4 | Coculture of regulatory T cells (Tregs) and PMNs after immune complex (IC) stimulation changes surface marker expression in neutrophils. Freshly isolated murine PMNs were stimulated in presence of mCOL7/anti-mCOL7 ICs for 1 h. Tregs were added for additional 4.5 h, and the surface expression of **(A)** CD18 and **(B)** CD62L expression was evaluated on $CD45^{pos}/Ly6G^{pos}/PI^{neg}$ neutrophils. Stimulation with ICs strongly increased the expression of CD18 and shedding of CD62L, but addition of Tregs inhibited only CD18 expression. **(C)** The survival of IC-stimulated PMNs was not affected by Tregs as indicated by measurement of propidium iodide (PI) negative $CD45^{pos}/Ly6G^{pos}$ cells. One-way ANOVA test with a Bonferroni *post hoc* test (*$p < 0.05$): the data are presented as medians (black line), 25th/75th percentiles (boxes), and max/min values (error bars). The dots represent actual results for each sample ($n = 7–8$/group).

be a possible mechanism to attract more neutrophil infiltrates in the skin. The fact that Tregs block CD18 expression in IC-stimulated neutrophils is in accordance with previous data where CD18-deficient mice were resistant to experimental EBA due to defective recruitment of PMNs into the inflamed dermis (31, 43). In addition, previous publications using a mouse melanoma model described that Tregs limit neutrophil accumulation and survival and thus, promoted survival of the inoculated tumor cells. This effect was associated with decreased expression of the neutrophil chemoattractants CXCL1 and CXCL2 (7). Further *in vitro* coculture studies of LPS-stimulated human Tregs and neutrophils demonstrated a decrease in CD62L shedding after 45 min of incubation and a decrease in IL-6, IL-8, and TNF-α production after 18 h of incubation. Neutrophil death was doubled in the presence of Tregs that had been stimulated with LPS (8). In our hands, the coculture was performed using IC-stimulated

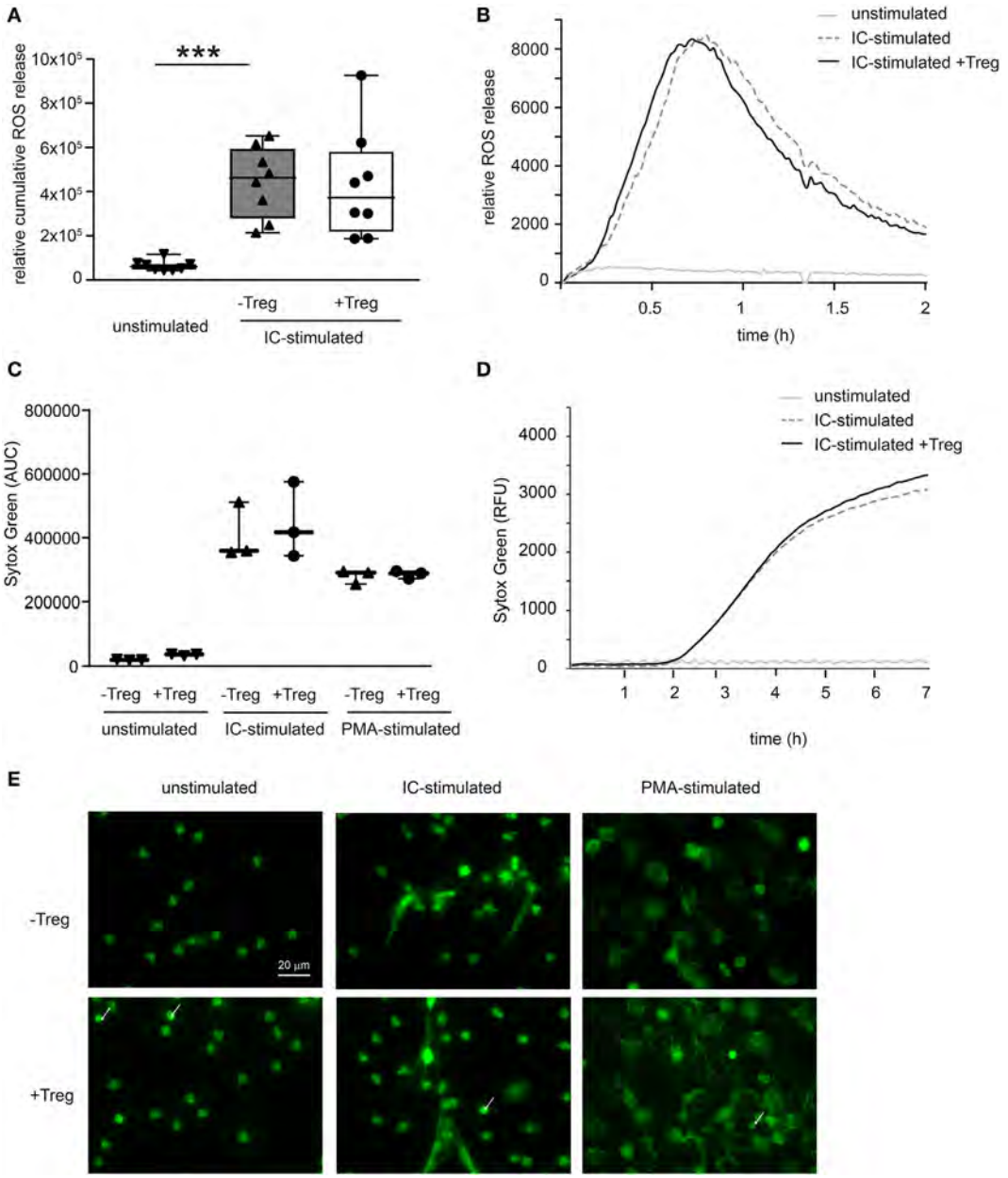

FIGURE 5 | Coculture of regulatory T cells (Tregs) and PMNs after immune complex (IC) stimulation does not affect reactive oxygen species (ROS) release and neutrophil extracellular trap (NET) formation. **(A)** Freshly isolated murine PMNs were pre-cultured with freshly isolated Tregs for 1 h followed by IC stimulation with addition of luminol stimulated in presence of mCOL7/anti-mCOL7 ICs for 2 h. Relative ROS release is indicated by chemiluminescence. Tregs have no influence on ROS release in PMNs. **(B)** Representative real-time kinetics of ROS release using mCOL7/anti-mCOL7 IC. **(C)** Human neutrophils were preincubated for 30 min under HEPES-buffered conditions at pH 7.4 and were then stimulated for 4 h with PMA, for 7 h with mCOL7/anti-mCOL7 IC, or left untreated w/o human Treg to induce NET formation. Area under the curve values (mean ± SD) of NET-dependent relative fluorescence intensities as measured by the SYTOXgreen assay and **(D)** representative real-time kinetics of NET release measured by staining with SYTOXgreen. **(E)** For fluorescence microscopy, cells were fixed and stained for DNA by using SYTOXgreen (green) Treg have no effect on NET formation. One-way ANOVA test with a Bonferroni *post hoc* test (***$p < 0.001$): the data are presented as medians (black line), 25th/75th percentiles (boxes), and max/min values (error bars). The dots represent actual results for each sample ($n = 3$–8/group).

neutrophils rather than LPS-activated neutrophils. During 4.5 h of incubation, ICs induced a significant increase in neutrophil cell death, but this observation was independent from Tregs. Still, it remains unclear whether the influence of Treg on IC-activated neutrophils is mediated by direct cell–cell contact or by Treg cytokines but earlier studies showed a possible effect of IL-10 on neutrophils (7).

These findings, however, do not allow to distinguish between cause and effect; i.e., the altered cytokine expression levels in DEREG mice may be either due to the absence of Tregs or they

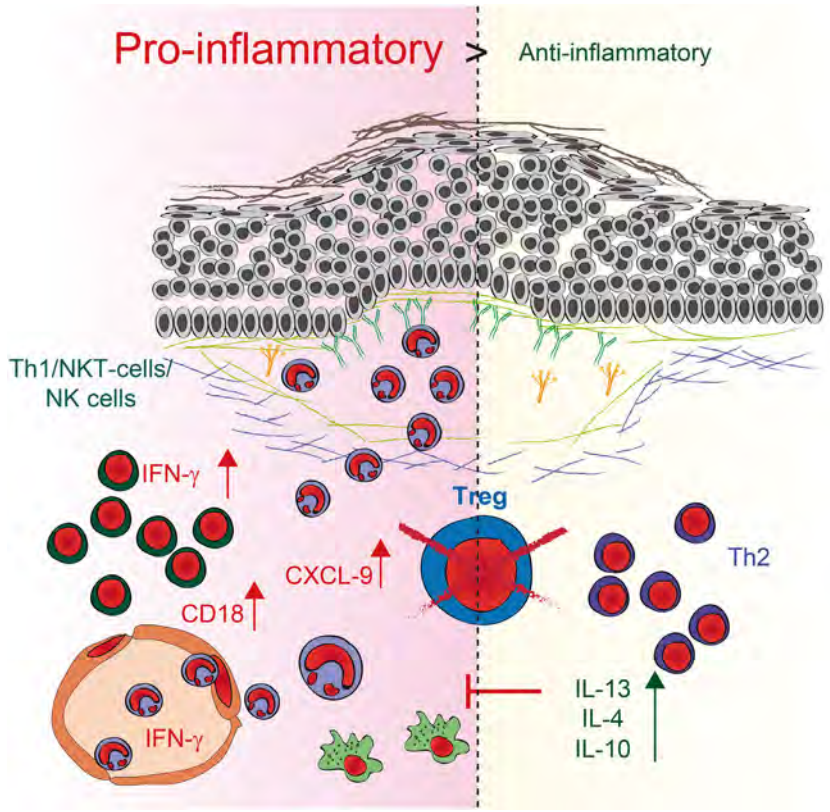

FIGURE 6 | Schematic illustration of regulatory T cell (Treg) action during pemphigoid disease. Reduction of Tregs in depletion of regulatory T cell mice induces two independent pathways. First, the expression of anti-inflammatory IL-10- and Th2-specific cytokines, such as IL-13 and IL-4, is enhanced in the skin. Second, higher expression of the pro-inflammatory Th1 cytokine IFN-γ as well as the chemoattractant CXCL9 is detectable in the skin, accompanied by an increase of IFN-γ in the serum. The number of neutrophils in the blood and the amount of infiltration increase. Direct interaction of Tregs with neutrophils also blocks CD18 expression on neutrophils, indicating that an increase in CD18 after Treg depletion could be a possible mechanism by which more neutrophils infiltrate the skin. By contrast, the increase in Th2 cytokines may be a rather ineffective counter mechanism induced by the absence of Tregs.

could merely reflect the degree of disease severity. Although, since in this study we compared the cytokine concentrations in lesional skin, the differential expression of cytokines is likely caused by the absence or presence of Tregs. Yet, further studies are needed to fully unravel the mechanisms by which Treg contribute to the inflammatory processes in PD. In addition, it is unclear whether these mechanisms are completely overlapping in humans and mice. It has been shown that the number of Tregs increase in mice and man under inflammatory conditions (44). In humans, specialized populations of Treg cells may be recruited to different types of inflammatory responses, and it has been discussed that these may share molecular characteristics with pro-inflammatory helper T cell populations (4). Therefore, in humans, the Foxp3-positive cells are more heterogeneous in function than mouse Foxp3-positive cells. This fact makes it difficult to use autologous Tregs transplantation as therapeutic targets (45).

In summary, we demonstrated that Tregs control myeloid cell-mediated skin inflammation in experimental PD. Furthermore, our data suggest this novel property of Tregs to be mediated by the modulation of cytokine production and by a change in the expression of neutrophil surface markers in the skin, thus regulating leukocyte extravasation into the skin.

ETHICS STATEMENT

This study was carried out in accordance with the recommendations of European Community rules for animal care. The protocol was approved by the Ministry for Energy, Agriculture, the Environment and Rural Areas, Kiel, Schleswig-Holstein, Germany. This study was carried out in accordance with the recommendations of the Declaration of Helsinki by the Ethical Committee of the Medical Faculty of the University of Lübeck with written informed consent from all subjects. All subjects gave written informed consent in accordance with the Declaration of Helsinki. The protocol was approved by the Ethical Committee of the Medical Faculty of the University of Lübeck.

AUTHOR CONTRIBUTIONS

KB and RL designed the research and wrote the manuscript. KB, SS, MW, AK, MB, FB, FS, NR, and RP performed experiments and analyzed data. KB, DZ, ES, EP, TL, TS, KK, and RL analyzed data and discussed the results. All the authors drafted the work critically and approved the final version. All the authors agreed to be accountable for all aspects of the work in ensuring that

questions related to the accuracy or integrity of any part of the work are appropriately investigated and resolved.

ACKNOWLEDGMENTS

The authors thank Lidija Gutjahr, Claudia Kauderer, Sonja Müller, and Astrid Fischer for their excellent technical support.

FUNDING

This work was supported by the Deutsche Forschungsgemeinschaft through Excellence Cluster "Inflammation at Interfaces" (EXC 306/2), the Research Training Group "Modulation of Autoimmunity" (GRK 1727/1 and 2), the Research Training Group "Genes, Environment and Inflammation" (GRK 1743/1 and 2), the Clinical Research Unit "Pemphigoid Diseases—Molecular Pathways and their Therapeutic Potential " (KFO303/1, project LU 877/12-1), and DFG LU 877/9-1.

SUPPLEMENTARY MATERIAL

The Supplementary Material for this article can be found online at http://www.frontiersin.org/article/10.3389/fimmu.2017.01628/full#supplementary-material.

REFERENCES

1. Wing JB, Sakaguchi S. Multiple treg suppressive modules and their adaptability. *Front Immunol* (2012) 3:178. doi:10.3389/fimmu.2012.00178
2. Jaffar Z, Ferrini ME, Girtsman TA, Roberts K. Antigen-specific Treg regulate Th17-mediated lung neutrophilic inflammation, B-cell recruitment and polymeric IgA and IgM levels in the airways. *Eur J Immunol* (2009) 39:3307–14. doi:10.1002/eji.200939498
3. Matsushima H, Takashima A. Bidirectional homing of Tregs between the skin and lymph nodes. *J Clin Invest* (2010) 120:653–6. doi:10.1172/JCI42280
4. Gratz IK, Campbell DJ. Organ-specific and memory Treg cells: specificity, development, function, and maintenance. *Front Immunol* (2014) 5:333. doi:10.3389/fimmu.2014.00333
5. Lahl K, Loddenkemper C, Drouin C, Freyer J, Arnason J, Eberl G, et al. Selective depletion of Foxp3+ regulatory T cells induces a scurfy-like disease. *J Exp Med* (2007) 204:57–63. doi:10.1084/jem.20061852
6. Kanangat S, Blair P, Reddy R, Daheshia M, Godfrey V, Rouse BT, et al. Disease in the scurfy (sf) mouse is associated with overexpression of cytokine genes. *Eur J Immunol* (1996) 26:161–5. doi:10.1002/eji.1830260125
7. Richards H, Williams A, Jones E, Hindley J, Godkin A, Simon AK, et al. Novel role of regulatory T cells in limiting early neutrophil responses in skin. *Immunology* (2010) 131:583–92. doi:10.1111/j.1365-2567.2010.03333.x
8. Lewkowicz P, Lewkowicz N, Sasiak A, Tchorzewski H. Lipopolysaccharide-activated CD4+CD25+ T regulatory cells inhibit neutrophil function and promote their apoptosis and death. *J Immunol* (2006) 177:7155–63. doi:10.4049/jimmunol.177.10.7155
9. Ludwig RJ, Vanhoorelbeke K, Leypoldt F, Kaya Z, Bieber K, McLachlan S, et al. Mechanisms of autoantibody-induced pathology. *Front Immunol* (2017) 8:603. doi:10.3389/fimmu.2017.00603
10. Ludwig RJ. Clinical presentation, pathogenesis, diagnosis, and treatment of epidermolysis bullosa acquisita. *ISRN Dermatol* (2013) 2013:25. doi:10.1155/2013/812029
11. Schmidt E, Zillikens D. Pemphigoid diseases. *Lancet* (2013) 381:320–32. doi:10.1016/S0140-6736(12)61140-4
12. Witte M, Koga H, Hashimoto T, Ludwig RJ, Bieber K. Discovering potential drug-targets for personalized treatment of autoimmune disorders – what we learn from epidermolysis bullosa acquisita. *Expert Opin Ther Targets* (2016) 20:985–98. doi:10.1517/14728222.2016.1148686
13. Hirose M, Kasprick A, Beltsiou F, Dieckhoff Schulze K, Schulze FS, Samavedam UK, et al. Reduced skin blistering in experimental epidermolysis bullosa acquisita after anti-TNF treatment. *Mol Med* (2016) 22:918–26. doi:10.2119/molmed.2015.00206
14. Liu Z, Sui W, Zhao M, Li Z, Li N, Thresher R, et al. Subepidermal blistering induced by human autoantibodies to BP180 requires innate immune players in a humanized bullous pemphigoid mouse model. *J Autoimmun* (2008) 31:331–8. doi:10.1016/j.jaut.2008.08.009
15. Kasprick A, Yu X, Scholten J, Hartmann K, Pas HH, Zillikens D, et al. Conditional depletion of mast cells has no impact on the severity of experimental epidermolysis bullosa acquisita. *Eur J Immunol* (2015) 45:1462–70. doi:10.1002/eji.201444769
16. Bieber K, Witte M, Sun S, Hundt JE, Kalies K, Drager S, et al. T cells mediate autoantibody-induced cutaneous inflammation and blistering in epidermolysis bullosa acquisita. *Sci Rep* (2016) 6:38357. doi:10.1038/srep38357
17. Antiga E, Quaglino P, Volpi W, Pierini I, Del Bianco E, Bianchi B, et al. Regulatory T cells in skin lesions and blood of patients with bullous pemphigoid. *J Eur Acad Dermatol Venereol* (2014) 28:222–30. doi:10.1111/jdv.12091
18. Arakawa M, Dainichi T, Ishii N, Hamada T, Karashima T, Nakama T, et al. Lesional Th17 cells and regulatory T cells in bullous pemphigoid. *Exp Dermatol* (2011) 20:1022–4. doi:10.1111/j.1600-0625.2011.01378.x
19. Kasperkiewicz M, Sadik CD, Bieber K, Ibrahim SM, Manz RA, Schmidt E, et al. Epidermolysis bullosa acquisita: from pathophysiology to novel therapeutic options. *J Invest Dermatol* (2016) 136:24–33. doi:10.1038/JID.2015.356
20. Schulze FS, Beckmann T, Nimmerjahn F, Ishiko A, Collin M, Kohl J, et al. Fcgamma receptors III and IV mediate tissue destruction in a novel adult mouse model of bullous pemphigoid. *Am J Pathol* (2014) 184:2185–96. doi:10.1016/j.ajpath.2014.05.007
21. Bieber K, Koga H, Nishie W. In vitro and in vivo models to investigate the pathomechanisms and novel treatments for pemphigoid diseases. *Exp Dermatol* (2017) 1–8. doi:10.1111/exd.13415
22. Behnen M, Leschczyk C, Moller S, Batel T, Klinger M, Solbach W, et al. Immobilized immune complexes induce neutrophil extracellular trap release by human neutrophil granulocytes via FcgammaRIIIB and Mac-1. *J Immunol* (2014) 193:1954–65. doi:10.4049/jimmunol.1400478
23. Behnen M, Moller S, Brozek A, Klinger M, Laskay T. Extracellular acidification inhibits the ROS-dependent formation of neutrophil extracellular traps. *Front Immunol* (2017) 8:184. doi:10.3389/fimmu.2017.00184
24. Stamm C, Barthelmann J, Kunz N, Toellner KM, Westermann J, Kalies K. Dose-dependent induction of murine Th1/Th2 responses to sheep red blood cells occurs in two steps: antigen presentation during second encounter is decisive. *PLoS One* (2013) 8:e67746. doi:10.1371/journal.pone.0067746
25. Barthelmann J, Nietsch J, Blessenohl M, Laskay T, van Zandbergen G, Westermann J, et al. The protective Th1 response in mice is induced in the T-cell zone only three weeks after infection with *Leishmania major* and not during early T-cell activation. *Med Microbiol Immunol* (2012) 201:25–35. doi:10.1007/s00430-011-0201-6
26. Sitaru C, Mihai S, Otto C, Chiriac MT, Hausser I, Dotterweich B, et al. Induction of dermal-epidermal separation in mice by passive transfer of antibodies specific to type VII collagen. *J Clin Invest* (2005) 115:870–8. doi:10.1172/JCI200521386
27. Sadeghi H, Lockmann A, Hund AC, Samavedam UK, Pipi E, Vafia K, et al. Caspase-1-independent IL-1 release mediates blister formation in autoantibody-induced tissue injury through modulation of endothelial adhesion molecules. *J Immunol* (2015) 194:3656–63. doi:10.4049/jimmunol.1402688
28. Colgan SP, Parkos CA, Delp C, Arnaout MA, Madara JL. Neutrophil migration across cultured intestinal epithelial monolayers is modulated by epithelial exposure to IFN-gamma in a highly polarized fashion. *J Cell Biol* (1993) 120:785–98. doi:10.1083/jcb.120.3.785
29. Vanheule V, Janssens R, Boff D, Kitic N, Berghmans N, Ronsse I, et al. The positively charged COOH-terminal Glycosaminoglycan-binding CXCL9 (74-103) peptide inhibits CXCL8-induced neutrophil extravasation and monosodium urate crystal-induced gout in mice. *J Biol Chem* (2015) 290:21292–304. doi:10.1074/jbc.M115.649855

30. Kulkarni U, Karsten CM, Kohler T, Hammerschmidt S, Bommert K, Tiburzy B, et al. IL-10 mediates plasmacytosis-associated immunodeficiency by inhibiting complement-mediated neutrophil migration. *J Allergy Clin Immunol* (2016) 137(1487–1497):e6. doi:10.1016/j.jaci.2015.10.018
31. Chiriac MT, Roesler J, Sindrilaru A, Scharffetter-Kochanek K, Zillikens D, Sitaru C. NADPH oxidase is required for neutrophil-dependent autoantibody-induced tissue damage. *J Pathol* (2007) 212:56–65. doi:10.1002/path.2157
32. Blair PJ, Bultman SJ, Haas JC, Rouse BT, Wilkinson JE, Godfrey VL. CD4+CD8- T cells are the effector cells in disease pathogenesis in the scurfy (sf) mouse. *J Immunol* (1994) 153:3764–74.
33. Danso MO, van Drongelen V, Mulder A, van Esch J, Scott H, van Smeden J, et al. TNF-alpha and Th2 cytokines induce atopic dermatitis-like features on epidermal differentiation proteins and stratum corneum lipids in human skin equivalents. *J Invest Dermatol* (2014) 134:1941–50. doi:10.1038/jid.2014.83
34. Esaki H, Brunner PM, Renert-Yuval Y, Czarnowicki T, Huynh T, Tran G, et al. Early-onset pediatric atopic dermatitis is TH2 but also TH17 polarized in skin. *J Allergy Clin Immunol* (2016) 138:1639–51. doi:10.1016/j.jaci.2016.07.013
35. Ju ST, Sharma R, Gaskin F, Fu SM. IL-2 controls trafficking receptor gene expression and Th2 response for skin and lung inflammation. *Clin Immunol* (2012) 145:82–8. doi:10.1016/j.clim.2012.07.015
36. Sehra S, Krishnamurthy P, Koh B, Zhou HM, Seymour L, Akhtar N, et al. Increased Th2 activity and diminished skin barrier function cooperate in allergic skin inflammation. *Eur J Immunol* (2016) 46:2609–13. doi:10.1002/eji.201646421
37. Billiau A, Matthys P. Interferon-gamma: a historical perspective. *Cytokine Growth Factor Rev* (2009) 20:97–113. doi:10.1016/j.cytogfr.2009.02.004
38. Meyer O. Interferons and autoimmune disorders. *Joint Bone Spine* (2009) 76:464–73. doi:10.1016/j.jbspin.2009.03.012
39. Pollard KM, Cauvi DM, Toomey CB, Morris KV, Kono DH. Interferon-gamma and systemic autoimmunity. *Discov Med* (2013) 16:123–31.
40. Ronnblom L. The importance of the type I interferon system in autoimmunity. *Clin Exp Rheumatol* (2016) 34:21–4.
41. Reinisch W, de Villiers W, Bene L, Simon L, Racz I, Katz S, et al. Fontolizumab in moderate to severe Crohn's disease: a phase 2, randomized, double-blind, placebo-controlled, multiple-dose study. *Inflamm Bowel Dis* (2010) 16:233–42. doi:10.1002/ibd.21038
42. Picard C, Belot A. Does type-I interferon drive systemic autoimmunity? *Autoimmun Rev* (2017) 16:897–902. doi:10.1016/j.autrev.2017.07.001
43. Mizgerd JP, Kubo H, Kutkoski GJ, Bhagwan SD, Scharffetter-Kochanek K, Beaudet AL, et al. Neutrophil emigration in the skin, lungs, and peritoneum: different requirements for CD11/CD18 revealed by CD18-deficient mice. *J Exp Med* (1997) 186:1357–64. doi:10.1084/jem.186.8.1357
44. Gratz IK, Rosenblum MD, Maurano MM, Paw JS, Truong HA, Marshak-Rothstein A, et al. Cutting edge: self-antigen controls the balance between effector and regulatory T cells in peripheral tissues. *J Immunol* (2014) 192:1351–5. doi:10.4049/jimmunol.1301777
45. Miyara M, Ito Y, Sakaguchi S. TREG-cell therapies for autoimmune rheumatic diseases. *Nat Rev Rheumatol* (2014) 10:543–51. doi:10.1038/nrrheum.2014.105

Conflict of Interest Statement: The authors declare that the research was conducted in the absence of any commercial or financial relationships that could be construed as a potential conflict of interest.

frontiers in Immunology

ORIGINAL RESEARCH
published: 23 November 2017
doi: 10.3389/fimmu.2017.01432

Development of Novel Promiscuous Anti-Chemokine Peptibodies for Treating Autoimmunity and Inflammation

Michal Abraham[1], Hanna Wald[1], Dalit Vaizel-Ohayon[1], Valentin Grabovsky[1], Zohar Oren[1], Arnon Karni[2,3], Lola Weiss[4], Eithan Galun[4], Amnon Peled[1,4] and Orly Eizenberg[1]*

[1] Biokine Therapeutics Ltd, Ness Ziona, Israel, [2] Department of Neurology, Tel Aviv Sourasky Medical Center, Tel Aviv, Israel, [3] Sackler Faculty of Medicine, Tel Aviv University, Tel Aviv, Israel, [4] Goldyne Savad Institute of Gene Therapy, Hebrew University of Jerusalem, Jerusalem, Israel

Chemokines and their receptors play critical roles in the progression of autoimmunity and inflammation. Typically, multiple chemokines are involved in the development of these pathologies. Indeed, targeting single chemokines or chemokine receptors has failed to achieve significant clinical benefits in treating autoimmunity and inflammation. Moreover, the binding of host atypical chemokine receptors to multiple chemokines as well as the binding of chemokine-binding proteins secreted by various pathogens can serve as a strategy for controlling inflammation. In this work, promiscuous chemokine-binding peptides that could bind and inhibit multiple inflammatory chemokines, such as CCL2, CCL5, and CXCL9/10/11, were selected from phage display libraries. These peptides were cloned into human mutated immunoglobulin Fc-protein fusions (peptibodies). The peptibodies BKT120Fc and BKT130Fc inhibited the ability of inflammatory chemokines to induce the adhesion and migration of immune cells. Furthermore, BKT120Fc and BKT130Fc also showed a significant inhibition of disease progression in a variety of animal models for autoimmunity and inflammation. Developing a novel class of antagonists that can control the courses of diseases by selectively blocking multiple chemokines could be a novel way of generating effective therapeutics.

Keywords: chemokines, autoimmunity, inflammation, phage display, peptibodies

OPEN ACCESS

Edited by:
Amanda E. I. Proudfoot, NovImmune, Switzerland

Reviewed by:
Jose Miguel Rodriguez Frade, Consejo Superior de Investigaciones Científicas (CSIC), Spain
Remo Castro Russo, Universidade Federal de Minas Gerais, Brazil

****Correspondence:***
Amnon Peled
peled@hadassah.org.il

Specialty section:
This article was submitted to Cytokines and Soluble Mediators in Immunity, a section of the journal Frontiers in Immunology

Received: *02 August 2017*
Accepted: *13 October 2017*
Published: *23 November 2017*

Citation:
Abraham M, Wald H, Vaizel-Ohayon D, Grabovsky V, Oren Z, Karni A, Weiss L, Galun E, Peled A and Eizenberg O (2017) Development of Novel Promiscuous Anti-Chemokine Peptibodies for Treating Autoimmunity and Inflammation. Front. Immunol. 8:1432. doi: 10.3389/fimmu.2017.01432

INTRODUCTION

Chemokines have been shown to be selective chemo-attractants for leukocyte sub-populations *in vitro* and to elicit a selective accumulation of immune cells *in vivo*. In addition to chemotaxis, chemokines mediate leukocyte degranulation (1) and adhesion receptor upregulation (2).

Chemokines are small (5–20 kDa, ~70–90 amino acids) proteins that are rich in basic amino acids and contain conserved cysteine motifs that form essential disulfide bonds between the first and third as well as the second and fourth cysteine residues. The numbers and spacing of the first cysteine residues in the amino acid sequence are used to classify chemokines into four subfamilies: CXC (or α), CC (or β), CX 3 C, and C chemokines. Currently, 20 chemokine receptors mediate the effects of more than 50 known chemokines (3). Interestingly, chemokines and their receptors have overlapping specificities for each other, unlike other types of G protein-coupled receptors. For this reason, the

chemokine system is often thought to show significant redundancy, as one receptor can bind multiple ligands, and conversely, a single ligand can bind several chemokine receptors (4, 5).

Chemokines and their receptors have received increased attention due to their critical roles in the progression of inflammation and associated conditions, such as asthma, atherosclerosis, graft rejection, AIDS, autoimmune conditions (e.g., multiple sclerosis, arthritis, myasthenia gravis, lupus, and AMD) and cancer (3). The role of chemokines has been thoroughly investigated in pathogen conditions, such as rheumatoid arthritis (RA) and multiple sclerosis (MS). RA is a chronic inflammatory disease that eventually leads to joint destruction. RA is characterized by the infiltration of neutrophils, T and B lymphocytes, and macrophages into the synovial membrane and fluid compartment (6). The infiltrating cells, such as macrophages, T cells, B cells, and dendritic cells, play important role in the pathogenesis of RA. Chemokines have an important role in the pathogenesis of RA by recruiting leukocytes and by controlling other important processes, such as release of mediators of inflammation, cell proliferation, and angiogenesis. Synovial fluid from actively involved joints contains a number of chemokines, including CCL2, CCL3, CCL5, CXCL8, and CXCL10. Both synovial-lining cells and infiltrating cells are sources of these chemokines. The receptors CCR2, CCR5, CXCR2, and CXCR3 have been detected in infiltrating cells. MS is an inflammatory, demyelinating disease of the central nervous system (CNS), suspected to be of autoimmune origin, in which CNS myelin proteins serve as autoantigens. MS is characterized by the recruitment of T lymphocytes (predominantly Th1/Th17) and macrophages into the CNS. Infiltration of these cells into the CNS contributes to the disease pathology and is mediated by several chemokines. The chemokines that were found to be involved in the pathogenesis of MS were CCL5, CCL2, CCL3, CCL4, CXCL9, CXCL11, and CXCL10 (7, 8).

Despite the extensive involvement of chemokines in many pathological conditions, except for selective CCR5 antagonists for HIV and a selective CXCR4 antagonist for stem cell mobilization, obtaining new therapeutics related to targeting single chemokine receptors and chemokines against autoimmunity, therapies for inflammation and cancer has been unsuccessful (5, 9). The lack of significance clinical results in these studies could be due to a variety of reasons, including the lack of predictability of animal models for inflammatory and autoimmune diseases, relevance of the target to the human disease, genetic diversity between the tested patient population, unsuitable PK/PD properties of the drug candidate which lead to reduced chemokine receptor coverage, ineffective dosing, and the redundancy of the chemokine/chemokine receptor system (4, 5).

Binding to multiple chemokines as a strategy for inhibiting inflammation is a natural phenomenon. As quoted by Heidarieh et al. (10), atypical chemokine receptors, such as ACKR1, ACKR2, or ACKR4, that bind multiple chemokines, do not transduce signals function as chemokine scavengers to control the magnitude of inflammation (11). Furthermore, pathogens such as herpesviruses, ticks, and the trematode *Schistosoma mansoni* secrete chemokine-binding proteins (CKBPs) that also inhibit inflammatory chemokines and inflammation (12).

The aim of this study was to use phage display peptide libraries to identify and develop novel promiscuous anti-chemokine-binding peptides to inhibit autoimmune and inflammatory disease progression. Since peptides are usually rapidly cleared due to the combined effects of having poor metabolic stability and hydrodynamic radii that fall below the limit of kidney glomerular filtration, we choose to present these peptides on mutated human Fc domain which have reduced antibody-dependent cell-mediated cytotoxicity (ADCC) and mitogenicity properties (13–15). This approach retains certain desirable antibody features, including increased apparent affinity through the avidity conferred by the dimerization of two Fcs and a prolonged PK. Peptide–Fc fusion or peptibodies are an attractive alternative therapeutic format to monoclonal antibodies and have already been used in the clinic (16).

MATERIALS AND METHODS

Materials

Amplification buffer was obtained from Invitrogen (CA, USA); Dextran T-500 was obtained from Pharmacosmos A/S (Denmark); Dulbecco's Modified Eagle's Medium (DMEM) was obtained from Biological Industries (Beit Haemek, Israel); ECL solution was obtained from Amersham Biosciences (Buckinghamshire, UK); EcoRI was obtained from New England Biolabs; enhancer solution was obtained from Invitrogen; EX-CELL® 293 medium was obtained from SAFC Biosciences; fetal calf serum (FCS) was obtained from Biological Industries (Beit Haemek, Israel); Ficoll 1077 was obtained from Sigma-Aldrich (Israel).

Freund's complete adjuvant (CFA) was obtained from Sigma-Aldrich or Difco; FuGENE® 6 was obtained from Roche; methylated bovine serum albumin (mBSA) was obtained from Sigma-Aldrich; NotI was obtained from New England Biolabs; NuPAGE® Bis-Tris gels were obtained from Invitrogen; the pIRESpuro3 vector was obtained from BD Biosciences Clontech; Protein A-Sepharose® beads were obtained from Amersham; RPMI medium was obtained from Biological Industries (Beit Haemek, Israel); Taq polymerase (Platinum® Pfx DNA polymerase) was obtained from Invitrogen; VCAM-1 (human) was obtained from R&D Systems, Inc. (Minneapolis, MN, USA); and all the recombinant human chemokines were ordered from PeproTech, Inc. (Rocky Hill, NJ, USA).

Phage Selection

Phage display libraries (Ph.D-12™ and Ph.D-C7C Peptide LibrariesKits) were purchased from New England Biolabs (Beverly, MA, USA). Peptides were fused to the N-terminus of the M13 phage gene III protein with a GGGS spacer.

For phage selection, 60 × 15 polystyrene Petri dishes were coated with CCL11, CXCL8, CXCL12, CXCL9, and CCL2 (1 ml, 0.1–1 μg/ml in 0.1 M $NaHCO_3$, pH 8.6) overnight at 4°C or 3–6 h at room temperature (RT) with gentle agitation in a humidified container. Coating the plates with the chemokine resulted in an immobilized, but still active (i.e., capable of binding), chemokine. The plates were blocked with BSA (5 mg/ml) in 0.1 M $NaHCO_3$ for 1 h at RT or overnight at 4°C. The plates were washed six

times with TBST (50 mM Tris–HCl (pH 7.5), 150 mM NaCl, 0.1% Tween), and incubated for 1 h at RT with the phage suspension [1 ml containing 10^9–10^{11} plaque forming units (PFU)]. Unbound phages were removed by washing with TBST 10 times. After each round of selection, bound phages were eluted with 1 ml of 0.2 M glycine-HCl (pH 2.2) and 1 mg/ml BSA for 10 min at RT with gentle rocking. Eluted phages were immediately neutralized in 150 µl of 1 M Tris–HCl (pH 9.1). Eluted phages were titered to assess the number of phages that were bound to the plate and then amplified by infection with an overnight ER2738 *Escherichia Coli* culture in LB medium (diluted 1:100) for 4.5 h at 37°C with vigorous shaking. Phages were obtained by double precipitation with a 1:5 polyethylene glycol (PEG)-NaCl solution (20% PEG, 2.5 M NaCl) and dissolved in TBS (50 mM Tris–HCl (pH 7.5), 150 mM NaCl) to a final concentration of ~10^{12} PFU/ml. In total, 3 or 4 rounds of selection were performed. Single phages from the third or fourth selection were analyzed for their ability to specifically bind the chemokine of interest using ELISA. The specific peptides were DNA sequenced.

Phage Titration

For phage titration, 200 µl of mid-log phase (OD_{600}~0.5) EП*2738 Escherichia Coli* cultures were infected with 10 µl of 10-fold serial phage dilutions in TBS for 1–5 min at RT. The infected cells were transferred to culture tubes containing 4 ml of 45°C melting top-agar and immediately poured onto pre-warmed LB/IPTG/X-Gal-coated plates. The phages were incubated overnight at 37°C. PFU values were calculated by counting the blue plaques that appeared on the plates.

ELISA for Phages

NUNC-immuno maxisorp plates were coated with the appropriate chemokine (0.1 ml/well, 0.1–1.0 µg/ml in 0.1 M $NaHCO_3$, pH 8.6) for 3 h at RT or overnight at 4°C. The plates were then blocked with 5 mg/ml BSA (0.2 ml/well) in 0.1 M $NaHCO_3$ (pH 8.6) overnight at 4°C or for 1 h at RT. Control wells were treated with blocking buffer alone with no target protein added. The plates were washed six times with TBST and then incubated with individually eluted phages (each representing individual peptides, 10^7–10^9 PFU in 0.1 ml of blocking buffer/well) for 45 min at RT. After the plates were washed six times with TBST, the bound phages were probed with an HRP/anti-M13 monoclonal conjugate [horseradish peroxidase conjugated to a mouse anti-M13 monoclonal antibody (mAb, Amersham Pharmacia Biotech, diluted 1: 5,000 to 1: 10,000 in blocking buffer, 0.1 ml/well)] for 45 min at RT. Target-bound phages were determined using a DAKO TMB one-step substrate system [3,3′,5,5′-tetramethlbenzidine, DAKO, CA USA (100 µl/well)]. The reaction was stopped by adding an HCl–H_2SO_4 mixture (1 N HCl, 3 N H_2SO_4). The results were analyzed by an ELISA reader (Anthos Labtec HT2, version 1.06) at OD_{450}.

DNA Purification and Sequence Analysis

In total, $10^{12–13}$ phages were amplified by infecting an overnight ER2738 *Escherichia Coli* culture diluted 1:100 in 10 ml of LB medium for 4.5 h at 37°C while vigorously shaking. Phages were obtained by precipitating with a 1:5 PEG–NaCl solution (20% PEG, 2.5 M NaCl). Single-stranded DNA (soda) was extracted by thoroughly suspending the phage pellet in 300 µl of iodide buffer (10 mM Tris–HCl (pH 8.0), 1 mM EDTA, 4 M NaCI) and then pelleting for 10 min. The pellet was incubated with 750 µl of ethanol and then centrifuged at RT for 10 min at 14,000 g. After being washed with cold 70% EtOH, the ssDNA pellet was re-suspended in 30 µl of water (double processed tissue culture water) (Sigma-Aldrich Co., Irvine KA, UK), and 0.5 µg of ssDNA was sequenced with a 10 pmol primer (5′-CCCTCATAGTTAGCGTAACG-3′, -96glll sequencing primer, New England Biolabs) by the Sequencing Unit at the Weizmann Institute of Science in Israel.

Peptide Synthesis

Peptides were synthesized at the Weizmann Institute of Science in Rehovot, Israel to perform characterization tests on their ability to influence the biological activity of chemokines. The format of the various synthesized peptides was as follows: Cyclic peptides ($ACX_7CGGGSK$-biotin-G) and linear peptides ($X_{12}GGGSK$-biotin-G) were used. The peptides were biotinylated at their C-termini; biotin served as the detector during the subsequent experiments. Each synthetic peptide was dissolved to a final concentration of 1 mg/ml (~0.6 mM) in 4% DMSO (dimethyl sulfoxide, Sigma).

ELISA of Synthetic Chemokine-Binding Peptides (CBPs)

NUNC-immuno maxisorp plates were coated with the appropriate chemokine (0.1 ml/well, 0.1–1.0 µg/ml in 0.1 M $NaHCO_3$, pH 8.6) and incubated overnight at 4°C. The plates were then blocked with 0.2 ml/well of 5 mg/ml BSA in 0.1 M $NaHCO_3$ (pH 8.6) for 3 h at RT. Control wells were treated with blocking buffer alone with no target protein added. The plates were washed six times with TBST, followed by incubation with 10-fold serial dilutions of the peptides (10 µg–10 pg in 0.1 ml TBST with 5 mg/ml BSA (TBST-BSA)/well) for 45 min at RT. After the plates were washed six times with TBST, the bound peptides were probed with either an HRP-SA conjugated antibody [horseradish peroxidase conjugated to streptavidin (R&D systems, diluted 1: 10,000 to 1: 20,000 in TBST–BSA, 0.1 ml/well) or AP-anti-biotin (alkaline phosphatase conjugated to a monoclonal anti-biotin antibody, clone BN-34, Sigma, diluted 1: 2,500 to 1: 5,000)] for 45 min at RT. The target-bound peptides that were probed with HRP-SA were determined using a DAKO TMB one-step substrate system (3,3′,5,5′-tetramethlbenzidine, DAKO) (100 µl/well). The reaction was stopped by the addition of an HCl–H_2SO_4 mixture (1 N HCl, 3 N H_2SO_4). The results were analyzed by an ELISA reader (Anthos Labtec HT2, version 1.06) at OD_{450}. The target-bound peptides that were probed with AP-anti-biotin were determined using a Sigma 104 phosphate substrate [(p-nitrophenyl phosphate, disodium, hexahydrate), 5 mg tablets, Sigma]. The 5-mg Sigma 104 tablets were dissolved in 10 ml of developing buffer (50 mM Na_2CO_3, 0.2 mM $MgCl_2$, pH 9.8) (100 µl/well). The results were analyzed by an ELISA reader (Anthos Labtec HT2, version 1.06) at OD_{405}.

Western Blot

Cell sample media were collected and centrifuged (1,000 rotations per minute, 7 min), and 1 ml of cell-deprived media was incubated with 50 µl of Protein A-Sepharose® beads for 45 min at RT. The proteins were then eluted from the beads with 50 µl of sample buffer containing 100 mM citrate phosphate buffer (pH 3.5) and 10 mM DTT (dithiothreitol). The samples were boiled for 3 min, and 25 µl of the samples was then loaded onto 12% NuPAGE® Bis-Tris gels. The proteins were transferred to nitrocellulose membranes and blocked with 10% low-fat milk in PBST (PBS supplemented with 0.05% Tween-20). The membranes were then blotted for 1 h with a human anti-IgG Fc fragment antibody followed by a goat anti-human antibody conjugated to HRP (horseradish peroxidase) diluted 1: 40,000 in blocking solution at RT. Following incubation with an ECL solution, the membrane was exposed to film.

Cloning the Peptides into Fc–Peptides (Peptibodies)

Two-Step PCR for Obtaining IL6-BKT Peptide DNA Fragments

In the first PCR step, the IL6 signal peptide DNA sequence was added to the DNA sequence corresponding to the first nine amino acids of each peptide. The product of this PCR was used in the second PCR step as the template to which a DNA sequence corresponding to the remaining three amino acids of the peptide, a spacer sequence, and a 3′-end BstBI restriction site was added.

IL6-Fc pIRES puro DNA served as the DNA template for all three of the first-step PCR. All three PCR were performed using the same forward primer (T7). Using the universal T7 primer resulted in a PCR product that contained multiple cloning sites at the 5′ end, including an NheI site, which was used for later sub-cloning. The reverse primers were specific for each peptide; ctgtggatgc tgtggctggg gatgctgggg ggcacggggg cagggg was used for BKT130, cacggtctga gggatagggt agtccagggg gggcacgggg gcagg was used for BKT120, and gtcgtagtcgaaagaaggtggtcacgggggcacgggggcagg. was used for BKT110Fc. BKT110 VTTFFDYDYGAPC-FC peptide was derived from the CCR2 n-terminal region and was used as a control peptibody.

The PCR conditions were as follows: 20 ng of DNA template, 5 µl of amplification X10 buffer, 0.2 mM of each deoxyribonucleotide (dNTP), 0.5 mM $MgSO_4$, 5 µl of X10 enhancer solution, 0.2 µM of each primer, 2.5 units of Taq polymerase, and water added to a total reaction volume of 50 µl.

Amplifications were performed with an initial denaturation step at 94°C for 3 min, followed by 30 cycles of 94°C for 30 s, 52°C for 30 s, and 72°C for 30 s, and a final step at 72°C for 10 min.

At the end of PCR amplification, 5 µl of each reaction mixture was analyzed on 2% agarose gels stained with ethidium bromide and visualized with UV light.

The PCR products obtained by the above procedures were used as templates for the second PCR step. The abovementioned T7 primer was used as the forward primer in all three reactions, while the reverse primer was specific for each peptide; SEQ cgcttcgaag cccttgctgc cgccgccggc cttggcgctg tggatgctgt ggctgg was used for BKT130, SEQ cgcttcgaag cccttgctgc cgccgccgtg gtgcagcacg gtctgaggga taggg was used for BKT120 and SEQ cgcttcgaagcccttgccgccgccgcatggggcgccgtagtcgtagtcgaagaagg was used for BKT110. Each reverse primer encoded amino acids 10–12 of the desired peptide, a hexapeptide spacer sequence (Gly Gly Gly Ser Lys Gly) and a BstB1 restriction site.

The PCR conditions were as follows: 0.5 µl of the DNA template; 5 µl of X10 amplification buffer, 0.2 mM of each dNTP, 0.5 µM $MgSO_4$, 5 µl of X10 enhancer solution, 0.2 µM of each primer, 2.5 units of Taq polymerase, and water added to a total reaction volume of 50 µl.

Amplifications and analysis of the PCR products were performed as described above for the first PCR step. After PCR amplification, the products were analyzed on 2% agarose gels stained with ethidium bromide and visualized with UV light. The PCR products were extracted from gels using a QiaQuick™ Gel Extraction kit (Qiagen™).

Ligation of IL6-BKT Peptide DNA Fragments to the Fc Sequence

Extracted IL6-BKT peptide DNA products were digested with NheI and BstBI, purified from agarose gels as described above, and ligated into Fc N297A pIRESpuro3 that was previously digested with the same enzymes.

This N297A Fc is a well-known mutation that prevents glycosylation and has a markedly decreased capacity to bind Fc receptors. This humanized Fc was found to be not mitogenic and circumvent the side effects that are linked to mitogenicity and ADCC (13–15).

The ligation mixture was then transformed into DH5a competent cells. Ampicillin-resistant transformants were screened, and positive clones were further analyzed by colony PCR.

DNA was extracted from ampicillin-resistant colonies and subjected to a 2-h digestion at 37°C with the EcoRI and NotI restriction enzymes. The reaction was resolved on an agarose gel. Positive colonies were expected to yield two bands corresponding to 5,123 and 868 bp. The positive colonies were verified by DNA sequencing.

Transfection

The constructs were transfected into HEK-293T cells using FuGENE 6 (Roche). Each BioPep construct was transfected into two wells of a 6-well plate. One well was dedicated for Western blot (WB) analysis, and the second well was dedicated for the establishment of a stable pool. The cells were plated in 6-well plates at a concentration of 500,000 cells per well. A day later, the cells were transfected with 6 µl of FuGENE and 2 µg of DNA (ratio of). Media from the wells that were dedicated for WB was replaced with serum-free media after 24 h and collected 48 h later. Media in the other wells was replaced with DMEM containing 10% FCS, and 48 h later, the cells were trypsynized and transferred to a T75 flask containing selection medium (DMEM, 10% FCS and 5 µg/ml puromycin) to obtain stable clones.

T Cell Purification from Fresh Blood

Briefly, 50 ml of blood was added to 10 ml of dextran [Dextran T-500, 6% w/v in phosphate buffered saline (PBS)] and 7 ml of

citrate buffer (25 g citrate and 8 g citric acid in 500 ml of PBS). The solution was incubated for 30 min at 25°C and separated using Ficoll 1077 (Sigma). The interphase was collected and washed twice with 8 ml of PBS-5% FCS, followed by centrifugation at 1,400 rpm for 5 min at 18°C. The cells were re-suspended in PBS-5% FCS at a concentration of less than 10^8/ml. Next, 2 ml of the cell solution was applied, and the mixture was incubated for 45 min at 25°C on a Perspex nylon wool column, which was pre-soaked in PBS-5% FCS. Each column was washed with 8 ml of PBS-5% FCS, and the cells (T cells and erythrocytes) were eluted using 50 ml of 5 mM EDTA in PBS. A red pellet was obtained by centrifugation at 1,400 rpm for 5 min at 4°C. To lyse the erythrocytes, the red pellet was re-suspended in 5 ml of lysis buffer (155 mM NH_4Cl, 10 mM $KHCO_3$, 0.1 mM EDTA, 0.1 M PBS) for 4 min, followed by the immediate addition of 50 ml of PBS–EDTA.

Following centrifugation at 1,400 rpm at 4°C for 5 min, the pellet was washed again with 50 ml of PBS–EDTA and re-centrifuged under the same conditions. The pellet was re-suspended in RPMI/10% FCS/L-glutamine/sodium pyruvate/antibiotics at a concentration of 3×10^6 cells/ml. The cells were incubated for 2 h at 37°C, and the non-adherent cells were collected. The cells were ready for use in experiments after overnight incubation at 37°C.

Preparation of Adhesive Subsites

Human VCAM-1 (1 μg/ml) and CXCL12 (intact or heat-inactivated) (2°μg/ml) were dissolved in PBS buffered with 20 mM bicarbonate (pH 8.5) and incubated on polystyrene plates overnight at 4°C. The plates were then washed three times and blocked with human serum albumin (HAS) (20 μg/ml in PBS) for 2 h at 37°C.

Biovalidation

Adhesion Assay Using Laminar Flow

Laminar flow assays were performed as described below. Polystyrene plates (Becton Dickinson) were coated with soluble VCAM-1 at 10 μg/ml in the presence of a 2 μg/ml HSA carrier. The plates were washed three times with PBS and blocked with HSA (20 μg/ml in PBS) for 2 h at RT. Alternatively, washed plates were coated with 10 μg/ml of the CCL2, CCL5, CCL11, CXCL8, CXCL9, MIG CXCL10, CXCL11, and CXCL12 chemokine in PBS for 30 min at RT before being blocked with HSA. The plates were assembled as the lower wall of a parallel wall flow chamber and mounted on the stage of an inverted microscope. The peptide, as described previously (10 μg/ml), was allowed to settle on the substrate-coated chamber wall for 10 min at 37°C and was then washed. T cells (5×10^6/ml, purity >98%) were suspended in binding buffer, perfused into the chamber and allowed to settle on the substrate-coated chamber wall for 1 min at 37°C. Flow was initiated and increased in 2- to 2.5-fold increments every 5 s, generating controlled shear stress on the wall. Cells were visualized using the 20× objective of an inverted phase-contrast Diaphot microscope (Nikon, Japan) and photographed with a long integration LIS-700 CCD video camera (Applitech, Holon, Israel) connected to a video recorder (AG-6730 S-VHS, Panasonic, Japan). The number of adherent cells resisting detachment by the elevated shear forces was determined after each interval by analyzing the videotaped cell images and was expressed as the percentage of originally settled cells. All the adhesion experiments were performed at least three times in multiple test fields.

ELISA for the Binding of BKT130 to Different Chemokines

ELISA assay was performed in order to evaluate the binding of BKT130Fc to different chemokines. Plates were pre-coated with different chemokines at concentration of 150 ng/well/100 μl in coating buffer (0.1 M Carbonate pH 9.5) and incubated over night at 4°C. Plates were than washed once with washing buffer (PBS with 0.05% Tween) and blocked with 200 μl of blocking buffer (4% BSA in PBS). Following 1 h of incubation at RT the plates were washed once with washing buffer and 100 μl of BKT130 (0, 1, 10, and 50 μg/ml) were added into each well. Following 2 h of incubation at RT plates were washed five times with washing buffer and second antibody (Goat anti-Human IgG HRP conjugate) was added at dilution of 1:1000 for 2 h at RT. Following incubation plates were washed five times with washing buffer and 3,3′-5,5′-tetramethylbenzidine (TMB) substrate was added (100 μl/well). 30 min later the reaction was stop with 50 μl of stop solution (1 M H_2SO4) and the absorbance was measured by ELISA Reader at wavelength of 450 nm.

BiAcore Analysis of Peptibodies

The binding of the peptibodies (BKT130Fc and BKT120Fc) to the chemokines CXCL11, CXCL10, CXCL9, CCL2, CCL11, and CCL5 was done using BiAcore analysis.

Biomolecular Interaction Analysis using surface plasmon resonance (SRP) was performed.

To immobilize the chemokines to the CM5 sensor chip (BIAcore), the carboxyl groups on the matrix were activated by adding 10 μl of 1:1 mixture of succinimide (NHS) and carbodiimide (EDC) to form active esters which react spontaneously with amine groups on the chemokines (BIAcore kit, according to the manufacturer orders). Then the chemokines were immobilized by using standard amine-coupling chemistry to a level of ~1,000 response units (RU; 1000 pg/mm^2) onto a CM5 sensor chip using a BIAcore 3000 biosensor.

In order to test the interaction of the peptibodies to the chemokines, serial dilutions of the peptibodies, 1, 0.5, 0.25, 0.125, and 0.032 mM were tested by the BIAcore analysis at a flow rate of 10 μl/min. Real-time binding data of the peptibodies to the different chemokines immobilized were plotted as the mass of peptide binding to immobilized chemokines in RU as a function of time. Data were globally analyzed with the analysis software BIAEVALUATION 3.0 (BIAcore) using a 1:1 mass transport mode. The equilibrium dissociation constant was calculated using the relationship between the mean values for Kon and Koff (K_D = Koff/Kon). To demonstrate reproducibility, sensorgrams of four concentrations of the peptide in question were overlaid.

In Vitro Migration Assay

The migration of cells *in vitro* toward the various chemokines was assessed using transmigration plates that were 6.5-mm in diameter and 5-μm in pore size (Costar). Migration toward CCL2 (10 ng/ml) and CCL5 (20 ng/ml) was assessed using THP-1

cell monocytes (ATCC cat# TIB202), while migration toward CXCL12 (100 ng/ml) was assessed using freshly isolated human CD4+ T cells, and migration toward CXC10 (500 ng/ml) and CXCL11 (500 ng/ml) was assessed using Jurkat cells overexpressing CXCR3. Briefly, 600 µl of RPMI supplemented with 1% FCS was added to the lower chamber of transwells supplemented with the different chemokines. The chemokines were incubated with BKT130Fc, BKT120Fc, or BKT110Fc (10 µg/ml) for 30 min prior to the initiation of the migration assay. After 30 min of incubation, 2×10^5 cells/well were added to the upper chambers of the transmigration plates in a total volume of 100 µl of RPMI plus 1% FCS. Cells that migrated to the bottom chamber of the transwell within 3 h were counted using FACScalibur.

When Jurkat-CXCR3 cells were used, the upper wells were pre-coated with fibronectin (10 µg/ml) for 1 h at 37°C prior to the migration assay.

CD4+ T cells were obtained from fresh whole blood using a RosetteSep Human CD4+T Cell Enrichment Cocktail (STEMCELL Technologies) according to the manufacturer's instructions.

In Vivo Assay

Animals

C57BL/6, SJL, and BALB/c mice (7–10 weeks old) were purchased from Harlan (Rehovot, Israel) and maintained under specific pathogen-free conditions at the Hebrew University Animal Facility (Jerusalem, Israel). All studies were carried out in accordance with the recommendations of Hebrew University Animal Facility (Jerusalem, Israel). The protocols were approved by the Animal Care and Use Committee of Hebrew University. The protocol numbers of the animal ethics committee that were used in this study are: MD-08-11724-2, MD-13-13659-3, MD-08-11460-4, MD-11-12355-5, and MD-09-12250-4.

Pharmacokinetics (PK) in Mice

Pharmacokinetic analysis of the peptibodies in mice was performed in C57BL/6 mice. First the mice were intravenously (i.v.) injected with different doses of BKT130Fc (25, 50, and 100 µg/mouse) The mice were bled for 2 h, 24 h, and 6 days post-injection, and serum was extracted. The level of peptibodies in their serum was tested using a Human Total IgG ELISA kit (ICL) according to the manufacturer's instructions.

Next the mice were i.v. injected with 50µg/mouse of BKT130Fc or BKT120Fc. The mice were bled for 2 h, 24 h, or 6, 11, and 18 days post-injection, and the level of peptibodies in their serum was tested using a Human Total IgG ELISA kit.

Production of Antibodies against BKT130Fc

C57BL/6 mice were i.v. injected with 50 µg of BKT130Fc once or twice a week for total of four injections. One-week after the last injection serum was extract and ELISA was performed.

ELISA assay was performed in order to evaluate the level of antibodies against BKT130Fc or BKT120Fc in the mice serum. Plates were pre-coated with either BKT130Fc, BKT120Fc or BSA at concentration of 150 ng/well/100 µl in coating buffer (0.1 M Carbonate pH 9.5) and incubated over night at 4°C. ELISA was done as described at section 2.12.2.

Delayed-Type Hypersensitivity (DTH)

Female BALB/c mice were sensitized on their shaved abdominal skin with 100 µl of 2% oxazalone dissolved in acetone/olive oil [4:1 (vol/vol)] applied topically (day 0). DTH sensitivity was elicited 6 days later by challenging the mice with 20 µl of 0.5% oxazalone in acetone/olive oil, with 10 µl being administered topically to each side of their right ears. BKT130Fc, BKT120Fc, or BKT110Fc were intravenously injected (50 µg/mouse) on day 0 and 24 h before the challenge (day 5) (total of 100 µg/mouse). Control group mice were subcutaneously injected with dexamethasone (100 µg/mouse in a total volume of 200 µl). Right ear swelling was measured 24 h after the challenge using a micrometer digital caliper (Mitutoyo Corp, Tokyo, Japan). Swelling of the left ear served as the control.

Antigen-Induced Arthritis (AIA)

Antigen-induced arthritis was induced as previously described by Coelho et al. (17). Briefly, the mice (8- to 10-week-old male C57BL/6 mice) were immunized intradermally at the base of their tail with 500 µg of mBSA (Sigma) in 100 µl of a saline emulsion and an equal volume of CFA (Difco Detroit, MI, USA) on day 0. Twelve days later, the mice were challenged with antigens. Each mouse received an injection of 10 µg of mBSA in 10 µl of sterile saline in their left knee joint (17, 18). In some mice, BKT130Fc or BKT120Fc (50 µg/mouse) were i.v. injected 24 h before the challenge. Naïve mice challenged with sham PBS served as the controls. Mice were killed 24 h after the antigen challenge.

The mouse knee cavities were washed with 3% BSA in PBS. The number of infiltrated cells was evaluated using FACScaliber. Periarticular tissue was removed from their joints to evaluate myeloperoxidase (MPO) activity.

For histology, the other knee joint form each mouse was removed and fixed with 8% paraformaldehyde for 12 h. The joints were then incubated in 20% EDTA at pH 7.2 for 6 days to decalcify the bones. Samples were washed with PBS and dehydrated. After being embedded in paraffin, the joints were sliced into 6-µm-thick sections and stained with hematoxylin and eosin (H&E) (17, 19).

The extent of neutrophil accumulation in the mouse tissues was measured by assaying MPO activity as described (20, 21). Briefly, the knee joint was removed and frozen at −20°C. Upon thawing of the sample, the tissue (0.1 gm of tissue per 1.9 ml of buffer) was homogenized and processed for the determination of MPO activity. The assay included 3,3′-5,5′ TMB (Sigma) in PBS as the color reagent.

Experimental Autoimmune Encephalomyelitis (EAE)

Experimental autoimmune encephalomyelitis was induced in female SJL and C57BL/6 mice. Mice were immunized subcutaneously in their flanks (day 0) with 100 µg of PLP139-151 or 250 µg MOG35-55, respectively. Proteolipid protein (PLP) and myelin oligodendrocyte glycoprotein (MOG) peptides were emulsified in an equal volume of CFA containing 800 µg of mycobacterium tuberculosis H37RA (Difco). Mice were injected intraperitoneally with 300 ng of pertussis toxin (PTX) on days 0 and 2.

Mice were i.v. injected once with either BKT130Fc, BKT120Fc, or BKT110Fc (50 µg/mouse) on day 9 post-immunization. Spinal

cord tissue samples were collected 30 days after the induction of disease, fixed in 4% paraformaldehyde, dehydrated and embedded in paraffin. Spinal cord sections were cut at 6 μm and processed for histological analysis by H&E staining to evaluate immune cell infiltration and by luxol fast blue to mark the area of demyelination.

Blood samples were collected on day 30 post-immunization, and serum was extracted for cytokine analysis. Cytokine levels were evaluated using a Mouse Th1/Th2 Cytokine kit/BD cytometric bead array according to the manufacturer's instructions.

Clinical assessment of EAE was performed according to the following criteria: 0, no disease; 1, decreased tail tone; 2, hind limb weakness or partial paralysis; 3, complete hind limb paralysis; 4, front and hind limb paralysis; 5, moribund state. For all EAE experiments, there were 10 to 12 mice per group.

Statistical Analysis

Data are presented as the mean ± SD. Statistical comparisons of the means were performed using two-tailed unpaired Student's *t*-tests. Differences of $p \leq 0.05$ were considered statistically significant.

RESULTS

Identification of CBPs that Inhibited the Chemokine-Induced Adhesion and Migration of Immune Cells

Phage display libraries were screened for their ability to bind five immobilized human chemokines CCL11, CXCL9, CXCL8, CXCL12, and CCL2 as described in the Section "Materials and Methods." Following three to four cycles of panning 156 different phages were identified (Table S1 in Supplementary Material). Sixty-nine different phages were further selected for their ability to bind CCL2 using ELISA assay (Table S2 in Supplementary Material). Whereas most of the CCL2-binding phages appeared in only one bacterial colony following three cycles of enrichment ($n = 65$), the phage carrying the BKT130 peptide appeared in 12 different colonies, suggesting a significant enrichment for this CCL2-binding phage throughout the process (Table S2 in Supplementary Material).

Next, we synthesized biotinylated peptides and analyzed their ability to bind CCL2. We found that BKT120, BKT130, and other peptides, interacted with CCL2 and, to a lesser extent, with CXCL12 (**Figure 1**). The ability of BKT120, BKT130, and peptide 23 [P23 that was fished from the library by another chemokine (CCL11)] to prohibit CCL2 (**Figure 2A**), CCL5 (**Figure 2B**), and CXCL12 (**Figure 2C**) from inducing immune cell-dependent adhesion to the endothelial adhesion molecule VCAM-1 was tested. BTK120 and BTK130 inhibit CCL2- and CCL5-mediated adhesion to VCAM-1 but have not effect on adhesion mediated by CXCL12 (**Figure 2**). Peptide 23 (P23), which was used as the control, did not affect the CCL2-, CCL5-, or CXCL12-dependent adhesion of T cells to VCAM-1.

Turning CBPs into Peptibodies Enhanced Their Biological Activity

Two of the CCL2-binding peptides (BKT120, BKT130) as well as control peptide (BKT110) were cloned into Fc-peptides (peptibodies). The BKT120, BKT130, and BKT110 peptibodies are composed of two moieties, a biologically active peptide and an Fc region. The effect of BKT120Fc and BKT130Fc on the ability of (**Figure 3A**), CCL5 (**Figure 3B**), CCL11 (**Figure 3C**), CXCL8 (**Figure 3D**), CXCL9 (**Figure 3E**) CCL2, CXCL10 (**Figure 3F**), CXCL11 (**Figure 3G**), and CXCL12 (**Figure 3H**) to induce immune cell-dependent adhesion to the endothelial adhesion molecule VCAM-1 was tested. BKT120Fc and BKT130Fc both inhibited the function of CCL2, CCL5, CXCL9, and CXCL11 but did not inhibit the function of CXCL8, CXCL12, and CCL11. BKT130Fc, but not BKT120Fc, inhibited CXCL10 function (**Figure 3F**). BKT110Fc did not inhibit the function of CCL2, CCL11, CXCL8, and CXCL10 (Figures S1A–D in Supplementary Material).

The effect of BKT110Fc, BKT120Fc, and BKT130Fc on the ability of CCL2, CCL5, CXCL10, CXCL11, and CXCL12 to induce the migration of immune cells was studied in more detail.

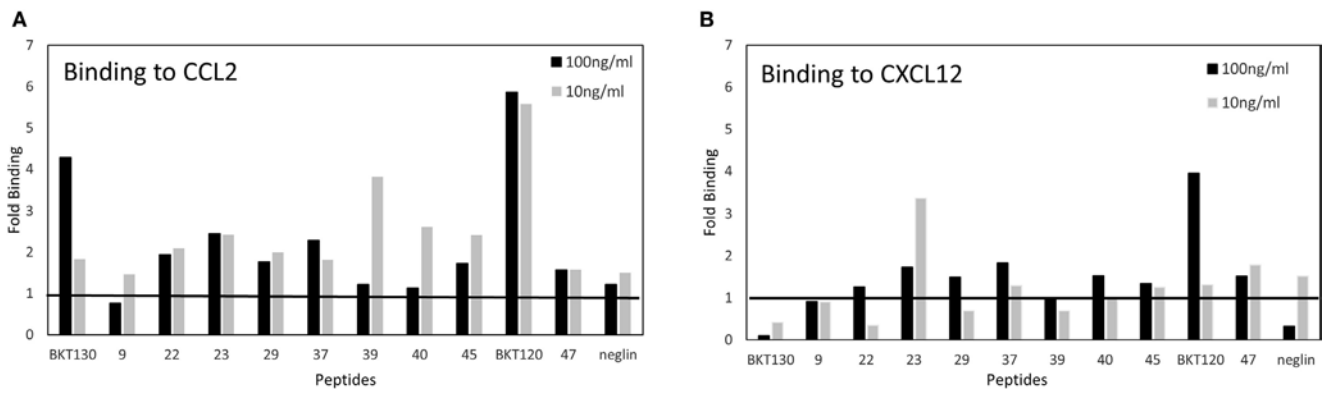

FIGURE 1 | ELISA of chemokine-binding peptides (CBPs) with CCL2 and CXCL12. ELISA was performed on biotinylated peptides to detect their interaction with **(A)** CCL2 or **(B)** CXCL12. The data are presented as the fold binding that was obtained using two concentrations of the various peptides (10 and 100 ng/ml).

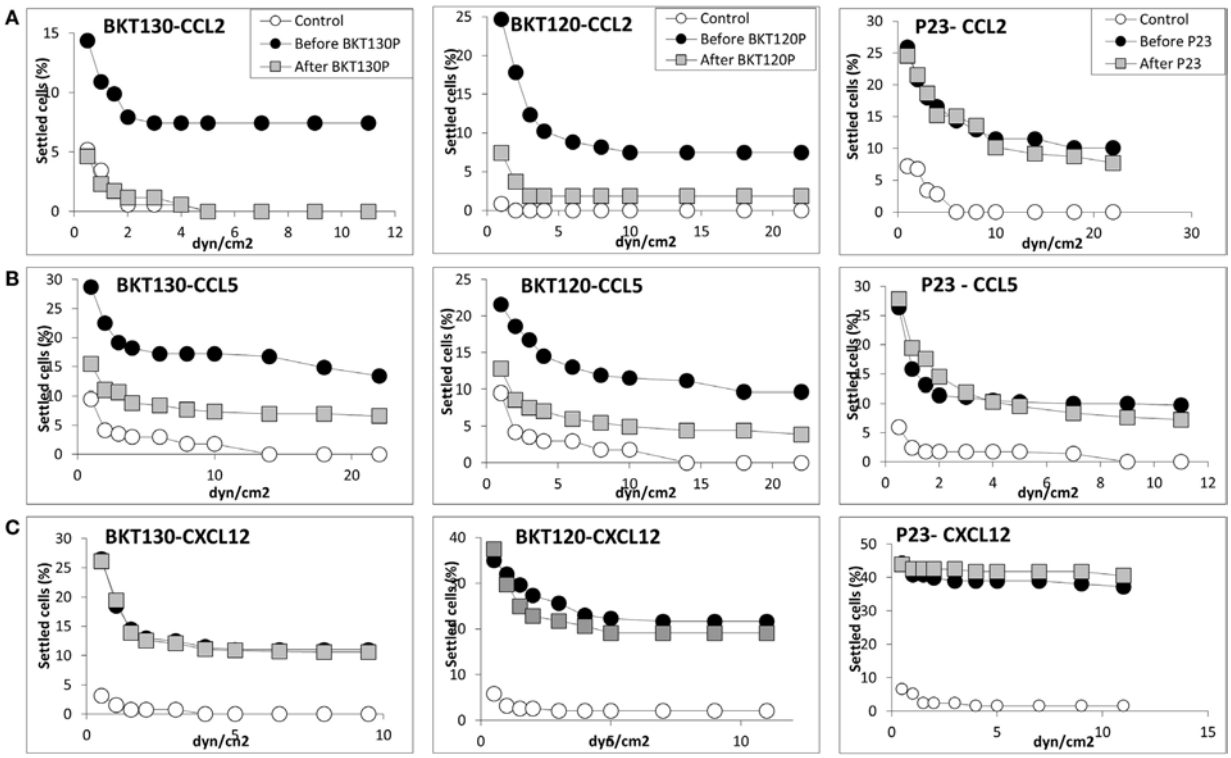

FIGURE 2 | Effect of various peptides on the chemokine-induced immune cell-dependent adhesion to VCAM-1. Adhesion was measured using the laminar flow assay. The number of adherent cells resisting detachment by elevated shear forces (dyn/cm^2) is expressed as the percentage of originally settled cells. The effects of the peptides BKT130, BKT120, and peptide 23 (P23) on the **(A)** CCL2-, **(B)** CCL5-, and **(C)**CXCL12-induced immune cell-dependent adhesion to VCAM-1 were measured. All the adhesion experiments were performed at least three times on multiple test fields.

BKT130Fc (10 μg/ml) was more effective then BKT120Fc in inhibiting the migration of immune cells in response to CCL2, CCL5, CXCL10, and CXCL11 but did not inhibit the migration of cells in response to CXCL12. BKT110 had no effect on the migration toward CCL2, CCL5, CXCL10, and CXCL11 whereas it has significant inhibition on the migration of cells in response to CXCL12 (**Figures 5A–E**).

Binding of BKT130Fc and BKT120Fc to Different Chemokines

In order to analyze the binding characteristics of the interaction between BKT130Fc/BKT120Fc and the chemokines CXCL11, CXCL10, CXCL9, CCL2, CCL11, and CCL5, a BiaCore assay was performed (**Table 1**). The affinity of BKT130Fc to CXCL11, CXCL10 and CCL5 was the highest with K_D of 8.3 E−0.8, 3.8 E−0.8, and 1.8 E−0.8, respectively. The K_D for CXCL9 binding was 1.3 E−0.7 and lower affinity binding to CCL2 and CCL11 with K_D of 6.5 E−0.6 and 2.7 E−0.5 were observed. The affinity of BKT120Fc to CXCL10, CCL2, and CXCL9 was the highest with K_D of 6.3 E−0.9, 4.6 E−0.8, and 1.8 E−0.8, respectively. The K_D for CXCL11 and CCL11 was lower with KD of 3.7 E−0.7 and 5 E−0.6, respectively (**Table 1**).

ELISA assay was developed to further study the binding of BKT130Fc to different chemokines (**Figure 4**). BKT130Fc demonstrated a strong binding to CXCL11, CXCL9, CCL5, and CXCL12 and lower binding to CXCL11 and CCL2. No binding of BKT130Fc was found to CCL11, CXCL8, CXCL13, CCL3, CCL19, CX3CL1, and CCL4.

The results obtained from the BiaCore and ELISA assays correlate with the ability of the peptibodies to inhibit the function of CCL5, CXCL9, CXCL10, CXCL11, and to lesser extent CCL2 (**Figures 3** and **5**). BKT130Fc/BKT120Fc did not bind or inhibit the function of CCL11 and CXCL8 (**Figures 3C,D**). BKT130Fc did not inhibit the migration and adhesion of immune cells in response to CXCL12 (**Figures 3H** and **5E**). However, BKT130Fc strongly bind CXCL12 suggesting that binding to chemokines does not always inhibit their function (**Figure 4A**). Similar results were obtained for BKT120 peptide (**Figure 1**) which interacts with CXCL12 in ELISA assay but do not inhibit its function (**Figure 2**).

PK of BKT130Fc and BKT120Fc in Mice

To evaluate the PK of BKT130Fc in mouse sera the peptibody was injected i.v once at three different doses of 25, 50, and 100 μg/mouse. The level of BKT130Fc in the sera was tested following 2h, 24h, and 6 days. The best PK for BKT130Fc was observed following injection of 50 and 100 μg of BKT130Fc. Injection of 25 μg/mouse gave a significant less effective PK for BKT130Fc (**Figure 5F**). Therefore, we choose to use the 50 μg/mouse of BKT130Fc throughout all the *in vivo* experiments. When 50 μg

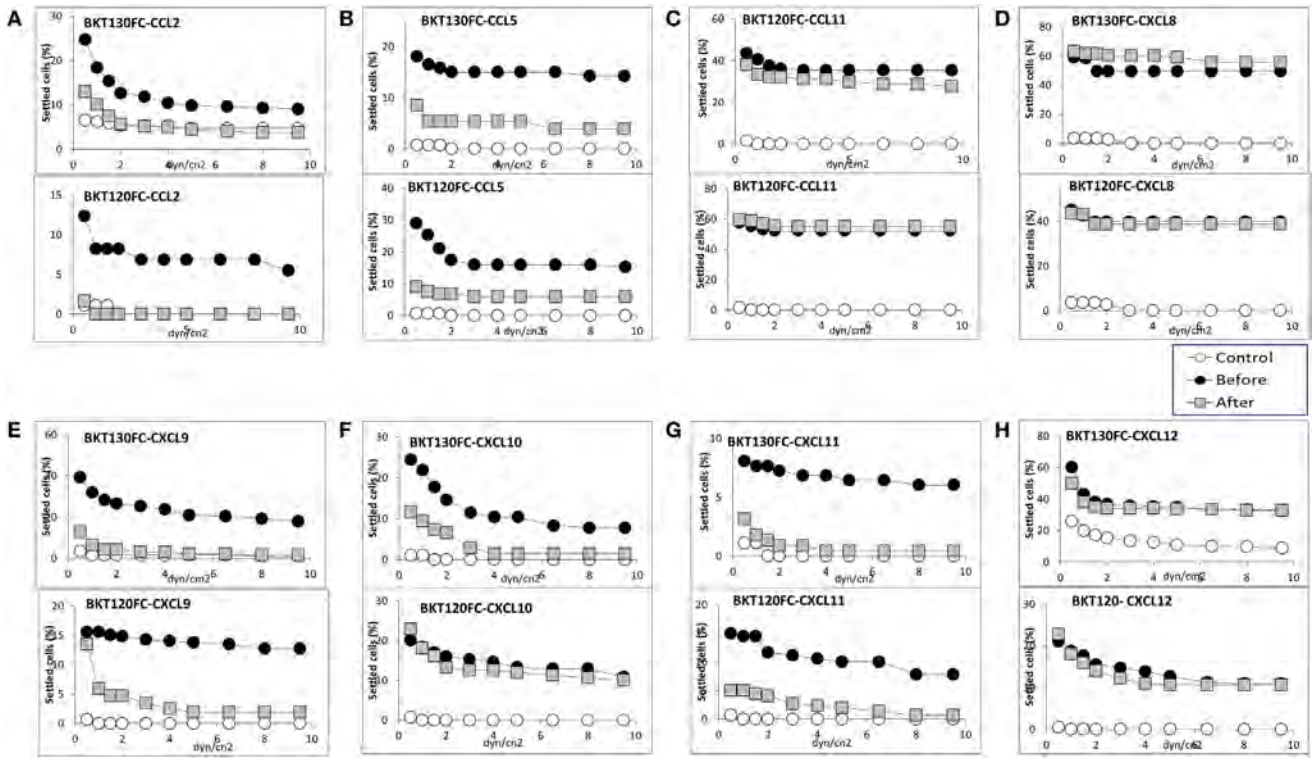

FIGURE 3 | Effect of the peptibodies BKT130Fc and BKT120Fc on the chemokine-induced immune cell-dependent adhesion to VCAM-1. Adhesion was measured using the laminar flow assay. The number of adherent cells resisting detachment by elevated shear forces (dyn/cm^2) is expressed as the percentage of originally settled cells. The effects of the peptibodies BKT130Fc and BKT120Fc on the **(A)** CCL2-, **(B)** CCL5-, **(C)** CCL11-, **(D)** CXCL8-, **(E)** CXCL9-, **(F)** CXCL10-, **(G)** CXCL11-, and **(H)** CXCL12-induced immune cell-dependent adhesion to VCAM-1 were measured. All the adhesion experiments were performed at least three times on multiple test fields.

TABLE 1 | BiAcore K_D Values for the interactions of BKT130Fc and BKT120Fc with various chemokines.

	BKT130Fc		BKT120Fc	
	BKT130Fc (K_D)	Chi-squared (χ^2)	BKT120Fc (K_D)	Chi-squared (χ^2)
CXCL11	8.3 E–0.8	0.51	3.7 E–0.7	0.76
CXCL10	3.8 E–0.8	1.05	6.3 E–0.9	0.99
CXCL9	1.3 E–0.7	1.05	1.8 E–0.8	0.61
CCL2	6.5 E–0.6	0.65	4.6 E–0.8	0.75
CCL11	2.7 E–0.5	1.2	5 E–0.6	0.51
CCL5	1.8 E–0.8	0.6		

of peptibodies were injected into mice, BKT120Fc and BKT130Fc retained certain desirable antibody features, including an increased apparent affinity through the avidity conferred by the dimerization of two Fcs and a prolonged PK, of IC50 = 6 days (**Figure 5G**).

Production of Antibodies against BKT130Fc

In order to check the immunogenicity of BKT130Fc, mice were i.v injected with BKT130Fc once or four times. Antibodies against BKT130Fc were not produced following single injection of 50 μg of BK130Fc. The level of antibodies against BKT130Fc was increased following four injections (Figure S2A in Supplementary Material). Interestingly, these antibodies could not recognize BKT120Fc (Figure S2B in Supplementary Material). These results suggest that the antibodies produced recognize the BKT130 peptide and not the Fc portion.

BKT130Fc and BKT120Fc Inhibited DTH

Delayed-type hypersensitivity is a process immunologically similar to cell-mediated immunity, and the inflammatory DTH reaction is mediated by effector TH1/TH17 memory T lymphocytes (22). In this *in vivo* assay, lymphocytes infiltrate to the injection site (ear) of an antigen against which the immune system has been primed. The inflammatory reaction is characterized by the redness and swelling of the ear following antigenic challenge. The chemokines CXCL10, CXCL9, CCL3, and CCL5 were shown to regulate this inflammatory process (23, 24). The ability of BKT110, BKT120Fc and BKT130Fc, i.v. administered at 50 μg/per a mouse once, on days 1 and 6, to inhibit the DTH response in mice 24 h before the second sensitization was tested. Dexamethasone, BKT130Fc, and BKT120Fc significantly inhibited the inflammatory process (80, 60, and 30%, respectively) (**Figure 5H**). Importantly, BKT110 had no effect on DTH. Overall, our results suggest that BKT130Fc has a more potent inhibitory effect than BKT120Fc on inflammatory chemokines *in vitro* and *in vivo*.

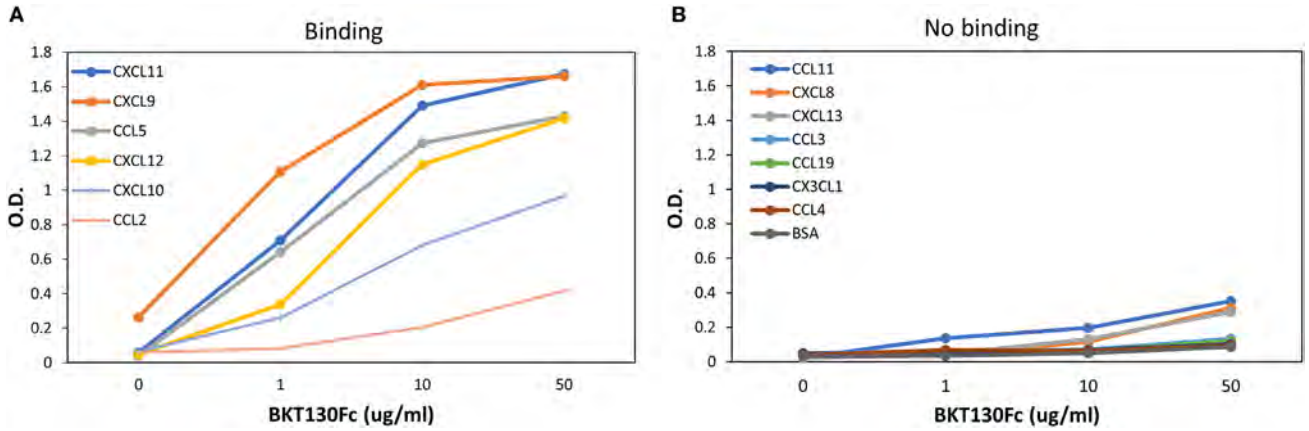

FIGURE 4 | ELISA for the binding of BKT130Fc to different chemokines. ELISA was performed with several dilutions of BKT130Fc (1, 10, and 50 μg/ml) to detect the interaction to different chemokines that were bound to the plates. The data are presented as the optical density (O.D.) obtained at wavelength of 450 nm. **(A)** presents the chemokines that demonstrate binding to BKT130Fc and **(B)** presents the chemokine with no binding to BKT130Fc.

BKT130Fc and BKT120Fc Inhibited the Infiltration of Inflammatory Cells into the Synovial Cavity in an Antigen-Induced Mouse Arthritis Model

The effect of BKT130Fc and BKT120Fc on RA was studied using an AIA model. BKT130Fc or BKT120Fc were i.v. administered once, at 50 μg/per a mouse 24 h before the challenge. BKT130Fc partially inhibited the infiltration of neutrophils into the synovial cavity, while it completely abrogated the infiltration of MNCs (including monocytes and lymphocytes) (**Figure 6**). BKT120Fc had less significant effect compare to BKT130Fc.

BKT130Fc and BKT120Fc Reduced the Severity of EAE by Inhibiting the Infiltration of Immune Cells into the CNS

The best animal model for MS is an EAE model, which can be induced by immunization using antigens derived from myelin, such as PLP fragments and MOGs.

The effect of BKT130Fc and BKT120Fc on EAE was studied in two different models. The PLP induced relapsing-remitting EAE and the MOG induced chronic EAE (25). BKT130Fc or BKT120Fc were intravenously administered once (50 μg/mouse) on day 9 after disease induction. In the SJL/PLP model, both BKT130Fc and BKT120Fc significantly prolonged the remission time and reduced the severity of the second relapse (**Figure 7A**), with an observed accumulating clinical score of 159 in the control group and an observed accumulating clinical score of 62 and 63 following BKT130Fc and BKT120Fc treatment, respectively. In the second relapse (starting from day 27), clinical signs appeared in 70–80% of the control mice compared to only 20% of the mice treated with BKT130Fc or BKT120Fc. This effect was accompanied by a lack of weight loss in the treated animals (data not shown). Histology of the spinal cord sections demonstrated that treatment with BKT130Fc or BKT120Fc inhibited the infiltration of immune cells into the CNS while also reducing the demyelination area (**Figure 7E**). Interestingly, BKT130Fc did not affect the peripheral balance between the Th1 and Th2 cytokine levels (**Figure 7F**).

Similar to the effect in the relapsing-remitting EAE model, a single i.v. injection of BKT130Fc (50 μg/mouse on day 9) significantly inhibited disease severity in the chronic EAE model (**Figure 7B**). BKT120Fc had less significant effect compare to BKT130Fc.

The control mice demonstrated an accumulating clinical score of 250.8 compared to 165.7 in mice treated with BKT130Fc and 193 following treatment with BKT120Fc. Importantly, BKT110 had no effect on MOG induced EAE with accumulating clinical score of 255 (**Figures 7C,D**).

The effect of BKT130Fc was accompanied by a lack of weight loss in the treated animals (data not shown). Like the first model, BKT130Fc did not affect the peripheral levels of Th1/Th2 cytokines (**Figure 7G**).

DISCUSSION

Effective inflammatory responses involve chemokine-dependent homing, retention, and the resolution of immune cell trafficking to damaged tissues (3). In addition to their physiological roles, chemokines and their receptors play a key role in the pathogenesis of autoimmune diseases, inflammation, viral infection, and cancer (3). However, except for selective CCR5 antagonists for HIV (Maraviroc) and a stem cell mobilizer (Mozobil), the promise of obtaining new therapeutics related to blocking chemokine receptor function in autoimmune diseases, inflammation, and cancer has not yet been realized.

In the past 15 years, several phase II/III clinical trials with antagonists against the chemokine receptors CCR1, CCR2, CCR3, CCR5, CCR9, CXCR1, CXCR2, and CXCR3 have failed to have significant clinical benefits in patients with autoimmune and inflammatory diseases, such as RA, multiple sclerosis (MS), IBD, psoriasis, and asthma (4, 5).

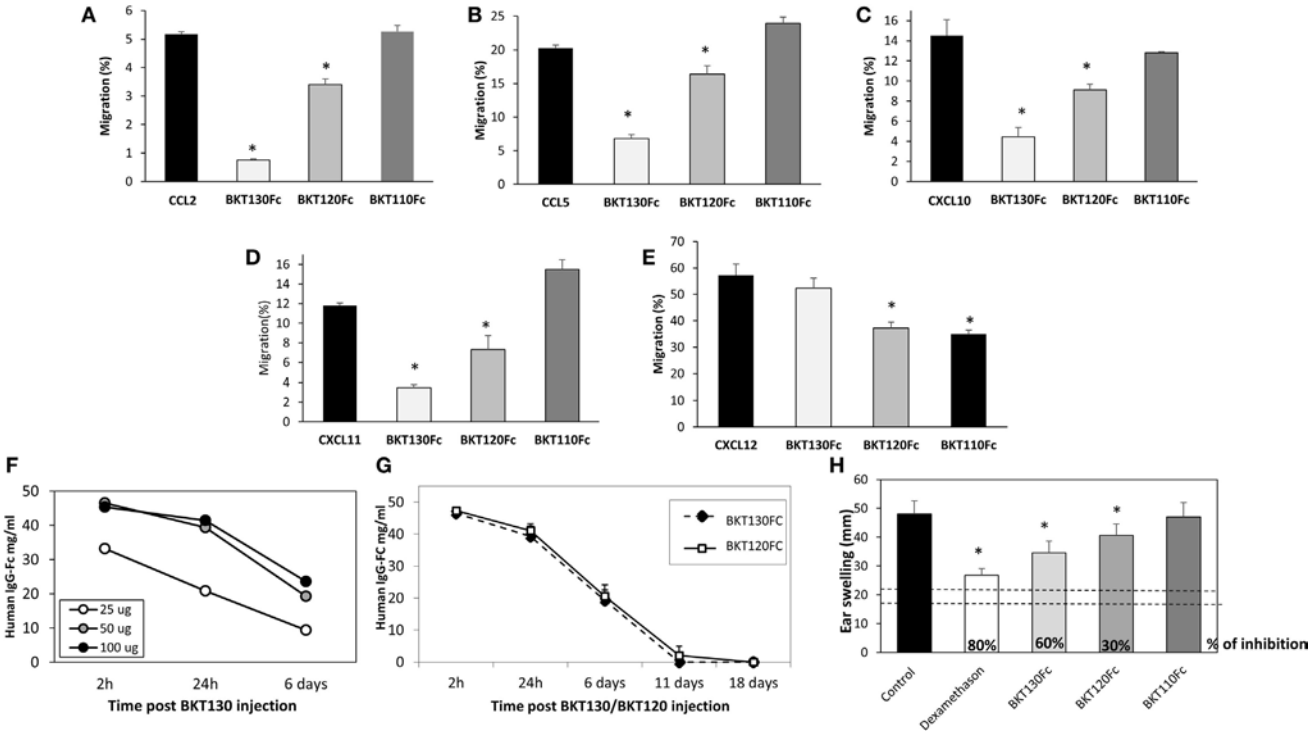

FIGURE 5 | The peptibodies BKT130Fc and BKT120Fc inhibit the *in vitro* migration of different chemokines. A transmigration assay was performed to study the effects of the BKT130Fc, BKT120Fc and BKT110Fc peptibodies on *in vitro* migration. **(A)** Migration toward CCL2 was assessed using THP-1 cells. **(B)** Migration toward CCL5 was assessed using THP-1 cells. **(C)** Migration toward CXCL10 was assessed using Jurkat cells overexpressing CXCR3. **(D)** Migration toward CXCL11 was assessed using Jurkat cells overexpressing CXCR3. **(E)** Migration toward CXCL12 was assessed using CD4+ T cells. BKT130Fc, BKT120Fc, and BKT110Fc were added at 10 μg/ml. The results, analyzed using Student's *t*-tests (*$p \leq 0.05$), are expressed as the mean percentage of migration ±SD. **(F)** Dosing of BKT130Fc pharmacokinetics (PK). C57BL/6 mice ($n = 3$) were intravenously (i.v.) injected with 25, 50, or 100 μg of BKT130Fc. The serum peptibody levels were tested after 2 h, 24 h, and 6 days. **(G)** PK of BKT130Fc and BKT120c in mice. C57BL/6 mice ($n = 5$) were i.v. injected with BKT120Fc or BKT130Fc at 50 μg/mouse. The serum peptibody levels were tested after 2 h, 24 h, and 6, 11, and 18 days. **(H)** BKT130Fc and BKT120Fc inhibited delayed-type hypersensitivity (DTH) *in vivo*. DTH model was established in female BALB/c mice ($n = 12$). BKT120Fc, BKT130Fc, or BKT110Fc were intravenously injected (50 μg/mouse) on day 0 and 24 h before the challenge (day 5) (total of 100 μg/mouse). Dexamethasone (100 μg/muse) served as the positive control. The two dotted lines indicate the normal range of ear swelling. The results, analyzed using Student's *t*-tests (*$p \leq 0.05$), are expressed as the mean ± SE of ear swelling (mm). All the DTH experiments were performed at least four times.

Reasons for such failures may be the lack of animal model predictability, relevance of the target to the human disease, diversity in the molecular and genetic drives of the disease within patient population, poor drug-like properties of small-molecule antagonists, ineffective dosing, target disease redundancy, and the use of multiple chemokine receptors (4, 5).

As quoted in the paper by Horuk et al. (5) CCR1, CCR2, CCR5, CCR6, and CXCR3 have all been implicated in the pathophysiology of MS. Moreover, MS is an extremely heterogeneous disease that consists of at least four distinct patterns of demyelination. Patients with MS that are enrolled in clinical trials could feasibly have varying pathophysiological subtypes that are perhaps driven by different chemokines and chemokine receptors. Multiple chemokine receptors, including CCR1, CCR2, CCR5, CXCR2, and CXCR3, seem to have roles in RA. Therefore, there is a strong possibility that receptor redundancy could account for the failure of CCR1 and CCR2 antagonists in RA clinical trials (4, 5).

In an elegant paper by Schall and Proudfoot the authors suggested that the chemokine/chemokine receptor system works as a network of signals in which redundancy is rare (26). They suggested that chemokine expression and chemokine receptor usage by immune cells is regulated in a cell type, time, and tissue-specific manner that is very specific and those not support the idea of redundancy in the system. It was, therefore, suggested that reasons for clinical failures is imbedded in the *in vivo* potency of the drug tested; in sufficient bioavailability, in sufficient metabolic stability and toxicity that prevented achieving high levels of free drug in the plasma. In addition, it was suggested that our miss understanding of the multidimensional nature of the inflammatory diseases, prevent us from effectively selecting the target and time of the intervention. It was, therefore, hypothesized that by deepen our understanding of the chemokine/chemokine receptor network in disease and improving our drugs a successful chemokine-targeted drugs for inflammatory diseases is visible.

Binding to multiple chemokines as a strategy for inhibiting inflammation is a phenomenon used by hosts as well as by different pathogens to reduce inflammation and immunity. Therefore, the inhibition of single chemokine receptors as an anti-inflammatory

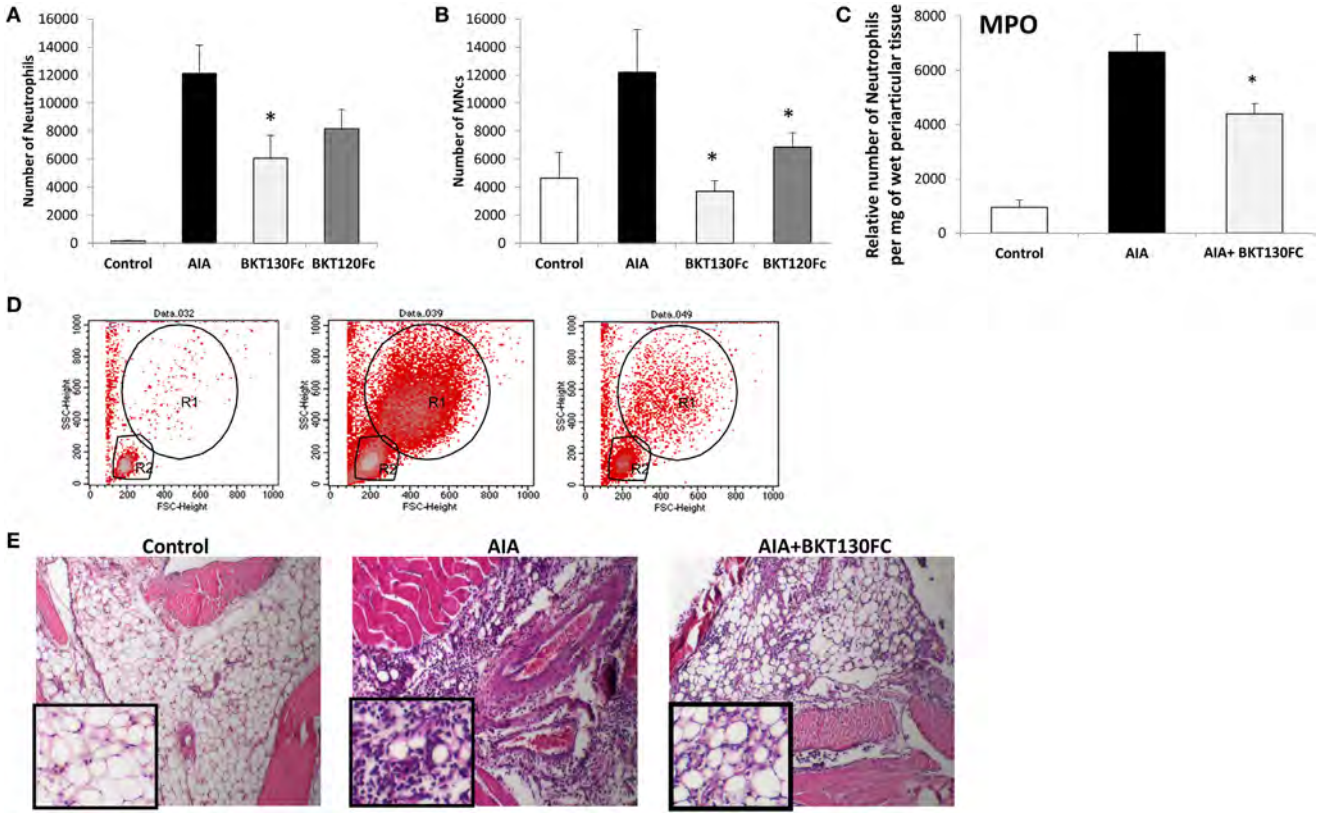

FIGURE 6 | BKT130Fc and BKT120Fc inhibited the infiltration of inflammatory cells into the synovial cavities of mice of the antigen-induced arthritis (AIA) model. Male C57BL/6 mice (n = 12) were immunized with methylated bovine serum albumin. BKT130Fc or BKT120Fc were administered *via* i.v. once at 50 µg/per a mouse, 24 h before the challenge. The control group represents normal mice, the AIA group represents untreated AIA mice and the BKT130Fc or BKT120Fc groups represent AIA mice treated with BKT130Fc or BKT120Fc, respectively. The number of infiltrated cells into the knee cavity was evaluated by FACScaliber: **(A)** number of neutrophils, **(B)** number of MNCs. Representative FACS analysis of cells within the knee cavity is presented in **(D)**. The R1 gate shows the neutrophil population and the R2 gate shows the MNCs. The level of myeloperoxidase (MPO) activity is presented in **(C)** as the relative number of neutrophils per mg of wet periarticular tissue. **(E)** Histology analysis of the knee joint shows the infiltration of inflammatory cells following hematoxylin and eosin (H&E) staining.

strategy most likely did not prevail during the evolution of hosts and pathogens.

As mentioned in the paper by Heidarieh (10), the immune system uses atypical chemokine receptors ACKR1, ACKR2, or ACKR4 that scavenge chemokine to control inflammation (27). These receptors are expressed mainly by erythrocytes and endothelial cells (11). ACKR1 (DARC) binds over 20 inflammatory chemokines (28) and is expressed by erythrocytes and endothelial cells (29). ACKR1 function as a scavenge receptor to limit excessive leukocyte trafficking (30). In addition, ACKR1 express on endothelial cells may reduce chemokine concentration in inflamed tissues and by that create a gradient that increases inflammation (11). ACKR2 which binds an inflammatory CC chemokines is also expressed lymphatic endothelial cells, placental trophoblasts, and leukocytes (31). ACKR2 is also a chemokine scavenger receptor (32, 33). ACKR2 control chemokine concentration by activating a β-arrestin without affecting its internalization rate (34, 35). ACKR2 promotes chemokine concentration by regulating lymphatic vessel function (36) and compactness (37), and ACKR2 KO mice in different pathological conditions show unregulated increased inflammation (38).

ACKR4 binds the homeostatic chemokines CCL19, CCL21, CCL25, and CXCL13 and is expressed by thymic epithelial cells, bronchial cells, and keratinocytes. ACKR4 is a constitutive internalization receptor with a chemokine-scavenging function (39). After chemokine binding, it recruits β-arrestin 2, but whether it activates signal transduction pathways is unknown. Few data are available on the *in vivo* role of ACKR4 in the context of inflammation. It appears to be important for the correct trafficking of dendritic cells to induce adaptive immune responses. Indeed, ACKR4 expression in lymph nodes is needed for generating a gradient of the CCR7 ligands CCL19 and CCL21 in the subcapsular sinus (40). In addition, ACKR4 KO mice were used to show that homeostatic chemokine clearance is necessary to control excessive Th17 responses that can lead to immunopathologys (41).

Herpesviruses have been shown to target the chemokine system (42, 43) by adopting and modifying chemokine and chemokine receptor genes to benefit their own survival and propagation (43–45). Interestingly, as quoted by Proudfoot et al. (46), two chemokine homologs with antagonistic activity were reported. The first one, MC148, is encoded by molluscum contagiosum

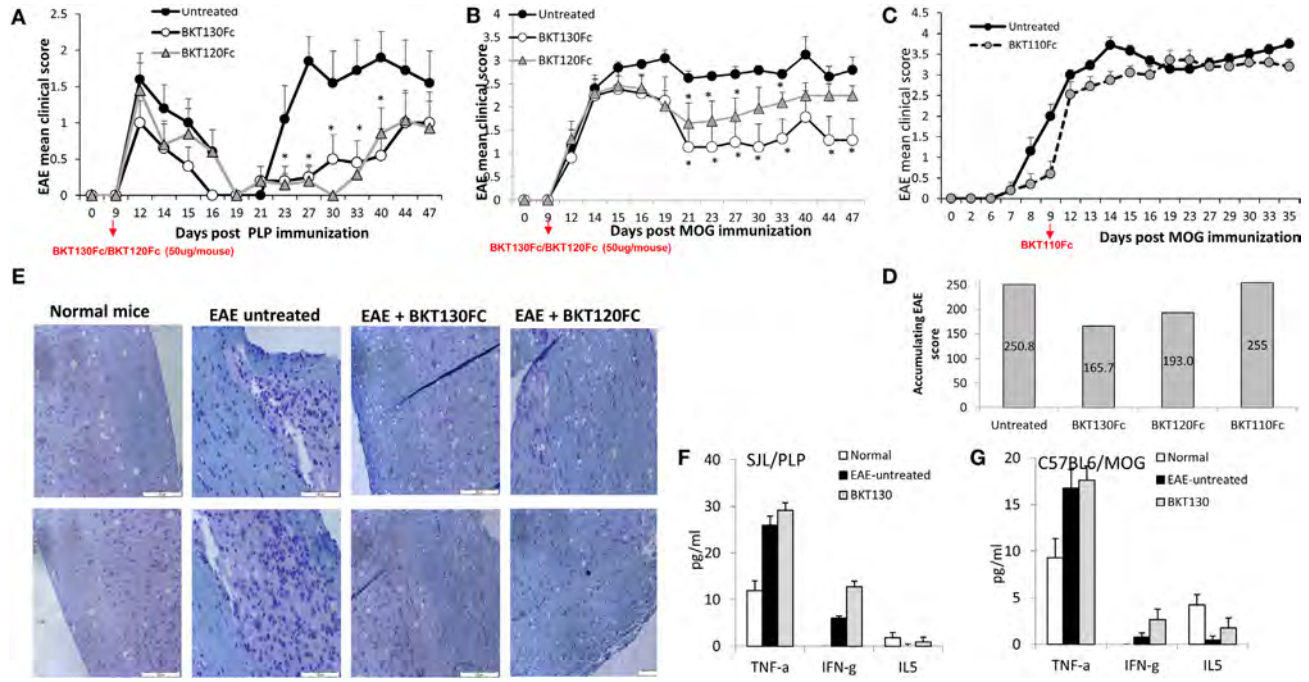

FIGURE 7 | BKT130Fc and BKT120Fc reduced the severity of experimental autoimmune encephalomyelitis (EAE) by inhibiting the infiltration of immune cells into the central nervous system (CNS). **(A)** Female SJL mice ($n = 12$) were immunized with the proteolipid protein (PLP) peptide to induce relapsing-remitting EAE. BKT130Fc or BKT120Fc were intravenously administered once (50 μg/mouse) on day 9 post-disease induction. **(B)** Female C57BL/6 mice ($n = 12$) were immunized with a myelin oligodendrocyte glycoprotein (MOG) peptide to induce chronic EAE. BKT130Fc or BKT120Fc were intravenously administered once (50 μg/mouse) on day 9 post-disease induction. The data are presented as the EAE mean clinical score measured for 47 days post-immunization. **(C)** Female C57BL/6 mice ($n = 8$) were immunized with a MOG peptide to induce chronic EAE. BKT110Fc was intravenously administered once (50 μg/mouse) on day 9 post-disease induction. **(D)** Accumulating score of MOG induced EAE after treating with BKT130Fc, BKT120Fc, or BKT110Fc. **(E)** Histology analysis of the spinal cords from SJL mice shows the infiltration of immune cells into the CNS following hematoxylin and eosin (H&E) staining and the area of demyelination marked with luxol fast blue (light blue staining = demyelination area). **(F–G)** Cytokine levels in the sera of mice on day 30 post-immunization as measured by the Mouse Th1/Th2 Cytokine Kit Array in **(F)** SJL mice immunized with PLP and **(G)** C57BL/6 mice immunized with MOG. The results, analyzed using Student's *t*-tests (*$p \leq 0.05$), are expressed as the mean ± SE. All the EAE experiments were performed at least three times.

virus 1, a poxvirus that infects humans and causes skin lesions lacking inflammatory cell infiltrates. MC148 does not induce by itself the migration of mononuclear cells (47, 48). However, it does inhibit the migration of immune cells mediated by CCL1, CCL2, CCL3, CCL5, CCL7, CXCL8, and CXCL12 (48, 49). The second viral chemokine, the viral macrophage inflammatory protein II (vMIP-II), also binds several chemokine receptors without inducing cell migration. vMIP-II compete with several chemokine receptors, including CCR1, CCR2, CCR5, CCR10, CXCR4, CX3CR1, and XCR1 (46).

Furthermore, in Heidarieh paper (10) it was mentioned that herpesviruses have been found to encode CKBPs to modulate the expression and function of chemokines (50–52). CKBPs were found to be expressed by non-viral pathogens. For example, a CKBP secreted by *Schistosoma mansoni* (53) interacts with chemokines such as CCL2, CCL3, CCL5, CXCL8, and CX3CL1, and inhibit their function (53). Another example is Evasins, which is expressed by ticks (54) and inhibit chemokine-induced inflammation (12). The main function of CKBPs is to inhibit chemokine activity and subsequently inhibit inflammation.

We hypothesize that lessons learned from our own immune system and from the anti-chemokine strategies that have evolved in pathogens will help us design potent and selective molecules with novel modalities that may have better success in the clinic in the future. We chose to screen for promiscuous CBPs using combinatorial libraries of random dodecapeptides (5×10^{12} for the linear library and 2×10^{13} for the circular library, of electroporated sequences) fused to a minor coat protein (pIII) of the M13 phage. We performed the screen on immobilized CCL11, CXCL9, CXCL8, CXCL12, and CCL2, and successfully identified two CBPs, BKT120 and BKT130, that could bind and inhibit the function of the chemokines CCL2 and CCL5. To improve the affinity and bioactivity of the peptides, we prepared BKT120 and BKT130 as peptide-Fc fusions protein (peptibodies). BKT130Fc peptibody bind at high affinity to inflammatory chemokines CXCL11, CXCL10, and CCL5 with K_D of 8.3 E−0.8, 3.8 E−0.8, and 1.8 E−0.8, respectively. BKT120Fc peptibody bind at high affinity to inflammatory chemokines CXCL10, CCL2, and CXCL9 was with K_D of 6.3 E−0.9, 4.6 E−0.8, and 1.8 E−0.8, respectively. Both inhibited cell adhesion in response to the inflammatory chemokines CCL2, CCL5, CXCL9, and CXCL11. BKT130Fc, also inhibited CXCL10 function, but both did not inhibit the function of the homeostatic chemokine CXCL12, the eosinophils chemokine CCL11 or the neutrophil chemokine

CXCL8. Cell migration inhibition in response to the inflammatory chemokines CCL2, CCL5, CXCL10, and CXCL11 was also demonstrated and was significantly better when BKT130Fc was used. *In vivo*, BKT120Fc and BKT130Fc had a prolonged PK in mice and were inhibitory to immune-mediated, chemokine-dependent DTH. Furthermore, we also demonstrated that both could inhibit immune cell migration, inflammation, and disease progression in RA and MS mouse models. Our work has demonstrated for the first time that CBPs can be identified and developed into potential therapeutic agents in diseases that are dependent on chemokines for their progression.

ETHICS STATEMENT

All studies were carried out in accordance with the recommendations of Hebrew University Animal Facility (Jerusalem, Israel). The protocols were approved by the Animal Care and Use Committee of Hebrew University.

AUTHOR CONTRIBUTIONS

MA—designed the study, performed experiments, data analysis, data interpretation, and wrote the manuscript. HW—performed experiments. DVO—performed experiments, data analysis. VG—performed experiments, data analysis. ZO—performed experiments, data analysis. AK—data analysis, data interpretation. LW—performed experiments. EG—data interpretation. AP—designed the study, data analysis, data interpretation, and wrote the manuscript. OE—designed the study, data interpretation.

SUPPLEMENTARY MATERIAL

The Supplementary Material for this article can be found online at http://www.frontiersin.org/article/10.3389/fimmu.2017.01432/full#supplementary-material.

FIGURE S1 | Effect of the peptibody BKT110Fc on the chemokine-induced immune cell-dependent adhesion to VCAM-1. Adhesion was measured using the laminar flow assay. The number of adherent cells resisting detachment by elevated shear forces (dyn/cm^2) is expressed as the percentage of originally settled cells. The effects of BKT110Fc on the **(A)** CCL2-, **(B)** CCL11-, **(C)** CXCL8-, **(D)** CXCL10-induced immune cell-dependent adhesion to VCAM-1 were measured. All the adhesion experiments were performed at least three times on multiple test fields.

FIGURE S2 | Production of antibodies against BKT130Fc. C57BL/6 mice were i.v. injected with 50 μg of BKT130Fc once or twice a week for total of four injections. One week after the last injection serum was extract and ELISA was performed. Sera were diluted at 1:5, 1:50, and 1:500 and loaded on plates that were pre-coated with **(A)** BKT130Fc, **(B)** BKT120Fc, or **(C)** BSA. The data are presented as the optical density (O.D.) obtained at wavelength of 450 nm.

REFERENCES

1. Baggiolini M, Dahinden CA. CC chemokines in allergic inflammation. *Immunol Today* (1994) 15:127–33. doi:10.1016/0167-5699(94)90156-2
2. Vaddi K, Newton RC. Regulation of monocyte integrin expression by beta-family chemokines. *J Immunol* (1994) 153:4721–32.
3. Griffith JW, Sokol CL, Luster AD. Chemokines and chemokine receptors: positioning cells for host defense and immunity. *Annu Rev Immunol* (2014) 32:659–702. doi:10.1146/annurev-immunol-032713-120145
4. Horuk R. Promiscuous drugs as therapeutics for chemokine receptors. *Expert Rev Mol Med* (2009) 11:e1. doi:10.1017/S1462399409000921
5. Horuk R. Chemokine receptor antagonists: overcoming developmental hurdles. *Nat Rev Drug Discov* (2009) 8:23–33. doi:10.1038/nrd2734
6. Firestein GS. Evolving concepts of rheumatoid arthritis. *Nature* (2003) 423:356–61. doi:10.1038/nature01661
7. Cardona AE, Li M, Liu L, Savarin C, Ransohoff RM. Chemokines in and out of the central nervous system: much more than chemotaxis and inflammation. *J Leukoc Biol* (2008) 84:587–94. doi:10.1189/jlb.1107763
8. Szczucinski A, Losy J. Chemokines and chemokine receptors in multiple sclerosis. Potential targets for new therapies. *Acta Neurol Scand* (2007) 115:137–46. doi:10.1111/j.1600-0404.2006.00749.x
9. Johnson Z, Schwarz M, Power CA, Wells TN, Proudfoot AE. Multi-faceted strategies to combat disease by interference with the chemokine system. *Trends Immunol* (2005) 26:268–74. doi:10.1016/j.it.2005.03.001
10. Heidarieh H, Hernaez B, Alcami A. Immune modulation by virus-encoded secreted chemokine binding proteins. *Virus Res* (2015) 209:67–75. doi:10.1016/j.virusres.2015.02.028
11. Bonecchi R, Graham GJ. Atypical chemokine receptors and their roles in the resolution of the inflammatory response. *Front Immunol* (2016) 7:224. doi:10.3389/fimmu.2016.00224
12. Bonvin P, Power CA, Proudfoot AE. Evasins: therapeutic potential of a new family of chemokine-binding proteins from ticks. *Front Immunol* (2016) 7:208. doi:10.3389/fimmu.2016.00208
13. Arnold JN, Wormald MR, Sim RB, Rudd PM, Dwek RA. The impact of glycosylation on the biological function and structure of human immunoglobulins. *Annu Rev Immunol* (2007) 25:21–50. doi:10.1146/annurev.immunol.25.022106.141702
14. Bolt S, Routledge E, Lloyd I, Chatenoud L, Pope H, Gorman SD, et al. The generation of a humanized, non-mitogenic CD3 monoclonal antibody which retains in vitro immunosuppressive properties. *Eur J Immunol* (1993) 23:403–11. doi:10.1002/eji.1830230216
15. Chao DT, Ma X, Li O, Park H, Law D. Functional characterization of N297A, a murine surrogate for low-Fc binding anti-human CD3 antibodies. *Immunol Invest* (2009) 38:76–92. doi:10.1080/08820130802608238
16. Hogarth PM, Pietersz GA. Fc receptor-targeted therapies for the treatment of inflammation, cancer and beyond. *Nat Rev Drug Discov* (2012) 11:311–31. doi:10.1038/nrd2909
17. Coelho FM, Pinho V, Amaral FA, Sachs D, Costa VV, Rodrigues DH, et al. The chemokine receptors CXCR1/CXCR2 modulate antigen-induced arthritis by regulating adhesion of neutrophils to the synovial microvasculature. *Arthritis Rheum* (2008) 58:2329–37. doi:10.1002/art.23622
18. Healy AM, Izmailova E, Fitzgerald M, Walker R, Hattersley M, Silva M, et al. PKC-theta-deficient mice are protected from Th1-dependent antigen-induced arthritis. *J Immunol* (2006) 177:1886–93. doi:10.4049/jimmunol.177.3.1886
19. Williams AS, Richards PJ, Thomas E, Carty S, Nowell MA, Goodfellow RM, et al. Interferon-gamma protects against the development of structural damage in experimental arthritis by regulating polymorphonuclear neutrophil influx into diseased joints. *Arthritis Rheum* (2007) 56:2244–54. doi:10.1002/art.22732
20. Barsante MM, Cunha TM, Allegretti M, Cattani F, Policani F, Bizzarri C, et al. Blockade of the chemokine receptor CXCR2 ameliorates adjuvant-induced arthritis in rats. *Br J Pharmacol* (2008) 153:992–1002. doi:10.1038/sj.bjp.0707462
21. Souza DG, Soares AC, Pinho V, Torloni H, Reis LF, Teixeira MM, et al. Increased mortality and inflammation in tumor necrosis factor-stimulated gene-14 transgenic mice after ischemia and reperfusion injury. *Am J Pathol* (2002) 160:1755–65. doi:10.1016/S0002-9440(10)61122-4
22. Kobayashi K, Kaneda K, Kasama T. Immunopathogenesis of delayed-type hypersensitivity. *Microsc Res Tech* (2001) 53:241–5. doi:10.1002/jemt.1090
23. Molesworth-Kenyon S, Mates A, Yin R, Strieter R, Oakes J, Lausch R. CXCR3, IP-10, and Mig are required for CD4+ T cell recruitment during the DTH response to HSV-1 yet are independent of the mechanism for viral clearance. *Virology* (2005) 333:1–9. doi:10.1016/j.virol.2005.01.005

24. Tumpey TM, Fenton R, Molesworth-Kenyon S, Oakes JE, Lausch RN. Role for macrophage inflammatory protein 2 (MIP-2), MIP-1alpha, and interleukin-1alpha in the delayed-type hypersensitivity response to viral antigen. *J Virol* (2002) 76:8050–7. doi:10.1128/JVI.76.16.8050-8057.2002
25. Aharoni R, Vainshtein A, Stock A, Eilam R, From R, Shinder V, et al. Distinct pathological patterns in relapsing-remitting and chronic models of experimental autoimmune enchephalomyelitis and the neuroprotective effect of glatiramer acetate. *J Autoimmun* (2011) 37:228–41. doi:10.1016/j.jaut.2011.06.003
26. Schall TJ, Proudfoot AE. Overcoming hurdles in developing successful drugs targeting chemokine receptors. *Nat Rev Immunol* (2011) 11:355–63. doi:10.1038/nri2972
27. Graham GJ, McKimmie CS. Chemokine scavenging by D6: a movable feast? *Trends Immunol* (2006) 27:381–6. doi:10.1016/j.it.2006.06.006
28. Novitzky-Basso I, Rot A. Duffy antigen receptor for chemokines and its involvement in patterning and control of inflammatory chemokines. *Front Immunol* (2012) 3:266. doi:10.3389/fimmu.2012.00266
29. Rot A. Contribution of Duffy antigen to chemokine function. *Cytokine Growth Factor Rev* (2005) 16:687–94. doi:10.1016/j.cytogfr.2005.05.011
30. Hansell CA, Hurson CE, Nibbs RJ. DARC and D6: silent partners in chemokine regulation? *Immunol Cell Biol* (2010) 89:197–206. doi:10.1038/icb.2010.147
31. Lee KM, Nibbs RJ, Graham GJ. D6: the 'crowd controller' at the immune gateway. *Trends Immunol* (2012) 34:7–12. doi:10.1016/j.it.2012.08.001
32. Weber M, Blair E, Simpson CV, O'Hara M, Blackburn PE, Rot A, et al. The chemokine receptor D6 constitutively traffics to and from the cell surface to internalize and degrade chemokines. *Mol Biol Cell* (2004) 15:2492–508. doi:10.1091/mbc.E03-09-0634
33. Fra AM, Locati M, Otero K, Sironi M, Signorelli P, Massardi ML, et al. Cutting edge: scavenging of inflammatory CC chemokines by the promiscuous putatively silent chemokine receptor D6. *J Immunol* (2003) 170:2279–82. doi:10.4049/jimmunol.170.5.2279
34. Borroni EM, Cancellieri C, Vacchini A, Benureau Y, Lagane B, Bachelerie F, et al. beta-arrestin-dependent activation of the cofilin pathway is required for the scavenging activity of the atypical chemokine receptor D6. *Sci Signal* (2013) 6:ra30, S31–3. doi:10.1126/scisignal.2003627
35. Bonecchi R, Borroni EM, Anselmo A, Doni A, Savino B, Mirolo M, et al. Regulation of D6 chemokine scavenging activity by ligand- and Rab11-dependent surface up-regulation. *Blood* (2008) 112:493–503. doi:10.1182/blood-2007-08-108316
36. McKimmie CS, Singh MD, Hewit K, Lopez-Franco O, Le Brocq M, Rose-John S, et al. An analysis of the function and expression of D6 on lymphatic endothelial cells. *Blood* (2013) 121:3768–77. doi:10.1182/blood-2012-04-425314
37. Lee KM, Danuser R, Stein JV, Graham D, Nibbs RJ, Graham GJ. The chemokine receptors ACKR2 and CCR2 reciprocally regulate lymphatic vessel density. *EMBO J* (2014) 33:2564–80. doi:10.15252/embj.201488887
38. Graham GJ, Locati M. Regulation of the immune and inflammatory responses by the 'atypical' chemokine receptor D6. *J Pathol* (2012) 229:168–75. doi:10.1002/path.4123
39. Comerford I, Milasta S, Morrow V, Milligan G, Nibbs R. The chemokine receptor CCX-CKR mediates effective scavenging of CCL19 in vitro. *Eur J Immunol* (2006) 36:1904–16. doi:10.1002/eji.200535716
40. Ulvmar MH, Werth K, Braun A, Kelay P, Hub E, Eller K, et al. The atypical chemokine receptor CCRL1 shapes functional CCL21 gradients in lymph nodes. *Nat Immunol* (2014) 15:623–30. doi:10.1038/ni.2889
41. Comerford I, Nibbs RJ, Litchfield W, Bunting M, Harata-Lee Y, Haylock-Jacobs S, et al. The atypical chemokine receptor CCX-CKR scavenges homeostatic chemokines in circulation and tissues and suppresses Th17 responses. *Blood* (2010) 116:4130–40. doi:10.1182/blood-2010-01-264390
42. Vischer HF, Vink C, Smit MJ. A viral conspiracy: hijacking the chemokine system through virally encoded pirated chemokine receptors. *Curr Top Microbiol Immunol* (2006) 303:121–54.
43. Rosenkilde MM, Waldhoer M, Luttichau HR, Schwartz TW. Virally encoded 7TM receptors. *Oncogene* (2001) 20:1582–93. doi:10.1038/sj.onc.1204191
44. Michelson S. Consequences of human cytomegalovirus mimicry. *Hum Immunol* (2004) 65:465–75. doi:10.1016/j.humimm.2004.02.002
45. Smit MJ, Vink C, Verzijl D, Casarosa P, Bruggeman CA, Leurs R. Virally encoded G protein-coupled receptors: targets for potentially innovative anti-viral drug development. *Curr Drug Targets* (2003) 4:431–41. doi:10.2174/1389450033491000
46. Proudfoot AE, Bonvin P, Power CA. Targeting chemokines: pathogens can, why can't we? *Cytokine* (2015) 74:259–67. doi:10.1016/j.cyto.2015.02.011
47. Krathwohl MD, Hromas R, Brown DR, Broxmeyer HE, Fife KH. Functional characterization of the C—C chemokine-like molecules encoded by molluscum contagiosum virus types 1 and 2. *Proc Natl Acad Sci U S A* (1997) 94:9875–80. doi:10.1073/pnas.94.18.9875
48. Damon I, Murphy PM, Moss B. Broad spectrum chemokine antagonistic activity of a human poxvirus chemokine homolog. *Proc Natl Acad Sci U S A* (1998) 95:6403–7. doi:10.1073/pnas.95.11.6403
49. Jin Q, Altenburg JD, Hossain MM, Alkhatib G. Role for the conserved N-terminal cysteines in the anti-chemokine activities by the chemokine-like protein MC148R1 encoded by Molluscum contagiosum virus. *Virology* (2011) 417:449–56. doi:10.1016/j.virol.2011.07.001
50. Alcami A. Viral mimicry of cytokines, chemokines and their receptors. *Nat Rev Immunol* (2003) 3:36–50. doi:10.1038/nri980
51. Rosenkilde MM. Virus-encoded chemokine receptors – putative novel antiviral drug targets. *Neuropharmacology* (2005) 48:1–13. doi:10.1016/j.neuropharm.2004.09.017
52. Seet BT, McCaughan CA, Handel TM, Mercer A, Brunetti C, McFadden G, et al. Analysis of an orf virus chemokine-binding protein: shifting ligand specificities among a family of poxvirus viroceptors. *Proc Natl Acad Sci U S A* (2003) 100:15137–42. doi:10.1073/pnas.2336648100
53. Smith P, Fallon RE, Mangan NE, Walsh CM, Saraiva M, Sayers JR, et al. *Schistosoma mansoni* secretes a chemokine binding protein with anti-inflammatory activity. *J Exp Med* (2005) 202:1319–25. doi:10.1084/jem.20050955
54. Deruaz M, Frauenschuh A, Alessandri AL, Dias JM, Coelho FM, Russo RC, et al. Ticks produce highly selective chemokine binding proteins with antiinflammatory activity. *J Exp Med* (2008) 205:2019–31. doi:10.1084/jem.20072689

Conflict of Interest Statement: By submitting this manuscript, the corresponding author accepts the responsibility that all authors have agreed to be so listed and have observed and approved the manuscript, its content, and its submission to Leukemia. This manuscript has not been published nor is it under consideration for publication elsewhere, including Internet publication. MA and OE are employees and shareholders of Biokine Therapeutics Ltd.; AP serves as consultant for Biokine Therapeutics and is also a shareholder. All other authors have no conflicts of interest to declare.

frontiers in Immunology

ORIGINAL RESEARCH
published: 21 November 2017
doi: 10.3389/fimmu.2017.01595

Antibodies against MYC-Associated Zinc Finger Protein: An Independent Marker in Acute Coronary Syndrome?

Diana Ernst[1], Christian Widera[2], Niklas T. Baerlecken[1], Wolfgang Schlumberger[3], Cornelia Daehnrich[3], Reinhold E. Schmidt[1], Katja Gabrysch[4], Lars Wallentin[5] and Torsten Witte[1]*

[1] Clinic of Rheumatology and Immunology, Hannover Medical School, Hannover, Germany, [2] Department of Cardiology, Heart Center Oldenburg, European Medical School Oldenburg-Groningen, Carl von Ossietzky University Oldenburg, Oldenburg, Germany, [3] Euroimmun, Medizinische Labordiagnostika AG, Lübeck, Germany, [4] Uppsala Clinical Research Center, Uppsala University, Uppsala, Sweden, [5] Department of Medical Sciences, Cardiology, Uppsala Clinical Research Center, Uppsala University, Uppsala, Sweden

OPEN ACCESS

Edited by:
Ralf J. Ludwig, University of Lübeck, Germany

Reviewed by:
Bruce Milne Hall, University of New South Wales, Australia
Unni Samavedam, University of Cincinnati, United States

***Correspondence:**
Diana Ernst
ernst.diana@mh-hannover.de

Specialty section:
This article was submitted to Immunological Tolerance and Regulation, a section of the journal Frontiers in Immunology

Received: *13 August 2017*
Accepted: *06 November 2017*
Published: *21 November 2017*

Citation:
Ernst D, Widera C, Baerlecken NT, Schlumberger W, Daehnrich C, Schmidt RE, Gabrysch K, Wallentin L and Witte T (2017) Antibodies against MYC-Associated Zinc Finger Protein: An Independent Marker in Acute Coronary Syndrome? Front. Immunol. 8:1595. doi: 10.3389/fimmu.2017.01595

Introduction: Atherosclerosis is considered the pathophysiology underlying cardiovascular (CVD), cerebrovascular, and peripheral vascular diseases. Evidence supporting an autoimmune component is emerging, with imaging studies correlating MYC-associated zinc finger protein antibody (MAZ-Ab) optical density (OD) with plaque activity. This study compares MAZ-Ab OD on ELISA testing among patients presenting with acute coronary syndromes (ACSs) to healthy controls and investigates the association of MAZ-Ab to traditional CVD risk factors.

Methods: Patients admitted with ACSs between August 2007 and July 2011 were included. Serum samples taken at presentation were retrospectively tested for MAZ-Ab and compared with serum from healthy volunteers with no CVD risk factors. Large-scale assessment of post-ACS prognostic relevance was performed using the established PLATO cohort.

Results: In total 174 ACS patients and 96 controls were included. Among ACS patients, median MAZ-Ab OD was higher compared with controls (0.46 vs. 0.27; $p = 0.001$). Although the majority of ACS patients (116/174; 67%) had suffered from a ST-elevation myocardial infarction, no significant differences in MAZ-Ab titers were evident between ACS subtypes ($p = 0.682$). No associations between MAZ-Ab OD and conventional CVD risk factors were identified. Large-scale testing revealed no prognostic stratification regarding reinfarction (OR 1.04 [95% CI: 0.94–1.16]; $p = 0.436$).

Conclusion: MAZ-Ab OD was higher or all ACS phenotypes compared with controls. Given current understanding of MAZ-Ab function, these findings support an autoimmune component to CVD independent of conventional risk factors and indeed the extent of end-organ damage.

Keywords: antibodies, MYC-associated zinc finger protein, acute coronary syndrome, cardiac risk factor, atherosclerosis

INTRODUCTION

Atherosclerosis is the pathophysiological process behind most cardiovascular, cerebrovascular, and peripheral vascular diseases. Consequently, it is associated with considerable morbidity and mortality (1). Numerous factors such as dyslipidemia, smoking, arterial hypertension, diabetes, and abdominal obesity appear to promote atherosclerotic plaque development within arterial vessel walls (2). Recently, the influence of multiple inflammatory and autoimmune promoters in atherosclerosis has been evaluated (3). While exact mechanisms remain unknown, autoantibodies such as anti-phospholipid antibodies, anti-oxidized low density lipid (oxLDL) antibodies, anti-phosphorylcholine antibodies, anti-apoA-1 IgG antibodies, and anti-heat shock protein antibodies have all demonstrated associations with atherosclerosis (3–5).

MYC-Associated Zinc Finger Protein (MAZ)

MAZ is a synonym for serum amyloid A binding protein 1 (SAF-1), the function of which appears variable and incompletely understood. Activation and induction of MAZ by minimally modified LDL and lipopolysaccharides have been shown, leading to expression of serum amyloid A (SAA), a known inflammation-responsive protein within macrophages (6, 7). SAA has been long considered influential in atherosclerosis, with SAA mRNA having been identified in the endothelial and macrophage foam cells of atherosclerotic lesions of coronary and carotid arteries. Subsequently, MAZ has proven to be a transcription factor in active macrophages within atherosclerotic plaques triggering the formation of matrix metalloproteinases (MMPs) (8). Active macrophages are the hallmark of vulnerable plaques, with a high tendency to rupture. Originally identified in patients with coexisting CVD and autoimmune disease, MAZ-Ab has recently been evaluated in atherosclerosis using ^{18}F-Fluorodeoxyglucose (^{18}F-FDG) positron-emission and computer tomography (9). ^{18}F-FDG uptake in vessel walls is known to correlate with macrophage activity in atherosclerotic plaques (10), with calculated plaque burden correlating with serum MAZ-Ab optical density (OD) (9).

Data regarding the further MAZ function have been emerging, with evidence supporting a role in certain cancers as regulator of oncogene transcription and angiogenesis (11–14). Furthermore, MAZ is known to regulate various inflammatory response genes (15), and associations to Alzheimer's disease have been suggested in transcription factor analysis of 1,372-probe gene expression signatures (16).

Study Aim

The aim of this study was to examine the clinical relevance of MAZ-Ab in patients with a confirmed cardiovascular event, compared with healthy controls. Furthermore, the relationship of MAZ-Ab to traditional cardiovascular risk factors and its prognostic value were evaluated.

MATERIALS AND METHODS

Acute Coronary Syndrome (ACS) Cohort

To assess the risk of premature ischemic heart disease, unselected adult patients below the age of 65 years admitted to Hannover Medical School between August 2007 and July 2011, and subsequently diagnosed with ACS were included. All patients provided both verbal and written informed consent before participation in the study, with the ethics committee of Hanover Medical School approving the study (Ethics Number: 2614). All patients completed a questionnaire assessing cardiac risk profile and provided a serum sample, which was subsequently used for MAZ-Ab testing. The questionnaire assessed age, gender, past-history of hypertension, hypercholesterolemia, statin treatment, diabetes, tobacco exposure, as well as previous vascular events including myocardial infarction and stroke. All patients underwent routine ACS diagnostics including laboratory investigations, electrocardiogram (ECG), and coronary angiography. Laboratory tests included N-terminal propeptide brain natriuretic peptide (NT-proBNP), cardiac TroponinT (cTnT), growth-differentiation factor-15 (GDF-15), total cholesterol, and low-density lipoproteins (LDL). Serum samples were stored at −70°C.

Acute coronary syndrome patients were divided into three groups: patients with ST-elevation myocardial infarction (STEMI), with non-ST elevation myocardial infarction (NSTEMI) and with unstable angina pectoris (AP).

Patients with AP required at least 1 angiographically documented stenosis ≥70% in a major coronary artery. Based on ECG changes and cTnT, using a decision threshold of 0.03 μg/L, STEMI or NSTEMI was diagnosed.

Control Group

Serum samples of an apparently healthy control group, which has previously been described in detail (17), underwent MAZ-Ab testing. Control patients received cardiac magnetic resonance imaging with dobutamine or adenosine stress, 12-lead ECGs, and physical examination without any pathological findings. In addition, all patients exhibited normal serum creatinine, aspartate aminotransferase, alanine aminotransferase, thyroid-stimulating hormone, hemoglobin concentrations, leukocyte, platelet counts, oral glucose tolerance test, and N-terminal pro-B-type natriuretic peptide (NT-proBNP) levels. None were in receipt of current medications and had no conventional cardiovascular risk factors. All were aged ≥18 years at inclusion and previously provided written informed consent.

MAZ-Ab Testing

MAZ-Ab has been detected via protein array technique in patients with CVD as described in an earlier publication (9). A specially developed anti-MAZ-antibody ELISA kit (EUROIMMUN AG, Lübeck, Germany) based on our previously described ELISA protocol was used to test serum for MAZ-Ab (9).

MAZ-Ab optical densities were compared between ACS patients and controls, as well as within the ACS groups. Furthermore, MAZ-Ab values were correlated to traditional risk factors. To rule out an influence on MAZ-Ab by statins, LDL and cholesterol values of all patients with and without statins were analyzed additionally.

Testing Prognostic Value of MAZ-Antibody after ACS

A well-defined group of 197 ACS patients, experiencing myocardial infarction, with up to 12 months subsequent follow-up

TABLE 1 | Summary of the relevant laboratory parameters at the time of hospital admission for an acute coronary syndrome.

	AP ($n = 14$)	NSTEMI ($n = 44$)	STEMI ($n = 116$)	p
MAZ-Ab	0.55 [0.22–1.14]	0.52 [0.27–1.07]	0.37 [0.18–1.05]	0.682
TroponinT	19.1 [16.7–34.2]	92.4 [26.5–520.6]	163.9 [37.1–711.1]	0.002
ProBNP	203 [128–508]	267 [80–934]	123 [56–588]	0.156
GDF-15	1,450 [1,077–2,367]	1,399 [1,141–1,749]	1,503 [1,139–2,180]	0.505
CRP	2.7 [0.7–7.2]	2.9 [1.3–7.4]	2.3 [1.0–7.9]	0.655
Creatinine (μmol/L)	79 [70–110]	76 [69–89]	78 [68–90]	0.572
Cholesterol	220 [174–275]	197 [176–213]	182 [166–220]	0.210
LDL	150 [101–196]	139 [117–155]	131 [101–149]	0.604

Values are grouped according to subsequently confirmed diagnosis. Other than an expected difference in Troponin, none of the other blood markers was associated with a particular diagnosis. In addition, none of these markers exhibited a quantitative correlation to MAZ-Ab titer.
MAZ-Ab, MAZ-antibody; AP, unstable angina pectoris; NSTEMI, non-ST elevation myocardial infarction; STEMI, ST-elevation myocardial infarction; GDF-15, growth-differentiation factor-15; LDL, low-density lipoproteins.

were identified within the Platelet Inhibition and Patient Outcomes (PLATO) database (http://www.ClinicalTrials.gov NCT00391872) (18). An equal number ($n = 199$) of patients surviving 12 months follow-up without a subsequent spontaneous myocardial infarction were randomly drawn from the same cohort. Being matched for initial STEMI/NSTEMI, age, gender, and nationality the latter acted as controls. Serum taken at the time of initial admission was tested for MAZ-Ab in both groups.

Statistical Analysis

Continuous variables were assumed non-parametric and tested using either the Mann–Whitney U test or Kruskal–Wallis test. Categorical variables were assessed using chi-square test or Fisher's exact test. Correction for age and gender between groups was performed using Propensity Score matching, employing logistic regression with nearest neighbor matching and a 0.2 caliper. Prognostic relevance regarding reinfarction was calculated in conditional logistic regression. All p-values are two-tailed, with 95% cutoff being the declared level of significance. Statistical analysis was performed using IBM SPSS Statistics for Macintosh, Version 23 (IBM Corp. Armonk, USA), Prism 7 (GraphPad Software, La Jolla, CA, USA), and R Version 3.2.3 (R Foundation for Statistical Computing, Vienna, Austria).

RESULTS

In total, serum from 270 individuals was tested for MAZ-antibody. Of these, 174 (64%) were performed on patients at the time of admission for a cardiac event (ACS group). The remaining 96 (36%) were randomly selected healthy volunteers (**Table 1**). The median MAZ-Ab OD was significantly higher among ACS patients compared with controls (0.46 vs. 0.27; $p = 0.001$).

Influence of Age and Gender on MAZ-Antibody

Taking the entire cohort, the median age of the controls was significantly lower than the ACS group (41 vs. 53 years; $p < 0.001$). Similarly, a far greater proportion of the ACS group was male (87 vs. 47%; $p = 0.001$). To eliminate these potential confounders, a logistic regression analysis was performed using propensity score matching for age and gender between groups. In total, 206/270 patients (76%) were included in the sub-analysis, 168 from the ACS group and 38 control patients. The median ages were 49 [45–57] years among the controls and 53 [47–60] years in the ACS group ($p = 0.46$). While improved, a significant disparity in gender composition remained between groups, with a significantly greater male domination in the ACS group (83 vs. 68%; $p = 0.003$). Having eliminated age as a confounder, a significant difference in MAZ-Ab between groups remained with significantly higher ODs in the ACS group (0.47 vs. 0.24; $p = 0.001$ **Figure 1**).

MAZ-Antibody Independent of ACS Phenotype

Within the ACS group, 116/174 patients (67%) were diagnosed with a STEMI, 44 patients (25%) with NSTEMI, and 14 (8%) with AP. Within the different ACS phenotypes, no differences in MAZ-Ab OD were observed between groups ($p = 0.682$), all of which proved higher than that observed among controls (**Figure 2**), suggesting that MAZ-Ab was independent of the extent of myocardial damage occurring. Supplementing this further, a comparison of all the relevant blood markers (**Table 1**) revealed no significant correlations between these and MAZ-Ab OD.

MAZ-Antibody and Traditional Cardiovascular Risk Factors

Comprehensive data relating to the incidence of hypertension, diabetes mellitus, hyperlipidemia including treatment with statins as well as smoking habits and family history of CVD were available for all patients. No known risk factors were present among the entire control group. In the ACS group, the most prevalent risk factors were tobacco consumption (84%), hypertension (56%) and hyperlipidemia (49%). For all CVD risk factors assessed, MAZ-Ab optical densities were lower among control patients than in ACS patients without a given risk factor (**Figures 3A–F**). With the exceptions of evident hyperlipidemia at original admission and preexisting HMG-CoA reductase inhibitor use, no differences in MAZ-Ab OD were evident within the ACS group. Taken collectively, these findings would strongly support that MAZ-Ab is independent of hypertension, diabetes, dyslipidemia, smoking, and family history in terms of generating cardiovascular risk.

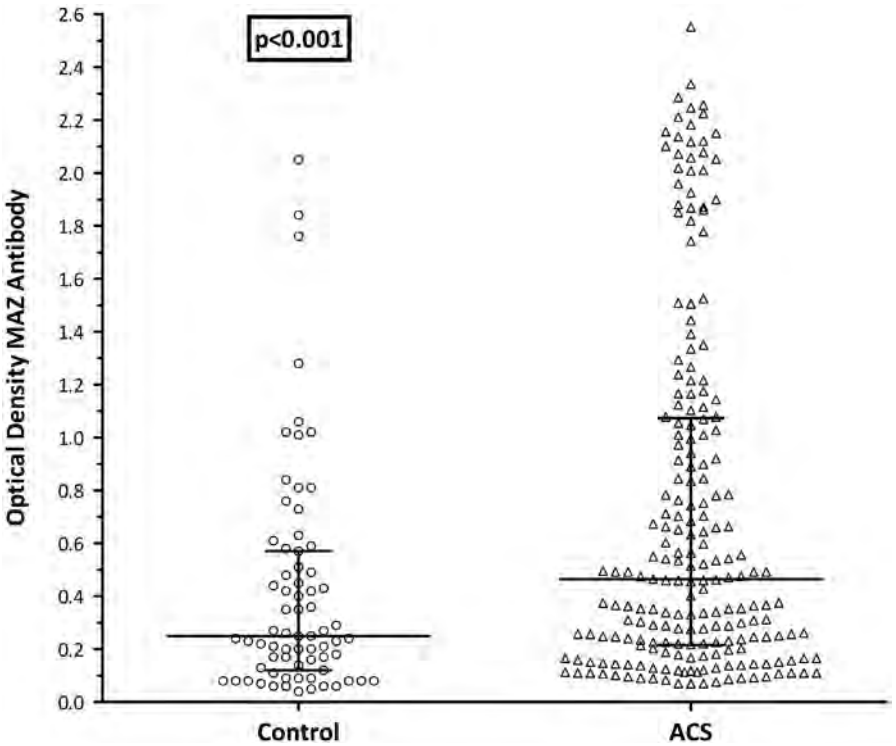

FIGURE 1 | MAZ-antibody ± ACS: propensity score matched (age and gender), ACS group had significantly higher MAZ-Ab titers than the healthy control group. Control, control group; ACS, acute coronary syndrome patients; MAZ-Ab, MAZ-antibody.

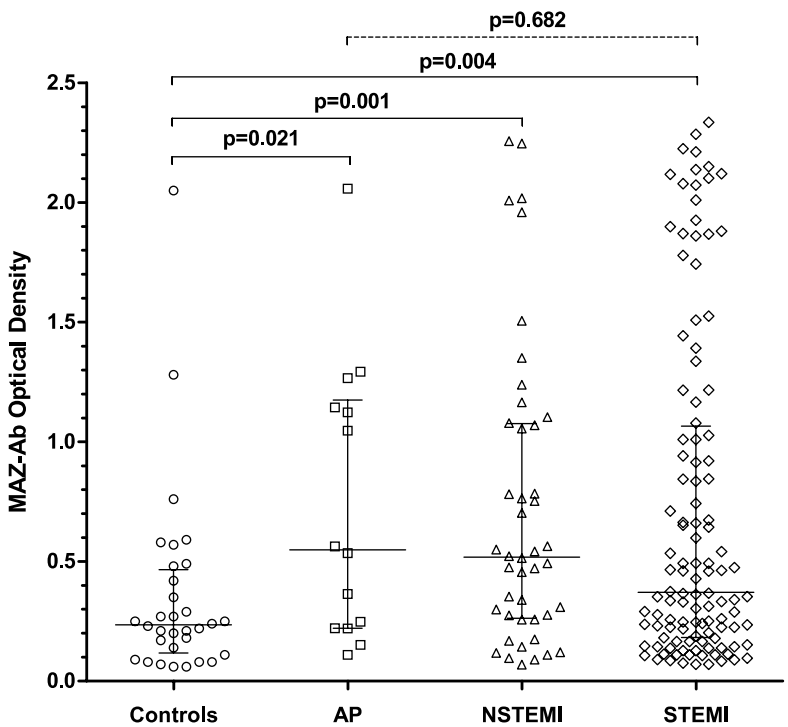

FIGURE 2 | Comparing MAZ-optical density (OD) in the control group with the various acute coronary syndrome (ACS) phenotypes. MAZ-Ab OD was significantly lower in the control group compared with each ACS subgroup. Between ACS phenotypes, no significant differences in MAZ-Ab OD were observed, suggesting that MAZ-Ab was independent of the extent of myocardial damage occurring. Key: MAZ-Ab, MYC-associated zinc finger protein antibody; AP, unstable angina pectoris; NSTEMI, non-ST elevation myocardial infarction; STEMI, ST-elevation myocardial infarction.

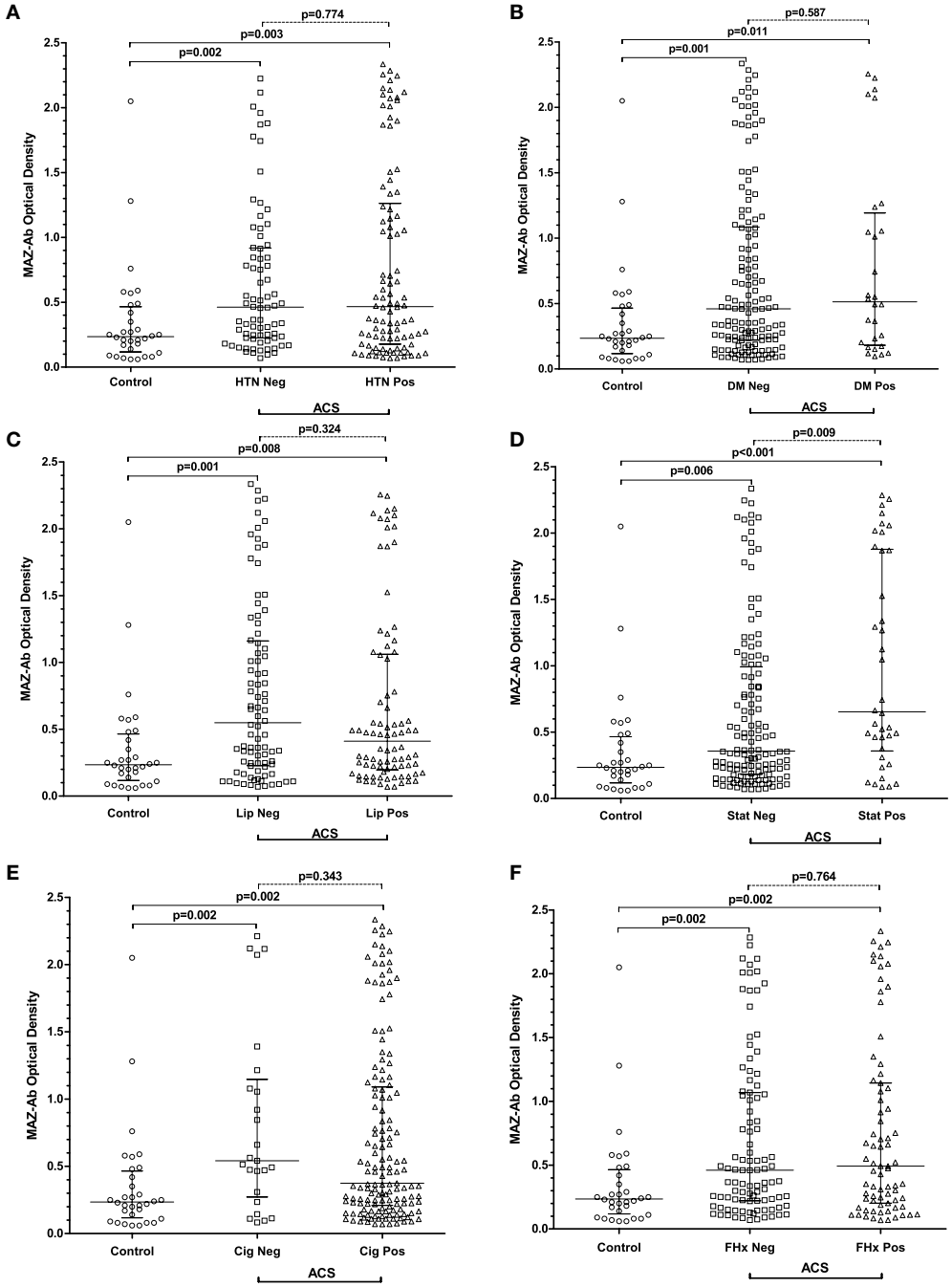

FIGURE 3 | **(A–F)** Summarizing MAZ-Ab optical densities in all patients, with patients in the acute coronary syndrome (ACS) group being sub-classified on the presence or absence of specific cardiovascular risk factors. For all risk factors, MAZ-Ab optical densities were higher in ACS patients regardless of risk factor status compared with controls. Among ACS patients, only statin use resulted in a difference in MAZ-Ab optical density, with treated patients having higher values. Key: MAZ-Ab, MYC-associated zinc finger protein antibody; HTN, arterial hypertension; DM, diabetes mellitus; LIP, dyslipidemia; STAT, current treatment with HMG-CoA reductase inhibitors; Cig, any smoking history; FHX, any first-degree family history of cardiovascular disease.

MAZ-Antibody Independent of Cholesterol Levels and Use of Statins

The findings regarding existing statin use are less clear (**Figure 3D**). In total, 35 patients in the ACS group were taking statins at admission. Considering the recommended European Society of Cardiology cutoff values for blood lipid concentrations (cholesterol <190 mg/dL, LDL <115 mg/dL), 6/35 (17%) still had elevated cholesterol at admission. 59/109 (54%) of those admitted without statin had an elevated cholesterol, showing no significant difference between the two groups ($p = 0.384$). Of those on statin 22/35 (63%) and 75/109 (69%) of those without had raised LDL levels at admission ($p = 0.59$).

Patients on statins did, however, have significantly higher MAZ-Ab ODs ($p = 0.009$). It is worth noting that while these patients were older 58 [52–60] vs. 52 [46–58] years ($p = 0.004$), no association between age and raised LDL ($p = 0.145$) or cholesterol ($p = 0.553$) was observed. Similarly, neither cholesterol >190 ($p = 0.945$) nor LDL >115 ($p = 0.946$) influenced MAZ-Ab OD. An alternative explanation, however, may exist that the findings are the result of a selection bias, in that only high MAZ-Ab patients on statins subsequently experienced an event. This, however, remains speculative and requires further evaluation in future studies.

MAZ-Antibody Has No Prognostic Relevance Regarding Reinfarction

Of the 197 PLATO patients experiencing a second cardiovascular event within one year of the initial ACS event, 42 died. No significant difference in MAZ-Ab OD between these patients and their 1997 matched controls was observed (OR 1.04 [95% CI: 0.94–1.16]; $p = 0.436$).

DISCUSSION

Taking a proven ACS as unequivocal evidence of atherosclerosis, this study clearly demonstrates a difference in MAZ-Ab OD on ELISA between these patients and healthy controls. This provides the first confirmed clinical association between MAZ-Ab OD and clinically apparent atherosclerosis. This augments existing data, which demonstrated an association between MAZ-Ab and the cumulative burden of inflammatory atherosclerosis on ^{18}F-FDG-PET/CT scanning (9).

Previous research has shown that MAZ production is promoted by inflammatory interleukins including IL-1 and IL-6, along with TNF-alpha and oxLDL (8), all of which are known to increase cardiovascular risk (3, 4). Although the exact role of the transcription factor MAZ remains unclear, it has been implicated in macrophage function within atherosclerotic plaques (8, 19). The principal functions appeared to include inducing MMPs involved in atherosclerotic plaque rupture. Other studies have suggested a wider MAZ effect, such as influencing angiogenesis and inducing VEGF expression. The latter appears integral in triple-negative breast cancer cells (13, 14) as well as regulation of inflammation-responsive genes (15).

It is important to reiterate that current data suggests that MAZ-Ab is a biomarker of atherosclerosis rather than a particular cardiovascular disease. This study highlights this, when the various ACSs included are considered. In essence, the current classification of ACSs reflects the extent of end-organ, myocardial, damage. The measured cTnT values confirm this, increasing sequentially from angina pectoris, non-ST elevation and STEMIs (**Table 1**). No perceptible difference in MAZ-Ab OD across these groups was evident. Furthermore, no correlation between all cTnT values and MAZ-Ab OD were observed (Spearman rank, $p = 0.391$). Further comparisons with other known biomarkers revealed no relationship to MAZ-Ab OD, again supporting the concept that MAZ-Ab is myocardium independent.

It is, however, noteworthy that MAZ-Ab OD was independent of GDF-15. GDF-15 is an accepted independent prognostic biomarker for NSTEMI and acute chest pain, with increasing levels impacting negatively on 1-year post-event survival (20, 21).

It is well recognized that traditional cardiovascular risk factors are inextricably linked to the development of atherosclerosis. Considering only the patients in the ACS group, MAZ-Ab OD was not influenced by hypertension, diabetes, lipid or smoking status. However, comparing ACS patients lacking a particular risk factor with healthy controls returned uniformly raised MAZ-Ab ODs among the former.

MAZ antibodies were associated with statin use. Sub-analysis within the current cohort failed to identify any clear explanation for our findings. The most likely explanation appears to be selection bias and the demographics for statin use. Furthermore, it is reasonable to assume that all of those treated were at some point either diagnosed with dyslipidemia of unknown duration or as secondary prevention following a previous cardiovascular event and that the actual duration of statin treatment is unknown. All of these characteristics are likely confounders of increased atherosclerosis risk.

Given the limited follow-up in the ACS group we collaborated with the PLATO trial group to evaluate the prognostic value of MAZ-Ab following a vascular event, both in terms of survival and treatment response. Among these 396 matched patients, actual MAZ-Ab OD demonstrated no prognostic relevance, again suggesting that. MAZ-Ab OD may be a better marker for atherosclerosis than myocardial damage. This complements current understanding of the pathophysiological role of MAZ, a known transcription factor in active macrophages within atherosclerotic plaques (8).

Given the single-center, retrospective nature of this study there are several incumbent limitations that require consideration. The number of patients included is comparatively small, and significant demographic differences were evident between the groups, limiting somewhat the validity of data analysis.

In conclusion, however, this study corroborates clinically the findings of previous imaging studies, demonstrating an association between MAZ-Ab OD and proven atherosclerotic disease in the form of ACSs. The exact autoimmune role of MAZ-Ab in atherosclerosis may be related to plaque macrophage activity but more research into the pathophysiological function of MAZ is needed. Most importantly, current evidence suggests that the association between MAZ-antibody and atherosclerosis is independent of established conventional risk factors of atherosclerotic disease.

AUTHOR CONTRIBUTIONS

DE: study design, data collection, analysis, and writing of the manuscript. CW: data collection, analysis, and reviewing the manuscript. NB: study design, data collection, and reviewing the manuscript. WS and CD: data collection and review of the manuscript (technical aspects only). RS: critical review of the manuscript. KG and LW: data collection, analysis, and review of the manuscript. TW: study design and critical review of the manuscript.

FUNDING

This project was supported by the Deutsche Forschungsgemeinschaft (DFG) Klinische Forschergruppe (KFO 250), grants TP03. The PLATO trial was funded by AstraZeneca.

REFERENCES

1. Laslett LJ, Alagona P Jr, Clark BA III, Drozda JP Jr, Saldivar F, Wilson SR, et al. The worldwide environment of cardiovascular disease: prevalence, diagnosis, therapy, and policy issues: a report from the American College of Cardiology. *J Am Coll Cardiol* (2012) 60(25 Suppl):S1–49. doi:10.1016/j.jacc.2012.11.002
2. Yusuf S, Hawken S, Ounpuu S, Dans T, Avezum A, Lanas F, et al. Effect of potentially modifiable risk factors associated with myocardial infarction in 52 countries (the INTERHEART study): case-control study. *Lancet* (2004) 364(9438):937–52. doi:10.1016/S0140-6736(04)17018-9
3. Szekanecz Z, Kerekes G, Vegh E, Kardos Z, Barath Z, Tamasi L, et al. Autoimmune atherosclerosis in 3D: how it develops, how to diagnose and what to do. *Autoimmun Rev* (2016) 15(7):756–69. doi:10.1016/j.autrev.2016.03.014
4. Carbone F, Nencioni A, Mach F, Vuilleumier N, Montecucco F. Evidence on the pathogenic role of auto-antibodies in acute cardiovascular diseases. *Thromb Haemost* (2013) 109(5):854–68. doi:10.1160/TH12-10-0768
5. Okada T, Ayada K, Usui S, Yokota K, Cui J, Kawahara Y, et al. Antibodies against heat shock protein 60 derived from Helicobacter pylori: diagnostic implications in cardiovascular disease. *J Autoimmun* (2007) 29(2–3):106–15. doi:10.1016/j.jaut.2007.05.004
6. Ray BK, Chatterjee S, Ray A. Mechanism of minimally modified LDL-mediated induction of serum amyloid A gene in monocyte/macrophage cells. *DNA Cell Biol* (1999) 18(1):65–73. doi:10.1089/104454999315637
7. Ray BK, Ray A. Involvement of an SAF-like transcription factor in the activation of serum amyloid A gene in monocyte/macrophage cells by lipopolysaccharide. *Biochemistry* (1997) 36(15):4662–8. doi:10.1021/bi9624595
8. Ray BK, Shakya A, Turk JR, Apte SS, Ray A. Induction of the MMP-14 gene in macrophages of the atherosclerotic plaque: role of SAF-1 in the induction process. *Circ Res* (2004) 95(11):1082–90. doi:10.1161/01.RES.0000150046.48115.80
9. Ernst D, Weiberg D, Baerlecken NT, Schlumberger W, Daehnrich C, Schmidt RE, et al. Anti-MYC-associated zinc finger protein antibodies are associated with inflammatory atherosclerotic lesions on 18F-fluorodeoxyglucose positron emission tomography. *Atherosclerosis* (2017) 259:12–9. doi:10.1016/j.atherosclerosis.2017.02.010
10. Joseph P, Tawakol A. Imaging atherosclerosis with positron emission tomography. *Eur Heart J* (2016) 37(39):2974–80. doi:10.1093/eurheartj/ehw147
11. Wang X, Southard RC, Allred CD, Talbert DR, Wilson ME, Kilgore MW. MAZ drives tumor-specific expression of PPAR gamma 1 in breast cancer cells. *Breast Cancer Res Treat* (2008) 111(1):103–11. doi:10.1007/s10549-007-9765-7
12. Jiao L, Li Y, Shen D, Xu C, Wang L, Huang G, et al. The prostate cancer-up-regulated Myc-associated zinc-finger protein (MAZ) modulates proliferation and metastasis through reciprocal regulation of androgen receptor. *Med Oncol* (2013) 30(2):570. doi:10.1007/s12032-013-0570-3
13. Ray A, Dhar S, Ray BK. Control of VEGF expression in triple-negative breast carcinoma cells by suppression of SAF-1 transcription factor activity. *Mol Cancer Res* (2011) 9(8):1030–41. doi:10.1158/1541-7786.MCR-10-0598
14. Ray A, Ray BK. Induction of Ras by SAF-1/MAZ through a feed-forward loop promotes angiogenesis in breast cancer. *Cancer Med* (2015) 4(2):224–34. doi:10.1002/cam4.362
15. Ray A, Dhar S, Shakya A, Ray P, Okada Y, Ray BK. SAF-3, a novel splice variant of the SAF-1/MAZ/Pur-1 family, is expressed during inflammation. *FEBS J* (2009) 276(15):4276–86. doi:10.1111/j.1742-4658.2009.07136.x
16. Gomez Ravetti M, Rosso OA, Berretta R, Moscato P. Uncovering molecular biomarkers that correlate cognitive decline with the changes of hippocampus' gene expression profiles in Alzheimer's disease. *PLoS One* (2010) 5(4):e10153. doi:10.1371/journal.pone.0010153
17. Widera C, Horn-Wichmann R, Kempf T, Bethmann K, Fiedler B, Sharma S, et al. Circulating concentrations of follistatin-like 1 in healthy individuals and patients with acute coronary syndrome as assessed by an immunoluminometric sandwich assay. *Clin Chem* (2009) 55(10):1794–800. doi:10.1373/clinchem.2009.129411
18. James S, Akerblom A, Cannon CP, Emanuelsson H, Husted S, Katus H, et al. Comparison of ticagrelor, the first reversible oral P2Y(12) receptor antagonist, with clopidogrel in patients with acute coronary syndromes: rationale, design, and baseline characteristics of the PLATelet inhibition and patient Outcomes (PLATO) trial. *Am Heart J* (2009) 157(4):599–605. doi:10.1016/j.ahj.2009.01.003
19. Schonbeck U, Mach F, Sukhova GK, Murphy C, Bonnefoy JY, Fabunmi RP, et al. Regulation of matrix metalloproteinase expression in human vascular smooth muscle cells by T lymphocytes: a role for CD40 signaling in plaque rupture? *Circ Res* (1997) 81(3):448–54. doi:10.1161/01.RES.81.3.448
20. Wollert KC, Kempf T, Peter T, Olofsson S, James S, Johnston N, et al. Prognostic value of growth-differentiation factor-15 in patients with non-ST-elevation acute coronary syndrome. *Circulation* (2007) 115(8):962–71. doi:10.1161/CIRCULATIONAHA.106.650846
21. Eggers KM, Kempf T, Allhoff T, Lindahl B, Wallentin L, Wollert KC. Growth-differentiation factor-15 for early risk stratification in patients with acute chest pain. *Eur Heart J* (2008) 29(19):2327–35. doi:10.1093/eurheartj/ehn339

Conflict of Interest Statement: DE, NB, and TW have recently patented the MAZ-antibody (PCT/EP2016/066588). WS and CD are employees of EUROIMMUN AG and shareholders in EUROIMMUN AG. Their role in the current project was, however, limited to developing the standardized ELISA test used and testing the PLATO cohort. They were in no way involved in designing the study, data collection, or analysis and provided only critical review of the manuscript related to their involvement. KG: institutional research grant from AstraZeneca. LW: institutional research grants, consultancy fees, lecture fees, and travel support from Bristol-Myers Squibb/Pfizer, AstraZeneca, GlaxoSmithKline, and Boehringer Ingelheim; institutional research grants from Merck & Co. and Roche Diagnostics; consultancy fees from Abbott; and holds a patent EP2047275B1 licensed to Roche Diagnostics, and a patent US8951742B2 licensed to Roche Diagnostics.

frontiers in Immunology

ORIGINAL RESEARCH
published: 20 November 2017
doi: 10.3389/fimmu.2017.01567

β1-Adrenergic Receptor Contains Multiple IA^k and IE^k Binding Epitopes That Induce T Cell Responses with Varying Degrees of Autoimmune Myocarditis in A/J Mice

*Rakesh H. Basavalingappa[1], Chandirasegaran Massilamany[1†], Bharathi Krishnan[1], Arunakumar Gangaplara[1†], Rajkumar A. Rajasekaran[1], Muhammad Z. Afzal[2], Jean-Jack Riethoven[3], Jennifer L. Strande[2], David Steffen[1] and Jay Reddy[1]**

[1] School of Veterinary Medicine and Biomedical Sciences, University of Nebraska-Lincoln, Lincoln, NE, United States,
[2] Department of Medicine, Division of Cardiology, Medical College of Wisconsin, Milwaukee, WI, United States,
[3] Center for Biotechnology, University of Nebraska-Lincoln, Lincoln, NE, United States

OPEN ACCESS

Edited by:
Satyajit Rath,
Agharkar Research Institute, India

Reviewed by:
Nagendra Singh,
Augusta University, United States
Ralf J. Ludwig,
University of Lübeck, Germany

***Correspondence:**
Jay Reddy
nreddy2@unl.edu

†Present address:
Chandirasegaran Massilamany,
Vaccine Branch, Center for Cancer Research, National Cancer Institute, Bethesda, MD, United States;
Arunakumar Gangaplara,
Laboratory of Immunology, National Institute of Allergy and Infectious Diseases, National Institutes of Health, Bethesda, MD, United States

Specialty section:
This article was submitted to Inflammation, a section of the journal Frontiers in Immunology

Received: 20 September 2017
Accepted: 01 November 2017
Published: 20 November 2017

Citation:
Basavalingappa RH, Massilamany C, Krishnan B, Gangaplara A, Rajasekaran RA, Afzal MZ, Riethoven J-J, Strande JL, Steffen D and Reddy J (2017) β1-Adrenergic Receptor Contains Multiple IA^k and IE^k Binding Epitopes That Induce T Cell Responses with Varying Degrees of Autoimmune Myocarditis in A/J Mice. Front. Immunol. 8:1567. doi: 10.3389/fimmu.2017.01567

Myocarditis/dilated cardiomyopathy (DCM) patients can develop autoantibodies to various cardiac antigens and one major antigen is β1-adrenergic receptor (β_1AR). Previous reports indicate that animals immunized with a β_1AR fragment encompassing, 197–222 amino acids for a prolonged period can develop DCM by producing autoantibodies, but existence of T cell epitopes, if any, were unknown. Using A/J mice that are highly susceptible to lymphocytic myocarditis, we have identified β_1AR 171–190, β_1AR 181–200, and β_1AR 211–230 as the major T cell epitopes that bind major histocompatibility complex class II/IA^k or IE^k alleles, and by creating IA^k and IE^k dextramers, we demonstrate that the CD4 T cell responses to be antigen-specific. Of note, all the three epitopes were found also to stimulate CD8 T cells suggesting that they can act as common epitopes for both CD4 and CD8 T cells. While, all epitopes induced only mild myocarditis, the disease-incidence was enhanced in animals immunized with all the three peptides together as a cocktail. Although, antigen-sensitized T cells produced mainly interleukin-17A, their transfer into naive animals yielded no disease. But, steering for T helper 1 response led the T cells reacting to one epitope, β_1AR 181–200 to induce severe myocarditis in naive mice. Finally, we demonstrate that all three β_1AR epitopes to be unique for T cells as none of them induced antibody responses. Conversely, animals immunized with a non-T cell activator, β_1AR 201–220, an equivalent of β_1AR 197–222, had antibodies comprising of all IgG isotypes and IgM except, IgA and IgE. Thus, identification of T cell and B cell epitopes of β_1AR may be helpful to determine β_1AR-reactive autoimmune responses in various experimental settings in A/J mice.

Keywords: autoimmunity, β1-adrenergic receptor, myocarditis, mouse model, T cells

INTRODUCTION

Myocarditis is one major cause of dilated cardiomyopathy (DCM) that can lead to heart failure in young adults in the developed countries. Approximately, half of those affected with DCM undergo heart transplantation due to lack of effective therapeutic options (1–4). Clinically, majority of DCM patients (up to 80%) are designated to be idiopathic DCM (IDCM), and the detection of heart

infiltrates in those affected suggests that immune dysfunction may be an underlying mechanism in the DCM pathogenesis (5–8). Growing evidence suggests that autoimmune responses may be an important trigger, since DCM patients can show autoantibodies for various antigens such as cardiac myosin, cardiac troponin I, adenine nucleotide translocator 1 (ANT), β1-adrenergic receptor (β_1AR), and branched chain alpha-ketoacid dehydrogenase (BCKD) (9–12). For example, β_1AR-reactive antibodies can be detected in 26–60% of IDCM patients as compared to ischemic cardiomyopathy (10–13%) or healthy controls (<10%) (6, 7, 13). While, DCM patients can show antibody reactivity to cardiac myosin heavy chain-α (Myhc) (66%) and troponin-I (50%), up to 80% of the end-stage IDCM patients or more than 90% of patients using left ventricular assist device were shown to be positive for antibodies to β_1AR (6, 7). These observations suggest that β_1AR may be a major autoantigen in the initiation and progression of DCM.

β-adrenergic receptors are classified into four subtypes with β_1AR being found primarily in the heart, whereas β_2AR is expressed in the lung, kidney, blood vessels and heart, and β_3AR-expression occurs primarily in the adipose tissue (14, 15). Although, mRNA and protein data are lacking, existence of β_4AR has been reported, which appears to represent the low-affinity state of β_1AR (16). Belonging to G-protein-coupled receptors, β_1AR contains three each of extracellular (EC) and intracellular loops. The natural ligands of β_1AR namely, adrenaline and noradrenaline trigger activation of cyclic adenosine monophosphate (cAMP) and protein kinase A leading to influx of calcium (Ca^{2+}) through L-type Ca^{2+} channel and cardiac contractility (17, 18). Similar events can be expected under conditions of autoimmunity as might occur with the presence of β_1AR-reactive autoantibodies. In fact, antibodies recognizing epitopes localized within the EC loops, particularly EC loop II (β_1AR 197–222), can agonistically trigger Ca^{2+} release and cAMP activation, without affecting interaction of β_1AR with its natural ligands (6, 19). Such antibodies have been detected in DCM patients indicating their pathological significance (13, 20).

Experimentally, monthly immunizations for 6–18 months with β_1AR 197–222 can result in the production of antibodies in various species such as rabbits, rats, and mice, and the immunized animals can develop features of cardiomyopathy during the course of ~1 year with little or no myocarditis (21–25). While, an assumption made in these studies that a single epitope of β_1AR can act as an immunogen in various species despite the major histocompatibility complex (MHC) alleles to be different was found valid, identification of other potential immunodominant epitopes, if any, was not explored. Likewise, it was unknown whether β_1AR possesses T cell epitopes and contributes to disease. This is particularly important because, for B cells to produce antibodies of different isotypes, T cell help is critical, and identification of T cell epitopes may thus provide another layer of evidence for pathologic importance of β_1AR in the DCM pathogenesis. To this end, we sought to characterize the T cell epitopes of β_1AR in A/J mice that are highly susceptible to lymphocytic myocarditis leading us to identify several epitopes that induce differential T cell and/or antibody responses. By testing for myocarditogenicity, we noted that the antigen-primed T cells could induce severe myocarditis in naive recipients, but the T cells needed to produce primarily, T helper (Th) 1 cytokines, in addition to Th17 cytokines.

Abbreviations: DCM, dilated cardiomyopathy; β_1AR, β1-adrenergic receptor; β_1AR_{Ac}, N-terminal acetylated β1-adrenergic receptor; IDCM, idiopathic dilated cardiomyopathy; ANT, adenine nucleotide translocator 1; BCKD, branched chain alpha-ketoacid dehydrogenase; Myhc, cardiac myosin heavy chain-α; EC, extracellular; cAMP, cyclic adenosine monophosphate; MHC, major histocompatibility complex; Th, T helper; RNase, bovine ribonuclease; HEL, hen egg lysozyme; MCC, moth cytochrome *c*; CFA, complete Freund's adjuvant; PT, pertussis toxin; H&E, hematoxylin and eosin; IHC, immunohistochemistry; Abs, antibodies; RT, room temperature; HRP, horseradish peroxidase; LV, left ventricle; LVID, left ventricular internal diameter; RWT, relative wall thickness; BSA, body surface area; ^{3}[H]-thymidine, tritiated-thymidine; cpm, counts per minute; SA, streptavidin; DELFIA, dissociation-enhanced lanthanide fluoroimmunoassay; LNCs, lymph node cells; 7-AAD, 7-aminoactinomycin-D; dext$^+$, dextramer$^+$; IL, interleukin; IFN, interferon; TNF, tumor necrosis factor; LPS, lipopolysaccharide; MNCs, mononuclear cells; *T. cruzi, Trypanosoma cruzi*.

MATERIALS AND METHODS

Mice

Six- to eight-week-old, female A/J mice (H-2^a) procured from the Jackson Laboratory (Bar Harbor, ME, USA) were maintained in accordance with the institutional guidelines of the University of Nebraska-Lincoln. Approval for animal studies was granted by the Institutional Animal Care and Use Committee, University of Nebraska-Lincoln, Lincoln, NE, USA (protocol #: 1398). Euthanasia was performed using a carbon dioxide chamber as recommended by the Panel on Euthanasia, the American Veterinary Medical Association.

Peptide Synthesis

An overlapping peptide library that included a total of 46 peptides of 20-mers, except one peptide, β_1AR 451–466 (16-mer) was created. In addition to these, bovine ribonuclease (RNase) 43–56 (VNTFVHESLADVQA), biotinylated hen egg lysozyme (HEL) 46–61 (YNTDGSTDYGILQINSR) (Neopeptide, Cambridge, MA, USA), and moth cytochrome *c* (MCC) 82–103 (FAGLKKANER ADLIAYLKQATK) (GenScript, Piscataway, NJ, USA) were synthesized by 9-fluorenylmethyloxycarbonyl chemistry. Where indicated, acetylated β_1AR (β_1AR_{Ac}) that contain acetyl group at the N-terminal end were used. All peptides were high-performance liquid chromatography-purified (>90%), and their identities were confirmed by mass spectroscopy. Ultrapure water was used to dissolve peptides and stored at −20°C.

Immunization Procedures

Peptide emulsions were prepared in complete Freund's adjuvant (CFA) containing *Mycobacterium tuberculosis* H37RA extract (Difco Laboratories, Detroit, MI, USA) to a final concentration of 5 mg/ml. To induce disease, animals were immunized twice s.c., in inguinal and sternal regions on days 0 and 7, and all animals received pertussis toxin (PT, List Biological Laboratories, Campbell, CA, USA; 100 ng/mouse) i.p., on days 0 and 2 after the first immunization (26–29). In pooled settings, 50 μg of each peptide was used, and when peptides were used individually,

100 μg was used per animal. To measure T cell responses in some experiments, a single dose of peptide emulsions were used.

Histology

Hearts, and non-cardiac tissues (brain, lung, liver, and kidney) collected at termination on day 21 postimmunization were fixed by immersing in 10% phosphate-buffered formalin (26, 28). Longitudinal tissue layers were cut from hearts, and also from non-cardiac tissues. Serial sections with 5 μm thickness were then obtained and stained with hematoxylin and eosin (H&E). Analysis was performed by a board-certified pathologist blinded to treatment. After ascertaining the inflammatory changes, total number of inflammatory foci were determined by sections with the largest number of foci or by adding non-overlapping foci across sections as reported previously (26, 28, 30, 31).

Immunohistochemistry (IHC)

To detect T cells in hearts, formalin-fixed paraffin-embedded tissue sections were stained with rabbit anti-mouse CD3 (clone SP7, 1:100, Abcam, Cambridge, MA, USA), rabbit anti-mouse CD4 (polyclonal, 1:100, Novus Biologicals, Littleton, CO, USA), and rabbit anti-mouse CD8 (clone EP1150Y, 1:100, Novus Biologicals) or their isotype controls. For non-T cells namely, neutrophils, macrophages, and B cells, rat anti-mouse Ly6G (clone 1A8, 1:250, Leinco Technologies, Fenton, MO, USA), rabbit anti-mouse CD11b (clone EPR1344, 1:3,500, Abcam) (30), and rat anti-mouse CD19 (clone 6OMP31, 1:1000, Thermo Fisher Scientific, San Diego, CA, USA) and their isotype controls were used, respectively. In brief, after deparaffinization, rehydration, and blockade of endogenous peroxidase activity, antigen retrieval was performed by treating the sections with 10 mM sodium citrate buffer (pH 6.0) in a water bath at 98°C for 15–40 min or using a pressure cooker. Sections were then blocked with 5% non-fat dry milk for 30 minutes, incubated with primary antibodies (Abs) at 4°C overnight; followed by incubation with horseradish peroxidase (HRP)-conjugated, goat anti-rabbit IgG or goat anti-rat IgG (Abcam) as secondary antibodies for 2 h at room temperature (RT). Diaminobenzoic acid was used as a substrate for color development before counterstaining with hematoxylin (26, 30). For quantitative analysis (T cells: $CD3^+$, $CD4^+$, and $CD8^+$; and non-T cells: $Ly6G^+$, $CD11b^+$, and $CD19^+$) in the heart, five random areas were selected from the representative sections and nuclear staining was confirmed using nuclear V9 software (Aperio Technologies, Vista, CA, USA). Cells positive for each marker were then enumerated and normalized to 1 mm^2 area using Aperio ImageScope Analysis Software (Leica Biosystems, MN, USA) as we have described previously (30).

Echocardiography and Image Analysis

Transthoracic echocardiography was performed in anesthetized animals immunized with or without a cocktail of β_1AR_{Ac} 171–190, β_1AR_{Ac} 181–200, and β_1AR_{Ac} 211–230 on day 20. Scanning was performed by a research sonographer, blinded to the study groups, using a commercially available echocardiography system (Vivid 7, General Electric, Wauwatosa, WI, USA) with an M12-L linear array transducer as we reported previously (30). The mice were anesthetized with isoflurane and images were captured in the short-axis view at the mid-left ventricle (LV) level, verified by the presence of prominent papillary muscles. Three consecutive cardiac cycles, defined from the peak of one R wave to the peak of the following R wave were measured and used for analysis as previously reported (30). In brief, linear measurements were performed using the M-mode view to assess width of the intraventricular septum at diastole and the internal diameter of the LV at diastole and systole. The Teichholz formula {LV volume = [7/2.4 + left ventricular internal diameter (LVID)] × $LVID^3$} was used to calculate end-diastolic and end-systolic volumes (30). The relative wall thickness (RWT) was calculated as the ratio of 2 × LV posterior wall thickness and LV internal diameter at end-diastole. The RWT normal range is between 0.32 and 0.42. Total body surface area (BSA) was calculated using the Meeh's formula (BSA = 10 × $[weight]^{2/3}$) (32). All measurements were indexed to BSA to account variation in size.

T Cell Proliferation Assay

At termination, lymph nodes (maxillary, mandibular, axillary, inguinal, and popliteal) and spleens were harvested from immunized animals to prepare single cell suspensions. Similarly, splenocytes were prepared from naive animals. After lysing the erythrocytes and washing, cell pellets were suspended in RPMI medium containing 10% fetal bovine serum, 1 mM sodium pyruvate, 4 mM L-glutamine, 1 × each of non-essential amino acids and vitamin mixture, and 100 U/ml penicillin–streptomycin (Lonza, Walkersville, MD, USA; hereafter called growth medium). In some experiments, CD4 T cells and CD8 T cells were enriched to a purity of ~95% by negative selection based on magnetic separation using IMAG (BD Biosciences, San Jose, CA, USA) (31). To stimulate CD4 and CD8 T cells, syngeneic naive irradiated splenocytes loaded with peptides were used as antigen-presenting cells at a ratio of 1:1. Cells were stimulated at a density of ~5×10^6 cells/ml in triplicates with or without the immunizing peptides (0–100 μg/ml) in growth medium. RNase 43–56 or HEL 46–61 were used as irrelevant controls. After 2 days, cells were pulsed with tritiated ^{3}[H]-thymidine (1 μCi/well; MP Biomedicals, Santa Ana, CA, USA), and 16 h later, proliferative responses were measured as counts per minute (cpm) using a Wallac liquid scintillation counter (Perkin Elmer, Waltham, MA, USA) (26, 28, 30).

MHC Class II-Binding Assay

A/J mice express two MHC class II alleles, IA^k and IE^k (33, 34), and to determine the affinities of β_1AR peptides, soluble IA^k and IE^k monomers were expressed (34, 35). In brief, the β-chain in each of IA^k and IE^k constructs contain sequence for class II-associated invariant-chain peptide 88–102 (VSQMRMATPLLMRPM) linked with thrombin cleavage site (34, 35). After expressing in the baculovirus, soluble IA^k and IE^k monomers were treated with thrombin (20 U/mg; Novagen, Madison, WI, USA) to release class II-associated invariant-chain peptide leading us to obtain empty IA^k and IE^k molecules. Reaction mixtures were prepared to include empty IA^k or IE^k monomers (0.35 μg), competitor peptides (β_1AR_{Ac} 171–190, β_1AR_{Ac} 181–200, β_1AR_{Ac} 201–220, and β_1AR_{Ac}

211–230) (0.00001–100 μM), and constant amounts of the biotinylated reference peptides HEL 46–61 (for IA^k) or MCC 82–103 (for IE^k) (1 μM) in a buffer containing 50 mM sodium phosphate pH 7.0, 100 mM sodium chloride, 1 mM EDTA, and 1 × protease inhibitor (Sigma-Aldrich, St. Louis, MO, USA) (36–38). After incubating overnight at RT, the mixtures were transferred to 96-well white fluorescence plates coated with anti-IA^k (clone 10-2.16, BioXcell, West Lebanon, NH, USA), and anti-IE^k (clone M5/114, BioXcell) Abs (10 μg/ml) in 0.2 M sodium phosphate buffer, pH 6.8, blocked with 2% bovine casein; and the plates were incubated on a rocker at RT for 1 h. Finally, after adding 100 μl of europium-labeled streptavidin (0.1 μg/ml) and dissociation-enhanced lanthanide fluoroimmunoassay (DELFIA) enhancement solution (Perkin Elmer) sequentially, fluorescence intensities were measured at excitation/emission wavelengths of 340/615 nm using a Victor Multilabel Plate Reader (Perkin Elmer). The IC_{50} values were determined based on the concentrations of competitor peptides needed to prevent 50% binding of the reference peptides as we have described previously (26, 28, 30).

Creation of MHC Class II/IA^k or IE^k Dextramers to Determine Antigen-Specificity of T Cells

To enumerate the frequencies of antigen-specific CD4 T cells, we created IA^k dextramers for β_1AR 171-190 and β_1AR 211–230, and IE^k dextramers for β_1AR 181–200. To create IA^k dextramers, the nucleotide sequence for β_1AR 171–190 (acgcgcgcgcgagcgcgggc-cctcgtgtgcacagtgtgggccatctcggcgttggtgtcc) and β_1AR 211–230 (aacgaccccaagtgctgcgatttcgtcaccaacagggcctacgccatcgcctcgtccgtc) was inserted into the IA^k-β construct that we had described previously (35, 39), whereas IA^k/RNase 43–56 (control) dextramers were readily available in our laboratory (30, 35, 40). The soluble, IA^k/β_1AR 171–190 and IA^k/β_1AR 211–230 molecules were expressed in sf9 cells using baculovirus expression system. After purifying through anti-IA^k-affinity column, the IA^k/β_1AR 171–190 and IA^k/β_1AR 211–230 monomers were biotinylated and dextramers were derived using streptavidin (SA)/fluorophore-conjugated dextran molecules as described previously (35, 39). IE^k/β_1AR 181–200 and IE^k/MCC 82–103 (control) dextramers were prepared based on peptide-exchange reaction as we have described previously (34).

To stain with dextramers, lymphocytes obtained from lymph nodes and spleens from immunized animals were stimulated with the immunizing peptides namely, β_1AR_{Ac} 171–190, β_1AR_{Ac} 181–200, and β_1AR_{Ac} 211–230 (20 μg/ml) for 2 days and growth medium containing interleukin (IL)-2 (IL-2 medium) was then added. After harvesting viable cells by ficoll density-gradient centrifugation on day 5, cells were rested in the IL-2 medium. During 7–10 days poststimulation, cells were stained with IA^k-[β_1AR_{Ac} 171–190 (37°C) or β_1AR_{Ac} 211–230 (RT), and RNase 43–56, control] or IE^k-dextramers [β_1AR_{Ac} 181–200 (RT) and MCC 82–103, control] followed by anti-CD4 and 7-aminoactinomycin-D (7-AAD). After washing, and acquisition by flow cytometry, percent dextramer$^+$ (dext$^+$) cells were analyzed within the live cells (7-AAD$^-$) using Flow Jo software (34, 35, 39).

Cytokine Secretion

Supernatants were obtained from lymph node cell (LNC) cultures prepared from immunized animals that were stimulated with or without acetylated or non-acetylated, β_1AR 171–190, β_1AR 181–200, and β_1AR 211–230 and RNase 43–56/HEL 46–61 (controls) (50–100 μg/ml) on day 3 poststimulations. Cytokine analysis was performed using beads conjugated with capture and detection Abs with the standard curves being derived from serial dilutions of mouse cytokine standard mixtures, consisting of IL-2, interferon (IFN)-γ, IL-4, IL-6, IL-10, IL-17A, and tumor necrosis factor (TNF)-α as recommended by the manufacturer's guidelines (BD Biosciences). Briefly, capture bead/cytokine antibody conjugates were first prepared, and the mixtures were added to a tube containing diluted standards or test samples, followed by addition of detection antibodies. After acquiring by flow cytometry, FCAP Array Software was used to analyze the data (BD Biosciences) (26, 30).

Induction of Myocarditis by Adoptive Transfer of Antigen-Sensitized T Cells

Lymph node cells obtained from animals immunized with individual peptides, β_1AR_{Ac} 171–190, β_1AR_{Ac} 181–200, or β_1AR_{Ac} 211–230 on day 21 postimmunizations were stimulated with the corresponding immunizing peptides (20 μg/ml) for 2 days followed by resting in IL-2 medium. In a separate set of experiments, animals were immunized with a mixture of β_1AR_{Ac} 171–190, 181–200, and 211–230 peptides and their lymphocytes were stimulated with the immunizing peptides individually (50 μg/ml) for 2 days and then IL-2 medium was added. On day 3, one of the two aliquots of cells were exposed to a mixture of Th1- and Th17-polarizing conditions by adding recombinant mouse IL-12 (20 ng/ml), IL-1β (30 ng/ml), IL-6 (30 ng/ml), IL-23 (50 ng/ml) (all cytokines were procured from BioLegend, San Diego, CA, USA), and human transforming growth factor-β1 (10 ng/ml; eBioscience, San Diego, CA, USA) as reported previously (41–44), and the other was maintained in IL-2 medium alone. Flow cytometrically, we analyzed the percentages of cytokine-producing cells on days 3 and 6 following polarization as we have described previously (28, 31, 40). Viable cells harvested on days 8–10 were administered through i.p., or retro-orbital sinus ($4–14 \times 10^6$ cells/animal) into naive mice primed with lipopolysaccharide (LPS, 25 μg/mouse i.p., day −4 and day 0). PT was administered i.p., (100 ng/mouse) on days 0 and 2 posttransfer (26, 30, 45). Saline recipients and the LPS/PT-primed naive mice were used as controls. Animals were euthanized on 14–21 days after transfer to collect hearts for histology.

Detection of Antibodies That React with β_1AR_{Ac} Peptides

ELISA was used to measure antibodies that react with β_1AR_{Ac} peptides in the serum samples collected from immunized animals at termination on day 21 as described previously (26). Microtiter polystyrene plates were coated with or without β_1AR_{Ac} 171–190, β_1AR_{Ac} 181–200, β_1AR_{Ac} 191–210, β_1AR_{Ac} 201–220, and β_1AR_{Ac} 211–230 or irrelevant control (RNase 43–56) (10 μg/ml) in 1 × coating buffer (eBioscience) and the plates were incubated

at 4°C overnight. After washing/blocking, serum samples (1:100) were added in duplicates, and the plates were incubated at 37°C for 1 h followed by addition of HRP-labeled goat anti-mouse immunoglobulins (Igs), IgG1, IgG2a, IgG2b, IgG3, IgM, IgA, and IgE (Southern Biotech, Birmingham, AL, USA) as secondary antibodies. Two hours after incubation at RT, 1 × tetramethylbenzidine solution was added as a substrate (eBioscience), and reactions were stopped using 1 M phosphoric acid. The plates were read at 405 nm using an automated ELISA reader (BioTek instruments, Winooski, VT, USA) to measure OD values (26, 46).

Statistics

Kruskal–Wallis test was used to compare differences in cytokine production, inflammatory foci and antibodies where more than two groups were involved. When significant differences were noted ($P < 0.05$), analyses were continued with *post hoc* tests *via* Dunn–Sidak multiple test correction. Differences in the incidence of myocarditis between groups were compared using the Fisher's exact test. Student's *t*-test was used to determine differences in the T cell proliferative responses, echocardiography parameters, MHC-binding affinities, frequencies of dext$^+$ cells, and cytokine producing cells.

RESULTS AND DISCUSSION

In this report, we describe identification of T cell epitopes of β_1AR in A/J mice that are highly susceptible to lymphocytic myocarditis induced by various cardiac antigens namely, Myhc (28), cardiac troponin I (47), ANT (26), and BCKD kinase (30). Importance of β_1AR in the cardiac disease has long been investigated in that patients with myocarditis/DCM, in particular, IDCM show β_1AR-reactive antibodies. Such a reactivity has been proposed to signify a marker of disease-progression and/or to predict prognosis (6, 20). β_1AR-reactive antibodies localized to EC loop II particularly for β_1AR 197–222 was also helpful to screen DCM patients in clinical settings (13, 48). Because the sequence of β_1AR 197–222 is found conserved with 100% identity between humans, mice and rats, and 96.1% with rabbits (Table S1 in Supplementary Material), perhaps, rodent studies were undertaken to determine the pathogenic significance of β_1AR 197–222 in the development of myocardial disease. Expectedly, rats and rabbits immunized with β_1AR 197–222 developed cardiac dysfunctions suggestive of DCM, with minimal or no heart infiltrates (21–25). But all these disease-inducing protocols required biweekly or monthly immunizations for a period of 6–18 months. In addition, animals immunized with β_1AR had agonistic antibodies of IgG isotype that trigger cardiac arrhythmias by activating cAMP/protein kinase A pathway and apoptosis of cardiomyocytes (19). In these conditions, however, relevance of β_1AR-reactive T cell responses in the causation of cardiac autoimmunity remained uninvestigated. Thus, we made efforts to identify T cell epitopes of β_1AR and their ability to induce myocarditis in A/J mice.

To identify T cell epitopes, we created an overlapping peptide library that included 46 peptides of 20-mers spanning the entire length of mouse β_1AR (466 amino acids; Table S2 in Supplementary Material). For initial screening, we made nine pools with four to five peptides in each, and immunized A/J mice using the standard myocarditis-inducing protocol by administering peptide emulsions twice with a week interval as we and others have reported for various cardiac antigens (26, 28, 49). These analyses revealed detection of myocarditis in animals that received peptides from pools namely, IV, VII, VIII, and IX, with a disease incidence of 20–40% and the inflammatory foci were in the range of 2–42 (Table S3 in Supplementary Material). However, by evaluating T cell responses using RNase 43–56 as an irrelevant control, a trend was noted in that animals receiving a pool of peptides starting from β_1AR 171–190 to β_1AR 211–230 (pool IV) had good T cell responses up to ~2- to 5-fold that also had diffused inflammatory foci in one animal (Table S3 in Supplementary Material). Similar pattern was noted for one other group (pool VII) with the proliferative responses noted up to two-fold for three peptides (β_1AR 321–340, β_1AR 351–370, and β_1AR 361–380), whereas T cell responses were not significant in the peptide pools, VIII and IX (Table S3 in Supplementary Material). Likewise, significant T cell responses although noted for few peptides in pools, I, II, III, V, and VI, inflammation was absent in the hearts of immunized animals (Table S3 in Supplementary Material). These observations suggest that occurrence of myocarditis might not be due to T cell responses in all the pools.

Since, our intent was to identify T cell epitopes which are capable to induce myocarditis, and the peptides spanning a stretch of 60 aa (β_1AR 171–230, pool IV; Table S3 in Supplementary Material) that also encompasses β_1AR 197–222 which was previously reported to be a B cell epitope (13, 48), we focused on all the five peptides from pool IV (Table S4 in Supplementary Material). For comparative analysis, we also randomly chose two other peptides from pool VIII namely; β_1AR 381–400 and β_1AR 391–410 that did not show T cell responses, but showed myocarditis (Table S3 in Supplementary Material). In the individual immunization settings, the disease incidence was noted to be 20–40%, but unexpectedly, none of the animals had significant disease, except two peptides that induced mild disease (β_1AR 181–200 and β_1AR 211–230) (Table S4 in Supplementary Material).

We and others had previously reported that the peptides modified to include acetyl group at N-terminal end can induce significant myocarditis such as Myhc 614–643 in Balb/c mice (26, 29). It has been proposed that acetylated peptides can be prevented from intracellular degradation leading to their stable binding to MHC molecules (29, 50). Thus, we decided to use the acetylated peptides, and focused only the peptides that were located within the stretch of β_1AR 171–230 (**Table 1**). While, some enhancement was noted with the ability of acetylated peptides (β_1AR_{Ac} 171–190 and β_1AR_{Ac} 181–200) to induce myocarditis, only 25% of animals had the disease (**Table 1**). Expectedly, hearts from control groups (naive and CFA/PT) were negative for inflammatory changes. The T cell responses however were consistently noted for β_1AR_{Ac} 171–190, β_1AR_{Ac} 181–200, and β_1AR_{Ac} 211–230 (**Figure 1**), whereas β_1AR_{Ac} 191–210 and β_1AR_{Ac} 201–220 remained as non-T cell activators (Figure S1A in Supplementary Material). The proliferative responses noted in the immunized animals were dose-dependent, and also specific to antigen, since responses to control antigen (RNase 43–56/HEL 46–61) were lacking (**Figure 1**). We then asked whether T cells primed with a pool of all three peptides that showed T cell responses (β_1AR_{Ac}

171–190, β_1AR_{Ac} 181–200, and β_1AR_{Ac} 211–230) can collectively contribute to myocarditis-induction. These experiments led us to note a significant increase in the disease incidence (63%), but the disease-severity remained unaltered (**Table 1**, $P = 0.03$).

Histologically, in contrast to normal heart sections, inflammatory foci consisting of mononuclear cells (MNCs) involving pericardium, myocardium and endocardium were detected in animals immunized with β_1AR_{Ac} 171–190, β_1AR_{Ac} 181–200, or β_1AR_{Ac} 211–230 individually or as a mixture, but necrosis or fibrosis were absent (**Figure 2A**). Consistent with these observations, echocardiographic analysis also revealed mild cardiac abnormalities as indicated by trends with increased heart rate relative to control animals (384.0 ± 10.10 vs. 337.67 ± 20.98 beats/min; $P = 0.08$, Table S5 in Supplementary Material). Immunized animals showed decreased LVID index at end-systole (0.26 ± 0.01 vs. 0.33 ± 0.01 mm; $P = 0.047$) and end-systolic volume (17.50 ± 2.89 vs. 33.33 ± 8.33 µl; $P = 0.09$, Table S5 in Supplementary Material) associated with an increase in left ventricular systolic function reported as ejection fraction and fractional shortening. The immunized mice showed the absence of hypertrophy and dilation as indicated by the lack of significant increase in the diastolic septal/posterior wall thickness indices and end-diastolic volume. However, the RWT of 0.43 in the immunized mice (normal RWT = 0.32–0.42) identifies concentric remodeling without hypertrophy whereas RWT of 0.39 identifies a normal morphology as seen in the naive mice (51). No differences with body weight (19.20 ± 0.32 vs. 18.23 ± 0.44 g), heart weight (87.25 ± 1.11 vs. 84.00 ± 1.73 mg) or heart/body weight ratio (4.55 ± 0.03 vs. 4.61 ± 0.07 mg/g) were observed between immunized and control groups (Figure S2 in Supplementary Material). Previous reports indicate that rats immunized with β_1AR 197–222 for a prolonged period showed early cardiomyopathic changes at 1 year, but with no necrosis or fibrosis including changes in heart to body weight ratios (21). Likewise, cardiac abnormalities could be detected in Balb/c mice only at 25 weeks but not at 14 weeks postimmunization (22). These observations support the notion that β_1AR-induced cardiomyopathy may be a slow progressive disease.

Nonetheless, we further characterized the immune cells by IHC and the analysis revealed that heart sections from animals immunized with a mixture of three peptides as indicated above had $CD3^+$ (136 ± 9 cells/mm^2), $CD4^+$ (92 ± 1 cells/mm^2), $CD8^+$ (66 ± 21 cells/mm^2) T cells, and $CD11b^+$ (65 ± 13 cells/mm^2) macrophages, whereas $Ly6G^+$ neutrophils, and $CD19^+$ B cells were absent (**Figure 2B**: bottom panel). Expectedly, sections from control groups were negative for all the markers tested except rare $CD11b^+$ cells. While, detection of T cells, mainly CD4 T cells and macrophages suggest the features of delayed-type hypersensitivity (DTH) reaction as noted with other myocarditis models (26, 28–30), detection of CD8 T cells was not expected although they can form a component of DTH reaction. This led us to test a possibility that both CD4 and CD8 T cells may have a role in myocarditis-induction. We sorted both subsets of T cells by magnetic separation from animals immunized with β_1AR_{Ac} 171–190, β_1AR_{Ac} 181–200, or β_1AR_{Ac} 211–230 to a purity of ~95% (Figure S3A in Supplementary Material), and tested their ability to respond to antigens in a proliferation assay. As shown in Figure S3B in Supplementary Material, both CD4 and CD8 T cells responded to the corresponding immunizing peptides dose-dependently, and also antigen-specifically, since responses to HEL 46–61 were lacking. While, these data suggest that the disease induced with β_1AR_{Ac} 171–190, β_1AR_{Ac} 181–200, and β_1AR_{Ac} 211–230 might have involved the mediation of both CD4 and CD8 T cells, existence of three CD8 T cell epitopes in as many CD4 T cell epitopes for a single autoantigen is unusual. But, we and others have previously reported that CD4 T cell epitopes of

TABLE 1 | Induction of myocarditis by β_1AR_{Ac} peptides.

Groups	Incidence (%)	Inflammatory foci[a]
Naive	0/6 (0)	0
CFA/PT	0/6 (0)	0
β_1AR_{Ac} 171–190	3/12 (25)	2.7 ± 1.2
β_1AR_{Ac} 181–200	3/12 (25)	3.7 ± 1.8
β_1AR_{Ac} 191–210	0/5 (0)	0
β_1AR_{Ac} 201–220	1/5 (20)	13
β_1AR_{Ac} 211–230	2/12 (17)	1.0 ± 0.0
β_1AR_{Ac} 171–190, 181–200, and 211–230	5/8 (63)*	2.8 ± 1.1

[a]*Represents mean ± SEM values derived from myocarditic animals.*
**P < 0.05 vs. controls.*

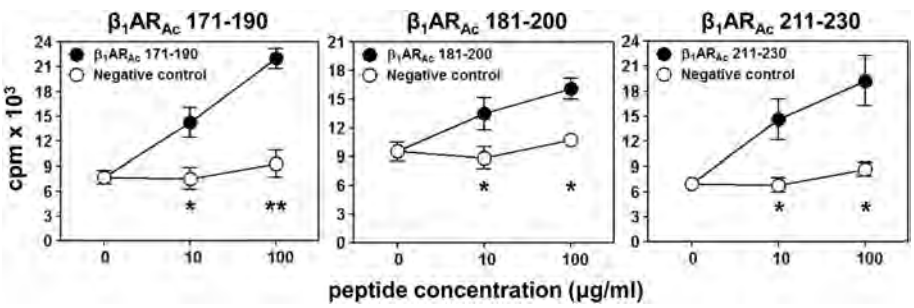

FIGURE 1 | T cell responses induced by β_1AR_{Ac} peptides. Lymph node cells (LNCs) obtained from animals immunized with β_1AR_{Ac} 171–190, β_1AR_{Ac} 181–200, and β_1AR_{Ac} 211–230 were restimulated with or without the corresponding peptides and RNase 43–56/HEL 46–61 (negative control) for 2 days. After pulsing with ^{3}[H]-thymidine for 16 h, proliferative responses were measured as cpm. Mean ± SEM values derived from three to four individual experiments, each involving three to eight mice are shown. *$P < 0.05$ and **$P < 0.01$ vs. negative controls.

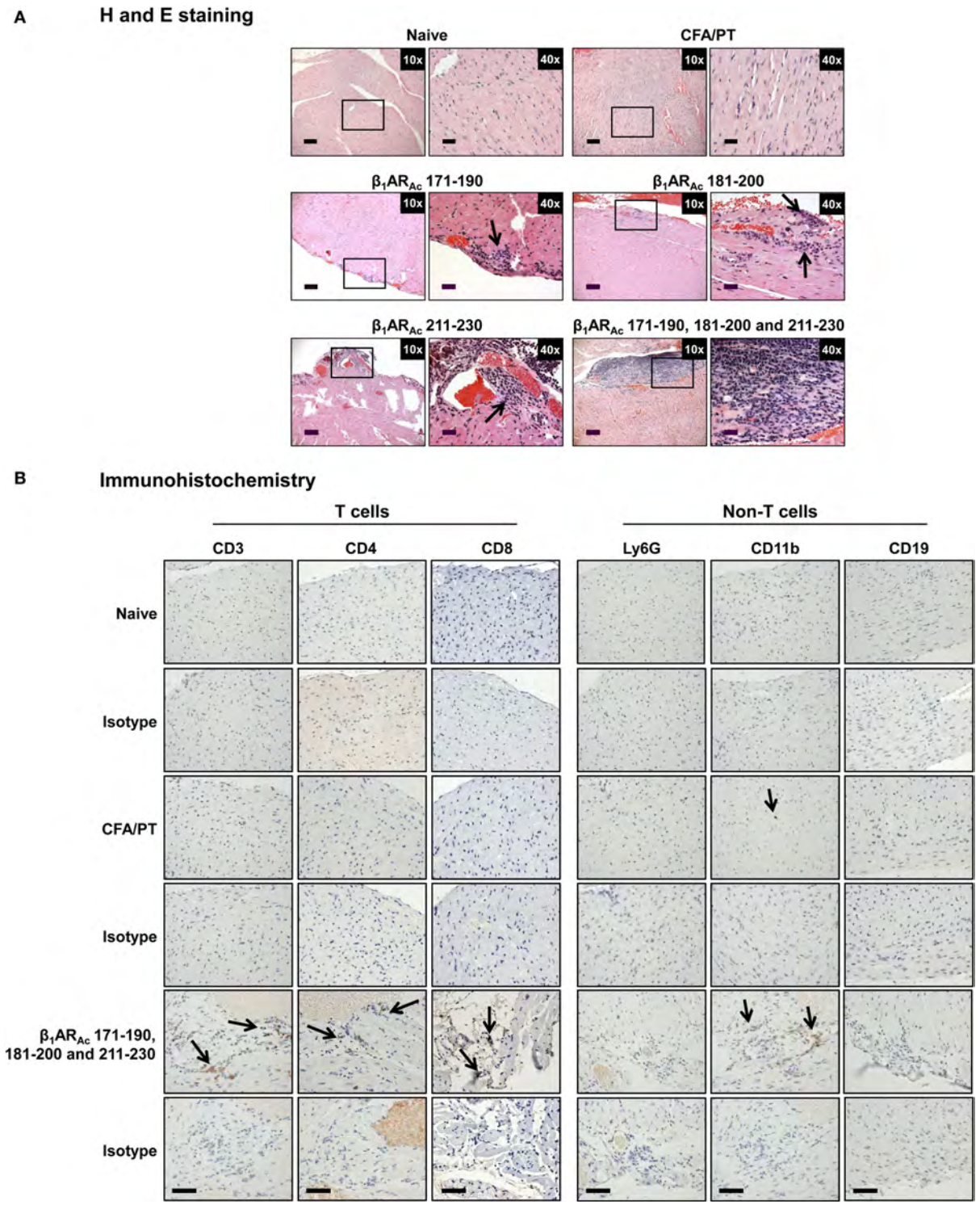

FIGURE 2 | Histological evaluation of hearts from animals immunized with β_1AR_{Ac} peptides. **(A)** Hematoxylin and eosin (H&E) staining. Groups of mice were immunized with or without indicated peptides in complete Freund's adjuvant (CFA) twice with an interval of 7 days. At termination on day 21, hearts were collected to determine inflammatory changes by H&E staining analysis. Mild myocarditis as indicated by infiltrates containing mononuclear cells (MNCs) were noted in all groups. Boxed areas are shown at higher magnifications to the right in each panel. Arrows, inflammatory foci. Scale bar: 120 µm (overview images, 10×), 30 µm (magnifications, 40×). **(B)** Immunohistochemistry. Heart sections obtained from animals immunized with a mixture of β_1AR_{Ac} 171–190, 181–200, and 211–230 were evaluated for the presence of T cells (CD3, CD4, and CD8) and non-T cells ($Ly6G^+$ neutrophils, $CD11b^+$ macrophages and $CD19^+$ B cells) using antibodies for each marker or their isotype controls. After washing and addition of horseradish peroxidase (HRP)-conjugated secondary antibodies, cells positive for each marker were identified as shown with arrows. Representative sections from groups involving five to eight mice are shown. Naive and CFA/PT, controls; and scale bar, 60 µm.

19–21-mers can act as common epitopes for both CD4 and CD8 T cells as shown with Myhc 334–352 (31), myelin oligodendrocyte glycoprotein 35–55 (52), and interphotoreceptor retinoid-binding protein 1–20 (53). In the present study however, we did not investigate localization of CD8 T cell epitopes in the β_1AR peptides, and such an identity may then create opportunities to determine how CD8 T cells independently or together with CD4 T cells can induce myocarditis, since their effector functions are distinct (CD8 cytotoxic vs. CD4 Th).

Further, we made efforts to characterize CD4 T cell responses as to their antigen-specificity. First, we determined MHC class II-binding affinities of β_1AR_{Ac} peptides using soluble MHC class-II/IA^k and IE^k monomers (26, 28, 30). These analyses revealed two of the three peptides that induced T cell responses (**Figure 1**) namely, β_1AR_{Ac} 171–190 and β_1AR_{Ac} 211–230 could bind IA^k molecules as indicated by their respective IC_{50} values, 26.14 ± 12.41 and 18.64 ± 1.23 μM, whereas the binding affinity of β_1AR_{Ac} 181–200 was low (97.15 ± 2.07 μM) (**Figure 3**, left panel; $P < 0.01$). Of note, in a comparative analysis, another peptide, β_1AR_{Ac} 201–220 that did not induce T cell response failed to bind IA^k molecule (Figure S1B in Supplementary Material), and it was not chosen for further characterization. Since, β_1AR_{Ac} 181–200, a T cell activator was found to be a poor binder of IA^k, we generated IE^k monomers to determine its ability to bind IE^k molecule, since A/J mice express both IA^k and IE^k molecules (33, 34). By using IE^k monomers, and MCC 82–103 as a reference peptide, we determined that β_1AR_{Ac} 181–200 to be a good binder of IE^k molecule as indicated by the IC_{50} value 6.12 ± 0.69 μM (**Figure 3**, right panel). Based on this information, we decided to create two sets of dextramers: IA^k dextramers for β_1AR_{Ac} 171–190 and β_1AR_{Ac} 211–230 with RNase 43–56 as control, and IE^k dextramers for β_1AR_{Ac} 181–200 and MCC 82–103 (control). Using these reagents, we tested the antigen-specificity of T cell responses in animals immunized with β_1AR_{Ac} 171–190, β_1AR_{Ac} 181–200, and β_1AR_{Ac} 211–230, respectively. CD4 T cells from cultures stimulated with the respective peptides were found to bind dextramers antigen-specifically, whereas the staining intensity obtained with the control dextramers was low as determined by flow cytometry (**Figure 4**). As we have reported previously for various self- and foreign-antigens (28, 34, 35, 54), we noted that the dextramers for all the three T cell epitopes of β_1AR were also preferentially found to bind activated CD4^{high} than CD4^{low} subset. The percent dext$^+$ CD4^{high} T cells were: β_1AR_{Ac} 171–190 (3.27 ± 0.56%) vs. RNase 43–56 (0.52 ± 0.08%) ($P = 0.049$, **Figure 4A**), β_1AR_{Ac} 181–200 (0.71 ± 0.09%) vs. MCC 82–103 (0.33 ± 0.03%) ($P = 0.028$, **Figure 4B**), and β_1AR_{Ac} 211–230 (0.51 ± 0.01%) vs. RNase 43–56 (0.12 ± 0.01%) ($P = 0.0003$, **Figure 4C**). The data point to a possibility that the antigen-sensitized CD4 T cells might be the mediators of disease.

Next, we sought to determine the pathogenic potential of T cells sensitized with β_1AR 171–190, β_1AR 181–200, or β_1AR 211–230 by analyzing their ability to produce various inflammatory cytokines (**Figure 5**). Supernatants from cultures stimulated with or without specific or control (RNase 43–56/HEL 46–61) antigens revealed the presence of all cytokines, except IL-4. Data revealed no striking differences for any of the cytokines except that IL-17A was tended to be elevated in β_1AR 171–190 and β_1AR 181–200 cultures ($P = 0.06$, **Figure 5**). Conversely, production of IFN-γ, another key cytokine was not altered including other pro-inflammatory (IL-6 and TNF-α) or anti-inflammatory (IL-4 and IL-10) cytokines. Accumulated literature suggests that IFN-γ can act as a disease-protective or disease-inducing cytokine in various myocarditis models, and such differential effects may be antigen-dependent (55). Likewise, IL-17A appears not to be required for initiating the disease, but plays a critical role for progression of myocarditis (56). We have also seen that cardiac-reactive T cells produce mostly IFN-γ (30) and/or IL-17A in addition to IL-6 and TNF-α in A/J mice (26, 28). Since, IFN-γ-production was found to be unaltered with β_1AR peptides, production of IL-17A alone might be insufficient to initiate myocarditis which is consistent with the observations made in Myhc 614–629-induced myocarditis (56). TNF-α and IL-6, being inflammatory cytokines may have a role in myocarditis (57, 58), but their amounts were low in cultures stimulated with β_1AR peptides to predict their impact. The finding that IL-4 or IL-10 were detected in insignificant amounts in all the cultures, suggests that the mild nature of disease in the

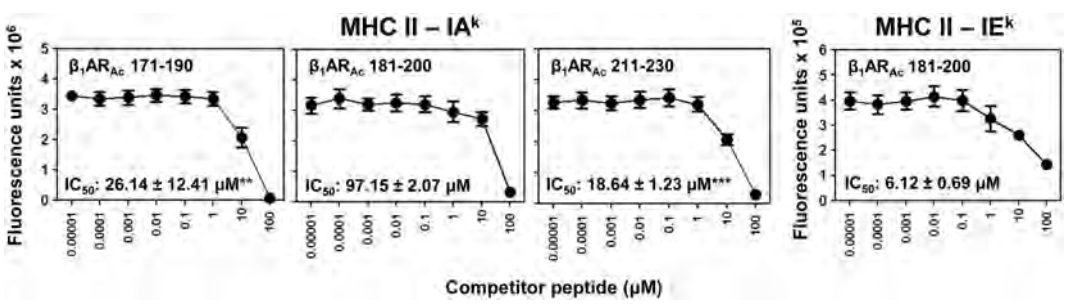

FIGURE 3 | Determination of major histocompatibility complex (MHC) class II-binding affinities of β_1AR_{Ac} peptides. Mixtures containing thrombin-cleaved IA^k and IE^k soluble monomers (0.35 μg), competitor peptides—β_1AR_{Ac} 171–190, β_1AR_{Ac} 181–200, and β_1AR_{Ac} 211–230 (0.00001–100 μM)—and biotinylated hen egg lysozyme (HEL) 46–61 (reference for IA^k) and moth cytochrome *c* (MCC) 82–103 (reference for IE^k) (1 μM) were prepared and added to fluorescence plates coated with anti-IA^k or IE^k in duplicates as described in the methods. After washing, and addition of europium-labeled streptavidin (SA) and dissociation-enhanced lanthanide fluoroimmunoassay (DELFIA) enhancer, fluorescence intensities were measured at excitation/emission wavelengths of 340/615 nm to calculate the IC_{50} values. Mean ± SEM values from three individual experiments with two replicates in each are shown. $^{**}P < 0.01$ and $^{***}P < 0.001$ vs. IC_{50} of IA^k/β_1AR_{Ac} 181–200.

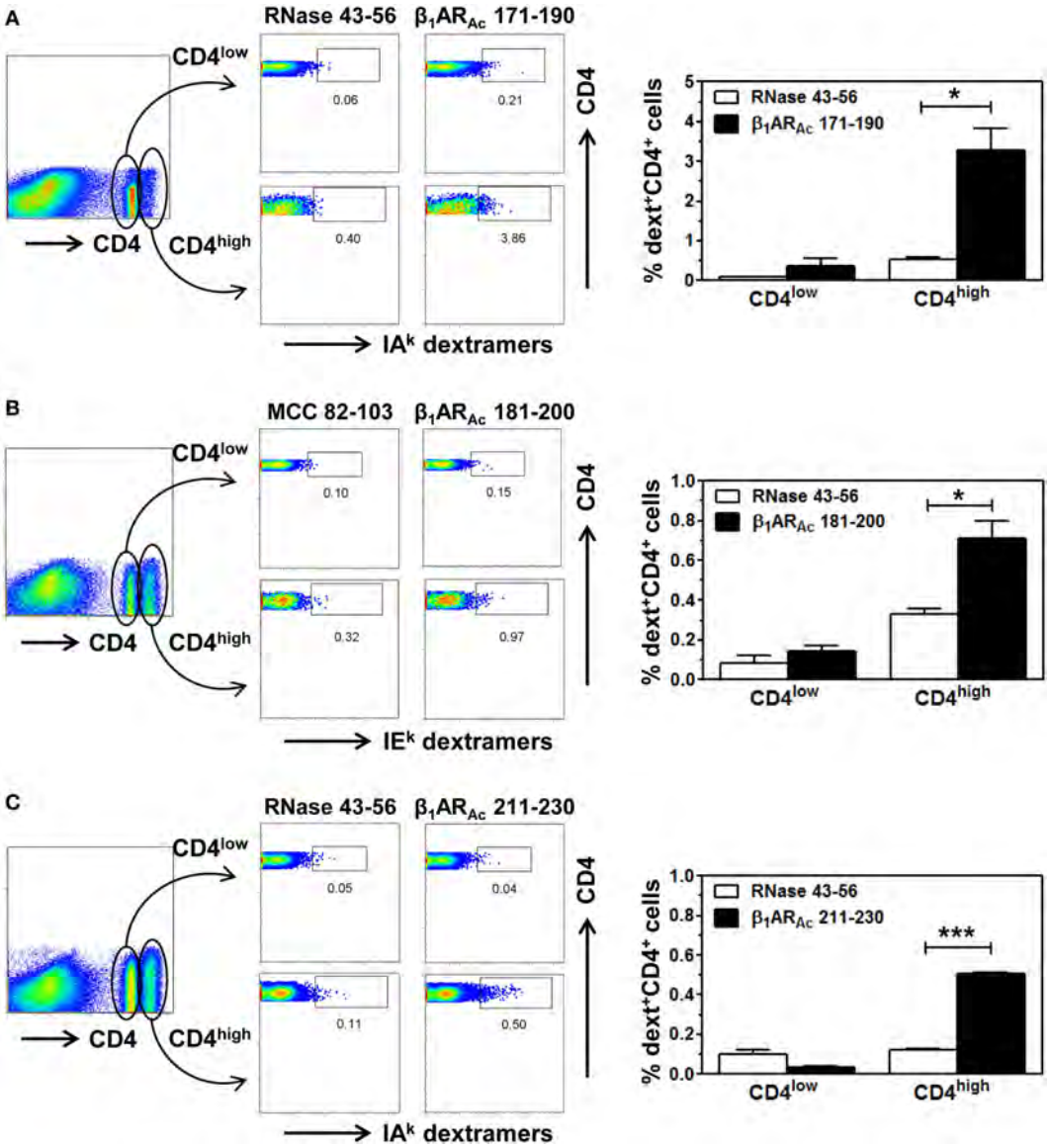

FIGURE 4 | Antigen-specificity of T cell responses induced by β_1AR_{Ac} peptides. Lymph node cells (LNCs) or splenocytes prepared from animals immunized with β_1AR_{Ac} 171–190, β_1AR_{Ac} 181–200, and β_1AR_{Ac} 211–230 were restimulated with the corresponding peptides for 2 days and cells were rested in interleukin (IL)-2 medium. Cells harvested on days 7–10 poststimulation were stained with three sets of dextramers namely, IA^k dextramers (β_1AR_{Ac} 171–190 and RNase 43–56 as control), panel **(A)**; IE^k dextramers [β_1AR_{Ac} 181–200 and moth cytochrome *c* (MCC) 82–103 as control], panel **(B)**; and IA^k dextramers (β_1AR_{Ac} 211–230 with RNase 43–56 as control), panel **(C)**; followed by staining with anti-CD4 and 7-aminoactinomycin-D (7-AAD). Cells were acquired by flow cytometry, and the dext$^+$ cells were analyzed corresponding to $CD4^{low}$ or $CD4^{high}$ populations using Flow Jo software (bar graphs on the right side in each panel). Representative flow cytometric plots are shown from two to three individual experiments, with two to five mice per group. $^*P < 0.05$ and $^{***}P < 0.001$ vs. control dextramers.

immunized animals appear not due to immune deviation occurring toward Th2 phenotype.

To investigate whether β_1AR-reactive cells producing differential amounts of Th1 and Th17 cytokines could determine the disease outcome, we performed adoptive transfer experiments using antigen-primed T cells treated with or without a cocktail of cytokines that polarize toward Th1 and Th17 responses (41–44). As shown in Figure S4 in Supplementary Material, we noted increase in the frequencies of cells expressing Th1 (IL-2 and IFN-γ) and Th17 (IL-17A and IL-22) including Th2 (IL-4 and IL-10) cytokines as reported by others (41–44, 59, 60). However, comparative analysis revealed Th1-producing cells to be significantly enhanced in β_1AR 181–200 cultures as opposed to Th2 cytokine-producing cells in β_1AR_{Ac} 171–190 and β_1AR_{Ac} 211–230 cultures but with no significant increase in the Th17 subset in any of the groups. **Table 2** shows that the naive animals receiving unpolarized lymphocytes specific to β_1AR_{Ac} 171–190 and β_1AR_{Ac} 211–230 had no inflammatory foci in their hearts, where as one animal receiving β_1AR_{Ac} 181–200-primed lymphocytes had heart lesions. When the cells were exposed

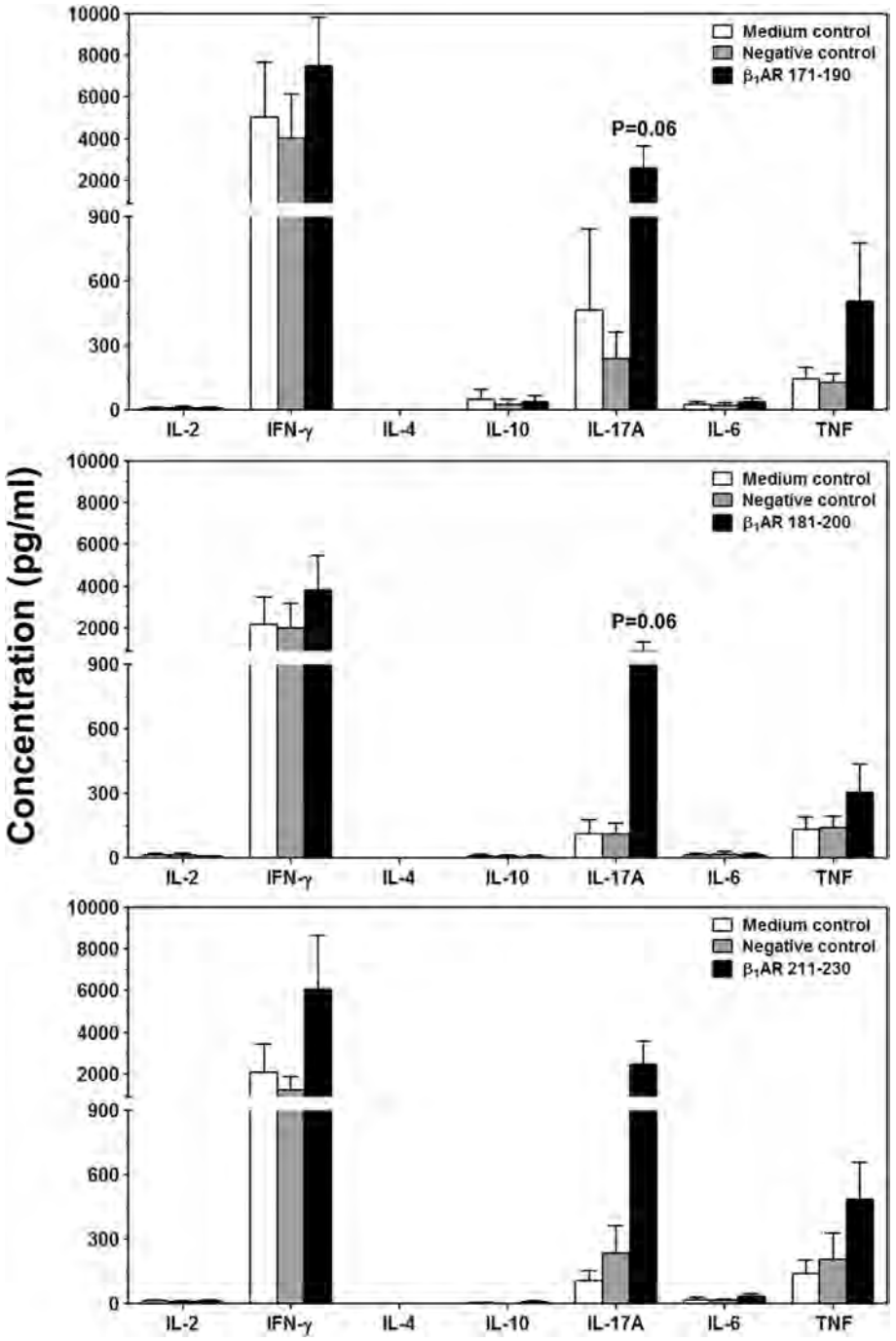

FIGURE 5 | Cytokine responses induced by β_1AR_{Ac} peptides. Lymph node cells (LNCs) were prepared from animals immunized with acetylated or non-acetylated β_1AR 171–190, β_1AR 181–200, or β_1AR 211–230, and after restimulating with or without the immunizing peptides or RNase 43–56/HEL 46–61 (negative controls), culture supernatants were harvested on day 3. Samples were analyzed for indicated cytokines by bead array analysis as described in the methods section. Each bar represents mean ± SEM values derived from four to five individual experiments, with three to eight mice per group.

to the polarizing conditions as described above, it was clear that the naive animals receiving β_1AR_{Ac} 181–200-primed lymphocytes had severe myocarditis (25.8 ± 7.4 foci; **Table 2**; **Figure 6A**; Figure S5 in Supplementary material). Under similar conditions, β_1AR_{Ac} 171–190-and β_1AR_{Ac} 211–230-responsive lymphocytes did not result in disease, which may be due to their enhanced ability to produce Th2 cytokines (**Table 2**; Figure S4 in Supplementary Material). Expectedly, heart sections from control groups (saline and LPS/PT) also were negative for inflammatory changes (**Table 2**; **Figure 6A**). Furthermore, by

TABLE 2 | Myocarditis induced by T cells sensitized with β_1AR_{Ac} peptides in naive A/J mice.

Groups	Incidence (%)	Inflammatory foci[a]
Saline	0/4 (0)	0
LPS/PT	0/4 (0)	0
Unpolarized cells		
β_1AR_{Ac} 171–190	0/4 (0)	0
β_1AR_{Ac} 181–200	1/4 (25)	6
β_1AR_{Ac} 211–230	0/4 (0)	0
Th1- and Th17-polarized cells		
β_1AR_{Ac} 171–190	0/4 (0)	0
β_1AR_{Ac} 181–200	4/4 (100)*	25.8 ± 7.4**
β_1AR_{Ac} 211–230	1/4 (25)	1

[a]*Represents mean ± SEM values derived from myocarditic animals.*
**P < 0.05 vs. control groups.*
***P < 0.01 vs. control groups.*

IHC analysis, we noted detection of $CD3^+$, $CD4^+$ and $CD8^+$ T cells and also $CD11b^+$ macrophages in heart sections from animals that received β_1AR_{Ac} 181–200-primed/polarized lymphocytes (**Figure 6B**). These findings may reinforce the notion that the disease induced with β_1AR_{Ac} peptides represents a T cell-mediated, disease as we have demonstrated with other antigens namely, Myhc, ANT, and BCKD kinase (26, 28, 30). While, cytokine-polarized experiments provided explanations as to why the disease-severity was mild in animals that received CFA/β_1AR_{Ac} peptide emulsions by active immunizations, occurrence of disease with only β_1AR_{Ac} 181–200-sensitized T cells, but not for two other peptides (β_1AR_{Ac} 171–190 and β_1AR_{Ac} 211–230) in adoptive transfer experiments may indicate that both Th1 and Th17 cytokines are critical for disease induction. Alternatively, it is possible that cytokines other than Th1 and Th17 subsets may have a role in the disease-mediation with β_1AR_{Ac} 181–200-sensitized T cells because comparison of frequencies of cytokine-producing cells between groups did not reveal striking differences for any of the cytokines tested.

Finally, we evaluated antibody responses for a panel of β_1AR_{Ac} peptides. These include peptides that induced both T cell responses and disease (β_1AR_{Ac} 171–190, β_1AR_{Ac} 181–200, and β_1AR_{Ac} 211–230), and those that did not induce T cell responses or disease (β_1AR_{Ac} 191–210 and β_1AR_{Ac} 201–220). Serum samples collected from immunized animals were tested for their reactivity to the immunizing peptides as indicated above or an irrelevant control, RNase 43–56. The analyses revealed detection of total Igs specific to β_1AR_{Ac} peptides, since such a reactivity was found lacking for RNase 43–56 (**Figure 7A**). However, comparison of antibody responses between different peptides revealed antibody response to β_1AR_{Ac} 201–220 and to some degree, β_1AR_{Ac} 191–210 (**Figure 7A**). By further characterizing various isotypes, we noted that the antibody response induced with β_1AR_{Ac} 201–220 involved the production of all IgG isotypes (IgG1, IgG2a, IgG2b, IgG3) including IgM, except IgA and IgE (**Figure 7B**). By being a non-T cell activator (Figure S1A in Supplementary Material), production of various isotypes of Abs specific to β_1AR_{Ac} 201–220 may mean that the antigen-specific B cells might have received cytokines from non-T cell sources for isotype switching to occur. One potential source is the adjuvant (CFA) that can promote isotype switching through the secretion of Type I IFNs from dendritic cells as shown previously (61). Furthermore, it is to be noted that β_1AR_{Ac} 201–220 encompasses 20 amino acids of the previously reported B cell epitope, β_1AR 197–222 that was shown to induce antibodies in various rodent species (21, 24, 25). Our data also supports this observation. Detection of antibodies to β_1AR_{Ac} 191–210 may be due to the presence of overlapping sequence between β_1AR_{Ac} 191–210 and β_1AR_{Ac} 201–220. However, the observation that β_1AR_{Ac} 201–220 failed to induce myocarditis in our model may not necessarily mean that the β_1AR_{Ac} 201–220-induced antibodies are not pathogenic. The reason for this discrepancy is that animals needed to be repeatedly immunized with β_1AR_{Ac} 197–222 for a period of 12 months in rats and rabbits, and mice were also to be immunized with six doses of CFA/peptide emulsions (21–25). We did not investigate whether A/J mice immunized for such a prolonged period can develop myocarditis, since we limited our focus to the extent of identifying T cell epitopes, and their ability to induce myocarditis in a standard disease-inducing protocol.

In summary, we demonstrate existence of multiple immunodominant epitopes that are unique to T cells or B cells, but not both. Use of a single motif, β_1AR 197–222 as a B cell epitope to determine the mechanisms of antibody-mediated myocardial disease in several rodent species was perhaps on the idea that the epitope was found conserved (Table S1 in Supplementary Material). Along the same lines, comparison of sequences between humans, mice, rats and rabbits revealed 100% identity for all T cell epitopes that we have described namely, β_1AR 181–200, and β_1AR 211–230 with only one residue being different for β_1AR 171–190 between humans and mice (Table S6 in Supplementary Material), suggest that these epitopes may be relevant to evaluate T cell responses in humans. In addition, we noted that splenocytes from naive animals responded to two out of three T cell epitopes namely, β_1AR_{Ac} 171–190, and β_1AR_{Ac} 181–200 (Figure S6 in Supplementary Material) indicating that the naive repertoire can contain a proportion of β_1AR-reactive T cells that might have responded in response to peptide immunizations. Reports suggest that β_1AR proteins are differentially expressed in the thymus with a predominant form being β_2AR (62). It is possible that the developing thymocytes may escape from thymic tolerance mechanisms due to low β_1AR-expression in the thymus leading to their emigration to the periphery. Thus, we speculate that the preexisting β_1AR-reactive T cells can be activated under conditions of self-tolerance to be broken by environmental triggers. Of note, cross-reactive immune responses have been noted between *Trypanosoma cruzi* and β_1AR and it might be interesting to determine whether such responses are directed against the T cell epitopes in A/J mice which are also highly susceptible to *T. cruzi* infection (63, 64). Additionally, we have demonstrated that the β_1AR-reactive T cells producing insufficient amounts of IFN-γ can become pathogenic under Th1-polarized conditions. Thus, we could envision a scenario that IL-12 produced by the innate immune cells such as macrophages and dendritic cells in response to intracellular pathogens like *T. cruzi* can possibly trigger IFN-γ-producing β_1AR-reactive T cells to become

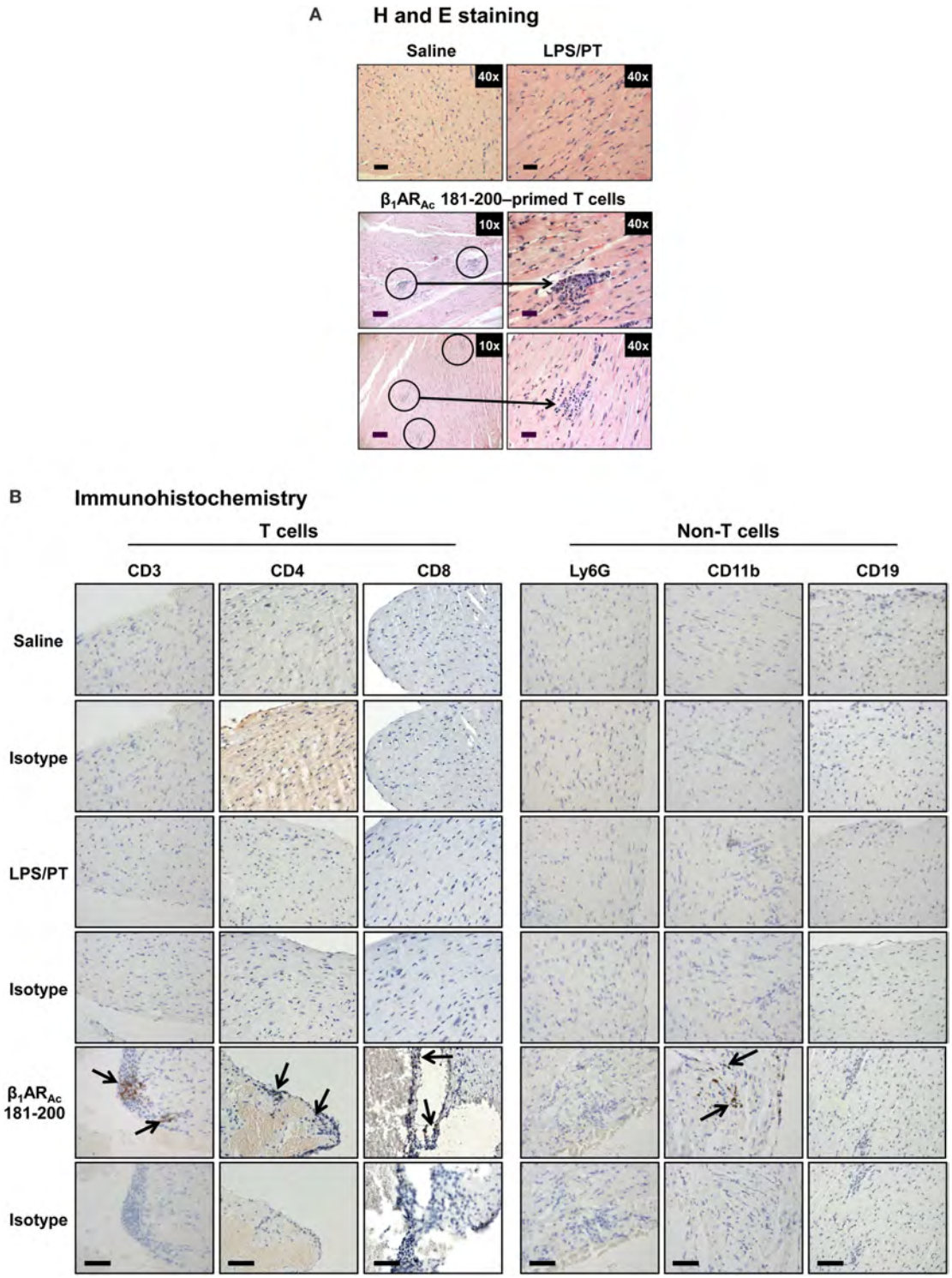

FIGURE 6 | Evaluation of hearts for inflammatory changes in naive recipients of T cells sensitized with β_1AR_{Ac} 181–200. **(A)** Hematoxylin and eosin (H&E) staining. Groups of mice were immunized with a mixture of β_1AR_{Ac} 171–190, β_1AR_{Ac} 181–200, and β_1AR_{Ac} 211–230 and after 14–21 days, lymph node cells (LNCs) were restimulated with the corresponding peptides for 2 days. After exposing to T helper (Th)1- and Th17-polarizing conditions, cells harvested on day 7 postpolarization and administered into naive mice primed with lipopolysaccharide (LPS). Representative normal heart sections in saline and LPS/PT controls are shown in the top panel. The bottom panel represents recipients of β_1AR_{Ac} 181–200-sensitized/polarized T cells. Circled areas are shown at higher magnifications to the right in each panel (arrows, inflammatory foci). Scale bar: 120 μm (overview images, 10×), 30 μm (magnifications, 40×). $n = 4$ mice per group. **(B)** Immunohistochemistry. Heart sections were examined for T cells and non-T cells using the antibodies for indicated markers. Detection of cells positive for each marker (arrows) was analyzed by adding HRP-conjugated secondary antibodies as described in the methods section. Representative sections from four animals in each group are shown. Scale bar, 60 μm.

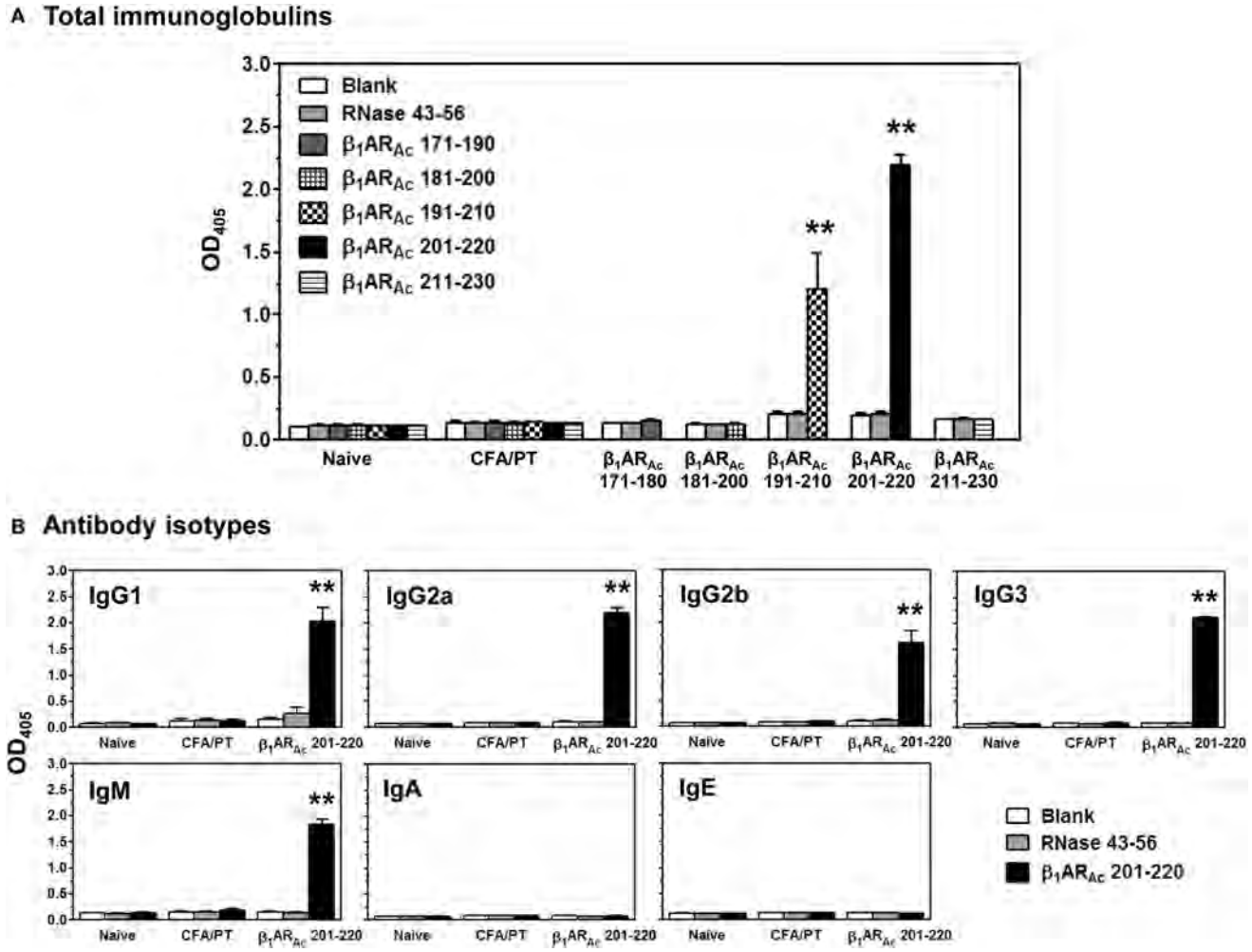

FIGURE 7 | Antibody responses induced by β_1AR_{Ac} peptides. Groups of mice were immunized with β_1AR_{Ac} 171–190, β_1AR_{Ac} 181–200, β_1AR_{Ac} 191–210, β_1AR_{Ac} 201–220, or β_1AR_{Ac} 211–230 and after 21 days, serum was collected. Samples with dilutions of 1:100 were added to low-binding plates coated previously with or without the above peptides or RNase 43–56 (control). After adding horseradish peroxidase (HRP)-conjugated, goat anti-mouse detection antibodies for Igs and different isotypes, plates were read at 405 nm to measure the OD values. Each bar represents mean ± SEM values derived from five animals per group. $^{**}P < 0.01$ vs. controls. **(A)** Total immunoglobulins and **(B)** antibody isotypes.

pathogenic. Such a possibility exists for three reasons: (a) β_1AR is preferentially expressed in the heart; (b) evaluation of non-cardiac tissues such as brain, liver, lung, and kidney in animals immunized with β_1AR peptides did not reveal any significant inflammatory changes relative to control groups (Table S7 in Supplementary Material); and (c) all the three T cell epitopes are unique to β_1AR because they share only 40–65% similarity with β_2AR and β_3AR (Table S8 in Supplementary Material). Thus, the pathogenic β_1AR-reactive T cells are expected to mediate damage preferentially in the heart.

ETHICS STATEMENT

All experiments with mice were performed in accordance with the regulations of and with the approval of the Institutional Animal Care and Use Committee, University of Nebraska-Lincoln, Lincoln, NE, USA (protocol #: 1398).

AUTHOR CONTRIBUTIONS

Conceived and designed the experiments: RHB, CM, AG, and JR. Performed the experiments: RHB, BK, CM, RAR, MZA, and JLS. Analyzed the data: RHB, BK, AG, J-JR, and DS. Wrote the article: RHB and JR.

ACKNOWLEDGMENTS

This work was supported by the National Institutes of Health (HL114669). We thank the sonographer, Leanne Harmman for the echocardiogram images.

SUPPLEMENTARY MATERIAL

The Supplementary Material for this article can be found online at http://www.frontiersin.org/article/10.3389/fimmu.2017.01567/full#supplementary-material.

REFERENCES

1. Centers for Disease Control and Prevention. Changes in mortality from heart failure – United States, 1980–1995. *JAMA* (1998) 280(10):874–5.
2. Basso C, Corrado D, Thiene G. Cardiovascular causes of sudden death in young individuals including athletes. *Cardiol Rev* (1999) 7(3):127–35. doi:10.1097/00045415-199905000-00009
3. Taylor DO, Edwards LB, Boucek MM, Trulock EP, Aurora P, Christie J, et al. Registry of the International Society for Heart and Lung Transplantation: twenty-fourth official adult heart transplant report – 2007. *J Heart Lung Transplant* (2007) 26(8):769–81. doi:10.1016/j.healun.2007.06.004
4. Virmani R, Burke AP, Farb A. Sudden cardiac death. *Cardiovasc Pathol* (2001) 10(5):211–8. doi:10.1016/S1054-8807(01)00091-6
5. Cihakova D, Rose NR. Pathogenesis of myocarditis and dilated cardiomyopathy. *Adv Immunol* (2008) 99:95–114. doi:10.1016/S0065-2776(08)00604-4
6. Dandel M, Wallukat G, Potapov E, Hetzer R. Role of beta(1)-adrenoceptor autoantibodies in the pathogenesis of dilated cardiomyopathy. *Immunobiology* (2012) 217(5):511–20. doi:10.1016/j.imbio.2011.07.012
7. Lappe JM, Pelfrey CM, Tang WH. Recent insights into the role of autoimmunity in idiopathic dilated cardiomyopathy. *J Card Fail* (2008) 14(6):521–30. doi:10.1016/j.cardfail.2008.02.016
8. Limas CJ, Goldenberg IF, Limas C. Soluble interleukin-2 receptor levels in patients with dilated cardiomyopathy. Correlation with disease severity and cardiac autoantibodies. *Circulation* (1995) 91(3):631–4. doi:10.1161/01.CIR.91.3.631
9. Caforio AL, Mahon NJ, Tona F, McKenna WJ. Circulating cardiac autoantibodies in dilated cardiomyopathy and myocarditis: pathogenetic and clinical significance. *Eur J Heart Fail* (2002) 4(4):411–7. doi:10.1016/S1388-9842(02)00010-7
10. Kaya Z, Leib C, Katus HA. Autoantibodies in heart failure and cardiac dysfunction. *Circ Res* (2012) 110(1):145–58. doi:10.1161/CIRCRESAHA.111.243360
11. Limas CJ, Goldenberg IF, Limas C. Autoantibodies against beta-adrenoceptors in human idiopathic dilated cardiomyopathy. *Circ Res* (1989) 64(1):97–103. doi:10.1161/01.RES.64.1.97
12. Ludwig RJ, Vanhoorelbeke K, Leypoldt F, Kaya Z, Bieber K, McLachlan SM, et al. Mechanisms of autoantibody-induced pathology. *Front Immunol* (2017) 8:603. doi:10.3389/fimmu.2017.00603
13. Wallukat G, Wollenberger A, Morwinski R, Pitschner HF. Anti-beta 1-adrenoceptor autoantibodies with chronotropic activity from the serum of patients with dilated cardiomyopathy: mapping of epitopes in the first and second extracellular loops. *J Mol Cell Cardiol* (1995) 27(1):397–406. doi:10.1016/S0022-2828(08)80036-3
14. Madamanchi A. Beta-adrenergic receptor signaling in cardiac function and heart failure. *Mcgill J Med* (2007) 10(2):99–104.
15. Ota A, Matsui H, Asakura M, Nagatsu T. Distribution of beta 1- and beta 2-adrenoceptor subtypes in various mouse tissues. *Neurosci Lett* (1993) 160(1):96–100. doi:10.1016/0304-3940(93)90922-8
16. Granneman JG. The putative beta4-adrenergic receptor is a novel state of the beta1-adrenergic receptor. *Am J Physiol Endocrinol Metab* (2001) 280(2):E199–202.
17. Jahns R, Boivin V, Lohse MJ. beta(1)-Adrenergic receptor function, autoimmunity, and pathogenesis of dilated cardiomyopathy. *Trends Cardiovasc Med* (2006) 16(1):20–4. doi:10.1016/j.tcm.2005.11.002
18. Lohse MJ, Engelhardt S, Eschenhagen T. What is the role of beta-adrenergic signaling in heart failure? *Circ Res* (2003) 93(10):896–906. doi:10.1161/01.RES.0000102042.83024.CA
19. Jane-wit D, Altuntas CZ, Johnson JM, Yong S, Wickley PJ, Clark P, et al. Beta 1-adrenergic receptor autoantibodies mediate dilated cardiomyopathy by agonistically inducing cardiomyocyte apoptosis. *Circulation* (2007) 116(4):399–410. doi:10.1161/CIRCULATIONAHA.106.683193
20. Nussinovitch U, Shoenfeld Y. The clinical significance of anti-beta-1 adrenergic receptor autoantibodies in cardiac disease. *Clin Rev Allergy Immunol* (2013) 44(1):75–83. doi:10.1007/s12016-010-8228-9
21. Buvall L, Bollano E, Chen J, Shultze W, Fu M. Phenotype of early cardiomyopathic changes induced by active immunization of rats with a synthetic peptide corresponding to the second extracellular loop of the human beta-adrenergic receptor. *Clin Exp Immunol* (2006) 143(2):209–15. doi:10.1111/j.1365-2249.2005.02986.x
22. Buvall L, Tang MS, Isic A, Andersson B, Fu M. Antibodies against the beta1-adrenergic receptor induce progressive development of cardiomyopathy. *J Mol Cell Cardiol* (2007) 42(5):1001–7. doi:10.1016/j.yjmcc.2007.02.007
23. Fukuda Y, Miyoshi S, Tanimoto K, Oota K, Fujikura K, Iwata M, et al. Autoimmunity against the second extracellular loop of beta(1)-adrenergic receptors induces early afterdepolarization and decreases in K-channel density in rabbits. *J Am Coll Cardiol* (2004) 43(6):1090–100. doi:10.1016/j.jacc.2003.09.057
24. Matsui S, Fu ML, Katsuda S, Hayase M, Yamaguchi N, Teraoka K, et al. Peptides derived from cardiovascular G-protein-coupled receptors induce morphological cardiomyopathic changes in immunized rabbits. *J Mol Cell Cardiol* (1997) 29(2):641–55. doi:10.1006/jmcc.1996.0307
25. Zuo L, Bao H, Tian J, Wang X, Zhang S, He Z, et al. Long-term active immunization with a synthetic peptide corresponding to the second extracellular loop of beta1-adrenoceptor induces both morphological and functional cardiomyopathic changes in rats. *Int J Cardiol* (2011) 149(1):89–94. doi:10.1016/j.ijcard.2009.12.023
26. Basavalingappa RH, Massilamany C, Krishnan B, Gangaplara A, Kang G, Khalilzad-Sharghi V, et al. Identification of an epitope from adenine nucleotide translocator 1 that induces inflammation in heart in A/J mice. *Am J Pathol* (2016) 186(12):3160–75. doi:10.1016/j.ajpath.2016.08.005
27. Donermeyer DL, Beisel KW, Allen PM, Smith SC. Myocarditis-inducing epitope of myosin binds constitutively and stably to I-Ak on antigen-presenting cells in the heart. *J Exp Med* (1995) 182(5):1291–300. doi:10.1084/jem.182.5.1291
28. Massilamany C, Gangaplara A, Steffen D, Reddy J. Identification of novel mimicry epitopes for cardiac myosin heavy chain-alpha that induce autoimmune myocarditis in A/J mice. *Cell Immunol* (2011) 271(2):438–49. doi:10.1016/j.cellimm.2011.08.013
29. Pummerer CL, Luze K, Grassl G, Bachmaier K, Offner F, Burrell SK, et al. Identification of cardiac myosin peptides capable of inducing autoimmune myocarditis in BALB/c mice. *J Clin Invest* (1996) 97(9):2057–62. doi:10.1172/JCI118642
30. Krishnan B, Massilamany C, Basavalingappa RH, Gangaplara A, Kang G, Li Q, et al. Branched chain alpha-ketoacid dehydrogenase kinase 111-130, a T cell epitope that induces both autoimmune myocarditis and hepatitis in A/J mice. *Immun Inflamm Dis* (2017). doi:10.1002/iid3.177
31. Massilamany C, Gangaplara A, Basavalingappa RH, Rajasekaran RA, Khalilzad-Sharghi V, Han Z, et al. Localization of CD8 T cell epitope within cardiac myosin heavy chain-alpha334-352 that induces autoimmune myocarditis in A/J mice. *Int J Cardiol* (2016) 202:311–21. doi:10.1016/j.ijcard.2015.09.016
32. Dawson NJ. The surface-area-body-weight relationship in mice. *Aust J Biol Sci* (1967) 20(3):687–90. doi:10.1071/BI9670687
33. Hirayama M, Azuma E, Jiang Q, Kobayashi M, Iwamoto S, Kumamoto T, et al. The reconstitution of CD45RBhiCD4+ naive T cells is inversely correlated with donor age in murine allogeneic haematopoietic stem cell transplantation. *Br J Haematol* (2000) 111(2):700–7. doi:10.1111/j.1365-2141.2000.02391.x
34. Massilamany C, Gangaplara A, Chapman N, Rose N, Reddy J. Detection of cardiac myosin heavy chain-alpha-specific CD4 cells by using MHC class II/IA(k) tetramers in A/J mice. *J Immunol Methods* (2011) 372(1–2):107–18. doi:10.1016/j.jim.2011.07.004
35. Massilamany C, Upadhyaya B, Gangaplara A, Kuszynski C, Reddy J. Detection of autoreactive CD4 T cells using major histocompatibility complex class II dextramers. *BMC Immunol* (2011) 12(1):1. doi:10.1186/1471-2172-12-40
36. Fremont DH, Dai S, Chiang H, Crawford F, Marrack P, Kappler J. Structural basis of cytochrome c presentation by IE^k. *J Exp Med* (2002) 195(8):1043–52. doi:10.1084/jem.20011971
37. Kasson PM, Rabinowitz JD, Schmitt L, Davis MM, McConnell HM. Kinetics of peptide binding to the class II MHC protein I– Ek. *Biochemistry* (2000) 39(5):1048–58. doi:10.1021/bi9921337
38. Wu LC, Tuot DS, Lyons DS, Garcia KC, Davis MM. Two-step binding mechanism for T-cell receptor recognition of peptide–MHC. *Nature* (2002) 418(6897):552–6. doi:10.1038/nature00920
39. Reddy J, Bettelli E, Nicholson L, Waldner H, Jang MH, Wucherpfennig KW, et al. Detection of autoreactive myelin proteolipid protein 139-151-specific T cells by using MHC II (IAs) tetramers. *J Immunol* (2003) 170(2):870–7. doi:10.4049/jimmunol.170.2.870

40. Gangaplara A, Massilamany C, Brown DM, Delhon G, Pattnaik AK, Chapman N, et al. Coxsackievirus B3 infection leads to the generation of cardiac myosin heavy chain-alpha-reactive CD4 T cells in A/J mice. *Clin Immunol* (2012) 144(3):237–49. doi:10.1016/j.clim.2012.07.003
41. Holley MM, Kielian T. Th1 and Th17 cells regulate innate immune responses and bacterial clearance during central nervous system infection. *J Immunol* (2012) 188(3):1360–70. doi:10.4049/jimmunol.1101660
42. Jager A, Dardalhon V, Sobel RA, Bettelli E, Kuchroo VK. Th1, Th17, and Th9 effector cells induce experimental autoimmune encephalomyelitis with different pathological phenotypes. *J Immunol* (2009) 183(11):7169–77. doi:10.4049/jimmunol.0901906
43. Kanakasabai S, Chearwae W, Walline CC, Iams W, Adams SM, Bright JJ. Peroxisome proliferator-activated receptor delta agonists inhibit T helper type 1 (Th1) and Th17 responses in experimental allergic encephalomyelitis. *Immunology* (2010) 130(4):572–88. doi:10.1111/j.1365-2567.2010.03261.x
44. Lee Y, Awasthi A, Yosef N, Quintana FJ, Xiao S, Peters A, et al. Induction and molecular signature of pathogenic TH17 cells. *Nat Immunol* (2012) 13(10):991–9. doi:10.1038/ni.2416
45. Hamada Y, Takata M, Kiyoku H, Enzan H, Doi Y, Fujimoto S. Monomethoxypolyethylene glycol-modified cardiac myosin treatment blocks the active and passive induction of experimental autoimmune myocarditis. *Circ J* (2004) 68(2):149–55. doi:10.1253/circj.68.149
46. Storck S, Delbos F, Stadler N, Thirion-Delalande C, Bernex F, Verthuy C, et al. Normal immune system development in mice lacking the Deltex-1 RING finger domain. *Mol Cell Biol* (2005) 25(4):1437–45. doi:10.1128/MCB.25.4.1437-1445.2005
47. Kaya Z, Goser S, Buss SJ, Leuschner F, Ottl R, Li J, et al. Identification of cardiac troponin I sequence motifs leading to heart failure by induction of myocardial inflammation and fibrosis. *Circulation* (2008) 118(20):2063–72. doi:10.1161/CIRCULATIONAHA.108.788711
48. Magnusson Y, Marullo S, Hoyer S, Waagstein F, Andersson B, Vahlne A, et al. Mapping of a functional autoimmune epitope on the beta 1-adrenergic receptor in patients with idiopathic dilated cardiomyopathy. *J Clin Invest* (1990) 86(5):1658–63. doi:10.1172/JCI114888
49. Afanasyeva M, Wang Y, Kaya Z, Park S, Zilliox MJ, Schofield BH, et al. Experimental autoimmune myocarditis in A/J mice is an interleukin-4-dependent disease with a Th2 phenotype. *Am J Pathol* (2001) 159(1):193–203. doi:10.1016/S0002-9440(10)61685-9
50. Zhao W, Wegmann KW, Trotter JL, Ueno K, Hickey WF. Identification of an N-terminally acetylated encephalitogenic epitope in myelin proteolipid apoprotein for the Lewis rat. *J Immunol* (1994) 153(2):901–9.
51. Fabiani I, Pugliese NR, La Carrubba S, Conte L, Antonini-Canterin F, Colonna P, et al. Incremental prognostic value of a complex left ventricular remodeling classification in asymptomatic for heart failure hypertensive patients. *J Am Soc Hypertens* (2017) 11(7):412–9. doi:10.1016/j.jash.2017.05.005
52. Leech MD, Carrillo-Vico A, Liblau RS, Anderton SM. Recognition of a high affinity MHC class I-restricted epitope of myelin oligodendrocyte glycoprotein by CD8(+) T cells derived from autoantigen-deficient mice. *Front Immunol* (2011) 2:17. doi:10.3389/fimmu.2011.00017
53. Shao H, Peng Y, Liao T, Wang M, Song M, Kaplan HJ, et al. A shared epitope of the interphotoreceptor retinoid-binding protein recognized by the CD4+ and CD8+ autoreactive T cells. *J Immunol* (2005) 175(3):1851–7. doi:10.4049/jimmunol.175.3.1851
54. Massilamany C, Marciano-Cabral F, Rocha-Azevedo B, Jamerson M, Gangaplara A, Steffen D, et al. SJL mice infected with *Acanthamoeba castellanii* develop central nervous system autoimmunity through the generation of cross-reactive T cells for myelin antigens. *PLoS One* (2014) 9(5):e98506. doi:10.1371/journal.pone.0098506
55. Fairweather D, Rose NR. Inflammatory heart disease: a role for cytokines. *Lupus* (2005) 14(9):646–51. doi:10.1191/0961203305lu2192oa
56. Baldeviano GC, Barin JG, Talor MV, Srinivasan S, Bedja D, Zheng D, et al. Interleukin-17A is dispensable for myocarditis but essential for the progression to dilated cardiomyopathy. *Circ Res* (2010) 106(10):1646–55. doi:10.1161/CIRCRESAHA.109.213157
57. Huber S. Tumor necrosis factor-alpha promotes myocarditis in female mice infected with coxsackievirus B3 through upregulation of CD1d on hematopoietic cells. *Viral Immunol* (2010) 23(1):79–86. doi:10.1089/vim.2009.0063
58. Tanaka T, Kanda T, McManus BM, Kanai H, Akiyama H, Sekiguchi K, et al. Overexpression of interleukin-6 aggravates viral myocarditis: impaired increase in tumor necrosis factor-alpha. *J Mol Cell Cardiol* (2001) 33(9):1627–35. doi:10.1006/jmcc.2001.1428
59. Jankovic D, Kugler DG, Sher A. IL-10 production by CD4+ effector T cells: a mechanism for self-regulation. *Mucosal Immunol* (2010) 3(3):239–46. doi:10.1038/mi.2010.8
60. McGeachy MJ, Bak-Jensen KS, Chen Y, Tato CM, Blumenschein W, McClanahan T, et al. TGF-beta and IL-6 drive the production of IL-17 and IL-10 by T cells and restrain T(H)-17 cell-mediated pathology. *Nat Immunol* (2007) 8(12):1390–7. doi:10.1038/ni1539
61. Le Bon A, Schiavoni G, D'Agostino G, Gresser I, Belardelli F, Tough DF. Type I interferons potently enhance humoral immunity and can promote isotype switching by stimulating dendritic cells in vivo. *Immunity* (2001) 14(4):461–70. doi:10.1016/S1074-7613(01)00126-1
62. Roggero E, Besedovsky HO, del Rey A. The role of the sympathetic nervous system in the thymus in health and disease. *Neuroimmunomodulation* (2011) 18(5):339–49. doi:10.1159/000329581
63. Ferrari I, Levin MJ, Wallukat G, Elies R, Lebesgue D, Chiale P, et al. Molecular mimicry between the immunodominant ribosomal protein P0 of *Trypanosoma cruzi* and a functional epitope on the human beta 1-adrenergic receptor. *J Exp Med* (1995) 182(1):59–65. doi:10.1084/jem.182.1.59
64. Joensen L, Borda E, Kohout T, Perry S, Garcia G, Sterin-Borda L. *Trypanosoma cruzi* antigen that interacts with the beta1-adrenergic receptor and modifies myocardial contractile activity. *Mol Biochem Parasitol* (2003) 127(2):169–77. doi:10.1016/S0166-6851(03)00003-3

Conflict of Interest Statement: The authors declare that the research was conducted in the absence of any commercial or financial relationships that could be construed as a potential conflict of interest.

frontiers in Immunology

ORIGINAL RESEARCH
published: 03 November 2017
doi: 10.3389/fimmu.2017.01366

Innate B-1 B Cells Are Not Enriched in Red Blood Cell Autoimmune Mice: Importance of B Cell Receptor Transgenic Selection

*Amanda L. Richards[1], Heather L. Howie[1], Linda M. Kapp[1], Jeanne E. Hendrickson[2], James C. Zimring[1,3,4] and Krystalyn E. Hudson[1]**

[1] Bloodworks Northwest Research Institute, Seattle, WA, United States, [2] Department of Laboratory Medicine and Pediatrics, Yale University, New Haven, CT, United States, [3] Department of Laboratory Medicine, Division of Hematology, University of Washington, Seattle, WA, United States, [4] Department of Internal Medicine, Division of Hematology, University of Washington, Seattle, WA, United States

OPEN ACCESS

Edited by:
Joanna Davies,
San Diego Biomedical Research Institute, United States

Reviewed by:
Raffi Gugasyan,
Burnet Institute, Australia
Maja Wallberg,
University of Cambridge, United Kingdom

***Correspondence:**
Krystalyn E. Hudson
krystalh@bloodworksnw.org

Specialty section:
This article was submitted to Immunological Tolerance and Regulation, a section of the journal Frontiers in Immunology

Received: 15 August 2017
Accepted: 05 October 2017
Published: 03 November 2017

Citation:
Richards AL, Howie HL, Kapp LM, Hendrickson JE, Zimring JC and Hudson KE (2017) Innate B-1 B Cells Are Not Enriched in Red Blood Cell Autoimmune Mice: Importance of B Cell Receptor Transgenic Selection. Front. Immunol. 8:1366. doi: 10.3389/fimmu.2017.01366

Autoimmune hemolytic anemia (AIHA) results from breakdown of humoral tolerance to RBC antigens. Past analyses of B-cell receptor transgenic (BCR-Tg) mice that recognize RBC autoantigens led to a paradigm in which autoreactive conventional B-2 B cells are deleted whereas extramedullary B-1 B cells escape deletion due to lack of exposure to RBCs. However, BCR-Tg mice utilized to shape the current paradigm were unable to undergo receptor editing or class-switching. Given the importance of receptor editing as mechanism to tolerize autoreactive B cells during central tolerance, we hypothesized that expansion of autoreactive B-1 B cells is a consequence of the inability of the autoreactive BCR to receptor edit. To test this hypothesis, we crossed two separate strains of BCR-Tg mice with transgenic mice expressing the BCR target on RBCs. Both BCR-Tg mice express the same immunoglobulin and, thus, secrete antibodies with identical specificity, but one strain (SwHEL) has normal receptor editing, whereas the other (IgHEL) does not. Similar to other AIHA models, the autoreactive IgHEL strain showed decreased B-2 B cells, an enrichment of B-1 B cells, and detectable anti-RBC autoantibodies and decreased RBC hematocrit and hemoglobin values. However, autoreactive SwHEL mice had induction of tolerance in both B-2 and B-1 B cells with anti-RBC autoantibody production without anemia. These data generate new understanding and challenge the existing paradigm of B cell tolerance to RBC autoantigens. Furthermore, these findings demonstrate that immune responses vary when BCR-Tg do not retain BCR editing and class-switching functions.

Keywords: B cell tolerance, red blood cells, autoimmunity, autoimmunity models, autoantibodies

INTRODUCTION

Establishment and maintenance of immunological tolerance is essential to prevent autoimmunity, and breakdown of tolerance to red blood cell (RBC) antigens may lead to autoantibody production. Development of anti-RBC autoantibodies can occur secondary to lymphoproliferative disorders, infections, or blood transfusions (1, 2); however, in some cases, autoantibodies to RBCs appear to be the result of primary immunodysregulation (3). The process of autoantibody generation to

RBC antigens occurs much more frequently than is generally appreciated, since the vast majority of RBC-specific autoantibodies do not cause any detectable hemolysis or illness. Indeed, up to one out of every 1,000 asymptomatic healthy blood donors have detectable autoantibodies specific for RBCs. However, in the instances where RBC autoantibodies do induce hemolysis, then autoimmune hemolytic anemia (AIHA) can ensue, leading to a severe and sometimes fatal disease (4).

Our understanding of the mechanisms by which B cell tolerance to self-antigens is established and maintained has been significantly advanced through the use of B-cell receptor transgenic (BCR-Tg) mice (5–8). Detailed analyses of BCR-Tg systems have established that developing B cells are tolerized to self-antigens in the bone marrow through receptor editing, deletion, and/or anergy. Applying this approach to the study of B cells specific for autoantigens on RBCs has been carried out in a series of elegant studies using the autoAb 4C8 BCR-Tg mouse model, in which transgenic mice carry immunoglobulin (Ig) genes derived from an anti-erythrocyte autoantibody, 4C8 (9). AutoAb 4C8 BCR-Tg mice show a relative absence of autoreactive conventional (B-2) B cells in the bone marrow and secondary lymphoid organs. By contrast, autoreactive B-1 B cells are enriched in the peritoneal cavity and lamina propria (10, 11). Experimental introduction of a B cell mitogen induces expansion of autoreactive B-1 B cells, correlating with increased autoantibody secretion (12). As a consequence of autoantibody production and hemolysis, the autoAb 4C8 BCR-Tg mice become anemic. Autoantibodies and disease pathology are resolved after elimination of B-1 B cells through hypotonic shock or antigen-induced cross-linking of the BCR (13). Together, these data lead to a model in which B-1 B cells represent a dangerous population in which BCRs specific for RBC autoantigens are not tolerized, presumably because B-1 B cells can develop in extramedullary spaces in which RBC antigens are not likely to be encountered. These data are the basis for the prevailing paradigm of B cell tolerance to RBC autoantigens.

Although the autoAb 4C8 BCR-Tg mouse model led to substantial generation of new knowledge, there are several limitations. The transgenic BCR of the autoAb 4C8 mouse recognizes Band 4.1 (14), a ubiquitous RBC antigen required for RBC membrane stability. Band 4.1 knockout mice are viable (15, 16); however, they exhibit moderate AIHA and their unstable RBC membranes result in abnormal morphology. As such, Band 4.1 knockout mice are not a good control to analyze the effects of the anti-RBC B cells in the absence of autoantigen in the autoAb 4C8 model. In addition, autoAb 4C8 BCR-Tg mice were designed with random integration, are genetically restricted to IgM, and cannot undergo BCR rearrangement, receptor editing, or class-switching. Finally, while the severe hemolysis and chronic inflammation resulting from autoantibody production models AIHA pathology, the presence of autoantibodies simultaneously complicate analysis of baseline immunology. To circumvent these limitations, we engineered a novel model of B cell tolerance to an RBC antigen by utilizing HOD transgenic mice. The HOD mouse expresses a triple fusion protein consisting of hen egg lysozyme (HEL), ovalbumin, and human blood group antigen Duffy (HOD), driven by an RBC-specific promoter (17). Similar to many human RBC autoantibodies, antibodies specific for the HOD antigen do not promote hemolysis.

Two separate BCR-Tg mice with specificity for HEL (contained within HOD) have been described (7, 18). IgHEL mice are random transgenic animals with heavy and light chains specific for HEL, and like autoAb 4C8 BCR-Tg mice, are incapable of undergoing BCR rearrangement, receptor editing, or normal class-switching (7). By contrast, the SwHEL mice were generated with the same Ig transgene as the IgHEL mice, but the heavy chain VDJ region was inserted into the Vh10 locus by homologous recombination; the same light chain was used in both IgHEL and SwHEL animals (18). In this way, anti-HEL B cells in the SwHEL mouse can undergo BCR editing in the bone marrow and can participate in germinal center reactions that result in class-switching to each of the natural antibody isotypes. To further study the mechanisms of B cell tolerance to an RBC autoantigen, we bred HOD mice with either IgHEL or SwHEL mice. This approach allows a direct juxtaposition of the experimental effects of allowing (or preventing) BCR receptor editing, recombination, and class-switching of an Ig specific for an RBC autoantigen.

RESULTS

Peritoneal B-1 B Cells Are Enriched in Autoreactive IgHEL But Not SwHEL Mice

Both IgHEL and SwHEL mice are on a C57BL/6 (B6) background and both were generated using the HyHEL10 heavy and light chain genes, which confer specificity for HEL (6, 18). Accordingly, BCR-Tg B cells found in either IgHEL or SwHEL mice express a BCR with the same HEL-specific paratope. To track and enumerate HEL-reactive B cells in either IgHEL or SwHEL mice, cells were stained with anti-B220 and tetramerized-HEL-APC (HEL-tet). Consistent with previously published data (18, 19), over 90% of B cells from IgHEL mice and 40–60% of B cells in SwHEL mice reacted with HEL-tet (**Figure 1A**, left and representative flow plots, right).

Previous data with the autoAb 4C8 BCR-Tg mouse model provided evidence that autoantibodies were a consequence of incomplete tolerance in the B-1 B cell compartment in the peritoneal cavity (10). To test the association of peritoneal autoreactive B-1 B cells in tolerance to RBC-specific autoantigens, both IgHEL and SwHEL mice were crossed with HOD mice, whereby HEL is part of the HOD fusion construct that has RBC-specific expression (20). B-1 B cells were defined as CD19+IgM+CD43+ events whereas B-2 B cells were defined as CD19+IgM+IgD+CD43− events. HEL-reactive B cells in these populations were determined by binding to HEL-tet.

Control B6 mice had fewer than 1,000 HEL-reactive B-1 B cells detectable in the peritoneum, representing the normal background staining for these mice (**Figure 1B**, left panel; Table S1 in Supplementary Material). No significant difference in this signal was observed in HOD, SwHEL, or IgHEL mice; thus, neither the presence of the HOD antigen nor a HEL-specific Ig transgene increased the number of HEL-reactive B-1 B cells in peritoneal cavity. Co-expression of the Ig transgene and the cognate autoantigen (HEL) in the IgHEL+HOD+ and SwHEL+HOD+ mice

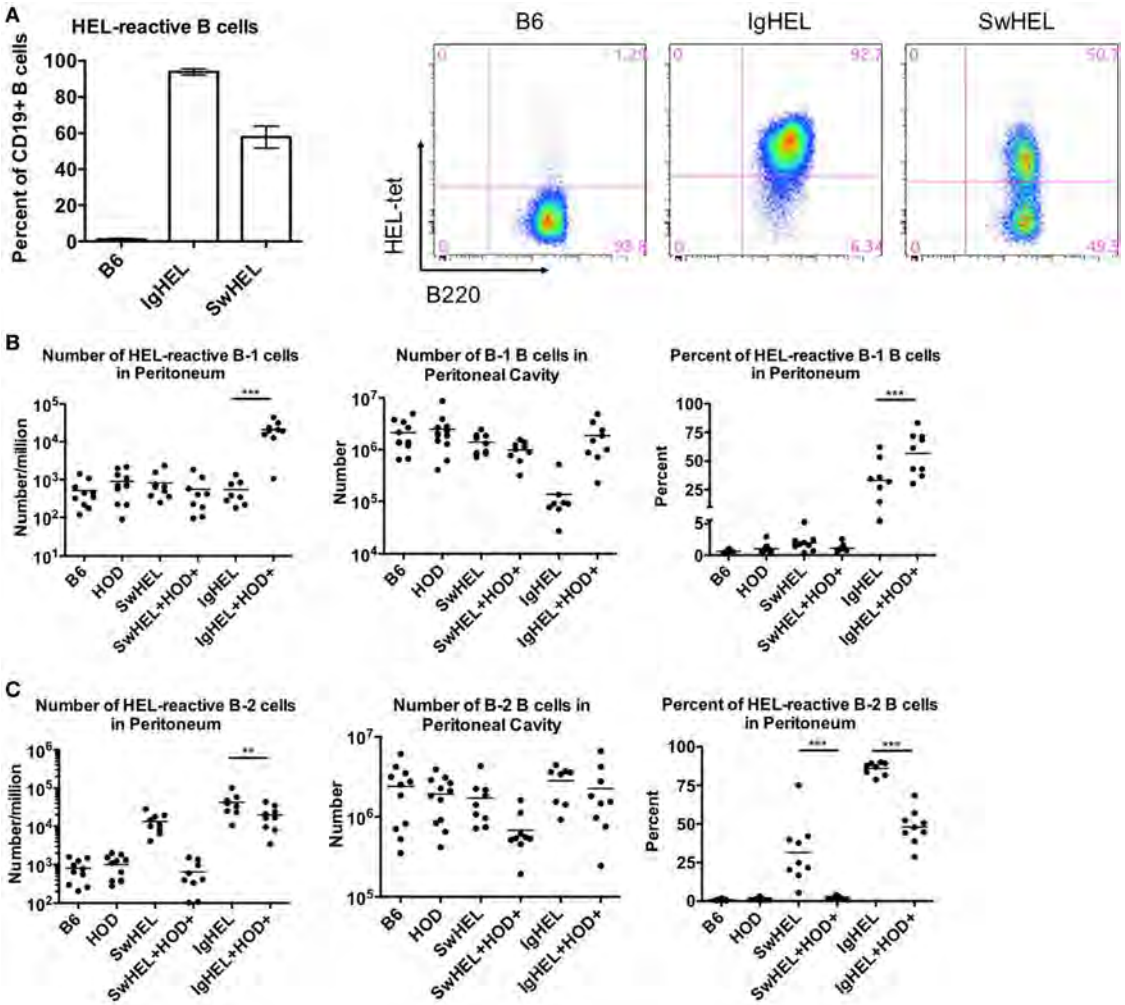

FIGURE 1 | B-1 B cells are enriched in autoreactive IgHEL+HOD+ but not SwHEL+HOD+. Splenocytes and peritoneal cells were harvested and evaluated for expression of cell surface markers to determine the number, frequency, and phenotype of hen egg lysozyme (HEL)-reactive B cells. **(A)** Splenocytes from B6 (left), IgHEL (middle), and SwHEL (right) mice were stained with anti-CD19, anti-B220, and fluorescently labeled HEL (HEL-tet) to determine the frequency of HEL-reactive B cells. Data are representative data from three independent experiments (with at least three mice per group), bar graphs are mean ± SD. Bar graphs and flow plots are gated on CD19+ cells. Peritoneal cells were stained with anti-CD19, anti-IgM, anti-CD43, anti-IgD, and HEL-tet to delineate **(B)** B-1 and **(C)** B-2 B cell subsets and to determine reactivity with HEL. Data shown in **(B,C)** are compiled from three independent experiments with at least three mice per group. Selective *p* values are shown on graphs and * ≤ 0.05, ** ≤ 0.01, and *** ≤ 0.001. For complete statistical analysis with all significant differences, see Table S1 in Supplementary Material.

yielded different observations; the number of HEL-reactive peritoneal B-1 B cells was similar between SwHEL and autoreactive SwHEL+HOD+ mice; however, unlike the observations made with SwHEL animals, there was a significant increase in HEL-reactive B-1 B cell numbers in IgHEL+HOD+ mice, compared to the IgHEL mice (**Figure 1B**, left panel; Table S1 in Supplementary Material).

The observed increase of HEL-reactive B-1 B cells in IgHEL+HOD+ mice was not due to a general increase in B-1 B cells, as the absolute number of peritoneal B-1 B cells (of any specificity) was not increased in IgHEL+HOD+ mice compared to other groups (**Figure 1B**, middle panel). On the contrary, a 10-fold decrease in absolute numbers of B-1 B cells was observed in IgHEL mice, compared to control strains; something not observed in SwHEL mice (**Figure 1B**, middle panel). However, within the decreased B-1 population in IgHEL mice, there was substantial enrichment in the percentage of B cells that were HEL-specific (**Figure 1B**, right panel), thus accounting for the decrease in total number of B-1 B cells but not in the number of HEL-specific B cells in IgHEL mice. Together, these data indicate that expression of the anti-HEL IgM Ig in the IgHEL mouse (in the absence of the HEL antigen) decreases total B-1 B cell numbers, but the surviving population has a high percentage of HEL-specific B cells. Furthermore, co-expression of HEL with the IgHEL BCR (IgHEL+HOD+ mice) resulted in significantly higher numbers of HEL-reactive peritoneal B-1 B cells. Thus, for

the IgHEL mouse, autoantigen promotes the expansion of autoreactive peritoneal B-1 B cells, consistent with the data obtained with the autoAb 4C8 mouse model.

Analysis of the SwHEL mouse gave a very distinct outcome compared to IgHEL. On its own, the SwHEL mouse was not significantly different from the B6 mice with regard to number of B-1 B cells (total or HEL-specific) in the peritoneum, with only a slight (but non-significant) increase in percentage of HEL-specific B-1 B cells (**Figure 1B**). In stark contrast to the IgHEL mouse, crossing SwHEL with HOD mice failed to significantly alter the number or percentage of B-1 B cells, either HEL specific or total. Moreover, the small increase in HEL-specific B-1 B cells in SwHEL mice was not increased by presence of HOD autoantigen (as observed in IgHEL+HOD+), but was decreased to baseline levels seen in control mice (**Figure 1B**, right panel). Together, these data draw a sharp distinction between the fates of autoreactive B-1 B cells in IgHEL vs. SwHEL mice, with a preferential increase in autoreactive peritoneal B-1 B cells in IgHEL+HOD+ but not SwHEL+HOD+ animals.

Analysis of B-2 B cells demonstrated that both B6 and HOD mice have similar numbers and percentages of B-2 B cells in the peritoneal cavity, both for absolute numbers and HEL-specific B-2 B cells (**Figure 1C**, left and middle panels). Consistent with carrying an anti-HEL Ig transgene, both the SwHEL and IgHEL mice have increased B-2 B cells specific for HEL (numbers and percentages) (**Figure 1C**, left and right panels), but in neither instance is this simply the result of increased total numbers of B-2 B cells as numbers of total B-2 B cells is unaltered in SwHEL or IgHEL mice compared to control strains (**Figure 1C**, middle panel). Crossing IgHEL or SwHEL with HOD gave distinct results. Numbers of HEL-reactive B-2 B cells were significantly reduced in IgHEL+HOD+ mice compared to IgHEL alone; however, despite this decrease, there remain a significantly elevated number of HEL-reactive B-2 B cells in IgHEL+HOD+ mice compared to controls (**Figure 1C**, left panel). By contrast, in SwHEL+HOD+ mice, HEL-reactive B-2 B cells were decreased (although this reduction was not statistically significant), returning to control baseline numbers. Some of the decrease in HEL-reactive B-2 B cells in SwHEL+HOD+ mice may be due to a reduction in the total number of B-2 B cells (**Figure 1C**, middle panel); however, analysis of percentages of HEL-reactive B-2 B cells shows a large percentage of HEL-reactive B-2 B cells in SwHEL mice that were absent in SwHEL+HOD+ animals. A similar trend was observed in the percentage of B-2 B cells that are HEL-reactive in IgHEL+HOD+ mice, but to a much lesser extent.

In aggregate, these findings demonstrate a significant enrichment of RBC autoreactive B-1 B cells in IgHEL+HOD+ mice that is absent in SwHEL+HOD+ mice. Moreover, RBC autoreactive B-2 B cells largely persisted in IgHEL+HOD+ mice, but were essentially absent in SwHEL+HOD+ mice. Thus, the question of how RBC autoantigens educate autoreactive B cells yields a very different answer depending upon whether the BCR transgene is a random integrant that cannot undergo BCR recombination, receptor editing, or class-switching vs. a knock-in that retains the ability to participate in these processes.

B Cell Development in the Bone Marrow Is Altered in IgHEL BCR-Tg Mice

To test the effects of RBC-specific antigen expression upon central tolerance mechanisms, B cell development in bone marrow was analyzed by flow cytometry. The baseline percentages of B cells in SwHEL mice was equivalent to B6 and HOD control strains, whereas a slight decrease was observed in IgHEL mice (**Figure 2A**; Table S2 in Supplementary Material). SwHEL+HOD+ had no decrease in B cell percentages in bone marrow compared to SwHEL mice; by contrast, IgHEL+HOD+ mice had a significant decrease in B cells compared to control B6 and HOD mice and a slight reduction compared to IgHEL+ mice (**Figure 2A**; Table S2 in Supplementary Material). Thus, the presence of autoantigen results in a decrease in B cell percentages for IgHEL+HOD+ but not SwHEL+HOD+ mice.

To analyze individual stages of B cell development, total B220+ cells were categorized into developmental Fractions A–F using surface expression of B220, CD43, BP-1, CD24, IgD, and IgM. Stages of B cell development consist of A = pre–pro-B, B = pro-B, C = early pre-B, D = IgM − IgD− late pre-B cells, E = new B, and F = antigen naïve, mature B (gating strategy shown in **Figure 2B**) (21, 22). Percentages of B cells in bone marrow from SwHEL mice (**Figure 2C**, top row) had similar frequencies of B cells in each developmental stage as was observed in control B6 and HOD mice (data not shown). By contrast, IgHEL mice had a significantly smaller percentage of B cells in Fraction C, the developmental stage for rearrangement of the heavy chain locus (**Figure 2C**, bottom row). In addition, IgHEL mice had a decrease in the percentage of B cells detected in Fraction D (pre-B cells with phenotype IgM − IgD−), during which light chain rearrangement occurs. Concomitantly, IgHEL mice had a significant increase in the percentage of cells detected in Fraction F, the final stage of B cell maturation where B cells express IgM+IgD+. Accordingly, IgHEL and SwHEL mice have different baseline B cells at each stage of development (in the absence of autoantigen), likely as a result of the different genetic constructs.

Bone marrow from IgHEL and SwHEL mice was juxtaposed with IgHEL+HOD+ and SwHEL+HOD+, respectively, to determine the effects of RBC autoantigen expression on B cell development (representative flow plots are shown in **Figure 2C**, right panels). Whereas B6, HOD, and SwHEL mice had a similar percentage of B cells in fraction F (mature B cells), a significant increase was observed in IgHEL mice (**Figure 2D**). The presence of autoantigen resulted in a 2-fold decrease in the percentage of B cells in Fraction F in SwHEL+HOD+ mice compared to SwHEL+ animals (**Figure 2D**). By contrast, IgHEL animals had a substantial increase in B cells in fraction F compared to controls, and only a slight decrease was observed in IgHEL+HOD+ mice compared to IgHEL animals (**Figure 2D**). Correlating with a decrease in mature B cells in SwHEL+HOD+ mice, the percentage of B cells reactive with HEL-tet was decreased 4-fold, compared to SwHEL [**Figure 2E**, average percentages: SwHEL+ (48%) and SwHEL+HOD+ (12%)]. Similarly, the percentage of B cells reactive with HEL was decreased 2.5-fold in IgHEL+HOD+ mice, compared to IgHEL [**Figure 2E**, average percentages: IgHEL (88%) and IgHEL+HOD+ (35%)]. Enumeration of HEL-reactive B cells

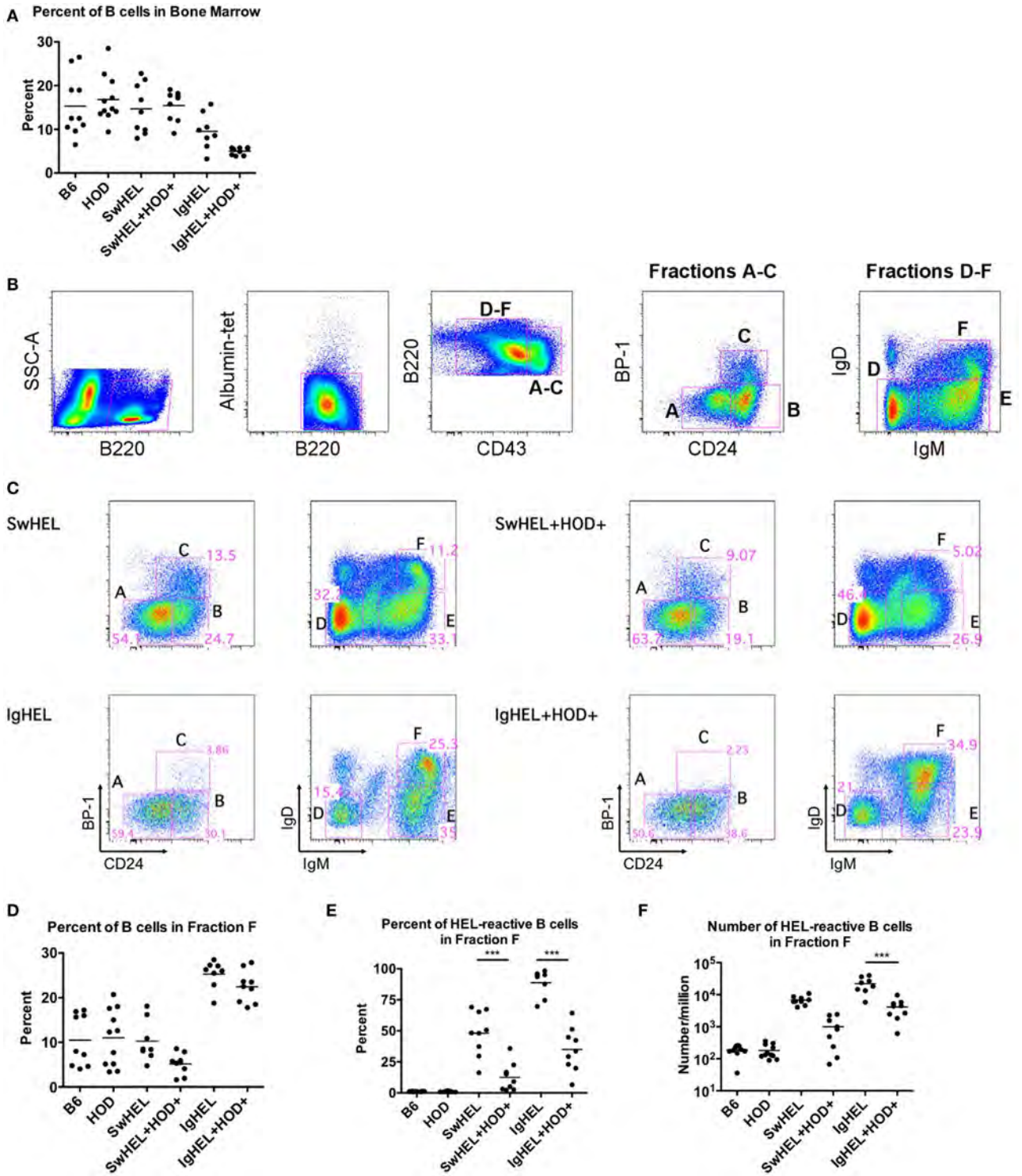

FIGURE 2 | Effect of red blood cell (RBC) autoantigen on B cell development in bone marrow. Bone marrow was harvested, RBCs were lysed, and residual cells were stained with anti-B220, anti-CD43, anti-CD24, anti-IgD, anti-IgM, anti-BP-1, HEL-tet, and control Albumin-tet to delineate the stages of bone marrow development. **(A)** The percentage of B cells in bone marrow was determined for each indicated genotype. **(B)** Bone marrow cells were evaluated for cell surface markers to determine the stages of B cell development, and **(C)** Fractions A–F are shown for each indicated genotype. **(D)** The percent of total B cells, and **(E)** percent and **(F)** number of hen egg lysozyme (HEL)-reactive B cells were determined for Fraction F, the final stage of bone marrow development. Flow plots are representative data from three independent experiments with at least three mice per group. Scatter dot plots in **(A,D–F)** are compiled data from three independent experiments with at least three mice per group. Selective *p* values are shown on graphs and * ≤ 0.05, ** ≤ 0.01, and *** ≤ 0.001. For complete statistical analysis with all significant differences, see Table S2 in Supplementary Material.

in Fraction F revealed a reduction of 6.8-fold in SwHEL+HOD+ and 5.4-fold in IgHEL+HOD+ mice compared to their respective BCR-Tg control mice [**Figure 2F**, mean HEL-reactive B cell numbers: SwHEL+ (6,789), SwHEL+HOD+ (998), IgHEL+ (22,172), and IgHEL+HOD+ (4,123)]. Thus, central tolerance mechanisms in both IgHEL+HOD+ and SwHEL+HOD+ mice decreased the numbers of autoreactive B cells to an RBC-specific antigen. However, while SwHEL+HOD+ mice appeared more efficient than IgHEL+HOD+ mice in decreasing HEL-specific B cells, mature autoreactive B cells were observed in both strain combinations.

HEL-Reactive Marginal Zone (MZ) B Cells Are Enriched in Autoreactive IgHEL Mice

The extent to which peripheral tolerance mechanisms act upon the mature autoreactive B cells detected in SwHEL+HOD+ and IgHEL+HOD+ mice was investigated by analyzing autoreactive splenic B cells that escaped central tolerance. IgHEL+HOD+ mice had significantly fewer splenic B cells, compared to all other groups, including IgHEL (**Figure 3A**; Table S3 in Supplementary Material). By contrast, no decrease in total B cells was detected in SwHEL+HOD+ mice compared to SwHEL mice. Once B cells leave the bone marrow, they pass though several transient transitional stages (T1, T2, and T3) in the spleen, which serve to dictate the final B cell maturation into follicular (FO) or MZ B cells (representative gating strategy shown, **Figure 3B**). There was no significant change in the percentage of T1 B cells in SwHEL+HOD+ mice compared to SwHEL mice, both of which were likewise similar to control B6 and HOD mice (**Figure 3C**). Analysis of the HEL specificity of B cells in these populations demonstrated that the percentage of HEL-specific B cells in T1 in SwHEL mice was significantly decreased in SwHEL+HOD+ mice (**Figure 3D**). Analysis of absolute numbers showed a similar pattern of decrease in HEL-reactive B cells in T1 in SwHEL+HOD+ compared to SwHEL, although to a lesser extent than predicted by percentage (**Figure 3E**). A similar trend was observed with percentages of total and HEL-reactive B cells in T2 (**Figures 3F,G**). The percentages of total and HEL-reactive B cells in T3 for SwHEL and SwHEL+HOD+ were similar to controls (**Figures 3H,I**). As T3 B cells have been correlated with anergy (23, 24), these findings make it unlikely that a large number of cells are arrested in an anergic T3 state in SwHEL+HOD+ mice.

In contrast to SwHEL, the percentage of B cells was significantly increased in T1 and T2 for IgHEL mice, compared to controls (**Figures 3C,F**, respectively). In the presence of HEL autoantigen, IgHEL+HOD+ mice had percentages of B cells in T1 similar to IgHEL. However, there was a significant decrease in the percentage of B cells in T2 compared to IgHEL (**Figure 3F**). Within T1 and T2, the frequency of HEL-reactive B cells was similar between IgHEL and IgHEL+HOD+ (**Figures 3D,G**) while the absolute number of HEL-reactive B cells in T1 and T2 were decreased in IgHEL+HOD+, compared to IgHEL (**Figure 3E** and data not shown). Together, these data suggest the peripheral tolerance mechanisms were initiated between T1 and T2. Coupled with the overall decrease of B cells observed in IgHEL+HOD+ mice but a similar percentage of HEL-reactive B cells within each transitional stage, it is hypothesized that clonal deletion occurred. Lastly, there were similar percentages of B cells in T3 from IgHEL mice and IgHEL+HOD+ mice (**Figure 3H**).

Functionally mature B cells in the spleen comprise FO and MZ B cell subsets; FO B cells localize in primary and secondary lymphoid follicles and require T cell help to secrete antibodies, class-switch, and establish memory B cells. SwHEL and SwHEL+HOD+ mice had statistically significant decreases in the percentage of FO B cells, compared to controls (**Figure 3J**). In addition, the B cells that comprised the FO B cell compartment were largely not HEL-reactive (autoreactive) (**Figure 3K**), which is consistent with previous data demonstrating that autoreactive B cells are excluded from participating in germinal center reactions (25, 26). Similarly, IgHEL and IgHEL+HOD+ had a statistically significant reduction in the percent of FO B cells (**Figure 3J**). However, the frequency of HEL-reactive B cells within FO remained high (**Figure 3K**, mean 55% for both groups). Again, correlating with the overall decreased numbers of B cells in IgHEL+HOD+ splenocytes, the absolute number of HEL-reactive B cells in FO were significantly reduced compared to IgHEL (**Figure 3L**).

Marginal zone B cells play a key role in early adaptive immune responses and share many similarities with B-1 B cells, including expression of a poly-reactive BCR and T cell-independent antibody secretion. SwHEL and SwHEL+HOD+ mice had similar frequencies of innate-like MZ B cells, compared to controls; however, the percent and absolute number of HEL-reactive MZ B cells was decreased in SwHEL+HOD+ autoantigen-expressing mice (**Figures 3M–O**). By contrast, while the percentage of MZ B cells in IgHEL was similar to controls, IgHEL+HOD+ had an increased frequency of MZ B cells (**Figure 3M**). IgHEL mice had a significant increase in percentage and number of HEL-reactive MZ B cells, compared to controls. However, despite HOD autoantigen expression, the frequency and number of autoreactive MZ B cells in IgHEL+HOD+ mice remained unaltered (**Figures 3N,O**, respectively).

In aggregate, these data demonstrate that SwHEL BCR-Tg mice follow a similar trend for B cell development as control mice but IgHEL BCR-Tg mice do not. IgHEL BCR-Tg mice had an abnormally high percentage of B cells in transitional stages, which result in decreased frequencies of mature B cells. In the presence of HOD, SwHEL B cells were reduced in each developmental stage and in the mature subsets of B cells. By contrast, autoreactive IgHEL B cells were increased in number in the MZ B cell compartment, a subtype that is most similar to B-1 B cells.

Autoantibodies Induce Anemia in IgHEL+HOD+ Mice But Not SwHEL+HOD+ Mice

To assess whether tolerance mechanisms employed in SwHEL+HOD+ and IgHEL+HOD+ mice were sufficient to prevent autoantibody production, sera was collected and assessed for anti-HOD autoantibodies by flow crossmatch.

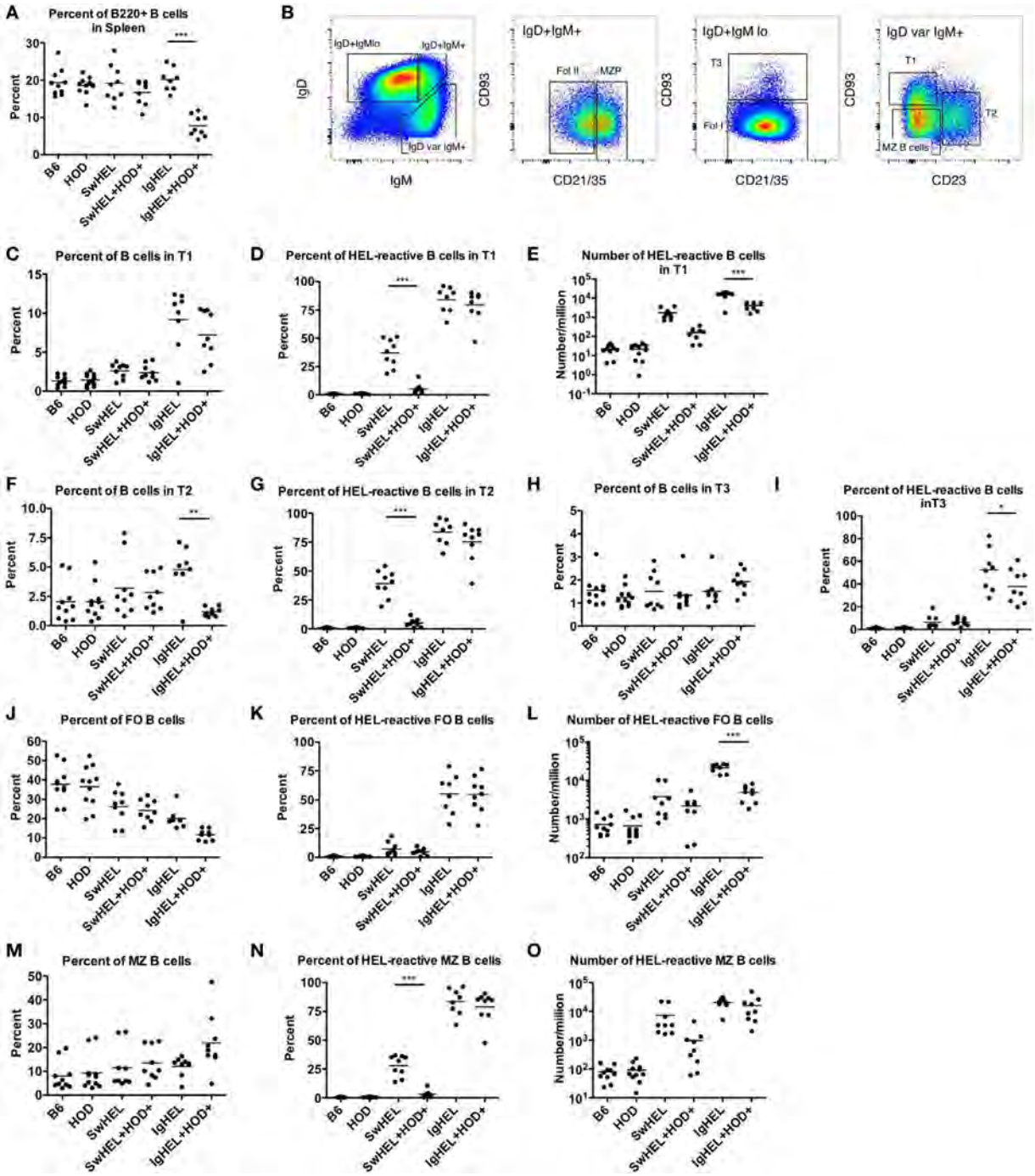

FIGURE 3 | Effect of red blood cell autoantigen on B cell transition and maturation. Splenocytes were harvested from mice and stained with antibodies against IgD, IgM, CD93, CD21/35, CD23, and B220 to define the stages of B cell development in the spleen. To evaluate reactivity to hen egg lysozyme (HEL), cells were stained with albumin-tet to control for nonspecific binding followed by HEL-tet. **(A)** The percentage of B220+ splenic B cells was determined and **(B)** the stages of B cell maturation was outlined. The **(C)** percentage of B cells, **(D)** frequency, and **(E)** absolute number of HEL-reactive B cells was computed for transitional stage 1 (T1). The **(F)** percent and **(G)** number of HEL-reactive B cells was assessed for transitional stage 2 (T2). Similarly, the percent of **(H)** total B cells and **(I)** HEL-reactive B cells was determined for transitional stage 3 (T3). Likewise, the **(J)** percentage of FO B cells, and **(K)** frequency, and **(L)** number of HEL-reactive mature FO B cells were evaluated. The **(M)** percent of MZ B cells was calculated and HEL-reactive MZ B cell **(N)** percentages and **(O)** numbers were determined. Flow plots in **(B)** are representative data from three independent experiments with at least three mice per group. Scatter dot plots in **(A)** and **(C–O)** are compiled data from three independent experiments with at least three mice per group. Selective *p* values are shown on graphs and * ≤ 0.05, ** ≤ 0.01, and *** ≤ 0.001. For complete statistical analysis with all significant differences, see Table S3 in Supplementary Material.

Briefly, experimental sera was tested for binding to control B6 and experimental HOD RBCs, as previously described in Ref. (27). No HOD-specific antibodies were detectable in control B6 or HOD mice (**Figure 4A**; Table S4 in Supplementary Material). Both SwHEL and IgHEL BCR-Tg mice had detectable anti-HOD antibodies in their sera. As a consequence of expression of the HOD antigen on RBCs, total anti-HOD antibodies decreased in SwHEL+HOD+ mice. Further analysis of antibody isotype and subtype revealed that SwHEL+HOD+ mice had significantly less circulating HOD-specific IgM and IgG2c antibodies compared to SwHEL BCR-Tg mice (**Figures 4B,D**). Similarly, anti-HOD IgG1 and IgG2b antibody subtypes were decreased in SwHEL+HOD+ mice compared to SwHEL BCR-Tg controls, but not significantly whereas anti-HOD IgG3 was slightly increased (**Figures 4E–G**). By contrast, a bimodal distribution of total anti-HOD autoantibodies was observed in IgHEL+HOD+ mice; elevated autoantibodies were detectable in a subset of IgHEL+HOD+ mice, compared to IgHEL controls (**Figure 4A**). Similarly, IgHEL+HOD+ mice had a bimodal distribution of anti-HOD IgM autoantibodies (**Figure 4B**). Given that the frequency of many autoimmune diseases are elevated in females (28, 29), anti-IgM titers in IgHEL+HOD+ mice were compared across gender; female IgHEL+HOD+ mice had significantly higher titers of anti-HOD IgM autoantibodies, compared to their male littermates thereby accounting for the bimodal distribution of autoantibodies (**Figure 4C**). No HOD-specific IgG antibodies were detected in IgHEL or IgHEL+HOD+ mice, as predicted due to the inability of the transgene to class-switch (data not shown).

The observation that lower levels autoantibodies were detectable in IgHEL+HOD+ compared to SwHEL+HOD+ mice was unexpected due to the enrichment of peritoneal B-1 B cells and incomplete deletion of B-2 HEL-reactive B cells (**Figures 1B** and **2D–F**). Modulation of circulating antibody levels is consistent with autoantibodies bound to their cognate antigen. Thus, to test the hypothesis that anti-HEL autoantibodies were bound to the RBCs in SwHEL+HOD+ and IgHEL+HOD+ mice, direct anti-globulin tests were performed. SwHEL+HOD+ RBCs had significantly more antibodies bound to their surface, compared to SwHEL controls (**Figure 5A**; Table S5 in Supplementary Material). Similarly, more antibodies were detected on RBCs from IgHEL+HOD+ mice, compared to IgHEL controls. However, there was a bimodal distribution of antibody-bound RBCs, with

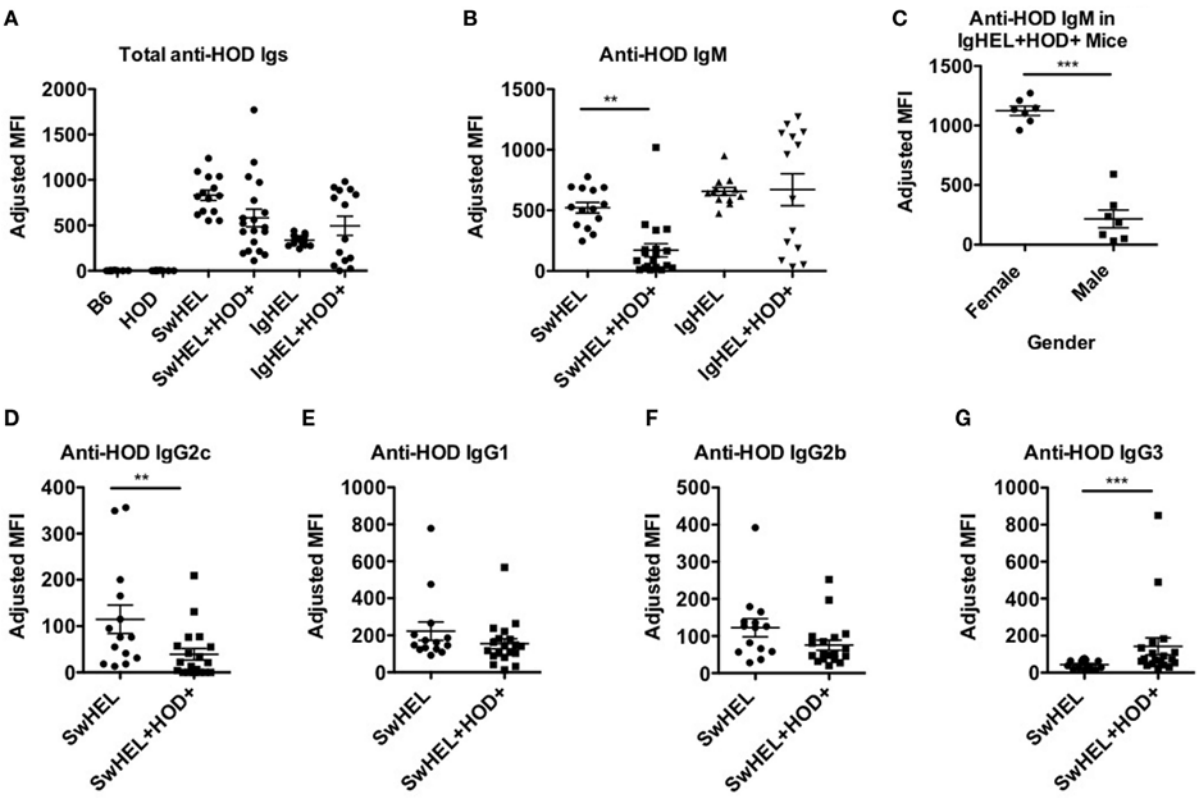

FIGURE 4 | Autoantibodies are detected in SwHEL+HOD+ and IgHEL+HOD+ mice. To evaluate whether B cells that escaped central and peripheral tolerance secreted autoantibodies, sera was collected from experimental mice and assayed for anti-HOD antibodies. **(A)** Total anti-HOD immunoglobulins (Igs) was determined by flow crossmatch against HOD and control B6 red blood cell targets. Anti-HOD IgM antibodies were evaluated in **(B)** BCR-Tg mice and **(C)** the role of gender in autoantibody production was assessed in IgHEL+HOD+ mice. Production of **(D)** IgG2c, **(E)** IgG1, **(F)** IgG2b, and **(G)** IgG3 subtype-specific antibodies were evaluated in SwHEL and SwHEL+HOD+ mice. Scatter dot plots shown are compiled from three independent experiments with at least three mice per group. Selective *p* values are shown on graphs and * ≤ 0.05, ** ≤ 0.01, and *** ≤ 0.001. For complete statistical analysis with all significant differences, see Table S4 in Supplementary Material.

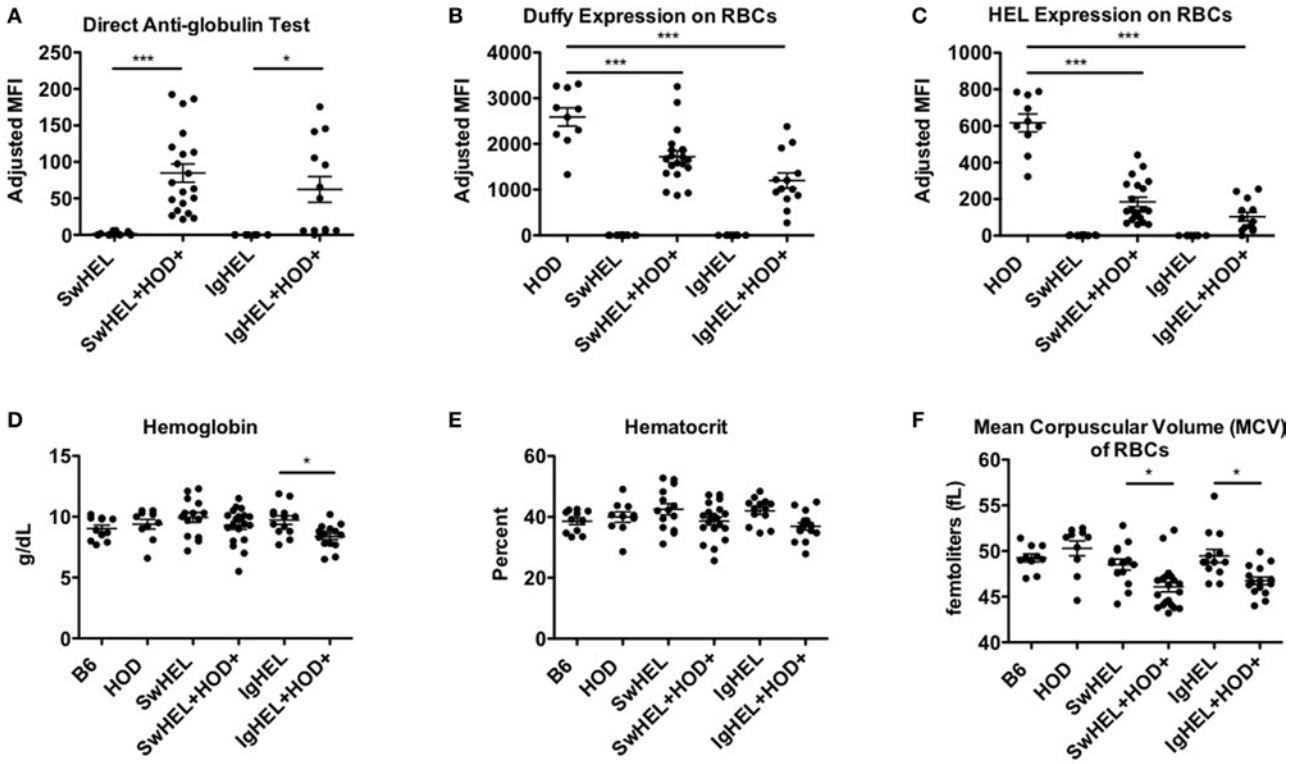

FIGURE 5 | Autoantibodies effect red blood cell (RBCs). To determine whether the presence of autoantibodies affected erythrocytes, RBCs from experimental mice were collected and assayed for **(A)** antibodies bound to their surface and surface expression of **(B)** Duffy and **(C)** hen egg lysozyme (HEL) antigens. To assess whether autoantibodies affect RBCs, a hematology profile was generated with a HemaVet. RBCs from experimental mice were evaluated for **(D)** hemoglobin, **(E)** hematocrit, and **(F)** mean corpuscular volume (MCV). Scatter dot plots shown are compiled from three independent experiments with at least three mice per group. Selective *p* values are shown on graphs and * ≤ 0.05, ** ≤ 0.01, and *** ≤ 0.001. For complete statistical analysis with all significant differences, see Table S5 in Supplementary Material.

some IgHEL+HOD+ RBCs not bound by antibodies. Presence of HOD-specific antibodies but absence of bound antibodies on RBCs suggest that circulating RBCs may not express the HOD antigen. Antigen loss is a well-described antibody-mediated phenomenon that occurs frequently to RBC antigens whereby RBCs cease to express that particular antigen and cannot re-synthesize new protein due to the absence of a nucleus (30). Thus, to test the hypothesis that expression of the HOD antigen is modulated in SwHEL+HOD+ and IgHEL+HOD+ mice, RBCs were stained with anti-Duffy and anti-HEL antibodies to detect components of the HOD antigen. RBCs from both SwHEL+HOD+ and IgHEL+HOD+ had significant reductions in the expression of both Duffy and HEL components of the HOD antigen, compared to naïve HOD mice, suggesting HOD antigen loss has occurred (**Figures 5B,C**).

Some RBC-specific antibodies can be pathogenic and lead to hemolysis. To determine whether the autoantibodies detected in SwHEL+HOD+ and IgHEL+HOD+ were pathogenic thereby resulting in anemia, whole blood samples were analyzed. No significant differences were detected in total RBC counts in any experimental group (data not shown). SwHEL+HOD+ mice had comparable levels of hemoglobin and hematocrit as B6, HOD, and SwHEL controls (**Figures 5D,E**), but decreased RBC mean corpuscular volume (MCV) (**Figure 5F**). By contrast, IgHEL+HOD+ mice had decreased hemoglobin, hematocrit, and MCV, compared to IgHEL BCR-Tg and control animals. Thus, taken together, RBCs in autoreactive IgHEL+HOD+ mice have altered hematological parameters consistent with anemia, which was not observed in SwHEL+HOD+ animals. In aggregate, these data suggest that the pathogenicity of RBC-specific autoantibodies is influenced by the ability of B cells to undergo class-switching; by extension, the method utilized in generating BCR-Tg mice (random integration vs. knock-in) may bias subsequent immune tolerance and responses.

DISCUSSION

The current understanding of tolerance to RBC-specific antigens has largely been generated using the autoAb 4C8 BCR-Tg mouse model, which has provided substantial data to support a paradigm in which B-1 B cells are the source of autoantibodies in AIHA (5–9). However, the autoAb 4C8 BCR-Tg mouse was constructed using a fully rearranged IgM, regulated by recombinant elements, and located outside the natural Ig locus due to random integration from pro-nuclear injection. While this approach was widely used in the first generation of BCR

transgenics, it has since been appreciated that more physiological data are obtained through homologous recombination of VDR domains into Vh regions of the Ig locus (knock-in BCR mice), to allow normal receptor editing and class-switching. In this report, we directly compare a random integrant vs. a knock-in BCR-Tg mouse in a model of RBC autoreactivity. In order to control for other variables, both BCR mice utilize the same VDR (anti-HEL HyHEL10) and are crossed with the same mouse expressing HEL epitopes on RBCs (HOD mouse) (6, 17, 18). In mice with intact receptor editing (SwHEL+HOD+ mice), autoreactive B-1 B cells were reduced to almost background levels, whereas autoreactive B-2 B cells were likewise decreased but to a lesser extent. By contrast, in mice with the inability to receptor edit (IgHEL+HOD+), there was a selective enrichment of B-1 B cells in the peritoneum and splenic MZ B cells, and a concomitant decrease in B-2 B cells. Moreover, anti-HOD autoantibodies are detected in both SwHEL+HOD+ and IgHEL+HOD+ mice, but autoantibodies significantly affect RBCs and may cause anemia only in IgHEL+HOD+ mice. Thus, these data demonstrate that the genetic approach to generate BCR-Tg mice significantly impacts the B cell repertoire and may not accurately recapitulate normal immune education and tolerance. Importantly, the existing paradigm for B cell education to RBC antigens rests almost entirely upon the autoAb 4C8 BCR-Tg mouse, which gives similar results to the IgHEL mouse, neither of which receptor edit or class-switch; whereas a very different outcome is observed with the SwHEL mouse, which retains the ability to receptor edit away from autoreactivity and class-switch into additional antibody isotypes and subtypes.

The data obtained from the IgHEL+HOD+ BCR-Tg model are similar to the findings reported by Murakami and colleagues with the autoAb 4C8 BCR-Tg system (10, 11). Of note, because the RBC antigen recognized by the autoAb 4C8 BCR-Tg mouse is essentially conserved in all known strains, the autoAb 4C8 BCR system has no control to study baseline B cells in the absence of autoantigen. In IgHEL BCR-Tg mice alone (no autoantigen), HEL-reactive B cells were detectable in secondary lymphoid organs and the peritoneal cavity demonstrating that there was not a preferential development of the B-1 B cell compartment at baseline. In addition, IgHEL B cells were observed in all stages of B cell development in the bone marrow and spleen. However, due to expression of a "fixed" BCR, there were significant increases in the numbers of IgHEL B cells in the bone marrow and transitional stages of B cell development in the spleen when compared to controls (**Figures 2D** and **3C,F**). This could be attributed to the forced expression of affinity matured IgM and IgD, the inability to undergo class-switching, or an altered regulation of expression of cell surface markers utilized to delineate subtype.

Analysis of IgHEL+HOD+ mice demonstrated that the absolute numbers of autoreactive HEL-specific B-2 cells are reduced in the bone marrow and spleen (**Figures 2A** and **3A**). This reduction is most likely due to clonal deletion, which has been observed in other BCR-Tg autoreactive models (31, 32). In contrast to the conventional B-2 B cells, there was a selective enrichment of B-1 B cells in the peritoneum. The increase of autoreactive B-1 B cells could be due to lack of exposure to the autoantigen due to development in extramedullary compartments. However, the substantial reduction of autoreactive B-2 B cells in the peritoneum, presumably due to encountering autoantigen, may argue against this notion (**Figure 1C**, right). Of course, we cannot rule out autoreactive B-2 but not B-1 B cells trafficking out of peritoneum to encounter autoantigen (thus prompting deletion), but B-1 B cells also have the capacity to migrate to and from the spleen (33, 34). An alternative explanation is that B-1 B cells have encountered autoantigen, but due to the inherent properties of B-1 B cells, they undergo activation and proliferation instead of deletion (35). This is plausible, as developmentally, newly forming B cells that receive a strong signal upon encounter with autoantigen are selected into the B-1 B cell compartment; B-2 B cells are more sensitive to ligation with autoantigen and are instructed to rearrange their BCR, undergo deletion, or become anergic.

In the SwHEL+HOD+ mouse, B-1 B cells are not preferentially enriched; on the contrary, autoreactive HEL-specific B cells are reduced to background levels (**Figure 1B**, right). Similar to IgHEL+HOD+ mice, numbers of autoreactive B-2 B cells in the peritoneum are significantly decreased (**Figure 1C**, right), suggesting that B-1 and B-2 B cells are capable of being tolerized upon autoantigen encounter. As such, we hypothesize that receptor editing plays a substantial role in tolerizing autoreactive B cells, as the total numbers of B cells in each population analyzed from SwHEL and SwHEL+HOD+ mice were similar to controls, but the frequency and number of autoreactive HEL-reactive B cells were significantly reduced in HOD+SwHEL+ mice. However, despite reductions in autoreactive B cells, autoantibodies were detectable in SwHEL+HOD+ mice. Autoantibody production in SwHEL+HOD+ mice was not predicted as Phan et al. observed anergy and significant reductions in autoantibodies in SwHEL mice that were bred with soluble HEL animals (18). Thus, these data further illustrate that the type of autoantigen may also influence B cell tolerance mechanisms.

An additional unexpected finding in our studies was a bimodal distribution of anti-IgM autoantibodies in IgHEL+HOD+ mice. Previously, Phan et al. demonstrated significant reductions of autoantibodies in IgHEL mice bred with soluble HEL animals (18). However, when IgHEL mice were bred with HOD mice, which express membrane-bound HEL antigen, a subset of IgHEL+HOD+ mice made higher titers of IgM autoantibodies compared to IgHEL controls. Upon further investigation, our data revealed sex-based differences in autoantibody production in IgHEL+HOD+ mice whereby females made significantly higher titers of anti-HOD IgM compared to their male littermates (**Figure 4C**). Despite the disparity in autoantibody titers, no significant sex-based differences were observed in other RBC parameters evaluated, such as hemoglobin, hematocrit, or MCV (data not shown). Moreover, the presence of autoantibodies did not affect B cell development as similar frequencies of total and HEL-reactive B cells in Fraction F of the bone marrow, splenic MZ, and FO B cells were observed between female and male IgHEL+HOD+ mice (data not shown). By contrast, no gender-based differences were observed in SwHEL+HOD+ mice. While a female predilection for autoimmunity has been described in many autoimmune models, it is unclear why a gender bias was observed in IgHEL but not SwHEL crosses. Regardless, these data

further draw a distinction between data obtained with the two BCR-Tg mice.

Taken together, these data reject the hypothesis that there is a single population or subset of B cells that serve as a reservoir for RBC-specific autoreactive B cells. Instead, the data suggest a more complex model, in which several phenotypes of B cells persist in the bone marrow and periphery despite tolerance mechanisms. Thus, these findings challenge the current paradigm that views B-1 B cells as the dangerous population of autoreactive B cells with respect to RBC antigens. Such a challenge also questions efforts to generate therapeutics for AHIA (either prophylactic or interventional) that specifically target B-1 B cells. Our findings demonstrate the necessity of a conceptual re-evaluation of B cell tolerance to RBC antigens and ongoing studies into baseline tolerance to RBCs, and the mechanisms by which it is lost in the pathogenesis of AIHA.

MATERIALS AND METHODS

Mice

C57BL/6 (B6) and IgHEL mice were purchased from Jackson Laboratories (Bar Harbor, ME, USA). IgHEL mice are listed as MD4 animals; IgHEL has been used in the current paper for clarity of nomenclature. SwHEL mice were a kind gift from Dr. Robert Brink. HOD (with RBC-specific expression of HEL, a portion of ovalbumin, and the human blood group antigen Duffy), IgHEL (also known as MD4), and SwHEL mice were bred at Bloodworks NW Vivarium. Mice were maintained on standard rodent chow and water in a temperature- and light-controlled environment and used at 8–12 weeks of age. All experiments were performed according to approved Bloodworks Northwest Institutional Animal Care and Use Committee (IACUC) procedures.

Tetramerization of HEL and Albumin

Hen egg lysozyme (Sigma) was resuspended to a concentration of 1 mg/mL in PBS and biotinylated with the EZ-Link Sulfo-NHS Biotinylation Kit according to the manufacturer's recommendations (Pierce). Albumin (Sigma) was similarly biotinylated. Both HEL and albumin were tetramerized with 10 additions of APC (Molecular Probes) and APC-Cy7 (Molecular Probes), respectively.

Staining Leukocytes

Bone marrow, splenocytes, and peritoneal cavity cells were harvested. RBCs were lysed with lysis buffer (Sigma). Leukocytes were stained with Albumin-APC-Cy7 for 30 min on ice followed by HEL-APC (HEL-tet). After cells were stained with both tetramers, organ-specific surface antibodies were added. Bone marrow cells were stained with antibodies against B220, CD43, BP-1, IgM, IgD, CD24, and CD93. Splenocytes were stained with antibodies directed against IgM, IgD, CD93, CD23, B220, CD19, and CD21/35. Peritoneal leukocytes were stained with antibodies against CD3, CD11b, CD5, IgD, IgM, F480, and CD43. All antibodies were purchased from eBioscience. Absolute cell counts were determined by use of APC beads (BD Biosciences). Cells were washed with FACS buffer [PBS + 0.2 mg/mL bovine serum albumin (Sigma) + 0.9 mg/mL EDTA (Sigma)] and analyzed on an LSRII flow cytometer.

Antibody Detection and RBC Analysis

Flow crossmatch and direct anti-globulin test were performed as previously described (27, 36). Isotype (IgM and IgG) and subtype-specific (IgG1, IgG2b, IgG2c, and IgG3) were utilized. To assess for HOD antigen expression, RBCs were stained with monoclonal antibodies specific for HEL (4B7) and Duffy (MIMA-29), as previously described (17, 20). Hemogram data on whole blood was collected with a HemaVet Hematology Analyzer (Drew Scientific).

Statistical Analysis and Graphing

Statistical significance for two groups was determined by an unpaired Student's *T*-test, whereas multiple groups were evaluated by a one-way ANOVA followed by a Bonferroni's multiple test comparison post-test was utilized for three or more groups. Significance was set at $p \leq 0.05$ and * ≤ 0.05, ** ≤ 0.01, *** ≤ 0.001. *P* values for selective groups are shown on graphs but for a more detailed and complete list of statistically significant differences, please refer to the Supplementary Tables. Flow plots were generated using Flow Jo software (TreeStar) and graphs were generated using Graphpad Prism (La Jolla, CA, USA).

ETHICS STATEMENT

All experiments were performed according to approved BloodworksNW Institutional Animal Care and Use Committee (IACUC) procedures.

AUTHOR CONTRIBUTIONS

AR, HH, LK, JH, JZ, and KH each performed experiments and analyzed data contained in this work. KH and JZ authored the manuscript and all authors read, corrected, and approved of the final manuscript.

FUNDING

This work was supported, in part, by the National Blood Foundation.

SUPPLEMENTARY MATERIAL

The Supplementary Material for this article can be found online at http://www.frontiersin.org/article/10.3389/fimmu.2017.01366/full#supplementary-material.

TABLE S1 | **Complete statistical analysis for data Figure 1**.

TABLE S2 | **Complete statistical analysis for data Figure 2**.

TABLE S3 | **Complete statistical analysis for data Figure 3**.

TABLE S4 | **Complete statistical analysis for data Figure 4**.

TABLE S5 | **Complete statistical analysis for data Figure 5**.

REFERENCES

1. Coutelier JP, Detalle L, Musaji A, Meite M, Izui S. Two-step mechanism of virus-induced autoimmune hemolytic anemia. *Ann N Y Acad Sci* (2007) 1109:151–7. doi:10.1196/annals.1398.018
2. Hoffman PC. Immune hemolytic anemia – selected topics. *Hematol Am Soc Hematol Educ Program* (2009) 2009:80–6. doi:10.1182/asheducation-2009.1.80
3. Arason GJ, Jorgensen GH, Ludviksson BR. Primary immunodeficiency and autoimmunity: lessons from human diseases. *Scand J Immunol* (2010) 71:317–28. doi:10.1111/j.1365-3083.2010.02386.x
4. Gehrs BC, Friedberg RC. Autoimmune hemolytic anemia. *Am J Hematol* (2002) 69:258–71. doi:10.1002/ajh.10062
5. Brombacher F, Köhler G, Eibel H. B cell tolerance in mice transgenic for anti-CD8 immunoglobulin mu chain. *J Exp Med* (1991) 174:1335–46. doi:10.1084/jem.174.6.1335
6. Goodnow CC, Crosbie J, Adelstein S, Lavoie TB, Smith-Gill SJ, Brink RA, et al. Altered immunoglobulin expression and functional silencing of self-reactive B lymphocytes in transgenic mice. *Nature* (1988) 334:676–82. doi:10.1038/334676a0
7. Hartley SB, Crosbie J, Brink R, Kantor AB, Basten A, Goodnow CC. Elimination from peripheral lymphoid tissues of self-reactive B lymphocytes recognizing membrane-bound antigens. *Nature* (1991) 353:765–9. doi:10.1038/353765a0
8. Tiegs SL, Russell DM, Nemazee D. Receptor editing in self-reactive bone marrow B cells. *J Exp Med* (1993) 177:1009–20. doi:10.1084/jem.177.4.1009
9. Okamoto M, Murakami M, Shimizu A, Ozaki S, Tsubata T, Kumagai S, et al. A transgenic model of autoimmune hemolytic anemia. *J Exp Med* (1992) 175:71–9. doi:10.1084/jem.175.1.71
10. Murakami M, Honjo T. Anti-red blood cell autoantibody transgenic mice: murine model of autoimmune hemolytic anemia. *Semin Immunol* (1996) 8:3–9. doi:10.1006/smim.1996.0002
11. Murakami M, Honjo T. B-1 cells and autoimmunity. *Ann N Y Acad Sci* (1995) 764:402–9. doi:10.1111/j.1749-6632.1995.tb55855.x
12. Murakami M, Tsubata T, Shinkura R, Nisitani S, Okamoto M, Yoshioka H, et al. Oral administration of lipopolysaccharides activates B-1 cells in the peritoneal cavity and lamina propria of the gut and induces autoimmune symptoms in an autoantibody transgenic mouse. *J Exp Med* (1994) 180:111–21. doi:10.1084/jem.180.1.111
13. Murakami M, Yoshioka H, Shirai T, Tsubata T, Honjo T. Prevention of autoimmune symptoms in autoimmune-prone mice by elimination of B-1 cells. *Int Immunol* (1995) 7:877–82. doi:10.1093/intimm/7.5.877
14. de Sá Oliveira GG, Izui S, Ravirajan CT, Mageed RA, Lydyard PM, Elson CJ, et al. Diverse antigen specificity of erythrocyte-reactive monoclonal autoantibodies from NZB mice. *Clin Exp Immunol* (1996) 105:313–20. doi:10.1046/j.1365-2249.1996.d01-772.x
15. Shi ZT, Afzal V, Coller B, Patel D, Chasis JA, Parra M, et al. Protein 4.1R-deficient mice are viable but have erythroid membrane skeleton abnormalities. *J Clin Invest* (1999) 103:331–40. doi:10.1172/JCI3858
16. Salomao M, Zhang X, Yang Y, Lee S, Hartwig JH, Chasis JA, et al. Protein 4.1R-dependent multiprotein complex: New insights into the structural organization of the red blood cell membrane. *Proc Natl Acad Sci U S A* (2008) 105:8026–31. doi:10.1073/pnas.0803225105
17. Desmarets M, Cadwell CM, Peterson KR, Neades R, Zimring JC. Minor histocompatibility antigens on transfused leukoreduced units of red blood cells induce bone marrow transplant rejection in a mouse model. *Blood* (2009) 114:2315–22. doi:10.1182/blood-2009-04-214387
18. Phan TG, Amesbury M, Gardam S, Crosbie J, Hasbold J, Hodgkin PD, et al. B cell receptor-independent stimuli trigger immunoglobulin (Ig) class switch recombination and production of IgG autoantibodies by anergic self-reactive B cells. *J Exp Med* (2003) 197:845–60. doi:10.1084/jem.20022144
19. Adams E, Basten A, Goodnow CC. Intrinsic B-cell hyporesponsiveness accounts for self-tolerance in lysozyme/anti-lysozyme double-transgenic mice. *Proc Natl Acad Sci U S A* (1990) 87:5687–91. doi:10.1073/pnas.87.15.5687
20. Hudson KE, Hendrickson JE, Cadwell CM, Iwakoshi NN, Zimring JC. Partial tolerance of autoreactive B and T cells to erythrocyte-specific self-antigens in mice. *Haematologica* (2012) 97:1836–44. doi:10.3324/haematol.2012.065144
21. Hardy RR, Carmack CE, Shinton SA, Kemp JD, Hayakawa K. Resolution and characterization of pro-B and pre-pro-B cell stages in normal mouse bone marrow. *J Exp Med* (1991) 173:1213–25. doi:10.1084/jem.173.5.1213
22. Hardy RR, Hayakawa K. B cell development pathways. *Annu Rev Immunol* (2001) 19:595–621. doi:10.1146/annurev.immunol.19.1.595
23. Merrell KT, Benschop RJ, Gauld SB, Aviszus K, Decote-Ricardo D, Wysocki LJ, et al. Identification of anergic B cells within a wild-type repertoire. *Immunity* (2016) 25:953–62. doi:10.1016/j.immuni.2006.10.017
24. Teague BN, Pan Y, Mudd PA, Nakken B, Zhang Q, Szodoray P, et al. Cutting edge: transitional T3 B cells do not give rise to mature B cells, have undergone selection, and are reduced in murine lupus. *J Immunol* (2007) 178:7511–5. doi:10.4049/jimmunol.178.12.7511
25. Chan TD, Wood K, Hermes J, Butt D, Jolly C, Basten A, et al. Elimination of germinal-center-derived self-reactive B cells is governed by the location and concentration of self-antigen. *Immunity* (2012) 37:893–904. doi:10.1016/j.immuni.2012.07.017
26. Ekland EH, Forster R, Lipp M, Cyster JG. Requirements for follicular exclusion and competitive elimination of autoantigen-binding B cells. *J Immunol* (2004) 172:4700–8. doi:10.4049/jimmunol.172.8.4700
27. Hudson KE, Lin E, Hendrickson JE, Lukacher AE, Zimring JC. Regulation of primary alloantibody response through antecedent exposure to a microbial T-cell epitope. *Blood* (2010) 115:3989–96. doi:10.1182/blood-2009-08-238568
28. Ngo ST, Steyn FJ, McCombe PA. Gender differences in autoimmune disease. *Front Neuroendocrinol* (2014) 35:347–69. doi:10.1016/j.yfrne.2014.04.004
29. Klein SL, Flanagan KL. Sex differences in immune responses. *Nat Rev Immunol* (2016) 16:626–38. doi:10.1038/nri.2016.90
30. Zimring JC, Cadwell CM, Spitalnik SL. Antigen loss from antibody-coated red blood cells. *Transfus Med Rev* (2009) 23:189–204. doi:10.1016/j.tmrv.2009.03.002
31. Brink R, Goodnow CC, Crosbie J, Adams E, Eris J, Mason DY, et al. Immunoglobulin M and D antigen receptors are both capable of mediating B lymphocyte activation, deletion, or anergy after interaction with specific antigen. *J Exp Med* (1992) 176:991–1005. doi:10.1084/jem.176.4.991
32. Lang J, Nemazee D. B cell clonal elimination induced by membrane-bound self-antigen may require repeated antigen encounter or cell competition. *Eur J Immunol* (2000) 30:689–96. doi:10.1002/1521-4141(200002)30:2<689::AID-IMMU689>3.0.CO;2-I
33. Ito T, Ishikawa S, Sato T, Akadegawa K, Yurino H, Kitabatake M, et al. Defective B1 cell homing to the peritoneal cavity and preferential recruitment of B1 cells in the target organs in a murine model for systemic lupus erythematosus. *J Immunol* (2004) 172:3628–34. doi:10.4049/jimmunol.172.6.3628
34. Moon H, Lee JG, Shin SH, Kim TJ. LPS-induced migration of peritoneal B-1 cells is associated with upregulation of CXCR4 and increased migratory sensitivity to CXCL12. *J Korean Med Sci* (2012) 27:27–35. doi:10.3346/jkms.2012.27.1.27
35. Grimaldi CM, Hicks R, Diamond B. B cell selection and susceptibility to autoimmunity. *J Immunol* (2005) 174:1775–81. doi:10.4049/jimmunol.174.4.1775
36. Zimring JC, Hair GA, Chadwick TE, Deshpande SS, Anderson KM, Hillyer CD, et al. Nonhemolytic antibody-induced loss of erythrocyte surface antigen. *Blood* (2005) 106:1105–12. doi:10.1182/blood-2005-03-1040

Conflict of Interest Statement: AR, HH, LK, JH, and KH have no conflicts of interest to declare. JZ serves on the Scientific Advisory Board for Rubius Therapeutics and consults for Surface Oncology and Sinopia Biosciences.

frontiers in Immunology

ORIGINAL RESEARCH
published: 24 October 2017
doi: 10.3389/fimmu.2017.01384

B Cells Are Indispensable for a Novel Mouse Model of Primary Sjögren's Syndrome

*Junfeng Zheng[1,2†], Qiaoniang Huang[1†], Renliang Huang[1†], Fengyuan Deng[1], Xiaoyang Yue[3], Junping Yin[1], Wenjie Zhao[1], Yan Chen[1], Lifang Wen[1], Jun Zhou[1], Renda Huang[1], Gabriela Riemekasten[2,4], Zuguo Liu[5], Frank Petersen[3] and Xinhua Yu[1,3]**

[1] Xiamen-Borstel Joint Laboratory of Autoimmunity, Medical College of Xiamen University, Xiamen, China, [2] Institute of Psychiatry and Neuroscience, Xinxiang Medical University, XinXiang, China, [3] Priority Area Asthma & Allergy, Research Center Borstel, Airway Research Center North (ARCN), Members of the German Center for Lung Research (DZL), Borstel, Germany, [4] Department of Rheumatology, University of Lübeck, Lübeck, Germany, [5] Eye Institute of Xiamen University, The Medical College of Xiamen University, Xiamen, China

OPEN ACCESS

Edited by:
Falk Nimmerjahn,
University of Erlangen-Nuremberg, Germany

Reviewed by:
Abdelhadi Saoudi,
Institut national de la santé et de la recherche médicale, France
Sylvie Lesage,
Université de Montréal, Canada

***Correspondence:**
Xinhua Yu
xinhuayu@fz-borstel.de

†These authors have contributed equally to this work.

Specialty section:
This article was submitted to Immunological Tolerance and Regulation, a section of the journal Frontiers in Immunology

Received: 18 August 2017
Accepted: 06 October 2017
Published: 24 October 2017

Citation:
Zheng J, Huang Q, Huang R, Deng F, Yue X, Yin J, Zhao W, Chen Y, Wen L, Zhou J, Huang R, Riemekasten G, Liu Z, Petersen F and Yu X (2017) B Cells Are Indispensable for a Novel Mouse Model of Primary Sjögren's Syndrome. Front. Immunol. 8:1384. doi: 10.3389/fimmu.2017.01384

Primary Sjögren's syndrome (pSS) is characterized by a panel of autoantibodies, while it is not clear whether B cells and autoantibodies play an essential role in pathogenesis of the disease. Here, we report a novel mouse model for pSS which is induced by immunization with the Ro60_316-335 peptide containing a predominant T cell epitope. After immunization, mice developed several symptoms mimicking pSS, including a decreased secretion of tears, lymphocytic infiltration into the lacrimal glands, autoantibodies, and increased levels of inflammatory cytokines. Disease susceptibility to this novel mouse model varies among strains, where C3H/HeJ (H2-k) and C3H/HeN (H2-k) are susceptible while DBA/1 (H2-q) and C57BL/6 (H2-b) are resistant. Depletion of B cells using anti-CD20 monoclonal antibodies prevented C3H/HeN mice from development of the pSS-like disease. In addition, HLA-DRB1*0803, a pSS risk allele, was predicted to bind to the hRo60_308-328 which contains a predominant T cell epitope of human Ro60. Therefore, this study provides a novel mouse model for pSS and reveals an indispensable role of B cells in this model. Moreover, it suggests that T cell epitope within Ro60 antigen is potentially pathogenic for pSS.

Keywords: primary Sjögren's syndrome, mouse model, T cell epitope, SSA, autoantibodies, B cells

INTRODUCTION

Primary Sjögren's syndrome (pSS) is an autoimmune disorder mainly targeting salivary and lacrimal glands and leading to xerostomia (dry mouth) and xerophthalmia (dry eye) (1). The pSS is characterized by lymphocytic infiltrates into the exocrine glands as well as by a specific panel of circulating autoantibodies (2). In contrast to the unknown disease-related autoreactive T cells, many autoantibodies have been identified in patients with pSS, including anti-SSA/Ro and anti-SSB/La autoantibodies, rheumatoid factor, anti-nuclear antibody, anti-muscarinic type 3 acetylcholine receptors (M3R), and anti-α fodrin antibodies (3). Although B cell hyper-activation resulting hypergammaglobulinemia and production of autoantibodies is a predominant feature of pSS, it is not clear whether B cells and autoantibodies are indispensable for the development of the disease. Clinical evidence from B cell-targeting therapy show an inconclusive result. Although several studies with small number

of patients have shown that Rituximab (anti-CD20 IgG) therapy can significantly improve the secretion function of the exocrine glands in pSS patients (4–6), a very recent large randomized controlled trial of Rituxmab did not confirm the effectiveness (7). In addition, since most B cell targeting therapies target CD20 (8), they are unable to deplete autoantibody-producing plasma cells, making it difficult to use this clinical evidence for reflecting the role of autoantibodies in pathogenesis of pSS.

Animal models provide a powerful tool for understanding the pathogenesis of disease. So far, several mouse models for pSS have been established and they provide some evidence for the role of autoantibodies in the disease pathogenesis (9). An essential role of B cells and autoantibodies in the impairment in secretion function of exocrine glands has been demonstrated NOD mouse model, where NOD.Igμ^{null} mice show no impairment in the secretion function (10). In addition, two mouse lines, mice overexpressing B cell activating factor and mice deficient in ACT1, a negative regulator of B cell survival, develop a pSS-like disease spontaneously (11, 12), also supporting an important role of B cell in the pathogenesis of experimental pSS. By contrast, in the *Id3−/−* mouse model (13) and the M3R immunization-induced mouse model (14), transfer of purified autoreactive T cells has been shown to be sufficient for inducing pSS-like symptoms, arguing that B cells and autoantibodies are dispensable in their pathogenesis. Since pSS is an autoimmune syndrome of which pathogenesis might differ from patient to patient, one animal model can only represent pathogenesis of a small part of patients. Therefore, to better explore the role of B cells, more animal models are required.

In 2013, Jonsson et al. reported that the presymptomatic presence of anti-SSA/Ro autoantibodies shows the highest odds ratio for the risk of development of pSS, followed by anti-SSB/La autoantibodies and ANA (15). This finding identifies anti-SSA/Ro autoantibodies as a good predictive marker of pSS but also suggests that immune response against SSA/Ro antigen might play a role in the development of pSS. Since no evidence has been shown so far that anti-SSA/Ro autoantibodies itself have pathogenic properties (16), an alternative possibility is that autoimmune response to T cell epitopes within SSA/Ro antigen play an important role in the pathogenesis of pSS. This notion is supported by the evidence that autoimmune response against the predominant T cell epitope within Ro60 antigen can induce production of autoantibodies against multiple antigens *via* intermolecular epitope spreading (17). In the latter study, Deshmukh et al. determined the T cell epitopes of both human and murine Ro60 protein by immunization of mice with the intact protein and a subsequent evaluation of the T cell response directed against small synthetic peptides derived from the Ro60 sequence. Using this strategy, the authors identified several regions within human Ro60 containing T cell epitopes, including the hRo60_316-335 peptide. Regarding murine Ro60, the most dominant T cell epitope was identified within the mRo60_311-330 peptide, which overlapped hRo60_316-355 (17). Furthermore, immunizing mice with mRo60_316-335 peptide resulted in the generation of a variety of autoantibodies against multiple antigens, confirming that this peptide contains a dominant T cell epitope of mRo60 (17).

In this study, we hypothesized that autoimmune response to the T cell epitope of SSA/Ro antigen contribute to the pathogenesis of pSS by producing pathogenic autoantibodies *via* intermolecular epitope spreading. To verify this hypothesis and to establish a novel mouse model for pSS, we immunized mice with a murine Ro60_316-335 peptide containing the predominant T cell epitope of Ro60 antigen (17). Furthermore, we investigated the role of B cells in this novel mouse model of pSS.

MATERIALS AND METHODS

Mice

All mice used in this study were female. C3H/HeJ, DBA/1J, and C57BL/6J mice were purchased from Shanghai SLAC laboratory Animal Co. (Shanghai, China), while C3H/HeN mice were purchased from Beijing Vital River Laboratory Animal Technology Co., Ltd. (Beijing, China). All mice were housed in the animal facility with a 12-h light–dark cycle at the Xiamen University. Mice were held at specific pathogen-free conditions and fed standard mouse chow and acidified drinking water *ad libitum*. Protocols of all animal experiments were approved by the Institutional Animal Care and Use Committee of Xiamen University.

Peptides and Immunization

Murine Ro60_316-335 (KARIHPFHVLIALETYRAGH) peptides used in this study were synthesized at Research Center Borstel, Germany. Mice of the age from 8 to 10 weeks were immunized at the hind footpad with 100 μg peptide emulsified (1:1) in non-ionic block copolymer adjuvant Titermax (Alexis Biochemicals, Lorrach, Germany). Control mice were treated with PBS emulsified in Titermax. The mice were followed until 12 weeks after immunization.

Measurement of Saliva and Tears

Mouse saliva and tears were measured at week 0, 6, and 12 after immunization as described previously (18), with slight modification. Briefly, mice were starved for 16– h before the measurement, deeply anesthetized, and stimulated by pilocarpine hydrochloride (0.5 mg/kg body weight) (Sigma-Aldrich). Saliva was collected with a sponge immediately after the injection of the pilocarpine for a duration of 20 min. Tears was collected using Phenol Red Thread (Jingming Ltd., Tianjin, China) at the 10 and 20 min time points after the injection of the pilocarpine. Since the body weight of mice increased during the time of the experiments (e.g., from 18.6 to 21.7 g mean body weight of C3H/HeJ mice during 12 weeks), both saliva and tears secretion volumes were normalized to their individual body weight.

Histopathological Assessment and Immunohistochemistry Staining

Histology of exocrine glands or kidney was evaluated by Hematoxylin and Eosin (H&E) staining with 6-μm-thick sections prepared from formalin-fixed tissues. Immunochemistry in exocrine gland specimens was performed using antibodies against murine CD3 (ab5690, Abcam) and B220 (RA3-6B, eBioscience) with 6-μm-thick paraffin sections.

Enzyme-Linked Immunosorbent Assay

An enzyme-linked immunosorbent assay (ELISA) was used to detect antibodies against mRo60_316-335 peptides. The SSA peptides (10 mg/ml in 0.5 M Na_2CO_3 buffer; pH 9.6) were absorbed onto Costar EIA/RIA Plates (Corning Incorporated, Corning, NY, USA), washed and blocked with 3% BSA in PBS with 0.05% Tween-20 (PBS-T), incubated with the respective mouse sera (1:200), and further washed with PBS-T. Bound antibodies were detected using peroxidase conjugated goat anti-mouse IgG antibodies (Sigma, USA) and tetramethylbenzidine (Solarbio, Beijing, China). Concentrations of IFN-γ, IL-17A, IL-4, and IL-10 in mouse sera were determined by commercially available ELISA kits (Peprotech, USA) according to the manufacturer's protocols. The detection range of the assay for IFN-γ, IL-17A, IL-4, and IL-10 was 7.5–1,000 pg/ml, 7.5–1,000 pg/ml, 40–5,000 pg/ml, and 15–2,000 pg/ml, respectively. All sera were diluted 1:3 before quantification.

Immunoblotting

Samples of total proteins extracted from lysates of salivary or lacrimal glands from healthy C57BL/6J mice were subjected a 10% SDS-PAGE gel and then separated proteins were transferred to PVDF membranes. Membranes were blocked using 5% defated milk in PBS-T for 2 h at room temperature. After washing, membranes were incubated with mouse sera (1:200 dilution in blocking buffer) from immunized or control mice overnight at 4°C and subsequently incubated with peroxidase conjugated goat anti-mouse IgG antibodies for 1 h at room temperature followed by visualization of bands using chemiluminescent substrate.

In Vivo B Cell Depletion

To deplete B cells, we injected C3H/He mice i.v. with 10 mg/kg anti-CD20 antibody 1 day before the immunization. To maintain the depletion, the same dose of anti-CD20 antibody was injected at the third, sixth, and ninth week after the immunization. Both anti-CD20 monoclonal antibody (18B12) and isotype control IgG were kind gift from Biogen (Biogen Inc., San Diego). Efficiency of depletion of the B cells was evaluated by determining B cells in the peripheral blood using FITC-conjugated anti-mouse CD19 IgG (6D5, Biolegend, USA).

Epitope Prediction and Sequence Similarity Search

The protein sequence of *Homo sapiens* Ro60 ribonucleoprote in isoform 3 (NP_001035829.2) was retrieved from the NIH database (http://www.ncbi.nlm.nih.gov/protein). By using the IEDB Analysis Resource Consensus tool (19), retrieved data were used to develop a prediction model that could identify the peptides binding to pSS-associated HLA-DR1*0803 allele. The percentile rank was applied for the output, and the binding affinity to the epitope was artificially set as 1/percentile rank. Amino acid sequence similarity search was performed by BLASTP software (https://blast.ncbi.nlm.nih.gov/).

Statistical Analysis

All analyses were performed with GraphPad Prism statistical software (GraphPad Software Inc., version 5.01, La Jolla, CA, USA). Normality and equality of variances of the quantitative data was determined first. At P values > 0.05, data were considered as normally distributed with equal variances. Depending on the quality of the data, data with normal distribution were further analyzed by unpaired Student's t-test with or without Welch's correction, while data displaying a non-parametric distribution were analyzed by using Mann–Whitney U test. P values below 0.05 were considered as statistically significant.

RESULTS

Induction of a pSS-Like Disease in C3H/HeJ Mice by Immunization with a Ro60-Derived T Cell Epitope

Previously, Deshmukh and colleagues reported that the predominant T cell epitope of mRo60 antigen is located within mRo60_316-335 peptide (17). We first investigated whether immunization with the mRo60_316-335 peptide could induce a pSS-like disease in mice. As described by others (13), tear secretion in control mice typically increased during the life span of the animals. As compared to the controls, C3H/HeJ mice immunized with mRo60_316-335 peptide showed a decreased production of tear at both 6 and 12 weeks after immunization (**Figure 1A**), suggesting an impaired function of the tear secretion. However, no significant difference was observed in the secretion of saliva between the two groups (**Figure 1B**).

Lymphocytic foci (LF), a hallmark of pSS, were observed in both lacrimal and salivary glands (**Figure 1C**). Unexpectedly, LF were observed in both groups of experimental mice, with a none-significant trend of higher incidence in Ro60_316-335 peptide-immunized mice (9 out of 17 in salivary gland and 5 out 17 in lacrimal gland) than in controls (5 out of 15 in salivary gland and 2 out 15 in lacrimal gland) (**Figure 1D**).

In the next step, we investigated the production of autoantibodies. As expected, C3H/HeJ mice immunized with the mRo60_316-335 peptide generated autoantibodies against the antigen while corresponding control mice did not (**Figure 2A**). To determine the interaction of serum-autoantibodies with glandular proteins, binding of antibodies to protein extracts derived from lacrimal or salivary glands of healthy mice were analyzed by western blot and bands were visualized by using a second antibody to murine IgG. While blots developed with sera from control mice showed only two major binds which corresponds to the heavy and light chains of murine IgG, sera from mRo60_316-335 peptide-immunized C3H/HeJ mice displayed multiple bands, suggesting that sera from mRo60_316-335 peptide-immunized C3H/HeJ mice contained multiple autoantibodies against exocrine glands-derived proteins (**Figure 2B**). Furthermore, immunochemistry staining of the salivary gland demonstrated that the LF were composed of both T cell and B cells, with a predominance of B cells (**Figures 2C,D**). Finally, we determined the serum levels of T cell associated cytokines, including IFN-γ, IL-17A, IL-4, and IL-10. Sera of C3H/HeJ mice immunized with mRo60_316-335 showed significantly higher levels of IFN-γ and IL-17A as compared to control mice, while no significant difference in the levels of IL-4 or IL-10 were observed between both groups (**Figure 2E**).

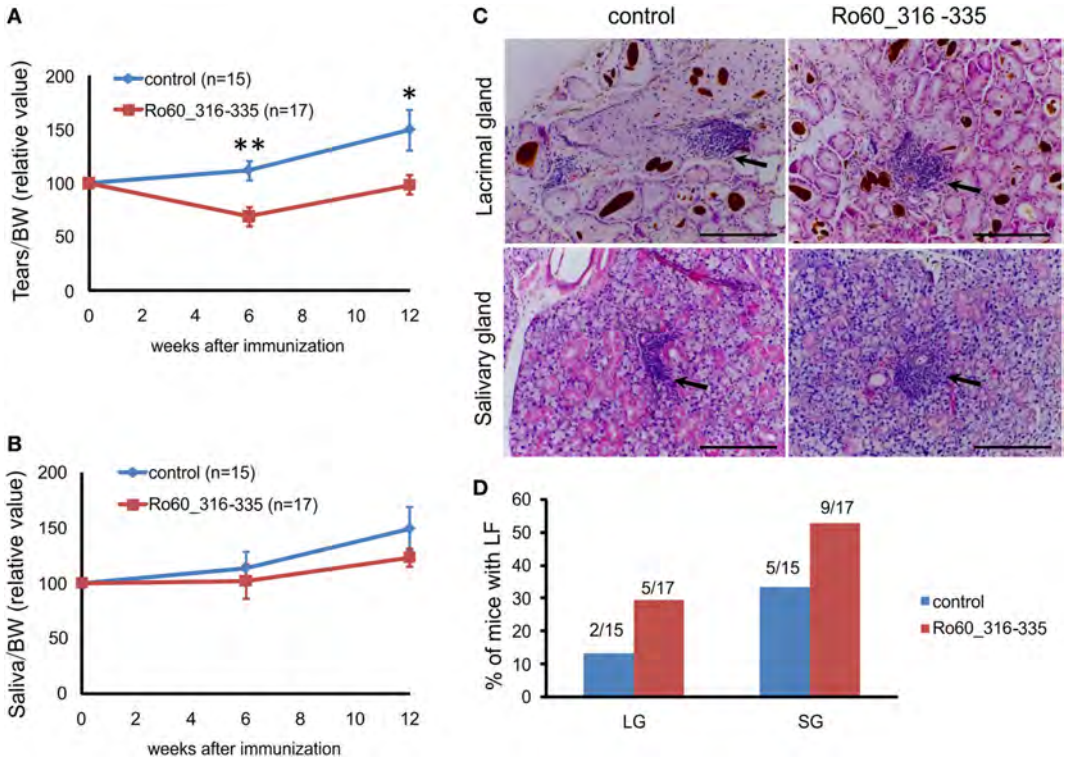

FIGURE 1 | Immunization with the Ro60_316-335 peptide induces a primary Sjögren's syndrome-like disease in C3H/He mice. C3H/HeJ mice were immunized with Ro60_315-336 ($n = 17$) or treated with PBS as control ($n = 15$) and secretion of tears **(A)** and saliva **(B)** was determined after pilocarpine stimulation. Values were normalized to the respective body weights and subsequently to the levels of secretion determined before immunization. Results two experiments were pooled and data are presented as mean ± SEM. Statistically significant differences between peptide-immunized mice and controls were calculated by using the Mann–Whitney *U*-test (*$p < 0.05$ and **$p < 0.01$). **(C)** Representative sections with lymphocytic foci (LF) derived from lacrimal (upper panel) and salivary glands (lower panel) of Ro60_315-336 immunized mice or controls after Hematoxylin and Eosin staining. Black arrows indicate LF. Bars, 100 µm. **(D)** Incidence of mice with LF in lacrimal and salivary glands. Numbers above bars indicate the ratio of number of mice with LF/total number of mice examined.

Since SSA autoantibodies are also found in systemic lupus erythematosus (SLE), we examined whether immunized mice express SLE-like symptoms. No obvious difference was observed in the H&E staining of kidney sections between the mRo60_316-335 peptide immunized mice and controls. In consistence with this, no significant difference was found in the concentration of proteins in the urine of the two groups of mice (Figure S1 in Supplementary Material). Therefore, immunization with Ro60_316-335 peptide induced a pSS-like disease in both, C3H/HeJ and C3H/HeN mice.

Development of the pSS-Like Disease among Mouse Strains

Since genetic background plays an important role in the development of experimental autoimmune disorders, we then investigated the development of the Ro60_316-335 peptide-induced pSS-like disease in other mouse strains. We first investigated C3H/HeN mice, a strain closely related to C3H/HeJ. Six weeks after immunization, C3H/HeN mice treated with the mRo60_316-335 peptide showed a significant decrease in the production of tears as compared to control mice (Figure S2A in Supplementary Material). No significant difference was observed in the secretion of saliva between the two groups (Figure S2B in Supplementary Material). Similar to C3H/HeJ mice, C3H/HeN mice immunized with mRo60_316-335 peptide generated autoantibodies against the peptide and protein extracts from lacrimal and salivary glands (Figure S2C,D in Supplementary Material). With regard to inflammatory cell infiltration, in C3H/HeN mice, LF were almost exclusively observed in Ro60_316-335 peptide-immunized mice but not in control mice, although the frequency of mice with LF was rather low (Figures S2E,F in Supplementary Material).

We next investigated other two mouse strains carrying different MHC allele, DBA1/J and C57BL/6J mice. DBA/1J mice treated with mRo60_316-335 peptide did not show any impairment in secretion function of salivary or lacrimal glands as compared to control mice. Furthermore, neither LF nor infiltrated cells was observed in the immunized mice. Although autoantibodies against Ro60_316-335 peptide can be detected in sera of DBA/1J mice treated with the peptide, no autoantibodies against proteins from lachrymal and salivary glands were detectable. In addition, serum levels of IL-17A but not IFN-λ, IL-4, or IL-10 was increased in peptide immunized mice as compared to control

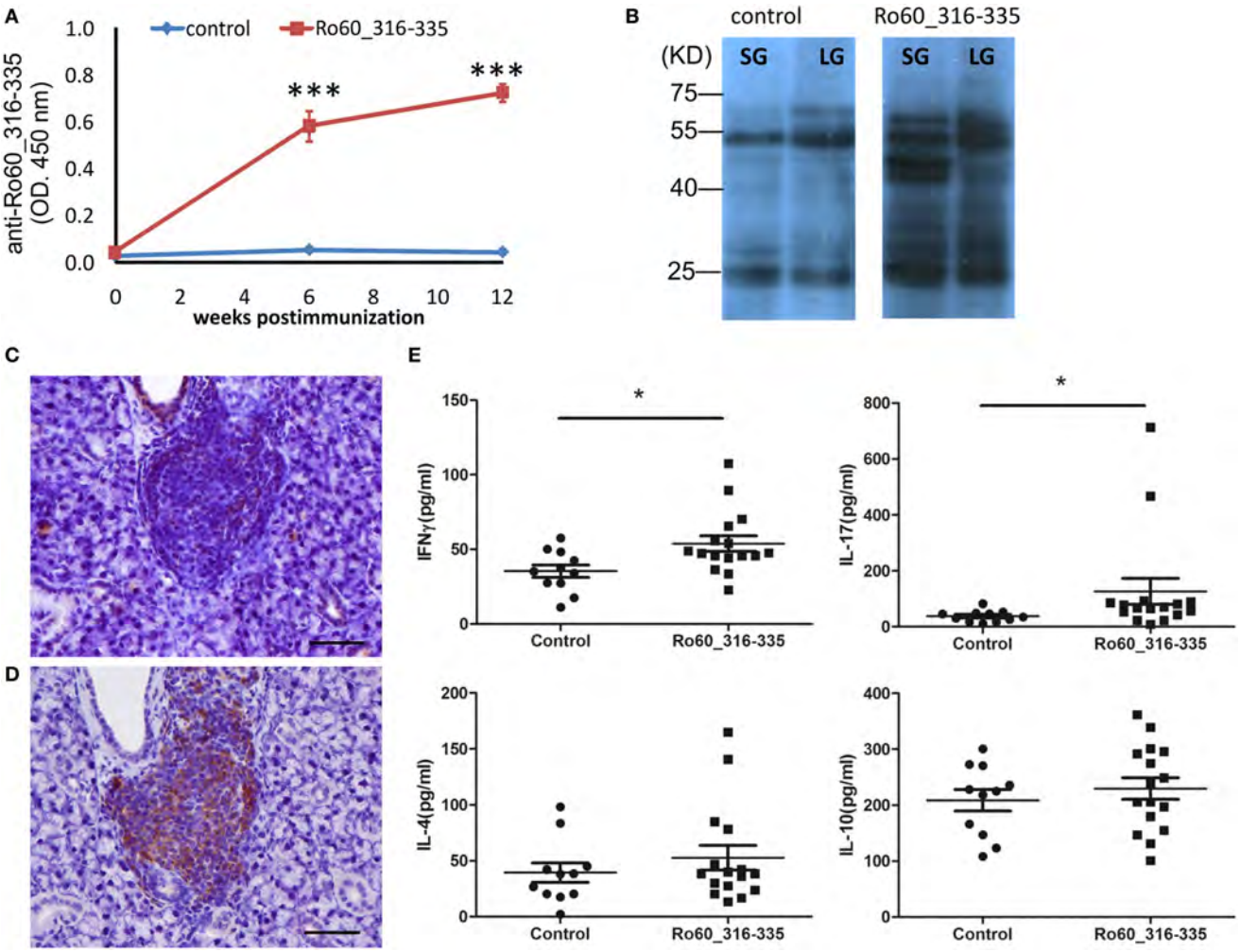

FIGURE 2 | Immunological features of the primary Sjögren's syndrome-like disease in C3H/He mice. **(A)** Autoantibodies against the Ro60_316-335 peptide in sera of Ro60_316-335 immunized ($n = 9$) C3H/HeJ mice or controls ($n = 9$). Results derived from one of two experiments performed are shown and data are presented as mean ± SEM. Statistically significant differences (*$p < 0.05$ and **$p < 0.01$) were calculated by using the Mann–Whitney *U*-test. **(B)** Immunoblotting of lacrimal glands (LG) or salivary glands (SG) tissue lysates from healthy mice with sera from control or Ro60_316-335 immunized mice. Representative results are shown. **(C,D)** immunochemistry staining of murine CD3 T cells **(C)** and CD19 B cell **(D)** in the lymphocytic foci (bar length = 50 μm). **(E)** Concentrations of IFN-γ, IL-17A, IL-4, and IL-10 in the sera of Ro60_316-335 immunized C3H/HeJ mice ($n = 16$) and controls ($n = 11$). Statistically significant differences (*$p < 0.05$) were calculated by the Mann–Whitney *U*-test.

mice (Figure S3 in Supplementary Material). Similar to DBA/1J mice, C57BL/6J mice were also resistant to the Ro60_316-335 peptide-induced pSS-like disease, without impairment in secretion of tears, infiltration of lymphocytes in exocrine glands or production of autoantibodies binding to proteins from exocrine gland (Figure S4 in Supplementary Material).

Table 1 summarizes the disease symptoms and immunological features in four tested mouse strains. Besides impairment in tears secretion, there are two major differences between susceptible C3H/He strains, and resistant strains, DBA/1J and C57BL/6J. One is that susceptible mice produced autoantibodies against proteins of the exocrine glands but resistant mice did not. The other is that lymphocytic infiltration into exocrine glands was observed in the susceptible mice but not resistant mice.

B Cell-Depletion Prevents the Development of pSS-Like Disease in C3H/He Mice

We next investigated the role of B cells in this novel mouse model of pSS. C3H/HeN mice were injected i.p. with anti-CD20 antibody before immunization as well as at third, sixth, and ninth weeks after immunization. We evaluated the efficiency of B cell depletion by detecting B cells in peripheral blood. As shown in **Figure 3A**, the percentage of CD19 + B cells in peripheral blood mononuclear cell decreased from 12.67% before depletion to 2.94% 1 week after the first anti-CD20 injection, further decreased to less than 1.5% 2 weeks after the anti-CD20 injection, and maintained at a level of lower than 1.5% during the whole experiment period,

while the B cell levels in mice treated with isotype IgG did not change significantly (**Figure 3A**). Furthermore, after immunization with Ro60_316-335 peptide, mice treated with anti-CD20 antibodies did not produce autoantibodies against the peptide, while animals which received irrelevant antibodies of the same isotype did (**Figure 3B**), confirming that B cells were depleted efficiently. Clinically, mice treated with isotype IgG showed a decreased production of tears at 6 weeks after the immunization with Ro60_316-335 peptide, while this impaired secretion function was not observed in mice treated with anti-CD20 IgG (**Figures 3C,D**), suggesting that B cell-depletion prevented the impairment in the tears secretion.

TABLE 1 | Summary of the development of the Ro60_316-335 induced primary Sjögren's syndrome -like disease among mouse strains.

	C3H/HeJ	C3H/HeN	DBA/1J	C57BL/6J
MHC II hyplotype	H2-d	H2-d	H2-q	H2-b
Tears secretion	Decreased	Decreased	Not affected	Not affected
Saliva secretion	Not affected	Not affected	Not affected	Not affected
Lymphocytic foci	Yes	Yes	No	No
Inflammatory cell infiltration	Yes	Yes	No	No
anti-Ro60_316-335 IgG	Yes	Yes	Yes	Yes
anti-exocrine gland lysate IgG	Yes	Yes	No	No
IFN-γ	Increased	–	Not affected	Increased
IL-17A	Increased	–	Increased	Not affected

–, *not evaluated.*

Prediction of Epitope within hRo60 for pSS-Associated HLA-DRB1 Alleles

Our data suggest a pathogenic role of the predominant T cell epitope of Ro60 in the development of pSS-like but not SLE-like disease in mice. Previously, we performed a comprehensive meta-analysis and demonstrated that HLA-DRB1*0301 and HLA-DRB1*0803 are two major alleles associated with an increased risk of pSS (20). We then investigated whether these two pSS-associated HLA alleles could bind the T epitopes within human Ro60 antigen using IEDB Analysis Resource Consensus tool. Within human Ro60, there is a predominant T cell epitope located within the amino acid sequence of 308aa–328aa (**Figure 4**), a region which has been shown to contain a T cell epitope of hRo60 (17). Another

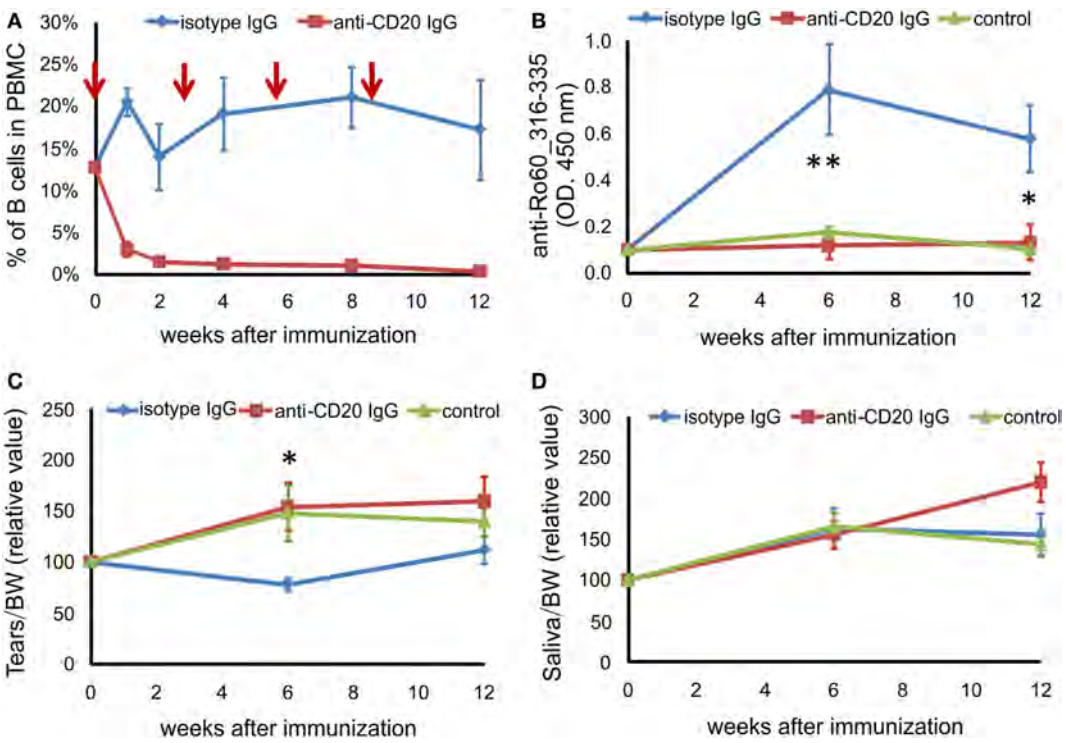

FIGURE 3 | B cell depletion prevents mice from Ro60_315-336-induced primary Sjögren's syndrome-like disease. Before and after immunization with Ro60_316-335 peptide, C3H/HeN mice were injected i.p. with anti-CD20 IgG (red line) or isotype IgG (blue line). The control group (green line) represents mice immunized with PBS and adjuvants alone. **(A)** Efficiency of depletion of murine B cells in C3H/HeN mice. The time points of B cell-depleting anti-CD20 antibody injection are indicated by red arrows, the percentage of B cells in the peripheral blood mononuclear cells were determined at 0, 1, 2, 4, 8, and 12 weeks after immunization using CD19 as marker for B cells. **(B)** Autoantibodies against the mRo60_316-335 peptides in sera of isotype IgG treated ($n = 7$) or anti-CD20 IgG treated ($n = 8$) mRo60_316-335-immunized C3H/HeN mice, or PBS-treated control mice ($n = 6$). Tears **(C)** and saliva **(D)** production in isotype IgG treated ($n = 7$) or anti-CD20 IgG treated ($n = 8$) mRo60_316-335-immunized C3H/HeN mice, or control mice ($n = 6$). Data are presented as mean ± SEM. Statistically significant differences between isotype IgG ($n = 7$) or anti-CD20 IgG treated ($n = 8$) mice were calculated by the unpaired Student's *t*-test with Welch's correction (*$p < 0.05$, **$p < 0.01$, unpaired Student's *t*-test).

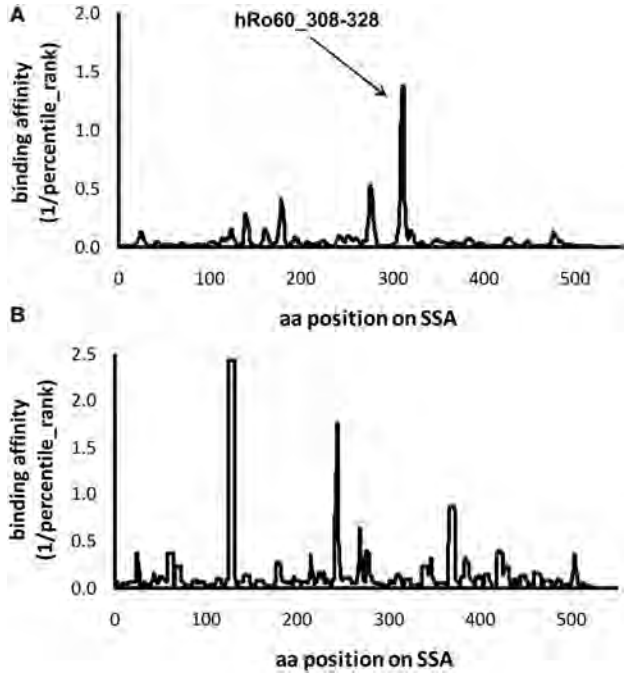

FIGURE 4 | Prediction of the epitopes for the primary Sjögren's syndrome (pSS)-risk associated HLA-DRB1 alleles within the hRo60 protein. The protein sequence of *Homo sapiens* Ro60 ribonucleoprote in isoform 3 (NP_001035829.2) was retrieved from the NIH database (http://www.ncbi.nlm.nih.gov/protein). By using the IEDB Analysis Resource Consensus tool, retrieved data were used to develop a prediction model that could identify the peptides binding to pSS-associated HLA-DRB1*0803 **(A)** and HLA-DRB1*0301 **(B)** alleles. The percentile rank was applied for the output, and the binding affinity to the epitope was artificially set as 1/percentile rank.

pSS associated allele, HLA-DRB1*0301, was predicted to bind three strong T cell epitopes within the hR60 antigen (**Figure 4**).

DISCUSSION

In this study, we induced a pSS-like disease by immunizing mice with a partial structure derived from the mRo60 protein, a peptide containing the predominant T cell epitope. Previously, Scofield et al. established a mouse model of pSS by repetitive immunization with Ro60 peptide containing predominant B cell epitopes (21). In the current study, susceptible mice developed pSS-like disease with only single immunization with peptide containing predominant T cell epitope, indicating that immunization with a T cell epitope might be more effective than a B cell epitope in induction of the disease. T cell epitopes within disease-associated autoantigens have been already identified in many systemic autoimmune disorders, e.g., SSc-associated topoisomerase I (22, 23) or SLE-associated histones (24). Therefore, the experimental approach in our current study might provide a good strategy for establishing further mouse models for different systemic autoimmune diseases.

The Ro60_316-335 peptide induced novel mouse model of pSS demonstrates that T cell epitope in this region is pathogenic in mice. Moreover, a T cell epitope in this section is predicted to bind to the pSS-risk associated HLA-DRB1*0803 allele, a HLA allele associated with pSS but not SLE (25), indicating that such epitope could indeed play a role in the development of pSS. Viral infections are currently seen as one potential risk factor in the development of autoimmune disease, including pSS (26). A reason for this may be sequence similarities between viral and host proteins leading to an unwanted immune response by molecular mimicry. A search of the sequence similarity between virus proteins and the hRo60 revealed that proteins from multiple virus proteins share five to six continuous amino acid residues with hRo60_310-335 peptide (**Figure 5**). Among those virus, human immunodeficiency virus type 1 (HIV-1) may be of specific interest since several lines of epidemiological and serological evidence suggest that HIV-1 represents a triggering factors for the development of SS (27, 28). Thus, a possible link between the HIV-1 infection and SS disease could be based on molecular mimicry.

As expected, different mouse strains show diverse susceptibility to these novel mouse models of pSS, which might reflect the situation in human where genetic factor contribute to the development of disease (29, 30). Therefore, examining differences among susceptible and resistant mouse strains can provide hints for understanding the pathogenesis of this mouse model. Notably, susceptible strains immunized with the mRo60_316-335 peptide did not only develop autoantibodies directed against the peptide but also some autoantibodies with a specificity unrelated to the antigen, indicating intermolecular antigen spreading (17). Since these autoantibodies produced *via* intermolecular antigen spreading were not observed in disease-resistant strains, these observations support our hypothesis that immunization with a T cell epitope might lead to intermolecular antigen spreading and to a consequent production of potentially pathogenic autoantibodies against further autoantigens which may mediate disease symptoms. Moreover, the susceptible strains carry H2-k (C3H/HeJ and C3H/HeN) in the MHC locus, while the resistant strains carry H2-q (DBA/1J) or H2-b (C57BL/6J), supporting the important role of the HLA in the development of the disease (20, 31). In addition, only susceptible strains but not resistant strains are characterized with lymphocytic infiltration in the exocrine glands, indicating a contribution of infiltrated lymphocytes.

Despite the similarities in the pathogenesis of experimental pSS in C3H/HeJ and C3H/HeN, it should be noted that there are some fine differences in the disease phenotypes developed in both substrains. For example, C3H/HeJ mice showed a higher level of inflammatory infiltration in exocrine glands in both Ro60_316-335 peptide immunized and PBS treated groups than C3H/HeN mice. Since the only known relevant genetic difference between these closely related substrains can be referred to the expression of TLR4, which is absent in C3H/HeJ but present in C3H/HeN mice (32), a contribution of TLR4 to the pathogenesis of pSS can be suggested.

Notably, in this new model, the mice developed specifically pSS-like but not SLE-like symptoms. In humans, the anti-SSA/Ro60 antibodies have been detected in the presymptomatic phases of both, pSS and SLE (15, 33). Our model provides a first hint to explain the fine difference between pSS and SLE in the immune response to SSA/Ro60. Previously, the observed difference between both disorders was explained by disease-specific

Species	protein	Accession no.	Start	Sequence	Stop
Human	Ro60	NP_001166995.1	310	NEKLLKKARIHPFHILIALETYKTGH	335
HIV-1	gag protein	ACN53507.1	55	NEKLLK**	62
HPV	E1	ACS73149.1	130	*EKLLKK*	137
HIV-1	rev protein	ADF86398.1	9	*EKLLK**	16
HIV-1	pol protein	ADZ73181.1	621	*EKL*KK*	628
MOCV	MC163R	NP_044114.1	499	*E*L*KKA	506
TANV	core protein P4a	YP_001497096.1	45	*HPF*ILI	52
CeHV-5	protein UL84	AEV80621.1	63	*HPF*IL*	70
MaHV-3	rh114	YP_068207.1	102	*HPF*IL*	109
HIV-1	vpu protein	AAK68077.1	2	*HP*HIL*	9
MARV	viral protein 35	AFV31387.1	13	**PFHIL*	20
SAdV-20	hexon	YP_007518079.1	537	I*PFHI**	544
RV-C	3D polymerase	ADL32209.1	66	*I*LETYK	73
RV-C	polyprotein	AEL31291.1	1987	*I*LETYK	1994
HIV-1	envelope glycoprotein	ADE87691.1	69	LIALET**	76
MOCV	MC129R	NP_044080.1	744	LIAL**YK	751

FIGURE 5 | Analysis of the sequence homology between hRo60_310-335 and human virus proteins. Sequence homologies were analyzed by BLASTP software (https://blast.ncbi.nlm.nih.gov/).

B cell epitopes (34). According to this hypothesis, autoantibodies against hRo60_169-190 should be specific for SLE and hRo60_211-232 for pSS (34). However, this idea was in contrast to further studies performed with larger numbers of samples (35). Results from our study provide a new explanation here: instead of disease-specific B cell epitopes, disease-specific T cell epitope on the Ro60 antigen may be responsible for the development of disease-specific pathologies.

Perhaps the most important finding of this study is that B cell-depletion prevents the impairment of secretion function of exocrine glands. However, this result may have two reasons. In autoimmune responses, B cells are involved in two essential processes, the presentation of antigen to T cells and producing autoantibodies. Since B cells were depleted before immunization and, thus, both processes were potentially affected, we are currently unable to delineate the individual contribution of each mechanism to the disease development. To address this issue, B cell depletion at different time points after the initiation of the immune responses will help to explore the underlying mechanism. The essential role of B cell in this novel mouse model of pSS provides some helpful evidence for clinical treatment of the human disease because it strongly argues for therapeutic approaches targeting B cells. Therefore, although the efficacy of current therapeutics targeting B cells have been proved not to be consistently effective (4, 5, 7), therapeutic approaches targeting plasma cells or autoantibodies might be of interest (36).

It should be mentioned that our model does not cover the entire pathology of pSS. First, disease symptoms are rather mild and impairment in secretion is observed only for tear but not for salivary glands. Second, although the formation of LF as a hallmark of pSS was observed in susceptible mice after immunization, no significant difference in incidence of LF between peptide-immunized mice and controls occurred. Finally, although the incidence of LF in salivary gland was higher than that in lacrimal glands, saliva production was found not to be impaired in this setting. This result argues against a direct association between LF development and secretion function which is not consistent with findings for the pSS in humans.

In conclusion, in the current study, we have established a novel mouse model of pSS based on a single immunization with a Ro60 peptide containing a predominant T cell epitope, demonstrating that T cell epitope within SSA/Ro60 antigen is potentially pathogenic. Furthermore, our results support that B cells play an essential role in the development of pSS.

ETHICS STATEMENT

All protocols of mouse experiments were approved by the Institutional Animal Care and Use Committee of Xiamen University.

AUTHOR CONTRIBUTIONS

XYu was involved in conception, design and supervision of the study. JZ, QH, RH, FD, XYue, YC, RH, WZ, LW and JY were involved in the performing experiment, acquisition of data and analysis of data. JZ, JY, and RH were involved in the bioinformatics analysis. XYu, GR, ZL and FP were involved in drafting of the manuscript.

FUNDING

This work was supported by the National Natural Science Foundation of China (No.81371325 and No. 81571593), the Deutsche Forschungsgemeinschaft, GRK1727 "Modulation of Autoimmunity" and the German Center for Lung Research (DZL).

SUPPLEMENTARY MATERIAL

The Supplementary Material for this article can be found online at http://www.frontiersin.org/article/10.3389/fimmu.2017.01384/full#supplementary-material.

REFERENCES

1. Patel R, Shahane A. The epidemiology of Sjogren's syndrome. *Clin Epidemiol* (2014) 6:247–55. doi:10.2147/CLEP.S47399
2. Moutsopoulos HM. Sjogren's syndrome: a forty-year scientific journey. *J Autoimmun* (2014) 51:1–9. doi:10.1016/j.jaut.2014.01.001
3. Kyriakidis NC, Kapsogeorgou EK, Tzioufas AG. A comprehensive review of autoantibodies in primary Sjogren's syndrome: clinical phenotypes and regulatory mechanisms. *J Autoimmun* (2014) 51:67–74. doi:10.1016/j.jaut.2013.11.001
4. Meijer JM, Meiners PM, Vissink A, Spijkervet FK, Abdulahad W, Kamminga N, et al. Effectiveness of rituximab treatment in primary Sjogren's syndrome: a randomized, double-blind, placebo-controlled trial. *Arthritis Rheum* (2010) 62(4):960–8. doi:10.1002/art.27314
5. Pijpe J, van Imhoff GW, Spijkervet FK, Roodenburg JL, Wolbink GJ, Mansour K, et al. Rituximab treatment in patients with primary Sjogren's syndrome: an open-label phase II study. *Arthritis Rheum* (2005) 52(9):2740–50. doi:10.1002/art.21260
6. vauchelle-Pensec V, Pennec Y, Morvan J, Pers JO, Daridon C, Jousse-Joulin S, et al. Improvement of Sjogren's syndrome after two infusions of rituximab (anti-CD20). *Arthritis Rheum* (2007) 57(2):310–7. doi:10.1002/art.22536
7. Bowman SJ, Everett CC, O'Dwyer JL, Emery P, Pitzalis C, Ng WF, et al. Randomized controlled trial of rituximab and cost-effectiveness analysis in treating fatigue and oral dryness in primary Sjogren's syndrome. *Arthritis Rheumatol* (2017) 69(7):1440–50. doi:10.1002/art.40093
8. Saraux A. The point on the ongoing B-cell depleting trials currently in progress over the world in primary Sjogren's syndrome. *Autoimmun Rev* (2010) 9(9):609–14. doi:10.1016/j.autrev.2010.05.007
9. Park YS, Gauna AE, Cha S. Mouse models of primary Sjogren's syndrome. *Curr Pharm Des* (2015) 21(18):2350–64. doi:10.2174/1381612821666150316120024
10. Robinson CP, Brayer J, Yamachika S, Esch TR, Peck AB, Stewart CA, et al. Transfer of human serum IgG to nonobese diabetic Igmu null mice reveals a role for autoantibodies in the loss of secretory function of exocrine tissues in Sjogren's syndrome. *Proc Natl Acad Sci U S A* (1998) 95(13):7538–43. doi:10.1073/pnas.95.13.7538
11. Groom J, Kalled SL, Cutler AH, Olson C, Woodcock SA, Schneider P, et al. Association of BAFF/BLyS overexpression and altered B cell differentiation with Sjogren's syndrome. *J Clin Invest* (2002) 109(1):59–68. doi:10.1172/JCI0214121
12. Qian Y, Giltiay N, Xiao J, Wang Y, Tian J, Han S, et al. Deficiency of Act1, a critical modulator of B cell function, leads to development of Sjogren's syndrome. *Eur J Immunol* (2008) 38(8):2219–28. doi:10.1002/eji.200738113
13. Li H, Dai M, Zhuang Y. A T cell intrinsic role of Id3 in a mouse model for primary Sjogren's syndrome. *Immunity* (2004) 21(4):551–60. doi:10.1016/j.immuni.2004.08.013
14. Iizuka M, Wakamatsu E, Tsuboi H, Nakamura Y, Hayashi T, Matsui M, et al. Pathogenic role of immune response to M3 muscarinic acetylcholine receptor in Sjogren's syndrome-like sialoadenitis. *J Autoimmun* (2010) 35(4):383–9. doi:10.1016/j.jaut.2010.08.004
15. Jonsson R, Theander E, Sjostrom B, Brokstad K, Henriksson G. Autoantibodies present before symptom onset in primary Sjogren syndrome. *JAMA* (2013) 310(17):1854–5. doi:10.1001/jama.2013.278448
16. Hernandez-Molina G, Leal-Alegre G, Michel-Peregrina M. The meaning of anti-Ro and anti-La antibodies in primary Sjogren's syndrome. *Autoimmun Rev* (2011) 10(3):123–5. doi:10.1016/j.autrev.2010.09.001
17. Deshmukh US, Lewis JE, Gaskin F, Kannapell CC, Waters ST, Lou YH, et al. Immune responses to Ro60 and its peptides in mice. I. The nature of the immunogen and endogenous autoantigen determine the specificities of the induced autoantibodies. *J Exp Med* (1999) 189(3):531–40. doi:10.1084/jem.189.3.531
18. Chen Y, Zheng J, Huang Q, Deng F, Huang R, Zhao W, et al. Autoantibodies against the second extracellular loop of M3R do neither induce nor indicate primary Sjogren's syndrome. *PLoS One* (2016) 11(2):e0149485. doi:10.1371/journal.pone.0149485
19. Wang P, Sidney J, Dow C, Mothe B, Sette A, Peters B. A systematic assessment of MHC class II peptide binding predictions and evaluation of a consensus approach. *PLoS Comput Biol* (2008) 4(4):e1000048. doi:10.1371/journal.pcbi.1000048
20. Huang R, Yin J, Chen Y, Deng F, Chen J, Gao X, et al. The amino acid variation within the binding pocket 7 and 9 of HLA-DRB1 molecules are associated with primary Sjogren's syndrome. *J Autoimmun* (2015) 57:53–9. doi:10.1016/j.jaut.2014.11.006
21. Scofield RH, Asfa S, Obeso D, Jonsson R, Kurien BT. Immunization with short peptides from the 60-kDa Ro antigen recapitulates the serological and pathological findings as well as the salivary gland dysfunction of Sjogren's syndrome. *J Immunol* (2005) 175(12):8409–14. doi:10.4049/jimmunol.175.12.8409
22. Oriss TB, Hu PQ, Wright TM. Distinct autoreactive T cell responses to native and fragmented DNA topoisomerase I: influence of APC type and IL-2. *J Immunol* (2001) 166(9):5456–63. doi:10.4049/jimmunol.166.9.5456
23. Veeraraghavan S, Renzoni EA, Jeal H, Jones M, Hammer J, Wells AU, et al. Mapping of the immunodominant T cell epitopes of the protein topoisomerase I. *Ann Rheum Dis* (2004) 63(8):982–7. doi:10.1136/ard.2003.008037
24. Lu L, Kaliyaperumal A, Boumpas DT, Datta SK. Major peptide autoepitopes for nucleosome-specific T cells of human lupus. *J Clin Invest* (1999) 104(3):345–55. doi:10.1172/JCI6801
25. Fernando MM, Stevens CR, Walsh EC, De Jager PL, Goyette P, Plenge RM, et al. Defining the role of the MHC in autoimmunity: a review and pooled analysis. *PLoS Genet* (2008) 4(4):e1000024. doi:10.1371/journal.pgen.1000024
26. Sipsas NV, Gamaletsou MN, Moutsopoulos HM. Is Sjogren's syndrome a retroviral disease? *Arthritis Res Ther* (2011) 13(2):212. doi:10.1186/ar3262
27. Ulirsch RC, Jaffe ES. Sjogren's syndrome-like illness associated with the acquired immunodeficiency syndrome-related complex. *Hum Pathol* (1987) 18(10):1063–8. doi:10.1016/S0046-8177(87)80223-X
28. Williams FM, Cohen PR, Jumshyd J, Reveille JD. Prevalence of the diffuse infiltrative lymphocytosis syndrome among human immunodeficiency virus type 1-positive outpatients. *Arthritis Rheum* (1998) 41(5):863–8. doi:10.1002/1529-0131(199805)41:5<863::AID-ART13>3.0.CO;2-F
29. Li Y, Zhang K, Chen H, Sun F, Xu J, Wu Z, et al. A genome-wide association study in Han Chinese identifies a susceptibility locus for primary Sjogren's syndrome at 7q11.23. *Nat Genet* (2013) 45(11):1361–5. doi:10.1038/ng.2779
30. Zheng J, Huang R, Huang Q, Deng F, Chen Y, Yin J, et al. The GTF2I rs117026326 polymorphism is associated with anti-SSA-positive primary Sjogren's syndrome. *Rheumatology (Oxford)* (2015) 54(3):562–4. doi:10.1093/rheumatology/keu466
31. Cruz-Tapias P, Rojas-Villarraga A, Maier-Moore S, Anaya JM. HLA and Sjogren's syndrome susceptibility. A meta-analysis of worldwide studies. *Autoimmun Rev* (2012) 11(4):281–7. doi:10.1016/j.autrev.2011.10.002
32. Poltorak A, He X, Smirnova I, Liu MY, Van HC, Du X, et al. Defective LPS signaling in C3H/HeJ and C57BL/10ScCr mice: mutations in Tlr4 gene. *Science* (1998) 282(5396):2085–8. doi:10.1126/science.282.5396.2085
33. Arbuckle MR, McClain MT, Rubertone MV, Scofield RH, Dennis GJ, James JA, et al. Development of autoantibodies before the clinical onset of systemic lupus erythematosus. *N Engl J Med* (2003) 349(16):1526–33. doi:10.1056/NEJMoa021933
34. Routsias JG, Tzioufas AG, Sakarellos-Daitsiotis M, Sakarellos C, Moutsopoulos HM. Epitope mapping of the Ro/SSA60KD autoantigen reveals disease-specific antibody-binding profiles. *Eur J Clin Invest* (1996) 26(6):514–21. doi:10.1046/j.1365-2362.1996.186316.x
35. Scofield AN, Kurien BT, Gordon TP, Scofield RH. Can B cell epitopes of 60 kDa Ro distinguish systemic lupus erythematosus from Sjogren's syndrome? *Lupus* (2001) 10(8):547–53. doi:10.1191/096120301701549679
36. Rosenberg AS, Pariser AR, Diamond B, Yao L, Turka LA, Lacana E, et al. A role for plasma cell targeting agents in immune tolerance induction in autoimmune disease and antibody responses to therapeutic proteins. *Clin Immunol* (2016) 165:55–9. doi:10.1016/j.clim.2016.02.009

Conflict of Interest Statement: The authors declare that the research was conducted in the absence of any commercial or financial relationships that could be construed as a potential conflict of interest.

frontiers in Immunology

ORIGINAL RESEARCH
published: 18 October 2017
doi: 10.3389/fimmu.2017.01364

Selective Limbic Blood–Brain Barrier Breakdown in a Feline Model of Limbic Encephalitis with LGI1 Antibodies

Anna R. Tröscher[1], Andrea Klang[2], Maria French[1], Lucía Quemada-Garrido[1], Sibylle Maria Kneissl[3], Christian G. Bien[4], Ákos Pákozdy[5†] and Jan Bauer[1†]*

[1] Department of Neuroimmunology, Center for Brain Research, Medical University of Vienna, Vienna, Austria, [2] Department for Pathobiology, Institute of Pathology and Forensic Veterinary Medicine, University of Veterinary Medicine, Vienna, Austria, [3] Diagnostic Imaging, Department for Companion Animals and Horses, University of Veterinary Medicine, Vienna, Austria, [4] Epilepsy Center Bethel, Krankenhaus Mara, Bielefeld, Germany, [5] Clinical Unit of Internal Medicine Small Animals, University of Veterinary Medicine, Vienna, Austria

Human leucine-rich glioma-inactivated protein 1 encephalitis (LGI1) is an autoimmune limbic encephalitis in which serum and cerebrospinal fluid contain antibodies targeting LGI1, a protein of the voltage gated potassium channel (VGKC) complex. Recently, we showed that a feline model of limbic encephalitis with LGI1 antibodies, called feline complex partial seizures with orofacial involvement (FEPSO), is highly comparable to human LGI1 encephalitis. In human LGI1 encephalitis, neuropathological investigations are difficult because very little material is available. Taking advantage of this natural animal model to study pathological mechanisms will, therefore, contribute to a better understanding of its human counterpart. Here, we present a brain-wide histopathological analysis of FEPSO. We discovered that blood–brain barrier (BBB) leakage was present not only in all regions of the hippocampus but also in other limbic structures such as the subiculum, amygdale, and piriform lobe. However, in other regions, such as the cerebellum, no leakage was observed. In addition, this brain-region-specific immunoglobulin leakage was associated with the breakdown of endothelial tight junctions. Brain areas affected by BBB dysfunction also revealed immunoglobulin and complement deposition as well as neuronal cell death. These neuropathological findings were supported by magnetic resonance imaging showing signal and volume increase in the amygdala and the piriform lobe. Importantly, we could show that BBB disturbance in LGI1 encephalitis does not depend on T cell infiltrates, which were present brain-wide. This finding points toward another, so far unknown, mechanism of opening the BBB. The limbic predilection sites of immunoglobulin antibody leakage into the brain may explain why most patients with LGI1 antibodies have a limbic phenotype even though LGI1, the target protein, is ubiquitously distributed across the central nervous system.

Keywords: hippocampus, amygdala, tight junctions, limbic encephalitis, neuroinflammation

OPEN ACCESS

Edited by:
Fabienne Brilot, University of Sydney, Australia

Reviewed by:
Tyler Cutforth, Columbia University Medical Center, United States
Pavan Bhargava, Johns Hopkins School of Medicine, United States

***Correspondence:**
Jan Bauer
jan.bauer@meduniwien.ac.at

[†]These authors share senior authorship.

Specialty section:
This article was submitted to Multiple Sclerosis and Neuroimmunology, a section of the journal Frontiers in Immunology

Received: *13 July 2017*
Accepted: *05 October 2017*
Published: *18 October 2017*

Citation:
Tröscher AR, Klang A, French M, Quemada-Garrido L, Kneissl SM, Bien CG, Pákozdy Á and Bauer J (2017) Selective Limbic Blood–Brain Barrier Breakdown in a Feline Model of Limbic Encephalitis with LGI1 Antibodies. Front. Immunol. 8:1364. doi: 10.3389/fimmu.2017.01364

Abbreviations: AMPAR, α-amino-3-hydroxy-5-methyl-4-isoxazolepoionic acid receptor; BBB, blood–brain barrier; FEPSO, feline complex partial seizures with orofacial involvement; FLAIR, Fluid attenuation inversion recovery; vWF, von Willebrand factor; $GABA_BR$, gamma aminobutyric acid B receptor; HN, hippocampal necrosis; HS, hippocampal sclerosis; LGI1, leucine-rich glioma-inactivated protein 1; MAP-2, myelin-associated protein 2; NeuN, neuronal nuclei; NMDAR, *N*-methyl-D-aspartate receptor; TG2, transglutaminase 2; TUNEL, terminal deoxynucleotidyl transferase dUTP nick end labeling; VGKC, voltage-gated potassium channel complex; ZO-1, zona occludens 1.

INTRODUCTION

In recent years, autoimmune epilepsies with antibodies against various antigens have been described. Among these are cases with antibodies targeting surface receptors such as the *N*-methyl-D-aspartate receptor (1), the α-amino-3-hydroxy-5-methyl-4-isoxazolepropionic acid receptor (2), the γ-aminobutyric acid-B receptor ($GABA_BR$) (3), or the voltage-gated potassium channel (VGKC) complex (4). For the latter, it is now known that, in most cases, the antibodies are directed to leucine-rich glioma inactivated protein 1 (LGI1) (5, 6). Patients with LGI1 antibodies typically develop limbic encephalitis and suffer from amnesia, confusion, personality change or psychosis, seizures, and often hyponatremia (7, 8).

In human LGI1 encephalitis, magnetic resonance imaging (MRI) studies have shown increased volume and T2 signal of temporomesial structures with the hippocampus most prominently affected. Initial swelling of these structures is often followed by atrophy (8, 9). Whereas seizures, amnesia, and confusion likely result from autoantibody-mediated inflammation and lesions in the hippocampus (10), the neuropsychiatric symptoms, such as personality changes, psychosis or mood disorders, can be explained by the involvement of the amygdala, which is known for its key role in processing emotions and behavior (11–14).

The involvement of the hippocampus in human LGI1 encephalitis has been confirmed in histopathological studies. Parenchymal T cell infiltrates are present, but sparse. In addition, neurodegeneration caused by immunoglobulin G and complement deposition has been shown (15, 16). Two different pathogenic mechanisms may play a role in the action of LGI1 antibodies. First, the LGI1 antibodies seem to bind to LGI1, resulting in a functional change in LGI1, which can be reversed as steroids and plasma exchange swiftly ameliorate the disease symptoms (8, 17). Second, complement-mediated neuronal destruction occurring in the hippocampus may contribute to temporomesial atrophy and persisting cognitive deficits in nearly all patients, despite treatment options (9, 11, 15).

Recently, we described an acute seizure disorder with orofacial involvement in cats. This disorder was coined feline complex partial seizures with orofacial involvement (FEPSO) (18). Besides the distinct clinical features, these cats in MRI scans showed bilateral hippocampal T2 signal increase. Importantly, cell-based assays revealed that almost all tested sera of these cats contained anti-LGI1 antibodies (16, 18–20). Subsequent analysis of the hippocampus of these animals revealed the presence of inflammatory T cells, B cells, and plasma cells in the parenchyma. Moreover, neurodegeneration in these animals was caused by immunoglobulin and complement deposition (16). Overall, clinical, neuropathological and MRI analysis, therefore, indicate that FEPSO is the feline equivalent of human LGI1 encephalitis and might be used as a natural model for this disease.

In both human LGI1 encephalitis and in FEPSO, little is known about pathologic changes outside the hippocampus. Extrahippocampal pathology is expected since human LGI1 antibody-positive sera not only bind to the hippocampus but also to other regions, including the molecular layer of the cerebellum where LGI1 is expressed in high amounts (6, 21, 22). Nevertheless, in human patients, cerebellar features such as ataxia have been found much less frequently than limbic affection (23, 24). MRI studies in LGI1 encephalitis have shown T2 signal increase and sclerosis of the whole mesial temporal lobe (6, 8) but also in the basal ganglia, which are thought to contribute to faciobrachial dystonic seizures (25–27). Less frequently, white matter atrophy (28) and blurring, suggestive of mild de- or hypomyelination, was shown (29).

Taken together, although the limbic system displays the most frequent and most prominent signs and symptoms, recent publications point toward the involvement of other brain areas. The limited amount of human material, especially of brain structures other than the impaired hippocampus, poses a problem in the study of these extrahippocampal structures.

Since a relatively high number of FEPSO brains are available, we took the opportunity to perform a detailed neuropathological analysis of limbic and non-limbic structures. Our analysis shows that inflammatory infiltrates can be found brain-wide. A disturbance of the blood–brain barrier (BBB), occurring with prominent loss of tight junctions and resulting in leakage of immunoglobulin and complement, however, was more restricted. This leakage was found in brain areas such as the hippocampus but also in the subiculum, amygdale, and piriform lobe and, to a lesser degree, in the basal ganglia and hypothalamus. Moreover, in these areas, immunoglobulin and complement deposition to neurons was present and was associated with severe neurodegeneration. Importantly, this finding suggests that BBB disturbance and immunoglobulin leakage does not depend on T cell inflammation but that other, yet unknown, mechanisms are responsible.

MATERIALS AND METHODS

Animals

In this study, 16 cats with FEPSO, characterized by facial seizures and hippocampal sclerosis or hippocampal necrosis (18), were included. Five of these cats were tested positive for serum antibodies against VGKC complex and showed positive reactivity to LGI1 in a cell-based binding assay as shown previously (16). The remaining 11 cats showed seizures typical of FEPSO but could not be tested for LGI1-reactive antibodies due to absence of sera. Throughout the manuscript, the definitive LGI1 antibody-positive FEPSO animals are indicated and separated from the FEPSO animals with unknown LGI1 antibody status. LGI1-positive animals are indicated in red and untested animals in black dots in all graphs. Of the 16 animals, 2 died spontaneously; all others were euthanized due to resistance to therapy or severe clinical course between 2 days and 34 months after onset of neurological signs. One cat (case 1) had papillary adenomas, whereas in the other cats, no tumors were found. Cats received antiepileptic therapy with phenobarbital, gabapentin, levetiracetam, potassium bromide, or a combination of those. Additionally, five cats were treated with prednisolone 1–2 mg/kg twice daily. For an epileptic control group, seven cats with epileptic seizures not fitting the classification of FEPSO (18) were used. Five suffered from temporal lobe epilepsy, four of which also had HS, one cat had an edema, and

one a meningioma. Additionally, seven cats without neurological implication, which died as a result of other, non-neurological problems, were selected for the normal control group. For animal details, please refer to Table S1 in Supplementary Material.

Ethics Approval

The project was discussed and approved by the institutional ethics committee (University of Veterinary Medicine, Vienna) in accordance with GSP guidelines and national legislation.

Neuropathology and Immunohistochemistry

In all cats, a general necropsy was performed, and brains were fixed in 4% neutral-buffered formalin, embedded in paraffin, and coronal sectioned. Immunohistochemistry was performed as shown previously (15) at the level of the frontal cortex, nucleus accumbens, amygdala, hippocampus, and cerebellum. Luxol Fast Blue-Periodic Acid Schiff staining was performed to study changes (demyelination or hypomyelination) in white matter. Immunohistochemistry was performed with antibodies for T lymphocytes (anti-CD3), endothelial cells [transglutaminase 2 (TG2)], early constituents of the complement cascade (C1q), fully assembled complement system end complex (C9neo), feline immunoglobulin, and neurons [neuronal nuclei (NeuN)], and myelin-associated protein 2 (MAP-2). Antigen retrieval was done by heating the sections for 45 min in EDTA (0.05 M) in tris(hydroxymethyl)aminomethane (Tris) buffer (0.01 M, pH 8.5) or citrate buffer (0.01 M, pH 6) in a household food steamer device for all antibodies except for C9neo, and immunoglobulin, in which case antigen retrieval was performed by incubating the tissue for 15 min in proteinase (bacterial proteinase Type XXIV, #SLBQ7212V, Sigma Life Science) at 37°C. For more detailed information regarding antibodies, dilutions used, and antigen retrieval, please refer to Table S2 in Supplementary Material.

Fluorescent Immunohistochemistry

We investigated BBB damage in more detail by double-labeling for the tight junction marker zona occludens 1 (ZO-1) and cat immunoglobulin in FEPSO animals in the hippocampus, the amygdala, basal ganglia, cortex, and cerebellum. Additionally, we investigated the hippocampus in normal and epileptic controls. Cats showing an average degree of BBB leakage were selected and investigated. To check for endothelial cell integrity of the blood vessels, we performed a triple staining for ZO-1, cat immunoglobulin, and von Willebrand Factor (vWF) as endothelial marker. Antigen retrieval was done with proteinase for 15 min at 37°C, and standard staining procedures were followed as described previously (15). For more detailed information regarding antibodies, dilutions used, and antigen retrieval, please refer to Table S2 in Supplementary Material.

Terminal Deoxynucleotidyl Transferase dUTP Nick End Labeling

Qualitative assessment of chronic cell loss was conducted in stained coronal sections at the level of the frontal cortex, basal ganglia, amygdala, hippocampus, and cerebellum. For the detection of cells with DNA fragmentation, TUNEL staining was performed with the *In Situ* Cell Death Detection Kit® (Roche, Basel, Switzerland) as described elsewhere (15) and developed with Fast Blue. To identify dying neurons, this step was followed by immunohistochemical staining for MAP-2 or NeuN, which was developed with 3-amino-9-ethylcarbazole as a substrate.

Quantification of Cells

$CD3^+$ cells were quantified by light microscopy using a morphometric grid in 1.25 mm^2 (20 grids in 400× magnification) or 2.5 mm^2 (40 grids in 400× magnification), depending on the number of brain slices containing the region of interest. $C9neo^+$ cells were counted in 1.25 mm^2 (20 grids in 400× magnification) for the cortex, cerebellum, and caudate nucleus. In the amygdala and the hippocampus, $C9neo^+$ cells were counted in the whole area. For the determination of cell loss, the number of $TUNEL^+$ cells among 100 cells was determined in the respective areas. For the determination of neuronal loss in the hippocampus, the number of $NeuN^+$ cells was counted in 0.75 mm^2 (3 grids in 200× magnification) of each hippocampal subfield in normal controls and FEPSO cats. The percentage of remaining $NeuN^+$ cells in comparison with normal controls was calculated for each subfield. The statistical difference to 100% (equal to "no neuronal loss") was calculated.

Quantification of Immunoglobulin

For quantification of immunoglobulin in different brain areas as well as in the hippocampus between FEPSO and controls, all slides were incubated and developed for the final color reaction for the exact same time. Images were analyzed using ImageJ by digital optical densitometry, as shown previously (30).

Magnetic Resonance Imaging

MR studies of two cats, acquired with a high-field MR unit (Magnetom Espree, 1.5T, Siemens Healthcare, Erlangen, Germany), were retrospectively evaluated. In each case, transverse T2-weighted fluid attenuation inversion recovery (FLAIR), sagittal 3D T2-weighted turbo spin echo (T2), transverse 2D and sagittal 3D pre- (T1) and post-contrast T1-weighted turbo spin echo images (T1C) were available. Slice thickness was 0.8–3 mm.

Graphical Presentation of Inflammation, Neurodegeneration, and Complement Deposition

For a full overview on neuropathological changes, a brain-wide investigation for inflammation, neurodegeneration, and complement deposition was performed. Graphical representations of coronal cat brain slices containing the hippocampus, amygdala, cortex, basal ganglia, and cerebellum, were produced with CorelDRAW X4 based on images present on www.brainmaps.org (31). Infiltrates, neurodegeneration, and complement deposition in 16 cats with FEPSO were drawn into the cat brain images using Adobe Photoshop CS4.

Statistical Analysis

For statistical analysis, GraphPad Prism 6 was used. First, we tested for differences between FEPSO animals positive for

LGI1 antibodies and FEPSO animals with unknown LGI1 antibody status. To this end, a two-way ANOVA was used, but no differences were found. Therefore, datasets were pooled for further analysis, which was performed with Kruskal–Wallis tests with Dunn's correction for multiple testing. Neuronal loss within the hippocampus was evaluated by the percentage of remaining neurons with regard to normal control hippocampal subareas (corresponding to 100% NeuN$^+$ cells). To this end, a Wilcoxon-signed rank test was performed. All graphical data are represented as medians with the interquartile ranges. Animals tested positive for LGI1 antibodies and animals with unknown status are graphically separated (data points and error bars). Data of LGI1 antibody positive animals indicated in red and animals with unknown status indicated in black. Results were considered statistically significant at $p \leq 0.05$.

RESULTS

Inflammation

In the hippocampus of normal controls, parenchymal inflammatory T lymphocytes were very rare (1.2 cells/mm^2). The hippocampus of epileptic controls showed higher numbers of T cells (2.4 cells/mm^2). These T cell numbers were comparable to T cell numbers in hippocampi of FEPSO animals (3.2 cells/mm^2). Statistical analysis of hippocampal T cell numbers between normal controls, epileptic controls, and FEPSO, possibly due to the high variance, however, revealed no significant difference. In brains of FEPSO animals, T cells were mostly found in perivascular cuffs and the meninges, with only moderate parenchymal infiltrating T cells. Parenchymal CD3$^+$ T cells were found in all investigated regions of the brain, including the hippocampus, amygdala, basal ganglia, cortex, and cerebellum (**Figures 1A–E** and **6**). T cell infiltrates, besides in gray matter, also were found in white matter tracts (**Figure 1F**). To determine if brain regions with high LGI1 abundance, such as the cerebellum or the hippocampus, showed increased levels of T cells, we quantified the number of CD3$^+$ T cells in these different regions. However, no significant difference in cell number was found (**Figure 1G**).

BBB Leakage

Immunoglobulin leakage was not found in the parenchyma of normal controls (**Figure 2A**). Epileptic controls, on the other hand, showed slightly increased levels of parenchymal immunoglobulin in the hippocampus and, to a lesser extent, in the cortex (**Figure 2B**). In FEPSO brains, leakage of immunoglobulin over the BBB was prominent in all limbic structures (**Figures 2C–F**). Most prominently affected were several nuclei of the amygdala, namely, the lateral and medial basal amygdala (N. basalis), the lateral (N. lateralis), medial (N. medialis) and central (N. centralis) amygdala, periamygdaloid area, and anterior cortical nucleus of the amygdala (N. corticalis) (**Figure 2D**), as well as, bilaterally, the hippocampus, adjacent subiculum, and entorhinal cortex (**Figure 2E**). These regions overlapped with signal and volume increase found in MR imaging (**Figure 2G**). In some animals, immunoglobulin leakage was also observed in the prepiriform cortex, putamen, claustrum, olfactory tubercle, nucleus accumbens, tenia tecta, septo-olfactory junction, hypothalamus, and anterior commissure (**Figure 6**). In the cerebellum, no significant immunoglobulin leakage was found (**Figure 2F**). Quantification of the mean optical density of immunoglobulin in the hippocampi confirmed the absence of immunoglobulin leakage of normal control cats. FEPSO cats showed a significant increase of immunoglobulin leakage compared to the baseline of normal controls (median of 70% increase). When compared with epileptic controls, no significant difference was found (**Figure 2H**). Within FEPSO animals, different brain areas showed large differences in immunoglobulin abundance. The amount of immunoglobulin in the hippocampus was significantly elevated compared to that in the basal ganglia, cortex, and cerebellum. Interestingly, we found no significant difference between the hippocampus and the

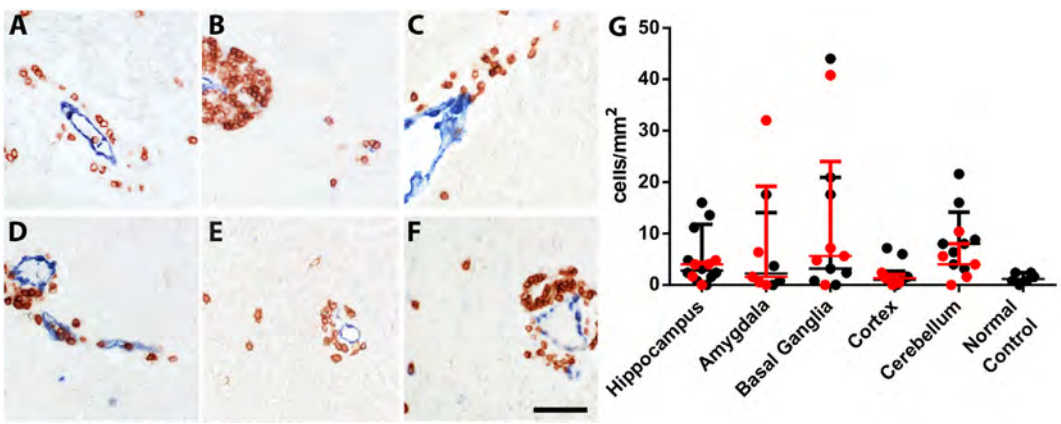

FIGURE 1 | Inflammatory infiltrates in FEPSO can be found all over the brain in gray and white matter. Immunohistochemical staining for CD3$^+$ and transglutaminase 2 showed that T cells are mainly located in perivascular cuffs with moderate parenchymal infiltrates in all inspected areas, namely the **(A)** hippocampus, **(B)** amygdala, **(C)** basal ganglia, **(D)** cortex, **(E)** cerebellum, and **(F)** white matter. **(G)** Quantification of parenchymal T cell infiltrates in the abovementioned areas did not reveal differences in T cell densities. Data shown as median with interquartile range, LGI1 antibody-positive animals are indicated in red and untested animals in black; (ns $p > 0.05$ Kruskal–Wallis test with Dunn's *post hoc* correction, hippocampus $n = 15$, amygdala $n = 9$, basal ganglia $n = 12$, cortex $n = 15$, cerebellum $n = 13$, normal controls $n = 6$) Scale bar corresponds to 50 µm.

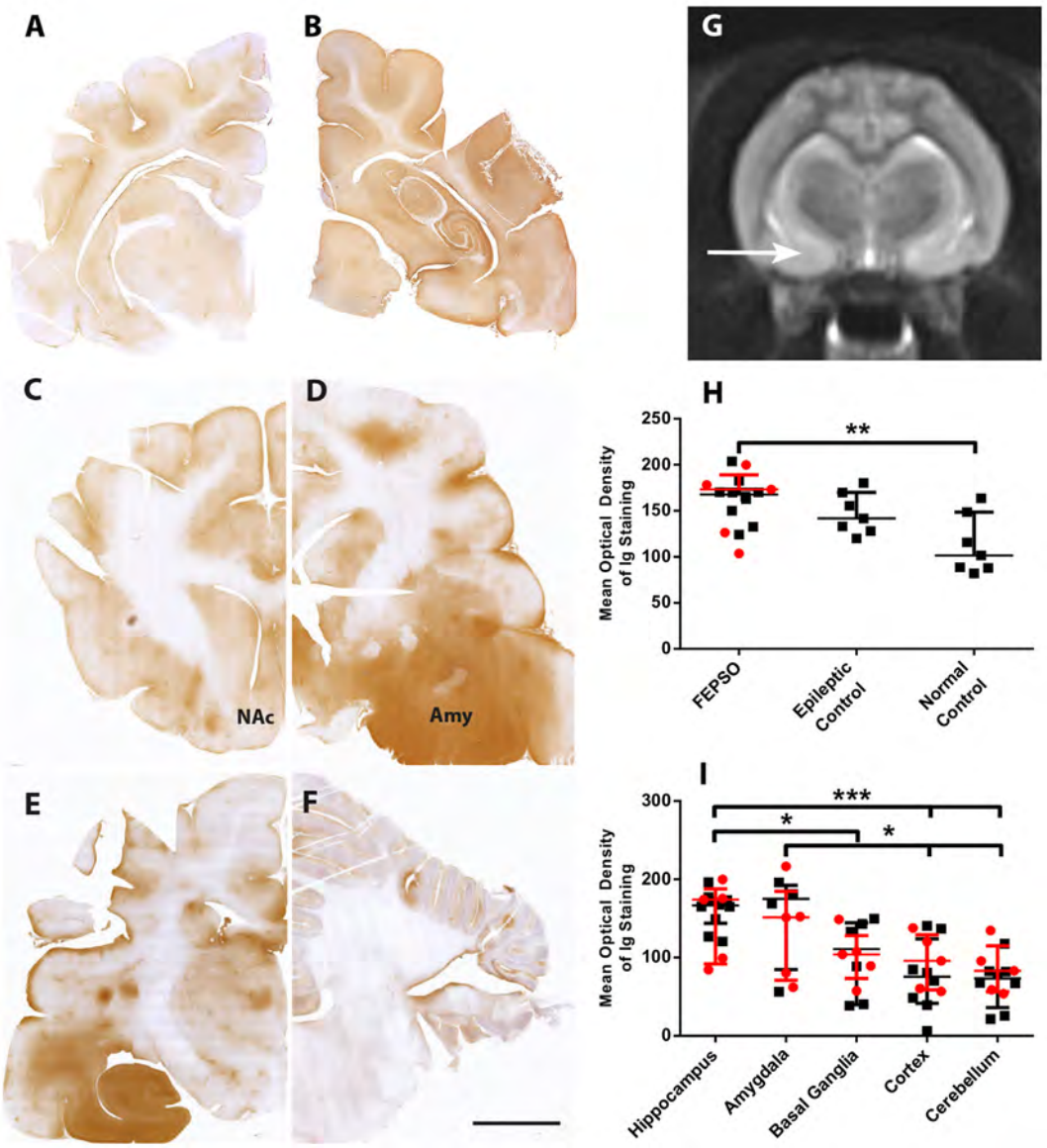

FIGURE 2 | Selective blood–brain barrier leakage overlaps with MR signal changes in the amygdala. **(A–F)** Staining for immunoglobulin in representative images of coronal brain sections in **(A)** normal controls, **(B)** epileptic controls, and in FEPSO at the level of **(C)** frontal cortex and nucleus accumbens, **(D)** amygdala and piriform lobe, **(E)** hippocampus, and **(F)** cerebellum. Immunoglobulin leakage is seen prominently in the hippocampus but also in the amygdala and adjacent regions. Scale bar corresponds to 5 mm. **(G)** Transverse T2-weighted MR image at the level of the hippocampus and piriform lobe in a 1-year-old female neutered European shorthair cat, orientated along the long axis of the hippocampus on a sagittal slice. The MR signal is bilaterally abnormally increased, and the area of the amygdala (arrow) appears bilaterally enlarged. **(H)** Optical density quantification of Ig leakage in FEPSO, epileptic, and normal control hippocampus. The hippocampi of FEPSO have higher values than normal controls. Data shown as median with interquartile range, LGI1 antibody-positive animals, are indicated in red and untested animals in black (**$p < 0.01$, Kruskal–Wallis test with Dunn's *post hoc* correction, FEPSO $n = 15$, epileptic controls $n = 7$, normal controls $n = 7$). **(I)** Significant elevation of immunoglobulin signal in hippocampus and amygdala in FEPSO cats compared to other brain areas of the same cats. LGI1 antibody-positive animals are indicated in red and untested animals in black. Data shown as median with interquartile range (*$p < 0.05$, ***$p < 0.001$; Kruskal–Wallis test with Dunn's *post hoc* correction, hippocampus $n = 15$, amygdala $n = 9$, basal ganglia $n = 12$, cortex $n = 15$, cerebellum $n = 13$).

amygdala, indicating comparable leakage in both areas. Moreover, the amount of immunoglobulin in the amygdala was significantly elevated compared with the cortex and the cerebellum (**Figure 2I**). We could not detect a significant difference in immunoglobulin signal intensities between hippocampal subareas.

Magnetic Resonance Imaging

Because our study revealed pathological changes outside the hippocampus, especially in the amygdala, we analyzed MRIs from two FEPSO brains (#2 and #15) to support our findings. Bilateral T2-weighted signal and volume increase changes were found in

the hippocampus as well as at the level of the amygdala and the piriform lobe (**Figure 2G**).

Tight Junction Breakdown in Blood Vessels

Blood–brain barrier disruption might be associated with a loss of tight junctions. We, therefore, decided to investigate these structures in our animals. In control animals, the tight junction marker ZO-1 was strongly expressed around vessels. When viewed in longitudinal sections of capillaries, a continuous staining could be observed. Double labeling with Ig showed that, in such vessels, no leakage was observed and Ig was only seen on the luminal side of the vessel (**Figure 3A**). Under pathological conditions, in the hippocampus of epileptic controls, ZO-1 reactivity was weaker and discontinuous. Here, moderate immunoglobulin leakage could be observed in the surrounding brain parenchyma (**Figure 3B**). In the hippocampus of FEPSO animals, we observed a drastic decrease in ZO-1 reactivity. Here, ZO-1 immunoreactivity was very weak and visible in small patches instead of showing a continuous staining pattern. Furthermore, this loss of ZO-1 was associated with severe immunoglobulin leakage in the surrounding parenchyma (**Figure 3C**). The ZO-1 reactivity in the amygdala was comparable to what was seen in the hippocampus, with severe loss of ZO-1 intensity and loss of integrity. Additionally, also in the amygdala, strong immunoglobulin immunoreactivity was observed in the parenchyma, showing similar BBB breakdown and leakage as in the hippocampus (**Figure 3D**). This was different in basal ganglia (**Figure 3E**), cortex (**Figure 3F**), and cerebellum (**Figure 3G**) of FEPSO animals where ZO-1 reactivity was strong and in a regular continuous staining pattern. Immunoglobulin in these regions again was restricted to the lumen of the vessels, and Ig leakage in the parenchyma could not be found. To indicate the endothelial lining of the blood vessels, vWF was added in the merged images.

Immunoglobulin and Complement Deposition

Normal control animals did not show any immunoglobulin deposition on neurons and epileptic controls showed immunoglobulin deposition in some cats. In FEPSO cats, brain areas with BBB leakage revealed strong membranous immunoglobulin deposition on severely damaged neurons. This was found in all limbic structures but was especially prominent in the hippocampus, (pre-) subiculum, entorhinal cortex, and amygdala. In some animals, immunoglobulin deposition was observed in the prepiriform cortex, putamen, claustrum, olfactory tubercle, nucleus accumbens, tenia tecta, septo-olfactory junction, hypothalamus, and anterior commissure. amygdala.

In order to analyze early constituents of the complement cascade, we stained for complement factor C1q. In normal controls, C1q was occasionally found on the surface of cortical neurons. However, in none of these animals, C1q was found on neurons in the hippocampus (**Figure 4A**). A similar staining pattern was observed in epileptic controls (**Figure 4B**). In FEPSO animals, besides on the surface of some cortical neurons, C1q was mostly present on the surface of hippocampal neurons while single neurons in addition showed granular staining in the cytoplasm (**Figure 4C**).

Complement activation, indicated by the complement end complex marker C9neo, was not seen in normal controls. In epileptic controls, although immunoglobulin deposition was observed in some of these brains, C9neo reactivity was completely absent. In cats with FEPSO, regions with Ig deposition also showed complement C9neo immunoreactivity in a punctate appearance on the membrane as well as inside of neurons. This was most prominently seen in the hippocampus (**Figures 4D,G**) and in the amygdala (**Figures 4E,H**). Neither in the basal ganglia nor in the cerebellum were C9neo$^+$ cells found (**Figures 4F,J**). Besides the entorhinal and prepiriform cortex, no complement deposition could be detected in the cortex (**Figure 4I**). Also, the white matter did not show any sign of complement activation (**Figure 4K**). In some animals, neurons with complement deposition were present in the dorsal hypothalamic area, tenia tecta, anterior prepiriform cortex, putamen, olfactory tubercle, and anterior commissure (**Figure 6**). Quantitative analysis of the number of C9neo$^+$ neurons revealed that complement deposition was significantly elevated in the hippocampus and amygdala compared to other brain areas such as basal ganglia, cortex, and cerebellum (**Figure 4L**).

Neurodegeneration and Neuronal Cell Loss

None of the normal control animals showed neuronal loss. Epileptic control animals, however, showed variable neuronal loss in the hippocampus and subiculum. In FEPSO animals, regions showing neurodegeneration largely correlated with immunoglobulin and C9neo deposition and were found in both hemispheres in the limbic structures (**Figure 6**). The hippocampus and the subiculum showed high numbers of TUNEL$^+$ cells, indicating a high degree of cell death (**Figures 5A,B**). Additionally, we found TUNEL$^+$ cells in the amygdala (**Figures 5C,D**). The affected areas comprised the lateral and medial basal amygdala (N. basalis), the lateral (N. lateralis), medial (N. medialis) and central (N. centralis) amygdala, periamygdaloid area, and anterior cortical nucleus of the amygdala (N. corticalis). In single animals, we also found neuronal loss and some TUNEL$^+$ cells in the tenia tecta, septo-olfactory junction, entorhinal cortex, anterior commissure, nucleus accumbens, claustrum, or the posterior prepiriform area (**Figure 6**). In none of the FEPSO animals was neurodegeneration observed in the cortex (except the entorhinal cortex, see above) or cerebellum (**Figures 5E–G**). Moreover, the white matter did not show any sign of hypo- or demyelination (**Figure 5H**). Quantification of the number of TUNEL$^+$ cells showed a significant increase of cell death in the hippocampus compared with the amygdala, basal ganglia, cortex, and cerebellum (**Figure 5I**).

Additionally, we questioned whether hippocampal subfields were equally affected. Quantification of neurons in these subfields in normal controls and FEPSO showed that CA4 was the most severely affected (median cell loss of 78.3%). In CA1, 52.2% were lost, and in CA2 and CA3, 37.5 and 46.7% were lost, respectively. The dentate gyrus, with a median of 98.2% remaining neurons, did not show significant neuronal loss, although three FEPSO

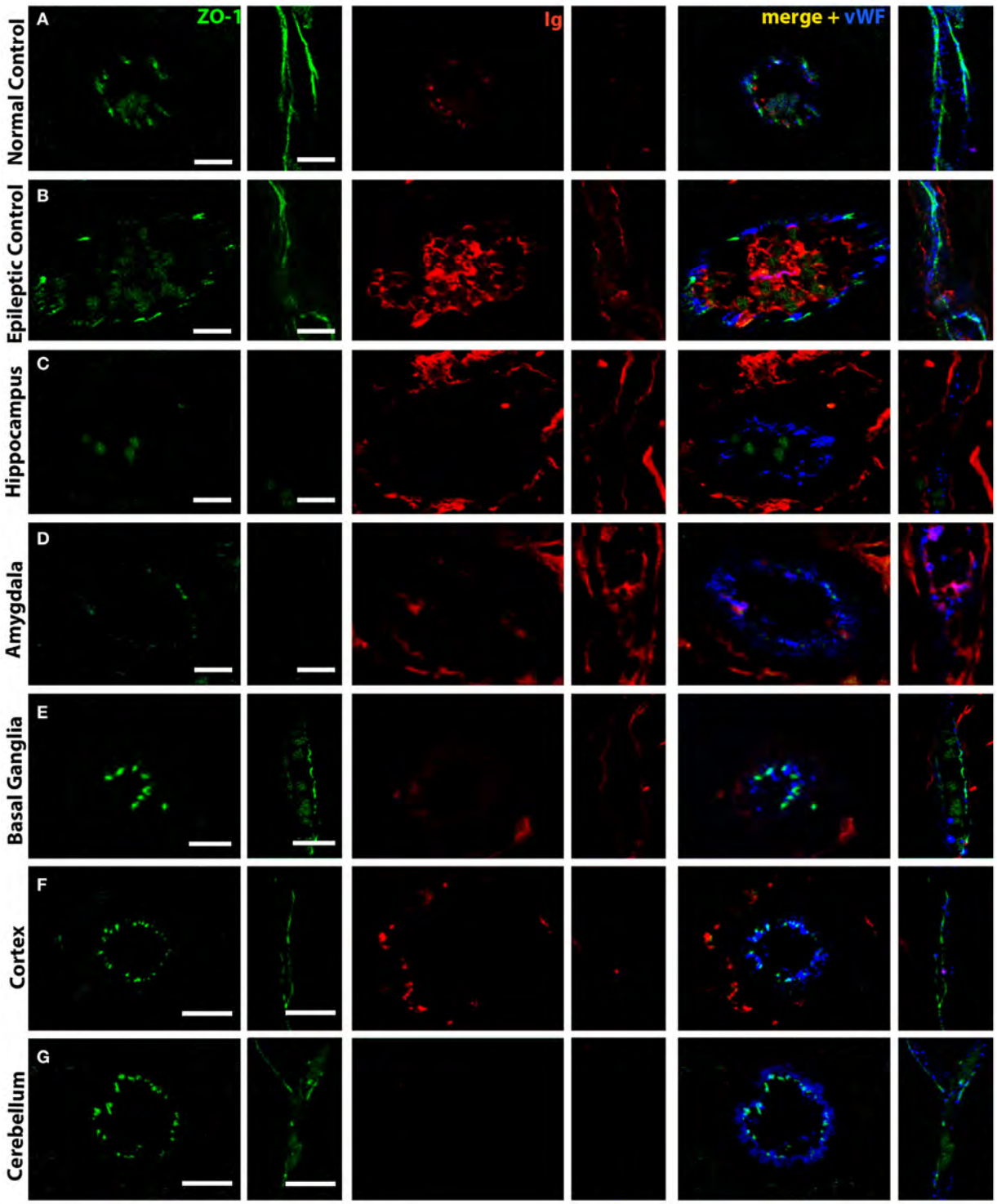

FIGURE 3 | Selective tight junction breakdown leads to blood–brain barrier leakage. Staining of tight junctions [zona occludens 1 (ZO-1), green], immunoglobulin (red), and von Willebrand Factor (blue) in **(A)** normal controls, **(B)** epileptic controls, and **(C–G)** FEPSO cats positive for LGI1 antibodies. The tight junction protein ZO-1 is found between endothelial cells in a strong and (in longitudinal cuts) continuous staining in **(A)** normal controls in the hippocampus. Therefore, weak immunoglobulin staining is restricted to the luminal side of the blood vessels. **(B)** In hippocampi of epileptic controls, the ZO-1 staining is weaker, less continuous, and associated with some immunoglobulin reactivity in the parenchyma. **(C)** In FEPSO, blood vessels in the hippocampus have very weak and discontinuous ZO-1 signal, indicating tight junction breakdown. Here, immunoglobulin has clearly leaked into the parenchyma. **(D)** In the amygdala, the same pattern of tight junction breakdown was seen, indicated by a weak and discontinuous ZO-1 staining, and immunoglobulin leakage into the parenchyma. In all other investigated brain areas such as **(E)** basal ganglia, **(F)** cortex, and **(G)** cerebellum, in FEPSO cats, no ZO-1 breakdown was observed and immunoglobulin only was found on the luminal side of the vessels or perivascular space. Scale bars correspond to 10 µm **(A–D,F,G)** or 5 µm **(E)**.

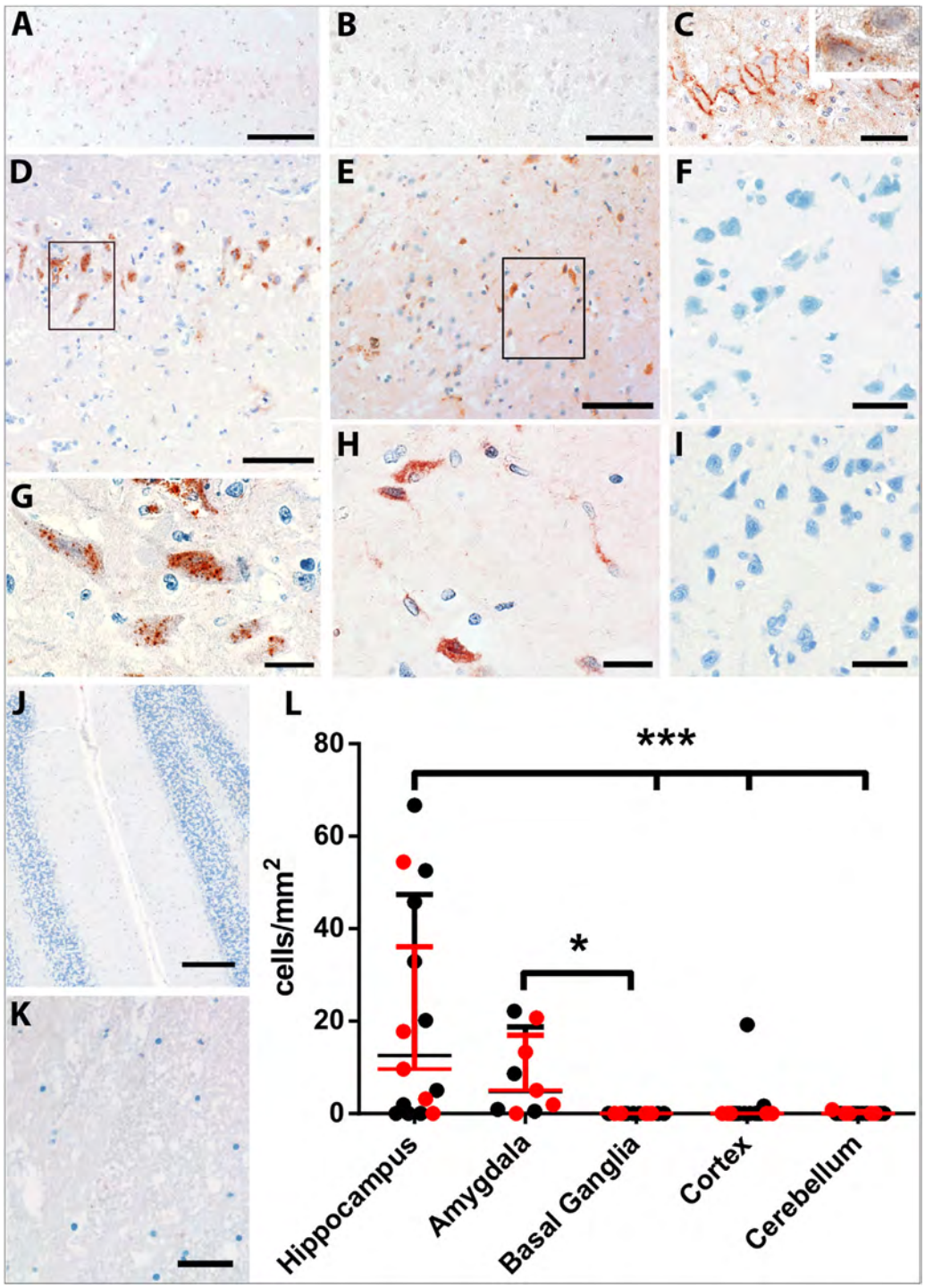

FIGURE 4 | Complement deposition in LGI1 antibody-positive FEPSO animals. Staining for early constituent, C1q of the complement cascade shows the absence of C1q on neurons of **(A)** the hippocampus of a normal control and **(B)** the hippocampus of an epileptic control animal. **(C)** The hippocampus of a FEPSO cat shows C1q reactivity on the surface of hippocampal neurons with occasional granular staining inside the cells (inset). **(D–K)** The brain areas affected by BBB leakage are also affected by complement activation as shown by immunohistochemistry for C9neo. **(D)** In the hippocampus, complement-positive cells are visible, which show a [**(G)**, enlargement] granular staining pattern inside the cells. **(E)** The amygdala shows very similar staining with C9neo positive cells, which [**(H)**, enlargement] show the same granular staining inside the cells. Neither **(F)** the basal ganglia, **(I)** cortex, **(J)** cerebellum nor **(K)** white matter showed any complement positive cells or structures. **(L)** Quantification of C9neo positive cells revealed significantly higher numbers in the hippocampus as well as in the amygdala. Data shown as median with interquartile range, LGI1 antibody-positive animals are indicated in red, and untested animals in black (*$p < 0.05$, Kruskal–Wallis test with Dunn's *post hoc* correction, hippocampus $n = 15$, amygdala $n = 9$, basal ganglia $n = 12$, cortex $n = 15$, cerebellum $n = 13$). Scale bars correspond to **(A,B,D,E)** 100 µm, **(C)** 50 µm, **(G,H)** 20 µm, **(F,I,K)** 25 µm, and **(J)** 200 µm.

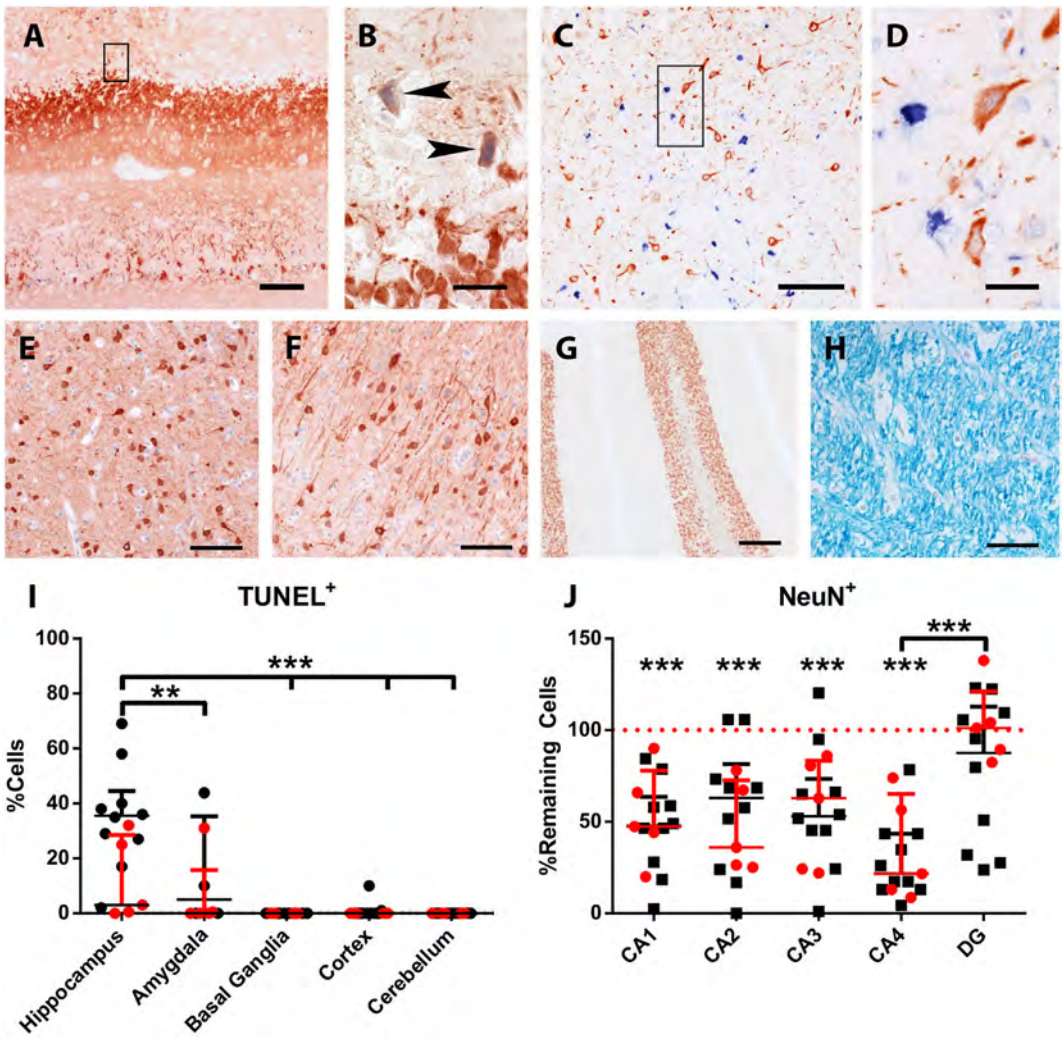

FIGURE 5 | Acute neuronal degeneration and cell loss in LGI1 antibody-positive FEPSO animals. Staining for terminal deoxynucleotidyl transferase dUTP nick end labeling (TUNEL) (blue) and MAP2/neuronal nuclei (NeuN) (red). **(A)** TUNEL+ cells and severe loss of neurons and processes is visible in the hippocampus. **(B)** Shows the areas indicated by the rectangle in **Figure 5A**, revealing TUNEL+ neurons and loss of myelin-associated protein 2 reactivity (arrowheads). **(C)** In the amygdala, a high number of TUNEL+ nuclei are visible, while in **(D)**, enlargement of rectangle in **Figure 5C** and loss of MAP2-reactivity around TUNEL + nuclei is observed. Neither in the **(E)** basal ganglia, **(F)** cortex, **(G)** cerebellum nor **(H)** white matter TUNEL+ cells or de-hypomyelination was observed. **(I)** The percentage of TUNEL+ cells in different areas was quantified. This graph shows significant cell loss in the hippocampus of FEPSO animals. Data are shown as median with interquartile range, LGI1 antibody-positive animals are indicated in red, and untested animals in black (***$p < 0.001$, Kruskal–Wallis test with Dunn's *post hoc* correction, hippocampus $n = 15$, amygdala $n = 9$, basal ganglia $n = 12$, cortex $n = 15$, cerebellum $n = 13$). **(J)** Hippocampal cornu ammonis (CA) subfields revealed severe loss of NeuN-positive cells compared with normal controls (equals 100%) in CA1-4, but not in DG. CA4 subfields exhibits reveal the most severe cell losses, which was significantly different from the loss in the DG. Data shown as median with interquartile range (***$p < 0.001$, Wilcoxon signed-rank test with hypothetical value: 100, $n = 14$, **$p < 0.01$, Kruskal–Wallis test with Dunn's *post hoc* correction for evaluation of inter-hippocampal differences, $n = 14$). Scale bar corresponds to **(A)** 200 µm, **(B,D)** 20 µm, **(C)** 100 µm, **(E,F,H)** 50 µm, and **(G)** 200 µm.

animals also showed severe neurodegeneration in the dentate gyrus with less than 50% of neurons remaining. Finally, CA4 showed significant neuronal loss compared with the dentate gyrus (**Figure 5J**). This neuronal loss in FEPSO corresponds to human hippocampus sclerosis type 1 according to the classification of the international league against epilepsy (32). One recent MRI study on human LGI1 encephalitis found volume loss in CA3 only (33), whereas another one found all areas except CA1 to be affected (9). These intrahippocampal differences, however, cannot be explained by differential expression of LGI1, as, at least in mice, it is most prominently expressed in CA3 and the dentate gyrus (22), and these two subareas in FEPSO strongly differ in the amount of neurodegeneration.

DISCUSSION

LGI1 encephalitis is a form of autoimmune epilepsy, an expanding group of disorders with antibodies against various neural

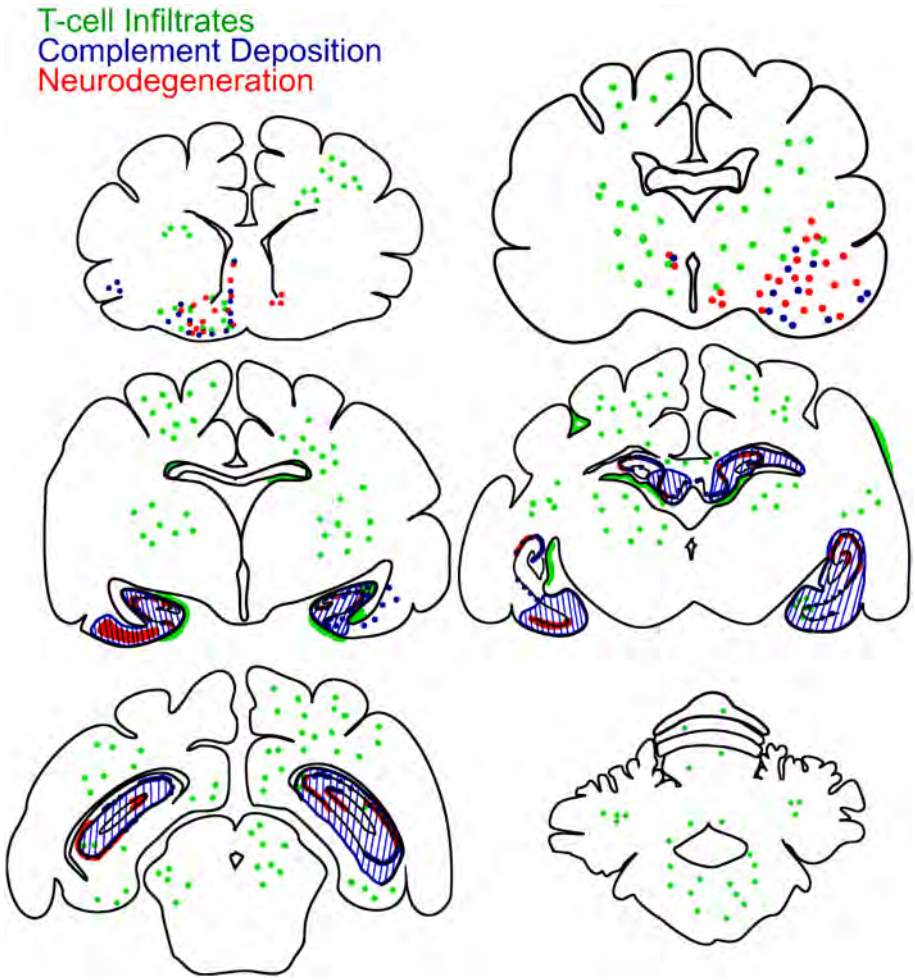

FIGURE 6 | Brain-wide mapping of pathological changes in FEPSO. Cumulative graphical presentation of T cell infiltrates (green), neurodegeneration (red), and complement deposition (blue) in the brains of 16 cats suffering from FEPSO. This presentation shows that inflammatory lesions are brain-wide. Neurodegeneration and complement deposition show strong overlap and is most prominent in the hippocampus, amygdale, and adjacent areas.

antigens and epileptic seizures as one of the broad range of neurological signs. The similarities between human LGI1 encephalitis and FEPSO have only recently been discovered (16, 20). These similarities comprise not only the presence of antibodies against LGI1 and the pathological changes seen in the hippocampus but also clinical symptoms such as radiological changes and facial seizures (15, 16).

The findings that human LGI1-positive sera show strong staining of the cerebellum and that human patients can (very rarely) develop cerebellar symptoms (24, 34) and the MRI studies that show involvement of the amygdala (35, 36) and basal ganglia (25–27) piqued our interest to investigate pathological changes in brain structures other than the hippocampus. Here, we show that inflammatory infiltrates are not restricted to the hippocampus but are also found in most other parts of the brain. Since inflammatory lesions do not overlap with areas affected by neurodegeneration, it can be assumed that T cells do not directly contribute to cell death. Interestingly, in human VGKC-limbic encephalitis, T cell infiltrates have also been found in the amygdala and the uncus in similar numbers as in FEPSO (15). The number of these infiltrating T cells is much lower than those found in T cell-mediated neurodegeneration, such as in paraneoplastic encephalitis in humans (15). In line with our results, a human MRI study found brain-wide metabolic changes, in gray as well as white matter, pointing toward brain-wide neuroinflammation (28). Here, we also found prominent T cell infiltrates in the white matter. This might explain the recently reported supratentorial white-matter blurring in MRI scans of human LGI1 encephalitis brains (29), since myelin breakdown and inflammatory infiltrates leading to localized edema can be difficult to distinguish in MRI scans (37).

Interestingly, in FEPSO, BBB disturbance was not purely restricted to the hippocampus but was also revealed in presubiculum, subiculum, amygdala, piriform lobe and, more rarely, in areas such as basal ganglia and hypothalamus. The larger limbic areas were also found to be affected in MR T2-weighted FLAIR scans showing signal as well as volume increase. In human LGI1 encephalitis, hippocampal and amygdaloidal swelling, followed

by atrophy of the affected areas, have been observed in MRI studies (35, 36, 38). Subsequently, considering the similarities in histopathology between human and feline hippocampi, and considering similar MRI changes in the human and feline hippocampus as well as amygdala, it can be assumed that in human LGI1 encephalitis, the amygdala might be similarly affected by BBB leakage and neurodegeneration as shown here in cats. Among patients with anti-LGI1 encephalitis, hypothalamic dysfunction in form of hyponatremia due to the syndrome of inappropriate antidiuretic hormone secretion [~60% of patients (5, 6)] and basal ganglia involvement in form of faciobrachial dystonic seizures [~50% of patients (8)] are readily known. Cerebellar affects have only rarely been reported in human LGI1 encephalitis cases (5, 23, 24). In our cats, hyponatremia and neurodegeneration of the hypothalamus as well as basal ganglia was seen occasionally. On the other hand, no cerebellar symptoms were observed, and we found neither BBB leakage and complement activation nor neurodegeneration in the cerebellum.

An important finding in this study of FEPSO is that BBB leakage was more restricted to specific areas associated with the limbic system, whereas T cell infiltrates were present brain wide. A clear finding in animal models of multiple sclerosis and neuromyelitis optica is that activated T cells can open the BBB and thereby enable antibodies to enter the CNS (39–44). Here, in FEPSO, however, T cell infiltrates and BBB leakage do not seem to overlap, since brain areas with high LGI1 abundance, such as the cerebellum (22), are spared of complement activation and neurodegeneration, despite a comparable number of infiltrating T cells. Therefore, this finding point toward another mechanism or an additional trigger that is required to induce local disturbance of the BBB. It has been shown repeatedly that cytokines, peripheral, or in the CNS, have a drastic effect on BBB permeability (45–49). Intrastriatal injection of interleukin-1β has been shown to profoundly alter BBB permeability, leading to complement activation in Lewis rats (46). Interferon-γ and tumor necrosis factor-α have been shown to decrease tight junction proteins, such as occludin (47, 50). Moreover, oxidative stress and cytokines have been reported to change phosphorylation patterns of various tight junction proteins, among them occludin, e-cadherin, and ZO-1, thereby dissociating the tight junction complexes (51, 52). However, to explain the selective breach of the BBB in FEPSO, other factors can also come into play. These are, for example, differences in permeability of the BBB, which have been reported in mice (53, 54). Moreover, differential expression of receptors on the microvasculature in the brain can lead to different alterations in BBB permeability (55). Furthermore, external factors can also be involved in the opening of the BBB. High adrenaline levels caused by trauma or extreme exercise, cocaine, and nicotine have an effect on BBB permeability (55). Animal studies with NR2-antibodies showed that additional factors, such as lipopolysaccharides and epinephrine, can open the BBB in distinct locations and, therefore, the same antibodies can cause different symptoms (56, 57). Finally, here, we showed increased immunoglobulin leakage in the hippocampus of cats with LGI1 antibodies when compared with normal control cats. However, compared with epileptic controls, no difference was found. This is not surprising as it has been shown repeatedly that BBB dysfunction can result in epilepsy and seizures, which in turn can lead to disturbances in the BBB, resulting in a vicious circle (58–62).

To summarize, in this naturally occurring animal model, we were able to show that BBB disturbance and neurodegeneration in FEPSO is restricted to the hippocampus and other limbic structures, but is not found in other areas such as the cerebellum despite the presence of T cell infiltrates. Our findings broaden the perspective on LGI1 encephalitis by not only looking at the target organ (the brain parenchyma) but also on the question of how the presumably pathogenic antibodies can enter it. This not only deepens the knowledge and understanding of LGI1 encephalitis but also leads to new questions regarding regional selectivity of dysfunctional BBB. These findings are not only of use in veterinary medicine but also are highly relevant to human disease. A better understanding of underlying disease mechanisms will help to ameliorate future treatments and hopefully minimize remaining cognitive deficits of patients.

ETHICS STATEMENT

The project was discussed and approved by the institutional ethics committee (University of Veterinary Medicine, Vienna) in accordance with GSP guidelines and national legislation. In addition, all animal owners have given their consent.

AUTHOR CONTRIBUTIONS

JB and AP designed and supervised the project. AT and JB prepared the manuscript. AT performed the statistical analysis and, together with JB, the data interpretation. AT, MF, and LQ-G performed immunohistochemical staining, cell quantification, and imaging. AK performed the necropsies. SK provided MRI scans and interpretation of those. CB contributed to the study design. All authors reviewed the manuscript.

ACKNOWLEDGMENTS

The authors thank Ulrike Köck, Marianne Leisser, and Angela Kury for skilled technical assistance.

FUNDING

This project was financially supported by the Austrian Science Fund (project number P 26179-B24).

SUPPLEMENTARY MATERIAL

The Supplementary Material for this article can be found online at http://www.frontiersin.org/article/10.3389/fimmu.2017.01364/full#supplementary-material.

REFERENCES

1. Dalmau J, Gleichman AJ, Hughes EG, Rossi JE, Peng X, Lai M, et al. Anti-NMDA-receptor encephalitis: case series and analysis of the effects of antibodies. *Lancet Neurol* (2008) 7:1091–8. doi:10.1016/S1474-4422(08)70224-2
2. Lai M, Hughes EG, Peng X, Zhou L, Gleichman AJ, Shu H, et al. AMPA receptor antibodies in limbic encephalitis alter synaptic receptor location. *Ann Neurol* (2009) 65:424–34. doi:10.1002/ana.21589
3. Lancaster E, Lai M, Peng X, Hughes E, Constantinescu R, Raizer J, et al. Antibodies to the GABAB receptor in limbic encephalitis with seizures: case series and characterisation of the antigen. *Lancet Neurol* (2010) 9:67–76. doi:10.1016/S1474-4422(09)70324-2
4. Vincent A, Buckley C, Schott JM, Baker I, Dewar B-KK, Detert N, et al. Potassium channel antibody-associated encephalopathy: a potentially immunotherapy-responsive form of limbic encephalitis. *Brain* (2004) 127:701–12. doi:10.1093/brain/awh077
5. Irani SR, Alexander S, Waters P, Kleopa KA, Pettingill P, Zuliani L, et al. Antibodies to Kv1 potassium channel-complex proteins leucine-rich, glioma inactivated 1 protein and contactin-associated protein-2 in limbic encephalitis, Morvan's syndrome and acquired neuromyotonia. *Brain* (2010) 133:2734–48. doi:10.1093/brain/awq213
6. Lai M, Huijbers MGM, Lancaster E, Graus F, Bataller L, Balice-Gordon R, et al. Investigation of LGI1 as the antigen in limbic encephalitis previously attributed to potassium channels: a case series. *Lancet Neurol* (2010) 9:776–85. doi:10.1016/S1474-4422(10)70137-X
7. Ariño H, Armangué T, Petit-Pedrol M, Sabater L, Martinez-Hernandez E, Hara M, et al. Anti-LGI1–associated cognitive impairment. *Neurology* (2016) 87:759–65. doi:10.1212/WNL.0000000000003009
8. van Sonderen A, Thijs RD, Coenders EC, Jiskoot LC, Sanchez E, de Bruijn MAAM, et al. Anti-LGI1 encephalitis. *Neurology* (2016) 87:1449–56. doi:10.1212/WNL.0000000000003173
9. Finke C, Prüss H, Heine J, Reuter S, Kopp UA, Wegner F, et al. Evaluation of cognitive deficits and structural hippocampal damage in encephalitis with leucine-rich, glioma-inactivated 1 antibodies. *JAMA Neurol* (2017) 74:50–9. doi:10.1001/jamaneurol.2016.4226
10. Navarro V, Kas A, Apartis E, Chami L, Rogemond V, Levy P, et al. Motor cortex and hippocampus are the two main cortical targets in LGI1-antibody encephalitis. *Brain* (2016) 139:1079–93. doi:10.1093/brain/aww012
11. Frisch C, Malter MP, Elger CE, Helmstaedter C. Neuropsychological course of voltage-gated potassium channel and glutamic acid decarboxylase antibody related limbic encephalitis. *Eur J Neurol* (2013) 20:1297–304. doi:10.1111/ene.12186
12. Kitten S, Gupta N, Bloch RM, Dunham CK. Voltage-gated potassium channel antibody associated mood disorder without paraneoplastic disease. *Biol Psychiatry* (2011) 70:e15–7. doi:10.1016/j.biopsych.2011.03.016
13. LeDoux J, Cardinal RN, Everitt BJ, Charney D, Davidson R, Erwin W, et al. The amygdala. *Curr Biol* (2007) 17:R868–74. doi:10.1016/j.cub.2007.08.005
14. Melzer N, Budde T, Stork O, Meuth SG. Limbic encephalitis: potential impact of adaptive autoimmune inflammation on neuronal circuits of the amygdala. *Front Neurol* (2015) 6:171. doi:10.3389/fneur.2015.00171
15. Bien CG, Vincent A, Barnett MH, Becker AJ, Blümcke I, Graus F, et al. Immunopathology of autoantibody-associated encephalitides: clues for pathogenesis. *Brain* (2012) 135:1622–38. doi:10.1093/brain/aws082
16. Klang A, Schmidt P, Kneissl S, Bagó Z, Vincent A, Lang B, et al. IgG and complement deposition and neuronal loss in cats and humans with epilepsy and voltage-gated potassium channel complex antibodies. *J Neuropathol Exp Neurol* (2014) 73:403–13. doi:10.1097/NEN.0000000000000063
17. Ohkawa T, Fukata Y, Yamasaki M, Miyazaki T, Yokoi N, Takashima H, et al. Autoantibodies to epilepsy-related LGI1 in limbic encephalitis neutralize LGI1-ADAM22 interaction and reduce synaptic AMPA receptors. *J Neurosci* (2013) 33:18161–74. doi:10.1523/JNEUROSCI.3506-13.2013
18. Pakozdy A, Gruber A, Kneissl S, Leschnik M, Halasz P, Thalhammer JG. Complex partial cluster seizures in cats with orofacial involvement. *J Feline Med Surg* (2011) 13:687–93. doi:10.1016/j.jfms.2011.05.014
19. Claßen AC, Kneissl S, Lang J, Tichy A, Pakozdy A. Magnetic resonance features of the feline hippocampus in epileptic and non-epileptic cats: a blinded, retrospective, multi-observer study. *BMC Vet Res* (2016) 12:165. doi:10.1186/s12917-016-0788-3
20. Pakozdy A, Halasz P, Klang A, Bauer J, Leschnik M, Tichy A, et al. Suspected limbic encephalitis and seizure in cats associated with voltage-gated potassium channel (VGKC) complex antibody. *J Vet Intern Med* (2013) 27:212–4. doi:10.1111/jvim.12026
21. Furlan S, Roncaroli F, Forner F, Vitiello L, Calabria E, Piquer-Sirerol S, et al. The LGI1/epitempin gene encodes two protein isoforms differentially expressed in human brain. *J Neurochem* (2006) 98:985–91. doi:10.1111/j.1471-4159.2006.03939.x
22. Herranz-Pérez V, Olucha-Bordonau FE, Morante-Redolat JM, Pérez-Tur J. Regional distribution of the leucine-rich glioma inactivated (LGI) gene family transcripts in the adult mouse brain. *Brain Res* (2010) 1307:177–94. doi:10.1016/j.brainres.2009.10.013
23. Irani SR, Michell AW, Lang B, Pettingill P, Waters P, Johnson MR, et al. Faciobrachial dystonic seizures precede Lgi1 antibody limbic encephalitis. *Ann Neurol* (2011) 69:892–900. doi:10.1002/ana.22307
24. Steriade C, Day GS, Lee L, Murray BJ, Fritzler MJ, Keith J. LGI1 autoantibodies associated with cerebellar degeneration. *Neuropathol Appl Neurobiol* (2014) 40:645–9. doi:10.1111/nan.12132
25. Boesebeck F, Schwarz O, Dohmen B, Graef U, Vestring T, Kramme C, et al. Faciobrachial dystonic seizures arise from cortico-subcortical abnormal brain areas. *J Neurol* (2013) 260:1684–6. doi:10.1007/s00415-013-6946-7
26. Flanagan EP, Kotsenas AL, Britton JW, McKeon A, Watson RE, Klein CJ, et al. Basal ganglia T1 hyperintensity in LGI1-autoantibody faciobrachial dystonic seizures. *Neurol Neuroimmunol Neuroinflamm* (2015) 2:e161. doi:10.1212/NXI.0000000000000161
27. López Chiriboga AS, Siegel JL, Tatum WO, Shih JJ, Flanagan EP. Striking basal ganglia imaging abnormalities in LGI1 ab faciobrachial dystonic seizures. *Neurol Neuroimmunol Neuroinflamm* (2017) 4:e336. doi:10.1212/NXI.0000000000000336
28. Szots M, Blaabjerg M, Orsi G, Iversen P, Kondziella D, Madsen CG, et al. Global brain atrophy and metabolic dysfunction in LGI1 encephalitis: a prospective multimodal MRI study. *J Neurol Sci* (2017) 376:159–65. doi:10.1016/j.jns.2017.03.020
29. Urbach H, Rauer S, Mader I, Paus S, Wagner J, Malter MP, et al. Supratentorial white matter blurring associated with voltage-gated potassium channel-complex limbic encephalitis. *Neuroradiology* (2015) 57:1203–9. doi:10.1007/s00234-015-1581-x
30. Hametner S, Wimmer I, Haider L, Pfeifenbring S, Brück W, Lassmann H. Iron and neurodegeneration in the multiple sclerosis brain. *Ann Neurol* (2013) 74:848–61. doi:10.1002/ana.23974
31. Mikula S, Trotts I, Stone JM, Jones EG. Internet-enabled high-resolution brain mapping and virtual microscopy. *Neuroimage* (2007) 35:9–15. doi:10.1016/j.neuroimage.2006.11.053
32. Blümcke I, Thom M, Aronica E, Armstrong DD, Bartolomei F, Bernasconi A, et al. International consensus classification of hippocampal sclerosis in temporal lobe epilepsy: a task force report from the ILAE commission on diagnostic methods. *Epilepsia* (2013) 54:1315–29. doi:10.1111/epi.12220
33. Miller TD, Chong TT-J, Aimola Davies AM, Ng TWC, Johnson MR, Irani SR, et al. Focal CA3 hippocampal subfield atrophy following LGI1 VGKC-complex antibody limbic encephalitis. *Brain* (2017) 140:1212–9. doi:10.1093/brain/awx070
34. Irani SR, Bien CG, Lang B. Autoimmune epilepsies. *Curr Opin Neurol* (2011) 24:146–53. doi:10.1097/WCO.0b013e3283446f05
35. Urbach H, Soeder BM, Jeub M, Klockgether T, Meyer B, Bien CG. Serial MRI of limbic encephalitis. *Neuroradiology* (2006) 48:380–6. doi:10.1007/s00234-006-0069-0
36. Wagner J, Schoene-Bake JC, Malter MP, Urbach H, Huppertz HJ, Elger CE, et al. Quantitative FLAIR analysis indicates predominant affection of the amygdala in antibody-associated limbic encephalitis. *Epilepsia* (2013) 54:1679–87. doi:10.1111/epi.12320
37. Barkovich AJ. Concepts of myelin and myelinization in neuroradiology. *Am J Neuroradiol* (2000) 21:1099–109. doi:10.1016/S0006-3223(01)01323-3
38. Wagner J, Witt J-A, Helmstaedter C, Malter MP, Weber B, Elger CE. Automated volumetry of the mesiotemporal structures in antibody-associated limbic encephalitis. *J Neurol Neurosurg Psychiatry* (2015) 86:735–42. doi:10.1136/jnnp-2014-307875
39. Babbe H, Roers A, Waisman A, Lassmann H, Goebels N, Hohlfeld R, et al. Clonal expansions of CD8(+) T cells dominate the T cell infiltrate in active multiple sclerosis lesions as shown by micromanipulation and single cell

polymerase chain reaction. *J Exp Med* (2000) 192:393–404. doi:10.1084/jem.192.3.393
40. Bradl M, Misu T, Takahashi T, Watanabe M, Mader S, Reindl M, et al. Neuromyelitis optica: pathogenicity of patient immunoglobulin in vivo. *Ann Neurol* (2009) 66:630–43. doi:10.1002/ana.21837
41. Jones MV, Huang H, Calabresi PA, Levy M. Pathogenic aquaporin-4 reactive T cells are sufficient to induce mouse model of neuromyelitis optica. *Acta Neuropathol Commun* (2015) 3:28. doi:10.1186/s40478-015-0207-1
42. Lassmann H, Brück W, Lucchinetti CF. The immunopathology of multiple sclerosis: an overview. *Brain Pathol* (2007) 17:210–8. doi:10.1111/j.1750-3639.2007.00064.x
43. Linington C, Bradl M, Lassmann H, Brunner C, Vass K. Augmentation of demyelination in rat acute allergic encephalomyelitis by circulating mouse monoclonal antibodies directed against a myelin/oligodendrocyte glycoprotein. *Am J Pathol* (1988) 130:443–54.
44. Zeka B, Hastermann M, Hochmeister S, Kögl N, Kaufmann N, Schanda K, et al. Highly encephalitogenic aquaporin 4-specific T cells and NMO-IgG jointly orchestrate lesion location and tissue damage in the CNS. *Acta Neuropathol* (2015) 130:783–98. doi:10.1007/s00401-015-1501-5
45. de Vries HE, Kooij G, Frenkel D, Georgopoulos S, Monsonego A, Janigro D. Inflammatory events at blood-brain barrier in neuroinflammatory and neurodegenerative disorders: implications for clinical disease. *Epilepsia* (2012) 53(Suppl 6):45–52. doi:10.1111/j.1528-1167.2012.03702.x
46. Kitic M, Hochmeister S, Wimmer I, Bauer J, Misu T, Mader S, et al. Intrastriatal injection of interleukin-1 beta triggers the formation of neuromyelitis optica-like lesions in NMO-IgG seropositive rats. *Acta Neuropathol Commun* (2013) 1:5. doi:10.1186/2051-5960-1-5
47. Minagar A, Alexander JS. Blood-brain barrier disruption in multiple sclerosis. *Mult Scler* (2003) 9:540–9. doi:10.1191/1352458503ms965oa
48. Pan W, Stone KP, Hsuchou H, Manda VK, Zhang Y, Kastin AJ. Cytokine signaling modulates blood-brain barrier function. *Curr Pharm Des* (2011) 17:3729. doi:10.2174/138161211798220918
49. Varatharaj A, Galea I. The blood-brain barrier in systemic inflammation. *Brain Behav Immun* (2017) 60:1–12. doi:10.1016/j.bbi.2016.03.010
50. Oshima T, Laroux FS, Coe LL, Morise Z, Kawachi S, Bauer P, et al. Interferon-γ and interleukin-10 reciprocally regulate endothelial junction integrity and barrier function. *Microvasc Res* (2001) 61:130–43. doi:10.1006/mvre.2000.2288
51. Nwariaku FE, Chang J, Zhu X, Liu Z, Duffy SL, Halaihel NH, et al. The role of p38 map kinase in tumor necrosis factor-induced redistribution of vascular endothelial cadherin and increased endothelial permeability. *Shock* (2002) 18:82–5. doi:10.1097/00024382-200207000-00015
52. Rao RK, Basuroy S, Rao VU, Karnaky KJ Jr, Gupta A. Tyrosine phosphorylation and dissociation of occludin-ZO-1 and E-cadherin-beta-catenin complexes from the cytoskeleton by oxidative stress. *Biochem J* (2002) 368:471–81. doi:10.1042/BJ20011804
53. Phares TW, Kean RB, Mikheeva T, Hooper DC. Regional differences in blood-brain barrier permeability changes and inflammation in the apathogenic clearance of virus from the central nervous system. *J Immunol* (2006) 176:7666–75. doi:10.4049/jimmunol.176.12.7666
54. Tonra JR, Reiseter BS, Kolbeck R, Nagashirma K, Robertson R, Keyt B, et al. Comparison of the timing of acute blood-brain barrier breakdown to rabbit immunoglobulin G in the cerebellum and spinal cord of mice with experimental autoimmune encephalomyelitis. *J Comp Neurol* (2001) 430:131–44. doi:10.1002/1096-9861(20010129)430:1<131:AID-CNE1019>3.0.CO;2-K
55. Diamond B, Huerta PT, Mina-osorio P, Kowal C, Volpe BT. Losing your nerves? Maybe it's the antibodies. *Nat Rev Immunol* (2009) 9:449–56. doi:10.1038/nri2529
56. Huerta PT, Kowal C, DeGiorgio LA, Volpe BT, Diamond B. Immunity and behavior: antibodies alter emotion. *Proc Natl Acad Sci U S A* (2006) 103:678–83. doi:10.1073/pnas.0510055103
57. Kowal C, DeGiorgio LA, Nakaoka T, Hetherington H, Huerta PT, Diamond B, et al. Cognition and immunity: antibody impairs memory. *Immunity* (2004) 21:179–88. doi:10.1016/j.immuni.2004.07.011
58. Friedman A. Blood-brain barrier dysfunction, status epilepticus, seizures, and epilepsy: a puzzle of a chicken and egg? *Epilepsia* (2011) 52:19–20. doi:10.1111/j.1528-1167.2011.03227.x
59. Marchi N, Granata T, Ghosh C, Janigro D. Blood-brain barrier dysfunction and epilepsy: pathophysiologic role and therapeutic approaches. *Epilepsia* (2012) 53:1877–86. doi:10.1111/j.1528-1167.2012.03637.x
60. Michalak Z, Lebrun A, Di Miceli M, Rousset M-C, Crespel A, Coubes P, et al. IgG leakage may contribute to neuronal dysfunction in drug-refractory epilepsies with blood-brain barrier disruption. *J Neuropathol Exp Neurol* (2012) 71:826–38. doi:10.1097/NEN.0b013e31826809a6
61. Van Vliet EA, Araújo SDC, Redeker S, Van Schaik R, Aronica E, Gorter JA. Blood-brain barrier leakage may lead to progression of temporal lobe epilepsy. *Brain* (2007) 130:521–34. doi:10.1093/brain/awl318
62. Vezzani A, Granata T. Brain inflammation in epilepsy: experimental and clinical evidence, brain inflammation in epilepsy: experimental and clinical evidence. *Epilepsia* (2005) 46:1724–43. doi:10.1111/j.1528-1167.2005.00298.x

Conflict of Interest Statement: CB gave scientific advice to Eisai (Frankfurt, Germany) and UCB (Monheim, Germany), undertook industry-funded travel with support of Eisai (Frankfurt, Germany), UCB (Monheim, Germany), Desitin (Hamburg, Germany), and Grifols (Frankfurt, Germany), obtained honoraria for speaking engagements from Eisai (Frankfurt, Germany), UCB (Monheim, Germany), Desitin (Hamburg, Germany), Diamed (Köln, Germany), Fresenius Medical Care (Bad Homburg, Germany), Biogen (Ismaning, Germany), and Euroimmun (Lübeck, Germany). He received research support from Diamed (Köln, Germany) and Fresenius Medical Care (Bad Homburg, Germany). He is a consultant to the Laboratory Krone, Bad Salzuflen, Germany, regarding neural antibodies and therapeutic drug monitoring for antiepileptic drugs. The other authors declare no competing financial interests.

frontiers in Immunology

REVIEW
published: 16 October 2017
doi: 10.3389/fimmu.2017.01292

Defective Suppressor of Cytokine Signaling 1 Signaling Contributes to the Pathogenesis of Systemic Lupus Erythematosus

Huixia Wang[1], *Jiaxing Wang*[2] *and Yumin Xia*[1]*

[1] Department of Dermatology, The Second Affiliated Hospital, School of Medicine, Xi'an Jiaotong University, Xi'an, China,
[2] Core Research Laboratory, The Second Affiliated Hospital, School of Medicine, Xi'an Jiaotong University, Xi'an, China

Systemic lupus erythematosus (SLE) is a complex autoimmune disease involving injuries in multiple organs and systems. Exaggerated inflammatory responses are characterized as end-organ damage in patients with SLE. Although the explicit pathogenesis of SLE remains unclear, increasing evidence suggests that dysregulation of cytokine signals contributes to the progression of SLE through the Janus kinase/signal transducer and activator of transcription (STAT) signaling pathway. Activated STAT proteins translocate to the cell nucleus and induce transcription of target genes, which regulate downstream cytokine production and inflammatory cell infiltration. The suppressor of cytokine signaling 1 (SOCS1) is considered as a classical inhibitor of cytokine signaling. Recent studies have demonstrated that SOCS1 expression is decreased in patients with SLE and in murine lupus models, and this negatively correlates with the magnitude of inflammation. Dysregulation of SOCS1 signals participates in various pathological processes of SLE such as hematologic abnormalities and autoantibody generation. Lupus nephritis is one of the most serious complications of SLE, and it correlates with suppressed SOCS1 signals in renal tissues. Moreover, SOCS1 insufficiency affects the function of several other organs, including skin, central nervous system, liver, and lungs. Therefore, SOCS1 aberrancy contributes to the development of both systemic and local inflammation in SLE patients. In this review, we discuss recent studies regarding the roles of SOCS1 in the pathogenesis of SLE and its therapeutic implications.

Keywords: suppressor of cytokine signaling 1, systemic lupus erythematosus, Janus kinase/signal transducer and activator of transcription pathway, cytokine, inflammation, lupus nephritis

OPEN ACCESS

Edited by:
Silvano Sozzani,
University of Brescia, Italy

Reviewed by:
Angela Ceribelli,
Humanitas Research Hospital, Italy
Raymond P. Donnelly,
United States Food and Drug Administration, United States

***Correspondence:**
Yumin Xia
xiayumin1202@163.com

Specialty section:
This article was submitted to Cytokines and Soluble Mediators in Immunity, a section of the journal Frontiers in Immunology

Received: *05 August 2017*
Accepted: *26 September 2017*
Published: *16 October 2017*

Citation:
Wang H, Wang J and Xia Y (2017) Defective Suppressor of Cytokine Signaling 1 Signaling Contributes to the Pathogenesis of Systemic Lupus Erythematosus. Front. Immunol. 8:1292. doi: 10.3389/fimmu.2017.01292

INTRODUCTION

As a complex autoimmune disease, systemic lupus erythematosus (SLE) is characterized by the presence of autoantibodies against self-antigens, including double-stranded (ds) DNA, as well as the risk of autoantibody-induced end-organ damage (1). Hematopoietic abnormalities, such as hyperactivation of T and B cells and overproduction of autoantibodies, exist in patients with SLE (2). Pathogenic autoantibodies may form immune complexes or directly deposit in the glomerular capillary, thus inciting irreversible glomerulonephritis, which is one of the most common complications in patients with SLE (3). In reality, numerous factors are implicated in the onset or progression of SLE. It is generally accepted that the deficiency in the clearance of apoptotic cells significantly contributes to the exposure of self-antigens, as well as subsequent autoimmune processes, such as

autoantibody production and inflammatory responses (4). Albeit the precise mechanisms underlying SLE are yet to be elucidated, emerging evidences indicate that the abnormal expression of proinflammatory cytokines plays an important role in local inflammation and in the development of end-organ injuries in SLE (5).

Cytokines are central in both innate and adaptive immunity. They are mostly synthesized by immune cells and in turn participate in the differentiation, maturation, and activation of diverse immune and hematopoietic cells. Abnormalities of various cytokines have been identified in patients with SLE and in murine lupus models (5). Moreover, it was found that in sera of SLE patients, the level of transforming growth factor (TGF)-β is decreased; whereas certain proinflammatory cytokines, such as interferon (IFN)-α, IFN-γ, interleukin (IL)-6, IL-12, IL-17, IL-23, and B-cell activating factor (BAFF), are all upregulated accordingly (6). The dysregulation of these cytokines mirrors the imbalance in diverse immune cell subsets, such as T helper (Th) 1, Th2, Th17, and T regulatory (Treg) cells. Many cytokines can activate the Janus kinase 2 (JAK2)/signal transducer and activator of transcription 1 (STAT1) signaling pathway. Upon ligand binding, the activated JAK2 phosphorylates the cytoplasmic domains of cognate receptors, thus providing docking sites for STAT1 (7). Furthermore, STAT1 can also phosphorylate at the tyrosine site and form dimers before translocating into the nucleus, where the dimers activate target genes that are related to the development, differentiation, and survival of hematopoietic cells (8). The suppressor of cytokine signaling 1 (SOCS1) is an inhibitive factor induced by relevant cytokines, and it negatively regulates immune responses by suppressing the activity of JAK2 (8). Under normal conditions, the expression level of SOCS1 is minimal, but it can be rapidly upregulated in a feedback manner through the activation of JAK2/STAT1 signals (9, 10). As cytokine signaling ceases, SOCS1 is rapidly degraded (9). Therefore, SOCS1 is essential for maintaining immune homeostasis in local tissues.

Recent studies have demonstrated that SOCS1 participates in the pathogenesis of SLE (11, 12). The mRNA expression level of SOCS1 is significantly decreased in peripheral blood mononuclear cells of patients with SLE (11). Patients with active SLE have lower expression of SOCS1 mRNA as compared to patients with inactive SLE, hence indicating that mRNA expression of SOCS1 is negatively correlated with lupus disease activity (11). SOCS1 is also involved in other pathological processes of SLE including activation of immune cells, production of proinflammatory factors, initiation of renal fibrosis, etc. (12). The upregulation of SOCS1 through alternative methods is beneficial to improve the conditions of SLE patients (12, 13). In this review, we summarized recent studies on the function of SOCS1 in the pathogenesis of SLE and elaborated its clinical significance and therapeutic implications.

THE STRUCTURAL BASIS OF SOCS1/JAK2 INTERACTION

The regulation of downstream signals by SOCS1 is triggered by the interaction between SOCS1-kinase inhibitory region (KIR) and JAK2 activation loop. Structurally, SOCS1 has an Src-homology-region 2 (SH2) with a central SH2 domain, an extended SH2 subdomain (ESS), and a KIR domain of 12 amino acids (**Figure 1A**) (10). The central SH2 domain has the most conserved sequence of SOCS1 protein. Mutations in the phosphotyrosine-binding residue Arg105 to Lys (R105K) or Glu (R105E) and deletion of the central SH2 domain can induce loss of function of SOCS1 (14). The ESS, comprising 12 residues, is essential for the interaction of SOCS1 with JAK2 (14). Substitution of conserved Ile68 with Glu (I68E) or Leu75 with Glu (L75E) in the ESS completely abolishes the binding of SOCS1 to JAK2 (14). KIR is responsible for the high-affinity binding of SOCS1 to the tyrosine kinase domain of JAK2, which further activates the kinase and transduces signals (10).

Janus kinase 2 is constitutively associated with the proline-rich, membrane proximal regions of cognate cytokine receptors, which are ubiquitously expressed in mammalian cells (15). Structurally, JAK2 can be roughly divided into an amino-terminal region (N region), followed by a catalytically inactive kinase-like domain and a tyrosine kinase domain (15). The N region participates only in cytokine receptor recognition and association; and the kinase-like domain of JAK2 is actually a pseudokinase domain that regulates only the catalytic activity of the tyrosine kinase domain, which is critical for the interaction of JAK2 with SOCS1 and for the catalytic activity of JAK2 as well (**Figure 1B**) (15). In humans, the amino acid sequence of autophosphorylation or activation loop in tyrosine kinase domain is ^{1001}LPQDKEYYKVKEP, which is so called as pJAK2 (1001–1013) (16). pJAK2 has phosphorylated tyrosine 1007, which reflects the activation status of JAK2; and phosphorylation of this tyrosine leads to conformational changes that facilitate substrate binding (16). Moreover, structure–function studies have demonstrated that SOCS1 solely binds to phosphopeptides with phosphorylated tyrosine 1007 (14).

Kinase inhibitory region sequence is somehow similar to JAK2 activation loop (8). Thus, KIR may act as a pseudosubstrate and mimic the activation region of JAK2 to prevent substrate binding at the catalytic cleft of JAK2 (14). Substitution mutations in KIR, such as phenylalanine at positions 56 or 59, aspartic acid at 64, or tyrosine at 65, can reduce the ability of SOCS1 to bind with JAK2 activation loop (16). Hence, KIR combines with the JAK2 activation loop and induces conformational changes of the JAK2 activation site, thus abrogating the phosphorylation of substrates (17). After binding to phosphorylated JAK2, SOCS1 dephosphorylates and forms a complex, with JAK2, which then leads to irreversible JAK2 degradation (**Figure 1C**) (18). Under these interactions, the phosphorylation of STAT1 is hindered and immune responses, such as IFN-γ signaling, inflammatory factor production, T cell development and activation, etc., are then, therefore, suppressed (19, 20).

THE PRINCIPLES OF SOCS1 REGULATION OF DOWNSTREAM SIGNALS *IN VIVO*

Insufficiency of SOCS1 expression and abnormalities in cytokine production are prominent in patients with SLE and in murine

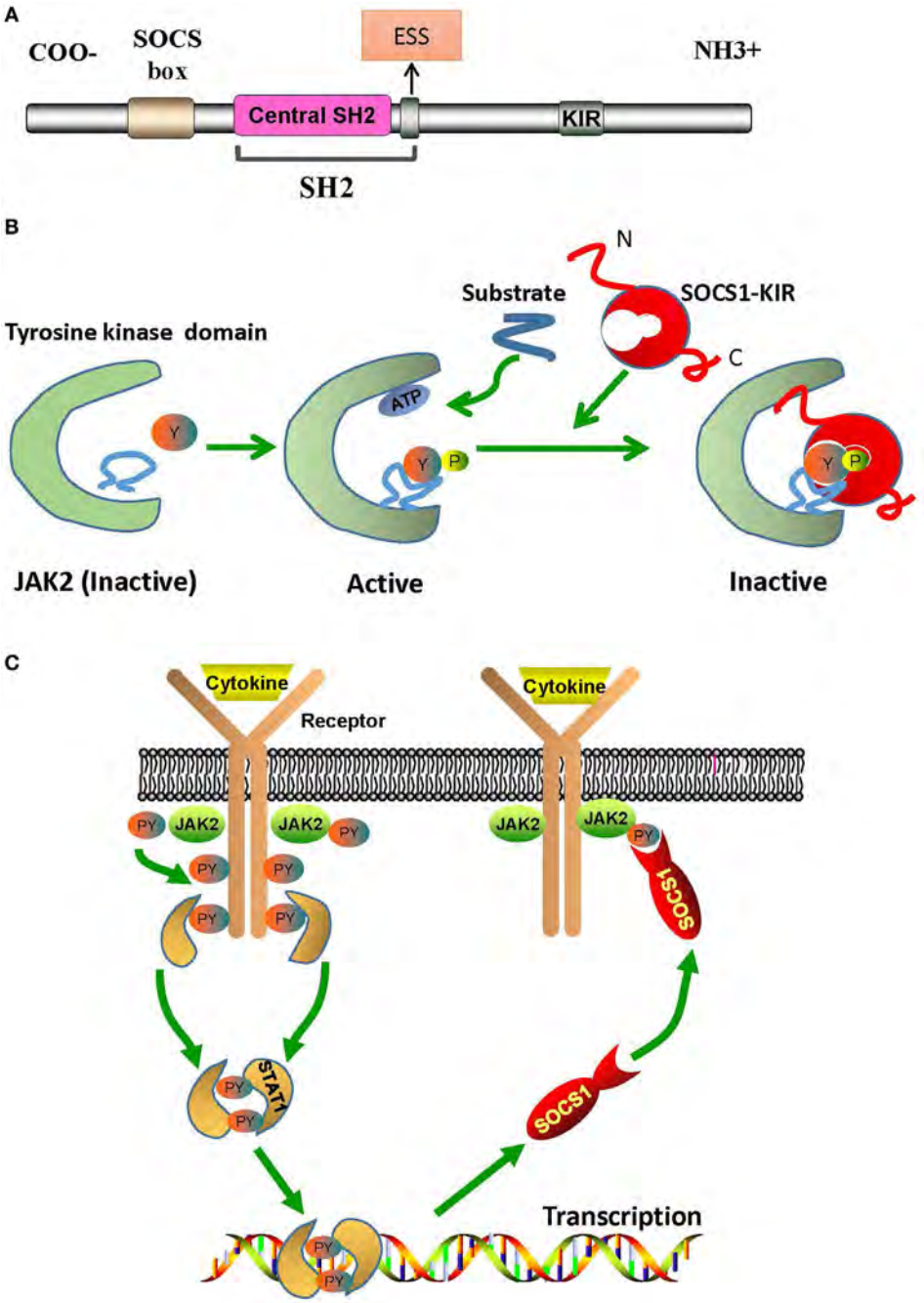

FIGURE 1 | The structural basis of SOCS1/JAK2 interaction. **(A)** The SOCS1 protein contains a C-terminal SOCS box motif, SH2 domain, KIR region, and N-terminal region of varied length and amino acid composition. **(B)** Model of tyrosine kinase domain activation and inhibition by SOCS1. Binding of SOCS1-KIR to the activation loop prevents the access of substrates to the catalytic pocket. **(C)** Mechanism of negative cytokine signaling regulation by SOCS1 protein. Cytokine binding with specific cytokine receptors leads to receptor dimerization and subsequent recruitment of JAK2. Activated JAK2 phosphorylate the cognate cytokine-receptor cytoplasmic domain, providing docking binding sites for STAT1 proteins. After phosphorylation by JAK2, STAT1 proteins form dimers and translocate to the nucleus. STAT1 signaling induces SOCS1 protein transcription. Following their translation, SOCS1 proteins suppress cytokine signaling by binding to phosphorylated JAK2. ESS, extended SH2 subdomain; JAK2, Janus kinase 2; KIR, kinase inhibitory region; PY, phosphorylated tyrosine; SH2, Src-homology-region 2; SOCS1, suppressor of cytokine signaling 1; STAT1, signal transducer and activator of transcription 1.

lupus models (6). A few *in vivo* studies have been carried out to reveal the effect of SOCS1 on downstream signals. IFN-γ plays an important role in patients with SLE, as it enhances the production of pathogenic autoantibodies and accelerates the progression of glomerulonephritis (21, 22). In fact, SOCS1 can directly bind to the IFN-γ receptor (IFNGR) to efficiently ensure the suppressive

effect of SOCS1 on IFN-γ signaling, even at low levels of SOCS1 expression (23). Full inhibition of IFN-γ signaling by SOCS1 requires the phosphorylation of tyrosine 441 in the IFNGR1 subunit, thus suggesting that SOCS1 interacts first with the IFNGR and then binds to JAK2 to inhibit its kinase activity (24). Excessive production of IFN-γ and aberrant control of the IFN-γ signaling pathway have been implicated in the pathogenesis of SLE in BWF1 mice (25). In lupus-prone (NZB × NZW) F1 mice, SOCS1 expression was decreased, whereas pSTAT1 was increased in spleen-derived lymphocytes, thus mirroring the results of SOCS1 expression in peripheral blood mononuclear cells of patients with SLE (12). hCDR1 is a tolerogenic peptide derived from the sequence of the first complementarity-determining region (CDR1) of anti-DNA immunoglobulin (Ig) G, and it can downregulate pathogenic cytokines, such as tumor necrosis factor (TNF)-α, IL-1β, and IFN-γ, and upregulate the immunosuppressive cytokine TGF-β in lupus-prone mice (25). In these murine models, SOCS1 was upregulated upon subcutaneous administration of hCDR1, accompanied by pSTAT1 downregulation and tempered IFN-γ signaling (25). Moreover, patients undergoing prednisone treatment exhibited higher SOCS1 protein levels than those not receiving prednisone (12). Therefore, these findings suggest that SOCS1 insufficiency results in unbridled downstream signaling and contributes to the development and progression of SLE, whereas upregulation of SOCS1 definitely alleviates the course of SLE.

Extensive studies have revealed the crucial roles of IFN-α in the pathogenesis of SLE (26). Exposure to IFN-α *in vivo* can induce lupus disease in lupus-prone NZB/NZW F1 mice but not in BALB/c mice (27). Moreover, lupus-prone NZB mice lacking type I IFN receptor exhibited significant decrease in both autoimmunity and mortality (28). In SLE patients, serum IFN-α induce monocytes to differentiate into IFN-dendritic cells (DCs), which then capture apoptotic cells or nucleosomes and present these autoantigens to $CD4^+$ T cells, thus initiating the proliferation of autoreactive T cells as well as the differentiation of autoantibody-producing B cells (29, 30). The dysregulation of IFN-α in SLE is also evident in gene expression profiles, including IFN-inducible genes, which correlate with the production of autoantibodies and the pathophysiology of SLE (31, 32). SOCS1 is an important inhibitor of IFN-α signaling *in vivo*. It associates with and regulates type I IFN receptor 1-specific signals, abrogates tyrosine phosphorylation of STAT1, and reduces the duration of antiviral gene expression—thus, SOCS1 balances the beneficial antiviral and detrimental proinflammatory effects of IFN-α (33). Furthermore, Toll/IL-1R-domain-containing adaptor protein inducing IFN-β–IFN-regulatory factor 3 pathway can rapidly induce type I IFN, which in turn activates secondary JAK/STAT1 pathway after stimulation with lipopolysaccharide and contributes, in combination with NF-κB, to the expression of IFN-inducible genes (34). Coincidentally, SOCS1 can effectively inhibit such process (35). Hence, SOCS1 deficiency in SLE patients might explain the excessive IFN-α signaling and high level of IFN-inducible genes, which subsequently contributes to the development of SLE.

Suppressor of cytokine signaling 1 deficiency is associated with the early death of mice, which were found to have severe lymphopenia, hyperactivation of peripheral T cells, fatty degeneration and necrosis of the liver, and inflammatory infiltration of liver and lungs (10). Partial restoration of SOCS1 can rescue Eμ-$SOCS1^{-/-}$ mice from early onset of fatal diseases (36). However, these Eμ-$SOCS1^{-/-}$ mice expressing insufficient SOCS1 spontaneously exhibited hyperactivation of T and B cells and DCs, produced anti-dsDNA antibodies, formed immune complexes in glomeruli, and eventually developed lupus-like disease (36). Moreover, SOCS1 deficiency induced prominent activation of STAT1, as well as hyperresponsiveness to IFN-γ, in mice models (12). However, IFN-γ deficiency can reverse the lupus phenotype of Eμ-$SOCS1^{-/-}$ mice, which again suggests the negative regulation of IFN-γ signaling by SOCS1 (37).

The SOCS1 transgenic mice were constructed by applying the *lck* proximal promoter to drive transgenic expression only in the T cell lineage (38). In these mice, tyrosine phosphorylation of STAT1 that is responsive to cytokines, such as IFN-γ, IL-6, and IL-7, was significantly suppressed; and the number of thymocytes decreased due to the blockade of development in the triple-negative stage, which consequently led to an increase in the percentage of $CD4^+$ T cells (38). Moreover, in these mice, peripheral T cells were spontaneously activated, and apoptosis was significantly increased (38). These phenomena strongly suggest that SOCS1 maintains the homeostasis of peripheral T cells by suppressing STAT1 activation. The effects of SOCS1 abnormalities on murine phenotypes and immune responses are illustrated in **Figure 2**.

SOCS1 PARTICIPATES IN THE HEMATOLOGIC ABNORMALITIES IN SLE

Eμ-$SOCS1^{-/-}$ mice express only a limited level of SOCS1 in their peripheral lymphocytes, thus allowing the excessive activation of STAT1, development of multiple organ inflammation, spontaneous activation of lymphocytes, production of autoantibodies such as anti-dsDNA IgG, and development of prominent glomerulonephritis, which are all reminiscent of murine lupus models (36). Therefore, appropriate SOCS1 expression is critical for the prevention of systemic autoimmune disease such as SLE. $CD4^+$ T cells were spontaneously activated in Eμ-$SOCS1^{-/-}$ mice and in diseased $SOCS1^{+/-}$ mice, and the T cells of $SOCS1^{+/-}$ mice proliferated more significantly in response to IL-2 (36). In T cell-specific SOCS1-conditional knockout mice, SOCS1-deficient $CD4^+$ naïve T cells mostly differentiated into Th1 cells, and Th17 differentiation was strongly suppressed (39); these mice eventually developed a lupus-like autoimmune disease (40). Previous studies have corroborated that Th1 polarization is primarily driven by IL-12 and IFN-γ, while Th2 polarization is primarily driven by IL-4 (41). As SOCS1 suppresses both IFN-γ and IL-4 signaling, SOCS1 upregulation may be an approach for the reciprocal inhibition of Th1 and Th2 cells. When IFN-γ is excessively expressed, IL-4 signaling through STAT6 can be blocked by SOCS1; however, when IL-4 is highly expressed, IFN-γ signaling through STAT1 is blocked by SOCS1 (39). Both IL-6 and TGF-β promote the production of IL-17 by naïve $CD4^+$ T cells, and this is essential for the development and differentiation of Th17 cells (42, 43). $SOCS1^{-/-}$ T cells are less responsive to

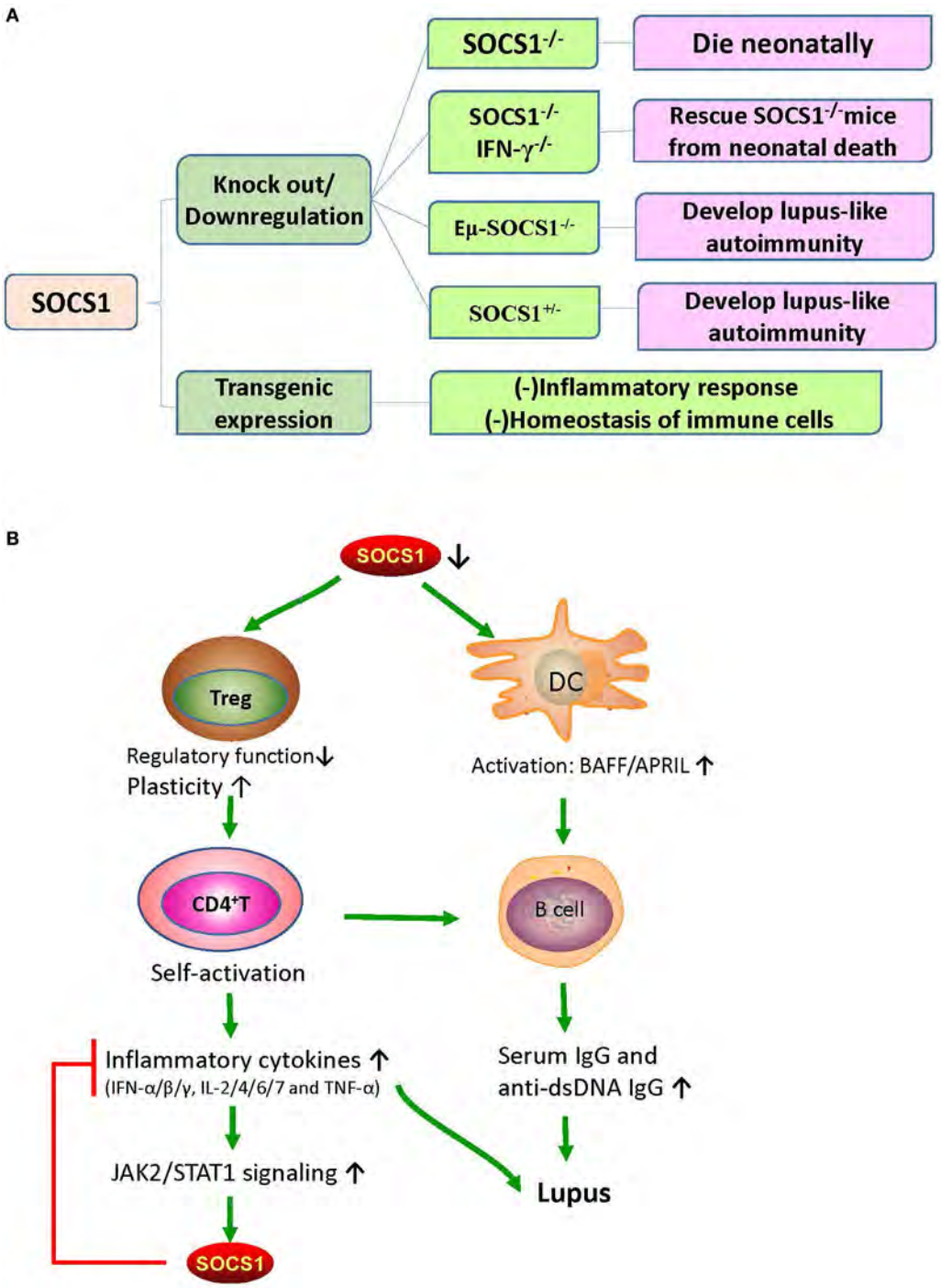

FIGURE 2 | The effects of SOCS1 abnormalities on murine phenotypes and immune responses. **(A)** The effects of different SOCS1 level on the immune system of mice model. SOCS1$^{-/-}$ mice died within 3 weeks after birth; and SOCS1$^{-/-}$IFN-γ$^{-/-}$ prevented the neonatal death of SOCS1$^{-/-}$ mice, thus suggesting that uncontrolled IFN-γ signaling has destructive effects. Eμ-SOCS1$^{-/-}$ and SOCS1$^{+/-}$ mice developed lupus-like autoimmunity with age, indicating that SOCS1 deficiency can initiate an autoimmune response. However, transgenic overexpression of SOCS1 suppresses the immune response and disturbs the homeostasis of immune cells. **(B)** Roles of SOCS1 in systemic lupus erythematosus (SLE). There is a deficiency in the expression of SOCS1 in SLE. SOCS1-deficient DCs express high levels of BAFF, which leads to abnormal B-cell growth and proliferation. Moreover, low SOCS1 levels correlate with reduced suppressive capacity and enhanced plasticity of Treg cells. These Treg cells maintain high numbers of hyperactivated B cells by promoting the interaction of self-reactive CD4^{+} T cells with B cells. This interaction leads to the production of diverse inflammatory cytokines and autoantibodies, leading to immune complex formation and tissue injury. Therefore, upregulated SOCS1 levels might play a protective role through the suppression of the destructive response of inflammatory cytokines. APRIL, a proliferation-inducing ligand; BAFF, B-cell activating factor; DC, dendritic cell; IFN, interferon; IL, interleukin; JAK2, Janus kinase 2; SOCS1, suppressor of cytokine signaling 1; STAT1, signal transducer and activator of transcription 1; TNF-α, tumor necrosis factor alpha; Treg, T regulatory cells.

TGF-β, and this possibly explains the inhibition of Th17 differentiation of SOCS1$^{-/-}$ T cells (39). Moreover, early differentiation of Th17 cells is inhibited by IFN-γ and IL-4 by depressing the production of IL-17 (39). Therefore, SOCS1 deficiency highly contributes to the imbalance of different Th cells and subsequent autoimmunity (**Figure 3**).

Suppressor of cytokine signaling 1 inhibition is important in the pathogenesis of SLE through the promotion of Treg cells plasticity (44). Dysregulation of Treg cells is highly implicated in the pathogenesis of SLE (45). T cell activation and autoantibody expression are accelerated in Treg cell-depleted lupus-prone mice (46). Transfer of Treg cells from normal mice into the murine lupus model can effectively suppress the progression of lupus autoimmunity such as anti-dsDNA antibody generation and lupus nephritis (LN) (47). However, SOCS1-deficient Treg cells usually lose Foxp3 expression and are converted into Th1-like cells, and this can be attributed to the hyperresponsiveness of Treg cells to IL-2 and IFN-γ, in which both accelerate the proliferation of Treg cells and its conversion into effector cells (48). As previously described, T cell-specific SOCS1-conditional knockout mice developed lupus-like diseases including spontaneous dermatitis, splenomegaly, lymphadenopathy, and serum positivity of anti-dsDNA antibodies (40). Treg-specific SOCS1-deficient mice also developed lupus-like phenotypes that are less serious than those in T cell-specific SOCS1-deficient mice, and many adult SOCS1$^{+/-}$ mice exhibited lupus-like manifestations as well (36). Splenic Treg cells from diseased SOCS1$^{+/-}$ mice showed less suppressive functions upon self-reactive T and B cells (36). Therefore, SOCS1 plays a crucial role in the interference of SLE development by maintaining the suppressive functions of Treg cells and by preventing Treg cells plasticity.

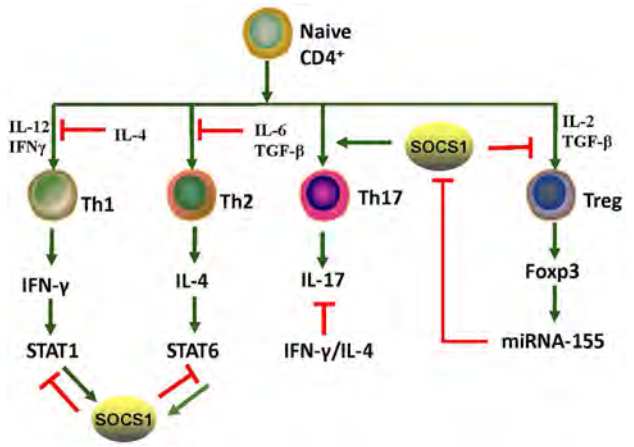

FIGURE 3 | Roles of SOCS1 protein in CD4+ T cell differentiation. T cell differentiation from naïve cells into the various functional subtypes, namely Th1, Th2, Th17, and Treg cells, primarily depends on the effect of cytokines. SOCS1 inhibits the differentiation of Th1, Th2, and Treg but promotes Th17 differentiation. IL-4 secreted by Th2 induces SOCS1 expression of STAT6; and correspondingly, SOCS1 suppresses IFN-γ-STAT1 signaling of Th1. IFN-γ secreted by Th1 induces SOCS1 expression of STAT1; SOCS1, in turn, suppresses IL-4-STAT6 signaling of Th2. Therefore, SOCS1 positively regulates Th17 cell differentiation by inhibiting the antagonistic effects of IFN-γ and IL-4. SOCS1 is a target of miRNA-155, and its deletion would impair the function of Treg cells. Upregulation of Foxp3 promotes expression of miRNA-155, which accelerates the proliferative potential of Treg cells through SOCS1 downregulation. The red and green lines denote inhibitory and activating signaling, respectively. IFN, interferon; JAK2, Janus kinase 2; IL, interleukin; miRNA, microRNA; SOCS1, suppressor of cytokine signaling 1, STAT, signal transducer and activator of transcription; TGF-β, transforming growth factor beta; Th, T helper cells; Treg, T regulatory cells.

Suppressor of cytokine signaling 1 regulates the maturation and activation of DCs. In Eμ-SOCS1$^{-/-}$ mice, DCs expressed higher levels of costimulatory molecules, such as CD80 and CD86 (36). Moreover, SOCS1-deficient DCs secreted more proinflammatory cytokines, such as IFN-γ, IL-6, IL-12, and TNF-α, and higher levels of major histocompatibility complex (MHC) class II molecules upon stimulation with lipopolysaccharide and CpG-containing DNA (49, 50). DCs are implicated in the development of systemic autoimmunity in aged SOCS1$^{-/-}$ mice (19). Transfer of SOCS1$^{-/-}$ DCs to wild-type mice induced the generation of autoantibodies due to the overexpression of BAFF in the donor DCs (19). It is known that failure of autoimmune tolerance accelerates the development of SLE (51). Self-tolerance can be disrupted by excessive IL-12 production of SOCS1$^{-/-}$ DCs (50). Therefore, SOCS1 inhibition participates in the pathogenesis of SLE by favoring the activation of DCs.

Systemic lupus erythematosus is characterized by serum positivity of anti-dsDNA autoantibodies, which are produced by B cell-derived plasma cells (52). Anti-dsDNA autoantibodies are instrumental in LN through recognition of multiple self-antigens and initiation of renal fibrosis (53–55). BAFF, which is a DC- and monocyte-derived cytokine of TNF family, is crucial in regulating B cell maturation, survival, and function (56). The expression level of BAFF/BLyS (B-lymphocyte stimulator) is increased in MRL/lpr mice during the onset and progression of lupus-like diseases (57). BAFF/BLyS-transgenic mice also had elevated serum titers of Ig and developed lupus-like autoimmunity (58, 59). Interestingly, high levels of BAFF/BLyS were detected in DCs but not in macrophages of SOCS1$^{-/-}$ transgenic mice, wherein transgenic SOCS1 was expressed in T and B cells but not in DCs (19). Furthermore, DCs induce Ig class switching through BLyS and a proliferation-inducing ligand (APRIL) (60). When BAFF/BLyS and APRIL are blocked by soluble B cell maturation antigen-Fc, as well as transmembrane activator and CAML interactor-Fc, the generation of IgG1 by B cells is partially restricted in the presence of SOCS1$^{-/-}$ DCs (60). Lipopolysaccharide induced more anti-dsDNA antibodies in the sera of C57BL/6 mice after they received DCs from SOCS1$^{-/-}$ transgenic mice (19). Thus, SOCS1 inhibition facilitates the activation of DCs, increases autoantibody generation and Ig class switching, and promotes the occurrence and development of SLE.

SOCS1 polymorphisms may also contribute to the development of SLE. It was found that the SLE patients have a lower frequency of SOCS1-1478del compared with those SLE patients without thrombocytopenia (61), suggesting that genetic background influences specific hematologic abnormalities in patients with SLE through regulating SOCS1 gene expression.

SOCS1 INHIBITION IS PIVOTAL IN THE PATHOGENESIS OF LN

Lupus nephritis is one of the most common complications in patients with SLE (3). It is primarily induced by renal deposition of pathogenic autoantibodies including anti-dsDNA IgG. It also involves the infiltration of immune cells, such as macrophages and lymphocytes, as well as the production of proinflammatory and profibrotic cytokines, namely IL-6, IL-12, IFN-γ, TNF-α, TGF-β, and monocyte chemoattractant protein-1, which accelerate renal injuries (21). In progressive LN, fibrosis is one of the main pathologies, and it contributes to the development of end-stage renal disease, which is evidenced by glomerular sclerosis (3). Wang et al. have demonstrated that SOCS1 expression is decreased in the glomeruli of LN patients and in MRL/lpr mice with anti-dsDNA IgG deposition as compared with their control groups (53). In MRL/lpr mice, STAT1 is overexpressed in glomerular mesangial, endothelial, and tubular epithelial cells, whereas SOCS1 is downregulated accordingly (62). In rat model of rapid focal segmental glomerulosclerosis, the expression levels of α-smooth muscle actin, collagen IV, and TGF-β1 were increased in the kidneys and were accompanied by reduced SOCS1 expression and activated JAK2/STAT1 signals (63).

Previous studies have shown that anti-dsDNA IgG binds to cell surface molecules, directly penetrates into kidney cells, and facilitates cell proliferation in the kidney (64). In addition, anti-dsDNA IgG participates in renal fibrosis through the induction of a myofibroblast-like phenotype of mesangial cells, as well as the production of proinflammatory cytokines and fibrotic factors in renal cells (65). Moreover, anti-dsDNA IgG can effectively catalyze DNA or peptides, depending on the structure of self-antigens (52). An interesting phenomenon is that anti-dsDNA IgG exhibits nephritogenicity through the blockade of SOCS1 signals. Anti-dsDNA IgG specifically binds to SOCS1-KIR and directly catalyzes KIR (53). Therefore, anti-dsDNA IgG competes with JAK2 activation loop for KIR, which leads to the blockade of signals from SOCS1 to the JAK2/STAT1 pathway. Downstream proinflammatory cytokines and profibrotic factors are upregulated in LN (53). In addition, ALW, which is a DNA-mimicking peptide with a sequence of ALWPPNLHAWVP, can restore SOCS1 expression by blocking the binding of anti-dsDNA IgG to antigens, thus further suppressing the JAK2/STAT1 pathway and attenuating LN (53, 54). These findings suggest that SOCS1 is involved in the nephritogenicity of anti-dsDNA IgG and that SOCS1 upregulation can ameliorate LN.

MicroRNAs (miRs) have been implicated in the pathogenesis of renal fibrosis (66). In patients with LN, miR-150 is overexpressed in resident cells of kidneys (67). SOCS1 is one of the potential targets of miR-150 (68). In proximal tubular and mesangial cells *in vitro*, miR-150 inhibited SOCS1 expression and increased the production of profibrotic proteins such as fibronectin, collagens I and III, and TGF-β1 (68). In podocytes, TGF-β stimulates miR-150 expression, accompanied by decreased SOCS1 and increased COL1 and COL3 expression (68). These findings are consistent with the facts that SOCS1 acts as an attenuator of renal immune responses, tubular epithelial–myofibroblast transdifferentiation, and tubulointerstitial fibrosis (69). Moreover, macrophage infiltration is a prominent feature of glomerulonephritis (70). SOCS1 regulates M1-macrophage activation, which mainly mediates inflammation and tissue damage by inhibiting IFN-γ-induced JAK2/STAT1 signaling in LN (71, 72). M1 macrophages of SOCS1-knockdown mice produced increased levels of proinflammatory cytokines, such as IL-6, IL-12, and MHC class II molecules, thus suggesting that SOCS1 limits the proinflammatory characteristics of M1 macrophages and regulates inflammatory balance (73).

Diabetic nephropathy is characterized by inflammation of the glomeruli and tubulointerstitial regions, accumulation of extracellular matrix (ECM), and subsequent focal and global glomerular sclerosis (74). Kidney infiltration of M1 macrophages in diabetic mellitus patients exacerbates renal cell damage (75). Numerous studies have demonstrated that dysregulated JAK/STAT signaling contributes to the onset and progression of diabetic chronic vascular complications, such as nephropathy (76). Interestingly, these features are similar to LN in a certain degree. Intraperitoneal administration of SOCS1 peptidomimetic (^{53}DTHFRTFRSHSDYRRI^{68}), which is a peptide that mimics the activity of the SOCS1 KIR region, in mice with diabetic nephropathy suppressed the activation of STAT1 signals, reduced serum creatinine and albuminuria levels, and ameliorated mesangial expansion, tubular injury, and renal fibrosis (77). Moreover, these SOCS1 peptidomimetic-treated mice exhibited significantly decreased T lymphocytes and M1 macrophages infiltration and reduced expression levels of monocyte- or T cell-derived chemokines such as C chemokine ligand (CCL) 2, CCL5, and TNF-α (77). Furthermore, SOCS1 peptidomimetic inhibits the expression of target genes induced under inflammation and reduces the migration and proliferation of mesangial and tubuloepithelial cells (77). Therefore, the correction of SOCS1 expression may be a promising method to suppress the development of inflammatory nephropathy such as LN. The role of SOCS1 signaling in the pathogenesis of LN is shown in **Figure 4**.

SOCS1 SIGNALS ARE INVOLVED IN OTHER END-ORGAN INJURIES IN SLE

Suppressor of cytokine signaling 1 is also involved in the function and injuries of other organs such as skin, central nervous system, liver, and lungs (78–80) (**Figure 5**). Cutaneous manifestations appear in most patients with lupus erythematosus, and IFN-γ is essential for the autoimmune responses in the skin of these SLE patients, as keratinocytes are highly susceptible to IFN-γ (81). Upon stimulation by IFN-γ, keratinocytes produce diverse chemokines, such as CCL2 and chemokine C–X–C motif ligand 10 (CXCL10), which promote the immigration of T cells, monocytes, and DCs into the inflamed skin, and CXCL8, which drives the chemoattractant activity of neutrophils (79, 81). However, SOCS1 suppresses the effect of IFN-γ on keratinocytes by inhibiting the JAK2/STAT1 pathway (79, 82). Keratinocytes overexpressing SOCS1 are less responsive to IFN-γ, as mirrored by the decreased activation of STAT1 and lowered production of CCL2, CXCL10, intercellular adhesion molecule-1, and MHC class II molecules (83). Evidently, SOCS1 protects keratinocytes

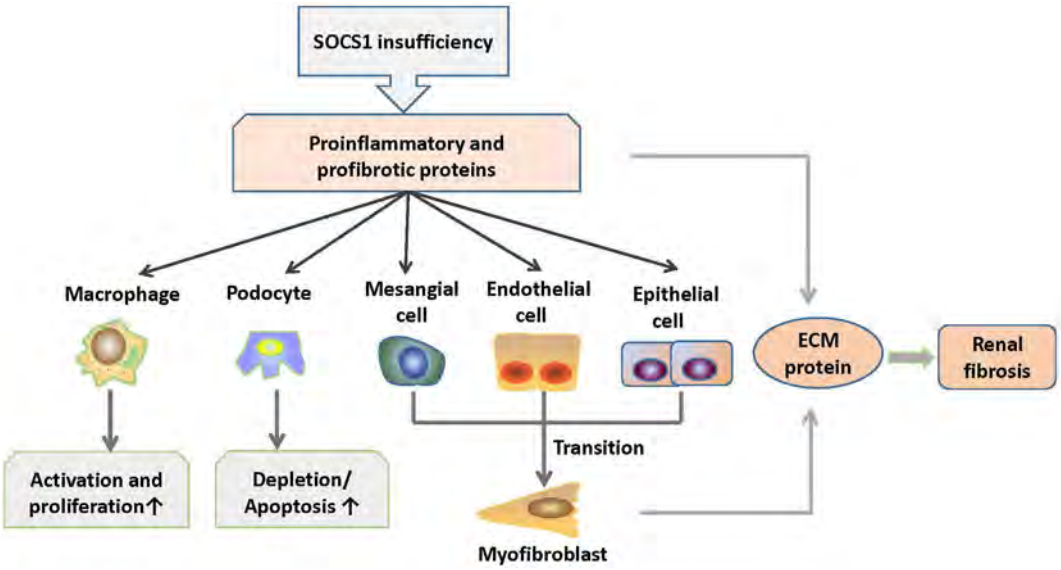

FIGURE 4 | Roles of SOCS1 in the pathogenesis of LN. SOCS1 deficiency results in excessive production of proinflammatory and profibrotic molecules, which further induces increased activation and proliferation of macrophages (M1) and depletion and apoptosis of podocytes. In addition, molecules, such as TGF-β, cause mesenchymal transition of renal cells and overexpression of ECM proteins in the kidney, which contribute to renal fibrosis. ECM, extracellular matrix; SOCS1, suppressor of cytokine signaling 1.

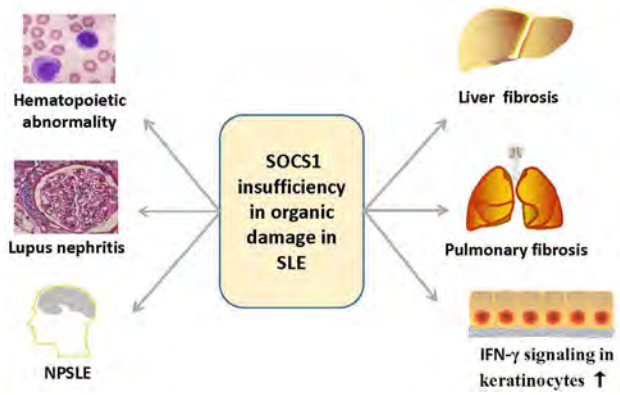

FIGURE 5 | Overview of the organ damage in systemic lupus erythematosus related with SOCS1 insufficiency. SOCS1 insufficiency contributes to the hematopoietic abnormalities such as spontaneous lymphocyte activation, production of autoantibodies, lupus nephritis, NPSLE, and liver or pulmonary fibrosis, and it also promotes autoimmune responses in skin *via* IFN-γ signaling. IFN, interferon; NPSLE, neuropsychiatric systemic lupus erythematosus; SOCS1, suppressor of cytokine signaling 1.

of SLE patients from autoimmunity induced by uncontrolled IFN-γ signaling.

Neuropsychiatric SLE (NPSLE) is a serious complication of SLE (84). Although the mechanism of NPSLE remains unclear, cytokines and chemokines, such as IFN-β and IFN-γ, are considered to be involved in the pathogenesis of NPSLE through the JAK/STAT signaling pathway (85–88). IFN-β-treated astrocyte *in vitro* was able to generate a large amount of chemokines, such as CCL2, CCL5, and CXCL10, and these chemokines can be negatively regulated by SOCS1 (89). The production of these chemokines apparently increased when SOCS1 is depleted by siRNA (78). Furthermore, the increase in chemokine expression correlates with enhanced migration of macrophages and $CD4^+$ T cells *in vitro*, indicating that SOCS1 might limit inflammatory cell migration within the central nervous system (89). Moreover, SOCS1 also inhibits IFN-γ-induced expression of MHC class II and CD40 in macrophages and microglia by blocking STAT1 activation (90, 91). Thus, SOCS1 inhibition contributes to the autoimmunity in the progression of NPSLE by affecting the production of inflammatory cytokines and chemokines, activation of microglia, macrophages and astrocytes, and infiltration of immune cells.

Aside from kidneys, skin, and central nervous system, the liver can also be affected in SLE (92). About 25–50% of SLE patients may present with abnormal liver function (93). Many studies demonstrated the ability of antiribosomal P antibodies to upregulate the expression of proinflammatory cytokines produced by peripheral monocytes in SLE, which can lead to the development of autoimmune hepatitis (94). In patients with hepatitis triggered by SLE, Treg cells are decreased in number and display impairment of suppressive function, along with elevated IFN-γ production *in vivo* (95). Diseased $SOCS1^{+/-}$ mice exhibited more severe liver fibrosis than wild-type littermates. Liver fibrosis is strongly correlated with SOCS1 gene silencing through DNA methylation, and this firmly supports that the inhibition of SOCS1 leads to the progression of autoimmune hepatitis in SLE (96).

Furthermore, a variety of cytokines and chemokines are involved in the pathophysiology of pulmonary fibrosis in SLE

(97, 98). It was reported that lower levels of SOCS1 mRNA and higher amounts of type I collagen were produced by fibroblasts from lungs of patients with pulmonary fibrosis as compared with those from healthy lungs (99). Moreover, SOCS1 deficiency in murine fibroblasts resulted in increased collagen production, whereas overexpression of SOCS1 suppressed collagen expression *in vitro* (99). Therefore, SOCS1 might suppress pulmonary fibrosis by inhibiting profibrotic cytokines and collagen synthesis of lung fibroblasts. The expression level of SOCS1 in bleomycin-injured lungs was significantly lower in SOCS1$^{+/-}$ mice than in wild-type mice (100). SOCS1$^{+/-}$ mice treated with bleomycin had significantly increased numbers of macrophages, lymphocytes, and eosinophils and elevated levels of IFN-γ, TNF-α, IL-4, IL-5, and monocyte chemoattractant protein-1 as compared with those of SOCS1$^{+/+}$ mice in bronchoalveolar lavage fluid (100). Exogenous SOCS1 delivered through adenoviral gene transfer ameliorated bleomycin-induced pulmonary inflammation and fibrosis in SOCS1$^{+/-}$ mice (100). These results highly suggest that SOCS1 inhibition is also involved in the progression of pulmonary fibrosis and that SOCS1 would be a novel target in treating lung fibrosis. The roles of SOCS1 in the different forms of lupus erythematosus are summarized in **Table 1**.

THERAPEUTIC POTENTIAL FOR TARGETING THE SOCS1 PATHWAY

Considering the abnormalities of SOCS1 expression in damaged tissues, as well as its role in the regulation of downstream cytokines, SOCS1 may be a novel therapeutic target in the treatment of patients with SLE. Administration of SOCS1 mimetics might affect the abnormal immune responses regulated by SOCS1. Tyrosine kinase inhibitory peptide (Tkip), which is a 12-amino acid peptide (WLVFFVIFYFFR), can specifically bind to the JAK2 activation loop (^{1001}LPQDKEYYKVKEP) and inhibit the activation of JAK2/STAT1 signaling (101). *In vivo* studies have demonstrated that subcutaneous administration of Tkip can block IFN-γ and TNF-α pathways and prevent the development of experimental autoimmune encephalomyelitis and multiple sclerosis (102). Moreover, the SOCS1-KIR mimetic peptide PS-5 (^{53}DTHFRTFRSHSDYRRI) ameliorates IFN-γ-induced inflammation in human keratinocytes by suppressing JAK2 kinase activity, as reflected by the inhibition of STAT1α phosphorylation and reduced expression of IFNGR1, CCL2, CXCL10, and intercellular adhesion molecule-1 (79). These strategies suggest that administration of SOCS1 mimetics is capable of ameliorating SLE.

TABLE 1 | The roles of SOCS1 deficiency in systemic lupus erythematosus (SLE).

Affected	Phenotype	Target	Effect	Reference
Hematological system	Hematopoietic abnormalities	Th cells Treg cells Dendritic cells Autoantibody	Spontaneous activation and proliferation; Th1↑/Th17 ↓ Cells plasticity ↑ Activation; BAFF ↑ IgG ↑; Ig class switching ↑	(36, 39) (36, 44, 48) (19, 36, 49, 50) (19, 60)
Kidney	Lupus nephritis	Anti-dsDNA IgG miRNA-150 Macrophages	Binds and catalyzes SOCS1-KIR SOCS1 expression ↓; renal fibrosis Renal inflammation	(53) (67) (70–72)
Skin	Cutaneous inflammation	Keratinocytes	Interferon-γ signaling ↑	(78, 81)
Brain	Neuropsychiatric SLE	Astrocytes Microglia Macrophages T cells	Activation ↑, inflammatory cytokines and chemokines ↑	(88–90)
Liver	Lupus hepatitis			(95)
Lung	Pulmonary fibrosis	Macrophages Lymphocyte	Activation ↑, profibrotic cytokines ↑, collagen synthesis ↑	(98, 99)

BAFF, B-cell activating factor; KIR, kinase inhibitory region; SOCS1, suppressor of cytokine signaling 1; Th, T helper cells; Treg, T regulatory cells.

TABLE 2 | Therapeutic potential for targeting SOCS1 pathway.

Pattern	Approach	Function	Mechanism	Implications	Reference
Upregulation of SOCS1	Adenoviral gene transfer	SOCS1 delivery	Upregulating SOCS1	Bleomycin-induced pulmonary fibrosis in SOCS1$^{+/-}$ mice	(99)
	Tyrosine kinase inhibitory peptide	SOCS1 mimetic	Competitive binding to the activation loop of JAK2	Experimental autoimmune encephalomyelitis and multiple sclerosis	(100, 101)
	PS-5	SOCS1-KIR analog	Competitive binding to the activation loop of JAK2	Psoriasis	(79)
	Edratide	SOCS1 inductor: a drug based on the CDR1 sequence of anti-DNA IgG		Systemic lupus erythematosus	(13, 25)

CDR1, complementarity-determining region 1; JAK2, Janus kinase 2; KIR: kinase inhibitory region; SOCS1, suppressor of cytokine signaling 1.

hCDR1 (Edratide), a peptide (GYYWSWIRQPPGKGEEWIG) based on the CDR1 sequence of anti-DNA monoclonal antibody, could ameliorate the progression of SLE (13). In SLE patients treated with Edratide subcutaneously, the expression of pathogenic cytokines, such as IL-1β, TNF-α, IFN-γ, and BLyS, were significantly downregulated, but the expression of anti-inflammatory cytokine TGF-β was increased (13). After the administration of hCDR1, NZB × NZW F1 mice showed increased SOCS1, decreased levels of pSTAT1, BAFF, anti-dsDNA autoantibodies, and MHC class II molecules on DCs, and better controlled IFN-γ signaling (25). Clinically, glomerular immune complex deposit was diminished and proteinuria levels were reduced in these lupus-affected mice upon injection of hCDR1 (25). It is, therefore, possible that part of the beneficial effects of hCDR1 is due to the induction of SOCS1 in hCDR1-treated mice and controlled IFN-γ signaling (25). The therapeutic strategies for targeting SOCS1 pathway are also summarized in **Table 2**.

Thus far, we have yet to fully understand the function of SOCS1 *in vivo*, because intracellular signaling pathways are complexly regulated by various factors. With the development of new technologies, the roles of SOCS1 in SLE will be explicitly elucidated, and SOCS1 signals can provide more therapeutic strategies for the treatment of SLE in the future.

CONCLUSION

The SOCS1 pathway is a key regulator of inflammatory cytokines, which are pivotal in the progression of SLE. The insufficient expression of SOCS1 in SLE is related with various pathological processes including hematologic abnormalities, generation of autoantibodies, and other end-organ damages such as LN. Although the explicit role of SOCS1 remains to be elucidated, SOCS1 insufficiency definitely contributes to the pathogenesis of SLE. The enhancement of SOCS1 signals, such as SOCS1 delivery or SOCS1 mimetics, can ameliorate the manifestations of SLE. Further investigation should focus on the design of SOCS1-mimicking molecules that may rectify SOCS1 insufficiency in SLE.

AUTHOR CONTRIBUTIONS

YX and HW conceived this review paper and prepared the manuscript. JW discussed the manuscript and contributed to the improvement of this paper. All the authors read and approved the final manuscript.

FUNDING

This study was supported by the National Natural Science Foundation of China (Projects No. 81472876 and No. 81630081) and the Fundamental Research Funds for the Central Universities (No. 2015qngz01).

REFERENCES

1. Golder V, Hoi A. Systemic lupus erythematosus: an update. *Med J Aust* (2017) 206(5):215–20. doi:10.5694/mja16.01229
2. Gottschalk TA, Tsantikos E, Hibbs ML. Pathogenic inflammation and its therapeutic targeting in systemic lupus erythematosus. *Front Immunol* (2015) 6:550. doi:10.3389/fimmu.2015.00550
3. Lech M, Anders HJ. The pathogenesis of lupus nephritis. *J Am Soc Nephrol* (2013) 24(9):1357–66. doi:10.1681/ASN.2013010026
4. Mahajan A, Herrmann M, Munoz LE. Clearance deficiency and cell death pathways: a model for the pathogenesis of SLE. *Front Immunol* (2016) 7:35. doi:10.3389/fimmu.2016.00035
5. Aleem A, Al Arfaj AS, Khalil N, Alarfaj H. Haematological abnormalities in systemic lupus erythematosus. *Acta Reumatol Port* (2014) 39(3):236–41.
6. Su DL, Lu ZM, Shen MN, Li X, Sun LY. Roles of pro- and anti-inflammatory cytokines in the pathogenesis of SLE. *J Biomed Biotechnol* (2012) 2012: 347141–56. doi:10.1155/2012/347141
7. Kershaw NJ, Murphy JM, Lucet IS, Nicola NA, Babon JJ. Regulation of Janus kinases by SOCS proteins. *Biochem Soc Trans* (2013) 41(4):1042–7. doi:10.1042/BST20130077
8. Yoshimura A, Yasukawa H. JAK's SOCS: a mechanism of inhibition. *Immunity* (2012) 36(2):157–9. doi:10.1016/j.immuni.2012.01.010
9. Kubo M, Hanada T, Yoshimura A. Suppressors of cytokine signaling and immunity. *Nat Immunol* (2003) 4(12):1169–76. doi:10.1038/ni1012
10. Liang Y, Xu WD, Peng H, Pan HF, Ye DQ. SOCS signaling in autoimmune diseases: molecular mechanisms and therapeutic implications. *Eur J Immunol* (2014) 44(5):1265–75. doi:10.1002/eji.201344369
11. Qiu LJ, Xu K, Liang Y, Cen H, Zhang M, Wen PF, et al. Decreased SOCS1 mRNA expression levels in peripheral blood mononuclear cells from patients with systemic lupus erythematosus in a Chinese population. *Clin Exp Med* (2015) 15(3):261–7. doi:10.1007/s10238-014-0309-2
12. Sukka-Ganesh B, Larkin J. Therapeutic potential for targeting the suppressor of cytokine signalling-1 pathway for the treatment of SLE. *Scand J Immunol* (2016) 84(5):299–309. doi:10.1111/sji.12475
13. Urowitz MB, Isenberg DA, Wallace DJ. Safety and efficacy of hCDR1 (Edratide) in patients with active systemic lupus erythematosus: results of phase II study. *Lupus Sci Med* (2015) 2(1):e000104. doi:10.1136/lupus-2015-000104
14. Yasukawa H, Misawa H, Sakamoto H, Masuhara M, Sasaki A, Wakioka T, et al. The JAK-binding protein JAB inhibits Janus tyrosine kinase activity through binding in the activation loop. *EMBO J* (1999) 18(5):1309–20. doi:10.1093/emboj/18.5.1309
15. Yeh TC, Pellegrini S. The Janus kinase family of protein tyrosine kinases and their role in signaling. *Cell Mol Life Sci* (1999) 55(12):1523–34. doi:10.1007/s000180050392
16. Ahmed CM, Larkin J, Johnson HM. SOCS1 mimetics and antagonists: a complementary approach to positive and negative regulation of immune function. *Front Immunol* (2015) 6:183. doi:10.3389/fimmu.2015.00183
17. Babon JJ, Kershaw NJ, Murphy JM, Varghese LN, Laktyushin A, Young SN, et al. Suppression of cytokine signaling by SOCS3: characterization of the mode of inhibition and the basis of its specificity. *Immunity* (2012) 36(2):239–50. doi:10.1016/j.immuni.2011.12.015
18. Zahn S, Godillot P, Yoshimura A, Chaiken I. IL-5-induced JAB-JAK2 interaction. *Cytokine* (2000) 12(9):1299–306. doi:10.1006/cyto.2000.0718
19. Hanada T, Yoshida H, Kato S, Tanaka K, Masutani K, Tsukada J, et al. Suppressor of cytokine signaling-1 is essential for suppressing dendritic cell activation and systemic autoimmunity. *Immunity* (2003) 19(3):437–50. doi:10.1016/S1074-7613(03)00240-1
20. Tamiya T, Kashiwagi I, Takahashi R, Yasukawa H, Yoshimura A. Suppressors of cytokine signaling (SOCS) proteins and JAK/STAT pathways: regulation of T-cell inflammation by SOCS1 and SOCS3. *Arterioscler Thromb Vasc Biol* (2011) 31(5):980–5. doi:10.1161/atvbaha.110.207464
21. Gigante A, Gasperini ML, Afeltra A, Barbano B, Margiotta D, Cianci R, et al. Cytokines expression in SLE nephritis. *Eur Rev Med Pharmacol Sci* (2011) 15(1):15–24.
22. Esmaeili SA, Mahmoudi M, Momtazi AA, Sahebkar A, Doulabi H, Rastin M. Tolerogenic probiotics: potential immunoregulators in systemic lupus erythematosus. *J Cell Physiol* (2017) 232(8):1994–2007. doi:10.1002/jcp.25748

23. Linossi EM, Babon JJ, Hilton DJ, Nicholson SE. Suppression of cytokine signaling: the SOCS perspective. *Cytokine Growth Factor Rev* (2013) 24(3):241–8. doi:10.1016/j.cytogfr.2013.03.005
24. Qing Y, Costa-Pereira AP, Watling D, Stark GR. Role of tyrosine 441 of interferon-γ receptor subunit1 in SOCS-1-mediated attenuation of STAT1 activation. *J Biol Chem* (2005) 280(3):1849–53. doi:10.1074/jbc.M409863200
25. Sharabi A, Sthoeger ZM, Mahlab K, Lapter S, Zinger H, Mozes E. A tolerogenic peptide that induces suppressor of cytokine signaling (SOCS)-1 restores the aberrant control of IFN-gamma signaling in lupus-affected (NZB x NZW)F1 mice. *Clin Immunol* (2009) 133(1):61–8. doi:10.1016/j.clim.2009.06.010
26. Hagberg N, Rönnblom L. Systemic lupus erythematosus-a disease with a dysregulated type I interferon system. *Scand J Immunol* (2015) 82(3):199–207. doi:10.1111/sji.12330
27. Mathian A, Gallegos M, Pascual V, Banchereau J, Koutouzov S. Interferon-α induces unabated production of short-lived plasma cells in pre-autoimmune lupus-prone (NZB×NZW)F1 mice but not in BALB/c mice. *Eur J Immunol* (2011) 41(3):863–72. doi:10.1002/eji.201040649
28. Braun D, Geraldes P, Demengeot J. Type I Interferon controls the onset and severity of autoimmune manifestations in lpr mice. *J Autoimmun* (2003) 20(1):15–25. doi:10.1016/S0896-8411(02)00109-9
29. Joo H, Coquery C, Xue Y, Gayet I, Dillon SR, Punaro M, et al. Serum from patients with SLE instructs monocytes to promote IgG and IgA plasmablast differentiation. *J Exp Med* (2012) 209(7):1335–48. doi:10.1084/jem.20111644
30. Blanco P, Palucka AK, Gill M, Pascual V, Banchereau J. Induction of dendritic cell differentiation by IFN-alpha in systemic lupus erythematosus. *Science* (2001) 294(5546):1540–3. doi:10.1126/science.1064890
31. Luo S, Wang Y, Zhao M, Lu Q. The important roles of type I interferon and interferon-inducible genes in systemic lupus erythematosus. *Int Immunopharmacol* (2016) 40:542–9. doi:10.1016/j.intimp.2016.10.012
32. Feng X, Wu H, Grossman JM, Hanvivadhanakul P, FitzGerald JD, Park GS, et al. Association of increased interferon-inducible gene expression with disease activity and lupus nephritis in patients with systemic lupus erythematosus. *Arthritis Rheum* (2006) 54(9):2951–62. doi:10.1002/art.22044
33. Fenner JE, Starr R, Cornish AL, Zhang JG, Metcalf D, Schreiber RD, et al. Suppressor of cytokine signaling 1 regulates the immune response to infection by a unique inhibition of type I interferon activity. *Nat Immunol* (2006) 7(1):33–9. doi:10.1038/ni1287
34. Qin H, Wilson CA, Lee SJ, Benveniste EN. IFN-beta-induced SOCS-1 negatively regulates CD40 gene expression in macrophages and microglia. *FASEB J* (2006) 20(7):985–7. doi:10.1096/fj.05-5493fje
35. Yoshimura A, Naka T, Kubo M. SOCS proteins, cytokine signalling and immune regulation. *Nat Rev Immunol* (2007) 7(6):454–65. doi:10.1038/nri2093
36. Fujimoto M, Tsutsui H, Xinshou O, Tokumoto M, Watanabe D, Shima Y, et al. Inadequate induction of suppressor of cytokine signaling-1 causes systemic autoimmune diseases. *Int Immunol* (2004) 16(2):303–14. doi:10.1093/intimm/dxh030
37. Marine JC, Topham DJ, McKay C, Wang D, Parganas E, Stravopodis D, et al. SOCS1 deficiency causes a lymphocyte-dependent perinatal lethality. *Cell* (1999) 98(5):609–16. doi:10.1016/S0092-8674(00)80048-3
38. Fujimoto M, Naka T, Nakagawa R, Kawazoe Y, Morita Y, Tateishi A, et al. Defective thymocyte development and perturbed homeostasis of T cells in STAT-induced STAT inhibitor-1/suppressors of cytokine signaling-1 transgenic mice. *J Immunol* (2000) 165(4):1799–806. doi:10.4049/jimmunol.165.4.1799
39. Tanaka K, Ichiyama K, Hashimoto M, Yoshida H, Takimoto T, Takaesu G, et al. Loss of suppressor of cytokine signaling 1 in helper T cells leads to defective Th17 differentiation by enhancing antagonistic effects of IFN on STAT3 and Smads. *J Immunol* (2008) 180(6):3746–56. doi:10.4049/jimmunol.180.6.3746
40. Takahashi R, Nishimoto S, Muto G, Sekiya T, Tamiya T, Kimura A, et al. SOCS1 is essential for regulatory T cell functions by preventing loss of Foxp3 expression as well as IFN-gamma and IL-17A production. *J Exp Med* (2011) 208(10):2055–67. doi:10.1084/jem.20110428
41. Blom L, Poulsen LK. In vitro Th1 and Th2 cell polarization is severely influenced by the initial ratio of naïve and memory CD4+ T cells. *J Immunol Methods* (2013) 397(1–2):55–60. doi:10.1016/j.jim.2013.08.008
42. Liu HP, Cao AT, Feng T, Li Q, Zhang W, Yao S, et al. TGF-β converts Th1 cells into Th17 cells through stimulation of Runx1 expression. *Eur J Immunol* (2015) 45(4):1010–8. doi:10.1002/eji.201444726
43. Chen DY, Chen YM, Wen MC, Hsieh TY, Hung WT, Lan JL. The potential role of Th17 cells and Th17-related cytokines in the pathogenesis of lupus nephritis. *Lupus* (2012) 21(13):1385–96. doi:10.1177/0961203312457718
44. Takahashi R, Nakatsukasa H, Shiozawa S, Yoshimura A. SOCS1 is a key molecule that prevents regulatory T cell plasticity under inflammatory conditions. *J Immunol* (2017) 199(1):149–58. doi:10.4049/jimmunol.1600441
45. Costa N, Marques O, Godinho SI, Carvalho C, Leal B, Figueiredo AM, et al. Two separate effects contribute to regulatory T-cell defect in SLE patients and their unaffected relatives. *Clin Exp Immunol* (2017) 189(3):318–30. doi:10.1111/cei.12991
46. Ahmadpoor P, Dalili N, Rostami M. An update on pathogenesis of systemic lupus erythematosus. *Iran J Kidney Dis* (2014) 8(3):171–84.
47. Weigert O, von Spee C, Undeutsch R, Kloke L, Humrich JY, Riemekasten G. CD4+Foxp3+ regulatory T cells prolong drug-induced disease remission in (NZBxNZW) F1 lupus mice. *Arthritis Res Ther* (2013) 15(1):R35. doi:10.1186/ar4188
48. Takahashi R, Yoshimura A. SOCS1 and regulation of regulatory T cells plasticity. *J Immunol Res* (2014) 2014:943149. doi:10.1155/2014/943149
49. Hanada T, Tanaka K, Matsumura Y, Yamauchi M, Nishinakamura H, Aburatani H, et al. Induction of hyper TH1 cell-type immune responses by dendritic cells lacking the suppressor of cytokine signaling-1 gene. *J Immunol* (2005) 174(7):4325–32. doi:10.4049/jimmunol.174.7.4325
50. Evel-Kabler K, Song XT, Aldrich M, Huang XF, Chen SY. SOCS1 restricts dendritic cells's ability to break self tolerance and induce antitumor immunityby regulating IL-12 production and signaling. *J Clin Invest* (2006) 116(1):90–100. doi:10.1172/JCI26169
51. Liao X, Reihl AM, Luo XM. Breakdown of immune tolerance in systemic lupus erythematosus by dendritic cells. *J Immunol Res* (2016) 2016:6269157. doi:10.1155/2016/6269157
52. Xia Y, Eryilmaz E, Zhang Q, Cowburn D, Putterman C. Anti-DNA antibody mediated catalysis is isotype dependent. *Mol Immunol* (2016) 69:33–43. doi:10.1016/j.molimm.2015.11.001
53. Wang P, Yang J, Tong F, Duan ZY, Liu XY, Xia LL, et al. Anti-dsDNA IgG participates in renal fibrosis through suppressing the SOCS1 signals. *Front Immunol* (2017) 8:610. doi:10.3389/fimmu.2017.00610
54. Xia Y, Eryilmaz E, Der E, Pawar RD, Guo X, Cowburn D, et al. A peptide mimic blocks the cross-reaction of anti-DNA antibodies with glomerular antigens. *Clin Exp Immunol* (2016) 183(3):369–79. doi:10.1111/cei.12734
55. Xia Y, Pawar RD, Nakouzi AS, Herlitz L, Broder A, Liu K, et al. The constant region contributes to the antigenic specificity and renal pathogenicity of murine anti-DNA antibodies. *J Autoimmun* (2012) 39(4):398–411. doi:10.1016/j.jaut.2012.06.005
56. Vincent FB, Morand EF, Mackay F, Morand EF, Schneider P, Mackay F. The BAFF/APRIL system in SLE pathogenesis. *Nat Rev Rheumatol* (2014) 10(6):365–73. doi:10.1038/nrrheum.2014.33
57. Zhou L, Sun L, Wu H, Zhang L, Chen M, Liu J, et al. Oridonin ameliorates lupus-like symptoms of MRL(lpr/lpr) mice by inhibition of B-cell activating factor (BAFF). *Eur J Pharmacol* (2013) 715:230–7. doi:10.1016/j.ejphar.2013.05.016
58. Kayagaki N, Yan M, Seshasayee D, Wang H, Lee W, French DM, et al. BAFF/BLyS receptor 3 binds the B cell survival factor BAFF ligand through a discrete surface loop and promotes processing of NF-kappaB2. *Immunity* (2002) 17(4):515–24. doi:10.1016/S1074-7613(02)00425-9
59. Fairfax KA, Tsantikos E, Figgett WA, Vincent FB, Quah PS, LePage M, et al. BAFF-driven autoimmunity requires CD19 expression. *J Autoimmun* (2015) 62:1–10. doi:10.1016/j.jaut.2015.06.001
60. Litinskiy MB, Nardelli B, Hilbert DM, He B, Schaffer A, Casali P, et al. DCs induce CD40-independent immunoglobulin class switching through BLyS and APRIL. *Nat Immunol* (2002) 3(9):822–9. doi:10.1038/ni829
61. Chan HC, Ke LY, Chang LL, Liu CC, Hung YH, Lin CH, et al. Suppressor of cytokine signaling 1 gene expression and polymorphisms in systemic lupus erythematosus. *Lupus* (2010) 19(6):696–702. doi:10.1177/0961203309357437
62. Dong J, Wang QX, Zhou CY, Ma XF, Zhang YC. Activation of the STAT1 signalling pathway in lupus nephritis in MRL/lpr mice. *Lupus* (2007) 16:101–9. doi:10.1177/0961203306075383

63. Liang Y, Jin Y, Li Y. Expression of JAKs/STATs pathway molecules in rat model of rapid focal segmental glomerulosclerosis. *Pediatr Nephrol* (2009) 24(9):1661–71. doi:10.1007/s00467-009-1163-4
64. Yung S, Chan TM. Mechanisms of kidney injury in lupus nephritis – the role of anti-dsDNA antibodies. *Front Immunol* (2015) 6:475. doi:10.3389/fmmu.2015.00475
65. Zhang Y, Yang J, Jiang S, Fang C, Xiong L, Cheng H, et al. The lupus-derived anti-double-stranded DNA IgG contributes to myofibroblast-like phenotype in mesangial cells. *J Clin Immunol* (2012) 32(6):1270–8. doi:10.1007/s10875-012-9724-x
66. Costa-Reis P, Russo PA, Zhang Z, Colonna L, Maurer K, Gallucci S, et al. The role of microRNAs and human epidermal growth factor receptor 2 in proliferative lupus nephritis. *Arthritis Rheumatol* (2015) 67(9):2415–26. doi:10.1002/art.39219
67. Yung S, Chan TM. Molecular and immunological basis of tubulo-interstitial injury in lupus nephritis: a comprehensive review. *Clin Rev Allergy Immunol* (2017) 52(2):149–63. doi:10.1007/s12016-016-8533-z
68. Zhou H, Hasni SA, Perez P, Tandon M, Jang SI, Zheng C, et al. miR-150 promotes renal fibrosis in lupus nephritis by downregulating SOCS1. *J Am Soc Nephrol* (2013) 24(7):1073–87. doi:10.1681/ASN.2012080849
69. Liu Q, Liu S, Shi Y, Li H, Hao J, Xing L, et al. Suppressors of cytokine signaling inhibit tubular epithelial cell-myofibroblast transdifferentiation. *Am J Nephrol* (2011) 34(2):142–51. doi:10.1159/000329325
70. Ma R, Jiang W, Li Z, Sun Y, Wei Z. Intrarenal macrophage infiltration induced by T cells is associated with podocyte injury in lupus nephritis patients. *Lupus* (2016) 25(14):1577–86. doi:10.1177/0961203316646861
71. Wilson HM. SOCS proteins in macrophage polarization and function. *Front Immunol* (2014) 5:357. doi:10.3389/fimmu.2014.00357
72. Qin H, Holdbrooks AT, Liu Y, Reynolds SL, Yanagisawa LL, Benveniste EN. SOCS3 deficiency promotes M1 macrophage polarization and inflammation. *J Immunol* (2012) 189(7):3439–48. doi:10.4049/jimmunol.1201168
73. Whyte CS, Bishop ET, Rückerl D, Gaspar-Pereira S, Barker RN, Allen JE, et al. Suppressor of cytokine signaling (SOCS)1 is a key determinant of differential macrophage activation and function. *J Leukoc Biol* (2011) 90(5):845–54. doi:10.1189/jlb.1110644
74. Wada J, Makino H. Inflammation and the pathogenesis of diabetic nephropathy. *Clin Sci (Lond)* (2013) 124(3):139–52. doi:10.1042/CS20120198
75. Anders HJ, Ryu M. Renal microenvironments and macrophage phenotypes determine progression or resolution of renal inflammation and fibrosis. *Kidney Int* (2011) 80(9):915–25. doi:10.1038/ki.2011.217
76. Brosius FC, He JC. JAK inhibition and progressive kidney disease. *Curr Opin Nephrol Hypertens* (2015) 24(1):88–95. doi:10.1097/MNH.0000000000000079
77. Recio C, Lazaro I, Oguiza A, Lopez-Sanz L, Bernal S, Blanco J, et al. Suppressor of cytokine signaling-1 peptidomimetic limits progression of diabetic nephropathy. *J Am Soc Nephrol* (2017) 28(2):575–85. doi:10.1681/ASN.2016020237
78. Baker BJ, Akhtar LN, Benveniste EN. SOCS1 and SOCS3 in the control of CNS immunity. *Trends Immunol* (2009) 30(8):392–400. doi:10.1016/j.it.2009.07.001
79. Madonna S, Scarponi C, Doti N, Carbone T, Cavani A, Scognamiglio PL, et al. Therapeutical potential of a peptide mimicking the SOCS1 kinase inhibitory region in skin immune responses. *Eur J Immunol* (2013) 43(7):1883–95. doi:10.1002/eji.201343370
80. Mak A, Isenberg DA, Lau CS. Global trends, potential mechanisms and early detection of organ damage in SLE. *Nat Rev Rheumatol* (2013) 9(5):301–10. doi:10.1038/nrrheum.2012.208
81. Carneiro JR, Fuzii HT, Kayser C, Alberto FL, Soares FA, Sato EI, et al. IL-2, IL-5, TNF-α and IFN-γ mRNA expression in epidermal keratinocytes of systemic lupus erythematosus skin lesions. *Clinics (Sao Paulo)* (2011) 66(1):77–82. doi:10.1590/S1807-59322011000100014
82. Madonna S, Scarponi C, Sestito R, Pallotta S, Cavani A, Albanesi C. The IFN-gamma-dependent suppressor of cytokine signaling 1 promoter activity is positively regulated by IFN regulatory factor-1 and Sp1 but repressed by growth factor independence-1b and Krüppel-like factor-4, and it is dysregulated in psoriatic keratinocytes. *J Immunol* (2010) 185(4):2467–81. doi:10.4049/jimmunol.1001426
83. Federici M, Giustizieri ML, Scarponi C, Girolomoni G, Albanesi C. Impaired IFN-gamma-dependent inflammatory responses in human keratinocytes overexpressing the suppressor of cytokine signaling 1. *J Immunol* (2002) 169(1):434–42. doi:10.4049/jimmunol.169.1.434
84. Govoni M, Bortoluzzi A, Padovan M, Silvagni E, Borrelli M, Donelli F, et al. The diagnosis and clinical management of the neuropsychiatric manifestations of lupus. *J Autoimmun* (2016) 74:41–72. doi:10.1016/j.jaut.2016.06.013
85. Ichinose K, Arima K, Ushigusa T, Nishino A, Nakashima Y, Suzuki T, et al. Distinguishing the cerebrospinal fluid cytokine profile in neuropsychiatric systemic lupus erythematosus from other autoimmune neurological diseases. *Clin Immunol* (2015) 157(2):114–20. doi:10.1016/j.clim.2015.01.010
86. Stock AD, Wen J, Putterman C. Neuropsychiatric lupus, the blood brain barrier, and the TWEAK/Fn14 pathway. *Front Immunol* (2013) 4:484. doi:10.3389/fimmu.2013.00484
87. Campbell IL. Cytokine-mediated inflammation, tumorigenesis, and disease-associated JAK/STAT/SOCS signaling circuits in the CNS. *Brain Res Brain Res Rev* (2005) 48(2):166–77. doi:10.1016/j.brainresrev.2004.12.006
88. Wen J, Xia Y, Stock A, Michaelson JS, Burkly LC, Gulinello M, et al. Neuropsychiatric disease in murine lupus is dependent on the TWEAK/Fn14 pathway. *J Autoimmun* (2013) 43:44–54. doi:10.1016/j.jaut.2013.03.002
89. Qin H, Niyongere SA, Lee SJ, Baker BJ, Benveniste EN. Expression and functional significance of SOCS-1 and SOCS-3 in astrocytes. *J Immunol* (2008) 181(5):3167–76. doi:10.4049/jimmunol.181.5.3167
90. O'Keefe GM, Nguyen VT, Ping Tang LL, Benveniste EN. IFN-gamma regulation of class II transactivator promoter IV in macrophages and microglia: involvement of the suppressors of cytokine signaling-1 protein. *J Immunol* (2001) 166(4):2260–9. doi:10.4049/jimmunol.166.4.2260
91. Wesemann DR, Dong Y, O'Keefe GM, Nguyen VT, Benveniste EN. Suppressor of cytokine signaling 1 inhibits cytokine induction of CD40 expression in macrophages. *J Immunol* (2002) 169(5):2354–60. doi:10.4049/jimmunol.169.5.2354
92. Takahashi A, Abe K, Saito R, Iwadate H, Okai K, Katsushima F, et al. Liver dysfunction in patients with systemic lupus erythematosus. *Intern Med* (2013) 52(13):1461–5. doi:10.2169/internalmedicine.52.9458
93. Chowdhary VR, Crowson CS, Poterucha JJ, Moder KG. Liver involvement in systemic lupus erythematosus: case review of 40 patients. *J Rheumatol* (2008) 35(11):2159–64. doi:10.3899/jrheum.080336
94. Nagai T, Arinuma Y, Yanagida T, Yamamoto K, Hirohata S. Anti-ribosomal P protein antibody in human systemic lupus erythematosus up-regulates the expression of proinflammatory cytokines by human peripheral blood monocytes. *Arthritis Rheum* (2005) 52:847–55. doi:10.1002/art.20869
95. Longhi MS, Ma Y, Grant CR, Samyn M, Gordon P, Mieli-Vergani G, et al. T-regs in autoimmune hepatitis-systemic lupus erythematosus/mixed connective tissue disease overlap syndrome are functionally defective and display a Th1 cytokine profile. *J Autoimmun* (2013) 41:146–51. doi:10.1016/j.jaut.2012.12.003
96. Yoshida T, Ogata H, Kamio M, Joo A, Shiraishi H, Tokunaga Y, et al. SOCS1 is a suppressor of liver fibrosis and hepatitis-induced carcinogenesis. *J Exp Med* (2004) 199(12):1701–7. doi:10.1084/jem.20031675
97. Nielepkowicz-Goździńska A, Fendler W, Robak E, Kulczycka-Siennicka L, Górski P, Pietras T, et al. The role of CXC chemokines in pulmonary fibrosis of systemic lupus erythematosus patients. *Arch Immunol Ther Exp (Warsz)* (2015) 63(6):465–73. doi:10.1007/s00005-015-0356-8
98. Nielepkowicz-Goździńska A, Fendler W, Robak E, Kulczycka-Siennicka L, Górski P, Pietras T, et al. Exhaled cytokines in systemic lupus erythematosus with lung involvement. *Pol Arch Med Wewn* (2013) 123(4):141–8.
99. Shoda H, Yokoyama A, Nishino R, Nakashima T, Ishikawa N, Haruta Y, et al. Overproduction of collagen and diminished SOCS1 expression are causally linked in fibroblasts from idiopathic pulmonary fibrosis. *Biochem Biophys Res Commun* (2007) 353(4):1004–10. doi:10.1016/j.bbrc.2006.12.128
100. Nakashima T, Yokoyama A, Onari Y, Shoda H, Haruta Y, Hattori N, et al. Suppressor of cytokine signaling 1 inhibits pulmonary inflammation and fibrosis. *J Allergy Clin Immunol* (2008) 121(5):1269–76. doi:10.1016/j.jaci.2008.02.003
101. Flowers LO, Johnson HM, Mujtaba MG, Ellis MR, Haider SM, Subramaniam PS. Characterization of a peptide inhibitor of Janus kinase 2 that mimics suppressor of cytokine signaling 1 function. *J Immunol* (2004) 172(12):7510–8. doi:10.4049/jimmunol.172.12.7510
102. Mujtaba MG, Flowers LO, Patel CB, Patel RA, Haider MI, Johnson HM. Treatment of mice with the suppressor of cytokine signaling-1 mimetic peptide, tyrosine kinase inhibitor peptide, prevents development of the acute

form of experimental allergic encephalomyelitis and induces stable remission in the chronic relapsing/remitting form. *J Immunol* (2005) 175(8):5077–86.

Conflict of Interest Statement: The authors declare that the research was conducted in the absence of any commercial or financial relationships that could be construed as a potential conflict of interest.

frontiers in Immunology

ORIGINAL RESEARCH
published: 06 September 2017
doi: 10.3389/fimmu.2017.01093

Targeted Delivery of Neutralizing Anti-C5 Antibody to Renal Endothelium Prevents Complement-Dependent Tissue Damage

*Paolo Durigutto[1], Daniele Sblattero[1], Stefania Biffi[2], Luca De Maso[1], Chiara Garrovo[2], Gabriele Baj[1], Federico Colombo[1], Fabio Fischetti[3], Antonio F. Di Naro[4], Francesco Tedesco[5] and Paolo Macor[1]**

[1] Department of Life Sciences, University of Trieste, Trieste, Italy, [2] Institute for Maternal and Child Health-IRCCS "Burlo Garofolo", Trieste, Italy, [3] Dipartimento Universitario Clinico di Scienze Mediche, Chirurgiche e della Salute, University of Trieste, Trieste, Italy, [4] ADIENNE Pharma & Biotech, Lugano, Switzerland, [5] IRCCS Istituto Auxologico Italiano, Milan, Italy

OPEN ACCESS

Edited by:
Massimo Triggiani, University of Salerno, Italy

Reviewed by:
Paul Proost, KU Leuven, Belgium
Diana Boraschi, Consiglio Nazionale Delle Ricerche (CNR), Italy
Vincenzo Montinaro, Azienda Ospedaliero Universitaria Consorziale Policlinico di Bari, Italy

***Correspondence:**
Paolo Macor
pmacor@units.it

Specialty section:
This article was submitted to Cytokines and Soluble Mediators in Immunity, a section of the journal Frontiers in Immunology

Received: *26 May 2017*
Accepted: *22 August 2017*
Published: *06 September 2017*

Citation:
Durigutto P, Sblattero D, Biffi S, De Maso L, Garrovo C, Baj G, Colombo F, Fischetti F, Di Naro AF, Tedesco F and Macor P (2017) Targeted Delivery of Neutralizing Anti-C5 Antibody to Renal Endothelium Prevents Complement-Dependent Tissue Damage. Front. Immunol. 8:1093. doi: 10.3389/fimmu.2017.01093

Complement activation is largely implicated in the pathogenesis of several clinical conditions and its therapeutic neutralization has proven effective in preventing tissue and organ damage. A problem that still needs to be solved in the therapeutic control of complement-mediated diseases is how to avoid side effects associated with chronic neutralization of the complement system, in particular, the increased risk of infections. We addressed this issue developing a strategy based on the preferential delivery of a C5 complement inhibitor to the organ involved in the pathologic process. To this end, we generated Ergidina, a neutralizing recombinant anti-C5 human antibody coupled with a cyclic-RGD peptide, with a distinctive homing property for ischemic endothelial cells and effective in controlling tissue damage in a rat model of renal ischemia/reperfusion injury (IRI). As a result of its preferential localization on renal endothelium, the molecule induced complete inhibition of complement activation at tissue level, and local protection from complement-mediated tissue damage without affecting circulating C5. The *ex vivo* binding of Ergidina to surgically removed kidney exposed to cold ischemia supports its therapeutic use to prevent posttransplant IRI leading to delay of graft function. Moreover, the finding that the *ex vivo* binding of Ergidina was not restricted to the kidney, but was also seen on ischemic heart, suggests that this RGD-targeted anti-C5 antibody may represent a useful tool to treat organs prior to transplantation. Based on this evidence, we propose preliminary data showing that Ergidina is a novel targeted drug to prevent complement activation on the endothelium of ischemic kidney.

Keywords: complement system, ischemia/reperfusion injury, targeted antibody-based therapy, *ex vivo* model, *in vivo* model

INTRODUCTION

The complement (C) system is an important humoral effector of innate immunity and is widely distributed in the circulation and at extravascular sites where it often provides the first line of defense against invading pathogens (1). C also plays a crucial role in maintaining homeostasis by contributing to clear apoptotic and necrotic cells, to remove immune complexes and to modulate

adaptive immune responses (2). These functions are usually fulfilled by biologically active products released as a result of C activation that act promoting opsonization, inflammation, and direct cell cytotoxicity. The effector molecules or complexes, however, are not selective for the targets to neutralize, whether foreign or altered self, and may easily diffuse out into surrounding tissues and attack bystander cells. Under normal circumstances, undesired effects of the C system are prevented by soluble and cell-bound regulators that inhibit its activation at various steps of the C sequence (1). Unrestrictive C activation is the result of either over-activation due to excessive amount of triggering factors or the consequence of defective or dysregulation of C regulatory proteins. Several pathological conditions, including autoimmune diseases and more generally inflammatory disorders, are associated with C activation leading to the release of biologically active products, which can cause extensive tissue destruction.

Different therapeutic strategies have been developed to prevent C-mediated cell and tissue damage using neutralizing antibodies or peptides. The only approved therapeutic molecules are the plasma-derived C1 inhibitor, indicated for the treatment of hereditary angioedema (3), and the C5-blocking antibody eculizumab (Soliris), currently used to treat patients with paroxysmal nocturnal hemoglobinuria (PNH) (4) and atypical hemolytic uremic syndrome (aHUS) (5). Other soluble inhibitors under development are Mubodina, a neutralizing miniantibody against C5 (6), compstatin and its analogs, peptides preventing C3 activation through the alternative pathway (7), mirococept, CR1 CCP1–3 fused with a membrane-targeting amphiphilic peptide (8) and others (see reviews by Ricklin and Lambris) (9, 10).

A problem that has not yet been solved in the control of C-mediated diseases is how to reduce and possibly avoid the side effects, which may be associated with chronic neutralization of the C system (11), in particular, the increased risk of common and opportunistic infections. Moreover, the high cost of long-term treatment of patients with these drugs to prevent C activation represents a major limitation to their clinical use.

We sought to solve these problems developing an alternative therapeutic approach consisting in the preferential delivery of the C inhibitor to the organ involved in the pathologic process. The kidney was selected as a target organ to protect from C-mediated damage given the broad range of renal diseases caused by C dysregulation, including antibody-mediated glomerulopathies, thrombotic microangiopathies, progressive kidney diseases, and ischemia/reperfusion injury (IRI) (12). To this purpose, we generated a recombinant protein (Ergidina®) obtained by fusing a cyclic-RGD peptide to a neutralizing antibody to C5 (Mubodina®) and tested its protective effect in a rat model of renal IRI. C activated through any one of the three pathways by danger-associated molecular patterns, neo-antigens, and immune complexes (13) is actively involved in IRI, inducing C-mediated cell lysis and tubule-interstitial injury (14), and C3a and C5a-dependent inflammatory response (15).

We now present data showing that Ergidina has a distinctive homing property for renal endothelial cells and is effective in controlling tissue damage caused by renal IRI.

MATERIALS AND METHODS

Production of Recombinant Proteins

Anti C5 scFv antibody (6) was cloned, using BssH2 and NheI restriction sites, into pMB-SV5 vector (16) containing human IgG1 Fc region to produce the scFv-Fc molecule called Mubodina (ADIENNE Pharma & Biotech). Ergidina was generated by replacing SV5 tag with the peptide RGD-4C (17). To this end, Mubodina was amplified with the following oligos pMBsense CTGCTTACTGGCTTATCG and pMB-RGD-anti GGTTTAAGCTTTTAGCCGCAGAAACAATCTCCTCGG CAGTCGCAGGCGCCTTTACCCGGGGACAGGGAGAG. The first oligo anneals on the vector pMB at the 5′ while the second anneals at the end of human CH3 region and introduce the RGD-4C sequence and the Hind III restriction site sequence. After PCR amplification, the fragments were cut with XbaI an Hind III restriction sites and cloned into pMB-SV5 vector. Finally, both Moubodina and Ergidina were subcloned into pUCOE (18) vector. All clones obtained were confirmed by sequencing.

Purified plasmid DNA was transfected with freestyle max reagent (Invitrogen) in CHO-S cells according to a standard protocol and the cells were grown in Pro-CHO 5 (Lonza). The recombinant scFv-Fcs were purified from cell-conditioned medium loaded on Protein A column and eluted with citric acid 0.1M pH 3. Fractions containing the recombinant proteins were selected by ELISA (6) and checked for purity by SDS-PAGE (19).

Hemolytic Assay

The hemolytic activity of the classical pathway of the C system was evaluated incubating human serum with sensitized sheep red blood cells in the presence of different amount of purified recombinant antibodies, as previously described (6).

Animals

Male Wistar rats weighing 240–270 g were obtained from a colony kept in the animal house at the University of Trieste. Male BALB/c mice weighing 20–24 g were purchased from Charles River Italy and maintained in our university facilities. The *in vivo* experiments were performed in compliance with the guidelines of the European (86/609/EEC) and Italian (D.L.116/92) laws, were approved by the Italian Ministry of Health and the Administration of the University Animal House, in line with NIH Guide for the care and use of laboratory animal, in order to minimize the number of animals used and their suffering.

Evaluation of Ergidina® Distribution using Time-Domain Near-Infrared Optical Imaging

Ergidina was labeled with N-hydroxysuccinimmide ester of the cyanine 5.5 (Cy5.5. Amersham Biosciences: Fluorolink Cy5.5 Monofunctional Dye 5-pack) following a previously reported procedure (19).

BALB/c mice received 0.05 mg of Ergidina labeled with 1 nmol of Cy5.5 in the tail vein. A small-animal time-domain Optix MX preclinical NIR-imager (Advanced Research Technologies)

equipped with a pulsed laser diode and a time-correlated single photon counting detector was used in this study for the *in vivo* and *ex vivo* evaluation of labeled Ergidina distribution, as previously detailed (20).

Binding of Ergidina to Ischemic Rat Kidney

Wistar rats were first anesthetized with sodium thiobarbital (Inactin, Sigma, 80 mg/kg) and then received i.v. 100–150 IU/kg of heparin (Ratiopharm, Germany).

The kidneys were excised and stored in ice for 24 or 48 h after perfusion with 5 ml of Celsior through a PE20 polyethylene catheter (Intramedic Clay-Adams, Sparks, MD, USA) inserted into the renal artery to remove blood.

Afterward, two groups of 18 kidneys each were infused with 1 ml of iso-osmotic physiologic sterile solution containing either 0.5 or 1 mg of Cy5.5-labeled Ergidina and stored at 4, 10, and 25°C for either 15 or 30 min. Three kidneys for each experimental condition were used and analyzed by time-domain optical imaging before and after washing with 20 ml of Celsior in order to quantify the amount of the initially injected and the remaining bound Ergidina after washing.

The kidneys were snap frozen in liquid nitrogen and kept at −80°C. Seven micrometer sections were also examined by confocal microscopy to confirm the data obtain using optical imaging.

Confocal Microscopy

Seven micrometer sections were also analyzed by confocal microscopy to confirm data obtained using optical imaging. Sections were examined using a Nikon C1-SI confocal microscope (TE-2000U) equipped with a 20× and 60× oil immersion lens. Light was delivered to the sample with an 80/20 reflector. The system was operated with a pinhole size of one airy disk (30 nm). Electronic zoom was kept at minimum values for measurements to reduce potential bleaching, collecting series of optical images at 2 μm *z* resolution step size. The unstained tissue was visualized using the 488 nm light line of the Argon laser and a 515 dichroic mirror with a 30 nm band emission filter was used. The Cy5.5 was exited using the 640 nm light coming from a diode laser and the fluorescence collected using a 650 long pass mirror. All images were acquired in the linear intensity window and with no visible saturation points. Representative images are *z*-projection performed using standard deviation algorithm in ImageJ software (NIH).

Model of Ischemia/Reperfusion in Rat

Two groups of six male Wistar rats were anesthetized with sodium thiobarbital (Inactin; 80 mg/kg) (Sigma) and underwent unilateral right nephrectomy following Pavone and Boonstra surgical procedure (21). After kidney excision, the animals were allowed to rest for 24 h, and then housed in metabolic cages for 24 h to collect urine 1 and 4 days after operation. Blood samples were drawn and analyzed to check glucose, blood cells, kidney, and liver functional parameters. Blood pressure was daily monitored using a tail sphygmomanometric device (22).

Two weeks after unilateral nephrectomy, all the rats underwent a second surgical intervention consisting in the exposition of left kidneys through a small flank incision and in the occlusion of both left renal artery and vein with a non-traumatic clamp for 45 min. At the end of the ischemic period, the clamp was released and the organ reperfused.

Before inducing ischemia, a PE20 polyethylen catheter (Intramedic Clay-Adams, Sparks, MD, USA) was inserted into the right femoral artery, gently pushed toward the iliac artery and abdominal aorta, and the tip of the catheter was finally placed at the origin of the left renal artery. Two groups of eight rats received 1 ml of Celsior containing 250 μg of either Ergidina or an unrelated miniantibody infused into the renal artery in a 5 min time.

Following IR procedure, the rats were housed in metabolic cages to collect daily excreted urine 1 and 4 days after operation, and blood samples were also obtained. The animals were sacrificed 4 days after surgery, and the kidneys were removed, embedded in OCT compound (Miles, Milan, Italy), snap frozen in liquid nitrogen, and kept at −80°C until used for immunofluorescence and histologic analysis.

Urinary proteins were analyzed using Bradfor solution (Sigma) and the serum creatinine level was quantified by Integrated System Dx 880 (Beckman Coulter).

Immunofluorescence Analysis

Ergidina binding to kidney or heart samples was evaluated using frozen sections (7 μm) that had been incubated with the antibody (10 μg/ml) for 60 min at room temperature followed by FITC-labeled goat anti-human IgG (Aczon, Monte SanPietro, Bologna, Italy).

Tissue deposition of C3 was assessed by incubating frozen kidney 7 μm sections with 1:200 goat IgG anti-rat C3 (Cappel, ICN Biomedicals, Milan, Italy) for 60 min at room temperature followed by FITC-labeled rabbit anti-goat IgG at a 1:200 dilution (DAKO, Glostrup, Denmark) for additional 60 min at room temperature. A similar approach was used to evaluate the presence of C9, using rabbit IgG anti-rat C9 (a kind gift from Prof. P. Morgan, Cardiff, UK) at a 1:1,000 dilution, followed by FITC-labeled swine anti-rabbit IgG (DAKO) at a 1:40 dilution.

The fluorescence intensity was evaluated in 10 different randomly selected areas (0.07 mm^2 each) of renal tissue. ImageJ image analysis software (National Institutes of Health) was used.

Histomorphologic Evaluation

The excised kidneys were preserved in phosphate-buffered 10% formalin, embedded in paraffin wax, cut into thin sections (7 μm), and stained with hematoxylin and eosin.

Histopathological changes were analyzed for tubular necrosis, proteinaceous casts, and medullary congestion, as previously described (23). Tubular necrosis and extension of proteinaceous casts were both graded as follows: no damage (0), mild (+1, unicellular, patchy isolated damage), moderate (+2, damage less than 25%), severe (+3, damage between 25 and 50%), and very severe (+4, more than 50% damage). The degree of medullary congestion was defined as follows: no congestion (0), mild (+1, vascular congestion with identification of erythrocytes by

+400 magnification), moderate (+2, vascular congestion with identification of erythrocytes by +200 magnification), severe (+3, vascular congestion with identification of erythrocytes by +100 magnification), and very severe (+4, vascular congestion with identification of erythrocytes by +40 magnification).

The tissue sections were analyzed in a blind fashion by two experienced observers.

Statistical Analysis

The results were expressed as mean ± SD. Data were compared by ANOVA using *post hoc* analysis for paired multiple comparisons with Fisher's corrected *t*-test. A non-parametric Mann–Whitney test was used to determine the significance of differences between tissue damage scores in the tested groups.

RESULTS

Production and *In Vitro* Characterization of Ergidina

We designed and cloned a novel recombinant antibody called Ergidina containing the neutralizing scFv to C5 (6, 24, 25) fused at the C terminal end to the Fc domains of human IgG1 (Hinge-CH2-CH3) to form Mubodina and the cyclic RGD-4C peptide (ACDCRGDCFCG) shown to bind avidly to the integrins αvβ3 and αvβ5 (26). A schematic picture of the two recombinant molecules, Mubodina and Ergidina, and the cyclic peptide RGD-4C used to generate Ergidina is presented in **Figure 1A**.

Analysis of Mubodina and Ergidina by SDS-PAGE and western blot revealed a major band of the expected size of 115–120 kDa, corresponding to the scFv-Fc dimers. Low amounts of monomers and degradation products were detected in all preparations of both Mubodina and Ergidina (Figure S1A in Supplementary Material). Moreover, Ergidina, examined by HPLC using SEC300 size exclusion column (Yarra), was eluted as a single peak corresponding to a protein of about 120 kDa (Figure S1B in Supplementary Material). Immunoenzymatic analysis showed that both miniantibodies were able to bind human C5, but failed to interact with human C3 (Figure S1C in Supplementary Material). We also tested the ability of Ergidina to neutralize C5 and to prevent C activation using a standard hemolytic assay. As shown in **Figure 1B**, Ergidina was found to be as efficient as the parent molecule Mubodina in inhibiting serum C hemolytic activity at similar concentration.

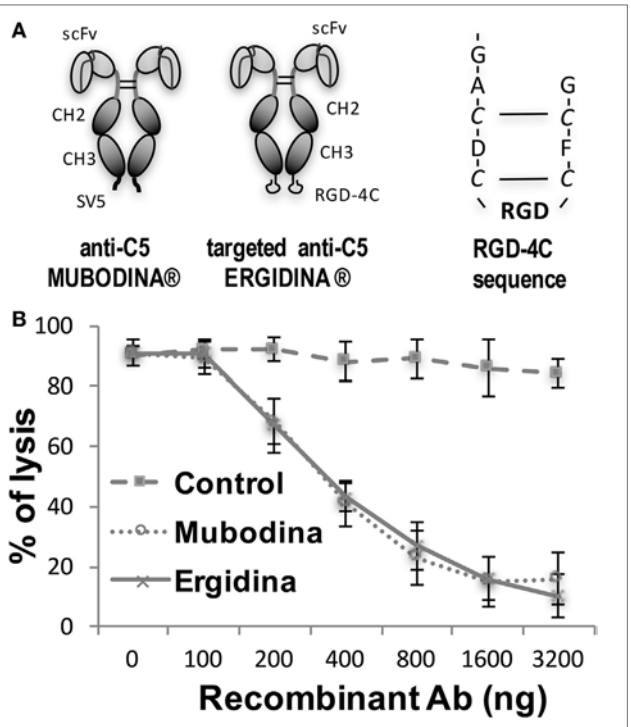

FIGURE 1 | Structure and function of recombinant anti-C5 antibodies. **(A)** Schematic representation of Mubodina, Ergidina, and the peptide RGD-4C. **(B)** Inhibition of hemolytic activity by Mubodina and Ergidina. Increasing amounts of recombinant antibodies were mixed with normal human serum (1 µl) and incubated for 15 min at room temperature prior to addition to 50 µl of sensitized sheep erythrocytes. The serum hemolytic activity is presented as mean ± SD of percent values obtained in three different experiments.

In Vivo Distribution of Ergidina

The distribution of the targeted anti-C5 recombinant antibody was first examined in healthy mice. The antibody (0.05 mg) labeled with 1 nmol Cy5.5 was injected intravenously (i.v.) into the tail vein, and its localization was examined by time domain optical imaging. Ergidina was diffusely distributed throughout the mouse body soon after i.v. administration followed, 6 h later, by a preferential accumulation in the kidney peaking at 24 h (**Figure 2A**). As already observed with the distribution pattern of other Cy5.5-labeled antibodies (19, 27), a proportion of the molecule was removed by the liver and the free dye was excreted through the kidney, thus explaining the visualization of fluorescent signals in the liver and bladder (**Figures 2A,B**). These data were confirmed by *ex vivo* analysis of the different organs performed 6 and 48 h after injection of the labeled molecule (**Figure 2C**). The pharmacokinetic profile of Ergidina was supported by confocal microscopy analysis of sections of different organs removed 6 h after antibody challenging that revealed specific near infrared fluorescent staining in the kidney and liver. The green fluorescence observed in both these organs was due to autofluorescence observed also in the lung that was examined as a control organ (Figure S2 in Supplementary Material).

Ex Vivo Binding of Ergidina to Ischemic Kidney

To investigate the extent of Ergidina deposition in isolated perfused rat kidney under various experimental conditions, the organ was removed from healthy animals and either fixed immediately or kept in ice for 24 h to mimic ischemic conditions prior to fixation in formalin. Tissue sections were then analyzed for antibody deposits. As shown in **Figure 3A**, Ergidina bound weakly to the endothelium and more strongly to the tubules of normal kidneys. Conversely, glomerular and vessel endothelium of ischemic kidney were heavily decorated by RGD-targeted antibody under ischemic conditions with levels of fluorescence intensity of glomeruli approximately sevenfold higher than that observed in control kidney (**Figure 3B**).

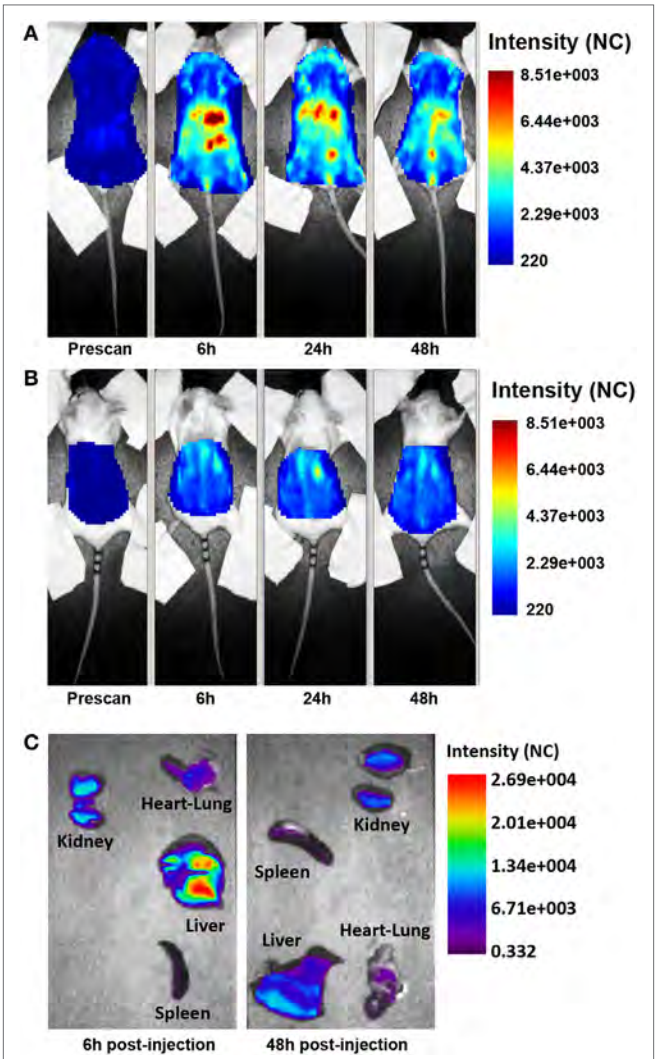

FIGURE 2 | Biodistribution of Cy5.5-labeled Ergidina. BALB/c mice received i.v. 50 µg of Cy5.5-labeled Ergidina and were analyzed by optical imaging. **(A)** Whole-body scans of a representative mouse in supine position; fluorescence intensity images were acquired at the indicated time post-injection and are displayed as normalized counts (NC). **(B)** The animal was placed in prone position, fluorescence emission in regions of interest encompassing the kidneys was acquired at indicated times postinjection and normalized. **(C)** *Ex vivo* imaging of organs collected 6 or 48 h after Ergidina-Cy5.5 administration.

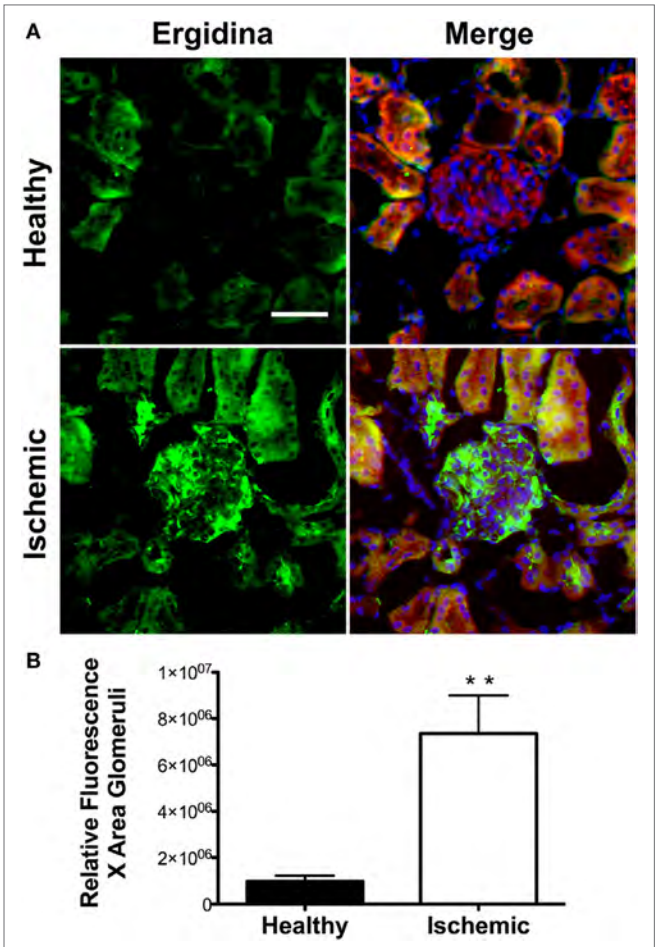

FIGURE 3 | Immunofluorescence analysis of Ergidina deposition on ischemic kidney. **(A)** Representative images from section obtained from healthy or ischemic kidneys incubated with Ergidina, followed by FITC-labeled anti-human IgG. Nuclei were counterstained with DAPI and tissue was visualized by orange autofluorescence. Original magnification: 200×. Scale bar: 100 µm. **(B)** ImageJ software was used to determine the fluorescence intensity/glomerular area of the images for each experimental group. Values are the mean ± SD. $^{**}P < 0.001$.

We then tested the capacity of Ergidina to decorate renal endothelium of kidneys kept under different ischemic conditions. To this end, 0.5 mg of Cy5.5-labeled Ergidina was injected into the renal artery of surgically removed kidneys that had been washed and stored at 4°C for 24 h in Celsius®. The fluorescence intensity was assessed before and after organ perfusion using time-domain optical imaging. As shown in supplemental Figure S3, approximately half of the antibody was still bound to the renal vessels after incubation for 15 min at 4°C followed by perfusion to wash out unbound antibodies. This percentage remained essentially unchanged when the incubation temperature was raised to 10 and 25°C (**Figure 4A**). The binding of RGD-targeted antibody to the vascular endothelium of kidney kept at 4°C for 24 h occurred in a short period of time reaching a plateau at 15 min (**Figure 4B**). The percentage of bound antibody was slightly increased when the cold ischemia time was prolonged from 24 to 48 h. However, the difference was not statistically significant (**Figure 4C**).

The amount of Ergidina bound to the kidney stored at 4°C for 24 h was related to the dose of administered antibody and increased from 0.26 to 0.48 mg using doses of 0.5 and 1 mg, respectively (**Figure 4D**). The analysis of frozen sections of these organs treated with 0.5 mg of cy5.5-labeled Ergidina by confocal microscopy showed that the antibody was widely distributed on all glomeruli and extraglomerular vessels and was undetectable on renal tubules (**Figure 5**).

To assess whether the binding of Ergidina to surgically removed organs was restricted to the kidney, we analyzed

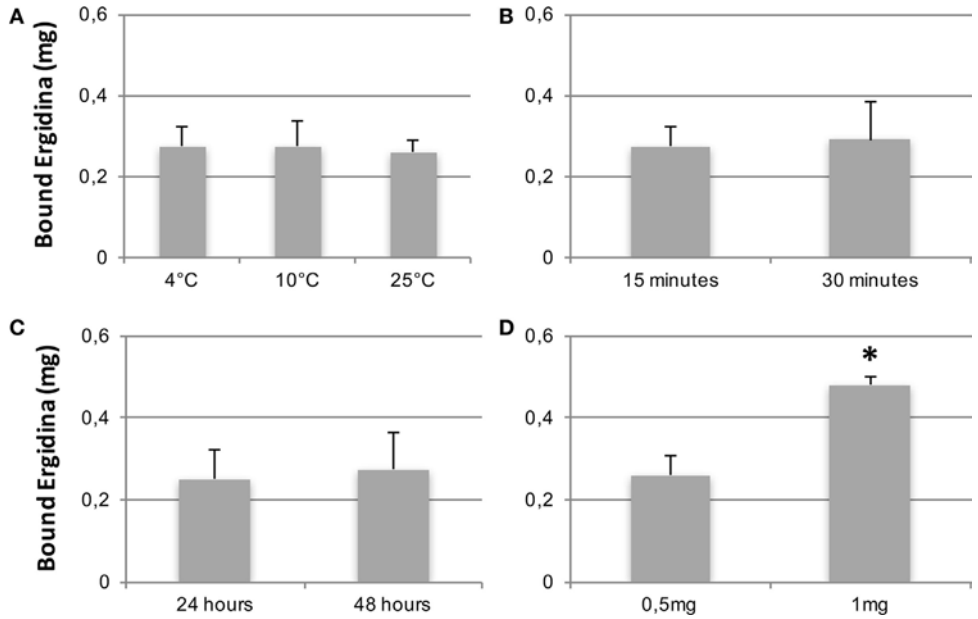

FIGURE 4 | CCharacterization of Ergidina binding to ischemic kidneys. Rat kidneys were excised, incannulated, and perfused as described in Section "Materials and Methods." Cy5.5-labeled Ergidina was injected through the renal artery. Each organ was visualized, washed, and analyzed again by time-domain optical imaging. Experimental conditions were maintained in all the groups except for the temperature of the binding **(A)**, the time of the binding **(B)**, the period of kidney ischemia **(C)**, or the amount of injected Ergidina **(D)**. Data are expressed as mean of the amount of bound antibody ± SD obtained from three organs per group. $^*P < 0.01$.

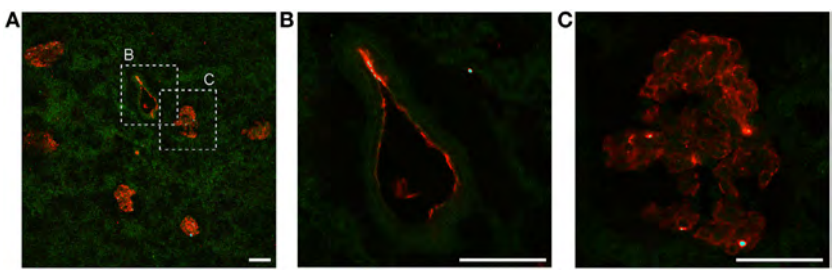

FIGURE 5 | Ergidina localization in ischemic rat kidney. **(A)** Representative images from section obtained from ischemic kidneys perfused with cy5.5-labeled Ergidina. Tissue was evidenced by green autofluorescence. Magnification 200×. Close up images at high magnification (600×) of a **(B)** vessel and **(C)** glomerular structure showing specific staining. Scale bar: 50 μm.

isolated perfused rat heart stored at 4°C for 24 h. Frozen sections of this organ were incubated with Cy5.5-labeled Ergidina and examined by confocal microscopy. Figure S4 in Supplementary Material shows that the endothelium of ischemic heart is covered by RGD-guided anti-C5 antibody.

Ergidina Prevents Tissue Damage in a Rat Model of Kidney Ischemia/Reperfusion

The finding that Ergidina preferentially accumulates in rat renal vessels *in vivo* suggested a potential use of the targeted antibody to prevent renal C-mediated damage. This hypothesis was tested in a rat model of kidney IRI described in Section "Materials and Methods."

Prior to the ischemic injury, the animals received 0.25 mg of Ergidina found in the *ex vivo* experiments to fully cover the renal endothelium. After 45 min of ischemia, the kidney was reperfused and samples of serum and urine were collected 24 and 96 h later for analysis. The data reported in **Figure 6** show clear signs of renal impairment in animals receiving the control antibody with marked increase in both protein excretion and serum creatinine level peaking 24 h after reperfusion. In contrast, Ergidina was able to completely prevent C-mediated damages, as revealed by the lack of significant changes in protein and creatinine concentrations that were comparable to those collected before IRI. The effect of Ergidina was still apparent 4 days after induction of ischemia despite the marked reduction in the protein and creatinine levels observed in the control group of rats.

We also investigated the ability of Ergidina to control C-mediated tissue damage in ischemic kidneys removed from rats treated with the C5 neutralizing and control antibodies. A strong C activation was observed in the ischemic rat model

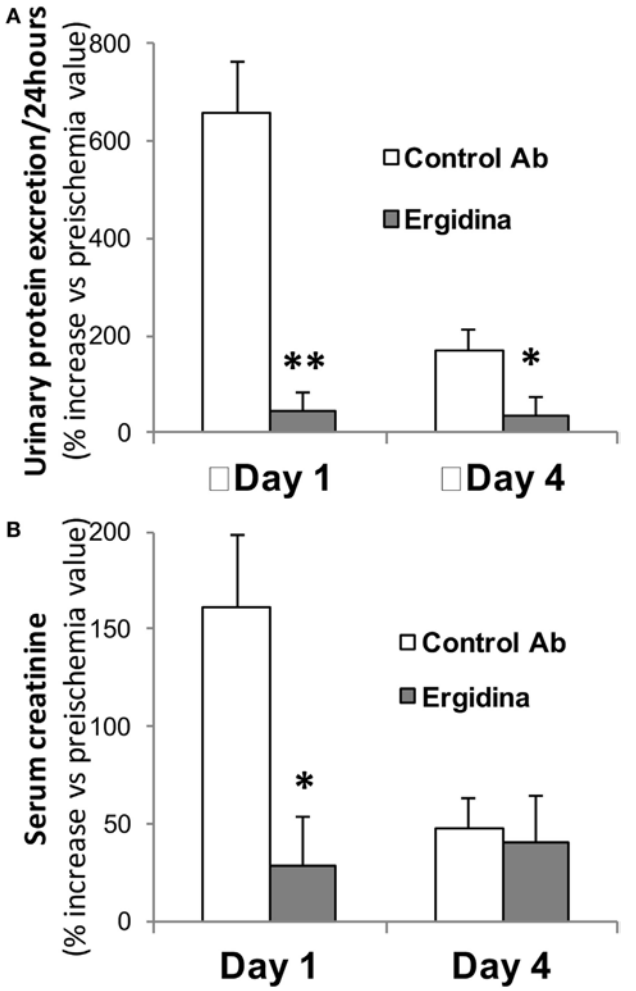

FIGURE 6 | Effect of Ergidina in an ischemia/reperfusion injury model in rat kidney. Two groups of four rats received Ergidina or control Ab before inducing renal ischemia, as described in Section "Materials and Methods." One or four days later, the animals were examined for **(A)** urinary protein excretion and **(B)** serum creatinine. Data are expressed as mean of the % increase vs preischemia value ± SD. *$P < 0.01$; **$P < 0.001$.

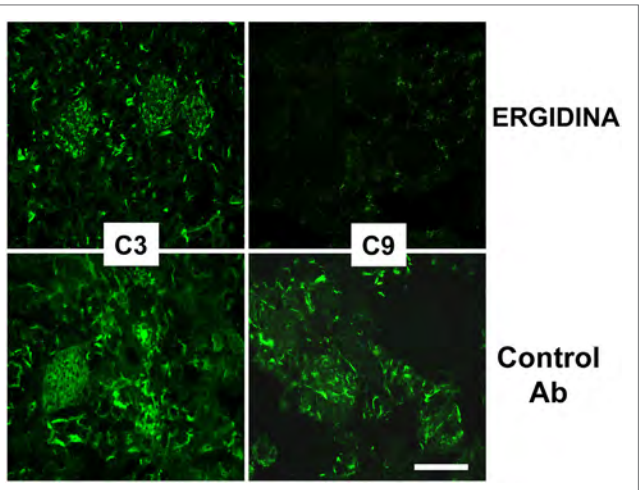

FIGURE 7 | Immunofluorescence analysis of C deposition in kidney ischemia/reperfusion injury model. Deposition of C3 and C9 was analyzed in cryosections of organs obtained from rat treated with Ergidina or control antibody using specific goat polyclonal antibodies and FITC-labeled secondary antibody. Scale bar: 50 μm.

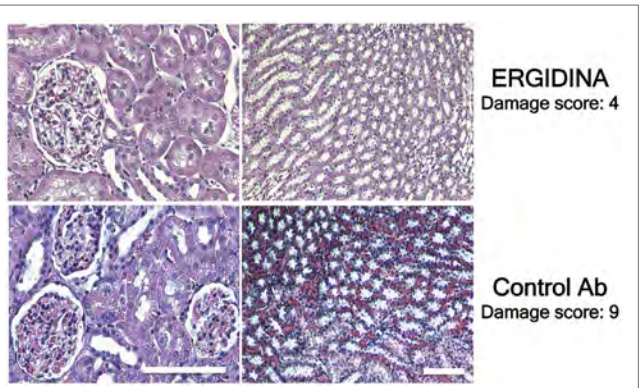

FIGURE 8 | Histological analysis of treated ischemic kidneys. Photomicrographs of kidney sections obtained from a representative rat treated with Ergidina or control Ab and sacrified 4 days after ischemia/reperfusion injury. Note the extensive necrosis of tubular cells, some glomerular hypercellularity and mesangial hyperplasia in control Ab samples that were absent in Ergidina treated animals. Scale bar: 50 μm. A tissue damage score was determined as described in Section "Materials and Methods." Values are the mean of four rats per group.

that proceeds to completion of the reaction sequence as documented by C3 and C9 deposition in the kidneys of rats receiving an irrelevant antibody. As expected, administration of Ergidina to rats undergoing renal IRI did not prevent C3 deposition but resulted in the complete inhibition of C5 activation and an undetectable localization of C9 on glomeruli and vascular endothelium (**Figure 7**).

Histologic analysis of ischemic kidney of rats treated with the control antibody revealed extensive necrosis of tubular cells, and some degree of glomerular hypercellularity and mesangial hyperplasia (**Figure 8**). Injection of Ergidina proved to be effective in preventing tissue injury both at glomerular and tubular level, reducing the damage score to more than half compared to that observed in the control group of rats.

The dose of Ergidina used in this study was sufficient to fully inhibit C5 activation at renal level preventing tissue injury and increase in serum creatinine and urine protein levels, and was not associated with any overt sign of toxicity.

DISCUSSION

Efforts are being made to develop drugs that preferentially localize in organs and tissues undergoing a pathologic process mediated by effector molecules present in the circulation and in the body fluids. C has been largely implicated in several pathologic conditions and C neutralization has been shown to exert beneficial effect in preventing tissue and organs damage in both experimental and clinical settings (1, 2). For example, targeting

C5 with the neutralizing antibody Eculizumab in humans has proved effective in controlling disease severity and progression in patients with PNH (4), aHUS (5), membranoproliferative glomerulonephritis (28), and antiphospholipid syndrome (29). Nevertheless, this therapeutic approach, though successful, is fraught with limitations due to the high cost and the possible side effects associated with generalized inactivation of the C system (30, 31). Our data indicate that this therapeutic strategy can be improved by developing a recombinant antibody that accumulates predominantly in the pathologic tissue.

To target endothelial cells with a neutralizing anti-C5 antibody, we used a recombinant human anti-C5 miniantibody recognizing C5 from human and other animal species (6) fused to the RGD-4C peptide at the Fc terminus. RGD-4C was selected for the study because this cyclic peptide offers several advantages over the linear peptide including increased structural stability, reduced susceptibility to degradation, and higher affinity for the target molecules (32).

Cyclic RGD has extensively been used in tumor-bearing mice to deliver imaging probes or drugs to tumor tissue for diagnostic and therapeutic purposes exploiting the ability of the peptide to recognize with high affinity αvβ3 integrin highly expressed in tumor vessels (33). The *in vivo* distribution of Ergidina observed in rats after i.v. administration suggests that RGD-4C can be used as a vehicle to deliver the neutralizing anti-C5 miniantibody to the kidney. The renal localization of Ergidina cannot be attributed to the clearance of the molecule, because its molecular weight of approximately 120 kDa is well above the size limit of the molecules filtering through the glomeruli under physiologic conditions. The weak fluorescent signal observed in the bladder is due to small amount of free fluorescent dye excreted in the urine (20, 27). A plausible explanation for the preferential homing of the neutralizing anti-C5 antibody to the kidney is that the recombinant molecule interacts with integrins expressing RGD-binding sites. Although αvβ3 and αvβ5 that bind RGD-4C peptide with high affinity are not expressed on quiescent endothelial cells, the mild staining of the vascular endothelium in normal kidney can possibly be justified by the presence of other integrins that bind less avidly RGD-4C, including α5β1 expressed on the endothelial cells of normal glomeruli (34, 35). The stronger immunofluorescence signal observed in the glomeruli of kidneys obtained from rats following IRI compared to untreated controls is consistent with the known ability of activated endothelial cells to express αvβ3 (35). This is also supported by the finding that RGD binding sites colocalize with αvβ3 on the intimal surface of vessels in ischemic kidneys (36).

The preliminary data collected in rat ischemic organs evidenced the capacity of this targeting approach to address activated endothelial cells of the kidney, but also on the heart and probably other organs; our attention was focused on kidneys and in particular in the prevention of tissue damages after IR.

Our failure to detect proteinuria, increased level of creatinine, and renal histologic alterations in rats undergoing IR treated with Ergidina is in line with the results of previous studies showing C involvement in the renal IRI (37–39). Evidence collected from various groups indicates that C is primarily activated through the lectin pathway in kidneys undergoing IR, as revealed by the early deposition of mannose-binding lectin (MBL) and prevention of tissue damage in MBL-deficient animals (40–42). More recently, Farrar and colleagues showed that the lectin pathway may also be triggered in ischemic kidney a few hours after reperfusion by collectin-11 found to colocalize with C3d to renal tubules (43). There has been some controversy about the contribution of the late C components to IRI through the action of C5a and/or the terminal C complex. C5b-9 was considered to play a predominant role in a mouse model of renal IRI based on the observation that C6-deficient mice were protected from tissue damage (39). Conversely, C5 inhibition failed to prevent IRI in Lewis rats raising the possibility that the involvement of the late C components in mediating renal IR may vary in different species (42). Our finding that C5 neutralization by Ergidina correlates with the prevention of renal IRI in Wistar rats does not support this hypothesis in agreement with recent data showing that antibody-mediated C5 inhibition markedly reduces tissue damage after reperfusion and prolongs graft survival in a syngeneic rat model of kidney transplantation (44).

The development of Ergidina falls within our tissue targeting approach to control C-mediated tissue damage. This strategy started with the generation of the recombinant molecule MT07 containing the C5 neutralizing antibody fused to a synovial-homing peptide that was effective at preventing joint inflammation (45). Similar to MT07, Ergidina has definite advantages over the non-targeting parent anti-C5 miniantibody that inhibits activation of circulating C5 (6). As a result of its delivery to renal endothelium, the drug guarantees local protection from the C-mediated tissue damage without affecting circulating C5 and consequently reducing the risk of infections associated with C5 depletion. This will be particularly important when treating patients with C-dependent chronic renal diseases, such as MPNG and aHUS (29), who require long-term therapy. In this case, treatment with the targeted recombinant molecule would be cost effective, since a limited amount of Ergidina (0.25 mg) corresponding to one-fourth of the dose required to partially inhibit circulating C5 (45) was sufficient to completely block the activation of C5 in the rat ischemic kidneys. The enhanced *ex vivo* binding to surgically removed kidney exposed to cold ischemia for 24 h followed by perfusion with the recombinant molecule supports its first therapeutic use to prevent posttransplant IRI, leading to delay of graft function. The contribution of C to this pathologic condition is suggested by the beneficial effect obtained perfusing the kidney with other C inhibitors including the membrane-binding C regulator APT070 (46) and, more recently, an anti-rat C5 (44) prior to transplantation. The finding that the *ex vivo* binding of Ergidina was not restricted to the kidney, but was also seen on ischemic heart, suggests that this membrane-binding anti-C5 antibody may represent a useful tool to treat surgically removed organs prior to transplantation to prevent posttransplant IRI.

In conclusion, we present a preliminary characterization of a recombinant molecule comprising a neutralizing anti-C5 antibody fused to RGD that preferentially binds *in vivo* and *ex vivo* to the ischemic vascular endothelium of surgically removed organs.

This membrane-binding molecule prevents C5 activation on the cell surface and kidney injury caused by IRI.

ETHICS STATEMENT

The *in vivo* experiments were performed in compliance with the guidelines of the European (86/609/EEC) and Italian (D.L.116/92) laws, were approved by the Italian Ministry of Health and the Administration of the University Animal House, in line with NIH Guide for the care and use of laboratory animal.

AUTHOR CONTRIBUTIONS

PD: performed *in vivo* experiment, composed pictures, and wrote the manuscript. DS: designed and produced vectors for protein production. SB: designed biodistribution study and analyzed data. LM: produced and characterized recombinant proteins. CG: performed biodistribution studies. GB: analyzed tissues using confocal microscopy. FC: characterized RGD interaction with the different tissues. FF: designed and analyzed functional studies. AN: designed the study and analyzed these data of the Ergidina/ischemic tissue interaction. FT and PM: designed the project, analyzed these data, and wrote the manuscript.

ACKNOWLEDGMENTS

This paper is dedicated to the memory of our colleague, Dr. Federica Ziller, whose valuable professional activity was also helpful in this study.

FUNDING

This project was supported by the contribution of Kathleen Fondazione Foreman-Casali (Trieste) and by the contribution of ADIENNE Pharma and Biotech.

SUPPLEMENTARY MATERIAL

The Supplementary Material for this article can be found online at http://journal.frontiersin.org/article/10.3389/fimmu.2017.01093/full#supplementary-material.

REFERENCES

1. Walport MJ. Complement. First of two parts. *N Engl J Med* (2001) 344(14):1058–66. doi:10.1056/NEJM200104053441406
2. Ricklin D, Hajishengallis G, Yang K, Lambris JD. Complement: a key system for immune surveillance and homeostasis. *Nat Immunol* (2010) 11(9):785–97. doi:10.1038/ni.1923
3. Longhurst H, Cicardi M. Hereditary angio-oedema. *Lancet* (2012) 379(9814):474–81. doi:10.1016/S0140-6736(11)60935-5
4. Hillmen P, Young NS, Schubert J, Brodsky RA, Socie G, Muus P, et al. The complement inhibitor eculizumab in paroxysmal nocturnal hemoglobinuria. *N Engl J Med* (2006) 355(12):1233–43. doi:10.1056/NEJMoa061648
5. Zuber J, Fakhouri F, Roumenina LT, Loirat C, Fremeaux-Bacchi V. Use of eculizumab for atypical haemolytic uraemic syndrome and C3 glomerulopathies. *Nat Rev Nephrol* (2012) 8(11):643–57. doi:10.1038/nrneph.2012.214
6. Marzari R, Sblattero D, Macor P, Fischetti F, Gennaro R, Marks JD, et al. The cleavage site of C5 from man and animals as a common target for neutralizing human monoclonal antibodies: in vitro and in vivo studies. *Eur J Immunol* (2002) 32(10):2773–82. doi:10.1002/1521-4141(2002010)32:10<2773::AID-IMMU2773>3.0.CO;2-G
7. Qu H, Ricklin D, Bai H, Chen H, Reis ES, Maciejewski M, et al. New analogs of the clinical complement inhibitor compstatin with subnanomolar affinity and enhanced pharmacokinetic properties. *Immunobiology* (2013) 218(4):496–505. doi:10.1016/j.imbio.2012.06.003
8. Souza DG, Esser D, Bradford R, Vieira AT, Teixeira MM. APT070 (mirococept), a membrane-localised complement inhibitor, inhibits inflammatory responses that follow intestinal ischaemia and reperfusion injury. *Br J Pharmacol* (2005) 145(8):1027–34. doi:10.1038/sj.bjp.0706286
9. Ricklin D, Lambris JD. Progress and trends in complement therapeutics. *Adv Exp Med Biol* (2013) 735:1–22. doi:10.1007/978-1-4614-4118-2_1
10. Ricklin D, Reis ES, Lambris JD. Complement in disease: a defence system turning offensive. *Nat Rev Nephrol* (2016) 12(7):383–401. doi:10.1038/nrneph.2016.70
11. Taylor PC, Feldmann M. Anti-TNF biologic agents: still the therapy of choice for rheumatoid arthritis. *Nat Rev Rheumatol* (2009) 5(10):578–82. doi:10.1038/nrrheum.2009.181
12. Noris M, Remuzzi G. Overview of complement activation and regulation. *Semin Nephrol* (2013) 33(6):479–92. doi:10.1016/j.semnephrol.2013.08.001
13. Danobeitia JS, Hanson MS, Chlebeck P, Park E, Sperger JM, Schwarznau A, et al. Donor pretreatment with IL-1 receptor antagonist attenuates inflammation and improves functional potency in islets from brain-dead nonhuman primates. *Cell Transplant* (2015) 24(9):1863–77. doi:10.3727/096368914X681045
14. Ponticelli C. Ischaemia-reperfusion injury: a major protagonist in kidney transplantation. *Nephrol Dial Transplant* (2014) 29(6):1134–40. doi:10.1093/ndt/gft488
15. Sacks SH. Complement fragments C3a and C5a: the salt and pepper of the immune response. *Eur J Immunol* (2010) 40(3):668–70. doi:10.1002/eji.201040355
16. Di Niro R, Ziller F, Florian F, Crovella S, Stebel M, Bestagno M, et al. Construction of miniantibodies for the in vivo study of human autoimmune diseases in animal models. *BMC Biotechnol* (2007) 7:46. doi:10.1186/1472-6750-7-46
17. Koivunen E, Wang B, Ruoslahti E. Phage libraries displaying cyclic peptides with different ring sizes: ligand specificities of the RGD-directed integrins. *Biotechnology (N Y)* (1995) 13(3):265–70.
18. Boscolo S, Mion F, Licciulli M, Macor P, De Maso L, Brce M, et al. Simple scale-up of recombinant antibody production using an UCOE containing vector. *N Biotechnol* (2012) 29(4):477–84. doi:10.1016/j.nbt.2011.12.005
19. Macor P, Secco E, Mezzaroba N, Zorzet S, Durigutto P, Gaiotto T, et al. Bispecific antibodies targeting tumor-associated antigens and neutralizing complement regulators increase the efficacy of antibody-based immunotherapy in mice. *Leukemia* (2015) 29(2):406–14. doi:10.1038/leu.2014.185
20. Capolla S, Garrovo C, Zorzet S, Lorenzon A, Rampazzo E, Spretz R, et al. Targeted tumor imaging of anti-CD20-polymeric nanoparticles developed for the diagnosis of B-cell malignancies. *Int J Nanomedicine* (2015) 10:4099–109. doi:10.2147/IJN.S78995
21. Pavone LV, Boonstra R. A technique for the surgical removal of a kidney from individuals of a feral population of small rodents. *Can J Zool* (1984) 62(11):2146–9. doi:10.1139/z84-311
22. Fabris B, Fischetti F, Carretta R, Narducci P, Piccinini C, Calci M, et al. Cardiac and nephroprotective effects of angiotensin converting enzyme inhibitor treatment in the renal ablation model. *J Hypertens Suppl* (1993) 11(5):S344–5. doi:10.1097/00004872-199312050-00151
23. Solez K, Kramer EC, Fox JA, Heptinstall RH. Medullary plasma flow and intravascular leukocyte accumulation in acute renal failure. *Kidney Int* (1974) 6(1):24–37. doi:10.1038/ki.1974.74
24. Durigutto P, Macor P, Ziller F, De Maso L, Fischetti F, Marzari R, et al. Prevention of arthritis by locally synthesized recombinant antibody neutralizing complement component C5. *PLoS One* (2013) 8(3):e58696. doi:10.1371/journal.pone.0058696
25. Fischetti F, Durigutto P, Macor P, Marzari R, Carretta R, Tedesco F. Selective therapeutic control of C5a and the terminal complement complex by anti-C5

single-chain Fv in an experimental model of antigen-induced arthritis in rats. *Arthritis Rheum* (2007) 56(4):1187–97. doi:10.1002/art.22492
26. Assa-Munt N, Jia X, Laakkonen P, Ruoslahti E. Solution structures and integrin binding activities of an RGD peptide with two isomers. *Biochemistry* (2001) 40(8):2373–8. doi:10.1021/bi002101f
27. Biffi S, Garrovo C, Macor P, Tripodo C, Zorzet S, Secco E, et al. In vivo biodistribution and lifetime analysis of cy5.5-conjugated rituximab in mice bearing lymphoid tumor xenograft using time-domain near-infrared optical imaging. *Mol Imaging* (2008) 7(6):272–82. doi:10.2310/7290.2008.00028
28. Smith RJ, Alexander J, Barlow PN, Botto M, Cassavant TL, Cook HT, et al. New approaches to the treatment of dense deposit disease. *J Am Soc Nephrol* (2007) 18(9):2447–56. doi:10.1681/ASN.2007030356
29. Meroni PL, Macor P, Durigutto P, De Maso L, Gerosa M, Ferraresso M, et al. Complement activation in antiphospholipid syndrome and its inhibition to prevent rethrombosis after arterial surgery. *Blood* (2016) 127(3):365–7. doi:10.1182/blood-2015-09-672139
30. Barnett AN, Asgari E, Chowdhury P, Sacks SH, Dorling A, Mamode N. The use of eculizumab in renal transplantation. *Clin Transplant* (2013) 27(3):E216–29. doi:10.1111/ctr.12102
31. Dmytrijuk A, Robie-Suh K, Cohen MH, Rieves D, Weiss K, Pazdur R. FDA report: eculizumab (Soliris) for the treatment of patients with paroxysmal nocturnal hemoglobinuria. *Oncologist* (2008) 13(9):993–1000. doi:10.1634/theoncologist.2008-0086
32. Noiri E, Romanov V, Forest T, Gailit J, DiBona GF, Miller F, et al. Pathophysiology of renal tubular obstruction: therapeutic role of synthetic RGD peptides in acute renal failure. *Kidney Int* (1995) 48(5):1375–85. doi:10.1038/ki.1995.426
33. Ruoslahti E. Antiangiogenics meet nanotechnology. *Cancer Cell* (2002) 2(2):97–8. doi:10.1016/S1535-6108(02)00100-9
34. Hafdi Z, Lesavre P, Nejjari M, Halbwachs-Mecarelli L, Droz D, Noel LH. Distribution of alphavbeta3, alphavbeta5 integrins and the integrin associated protein – IAP (CD47) in human glomerular diseases. *Cell Adhes Commun* (2000) 7(6):441–51. doi:10.3109/15419060009040302
35. Liu S. Radiolabeled cyclic RGD peptide bioconjugates as radiotracers targeting multiple integrins. *Bioconjug Chem* (2015) 26(8):1413–38. doi:10.1021/acs.bioconjchem.5b00327
36. Romanov V, Noiri E, Czerwinski G, Finsinger D, Kessler H, Goligorsky MS. Two novel probes reveal tubular and vascular Arg-Gly-Asp (RGD) binding sites in the ischemic rat kidney. *Kidney Int* (1997) 52(1):93–102. doi:10.1038/ki.1997.308
37. Gorsuch WB, Chrysanthou E, Schwaeble WJ, Stahl GL. The complement system in ischemia-reperfusion injuries. *Immunobiology* (2012) 217(11):1026–33. doi:10.1016/j.imbio.2012.07.024
38. Thurman JM, Ljubanovic D, Edelstein CL, Gilkeson GS, Holers VM. Lack of a functional alternative complement pathway ameliorates ischemic acute renal failure in mice. *J Immunol* (2003) 170(3):1517–23. doi:10.4049/jimmunol.170.3.1517
39. Zhou W, Farrar CA, Abe K, Pratt JR, Marsh JE, Wang Y, et al. Predominant role for C5b-9 in renal ischemia/reperfusion injury. *J Clin Invest* (2000) 105(10):1363–71. doi:10.1172/JCI8621
40. de Vries B, Walter SJ, Peutz-Kootstra CJ, Wolfs TG, van Heurn LW, Buurman WA. The mannose-binding lectin-pathway is involved in complement activation in the course of renal ischemia-reperfusion injury. *Am J Pathol* (2004) 165(5):1677–88. doi:10.1016/S0002-9440(10)63424-4
41. Moller-Kristensen M, Wang W, Ruseva M, Thiel S, Nielsen S, Takahashi K, et al. Mannan-binding lectin recognizes structures on ischaemic reperfused mouse kidneys and is implicated in tissue injury. *Scand J Immunol* (2005) 61(5):426–34. doi:10.1111/j.1365-3083.2005.01591.x
42. van der Pol P, Schlagwein N, van Gijlswijk DJ, Berger SP, Roos A, Bajema IM, et al. Mannan-binding lectin mediates renal ischemia/reperfusion injury independent of complement activation. *Am J Transplant* (2012) 12(4):877–87. doi:10.1111/j.1600-6143.2011.03887.x
43. Farrar CA, Tran D, Li K, Wu W, Peng Q, Schwaeble W, et al. Collectin-11 detects stress-induced L-fucose pattern to trigger renal epithelial injury. *J Clin Invest* (2016) 126(5):1911–25. doi:10.1172/JCI83000
44. Yu E, Ueta H, Kimura H, Kitazawa Y, Sawanobori Y, Matsuno K. Graft-versus-host disease following liver transplantation: development of a high-incidence rat model and a selective prevention method. *Am J Transplant* (2016) 17(4):979–91. doi:10.1111/ajt.14077
45. Macor P, Durigutto P, De Maso L, Garrovo C, Biffi S, Cortini A, et al. Treatment of experimental arthritis by targeting synovial endothelium with a neutralizing recombinant antibody to C5. *Arthritis Rheum* (2012) 64(8):2559–67. doi:10.1002/art.34430
46. Patel H, Smith RA, Sacks SH, Zhou W. Therapeutic strategy with a membrane-localizing complement regulator to increase the number of usable donor organs after prolonged cold storage. *J Am Soc Nephrol* (2006) 17(4):1102–11. doi:10.1681/ASN.2005101116

Conflict of Interest Statement: AN is chairman and president of ADIENNE Pharma and Biotech, owner of Mubodina® and Ergidina® patent, and partially supporter of the study. All other authors declare that the research was conducted in the absence of any commercial or financial relationships that could be construed as a potential conflict of interest.

frontiers in Immunology

PERSPECTIVE
published: 05 September 2017
doi: 10.3389/fimmu.2017.01022

Crosstalk between Signaling Pathways in Pemphigus: A Role for Endoplasmic Reticulum Stress in p38 Mitogen-Activated Protein Kinase Activation?

*Gabriel A. Cipolla[1,2], Jong Kook Park[3,4], Robert M. Lavker[3] and Maria Luiza Petzl-Erler[1]**

[1] Department of Genetics, Federal University of Paraná, Curitiba, Brazil, [2] CAPES Foundation, Ministry of Education of Brazil, Brasília, Brazil, [3] Department of Dermatology, Feinberg School of Medicine, Northwestern University, Chicago, IL, United States, [4] Department of Biomedical Science and Research, Institute for Bioscience and Biotechnology, Hallym University, Chuncheon, South Korea

Pemphigus consists of a group of chronic blistering skin diseases mediated by autoantibodies (autoAbs). The dogma that pemphigus is caused by keratinocyte dissociation (acantholysis) as a distinctive and direct consequence of the presence of autoAb targeting two main proteins of the desmosome—desmoglein (DSG) 1 and/or DSG3—has been put to the test. Several outside-in signaling events elicited by pemphigus autoAb in keratinocytes have been described, among which stands out p38 mitogen-activated protein kinase (p38 MAPK) engagement and its apoptotic effect on keratinocytes. The role of apoptosis in the disease is, however, debatable, to an extent that it may not be a determinant event for the occurrence of acantholysis. Also, it has been verified that compromised DSG trans-interaction does not lead to keratinocyte dissociation when p38 MAPK is inhibited. These examples of conflicting results have been followed by recent work revealing an important role for endoplasmic reticulum (ER) stress in pemphigus' pathogenesis. ER stress is known to activate the p38 MAPK pathway, and *vice versa*. However, this relationship has not yet been studied in the context of activated signaling pathways in pemphigus. Therefore, by reviewing and hypothetically connecting the role(s) of ER stress and p38 MAPK pathway in pemphigus, we highlight the importance of elucidating the crosstalk between all activated signaling pathways, which may in turn contribute for a better understanding of the role of apoptosis in the disease and a better management of this life-threatening condition.

Keywords: pemphigus, autoimmunity, p38 mitogen-activated protein kinase, endoplasmic reticulum stress, apoptolysis

OPEN ACCESS

Edited by:
Junji Yodoi,
Kyoto University, Japan

Reviewed by:
Ralf J. Ludwig,
University of Lübeck, Germany
David Dombrowicz,
Institut national de la santé et de la recherche médicale, France

****Correspondence:***
Maria Luiza Petzl-Erler
perler@ufpr.br

Specialty section:
This article was submitted to Inflammation, a section of the journal Frontiers in Immunology

Received: *25 March 2017*
Accepted: *08 August 2017*
Published: *05 September 2017*

Citation:
Cipolla GA, Park JK, Lavker RM and Petzl-Erler ML (2017) Crosstalk between Signaling Pathways in Pemphigus: A Role for Endoplasmic Reticulum Stress in p38 Mitogen-Activated Protein Kinase Activation? Front. Immunol. 8:1022. doi: 10.3389/fimmu.2017.01022

INTRODUCTION

Pemphigus encompasses various chronic autoimmune blistering skin diseases with acute stages often controlled by the administration of glucocorticosteroid drugs, especially when co-administrated with an adjuvant (1). However, the lack of specificity and the broad effect of steroid treatment may impact patient's homeostasis. The side effects of short- and long-term treatments with glucocorticosteroid drugs are well documented and may even include death

[reviewed in Ref. (2–6)]. Successful clinical trials with more specific drugs have been reported, such as rituximab (anti-CD20) and protein A immunoadsorption (7, 8). However, our limited knowledge of the disease has hampered the development of highly specific therapeutic agents that would ultimately minimize the use of glucocorticosteroid drugs as therapeutic agents.

Historically, pemphigus is identified by pathogenic IgG autoantibodies (autoAbs) targeting adhesion molecules of keratinocytes. These autoantigens are mainly two desmosomal cadherins: desmoglein (DSG) 1 and/or DSG3. Two main forms of pemphigus usually associate to autoAb profiles (9–12). In pemphigus foliaceus (PF), typically only anti-DSG1 autoAb, superficial blistering and erosions are observed. In contrast, pemphigus vulgaris (PV) patients may exhibit anti-DSG3 or anti-DSG3 and anti-DSG1 autoAb, known to specify the suprabasal blistering of mucous membranes or a mucocutaneous form, respectively [reviewed in Ref. (13, 14)]. While the anti-DSG profiles are highly indicative of the clinical form, the observation that reduction of disease activity toward a remitting stage may be followed by the maintenance of high anti-DSG titers remains a conundrum (15). However, the molecular mechanisms that comprise anti-DSG autoAb and lead to the loss of adhesion between keratinocytes in pemphigus are a major puzzle. Here, we review what has been generally proposed for pemphigus' pathogenesis, while suggesting a potentially p38 mitogen-activated protein kinase (p38 MAPK)-co-shared central role for endoplasmic reticulum (ER) stress in the disease.

CONCEIVABLE MOLECULAR MECHANISMS FOR LOSS OF CELL ADHESION IN PEMPHIGUS

Two main explanations, the first one simpler and more intuitive and the latter more recently proposed, have been put together as our knowledge of the disease has evolved. The simpler model proposes that pemphigus pathogenic autoAb inhibit, either sterically or allosterically, the interaction of DSG1 and DSG3 from desmosomes of adjacent keratinocytes (trans-interaction), inducing loss of cell adhesion. Such hindrance would take place at the extracellular (EC) domains 1 and 2 located in the NH_2-terminal region of DSGs, where pathogenic autoAb have been shown to bind specifically (16–20). Importantly, at least one of these EC domains is believed to allow for cis- and trans-interactions necessary for robust binding between adjacent keratinocytes (21).

In clinical terms, this model has been corroborated by the main findings that, in a Brazilian endemic form of PF known as *fogo selvagem*, patients in the preclinical stage exhibit IgG1 autoAb against the EC5 domain of DSG1, and that the onset of disease is accompanied by the emergence of IgG4 autoAb recognizing the EC1 and EC2 domains of the molecule (22). Similarly, mucosal PV is suggested to evolve to mucocutaneous PV upon intramolecular epitope spreading of autoAb against EC domains of the COOH-terminal region to autoAb against EC domains of the N-terminus portion of DSG3, as the former autoAb fail to recognize human skin and the latter autoAb have affinity for this tissue (23). This intramolecular epitope spreading in DSG3 is believed to precede an intermolecular epitope spreading from DSG3 to DSG1, an autoAb profile that correlates with the mucocutaneous form of PV (9). However, that autoAb against the EC C-terminus portion of DSG3 can be pathogenic themselves and that PV patients may have anti-DSG3-N-terminus portion autoAb without showing skin lesions suggest another layer of complexity to this model of pemphigus' pathogenesis (23). The fact that some PF and PV patients also exhibit IgG or other isotypes of autoAb with specificity to different keratinocyte adhesion and/or non-adhesion molecules also argues in favor of a more complex pathogenesis [reviewed in Ref. (24, 25)]. Moreover, DSG1 and DSG3 have been shown to be targeted also by other immunoglobulin isotypes, specifically by IgE and IgM autoAb, which may as well play a role in disease development [reviewed in Ref. (26, 27)].

The rather simple explanation of pemphigus' pathogenesis through steric hindrance relies on the DSG compensation hypothesis, which states that the distribution of DSG1 and DSG3 in the epidermis determines the site of blistering in pemphigus skin. Based on what has been discussed so far, this suggests that either DSG1 or DSG3 could solely account for epidermal cohesion. However, a new concept for the pathogenesis of pemphigus derives from a series of observations of signaling pathways activated by PF and PV autoAb [reviewed in Ref. (24)]. Among these activated pathways, researchers have described involvement of cyclic adenosine monophosphate (cAMP), epidermal growth factor receptor kinase (EGFRK), heat shock protein 27 (HSP27), c-Jun N-terminal kinases (JNK), mechanistic target of rapamycin, phospholipase C, protein kinases A and C, p38 MAPK, tyrosine-protein kinase SRC, and other tyrosine kinases (28–36). This new model has been termed apoptolysis, referring to the loss of epidermal cell adhesion (acantholysis) as a main outcome of the activation of keratinocyte intracellular apoptotic enzymes following the binding of distinctive autoAb profiles in pemphigus (36, 37).

It is not clear, however, whether apoptosis is a necessary preceding event for the pathognomonic acantholysis in pemphigus patients. In fact, in a large-scale electron microscopy study of pemphigus skin and mucosa, no cellular changes compatible with apoptosis were observed in lesional or non-lesional tissue (38). Moreover, molecular evidences have also argued against the role of apoptosis in blistering given the lack of consistent TUNEL positivity and detection of apoptotic markers, such as cleaved caspase 3, in pemphigus biopsies (39, 40). In a review on the topic, Schmidt and Waschke reported that most of the experiments suggesting a role for apoptosis in pemphigus were based on keratinocyte culture assays and their incubation with PV-derived IgG (41). This has been interpreted as a consequence of the high levels of Fas ligand present in pemphigus sera, which would be a trigger for the extrinsic apoptotic pathway (42). Independently of apoptosis being a primary or secondary, or even an irrelevant event in pemphigus' pathogenesis, the signal transducing component of the apoptolytic theory is a well-supported and expected sequence of events, as illustrated below by the role of p38 MAPK pathway engagement in pemphigus. In summary, the concept of altered signaling involves the following events: (i) phosphorylation of adhesion or non-adhesion

molecules with desmosome disassembly, (ii) derangement and collapse of the cytoskeleton, and (iii) impaired formation of new intercellular desmosomes and/or keratinocyte apoptosis [reviewed in Ref. (24, 41)].

Although the apoptolysis hypothesis was initially proposed based on direct observations, as the DSG compensation hypothesis fails to explain the mismatch between the autoAb pattern/DSG1 and DSG3 distribution and the morphological blistering phenotype observed in PV (24), the apoptolytic mechanism considers several other events also observed in PF. Initially, cell culture and cell-free assays showed that anti-DSG1 autoAb derived from PF patients induce keratinocyte dissociation without direct inhibition of DSG1 trans-interaction, possibly requiring cell-dependent signaling mechanisms (43). Furthermore, PF IgG also activated the p38 MAPK pathway and induced blister formation in a murine model of PF (44). More recently, a careful inspection of the ultrastructure of PF lesional skin revealed: almost detached keratinocytes with severe stretching of plasma membranes in pre-acantholytic areas; desmosomes still attached but beginning to tear off from cell membranes; and full desmosomes torn off from keratinocytes (45). This would agree with the third and fourth steps of the apoptolytic mechanism, after transduction of apoptolytic signals from plasma membranes (step 1), and elevation of intracellular calcium and launching of cell death cascades (step 2): "collapse and retraction of the tonofilaments … while most of desmosomes remain intact" (step 3); and "collapse of the cytoskeleton and tearing off desmosomes from the cell membrane" (step 4) (37). Another recent finding supporting the apoptolysis model, where p38 phosphorylation is presumed to have a central role (**Figure 1**), comes from the observation that hampered DSG trans-interaction does not result in keratinocyte dissociation when p38 MAPK signaling is inhibited (46). Very recently, in fact, it has been shown that blockage of p38 MAPK prevents PV-IgG-induced blistering (47) and PF-IgG-induced desmosomal changes (48) both in human skin.

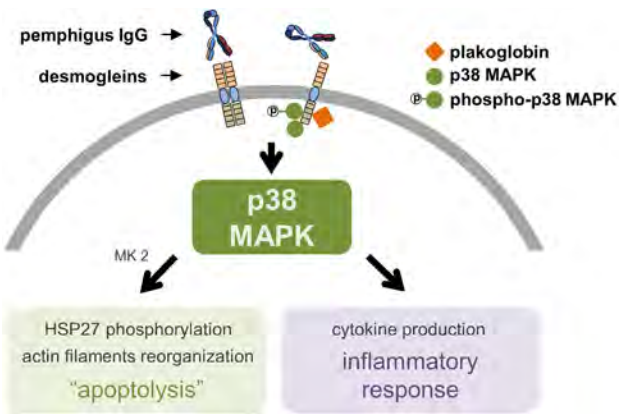

FIGURE 1 | The proposed central role of p38 mitogen-activated protein kinase (p38 MAPK) in pemphigus' pathogenesis. The molecular complex supposed to be formed by desmoglein (DSG, specifically DSG3, as of the gap for data on DSG1), plakoglobin, and p38 MAPK induces keratinocyte apoptolysis and a local inflammatory response after binding of pemphigus IgG to extracellular domains of DSG. A phosphorylation cascade involving p38 MAPK, MAPK activated protein kinase 2 (MK2), and heat shock protein 27 (HSP27) leads to the collapse of the cytoskeleton and ultimately to keratinocyte apoptosis. The central role of p38 MAPK includes the production of pro-inflammatory cytokines.

More sophisticated studies have corroborated the simpler understanding that pemphigus autoAb induce loss of cell adhesion through steric hindrance. In another ultrastructural inspection of pemphigus skin and mucosa, two interesting findings have been reported for the first time in PF: the lack of desmosomes surrounding spontaneous blisters; and blistering in the below-granular layers when force was applied (38). According to the authors, these observations best fit the non-assembly depletion hypothesis, which may be considered a complementation of the steric hindrance hypothesis (25). It has also been verified that, among isolated monoclonal antibodies (mAb) of a PF patient, the single DSG1-specific pathogenic mAb recognizes exclusively the mature form of DSG1 lacking the N-terminal prosequence, while those non-pathogenic mAb were able to bind preferably the precursor form. Among all mAb, only the pathogenic mAb showed binding to the mature DSG1 region thought to be responsible for DSG trans-interaction (49). DSG1 maturation has been known to be regulated by furin, a proprotein convertase, *via* proteolytic cleavage of the prosequence (49, 50). Transcription of *FURIN* can be positively regulated by nuclear factor kappa-light-chain-enhancer of activated B cells (NFκB) (51) and cAMP-responsive element-binding protein (52), both of which are activated by p38 MAPK signaling pathways (51, 53). ER stress, in turn, has been very recently associated to PV's pathogenesis (54). Therefore, considering that ER stress seems to be involved in pemphigus' pathogenesis, while being known as an activator of the p38 MAPK pathway, which in turn has been reported to lead to ER stress, we focus on the potential connection between these pieces by suggesting that they may be linked as a positive feedback loop (**Figure 2**).

p38 MAPK SIGNALING PATHWAY IN PEMPHIGUS

The importance of the p38 MAPK pathway involvement in pemphigus pathogenesis has been consistently reported throughout the literature (28, 29, 44, 46–48) and extensively reviewed elsewhere (55). The observations that DSG3 and p38 MAPK are in close proximity and that plakoglobin, p38 MAPK, and DSG3 can be co-immunoprecipitated have suggested the existence of a signaling complex formed by these molecules and its importance for the anchorage of the desmosomal plaque to the keratinocyte cytoskeleton (**Figure 1**) (56). Interestingly, phosphorylation of p38 MAPK induced by incubation of cultured keratinocytes with PV IgG can take place as early as 15 min, corroborating DSG3 and p38 MAPK association (32). However, this same study showed that, for the majority of patient-derived PV IgG, phosphorylated p38 MAPK did not reach its peaks until after 240 min from incubation. Such peaks were observed after an important reduction of p38 MAPK and increase of EGFRK and

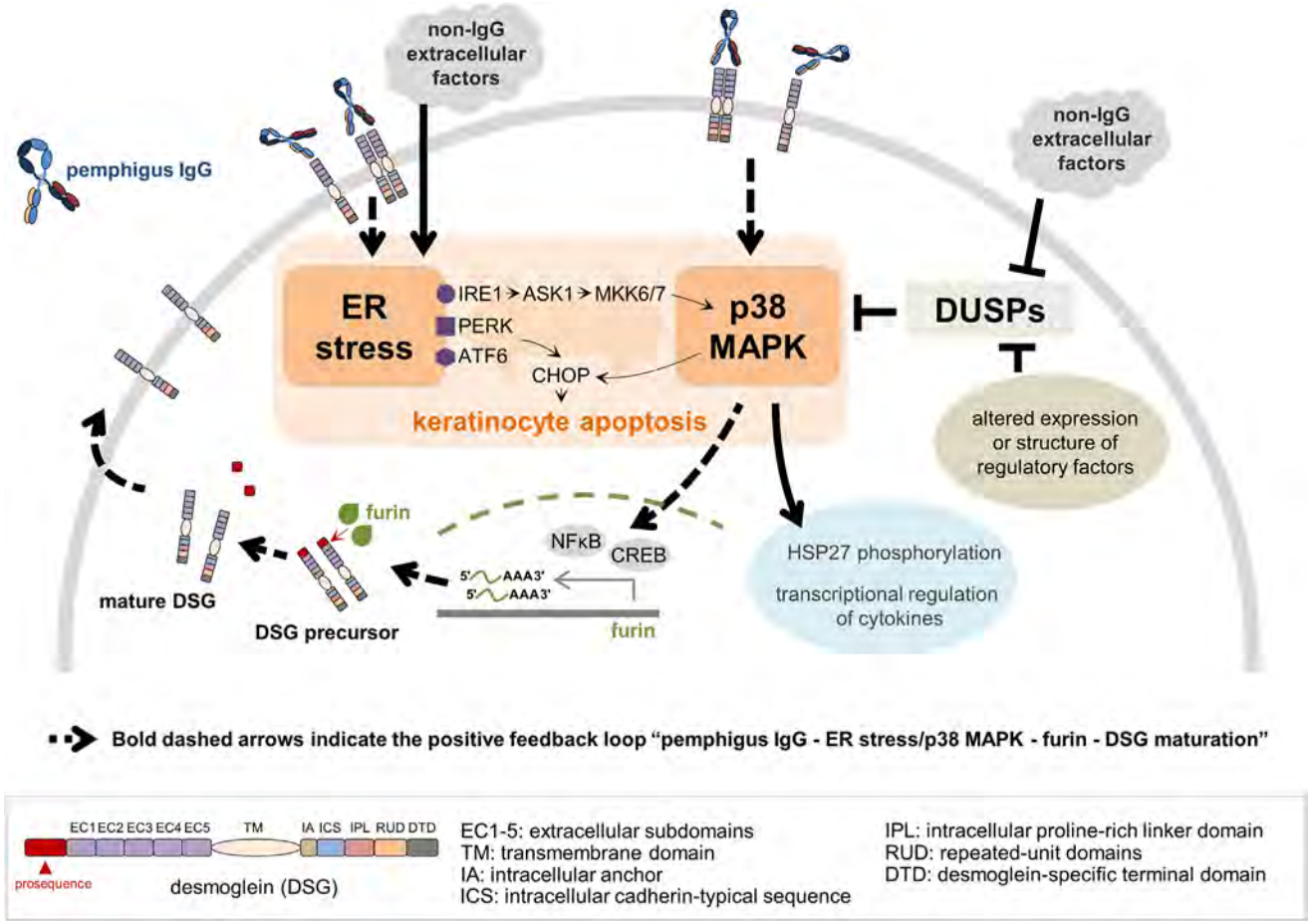

FIGURE 2 | A model for a crosstalk between endoplasmic reticulum (ER) stress and p38 mitogen-activated protein kinase (p38 MAPK) pathway in the context of pemphigus. Both pemphigus IgG and non-IgG extracellular factors lead to ER stress resulting in C/EBP-homologous protein (CHOP) induction *via* protein kinase R-like ER kinase (PERK) and activating transcription factor 6 (ATF6). ER stress activates p38 MAPK through the inositol-requiring kinase 1 (IRE1)-apoptosis signal-regulating kinase 1 (ASK1)-MKK6/7 signaling pathway, and CHOP is activated by p38 MAPK. Pemphigus IgG binding preferentially to mature desmoglein (DSG) 1 and/or 3 activates the p38 MAPK pathway, which in turn induces ER stress. Dual-specificity phosphatases (DUSPs), negative regulators of p38 MAPK activation, can be targeted by either non-IgG extracellular factors or intracellular regulatory factors, such as RNAs and proteins, with altered expression or structure. ER stress and p38 MAPK play a critical role in keratinocyte apoptosis, heat shock protein 27 (HSP27) phosphorylation and transcriptional regulation of cytokines. In addition, activation of nuclear factor kappa-light-chain-enhancer of activated B cells (NFκB) and cAMP-responsive element binding protein (CREB) by p38 MAPK signaling pathway positively regulates *FURIN* transcription, which ultimately facilitates the DSG maturation process. As more mature DSG becomes available on the keratinocyte's plasma membrane, the entire process restarts, characterizing the positive feedback loop.

SRC phosphorylation at 60 min. Comparable findings had been reported previously (30). Meanwhile, it has been documented that p38 knockdown seems to prevent loss of desmosomal DSG3 and exogenous p38 activation appears to induce DSG3 internalization, both in PV IgG-treated keratinocyte cultures (57). Therefore, the late p38 phosphorylation peak has been interpreted as a consequence of internalized and processed DSG3, which in turn would not be primary for the loss of keratinocyte adhesion in PV, but actually an enhancer for blistering through DSG3 endocytosis.

Nonetheless, it is conceivable that such late peaks of p38 phosphorylation represent the activation of distinct pathways that converge to p38 MAPK *de novo* engagement, as in a positive feedback loop. In fact, negative feedback mechanisms insure that MAPKs are not uninterruptedly active. This task is undertaken by dual-specificity phosphatases (DUSPs), proteins with precise phosphorylating and dephosphorylating functions and with discrete cell-type distribution and subcellular localization (58). DUSP1, also known as MAP kinase phosphatase 1 (MKP1), is a well-known regulator of p38 MAPK activation, which may in turn induce a DUSP1-dependent negative feedback (59, 60). Besides the conceivable existence of a positive feedback loop downstream of a p38 phosphorylation and dephosphorylation cycle by DUSPs, these are themselves potentially associated with autoimmune diseases. DUSP1, for example, is underexpressed in psoriatic skin lesions in comparison to their normal-appearing counterparts (61), and this is believed to contribute to the inflammatory condition observed in the disease. Such an assumption derives from reports indicating reduced production of cytokines when inhibiting signaling through MAPKs.

The PV-associated interleukin (IL)-8, for instance, seems to be downregulated with MKP1-dependent inhibition of p38 MAPK (62, 63). Finally, given the limited repertoire of known p38 dephosphorylators, regulatory RNAs that putatively target DUSPs could be comprehensively validated as such. Specifically, pemphigus-overexpressed microRNAs (miRNAs) putatively targeting DUSPs could be validated in light of their role in fine-tuning gene expression at the posttranscriptional level. This approach would be of special importance for validating the existence of a positive feedback loop, because of the expected upregulation of DUSP expression downstream of p38 MAPK activation and the potential existence of an abnormal miRNA profile in pemphigus keratinocytes. Again, such abnormal profile could include upregulated miRNAs that target DUSPs' messenger RNA, therefore interfering with the negative feedback between newly synthesized DUSPs and p38 MAPK.

THE EMERGING ROLE OF ER STRESS IN PEMPHIGUS

In contrast with the well-established role of p38 MAPK in pemphigus, the importance of ER stress in the disease has not yet undergone scrutiny. However, a link between ER stress and apoptosis has been demonstrated. During ER stress, proapoptotic transcription factor C/EBP-homologous protein (CHOP, or DNA damage-inducible transcript 3, DDIT3) is induced by PKR-like endoplasmic reticulum kinase (PERK) and activating transcription factor 6 (ATF6) on ER membranes. Inositol-requiring kinase 1 (IRE1α) on ER membranes is also activated by ER stress resulting in activation of p38 MAPK *via* apoptosis signal-regulating kinase 1 (ASK1) and MKK6/7. p38 MAPK in turn activates CHOP (**Figure 2**) [reviewed in Ref. (64)]. Engagement of p38 MAPK and JNK pathways were reported to take place initially after stimulation of Epstein–Barr virus-transformed B cells with anti-CD70—a treatment that leads to ER stress-mediated apoptosis of these cells—while inhibition of both pathways blocked upregulation of ER stress markers, such as CHOP (65). Also, p38 MAPK can function as an upstream inducer of ER stress (66, 67). This is indicative of the existence of an ER stress response *via* p38 MAPK and JNK pathways, suggesting that at least ER stress and p38 MAPK might be connected by a two-way route (**Figure 2**).

Some studies have investigated the involvement of ER stress in pemphigus pathogenesis. The ER stress pathway represented by the activation of PERK was shown to be engaged when exposing cultured keratinocytes to PV serum (68), which had been previously shown to upregulate PERK (69). Moreover, downregulation of PERK expression through small interfering RNA restricted the changes in keratinocyte cell cycle and viability typically observed after treatment of these cells with pemphigus serum (68). Interestingly, PERK phosphorylation can occur independently of PV IgG, i.e., when treating keratinocytes with total or Ig-depleted PV serum (68). However, by looking at the isolated effects of both anti-DSG1 and anti-DSG3 PV autoAb on ER stress induction, it was also reported that overexpression of CHOP may be anti-DSG1 dependent (54). These apparently conflicting results might be interpreted in light of the different intracellular signaling events triggered by the heterogeneous autoAb profiles of pemphigus patients (36). Moreover, in contrast with DSG3, it is unknown whether DSG1 is in association with p38 MAPK or not. Thus, the specific signaling complexes formed by both of these molecules could also explain such results.

Besides stimulating or being stimulated by the p38 MAPK pathway, ER stress could be contributing to the activation of HSP27 in pemphigus. Phosphorylation of this protein, known to occur in pemphigus and downstream of p38 MAPK and MAPK-activated protein kinase 2 (MK2, or MAPKAPK2) (70), has been reported to be induced by ER stress (71). Although environmental factors may play an important role in the pathogenesis and course of pemphigus, the contribution of viral infections to the disease remains unclear (72). Nonetheless, it has been reported that a hepatitis B virus envelope protein is capable of activating the p38 MAPK and NFκB pathways in an ER stress-dependent manner (73), being therefore an example of how viral factors could directly contribute to a connected ER stress induction and p38 MAPK activation. Altogether, by adding ER stress to the understanding of pemphigus pathogenesis, an entirely new set of hypotheses and connections can be made in the context of the signaling pathways activated in the disease. Hence, we have put together a model in which ER stress has a potential central role in pemphigus (**Figure 2**). In summary, we suggest that ER stress may be triggered more directly by non-IgG factors, secondarily by anti-DSG1 autoAb—given the anti-DSG1-dependent induction of ER stress found by Mihailidou and collaborators (54)–or indirectly by pemphigus IgG *via* p38 phosphorylation. Once ER stress has been triggered, it can act as positive regulator of p38 phosphorylation. In addition, we suggest that pemphigus patients may produce factors that also, directly or indirectly, downregulate DUSP levels and act in conjunction with ER stress, for example, to allow for a secondary, but strong p38 MAPK engagement.

CONCLUDING REMARKS

The existence of consistent data favoring either one of the molecular mechanisms explaining the loss of cell adhesion in pemphigus is consistent with its intricate pathogenesis. Indeed, histopathology may develop as a consequence of anti-DSG antibodies, both, impairing DSG trans-interaction through steric hindrance and subsequently transducing intracellular signals leading to keratinocyte apoptosis. However, non-IgG factors may also contribute to histopathology by inducing additional pathways, including ER stress, which may in turn activate the p38 MAPK signaling pathway of great importance in pemphigus. By connecting both, the ER stress and the p38 MAPK pathway, we put in perspective a potential positive feedback loop between these events in which, in an IgG-dependent manner, p38 MAPK activation leads to ER stress, which in turn stimulates p38 phosphorylation. We also suggest that, independently of autoAbs, i.e., also through factors such as viral particles, cytokines, metabolites, and/or regulatory RNAs and proteins, ER stress would primarily induce p38 MAPK activation, which would then prompt the positive feedback loop through the same intracellular signaling cascades. Finally, this is suggestive of a central role for ER stress

in pemphigus pathogenesis and, by bringing this to light, we hope to inspire researchers in the field to deepen the understanding of this life-threatening disease.

AUTHOR CONTRIBUTIONS

All authors contributed substantially to the conception of the work. GC and JP drafted the work. RL and MP-E revised the work critically for intellectual content. All authors approved the final version of the work. All authors agreed to be accountable for all aspects of the work.

ACKNOWLEDGMENTS

The authors would like to thank Professors Daniela Fiori Gradia, Karin Braun-Prado, Marcelo Távora Mira, and Wanderson Duarte da Rocha for all corrections and suggestions that contributed to the improvement of the manuscript. GC would like to thank the Coordenação de Aperfeiçoamento de Pessoal de Ensino Superior (CAPES Foundation) for the international scholarship [Bolsista CAPES—Processo 99999.006318/2015-00].

FUNDING

This work was funded by the National Institutes of Health [grant number EY019463] to RL; Conselho Nacional de Desenvolvimento Científico e Tecnológico (CNPq) [grant numbers 478907/2013-3 and 446973/2014-9] to MP-E; Fundação Araucária/CNPq [PRONEX convênio 251/2013 protocolo 24.652] to MP-E; and Coordenação de Aperfeiçoamento de Pessoal de Ensino Superior (CAPES) [Bolsista CAPES—Processo 99999.006318/2015-00] to GC.

REFERENCES

1. Carson PJ, Hameed A, Ahmed AR. Influence of treatment on the clinical course of pemphigus vulgaris. *J Am Acad Dermatol* (1996) 34(4):645–52. doi:10.1016/S0190-9622(96)80066-1
2. Bystryn JC, Steinman NM. The adjuvant therapy of pemphigus. An update. *Arch Dermatol* (1996) 132(2):203–12. doi:10.1001/archderm.1996.03890260105016
3. Kneisel A, Hertl M. Autoimmune bullous skin diseases. Part 2: diagnosis and therapy. *J Dtsch Dermatol Ges* (2011) 9(11):927–47. doi:10.1111/j.1610-0387.2011.07809_suppl.x
4. Lehmann P, Zheng P, Lavker RM, Kligman AM. Corticosteroid atrophy in human skin. A study by light, scanning, and transmission electron microscopy. *J Invest Dermatol* (1983) 81(2):169–76. doi:10.1111/1523-1747.ep12543603
5. Rosenberg FR, Sanders S, Nelson CT. Pemphigus: a 20-year review of 107 patients treated with corticosteroids. *Arch Dermatol* (1976) 112(7):962–70. doi:10.1001/archderm.112.7.962
6. Zheng PS, Lavker RM, Lehmann P, Kligman AM. Morphologic investigations on the rebound phenomenon after corticosteroid-induced atrophy in human skin. *J Invest Dermatol* (1984) 82(4):345–52. doi:10.1111/1523-1747.ep12260665
7. Kolesnik M, Becker E, Reinhold D, Ambach A, Heim MU, Gollnick H, et al. Treatment of severe autoimmune blistering skin diseases with combination of protein A immunoadsorption and rituximab: a protocol without initial high dose or pulse steroid medication. *J Eur Acad Dermatol Venereol* (2014) 28(6):771–80. doi:10.1111/jdv.12175
8. Joly P, Maho-Vaillant M, Prost-Squarcioni C, Hebert V, Houivet E, Calbo S, et al. First-line rituximab combined with short-term prednisone versus prednisone alone for the treatment of pemphigus (Ritux 3): a prospective, multicentre, parallel-group, open-label randomised trial. *Lancet* (2017) 389(10083):2031–40. doi:10.1016/S0140-6736(17)30070-3
9. Ding X, Aoki V, Mascaro JM Jr, Lopez-Swiderski A, Diaz LA, Fairley JA. Mucosal and mucocutaneous (generalized) pemphigus vulgaris show distinct autoantibody profiles. *J Invest Dermatol* (1997) 109(4):592–6. doi:10.1111/1523-1747.ep12337524
10. Harman KE, Seed PT, Gratian MJ, Bhogal BS, Challacombe SJ, Black MM. The severity of cutaneous and oral pemphigus is related to desmoglein 1 and 3 antibody levels. *Br J Dermatol* (2001) 144(4):775–80. doi:10.1046/j.1365-2133.2001.04132.x
11. Ishii K, Amagai M, Hall RP, Hashimoto T, Takayanagi A, Gamou S, et al. Characterization of autoantibodies in pemphigus using antigen-specific enzyme-linked immunosorbent assays with baculovirus-expressed recombinant desmogleins. *J Immunol* (1997) 159(4):2010–7.
12. Oliveira LA, Marquart-Filho A, Trevilato G, Timoteo RP, Mukai M, Roselino AM, et al. Anti-desmoglein 1 and 3 autoantibody levels in endemic pemphigus foliaceus and pemphigus vulgaris from Brazil. *Clin Lab* (2016) 62(7):1209–16. doi:10.7754/Clin.Lab.2015.150628
13. Groves RW. Pemphigus: a brief review. *Clin Med (Lond)* (2009) 9(4):371–5. doi:10.7861/clinmedicine.9-4-371
14. Stanley JR, Amagai M. Pemphigus, bullous impetigo, and the staphylococcal scalded-skin syndrome. *N Engl J Med* (2006) 355(17):1800–10. doi:10.1056/NEJMra061111
15. Hammers CM, Stanley JR. Patients with pemphigus foliaceus may retain antibody reactivity against calcium-stabilized, distal desmoglein 1 domains in remission. *Br J Dermatol* (2016) 174(1):17–8. doi:10.1111/bjd.14262
16. Di Zenzo G, Di Lullo G, Corti D, Calabresi V, Sinistro A, Vanzetta F, et al. Pemphigus autoantibodies generated through somatic mutations target the desmoglein-3 cis-interface. *J Clin Invest* (2012) 122(10):3781–90. doi:10.1172/JCI64413
17. Payne AS, Ishii K, Kacir S, Lin C, Li H, Hanakawa Y, et al. Genetic and functional characterization of human pemphigus vulgaris monoclonal autoantibodies isolated by phage display. *J Clin Invest* (2005) 115(4):888–99. doi:10.1172/JCI24185
18. Sekiguchi M, Futei Y, Fujii Y, Iwasaki T, Nishikawa T, Amagai M. Dominant autoimmune epitopes recognized by pemphigus antibodies map to the N-terminal adhesive region of desmogleins. *J Immunol* (2001) 167(9):5439–48. doi:10.4049/jimmunol.167.9.5439
19. Tsunoda K, Ota T, Aoki M, Yamada T, Nagai T, Nakagawa T, et al. Induction of pemphigus phenotype by a mouse monoclonal antibody against the amino-terminal adhesive interface of desmoglein 3. *J Immunol* (2003) 170(4):2170–8. doi:10.4049/jimmunol.170.4.2170
20. Wheeler GN, Parker AE, Thomas CL, Ataliotis P, Poynter D, Arnemann J, et al. Desmosomal glycoprotein DGI, a component of intercellular desmosome junctions, is related to the cadherin family of cell adhesion molecules. *Proc Natl Acad Sci U S A* (1991) 88(11):4796–800. doi:10.1073/pnas.88.11.4796
21. Al-Amoudi A, Diez DC, Betts MJ, Frangakis AS. The molecular architecture of cadherins in native epidermal desmosomes. *Nature* (2007) 450(7171):832–7. doi:10.1038/nature05994
22. Li N, Aoki V, Hans-Filho G, Rivitti EA, Diaz LA. The role of intramolecular epitope spreading in the pathogenesis of endemic pemphigus foliaceus (fogo selvagem). *J Exp Med* (2003) 197(11):1501–10. doi:10.1084/jem.20022031
23. Salato VK, Hacker-Foegen MK, Lazarova Z, Fairley JA, Lin MS. Role of intramolecular epitope spreading in pemphigus vulgaris. *Clin Immunol* (2005) 116(1):54–64. doi:10.1016/j.clim.2005.03.005
24. Grando SA. Pemphigus autoimmunity: hypotheses and realities. *Autoimmunity* (2012) 45(1):7–35. doi:10.3109/08916934.2011.606444
25. Ludwig RJ, Vanhoorelbeke K, Leypoldt F, Kaya Z, Bieber K, McLachlan SM, et al. Mechanisms of autoantibody-induced pathology. *Front Immunol* (2017) 8:603. doi:10.3389/fimmu.2017.00603

26. Ahmed AR, Carrozzo M, Caux F, Cirillo N, Dmochowski M, Alonso AE, et al. Monopathogenic vs multipathogenic explanations of pemphigus pathophysiology. *Exp Dermatol* (2016) 25(11):839–46. doi:10.1111/exd.13106
27. Qian Y, Culton DA, Jeong JS, Trupiano N, Valenzuela JG, Diaz LA. Non-infectious environmental antigens as a trigger for the initiation of an autoimmune skin disease. *Autoimmun Rev* (2016) 15(9):923–30. doi:10.1016/j.autrev.2016.07.005
28. Berkowitz P, Hu P, Liu Z, Diaz LA, Enghild JJ, Chua MP, et al. Desmosome signaling. Inhibition of p38MAPK prevents pemphigus vulgaris IgG-induced cytoskeleton reorganization. *J Biol Chem* (2005) 280(25):23778–84. doi:10.1074/jbc.M501365200
29. Berkowitz P, Diaz LA, Hall RP, Rubenstein DS. Induction of p38MAPK and HSP27 phosphorylation in pemphigus patient skin. *J Invest Dermatol* (2008) 128(3):738–40. doi:10.1038/sj.jid.5701080
30. Chernyavsky AI, Arredondo J, Kitajima Y, Sato-Nagai M, Grando SA. Desmoglein versus non-desmoglein signaling in pemphigus acantholysis: characterization of novel signaling pathways downstream of pemphigus vulgaris antigens. *J Biol Chem* (2007) 282(18):13804–12. doi:10.1074/jbc.M611365200
31. Frusic-Zlotkin M, Raichenberg D, Wang X, David M, Michel B, Milner Y. Apoptotic mechanism in pemphigus autoimmunoglobulins-induced acantholysis – possible involvement of the EGF receptor. *Autoimmunity* (2006) 39(7):563–75. doi:10.1080/08916930600971836
32. Marchenko S, Chernyavsky AI, Arredondo J, Gindi V, Grando SA. Antimitochondrial autoantibodies in pemphigus vulgaris: a missing link in disease pathophysiology. *J Biol Chem* (2010) 285(6):3695–704. doi:10.1074/jbc.M109.081570
33. Pretel M, Espana A, Marquina M, Pelacho B, Lopez-Picazo JM, Lopez-Zabalza MJ. An imbalance in Akt/mTOR is involved in the apoptotic and acantholytic processes in a mouse model of pemphigus vulgaris. *Exp Dermatol* (2009) 18(9):771–80. doi:10.1111/j.1600-0625.2009.00893.x
34. Sanchez-Carpintero I, Espana A, Pelacho B, Lopez Moratalla N, Rubenstein DS, Diaz LA, et al. In vivo blockade of pemphigus vulgaris acantholysis by inhibition of intracellular signal transduction cascades. *Br J Dermatol* (2004) 151(3):565–70. doi:10.1111/j.1365-2133.2004.06147.x
35. Spindler V, Vielmuth F, Schmidt E, Rubenstein DS, Waschke J. Protective endogenous cyclic adenosine 5'-monophosphate signaling triggered by pemphigus autoantibodies. *J Immunol* (2010) 185(11):6831–8. doi:10.4049/jimmunol.1002675
36. Walter E, Vielmuth F, Rotkopf L, Sardy M, Horvath ON, Goebeler M, et al. Different signaling patterns contribute to loss of keratinocyte cohesion dependent on autoantibody profile in pemphigus. *Sci Rep* (2017) 7(1):3579. doi:10.1038/s41598-017-03697-7
37. Grando SA, Bystryn JC, Chernyavsky AI, Frusic-Zlotkin M, Gniadecki R, Lotti R, et al. Apoptolysis: a novel mechanism of skin blistering in pemphigus vulgaris linking the apoptotic pathways to basal cell shrinkage and suprabasal acantholysis. *Exp Dermatol* (2009) 18(9):764–70. doi:10.1111/j.1600-0625.2009.00934.x
38. Sokol E, Kramer D, Diercks GF, Kuipers J, Jonkman MF, Pas HH, et al. Large-scale electron microscopy maps of patient skin and mucosa provide insight into pathogenesis of blistering diseases. *J Invest Dermatol* (2015) 135(7):1763–70. doi:10.1038/jid.2015.109
39. Schmidt E, Gutberlet J, Siegmund D, Berg D, Wajant H, Waschke J. Apoptosis is not required for acantholysis in pemphigus vulgaris. *Am J Physiol Cell Physiol* (2009) 296(1):C162–72. doi:10.1152/ajpcell.00161.2008
40. Janse IC, van der Wier G, Jonkman MF, Pas HH, Diercks GF. No evidence of apoptotic cells in pemphigus acantholysis. *J Invest Dermatol* (2014) 134(7):2039–41. doi:10.1038/jid.2014.60
41. Schmidt E, Waschke J. Apoptosis in pemphigus. *Autoimmun Rev* (2009) 8(7):533–7. doi:10.1016/j.autrev.2009.01.011
42. Puviani M, Marconi A, Cozzani E, Pincelli C. Fas ligand in pemphigus sera induces keratinocyte apoptosis through the activation of caspase-8. *J Invest Dermatol* (2003) 120(1):164–7. doi:10.1046/j.1523-1747.2003.12014.x
43. Waschke J, Bruggeman P, Baumgartner W, Zillikens D, Drenckhahn D. Pemphigus foliaceus IgG causes dissociation of desmoglein 1-containing junctions without blocking desmoglein 1 transinteraction. *J Clin Invest* (2005) 115(11):3157–65. doi:10.1172/JCI23475
44. Berkowitz P, Chua M, Liu Z, Diaz LA, Rubenstein DS. Autoantibodies in the autoimmune disease pemphigus foliaceus induce blistering via p38 mitogen-activated protein kinase-dependent signaling in the skin. *Am J Pathol* (2008) 173(6):1628–36. doi:10.2353/ajpath.2008.080391
45. van der Wier G, Jonkman MF, Pas HH, Diercks GF. Ultrastructure of acantholysis in pemphigus foliaceus re-examined from the current perspective. *Br J Dermatol* (2012) 167(6):1265–71. doi:10.1111/j.1365-2133.2012.11173.x
46. Vielmuth F, Waschke J, Spindler V. Loss of desmoglein binding is not sufficient for keratinocyte dissociation in pemphigus. *J Invest Dermatol* (2015) 135(12):3068–77. doi:10.1038/jid.2015.324
47. Egu DT, Walter E, Spindler V, Waschke J. Inhibition of p38MAPK signaling prevents epidermal blistering and alterations of desmosome structure induced by pemphigus autoantibodies in human epidermis. *Br J Dermatol* (2017). doi:10.1111/bjd.15721
48. Yoshida K, Ishii K, Shimizu A, Yokouchi M, Amagai M, Shiraishi K, et al. Non-pathogenic pemphigus foliaceus (PF) IgG acts synergistically with a directly pathogenic PF IgG to increase blistering by p38MAPK-dependent desmoglein 1 clustering. *J Dermatol Sci* (2017) 85(3):197–207. doi:10.1016/j.jdermsci.2016.12.010
49. Yokouchi M, Saleh MA, Kuroda K, Hachiya T, Stanley JR, Amagai M, et al. Pathogenic epitopes of autoantibodies in pemphigus reside in the amino-terminal adhesive region of desmogleins which are unmasked by proteolytic processing of prosequence. *J Invest Dermatol* (2009) 129(9):2156–66. doi:10.1038/jid.2009.61
50. Posthaus H, Dubois CM, Muller E. Novel insights into cadherin processing by subtilisin-like convertases. *FEBS Lett* (2003) 536(1–3):203–8. doi:10.1016/S0014-5793(02)03897-8
51. Kumar V, Behera R, Lohite K, Karnik S, Kundu GC. p38 kinase is crucial for osteopontin-induced furin expression that supports cervical cancer progression. *Cancer Res* (2010) 70(24):10381–91. doi:10.1158/0008-5472.CAN-10-1470
52. Zhou Z, Wang R, Yang X, Lu XY, Zhang Q, Wang YL, et al. The cAMP-responsive element binding protein (CREB) transcription factor regulates furin expression during human trophoblast syncytialization. *Placenta* (2014) 35(11):907–18. doi:10.1016/j.placenta.2014.07.017
53. Tan Y, Rouse J, Zhang A, Cariati S, Cohen P, Comb MJ. FGF and stress regulate CREB and ATF-1 via a pathway involving p38 MAP kinase and MAPKAP kinase-2. *EMBO J* (1996) 15(17):4629–42.
54. Mihailidou C, Katsoulas N, Panagiotou E, Farmaki E, Sklavounou A, Kiaris H, et al. Endoplasmic reticulum stress is associated with the pathogenesis of pemphigus vulgaris. *Exp Dermatol* (2016) 25(9):731–3. doi:10.1111/exd.13026
55. Mavropoulos A, Orfanidou T, Liaskos C, Smyk DS, Spyrou V, Sakkas LI, et al. p38 MAPK signaling in pemphigus: implications for skin autoimmunity. *Autoimmune Dis* (2013) 2013:728529. doi:10.1155/2013/728529
56. Spindler V, Rotzer V, Dehner C, Kempf B, Gliem M, Radeva M, et al. Peptide-mediated desmoglein 3 crosslinking prevents pemphigus vulgaris autoantibody-induced skin blistering. *J Clin Invest* (2013) 123(2):800–11. doi:10.1172/JCI60139
57. Mao X, Sano Y, Park JM, Payne AS. p38 MAPK activation is downstream of the loss of intercellular adhesion in pemphigus vulgaris. *J Biol Chem* (2011) 286(2):1283–91. doi:10.1074/jbc.M110.172874
58. Lang R, Hammer M, Mages J. DUSP meet immunology: dual specificity MAPK phosphatases in control of the inflammatory response. *J Immunol* (2006) 177(11):7497–504. doi:10.4049/jimmunol.177.11.7497
59. Hu JH, Chen T, Zhuang ZH, Kong L, Yu MC, Liu Y, et al. Feedback control of MKP-1 expression by p38. *Cell Signal* (2007) 19(2):393–400. doi:10.1016/j.cellsig.2006.07.010
60. Lasa M, Abraham SM, Boucheron C, Saklatvala J, Clark AR. Dexamethasone causes sustained expression of mitogen-activated protein kinase (MAPK) phosphatase 1 and phosphatase-mediated inhibition of MAPK p38. *Mol Cell Biol* (2002) 22(22):7802–11. doi:10.1128/MCB.22.22.7802-7811.2002
61. Kjellerup RB, Johansen C, Kragballe K, Iversen L. The expression of dual-specificity phosphatase 1 mRNA is downregulated in lesional psoriatic skin. *Br J Dermatol* (2013) 168(2):339–45. doi:10.1111/bjd.12020
62. Dauletbaev N, Eklove D, Mawji N, Iskandar M, Di Marco S, Gallouzi IE, et al. Down-regulation of cytokine-induced interleukin-8 requires inhibition of p38 mitogen-activated protein kinase (MAPK) via MAPK phosphatase 1-dependent and -independent mechanisms. *J Biol Chem* (2011) 286(18):15998–6007. doi:10.1074/jbc.M110.205724

63. King EM, Holden NS, Gong W, Rider CF, Newton R. Inhibition of NF-kappaB-dependent transcription by MKP-1: transcriptional repression by glucocorticoids occurring via p38 MAPK. *J Biol Chem* (2009) 284(39):26803–15. doi:10.1074/jbc.M109.028381
64. Kim I, Xu W, Reed JC. Cell death and endoplasmic reticulum stress: disease relevance and therapeutic opportunities. *Nat Rev Drug Discov* (2008) 7(12):1013–30. doi:10.1038/nrd2755
65. Park GB, Kim YS, Lee HK, Song H, Cho DH, Lee WJ, et al. Endoplasmic reticulum stress-mediated apoptosis of EBV-transformed B cells by cross-linking of CD70 is dependent upon generation of reactive oxygen species and activation of p38 MAPK and JNK pathway. *J Immunol* (2010) 185(12):7274–84. doi:10.4049/jimmunol.1001547
66. Yang G, Yang W, Wu L, Wang R. H2S, endoplasmic reticulum stress, and apoptosis of insulin-secreting beta cells. *J Biol Chem* (2007) 282(22):16567–76. doi:10.1074/jbc.M700605200
67. Koeberle A, Pergola C, Shindou H, Koeberle SC, Shimizu T, Laufer SA, et al. Role of p38 mitogen-activated protein kinase in linking stearoyl-CoA desaturase-1 activity with endoplasmic reticulum homeostasis. *FASEB J* (2015) 29(6):2439–49. doi:10.1096/fj.14-268474
68. Lanza A, Lanza M, Santoro R, Soro V, Prime SS, Cirillo N. Deregulation of PERK in the autoimmune disease pemphigus vulgaris occurs via IgG-independent mechanisms. *Br J Dermatol* (2011) 164(2):336–43. doi:10.1111/j.1365-2133.2010.10084.x
69. Lanza A, Cirillo N, Rossiello R, Rienzo M, Cutillo L, Casamassimi A, et al. Evidence of key role of Cdk2 overexpression in pemphigus vulgaris. *J Biol Chem* (2008) 283(13):8736–45. doi:10.1074/jbc.M702186200
70. Mao X, Li H, Sano Y, Gaestel M, Mo Park J, Payne AS. MAPKAP kinase 2 (MK2)-dependent and -independent models of blister formation in pemphigus vulgaris. *J Invest Dermatol* (2014) 134(1):68–76. doi:10.1038/jid.2013.224
71. Ito H, Iwamoto I, Inaguma Y, Takizawa T, Nagata K, Asano T, et al. Endoplasmic reticulum stress induces the phosphorylation of small heat shock protein, Hsp27. *J Cell Biochem* (2005) 95(5):932–41. doi:10.1002/jcb.20445
72. Sagi L, Sherer Y, Trau H, Shoenfeld Y. Pemphigus and infectious agents. *Autoimmun Rev* (2008) 8(1):33–5. doi:10.1016/j.autrev.2008.07.021
73. Li YX, Ren YL, Fu HJ, Zou L, Yang Y, Chen Z. Hepatitis B virus middle protein enhances IL-6 production via p38 MAPK/NF-kappaB pathways in an ER stress-dependent manner. *PLoS One* (2016) 11(7):e0159089. doi:10.1371/journal.pone.0159089

Conflict of Interest Statement: The authors declare that the research was conducted in the absence of any commercial or financial relationships that could be construed as a potential conflict of interest.

frontiers in Immunology

ORIGINAL RESEARCH
published: 14 August 2017
doi: 10.3389/fimmu.2017.00978

Cytokine and Chemokines Alterations in the Endemic Form of Pemphigus Foliaceus (Fogo Selvagem)

*Rodolfo Pessato Timóteo[1], Marcos Vinicius Silva[1], Djalma Alexandre Alves da Silva[1], Jonatas Da Silva Catarino[1], Fernando Henrique Canhoto Alves[2], Virmondes Rodrigues Júnior[1], Ana Maria Roselino[2], Helioswilton Sales-Campos[1] and Carlo José Freire Oliveira[1]**

[1]Laboratory of Immunology, Institute of Natural and Biological Sciences, Federal University of Triângulo Mineiro, Uberaba, Brazil, [2]Division of Dermatology, Department of Medical Clinics, Ribeirão Preto Medical School, University of São Paulo, Ribeirão Preto, Brazil

OPEN ACCESS

Edited by:
Heiko Mühl,
Goethe University Frankfurt, Germany

Reviewed by:
Robert Gniadecki,
University of Alberta, Canada
Ralf J. Ludwig,
University of Lübeck, Germany
Hiroshi Koga,
Kurume University School of Medicine, Japan

***Correspondence:**
Carlo José Freire Oliveira
carlo.oliveira@uftm.edu.br

Specialty section:
This article was submitted to Inflammation, a section of the journal Frontiers in Immunology

Received: 09 June 2017
Accepted: 31 July 2017
Published: 14 August 2017

Citation:
Timóteo RP, Silva MV, da Silva DAA, Catarino JDS, Alves FHC, Rodrigues Júnior V, Roselino AM, Sales-Campos H and Oliveira CJF (2017) Cytokine and Chemokines Alterations in the Endemic Form of Pemphigus Foliaceus (Fogo Selvagem). Front. Immunol. 8:978. doi: 10.3389/fimmu.2017.00978

Introduction: The endemic form (fogo selvagem—FS) of pemphigus foliaceus is an autoimmune disease characterized by the presence of IgG autoantibodies against desmoglein-1. Despite the array of findings, the role of chemokines and cytokines that dictate the immune response and disease outcome is still poorly investigated.

Materials and methods: Serum from 64 patients diagnosed with FS was used to draw and establish the levels of these molecules on this disease and establish the levels of these molecules with the severity of FS, and influence of treatment.

Results: In comparison to healthy subjects, FS patients, newly diagnosed and still without therapeutic intervention, had higher levels of IL-22 and CXCL-8, and reduced levels of IFN-γ, IL-2, IL-15, and CCL-11. Furthermore, treatment using immunosuppressant drugs augmented the production of IFN-γ, IL-2, CCL-5, and CCL-11 besides reducing the levels of IL-22 and CXCL-10. Immunosuppressive therapy seemed to have long-lasting effects on the production of higher amounts of IFN-γ, IL-2, and CCL-5, besides keeping lowered the levels of IL-22 in remission FS patients.

Conclusion: Taken together, our findings suggest a putative role of IL-22 in the pathogenesis of FS. Finally, data presented here may contribute for better understanding the immune aspects that control disease outcome.

Keywords: pemphigus foliaceus, fogo selvagem, IL-22, cytokines, chemokines, pathogenesis

INTRODUCTION

Pemphigus is a severe and rare autoimmune disease characterized by antibodies targeting desmosomal proteins that are crucial to mucosal and epidermal integrity. So far, two major types of pemphigus were described, pemphigus vulgaris and pemphigus foliaceus (PF), and in some cases, these diseases can be subcategorized or present variants (1). PF can be found in all continents, but its endemic form known as "fogo selvagem" (FS) is more frequently found in Brazil, where the disease is up to 20 times more frequent than in other committed countries such as Peru, Colombia, Algeria, and Tunisia (2). Particularly in Brazil, autoimmune blistering diseases, such as PF, are more frequently associated with black subjects living in rural areas (1, 3, 4).

Fogo selvagem shares clinical and immunopathological features to the non-endemic form and is characterized by the presence of pathogenic autoantibodies (primarily IgG4) against the desmoglein-1 (Dsg1), resulting in loss of organization between keratinocytes (acantholysis) that leads to the formation of intraepidermal vesicles (1, 5, 6). Despite the role of antibodies targeting desmoglein, several other aspects are associated with the complex pathogenesis and susceptibility of pemphigus. Increased levels of T helper-2 (Th2) cytokines such as IL-4, IL-10, and IL-13 were already shown to be involved in the production of IgG4 by B-lymphocytes in both PF and PV patients. Those patients also exhibited reduced levels of IL-2 and IFN-γ, resulting in suppressed expansion of Th1 lymphocytes, which suggests an inhibitory effect of Th2-cytokines, thus contributing to disease worsening (7).

Owing to the immune imbalance, pharmacological treatment of pemphigus, especially in underdeveloped and developing countries, is mainly based on immune modulatory and anti-inflammatory drugs such as glucocorticoids (GC). However, some patients are refractory or may present some side effects (8). This poor responsiveness could be related to elevated levels of the inflammatory cytokines IL-6 and TNF-α, which can induce GC resistance observed in peripheral blood mononuclear cells (PBMCs) isolated from pemphigus subjects (8). Furthermore, augmented levels of IL-10 and IL-12 concomitant to reduced levels of IL-2, IL-4, IL-5, and IFN-γ were found in PF patients without treatment, when compared to their control counterparts (9). On the other hand, PBMCs isolated from PF patients treated with GC, showed increased levels of both the inflammatory cytokine IL-1β or in the IL-5/IFN-γ, when compared to their healthy counterparts (10). Taken together, the few studies conducted so far only describe cytokines related to Th1 and Th2 pattern of immune response. In other words, these findings do not permit a clear definition of the entire immune aspects related to the onset, treatment, and remission of the disease.

In the last years, other cytokines such as IL-9, IL-17, and IL-22 have been implicated in the pathogenesis of inflammatory and autoimmune diseases affecting skin, such as psoriasis, for example (11, 12). IL-9 seems to act synergistically with IL-17 and IL-22, which can be related to disease worsening (12). Though skin diseases such as psoriasis can be associated with the development of pemphigus (13, 14), the latter still requires more clarification regarding cytokine interplay, immune profile, and the impact of treatment on disease outcome.

Thus, given the lack of data concerning the immune profile of FS patients in different clinical stages of disease as well as the impact of treatment in this context, this study aimed to elucidate the cytokine/chemokine interplay in those subjects.

MATERIALS AND METHODS

Patients

The study was conducted with patients from a hospital for blistering diseases located in Uberaba, state of Minas Gerais, Brazil, from January 2013 to December 2015. Serum from 64 patients diagnosed with FS was used in this study (**Table 1**; **Figure 1**). Samples were collected during the consultation of patients in different stages of treatment (before, during, and after treatment) in the hospital for blistering disease. For all patients, peripheral blood samples were collected by venipuncture in an EDTA-coated vacutainer tube (BD Biosciences, San Jose, CA, USA) and kept in ice until plasma separation (within 30 min). Blood was centrifuged at 1,000 × *g* for 10 min and plasma was aliquoted (0.5 ml per tube) and stored at 80°C until analysis. Among them, 9 did not receive treatment by the time they were diagnosed and samples were collected (untreated subjects), 45 were under treatment with immunosuppressant drugs (treated subjects) (Table S1 in Supplementary Material), and 10 remissive subjects were treated at least 1 year before samples were collected, did not display any features of disease activity nor were taking any further medication (post-treatment subjects). Treated subjects ($n = 45$) were further subcategorized in three groups (group I—29, II—6, and III—10 patients) according to the level of cutaneous lesions. The extension of cutaneous damage was assessed according to the Wallace's rule of nines (15). 39 subjects, age-matched, originated from the same areas without diagnosis of autoimmune, inflammatory or infectious diseases, neoplastic disorders, or allergies, composed the control group. Furthermore, none of the individuals from the control group had any familial case of pemphigus. Patients diagnosed with FS had clinical, pathological, and/or serological diagnosis. Informed consent was obtained for experimentation with all human subjects. The median age of FS patients in our study was 36 years old with no predominance of sex. The majority of patients were white or mulattoes (76.6%). The number of patients from urban area (40.6%) or from urban area with frequent contact with rural areas (51.6%) was higher than those living in rural area (7.8%) (**Table 1**).

All procedures were conducted in accordance with the Declaration of Helsinki, with full patient compliance and approved human practices as defined by the Ethics Committee for Human Experimentation of the Federal University of Triângulo Mineiro (UFTM), Uberaba, Minas Gerais, Brazil, protocol number 1.311.730.

TABLE 1 | Gender, skin color, and housing area of fogo selvagem patients and their control counterparts.

	Control	PF patients	*p* Value
Age (±SD years)	37.85 ± 13.75	37.73 ± 18.51	0.97[a]
Gender	17M/22F	32M/32F	0.2[b]
Skin color			
Mulattoes (*n*)	10	20	
White (*n*)	23	29	0.38[c]
Black (*n*)	6	15	
Housing area			
Urban area (*n*)	18	26	
Urban and rural areas (*n*)	15	33	0.55[c]
Rural area (*n*)	4	5	

[a]*Unpaired t test.*
[b]*Fisher's exact test.*
[c]*Chi-square test.*
n, number of individuals in each condition; PF, pemphigus foliaceus; M, male; F, female.

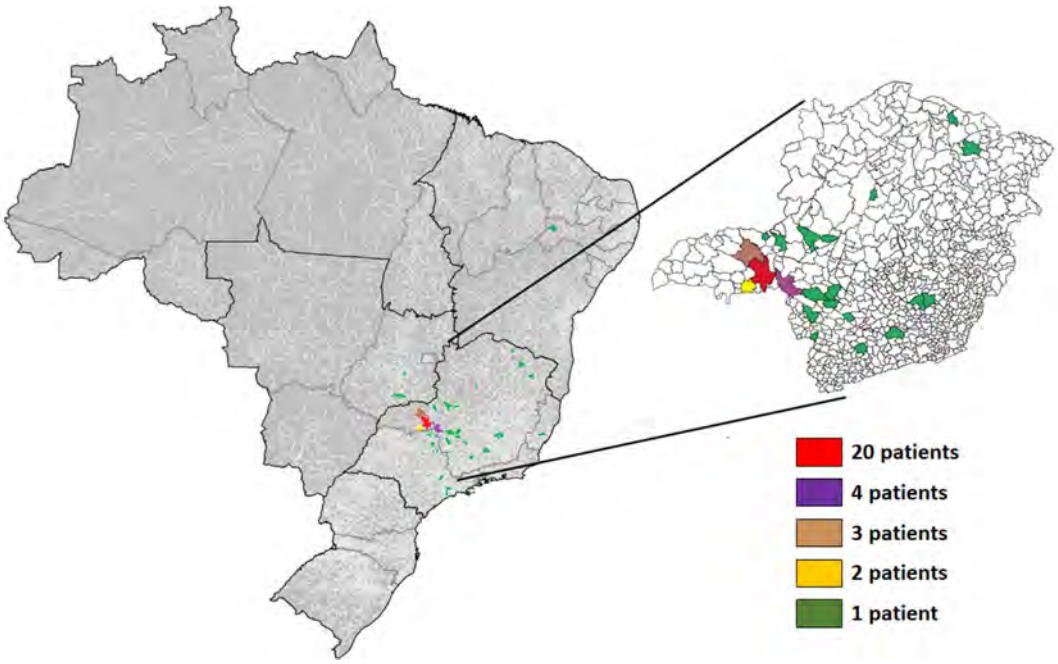

FIGURE 1 | Geographical distribution of patients with the endemic form (fogo selvagem) of pemphigus foliaceus. The respective colors represent the number of patients from each municipality. Highlight to the state of Minas Gerais.

Chemokine and Cytokine Production

The production of IL-1β, IL-5, IL-12, IL-13, IL-15, IL-22, IL-23, IL-33, CCL-10 (IP-10), CCL-2 (MCP-1), and CCL-11 (Eotaxin-1) was assessed in plasma using the enzyme-linked immunosorbent assay (R&D Systems®, San Diego, CA, USA), following the manufacturer's instructions. Cytometric Bead Array (BD Biosciences, San Jose, CA, USA) was used for simultaneous detection of TNF-α, IFN-γ, TGF-β, IL-2, IL-4, IL-6, IL-9, IL-10, IL-17A, CCL-5 (RANTES), CXCL-8 (IL-8), and CCL3 (MIP-1α).

Data Analysis and Statistics

For all variables, normal distribution and homogeneous variance were tested. The *D'Agostino-Pearson* test was used to assess normality for all variables. In cases of non-Gaussian distribution of data, the non-parametric Mann–Whitney test was applied. Multiple comparisons relating to the medians of values for more than two groups were made using the Kruskal–Wallis non-parametric test followed by Dunn's test. For correlations the Spearman test was used. The observed differences were considered significant when $p < 0.05$ (5%). Statistical analysis was performed using the Graphpad Prism software (GraphPad Software 6.0, La Jolla, CA, USA).

RESULTS

Cytokine and Chemokine Profile in Treated and Non-Treated Subjects

Because of the importance of cytokines and chemokines on different physiological and pathological aspects, and due to the lack of a more consistent data concerning the production of these molecules in FS patients, the level of cytokines and chemokines was assessed in untreated FS patients and their healthy control counterparts. Thus, FS patients had lower levels of IFN-γ (**Figures 2A,R**), IL-2 (**Figure 2H**), IL-15 (**Figure 2K**), and CCL-11 (**Figures 2P,R**) when compared to their control counterparts. On the other hand, the levels of IL-22 (**Figure 2G**) and CXCL-8/IL-8 (**Figures 2M,R**) were significantly elevated in FS patients. No differences were detected for the levels of IL-17 (**Figure 2B**), IL-6 (**Figure 2C**), IL-23 (**Figure 2D**), IL-5 (**Figure 2E**), IL-10 (**Figure 2F**), TNF-α (**Figure 2I**), IL-12 (**Figure 2J**), IL-33 (**Figure 2L**), CCL-2 (**Figure 2N**), CCL-5 (**Figure 2O**), and CXCL-10 (**Figure 2Q**). The following cytokines/chemokines were not detected: IL-13, TGF-β, IL-4, IL-9, and CCL3 (data not shown). These results suggest a complex interplay between cytokines and chemokines in the pathogenesis of FS.

The Relationship between Cytokines, Chemokines, and Disease Severity

To check for a relationship between disease severity and the levels of cytokines and chemokines, FS patients were stratified according to the extension of lesion (**Figure 3A**). The greater severity of disease, which means patients with more than 90% of compromised skin (group III), was associated with higher levels of IFN-γ (**Figure 3B**), IL-2 (**Figure 3C**), and CCL-5 (**Figure 3H**), when compared to the untreated patients. Furthermore, higher levels of IL-22 (**Figure 3G**) were also verified in group III, when compared to group I, and in untreated patients compared to group I. The greater severity of disease was also related to higher levels of IL-10

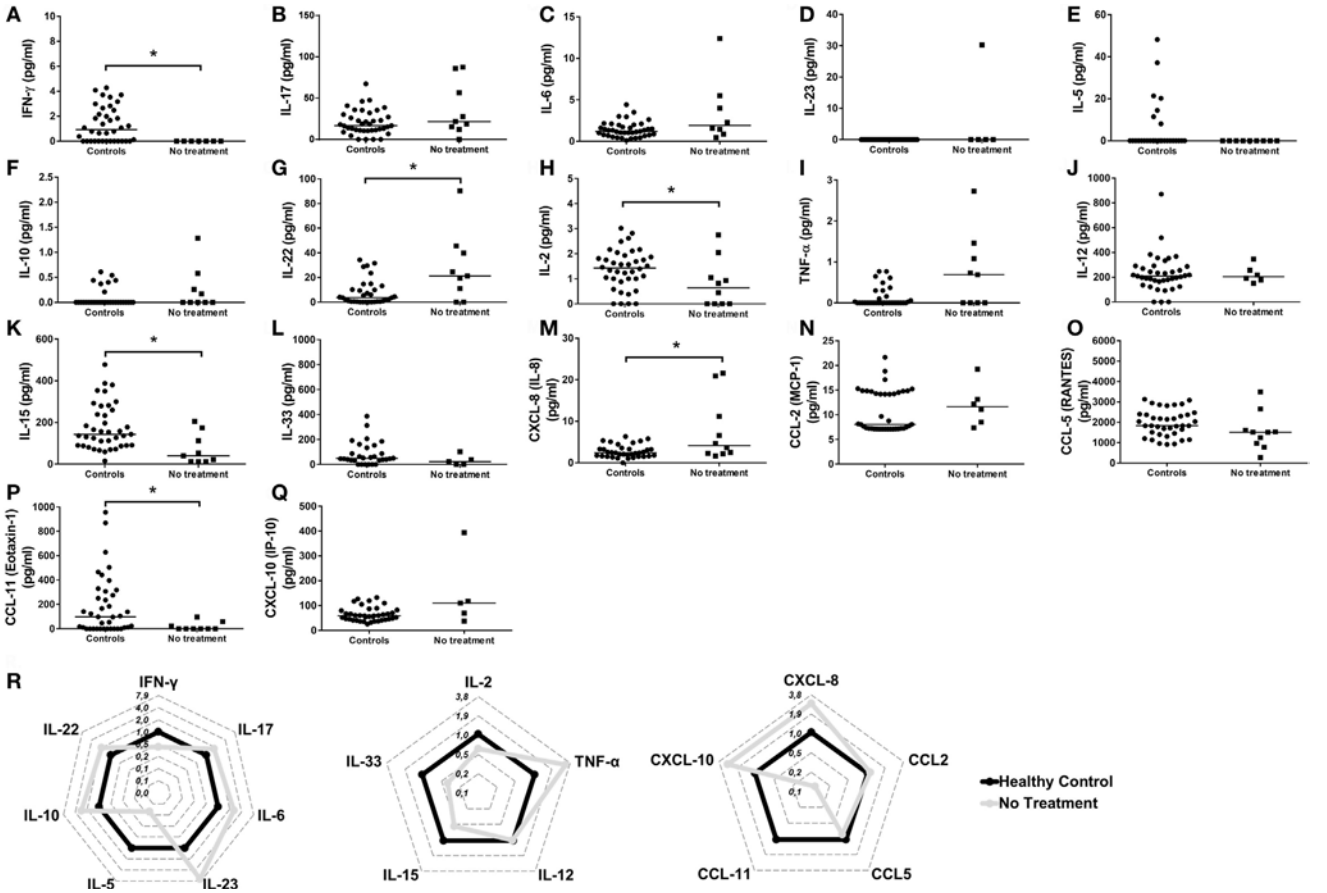

FIGURE 2 | Serum profile of cytokines and chemokines in the pathogenesis of the endemic form (fogo selvagem) of pemphigus foliaceus. Levels of **(A)** IFN-γ, **(B)** IL-17, **(C)** IL-6, **(D)** IL-23, **(E)** IL-5, **(F)** IL-10, **(G)** IL-22, **(H)** IL-2, **(I)** TNF-α, **(J)** IL-12, **(K)** IL-15, **(L)** IL-33, **(M)** CXCL-8/IL-8, **(N)** CCL-2/MCP-1, **(O)** CCL-5/RANTES, **(P)** CCL-11/eotaxin-1, and **(Q)** CXCL-10/IP-10 from healthy donors (controls) and untreated patients with the endemic form (fogo selvagem) of pemphigus foliaceus (no treatment). Lines represent median. *$p < 0.05$, Mann–Whitney test. **(R)** Radar plot representation of serum cytokine and chemokine profile. Lines highlight the fold change in cytokine levels in pemphigus foliaceus patients (gray line) in relation to healthy donors (black line). Data were obtained by calculating the ratio between the median concentration of each cytokine in the pemphigus foliaceus (fogo selvagem) group and in the healthy group.

when compared to group II and untreated patients (**Figure 3F**). No differences were registered for the levels of IL-6 (**Figure 3D**), CXCL-8/IL-8 (**Figure 3E**), and CCL-10/IP-10 (**Figure 3I**). The following cytokines/chemokines were not detected: TGF-β, IL-4, IL-9, IL-23, IL-13, and CCL3 (data not shown). These results pointed to an influence of severity of disease on cytokine and chemokine production in FS patients.

Cytokine and Chemokine Interplay after Treatment with Immunosuppressant Drugs

Next, to verify if immunosuppressant therapy may induce long-lasting effects on cytokine and chemokine levels, we evaluated the cytokine and chemokine levels in remissive patients and compared it with FS subjects before and during treatment with immunosuppressive therapy. Treatment induced and maintained the production of IFN-γ and IL-2 (**Figures 4A,H**, respectively). However, though the production of IL-33 (**Figures 4L,R**) and CCL-11 (**Figures 4P,R**) was induced by treatment, the higher levels of these molecules were not kept after withdrawal of therapy. The levels of the chemokine CCL-5 (**Figure 4O**) were higher in FS patients after treatment. The absence of treatment in FS patients was especially associated with higher levels of IL-22 (**Figures 4G,R**). No differences were observed between the conditions of treatment for the production of IL-17 (**Figure 4B**), IL-6 (**Figure 4C**), IL-23 (**Figure 4D**), IL-5 (**Figure 4E**), IL-10 (**Figure 4F**), TNF-α (**Figure 4I**), IL-12 (**Figure 4J**), IL-15 (**Figure 4K**), CXCL-8 (**Figure 4M**), CCL-2 (**Figure 4N**), and CCL-10/IP-10 (**Figures 4Q,R**). The following cytokines/chemokines were not detected: IL-13, TGF-β, IL-4, IL-9, and CCL3 (data not shown). These results suggest that immunosuppressant therapy may induce long-lasting effects on the production of cytokines and chemokines.

DISCUSSION

In recent years, some efforts have been made to elucidate the role of cytokines and chemokines in the pathogenesis of FS; however,

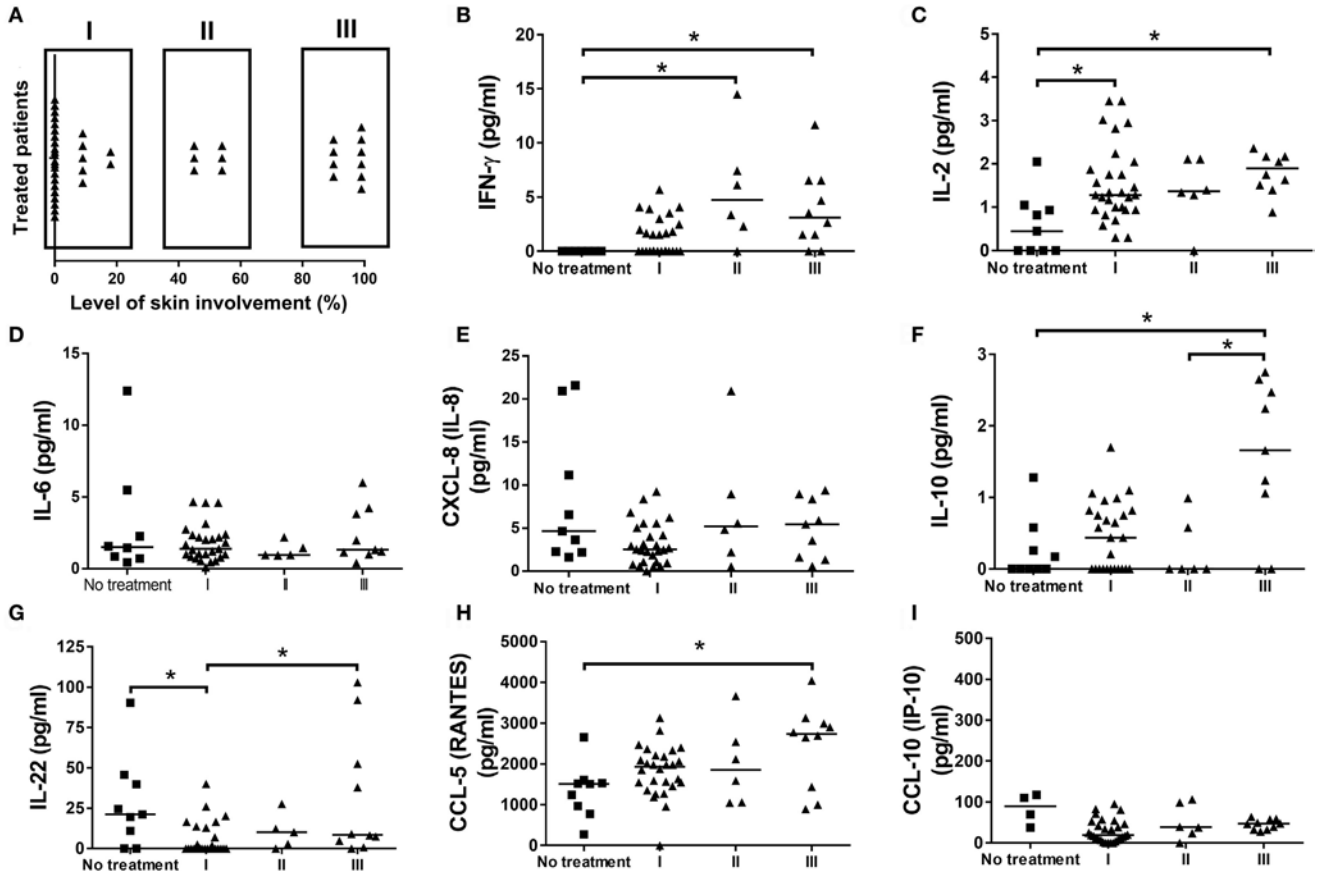

FIGURE 3 | The profile of cytokines, chemokines, and disease severity in patients with the endemic form of pemphigus foliaceus. **(A)** Stratification of fogo selvagem (FS) patients according to the extension of skin lesions. Levels of **(B)** IFN-γ, **(C)** IL-2, **(D)** IL-6, **(E)** IL-8, **(F)** IL-10, **(G)** IL-22, **(H)** CCL-5/RANTES, and **(I)** CCL-10/IP-10, from patients with the endemic form (FS) of pemphigus foliaceus without treatment (No treatment) compared to those taking immunosuppressive therapy with different degrees of lesions in skin (I-III). Lines represent median. *$p < 0.05$, Kruskal–Wallis test followed by Dunn's test.

the findings described so far are limited, and their implications in disease outcome were not fully elucidated yet. In our study, the plasma levels of over 17 cytokines and 6 chemokines were evaluated in FS patients. The results pointed to a putative role of IL-22 in the pathogenesis of FS, and to a supposed protective function of especially Th1-related cytokines and Th2 chemokines in serum.

The most affected regions in Brazil include the mid-western and the southeastern states, including Minas Gerais (3, 16), where the majority of patients analyzed in our study came from. Furthermore, FS has been primarily described as predominant over people from rural areas, being uncommonly described in urban areas (3). Since its first description, the etiology of FS has been mainly attributed to environmental triggers present in rural areas, which can be different based on geographical distribution and genetic inheritance (17, 18). Despite the description of FS as primarily found in rural areas, our study suggested an urbanization of this disease. This scenario could be at least partly attributed to the presence of strong environmental triggers in urban areas, including stress, lifestyle, and pollution, which were already described as potential triggers for other autoimmune diseases such as those affecting thyroid (19), systemic lupus erythematosus, and type 1 diabetes (20), for example. Additionally, the saliva of sand flies contains some components like LJM11, which is a salivary protein from the sand fly *Lutzomyia longipalpis* (21), able to cross-react to anti-Dsg1 monoclonal autoantibodies from FS patients. This phenomenon, in turn, induced a production of autoantibodies targeting Dsg1 in mice previously immunized with the salivary protein (1, 21, 22). Accordingly, the so-called "urbanization" of FS observed in our study, can be also attributed to changes in the behavior of the insects moving from sylvatic areas to urban areas as a consequence of social–environmental alterations (23, 24). Therefore, it is possible to consider the role of insect-derived saliva proteins, like LJM11, in the onset of a pathogenic response, leading to FS.

The complex interplay between cytokines and chemokines that dictates disease outcome in FS is still a matter of investigation. In our study, the comparison between healthy subjects and FS patients suggested a role of IL-22, and to a less extent IL-8, in the FS. Healthy subjects had higher levels of IFN-γ and IL-2. Similarly, elevated levels of IFN-γ and IL-2, along with a reduction in IL-22, were observed in FS patients under treatment or after treatment withdrawn, when compared to untreated patients. A different study, also pointed to a reduction in serum

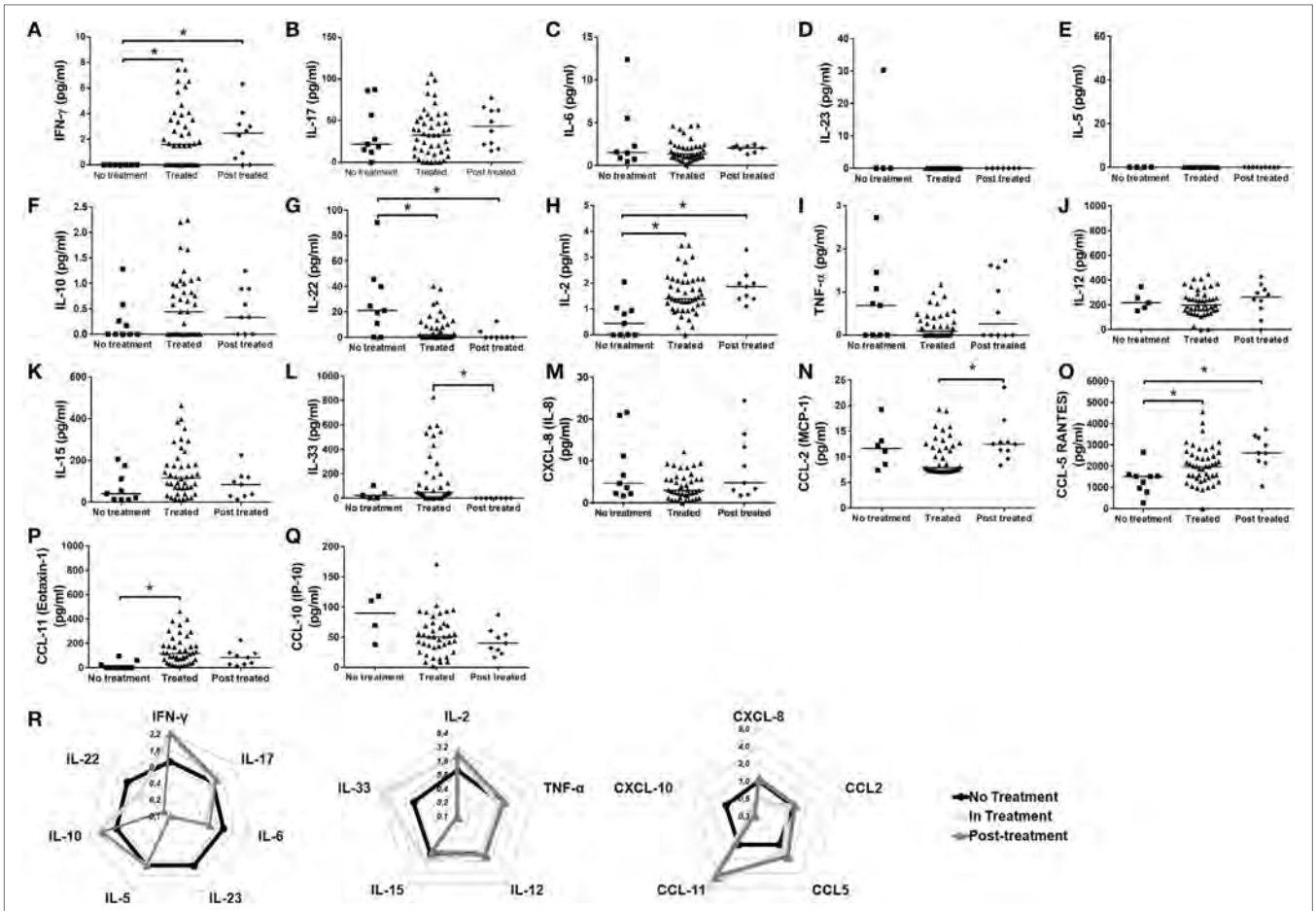

FIGURE 4 | Cytokine and chemokine interplay after treatment with immunosuppressant drugs. Levels of **(A)** IFN-γ, **(B)** IL-17, **(C)** IL-6, **(D)** IL-23, **(E)** IL-5, **(F)** IL-10, **(G)** IL-22, **(H)** IL-2, **(I)** TNF-α, **(J)** IL-12, **(K)** IL-15, **(L)** IL-33, **(M)** CXCL-8/IL-8, **(N)** CCL-2/MCP-1, **(O)** CCL-5/RANTES, **(P)** CCL-11/eotaxin-1, and **(Q)** CXCL-10/IP-10 from patients with the endemic form (fogo selvagem—FS) of pemphigus foliaceus under different conditions of treatment (no treatment, treated, and post-treatment). Lines represent median. *$p < 0.05$, Kruskal–Wallis test followed by Dunn's test. **(R)** Radar plot representation of serum cytokine and chemokine profile of not treated (black lines), in treatment (light gray) and post-treatment (dark gray) FS patients. Data were obtained by calculating the ratio between the median concentrations of each cytokine in the pemphigus foliaceus (FS) patients under- or post-treatment versus the untreated group.

of IL-2 and IFN-γ in FS patients when compared to their healthy control counterparts (9). Though in a different pemphigus entity, PV-treated patients also showed elevated levels of IFN-γ (25). Additionally, the inverse relationship between IL-22 and IFN-γ was described in patients with active psoriasis (26). IL-22 is especially produced by Th17 and Th22 cells (27) and is involved in several processes including the regulation of tissue cells in skin, kidney, pancreas, small intestine, liver, colon, and respiratory system (26). Despite the beneficial role of IL-22 in the aforementioned tissues, this cytokine, depending on the context, may present a pro-inflammatory role. For this reason, it has been implicated in the pathogenesis of different inflammatory skin disorders including atopic dermatitis (28), psoriasis (29) and systemic lupus erythematosus with skin manifestations (30). However, the participation of IL-22 in the pathogenesis of FS is still not elucidated and needs to be further explored. In skin, despite the absence of effect over skin fibroblasts, endothelial cells, and melanocytes, proliferation of keratinocytes, epidermal hyperplasia, and abrogated keratinocyte terminal differentiation are mediated by IL-22, mainly derived from Th22 cells (31). IL-22 has shown *in vitro*, great ability to downregulate key genes in keratinocyte differentiation, including loricrin, filaggrin, and involucrin, which resulted in striking acanthosis (32, 33). Because of the effect of IL-22 in skin, higher levels in both skin and serum have been related to disease worsening in patients with active psoriasis (34, 35). Even though psoriasis and PF are considered to be distinct entities, in some cases, they can occur together in the same patient. In these cases, PF has been developed in untreated or chronic psoriatic patients (36–42). However, we cannot exclude the participation of genetics in this context, the presence of HLA DRB1 alleles, which have been described to be related with both psoriasis (43) and PF/FS (44, 45), could possibly explain the concomitant occurrence of both diseases. Although we have not determined the presence of the HLA DRB1 alleles in our study, the importance of IL-22 in the pathogenesis of FS cannot be underestimated and needs to be further explored. Additionally, we cannot underestimate the importance of the balance between IL-22, IL-2, and IFN-γ, neither the role of IL-22, on disease onset

and progression. As we have pointed out here, in treated patients (even after treatment withdrawn), the opposite relationship between the higher levels of IL-2 and IFN-γ and lower levels of IL-22, appeared to be related to disease amelioration. We believe that in FS, IL-2 and IFN-γ may exert a protective role antagonizing the effects of IL-22.

Despite the crucial role of cytokines in the pathogenesis of FS, chemokines are also important players in this scenario. Our results pointed to higher levels of CXCL-8/IL-8 in FS patients. IL-8 is a chemokine produced during inflammatory stimulation, and its main function is to chemoatract and activate neutrophils (46). Though this chemokine is widely studied owing to its role in neutrophil recruitment and inflammation, data concerning the participation of IL-8 in the pathogenesis of FS still needs to be clarified. In a rare subset of pemphigus, known as pemphigus herpetiformis (PH), in which IgG autoantibodies targeting Dsg1 seems to be related to the development of disease, it was suggested that these autoantibodies were able to induce overexpression of IL-8 in keratinocytes (47). Cultured keratinocytes from these patients showed increased production and secretion of cytoplasmic IL-8 after stimulation with autoantibodies derived from PH patients (47), which reinforces the effect of autoantibodies targeting Dsg1 on the production of IL-8. Similarly, the blister formation in bullous pemphigoid was associated with higher levels in serum of IL-6 and IL-8 (48, 49). In contrast, in other subsets of pemphigus, pemphigus vulgaris, higher levels of IL-8 were observed in PV-treated patients (25). Although we have not investigated the relationship between the effects of autoantibodies targeting Dsg1 on the production of IL-8 in our study, we cannot exclude this possibility. Moreover, though not as important as IL-22, IL-8 seems also to be related to disease activity, and together with the former, may represent a potential target for new therapeutic approaches. However, such role of IL-22 and IL-8 in FS pathogenesis needs to be further clarified.

In our study, CCL-5/RANTES was induced and maintained by immunosuppressant drugs even after treatment withdrawn. However, its role in the development of FS is not fully explored. CCL-5 is a chemokine with strong capacity to recruit monocytes, T cells, and eosinophils, acting via the receptors CCR1, CCR3, and CCR5 (50). Its expression in other forms of pemphigus is controversial. Patients diagnosed with bullous pemphigoid, pemphigus, and dermatitis herpetiformis showed no differences for the presence of IL-8 and RANTES in the skin lesions (51) or in serum (52), when compared to their control counterparts. Interestingly, the higher levels of CCL-5, IFN-γ, and IL-2 found in treated patients in our study were followed by a reduction in IL-22. In patients with lung inflammation, higher levels of IL-22 were shown to be able to suppress IFN-γ-induced secretion of CCL-5 (53). The effects of immunosuppressant drugs like prednisone, one of the most prescribed therapies to treat FS, were shown to be involved in the reduction of IL-22 in patients with systemic lupus erythematosus (54). Therefore, we believe that immunosuppressive therapy influenced this balance, reducing the levels of IL-22, and thus favoring the production of IFN-γ-derived CCL-5. Nevertheless, the mechanisms behind this modulation were not explored in our study. Additionally, it is difficult to address the consistencies/inconsistencies between different subtypes of pemphigus. This is probably due to the distinctions in etiology, physiopathology, geographical area, incidence, and prevalence observed in each case.

We believe that our study is the most detailed and complete study on the effects of cytokines and chemokines in the pathogenesis of the endemic form (FS) of PF. Our results pointed to a putative role of IL-22 in the pathogenesis of FS, and to the importance of immunosuppressive therapy to reestablish the immune balance in FS patients. Ultimately, we believe that this study may provide a better knowledge of the cytokines and chemokines involved in disease outcome, besides suggesting IL-22 as a hypothetical target to be explored in future studies. Moreover, our study demonstrates, for the first time, the urbanization of the disease. These data are also important because future preventive decisions must take into account the environmental triggers in urban areas that may be related with the onset of the disease.

ETHICS STATEMENT

This study was carried out in strict accordance with the principles and guidelines adopted by the Declaration of Helsinki, with full patient compliance and approved human practices as defined by the Ethics Committee for Human Experimentation of the Federal University of Triângulo Mineiro (UFTM), Uberaba, Minas Gerais, Brazil, protocol number 1.300.898.

AUTHOR CONTRIBUTIONS

RT, MS, FA, VJR, AR, HS-C, and CO conceived and designed the experiments; RT, HS-C, and CO wrote the paper with the assistance of all the authors. RT, MS, DS, JC, and HS-C performed the experiments. RT, MS, DS, JC, FA, VJR, AR, HS-C, and CO analyzed the data. RT, MS, DS, JC, FA, VJR, AR, HS-C, and CO provided critical review for important intellectual content. The final version of the manuscript was approved by all authors.

FUNDING

This study was supported by *Fundação de Amparo à Pesquisa do Estado de Minas Gerais* (*FAPEMIG*), *Coordenação de Aperfeiçoamento de Pessoal de Nível Superior* (*CAPES*), and *Conselho Nacional de Desenvolvimento Científico e Tecnológico* [grant number: 150075/2016-2]. The funding sources had no involvement in study design; in the collection, analysis, and interpretation of data; in the writing of the report; and in the decision to submit the article for publication.

SUPPLEMENTARY MATERIAL

The Supplementary Material for this article can be found online at http://journal.frontiersin.org/article/10.3389/fimmu.2017.00978/full#supplementary-material.

REFERENCES

1. Aoki V, Rivitti EA, Diaz LA; Cooperative Group on Fogo Selvagem Research. Update on fogo selvagem, an endemic form of pemphigus foliaceus. *J Dermatol* (2015) 42:18–26. doi:10.1111/1346-8138.12675
2. Alpsoy E, Akman-Karakas A, Uzun S. Geographic variations in epidemiology of two autoimmune bullous diseases: pemphigus and bullous pemphigoid. *Arch Dermatol Res* (2015) 307:291–8. doi:10.1007/s00403-014-1531-1
3. Diaz LA, Sampaio SA, Rivitti EA, Martins CR, Cunha PR, Lombardi C, et al. Endemic pemphigus foliaceus (fogo selvagem): II. Current and historic epidemiologic studies. *J Invest Dermatol* (1989) 92:4–12. doi:10.1111/1523-1747.ep13070394
4. Silvestre MC, Netto JCA. Endemic pemphigus foliaceus: social and demographical characteristics and incidence in the microregions of Goias, based on patients seen at the Tropical Diseases Hospital, Goiania-Goias. *An Bras Dermatol* (2005) 80:261–6. doi:10.1590/S0365-05962005000300006
5. Oliveira LA, Marquart-Filho A, Trevilato G, Timoteo RP, Mukai M, Roselino AM, et al. Anti-desmoglein 1 and 3 autoantibody levels in endemic pemphigus foliaceus and pemphigus vulgaris from Brazil. *Clin Lab* (2016) 62:1209–16. doi:10.7754/Clin.Lab.2015.150628
6. Ludwig RJ, Vanhoorelbeke K, Leypoldt F, Kaya Z, Bieber K, McLachlan SM, et al. Mechanisms of autoantibody-induced pathology. *Front Immunol* (2017) 8:603. doi:10.3389/fimmu.2017.00603
7. Satyam A, Khandpur S, Sharma VK, Sharma A. Involvement of T(H)1/T(H)2 cytokines in the pathogenesis of autoimmune skin disease-pemphigus vulgaris. *Immunol Invest* (2009) 38:498–509. doi:10.1080/08820130902943097
8. Chriguer RS, Roselino AM, de Castro M. Glucocorticoid sensitivity and proinflammatory cytokines pattern in pemphigus. *J Clin Immunol* (2012) 32:786–93. doi:10.1007/s10875-012-9679-y
9. Zeoti DM, Figueiredo JF, Chiossi MP, Roselino AM. Serum cytokines in patients with Brazilian pemphigus foliaceus (fogo selvagem). *Braz J Med Biol Res* (2000) 33:1065–8. doi:10.1590/S0100-879X2000000900012
10. Rocha-Rodrigues DB, Paschoini G, Pereira SA, dos Reis MA, Teixeira Vde P, Rodrigues Junior V. High levels of interleukin-1 in patients with endemic pemphigus foliaceus. *Clin Diagn Lab Immunol* (2003) 10:741–3. doi:10.1128/CDLI.10.5.741-743.2003
11. Singh TP, Schon MP, Wallbrecht K, Gruber-Wackernagel A, Wang XJ, Wolf P. Involvement of IL-9 in Th17-associated inflammation and angiogenesis of psoriasis. *PLoS One* (2013) 8:e51752. doi:10.1371/journal.pone.0051752
12. Mabuchi T, Takekoshi T, Hwang ST. Epidermal CCR6+ gammadelta T cells are major producers of IL-22 and IL-17 in a murine model of psoriasiform dermatitis. *J Immunol* (2011) 187:5026–31. doi:10.4049/jimmunol.1101817
13. Grattan C. Evidence of an association between bullous pemphigoid and psoriasis. *Br J Dermatol* (1985) 113:281–3. doi:10.1111/j.1365-2133.1985.tb02079.x
14. Tsai TF, Wang TS, Hung ST, Tsai PI, Schenkel B, Zhang M, et al. Epidemiology and comorbidities of psoriasis patients in a national database in Taiwan. *J Dermatol Sci* (2011) 63:40–6. doi:10.1016/j.jdermsci.2011.03.002
15. Hettiaratchy S, Papini R. Initial management of a major burn: II – Assessment and resuscitation. *BMJ* (2004) 329:101–3. doi:10.1136/bmj.329.7457.101
16. Hans-Filho G, dos Santos V, Katayama JH, Aoki V, Rivitti EA, Sampaio SA, et al. An active focus of high prevalence of fogo selvagem on an Amerindian reservation in Brazil. Cooperative Group on Fogo Selvagem Research. *J Invest Dermatol* (1996) 107:68–75. doi:10.1111/1523-1747.ep12298213
17. Empinotti JC, Aoki V, Filgueira A, Sampaio SA, Rivitti EA, Sanches JA Jr, et al. Clinical and serological follow-up studies of endemic pemphigus foliaceus (fogo selvagem) in Western Parana, Brazil (2001–2002). *Br J Dermatol* (2006) 155:446–50. doi:10.1111/j.1365-2133.2006.07302.x
18. Sampaio SA, Rivitti EA, Aoki V, Diaz LA. Brazilian pemphigus foliaceus, endemic pemphigus foliaceus, or fogo selvagem (wild fire). *Dermatol Clin* (1994) 12:765–76.
19. Brent GA. Environmental exposures and autoimmune thyroid disease. *Thyroid* (2010) 20:755–61. doi:10.1089/thy.2010.1636
20. Schmidt CW. Questions persist: environmental factors in autoimmune disease. *Environ Health Perspect* (2011) 119:A249–53. doi:10.1289/ehp.119-a248
21. Qian Y, Jeong JS, Maldonado M, Valenzuela JG, Gomes R, Teixeira C, et al. Cutting edge: Brazilian pemphigus foliaceus anti-desmoglein 1 autoantibodies cross-react with sand fly salivary LJM11 antigen. *J Immunol* (2012) 189:1535–9. doi:10.4049/jimmunol.1200842
22. Qian Y, Jeong JS, Abdeladhim M, Valenzuela JG, Aoki V, Hans-Filhio G, et al. IgE anti-LJM11 sand fly salivary antigen may herald the onset of fogo selvagem in endemic Brazilian regions. *J Invest Dermatol* (2015) 135:913–5. doi:10.1038/jid.2014.430
23. Desjeux P. The increase in risk factors for leishmaniasis worldwide. *Trans R Soc Trop Med Hyg* (2001) 95:239–43. doi:10.1016/S0035-9203(01)90223-8
24. Harhay MO, Olliaro PL, Costa DL, Costa CH. Urban parasitology: visceral leishmaniasis in Brazil. *Trends Parasitol* (2011) 27:403–9. doi:10.1016/j.pt.2011.04.001
25. Timoteo RP, da Silva MV, Miguel CB, Silva DA, Catarino JD, Rodrigues Junior V, et al. Th1/Th17-related cytokines and chemokines and their implications in the pathogenesis of pemphigus vulgaris. *Mediators Inflamm* (2017) 2017:7151285. doi:10.1155/2017/7151285
26. Wolk K, Kunz S, Witte E, Friedrich M, Asadullah K, Sabat R. IL-22 increases the innate immunity of tissues. *Immunity* (2004) 21:241–54. doi:10.1016/j.immuni.2004.07.007
27. Trifari S, Kaplan CD, Tran EH, Crellin NK, Spits H. Identification of a human helper T cell population that has abundant production of interleukin 22 and is distinct from T(H)-17, T(H)1 and T(H)2 cells. *Nat Immunol* (2009) 10:864–71. doi:10.1038/ni.1770
28. Nograles KE, Zaba LC, Shemer A, Fuentes-Duculan J, Cardinale I, Kikuchi T, et al. IL-22-producing "T22" T cells account for upregulated IL-22 in atopic dermatitis despite reduced IL-17-producing TH17 T cells. *J Allergy Clin Immunol* (2009) 123:1244–52.e2. doi:10.1016/j.jaci.2009.03.041
29. Benham H, Norris P, Goodall J, Wechalekar MD, FitzGerald O, Szentpetery A, et al. Th17 and Th22 cells in psoriatic arthritis and psoriasis. *Arthritis Res Ther* (2013) 15:R136. doi:10.1186/ar4317
30. Yang XY, Wang HY, Zhao XY, Wang LJ, Lv QH, Wang QQ. Th22, but not Th17 might be a good index to predict the tissue involvement of systemic lupus erythematosus. *J Clin Immunol* (2013) 33:767–74. doi:10.1007/s10875-013-9878-1
31. Wolk K, Haugen HS, Xu W, Witte E, Waggie K, Anderson M, et al. IL-22 and IL-20 are key mediators of the epidermal alterations in psoriasis while IL-17 and IFN-gamma are not. *J Mol Med (Berl)* (2009) 87:523–36. doi:10.1007/s00109-009-0457-0
32. Sa SM, Valdez PA, Wu J, Jung K, Zhong F, Hall L, et al. The effects of IL-20 subfamily cytokines on reconstituted human epidermis suggest potential roles in cutaneous innate defense and pathogenic adaptive immunity in psoriasis. *J Immunol* (2007) 178:2229–40. doi:10.4049/jimmunol.178.11.7487-a
33. Boniface K, Bernard FX, Garcia M, Gurney AL, Lecron JC, Morel F. IL-22 inhibits epidermal differentiation and induces proinflammatory gene expression and migration of human keratinocytes. *J Immunol* (2005) 174:3695–702. doi:10.4049/jimmunol.174.6.3695
34. Boniface K, Guignouard E, Pedretti N, Garcia M, Delwail A, Bernard FX, et al. A role for T cell-derived interleukin 22 in psoriatic skin inflammation. *Clin Exp Immunol* (2007) 150:407–15. doi:10.1111/j.1365-2249.2007.03511.x
35. Wolk K, Witte E, Warszawska K, Schulze-Tanzil G, Witte K, Philipp S, et al. The Th17 cytokine IL-22 induces IL-20 production in keratinocytes: a novel immunological cascade with potential relevance in psoriasis. *Eur J Immunol* (2009) 39:3570–81. doi:10.1002/eji.200939687
36. Lee CW, Ro YS, Kim JH, Kim JH. Concurrent development of pemphigus foliaceus and psoriasis. *Int J Dermatol* (1985) 24:316–7. doi:10.1111/j.1365-4362.1985.tb05792.x
37. Tomasini D, Cerri A, Cozzani E, Berti E. Development of pemphigus foliaceus in a patient with psoriasis: a simple coincidence? *Eur J Dermatol* (1998) 8:56–9.
38. Perez GL, Agger WA, Abellera RM, Dahlberg P. Pemphigus foliaceus coexisting with IgA nephropathy in a patient with psoriasis vulgaris. *Int J Dermatol* (1995) 34:794–6. doi:10.1111/j.1365-4362.1995.tb04400.x
39. Yokoo M, Oka D, Ueki H. Coexistence of psoriasis vulgaris and pemphigus foliaceus. *Dermatologica* (1989) 179:222–3. doi:10.1159/000248369
40. Giomi B, Cardinali C, Pestelli E, Caproni M, Fabbri P. Pemphigus foliaceus developing on pre-existing psoriasis: a supposed pathogenetic linkage. *Acta Derm Venereol* (2004) 84:82–3. doi:10.1080/00015550310020567

41. Lee CW, Ro YS. Pemphigus developed on preexisting dermatoses. *J Dermatol* (1994) 21:213–5. doi:10.1111/j.1346-8138.1994.tb01724.x
42. Kwon HH, Kwon IH, Chung JH, Youn JI. Pemphigus foliaceus associated with psoriasis during the course of narrow-band UVB therapy: a simple coincidence? *Ann Dermatol* (2011) 23:S281–4. doi:10.5021/ad.2011.23.S3.S281
43. Cardoso CB, Uthida-Tanaka AM, Magalhaes RF, Magna LA, Kraemer MH. Association between psoriasis vulgaris and MHC-DRB, -DQB genes as a contribution to disease diagnosis. *Eur J Dermatol* (2005) 15:159–63.
44. Pavoni DP, Roxo VM, Marquart Filho A, Petzl-Erler ML. Dissecting the associations of endemic pemphigus foliaceus (fogo selvagem) with HLA-DRB1 alleles and genotypes. *Genes Immun* (2003) 4:110–6. doi:10.1038/sj.gene.6363939
45. Brochado MJ, Nascimento DF, Campos W, Deghaide NH, Donadi EA, Roselino AM. Differential HLA class I and class II associations in pemphigus foliaceus and pemphigus vulgaris patients from a prevalent Southeastern Brazilian region. *J Autoimmun* (2016) 72:19–24. doi:10.1016/j.jaut.2016.04.007
46. Xie K. Interleukin-8 and human cancer biology. *Cytokine Growth Factor Rev* (2001) 12:375–91. doi:10.1016/S1359-6101(01)00016-8
47. O'Toole EA, Mak LL, Guitart J, Woodley DT, Hashimoto T, Amagai M, et al. Induction of keratinocyte IL-8 expression and secretion by IgG autoantibodies as a novel mechanism of epidermal neutrophil recruitment in a pemphigus variant. *Clin Exp Immunol* (2000) 119:217–24. doi:10.1046/j.1365-2249.2000.01104.x
48. Inaoki M, Takehara K. Increased serum levels of interleukin (IL)-5, IL-6 and IL-8 in bullous pemphigoid. *J Dermatol Sci* (1998) 16:152–7. doi:10.1016/S0923-1811(97)00044-3
49. Schmidt E, Reimer S, Kruse N, Jainta S, Brocker EB, Marinkovich MP, et al. Autoantibodies to BP180 associated with bullous pemphigoid release interleukin-6 and interleukin-8 from cultured human keratinocytes. *J Invest Dermatol* (2000) 115:842–8. doi:10.1046/j.1523-1747.2000.00141.x
50. Schall TJ, Bacon K, Toy KJ, Goeddel DV. Selective attraction of monocytes and T lymphocytes of the memory phenotype by cytokine RANTES. *Nature* (1990) 347:669–71. doi:10.1038/347669a0
51. Bornscheuer E, Zillikens D, Schroder JM, Sticherling M. Lack of expression of interleukin 8 and RANTES in autoimmune bullous skin diseases. *Dermatology* (1999) 198:118–21. doi:10.1159/000018085
52. Nakashima H, Fujimoto M, Asashima N, Watanabe R, Kuwano Y, Yazawa N, et al. Serum chemokine profile in patients with bullous pemphigoid. *Br J Dermatol* (2007) 156:454–9. doi:10.1111/j.1365-2133.2006.07601.x
53. Pennino D, Bhavsar PK, Effner R, Avitabile S, Venn P, Quaranta M, et al. IL-22 suppresses IFN-gamma-mediated lung inflammation in asthmatic patients. *J Allergy Clin Immunol* (2013) 131:562–70. doi:10.1016/j.jaci.2012.09.036
54. Lin J, Yue LH, Chen WQ. Decreased plasma IL-22 levels and correlations with IL-22-producing T helper cells in patients with new-onset systemic lupus erythematosus. *Scand J Immunol* (2014) 79:131–6. doi:10.1111/sji.12135

Conflict of Interest Statement: The authors declare that the research was conducted in the absence of any commercial or financial relationships that could be construed as a potential conflict of interest.

Advantages of publishing in Frontiers

OPEN ACCESS
Articles are free to read for greatest visibility and readership

FAST PUBLICATION
Around 90 days from submission to decision

HIGH QUALITY PEER-REVIEW
Rigorous, collaborative, and constructive peer-review

TRANSPARENT PEER-REVIEW
Editors and reviewers acknowledged by name on published articles

Frontiers
Avenue du Tribunal-Fédéral 34
1005 Lausanne | Switzerland

Visit us: www.frontiersin.org
Contact us: info@frontiersin.org | +41 21 510 17 00

REPRODUCIBILITY OF RESEARCH
Support open data and methods to enhance research reproducibility

DIGITAL PUBLISHING
Articles designed for optimal readership across devices

FOLLOW US
@frontiersin

IMPACT METRICS
Advanced article metrics track visibility across digital media

EXTENSIVE PROMOTION
Marketing and promotion of impactful research

LOOP RESEARCH NETWORK
Our network increases your article's readership